Y 3. At 7: 16/19-11

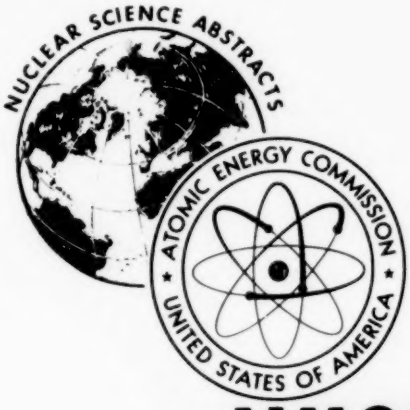

NUCLEAR SCIENCE ABSTRACTS

JUN 28 1965

Volume 19 Number 11

Abstracts 19455–21785

June 15, 1965

UNITED STATES ATOMIC ENERGY COMMISSION
Division of Technical Information

MIAMI UNIVERSITY LIBRARY

USAEC DEPOSITORY LIBRARIES

Collections of USAEC reports are maintained in the libraries of the organizations listed below for reference use by the general public. Facilities for making photocopies are available. The USAEC also makes available through these libraries atomic energy reports of countries other than the U. S. that are abstracted in *Nuclear Science Abstracts*.

ALABAMA
Auburn, Auburn University
Birmingham, Public Library

ARIZONA
Tucson, University of Arizona

ARKANSAS
Fayetteville, University of Arkansas

CALIFORNIA
Berkeley, University of California
Davis, University of California
Los Angeles, University of California
San Diego, Public Library
Stanford, Stanford University

COLORADO
Boulder, University of Colorado
Denver, Public Library

CONNECTICUT
New Haven, Yale University

DELAWARE
Newark, University of Delaware

DISTRICT OF COLUMBIA
Washington, Library of Congress

FLORIDA
Coral Gables, University of Miami
Gainesville, University of Florida

GEORGIA
Atlanta, Georgia Institute of Technology

HAWAII
Honolulu, University of Hawaii

ILLINOIS
Chicago, John Crerar Library
Chicago, University of Chicago
Evanston, Northwestern University
Urbana, University of Illinois

INDIANA
Bloomington, Indiana University
Lafayette, Purdue University

IOWA
Ames, Iowa State University

KANSAS
Manhattan, Kansas State University

KENTUCKY
Lexington, University of Kentucky
Louisville, University of Louisville

LOUISIANA
Baton Rouge, Louisiana State University
New Orleans, Tulane University

MARYLAND
Baltimore, Johns Hopkins University
College Park, University of Maryland

MASSACHUSETTS
Cambridge, Harvard University
Cambridge, Massachusetts Institute of Technology

MICHIGAN
Ann Arbor, University of Michigan
Detroit, Public Library
East Lansing, Michigan State University

MINNESOTA
Minneapolis, University of Minnesota

MISSISSIPPI
State College, Mississippi State University

MISSOURI
Kansas City, Linda Hall Library
Rolla, University of Missouri School of Mines and Metallurgy
St. Louis, Washington University

MONTANA
Bozeman, Montana State College

NEVADA
Las Vegas, Nevada Southern University
Reno, University of Nevada

NEW JERSEY
Princeton, Princeton University
Teaneck, Fairleigh Dickinson University

NEW MEXICO
Albuquerque, University of New Mexico

NEW YORK
Albany, The University of the State of New York
Buffalo, State University of New York at Buffalo
Ithaca, Cornell University
New York, Atomic Industrial Forum, Inc.
New York, Columbia University
New York, New York University
Rochester, University of Rochester
Schenectady, Union College
Syracuse, Syracuse University
Troy, Rensselaer Polytechnic Institute

NORTH CAROLINA
Charlotte, Public Library of Charlotte and Mecklenburg County
Durham, Duke University
Raleigh, North Carolina State College

NORTH DAKOTA
Grand Forks, University of North Dakota

OHIO
Cincinnati, University of Cincinnati
Cleveland, Public Library

OHIO (CONT.)
Columbus, Ohio State University
Toledo, University of Toledo
Youngstown, Youngstown University

OKLAHOMA
Norman, University of Oklahoma
Stillwater, Oklahoma State University

OREGON
Corvallis, Oregon State University
Portland, Reed College

PENNSYLVANIA
Philadelphia, University of Pennsylvania
Pittsburgh, Carnegie Library
University Park, Pennsylvania State University

PUERTO RICO
Rio Piedras, University of Puerto Rico

RHODE ISLAND
Providence, Brown University

SOUTH CAROLINA
Columbia, University of South Carolina

TENNESSEE
Knoxville, University of Tennessee
Memphis, Public Library
Nashville, Joint University Libraries
Oak Ridge, Oak Ridge Institute of Nuclear Studies

TEXAS
Austin, University of Texas
College Station, Texas A & M University
Dallas, Southern Methodist University
Houston, Rice University
Lubbock, Texas Technological College
San Antonio, Public Library

UTAH
Salt Lake City, University of Utah

VIRGINIA
Blacksburg, Virginia Polytechnic Institute
Charlottesville, University of Virginia
Norfolk, Old Dominion College

WASHINGTON
Pullman, Washington State University
Seattle, University of Washington

WEST VIRGINIA
Morgantown, West Virginia University

WISCONSIN
Madison, University of Wisconsin
Milwaukee, Public Library

WYOMING
Laramie, University of Wyoming

Volume 19, Number 11, June 15, 1965

NUCLEAR SCIENCE ABSTRACTS

A semimonthly publication of the USAEC Division of Technical Information, Edward J. Brunenkant, Director.
Published by the USAEC Division of Technical Information Extension, Robert L. Shannon, Extension Manager.

Nuclear Science Abstracts covers the international literature on nuclear science and technology and provides the only comprehensive abstracting and indexing of this body of information. Published twice each month since 1947, *NSA* covers technical reports of the U. S. Atomic Energy Commission and its contractors, technical reports of U. S. Government agencies and other governments, universities, industrial and research organizations, as well as patents, books, and journal literature on a world-wide basis. Nearly 300,000 abstracts have appeared in *NSA* through Volume 18. The subject matter covered in *NSA* is described in issue Number 1 and in TID-4552, *Subject Scope of Nuclear Science Abstracts*, available free from the U. S. Atomic Energy Commission, Division of Technical Information Extension, P. O. Box 62, Oak Ridge, Tennessee 37831.

Abstracts are arranged according to a number of subject categories and subcategories. Definitions of categories appear in issues Number 1 and 13. If the language of the original item is not English, the language will be indicated. Translations are not abstracted where an abstract of the original item has appeared in *NSA*.

INDEXES TO NSA

Corporate author, personal author, subject, and report number indexes appear in each issue and are cumulated quarterly, semiannually, and annually. At the end of Volume 19, report number indexes will be cumulated in two separate publications. Indexes for Vols. 1–15 will be reissued with the latest public availability known at that time. This index will not be reissued. Indexes for Vols. 16–19 will be cumulated as a separate issuance and will be reissued annually to include all volumes beginning with Volume 16.

AVAILABILITY OF PUBLICATIONS ABSTRACTED

The public availability of all U. S. Atomic Energy Commission reports is indicated in the report number indexes. The availability of other reports, when known, is also indicated. The availability of some unnumbered reports is given in the abstract.

Dissertations abstracted in *Dissertation Abstracts* and included in *NSA* are available from University Microfilms, Inc., 315 N. First Street, Ann Arbor, Michigan.

Most of the published literature abstracted in *NSA* is on deposit at the Oak Ridge Institute of Nuclear Studies Library, Oak Ridge, Tennessee, (a USAEC depository library) and is available through interlibrary loan. When requesting papers from this source, it is important that *NSA* volume and abstract number be cited.

HOW TO OBTAIN NUCLEAR SCIENCE ABSTRACTS

NSA is available on an exchange basis to universities, research institutions, industrial firms, and publishers of scientific information. Inquiries should be directed to the U. S. Atomic Energy Commission, Division of Technical Information Extension, P. O. Box 62, Oak Ridge, Tennessee 37831.

Government agencies may obtain *NSA* free of charge.

NSA is available to the general public on a subscription basis from the Superintendent of Documents, U. S. Government Printing Office, Washington, D. C. 20402, as follows:

For the 24 regular issues, $30.00 domestic, $37.00 foreign. A single issue costs $1.75, plus 25 per cent for foreign mailing. Domestic rates apply to the United States, Canada, Mexico, and Central and South American countries except Argentina, Brazil, British and French Guiana, Surinam, and British Honduras. Foreign rates apply to the countries excepted above and to all other countries throughout the world.

For the quarterly, semiannual, and annual indexes, $22.00 domestic, $25.00 foreign.

Multivolume subject and author indexes are available as follows:

Vols. 1–4 (1948–1950) Johnson Reprint Corporation, 111 Fifth Avenue, New York, N. Y. 10003, $30.00.

Vols. 5–10 (1951–1956) Superintendent of Documents, U. S. Government Printing Office, Washington, D. C. 20402, $5.25.

Vols. 11–15, Subjects, Superintendent of Documents, U. S. Government Printing Office, Washington, D. C. 20402, $19.00.

Vols. 11–15, Personal Authors, Superintendent of Documents, U. S. Government Printing Office, Washington, D. C. 20402, $14.25.

Vols. 11–15, Corporate Authors, Superintendent of Documents, U. S. Government Printing Office, Washington, D. C. 20402, $2.50.

Cumulative Report Number Index, Vols. 1–18, is available from the Superintendent of Documents, U. S. Government Printing Office, Washington, D. C. 20402, $5.75.

Annual Indexes are available separately from the U. S. Government Printing Office as follows:

Vol. 16, Subject and Authors, $9.75.
Vol. 17, Subject and Authors, $12.25.
Vol. 18, Subject and Authors, $12.50.

ACKNOWLEDGMENTS

Agreements between the United States Atomic Energy Commission and the following organizations with regard to providing continuing services and specific literature coverage for *Nuclear Science Abstracts* are gratefully acknowledged:

American Institute of Physics; Atomic Energy of Canada Limited; Atomic Energy Research Establishment, United Kingdom; European Atomic Energy Community (EURATOM); Gmelin Institute; International Atomic Energy Agency; Japan Atomic Energy Bureau — Japan Atomic Energy Research Institute; Netherlands Patent Office; Reactor Centrum Nederland.

TABLE OF CONTENTS

Volume 19, Number 11, June 15, 1965

Category	Page
BIOLOGY AND MEDICINE	2377
General	2377
Ecology	2378
Metabolism, Tissue Distribution, and Toxicology	2378
Radiation Effects	2382
Radiation Effects Therapy and Countermeasures	2400
Radiation Hazards and Protection	2405
Radiotherapy and Radiodiagnosis	2406
CHEMISTRY	2420
General	2420
Analytical Procedures	2420
Inorganic and Physical Chemistry	2430
Organic Chemistry	2443
Radiation Chemistry	2444
Radiochemistry	2452
Separation Processes and Procedures	2454
ENGINEERING	2462
General	2462
Applications of Nuclear Explosions	2462
Facilities and Equipment	2462
Heat Transfer and Fluid Flow	2464
Materials Testing	2467
Protective Structures	2469
Space Propulsion	2469
Vacuum Engineering	2469
GEOLOGY AND MINERALOGY	2471
General	2471
Natural Radioactivity and Fallout	2471
Techniques and Equipment	2473
Thorium and Uranium Minerals	2475
HEALTH AND SAFETY	2477
INSTRUMENTATION	2485
General	2485
Radiation Detection	2491
Radiation Effects	2500
ISOTOPE TECHNOLOGY	2502
General	2502
Industrial Applications	2502
Power Application	2504
Separation and Production	2505
MATHEMATICS AND COMPUTERS	2507
METALS, CERAMICS, AND OTHER MATERIALS	2509
General	2509
Corrosion	2511
Fabrication	2516
Properties and Structure	2521
Radiation Effects	2531
METEOROLOGY	2537
PHYSICS	2538
General	2538
Accelerators	2544
Astrophysics and Cosmology	2548
Atomic Physics	2554
Cosmic Radiation	2561
Direct Energy Conversion	2565
Elementary Particles and Radiations	2567
Field Theory and Quantum Mechanics	2583
Geophysics	2588
Low Temperature Physics	2593
Neutron Physics	2596
Nuclear Properties and Reactions	2599
Plasma Physics and Thermonuclear Processes	2624
Shielding	2642
Solid State Physics	2643
REACTOR TECHNOLOGY	2644
General	2644
Auxiliaries and Components	2644
Criticality Studies	2647
Design and Feasibility	2649
Fuels	2650
Power and Power-Breeder Reactors	2652
Process Heat Reactors	2656
Production Reactors	2657
Propulsion and Space	2657
Research and Test Reactors	2658
WASTE DISPOSAL AND PROCESSING	2662
GENERAL AND MISCELLANEOUS	2664
CORPORATE AUTHOR INDEX	INDEX-1
PERSONAL AUTHOR INDEX	INDEX-11
SUBJECT INDEX	INDEX-58
REPORT NUMBER INDEX	INDEX-149

STAFF OF NUCLEAR SCIENCE ABSTRACTS

MANAGING EDITOR

John W. Norris

ASSISTANT MANAGING EDITOR

Donald D. Davis

ASSOCIATE EDITORS

Lawrence T. Whitehead
David E. Bost
Robert C. Kelly
Lee M. Thompson

SUBJECT INDEX EDITOR

Everett J. Hoffman

EVALUATORS

William D. Matheny
John H. Mitchell
Mary H. Newman

ABSTRACTORS

F. S. Armstrong (AECL)
Jane G. Buchanan
D. Lamar Cason
Helen G. Donald
James R. Dulaney
Wells L. Green
Bernard O. Griggs
Mary Catherine Grissom
Phyllis C. Hansen
Thomas F. Heagerty
Carolyn D. Houston
Rose V. Jermain
Betty L. McDowell
Mona H. Raridon
Julia Redford
Lila B. Smith
Charles E. Stuber
Martha J. Thomas
Anne G. Ward
David C. West

SUBJECT HEADING SPECIALIST

Robert E. Upchurch

CORPORATE AUTHOR SPECIALIST

Clara L. Fox

DESCRIPTIVE CATALOGING SPECIALIST

J. Paul Meredith

SCHEDULING AND PUBLISHING COORDINATOR

Henry H. Lansford

Communication concerning the editorial policy and content of *NSA* should be addressed to the Managing Editor, *Nuclear Science Abstracts*, AEC Division of Technical Information Extension, P. O. Box 62, Oak Ridge, Tennessee 37831.

Use of funds for printing this publication approved by the Director of the Bureau of the Budget, May 20, 1963

Volume 19, Number 11 June 15, 1965

NUCLEAR SCIENCE ABSTRACTS

BIOLOGY AND MEDICINE

General

Refer also to abstract 20324.

19455 (CONF-640204(p.44-62)) FRONTIERS IN BIOLOGICAL APPLICATIONS OF ELECTRON MICROSCOPY. Michael Beer (Johns Hopkins Univ., Baltimore, Md.).

The importance of structural information in biology is pointed out. The structure of the nucleic acids is discussed, and the problems (support, dessication, etc.) of determining their structure with electron microscopy are discussed. A group discussion is included. (D.L.C.)

19456 (LF-21) TRANSPORT OF RELATIVELY INSOLUBLE MATERIALS FROM LUNG TO LYMPH NODES. R. G. Thomas (Lovelace Foundation for Medical Education and Research, Albuquerque, N. Mex.). Jan. 1965. Contract AT(29-2)-1013. 18p. Dep.; $0.50(cy), 1(mn) CFSTI.

The concentration of relatively insoluble materials in the lung apparently bears a linear logarithmical relationship to that in the pulmonary lymph nodes after either single or repetetive inhalation exposures. This has been shown with experimental data in which compounds of uranium, thorium, plutonium, and polonium have been inhaled by various species. Theoretical functions based upon logical postulates have been derived for predicting the concentration of materials in lung and lymph nodes following inhalation exposure. The calculations yield ratios between the two organs which closely approximate those from the experimental studies. An extremely long half-life component is postulated for lung (10,000 days) and an infinite residence time in lymph nodes has been assumed. Even though complicated biological processes may be involved in the transport from lung to lymph nodes, it appears that until more data are collected simple schemes like those presented could be employed. (auth)

19457 (NP-14886) A BIOLOGICAL TOOL FOR STUDY OF CELLULAR RADIATION DAMAGE. (Avco Corp., Tulsa, Okla.). [1964]. Contract NASw-782. 15p.

A versatile new technique is reported by which living tissue can be simulated for studies involving radiation quality and related three dimensional interactions between living cells and tissue penetrating radiations. The technique has the advantages of ease of preparation, stability, versatility as to choice of living cells, and requires a single radiation exposure to obtain data for dosages from only a few to several thousand rad. No specilized equipment is necessary and only the standard equipment found in most biological laboratories is required by the technique. (auth)

19458 (JPRS-27940) PLANT PHYSIOLOGY AND THE EFFECT OF FERTILIZERS ON CROPS AND BUILD-UP OF RADIOACTIVE PRODUCTS. Translated from Vestn. Mosk. Univ., Ser. VI: Biol., Pochvoved., No. 5, 3-10; 57-62; 70-9(Sept.-Oct. 1964). 32p. (TT-64-51982). $2.00 (CFSTI).

A separate abstract was prepared for one paper in this translation of selected papers. Other papers discuss the relation of plant physiology to intensification of crop production and the effects of fertilizers on the yield and quality of lettuce. (C.H.)

For an abstract of the individual section see: 19475.

19459 (JPRS-29250) BULLETIN OF EXPERIMENTAL BIOLOGY AND MEDICINE. Translation of Byulleten Eksperimental'noi Biologii i Meditsiny, 59: No. 1, 6-10; 33-5; 52-5; 86-93 (Jan. 1965). 35p. (TT-65-30569). $2.00(CFSTI).

Separate abstracts were prepared on two sections of this translation of selected articles. Other articles discuss electrical stimulation of nerve impulses, immune reactions in the homotransplantation of extremities in canines, and bone marrow transplantation in tumor-bearing rats. (C.H.)

For abstracts of individual papers see: 19509 and 19510.

19460 (JPRS-29364) STUDIES IN LIVER AND LUNG CHOLESTEROL EXCHANGE AND SKIN PERMEABILITY. Translated from Dokl. Akad. Nauk Belorussk. SSR, 8: 675-6; 680-81(1964). 10p. (TT-65-30622). $1.00(CFSTI).

A separate abstract was prepared for one paper included in this translation. The other paper discusses the pathology and treatment of industrial dermatitis. (C.H.)

For an abstract of the individual section see: 19511.

19461 ADVANCES IN RADIATION BIOLOGY. VOLUME 1. Leroy G. Augenstein, Ronald Mason, and Henry Quastler, eds. Advan. Radiation Biol., 1: 1-285(1964). New York, Academic Press, 1964.

Separate abstracts were prepared on five chapters. One chapter was abstracted previously in NSA Vol. 18 as number 15714. (C.H.)

For abstracts of individual chapters see: 19515, 19516, 19517, 19968, and 19969.

19462 SIXTH INTERNATIONAL TRANSPLANTATION CONFERENCE, FEBRUARY 6, 7, AND 8, 1964. PART II. Harold E. Whipple, ed. Ann. N. Y. Acad. Sci., 120: 447-806(Nov. 30, 1964). (CONF-641113(Pt.II))

Separate abstracts were prepared for six papers. Other papers discuss organ preservation, surgical techniques for organ transplantation, the present status of artificial internal organs, and results of experimental and clinical studies on organ and tissue transplantation. (C.H.)

For abstracts of individual papers see: 19463, 19519, 19520, 19521, 19522, and 19523.

19463 STUDIES OF RENAL HOMOTRANSPLANTATION IN MAN. D. M. Hume, J. H. Magee, G. R. Prout, Jr., H. M. Kauffman, Jr., R. H. Cleveland, J. D. Bower, and H. M. Lee (Medical Coll. of Virginia, Richmond). Ann. N. Y. Acad. Sci., 120: 578-606(Nov. 30, 1964).

Various studies and observations of renal homotransplants in man are presented. Although the results thus far are encouraging, they are by no means perfect. Much

more work remains to be done in the field of cadaver transplantation, and better methods to obtain permanent acceptance of the transplant must continually be sought clinically and in the experimental laboratory. (43 references.) (auth)

19464 A NONKILLER RESISTANT KAPPA AND ITS BEARING ON THE INTERPRETATION OF KAPPA IN PARAMECIUM AURELIA. Dorothea J. Widmayer (Indiana Univ., Bloomington). Genetics, 51: 613-23(Apr. 1965). (COO-235-16)

Kappa 51m43, obtained by two successive mutations from 51 hump kappa, is a nonkiller kappa which confers full resistance against hump killing activity of Paramecium aurelia. B kappa, the type associated with hump killing activity, is totally absent from populations of 51m43 kappa. The absence of B kappa accounts for the nonkiller aspect of the stock 51m43 phenotype. The resistant aspect of the phenotype is related to the presence of a multiplicity of N kappa, the type of kappa shown by this study to confer resistance against toxic kappa activity. It is not known whether all 51m43 N kappa contribute to protective action or whether the capacity to do so develops in 51m43 kappa as a part of the developmental sequence of N kappa to B kappa, a sequence blocked by mutation in kappa 51m43 prior to morphological differentiation into B kappa. An additional step in the degradational-mutational series of mutation affecting killing action has been identified. (auth)

19465 THE USE OF LABELED ANTIBODIES IN ULTRASTRUCTURAL STUDIES. G. B. Pierce, Jr., J. Sri Ram, and A. R. Midgley, Jr. (Univ. of Michigan, Ann Arbor). Intern. Rev. Expti. Pathol., 3: 1-34(1964).

The relative merits and limitations of various labels for antibodies used in electron microscopic studies of macromolecules against which specific antibodies may be obtained are discussed. Methods of conjugating antibodies with suitable tags and methods of utilizing the tagged antibodies are described. Emphasis is placed on the use of ferritin as a label for antibodies. (77 references.) (C.H.)

19466 TERATOGENIC EFFECTS OF IONIZING RADIATIONS ON THE EMBRYONIC DEVELOPMENT OF THE HIGHER VERTEBRATES. Jean-Michel Kirrmann and Etienne Wolff (C.N.R.S., Paris and College de France, Paris). Intern. Rev. Expti. Pathol., 3: 365-408(1964).

Data are reviewed from a number of studies on the effects of x and γ radiation on embryonic development in chicks, mice, rats, rabbits, hamsters, goats, and man. The results emphasize the wide diversity of types of malformations obtained by means of ionizing radiations in upper vertebrate embryos. The majority of known spontaneous monstrosities have been reproduced by irradiation and their embryological mechanisms have been studied. The radiation doses required and the sensitive stages for the different animal species are discussed for both total-body and localized irradiation. The protective effects of cysteamine, cystamine, and anoxia against radiation injuries of embryos were evaluated and it was concluded that the majority of malformations produced by ionizing radiation can be avoided or diminished by the application of radioprotective treatments to the mother before irradiation. The treatments had no effect on reducing the teratogenic effect of radiation once it has taken place. The problems encountered in the extrapolation of data from studies in lower mammals to human studies are considered. The data indicate that the teratogenic effects of ionizing radiations in the mammalian embryo depend largely on the embryonic stage at which irradiation is administered, the size of the radiation dose, the length of time of the animals exposure, and the radiosensitivity of the strain or species involved. (120 references.) (C.H.)

19467 OCEANOGRAPHY AND MARINE BIOLOGY. AN ANNUAL REVIEW. VOLUME 2. Harold Barnes, ed. New York, Hafner Publishing Co., 1964. 548p.

Information is included on: turbulence; turbidity currents; physical oceanography in Arctic Canada; beach studies; advances in the estimation of salinity; the mud-water interface; nitrogenous constituents of the plankton; lipids of marine organisms; the chlorophyta; temperature and salinity effects on marine and brackish water animals; planktonic bioluminescence; marine zoology in the Baltic area in 1953–62; Echinoderms; biological aspects of underwater sound; and ethology and marine zoology. One chapter on artificial and natural radioisotopes in the marine environment was abstracted separately in NSA. (P.C.H.)

For an abstract of the individual chapter see: 20226.

19468 FETAL HEMOPOIETIC CELLS: ARE THEY TOLERANT? H. E. M. Kay (Royal Marsden Hospital, London). 11p. (CONF-717-11)

From CNRS Meeting on Graft of Allogenic Hematopoietic Cells, Paris, Sept. 1964.

The production of globulins in animal fetal hemopoietic cells is discussed in relation to the development of immune capacity in the human fetus. Recent evidence relating to the pre-natal period is described with emphasis on aspects that may be of practical importance to hemopoietic transplantation. (P.C.H.)

Ecology

19469 THE ATOM FISHERS. Michael Bernhard (Laboratory for the Study of Radioactive Contamination of the Sea, Fiascherino, Italy). Euratom Bull., 4: No. 1, 8-11 (Mar. 1965).

The activities of the Laboratory for the Study of the Radioactive Contamination of the Sea at Fiascherino, Italy, are outlined. The distribution, level, and uptake of radioisotopes by marine organisms are studied in view of the hazards for man. (D.C.W.)

Metabolism, Tissue Distribution, and Toxicology

Refer also to abstracts 19739, 19793, 20026, and 20165.

19470 (ANL-6938(p.141-61)) CALCIUM ACCRETION AND BONE FORMATION IN DOGS. AN EXPERIMENTAL COMPARISON BETWEEN THE RESULTS OF Ca^{45} KINETIC ANALYSIS AND TETRACYCLINE LABELING. W. R. Lee, J. H. Marshall, and H. A. Sissons (Argonne National Lab., Ill.).

The rates of bone formation in a number of skeletal sites in a puppy and in an adult dog were directly measured by double tetracycline labeling. In the same animals the Bauer-Carlsson-Lindquist accretion rate was measured using ^{45}Ca. Accretion rates were calculated five days after injection. Data for shorter times of calculation are included. In the rapidly-growing puppy the accretion rate was comparable to the bone formation rate at all sites studied. In the adult dog, the values were comparable in cancellous bone, but in cortical bone the accretion rate was two to three times the bone formation rate. Most of the difference between accretion rate and bone formation rate in adult cortical bone was due to the diffuse component and, hence, to long-term exchange. The ratio of the diffuse component to the uniform label in the puppy was about one-tenth, and in the dog was about one-sixth, based on data from femora and humeri six days after ^{45}Ca injection. Despite the important differences between the accretion rate and the bone formation rate that were found to exist in regions where there was only a small amount of bone formation, there was a strong correlation between the two rates. The value of the accretion rate as a parameter of bone metabolism is clear. (auth)

19471 (ANL-6938(p.162-78)) OSTEOLATHYRISM IN MICE AND INHIBITION OF THE ENDOSTEAL BONE REACTION IN ESTROGEN-TREATED MICE BY AMINOACETONITRILE. D. J. Simmons, A. M. Pankovich, and A. M. Budy (Argonne National Lab., Ill.).

The effect of aminoacetonitrile (AAN) on the skeletons of young mice injected with estrogen was studied histologically and microradiographically. AAN (0.5, 2.5, 5, 10, or

20 mg) was administered daily during the first week of treatment alone or in combination with a single injection of 1 mg estradiol valerate on the first day. The animals were sacrificed at intervals of 7 days for a period of 4 weeks. The bone reaction leading to ossification of the marrow cavities as a consequence of estrogen treatment was diminished by 5 to 20 mg AAN, and the effect was roughly proportional to the dose of the nitrile. The metaphyseal trabeculae (distal femur) of the AAN-treated mice developed a mosaic appearance. While administration of the nitrile alone induced the formation of periosteal hyperostotic and osteocartilaginous hyperostotic fibrous bone tissue over the femoral shafts late in the posttreatment recovery period; combined treatment with estrogen potentiated these changes during the treatment period itself. The cortical bone tissue was also demineralized by combined treatment, and fused osteocyte lacunae regularly appeared as an apparent sequela of both cell enlargement and degradation of perilacunar matrix. Conversely, estrogen completely protected the epiphyseal cartilages against degenerative changes (abnormal vascular invasion, rents, etc.) after low doses of AAN (0.5 to 2.5 mg) during the treatment period, but the hormone was only partially effective after higher doses of AAN. It was suggested that aminoacetonitrile disrupts both the formation of new bone collagen and the integrity of collagenous structures deposited prior to the treatment. (auth)

19472 (ANL-6938(p.179-93)) DIURNAL VARIATIONS IN THE METABOLIC ACTIVITY OF BONE AND CARTILAGE. David J. Simmons and George Nichols, Jr. (Argonne National Lab., Ill.).

In vivo and in vitro studies of the metabolism of bone cells in the metaphyses of the rat femur (distal) and tibia (proximal) have established that collagen synthesis and new bone formation are diurnally regulated. Significantly greater amounts of glycine-1-^{14}C were initially incorporated by osteogenic cells (principally osteoblasts) at 10:00 hrs than at 03:00 hrs, and the subsequent rate of bone formation by these cells was also faster at 10:00 hrs. While DNA values did not vary at these clock hours, the content of RNA was significantly higher at 10:00 hrs, consistent with the increased bone protein synthesis. The greatest production of bone lactate and the maintenance of a higher steady-state distribution of Ca between the bone and the incubation medium (release of Ca^{2+} from the tissue) also occurred at 10:00 hrs. It was concluded that the daily periods of most active metaphyseal bone formation and bone resorption are perhaps coincident, and that tissue remodeling is most intense in rats during the early part of the environmental photoperiod. (auth)

19473 (UR-661) RETENTION OF STRONTIUM-90 BY FETAL AND NEWBORN RATS. B. J. Hopkins, R. C. Baxter, and L. W. Tuttle (Rochester Univ., N. Y. Atomic Energy Project). Nov. 9, 1964. Contract W-7401-eng-49. 15p. $1.00(cy), 1(mn) CFSTI.

The effect of dose size, maternal age at conception, and gestational age at the time of injection upon the retention of strontium in rat fetuses and newborn was investigated. Examination of the offspring from 60 pregnant females of the Long-Evans strain injected with ^{90}Sr showed that the fraction of the dose retained by the developing fetus or newborn was not influenced markedly by the size of the dose injected to the dam over the range of 24 to 382 microcuries. When 191 or 382 microcuries was injected to the dam on day 2 post-conception, 0.05 and 0.04 percent of the dose was retained respectively by the litter on the 20th day post-conception. The percentage retained was similar, though slightly higher, when these doses were injected on day 10 post-conception. The percentage retained in the litter at parturition following injection on day 17 post-conception was 3.5, 4.0 and 3.9 percent of total doses of 24, 191, or 382 microcuries of strontium-90, respectively. The dose fraction retained by the newborn was greatly influenced by the gestational age at the time of injection to the mother. Litter content increased from 4.0 percent of the maternal dose following injection on day 17 post-conception to 20.7 percent following injection on day 22 for a dose of 191 microcuries of ^{90}Sr to dams that were 105 days of age at conception. When maternal age at conception was increased from 105 to 370 days, the dose fraction retained by offspring at parturition decreased by a factor of 2.5, but the ratio of body burden in the newborn to maternal content was independent of the age of the dam for a given dose and gestational age. (auth)

19474 (CEA-tr-A-1616) ETUDE DE LA SORPTION DU STRONTIUM DANS LES SOLS DU SCHLESWIG-HOLSTEIN. (Study on the Sorption of Strontium in Schleswig-Holstein Soils). H. [Graff von] Reichenbach and G. [Preimerr von dem] Bussche. Translated into French by M. Maire from Z. Pflanzenernaehr. Dueng. Bodenk., 101: 24-33(1963). 19p. Dep.(mn).

The distribution of low quantities of strontium added to the soil between the water-soluble, exchangeable, and non-exchangeable fractions was studied in 165 samples of soils from Schleswig-Holstein. The relations of this distribution with the properties of soils, exchange capacity, pH, clay content, and carbon content were determined with the aid of the calculation of multiple corrections. Under the conditions existing in the soil, the water-soluble fraction is low with respect to the quantity of strontium added; the strontium is then fixed in the upper layer of the soil, several centimeters thick only, and in a fashion almost independent of the properties of the soil. It then avoids the displacement action of percolation caused by precipitations, and a part of the strontium is transferred under a non-exchangeable form. The importance of the non-exchangeable fractions depends on properties of the soils, particularly on the nature of the soil exchangers. When the contents in carbon or humus increase or when the exchange capacity increases, the non-exchangeable fraction of strontium increases; it decreases in a slighter measure when the clay content and the pH increase. The importance of these results for the mobilization of strontium by plants is discussed. (tr-auth)

19475 (JPRS-27940(p.10-17)) ON THE EFFECTS OF POTASSIUM PHOSPHATE AND LIME ON THE ACCUMULATION OF STRONTIUM-90 BY PLANTS DEPENDING ON THE STABLE STRONTIUM CONTENT IN THE SOIL. N. M. Skadchenko. Translated from Vestn. Mosk. Univ., Ser. VI: Biol., Pochvoved., No. 5, 57-62(Sept.-Oct. 1964).

The effects of various doses of stable Sr, phosphate and lime on the accumulation of ^{90}Sr in the vegetative parts and grain of oats were studied. Results showed that the addition of stable Sr to the soil caused an increase in ^{90}Sr in oat plants, especially in the stalks; the addition of K_3PO_4 to the soil decreased the deposition of ^{90}Sr in both vegetative plant parts and grain: and the greatest reduction of ^{90}Sr in grain and vegetative plant parts was produced by the addition of lime to the soil. (C.H.)

19476 THE EFFECT OF CORTISONE AND ANABOLIC STEROIDS ON THE RETENTION OF RADIOACTIVE CALCIUM AND STRONTIUM IN RATS. H. H. Bohr and S. G. Dawids (Orthopathological Hospital, Copenhagen). Acta Endocrinol., 47: 223-30(1964).

Experiments with adult rats treated with dexamethasone showed a decreased retention of radioactive calcium-47 and strontium-85 as compared with the controls. In addition a marked reduction in weight was observed probably due to dehydration. In animals that had additional injections of nortestosterone compounds, Durabolin and Anadur, the effects of cortisone were not counteracted although animals treated with nortestosterone compounds alone showed an increased retention of radioactive calcium as compared with the control animals. (Excerpta Med., Sect. XXIII, 2: No. 3, (Mar. 1965))

19477 SECRETION OF RADIOIODINE IN MILK FOLLOWING A SINGLE ORAL ADMINISTRATION IN THE COW. C. B. Thorell (Royal Veterinary Coll., Stockholm). Acta Vet. Scan., 5: 217-23(1964).

The secretion of radioiodine in cow's milk following the administration of a single oral dose was studied using ^{131}I. All of the values were corrected for the physical decay of the isotope. ^{131}I began to appear in the milk 30 minutes after administration with a maximal concentration of, on the

average, 1.7% of the given dose per l of milk at about six hours following administration. The subsequent reduction in the concentration showed a two-exponential course with biological half lives of 0.6 and 10 days, respectively. The total secretion in the milk was between 10 and 27% of the given dose of ^{131}I in six days. The total secretion of radioiodine in the milk was seen to be dependent upon the cow's milk production. (Excerpta Med., Sect. XXIII, 2: No. 3, (Mar. 1965))

19478 THE RELATIONSHIP BETWEEN AND THE IMPORTANCE OF THE DIMENSIONS OF URANIUM PARTICLES DISPERSED IN AIR AND THE EXCRETION OF URANIUM IN THE URINE. Robert L. Fischoff (National Lead Co. of Ohio, Cincinnati). Am. Ind. Hyg. Assoc. J., 26-33(Jan.-Feb. 1965).

Studies showed that the excretion of uranium in the urine of workmen is related to the concentration of uranium dispersed in the air of their work places, when the dispersed particles are separated into the respirable and nonrespirable fractions. Discussion of and conclusions from the results obtained and published literature are made as related to uranium for the control value, biological effects, particle size and distribution, solubility, ICRP recommendations, and usefulness of two-stage air sampling data. (auth)

19479 THE SITE OF UPTAKE OF IODINE BY HAIR. E. A. Wright (Saint Mary's Hospital, London). Arch. Exptl. Pathol. Pharmakol., 248: 417-25(1964)

The uptake of radioactive iodide by the vibrissal hairs of the mouse was studied using a dry autoradiographic technique. Iodide first appeared in the hairshaft just deep to the orifice of the sebaceous gland 0.2 to 0.5 mm below the skin surface. L-cystine-^{35}S on the other hand was taken up in the deeper parts of the hair root in the region of the site of the dermal papilla. Even with heavy uptakes of both substances little overlap occurred. (Excerpta Med., Sect. XXIII, 2: No. 3, (Mar. 1965))

19480 DETERMINATIONS OF BODY WATER IN HUMANS WITH THE AID OF TRITIUM. M. Paerisch, K. Buettner, H. Langer, and H.-K. Bothe (Deutsche Hochschule für Koerperkultur, Leipzig). Arch. Ges. Physiol., 281: 374-8(1964). (In German)

Body water in humans was measured by comparison of ^{3}H specific activity in expired air, serum, and urine samples after oral administration of $^{3}H_2O$. The measurement accuracy of the ionization chamber used was greatest when the ^{3}H in serum was estimated, and for this reason serum was probably the best indicator of changes in body water concentrations. The average value of the quotient air/urine was 1.02. The average value of the quotient air/serum was 0.98. The values obtained for the total-body water were slightly higher than those accepted as normal. There was a wide variation in the values obtained from urine measurements, but probably this was because excretion was not sampled continuously and also because the amounts of ^{3}H it contained were small. Other measurements showed that the concentration of ^{3}H in expired air was a sensitive measure of body water changes. It also had the advantages that it was easily sampled and fluctuated the least. Measurement of ^{3}H in expired air permits estimation of body water to be carried out continuously over long periods of time, so that changes in body water amounting to several kg can be assessed accurately. Relatively small losses of body water of from 0.5 to 1.5 l, which may result from brief participation in sports cannot be measured accurately by this method. (BBB)

19481 INFLUENCE OF PETHIDINE UPON BREATHING AND METABOLISM OF RATS AND PETHIDINE METABOLISM DURING ACUTE IRRADIATION DISEASE. J. Kvetina and O. Peca (Charles Univ., Hradec Kralove, Czechoslovakia). Cesk. Fysiol., 13: 517-18(Dec. 1964).

Pethidine decreased breathing efficiency in irradiated rats. The products of its metabolism did not show any influence upon breathing. The experimental apparatus and results obtained are discussed. (CFSTI)

19482 THEORETICAL STUDY OF THE DOSE DELIVERED TO TISSUE SUPERFICIALLY CONTAMINATED WITH AN α-EMITTER. M. Dousset and J. Le Grand (Commissariat a l'Energie Atomique, Paris). Health Phys., 11: 171-8(Mar. 1965). (In French)

Variation with depth of the absorbed dose rate in a tissue superficially contaminated with an α-emitter was studied. The calculation takes into account not only the decrease of the particle flux density with the distance from the contaminated surface but also the variations of the linear energy transfer as a function of the distance covered by the particles. The results are shown by curves for α-emitters of 4, 5, 6, and 7 Mev. (auth)

19483 BETA RADIATION FROM RADIOACTIVE IODINE (I^{131})—MEASUREMENT OF ONE HUNDRED HUMAN OVARIES. D. L. Weijer (University Hospital, Edmonton, Alberta, Can.). J. Can. Assoc. Radiologists, 15: 153-60 (Dec. 1964).

The β-radiation to the whole blood and to plasma were calculated for the first seventy-two hours after ingestion of a tracer dose of ^{131}I in a series of twenty euthyroid volunteers. One hundred human ovaries were also assayed for ^{131}I content immediately after removal from patients who had received a prior ^{131}I tracer drink. It was assumed that an immediate equilibrium was established between the ^{131}I in the whole blood, plasma, and ovary. On the basis of ^{131}I content curves deduced for each of the one hundred ovaries, the average β-radiation levels were found to be: to fifty-two pre-menopausal normal ovaries, 9.4 mR/100 μC administered; to fourteen post-menopausal normal ovaries, 9.4 mR/100 μC administered; to twenty-seven pre-menopausal abnormal ovaries, 9.8 mR/100 μC administered and to seven post-menopausal abnormal ovaries, 10.5 mR/100 μC administered. The β-radiation to the whole blood and plasma in the euthyroid series was 9.9 and 12.6 mR/100 μC, respectively. It was thought that the β-radiation after the first seventy-two hours would exceed these figures by no more than 20%. The ^{131}I content of thirty-one cysts was measured and the results have been discussed in the light of ^{131}I transfer through membranes and the consequent dose to the ovum. (auth)

19484 SOME STUDIES OF WOUND HEALING: EXPERIMENTAL METHODS, EFFECT OF ASCORBIC ACID AND EFFECT OF DEUTERIUM OXIDE. S. M. Levenson, L. V. Crowley, E. F. Geever, H. Rosen, and C. W. Berard (Yeshiva Univ., New York). J. Trauma, 4: 543-66(1964).

Procedures are described for the evaluation of experimental wound healing; paravertebral skin wound and polyvinyl alcohol sponge implants were used, and each animal's local response was appraised by physical, biochemical and histopathologic methods. Breaking strength was measured by a mechanical electronic device; skin thickness by several methods, both in situ and on the excised skin strip; hydroxyproline was determined after isolation by column chromatography; comparative histopathologic studies were made with special stains. It was found that the breaking strength of a wound becomes most meaningful when related to cross-sectional area of the wound and adjacent skin, i.e. tensile strength, and to the strength of the unwounded skin of the experimental animal. Column chromatography was found to yield results for hydroxyproline in granulation tissue usually lower than when hydroxyproline was estimated by the Neuman-Logan method without prior isolation. Using this method on sponges from normal, scorbutic, and partially repleted guinea pigs, it was found that neutral salt soluble collagen was greatest early in the normal healing period, and partial repletion of scorbutic animals with 2 mg ascorbic acid per day led to a surge of synthesis that approached but did not overtake the normals after 21 days. Acetic acid soluble collagen from rat tail tendons and skin was fractionated by column chromatography to yield three high molecular weight fractions, and a complex of hydroxyproline-poor peptides. It is possible that ascorbic acid acts to catalyze the formation of these peptides, and/or to catalyze their conversion to hydroxyproline-rich types with simultaneous polymerization. Twenty-five per cent deute-

rium oxide fed to rats induced collagen abnormalities and wound healing defects; these defects were postulated to be caused by interference with the hydration shell of in vivo collagen and/or the interaction of collagen and ground substance. (Excerpta Med., Sect. XXIII, 2: No. 3, (Mar. 1965))

19485 RECOVERY FROM THE "LETHAL" EFFECTS OF CROSS-LINKING ALKYLATION. A. Loveless, Judy Cook, and Pamela Wheatley (Royal Cancer Hospital, London). Nature, 205: 980-3(Mar. 6, 1965).

The phenomenon of recovery in E. coli strains B, B/r, and K-12 and phage T 2 in vitro treated with mustard gas (di(2-chloroethyl)sulfide, H) was investigated. Untreated cells of strain B proved wholly stable in buffer at 37°C, showing no significant fluctuation in viable count up to 28 hr. H-treated cells gave steadily rising viable counts that took longer to reach a maximum the more severe the treatment. As with strain B, treated cells of B/r showed an appreciable recovery at all doses, but the erratic control prevented any conclusion regarding the positions of the maxima. Experiments with HN_2 are also described. The results left little doubt that the recovery of bacteria from treatment by mustard gas is metabolically mediated. (P.C.H.)

19486 SALIVARY SECRETION OF CAESIUM-131. Franz K. Bauer, Nancy Telfer, and Brita Hetter (Harbor General Hospital, Torrance, Calif. and Univ. of California, Los Angeles). Nature, 205: 1014-15(Mar. 6, 1965).

Experiments showed that ^{131}Cs is secreted in the saliva in an unpredictable manner as compared with ^{39}K and that at no time does there appear to be complete equilibration. The fluctuations of ^{131}Cs excretions in saliva from one collection period to the next were much greater than those of ^{39}K. An unexplained transient dip in specific activity and rise in exchangeable potassium values after 20 hr was noted in 4 of 5 tests in which multiple collections were done. Since the rate of equilibration of these two isotopes in saliva is similar, the reduced secretion of ^{131}Cs must be due to a mechanism other than delayed equilibration. It was concluded that ^{131}Cs cannot be used for salivary estimation of exchangeable potassium. (P.C.H.)

19487 SIGNIFICANCE OF FORMATION OF ANTI-ENDOTOXINS AGAINST E. COLI IN INVOLUTION OF THE HEMORRHAGIC SYNDROME IN RADIATION SICKNESS. P. N. Kiselev, K. I. Nikitina, and Shao-chang Cheng (Central Research Inst. of Medical Radiology, Moscow). Radiobiologiya, 5: 87-92(1965). (In Russian)

A hemorrhagic syndrome typical of radiation sickness appeared in guinea pigs after long treatment with E. coli endotoxin. The beginning of the involution of the hemorrhagic events coincided with the appearance in the blood of specific antibodies (antiendotoxin and agglutinin) to self-strains of intestinal bacteria. This relation indicates the important role of autoinfection in the origin and development of the hemorrhagic syndrome. (tr-auth)

19488 TOXICITY OF INTRAVENOUSLY INJECTED URANIUM IN GUINEA PIGS. Daniel R. Farnell (Auburn Univ., Ala.). Toxicol. Appl. Pharmacol., 7: 32-6(Jan. 1965).

Two experiments were performed, one to determine renal lesions in guinea pigs given a single injection of uranyl acetate, $UO_2(C_2H_3O_2)_2 \cdot 2H_2O$; the second was a dose-response test in which guinea pigs given varying single doses of U were observed for 33 days to detect signs of toxicity. Kidney lesions and plasma creatinine were followed in the first group of guinea pigs injected intravenously five days previously with doses of U acetate corresponding to either 1.5, 3.0, or 6.0 mg U/kg of body weight. Extensive lesions of nephritis, including both glomerular and tubular damage, were seen at all three dose levels. Plasma creatinine increased noticeably as the dose increased. In another group of animals given U at the same dose levels as the first group, a dose of U acetate of 2.67 mg/kg (1.5 mg U/kg) caused no deaths during a 33-day observation period. More than half of the animals survived the higher doses. It was concluded that an effective, nonlethal intravenous dose of U acetate for producing nephritis in guinea pigs is 2.67 mg/kg. These and earlier experiments show that uranium nitrate hexahydrate is more toxic intravenously than an equal quantity of U acetate. The total content of U is slightly higher in the acetate; therefore, it is possible that the nitrate ion is responsible for the greater toxicity of uranium nitrate hexahydrate. (BBB)

19489 CHANGES IN THE ERYTHROGRAMS OF RATS SUBJECTED TO THE ACTION OF THE SYNTHETIC RADIOMIMETIC EMBIKHIN. E. V. Burlakova, E. N. Goncharenko, and Yu. B. Kudryashov (Moscow State Univ.). Vestn. Mosk. Univ., Ser. VI, Biol., Pochvoved., No. 5, 18-21(Sept.-Oct. 1964).

Embikhin, $CH_3N(CH_2CH_2Cl)_2$, a synthetic radiomimetic substance of the nitrogen mustard type, was infected into the jugular vein of male rats in doses of 0.02 to 0.8 mg a single time or repeatedly. Embikhin injected in amounts above the minimum active dose (0.02 mg) produced a shift of the maximum of erythrogram curves to the left on the time axis. This showed a reduced stability of erythrocytes to the action of hemolysins, indicating a disturbance of the normal balance between blood formation and blood destruction. Similar changes in the blood of animals were observed in acute radiation sickness. A shift of the maximum of erythrogram curves to the right in later periods, such as that observed following restoration of the functioning of the bone marrow in radiation sickness, did not take place after administration of embikhin. (CFSTI).

19490 URANIUM CONTENT IN THE SURROUNDING MEDIUM AND HUMAN ELIMINATION. A. V. Berdnikova. Vopr. Pitaniya, 23: No. 4, 17-20(1964).

The migration of uranium from soil and water into plants, food products, and the human organism was followed. The study was conducted in 2 representative rural settlements, selected because of their different uranium content in water and soil, which was 28 and 6 times respectively higher in the test locations, six hundred specimens of soil, water, plants, food, human urine and feces, were analyzed by means of fluorometry. Results are tabulated. A direct relationship was observed between the contents in water and soil and in the food products. Uranium accumulated evenly on the surface as well as in the interior of plants where its total was higher than in meat and dairy products. Uranium entering the body is apparently accumulated; total absorption was $3.045.10^{-4}$ as against $4.3.10^{-5}$ elimination in g/24 hours in the test location. The main source of uranium entering the body was water; food stuffs supplied only 1 to 5% of the daily total intake. Elimination was mainly in the feces. Uranium found in the urine was considered to indicate its possible absorption and penetration into the blood circulation. Uranium contents were found constant over the seasons. (CFSTI)

19491 IODINE STORAGE BY THE HUMAN FOETAL THYROID. L. Lampe, L. Kertesz, and J. Dzvonyar (Medical Univ., Debrecen, Hungary). Zentr. Gynaekol., 86: 905-8(1964)

Storage of iodine in the human fetal thyroid starts after the 12th week and increases as pregnancy progresses. Studies showed that the uptake of iodine by the thyroid is some 10-100 times that of other fetal organs. Attention is drawn to the risks of ^{131}I therapy during a pregnancy. (Excerpta Med., Sect. XXIII, 2: No. 3, (Mar. 1965))

19492 PROFILE COUNTING STUDIES OF HEPATIC UPTAKE OF LABELLED MATERIALS IN MAN. E. E. Pochin (University Coll. Hospital, London). p.447-55 of "STI/PUB/82(Vol. II)."

The value of a rapid and quantitative method for measuring the total radioisotope content of an organ is illustrated by profile-counting studies on the hepatic uptake of various radionuclides or labeled compounds in man. The method is likely to have wider application to the examination of uptake or turnover of materials in organs in which they are selectively concentrated. After an intravenous injection of ^{131}I-labeled thyroxine (T_4) or tri-iodothyronine (T_3) in man, serial profile or linear scans combined with blood sampling allow a determination of the distribution space of these hormones within the liver, and of the speed with which they

enter and leave the organ. Concentration ratios between liver and plasma of three for T_4 four for T_3 were observed in normal subjects and evidence was obtained that a large proportion of the circulating hormones enter and leave the liver during every hour. The rapidity with which profile scans can be obtained, and the accuracy with which hepatic contents can be estimated by these methods, facilitate such quantitative analyses. The hepatic concentration of endogenously produced hormone in hyperthyroidism was similarly examined by serial profiles in the days following test doses of radioiodine, given as iodide, and showed proportionality with levels of circulating protein-bound radioiodine. Following therapeutic doses of radioiodine to such patients, a lower proportionality was observed suggesting the liberation of metabolites from the irradiated thyroid, which were less actively concentrated in the liver. Similar methods were used to examine the hepatic uptake of circulating metabolites during radioiodine ablation of normal thyroid tissue in patients with thyroid cancer, and during the treatment of functioning thyroid cancer with radioiodine, when the detection of hepatic radioactivity at several days after a test dose of ^{131}I appears to give useful evidence of the presence or persistence of iodine-concentrating tumor tissue within the body. Estimates of hepatic content of ^{198}Au or ^{90}Y may be used to estimate the hepatic uptake or retention of injected particulates. (auth)

19493 MODIFICATION OF IMMUNOLOGIC TOLERANCE WITH THE TRANSPLANTATION OF ALLOGENIC HEMATOPOIETIC CELLS. J. Parra, J. A. Torres, F. Alvarez, and R. Vela (Instituto de Investigaciones Clinicas y Medicas Fundacion Jimenez Diaz, Madrid). 8p. (CONF-717-16)

From CNRS Meeting on Graft of Allogenic Hematopoietic Cells, Paris, Sept. 1964.

Different methods were used to produce bone marrow and lymphoid cell chimeras, in order to study their effect on the grafted kidney in dogs. The studies began with the radiation chimera and then several antimitotic drugs in different systems were used. With cumulative implantation of bone marrow from the same donor, the longest tolerance of grafted kidney was obtained. This method gave better results than when specifically competent lymph cells were employed. The interpretation and discussion of the results open the question of the difference between the transplanted kidney (where only physiological function is expected) and grafted bone marrow from which, besides the hematopoietic function, immunogenetic activity was also sought by the simultaneous existence of two immune systems, as is seen in acquired embryonic tolerance. (P.C.H.)

19494 DECONTAMINATION OF RADIOACTIVE MATERIALS FROM THE SKIN. T. A. Lincoln (Oak Ridge National Lab., Tenn.). 3p. (CONF-705-3)

From 14th International Congress of Occupational Health, Madrid, Sept. 1963.

Considerations to be taken by the industrial physician in the approach to skin decontamination are discussed. These include understanding of the special physical and biological problems involved and awareness of the mechanisms of skin contamination and the limitations of instruments used. A careful estimate of the dose rate to the epidermis should be made before any excision is contemplated. It is also recommended that the physician include the normal renewal time of the skin in the estimate of the probable total dose. (P.C.H.)

19495 GONADAL EXPOSURE TO POLONIUM-210 IN MOUSE AND MAN. L. D. Samuels, V. R. Hunt, J. P. Little, and E. P. Radford, Jr. (Harvard School of Public Health, Boston). 6p. (CONF-640802-2)

From American Institute of Biological Sciences 15th Annual Meeting, Boulder, Colo.

Polonium-210 was found to be a component of tobacco smoke, constituting a significant source of α radioactivity in the environment. Polonium-210 was found to be present in human tissues from both smokers and non-smokers, and smokers have considerably more ^{210}Po than non-smokers in lung, blood, and semen and possibly in ovary. Results of studies in mice showed that ^{210}Po is selectively localized in the gonads. The possible effects of this localization are discussed. (C.H.)

Radiation Effects

19496 (ANL-6938(p.49-56)) RECOVERY FROM DIVISION DELAY IN IRRADIATED GAMETES OF ARBACIA PUNCTULATA. Patricia McClement Failla (Marine Biological Lab., Woods Hole, Mass.).

The recovery from radiation-induced cleavage delay that occurs when the first cell division cycle is prolonged in the zygote of Arbacia punctulata was studied. Results of the study indicate that the recovery rate is independent of radiation dose and is approximately the same when either the egg or sperm is irradiated; it is also the same for anoxically and aerobically irradiated sperm. The pre- and postfertilization process is still operative in eggs irradiated in vivo and removed from the animal up to at least 28 hours after irradiation. The recovery rate is reduced at 0°C, but is insensitive to treatment of the zygote with D_2O or puromycin. (auth)

19497 (ANL-6938(p.127-39)) THE RELATIVE ACTIVITIES OF THORIUM DAUGHTER ISOTOPES IN THE TISSUES OF THOROTRAST PATIENTS. A Progress Report. Robert M. Parr (Argonne National Lab., Ill.).

Thorotrast is a colloidal preparation of ThO_2 which was used extensively as a contrast medium in diagnostic radiology between the years 1930 and 1945. It is a radioactive substance containing isotopes of the ^{232}Th decay series which, depending on the exact mode of administration, may be retained in the body over long periods of time. The patients who received injections of this material during the years it was in common usage now constitute an invaluable and irreplaceable source of data on the clinical effects of long-term irradiation in man. As an initial step in determining the radiation doses received by the tissues of thorotrast patients, procedures were developed for elucidating the equilibrium status of Th daughter-isotopes in small samples of tissue. These methods were applied to the analysis of tissues from thorotrast patients and from a small number of animals which were injected with this material. Results of analyses are discussed. (J.R.D.)

19498 (LA-3204) CALCULATION OF RETINAL DOSE DUE TO VISIBLE RADIATION FROM NUCLEAR EXPLOSIONS. Robert D. Cowan (Los Alamos Scientific Lab., Univ. of California, N. Mex.). Oct. 6, 1964. Contract W-7405-eng-36. 101p. Dep.; $4.00(cy), 2(mn) CFSTI.

Calculation of the maximum energy density received by any portion of the retina due to radiation from an incompletely resolved source requires knowledge of the point-source retinal-image-spread function. For a uniform circular source, one requires more specifically the point-source effective image radius a_0, and the normalized integral $g(a/a_0)$ of the image spread function out to the geometrical image radius a. The function g tends to a^2/a_0^2 for small a, to unity for large a, and in intermediate regions may be roughly characterized by its value at $a = a_0$. Experimental measurements on human eyes appear to indicate $a_0 > 6$ microns and $g(1) \cong 0.5$, but these values are uncertain. A theoretical calculation assuming only diffraction and chromatic aberration gives $a_0 = 3.5\mu$ and $g(1) \cong 0.15$ for large pupils (nighttime conditions) and $a_0 = 4\mu$, $g(1) \cong 0.4$ for small pupils (daytime). Less conservative results, in which effects of other aberrations have been incorporated, are $a_0 \cong 7\mu$, $g(1) \cong 0.5$ for any size pupil, which is in reasonable agreement with experiment. The dose from a hypothetical high-altitude explosion is calculated to illustrate use of these results. (auth)

19499 (NP-14899) FINAL PROGRESS REPORT [ON HEMATOPOIETIC REGENERATION OF IRRADIATED ANIMALS]. Srdan Hajdukovic (Institut za Nuklearne Nauke "Boris Kidric," Belgrade (Yugoslavia)). [196?]. 12p. Dep.(mn)

Results are reported from studies on the effects of sublethal, lethal, and supralethal doses of x radiation on erythropoietin induction and on the behavior of previously

existing erythropoietin in rats and rabbits. Iron-59 was used as a tracer of erythropoiesis in anemic animals and in animals exposed to doses of 700 to 3,000 R x radiation. The effects of plasma from irradiated and anemic donors on the reticulocyte count in rats was determined. (C.H.)

19500 (NP-14907) THE DEPOSITION OF Ba OR Sr IN AORTIC TISSUE. Final Report. R. Brinkman, H. B. Lamberts, and J. G. van Andel (International Atomic Energy Agency, Vienna). [1963]. Contract 112/R2/RB. 9p. Dep.(mn).

The deposition of ^{140}Ba in the aorta, skin, lungs, and tibia of rats was determined at intervals of 1 to 14 weeks after subcutaneous injection. A preferential deposition of ^{140}Ba in the aorta wall was demonstrated. A similar deposition pattern was found using ^{85}Sr. The effects of x radiation on the permeability of blood vessels by macromolecules was demonstrated in rabbits in which $^{140}BaCl_2$ was injected before the x ray exposure of the left carotic artery. The activity of both carotic arteries was measured after 3 days and the left carotic was 3 times as active as the control. The possible effects of β particles from deposited ^{140}Ba and ^{85}Sr on arterial permeability are discussed. (C.H.)

19501 (NP-14931) THE INFLUENCE OF ULTRAVIOLET AND IONIZING RADIATION AND RADIOMIMETIC CHEMICALS ON TRANSDUCTION IN PSEUDOMONAS AERUGINOSA. Progress Report No. 1, December 27, 1960–June 26, 1961. (Melbourne Univ., Parkville (Australia). Dept. of Bacteriology). Contract No. 86. 30p. Dep.(mn).

Transduction in Pseudomonas aeruginosa is a genetic process in which fragments of the bacterial chromosome are transferred by means of a bacteriophage. It has previously been shown that ultraviolet irradiation of the phage prior to its adsorption to the acceptor bacterium results in elevated frequencies of transduction. It has now been shown that irradiation of the phage with gamma rays from a ^{60}Co source results in similar stimulation, as does treatment with ethyl methane sulphonate. These three agents are thought to act genetically by cross-linking deoxyribonucleic acid molecules and this explanation has been adopted as a working hypothesis. Results are reported from studies that show that agents which affect the purine and pyrimidine bases of the nucleic acid, such as nitrous acid, β-propiolactone, and methyl methane sulphonate cause a rapid inactivation of the transducing titre of the phage without any drop in the plaque forming titre. (C.H.)

19502 (NP-14932) THE INFLUENCE OF ULTRAVIOLET AND IONIZING RADIATION AND RADIOMIMETIC CHEMICALS ON TRANSDUCTION IN PSEUDOMONAS AERUGINOSA. Report No. 2, June 27–December 26, 1961. (Melbourne Univ., Parkville (Australia). Dept. of Bacteriology). Contract No. 86. 10p. Dep.(mn).

Results are reported from studies on the effects of ultraviolet radiation, visible light, acridine orange, temperature, and the combined effects of γ and uv radiations on bacteriophage and other transduction systems in Pseudomonas aeruginosa. (C.H.)

19503 (NP-14933) THE INFLUENCE OF ULTRAVIOLET AND IONIZING RADIATION AND RADIOMIMETIC CHEMICALS ON TRANSDUCTION IN PSEUDOMONAS AERUGINOSA. Final Report. Report No. 4, June 27–December 26, 1962. B. Holloway (Melbourne Univ., Parkville (Australia). Dept. of Bacteriology). Contract No. 86. 15p. Dep.(mn).

Results are summarized from studies on the various effects of radiation on transduction and the relationship of these modifications to nucleic acid content in Pseudomonas aeruginosa. The data provide information for understanding the effects of different types of radiation on genetic recombination and also provide a system for use in studies on the modifying effects of chemical and physical agents on this radiation damage. The radiation effects observed include loss of plaque-forming ability of the bacteriophage, changes in frequency of complete transduction, and changes in frequency of joint transduction, or simultaneous transfer of more than one genetic marker. (C.H.)

19504 (RM-2801-PR) ECOLOGICAL PROBLEMS AND POSTWAR RECUPERATION. A PRELIMINARY SURVEY FROM THE CIVIL DEFENSE VIEWPOINT. H. H. Mitchell (RAND Corp., Santa Monica, Calif.). Aug. 1961. Project RAND. 40p. (AD-606326). $2.00(CFSTI).

The need for assessing and solving ecological problems in the post-attack environment as an integral part of civil defense is discussed. Basic ecological principles involving food chain relationships, climax growth, biological and environmental relationship, and land management are considered. The large-scale damage due to fire, drought, flood and other things has already presented the world with problems of reconstruction and reconstitution of biotic communities which are similar to those envisioned in the post-attack environment. The only qualitatively new element in the post-attack situation will be the effects of radiation. The available information on this subject is summarized and the need for extensive further research is pointed out. (auth)

19505 (TID-3580) BIOLOGICAL APPLICATIONS OF GAMMA RADIATION. Helen L. Ward, comp. (Division of Technical Information Extension, (AEC), Oak Ridge, Tenn.). Jan. 1965. 97p. Dep.; $3.00(cy), 2(mn) CFSTI.

This bibliography contains nine hundred and sixty-two selected references to literature published from 1958 through 1963 on the uses of gamma radiation in all fields of biological and medical research. Author and report number availability indexes are included. (C.H.)

19506 (TID-21703) THE RADIATION DOSE RATE DEPENDENCE OF DNA SYNTHESIS (IN VIVO) SYNCHRONOUS LIVER CELL POPULATION AND AN ASYNCHRONOUS INTESTINAL CELL POPULATION. W. B. Looney (Virginia Univ., Charlottesville. Radiobiology and Biophysics Lab.). [nd]. Contract AT(40-1)-2889. 8p. Dep.(mn); $1.00(cy), 1(mn) CFSTI

Results are reported from studies on the effects of a total dose of 1500 R x radiation, given at dose rates varying from 12.5 to 300 R/min, on DND synthesis in rat liver, considered to be radioresistant, and rat intestine, considered to be radiosensitive. Results indicate that the mechanism of action of radiation on DNA synthesis is similar in cells in all stages in the replication period. Results also indicate that the mechanism of action of radiation on DNA synthesis is similar in both liver and intestinal cells. (C.H.)

19507 (TID-21712) THE EFFECT OF IRRADIATION ON THE MORPHOLOGICAL AND BIOCHEMICAL CHANGES ACCOMPANYING PHAGOCYTOSIS BY LEUKOCYTIC CELLS. Progress Report, June 1964–March 1965. (Saint Margaret's Hospital, Boston, Mass.). Contract AT(30-1)-3240. 40p. Dep.(mn); $2.00(cy), 1(mn) CFSTI.

Results are reported from a number of studies on the effects of x radiation on phagocytosis by leukocytes. Emphasis was placed on morphological and biochemical changes accompanying phagocytosis and tracer studies of metabolic changes in leukocytes during phagocytosis. Data are included from studies on the effect of irradiation on the metabolic activities of guinea pigs peritoneal exudates in the absence and presence of particles; the phagocytic and bactericidal activities of peritoneal exudate cells from guinea pigs; the metabolic activities of rabbit alveolar macrophages in the absence and presence of particles; the effects of irradiation on rabbit alveolar macrophages; the effects of irradiation on phagocytosis and metabolism of rabbit peritoneal exudate; and phagocytic, bactericidal, and metabolic activities of leukocytes in patients undergoing x ray therapy. (41 references.) (C.H.)

19508 (JPRS-28977) STUDY OF THE AFTER-EFFECTS OF RADIOACTIVE FISSION PRODUCTS ON THE HARVEST AND THE QUALITY OF THE GRAIN OF CERTAIN CROPS. G. V. Il'ina, S. G. Rydkii (Rydkiy), and N. N. Kuznetsova. Translated from Agrokhimiya, No. 5, 83-90 (May 1964). 13p. (TT-65-30432). $1.00(CFSTI).

Results are reported from field and greenhouse experiments on the effects of a mixture of fission products, in which ^{90}Sr and ^{90}Y predominated, added to the soil at a dose of 1.0 $\mu c/m^2$ on the growth and yield of oats, mustard, buck-

wheat, and millet during 3 generations. An inhibition of growth and development was observed in some first generation plants, but no changes in growth, development, harvest yield, or grain quality were noted in second and third generation plants grown from seed of the plants used in the first experiment. (20 references.) (C.H.)

19509 (JPRS-29250(p.9-13)) EFFECT OF IONIZING RADIATION ON THE NEUROSECRETION OF NUCLEI IN THE HYPOTHALAMIC AREA. L. A. Andrianova. Translated from Byul. Eksperim. Biol. i Med., 59: No. 1, 33-5 (Jan. 1965).

The changes induced in the functional state of the hypothalamic region of the brain were investigated in rabbits exposed to doses of 400 R ^{60}Co γ radiation. Animals were killed at intervals of 3, 24, and 72 hr after irradiation, the brains were removed, and sections for microscopic examination were stained with differential dyes for the identification of basophylic and oxyphylic substances. The material secreted by nuclei of the hypothalamic region is a lipoprotein or lipoglucoprotein complex with phospholipids the main component and this material gave a characteristic basophylic reaction. Results indicate that initially after irradiation stimulation occurs in the secretory activity of nuclei of the hypothalamic area that influence regulatory mechanisms of the autonomic nervous system. Additional studies were performed in rabbits given aminazine, a drug that affects the activity of the autonomic nervous system, before irradiation. Aminazine blocked the activating effects of irradiation on the autonomic nervous system. (C.H.)

19510 (JPRS-29250(p.27-32)) DAILY RHYTHM OF MITOTIC ACTIVITY IN THE REGENERATING LIVER DURING ACUTE RADIATION SICKNESS. V. I. Bulgak. Translated from Byul. Eksperim. Biol. i Med., 59: No. 1, 90-3(Jan. 1965).

Results are reported from studies of the daily mitotic rhythm in cells of the regenerating liver of rats exposed to doses of 600 R x radiation. Wide variations were observed in the mitotic activity of cells in the regenerating liver of irradiated and non-irradiated rats. No regularity of daily variations was observed. (C.H.)

19511 (JPRS-29364(p.1-4)) CHOLESTEROL METABOLISM IN THE LIVER AND LUNGS DURING IONIZING RADIATION AND HYPOTHYREOSIS. M. A. Kil'chevskaya. Translated from Dokl. Akad. Nauk Belorussk. SSR, 8: 675-6(1964).

Results are reported from studies on the effects of x radiation and hypothyroidism on cholesterol metabolism in the liver and lungs of rats. Irradiation of rats caused an increase in the content of fast-acting sterols and a decrease in the cholesterol content of both liver and lungs. In hypothyroidism, there was a noticeable change in cholesterol metabolism in the liver while the changes in the lungs were less pronounced. (C.H.)

19512 EFFECT OF X-RAY IRRADIATION ON LIVER REGENERATION. E. Czeizel, G. Vaczo, and P. Kertai (State Inst. of Public Health, Budapest). Acta Physiol. Acad. Sci. Hung., 24: Suppl., 62-3(1964).

Total-body irradiation with 500 R reduced the weight of the liver regenerated after partial hepatectomy. This inhibitory effect can be prevented by the administration of bone marrow and splenic cell suspension. Irradiated bone marrow and splenic cell suspensions have no such protective effect. Irradiated bone marrow and splenic cell suspensions were injected into nonirradiated, partially hepatectomized rats. The irradiated splenic cell suspension inhibited the regeneration of the liver slightly, whereas the irradiated bone marrow suspension inhibited it significantly. Irradiated suspensions of muscle, liver, embryonic liver, leucocytes, and erythrocytes, as well as irradiated blood, had no such effect. So-called radiotoxins are formed in the tissues and the irradiated bone marrow may form a particularly strong radiotoxin, or possibly some other substance responsible for the effect. (BBB)

19513 EFFECTS OF ^{60}Co γ RADIATION ON RED BLOOD CELLS IN STORED HUMAN BLOOD. Tadeusz Dorobisz, Stanislaw Przestalski, Michal Masiak, Edward Bielinski, and Andrzej Gradzinski (Provincial Blood Diffusion Station, Wroclaw, Poland). Acta Physiol. Polon., 15: 85-92(1964). (In Polish)

The following parameters were compared in irradiated and nonirradiated blood stored at 4°C: red cell uptake of ^{32}P-phosphate, osmotic resistance to hemolysis, degree of homolysis, and plasma levels of total protein, Na, K, Ca, and inorganic P. The human bank blood had been submitted to doses of 2×10^5 R of γ rays and was then stored for four weeks. Significant differences in the penetration of phosphate ions into the red blood cells of irradiated and control blood, hemoglobin content, or hematocrit indexes were not observed. In irradiated blood a slight shift in pH toward the alkaline side and somewhat lower values of p_{CO_2} were found. After eight days osmotic resistance of the red cells of irradiated blood showed a sharp decrease, accompanied by marked hemolysis. The plasma K levels of irradiated blood increased sevenfold 24 hr after irradiation, but further elevation did not occur. In control blood after eight days the K levels were two times higher than initially, and after four weeks, four times. Sodium levels were lowered in the plasma of both groups of blood in parallel to the elevation of K levels. Inorganic P was increased in proportion to degree of hemolysis, especially in irradiated blood. Calcium levels in plasma showed only slight increases during storage, similar to degree in control and irradiated samples. Hemolysis was most pronounced from the 8th to the 20th day in irradiated blood, but rose only slightly in nonirradiated blood. (BBB)

19514 CHANGES OF ELECTROSHOCK SEIZURES IN RATS AFTER IRRADIATION. J. Farsky, S. Komenda, and B. Schober (Univ. of Palackeho, Olomouc, Ger.). Acta Univ. Palackianae Olomuc., 33: 249-61(1963).

Wistar rats, siblings of the same sex and approximately the same weight, were used in order to study the influence on some parameters of electroshock seizures including their dependence on time by means of: x irradiation; doses of irradiation; cysteine; and repeated electroshocks. Under the conditions of the experiment, the duration of tonic seizures was found to be the best parameter: x irradiation shortens the duration of tonic seizures. The shortening was also dose-dependent. After 700 R a statistically significant difference was observed when compared with the controls. In x irradiated rats, administration of cysteine resulted in a statistically significant prolongation of the duration of tonic seizures. Repetition of the electroshock after 24 hours was followed by a shortening of the duration of tonic seizures. It was concluded that the electroshock seizure threshold is a reliable indicator only under the conditions used. Optimal conditions of electroshocking and the registration of seizures are presented. (Excerpta Med., Sect. XXIII, 2: No. 3, (Mar. 1965))

19515 EFFECTS OF INTRACELLULAR IRRADIATION WITH TRITIUM. Donald E. Wimber (Brookhaven National Lab., Upton, N. Y.). Advan. Radiation Biol., 1: 85-115 (1964).

The radiobiological effects produced by intracellular tritium incorporation are discussed. The physical properties of tritium are reviewed and the effects of β particles from tritium incorporated into cells are described. Results are reported from a number of studies using tritiated nucleic acid precursors as tracers. These include studies of chromosome breakage, mutations, cell population kinetics, root morphogenesis, the toxic effects of tritium in cells, the effects of tritium on DNA synthesis, and comparative studies using tritiated water and ^{3}H–thymidine. (87 references.) (C.H.)

19516 EFFECTS OF SMALL DOSES OF IONIZING RADIATIONS. Arne Forssberg (Karolinska Institutet, Stockholm). Advan. Radiation Biol., 1: 117-56(1964).

Results are reviewed from a number of studies on the somatic effects of small doses of ionizing radiation, at doses of tens of rads or less, on cells, tissues, plants, and animals. The studies include radioinduced cytological lesions, cell death, and growth rate changes, the biochemical effects of radiation in biological systems, and biophysi-

cal effects of radiation in animals and plants. (101 references.) (C.H.)

19517 THE RELATIVE ROLES OF IONIZATION AND EXCITATION PROCESSES IN THE RADIATION INACTIVATION OF ENZYMES. Leroy G. Augenstein (Michigan State Univ., East Lansing), Tor Brustad, and Ronald Mason. Advan. Radiation Biol., 1: 227-66(1964).

A review is presented of a number of studies on the effects of temperature on radioinduced enzyme reactions. Topics discussed in detail include the effects of temperature on inactivation yields, physical processes that exhibit the observed thermal coefficients, the nature of initial interactions between ionizing radiations and biological materials, and the possible implications of the present conclusions to more complex biological systems. (135 references.) (C.H.)

19518 SOMATIC MUTATIONS IN POTATOES INDUCED BY GAMMA RADIATION. A. Benvenuti, M. Buiatti, F. D'Amato, and R. Ragazzini. Agr. Inal., (Pisa), [63]: 449-56(Dec. 1963). (In Italian)

Investigations were made on the effects of acute gamma irradiation from ^{60}Co on the potato varieties Allerfrüheste gelbe and Blu di Arabba, the first with white and the second with dark red tubers. Tubers in an initial stage of sprouting were halved and of the two halves one was irradiated and the other served as control. The following doses were applied: 2500, 5000, and 7500 R. The irradiated and unirradiated tuber halves were grown in the field side by side. In R_1 (generation raised from irradiated tubers), in addition to morphological effects (fasciation, changes in leaf morphology, increased fleshiness, etc.), a general inhibitory effect on growth and tuber production was ascertained. Moreover, in Blu di Arabba, it was also possible to calculate the mutation frequency for tuber color. This was found to be roughly proportional to dose and to reach values as high as 20.43% on a plant progeny basis. Through cloning of the irradiated material (vR_2) and scoring of seed plants (R_2) the following mutant types were isolated: convolvulus-leaf, light green leaf, wilding, and feathery-wilding. Other morphological mutants were also obtained; of special interest appears a mutant showing thickened leaves with dark green sectors. A few histological observations on the irradiated shoots (R_1) are also reported. (auth)

19519 KIDNEY HOMOGRAFTS: INDUCTION OF SPECIFIC TOLERANCE THROUGH THE LYMPHOID TISSUES. J. Parra, J. A. Torres, F. Alvarez, R. Vela, C. Albert, and H. Oliva (Ciudad Universitaria, Madrid). Ann. N. Y. Acad. Sci., 120: 524-34(Nov. 30, 1964).

Kidney transplantation was performed in 165 dogs treated with splenectomy; spleen irradiation; injections of RNA from spleen of donor; injection of cells from specifically competent lymph tissues; irradiation of area of implantation; irradiation of donor kidney before and after graft; bone marrow transplant with x irradiation and antimitotic drugs; antimitotic drugs; and antimitotic drugs and x irradiation. Typical pathological and histological results are summarized. The possible value of the methods in clinical trials is discussed. (C.H.)

19520 CURRENT EVALUATION OF HUMAN KIDNEY TRANSPLANTATION. Joseph E. Murray, John P. Merrill, Gustave J. Dammin, J. Hartwell Harrison, Edward B. Hager, and Richard E. Wilson (Peter Bent Brigham Hospital, Boston and Harvard Medical School, Boston). Ann. N. Y. Acad. Sci., 120: 545-57(Nov. 30, 1964).

Results are evaluated for 81 patients receiving kidney transplants. This included 24 sets of twins. Whole-body irradiation for immune suppression was abandoned because of repeated failures. Immunosuppressive drug therapy was used in 31 patients. Removal of the host's spleen at the time of transplant allowed higher drug dosage during the first 10 postoperative days. Rejection crises were treated with high doses of corticosteroids or actinomycin C alone or in combination. Twelve kidneys continued to function well, but only 5 of the cases were 6 mo. post-operative. The use of cadavers as a kidney source is discussed. (C.H.)

19521 SPLENIC TRANSPLANTATION IN THE DOG. George L. Jordan, Jr., W. Guy Fiscus, John J. Trentin, Riley P. Foster, Vincent P. Collins, and Harry L. Barton (Baylor Univ., Houston, Tex. and Veterans Administration Hospital, Houston, Tex.). Ann. N. Y. Acad. Sci., 120: 612-25(Nov. 30, 1964).

Splenic autografts and homografts, as total transplants with vascular anastomoses and as intravenous suspension of splenic cells, were performed in 92 dogs. Some dogs were unmodified recipients, while others were subjected to varying doses of total-body irradiation. Total-splenic transplants and free transplants in the peritoneal cavity were rejected and, if left undisturbed, totally resorbed by the unmodified recipient. Autologous splenic cells injected intravenously protect animals against lethal effects of total-body irradiation, while homologous cells do not. Following sublethal doses of irradiation, total-splenic transplants had a deleterious effect upon the formed elements in the peripheral blood and upon the survival of the animal, while intravenous injections of homologous spleen cells did not. The differences observed in the effects of these two methods of transplantation and the differences observed in the dog as compared to some other animals are not fully understood. (auth)

19522 SPLENIC HOMOTRANSPLANTATION. Thomas L. Marchioro (Univ. of Colorado, Denver and Veterans Administration Hospital, Denver), David T. Rowlands, Jr., David Rifkind, William R. Waddell, Thomas E. Starzl, and Hugh Fudenberg. Ann. N. Y. Acad. Sci., 120: 626-51(Nov. 30, 1964).

Results are reported from a series of canine splenic homografts performed. Animals pretreated with total-body irradiation showed markedly shortened red cell half-life and sharp drops in hematocrit with no potentiation of homograft survival. Those dogs treated with azathioprine had no change in red cell half-life, hematocrit changes were much less than in the irradiated animals, and homograft survival was increased as judged by pathologic studies. In another series of animals, simultaneous renal and splenic homografts were performed to bilaterally nephrectomized dogs. Function of both transplanted organs was inferred from the behavior of the renal homograft. Control animals receiving no therapy showed a somewhat delayed rejection. Those dogs treated with total-body irradiation frequently developed severe hemolytic anemia and graft survival was less than in untreated animals. Both the spleen and the kidney appeared to be particularly susceptible to the rejection reaction in this series, and of the two organs, the spleen appeared to be more damaged than the kidney. When azathioprine was used as the immunosuppressive agent, survival of both renal and splenic homografts was obtained to as long as seven and one-half months. Anemia was not noted in these animals after the first month and gross and microscopic examination at seven months revealed both organs to be viable. No evidence of secondary disease was observed in these dogs. In one animal, azathioprine was discontinued after 120 days. He remains alive, three and one-half months later. In addition, whole-organ spleen homotransplantation was carried out in five patients. In four instances the purpose was to provide a continuous endogenous source of antibody against a malignant tumor. In the fifth case, it was hoped that the homograft would supply the immunologic deficiency in a child with congenital sex-linked hypogammaglobulinemia. The clinical experience was disappointing. In the patients with tumor, no alteration of the progression of the disease was obtained. In one patient of A+ blood type, who received a spleen from an O+ donor, severe hypersplenism developed shortly after transplantation. One patient is alive 11 months post-operatively with radiographic evidence of progression of his alveolar cell carcinoma. In the child with hypogammaglobulinemia, evidence for production of gamma globulin by the homografted spleen could not be obtained by a variety of techniques. (auth)

19523 LUNG TRANSPLANTATION IN THE DOG. David A. Blumenstock, John A. Collins, Herbert B. Hechtman, David J. Hosbein, Neil Lempert, E. Donnell

Thomas, and Joseph W. Ferrebee (Mary Imogene Bassett Hospital, Cooperstown, N. Y.). Ann. N. Y. Acad. Sci., 120: 677-88(Nov. 30, 1964).

Results are reported from a series of 45 homotransplants of the lung in dogs. Eight untreated control animals evidenced rejection of the lung in four to six days and died within 14 days. When animals of this study, dying before the fifth month after transplantation, are eliminated from consideration, results can be stated as follows: (a) A single animal out of eight treated with methotrexate after transplantation of the lung is alive 38 months after transplantation. There is no evidence of function in the transplanted lung. (b) One of the 12 animals treated with azathioprine after transplantation survived eight months. Oxygen consumption of the transplant two months after transplantation was 32 per cent of the total. This decreased to seven per cent at eight months. (c) One animal of 11 survived six months after supralethal whole-body irradiation followed by homotransplantation of bone marrow and lung. The animal was so debilitated after transplantation that pulmonary function studies were not attempted. (d) Five of six animals pretreated with unirradiated donor blood before transplantation while immune responses were depressed with methotrexate and/or sublethal irradiation, survived five months or more after transplantation. Pulmonary function was demonstrated up to two years after transplantation. Skin grafts were exchanged between two donor-recipient pairs one and one-half and two and one-half years after lung transplantation. The donor to recipient grafts survived 30 and 101 days, while back grafts from recipients to donor survived 10 and 12 days. The lung recipients rejected an indifferent skin graft in the normal time. (auth)

19524 RADIATION DERMATITIS AND RADIOGENIC NEOPLASMS OF THE HANDS. Shattuck W. Hartwell, Jr. (Cleveland Clinic), William Huger, Jr., and Kenneth Pickrell. Ann. Surg., 160: 828-34(Nov. 1964).

Clinical experience with 39 cases of radiogenic dermatitis and neoplasms of the hand in the Duke Univ. Medical Center between 1945 and 1960 is reviewed and the findings tabulated. Over one-half of the patients were physicians, dentists, and veterinarians, and injury from radiation was due in every instance, except one, from their carelessness in the professional use of x-ray equipment. The other patients were treated by x ray for some skin disorder; the most common lesion was warts and next most common were rashes of the hands attributed to allergic states or eczema. Nearly half of the patients were exposed over a period of four or more years. An analysis of the varieties of treatment used among the 26 patients with radiodermatitis shows that nearly half received no operative treatment, such as (1) simple excision, (2) excision coupled with resurfacing the defect with a free or pedicled graft, or (3) amputation. Nearly a third of this series (12/39) developed radiogenic neoplasia; among these 12 are three different histopathologic types. Squamous cell carcinoma is the most common, then fibrosarcoma, and a case of undifferentiated malignant tumor of the skin. Photographs of hands are provided, showing the manifestations of radionecrosis, radiodermatitis, and radiogenic cancer. Reconstructive technics in the hand are described. When operation is indicated it is usually to clear an area of unserviceable and easily injured tissue or tissue which has become painful, precancerous, or cancerous. Such operations are complicated by infection and languid healing; poor blood supply and indolent reparative processes in these areas impair hopes of good functional improvement in many patients. Frequently, changes in peri-articular tissues and in joints are not remedied by graft or flap, and imperfect function remains. (BBB)

19525 HEMATOLOGIC OBSERVATION OF PERSONNEL EXPOSED TO X RAYS IN HOSPITALS. J. Bourret and R. Detry (Universite de Medecine du Travail, Lyon). Arch Maladies Profession., [Med. Travail Securite Sociale], 24: 919-22(Dec. 1963). (In French)

Hospital personnel may be exposed to slight doses of irradiation over a long period of time. A detailed analysis of 650 hematological examinations of personnel was made to determine the effects of such exposure. The exposed personnel were divided into categories according to the results obtained by the analysis of dosimetric films carried by them for three years. The limits of normal variation in blood cells and hemoglobin were established with nonirradiated personnel as a reference. The hematological anomalies in the exposed personnel within the different categories corresponded to the degree of exposure. The blood cell formulas of the groups were within the normal range, only slight anomalies being provoked by indirect irradiation. No important anomalies were observed in erythrocytes. The change in white blood cells was manifested generally as leucocytosis or, more rarely, as leucopenia. The latter is indicative of heavier irradiation. The number of white blood cells increased to 15,000 to 20,000 per mm^3 from a normal count of 5800 to 8300, but decreased again in several weeks, which might indicate a factor independent of the ionizing radiations. The number of anomalies in the eosinophils seemed to become greater as the exposure of the personnel increased. Basophils appeared in the exposed groups and increased in number with more intense radiation. The number of lymphocytes and large monocytes was not modified significantly with exposure to x rays. With increasing irradiation the medium monocytes increased in number. It is suggested that hematologic examinations properly interpreted constitute one of the best techniques in preventive medicine for personnel exposed to irradiations in hospitals. (BBB)

19526 AUTOPSY STUDY OF LEUKEMIA IN HIROSHIMA. Robert E. Anderson, Tsutomu Yamamoto, Atsushi Yamada, and Drake W. Will (Atomic Bomb Casualty Commission, Hiroshima). Arch. Pathol., 78: 618-25 (Dec. 1964).

Consideration is given to 157 cases of leukemia autopsied by the Atomic Bomb Casualty Commission (ABCC) from 1949 to 1962 inclusive. Correlations were made between exposure status and type of leukemia, age, duration of symptomatology, and degree of organomegaly. The cases were classified as: proximally exposed (0 to 399 m from the hypocenter), distally exposed (1400 to 10,000 m), and nonexposed (not in Hiroshima at the time of the bombing). Approximately 40% of all patients with leukemia known to have died prior to Jan. 1, 1963, were autopsied by ABCC. The distribution of leukemia cases by exposure status and age at death showed that there were proportionately more nonexposed persons in the 0- to 19-year age group in comparison with the other age groups and fewer in the 60+ year group. In addition, the male:female ratio in the nonexposed group was almost double that in the exposed group (1.9:1 vs 1.1:1). The cases of leukemia were distributed as follows: acute myelogenous 48, subacute myelogenous 16, chronic myelogenous 41, acute lymphatic 30, subacute lymphatic 3, and all others 19. Of the 157 cases of leukemia, 30 were in the proximally exposed group, 33 in the distally exposed group, and 94 were not in the city at the time of the bomb. With the exception of acute lymphatic leukemia, the mean age at death in the proximally exposed group was the same for distally exposed individuals. The duration of the estimated total clinical course in myelogenous leukemia was shorter in the proximally than in the distally exposed; this was true for both the acute form where the average difference was 1.8 months and the chronic form where the comparable figure was 11.2 months. No significant differences were observed with respect to associated diseases or tumors, terminal complications of the leukemic process, or the magnitude or character of the leukemic infiltrates other than those noted previously. No morphologic changes were evident to enable identification of an individual case as radioinduced. (TCO)

19527 COMPARATIVE CYTOLOGICAL AND PHYSIOLOGICAL INVESTIGATION OF MAIZE LINES TREATED WITH IRRADIATION AND WITH ETHYL METHANE SULFONATE (EMS). Andor Balint, Jozsef Sutka, and Geza Kovacs (Univ. of Agrarian Sciences, Hungary). Biol. Kozlemen., 12: No. 1, 11-15(1964).

The cytological and physiological effects of the various mutagens were studied on two inbred maize lines. The results indicate a linear increase in the number of chromosome aberrations with the increase of irradiation dosage

rates. Similar correlations were not observed with the concentration of EMS used. One line was found to be more sensitive to irradiation while the other was more sensitive to the EMS treatment. Depending on the treatment used, the ^{32}P uptake increased in one line. This can be explained by the degenerative increase in the metabolic process. The study of bios substances indicates that larger doses or irradiation destroys part of these substances. (CFSTI)

19528 INFLUENCE OF GAMMA IRRADIATION ON THE GERMINATION AND FIRST DEVELOPMENTAL STAGES OF MAIZE. Karol Erdelsky (Comenius Univ., Bratislava). Biologia, 15: 890-4(1960). (In Czech)

Maize seeds were exposed to ^{60}Co γ radiation to total doses of 500, 1000, 3000, 5000, 10,000, and 20,000 R. The dry seeds were irradiated, then moistened, following which the rate of germination, growth anomalies, and length of the roots and coleoptiles were examined. The rate of germination, compared with a value of 84.0% for unirradiated seeds, was as follows for the seeds irradiated 96 hr earlier at the aforementioned six doses: 80.0, 80.0, 81.0, 82.0, 77.0, and 65.0%. There was a slight stimulation of increase of root length at the lowest radiation dose; the length at 96 hr was 3.9% greater than that of the unirradiated controls. At the five higher doses the root lengths were 99.9, 63.5, 49.1, 31.1, and 28.3% that of the control length. Hence, it is seen that at doses of 1000 R and higher, inhibition of root growth is dose dependent. Germination, however, was significantly inhibited only at the two highest doses (10,000 and 20,000 R). Coleoptile growth was inhibited in a dose-dependent way, similar to that seen with the roots. (BBB)

19529 THE TRANSITIONAL PROCESS AND REVERSIBLE ATTACHMENT OF OXYGEN TO HAEMOGLOBIN. I. V. Vysochina (Inst. of Biology and Physics, Moscow). Biophysics (USSR) (English Transl.), 8: No. 3, 421-7(1963). Translated from Biofizika, 8: No. 3, 361-6 (1963).

Reversible attachment of oxygen to hemoglobin is a transitional process in four equivalent steps. To calculate the oxyhemoglobin dissociation curves, a transitional process equation is proposed containing only one constant, distinguishing it from all the other existing equations for the reaction of oxygenation that have two or more constants. The constant τ as well as relating the content of oxygen in the blood to partial O_2 pressure, characterizes the state of hemoglobin, and its ability to bind oxygen. As a result, the proposed equation may be used in medical practice for investigating dissociation curves in pathology since to construct the whole curve, it suffices to have only two experimental points. The results of experiments on rabbits before and after whole-body x irradiation to doses of 900–1300 R were analyzed using the equation. Data are tabulated. (P.C.H.)

19530 RADIATION-INDUCED LEUKEMIA IN WISTAR RATS AFTER FRACTIONATED TOTAL-BODY IRRADIATION. W. Hunstein, E. Stutz, and U. Reincke (Universitat, Freiburg i. B.). Blut, 9: 389-404(Dec. 1963). (In German)

Chronic irradiation experiments were conducted on 220 male and female Wistar rats of a single inbred strain. Starting on the 100th day of life they were given fractionated whole-body irradiation, the total dose being 900 R. Series A were given 6 doses of 10 R at weekly intervals, for a total dose of 90 times 10 R. Series B were given 3 doses of 300 R at monthly intervals. All the irradiated rats were kept under identical conditions until moribund or dead. In addition to a variety of epithelial and mesenchymal radiation tumors, both benign and malignant, changes in the hemopoietic system were observed. The reticuloses or reticuloendothelioses that developed in four animals are described in detail, one being a malignant reticulosis with mast-cell differentiation associated with a leukemic blood picture. Five animals presented a picture of an immature-cell acute leukemia with characteristic infiltrations in the liver, spleen, and bone marrow, and with involvement of some lymph nodes. These leukemias were considered to be due to radiation. Whole-body irradiation could, thus, produce leukemoid and leukemic states in the reticular organs, and these effects were manifested at various stages of the cellular differentiation of the reticular tissues. Correlation of these findings with those in human leukemia and other evidence of the leukemogenic action of radiation are discussed. (BBB)

19531 EFFECT OF CHLORAMPHENICOL ON UV-INDUCED STREPTOMYCIN-, NOVOBIOCIN- AND PENICILLIN-RESISTANCE IN STAPHYLOCOCCUS AUREUS STRAIN 209P. W. T. Dobrzanski (Dept. of Microbiology and Hygiene, School of Medicine, Warsaw). Bull. Acad. Polon. Sci., Ser. Sci. Biol., 12: 561-7(1964).

Results are reported from studies on the effects of chloramphenicol on ultraviolet-induced mutations of Staphylococcus aureus resistant to streptomycin, novobiocin, and penicillin. Data indicate that chloramphenicol blocks the phenotypic expression of uv-induced mutants resistant to these three antibiotics. Possible mechanisms involved are discussed. (C.H.)

19532 EFFECT OF VARIOUS POST-IRRADIATION TREATMENTS ON UV-INDUCED MUTATIONS TO ANTIBIOTIC-RESISTANCE IN STAPHYLOCOCCUS AUREUS STRAIN 209P. W. T. Dobrzanski (Dept. of Microbiology and Hygiene, School of Medicine, Warsaw). Bull. Acad. Polon. Sci., Ser. Sci. Biol., 12: 569-74(1964).

The influence of various kinds of post-irradiation treatment on uv-induced mutants resistant to three antibiotics in Staphylococcus aureus strain 209P and on uv-induced prototrophic mutants in various E. coli B strains is different in a number of cases. Results are reported from studies that indicate that the uv-induced premutants resistant to three antibiotics in strain 209P are more stable than the prototrophic premutants induced by uv in E. coli B and B/r and/or that the processes leading to the phenotypic expression of mutation of antibiotic-resistance are less sensitive to various agents and that there exists a certain similarity in the response to various post-irradiation treatments in the uv-induced SM-R mutations in the strain 209P and in E. coli strains. (auth)

19533 HOW MAY THE INTERNIST DETECT PHARMACOGENIC TERATOGENIC HAZARDS IN THE CLINIC. L. Justin-Besancon, H. Pequignot, and C. Roux. Bull. Schweiz. Akad. Med. Wiss., 20: 527-43(Sept. 1964). (In French)

Fetal anomalies caused by drugs, ionizing radiations, and other teratogenic agents are discussed. (BBB)

19534 THE EFFECT OF IONIZING RADIATION ON PHYSIOLOGICAL CHANGES IN THE CONTENT OF MINERAL COMPONENTS IN THE BRAIN DURING DEVELOPMENT. M. Wender (Neurological Clinic, Medical Academy, Poznan, Poland). Bull. Soc. Amis. Sci. Letters, Ser. C, 13: 13-22(1964).

Investigations were made on the influence of x irradiation, applied as a single dose of 400 R, on concentration changes of mineral components in the brains of guinea pigs during development. The physiological changes of water content in the brain due to maturation were unaltered by the ionizing radiation, which caused only negligible modifications in the composition of electrolytes in the developing cerebral white matter. However, the ionizing radiation, applied at the final stage of intrauterine life influenced markedly the developmental concentration changes of mineral components in the cerebral cortex, where a distinct shift of the motor Na/K ratio was observed. These changes in electrolyte composition, resulting from irradiation may lead to important functional disturbances in the developing cerebral cortex. (Excerpta Med., Sect. XXIII, 2: No. 3, (Mar. 1965))

19535 FATAL SHOCK IN IRRADIATED RABBITS AS A RESPONSE TO ADMINISTRATION OF HOMOLOGOUS GAMMA-GLOBULIN. V. F. Sosova. Byul. Eksperim. Biol. i Med., 58: No. 10, 31-3(Oct. 1964).

Administration of homologous gamma-globulin (50 mg in 10 ml of physiological saline solution) to rabbits 1 hour after irradiation with 800 R was fatal for eight out of nine rabbits. The clinical symptoms of fatal shock are described. The same injection 3 days after irradiation did not cause shock as was also the case in intramuscular injection one hour after irradiation. These results to the

varying reactivity of the organism in various phases of radiation sickness and to the involvement of high gamma-globulin concentrations in the blood in the advent of shock. (OTS)

19536 CHARACTERISTICS OF THE HIGHER NERVOUS ACTIVITY OF ADULT DOGS SUBJECTED TO THE ACTION OF IONIZING RADIATION IN VARIOUS PERIODS OF ANTENATAL DEVELOPMENT. I. A. Piontkovskii and M. G. Ayrapetyants (Inst. of Higher Nervous Activity and Neurophysiology, Academy of Sciences, Moscow). Byul. Eksperim. Biol. i Med., No. 11, 29-33(Nov. 1964).

Higher nervous activity was studied by the method of salivary conditioned reflexes in dogs 1–2 yrs old that had been subjected to x irradiation in a dose of 200 R on the 13th, 20th, 45th, and 55th days of antenatal development. The time required for elaboration of positive and negative conditioned reflexes was determined. The tests indicated that the higher nervous activity of antenatally irradiated dogs was characterized by slowness of the principal nervous processes, reduced capacity for differentiation, and inertia. While the time required for formation of conditioned reflexes in irradiated dogs was not much longer than in control animals, the training that had to be applied before these reflexes were firmly established was much more extensive, i.e., the nervous processes of the experimental animals were deficient with respect to concentration. The irradiated animals reacted to an exceptionally strong irritant with short-lived failure of reflexes, which was exhibited on the day of the test only, while disturbances of conditioned reflex activity persisted in control animals for 4-8 days. The maximum disturbance of cerebral functions was observed in animals irradiated on the 13th day of antenatal development and the minimum disturbance in those irradiated on the 55th day. Visual analyser disturbances predominated in dogs irradiated on the 20th day of embryogenesis. (OTS)

19537 EFFECTS OF IRRADIATION WITH X RAYS ON THE FREQUENCY OF GENETIC RECOMBINATIONS AND THE PROPERTIES OF RECOMBINATIONS IN E. COLI. A. P. Pekhov and E. V. Yudin (Inst. of Experimental Biology, Academy of Medical Sciences, Moscow). Byul. Eksperim. Biol. i Med., No. 11, 73-6(Nov. 1964).

The effects produced by x irradiation on genetic recombination in E. coli were studied. The donor strain, E. coli Hfr, which was x irradiated in doses of $0-150 \times 10^3$ R before being crossed with the recipient strain, was thiamine-dependent and sensitive to streptomycin (S^s), phages of group T, and gamma phage. The order of transmission by it of characteristics to the recipient cells was threonine (T)–leucine (L)–lactose (Lac)–galactose (Gal). The recipient strain, E. coli PA678F, was resistant to streptomycin (S^r) and had lost the capacity to synthesize threonine, leucine, and thiamine (i.e., thiamine was added to the medium for the derived strain in every instance) or to ferment lactose, galactose, xylose, mannose, or maltose. It was resistant to phages T_1, T_5, T_6, and gamma. The initial doses (up to $20 \times 10^3 - 30 \times 10^3$ R) produced an increase in the number of $T^+L^+S^r$, L^+S^r, and T^+S^r recombinations. With increasing doses of radiation, the number of these recombinations then decreased. The number of Gal^+S^r recombinations began to decrease beginning with the smallest doses of radiation. With increasing doses of radiation, the number of $T^+L^+S^r$ recombinations with Lac^+ and Gal^+ decreased. The number of Gal^+S^r with Lac^+ first increased and then decreased. The percentage of T^+ and gamma^s showed a general tendency to decrease with increasing doses of radiation. The T^+L^+ linkage of characteristics was disturbed by irradiation: the number of T^+S^r recombinations that inherited the capacity to synthesize leucine decreased with increasing doses of radiation, while that of L^+S^r recombinations with an inherited capacity to synthesize threonine did not decrease. This was due to the fact that L^+ was transmitted to recipient cells after T^+. An estimation of the relative extent of transmission of non-selective characteristics showed that with increasing distance of the locus of the characteristic from the initial segment of the donor chromosome that was transferred, the radiosensitivity of the characteristic increased. (OTS)

19538 PENTOSE CYCLE AND RADIATION DISEASES. J. Sonka*, J. Pospisil, Z. Dienstbier, J. Charvat, and Z. Dienstbier (*Charles Univ., Prague). Casopis Lekaru Ceskych., 103: 1343-4(Nov. 27, 1964).

The pentose cycle of glucose metabolism was studied. It is important in radiation diseases because it is the only source of ribose-6-phosphate, and it is the main source of the reduced nicotine amino-adenine-dinucleophosphate. Stimulation of the cycle facilitates regeneration processes; irradiation reduces the activity of the cycle; this lasts a few days, and causes delays in the regeneration of nucleic acids. Sublethal irradiation increases activity of enzymes, and therefore the damage is probably due to the co-enzymes. (CFSTI)

19539 STUDY OF OXYGEN REQUIREMENTS OF IRRADIATED RATS OF VARIOUS AGE. M. Tusl, V. Kaut, and S. Svorcova (Charles Univ., Hradec Kralove, Czechoslovakia). Cesk. Fysiol., 13: 524(Dec. 1964).

Female rats aged 3, 9, and 24 months were used. A single dose of irradiation of 600 R was used, and oxygen consumption in the presence of up to 8% of CO_2 was measured after 1, 3, 6, and 10 days. Young rats were less influenced by CO_2, but more by the irradiation than the old rats. Oxygen requirement is a good indication for the prognosis of recovery from irradiation disease. (OTS)

19540 Mn, Ni, AND Cr IN EXPERIMENTAL RADIATION SICKNESS IN GROWING ANIMALS. V. A. Boiko. Dokl. Akad. Nauk Belorussk. SSR, 8: 332-3(1964). (In Russian)

Changes were determined in the content of Mn, Ni, and Cr in the blood, heart, lungs, liver, spleen, kidney, small intestine, and sternum of 20 young dogs with radiation sickness provoked by single x-irradiation of 500 R. All experimental animals died within 13 to 54 days following irradiation and the Mn, Ni, and Cr in the organs were determined. The Mn, Ni, and Cr in the blood of control animals were 21, 28.2, and 11 γ%, respectively. In the irradiated animals they were 30, 15.7, and 6.3 γ%, respectively. In the liver of irradiated animals the Mn increased, while the Ni and Cr decreased. The Mn in the bones increased following irradiation, while the Cr decreased. The greatest changes in the content of Mn, Ni, and Cr were found in the blood, liver, spleen, and sternum. (C.H.)

19541 KINETIC CHARACTERISTICS OF THE DECAY OF PEROXIDES IN IRRADIATED DNA SOLUTIONS. G. P. Zhizhina, D. L. Zybina, K. E. Kruglyakova, and N. M. Emanuel' (Inst. of Physics and Chemistry, Academy of Sciences, USSR). Dokl. Akad. Nauk SSSR, 158: 935-8 (Oct. 11, 1964). (In Russian)

Aqueous solutions of DNA, 0.1%, prepared from rat spleens were x irradiated to 70 kR at 52 to 90°C. The linear part of a semilogarithmic plot of DNA concentration vs time was extrapolated to zero, and the destruction rate constants (k_1 and k_2) of a less- and a more-stable DNA peroxide were determined. The activation energies of decay were calculated to be 13 and 24 kcal/mole, respectively. The Arrhenius plot of k_1 was less steep than that of k_2. Similar studies on thymine and cytosine showed a significantly higher decay rate of cytosine peroxide than of thymine, e.g. 0.51 and 0.0038 min^{-1} at 52°C. The Arrhenius plot of the thymine k was about the same as that of the DNA k_2. It is therefore proposed that the more stable peroxide in the DNA solution is thymine peroxide and that the less stable possibly is cytosine. The activation energy value of 13 kcal/mole agrees with the value of 11 kcal/mole found from chemiluminescent data, and the agreement indicates that DNA decay may be the source of the luminescence. The kinetic curves for change in viscosity of irradiated DNA solutions were found to be similar to those for DNA peroxide decay, which may indicate a role of peroxide compounds in secondary radiation phenomenons. (TTT)

19542 MUTAGENESIS ON ISOLATED DNA, INDUCED BY ULTRAVIOLET RADIATION AND CHEMICAL AGENTS. S. E. Bresler and D. A. Perumov (Inst. of High Molecular Compounds, Academy of Sciences, USSR). Dokl. Akad. Nauk SSSR, 158: 967-9(Oct. 11, 1964). (In Russian)

The results of experiments on mutagenesis in vitro resulting from the action of uv irradiation on isolated DNA of B. subtilis are presented and compared with the mutagenic action of nitrous acid and hydroxylamine. In 5000 colonies obtained in the transformation of bacteria by irradiated DNA, 36 fluorescing mutants were found. With nonirradiated DNA not one mutant was found. For determining whether free radicals act in the irradiation of DNA, 0.1% cystamine was added to some cultures, but no differences were observed in the inactivation curves. This indicates a direct action of ultraviolet radiation on DNA. Similar experiments were made with nitrous acid and hydroxylamine as mutagenic agents, and a mathematical expression was developed for comparing the action of the three agents. The results show that the mutagenic action of ultraviolet radiation is less efficient than that of the two chemicals. The dependence of the decrease in the number of transformations on time was calculated from the equation and found to agree well with the experimental data. (TTT)

19543 THE EFFECT OF ULTRA-VIOLET RADIATION ON THE DARK PHASE OF THE ACTINORHYTHMIC REACTION IN PLANTS. B. S. Moshkov and A. P. Mikhailov (Scientific Research Inst. of Agronomical Physics, Leningrad). Dokl. Akad. Nauk SSSR, 158: 990-2(Oct. 11, 1964). (In Russian)

Ultraviolet regions were defined as short, 253.7 mμ; medium, 290–320 mμ; and long, 330–390 mμ. Perilla, a short-day plant, after 20 days' growth in continuous light, was subjected to a regime of a 14-hr day and 10-hr night. Controls budded after 18 days. When the night was broken by a 60-min exposure to white light (400–800 mμ) at 0.2 watt/m^2, the dark processes of the actinorhythmic reaction were prevented. Ultraviolet from 390 to 253 mμ at the same energy did not interfere, but that from 390 to 330 mμ at 12 watts/m^2 did. Short- and medium-wavelength ultraviolet at 0.6–1 watt/m^2 killed the plants. The perilla plants did not flower under experimental conditions. Abyssinian cabbage, a long-day plant, grew well on exposure to 150 to 200-watts/m^2 light but reproduced only when the day was increased by 150 min. With a 10-hr night interrupted by medium- or short-ultraviolet radiation for 150 min, the plants died with 0.25- to 0.50-watt/m^2 light. Long-wave uv had no lethal effect even at 90 watts/m^2, and plants bloomed at the same time as those in a regime where the 10-hr night was broken by a 150-min interval of visible light at 80 watts/min. (TTT)

19544 CAUSES UNDERLYING THE LOSS OF REGENERATION CAPACITY BY SALAMANDER EXTREMITIES, AFTER EXPOSURE TO X-RAYS. S. J. Tuchkova (Severtsov Inst. of Morphology of Animals, Academy of Sciences, USSR). Dokl. Akad. Nauk SSSR, 158: 1420-3(Oct. 21, 1964). (In Russian)

Sixty 10 months old, 12 to 15 cm long salamanders, were used. The experimental animals were x-irradiated, on the posterior extremities only, to 10,000 R at a rate of 480 R/min. Nineteen days later the limbs were removed and then observed for up to 60 days. The results indicated that failure of the limbs to regenerate after x irradiation is due to changes in the molecular structure of the cell and loss of its ability to differentiate and form new structures rather than to growth of connective tissue in the wound or to suppression of the mitotic activity. Details of the microstructure of the cultured limbs are shown in a series of photomicrographs, and differences in control and experimental animals throughout the observation period are discussed. Immediately after amputation there is intensive tissue destruction, which is paralleled by regenerative processes in the controls. In the experimental animals the cells do not differentiate. At first nonmitotic the regenerative process later becomes one of mitotic multiplication. Cellular material accumulates under the epithelium of the wound surface and degenerates, and is replaced by scar tissue. This is more resistant than some of the other tissue, and it grows into the distal part of the culture because of the absence of regeneration. (TTT)

19545 EFFECT OF RADIATION INTENSITY ON THE DEVELOPMENT AND GROWTH OF PLANTS, AS A FUNCTION OF THE LENGTH OF PHOTOPERIOD AND TEMPERATURE. I. A. Shul'gin and V. Z. Podol'nyi. Dokl. Akad. Nauk SSSR, 158: 1439-42(Oct. 21, 1964). (In Russian)

The time between the seedling and the flowering stages in two varieties of wheat decreased at a given temperature as the intensity of the light (400–700 mμ) to which they were exposed increased from 55×10^3 to 200×10^3 ergs/cm^2 sec. For a given intensity, increasing the temperature within the limits 16–27°C also decreased the time. Probably with further increase in temperature, a point would be reached where the intensity would not affect the development rate. The effects of intensity and temperature were much more marked in some stages than in others. In the earlier stages, the dry weight of the plant increased more at higher temperatures and intensities. For the same radiation intensity, the greatest growth was at lower temperatures. The average daily growth from seedling to flowering stage at all temperatures studied was maximum for intermediate light intensities. (TTT)

19546 VARIATION IN THE CONTENT OF NUCLEIC ACIDS, ACCOMPANYING SUPPRESSED REGENERATION OF EXTREMITIES IN SALAMANDERS FOLLOWING X-RAY TREATMENT. S. J. Tuchkova (Severtsov Inst. of Animal Morphology, Academy of Sciences, USSR). Dokl. Akad. Nauk SSSR, 159: 215-18(Nov. 1, 1964). (In Russian)

Salamanders, 10 months old and 12 to 15 cm long, were x-irradiated on the posterior extremities to 8000 R at a rate of 480 R/min. Nineteen days later their limbs were removed and they were observed for up to 60 days. The highest concentration of RNA was found in the cytoplasm of the nondifferentiated cells of the blastema. This lasted until they differentiated, but then it gradually decreased with forming and differentiation of tissue. DNA was high in all cells throughout the regeneration process. In the regenerating cells chromatin was in small clumps, and its Feulgen staining was less intense than in the compact nuclei of the differentiated cells. In the experimental animals, tissue differentiation was absent and regenerating cells of the embryonal type did not form under the epithelium of the wound surface. There was no increase in cytoplasmic RNA in the cells released from the tissue. The data verified suggestions with regard to changes in the molecular structure of irradiated cells, which lose the ability to synthesize and accumulate RNA and in which the DNA distribution is changed. The histochemical data agreed with biochemical data, which showed a regularity in the decreased amounts of RNA and DNA in tissue after irradiation and amputation of salamander limbs. (TTT)

19547 THE GENETICS OF SORDARIA BREVICOLLIS. I. DETERMINATION OF SEVEN LINKAGE GROUPS. Kuo-chun Chen (Columbia Univ., New York). Genetics, 51: 509-17(Apr. 1965).

Twenty-seven mutants affecting ascospore color and mycelial morphology were obtained following ultraviolet irradiation of microconidia. These and the mating type alleles have been mapped at not fewer than 21 loci making up seven linkage groups linked to seven independent centromeres. The ascospore color mutants are autonomous in their expression. Four yellow spored mutants belong to a compound locus concerned with a single phase in ascospore pigment development, while three hyaline spore-color mutants at another compound locus involve an earlier stage in pigmentation. (auth)

19548 INDUCED PREMEIOTIC EXCHANGE OF LINKED MARKERS IN THE ANGIOSPERM ARABIDOPSIS. Y. Hirono and G. P. Redei (Univ. of Missouri, Columbia). Genetics, 51: 519-26(Apr. 1965).

Plants of Arabidopsis thaliana heterozygous for linkage group 4 markers, when x irradiated, developed somatic sectors and occasional twin spots. In the sexual progenies of the sectors, premeiotic exchange between linked markers has been demonstrated by a test comparable to half-tetrad

analysis. Since this recombination is associated with chromosomal aberrations, it appears that a recombination mechanism different from meiotic crossing over is involved. (auth)

19549 CHARACTERIZATION ON A HEREDITABLE VARIANT IN HEMAGGLUTININ PRODUCTION IN VACCINIA VIRUS. Yoshihisa Fujio (Osaka Univ.). Idengaku Zasshi, 39: 41-54(June 1964).

Some cytopathic changes in L cells infected with the HA^+ and HA^- viruses and with mixture of both viruses were examined. The HA^+ virus produced cell clumping and hemadsorption of fowl red blood cells around the infected cells, whereas the HA^- virus produced polynucleated giant cells without hemadsorption. The production of hemagglutinin in cells infected with the HA^+ virus first became appreciable 10 hours after infection and a parallelism was found between the growth of virus and the production of hemagglutinin. The cells infected with the heat and UV-treated HA^+ virus showed no hemagglutinin production. Inhibition of the production of hemagglutinin by actinomycin and puromycin indicates that viral DNA-dependent RNA and protein synthesis are indispensable for the production of hemagglutinin. The HA^+ virus produced cell clumping whereas the HA^- virus produced polynucleated giant cells 6 hours after infection and their formation depended on multiplicity of viruses. The formation of polynucleated giant cells was not affected by mitomycin C and actinomycin but inhibited by puromycin. Although the heat-treated viruses produced no morphological changes in their host cells, the uv-irradiated HA^+ and HA^- viruses produced cell clumping and polynucleated giant cells respectively. The fact that dual infection with both HA^+ and HA^- viruses produced cell clumping but no polynucleated giant cells indicates that the changes produced by the HA^+ virus were dominant. (auth)

19550 RESTORATION OF ESCHERICHIA COLI STRAIN B AFTER γ-IRRADIATION. A. J. Forage and N. E. Gillies (Middlesex Hospital Medical School, London). J. Gen. Microbiol., 37: 33-9(Oct. 1964).

The effect on survival of depriving the bacteria of proline for an initial period after exposure to γ rays was studied by incubating the irradiated bacteria for various periods on a nutrient medium which lacked proline, before transferring them to one containing proline. The viable fraction of bacteria of a proline-requiring auxotrophic strain of Escherichia coli B after exposure to γ rays under anoxic conditions was markedly increased when the organisms were deprived of proline or were treated with chloramphenicol for the initial period after irradiation. Either treatment was equally effective and the maximum degree of survival which was obtained was above that observed when the cells had been incubated throughout on a proline + inorganic salts + glucose medium. The depression in survival caused by including NaCl in the defined nutrient medium, on which the irradiated bacteria were grown, was completely eliminated by both treatments. Rescue appears to depend on the temporary inhibition of protein synthesis. The modes of action by which the two treatments inhibit protein synthesis, however, are probably not identical. Proline deprivation will lead to inhibition of synthetic reactions which involve proline, whereas chloramphenicol appears to act by preventing the attachment of messenger RNA to ribosomal RNA. The fact that the extent of rescue effected by the two methods is the same may be fortuitous, for the efficiency and pattern of rescue obtained by chloramphenicol is dependent on the concentration of inhibitor used. Previous data suggested that treatment with chloramphenicol was more effective in promoting rescue than was deprivation of proline, but this finding was not supported by the present work in which incubation without proline was as efficient in increasing survival as was chloramphenicol treatment. (BBB)

19551 THE BIOLOGICAL EFFECT OF IONIZING RADIATION. Jozsef Tigyi (Medical Univ., Pecs, Hungary). Magy. Tud. Akad. Biol. Tud. Oszt. Kozlemen., 7: 223-41 (1964).

Experiments, performed mainly on heart and striated muscles, indicated that several radiation effects can be observed on muscle. The development of a positive radiation effect is, in general, accompanied by a change in the electric properties of the tissue. These phenomena cannot be explained simply on the basis of classical radiobiological theories. A satisfactory theoretical explanation can be found only by studies of basic phenomena in radiophysics and radiochemistry and analogous processes must be sought. One must take into consideration the laws known to govern fluid, solid, semiconductor, and polymer systems, and, starting out from these, long-range hypotheses can be developed which will advance research. (CFSTI)

19552 INFLUENCE OF BETA RADIATION ON THE METABOLISM OF THE CORNEA. Karoly Korecz and Eva Szirmak (Peterfy Sandor Utcai Korhaz, Budapest). Magy. Radiol., 16: 342-5(Dec. 1964). (In Hungarian)

Attempts were made to determine the effects of β radiation on the O_2 consumption and anaerobic glycolysis of rabbit corneas. The experiments were conducted on rabbits which received 1000 rep in fractions delivered to the right eye every other day. The left eye served as control; irradiation was administered with a ^{90}Sr source giving a dose rate of 120 rep/min. Measurements made by the Warburg method gave the following average results: after 1000 rep the Q_{O_2} was −0.89 in the irradiated eye and −0.80 in the control eye; after 1500 rep the respective figures were −0.96, and −0.98; after 3000 rep, −0.83, −0.93; after 5000 rep, −0.56, −1.01. Data for anaerobic glycosysis were as follows: at 1000 rep, Q_{O_2} +1.87, controls +1.75; after 1500 rep, +1.94, +1.95; after 3000 rep, +1.80, +1.85; after 5000 rep, +1.19, +1.84. These values indicate that no significant changes were observed after 1000 and 1500 rep. After 3000 rep, O_2 consumption was 13.6% higher in the control eye, and 45% higher after 5000 rep in the control than in the irradiated eye. CO_2 production was higher by 35% in the control eye only after 5000 rep; at lower doses no appreciable change was noted. In only one instance did the contralateral eye show changes after irradiation. Qualitative and quantitative blood tests conducted before and after irradiation showed no significant changes. (BBB)

19553 ACUTE RADIATION SYNDROME. Mechali. Maroc Med., 43: 177-82(1964).

The symptoms occurring following the exposure of humans to different doses of acute radiation are described. The general syndrome of radiation sickness is discussed and a brief description of the gastrointestinal and hematological changes are given. Methods of diagnosis and treatment are also mentioned. (Excerpta Med., Sect. XXIII, 2: No. 3, (Mar. 1965))

19554 NUCLEAR WEAPONS, WAR, AND SURVIVAL. Thomas R. Ostrom (Headquarters, Seventh Army, APO 46). Med. Bull. U. S. Army Europe, 21: 124-5(Apr. 1964).

The effects of nuclear weapons and their influence upon medical operations and patient care are briefly reviewed. Consideration is given to prompt and residual weapons effects, shelter design, food, water, patient care, and the development and implementation of plans. The prompt effects occur in the first minute as blast, thermal, and initial radiation. Casualty estimates utilizing computer techniques reveal that the use of nuclear weapons will result in an increase in killed in action as well as a reversal of the present downward trend in died of wounds cases. Increased difficulty will be experienced both in locating and recovering casualties, and this will affect the number of killed in action. Computer data further reveal that the patients will be suffering from combined blast, thermal, and radiation injuries. With such multiple injuries and delayed treatment, the number of casualties from wounds will increase and, therefore, the load placed on treatment resources will be far greater than ever experienced. Under such circumstances, medical treatment units cannot be expected to provide personnel for search, rescue, and first-aid work. Unit level medical service will continue, though, to perform its normal role including first aid, search, and rescue. Fallout will provide much more serious obstacles to effective medical operations than prompt effects, for several reasons: fallout involves a greater area; the ra-

diation lasts for days; fallout increases the possible patient load; and it interferes with movement. Protection factors are considered in relation to fallout. Shelters that have been used in Seventh Army exercises are basements, tunnels, caves, and old fortifications. In selecting any of these shelters the first operational consideration is that the medical unit should function outside the shelter until forced into it. Medical units suffer a great loss in efficiency once an operation is begun in a shelter. Also considered are adequacy of shielding, ventilation, food, water, waste disposal, and traffic control. Analysis has revealed that the internal dose received from consumption of contaminated rations is less than one tenth the external exposure received from the environment from which the food or water was obtained. With the program of training and a standard operating procedure which has been developed, emphasis is placed on the proper time to move into shelters, priorities of movement of personnel and equipment, monitoring procedures, radiation exposure control measures, communications links, and traffic control in shelters. (BBB)

19555 A REVIEW OF THE LITERATURE ON BURNS AND TRAUMA, SEPTEMBER 1962 TO AUGUST 1963. D. A. Kernahan (Univ. of Manitoba, Can.). Med. Serv. J. (Can.), 20: 315-51(Apr. 1964).

An extensive review of the literature on burns and trauma, including 528 references, was prepared for the Defence Medical Research Advisory Committee of Canada. In addition to a review of thermal burns, burns and other injuries caused by radiation are discussed. The injuries which may result from thermonuclear weapons are described. At a distance of 15 miles from a 20-Mt explosion, glass fragments would have a velocity of 170 ft/sec. At 4.8 miles from ground zero the heat on an exposed surface would be 700 cal/cm^2, and 10 cal/cm^2 gives a severe second-degree burn. The leucocyte count is given as the most reliable prognostic indicator after irradiation. There is a consistent correlation between depression of the leucocyte count and death in the third to fifth week after injury. Reports on the environmental effects of radiation are cited. Natural radiation still is far in excess of that resulting from fallout. Two weeks after a detonation the radiation effects of a 20-Mt weapon would be reduced by a factor of 1000. Other topics discussed include ^{90}Sr levels in human bones, preponderance of girls over boys in children of Japanese survivors (indicating sex-linked mutations), treatment of radiation sickness, and effect of oxygen on radiosensitivity. (BBB)

19556 VARIABILITY OF PENICILLIUM NIGRICANS, THE PRODUCER OF GRISEOFULVIN, ON ULTRAVIOLET AND X-RAY IRRADIATION AND ETHYLENIMINE ACTION. A. G. Romankova, M. V. Fursenko, and A. D. Kommunarskaya (Antibiotic Research Inst., Leningrad). Mikrobiologiya, 33: 382-6(1964). (In Russian)

The resistance of the conidia of P. nigricans to ultraviolet, x irradiation, and ethylenimine was studied. The ultraviolet causes profound morphological changes without affecting griseofulvin (I) production, while x irradiation (100,000 R) markedly affects the I production. (C.H.)

19557 HISTOLOGICAL AND HISTOCHEMICAL FINDINGS IN IRRADIATED RAT PLACENTA. II. THE EFFECT OF PHYSICAL AND CHEMICAL PROTECTION. G. Sinistrero, G. Agati, I. M. Stoppa, V. Aimone, and P. F. Carazzone (Universita, Turin and Sant' Anna Obstetric and Gynaecological Hospital, Turin). Minerva Radiol., Fisioterap. Radiobiol., 9: 571-5(Dec. 1964). (In Italian)

A study was made in pregnant rats, of the effect of radiation on the placenta protected physically by lead shielding and chemically by cysteamine. From weight measurement and histological and histochemical examination it was found that lead shielding affords almost complete protection, whereas cysteamine was highly effective but not to the same extent. With chemical protection the radiation effects are, from a qualitative standpoint similar to those observed during irradiation without protection. The results are briefly discussed. (auth)

19558 EFFECTS OF ROENTGEN IRRADIATION ON FUNGAL SPORES. E. Delorenzi and U. Tosco (Universita, Turin and Dept. of Hygiene, Turin). Minerva Radiol., Fisioterap. Radiobiol., 9: 580-2(Dec. 1964). (In Italian)

Irradiation of conidia and conidiophores of various species of fungi with the 15 and 50 kv plesiotherapeutic technique revealed a considerable resistance of these organisms to irradiation, an initial delay in the development of cultures from these irradiation spores, a variable sensitivity to irradiation according to the strain and season, and difference in the morphologic aspect of the cultures such as color, aspect of the mycelium, and formation of a secondary aerial mycelium. (auth)

19559 BEHAVIOUR OF FUNGAL SPORES IN A CONFINED IRRADIATED ENVIRONMENT. E. Delorenzi and U. Tosco (Universita, Turin and Dept. of Hygiene, Turin). Minerva Radiol., Fisioterap. Radiobiol., 9: 582-4(Dec. 1964). (In Italian)

Attention is drawn to the fact that in radiobiological research certain changes may be attributed to irradiation alone whereas other, less apparent factors may be involved. Thus, in the present investigation, statistically significant results were found to be due to a confined environment rather than to irradiation. Fungal spores were found to be very resistent to irradiation. A decreased size of the conidia and, in some species, the appearance of secondary or tertiary aerial mycelia not characteristic for the species were observed. These perhaps represent poorly viable mutations which are ultimately overcome by the normal fungi. (auth)

19560 LATE LIVER CIRRHOSIS FROM THOROTRAST. Setsuya Naito, Koji Shiga, and Shigekuni Sirahama (Univ. of Kyushu, Fukuoka). Naika, 12: 955-60(Nov. 1963). (In Japanese)

The case history of a 67-yr-old male patient who died of liver cirrhosis is described. The patient had had an operation for prostate hypertrophy (with intravenous injection of a contrast medium for abdominal roentgenography) 8 yr ago, before he was hospitalized in May 1963 for liver cirrhosis. The patient had been hospitalized for three times since 1961 for disease of the liver without subsequent improvement of its function. At the last admission, the patient looked somewhat undernourished, his skin and eyes showing jaundice. The abdomen was swollen and protruded. A series of extensive liver function tests had been undertaken for the period from May 1961 through June 1963. During the last hospitalization, the patient was given general treatment for liver disease and administered anti-aldosterone agents and thiazide diuretics. On several occasions fluid was removed from the pleural cavity to alleviate difficult breathing. When the patient died in August 1963, the autopsy showed liver cirrhosis and atrophy of spleen due to Thorotrast deposits, pulmonary edema, and jaundice. Surface of the liver was granular and coarse and indented irregularly with opaque grey-white patches. The Glisson capsule was thickened and contained many phagocytes containing deposits of light brownish Thorotrast particles. The liver lobules were irregularly divided into pseudo-lobules. Nodular development was seen widely. Thorotrast grains were also found in Kupffer cells in the sinusoids. The liver was generally contracted, and part of the parenchyma was atrophied and part necrotic. Brownish pigment was seen generally in the cells. Spleen showed marked atrophy. The hardened surface was irregularly indented with greyish white fibrotic areas, and hardened arteries protruded on the surface. Two or three grey-white granulated lymph nodes were seen in the hilum; many phagocytes containing Thorotrast granules were seen in the red and white pulp; and supporting structures were thickened and partly calcified. The red and white pulp was completely destroyed around these granular deposits. It was considered that the diagnostic use of Thorotrast took place much earlier than the eight years ago suggested by the patient. Radiation intensities of 401 cpm were registered 20-cm from the liver and 86 cpm from the spleen, as evidence of deposition of radioactive material (ThO_2) in these organs. (BBB)

19561 CANCER PRODUCTION BY CHRONIC EXPOSURE TO PENETRATING GAMMA IRRADIATION. R. H. Mole (Medical Research Council Radiobiological Research Unit, Harwell, Berks, Eng.). Natl. Cancer Inst. Monograph., 14: 271-90(May 1964).

In experiments in which female CBA mice were exposed to fractionated whole-body γ radiation over a 4-week period to total doses of 1000 or 2000 R, the leukemogenic effect appeared early and was exhausted within 2 years. In the same experiment radiation seemed to act differently in the induction of other kinds of tumors, malignant or benign. The age-specific mortality rates for these lesions appeared to be increased in a constant proportion at all ages, i.e., radiation had a multiplicative action. There was none or very little reduction in this carcinogenic action even in advanced old age and hence no exhaustion of effect with time. Thus, over-all tumor incidence may be a misleading index of carcinogenicity; this experimental difference between leukemia and other forms of neoplasia is also seen in humans. The hypothesis is advanced that carcinogenesis depends on two successive cellular events, each of which can occur spontaneously and can be caused by radiation, with the additional assumption that the relative probabilities of these events are different for leukemia and for the other kinds of tumors. An adequate hypothesis for carcinogenesis must explain how an increase in amount of carcinogenic exposure (radiation) can fail to lead to a further increase in tumor rate. Both leukemia and the other kinds of tumors show this saturation type of response. It is suggested that, although there may be no fundamental difference in the nature of acute leukemia and cancer, there is a marked difference in their epidemiology because of the difference between reticular and other stem cells in the relative probabilities of the first and second events (either spontaneous or radiation-induced) which are needed before cells behave as malignant cells. It is possible that chronic lymphatic leukemia of man and some, if not all, chronic myeloid leukemias of man are not fully developed malignant diseases but halfway states in which the first event only has occurred. Acute leukemic transformation of such chronic and only mildly disabling conditions would correspond to the occurrence of the second kind of event. (BBB)

19562 THE EFFECT OF RADIATIONS ON LIVE SUBSTANCES. I. Hirlea. Natura Ser. Biol., 16: No. 5, 27-35 (Sept.-Oct. 1964).

The author summarizes the effects of nuclear radiations on various tissues, examining both somatic and genetic changes, and discussing the influence of the type of radiation, the duration of exposure, and the dosage on the extent of damage done and on whether a regenerative process will or will not take place. (CFSTI)

19563 INHIBITION OF INTERFERON SYNTHESIS AND STIMULATION OF VIRUS PLAQUE DEVELOPMENT IN MAMMALIAN CELL CULTURES AFTER ULTRA-VIOLET IRRADIATION. Jaqueline De Maeyer-Guignard and Edward De Maeyer (Univ. of Louvain, Belg.). Nature, 205: 985-7 (Mar. 6, 1965).

The inhibition of interferon synthesis and the enhancement of virus plaque development in rat embryo cell cultures after uv irradiation was investigated. The results showed a significant increase in virus plaque size in cultures previously exposed to uv rays. The irradiation dose enhancing plaque size did not exert any lethal effect on the cells when fully developed (5-day-old) cultures were irradiated. However, if one-day-old cultures were irradiated, a 30% decrease in growth rate was observed. The higher susceptibility to virus infection of mammalian cells under agar after uv irradiation resembled the effect observed with some carcinogens. Experiments also showed that irradiation of cells before addition of Newcastle Disease virus completely inhibited interferon production, whereas a considerable amount of interferon was produced in non-irradiated control cultures. Indirect evidence in favor of the hypothesis that there might be a causal relation between the inhibition of interferon synthesis and enhancement of plaque size was obtained and is described. (P.C.H.)

19564 THEORETICAL APPROACH TO LIFE SPAN SHORTENING INDUCED BY RADIATION. 4. A MODEL FOR RADIATION INJURY. F. Sato (National Inst. of Radiological Sciences, Chiba, Japan). Nippon Igaku Hoshasen Gakkai Zasshi, 24: 211-37(June 1964).

Various models that have been proposed to explain radiation injury are reviewed. The two previous models for radiation injury may be classified as phenomenological and statistical. The phenomenological approach is mostly concerned with population means such as mean survival time, but not with survival curves or types of distribution around mean values. The phenomenological approaches may explain dose-effect curves but they do not clarify which organ or organ system is responsible for the effects. The statistical approaches based on somatic mutation theory also give no attention to organ specificity. In the model for the radiation injury proposed here, consideration is given to the injury of organs and the interaction between organs. At present, experimental data relating to these problems are few and it is not possible to compare quantitatively the model with the data. In the mathematical model for radiation injury developed here, assuming organ injury and organ-organ interaction, a normal distribution is assumed for individual fluctuations in radiosensitivity. The time-dependence of the injury is included in the model by considering retardation of transfer of the interaction. The model has the form of a vector-matrix. It was compared with experimental data as to mode of death, recovery, LD_{50} of partial-body irradiation, and temporal death distribution. Some qualitative agreements were detected in the comparisons made. References cited, 115. (BBB)

19565 BASIC STUDIES ON RADIATION INJURY TO DOMESTIC ANIMALS BY RADIOACTIVE MATERIALS. II. DISTURBANCE BY IRRADIATION OF P^{32} LOCALLY APPLIED TO THE DIGESTIVE TRACT. O. Matsuoka, et al. Nippon Juigaku Zasshi, 24: 135-40(1962). (In Japanese)

Using a special method to achieve even distribution of isotopes in the body, a study was made on the effects of ^{32}P on the digestive tract. A lethal dose of ^{32}P was wrapped with thin layer (0.02–0.04 mm) polyethylene capsules. The experiments were carried out on white rats in four groups: (1) subcutaneous insertion; (2) abdominal cavity insertion; (3) liver insertion; and (4) intraperitoneal implantation. Control was made in every group on a certain number of white rats (treated in the same way with no ^{32}P in the capsules). In Trial (1), there was no remarkable clinical change in the animals, only slight inflammatory change in the inserted places. In (2), marked emaciation, loss of appetite, and diarrhea occurred; the animals died eventually. There were inflammation in the digestive tract and atrophy of spleen but no significant change in the bone marrow. In (3), one had diarrhea on the 9th day and died on the 17th. Autopsy revealed that the irradiation source had moved from liver to intestine and there was marked inflammatory change in the digestive tract. The rest survived. Autopsy found that the irradiation source was in the lobuli hepatis and there was only fibrosis with no other change. However, the ratio between the weights of the liver and the body had increased. In (4), the animals had loss of appetite or even refused to eat, suffered from marked diarrhea, and died eventually. The number of red blood cells increased and that of the white blood cells decreased. Post-mortem examination showed that the irradiation source was well fixed and there was no fibrosis. There were marked congestion in the abdominal wall and inflammation in the irradiated digestive tract. No increase in the ratio between the weights of the liver and the body was observed. Based on the results, it was reasoned that the effect of ^{32}P on tissues was highly local and was directly related with the depth of the insertion. It was suggested that the injury caused by β rays was no different essentially from the injury caused by x or γ rays. However, the features were not entirely identical, because distribution of ^{32}P and other β sources in the body was not even. (TCO)

19566 PHYSICOCHEMICAL STUDIES ON DNA IRRADIATED WITH IONIZING RADIATIONS WITH CONSIDERATIONS OF SOME RELATED BIOLOGICAL PROBLEMS. Nobutane Mori (Nihon Univ., Japan). Nippon Univ. J. Med., 5: 175-201(June 1963).

A review is presented on studies on radiation effects on DNA conducted in the past several years at the Nihon Univ. School of Medicine. The studies were focused mainly on the mechanism of radiation effects on DNA in vitro and in vivo. The results showed that: irradiation reduced the amounts of DNA in living tissues; phosphorus renewal always took place in DNA metabolism in trace experiments using ^{32}P; the rate of phosphorus renewal in DNA was great particularly in proliferative cells, such as Yoshida sarcoma cells; the growth of tumor was inhibited by irradiation of tumor-inoculated animals, at which time there was a striking reduction in the rate of phosphorus renewal in DNA; and radiation caused changes in the molecular structure of DNA, e.g., changes in the viscosity of DNA solution and liberation of inorganic phosphate and nitrogen. The results are discussed in relation to previous findings. (P.C.H.)

19567 INJURY TO BONE MARROW AFTER THOROTRAST. Sten Halvorsen and Sten Sander (Rikshospitalet, Oslo). Nord. Med., 70: 1320-1(Dec. 5, 1963). (In Norwegian)

The case history is reported of a 46-yr-old female epileptic patient who 17 yr after cerebral angiography with Thorotrast developed a regenerative anemia with leucopenia and thrombopenia. She died in a septic state and necropsy revealed generalized plasma cell infiltration in the bone marrow. Deposits of Thorotrast were demonstrated in the spleen, lymph nodes, liver, and bone marrow. Autoradiography of tissue sections revealed α-particle tracks attributable to the ThO_2 deposits. Spleen and lymph nodes showed more α activity than liver. Marked fibrosis of the spleen was evident. It is suggested that x-ray photographs reveal a characteristic picture of Thorotrast deposition in the liver, spleen, and lymph nodes, that is readily distinguished from other liver disorders. The patient's history indicates that she received a 40-ml dose of Thorotrast, injected into the carotid artery, for cerebral angiography. Thorotrast consits of a 20% suspension of ThO_2 stabilized by dextrin. The radiation emitted by Th consists of α, β, and γ in the ratio of 90:9:1. Thus most of the tissue injury is localized around reticuloendothelial cells which take up ThO_2. (BBB)

19568 GENETIC EFFECTS OF X IRRADIATION. Sandor Igali. Orv. Hetilap, 104: 2121-2(Nov. 10, 1963). (In Hungarian)

Arguments are raised against x-ray screening tests of large segments of the infant population to detect cases of dysplasia of the hip joint. It is pointed out that such pelvic irradiation reaches the reproductive organs of both boys and girls, particularly girls, and mutation of genes may occur that will influence future generations. Several facts known about radioinduced mutations are pointed out, namely that there is an apparent linear relation between the amount of irradiation and the frequency of mutations; and that genetic material bears the imprint of irradiation and repeated small doses will do as much damage as one large dose, although there is some dispute on this subject. As a hypothetical case to illustrate the danger of genetic damage from excessive medical irradiation, it is cited that if the infant population of Hungary were radiographically screened using the most advanced gonad protection, and each infant would receive an estimated 250-mR gonad dose, and if this program were carried on for ten consecutive years, 10 million people would suffer genetic death, and 10% of them would be seriously injured. Such a program carried on indefinitely could do untold damage. The benefits of x-ray examination are not discounted, but it is emphasized that screening entire segments of the population without valid medical reasons is harmful. (TCO)

19569 MORPHOLOGIC CHANGES IN THE THYROID OF RATS TREATED WITH IONIZING RADIATION. Z. Lewicki (Inst. of Experimental Pathology, Academy of Sciences, Warsaw). Polish Med. J., 3: 279-86(1964).

Seventy-five Wistar rats were irradiated with a sublethal dose of 500 R or a lethal one of 900 R. The thyroid glands of these rats were examined microscopically. The changes consisted in vacuolization and degeneration of thyroid epithelium. Some cells or groups of them became necrotic and desquamated into the acinar lumen. These changes developed during the first ten days after irradiation. In the second and third week the regenerative and hyperplastic processes predominated resulting in the restitution of normal thyroid structure. (Excerpta Med., Sect. XXIII, 2: No. 3, (Mar. 1965))

19570 THE EFFECT OF ACUTE CHEMICAL INTOXICATIONS AND PROTRACTED IONIZING RADIATIONS ON ALKALINE PHOSPHATASE ACTIVITY IN HUMAN GRANULOCYTES. J. Lyko. Polski Tygod. Lekar, 19: 1018-20 (1964).

The behavior of the alkaline phosphatase scores in granulocytes of 90 persons was investigated by the Kaplow method, according to the modification of Cichocki. The material was arranged in three groups. In 26 healthy persons scores ranged from 8 to 80 (average 32), which confirmed normal range of scores according to Cichocki. In 42 cases of different acute chemical intoxications scores ranged from 6 to 267 (average 82). In this group scores were especially elevated in barbital, azotox, and carbon tetrachloride intoxications. In 22 radiologists occupied for over 5 years in using ionizing radiations scores ranged from 15 to 183 (average 96). Average scores in cases of chemical intoxications especially in radiologists were distinctly higher in comparison with the normal values, which is statistically significant. The determination of granulocyte alkaline phosphatase scores can be helpful in estimation of the functional state of the granulocytic system. (Excerpta Med., Sect. XXIII, 2: No. 3, (Mar. 1965))

19571 REMOVAL OF THE ASTRINGENCY IN KAKI BY GAMMA RADIATION. Hirotoshi Kitagawa, Hiroyasu Yamane, and Masahisa Iwata (Kyoto Univ.). Proc. Am. Soc. Hort. Sci., 84: 213-16(1964).

The astringency of mature Kaki fruit was removed by gamma radiation of more than 150×10^4R. As the radiation dosage increased, firmness and astringency decreased, and water soluble pectin increased. The fruit that lost astringency became soft like overripe fruit. Gamma radiation seemed to accelerate the ripening of the fruit. The mechanism of removal of the astringency was the same as in overripe fruits. (auth)

19572 POSTSCRIPT TO BEHAVIORAL EFFECTS OF IONIZING RADIATIONS: 1955-61. Ernest Furchtgott (Univ. of Tennessee, Knoxville). Psychol. Bull., 61: 236-8(Mar. 1964).

Comments are made on Garcia and Buchwald's concept of the stimulus characteristics of radiation. They object to considering radiation as an unconscious stimulus. Several studies, including those of Garcia and coworkers, have shown that, in conditioning, radiation acts primarily through the interoceptors and that exclusion of visual and olfactory receptors does not affect the phenomena in which radiation acts as the unconditioned stimulus. Whether it is accurate to refer to radiation as unconscious stimulus depends upon definitions of the term. Secondly, Garcia and Buchwald attempt to account for the stimulus properties of radiation by pointing out that it leads, as do most other conventional stimuli, to arousal which may be detected electrophysiologically or behaviorally. That radiation leads to electroencephalographic changes which resemble those usually associated with the sensory induced arousal has been previously suggested by some investigators, but behavioral arousal after low doses, however, was not definitely demonstrated until a year ago. Thirdly, to account for the diverse Soviet data on the effect of irradiation in condition ing studies in terms of the short-term arousal effect proposed by Garcia and coworkers is too simplified an explanation. Illustrations are given of some of the difficulties encountered in trying to elucidate the role of radiation in conditioning. In all of the radiation-induced spatial avoidance conditioning studies the effects can not be obtained with doses of less than 100 R. Furthermore, the phenom-

enon was always observed either immediately following irradiation or within a period of less than 36 hr. In the Soviet studies, changes in conditioning were observed after exposures of a few roentgens or less, and these changes sometimes lasted for several days after the cessation of exposure or even for one yr in one case. Also, the changes involve different parameters of conditioning in different studies. To state that the diverse phenomena observed by Soviet conditioning investigators can be explained on the basis that irradiation affects the arousal mechanism does not sufficiently account for the diversity of changes which has been observed. (BBB)

19573 EFFECTS OF THE IONIZING RADIATION ON PHYSIOLOGICAL CHANGES IN THE ACTIVITY OF 3.1.6.1 ARYL-SULPHATE SULPHOHYDROLASE IN THE BRAIN DURING DEVELOPMENT. M. Wender and A. Wenclewski (Medical Academy, Poznan, Poland). Radiobiol. Radiotherap., 5: 679-84(1964).

Investigations were made concerning the effects of x irradiation, applied as a single dose of 400 R, on the activity of 3,1,6,1-aryl-sulfate sulfohydrolase in the brain and liver of guinea pigs during onthogenesis. The decisive period of myelination paralleled with the increase of activity of aryl-sulfate sulfohydrolase in the cerebral white matter. The ionizing radiation, applied at the final stage of intrauterine life caused a decrease in the activity of aryl-sulfate sulfohydrolase in the brain, what has a transitory character, since it was compensated during the further period of development. (auth)

19574 HISTOCHEMICAL STUDIES ON ALKALINE AND ACID PHOSPHATASES, NON-SPECIFIC, AND E 600-RESISTANT ESTERASE IN SKELETAL MUSCLES AT DIFFERENT STAGES OF RADIATION DISEASE. S. Kosmider, J. Jonak, and H. Grzybek (Silesian Medical School, Zabrze, Poland). Radiobiol. Radiotherap., 5: 685-93(1964).

Histochemical studies on alkaline and acid phosphatases, non-specific esterase, and on E 600-resistant esterase in striated muscles of guinea-pigs were performed at certain stages of radiation disease induced by x rays. Results obtained revealed a decline in alkaline phosphatase activity in the endothelium of muscular blood vessels which may implicate active transport of serumal substrates into the sarcoplasm. Coincident increase of acid phosphatase activity indicates catabolic activation in the vascular endothelium. Decrease of thiolacetic esterase in the muscles, as a later radiation response, may be related to disturbances in the metabolism of fatty acids. Detected activity increase of E 600-resistant esterase may signify intensifying proteolytic action in muscle fibers. The experimental results revealed multilateral disturbances of the metabolism in skeletal muscles. (auth)

19575 THE GENERAL GRAPHIC RELATION BETWEEN HALF LETHAL DOSE ($LD_{50/30}$) AND THE AGE OF IRRADIATED RATS. V. V. Cholin (Institut fur Arztliche Fortbildung, Leningrad). Radiobiol. Radiotherap., 5: 695-7 (1964). (In German)

A dependence of half lethal dose ($LD_{50/30}$) on age was found in rats. It shows an increase of radioresistance from the new-born period up to puberty. (auth)

19576 DESTRUCTION OF BACTERIUM COLI COMMUNE DEOXYNUCLEOPROTEIN BY X IRRADIATION. G. V. Korotkova and E. V. Moiseenko (Inst. of Biological Physics, Moscow). Radiobiologiya, 5: 21-4(1965). (In Russian)

The action of x rays in destroying deoxynucleoprotein (DNP) isolated from E. coli was studied. The irradiation and subsequent treatment were carried out at 3 to 5°C. DNP was determined from the DNA released from the complex. The addition of Versene and $MgSO_4$ did not change the magnitude of the effect. For nucleoproteins, the limiting value of the effect did not change with an increase in the dose above 10 kR and corresponded to 30 to 40% release of DNA from preparations containing it. Radiosensitivity was highest in preparations of nucleoproteins and homogenate, was an order of magnitude lower for protoplasts, and very low for whole cells. (tr-auth)

19577 IONIC PENETRABILITY OF IRRADIATED ERYTHROCYTES. Z. N. Nahilnitskaya (Inst. of Biological Physics, Moscow). Radiobiologiya, 5: 25-31(1965). (In Russian)

X irradiation, 10^5 to 5×10^4 R, of a thick suspension of nucleated (rats) and nonnucleated (rooster) erythrocytes decreased the low-frequency ohmic resistance and changed the capacity, as a function of dose. The decrease in resistance was the same for the two types of nuclei, but differences in the postirradiation dynamics indicated a greater radiosensitivity of the erythrocytes. The lowering of the resistance was consistent with the higher potassium ion content in a medium not containing electrolytes. The resistance decrease occurred in nonnucleated erythrocytes that had been washed with isotonic sucrose; those washed with isotonic NaCl showed a higher resistance. Capacity, although its changes were less regular, increased in the sucrose-washed nonnucleated cells but in the NaCl-washed ones increased and then decreased. In the nucleated cells, it decreased. (tr-auth)

19578 BIOLOGICAL ACTION OF PROTONS OF 510-Mev ENERGY IN IRRADIATION OF DOGS. A. V. Lebedinskii, Yu. G. Nefedov, M. P. Domshlak, N. I. Ryzhov, N. G. Darenskaya, A. F. Bibikova, A. N. Ganshina, and B. I. Lebedev. Radiobiologiya, 5: 72-6(1965). (In Russian)

Dogs irradiated several times with 510-Mev protons to 650-690 rads developed acute radiation symptoms. The characteristic functional and morphological changes were similar to those caused by x irradiation, but the hemorrhagic syndrome was more developed. The animals died with a relatively high leukocyte count in the peripheral blood and some decrease in blood production in the marrow and serious damage to the erythroblastic cells. (tr-auth)

19579 COMPARISON OF MITOSIS SUPPRESSION BY SEPARATE IRRADIATION OF NUCLEUS AND CYTOPLASMIC STRUCTURES. V. N. Saharov, V. A. Otroschenko, and L. N. Voronkova (Kurchatov Inst. of Nuclear Physics, Academy of Sciences, USSR and Inst. of Chemical Physics, Academy of Sciences, USSR). Radiobiologiya, 5: 93-6(1965). (In Russian)

Cells of Tradescantia paludosa in a sensitive stage of mitosis (between early and mid prophase) were exposed to uv (280 mμ) light. The results showed threshold values of light, above which mitosis does not go beyond the first half of late prophase. When cells were irradiated in the sensitive phase with identical absorption of light energy, the results were the same for irradiation of any cell structure, regardless of its function. Therefore suppression of mitosis by irradiation of the all in the early stages of mitosis is not due to direct interference with the function of any structure. (IIC-M.G.)

19580 CULTIVATION OF COTTON MUTANTS UNDER THE INFLUENCE OF ^{32}P. N. N. Nazirov and F. Dzhanikulov (Inst. of Plant Genetics and Physiology, Tashkent). Radiobiologiya, 5: 108-11(1965). (In Russian)

Administration of a small dose of ^{32}P through the leaves in a 2-year short-day cotton plant while the boll was developing and selection gave a series of mutants. Some produced the first year under natural conditions. Most of the mutants had large bolls and some had colored fibers. (tr-auth)

19581 AFTER-EFFECTS OF FAST NEUTRON IRRADIATION IN CREPIS CAPILLARIS SEEDS. L. S. Nemtseva (Inst. of Biological Physics, Moscow). Radiobiologiya, 5: 126-9(1965). (In Russian)

Postirradiation effects depended on the moisture in the seeds both at the time of irradiation and during storage. The relationship was characteristic for density and sparsely ionizing radiation. Effects were greatest for sparsely ionizing radiation in seeds with a low moisture content. Seeds kept under room conditions were less affected than those in a desiccator. The possibility that the nature of the after effects is related to the appearance of chemical mutagens of delayed action was excluded by the facts. (ICC-M.G.)

19582 ON THE CAUSE OF VARIOUS RADIOSENSITIVITIES OF KINDRED PLANTS. PART II S. A. Valeva (Inst. of Biological Physics, Moscow). Radiobiologiya, 5: 130-5(1965). (In Russian)

Treatment of sprouting maize seeds with 2,4-dinitrophenol that had been irradiated with gamma rays and fast neutrons showed that exclusion of ATP from the cell metabolic system suppresses the postirradiation recovery of the chromosomes in the case of gamma irradiation but has no effect on the fast-neutron-irradiated seeds. One cause of the difference in sensitivity of plants to low-linear-density ionizing irradiation may be a difference in the post-irradiation recovery, which depends on the intensity of the cell processes. The difference in radiosensitivity of the two varieties studied does not depend on a predominance in the interphase of the resting nucleus of a stage that differs from other stages in its radiosensitivity. It is determined by a specific stability of the nucleus to direct irradiation. Interphase stages in the nuclei of the seedling are not identical in sensitivity to direct irradiation with fast neutrons. The most sensitive is the synthetic autoreproduction and then the presynthetic. (tr-auth)

19583 PROBLEM OF SOLUBLE DNA LOCALIZATION IN LYMPHOID APPENDIX TISSUE SHORTLY AFTER WHOLE-BODY GAMMA IRRADIATION. N. V. Ermolaeva and A. L. Pozdnyakov. Radiobiologiya, 5: 147-8(1965). (In Russian)

The luminescence of both lymphocytes and separated nuclei of rabbit appendix increased with time after lethal gamma irradiation Of 500 cells, 42% were damaged after 1 hr, 60% after 2 hr, and 88% after 6 hr. The nuclear luminescence changed from green to yellow-green and yellow, probably due to depolymerization of the DNA. The results indicate that DNA moves from the nucleus to the cytoplasm, is depolymerized, degraded by DNAase, and liberated from the cell granules by the radiation. (IIC-M.G.)

19584 INCREASE OF OXYGEN ASSIMILATION DURING IRRADIATION AS A NONSPECIFIC REACTION REALIZED THROUGH ADRENAL CORTEX. Yu. A. Medvedev, G. A. Vasilev, and V. A. Belyaev. Radiobiologiya, 5: 149-50(1965). (In Russian)

A small but statistically significant decrease in adrenal weight was accompanied by a fall in the ascorbic acid and cholesterol content. The results showed that during irradiation the adrenal cortex function increased, resulting in increased synthesis of the steroid hormones and release of them to the blood. The increase in oxygen consumption is related to the hypophysis-adrenal cortex system. (tr-auth)

19585 COMPARATIVE RADIATION SENSITIVITY OF WISTAR AND NONPEDIGREED RATS. G. M. Pravdina and N. G. Darenskaya. Radiobiologiya, 5: 150-1(1965). (In Russian)

Wistar strain rats were found to be more sensitive to radiation than nonpedigreed rats. Differences were apparent in length of life as well as in clinical symptoms of radiation sickness. (tr-auth)

19586 CHRONIC GAMMA-IRRADIATION EFFECT ON PEA AND VETCH. N. M. Makarov (Inst. of Biology, Sverdlovsk, USSR). Radiobiologiya, 5: 152-5(1965). (In Russian

Daily irradiation from 1 to 5 R of pea and vetch proportionally stimulated all plant organs. With further increase in the irradiation intensity progressive depression of the organs was observed, which was opposed by a compensatory increase in the vegetative mass. Doses greater than 100 R/day had a lethal effect. Vetch was twice as resistant to radiation as pea. (tr-auth)

19587 USE OF RADIOACTIVE IODINE IN THYROID PATHOLOGY. C. Godon. Rev. Med. Liege, 19: 401-4 (June 15, 1964). (In French)

Among other aspects, hazards of the use of ^{131}I in thyroid diseases are discussed. (BBB)

19588 IRRADIATION AND INCOMPATIBLE GRAFTS. P. Ponthus. Rev. Med. Moyen-Orient, 21: 131-48(1964).

A general review of the problem of natural and acquired tolerance for medullary and organ grafts is presented. The role of whole-body irradiation is especially discussed, as are other methods for non-specific conditioning of the receptor organism (adrenocortical hormones, antimitotic drugs) and for specific conditioning. The clinical use of transfusion of bone marrow and organ grafts is also discussed. (Excerpta Med., Sect. XXIII, 2: No. 3, (Mar. 1965))

19589 ANTIBODY FORMATION AND INHIBITION OF THE IMMUNE RESPONSE. A. Cruchaud (Hospital Cantonal, Geneva). Rev. Med. Suisse Romande, 84: 305-13(May 1964). (In French)

Inhibition of immunogenesis by ionizing radiations and other agents is reviewed. (BBB)

19590 RADIOSENSITIVITY OF MICROORGANISM: PRACTICAL CONSEQUENCES. Chr. Stellmann. Rev. Pathol. Gen. Physiol. Clin., 64: 83-91(Feb. 1964). (In French)

Radiosensitivity is the interference of radiation with various factors at all stages of cellular growth. These factors are analyzed with respect to irradiation of microorganisms. The general terms of radiobiology are defined. (J.S.R.)

19591 THE MORPHOLOGICAL CHANGES INDUCED BY IONIZING RADIATIONS IN SOME SUBCUTANEOUS NERVOUS STRUCTURES IN LIGHT OF RECENT KNOWLEDGE OF THE PHYSIOPATHOLOGY OF THE PERIPHERAL NERVOUS SYSTEM. M. Guarino and L. Peroni (Istituto Nazionale per lo Studio e la Cura dei Tumori, Milan). Riv. Anat. Patol. Oncol., 19: 359-90(Apr. 1961). (In Italian)

Biopsy material from nine patients with radiodermatitis, who received x-ray therapy varying in dose from 4000 to 6000 R, was examined. The material was prepared according to the Weigert staining method, and the amyelinic neural endings of the pacinian corpuscles were observed. The corpuscles showed hypertrophic and degenerative alterations, the morphological alterations consisting mostly of vacuolation of the cytoplasm, shrivelling of the nuclear membrane, volumetric increase of the entire cell, rupture of cytoplasmic membrane, as well as multinuclear cells. The nerve bundles showed degeneration of the connective tissue hyaline membrane, and considerable thickening of the arteriole wall was observed. The endoneural connective tissue cells showed hyperchromic and hypertrophic nuclei. An edematous swelling in endoneural structures and twisting of the lamellar structure were observed. The pacinian cells showed late inflammatory, sclerotic changes and the Schwann cell nuclei also showed structural disorders. The radionecrotic lesion probably is preceded by a phase of increased cell proliferation induced by physiologic stimulation; this would explain the numerical increase of the outer lamellar cells of the pacinian corpuscles and the thickening of the perineural fiber sheath. The patients' complaint of pain, sometimes intense and not in relation to the extent of the radiodermitis lesions, could be explained through a not yet clearly defined mechanism whereby ionizing irradiation decreases the stimulation threshold of the neural receptors. The sensitivity of these receptors was tested piezometrically. Some pacinian corpuscles with double axial centers, which were only observed in radiodermitis lesions, may reflect the regenerative capacity of these structures. (BBB)

19592 THE EFFECT OF REPEATED CHEST X-RAY EXAMINATIONS OF WOMEN ON THE DEVELOPMENT OF THE NEXT GENERATION. J. Musil (Medical School, Olomour, Czechoslovakia). Rozhledy Turberk., 22: 164-9 1962). (In Czech)

This study was undertaken in 163 women with tuberculosis to determine whether repeated x-ray examinations in the course of temporary lung collapse resulted in increased incidence of developmental abnormalities in their offspring. In a total of 113 children born during the course of temporary lung collapse, congenital abnormalities were found four times and possibly two times, with reduced resistance against infections or physical debility eight times. Treatment preceding pregnancy lasted 4.2 yr on an average. In

154 children born after termination of treatment lasting an average of 4.7 yr, congenital abnormalities were found four times, possibly once, and reduced resistance or physical debility five times. In a control group of 90 children born to the same mothers before treatment, congenital abnormalities were found once and reduced resistance or physical debility twice. The estimated gonadal dose of radiation received by the mother probably did not exceed an average of one R for the whole treatment. The statistical significant increase in incidence of developmental abnormalities, as well as reduced resistance and physical debility was shown for the children born in the course of temporary lung collapse treatment of their mothers. The deleterious effect of direct irradiation of the fetus during chest x-ray examination of the mother may also be manifested in these children. Radiation sequelae may become evident to a greater degree in further generations. Recommendations for employing all available methods of protecting women, particularly pregnant women, from radiation exposure are made. In view of the possible side-effects on the offspring, every diagnostic radiologic test should be evaluated for its necessity and avoided whenever possible in women of child-bearing age. (BBB)

19593 TRICARBOXYLIC ACID CYCLE MUTANTS IN SACCHAROMYCES: COMPARISON OF INDEPENDENTLY DERIVED MUTANTS. M. Ogur, A. Roshanmanesh, and S. Ogur (Southern Illinois Univ., Carbondale). Science, 147: 1590(Mar. 26, 1965).

A yeast mutant, induced by ultraviolet radiation independently isolated as a glutamate auxotroph (glt_{2-1}), was similar to the glt_{1-1} mutant in exhibiting a blocked tricarboxylic acid cycle due to the lack of aconitate hydratase. This mutant differed by exhibiting blocks in lysine and cytochrome biosynthesis, which segregated together with the glutamate requirement. (auth)

19594 HEPATOMAS IN MICE: INCIDENCE INCREASED AFTER GAMMA IRRADIATION AT LOW DOSE RATES. Peter C. Nowell (Univ. of Pennsylvania, Philadelphia) and Leonard J. Cole. Science, 148: 96-7(Apr. 2, 1965).

Irradiation of LAf_1 mice with gamma rays (total doses of 618 to 1335 rad) at a rate of 1.45 rad per hour markedly increased the incidence of hepatomas and ovarian adenomas, compared with incidence of these tumors in mice irradiated with x rays at 30 rad per minute. This was somewhat unexpected, since chromosome aberrations in the liver cells were less frequent after irradiation at the low dose rate. Other types of tumors were not increased by irradiation with gamma rays at the low dose rate. It is suggested that indirect hormonal mechanisms may contribute to the production of the hepatomas as well as of the ovarian adenomas. (auth)

19595 EFFECT OF X-RAYS ON MECHANICAL RESISTANCE OF ERYTHROCYTES. J. Polcakova and L. Vacek. Scripta Med. Fac. Med. Univ. Brun. Olomuc., 37: 215-20(1964).

The effects of x rays on the mechanical resistance of human erythrocytes was investigated: the doses were 500 and 1000 R, and the influence was observed 2 and 24 hr subsequent to irradiation. The irradiation reduced the mechanical resistance of erythrocytes, the effect being more manifest with erythrocytes investigated 24 hours after irradiation. This prospective reduction of resistance by proposed x-ray treatment should be taken into account especially in such cases when the resistance of erythrocytes has already been reduced in the patients by the existing disease. (Excerpta Med., Sect. XXIII, 2: No. 3, (Mar. 1965))

19596 CHROMOSOMAL ABERRATIONS OF HUMAN LEUKOCYTES IRRADIATED IN VITRO (CHINESE). Anchi Wong and Shing-ting Chou (Inst. of Genetics, Academy of Sciences, Peking). Shih Yen Sheng Wu Hsueh Pao, 9: 178-83(1964).

Human leukocytes were irradiated in vitro with different doses of x rays (25 to 200 R), then cultured. Chromosomal aberrations were scored at metaphase. The coefficient of aberration production for total breakages obtained was 0.0027 ± 0.001/cell/R. Spontaneous aberration rate was 0.003 ± 0.0017/cell. Hence, the double dose for human leucocytes in vitro was calculated out to be 1.11 ± 0.64 R. It was demonstrated that for purposes of biological dosimetry, the formula of regression for total chromosomal breakage rate appears to be more accurate than that of dicentrics and rings as suggested by others. (Excerpta Med., Sect. XXIII, 2: No. 3, (Mar. 1965))

19597 THE EXPOSURE OF MAN TO IONIZING RADIATION ARISING FROM MEDICAL PROCEDURES; WITH SPECIAL REFERENCE TO SOMATIC INJURY. K. Koren, S. Maudal, J. Flatby, and L. Berteig (Statens Institutt for Stralehygiene, Oslo). Tidsskr. Norske Laegeforen., 82: 78-9(Jan. 15, 1962). (In Norwegian)

The relation of absorbed tissue doses of radiation therapy techniques and the recommended maximum acceptable doses of the International Commission on Radiological Protection (1959) is discussed. The absorbed doses in bone marrow and thyroid gland resulting from x irradiation of benign lesions were measured. Small ionization chambers were introduced into the sites of interest in a tissue-like (Mix-D) phantom for the measurements. The radiation absorbed in these organs was evaluated on the basis of a skin dose of 100 R. Owing to the variations in irradiation technique in the five therapy centers investigated in Norway, no true mean values could be found. The doses are represented by dose ranges. The absorbed doses are related to the number of patients and their age and sex distribution in the therapy centers. These results are integrated into the United Nations publication: The Exposure of Man to Ionizing Radiation Arising from Medical Procedures with Special Reference to Radiation-Induced Diseases: An Inquiry into Methods of Evaluation, published by the International Commission on Radiological Protection and the International Commission on Radiological Units and Measurements, December 1960. (BBB)

19598 THE PROTEIN FRACTIONS OF THE BLOOD SERUM IN RADIO-INDUCED DERMATITIS (RUSSIAN). A. Ya. Prokopchuk and A. T. Sosnovskii (Belorussian Dermovenereol. Research Inst., Minsk). Vestn. Dermatol. i Venerol., 7: 33-40(1964).

Changes in the protein fractions of the blood serum were studied in rabbits with radioinduced dermatitis (single dose of 3000 R to an area of 50 cm^2), in patients with radiodermatitis, and in healthy subjects, by means of paper electrophoresis and refractometry. In the rabbits, at 4-6 weeks after irradiation the albumin level increased, the α_1-, α_2- and β-globulins decreased, and γ-globulins decreased slightly; the A/G ratio increased from 1 to 1.5. At 8-9 weeks the albumins decreased slightly; the α-globulins and β-globulins increased slightly, while the γ-globulins increased to above the normal level; the A/G ratio decreased somewhat. At 3 months there was further decrease of albumins to near-normal levels; the α-globulins returned to normal level; the α_2- and β-globulins remained subnormal; γ-globulins continued to increase. At 4.5 months there were no appreciable changes except for a further increase of the γ-globulins, a slight decrease of α_1-globulins and a slight increase of β-globulins as compared with the previous analysis. At 6.5 months the albumins were normal while the α_1-, α_2- and β-globulins were slightly subnormal and the γ-globulins remained supranormal. In the dermatitis patients there was a decrease of albumins, a distinct increase of α_1-globulins, an increase of α_2-globulins and no appreciable changes in the β- and γ-globulins and the A/G ratio. It was noted that the A/G ratio was lower when derived electrophoretically than when determined refractometrically, due to admixture of some α- and β-globulins with the albumin in the latter method. (Excerpta Med., Sect. XXIII, 2: No. 3, (Mar. 1965))

19599 THE PROBLEM OF THE FORMATION OF TOXIC (HEMOLYTIC) LIPIDS IN RADIATION SICKNESS OF ANIMALS. M. L. Kakushkina (Moscow State Univ.). Vestn. Mosk. Univ., Ser. VI, Biol., Pochvoved., No. 5, 11-17(Sept.-Oct. 1964).

Male rabbits were irradiated with γ-rays at doses of 1000 and 3000 R. To eliminate the effects of food on the

state of lipids in the organism, the animals were not fed after irradiation. Three days after irradiation, the lipids of the liver of irradiated animals were extracted and the phospholipids separated with acetone. The presence of the hemocytotoxic factor formed in the lipids as a result of irradiation of the animals was established by determining the hemolytic effect on erythrocytes. The toxicity of the lipid fraction soluble in acetone was markedly increased as compared with controls. The phospholipid fraction, on being added to the acetone-soluble lipids, protected the erythrocytes from hemolysis. Addition of cysteamine to the erythrocyte suspension also protected the erythrocytes from hemolysis due to the effect of the toxic lipids. The protective effect was highest at cysteamine concentrations equal to, or above, 0.013 M; at concentrations of cysteamine lower than 0.013 M, a sensitizing effect on erythrocytes was observed. Both phospholipids and cysteamine have an antioxidizing effect on lipids. (CFSTI)

19600 HEMOPOIESIS IN SHEEP EXPOSED TO SUBLETHAL DOSES OF X RAYS. Angel Vrigazov, Ivan Ivanov, Boris Stamenov, and Krusto Surtmadzhiev. Vet. Sbirska, 61: No. 10, 20-1(1964).

Studies were made on 14 healthy sheep aged 2 to 4 years irradiated 250 or 300 R (4 sheep) with 180 kw, 15 mA, 120 cm focal skin distance, 6.7 R/min. A light form of radiation disease that ensued is described; Patterns of lymphocytes, leukocytes, polymorphs, monocytes, eosinophils and staffs over succeeding days are illustrated graphically. Lymphocytes were most sensitive. The only difference in the 2 groups was that the changes were more pronounced in the 4 sheep that received 300 R. (OTS)

19601 TISSUE ACTIVATION DURING MIXED NEUTRON IRRADIATION. D. Draev and K. Nikolov. Voenno Med. Delo, 19: No. 5, 24-8(1964).

The radioactivity in the tissues of rats exposed to 720 R mixed neutron and γ radiation was determined at various times after exposure. The animals were killed 14, 24, or 48 hr after irradiation and daily counts were made on samples of blood, heart, brain, stomach, and intestine. Results showed that most of the radioactivity was present in the blood, heart, brain, stomach, and intestine. The contribution of the short-lived radioisotopes to total radioactivity was minimal. (C.H.)

19602 EFFECT OF RADIATION ON RNA AND RNA METABOLISM IN HUMAN CANCEROUS TUMOR CELLS. E. V. Budnitskaya, M. Bryunfo, and M. Errera. Vopr. Med. Khim., 10: 179-84(1964)

The effects of x irradiation on RNA radiosensitivity and metabolism were investigated in labeled cancerous tumor cells (HeLa cells) in two experimental series. In the first series, groups of HeLa cells were incubated for 10 min, 60 min, and 24 hrs in a medium containing cytidine-^{3}H (360 microcuries/mM) before x irradiation with single 100, 300, and 900 R doses. After x irradiation the cells were fixed and prepared for radioautographic investigation to determine RNA radiosensitivity by the number of granules in the nucleolus, nonnucleolus part of the nucleus, and the cytoplasm, and the total number of granules in a cell (30 cells counted in each sample). In the second series incubation and irradiation were reversed. Results showed that RNA is radiosensitive immediately after formation and nucleolar RNA is more sensitive than the rest of the nucleus. Depressed RNA radioactivity in irradiated cells incubated in a cytidine-^{3}H medium for a short period indicated that injury of the RNA synthesis mechanism is restorable. Migration of labeled RNA from the nucleus into the cytoplasm was inhibited in cells incubated in a cytidine-^{3}H medium before irradiation and then transferred to a nonradioactive medium. (TCO)

19603 ON THE CAUSES OF IMPAIRMENT OF SYNTHESIS OF SERUM ALBUMIN IN RAT LIVER IN ACUTE RADIATION SICKNESS. O. G. Zamyatkina (Inst. of Biological and Medical Chemistry, Moscow). Vopr. Med. Khim., 10: 362-6(July-Aug. 1964).

Studies were made to determine whether the lowering of serum albumin synthesis (SAS) in rat liver on the 3rd–6th day after irradiation was caused by irradiation per se or because of loss of appetite and disturbance of the GI tract of the animals. Part of the animals were x irradiated at 900 R, they were kept in separate cages and their food intake was measured daily. The controls were given 50 g of a mixed diet daily. Both groups were weighed daily. Incubation of liver slices in vitro in a salt medium to which 0.15% of glucose solution was added and determination of SAS was performed on both groups. A mixture of several amino acids was added to the incubation medium within the period of irradiation disease. It was concluded that the decrease in food ingestion during the first 3 days of acute radiation sickness in rats leads to a moderate inhibition of serum albumin synthesis in liver slices incubated in vitro. Addition of amino acid mixtures to the incubation medium within this period of radiation sickness increased the synthesis of serum albumin. During the most severe period of irradiation disease, at the 4th–6th day after irradiation, almost complete inhibition of serum albumin biosynthesis was independent upon restricted food ingestion by irradiated animals. No increase in serum albumin synthesis could be observed after addition of the amino acid mixture into the incubation media containing liver slices obtained from the rats within this period of irradiation disease. In rats surviving the 8th day post-irradiation, both ingestion of food and synthesis of serum albumin in liver slices incubated in vitro were observed. Addition of an amino acid mixture into the incubation medium in these experiments increased serum albumin biosynthesis. (TCO)

19604 INCORPORATION OF METHIONINE–S^{35} INTO THE PROTEINS OF BONE MARROW AND SPLEEN IN ACUTE RADIATION SICKNESS. V. A. Revis (Kalinin Medical Inst., USSR). Vopr. Med. Khim., 513-19(Sept.-Oct. 1964).

Acute radiation sickness was induced in rabbits by exposure to whole-body x radiation applied in doses of 1100 R. Indicator doses of methionine–^{35}S were administered to the rabbits subcutaneously at different periods of development of the disease. Within 2 hours after each administration of the methionine–^{35}S, the animals were sacrificed, suspensions of bone marrow were prepared, and then examined. It was found that the intensity with which the labeled methionine is incorporated into the proteins of bone marrow and spleen was sharply decreased in the course of acute radiation sickness. The decrease reached its maximum intensity about two weeks after irradiation. The process was then reversed, with the intensity of the incorporation of amino acid being restored to an almost normal level within one month. A histoautoradiographic method of investigation indicated that the basis of the changes that took place in the intensity of the incorporation of the labeled methionine into the proteins of the hemopoietic organs are morphological and biochemical modifications of the organs as a result of radiation sickness. (CFSTI)

19605 ON THE TREATMENT OF ULCERATED AFTER-EFFECTS OF X RAY IN THE SKIN OF HUMANS. H. C. Friedrich and J. Thomas (Universitats-Hautklinik, Tubingen, Ger.). Z. Haut-Geschlectskrankh., 35: 42-62 (July 15, 1963). (In German)

Ulcerated postirradiation skin defects require treatment to restore function. In untreated ulcerated areas of this kind, infections of deep lying tissues may give rise to bone necrosis, brain abcess, meningitis, infections of the pleura and pericardium, intestinal fistulas, etc. Continuous loss of protein from radiation ulcers may produce hypoproteinemic conditions. Although there is some question whether radiation ulcers are obligatorily precancerous, it is probably not the ulcers that are the starting points for carcinoma, but instead the atrophic, papillary keratotic growths. Probably as many as 30% of all patients with radioinduced lesions would develop carcinoma if they survived for a long enough time. The best prophylaxis to prevent development of malignant ulcers is total surgical removal of ulcerated skin lesions that appear after irradiation. The amount of tissue to be excised can be estimated visually. To replace the tissue removed, and

repair the resulting defects, skin transplants should be made. The results obtained by this type of repair are generally much more successful in an esthetic and functional sense than are those that can be obtained by other, conservative treatment measures. (BBB)

19606 THE ALTERATION OF CARCINOGENESIS BY THE USE OF IONIZING RADIATION DURING EMBRYONIC DEVELOPMENT. E. Diener (Universitat, Zurich). Z. Krebsforsch., 65: 607-19(Oct. 4, 1963). (In German)

Attempts were made to detect a synergistic action of prenatal ionizing irradiation on cancer induction by a chemical carcinogen. Three experimental groups of rats of an inbred tumor-free strain were treated as follows: (1) 2-acetylaminofluorene (AAF) was fed in doses of 300 mg to young rats, weighing 60 g. (2) 10-day-old embryos were exposed to x irradiation doses of 75, 100, and 200 rad from a 31-Mev betatron. (3) 10-day-old embryos were exposed to irradiations of 75, 100, 150, and 200 rad, followed by postnatal feeding of AAF to young rats weighing 60 g. All irradiated groups showed malformations of the eyes, nervous system, and hind extremities. These malformations varied with the dose of the irradiation. Single irradiation beside causing malformations produced also benign tumors. In utero irradiation with doses of 75 rad increased AAF-induced carcinogenesis significantly. This carcinogenesis-promoting effect decreased with the increasing irradiation dose. Thus after 150 and 200 rad no synergistic carcinogenic effect was observed. A life-shortening effect of irradiation was seen. It was more pronounced at 200 than 75 and 100 rad. No relation was found between the incidence of malformations and tumors in individual organs. (BBB)

19607 THE IMPORTANCE OF OEDEMA IN ACUTE RADIATION INJURY TO THE CEREBRAL CORTEX OF RATS: AN ELECTRON MICROSCOPE STUDY. T. F. McDonald (Argonne National Lab., Ill.). Z. Zellforsch., 64: 119-28(1964).

Edematous changes in the cerebral cortex of rats after acute irradiation are described. The importance of these changes in the over-all injury is discussed. Swelling and rupture of clear glial cells without expansion of the extracellular space were seen during the early phases of injury. Not all of the clear glia became swollen, but those that did eventually underwent complete dissolution, initiating small foci of severe damage. The necrosis that ultimately encompassed the entire irradiated field may spread from these initial sites of injury. Clear glial cells that did not undergo swelling showed an unusual type of reaction before they became necrotic. (Excerpta Med., Sect. XXIII, 2: No. 3, (Mar. 1965))

19608 EFFECTIVENESS OF PREVENTIVE TETANUS VACCINATION IN EXPERIMENTS ON MONKEYS AFTER PROLONGED IRRADIATION WITH LOW DOSES. E. K. Dzhikidze and A. S. Aksenova (Inst. of Experimental Pathology and Therapy, Academy of Medical Sciences, USSR). Zh. Mikrobiol., Epidemiol. i Immunobiol., No. 12, 29-31 (Dec. 1964).

Studies showed that prolonged irradiation with doses of 630-750 R did not interfere with the processes of immunogenesis in monkeys, unlike the situation caused by acute irradiation. Tetanus vaccination of irradiated monkeys led to the development of immunity equal to that in the control animals. The results were compared with those obtained in experiments on postvaccinal immunity to gas gangrene and it was concluded that active prophylaxis of wound infections under these conditions is quite effective. (CFSTI)

19609 CHANGE IN CHOLINESTERASE ACTIVITY AFTER IMMUNIZATION AND IRRADIATION. G. P. Zolotnikova and V. A. Krzhivokol'skii (Kursk Inst. of Medicine, USSR). Zh. Mikrobiol., Epidemiol. i Immunobiol., No. 12, 71-4(Dec. 1964).

Cholinesterase activity in immunized and irradiated rabbits was investigated. During the process of immunogenesis (under the influence of corpuscular and soluble antigens), cholinesterase activity decreased in the blood serum, liver, lung, and spleen of the animals. An inverse relationship was noted between the degree of reduction of enzyme activity and increase in antibody titers. The decrease in cholinesterase activity in the serum and organs of the experimental rabbits became more pronounced in the animals exposed to ionizing radiation before immunization than in those immunized but not irradiated. (OTS)

19610 LIPID METABOLISM IN ACUTE RADIATION INJURY — EFFECTS OF RADIATION ON BRAIN BIOCHEMISTRY. John G. Coniglio, James T. Davis, Frank Windler, and Vera Hsiung. p.377-87 of "Response of the Nervous System to Ionizing Radiation." Boston, Little, Brown and Co., Inc., 1964. (TID-18958)

Studies were conducted in an attempt to define biochemical changes in brain lipids 24 hours after a 10,000 R dose of whole-body gamma irradiation to newborn and to weanling rats. In general, very few statistically significant alterations were observed, although there were suggestive changes. Among the former group were decreased total fatty acid concentrations in irradiated newborn rats, increased palmitic and palmitoleic acid concentrations, and altered hexaenoic acid concentrations in irradiated weanling rats. Slightly suggestive changes were decreased arachidonic acid in irradiated newborn animals and slightly increased vinyl ether plasmalogens in irradiated weanlings. No measurable differences were observed between irradiated and control animals in brain weights, phospholipid phosphorus, and ^{14}C content of total lipids or total fatty acids (brain lipids labeled by administration of acetate-^{14}C 24 hours before irradiation). (P.C.H.)

19611 STUDIES OF BRAIN LYSOSOMES. Harold Koenig. p.403-17 of "Response of the Nervous System to Ionizing Radiation." Boston, Little, Brown and Co., Inc., 1964.

Histochemical and biochemical data are presented to show that lysosomes occur in the central nervous system. Special attention is given to the matrix of brain lysosomes, which consists of glycolipid and phospholipid components associated with proteolipid protein, and displays a natural fluorescence. A lysosome-rich fraction was prepared from rat brain homogenates by density-gradient centrifugation which contained practically no succinic dehydrogenase activity, and showed a twofold to sixfold increase in specific activity of acid phosphatase, beta-glucuronidase, acid RNase, acid DNase, and cathepsin. In addition to disruptive treatments, a wide assortment of cationic molecules induce a release of latent, particulate lysosomal enzymes in vitro. The release is accompanied with a binding of some cations to lysosomal matrix and evidently represents a cation exchange reaction. The releasing experiments implicate electrostatic forces in the structural latency of acid hydrolases. It is hypothesized that acid hydrolases are labile constituents of lysosomes, the distinctive feature of the particles being their negatively charged lipoprotein matrix. It is also proposed that a primary effect of radiation may be a cleavage of nuclear histones from nucleoprotein. Upon diffusing into the cytoplasm, histones may bind to lysosomes and bring about a release of acid hydrolases, and possibly other substances, through a cation exchange reaction analogous to that occurring in vitro. (P.C.H.)

19612 THE RELATIVE BIOLOGICAL EFFECTIVENESS OF 1.2 Mev GAMMA RADIATION AND 200 kv X-RADIATION FOR CATARACT INDUCTION. Elizabeth Florence Focht. Thesis, New York, Columbia Univ., 1964. 76p.

A study of the induction of radiation cataract in the rat lens was limited to six-month-old White Sherman rats and to two dosage schedules. The x-rays were produced at 200 kv, with a half value layer of 1.0 mm Cu, at a rate of 180 R per minute, at 60 cycles per second, and had a mean energy deposition of 1.8 kilo electron volts per micron of path in water. The gamma rays of cobalt had an average of 1.2 Mev, with a continuous rate of about 130 R per minute, and an energy deposition of about 0.27 kilo electron volts per micron of water. Lead shielding devices always limited the radiation to one eye only. Each group subjected to a different radiation quality or schedule consisted of 25 to 30 rats. Doses of 1500 R were given for both x rays and cobalt gamma rays in a single treatment, and also on a divided schedule of 500 R on the first, third, and sixth days for

each radiation. Each cataract was graded 0, 1, 2, 3, or 4 according to increasing degrees of severity. The "average" cataract for the group was plotted against the time in weeks. Another analysis of the same data was made by plotting for each group the percentage which had reached 1 or greater, 2 or greater, etc., thus giving four curves for each irradiation. The curves for either method appeared to represent normal sigmoid curves. The results for the x radiation and the gamma radiation of cobalt agreed with each other within 95% fiducial limits for both the single and divided treatment, and by either method of analysis. The RBE of radioactive cobalt gamma radiation compared to 200-kv x radiation is therefore estimated as one for these experiments. (A.G.W.)

19613 MECHANISM OF THE INHIBITING EFFECTS OF IONIZING RADIATION ON CELL DIVISION. A. V. Lebedinskii, V. M. Mastryukova, and A. D. Strzhizhovskii. p.157-65 of "Pervichnye i Nachal'nye Protsessy Biologicheskoga Deystviya Radiatsii." Moscow, Academy of Sciences, 1963.

The relation between the effects of ionizing radiation, mitotic activity, and extracellular influences on metabolism in cell nuclei are discussed. The effects of neural and hormonal factors on the state of DNA, radiation effects on genetic mechanisms, irreversible changes induced by radiation, and metabolic activity are considered. The inhibition and recovery of mitotic activity in a number of irradiated biological systems are compared. (C.H.)

19614 PRIMARY AND INITIAL PROCESSES OF THE BIOLOGICAL ACTION OF RADIATION. GENERAL DISCUSSION. p.243-70 of "Pervichnye i Nachal'nye Protsessy Biologicheskoga Deystviya Radiatsii." Moscow, Academy of Sciences, 1963.

The use of electron paramagnetic resonance in studies of the role of free radicals in primary radiation effects in biological materials; the relation between damage to DNA synthesis and retardation of mitosis in irradiated cells; reparation of radiation injuries by natural metobolic processes and artificial factors; radioinduced chromosome aberrations; radiation injuries in cells; the effect of oxygen on radiosensitivity; and the mechanisms involved in the action of chemical radioprotective agents are discussed. (C.H.)

19615 HOST-CELL INTERACTIONS IN MICE BEARING ISOLOGOUS HEMOPOIETIC GRAFTS. E. A. McCulloch, J. E. Till, and L. Siminovitch (Univ. of Toronto and Ontario Cancer Inst., Toronto). 25p. (CONF-717-14)

From CNRS Meeting on Graft of Allogenic Hematopoietic Cells, Paris, Sept. 1964.

The results of experiments that define three of the features of cells, hosts, and the interaction between them that are required for colony formation are reported. The features are based on studies of mice bearing specific mutations affecting hemopoietic function. The help these studies offer in the elucidation of the nature of the control mechanisms involved in the proliferation and differentiation of hemopoietic cells is indicated. The three loci studied were the W locus, the Sl locus, and the F locus. From the results it was concluded that the mutations studied do not prevent the production of erythroblasts, but rather change the pattern of differentiation, so that these red cell precursors are produced at a later time during the growth of the transplanted cells. From this point of view, the curing, observed during the growth of the mice, results from the late appearance of erythrocytic precursors. If this interpretation of the experiments is correct, then the F locus may be considered to control a late function in colony formation, one that directs the pattern of differentiation within a colony, rather than providing the genetic information needed to produce any specific cell type. (P.C.H.)

19616 BIOLOGICAL EFFECTS OF PROTONS AND NEUTRONS IN LARGE ANIMALS. S. Tom Taketa (Ames Research Center, Moffett Field, Calif.). 39p. (CONF-720-15)

From 2nd Symposium on Protection Against Radiation Hazards in Space, Gatlinburg, Tenn., Oct. 1964.

Studies were made on the biological effects of high energy protons compared to ^{60}Co gamma rays in whole-body irradiated monkeys. The exposure set-up used was unique in that it provided omnidirectional exposure. Proton exposures ranged from 200 to 950 Rads midpoint air dose; gamma exposures, 195 to 1065 Rads. The results of depth-dose measurements showed: a dose falloff at midpoint in gamma exposures, but a dose buildup in proton exposures; tissue doses at various loci varied, with respect to the midpoint dose, from 96 to 114% and 71 to 104% in gamma and proton exposures, respectively; and the midpoint tissue dose (MTD) was 60 to 70% of midpoint air dose (MAD) in gamma exposures, and about 120 to 130% in proton exposures, indicating that for a given MAD the MTD for protons was about twice that for gamma rays. The relative biological effectiveness (RBE) of protons was compared with gamma rays for lethality and white blood cell (WBC) depression. The survival times of the decendents were essentially similar for the two types of radiation and ranged predominantly from the 10th to the 20th post-exposure days, which suggests prominence of the hematological syndrome. It was concluded on the basis of existing MTD data that for hematological effects, the effectiveness of high energy protons in large animals may be somewhat less than that of gamma rays, x rays, or fast neutrons, and that appropriate experimental data are lacking to even consider a maximum permissible emergency exposure for space explorers. (P.C.H.)

19617 STABLE-FLOW FREE BOUNDARY FRACTIONATION OF SPLEEN-COLONY-FORMING CELLS FROM MOUSE BONE MARROW. Howard C. Mel and John C. Schooley (Univ. of California, Berkeley). 5p. (CONF-717-12)

From CNRS Meeting on Graft of Allogenic Hematopoietic Cells, Paris, Sept. 1964.

The Till and McCulloch (Radiation Res., 14: 213(1961)) spleen colony technique for assaying viable stem cells was applied to the study of fractions separated from mouse bone marrow by stable-flow free boundary (STAFLO) sedimentation. The fractions were injected intravenously into lethally irradiated C3H female mice using 12-15 animals per group. A known number of viable nucleated cells, determined by the eosin exclusion test, was injected into each recipient mouse. A control group for endogenous colony formation was also included. After 8 days the spleens were removed and the colonies counted under a dissecting microscope. Viability (eosin exclusion) and colony-forming ability of mouse bone marrow cell suspensions were maintained throughout the fractionation and handling procedures. Significant enrichment (as well as significant depletion) of colony-forming cells was achieved in different fractions, relative to the initial marrow suspension. Major morphological differences were seen between cells in the different collection fractions. A relationship was noted between colony-forming ability and cell morphology. Thus, fractions containing more than 60% small round mononuclear cells were found to contain fewer colony formers than fractions having less than half this percentage. (P.C.H.)

19618 X-IRRADIATION OF THE 36-HOUR RAT EMBRYO: NEONATAL MORTALITY AND POSTNATAL ACTIVITY, LEARNING, AND SEIZURE SUSCEPTIBILITY. Joan M. Havlena, Jack Werboff, and Melvin R. Sikov. 10p. (CONF-556-19)

From 12th Annual Meeting of the Radiation Research Society, Miami, Fla., May 1964.

Pregnant albino rats of the Sprague-Dawley strain were exposed to x radiation in doses of 5 to 100 R at 9:00 a.m. of the day following the day on which a positive vaginal smear was observed. This is equivalent to 24 hr after fertilization. Only in the 100 R group was litter size significantly reduced during the first 30 days of life. Litter size was not affected in the other irradiated groups as compared to the control group and no gross abnormalities were observed in any of the groups. At the age of 26 days, all of the offspring were tested for activity level on the inclined plane test. No consistent differences were observed. From these results and those from learning tests and seizure susceptibility, it was concluded that prenatal x irradiation

at this time of gestation has no consistent effects on the subsequent behavior of the offspring. (P.C.H.)

19619 HEMATOLOGICAL CHANGES IN GERMFREE MICE FOLLOWING WHOLE-BODY X-IRRADIATION. Raphael Wilson, Taiju Matsuzawa, and St. James Connell (Univ. of Notre Dame, Ind.). 11p. (CONF-556-22)

From 12th Annual Meeting of the Radiation Research Society, Miami, Fla., May 1964.

In order to separate the damage to the hematopoietic system due directly to irradiation from that due to post-irradiation infection and an altered relation to intestinal microorganisms, the peripheral blood changes in germ-free and conventional Swiss-Webster mice were compared for 24 days after whole-body x irradiation Total red cell counts, total and differential white cell counts, reticulocyte counts, platelet counts and hematocrit values were determined following doses of 850, 710, 200, and 100 R. Germ-free mice were found to have total white cell, lymphocyte, reticulocyte, platelet, and hematocrit values lower than those of conventionals by about 10%. In general, it appeared that the presence of bacteria in irradiated animals contributed in part to damage to the bone marrow as evidenced by a decrease in the peripheral count of cells originating in myeloid tissue, but did not alter the effect on lymphoid tissue. (P.C.H.)

Radiation Effects Therapy and Countermeasures

19620 (JPRS-29200(p.96-106)) CHEMICAL PROTECTIVE DRUGS AGAINST IONIZING RADIATION. Chi-chick Hsiao. Translated from Yao Hsueh T'ung Pao, 10: 337-41(Aug. 1964).

Radioprotective compounds that have been proven to be effective against radiation injury are reviewed. The chemical structure and mechanisms of protective effects are described. The various types of chemical protective drugs discussed include sulfur containing drugs, amino acids and amines without sulfur, substances that induce anoxia, and chelating agents used for the removal of metal ions. Criteria for radioprotective compounds are summarized. (66 references) (C.H.)

19621 THE EFFECT OF SH-INHIBITORS ON THE RADIATION SENSITIVITY OF PROTEINS AND AMINO ACIDS. Sandor Damyanovich, Marton Szabolcs, and Imre Szati (Medical Univ., Debrecen, Hungary). Acta Physiol. Acad. Sci. Hung., 25: 307-17(1964).

Proteins and amino acids were made sensitive to indirect radiation injury by means of SH-inhibitors of different specificity. The extent of radiation injury was determined by spectrophotometric and sedimentation studies. Experiments were also carried out under conditions in which the radiation effect was simulated by the use of OH groups liberated from H_2O_2. The possible mechanisms of the radiosensitizing effect of SH-inhibitors are discussed. (OTS)

19622 FURTHER EXPERIMENTAL INVESTIGATIONS ON THE CHEMOTHERAPY OF RADIATION SICKNESS. M. A. Tumanyan and A. V. Izvekova. Antibiotiki, 9: 719-22(1964).

Results are reported from studies on the effectiveness of antibiotic therapy in the control of infections associated with radiation sickness. Data are presented on the effects of penicillin alone, and in combination with other antibiotics, on infections in rats and rabbits exposed to lethal and sublethal doses of ^{60}Co γ radiation. It was concluded that phenoxypenicillin, mycerin, monomycin, and pthalazole sulfamide reduce infectious complications of radiation sickness. (C.H.)

19623 CLINICAL DIAGNOSIS AND THERAPY OF CHRONIC RADIATION INJURIES. L. S. Vaskov (Inst. of Radiobiology, Sofia). At. Energy Rev., 2: No. 4, 59-94 (1964). (In Russian)

Radiation injuries and their diagnosis and therapy are reviewed. Attention is paid primarily to the classification, causal mechanism, and clinical picture of chronic radiation injuries, and to their differential diagnosis. Differences in the views of a number of problems relating to the pathogenesis of radiation injury are indicated. The present status of research on indices for clinical use and methods of treatment is covered. (270 references.) (auth)

19624 THE INFLUENCE OF 19-NORANDROSTENOLONE UPON THE COURSE OF ACUTE IRRADIATION DISEASE IN RATS. M. Dostal, I. Vodicka, and J. Zachvej (Military Medical Research and Training Inst., Hradec Kralove, Czechoslovakia). Cesk. Fysiol., 13: 519(Dec. 1964).

Caprinate of 19-norandrostenolone was administered as a single dose before whole-body x irradiation of rats at 600 to 700 R. The drug administered 7 days before irradiation had no effect; administration 1 hour before irradiation substantially increased the death rate; administration 1 hour or 7 days after irradiation increased the death rate slightly. When a streptomycin sulfate was administered, there was no increase in death rate due to administration of norandrostenolone. N-N'-tetramethyl cystamine and neomycine sulfate offered similar protection. (OTS)

19625 NUTRITION AND RADIATION. THE PROTECTIVE EFFECT OF FAT IN RADIATION SICKNESS. R. Eichnerova V. Nemec and M. Ovecks. Cesk. Gastroenterol. Vyziva, 18: 402-8(1964).

The effects of diets of different unsaturated fat content on the course of experimentally induced radiation sickness were studied in rats. The best criterion of the course of radiation sickness was the survival of rats where statistically significant differences were obtained on the 30th and 60th day after irradiation when comparing diets containing lard (16.3% cal volume) and sunflower seed oil (26.3% cal volume). Animals fed lard survived significantly longer than animals receiving sunflower seed oil. Similarly the lard diet proved best with regard to the blood count and the dynamics of radiation sickness during the first days of its development. Least satisfactory was the diet with the high sunflower seed oil content, where a deterioration of the animals' health was recorded. It is emphasized that a diet that exerts a protective effect in radiation sickness must contain only an appropriate amount of unsaturated fatty acids, as excessive amounts cause deterioration of the animals' health. This deterioration is due to the accumulation of peroxides which are formed from unsaturated fatty acids accumulated in the organism and which exert an adverse effect on the animals. (Excerpta Med., Sect. XXIII, 2: No. 3, (Mar. 1965))

19626 INFLUENCE OF TEMPERATURE ON THE RECOVERY OF THE REPRODUCTIVE FUNCTION OF YEAST CELLS DAMAGED BY ULTRAVIOLET RADIATION. N. V. Kovyazin, I. N. Polykova, and V. I. Pochtareva (Moscow State Univ.). Dokl. Akad. Nauk SSSR, 159: 1411-14 (Dec. 21, 1964). (In Russian)

The postradiation treatment of exposed cells is known to affect their chances for survival. It was previously shown that keeping uv-irradiated diploid yeast cells in aqueous nonnutritive medium at 30°C led to a partial regeneration of their reproductive functions. The dependence of the recovery process on the length and temperature of incubation is investigated in order to complement the previous findings. Recovery is maximal in a temperature range of 20–40°C. A reduction in temperature (down to 10°C) which reduces the metabolic rate also slows down the recovery processes within the cells. Various reactions seem to take place simultaneously and the recovery process requires a minimum background temperature for a successful regeneration of the reproductive capacity. In addition to a predetermined temperature, these reactions also require a definite interval of time, which is longer at higher doses of radiation. (ATD)

19627 DELAYED CHANGES IN ANIMALS WHICH SURVIVED LETHAL IRRADIATIONS AS A RESULT OF RADIATION PROTECTORS. L. Dimitrov (Higher Medical Inst., Sofia). Dokl. Bolgar. Akad. Nauk, 17: 969-72(1964).

The percentage of experimental animals that survived lethal irradiation doses with the help of radiation protectors was established. Clinical observations for the search of pathomorphologic and biochemical changes over 6–7

months following the irradiation were also made. The animals were treated initially by serotonine (5-HT), or a combination of serotonine with beta-mercaptoethylamine (MEA) and aminoethylisothiouronium (AET). Tests were carried out on 984 white mice of both sexes. A detailed account of the experiments is given. (OTS)

19628 NUTRITION AND EFFECT OF γ-RAY EXPOSURE. A. Kenmoku and H. Iwao. Eiyogaku Zasshi, 20: No. 2, 70-6(1962). (In Japanese)

In view of the increasing possibilities of contact with radiation in recent years, the series of experiments were carried out for the purpose of determining the proper food supply to be given in daily meals that would be of some aid in reducing the hazard of radiation to organisms. Studies were made on the effects of ingestion of different levels of dietary protein on the protection against radiation, in the light of urinary nitrogen excreted. 20 Male adult albino rats, weighing 260 g each, were divided into two groups fed with 8 and 25% casein diets, respectively. Other components of the feed were: 10% hydrogenated oil, vitamin-mineral mixture, and dextrin. After 10 days on the above diets, the two groups of rats were each sub-divided into exposed and non-exposed groups with the latter as controls. The same diets were maintained for 7 days. ^{60}Co gamma irradiation was given in a dosage of 600 R, and continuous exposure of the entire body was maintained for 1 hr. Urine was collected for 24 hours right after the radiation and daily values of urinary total nitrogen, urea, and allantoin were determined for 6 days. The body weight of the controls in the 8% casein group remained unchanged, while that of the exposed animals decreased by 3 g. In the 25% casein group, the body weight of the exposed rats was almost unaffected, but that of the controls increased by 1.5 g. The urinary nitrogen of the exposed animals of the 8 and 25% casein groups totaled 135.3 mg and 424.1 mg, respectively, while that of the controls amounted to 83.5 and 337.9 mg, respectively, the increases of urinary total nitrogen after irradiation in the two groups being 62 and 24%, respectively. The excretions of urea of the exposed animals in both groups were 72.9 and 385.9 mg, respectively, while those of the controls were 53.9 and 298.5 mg, respectively, the increases in this connection after irradiation being 35 and 29%, respectively for the 8 and 25% casein animals. The excretions of allantoin were 11.0 and 9.4 mg, respectively for the exposed animals and 7.2 and 8.0 mg for the controls, respectively, the increases being 53 and 17%, respectively for the 8 and 25% casein groups. Thus after exposure the animals of the 8% casein group had a higher excretion of urinary total nitrogen, urea, and allantoin than those of the 25% casein group. The increase of urinary nitrogen output of the exposed animals in the 25% casein group was mainly due to urea, whereas in the 8% casein group the ratio between urea and urinary total nitrogen of the exposed animals was smaller than with the case of the controls. It was concluded that ingestion of a high protein diet might be of some aid in reducing the hazard of ionization radiation. (TCO)

19629 BIOLOGICAL PROPHYLAXIS OF ACUTE RADIATION DISEASE WITH LYOPHILIZED ROYAL JELLY. Ts. N. Tsochev (Scientific Inst. for Research in Radiology and Radiation Hygiene, Sofia). Eksperim. Med. i Morfol., 3: 219-23(1964).

Studies using the lyophilized Bulgarian royal jelly apitonin and cystamine chloride in 280 rats irradiated with LD_{90} to LD_{100} (750-850 R) revealed that a dose of 0.8 to 1 g/kg daily for 6 days (with irradiation on day 3) protected rats more effectively than an optimal (nearly toxic) dose of cystamine; 55% survival ($p < 0.05$), compared with 50% for cystamine. Only 10% of the untreated controls survived. (OTS)

19630 PRESENT THOUGHT ON THE MANAGEMENT OF IRRADIATION CASUALTIES. T. L. Fallowfield (Royal Naval Medical School, Alverstoke, Eng.). J. Roy. Naval Med. Serv., 50: 47-50(Spring 1964).

Medical handling of heavily irradiated persons is considered, with special reference to casualties resulting from reactor accidents. One problem is that there has not been a sufficient number of accidents to allow reasonable prediction of the number of persons likely to be involved and the dose range which might be encountered. In an incident such as an accidental reactor excursion, a high radiation flux may be indicated by the reactor alarm system, but there is no way of telling, at that time, who, out of the large number of people who may be present, has received a potentially harmful dose of radiation. The first requirement is therefore an initial sorting on the basis of dose estimation. This can be carried out quickly and easily with regard to the neutron dose by measuring the activity of the indium foil carried by radiation workers. Classification by this method would be fairly rough: into high, medium, and low dose groups. The division between the groups might be over 100 rem for the high dose group and less than 25 rem for the low dose group. According to the degree of irradiation, disposal of the evaluated cases would take different routes. Those found to have suffered supralethal doses and showing early distress should not be subjected to long journeys and therefore should be admitted to the nearest hospital. High external contamination and physical injury together form the most serious problem. The emergency treatment required before transfer of the patient to a hospital unit might be extensive. Therefore, for the reception of irradiation casualties a clinical unit should be designed for this purpose. The design must be based on the necessity for strictest bacteriological isolation. Although there is no specific treatment for the acute radiation syndrome, an unfavorable prognosis can be altered by therapy. Immediate bed rest, bland diet, and good nursing are the first requirements. Antiemetics are indicated almost at once for the severe nausea and vomiting, while intravenous feeding may be necessary both for nourishment and to maintain hydration. The maintenance of pH and electrolyte balance depends on the indices of the serum pH, acid-base, and electrolyte estimations. In the second or third week, with the increasing depression of hemopoiesis, isolation and aseptic techniques become of the highest importance. Bactericidal antibiotics should be administered parenterally in high doses at the slightest sign of infection, because in these conditions the infection will progress most rapidly to a fulminating state. Hemorrhagic manifestations are treated by the appropriate transfusion therapy. Severe pancytopenia produced by the suppression of hemopoiesis may require bone marrow transfusion using cells from a donor of the same sex and matched, not only in the major groups, but in most of the minor ones. However, the benefit of this form of treatment is not yet established and it involves a risk of producing secondary disease. It is concluded that the requirements for the ideal management of irradiation casualties, according to present state of knowledge, are a reliable system of classification based on the clinical evaluation, and a hospital unit designed for the reception of these casualties, staffed by a co-ordinated team and provided with treatment facilities to cope with all facets of radiation injury. (BBB)

19631 ON THE RADIOPROTECTIVE POWER OF PROCHLORPERAZINE IN EXPERIMENTAL PANIRRADIATION WITH COBALT 60. R. Bergonzini, L. Vendrame, D. De Maria, C. Canossi, and M. Morini (Universita, Modena, Italy). Minerva Radiol., Fisioterap. Radiobiol., 9: 560-4 (Dec. 1964). (In Italian)

Reference is made to experimental research carried out on albino mice panirradiated with telecobaltotherapy. Initially this research was directed to the determination of the $LD_{50/30}$ days and later to the study of the radioprotective power of prochlorperazine (PCP), a phenothiazinic which has recently been applied clinically because of its beneficial effect on some symptoms of radio-intolerance. Particular care was taken to standardize irradiation conditions and the biological material used (in total 780 animals of selected stock). PCP and the control solutions were injected by the endoperitoneal way before irradiation. Having established $LD_{50/30}$ days at a dosimetrical value of 609 R, it was seen that PCP at a dose of 0.5 mg protects mice panirradiated with sublethal doses (700 R) to the extent of 85% while only 30% of the controls sur-

vived; for lethal and supralethal doses (800 and 850 R) on the other hand, this action is much more modest. This differentiates it from cysteamine which even in these experimental conditions preserves its radioprotective power. It is believed that PCP acts on the tissue metabolism of the irradiated animal, provoking a reduction in oxygen consumption and possibly cytological hypoxia; also to be presumed is an interference on the syndrome of post-irradiatory adaptation; this takes place up to a particular dosimetrical level beyond which more serious organic phenomena, which the drug cannot dominate, come into play. (auth)

19632 WEIGHT CHANGES IN ALBINO MICE AFTER TOTAL BODY IRRADIATION WITH Co^{60} AND TREATMENT WITH DIFFERENT DOSES OF PROCHLORPERAZINE. R. Bergonzini, D. De Maria, M. Morini, R. Reggiani, and L. Vendrame (Universita, Modena, Italy). Minerva Radiol., Fisioterap. Radiobiol., 9: 565-71(Dec. 1964). (In Italian)

The radioprotective capacity of prochlorperazine was analyzed experimentally by determining the survival of totally irradiated mice. The body weight drop observed in the same animals after total-body irradiation and treatment with this substance is analyzed statistically. It was found that at all the dose levels tested (0.21, 0.50, 1.00, and 2.00 mg for mice weighing 21 g irradiated with 700 roentgen units) prochlorperazine delays and reduces the severity and rate of the initial acute body weight drop which represents a typical expression of the effects of irradiation, but also delays the secondary general recovery of the body weight. Only with 1 mg of prochlorperazine does this recovery occur in the same time as in irradiated untreated controls. Thus, as regards the body weight changes, a dose of 1 mg of prochlorperazine exhibits the specific capacity to rapidly and permanently counteract the harmful effects of radiation. Considering that the total ultimate mortality rate is reduced with all the doses considered, it was concluded that although prochlorperazine has a toxic effect, demonstrated by the acceleration of death in the more sensitive animals, its pharmacologic effectiveness is such that the overall death rate is diminished. The findings are described and discussed. (auth)

19633 THE USE OF A NEW DRUG IN THE TREATMENT OF RADIODERMATITIS. F. Coucourde and A. Schifino (Universita, Pavia, Italy). Minerva Radiol., Fisioterap. Radiobiol., 9: 585-90(Dec. 1964). (In Italian)

Fifty patients presenting various degrees of radiodermatitis were treated with Solcoseryl; 5 were given preoperatory therapy and did not have radiodermatitis. The results were very satisfactory especially as regards cicatrization which began and was completed fairly rapidly with trophic cutis. It is concluded that Solcoseryl constitutes a valid therapeutic method in the treatment of radiodermatitis. (auth)

19634 APPLIANCES PROTECTING AGAINST IONIZING RADIATIONS IN THE GYNAECOLOGICAL RADIUM APPLICATION ROOM. K. Jach and S. Skowronski (Onkological Center, Poznan, Poland). Nowotwory, 14: 305-9(1964).

A system of protecting appliances constructed in the gynecological radium application room is described. Protecting appliances include: preparatory table with radium safe and with containers closing automatically, lead radium transporter resembling a railway carriage moving on rails, transporting applicators to the physicians' post, protecting table close to the physicians' post, and mobile protecting screen for the physician. After construction of these appliances and their automation, together with some improvements, it was possible to eliminate the assistance of nursing staff during procedures. Considerable decrease of ionizing radiation doses to the working staff was achieved. (Excerpta Med., Sect. XXIII, 2: No. 3, (Mar. 1965))

19635 THE COMPARATIVE PROTECTIVE ACTIONS OF AET (β-AMINOETHYLISOTHIURONIUM) OR SEROTONIN IN EXPERIMENTAL BETA RADIATION INJURY. O. M. Meredith, Eveline G. Bowers, and J. T. Heintzelman (Lockheed Missiles and Space Co., Palo Alto, Calif.). Proc. Western Pharmacol. Soc., 7: 15-18(1964).

CF_1 male mice were exposed to 1-Mev electrons. The drugs were administered intraperitoneally 5 min prior to their radiation. Serotonin creatine sulfate was administered at 50 mg/kg and AET at 250 mg/kg. Either the ventral or dorsal surface of animals was exposed to an electron beam at a rate of 3000 rad/minute, but protective effects were studied only in animals receiving ventral exposures. Radiation injury caused by whole-body exposure to a 1-Mev electron flux is unique due to factors not found with deeply penetrating x or γ radiations. The important differences are the short range of penetration in soft tissue, abrupt loss of energy (mainly by collisional losses) to the tissues, and no secondary radiation or bremsstrahlung. Higher energy deposition occurs in the tissue penetrated than with deeply penetrating x radiation having comparable energy. Two distinct patterns of lethal response were observed. At the radiation level (1500 rad) employed, the lethal response among animals irradiated over the ventral surface was much greater. The discrepancy in response is reasonable since the bony mass of the spinal column would reduce significant penetration of the particulate beam to deeper tissues and irradiation from the ventral aspect causes exposure of the highly radiosensitive intestine. Direct estimates of intestinal injury were gauged by the comparison of intestinal weights at two days postirradiation. The differences established that some protective effect was achieved with serotonin only, and that intraperitoneal injection of agents used had a depressive effect on the intestinal mass. A more significant role of the protective agents appears from body weight data. Both drugs suppressed weight loss in comparison to that seen with control animals. The agents had no significant protective action upon the 30-day cumulative mortality after 1500-rad ventral whole-body radiation with 1-Mev electrons. These data indicate a unique therapeutic problem where relatively low-energy electrons are involved. The results agree with a finding that sufficient x irradiation of 50% of the mouse intestinal mass will produce death. A similar or lesser requirement may exist for 1-Mev β particles, since they create a greater local energy dissipation where they penetrate. Possible mechanism of radiation protection by AET or serotonin are discussed. Serotonin reduces the oxygen level in walls of the small intestine and spleen, and AET acts as a free radical scavenger. (BBB)

19636 DECREASE OF IRRADIATION DAMAGE OF ISOLATED CELLS OF MAMMALIA BY SOME AMINO ACIDS. I. F. Bregadze (Inst. of Biological Physics, Moscow). Radiobiologiya, 5: 97-102(1965). (In Russian)

Arginine and α- and β-alanine, in a wide range of concentrations, protected nuclear structures of the cells of Ehrlich ascites carcinoma (from mice) from damage by ionizing radiation. α- and β-alanine were effective not only when administered before irradiation but when given immediately after. (tr-auth)

19637 USE OF EMBRYONIC BLOOD-FORMING LIVER CELLS IN ACUTE RADIATION SYNDROME. M. N. Trushina and A. L. Pozdnyakov. Radiobiologiya, 5: 103-7(1965). (In Russian)

Administration of a suspension of embryonic blood-forming cells from the liver to rats gamma irradiated to 600 R did not prevent death or even show any favorable effect on the course of the syndrome. When biomycin was used with the cell suspension, the treatment was somewhat effective; the survival rate of the animals was a function of the amount of cells given. (tr-auth)

19638 VERSENE PROTECTIVE ACTION AGAINST UV DAMAGES OF SOME PHAGES OF BACTERIUM COLI COMMUNE. V. I. Ivanov, G. B. Zavilgelskii, and A. S. Kriviskii (Inst. of Radiation and Physico-Chemical Biology, Moscow). Radiobiologiya, 5: 112-18(1965). (In Russian)

Versene was found to have a protective effect against uv irradiation of some bacteriophages but not others. The phage was protected only when Versene was introduced into suspension during the irradiation. When added before or after, it had no effect. The addition of Mg^{2+} to the Versene eliminated its protective action. The data ob-

tained plus literature data indicate that the protective effect is due to interaction of the active carboxyl groups of Versene with the primary damaged DNA molecules of the phage. (tr-auth)

19639 PARTIAL RECOVERY OF BARLEY SEEDS FROM RADIATION DAMAGE. V. V. Hvostova and K. A. Elshuni (Inst. of Biological Physics, Moscow). Radiobiologiya, 5: 136-9(1965). (In Russian)

Supplementary treatment of barley seeds (irradiated in dry ice, temperature shock 60°C, moistening with boiled distilled water) following ^{137}Cs gamma irradiation decreased the radiation damage, as determined by the number of chromosome rearrangements in the rootlets of the sprouted seeds. Field germination of seeds treated after 40 kR irradiation was 33.8%. Twenty-seven percent of the plants yielded seeds. Treatment of seeds that had been fast-neutron irradiated to 200 Rad (+120 Rad gamma) had no effect. (tr-auth)

19640 THE VALUE OF SULFHYDRYL COMPOUNDS AS RADIOPROTECTIVE SUBSTANCES IN THE LIGHT OF MODERN RADIOBIOLOGICAL RESEARCH. Z. R. Zsebok (Medical Univ., Budapest). Therapia Hung., 11: 14-19 (1963).

Postulated primary radiation reactions to explain radiobiological effects are discussed and the pertinent literature reviewed. The possible involvement of proteins and nucleic acids as the target of radiation injury is considered, as well as the role of radiolysis of water and the resulting products in damage to these macromolecules. Other constituents of the cells which can give rise to radicals are enumerated. Electrolyte disequilibrium may also play a role in the body's response to radiation. The role of the liver in injury and of infection from intestinal bacteria is reviewed. Injury of blood and marrow cells and induction of hemorrhagic phenomena by radiation are cited as complicating factors, and as weakening body defenses. Point of action of radioprotectant chemical agents is considered, with particular reference to sulfhydryl compounds. Some experiments of the author on this problem are presented. Thus, if cysteamine is administered 30 sec after irradiation, its radioprotective effect fails to materialize. Neither cysteine, cysteamine, nor cystamine was capable of entirely preventing the disintegration of white blood cells; they merely promoted the regeneration of the leukopoietic system as compared with that of nontreated animals, nor could they prevent the decrease in weight after a lethal radiation dose. In animal experiments it was found that cysteamine given intraperitoneally afforded, after an LD_{100}, effective protection for rats subjected to total-body irradiation inasmuch as the animals given previous doses were alive after six months. Experiments with other sulfhydryl agents are described and their use in humans subjected to radiotherapy is considered. (BBB)

19641 TRANSPLANTATION OF FRESH AND PRESERVED BONE MARROW TO ANIMALS WITH ACUTE RADIATION SICKNESS. N. S. Pushkar and L. I. Simonova. III Tretyaya Vses. Konf. po Peresadke Tkanei i Organov, Erevan, 1963, 223-4(1963).

Sixty-five white rats were subjected to irradiation with x-rays. In the control group of animals the average duration of life was 10.5 days and the average loss of weight was 65 g. To rats of the second group, fresh homologous bone marrow was administered intravenously, and to rats of the third group, bone marrow that had been preserved for a long time at minus 196° in Hank's solution and contained 15% glycerol as well as serum and antibiotics. The average duration of life of rats of the second group was increased by 5.5 days, while their weight decreased an average of 31 g. In the third group of animals, 13 animals survived, while the average duration of their life increased by 13 days and no loss of weight was observed. Histological investigation indicated that there was normalization of hemopoiesis after administration of preserved bone marrow. It was concluded that bone marrow preserved at low temperatures retains its capacity to survive, and after transplantation into an irradiated organism, becomes adapted and participates in regeneration. The superior therapeutic effect obtained on transplantation of preserved bone marrow is explained by the assumption that antigenic properties decreased under the effect of the low temperatures. (CFSTI)

19642 THE TREATMENT OF RADIATION SKIN LESIONS WITH FRESH AUTOFIBRIN FILMS. I. I. Kotlyarov, E. F. Plute, A. J. Ritter, and O. V. Romanova (Medical Inst. and Regional Oncological Dispensary, Krasnoyarsk, USSR). Vopr. Onkol., 10: No. 10, 97-100(Oct. 1964).

On the basis of the assumption that fresh blood fibrinogen possesses healing properties in inflammatory processes and tissue defects of various origin, autofibrin films were used in the treatment of skin lesions appearing as the result of radiation therapy of malignant neoplasms. The film is obtained from venous blood taken from the patient. After the blood has been stirred about with a fine glass rod toward the bottom and walls of the test tube, a fibrin film is formed on the rod. One cm^2 of film is obtained from 1 ml of blood. The film is placed on the surface of the wound, which has previously been cleansed with physiological solution, and is covered with a layer of gauze moistened with physiological solution. A light bandage is applied. Thirty-two patients, 18 men and 12 women of older age and a 12-year-old girl, were treated. Twelve patients had an oozing dermatitis following radiotherapy with a total dose of 7000–8000 R, and 20 patients had ulcers that appeared 3 to 8 years subsequent to radiotherapy. The results of these treatments were very satisfactory and are described. The application of fresh autofibrin films significantly decreased the period of healing of epidermitis appearing in radiotherapy of malignant neoplasms. Within a period of some weeks or months these films provoked healing of late radiation ulcers. In such cases the tissue defects were completely closed by epithelial tissue, while teleangiectasis and atrophy of the skin developed after routine ointment therapy of epidermitis were found to decrease. No side effects were noted. (auth)

19643 ON THE PROBLEMS OF SO-CALLED RADIATION PROTECTIVE AGENTS. G. Pliess (Universitaet, Hamburg). Zentr. Allgem. Pathol. Pathol. Anat., 106: 226(Aug. 31, 1964). (In German)

A brief discussion is presented of the tissue distribution, species-specificity, postulated mechanisms of action, and possible use in man of radioprotective drugs. It is concluded that experiments so far performed in small laboratory animals do not provide adequate data to allow definite conclusions as to their effectiveness in humans. (BBB)

19644 THE RECOVERY IN ERYTHROPOIESIS AND ERYTHROPOIETIC CAPACITY FOLLOWING WHOLE BODY IRRADIATION, USING ^{59}Fe AND BONE MARROW TRANSPLANTATION. N. M. Blackett and P. J. Roylance (Royal Cancer Hospital, London). 13p. (CONF-717-15)

From CNRS Meeting on Graft of Allogenic Hematopoietic Cells, Paris, Sept. 1964.

The change in the erythroid repopulating ability (stem cells?) of bone marrow following irradiation of rats was determined using a bone marrow transplantation technique. This property of bone marrow was compared with changes in the bone marrow cell population and with the change in red cell production as measured by the incorporation of ^{59}Fe into hemoglobin synthesizing cells. The response of rats was followed for 50 days after 200 and 450 R acute whole-body irradiation. The results demonstrated the complexity of the process of recovery of erythropoiesis following whole-body irradiation. After 200 R the repopulating ability did not return to normal until after the recovery in red cell production and then fell to a minimum at 25 days after irradiation without any evidence of a change in red cell production from normal. At 450 R the repopulating ability followed the change in red cell production somewhat more closely but was always less than the red cell production. The erythroid bone marrow cells showed a sharp peak in numbers 9 days after 450 R; this was due to a piling up of early erythroid precursors as a result of the decrease in red cell production between 7 and 10 days, although recovery was rapid before and after this interval. (P.C.H.)

19645 TRANSPLANTATION POTENTIAL OF MARROW FROZEN AT PROGRAMMED COOLING RATES. Jerry P. Lewis, Mitchell Passovoy, and Frank E. Trobaugh, Jr. (Presbyterian–St. Luke's Hospital, Chicago and Univ. of Illinois, Chicago). 13p. (CONF-717-13)

From CNRS Meeting on Graft of Allogenic Hematopoietic Cells, Paris, Sept. 1964.

Studies were made on the effects of controlled rate cooling on the preservation of stem cells. The bioassay of stem cells used was based on the colony producing potential of hematopoietic tissue injected into lethally irradiated mice. Femoral marrow was suspended in 12% glycerol, and three samples were cooled simultaneously at three different rates. Following this, each sample was thawed, deglycerolized, and injected into mice that had just received heavy irradiation. Nine days later, the spleens of these animals were removed, fixed in Bouin's, and the colonies of proliferating hematopoietic tissue on the spleen counted. The number of colonies is a function of the dose of the inoculum providing a basis for a bioassay. This bioassay yields quantitative rather than quantal data and is 25 times as efficient as the animal survival assay. Marrow was suspended in glycerol as it was cooled from room temperature to −100°C. The cooling was divided into five phases, and each phase was studied independently. Within three of the five ranges studied (the rate of cooling to freezing, the duration of pre-freezing plateau, and the temperature at which freezing was initiated), marrow viability was not affected. In two other ranges, prolonging the post-freezing plateau significantly decreased viability, and increasing the rate of cooling from the post-freezing plateau to −100°C decreased the viability of marrow. Through such studies, it is hoped that the formulation of optimal conditions for the freezing and storage of mammalian marrow will be possible. (P.C.H.)

19646 ALLOGENIC CHIMERIC BONE MARROW: ITS CAPACITY TO REPOPULATE THE LYMPHATIC TISSUES OF AN IRRADIATED SYNGENEIC HOST. O. Brocades Zaalberg (National Defense Research Council TNO, Rijswijk, Netherlands). 18p. (CONF-717-7)

From CNRS Meeting on Graft of Allogenic Hematopoietic Cells, Paris, Sept. 1964.

Bone marrow and lymph node cells from (CBA × C57B1)F_1 chimeras, that had been given respectively 0.2, 1-2, and 50×10^6 CBA bone marrow cells, were transferred to irradiated CBA mice. It was found that transfer of tolerance with such bone marrow and lymph node cell suspensions was successful when these cells were obtained from the group of chimeras treated with 0.2 or $1\text{-}2 \times 10^6$ CBA bone marrow cells. No tolerance was found in the CBA host when the bone marrow and lymph node cells were taken from chimeras treated with 50×10^6 CBA bone marrow cells. Transfer of tolerance from this group of chimeras was possible only if the CBA host had been thymectomized prior to irradiation. From these results it was concluded that the bone marrow from the chimeras treated with a large number of bone marrow cells had a stronger tendency to repopulate the lymphatic tissues of the second host and in this way to replace the tolerant lymph node cell population by nontolerant cells than bone marrow from the other two groups of chimeras. (P.C.H.)

19647 SECONDARY DISEASE IN DIFFERENT SPECIES AND ITS MODIFICATION. L. M. van Putten (Radiobiological Inst. TNO, Rijswijk, Netherlands). 13p. (CONF-717-9)

From CNRS Meeting on Graft of Allogenic Hematopoietic Cells, Paris, Sept. 1964.

In view of the similarity in the clinical syndrome noted in monkeys and in man, studies were made on the possibilities of modifying secondary disease in the monkeys by various methods that have previously been found to be effective in rodents. None of the methods alone (modification of donor cell suspensions, pooling marrow from several donors, fetal hemopoietic tissue, and chemotherapy) provided a directly useful result, and it was concluded that secondary disease in primates is much more difficult to prevent than in rodents. (P.C.H.)

19648 COMPARATIVE SURVIVAL OF SUBSTRAINS C3HeB AND C3HfB FOLLOWING MIDLETHAL IRRADIATION AND ALLOGENIC MARROW INOCULATION. Delta E. Uphoff and Margaret K. Deringer (National Cancer Inst., Bethesda, Md.). 18p. (CONF-717-4)

From CNRS Meeting on Graft of Allogenic Hematopoietic Cells, Paris, Sept. 1964.

Following midlethal x irradiation and allogenic marrow inoculation of mice, survival varied with different donor-host combinations but constituted a host-versus-graft response. C3HfB and C3HeB, both closely related substrains of C3H, responded quite differently to this treatment. The substrains used were genetically C3H/He, differing only in fetal environment. Survival following 500 R for both substrains was 76-81%. Survival following 500 R and reciprocal marrow inoculation from either C3HfB or C3HeB was 80-88%. Only 28% of the C3HfB exposed to 500 R and inoculated with C57BL($\underline{H\text{-}2^b}$) marrow survived, while 72% of the C3HeB mice survived. With marrow from C57L($\underline{H\text{-}2^b}$) donors, 67% of the C3HfB and 95% of the C3HeB mice survived. Again, with (C57BL × C3Hf)F_1 marrow, more C3HeB (42%) mice survived than C3HfB (4%). The opposite effect was seen with C57BL/$\underline{10\text{-}H\text{-}2^d}$ marrow when 23% of the C3HfB mice survived but all of the C3HeB mice died. With the inoculation of $\underline{H\text{-}2^b}$ marrow or (C57BL × C3H)F_1 hybrid marrow, the difference between these substrains was toward better survival of the C3HeB than the C3HfB. The effect was reversed following the inoculation of $\underline{H\text{-}2^d}$ marrow. Both reciprocal hybrids between C3HfB and C3HeB were more sensitive to irradiation than either parental strain. Survival following 500 R was 44% for (C3HeB × C3HfB)F_1, 19% for (C3HfB × C3HeB)F_1, and 19% for (C3HfB × C3HeD)F_1. The recent development of the C3HeD substrain indicates that the altered radiosensitivity occurred at the time the ova were transferred. This would indicate that the alteration(s) once established was perpetuated over many generations and was apparently transferred by males as well as females. (auth)

19649 THE DEPENDENCE OF THE RADIATION SENSITIVITY OF SERRATIA MARCESCENS ON RELATIVE HUMIDITY AND THE PRESENCE OF INOSITOL. Gail Morrison, D. V. Cormack, and S. J. Webb (Univ. of Saskatchewan, Saskatoon). 8p. (CONF-556-21)

From 12th Annual Meeting of the Radiation Research Society, Miami, Fla., May 1964.

The effects of humidity and inositol on the radiosensitivity of Serratia marcescens were investigated. The cells were found to be much more sensitive at very high humidities and in suspension than at low humidities. A sharp drop in sensitivity occurred between 80 and 70%. At relative humidities between 65 and about 50%, the sensitivity increased again. The inositol was seen to protect the cells from damage to some extent throughout the relative humidity range, its effect being most pronounced at humidities from 20-50%. (P.C.H.)

19650 AMYLOIDOSIS IN RADIATION CHIMERAS AND ITS RELATIONSHIP TO LYMPHOID HYPOPLASIA. H. S. Micklem and S. Bradbury (Medical Research Council, Harwell, Berks, Eng. and Dept. of Human Anatomy, Oxford). 8p. (CONF-717-8)

From CNRS Meeting on Graft of Allogenic Hematopoietic Cells, Paris, Sept. 1964.

CBA/H mice were x irradiated with an LD_{99} of 1000 Rads to the whole-body. Within four hours of irradiation they were injected intravenously with syngeneic or allogeneic bone marrow or fetal liver. The incidence of hyaline deposits in the spleen and liver of a series of radiation chimeras which died, or were found moribund, with secondary disease, and of a smaller series which were killed at various stages before or during the development of the disease was investigated. The incidence of other common histologic features was investigated in parallel, and the effects of injecting histocompatible lymphoid cells were noted. The hyaline deposits were identified as being amyloid in nature, closely comparable to secondary amyloid in man, by a variety of histochemical techniques and by electron microscopy. (P.C.H.)

19651 SOME MEANS OF COUNTERACTING THE KILLING EFFECT OF FOREIGN CELLS. V. Stankovic, M. Boranic, and I. Hrsak ("Ruder Boskovic" Inst., Zagreb). 10p. (CONF-717-5)

From CNRS Meeting on Graft of Allogenic Hematopoietic Cells, Paris, Sept. 1964.

Spleen cells of C57BL or C57BR mice (ca 15 or 30 million cells which were injected intravenously into CBA mice 1 day after the hosts were sublethally whole-body x irradiated at 500 R) induced death of nearly all recipients within the 2nd and 3rd week. The same irradiation dose was lethal for only some of the exposed mice. Lymphatic atrophy together with bowel or lung affections were always present in animals that died. It seemed logical to postulate breakdown of immunologic defense as one of the main reasons of mortality. Mortality, viz. immunologic breakdown, is attributable to an immune reaction by the immunocompetency of injected spleen cells against the host. Attempts were made to determine the possibility of inhibiting or reducing lethality that follows as a result of spleen cells implantation. Results with antisera seemed to indicate that lethality is due to graft-versus-host reaction. By treating the host animals with an antibiotic (Geomycin "Pliva", an oxytetracycline) life was prolonged for only about 1 week. Similar postponement of the lethal outcome was induced when acceptor mice were injected with methyl cellulose. It was concluded that the lethal outcome of the foreign spleen cell effect in CBA mice can be delayed but not inhibited by assisting the host's unspecific immunologic defense. Death can only be avoided when the foreign cells are specifically attacked by preformed antibodies which must be applied early enough after the administration of the foreign cells. (P.C.H.)

19652 IMMUNOLOGIC REACTIVITY AND SPECIFIC TOLERANCE OF THE GRAFT IN RADIATION CHIMERAS AND THE INFLUENCE OF THE THYMUS. D. W. van Bekkum (Radiobiological Inst. TNO, Rijswijk, Netherlands). 23p. (CONF-717-6)

From CNRS Meeting on Graft of Allogenic Hematopoietic Cells, Paris, Sept. 1964.

An investigation was made on the immunologic activity of grafted cell populations in radiation chimeras as estimated by way of the Simonsen assay. This method permits the semi-quantitative determination of anti-host, and of anti-third party activity of the cells under investigation. In a number of different host-donor combinations the anti-host reactivity was correlated with secondary disease in the chimeras. In compatible $P \rightarrow F_1$ or homologous combinations, anti-host activity is not apparent at any time, while anti-third party activity returns within about 1 month after transplantation. In thymectomized chimeras, the return of anti-third party activity was found to be greatly retarded and normal levels of activity were only rarely recorded within the observation time of 200 days. However, in those cases where the latter activity returned, the anti-host tests were always negative, showing that specific immunologic tolerance towards the host can develop in the absence of the thymus. The implications of these results with regard to the function of the thymus and the mechanism of secondary disease are discussed. (auth)

19653 EFFECT OF BLOOD TRANSFUSIONS ON A SUBSEQUENT MARROW TRANSPLANT IN IRRADIATED MICE. H. Da Costa (Atomic Energy Establishment, Bombay) and F. Lapeyraque. 8p. (CONF-717-10)

From CNRS Meeting on Graft of Allogenic Hematopoietic Cells, Paris, Sept. 1964.

An investigation was made on the effects of blood transfusions on a subsequent homologous bone marrow transplant in mice. Groups of animals were transfused two, four, six, eight, nine, or ten times with 0.2 ml whole blood at intervals of 3-4 days and 950 R whole-body x radiation followed by an immediate marrow transplant was administered 15-60 days after the last transfusion. An adverse effect on the incidence of early mortality was noted in all the groups as compared with the control animals. Antibodies against donor red cells could, however, be demonstrated only in those transfused eight times or more. Selective cell transfusions subsequently carried out incriminated both the red and the white cell series. Histologic examination showed that the myeloid population of the transfused mice compared unfavorably with that of the control group a week after transplantation. The observations indicate a detrimental effect of blood transfusions on a subsequent homologous marrow transplant in irradiated animals and are reminiscent of the poor results obtained in transfused leukemic subjects as contrasted with those of nontransfused reactor accident patients. (auth)

Radiation Hazards and Protection

See *also* HEALTH AND SAFETY.

19654 RADIATION PROTECTION IN CANADA. PART VI. PROBLEMS IN THE ASSESSMENT OF GENETIC DAMAGE FROM EXPOSURE TO INDIVIDUALS AND POPULATIONS TO RADIATION. Howard B. Newcombe (Atomic Energy of Canada Ltd., Chalk River, Ont.). Can. Med. Assoc. J., 92: 171-6(Jan. 23, 1965).

Estimates of the genetic damage from radiation exposures of human populations are discussed. In addition to the three Rads per generation received by the gonads from natural sources, a similar amount is currently contributed by medical radiology and a further five Rads per generation has been suggested as an upper limit for exposures from the future peaceful uses of atomic energy. Two methods of estimating the genetic damage from such an increase suggest that there might be in the vicinity of 250 to 800 severely affected individuals per year in a population of 20 million people, or within an order of magnitude of the current highway fatality rate for Canada of about 4000 per year. Although the true value may be less, or greater, by as much as tenfold, the effect is in any case large enough to justify continued scrutiny. (auth)

19655 THE NEW RADIATION CONTROL REGULATIONS OF THE STATE OF CALIFORNIA. F. R. Holden and E. Tochilin. J. Calif. State Dental Assoc., 38: 185-90 (June 1962).

The California State legislature developed and the governor has approved: regulations for the registration of sources of radiation; the licensing of users of radioactive materials; and standards for protection against radiation. Administration of these regulations by the State Department of Public Health was authorized. The Radiation Control Law regulates the use of x rays in dentistry through provisions for preventing unnecessary exposure of patients and dental personnel to nonuseful radiation. Every dentist having x-ray equipment (or any source of ionizing radiation) must register it, pay a fee, and maintain records for inspection by the Department. Advanced notice is required for testing his equipment. The standards for protection against radiation require: maximum permissible exposure to personnel of 1250 mRem in any quarter of a year; personnel monitoring (if, after one quarter, exposure is less than 25% of maximum exposure, further monitoring is not required); notice to employees of exposure; diaphragm for a 3-in. beam or less; cone distance not less than 7 in. above 50 kvp or 4 in. below 50 kvp; total filtration of 1.5 mm of aluminum up to 70 kvp and at least 2.5 mm above 70 kvp; a protective barrier for the operator or arrangement for the operator to stand at least 6 ft from the patient and the useful beam; primary barriers at all areas struck by the useful beam; and a protective apron of not less than 0.25 mm lead equivalent to cover the gonadal area of the patient. Surveys revealed that patients and personnel were receiving needless exposure that could be corrected by collimation, filtration, and lead aprons. Education of technicians reduced radiation exposure. (BBB)

19656 DIAGNOSIS AND TREATMENT OF RADIOACTIVE CONTAMINATION. Lafuma. Maroc Med., 43: 183-7(1964).

Methods of determining the severity of external and internal contamination by radioactive substances are reviewed. A short description of α, β, and γ contaminants

is given. Methods of determining the amount of contamination are mentioned. This is followed by a review of treatment particularly by use of chelating agents. (Excerpta Med., Sect. XXIII, 2: No.3, (Mar. 1965))

Radiotherapy and Radiodiagnosis

19657 (ANL-6938(p.97-119)) GENERAL TECHNICAL PROBLEMS IN RADIOLOGICAL PHYSICS. Leonidas D. Marinelli (Argonne National Lab., Ill.).

A review of problem areas associated with x-ray diagnosis, radiotherapy, and nuclear medicine is presented. The measurements of exposure and absorbed dose in patients undergoing diagnostic procedures are discussed. The role of dosimetry in radiation therapy is also discussed along with measuring methods. Other discussion is included on those fields of medical research, diagnosis, and therapy in which radioactive isotopes are administered internally. (J.R.D.)

19658 INTRALYMPHATIC RADIOACTIVE THERAPY FOR PELVIC CANCER. Peter Siegel and Edwin J. Liebner (Univ. of Illinois, Chicago). Am. J. Obstet. Gynecol., 90: 122-31(Dec. 15, 1964).

By incorporating a radioactive substance into contrast material, it is possible to deliver intense localized radiation directly into the pelvic and abdominal lymph nodes. A study was made on the feasibility of employing radioactive lymphography as a routine therapeutic adjunct in the hope of improving survival in patients with cervical or vulvar cancer. In diagnostic lymphography, the commonly used radiopaque substance is Ethiodol. It remains uniformly distributed and fixed in the lymph nodes for long periods (more than six months). The isotope to be used therapeutically in radioactive lymphography should have the following characteristics: it should be firmly bound to Ethiodol; it should have a reasonably short half-life so as not to preclude subsequent surgery; it should be primarily a β emitter so that its radiation effect is localized; and its degradation products must be nontoxic. Radioactive lymphography employing ^{131}I Ethiodol was done in 18 patients with pelvic cancer. The patients were given from 9 to 22 mC of ^{131}I, with more than half of the patients receiving from 15 to 22 mC. In general, the procedure was well tolerated. Histologically, marked radiation changes were seen, giving a skeletonized appearance to the lymph nodes with fibrosis and loss of lymphocytes. Pronounced vascular changes were also evident with disruption of the collagen and smooth muscle elements of the vessel wall. It was concluded that radioactive lymphography with ^{131}I is safe, well tolerated, and delivers uniformly high radiation to all the retroperitoneal lymph nodes. (TCO)

19659 THE CURRENT STATUS OF RADIOTHERAPY IN CARCINOMA LARYNGIS. L. Henry Garland. Ann. Otol. Rhinol. Laryngol., 73: 488-500(June 1964).

Results and complications of irradiation of laryngeal cancer are described with reference to 132 cases. Most patients with localized cancer, previously untreated, were advised to have radical radiotherapy, the cure rate being as good as that obtained with surgery, and the voice is preserved. The results with orthovoltage (200- to 300-kv) x rays were as good as if not superior to those obtainable with ^{60}Co and other modalities. The radiation absorbed, not the radiation applied, is important. By careful application of orthovoltage x rays, a carcinocidal dose could be applied to most localized laryngeal cancers, without the undesirable deep side-effects common with megavoltage (such as connective tissue injury and more marked late deep tissue changes). The warning skin erythema of orthovoltage was useful, and is absent with megavoltage. The late superficial telangiectasis often present after properly given orthovoltage x-ray therapy was not serious. Most squamous cell carcinomas of the glottis were treated by cross-fire technique, using opposing circular or rectangular beams about 5 cm in diameter. One field was treated daily. Midtumor dose ranged from 5000 Rad in about four weeks to 6000 Rad in about six weeks. This requires from 3000- to 3300-R air doses to each of the two lateral fields delivered in 24 to 42 treatment days. Daily dosage and total dosage were individualized to produce a mild mucositis in about the fourth week. Premature or intense reactions were avoided, and dosage was sometimes reduced in the fourth week because of painful pharyngitis. Pain and skin reaction usually subsided even though treatment was continued. The tolerance of the deep tissues paralleled that of the epidermis under the conditions described. An advantage of orthovoltage treatment was that dosage could be adjusted accordingly. If large fields (7 by 8 cm) were necessary to encompass the tumor, the total dose had to be reduced, and a carcinocidal level could not be attained with safety. The epidermitis present at or near the end of treatment usually equaled the degree of mucositis present in the larynx. With conservative management both cleared up within two or three weeks, the mucosa more speedily than the skin. In favorable cases, the tumor was greatly reduced in size or gone by the time this mucosal reaction has subsided. When palliation alone was intended, a tumor dose of 3000 to 4000 R was usually adequate. Occasional cures were obtained with doses as small as 4000 R in four to five weeks. Most curable cases of laryngeal cancer were controlled with doses in the range of 4500- to 5500-Rad doses of orthovoltage x rays in four to six weeks. There was some evidence that therapy on alternate days (three times a week) was more effective than daily treatments. When telecobalt therapy is used, a similar two-field, opposing-beam technique is usually recommended. With radical treatment courses the midtumor dose was 6000 to 7000 R in six weeks. The daily dose was about 300 R in air with small fields, suitably reduced with larger fields. This was given to alternate sides of the neck daily for five days each week. Of 132 cases, 56 five-year survivors gave a relative cure rate of 42%. (BBB)

19660 THE USE OF RADIOACTIVE YTTRIUM FOR DESTRUCTION OF THE PITUITARY GLAND. A. P. M. Forrest and H. J. Stewart (Welsh National School of Medicine, Cardiff, Wales). Bull. Soc. Intern. Chir., 23: 224-6 (1964).

The physical aspects of yttrium-90 that make it suitable for an implant to destroy the pituitary gland are described. The techniques of implantation are outlined. Initially two rods of yttrium-90, each of 5 millicurie activity, were introduced in the pituitary fossa through a cannula passed through each nostril. With this technique the yttrium frequently became misplaced and the technique has now been modified. Each yttrium rod is encased in nylon and fixed into a small stainless-steel screw-threaded base. The hole through which the unit is inserted into the pituitary fossa is thus plugged by the screw which, with its attached yttrium, remains permanently in position. The latter technique has reduced the complication rate approximately 50%. In advanced breast cancer the remission rates and duration of remission compare favorably with patients having oophorectomy and adrenalectomy. (Excerpta Med., Sect. XXIII, 2: No. 3, (Mar. 1965))

19661 CLINICAL USE OF RADIOISOTOPES: INTRA-ARTERIAL INJECTION. David S. Sklaroff (Albert Einstein Medical Center, Philadelphia). Current Therap. Res., 7: 50-3(Jan. 1965).

Five new radiotherapeutic techniques are discussed. The first concerns intratumor injection of ^{32}P or ^{51}Cr, bound to minute spheres of resin, into the main artery to the tumor. The resin microspheres range in diameter from 30 to 80 μ and give varying amounts of radiation, depending on types and sites of tumors. The microspheres lodged in the arterial capillaries around and in the tumor, exposing the malignant cells to γ rays emitted by the isotopes. In 115 patients treated to date, best results have been obtained in tumors of the tongue, breast, and cervix uteri. Tumor shrinkage is noted within a few days, and complete destruction in about two months. One weakness of this technique is the problem of obtaining an equal homogeneous distribution of the radiation. In the second technique, for treatment of thyroid malignancy, after surgery, ^{131}I concentration is carefully sought by scanning, and residual thyroid tissue and significant disease is abolished by therapeutic doses of radioactive ^{131}I. Desiccated thyroid is then administered

to keep the patient euthyroid. The usual dose of ^{131}I necessary is ~100 to 150 mC, ranging up to a total dose of 660 mC. Bone marrow suppression is a complication of treatment. In the third method, neoplastic pleural effusions are treated by radioactive colloidal gold. The periods of relief last from a few months to over two years. The usual dose is between 50 and 100 mC. The fourth concerns the intralymphatic administration of radioisotopes, microspheres (1-4 γ in diameter) containing ^{90}Y in the treatment of patients with lymphoma, as well as Ethiodol-tagged ^{131}I and colloidal ^{198}Au. In the fifth method, treatment of polycythemia and leukemia with ^{32}P results in normal life expectancy and successful control of the disease in polycythemia with a median age at death of 69 years and 38% survival in leukemia. (BBB)

19662 DETECTION OF LIVER METASTASES THROUGH CONTINUOUS MEASUREMENT OF HEPATIC RADIOACTIVITY FOLLOWING RECTAL ADMINISTRATION OF I^{131}. H. Ernst and U. Bauer (Freie Univ., Berlin). Fortschr. Gebiete Rontgenstrahlen Nuklearned., 100: 701-2(1964).

Liver metastases were verified with great accuracy by a simple method. A small amount of ^{131}I was infused into a bowel, and the rise in activity was recorded above the liver. In normal patients the equilibrium level was reached within less than 9 minutes, whereas patients with liver tumors exhibited a significant increase in equilibration time. One false positive result was encountered, and five results were ambiguous in a series of 30 patients. (Excerpta Med., Sect. XXIII, 2: No. 3, (Mar. 1965))

19663 CRITICAL CONSIDERATIONS IN TELECOBALT TREATMENT OF UTERINE CARCINOMA. H.-J. Frischbier and H. Kuttig (Universität, Heidelberg). Geburtsh Frauenheilk., 24: 761-70(Sept. 1964). (In German)

When Ra implants are used with percutaneous stationary or pendulum ^{60}Co irradiation of uterine carcinoma, excessive localized irradiation may damage the ureters. Also, if the uterus is displaced from the central axis of the body, the irradiation dose administered may vary widely from what is expected. Even though procedures may be used which try to take these problems into account, the combination of two methods of irradiation is unwise, and often results in exposures that exceed the capacities of rather extensive radioprotective measures. One way to reduce the hazard of internal injury from Ra implants would be to omit their use completely. Because of the characteristics of its absorption by tissue, the intensity of radiation from Ra falls abruptly within short distances in tissue. As a result, sometimes as much as 20000 to 30000 R must be administered in order to provide adequate irradiation of the endometrium. This amount is unnecessary for treatment of squamous cell carcinoma. If telecobalt therapy alone is used it would eliminate many uncertainties in dose distribution and the possibility of damage to healthy tissue of adjacent organs. Fractionation of the dose can be more easily measured and controlled. In the authors' experience, pendulum irradiation from two axes at a distance of 6 cm, with an angle of 160° on both sides, produces a summation of the isodose at the center of the pelvis, with optimum dose distribution, decreased irradiation of adjacent organs, and simplicity of operation. (BBB)

19664 ISOTOPE HYPOPHYSECTOMY. L. Zoltan. Ideggyogy Szemle, 17: 193-205(1964).

The results of isotope hypophysectomy are reported. Stereotactic introduction of ^{90}Y, a pure β-emitter, into the anterior part of the sella is considered the best method. The main advantages are discussed. With the instrument used the method is practically without danger and can be done even if the patient's general condition is poor. In some patients with disseminated cancers survival is prolonged and a definite regression of the metastases and disseminations is seen. In hypophyseal tumors where there are contraindications for operation and in Cushing's syndrome good results are also obtained. As regards other tumors neither previous data no personal experience permit an evaluation of the method. In patients with disseminated cancer isotope hypophysectomy should be done as soon as metastasization has started as this improves the results. In mammary cancer a preventive isotope hypophysectomy may be valuable in addition to classic treatment by surgery and irradiation to delay or prevent metastases or dissemination and prolong survival. 82 references are included. (Excerpta Med., Sect. XXIII, 2: No. 3, (Mar. 1965))

19665 RADIOACTIVE IODINE AND SURGERY OF THE THYROID. Morris T. Friedell (Jackson Park Hospital, Chicago). J. Am. Geriat. Soc., 12: 737-48(Aug. 1964).

Uses of ^{131}I in the management of thyroid disease, assessment of thyroid function, and differential diagnosis of nodules located within the thyroid gland are discussed. The value of radioiodine as a diagnostic tool in the management of thyroid enlargement is emphasized. Two methods are discussed: (1) the 24-hr ^{131}I uptake for the assessment of thyroid function, and (2) scintillation scanning of the thyroid for differentiation of various areas of functioning thyroid tissue. Proper analysis of the scan in relation to ^{131}I uptake will increase the preoperative diagnostic accuracy regarding the cause of enlargement. A so-called cold nodule in a hot (hyperthyroid) gland is not necessarily malignant but should be considered as such until proved otherwise. A hot nodule is probably never malignant. Unilateral enlargement can be assessed by the scanning process and a differential diagnosis of carcinoma established with increased certainty. A cold nodule in a female whose 24-hr thyroidal ^{131}I uptake is less than 30% will prove to be malignant about once in four times. The chances of malignancy will be about doubled if the patient is a male. Bilateral thyroid enlargements containing several hot or cold areas are usually caused by multinodular goiter and are invariably benign. The same picture, but with a more patchy and usually less discrete scan differentiation, is presented by thyroiditis. It can be assumed that both such enlargements are benign when thus depicted by the scan pattern. Total lobectomy on the affected side is justified when the scan shows a cold nodule in a unilaterally enlarged thyroid. It is concluded that application of radioiodine diagnostic technics is of great help to the surgeon in determining if surgery is indicated and, if so, what type of operation should be employed. Radioiodine as a preoperative therapeutic agent does not interfere with subsequent surgery. It was found to be a rapid and convenient means of preparing patients for thyroid surgery when a clinical and lab diagnosis of hyperthyroidism had been established. Even in severely thyrotoxic patients, operation could be safely performed within three to four weeks after the initiation of treatment with ^{131}I. (BBB)

19666 DIAGNOSIS OF BONE METASTASIS BY PHOTOSCANNING WITH STRONTIUM-85. David M. Sklaroff and N. David Charkes (Albert Einstein Medical Center, Philadelphia). J. Am. Med. Assoc., 188: 1-4(Apr. 6, 1964).

The relative advantages and disadvantages of ^{45}Ca, ^{47}Ca, ^{85}Sr, ^{89}Sr, and ^{90}Sr for the study of bone metabolism are discussed. Calcium-45, a pure β-emitter, cannot be followed externally because of lack of γ emission. High-specific activity ^{47}Ca is available, but again its use appears limited because of the high energy of its γ ray and consequent collimation problems. Both ^{89}Sr and ^{90}Sr are pure β-emitters and therefore unsuitable for external detection studies in humans. Strontium-85, however, is well suited for photoscanning since in its decay by electron capture to stable ^{85}Rb a single γ photon of 0.513 Mev is emitted. There is no associated corpuscular emission. Strontium (^{85}Sr) nitrate was administered intravenously, 50 μC to adults and 20 μC to patients under 20 years of age. This dose results in an estimated total-body dose to a standard man of about 0.33 rad and a total bone dose of 2.3 rad. Twenty-four to 48 hr after the intravenous administration of ^{85}Sr the patients were scanned with a photoscanner equipped with a 3- × 2-in. thallium-activated sodium iodide crystal, pulse-height analyzer, and 19-hole focusing collimator. Four cases are described using ^{85}Sr for the demonstration of bone metastases by photoscanning, and a total of 40 cancer patients were studied for the presence of suspected or known metastatic involvement of bone. In 18

patients both the scan and the x ray were positive; both osteolytic and osteoblastic lesions were included. The degree of osteogenic activity is of considerable importance in Sr deposition, particularly in small lesions. These results confirm that radiostrontium can be detected in increased amounts in bone prior to demonstrable roentgenographic changes in patients with metastatic cancer. The photoscanning technique presents the data in a form which is readily interpreted, and areas of abnormal osteogenesis can be easily detected by this means. In many instances, the scan is positive despite absence of symptoms and negative x-ray findings. Bone biopsies demonstrated that the cause of the abnormal Sr deposition is metastatic tumor in the scan-positive site; counting of the specimens in a scintillation well-counter confirmed the photoscan findings. Strontium scanning is of particular aid to the radiation therapist in the planning of treatment portals, revealing knowledge of areas of abnormal osteogenesis. The radiation dose to bone may be high (2.3 rad from a 50 μC dose), but it is comparable to organ doses produced by diagnostic x rays during gastrointestinal or genitourinary examinations. On the basis of these studies, an increase in the ^{85}Sr dose to 100 μC is recommended to decrease the scanning time and also to increase resolution. Another isotope, ^{87m}Sr, produces comparable scans with a radiation dose less than 1% that of ^{85}Sr, and with ^{87m}Sr it should be possible to evaluate the osteogenic response to therapy and to undertake studies of nonmalignant bone disorders, including those of children. (BBB)

19667 THERAPEUTIC PITUITARY ABLATION BY IMPLANTING RADIOACTIVE SEEDS (^{90}Y OR ^{198}Au). R. Fraser (Postgraduate Medical School, London). Leech, 34: No. 4, 99-102(1964).

The use of ^{90}Y and ^{198}Au seeds for therapeutic pituitary ablation is described. Results obtained were encouraging and showed that this method of intensive localized radiotherapy has a place both in the treatment of pituitary diseases and also for modifying other diseases whose progress can be pituitary-dependent. (TCO)

19668 MEASUREMENT OF CORONARY CIRCULATION WITH A NEW ISOTOPE TECHNIQUE. G. Bluemchen, A. Cohen, J. Gallagher, E. Zaleski, E. Bassenge, and R. J. Bing (Wayne State Univ., Detroit). Med. Klin. (Munich), 59: 1123-6(1964).

Description is given of a new method for the diagnosis of coronary insufficiency and measurement of myocardial circulation in man by means of an isotope technique. By this method the clearance equivalents of ^{86}Rb are determined as a function of coronary perfusion. The curves are evaluated by a computer and thus the clearance equivalent before and after administration of trinitroglycerol and significance of the increase are calculated. (TCO)

19669 A COMPARATIVE STUDY OF SOME ANABOLIC STEROIDS DURING RADIATION THERAPY. F. Kleibel (Universitat, Heidelberg). Med. Klin. (Munich), 59: 1205-8 (1964).

Clinical and hematological studies and the proteinogram clearly showed that 4-chloro-testosterone acetate, 4-hydroxy-17-methyl-testosterone, and a combination of prednisolone and 4HMT had an anabolic effect. The studies were made on 96 patients with tumors, of both sexes, and treated with irradiation, cytostatics, or a combination. The body weight, appetite, hematological findings (hemoglobin and erythrocytes), hypoproteinaemia and dysproteinaemia showed an improvement in the majority of patients. These anabolic steroids have a significant protective effect against radiation reactions. A certain economy in cortisone was also seen. There was a good correlation between the laboratory findings and the clinical improvement. (Excerpta Med., Sect. XXIII, 2: No. 3, (Mar. 1965))

19670 RADIATION HAZARD IN THE DIAGNOSTIC USE OF RADIOACTIVE ISOTOPES. Istvan Krasznai and Janos Foeldes (Orvostudomanyi Egyetem, I. sz. Belgyogyaszati Klinika, Budapest). Nepegeszegugy, 44: 91-3(Mar. 1963). (In Hungarian)

Attempts were made to determine the amount of radiation reaching the gonads and other organs, especially those which contained the largest amount of the given isotope, after radioisotope diagnostic methods, and to compare these figures with those published by the National Radiation Institute on gonad doses resulting from x ray examinations. There appears considerable difference of opinion among authorities on the dangers of radioisotope diagnosis. A table shows the doses received by critical organs and the gonads in various types of isotope examinations to be as follows: for ^{131}I uptake by and elimination from the thyroid after administration of 5 to 10 μC the gonad dose in mrad is 0.6 to 3.7 in euthyroid persons and 0.6 to 3.6 in hyperthyroid patients; the dose reaching the critical organ (thyroid gland), in rad, is 11 to 22 in euthyroid and 7 to 14 in hyperthyroid patients. The respective figures for other examinations were: in ^{131}I tests for determining protein-bound plasma activity, 20 to 50 μC, gonad doses 2.5-18.4, 2.3-17.00, thyroid doses 44-110, 29-73; ^{131}I for a thyroid scintillogram, 100-200 μC, gonad doses 12.5-74, 11.2-71.5, thyroid doses 220-440, 146-292; ^{132}I for thyroid examination, 10-20 μC, gonad doses 1.2-2.34, 0.6-1.1, thyroid doses 0.3 to 0.7, 0.5-1.00; ^{131}I-albumin for circulation studies, 20-30 μC, the gonad dose is 20-45 mrad, the dose for critical organs is 0.1-0.2 rad; ^{51}Cr for red blood cell studies, 100 μC, gonad dose is 30 mrad, 0.04 rad for whole body, 0.4 rad for spleen and blood; ^{198}Au for liver scintillogram, 200 to 400 μC, gonad dose 40-120 mrad, 8-16 rad for liver, 10-20 rad for spleen. It is observed that, with the exception of ^{131}I thyroid examinations, the dose reaching the critical organ is under 10 rad and the gonad dose is under 30 mrad. Although thyroid examinations constitute 80 to 90% of the radioisotope diagnostic examinations conducted in Hungary, they have not shown a tendency to cause carcinoma or leukemia and even doses as high as 8000 to 10,000 rad are considered safe. A table showing the various doses from x ray examinations gives the following gonad doses: thoracic radiographs, men, 0.04 mR, thoracic fluoroscopy, women, 1.2 mR; abdominal series, men 65.0, women, 48.0; intravenous pyelography, men, 380.0, women, 291.0; pelvic radiography men 480.0, women 242.0. The dose reaching the critical organs is considered to be 5 to 15 R. It is concluded that the gonad dose may be much higher when x ray examinations are conducted as compared with diagnostic radioisotope examinations. Caution is recommended, however, in the use of radioisotopes, in order to reduce the amount of radiation reaching the population; the manufacture of more sensitive radiation-measuring devices is urged and the use of isotope preparations with the shortest half lives is recommended. (BBB)

19671 STUDIES ON HOMOGENEITY OF THE DOSE DISTRIBUTION IN TUMORS. (1ST REPORT). HETEROGENEITY INDEX. Nobuo Yamashita (Tohoku Univ., Sendai). Nippon Igaku Hoshasen Gakkai Zasshi, 22: 750-4(1962). (In Japanese)

It is pointed out that in the study of the dose distribution in tissue at least three factors, i.e. tumor dose, tumor volume dose ratio, and distribution ratio of tumor dose, should be taken into consideration. Tumor dose and tumor volume dose ratio have been well studied; however, there is little data on the distribution ratio of tumor dose. In this study, information on this problem was sought. Since the dose at various points in tumor is not homogeneous, the concept of a heterogeneity index was introduced to indicate the deviation ratio of dose distribution in the tumor. This concept is mathematically expressed in terms of the location and volume of tumor. However, the derived equation is very difficult to calculate in its present form; therefore, attempts were made to obtain an approximate value of the heterogeneity index by integral calculation. The results are reported in the next abstract. (BBB)

19672 STUDIES ON HOMOGENEITY OF THE DOSE DISTRIBUTION IN TUMORS. (2ND REPORT). 200-kv X-RAY THERAPY. Nobuo Yamashita (Tohoku Univ., Sendai). Nippon Igaku Hoshasen Gakkai Zasshi, 22: 1125-30(Jan. 25, 1963). (In Japanese)

The dose distribution in tumors with 200-kv x rays was calculated from the data of Worthley & Wheatley, Johns,

and Mayneord & Lamerton. Heterogeneity index, as defined in the previous abstract, was calculated from their data under the following condition: focus-skin distance (F.S.D.) 50 cm, half-value layer (H.V.L.) 1.0, 1.5, and 2.0 mm Cu, assuming the radius of the tumor sphere to be from 1 to 4 cm. For single-field irradiation, when H.V.L. and F.S.D. were constant, the heterogeneity index increased with increase of tumor radius. When the tumor depth in the body was changed, heterogeneity index changed slightly, while the change of x-ray quality caused little variation of the index. For two-field irradiation the heterogeneity index was less than that for one-field irradiation. For four-field irradiation the heterogeneity index was under 1%. (BBB)

19673 THE ROLE OF LINEAR ACCELERATORS AND OF THE BETATRON IN MODERN RADIOTHERAPY. Felix Wachsmann (Universität, Erlangen-Nuernberg, Ger.). Nippon Igaku Hoshasen Gakkai Zasshi, 23: 375-86(July 25, 1963).

The relative therapeutic effectiveness, based on depth dose considerations, is discussed for radiation sources of various energy levels. When deep-seated lesions are to be treated, conventional radiotherapy of the energy range up to about 250 kv is not sufficient to obtain the required dose distribution. As human skin has a tolerance of about 3000 R for a fractionated treatment spread over 30 days, and since certain types of tumors need for a successful cure 6000 R or more, the depth dose has to be at least two to three times as large as the skin dose whenever deep-seated lesions are concerned. The obtainable percentage depth dose increases with increasing energy; for instance, with the hard γ radiation of a ^{60}Co teletherapy unit, the minimum requirement of attaining a 50% depth dose at a depth of 15 cm can be met. The construction and characteristics of linear accelerators are discussed. Large linear accelerators have been built mainly for electron therapy; to reach deep-seated lesions, energies of at least 40 Mev are required. Such accelerators having accelerator tubes of 3-m length and more are immobile, but to obviate this drawback, a deflecting and defocussing magnet has been designed. The betatron is designed for energies of up to hundreds of Mev; with energies in excess of 300 Mev difficulties arise. Some difficulties are encountered with the betatron with reference to the dose required in therapy. Since the electrons are captured only in a fraction of the time available for acceleration (about 1/10000) and since the capacity of the accelerator vessel for electrons is limited for reasons of the space charge, the required dose rates can only be reduced with larger machines. In addition, since the efficiency of the radiation rises markedly with energy, the dose rate obtained with the betatron increases by an amount raised to the third power of the energy if machines of equivalent designs are used. With machines built for high energies, a sufficiently high dose rate is obtained but never that yielded by a linear accelerator. The smallest betatron for medical purposes both with reference to energy and dimensions is manufactured in Germany by Siemens-Reiniger-Werke, Erlangen. It is operated on 50 cycles a-c and was initially destined for an energy of 12 Mev. However, its output was later increased to 18 Mev without changing the outer dimensions. This betatron design is unique in that it yields a relatively high dose rate despite the fairly low energy for which it is built. The ultrahard radiation from 15 to 20 Mev represents, it is suggested, the practical optimum for deep therapy because the entry and exit dose are about equal in the case of medium-size fields. This betatron can be switched in a matter of seconds from roentgen to electron radiation. Electron radiation from 6 to 18 Mev is optimal for treatment of lesions at a depth of about 2 to 6 cm. Higher electron energies are of less interest. The dose rate of the 18-Mev Siemens betatron is particularly high in comparison to the dimensions of the machine. With roentgen radiation and with a distance of 50 cm from the target it amounts to about 80 to 120 R/min with small fields and about 60 R with large fields and flattening filters. Of this dose, about 80% penetrates into a depth of 10 cm and 60% into a depth of 15 cm so that the min requirements are more than met. The 42-Mev Siemens betatron is also described and illustrated. Costs of providing supervoltage radiation are discussed, and it is concluded that the cost per R at the tumor rise with growing radiation energy and is three times as high for the linear accelerator and betatron as with conventional machines or two times higher than with ^{60}Co. Between the linear accelerator and betatron, however, no significant differences exist in expenses involved. (BBB)

19674 A SLIT TYPE SCREEN FOR TELECOBALT THERAPY. Morimasa Maeda, Takatoshi Kobayashi, Jiro Nakatsuka, and Chikahisa Yamada (Kyoto Prefectural Univ.) Nippon Igaku Hoshasen Gakkai Zasshi, 24: 107-10(May 1964). (In Japanese)

Dosimetric data are provided for γ-ray exposure of patients by the use of newly developed slit type screen. This screen differs from the usual sieve type consisting of multiple holes. Depth doses at open and shielded areas with this screen, as well as inhomogeneity ratios, are tabulated. This telecobalt screen consists of lead plates of 5-mm thickness, 60-mm width, and 50-mm height, arranged parallel to the direction of radiation. The upper surfaces of the lead plates are parallel to each other with a space of 5 mm between them on the circumference of a circle drawn with the center at the source and a radius of 45 cm. Consequently, the area of the openings is 50% of the whole area of the screen on the source side and 54.5% on the patient side. Although the entire area of the upper surface of the screen is 6×12 cm^2, the field size suitable for the lesion can be obtained by adjusting the collimator of the telecobalt unit. Such a telecobalt screen can be made more easily than a sieve with many holes, and construction of a fine telecobalt screen would not be difficult. The dose distribution in a water phantom measured with a fluoroglas dosimeter gave results which were similar to those obtained previously with a telecobalt sieve in this clinic. The telecobalt screen with a narrow field is considered especially suitable for irradiation of esophagus cancer. (BBB)

19675 LOCALIZATION OF PRIMARY AND SECONDARY BONE TUMORS BY Sr^{85}. M. Erjavec (Inst. of Onkology, Ljubljana, Yugoslavia). Nowotwory, 14: 259-64 (1964).

The use of ^{85}Sr for localization of primary and secondary bone tumors is discussed. 30 patients with neoplastic changes in the osseous system were examined. Various external measurements were performed using the improved method of scanning, with applications of additional screens and changed methods of collimation. With this type of examination, it is possible to improve the diagnosis of doubtful cases, determine the extension of changes in the osseous system, and detect osseous metastases several months prior to the detection by radiological examination. (TCO)

19676 DENTAL X-RAY EXPOSURE OF SITES WITHIN THE HEAD AND NECK. A. G. Richards and R. L. Webber (Univ. of Michigan, Ann Arbor). Oral Surg., Oral Med., Oral Pathol., 18: 752-6(Dec. 1964).

This investigation determined the amount of radiation to which selected sites within the patient's head and neck are exposed during dental x-ray examinations. Measurements were obtained by miniature condenser-type ionization chambers located within an adult-sized phantom head. The phantom head consisted of an adult human skull, with complete dentition, located in a head-shaped plastic container filled with water. The sinuses and other air passages were filled with plastic foam to prevent the water from filling them. A medium-speed film (A.S.A. speed group B) was used for the bitewing examination, and a high-speed film (A.S.A. speed group D) for the periapical examination. Filtration of the x-ray beam was equivalent to 2 mm of aluminum. The half-value layers (HVL) of the beam were 1.85 and 2.60 mm of aluminum at 65 and 90 kvp, respectively. The times of exposure employed with 90 kvp were 0.4 times the 65-kvp exposures. The dia of the x-ray beam was 2.9 in. measured at the tip of the pointed plastic cone, 8.2 in. from the focal spot of the x-ray tube. A table lists the average

radiation exposures, recorded at nine sites within the head and neck, in a posterior bitewing examination of one exposure made of each side of the face. The doses varied from 333 mr for the tongue to 8 mr for the spinal cord. Another table lists the average radiation exposures, recorded at nine sites within the head and neck, resulting from a 14-film periapical x-ray examination, as well as the percentage of the total exposure at each of the nine sites. The doses varied from 427 mr for the tongue to 16 mr for the spinal cord (at 65 kvp). With few exceptions, the exposures made with 65 and 90 kvp were comparable, and all were relatively low compared with earlier studies. All tissues lying in front of the plane of the film received less exposure and all tissues lying beyond the plane of the film received more exposure with 90 kvp than with 65 kvp. This accounts for the reduced entrance exposure of the patient's skin when the higher voltage was employed, but at the same time the exit exposure of the skin on the far side of the face was increased. With the radiation exposure data for posterior bitewing and periapical examinations made with 65 and 90 kvp the experimental error (±20%) was sufficient to mask, in most instances, the differences in the exposure of the various organs resulting from the use of the two voltages. In general, the exceptions occurred at sites located deep within the phantom (for example, the pituitary gland) where the greater penetrating power of the 90 kvp radiation resulted in measurably higher exposures. (BBB)

19677 PROTECTING CHILDREN AGAINST RADIATION INJURY IN PELVIC X-RAY EXAMINATIONS. Janos Barany. Orv. Hetilap, 104: 2123-4(Nov. 10, 1963). (In Hungarian)

It is strongly emphasized that x-ray examinations of the pelvic joints should only be conducted at the direction and under the supervision of orthopedic specialists. Screening of the infant population should be avoided as these measures expose the infants and their descendants to possible genetic damage. If physical examination suggests pelvic dysplasia, an x-ray examination is recommended, with utmost precautions being taken to expose only the necessary areas of the body to x irradiation. It is pointed out that the standard 12-cm cone allows irradiation over a 50-cm circle, in which case a 50-cm tall child will receive irradiation over his entire body, a 75-cm tall child from nose to ankles, a 100-cm child from neck to mid-calf, thus all endocrine glands, reproductive organs, and blood-producing tissues will receive irradiation. However, it is possible to use a shield with a slit 3-cm wide for a small child, and 4-5 cm wide for an older child, which would eliminate most of the scattered radiation reaching the gonads. This method of shielding, if executed with precision and vigilance, would reduce the hazard and give satisfactory pictures. Testes should further be protected by a lead bag which can be produced at the radiologic clinic with little trouble. Protection against scattered radiation in girls is more difficult, but a kidney-shaped lead shield covering the lower pelvic area is helpful. Data on fractions of radiation, in percentage values, reaching ovaries when various methods of protection are used are tabulated. (TCO)

19678 REMARKS CONCERNING X-RAY SCREENING OF PELVIC DYSPLASIA. Zoltan Hrabovszky. Orv. Hetilap, 104: 2124-5(Nov. 10, 1963). (In Hungarian)

Various interested groups of technical personnel discussed this subject and the following recommendations were summarized: (1) General screening of infants to detect pelvic dysplasia is unnecessary and submits both the child and the population to harmful doses of radiation. (2) No x ray examinations should be made before three months of age as neither these results nor clinical examinations allow the positive diagnosis of dysplasia. Very often early dysplasia will correct itself by proper care and exercise. (3) Up to age 4 months pediatricians may detect dysplasia and should then consult orthopedic specialists. (4) Orthopedic specialists should examine the patient and only he should order an x ray series if he feels it is warranted. (5) The healing of pelvic dysplasia, subluxation, or luxation can be checked by clinical examination and no control x rays need or should be taken. (6) Optimal corditions for dose reduction should prevail at the time of the x ray examination in both positioning of the child and in the equipment available. Personnel in the x-ray department should not hold the child during the examination. (7) Evaluation of the results should be done in close cooperation between the radiologist and the orthopedic specialist. (8) Shielding of the entire body should be maintained, leaving only the areas to be examined exposed. (BBB)

19679 LABELLED TRIIODOTHYRONINE IN VITRO TEST FOR THYROID FUNCTION USING DIALYSIS TECHNIQUE. M. Ahmad Shahid (Atomic Energy Commission, Pakistan). Pakistan Med. J., 14: 383-8(1964).

The accuracy and safety of the in vitro labeled-triiodothyronine test using the dialysis technique for evaluation of the thyroid function is discussed. It is hoped that in the future this test will replace the $PB^{131}I$ test in order to avoid any radiation to thyroid patients for diagnostic purposes, or to reduce the amount. (TCO)

19680 THE EFFECT OF RADIOACTIVE STRONTIUM ON THE TREATMENT OF EXPERIMENTAL RICKETS IN RATS WITH VITAMIN D_2. T. Giza, M. Hanicka, N. Hornik, A. Jelonek, and H. Rembiesowa. Polski Tygod. Lekar. Wiadomosci Lekar., 19: 1030-1(1964).

Thirty rats kept on McCollum's rachitogenic diet were subjected from the sixth week of feeding to treatment with vitamin D_2. The animals were divided into three groups of ten each, of which Group I was given a single dose of 5 μC ^{90}Sr, Group II received 1 μC ^{90}Sr five times with one day's interval between each dose, and Group III served as controls. The criteria accepted for the evaluation of healing were: measurement of the space between the visible end of the shaft of the tibia and the adjacent epiphyseal ossification center on x-ray films before and during treatment, after 5, 10, and 15 days; and determination of the serum alkaline phosphatase activity and of the inorganic phosphorus at the beginning and end of the experiment. Analysis of the results showed a statistically significant retardation in the healing of the bone changes and in the normalization of disturbed chemical processes in the groups of rats receiving radiostrontium as compared with the control group. A relation between certain vitamin D_2 resistant rickets and contamination with radioactive substances is proposed. (Excerpta Med., Sect. XXIII, 2: No. 3, (Mar. 1965))

19681 RADIATION THERAPY FOR CANCER OF THE UTERINE CERVIX. Gilbert H. Fletcher (Univ. of Texas, Houston). Postgrad. Med., 35: 134-42(Feb. 1964).

Various aspects are considered, including dosimetry, radiosensitivity of cervical cancer, and radioinduced injuries. Dosimetry based on calculating the doses at point A and point B is unsatisfactory, since it has been shown that the alleged correlation of point A and point B with specific pelvic structures does not exist. No correlation with successes, failures, or complications was found in the present series in which doses at point A and point B were calculated from radiographs of the actual radium insertions. Bladder and rectal measurements with a probe are useful in detecting faulty insertions and in preventing excessive doses to these organs. In addition to Ra implantation, transvaginal x-ray therapy is useful to stop profuse bleeding; therapy may consist of 500 R given on two consecutive days with a 140-kv unit. Also, transvaginal therapy is sometimes used in lieu of intracavitary Ra in recurrences after surgical procedures. Since the tolerance of tissues to irradiation is an inverse function of the volume irradiated, the portals should be no larger than necessary to cover the tumor-bearing area. With 2-Mev x-ray of ^{60}Co units it is unsafe to give more than 4000 rad with parallel opposing open portals, as the dose becomes excessive to subcutaneous tissue, muscle, and fat. Biaxial rotation technics should be used for 5000 or 6000 rad. If energies of 20-Mev or more are available, anterior, posterior, and lateral fields should be used for high-dose irradiation of the whole pelvis. In pregnant patients, up to three or four months of gestation, the whole-pelvis technic is employed to deliver at least 4000 rad. The patient may abort during or after external irradiation. In the late second or the third trimester of pregnancy, a cesarean section usually is performed, followed immediately by whole-pelvis irradiation, diminished Ra doses, and hysterectomy. Complications in radiation ther-

apy for cervical cancer are described with reference to 1811 patients. In cases in which primary intracavitary Ra therapy was given alone or supplemented by external irradiation to the regional nodes, the incidence of rectovaginal or vesicovaginal fistula was less than 1% among white patients and 5% among Negro patients. There was a low incidence of rectal and bladder ulcers, usually traced to local high doses. With conventional voltages, skin complications appeared, sometimes years later, in the more advanced stages where high skin doses had to be given in order to achieve sufficient tumor dose to the parametrium and regional nodes. The 22-Mev betatron eliminated this type of complication. Necrosis of the small bowel did not occur but rectosigmoiditis of various degrees from spasm to constriction was seen as a complication. With a dose of 4000 rad given to the whole pelvis the incidence was ~5%; it was 10% with 6000 rad. In addition to being twice as frequent with the larger doses, the complication generally was more severe. (BBB)

19682 SOME PROBLEMS IN ESTABLISHING A RADIOACTIVE IODINE UPTAKE DIAGNOSTIC SERVICE. R. A. Carter (East Birmingham Hospital, Eng.). Proc. Assoc. Clin. Biochemists, 3: No. 2, 52-4(1964).

The procedure for establishing a limited clinical isotope service in Great Britain is outlined. The relative merits of ^{131}I and ^{132}I for routine iodine uptake tests is discussed from economic, technical, and patient welfare viewpoints. The use of ^{132}I is technically much more demanding but results in much lower radiation dose to the subject. The very short half life of ^{132}I (2.5 hr) limits its use to short term tests. It is recommended only in pediatric practice. Since most patients requiring investigation are equivocal by other tests, a full scheme of testing with radioactive iodine including 24 hr uptake and possibly thyroidal and plasma iodine dynamics is indicated, and is possible only by using ^{131}I. (Excerpta Med., Sect. XXIII, 2: No. 3, (Mar. 1965))

19683 ROENTGENOLOGICAL EXAMINATION OF THE RADIATION RESPONSE OF THE LUNG AFTER INTENSIVE TELECOBALT THERAPY. B. Mateev (Robert-Rossle-Klinik, Berlin). Radiobiol. Radiotherapy., 5: 665-72(1964). (In German)

From 120 cases the course of radiation response was studied in the healthy pulmonary tissue that was irradiated with the tumor, especially the time when radiation pneumonitis and radiation fibrosis occurred. The maximum frequency of radiation pneumonitis with irradiation in one series was about one month after irradiation had been terminated, the maximum frequency was then about 4 months after irradiation had been terminated. Dividing the dose into two series of irradiations the maximum frequency of radiation pneumonitis as well as of radiation fibrosis was postponed by about 1–2 months. The importance of an antipneumonitic treatment of secondary infections in order to avoid later severe radiation fibrosis is emphasized. (auth)

19684 THE INFLUENCE OF X-RAY THERAPY ON THE HEPATIC FUNCTION OF PERSONS SUFFERING FROM CANCER. L. Teltscharov, K. Vlachov, and Th. Marovski (Hohes Medical Inst., Plovdiv, Bulgaria). Radiobiol. Radioterap., 5: 673-7(1964). (In German)

In deep x-ray therapy hepatic function is influenced to various extents. The results of examination are, of course, partly masked by the primary disease of the patients, an influence of the liver by irradiation, however, is not to be doubted. The best information about the radioinduced changes is hippuric acid test and urobilinogen test. Considering that each of these tests reflects a certain function of the liver that may be disturbed more or less severely without the other functions being involved, it will be evident that an accordance of all tests cannot be expected. The determined normalization of serum protein fraction is considered as a compensation phenomenon that protein metabolism is capable of in abnormal states. Compensatory phenomena, means pathological compensation. Examples of such a pathological compensation in patients are a decrease of chlorides in the blood and an increase of blood-sugar caused by changes of proteins and an increase of adrenalin, respectively. These phenomena as well as changes of the blood-forming mesenchyma are general reactions of adaptation and possibly also autoimmune reactions that show a distinct conversion of reactivity under the effect of the radiation doses used. Further examinations must show if this compensation is a functional overexertion of the liver and consequently later on leads to hepatic insufficiency. (P.C.H.)

19685 EXPERIENCES IN THE TREATMENT OF EUTHYROID GOITERS WITH I^{131}. J. Loebe (Karl-Marx-Universitat, Leipzig). Radiobiol. Radiotherap., 5: 703-11 (1964). (In German)

The use of ^{131}I in the fractionated treatment of 17 patients with euthyroid goiters that could not be operated on for different reasons is reported. With good functional, final results a subjective and objective improvement of the symptoms existing before treatment was achieved. On an average a total activity of 45 mC was necessary for treatment, the radiation doses being between 11,000 and 35,000 Rad. A dependence between radiation dose and result of treatment did not exist. There were no symptoms of a medullary damage due to therapy with radioiodine either during the treatment or in later controls. (auth)

19686 THE IMPORTANCE OF DISTRIBUTING THE DOSE FIELD IN TELEGAMMA THERAPY OF COLLUM CARCINOMA. K. N. Kostromina. Radiobiol. Radiotherap., 5: 739-53(1964). (In German)

The distribution of isodoses in telegamma irradiation of patients with uterine carcinomas under different conditions is discussed. For irradiation, the Soviet Gut-400 gamma unit was used with an open cone that permits a high dose to be delivered to the tumor without severer changes of the skin. For the production of isodose charts considering the topography of the malignant process sagittal and lateral roentgenograms of the pelvis after introduction of an empty applicator into uterus and vagina with contrast representation of the urinary bladder and the rectum were used. Thirteen cross-sections of the female pelvis with a distribution of radiation energy depending on the angle of inclination of the cone, on the position of irradiation fields to the mid-line of the body, field-size, radiation source-skin distance and other factors are quoted. In the performance of telegamma therapy it is important to protect the area of point A, ureters, urinary bladder, and rectum, which are irradiated in the intracavitary gamma therapy with a sufficient dose. Setting up isodose charts gives an idea of the distribution of radiation energy and permits the choice of the most favorable conditions of irradiation for each patient. (auth)

19687 MEDICAL REQUIREMENTS OF THE IRRADIATION PLAN. H.-J. Eichhorn (Robert-Rossle-Klinik, Berlin). Radiobiol. Radiotherap., 6: 1-9(1965). (In German)

The irradiation plan documents individually for each case of treatment to be established including calculation of compromise between aim, technical possibility, and risk of treatment. It results from three operations: localization, adaptation of dose, and determination of risk. The plan includes three requirements: enabling a measurement of tumor sizes and position by means of distant roentgenograms in two planes; calculated adaptation of dose distribution to the shape of tumor and of focal space, respectively, and its representation in isodose curves of natural size for the cross-section of the body; and making of an individual picture of body cross-section in the irradiation region for representing the topographical relations between tumor and focal space, respectively, neighboring organs, and isodose curve in natural size in order to find unintended side-irradiation. Some aids for roentgenological localization of the tumor, calculation of isodoses, and making of cross-sectional pictures are described. It is emphasized that complete modern diagnostical equipment must be available for each therapeutical department and the radiation therapist must do localization diagnostics for himself for reasons of economy and, above all, of responsibility. Today, cooperation of the roentgenologist and radiation physicists in preparing an intensive therapy of

the tumor is just as urgently necessary as in the operative field of surgeon and anaesthetist. (P.C.H.)

19688 COMPARATIVE PHYSICAL CONSIDERATIONS OF MODERN WAYS OF IRRADIATION. W. Degner and H. Hegewald (Humboldt-Universitat, Berlin). Radiobiol. Radiotherap., 6: 11-15(1965). (In German)

The properties of types of radiation available today are compared with the requirements of modern radiotherapy. Different principles in the use of the individual radiation sources result from these; the possibilities of which complement one another in practical radiation therapy. Referring to the discussion of some problems and questions, it is emphasized that high-energy radiotherapy may build up. For the present the medical results are, of course, not necessarily proportional to these better presuppositions. (auth)

19689 NEW MEASUREMENTS ABOUT TISSUE FACTOR WITH DIFFERENT RADIATION QUALITIES AND DETAILS ABOUT ITS CONSIDERATION IN IRRADIATION PLANNING. F. Wachsmann and H. L. Keller (Universitat, Erlangen, Ger.). Radiobiol. Radiotherap., 6: 29-34(1965). (In German)

The tissue factors used for considering the influence of attenuating tissues (not water-equivalent) were determined for radiation of 1 and 4 mm of copper half-value layer as well as for ^{60}Co and 17 Mev betatron radiation. The run of tissue factor within the transirradiated section of the body are considered, and the minimum, maximum, and medium tissue factors for practical use in radiotherapy are tabulated. (auth)

19690 THE INFLUENCE OF DOSE DISTRIBUTION BY INDIVIDUAL FILTER TECHNIQUE IN COBALT^{60}-RADIATION THERAPY. L. Sundbom (Karolinska Sjukhuset, Stockholm). Radiobiol. Radiotherap., 6: 35-48(1965). (In German)

In order to obtain a homogeneous tumor dose and simultaneously to spare those organs that are sensitive to irradiation it is necessary in many cases to influence the dose distribution of the given radiation field. This may be achieved by introducing filters into standard radiation fields in order to be able to reproduce and modify standard dose distribution. The use of standard filters and individually shaped filters is discussed. Special consideration is given to the problems that arise if the radiation field has an oblique incidence and/or incides an irregular surface of the body, if the beam passes pulmonary tissue, and if a region that formerly was intravaginally and/or intrauterinely irradiated with radium is to be spared. (auth)

19691 A NEW PROCEDURE FOR THE DETERMINATION OF DOSE DISTRIBUTION AND DOSE RATE IN PENDULUM IRRADIATION. H. L. Keller (Universitat, Erlangen, Ger.). Radiobiol. Radiotherap., 6: 55-60(1965). (In German)

Attempts were made to develop a procedure in which the dose distribution in pendulum irradiation may be gathered from systematically elaborated data so that time consuming dose measurements with phantoms may be avoided in individual irradiation planning. This was achieved by determining the dose distribution along the half line of pendulum angle with four different radiations (between 200 kv and 17 Mev) and with a variety of irradiation conditions of water phantoms and registering the obtained results, all referred to the roentgen-value as a common base, in diagrams in such a way that also for any individual irradiation conditions dose distribution may be interpolated with sufficient accuracy. (auth)

19692 THE DETERMINATION OF ISODOSES BY MEANS OF COMPUTERS. J. Richter and D. Schirrmeister (Robert-Rossle-Klinik, Berlin). Radiobiol. Radiotherap., 6: 61-7(1965). (In German)

The calculation of dose distribution based on the use of stationary field-dose distributions is discussed. A method developed is described and the practical measures in stationary field-, rotation, or pendulum irradiation are represented. (auth)

19693 THE VALUE OF PHOTOGRAPHIC DETERMINATION OF DOSE DISTRIBUTION FOR IRRADIATION PLANNING. A. Rakow (Institut fur Biophysik, Berlin). Radiobiol. Radiotherap., 6: 69-76(1965). (In German)

Photographic density distributions may be analyzed quickly and cheaply without additional devices into curves of the same density by means of repeated printing (Sabattier-effect). This possibility was used for establishing isodose curves and a calibration method is given that eliminates nearly all photographic errors. The advantages of this method for irradiation planning in radiotherapy are discussed. The disadvantage of energy dependence of the photographic reaction in the most practical procedure only leads to unimportant errors. (auth)

19694 RADIATION PHYSICAL PROBLEMS OF THERAPY WITH HIGH-ENERGY ELECTRONS. E. Walter (Siemens-Reiniger-Werken AG, Erlangen, Ger.). Radiobiol. Radiotherap., 6: 77-87(1965). (In German)

Demonstrable physical peculiarities of electrons for radiotherapy are discussed. Compared with photons electrons permit a much greater possibility of dose distribution and this by farp even with one and the same generator. Inexplicable differences compared with photons are considered and the methods of investigation referring to these and hitherto existing results are described. (P.C.H.)

19695 NEW RESULTS OF MEASUREMENTS OF HIGH-ENERGY ELECTRONS. W. Seidel (Humboldt-Universitat, Berlin). Radiobiol. Radiotherap., 6: 89-95(1965). (In German)

General considerations are made concerning the dose run with high-energy electrons of a betatron and the resulting applicability in radiotherapy. Data from different sources on the situation of the 80% isodose in dependence on energy as well as the different data of surface dose are graphically represented and discussed from a special example. The influence of scattering foils on energy is pointed out. (auth)

19696 A CONTRAST INCREASING ELECTRONIC DEVICE FOR THE AUTOMATIC SCINTILLATION SCANNER. J. Snajder and M. Erjavec (Inst. of Oncology, Ljubljana, Yugoslavia). Radiobiol. Radiotherap., 6: 109-17(1965).

An electronic digital device was developed to enhance contrast in isotope dot scanning records. Instead of a simple cut-off principle, it increases contrast over a considerable range of count rates and thus improves the legibility of the printed pictures. The device may be incorporated into any commerical scintillation scanning system and is easy to operate. It has been successfully employed in thyroid, bone, kidney, brain, and particularly in liver scanning. (auth)

19697 SCINTILLATION SCANNING OF BONE TUMORS AND METASTASES BY THE USE OF Sr 85. M. Erjavec (Inst. of Oncology, Ljubljana, Yugoslavia). Radiobiol. Radiotherap., 6: 119-26(1965).

The possibilities of an early discovery of skeletal metastases by means of a simple commercial scintiscanning device were investigated. By means of ^{85}Sr administration and scintiscanning about 7 days later, it was possible in some cases to discover bone metastases several months earlier than by radiography. In a series of 30 patients the diagnosis by ^{85}Sr was correct in 22 cases and incorrect in only 2. In the remaining 6 cases a definite diagnosis was not established. The method of examination and its diagnostic value are discussed. Schematic representation of the scanning device and some typical records are given. (P.C.H.)

19698 RADIOPELVIMETRY. S. Nelken. Rev. Franc. Gynecol. Obstet., 59: 549-52(Sept. 1964). (In French)

Possible danger to the fetus from the use of radiopelvimetry is discussed. (BBB)

19699 CURRENT DATA ON THE RISKS FOR THE EMBRYO, FETUS, AND INFANT FROM MEDICAL RADIOLOGY. M. Tubiana, M. Mayer, J. Lejeune, J. De Grouchy, and O. Rethore (Institut Gustave Roussy, Villejuif, France). Rev. Hyg. Med. Sociale, 11: 751-61(Dec. 1963). (In French)

The chances of irradiation causing malformations in an

embryo are greatest 1.5 to seven weeks after conception. For an older embryo or fetus the greatest risk is believed to be an increase in the frequency of leukemia and neoplasia. However, a review of studies done on infants irradiated in utero showed, in the authors' opinion, that while caution is necessary in the use of x rays, there is no confirmation that irradiation in utero increases the frequency of leukemia. Nor has it been proven conclusively that in utero irradiation increases mongolism or the frequency of retinoblastomas. A study of anomalies of iris pigmentation and of the presence in the hair of brown patches showed that the frequency of heterochromatic irises is ten times greater in infants irradiated in utero, while brown hair patches were observed only in the irradiated infants. There was no occurrence of them in a nonirradiated control group. Thus, weak doses of x rays are capable of modifying the genetic material of somatic cells. All humans receive natural irradiation at the rate of about 5 r/30 yr. It is estimated that the max permissible dose, with regard to the genetic risk, is double this amount. As to the somatic risk, it is estimated that 100 rad delivered to 10,000 subjects will cause ~35 cases of thyroid cancer, 20 cases of leukemia, and 120 cases of other cancers. To avoid exposing an embryo to x rays, it should be determined that a woman is not pregnant before x raying her pelvic region. In a woman exposed to irradiation occupationally, the dose must not exceed 100 mR/week. If tuberculosis is suspected during pregnancy, the radiologist should substitute radiophotography for fluoroscopy and shield the abdomen. X rays are useful for detecting congenital disorders in infants, but repeated x rays are rarely necessary. To minimize irradiation danger to a patient, technicians should: limit irradiation to the essential area, reduce the proportion of the rays absorbed by the body by use of more penetrating rays and filtration of the beam, and use more sensitive, high-speed film. (BBB)

19700 TREATMENT OF UTERINE FIBROMAS OUTSIDE PREGNANCY. G. Cerebonnet. Rev. Praticien, 13: 3145-55(Oct. 11, 1963). (In French)

The occurrence of hemorrhage after radiotherapy for benign tumors of the uterus is considered. (BBB)

19701 BRAIN INJURIES RESULTING FROM RADIOTHERAPY FOR EYE TUMORS. Hiroyoshi Ohara (Nagoya Railway Hospital, Japan), Syunichi Akatsuka, Kazuo Nakamura, Sumiyoshi Akutsu, and Noriyoshi Matsui. Rinsho Ganka, 17: 313-16(Mar. 1964). (In Japanese)

Two women with eye tumors were subjected to a study for possible brain damage resulting from radiotherapy for these tumors. The two patients, one 44 years old with lacrimal adenocarcinoma and another 43 years old with retinoblastoma, were operated on for removal of the tumors, and both were subjected to a postoperative radiotherapy with a total dose of 10,200 R for the former and 4600 R for the latter. The histologic examination of the lacrimal tumor revealed a carcinoma and the patient was given isotope radiation therapy of semiweekly dose of 200 R over 18 min to a total of 3000 R extending through 55 days. The tumor recurred about three years later, and spread to anterior and posterior lymph nodes and to upper portion of the orbital cavity. About 600 R was given before the second operation and the irradiation was continued after the operation every other day from front and right portals to a total of 7200 R from each direction. During therapy, headache and hearing difficulty and inflammation in right ear occurred. After therapy, inflammation occurred in the left middle ear. There was, however, no sensory or locomotive disorder in other parts of the body and no speech disorder. About eight months later, radiographic examination of brain arteries revealed no abnormality, and the cerebrospinal fluid showed fluid pressure of 180 mm H_2O. An electroencephalographic (EEG) examination of brain wave pattern revealed that the α rhythm was low in frequency with normal recovery pattern with hyperventilation. The reaction to restamin (60 mg) was normal. A single wave was noted in the tests with 4% chloral hydrate (40 ml). Thus, the EEG tracing showed abnormality in the irradiated side. The other patient, with retinoblastoma, was irradiated over the anterior visual nerve bundle with the total radiation dose of 4600 R (area 6 × 6 cm). An irradiation dose of 400 R on the skin or 200 R on the affected area was given for 12 min every day frontally and laterally (left side for 35 days). During therapy the patient complained of occasional headache, and inflammation developed in the left middle ear and an ulcer on the tongue. Two years later, examination of spinal fluid showed fluid pressure of 180 mm H_2O. Radiographs of brain arteries were normal, and locomotive and sensory disorders were absent. Four months later, EEG examination revealed a normal wave pattern when at rest, and a slightly slow but normal θ wave was detected when restamin (60 mg) and 4% chloral hydrate (40 ml) were given. Seven months later, a second EEG test showed that the resting α wave pattern with single electrode indicated a lower potential in the left temporal and left frontal lobe area compared to the right side. With double electrodes, a lower potential was noted in the left lobes than in the right. Hyperventilation recovery was normal, but the restamin test showed a slight strengthening of the above-mentioned differences of potential. To prevent these brain injuries, it was concluded that the rotation or pendulum irradiation methods should be introduced in radiotherapy in ophthalmology and rhino-otology. (BBB)

19702 THE PROBLEM OF RADIOBIOLOGY IN THE FIELD OF RADIOTHERAPY. A. Zuppinger (Universität und des Inselspitals, Bern). Schweiz. Med. Wochschr., 93: 845-8(June 15, 1963). (In German)

Physical research has provided a variety of radiations that can be used for treatment of human cancer. Chemistry and biology have shown that the ultimate growth of tumors can be influenced only infrequently. Radiations and chemicals vary in their type, their use, and the possible combinations in which they can be studied in humans. Frequently, in order to test treatment effectivity, studies that extend over 3 to 10 yr are required. Sometimes the results are hard to ascertain, because a single treatment is almost never used alone, but often, in addition to irradiation other medications, such as sulfonamides, antibiotics, cytostatics, and hormones, are also used so it is difficult to tell if the irradiation is causal, curative, or only palliative. Studies made on bacteria, phage, plants, and animals sometimes lead to useful conclusions on the method of effect of irradiation. Relative differences between normal and tumor tissues are important, but it is difficult to quantitate effects on tissues and tumors. The relative biological effect of various radiations is one useful measure, but numerous questions about its actual significance for mammals, in terms of whole-body and localized irradiation, remain to be answered. Incentive for this is provided by the requirements of practical radiotherapy to develop methods for treatment of organs and tumors. Studies of radioisotope metabolism in tissues and organs should reveal many more accurate answers to the question of the effect of supplementary medication on irradiation effects. Uptake of ^{45}Ca is reduced by cortisone administered prior to irradiation, but when administered after irradiation it only diminishes uptake, without influencing the irradiation effect. With $^{3}H_2O$ it is possible to demonstrate irradiation effects at points remote from irradiated sites in bone and skin. (BBB)

19703 RADIOTHERAPY AND SURGERY. William T. Moss (Chicago Wesley Memorial Hospital). Surg. Clin. North Am., 44: 91-6(Feb. 1964).

Some problems encountered when irradiation precedes or follows surgical removal of tumors are discussed. Intensive irradiation and radical surgery, regardless of the sequence, increases problems related to healing. Previous radical surgery increases the incidence of postirradiation sequelae just as previous high-dose irradiation increases the incidence of postoperative complications. The nature of these complications vary with site, type of procedure, age and general condition of the patient. These additional risks are usually accepted if there is a reasonable possibility of cure. Skin-sparing qualities of ^{60}Co and supervoltage radiations have renewed interest in preoperative irradiation. With medium voltage x rays, high skin doses are unavoidable if adequate doses are to be given to the underlying tu-

mor. Supervoltage and ^{60}Co radiations have skin-sparing characteristics and with such radiations subcutaneous vasculoconnective tissues retain much of their healing ability. These factors have accounted for a decrease in radiation-induced wound complications, and are largely responsible for the justified renewed interest in the possibilities of preoperative irradiation. Radical surgery after curative doses of radiations is possible with an acceptable though increased incidence of wound complications. The zone of preoperative irradiation is usually larger than the anticipated limits of surgical excision. The dose is rarely of a curative level and there is rarely an intent to cure the patient by irradiation alone, even though residual cancer may not be found in the operative specimen. An interval of three to six weeks is usually allowed between the two procedures. Preoperative irradiation delays surgery, but the delay may not be detrimental. Preoperative irradiation can be recommended for rendering nonviable, malignant cells that might later be implanted in the operative wound or circulatory system. There is experimental evidence to justify this view. Irradiation of a tumor even with very low doses decreases the frequency with which it will subsequently take and metastasize. Another aim of preoperative irradiation is to render normal tissue somewhat immune to subsequent cancer invasion; there is also experimental evidence to support this aim. In some combined radiotherapeutic and surgical procedures radiotherapy plays the major role and surgery is an adjuvant. Thus, in the treatment of medulloblastomas and many tumors metastatic to the spinal cord, initial surgery with decompression is essential, yet the major treatment of the neoplasm is irradiation. (BBB)

19704 SOME PROBLEMS OF THE INVESTIGATION OF RADIATION PARAMETERS OF POWERFUL GAMMA DEVICES FOR RADIOTHERAPY (E. G. THE VOLFRAM DEVICE TEST). A. V. Bibergal, T. G. Ratner, Yu. P. Nikulin, and V. L. Lipis (Inst. of Biological Physics, Moscow). Radiobiologiya, 5: 140-6(1965). (In Russian)

The advantages and the deficiencies of the Russian Volfram radiotherapy apparatus are discussed. (IIC-M.G.)

19705 EXPLORATION OF CARDIAC DYNAMICS WITH RADIOACTIVE TRACERS. M. Berger. Rev. Lyon. Med., 13: 441-51(1964).

A description is given of the technique of exploration of cardiac dynamics using radioactive tracers, especially the radiocardiogram and its interpretation, measurement of cardiac output, and detection of communication between the right and left heart. (Excerpta Med., Sect. XXIII, 2: No. 3, (Mar. 1965))

19706 RADIOISOTOPE THERAPY IN NUCLEAR MEDICINE. E. R. King (Medical Coll. of Virginia, Richmond). Virginia Med. Monthly, 91: 93-101(1964).

A clinical review is presented on the common therapeutic applications of the artificial radioisotopes of iodine, phosphorus, gold, yttrium, gallium, and sulfur and the possible uses of radioactive strontium, calcium, mercury, and zinc. Contraindications, dosage, and complications of therapy are presented for the treatment of hyperthyroidism, cardiac disease, polycythaemia, rubra vera, chronic leukemia, skeletal metastases from carcinoma of breast and prostate, malignant effusions, and thyroid carcinoma. Results in some conditions are presented rather optimistically, a good response or improvement being reported in 60% of cardiacs and 50-80% of various malignancies. Less benefit is expected in chronic pulmonary disease, paralysis agitans, chondrosarcoma, lymphoma, hepatic tumours, breast cancer, and primary bone tumors. Future possibilities in using radioactive strontium and calcium in bone tumors, radioactive mercury, labelled amino acids for cancer of the pancreas, and radioactive zinc for cancer of the prostate are discussed. (Excerpta Med., Sect. XXIII, 2: No. 3, (Mar. 1965))

19707 RADIATION DAMAGE AND TUMOUR GROWTH FOLLOWING THOROTRAST PYELOGRAPHY. CASUISTIC CONTRIBUTION. F. Laetsch and W. Klug. Z. Urol., 57: 505-6(1964).

A report on 2 cases of radiation damage following Thorotrast pyelography is presented. In one case the damage (malignant tumor growth) was unilateral, and in the second case, Thorotrast residues were demonstrable in both kidneys, with severe functional impairment and suspicion of malignant degeneration in one kidney. (Excerpta Med., Sect. XXIII, 2: No. 3, (Mar. 1965))

19708 DOSAGE PROBLEMS IN THE TREATMENT OF UTERINE CARCINOMA WITH ^{60}COBALT PEARLS. Endre Kuhn (Medical University, Pecs, Hungary). Zentr. Gynaekol., 86: 63-8(Jan. 11, 1964). (In German)

Radiation dosage from ^{60}Co beads inserted into the uterine cavity and cervical canal was measured by probes placed in the urinary bladder and rectum. When the treatment was fractionated, the dosage in these locations was about 2400 rep. On the basis of 3-yr experience with 53 intrauterine irradiations using pearls the radiation exposure of the bladder was twice as great as the dosage in the rectum, except for cases of retroflexed uterus. The point of maximal dose rate is near the trigonum, and in the rectum it is at a height of from 6 to 10 cm. These dose rates vary widely between individuals, depending on the location and number of the pearls used, musculature, etc. Studies made with phantoms indicated that the contact dose at the uterine mucosa was 3 to 5 times as great as the max measured in the bladder or rectum, and the dose at the outer surface of the uterine musculature was about double this maximum. This indicates that the order surface of the uterine wall is irradiated with a total of between 12000 and 15000 rep. The cancerocidal dose has been reported to be from 10000 and 15000 rep. According to this, adjacent organs may receive as much as 7200 to 7500 rep, which is close to what may be considered permissible. Past experience shows that with treatments at these radiation levels there is no recurrence of the tumor treated, and the bladder and rectum are not injured. (BBB)

19709 MEDICAL RADIOISOTOPE SCANNING. Proceedings of the Symposium, Athens, 20-24 April 1964. (International Atomic Energy Agency, Vienna (Austria)). Proceedings Series. Oct. 1964. 477p. (STI/PUB/82(Vol. II); CONF-453(Vol. II)). $9.50; S 199,50; £2.17.0; F.Fr. 38,-; DM 33,25(IAEA).

Twenty-seven articles are included; separate abstracts were prepared for 22. The remaining 5 articles were previously abstracted in NSA as 18: 19814, 19834, 35433, 35434, and 35435. (P.C.H.)

For abstracts of individual papers see: 19492, 19710, 19711, 19712, 19713, 19714, 19715, 19716, 19717, 19718, 19719, 19720, 19721, 19722, 19723, 19724, 19725, 19726, 19727, 19728, 19729, and 19730.

19710 ORGAN VISUALIZATION BY PHOTOSCANNING USING MICRO- AND MACRO-AGGREGATES OF RADIO-ALBUMIN. G. V. Taplin, D. E. Johnson, E. K. Dore, and H. S. Kaplan (Univ. of California, Los Angeles and Los Alamos County Harbor General Hospital, Torrance, Calif.). p.3-31 of "STI/PUB/82(Vol. II)."

Micro aggregates (10-20 nm) of ^{131}I-labeled human serum albumin were found to be superior to other agents for liver-spleen photoscanning. Radiation exposure to these organs is minimized and the test agent can be prepared with relative ease and simplicity. Also the heart, stomach, and salivary glands may be clearly visualized with the same material. The techniques and physiological basis for performing and interpreting scans of these organs are described. Their diagnostic value is illustrated. The physiological basis for using macro albumin aggregates (1-10 μm) for visualization of the lungs is presented, along with typical scans in dogs. Toxicity studies and related pathophysiological investigations in animals demonstrate a wide margin of safety for using the large-particle test agents in man. Preliminary experiments in dogs indicate the feasibility of performing lung scans following the inhalation of an aerosol of the same material. This technique is simple, painless, and entirely safe. Photoscans are presented from patients with a wide variety of pulmonary disorders. (auth)

19711 SCANNING WITH IODINE-125. M. Ben-Porath, A. Hochman, and J. Gross (Hadassah Univ. and Hebrew Univ., Jerusalem). p.71-7 of "STI/PUB/82(Vol. II)."

The use of ^{125}I as ^{125}I-iodide for scanning of the thyroid

and of thyroid carcinoma metastases and as ^{125}I-labeled Rose Bengal for scanning of the liver was investigated. In some patients, the thyroid scans and the scans of thyroid carcinoma metastases were repeated with ^{131}I. The liver scans were repeated with colloidal ^{198}Au. Cold nodules in the thyroid that could not be detected with ^{131}I were clearly seen with ^{125}I. Anterior metastases in the lungs could be differentiated from posterior metastases with ^{125}I, while with ^{131}I this was not possible. Using the same doses of radioactivity the background with ^{131}I was much higher and could not be eliminated, as this would have reduced the counting rate over the lesions to levels that could not be detected. Some of the photoscans and mechanical scans of livers carried out with colloidal ^{198}Au could not be interpreted. However, cold lesions were clearly seen on the scans of the same livers with ^{125}I-labeled Rose Bengal. (auth)

19712 DESIGN AND FUNCTION OF A BRAIN SCANNER FOR CLINICAL USE. W. Paul and T. P. Morley (Univ. of Toronto). p.81-94 of "STI/PUB/82(Vol. II)."

A scanner is described that was designed to be used as a screening device for brain-tumour suspects, so that high sensitivity, simplicity of patient preparation, and ease of reading and interpretation were primary requirements. Brownell's equation relating radioactivity concentration to diameter of resolution indicates that the required radioactivity per unit volume is inversely related to the sixth power of the resolution diameter. Accordingly, a maximum permissible diameter of resolution was chosen consistent with satisfactory localization of areas of increased radioactivity. Precise delineation was not required. Since the number of detected disintegrations per unit time is an inverse function of the square of distance, two detectors each with a short focus are used rather than one detector that must be made optimal for the mid-sagittal plane. The 2 in. dia. crystal and photomultiplier assemblies are mounted opposite one another on a rigid scanning frame, each fitted with a seven-hole (hexagonal) focusing collimator designed for a 1.5-cm resolution diameter and a focus 8 cm from the collimator face. The frame scans rectilinearly in the sagittal plane. The scan record is presented as an asymmetrogammagram and as separate left and right photographic two-dimensional displays. Pulses from each detector are fed to an amplifier-discriminator circuit and thence to a difference circuit which prints a left or right marker to indicate a predominance of left or right radioactivity. Pulses from each amplifier-discriminator circuit also go to count-rate meters which in turn activate lamps mounted in a lighttight housing. The two lamps, the light intensity of which is a function of activity measured by the respective detectors, are mounted on a common arm moved by Selsyn motors synchronous with Selsyn generators on the detector frame, thus permitting the use of a remotely placed recording unti. Cylindrical lenses focus the lamp sources on film, both right and left records being made simultaneously on an 11 in. × 14 in. x-ray film. Although the operator may adjust mean lamp current to a proper predetermined value over a wide range of count rate, a great deal of latitude is given the operator by the inclusion of three sheets of film in the cassette each providing optimum contrast for a different range of count rate. Patients are given 350 μC of ^{131}I human serum albumin after previous treatment with Lugols solution and scanning is performed between 24 and 72 hr later. A single scan is usually sufficient. Scans on some patients are repeated in the antero-posterior direction. On 653 patients 789 scans were made from September 1961 to November 1962. There was a confirmed diagnosis in 109 of these patients, 88 having tumors. Twenty-three of 30 glioblastomas and 15 of 19 meningiomas were clearly located. (auth)

19713 RESULTS OF POSITRON SCANNING IN 1200 CASES FOR DIAGNOSIS OF INTRACRANIAL LESIONS. O. Wilcke (Universitat, Cologne). p.95-107 of "STI/PUB/82 (Vol. II)."

The positron scanning method with ^{64}Cu and ^{74}As for the diagnosis of brain tumors has the advantage over γ scanning methods that it needs a shorter test time and moreover involves less irradiation hazards. This is especially true with ^{64}Cu (half life 12.8 hr), which may be used in studies on outpatients. From the degree of concentration of the radioactive substance in the tumor, its type may be determined. In combination with cerebral angiography, the diagnosis of the type of tumor is still better established, a fact that is very important in determining the indication for operation. In the results reported, the exactness of the diagnosis amounted to 75-80% of all cases of brain tumors. The most easily recognized lesions, through their high ability to concentrate the isotopes, were the meningiomas, abscesses, and glioblastomas, while the oligodendrorogliomas and astrocytomas showed less ability to concentrate the radioactive substance and hence were less easily recognizable. A group of astrocytomas and almost all epidermoid tumors did not show any ability to concentrate the radioactive substance and in this group the combination with cerebral angiography is important for determining the diagnosis. The method of positron-scanning has proved of great value in excluding tumors in cases of suspected symptomatic epilepsy; the exactness of diagnosis here amounted to 90%. The combination of electroencephalography with scanning showed similar accuracy in tumor diagnosis as well as tumor exclusion, so that arteriography and/or hospital admission could be dispensed with whenever combined negative findings and lack of clinical symptoms were found. The value of this method in examination of out-patients is thus clearly demonstrated. (auth)

19714 SCANNING TECHNIQUES FOR BRAIN-TUMOUR LOCALIZATION. M. H. Duggan, J. Brice, E. Jones, J. R. Mallard, and M. I. Myers (Hammersmith Hospital, London). p.121-45 of "STI/PUB/82(Vol. II)."

The color scanner was used to scan two small clinical series of brain tumor cases, one by means of ^{74}As using positron detection, the other with ^{131}I-labeled albumin using gamma detection and a focusing collimator. The results of these series are given and the value of the procedure to the clinician is presented. A preliminary attempt was made to scan with ^{206}Bi citrate using gamma detection and a focusing collimator. The results are presented. The focusing collimators used with the gamma-emitting isotopes have a deep geometrical focus and isocount responses are obtained on point sources that are almost depth independent for 20 cm. Experimental results on a series of collimators led to design data for building such collimators to a given specification. Stationary detector scanning has been carried out on brain-tumor cases using a gamma camera with storage-tube display. The advantages of such machines lie in greater sensitivity and more rapid visualization of the pattern of distribution of radioactivity, which in turn enables dynamic studies to be carried out. Problems that occur with such machines include the difficulty in marking anatomical features and the geometric distortions that occur. These are compared for pin-hole and matrix viewing apertures. The improvement in performance resulting from circuit modifications to remove the dependence of picture size on gamma energy is discussed. The analysis of cerebral scans presents difficulties when the suspected region is only slightly greater in count-rate than its surroundings. A normal count-rate pattern for a head has been determined by dividing scans into regions that are approximately anatomically equivalent from patient to patient, and counting scintiscan marks in each region. Any abnormal scan may then be compared with this pattern. Such analysis lends itself to computer techniques. The use of continuous averaging techniques may also prove to be of value in improving the perception of abnormalities near the limits of detection in moving detector systems. The possible use of multichannel analysers to apply this and at the same time make possible a valuable new display system for both moving and stationary systems is presented. (auth)

19715 SELECTIVE NEOPLASM LOCALIZATION WITH MERCURY-197 NEOHYDRIN. D. B. Sodee (Doctors Hospital and Renner Clinic Foundation, Cleveland Heights, Ohio). p.147-57 of "STI/PUB/82(Vol. II)."

Mercury-197, a low-energy x- and gamma-ray emitter (2.7-d half life, 69-kev conversion x rays, 77-kev gamma

rays) was tested as a scanning agent in a large series of patients. Five hundred patients suspected of neuro-surgical disease were scanned with ^{197}Hg-Neohydrin. Utilizing photoscanning techniques that brought out vascular lesions as well as tumors, this procedure had a 96% correlation with the final diagnostic evaluation. The screening procedure was done before all other diagnostic tests. As an outgrowth of this brain-scanning procedure, localization of ^{197}Hg-Neohydrin was found in lymphomas as well as in carcinomas. There seems to be selective deposition of the radioactive substance intercellularly. Areas of increased uptake of radioactivity can easily be delineated with standard commercial scanners. ^{197}Hg-Neohydrin was also found to be useful as a screening agent in the differentiation of eye tumors in a series of 88 patients and recently this low-energy radiopharmaceutical was found to concentrate in nasopharangeal tumors which could then be delineated by photoscanning. The diagnostic dose of ^{197}Hg-Neohydrin for brain scanning delivers a radiation dose of 3 Rad to the kidneys as compared to the 70 Rad delivered to the kidneys by that of ^{203}Hg-Neohydrin. The high counting efficiency and ease of collimation of ^{197}Hg make this isotope far better for scanning purposes than all other standard diagnostic scanning agents. (auth)

19716 RADIOIODINATED (I^{131} AND I^{125}) FIBRINOGEN FOR THE DETECTION OF MALIGNANT TUMOURS IN MAN. G. Monasterio, M. F. Becchini, and N. Riccioni (Universita, Pisa, Italy). p.159-72 of "STI/PUB/82(Vol. II)."

Human fibrinogen labeled with ^{131}I and ^{125}I was tested as a possible agent for detecting malignant tumors in man. The uptake of radioiodinate fibrinogen was studied in malignant and benign tumors, as well as non-neoplastic space-occupying lesions. Seventy-three cases were examined; 53 of these were represented by malignant tumors localized in the skeleton, lungs, brain, abdominal organs etc. The ^{131}I-fibrinogen uptake test gave correct results in 79% of the cases examined; no false positive results were obtained in the whole series. The technique and the results are briefly discussed. From the data obtained, it seems that fibrinogen-^{131}I may be successfully applied for the early detection of malignancies in man; possible improvements of the detection technique may markedly increase the diagnostic value of the method. (P.C.H.)

19717 STUDY ON THE LOCALIZATION OF IODINE IN THE STOMACH. W. H. Clode, M. Simao Rodrigues, M. A. Perez Fernandez, M. A. Murteira, and A. M. Baptista (Instituto Portugues de Oncologia, Lisbon). p.175-92 of "STI/PUB/82(Vol. II)."

The localization of iodine in the stomach after intravenous injection of ^{131}I-iodide, using a high-contrast photoscanning system, was investigated. The study was performed at different times after injection (ordinarily 2, 24, and 48 hr) in patients without any gastric disease, in patients with cancer of the stomach, and in patients with peptic ulcers. The distribution of radioiodine was also studied in dog and human stomachs surgically removed at different times after the radioiodine injection. In the surgically removed stomachs, the specific activity of the tissue corresponding to areas of interest revealed by scanning was determined in order to assist in interpreting the findings. It was concluded that there are certain areas of the normal stomach that play a particular part in iodine metabolism. Localization of the zones of highest radioactivity concentration suggests more than one mechanism for iodine excretion. These observations support the findings of others using different methods. Scanning at 24 hr after administration of ^{131}I allows gastric cancer to be detected in most of the patients with this disease who were studied. The explanation of the results is not only related to the iodine concentration by the tumor cells but also to some retention of iodine in the stomach walls. In most cases the radioiodine concentration in the tumor was not higher than in the normal mucosal areas where increased iodine uptake occurs. (auth)

19718 BONE-MARROW SCANNING AFTER INTRAVENOUS INJECTION OF COLLOIDAL Au^{198}. I.-G. Larsson and I. Jonsson (Univ. of Umea, Sweden). p.193-205 of "STI/PUB/82(Vol. II)."

Bone-marrow uptake of ^{198}Au was studied in a large number of patients by means of whole-body scintigrams and whole-body profile counting. Three main patterns of distribution could be distinguished. Normal pattern: In patients without bone-marrow disease, uptake of ^{198}Au was limited to the central parts of bone system (thorax, spine, pelvis, skull, and proximal epiphyses of femur and humerus), i.e. normal sites for active red bone marrow. With the exception of the proximal epiphyses of femur and humerus no, or only a very slight, uptake was found in the bones of arms and legs. Hyperplastic pattern: This type of distribution was found in polycythaemia vera and haemolytic conditions. Bone-marrow uptake was increased and, besides the central parts of bone system, considerable uptake was often demonstrated in the long bones of arms and legs. Destructive pattern: This pattern was regularly found in myelofibrosis and very often in leukemia, bone marrow carcinomatosis and malignant lymphoma with bone marrow involvement. It was characterized by general reduction of bone marrow uptake in central parts of the body, combined with increased uptake in the long bones of legs and arms due to compensatory peripheral hematopoiesis. All degrees of bone marrow destruction and compensatory peripheral hyperplasia could in this way be visualized. By means of whole-body profile counting it was possible to obtain a more quantitative and reproducible expression for bone marrow uptake. Repeated examinations were performed in cases of polycythaemia vera; in some cases it was possible to follow the changes in bone marrow uptake that occurred when polycythaemia vera developed into a stage of myelofibrosis. In detailed scintigrams of the pelvis, it was also possible to study the extent of local abnormalities, such as bone tumors and bone metastases. Some improvements regarding collimator design and method of registration are also reported. (auth)

19719 INDIRECT LYMPHOGRAPHY AND ITS IMPORTANCE IN ONCOLOGY. B. Delaloye and P. Magnenat (Universitat, Lausanne, Switzerland). p.227-36 of "STI/PUB/82(Vol. II)."

Indirect lymphography, which only requires a subcutaneous injection of colloidal gold-198 with a particle diameter of 50 A in the tributary region of the lymphatic system being explored, makes possible, by scintigraphic recording, a clear representation of the ganglionic lymphatic chains. The problems of collimation in getting optimum definition are discussed. With this method of investigating the lymphatic system, measurement of the time of appearance of the gold in the blood yields indirect information regarding the rate of transit of the colloidal gold particles in the lymphatic vessels. Useful information was also obtained on neoplastic infiltrations of the ganglia and hence it was possible to determine the extent of a metastatic infiltration. Clinical examples are described. In addition, a new technique for hepatic lymphography by the transcutaneous, sub-capsular injection of colloidal gold-198 is described. This technique reveals the anterior and posterior mediastinal lymphatic chains. (auth)

19720 DIAGNOSIS OF INTRASPINAL NEUROLOGICAL SYNDROMES BY MYELOSCINTIGRAM. G. Pantazis, J. Taptas, H. Mikropoulos, N. Kordiolis, V. Samaras, E. Parashou, C. Savvas, and F. Dermentzoglou (Democritus Centre and Aghios Savvas Hospital, Athens). p.237-55 of "STI/PUB/82(Vol. II)."

Thirty-eight patients presenting signs of intraspinal neurological syndromes were examined by myeloscintigram at the Greek Anticancer Institute. They were suffering from intervertebral disc protrusions, tumors, and congenital and inflammatory lesions. Studies with myelograms as well and the relative advantages of the two methods are discussed. The findings of the myeloscintigram consisted either in decrease or increase of radioactivity locally, depending on the different types of lesions. Provided a careful and detailed examination is done the myeloscintigram may, in a large proportion of cases, prove considerably helpful in the diagnosis of intraspinal lesions. (auth)

19721 RENAL SCINTISCANNING WITH Hg^{203}–NEOHYDRIN IN UROLOGIC DISEASES. V. Bollini and G. Tori (Universita, Bologna). p.257-72 of "STI/PUB/82(Vol. II)."

Renal scintiscanning was carried out using ^{203}Hg-labeled Neohydrin. The Nuclear Chicago Isotope Scanner Type 1700 with 2 × 2-in. crystal and a 7-cm focal-length honeycomb collimator was used. Usually the scintigrams are registered both on paper and on photographic film. ^{203}Hg-labeled Neohydrin is usually employed in doses of 120-160 μC (about 2 μC/kg). The scanning examination starts about 2 hr after the injection and lasts about 40-50 min. The selective storage of labeled Neohydrin at the level of the renal cortex makes it possible to obtain a graphic representation of the two kidneys and to identify their position, orientation and shape, and the homogeneity of the actively functioning parenchyma. In some cases, autoradiographic investigations were carried out on diseased kidneys after surgical removal. By this method anomalies in position and orientation, both congenital and acquired, can be ascertained. As regards shape, the limits of the renal patterns are the more clearly defined as the renal function is better. Technical aspects such as the width of the crystal, type of collimator (whose focal plane should pass through the transverse medial plane of the kidneys), and dose, which should be not too high nor too low, are essential conditions for a correct graphic reproduction of the renal patterns. Failure in tabular activity in the parenchyma is shown by a lack in the uptake of radioactivity. The position, extent, and shape of such defects in uptake vary according to the entity of the renal structures and their derangement due to various pathological processes: tumors, cysts, hydronephrosis, tuberculosis etc. In normal subjects a homogeneous scintigram is usual, although a clearer hilar region is not a rare occurrence. Any circumscribed decrease of scintigraphic density outside the hilum is the expression of a less actively functioning zone. Among kidney patterns larger than normal, the homogeneous ones that point to a compensatory hypertrophy should be distinguished from the dishomogeneous and irregular ones. These pictures suggest the presence of large hydronephroses, tumors, or multiple cysts. In renal vascular disease, the character of the uptake in the two kidneys can be of significant value in assessing the reduced function and in differentiating unilateral from bilateral diseases. Renal scintiscanning thus shows promise of proving a useful clinical technique, particularly if combined with radiological examination of the kidneys by traditional means (urography, ascending pyelography, retropneumoperitoneum, tomography, aortography, etc.). (auth)

19722 PANCREAS SCANNING WITH Se^{75}–SELENOMETHIONINE. M. Blau (Roswell Park Memorial Inst., Buffalo). p.275-87 of "STI/PUB/82(Vol. II)."

The chemical similarity of selenium and sulfur suggested that the selenium analogue of methionine might resemble methionine closely enough to take its place in protein synthesis. Se^{75} (half-life, 128 d; principal gamma ray, 0.27 Mev) was found to be suitable for scanning. Selenium-75-selenomethionine was prepared by yeast biosynthesis. The yeast was grown on a low sulfur medium containing high specific activity ^{75}Se as selenite. After extraction with ether and hot trichloracetic acid, the protein residue was hydrolyzed with hydrochloric acid. The resulting amino acid mixture was separated by column chromatography. Selenium-75-selenomethionine prepared in this manner showed biological properties of a natural amino acid. The uptake in pancreas was about 7% of the administered dose and the concentration in a gram of pancreas was seven times that in a gram of liver. Blood and other organs had even lower uptakes. The clinical usefulness of pancreas scanning is now being evaluated. Tumors of the pancreas were found as areas of decreased uptake. There was no concentration of selenomethionine in cases of acute pancreatitis. It is too early to give a statistical estimate of the ability to find tumors of the pancreas by this technique. The estimated whole-body dose from this procedure is less than 1 Rad. The selenium dose is only a few micrograms and represents no toxicity hazard. (P.C.H.)

19723 RADIOISOTOPE SCANNING OF THE PANCREAS WITH SELENOMETHIONINE-Se^{75}. D. B. Sodee (Doctors Hospital and Renner Clinic Foundation, Cleveland Heights, Ohio). p.289-302 of "STI/PUB/82(Vol. II)."

Photoscanning of the pancreas utilizing selenomethionine-^{75}Se has recently been shown to be a practical technique. In a series of 100 patients who underwent 250 such photoscans, the pancreas was visualized in 90% of the cases. The physiological stimulation of the pancreas was found to be the most important factor in pancreatic selenomethionine-^{75}Se concentration. Utilizing a 30-g protein meal, physiological stimulation of the pancreas was begun one hour before the intravenous administration of 3 to 4-μC/kg selenomethionine-^{75}Se. Fifteen minutes later continued stimulation of the pancreas was ensured by the oral administration of 900 μg of glutamic acid hydrochloride. Before scanning the pancreas, a $\frac{3}{8}$-in. curved lead shield was placed over the liver bed previously outlined by an ^{198}Au liver scan. This lead shield blocks the radiation from the concentration of selenomethionine-^{75}Se in the liver that in the past impaired accurate delineation of the pancreas. A 5-in. by 3-in. crystal and a 121-hole lead collimator with a 5-in. focal distance was used. This has further improved delineation of the pancreas and, as the technique is perfected, smaller lesions at greater depths may be visualized. The results show that pancreatic carcinoma does not concentrate selenomethionine-^{75}Se as well as normal tissue. Five of six patients with pancreatic carcinoma had their disease correctly interpreted by this procedure. The smallest carcinoma not visualized was obscured by an enlarged liver. Acute and chronic pancreatitis were also confirmed by the pancreatic scan as the impaired cells of the pancreas do not concentrate selenomethionine-^{75}Se. Selective uptake of selenomethionine-^{75}Se by parathyroid tissue is also reported. Utilizing the same scanning technique parathyroid adenomas in a small group of hyperparathyroid patients were visualized. Photoscanning of the pancreas is already a practical technique and an investigation of photoscanning of the parathyroid is now being undertaken. (auth)

19724 DIAGNOSIS OF MASSIVE PULMONARY EMBOLISM IN MAN BY RADIOISOTOPE SCANNING. H. N. Wagner, Jr., D. C. Sabiston, Jr., and J. K. Langan (Johns Hopkins Univ., Baltimore). p.303-24 of "STI/PUB/82(Vol. II)."

Macroaggregated human-serum albumin particles labeled with either ^{131}I or ^{51}Cr were used to determine regional blood flow to the lungs in dogs and man. Following intravenous injection, the particles accumulated in the lung, permitting clear delineation of the lung fields by scintillation scanning. In patients with lung abscess, pneumonia, atelectasis, tumors, and thromboembolic disease of the lung, there was a decreased accumulation of the radioactivity in the regions of the lungs involved. The technique was found to be clinically useful in the diagnosis of massive pulmonary emboli in man and in the demonstration of vascular occlusion in certain patients with cor pulmonale. Studies in dogs made possible the determination of the rate at which revascularization occurred following experimental pulmonary emboli. Scintillation scanning was carried out at various times after the removal of the experimental emboli. The circulation was restored through the lungs within a period of several weeks after the removal of chronic pulmonary emboli in dogs. Although aggregated human-serum albumin retained its antigenicity in rabbits, guinea pigs and dogs, extensive studies failed to reveal any antigenicity of the particles to man. Because of the rapid metabolism of the macroaggregated albumin particles, the radiation to the patient was well within permissible levels. The use of albumin of high specific activity permitted injections of small chemical quantities; consequently no cardiovascular effects, such as increases in pulmonary artery pressure, changes in electrocardiogram, or respiratory rate, were noted. (auth)

19725 PHOTOSCANNING OF THE SPLEEN BY HEAT-TREATED Cr^{51}-LABELLED ERYTHROCYTES IN CONGENITAL HAEMOLYTIC ANAEMIAS. H. Gyftaki, C. Proukakis, D. Binopoulos, C. Elias, and V. Alevizou (Athens Univ.). p.325-35 of "STI/PUB/82(Vol. II)."

The delineation of the spleen by photoscanning after the intravenous injection of heat-treated ^{51}Cr-labeled erythrocytes is valuable when investigating congenital hemolytic anemias, especially thalassemia, a disease which is recognized as one of the most important public health problems in Greece. Heat-treated ^{51}Cr-labeled erythrocytes were prepared as follows: blood was taken from the subject by venepuncture and delivered into a sterile bottle containing acid citrate dextrose. The red cells were separated by centrifugation and the plasma discarded. 50–150 μC ^{51}Cr-chromate was added to the red cells and the mixture allowed to stand for 30 min at room temperature. The labeled cells were washed once with saline and re-suspended in saline. The suspension was heated at 49.5°C for one hour. The heated cells were washed once with saline and re-suspended in saline. The suspension was then injected intravenously into the subject. Scanning was performed one hour later. Cases of thalassemia major, sickle cell hemoglobin/thalassemia and thalassemia trait were investigated by this method. All the cases studied, with the exception of one carrier of thalassemia trait, whose spleen was not palpable, showed varying degrees of splenomegaly. The size and configuration of the spleen could be well demonstrated. A constant finding in spleen scans on patients with congenital hemolytic anemia, not observed in scans on normal subjects, was the presence of regions of lower average radioactivity throughout the organ. The interpretation of this finding is discussed. (auth)

19726 RESULTS OF CLINICAL APPLICATION OF SCINTILLATION SCANNING OF THE SPLEEN ON 500 PATIENTS: POSSIBILITIES AND LIMITS. J. Fischer and R. Wolf (Universitat, Mainz). p.337-53 of "STI/PUB/82(Vol. II)." (In French)

After injecting erythrocytes marked with radioactive substances and artificially damaged there is a rapid clearance of these cells from the blood stream and sequestration in the spleen. The resultant high concentration of radioactivity in the spleen permits a good scintigraphic demonstration of the organ. For many reasons $Na_2{}^{51}CrO_4$ seems at present to be the most suitable substance for labeling erythrocytes, and alteration by heat the most practical means of damaging the cells. The systematic application of spleen scintigraphy on over 500 patients showed: demonstration of enlargement of the spleen is not possible by clinical or roentgenological methods; verification of tumors in the upper left abdominal region; demonstration of accessory spleens after splenectomy; demonstration of ectopic spleens (situs inversus, ptosis); and demonstration of parenchymal defects in the spleen (e.g. intrasplenic bleeding, infarcts of the spleen, and necrosis of the spleen, and intrasplenic cysts). By planimetric measurements of the scintigram area and by calculating the splenic surface area index (= scintigram area/body surface of the patient) a good quantitative estimation of the extent of spleen enlargement may be obtained. In healthy persons the surface area of the scintigram does not exceed 70–80 cm^2 and the splenic surface-area-index lies normally within $2.5-4.5 \times 10^{-3}$. A comparison with the clinical findings showed that only one third of the spleens that were found by scintigraphy to be positively enlarged could be detected by percussion and palpation. In various diseases the clinical estimation of spleen enlargement is false in an even higher percentage of the cases. Only when the spleen has completely lost the ability to sequestrate heat-altered erythrocytes is the scintigraphic depiction of the spleen impossible. Such cases, however, seem to be extremely rare; only one has been observed so far. Up to now the information on form, size, position, and parenchymal defects that are afforded by scintigraphy, cannot be obtained by any other method, including special roentgenological methods. The process makes few demands on the patient, so that even very ill persons can tolerate it; it is not dangerous and can be performed on walking patients. The load of radiation dose to the patient is slight. For the spleen, depending on the volume, it is of the order of a few Rad. The dose to the sex organs and the whole body is on the average 40 mRad, which is far less than arises in many simple routine roentgenological examinations. (auth)

19727 SCINTILLATION SCANNING OF THE SPLEEN WITH RED CELLS LABELLED WITH CHROMIUM-51. F. Spinelli-Ressi (Ospedale Maggiore, Milan). p.355-69 of "STI/PUB/82(Vol. II)."

Satisfactory scintiscans of the spleen were obtained using chromium-51-labeled red cells, modified by two methods. Initially red cells were sensitized in vitro by coating with incomplete anti-D antibody. In this method the concentration of sensitized red cells in the spleen is proportional to the volume of anti-D serum employed in the sensitization procedure. Satisfactory scintiscans were obtained using 0.50 ml of a 1:128 dilution of anti-D serum, having an original titer of 1:512/ml of red cells. In spite of good results, the sensitization method, utilizable only in Rh positive patients, was replaced by the method using red cells modified by heating, which is technically easier and may be used also in Rh negative patients. The image of the spleen is clearly delineated in all the cases, without interference from hepatic radioactivity. The spleen: liver ratio ranges between 5:1 and 10:1. To date scintillation scans of the spleen have been performed in about 60 patients. No immediate or delayed clinical reactions have been observed in the patients after the injection of sensitized or heated red cells. Since the radiation dose delivered to the patient is lower than the dose delivered in many radiological and clinical examinations with radioactive isotopes, the scanning procedure has been widely used in the differential diagnosis of the masses of the left abdomen. Among the cases studied, it is worth while mentioning two cases of splenomegaly associated with a tumor of the left kidney, one case of Banti's disease in a patient, in which a neoplasm of descending colon was suspected, and a case of neuroblastoma in a patient two years old, in which the scintiscan of the spleen and that of the kidneys were of great help in making the correct diagnosis. Further, the scintiscan has been of unique utility in ruling out an accessory spleen and to demonstrate the spleen in congenital malformations, like situs inversus viscerum. In patients affected by chronic leukemia the scanning procedure has been used in objectively demonstrating modifications in spleen size after roentgen therapy. (auth)

19728 USE OF THE SCINTIGRAPHIC METHOD IN MORPHOLOGICAL EXPLORATION OF THE LIVER DURING AMOEBIASIS. R. Gongora and H. Jammet (Foundation Curie, Paris). p.373-87 of "STI/PUB/82(Vol.II)." (In French)

Statistics of morphologic examinations of the amoebic liver by the scintigraphic method are quoted and results are discussed. The technique is described, including choice of materials (^{131}I-labeled Rose Bengal and ^{198}Au in colloidal solution), apparatus used, actual performance of the examination, and repetition of the examination after an interval of several months. The scintigraphic semeiology of hepatic localizations of amebiasis is discussed, including analysis of elementary abnormal images, topography, and associations in the case of hepatitis and amoebic abscess. The development of these images with time was studied, and a number of cases for which the scintigraphic examination was repeated after an interval of several weeks or months are reported. Applications of the method, which provides essential data for the positive diagnosis of amoebic abscess of the liver and for topographical and morphological diagnosis, and which makes it possible to observe the progress of the disease and the healing of the abscess after medical treatment, are indicated. (P.C.H.)

19729 THE VALUE OF LIVER SCANNING IN THE DIAGNOSIS OF ECHINOCOCCUS DISEASE OF THE LIVER. T. Doxiades, P. Gatsou, D. Ikkos, G. Merikas, and A. Nastou (Evangelismos Hospital, Athens). p.389-400 of "STI/PUB/82(Vol.II)."

Echinococcus disease of the liver is quite common in Greece. During the past year, liver scanning was carried out in 40 patients with proven hyatid cysts of the liver. These cysts appear as defects in the scan. Therefore, it is impossible to attribute with absolute certainty a liver-scan defect to a hydatid cyst without the help of clinical and/or laboratory data. However, in the scans signs exist

that help to decide whether a defect is probably due to a cyst or not. Experience has shown that liver scanning is a valuable method in the diagnosis of Echinococcus disease of the liver for the following reasons: it shows the presence or absence of a clinically important cyst; it defines satisfactorily the number, size, and localization of cysts of clinically important size; and it is the only available method by which it can be decided whether an elevation of the right hemidiaphragm is due to an Echinococcus cyst or a normal variation in the shape and/or location of the liver. (auth)

19730 SCANNING STUDY OF 700 LIVERS. EVALUATION OF EXISTING DIAGNOSTIC PROCEDURES. P. Czerniak (Government Hospital, Tel-Hashomer, Israel). p.401-30 of "STI/PUB/82(Vol.II)."

Clinical studies, laboratory tests, roentgenographic examinations, and liver-scanning studies were performed on 700 patients. The patients were followed up and finally an objective diagnostic confirmation was obtained in most cases. In this way an evaluation of the performed tests was established. The liver scanning was done using ^{198}Au, ^{131}I-Rose Bengal, and ^{131}I PVP. Apart from the classical AP technique, special methods were utilized, such as tri- or bi-plane stereoscanning and combined isotope studies with ^{198}Au and ^{131}I-Rose Bengal leading to a determination of the RLC (radioisotope liver coefficients). The patients were divided into eight clinical groups and the diagnostic data were accordingly compiled and evaluated. Each clinical group was separately analyzed. For example, a space-occupying lesion was detected in 95% of the 65 cases of Echinococcus disease. X-ray examination detected calcifications in only 35% of these cases, but also in 14% of other liver diseases. Weinberg and Casoni reactions were positive in 64% of the cases of Echinococcus, but also in 22% of other diseases. In hepatic malignancy, a space-occupying lesion was detected in 44% of cases, a foggy scan in 30% and morphological changes in 29%. In two of the 158 tumor cases the scan falsely appeared to be normal, but in 40% of the same cases the laboratory results were negative. By using the bi- and tri-plane stereoscanning technique, new and supplementary information on the state of the liver was obtained in 45% of cases. Liver scanning was also used in the follow-up study. It was found that: after Echinococcotomy, a definite scar persists as a space-occupying lesion; three months after a treated amoebic abscess, complete regeneration occurs; after a porto-caval shunt, the liver scan becomes smaller and the spleen larger—even when the general condition is satisfactory; cytostatic agents may be temporarily effective in some diffuse hepatic lesions; and a rescanned suspected lesion may reappear as a space-occupying lesion or disappear. Thus the time of scanning may affect the diagnosis. It was concluded that liver scanning can be considered as a very useful method for clinical, morphological, and topographical diagnosis in hepatopathology. (auth)

19731 A STUDY OF THYROID UPTAKE OF THE DISASSOCIATED I-131 FROM LABELLED PREPARATIONS. Yen Wang. 9p. (CONF-640609-4)

From Society of Nuclear Medicine 11th Annual Meeting, Berkeley, Calif.

The stability of the various ^{131}I labeled compounds which are currently employed in the medicine was evaluated by ^{131}I thyroid uptake. Iodine-131-Rose Bengal and ^{131}I-Hippuran showed the least ^{131}I thyroid uptake and are proven to be most stable compounds. They are the ideal compound for clinical use. Four doses of Lugol solution, five drops each, completed in one day was found to be satisfactory for the blockage of thyroid in preparing patient for a large tracer dose of ^{131}I-serum albumin and ^{131}I-triolein. (auth)

19732 THE PRE-OPERATIVE LOCALIZATION OF PARATHYROID ADENOMATA. Joseph B. Workman and Thomas B. Connor (Univ. of Maryland, Baltimore). 6p. (CONF-640609-2)

From Society of Nuclear Medicine 11th Annual Meeting, Berkeley, Calif.

Eight patients with hyperfunctioning parathyroid adenomata were studied using ^{57}Co-labeled vitamin B-12 in attempts at pre-operative localization. Positive identification by external scintillation scanning was unsuccessful in all 8 patients, possibly due to the small size of the tumors and to the low dosage of isotope used. Cobalt-58 appears to have no advantage over ^{57}Co-labeled Vitamin B-12 in the three patients in whom it was used. Positive identification at the time of surgery was possible in 50% of the patients in whom it was attempted. The use of a small crystal scintillation detector at the time of surgery may be of decisive help in localization in the patient with hyperparathyroidism due to a small or unusually located adenoma. (C.H.)

19733 ISODOSE CHARTS FOR OBLIQUELY INCIDENT WEDGE-FILTERED Co^{60} TELETHERAPY BEAMS. E. M. Campbell and Than Tun (Manitoba Cancer Treatment and Research Foundation, Winnipeg, Can.). 15p. (CONF-640611-5)

From Canadian Assn. of Physicists, Division of Medical and Biological Physics, Annual Meeting, Halifax, Nova Scotia, Can.

A method is described for modifying normal incidence ^{60}Co isodose charts for use with oblique beams for both wedge and non-wedge filtered fields. The method affords the advantages of simplicity, rapidity, and accuracy and results in obtaining complete isodose charts for use in radiotherapy. (C.H.)

CHEMISTRY

General

19734 (UCRL-11757) COMPUTATIONAL STUDIES OF TRANSIENTS IN PACKED TABULAR CHEMICAL REACTORS (thesis). John Earl Crider and Alan S. Foss (Lawrence Radiation Lab., Univ. of California, Berkeley). Jan. 1965. Contract W-7405-eng-48. 195p. Dep.(mn); $5.00(cy), 3(mn) CFSTI.

Concentration and temperature transients in a packed bed tubular chemical reactor were calculated for three different mathematical models of the reactor. Two of the models represent the reactor as an array of continuous perfectly mixed stages; one model is two-dimensional, the other is one-dimensional. The third model is a one-dimensional differential representation without axial fluid dispersion. The chemical reaction is an exothermic, homogeneous, liquid-phase, second order reaction. Machine calculations of transients following step changes in feed temperature or concentration showed that the effects of axial fluid dispersion are small compared with the dispersive effects of finite rates of heat transfer between fluid and packing. Cases were found in which the transient concentration initially moved in the direction leading away from the final steady state. Such behavior, which derives from the coupling of concentration and temperature in exothermic reactions, can make the control of reactors difficult. Radial concentration and temperature gradients, arising from incomplete radial mixing, are shown to be small, and their effect upon transients is imperceptible in the cases treated. The results show that mathematical models that adequately simulate chemical reactors in unsteady state must incorporate the following phenomena: thermal capacity of the packing, finite (as distinguished from infinite) rates of heat transfer between fluid and packing, and coupling between concentration and temperature. (auth)

19735 (UCRL-11828) NUCLEAR CHEMISTRY DIVISION ANNUAL REPORT, 1964. J. M. Hollander, F. Reynolds, and B. B. Cunningham, eds. (Lawrence Radiation Lab., Univ. of California, Berkeley). Jan. 1965. Contract W-7405-eng-48. 289p. Dep.; $6.00(cy), 5(mn) CFSTI.

A total of 180 short articles are presented on topics in radioactivity and nuclear structure, fission, nuclear reactions and scattering, physical chemistry, instrumentation, and chemical engineering. Fourteen thesis abstracts are also included, along with author indexes to the articles and to papers and reports published in 1964. Abstracts were prepared of 43 of the articles which were not abstracts or condensations of published literature. (D.L.C.)

For abstracts of individual papers see: 19775, 19845, 19846, 19847, 19848, 20281, 20282, 20283, 20284, 20285, 20286, 20287, 20288, 20327, 20328, 20736, 20807, 20938, 21162, 21247, 21248, 21249, 21250, 21251, 21252, 21253, 21254, 21255, 21256, 21257, 21258, 21259, 21260, 21261, 21262, 21263, 21264, 21265, 21266, 21267, 21268, 21269, and 21270.

19736 ON THE NOMENCLATURE OF ISOTOPES OF CHEMICAL ELEMENTS AND OF ISOTOPICALLY LABELLED CHEMICAL COMPOUNDS. H. Huebner (Deutsche Akademie der Wissenschaften, Berlin). Chem. Listy, 58: 1273-82(1964). (In Czech.)

Previous publications on the nomenclature of isotopes and isotopically labeled compounds are reviewed. Six rules to be followed in writing formulas and naming isotopes and isotopically labeled compounds are presented and examples given. The rules cover the symbols and names for isotopes of the elements, formulas, and names for simple inorganic and organic compounds including the designation of the position of labeling, the indication of the extent of labeling, structural formulas of some labeled inorganic and organic compounds and their naming, the designation of compounds labeled in unknown positions, and suggestions for resolving cases of ambiguity arising from the application of the other rules. (TTT)

19737 THE NOMENCLATURE OF ORGANIC LABELLED MOLECULES. C. Parkanyi. Chem. Listy, 58: 1283-5(1964). (In Czech.)

The recommendations of the IUPAC Commission on the Nomenclature of Organic Chemistry for writing the formulas, naming, and indicating position of labeling for isotopically labeled organic compounds are presented. The recommendations are presented in the form of a series of six rules with several examples of the application of each rule. (TTT)

19738 RARE EARTHS–NUCLEAR CHEMISTRY. Jean-Pierre Adloff. French Bibliographical Digest. No. 36. Series II. Translated by Alexandre Berlin. New York, The Cultural Center of the French Embassy, 1962. 96p.

Three hundred and ninety-two papers by French authors on the chemistry of rare earths and on nuclear chemistry, published between Jan., 1956 and May, 1961 are listed. The papers on rare earths are limited to those on separation of the elements, chemical properties of the elements, and properties of their compounds. Papers on nuclear chemistry cover the following topics: natural radioactive elements uranium and thorium, artificial radioactive elements and nuclear reactions, chemical effects associated with nuclear transformations, chemical effects of ionizing radiations, and applications of radioisotopes. An author index is included. (M.C.G.)

Analytical Procedures

Refer also to abstracts 19490, 19656, 20162, and 21667.

19739 (AERE-AM-101) ANALYTICAL METHODS FOR THE DETERMINATION OF RADIOSTRONTIUM IN BIOLOGICAL MATERIALS. A. Parker, E. H. Henderson, and G. S. Spicer (Atomic Energy Research Establishment, Harwell, (England)). Jan. 1965. 40p. Dep.; $1.10(BIS), 5s. 6d. (HMSO).

Detailed procedures are described for the isolation, radiochemical purification, counting, and calculation of ^{89}Sr and ^{90}Sr in biological materials. These include bones, teeth, milk, vegetable ashes, and soils. (C.H.)

19740 (ANL-7005) GRAVIMETRIC METHOD FOR THE DETERMINATION OF THORIUM AND PHOSPHORUS IN THORIUM PHOSPHIDES. R. E. Telford and Y. Baskin (Argonne National Lab., Ill.). Feb. 1965. Contract W-31-109-eng-38. 9p. Dep.; $1.00 (CFSTI).

Thorium was precipitated as the oxalate and ignited to the oxide after dissolving the sample in a HNO_3-Br_2 solution. Phosphorus was determined in the filtrate by precipitation and weighing as $MgNH_4PO_4 \cdot 6H_2O$. (auth)

19741 (CEA-R-2539) CONTRIBUTION A L'ANALYSE DES ELEMENTS LEGERS PAR FLUORESCENCE X EXCITEE AU MOYEN DE RADIOELEMENTS (theses). (Contribution to the Analysis of Light Elements Using X Fluorescence Excited by Radioelements (thesis)). André Robert (Commissariat à l'Énergie Atomique, Saclay (France). Centre d'Études Nucléaires). 1964. 102p. Dep.(mn).

In order to study the possibilities of using radioactive sources for the x-fluorescence analysis of light elements, the principle is given, after a brief description of x-fluorescence, of the excitation of this phenomenon by x, β, and α emission from radio-elements. The operation and use of the proportional gas counter for x-ray detection is described. A device has been studied for analyzing the elements of the 2nd and 3rd periods of the Mendeleev table. It makes it possible to excite the fluorescence with a radioactive source emitting x rays or α particles; the x-ray

fluorescence penetrates into a window-less proportional counter, this being made possible by the use of an auxiliary electric field in the neighborhood of the sample. The gas detection pressure leading to the maximum detection yield is given. Spectra are given for the K_α lines of 3rd period elements excited by ^{55}Fe, $^{3}H/Zr$, and ^{210}Po sources; for the 2nd period the K_α spectra of carbon and of fluorine excited by the α particles of ^{210}Po. (auth)

19742 (CEA-R-2592) ETUDE THERMODYNAMIQUE DU TRAITEMENT DES ALLIAGES URANIUM–ZIRCONIUM POUR LA RECUPERATION DE LEURS COMPOSANTS. (Thermodynamic Study of the Treatment of Uranium–Zirconium Alloys for Recovering Their Constituents). Alfred Lecocq (Commissariat à l'Énergie Atomique, Fontenay-aux-Roses (France). Centre de Études Nucléaires). Jan. 1965. 35p. Dep.(mn).

Studies were made on favorable conditions of attack reactions for the separation and recovery of U and Zr contents in enriched U–Zr alloys. The Zircex process was used for the separation. The attack reactions were studied from the thermodynamic point of view. The results showed that the reactions considered for the separation of U from U–Zr alloys are chemically very reliable. Very stable products are obtained. (P.C.H.)

19743 (CEA-R-2619) AMELIORATION DE L'ANALYSE SPECTROGRAPHIQUE PAR L'UTILISATION D'UN TASSEUR MECANIQUE DANS LA METHODE DE DISTILLATION DANS L'ARC. (Improvement of Spectrographic Analyses by the Use of a Mechanical Packer in the Arc Distillation Technique). Michel Buffereau, Suzanne Deniaud, Bernard Pichotin, and Regis Violet (Commissariat à l'Énergie Atomique, Saclay (France). Centre d'Études Nucléaires). 1965. 41p. Dep.(mn).

A study was made of the improvement of spectrographic analysis by the "carrier distillation" method with the help of a mechanical device. Experiments and advantages of such an apparatus are given (precision and reproducibility improvement, operator factor suppression). A routine apparatus (French patent n° 976.493) is described. (auth)

19744 (CEA-R-2622) COMPARAISON DES CASCADES A FLUX TOTAL MINIMUM. (Comparison of Cascades With Total Minimum Flux). Georges-Marie Bouligand (Commissariat à l'Énergie Atomique, Saclay (France). Centre d'Études Nucléaires). Dec. 1964. 117p. Dep.(mn).

A theoretical method, illustrated by numerical computations, is given to compare the plant parameters of gaseous diffusion cascades of minimum total flux. These parameters are total flux, total number of stages, surface of porous membrane, power consumption, etc. For fixed process conditions and for a choosen mode of recyclage the steady state of concentrations is described by differential equations depending on two parameters. These two parameters also characterize the comparison relations. The design of the different recyclage models was determined by simple geometric structure or by a simple criterium. The results give, by elementary computations, the method of choosing the most advantageous one between all the possible models. (auth)

19745 (CEA-R-2712) SEPARATION RADIOCHIMIQUE QUANTITATIVE DE CALCIUM–STRONTIUM–BARYUM. (Quantitative Radiochemical Separation of Calcium, Strontium, and Barium). Marie-Claire Dupuis, Michel Dupuis, Monique Le Nagard, and Helene Michot (Commissariat à l'Énergie Atomique, Saclay (France). Centre d'Études Nucléaires). Feb. 1965. 10p. Dep.(mn).

A method for separation of ^{45}Ca, ^{89}Sr, and ^{140}Ba was developed for the radiochemical determination of these isotopes in a fission products solution with a large concentration of mineral salts. After removal of most fission products by solvent extraction (thénoyltrifluoroacetone–méthylisobutylkétone) at different pH, the alkaline earths are extracted from the aqueous phase at pH 9. After recovery with diluted hydrochloric acid, the three elements are adsorbed on cationic resin Dowex 50 and eluted sequentially with ammonium α-hydroxyisobutyrate using gradient concentration and pH. ^{45}Ca and ^{89}Sr are measured by β counting and ^{140}Ba by γ spectrometry. The chemical yield approximates 80 per cent for calcium, and 70 per cent for strontium and barium. The decontamination factor is 10^5 for most fission products. Four separations can be performed in twenty hours. (auth)

19746 (CEA-R-2728) MICROANALYSE X—DETERMINATION DE QUELQUES FACTEURS CORRECTIFS DUS AU RALENTISSEMENT DES ELECTRONS. (X-Ray Microanalysis—Determination of Some Correction Factors. The Penetration Factor). Daniel Calais, Guy Moreau, and Annick Van Craeynest (Commissariat à l'Énergie Atomique, Fontenay-aux-Roses (France). Centre de Études Nucléaires). Dec. 1964. 34p. Dep.(mn).

Correction factors owing to electron penetration were determined according to the following scheme. Let $C_{\theta A}$ be the measured concentration of element A in an alloy AB. Then, the absorption correction can be carried out following Philibert's method. Neglecting fluorescence absorption, $C_{\theta'A} = 1/\{1 + (C_{OB}/C_{OA})(S_B/S_A)[(1 - R_A\xi_A)/(1 - R_B\xi_B)]\}$ where C_O is the true mass concentration of element A in AB, S the stopping power which determines the penetration of an electron. R the back-scatter coefficient, and ξ the fraction of backscattered electrons lost for ionization. Integers of ξ (1 or 0) enable the penetration yield to be calculated, choosing methods are proposed, the results are tabulated. The values are compared to Nelms' (obtained assuming Bethe's law) and to those which can determine from Kulenkampff's experiments about energy spectrum of backscattered electrons. (auth)

19747 (CONF-650214-1) X-RAY EMISSION ANALYSIS. P. D. Zemany (Knolls Atomic Power Lab., Schenectady, N. Y.). [Feb. 18, 1965]. Contract [W-31-109-eng-52]. 11p. Dep.(mn); $1.00(cy), 1(mn) CFSTI.

From American Chemical Society, Troy, N. Y.

The technique of x-ray beam emission by the x-ray emission spectrograph and the electron beam microprobe is discussed. Some experimental results on measurements of small quantities of cobalt are illustrated. (P.C.H.)

19748 (DP-933) DETERMINATION OF ^{95}Zr AND ^{95}Nb IN MIXTURES OF THE TWO NUCLIDES. E. Kenneth Dukes, M. Yates Donnan, and Richard M. Wallace (Du Pont de Nemours (E. I.) & Co., Aiken, S. C. Savannah River Lab.). Feb. 1965. Contract AT(07-2)-1. 15p. Dep.; $1.00(cy), 1(mn) CFSTI.

A method based on decay measurements was developed to determine the relative amounts of zirconium-95 and niobium-95 in mixtures of the two nuclides. The method was tested on synthetic and process solutions; plutonium and ruthenium did not interfere. (auth)

19749 (EUR-2118.f) METHODES SPECIALES POUR LA MESURE DE LA RADIOACTIVITE DES EAUX USEES. (Special Methods for the Determination of Waste Water Radioactivity). A. Malvicini (European Atomic Energy Community, Ispra (Italy). Joint Nuclear Research Center. Feb. 1965. 15p. (CONF-640506-1). Dep.(mn).

From Biomathematics Symposium, Houston, Tex.

After a short introduction stressing the importance of the problem, a review is presented of the methods of control and measurement of radioactivity in waste waters. Strontium and cesium determination in such waters is also described in detail. (auth)

19750 (EUR-2286.f) DOSAGE DE Al, Al_2O_3, Fe, Si, Zn, C DANS LES POUDRES DE SAP COMPARAISON ENTRE LABORATORIES. (Determination of Al, Al_2O_3, Fe, Si, Zn, and C in SAP Powders. Comparison Between Laboratories). J. L. Collin and A. Hubaux (European Atomic Energy Community, Ispra (Italy). Joint Nuclear Research Center). 1965. 28p. Dep.(mn).

A comparative statistical study concerning the determination of Al, Al_2O_3, Fe, Si, Zn, and total Carbon in SAP powders is reported. The results are given in tables and graphs. A short description on the statistical calculations is also included. (auth)

19751 (GA-5982) DEVELOPMENT OF NEUTRON ACTIVATION ANALYSIS PROCEDURES FOR THE DE-

TERMINATION OF OXYGEN IN POTASSIUM. Final Report, Period Ending December 15, 1964. E. L. Steele, H. R. Lukens, Jr., and V. P. Guinn (General Atomic, San Diego, Calif.). Contract NAS3-2537. 51p. (NASA-CR-54100)

The development of neutron activation analysis procedures for the determination of oxygen in potassium has produced an analytical system that is representive of the state of the art. The oxygen sensitivity of detection is approximately 2000 photopeak counts per milligram of oxygen. The lower limit of detection is 25 μg. The system will produce precisions of 1% at the higher oxygen levels and very near the theoretical value (based on just the counting statistics) at the lower limit of 25 μg (26% versus 24% theoretical). The dual transfer system, which essentially eliminates timing and neutron production monitoring errors; the automatic control unit, which eliminates operator errors; and the spinning terminal end, which averages the non-uniform flux gradient, all contribute to precision and accuracy. Understanding of the other sources of error, such as recoil, pulse pileup, and electronic discrimination, also helps in this respect. (auth)

19752 (IS-T-2) REVERSED-PHASE CHROMATOGRAPHIC SEPARATION OF ZIRCONIUM AND HAFNIUM (thesis). Russell Thomas Frazee (Ames Lab., Iowa State Univ. of Science and Tech.). Feb. 1965. Contract W-7405-eng-82. 41p. Dep.(mn); $2.00(cy), 1(mn) CFSTI.

A method is presented for the separation of zirconium (IV) and hafnium (IV) by reversed-phase chromatography using Teflon-6 as the solid support. The stationary phase is methyl isobutyl ketone equilibrated with 3M thiocyanic acid. Zirconium(IV) is eluted with an aqueous ammonium thiocyanate-ammonium sulfate solution. A 1.2M ammonium sulfate or 1M sulfuric acid solution is used to strip the hafnium from the column. Using a 4.0M ammonium thiocyanate-0.2M ammonium sulfate eluting solution, ratios of zirconium(IV) to hafnium(IV) from 1:1 to 25:1 were separated quantitatively. Using radioactive ^{181}Hf isotopes and the same eluting solution, a ratio of zirconium(IV) to hafnium(IV) of 500:1 was separated quantitatively. The column loading for zirconium(IV) ranged from 50 μmoles to 250 μmoles and that of hafnium(IV) from 0.5 μmoles to 50 μmoles. (auth)

19753 (IS-T-3) PREPARATION AND SOME ANALYTICAL APPLICATIONS OF TRI-N-OCTYLPHOSPHINE SULFIDE (thesis). Donald Edward Elliott (Ames Lab., Iowa State Univ. of Science and Tech.). Feb. 1965. Contract W-7405-eng-82. 55p. Dep.(mn); $3.00(cy), 1(mn) CFSTI.

The extraction of several metal nitrates and chlorides with tri-n-octylphosphine sulfide (TOPS) from HNO_3 and HCl solutions, respectively was studied by both reversed-phase partition paper chromatography and liquid-liquid extraction techniques. TOPS was found to be a more selective extractant from HCl than from HNO_3 solutions. It also appears to be a more generally applicable extractant when used as the stationary phase in reversed-phase partition paper chromatography. Ag(I), Hg(II), and Pd(II) were selectively extracted from HNO_3 solutions by the two different experimental techniques used. Au(III), Hg(II), Pd(II), and Pt(IV) were completely retained from HCl by reversed-phase partition paper chromatography. Only Au(III) and Hg(II) were completely extracted by liquid-liquid extraction. Several separations were performed easily and efficiently by solvent extraction with TOPS. However, there are two major disadvantages associated with TOPS. These are preparation time and commercial availability. The extracting properties of TOPS as compared with those of tri-n-octylphosphine oxide are discussed. (P.C.H.)

19754 (JEN-134-DQ/I-39) APPLICATION DE LA SPECTROMETRIE DE FLUORESCENCE DE RAYONS X A LA DETERMINATION DE NIOBIUM, TANTALE ET URANIUM DANS NIOBIOTANTALITES. (Determination of Niobium, Tantalum, and Uranium in Tantalite–Columbite Ores by X-ray Fluorescence Spectrometry). O. Latorre and J. Bermúdez Polonio (Junta de Energía Nuclear, Madrid (Spain). División de Química). 1964. 12p. Dep. (mn).

A simple and quick procedure is carried out to determine niobium, tantalum, and uranium employing the internal standard technique; zinc as internal standard for tantalum and molybdenum for niobium and uranium were selected. Some interelement effects were studied and the ratios ($TaL_{\alpha_1}^{II}/ZnK_{\alpha}^{II}$), ($NbK_{\beta_1}/MoK_{\beta_1}$), and ($UL_{\gamma_1}/MoK_{\beta_1}$) were found to be unchangeable. The precision of the method is about 5%. Time consumption for each sample, excluding grinding time, is about 45 minutes. (auth)

19755 (KFK-252) ABSOLUTEICHUNG VON RADIONUKLIDEN MIT DEM 4π-ZAHLER. (Absolute Measurement of Radionuclides with the 4π Counter). J. Lange and H. Muenzel (Kernforschungszentrum, Karlsruhe (West Germany). Institut fur Radiochemie). Feb. 1964. 45p. Dep.(mn).

In carrying out absolute measurements, the properties of the measurement solution, the measurement sample, and the counting arrangement are of decisive importance. Each of these factors was considered individually in a literature search as complete as possible. Experiments using a simple 4π arrangement to determine whether satisfactory results could be obtained with low β energies (^{35}S, ^{99}Tc, ^{90}Sr, ^{137}Cs, and ^{103}Ru) were recorded. The results show that all calibrations agree with the theoretical values. The calibration values determined from diluted solution generally agreed better with the theoretical value. Extrapolation methods lead to better results in most cases. (J.S.R.)

19756 (LA-3193) DETERMINATION OF BORIC ACID IN ADMIXTURE WITH CYANURIC ACID. Raymond N. Rogers (Los Alamos Scientific Lab., Univ. of California, N. Mex.). Oct. 30, 1964. Contract W-7405-eng-36. 16p. Dep.; $1.00(cy), 1(mn) CFSTI.

Boric acid can be separated from cyanuric acid by methanol vapor distillation. Procedures for the separation and for a coulometric titration of the boric acid are described. Consistent recoveries of greater than 99.7% with a standard deviation of $\pm$0.21% are obtained. (auth)

19757 (LA-3213) SPECTROPHOTOMETRIC DETERMINATION OF RHENIUM IN TANTALUM–RHENIUM ALLOYS. K. S. Bergstresser (Los Alamos Scientific Lab., Univ. of California, N. Mex.). Dec. 1964. Contract W-7405-eng-36. 13p. Dep.; $1.00(cy), 1(mn) CFSTI.

A method is described for the determination of 1 to 6% rhenium in binary alloys of tantalum. Samples of the alloy are dissolved with hydrofluoric acid and a mixture of hydrochloric acid and hydrogen peroxide. After excess acid and peroxide are removed by evaporation, an aliquot of the dissolved sample containing no more than 200 micrograms of rhenium is used for color development. The fluoride in a properly diluted aliquot is complexed with borate, and rhenium is reduced with stannous chloride in the presence of the color reagent, furil dioxime. Absorbance of the red, rhenium-dioxime complex is measured with a spectrophotometer at 532 millimicrons. The standard deviation of a single measurement was estimated to be 0.5 micrograms of rhenium from data obtained in analyzing 16 solution samples containing tantalum and from 20 to 200 micrograms of rhenium. The method was successfully applied to the analysis of 1 and 5% tantalum-rhenium alloys. (auth)

19758 (LA-3225) THE GRAVIMETRIC DETERMINATION OF HYDROGEN IN MOLYBDENUM METAL. Ross D. Gardner, William H. Ashley, and Paul Bergstresser (Los Alamos Scientific Lab., Univ. of California, N. Mex.). Jan. 1965. Contract W-7405-eng-36. 10p. Dep.; $1.00 (cy), 1(mn) CFSTI.

The combustion-gravimetric method for the determination of hydrogen was modified and adapted to the measurement of hydrogen in molybdenum metal. The sample is burned in oxygen at 1100°C. Fused magnesium oxide sand is used to absorb the molybdic oxide produced and prevent its sublimation in the combustion tube. The water produced by oxidation of the hydrogen present is absorbed in anhydrous magnesium perchlorate and weighed. An

average recovery of 99.1% with a standard deviation of 8 ppm was obtained for the analysis of 62 samples containing known amounts of hydrogen in the 10 to 500 ppm range. (auth)

19759 (LA-3226) THE SPECTROPHOTOMETRIC DETERMINATION OF URANIUM IN MIXTURES OF URANIUM AND MOLYBDENUM. A. D. Hues and A. L. Henicksman (Los Alamos Scientific Lab., Univ. of California, N. Mex.). Jan. 1965. Contract [W-7405-eng-36]. 22p. Dep.; $2.00(cy), 1(mn) CFSTI.

The spectrophotometric determination of uranium with 3-(2-arsonophenyl-azo)-4,5-dihydroxy-2,7-naphthalenedisulfonic acid was modified and applied in the presence of large amounts of molybdenum, which is shown to be without effect. An extensive investigation was made of the interference of numerous foreign ions. The usual masking reagent is ethylenediaminetetraacetic acid. The use of sodium cyanide as a supplementary complexing agent was found to give significant improvement in the tolerance for cadmium, cobalt, copper, gold, iron, mercury, nickel, ruthenium, and zinc. The relative standard deviation of the procedure is shown to be less than 0.4% for a single determination. (auth)

19760 (NASA-TM-X-1085) ANALYSIS OF OXYGEN IN POTASSIUM. NASA Round-Robin Meeting Held June 4, 1964. (Lewis Research Center, National Aeronautics and Space Administration, Cleveland, Ohio). Mar. 1965. 32p. $2.00(CFSTI).

A meeting was held to discuss the results of the NASA-sponsored round-robin analysis of oxygen in potassium. The minutes of the meeting are presented. The analyses of low- and high-oxygen potassium are given, and the analytical procedures used by the participants are described. (D.L.C.)

19761 (NP-14876) THE DETERMINATION OF BORON IN REFRACTORY BORIDES BY PYROHYDROLYSIS. Technical Report No. C-28. G. J. McKinley and H. F. Wendt (Union Carbide Research Inst., Tarrytown, N. Y.). Jan. 1965. Contract DA-30-069-ORD-2787. 16p.

An analytical method was developed for the determination of boron in the refractory borides of titanium, zirconium, niobium, and tantalum. Pyrohydrolysis of the refractory boride forms boric acid which is distilled, collected, and titrated by a mannitol-sodium hydroxide procedure. The method is precise and accurate, and its simplicity of operation makes it attractive for use as a routine procedure. (auth)

19762 (RPI-2714-6) ELECTRODE KINETIC STUDIES OF THORIUM. N. D. Greene and L. E. Kindlimann (Rensselaer Polytechnic Inst., Troy, N. Y. Dept. of Materials Engineering). Mar. 1965. Contract AT(30-1)-2714. 19p. Dep.(mn); $1.00(cy), 1(mn) CFSTI.

Electrode kinetic characteristics of thorium in acid and alkali solutions were measured by potentiostatic and galvanostatic techniques. Electrode kinetic measurements indicate that a very stable barrier film on the surface of thorium retards dissolution. Application of these data to the separation of uranium–thorium alloys is discussed. (P.C.H.)

19763 (TEES-2671-4) INVESTIGATIONS IN AUTOMATED ACTIVATION ANALYSIS. Richard E. Wainerdi, Manchery P. Menon, Lloyd E. Fite, et al. (Texas Engineering Experiment Station, College Station). Jan. 1, 1965. Contract AT(40-1)-2671-1. Dep. (CFSTI).

Investigations in automated activation analysis are described in chapters on neutron activation analysis, Mark II computer-coupled activation analysis system, communications theory in neutron activation analysis, detector research, sodium separation, application of linear estimation of chemical mixture problems, program for digital computer analysis of pulse-height spectra, and public benefit utilizations. Separate abstracts were prepared for each chapter. A chapter on P determination by fast neutron activation analysis was previously abstracted in NSA as 18: 19850. (J.R.D.)

For abstracts of individual chapters see: 19764, 19765, 19766, 19767, 19768, 19769, 19770, and 19771.

19764 (TEES-2671-4(Chap.1)) [NEUTRON ACTIVATION ANALYSIS]. M. P. Menon (Texas Engineering Experiment Station, College Station). 7p.

An introduction to information presented in the report is given. The research is mainly concerned with technique and equipment improvement. (J.R.D.)

19765 (TEES-2671-4(Chap.2)) MARK II AUTOMATIC COMPUTER-COUPLED ACTIVATION ANALYSIS SYSTEM. L. E. Fite (Texas Engineering Experiment Station, College Station). 82p.

Design and operation of the system is described; control circuitry is emphasized. (J.R.D.)

19766 (TEES-2671-4(Chap.3)) COMMUNICATION THEORY IN NEUTRON ACTIVATION ANALYSIS. W. W. Wilkins (Texas Engineering Experiment Station, College Station). 40p.

Investigations of a class of nonstationary random signals are described. Solution of the equation $Y = f(x,t)h(x,t,z)$ is studied where x and t are random variables, z is a fixed function of x, and f and h describe nonstationary random processes. (J.R.D.)

19767 (TEES-2671-4(Chap.4)) DETECTOR RESEARCH. C. F. Lam (Texas Engineering Experiment Station, College Station). 15p.

A detector assembly study is described in which the application of dual crystal-single photomultiplier systems with pulse-shape descrimination techniques is made for Compton background reduction. Results of assembly tests indicate that significant reductions can be achieved in the Compton-region gamma spectra by its use. (J.R.D.)

19768 (TEES-2671-4(Chap.6)) SODIUM SEPARATION. M. P. Menon (Texas Engineering Experiment Station, College Station). 13p.

The method is based on precipitation of sodium chloride from small volumes of irradiated samples in n-butyl alcohol-HCl solutions. Results show that yields of greater than 80% are possible with most elements using a single precipitation. (J.R.D.)

19769 (TEES-2671-4(Chap.7)) APPLICATION OF LINEAR ESTIMATION TO A CHEMICAL MIXTURE PROBLEM. L. H. Smith and H. O. Hartley (Texas Engineering Experiment Station, College Station). 42p.

Results of investigations concerning the use of statistical methods in estimating the weights of chemical mixture components are described. Statistical concepts are discussed and related to activation analysis problems. Procedures recommended for activation analysis are given along with examples. (J.R.D.)

19770 (TEES-2671-4(Chap.8)) A NEW PROGRAM FOR THE DIGITAL COMPUTER ANALYSIS OF PULSE-HEIGHT SPECTRA. H. R. Phillips, J. L. Alexander, and D. D. Drew (Texas Engineering Experiment Station, College Station). 56p.

A description of the AA-6 computer program for analyzing pulse-height spectra associated with activation analysis is presented. AA-6 sub-programs are also described along with a users guide. (J.R.D.)

19771 (TEES-2671-4(Chap.9)) PUBLIC BENEFIT UTILIZATIONS. P. Jimenez and M. Y. Cuypers (Texas Engineering Experiment Station, College Station). 55p.

Analytical work involving public interest and benefit is described. Samples of cottonseed, pesticides, feed, grain, and liver were analyzed along with geological specimens. (J.R.D.)

19772 (TID-7022(Vol.I)(Bk.2)) ANALYTICAL CHEMISTRY MANUAL OF THE FEED MATERIALS PRODUCTION CENTER. GENERAL ANALYTICAL METHODS: INSOLUBLE SOLIDS THROUGH ZIRCONIUM. (National Lead Co. of Ohio, Cincinnati). Dec. 1964. Contract AT(30-1)-1156. 338p. Dep.; $3.50(cy), 5(mn) CFSTI.

A compilation of general methods used by the Wet Chemical Analytical Section is presented. The compilation begins with constituents beginning with "I," and ends with constituents beginning with "Z." (D.L.C.)

19773 (TID-20467) ACTIVATION ANALYSIS AS APPLIED TO THE PETROLEUM EXPLORATION INDUSTRY.

Richard Elliott Wainerdi and Lloyd E. Fite (Texas Agricultural and Mechanical Univ., College Station. Activation Analysis Research Lab.). [nd]. Contract AT(40-1)-2671. 16p. Dep.(mn); $1.00(cy), 1(mn) CFSTI.

After a brief discussion of methods used in activation analysis, the Mark I-Ia and II automatic activation systems and their operation are described. The design of a unit for activation analysis of lunar rock is considered. (D.L.C.)

19774 (UCRL-7962) GALLIUM OXIDE—A VERSATILE COMPOUND IN SPECTROGRAPHIC PROCEDURES. W. Morris (Lawrence Radiation Lab., Univ. of California, Livermore). Jan. 22, 1965. Contract W-7405-eng-48. 12p. Dep.; $1.00(cy), 1(mn) CFSTI.

Four spectrographic methods are described which show the versatility of Ga_2O_3. One method employs Ga_2O_3 as a carrier (analysis of BeO for impurities), while the other methods uses it as a collector (analysis of pure water, organic materials, and boron for impurities). (D.L.C.)

19775 (UCRL-11828(p.197-9)) NONDESTRUCTIVE ACTIVATION ANALYSIS WITH LITHIUM-DRIFTED GERMANIUM DETECTORS. S. G. Prussin, J. A. Harris, and J. M. Hollander (Lawrence Radiation Lab., Univ. of California, Berkeley).

In order to assess the potential of high-resolution Li-drifted Ge detectors for activation analysis, the concentrations of several trace metals (Na, Cu, Mn, and Ga) were determined in 99.9 and 99.999% pure Al. The gamma spectra of the irradiated 99.9% pure Al are compared with that obtained using a NaI(Tl) crystal. (D.L.C.)

19776 (UCRL-12169) THE GAS ANALYTICAL APPARATUS FOR PROJECT DRIBBLE. J. Frazer, V. DuVal, and Clarence Morris (Lawrence Radiation Lab., Univ. of California, Livermore). Jan. 6, 1965. Contract W-7405-eng-48. 19p. Dep.; $1.00(cy), 1(mn) CFSTI.

A gas chromatographic apparatus was developed for analyzing the vented gas from the Salmon event for H_2, CO, CO_2, SO_2, O_2, N_2, CH_4, C_2H_6, and H_2O. The design and operating characteristics of the apparatus are described in some detail. (D.L.C.)

19777 (USNRDL-TR-819) A RAPID RADIOCHEMICAL PROCEDURE FOR INDIUM. D. Sam and D. L. Love (Naval Radiological Defense Lab., San Francisco, Calif.). Jan 29, 1965. Contract AT(49-2)-1167. 16p. Dep.(mn); $1.00(cy), 1(mn) CFSTI.

A rapid radiochemical procedure was developed for the separation of indium radionuclides from a mixed-fission-product solution. An alcoholic pyridine solution is added to a uranium solution containing indium and tin carriers. The resulting tin precipitate is separated from the indium-containing solution by filtering through a cellulose membrane filter under 75 psig. The decontamination factor for tin is 2×10^3. Other fission products are only partially removed. The chemical yield of indium is about 44%, and the time required for the separation is about 10 seconds. After the tin-separated indium has decayed, the tin daughters of indium are removed from all the other fission products at a specified time by a procedure involving the volatilization of stannane from an alkaline borohydride solution. Measurements of the quantity of tin daughters of indium permits determination of the number of atoms of indium present at the time of the tin precipitation. (auth)

19778 (JPRS-29037(p.58-68)) COLORIMETRIC DETERMINATION OF TOTAL MINUTE AMOUNT OF RARE EARTH ELEMENTS AND THORIUM IN ORE. Kuo-t'ai Yü. Translated from Hua Hsueh Shih Chieh, No. 12, 565-8(Dec. 1964).

Methods for the colorimetric determinations of rare earths and thorium using uranium reagent I and uranium reagent III, respectively are described. The method has high sensitivity and is suitable for determinations of the total amount of the rare earths and thorium of 0.001–1.0%. The method also satisfies the requirements of mass production in plant laboratories and also the principles of quantity, speed, excellence, and thrift. Within certain ranges no interference was found in the presence of Fe, Nb, Ta, Zr, Ti, and Ca. (P.C.H.)

19779 USE OF EDTA IN THE QUANTITATIVE ANALYSIS OF INORGANIC COMPOUNDS. III. NEW SPECIFIC ATTEMPT FOR THE IDENTIFICATION OF THE URANYL CATION AND IMPROVEMENTS IN THE SELECTIVITY OF THE REACTION OF THE Mg^{2+} AND Zn^{2+} CATIONS WITH TITANIUM YELLOW AND MERCURY CYANATE, RESPECTIVELY. S. Arribas Jimeno and M. L. Alvarez Bartolome (Universidad de Oviedo, Spain). Anales Real Soc. Espan. Fis. Quim. (Madrid), Ser. B, 60: 541-6(July-Aug. 1964). (In Spanish)

On the basis of the good occultation properties of EDTA and on the basis of the line of study established in previous investigations, a specific reaction was proposed for U^{6+}. The selectivity of the identification reaction of Mg^{2+} with titanium yellow was improved. The strong interference that copper produces in the detection of zinc was eliminated. A system, which makes it possible to represent graphically the variation of the sensitivity as a function of the strange cation that can decrease it, was proposed. (tr-auth)

19780 THE DETERMINATION OF ZIRCONIUM (AND HAFNIUM) IN NIOBIUM AND OTHER METALS WITH CATECHOL VIOLET. D. F. Wood and J. T. Jones (Imperial Metal Industries (Kynoch) Ltd., Birmingham, Eng.). Analyst, 90: 125-33(Mar. 1965).

A procedure, based on the extraction of zirconium ions with a solution of tri-n-octylphosphine oxide in cyclohexane, and the formation of a zirconium-catechol violet complex in the organic extract, was successfully applied to the determination of zirconium, over the range 20 to about 1000 ppm, in niobium. Alloying amounts of chromium, cobalt, molybdenum, and tungsten did not interfere. The procedure was also satisfactorily applied to the determination of zirconium in complex nickel-base alloys, and tests showed that the method should be equally applicable to the determination of zirconium in aluminum, copper, iron, stainless steels, magnesium, titanium, tantalum, tungsten, and vanadium. In the analysis of tantalum- or tungsten-base materials, a preliminary separation of zirconium from the parent metal is necessary. Hafnium ions are also extracted into a solution of tri-n-octylphosphine oxide in cyclohexane, and produce a colored complex with catechol violet in the organic extract; the procedure is, therefore, equally applicable to the determination of hafnium provided that zirconium is absent. (auth)

19781 THE POLAROGRAPHIC DETERMINATION OF MOLYBDENUM IN NIOBIUM-BASE ALLOYS. J. B. Headridge and D. P. Hubbard (Univ. of Sheffield, Eng.). Analyst, 90: 173-5(Mar. 1965).

A polarographic method was developed for determination of molybdenum in niobium alloys. Six standard molybdenum solutions were prepared and polarograms were recorded. The anode was a still mercury pool. A plot of diffusion current versus molybdenum concentration produced a straight-line graph that passed through the origin. The relative standard deviation in determinations was found to be about 1%. (M.C.G.)

19782 RECENT ADVANCES IN PHYSICAL METHODS OF ANALYSIS. Robert G. Keenan (Public Health Service, Cincinnati). Arch. Environ. Health, 10: 583-92(Apr. 1965).

Discussion is presented on the present state of the art of neutron activation analysis, radiotracer techniques, atomic absorption spectrophotometry, mass spectrometry, and emission spectroscopy in the solution of industrial hygiene problems. Recent advances in instrumentation for the separate techniques, the advantages and limitations of the methods, and typical applications are included. (auth)

19783 SUBSTOICHIOMETRY IN RADIOCHEMICAL ANALYSIS. J. Ruzicka and J. Stary (Dept. of Nuclear Chemistry, Faculty of Technical and Nuclear Physics, Prague). At. Energy Rev., 2: No. 4, 3-58(1964).

Substoichiometric separation is more selective than other radiochemical separation procedures, for it is based on the use of strictly controlled amounts of reagent (chelating, extracting, precipitating) in quantities less than those which stoichiometrically correspond to the amount of the element to be separated. Moreover, the substoichio-

metric principle avoids the necessity of determining the chemical yield. The theory is given from which the best conditions can be calculated for attaining maximum selectivity and reproducibility of determination. The use of substoichiometry in activitation analysis, isotope dilution, and radiochemical analysis of mixtures of radioitosopes, such as radioactive preparations and fission products, is explained. Optimum conditions for determinations of traces of 24 metallic elements are given. Advantages, disadvantages, and trends in substoichiometry are discussed. (auth)

19784 THE DETERMINATION OF COBALT IN STEEL BY NEUTRON ACTIVATION AND GAMMA RAY SPECTROMETRY. Francesco Girardi, Jules Pauly, and Enrico Sabbioni (EURATOM, Ispra, Italy). Bull. Soc. Chim. France, 1439-45(1964). (In French) (EUR-2134.f)

The determination of cobalt in steel was carried out by irradiating in a nuclear reactor and counting the ^{60}Co sum peak at 2.50 Mev in a crystal gamma spectrometer. In order to obtain a high sensitivity and avoid the perturbations produced by other activities, the measurements were made in a gold absorber placed into a well-type crystal. The concentrations were deduced by comparing the measured activity to that of a cobalt comparator or to the activity of ^{59}Fe produced by the activation of the iron of the steel to be analyzed. A sensitivity of a few parts per million could be obtained by both methods. The reproducibility in terms of mean deviation was better than 2.5%. The method described is suitable for the analysis of steel for nuclear applications. No chemical treatment is needed and it can be applied to samples having a very small weight. (auth)

19785 ANALYSIS OF URANIUM TETRAFLUORIDE. Evzen Singer (Research Inst. for Inorganic Chemistry, Usti nad Labem, Czechoslovakia). Chem. Listy, 59: 225-32(1965). (In Czech.)

A method of analysis was developed and tested, which is suitable for production control of uranium tetrafluoride. With the described method the total contents of the fluorine, water, uranyl fluoride, uranium tetrafluoride, and uranium dioxide could be determined with satisfactory accuracy. (tr-auth)

19786 DETERMINATION OF THE SODIUM CONTENT OF FILTER PAPERS BY THE NEUTRON ACTIVATION METHOD. M. Rakovic and H. Talpova. Chem. Prumysl, 14: 152(Mar. 1964). (In Czech.)

The ^{23}Na impurity in filter papers was activated to ^{24}Na by a neutron flux of 1.5×10^{12} n/cm^2/sec. The activity was measured 5 hr later by a scintillation probe with a photomultiplier. The interfering β and soft γ radiations of the other impurities, which became activated at the same time, were filtered out with a Cu-plated sheet metal filter of 2640 mg/cm^2 thickness. The Na content was calculated from the number of impulses. Test results showed that one filter paper (0.0171 g/cm^2 surface wt) contained 0.016 μg/cm^2 of Na and another filter paper (0.0085 g/cm^2 surface wt) contained 0.063 μg/cm of Na. (OID)

19787 USE OF REFLECTED β-RADIATION FOR THE DETERMINATION OF END-POINTS IN PRECIPITATION TITRATIONS. J. Toelgyessy and S. Varga (Inst. of Chemistry and Technology, Bratislava). Chem. Zvesti, 17: 779-86(1963).

The principle of the method and its application to the titration of Ag^+ with 0.1N HCl, and $Fe(CN)_6^{4-}$ with 1.1N $Pb(NO_3)_2$, are described. (Anal. Abstr., 12: No. 2(Feb. 1965))

19788 MODIFICATION OF THE VOLUMETRIC DETERMINATION OF MICRO AMOUNTS OF FLUORIDE. V. Delmarova, L. Machu, M. Malinovsky, and A. Moncmanova (Inst. of Chemistry and Technology, Bratislava). Chem. Zvesti, 17: 787-94(1963).

The fluoride sample, with added 2,5-dinitrophenol, was neutralized with 0.1N HCl and the pH adjusted to 4. Alizarin red S solution, 2N NaCl, and 0.1N HCl were added to pH 2.63. The solution was titrated with 0.004N $Th(NO_3)_4$, containing 72 ml of 0.1N HCl per liter, to the appearance of a pink color. The standard deviation for up to 80 μg of F^- was 1.07 to 0.1%. (Anal. Abstr., 12: No. 2, (Feb. 1965))

19789 RADIOCHEMICAL METHOD FOR THE ANALYSIS OF STRONTIUM-90 IN BONES IN THE PRESENCE OF RADIOACTIVE CONTAMINANTS. Pierre Lerch, Jean-Jacques Geering, and Alain Delay (Universite, Lausanne, Switzerland). Chimia (Aarau), 19: 43-4(Jan. 15, 1965). (In French)

A method of radiochemical determination of low-level ^{90}Sr in human bones is described. This method permits the elimination of the contamination by unwanted radioactive isotopes, such as other fission products. The Sr is first separated from the other alkaline earth metals, the rare earths, and Y. The chemical yield of both separations was determined by isotopic dilution. The decrease of the radioactivity was followed for 8 to 10 days and did not differ from the ^{90}Y by more than 8%. The residual activity remaining after 15 days was 0.06 ± 0.02 pulse/min, after subtraction of the background (0.245 pulse/min). The reproducibility was about 8% (95% confidence level). (tr-auth)

19790 DETERMINATION OF MIXED FISSION PRODUCTS IN THE LIGURIAN SEA WATER. S. Kanitz, G. Orlando, and R. Pavanello (Univ., Genoa). Giron. Igiene Med. Prevent., 5: No. 2, 99-104(1964).

A technique employed for the determination of mixed fission products in sea water is described. Some results are given. (Excerpta Med., Sect. XXIII, 2: No. 3, (Mar. 1965))

19791 DETERMINATION OF POLONIUM-210 IN URINE BY TRACK COUNTING. M. P. Taylor, P. Hibbert, and B. E. Lambert (Radiological Protection Service, Belmont, Surrey, Eng.). Intern. J. Appl. Radiation Isotopes, 15: 665-9(Nov. 1964).

An autoradiographic technique that has proved to be sensitive and useful in the estimation of very low concentrations of ^{210}Po in urine is described. Chemical separation of the polonium is described in detail. Although the overall time for the assay of a sample is long, the technique can be used to advantage when there are a considerable number of samples. Furthermore, for samples containing up to 1 $\mu\mu$C/l of urine, the length of time taken, in the autoradiographic method described, is no more than that required to obtain comparable accuracy by conventional α-scintillation techniques. (auth)

19792 COMPARATIVE STUDY OF THE MEASUREMENT OF β-ACTIVITIES OF THIN CHROMATOGRAPHIC LAYERS; INFLUENCE OF THE DETECTOR, OF THE NATURE OF THIN LAYER AND OF THE β-RAY ENERGY. J. C. Roucayrol (Universite, Paris), J.-A. Berger, G. Meyniel, and J. Perrin. Intern. J. Appl. Radiation Isotopes, 15: 671-7(Nov. 1964). (In French)

The use of a Geiger-Müller counter or gel scintillator combined with a photomultiplier for measurement of β-activities on thin chromatographic layers of adsorbent or of ion-exchange resins is described. The method of preparing the thin layers is given particularly those of exchange resin, and also their treatment with a gel scintillator. The effect of three factors (thickness of the fluorescent gel, β energy, and nature of the thin layer) were investigated on the relative statistical note which is defined as the ratio: {[(efficiency)^2/proper movement] gel scintillator/[(efficiency)^2/proper movement] Geiger-Müller}. It is shown that the detection efficiency for ^{14}C on a thin layer of silica may exceed 75% with a gel scintillator and that the fluorescence photons are not diffused in the thin layer, which is a condition for a satisfactory resolving power. (auth)

19793 SIMULTANEOUS DETERMINATION OF 30 TRACE ELEMENTS IN CANCEROUS AND NON-CANCEROUS HUMAN TISSUE SAMPLES BY NEUTRON ACTIVATION ANALYSIS. K. Samsahl (Aktiebolaget Atomenergi, Stockholm), D. Brune, and P. O. Wester. Intern. J. Appl. Radiation Isotopes, 16: 273-81(Apr. 1965).

The following trace elements were quantitatively determined by γ-ray spectrometry in 6 samples of non-cancerous and 4 samples of cancerous human tissues: As, Au, Br,

Ca, Cd, Co, Cr, Cs, Cu, Fe, Hg, La, Mo, P, Rb, Sb, Se, and Zn. In some of the samples the following elements were qualitatively determined: Ag, Ba, Ce, Ga, Hf, In, Na, Os, Pt, Sr, Ti + Sc, and U. Most of the trace elements were found to be present in higher concentrations in the noncancerous than in the corresponding cancerous samples. In a typical run one sample each of cancerous and noncancerous tissue was irradiated together with standards of the elements to be determined in a thermal flux of 2×10^{13} n/cm^2 sec for 24 hr. The radioactive trace elements were separated into 16, and in some cases 18, groups by means of a chemical group-separation method. Subsequently, γ-spectrometric measurements were performed. A new method of comparing unknown samples with standards was developed. (auth)

19794 ION EXCHANGE ON A NATURAL CLAY MINERAL: A DEMONSTRATION EXPERIMENT. Joseph F. Mucci, Charlotte Hollister, and Louise R. Marshall (Vassar Coll., Poughkeepsie, N. Y.). J. Chem. Educ., 41: 602-3 (Nov. 1964).

The exchange properties of the natural clay mineral montmorillonite as well as the relative ease of replacing Cs by Co and Co by Cs while using this exchanger are demonstrated. The quantitative aspects of the process were followed by use of ^{137}Cs and ^{60}Co. A small column (5-in. long and 1.25-in. dia) containing 2 g of montmorillonite clay mixed with asbestos was used. A 0.020N aqueous solution of CsCl, labeled with enough ^{137}Cs (half life ~30 yr) to give ~100 counts/sec, is allowed to flow through the column at the rate of 1 ml/3 min. Fractions of the effluent are collected and counted. When the column is saturated with Cs, water is introduced to wash the excess Cs^+Cl^- from the column. At this point a 0.020N $CoCl_2$ (not radioactive) solution is allowed to run through the column. The Co is present as $Co(H_2O)_6^{++}$. Samples of the effluent are collected and counted for ^{137}Cs. Next, a 0.020N $CoCl_2$ solution (labeled with ^{60}Co to give about 100 counts/sec) is allowed to flow through the column. When the column is saturated with radiocobalt, the excess $CoCl_2$ is washed off with distilled water. At this point, 0.020N CsCl solution (not radioactive) is introduced into the column and the effluent is checked for radioactive Co. The normality of Co being displaced by Cs^+ vs the effluent volume is plotted. The number of meq of Co displaced was 2.01. Enough counts were taken to give about 0.5% counting statistics; background and resolving time corrections were made throughout. The use of a clay mineral as an exchanger was demonstrated and the reaction Co^{2+} + Cs_2-Mont → Co-Mont + $2Cs^+$ is seen to be much more difficult to carry out than $2Cs^+$ + Co-Mont → Cs_2-Mont + Co^{2+}. (BBB)

19795 CHEMICAL ANALYSIS OF SURFACES USING ALPHA PARTICLES. James H. Patterson (Argonne National Lab., Ill.), Anthony L. Turkevich, and Ernest Franzgrote. J. Geophys. Res., 70: 1311-27(Mar. 15, 1965).

The chemical analysis of surfaces using α-particle interactions was investigated. Simple instruments incorporating ^{242}Cm α sources and semiconductor silicon detectors are described. The characteristic energy spectra of α particles scattered at large angles from thick targets of different elements were determined. The relative intensities of scattering by different elements were established. They show large enhancement due to nuclear effects over Rutherford scattering for elements lighter than sodium. The production of protons from (α,p) reactions in certain elements increases the sensitivity of the method for these elements. The theoretical basis for the quantitative interpretation of scattering spectrums from complex materials is developed. The technique appears to be suitable for instrumented space missions. (auth)

19796 ACTIVATION ANALYSIS OF METALS. L. Poecze. Kohasz. Lapok, 96: 179-83(Apr. 1963). (In Hungarian)

Concentrations as low as 10 ppb can be detected by activation analysis by exposure to a neutron flux. It is possible to measure the radiation level of individual components of a mineral by using appropriate activation and cooling periods without employing chemical analyses. A 50-channel scintillation spectrometer was used to obtain the γ spectrum of Si. Using a 10^4 n/sec/sq cm flux, one group of trace elements in Al could be detected in 10^{-7} μg quantities, while 50 other elements were detectable in 10^{-4} μg quantities. In Mn : Ni analysis, the irradiation lasted 10 min and measurements began 4 hr later. The half lives of Mn and Ni are similar, but their activation cross sections differ. A 1.5-Mev discriminator was used in these analyses. Cu, Sb, As, and rare earth impurities in pure Bi were measured. Impurities in Sb, Ag, Ni, and Au were also measured along with other elements in Fe_2O_3 and in NiO. Side reactions in activation analysis interfered with the evaluations. Chemical separation analyses showed different results by 10 to 25%. (O.L.D.)

19797 POLAROGRAPHIC DETERMINATION OF U(VI) IN AQUEOUS SOLUTIONS IN THE PRESENCE OF SO_4^{--}, NO_3^- AND CH_3COO^- ANIONS. Ervin Schiff. Magy. Kem. Folyoirat, 71: 18-20(Jan. 1965). (In Hungarian)

A method was developed, which makes it possible to determine U(VI) in the presence of NO_3^- and SO_4^{--} anions and acetic acid with an accuracy of 2%. The accuracy does not decrease if the solution to be analyzed contains an excess of 250 equivalents of nitrate and sulfate anions and an excess of 500 equivalents of acetic acid for one equivalent of uranyl cations. In the concentration range studied, with uranium contents of 21.2 to 90.5 γ/ml U(VI) the calibration curve is a straight line. The method is suitable for routine analyses. (auth)

19798 DETERMINATION OF PHOSPHORUS, SULFUR, AND CHLORINE BY ACTIVATION ANALYSIS. W. Roehnsch (Institut fur Angewandte Radioaktivitat, Leipzig). Mikrochim. Ichnoanal. Acta, No. 1, 10-16(1965). (In German)

Double irradiation and measurement of the ^{32}P and ^{33}S activities permit determination of phosphorus, sulfur, and chlorine in the presence of each other by activation analytical procedures. Determination in selenium is described. (auth)

19799 PHOTOMETRIC DETERMINATION OF NICKEL TRACES IN PURE MOLYBDENUM AND TUNGSTEN. Richard Pueschel and Erik Lassner (Metallwerk Plansee AG, Reutte Tirol, Austria). Mikrochim. Ichnoanal. Acta, No. 1, 17-20(1965). (In German)

The red nickel-PAN-complex (PAN = 1-(2-pyridylazo)-2-naphthol) is extracted with chloroform at pH 10. Interfering iron and copper are masked with Tiron. Standard deviations in samples of molybdenum and tungsten containing 5 to 100 ppm nickel were ±1.6 ppm Ni. (auth)

19800 ANALYSIS OF PURIFIED URANIUM COMPOUNDS FOR NANOGRAM QUANTITIES OF BERYLLIUM AND CERTAIN RARE EARTHS. CHEMICAL SEPARATION AND SPECTROGRAPHIC DETERMINATION. R. Krefeld, G. Rossi, and Z. Hainski (EURATOM CCR, Ispra, Italy). Mikrochim. Ichnoanal. Acta, No. 1, 133-40(1965).

A 2−1 method was established for determination of traces of Be, La, Eu, Gd, Dy, Sm, and Er in purified uranium compounds. The elements were first separated from uranium by means of a column of TNOA (tri-n-octylamine) supported by SiO_2, followed by a spectrographic determination. By using a modified copper spark technique detection limits between 7×10^{-4} μg Be and 1×10^{-2} μg Sm were achieved. (auth)

19801 A COMMERCIAL SPECTROMETER MODIFIED FOR X-RAY SPECTROSCOPY OF THE LIGHT ELEMENTS. Ralph W. G. Wyckoff and Franklin D. Davidson (Univ. of Arizona, Tucson). Nature, 205: 969-71(Mar. 6, 1965).

A simple modification of a commercial x-ray spectrometer is described that permits the analysis of the lighter elements through boron. Typical spectra obtained with the modified spectrometer are illustrated; backgrounds are low and peak-to-background ratios satisfactory. (P.C.H.)

19802 SEPARATION AND DETERMINATION OF ZIRCONIUM, THORIUM, TITANIUM AND THE RARE-EARTH METALS. R. Pribil (Anal.-Chem. Lab., Polarograph. Inst., Prague). Oesterr. Chemiker-Ztg., 64: 334-7(1963).

Conditions are described in which the various complexing powers of EDTA, diethylenetriaminepentaacetic acid, and triethylenetetraaminehexaacetic acid are utilized to determine Zr, Th, Ti, and the rare earth elements, either separately or in mixtures. (Anal. Abstr., 12: No. 2, (Feb. 1965))

19803 TITRATION OF BERYLLIUM IN GLACIAL ACETIC ACID. S. M. Ali (Univ. of Peshawar, Pakistan) and Rab Nawaz. Pakistan J. Sci. and Ind. Res., 7: 224-6(July 1964).

A study was made of the titration of beryllium in glacial acetic acid to develop a method for determination of beryllium in non-aqueous medium. No satisfactory end point could be obtained on titrating basic beryllium acetate directly with perchloric acid. Therefore, a measured excess of the standard perchloric acid was added to an aliquot containing 3 to 15 mg of beryllium and the volume of perchloric acid consumed was determined by back titration with standard sodium acetate solution. The amount of Be found by titration in each case was 25% of the quantity actually taken. The values were fairly constant over a four-fold increase in concentration, indicating a stoichiometric reaction between basic beryllium acetate and perchloric acid. The proposed mechanism of the reaction indicated that the reaction of perchloric acid takes place only with the basic portion of the acetate and that normal beryllium acetate remains undissociated in acetic acid and does not react. It was concluded that this method may be used for determination of beryllium by multiplying the results by four. (M.C.G.)

19804 IONIZATION DETECTORS IN GAS CHROMATOGRAPHY. J. Krugers. Philips Res. Rept., Suppl., No. 1, 1-133(Feb. 1965).

The more important types of ionization detectors in gas chromatography are described. Their function is related to phenomena well-known in nuclear radiation detectors. These are dealt with as far as they are used in combination with a gas chromatograph. A literature survey was made. The references were obtained from four different fields of information, gas chromatography, combustion, nuclear physics, and, partly, spectroscopy. The flame ionization detector is explained qualitatively. Development of the cyanogen detector is described. A series of instruments for the testing of detectors was developed. Results obtained with these instruments are given. It was concluded that the flame ionization detector is a nearly ideal detector, and that its simple operation seems to have excluded its complicated mechanism. It is necessary to introduce the burning velocity, the width of the reaction zone, and the presence of a radical CHO^*. The efficiency of this detector seems to be determined by the competition between the oxidation of CH by O_2 and chemi-ionization by O. The importance of adjustment (e.g. for the dynamic range) of the gas velocities for the flame ionization detector to optimum values was found to be underestimated. A large dynamic range appeared to demand a minimum critical value of the nitrogen gas velocity. It is therefore recommended that the detector always be supplied with a hydrogen/nitrogen mixture containing a minimum amount of nitrogen. Detectors giving a Gaussian noise required an amplifier with a variable time constant to provide the minimum detection limit for every peak width. A logarithmic gas dilution system was further developed; its improvement was of value in measuring the response of a detector as a function of the concentration of the component. This function gives also information about reaction mechanisms. It was concluded that a detector using an excitation reaction instead of an ionization reaction may have better characteristics than existing detectors. A few preliminary experiments indicated the method that may be followed to determine this. (auth)

19805 RAPID DETERMINATION OF CESIUM-137 IN RADIOACTIVE DUSTS BY MEANS OF AMMONIUM PHOSPHOMOLYBDATE. E. Van der Stricht (CCR, Euratom, Ispra, Italy). Radiochim. Acta, 3: 193-9(Dec. 1964). (In Italian)

A rapid method for determination of ^{137}Cs is described, which is based on the use of thin layers of ammonium phosphomolybdate. The procedure was developed for samples like milk, plants, soil, fish, water, radioactive dust, but it was concluded that its generalization to other types of samples should not be difficult. (auth)

19806 RADIOACTIVATION ANALYSIS OF MANGANESE BY COUNTING DEUTERIUM PHOTONEUTRONS. S. Amiel and Z. Stuhl (Soreq Research Establishment, Israel Atomic Energy Commission, Yavne). Radiochim. Acta, 3: 199-204(Dec. 1964).

A method is described for the assay of 2.58-hr ^{56}Mn in different radioactive samples by counting photoneutrons. The high-energy portion of the gamma radiation of ^{56}Mn, produced by neutron activation of samples containing manganese, causes emission of photoneutrons from a D_2O reservoir incorporated in a 4π neutron counting assembly. To cause photoneutron emission from D_2O the gamma energy must exceed 2.23 Mev and thus the method discriminates efficiently against all gamma rays of lower energies. The photoneutron activity is proportional to the ^{56}Mn content of the sample, and submilligram quantities of manganese were determined with a precision of ~1%. Sensitivities of ~1 μg and better were indicated. The only serious sources of interference were sodium and fissionable elements, when present in large proportions. The method is rapid and can be used to determine manganese in complex matrices, without any chemical processing. The neutron counting apparatus required is relatively cheap, simple, and versatile. (auth)

19807 ROUTINE DETERMINATION OF COPPER IN BIOLOGICAL MATERIALS BY NEUTRON ACTIVATION. K. Fritze, N. Aspin, and T. H. Holmes (McMaster Univ., Hamilton, Ont.; Univ. of Toronto; and Hospital for Sick Children, Toronto). Radiochim. Acta, 3: 204-6(Dec. 1964).

A method was developed, which allows the simultaneous separation of ^{64}Cu from a large number of neutron-irradiated tissue samples. Based on the use of a chelating resin the procedure provides a fast and quantitative recovery of the copper, thus eliminating determination of chemical yields. (auth)

19808 RADIO THIN-LAYER CHROMATOGRAPHY. F. W. Koss and D. Jerchel. Radiochim. Acta, 3: 220-4 (Dec. 1964). (In German)

The combination of thin layer chromatography and radioanalysis is described. Examples for the different methods are given. (auth)

19809 CONCENTRATION OF RADIOACTIVE STRONTIUM AND CESIUM FROM WATER BY ELECTRODIALYSIS. M. M. Golutvina, Yu. M. Nikolaev, T. A. Kazakova, and G. A. Kuznetsova. Radiokhimiya, 6: 738-42(1964). (In Russian)

An electrodialysis method was developed for concentrating the isotopes ^{89}Sr, ^{90}Sr, and ^{137}Cs, present in rain water, snow, and natural water reservoirs. The electrodialyzer used is illustrated and described. Efforts were made to achieve a maximum rate of the process and to use the most readily available materials and equipment. In one hour, the method makes it possible to achieve a 60- to 70-fold concentration of radiostrontium and radiocesium; this represents a great time gain over the evaporation, ion-exchange, and coprecipitation techniques used for concentrating these isotopes. A scintillation gamma spectrometer was used to determine the radiochemical purity of ^{89}Sr, ^{90}Sr, and ^{137}Cs isolated from rain water; no extraneous gamma emitters were found in any of these products. Thus, other radionuclides were found to be eliminated by the electrodialysis method. (ATD)

19810 EXPERIMENTAL FACTORS IN THE PAPER ELECTROPHORESIS OF YTTRIUM IN HYDROCHLORIC ACID SOLUTION. C. G. Gonzalez and R. A. Guedes de Carvalho (Univ. of Oporto, Portugal). Rev. Port. Quim., 5: 188-93(1963).

Factors affecting the mobility and spot area in the electrophoresis of Y in 0.1M HCl, viz, the amount of material applied, the concentration of the solution, the acidity, voltage, and time, were examined. (Anal. Abstr., 12: No. 2, (Feb. 1965))

19811 CONTRIBUTIONS TO THE DETERMINATION OF URANIUM AND THE ELEMENTS THAT ACCOMPANY IT. NOTE I. THE PHOTOCOLORIMETRIC DETERMINATION OF URANIUM IN THE PRESENCE OF IRON AND OF IRON IN THE PRESENCE OF URANIUM. Raluca Ripan, I. Eger, and N. Bojan (Institut de Chimie, Academie de la Republique Populaire Roumaine, Cluj). Rev. Roumaine Chim., 9: 829-33(Dec. 1964). (In French)

A photocolorimetric method for the determination of iron in the presence of uranium and of uranium in the presence of iron is given. For determination of iron, Fe^{3+} was reduced to Fe^{2+} with hydroquinone, and it was determined colorimetrically at pH 4.5 using the blue filter. The sensitivity of the method was 0.063 γ Fe. The reagent used was 1,10-phenanthroline. For determination of uranium, ascorbic acid, which reduced Fe^{3+} to Fe^{2+} and at the same time was the reagent for uranium, was used. The determination was made at pH 4.5, using the blue filter. The sensitivity of the method was 0.9 γ U. (tr-auth)

19812 5,5′-THIODISALICYLIC ACID AS AN ANALYTICAL REAGENT. Mary L. Good and Suresh C. Srivastava (Louisiana State Univ., New Orleans). Talanta, 12: 181-5 (Feb. 1965). (TID-21162)

The reactions of 5,5′-thiodisalicylic acid with various metal ions were studied. The reagent produced colored complexes with Rh(III), Pd(II), Fe(III), Ru(III), and UO_2(II), and precipitates with Pb(II), ZrO(II), In(III), Th(IV), Ce(III), Ce(IV), and the rare earths under suitable conditions. The reagent showed promise as a spectrophotometric, as well as gravimetric, reagent for various metal ions. (auth)

19813 TETRAETHYLENEPENTAMINE-N,N,N′,N″,N‴,N⁗,N⁗′-HEPTA-ACETIC ACID AS A TITRIMETRIC REAGENT. Rudolf Pribil and Vladimir Vesely (Polarographic Inst. of J. Heyrovsky, Czechoslovak Academy of Sciences, Prague). Talanta, 12: 191-3(Feb. 1965).

A study was made, from an analytical point of view, of tetraethylenepentamine-N,N,N′,N″,N‴,N⁗,N⁗′-heptaacetic acid (TPHA). A good end-point was obtained in its use for titration of Al, Th, Pb, Zn, and Ni, adequate endpoints for Cd, Cr, Ca, and Mn, and poor results for Bi, La, Fe, Sc, Ce, Nd, Pr, and Mg. It was concluded that, with a few exceptions, TPHA is not a suitable titrant in aqueous solutions. (M.C.G.)

19814 DERIVATIVES OF 2-(2-THIAZOLYLAZO) PHENOL AS ANALYTICAL REAGENTS. VII. SPECTROPHOTOMETRIC DETERMINATION OF ZINC WITH 1-(2-THIAZOLYLAZO)-2-NAPHTHOL. Akira Kawase (National Research Inst. for Metals, Tokyo). Talanta, 12: 195-210 (Mar. 1965).

The spectrophotometric determination of trace amounts of zinc using derivatives of 2-(2-thiazolylazo)phenol was studied. With zinc these compounds form blue or red-violet chelates, which are mostly extractable with chloroform to give solutions exhibiting an absorption maximum near 600 mμ. 1-(2-Thiazolylazo)-2-naphthol (NT) is recommended for the determination of zinc down to 0.1 μg. Sandell's expression of the sensitivity is 0.0013 μg of zinc/cm^2. The interference of 29 cations and 11 anions was examined in the presence and absence of ammonium citrate and demethylglyoxime. Mercury(II), manganese(II), cadmium(II), uranium(VI), EDTA, cyanide, and pyrophosphate interfere, but mercury(II) and manganese(II) can be masked by the addition of thiosulfate and periodate, respectively. NT was applied to the determination of zinc in thorium oxide and magnesium. (auth)

19815 NEUTRON-ACTIVATION ANALYSIS OF COPPER IN LEAD. F. Adams and J. Hoste (Ghent Univ., Belg.). Talanta, 12: 221-5(Mar. 1965).

Submicrogram quantities of copper were determined in lead samples using neutron activation analysis. The chemical separation of copper was performed by extraction with 2,2′-diquinolyl (cuproïne) in isoamyl alcohol. No minor or trace constituents in the lead samples interfered with the copper determinations. (auth)

19816 POLAROGRAPHIC STUDY OF URANYL PYROPHOSPHATE COMPLEX IN THE PRESENCE OF VARIOUS SURFACE-ACTIVE SUBSTANCES. Tsai-teh Lai and Songjey Wey (Cheng Kung Univ., Tainan, Formosa). Talanta, 12: 269-76(Mar. 1965).

The effects of various surface-active substances on the characteristics of the polarograms of uranyl-pyrophosphate complexes were studied. In the absence of surface-active substances, reversible and diffusion-controlled reduction waves were obtained when the ligand concentration was 0.05 to 0.30M and the pH 1.05 to 4.0. Beyond pH 4.0, the irreversible waves were rendered reversible by the addition of 0.04% α-naphthol, 0.02% β-naphthol, and 0.002% Triton X-100 and 0.18% camphor, shifting the waves to a more negative potential. The formation of a 1:1 complex was confirmed by conductometry. (auth)

19817 EXTRACTION OF URANIUM AS URANYL ACETATE BY MEANS OF ANILINE AND ITS SOLUTIONS IN ORGANIC SOLVENTS. A. A. Nemodruk. Tr. Komis. po Analit. Khim., Akad. Nauk SSR, [Inst. Geokhim. i Analit. Khim.]. 14: 141-7(1963).

The extraction of U from solutions containing 1 ml of acetic acid by aniline (I) (distribution coefficient 4.3) and solution of I in organic solvents was studied. The distribution coefficient was highest with ketones and decreased in the series esters, ethers, aliphatic chlorohydrocarbons, and aromatic and aliphatic hydrocarbons. The percentage extraction of U decreased with decreasing concentration of I in the organic phase. To the aqueous solution 1% of EDTA was added to increase the selectivity of the extraction. Optimum conditions were pH 3.5 to 4.2 and an acetic acid concentration of 1 to 2M. Under these conditions, only Mo and W were extracted with U. The distribution coefficient for U increased if inorganic salts were added to the solution. The greatest increase was found with NaCl or NH_4Cl. After extraction from a solution containing NaCl and EDTA, U was re-extracted into ammonium carbonate solution and determined photometrically with chlorphosphonazo III. (Anal. Abstr., 12: No. 2, (Feb. 1965))

19818 ARSENATE METHOD FOR THE IODIMETRIC DETERMINATION OF ZIRCONIUM IN THE PRESENCE OF ALUMINIUM AND IRON. G. B. Shakhtakhtinskii and A. S. Sarkisyan. Uch. Zap. Azerb. [Gos.] Univ., Ser. Khim. Nauk, No. 2, 73-6(1963).

The arsenate method (Anal. Abstr., 11: 929(1964)) may be used to determine 2 to 20 mg of Zr in the presence of <8-fold amounts of Fe and Al. The precipitant solution should be added in small portions, with stirring. The reproducibility is good. (Anal. Abstr., 12: No. 2, (Feb. 1965))

19819 COLORIMETRIC DETERMINATION OF CERIUM WITH DIANTIPYRINYL-p-NITROPHENYLMETHANE. V. P. Zhivopistsev and V. V. Parkacheva. Uch. Zap. Permsk. [Gos.] Univ., 25: 104-7(1963).

The determination of cerium is based on the oxidation, by Ce^{4+}, of the colorless diantipyrinyl-p-nitrophenylmethane (I) to diantipyrinyl-p-nitrophenylmethanol, which is orange-red and exhibits maximum extinction at 495 mμ. To 15 to 20 ml of the sulfate solution (10 to 30 μg of Ce) a little PbO_2 is added (to oxidize Ce^{3+} to Ce^{4+}). The excess PbO_2 is filtered off. To the filtrate 0.5 ml of 0.5% ethanolic I is added, and after a few minutes, the extinction is measured in a 2-cm cell with a blue filter. In the presence of Fe, after oxidizing Ce and removing the excess PbO_2, 5 ml of 80% H_3PO_4 are added, and, after 1 to 2 min, the ethanolic I is added, and the process is continued as described. There was no interference from alkali, alkaline earth or rare earth elements, Sc, Y, Ga, In, Al, Ti, Be, Mg, Cu, Pb, Zr, Hg, Zn, Cd, As or Ni; Mn(VII) and Cr(VI) interfere. The error is ±2.5%. (Anal. Abstr., 12: No. 2, (Feb. 1965))

19820 ANALYTICAL CHEMISTRY OF TECHNETIUM. A. A. Pozdnyakov (Inst. of Geochemistry and Analytical Chemistry, Academy of Sciences, USSR). Usp. Khim., 34: 300-21(Feb. 1965). (In Russian)

The recently uncovered anticorrosive properties of the pertechnate ion suggest the use of this ion as a corrosion inhibitor for ferrous alloys, specifically protecting components of boiling-water reactors. Metallic Tc and some of its alloys are superconductors at low temperatures and could be used to replace high-purity Nb in inertial guidance

systems. In view of these potential applications, the analytical chemistry of the element becomes important. Techniques are described for separating Tc from irradiated Mo and from U fission products. Methods used for prospecting for Tc in minerals are also discussed, together with separation methods used to remove the element from Re, Mo, and Ru. Precipitation, extraction, and chromatographic methods are reviewed, along with the method based on selective electrolytic reduction and precipitation of Tc on electrodes. For analysis, gravimetric, spectrophotometric, radiometric, spectroscopic, polarographic, mass-spectroscopic, and neutron-activation methods were found to be available. It is recommended that an economical method for concentrating Tc from very dilute solutions containing high concentrations of other salts be developed. Ion-exchange chromatography based on highly basic anion-exchange resins appears to be very promising for this purpose. The extraction method seems to be useful for purifying the element and for carrying out preliminary concentration steps. (Review article, 118 references). (TTT)

19821 DETERMINATION OF CERIUM IN A MIXTURE OF RARE EARTHS BY MEANS OF FILM POLAROGRAPHY. Kh. Z. Brainina and T. A. Rygailo (All Union Research Inst. of Chemical Reagents and Pure Chemicals, USSR). Zavodsk. Lab., 31: 28-30(1965). (In Russian)

The method consisted in the concentration of cerium (IV) hydroxide on graphite electrodes in acetate buffered solutions with subsequent electrodiffusion of the precipitate. The maximum size of the cathode current was proportional to the concentration of Ce(III) ions in solution. The sensitivity of the determination was 4×10^{-5} to 1×10^{-3}%. (tr-auth)

19822 NUCLEAR TECHNIQUES IN ANALYTICAL CHEMISTRY. Alfred J. Moses. A Pergamon Press Book. International Series of Monographs on Analytical Chemistry. Volume 20. New York, The Macmillan Company, 1964. 147p.

Nuclear techniques for increasing sensitivity in analytical methods are discussed. Topics covered include: safe handling of radioactivity, nuclear instrumentation, sources of radiation, radiochemical techniques, measurement of natural radioactivity, principles of activation analysis, neutron activation analysis, positive ion and gamma activation analysis, radiation scattering and absorption, isotope dilution, tracer investigations of analytical techniques, radiometric measurements, exchange reactions, geochronology, cosmochronology, and other nuclear techniques. Neutron activation data are presented in appendixes. (M.C.G.)

19823 URAN–METODY EGO OPREDELENIYA. (Uranium: Methods for Determination). V. K. Markov, E. A. Vernyi, A. V. Vinogradov, S. V. Elinson, A. E. Klygin, and I. V. Moiseev. Moscow, Atomizdat, 1964. 504p.

The analytical chemistry of U treated in detail. Physical and chemical properties of the element are described, its most important ores indicated, and radiological characteristics of the natural and artificial U isotopes discussed. The decay products of the U–Ra family are identified. On the basis of the properties of the element and its compounds, the precipitation, extraction, chromatographic, volumetric, photometric, electrometric, luminescence, and radiometric methods of determination and separation are described. Determination of impurities in U and U compounds and alloys is also discussed. Analytical procedures are given for the following elements that may be present in pure U compounds: N, H, and O (determination of the gases by vacuum melting, titrimetric and colorimetric determination of N); Al (complexometric and photometric determination); Be (photometric and gravimetric method); B (photometric method, curcumin, quinalizarin, and other methods); As and V (titrimetric and photometric methods); W, Nb, P, and Cr (photometric determination); Fe and Co (complexometric and photometric analysis); Si, Mn, and Ta (photometric determination); Mg (photometric and titrimetric methods); Mo (photometric, volumetric, gravimetric, and complexometric methods); Ni (volumetric and photometric methods); Pu (nuclear and chemical properties, recommended working conditions, dissolution processes for materials containing Pu and U, gravimetric, spectrometric, polarographic, and radiometric methods); rare earth elements (separation of U from rare earths and subsequent spectroscopic and roentgenospectroscopic determination); Ti (complexometric and photometric methods); Th (complexometric and photometric analysis); C (microeudiometric and conductometric determination); F (total F in UF_4); and Zr (complexometric and photometric methods). An extensive bibliography is given after each chapter. (TTT)

19824 THERMOGRAVIMETRIC INVESTIGATION OF INORGANIC SALTS OF 5-NITROBARBITURIC ACID. Milton Ward Goheen. Thesis, Seattle, Univ. of Washington, 1964. 83p.

Thermolysis curves for lithium, sodium, and cesium dilituates (5-nitrobarbiturates), for calcium, strontium and barium dilituates, for scandium, yttrium, lanthanum, cerium(III), neodymium, samarium, gadolinium, dysprosium, and erbium dilituates, and for the dilituates of manganese(II), silver, and thorium were obtained. All of the dilituates formed hydrates from aqueous solution except cesium. The dilituates are all quite stable to heat. Manganese(II) dilituate, the least stable dilituate studied, starts to decompose at 225°C. The solubilities of lithium, sodium, rubidium and cesium dilituates and of manganese(II) and thorium dilituates in water were determined. The solubilities of a number of the rare earth dilituates were determined and were found to vary regularly with atomic numbers; consequently the solubilities of rare earth dilituates not determined could be predicted. From the results of the solubilities of the dilituates and of the thermolysis curves, methods for the thermogravimetric determination by precipitation with dilituric acid for rubidium, cesium, calcium, strontium, barium, manganese(II), thorium, yttrium, lanthanum, neodymium, samarium, gadolinium, dysprosium, and erbium were developed. (Dissertation Abstr., 25: No. 5, Nov. 1964)

19825 RADIOMETRIC SENSING OF ATOMIC HYDROGEN IN TRACE QUANTITIES. Richard L. Bersin (Tracerlab, Inc., Richmond, Calif.). 26p. (CONF-654-80)

From American Nuclear Society Meeting, San Francisco, Nov.-Dec. 1964.

This study was undertaken to evaluate a radiometric technique for sensing atomic hydrogen in trace quantities at low pressure, for possible application to upper atmosphere measurements. Radioactive ^{74}As surfaces, which when exposed to trace quantities of atomic hydrogen evolved $^{74}AsH_3$ gas, were used. The technique requires no pretreatment of the sample with the usual associated ionization, decomposition, or recombination to destroy the sample integrity. (auth)

19826 DETERMINATION OF CHLORINE BY INSTRUMENTAL NEUTRON ACTIVATION ANALYSIS. R. A. Johnson and B. E. Gordon (Shell Development Co., Emeryville, Calif.). 21p. (CONF-654-81)

From American Nuclear Society Meeting, San Francisco, Nov.-Dec. 1964.

Instrumental neutron activation analysis was successfully used for determination of chlorine in a wide variety of sample types. Under favorable conditions the standard deviation was 2 to 3%, relative. The limit of detection was 20 to 40 μg chlorine. The selectivity was favored by the relatively high energies of the ^{38}Cl γ rays and by relatively great differences between the half life of ^{38}Cl and the half lives of other activation products with interfering gamma rays. Unusual nuclear properties of chlorine presenting special analytical problems are the high neutron capture cross section and the emission of relatively high energy beta particles. (auth)

19827 THE DETECTION AND ESTIMATION OF SOME TRACE ELEMENTS BY DC ARC EXCITATION USING THE VACUUM CUP TECHNIQUE. Eleanor E. Bevege and Robert E. Gallion (Ultra Carbon Corp., Bay City, Mich.). 14p. (CONF-313-12)

From 2nd National Meeting of the Society for Applied Spectroscopy, San Diego, Calif., Oct. 1963.

The d-c arc excitation of aqueous hydrochloric acid solutions of various elements was studied. Teflon cups of the Zink type were employed. Using the 3089 line of the OH band or gallium as internal standard, boron, mercury, tin, chromium, iron, aluminum, manganese, copper, and zinc in the ppm range were determined. (auth)

19828 THE DETERMINATION OF PHOSPHORUS BY FAST NEUTRON ACTIVATION ANALYSIS. To-on Maen (Agricultural and Mechanical Univ., College Station, Tex.). 124p. (CONF-654-83)

From American Nuclear Society Meeting, San Francisco, Nov.-Dec. 1964.

The determination of phosphorus by fast neutron activation analysis was found to be feasible. The technique utilizes the reaction $^{31}P(n,\alpha)^{28}Al$. The half life of ^{28}Al is 2.3 minutes, and the 1.78-Mev gamma was detected by scintillation spectrometry. Possible interferences are the $^{28}Si(n,p)^{28}Al$ and $^{27}Al(n,\gamma)^{28}Al$ reactions. Interferences of both reactions were studied. The latter reaction can be eliminated by use of cadmium shielding. The former, when the weight ratio Si/P is greater than 0.65%, can only be eliminated by pre-irradiation removal of the silicon. The technique was tested on the following samples: ammonium dihydrogen phosphate, soluble phosphate, lubrication oils, biological materials, mixtures of ammonium dihydrogen phosphate and silicon dioxide, fertilizer, and phosphate rock samples. (auth)

19829 THE MEASUREMENT OF LONG-LIVED ACTIVATION PRODUCTS IN SOIL BY GAMMA SPECTROSCOPY. Herman L. Krieger (Robert A. Taft Sanitary Engineering Center, Cincinnati). 18p. (CONF-642-27)

From Health Physics Society, Cincinnati, June 1964.

Soil samples collected at the site of the 1957 balloon-type nuclear detonation in Nevada were periodically analyzed to determine specific nuclides and to observe changes in spectrum configurations resulting from decay of the shorter lived gamma activities. In 1963, ^{134}Cs, ^{60}Co, ^{152}Eu, and ^{154}Eu were separated by radiochemical analysis and identified by gamma spectrometry. Both manual stripping of the identified nuclides and matrix calculations, in which identical geometric configurations were used, corroborated the presence of these nuclides in the soil sample. Photopeaks of the induced short-lived ^{46}Sc, which were evident in the 1957 spectrum, were not evident in the new gamma scan. No ^{90}Sr, ^{137}Cs, or other fission products were detected; all the nuclides present evidently were produced by neutron activation of their stable precursors. Repeated acid leaching removed only about 70% of the activities of the nuclides present, indicating a very strong attachment of these nuclides to the soil. Estimations of the relative individual activities were calculated by use of computer matrix solutions developed from calibrated standards. (auth)

19830 A COMMENTARY ON THE SPARK SOURCE MASS SPECTROGRAPH. G. G. Cookson, W. Fletcher, and R. Tushingham. 16p. (CONF-721-9)

From 8th Conference on Analytical Chemistry in Nuclear Technology, Gatlinburg, Tenn., Oct. 1964.

The use of spark source mass spectrographs in analyses in atomic energy programs is discussed. Methods of preparing samples are described. Analysis of pure graphite, stainless steels, sodium, uranium, and polyurethane resin are discussed. Methods of comparative analysis, determining gas content of solids, and analysis of rare earths are considered. The precision, expressed as the standard deviation, of analysis was usually between 20 and 30%. (M.C.G.)

19831 DETERMINATION OF HYDROGEN IN ZIRCONIUM ALLOYS BY ISOTOPIC EQUILIBRATION. R. W. Ashley and A. S. Denovan. 9p. (CONF-721-11)

From 8th Conference on Analytical Chemistry in Nuclear Technology, Gatlinburg, Tenn., Oct. 1964.

Determination of hydrogen in zircaloy-2 and titanium by isotopic equilibration methods is discussed. The analyses were carried out using 10-min. equilibration at 800°C. This method was found to be much more efficient than hot vacuum extraction or vacuum fusion when only a few samples were involved and results could be obtained in a shorter time. (M.C.G.)

Inorganic and Physical Chemistry

Refer also to abstracts 19742, 20191, 20258, 20530, 20537, 20538, and 20807.

19832 (CEA-R-2591) PREPARATION D'OXALATE DE BERYLLIUM TRIHYDRATE DE PURETE NUCLEAIRE. (Preparation of Nuclear-Pure Beryllium Oxalate Tri-Hydrate). Michele Delcorte, Alfred Lecocq, and Andre Rigaud (Commissariat à l'Énergie Atomique, Fontenay-aux-Roses (France). Centre de Études Nucléaires). Dec. 1964. 29p. Dep.(mn).

Information is presented which was acquired in the preparation of beryllium oxalate in the first half year of 1962. Bibliographic data are first given, and a description is given of the original process and the production techniques used in the semi-large operative units. Results are presented on the quantities produced and the purity obtained. (D.L.C.)

19833 (CEA-R-2628) REACTIONS D'ECHANGE ENTRE UN SEL FONDU ET UNE SOLUTION DE PHOSPHATE DE TRIBUTYLE DANS UN SILICONE LIQUIDE. (Exchange Reactions Between a Molten Salt and a Solution of Tri-Butyl Phosphate in a Liquid Silicone). Daniel Hertzog (Institut National des Sciences et Techniques Nucléaires, Paris (France) and Commissariat à l'Énergie Atomique, Saclay (France). Centre d'Études Nucléaires). Dec. 1964. 43p. Dep.(mn).

Present interest centered around molten salts can be explained by their possible use in the field of nuclear energy, in particular as a support for fuels and also as reprocessing agents. It seemed of interest to consider the molten salt as a solvent and to study partition phenomena with a second phase stable at high temperatures. The salt chosen is a ternary eutectic of alkali nitrates and the second phase is a solution of tri-butyl phosphate in a liquid silicone. The working temperature is fixed at 150°C, and the stability of the two phases and their mutual solubilities at this temperature were studied. It was shown that the two solvents are immiscible and stable. The extraction by the silicone solution of various products in solution in the salt phase was described, and the partition coefficients and the formulas of the extracted molecules were determined. It was possible to calculate the partition coefficients of the following ions extracted as nitrates: Li^+, Na^+, K^+, Sr^{2+}, Ca^{2+}, Ba^{2+}, Hg^{2+} whose partition coefficients are very low; Mg^{2+}, Ni^{2+}, Co^{2+}, Co^{2+}, Zn^{2+} whose extraction yields are greater than 50 percent; and finally Ce^{3+}, La^{3+}, UO_2^{2+}, highly extracted. Also the following anions have been extracted in the form of alkali salts: F^-, Cl^-, Br^-, I^-, IO_3^-, CN^-, $SO_4^=$, $C_2O_4^=$, NO_2^-. Amongst these, only the halogens have non-negligible partition coefficients. In certain particular cases, the influence of complex formation on the extraction phenomena was studied. Two applications are described: The separation of two products by complex formation and extraction (separation of magnesium from cobalt, nickel, and zinc), and the calculation of the equilibrium constant of a complex by measurement of the variation in the partition coefficient of the ion complexed. The equilibrium constants for the reactions: (I) $Co^{2+} + CN^- \rightarrow CoCN^+$; (II) $Co^{2+} + Cl^- \rightarrow CoCl^+$ were determined: $K_1 = 10^{-4}$, $K_2 = 0.16$. (auth)

19834 (HW-74393) A 709/7090 PROGRAM FOR INDEXING X-RAY DIFFRACTION POWDER PATTERNS. I. THE CUBIC CASE. J. B. Goebel and A. S. Wilson (General Electric Co., Richland, Wash. Hanford Atomic Products Operation). July 12, 1962. Contract AT(45-1)-1350. 19p. Dep.(mn); $1.00(cy), 1(mn) CFSTI.

A set of two theta reflections where theta is the Bragg angle, as measured by a diffractometer from powdered crystalline samples, is used as input data for the program. The program indexes the set of reflections on the basis of a cubic system. The least squares method is used to de-

termine an $\mathring{A} = (\lambda^2/4a_0^2)$, where a_0 is the lattice constant and λ the x-ray wave length. The program prints $\mathring{A}$, the lattice constant a_0 in Angström's, the observed 2Θ's, and the corresponding $\sin^2\Theta$'s calculated from the assigned Miller indices using the calculated $\mathring{A}$. The difference between the observed and calculated $\sin^2\Theta$'s and an error term, E, are also printed. The value of E indicates to the crystallographer the validity of the cubic indexing. (auth)

19835 (HW-89062) A 709/7090 PROGRAM FOR INDEXING X-RAY DIFFRACTION POWDER PATTERNS. III. THE ORTHORHOMBIC CASE. J. B. Goebel and A. S. Wilson (General Electric Co., Richland, Wash. Hanford Atomic Products Operation). June 2, 1964. Contract AT (45-1)-1350. 48p. Dep.(mn); $2.00(cy), 2(mn) CFSTI.

Input data for the program are the 2Θ reflections where Θ is the Bragg angle as measured by a diffractometer from powdered crystalline samples. The program indexes the set of reflections on the basis of the orthorhombic system then calculates all lattice constants by the method of least squares. The printed output includes the lattice constants and their standard deviations, the observed and calculated $\sin^2\Theta$ values, and the difference between the latter two. An error term, E, is also printed. The value of E and the standard deviations indicate to the crystallographer the validity of the indexing. The miller indices, hkl, are printed in the form h^2, k^2, and l^2. (auth)

19836 (HW-SA-3476) RATE AND FORMATION CONSTANTS FROM OXIDATION-REDUCTION REACTION DATA. J. C. Sheppard (General Electric Co., Richland, Wash. Hanford Atomic Products Operation). May 4, 1964. Contract AT(45-1)-1350. 6p. (CONF-606-5). Dep.(mn); $1.00(cy), 1(mn) CFSTI.

From American Chemical Society Northwest Regional Meeting, Spokane, Wash., June 1964.

It is shown that for many anion-catalyzed redox reactions, the data can be used to calculate formation as well as rate constants, if only one of the reactants is complexed and the rate equation is $k_0[N][M] + k_1[N][MA] + k_2[N][MA_2] +$ ---. Calculations were made using the Yatsimirskii-Budarin equation for several redox equations, and the results are compared with experimental results. (D.L.C.)

19837 (IA-1000) ION EXCHANGE STUDIES OF COMPLEX FORMATION. Y. Marcus (Israel Atomic Energy Commission, Yavne. Soreq Nuclear Research Establishment). Oct. 1964. 57p. Dep.(mn).

The well-established cation exchange method of studying complex formation in solution was carefully analyzed. The importance of considering the sorption of cationic complexes is discussed. Stoichiometric methods, such as equivalent accounting, seem to be of little value, because of the many restrictions required. The applicability of anion exchange methods at high ligand concentrations is discussed in detail, and the effects of variables such as the crosslinking of the resin and acidity in solution are analyzed. Many outstanding problems pertaining to this method are outlined. Some other applications of ion exchangers to the study of metal complexes, such as cases involving uncharged ligands or complexing with resin functional groups, are briefly discussed. 133 references are included. (auth)

19838 (IS-1070) APPLICATION OF AN ADIABATIC CALORIMETER TO THE DETERMINATION OF THE HEATS OF FUSION AND HEATS OF FORMATION OF SEVERAL METALLIC COMPOUNDS. Gerald J. Gartner and Premo Chiotti (Ames Lab., Iowa State Univ. of Science and Tech.). Feb. 1965. Contract W-7405-eng-82. 71p. Dep.; $3.00 (cy), 2(mn) CFSTI.

The general operating principles of a commercial adiabatic calorimeter are summarized; its application to the measurement of heats of fusion and transformation of materials, and heats of formation of intermetallic phases is described. The results of the heat of formation experiments are: $MgZn_2$ @ 863°K, −4.30 kcal/g-atom; $CaMg_2$ @ 532°K, −3.12 kcal/g-atom; and CeZn @ 623°K, −10.6 kcal/g-atom. The results of the heat of fusion of the materials are: $MgZn_2$, 9.687 kcal/mole; $CaMg_2$, 11.744 kcal/mole; CeZn, 7.826 kcal/mole. The average values for the heats of fusion are accurate to ±2%. (P.C.H.)

19839 (K-1627) KINETICS AND MECHANISM OF THE FLUORINATION OF COPPER(I) OXIDE AND COPPER(II) OXIDE. Robert Lucien Ritter (Oak Ridge Gaseous Diffusion Plant, Tenn.). Mar. 29, 1965. Contract W-7405-eng-26. 247p. Dep.; $6.00(cy), 5(mn) CFSTI.

The reaction rates were measured gravimetrically, using a continuously recording totally enclosed thermobalance. The oxide samples employed were relatively high surface area powders whose particles could be closely approximated by a spherical geometry. A series of five copper(I) oxide samples, with specific surface areas ranging from 6.5 to 29.3 square meters per gram, and a series of three copper(II) oxide samples, with specific surface areas of 11.8, 18.6, and 25.8 square meters per gram, were investigated. The reaction of fluorine with copper(II) oxide was found to take place by a diffusion-controlled mechanism at temperatures between 82 and 151°C and at fluorine pressures between 40 and 80 mm Hg. The data obeyed the kinetic law given by the equation $(-dN_R/dt) = (k_p 4\pi r_R r_T/r_T - r_R)$, where N_R is the moles of solid reactant, t is the time, k_p is the rate constant, r_R is the radius of the solid reactant particle, r_T is the total radius of the solid particle, and $r_T - r_R$ is the thickness of the film of copper(II) fluoride. The activation energy for the reaction was 16.3 kilocalories per mole. In the pressure range investigated, the reaction rate was proportional to the square root of the fluorine pressure. The reaction of fluorine with copper(I) oxide was found to occur through a two-step mechanism given by the reactions $Cu_2O + F_2 \rightarrow CuF_2 + CuO$ and $CuO + F_2 \rightarrow CuF_2 + \frac{1}{2} O_2$. Using a graphical method of data analysis, it was shown that the initial reaction in this two-step mechanism probably exhibits linear reaction kinetics in the temperature range of 152 to 207°C and at fluorine pressures between 50 and 800 mm Hg. The activation energy for the reaction was 19.7 kilocalories per mole. In the pressure range investigated, the reaction rate was proportional to the 0.63 power of the fluorine pressure. Possible reaction mechanisms are presented to explain the observed pressure dependence of the reaction rate for copper(I) and (II) oxides. (D.L.C.)

19840 (LA-3250) THE COMPRESSIBILITY OF GASEOUS MIXTURES OF HELIUM–NITROGEN AND HELIUM–DEUTERIUM AT HIGH PRESSURES. James D. Cramer (Los Alamos Scientific Lab., Univ. of California, N. Mex.). Feb. 15, 1965. Contract W-7405-eng-36. 21p. Dep.; $2.00(cy), 1(mn) CFSTI.

The compressibilities of gaseous mixtures of helium-nitrogen and helium-deuterium were determined in the pressure range from 100 to 1400 atm. at 25°C. The compressibility of pure helium was also determined in the same pressure range at 25°C. The experimental data are fitted to a four-term virial equation by the method of least squares, and the resulting virial coefficients are listed. Some of the experimental compressibility factors were then compared with the corresponding compressibility factors determined by an additive volume method. (auth)

19841 (MIT-1965-18) THERMODYNAMIC, SPECTRAL AND STRUCTURAL STUDIES OF COMPLEX IONS. Annual Report, September 16, 1964–September 14, 1965. (Massachusetts Inst. of Tech., Cambridge). Mar. 31, 1965. Contract AT(30-1)-1965. 17p. Dep.(mn); $1.00(cy), 1(mn) CFSTI.

Developments in research on the nature of Rh(III) chloride, compounds containing both Re_3Br_9 and $ReBr_3^{2-}$, structure of the $(Re_2Cl_8)^{3-}$ ion, structure of the $(Tc_2Cl_8)^{3-}$ ion, monomeric Re(III) complexes, binuclear Re(III) species, and the $(Mo_6Cl_{14})^{2-}$ ion are reported. (P.C.H.)

19842 (NASA-SP-3014) EQUILIBRIUM THERMODYNAMIC PROPERTIES OF CARBON DIOXIDE. Harry E. Bailey (Ames Research Center, National Aeronautics and Space Administration, Moffett Field, Calif.). 1965. 68p. $3.00(CFSTI).

Entropy, enthalpy, pressure, and speed of sound of carbon dioxide computed for wide ranges of temperature and density are presented graphically. The temperature range is $250°K \leq T \leq 25,000°K$ ($\Delta T = 250°K$). The density range is $-7.0 \leq \log \rho/\rho_0 \leq +3.0$ ($\Delta \log \rho/\rho_0 = 0.2$). (auth)

19843 (ORNL-TM-1071) HIGH-PURITY POTASSIUM CHLORIDE. R. B. Quincy, Jr., and D. E. LaValle (Oak Ridge National Lab., Tenn.). Mar. 1965. Contract W-7405-eng-26. 16p. Dep.(mn); $1.00(cy), 1(mn) CFSTI.

The preparation of high-purity potassium chloride is described. Reagent grade starting material is recrystallized once, redissolved, and the solution extracted with a solution of thenoyltrifluoroacetone (TTA) in 4-methyl-2-pentanone (hexone). The potassium chloride is recovered by crystallization, dried, and fused in a quartz filtration tube. A mixture of chlorine and hydrogen chloride gases is passed upward through the melt which is finally filtered and collected in an attached bulb cooled with Dry Ice. The total impurities remaining after these treatments are of the order of 25 ppm. (auth)

19844 (PAN-550/XVII) THEORETICAL INVESTIGATION OF THE OXYGEN HYDRIDES BY USING THE UNITED ATOM METHOD. Krzysztof Pecul (Polish Academy of Sciences, Warsaw. Inst. of Nuclear Research). July 1964. 29p. Dep.

The energies and one-center single determinant wave functions of OH_M^p oxygen hydrides and of some isoelectronic systems were calculated. Orthonormalized Slater type orbitals were employed. It was found that they give more accurate energies and bond lengths than the Fock-Petrashen type orbitals. Using semi-empirical corrections, OH bond lengths for OH^-, H_3O^+, and H_3O^+ were estimated. The accuracy of the approximations and the possibilities of further applications of the model are discussed. (auth)

19845 (UCRL-11828(p.146)) THE CRYSTAL STRUCTURE OF CESIUM AQUOPENTACHLORORUTHENATE. Ted E. Hopkins, Allan Zalkin, David H. Templeton, and Martyn G. Adamson (Lawrence Radiation Lab., Univ. of California, Berkeley).

The unit cell contains four formula units of $Cs_2RuCl_5H_2O$ and is face-centered orthorhombic with a = 7.986 A, b = 17.289 A, c = 7.400 A, D_x = 3.65 g/cm^3, and space group = Amam. Cs–Ru and Ru–Cl vectors were identified in the three-dimensional Patterson function. Bond angles, distances, and packing are illustrated. (D.L.C.)

19846 (UCRL-11828(p.158-9)) THE CRYSTAL STRUCTURE OF OSMIUM TETROXIDE. Tatzuo Ueki, Allan Zalkin, and David H. Templeton (Lawrence Radiation Lab., Univ. of California, Berkeley).

The complete crystal structure of OsO_4 was established with new data on the oxygen positions. The space group is C 2/c, with a = 9.379 A, b = 4.515 A, c = 8.632 A, β = 116.6°, and V = 330.7 A^3. The bond distances and packing are described. Atomic coordinates are tabulated. (D.L.C.)

19847 (UCRL-11828(p.182-3)) A STUDY ON THE STABILITY OF XENON TRIOXIDE IN BASIC SOLUTIONS. Charles W. Koch and Stanley M. Williamson (Lawrence Radiation Lab., Univ. of California, Berkeley).

A study was made of the stoichiometry of the reaction between XeO_3 and KOH in solution. The results show that the reaction is more complex than the simple disproportionation of XeO_3 followed by decomposition of Xe(IV). A 25 to 33% yield of perxenate is obtained for 0.3 to 3 M KOH, and the evolved O_2/Xe is greater than unity. As the decomposition progresses, a yellow, insoluble, explosive compound is formed. In one experiment, when the solution was reduced by vacuum distillation, $K_4XeO_6 \cdot 9H_2O$ was formed. (D.L.C.)

19848 (UCRL-11828(p.193-7)) MOLECULAR BEAM ELECTRIC RESONANCE EXPERIMENTS ON LiF, LiCl, LiBr, LiI, AND NaF. Alvin J. Hebert, Troy L. Story, Jr., Francis W. Breivogel, Jr., Craig D. Hollowell, and Kenneth Street, Jr. (Lawrence Radiation Lab., Univ. of California, Berkeley).

The molecular beam electric resonance method was used to study the molecular properties of $^6Li^{19}F$, $^7Li^{19}F$, $^6Li^{35}Cl$, $^6Li^{37}Cl$, $^6Li^{79}Br$, $^6Li^{81}Br$, $^7Li^{79}Br$, $^6Li^{127}I$, and $^{23}Na^{19}F$. Values are reported for rotational constants, dipole moments, quadrupole coupling constants, and spin-rotation and spin-spin interaction constants of molecules in different vibration states and in low rotational states. (D.L.C.)

19849 (WAPD-T-1760) THE RAMAN SPECTRUM OF ZIRCONIUM OXIDE. C. J. Emert and S. Milani (Bettis Atomic Power Lab., Pittsburgh, Pa.). Feb. 1965. Contract AT-11-1-GEN-14. 7p. Dep.(mn); $1.00(cy), 1(mn) CFSTI.

The Raman spectrum of ZrO_2 was measured in the Stokes region to 5000 cm^{-1} displacement. Raman lines were observed at 340, 384, 477, 559, 618, and 642 cm^{-1}. Very weak lines detected at 748, 1013, and 1352 cm^{-1} are probably combinational levels. Only the 477 cm^{-1} anti-Stokes line could be reliably detected. Upon an increase in sample temperature the peak intensity of this line was reduced and the line appeared considerably broadened. (auth)

19850 (NP-tr-1230) INVESTIGATION OF THE DECOMPOSITION POTENTIAL OF THE SYSTEM K_2ZrF_6–NaCl–KCl. I. N. Sheiko and V. G. Feshchenko. Translated by E. B. Uvarov (Atomic Energy Research Establishment, Harwell (England)), from Ukr. Khim. Zh., 25: 166-72(1959). (Includes original, 3p.). Dep.(mn); $1.00(cy), 1(mn) CFSTI; $1.60(fs), $0.80(mf) JCL.

The decomposition potentials, polarization back-emf, and cathode potentials were investigated in fused potassium fluozirconate and in the system K_2ZrF_6–KCl–NaCl in relation to the temperature, the gas over the melt in the cathode space, and the K_2ZrF_6 concentration. Three decomposition potentials were found for electrolysis of fused potassium fluozirconate: the first corresponds to electrolytic reduction of the zirconium salt to the lowest valency state, the second to liberation of metallic zirconium at the cathode, and the third to decomposition of potassium fluoride and liberation of metallic potassium at the cathode. The lowest decomposition potentials were found with air in the cathode space over the melt, and the highest were obtained in argon. Under constant measurement conditions, the decomposition potentials showed good reproducibility. Data are tabulated. (C.H.)

19851 (ORNL-tr-491) DIELECTRIC LOSSES IN OXIDES AND HALIDE COMPOUNDS OF GROUP II ELEMENTS. A. A. Vorobev and A. P. Nakhodova. Translated by A. L. Monks (Oak Ridge National Lab., Tenn.), from Izv. Tomsk. Politekhn. Inst., 95: 306-13(1958). 10p. Dep.(mn); $1.00 (cy), 1(mn) CFSTI; $1.10(fs), $0.80(mf) JCL.

The temperature and frequency dependence of tg δ of BeO, MgO, CaO, SrO, BaO, CaF_2, SrF_2, BaF_2, $CaCl_2$, $SrCl_2$, and $BaCl_2$ was determined at 25 to 480°C in vacuum. It is concluded that the angle of dielectric loss at 25°C in vacuum is relatively small, the dielectric loss is greater in air than in vacuum, the tangent is inversely proportional to the frequency, and the losses increase with temperature for samples of 65 to 70% density. A temperature maximum was observed for samples with a high density. (D.L.C.)

19852 THE CRYSTAL STRUCTURE OF DOUBLE NITRATE OCTAHYDRATES OF THORIUM AND BIVALENT METALS. S. Scavnicar and B. Prodic (Faculty of Science, Zagreb and Institute "Rudjer Boskovic," Zagreb). Acta Cryst., 18: 698-702(Apr. 10, 1965).

The x-ray crystal structure analysis of magnesium thorium nitrate hydrate, previously given the formula $MgTh(NO_3)_6 \cdot 8H_2O$, showed that the compound (in the crystal state) is hexa-aquomagnesium hexa-nitratothorate dihydrate, $Mg(H_2O)_6 \cdot Th(NO_3)_6 \cdot 2H_2O$. It is a monoclinic holohedral with the space group $P2_1/c(C_{2h}^5)$. The unit cell, with a = 9.08, b = 8.75, and c = 13.61 Å and β = 97°, contains two formula units. The coordinates of all atoms (except hydrogen) were obtained by means of Patterson projections and Fourier and difference Fourier syntheses along [010] and [100]. The crystal structure contains two types of polyhedra around thorium and magnesium atoms (both at the centers of symmetry). Each thorium atom is surrounded by twelve oxygen atoms, which belong to six nitrate ions. The average Th–O distance is 2.63 Å. These oxygen atoms are at the corners of an irregular icosahedron. Each magnesium atom is octahedrally surrounded by six water molecules; the average Mg–O distance is 2.12 Å. The connection between the polyhedra themselves as well as the polyhedra and the remaining (one quarter) isolated water molecules is realized through the weak hydrogen bonds. A series of compounds of general formula $M^{II}Th(NO_3)_6 \cdot 8H_2O$ (M^{II} = Zn,

Co, Ni, Mn) is isomorphously related to the described magnesium thorium nitrate hydrate. (auth)

19853 LUMINESCENCE. PROCEEDINGS OF THE INTERNATIONAL CONFERENCE ON LUMINESCENCE HELD AT TORUN, SEPTEMBER 1963. Acta Phys. Polon., 26: 311-893(Sept.-Oct. 1964). (CONF-630907)

Proceedings of the International Conference on Luminescence are presented. Seventy-five papers and 15 abstracts of papers are included. Separate abstracts were prepared for eight papers. Two papers were previously abstracted for NSA and appeared as abstracts 17: 8115 and 18: 23580. (M.C.G.)

For abstracts of individual papers see: 19854, 19855, 19962, 19963, 19964, 19965, 19966, and 19967.

19854 LUMINESCENCE OF TRI- AND BIVALENT IONS OF THE RARE EARTHS IN CRYSTALS OF FLUORITE TYPE. P. P. Feofilov (Academy of Sciences, Leningrad). Acta Phys. Polon., 26: 331-43(Sept.-Oct. 1964). (In Russian)

A survey was made of the spectral-luminescence characteristics of alkaline earth fluoride crystals, MeF_2, where Me = Ca, Sr, and Ba (crystallized into fluoride type cubic system), activated by rare earths as di- and trivalent luminophors with characteristic spectra. Physicochemical conditions of the appearance of luminescence centers, structure of activated centers, luminophor energy levels, and excitation processes were analyzed. The lowest excitation therms of the isoelectron ions TR^{2+} and TR^{3+} were tabulated. It is shown that the divalent Sm, Eu, and Yb ions influence the optical (absorption and luminescence) properties of natural fluorites. The observed green coloring of the fluorite is provided by the presence of Sm^{2+}. The presence of formerly unknown divalent Dy, Ho, Er, and Tm and the data on Nd^{2+} suggested that certain colorings in the natural fluorite are related to the presence of these ions. (R.V.J.)

19855 NUCLEAR RESONANCE ABSORPTION AND PROPERTIES OF THE LUMINESCENCE OF Fe^{57} IN ZnS-PHOSPHORS. K. Luchner and J. Dietl (Technische Universitat, Munich). Acta Phys. Polon., 26: 697-701 (Sept.-Oct. 1964).

The spectrum of nuclear resonance absorption of the 14.4-kev γ line of ^{57}Fe, incorporated in various ZnS phosphors was observed. It was found, that iron can be incorporated as a trivalent ion at two different lattice sites. At a firing temperature of about 600°C iron incorporation at a regular lattice site prevailed; after firing at around 900°C, however, the iron was mostly found at lattice sites characterized by an electric field gradient, as could be seen from quadrupole-splitting. Both these states of iron could be assigned to two well-known luminescent properties of iron. The quenching action of iron could be explained by the following model: A Fe^{3+} ion sits at a Zn^{2+} site, in the next neighborhood of a luminescence center. The polarization of the lattice in the vicinity of a luminescence center allowed this constitution to be formed only at a relatively high temperature (900°C). The order of magnitude of the measured electric field gradient could only be explained by a lattice vacancy (one charge missing, luminescence center in the next neighborhood of the Fe^{3+}). This model was supported by a strong dependence of the luminescence band width on the concentration of iron in the state reached by firing around 900°C (no dependence after firing around 600°C). The non-radiative transition within this center could take place via a double Franck-Condon-Process. This process is possible only if an electron, trapped at Fe^{3+}, finds a hole to recombine with before the binding energy of the electron is dissipated. This hole is available in the proposed model: during excitation it is trapped at the luminescence center in the vicinity of Fe^{3+}. (auth)

19856 A KINETIC STUDY OF THE ISOTOPIC EXCHANGE OF THALLIUM(III) BETWEEN THE THALLIUM-(III) ION AND THE THALLIUM N-2-HYDROXYETHYL-ETHYLENEDIAMINE-N,N',N'-TRIACETATE COMPLEX IN WATER. Michiko Tsuchimoto (Tokyo Univ.). Bull. Chem. Soc. Japan, 38: 478-85(Mar. 1965).

The kinetics of the isotopic exchange of the thallium(III) EDTA-OH complex with uncomplexed thallium(III) was studied in acid, neutral, and weakly basic solutions, with ^{204}Tl as tracer. The exchange rate was independent of the concentration of uncomplexed thallium and proportional to that of the EDTA-OH complex, giving the relationship $R = k \cdot b$ under appropriate conditions throughout the pH range. In a basic solution buffered by ammonia or barbiturate, the k was proportional to $[OH^-]$ and [TEA] and was little affected by the concentration of buffers. The Arrhenius activation energy was 29 kcal/mole. In a neutral solution, near pH 7, the rate was small but measurable. It was independent of the pH value but proportional to the concentration of TEA, and it was little affected by the concentration of barbiturate. The activation energy was 22 kcal/mole. In an acid solution buffered by acetate, the k was proportional to $[H^+]$, and $[Cl^-]^{1.5}$ and was little influenced by the concentration of acetate. The Arrhenius activation energy was 11 kcal/mole. The features of the isotopic exchange of the thallium EDTA-OH complex were very similar to those of the thallium(III) EDTA complex. (auth)

19857 RADIOCRYSTALLOGRAPHIC ANALYSIS OF SULFATES OF CERIUM NONAHYDRATE $[Ce_2(SO_4)_3 \cdot 9H_2O]$ AND OCTAHYDRATE $[Ce_2(SO_4)_3 \cdot 8H_2O]$. Guy Pannetier and Andre Dereigne (Universite, Paris). Bull. Soc. Chim. France, No. 1, 102-8(Jan. 1965). (In French)

X-ray diffraction on powder and monocrystals of cerium sulfates with 9 and 8 water molecules made it possible to determine special systems, parameters, and groups: $Ce_2(SO_4)_3 \cdot 9H_2O$, a hexagonal system with $\underline{a}$ = 11.08 and $\underline{c}$ = 8.08 Å and P $6_3/m$: C_{3h}^2 and $Ce_2(SO_4)_3 \cdot 8H_2O$, with $\underline{a}$ = 9.92$_8$, $\underline{b}$ = 9.51$_3$, and $\underline{c}$ = 17.32$_9$ Å and Cmca : D_{2h}^{19}. (tr-auth)

19858 MECHANISM OF HYDROLYSIS OF THE URANYL ION. Yigal Julius Israeli (Universite Hebraique, Jerusalem). Bull. Soc. Chim. France, No. 1, 193-6(Jan. 1965). (In French)

The hydrolysis of the uranyl ion is produced in several steps. The equilibrium constants relative to the following reactions were determined: $2\ UO_2^{2+} + 2\ OH^- \rightarrow (UO_2OH)_2^{2+}$, $(UO_2OH)_2^{2+} \rightarrow 2\ UO_4H_2$, $2\ UO_4H_2 + (UO_2OH)_2^{2+} \rightarrow U_4O_9(OH)_2^{2+}$, $U_4O_9(OH)_2^{2+} + 2\ OH^- \rightarrow 4\ UO_4H_2$, $UO_4H_2 + OH^- \rightarrow UO_4H^- + H_2O$, and $2\ UO_4H_2 + 2\ OH^- \rightarrow U_2O_7^{2-} + 3\ H_2O$. It is shown that these reactions can explain the products obtained by precipitation as well as the spectroscopic curves. (tr-auth)

19859 ULTRAVIOLET AND VISIBLE SPECTRA OF THE URANYL ION. Yigal Julius Israeli (Universite Hebraique, Jerusalem). Bull. Soc. Chim. France, No. 1, 196-9(Jan. 1965). (In French)

Seven maxima were observed in the spectrum of the uranyl ion and all these transitions were produced by electron charge transfer of the Π_g orbital located on the two oxygen atoms at the f orbitals located principally on U(VI). The first three maxima observed at 22100, 24200, and 28000 cm^{-1} were produced by the singlet-triplet transition $^1\Sigma_g^+ \rightarrow {}^3\Pi_u$. The fourth maximum, observed at 29000 cm^{-1}, was produced by the transition $^1\Sigma_g^+ \rightarrow {}^1\Delta_u$, which was made possible by the Π_u vibration. The other three maxima were characterized by the following transitions: 34500 cm^{-1}, $^1\Sigma_g^+ \rightarrow {}^1\Pi_u$; 42600 cm^{-1}, $^1\Sigma_g^+ \rightarrow {}^1\Sigma_u^+$; and 53000 cm^{-1}, $^1\Sigma_g^+ \rightarrow {}^1\Pi_u$. The maximum at 24200 cm^{-1} was split into two maxima when $U_2O_4(OH)_3^+$ was dimerized and the phenomenon can be explained by the theory of molecular excitons. (tr-auth)

19860 COMPLEX OF URANIC ACID WITH MONOSODIUM DIMETHYLGLYOXIME. Yigal Julius Israeli (Universite Hebraique, Jerusalem). Bull. Soc. Chim. France, No. 1, 199-201(Jan. 1965). (In French)

Uranic acid H_2UO_4 forms with monosodium dimethyl glyoxime (HA) a complex whose formula is $(HA)H_2UO_4$. The formation constant of this complex, 2.7×10^3, was determined by spectrophotometry. In the hydroxyl derivatives, the coordination number of U(VI) is six. (tr-auth)

19861 INFLUENCE OF CONDITIONS OF PRECIPITATION OF A SALT ON THE TEXTURE OF ITS THERMAL DECOMPOSITION PRODUCT. CASE OF THORIUM OXALATE. Michele Breysse, Bernard Claudel, and Yves

Trambouze (Institut de Recherches sur la Catalyse, Villeurbanne, France). Bull. Soc. Chim. France, No. 1, 201-4 (Jan. 1965). (In French)

The different factors affecting the size of the crystals of thorium oxalate precipitated from nitrate solutions were studied. The study of the texture of the thoria obtained by calcination of the oxalate led to the conclusion that the oxide has a larger specific area when the oxalate crystals have larger dimensions. (tr-auth)

19862 CRYSTALLOGRAPHIC STUDY OF SULFIDES OF RARE EARTHS AND SODIUM. R. Ballestracci and E.-F. Bertaut (Centre d'Etudes Nucleaires, Grenoble, France). Bull. Soc. Franc. Mineral. Crist., 87: 512-17 (Oct.-Dec. 1964). (In French)

Two categories of sulfides of rare earths and sodium are described. In the two cases, the rare earth (T) and the Na ion have the coordination six. The first category contains the rare earths T = La, Ce, Pr, and Nd. The structure can be considered as the NaCl type, with lacuna, and disordered. The S anions form a compact cubic lattice while the cations occupy at random the sites of the Na in the same fashion as in $BiNaS_2$. In the second category, containing the rare earths T = Nd, Sm, Eu, Gd, Tb, Dy, Ho, Er, and Y, the structure is rhombohedric deformed, but still belonging to the NaCl type. The space group is R $\bar{3}$m- (D^5_{3d}). In the compact, almost cubic lattice of the anions S at c, the cations T occupy the sites a and the cations Na the sites b, forming thus a structure type of the formula $TNaS_2$ analogous to that of $CrNaS_2$. (tr-auth)

19863 LUMINESCENCE OF URANYL IONS DISSOLVED IN WATER AND GLYCEROL WATER MIXTURES AT LOW TEMPERATURES. Sohachiro Hayakawa, Masao Hirata, Shigeo Kobayashi, and Tokihisa Nakamura. Bull. Tokyo Inst. Technol., No. 54, 19-30(1963).

Fluorescence spectra of uranyl ions embedded in some host substances consist of narrow bands characteristic of the uranyl ion and its vibration modes, which are affected by the surroundings. The spectra in water and water-glycerol mixtures were observed at the temperature range from −190 to 0°C. Their fine structures depended on the temperature, the concentration of uranyl ion, and the constitution of solvent. The solid state of host substance is thought to affect the spectra. The dielectric property was also measured in the same range of temperature. The frequency of the applied field was changed between 120 c/sec and 10 kc/sec. Some relation between the luminescent and dielectric properties was observed. (auth)

19864 DISTRIBUTION OF DEUTERIUM BETWEEN WATER AND ANION EXCHANGER. I. THE SYSTEM OF WATER—HIGH MOLECULAR WEIGHT TERTIARY AMINES. Hiroshi Fukutomi, Takashi Kojima, and Hidetake Kakihana. Bull. Tokyo Inst. Technol., No. 54, 81-92(1963).

The distribution of deuterium was measured by equilibrating amine salts of tri-n-octylamine and n-benzyldilaurylamine with water containing deuterium at 25°C. The separation factors of hydrogen isotopes in the system are evaluated and interpreted on the basis of equilibria of deuterium exchange reaction between amine and water phases. (auth)

19865 DISTRIBUTION OF DEUTERIUM BETWEEN WATER AND ANION EXCHANGER. II. THE SYSTEM OF WATER—ANION EXCHANGE RESIGN. Hiroshi Fukutomi, Takashi Kojima, and Hidetake Kakihana. Bull. Tokyo Inst. Technol., No. 54, 93-7(1963).

The distribution of deuterium was investigated by equilibrating an anion exchange resin with water containing deuterium at 25°C. The separation factors of hydrogen isotopes in the system were evaluated and discussed on the basis of deuterium exchange reaction between anion exchange resin and water phases. (auth)

19866 ON TWO KINDS OF ZIRCONIUM CARBIDE. Hiroshige Suzuki, Shiushichi Kimura, and Takuo Hozaka. Bull. Tokyo Inst. Technol., No. 54, 159-61(1963).

Problems encountered in the synthesis of zirconium carbide are discussed. From a mixture of zirconium oxide and graphite, zirconium carbide was formed. By changing the ratio of Zr/C in the mixture, two kinds of zirconium carbide could be formed. Examinations are being made to determine whether they are the compounds or belong to solid solutions. (auth)

19867 FLUIDIZED-BED CONVERSION OF URANIUM OXIDE FUEL TO URANIUM HEXAFLUORIDE. R. Heremans and J. Schmets (Centre d'Etude de l'Energie Nucleaire, Mol-Donk, Belg.). Chem. Eng. Progr., Symp. Ser., 60: No. 47, 90-5(1964). (BLG-287)

The conversion of ceramic nuclear fuels, especially uranium dioxide, into uranium hexafluoride is discussed. The equipment used and the operations performed on laboratory pilot plant scale are described. (auth)

19868 PROBLEMS OF CHEMICAL ENGINEERING IN HIGH TEMPERATURE TECHNOLOGY. Leopoldo Massimilla and Massimo Diana (Universita, Naples). Chim. Ind. (Milan), 46: 929-38(Aug. 1964). (In Italian)

Studies are being made on phenomena taking place in systems at temperatures from 5,000 to 30,000°C by the methods of chemical engineering. Developments in the field of high-temperature systems are reviewed, with special reference to the study of thermodynamic equilibrium conditions in ionized gases to the definition of their transport properties, and to the design and operation of plasma reactors. (auth)

19869 CHEMICAL DIFFUSION IN THE PLUTONIUM–URANIUM SYSTEM. Michel Dupuy and Daniel Calais. Compt. Rend., 260: 1412-15(Feb. 1, 1965). (In French)

The chemical diffusion coefficients D relative to the U–Pu system obeyed the Arrhenius law $D = D_0e^{-Q/RT}$ for Pu concentrations below 17.5% and at temperatures from 400 to 540°C. D_0, the factor of frequency, varied from 0.15 to 2.5×10^{-7} cm^2sec^{-1}, and Q, the energy of activation, varied from 13 to 20 kcal/mole. (tr-auth)

19870 PRECIPITATION AND HYDROLYSIS OF URANIUM(VI) IN AQUEOUS SOLUTIONS. II. URANYL NITRATE–SODIUM CARBONATE–ALKALINE EARTH CHLORIDES. H. Fueredi and B. Tezak (Institut "Rudjer Boskovic", Zagreb). Croat. Chem. Acta, 36: 119-31(1964).

The precipitation systems of uranyl nitrate (2×10^{-3}N) with sodium carbonate and Me chlorides (Me = Ba, Sr, Ca, and Mg) were investigated and compared. The corresponding precipitation diagrams were constructed by plotting the percentage of uranium precipitated as a function of the concentrations of sodium carbonate and alkaline earth chloride. Solid phase formation started in all systems at sodium carbonate concentration of 1.6×10^{-3}N and pH ~ 5, when a critical concentration of the particular alkaline earth chloride, necessary for precipitation, was exceeded. A precipitation maximum with more than 80% of uranium precipitated occurred at 3×10^{-3}N of sodium carbonate and pH ~ 6. At high concentrations of both sodium carbonate and alkaline earth chloride uranium was coprecipitated with the corresponding alkaline earth carbonate. The coprecipitation regions were shifted to higher concentrations of the precipitating components in the normal order of alkaline earth ions. A region with less than 15% of uranium precipitated separated the regions of precipitation and coprecipitation of uranium in the presence of strontium, calcium, and magnesium chloride. With barium chloride in solution, this minimum was replaced by a transitional precipitation region with 55 to 95% of uranium precipitated. When sodium carbonate was present in concentrations higher than the concentrations of soluble alkaline earth chloride complex, uranyl carbonates prevailed in all systems. (auth)

19871 THE PREPARATION AND CRYSTAL STRUCTURE OF SOME TERNARY SILICIDES CONTAINING URANIUM AND TRANSITION METALS. Z. Ban and M. Sikirica (Institut "Rudjer Boskovic", Zagreb). Croat. Chem. Acta, 36: 143-9(1964).

Compounds of the general composition $U_4M_5Si_3$ (M = Mo, Cr, Mn, and Fe) were prepared in an electron-beam melting apparatus. Mixtures of corresponding elements were hydrogenated in order to secure good mixing before pressing the specimens for melting. The x-ray-powder-diffraction method yielded C14($MgZn_2$) type structure with a

statistical distribution of both kinds of smaller atoms. The space group is P 6/mmc (D_{6h}^1) and the unit cells contain one formula unit. The a and c dimensions are: for Mo: 5.370, 8.582; for Cr: 5.199, 8.098; for Mn: 5.158, 7.972; and for Fe: 5.142, 7.759, with ±0.002 and ±0.005 Å for the two respective standard deviations. The chemical composition of the monophase specimens is considered to be probably temperature dependent. At lower temperatures it may approach the formula U_2M_3Si. In some of these systems ternary compounds UM_2Si_2 were also identified as being isostructural with the previously reported ThM_2Si_2 series. (auth)

19872 ISOTOPIC EXCHANGE OF OXYGEN IN THE γ-Al_2O_3–O_2 SYSTEM. G. K. Boreskov, V. S. Muzykantov, V. V. Popovskii, and N. D. Goldstein (Inst. of Catalysis, Academy of Sciences, Siberian SSR). Dokl. Akad. Nauk SSSR, 159: 1354-6(Dec. 21, 1964). (In Russian)

Oxygen exchange on γ-Al_2O_3 at low and high temperatures and the ratio between homomolecular exchange and isotopic exchange with oxygen of the oxide were investigated. In freshly prepared specimens of γ-Al_2O_3 homomolecular exchange at temperatures below 350°C was not observed. The initial activity of the specimen as a function of the temperature was plotted showing the variations with exchange in specimens degassed at 350, 400, 450, and 500°C. Treatments below 350°C did not produce activation, while treatment at 600°C resulted in high activation. Isotopic exchange of molecular oxygen with the oxygen of specially treated oxides was observed at 350°C and coincided with the minimum activation temperature of γ-Al_2O_3 for low temperature homomolecular oxygen exchange. Isotopic exchange activation energy at 425 to 475°C was 40 kcal/mole. The temperature dependence of homomolecular exchange was not uniform; the minimum observed at 150° was obviously related to various oxygen exchange mechanisms. The rate of isotopic and homomolecular exchange as a function of oxygen pressure was studied at –78, 25, 300, and 450°C. At all temperatures, except –78°, the order in terms of oxygen pressure was equal to unity and for –78° it was below unity. The results showed that the rate of homomolecular exchange in all examined γ-Al_2O_3 specimens is considerably higher than the rate of isotopic exchange between molecular oxygen and oxygen of the oxide. At low temperatures the specially treated specimens of γ-Al_2O_3 exhibited a stable activity in relation to the homomolecular oxygen exchange. (R.V.J.)

19873 INVESTIGATION OF THE SYSTEM UO_2–UO_3. V. V. Rachev, L. M. Kovba, and E. A. Ippolitova (Moscow State Univ.). Dokl. Akad. Nauk SSR, 159: 1371-3(Dec. 21, 1964). (In Russian)

The results of the investigation are given of the system UO_3–U_3O_8 by the method of x-ray-diffraction analysis at high temperatures. By studying different uranium oxides at high temperatures (up to 1150°C) a phase diagram is suggested for the condensed state of the system UO_2–UO_3 consisting of only stable oxides. The diagram is based on the results of the present investigation and on the critical appraisal of data previously published. (ATD)

19874 FORMATION OF COMPLEXES FROM YTTRIUM, LANTHANUM AND RARE-EARTH ELEMENTS WITH SERINE. V. D. Panasyuk and V. A. Golub (Kiev State Univ.). Dopovidi Akad. Nauk Ukr. RSR, No. 2, 231-4 (1965). (In Ukrainian)

It is shown that the pH-potentiometric titration method with a glass electrode can be used for the investigation of the complexing of the elements of the scandium subgroup with serine. The formation of complexes of thirteen elements was investigated. The composition and the stability of the complex compounds formed were determined by Bjerrum's method. (auth)

19875 ELECTRODE REACTION KINETICS FOR HYDROGEN EVOLUTION IN MOLTEN KHF_2. S. Pizzini and A. Magistris (C.C.R. EURATOM, Ispra, Italy). Electrochim. Acta, 9: 1189-96(1964). (EUR-2123.e)

A potassium acid fluoride melt at 250°C, in which minor amounts of water were dissolved, was electrolyzed in order to investigate the kinetics of the hydrogen evolution at bright Pt electrodes. The following electrode reactions are discussed: (α) $HF + e \rightarrow \frac{1}{2}H_2 + F^-$ and (β) $H_3O^+ + e \rightarrow \frac{1}{2}H_2 + H_2O$. In the cd range where reaction (β) applies, overvoltages can be ascribed to a Volmer-Tafel mechanism. (auth)

19876 THE DEPHOSPHORYLATION OF SUGAR PHOSPHATES AND NUCLEOTIDES BY GROUP-IV METAL IONS. Heinz Trapmann and Muljibhai Devani (Universitat, Munich). Enzymologica, 28: 65-84(Dec. 31, 1964). (In German)

The nonenzymic dephosphorylation of the following sugar phosphates and nucleotides by Th ion (added as $Th(NO_3)_4$) and Zr ion ($ZrOCl_2$) was studied: glucose-1-phosphate, -6-phosphate; fructose-6-phosphate, -1,6-diphosphate; 3-phosphoglyceric acid; glycerol-α-phosphate; adenosinetriphosphate, -2′-phosphate, -3′-phosphate, -5′-phosphate; guanosine-3′-phosphate; and uridine-3′-phosphate. pH-activity curves for these substrates with Th and Zr ions are shown extending over a range of pH 2 to 10. Ions of both the elements possess catalytic activity within this range; they show pH optima in acid and alkali medium. Particularly when the substrates possess a free carbonyl group and Th ions catalyze the dephosphorylation, pH optima in acid medium are seen. The appearance of a pH optimum is due to various active forms of metal hydroxides. The acidities of substrate and catalyst are responsible for the shifting of the pH optimum; with increase in acidity of one of the two or both factors, the pH optimum shifts towards a more acid range. Detailed investigations with 3-phosphoglyceric acid show the influence of the carboxyl group in the molecule. The undissociated carboxyl group (pH <3.5) accelerates the phosphatasic activity of the catalyst, whereas the dissociated carboxyl group (pH >3.5) diminishes it. Aminopurine nucleotides are hydrolyzed faster than the aminopyrimidine nucleotides. Theoretical considerations led to the conclusion that the substrates undergo an intramolecular change due to the electrophilic attack of cationic metal hydroxides in acid medium; the consequence is a progressive enolization up to isomerization of the substrate molecule. The phosphate bond will thereby be weakened and can be hydrolyzed with increased speed. The active state of Th in these reactions appears to be the $Th(OH)_2^{3+}$ ion. Reaction mechanisms are shown indicating the intermediate states involved. (BBB)

19877 FORMATION OF α-SOLID SOLUTION OF NITROGEN IN ZIRCONIUM AT HIGH TEMPERATURE. S. E. Salibekov, Yu. V. Levinskii, V. D. Khvostikov, and M. Kh. Levinskaya. Fiz. Metal. i Metalloved., 18: 858-61(Dec. 1964). (In Russian)

Metallographic and x-ray analyses, together with measurements of microhardness, made it possible to conclude that by nitration of zirconium in the interval from 1400 to 1700°C dense layers of α-solid solutions and ZrN were formed. The velocity of the growth of the external nitrated layers depended on the time and temperature. (tr-auth)

19878 THE HYDROLYSIS OF THORIUM(IV) AT 0 AND 95°. C. F. Baes, Jr., Norman J. Meyer, and C. E. Roberts (Oak Ridge National Lab., Tenn.). Inorg. Chem., 4: 518-27(Apr. 1965).

The hydrolysis of thorium(IV) in 1M (Na)ClO_4 was measured at 0 and 95°C to better establish the reactions that occur and their temperature coefficients. Potentiometric measurements were made primarily with the quinhydrone electrode at 0°C and with the glass electrode at 95°C. Measurements of the solubility of ThO_2 as a function of acidity together with the potentiometric results at low hydrolysis were consistent with formation of $ThOH^{3+}$, $Th(OH)_2^{2+}$, and $Th_2(OH)_2^{6+}$, initial hydrolysis products proposed at 25°C by previous investigators. Their results along with the present measurements were compared with numerous possible schemes of hydrolysis products, $Th_x(OH)_y^{(4x-y)+}$, by means of a general least-squares computer program. Two schemes of four species, (I) x,y: 1,1; 1,2; 2,2; 5,12 and (II) x,y: 1,1; 1,2; 2,3; 6,15, approximate the data, but yield systematic deviations, which are similar at all three temperatures. Two schemes of five species, (III) x,y: 1,1; 1,2; 2,2; 3,6; 6,15 and (IV) x,y: 1,1; 1,2; 2,2;

4,8; 6,15, fit the data within the expected experimental error, with scheme IV the better. The assumption of six or more hydrolysis products was not justified by the accuracy of the measurements. The equilibrium quotients found for the formation of the five species in scheme IV from Th^{4+} and H_2O were: log $Q_{x,y}$ = (0°C) −4.32, −8.48, −5.60, −22.79, and −43.84; (25°C) −4.12, −7.81, −4.61, −19.01, and −36.76; and (95°C) −2.29, −4.50, −2.55, −10.49, and −20.63. The indicated average enthalpy and entropy changes per OH^- bound in the polymeric species were nearly constant at ~7.3 kcal and ~13.6 cal/°K, respectively. (auth)

19879 THE PHASE EQUILIBRIA AND CRYSTAL CHEMISTRY OF THE RARE EARTH GROUP VI SYSTEMS. I. ERBIUM–SELENIUM. D. J. Haase, H. Steinfink, and E. J. Weiss (Univ. of Texas, Austin). Inorg. Chem., 4: 538-40(Apr. 1965).

The phases occurring in the erbium–selenium system are: ErSe, fcc, a = 5.662 Å, mp 1630°C; the solid solution series, Er_2Se_3–Er_3Se_4, orthorhombic, Fddd, a = 11.38, b = 8.09, and c = 24.20 Å, mp 1400 to 1440°C; α-$ErSe_2$, orthorhombic, Cmma, a = 16.22, b = 15.80, and c = 11.88 Å, transition to β-$ErSe_2$ at 890°C; β-$ErSe_2$, orthorhombic, Immm, a = 4.016, b = 5.571, and c = 13.16 Å, peritectic at 1010°C. Two eutectics were observed at approximately 3 at. % selenium and 1310°C and approximately 55.5 at. % selenium and 1370°C. (auth)

19880 THE PHASE EQUILIBRIA AND CRYSTAL CHEMISTRY OF THE RARE EARTH GROUP VI SYSTEMS. II. ERBIUM–TELLURIUM. D. J. Haase, H. Steinfink, and E. J. Weiss (Univ. of Texas, Austin). Inorg. Chem., 4: 541-3(Apr. 1965).

The phases occurring in the erbium–tellurium system are: the solid solution series ErTe–Er_2Te_3, orthorhombic Fddd, a = 12.096, b = 8.553, and c = 25.659 Å, the lattice constants vary throughout the solid solution series, mp 1525 to 1460°C; $ErTe_3$, orthorhombic, Cmc2, a = 4.31, b = 25.45, and c = 4.31 Å, peritectic at 575°C. A eutectic was observed at approximately 13 at. % tellurium and 1270°C. The influence of the ionic ratio on the stability of the structures is discussed. (auth)

19881 SYSTEMS OF LITHIUM HYDRIDE WITH ALKALINE EARTH AND RARE EARTH HYDRIDES. Charles E. Messer and Ira S. Levy (Tufts Univ., Medford, Mass.). Inorg. Chem., 4: 543-8(Apr. 1965). (TID-20907)

Solid-liquid equilibrium was investigated by thermal analysis of systems of lithium hydride with the dihydrides of strontium, barium, europium, ytterbium, scandium, lanthanum, cerium, and samarium. The compound $LiSrH_3$, with the congruent melting point 745°C, was found. Eutectic temperatures and compositions found, in mole % MH_2, were: SrH_2 644.6°C, 11.2%; BaH_2 670.8°C, 5.0%; EuH_2 664.1°C, 6.8%; and YbH_2 668.7°C, 6.8%. The dihydrides of the other rare earth metals, and also $LaH_{2.8}$, did not affect the freezing point of LiH within experimental error. The soluble hydrides were the saline ones; the insoluble ones had metallic conduction electrons, which contributed an interaction unfavorable to solubility in the saline molten LiH. The apparatus is described, and the purity and melting point of the lithium hydride are discussed. (auth)

19882 THE EFFECT OF TUNGSTEN ON THE HYDROLYSIS OF URANIUM DICARBIDE. Mildred J. Bradley and Leslie M. Ferris (Oak Ridge National Lab., Tenn.). Inorg. Chem., 4: 597-9(Apr. 1965). (ORNL-P-725)

Tungsten, as an impurity in UC_2, was found to have a pronounced effect on the hydrolysis reaction. It catalyzed the polymerization of the C_2 units to wax during the hydrolysis. (M.C.G.)

19883 HYDROGEN EXCHANGE OF AZULENES. V. THE KINETICS OF PROTON TRANSFER IN ACIDIC AQUEOUS MEDIA. B. C. Challis and F. A. Long (Cornell Univ., Ithaca, N. Y.). J. Am. Chem. Soc., 87: 1196-1202(Mar. 20, 1965).

The rates of proton transfer to and from azulene in aqueous solution were studied as a function of temperature and acidity using a continuous fast-flow apparatus of the Hartridge-Roughton type. Parallel determination of the equilibrium protonation permitted calculation of the separate values of k_f and k_r, the first-order rate coefficients for protonation and deprotonation. At 7.3°C and for the acidity range from 1.5 to 4.0M perchloric acid, $k_f = 1.52h_0^{1.28}$ and $k_r = 110h_0^{-0.68}$, where h_0 is the Hammett acidity function. In 1.93M perchloric acid the Arrhenius parameters were: for protonation (sec^{-1} units), $\Delta F^* = 16.0$ kcal, $\Delta H^* = 15.0$ kcal, and $\Delta S^* = -3.2$ e.u.; for deprotonation (sec^{-1} units), $\Delta F^* = 15.6$ kcal, $\Delta H^* = 12.4$ kcal, and $\Delta S^* = -11.0$ e.u. The protonation rate, extrapolated to a 0.1M aqueous electrolyte solution, agreed closely with a protonation rate for the same medium derived from isotopic hydrogen exchange data for low acidities. This and the Arrhenius data for the protonation provided direct, semi-quantitative support for a two-stage A-Se2 mechanism for the detritiation of azulene-1-t and thus confirmed earlier proposals. (auth)

19884 MELTING PROPERTIES OF THE ALKALI NITRATES TO 10 000 ATMOSPHERES. B. B. Owens (Atomics International, Canoga Park, Calif.). J. Chem. Phys., 42: 2259-62(Apr. 1, 1965).

The melting points and the volumes of fusion of the alkali nitrates were determined at pressures up to 10,000 atm. $LiNO_3$, $NaNO_3$, and $CsNO_3$ had normal melting curves. However, the $RbNO_3$ melting curve exhibited an initial negative slope followed by normal behavior at higher pressures, whereas the KNO_3 melting curve was initially normal, but went through a maximum at elevated pressures. The results of this investigation indicated that the $RbNO_3$ liquidus curve has two triple points, one at 310°C and 200 atm and the other at 315°C and 1900 atm. (auth)

19885 ELECTRON ENERGY FOR H_2^+ IN THE GROUND STATE. H. Wind (Culham Lab., Abingdon, Berks, Eng.). J. Chem. Phys., 42: 2371-3(Apr. 1, 1965). (CLM-P-58)

The $1s\sigma_g$ state of the hydrogen molecular ion was investigated. The result is given as a table in which the electronic energy for a two-Coulomb center is given in seven decimal places for values of internuclear separation R up to 20 in steps of 0.05 au. (auth)

19886 CRYSTAL-FIELD SPLITTING IN Tm^{3+} CHELATES. W. G. Perkins and G. A. Crosby (Univ. of New Mexico, Albuquerque). J. Chem. Phys., 42: 2621-3(Apr. 1, 1965).

The absorption spectrum of a CCl_4 solution of thulium trisbenzoylacetonate dihydrate was measured in the region of 4500 to 18000 Å. Weak absorptions were observed at the positions expected for intra-4f transitions. The bands corresponding to transitions from $^3H_6$ to the $^1G_4$ and ^3F levels displayed very poor structure, and accurate measurements of the splittings were impossible. Emission spectra were also obtained. Analysis of the absorption and emission data permitted location of crystal components of the various terms. The electrostatic theory of the ligand field gave a better account of splittings for the complete set of terms than the sigma-antibonding model. (M.C.G.)

19887 SMALL-CROSS-SECTION EXOTHERMIC ION-MOLECULE REACTIONS. $He^+ - H_2$, $Ne^+ - H_2$. L. Friedman and T. F. Moran (Brookhaven National Lab., Upton, N. Y.). J. Chem. Phys., 42: 2624-5(Apr. 1, 1965). (BNL-8684)

The $H_2 - He^+$ and $H_2 - Ne^+$ systems were studied using deuterium isotope techniques, and a reversed repeller technique was used to discriminate between the H^+ ions formed by electron impact and those formed in dissociative charge-transfer processes. Cross sections indicated that most of the ion–molecule collisions are elastic. (M.C.G.)

19888 INTERMOLECULAR INTERACTIONS AND THE ELECTRON COUPLING OF NUCLEAR SPINS. H. S. Gutowsky, J. Jonas, Fu-ming Chen, and R. Meinzer (Univ. of Illinois, Urbana). J. Chem. Phys., 42: 2625-6(Apr. 1, 1965).

Some observations were made of temperature and solvent effects on the internuclear coupling constant J_{FF} between the 2.6 and CF_3 group fluorines in perfluorotoluene and to suggest that the effects result mainly from an intermolecular fluorine-fluorine interaction. It was found that J_{FF} increases with increasing temperature in both the pure liquid

and in a 20% vol/vol solution in CCl_4. However, J_{FF} at a given temperature decreased monotonically by as much as 0.7 cps on the addition of solvent. It was concluded that intermolecular interactions are responsible for the solvent effects and for most, if not all, of the temperature dependence. (M.C.G.)

19889 CONCERNING THE INFLUENCE OF OXYGEN ON THE VAPOR PRESSURE OF URANIUM. J. Drowart, A. Pattoret, and S. Smoes (Universite Libre, Brussels). J. Chem. Phys., 42: 2629-30(Apr. 1, 1965).

The heat of sublimation of U was found to be 125.5 ± 2.5 kcal/g-atom in the presence of oxygen. Partial pressures over U(l) + UO_2(s) and pure uranium were measured. (M.C.G.)

19890 COMMENTS ON PRESSURE OF URANIUM OVER URANIUM–URANIUM DIOXIDE SYSTEM. R. J. Ackermann, E. G. Rauh, and R. J. Thorn (Argonne National Lab., Ill.). J. Chem. Phys., 42: 2630-1(Apr. 1, 1965).

In the case of uranium and uranium dioxide at 1900°K data yielded a value of 10^{-6} for the ratio of the partial pressure of uranium in equilibrium with congruently vaporizing uranium dioxide to the vapor pressure of the metal. Measurements established the absolute effusion rate of the uranium-bearing species in the diphasic region and the relative intensities of the gaseous species UO_2, U, and UO as determined mass spectrometrically. (M.C.G.)

19891 EQUILIBRIUM BETWEEN LIGHT AND HEAVY WATER. Ralph E. Weston, Jr. (Brookhaven National Lab., Upton, N. Y.). J. Chem. Phys., 42: 2635-6(Apr. 1, 1965). (BNL-8586)

The equilibrium constant for the reaction $H_2O + D_2O \rightarrow 2HDO$ is discussed and data from various sources are considered. (M.C.G.)

19892 COMPLEX COMPOUNDS OF QUADRIVALENT AND TERVALENT MOLYBDENUM. E. A. Allen, K. Feenan, and G. W. A. Fowles (Univ. of Southampton, Eng.). J. Chem. Soc., 1636-42(Mar. 1965).

A series of complex compounds of quadrivalent molybdenum of the types $MoCl_4$,2L and $MoCl_4$,B were prepared, where L is one of a wide range of monodentate ligands and B is 2,2′-bipyridyl or 1,10-phenanthroline. Several complex compounds of tervalent molybdenum of the types $MoBr_3$,3L and $MoBr_3$,2L,RCN were also prepared. The physical properties of these compounds, particularly spectra and magnetic susceptibilities, were examined and the results interpreted. (auth)

19893 ISOTOPE EFFECTS IN GAS-LIQUID CHROMATOGRAPHY OF STEROIDS. Marvin A. Kirschner and Mortimer B. Lipsett (National Cancer Inst., Bethesda, Md.). J. Lipid Res., 6: 7-9(Jan. 1965).

In the combined use of radiolabeled compounds and gas-liquid chromatography (GLC) in biological research, it has been assumed that labeled and unlabeled molecules behave identically. However, a nonuniform distribution of isotope ratios was observed within fractions of the effluent peak of steroid derivatives. This is important when double-isotope derivative techniques are used with GLC, since a classical criterion of radiohomogeneity of the final steroid derivative is the constancy of the isotope ratios throughout the chromatographic peak. Tests were conducted on testosterone-4-^{14}C and dehydroepiandrosterone-4-^{14}C acetylated with acetic anhydride-1-^{3}H, and with testosterone-1,2-^{3}H and dehydroepiandrosterone-7α-^{3}H acetylated with acetic anhydride-1-^{14}C. GLC was performed by glass coiled columns, 6 ft × 3.4 mm, packed with either 1% neopentyl glycol succinate, 2% XE-60, or 2.5% SE-30 on Gas Chrom P and operated at 200 to 240°C. The $^{3}H/^{14}C$ ratio of the doubly labeled steroid was unchanged by GLC when the ratio of the entire effluent peak was measured, but when fractions were collected every 20 sec throughout the steroid peak, the $^{3}H/^{14}C$ ratio varied among the fractions. In all studies the observed $^{3}H/^{14}C$ ratios of counts were higher in the early fractions of the peak. The $^{3}H/^{14}C$ ratio progressively decreased to values lower than the ratio obtained before GLC. Often, the ratio increased again in the tail of the peak. The results showed that GLC with columns of 2000 to 3000 theoretical plates containing frequently used polar and nonpolar phases has sufficient resolving power to partially segregate isotopic species that differ in molecular weight by less than 6 parts in 350, or 2%. Thus an important criterion of radiohomogeneity, namely a constant $^{3}H/^{14}C$ ratio within a steroid peak, cannot be applied when GLC is used in combination with the double isotope derivative technique. (BBB)

19894 THE ABSORPTION SPECTRA OF THE MOLECULES H_2, HD, AND D_2. PART VI. RATIONAL ANALYSIS OF THE B′, B″, D, D′, AND D″ STATES. A. Monfils (Institut d'Astrophysique, Cointe-Sclessin, Belg.). J. Mol. Spectr., 15: 265-307(Mar. 1965).

The rotational levels belonging to the B′, B″, D, D′, D″ states were computed from the absorption spectra of H_2, HD, and D_2. The rotational analysis was worked out for these states as well as for the higher vibrational levels of the B and C states. B_ν, D_ν, and H_ν constants were computed by least square analysis. From these data, the equilibrium constants B_e and D_e, as well as the coupling constants α_e, β_e, γ_e, δ_e, and ϵ_e, were determined. The interatomic distances at equilibrium r_e were computed and an average value for the three molecules is given for each substate. The evolution of $\bar{r}_e$ with the principal quantum number n is shown. (auth)

19895 INFLUENCE OF CRYSTAL FIELDS ON THE MAGNETIC PROPERTIES OF THE RARE-EARTH NITRIDES. G. Busch, P. Junod, F. Levy, A. Menth, and O. Vogt (Eidgenossische Technische Hochschule, Zurich). Phys. Letters, 14: 264-6(Feb. 15, 1965).

Stoichiometric specimens of the rare earth nitrides were prepared by direct reaction of the components, and measurements were made of the magnetization up to 130 kOe and of the magnetic susceptibilities at 1.5°K to 600°K. It is shown that the Curie-Weiss law does not hold at low temperatures for compounds with an even number of 4f electrons, and that the susceptibilities tend to a temperature independent value. For the high temperature region, where the crystalline field splittings are smaller than kT, the nitrides of Pr, Gd, Tb, Dy, Ho, Er, and Tm obey the Curie-Weiss law. The results are compared with the experimental results of Child et al. and the predictions of Trammell. The physical properties are tabulated. (L.B.S.)

19896 PARAMAGNETIC RESONANCE OF HYDROGEN ATOMS IN CaF_2 AND KCl. R. G. Bessent, W. Hayes, and J. W. Hodby (Oxford Univ.). Phys. Letters, 15: 115-16 (Mar. 15, 1965).

The CaF_2:H crystals were x-irradiated in an X-band microwave cavity at 77°K and the electron paramagnetic resonance spectrum of hydrogen atoms on fluorine sites was observed. The parameters of the spin hamiltonian are tabulated. It is found that on warming the crystals to 124°K the substitutional hydrogen atoms move into interstitial sites with a time constant of ~6 min and then give rise to the EPR. Similar measurements on KCl:H crystals at 4°K showed intense EPR spectra of H centers and U_2 centers. U_3 centers were also observed, which convert to U_4 centers upon warming to 40°K. It is suggested that the U_3 centers may be an interstitial hydrogen atom associated with a chlorine vacancy. (L.B.S.)

19897 SPIN LATTICE RELAXATION TIME OF F^{19} IN CaF_2 BELOW 1°K. B. T. Beal and J. Hatton (Oxford Univ.). Phys. Letters: 15: 210-11(Apr. 1, 1965).

The spin lattice relaxation time of ^{19}F in a crystal of natural fluorite was measured as a function of temperature between 0.07 to 0.5°K during NMR studies of ^{3}He in which the magnetic susceptibility of the fluorine was used to measure temperature. The magnetic field dependence of the relaxation time was also studied. An empirical relation for the relaxation behavior was obtained. (D.C.W.)

19898 MAGNETIC HYPERFINE INTERACTIONS AND RELAXATION PHENOMENA IN Dy_2O_3; THEORY. I. Nowik (Israel Atomic Energy Commission, Yavne, Israel). Phys. Letters, 15: 219-20(Apr. 1, 1965).

The magnetic hyperfine interactions in Dy_2O_3 are investigated, considering only the Dy^{3+} ion in the C_2 symmetry

site. The spin-lattice and spin-spin relaxation times are found to be much longer than 10^{-3}sec below 70°K. (D.C.W.)

19899 ISOTOPIC EFFECT IN THE RESONANCE DISSOCIATIVE CAPTURE OF AN ELECTRON AND QUASI-STATIONARY STATES OF MOLECULES. Yu. N. Demkov (Leningrad State Univ.). Phys. Letters, 15: 235-6(Apr. 1, 1965).

The dissociative capture of electrons by molecules with the formation of a quasistationary molecular ion is discussed. Both resonance capture and negative ion formation are considered. A strong decrease in the resonance peaks when D_2 is substituted for H_2 in the hydrogen process is predicted. (D.C.W.)

19900 THE TRANSITION ENERGY FOR THE POLYMORPHIC TRANSFORMATION OF CsCl. Jorma Poeyhoenen and Kauko Mansikka (Univ. of Turku, Finland). Physik Kondensierten Materie, 3: 218-26(1965).

The transition energy of CsCl for the transformation I ⇌ II was determined by theoretical and experimental methods. The theoretical method was based on a generalized expression of the repulsion energy introduced by Wasastjerna and used in his theory of ionic solid solutions. The theoretical value of the transition energy obtained, 880 ± 220 cal/mole, was considerably smaller than previous theoretical results and agreed well with the experimental value, 690 ± 28 cal/mole. (auth)

19901 THE DETERMINATION OF SIZE DISTRIBUTION OF PARTICLES IN SUSPENSION BY A DIFFUSION TECHNIQUE. H. Reinhardt, J. O. Liljenzin, and R. Lindner (CCR Euratom, Ispra, Italy). Radiochim. Acta, 3: 215-19 (Dec. 1964).

Under the assumption of a logarithmic particle-size distribution, the geometric mean radius F and the geometric standard deviation σ can be determined by means of radial diffusion transport and wall adsorption within a capillary. The possibility of simultaneous sedimentation is taken into account. The best fit of the experimental results to calculated curves confirmed earlier estimates of the size of radiocolloids and Al_2O_3 powder. (auth)

19902 ELECTRODEPOSITION OF ACTINIUM. R. H. Iyer, H. C. Jain, M. V. Ramaniah, and C. L. Rao (Atomic Energy Establishment, Trombay, India). Radiochim. Acta, 3: 225(Dec. 1964).

An investigation was made of the conditions suitable for quantitative electrodeposition of actinium with a view to preparing thin adherent targets of ^{227}Ac on platinum backing for use in fission studies. ^{228}Ac was used in the study and the amount of actinium electrodeposited was determined by beta counting. It was found that quantitative electrodeposition of carrier-free ^{228}Ac can be obtained from a nitrate solution at pH 2.0 with a current density of about 200 ma/cm^2 in about an hour. (M.C.G.)

19903 COMPLEXING OF URANYL ION WITH SALICYLIC ACID. I. SPECTROPHOTOMETRIC STUDIES OF COMPLEXING IN SOLUTIONS. V. I. Paramonova, N. B. Platunova, and V. S. Dubrovin. Radiokhimiya, 6: 505-13 (1964). (In Russian)

The complexing of U^{6+} in solutions with salicylic acids was studied by the spectrophotometric method. It was established that the uranyl ion formed complexes only with ions of the second order of dissociated salicylic acid. Complexes with the composition UO_2Sal, $UO_2Sal_2^{2-}$, and $UO_2Sal_3^{4-}$ (Sal = salicylate) were detected. The equilibrium constants were $k_1 = (1.5 \pm 0.6) \times 10^{-12}$, $k_2 = (4 \pm 2) \times 10^{-22}$, and $k_3 = (2 \pm 2) \times 10^{-30}$M, respectively. Polymerizations in the salicylic acid at concentrations from 1.6×10^{-3} to 2.17×10^{-2}M and at total concentrations of uranyl ion of 1.22×10^{-3} to 7.32×10^{-3}M at pH 3 were not detected. (tr-auth)

19904 COMPLEXING OF URANYL ION WITH SALICYLIC ACID. II. STUDIES OF COMPLEXING IN SOLUTIONS BY ION EXCHANGE METHOD. V. I. Paramonova, N. B. Platunova, and E. D. Baklanovskii. Radiokhimiya, 6: 513-18(1964). (In Russian)

A study of the comparative absorption curves of cationites and anionites established that under the conditions used ($C_{UO_2^{2+}} = 4.7 \times 10^{-4}$ g-ions/l, $C_{Sal^{2-}} = 10^{-13}$ to 10^{-8} g-ions/l) uranyl formed, in solutions of salicylic acid (Sal), complexes with the composition UO_2Sal and $UO_2Sal_2^{2-}$. Numerical values of the total and stepped dissociation constants were determined for these compounds. $K_1 = (5 \pm 0.9) \times 10^{-12}$, $k_{2-1} = (4 \pm 1) \times 10^{-10}$, and $k_{2-0} = 2.1 \times 10^{-21}$. Complexes of uranyl with $HSal^-$ were not detected under the conditions studied. (tr-auth)

19905 HYDROLYSIS OF POLONIUM IN PERCHLORIC ACID. I. E. Starik, N. I. Ampelogova, and B. S. Kuznetsov. Radiokhimiya, 6: 519-24(1964). (In Russian)

In studies of the extraction of polonium solutions of acetylacetone in benzene from $HClO_4 + NaClO_4$ ($\mu = 0.1$) solutions, the Po^{4+} complexing constants with acetylacetone were determined. The formation constants for mixed hydroxyacetylacetone complexes of $Po[POH]^{3+}$, $[Po(OH)_2]^{2+}$, $[Po(OH)_3]^{+}$, and $Po(OH)_4$ were calculated as $(5 \pm 2) \times 10^{12}$, $(2.5 \pm 1) \times 10^{25}$, $(2.2 \pm 2) \times 10^{38}$, and $(2.5 \pm 1) \times 10^{50}$, respectively. The constants of successive hydrolysis reactions of Po by ions of strong solutions were calculated as 0.1: $K_1 = 0.08$, $K_2 = 6.3 \times 10^3$, $K_3 = 8.7 \times 10^{-4}$, and $K_4 = 1.6 \times 10^{-5}$. The effects of pH on the percentage content of different hydrolysis products of Po was calculated. (tr-auth)

19906 COMPLEXING OF POLONIUM WITH CHLORIDE IONS IN AQUEOUS AND AQUEOUS-ACETONE SOLUTIONS. I. E. Starik, N. I. Ampelogova, and B. S. Kuznetsov. Radiokhimiya, 6: 524-7(1964). (In Russian)

The possibility of using the ion exchange method on cationite for determination of the stability constant of Po chlorocomplexes in $HCl + HClO_4$ solutions was determined. The formation constants of the chloride complexes $Po[PoCl_i]^{(4-i)+}$, where i = 1, 2, ... 6, in aqueous solutions $\mu = 1$ and in aqueous acetone solutions were calculated. It is shown that the stability of Po complexes with chloride ions increases in the presence of acetone during which the stability of some complexes (i = 5 to 6) increased very sharply. (tr-auth)

19907 INVESTIGATION OF HETEROGENEOUS EQUILIBRATES IN A TERNARY SYSTEM OF $UO_2(NO_3)_2-HNO_3-H_2O$. II. VAPOR-SOLUTION EQUILIBRIUM IN A BINARY HNO_3-H_2O SYSTEM AT 25, 35, AND 50°C. M. A. Yakimov and V. Ya. Mishin. Radiokhimiya, 6: 543-8(1964). (In Russian)

The solution-vapor equilibrium of the binary system HNO_3-H_2O was investigated at 25, 35, and 50°C. From the data obtained by dynamic methods the partial pressures of the water vapor and nitric acid were calculated in the concentration range from 0 to 80 wt % HNO_3. From data on pressures of water vapor and acid the chemical potentials of the components and the free energy of solutions formed were calculated. It was indicated that the change of chemical potentials of the components in the temperature interval studied does not depend on temperature. It was established that the vapor phase of the binary system HNO_3-H_2O at 20°C contracts as an ideal gas down to 80 wt % nitric acid. Therefore the study of the solution-vapor equilibrium above this acid concentration by dynamic methods without the knowledge of the virial coefficients is impossible. (tr-auth)

19908 INVESTIGATION OF HETEROGENEOUS EQUILIBRATES IN A TERNARY $UO_2(NO_3)_2-HNO_3-H_2O$ SYSTEM. III. VAPOR-SOLUTION EQUILIBRIUM IN A BINARY SYSTEM $UO_2(NO_3)_2-H_2O$ AT 25 AND 50°C. M. A. Yakimov, V. Ya. Mishin, and V. K. Filippov. Radiokhimiya, 6: 548-52(1964). (In Russian)

On the basis of the pressures measured for water at eutectic points in $UO_2(NO_3)_2-HNO_3-H_2O$ systems the free energies of formation ($\Delta\phi$) of uranyl nitrate crystal hydrates from pure components at 25 and 50°C were calculated. It is shown that the suggested method of calculation is equivalent to the calculation of $\Delta\phi$ from pressures for the crystal hydrate. The chemical potentials of the components and $\Delta\phi$ of the solutions formed from water and anhydrous uranyl nitrate were calculated for 25 and 50°C. (tr-auth)

19909 INVESTIGATION OF HETEROGENEOUS EQUILIBRATES IN A TERNARY $UO_2(NO_3)_2-HNO_3-H_2O$ SYSTEM.

IV. VAPOR-SOLUTION EQUILIBRIUM IN URANYL NITRATE–NITRIC ACID–WATER SYSTEM AT 25 AND 50°C. M. A. Yakimov, V. Ya. Mishin, N. F. Nosova, and V. K. Filippov. Radiokhimiya, 6: 552-8(1964). (In Russian)

From the pressures of the water vapor and nitric acid, the chemical potentials of uranyl nitrate at 25 and 50°C were calculated. It was established that the chemical potentials of water and nitric acid conform to additional conditions and determine the boundary conditions of the system (in binary systems and at the solubility isotherm). Some thermodynamic regularities concerning the pattern of the isopotentials of the components in ternary system were investigated. The hypothesis of the process of overdistribution of water in solutions between uranyl nitrate and nitric acid and, therefore, of the association of these components as the dominant process in the composition range studied, was formulated. (tr-auth)

19910 ANION URANYL PERCHLORATE COMPLEXES. V. M. Vdovenko, A. I. Skoblo, and D. N. Suglubov. Radiokhimiya, 6: 677-82(1964). (In Russian)

Complex compounds of $R_4NUO_2(ClO_4)_3$ and $(R_4N)_2UO_2(ClO_4)_4$ were formed by reactions of uranyl perchlorate with tetradicylammonium perchlorate benzene solutions. The constant for reaction $R_4NClO_4 + R_4NUO_2(ClO_4)_3 \rightarrow (R_4N)_2\ UO_2(CLO_4)_4$ was 34 ± 4 at 20°C. Infrared absorption spectra were measured and the frequency of the compounds determined. It was found that perchlorate groups in triperchlorate complexes coordinated by bidentate complexing (with the coordinate uranyl number 6) and by monodentate complexing in tetraperchlorate (with coordinate number 4). The visible part of the $R_4NUO_2(ClO_4)_3$ spectrum had a clear oscillatory structure. Two electron transitions with different excited uranyl oscillation frequencies were observed in $R_4NUO_2(ClO_4)_2$ and $(R_4N)_2\ UO_2(ClO_4)$ spectra. (R.V.J.)

19911 INFRARED ABSORPTION SPECTRA OF CERTAIN COMPLEX URANYL COMPOUNDS WITH HYDROXY ACIDS. Yu. Ya. Kharitonov and Z. M. Alikhanova. Radiokhimiya, 6: 702-13(1964). (In Russian)

Infrared absorption spectra (~650 to 4000 cm^{-1}) of polycrystalline specimens of uranyl compounds with malic, tartaric, and trioxyglutaric acid radicals, and spectra of these acids, their potassium salts, and their deuterium-substituted salts showed that carboxyl groups participate in complexing of all uranyl ions. In uranyl complexes with malic acid radicals, non-dissociated oxy-groups formed coordinating bonds with uranium atoms. In a similar complex with tartaric acid radicals, one oxy-group participated in the complexing process and the second did not. In complexes with trioxyglutaric acid neither of the three non-dissociated oxy-groups formed coordinate bonds with uranium atoms. The structures of complexes (with trioxyglutaric acid radical) and the composition: $(UO_2)_2\ C_5H_4O_7 \cdot 4H_2O$ and $K(UO_2)_2C_5H_3O_7 \cdot 3H_2O$ were identical with the acid radical configurations and with their bonding to the uranyl groups. (R.V.J.)

19912 FACTORS DETERMINING THE OXIDIZING ACTIVITY OF NITRIC ACID DURING THE REACTION WITH URANIUM DIOXIDE. E. A. Kanevskii and A. P. Filippov. Radiokhimiya, 6: 732-7(1964). (In Russian)

An attempt was made to examine the principal factors determining the oxidizing activity of nitric acid in sulfuric acid solutions in the interaction with uranium dioxide and to offer an explanation for the regularities observed. The effect of nitric and sulfuric acid concentrations was established. Temperature was found to be a decisive factor in enhancing the oxidative properties of nitric acid, and its effect was studied together with the rate of stirring of the reaction mixture. It was postulated that some of the products of decomposition of nitric acid are strong oxidants. The kinetics of establishment of oxidation-reduction potentials in the system $UO_2–HNO_3–H_2SO_4–H_2O$ and the kinetics of the simultaneous dissolution of UO_2 were studied. No direct relation was found to exist between these two phenomena, but it was concluded that the dissolution of UO_2 is probably related to an acceleration of the decomposition of HNO_3 under the catalytic influence of the products of reduction of this acid. (ATD)

19913 ISOTHERMAL SOLUBILITY IN $NH_4F–UO_2–H_2O$ SYSTEM. A. A. Opalovskii and Z. M. Kuznetsova. Radiokhimiya, 6: 743-9(1964). (In Russian)

Isothermal solubility in the $NH_4F–UO_2–H_2O$ system was studied at 25°C. The solid phase composition in $NH_4^+–UO_2^{2+} + H_2O$ ion system was determined. Separation of triammoniumuranylpentafluoride was achieved by direct reaction between hydrous ammonium fluoride and uranium trioxide without using hydrogen fluoride. Reactions in $NH_4F–MeO_3–H_2O$ systems were compared to reactions in $HF–MeO_3–H_2O$ systems where Me = Mo, W, or U. (R.V.J.)

19914 STRUCTURE REFINEMENT FOR $Pr(NO_3)_3 \cdot 6H_2O$. I. M. Rumanova, G. F. Volodina, and N. V. Belov (Inst. of Crystallography, Academy of Sciences, USSR). Soviet Phys.-Cryst. (English Transl.), 9: 545-52(Mar.-Apr. 1965). Translated from Kristallografiya, 9: 642-54 (Sept.-Oct. 1964).

$Pr(NO_3)_3 \cdot 6H_2O$ is triclinic and has the following cell parameters: a = 9.19, b = 11.70, c = 6.78 Å, α = 89°, β = 110°40′, γ = 110°10′, and Z = 2; the space group $C_i^1 = P\bar{1}$. The structure was determined and refined by the use of differential ordinary and phase Fourier projections. The Pr atom lies within a figure having ten vertices and consisting of oxygen atoms. The figure is linked via common edges to three NO_3 triangles. These together give the neutral complex $Pr(NO_3)_3 \cdot 4H_2O$. The structure consists of these complexes joined by hydrogen bonds either directly or via 2 molecules of H_2O, which do not form part of any complex. (auth)

19915 X-RAY AND THERMOGRAVIMETRIC STUDIES OF THE OCTAHYDRATES OF THE SULFATES OF THE LANTHANIDES AND YTTRIUM. V. I. Ivanov (Vernadskii Inst. of Geochemistry and Analytical Chemistry, Moscow). Soviet Phys.-Cryst. (English Transl.), 9: 553-6(Mar.-Apr. 1965). Translated from Kristallografiya, 9: 655-9(Sept.-Oct. 1964).

A systematic study was made of the lanthanide contraction in rare earth octahydrates (Pr to Lu, including Y) on the basis of precision unit-cell measurements. The parameters showed a monotonic course, with no inflection near Gd. The bond type for the water was examined by thermogravimetric analysis for some of these compounds. (auth)

19916 SODIUM ZIRCONOSILICATE AND HAFNOSILICATE CRYSTALS. Yu. M. Polezhaev, L. Ya. Pivnik, and V. G. Chukhlantsev (Ural Polytechnic Inst., USSR). Soviet Phys.-Cryst. (English Transl.), 9: 630-1(Mar.-Apr. 1965). Translated from Kristallografiya, 9: 747-9(Sept.-Oct. 1964).

Studies were made of Na_2ZrSiO_5 and Na_2HfSiO_5 crystals obtained by crystallization from sodium silicate melts containing ZrO_2 or HfO_2. It was established that the crystals first form in the shape of small prisms and that they grow most rapidly in the direction of the c axis and least in the direction of the a axis. Therefore, as the crystal grows it takes on the shape of an extended lamina. The crystals were colorless with a glassy luster. They are optically biaxial and positive; the optical sign of the principal zone is positive. (M.C.G.)

19917 SCATTERING FILTERS IN THE FAR INFRARED. T. R. Manley and D. A. Williams (Rutherford Coll. of Tech., Newcastle-upon-Tyne, Eng.). Spectrochim. Acta, 21: 737-45(Apr. 1965).

The transmission spectra of suspensions of several metal oxides and halides in thin films of linear polythene were examined in the region from 1 to 500 μ using grating instruments and a Michelson interferometric spectrometer. The films studied act as convenient long wave cut-on filters. (auth)

19918 THERMODYNAMICS AND SOLUBILITY OF OXYGEN IN LIQUID METALS FROM E.M.F. MEASUREMENTS INVOLVING SOLID ELECTROLYTES. PART 2. TIN. T. N. Belford and C. B. Alcock (Royal School of Mines, London). Trans. Faraday Soc., 61: 443-53(Mar. 1965).

Electromotive force measurements on galvanic cells involving oxide electrolytes were made in order to obtain the standard free energy of formation of SnO_2 in the range of 500 to 710°C, and the standard free energy of solution and solubility of oxygen in Sn at 536, 600, 700, and 751°C. Values of −43,870 ± 1000 cal/g atom and −15.74 ± 1.10 cal/g atom degree were deduced for the partial enthalpy and excess entropy of solution of oxygen in Sn, respectively. The solutions of oxygen in Sn obeyed Henry's law. The oxygen content of the Sn was varied by solid state coulometry. On adding oxygen to pure Sn it was found that the concentration of dissolved oxygen could apparently be increased beyond that at which solid SnO_2 normally separates and some evidence of a limiting potential was obtained at oxygen activities corresponding to those expected for unstable solid SnO. (auth)

19919 ON PHOSPHORESCENCE OF BORON–URANIUM PHOSPHORS. G. M. Kislyak and G. M. Lysenko (Korolenko Poltava Pedagogical Inst., [Ukrainian SSR]). Ukr. Fiz. Zh., 9: 1256-60(Nov. 1964). (In Ukrainian)

On change of temperature from −183 to 0°C for uranium in boric acid and in aluminum alums at a temperature of −70°C, an abrupt change in τ and the phosphorescence spectrum maximum is observed. This is accompanied by a change in the afterglow color. A similar phenomenon was also observed for anthranilic and sulfanilic acid in boric glacials. This phenomenon is explained by the presence in the molecules of an activator of two metastable levels, the emissive transitions from which go on in the normal state only at definite temperatures. (auth)

19920 ON THE THEORY OF ELECTRON-NUCLEAR DOUBLE RESONANCE (ENDOR) OF F-CENTERS IN NaCl TYPE CRYSTALS. A. B. Roitsin (Inst of Semiconductors, Kiev). Ukr. Fiz. Zh., 10: 147-52(Feb. 1965). (In Ukrainian)

The role of electron spin in reorientation of nuclei is considered. The square of the matrix element of spin-nuclear transitions is calculated for the systems in question. The Zeeman energy of the electron and nucleus is regarded as a perturbation operator inducing the transitions. As a result the matrix element also depends on the hyperfine interaction constants, which leads to the dependence of the ENDOR line intensity on the orientation of the magnetic vector (static and time-dependent) in the crystal. The effect of static and alternating electric fields on the ENDOR spectra is also considered. The spin-hamiltonian of the interaction of nuclei with the electric field is obtained. The corrections to the frequencies of the spin-nuclear transitions in static electric fields are determined, and the matrix elements of the transitions due to the radio-frequency field are calculated. The static electric field lifts the degeneration due to the equivalence of the two nuclei located on one axis. The alternating field causes transitions with the selection rules $\Delta m = \pm 1, \pm 2$. The corresponding matrix elements are very sensitive to the orientation in the crystal of the static magnetic field and the electric field inducing the transitions. (auth)

19921 INVESTIGATION OF THE CIRCULAR LUMINESCENCE OF A SODIUM URANYL ACETATE CRYSTAL. M. S. Brodin and V. Ya. Reznichenko (Inst. of Physics, Kiev). Ukr. Fiz. Zh., 10: 178-86(Feb. 1965). (In Ukrainian)

Measurements of the degree of polarization of sodium uranyl acetate crystal luminescence bonds polarized on a circle were conducted at low temperatures (20 and 77° K). In contrast to the accepted point of view, based on quantitative investigations by Samoilov, the degree of polarization of these bands proved incomplete, and does not exceed 0.63 in the investigated samples. It is less than the degree of circular dichroism of the respective actinic bands in the absorption spectrum. A rise in temperature, as well as aging of the crystal, leads to a marked decrease in the degree of polarization without disturbing the resonance coincidence of the initial luminescence and absorption bands. All these facts furnish grounds for the inference that in the mechanism of deexcitation of the investigated crystals defects play a double role. On the one hand they further exciton de-excitation without localization of energy. The great circular dichroism is connected with this. On the other hand, with the concentration used the defects evidently lead to an increase in the interaction between the zones of the left and right excitons. This factor leads to a decrease in the degree of circular polarization. (auth)

19922 HYDROXO-COMPLEXES OF THORIUM(IV). B. I. Nabivanets and L. N. Kudritskaya (Inst. of General and Inorganic Chemistry, Academy of Sciences, Ukrainian SSR). Ukr. Khim. Zh., 30: 891-5(1964). (In Russian)

The dependence of the solubility of freshly precipitated thorium hydroxides on pH was studied at $\mu = 0.1$. It was established that at pH ≥ 6 only the molecule $Th(OH)_4$ develops in solution and its concentration in equilibrium solutions is 4.8×10^{-7} mole/g. From the magnitude of the solubility, the individual (k) and total (K) instability constants of hydroxy complexes of Th were calculated at 17°C: $K_1 = 4.0 \times 10^{-10}$, $K_2 = 5.6 \times 10^{-19}$, $K_3 = 1.8 \times 10^{-27}$, and $K_4 = 1.5 \times 10^{-35}$. According to the instability constants found, the effects of pH on the distribution of Th between the different forms was calculated. The solubility product of thorium hydroxide was calculated: $SP_{Th(OH)_4} = [Th^{4+}][OH^-]^4 = 7.2 \times 10^{-42}$ ($\mu = 0.1$). (tr-auth)

19923 STUDY OF THE STATE OF THORIUM IN SOLUTIONS OF PERCHLORIC, HYDROCHLORIC, AND NITRIC ACIDS BY THE METHODS OF ELECTRODIALYSIS AND ION-EXCHANGE CHROMATOGRAPHY. B. I. Nabivanets and L. N. Kudritskaya (Inst. of General and Inorganic Chemistry, Academy of Sciences, Ukrainian SSR). Ukr. Khim. Zh., 30: 1007-16(1964). (In Russian)

By the methods of electrodialysis and ion exchange the state of thorium in HCl, HNO_3, and $HClO_4$ solutions was studied. The regions for the existence of cationic and anionic forms of Th in perchloric and nitric acid solutions were determined. It was established that at HCl ≤ 6M and HNO_3 ≤ 5M Th is found in the cationic form; at HCl > 6 to 7M and HNO_3 > 5M anionic complexes are formed. In $HClO_4$ solutions thorium is found only in the cationic form. By the Fronaeus and Paramonovoi methods the stability constants of chloride and nitrate complexes of thorium were calculated, and the distributions of the complex forms of thorium in the presence of concentrated HCl and HNO_3 were obtained from the diagrams calculated. (tr-auth)

19924 COMPARATIVE INTERPRETATION OF ABSORPTION SPECTRA OF TECHNETIUM(IV) AND RHENIUM(IV) HEXAHALIDES. Chr. Klixbuell Joergensen (Cyanamid European Research Inst., Cologne) and Klaus Schwochau. Z. Naturforsch., 20a: 65-75(Jan. 1965).

Absorption spectra of aqueous solutions of TcX_6^{2-} and ReX_6^{2-} (X = F, Cl, Br, I) are measured between 8,000 and ~50,000 cm^{-1} and theoretically discussed. The electron transfer spectra indicate the optical electronegativity x_{opt} = 2.25 for Tc(IV) and 2.05 for the less oxidizing Re(IV). The spectrochemical parameter Δ is determined to 28,400 cm^{-1} in TcF_6^{2-} and 32,800 cm^{-1} in ReF_6^{2-}. The nephelauxetic effect is evaluated from the spin-forbidden intra-sub-shell transitions in all eight species, and from the two spin-allowed bands of TcF_6^{2-}. The vibrational structure of the narrow absorption bands and the possible weak distortion from octahedral symmetry of Tc(IV) hexahalides are discussed. (auth)

19925 POLYMORPHISM OF ZrO_2 AND PRODUCTION OF RARE EARTH ZIRCONATES BY MEANS OF COMPLEX THERMOANALYSIS. A. K. Kuznetsov, E. K. Keler, and Fui-k'ang Fan. Zh. Prikl. Khim., 38: 233-41(Feb. 1965). (In Russian)

Complex thermal and x-ray analyses showed that ZrO crystallized from the amorphous state into the metastable cubic modification, which at 600°C transformed into a monocline formation. The existence of $La_2Zr_2O_7$, $Nd_2Zr_2O_7$, and $Ce_2Zr_2O_7$ compounds, with pyrochloride structures, was confirmed and the mechanism of formation of the zirconate compounds from precipitated hydroxides was investigated. In contrast to $La_2Zr_2O_7$ and $Nd_2Zr_2O_7$, the cerium zirconate, $Ce_2Zr_2O_7$, oxidized in air and trans-

formed into a cubic solid solution of the fluorite type between ZrO_2 and CeO_2. The temperature of the coprecipitation of zirconate compounds with the rare earths was much lower than the temperature of zirconate crystallization. It was postulated that the formation of the compounds begins during the precipitation process. (R.V.J.)

19926 ON THE LANTHANUM BOROCARBIDES. L. Ya. Markovskii, N. V. Vekshina, and G. F. Pron. Zh. Prikl. Khim., 38: 245-51(Feb. 1965). (In Russian)

The composition of the high-temperature boron carbide phase of LaC_4B_2 formed at 2000°C was studied. The synthesis of 93 to 96% pure LaC_4B_2 by boron and carbon reactions with metallic lanthanum, its oxide, and carbide and by mixed LaC_2 and carbon reaction with boron and boron anhydride is described. It is shown that lanthanum boron carbides are subject to easy hydrolytical disintegration under the effects of dilute oxides. Lanthanum and boron pass into solution and form gaseous and solid substances. The experiments also confirmed the existence of other rare earth boron carbides similar in composition and properties to La boron carbides. (R.V.J.)

19927 APPLICATION OF CARBON DISULFIDE AS SULFONATING AGENT IN THE SYNTHESIS OF RARE EARTH SULFIDES. L. Ya. Markovskii, E. Ya. Pesina, and R. I. Smirnova (State Inst. of Applied Chemistry, USSR). Zh. Prikl. Khim., 38: 411-14(Feb. 1965). (In Russian)

Experiments on the preparation of rare earth sesquisulfides by sulfonation of oxides (CeO_2 and La_2O_3 of 99.5 and 99.7% purity were basic materials) in a carbon disulfide vapor stream showed that the sulfonation by means of carbon disulfide was more efficient than by hydrogen sulfide and resulted in more energetic reactions. The content of Ce_2S_3 and La_2S_3 in the final products was tabulated as a function of the temperature and duration of sulfonation. The reaction of carbon disulfide with Pr and Sm under identical conditions of sulfonation resulted in praseodymium and samarium sesquisulfides containing 98.3 and 97.5% of the base material, respectively, indicating that the method can be adapted to other rare earth materials. (R.V.J.)

19928 OPTICAL PROPERTIES OF RARE EARTH OXIDES. II. POLYTHERMAL STUDIES OF Nd_2O_3. S. S. Batsanov, G. N. Kustova, E. D. Ruchkin, and V. S. Grigor'eva (Inst. of Inorganic Chemistry, Academy of Sciences, Novosibirsk, Siberian SSR). Zh. Strukt. Khim., 6: 58-65(Jan.-Feb. 1965). (In Russian)

Refractometric, spectroscopic, and x-ray analyses of Nd_2O_3, prepared by annealing neodymium nitrate, oxalate, and sulfate at 600 to 1300°, indicated that pure oxide is formed at 1100°C. Neodymium oxysulfate, $Nd_2O_2SO_4$, was prepared and studied. A polymorphic transformation was revealed in the oxalate at 700 to 800°C and in the nitrate at 800 to 900°C. During the thermal disintegration process the intensity of the (Nd–O) absorption band first increases due to the increase of the Nd_2O_3 concentration then drops due to the reduced defects in the structure. (R.V.J.)

19929 STRUCTURE OF URANIUM OXIDE SOLID SOLUTIONS AT α-UO_3–U_3O_8 REGION. A. R. Beketov, V. N. Strekalovskii, and V. G. Vlasov (Ural Polytechnic Inst., USSR). Zh. Strukt. Khim., 6: 75-8(Jan.-Feb. 1965). (In Russian)

Studies of structural transformation in the α-UO_3–U_3O_8 transition process indicated the possible existence of a transition solution with composition from $UO_{2.90}$ to $UO_{2.82}$ ($UO_{2.76}$) in addition to the solid solutions with UO_3 (hexagonal) and U_3O_8 (rhombic) structures. (R.V.J.)

19930 STRUCTURE OF GAMMA-URANIUM TRIOXIDE. A. R. Beketov, V. N. Strekalovskii, and V. G. Vlasov (Ural Polytechnic Inst., USSR). Zh. Strukt. Khim., 6: 164-5 (Jan.-Feb. 1965). (In Russian)

Data from x-ray analyses of γ-UO_3 structure made by Perio, Connoly, de Wolf, and Dawson were correlated and compared to experimental data obtained on a γ-UO_3 specimen prepared by annealing hexahydrous uranium nitrate at 550°C for 4 hr. Results of the analysis were inconclusive. (R.V.J.)

19931 RESONANCE CHARGE EXCHANGE IN INERT GASES. B. M. Smirnov and M. I. Chibisov. Zh. Tekhn. Fiz., 35: 117-22(Jan. 1965). (In Russian)

The cross section for resonance charge exchange between a noble gas ion and its atom was calculated as a function of collision velocity of He, Ne, Ar, Kr and Xe, and the results were compared with experimental data from many sources. The formula of Firsov and Smirnov for the charge exchange cross section was used. The calculations were performed in the one-electron approximation with asymptotic Coulomb wave functions which were normalized by fitting them to the corresponding Hartree-Fock wave functions at the boundary of the atom. It was found that the resonance charge exchange cross section depends only weakly on the angular momentum of the incident ion. Reasonably good agreement with experiment was found, and it is concluded that the relatively simple Firsov model is adequate. (ATD)

19932 PEREKIS' LITIYA. (Lithium Peroxide). T. A. Dobrynina. [Moscow], Izdatel'stvo "Nauka," 1964. 49p.

A biblographic review of research on lithium peroxide is presented. The discovery and preparation of lithium peroxide and the question of the existence of higher oxygen compounds of lithium are considered. (73 references) (J.S.R.)

19933 TABLES OF THERMODYNAMIC DATA. (International Atomic Energy Agency, Vienna (Austria)). Technical Reports Series No. 38. 1964. 98p. (STI/DOC/10/38) $2.50; S 52.50; 15/-stg; F.Fr.10,-; DM 8 (IAEA)

A compilation is presented of data on the thermodynamic properties of materials of interest for nuclear technology. The data were released in the Symposium on the Thermodynamics of Nuclear Materials, which was held in May 1962. (D.L.C.)

19934 DIFFUSION OF HELIUM IN SOLIDS. Lars Christian Luther. Thesis, Bloomington, Ind., Indiana Univ., 1964. 276p.

The evolution of helium in the temperature range 650 to 850°C from Brazilian tourmaline was studied. The evolution curves are in agreement with the assumption that the helium is concentrated in the surface layer of the crystal. The method of introducing helium into solids by means of neutron-induced nuclear transmutation reactions was studied using lithium- and boron-doped aluminum. Bubbling of the annealed material interfered with diffusion studies. The diffusion coefficients of helium in silicon, germanium, and diamonds were determined from the rate of evolution of the gas at elevated temperatures from the boron-doped neutron-irradiated materials. At low temperatures and high helium concentrations appreciable amounts of helium were trapped in the silicon. At higher temperatures the helium retention was small. No correlation between helium retention and diffusion coefficients was observed. The Arrhenius expressions for the diffusion coefficients obtained from the helium evolution curves are given. Unlike inert gas interaction potentials of the exp-six form and the elastic coefficients of diamond, silicon, and germanium were used to derive theoretical values for the solubilities, the heats of solution, and the diffusion activation energies. The complete theoretical Arrhenius expressions for solubilities and diffusion coefficients are given. The diffusion of helium into silicon targets bombarded with helium ions at 200 to 300°C was studied. The distribution of helium in the targets was obtained from measurements of helium remaining after etching. (A.G.W.)

19935 INFRARED SPECTRA OF SOLID ACETYLENE. Gary Lee Bottger. Thesis, Seattle, Univ. of Washington, 1964. 87p.

The infrared absorption spectra of polycrystalline films of C_2H_2, C_2HD, and C_2D_2 were examined at 63°K in the frequency range between 4500 and 450 cm^{-1}. The spectra of the solid-state and the gas phase of the various acetylenes are compared and the appropriate vibrational assignments are made. Several absorptions attributable to combinations of lattice modes and molecular fundamentals were found. The observed multiplet structure of the fundamental vibrations indicates that in the low-temperature modifica-

tion of C_2H_2 and C_2D_2 the molecules are located at sites of C_{2h} symmetry. Spectra of various solid solutions composed of mixtures of isotopic species were obtained and their significance is discussed. The effect of isotopic substitution on the splittings in the ν_5 fundamental region led to the conclusion that the dipole-dipole coupling model is sufficient to explain the observed spectra. The spectrum of the ν_5 fundamental of acetylene was found to have a pronounced temperature dependence. Nonreversible spectral changes observed when the polycrystalline films were annealed could not be explained merely in terms of an increase in sample crystallinity. The spectrum was also found to be sensitive to the temperature at which the acetylene was deposited. Matrix isolation studies of the infrared spectra of acetylene in various solid rare-gas crystals at 22°K are presented. The ν_5 adsorption frequencies of monomeric acetylene suspended in krypton and xenon solid solutions were obtained. The rather gross effects that occur when the rate of sample deposition is varied are described in detail. A careful investigation was made of certain concentration-dependent multiple absorptions found in the spectra. (Dissertation Abstr., 25: No. 5, Nov. 1964)

19936 A STUDY OF THE HIGH-RESOLUTION INFRARED ADSORPTION SPECTRUM OF $C^{12}O_2^{18}$ BETWEEN 1800 AND 5000 CM^{-1}. Charles Chackerian, Jr. Thesis, Seattle, Univ. of Washington, 1964. 103p.

A sample of carbon dioxide ninety-five per cent of which is $C^{12}O_2^{18}$ was prepared, and a number of vibration-rotation infrared absorption bands of this molecule was measured using a 1.5-meter Ebert spectrometer in the region between 1800 and 5000 cm^{-1}. Quadratic and cubic vibrational anharmonicity constants calculated from the corresponding constants in normal carbon dioxide via simple isotopic substitution rules were used to calculate vibrational band centers, and the agreement with experimentally determined band centers is good. A set of Fermi resonance parameters was determined to fit the seven bands involved in Fermi resonance, which have been observed ($\lambda_1 = 0.05$ cm^{-1}, $\lambda_2 = 0.39$ cm^{-1}, $\lambda_3 = 0.72$ cm^{-1}, and $W_e = 54.64$ cm^{-1}), and the anomalous increase in the Fermi resonance interaction in going from $^{12}C^{16}O_2$ to $^{12}C^{16}O^{18}O$ (Courtoy, Ann. Soc. Sci. Bruxelles, 73: 1959) is seen to be extended in going from $^{12}C^{16}O^{18}O$ to $^{12}C^{18}O_2$. The constants α_1, α_2, and α_3, which are necessary to calculate the rotational constant in a state other than the ground vibrational state, were determined for $^{12}C^{18}O_2$: $\alpha_1 = 91 \times 10^{-5}$ cm^{-1}, $\alpha_2 = -61 \times 10^{-5}$ cm^{-1}, $\alpha_3 = 273 \times 10^{-5}$ cm^{-1}, and also α_3 for $^{12}C^{18}O_2 = 261 \times 10^{-5}$ cm^{-1}. (Dissertation Abstr., 25: No. 5, Nov. 1964)

19937 REACTIONS OF HYDROCARBONS INITIATED BY EXCITED HELIUM. Norman Roy Greiner. Thesis, Austin, Tex., Univ. of Texas, 1964. 87p.

Gaseous hydrocarbons (methane and some simple aromatics) were allowed to interact with a stream of helium emerging from a microwave discharge at near-sonic velocity. The long-lived excited helium species transported out of the active discharge caused the hydrocarbons to be decomposed, sometimes into excited fragments. Stable hydrocarbon products were subsequently formed in the system and trapped in a cold trap for analysis. The results showed that aromatic rings were broken in as many as three places and that substituent groups were probably removed. The methane reaction produced acetylene, ethylene, ethane, and propane in varying amounts, depending on conditions. Previous spectroscopic work by Collins and Robertson has shown that CH^+ ions and CH ($^2\Delta$, $^2\Sigma$ and $^2\pi$, the ground state) radicals are present in the flame-like interaction zone, the radicals being formed from the ions thru recombination with electrons and subsequent emission of light quanta. It was shown that of these CH species only CH ($^2\pi$) reacts to form any appreciable amount of product. Evidence that acetylene is produced in this system from two CH ($^2\pi$) radicals is presented. The mechanism of energy transfer from the excited helium species has been shown to involve charge transfer. A treatment of resonant, non-symmetrical charge transfer in quantum mechanical terms is presented, and the cross section for charge transfer from hydrogen atoms to helium nuclei (α-rays) is calculated as an illustration of this kind of charge transfer. The values obtained compare well with cross sections calculated by Gurnee and Magee for similar reactions. The theory of molecular dissociation caused by ionization is discussed. (Dissertation Abstr., 25: No. 5, Nov. 1964)

19938 SECONDARY ISOTOPE EFFECTS AND COLLISIONAL ENERGY TRANSFER IN CHEMICAL ACTIVATION SYSTEMS. John Wesley Simons. Thesis, Seattle, Univ. of Washington, 1964. 181p.

The decomposition of chemically activated sec-butyl-d_8 and -d_9 radicals, produced by H- and D- atom addition to cis-butene-2-d_8, was studied at 195 and 300°K over a range of pressures. These measurements, as well as internal comparison experiments with cis-butene-2-d_0, reveal a large normal secondary intermolecular kinetic isotope ratio, which varies with the pressure and temperature, whose minimum value is a factor of 4, and whose maximum value averages around 7. Evidence against a significant mechanistic isotope effect on the energetics is presented. Calculated isotope effects for all of the possible sec-butyl radical systems, to be formed by H- and D-atom addition to butene-d_0 and -d_8 isomers, are given. A study of the geometric and structural isomerization reactions of chemically activated cis-1,2-dimethylcyclopropane-d_0 (dmc-d_0) and dmc-d_8 is reported. The measured intermolecular isotope effects for the geometric isomerization and for one of the structural isomerization reactions are, for the most part, secondary quantum statistical-weight effects. The effect on the other structural isomerization processes is a mixed primary-secondary isotope effect. Theoretical calculation of rates and of isotope effects are in fairly good agreement with experimental values. Isotope effects in the singlet methylene radical C-D insertion and C = C addition reactions with cis-butene-2-d_8 were determined. Vibrationally excited cyclopropane molecules were produced by chemical activation at ~100 kcal $mole^{-1}$ above the ground level; methylene radicals were formed by photolysis of ketene at 3200 Å and were added to ethylene. Collisional deactivation was studied at 298 and 423°K, with ethylene as the inert deactivator, and at 298° with He, Ar, and N_2 as deactivators. (A.G.W.)

19939 CONTINUOUS FLUORINATION OF PLUTONIUM (Engineering Materials). (Rocky Flats Plant, Dow Chemical Co., Denver, Colo.). 35 drawings. (CAPE-1181)

The hydrofluorinator described is used to continuously convert plutonium oxide to plutonium tetrafluoride. Also included are drawings describing a feed hopper, lined tube, product solids receiver, dry boxes, movable neutron shielding, a conveyor system, and piping. (For details, see TID-400). (M.C.G.)

19940 NUCLEAR QUADRUPOLE RESONANCE OF Bi^{209} IN $BiBr_3$. Elizabeth D. Swiger, Paul J. Green, Gary L. McKown, and Jack D. Graybeal (Univ. of West Virginia, Morgantown). 9p. (CONF-571-29)

From American Chemical Society 148th National Meeting, Chicago, Aug.-Sept. 1964.

An investigation of the nuclear quadrupole coupling of the ^{209}Bi nucleus in solid $BiBr_3$ was undertaken in order to determine if the crystal structure was related to either that of $BiCl_3$ or that of BiI_3. A 50 g sample of anhydrous $BiBr_3$, prepared by the direct reaction of Bi and Br_2, was investigated between 20 and 40 Mc/sec using a super-regenerative spectrometer. Three of the four allowed transitions of the ^{209}Bi nucleus were measured. By plotting calculated frequency ratios vs. asymmetry parameters and by plotting relative frequency factors vs. asymmetry parameters, the experimental values for the asymmetry parameter and the nuclear quadrupole coupling constant of the ^{209}Bi nucleus were determined to be 0.553 and 340.5 Mc/sec, respectively. Assuming an ionic character of 15%, these data indicated that there is 5.8% s-character in the bonds to the Bi atom and that the Br-Bi-Br bond angle is 93.5°. The large value of the asymmetry parameter indicated considerable cross bonding among the $BiBr_3$ molecules in the solid. (auth)

19941 HIGH-TEMPERATURE VISCOSITIES AND DIFFUSIVITIES OF IONIZED HYDROGEN–URANIUM MIXTURES. S. B. Schneiderman (United Aircraft Corp., East Hartford, Conn.). 51p. (CONF-641208-8).

From 3rd Conference on Performance of High Temperature Systems, Pasadena, Calif.

A method for calculating theoretical values for the coefficients of viscosity and diffusion appropriate to high-temperature ionized or partially ionized mixtures is presented. This method, which is based on the classical perturbation solution to the integro-differential Boltzmann transport equation, permits evaluation of certain effective diffusivities based on a simplified picture of the transport process, in addition to evaluation of the usual viscosity and diffusion terms. The validity of the Boltzmann equation analysis is discussed, a method for insuring the neutrality of flow in the calculation of the simplified diffusion terms is developed, and general relationships between the various coefficients of diffusion in a multicomponent mixture and between the diffusive flux of each component relative to the mixture as a whole and relative to a fixed laboratory coordinate system are derived. Typical results of transport property calculations, which were performed for a number of high-temperature, high-pressure hydrogen-uranium equilibrium mixtures, are discussed. These calculations were performed on an IBM 7094 computer using a program written to handle any type of ionized mixture and certain partially ionized mixtures. (auth)

19942 METHOD FOR PRODUCING THORIUM OXIDE–URANIUM OXIDE MIXTURES OF CERAMIC QUALITY. Alberto Cacciari, Ruggero de Leone, Sergio Ferrari, and Guido Cogliati (to Comitato Nazionale per l'Energia Nucleare). German Patent 1,176,632. Aug. 27, 1964. Priority date Dec. 5, 1961, Italy.

The thorium oxide–uranium oxide mixtures are obtained from a solution containing thorium and uranyl nitrates with less than 1.5 mol/l free nitric acid. The uranyl nitrate is reduced with gaseous hydrogen in the presence of a catalyzer to uranium(IV) nitrate, thorium and uranium(IV) oxalate precipitated with an excess of oxalic acid, and the precipitates baked at a temperature of more than 400°C. (Gmelin Inst.)

Organic Chemistry

19943 (BNL-8243) THE MECHANISM OF THE THERMAL DECOMPOSITION OF α-PHENYLETHYLAZOMETHANE. A TWO-STEP REACTION. Stanley Seltzer and F. T. Dunne (Brookhaven National Lab., Upton, N. Y.). [1964]. Contract AT(30-2)-Gen-16. 28p. (CONF-322-16). Dep.(mn); $2.00(cy), 1(mn) CFSTI.

From American Chemical Society 146th National Meeting, Denver, Jan. 1964.

α-Phenylethylazomethane (IIIa), α-phenylethyl-α-d-azomethane (IIIb), and α-phenylethylazomethane-d_3 (IIIc) were prepared. The isotope effects in the thermal decomposition, $k_{IIIa}/k_{IIIb} = 1.13$ and $k_{IIIa}/k_{IIIc} = 0.97$, were found. In addition, the C^{13}-effect in the decomposition of α-phenyl-ethylazomethane-^{13}C is $k_{12}/k_{13} = 1.0068$. From these results it is concluded that the slow step involves rupture of only the α-phenylethyl-carbon-nitrogen bond; the breaking of the methyl-nitrogen bond in the unstable methylazo radical occurs in a subsequent fast step. An estimate of the lower limit of the rate constant for the second step is obtained from the results. The energy and entropy of activation are discussed. (auth)

19944 (ORINS-50) COBALT MOLYBDATE CATALYST FOR AMBIENT TEMPERATURE SYNTHESIS OF BENZENE FOR LIQUID SCINTILLATION RADIOCARBON DATING. John E. Noakes, Stephen M. Kim, and L. K. Akers (Oak Ridge Inst. of Nuclear Studies, Inc., Tenn.). Contract AT-40-1-GEN-33. 15p. Dep.; $1.00(cy), 1(mn) CFSTI.

A method for synthesizing acetylene gas to liquid benzene in quantitative yields for liquid scintillation radiocarbon dating was developed. The ambient temperature catalysis is accomplished using a cobalt molybdate alumina catalyst which requires no pretreatment other than dehydration. The synthesized benzene was checked by gas chromatography and infrared analysis and found to be pure. $^{13}C/^{12}C$ mass spectrometric analysis of the benzene and the acetylene from which it was derived show no carbon isotope fractionation. (auth)

19945 (UCRL-11864) THE ELECTRON SPIN RESONANCE SPECTRA OF RADICAL ANIONS IN LIQUID AMMONIA (thesis). Donald Harris Levy (Lawrence Radiation Lab., Univ. of California, Berkeley). Jan. 1965. Contract W-7405-eng-48. 142p. Dep.(mn); $4.00(cy), 3(mn) CFSTI.

A new technique for the generation of pi-bonded radical anions by means of continuous electrolysis in liquid ammonia was developed, and the experimental procedures are described in detail. The radical anion of 1,3-butadiene was prepared by this method and its electron spin resonance spectrum was observed. The measured proton hyperfine coupling constants are compared to those predicted by several theoretical calculations. The radical anions of isoprene, 1,3-cyclohexadiene and 2,3-dimethylbutadiene were prepared and their ESR spectra were observed. A theory for deriving methyl and methylene proton coupling constants from a knowledge of the unpaired spin density distribution is developed and used to predict the coupling constants of these and other methyl and methylene containing radical anions. The unpaired spin distribution is calculated using a hyperconjugation model and several simple LCAO molecular orbital theories. A small correction for spin exchange polarization is taken into account. It is shown that a simple extension of Huckel theory can be used to successfully predict the methyl and methylene proton coupling constants of all the radical anions considered. An inequivalence of the methylene protons in dimethylbutadiene radical anion was observed. To explain this, the usual molecular orbital treatments were modified by using an expanded basis set including the 3d carbon atomic orbitals. These are shown to be of the correct symmetry to account for the observed anisotropy. The radical anion of 1,3,5-cycloheptatriene was prepared and the hyperfine coupling constants measured. The methylene proton coupling constant was assigned by monodeuteration of the methylene group. The wavefunction of the unpaired electron in this molecule is shown to have a node at the methylene protons and consequently any hyperfine coupling is due to a combination of spin exchange polarization and electron correlation. The small contribution of electron correlation is estimated by an approximate self-consistent field calculation, and the remaining hyperfine coupling is taken as a measure of the spin exchange polarization. A correction term useful for accounting for spin polarization effects in other radicals is derived. The fact that this term is small provides a justification of the hyperconjugation model used previously. The ESR spectra of the nitrosobenzene and nitrobenzene radical anions were observed in liquid ammonia. The nitrosobenzene radical anion shows two ortho and two meta proton coupling constants which may be explained by either of two simple theoretical models. One model involves non-bonded interactions introducing off-diagonal Hamiltonian matrix elements between non-bonded atoms, and the other involves an electron polarization effect which produces small changes in the on-diagonal matrix elements. These have been described previously as the β- and α-effects. The nitrobenzene radical anion was prepared in liquid ammonia as a reference and to compare solvent shifts. The radical anion of cyclooctatetraene was prepared in liquid ammonia and is shown to be much more stable in this solvent than in any previously used. Small coupling constant solvent shifts were observed which, because of the symmetry of the molecule, can only be attributed to a solvent perturbation of the Σ-π interaction. (auth)

19946 (UCRL-11950) CHEMICAL EVOLUTION. Melvin Calvin (Lawrence Radiation Lab., Univ. of California, Berkeley). Aug. 1964. Contract W-7405-eng-48. 20p. (CONF-640809-1). Dep.(mn); $1.00(cy), 1(mn) CFSTI.

From 10th International Botanical Congress, Edinburgh.

Darwin's recognition of chemical evolution as a logical backward extrapolation of his concept of organic evolution is pointed out. The two approaches being used in the ex-

amination of the period of chemical evolution are discussed: search for evidence for organic materials in ancient rocks, and attempts to reproduce in the laboratory chemical processes induced by various radiations. The results obtained by these two approaches are described. The possibility of evidence in nonterrestrial materials (meteorites, moon, etc.) is considered briefly. (D.L.C.)

19947 SECONDARY α-DEUTERIUM ISOTOPE EFFECT IN THE REACTION OF 2-PHENYLETHYLTRIMETHYLAMMONIUM ION BY HYDROXIDE ION IN AQUEOUS SOLUTION AND BY ETHOXIDE ION IN ETHANOL. S. Asperger, L. Klasinc, and D. Pavlovic (Institut "Rudjer Boskovic," Zagreb and Univ. of Zagreb). Croat. Chem. Acta, 36: 159-63(1964).

Secondary α-deuterium isotope effects in the reaction of 2-phenylethyltrimethylammonium iodide with hydroxide ions in aqueous solutions at 97.0°C and with ethoxide ions in ethanol at 40.0°C were found to be very small. The results suggested that the hydrogen compound reacts slightly faster than the deuterium compound. The secondary α-deuterium isotope effect in the reaction of 2-phenylethyl bromide with sodium ethoxide in ethanol, determined previously, was appreciably larger and amounted to 9% per deuterium atom at 59.8°C. The mechanistic implications of these results are discussed. (auth)

19948 EFFECTS OF NONPOLAR SOLVENTS ON AN IONIC REACTION. II. CATALYST BASICITY, ACTIVATION PARAMETERS, SALT EFFECTS, AND DEUTERIUM ISOTOPE EFFECTS IN THE IONIC DECOMPOSITION OF t-BUTYLPEROXY FORMATE. Richard E. Pincock (Univ. of British Columbia, Vancouver). J. Am. Chem. Soc., 87: 1274-9(Mar. 20, 1965).

Formate C–H bond breakage in the initial step for base-catalyzed decomposition of t-butylperoxy formate to carbon dioxide and t-butyl alcohol in nonhydroxylic solvents was established by kinetic deuterium isotope effect ratios $(k_H/k_D = 4.1$ for the pyridine-catalyzed reaction in heptane or chlorobenzene at 90°C). For a wide variety of bases, the Brønsted relation (with $\log k_2 = 0.64pK_a - 5.35$) was followed in chlorobenzene with no steric effect observed for ortho-substituted bases. Triethylamine was 660 to 1380 times more effective as a catalyst than pyridine but the pattern of solvent effects remained the same (heptane << benzene < chlorobenzene < nitrobenzene). Changes in media by addition of salts to polar solvents ($LiClO_4$ to acetonitrile) or polar compounds to nonpolar solvents (pyridine to heptane) caused small increases in rates. The rates in heptane–benzene mixtures and the lower activation energies and more negative activation entropies found in benzene were consistent with the expected effect of polarization of solvent. Solvent effects in some other dipolar reactions in nonhydroxylic solvents were similar to those found in ionic decomposition of t-butylperoxy formate, but no general relationship was found. (auth)

19949 HYDROGEN PARTICIPATION IN cis-4-t-BUTYLCYCLOHEXYL BROSYLATE SOLVOLYSIS. V. J. Shiner, Jr. and John G. Jewett (Indiana Univ., Bloomington). J. Am. Chem. Soc., 87: 1382-3(Mar. 20, 1965).

The effect of substitution of deuterium for each of the four β-hydrogen atoms on the rate of solvolysis of cis-4-t-butylcyclohexyl-p-bromobenzenesulfonate (brosylate). The products of aqueous ethanolysis consisted of 86% t-butylcyclohexene, 3% ethers, 9% trans-4-t-butylcyclohexanol, and 2% t-butylcyclohexanol. Complete deuteration of the β-positions did not substantially lower the olefin fraction of the product. Data indicated that successive β-deuterium substitution at conformationally equivalent sites does not lead to cumulative isotope effects, i.e., the solvolytic rate retardation caused by 2,6-diaxial deuteration exceeded the square of that caused by monoaxial deuteration. (M.C.G.)

19950 NONCHAIR TRANSITION STATE CONFORMATION IN trans-4-t-BUTYLCYCLOHEXYL BROSYLATE SOLVOLYSIS. V. J. Shiner, Jr. and John G. Jewett (Indiana Univ., Bloomington). J. Am. Chem. Soc., 87: 1383-4 (Mar. 20, 1965).

The rate retardation caused by the substitution of deuterium for each of the four β-hydrogen atoms in aqueous ethanolysis of trans-4-t-butylcyclohexyl-p-bromobenzenesulfonate (brosylate) is reported. The products from solvolysis consisted of 67% 4-t-butylcyclohexene, 27% t-butylcyclohexanols, and 6% ethers. The alcohol fraction consisted of 94% cis-4-t-butylcyclohexanol. The isotope effects due to equatorial deuterium substitution were larger and very nearly cumulative. The two equatorial β-hydrogen atoms seemed to be equivalent in the solvolytic transition state, and the two axial β-hydrogen atoms seemed to be nonequivalent. (M.C.G.)

19951 STUDY OF ^{13}C CHEMICAL SHIFTS IN SUBSTITUTED BENZENES. Gary E. Maciel and J. John Natterstad (Univ. of California, Davis). J. Chem. Phys., 42: 2427-35 (Apr. 1, 1965).

Carbon-13 chemical shifts of several monosubstituted benzenes and para-substituted fluorobenzenes were determined. The shifts of the para carbons in monosubstituted benzenes were to correlate with Taft's resonance parameters, especially when the shifts were corrected by the amount of the meta shifts. A much less precise correlation was found between the ^{19}F chemical shifts in the para-substituted fluorobenzenes and the $^{13}C-F$ chemical shifts in the same set of compounds than between the ^{19}F shifts and the para ^{13}C shifts in monosubstituted benzenes. The relationships between the ^{13}C and ^{19}F shifts were considered in terms of the available theories of Karplus and Pople, Karplus and Das, and Prosser and Goodman, and are discussed in terms of π-electron densities. It was concluded that both ^{13}C shifts in monosubstituted benzenes and ^{19}F shifts in para-substituted fluorobenzenes are useful indices of the π-electron densities in para positions. (auth)

19952 DIFFUSE INTERFACE IN A CRITICAL FLUID MIXTURE. G. H. Gilmer, W. Gilmore, J. Huang, and W. W. Webb (Cornell Univ., Ithaca, N. Y.). Phys. Rev. Letters, 14: 491-4(Mar. 29, 1965).

The reflectivity of the interface between the two phases in equilibrium just below the critical consolute temperature of the binary fluid mixture was measured. The binary system cyclohexane plus methanol was studied. It was found that the interface was diffuse with an effective thickness ~1000 Å at 0.38°C below the critical temperature by comparison with the Fresnel reflectivity calculated for a sharp boundary. The temperature dependence of the effective thickness was found to be near that predicted by lattice-gas models for the range of correlations in critical fluids. (L.B.S.)

Radiation Chemistry

See *also* BIOLOGY AND MEDICINE — Radiation Effects.

Refer also to abstracts 20329 and 20409.

19953 (AERE-R-4201) INHIBITORS FOR THE CO_2–GRAPHITE REACTION IN REACTORS: PRELIMINARY SURVEY. M. Tomlinson and J. Wright (Atomic Energy Research Establishment, Harwell (England)). Dec. 1964. 27p. Dep.; $0.80(BIS) 4s(HMSO).

Preliminary experiments in sealed tubes at 140 and 500°C in BEPO, with a gas density of about 50 mg cm^{-3} and conditions favoring attack by irradiated gas in the interstices of a powder, show that some gaseous additives present at about 2% in CO_2 can reduce the radiolytic oxidation of carbon. Carbon monoxide was not very effective, but SO_2, Cl_2, and (less certainly) I_2 reduced the rate of gasification by factors of 5 to 15. At the higher temperature the halogens required the simultaneous presence of CO in order to be effective. Hydrocarbons and organic additives generally produced heavy carbonaceous deposits. Lighter deposits were also found in tubes containing appreciable carbon monoxide either added initially or built up during the irradiation. It is not possible, from these preliminary experiments, to distinguish between inhibition due to recombination or scavenging processes in the gas phase, and effects

of additive molecules adsorbed on the carbon surfaces. Sealed-tube experiments with methane additive show a small reduction in oxidation rate, but the sealed-tube technique is more suitable for studies of additives which affect the gas phase steps in the oxidation than those (like methane) which interfere with processes on the graphite surface. For studies of the latter kind, gas flow experiments are required. (auth)

19954 (AERE-R-4839) THE EFFECT OF HYDROGEN AND WATER ON THE RADIATION INDUCED REACTION OF CARBON DIOXIDE WITH GRAPHITE. H. B. F. Gow and W. R. Marsh (Atomic Energy Research Establishment, Harwell (England)). Jan. 1965. 34p. Dep.; $1.00(BIS); 5s. (HMSO).

The radiation-induced reaction of carbon dioxide with graphite was studied in the presence of added hydrogen and water at temperatures between 100 and 600°C. At 600°C, hydrogen reacts rapidly and an equimolar amount of carbon monoxide is formed, the only other product of the reaction being water. The reaction is temperature-dependent having an apparent "activation energy" of 21 kcal/mole. The subsequent rate of production of carbon monoxide after complete reaction of hydrogen is the same as that from pure carbon dioxide. At 100°C, the reaction rate is slower but still much greater than that due to thermal processes which are negligible at this temperature. The effect of added water is also temperature-dependent. Above 350°C, there is little effect of the addition of water on the production of carbon monoxide, but at 100°C a much lower rate of carbon monoxide production is observed, and, in addition, hydrogen is formed. (auth)

19955 (ANL-6938(p.21-2)) AN APPARATUS FOR MEASURING PHOTOIONIZATION EFFICIENCIES AS A FUNCTION OF ENERGY. James C. Person (Argonne National Lab., Ill.).

The apparatus consists of a monochromatic light source and a means of measuring I_0/I, where I_0 is the light intensity in photons/sec when there is no sample in the light path and I is the light intensity after passing through a length (l) of a sample of n molecules/cm^3. An ionization chamber and vacuum system are included in the apparatus to measure the saturated ion current and the electric charge. (J.R.D.)

19956 (ANL-6938(p.27-35)) INTRAMOLECULAR EXCIMER FORMATION IN DIPHENYL- AND TRIPHENYL-ALKANES. Fumio Hirayama (Argonne National Lab., Ill.).

The mechanisms involved in the association of electronically excited molecules and unexcited ones (excimers) were studied by examining the fluorescence spectra of diphenyl- and triphenyl-alkanes in liquid solution. The results indicate that intramolecular excimers can be formed in these compounds only when a favorable steric condition exists. (J.R.D.)

19957 (BNL-8993) PRELIMINARY COST ESTIMATE FOR A Co^{60} GAMMA RADIATION-INDUCED ETHYLENE POLYMERIZATION PROCESS. M. Steinberg, B. Manowitz, and L. E. Kukacka (Brookhaven National Lab., Upton, N. Y.). Mar. 1965. Contract AT(30-2)-Gen-16. 31p. Dep.(mn); $2.00(cy), 2(mn) CFSTI.

Preliminary estimates of capital investment and production costs were made for the ^{60}Co gamma radioinduced polymerization of ethylene based on designs obtained from laboratory-scale data. Two processes for the conversion of ethylene to polyethylene are considered. One operates at temperatures below the melting point of the polymer, ~120°C, forming solid polymer having an intermediate density, high molecular weight, and low melt index. The second process is carried out above the melting point and produces a low density polyethylene comparable to that formed in the conventional high-pressure process. It was concluded that the cost of ^{60}Co, although appreciable, is not a large factor in the conversion cost. The cost of the ^{60}Co source is less than 16% of the total plant investment. The ability to operate at high rates at pressures in the range of 680 to 1360 atm permits a significant reduction in investment and in production cost for low-density polyethylene. Thus, there appears to be sufficient evidence for continued development of radioinduced ethylene polymerization processes. (P.C.H.)

19958 (CEA-R-2348) EVOLUTION DES QUANTITES DE NUCLEIDES LORS DE TRANSFORMATIONS RADIOACTIVES. II. RESOLUTION DE L'EQUATION MATRICIELLE. (Determination of the Amounts of Nuclides During Radioactive Transformations. II. Resolution of the Matrix Equation). Ginette Guillou, Jean-Paul Boujot, Andre Guillou, and Franck Roche (Commissariat à l'Énergie Atomique, Fontenay-aux-Roses (France). Centre de Études Nucléaires). 1964. 18p. Dep.(mn).

Resolution of the linear differential system to which the physical method leads is reported. This amounts to a presentation of the integration formulas having a large stability radius. (auth)

19959 (CONF-571-37) THE RADIATION POLYMERIZATION OF CRYSTALLINE TRITHIANE. J. B. Lando and V. Stannett (Camille Dreyfus Lab., Research Triangle Inst., Durham, N. C.). Nov. 1964. Contract AT(40-1)-2513. 18p. Dep.(mn); $1.00(cy), 1(mn) CFSTI.

From American Chemical Society 148th National Meeting, Chicago, Aug.-Sept. 1964.

The polymerization of single crystals and finely powdered samples of trithiane (m.p. 215-16°C) was accomplished by irradiation of the samples at room temperature with ^{60}Co gamma radiation to doses of from 1 to 10 Mrads. Polymerization occurred during subsequent heating of the samples at 180°C. The conversion to polythiomethylene after a given time of heating at 180°C is dependent on radiation dose, the G values for conversion being higher at lower doses. Purified polymer samples were studied by means of differential thermal analysis. Polymerized single crystals of trithiane were found to retain their orientation in three dimensions, although the polymer samples were systematically twinned. The directions of greatest chain growth were along the diagonals in the (ab) plane of the monomer. This reaction can be classified as topotactic; that is, the molecular orientations of the product are correlated with the molecular orientation in the reactant crystal. The relationship between the polymer structure and that of the monomer is evaluated. (auth)

19960 (VDDIT-93) RADIATION-INDUCED GRAFT POLYMERIZATION ON CELLULOSE. A Literature Survey. Hans I. Holm (Aktiebolaget Atomenergi, Stockholm (Sweden)). Feb. 1965. 41p. Dep.(mn).

A total of 94 references, most with appended abstracts, is presented to reports and published literature in the time period 1959 to 1964. A subject index is included. (D.L.C.)

19961 (CEA-tr-A-1741) IRRADIATION DE LA CELLULOSE ET DES DERIVES DE LA CELLULOSE. (Irradiation of Cellulose and Cellulose Derivatives). F. Munzel and J. Schenkel. Translated into French by M. Chabrillac from a Paper Presented at Communication au Symposium de Lindau, 8-10 Juillet 1964. Dec. 8, 1964. 21p. Dep.(mn); $2.60(fs), $0.83(mf) JCL.

An attempt is made to show that radiation chemistry is in a state of evolution. The effects of radiation on cellulose and its derivatives are then investigated. It is shown that it is premature to pass a definitive judgement on the possibilities of development of irradiation in the sector of cellulose and its eventual industrial applications. (tr-auth)

19962 APPLICATION OF THE "UNIQUE PHOTOELECTRON TECHNIQUE" FOR THE DETERMINATION OF EMISSION SPECTRA AND TIME CONSTANTS OF ORGANIC SCINTILLATORS. G. Laustriat, G. Pfeffer, H. Lami, and A. Coche (Centre de Recherches Nucleaires, Strasbourg). Acta Phys. Polon., 26: 449-53(Sept.-Oct. 1964). (In French)

The radioluminescence of liquid and plastic scintillators is characterized by weak intensity (several thousands of photons) and extremely rapid decay (within a few nsec). The use of photomultipliers in the study of these phenomena is limited by their relatively high background noise and by their transit-time fluctuations, which have a considerable effect on the form of the electric pulse with respect to that

of the light pulse. By using high-gain fast photomultipliers (56 AVP or UVP), following the "unique photoelectron technique", it is nevertheless possible to evade these difficulties. A description is given of two experimental setups that are particularly useful in the study of scintillators: a very sensitive spectrophotometer that permits radioluminescence spectra to be obtained; and an apparatus that makes possible reproduction of the curve giving the intensity variations of the scintillations as a function of time. (tr-auth)

19963 LUMINESCENCE DECAY OF PYRENE-, DIBENZYL- AND DIBENZYL TETRACENE-CRYSTALS AT EXCITATION WITH ELECTRON PULSES AND α-PARTICLES. A. Schmillen and J. Kohlmannsperger (Universität, Giessen, Ger.). Acta Phys. Polon., 26: 495-500(Sept.-Oct. 1964).

When excited with electrons of approximately 30 kev or with alpha particles from a Po sample, pyrene and dibenzyl showed inverse behavior. After electron excitation, pyrene decayed exponentially with $\tau = 145$ nsec; it decayed non-exponentially after α excitation. Dibenzyl decayed exponentially after α excitation with $\tau = 1.9$ nsec and non-exponentially when excited by electrons. About 97% of the total luminescence of dibenzyl was in the case of electron excitation, emitted in a component with $\tau = 1.9$ nsec, the remainder was emitted in a mixture of components with $\tau > 100$ nsec. The importance of this behavior for particle discrimination is discussed. (auth)

19964 INFLUENCE OF IRRADIATION ON LUMINESCENCE AND ELECTRONIC EMISSION OF ALKALI CHLORIDES WITH COPPER. A. Bohun and J. Dolejsi (Inst. of Solid State Physics, Czechoslovak Academy of Sciences, Prague). Acta Phys. Polon., 26: 557-63(Sept.-Oct. 1964). (In German)

The luminescence of NaCl and KCl crystals doped with copper vanished when the crystals were exposed to large doses of x radiation. It reappeared after bleaching of the crystals. The high-temperature peaks of thermostimulated luminescence and electronic emission were at higher temperatures as in the case of more weakly irradiated crystals. The causes of these effects are discussed from the standpoint of color centers formation rate. (auth)

19965 INFLUENCE OF INFRARED RADIATION ON ROENTGENOLUMINESCENCE. H. Roeppischer and H. Winkler (Technische Hochschule, Ilmenau, Ger.). Acta Phys. Polon., 26: 779-84(Sept.-Oct. 1964). (In German)

Investigations on ZnCdS–Mn–In phosphors excited by x rays (50 kv, tungsten anode), simultaneously irradiated by infrared light are considered. Infrared radiation from 700 to 1200 nm intensified the roentgenoluminescence of yellow manganese band over the whole temperature range from 90 to 300°K under investigation. At low temperatures an appreciable stimulation was observed. The experimental results are discussed. (auth)

19966 ON THE TEMPERATURE QUENCHING OF RADIOLUMINESCENCE OF SOME THALLIUM ACTIVATED ALKALI HALIDES. K. K. Schwarz, E. D. Aluker, and I. P. Mezina (Inst. of Physics, Academy of Sciences, Latvian SSR). Acta Phys. Polon., 26: 795-9(Sept.-Oct. 1964).

The temperature dependence of stationary luminescence radiation and growth curves was investigated. The thermoluminescence of KCl(Tl), KBr(Tl), and KI(Tl) crystals excited by x rays and pile irradiation. A sharp decrease in luminescence efficiency for KCl(Tl) and KBr(Tl) crystals in the low-temperature region was found. There were glow peaks in the region of this decrease. There were two distinct decreases in the region of high temperatures in the crystals. Results were almost the same for x-ray and pile irradiations. (M.C.G.)

19967 INFLUENCE OF FAST NEUTRONS ON LUMINESCENCE OF ZnS SINGLE CRYSTALS GROWN IN A REDUCING ATMOSPHERE. A. Wrzesinska (Nicholas Copernicus Univ., Torun, Poland). Acta Phys. Polon., 26: 861-8(Sept.-Oct. 1964).

Thermal quenching, the spectrum of luminescence, and the thermoluminescence of single crystals of ZnS grown in an atmosphere of H_2 at a temperature of 1200 to 1100°C were investigated. The green band was much stronger than the blue one in the emission of this crystal. The measurement made a few days after a 25-min irradiation in the Ewa reactor showed that the influence of neutron bombardment on the thermal quenching and thermoluminescence is much smaller than for the blue luminescent self-activated ZnS powder. This influence seemed to be as small as that for the ZnS (Cu) 10^{-4} g/g powder, after similar irradiation in the reactor. However, when the measurements were repeated about 18 months after irradiation in the reactor a change in thermal quenching, thermoluminescence, and in the spectrum of ZnS crystals was found. No such change for ZnS (Cu) was observed. (auth)

19968 RECENT RESEARCH ON THE RADIATION CHEMISTRY OF AQUEOUS SOLUTIONS. Harold A. Schwarz (Brookhaven National Lab., Upton, N. Y.). Advan. Radiation Biol., 1: 1-32(1964).

Recent studies on the nature of radioinduced free radicals in water and the rates of some of the reactions of the radicals are reviewed. Topics discussed include the nature of the radical species generated in the radiolysis of water; methods of measuring rate constants for the reaction of a given radical with all the solutes in a mixture in order to predict the extent to which a reaction will occur; rate constants for a number of reactions; the diffusion model of the spur; other sources of chemical effects; and applications of the radical model in studies of the inactivation of trypsin in solutions of HCl, H_2SO_4, and HNO_3. (85 references.) (C.H.)

19969 THE RADIATION CHEMISTRY OF AMINO ACIDS. J. Liebster and J. Kopoldova (Inst. for Biological Research, Czechoslovak Academy of Sciences, Prague). Advan. Radiation Biol., 1: 157-226(1964).

Results are reported from studies of the behavior of amino acids in aqueous solutions under the influence of radiation. Emphasis was placed on the radiation chemical behavior of the components of the primary amino acids, the possible role of radiation chemistry of amino acids in reactions connected with the origin of life, and the use of radioinduced reactions of amino acids for various synthetic purposes. (111 references.) (C.H.)

19970 INTERACTION OF EXCITED BIOMOLECULES WITH OXYGEN. II. QUENCHING BY OXYGEN AND NITRIC OXIDE OF RADIOFLUORESCENCE OF TRYPTOPHAN AND TYROSINE. G. M. Barenboim and A. N. Domanskii (Inst. of Cytology, Leningrad). Biophysics (USSR) (English Transl.), 8: No. 3, 377-88(1963). Translated from Biofizika, 8: No. 3, 321-30(1963).

Studies were made on the reactions of oxygen with tryptophan and tyrosine excited by x radiation, and the possible role of this phenomenon in the radiobiological effect of oxygen was considered. In view of this, quenching with oxygen and nitric oxide of the radiofluorescence of the aromatic amino acids, tryptophan and tyrosine, was investigated. The results showed that the amino acids, in solutions at room temperature, fluoresce in response to x irradiation and that the spectra of radio- and photofluorescence coincide. The rate of radiofluorescence quenching by oxygen and nitric oxide depends on the amino acid, the solvent, and quenching agent increasing linearly with the concentration of the latter. Interpolation of the results to the normal partial pressures in air and in the cell showed that the direct interaction of the singlet excited molecules and oxygen play practically no role in the oxygen radiobiological effect. (P.C.H.)

19971 DYNAMIC MECHANICAL STUDIES OF IRRADIATION EFFECTS IN POLYTETRAFLUOROETHYLENE. K. G. McLaren (Defence Standards Labs., Alexandria, New South Wales, Australia). Brit. J. Appl. Phys., 16: 185-93(Feb. 1965).

Dynamic mechanical measurements were made with a low frequency (~1 c/s) torsion pendulum at temperatures from –170 to 150°C, on thin polytetrafluoroethylene (PTFE) sheet irradiated in vacuum at 23°C with doses up to 5 mega-

rads of gamma radiation. Marked radiation-induced increases in shear modulus and decreases in amorphous and crystalline damping peaks were observed. Irradiation increased the density of the polymer, and x-ray and infrared measurements indicated an increase in the overall crystallinity of low density PTFE. Low crystallinity material showed bigger changes in modulus, damping, and density than highly crystalline PTFE; and this may be due to the lower mobility of excited species or free radicals in the more crystalline regions of the polymer. Irradiation reduced the tensile strength of the PTFE mainly by reducing the strain-hardening contribution to the strength. With ductile low crystallinity material where strain-hardening was marked, irradiation produced a 52% decrease in ductility and a 35% decrease in tensile strength. By contrast highly crystalline PTFE which was not so ductile and showed little strainhardening initially, lost all ductility, but its tensile strength was little affected. The results suggest that although some chain scission occurs during irradiation, crosslinking is prominent, and this, together with the unusual increase in crystallinity, makes the polymer more rigid and brittle. Specimens irradiated in air rapidly lost mechanical strength; changes in dynamic modulus and damping were similar to those resulting from vacuum irradiation, but increases in density and crystallinity of low density PTFE were greater when air was present during irradiation. (auth)

19972 SOLID STATE POLYMERIZATION OF BINARY COMPONENT SYSTEM. Masatoshi Miura, Takako Hirai, and Shunji Kawamatsu (Hitachi Central Research Lab., Tokyo). Bull. Chem. Soc. Japan, 38: 344-51(Mar. 1965).

The γ irradiation of a solid solution of 3-chloromethyl-3-ethyloxetane and 3,3-bis-(chloromethyl)oxetane gave a copolymer with the same composition as that of the initial monomer mixture, while a BF_3-catalyzed copolymerization formed a copolymer with a different composition from that of the initial monomer mixture. In the polymerization, the solid solution behaved like each single component crystal in respect to the relation of polymer yield to the irradiation temperature and to the crystal state of the monomers. The copolymer obtained from small crystals grown by rapid cooling was found to have a narrower distribution of composition than that obtained from large crystals. With a solid solution of 3-chloromethyl-3-ethyloxetane and 3-fluoromethyl-3-ethyloxetane, the polymerization was studied and similar results obtained. The mixed crystal of 3-chloromethyl-3-ethyloxetane and diketene gave a polymer bland. The curve of the polymer yield versus the irradiation temperature was a superposition of those for each component crystal. The mixed crystals of 3-chloromethyl-3-ethyloxetane and trioxane gave only a homopolymer of oxetane, and the temperature dependence of the yield was similar to that of oxetane, even in an eutectic composition. (auth)

19973 CHEMICAL EFFECTS FOLLOWING THE ISOMERIC TRANSITION OF ^{80m}Br IN PENTAMMINECOBALT(III) BROMIDES. Nobufusa Saito, Shizuko Ito, and Takeshi Tominaga (Tokyo Univ.). Bull. Chem. Soc. Japan, 38: 504-5(Mar. 1965).

The recoil reactions following isomeric transition of ^{80m}Br in ^{80m}Br-labeled cobalt ammine bromides were studied and compared with results obtained with the (n,γ) reaction. The ligand yield of ^{80}Br produced in the isomeric transition tended to increase with decreases in the frequency of the maximum in the first absorption band. (M.C.G.)

19974 THE RADIOLYSIS OF COBALTAMMINE COMPLEXES. Nobufusa Saito and Takeshi Tominaga (Tokyo Univ.). Bull. Chem. Soc. Japan, 38: 505-6(Mar. 1965).

The radiolysis of 23 kinds of crystalline cobaltammine complexes was studied using ^{60}Co gamma rays. After irradiation, each complex was dissolved in water, and the cobalt(II) present in the solution was determined spectrophotometrically. For a series of nitroammine complexes which contained the same outer anion, the $G(Co^{2+})$ value decreased with increases in the number of NO_2 groups in the ligands. For a series of pentammine complexes containing the same outer anion and a different acidic ligand, the $G(Co^{2+})$ value decreased with increasing stability in the spectrochemical series. In a group of salts composed of the same complex cation and a different outer anion, the $G(CO^{2+})$ value was greatly affected by the kind of outer anion. (M.C.G.)

19975 THE REDUCTION OF GAMMA-IRRADIATED NICKEL OXIDE BY HYDROGEN. Toshiro Yamashina and Takaaki Nagamatsuya (Hokkaido Univ., Sapporo, Japan). Bull. Chem. Soc. Japan, 38: 507-8(Mar. 1965).

A gamma-irradiated nickel oxide was found to behave in an unusual manner in reduction by hydrogen, depending on radiation dose. The reduction rates were found to decrease following irradiation. The curves of induction periods and reduction rates, plotted as a function of radiation dose, both changed abruptly at radiation doses above 5×10^7 R. Abrupt increases of excess oxygen were also observed above 5×10^7 R. (M.C.G.)

19976 INFLUENCE OF NUCLEAR REACTOR RADIATION ON THE ELECTRICAL CONDUCTIVITY OF GLASSES. K. Schwabe and J. Luedenbach (Technische Universitat, Dresden). Chem. Tech. (Leipzig), 17: 42(Jan. 1965). (In German)

Glass foils and electrodes were exposed to reactor irradiation at a neutron flux at 10^{13} n/cm^{2}sec for time periods of 1, 5, 10, or 100 hrs. Only MacInnes glass showed an increase in specific resistance. LiBa glass shows no variation of the electrical resistance, and in NaBa glass the electrical resistance decreased only slightly. The time period of irradiation had no visible effect. (J. S. R.)

19977 FUNDAMENTALS OF RADIATION CHEMISTRY. Tino Gaeumann (Eidgenossische Technische Hochschule, Zurich). Chimia (Aarau), 19: 1-4(Jan. 15, 1965). (In German)

The physical process of energy absorption is described, and radiation energy is compared with other types of energy. The chemical process of energy absorption is reviewed. The special problems of radiation chemistry, the G value, absorbed dose, effect of the type of radiation, and energy and charge transfer, are summarized. (J.S.R.)

19978 THE EFFECTS OBTAINABLE BY IRRADIATION OF POLYMERS. J. Schenkel (Internationale Forschungs-Gesellschaft, Schwerzenbach, Switzerland). Chimia (Aarau), 19: 34-42(Jan. 15, 1965). (In German)

The radioinduced cross-linking, decomposition, grafting, and polymerization of polymers are the principal effects of irradiation. Each of these processes is reviewed extensively on the basis of a literature search. (J.S.R.)

19979 COLOR CENTERS PRODUCED BY A BEAM OF ELECTRONS IN CRYSTALS OF KCl AND KBr. I. Agarbiceanu and G. Teodorescu (Polytechnic Inst., Bucharest). Commun. Acad. Rep. Populare Romine, 13: 1047-9(1963). (In Romanian)

The formation of color centers in monocrystals of KCl and KBr, under the action of a beam of electrons of 60 kv and 40 μamp intensity, was studied. The centers thus formed were identified by spectral analysis of the transmission between 3600 and 9000 Å. (tr-auth)

19980 RADIATION THERMAL TRANSFORMATIONS OF NORMAL ALKANES IN THE LIQUID PHASE. A. M. Brodskii, K. P. Lavrovskii, V. B. Titov, and A. Kh. Eglit (Topchiev Inst. of Petroleum-Chemical Synthesis, USSR). Dokl. Akad. Nauk SSSR, 159: 1319-22(Dec. 21, 1964). (In Russian)

Characteristics of radiation thermal transformation and concentration of n-alkanes following radical thermalization were studied during $C_{34}H_{70}$ n-paraffin radiolysis at various temperatures. Experiments carried out in a reactor channel with heated quartz capsules at integral doses of 6×10^{21} ev/g and 150, 250, 280, 315, and 380° temperature showed, within the limits of the analysis, a linear dependence between the dose and trans-olefin groups, formed with 4 to 8% concentration, which did not vary at increased temperatures. Vinyl groups of the $HC = CH_2$ type with 1 to 2% concentration appeared at temperatures over 300°C. It was

also observed that with increasing temperature the number of methyl groups in the solid products increased; at 150°C an average of 2 methyl groups formed per molecule of the initial tetratriacontane and 3 to 4 groups at 380°C. Effective activation energy of the process was equal to 10 kcal/mole. An increase of temperature at the same integral dose inhibited increasing polymer molecular weight. At 150 to 200°C polymer molecular weight was double the initial hydrocarbon weight, at 380°C the weight was reduced 25%. Solutions of n-terphenyl in tetratriacontane (from 10^{-1} to 10^{-6}M n-terphenyl) were studied in addition to the tetratriacontane. Inhibiting effects of n-terphenyl were observed only during formation of diene compounds. (R.V.J.)

19981 THE MECHANISM UNDERLYING THE RADIOLYSIS OF AQUEOUS NITRATE SOLUTIONS. B. G. Ershov, A. K. Pikaev, G. G. Ryabchikova, and Vict. I. Spitsyn (Inst. of Physics and Chemistry, Academy of Sciences, USSR). Dokl. Akad. Nauk SSSR, 159: 1357-60 (Dec. 21, 1964). (In Russian)

The mechanism of ionizing radiation effects on dilute nitrate solutions, in which the chemical transformation of NO_3^- ions depends mainly on e^-_{aq}, H, and OH, was studied using ^{60}Co γ radiation. The absorbed dose determined with a ferrosulfate dosimeter was 2.8×10^{16} ev/ml sec. Graphs are given of the $G(NO_2^-)$ dependence on pH for 5×10^{-3}M of deaerated and air-saturated $NaNO_3$ solution. Radiolytic transformations in alkaline 5×10^{-3}M $NaNO_3$ solutions showed that with increasing pH $G(NO_2^-)$ increased; at pH 13.2 $G(NO_2^-)$ was 1.9 to 2.0. The yield of molecular hydrogen did not vary in alkaline media, and was equal to 0.35 to 0.40. The increase of $G(NO_2^-)$ was the result of OH radical dissociation and the increase of $G_{e^-_{aq}}$ in alkaline media. Assuming G_{H_2} equal to 0.45 and $G(NO_2^-) = \frac{1}{2} G_{e^-_{aq}}$ at pH 13.2, the results were $G_{e^-_{aq}} = 3.7$ to 3.8 and $G_{-H_2O} = 4.6$ to 4.7, which is in good agreement with published results for radiolysis of NO_2 solutions. (R.V.J.)

19982 RADIATION SYNTHESIS OF POLYMERS BASED ON TRIMERIC CYCLIC DIMETHYLPHOSPHINOBORINE. V. A. Zamyatina, V. V. Korshak, A. I. Solomatina, Yu. G. Chikishev, B. L. Tsetlin, S. R. Rafikov, and P. Yu. Glazunov (Inst. of Elementary and Organic Compounds, Academy of Sciences, USSR). Dokl. Akad. Nauk SSSR, 159: 1361-3 (Dec. 21, 1964). (In Russian)

Radiative yields of dimethylphosphinoborine polymers were studied using trimeric cyclic dimethylphosphinoborine irradiated at 6.5×10^4 Rad/sec in a 800-kev electron accelerator. At 4×10^{18} ev/g sec nearly 70% of the initial monomer transformed into two types of polymer products. One of the polymers, a white, hard substance with a molecular weight of 5200, was soluble in benzene and other ordinary solvents. After heating in dimethylformamide and tricresol the polymer differed from the initial dimethylphosphinoborine by lower hydrogen content (approximately three atoms per one trimeric cycle). The other polymer was a vitreous substance easily soluble in benzene, with a molecular weight of 4700 and a composition only slightly different from the initial composition. After prolonged heating in a vacuum at 350°C most of the polymer (67%) transformed into sublimated trimeric cyclic dimethylphosphine. Analysis of the two parallel processes showed that the irradiated trimeric cyclic dimethylphosphinoborine formed products of linear and polycyclic structures. (R.V.J.)

19983 LONG AFTERGLOW IN AQUEOUS SOLUTIONS OF PROTEINS AND SYNTHETIC POLYMERS IRRADIATED BY X-RAYS. I. I. Sapezhinskii, Yu. V. Silaev, and N. M. Emanuel (Inst. of Chemistry and Physics, Academy of Sciences, USSR). Dokl. Akad. Nauk SSSR, 159: 1378-80 (Dec. 21, 1964). (In Russian)

Thermoluminescence of proteins and synthetic polymers was studied using six proteins and enzymes (bovine albumin, hemoglobin, hyaluronidase, ribonuclease, trypsin, and cytochrome C) and three water-soluble polymers (polyethyleneoxide, polyvinylpyrrolidone, and polyvinyl alcohol), x-irradiated at 77 Rad/sec at various temperatures. Effects of oxygen, cysteine, and free radical inhibitors (propylgallate and isopropylgallate) on the thermoluminescence processes indicated their inhibiting influence on the afterglow intensity in proteins and synthetic polymers. It is shown that x- and ultraviolet radiation have identical effects on thermoluminescence in the materials examined. It is postulated that the afterglow is induced by recombinations of protein and polymer peroxide radicals. (R.V.J.)

19984 STUDY OF RADIOLYSIS OF AMMONIA ADSORBED ON SOLIDS BY THE METHOD OF ELECTRONIC PARAMAGNETIC RESONANCE. Yu. A. Sorokin, A. G. Kotov, and S. Ya. Pshezhetskii (Karpov Inst. of Physics and Chemistry, Moscow). Dokl. Akad. Nauk SSSR, 159: 1385-8(Dec. 21, 1964). (In Russian)

The effectiveness of utilization of the energy of nuclear radiation for chemical reactions is increased by the use of solid sorbents. However, the mechanism of the sensibilization is not clear. Processes which take place on γ irradiation of ammonia absorbed in zeolite were investigated. Specimens of zeolite with adsorbed ammonia were irradiated with ^{60}Co at the temperature of liquid nitrogen. The EPR spectrum was recorded. The spectrum of zeolite is a weakly anisotropic singlet. The spectrum of zeolite with adsorbed ammonia shows a fine structure. With the increase of ammonia amount, this distortion is increased, and the original singlet disappears. The radical NH_2 in argon shows a different EPR spectrum (triplet) than in water and in zeolite. The differences could be explained by the effect of the matrix on the rotational degrees of freedom of NH_2. The formation of NH_2 apparently depends not only on the direct radiolysis, but also on the energy transfer from zeolite. (ATD)

19985 METHYL-C^{14} RADICAL AS A SCAVENGER IN STUDIES OF THE RADIOLYSIS OF SATURATED AND UNSATURATED HYDROCARBONS. R. A. Holroyd and G. W. Klein (Mellon Inst., Pittsburgh). Intern. J. Appl. Radiation Isotopes, 15: 633-40(Nov. 1964). (RRL-129)

A scavenging technique is described for determining the yields of radical species produced in the radiolysis of reactive solvents such as olefins. The scavenger, methyl-^{14}C radical, is generated from $^{14}CH_3I$ present in low concentrations. These studies are necessarily carried out either at high dose rates or low temperatures so that $^{14}CH_3$ radicals react with the various radical intermediates. From the yields of labeled hydrocarbons formed, the individual radical yields are calculated. In liquid ethylene ethyl, vinyl, and 3-butenyl radicals were detected with yields of $G_{ethyl} = 1.7$ and $G_{vinyl+3\text{-}butenyl} = 0.8$. Relative radical yields were determined for n-pentane and found to be in good agreement with yields reported using several other radical scavengers. The results for pentane suggest that $^{14}CH_3$ radicals are generated from $^{14}CH_3I$ by the reaction: $H + {}^{14}CH_3I \rightarrow {}^{14}CH_3 + HI$. (auth)

19986 RADIATION EFFECTS ON THE THERMAL PROPERTIES OF ALKALI-HALIDE CRYSTALS AND THEIR SOLID SOLUTIONS. I. N. Anokhina, M. S. Ivankina, and P. A. Savintsev (Tomsk Polytechnic Inst., USSR). Izv. Vysshikh Uchebn. Zavedenii, Fiz., No. 1, 47-9(1965). (In Russian)

Irradiation of alkali-halide crystals from a Ra–Be source with a dose of 4.2×10^{10} n/cm^2 expanded NaCl, KCl, KBr, and KI crystals. Correlations of the relative changes in alkali halide crystals and their lattices showed the highest change in crystals with a stronger ion bond (NaCl and KCl). Measurements of linear temperature expansion in 0.5 KCl + 0.5 KBr irradiated with 4.8×10^6 n/sec and γ ray 10 R/min indicated a reduced coefficient of linear expansion and increased coefficient of thermal conductivity. The possibility of reducing structural defects by irradiation was postulated. (R.V.J.)

19987 INVESTIGATION OF THE STORED ENERGY OF NaCl, KCl, KBr, AND KI ALKALI-HALIDE CRYSTALS FOLLOWING γ IRRADIATION AT ROOM TEMPERATURE. E. K. Zavadovskaya and A. V. Kuz'mina (Komi State Teacher's Univ., USSR). Izv. Vysshikh Uchebn. Zavedenii, Fiz., No. 1, 175-6(1965). (In Russian)

The results showed that the magnitude of stored energy in irradiated alkali-halide crystals NaCl, KCl, KBr, and KI

depends on the energy of their lattices; the larger the lattice energy the higher is the stored energy. (R.V.J.)

19988 ION-MOLECULE REACTIONS IN ACETYLENE. G. A. W. Derwish, A. Galli, A. Giardini-Guidoni, and G. G. Volpi (CNEN, Rome and Universita, Rome). J. Am. Chem. Soc., 87: 1159-68(Mar. 20, 1965).

Ion-molecule reactions occurring in acetylene were studied up to a pressure of 0.3 torr inside the ion source of a mass spectrometer. Long-chain ionic reactions were recognized leading to the formation of high-order ions. A full kinetic study was carried out, and a mechanism is proposed for these reactions. (auth)

19989 EFFECT OF pH ON THE γ-RAY-INDUCED CHAIN REACTION BETWEEN FORMIC ACID AND HYDROGEN PEROXIDE. Ather Husain and Edwin J. Hart (Argonne National Lab., Ill.). J. Am. Chem. Soc., 87: 1180-6(Mar. 20, 1965).

The effects of pH on carbon dioxide, carbon monoxide, and hydrogen yields is reported for the chain radiolysis of dilute aqueous formic acid-hydrogen peroxide solutions. In the pH range from 1 to 13, $G(CO_2)$ reached a maximum yield of 300 at pH 4.4, and G(CO) a maximum yield of 1.5 at pH 2.5. $G(H_2)$ was unchanged from pH 0.4 to 3.0 and then decreased to a constant value of 0.6 at pH 5.0. Oxygen was a powerful inhibitor, but carbon monoxide, formaldehyde, and glyoxylic acid also retarded the chain reaction. The mechanism is discussed in terms of ionization of the carboxyl, hydroperoxy, and hydroxyl radicals, as well as of the formic acid. (auth)

19990 A MARKED EFFECT OF CONFORMATION IN THE RADIOLYSIS OF POLY-α-L-GLUTAMIC ACID IN AQUEOUS SOLUTION. Harvey A. Sokol, Winifred Bennett-Corniea, and Warren M. Garrison (Univ. of California, Berkeley). J. Am. Chem. Soc., 87: 1391-2(Mar. 20, 1965). (UCRL-11733)

Studies were made of the gamma-induced oxidation of poly-α-L-glutamic acid (PGA) over the pH range from 3.5 to 9. Pyruvic and α-ketoglutaric acids were identified as the major carbonyl products. Acetaldehyde and glyoxylic acid were detected in low yield. The yield of ammonia and α-keto acids increased abruptly with increasing pH from ≈4.5 to ≈6 pH. Reaction mechanisms are discussed. (M.C.G.)

19991 RADIOLYSIS OF HEXAFLUOROETHANE. Larry Kevan and Peter Hamlet (Univ. of Chicago). J. Chem. Phys., 42: 2255-8(Apr. 1, 1965). (COO-1365-2)

The radiolysis of C_2F_6 at 3 atm was examined. The products and 100-ev yields were CF_4 (1.6), cyclo-C_3F_6(0.30), C_3F_8(0.21), C_4H_{10}(0.14), and C_2F_2(0.03). Good material balance was obtained; the F/C ratio in the products was 3.0. Experiments using radical scavengers indicated that 50% of the CF_4 comes from radical reactions and 50% from nonradical reactions, that C_3F_8 and C_4H_{10} are entirely formed by radical reactions, and that C_2F_2 and cyclo-C_3F_6 are probably formed by ionic reactions. In Ar–C_2F_6 mixtures energy transfer, thought to be charge transfer, was observed and ionic production of C_3F_8 was seen. C_2F_6 was about one-fifth as sensitive to radiation decomposition as C_2H_6. It was concluded that excited molecule decompositions, particularly those giving molecular fluorine, are relatively unimportant in the radiolysis of perfluoroalkanes. (auth)

19992 DETERMINATION OF THE EXCITATION FUNCTIONS FOR FORMATION OF METASTABLE STATES OF SOME RARE GASES AND DIATOMIC MOLECULES BY ELECTRON IMPACT. John Olmsted, III, Amos S. Newton, and K. Street, Jr. (Univ. of California, Berkeley). J. Chem. Phys., 42: 2321-7(Apr. 1, 1965). (UCRL-11631)

An apparatus for the determination of the excitation functions for formation of metastable states by impact of electrons of precisely defined energies in the energy range from threshold to the ionization potential is described. Results are given for Ne, Ar, Kr, H_2, N_2, and CO. Two sharp resonances were observed in each of the rare gas excitation functions, which corresponded to excitation with electron exchange of the first two excited configurations of these atoms. For diatomic molecules, no such resonances were observed, except in nitrogen, where there was a resonance process with an onset energy of 11.8 ev. A partial explanation for the shapes of the excitation functions is offered, based on the location and character of the various excited triplet states of the molecules studied. (auth)

19993 RADIOLYSIS OF ETHYLENE. IV. UNIMOLECULAR DISSOCIATION OF INTERMEDIATE ION-MOLECULE COMPLEXES. G. G. Meisels (Union Carbide Corp., Tuxedo, N. Y.). J. Chem. Phys., 42: 2328-34(Apr. 1, 1965).

Kinetic analysis of free-radical reactions in the radiolysis of ethylene demonstrated that the relative extent of radical addition to ethylene can be held constant by maintaining the ratio of accelerator beam current to ethylene pressure invariant. The pressure dependence of the methane and methyl radical yields when this ratio was constant revealed that the mechanism of their formation includes competition between unimolecular dissociation of an intermediate ion and its participation in an ion–molecule reaction. Consideration of known ion–molecule reactions suggested that the species involved in the competing steps are $[C_6H_{11}^+]$ (methane formation) and $[C_6H_{12}^+]$ or $[C_4H_9^+]$ (methyl radical formation). Rate constants of 4.2×10^8 and 1.0×10^9 sec^{-1}, respectively, were calculated for the dissociation processes on the basis of collision efficiency for the competing ion-molecule reactions. About one-fourth of the methane and one-half of the methyl radicals were formed by reactions, which were independent of pressure below 1 atm. This could be ascribed to rate constants larger than 10^{10} sec^{-1} for dissociation of $[C_8H_{15}^+]$ and $C_8H_{16}^+]$ ion, respectively, or to the existence of at least two discrete energy levels for the dissociating species. Relative dissociation probabilities of intermediate ion–molecule complexes, determined by mass spectrometry, were used to estimate $G(C_2H_4^+) \approx 1.5$ and $G(C_2H_3^+) \simeq 1.0$ ions/100 ev at approximately atmospheric pressure, in good agreement with values of 1.51 and 0.96, respectively, which could be calculated from W and fragmentation patterns for 70-ev electrons. (auth)

19994 ELECTRON SPIN RESONANCE STUDY OF IRRADIATED ANHYDROUS MALTOSE. J. N. Herak, K. Adamic, and R. Blinc (Institut "Rudjer Boskovic," Zagreb and Nuclear Institute "Jozef Stefan," Ljublijana, Yugoslavia). J. Chem. Phys., 42: 2388-91(Apr. 1, 1965).

The electron spin resonance spectra of γ-irradiated powdered anhydrous α-maltose were measured. By temperature annealing it was found that: the room temperature ESR spectrum consists of at least three different types (A, B, C) of radioinduced damage centers. Type A centers seemed to result from a rupture of the C-1–H bond. They transformed into Type B centers with a half life of about 110 min (in air at room temperature). The most probable type of transformation seemed to be a change in configuration of the pyranose ring. Whereas Type B centers recombined under these conditions with a half life of about 26 hr, the half life of Type C centers exceeded a month. There were some indications that Type C centers are connected with a breaking of the glycosidic bond between two pyranose rings. (auth)

19995 CROSS SECTIONS AND INTRAMOLECULAR ISOTOPE EFFECTS ON AB–HD ION-MOLECULE REACTIONS. T. F. Moran and L. Friedman (Brookhaven National Lab., Upton, N. Y.). J. Chem. Phys., 42: 2391-2405(Apr. 1, 1965). (BNL-8598)

Isotopic ion–molecule reactions producing ABH^+ and ABD^+ ions (AB = N_2, CO, O_2, and CO_2) when AB–HD mixtures are subjected to electron bombardment in a mass-spectrometer ion source were studied as a function of reactant ion velocity. Good agreement between the experimental and theoretical cross sections for secondary ion formation was obtained when both AB^+–HD and HD^+–AB interactions were taken as possible reaction paths. Ionization efficiency curves of the secondary ion products furnished supporting evidence for the assumed reaction mechanisms. Identification of reactant ions by ionization efficiency curves was not sufficient to establish the ther-

mochemistry of the ion–molecule reaction; distributions of vibronic states produced by electron impact were also required. The vibrational population of excited reactant ions formed in the electron impact process was estimated from the squares of the overlap integrals of respective ground and excited ionized states. Data taken from published photoionization experiments were used to estimate the distribution of electronic excitation in the N_2^+, CO^+, and O_2^+ reactant ions. These data served to better define the reactant ion species in these ion–molecule interactions and aided in the analysis of energy transfer processes and intramolecular isotope effects in the reactions. Intramolecular isotope effects showed an increase in the ratio of ABH^+/ABD^+ with increasing reactant ion velocity. The isotope effects are described in terms of a unimolecular decomposition of the collision complex and ion or atom transfer mechanisms. The isotope effects indicated that atom transfer mechanisms are favored both in reactions of ions with high kinetic energy and in strongly exothermic reactions of relatively slow ions. (auth)

19996 TRANSITION PROBABILITY OF $^2\Pi_u \rightarrow X\ ^2\Pi_g$ SYSTEM OF CO_2^+. R. P. Schwenker (E. I. du Pont de Nemours and Co., Wilmington, Del.). J. Chem. Phys., 42: 2618-19(Apr. 1, 1965).

The emission spectrum obtained from the bombardment of CO_2, at a pressure of 5μ by 200-ev electrons is shown. This spectrum was previously identified as due to the $^2\Pi_u \rightarrow X\ ^2\Pi_g$ transition of CO_2^+. A mean radiative lifetime of $(13.9 \pm 1.0) \times 10^{-6}$ sec was measured for the $^2\Pi_u$ state. An oscillator strength of $(1.18 \pm 0.1) \times 10^{-2}$ was calculated for the system. (M.C.G.)

19997 DEACTIVATION OF GAS CHROMATOGRAPHIC SUPPORT BY RADIATION INDUCED COPOLYMERIZATION. Paul Urone and Jon F. Parcher (Univ. of Colorado, Boulder). J. Gas Chromatog., 3: 35-6(Jan. 1965).

An inert gas chromatographic support was obtained by radioinduced copolymerization of hexamethyldisilazane on 60/80 mesh acid-washed firebrick. Cleaned and vacuum dried firebrick was exposed to a dosage of 50 MR of gamma radiation after which the firebrick was recovered by filtration and drying. The deactivated support gave nearly symmetrical elution curves and specific retention volumes of less than one ml/g at 70°C for the normal alcohols through butanol. Non-deactivated firebrick columns under the same conditions gave exceedingly poor elution curves and very long retention times for the more polar solutes. Efficiencies were compared for both polar and non-polar liquid phases, with better results obtained on the treated support. (M.C.G.)

19998 INFLUENCE OF IMPURITIES ON THE OPTICAL PROPERTIES OF IRRADIATED LITHIUM FLUORIDE. M. Dubois, P. Berge, M. Benveniste, and G. Blanc (Centre d'Etudes Nucleaires, Saclay, France). J. Phys. (Paris), 25: 1017-22(Dec. 1964). (In French)

The optical properties of LiF are dependent on the divalent positive impurities, such as magnesium, present in the crystal. The magnesium increases the rate of F-center formation and influences the bleaching of this center. In some cases, a Z band at 2 220 Å, and a band at 3 400 Å which could be due to a V center were observed. These results can be related to the state of the magnesium in the lattice. (auth)

19999 DETERMINATION OF FORMATION ENERGY OF M CENTER IN KCl. Yoshiki Sato and Toru Nakano (Japan Atomic Energy Research Inst., Tokyo). J. Phys. Soc. Japan, 20: 173(Jan. 1965).

A KCl crystal was irradiated with from 2.01×10^5 to 16.4×10^5 R ^{60}Co gamma radiation at temperatures from 33 to 77°C. Optical absorption measurements were made to determine the ratio of the absorption coefficient for M centers to the square of that for F centers. Equilibrium constants are calculated from a thermodynamic equation, and the heat and entropy changes are determined. (M.J.T.)

20000 DIELECTRIC BEHAVIOR OF POLY(β-PROPIOLACTONE) PREPARED BY RADIATION INDUCED SOLID STATE POLYMERIZATION. Yoichi Ishida, Masato Matsuo, Masao Onga, and Motow Takayanagi (Kyushu Univ., Fukuoka). J. Polymer Sci., Pt. B, 3: 301-4(Apr. 1965).

Gamma rays from a ^{60}Co source were used to irradiate β-propiolactone at −78°C for 46 hr under vacuum. The dose rate was 10^5 R/hr. The polymer formed was isolated from the residual monomer and the samples for dielectric measurement were prepared by pressing at room temperature. Data indicated that the sample prepared by solid-state polymerization contains a defective region capable of local twisting motion, but contains no relaxed amorphous region, which is capable of the segmental motion. The data are presented in graphs. (M.C.G.)

20001 DYNAMIC VISCOELASTIC PROPERTIES OF GRAFT COPOLYMERS. 2. THE PECULIAR THERMAL HYSTERESIS OF PVF-St GRAFT COPOLYMER. T. Honjo and S. Ogawa. Kogyo Gijutsuin Sen'i Kogyo Shikenjo Kenkyu Hokoku, No. 67, 13-18(Mar. 1964). (In Japanese)

Samples of polyvinyl fluoride-styrene (PVF-St) graft copolymer were irradiated with ^{60}Co γ rays at 40 or 60°C. The viscoelasticities were measured at 20 cps and at 1°C/min for increasing or decreasing temperatures between 20 and 170°C at a constant surface pressure. The results obtained for the PVT-St graft copolymer with a large graft ratio (5.31) are discussed. Tan δ temperature curves obtained for increasing temperatures showed 2 peaks at 75 and 110°C and one large peak at 120°C corresponding to the main dispersion of PSt for decreasing temperatures. The graft copolymer heat-treated above the glass transition temperature of PSt did not exhibit thermal hysteresis and showed the same curve as that for decreasing temperatures of the untreated copolymer. However, it recovered the original hysteresis when it was washed in the solvent (benzene). Various factors responsible for this phenomenon are discussed. (OID)

20002 SOME ELEMENTARY PROCESSES IN RADIATION- AND PHOTO-CHEMISTRY REVEALED BY ELECTRON SPIN RESONANCE. P. B. Ayscough, R. G. Collins, and F. S. Dainton (Univ. of Leeds, Eng.). Nature, 205: 965-9(Mar. 6, 1965).

The ESR spectra of various odd electron species produced by γ rays or light and trapped in various glassy matrices at 77°K are described. The glassy materials include aqueous alkaline, aqueous acid, and non-aqueous glasses. (P.C.H.)

20003 PARAMAGNETIC RESONANCE OF THE V_F CENTER IN CaF_2. Jerome Sierro (Argonne National Lab., Ill.). Phys. Rev., 138: A648-50(Apr. 19, 1965).

Natural CaF_2 crystals subjected to x rays at 77°K and then warmed to a temperature above 138°K contain V_F centers. The electronic structure of this electron-deficient center was investigated by electron paramagnetic resonance. The parameters of the appropriate spin hamiltonian were determined. The center appears to consist of an F_2^- molecule ion associated with a Ca^{2+} vacancy. (auth)

20004 CHEMICAL EFFECTS OF THE $^{35}Cl(n,p)^{35}S$ REACTION. I. PROTECTION EFFECTS AGAINST SULFUR OXIDATION. Kenji Yoshihara, Ting-chia Huang, Hiroshi Ebihara, and Nagao Shibata (Japan Atomic Energy Research Inst., Tokyo). Radiochim. Acta, 3: 185-91(Dec. 1964).

Chemical effects of the $^{35}Cl(n,p)^{35}S$ reactions in various alkali chlorides, in hydrazine hydrochloride, and in hydroxylamine hydrochloride were investigated. Protection effects of carriers, reducing groups, and solvents were found to be very important in determinating the chemical fate of radiosulfur. Low-valency sulfur species survived even carrier-free dissolution of the neutron-irradiated hydrazine hydrochloride. The oxidation mechanism of radiosulfur according to Koski's explanation did not fit the experimental results. The possibility that certain molecules may occur in the neighborhood of the recoil atoms, which easily oxidize sulfur is considered. The assumption that chlorine atoms act as strong oxidants at the moment of dissolution is discussed. (auth)

20005 THE CHEMICAL STATE OF IODINE IN TELLURIUM COMPOUNDS AFTER NEUTRON IRRADIATION.

L. Kronrad (Nuclear Research Inst., Academy of Sciences, Rez, Czechoslovakia). Radiochim. Acta, 3: 191-3(Dec. 1964).

The activity distribution of ^{131}I between the iodide-elementary fraction and the iodate-periodate fraction in irradiated tellurium compounds as a function of irradiation length was investigated. The change in activity distribution of ^{131}I in thermally annealed tellurium dioxide was observed. (auth)

20006 THE ELECTRON SPIN RESONANCE SPECTRA OF γ-IRRADIATED SINGLE CRYSTAL OF CYANOACETIC ACID. De-liang Kuo. Sci. Sinica (Peking), 14: 469-71 (Mar. 1965).

The results of a study on the ESR spectra of a gamma-irradiated single crystal of cyanoacetic acid are presented. Crystals of cyanoacetic acid were grown from an aqueous solution. A single crystal with dimensions of a = 3 mm, b = 2.5 mm, c = 5 mm was irradiated at room temperature with a ^{60}Co γ source at a dose of 3.99×10^6 R. After irradiation, the crystals turned purple. The ESR spectra were recorded from a paramagnetic resonance spectrometer. The results confirmed that the free radical trapped in the irradiated single crystal is in the form of NCCHCOOH. The free radical may be clearly represented by overlapping a carbon 2p-orbital with the π-bond of the nitrile bond to form a π-conjugation bond. The unpaired electron is localized in the π-conjugation bond, and the large ^{14}N-hyperfine splitting is produced by direct interaction with the ^{14}N nucleus. (P.C.H.)

20007 THE THERMOLUMINESCENCE OF IRRADIATED HIGH POLYMERS. I. DETERMINATION OF GLOW PEAKS AND THEIR ACTIVATION ENERGIES OF γ-IRRADIATED POLYETHYLENE. Wen-shang Yang, Guan-yin Chien, Guang-chi Lai, and Pao-kung Chien. Sci. Sinica (Peking), 14: 473-6(Mar. 1965).

Studies were made to determine the number of glow peaks of irradiated polyethylene, to observe the change of intensities of the glow peaks, and also to determine the activation energies of luminescent processes. The results were compared with those from differential thermal analysis. Low density polyethylene samples were irradiated by a 20,000 gram radium equivalent ^{60}Co γ source at 50 R/sec at liquid nitrogen temperature. Three main peaks appeared at 126, 179, and 232°K on the glow curve of a polyethylene specimen irradiated under high vacuum with a total dose of 9×10^5 Rad. The number of main peaks and their intensity changed with irradiation dose in the region from 5×10^4 to 1.1×10^7 Rad. Data on activation energies are tabulated. From the DTA tests it was concluded that the factors that give rise to the glow peak at 126°K and the DTA peak are not the same; what causes the appearance of the DTA peak may be decreased or eliminated by a single irradiation or DTA test. However, it is possible that the factors determining the position of the two peaks might be the same. (P.C.H.)

20008 POLONIUM^{210} PRODUCTION BY THE NEUTRON IRRADIATION OF BISMUTH. D. Nemoda. Tehnika (Belgrade), 19: 428-31(Mar. 1964). (In Serbo-Croatian)

The methods and apparatus used for ^{210}Po production in quantities of a few tenths of a millicurie are described. Po is produced by exposing metallic Bi to neutron irradiation in a nuclear reactor. For separation of Po from Bi, the O. Erbacher method of electrochemical Pu deposition on Pt from a natural mixture with Pb and Bi was used (Naturwissenschaften, 20: 391(1932)). It was established that it is possible to separate the greater part of Po (about 90%) by spontaneous electrolysis from a 12% solution of HCl, which contains about 0.33 g Bi/ml and traces of Po (about 7×10^{-8} g Po/g Bi). Also, some radiochemical and electrochemical properties of ^{210}Po are described as well as the method used for its production. (OID)

20009 SPECTROSCOPIC STUDIES OF REACTIONS OF THE OH RADICAL IN AQUEOUS SOLUTIONS. REACTION OF OH WITH THE FERROCYANIDE ION. G. E. Adams, J. W. Boag, and B. D. Michael (Mount Vernon Hospital, Northwood, Middx., Eng.). Trans. Faraday Soc., 61: 492-505(Mar. 1965).

A study of the pulsed radiolysis of aqueous oxygenated solutions of ferrocyanide ion showed that the oxidation proceeds in distinct stages. The yield of ferricyanide ion, measured spectroscopically, immediately after a 2-μsec pulse of electron irradiation, was equal to G(OH). Over a period of several msec, an additional yield was observed, which was due to oxidation of the solute by HO_2 radicals. The effect of ethanol and N_2O was investigated in order to determine the nature and yield of the primary species as a function of pH. It was concluded that above pH 4, G(OH) = 3.2, G(e^-_{aq}) = 3.16, and G(H) = 0.6-0.8. Relative reactivities of OH and O^-, the basic form of OH, were determined, and the absolute rate constant for the oxidation of ferrocyanide ion by HO_2 was measured. (auth)

20010 LUMINESCENCE APPEARING IN CRYSTALS OF SODIUM URANYL ACETATE IRRADIATED BY A RUBY LASER BEAM. M. S. Brodin, V. M. Vatul'ov, and S. V. Zakrevskii (Inst. of Physics, Kiev). Ukr. Fiz. Zh., 9: 1150-1(Oct. 1964). (In Ukrainian)

The high intensity of laser beams makes it possible to observe and investigate a series of nonlinear effects. It also makes the observation of luminescence possible when a substance becomes transparent to the frequency of the exciting light. To investigate nonlinear effects, sodium uranyl acetate single crystals and crystalline powders were irradiated with the focused beam of a ruby laser and the luminescence spectra were photographed. Irradiation of crystals with a focused laser beam caused the formation of cavities or through-holes. The destruction of the crystals may be due to mechanical forces or to thermal effects. One may conclude that the line-structured single crystal spectrum is associated with laser excited luminescence resulting from two-photon absorption or absorption of light of another harmonic. It also is possible that this spectral structure is due to luminescence of several defect centers which are formed when the crystal is irradiated by a laser beam. Large overlapping of absorption and luminescence spectra in the case of a single crystal can be associated with the fact that a crystal region which radiates is heated to a high temperature, or that luminescence is superposed by radiation with a continuous spectrum which penetrates through a layer of crystal. (ATD)

20011 THE EFFECTS OF X-RAY IRRADIATION ON THE SELF-FRICTION OF POTASSIUM CHLORIDE. Earl Zwicker and G. H. Jirgal, Jr. (Illinois Inst. of Tech., Chicago). Wear, 7: 39-47(1964).

The effects of x-ray irradiation on the sliding and static friction of polished KCl were studied. The sliding friction obeyed a law with both adhesive and plowing terms, and the static friction obeyed the classical law, $F = \mu N$. It was found that x-ray irradiation for 12 hours from a 40 kv, to ma silver target source doubled the values of the adhesive and plowing terms for sliding friction of non-annealed KCl with powdered KCl surface debris, and static friction was increased by 65%. Pre-irradiation annealing of the crystals with surface debris lowered the radioinduced increase in friction to 14%. Removal of surface debris prior to irradiation of annealed crystals resulted in a 20% decrease in static friction with x-ray irradiation. Explanations for the static friction results were devised by combining the ideas of Bowden and Tabor with those of Archard. The behavior of sliding friction with irradiation could be explained successfully by Archard's theory. (auth)

20012 RADIOLYSIS OF FROZEN AQUEOUS SOLUTIONS OF SOME AMINO ACIDS AND PEPTIDES. V. A. Sharpatyi, K. G. Yanova, A. V. Topchiev, and A. P. Ibragimov (Karpov Inst. of Physics and Chemistry, Moscow). Zh. Fiz. Khim., 39: 232-5(Jan. 1965). (In Russian)

The electron paramagnetic resonance method was used for determining the nature of radicals formed during radiolysis of frozen aqueous solutions of amino acids and peptides. The G_R magnitudes were found for some amino acids and peptides (glycine, α-alanine, and glycine-glycine, α-alanine-α-alanine, and β alanine-β alanine peptides) in frozen 1M solutions and for dry polycrystalline specimens. (R.V.J.)

20013 EFFECT OF RADIOACTIVE S^{35} RADIATION ON THE CATALYTIC DEHYDRATION OF CYCLOHEXANOL.

A. A. Balandin, Vikt. I. Spitsyn, N. P. Dobrosel'skaya, I. E. Mikhailenko (Moscow State Univ. and Inst. of Physics and Chemistry, Moscow). Zh. Fiz. Khim., 39: 258-61(Jan. 1965). (In Russian)

Processes of heterogenic catalysis with radioactive catalysts and ionizing radiation were studied using a specially designed vertical catalytic installation. It was confirmed that, in contrast to the self-irradiating catalyst, irradiation with fast electrons from external sources produced a negligible effect. The radioactive catalysts $Mg^{35}SO_4 + Na_2{}^{35}SO_4$ were prepared. A certain amount of radioactive Na_2SO_4 was added to $MgSO_4 \cdot 7H_2O$ at room temperature after which the sulfate solution was evaporated at 400°C and the residue crushed into dry 2 mm granules. Comparisons of specific surfaces of non-radioactive specimens showed that the surface of Na_2SO_4 was 22 times smaller than $MgSO_4$. The higher the amount of Na_2SO_4 the smaller the surface of the sulfate catalysts, indicating that the slow crystallization of $MgSO_4$ with Na_2SO_4 formed denser crystal structures. Radioactivity from ^{35}S β emission did not affect the surface. The highest specific catalytic activity was observed with the smallest (2 m^2/g) surface area and highest specific radioactivity (105.2 $\mu C/g$). Graphs of the catalytic activity of ^{35}S-labeled $MgSO_4$ + 21.87% Na_2SO_4 in cyclohexanol dehydration at time lengths of 1 day (105.2 $\mu C/g$), 315 days (8.5 $\mu C/g$), and 503 days (1.9 $\mu C/g$) are plotted. (R.V.J.)

20014 EFFECT OF POLYETHYLENE GLYCOLS ON NUCLEAR PHOTOGRAPHIC EMULSIONS. A. P. Zhdanov, A. L. Kartuzhanskii, G. G. Martysh, and L. I. Shur. Zh. Nauchn. i Prikl. Fotogr. i Kinematogr., 9: 300-2(1964). (In Russian)

The effect of polyethylene glycols (PEG) on nuclear emulsions during exposure to light and to ^{210}Po α particles, ^{14}C β particles, and relativistic electrons. The sensitivity to light increased noticeably, but the sensitivity to particles did not increase. The PEG reduced only the time of development during which the limit value was attained, and it had an apparent sensitizing effect in short-time or incomplete development. Reasons of the difference in sensitivity to light and to ionizing particles are discussed. (M.C.G.)

20015 EFFECTS OF IONIZING RADIATION ON THE AQUEOUS SOLUTION OF GLYCOGEN IN OXYGEN AND IN VACUUM. E. A. Kuzicheva and M. A. Khenokh. Zh. Obshch. Khim., 35: 7-14(Jan. 1965). (In Russian)

Following previous studies, which revealed that irradiation of glycogen results in a decrease of its molecular weight from 6.5×10^6 to 0.5×10^6 and in the hydrolytic decomposition of the polysaccharide structure, the effects of its exposure to γ radiation were investigated. The effects of OH· and HO_2· radicals were especially studied. It was found that the exposure causes a strong decomposition, yielding dextrin-like substances but no glucose or maltose. The radiolytic products, such as carbonyl compounds, organic acids, formaldehyde, reducing compounds, and dihydroxyacetone were identified as the primary products of radiation. The presence of O during the irradiation increased the yield of the products of radiolysis by 10 to 20%, as compared with irradiation in vacuum. This indicated that the OH· radicals are more active than the HO_2· radicals. Irradiation in a vacuum in the presence of H_2O_2 enhanced the effects of radiolysis. The radioinduced decomposition was stronger in acid than in alkaline media. (TTT)

20016 EFFECT OF IONIZING RADIATIONS ON METHYLENE BLUE IN GLYCEROL SOLUTION. R. Ducousso. Thesis, Bordeaux, Faculte de Pharmacie, 1963. (In French)

20017 ELECTROPHYSICAL PROPERTIES OF IRRADIATED AND HEAT-TREATED POLYETHYLENE. A. V. Vanikov, V. D. Bityukov, and N. A. Bakh. p.41-7 of "Khimicheskiye Svoystva i Modifikatsiya Polimerov." Moscow, Izd-vo Nauka, 1964.

20018 THE EFFECT OF OXYGEN ON THE RECOIL REACTIONS OF CARBON-11 IN HYDROCARBONS. Dale Byron De Vries. Thesis, Ames, Iowa, Iowa State Univ. of Science and Tech., 1964. 80p.

The recoil reactions of carbon-11 produced by the $^{12}C(\gamma,n)^{11}C$ reaction in benzene, cyclohexane, and n-hexane were studied. The yields of carbon-11 labeled methane, ethane, ethylene, and acetylene were determined. The effect of radiation dose and oxygen scavenger on these yields was investigated. With the exception of acetylene, all the yields observed were found to be sensitive to radiation dose. It was also observed that the extrapolation of product yield versus dose curves to "zero" dose gave the same value for the product yield that was found with oxygen scavenger present. It was found that the acetylene yield increased from benzene to cyclohexane to n-hexane. Very small amounts of methane and no two-carbon products other than acetylene were observed for benzene. The methane yield was larger in cyclohexane than in n-hexane, but the yields of ethane and ethylene were smaller in cyclohexane. These results are discussed in terms of the nature of the recoil carbon-11 atom as it dissipates its kinetic energy in the system. The results are consistent with a mechanism involving the insertion of a $[\cdot{}^{11}\ddot{C}]$, $[\cdot{}^{11}\ddot{C}H]$, or $[:{}^{11}CH_2]$ recoil fragment into a carbon-hydrogen bond of the parent hydrocarbon. The trends observed in the yields of specific products indicate that the insertion reactions take place at energies higher than thermal equilibrium values, and that the most important product determining factor is the nature of the intermediate formed in the insertion process. (Dissertation Abstr., 25: No. 5, Nov. 1964)

20019 RADIATION EFFECTS IN OPTICAL MATERIALS. W. E. Spicer (Stanford Univ., Calif.). 21p. (CONF-720-19)

From 2nd Symposium on Protection Against Radiation Hazards in Space, Gatlinburg, Tenn., Oct. 1964.

Mechanisms involved in radiation damage to optical materials and their practical consequences are discussed. Three types of damage and their thresholds are considered: direct electronic displacement damage, direct atomic displacement damage, and indirect atomic displacement damage. Spatial distribution of damage and the importance of perfection of the sample are discussed. Radiation effects on quartz, CdS, ZnO, alkali metal halides, and pigmented thermal control surfaces are considered. (M.C.G.)

Radiochemistry

See also Separation Processes and Procedures.

Refer also to abstract 21741.

20020 (IA-907) A CRITERION FOR SELECTIVITY IN RECOIL LABELING. S. Amiel and Y. Paiss (Israel Atomic Energy Commission, Yavne. Soreq Nuclear Research Establishment). Dec. 1964. 15p. Dep.(mn).

An examination of physical properties was made with the aim of deriving parameters related to selectivity in hot displacement reactions when atoms produced by different nuclear processes recoil into appropriate stopping media. Different probabilities of labeling were inferred from revised versions of the Billiard-Ball Collision Model and scavenging effects. The conclusions were examined in the light of experimental results obtained for the reaction $I^* + CH_3I \rightarrow CH_3I^* + I$ where the labeling atom is either a fission fragment, an atom recoiling after neutron capture, or a beta decay product. Possible applications of selective labeling for the separation of primary nuclear reaction products from the same nuclides produced by radioactive decay, are discussed. (P.C.H.)

20021 (NP-14900) UN NUEVO METODO DE PREPARACION DE ^{32}P SIN PORTADOR. Informe No. 128. (On a New Method of Preparation of Carrier-Free ^{32}P. Report No. 128). R. P. Goso and R. Radicella (Comision Nacional de Energia Atomica, Buenos Aires (Argentina)). 1964. 11p. Dep.(mn).

A description is given of the method utilized for preparing carrier-free ^{32}P-orthophosphate by solution of the irradiated sulfur in carbon sulfide, followed by the adsorption of phosphorus-32 in a powered glass column and elu-

tion with distilled water. The chemical yield is 90%. The radioactive purity is better than 99.95% and the radiochemical purity is higher than 99.5% after heating the solution (0.01 N, hydrochloric acid) for 1 hour, at 120°C. (auth)

20022 (JPRS-29258) ON THE NEW PROCEDURES FOR PRODUCING RADIOACTIVE COLLOIDAL GOLD ^{198}Au IN THE "BORIS KIDRIC" INSTITUTE AT VINCA. Rade Draskovic, Jelisaveta Cvoric, Sreten Vukicevic, and Ratko Ilic. Translated from Tehnika (Belgrade), 20: 228-33(1965). 16p. (TT-65-30572). $1.00(CFSTI).

Constant modification of Henry's method was used to produce radioactive colloidal ^{198}Au with an activity of 25 to 50 mC/ml and a dispersal of 200 ± 50 A. Results of chemical and biological controls of the product are given. Procedures are also given for the production of diluted radiocolloid and of a radiocolloid with a dispersal of 40 to 50 A. (D.L.C.)

20023 (ORNL-tr-556) PREPARATION OF ^{115}mIn IN A SMALL AMOUNT OF CARRIER. H. Laurent. Translated by Martha Gerrard and J. J. Pinajian (Oak Ridge National Lab., Tenn.), from J. Chim. Phys., 48: 412-4 (1951). 8p. Dep.(mn); $1.10(fs), $0.80(mf) JCL.

A method for separating indium from cadmium was developed for use in preparing ^{115m}In, obtained by β^- decay from ^{115}Cd. The cadmium is converted to an amino complex and the indium hydroxide is precipitated with alkali. The method is fast and gives indium of high radiopurity containing a small amount of carrier. (auth)

20024 ENZYMIC PREPARATION OF RADIOACTIVE OROTIDINE 5'-PHOSPHATE. Thomas I. Pynadath and Robert M. Fink (Univ. of California, Los Angeles). Biochim. Biophys. Acta, 95: 355-6(Feb. 8, 1965).

An efficient and convenient orotidine 5'-phosphate synthesizing system devoid of orotone-5'-phosphate decarboxylase activity was obtained from a pyrimidine-requiring mutant, strain 36601, of Neurospora crassa. The method resulted in 79% yield of (7-^{14}C) orotidine-5'-phosphate. A typical preparation is described. (P.C.H.)

20025 SYNTHESIS OF 1,2-$^3H_2$-MEDROXYPROGESTERONE ACETATE (17α-ACETOXY-6α-METHYL-1,2-$^3H_2$-PREGN-4-ENE-3,20-DIONE) AND 1,2-$^3H_2$-PREGNA-4,6-DIENE-3,20-DIONE). G. Cooley and A. E. Kellie (British Drug Houses Ltd., London). Biochem. J., 93: 8c-9c(Oct. 1964).

The syntheses of these compounds, at high specific activity is described. For preparation of the first compound, 17α-acetoxy-6α-methylpregna-1,4-diene-3,20-dione (384 mg, 1 mmole) was reduced with carrier-free tritium in the presence of 5% palladium-charcoal catalyst. Approximately 15.5 ml of tritium (40 μC) was absorbed and the product, which consisted of a mixture of starting material, the required 4-en-3-one (medroxyprogesterone acetate), the 1-en-3-one and the saturated 3-one, was separated by partition chromatography of Celite 535 in the system light petroleum ether-methanol-water (5:4:1, by vol). Fractions containing medroxyprogesterone acetate were recrystallized from acetone-light petroleum ether. The sample was then purified by adsorption chromatography on alumina and recrystallized with the same solvents. The yield was 35.7 mg with a specific activity of 95 μC/μg (35.3–38.0 C/mmole). For preparation of 17α-acetoxy-6-methyl-1,2-$^3H_2$-pregna-4,6-diene-3,20-dione, medroxyprogesterone acetate (46.2 mg of the 1,2-$^3H_2$-labeled compound and 23.1 mg of the unlabeled compound) was refluxed with chloranil (69 mg) and p-nitrophenol (7 mg) in butan-2-ol (1.5 ml) for 8 hr. After cooling, the contents were transferred with methylene chloride (2 × 4 ml) to a stoppered tube, and the solution was washed with 0.35N KOH (4 × 3 ml) and subsequently with water until neutral. The methylene chloride solution was dried and the solvent removed. The yellow-brown residue, dissolved in methanol (3 × 1 ml) was concentrated to 1.5 ml; on cooling, yellow crystals separated. This radioactive megestrol acetate (27 mg) was further purified on a column of Celite 535 in the light petroleum ether-methanol-water system. The yield was 16.8 mg with a specific activity of 92 μC/μg (33.3–37.4 C/mmole). (TCO)

20026 THE CHROMIUM-51 COMPLEX OF ETHYLENEDIAMINETETRAACETIC ACID AS A SOLUBLE RUMEN MARKER. A. M. Downes and I. W. McDonald (Ian Clunies Ross Animal Research Lab., Prospect, Australia). Brit. J. Nutr., 18: 153-62(1964).

Preparation of ^{51}Cr-EDTA is described. Chromic chloride (0.80 g $CrCl_3 \cdot 6H_2O$) dissolved in water (10 ml) was labeled by the addition of an aqueous solution of ^{51}Cr-chromic chloride (1-2 mC). A solution of disodium EDTA (1.00 g in 20 ml H_2O) was then added and the mixture heated at 100° for 1 hr. The excess chromic ions were then precipitated as $Cr(OH)_3$ by adding a slight excess of NH_4OH to the hot solution. The suspension was cooled, filtered, and washed with water. The filtrate, containing ^{51}Cr-EDTA, was diluted to 100 ml, and suitable portions were used as required. It was tested as a soluble marker for experiments on gastrointestinal function of sheep, and compared as to rate of disappearance from the rumen with polyethylene glycol (PEG-4000, Carbowax), a widely used marker. The two markers gave the same results within experimental error, the concentration of each decreasing exponentially, with half-times ranging from 8 to 48 hr. It was concluded that ^{51}Cr-EDTA is a satisfactory soluble marker in spite of a slight absorption and subsequent excretion in the urine. The estimation of ^{51}Cr is simple, accurate, and specific. Since ^{51}Cr has a half life of 27.8 days, each preparation can be used over a period of several months. This marker should prove equally valuable in studies of gastrointestinal function in other species. (TCO)

20027 PREPARATION OF RADIOACTIVELY LABELLED CONDENSATION AEROSOLS. I. AEROSOLS OF SODIUM CHLORIDE, SILVER IODIDE AND SULPHURIC ACID. K. Spurny and V. Hampl (Inst. of Physical Chemistry, Czechoslovak Academy of Sciences, Prague). Collection Czech. Chem. Commun., 30: 507-14(Feb. 1965).

Methods and equipment are described for the preparation of condensation aerosols of sodium chloride, silver iodide, and sulfuric acid labeled with ^{24}Na, ^{131}I, ^{110}Ag, and ^{35}S. Some physico-chemical properties of these aerosols are given, e.g., the dependence of the concentration and the mean particle size on the temperature of evaporation. Suitable methods for the sampling of these aerosols were worked out for electron-microscopic studies. (auth)

20028 THE PREPARATION OF SODIUM PERCHLORATE LABELLED WITH CHLORINE-36. M. Vlatkovic and R. Despotovic (Institut "Ruder Boskovic", Zagreb). Croat. Chem. Acta, 36: 171-2(1964).

The preparation of sodium perchlorate labeled with ^{36}Cl is performed by anodic oxidation of $Ca^{36}Cl_2$. The total volume of calcium chloride solution used was 5 cc at an electric current 100 ma. After electrolysis separation of sodium perchlorate from calcium chloride was performed by means of precipitation and solvent-extraction. Yields up to 94.7% were obtained. (auth)

20029 PREPARATION OF I^{131} FROM IRRADIATED URANIUM OXIDE. S. Abrashkin and R. Radicella (Comision Nacional de Energia Atomica, Buenos Aires). Intern. J. Appl. Radiation Isotopes, 15: 695(Nov. 1964).

A dry distillation method is described for the preparation of ^{131}I directly from irradiated enriched uranium. The simplicity of the method makes it especially suitable for remote control operations. ^{131}I is distilled from UO_3 in a current of air at a temperature of 800°C with a yield of about 70%. Under these conditions, the ruthenium isotopes also distill, but contamination of ^{131}I was completely avoided by passing the distillate through iron shavings heated to 700°C. The radioactive purity of ^{131}I was greater than 99%. (P.C.H.)

20030 THE DEVELOPMENT OF OIL-SOLUBLE GOLD-198 COMPOUNDS FOR INDUSTRIAL RADIOTRACING. B. L. Campbell and W. R. Ellis (Australian Atomic Energy Commission, Sutherland, New South Wales). In-

tern. J. Appl. Radiation Isotopes, 16: 257-9(Apr. 1965). (AAEC/TM-247)

The extraction of gold from gold(III) chloride/HCl solutions by primary, secondary, and tertiary amines was studied. The amine–gold salts so formed were shown to be stable under certain conditions. Industrial applications of organic soluble ^{198}Au salts are briefly discussed. (auth)

20031 DEMONSTRATION OF A PARENT-DAUGHTER RADIOACTIVE EQUILIBRIUM USING ^{137}Cs-^{137m}Ba. Gregory R. Choppin and Carson L. Nealy (Florida State Univ., Tallahassee). J. Chem. Educ., 41: 598-600(Nov. 1964).

It is possible to show the relation between radioactive half life and both the rate of decay and of growth of a radioactive daughter with the ^{137}Cs-^{137m}Ba system. It also has the advantage of a short-lived daughter separable by simple techniques without requirement of an activation source. Furthermore, since γ emission is associated only with the ^{137m}Ba, its behavior can be followed directly by scintillation counting with a NaI(Tl) crystal in the presence of ^{137}Cs. The ^{137m}Ba ($t_{\frac{1}{2}}$ = 2.6 min) in equilibrium with its parent, ^{137}Cs ($t_{\frac{1}{2}}$ = 30 yr) is separated by precipitation of $BaSO_4$ and its decay followed in a well-type scintillation counter. The separation is repeated on the same ^{137}Cs solution and the supernatant liquid counted. This fraction shows the growth of ^{137m}Ba. The relation between growth rate and the half life is shown by plotting the difference between the observed count rate and the saturation count rate (taken on the supernatant solution 15 min after the $BaSO_4$ precipitation) vs time. This experiment illustrates the parent-daughter relation for the case of secular equilibrium. The long-lived ^{137}Cs parent shows no change in decay rate during the period of the experiment and, consequently, the ^{137m}Ba grows to a constant value. The rate at which it grows to this constant value is a function of the half life of ^{137m}Ba and not of ^{137}Cs. Equations expressing the decay constants are derived. (BBB)

20032 MÖSSBAUER EVIDENCE FOR HIGHLY CHARGED STATES FOLLOWING Co^{57} ELECTRON CAPTURE IN HYDRATED COBALT COMPOUNDS. R. Ingalls and G. Depasquali (Univ. of Illinois, Urbana). Phys. Letters, 15: 262-4(Apr. 1, 1965). (COO-1198-254)

The Mössbauer spectra of ^{57}Co in powdered $CoCl_2 \cdot 6H_2O$, $CoSO_4 \cdot 7H_2O$, $CO(NH_4SO_4)_2 \cdot 6H_2O$, and $CoSiF_6 \cdot 6H_2O$ were measured at various temperatures using an absorber of enriched stainless steel. The isomer shifts were also obtained. Evidence for the formation of Fe^{3+} and in some cases Fe^{4+}, as well as Fe^{2+}, was observed. (D.C.W.)

20033 25 YEARS OF NUCLEAR FISSION. METHODS AND RESULTS OF CHEMICAL STUDIES. 1. HISTORICAL BACKGROUND, FISSION PRODUCTS. Guenter Herrmann (Universitat, Mainz). Radiochim. Acta, 3: 169-85(Dec. 1964). (In German)

Methods and results of chemical studies on low-energy fission of heavy nuclei are reviewed. Topics covered include: historical background, scheme of the fission process, fission chains, products of ternary fission, and unknown fission products. (auth)

20034 A SIMPLE PREPARATION OF DEUTERIUM LABELLED O-METHYL GROUPS FOR MASS SPECTROMETRY. K. F. van der Merwe, P. S. Steyn, and S. H. Eggers (National Chemical Research Lab., Pretoria, South Africa). Tetrahedron Letters, No. 52, 3923-5(1964).

A partial deuteration method is described that is effected by methylation of an acid or phenol with diazomethane in the presence of an excess of D_2O. Mass spectra of the reaction products showed the introduction of mainly three D atoms per O-methyl group in addition to smaller amounts of the partially deuterated species. The NMR spectrum of diazomethane in chloroform at 5°C showed a single peak at τ 6.72 that was not altered by treatment with an excess of D_2O over 10 min. On subsequent addition of catalytic amounts of either benzoic acid, propionic acid, phenol, or ammonium chloride, yellow solutions resulted that showed practically no absorption in the τ 6.6 to 6.8 region, but still reacted vigorously with large amounts of acid. These results suggest that exchange of the H atoms of diazomethane for D is acid catalyzed. Methylation of an acid or phenol is preceded by a much faster, and reversible, protonation of diazomethane. The following simple procedure is recommended to give at least a 50% yield of trideuterated O-methyl compounds. An ethereal diazomethane solution is prepared in the standard way from N-nitroso-N-methyltosylamide or N-nitroso-methylurea and dried over solid KOH. The diazomethane is then carried over into dry dioxane in a stream of dry nitrogen. An excess of D_2O is added to this diazomethane solution followed by a slow addition of a dioxane-D_2O solution of the acid or phenol over a period of at least 10 min. Substitution of chloroform or ether for dioxane results in the formation of two phases and a corresponding decrease in the efficiency of D exchange. Groups unreactive towards diazomethane but which might have become deuterated during the reaction can be re-exchanged by treatment of the deuterio-methylated product with water. (BBB)

Separation Processes and Procedures

See also Analytical Procedures.

Refer also to abstracts 20203 and 20481.

20035 (BNWL-4) RECOVERY OF STRONTIUM FROM STORED PUREX WASTE BY LEAD SULFATE CARRIER PRECIPITATION— PILOT PLANT STUDIES. G. L. Richardson (Battelle-Northwest, Richland, Wash. Pacific Northwest Lab.). Jan. 15, 1965. Contract AT(45-1)-1830. 32p. Dep.(mn); $2.00(cy), 1(mn) CFSTI.

Pilot plant runs that were designed to test and optimize a flowsheet for lead sulfate scavenging process for isolating strontium crud fraction from wastes on a 100 to 700-liter scale and to evaluate alternate methods of separating the precipitate from the supernatant liquid are described. The tests were restricted to Purex-type wastes, but the results should be approximately the same for Redox wastes. Strontium losses of 5% or less were demonstrated. High iron concentration (0.35M) in one series of runs was believed to have contributed to high strontium losses (ranging from 6 to 28%) through sulfate depletion by complexing and ferric sulfate precipitation. The precipitate, after digestion, proved to be quite insoluble and could be washed with cold water or very dilute nitric acid (pH > 1) with no significant solubility losses for either strontium or cerium. The precipitate was satisfactorily metathesized to the acid-soluble carbonate by using a mixture of sodium hydroxide and carbonate as the metathesis solution. Best results were obtained when the hydroxide/lead mole ratio was 15 or above. As little as 0.2M carbonate was sufficient to prevent strontium solubility losses. Overall product decontamination factors for some of the feed constituents were obtained. Under optimum washing conditions, the DF's ranged from 30 to 460 for iron, aluminum, calcium, magnesium, manganese, and nickel. Lead decontamination factors of 3 and 8 were obtained using hydroxide/lead mole ratios of 15 and 17, respectively, in the metathesis solutions. Centrifugation, continuous decantation, and batch settling and decantation proved to be feasible methods for removing the supernate from the precipitate. (P.C.H.)

20036 (BNWL-25) VALUES IN SPENT FUEL FROM POWER REACTORS. C. A. Rohrmann (Battelle-Northwest, Richland, Wash. Pacific Northwest Lab.). Mar. 1965. Contract AT(45-1)-1830. 53p. Dep.; $3.00(cy), 1(mn) CFSTI.

Studies were made with the objective of appraising the magnitude of future amounts of by-products available from discharged reactor fuels, establishing the candidate materials that are most likely to have value, utilizing some simplified ground rules for appraising value and recovery cost, estimating in a preliminary way the value of candidate materials in unprocessed fuels, and defining the chemistry and technology of economical recovery pro-

cesses. In general it was concluded that there is expectation of only modest credit to the reactor operator or fuel owner for fission products. (P.C.H.)

20037 (CEA-R-2654) ELEMENTS DE SECURITE TIRES DE SIX ANNEES D'EXPLOITATION DE L'USINE DE TRAITEMENT DE COMBUSTIBLES IRRADIES DU CENTRE DE MARCOULE. (Elements of Safety Precautions Derived from Six-Year Experience of the Marcoule Center Reprocessing Plant for Irradiated Fuels). Jean Rodier (Commissariat à l'Énergie Atomique, Chusclan (France). Centre de Production de Plutonium de Marcoule). Dec. 1964. 14p. Dep.(mn).

The safety elements inherent in the design of the installations are examined from the point of view of both radioactive and conventional protection. Great attention must be paid to the problems arising from the confinement of materials, radioactivity, and the risks of criticality. The general principles of the technical prevention of radioactive risks must be applied as soon as the plans are drawn up for the installations, by taking into account: the design and construction of the installations with respect to the risks mentioned above, the division of the plant into zones, the circulation of personnel and material, and ventillation and purification of the air. The technical safety factors however, are not sufficient in themselves. However good the material and the degree of automation achieved, the smooth running of a factory depends on the man responsible for supervision and repair work or who takes initiatives. Technical safety is never definitive and must be continually maintained. The collaboration of the workers is necessary to its efficiency. Psychological measures must thus be taken as an addition to the technical precautions. This psychological prevention is based on: education of the personnel, organization of the work and definition of the safety rules, checking on obedience to the rules and behaviour of the personnel, and constant reminders of the necessity for the prevention of radioactive risks. Six years' operation of the irradiated fuel processing plant at Marcoule have shown the importance of close collaboration between workers and technique. The results obtained from an organization of the work aimed at eliminating the causes of incidents are analyzed. The following points were investigated in particular: frequency of entry into forbidden zones during normal functioning, the distribution of exceptional tasks, the prevention of criticality risks, zone contamination incidents, the volume and nature of decontaminated material and eliminated residues, the evolution and distribution of external irradiation doses received by the workers, the frequency of cases of body contamination, and internal contamination fixed in the organisms of workers. Conclusions are drawn from the different incidents which have occurred during the years of operating the plant. (auth)

20038 (EUR-2245.e) LIQUID-LIQUID EXTRACTION OF FERRIC CHLORIDE BY TRI-n-LAURYLAMINE HYDROCHLORIDE. W. Mueller (European Atomic Energy Community), G. Duyckaerts (Liege Univ. (Belgium)), and F. Maino (European Atomic Energy Community). 1965. Contract 003-61-2-TPUB. 67p. Dep.(mn).

The extraction from hydrochloric acid or from lithium chloride solutions was studied, using a tracer technique (Fe-59). From a slope analysis of the curves log E_a^0 = f(log C)—where E_a^0 is the extraction coefficient, C is the total amine concentration in the organic phase—it can be concluded that a 2:1 complex (ratio of amine salt to ferric chloride) is extracted from dilute hydrochloric acid or chloride solution. For concentrated chloride solutions, a 1:1 complex is extracted. For aqueous phases which are not too concentrated ($[HCl]_a \leq 5\underline{M}$; $[LiCl]_a \leq 7\underline{M}$) the extraction coefficient E_a^0 of ferric chloride increases to approximately the 3rd power dependence of chloride ion activity a_{Cl^-} defined as $\sqrt{c^2 \cdot \gamma_\pm^2}$. c and $\gamma_\pm^2$ being the molar concentration and the mean molar activity coefficient of the 1:1 electrolyte. The decrease of iron extraction with increasing acid concentration in pure hydrochloric acid or in mixtures with chlorides can be explained by competition between metal and acid extraction, the latter leading to amine dihydrochloric formation. Americium extraction from highly concentrated chloride was studied for purposes of comparison and shows approximately the same 3rd power dependence of E_a^0 on chloride ion activity as observed with iron extraction. Again, the decrease of the americium extraction coefficient can be ascribed to competition between amine dihydrochloride and metal complex formation which leads, however, to a 2:1 complex—in contrast to the 1:1 iron complex formed under comparable conditions. (auth)

20039 (EUR-2246.e) DILUENT INFLUENCE ON LIQUID-LIQUID EXTRACTION BY TRILAURYLAMINE HYDROCHLORIDE. W. Mueller (European Atomic Energy Community) and G. Duyckaerts (Liege Univ. (Belgium)). 1965. Contract 003-61-2-TPUB). 85p. Dep.(mn);

The diluent influence on liquid-liquid extraction of trivalent metals by trilaurylamine hydrochloride was investigated by means of solubility measurements, infrared absorption spectroscopy, and by a study of the equilibria between trilaurylamine and hydrogen chloride. In general, the solubilities of water, hydrogen chloride, and trilaurylamine chloride increase with increasing polarizability or polarity of diluents. With few exceptions, water and hydrogen chloride solubilities are proportional to their activities in the aqueous phase, and independent of each other. Hydration favours amine salt solubility. Monohydrated amine hydrochloride is formed in benzene, toluene, nitrobenzene and cyclohexane. In carbon tetrachloride and in chloroform, the hydration of the amine salt is not complete. The analytical results are supported by infrared spectroscopy. The equilibrium constants for the formation of the amine monohydrochloride from organic amine solutions and aqueous hydrochloric acid increase with increasing polarizability or polarity of the diluents. The formation constants of the amine dihydrochloride, however, decrease with increasing polarity (exception: nitrobenzene). Extraction of ferric or americium chloride from hydrochloric acid or lithium chloride solutions, decrease with increasing polarity of diluents, with the exception of nitrobenzene whose extracting power is comparable to that of cyclohexane. Infrared spectra do not reflect the interaction between the diluent and the amine salt or the extracted metal complex. (auth)

20040 (HW-84085) ENGINEERING STUDY—INCREASED PROCESSING FLEXIBILITY—PUREX. PART II. R. D. Ehrlich, J. R. La Riviere, J. H. Nordahl, and J. C. Willi (General Electric Co., Richland, Wash. Hanford Atomic Products Operation). June 24, 1964. Contract AT(45-1)-1350. 55p. Dep.(mn); $3.00(cy), 2(mn) CFSTI.

The additional changes required for increased processing flexibility at the Purex Plant are defined. These changes are as follows: (1.) Installation of two new tanks in the F7 Canyon location for 1WW and 1WF holdup and supplementary routings to permit usage of TK-F12 and E-F11-1 for 3WB storage between processing campaigns. (2.) Installation of a new critically safe 2AF tank. (3.) Modifications to Canyon Sumps SJ and SK to permit higher nuclear safety limits. (4.) Installation of sump piping and instrumentation for the new SNA Sump in N Cell. (5.) Installation of additional weight factor controls for each of the two uranium concentrators. (6.) Installation of backup flow measuring instrumentation and additional flow alarm systems (for critical process streams). (7.) Installation of nuclear blanks to prevent the addition of extraneous precipitating agents to the process. (auth)

20041 (HW-84352) ION EXCHANGE PURIFICATION OF AMERICIUM-241 IN THE 222-S BUILDING I-F CUBICLE. J. S. Buckingham (General Electric Co., Richland, Wash. Hanford Atomic Products Operation). Oct. 6, 1964. Contract AT(45-1)-1350. 7p. Dep.(mn); $1.00(cy), 1(mn) CFSTI.

With minor modifications and additions, the same equipment used for the chromatographic ion exchange purification of promethium can be used for americium purification. One feed tank in the cubicle will be converted to a combustion feed tank and concentrator by connecting an existing steam coil and adding a condenser. Concentration of the

americium is necessary to reduce the amount of nitric acid in the feed material. The americium will be loaded on a 2-in.-dia column and eluted in sequence through a 2-in.-dia column and a 1-in.-dia column using diethylenetriaminepentaacetic acid. Adequate flushing of the lines and separate receiver tanks for the purified products will keep cross contamination to a minimum. A flowsheet for the purification of americium is presented. (P.C.H.)

20042 (IDO-14646) CHEMICAL PROCESSING TECHNOLOGY. Quarterly Progress Report, April–June 1964. J. R. Bower, ed. (Phillips Petroleum Co., Idaho Falls, Idaho. Atomic Energy Div.). Jan. 1965. Contract AT(10-1)-205. 38p. Dep.; $2.00(cy), 1(mn) CFSTI.

The modified ICPP zirconium processing facilities are being prepared for cold start-up testing. The flowsheet is presented for the new process. In aluminum fuel processing studies, the potential usefulness of dissolved cadmium (nitrate) as a nuclear poison in nitric acid dissolver solutions was demonstrated. Sample ATR fuel plates and Type 6061-T0 aluminum were shown to resist corrosion in the fuel storage basin water. Electrolytic dissolution of kilogram quantities of actual HTRE-3 fuel elements and APPR fuel plates was successfully demonstrated in the Model 2 pilot plant dissolver. The operation of the dissolver is described. Laboratory studies characterized the sludge produced during electrolytic dissolution as consisting of grains dropped from the dissolving surface and silica produced by polymerization following dissolution. The ICPP Waste Calcining Facility (WCF) has operated very smoothly; only 55 hours of down time have been experienced since starting radioactive operation in December 1963. The successful calcination of zirconium–aluminum–fluoride wastes from the ICPP hydrofluoric acid process for zirconium–based fuels was demonstrated in WCF pilot plant equipment. Additional waste management studies indicate that alumina calcine deposits yield to nitric acid decontamination and that phosphate glasses prepared from calcined alumina were blackened, but otherwise unaffected, by gamma irradiation to 10^{10} R. Other plant improvement projects are described. (D.L.C.)

20043 (IEA-77) TECHNOLOGY OF PULSED SIEVE-PLATE EXTRACTION COLUMNS. PART I. CARTRIDGE DESIGN. PART II. INTERFACE LEVEL CONTROL. Kazimierz J. Bril and Eduardo C. Costa (Instituto de Energia Atômica, São Paulo (Brazil)). Nov. 1964. 56p. Dep.(mn).

The performance of several cartridges was studied in the extraction of HNO_3 from a 3N aqueous solution into 45 vol % TBP–Varsol. Results were compared with the ones obtained with the same cartridges containing intermediate settling zones (ISZ). Intermediate settling zones, as studied, did not improve column performance as expected, and caused an undesirable shifting of both HETS and flooding capacity curves toward the high-energy region. The Lucite cartridge did show a small increase both in capacity and efficiency. The effect of temperature on the flooding capacity of the stainless steel, Lucite, and mixed cartridges was also studied. Flooding curves were determined at 22, 25, and 30°C, and show an appreciable increase in capacity with increasing temperature in the case of the stainless steel and Lucite cartridges. Thus, temperature proved to be an important operating parameter. The performance of a conductivity-probe interface level controller is discussed. The controller operated for 80 hours in actual service and seems to depend to a large extent on proper electrode design for reliable operation. (auth)

20044 (IS-T-1) CONCENTRATION OF CESIUM FROM POLLUCITE (thesis). Tommy Lee Young (Ames Lab., Iowa State Univ. of Science and Tech.). Feb. 1965. Contract W-7405-eng-82. 123p. Dep.(mn); $4.00(cy), 3(mn) CFSTI.

Three different treatments of pollucite ore were developed. The hydrogen fluorination treatment does not appear to hold much promise, unless a means by which cesium can be conveniently separated from the water insoluble residue is found. This gaseous treatment does, however, produce essentially complete destruction of pollucite and is much more easily controlled than the aqueous hydrofluoric acid treatment. The sulfur chloride-chlorine treatment renders most of the cesium in pollucite water-soluble. The cesium chloride produced by this treatment could be purified by several processes, and good quality metal could be produced by calcium or lithium reduction of the purified salt. The aluminum reduction of pollucite to give a crude cesium product was developed adequately to demonstrate the efficiency of this process. Known reserves of pollucite are estimated to contain over 75,000 tons of cesium. Thus, this treatment of pollucite, used in combination with fractional distillation of cesium from the crude product, should assure low cost cesium when the demand for the metal becomes relatively large. (auth)

20045 (LA-2838) PROCESSING OF PLUTONIUM BY ION EXCHANGE. III. THE CALCULATION OF FIXED-BED COLUMN PERFORMANCE. D. B. James and R. S. Cooper (Los Alamos Scientific Lab., Univ. of California, N. Mex.). July 1964. Contract W-7405-eng-36. 15p. Dep.; $1.00(cy), 1(mn) CFSTI.

Parameters and equations are presented which permit the numerical duplication of the sorption of plutonium on nitrate-form Dowex 1 × 4 from 7M nitric acid. A mass-action description of the two-phase equilibria and an empirical expression for the sorption rate are coupled with the fundamental partial differential equation which describes the operation of a fixed-bed ion-exchange column to produce a system that is only numerically solvable. The calculation and experiment are in good agreement. (auth)

20046 (LA-3188) THE PROCESSING OF PLUTONIUM BY ION EXCHANGE. V. EQUILIBRIUM ANION-EXCHANGE SORPTION FROM MIXED NITRIC ACID–ALUMINUM NITRATE SOLVENTS. D. B. James (Los Alamos Scientific Lab., Univ. of California, N. Mex.). Sept. 1964. Contract W-7405-eng-36. 15p. Dep.; $1.00(cy), 1(mn) CFSTI.

A method is described for calculating the trace-loading equilibrium distribution coefficients, K_D^0, for the sorption of plutonium (IV) on Dowex 1 × 4 anion-exchange resin from mixed aluminum nitrate–nitric acid solutions. Published data for sorption from salt solutions and from acid solutions are used to obtain the dependence of K_D^0 upon the molar concentration of nitrate ion and upon the mole ratio of hydronium ion to water. These parameters are calculated according to a published technique for twenty-two mixed solutions. Values of K_D^0, calculated from theoretical equations, were compared to experimental measurements of K_D^0 for these solutions. (auth)

20047 (MLM-734) BISMUTH RECOVERY PROCESS. Engineering Research Final Report. W. J. Raiff, P. M. Engle, and M. McEwen (Mound Lab., Miamisburg, Ohio). Aug. 5, 1952. Contract AT(33-1)-Gen-53. 45p. Dep.(mn); $2.00(cy), 1(mn) CFSTI.

Waste solutions from the concentration cells of the primary process of Mound Laboratory are disposed of by removing the bismuth as an oxychloride sludge and allowing the liquid wastes to enter the general plant waste-disposal system. This removal operation calls for an annual expenditure with no return. It also calls for the scrapping of bismuth, which is a critical and valuable metal. The bismuth-recovery program is designed to salvage this valuable metal. It also provides for the recovery of bismuth from the accumulated oxychloride sludge from past operations. The bismuth-recovery program promises not only to save money on current operations when compared to the present system, but also to produce an income while the stored sludge is being recovered. The process adopted for the bismuth recovery, after consideration of pyrometallurgy and electrochemical reduction, is the electrodeposition of the bismuth from solution. This process is completed with the melting and casting of the metal in the required slug form. These slugs will then be reirradiated and recycled through the process so that the requirements of this project for new bismuth will be greatly reduced. Due to the small size of the proposed plant, a full-size plant is proposed with all necessary developmental changes to be

made on the full plant itself. The best location for this plant is the "HH" Building, where the necessary installation can be made with a minimum of interference to present operations. Flowsheet, equipment layout plan, charts, specifications for equipment, and a general process description for plant operation for the electrolytic section of the plant are included, along with a history and justification. (auth)

20048 (NAA-SR-9335) COMPARATIVE FUEL CYCLE EVALUATIONS, LOW DECONTAMINATION PYROPROCESSING, AND AQUEOUS REPROCESSING. PART II. UC FUEL IN A THERMAL REACTOR. K. L. Mattern and L. J. Colby, Jr. (Atomics International, Canoga Park, Calif.). Feb. 15, 1965. Contract AT-11-1-GEN-8. 41p. Dep.; $1.00 (cy), 1(mn) CFSTI.

Fuel cycle cost studies for recycle of UC fuel indicate an economic advantage for the CARBOX Process (reconstitution of spent carbide fuel via oxidative decladding, reenrichment, and carbothermic reduction of the resultant oxides to recycle UC fuel material) relative to a fuel cycle using aqueous decontamination. Although ^{235}U burnup and inventory charges are higher for the CARBOX cycle than for cycles entailing the complete removal of fission products prior to refabrication, they are more than offset by the savings incurred via the simple process flowsheet and integrated facilities. These fuel cycle cost studies were undertaken for a 1000-Mw(e) complex, based on an SCR Reference Reactor system. Preliminary cost estimates for fuel cycles using both aqueous and CARBOX reprocessing are presented. (auth)

20049 (NP-14834) ANORGANISCHE ODER ORGANISCHE CHELATBILDNER ALS ELUTIONSMITTEL ZUR TRENNUNG DER SELTENEN ERDEN AN IONENAUSTAUSCHERN? VERSUCHE MIT KONDENSIERTEN PHOSPHATEN. (Inorganic or Organic Chelate Formers as Elution Medium for the Separation of Rare Earths on Ion Exchangers? Tests with Condensed Phosphates (thesis)). Werner Pippig (Johannes-Gutenberg-Universitat, Mainz (West Germany)). 1963. 172p.

A series of condensed phosphates are commercially prepared and therefore easily available. These polyphosphates are very effective complexing agents and in their behavior relatively easily as few supplementary reactions—as in other iso- or heteropoly acids—occur. The suitability of this chelate builder was investigated in comparison with the organic elution media in the separation of rare earths on cation exchangers. The equilibrium method could lead to a faster orientation of the best conditions for a separation, but it is not usable with condensed phosphates, principally because of the following sources of error: pH displacements, loss of tracer masses, and dependence of the distribution coefficients on the ratio of resin to solution. On the anion exchanger, the formation of negative rare earth phosphate complexes could be detected in which a return of the normal elution sequence occurred. The best separations on cation exchanger columns were obtained with pyrophosphate solution of pH 0.9 and pH 5.0 at a temperature of 85°C. In the alkali range, perturbations occur both in weighable and unweighable masses. Because of a slow step in the complex dissociation, the flow-through of the elution solution must be very slow. The peak edge of the rare earths is however no worse in the application of low molecular phosphates than in organic complex builders. The separation factors, however, remain small. (tr-auth)

20050 (ORNL-3695) DISSOLUTION OF HIGH-DENSITY UO_2, PuO_2, AND UO_2–PuO_2 PELLETS IN INORGANIC ACIDS. Armando L. Uriarte and Robert H. Rainey (Oak Ridge National Lab., Tenn.). Apr. 1965. Contract W-7405-eng-26. 82p. Dep.; $3.00(cy), 2(mn) CFSTI.

A laboratory study was made of the initial instantaneous dissolution rates (IDR) and total dissolution times of unirradiated, commercially prepared UO_2, PuO_2, and PuO_2–UO_2 pellets in boiling nitric acid alone and with additives. The UO_2 dissolved readily in nitric acid alone; PuO_2 dissolved slowly even with the addition of fluoride. Pellets containing as much as 28% PuO_2 in UO_2 dissolved in nitric acid alone when fabrication procedures indicated that solid solutions were formed, but part of the plutonium remained undissolved from pellets which were probably not solid solutions. Since the present state of the art of pellet fabrication does not ensure that the plutonium will be in solid solution in all pellets, and since complete dissolution of plutonium is required in commercial fuel processing, the use of fluoride for the dissolution of PuO_2–UO_2 pellets is indicated. Empirical equations for approximating the dissolution rates are as follows: $IDR_{UO_2} = 480\ (\underline{M}\ HNO_3)^2 e^{-0.091\ (\%TD)}$; $IDR_{PuO_2} = 5 \times 10^3 (\underline{M}\ HNO_3)^4 e^{0.27\ (\%TD)} + 4 \times 10^7 (\underline{M}\ HNO_3)^4 (\underline{M}\ HF)^{1.4} e^{-0.27\ (\%TD)}$; and $IDR_{PuO_2-UO_2} = (IDR_{PuO_2})^n (IDR_{UO_2})^{1-n}$, where (% TD) is the percent of theoretical density of the pellet, ($\underline{M}$ HNO_3) and ($\underline{M}$ HF) are the molar concentration of the acids, and (n) is the mole fraction of PuO_2 in the UO_2–PuO_2 solid solution. Due to roughening of the pellets while dissolving, the time to dissolve 95% was only about a third the time that would be calculated from these rates. It was concluded that PuO_2–UO_2 pellets presently considered for power reactors can be dissolved in a reasonable time. For example, 28% PuO_2–72% UO_2 solid solution pellets (0.17 cm × 0.55 cm diameter) with densities that were 93% of theoretical dissolved in less than 6 hr in 6 $\underline{M}$ HNO_3 to produce a solution 0.57 $\underline{M}$ in plutonium, 1.25 $\underline{M}$ in uranium, and 3 $\underline{M}$ in HNO_3. (auth)

20051 (ORNL-3773) ADSORPTION OF PROTACTINIUM ON UNFIRED VYCOR: INITIAL HOT-CELL EXPERIMENTS. J. G. Moore, J. H. Goode, J. W. Ullmann, R. H. Rainey, and J. R. Flanary (Oak Ridge National Lab., Tenn.). Apr. 1965. Contract W-7405-eng-26. 25p. Dep.; $2.00(cy), 1(mn) CFSTI.

A process for recovering ^{233}Pa by adsorbing it on unfired Vycor glass was demonstrated using thorium–uranium fuel specimens that had been irradiated to 75,000 Mwd/metric ton in an average neutron flux of 2×10^{14} and allowed to decay 26 days. Over 99% of the fuel dissolved in refluxing 13 $\underline{M}$ HNO_3–0.05 $\underline{M}$ HF, leaving a residue containing less than 0.1% of the uranium and up to 20% of the protactinium. The protactinium losses could be minimized by cyclic dissolution in a process application. About 99.6% of the protactinium was adsorbed from a solution, which contained 69 mg/ml Th, 1.80 mg/ml U, 30 mg/liter ^{233}Pa, 10.1 $\underline{M}$ HNO_3, 0.05 $\underline{M}$ HF, 0.1 $\underline{M}$ $Al(NO_3)_3$, and 1.7×10^{11} counts min^{-1} ml^{-1} gross gamma by passing the solution through a bed 0.9 cm in diameter and 17 cm long, containing 8 g of 60- to 80-mesh unfired Vycor glass. The flow rate was 1 ml/min. Less than 0.1% of the adsorbed protactinium was removed by washing the column with 10 $\underline{M}$ HNO_3–0.1 $\underline{M}$ $Al(NO_3)_3$. Ninety-two percent of the protactinium was recovered at a concentration equivalent to 5.5 times the protactinium concentration in the feed solution. The product had been decontaminated from zirconium–niobium, ruthenium, and total rare earths by factors of 9, 2.87×10^3, and 6.03×10^3, respectively. Several gross inconsistencies were observed in results from protactinium analyses. These difficulties indicate that the analytical procedures for protactinium and the stability of solutions containing protactinium in the presence of macro concentrations of fission products need to be reinvestigated. (auth)

20052 (ORNL-TM-1035) THE SEPARATION OF LONG-LIVED FISSION PRODUCT ELEMENTS BY USING ETHYLENEDIAMINETETRAACETATE IN AN ELECTRODIALYSIS CELL. A. Facchini and R. H. Rainey (Oak Ridge National Lab., Tenn.). Feb. 17, 1965. Contract W-7405-eng-26. 28p. Dep.(mn); $2.00(cy), 1(mn) CFSTI.

The migration of long-lived fission product elements in a nitrate solution containing ethylenediaminetetraacetate in an electrodialysis cell was determined as a function of pH. The pH's at which 90% of the Zr–Nb, Ru, Eu, Ce, Sr, and La transferred to the anodic compartment were <0.5, 1.4, 1.75, 2.20, 2.35, and 3.55, respectively. Cesium continued to be cationic even at pH 10.8. By regulating the pH, rough separations of these elements were obtained. (auth)

20053 (UJV-1202/64) CHEMICKE PODKLADY EXTRAKCE URANOVYCH RUD SE ZAMERENIM NA POUZITÍ

AMINU A KYSELÝCH ORGANOFOSFÁTŮ. (Chemical Extraction of Uranium From Ores by Means of Aliphatic Amines and Acidic Organophosphorous Compounds). J. Kadlec (Ústav Jaderného Výzkumu, Ceskoslovenská Akademie Věd, Rêz (Czechoslovakia)). Dec. 1964. 68p. Dep.(mn).

The use of amines and acidic organophosphorus compounds to recover U from leach solutions of U ores is discussed. The use of these extractants to recover other metals, to process irradiated fuels and wastes, and to prepare transuranium elements is also considered. The treatment of U ores by leaching, etc., for U recovery is described. A bibliography with appended notes is included. (D.L.C.)

20054 SEPARATION OF NIOBIUM FROM TANTALUM ON ANION-EXCHANGE RESINS. C. Dragulescu, I. Kyri, and M. Oprescu. Acad. Rep. Populare Romine, Baza Cercetari Stiint. Timisoara, Studii Cercetari, Stiinte Chim., 10: 55-9(1963).

The use of Amberlite IRA-410 (50 to 100 mesh) for separation of Nb from Ta with oxalic acid–HCl as eluent was investigated. The most effective separation was attained with 0.3M oxalic acid–1M HCl. Complete separation was possible with a column, 21 cm × 0.8 cm, packed with 5.5 g of dry resin, with an eluent flow rate of 0.75 ml per min. The rate of elution was increased by using 2M HCl to elute Ta after the elution of Nb with the mixed solvent. The separation was effective at ratios of Nb_2O_5 to Ta_2O_5 ranging from 3:1 to 1:3, for 10 to 30 mg of ion adsorbed. (Anal. Abstr., 12: No. 2, (Feb. 1965))

20055 STUDY OF IONIC SPECIES OF PROTACTINIUM IN AQUEOUS SOLUTION. II. RESEARCH ON THE SYNERGISTIC EFFECT IN THE PARTITION OF Pa(V) BETWEEN AN AQUEOUS PERCHLORIC SOLUTION AND AN AROMATIC SOLUTION OF THENOYL 2-TRIFLUOROACETONE AND TRI-n-BUTYLPHOSPHATE. Robert Guillaumont (Universite de Paris, Arcueil, France). Bull. Soc. Chim. France, No. 1, 132-4(Jan. 1965). (In French)

A synergistic effect was shown in the partition of Pa(V) between a 3N $HClO_4$ solution and a benzene solution of TTA and TBP. This effect seemed to be due to the formation of the species $Pa(OH)_3A_2 \cdot 2TBP$ beginning from the chelate $Pa(OH)_3A_2 \cdot 2HA$ extracted in the presence of TTA alone. (tr-auth)

20056 STUDY OF IONIC SPECIES OF PROTACTINIUM IN AQUEOUS SOLUTION. III. CALCULATION OF HYDROLYSIS CONSTANTS OF Pa(V) AND OF FORMATION CONSTANTS OF ITS COMPLEXES WITH THENOYL 2-TRIFLUOROACETONE. Robert Guillaumont (Universite de Paris, Arcueil, France). Bull. Soc. Chim. France, No. 1, 135-9(Jan. 1965). (In French)

The first hydrolysis constant K_1 of the ion $Pa(OH)_3^{4+}$, as well as some of the formation constants of its complexes with thenoyl-2-trifluoroacetone, was calculated; $K_1 = [Pa(OH)_4^{+}]\,[H^+]\,[Pa(OH)_3^{4+}]^{-1} = 9 \times 10^{-2}$ at 25°C. (tr-auth)

20057 THERMODYNAMIC THEORY OF ION EXCHANGE. III. ION EXCHANGE EQUILIBRIUM IN MIXED SOLVENT SYSTEM. Hidetake Kakihana and Takashi Kojima. Bull. Tokyo Inst. Technol., No. 54, 75-80(1963).

Ion exchange equilibrium in a mixed solvent system was theoretically studied considering not only the hydration but also the solvation of an organic solvent. A series of fundamental equations was derived. Based on these equations, the characteristics of the ion exchange reactions are discussed for mixed solvent systems as well as for aqueous solvent systems. (auth)

20058 SOLVENT EXTRACTIONS OF CESIUM AND FRANCIUM WITH TETRAPHENYLBORON. Kanji Haruyama and Takashi Ashizawa (Atomic Fuel Corp., Tokyo). Bunseki Kagaku, 14: 120-4(Feb. 1965). (In Japanese)

A micro amount of cesium was extracted by benzene as its salt of tetraphenylboron (TPB) from a solution with pH higher than 2. Addition of calcium ions prevented emulsification. Interference from traces of potassium could be avoided by the use of a mixture of benzene and methyl isobutyl ketone. Radioactive ^{134}Cs added to a solution (pH 5) from pitchblende (corresponding to 20 mg of U) was recovered quantitatively by extraction with mixed benzene and methyl isobutyl ketone (1 + 1). Francium and thallium were extractable under the same conditions as those for cesium. (auth)

20059 PILOT PLANT STUDIES OF A DIRECT FLUORINATION PROCESS APPLIED TO URANIUM DIOXIDE REACTOR FUELS. W. J. Mecham, J. D. Gabor, and A. A. Jonke (Argonne National Lab., Ill.). Chem. Eng. Progr., Symp. Ser., 60: 76-83(1964).

The direct fluorination volatility process is being developed to recover uranium and plutonium from spent uranium oxide, Zircaloy-clad fuel elements. The process consists of vapor-phase chemical decladding, fluorination of uranium and plutonium oxides, and separation and decontamination of the uranium hexafluoride and plutonium fluoride products. Although the dense oxide pellet fuel is not directly fluidizable, fluid bed techniques with inert materials were applied to aid in heat removal and in product handling steps. Results are presented of pilot plant fluorination studies in a 3-in. dia reactor and on supporting work on heat transfer in this process. (auth)

20060 CHEMISTRY OF THE REPROCESSING OF CERAMICS BY VOLATILIZATION. Jean Schmets, Rene Heremans, Aldo Francesconi, and Philippe Speeckaert (Centre d'Étude de l'Énergie Nucléaire, Mol-Donk, Belg.). Chem. Eng. Progr., Symp. Ser., 60: No. 47, 20-30(1964). (BLG-288)

The chemistry of the following reactions is discussed: oxidation of sintered uranium dioxide, reduction of uranium octoxide, oxidation of uranium monocarbide, hydrofluorination of uranium monocarbide, and fission products behavior during the volatilization. (auth)

20061 LIQUID ION EXCHANGERS: SEPARATIONS ON INERT SUPPORTS IMPREGNATED WITH LIQUID ION EXCHANGERS. Enrico Cerrai (Laboratorio del Centro Informazione Studi Esperience CISE, Milan). Chromatog. Rev., 6: 129-53(1964).

The general principles of liquid ion exchangers are discussed, along with chromatography on supports impregnated with liquid ion exchangers. Studies indicated that almost inert supports, such as sheet or powder cellulose or other granular water-insoluble substances, can hold fixed any organic compound belonging to the class of ion exchangers or of extracting materials in general, and that in this way many of the inorganic separations predictable on the basis of the data provided by liquid-liquid processes can be carried out. It was found that, in particular, supports treated with liquid amines behave analogously to anion exchange resins. The development of these techniques allows not only the separation of many similar elements from one another, but also the separation of ions of the same element, present in two different states of valency. (M.C.G.)

20062 PURIFICATION OF EUROPIUM BY DISTILLATION OF THE HALOGENIDES. Gerard Schiffmacher (C.N.R.S., Bellevue, France). Compt. Rend., 260: 182-5 (Jan. 4, 1965). (In French)

The difference in vapor pressure of the rare earth halogenides was investigated for utilization in the separation of the various elements, with emphasis on europium. The volatility differences between the halogenides of valence II and valence III and, for the chlorides, the tendency to reduction by hydrogen were studied. After distillation under vacuum at 1000, 950, and 900°C, respectively, for the chlorides, bromides, and iodides the separation was determined. The experimental and theoretical values of α (the ratio of the vapor pressures) did not agree. This difference can be explained by the possibility of a dismutation $EuX_2 \rightleftharpoons Eu + EuX_3$. (J.S.R.)

20063 STUDY OF THE HYDROLYSIS OF TETRAVALENT PROTACTINIUM. Robert Guillaumont (Universite de Paris, Arcueil, France). Compt. Rend., 260: 1416-18 (Feb. 1, 1965). (In French)

The partition of tetravalent protactinium between $HClO_4$–$LiClO_4$ aqueous solutions with ionic force 3 and benzene

solutions of thenoyltrifluoroacetone was studied. In 3N perchloric medium, the dominant ion was Pa^{4+}. The species $Pa(OH)^{3+}$, $Pa(OH)_2^{2+}$, and $Pa(OH)_3^{+}$ appeared when the acidity decreased. (tr-auth)

20064 WORLD'S CHEAPEST ATOM FUEL PROCESSING SERVICE. Elec. Export Rev., 4: 1-2(Jan.-Mar. 1965).

Following the completion by the UKAEA of the world's largest fuel processing plant, a contract for the reprocessing of the spent fuel elements from Latina (Italy) and the recovery of plutonium was signed in November 1964 by ENEL (the nationalized Italian State electricity supply organization) and the UKAEA. This contract is worth about $5 million per annum. The Authority's new $13 million separation plant at Windscale has a design throughput of 1500 tons of spent fuel per annum which is sufficient to meet the requirements of all nine magnox nuclear power stations of Britain's first nuclear power program. The plant is capable of a 30% increase in throughput which, together with the latest guaranteed increase in magnox element irradiation from 3000 to 4000 Mw d/t, will provide considerable spare capacity for overseas contracts. With the addition of a preprocess plant, estimated to cost $1¼ million, the Windscale works will be able to reprocess over 300 tons per year of enriched uranium oxide fuel discharged from reactors. The only other comparable reprocessing plant, being built in the U.S.A., will not be commissioned until 1966. It will have a capacity of 225 tons per yr of spent oxide fuel. Under the Italian contract, ENEL will obtain Pu at a cost equivalent to the price for ^{235}U used for power generation, and the UKAEA eventually expect to reduce Pu recovery cost below that for ^{235}U. The Authority's ability to provide cheap reprocessing service is mainly due to the size of the plant. In offering reprocessing services to foreign countries, the UKAEA had to overcome practical problems of transporting the highly active spent fuel. A 1000-ton ship has been chartered which is fitted with refrigeration plant for this purpose, and the first shipment from Latina is expected to be made in September 1965. (BBB)

20065 TRIFLUORIDE PROCESSING OF PLUTONIUM METAL RECYCLE. J. M. Cleveland (Dow Chemical Co., Golden, Colo.). Ind. Eng. Chem., Process Design Develop., 4: 230-1(Apr. 1965).

Plutonium metal recycle may be reprocessed by a one-step method, involving simultaneous dissolution and precipitation as the trifluoride with a hydrochloric acid–hydrofluoric acid mixture. After filtration and drying, the trifluoride may be reduced with calcium to plutonium metal (using iodine booster), or converted to PuF_4 and reduced to metal (without booster) in yields averaging 98%. Filtrate losses are of the order of 10 ppm of the metal processed. The process achieves good purification with respect to iron and carbon, but is only 25 to 60% effective in removing aluminum. (auth)

20066 TRANSFER OF SOLUTES BETWEEN LIQUID ALLOYS IN MUTUAL CONTACT WITH A FUSED SALT. APPLICATION TO FUEL REPROCESSING. Premo Chiotti and J. S. Klepfer (Iowa State Univ., Ames). Ind. Eng. Chem., Process Design Develop., 4: 232-9(Apr. 1965).

A purification process based on the transfer of solutes between two liquid metal alloys in mutual contact with a fused salt is described. Transfer depends on the relative chemical potentials of the solutes in the two alloys; the fused salt serves as a contact medium and as a carrier for an oxidizing agent. A Mg–40% Th alloy containing yttrium and lanthanide elements was decontaminated in a simple, single-stage, batch extractor. Impurities in the alloy were selectively oxidized by $MgCl_2$ in a KCl–44.5% LiCl eutectic salt and simultaneously reduced from the salt by a Zn–Mg scrub alloy. The optimum reducing power of the scrub alloy occurred at a composition of 4 to 8% magnesium in zinc. Large quantities of impurities could be extracted into the scrub alloy and still attain low levels of impurities in the Mg–Th alloy. For a Mg–40% Th/KCl–LiCl–25% $MgCl_2$/Zn–7% Mg system at 600°C, the concentration of each solute, yttrium, cerium, and neodymium, was reduced from 1000 to a minimum of less than 30 ppm in about 7 hours. Over 95% of the solutes were extracted in 2 hours. The amount of thorium concurrently transferred to the zinc-rich alloy was small and in 7 hours was approximately equivalent to the total mass of solutes transferred. An appreciably larger quantity of magnesium may be transferred. (auth)

20067 EXTRACTION OF URANIUM(VI) FROM NITRIC ACID SOLUTIONS BY LONG-CHAIN ALIPHATIC AMINES. Taichi Sato (Government Chemical Industrial Research Inst., Tokyo). J. Appl. Chem. (London), 15: 92-8 (Feb. 1965).

The partition of uranium(VI) between nitric acid solutions and organic solutions of long-chain aliphatic amines was investigated at different concentrations of nitric acid and solvent, and at different temperatures. The effects of amine structure and of organic solvent and the mechanism of uranium extraction are discussed on the basis of the results obtained. It is postulated, from infrared spectroscopy measurements, that the complex formed in the extraction of uranium(VI) from nitric acid solution by tri-n-dodecylamine in benzene is a nitrato complex of uranium. (auth)

20068 EFFECT OF SURFACE TREATMENT ON THE EFFICIENCY OF STAINLESS STEEL PACKINGS. P. J. King and P. N. Walmsley (Manchester Coll. of Science and Tech., Eng.). J. Appl. Chem. (London), 15: 98-104(Feb. 1965).

The separation efficiency of triangular-pyramid-type Stedman packing made from stainless steel gauze was investigated with both organic and aqueous test mixtures at atmospheric and under reduced pressure. For the organic system the packing was found to be most efficient at 310 mm Hg. With the aqueous test mixture, scatter and irreproducible results were obtained and it was found that this was due to the wetting characteristics of the stainless steel gauze. Untreated stainless steel packing was unsuitable for heavy water preparation. Improvement in the wetting properties of the gauze by treatment with potassium permanganate led to similar efficiency with both aqueous and organic test mixtures. (auth)

20069 THIN LAYER CHROMATOGRAPHY IN SALTS OF HETEROPOLYACIDS. K. Buchtela and Margrit Lesigang (Universitat, Vienna). Mikrochim. Ichnoanal. Acta, No. 1, 67-74(1965). (In German)

An investigation was made of the possibility of employing oxine germanomolybdate and pyridine germanomolybdate as thin layer carrying materials in the separation of uranium fission products. A specific separation of cesium from the fission products $^{95}Zr/^{95}Nb$, ^{106}Ru, $^{90}Sr/^{90}Y$, and ^{144}Ce was carried out with the aid of 0.01M ammonium acetate-EDTA or 0.001M ammonium acetate-EDTA solutions. (auth)

20070 PURIFICATION OF BERYLLIUM BY ACETYLACETONE-EDTA SOLVENT EXTRACTION: PROCEDURE AND CHEMISTRY. C. E. L. Bamberger, H. F. McDuffie, and C. F. Baes, Jr. (Oak Ridge National Lab., Tenn.). Nucl. Sci. Eng., 22: 14-19(May 1965). (ORNL-P-663)

A procedure, described previously, for the preparation of high purity beryllium hydroxide was improved and demonstrated on a kilogram scale, and a systematic study of its chemistry was carried out. The $Be(OH)_2 \cdot xH_2O$ starting material is dissolved in acetylacetone (HX) as BeX_2, scrubbed with aqueous EDTA to remove metallic impurities stripped with nitric acid, and precipitated with ammonia. The dried $Be(OH)_2 \cdot 0.3\ H_2O$, a granular, free-flowing powder, was obtained in 85% yield. Detectable metallic impurities totalled <5 parts/10^6. The variation of BeX^+ and BeX_2 formation quotients with ionic strength as well as the variation of BeX_2 and HX distribution coefficients with both aqueous ionic strength and organic phase composition are summarized. Decontamination efficiencies for some 13 cations were estimated to be very high. Effective purification was demonstrated on a sample of $Be(OH)_2$ starting material which was contaminated with 1000 parts/10^6 parts BeO of Na^+, Mg^{2+}, B(III), Cu^{2+}, Al^{3+}, Fe^{3+}, and Cr^{3+}. (auth)

20071 SIMPLE QUANTITATIVE SEPARATION OF BERKELIUM FROM CERIUM. J. Kooi and R. Boden (CEN, Mol, Belg.). Radiochim. Acta, 3: 226(Dec. 1964).

Results obtained in the separation of tracer amounts of ^{249}Bk (~12000 cpm on a 2π proportional counter) and 2 mg of cerium, labeled with ^{144}Ce, by extraction chromatography are presented. Dilute (0.5M) HCl was used to successively elute the elements from kieselguhr columns loaded with di-(2-ethylhexyl)orthophosphoric acid. Adsorption took place from 0.1M HCl and no oxidizing or reducing agents were used. (M.C.G.)

20072 URANYL NITRATE SOLUBILITY IN MIXED SOLVENTS. V. M. Vdovenko, I. G. Suglobova, I-Wui Wang, and D. N. Suglobov. Radiokhimiya, 6: 533-8(1964). (In Russian)

The solubility of uranyl nitrate dihydrates in mixtures of ethyl, butyl, and β,β'-dichlorodiethyl ethers with benzene (toluene, xylene), chloroform, carbon tetrachloride, and heptane was measured at 25°C. From the data obtained it was established that the activity coefficients of active solvents and solvates fluctuate symbatically. An approximate calculation of the size of molecules correlated the solubility curves. Relatively high solubilities in mixtures with benzene and chloroform made possible weak interaction of this material with molecules of the solute. The mean number of esters of solvated uranyl nitrate dihydrate molecules M was determined, and found to increase with increased acidity of the esters and the tendency of diluent molecules to intermolecular interactions. (tr-auth)

20073 SOLUBILITY OF URANYL PERCHLORATE TRIHYDRATE IN MIXED SOLVENTS. V. M. Vdovenko, I. G. Suglobova, and D. N. Suglobov. Radiokhimiya, 6: 539-42(1964). (In Russian)

The solubility of $UO_2(ClO_4)_2 \cdot 3H_2O$ in mixtures of n-dibutyl ether and diluents at 25°C in ether concentration intervals from 0.07 to 1M (in systems with CCl_4 at 3M) was determined. The solubility decreased and the number of solvated molecules of ether salts in solution increased in the sequence 2-chloropropane, 1-chloropropane, benzene, chloroform, CCl_4, and cyclohexane. High solubility of uranyl perchlorate in chloropropane and chloroform indicated the contribution to solubility of dipole-dipole interactions of diluent with solvate. (tr-auth)

20074 ADSORPTION OF COMPLEX URANIUM COMPOUNDS FROM AQUEOUS SOLUTIONS. I. D. Muzyka, E. D. Romanenko, and N. N. Tananaeva. Radiokhimiya, 6: 633-40(1964). (In Russian)

Some of the results obtained in an adsorption and physicochemical study of the system $UO_2(NO_3)_2-NaK-H_2O$ are reported. It was found that the predominant complex present in this system has the composition UO_2K_2. The optimum conditions for the stability of the complex correspond to a pH of 5.5 to 6.5. At pH $\leq$ 1.5, the complex decomposes almost completely into its components. The adsorption of this complex on activated charcoal from aqueous solutions was investigated. The complex was found to have a high uranium-adsorbing capacity (about 320 mg of uranium per g of carbon), and can therefore be used for the simultaneous recovery and concentration of uranium from salt systems. The adsorbed uranium may be recovered either by burning off the carbon to obtain uranium oxide, or by desorbing the uranium with a mineral acid such as sulfuric acid. Following the desorption, the charcoal may be reused for the absorption of more uranium. The study established the possibility of obtaining uranium compounds of high purity, particularly with respect to cadmium, one of the most harmful impurities in uranium. (ATD)

20075 EXTRACTION OF ACTINIDE ELEMENTS WITH DIALKYL PHOSPHORIC ACIDS. E. S Gureev, V. N. Kosyakov, and G. N. Yakovlev. Radiokhimiya, 6: 655-65(1964). (In Russian)

The extraction of uranium(VI), neptunium(V), plutonium(IV), americium(III), and cerium(III) with dialkyl prosphates from nitric acid solutions and the influence on the extraction of such factors as the length and degree of branching of the carbon atom chain of the alkyl radical, concentration of the extracting agent in the organic phase, concentration and type of the acid in the aqueous phase, and type of the neutral diluent were studied. The nature of the dependence of the distribution coefficients of Am(III), Pu(IV), and U(VI) on the concentration of the extracting agent in the organic phase and on the content of hydrogen ions in the aqueous phase was elucidated. It was found that when the carbon chain of the radical in the dialkyl phosphate increases in length, the extractability of these elements increases slightly, and that branching of the chain causes a decrease in the distribution coefficients. The nature of the diluent also has a pronounced effect on the extraction. (ATD)

20076 COMPLEXING OF AMERICIUM WITH NEUTRAL ORGANOPHOSPHORUS COMPOUNDS. PART II. V. I. Zemlyanukhin, G. P. Savoskina, and M. F. Pushlenkov. Radiokhimiya, 6: 694-701(1964). (In Russian)

The extraction of americium from nitric acid solutions and the influence of both the diluent and the chain length of radicals in the extracting agents were studied. The extraction of americium from 1M HNO_3 solutions was found to increase in the series TBP < DBEBP < BEDBP < TBPT. The extraction of nitric acid also increased in the same order, but to a much lesser extent. As the chain length of the aliphatic radicals increased in the phosphate extracting agents, the electronegativity of the P-O group rose, causing steric hindrance, and hence the conditions for complexing became less favorable. The effective constant of complex formation by americium and HNO_3 with neutral organophosphorus compounds depended on the nature of the diluent. The effective complexing constant of americium (K_{Am}) was higher the more dilute the extracting agent; the opposite was true in the case of K_{HNO3}. (ATD)

20077 COMPLEX FORMATION OF TRANSURANIC NITRATES WITH NEUTRAL ORGANO-PHOSPHORUS COMPOUNDS. V. I. Zemlyanukhin, G. P. Savoskina, and M. F. Pushlenkov. Radiokhimiya, 6: 714-32(1964). (In Russian)

Complex formation of transuranic nitrates with organic phosphorus compounds TBP, DBEBP, and BEDBP (tri-n-butyl phosphate, di-n-butyl ester of butyl phosphinic acid, and n-butyl ester of di-n-butyl phosphinic acid) was studied by 100% extraction. Distribution curves of U(IV), Np(VI), Pu(VI), and Pu(IV) were plotted for neutral TBP-DBEBP-BEDBP compounds at 0.1 to 18M HNO_3. Complexing agents found for $UO_2(NO_3)_2 \cdot 2T$, $NpO_2(NO_3)_2 \cdot 2T$, $PuO_2(NO_3)_2 \cdot 2T$, and $Pu(NO_3) \cdot 2T$ (where T = TBP, DBEBP, or BEDBP) showed that the bonding energy increased proportionally with the number of ester radicals replaced by alkyls and with the number of extraction agent molecules connected to the metal nitrate. An analysis was made of the extraction behavior of nitrates in highly acidic organic phosphorus compounds, simple acid compounds, and tertiary amines. The mean activity coefficients were calculated for U(VI), Np(VI), Pu(VI), and Pu(IV) nitrates in aqueous solutions in the presence of 0.1 to 5M HNO_3. (R.V.J.)

20078 ISOLATION OF NEUTRON-DEFICIENT ISOTOPES OF ELEMENTS IN THE CERIUM GROUP OF RARE EARTHS FROM ERBIUM IRRADIATED WITH 680 Mev PROTONS. E. Kherrmann, Kh. Grosse-Ryuken, N. A. Lebedev, and V. A. Khalkin. Radiokhimiya, 6: 756-62(1964). (In Russian)

Erbium was bombarded with 680-Mev protons to obtain neutron-deficient isotopes of light lanthanides. In order to separate these elements from erbium, use was made of partition chromatography on silica gel with bis(2-ethylhexyl)orthophosphoric acid as the extracting agent. The method is suitable for remote-control operations. The following light lanthanides were separated chromatographically: Dy, Tb, Gd, Eu, Sm, Pm, Nd, Pr, and Ce. The separation on a cation-exchange column was begun 2 hours after the proton irradiation ended. When the isolated products were measured with magnetic β spectrometers and β spectrographs in the soft region (<100 kev), no broadening of the lines of conversion electrons was observed. From this it was concluded that the purification of erbium

by partition chromatography makes it possible to eliminate light rare earths virtually completely. (auth)

20079 EXTRACTION OF RARE-EARTH ELEMENTS AS THE TERNARY SALICYLATE–PYRIDINE COMPLEXES. N. S. Poluektov. Tr. Komis. po Analit. Khim., Akad. Nauk SSSR, [Inst. Geokhim. i Analit. Khim.], 14: 154-9(1963).

Addition of salicylic acid (I) to solutions of rare earth salts containing >10% of pyridine (II) produced precipitates soluble in organic solvents. By extraction with 10 ml of $CHCl_3$ from an equal volume of aqueous solution (containing 50 mg of the element oxide, 5 ml of II, 0.4 g of I, and 0.2 ml HCl), Er, Nd, Ce, and La were completely extracted at pH ≈ 6. The absorption spectra of the Nd and Er extracts are given. In the extracts, the relative extinctions at the maxima were 2 to 3.5 times those in aqueous solutions. For Nd, it is shown that the ratio of metal to I is 1:3. (Anal. Abstr., 12: No. 2, (Feb. 1965))

20080 EXTRACTION SEPARATION OF SCANDIUM FROM OTHER ELEMENTS AS THE THIOCYANATE COMPLEX WITH DIANTIPYRINYLMETHANE. V. P. Zhivopistsev and I. S. Kalmykova. Uch. Zap. Permsk. [Gos.] Univ., 25: 120-2(1963).

In the presence of SCN^- and diantipyrinylmethane (I), Sc^{3+} formed a complex, which is readily soluble in $CHCl_3$. The influence of the concentration of HCl, SCN^-, and I on the extraction of Sc was studied, and a method was developed for the separation of Sc from accompanying elements. To the test solution (1 to 10 mg of Sc; 0.5 to 1.5N in HCl) 0.9 to 1 g of NH_4SCN, 15 ml of $CHCl_3$, and 1 g of I were added. The organic layer is removed, and 10 to 15 ml of $CHCl_3$ and 0.3 to 0.5 g of I added to the aqueous phase and the extraction repeated. To the combined extracts 20 to 50 ml of 0.0125M EDTA and 2 to 3 ml of aqueous NH_3 are added. The organic layer is separated and washed with H_2O. The combined aqueous phases are titrated with $ZnSO_4$ solution in the presence of Chromogen black ET-00. The method can be used to separate Sc from Y, Al, La, Ce, Pr, and Nd. The error in the determination of Sc is ±2%. (Anal. Abstr., 12: No. 2, (Feb. 1965))

20081 ON THE SCANDIUM SEPARATION FROM PYROXENITES. L. N. Komissarova, L. F. Borisenko, and V. M. Shatskii. Zh. Prikl. Khim., 38: 241-4(Feb. 1965). (In Russian)

Extraction of Sc from pyroxenites and blast furnace slags was studied with materials containing 50 wt % SiO_2, 10 wt % Fe_2O_3, 15 wt % MgO, 20 wt % CaO, 1.5 wt % Al_2O_3, and 0.016 wt % Sc_2O_3. After solvent partition by sulfuric acid, hydrochloric acid, sodium bisulfate, and sodium hydroxide the partition from pyroxenites was followed by carbonate treatment. The resulting concentrates contained 4 to 7% ScO_3 indicating 80% extraction. Further treatment of the scandium concentrate, combined rhodonite extraction with oxalate precipitation, resulted in a 70 to 75% yield of 99.9% scandium oxides. (R.V.J.)

20082 SELECTIVE EXTRACTION OF SCANDIUM BY ALKYL PHOSPHORIC ACIDS. M. L. Navtanovich, A. S. Chernyak, and Yu. E. Suryrin. Zh. Prikl. Khim., 38: 345-8(Feb. 1965). (In Russian)

Solvent extraction of Sc by partition with alkyl phosphoric acid was studied using tungsten concentrate disintegration residue, containing 0.3 to 0.4% Sc, tin slags with 0.05 to 0.10 and 0.3 to 0.6% Sc, and black scandium oxide with various contents of Sc metal. A freshly prepared, from n-octanol, octyl phosphoric acid (0.85M solution in kerosene) and mixtures of other alkyl phosphoric acid were used as extractants. The extraction was achieved according to the scheme: $nSc^{3+} + 3H_nX \rightarrow Sc_nX_3 + 3nH^+$ (where H_nX is the corresponding alkyl phorphoric acid $H_nR_{3-n}PO_4$ and $H_nR_{4-n}P_2O_7$). The re-extraction carried out with concentrated HF resulted in a white scandium fluoride residue: $Sc_nX + 3_nHF \rightarrow nSc_nF_3 + 3H_nX$. Further treatment resulted in an oxide precipitate of 99.0% Sc_2O_3 (Sc ~ 65%). (R.V.J.)

20083 RESIDUE LEACHING FACILITY (Engineering Materials). (Rocky Flats Plant, Dow Chemical Co., Denver, Colo.). 69 drawings. (CAPE-1179)

The facility used to recover plutonium values from leachable residues is described. Included is equipment used in extraction, calcining, and tantalum leaching. Also included are descriptions of hydraulic and vacuum pumps, storage tanks and piping, conveyer systems, scrubber systems, and a glove box. (For details, see TID-4100). (M.C.G.)

20084 METHOD OF PRE-DECONTAMINATING NUCLEAR FUEL TO BE REPROCESSED. Warner Baehr and Hubert Vogg (to Gesellschaft fur Kernforschung mbH). German Patent 1,184,503. Dec. 31, 1964. Filed May 9, 1964.

The pre-decontamination of nuclear fuel to be reprocessed is carried out by separating fission products such as cerium, ruthenium, zirconium, and niobium. The nuclear fuel is decomposed in an oxidizing alkaline melt, the liquefied material obtained is leached with water or sodium hydroxide, and the remaining nuclear fuel is mixed with dilute acid in which the nuclear fuel is dissolved and the fission nuclides remain behind as residues. (Gmelin Inst.)

ENGINEERING

General

Refer also to abstracts 19734, 21618, 21619, and 21620.

20085 (CONF-640204(p.93-105)) HIGH-VOLTAGE POWER SUPPLIES AND THEIR REGULATION. P. Livdahl (Argonne National Lab., Ill.).

A summary is presented of the state of the art of high-voltage power supplies and their regulation. The problem of stability and its measurement is discussed. Commercial power supplies for use at 1 to 5 million volts are described. The possibilities of improving the power supplies are discussed. (D.L.C.)

20086 (GAMD-5926) ITERATIVE TECHNIQUE FOR THE STRESS ANALYSIS OF PCR STRUCTURES USING THE FINITE ELEMENT METHOD. D. C. Cornell (General Atomic, San Diego, Calif.). Nov. 30, 1964. Contract AT(04-3)-167. 21p. Dep.(mn); $1.00(cy), 1(mn) CFSTI.

A straight-forward application of the TARGET code that appears to be readily adaptable to programming for the IBM digital computer is outlined. The technique of overlapping the blocks and inputing the iterated boundary conditions is performed by hand, presently. The method is general for structural problems with a large system of equations in which the links between blocks are relatively uncomplicated. (P.C.H.)

20087 (GAT-P-33) CAN YOU AFFORD YOUR COOLING WATER TREATMENT PROGRAM? D. B. Jones (Goodyear Atomic Corp., Piketon, Ohio). June 30, 1964. Contract AT(33-2)-1. 17p. (CONF-492-10). Dep.(mn); $1.00(cy), 1(mn) CFSTI.

From National Association of Corrosion Engineers, Chicago, Mar. 1964.

A discussion is presented of various ways to reduce the costs of water treatment programs. The date required to determine true operating costs and their possible reduction are discussed. Methods of conserving chemicals are considered. Some examples of water treatment problems and their solutions are given. (D.L.C.)

20088 NUCLEAR MEASUREMENTS. Jozef Spaepen (European Central Bureau for Nuclear Measurements, Geel, Belg.). Euratom Bull., 4: No. 1, 2-7(Mar. 1965).

The activities of the Euratom standards bureau for nuclear measurements are outlined, including preparation of samples and standards; development of counting techniques; and research on threshold reactions, dosimetry, fast neutron scattering, boron, and preparation of foils containing fissile isotopes. The facilities of the bureau are briefly considered. (D.C.W.)

Applications of Nuclear Explosions

20089 (NP-14887) METHOD FOR PREDICTING THE SHAPE OF EXPLOSION-PRODUCED CRATERS. J. N. Strange and A. J. Hendron, Jr. (Army Engineer Waterways Experiment Station, Vicksburg, Miss.). Oct. 1964. 23p. (MP-1-677)

This report is concerned with defining the geometry (shape) of explosion-produced craters. A representative group of averaged half-crater profiles was studied, and the crater geometries were normalized so as to be representative of a wide range of explosion yields, types of earth materials cratered, and charge depths of burial. From the normalization study, a shape equation was developed which specifies the apparent crater profile as a function of the apparent crater depth and radius. Thus, the shape of the crater immediately after the shot can be defined by substituting into the shape equation the predicted values of the apparent crater depth and radius. The problem of assessing the stability of the crater slopes is rendered amenable to solution by means of classical slope-stability analysis techniques utilizing the predicted crater geometry derived from the shape equation. (auth)

20090 (SC-RR-65-41) A SMALL-SCALE INVESTIGATION OF THE POSSIBILITY OF CONSTRUCTING LOW-RELIEF EARTH-FILL DAMS USING NUCLEAR EXPLOSIVES. L. J. Vortman (Sandia Corp., Albuquerque, N. Mex.). Feb. 1965. Contract AT(29-1)-789. 35p. Dep.; $2.00(cy), 1(mn) CFSTI.

The experiment described herein has shown that the concept of low dams produced by ballistic collision of ejecta from simultaneous detonation of properly spaced parallel rows of charges is a feasible one. Rows of 8-pound charges were buried 3 feet deep with 4-foot spacing between charges. When two such rows of charges were placed parallel and 17.5 feet apart, the maximum height of the dam was achieved. The spacing of 17.5 feet between rows corresponds to 4.7 times the crater radius of one 8-pound charge at the burial depth which maximizes the single-charge crater. The extrapolation of these results to larger explosions and the use of nuclear explosives is discussed. The height decreases and the width increases as the spacing between rows is further increased. The mass of material in the dam cannot exceed that in the crater of one of the rows. At the spacing between rows which maximizes height, the volume of the dam is about 50 percent of maximum volume theoretically achievable. At wider spacings, the volume increases to 75 percent. (auth)

20091 ISTHMIAN SEA-LEVEL CANAL. John Hurd. Nucl. News, 8: No. 4, 22-7(Apr. 1965).

The routes and excavations being proposed for the sea-level canal are discussed, with consideration of the canal specifications and the technology of nuclear cratering. (D.C.W.)

Facilities and Equipment

Refer also to abstracts 20347 and 21610.

20092 (ANL-6938(p.91-6)) THE LOW-LEVEL GAMMA COUNTING ROOM: RADON REMOVAL AND CONTROL. Henry F. Lucas, Jr. (Argonne National Lab., Ill.).

An underground counting room was constructed for use in studies requiring the quantitative assay of very low intensity gamma-ray-emitting sources. The room was placed underground to provide increased shielding from sources of fast neutrons and from the nucleonic component of cosmic rays. Airborne radioactive particles are removed from the air supply by filtration, and the radioactive gases ^{41}Ar and ^{222}Rn are eliminated either by aging for several half-lives in large steel tanks or by adsorption on cooled charcoal. Results of an investigation show that the air lock system should be made more effective and that other sources of leakage should be reduced to a minimum. Increased pressure should eliminate all external sources of radon and allow the concentration in the vault air to approach an expected level of 10^{-14} C/l or lower. (J.R.D.)

20093 (ANL-6938(p.194-205)) AN UNDERGROUND LABORATORY FOR HIGH-SENSITIVITY GAMMA-RAY COUNTING. Harold A. May, John B. Corcoran, and Paul Hess (Argonne National Lab., Ill.).

Tests made in an underground laboratory designed to reduce the background contributed by cosmic nucleons to a negligible amount are discussed. The laboratory design is also discussed. (J.R.D.)

20094 (BNL-8969) ELECTRONIC PEAKERS. W. Michaelson (Brookhaven National Lab., Upton, N. Y.). [1964]. Contract AT-30-2-GEN-16. 6p. (CONF-650306-17). Dep.(mn); $1.00(cy), 1(mn) CFSTI.

From Particle Accelerator Conference, Washington, D. C.

A reliable system has been designed and built for the variable-phase generation of pulses for the firing of ignitrons. These ignitrons rectify the a-c output of a motor generator set for application of d-c power to the main magnets of the Alternating Gradient Synchrotron at Brookhaven National Laboratory. It is possible to shift the phase of the ignitron firing so that the current in the main magnets either increases in a linear manner (rectify mode), decreases in a linear manner (invert mode), or stays constant at any desired level (flat-top mode). In addition, time interval pulses can be applied to the electronic peakers so that the main magnet current can be made to be any combination of the rectify, flat-top, and invert modes. The electronic peakers have been in operation for a little over a year without a failure. (auth)

20095 (BNL-8976) COBALT-60 RESEARCH IRRADIATORS. B. Manowitz, O. Kuhl, A. Oltmann, L. E. Kukacka, and M. Steinberg (Brookhaven National Lab., Upton, N. Y.). Sept. 17, 1964. Contract AT-30-2-GEN-16. 28p. Dep.(mn); $2.00(cy), 2(mn) CFSTI.

Four pool-type gamma irradiation units and one portable lead-shielded irradiator have been designed and built. Figures on construction, operating, and maintenance costs are given. (auth)

20096 (NAA-SR-Memo-10729) MERCURY RANKINE PROGRAM THERMOELECTRIC PUMP DATA ANALYSIS AND CORRELATION. J. M. Hochman (Atomics International, Canoga Park, Calif.). Nov. 17, 1964. Contract AT (11-1)-Gen-8. 16p. Dep.(mn); $1.00(cy), 1(mn) CFSTI.

An analytic technique has been developed which gives good correlation of the mercury Rankine-cycle powerplant thermoelectric pump data. This correlation showed that the recorded performance is real and that the present design equations adequately describe the system in conjunction with a calculated "effective Seebeck coefficient." (auth)

20097 (NASA-SP-5019) ADVANCED VALVE TECHNOLOGY. Technology Survey. Kenneth D. May (Midwest Research Inst., Kansas City, Mo.). Feb. 1965. 189p. $5.00(CFSTI).

This book has the purpose of disseminating advanced valve technology throughout industry. Limitations of commerically available valves are identified, and technological advancements are described. The technology is grouped into several categories such as leakage, materials, compatibility, etc. (D.L.C.)

20098 (TID-21633) BASIC STUDIES IN GAS-SOLID SUSPENSION, Quarterly Report No. 64-2, April 1–October 1, 1964. Richard L. Peskin (Rutgers–The State Univ. of New Jersey, New Brunswick. Bureau of Engineering Research). Oct. 15, 1964. Contract AT(30-1)-2930. 18p. Dep.(mn); $1.00(cy), 1(mn) CFSTI.

Current experimental research under the program of basic studies in gas-solid suspension is reported. The current projects in helium diffusion study, instrumentation development, electrostatic study, heat transfer, and cooling are discussed. Experimentation was carried out in the field of electrostatic effects on gas-solid suspension flow. In general it was preliminarily concluded that the solid particles do become charged provided the carrier gas is dry and nonconducting. It was concluded from this and other work that the charge on the particles effects the density distribution more severely than the mass flux distribution. Instrumentation techniques consisted of further development and initial trial of the discharge anemometer, further improvements on the optical density measuring devices, and an evaluation of the Bureau of Mines mass flux meter with the optical mass flux metering system. Also a large amount of time was spent in developing instrumentation for heat transfer and cooling research. The major research effort was devoted to the construction of a modified gas-solid suspension loop designed for heat transfer experiments. This included the acquisition of radiant heaters the fabrication of new circular test sections, a new return line, a water jacket cooler, installation of major power substation controls, installation of a temperature controlling device, and installation of safety equipment. (P.C.H.)

20099 (TID-21644) GANTRY AND TROLLEY FOR FUEL HANDLING CASK. J. deArrieta (Atomics International, Canoga Park, Calif.). July 17, 1959. Revised Oct. 9, 1959. Contract [AT(11-1)-Gen-8]. 18p. Dep. (mn); $1.00(cy), 1(mn) CFSTI.

Specifications are given for the gantry and trolley for transferring reactor components to and from the Hallam reactor core. Operational requirements, structural design, equipment details, etc., are specified. (D.L.C.)

20100 (UCRL-12203) AN EXPLOSIVELY DRIVEN PIPE CLOSURE. Donald H. Gipson (Lawrence Radiation Lab., Univ. of California, Livermore). Feb. 15, 1965. Contract W-7405-eng-48. 9p. Dep.; $1.00(cy), 1(mn) CFSTI.

The design of explosively driven pipe closure is given. It is an 8-foot-long, 6,000-pound, hollow steel cylinder having an inner bore of 9½ inches and an outer diameter of 18 inches. A laminate charge of high explosives drives a portion of the wall thickness radially inward to form a solid rod of steel centered on the original long axis of symmetry. This solid rod is approximately 10 inches in outer diameter by 40 inches in length. The closure operation is completed within a time period of 335 ± 5 microseconds. (auth)

20101 (ORNL-tr-442) CENTRIFUGAL PUMP FOR SAMPLING RADIOACTIVE LIQUIDS. Translated by A. L. Monks (Oak Ridge National Lab., Tenn.), from French Patents 818,520 and 1,248,341. Feb. 15, 1960. 10p. Dep.(mn); $1.10(fs), $0.80(mf) JCL.

A description is given of a centrifugal pump and an apparatus for taking samples from radioactive liquids. The pump contains a shaft carrying an impeller and supported on an air-lubricated thrust bearing centralized by air-lubricated journal bearings and rotated by an air-powered turbine rotor. The apparatus consists of a biological shield containing a pipe for radioactive liquors and one outside the shield for liquor drawn off from the interior pipe. The pump inlet and outlet communicate with the interior and outside pipes, respectively. The pump is located within a casing extending from the outside to a position integral with the pipe inside the shield. (D.L.C.)

20102 AN AUTOMATICALLY CONTROLLED OUTDOOR GAMMA IRRADIATION FACILITY AT EMORY UNIVERSITY. R. B. Platt, J. T. McGinnis, and J. J. Cowan (Emory Univ., Atlanta). Bull. Georgia Acad. Sci., 22: 75-80(Sept. 1964).

The construction and operation of a 2500-C ^{137}Cs radiation source for field radiobiology studies are described. The facility is located in a populous, urban area and is equipped with fully automatic and integrated operating and safety systems. Earthen bunkers 16 ft in height around the perimeter of the elliptical field combine with the source shielding to reduce direct and scattered radiation to safe levels for the nearby residences. A steel and lead sky shield attenuates upward radiation by a factor of 10^8. Automatic operation may be programmed through a time clock, or the source may be raised and lowered by push-button manual control. Emergency switches located in the control building and in the field permit immediate dropping of the source into the 30 in. of oil in its underground well by de-energizing the electromagnet that holds the source. The entire perimeter of the field outside the earthen bunker is protected by a commercial burglar alarm infrared system. Radiation is attenuated to 192 R/hr at 1M in all except one 30° sector, in which a 800 R/hr beam is directed. In the high-flux sector, the terrain drops sharply beyond the field and there are no buildings within a half-mile and no free access areas for 840 ft. Wedge-shaped lead bricks are attached about the source pipe when further attenuation of the γ radiation is required for experimental purposes. A lead cylinder surrounding the source pipe minimizes the environmental dose rate during the 27-sec up or down transit time of the source. Portable controlled

environment chambers are being installed, to provide facilities for irradiation of organisms under many combinations of programmed environmental conditions. Doses within the field vary from 800 R/hr at 1M to background levels, thus permitting both acute and chronic irradiation procedures. Operation is on a 20-hr day schedule. (TCO)

20103 AUTOMATIC SAFETY CONTROL EQUIPMENT FOR POWER PLANTS, CLASSICAL AND NUCLEAR. Ch. Kaplan (C.D.C., Paris). Paper 5, Session 14, 12p. of "Mesucora 63. Congres International Mesure-Controle Regulation-Automatisme. Tome II." Paris, Mesucora, [1964]. (In French)

Two safety control devices that can be used on both conventional and nuclear power plants are described. One measures directly the stresses in the metal taking into consideration the pressure in the vessel and the temperature differences across the wall thickness and between different parts of the envelop. The other device measures the derivative of the temperature with respect to time at some critical points of the installation in order to maintain the thermal drop within safe limits. The design and principles of both devices are discussed in detail. (J.S.R.)

20104 ALVA 12 IN. BALL VALVE MODIFICATION (Engineering Materials). (California. Univ., Livermore. Lawrence Radiation Lab.). 9 drawings. (CAPE-1120)

The 12-in., 250-psi valve was modified to include a closing system, which consists of a tension spring actuator and a Conax explosive latch pin. The valve, which is held in the open position until detonated by an electrical signal, closes in about 0.5 sec. The valve was evacuated to a pressure of less than 100μ of Hg and hydrostatically tested to 1000 psi without leaking. (For details, see TID-4100.) (M.C.G.)

20105 IMPROVEMENTS IN MEANS FOR OBSERVING SPECIMENS CONTAINED IN A FLUID-TIGHT CHAMBER. Albert Guinard and Pierre Rosseau (to Commissariat a l'Energie Atomique). British Patent 976,045. Nov. 25, 1964. Priority date Feb. 2, 1962, France.

An apparatus for observing specimens contained in a fluid-tight chamber includes a specimen holder connected to the chamber by a flexible fluid-tight coupling through which the specimen can be moved to the specimen holder from the chamber and vice versa. The specimen holder has an optical window through which the specimen may be observed using a microscope outside the chamber. The flexible coupling ensures that the specimen holder can be correctly adjusted relative to the objective of the microscope. The specimen may be observed either dry or partially immersed in a liquid. The objective on the microscope is spring-mounted or includes a stop mechanism to prevent the objective from breaking the viewing window. (A.G.W.)

20106 IMPROVEMENTS IN OR RELATING TO CLOSURE MEANS FOR PRESSURE VESSELS. Harry William Norton (to Geartight Unions Ltd.). British Patent 976,501. Nov. 25, 1964. Filed Dec. 18, 1959.

A closure means for an opening in a pressure vessel consists of two portions capable of limited relative movement in a direction substantially axial to the opening. A plurality of members angularly separated with respect to the axial direction is arranged on one portion, and when the plates are separated the members are withdrawn into the one portion. As the portions move toward each other, the locking members are extended and locked in the extended position by a locking surface on the other portion. At least one of the portions is provided with a mechanical or electrical means for interlocking the two portions and for indicating when they are completely engaged and locked. The interlock may be arranged to engage a grab by which the closure means is positioned and to prevent disengagement of the grab until the locking means are locked. (A.G.W.)

Heat Transfer and Fluid Flow

See also PHYSICS — General.

20107 (BAW-1280-22) SODIUM-HEATED STEAM GENERATOR DEVELOPMENT. Progress Report No. 20. (Babcock and Wilcox Co., Barberton, Ohio. Boiler Div.). Dec. 1964. Contract AT(11-1)-1280. 55p. Dep.(mn); $3.00(cy), 1(mn) CFSTI.

The design criteria for the once-through type steam generator are outlined. The preliminary design of the full-size steam generator has been completed, while that of the prototype is approximately 70% complete. In the model steam generator test for studying carbon and mass transfer effects, piping specimens were removed after exposure to sodium for 4000 hr. The specimens showed no further change in the microstructure of Type 316 stainless steel, while decarburization of Croloy 2¼ occurred to a depth of of 10 mils. The objectives, scope, and present status are reported for the following projects: corrosion rates of Croloy 2¼ steel in products of sodium-water reaction, welding of tubes to backside of tube sheet, and chemical simulation of sodium environment for leak testing. The analysis to be done on sodium-water reaction problems in the steam generators is outlined, and progress is reported. (D.L.C.)

20108 (BNWL-31) FLOW VISUALIZATION: A COMPARISON OF STREAMING BIREFRINGENCE WITH OTHER TECHNIQUES. D. H. White (Battelle-Northwest, Richland, Wash. Pacific Northwest Lab.). Mar. 1965. Contracts AT(45-1)-1350 and AT(45-1)-1830. 88p. Dep.; $3.00(cy), 2(mn) CFSTI.

The flow visualization technique known as streaming birefringence (SBR) was studied by direct comparison with three other techniques; small spherical plastic tracers, cotton thread surface tufts, and dye injection. Comparative tests on four differently shaped, two-dimensional models were run. Reynolds numbers for the incompressible fluids varied from about 1000 to about 6000. These tests showed that an SBR solution of bentonite clay compared favorably with other visualization techniques for the (a) flow separation around a cylinder, (b) flow separation at the throat of a restrictor, (c) vena contracta of an orifice, and (d) transverse flow in a rectangular channel. The SBR fluid compares unfavorably or questionably for diffuser separation and circular eddies. It is concluded that the SBR flow visualization technique has potential for use as a visualization tool, requires skill and care in use, and should be investigated in greater depth. (auth)

20109 (CER-D1703) STUDY PROGRAM FOR HF, VHF, AND UHF ANTENNAS FOR 1- TO 50-PSI OVERPRESSURE RANGE. Final Report, July 1, 1962–September 30, 1963. (Collins Radio Co., Dallas, Tex.). Contract OCD-05-62-199. 333p. (AD-422652). $19.75(CFSTI).

An investigation was made of various approaches toward providing receiving and transmitting hf, vhf, and uhf antennas capable of surviving 1 to 50 psi overpressure either while in place or while stowed, to be put in place after the blast. The additional requirement was made that the antennas be as economical as possible, especially in the vhf and uhf ranges. Several antenna types were evolved that are suitable for meeting these requirements. In addition, an evaluation of commercially available antennas has been made. A study of the hardening possibilities of an antenna has necessitated a study of the material and structure of which the antenna is made and upon which it is placed. (auth)

20110 (GAMD-5432) THERMAL PROTECTION OF CONCRETE PRESSURE VESSEL BY LAMINATED INSULATION AND INTERNAL COOLING. L. Cavallaro (General Atomic, San Diego, Calif.). June 1964. Contract AT(04-3)-167. 44p. Dep.(mn); $1.00(cy), 1(mn) CFSTI.

To preserve the integrity of a concrete pressure vessel, the temperature must be kept within the limit of 150°F. This requires removal of the gamma heat generated in the concrete, and of the heat transmitted by the reactor and primary loop to the inner liner of the vessel. Water cooling of the liner is provided for this purpose; however, in order to make the cooling practical, it is imperative that the quantity of heat transmitted to the liner be kept at a low level. Two alternate means to achieve this limitation are considered: applying a laminated insulation to the liner; and cooling the space between the primary loop and the

pressure vessel. Using the TARGET design as a reference, an approximated evaluation of the economics of the two systems was carried out, and the areas requiring further, more detailed investigation are outlined. As far as insulation is concerned, it appears that an effort should be made to reduce the fixed costs, by a careful and detailed design directed toward more economical fabrication and installation. An internal cooling system, on the other hand, may present a better economic potential than the insulation, if operated with very low cooling flows, so as to reduce the heat transfer from the hot surfaces to the cooling gas. Such a cooling scheme, however, involves important hydrodynamic problems; these may require a substantial developmental effort, whose cost is not easily predictable. (auth)

20111 (NAA-SR-Memo-10224) WETTING OF MERCURY-RANKINE BOILER TUBE SURFACES. I. E. Randall (Atomics International, Canoga Park, Calif.). July 16, 1964. Contract AT-11-1-GEN-8. 28p. Dep.(mn); $2.00 (cy), 1(mn) CFSTI.

The mercury wetting conditions for the Mercury Rankine system boiler were tested by observing the contact angle of mercury on Haynes alloy 25 surfaces treated in two different ways. A sessile drop apparatus was used in which mercury drops were placed on samples and the contact angles were measured from photographs. The tests were the preliminary ones of a proposed complete program. Boiler tube surface conditions were simulated by cleaning the test samples in the same manner as the boiler tubes. Two cleaning processes were used, a pickling process and a hydrogen annealing process. The surface which was cleaned by pickling was mercury wet of 710°F ± 20°F and non-wetting of the hydrogen annealed surfaces was observed up to 720°F ± 20°F, the temperature limit of the apparatus after it had partially failed. The tests indicate that the pickling process is the better one, and that tubes cleaned by pickling will be wet by mercury, at least initially, at the boiler operating temperature. (auth)

20112 (NAA-SR-Memo-10315) MERCURY WETTING AND ITS EFFECTS ON HEAT TRANSFER. J. M. Hochman (Atomics International, Canoga Park, Calif.). Aug. 21, 1964. Contract AT-11-1GEN-8. 28p. Dep.(mn); $2.00(cy), 1(mn) CFSTI.

A literature review was conducted on mercury wetting to evaluate its effect on heat transfer. The various surface effects cannot be separated, but reliable nucleate boiling can be attained under wetting conditions. Wetting may be attained under proper conditions without the use of additives by the use of sufficiently clean surfaces and clean mercury. It is concluded that the desired goal is a wetted system obtained by proper pretreatment. (D.L.C.)

20113 (NP-14895) FILM BOILING OF SATURATED LIQUID FLOWING UPWARD THROUGH A HEATED TUBE: HIGH VAPOR QUALITY RANGE. Technical Report No. 9857-32. William F. Laverty and Warren M. Rohsenow (Massachusetts Inst. of Tech., Cambridge. Dept. of Mechanical Engineering). Sept. 1964. 106p.

Film boiling of saturated liquid flowing upward through a uniformly heated tube was studied for the case in which pure saturated liquid enters the tube and nearly saturated vapor is discharged. This investigation was concentrated on film boiling in the region where the vapor quality is greater than 10 percent. Visual studies of film boiling of liquid nitrogen flowing through an electrically conducting pyrex tube were made to determine the characteristics of the two-phase flow regimes which occur as a result of the film boiling process. It was found that the annular flow regime with liquid in the core and vapor between the liquid and the tube wall, which exists at very low qualities, is broken up at higher qualities to form a dispersed flow of droplets and filaments of liquid carried along in a vapor matrix. A stainless steel test section having a 0.319 inch ID and heated electrically, was used to obtain experimental data of wall temperature distributions along the tube and local heat transfer coefficients for different heat fluxes and flow rates with liquid nitrogen as the test fluid. Heat flux was varied from 3500 to 30000 Btu/hr-ft^2 and mass velocity from 70000 to 210000 lbm/hr-ft^2. From these tests, values of wall superheat, ($T_w - T_s$), from 200 to 975°F and heat transfer coefficients from 11.1 to 65.5 Btu/hr-ft^2-°F were obtained. A theoretical derivation using the Dittus-Boelter equation as an asymptote for the heat transfer to pure vapor demonstrated that a significant amount of vapor superheat is present throughout the film boiling process. The mechanism of the heat transfer process in the dispersed flow region was described by a two step theory in which (1.) all of the heat from the wall is transferred to the vapor and (2.) heat is transferred from the vapor to the liquid drops. A method was given by which both an upper bound of the heat transfer coefficient to the dispersed flow and an estimate of its true value may be calculated. (auth)

20114 (NP-14920) ENTRANCE FLOW AND TRANSITION FROM LAMINAR TO TURBULENT FLOW IN VERTICAL TUBES WITH COMBINED FREE AND FORCED CONVECTION (thesis). W. Thompson Lawrence (Massachusetts Inst. of Tech., Cambridge. Dept. of Mechanical Engineering). Feb. 1965. 108p. (DSR-9365)

This investigation deals with entrance flow in vertical tubes. A theoretical solution to this problem was obtained using a finite difference method. The theoretical solution solves both upflow and downflow problems for the constant heat flux or constant wall temperature case using an IBM 7094 computer. All the results were obtained for a uniform entrance velocity, but any nonuniform velocity profile can be used at the entrance. Using water, the solution was verified by experimental measurements made for upflow with uniform heating. By a comparison of theoretical and experimental results it was found that to obtain an accurate solution the density must be represented by a quadratic function of temperature and viscosity must be treated as a function of temperature. The results show that the velocity profiles continue to develop as the fluid moves downstream. Thus in treating a real fluid, it is inadequate to consider the fully developed case in which both velocity and temperature profiles are assumed to stop changing after some axial position in the tube. The transition from laminar to turbulent flow was studied. Experimental measurements with uniform heat flux and upflow in a tube demonstrated that the transition process depends on developing velocity profiles. The velocity profiles constantly change along the tube until a profile shape occurs which is unstable for the entrance Reynolds number. Thus transition will always occur at some axial position if the tube is long enough, and, for a given entrance temperature, the distance to transition is fixed by the fluid flow rate and heat flux at the wall. Finally, using the theoretical solution to obtain developing velocity and temperature profiles corresponding to cases for which experimental transition data was available, a tentative transition criterion was obtained. This criterion gave a correlation between the entrance Reynolds number and a transition parameter based only on the velocity profile shape and fluid viscosity for the experimental results obtained. (auth)

20115 (ORNL-TM-1093) A COMPUTER PROGRAM FOR FLOW CALCULATIONS. E. G. Davisson (Oak Ridge National Lab., Tenn.). Feb. 3, 1965. Contract [W-7405-eng-26]. 37p. Dep.(mn); $2.00(cy), 1(mn) CFSTI.

A computer program is described for precise calculation of liquid, gas, steam, and vapor flows for flange, pipe, corner, radius, vena contracta, and venturi taps when used with a dry meter, a dry-calibrated mercury meter, a wet-calibrated mercury meter, or a U-tube manometer. The program provides an option of specifying either the orifice diameter or the maximum flow desired. The program assumes that the pipe size and meter range have been selected in advance. Also required as input data are the physical properties and flowing conditions of the fluid. (auth)

20116 (SAN-409-12) HIGH ACCELERATION FIELD HEAT TRANSFER FOR AUXILIARY SPACE NUCLEAR POWER SYSTEMS. Annual Technical Report, September 1, 1963–August 31, 1964. (Geoscience Ltd., Solana Beach, Calif.). Contract AT(04-3)-409. 159p. (GLR-27). Dep. (mn); $5.00(cy), 3(mn) CFSTI.

High-temperature liquid-metal heat and momentum transfer processes were investigated in studies of analytical and experimental liquid-metal boiling and condensing with emphasis on high gravity or helical flow in the high vapor quality and superheated regions. Design criteria which are applicable to the SNAP Project are being developed so that nuclear reactor and heat exchanger performance can be predicted. A boiling heat transfer analysis was made for alternate slugs of liquid and vapor flowing through boiler tubes. An analysis was made of helical, forced-flow pressure drop for single-phase flow in tubes. An equation was derived for convective heat transfer in helical, single-phase flow; the analysis accounts for improved heat transfer as a result of both forced- and free-convection phenomena. The stationary droplet vaporization model was extended to the forced-flow case. Experimental forced-flow boiling Hg heat transfer and pressure drop measurements were made under linear flow conditions. Experimental forced-flow boiling Hg heat transfer and pressure drop measurements were made under helical flow conditions. Forced-flow boiling Hg heat transfer and pressure drop measurements in linear and helical flow were completed. Preliminary forced-flow K boiling heat transfer measurements were obtained. Droplet vaporization lifetimes were measured and compiled for Hg, Freon, and benzene. Forced-flow Freon boiling measurements were made; six different fluid flow regimes were identified and quantitative heat transfer conductances were obtained as a function of vapor quality and flow rate. Comparisons were made of some of the experimental forced-flow boiling liquid-metal heat transfer data found in the literature; similarities and differences were pointed out. The thermodynamic properties of K vapor in the superheated region were extended analytically to higher temperatures. A kinetics study was made of the effect of a temperature perturbation at the coolant channel wall on the reactor criticality; the phase lag and amplitude reduction in the fuel region were considered. (auth)

20117 (SU-247-4) THE EFFECT OF LARGE TEMPERATURE GRADIENTS ON TURBULENT FLOW OF GASES IN THE THERMAL ENTRANCE REGION OF TUBES. Patrick M. Magee (Stanford Univ., Calif. Nuclear Technology Lab.). Oct. 1964. Contract AT(04-3)-247. 243p. Dep.(mn); $6.00(cy), 5(mn) CFSTI.

The results of an experimental and analytical investigation of the thermal entrance region for gases flowing turbulently through smooth, electrically heated, circular tubes are described. Emphasis is placed upon high heat-flux levels where the variations of fluid properties, due to large temperature gradients, must be considered. Local measurements for air and helium are made at entering Reynolds numbers from 10^4 to 2×10^5. Previous studies have shown that integral boundary-layer analyses underestimate the entrance-region heat-transfer effects for low heat-flux conditions. The present experimental study indicates that these analyses also underestimate entrance effects for cases of large heat flux. As an alternative, the use of finite-difference solutions to the two-dimensional energy equation, including variable gas properties, is proposed. The resulting analysis is in substantially better agreement with the experimental data at low heat flux than are the former variable-properties analyses and is in as good agreement with the data at high heat-flux as are the former analyses. A method of correlating entrance-region heat-transfer data, that is successful both at low and high heat-flux levels, is proposed. It is shown experimentally and analytically that the parameter characterizing entrance region behavior is strongly dependent upon the wall-to-bulk temperature ratio as well as upon the distance-diameter ratio. In the flow range under investigation, the entrance parameter does not vary significantly with entering Reynolds number. Local friction factors are experimentally measured in the thermal entrance region, beginning at a distance-diameter ratio of five. Although a fully developed velocity profile is always established prior to the initial point of heating, the friction factors vary within the thermal entrance region and for a considerable distance downstream; the magnitude of the variation increases with the heat-flux level. An empirical equation, involving the wall-to-bulk temperature ratio and the distance-diameter ratio, is proposed to correlate the air data. (auth)

20118 TURBULENT HEAT TRANSFER IN A PIPE WITH ARBITRARY HEAT FLUX. Shigebumi Aoki, Tadao Takahashi, and Hisashi Shimazu. Bull. Tokyo Inst. Technol., No. 61, 1-11(1964).

Turbulent heat transfer in a round pipe is considered. Attempts were made to obtain the experimental formula of heat transfer coefficient when the heat flux along the pipe varies sinusoidally. The local Nusselt number obtained is expressed as follows: $Nu = 0.023\ Re^{0.8}(1 + 0.1 \cot (x/Lo)\pi)$. The maximum deviation of this formula from the experimental data was 15%, except at the end of the pipe. (auth)

20119 SIMILITUDE CRITERION OF MAGNETOHYDRODYNAMIC PHENOMENA AND ELECTROMAGNETIC-POWER LOSSES IN A LAYER OF CONDUCTING LIQUID BETWEEN THE ROTOR AND STATOR IN AN INDUCTION MOTOR. A. V. Ivanov-Smolenskii and G. S. Tamoyan. Izv. Vysshikh Uchebn. Zavendenii, Energ., No. 6, 32-9 (1964).

This problem is treated by simulating the driving motor of a completely sealed turbine-type pump handling a liquid metal or other conducting liquid. By adapting the classical Navier-Stokes fluid-motion equations to the specific conditions of the sealed-pump motor, these similitude criteria are developed: s_p = idem, $\Delta B\sqrt{\sigma/\rho\nu}$ = idem. (Hartmann's criterion, M), where s_p is the slip of the rotor boundary in the magnetic field, Δ is the gap thickness, B is the magnetic induction, σ is the electric conductivity, ρ is the liquid density, and ν is the kinematic viscosity. Scale factors for determining power losses in the motor are calculated. The above criteria were experimentally corroborated on a universal induction-motor model with a liquid metal in its air-gap; tests were conducted for a wide range of M. Theoretical and experimental unit-electromagnetic-power-vs-M curves are presented. (ATD)

20120 SEVEN-ROD BUNDLE, NATURAL-CIRCULATION, STABILITY AND BURN-OUT TESTS WITH WATER AT UP TO 28 ATMOSPHERES PRESSURE. R. W. Bowring (Institutt for Atomenergi, Halden, Norway) and C. L. Spigt. Nucl. Sci. Eng., 22: 1-13(May 1965).

Stability and burnout natural-circulation tests on an electrically heated 7-rod cluster were carried out to obtain data relevant to the Halden II reactor. The object of the tests was to measure the maximum channel powers obtainable without burnout at pressures up to 28 atm and various inlet subcoolings. The test-section heat flux was essentially uniform, but local heat-flux peaks were introduced at hot patches to probe burnout. It was found that at 28 atm and up to 6°C inlet subcooling, a channel power of nearly 600 kw could be reached without burnout or instability; increasing the subcooling further reduced the burnout power. The instability channel power threshold was investigated and found to decrease with decreasing pressure. In addition, the natural-circulation inlet velocity was measured at various constant pressures and values of inlet-subcooler heat removal, as a function of channel power up to and in the hydraulic instability region. Flow oscillations of about 1-sec period were observed and recorded together with the burnout detector signal at trip under these conditions. (auth)

20121 FLOW INSTABILITY IN A NATURALLY CIRCULATING BOILING WATER REACTOR. Mark Arthur McDermott. Thesis, Ames, Iowa, Iowa State Univ. of Science and Tech., 1964. 122p.

The coolant flow oscillations in a naturally circulating boiling water reactor were analyzed by comparing the reactor to a naturally circulating boiling loop with two risers and a single downcomer. The flow in the boiling loop is calculated by solving the energy, continuity, and momentum equations for two-phase flow with an additional equation that describes the relation between the two phases. The relation between the two phases is described in terms of Kholodovskiy's prediction equation after his equation has been modified to allow for the relative velocity of bubbles in

regions of low flow or low void fractions. The resulting partial differential equations are solved on a digital computer. One model, which is hydraulically similar to EBWR, is analyzed. No regions of flow instability are found in the investigation. Flow reversals are obtained in one channel by setting the heat release rate to zero and then adding heat to the channel. This heat addition produces a flow surge, which returns to a steady-state value. A five percent power oscillation in one channel shows that the circulation rate response is dependent on the frequency of the power oscillation. The maximum flow disturbance is observed when the period of the oscillation is nearly twice the time required for a bubble to travel from the center of the boiling region to the riser exit. This corresponds to a condition where the acceleration of the fluid in the riser due to pressure change from temporal acceleration and due to an increase in void generation reinforce each other in the region above the section where the heat is released. The steady-state circulation rates and void fraction are in good agreement with the observed values in EBWR. (Dissertation Abstr., 25: No. 5, Nov. 1964)

20122 SIMILAR SOLUTIONS FOR MAGNETOGASDYNAMIC LAMINAR COMPRESSIBLE BOUNDARY LAYERS. James Delano Iversen. Thesis, Ames, Iowa, Iowa State Univ. of Science and Tech., 1964. 89p.

A theoretical investigation is made of the laminar compressible boundary layer along a flat plate with an applied magnetic field for an electrically conducting fluid. The fluid is assumed to be a perfect gas. The boundary layer approximations are used to derive equations for two different magnetic field configurations. For the crossed-field configuration the magnetic field component perpendicular to the plate is an order of magnitude larger than the streamwise component. For the aligned-field configuration the streamwise component is an order of magnitude larger than the component perpendicular to the plate. The permissible orders of magnitude for the magnetic Reynolds number and the magnetic pressure number were determined for both configurations. A similar solution technique is employed in which the temperature, density, velocity, and magnetic field can be made functions of a single similar independent variable so that the equations to be solved are ordinary differential equations. Solutions are obtained by numerical integration with the use of a digital computer. The results of the numerical solution show that the velocity gradient at the wall and therefore the viscous skin friction is reduced by application of a magnetic field. The total drag (magnetic plus viscous) may increase, however, depending upon the value of the streamwise component at the wall. For the cold wall problem, the temperature gradient at the wall, and therefore the heat transfer to the wall, is reduced by application of the magnetic field. For the adiabatic wall problem, the wall temperature is increased slightly with increase in magnetic field strength. The value of the magnetic interaction parameter at which separation of the boundary layer occurs is shown to decrease with an increase in Mach number. (Dissertation Abstr., 25: No. 5, Nov. 1964)

20123 HEAT TRANSFER TO LIQUID METALS FLOWING TURBULENTLY IN ECCENTRIC ANNULI. Wen-shi Yu. Thesis, Brooklyn, Polytechnic Inst., 1964. 151p.

Heat transfer to liquid metals flowing turbulently in eccentric annuli with uniform heat flux from the inner wall was studied analytically. It was shown that the heat transfer rate might be reduced from that of a concentric annulus by 95% with maximum eccentricity. Present correlations of the friction factor were extended, and the velocity correlation for flow of fluids in concentric annuli was modified to predict turbulent velocity profiles in eccentric annuli. Effective thermal conductivity values were calculated by using the analogy between heat transfer and momentum transfer. Temperature distributions were determined. Local and average heat transfer coefficients were obtained under given conditions. Results make it possible to predict Nusselt numbers for liquid metals flowing through eccentric annuli under conditions of uniform heat flux from the inner wall and fully-established flow. The major conclusions are summarized as follows: (1) Increase in eccentricity causes a large reduction in average Nusselt number, other things being equal. (2) The fractional reduction in average Nusselt number from the concentric value is independent of the Peclet number for given values of the radius ratio and the eccentricity. (3) At low R values such as R = 1.5, negative local coefficients occur in the region of widest separation, where the surface temperature is less than the average bulk temperature of the fluid. At the points where the surface temperature is equal to the average bulk temperature of the fluid, the local coefficients are infinite. The larger the radius ratio, the smaller is the effect of the eccentricity in reducing the average Nusselt number. (A.G.W.)

20124 EXPERIMENTAL EQUILIBRIUM CONDITIONS OF DISSOCIATED AND IONIZED HYDROGEN HYPERSONIC FLOWS. D. E. Bloxsom, Jr. (Rhodes and Bloxsom, Canoga Park, Calif.). 6p. (CONF-641208-7)

From 3rd Conference on Performance of High Temperature Systems, Pasadena, Calif.

Hydrogen to 13,000°K and 1000 atm was prepared by electric arc heating techniques. This hydrogen is in equilibrium, partially dissociated and ionized. Flow of this hydrogen in wind tunnel nozzles was investigated as to gas velocities by means of acceleration of small particles to the stream velocity. This terminal velocity permits equilibrium state of the nozzle flows to be determined. Some such flows are in equilibrium, others are not, and still others are mixed. Experimental data are presented with correlation to the high-temperature hydrogen equation of state. (auth)

20125 IMPROVEMENTS IN AND RELATING TO HEAT EXCHANGING ELEMENTS. Clement John Richards (to English Electric Co. Ltd.). British Patent 975,934. Nov. 25, 1964. Filed Apr. 26, 1960.

The heat exchange element patented includes parallel hollow longitudinal members and a plurality of separate flat baffles arranged on the outside of the longitudinal members. The longitudinal members are arranged in at least two groups in longitudinally intersecting planes. Each group has at least one longitudinal member and each baffle of each group extends across the whole group at an angle to the longitudinal direction. Preferably, there are an even number of groups, and the baffles in adjacent groups are inclined to the longitudinal members in opposite senses. The hollow longitudinal members may be hollow fuel cans for containing a nuclear fuel; or in the case of a steam condenser, the steam to be condensed would flow around the outside of the element and the cooling water or feed water through the interior of the tubes. (A.G.W.)

Materials Testing

20126 (DPSPU-65-30-11) NONDESTRUCTIVE TESTING OF REACTOR FUEL, TARGET, AND CONTROL ELEMENTS. Robert H. McKane and David L. Honkonen (Du Pont de Nemours (E. I.) & Co., Aiken, S. C. Savannah River Plant). [Mar. 1965]. Contract AT(07-2)-1. 15p. (CONF-650509-1; SM-63/43). Dep.(mn); $1.00(cy), 1(mn) CFSTI.

From IAEA Symposium on Nondestructive Testing in Nuclear Technology, Bucharest.

The method and equipment used for the nondestructive testing of uranium fuel elements, U–Al alloy fuel tubes, and Li–Al alloy target and control rods used in production reactors are described. Measurements are made on outside diameter, inside diameter, length, and warp. The equipment used include nickel gage, nickel detector, end cladding thickness gage, grain size tester, nonbond detector, and nuclear test gage. (P.C.H.)

20127 (IITRI-N213-23) NONDESTRUCTIVE METHODS OF EVALUATING COATING-METAL BONDS. Eighth Quarterly Report. W. E. Lawrie (IIT Research Inst., Chicago, Ill.). Oct. 19, 1964. Contract AF33(657)-8938. 31p.

The development of ultrasonic and nuclear methods for the nondestructive evaluation of coated refractory metals is reported. The objective was not limited to the develop-

ment of nondestructive methods, but also to determine the coating parameters which should be measured. Special attention was given to technique development. The extension of ultrasonic nondestructive methods to the very high frequency spectrum requires careful assessment of all factors effecting high frequency ultrasonic wave generation and propagation in laminar polycrystalline materials. Transducers were improved, and a procedure established for isolating and overcoming each of the experimental obstacles. The adjustable energy spectrometer for obtaining nearly monoenergetic electrons from a ^{90}Sr beta source was modified and improved. Backscatter apparatus was developed to permit backscattering of effectively monoenergetic incident electrons and measuring their backscattered spectrum without background correction and without the need for special health physics precautions. A series of measurements and subsequent analysis for two layer coating systems confirmed feasibility of spectrum analysis as a means for measurement of unknown thicknesses rather than only nominally known thicknesses as before. The investigations resulted in a clearly defined procedure for obtaining, displaying, and utilizing parametric data to be obtained on three layer systems. (P.C.H.)

20128 MANIFESTATION OF METALLIC URANIUM DEFECTS IN LINEAR ELECTRON ACCELERATOR. Kholi San'yu and Kanati Tolu. Genshiryoku Kogyo, 9: No. 1, 57-61(1963). (In Japanese)

A review is given of various methods for determining internal metal defects by ultrasonics, electromagnetic methods, and radiography. Defects in uranium specimens were determined using the incident x-ray activity as a function of the specimen thickness using various concentrations of emulsions. The specimen thickness was 10, 20, 40, and 50 mm, and their purity and density were 99.9% and 19g/cm^3, respectively. Experimental radiography was carried out 1.5 m from the target. A defect of 2 mm in diameter and 1 mm in depth was found. (R.V.J.)

20129 NEUTRON RADIATION PHOTOGRAPHY. M. Kobayashchi. Genshiryoku Kogyo, 10: No. 2, 17-21(1964). (In Japanese)

Problems in neutron photography using the direct exposure and the direct image transformation are analyzed. Suggestions are made for proper selection of screen materials, considering activation of particles in the ordinary photographic emulsion, the density of thermal neutrons used for activation, resonance interference, etc. It is shown that neutron photography can be used in irradiated fuel radiography and material defect studies. (R.V.J.)

20130 STRESSES AND DEFLECTIONS OF THICK, CURVED PLATES. D. S. Griffin (Westinghouse Electric Corp., Pittsburgh). New York, American Society of Mechanical Engineers, 1964. Paper No. 64-WA/MD-8, 6p. (CONF-763-44)

From American Society of Mechanical Engineers Winter Meeting, New York, Nov.-Dec. 1964.

A solution was obtained using the linear theory of elasticity for the stresses in a long, thick, uniformly curved plate due to pressures on the curved surfaces and forces or deflections specified on the straight edges. The maximum stresses were compared with those obtained by the elementary thin beam theory, showing the range of applicability of the simpler theory. In general, the accuracy of the elementary theory depended on the total plate angle (α) as well as the mean radius-to-thickness ratio (r_m/t). (auth)

20131 ULTRASONIC INSPECTION DEVICE (Engineering Materials). (Oak Ridge National Lab., Tenn.). 2 drawings. (CAPE-1140)

A through-transmission, ultrasonic inspection device was designed to assure greater quality of small-diameter tubing for leak detector lines, purge gas lines, and other nuclear uses. The pulse-echo technique specified by industry cannot be used for tubing less than 0.250 in. in dia. This device transmits a very narrow beam of sound at ultrasonic frequencies into the tube wall and received this sound with a piezoelectric crystal after it has passed through a segment of the tube wall. The signal is electronically amplified and monitored. A decrease in the received signal, due to anomalies in the tube wall, is evaluated as a measure of tube quality. Cracks, seams, and eccentricity, which cause a 10% or greater reduction in effective wall thickness, can be detected. Tube sizes as small as 0.090 in. in dia. were inspected. (For details, see TID-4100.) (M.C.G.)

20132 PHASE SENSITIVE EDDY-CURRENT CONCENTRATOR (Engineering Materials). (Oak Ridge National Lab., Tenn.). 3 photographs, 6 drawings. (CAPE-1139)

This non-destructive testing instrument was originally designed to inspect graphite spheres; however, it is also useful in detecting flaws in any non-magnetic material. The device generates an electromagnetic wave, which induces eddy currents in the conductor being tested. The transmitted or reflected wave is measured by a pickup coil. The voltage differential between the driving and pickup coils permits accurate measurement of stainless steel thickness as great as 1.25 cm (0.5 in.). (For details, see TID-4100.) (M.C.G.)

20133 TEMPERATURE VERIFICATION SYSTEM (Engineering Materials). (Dow Chemical Co. Rocky Flats Plant, Denver). 11 drawings. (CAPE-1186)

The temperature verification system described is used to determine and minimize temperature effects during inspection and certification of production parts. The maximum allowable gaging error attributed to temperature cannot exceed 10% of the part tolerance. The 10% must include uncertainties of coefficients of linear expansion and "drift" rates. The instrument consists of two glass bead thermistors; one mounted in the outer tool holder of the rotary gage and the other on a sensing head. These are plotted by a chart recorder showing the temperature difference between the gage and the part. Electronics consist of two parts: one unit has all heat producing parts including power supplies and relays, and the other has heat sensitive parts including calibration resistors and an operational amplifier. The entire unit fits into a standard 19-in. rack. The total height is 7 in. (For details, see TID-4100.) (M.C.G.)

20134 BETA SOURCE SHIELD (Engineering Materials). (Oak Ridge National Lab., Tenn.). 3 drawings. (CAPE-1193)

The beta source shield was designed to contain 80 C of ^{90}Sr to study the radiation effects on solid catalysts. The beta particles that are released have a very short range and are most suitable for use with thin layers of solid or liquid samples. The energy can be deposited more efficiently for gases. Dose rates were measured from 0.7 to 4.26 Mr. The shield is 11.5 in. high, 9.5 in. OD at the base, and 6 in. OD at the top. It is fabricated of stainless steel and lead. The source container is 1.38 in. high and 1.38 in. OD. (For details, see TID-4100) (M.C.G.)

20135 X-RAY ANALYSIS SYSTEM WITH MEANS TO DETECT ONLY THE COHERENTLY SCATTERED X-RAYS. Charles A. Ziegler (to Electronics, Inc.). U. S. Patent 3,154,684. Oct. 27, 1964. Filed June 22, 1960.

An apparatus for the accurate, economic, and nondestructive determination of the position and shape of the U core in a reactor fuel element is described. The apparatus includes the following: a conventional type x-ray generator having a spectral peak in the region from 85 to 135 kv and adapted to provide a beam of x rays within a confined locus on the surface of the reactor fuel element; detector means adapted to respond only to that portion of the x-ray beam that is coherently scattered from the confined locus at a predetermined angle (120°) with respect to the axis of the primary x-ray beam; transversing means adapted to move the fuel element in such a manner that the x-ray beam scans the surface; and readout means coupled to the detector and adapted to provide an indication of the response of the detector to the scanning x-ray beam. More generally, the apparatus is applicable for determining the position of any core formed of high-Z material within a casing formed of lower-Z material. (A.G.W.)

Protective Structures

20136 (AFWL-TDR-64-13) THE RESPONSE OF BURIED CYLINDERS TO QUASI-STATIC OVERPRESSURES. B. A. Donnellan (New Mexico Univ., Albuquerque). Sept. 1964. Contract AF29(601)-6002. 98p. (AD-606685). $3.00(CFSTI).

An experimental investigation was conducted into the response of small buried aluminum cylinders to quasistatic overpressures. The cylinders were buried with their axes horizontal in dense, dry, 20-30 Ottawa sand. Cylinders of two stiffnesses were tested at depths ranging from zero to two cylinder diameters. Their behavior was evaluated quantitatively by radial displacement gages and tangential strain gages. Data at five overpressure levels up to 140 psi are presented. This maximum value exceeded the theoretical in-air primary buckling pressure of the cylinders by factors of 9.4 and 99. Destructive tests were conducted on noninstrumented cylinders of six stiffnesses. This maximum applied overpressure was 160 psi, 470 times the theoretical in-air primary buckling pressure of the most flexible cylinder. The overpressure required to cause collapse of the various-cylinders was determined for as many depths of burial as the maximum overpressure would allow. The destructive tests demonstrate the great resistance to collapse imparted to a cylinder by burial. The nondestructive tests afford a comparison between the behavior of stiff and flexible cylinders as the depth of burial and the overpressure are changed. Two zones of burial, deep and shallow, are defined. (auth)

Space Propulsion

See also REACTOR TECHNOLOGY — Propulsion and Space.

20137 (NASA-CR-59332) A COMPARATIVE MISSION ANALYSIS FOR SOLAR-HEATED HYDROGEN PROPULSION SYSTEM. VOLUME I. SYSTEM ANALYSIS. Final Report. (Aerojet-General Corp., Azusa, Calif.). Mar. 1964. Contract NAS-7-230. 303p. (N64-33809; LO774-01-9(Vol.I)). $6.00(CFSTI).

A comparative missions analysis for a solar heated hydrogen propulsion system is presented in two volumes. Volume I, "System Weight Analysis," presents an analytic tool and computational procedure for evaluating three functionally equivalent solar hydrogen propulsion systems. Specific numerical examples are presented and comparisons are made. The combination of components that produces the lowest system weight is defined. The basic vehicle-SHPS integration problems are discussed and a model that is the basis for all computations is selected. System weights, in terms usable for mission analysis, are prepared for advanced chemical and nuclear-heated hydrogen systems. Weights of the Nuclear Electric Propulsion System and the Solar Electric Propulsion System are also presented. Volume II, "Mission Analysis," presents the energy requirements for the space maneuvers and also presents a method of comparing the various propulsion systems of interest. (auth)

20138 (NASA-TN-D-2173) EVALUATION OF FILAMENT DETERIORATION IN ELECTRON-BOMBARDMENT ION SOURCES. Nelson L. Milder and William R. Kerslake (Lewis Research Center, National Aeronautics and Space Administration, Cleveland, Ohio). May 1964. 41p. $1.00 (CFSTI).

The attrition of refractory-metal (tantalum) filaments operating in electron-bombardment ion sources using mercury as the propellant was measured from the time variation of filament resistance. Two basic filament geometries, ribbon and wire, were studied in two separate facilities under varying conditions of ion discharge voltage and emission current density. The results indicate that the primary factors contributing to filament deterioration were the sputtering caused by ion bombardment and the chemical action of residual gases in the facility on the hot filament surface. The presence of mercury vapor had negligible effect on the initial attrition rate in the absence of an ion discharge. A correlation was found among the initial attrition-rate, the ion discharge voltage, and the emission current density. The maximum filament lifetime attained in this study was 1500 hours. There was evidence that possibly as much as an order of magnitude improvement could be attained for filament operation in ultrahigh vacuum. It appears, however, that such long lifetimes for refractory-metal filaments can only be realized at the expense of propellant utilization efficiency and overall thrustor power efficiency. (auth)

20139 ADVANCES IN THE HIGH TEMPERATURE ACCELERATION OF PROPELLANTS. Adriano C. Ducati, Gabriel M. Giannini, Erich Muehlberger, and James P. Todd (Giannini Scientific Corp., Santa Ana, Calif.). 21p. (CONF-641208-6).

From 3rd Conference on Performance of High Temperature Systems, Pasadena, Calif.

Advances in one particular category of high temperature propulsion devices, the electrothermal thrustor, which includes the resisto-jet, arc-jet, and thermo-ionic configurations, are reviewed. The lower temperature considered for propulsion purposes is the cold gas thrustor (300°K) in which the electrical input power is zero. The resisto-jet therefore theoretically can operate over a wide range between room temperature (zero power) and the melting point of tungsten. The conventional arc-jet is used in the intermediate specific impulse range, and the thermo-ionic design is used for the very high temperature range (up to 100,000°K at the present state-of-the-art). The very high temperature acceleration in the thermo-ionic thrustor is presented only for hydrogen. A forecast of plasma propulsion progress, which was extrapolated from recent experimental results, is given. (auth)

Vacuum Engineering

20140 (ORNL-3760(p.94-7)) VACUUM SYSTEMS, TECHNIQUES, AND MATERIALS STUDIES. D. M. Richardson and R. A. Strehlow (Oak Ridge National Lab., Tenn.).

The composition of gas which evolves from a sputter-ion pump after the pump is turned off was found to be strongly dependent on the water partial pressure in the vacuum system. Although methane and ethane were observed to be evolved at constant rates, H_2 and CO constituted 60% of the gas at a water pressure of 3×10^{-7} torr but less than 1% at a water pressure of about 3×10^{-9} torr. A study was made to distinguish between surface diffusion and vaporization transport processes for diffusion pump oil in specially designed apparatus. Surface diffusion was found to be the dominant process. An attempt to measure the heat of activation for the process yielded a value of 14 kcal/mole, which agrees with the value estimated for surface diffusion. The response of ionization gages to the local presence of oil was studied by measuring the H_2 partial pressure at various gage emission currents. The H_2 pressure was found to be a linear function of emission with some H_2 being produced even at very low emissions, presumably by pyrolysis at the hot filament. (auth)

20141 SYNTHETIC ZEOLITES AND THEIR APPLICATION IN HIGH VACUUM TECHNOLOGY. W. Espe. Exptl. Tech. Physik, 12: 293-308(1964). (In German)

A brief review on the application of artificial zeolites in high vacuum technology, especially in test methods and instruments, and the results obtained is given. Non-refrigerated isolation traps and dry pumping system are treated principally. (tr-auth)

20142 A REVIEW OF LOW PRESSURE MEASUREMENT FROM AN INDUSTRIAL VIEWPOINT. W. Steckelmacher (Edwards High Vacuum International Ltd., Crawley, Sussex, Eng.). J. Sci. Instr., 42: 63-76(Feb. 1965).

Recent advances in the measurement of total pressures and their equivalent both by direct and indirect methods over the whole vacuum range are reviewed from an indus-

trial viewpoint. Mechanical manometers, together with suitable transducers, measure total gas pressure in a more fundamental way than other vacuum gages and hence the development of micromanometers has been given some attention. The review includes brief discussions on viscosity gages, especially of the resonance types, recent work on thermal conductivity gages, the possible application of radiometer and Knudsen type gages, and improvements in cold-cathode ionization gages using radioactive materials. Cold-cathode ionization gages operating in a magnetic field are used widely in industrial vacuum systems and have been subject to a number of investigations. The consolidation of the Bayard–Alpert type ionization gages has led to many investigations into the physical and chemical interactions between gages and the gases in vacuum systems leading to developments in gage construction which are discussed. Finally, some consideration is given to developments of thermionic ionization gages to extend their range to lower pressures. (auth)

20143 DIFFUSION PUMP OIL DEPOSITION MEASUREMENTS UTILIZING RADIOACTIVE TRACERS. J. G. Carter, J. A. Elder, R. D. Birkhoff, and A. K. Roecklein (Oak Ridge National Lab., Tenn.). J. Vacuum Sci. Technol., 2: 59-62(Mar.-Apr. 1965).

A radioactive tracer technique is proposed as a quick, simple, nondestructive method for measuring the deposition of diffusion pump oil and as a possible means of evaluating the efficiency of vacuum components. A simple bell jar vacuum system was assembled consisting of a 4-in. oil diffusion pump, a multicoolant baffle, a 4-in. gate valve, and a bell jar with associated gauges. Ten milliliters of Dow Corning 704 oil were irradiated in the low-intensity test reactor at ORNL for 2.6 hr. The $^{30}Si_{14}$, comprising 0.54% by weight of the oil, becomes activated to $^{31}Si_{14}$. The system utilizing various baffle coolants, was operated for certain time intervals. The results indicate the presence of an initial backstreaming surge and also show the relative effectiveness of air-, water-, and liquid-nitrogen-cooled baffles. Deposition rates of a few Å/h were measured. (auth)

20144 ADSORPTION-DESORPTION OF RESIDUAL GASES IN HIGH VACUUM. David Lichtman (Honeywell Research Center, Hopkins, Minn.). J. Vacuum Sci. Technol., 2: 70-4(Mar.-Apr. 1965).

Measurements were made on the adsorption and desorption of residual gases in an ultrahigh-vacuum ion-pumped system using mass spectrometer analysis. The predominant residual gases in the system are hydrogen, carbon monoxide, and water vapor at a total pressure of about 5×10^{-10} Torr. Mass analysis indicates two hydrogen peaks, one carbon monoxide peak, and no water vapor peak on thermally heating a molybdenum ribbon from room temperature to 1000°C. Desorption and readsorption are observed continuously by monitoring ion desorption induced by an extremely low density ($\sim 10^{-7}$ A/cm^2) electron beam. Data obtained by this technique correlated very well with that obtained by thermal flashing and aids in understanding the reactions that are occurring. The use of electron-induced ion desorption coupled with mass analysis is seen to be a very useful tool in studying adsorption-desorption phenomena in high vacuum by allowing continuous observation as substrate conditions are changed. (auth)

20145 MODIFIED HOKE VALVE FOR ULTRAHIGH-VACUUM USE. Richard W. Roberts and Edward L. Bahm (General Electric Research Lab., Schenectady, N. Y.). J. Vacuum Sci. Technol., 2: 89(Mar.-Apr. 1965).

A modified Hoke valve is described, which can be closed with a torque of about 120 in.-lb without distortion of the valve stem. (D.C.W.)

20146 HELIUM MEMORY EFFECTS OBSERVED WITH TANDEM MASS SPECTROMETER. A. E. Barrington, R. F. K. Herzog, and G. O. Sauermann (Geophysics Corp. of America, Bedford, Mass.). J. Vacuum Sci. Technol., 2: 89-90(Mar.-Apr. 1965).

A signal was registered at the helium peak when a stigmatic-focusing magnetic tandem helium mass spectrometer, equipped with a Nier-type ion source and an electron multiplier, was operated on pure oxygen immediately after a run on air at 10^{-4} Torr. It was established that this signal was due to helium which originated in the ionization gages used to monitor the system pressure. (D.C.W.)

20147 LOW-PRESSURE LIMITS OF HOT-FILAMENT IONIZATION GAUGES. J. P. Hobson and P. A. Redhead (National Research Council, Ottawa). J. Vacuum Sci. Technol., 2: 93(Mar.-Apr. 1965).

The processes which have been identified as causes of low-pressure limits in hot-filament ionization gages are summarized, together with the limits of specific gages. (D.C.W.)

20148 OUTGASSING PROCEDURES FOR GLASS ULTRAHIGH-VACUUM SYSTEMS. J. H. Singleton and W. J. Lange (Westinghouse Research Labs., Pittsburgh). J. Vacuum Sci. Technol., 2: 93-4(Mar.-Apr. 1965).

A technique for processing Pyrex ultrahigh vacuum systems is described, which effectively reduces the content of residual carbon dioxide in such systems. (D.C.W.)

20149 ULTRAHIGH VACUUM. Richard W. Roberts and Leon E. St. Pierre (General Electric Research Lab., Schenectady, N. Y.). Science, 147: 1529-42(Mar. 26, 1965).

Applications and techniques of ultrahigh vacuums are discussed. Materials, pumps, gases, seals, and valves are described and typical diagrams given. (M.C.G.)

GEOLOGY AND MINERALOGY

General

20150 (TEI-859) GEOLOGIC MAP AND SECTIONS OF THE THIRSTY CANYON SE QUADRANGLE, NYE COUNTY, NEVADA. P. W. Lipman, W. D. Quinlivan, W. J. Carr, and R. E. Anderson (Geological Survey, Washington, D. C.). Feb. 1965. 16p. Dep.(mn); $1.00(cy), 1(mn) CFSTI.

20151 (TEI-860) GEOLOGIC MAP OF THE QUARTET DOME QUADRANGLE, NYE COUNTY, NEVADA. K. A. Sargent, S. J. Luft, A. B. Gibbons, and D. L. Hoover (Geological Survey, Washington, D. C.). Apr. 1965. 16p. Dep. (mn); $1.00(cy), 1(mn) CFSTI.

20152 SIZE EFFECT OF OXYGEN ANION ON PARTITION COEFFICIENTS. Akimasa Masuda (Tokyo Univ.). Nature, 205: 971-2(Mar. 6, 1965).

The size effect of oxygen anion on partition coefficients of lanthanide and other elements in basic rocks is discussed. Using previously obtained data it was found that the size limits for partition are comparable with that of the oxygen anion. In addition, it seemed to be significant that the size limit for partition of elements with increasingly larger electric positive charge becomes smaller. This can be interpreted as suggesting that the oxygen anion behaves as a smaller sphere towards the cation with higher electric charge. Using the value of 1.76 Å of oxygen for a univalent crystal and 1.40 Å of oxygen for a polyvalent crystal, a graph on the dependence of size limit for partition on valency can be interpreted as reflecting the Coulomb effect. However, it is believed that the possibility cannot be ruled out that compressibility may be connected to a lesser extent with this phenomenon. (P.C.H.)

20153 NEXT THE SECOND-PHASE MOHOLE PROJECT. Rivoluzione Ind., No. 143, 31-4(Dec. 1964). (In Italian)

The scientific objectives of the Mohole Project and the characteristics of phase I and phase II are described. The criteria used, site selection, and the principal engineering problems are reviewed. The system components are also considered. (J.S.R.)

Natural Radioactivity and Fallout

Refer also to abstract 20657.

20154 (HASL-158) FALLOUT PROGRAM. Quarterly Summary Report, December 1, 1964–March 1, 1965. Edward P. Hardy, Jr., and Joseph Rivera (Health and Safety Lab., New York Operations Office (AEC), N. Y.). Apr. 1, 1965. 330p. Dep.; $4.00(cy), 9(mn) CFSTI.

Current data on fallout radioactivity during 1964 and early 1965 are summarized from results obtained by the HASL Fallout Program, the National Radiation Laboratory in New Zealand, and Argonne National Laboratory. Radionuclide levels in monthly fallout, milk, tap water, diet, and upper air samples are given in tabular form. Data collected since 1947 are included for comparison. Also, included are interpretive reports and notes dealing with HASL inter and intra laboratory quality control programs, fallout over the Atlantic Ocean, equivalence of the pot and ion-exchange collectors, dietary intakes of Cs-137, and SNAP-9A debris in the stratosphere. A bibliography of recent literature pertinent to nuclear debris studies is given at the end of the report. (C.H.)

20155 (HASL-159) CARBON-14 MEASUREMENTS IN THE ATMOSPHERE—1953 TO 1964. F. T. Hagemann, James Gray, Jr., and Lester Machta (Health and Safety Lab., New York Operations Office (AEC), N. Y.). Apr. 1, 1965. 124p. Dep.; $4.00(cy), 4(mn) CFSTI.

A ^{14}C sampling program has been conducted by the U. S. Air Force, U. S. Atomic Energy Commission, and U. S. Weather Bureau since 1953 using balloons and aircraft. Whole air collections have been obtained from ground level to greater than 100,000 ft. Over 3,000 results of both the total and bomb produced ^{14}C concentration in CO_2 are presented together with auxiliary $\delta\ ^{13}C$ and CO_2 concentration determinations. It is expected that the findings subsequent to 1964 will be published periodically. A few ^{14}C in CO determinations are also given and interpreted. (auth)

20156 (IS-1098) SURVEY OF ENVIRONMENTAL RADIOACTIVITY. Milo D. Voss and Emery E. Sobottka (Ames Lab., Iowa State Univ. of Science and Tech.). Dec. 1964. Contract W-7405-eng-82. 35p. Dep.(mn); $2.00 (cy), 1(mn) CFSTI.

This environmental monitoring program of the Ames Laboratory of the USAEC is the pre-operational program for the Ames Laboratory Research Reactor (ALRR). The pre-operational environmental program consists of gross alpha and beta determinations of air, soil, vegetation, river water, bottom sediment, precipitation, and well water samples. Data are presented for the period January 1, 1964 to December 31, 1964. As of December 31, 1964 the ALRR was still under construction. There were no appreciable contributors to environmental radioactivity levels in the Ames area. Radioactivity levels recorded represent background conditions from atmospheric fallout. (auth)

20157 (NP-14697) ISSKUSTVENNAYA RADIOAKTIVNOST PRIZEMNOGO SLOYA ATOMSFERY NA O. KHEISA ZEMLI FRANTS-IOSIFA V 1960–1961 GG. (Artificial Radioactivity of Ground-Level Air on Hayes Island (Franz Josef Land) in 1960 and 1961). E. N. Davydov and S. G. Malakhov (Gosudarstvennyĭ Komitet po Ispol'zovaniyu Atomnoi Energii SSSR). 1963. 12p. Dep.(mn)

Tabulated data are given of the concentration of β-activity aerosols in the troposphere along the Hayes island (80°37′ latitude-north and 58°03′ longitude east). The mean monthly concentrations of ^{144}Ce and ^{137}Cs during 1960 at various points of the northern hemisphere were compared with the concentrations in the air along the Hayes island. The graphs of ^{90}Sr concentration in the air along the 80th meridian are also included. (R.V.J.)

20158 (NP-14712) NEKOTORYE DANYE PO KONTSENTRATSII RADIOAKTIVHYKH PRODUKTOV NAD INDIISKIM I TIKHIM OKEANAMI V 1961-1962 GG. (Some data on the Concentration of Radioactive Products Over the Indian and Pacific Oceans in 1961 and 1962 gg). Yu. V. Krasnopevtsev (Gosudarstvennyĭ Komitet po Ispol'zovaniyu Atomnoi Energii SSSR). 1963. 12p. Dep.(mn)

Data on the concentration of radioactive products over the Indian and Pacific Ocean measured from Sept. 20, 1961 to Jan. 25, 1962 were analyzed. The graphs of the γ spectra from the samples collected Sept. 25, 1961 over the South-China Sea (23°5′ latitude north) indicated the presence of fresh fission products: ^{95}Zr, ^{95}Nb, ^{141}Ce, and ^{103}Ru. The analysis of the samples collected from Oct. to Nov. revealed only the old fission products (^{137}Cs, ^{144}Ce, and ^{106}Ru. Graphs plotted for isotope concentrations according to the latitudes showed the maximum concentrations near the 25° latitude north. A higher isotopic concentration was found in the air of the northern hemisphere than in the southern hemisphere. An analysis of the data fixed the time of radioactive product transit through the equatorial zone as 3 to 4 months. (R.V.J.)

20159 (NP-14726) STRONTSII-90 V VODAKH TIKHOGO OKEANA. (Strontium-90 in the Waters of the Pacific Ocean). N. I. Popov, S. A. Patin, and V. A. Pchelkin, and R. M. Polevoi (Gosudarstvennyĭ Komitet po Isopol' zovaniyu Atomnoi Energii SSSR). 1963. 11p. Dep.(mn)

Radiochemical analysis of the western and central Pacific surface waters showed a more uniform distribution of ^{90}Sr in 1961 than in previous years. The mean concentra-

tion was obviously reduced by the turbulence diffusion processes and by vertical and horizontal water mixing. The mean activity of ^{90}Sr surface water between the equatorial Pacific and 35° latitude north was 51 decay/min per 100 l and between the equator and 20° latitude south 30 decay/min or 0.23 pC/l and 0.14 pC/l, respectively. (R.V.J.)

20160 (NP-14728) STRONTSII-90 V VODE PRESNYKH VODOEMOV SOVETSKOGO SOYUZA V 1961–1962 GG. (Strontium-90 in Fresh-Water Reservoirs in the Soviet Union in 1961 and 1962). G. A. Sereda and Ts. I. Bobovnikova (Gosudarstvennyĭ Komitet po Ispol'zovaniyu Atomnoĭ Energii SSSR). 1963. 28p. Dep.(mn)

Measurements were made of the content of ^{90}Sr in rivers and fresh water basins in Moscow region and European and Aseatic parts of USSR during 1961 and 1962. The tabulated data indicated that the ^{90}Sr run off in rivers was small and comprised only 0.4 to 2% (per year) of its storage in the soils of water basins. The ratio of ^{90}Sr to the calcium diminished considerably during the transport of ^{90}Sr from the soil to the river. In the northern water basins of USSR the ratio of ^{90}Sr to calcium (in strontium units) was 2 to 11 times higher than in the basins of the moderate and southern latitudes. Thus, at identical conditions the global contamination of northern regions results in higher contamination of the flora and fauna of water basins than in the southern regions. (R.V.J.)

20161 (NP-14869) DATA FROM RADIATION PROTECTION PROGRAMS. Volume 3, Number 1. (Department of National Health and Welfare, Ottawa (Ontario). Radiation Protection Div.). Jan. 1965. 71p. Dep.(mn).

Recommendations of the International Commission on Radiological Protection concerning radiation exposure are reviewed. Data are presented on fallout radioactivity in samples of air, milk, and precipitation collected during 1964. Data on samples collected in 1963 are included for comparison. Rain water was analyzed for ^{90}Sr, ^{137}Cs, and ^{95}Zr, and milk samples were analyzed for ^{137}Cs and ^{90}Sr. The Chinese nuclear test in Oct. 1964 caused a slight rise in radioactivity of air samples and of ^{131}I in milk samples for a few days but average values for the month were not affected. Environmental monitoring studies were conducted near the sites of the Chalk River reactors, the Nuclear Power Demonstration Reactor and the Candu Reactor. Activities of the Safety Assessment and Control Section are reviewed. The development of a nuclear emulsion neutron dosimeter is reported. The dosimeter is a film badge employing a special nuclear emulsion and neutron exposure is evaluated by counting the tracks of protons produced in the emulsion. Results are reported from a study of tritium leakage from luminous points. Analytical techniques are described. (C.H.)

20162 (NYO-3276-9) HIGH-ALTITUDE BALLOON SAMPLING PROGRAM FOURTH QUALITY CONTROL. Progress Report, [July–December 1964]. John M. Matuszek, Jr., and Colin G. Sanderson (Health and Safety Lab., New York Operations Office (AEC), N. Y.). Mar. 31, 1965. Contract AT(30-1)-3276. 20p. Dep.(mn); $1.00(cy), 1(mn) CFSTI.

The comprehensive quality control program for the high-altitude balloon fallout sampling program is reviewed. Standard control samples are prepared by pipetting appropriate volumes of radiochemically pure fission product solutions onto filter paper. The samples are ashed and counted with a γ spectrometer. Data are compared with that obtained from balloon samples. Results obtained from July to Dec. 1964 are presented. The limits of detection and counting systems are discussed. (C.H.)

20163 (RRA-M42) GAMMA-RAY ENERGY AND ANGULAR DISTRIBUTIONS NEAR THE AIR/GROUND INTERFACE FROM PLANE FALLOUT AND POINT Co^{60} SOURCES. R. L. French and C. W. Garrett (Radiation Research Associates, Inc., Fort Worth, Tex.). June 1, 1964. Contract DA-49-146-XZ-254. 28p. (CONF-642-28)

From Health Physics Society, Cincinnati, June 1964.

Monte Carlo techniques were applied in a detailed study of the gamma radiation environment three feet above the air/ground interface from two types of gamma sources namely fallout uniformly distributed on the ground surface, and a ^{60}Co point source also three feet above the ground at separation distances of 100 to 800 feet. In each case, the scattered and direct-beam fluxes were computed in each of ten receiver energy intervals between 0.04 and 3.5 Mev and eighteen equal receiver angle intervals between 0 (nadir) and 180° (zenith). All results were integrated over azimuthal angles at the receiver to reflect distribution in polar angles only. The source energy was used as a parameter in the fallout calculations and the results thus computed for each of ten different source energies may be weighted and combined to obtain data for fallout of any desired age. Comparisons of the Monte Carlo data with measured data and with other calculated data, both for fallout and for ^{60}Co point sources, show favorable agreement. (auth)

20164 (TID-3086(Suppl.2)) RADIOACTIVE FALLOUT. A Bibliography of the World's Literature. William E. Bost and Hugh E. Voress, comps. (Division of Technical Information Extension (AEC), Oak Ridge, Tenn.). Feb. 1965. 272p. Dep.; $6.00(cy), 5(mn) CFSTI.

Included are 1953 references to unclassified reports, journal articles, and other literature on the radioactive materials produced by nuclear explosions. The interactions of these materials with the biosphere and with its inhabiting organisms are the primary concern, but an attempt has also been made to cover contiguous areas. A subject arrangement of the references is employed, and author and report availability indexes are provided. This supplement covers the period from February 1962 through December 1963. Two prior reports in this series bear the numbers TID-3086 and TID-3086 (Supplement 1) and were published in March 1961 and July 1962, respectively. (auth)

20165 (TID-21711) STRONTIUM-90 LEVELS IN THE DIETS AND BONES OF CHILDREN. Progress Report, 1965. (Comisión Nacional de Energia Atómica, Buenos Aires (Argentina)). Contract AT(30-1)-2753. 21p. Dep.(mn); $1.00(cy), 1(mn) CFSTI.

Data are presented on the ^{90}Sr content in diet of individuals residing in Buenos Aires, Argentina, during 1964. Data are included from a survey of the Ca content in the diet of infants. Results are presented from the analysis of 140 bone samples from children, collected during 1964, for ^{90}Sr content. The bone samples included those from the population for which diet history could be estimated with some degree of certainty and other bone samples. The data were used to estimate the turnover and discrimination of Sr in bone. (C.H.)

20166 DETERMINATION OF RADIOGENIC ARGON ACTIVATION ENERGY. E. A. Denisenko. Geokhimiya, No. 1, 110-13(Jan. 1965). (In Russian)

The activation energy of radiogenic argon must be known for studying the mechanism of separation of this material from minerals and for correcting the absolute age values. To determine the activation energy the mineral was heated to the necessary temperature, which was measured by a chromel-alumel thermocouple. The temperature was constant for about 2 hr and then increased sharply to a second temperature and then again remained constant. After 20 min, the released argon was collected on activated carbon cooled with liquid air and then was analyzed by an isotopic dilution method. The rate of release was determined for the 20-min period, and the results plotted as the logarithm of the separation versus time. The equation for the calculations is presented together with data for several mineral samples. The results agreed with earlier data for muscovite but were too low for biotite. The value obtained for the activation energy depended partly on the location of the argon in the mineral. Besides giving activation energy values, the method permits studying the dependence of the number of defects of a given type per unit volume as a function of time and temperature. (TTT)

20167 RADIOCHEMICAL EVIDENCE FOR ANTLER SHOT CONTRIBUTION TO THE SEPTEMBER 1961 FALLOUT. E. A. Martell, J. P. Shedlovsky, and C. A. Watkins

(National Center for Atmospheric Research, Boulder, Colo.). J. Geophys. Res., 70: 1295-1302(Mar. 15, 1965).

In an attempt to resolve contradictory conclusions based on meteorological conditions, radiochemical data bearing on the origin of the unusually high radioactive fallout over southeastern United States during the period September 17 to 22, 1961 is presented. The isotopic composition of the escaping cloud from the vented Antler underground shot affords an explanation for the marked enrichment of ^{141}Ce relative to ^{144}Ce in Washington, D. C., fallout samples. The appreciable enrichment of ^{141}Ce, ^{140}Ba, and ^{90}Sr relative to ^{144}Ce in the fallout over southeastern United States on September 18 and thereafter seems explainable only by the contribution of fractionated debris from the vented underground Antler shot. The radiochemical data are inadequate for an assessment of the relative proportion of Antler shot debris and Soviet atmospheric test debris in the fallout mixture. (auth)

20168 STRONTIUM 87 ABUNDANCE IN A SUITE OF HAWAIIAN VOLCANIC ROCKS OF VARYING SILICA CONTENT. J. L. Powell, G. Faure, and P. M. Hurley (Oberlin Coll., Ohio; Ohio State Univ., Columbus; and Massachusetts Inst. of Tech., Cambridge). J. Geophys. Res., 70: 1509-13 (Mar. 15, 1965).

The mean initial $^{87}Sr/^{86}Sr$ ratio of four volcanic rock specimens from Oahu which have low SiO_2 concentrations is significantly lower than that of four specimens from Hawaii which have higher SiO_2 contents. This difference may reflect the fact that the source regions of magmas under Oahu have lower $^{87}Sr/^{86}Sr$ ratios than those under Hawaii. Alternatively, it may indicate that the strongly undersaturated rocks of the Hawaiian Islands are formed independently of both tholeiite and alkali olivine basalt magma. The initial $^{87}Sr/^{86}Sr$ ratios of the individual specimens are (weight % SiO_2 shown in parentheses): melilite-nepheline basalt I (36.3), 0.7030; melilite-nepheline basalt II (37.2), 0.7031; nepheline basalt (38.6), 0.7031; basanitoid (43.1), 0.7033; alkali olivine basalt (46.5), 0.7040; hawaiite (48.0), 0.7043; tholeiite (51.9), 0.7041; trachyte (62.0), 0.7043. With one exception corrections for radiogenic strontium were not required. The $^{87}Sr/^{86}Sr$ ratios are the means of duplicate and triplicate analyses and their standard deviation is estimated to be ±0.0004. All $^{87}Sr/^{86}Sr$ ratios are normalized to $^{86}Sr/^{88}Sr = 0.1194$. A value of 0.7073 was obtained for the $^{87}Sr/^{86}Sr$ ratio of the Eimer and Amend interlaboratory strontium standard. (auth)

20169 DIRECT MEASURING OF AIR β-ACTIVITY. N. N. Aleksandrov. Tr. Gl. Geofiz. Observ., 158: 128-35 (1964). (In Russian)

Measurements of beta activity in air with a spherical counter set directly into the medium to be studied are discussed. A method of calculating counter efficiency for various boundary values of the energy of the β sprectra at various counter sizes is described. A table for calculation of counter efficiency for 0.24 to 12 Mev is given. Efficiencies for various isotopes are also given. (M.C.G.)

20170 ASSAY OF STRONTIUM-90 IN HUMAN BONE IN THE UNITED KINGDOM, RESULTS FOR 1963, PART II. Medical Research Council Monitoring Report Series No. 9. (Medical Research Council, London (England)). Aug. 1964. 20p. (A/AC.82/G/L.973). $0.40(BIS); 2s. (HMSO).

Data are presented on the ^{90}Sr content in samples of human bone from residents of Great Britain who died in the second half of 1963. Data are compared with corresponding figures for 1962 and results for 1963 as a whole are compared with those of 1962. Data are included on the ^{90}Sr content of the bones of infants under one year of age from 1959 through 1963. Results show a rise in the mean ^{90}Sr content of bone, and especially in that of infants. (C.H.)

Techniques and Equipment

20171 (AFCRL-64-659) THE BILLIKEN CALIBRATION SHOT IN SOUTHEAST MISSOURI. Scientific Report 4. William Stauder, John Dowling, and Wayne H. Jackson (Saint Louis Univ., Mo.). Aug. 1964. Contract AF10(604)-7399. 30p. (AD-606573) $2.00(CFSTI).

A high-explosive "calibration shot" was detonated near the epicenter of a regional earthquake of 3 March 1963. The purpose of the explosion was to check the accuracy of the epicenter location and to test a calibration procedure suggested as an on-site inspection technique for investigating a suspicious event. The accuracy of the epicenter location is confirmed. Data from the shot are also used to obtain an indication of focal depth from earthquakes in the region. (CFSTI)

20172 (NP-14877) SEISMIC DATA LABORATORY SEMI-ANNUAL TECHNICAL SUMMARY REPORT. (United Electrodynamics, Inc., Alexandria, Va. Earth Sciences Div.). Oct. 15, 1964. Contract AF33(657)-12447. 53p.

Progress is reported on seismic signals and noise as a function of depth in wells, seismic noise attenuation in unconsolidated material, teleseismic models of earthquakes and explosions, analysis of errors in seismic event location determination, and identification of nuclear explosions. A comparative study of the SHOAL event, the FALLON earthquake, and the HARDHAT event is described. Research on wave equations and on recursive numerical filters with specified impulse response is described. Other work is in progress on design of seismometer arrays, array signal variance analysis, and determination of the maximum seismometer array size. (J.R.D.)

20173 (VESIAC-4410-83-X) VESIAC CONFERENCE PROCEEDINGS: PROGRESS OF VELA UNIFORM BOREHOLE RESEARCH. (Michigan Univ., Ann Arbor. Acoustics and Seismics Lab.). Oct. 1964. Contract SD-78. 180p.

Nine papers are included which were presented at the VESIAC conference, held 9 and 10 March 1964, to outline progress in deep borehole research since the conference of 9 October 1961. Also included are transcripts of summary comments by the conference participants at the closing session of the meetings. (auth)

20174 (CEA-tr-A-1729) LE TRITIUM DES BOMBES ATOMIQUES COMME INDICATEUR EN HYDROLOGIE. (Tritium of Atomic Bombs as an Indicator in Hydrology). K. O. Munnich. Translated into French from Physik. Bl., 19: 418-21(1963). 10p. Dep.(mn); $1.10(fs), $0.80(mf) JCL.

The use of tritium, produced by nuclear explosions, as a tracer in hydrology is discussed. The methods used to measure tritium are indicated, and the tritium concentration in rain is shown graphically. The use of tritium as a tracer in the determination of subterranean and source waters, the distinction between subterranean and rain waters in rivers, the determination of the point of penetration of fluvial water into the subterranean water, and the measurement of the vertical profiles of the upper layers of the soil are considered. (J.S.R.)

20175 SEISMIC MEASUREMENTS OF LARGE UNDERWATER SHOTS. D. E. Willis (Univ. of Michigan, Ann Arbor). Bull. Seismol. Soc. Am., 53: 789-809(July 1963).

A series of 10,000 pound high-explosive shots was fired at various water depths off San Clemente Island, California, during August 1961. These shots were recorded on magnetic tape at one fixed station (123 km) and at portable stations located at 180, 196, 500, and 518 km. The effect of water depth on the amplitude and spectra of the seismic waves generated by these shots is discussed, and a comparison is made with the maximum displacement of underground shots. A spectral comparison is also made with a local earthquake recorded at two of the shot recording sites. (auth)

20176 ABSOLUTE AGE OF PEGMATITE OF BIRYUSA (EASTERN SAYAN). A. V. Milovskii, S. I. Zykov, and N. I. Stupnikova (Moscow State Univ.). Geokhimiya, No. 1, 105-8(Jan. 1965). (In Russian)

The absolute age of pegmatites was determined by the lead isotope method from the orthite and oligoclase present. The veins used were selected because of their significant contents of orthite. The results on orthite indicated an age of 630 to 810 million years, with an average of 730 million

years. The scatter of the data indicated a partial loss of uranium, and therefore of lead. The isotopic composition of lead in the oligoclase indicated an age of 600 to 900 million years. Thus the Biryusa pegmatites are of the Precambrian era. The surrounding metamorphic rock was found to be older than the pegmatites. The orthite and oligoclase were formed earlier than the micas. The radiological method thus verified the fact that the pegmatoids are replaced by quartz-muscovite complexes. In the lower Paleozoic era, metasomatic processes took place. The development of the quartz-muscovite complex is related to these processes. (TTT)

20177 DETECTING EXPLOSIONS. H. I. S. Thirlaway. Intern. Sci. Technol., No. 40, 48-50; 52; 55-6; 58 (Apr. 1965).

Distinguishing earthquakes that occur at the very shallow depths in the earth's crust at which clandestine nuclear explosions are likely to be carried out from nuclear explosions are discussed. It was found that perhaps 90% or so can be distinguished from explosions by the characteristically more complex seismic records, which they produce, at some stations, provided, first, that these stations consist of a score or more of individual seismometers laid out in an array, and second, that the stations are located 2000 to 6000 miles from the shock source. Arrays permit weak incoming signals to be phased and otherwise processed so as to minimize interfering signals and earth noise. Seismic waves emerging at 2000 to 6000 mile ranges travel mostly through the earth's homogeneous deep mantle, and their records are freer from complexities introduced at shorter ranges by heterogeneities along shallower propagation paths through the crust. Detection at longer ranges is at least as good, statistically, as it is at closer ranges. (auth)

20178 ZIRCON URANIUM–LEAD AND THORIUM–LEAD AGES AND MINERAL POTASSIUM–ARGON AGES OF LA SAL MOUNTAINS ROCKS, UTAH. T. W. Stern (Geological Survey, Washington, D. C.), M. F. Newell, R. W. Kistler, and D. R. Shawe. J. Geophys. Res., 70: 1503-7(Mar. 15, 1965).

Krypton–argon ages of 23 and 26 × 10^6 yr for pyroxene and $^{206}Pb/^{238}U$ ages of 32 × 10^6 yr for zircon were determined for monzonite and soda syenite porphyries. A K–Ar age of 55 × 10^6 yr for hornblende and a $^{206}Pb/^{238}U$ age of 494 × 10^6 yr for zircon from diorite porphyry are interpreted as due to incomplete degassing of Precambrian hornblende and the presence of Precambrian zircon xenocrysts. Feldspar-lead is similar in isotopic composition to galena from the uranium ore deposits of the Colorado plateau. (auth)

20179 ISOTOPE EFFECT IN THE BENZENE SYNTHESIS FOR RADIOCARBON DATING. M. A. Tamers and F. J. Pearson, Jr. (Instituto Venezolano de Investigaciones Cientificas, Caracas and Univ. of Texas, Austin). Nature, 205: 1205-7(Mar. 20, 1965).

Evidence is given to support the absence of an important non-reproducible isotope effect in the benzene liquid scintillator method for radiocarbon dating. It is postulated that in all respects this method is as reliable as the gas counter procedures. It was concluded that variations in the measured radioactivities due to causes other than the random nature of the disintegration process amount to certainly less than 1.0% and probably less than 0.5%, which is insignificant for all purposes of radiocarbon dating. (P.C.H.)

20180 QUANTITATIVE DETERMINATION OF HEAVY ELEMENTS FROM THE COMPOSITION OF NATURAL γ-RADIATION FROM ROCKS. M. M. Sokolov, P. P. Klevtsov, P. P. Khitev, and A. A. Fedorov. Vopr. Razved. Geofiz., Sb., 64-7([1962]). Leningrad, Gos. Izd. Neft. i Gorno-Toplivn. Prom., 1962.

The possibility of using the gamma radiation from rocks for determination of their heavy element content was studied. Spectrometry of gamma rays from rocks containing uranium showed that the presence of heavy elements, especially lead, decreased the intensity of the soft component (≤ 200 kev) and caused practically no change in the hard component (≥ 300 to 400 kev). The ratio of the soft to hard components was found to depend substantially on their lead content. The threshold of sensitivity to lead was 0.2%. (M.C.G.)

20181 Th^{230}–U^{234} DATING OF CARBONATES FROM LAKES LAHONTAN AND BONNEVILLE. Aaron Kaufman. Thesis, New York, Columbia Univ., 1964. 292p.

Several investigators have reported that marine carbonates can apparently be dated by determining the degree of disequilibrium among the isotopes in the ^{238}U decay series. The ^{230}Th–^{234}U ratio is very low at the time of formation of the carbonate and approaches the theoretical limit of 1.00 with increasing age. In general, the age calculated for a given sample is reasonable stratigraphically and is in fair agreement with the ^{14}C age where the latter is available. The reliability of such ages for pluvial lake carbonates is studied. Fifty-one 1000- to 400,000-year-old samples (forty-one were between 10,000 and 20,000 by ^{14}C) were analyzed for ^{238}U, ^{234}U, ^{234}Th, ^{232}Th, ^{230}Th, ^{228}Th, and ^{226}Ra and their ^{14}C ages were determined. Of the six types of carbonates considered, mollusks are the lowest in ^{232}Th and hence most suited to age determinations based on ^{230}Th–^{234}U ratios. Where ^{232}Th is significant, the amount of ^{230}Th which accompanies it seems to be consistently 1.6 times as high and may therefore be corrected for. $^{234}U/^{238}U$ is consistently about 1.45 in Lake Lahontan and varies from 1.6 to 1.9 in Lake Bonneville. $^{228}Th/^{232}Th$ is essentially at equilibrium for non-mollusks and varies from 1.1 to 1.7 among mollusks. Most of the 10,000- to 20,000-year-old samples show at least rough agreement among ^{226}Ra ages, ^{230}Th ages, and ^{14}C ages. Where discordance occurs, the data can generally be explained by the recent loss of ^{230}Th. Six samples beyond the ^{14}C range (> 25,000 years old) yield U disequilibrium ages between 33,000 and 400,000 years old. The analytical uncertainties for samples less than 2000 years old are too high to determine whether or not concordance exists. (Dissertation Abstr., 25: No. 5, Nov. 1964)

20182 SOIL PROFILE MEASUREMENTS WITH RADIOACTIVITY. Paul E. James and Dale E. Wilkins (Dept. of Agriculture, Beltsville, Md.). St. Joseph, Mich., American Society of Agricultural Engineers, 1964, Preprint Paper No. 64-824, 11p. (CONF-641207-1).

From American Society of Agricultural Engineers, Winter Meeting, New Orleans.

Studies were made to determine the location of surface soil after it was plowed under in order to determine if radioactive fallout that might settle on farmland could be plowed to a less objectionable location. A short-lived radioactive dust was distributed on the surface of the soil and then plowed under. The distribution of the radioactivity in the soil profile was then determined. ^{198}Au was used as the tracer. Four different methods of analyzing radioactivity in the soil profile were used: removing soil samples and measuring the activity in them; observing the reading on a survey meter as it is moved along the profile; slowly moving a scintillation probe up a track while sending a signal back to a counter and x-y recorder; and moving a scintillation probe up a track as the signal is sent to an analyzer, which records the counts every fraction of a second. Advantages and disadvantages of each method are discussed. (M.C.G.)

20183 SCANDIUM AS A TRACER OF THE MOVEMENT OF CLAY SUSPENSIONS IN COLUMNS OF POROUS MEDIA. R. Bruce Curry (Ohio Agricultural Experiment Station and Ohio State Univ., Wooster). St. Joseph, Mich., American Society of Agricultural Engineers, 1965, Preprint Paper No. 64-822, 12p. (CONF-641207-3).

From American Society of Agricultural Engineers, Winter Meeting, New Orleans.

A method was developed to determine the distribution of clay from suspensions, which are passed through columns of porous media. ^{46}Sc, a gamma-emitting isotope, was found to be satisfactory for tagging the clay suspensions. The scandium is held tightly to the exchange complex of the clay. A single-channel scintillation spectrometer was found to be the best suited detection system for ^{46}Sc. Using an

activity level of 0.15 μC of ^{46}Sc per liter of 1% suspension of bentonite clay and deionized water, a sensitivity of 1×10^{-4} g of clay/cm^3 of porous media was achieved. The low activity levels needed plus the relatively short half life (84) days of ^{46}Sc made the method advantageous from the radiation safety standpoint. (auth)

20184 A TECHNIQUE FOR SIMULATING AIR-BLAST-INDUCED GROUND MOTIONS. Gerald P. D'Arcy, Harry E. Auld, and Gerald G. Leigh (Air Force Weapons Lab., Kirtland AFB, N. Mex.). 23p. (CONF-592-2)

From 9th Symposium on Ballistic Missile and Space Technology, San Diego, Calif., Aug. 1964.

A technique for simulating air-blast-induced ground motions from a nuclear weapon with a detonation wave is discussed. A nuclear blast environment is described and the necessary simulation parameters are discussed. Detonation waves were studied from a theoretical standpoint and the concept of substituting a detonation wave for an air shock wave was developed into a simulation technique. The technique was then critically evaluated. (auth)

Thorium and Uranium Minerals

20185 (JEN-132-SIG/I-3) CONSIDERACIONES SOBRE LA GENESIS DE LOS YACIMIENTOS URANIFEROS. I. (On the Genesis of the Uraniferous Deposits. [Part] I). E. Mingarro (Junta de Energia Nuclear, Madrid (Spain). Laboratorio de Mineralogia). 1964. 34p. Dep.(mn).

The main problems in the genesis of uranium deposits as hydrothermals are objectively considered under three aspects: uranium source, transport, and deposition. The transport of uranium can be effected under a tetravalent form, or as complex ions of hexavalent uranium: as uranyl ion $(UO_2)^{2+}$ or under complex carbonic or sulfuric forms, such as $UO_2(XO_n)_2^{2-}$ or $UO_2(XO_n)_3^{4-}$. These three ways of transport correspond to the three basic geochemical paragenesis of uranium: uranium-titanium, uranium-cobalt, uranium. Deposition is currently made by reduction and in some way is no dependent of mineralogical association. The source of uranium is not yet satisfactorily established, but in no way is it necessary to revert to hypogene sources. (auth)

20186 URANIUM ORE ROLLS— AN ANALYSIS. D. R. Shawe and H. C. Granger (Geological Survey, Denver). Econ. Geol., 60: 240-50(Mar.-Apr. 1965).

Sharply discordant, curved uranium ore layers in sedimentary rocks are commonly called rolls and can be either a subsidiary or dominant form of a deposit. Although environmental differences among rolls were not previously described, at least two types can be distinguished. Rolls of the Colorado Plateau type are surrounded by a wide halo of reduced altered rock. It was concluded that they probably formed in favorable strata before or during maximum burial prior to major structural deformation and are not genetically related to uplift and denudation. Rolls of a type found in the Tertiary basins of Wyoming are bounded on one side by relatively oxidized altered rock and on the other by relatively reduced rock. It was concluded that they probably formed near the surface following major deformation, uplift, and denudation. It appeared probable that the ore-bearing solutions that formed the Colorado Plateau type of roll flowed parallel to the roll axis, whereas it is possible that solutions flowed through the roll front in the type of roll common in the Tertiary basins. This conclusion was supported by studies of similar rolls in the USSR. The various spatial relations between roll-type deposits and altered rock are discussed. (auth)

20187 ISOTOPIC FRACTIONATION OF URANIUM IN SANDSTONE, POWDER RIVER BASIN, WYOMING, AND SLICK ROCK DISTRICT, COLORADO. J. N. Rosholt (Geological Survey, Denver), A. P. Butler, E. L. Garner, and W. R. Shields. Econ. Geol., 60: 199-213(Mar.-Apr. 1965).

Considerable isotope fractionation of uranium was found in sandstone-type deposits in the Powder River Basin, Wyoming. Uranium deposits, protected from surface weathering and only partly oxidized, occurred in roll ore bodies in the zone of oxidation above the water table. ^{234}U deficiencies of 40 to 60% were found in ore, and slight ^{234}U excess was found in samples directly below ore. The large magnitude of isotope fractionation appeared to be the result of the slightly oxidizing environment. The roll ore body in the Slick Rock District occurred below the zone of oxidation, and the uranium ore was varied only from that which was 5% deficient in ^{234}U to that which was 2% in excess of ^{234}U. Of the roll ore bodies below the zone of oxidation and studied for isotopic fractionation of uranium, the Slick Rock roll had the least amount of fractionation. The relative lack of preferential leaching of ^{234}U was attributed to the high reducing potential of the environment. (auth)

20188 ISOTOPIC ANALYSIS OF URANIUM USING AN INTERNAL STANDARD. R. G. Ridley, N. R. Daly, and M. H. Dean (Atomic Weapons Research Establishment, Aldermaston, Berks, Eng.). Nucl. Instr. Methods, 34: 163-4(Apr. 1965).

An internal standard technique was applied to the precise measurement of uranium-235/-238 ratios. In the internal standard technique a mixture of isotopes C and D is added to the sample A and B and the ratio of ratios (A/B)/(C/D) is measured where $M_A - M_B = M_C - M_D$, i.e. the mass differences are equal. In the case of uranium suitable isotopes for the mixed spike are uranium-233 and -236. (C.E.S.)

20189 ON A RADIOACTIVE EQUILIBRIUM IN ACCESSORY MONAZITES. L. V. Komlev and K. S. Ivanova. Radiokhimiya, 6: 585-94(1964). (In Russian)

The series of the occurrence of noticeable disturbances of radioactive equilibrium in the accessory monazites of the Ukraine, taken from zones of weathering of mountainous rock, was established. But the matrix of aged samples of monazites was characterized by states of complete radioactive equilibrium between uranium and radium, and thorium. Displacement of the radioactive equilibrium by 10 to 16% often developed in the uranium–radium series and was determined to be significant for the thorium series. In all cases the disturbances of the radioactive equilibrium in monazites established the loss of radium and its isotopes by the relation to the equilibrium quantity of uranium and thorium. The loss from monazites of radium and its short-lived isotopes testified to the development of contemporary processes of mineral modifications combined with weathering. The increased values obtained for monazite with disturbed radioactive equilibrium were characterized by great dispersion. The nearest approach to the established age was given by the ratio $^{207}Pb/^{206}Pb$. The nature of the dispersal gave evidence of the development of multiple complex processes of conversion of monazites. The values of the emission coefficients for monazites did not exceed 0.1 to 0.2% and only for transformed samples with disturbed radioactive equilibrium did it reach 1%. In this way, the occurrences of emissions themselves alone could not cause significant losses of the final products, lead isotopes. It was concluded that the disturbance of radioactive equilibrium, combined with partial loss of radium and its isotopes from monazites, in most cases can be investigated as an indicator of very profound changes in the mineral. The establishment of a marked displacement of the radioactive equilibrium in accessory monazites of zones of weathering is required for an increase in the precision of old data used direct methods for the determination of uranium and thorium together with emission. (tr-auth)

20190 MINERALOGIYA I GEOKHIMIYA REDKIKH ELEMENTOV VISHNEVYKH GOR. (Mineralogy and Geochemistry of Rare Elements in Cherry Mountains (Urals)). E. M. Es'kova, A. G. Zhabin, and G. N. Mukhitdinov. Moscow, Izdatel'stvo "Nauka," 1964. 318p.

Work done in 1956-63 in the northern part of the Urals is reported in three parts: the geochemical structure and characteristics of the composition of alkaline complexes, the mineralogy of the rare elements, and the geochemistry of the individual elements (Li, Rb, Cs, Be, Sr, Ba, Sc, Ga, Y, In, rare earths, Tl, Ti, Ge, Zr, Hf, Th, Nb, Ta, Se, Te,

U, and Re). Data were obtained on the geology, petrography, mineralogy, and geochemistry of the region. The distribution of the rare metals and their concentrations were determined and the hypogene aureoles were studied. Data on the classification of the alkaline pegmatites are presented, and numerous minerals are described. The basic distribution patterns of the rare elements are clarified with regard to the various mineralization processes, and the geochemistry of most of the rare elements is summarized. (84 non-Russian references and 156 Russian). (TTT)

HEALTH AND SAFETY

See also BIOLOGY AND MEDICINE — Radiation Hazards and Protection.

Refer also to abstracts 19478, 19790, 19829, 20037, 20156, 20161, 20170, 20317, 20330, 20338, and 21605.

20191 (AERE-R-4635) SOME EXPERIMENTS TO DETERMINE THE RESUSPENSION FACTOR OF PLUTONIUM FROM VARIOUS SURFACES. I. S. Jones and S. F. Pond (Atomic Energy Research Establishment, Harwell (England)). May 1964. 19p. (CONF-555-16). Dep.(mn).

From International Symposium on Surface Contamination, Gatlinburg, Tenn., June 1964.

Experiments were carried out in which the radioactivity in the air of a laboratory was measured under various degrees of disturbance of the floor which had previously been contaminated with measured amounts of plutonium deposited as oxide powder or as a nitrate solution. Measurements were made using a 15-head air sampler to achieve representativeness of sample and the types of floor surface studied consisted of waxed and unwaxed linoleum, PVC sheet, and bituminised paper. The resuspension factors for plutonium oxide are about an order of magnitude higher than those for the nitrate, but the values found so far tend to confirm that the current derived working levels for surface contamination in use in the Authority are reasonable under normal working conditions. (auth)

20192 (ANL-6938) RADIOLOGICAL PHYSICS DIVISION ANNUAL REPORT, JULY 1963 THROUGH JUNE 1964. (Argonne National Lab., Ill.). Contract W-31-109-eng-38. 278p. Dep.; $6.00(cy), 5(mn) CFSTI.

Progress is reported in sections on scintillation studies of $Ar-N_2$ mixtures, development of a measuring apparatus for photoionization, measurement of inelastic collision cross sections for Ne and Ar, radiation effects on Arabacia Punctulata, measurement of environmental dose rates, measurement of cosmic neutron background, low-level gamma counting, analysis of radiological physics problems, lead-210 measurement in Puerto Ricans, determination of thorium daughters in thorotrast patients, calcium accretion and bone formation in dogs, studies of osteolathyrism in mice, measurement of diurnal variations in bone and cartilage metabolism, development of multichannel data processing, stack plume rise determinations, determination of air turbulence, development of instruments for turbulence studies, and scale-model plume-rise studies. Separate abstracts were prepared for each section. A section concerning the gamma response of ionization chambers was previously abstracted in NSA. Other sections in the report for which no abstracts were prepared are concerned with fluorescence decay-times of deuterated compounds, nanosecond decay-time measurements, excitation migration in linear chains of molecules, exciton effects in radiation chemistry, energy transfer and quenching in plastic scintillators, excimer formation in alkanes, effects of inelastic collisions, electron mobility in noble gases, electron velocities in noble gases, ^{90}Sr beta dosimetry using fluororods, primary ionization by beta particles, radium toxicity, alkaline earth tracer metabolism and determination of Pb in bone ash. (J.R.D.)

For abstracts of individual sections see: 19470, 19471, 19472, 19496, 19497, 19657, 19955, 19956, 20092, 20093, 20193, 20313, 20314, 20315, 20653, 20654, 20655, 20656, 20804, and 20872.

20193 (ANL-6938(p.120-4)) Pb^{210}(RaD) IN INHABITANTS OF A CARIBBEAN ISLAND. Richard B. Holtzman (Argonne National Lab., Ill.).

The mean concentration of lead-210 in vertebrae of Puerto Ricans was 0.118 pC/g ash. The value in males, 0.133 pC/g ash, was significantly higher than the 0.088 pC/g ash in females. These values are significantly lower than those in similar groups of mid-continent (midwestern U. S.) residents, 0.196 for males and 0.156 for females. The lower values in island dwellers are attributed to the lower atmospheric concentration of ^{210}Pb over the oceans. (auth)

20194 (BLG-280) LABORATOIRE TRITIUM — ETUDE DE L'ACCIDENT MAXIMUM CROYABLE. (Tritium Laboratory. Study of the Maximum Possible Accident). G. Penelle and O. Corbisier (Centre d'Étude de l'Énergie Nucléaire, Brussels (Belgium)). July 1964. 9p. Dep.(mn).

In the case of the tritium laboratory the maximum credible accident is defined as a fire that would destroy the different rooms and release to the atmosphere all the tritium contained in the laboratory; the quantity of tritium supposed to be in the laboratory when the fire starts is the maximum foreseeable quantity with respect to the existing installations. The doses by direct radiation from the radioactive cloud and the inhalation doses were calculated and found to be smaller than the corresponding guide-levels. (P.C.H.)

20195 (BLG-281) LABORATOIRES DE PRODUCTION DES RADIOISOTOPES. ETUDE DE L'ACCIDENT MAXIMUM CROYABLE. (Laboratories for Production of Radioisotopes. Study of Maximum Possible Accident). G. Penelle and O. Corbisier (Centre d'Études de l'Énergie Nucléaire, Brussels (Belgium)). July 1964. 31p. Dep.(mn).

In the case of laboratories for the production of radioisotopes the maximum possible accident is defined as a fire that would destroy part of the laboratory. The quantity of radioisotopes assumed to be in the laboratory when the fire starts are the maximum foreseeable quantities with respect to the existing installations. The doses by direct radiation from the radioactive cloud, the inhalation doses, and the surface depositions were calculated for the different isotopes and compared to the corresponding guide-levels; it appears from this comparison that a fire in the gamma laboratory could result in a rather slight problem of iodine inhalation and deposition. (P.C.H.)

20196 (CONF-650103-6) INVESTIGATION OF LOW-LEVEL RADIOACTIVE WASTE CONTAINERS IN AN ACCIDENT ENVIRONMENT. Joseph E. Minor and Leonard U. Rastrelli (Southwest Research Inst., San Antonio, Tex.). Jan. 14, 1965. Contract AT(30-1)-2140. 28p. Dep.(mn); $2.00(cy), 1(mn) CFSTI.

From International Symposium on Packaging and Transportation of Radioactive Material, Albuquerque, N. Mex.

A summary is presented of the work accomplished during an AEC-sponsored effort to investigate the structural integrity of low-level radioactive waste containers in an accident environment. The effort associated with this program was concentrated in two major areas: (1) a survey of current practice for low-level radioactive waste transport and disposal and (2) the structural analysis of typical low-level radioactive waste containers in an accident environment. Each of these areas is discussed and summarized, and conclusions concerning the dynamic response of typical containers are outlined. (auth)

20197 (COO-281) RADIOLOGICAL ASSISTANCE PLAN HANDBOOK. Region Five. A. Wendell, comp. and Donald M. Gardiner, ed. (Chicago Operations Office (AEC), Ill.). Feb. 1965. 80p. Dep.(mn); $3.00(cy), 2(mn) CFSTI.

A nuclear incident is defined as any occurrence causing bodily injury, sickness, disease, death, or loss of property arising out of or resulting from the radioactive, toxic, explosive, or other hazardous properties of source, special nuclear, or by-product material. The United States is divided into 8 regions for providing radiological assistance in the event of a nuclear incident. Procedures are outlined that are to be followed when the Chicago Operations Office

of the AEC is requested to provide assistance following a radiological incident in the area designated as Region 5. A team of specialists will be dispatched immediately to the incident site where they will evaluate the hazard, take action to counteract and control any acute hazard, and establish a line of communication with local authorities and the press. The procedures outlined are intended to be used as a guide and are designed for the most probable set of circumstances that might be met in connection with incidents involving radioactive materials. (C.H.)

20198 (HASL-157) THE BOUNDARY EFFECT ON GAMMA-RAY TRANSPORT FROM A POINT SOURCE. Keran O'Brien and James E. McLaughlin (Health and Safety Lab., New York Operations Office (AEC), N. Y.). Jan. 1965. 28p. Dep.; $2.00(cy), 1(mn) CFSTI.

The density interface effect on γ intensities resulting from a point source was measured at 0.66 and 1.25 Mev. Source-detector separations from about 10 to 900 meters were employed. A phenomenological representation is suggested of this effect, based on a 2-dimensional diffusion equation, which reasonably describes the behavior both of the present results and those of others. (auth)

20199 (HI-388-RR(Pt.III)) SPECIAL ASPECTS OF ENVIRONMENT RESULTING FROM VARIOUS KINDS OF NUCLEAR WARS. PART III. OVERVIEW. Robert U. Ayres (Hudson Inst., Inc., Harmon-on-Hudson, N. Y.). Nov. 30, 1964. Contract OCD-OS-62-218. 92p.

Includes Annex I and II.

The possible effects of nuclear warfare on man's environment are considered. The significance of various problems that may arise in a post-attack environment is evaluated. It is pointed out that it will take many years for the response of the ecosystem to such a disturbance to be ameliorated. The relation between ecosystem recovery and the economy is discussed. Historical examples of ecological disasters cited for comparative purposes include fires, flooding, erosion, pest outbreaks, outbreaks of epidemic disease, and extreme conditions of weather and climate. Estimates are included of the surviving population, surviving industry and property, and surviving biological and agricultural resources after nuclear attack. (C.H.)

20200 (HW-83668) A REVIEW OF RESEARCH ON PLUTONIUM RELEASES DURING OVERHEATING AND FIRES. J. Mishima (General Electric Co., Richland, Wash. Hanford Atomic Products Operation). Aug. 1964. Contract AT(45-1)-1350. 22p. Dep.; $2.00(cy), 1(mn) CFSTI.

Articles and documents are reviewed which are concerned with oxidation and ignition temperatures of metallic and delta-phase stabilized plutonium, particle size distribution of oxide produced by heating plutonium and some of its compounds, deposition from turbulent streams, resuspension of plutonium dioxide particulate material from various surfaces, or release of plutonium during experimental and accidental fires. In most instances, plutonium oxidation rates are found to increase with increasing temperature and humidity. A minimum rate is found in the delta-phase region due to changes in the oxide layer. Ignition can occur at temperatures above 100°C depending upon the conditions of the metal and heating. The rate of release of plutonium dioxide aerosol increases with increasing temperature and gas velocity. Conditions in and around fires are variable and forces affecting the deposition of particles, complex. Once deposited in the soil, particulate material shows little tendency to resuspend. Several plutonium resuspension factors embracing many types of circumstances are listed. (auth)

20201 (HW-SA-3525) NEUTRON SPECTRUM MEASUREMENTS AT HANFORD WORK LOCATIONS. G. W. R. Endres (General Electric Co., Richland, Wash. Hanford Atomic Products Operation). May 15, 1964. Contract AT(45-1)-1350. 31p. (CONF-642-33). Dep.(mn); $2.00 (cy), 1(mn) CFSTI.

From Health Physics Society, Cincinnati, June 1964.

Hanford occupational exposures to neutron radiation are due mainly from two types of neutron sources, production reactors and plutonium in chemical processing facilities. A knowledge of the incident neutron spectrum is necessary to interpret data obtained from the nuclear-track-type personnel neutron dosimeters accurately. The basic device used to measure the spectrum was a surface-barrier sandwich detector with neutron converters of either ^{6}Li or ^{3}He. The energy deposited in each surface barrier detector, by the reaction products, was added electronically to obtain the initial neutron energy. The neutron spectra measurements obtained are typical of PuF_4 isotopic sources, shielded plutonium production reactors, and plutonium metal with a significant neutron emission by spontaneous fission of ^{240}Pu. An explanation of the data analysis is given along with appropriate curves showing the results. The plutonium fluoride spectrum has a broad peak at about 0.9 Mev, slightly lower than the theoretical peak of 1.2 Mev. The plutonium metal spectrum has a rather sharp peak at about 1.1 Mev. The spectra inside and outside the reactor shielding show how the neutron spectrum is degraded in going through the shield. Attempts to measure the plutonium–beryllium source spectrum were only partially successful owing to the activation of the silicon in the surface barrier detectors by the high energy (>3 Mev) neutrons from the source. (auth)

20202 (ORNL-P-1093) CIVIL DEFENSE RESEARCH AT OAK RIDGE NATIONAL LABORATORY. J. C. Bresee (Oak Ridge National Lab., Tenn.). [1965]. Contract W-7405-eng-26. 31p. (CONF-650211-1). Dep.(mn); $2.00 (cy), 1(mn) CFSTI.

From New York State Radiological Officers Conference, Albany.

The technical feasibility and cost estimates of urban civil defense shelters are discussed. The tunnel-grid shelter concept is reviewed and design and engineering data are presented for a city in which one million people live. The interconnected tunnel grid could house all inhabitants and is based on the use of standard 8-ft-diameter reinforced concrete pipe with an 8-in.-wall. The tunnel would include bunk space for 4 adults every 6 ft, or 3500/mile. With all bunks folded back, walking space 5 ft wide would be available, and with one bunk folded down on aisle space of 3 ft and seating space for 4 in 6 ft would be provided. Forced air ducts, water pipes, and electrical power cables are located under the floor. The cost for an elaborate system with refrigeration and power plants was estimated at $400 to $500 per person and more austere systems could be built for $300 to $400 per person. A number of dual uses for a tunnel-grid shelter system are suggested that would help to minimize the cost. (C.H.)

20203 (ORNL-TM-988) DESCRIPTION OF FACILITY RADIATION AND CONTAMINATION ALARM SYSTEMS INSTALLED IN RADIOCHEMICAL PROCESSING PILOT PLANT BUILDING 3019. J. A. Russell, Jr. and D. J. Knowles (Oak Ridge National Lab., Tenn.). Mar. 16, 1965. Contract [W-7405-eng-26]. 19p. Dep.(mn); $1.00(cy), 1(mn) CFSTI.

Facility Radiation and Contamination Systems were installed to continuously and automatically monitor gamma radiation (by sixteen gamma monitrons), neutron radiation (by three neutron dose-rate-burst detectors), and air contamination (by seven beta-gamma and four alpha constant air monitors) in the entire facility. These instruments and other components in the network provide health physics monitoring information, sound local alarms when abnormal conditions occur, and indicate the abnormal conditions on a central panel board. Operating personnel are first given warning when a caution level of 7.5 MR/hr or 1000 counts/min is detected by a monitron or beta-gamma air monitor, respectively. A second warning is given when a high level is detected, i.e., 23 MR/hr by a monitron, 4000 counts/min by a beta-gamma air monitor, or 800 counts/min by an alpha air monitor. The neutron detectors operate rate alarms when a level of 23 MRem/hr is detected or operate burst alarms when a current pulse of 3×10^{-6} amp with a rise time of 100 μsec is exceeded. The building is automatically contained when two or more monitrons or two or more air monitors detect a caution level of radiation or air contamination. The building evacuation system operates automatically when two or more moni-

trons or two or more air monitors detect a high level of radiation or air contamination, or when two or more neutron monitors detect a neutron burst or a high-rate level. (auth)

20204 (RPI-328-25) RADIOACTIVE GAS PRODUCTION FROM THE R.P.I. ELECTRON LINEAR ACCELERATOR. James E. Russell and Robert M. Ryan (Rensselaer Polytechnic Inst., Troy, N. Y. Dept. of Nuclear Engineering and Science). [1965]. Contract AT(30-3)-328. 7p. (CONF-650306-22). Dep.(mn); $1.00(cy), 1(mn) CFSTI.

From Particle Accelerator Conference, Washington, D. C.

Descriptions are given of the air handling and monitoring systems, measurement of the gaseous activities, concentration guides developed at R.P.I. for ^{13}N and ^{15}O, and operating procedures used for control of the activity. The nuclear reactions responsible for the generation of the isotopes are $^{16}O(\gamma,n)^{15}O$ and $^{14}N(\gamma,n)^{13}N$. (P.C.H.)

20205 (SC-TM-64-1722) IMPROVEMENTS IN USE OF THE INDIUM ADHESION TEST FOR SURFACE CLEANLINESS. G. L. Krieger (Sandia Corp., Albuquerque, N. Mex.). Nov. 1964. Contract AT(29-1)-789. 17p. Dep. (mn); $1.00(CFSTI).

Better techniques that were developed for the indium adhesion test of surface cleanliness are reported. Shorter holding times (<1 sec) resulted in increased sensitivity and a large response to previously unsensed contaminants. A second change made was the repeated use of an indium tip in testing a given specimen. Specifications for the determination of surface cleanliness are appended. (P.C.H.)

20206 (TID-7698(Pt.I)(p.31-2)) NUCLEAR SAFETY — STANDARDS AND EVALUATION. J. A. Lieberman (Division of Reactor Development (AEC), Washington, D. C.).

An outline is presented of guides and hazards evaluation for nuclear devices in space. A chart for aerospace nuclear power safety reviews and approval for use is included. (D.L.C.)

20207 (USNRDL-TR-797) REMOVAL OF SIMULATED FALLOUT FROM PAVEMENTS BY CONVENTIONAL STREET FLUSHERS. D. E. Clark, Jr., and W. C. Cobbin (Naval Radiological Defense Lab., San Francisco, Calif.). June 18, 1964. 84p.

A conventional motorized street flusher was evaluated as a suitable decontamination tool to be used in the operational recovery of extensive paved areas contaminated with fallout from a land-surface nuclear detonation. The selection of fallout parameters such as particle size and initial mass levels was based on a theoretical fallout model. The flusher nozzle orientation was adjusted for maximum decontamination effectiveness. This adjustment can be applied to any flusher to be used for similar purposes. Using a fixed set of flusher adjustments and constant-size test area, the effects of 4 particle size ranges, 3 mass levels, and 2 types of surfaces on removal effectiveness were determined. The least effective removal by flushing (2.2 g/ft^2 residual mass) for a given expenditure of effort was obtained at high initial mass loadings (100 to 600 g/ft^2) on asphalt surface using small particles (44 to 88 μ and 88 to 177 μ). The best removal effectiveness by flushing (0.06 g/ft^2 residual mass) for the same expenditure of effort was obtained using low initial mass loading (20 g/ft^2) on concrete surface with 350 to 700 μ particle sizes. A majority of the tests conducted were in agreement with previously developed theoretical equations describing decontamination in terms of residual mass as a function of expended effort. (auth)

20208 RADIATION HAZARD FROM CONTAMINATED AIRCRAFT. R. E. Luehrs (U.S.S. Enterprise, U. S. Navy). Aerospace Med., 36: 54-5(Jan. 1965).

Routine checking for radioactivity in the spaces and on the outer surfaces of the USS Enterprise CVA(N)-65 disclosed a sudden increase in October 1961. It was determined that rain showers had washed radioactive fallout onto the decks of the ship. The level of contamination was low and constituted no danger to the crew. Spot checks of aircraft were conducted during the ensuing months followed by systematic monitoring for radioactivity during the period 7 February through 2 August 1963. Four high performance aircraft were checked weekly for radioactive contamination. Preliminary tests showed that only jet intakes and first compressor stages were measurably contaminated. From February to early April swipes from jet intake showed less than 15,000 $\mu\mu$C/ft^2 (equivalent to 4167 disintegrations/min). On 10 April one swipe disclosed a contamination of 30,000 $\mu\mu$C/ft^2. In late April swipes of exposed jet engines (torn down for inspection and maintenance) showed highest contamination in the first compressor stage to be 2940 and the highest contamination in the bottom of the intake to be 6200 $\mu\mu$C/ft^2. Surveys of maintenance personnel for fixed and loose radioactive contamination taken during June, July, and August disclosed the highest swipe to be from the hands of maintenance personnel, 258 $\mu\mu$C/ft^2 of hand surface, and the highest $\beta-\gamma$ concentration on shoes to be 0.12 mR/hr. None of several hundred film badges from cockpits and aircrew personnel showed any exposure attributable to passing through radioactive fallout contamination. (BBB)

20209 DESIGN FOR RADIATION SAFETY. W. J. Thon. Air Conditioning, Heating, Ventilating, 61: 87-93(Oct. 1964).

Present operations with radiochemical materials by Atomic Energy Commission contractors demonstrate that materials which present a potential radiation hazard to working personnel can be handled safely if the proper techniques and facilities are used. This paper is a guide to those techniques and facilities. Public Health Eng. Abstr., 45: (Feb.-Mar. 1965).

20210 THE TOXIC HAZARD ASSOCIATED WITH BARIUM CHLORIDE AS A CONSTITUENT OF A TERNARY EUTECTIC SALT USED AS A FIRE EXTINGUISHANT. N. L. Spoor (United Kingdom Atomic Energy Authority, Harwell, Berks, Eng.). Ann. Occupational Hyg., 7: 369-72(Dec. 1964). (AHSB(RP)M-24)

The Ternary Eutectic Salt discovered and developed by others for the purpose of extinguishing uranium or plutonium fires contains about 50% barium chloride. Some doubt has been expressed concerning the suitability of this mixture for the general control of uranium and magnesium fires, on the ground that barium chloride is a toxic material. An assessment of the available information shows that the toxicological hazard resulting from the barium chloride should not be regarded as unduly restricting. The use of Ternary Eutectic Salt in fire-fighting operations without respiratory protection must be restricted however to exposures of not more than a few minutes. (auth)

20211 APPARATUS AND MEASURING TECHNIQUES FOR ENSURING COMPLIANCE WITH THE 1st SSVO. PART II. S. Mueller. Atomwirtschaft, 10: 82-6(Feb. 1965). (In German)

The monitoring of environmental radioactivity in air is described. The fulfillment of requirements demanded by the First Radiation Protection Regulation (1stSSVO) within the framework of German Atomic Legislation gives rise to measurement difficulties. Particular problems in the assessment of the activity of water and the atmosphere raised the question as to which methods can be used for the measurement of the highest permissible concentration values assigned to non-analyzed mixtures. A concentration value of $1 \times 10^{-7}\mu$C/cm^3 was fixed for radioactive materials or mixtures of such materials in water, which was not analyzed. This regulation demands measuring equipment, which would cover all kinds of radiation in an equal manner. Further, determination of the activity must be completely independent of the kind and energy and even of the emission probability of the radiation. It is shown that it is sufficient to discover methods of measurement, which cover the concentration values of all the possible radionuclides that can occur in water. If monitoring is limited to these radionuclides then not only is the financial expenditure held within bearable limits but safety is also increased. (auth)

20212 RADIATION PROTECTION IN CANADA. PART VII. SETTING STANDARDS FOR RADIATION PROTECTION. F. D. Sowby. Can. Med. Assoc. J., 92: 505-7 (Mar. 1965).

The recommendations of the International Commission on

Radiological Protection have as a basic objective the limitation of radiation dose to "that which involves a risk that is not unacceptable to the individual and to the population at large." The problem is to decide what degree of risk is acceptable, in relation to the benefits of a practice that necessitates radiation exposure. Routh estimates of some of the risks of exposure to radiation were made and compared with some of the other risks tolerated by society. On the assumption that it would be possible to make quantitative assessments of both the benefits and the risks, the question is raised as to how and by whom an appropriate balance should be made. (auth)

20213 DOSIMETRY AND RADIATION PROTECTION. W. Minder (Radiuminstitut, Bern). Chimia (Aarau), 19: 12-17(Jan. 15, 1965). (In German)

The purpose of dosimetry is to determine the energy absorbed by any body from a radiation field of any nature and field strength distribution during any period of time. The difficulties of this determination are indicated. The methods used for dose measurement and dose calculation are summarized. The fundamentals of radiation protection are briefly reviewed. The specific cases of γ cells and electron accelerators are considered. (J.S.R.)

20214 MEDICAL SUPERVISION OF PERSONNEL OCCUPATIONALLY EXPOSED TO RADIATION. A. Morczek (Strahleninstitut der Medizinische Akademie, Magdeburg, Ger.). Deut. Gesundheitsw., 19: 20-6(Jan. 1964). (In German)

The physician who is concerned with problems of radioprotection must ensure that persons whose health or physical condition might be affected seriously should not be permitted to work in occupations where radiation is used. In addition, he should take steps to ensure that he will be able to detect any radiation injury at an early stage in order that appropriate corrective measures can be taken promptly. The methodology of radioprotection requires that, in effect, minor symptoms of radiation sickness must be detected and treated. This requires consideration of both the anamnestic history of the patient and the clinical evaluation of symptoms. The main symptomatic evidence is found in hematological studies and evaluation of the blood picture. This may include total leucocyte count, segmented nuclear cells, eosinophiles, rod cells, basophils, lymphocytes, monocytes, binuclear lymphocytes, and monocytoid cells. Under certain conditions the skin may be the first organ to show evidence of radiation injury, or when heavy radiation particles are involved, the lens of the eye is an organ that may deserve particular attention because of its extreme sensitivity to this type of radiation. One problem encountered in efforts to detect early changes in liver and kidney is that their radiosensitivity is low compared to other organs, such as the gonads, so that it is difficult to evaluate injury. Standard clinical tests are often the only way to measure this. Closely related to this is the problem of incorporation of radioisotopes in the body. For this, physical methods of radioprotection are most sensitive and relatively accurate when compared to biological methods, which are often nonspecific. (BBB)

20215 DISTRIBUTION OF Sr^{90} AND Cs^{137} CONCENTRATION IN THE BULL (JAPANESE). H. Danbara, T. Mitsuhashi, and H. Nozaki (National Inst. of Animal Industries, Chiba, Japan). Eiyo To Shokuryo, 16: No. 6, 9-11(1964).

In order to detect contamination of animal products due to the nuclear tests and to ascertain the distribution of ^{137}Cs in soft tissues of bulls, K and ^{137}Cs were measured in organs and muscles of 18-month-old bulls under normal feeding conditions. The organs and muscles were rumen, intestine, liver, kidney, pancreas, lung, heart, etc., and 6 kinds of muscles of best quality for food. Ca and ^{90}Sr contents in some of the organs were also assayed. ^{90}Sr was detected only in the rumen, kidney, and large intestine, whereas ^{137}Cs was detected in amounts from 2 to 15 CU in all the organs and muscles, although there was no definite pattern of distribution of ^{137}Cs in the tissues. (Excerpta Med., Sect. XXIII, 2; No. 3, (Mar. 1965))

20216 ^{226}Ra IN HUMAN EMBRYONIC TISSUE, RELATIONSHIP OF ACTIVITY TO THE STAGE OF PREGNANCY, MEASUREMENT OF NATURAL ^{226}Ra OCCURRENCE IN THE HUMAN PLACENTA. B. Rajewsky, V. Belloch-Zimmermann, E. Loehr, and W. Stahlhofen (Max-Planck Institut für Biophysik, Frankfurt am Main). Health Phys., 11: 161-9(Mar. 1965).

The natural ^{226}Ra activity in human fetal bone ash remained constant from the fourth to the tenth month of pregnancy. The ^{226}Ra content was equal to that determined in the bone ash of adults, found to be $1.3 \cdot 10^{-14}$ C/g of bone ash. An analogous identity in the ^{226}Ra content of soft tissue of fetuses and adults was also found. For both embryonic and adult tissues the specific activity was $1 \cdot 10^{-16}$ C/g of fresh tissue. From comparison of the specific values of the ^{226}Ra content in bone and soft tissue it may be derived that the major portion of the ^{226}Ra content of the fetus is in the skeleton. Therefore the specific ^{226}Ra activity of ashed total fetuses is of the same order of magnitude as the value in fetal bones. The ^{226}Ra activity of placental tissue was about $2 \cdot 10^{-16}$ C/g of fresh tissue. The discrimination factor between the placenta and the fetal bones, and the placental transfer of ^{226}Ra are discussed. The specific radium level of both the placenta and the embryonic tissue proved to be comparable. In consequence the placenta does not act as a barrier for the natural ^{226}Ra content, that is to say there seems to be no discrimination in the passage of this radionuclide. (auth)

20217 SPATIAL DOSE DISTRIBUTION IN AIR-OVER-GROUND GEOMETRY. F. F. Haywood (Oak Ridge National Lab., Tenn.). Health Phys., 11: 185-92(Mar. 1965).

Spatial distributions of gamma exposure and neutron dose were measured using a point ^{60}Co source (800 C) and the ORNL Health Physics Research Reactor as a small fission source. The sources were supported on a 1527-ft tower, at the Nevada Test Site, at heights ranging from 27 to 1500 ft. Neutron dose rate was measured (independently of the gamma exposure rate) with a recoil proton proportional counter, and the gamma exposure rate was measured (independently of the neutron dose rate) with a halogen-quenched geiger tube, which was surrounded by a filter (tin and lead) such that the response was proportional to exposure in roentgens over a broad range of photon energies. Measurements were made in a plane 4500 ft long and 100 ft high which extended eastward from the base of the tower. At large source-detector separations, a significant decrease in intensity was noticed at a detector height of 2 ft, relative to the intensity at ground level, for both neutrons and gamma rays. For a given slant range greater than about one relaxation length, there is an increase in neutron dose rate at the interface by a factor of 2.4 as the reactor is raised from 27 to 1500 ft above the ground; and, similarly, there is an increase in gamma exposure rate by a factor of 2.1. These increases appear fixed for source-detector separations greater than about 400 yards. An effect of the presence of the interface was observed by comparing experimentally determined values of the exposure buildup factor for ^{60}Co gamma rays to calculated buildup factors in an infinite medium. Boundary correction factors K(exp) were determined experimentally. K(exp) is defined as the ratio of dose in the finite air medium to dose in the infinite air medium at the same slant range. The dependence of neutron dose rate on variation of detector heights and on variation of source heights is compared to theoretical models with satisfactory agreement. (auth)

20218 MEASUREMENT OF ENVIRONMENTAL GAMMA RADIATION IN NORWEGIAN HOUSES. A. Storruste, A. Reistad, T. Rudjord, A. Dahler, and I. Liestoel (Universitetet, Oslo). Health Phys., 11: 261-9(Apr. 1965).

Results of measurements of the environmental radiation inside Norwegian houses are reported. Three types of measuring equipment were used, i.e. a scintillation rate meter specially designed for low intensity measurements, a Geiger counter with a rate meter, and an ionization chamber. The average dose rate in air due to environmental radiation was found to be 87 mrad/year inside houses with outer walls of wood, 115 mrad/year for buildings with outer walls of concrete, and 129 mrad/year for buildings with outer walls of brick. The average of all the 2026 measure-

ments inside Norwegian houses is 83 mrad/year for the dose rate due to gamma rays, when 25 mrad/year due to cosmic rays is subtracted. (auth)

20219 THE PROFESSIONAL RESPONSIBILITIES OF THE HEALTH PHYSICIST OR VIRTUE IN COMPROMISE. H. J. Dunster (United Kingdom Atomic Energy Authority, Harwell, Berks, Eng.). Health Phys., 11: 307-11(Apr. 1965).

The aims of the health physicist are summarized. These aims are discussed in the context of the responsibility of the health physicists in view of uncertain dose-effect and dose-risk relationships. One implication is that the profession has to be increasingly concerned with such subjects as acceptibility of risk, the cost of safety measures, and labor-management relationships. (C.H.)

20220 RADIUM CONTAMINATION AT THE JORDAN RIVER DELTA OF THE GREAT SALT LAKE. Robert C. Pendleton*, R. D. Lloyd, C. W. Mays, D. R. Atherton, and N. V. Chamberlain (*Univ. of Utah, Salt Lake City). J. Water Pollution Control Federation, 36: 925-7(July 1964).

An environmental survey of the Jordan River Delta area was made to determine the extent and levels of contamination resulting from an accidental release of wastes from a uranium ore refining plant. Silt deposits, blue-green algae, and weeds were analyzed and found to contain varying but appreciable amounts of ^{226}Ra and ^{228}Th. Muskrat bones were found to be accumulating radium to relatively high levels. A high degree of control to prevent future releases is recommended. Public Health Eng. Abstr., 45: (Jan. 1965).

20221 SAFETY STANDARDS. M. Dousset. Maroc Med., 43: 147-55(1964).

Four different categories of exposed people are distinguished, the worker who is only occasionally exposed, the professionally exposed, people living in the vicinity of an atomic plant, and the population at large. The maximal permissible doses of external radiation are given for all these categories under normal and exceptional exposures, together with the method of calculating the maximal permissible doses for internal uptake of radioisotopes for the same groups. The recommendations are based on those of the I.C.R.P. and Euratom. (Excerpta Med., Sect. XXIII, 2: No. 3, (Mar. 1965))

20222 GENERAL PRINCIPLES OF THE ORGANIZATION OF PROTECTION. H. Jammet. Maroc Med., 43: 198-206(1964).

The general principles of radiation protection are discussed. The degree of protection required is determined by the many factors contributing to the degree of exposure in both the general population and in those exposed in their work. A general approach is suggested for developing a flexible organization to handle the problems of radiation protection. (Excerpta Med., Sect. XXIII, 2: No. 3, (Mar. 1965))

20223 THE "KNEE" OF A FALLOUT DECAY CURVE. James T. Brennan (National Naval Medical Center, Bethesda, Md.). Med. Bull. U. S. Army Europe, 18: 32-5 (Feb. 1961).

For the use of military units operating under fallout conditions, a system is presented for designating categories of hazard in a fallout field based on an analysis of the fallout decay curve. The point of max curvature of the dose rate vs time curve is defined as the "knee." Before the knee, in the upper leg region, is the time period in which dose rates are decreasing rapidly and passive defense is indicated. After the knee, in the lower leg region, relatively less benefit is derived from shelter. The upper leg is relatively short in duration. In most cases, the knee occurs in $\frac{1}{2}$ day or less after time of burst. The lower leg and the toe are indefinitely long. While giving this presentation to military units, it was found that the knee is an idea which is readily grasped as a matter of immediate intuition. No special technical training is necessary. This led to an investigation of the nature of the knee and an attempt to develop from it simple rules of action that may have value as tactical doctrine. Mathematical proof of the existence of the knee is derived. Using the equations derived it was shown that a fallout pattern on the ground may be divided, or zoned, according to the value of T_{kn}, the time of occurrence of the knee. T_{kn} increases as one approaches ground zero. From a table provided it is seen that a knee time of 5 hr is always associated with an upper leg dose of 50 R; a knee time of 7 hr indicates an upper leg dose of 100 R, and so on. The medical and tactical significance of the doses received in each zone are discussed. If the field commander can tolerate a delay, he should wait for the knee. There are situations, however, which do not permit delay. The zone concept is used to classify the degree of hazard resulting from operation in the open before the knee. It is concluded that analysis of fallout patterns in terms of the knee and zone concepts lead to a method of reporting radiac situation meaningful to the tactician and containing no technical terms such as Roentgen or reference dose rate. (BBB)

20224 NATIONAL HEALTH GRANTS, 1948–1961. IX. GENERAL PUBLIC HEALTH GRANT. RADIATION CONTROL. Med. Serv. J. (Can.), 20: 54-6(Jan. 1964).

This survey is based on a report of the Department of National Health and Welfare (National Health Grants, 1948–1961. Queen's Printer, Ottawa. 1962). Since 1948, with the development of the atomic energy industry in Canada and the increasing use of artificially-produced radioisotopes in industry, medicine, and research, health departments became increasingly involved with occupational health hazards. About 50% of the money expended in grants for radiation control in Canada has been used by provincial health departments for setting up laboratory programs for measuring radioactivity in the environment and for field programs and associated laboratory facilities for inspecting and measuring exposures from x-ray equipment. Most of the remainder of the expenditures has been for research in universities, mainly in departments where there is close liaison with groups in provincial health departments concerned with radiation protection problems. Tuberculosis Control and the Laboratory and Radiological Services Grants were made for purchase of attachments designed to reduce the exposure to both the operators of x-ray equipment and persons having diagnostic x rays. About 5% of the money for grants in this field was used for training courses for technical and professional personnel working in health departments or rendering services to health departments in radiation protection. Most of the administrative responsibility in radiation protection is being assumed by health departments. Legislative control of the use of radioisotopes is federal (Atomic Energy Control Board) with health aspects being administered mainly by health departments. Services are provided by the federal health department in areas where the need is common to all provinces, and provincial health departments provide services of particular need in their provinces. Fallout measurement has been largely managed by the Department of National Health and Welfare, with assistance from other federal departments. Other current problems of major importance (requiring activity mainly by the provinces) are control of the use of x rays; improved protection in institutions, such as hospitals or group clinics, where there may be a radiation hazard to staff and to the general public; environmental radiation surveys related to nuclear reactors and mines, such as uranium mines; radioactive waste disposal; medical supervision of radiation workers; education concerning the nature and effects of radiation; and the training of technical and professional personnel in radiological health. (BBB)

20225 SODIUM-22 AND CESIUM-134 IN FOODS, MAN, AND AIR. R. W. Perkins and J. M. Nielsen (General Electric Co., Richland, Wash.). Nature, 205: 866-7 (Feb. 27, 1965).

The radioisotopes ^{22}Na and ^{134}Cs were measured in air filter samples and other materials during the past few years as part of a comprehensive investigation of fallout materials. Special attention was given to studies on the route by which ^{22}Na finds its way to man. The major sources of ^{22}Na in foods considered were meat, milk, wheat, and freshwater fish, with smaller contributions coming from vegetables. Although the few foods considered

are not sufficient to give a complete picture of man's ^{22}Na intake, they do indicate the relative importance of different foods and suggest that the foods that carry ^{137}Cs to man are also the main sources of ^{22}Na. The results also indicated that the major injection of ^{134}Cs into the atmosphere occurred in tests prior to the 1961-62 nuclear test series. (P.C.H.)

20226 ARTIFICIAL AND NATURAL RADIOISOTOPES IN THE MARINE ENVIRONMENT. J. Mauchline and W. L. Templeton (Marine Station, Millport, Scotland and United Kingdom Atomic Energy Authority, Windscale Works, Eng.). Oceanogr. Mar. Biol. Ann. Rev., 2: 229-79(1964).

A review is presented on the content, measurement, behavior, and source of artificial and natural radioisotopes in the marine environment. Approximately 600 references are included. (P.C.H.)

20227 RADIATION EXPOSURE OF THE INHABITANTS OF MOSONMAGYAROVAR IN 1961. Gyoergy Luzsa (Varosi Tanacs Korhaza, Mosonmagyarovar, Hungary). Orv. Hetilap, 104: 642-5(Apr. 7, 1963). (In Hungarian)

A general survey made by the local health department determined the approximate amount of irradiation received by the 65,000 residents of the city and county of Mosonmagyaróvár. There were a total of 29,825 fluoroscopic examinations with a total gonad dose of 502 R, and 11,218 x-ray pictures were taken with a gonad dose of 380 R. There were a total of 41,043 x-ray examinations in the year 1961, giving a per capita rate of 0.63 examinations. The per capita gonad exposure in the 0- to 30-yr age group was 12.8 mRem. A table shows the number of various types of examinations conducted, on the basis of male and female exposures, with the approximate gonad dose in each instance. It was found that the use of x-ray film in Hungary doubled in the period from 1955 to 1959, whereas in this locality the increase was 3.16-fold from 1955 to 1961. Both the number of films used and the increased film area indicate an increase in x-ray examinations with a resultant increased exposure of the population. On a nationwide basis it was estimated that 160,000 to 180,000 needless chest x-ray examinations are conducted annually on patients complaining of chest ailments. (TCO)

20228 NOTE CONCERNING FILTRATION MATERIALS FOR RESPIRATORS DESIGNED FOR PROTECTION AGAINST RADIOACTIVE AEROSOLS. Kvetoslav Spurny (Inst. of Physical Chemistry, Czechoslovak Academy of Sciences, Prague). Pracovni Lekar., 17: 22-3(Jan. 1965). (In Czech)

Radioactive labeled NaCl aerosol with a medium size of particles (R = 0.3 microns) was used to test the effective absorption of submicron particles by the Lepestok Filter (Chlorinated PVC). The filter was found to be 99.99% effective. (CFSTI)

20229 ON THE POSSIBILITY OF DOSAGE REDUCTION IN X-RAY DIAGNOSIS BY THE PROPER SELECTION OF FILM. Wilfried Angerstein (Forschungsinstitut fuer Tuberkulose and Lungenkrankheiten, Berlin). Radiol. Diagn., 4: 387-91(1963). (In German)

From the standpoint of radioprotection the sensitivity of film is extremely important. Twelve different types of commercially available films were compared in terms of their sensitivity, granulosity, and resolution of detail. Sensitivity was measured as a function of tube amperage used, and estimated by the comparison with a scale of gray shades. The granulosity was estimated with the aid of photomicrographs. The detail resolution was measured by photographic studies of Landoldt rings and small cylinders placed behind a scattering body, and by averaging the estimates of test observers. There was a wide range of gradation between the amperage required to obtain a similar degree of blackening in the films designed to be used with foils. The proportional difference in this group was in a ratio of 1:4. For the two film types that were to be used without foils there was a considerable difference in sensitivity. However, there was little difference in the measured visibility of detail between any of the films tested. One feature that would increase the efficiency of film use at the present time would be to strengthen the filter on the dark chamber lamp. In every instance fresh film should be used always. (BBB)

20230 A STUDY OF THE EXPERIMENTAL CONTAMINATION OF CERTAIN MEDITERRANEAN SHELLFISH CURRENTLY CONSUMED. M. Leandri*, J. Charrel, and D. Omes (*Inst. d'Hyg. Trop. et de Med. Soc., Marseille). Rev. Hyg. Med. Sociale, 11: 401-10(1963).

The experimental contamination of edible Mediterranean shellfish by ^{131}I and ^{59}Fe showed that contamination is at its maximum between the 4th and 7th day in polluted water, varies with the type of shellfish, and is maximum on the shell, the body only fixing 1/50 to 1/10 of the ^{131}I in the Mytilus galloprovincialis. Public Health Eng. Abstr., 45: (Jan. 1965).

20231 THE EFFECTS OF THE EXPOSURE OF DRUGS TO NUCLEAR BOMB EXPLOSION. M. Vartolomei and R. Zdrafcovici. Rev. Sanit. Mil., 60: 851-6(Sept.-Oct. 1964).

Data on the effects of nuclear explosions on the more common types of drugs are reviewed. The tests described determined the radioactivity of the products after the explosion, their chemical composition, and biological and bacteriological data. (CFSTI)

20232 RADIATION SCATTERING AND LEAKAGE FROM MEDICAL AND INDUSTRIAL X-RAY INSTALLATIONS AND X-RAY DIFFRACTION EQUIPMENT AND ELECTRON MICROSCOPES. Kikuzi Kimura and Toyohiko Miura. Rodo Kagaku, 40: 121-9(Mar. 1964). (In Japanese)

A five-year study of radiation scattering and leakage measurements in radiology clinics and industrial laboratories, and their hazards to the workers involved is reported. An ionization chamber was used for measuring x rays scattered during diagnostic irradiation procedures, and x-ray sensitive film badges were worn by workers or hung on walls for measuring long-term exposure to scattered radiation. It was found that the x-ray scattering during diagnostic irradiation at a clinic registered less than 10 mR/hr (the badge's minimum sensitivity) in front of the fluoroscopic plate, and several hundred mR/hr at lateral sites often occupied by aides. Scattering from stratigraphy was over 2000 mR/hr at a one-distance, 100 to 1000 mR/hr at 2 m, and around 100 mR/hr at 4 m from the body area irradiated. Scattering from direct chest radiography was around 2000 mR/hr at 1 m, and several hundred mR/hr at 2 m. Scattering from indirect radiography (used usually for screening a large group) was over 2000 mR/hr at 2 m, 500 to 1000 mR/hr at 3 m from the area irradiated. Film badges worn by workers registered less than 30 mR (the badge's minimum sensitivity) in all cases of technicians wearing them for 7 to 19 days and after taking several hundred radiographs. X-ray scattering around x-ray diffraction equipment registered dose rates of 8 to 12.8 mR/hr, 1 to 17 mR/hr on the operator's hands, 1 to 15 mR/hr on the operator's eyes, 16 to 17.3 mR/hr at 0.5 m from the diffractor without a shield, 0.8 to 0.9 mR/hr with a shield, 2 to 3.5 mR/hr at 30 cm from specimen without a shield and 0 to 0.5 mR/hr with shield. Film badges worn for two weeks by 17 industrial x-ray technicians registered in most cases less than 10 mR/hr. X-ray scattering from electron microscopy in front of the electron gun registered 3.5 mR/hr, 11 to 40 mR/hr at lateral regions when focusing, and zero radiation doses on the operator's hand when viewing sections. (TCO)

20233 PROGNOSIS OF RADIOACTIVE FALLOUT IN 1964 AND 1965. Ugeskrift Laeger, Suppl. No. 17, 193 (1964).

A prognosis for radioactive fallout that can be expected from explosions during and before 1962 was worked out on lines similar to those of spring 1962 and 1963. (Excerpta Med., Sect. XXIII, 2: No. 3, (Mar. 1965))

20234 GUIDING RADIOACTIVE SEWAGE INTO SURFACE WATERS. [PART] II. Wasser, Luft Betrieb, 8: 469-73[1964].

Information presented during a specialized conference on the subject of radioactive contamination of surface waters

and treatment and monitoring of liquid radioactive wastes from atomic plants and radioisotope laboratories is summarized. (Excerpta Med., Sect. XXIII, 2: No. 3, (Mar. 1965))

20235 INVESTIGATIONS INTO THE RADIOACTIVITY OF ATMOSPHERIC SEDIMENTS. F. Peter and E. Jeney (Medical Univ., Debrecen, Hungary). Z. Ges. Hyg. Ihre Grenzgebiete, 10: 448-54(1964).

The radioactivity of the air in Debrecen has been studied since 1958. The relative activity and the semi-value time of the sediment substances collected for sampling from 12 places were measured by means of GM-tubes of 2 mg/cm^2. The absolute activity as compared to standard ^{40}K with 100 $\mu\mu$C was calculated by way of comparisons. The direct detection of the dust activity and the selection of the grains was effected by autoradiography. Absorption measurements made by using aluminium foils permitted conclusions as to the energy of radiation. In January 1963 the activity of the sediment substances amounted to $1.2 \cdot 10^{-7}$ C/m^2. The highest values per day were measured in May and June 1963: they reached the order of 5×10^{-8} C. Several grains of dust with a high activity (10^{-9} C) and with a diameter of some μ, were isolated. The respective results indicate the correlation between the reduced sedimentation and the occurrence of the activity. (Excerpta Med., Sect. XXIII, 2: No. 3, (Mar. 1965))

20236 COMPARATIVE MEASUREMENTS OF ACTIVITY TO DETERMINE THE TRAPPING OF DUST BY FOILS. W. Altvater and W. Schneider. Zentr. Biol. Aerosol. Forsch., 12: 12-23(1964).

In contrast to studies in other regions of Germany, foils were found more effective in trapping of dust than instruments for collection of rain in regions with serious atmospheric pollution by dust, provided the foils were renewed each week. The total beta activity of dust samples in the German Federal Republic cannot be assessed absolutely. It depends on the method used (e.g. on the type of examination of air-borne dust or measurement of sedimenting dust), the unit of measurement adopted (relation to m^2 or to 1 g of dust), and the local conditions and chemical composition of the dust. As in regions with serious air pollution foils are more effective for collection of sedimenting dust than instruments for collecting rain; the values obtained by the former method are more representative in industrial regions. Foils are, therefore, especially suitable. This finding agrees with the fact that foils are also generally superior for determination of radiation exposure in polluted regions. (Excerpta Med., Sect. XXIII, 2: No. 3 (Mar. 1965))

20237 THE STATE OF THE BLOOD COAGULATING SYSTEM AND BASIC HEMATOLOGICAL INDICES DURING CONTINUOUS WORK WITH VARIOUS PARTICLE ACCELERATORS. M. P. Strakhova and A. G. Likhacheva. p.103-10 of "Deistvie na Organizm Vyskoenergicheskogo Izluchen-iya (Tomsk: Tomsk Univ.), Sbornik, 1962. (In Russian)

The blood picture was observed for 10 months in 24 men who had worked in the betatron laboratory and 17, in the cyclotron. In the betatron group coagulation time, recalcification time, prothrombin content, thromboplast, and antithrombin activities, and proconvertin were high. The Ac-globulin content was slightly low. There was no indication that prolonged work with the betatron was very harmful. In the cyclotron group changes were not found or were less pronounced. (IIC-M.G.)

20238 RECENT DEVELOPMENTS IN THE INTERPRETATION AND THE REPORTING OF CARBON-14 ACTIVITY MEASUREMENTS FROM NEW ZEALAND. T. A. Rafter (Inst. of Nuclear Sciences, Lower Hutt, N. Z.). p.33-41 of "Radioactive Tracers in Oceanography. I.U.G.G. Monograph No. 20."

Measurements on ^{14}C activity in atmosphere, ocean water, and the Kauri tree in New Zealand are reported. Equations for standardization of ^{14}C activity measurements are given. The results showed that since nuclear testing ceased in 1958 the activity in the atmosphere has started to decrease. Previously there was an approximately linear increase (r) of 37% per year over New Zealand since 1953. Surface ocean ^{14}C measurements showed a decrease in ^{14}C with latitude. In the Kauri tree, results showed a gradual increase in the ^{14}C activity since 1030 A.D. and more rapid increase between 1550 and 1650 A.D. Data are tabulated. (P.C.H.)

20239 SPECIAL PROBLEMS FROM THE VIEWPOINT OF BRIDGE, TUNNEL AND TURNPIKE AUTHORITIES. Phillip B. Lee (New York State Thruway Authority). 21p. (CONF-650103-8)

From International Symposium on Packaging and Transportation of Radioactive Material, Albuquerque, N. Mex.

Special problems involved in the transportation of radioactive materials in truck using toll roads, bridges, and tunnels in the U. S. and other countries are discussed. It is pointed out that present regulations generally permit the shipment of radioactive materials on toll roads and bridges, but not through tunnels. Packaging requirements for resistance to the high-powered shock and the gasoline fires that must be anticipated in accidents under modern high-speed travel conditions are discussed. Special precautions to reduce accident hazards during the transport of radioactive materials are outlined. It is pointed out that present packaging standards for radioactive materials evince for more concern with the prevention of radiation injury to persons than with the prevention of contamination of property. It is suggested that materials particularly hazardous to toll facilities must be packaged in whatever manner is necessary to prevent the destruction of property if they are to travel on toll facilities under high-speed accident conditions. (C.H.)

20240 PROTECTING FOODS AND WATER AGAINST RADIOACTIVE CONTAMINATION. Frank A. Todd (Dept. of Agriculture, Washington, D. C.). 24p. (CONF-631105-1)

From Seminar on Protection of the Public in the Event of Radiation Accidents, Geneva.

Information is reviewed on protective measures and countermeasures for the protection of foods and water supplies that can be considered for use under emergency conditions. Emphasis is placed on the removal of ^{137}Cs, ^{131}I, and ^{90}Sr from milk and other foods, the protection of stored food stocks, and the decontamination of water supplies. It is pointed out that as research continues, the fund of dependable knowledge increases and improved methods for the protection of foods and food resources against radioactive materials are being developed. (33 references.) (C.H.)

20241 RADIATION EXPOSURE TRENDS FROM FILM MONITORING DATA, 1958-60. P. M. Bird (Dept. of National Health and Welfare, Ottawa). 15p. (CONF-640611-2)

From Canadian Assn. of Physicists, Division of Medical and Biological Physics, Annual Meeting, Halifax, Nova Scotia, Can.

Radiation exposure punch card records for the years 1958 to 60 were statistically analyzed according to six occupational classifications. A special study was undertaken to determine an average exposure which could be used to compute overall averages allowing for the large number of films which had previously been recorded as below reportable limits. Two techniques have been used for evaluating the exposure records. One involves an assessment of the average annual cumulative exposure per individual in a given occupational class, and the other an assessment of the average exposure per film used in that class. Both techniques indicate that radiation exposures in industry are higher than in any other class but still substantially less than that recommended as maximum permissible by the ICRP. The records show that in all but one class there has been a steady decline in radiation exposures by either technique during the three year period under study. (auth)

20242 FILMBADGE MONITORING FOR RADIATION. Herbert R. Isenburger (St. John X-Ray Lab., Califon, N. J.). 14p. (CONF-705-2)

From 14th International Congress of Occupational Health, Madrid, Sept. 1963.

The use of film badges for radiation monitoring of personnel is discussed. Some of the advantages of film badge monitoring are listed. The importance of film badge monitoring lies in the fact that it provides a warning signal of radiation exposure. An AEC list of procedures for issuance and processing of film badges is included, along with a film badge report sheet. (P.C.H.)

20243 FILM MONITORING PROCEDURES FOR RADIATION WORKERS. P. M. Bird (Dept. of National Health and Welfare, Ottawa). 20p. (CONF-640611-3)

From Canadian Assn. of Physicists, Division of Medical and Biological Physics, Annual Meeting, Halifax, Nova Scotia, Can.

A review is presented of various forms and procedures used in the Canadian Radiation Protection Division's film monitoring service. Emphasis is placed on the need for following instructions carefully as a major contribution to the smooth and efficient operation of this rapidly expanding service. Small points which seem insignificant individually combine to formidable proportions in the operation of a service already extended to some 16,000 Canadian radiation workers. Automatic handling techniques have been developed to improve the value of the service and to make it possible to report as a matter of routine cumulative exposure data in conformity with the Recommendations of the International Commission on Radiological Protection. (auth)

20244 DEVICE FOR SIMULATION OF THE INFLUENCE OF RADIOACTIVITY IN THE ENVIRONMENT OF AN ASSUMED ATOMIC EXPLOSION ON TRACKING APPARATUS FOR RADIATION. Robert Favre (to Landis and Gyr). German Patent 1,178,150. Sept. 17, 1964. Priority date July 14, 1960, Switzerland.

The radioactivity is simulated by the electromagnetic waves of a transmitter and the monitors are simulated by receivers for these electromagnetic waves. The transmitter is provided with a control device for emitting a succession of pulses of variable pulse frequency in which the pulse height varies continuously between a maximum and a minimum value. The receivers are equipped with pulse height discriminators so that only pulses above a given height are recorded. (Gmelin Inst.)

INSTRUMENTATION

General

Refer also to abstracts 20419 and 21664.

20245 (CEA-R-2718) APPAREIL DE MESURE A HAUTE TEMPERATURE DU FROTTEMENT INTERIEUR D'EPROUVETTES RIGIDES. (Apparatus for the High Temperature Measurement of the Interior Friction in Rigid Samples). Jean Delaplace, Jacques Hillairet, and Louis Trabut (Commissariat à l'Énergie Atomique, Saclay (France). Centre d'Études Nucléaires). Feb. 1965. 35p. Dep.(mn).

The apparatus described is an inverted pendulum making it possible to measure the internal friction in rigid samples at temperatures of between 20 and 600°C. This apparatus is well suited to the study of metals and alloys from which it is difficult to prepare samples in the form of wire. The various improvements made for facilitating the setting up the apparatus are applicable to any torsion pendulum. Certain results obtained with beryllium and an iron–aluminium alloy are described. (auth)

20246 (CONF-640204) PROCEEDINGS OF THE AMU–ANL HIGH-VOLTAGE ELECTRON MICROSCOPE MEETING HELD AT ARGONNE NATIONAL LABORATORY, FEBRUARY 13-14, 1964. (Argonne National Lab., Ill.). Contract W-31-109-eng-38. 144p. Dep.(mn); $4.00(cy), 3(mn) CFSTI.

Eleven papers are presented on the following topics: commercial instruments, research and development, metallurgical applications, biological applications, scanning techniques, aberrations of quadrupole magnets, power supplies, electron scattering, etc. Separate abstracts were prepared for all the papers. (D.L.C.)

For abstracts of individual papers see: 19455, 20085, 20247, 20248, 20249, 20250, 20251, 20252, 20253, 20254, and 20548.

20247 (CONF-640204(p.1-16)) STATE OF THE ART OF CONVENTIONAL COMMERCIAL INSTRUMENTS. John H. Reisner (Radio Corp. of America, Camden, N. J.).

A survey is presented of commercial electron microscopes and the ways they are being used to advance the state of art. The four phases of development of the instruments are outlined: research, developmental, commercialization, and engineering. Resolving power and contamination problems are discussed. A group discussion is included. (D.L.C.)

20248 (CONF-640204(p.17-19)) SUPERVOLTAGE ELECTRON MICROSCOPY OUTSIDE THE UNITED STATES. R. A. Dodd (Wisconsin Univ., Madison).

The features of the 1.5-million-volt instrument at Toulouse, France, are reviewed. The difficulties in the design of super-high-voltage microscopes are considered. Such instruments are not being developed in England because they hold little advantage for crystalline materials. The Hitachi 300-kv microscope in Japan is described briefly. (D.L.C.)

20249 (CONF-640204(p.20-5)) THE MIT PROGRAM IN ELECTRON MICROSCOPY. Robert E. Ogilvie (Massachusetts Inst. of Tech., Cambridge).

The use of high-voltage instruments to study defect structures in metallurgical samples is considered. Lenses with higher magnetic field strengths would be needed, and the fields that would be required to produce magnetic lenses with the desired spherical aberration constants are calculated. The high fields indicate that superconductive materials may have to be used in the windings. A brief group discussion is included. (D.L.C.)

20250 (CONF-640204(p.26-34)) THE ORNL PROGRAM IN ELECTRON MICROSCOPY. T. A. Welton (Oak Ridge National Lab., Tenn.).

Studies are being made of the problem of how to improve resolution in electron microscopy for studies of molecular structure. The reduction of the aperture defect to obtain 1-angstrom resolution is discussed. The problem of eliminating aberration is considered, and the application of the computer to the problem is discussed. The annular beam is discussed briefly. (D.L.C.)

20251 (CONF-640204(p.63-81)) SCANNING TECHNIQUES FOR HIGH-VOLTAGE MICROSCOPES. Albert V. Crewe (Argonne National Lab., Ill.).

The problems of conventional electron microscopes are discussed with respect to scanning electron microscopes. The tungsten tip electrode, lens system, spectrometer, display system, and vacuum system are discussed. The problem of going to high energies is considered. Some preliminary results are given. A group discussion is included. (D.L.C.)

20252 (CONF-640204(p.82-92)) ABERRATIONS OF QUADRUPOLE MAGNETS. Philip F. Meads, Jr. (Midwestern Universities Research Assn., Stoughton, Wis.).

A treatment is given of aberrations in quadrupole magnetic lenses. Some of the aberration terms are discussed, and an expression is given for the root-mean-square aberration. The case of the image of a point source is considered, and typical aberration figures are given. Octupole correction of aberrations is discussed. A group discussion is included. (D.L.C.)

20253 (CONF-640204(p.106-22)) SOME CONSIDERATIONS AND OBSERVATIONS ON HIGH-VOLTAGE ELECTRON MICROSCOPY. E. H. Zeitler and G. F. Bahr (Armed Forces Inst. of Pathology, Washington, D. C.).

A discussion is presented of the theoretical advantages and limitations of an increase of the acceleration voltage. Some results of measurements are given. It is shown that the choice of electron microscopic conditions is determined by the information sought from the object. (D.L.C.)

20254 (CONF-640204(p.123-36)) ELASTIC AND INELASTIC SCATTERING OF ELECTRONS AT HIGH ACCELERATING VOLTAGES. Robert D. Heidenreich (Bell Telephone Labs., Murray Hill, N. J.).

A simple treatment is presented of the phase contrast of the electron microscope and how it varies with electron velocity. Calculations are made for carbon and nickel. The increase of contrast by use of phase plates is discussed. A group discussion is included. (D.L.C.)

20255 (EUR-2119.e) STUDIES OF MAGNETIC TAPE INSTRUMENTATION FOR ON-LINE RECORDING AND OFF-LINE ANALYSIS OF DATA FROM MULTIPARAMETER NUCLEAR EXPERIMENTS. B. Idzerda (European Atomic Energy Community, Ispra (Italy). Joint Nuclear Research Center and European Atomic Energy Community, Geel (Belgium). Central Nuclear Measurements Bureau). 1965. 19p. Dep.(mn).

A 4-track, ¼ inch magnetic tape was used as a storage medium for 8-bit words in the series parallel mode. Stepwise tape transport by means of a stepping motor was applied in order to get high bit-packing densities at low data rates. For higher rates, the use of the original continuous speeds is still possible. The studies of stepping techniques have shown that stepping motors with the smallest stepping angle allow the highest packing density (i.e., 250 bits per inch). A simple test of the realized unit shows a failure rate of 1.5%. Experiences gained from these preliminary studies were used for the modification of a 1 inch, 24 track tape deck delivered by the firm E.M.I. First measurements have shown that the realization of the following specifications may be expected to be possible: a bit density of 250 bits per inch at stepping rates down to zero and up to 300 steps per second, together with a simple switch-over facility to continuous speeds. (auth)

20256 (HASL-151) DETERMINATION OF ENERGY DISTRIBUTION OF X-RAY BEAMS FROM A 250 KV CONSTANT POTENTIAL MACHINE. Arthur Shambon (Health and Safety Lab., New York Operations Office (AEC), N. Y.). Nov. 1964. 40p. Dep.; $2.00(cy), 1(mn) CFSTI.

An x-ray facility suitable for the energy calibration of radiation detection devices is described. The energy distribution of the useful beam from a 250 kv constant potential x-ray machine is established through the evaluation of the x-ray machine's kilovoltage scale and the determination both theoretically and experimentally of the inherent filtration. The radiation fields at three positions in both filtered and unfiltered beams are found and the transmitted energy passing through materials of the x-ray machine and other filters is calculated. (auth)

20257 (IPP-1/19) MAGNETFELDMESSUNGEN MIT HILFE DES ZEEMANEFFEKTES. (Magnetic Field Measurement With the Help of the Zeeman Effect). K. Huebner (Institut fur Plasmaphysik, G.m.b.H., Garching (West Germany)). Jan. 1964. 52p. Dep.(mn).

A method for the determination of non-constant magnetic fields from the Zeeman effect of time-fluctuating line radiation was described. In this method, both components of the normal longitudinal Zeeman effect could be separated by virtue of their different polarizations. With cleavages to the line flank, their intensity difference was measured in a given wave length interval. This difference is proportional to the magnetic field and flank inclination. The contribution of the flank inclination was separately but simultaneously determined. The method is independent of the line form and the cleavage profile and does not depend on variations of the intensity and line width so long as the Zeeman displacements are small with respect to the line width. Line asymmetries and double displacements that are small with respect to the line width play no role. The sensitivity of the method depends on a suitable dimensioning of the input and output slit and is given, in the long run, by the available radiation output and by the necessary band width. The accuracy of the measurement is limited by the stability of the electronics and is determined by the relative intensity changes in the slit. The method was tested on a nitrogen discharge in a homogeneous magnetic field of frequency 130 kHz. A threshold value of 650 gauss could be attained at a band frequency of 1 Mc, and the measurement error was less than 18% at the field maximum. In measurements of inhomogeneous fields from spatially nonconstant line emission the mean value of the field was not obtained, but only a value that lies between the maximum and the minimum of the field and which is dependent on the space distribution of the line emission. Experimentally reproducible values on a small fast theta pinch were obtained on discharges in hydrogen with 10% nitrogen with application of a N II line emitted only by the plasma layer. (tr-auth)

20258 (JAERI-1070) CONSTRUCTION OF RECORDING THERMOBALANCE FOR FLUORINE GAS AND VAPORS OF REACTIVE FLUORIDES. Shigeo Tsujimura, Ginji Fujisawa, and Akira Takahashi (Japan Atomic Energy Research Inst., Tokyo). Oct. 3, 1964. 28p. (In Japanese). Dep.(mn).

A recording thermobalance is described which was developed for studies of chemical reactions involving fluorine gas or vapors of reactive fluorides. Phosphor bronze spring was used as a sensing element; the extension of the spring was measured by a differential transformer. The characteristics of the thermobalance are: (1) capacity of sample, 5 g; (2) limit of weight change, 600 mg; (3) accuracy, 0.5 ~ 1.0 mg for weight changes up to 100 ~ 200 mg, 0.5% for changes 100 ~ 200 mg and more; (4) sensitivity, better than 0.5 mg. The structure of the thermobalance is so simple that its assembly, repair, and decontamination of radioactive materials are very easy. It can be easily used in a hood or glove box because of simplicity of its operation. The results of measurements of following reactions are given as examples of uses of the thermobalance: (1) $NaF \cdot xUF_6 = NaF + xUF_6$; (2) absorption of F_2 and HF by soda-lime; and (3) $UF_4 + F_2 = UF_6$. (auth)

20259 (JAERI-1074) CONSTRUCTION OF FLOWMETER FOR FLUORINE GAS AND VAPORS OF REACTIVE FLUORIDES. Shigeo Tsujimura, Ginji Fujisawa, Akira Takahashi, and Keizo Suzuki (Japan Atomic Energy Research Inst., Tokyo). Nov. 1964. 17p. Dep.(mn).

Descriptions are given of flowmeters which were developed for measuring the flow rates of F_2 gas and reactive fluoride vapors. For F_2 gas, two flowmeters were constructed: (1) A manganin heating element was wound on a Ni tube through which F_2 flows. The flow rate was measured using Pt resistance thermometers on both sides of the heating element. (2) A Ni filament was placed directly in the F_2 gas, and its resistance variation was used to measure the flow rate. The flow rate range is 0 to 200 and 3000 cc/min, the sensitivity for F_2 is 0.8 and 0.01 μa/(cc/min), and the response time is 2 min and 5 sec, respectively, for the above flowmeters. A third flowmeter for anhydrous HF vapor was constructed in which the vapor was bubbled through fluorinated oil. (D.L.C.)

20260 (JINR-P-1948) ELEKTROMAGNITNII MASSSEPARATOR LABORATORII YADERNYKH REAKTSII. 1. RASCHET MAGNITNOGO ANALIZATORA MASSSEPARATORA. (An Electromagnetic Mass-Separator of the Laboratory of Nuclear Reactions (Joint Institute for Nuclear Research). I. A Calculation of the Magnetic Analyzer for the Mass Separator). N. I. Tarantin and A. V. Dem'yanov (Joint Inst. for Nuclear Research, Dubna (USSR). Lab. of Nuclear Reactions). 1965. 8p. Dep.(mn).

A calculation is given of a magnetic analyzer for the mass separator. This analyzer is meant for the mass identification of the radioactive nuclei bombarded with accelerated heavy ions. (auth)

20261 (JINR-P-1949) ELEKTROMAGNITNII MASSSEPARATOR LABORATORII YADERNYKH REAKTSII. II. OPISANIE MASS-SEPARATORA I EGO KHARAKTERISTIKI. (An Electromagnetic Mass-Separator of the Laboratory of Nuclear Reactions (Joint Institute for Nuclear Research). II. A Description of Mass Separator and Its Characteristics). A. V. Dem'yanov, N. I. Tarantin, Yu. A. D'yachikhin, and A. P. Kabachenko (Joint Inst. for Nuclear Research, Dubna (USSR). Lab. of Nuclear Reactions). 1965. 16p. Dep.(mn).

A mass separator made on the basis of the available commercially CП-57 electromagnet with the magnetic screens at the input and output of the magnetic analyzer is described. The mass separator is meant to analyze the nuclear reaction products with mass number up to M = 260. The ionic optical characteristics of the mass separator are given, and the results of experiments on ^{205}Tl and ^{203}Tl isotope separation are presented. (auth)

20262 (KFK-259) GERATE- UND BAUSTEINPROGRAMM. (Instrument and Unit Program). E. Neuburger (Kernforschungszentrum, Karlsruhe (West Germany)). Nov. 1964. 24p. Dep.(mn).

Part of the electronic devices necessary in nuclear physical experiments has the same form in every experiment. Therefore it is helpful to have available standard electronics. An instrument and unit program for preparing such standard electronics is summarized. The characteristics of the apparatus and units are given. The development stage (pilot series fabricated, pilot series under construction, prototype fabricated, and prototype under construction) is indicated. (J.S.R.)

20263 (ORNL-3649(Vol.2)(Sect.2.1)) SMOOTHED THERMOCOUPLE TABLES OF EXTENDED SIGNIFICANCE (°C). VOLUME 2. PLATINUM VS. PLATINUM–10% RHODIUM THERMOCOUPLES. R. K. Adams and E. G. Davisson (Oak Ridge National Lab., Tenn.). Mar. 1965. Contract W-7405-eng-26. 53p. Dep.; $3.00(cy), 2(mn) CFSTI.

Tables of emf (absolute millivolts) vs temperature (°C) are presented for Pt/Pt–10% Rh thermocouples. Emf differences are also tabulated. The tables were derived from NBS reference tables and are expressed to the nearest 0.001 microvolt. (D.L.C.)

20264 (ORNL-3649(Vol.2)(Sect.2.2)) SMOOTHED THERMOCOUPLE TABLES OF EXTENDED SIGNIFICANCE (°C). VOLUME 2. PLATINUM VS. PLATINUM–13% RHODIUM THERMOCOUPLES. R. K. Adams and E. G. Davisson (Oak Ridge National Lab., Tenn.). Mar. 1965. Contract W-7405-eng-26. 51p. Dep.; $3.00(cy), 1(mn) CFSTI.

Tables of emf (absolute millivolts) vs temperature (°C) are presented for Pt/Pt–13% Rh thermocouples. Emf differences are also tabulated. The tables were derived from NBS reference tables and are expressed to the nearest 0.001 microvolt. (D.L.C.)

20265 (ORNL-3649(Vol.2)(Sect.2.3)) SMOOTHED THERMOCOUPLE TABLES OF EXTENDED SIGNIFICANCE (°C). VOLUME 2. CHROMEL–ALUMEL THERMOCOUPLES. R. K. Adams and E. G. Davisson (Oak Ridge National Lab., Tenn.). Mar. 1965. Contract W-7405-eng-26. 51p. Dep.; $3.00(cy), 1(mn) CFSTI.

Tables of emf (absolute millivolts) vs temperature (°C) are presented for Chromel/Alumel thermocouples. Emf differences are also tabulated. The tables were derived from NBS reference tables and are expressed to the nearest 0.001 microvolt. (D.L.C.)

20266 (ORNL-3649(Vol.2)(Sect.2.4)) SMOOTHED THERMOCOUPLE TABLES OF EXTENDED SIGNIFICANCE (°C). VOLUME 2. IRON–CONSTANTAN THERMOCOUPLES. R. K. Adams and E. G. Davisson (Oak Ridge National Lab., Tenn.). Mar. 1965. Contract W-7405-eng-26. 32p. Dep.; $2.00(cy), 1(mn) CFSTI.

Tables of emf (absolute millicolts) vs temperature (°C) are presented for iron/constantan thermocouples. Emf differences are also tabulated. The tables were derived from NBS reference tables and are expressed to the nearest 0.001 microvolt. (D.L.C.)

20267 (ORNL-3649(Vol.2)(Sect. 2.5)) SMOOTHED THERMOCOUPLE TABLES OF EXTENDED SIGNIFICANCE (°C). VOLUME 2. COPPER–CONSTANTAN THERMOCOUPLES. R. K. Adams and E. G. Davisson (Oak Ridge National Lab., Tenn.). Mar. 1965. Contract W-7405-eng-26. 26p. Dep.; $2.00(cy), 1(mn) CFSTI.

Tables of emf (absolute millivolts) vs temperature (°C) are presented for Cu/constantan thermocouples. Emf differences are also tabulated. The tables were derived from NBS reference tables and are expressed to the nearest 0.001 microvolt. (D.L.C.)

20268 (ORNL-3649(Vol.2)(Sect.2.6)) SMOOTHED THERMOCOUPLE TABLES OF EXTENDED SIGNIFICANCE (°C). VOLUME 2. CHROMEL–CONSTANTAN THERMOCOUPLES. R. K. Adams and E. G. Davisson (Oak Ridge National Lab., Tenn.). Mar. 1965. Contract W-7405-eng-26. 36p. Dep., $2.00(cy), 1(mn) CFSTI.

Tables of emf (absolute millivolts) vs temperature (°C) are presented for Chromel/constantan thermocouples. Emf differences are also tabulated. The tables were derived from NBS reference tables and are expressed to the nearest 0.001 microvolt. (D.L.C.)

20269 (ORNL-3649(Vol.2)(Sect. 2.7)) SMOOTHED THERMOCOUPLE TABLES OF EXTENDED SIGNIFICANCE (°C). VOLUME 2. TUNGSTEN VS. TUNGSTEN–26% RHENIUM THERMOCOUPLES. R. K. Adams and E. G. Davisson (Oak Ridge National Lab., Tenn.). Mar. 1965. Contract W-7405-eng-26. 67p. Dep.; $3.00(cy), 2(mn) CFSTI.

Tables of emf (absolute millivolts) vs temperature (°C) are presented for W/W–26% Re thermocouples. Emf differences are also tabulated. The tables are expressed to the nearest 0.001 microvolt. (D.L.C.)

20270 (ORNL-3649(Vol.2)(Sect.2.8)) SMOOTHED THERMOCOUPLE TABLES OF EXTENDED SIGNIFICANCE (°C). VOLUME 2. TUNGSTEN–5% RHENIUM VS. TUNGSTEN 26% RHENIUM THERMOCOUPLES. R. K. Adams and E. G. Davisson (Oak Ridge National Lab., Tenn.). Mar. 1965. Contract W-7405-eng-26. 66p. Dep.; $3.00(cy), 2(mn) CFSTI.

Tables of emf (absolute millivolts) vs temperature (°C) are presented for W–5% Re/W–26% Re thermocouples. Emf differences are also tabulated. The tables are expressed to the nearest 0.001 microvolt. (D.L.C.)

20271 (ORNL-3649(Vol.2)(Sect.2.9)) SMOOTHED THERMOCOUPLE TABLES OF EXTENDED SIGNIFICANCE (°C). VOLUME 2. TUNGSTEN–3% RHENIUM VS. TUNGSTEN–25% RHENIUM THERMOCOUPLES. R. K. Adams and E. G. Davisson (Oak Ridge National Lab., Tenn.). Mar. 1965. Contract W-7405-eng-26. 68p. Dep.; $3.00(cy), 2(mn) CFSTI.

Tables of emf (absolute millivolts) vs temperature (°C) are presented for W–3% Re/W–25% Re thermocouples. Emf differences are also tabulated. The tables are expressed to the nearest 0.001 microvolt. (D.L.C.)

20272 (ORNL-3649(Vol.2)(Sect.2.10)) SMOOTHED THERMOCOUPLE TABLES OF EXTENDED SIGNIFICANCE (°C). VOLUME 2. GOLD–2.1% COBALT VS. COPPER CRYOGENIC THERMOCOUPLES. R. K. Adams and E. G. Davisson (Oak Ridge National Lab., Tenn.). Mar. 1965. Contract W-7405-eng-26. 13p. Dep.; $1.00(cy), 1(mn) CFSTI.

Tables of emf (absolute millivolts) vs temperature (°K) are presented for Au–2.1% Co/Cu cryogenic thermocouples. Emf differences are also tabulated. The tables are expressed to the nearest 0.001 microvolt. (D.L.C.)

20273 (ORNL-3649(Vol.2)(Sect.2.11)) SMOOTHED THERMOCOUPLE TABLES OF EXTENDED SIGNIFICANCE (°C). VOLUME 2. CONSTANTAN–COPPER CRYOGENIC THERMOCOUPLES. R. K. Adams and E. G. Davisson (Oak Ridge National Lab., Tenn.). Mar. 1965. Contract W-7405-eng-26. 13p. Dep.; $1.00(cy), 1(mn) CFSTI.

Tables of emf (absolute millivolts) vs temperature (°K) are presented for constantan/copper cryogenic thermocouples. Emf differences are also tabulated. The tables are expressed to the nearest 0.001 microvolt. (D.L.C.)

20274 (ORNL-3649(Vol.2)(Sect.2.12)) SMOOTHED THERMOCOUPLE TABLES OF EXTENDED SIGNIFICANCE (°C). VOLUME 2. ALUMEL–CHROMEL CRYOGENIC THERMOCOUPLES. R. K. Adams and Davisson (Oak Ridge National Lab., Tenn.). Mar. 1965. Contract W-7405-eng-26. 12p. Dep.; $1.00(cy), 1(mn) CFSTI.

Tables of emf (absolute millivolts) and emf differences vs temperature (°K) are presented for Alumel/Chromel cryogenic thermocouples. The tables are expressed to the nearest 0.001 microvolt. (D.L.C.)

20275 (ORNL-3649(Vol.2)(Sect.2.13)) SMOOTHED THERMOCOUPLE TABLES OF EXTENDED SIGNIFICANCE (°C). VOLUME 2. CONSTANTAN (JN)–IRON (JP) CRYOGENIC THERMOCOUPLES. R. K. Adams and E. G. Davisson (Oak Ridge National Lab., Tenn.). Mar. 1965. Contract W-7405-eng-26. 12p. Dep.; $1.00(cy), 1(mn) CFSTI.

Tables of emf (absolute millivolts) and emf differences vs temperature (°K) are presented for constantan(JN)/iron(JP) cryogenic thermocouples. The tables are expressed to the nearest 0.001 microvolt. (D.L.C.)

20276 (ORNL-3649(Vol.2)(Sect.2.14)) SMOOTHED THERMOCOUPLE TABLES OF EXTENDED SIGNIFICANCE (°C). VOLUME 2. CONSTANTAN (YN)–IRON (YP) CRYOGENIC THERMOCOUPLES. R. K. Adams and E. G. Davisson (Oak Ridge National Lab., Tenn.). Mar. 1965. Contract W-7405-eng-26. 12p. Dep.; $1.00(cy), 1(mn) CFSTI.

Tables of emf (absolute millivolts) and emf differences vs temperature (°K) are presented for constantan(YN)/iron(YP) cryogenic thermocouples. The tables are expressed to the nearest 0.001 microvolt. (D.L.C.)

20277 (ORNL-P-1068) DYNAMIC GAS THERMOMETRY. E. W. Hagen (Oak Ridge National Lab., Tenn.). [nd]. Contract W-7405-eng-26. 8p. (CONF-650204-5). Dep.(mn); $1.00(cy), 1(mn) CFSTI.

From Meeting on Thermocouple Technology and the Effects of Nuclear Radiation on Thermocouples, Washington, D. C.

An investigation is being conducted to develop nozzles for measuring high temperatures in the EGCR. Tests were made on the long-term stability and accuracy of nozzles for this application. Nozzle materials studied included types 304 and 321 stainless steels, Inconel, chromium carbide, and tungsten carbide. A facility was constructed for studying the stability of EGCR-PTM nozzles. (D.L.C.)

20278 (ORNL-P-1069) HIGH-TEMPERATURE HIGH-VACUUM THERMOCOUPLE DRIFT TESTS. J. W. Hendricks and D. L. McElroy (Oak Ridge National Lab., Tenn.). [1964]. Contract [W-7405-eng-26]. 30p. (CONF-650204-3). Dep.(mn); $2.00(cy), 1(mn) CFSTI.

From Meeting on Thermocouple Technology and the Effects of Nuclear Radiation on Thermocouples, Washington, D. C.

Tests at 1200 to 1450°C and 10^{-6} to 10^{-8} torr pressure for times up to 1012 hr, were conducted on Pt–Rh/Pt, Pt–Rh/Pt–Rh, W/W–Re, and W–Re/W–Re thermocouples. No drift was observed in the thermal emf of the thermocouples, although drifts were produced in several cases by reaction of thermoelements with Nb and MgO. (D.L.C.)

20279 (RTD-TDR-63-4001) STUDY TO INVESTIGATE AND DEMONSTRATE FEASIBILITY OF A NUCLEAR GYRO. C. D. Bock (Arma Div., American Bosch Arma Corp., Garden City, N. Y.). Nov. 1963. Contract AF33 (657)-8804. 104p. (AD-424670; DS-63-R531-55). $4.00 (CFSTI).

An investigation into the applicability of solids in a nuclear gyroscope was made. The performance of rate and position gyroscopes was evaluated using experimentally determined characteristics of representative types of solids and some liquids, and a breadboard pulsed-coil position gyro was fabricated to test principles and to provide direct experimental data on materials. It was concluded that normal solids would not admit inertial quality performance. One exception was found. It was further noted that liquids categorically allow performance superior to solids. (auth)

20280 (SCL-DR-64-128) A TRANSISTORIZED, 25-AMPERE CONSTANT-CURRENT BATTERY DISCHARGER. G. E. Overturf (Sandia Corp., Livermore, Calif.). Nov. 1964. Contract AT(29-1)-789. 15p. Dep.(mn); $1.00(cy), 1(mn) CFSTI.

The unit is found to be a convenient and versatile telemetry battery testing device. Constant current discharge levels of 5, 10, 15, 20, and 25 amperes may be selected. The test is automatically terminated at the 24-volt level. Test-run time is recorded by an elapsed-time clock. (auth)

20281 (UCRL-11828(p.204-7)) CONTROL OF RESPONSE SENSITIVITY IN GAS CHROMATOGRAPHY USING HOT-WIRE THERMAL CONDUCTIVITY DETECTORS. Amos S. Newton and Aldo F. Sciamanna (Lawrence Radiation Lab., Univ. of California, Berkeley).

A study was made of the variables affecting the sensitivity of response of a hot-wire thermal conductivity cell with a helium flow. The sensitivity was found to be proportional to the 3.05 power of the bridge current and to the inverse of the carrier gas flow rate. It also increases slightly with cell block temperature. The conditions for controlling the sensitivity to within 1% are discussed. (D.L.C.)

20282 (UCRL-11828(p.218-19)) EXPERIMENTAL INSTRUMENTATION FOR THE 88-INCH CYCLOTRON. F. S. Goulding, D. A. Landis, and R. P. Lothrop (Lawrence Radiation Lab., Univ. of California, Berkeley).

Some of the recent advances in the instrumentation for experiments and in the accuracy of energy measurements are summarized: particle identification, analyzer routing, multiple single-channel analyzers, multiple-detector experiments, pulse generators for energy calibration, and energy resolution in cyclotron experiments. (D.L.C.)

20283 (UCRL-11828(p.221)) SUBGROUPING MULTICHANNEL ANALYZERS ON A PERIODIC BASIS. Richard G. Leres (Lawrence Radiation Lab., Univ. of California, Berkeley).

A device was developed for subgrouping multichannel analyzers at accelerator beam rates. The device, a Gating and Sequential Subgrouping External Router (GASSER), works on four RIDL model 34-12B 400-channel analyzers. Its capabilities and flexibilities are described briefly. (D.L.C.)

20284 (UCRL-11828(p.222-3)) A NEW TYPE OF BEAM INTEGRATOR. D. A. Landis and F. S. Goulding (Lawrence Radiation Lab., Univ. of California, Berkeley).

A new beam-integrator circuit was developed for the 88-inch cyclotron. A diode pump and capacitor arrangement is used to restore the charge at the end of each integrating period, and the dump rate can be quite high, up to 500 cps. The operation and stability of the circuit are described. (D.L.C.)

20285 (UCRL-11828(p.229)) HEWLETT-PACKARD DIGITAL RECORDER MODEL 562A INSIGNIFICANT-ZERO SUPPRESSION. A. A. Wydler (Lawrence Radiation Lab., Univ. of California, Berkeley).

A circuit was designed for eliminating insignificant zeros in the Model 562A recorder. The circuit uses "AND" gates to detect zeros, and a character is substituted for the suppressed zero. (D.L.C.)

20286 (UCRL-11828(p.230)) HEWLETT-PACKARD DIGITAL RECORDER MODEL 562A MODIFICATION TO PRODUCE LEADER PAPER. A. A. Wydler (Lawrence Radiation Lab., Univ. of California, Berkeley).

A method is given for automatically inserting ten spaces between each group of data in the automatic, unattended operation of the Model 562A recorder. The method uses a circuit board and a reed relay. (D.L.C.)

20287 (UCRL-11828(p.230-2)) INSTRUMENT DEVELOPMENT PROGRAM. W. W. Goldsworthy (Lawrence Radiation Lab., Univ. of California, Berkeley).

A summary is presented of the development of a linear amplifier in modular package, a semilogarithmic amplifier system, and modular packaging of several instruments. (D.L.C.)

20288 (UCRL-11828(p.232-3)) AUTOMATIC SPECTROGRAM MEASURING AND RECORDING. Kenneth C. Ward and Michiyuki Nakamura (Lawrence Radiation Lab., Univ. of California, Berkeley).

A spectrogram measuring and recording system was developed for use with the Grant Instruments Spectrum Line Comparator. The centers of the lines are automatically detected and recorded on magnetic data, and reading of the spectra is very rapid, up to 16 spectra per second. The electrical components of the comparator and the operation are described. (D.L.C.)

20289 ALTERNATIVES TO THERMIONIC EMISSION. P. Schagen (Mullard Research Labs., Surrey, Eng.). Brit. J. Appl. Phys., 16: 293-303(Mar. 1965).

Applications of thermionic emission are reviewed, together with alternatives to thermionic emission. (D.C.W.)

20290 A DEVICE FOR MEASURING ELECTRIC FIELD IN THE PRESENCE OF IONIZATION. P. J. L. Wildman (Univ. of Durham, Eng.). J. Atmospheric Terrest. Phys., 27: 417-23(Mar. 1965).

A device was developed related to the Malan–Schonland electric field mill, which allows the determination of electrostatic fields when a charged particle flux is acting upon the field sensors. The value of this flux may also be determined. Examples of the calibrations of such a device are given. (auth)

20291 A FINE FOCUS, HIGH INTENSITY, MEDIUM ENERGY X-RAY SOURCE. K. Gugan (Imperial Coll. of Science and Tech., London). J. Sci. Instr., 42: 86-9(Feb. 1965).

An x-ray tube is described whose attributes of beam coherency, low penetrating power and high intensity were required for the radiography of cigarettes, but it is thought to have a potential usefulness also in the field of radiobiology and medium energy crystallography. At full load the tube has a rating of 300 w at 15 kv. The diameter of the source, as determined by resolution experiments, is 0.61

mm, so that the specific target loading is 1.03 kw mm^{-2}. (auth)

20292 A PIEZOELECTRIC VACUUM VIBRATOR AS A SOURCE OF IONS IN A MASS SPECTROMETER. R. J. Conzemius and H. J. Svec (Ames Lab., Ames, Iowa). J. Sci. Instr., 42: 136-9(Mar. 1965). (IS-953)

A piezoelectric crystal of lead zirconate–titanate was used as a means of vibrating nickel electrodes in a vacuum vibrator ion source. Ion currents of 3×10^{-9} amp were obtained. No electrical noise was observed; thus electrical ion detection can be used. (auth)

20293 A TRANSISTORIZED METHOD FOR THE RESPONSE MEASUREMENT OF A MAGNETIC PROBE. F. Yenicay, S. Sinman, A. Sinman, and S. Goekgoer (Univ. of Istanbul). J. Sci. Instr., 42: 147-9(Mar. 1965).

A method for measurement of the responses of a magnetic probe, based on a transistorized circuit, is described. The overall sensitivity of the system is 1 mv g^{-1} for 10 msec RC time. (auth)

20294 OUT-OF-PILE STEAM-FRACTION DETERMINATION BY NEUTRON-BEAM ATTENUATION. William T. Sha and Charles F. Bonilla (Columbia Univ., New York). Nucl. Appl., 1: 69-75(Feb. 1965).

A method for determining the steam, or void, fraction in a boiling-water out-of-pile test section was theoretically analyzed and experimentally verified with air voids at room temperature. The method uses the combined moderation and attenuation of neutrons from an Sb-Be source by the boiling water in which boron has been dissolved. It was found that the method is applicable to multi-rod test sections with void fractions up to 25% or more and is sensitive enough to detect void fractions as small as 3% or less. (auth)

20295 A DIGITAL DECIMAL PULSE RATEMETER. M. Werner (Israel Atomic Energy Commission, Tel-Aviv, Israel). Nucl. Instr. Methods, 34: 103-8(Apr. 1965).

A digital version of the conventional analog linear pulse ratemeter is described, which may be organized for either binary or decimal readout. Wide ranges of full-scale readings and time constants, desired accuracy and linearity and binary coded decimal or decimal readout are some of the advantages of the proposed system. In addition, it may be easily converted into a scaler or timer. The described system may be designed to measure very low or very high pulse rates, thus being a very convenient laboratory instrument. (auth)

20296 A NOVEL FAST SCALE-OF-FIVE CIRCUIT AND ITS APPLICATIONS. S. Sinman (Istanbul Univ.). Nucl. Instr. Methods, 34: 155-6(Apr. 1965).

A scale-of-five circuit with a double pulse resolution of 0.1 and overall recovery time of less than 0.2 μsec is described, and its applications are discussed. (C.E.S.)

20297 ATTAINMENT OF HIGH RESOLUTIONS IN HOLOGRAPHY BY MULTI-DIRECTIONAL ILLUMINATION AND MOVING SCATTERERS. George W. Stroke and David G. Falconer (Univ. of Michigan, Ann Arbor). Phys. Letters, 15: 238-40(Apr. 1, 1965).

A method for attaining high resolution in holography is discussed in which the phase problem is solved by multi-directional illumination using moving mirrors (or scatterers). The theory of multi-directional illumination is given by a one-dimensional model, and an image of a two-dimensional grating reconstructed from a hologram illuminated through a moving scatterer is considered. (D.C.W.)

20298 TIME ANALYZER BASED ON AI-100. V. G. Varlamov and Yu. M. Grashin (Inst. of Physics and Engineering, Moscow). Pribory i Tekhn. Eksperim., No. 4, 148-52(1964).

The development of 100-channel time analyzer based on the standard AI-100 pulse-height analyzer (less its input part) is reported. Its essential addition is a time-amplitude-time-code (pulse train) converter. The analyzer has four ranges: 0.5, 1, 2, and 4 microsec. The analyzer has been in operation since autumn, 1962, on the pi-meson beam of the OIYaI synchrocyclotron; it was often in continuous use for 20 to 30 hrs. Under these conditions, its nonlinearity (variation of channel width with the range) was ±0.3% and the time-reading zero drift was ±0.3%; the dead time is 30 to 130 microsec. A block diagram of the time analyzer and a simplified connection diagram of its converter are supplied. A check characteristic within 0 to 1 microsec, at a channel width of 10 nsec, reveals that channels 10 to 95 are operable. (CFSTI)

20299 A HIGH-SPEED BINARY ANALOGUE-DIGITAL CONVERTER FOR PULSE HEIGHT ANALYSES IN NUCLEAR RADIATION SPECTROMETRY. K. Fraenz and J. Schulz. Telefunken Ztg., 37: 210-20(Nov. 1964). (In German)

After an analysis of the requirements for an analog-digital converter suitable for multichannel pulse-height analyses, a converter based on the principle of binary weighing is described, together with its operation. (D.C.W.)

20300 THE QUADRUPOLE MASS ANALYZER AND ITS APPLICATION TO CHEMICAL AND ISOTOPIC ANALYSIS. A. E. Rafal'son. Zh. Tekhn. Fiz., 35: 3-13(Jan. 1965). (In Russian)

The theory of the instrument is briefly derived, and a number of articles are reviewed in which are described applications of the instrument to such diverse problems as chemical analysis, the precise measurement of mass, the determination of residual vapors in high vacuum systems, and the analysis of the upper regions of the atmosphere. The principal characteristics of a number of instruments are tabulated; these instruments range in length from 12.75 cm to 5.82 m and in resolving power from 40 to 20,000. (ATD)

20301 IMPEDANCE OF A PLANE CAPACITOR COMPLETELY OR PARTLY FILLED WITH PLASMA. [PART] I. A. F. Aleksandrov (Moscow State Univ.). Zh. Tekhn. Fiz., 35: 35-42(Jan. 1965). (In Russian)

The impedance of a plane capacitor containing a nonuniform plasma is calculated with space dispersion taken into account. The impedance of a capacitor filled with a uniform plasma is calculated first. The ion motions are neglected and the effect of electron collisions is taken into account by means of a linear damping term in the electron equation of motion. The case of a nonuniform plasma is then treated by integrating the impedance for a uniform plasma across the width of the capacitor. The integration is performed for a parabolic electron density distrubution, and the resulting expressions are simplified for the case in which the Langmuir frequency greatly exceeds both the applied and the electron collision frequency. The effect of space dispersion is taken into account. The linearized hydrodynamic equation of motion is employed for the electrons, and Poisson's equation is introduced. The resulting expression for the impedance is discussed in some detail for values of the parameters appropriate to experimental conditions. A resonance increase in the resistance is found to occur; this is due to the excitation of plasma waves. The motion of the ions is expected to give rise to a similar increase in the resistance due to the excitation of the low-frequency branch of the plasma waves. (ATD)

20302 OPTICAL PROPERTIES OF MAGNETS FOCUSING THE ATOMIC BEAM INTO A CAVITY OF A HYDROGEN MASER. D. L. Kaminskii (Ioffe Inst. of Physics and Tech., Leningrad). Zh. Tekhn. Fiz., 35: 140-4(Jan. 1965). (In Russian)

The potentialities of six-pole magnets for focusing hydrogen beams are investigated. Equations are written for the field configuration of a six-pole magnet. The general equations of motion of an atom with a magnetic moment in such a field are then derived. The motion is considered using matrix formalism. Depending on the direction of the atomic moment of the particles, the magnet may be either focusing or defocusing (it may act either as a converging or a diverging lens). It is noted that in classical optics a combination of a converging and a diverging lens with different refractive indices can yield an achromatic system. Hence, by using two six-pole magnets with appropriate parameters, a magnet system that is basically achromatic can also be

assembled. Admittedly, solution of the pertinent equations in the double six-pole magnet case is difficult in the general case, but solutions can be arrived at in particular cases. The Zeeman splitting of the ground state of the hydrogen atom is then described, and it is noted that if a hydrogen atom beam is sent through a system of two consecutive magnets there will pass through the first magnet only the atoms in the upper Zeeman states. In the second magnet the upper state splits into three levels. As a result, the magnet operates as a diverging lens with an ensuing great loss of hydrogen atoms. If the conditions for achromatic operation are chosen, 17% of particles entering the first magnet, will be focused, which should yield a considerable enhancement of the output. Ways of realizing this improvement are suggested in principle. (ATD)

20303 MESUCORA 63. CONGRES INTERNATIONAL MESURE-CONTROLE REGULATION-AUTOMATISME, PARIS DU 15 AU 22 NOVEMBRE 1963. TOME I. (International Congress on Measurement, Control, Regulation, and Automation, Paris, 15-22 November, 1963. Vol. I). Paris, Mesucora, [1964]. 240p.

Forty-two articles are included; separate abstracts were prepared for 10. The remaining 32 articles include information on measurement of geometrical quantities; matters about bearings; little displacements; numerical control of machine tools; optical measurement and spectroscopic analysis; electrical measurement; teletransmission techniques; and electronic measurement. (P.C.H.)

For abstracts of individual papers see: 20304, 20380, 20381, 20382, 20383, 20384, 20385, 20386, 20387, and 21591.

20304 MEASUREMENTS IN NANOSECOND ELECTRONICS. Georges Klein (Etudes Atomiques au Centre de Recherches de la C.G.E., Paris). Paper 4, Session 7, 8p. of "Mesucora 63. Congres International Mesure-Controle Regulation-Automatisme. Tome I." Paris, Mesucora, [1964]. (In French)

The specific measurement problems in nanosecond electronics and the particular aspect taken by some types of classical measurements when they are applied to the nanosecond range were examined. Measurements on elements of circuits, groups of pulses, and pulses themselves are considered. (J.S.R.)

20305 MESUCORA 63. CONGRES INTERNATIONAL MESURE-CONTROLE REGULATION-AUTOMATISME, PARIS DU 15 AU 22 NOVEMBRE 1963. TOME II. (International Congress on Measurement, Control, Regulation, and Automation, Paris, 15-22 November, 1963. Vol. II). Paris, Mesucora, [1964]. 240p.

Forty-one articles are included; separate abstracts were prepared for 3. The remaining 38 articles include information on: general problem of connecting regulators with computers; applications in chemical industry; applications in power plants and in gas distribution networks; applications in iron works; and problems in automation. (P.C.H.)

For abstracts of individual papers see: 20103, 20416, and 20452.

20306 10-MEGACYCLE SCALER (Engineering Materials). (California. Univ., Berkeley. Lawrence Radiation Lab.). 24 drawings. (CAPE-1058)

The 10-Mc scaler with serial and readout facilities has: 23 printed circuit boards, including a discriminator; twelve 10-Mc decade scalers; 2 scan gates and a master scan gate; a Nixie decoder and gate, which is a decimal visual indication used to show the contents of any scaler; a station control; a sequence generator; a binary, 16-output decimal decoder; a program card; and a miscellaneous card. The chassis is constructed of 14GA (0.064) Al, and is approximately 16 × 11 × 7 in. (For details, see TID-4100). (M.C.G.)

20307 RESISTANCE BRIDGES (Engineering Materials). (Brookhaven National Lab., Upton, N. Y.). 2 drawings. (CAPE-1115)

Resistance bridges were designed for low-temperature resistance thermometers. They operate at 30 cps. The 30 cps waveform was derived by dividing the line frequency by two with a binary scaler so that the resultant waveform was perfectly symmetrical with no even harmonics. Preceeding the meter circuit is a phase sensitive detector, which is synchronized by the symmetrical waveform and is sensitive only at 30 cps and at its odd harmonics. The amplifier input circuit consists of a well-shielded, step-up transformer and a high-input impedance field-effect transistor. The amplifier includes a stage tuned to 30 cps and a 60-cps rejection filter to prevent overload on noise and pickup before the phase detector. One bridge is used for measuring two terminal resistors in the 10 Ω and above range. The other bridge, which has a four-terminal configuration is preferred when the resistance of the leads to the resistor in the cryostat is a significant part of the total. (For details see TID-4100) (M.C.G.)

20308 TURBINE DRIVEN MIRRORS, MODELS 231 AND 232 (Engineering Materials). (Los Alamos Scientific Lab., N. Mex.). 10 drawings. (CAPE-1184)

The turbine driven mirrors described are used with the Framing Camera, Model II. The model-231 mirror has a speed of 11,000 rps and the faces of the mirror are 20 × 20 mm. The model-232 mirror has a speed of 10,000 rps and the faces of the mirror are 25 × 38 mm. (For details, see TID-4100) (M.C.G.)

20309 IMPROVEMENTS IN OR RELATING TO PULSE GENERATORS. Richard Anthony Fitch and Vernon Thomas Seymour Howell (to United Kingdom Atomic Energy Authority). British Patent 975,911. Nov. 25, 1964. Filed May 18, 1961.

A single-unit pulse generator is patented that can generate pulses having peak voltage up to 100 times the charging voltage. The generator consists of two sheets of electrically conductive material and two sheets of electrically insulating material (all thin foils) arranged alternately and wound together into a roll around a core of highly inductive material to form two open-end strip transmission lines having in common a sheet of electrically conductive material. Means for connecting the sheets of conductive material to an electrical source to charge the transmission lines, a load connected across opposite ends of one of the conductors, a switch located at substantially the midpoint of the transmission line, and means for connecting the two sheets of conductive material together through the switch to discharge not more than one of the two transmission lines are also provided. One of the sheets of conductive material may be longer than the other and extend around the roll to separate the ends of the sheets by substantially 180°. The width of the sheets of conductive material decreases toward one or both ends in order to avoid unwanted reflection in the transmission lines. The duration of the pulse increases as the pulse voltage becomes a higher multiple of the charging voltage, and the shape of the pulse is triangular rather than square. (A.G.W.)

20310 RESISTOR EMPLOYING IRRADIATED GAS. Roy S. Sennett and Alan K. Knowles (to N. V. Philips' Gloeilampenfabrieken). Canadian Patent 679,254. Feb. 4, 1964. Filed May 6, 1959.

The resistor consists of a ceramic capsule of gas at slightly less than atmospheric pressure, pierced by two electrodes of similar work function. Incorporated into the case is a radioactive source of less than 0.5 microcuries that enables the gas to act as a resistor in the million megohm range. Over-voltage leading to self-ionization must be avoided. Provision for varying the resistance is included. (F.S.A.)

20311 SELECTIVE RAY ENERGY UTILIZATION IN RADIATION GAUGING SYSTEMS HAVING SPECTRAL-ENERGY RAY SOURCES. George B. Foster (to Industrial Nucleonics Corp.). U. S. Patent 3,154,685. Oct. 27, 1964. Filed May 5, 1961.

A method and apparatus for using subatomic particles, particularly β particles, in gaging physical properties of materials are patented. A beam of particles of varying energy from a radioactive source such as ^{90}Sr is directed toward a sample of the material to be investigated. A ra-

diation detector is positioned to detect the particles passing through the sample. Before impinging on the sample the particle beam is subjected to a time-varying electromagnetic field whose strength can be so adjusted that all particles below a predetermined energy level are periodically swept beyond the face of the radiation detector. Thus the electrical output of the radiation detector has a steady component and a time-varying component, which components may be separated by known means. This effect of a change in the energy-emission spectrum of a given radioactive source permits measurements on thinner and thicker materials than can ordinarily be measured with the same source. (A.G.W.)

Radiation Detection

Refer also to abstracts 20203, 20872, and 21202.

20312 (AERE-R-4525) A FAST NEUTRON DOSE-EQUIVALENT RATE MONITOR. J. W. Leake (Atomic Energy Research Establishment, Harwell (England)). Jan. 1965. 18p. Dep.; $0.80(BIS); 4s. (HMSO).

A fast neutron dose equivalent ratemeter has been developed to cover the neutron energy range from 3 to 25 Mev. The neutron dose equivalent is estimated by measuring the total light emission from a liquid organic scintillator, NE 213. Dose equivalent indication is given by means of a rate meter whose output is directly proportional to the product of the amplitude of the light pulses and their frequency. The gamma ray discrimination properties can be adjusted so that a gamma ray exposure rate of 10 mR/hour from radium-226 gives a response which is less than that due to 0.25 mRem/hr of AmBe neutrons. The sensitivity of the instrument, using a 1 inch diameter scintillator, is such that 1 mRem/hr of Am–Be neutrons produces a count rate of about 3 pps, (for a 1-Mev neutron bias). The sensitivity may be increased by about a factor of 5 by enlarging the scintillator size to 2" in diameter, but this reduces the neutron/gamma ray rejection ratio. In addition to a meter display calibrated in mRem/hour, the indicator unit also provides a linear pulse output signal, which may be fed into an external pulse height analyzer to give the proton recoil spectrum, from which the neutron energy spectrum can be subsequently calculated. Alternatively, the system may be used to measure the neutron flux density from monoenergetic neutron sources. (auth)

20313 (ANL-6938(p.9-20)) SCINTILLATIONS IN ARGON–NITROGEN MIXTURES: EFFECT OF CONCENTRATION AND PRESSURE. H. A. Schultz (Argonne National Lab., Ill.).

Results are presented of a pulse height study of scintillations produced by alpha particles in Ar–N_2 mixtures with concentrations ranging from 100% Ar to 100% N_2 and total pressures from 3 to 6 atmospheres. (auth)

20314 (ANL-6938(p.62-70)) INTERNAL Sr^{90} BETA RAY DOSIMETRY WITH FLUORODS. Jacob Kastner, Donald R. Roberts, and William Prepejchal (Argonne National Lab., Tenn.).

Results of an investigation are described in which it was found that the use of Schulman and Etzel fluorods for in vivo and in vitro dosimetry for ^{90}Sr beta rays is feasible, provided careful precalibration is carried out on a sample of the specific batch of dosimeters to be used. A reproducible technique for calibration employing gelatin phantoms is described. The convenience in practice of using such gelatin techniques for calibrating beta-ray applicators is noted. Comparison with the work of other laboratories can be made if a ^{60}Co gamma-ray calibration is included. The response is linear with dose over a large range and is also independent of dose rate, at least from 24 R/hr to 2400 R/min. If low-Z fluorods are used the fluorescence does not fade over many months. Of the two commercially available materials, the Toshiba fluorods are superior with regard to sensitivity and low pre-dose reading; however, both the Toshiba and the B and L products offer good reproducibility if the B and L reader is slightly modified to provide better alignment of the fluorods. (auth)

20315 (ANL-6938(p.206-8)) MULTICHANNEL ANALYZER DATA PROCESSING ON THE CDC 160-A COMPUTER. J. B. Corcoran (Argonne National Lab., Ill.).

An approach to multichannel analyzer data processing through a system for generating special-purpose computer programs is described. The system is intended to provide the full range of computer facilities to any multichannel analyzer application regardless of the anticipated volume or the stage of development of the application. (J.R.D.)

20316 (ANL-6984) AN ITERATIVE UNFOLDING METHOD FOR RESPONSE MATRICES. Raymond Gold (Argonne National Lab., Ill.). Dec. 1964. Contract W-31-109-eng-38. 40p. Dep.; $2.00(cy), 1(mn) CFSTI.

The problem of unfolding the output data of a detection system is reviewed. Physical implications of the matrix representation of a detection system are discussed. An iterative method of solution is presented. The properties of the iterative method are investigated, and proof of convergence to the exact solution is given for two-dimensional, triangular, and positive-definite response matrices. The unfolding characteristics of the method are examined by applying the iterative process to the results of a neutron detection system. Limitations of the iterative method are discussed. (auth)

20317 (HW-82369) RADIATION MONITORING OF PERSONNEL BY DOSE RATE TELEMETERING. M. L. S Smith and P. J. Horvath (General Electric Co., Richland, Wash. Hanford Atomic Products Operation). June 8, 1964. Contract AT(45-1)-1350. 18p. (CONF-642-32). Dep.(mn); $1.00(cy), 1(mn) CFSTI.

From Health Physics Society, Cincinnati, June 1964.

A new technique is described for monitoring of personnel in reactor areas by dose rate telemetering systems with the radiation monitor located out of the radiation zone. A detector-transmitter is placed on each worker entering the radiation zone and this package telemeters the radiation intensity to a central monitoring station where a monitor follows the dose rate and dose of each worker and observes the work being performed by closed-circuit television. The receiver system sounds an alarm when the signal is lost, when a pre-set dose rate is exceeded, or when a preset dose is reached. Circuit diagrams and test results are included. (C.H.)

20318 (HW-SA-3526) THE STATUS OF NEW PERSONNEL NEUTRON DOSIMETER DEVELOPMENT. C. M. Unruh (General Electric Co., Richland, Wash. Hanford Atomic Products Operation). May 15, 1964. Contract AT(45-1)-1350. 12p. (CONF-642-34). Dep.(mn); $1.00(cy), 1(mn) CFSTI.

From Health Physics Society, Cincinnati, June 1964.

A neutron dosimeter sensitivity to a full energy spectrum of fast and intermediate energy neutrons is required for personnel neutron dosimetry. A variety of approaches to personnel neutron dosimetry are under investigation. Investigations consider the use of silicon diodes, tissue equivalent chambers, thermoluminescent materials, and fission fragment material damage for personnel fast-neutron dosimetry. The advantages and disadvantages as well as the state of development of each of these dosimetry principles are reviewed. Two systems, thermoluminescence and fission-fragment material damage, offer promising performance for applications in personnel neutron dosimetry. The current rate of development of these two dosimeter principles may lead to the general use of one of these systems for personnel fast-neutron dosimeters in 1965 or 1966. (auth)

20319 (IDO-17059) A TRANSISTORIZED BIDIRECTIONAL DECADE COUNTER. K. D. Smith (Phillips Petroleum Co., Idaho Falls, Idaho. Atomic Energy Div.). Jan. 1965. Contract AT(10-1)-205. 18p. Dep.; $1.00(cy), 1(mn) CFSTI.

A transistorized bidirectional decade counter utilizing a binary and a quinary circuit is described: The elimination of feedback requirements, the minimization of the readout logic, and the symmetrical properties of the ten logical states produce an attractive counter. The logical design of the device is presented. The electrical equivalent

circuit of the quinary is analyzed in detail and the conditions necessary for successful operation are described. (auth)

20320 (IS-989) WRITING TOPOLOGICAL PROGRAMS FOR I.S.U. GUTS. William J. Kernan, William J. Higby, and Iva H. Boessenroth (Ames Lab., Iowa State Univ. of Science and Tech.). Sept. 1964. Contract W-7405-eng-82. 49p. Dep.; $2.00(cy), 1(mn) CFSTI.

This paper is devoted to the analysis of bubble chamber data through the use of a computer program, GUTS. This system is designed in a general manner. That is, a wide variety of interactions in bubble chambers may be studied by writing control programs describing the interaction. The techniques employed and the method of writing these programs will be presented. (auth)

20321 (ISS-64/28) CATALOGO DELLE APPARECCHIATURE ELETTRONICHE STANDARDIZZATE DA E91 A E100. (Electronic Service—Circuit Diagrams and Characteristics of Standard Electronic Equipment E91 to E100). (Istituto Superiore di Sanita', Rome (Italy). Laboratori di Fisica). July 12, 1964. 41p. Dep.(mn).

A catalog of circuit diagrams and characteristics of electronic equipment is presented. The main purpose of this catalog is a practical one: that is to give to the experimenter a short account of equipment available off the shelf. (auth)

20322 (LA-DC-6397) A SEMICONDUCTOR ANTICOINCIDENCE DETECTOR SYSTEM. Dale M. Holm and William Mort Sanders (Los Alamos Scientific Lab., Univ. of California, N. Mex.). [nd]. Contract [W-7405-eng-36]. 10p. (CONF-641001-54). Dep.(mn); $1.00(cy), 1(mn) CFSTI.

From Symposium on Radiochemical Methods of Analysis, Salzburg, Austria.

An anticoincidence lithium-drifted germanium detector system is described. A block diagram of the circuitry is included. Features and applications of the detector are also discussed. (C.E.S.)

20323 (NYO-3246-4) STUDY OF SURFACE CONTOURING AS APPLIED TO SEMICONDUCTOR RADIATION DETECTORS. Semiannual Report, June 1964–January 1965. Gerald C. Huth, James B. Trice, Robert J. Locker, and Russell A. McKinney (General Electric Co., King of Prussia, Pa. Space Sciences Lab.). Contract AT(30-1)-3246. 63p. Dep.(mn); $3.00(cy), 2(mn) CFSTI.

Studies are reported of semiconductor p-n junctions, utilizing geometrical surface-field control, and possessing sufficiently high values of internal electric field to cause carrier multiplication and thus pulse amplification. Specific topics studied include: the effect of directionality of response of the detector junction in the amplifying mode; the effects of variations in the base resistivity (and thus the field-distance relation); development of surface-field-controlled P + NN + devices; development of a tunnel-diode univibrator for use with amplifying detectors; and measurement and resolution of the 5.6-kev Kα x ray from Mn produced by decay of ^{55}Fe. (T.F.H.)

20324 (ORNL-P-1094) THEORETICAL AND EXPERIMENTAL ASPECTS OF QUENCHING VARIABLES FROM BIOMEDICAL SAMPLES IN LIQUID SCINTILLATOR SYSTEMS. Harley H. Ross (Oak Ridge National Lab., Tenn.). [1963]. Contract [W-7405-eng-26]. 23p. (CONF-650507-1). Dep.(mn); $1.00(cy), 1(mn) CFSTI.

For presentation at IAEA Symposium on Radioisotope Sample Measurement Techniques in Medicine and Biology, Vienna.

The usual methods used for the preparation of samples of biological materials for liquid scintillation counting result in quenching variables that affect the results of the radiochemical analysis. Two different approaches to determine the amount of color quenching in a sample are described. The first method illustrates a general mathematical model for color quenching as a function of the spectrophotometric properties of the system, and the second method provides a simple experimental technique to evaluate color quenching directly. Comparisons were of calculated and observed quenching for various colored substances, various methods of color quench correction for a number of dyes, and the separation of color and chemical quenching effects using several quenchers. Results are reported from applications of the methods in the analysis of ^{14}C-labeled samples of liver, blood, and urine. It is pointed out that the quenching effect is dependent upon the disintegration energy of the particular radioactive tracer being counted and that different quenching coefficients will be obtained for different isotopes and for the same radioisotopes in different liquid scintillation systems so that quenching coefficients are valid only for a specified isotope in a specified scintillation system. (C.H.)

20325 (UCRL-11624) ARTIFICIAL CONSTRUCTION OF PARTICLE TRACKS BY A MONTE CARLO METHOD. Francis M. Smith, Hla Shwe, and Walter H. Barkas (Lawrence Radiation Lab., Univ. of California, Berkeley). Aug. 21, 1964. Contract W-7405-eng-48. 5p. Dep.(mn); $1.00(cy), 1(mn) CFSTI.

A Monte Carlo method is given for successively generating the grain coordinates of particle tracks in emulsion. For such a calculation one needs to know three parameters of the distribution functions of the grain variables. These are the parameters of multiple scattering, grain noise, and grain spacing. To generate equivalent tracks, the parameters for the distributions of these three random variables may be experimentally determined from a fair sample of real tracks. The method was developed for an emulsion application, but it is readily adapted to other instruments such as the bubble chamber, and to problems of the spatial distribution of ionization in a beam of particles penetrating matter. Also, a brief description is given of the IBM 7094 program for performing such Monte Carlo calculations of particle track grains. (auth)

20326 (UCRL-11787) VELOCITY SPECTROMETERS USED IN BEVATRON DEFLECTED-BEAM RESEARCH. George W. Edwards and Robert D. Watt (Lawrence Radiation Lab., Univ. of California, Berkeley). Feb. 4, 1965. Contract W-7405-eng-48. 11p. (CONF-650306-10). Dep.(mn); $1.00(cy), 1(mn) CFSTI.

From Particle Accelerator Conference, Washington, D. C.

Two ten-ft, glass-cathode, parallel-plate velocity spectrometers have been used in particle research at 500 kv for about 3000 hr each without maintenance. Current consumption, including power supply, is approximately 100 μA on each plate (<200 μA total). The units do not appear to be gap-sensitive, because one was operated with a 2-in. gap and the other with a 4-in. gap. No significant operating differences are apparent. (auth)

20327 (UCRL-11828(p.221-2)) MÖSSBAUER EFFECT INSTRUMENTATION. Ronald Zane (Lawrence Radiation Lab., Univ. of California, Berkeley).

A method was developed for performing Mössbauer effect experiments in the multiscaler mode operation of pulse-height analyzers. Results are given for the ^{57}Fe spectrum. (D.L.C.)

20328 (UCRL-11828(p.225-6)) SILICON RADIATION DETECTORS. Robert P. Lothrop, Morris D. Roach, and Harry E. Smith (Lawrence Radiation Lab., Univ. of California, Berkeley).

A fabrication process for diffused silicon devices is described in which control of surface states is effected by means of the gaseous ambient during the end of the final high-temperature diffusion. Progress in the fabrication of Li-drifted silicon devices is also summarized. (D.L.C.)

20329 (USNRDL-TR-806) THE NITROUS OXIDE DOSIMETER—INFLUENCE OF CELL DIAMETER ON THE NITROGEN YIELD. D. A. Kubose (Naval Radiological Defense Lab., San Francisco, Calif.). Jan. 5, 1965. 12p.

The effect of cell diameter on the nitrogen yield from ^{60}Co gamma-irradiated gaseous nitrous oxide was examined. The Fricke dosimeter was used as the reference of absorbed dose. The dose actually absorbed by the gas was calculated by the Bragg-Gray principle. The results obtained indicate there is no significant dependence of $G(N_2)$ on cell diameter. The mean $G(N_2)$ of 11.4 ± 0.8 obtained

compared well with values reported by other workers. (auth)

20330 (AEC-tr-6547) DETECTION OF CRITICAL ACCIDENTS AT THE COMMISSARIAT A L'ENERGIE ATOMIQUE. A. Barthoux, G. Debrie, P. Desneiges, J. M. Lavie, and M. Planque ([Comnissariat à l'Énergie Atomique, Saclay (France). Centre d'Etudes Nucléaires]). Translated by Myra S. Feldman (E. I. du Pont de Nemours and Co., Aiken, S. C.). 1964. 6p. Dep.(mn); $1.10(fs), $0.80(mf) JCL.

Design features are described of a dose integrating radiation detector for use in the event of a criticality accident. The instrument incorporates an ionization detector, a semiconductor detector, and a scintillation detector with a photomultiplier assembly for the simultaneous detection of γ radiation and neutrons. An alarm system is activated by coincidence of signals originating from at least two probes of the detector. The instrument gave satisfactory performance when tested under conditions of a reactor excursion. The instrument is commercially available and is recommended for use in installations using fissile materials. (C.H.)

20331 A NEUTRON CHOPPER OF THE RESEARCH REACTOR GEESTHACHT I FOR MEASUREMENT OF TOTAL CROSS SECTIONS. PART II. G. Richter and E. Bagge (Universität, Kiel). Atomkernenergie, 9: 395-410 (Nov.-Dec. 1964). (In German)

The resolution function of the neutron chopper is calculated with consideration of the effects of a rotating rotor with parallel-channels on a divergent neutron beam; of the rotor and the collimator-detector arrangement on the neutron beam; and of detector length, counter reading delay, and channel width of the time-of-flight analyzer. (J.S.R.)

20332 QUENCHING CORRECTION IN LIQUID SCINTILLATION COUNTING. C. T. Peng (Univ. of California, San Francisco). Atomlight, No. 44, 1-9(Mar. 1965).

Several methods for quenching correction in homogeneous samples are summarized, together with their merits. Their usefulness for assaying singly, doubly, or triply labeled samples is indicated. Background counts, counting modes, and instrument settings are briefly considered. (D.C.W.)

20333 THE MEASUREMENT OF THE ANGULAR DISTRIBUTION OF THE PHOTONEUTRONS BY MEANS OF A HIGH EFFICIENCY DETECTOR. S. Costa (Universita, Turin). Atti Accad. Sci. Torino, I, Classe Sci. Fis., Mat. Nat., 99: 77-83(1964-65). (In Italian)

A possible method is suggested for the measurement of the angular distribution of photoneutrons and, in particular, the asymmetric term of this distribution, assumed to be of the type $A + \underline{b} \sin^2\theta + \underline{c} \cos\theta$. The method is based on the symmetry property possessed by the thermal neutron detector described. The essential value of the method consists in the possibility of using the high efficiency of the detector to measure, with good statistics, C as a function of E_γ, by detecting the neutrons emitted at various angles by means of the reactions induced. (tr-auth)

20334 SPECTROMETRY OF FAST NEUTRONS BY SURFACE BARRIER JUNCTIONS AND LITHIUM-6. J.-P. Noel (CEA, Paris), S. Passe, C. Beets, S. De Leeuw, and G. Gierts. Bull. Inform. Sci. Tech. (Paris), No. 81, 1-14 (1964). (In French). (EUR-935.f)

The reaction $Li^6(n,\alpha)H^3$ can be used for fast neutron spectrometry. With silicon diodes two different methods (according to the neutron energy range being studied) may be used for the detection of the charged particles created and for the measurement of their energy. These two methods are described in detail. (auth)

20335 MEASUREMENT OF WEAK ACTIVITIES OF $^{137}CsClO_4$, $^{90}SrSO_4$, AND $Ag^{131}I$ IN SUSPENSION IN SCINTILLATION GELS. Georges Germai. Bull. Soc. Roy. Sci. Liege, 33: 672-7(1964). (In French)

The efficiencies of counting $^{137}CsClO_4$, $^{90}SrSO_4$, and $Ag^{131}I$ in suspension in a gel composed of toluene, PPO, POPOP, naphthalene, and Aerosil were determined. The factors influencing the counting were established, and the optimum conditions for counting with the photomultiplier system used were studied. The activities of ^{137}Cs and ^{90}Sr in rainwater were determined as an example of the application of the method. (D.C.W.)

20336 METHOD FOR DIRECT DETECTION OF THE CENTER OF GRAVITY OF THE CURRENT PULSES OF A SCINTILLATION COUNTER. Raymond Richert (Centre de Recherches Nucleaires, Strasbourg). Compt. Rend., 260: 508-9(Jan. 11, 1965). (In French)

This method takes into account directly the form of the current pulses. It makes it possible to visualize the time fluctuations introduced by the counter and, by discrimination, gives more precise time information. (tr-auth)

20337 DETERMINATION OF THE INTENSITY AND THE FINAL ENERGY OF THE BREMSSTRAHLUNG OF A BETATRON USING IONIZATION CHAMBERS. F. Klapper and G. Geske (Friedrich-Schiller-Universitat, Jena, Ger.). Exptl. Tech. Physik, 12: 331-42(1964). (In German)

The intensity of a high-energy bremsstrahlung has been estimated usually by the ion dose produced in an absorber. Since the magnitude is dependent on the detector properties, the intensity is determined more and more in absolute units (W/cm^2). The sensitivity of a thick-walled ionization chamber was recalculated. It could be shown that an ionization chamber with a 4 to 5 cm thick wall measures almost independently of energy for bremsstrahlung spectra with a boundary energy of 7 to 30 Mev. The filter analysis has been used for a long time in the x-ray range. The possibilities and limits of this method for the characterization of high-energy bremsstrahlung was investigated. For the determination of the boundary energy from the effective energy, a relation was devised that is valid for energies from 10 to 25 Mev. For the determination of isodoses of a betatron cone of rays, photographic method was used. It is distinguished from the point measurement of the cone of rays by a very low cost. (tr-auth)

20338 PERSONAL MONITORING OF EXPOSURE TO RADIATION. Kenji Takeshita (Kyushu Univ., Fukuoka, Japan). Fukuoka Igaku Zassi, 55: 65-8(Feb. 1964). (In Japanese)

Two standard types of radiation exposure monitoring devices, the pocket chamber and film badge, were tested for their performance under various conditions. Five film badge samples used for γ- and x-ray monitoring, and five pocket chamber samples were tested. The test radiation doses ranged from 30 to 200 mR. The ratio of measured values to the standard exposure doses was determined for both x and γ radiation. It was found that the pocket ionization chamber registered 10 to 20% larger doses than the standard x-ray exposure doses, with only small variations with each measurement. Film badges registered 20 to 40% larger doses than the actual exposure doses with relatively large variations. In regard to Ra radiation, the pocket chambers read 80 to 120% larger doses, and the film badges 30 to 40% smaller doses than the actual exposures. In regard to ^{60}Co radiation, the picket chambers read 20% larger, and the film badges 10 to 30% larger doses than the true exposures. Judging from these results, pocket chambers gave relatively stable values (excluding the data with Ra radiation), whereas film badges showed larger variation of readings owing to varying conditions of film processing. There was a linear relation between standard radiation doses and the measured values irrespective of type of device used, the reading variations tending to increase with the increase of irradiation doses. In general, film badge readings tended to register lower values with the prolonged use owing to regression of the latent image, emulsion characteristics, processing condition, directional bias, etc.; while pocket chambers tended to register higher values due to mechanical shock, leakage, reading bias, directional bias, etc. It was considered desirable to use two different types of monitoring devices: pocket chambers in each radiation installation for taking hourly readings when in operation, and film badges worn by individuals to register accumulated exposure over a two-week interval. In any case, a

reading bias of 30 to 40% is considered inevitable. It is also important to use the same monitoring device repeatedly for x or γ radiation, and not for x and γ radiation interchangeably. (BBB)

20339 METHOD FOR MEASURING THE IONIZING POWER OF AN INCIDENT CHARGED PARTICLE WITH A DISCHARGE BOX. Shigenori Miyamoto (Osaka City Univ.). Genshikaku Kenkyu, 8: 401-6(Aug. 1963). (In Japanese)

Investigations are made of the possibility of making a discharge box in which the sparking efficiency is changed according to the ionizing of the incident charged particle. There are two systems, for the determination of the ionizing power of an incident charged particle by the change of the detection efficiency in the discharge box: 1) to maintain the spark efficiency per gap in the range of 10–60% when the particle of the minimum ionizing power has passed by reducing the intensity of the pulsed field; 2) to drop the spark efficiency by reducing the number of effective electrons through mixing the sealed gas with an electronegative gas. (NSA of Japan)

20340 A TWO-URANIUM-FOIL SYSTEM FOR USE IN NUCLEAR ACCIDENT DOSIMETRY. E. Roberts, Jr. (Union Carbide Corp. Y-12 Plant, Oak Ridge, Tenn.). Health Phys., 11: 255-60(Apr. 1965). (Y-KB-32)

A system is described whereby two uranium foils of different ^{235}U enrichments may be used in nuclear accident dosimetry. Data are presented showing that a ^{10}B shielded uranium foil in the threshold detector measures within 36 to 65 per cent of the total neutron dose for a variety of measured neutron spectra. However, the expense of ^{10}B shields precludes their extensive field use. Experiments were conducted using a combination of normal and depleted uranium foils to determine the feasibility of measuring the dose from neutrons above 1.5 Mev using the ^{238}U fission activity. Two different foils were used to compensate for the activity from thermal neutron absorption by ^{235}U and therefore eliminate the need for the ^{10}B shield. More than fifty observations were made in which the results of the two foils were compared with the results from the ^{10}B shielded foil. These observations were made for various neutron doses and several different neutron energy spectra. The results for the two-foil measurement method differed from the shielded reference foils by -7.8 ± 4.9 per cent. The 95 per cent confidence interval associated with a single count using the two-foil system is ±14.8 per cent. It is concluded that this system can be used independently to measure the neutron tissue dose in air. (auth)

20341 A SIMPLE AND RAPID METHOD OF CYCLOHEXANE DOSIMETRY. E. Proksch and H. Bildstein (Institut fur Chemie, Seibersdorf, Austria). Intern. J. Appl. Radiation Isotopes, 16: 56-8(Jan. 1965). (In German)

The $G(H_2)$ value in the radiolysis of cyclohexane is known to be independent of irradiation temperature, type of radiation, and dose output. Therefore the use of cyclohexane for the fast, simple determination of the radiation dose was investigated. The hydrogen formed in the irradiation was determined by gas chromatography. The results showed that cyclohexane is suitable for γ dosimetry in the range from 0.5 to 5 Mrad. (J.S.R.)

20342 GAMMA-GAMMA COINCIDENCE SETUP WITH ENERGY ANALYSIS OF THE COINCIDING RADIATIONS. V. R. Burmistrov, A. Kh. Abil'daev, and V. A. Shilin. Izv. Akad. Nauk Kaz. SSR, Ser. Fiz.-Mat. Nauk, No. 1, 60-6 (1964).

An installation was developed for γγ coincidences, with energy analysis of the coincident radiations in the energy range 100 kev to 3 Mev. A block diagram of the fast-slow coincidence setup, the associated fast-coincidence circuit, is described. The detectors used are NaI(Tl) crystals with FEU-11 photomultipliers. The output of the fast coincidence circuit is fed to a single-channel type AADO-1 analyzer, whose slow-coincidence circuit output is shaped and fed to the control circuit of a pulse height analyzer (AI-100-1). The discriminator window is adjusted in such a way that the circuit remains the same during the adjustment and during the performance of the experiment. The circuit was used to investigate the influence of the resolution time on the dynamic range and to determine the spectra of ^{60}Co, ^{134}Cs, and ^{65}Zn at a coincidence-circuit resolution time 0.04 to 0.1 μsec. The dynamic range increased from about 4 at 0.04 μsec to 12 at 0.1 μsec, depending on the pulse amplitudes in the control and analysis channels. Plots of the different spectra are included. (ATD)

20343 RADIATION STUDY BY COSMOS 17. S. N. Vernov, A. E. Chudakov, P. V. Vakulov, et al. Izv. Akad. Nauk SSSR, Ser. Fiz., 28: 2058-74(Dec. 1964). (In Russian)

Equipment used in the flight of Cosmos-17 (apogee, 788 km; perigee, 260 km) for investigating the earth's radiation belts and primary cosmic radiation are described. The equipment consisted of two scintillation counters (with NaI and CsI crystals) and a STS-5 gas-discharge counter. The cylindrical NaI counter (20 × 20 mm) was mounted under the shell of the satellite and was fitted with aluminum shielding (1 g/cm²). On one channel it recorded ionization produced in the crystal by radiation; on the two others, it registered the number of pulses with energy release in the crystal over the specified thresholds (50 kev and Mev). The effective cross section of the NaI crystal for particles registered along the ionization and first threshold channels was approx. 4.7 cm²; for the second channel, it was roughly 5% smaller for particles with quadruple ionization and 20% smaller for relativistic particles. The STS-5 gas-discharge counter has an effective cross section of 4.3 cm². It was placed inside the device containing the scintillation counter and was not fitted with any special protection. Up to counting rates of 3×10^3 pulse/sec, the counter registered virtually all particles. At higher rates, the count became less reliable. The flat CsI counter (crystal diameter, 6 mm; thickness, 3 mm) was mounted outside the container. For protection from light, the crystal was covered with aluminum foil (2 mg/cm²). For protection against bremsstrahlung, the photomultiplier and the crystal were shielded with 5 mm of lead and 11 mm of aluminum, except for the front of the photomultiplier, which had a conical opening for particle incidence (aperture angle, 40°). This counter carried out ionization measurements and particle registration at energy release in the crystal of 45 and 160 kev and 5.4 and 8.5 Mev. Both electrons and protons could be registered along the first two (45 and 160 kev) channels. Along the other two (5.4 and 8.5 Mev) channels, the count was mainly of protons; at an electron path perpendicular to the crystal surface energy losses were about 2 Mev and oblique paths were precluded by the thickness of the shielding. The minimal particle energies registered by the counters were tabulated. (ATD)

20344 A STUDY OF THE ACCURACY OF LOCATING A PARTICLE IN A SPARK CHAMBER AND OF DETERMINING ION DRIFT IN A WILSON CHAMBER. Yu. A. Eremenko, Yu. T. Lukin, A. M. Machekhin, M. I. Pak, and A. Kh. Tsoi (Inst. of Nuclear Physics, Academy of Sciences, Kazakh USSR). Izv. Akad. Nauk SSSR, Ser. Fiz., 28: 2075-6(Dec. 1964). (In Russian)

The experimental unit was so arranged that each charged particle passing through a telescope of Geiger-Muller counters connected in coincidence passes through a Wilson chamber and the sensitive volume of a spark chamber. A Wilson chamber track in the plane of photography is hardly displaced at all on expansion, and this fact is utilized in estimating the location of a particle by means of a spark chamber. Because of the small dimensions of the spark chamber and the Wilson cloud chamber, it is possible to obtain a trace in the Wilson chamber and a spark in the spark chamber on the same photograph. Thus, it is possible to measure directly the deflection of the spark from the trace. The accuracy in determining the relative displacement of the spark and trace is better than 0.1 mm. Two identical spark chambers are placed over and above the Wilson chamber in determining ion drift during expansion of the Wilson chamber. Photographs are taken of the spark chambers, and of the upper and lower parts

of the Wilson chamber. The depth coordinates of the two sparks is taken as Z_{true}, and the depth coordinates of the trace in the Wilson chamber is taken as Z_{meas}. The difference between Z_{true} and Z_{meas} gives ΔZ, which is the value of the ion drift. The ion drift is described by the following formula: $Z_{true} = Z_{meas}/(1 + \alpha)$, where α is the degree of expansion. (TTT)

20345 METHOD FOR REDUCTION OF ERRORS DUE TO MISSES AND ACCIDENTIAL COINCIDENCES IN COUNTER TELESCOPES. I. N. Kapustin. Izv. Akad. Nauk SSSR, Ser. Fiz., 28: 2082-4(Dec. 1964). (In Russian)

One of the significant sources of error in recording cosmic ray and similar data by means of counter telescopes is misses, i.e., failure to detect pulses owing to the dead time of the counters. Use of quenching reduces but cannot eliminate this error. A method for compensating for the misses, based on the use of feedback is described. In such compensation there is automatically taken into account the intrinsic background of the counters and the dead time of the input devices, which must be chosen greater than the dead time of the counters. For the dead-time shaping circuits one can use appropriate quenching circuits, which should prolong the effective service life of the counters. The delayed feedback is provided by delay circuits with delay times greater than the dead time of the shaping circuits. A block diagram of the proposed arrangement is given; in addition to the above mentioned components, it comprises a coincidence circuit, two anticoincidence circuits, and the usual scaler and register. A brief mathematical analysis is given to illustrate the probable reduction in error. There is also proposed a multiple trigger circuit to minimize accidental coincidences; this also incorporates a dead-time shaper. Its operation is based on pulse shifting. (ATD)

20346 RADIO PROBE FOR THE MEASUREMENT OF COSMIC-RAY DENSITY IN THE STRATOSPHERE. L. L. Lazutin and E. T. Frantsuz. Izv. Akad. Nauk SSSR, Ser. Fiz., 28: 2085-6(Dec. 1964). (In Russian)

A new radio probe for measuring cosmic-ray density in the ionosphere, particularly solar radiation, is described. The design of the RKL-4 probe was based on experimental data collected during the IGY. Registration of charged particles is accomplished with either a single STS-6 gas-discharge counter or a two-counter telescope. In the RKL-4 with a single counter, the keying circuit is eliminated; a pulse from the counter directly triggers the blocking-oscillator. In this case the shaping circuit is blocked by the barograph contact, and the counting ceases. Substitution of a copper chloride–magnesium battery for the usual dry-battery set sharply increases the utilization factor of the chemical supply source. Tests carried out during the second and third quarters of 1963 demonstrated the reliability of the RKL-4 probe for 7–8-hr operation. Steady signal reception was secured in ascent, descent, and even drift (4–5 hr) at 25–30 km. Maximum altitude was 35 km. Since January 1964, regular daily flights of the probe have been made. (ATD)

20347 DESCRIPTION OF THE MODERNIZED COMPLEX INSTALLATION FOR STUDY OF EXTENSIVE AIR SHOWERS. S. N. Vernov, G. B. Khristiansen, A. T. Abrosimov, V. B. Atrashkevich, I. F. Belyaeva, G. V. Vedeneev, and V. A. Dmitriev. Izv. Akad. Nauk SSSR, Ser. Fiz., 28: 2087-92(Dec. 1964). (In Russian)

During the past two years the installation for comprehensive investigation of extensive air showers and high-energy muons has been greatly improved. The installation is located at Moscow State University and covers an area of about 10 acres; it consists of a large number of stationary and mobile laboratories. In the mobile laboratories and in the stationary laboratories and in the main building the old system of hodoscopic counters has been supplemented by an array of 20 scintillation counters with an area of 0.5 m^2 each, which make it possible to determine the strength of a shower and the orientation of its axis in space. In the underground laboratory the area of the muon detector has been increased from 6 to 45 m^2 and there has been installed a new system of 240 ionization chambers shielded by an absorber, intended for statistical measurements of the energy of muon fluxes. Diagrams of some of the counter and chamber arrays are given, and some of the specific design features of the detectors and associated electronic equipment are described. A few typical curves are reproduced. The underground installation is characterized by an exceptionally large area, good continuity, and a high resolution. (ATD)

20348 A TWO-METRE GRAZING-INCIDENCE SPECTROMETER FOR USE IN THE RANGE 5-950 Å. A. H. Gabriel, J. R. Swain, and W. A. Waller (Atomic Weapons Research Establishment, Aldermaston, Berks, Eng.). J. Sci. Instr., 42: 94-7(Feb. 1965).

An instrument is described for the photographic recording of spectra down to 5 Å. A 600 line per mm blazed grating is used and the instrument can be set to angles of incidence of 86, 88, or 89°. Plates are cassette loaded. Spectra were recorded from an x-ray tube, a 45 kj theta-pinch, and a carbon vacuum spark. An attachment is provided to convert the instrument for photoelectric recording. (auth)

20349 A NEW FAST QUENCHING CIRCUIT FOR SELF-QUENCHED GEIGER-MÜLLER COUNTERS. K. W. Ettinger and A. Zastawny (Technical Univ. of Gdansk, Poland). J. Sci. Instr., 42: 125-6(Feb. 1965).

A simple quenching circuit for Geiger–Müller counters filled with quenching vapor is described. A circuit, based on a modified Kandiah low-level discriminator, delivers pulses with about 90 v amplitude and 0.2 μsec rise time. The threshold level is 100 mv or slightly lower. (auth)

20350 A PULSE-LENGTHENING CIRCUIT. R. N. Thomas (Univ. of London). J. Sci. Instr., 42: 169(Mar. 1965).

A transistor circuit for lengthening pulses derived from nuclear particle detectors is described. A linear relation exists between the input and output pulse amplitudes, and the output pulse length may be set to a time duration suitable for the operation of a pulse-height analyzer or similar instrument. (auth)

20351 FACTORS AFFECTING ENERGY RESOLUTION IN LIQUID SCINTILLATION COUNTING. A. Guillon, J. Pintena, and R. Sauvagnac (Commissariat a l'Energie Atomique, Saclay, France). Nature, 205: 1200(Mar. 20, 1965).

Factors that affect energy resolution when using β-conversion electron peaks to calibrate a liquid scintillation β-spectrometer are discussed. These factors include: selection of photomultiplier tube; solution purity; composition of liquid scintillator; and transparency of vile surrounded by a reflecting material. By considering these factors, the 0.625-Mev conversion electron peak of ^{137m}Ba for calibration of the β-spectrometer gave a resolution of 25%. (P.C.H.)

20352 ON THE PROPERTIES OF RETINA-LIKE COUNTER. K. O. Thielheim (Christian-Albrechts-Universitat, Kiel). Nucl. Instr. Methods, 31: 341-2 (Dec. 11, 1964).

The distribution function, the parameter of the distribution function, and the maximum-likelihood estimation of $\underline{k}$ of retina-like counters are calculated. (J.S.R.)

20353 A LOW BACKGROUND GAS-FLOW COUNTER ASSEMBLY. M. N. Rao, J. K. Samuel, and M. R. Ponkshe (Atomic Energy Establishment, Trombay, India). Nucl. Instr. Methods, 34: 10-12(Apr. 1965).

For low-level β^- measurements, an anti-coincidence counting assembly was set up, which consisted of a flow-type rectangular perspex sample counter, surrounded by a ring counter (12 G.M. counters). The counters were shielded against cosmic radiation with a 6" mild steel frame. The counting gas used was argon + isopropylalcohol, cooled to 0°C. The anti-coincidence circuit used was of the standard "Putmann-Cooke Yarborough type." This assembly gave a reproducible background of about 1 cpm with a sample counter of 12.6 cm^2 counting area. (auth)

20354 FILMLESS AUTOMATIC PROCESSING OF NUCLEAR TRACKS USING STANDARD EQUIPMENT.

A. Seidman (Univ. of Southampton, Eng.). Nucl. Instr. Methods, 34: 13-20(Apr. 1965).

A system is proposed for filmless digitizing of the location of patterns of nuclear tracks. It also stores the information, and reads it out in a computer-compatible form, using standard nuclear-physics laboratory equipment in general use and associated electronic circuits. The system is able to resolve tracks close together and to deal with an arbitrary number of tracks. It is flexible and suitable for adaptation to a large variety of experiments. It can also be used for scanning photographs. One version of the system is in a final stage of realization. (auth)

20355 A LOW THRESHOLD NEUTRON DETECTOR FOR NANOSECOND TIME OF FLIGHT SPECTROMETRY. J. M. Adams, E. Barnard, A. T. G. Ferguson, W. R. McMurray, and I. J. Van Heerden (Atomic Energy Research Establishment, Harwell, Berks, Eng.). Nucl. Instr. Methods, 34: 21-8(Apr. 1965).

An efficient low threshold neutron detector for nanosecond time of flight spectrometry is described. It consists of a twin photomultiplier system in an unusual geometrical arrangement. Photomultiplier noise is reduced by fast coincidence to less than one per second, with useful neutron detection efficiency below 75 kev. Its timing and efficiency characteristics were measured as a function of neutron energy. With energetic radiations its timing resolution was 0.7 ns, and an example is presented of its high resolution capabilities for inelastic scattering of fast neutrons. To simplify future detector calibrations, the measured relative efficiency of the detector was used to obtain standard spectra for energetic protons on very thick targets of ^{55}Mn and ^{65}Cu. (auth)

20356 UNIFORM SPECTRAL SENSITIVITY PHOTON COUNTER. A. M. Ghose (Bose Inst., Calcutta). Nucl. Instr. Methods, 34: 45-53(Apr. 1965).

It is shown that a photon counter, the efficiency of which is independent of the energy of the photon over a wide range can be obtained by combining a suitable filter with a conventional NaI(Tl) scintillation counter. A theory is developed which makes it possible to choose the constitution as well as the optimum thickness of the filter for a particular dimension of the crystal. Performance of the system for paraxial as well as wide beam geometries were considered. Experimental investigations for verifying the theory have been given. (auth)

20357 A TRANSISTORIZED STABILIZED HIGH VOLTAGE POWER SUPPLY 650-3000 V, 10 MA, FOR SUPPLYING PHOTOMULTIPLIERS. L. Frevert and W. D. Kreisel (Universitat, Gottingen, Ger.). Nucl. Instr. Methods, 34: 69-71(Apr. 1965). (In French)

A transistorized stabilized high voltage power supply 650–3000 v, 10 mamp is described. The performances of the instrument are as follows: long time drift less than 0.01%, regulation better than 0.003% for ±10% mains voltage variation, temperature stability better than 0.003%/°C, output voltage ripple less than 30 mv rms, internal resistance less than 50Ω, stabilization against load changes within 0.1 sec. (auth)

20358 PHOTOPEAK EFFICIENCIES OF NaI(Tl) CRYSTALS. R. M. Green and R. J. Finn (Australian Atomic Energy Commission, Sutherland, New South Wales). Nucl. Instr. Methods, 34: 72-6(Apr. 1965).

Experimental results of photopeak efficiencies for NaI(Tl) crystals for gamma rays ranging in energy from 0.279 to 1.52 Mev are given. The crystals considered are 8″ dia. × 4″, 5″ dia. × 4″, and 3″ dia. × 3″. The sources are placed on the crystal axis at distances ranging from 5 mm to 60 cm from the crystal face. These results are compared with the results of others. (auth)

20359 THE MOBILITY OF HOT ELECTRONS AND THEIR INFLUENCE ON THE RISE TIME OF THE PULSES OF n-SILICON SEMICONDUCTOR COUNTERS. O. Meyer and H. J. Langmann (Kernforschungszentrum, Karlsruhe, Ger.). Nucl. Instr. Methods, 34: 77-8(Apr. 1965). (In German)

The rise time of the pulses in semiconductor counters excited by alpha particles is calculated and compared with measurements on counters fabricated of high resistance n-silicon. The calculation is effected including the strong dependence of the mobility of charge carriers on the high electric field in a semiconductor counter. The case of overvoltage on a fully depleted counter was taken into account, too. Calculated and measured rise times agreed reasonably well, using a fixed set of constants for all counters. For low electric field strengths of the order of 1000 v/cm the governing time constant is the plasma time. Its value for alpha particles was empirically determined to be 1.9×10^{-2} sec · v²/cm². For an average field strength the rise time is strongly influenced by integration of the pulses by the resistance of the counter base together with the input capacitance of the measuring equipment, provided the depletion layer is not extended up to the back contact. Only in a fully depleted counter the rise time is proportional to the transient time of the charge carriers. This transient time even in a not fully depleted counter will depend on the electric field strength in as much as the mobility itself is field dependent. For field strengths of about 30,000 v/cm the transient time and thus the drift velocity are constant, the mobility therefore is inversely proportional to the field strength. The value determined for this maximum drift velocity v_m for conduction electrons amounts to 7.4×10^6 cm/sec, and for defect electrons to 4.8×10^6 cm/sec. (auth)

20360 STUDIES OF BETA SPECTRA USING A SOLID STATE SPECTROMETER. P. Charoenkwan (Univ. of California, Los Angeles). Nucl. Instr. Methods, 34: 93-9 (Apr. 1965).

The lithium drifted detectors of different depletion depths were used as beta spectrometers studying beta spectra of both allowed and forbidden shapes. Distortions to the beta spectra are mainly due to the backscattering effect of the detectors. Corrections to this effect were performed by using the backscattering coefficient independent of the primary energy and by using a standard source as a reference. This technique gives very satisfactory results in the study of beta spectra of medium energy range. (auth)

20361 HIGH PRESSURE GAS SCINTILLATION COUNTERS. PART II. J. G. Jenkin and R. E. Shamu (Australian National Univ., Canberra). Nucl. Instr. Methods, 34: 116-20(Apr. 1965).

A gas scintillation counter which has a high resolution is described. For a filling of about 30 atm xenon and about 100 atm helium the spread in pulse heights of 14.5-Mev recoil alpha particles was observed to be less than 5%. The linearity of scintillation response to alpha particles was studied for several mixtures of helium and xenon by bombarding the counter with mono-energetic neutrons. For a mixture of 42 atm helium and 8 atm xenon the pulse height of the maximum energy helium recoils was found to be directly proportional to energy for the neutron energy range 1 to 8 Mev, a result consistent with earlier work. However, for mixtures containing 34 atm xenon, the response was observed to be nonlinear for neutron energies less than 4 Mev. The scintillation response of helium–xenon mixtures to electrons and alpha particles was studied as a function of helium pressure. The results suggest that the response of a helium–xenon mixture to a charged particle can depend on the dE/dx of the particle. (auth)

20362 LOW-BACKGROUND PREAMPLIFIER-AMPLIFIER SYSTEM FOR PROPORTIONAL COUNTERS. F. May and F. Semturs (Elektronikinstitut d. Osterr. Studiengesellschaft fur Atomenergie, GmbH Reaktorzentrum, Seibersdorf, Austria). Nucl. Instr. Methods, 34: 121-4(Apr. 1965).

In some experiments only small counting rates of detected particles are available. In those cases there must not be any electrical disturbances which would distort experimental results. Here, a preamplifier-mainamplifier and discriminator counting system is described which counts only 1 or 2 pulses within 24 h generated by electrical disturbances. In this case the discriminator level

is set at 0.2–0.3 mv referring to preamplifier input. The reasons for electrical disturbances are to be found in earth loops, in corona discharges, and punch through effects. The preamplifier was constructed for inelastic scattering experiments with neutrons. Therefore the counting tube is a BF_3 proportional counter for neutron detection. (auth)

20363 EFFICIENCIES OF A COINCIDENCE SPECTROMETER FOR POSITRON ANNIHILATION RADIATION. M. L. Verheijke (Philips' Gloeilampenfabrieken, Eindhoven, Netherlands). Nucl. Instr. Methods, 34: 132-6(Apr. 1965).

The efficiency of a coincidence spectrometer with two NaI(Tl) scintillation crystals in line is considered for the special case of β^+-annihilation radiation. Calculated efficiencies for a set-up of 1¾" dia. × 2", 2" dia. × 2", and 3" dia. × 3" crystals are given. Experiments by means of a ^{64}Cu "point"-source were carried out for the case of 1¾" dia. × 2" crystals and the agreement with the calculated values is good. Further the influence of eccentric positioning and the finite dimensions of the source on the efficiency is considered. (auth)

20364 DETECTOR TIME JITTER IN He^3 AND BF_3 PROPORTIONAL COUNTERS. O. K. Harling (General Electric Co., Richland, Wash.). Nucl. Instr. Methods, 34: 141-5(Apr. 1965). (HW-SA-3366)

The delayed-coincidence technique was used to measure the electronic time jitter for a number of neutron-detecting proportional counters. A selection of BF_3 counters with filling pressures of 1–2 atm and cathode diameters of one and two inches were investigated. Several 1" diameter-^3He counters with fillings of helium and various polyatomic gas additives in pressures up to 12 atm were also studied. Procedures for the use of these results in the design of neutron time-of-flight detectors are discussed. (auth)

20365 THE THIRD-ORDER ABERRATIONS IN A BROAD RANGE SPECTROMETER WITH A UNIFORM-FIELD SECTORIAL MAGNET AND A PRECEDING QUADRUPOLE-MAGNET DOUBLET. K. Yagi (Tokyo Univ.). Nucl. Instr. Methods, 34: 146-54(Apr. 1965).

The third-order aberrations due to a quadrupole-magnet doublet are formulated for the combined spectrometer. These aberrations arise from the third-order terms of the trajectory equations in the quadrupole-magnet doublet. The aberrations are expressed by simple analytic functions. The cross section of the trajectory envelope at the first order focusing point of the spectrometer is calculated numerically. The result shows that these aberrations can be neglected in the spectrometer which was designed to have an energy resolution of 0.1% and a solid angle of 3.0×10^{-3} sr. (auth)

20366 INFLUENCE OF NON-CONSTANT CARRIER MOBILITY ON THE CHARGE TRANSPORT TIME IN SEMICONDUCTOR DETECTORS. K. Falk, P. A. Tove, and M. Madakbas (Uppsala Univ.). Nucl. Instr. Methods, 34: 157-9(Apr. 1965).

The influence of non-constant carrier mobility on the charge transport time in semiconductor detectors was calculated. Two main conditions are considered: non-fully depleted detectors and fully depleted detectors, with applied overvoltage. Approximation formulas for the pulse rise time are given for special cases. It is found that the transport time calculated under the assumption of constant mobility is modified by an appreciable factor, under some conditions, especially when a high voltage is applied to low-resistivity diodes. (auth)

20367 AN IONIZATION CURRENT INTEGRATOR AND ITS APPLICATION TO THE MEASUREMENT OF THE ENERGY DEPENDENCE OF THE CORNELL THICK-WALLED IONIZATION CHAMBER. Th. W. Aitken (Glasgow Univ.). Nucl. Instr. Methods, 34: 160-2(Apr. 1965).

A current integrator circuit, which was developed for use with ionization chambers for monitoring bremsstrahlung beams, is discussed. The ionization chambers used were the standard Cornell thick-walled chamber and the Wilson quantameter. These produce typical currents of 10^{-9} amp, but in many instances the output may be less. The design and performance of the current integrator are outlined. (C.E.S.)

20368 DIRECT RECORDING OF PARTICLE TRACKS OF SPARK CHAMBER ON X-RAY FILMS. R. Kajikawa, K. Kikuchi, F. Makino, A. Masaike, Y. Ohashi, and K. Yokoi (Nagoya Univ., Japan). Nucl. Instr. Methods, 34: 165-6 (Apr. 1965)

Results of a preliminary experiment on the method of direct recording of particle tracks on x-ray films placed on the inner surface of the spark electrode are reported. Spark tracks were recorded on the film directly by photons and electrons in the spark. (C.E.S.)

20369 PRELIMINARY RESULTS ABOUT THE INFORMATION AVAILABLE FROM RISE-TIME OF THE PULSES SUPPLIED BY SEMICONDUCTOR DETECTORS. A. Alberigi Quaranta, M. Martini, G. Ottaviani, and G. Zanarini (Istituto Nazionale di Fisica Nucleare, Bologna and Istituto di Fisica, Bologna). Nucl. Instr. Methods, 34: 167-8(Apr. 1965).

The possibility of obtaining information about the impact angle of ionizing particles on a semiconductor detector by means of a measurement of the pulse rise time is discussed. Experiments were performed with proton beams and the possibility of distinguishing, by a direct measurement of the pulse rise times, protons with different impact angles or protons from other charged particles of the same energy but with different ranges in the detector is confirmed. (C.E.S.)

20370 IMPROVED PULSE SHAPE DISCRIMINATOR. R. Basse, W. Kessel, and G. Majoni (Universitat, Frankfurt am Main). Nucl. Instr. Methods, 34: 169-70(Apr. 1965).

Circuit modifications on a pulse shape discriminator for particle separation and pile-up suppression are described. (C.E.S.)

20371 ON THE ACCURACY OF THE CALIBRATION TECHNIQUES USED WITH SEMICONDUCTORS. F. E. Emery and T. A. Rabson (Rice Univ., Houston, Tex.). Nucl. Instr. Methods, 34: 171-2(Apr. 1965).

A fairly common technique used to calibrate amplifier chains used in semiconductor detector spectroscopy is to use a fast rise time mercury relay pulser. The signal is fed through a series capacitor to the input of the charge sensitive preamplifier. Accurate determinations of the pulse height may be made conveniently if a capacitor is charged for several time constants and then discharged. Two simple multiplicative errors were found in this technique and are discussed. (C.E.S.)

20372 LUMPED DELAY LINE SPARK CHAMBER. G. F. Bertsch (Princeton Univ., N. J.). Nucl. Instr. Methods, 34: 175-6(Apr. 1965). (PPAD-2137-538)

The design and performance of an automatic-recording spark chamber is presented. The principle of operation is to convert the position of the spark into a delay with a lumped-constant electrical delay line. To do this, one of the plates consists of a series of strips; each strip is connected to the delay line. (C.E.S.)

20373 MIXED RADIATION FIELD MEASUREMENT BY MEANS OF IONIZATION CHAMBERS FILLED WITH DIELECTRIC LIQUIDS. M. Ladu, M. Pelliccioni, and M. Roccella (Comitato Nazionale per l'Energia Nucleare, Frascati, Italy). Nucl. Instr. Methods, 34: 178(Apr. 1965).

The previously observed linearity between the ionization current and voltage in a spark chamber for the same kind of ionizing radiation was confirmed, and the possibility is suggested of using spark chambers filled with dielectric liquids in order to measure the intensity of the different components of a mixed radiation field. (C.E.S.)

20374 MEASUREMENT OF ANISOTROPIC FAST-NEUTRON SPECTRUM WITH NUCLEAR EMULSION. Tsutomu Iijima and Shoji Nomoto (Japan Atomic Energy Research Inst., Tokyo). Nucl. Sci. Eng., 22: 102-110(May 1965).

A new method for determining the angular and energy

distributions of an anisotropic fast-neutron flux by using nuclear emulsions based on the proton-recoil method is proposed. The relation between the distributions of neutron flux and proton-recoil tracks is analyzed, and formulas for obtaining the angular distribution and energy spectrum of the neutron flux from the measurement of proton-recoil tracks are derived. Measurements were made to investigate the accuracy of this method with the emulsion plate, which was irradiated inside a natural uranium system. The experimental results show that the measurement of the anisotropic component, which hitherto could not be measured, is possible. (auth)

20375 NEW METHOD FOR MEASUREMENT OF NEUTRON FLUX DENSITY AND NEUTRON DOSE WITH SCINTILLATION COUNTER AND SPHERICAL MODERATOR. D. Nachtigall and F. Rohloff (Kernforschungsanlage, Julich, Ger.). Nukleonik, 6: 330-5(Nov. 1964). (In German)

It was shown that the neutron scintillation measurement head, described by Bramblett, Ewing, and Bonner, with a LiI(Eu) crystal and polyethylene moderator spheres can be used for flux density and dose output measurements. With a 3-sphere combination (2″, 3½″, and 11″ diameter) energy- and direction-independent flux densities can be measured in the region from 0.5 ev to 7 Mev. A 2-sphere combination (2¼″ and 11¾″ diameter) and weight factors approximate the energy-dose curve in the energy range of thermal neutrons up to 7 Mev. With a 3-sphere combination (5″, 7″, and 12″ diameter) and weight factors, the neutron dose output equivalent can be determined completely in the neutron energy range of practical interest in radiation protection. A biological dose curve, that can be calculated with the help of the Bond and Bateman quality factors, can be satisfactorily approximated with a 3-sphere combination (2″, 4″, and 7″ diameter) and weight factors. With other sphere combinations, each future variation of the biological dose curve can be considered by measurement techniques. (tr-auth)

20376 MEASUREMENT OF THE GAS AMPLIFICATION IN METHANE AT LOW PRESSURES WITH A TRANSMISSION PROPORTIONAL COUNTER FOR FISSION PRODUCTS. H. J. Specht and P. Armbruster (Technische Hochschule, Munich). Nukleonik, 7: 8-14(Jan. 1965). (In German)

For the registration of fission products on the mass separator of the FRM, a transmission proportional counter was built. It works in the proportional range with methane at a pressure of 1 torr and a voltage of 500 v; the plateau rise is therefore inmeasurably small. Al-evaporated formvar windows of layer thickness 50 $\mu g/cm^2$ limit the energy loss of fission products passing through to about 6 Mev. The high specific ionization of the fission products makes possible a measurement of the gas amplification of methane in the pressure range $0.3 < p < 10$ torr. The results were compared with various theories; the best agreement is obtained with the formula of Rose and Korff. The remaining deviations were discussed. (tr-auth)

20377 A WHOLE BODY COUNTER EMPLOYING EIGHT UNITS OF PLASTIC SCINTILLATION DETECTORS. 1. γ-RAY PERFORMANCE OF A PLASTIC SCINTILLATION DETECTOR UNIT. Takeshi A. Iinuma, Norimasa Nohara, Eiichi Tanaka, Toshiyuki Hiramoto, and Tomio Ishihara (National Inst. of Radiological Sciences, Chiba, Japan). Radioisotopes (Tokyo), 14: 1-7(Jan. 1965). (In Japanese)

A whole-body counter was built utilizing eight units of plastic scintillation detectors. A detector unit is made of a plastic scintillator (50 cm × 50 cm × 15 cm) and four 5 in. dia photomultipliers which are optically coupled to a surface of the scintillator via light guides. The response of the unit to four kinds of monochromatic γ rays (^{137}Cs, ^{65}Zn, ^{40}K, and ^{208}Tl) in the energy range between 0.662 and 2.62 Mev is described. Each γ spectrum obtained showed an asymmetrical peak having a broad tail on the low energy side. A linear relationship was observed between pulse heights at the peak and the maximum energies of Compton-recoiled electrons at first collision, intersecting the energy axis at about 50 kev. Half-Resolution, that is the relative half-width at half-maximum in the high energy side of the peak, was calculated for the four spectra, and found to be 28.6% for ^{137}Cs, 18.3% for ^{65}Zn, 15.7% for ^{40}K, and 12.1% for ^{208}Tl, respectively. The Half-Resolution was analyzed and it was found that the observed Half-Resolution was reasonable for the present set-up of the detector. Several modifications are suggested in order to extract better performance from the detector. (auth)

20378 A SPARK CHAMBER. V. G. Vlasenko, V. V. Lubyani, V. I. Petran, and A. I. Shpetnii (Khar'kov Inst. of Physics and Tech.). Ukr. Fiz. Zh., 10: 21-6(Jan. 1965). (In Ukrainian)

The spark chamber efficiency at a helium pressure of 760 mm Hg as a function of the voltage and clearing field was determined at various gap lengths. (auth)

20379 EXPERIMENTS ON DISCHARGE BROADENING IN SELF-QUENCHING COUNTING TUBES. H. G. Franke, E. Huster, O. Krafft, and K. H. Rohe (Universitat, Munster, Ger.). Z. Naturforsch., 19a: 1416-19(Dec. 1964). (In German)

The mechanism of the discharge broadening in self-quenching counting tubes was investigated on three types of tubes: lattice counting tubes, counting tubes with various degrees of covering of the cathode, and counting tubes with multiply divided cathodes. The experimental conditions and the results are reported. The results show that the discharge is propagated by the photoeffect in the gas in a zone near the wire in small steps of about 1 mm length and by the photoeffect on the cathode in smaller steps (the wire and mantel components). (J.S.R.)

20380 QUICK COUNTING SCALES FOR NUCLEAR PHYSICS. M. R. Peincenat (C.F. Thomson-Houston, Paris). Paper 1, Session 8, 3p. of "Mesucora 63. Congres International Mesure-Controle Regulation-Automatisme. Tome I." Paris, Mesucora, [1964].

The development and characteristics of a 100 Mc counting prescaler, capable of discriminating between two pulses separated by a time interval of 10 nsec, are described. (J.S.R.)

20381 A NEW SURVEILLANCE MONITOR FOR URANIUM AND PLUTONIUM IN THE ATMOSPHERE. D. Allerden and S. E. Hunt (Associated Electrical Industries Ltd., Manchester, Eng.). Paper 2, Session 8, 5p. of "Mesucora 63. Congres International Mesure-Controle Regulation-Automatisme. Tome I." Paris, Mesucora, [1964].

The design and performance of a monitor for uranium and plutonium in the atmosphere is described. It is capable of rejecting the natural background activity and can discriminate between the U and Pu radiations. It evaluates the true biological hazard even when this comes from a mixture of the two elements in any proportions. The time required to give an alarm is 6 MPC in 10 min or 1.5 MPC in 25 min. (J.S.R.)

20382 A NEW MEASUREMENT DEVICE FOR LOW β ACTIVITIES. Y. Coutarel (Societe Intertechnique, Paris). Paper 3, Session 8, 10p. of "Mesucora 63. Congres International Mesure-Controle Regulation-Automatisme. Tome I." Paris, Mesucora, [1964]. (In French)

The design, characteristics, and performance of a complete radiation detector for low β activities are described. The weight, detectors, measurement chamber, operational safety, and automation of the device are discussed. (J.S.R.)

20383 SOME GENERAL CONSIDERATIONS ON THE METHODS FOR THE MEASUREMENT OF ALPHA AND BETA RADIOACTIVITY. S. Vuccino (Faculte des Sciences, Reims, France). Paper 4, Session 8, 4p. of "Mesucora 63. Congres International Mesure-Controle Regulation-Automatisme. Tome I." Paris, Mesucora, 1964. (In French)

The various factors that must be considered in the measurement of α and β activity are briefly indicated. The design and characteristics of the air pulse chamber, constructed for the relative measurement of very low α activities (of the order of 1/100 μc), are described. (J.S.R.)

20384 THE STANDARDIZATION OF ELECTRON CAPTURE NUCLIDES. R. A. Allen (Atomic Energy Research Establishment, Wantage, Berks, Eng.). Paper 4, Session 8, 4p. of "Mesucora 63. Congres International Mesure-Controle Regulation-Automatisme. Tome I." Paris, Mesucora, [1964].

A method, using 4-π proportional counting, for the measurement of x rays accompanying the processes of electron capture is described for the standardization of electron capture nuclides. (J.S.R.)

20385 ABSOLUTE MEASUREMENT OF THE ACTIVITY OF RADIONUCLIDES BY THE METHOD OF 4-π β-γ COINCIDENCES. CORRECTION OF DECAY SCHEME. Ianca Asavinei, Leon Grigorescu, Cristion Lazarovici, and Mircea Oncescu (Inst. of Atomic Physics, Bucharest). Paper 4, Session 8, 4p. of "Mesucora 63. Congres International Mesure-Controle Regulation-Automatisme. Tome I." Paris, Mesucora, [1964]. (In French)

The explicit calculation of K_ϵ, in the case of radionuclides with decay schemes of the ^{60}Co or ^{24}Na type, was made. The effect of the difference of value between the efficiencies of detection of the two quanta was indicated. The measurement of K_ϵ for gas and liquid scintillator 4-π counting is discussed. (tr-auth)

20386 ABSOLUTE MEASUREMENT OF THE ACTIVITY OF RADIONUCLIDES BY THE BETA-GAMMA COINCIDENCE METHOD. CORRECTIONS OF THE INSTRUMENTAL COINCIDENCES AND THE DEAD TIME. Leon Grigorescu (Inst. of Atomic Physics, Bucharest). Paper 4, Session 8, 10p. of "Mesucora 63. Congres International Mesure-Controle Regulation-Automatisme. Tome I." Paris, Mesucora, 1964. (In French)

A correct demonstration for the formula of instrumental coincidences C_i, including the τ^2 term, is proposed. A simple demonstration for the correction of the dead time of the coincidence way is also given. In the case where the terms of a degree higher than 2 can be neglected, these two demonstrations become very simple. The correct expression of the correct formula, and some errors in the formulas of C_i found in the literature are emphasized. (tr-auth)

20387 METHODS FOR THE MEASUREMENT OF RADIOACTIVITY USED AT THE LABORATORY OF THE AGENCE INTERNATIONALE DE L'ENERGIE ATOMIQUE. A. Sanielevici and H. Houtermans (International Atomic Energy Agency, Vienna). Paper 4, Session 8, 12p. of "Mesucora 63. Congres International Mesure-Controle Regulation-Automatisme. Tome I." Paris, Mesucora, [1964]. (In French)

Practical measurement methods used for the calibration of solutions of radioisotopes distributed by the International Agency of Atomic Energy are reviewed. The methods discussed are 4-π proportional counting, β-γ coincidence counting, extrapolation method, tracer of efficiency method, use of liquid scintillators, and calibration of nuclides with electron capture by x-γ coincidence counting. (J.S.R.)

20388 THE PROPERTIES OF A SECONDARY EMISSION MULTIPLIER WITH INCIDENCE OF ELECTRONS, RARE GAS IONS, AND ATOMS ON THE FIRST DYNODE AND ITS APPLICATION TO SECONDARY EMISSION STUDIES. E. Brinkmann. Thesis, Mainz, Universitat, 1963. 106p. $2.00(Gmelin, AED-DISS. 63-736). (In German)

The properties of an Allen type electron multiplier are investigated. Pulse height spectra and yields for electrons (500 to 2500 ev) and ions, which are incident on the first dynode, are given. Threshold energies for electron emission by rare gas atoms were measured. (Gmelin Inst.)

20389 RADIATION ABSORPTION AND CHARGE SEPARATION IN CRYSTAL COUNTERS AND THEIR OPERATION WITH HIGH FREQUENCY ALTERNATING VOLTAGE. H. de Vries. Thesis, Marburg, Ger., Universitat, 1963, 75p. $2.00(Gmelin, AED-DISS. 63-693). (In German)

The spatial distribution of a track of high electron-hole concentration, as produced by the absorption of heavy charged particles in a crystal counter, was studied. Charge separation by the electrical field and by diffusion is treated in detail. Diffusion is described by a second-order differential equation. Application of high-frequency-operated crystal counters is limited to arrangements with very small electrode distance. (Gmelin Inst.)

20390 THRESHOLD DETECTOR PLACEMENT CONTAINER (Engineering Materials). (Oak Ridge National Lab., Tenn.). 1 drawing. (CAPE-926)

The container described is used with a threshold detector. It consists of a cover plate and a retainer plate, which are fabricated of Al 100. Special locations are provided in a pan 0.5-in deep for the Cd filter, and Au and S samples. A sphere, which is built half way in the cover and retainer plates, holds the ^{10}B threshold detector. (For details, see TID-4100) (M.C.G.)

20391 IRRADIATION DOSIMETERS. (to Landis & Gyr AG). British Patent 975,468. Nov. 18, 1964. Priority date May 19, 1961, Switzerland.

A small portable irradiation dosimeter consists of an ionization chamber that is a flat oblong in a cross-sectional shape and has two electrodes separated by insulation bounding opposite sides of the chamber and two electrically separated capacitors. Each capacitor is connected to a switch, and one capacitor supplies voltage to the chamber while the other serves to integrate the ionization chamber current. One capacitor is connected between the chamber and one of the electrodes, the other capacitor between the other electrode and the casing. A guard electrode maintained at a reference potential (earth potential) is interposed in the insulation to break the continuity between the electrodes. The capacitors may take the form of physically separated capacitors or single capacitors of a double capacitor constructed from conductor surfaces separated by insulating foils. The dosimeter is suitable for use as a pocket meter or as a flat medallion-type meter. It may be read with the aid of an external measuring instrument or by means of a quartz thread electrometer fitted in the dosimeter. (A.G.W.)

20392 IMPROVEMENTS IN OR RELATING TO DEVICES FOR DETECTING RADIO-ACTIVE RADIATION. James Robert Brown (to Electric & Musical Industries Ltd.). British Patent 975,554. Nov. 18, 1964. Filed Mar. 10, 1960.

A device for detecting radiation consists of a lighttight casing including a fluorescent screen sensitive to the radiation and having at least one rectilinear edge, a light-reflecting surface inside the casing and facing the screen, and a photosensitive device. The photosensitive device has a photosensitive target disposed in the casing to receive light from the screen and the reflecting surface. The target is so shaped as to receive light from directions parallel to and perpendicular to the rectilinear edge, and is so located that the response of the photosensitive device to radiation incident near the edges of the screen is substantially the same as the response of the device to radiation incident near the center of the screen. (A.G.W.)

20393 IMPROVEMENTS IN OR RELATING TO DEVICES FOR DETECTING RADIO-ACTIVE RADIATION. James Robert Brown (to Electric & Musical Industries Ltd.). British Patent 975,555. Nov. 18, 1964. Filed Mar. 10, 1960.

A scintillation-type radiation detecting device has fluorescent and light-opaque screens mounted in a manner that ensures light tightness and yet allows them to be removed when required. The casing of the device has a rectangular opening and an inwardly projecting flange to hold a first resilient rectangular ring. On this ring rests the fluorescent screen of a material such as ZnS on a methyl methacrylate support for α radiation or a plastic phosphor having a layer of ZnS for α and β radiation. Adjacent to this and separated from it by another resilient ring rests the light-opaque screen of "Melinex" suitability aluminized. The screens are protected by a grill integral with a rectangular frame that carries another resilient ring and serves to hold the screens in lighttight contact. The grill frame is provided with apertured spring fingers arranged to engage pins projecting from the casing. (A.G.W.)

20394 IMPROVEMENTS IN APPARATUS FOR MEASURING AND RECORDING IONIZING RADIATION. Rolf Maximilian Sievert (to Radiofysiska Institutionen). British Patent 975,956. Nov. 25, 1964. Priority date Apr. 13, 1960, Sweden.

A compact, lightweight apparatus is patented for measuring and recording not only the total quantity of ionizing radiation during a period of time but also the highest intensities of radiation and the times at which they occur. The apparatus consists of an ion chamber with an inner and outer electrode, an electrometer tube, an electromagnet adapted to be energized when the anode current of the electrometer tube attains a predetermined value, and an armature of the electromagnet adapted to actuate marking means upon a moving record carrier operated by the energized electromagnet. The electrometer tube has an anode and a control grid connected permanently to the inner electrode of the ion chamber so that when the charge on the inner electrode attains a predetermined value from an initial potential due to ionizing radiation, the control grid causes the anode current of the electrometer tube to attain a predetermined value. The armature of the electromagnet is adapted to connect the inner electrode of the ion chamber selectively to a higher or lower potential, and the value of the potential determines the quantity of radiation needed to bring the charge on the inner electrode to the predetermined value. (A.G.W.)

20395 DEVICE FOR THE CALIBRATION OF DETECTION INSTRUMENTS FOR RADIOACTIVE RADIATION. Alfred Stebler and Franz Humbel (to Landis and Gyr A.G.). German Patent 1,180,465. Oct. 29, 1964. Priority date July 27, 1960, Switzerland.

A detection instrument comprising a counter tube, a pulse rate meter, and a pulse height discriminator can be calibrated by means of a radioactive preparation, the radiation of which is shut off from the detector by movable shielding, which is brought between the preparation and the tube. The mechanism for moving this shielding is coupled to the discriminator in such a way that the pulse heights of the counter tube are reduced during the calibration. By this reduction of the pulses the more unfavorable conditions of the environment influencing the counter in action are simulated. (Gmelin Inst.).

20396 METHOD OF MEASURING THE DOSAGE RATE OF PARTICLE OR ELECTROMAGNETIC RADIATION. Christian Loeber (to VEB Vakutronik). German Patent 1,186,563. Feb. 4, 1965. Filed Mar. 16, 1961.

The method of measuring the dose rate of particle or electromagnetic radiation is based on the principle of measuring the pulse density at which the measuring device is automatically and continuously calibrated by means of an additional, periodically modulated radiation from an auxiliary preparation. The method comprises the steps of normalizing and integrating the pulses obtained from the detector, of separating that part of the integration voltage that originates from the auxiliary radiation, of comparing it with a given voltage, and of controlling the contribution of the normalized pulses to the integration voltage by means of the difference voltage obtained so that the alternating portion of this voltage remains constant. (Gmelin Inst.)

20397 PORTABLE GAMMA INTENSITY TIME RECORDER. Harry A. Zagorites, Marko I. Lipanovich, and Laurence A. Perrine. U. S. Patent 3,154,686. Oct. 27, 1964. Filed Mar. 6, 1962.

A portable gamma intensity time recorder consists of a plurality of radiation detectors, a hybrid electrometer blocking oscillator associated with each detector, and time-signal generating means, all of which are recorded as separate tracks on a single magnetic tape recorder. The detectors cover different but overlapping ranges and the output from each detector triggers a recycling electrometer. The output pulses are amplified and shaped efficiently by the electrometer-transistor hybrid blocking oscillator with the voltage and power requirements associated with it kept at a strict minimum. The use of zener diodes in the initial biasing arrangement on the electrometer tubes holds the dose accuracy at a maximum, and the unique start-stop circuitry that controls operating power to the entire equipment not only holds down control power requirements but insures start and stop tracking of the entire system. The inherent ruggedness and compactness of the magnetic tape recorder overcomes some of the major limitations of the paper chart system. (A.G.W.)

Radiation Effects

20398 (FZK-214) INDUCED-VOLTAGE STUDIES IN A COBALT-60 GAMMA IRRADIATOR. L. W. Nelms (General Dynamics/Fort Worth, Tex.). Feb. 1965. Contract AF29(601)-6213. 54p. (WL-TR-64-149). CFSTI.

An investigation into the basic mechanism of gamma-radiation induced current and voltage in electrical systems has been started by using the NARF 1500-curie ^{60}Co radiation source. Steady-state measurements of electric potentials induced in a specially constructed hollow cylindrical capacitor as a function of gamma field direction, gamma field strength, and apparatus temperature are described. From these data, it is concluded that the Compton process is the dominant mechanism involved. A theory is developed explaining in detail how electrons from Compton collision might produce currents in a simple insulator-conductor system. The validity of the developed equations was tested by experimentally investigating the dependence of induced current upon gamma field intensity and upon thickness of dielectric interposed between the electrode and the radiation source. It was found that, within the narrow range of gamma field intensity available, the induced current depended linearly upon field intensity as the equation predicted. The tests of the dependence of induced current are not complete, but early data show a trend consistent with results predicted by the equation. (auth)

20399 (NP-14946) ELECTRON TUBES, RADIATION-RESISTANT. PILOT-LINE PRODUCTION. Quarterly Progress Report No. 6, September 1–November 30, 1964. John Grimm (Tung-Sol Electric Inc., Bloomfield, N. J. Electron Tube Div.). Dec. 31, 1964. Contract DA-36-039-AMC-01476(E). 69p.

Fabrication and processing of all four tube types have continued, so that sample tubes may be subjected to the various destructive tests specified. High temperature life testing (500°C bulb temperature) has been concluded on 6080WB Alumino-Silicate tubes, twenty-one now having successfully completed 500 or more hours of operation. Testing of Alumino-Silicate 6360 tubes was discontinued owing to premature life failure of the entire lot. The 1000-hour steady-state nuclear radiation exposure test has been completed on both conventional and Alumino-Silicate tubes of all four types. The irradiated tubes are still too radioactive to test. Thermal Shock and Moisture Resistance tests have been run successfully on representative tubes of all four types, in both conventional and Alumino-Silicate glass. The pulsed radiation exposure test, postponed due to trouble with the associated potted component circuitry, has been revised to provide additional information. New approaches are being attempted in an effort to improve the low yield on 5886 and 6205 types meeting initial electrical characteristics. Both of these tubes are running 85 to 90% shrinkage. Radical departures from the present design are being followed in order to eliminate low emission. (auth)

20400 (NP-14955) NUCLEAR-RESISTANT TRANSMITTER. Final Progress Report. R. Basiago and J. R. Borbas (Thomas A. Edison Research Lab., West Orange, N. J.). Dec. 1960. Contract AF33(600)-40324. 30p.

Nuclear testing programs were carried out to obtain proof of operation of a miniature high temperature pressure transmitter at high temperature and in a relatively intense nuclear radiation environment for future Air Force requirements. The results indicated that the pressure transmitter operation was negligible affected by a nuclear environment. Activation data of the transmitter after irradiation indicated that some further effort should be made to reduce the nickel content of the transmitter so that the decay rate would be faster and thus be less lethal upon re-

moval from the radiation field. It is suspected that the magnetic structure and the diaphragm are the two parts that become most highly activated because of their high nickel content. (P.C.H.)

20401 (ORNL-P-1065) SUMMARY OF EXPERIENCE WITH HIGH-TEMPERATURE THERMOCOUPLES USED IN THE ORNL-GCR PROGRAM FUEL IRRADIATION EXPERIMENTS. N. H. Briggs, E. L. Long, Jr., and F. R. McQuilkin (Oak Ridge National Lab., Tenn.). [1964]. Contract W-7405-eng-26. 22p. (CONF-650204-6). Dep.(mn); $1.00(cy), 1(mn) CFSTI.

From Meeting on Thermocouple Technology and the Effects of Nuclear Radiation on Thermocouples, Washington, D. C.

Experience is reported with 44 high-temperature thermocouples used in about 40 irradiation tests of encapsulated fuel materials. Information is presented on the design of thermocouple assemblies and their compatibility with fuel materials. The thermocouples were classified into six groups with subtypes; the wires were Pt/Pt–Rh, W/Re, or W–Re/W–Re. (D.L.C.)

ISOTOPE TECHNOLOGY

General

20402 (TID-7698(Pt.I)(p.17-30)) ISOTOPIC POWER DATA SHEETS. S. J. Rimshaw, comp. (Oak Ridge National Lab., Tenn.).

Nuclear and physical properties are listed for ^{60}Co, ^{90}Sr, ^{137}Cs glass, ^{144}Ce, ^{147}Pm, ^{242}Cm, and ^{244}Cm. (D.L.C.)

Industrial Applications

Refer also to abstract 20310.

20403 (AD-606253) RECENT APPLICATIONS OF RADIOISOTOPES. Technical Note N-606. Leonard B. Gardner (Naval Civil Engineering Lab., Port Hueneme, Calif.). Aug. 1964. 13p. $1.00(CFSTI).

A summary is presented of applications found during a literature search which are suitable for Naval use. Prime emphasis has been placed on determining those applications suitable for field applications. Secondary consideration is given to research applications. Specifically excluded from this report is the application of radioisotopes to space heating. During the literature search, applications were sought which would reduce costs, improve efficiency and quality control, and open new fields for the Naval Shore Establishment. (auth)

20404 (IA-999) SOME EFFECTS OF Co^{60} GAMMA RAYS ON GREEN AND RIPE SHAMOUTI ORANGES. R. S. Kahan, Y. Aharoni, and S. F. Lattar (Israel Atomic Energy Commission, Yavne. Soreq Nuclear Research Establishment). Oct. 1964. 11p. Dep.(mn).

Green Shamouti oranges irradiated with 21 to 175 krad γ radiation suffered severe skin damage and retardation in ripening. Ripe Shamouti fruit showed no skin damage. There were no textural or other macroscopic changes in the pulp of either green-skinned or ripe oranges. Irradiation caused increased respiration in both green and ripe freshly picked fruit; the increases were much smaller in fruit stored for one month before irradiation. The maximum increase in respiration rate occurred during the first 24 hours after irradiation. Radiation caused increased loss in weight of stored oranges, and this increase depended on the interval between picking and irradiation. Irradiation within 4 to 5 hours of picking caused a weight loss several-fold that occurring after a 24-hour interval. There was almost no weight loss due to irradiation applied one month after picking. (auth)

20405 (MND-3180-1) A RADIOISOTOPE-POWERED UNDERWATER ACOUSTIC BEACON. PHASE I FINAL REPORT. FEASIBILITY STUDY. Marvin P. Norin (Martin Co., Baltimore, Md. Nuclear Div.). Jan. 1965. Contract AT(30-1)-3180. 69p. Dep.(mn); $3.00(cy), 2(mn) CFSTI.

For drawings, see CAPE-1240.

A conceptual study was performed on a radi· sotope-powered underwater acoustic beacon wherein heat of decay is converted to acoustic energy by fluid-. hanical means. A concept was selected which utilized components within state-of-the-art technology. This was followed by the design and fabrication of an electrically heated proof-of-principle model for experimental verification of system feasibility. Component and system laboratory tests were performed. It was found that the concept is feasible and offers a new technique for the use of a radioisotope to power an underwater acoustic beacon. Characteristics of the model system are: signal frequency, approximately 5000 cycles per second; duration of signal, adjustable from about 15 to 30 milliseconds; time between signals, adjustable from about 15 to 45 seconds; range, 20 miles; weight, 1300 pounds; design depth, up to 200 feet. (auth)

20406 (NP-14928) DEVELOPMENT OF READY-TO-EAT RATION-TYPE BEEF ITEMS. Technical Report FD-5. F. L. Kauffman and J. W. Harlan (Swift and Co., Chicago, Ill. Research Labs.). Feb. 1965. Contract DA19-129-QM-1897. 27p.

Beef cooked in barbecue sauce, beef sauce, or mushroom sauce had reduced irradiation flavor compared to untreated controls and had a fair acceptability in consumer tests. Some spices added to beef resulted in a product having a lower overall irradiation flavor, but no space was found that was satisfactory. Protein hydrolysates pumped into the beef before slicing also lowered ultimate irradiation flavor. Beef must be enzyme-inactivated in order to make it shelf-stable. This enzyme inactivation has been done by heating to 77°C and results in a partially cooked product. When it is reheated prior to serving it has a warmed over flavor that is not desirable. To improve this aspect of beef steak quality steak preparation methods were evaluated based on lower temperatures for longer times. It was found that steaks heat-enzyme-inactivated at 65°C and 50% relative humidity for 15 minutes, or at 57°C and 90% relative humidity for 60 minutes, had a better flavor. (auth)

20407 (ORO-626) RADIATION PASTEURIZATION OF SHRIMP AND OYSTERS. Final Summary Report, January-December 1964. Arthur F. Novak (Louisiana State Univ., Baton Rouge. Dept. of Food and Science and Technology). Jan. 15, 1965. Contract AT(40-1)-2951. 29p. Dep.; $2.00 (cy), 1(mn) CFSTI.

Low-dose ^{60}Co γ radiation can be used to extend the storage life of iced raw shrimp from 7 to 14 days and the storage life of iced raw, shucked oysters from 5 to 10 days. Results of numerous field trials of radiation pasteurized shrimp and oysters showed good public acceptance. (C.H.)

20408 RADIATION SOURCES FOR RESEARCH AND INDUSTRY. F. Muenzel (Internationale Forschungsgesellschaft, Schwerzenbach, Switzerland). Chimia (Aarau), 19: 4-11(Jan. 15, 1965). (In German)

The characteristics and examples of reactors, isotopes, and accelerators used as radiation sources are discussed. The possibilities of the installation and use of isotope radiation sources and accelerators are compared. In conclusion the economics of irradiation are considered. (J.S.R.)

20409 APPLICATION OF HIGH-ENERGY RADIATION TO CHEMICAL PRODUCTION. J. Hoigne (Eidgenossische Technische Hochschule, Zurich). Chimia (Aarau), 19: 18-21(Jan. 15, 1965). (In German)

Methods of the selective radiochemical production of specific compounds are summarized and compared with photochemical and catalytic methods. The production costs are also considered. (J.S.R.)

20410 CONSERVATION OF FOODS AND STERILIZATION OF MEDICAL AND PHARMACEUTICAL PRODUCTS. H. Mohler (Universitat, Basel). Chimia (Aarau), 19: 21-34 (Jan. 15, 1965). (In German)

The causes of food spoilage and the preventive effects of sterilization and pasteurization are reviewed. The use of γ and electron irradiation and their effects are discussed. Food irradiation methods with high, medium, and low doses are reviewed. The sterilization of medical and pharmaceutical products is discussed. The concept of wholesomeness in an evaluation of the effectiveness of irradiation sterilization is defined. (J.S.R.)

20411 RADIOISOTOPES AND RADIATIONS IN THE TEXTILE INDUSTRY. George Propstl. Euratom Bull., 4: No. 1, 24-9(Mar. 1965).

The Euratom program for the promotion of the use of techniques involving radiations and radioisotopes by the textile industry is discussed. (D.C.W.)

20412 TRANSMISSION TYPE RADIOACTIVE MEASURING DEVICES. T. Vashchinu. Genshiryoku Kogyo, 9: No. 4, 49-54(1963). (In Japanese)

A review of the theoretical data and construction of transmission type radioactive measuring devices (level gauges and densitometers) is presented. The standard deviations caused by statistical variations at the entrance of detector output pulses into the counter are analyzed. The ratio of the minimum count rate was calculated with the accuracy order of 99.7%, and the relation between the penetration coefficient and the maximum count rate was found. The length of γ ray paths through a liquid was measured by an inclined level gauge. Densities measured using ^{137}Cs and ^{60}Co sources are discussed. (R.V.J.)

20413 FACTORS AFFECTING THE STORAGE TIME AND QUALITY OF FRESH FRUIT, BERRIES, AND VEGETABLES TREATED WITH GAMMA RAYS. L. P. Koval'skaya. Konserun. i Ovshchesushil'n. Prom., 18: No. 10, 22-6(1963). (In Russian)

The use of ionizing radiation for increasing the storage life of fresh fruit, berries, and vegetables is discussed. Various species of yeast and mold fungi causing decay, lethal doses of γ radiation required for prevention or retardation of microbiological decay, and effects of specific radiation doses on various types of fruit and berries were examined. An evaluation of research data and a comparison of graphs showing the storage life dependence of the applied radiation on specific types of fruit and berries indicated that various fungi require various radiation treatments and the radiation treatment has not only a preventive effect but in contrast under specific circumstances it reduced the natural immunity of fruits against recurrent fungi infestation. The most suitable doses are considered to be 100 to 600×10^3 rad because lower radiation doses do not suppress the development of microorganisms and may even aggrevate the storage conditions. Higher doses cause unsatisfactory changes in the organoleptic properties of fresh berries and vegetables. Data are given on the applied radiation and storage time for tests made on strawberries, cherries, peaches, apricots, tomatoes, apples, tangerines, and grapes. (OID)

20414 THE EFFECT OF γ-RADIATION ON RAW HIDES AND LEATHER. G. Pastuska, R. Hoehn, and R. Krueger. Leder, 15: 212-16(Sept. 1964). (In German)

Air-dried South American sheepskins (8% H_2O) were cut longitudinally. Half of the hides were exposed to ^{60}C γ radiation, and the other half of the hides were not irradiated. Then both sample groups were chrome-tanned. The radiation dose was 0.1 Mr/hr; the total doses received were 0.01, 0.05, 0.1, 0.5, 1.0, 5.0, 10, 50, and 100 Mr. Visibly, the irradiated samples could not be distinguished from the unirradiated ones except that the samples that received 100 Mr became brittle, yellowish-colored, and lost the hair cover. At extremely low radiation doses, the tensile strength increased with the ratio of doses received, reached a maximum at 0.05 Mr, and decreased slowly up to 0.5 Mr and then rapidly at 5 Mr. Doses (1 to 4 Mr) needed to destroy the bacteria appeared feasible for sterilizing the hides to prevent spreading disease and at the same time maintaining the usefulness of the tanned hides. Leather impregnated with dimethylsilicone was used to determine whether low dose ionizing radiation improved the leather quality by initiating intramolecular lacing. The impregnated samples were exposed to 1, 5, 10, and 50 Mr; one sample was not irradiated. The tensile strength of silicone-impregnated samples increased with the total radiation dose received between 1 and 10 Mr. The water permeability of impregnated leather remained the same up to 10 Mr; unimpregnated leather became increasingly permeable with increasing doses. (OID)

20415 REVOLUTION IN POWER GENERATION. G. E. Hare (Atomic Energy Research Establishment, Harwell, Berks, Eng.). Mod. Power Eng., 59: 62-3(Jan. 1965).

The economics of power generation by radioisotopes is discussed. It is felt that the most likely commercial application is in the communications field, where reliable power sources are needed in remote locations. (P.C.H.)

20416 THE INDUSTRIAL APPLICATIONS OF RADIOACTIVE ISOTOPES IN THE FUTURE OF AUTOMATION. S. Margolinas (S.A.I.P., Paris). Paper 5, Session 13, 6p. of "Mesucora 63. Congres International Mesure-Controle Regulation-Automatisme. Tome II." Paris, Mesucora, [1964]. (In French)

The industrial applications of radioactive isotopes in automation are reviewed with consideration to the types of radiation, the operations performed, and the economic aspects. (J.S.R.)

20417 LES APPLICATIONS INDUSTRIELLES DES RADIOELEMENTS. (Industrial Applications of Radioelements). A. Blondel, R. Colas, R. Cornuet, et al. Paris, Editions Eyrolles and Editions Gauthier-Villars, 1962. 352p.

The industrial uses of radioisotopes are summarized to give a broad outline of the specific applications that radiation finds in various industries. The methods used for the detection of radiation, characteristics of intense radiation sources, activation analysis, autoradiography, gammagraphy, and thickness gages are general topics considered, and techniques used in many industries are also discussed. The applications of radiations to treatments of high polymers and for the study of industrial metallurgical processes are discussed. The utilization of radioelements in the chemical, cement, petroleum, glass, textile, and coal mining industries is described. The uses of radioisotopes in the study of waters and shielding are considered. Radiation protection and legal aspects in their use are discussed. (J.S.R.)

20418 RADIOIZOTOPNYE METODY ISSLEDOVANIYA VNUTRIKOTLOVYKH PROTSESSOV. (Radioisotopic Methods for Investigation of Processes Inside Boilers). M. I. Reznikov and Z. L. Miropol'skii. Moscow and Leningrad, Izdatel'stvo "Energiya," 1964. 215p.

In order to ensure the reliable operation of the high-power steam generators used in modern power stations and to maintain the required high purity of the produced steam, the hydrodynamic, thermal, and physicochemical processes occurring inside boilers must be closely examined. Use of the radioactive isotope methods made it possible to broaden the range of the measurement of moisture carried by the steam and of the materials dissolved in the liquid and vapor phases; very small amounts could thus be determined conveniently. Nuclear engineering design requires exact knowledge of the true vapor content and radioactive methods were found satisfactory for obtaining the needed data. The basic principles involved in the phase concentration within the boundary layer of boiling liquids were clarified by using narrow β or γ beams. Composition of water–steam mixtures and the location of the liquid level could also be successfully determined by using isotopes. The experiments are discussed. The basic principles of radioactivity, methods for detecting and recording it, unclear measurements, determination of the true steam content, level determinations, radioactivity methods for controlling the purity of the steam and feed water, radiometric apparatus, shielding, and auxiliary equipment are discussed. Instructions are given for carrying out the experiments under safe conditions. (TTT)

20419 SEDIMENT DENSITY METER (Engineering Materials). (Lane-Wells Co., Houston, Tex.). 214 drawings. (CAPE-1176)

A sediment density meter was developed for in situ measurement of ocean-bottom materials ranging from ~1.0 to ~2.0 g/cm^3. The measurement is based on scattering of gamma rays from a radiation source contained in the device, which is lowered on a cable into unconsolidated sediments. A ^{137}Cs source, with a strength of 100 mC, is screwed into the end of the traveling shield. The gamma intensity is measured by a detector assembly consisting of 30 G-M tubes, a high-voltage power supply, pulse discriminator module, pulse shaper module, and two stages of binary division. Data is photographically recorded by a camera in the instrument while the sensing probe is moved stepwise upward from solid bottom through a range of 11 ft of sediments. A picture is taken of the target data at

each of the measuring stations at 2 ft increments of travel in an upward direction. The device is ~26 ft long and is powered by self-contained batteries. (For details see TID-4100) (M.C.G.)

20420 PRINCIPLES OF MICROBIOLOGICAL SAFETY AND STABILITY OF RADIATION STERILIZED FOODS. Hamed M. El-Bisi (Army Natick Labs., Mass.). 17p. (CONF-640909-6)

From International Conference on Radiation Preservation of Foods, Boston.

Applications of ionizing radiation in food processing are compared with thermoprocessing procedures. Terms and standards used by the food processing industry are defined. It is pointed out that x or γ radiation may be used to extend the shelf-life of perishable foods by reduction of the dominant spoilage microflora, to free the food from major microbial pathogenic agents, or a combination of these two objectives for the indefinite preservation of food under common ambient conditions. Minimal radiation dose requirements and principles underlying the safety and stability of radiation processed foods are discussed. (C.H.)

20421 PACKAGING ASPECTS OF RADIATION PRESERVATION OF FOODS. George O. Payne, Jr. and Charles J. Spiegl. 16p. (CONF-640909-3)

From International Conference on Radiation Preservation of Foods, Boston.

The packaging requirements for food irradiated at 4 to 6 megarad levels are reviewed and results are reviewed for studies on metal containers with interior finish. Results are reported from studies on the development of flexible laminate packages for long-term storage of irradiated foods without refrigération. Emphasis was placed on determinations of the nature and amount of extractives released into foods from flexible packaging materials subjected to 6 megarad doses of ionizing radiation. The nature and concentration of extractives were determined for 6 widely used commercially available contacting films. Results showed that no significant change in extractability was induced by irradiation of these polymeric materials. Polyester, polyamide, and polyolefin flexible laminate pouches were developed for use as single-service packaging for chicken, ham, and bacon during radiation processing and storage. (C.H.)

20422 ELECTRON ACCELERATORS FOR FOOD PROCESSING. H. W. Koch and E. H. Eisenhower (National Bureau of Standards, Washington, D. C.). 59p. (CONF-640909-9)

From International Conference on Radiation Preservation of Foods, Boston.

Developments in the radiation processing of foods are reviewed. The characteristics of intense electron beams and their sources are discussed. Advantages to be gained from the use of electron accelerators as radiation sources for commercial food irradiation facilities are pointed out. Cost figures are presented that indicate the cost of complete sterilization would be about 10 cents/lb, while surface pasteurization would cost about 0.05 cents/lb using electrons. Presently available electron accelerators that could be used to sterilize food products up to several feet thick at a plant capacity of up to 2 tons/hr are reviewed and plans for future developments are discussed. (20 references.) (C.H.)

20423 WHOLESOMENESS CONSIDERATIONS IN THE RADIATION PRESERVATION OF FOODS. H. F. Kraybill (Public Health Service, Washington, D. C.). 14p. (CONF-640909-8)

From International Conference on Radiation Preservation of Foods, Boston.

Comprehensive biomedical studies during the last fifteen years have failed to demonstrate that radiation processed foods are less safe for human consumption than conventional heat processed foods. Some precautionary procedures must be observed with respect to microbiological safety in order to insure that no bacterial toxins prevail either through inadequate processing at radiation sterilization dose or through maintenance of temperature control at low dose radiation pasteurization. Nutrient alteration in radiation processed foods does not, in general, differ from that of thermal processed foods or are there any significant biological responses which may be considered adverse to man. Under the conventional toxicological and biological methodology employed, investigations on several test animal species have failed to show any toxic, mutagenic, or carcinogenic activity from feeding a series of individual irradiated foods in conjunction with a synthetic ration or a composite of irradiated foods as the complete diet. The potential presence of peroxides and epoxides found in highly processed foods and food components has been postulated. From theoretical considerations, confirmation as to their absence and proof of their non mutagenic or carcinogenic potential would require further biological assessment employing the most sophisticated methodological approaches of subliminal or subthreshold toxicology. The synergistic role of these types of compounds at the levels potentially present in irradiated foods has not been explored in terms of other contaminants known to be present in foods under certain conditions. These possibilities present intriguing prospects for future research. (auth)

20424 SPROUT INHIBITION OF VEGETABLES USING GAMMA RADIATION. K. F. MacQueen (Atomic Energy of Canada Ltd., Ottawa). 23p. (CONF-640909-1)

From International Conference on Radiation Preservation of Foods, Boston.

Results are summarized from an eight-year study on the use of gamma radiation to inhibit sprouting in potatoes, onions, and carrots. Preliminary experiments were undertaken to determine optimum dose levels and their effects on product quality. These were followed by pilot plant feasibility studies in which a mobile irradiator was employed, and commercial irradiation by private industry. Some details of the food irradiation facility are described. (C.H.)

20425 RADIATION PRESERVATION OF FRESH MEAT AND POULTRY. Walter M. Urbain (Swift & Co., Chicago). 20p. (CONF-640909-4)

From International Conference on Radiation Preservation of Foods, Boston.

Results are reviewed from a number of studies on the radiation processing of fresh meat and poultry. It was concluded that the principal problem with sterilized meat is the flavor change induced by irradiation. This is not serious for pork and chicken irradiated at 4.5 megarad but this radiation level makes beef unacceptable. Irradiation at liquid nitrogen temperatures (approximately –196°C) prevents the development of flavor changes in beef. Data are included on the cause and reduction of flavor, color, odor, and texture changes induced by irradiation of meats, the radiosensitivity of bacteria causing spoilage of meats, and cost estimates for irradiation facilities for commercial radiation processing of meats. (C.H.)

Power Application

20426 (TID-7698(Pt.I)) [CONFERENCE ON ISOTOPIC POWER DEVELOPMENT, GERMANTOWN, MARYLAND, JUNE 1964]. (Division of Isotopes Development (AEC), Washington, D. C.). 284p. Dep.; $6.00(cy), 5(mn) CFSTI.

Six papers are presented on the following subjects: fission products for use as heat sources, property data on isotopes as power sources, nuclear safety in space, shielding of isotopic power sources, SNAP 9A and 19, and radioisotope propulsion in space. Separate abstracts were prepared for all six papers. (D.L.C.)

For abstracts of individual papers see: 20206, 20402, 20427, 20428, 20431, and 21595.

20427 (TID-7698(Pt.I)(p.249-56)) SNAPS 9A AND 19. Charles R. Fink and Jerome G. Morse (Martin Co., Baltimore, Md. Nuclear Div.).

SNAP 9A is reviewed from launch approval to the present. SNAP 19 is reviewed with respect to the design and test program planned for it. (auth)

20428 (TID-7698(Pt.I)(p.257-76)) RADIOISOTOPE SPACE PROPULSION SYSTEMS. John S. Martinez (TRW Space Technology Labs., Thompson Ramo Wooldridge Inc., Redondo Beach, Calif.).

Some of the potential non-electric-power-producing radioisotope applications in space are outlined. A detailed discussion is given on the direct-cycle radioisotope propulsion system. Thrusters heated by α-, β-, and γ-emitters are considered; the α- and β-heated thrusters are called POODLE. The major advantage of POODLE is its high specific impulse. Several versions of the POODLE thruster are described, and control of internal temperatures are discussed. The mission applications and payload capabilities of POODLE are discussed, and the possible cost savings through the use of POODLE in upper stages are estimated. (D.L.C.)

Separation and Production

See also CHEMISTRY — Separation Processes and Procedures.

Refer also to abstract 19865.

20429 (MLM-1214) AN EVALUATION OF THE PHOTOCHEMICAL METHOD OF SEPARATING MERCURY ISOTOPES. D. L. Coffey and F. X. Haas (Mound Lab., Miamisburg, Ohio). Dec. 11, 1964. Contract AT-33-1-GEN-53. 11p. Dep.; $1.00(cy), 1(mn) CFSTI.

A source lamp containing mercury of natural isotopic abundance was used to determine the order of magnitude of the production rate for mercury isotopes in a study of the feasibility of photochemically separating isotopes. The maximum production rate achieved from the reaction of photoexcited mercury with water vapor was 53 micrograms of reacted mercury per hour. Modifications to the apparatus and procedures could be expected to increase this rate to approximately 75 micrograms per hour. This rate probably would be reduced to approximately 35 to 40 micrograms per hour under conditions which give high isotope separation factors. The factors influencing production rate are discussed, together with a production rate anomaly which appears to be associated with the transition from laminar to turbulent flow. (auth)

20430 (P-1231(RAND)) A LINEAR PROGRAMMING MODEL OF THE GASEOUS-DIFFUSION ISOTOPE-SEPARATION PROCESS. Donald Fort (RAND Corp., Santa Monica, Calif.). Dec. 12, 1957. 26p. (AD-606605). $2.00 (CFSTI).

A linear programming model of the gaseous diffusion process for separating uranium isotopes is developed using the theoretical or engineering approach. A brief description is given of the physical separation process. It is shown how the physical relationships may be translated into linear programming terms. The application of the model in larger models of the nuclear materials and power industry is considered. (D.L.C.)

20431 (TID-7698(Pt.I)(p.1-16)) THE FISSION PRODUCTS. C. A. Rohrmann (Hanford Atomic Products Operation, Richland, Wash.).

Of the 12 or 14 radioisotopes which have potential as heat sources, four are fission products (^{90}Sr, ^{137}Cs, ^{144}Ce, and ^{147}Pm). The properties of these radioisotopes and fission products are tabulated. The Hanford Waste Management Program is described briefly. The cost results of the engineering study for the Hanford Isotope Plant are discussed. The separation of isotopes from irradiated power reactor fuels is considered. (D.L.C.)

20432 (ORNL-tr-295) PRODUCTION OF RADIOACTIVE ISOTOPES IN SPAIN. G. Dominguez, F. de la Cruz, and M. del Val (Junta de Energia Nuclear, Madrid (Spain)). Translated by A. L. Monks (Oak Ridge National Lab., Tenn.), Apr. 1964. 32p. Dep.(mn); $3.60(fs), $1.16(mf) JCL.

Methods used in Spain for the production of ^{32}P, ^{35}S, ^{51}Cr, ^{58}Co, ^{131}I, and colloidal and granular ^{198}Au are described. Irradiation conditions, chemical treatment, analysis, and product uses are discussed individually for each of these isotopes. (D.L.C.)

20433 THE SEPARATION FACTORS OF NITROGEN ISOTOPES WITH ION EXCHANGERS AND THE ESTIMATION OF ISOTOPIC DIFFERENCE OF DISSOCIATION CONSTANTS OF AMMONIA. Terunosuke Nomura (Sophia Univ., [Tokyo]) and Hidetake Kakihana. Bull. Tokyo Inst. Technol., No. 61, 51-8(1964).

The separation factors of nitrogen isotopes, $^{15}S_{14}$ (N), for 0.1M NH_3 and NH_4Cl in acetone-water (ethanol-water) mixtures were determined with differently crosslinked sulfonated polystyrene-divinylbenzene copolymers and a synthetic inorganic ion exchanger. The values for $^{15}S_{14}$ (N) for NH_3 systems were between 1.023 and 1.036. The highest values, 1.036 and 1.033, were obtained for 40% acetone with 55% DVB (divinylbenzene) exchanger and 80% acetone with inorganic exchanger, respectively. The values for $^{15}S_{14}$ (N) for NH_4Cl systems were between 0.999 and 1.008. It was indicated that the isotopic differences of dissociation constants for ammonia (or the equilibrium constant for the isotopic exchange reaction between NH_3 and NH_4^+ ion), $^{15}_{14}K_{NH_3}$, in ethanol (or acetone)-water mixed solvent is not significantly different from 1.027, the value obtained for the aqueous solution. (auth)

20434 SEPARATION OF ISOTOPE GAS MIXTURE IN A SUPERSONIC JET. Hisashi Mikami and Yooichi Takashima. Bull. Tokyo Inst. Technol., No. 61, 67-89(1964).

The separation effect of nozzle process was calculated theoretically on the basis of the assumptions that the flow of gas from a nozzle outlet can be regarded as a continuum flow, and pressure diffusion causes separation. An approximate expression is presented, which gives the separation effect in the form of a function of the cut and Mach number. It was necessary to solve the equation of motion for a supersonic jet before calculation were made of the separation effect, and the equation of motion in the modified hodograph plane was solved with the aid of an analog computer. The results of calculation, which give the relation between the separation effect and the cut with Mach number as a parameter, show characteristics of the process. In the case of infinite Mach number, the maximum separation effect available by the process was obtained. (auth)

20435 SEPARATION AND ANALYSIS OF VARIOUS FORMS OF HYDROGEN BY ADSORPTION AND GAS CHROMATOGRAPHY. Sayeed Akhtar and Hilton A. Smith (Univ. of Tennessee, Knoxville). Chem. Rev., 64: 261-76(1964). (TID-20261)

The separation of the isotopes of hydrogen, their spin isomers, and their interisotopic molecular forms is discussed. Methods of detecting the spin isomers and isotopes are described. These include: thermal conductivity, mass spectroscopy, and radioactivity. Absorption and chromatography used to separate the isotopes and spin isomers are described and experimental developments reviewed. (M.C.G.)

20436 THE MANUFACTURE OF OPEN RADIOACTIVE PREPARATIONS IN EAST GERMANY. P. Knoll. Tehnika (Belgrade), 19: 221-3(Feb. 1964). (In Serbo-Croatian)

A brief history is presented on the production of open radioactive preparations in the German Democratic Republic in the Rossendorf Reactor since the reactor became critical in Dec. 1957. Ethyl bromide-^{80m}Br was produced in Nov. 1958, and in 1959, the radioisotopes, ^{82}Br, ^{24}Na, ^{124}Sb, and ^{115}Cd, were prepared. Buildings for storage of radioisotopes; laboratories for manufacturing high-energy γ emitters, gammagraphy, handling "hot" material, producing ^{14}C and ^{35}S and preparing compounds labeled with these radioisotopes, producing ^{131}I and its compounds, dosage and absolute activity measurements, are described, and several analytical and accessory laboratories are described. In 1961, several isotopes (^{110m}Ag, ^{65}Zn, and ^{60}Co) were produced by the (n,γ) reaction. Present practices used in the production of radioisotopes in a water-cooled reactor with a neutron flux of 2×10^{13} n/cm^2/sec are dis-

cussed. The radiation techniques and the processing of the irradiated targets and isolation of radioisotopes are described. A statistical survey is given of the production activity from 1958 to 1963 with data on the activities of each radioisotope produced and the shipments made in each year. (auth)

20437 SOURCE FABRICATION EQUIPMENT (Engineering Materials). (Oak Ridge National Lab., Tenn.). 8 drawings. (CAPE-1175)

The equipment described is used in preparing ^{90}Sr and ^{144}Ce sources. It includes a precipitate filter, dies, and presses for ^{90}Sr. Also included are a V-band clamp and filter alterations necessary to handle ^{144}Ce sources. The ^{90}Sr filter is a ceramic thimble 110 mm in dia, 300 mm long, with a 3 mm thick wall. It is housed in a pot 12.625 in. high with walls 0.1875-in. thick. The OD of the flange is 8.125 in, and the OD of the pot is 7 in. The filter housing used for ^{144}Ce is 9.625 in. OD at the flange and is constructed of stainless steel. The stainless steel V band clamp has a radius of 4.906 in. The clamp is 1.375 in. × 1 in. (For details, see TID-4100). (M.C.G.)

MATHEMATICS AND COMPUTERS

Refer also to abstracts 19692, 21078, and 21228.

20438 (ANL-7016) PROGRAM CATALOG WITH PERMUTED DESCRIPTION INDEX FOR CDC CO-OP COMPUTERS. N. J. Purcell (Argonne National Lab., Ill.). Mar. 1965. Contract W-31-109-eng-38. 92p. Dep.; $3.00(cy), 3(mn) CFSTI.

A catalog of current program descriptions for Control Data Corporation large scale computers is presented. Each source entry represents one line of printed matter and is permuted in an end-around fashion so that one line of printing results for each significant word in the entry (the classification code and installation field are excluded from this permutation and remain fixed). The result is that a program may be recovered by knowing only one nontrivial word from the description field or one of the other fields. The source entry is divided into eight subfields: title, machine, language, material available, system, date, description, classification code and installation. Program abstracts are also included. (C.E.S.)

20439 (COO-614-31) ICR QUARTERLY REPORT NUMBER 4, FEBRUARY 1, 1965. Nicholas Metropolis (Chicago Univ., Ill. Inst. for Computer Research). Contract AT(11-1)-614. 89p. Dep.(mn); $3.00(cy), 2(mn) CFSTI.

The Maniac III computer was operated in cyclotron on-line experiments around the clock for an extended period. Modifications of the Algol compiler are reported along with certification of algorithm TREESORT 3 by its use in sorting randomly ordered lists. Information is included on methods for the solution of linear equations with unbounded operators. Investigations of the positional correlations of nearby stars are described, and an estimate of systematic errors in the Hiltner-Williams-Dennison tracing isophotometer for nebular isophotes is presented. An analysis of a quadded logic system is included in which the ability of this system to correct single errors occurring in any logical unit is discussed. (J.R.D.)

20440 (EUR-2251.i) LEGGE DI DISTRIBUZIONE DEL PRODOTTO DI VARIABILI CASUALI SECONDO UNA NUOVA LEGGE DI COMPOSIZIONE. (Distribution Law of the Product of Random Variables According to a New Composition Law). F. Brambilla (Universita Commerciale Luigi Bocconi, Milan). 1965. 8p. Dep.(mn).

Certain characters may be measured considering many elementary measures composed by the law $\lambda(^2) = (\lambda_1\lambda_2/\lambda_1\lambda_2 + (1-\lambda_1)(1-\lambda_2))$ where λ_1 and λ_2 are two elementary measures. A particular distribution function for λ_1 and the statistical properties of $\lambda(^2)$ are studied. (auth)

20441 (JINR-P-1958) SVEDENIE MINIMIZATSII KVADRATICHNOGO FUNKTSIONALA S USLOVIYAMI SVYAZI S DOPOLNITELNYM KVADRATICHNYM CHLENOM. (A Reduction of Minimization of the Quadratic Functional with the Coupling Conditions to Minimization of the Functional with an Additional Quadratic Term). V. I. Moroz (Joint Inst. for Nuclear Research, Dubna (USSR). Lab. of High Energy). 1965. 9p. Dep.(mn).

If P'C belongs to a geometric place of points (GPP) given by a system of linearized equations $f_k(\ldots, p_i, \ldots) = 0 (i = 1, \ldots, n; k = 1, \ldots, k; n > k)$ and such that $\chi^2_{min} = \Sigma[(P_i - P_i')^2/(\Delta P_i)^2] = \min_{GPP} \Sigma[(P_i - P_i)^2/(\Delta P_i)^2]$, $\chi^2_{min} = [A^2_{(T)} + T\Sigma\{f_k^2/(\Delta f_k)^2\}] \to 0$ like $1/T^2$ when $T \to \infty$, $[P_i' - P_{i(T)}] = \delta P' \to P_i$ like $1/T$ when $T \to \infty$, where the following designations are made $A^2_{(\ldots,P_i,\ldots)} = \Sigma[(P_i - P_i)^2/(\Delta P_i)^2] + T\Sigma\{f_k^2/(\Delta f_k)^2\}$; $A^2_{(T)} = \min A^2_{(\ldots,P_i\ldots)} = \Delta^2_{(\ldots,P_i(T))}$.

It is suggested to use this method for the identification of the reaction channel. (auth)

20442 (NAA-SR-Memo-9729) HARMONIC ANALYSIS FOURIER SERIES CURVE FIT. Elizabeth Lee Bramblett (Atomics International, Canoga Park, Calif.). Mar. 1964. Contract AT-11-1-GEN-8. 22p. Dep.(mn); $1.00(cy), 1(mn) CFSTI.

A program is described that calculates the Euler coefficients of the Fourier series of a discretely defined function. In addition, a curve fit using these coefficients is calculated. A subroutine is also described that performs the coefficient calculation. (auth)

20443 (UCRL-12256) OCTOPUS/6600 USERS' MANUAL. R. P. Abbott (Lawrence Radiation Lab., Univ. of California, Livermore). Jan. 1965. Contract W-7405-eng-48. 64p. Dep.(mn); $3.00(cy), 2(mn) CFSTI.

Instructions are presented for the use of OCTOPUS/6600, which is a programming system for time-shared remote-console use of the CDC 6600. A brief description of the programming system and its current state is also included. (C.E.S.)

20444 (UCRL-12293-T) PARALLELISM IN COMPUTING SYSTEMS. S. Fernbach and Joseph E. Wirsching (Lawrence Radiation Lab., Univ. of California, Livermore). [1964]. Contract W-7405-eng-48. 16p. (CONF-650213-1). Dep.(mn); $1.00(cy), 1(mn) CFSTI.

From IEEE Sixth Winter Convention on Military Electronics, Los Angeles.

An outline is given of several attempted techniques for increasing computer speed and efficiency by means of parallelism. The successes and shortcomings of these techniques are discussed. Proposals for highly parallelized computing systems are described. (T.F.H.)

20445 ON THE NUMERICAL SOLUTION OF ONE CLASS OF NONLINEAR INTEGRAL EQUATIONS OF THE DISPERSION TYPE. I. Nedyalkov and G. Penchev. Izv. Fiz. Inst. s Aneb, Bulgar. Akad. Nauk., 12: 143-51(1964).

The shortcomings of the N/D method and of the Chew-Low-Salzman method for the numerical solution of singular nonlinear integral equations of the Low type, utilizing the preliminary regularization of those equations, are analyzed. The method is presented for the direct numerical solution (without preliminary regularization) of one particular class of Low-type integral equations—the Chew-Low equation, which describes the P-wave resulting from the pion-nucleon interaction under the assumption that the nucleon is fixed. By utilizing certain substitutions of variables, the Chew-Low equation is transformed to a form for which solutions are derived by the method of successive approximations. Measures for eliminating the instability from the iterative process are indicated. It is explained how the proposed method can be used to obtain adiabatic and resonance solutions of the Chew-Low equation. It is shown that the adiabatic solution ceases to be analytic when the coupling constant $f^2 = 0.07$. Some numerical results are presented. (ATD)

20446 ON A CLASS OF K-p,d AND NON-K-p,d OPERATORS AND OPERATOR EQUATIONS. W. V. Petryshyn (New York Univ., New York). J. Math. Anal. Appl., 10: 1-24(Feb. 1965).

Solvable extensions are developed for a large class of nonsymmetric linear and unbounded operators in a complex or real Hilbert space, and are applied to the investigation of the convergence and the error estimates of certain iterative and direct methods and to the theory of the H_0-bounded operators. (L.B.S.)

20447 SOME OBSERVATIONS ON SYSTEMS FOR AUTOMATIC ACQUISITION AND REDUCTION OF NUCLEAR DATA AND A PRELIMINARY REPORT ON THE COMPUTER SYSTEM TRASK. S. Hultberg (Research Inst. for Physics, Stockholm). Nucl. Instr. Methods, 34: 125-31(Apr. 1965).

Along with the more usual equipment used for the collection and reduction of nuclear data, small digital computers are rapidly gaining in importance as extremely versatile tools in nuclear physics experimentation. To help in making

the physicist become more familiar with computer concepts in relation to standard fixed-program machines and tape recorders (which may be used to great advantage together with computers), some computer features are discussed. A new transistorized computer TRASK, using a 24K 40-bit word memory (5 μs cycle) and floating point arithmetics (K = 1024) is described. TRASK will also be used as a two-dimensional analyzer, organizing the memory as a 48K 20-bit word store where each word represents one channel. TRASK will be installed at the Research Institute for Physics and is scheduled to be operating in May 1965. (auth)

20448 AN INVARIANT DERIVATION OF SU(6) SYMMETRY. Y. Ne'eman (California Inst. of Tech., Pasadena). Phys. Letters, 14: 327-9(Feb. 15, 1965).

SU(6) symmetry is covariantly defined, independently of an explicit expression in terms of specific fields. A real six-dimensional manifold which is orthogonal to the Minkovsky at every point of space and time is considered, and a particular Lorentz group in 24 real dimensions is defined. Commutation relations are derived for the constants of motion in the physical world, which reduce to the total momentum operators and SU(3) tensors. The advantages of the approach are pointed out. (L.B.S.)

20449 INTERNAL SYMMETRY AND LORENTZ INVARIANCE. L. O'Raifeartaigh (Syracuse Univ., N. Y.). Phys. Rev. Letters, 14: 332-4(Mar. 1, 1965). (NYO-3399-15)

The most general conditions under which a combination of internal symmetry and Lorentz invariance is possible are considered. The result is used that any Lie algebra E can be expressed as the semidirect sum of a semisimple subalgebra G and an invariant solvable subalgebra S. It is proved that, for R the vector space of any irreducible representation of E, and for R_m any subspace of R which is an eigenspace of the mass operator $p_\mu p^\mu$ belonging to the discrete eigenvalue m^2, then the space R_m is invariant with respect to E, in the cases where S = P or where S is abelian, but larger than and containing P, P being the translation part of the inhomogeneous Lorentz group. (M.J.T.)

20450 AN APPROXIMATE FUNCTIONAL EQUATION FOR DIRICHLET L-FUNCTIONS. D. Davies (Univ. of Manchester, Eng.). Proc. Roy. Soc. (London), Ser. A, 284: 224-36(Feb. 23, 1965).

An asymptotic formula is derived for the computation of Dirichlet L-functions, $L(s,\chi)$, where $s = \sigma + it$. The formula is applicable for large values of t and was used on the Mercury computer at Manchester University to calculate the zeros of the L-functions with moduli 3 and 4 on the line $\mathcal{R}s = \frac{1}{2}$. The results were placed in the Royal Society Depository for Unpublished Mathematical Tables (No. 83). (auth)

20451 THEOREMS ABOUT THE BEHAVIOR OF THE GREEN FUNCTION OF A FINITE-DIFFERENCE ANALOGUE OF THE STURM-LIOUVILLE BOUNDARY VALUE PROBLEM AND THEIR APPLICATION TO THE INVESTIGATION OF DIFFERENTIAL EQUATIONS. A. L. Teptin and N. N. Yuberev. Sibirsk. Mat. Zh., No. 5, 1163-80 (Sept.-Oct. 1964).

Conditions for fixed sign of the Green function of a linear difference boundary value problem, analogous to the Sturm-Liouville problem, are investigated. The results obtained are used to prove a theorem about the differential inequality for a nonlinear differential equation with boundary conditions of the Sturm type. It is noted that theorems of the Chaplygin type on differential inequalities make possible various evaluations of solutions of functional equations. (ATD)

20452 AUTOMATIC TRANSLATION. Ernest H. Goldman (International Business Machines Corp., Yorktown Heights, N. Y.). Paper 8, Session 11, 9p. of "Mesucora 63. Congres International Mesure-Controle Regulation-Automatisme. Tome II." Paris, Mesucora, [1964].

A summary is given of the research being undertaken in the field of automatic translation. The theoretical steps, equipment required, and the present state of development are discussed. Some specific results obtained on the translation of Russian, machine shorthand, and Chinese are indicated. (J.S.R.)

METALS, CERAMICS, AND OTHER MATERIALS

General

Refer also to abstracts 20111 and 21690.

20453 (CEA-R-2572) TENUE DES TUBES D'URANIUM METALLIQUE A LA PRESSION EXTERIEURE. (Resistance of Metallic Uranium Tubes to External Pressure). Paul Delpeyroux, Claude Thomas de Montpreville, Henri Viallet, and Raymond Sifferlen (Commissariat à l'Énergie Atomique, Saclay (France). Centre d'Études Nucléaires). Aug. 1964. 62p. Dep.(mn).

After certain indications obtained from a simplified theoretical analysis of the deformation to be expected in a closed tube subjected to an exterior pressure are given, out-of-pile experimental results obtained on fuel elements based on metallic uranium are presented. Experiments carried out on tubes and on the end-pellets which enclose them have made it possible to show the importance of the parameters: time, temperature, thermal cycling, geometry, nature of the alloy, radial thermal gradient. They have also made it possible to determine the shapes of projected fuel elements. Systematic tests are now being carried out both in-pile and out-of-pile with a view to define tubular elements having any shape whatever. (auth)

20454 (CONF-650212-1) ELECTROMAGNETIC TESTING OF THIN-WALL, REFRACTORY METAL TUBING. A. W. Bauer and J. P. Clark (General Electric Co., Cincinnati, Ohio. Nuclear Materials and Propulsion Operation). Oct. 14, 1964. Contract AT(40-1)-2847. 18p. Dep.(mn); $1.00(cy), 1(mn) CFSTI.

From The Society for Non-Destructive Testing Spring Convention, Los Angeles.

The development of a multi-purpose electromagnetic test instrument along with associated accessories is presented. Applications of this instrument to the inspection of thin wall, refractory metal tubing are also discussed. Various encircling coil mountings have been used to provide for: (1) a special circuit for rapid scanning; (2) differential coils for hand sorting and accurately locating defective areas; (3) an absolute coil with both amplitude and phase readouts for detecting long seams and monitoring dimensional variations. Leak tests, penetrants, radiography, ultrasonics, and metallographic sectioning are utilized as complementary tests and as aids in the interpretation of results. A discussion of quality levels and calibration procedures is presented. Justification of these quality levels is established by studying the propagation of small defects when the tubing is submitted to service stresses. (auth)

20455 (DCAS-TDR-62-192) MATERIALS AND STRUCTURES. Applied Ceramic Research Program. Semiannual Technical Report, January 1–June 30, 1962. E. G. Kendall (Aerospace Corp., El Segundo, Calif.). Oct. 12, 1962. Contract AF04(695)-69. 26p. (AD-606422). $2.00(CFSTI).

The major construction phase of the ceramic laboratory has been completed, and descriptions of key equipment are given. High-purity elemental materials and commercial carbide and boride powders have been obtained. Some work was done on the purification of boron and on the preparation and casting of titanium carbide. (D.L.C.)

20456 (EUR-2111.d) VERSUCHE ZUM PLATTIEREN VON URAN UND ALUMINIUM MIT NIOB. (Attempts at Plating Uranium and Aluminum With Niobium). H. Venker (European Atomic Energy Community, Ispra (Italy). Joint Nuclear Research Center). Oct. 1964. 46p. Dep.(mn).

In an attempt to create a diffusion barrier of niobium between uranium and aluminum, investigations were carried out concerning the deposition of niobium by two fundamentally different methods. In the first part of the work, tests are being carried out to determine whether metal is detached from the anode by erosion during an electric gas discharge and can be deposited uniformly on the cathode. Tests with silver and copper showed that such a process is perfectly feasible, but it was found that the method cannot be used for metals having a high melting point, such as niobium. The second section is devoted to tests on the reduction of $NbCl_5$. With the aid of an electric discharge, reduction by hydrogen can be carried out at temperatures which are so low that a complete reaction would not take place without discharge. Tests on the reduction of $NbCl_5$ with zinc vapor yielded uniform adherent layers of niobium at temperatures in the 400-600°C range. (auth)

20457 (GAMD-4814) GAS TRANSPORT PROPERTIES AND PORE STRUCTURE OF SOME NUCLEAR GRAPHITES. A. Riedinger (General Atomic, San Diego, Calif.). June 25, 1964. Contract AT(04-3)-167. 36p. Dep.(mn); $2.00(cy), 1(mn) CFSTI.

Studies were made to evaluate the effectiveness of backsweeping in reducing diffusion of fission products through graphite. Measurements of helium permeability and mercury porosimetry were made on a number of graphites, and noble gas transport through graphite septa was studied. The results show that: (1) Impregnation of graphite decreases the pore size. (2) Heating impregnated graphite to 2650°C produces a larger pore size than does heating to 2000°C. (3) The pore structure as measured by the mercury porosimetry is indicative of the helium permeability and/or back diffusion, but the relationship is not quantitative. (4) Helium permeability behavior is indicative of the back-diffusion behavior, but again, the relationship is not quantitative. (5) The model which appears to best describe the pore structure of graphite is one with "large" voids randomly interconnected with a large number of "small" pores. A variation of this comprising the same type of structure, except penetrated by a relatively small number of intermediate size pores, may be more applicable for the impregnated HLM-85. (D.L.C.)

20458 (GEAP-4283) EXPERIMENTAL STUDIES OF SODIUM LOGGING IN FAST CERAMIC REACTOR FUELS. G. L. O'Neill, P. E. Novak, M. L. Johnson, and W. E. Baily (General Electric Co. San Jose, Calif. Atomic Power Equipment Dept.). Sept. 1963. Contract AT(04-3)-189. 125p. Dep.; $4.00(cy), 2(mn) CFSTI.

The experimental determination of the effects of sodium ingress on high-performance oxide fuels is described. Short-term tests of UO_2 and PuO_2–UO_2 solid solution fuels are described which show that the sodium-logging effect should not be a major criterion for setting high-density fuel performance limits. Fuel performance characteristics were tested to power levels which produced central fuel temperatures above the fuel melting point, yet sodium present inside the fuel rod did not create significant damaging effects. The tests gave evidence of an improvement in fuel thermal conductivity as well as improved gap conductance as a result of the presence of sodium within the clad. Capsule design, fabrication, irradiation, examination, and analysis are described in detail. (auth)

20459 (IITRI-B6019-6) HIGH-TEMPERATURE OXIDATION PROTECTIVE COATINGS FOR VANADIUM-BASE ALLOYS. Final Report, October 1, 1963–September 30, 1964. (IIT Research Inst., Chicago, Ill.). Dec. 1, 1964. Contract NOw 64-0140-c. 44p.

The objective of this program was the development of oxidation-protective coatings for vanadium-base alloys for use at 1800 to 2500°F. Specifically, the effect of the pack-siliconizing process and the silicide coating itself on the mechanical properties of 0.020-in.-thick sheet of V–60 Nb–1Ti (weight per cent) was studied. Results indicate that both of the above parameters have little effect on strength, but causes some reduction in tensile ductility. However, the tensile transition temperature remains less than –320°F after coating. Also, there is little or no embrittlement of this coated sheet after twenty-five 4-hr oxidation cycles at

temperatures up to 2300°F in static laboratory air. At reduced pressures, 100-1,000 μ, useful life is at least ten 2-hr cycles at the above temperatures. Initial development of an oxidation-resistant slurry or liquid cementation type of coating for V–60 Nb–1Ti was completed. Slurry compositions containing tin, silicon, silver, copper, aluminum, and niobium were investigated; several of these show good coverage, even at corners and edges. The static oxidation life of other vanadium-base alloys, coated by the pack-siliconizing process, was investigated. V–40Nb–30Ta–1Ti, the most promising of these alloys, has an oxidation life of about 50 hr at 2200°F, and less under cyclic conditions. (auth)

20460 (NAA-SR-Memo-9761) PREPARATION OF CERAMOGRAPHIC SECTIONS OF BERYLLIUM OXIDE. V. C. Davis and R. L. Eichelberger (Atomics International, Canoga Park, Calif.). June 29, 1964. Contract AT-11-1-GEN-8. 13p. Dep.(mn); $1.00(cy), 1(mn) CFSTI.

Procedures have been developed for the preparation of polished sections and thin sections of BeO to permit microscopic examination in reflected and transmitted light. Special procedures are necessary because of the extreme hardness of BeO and the tendency for whole grains to pull out of a specimen during grinding and polishing. High quality sections may be prepared from either high density or low density samples by the procedures described. (auth)

20461 (NP-14893) DEVELOPMENT OF REFRACTORY CERAMICS THAT CAN BE PROCESSED AT TEMPERATURES CONSIDERABLY LOWER THAN THEIR MAXIMUM USE TEMPERATURE. Final Report. Edward J. Smoke and John H. Koenig (Rutgers–The State Univ. of New Jersey, New Brunswick. School of Ceramics). Dec. 31, 1964. Contract NOw 64-0040-d. 127p.

The objective of this study is to determine the compositions, mechanisms, and procedures necessary to lower the firing temperature of high quality ceramics which approach true density, yet retain all engineering properties including refractoriness. The effort was divided into three temperature ranges. In the highest range, 3000°F and higher, the sintering characteristics of pure alumina, and plus additives, and pure spinel were studied. The variables include firing temperature, firing time, and firing atmosphere. The effects were determined by property and structure evaluations. Pure alumina plus minor additions of magnesia have attained maturity at 2840°F. Matured spinel has been realized at 2650°F. In the temperature range 2600 to 3000°F, the presintered approach to the prereacted materials technique was being used. Compositions in the high alumina portion of the $CaO \cdot Al_2O_3 \cdot SiO_2$ system were evaluated and compared to the earlier work in the $MgO \cdot Al_2O_3 \cdot SiO_2$ system. Properties, mechanisms, and structure are discussed. In the lowest temperature range, the devitrification approach to the prereacted raw materials technique was utilized. Cordierite ($2MgO \cdot 2Al_2O_3 \cdot 5SiO_2$) was the crystalline phase studied. Two approaches were used. In the first, the whole composition is fritted and used as the sole raw material from which specimens were prepared. Compositions in the $MgO \cdot Al_2O_3 \cdot SiO_2$ system were studied. In the second, two devitrifiable frits are prepared and used. The first results in cordierite and the second supplies the glass for maturity and then devitrifies. Compositions have resulted which mature from 1900 to 2450°F, with sufficient firing range, and exhibit coefficients of linear thermal expansion less than 1.88×10^{-6} in./in/°C. (auth)

20462 (NRL-6258) METALLURGICAL CHARACTERISTICS OF HIGH STRENGTH STRUCTURAL MATERIALS. Sixth Quarterly Report. W. S. Pellini, R. J. Goode, R. W. Huber, et al. (Naval Research Lab., Washington, D. C.). Dec. 1964. 95p. $2.25(CFSTD.

A progress report covering research studies in high strength hull structural materials, conducted in the period September 1964 to December 1964, is presented. Included in the report are fracture toughness studies on: (1) titanium alloys as related to processing variables (including diffusion-bonding), thickness, and heat-treatment, (2) aluminum, (3) high strength steels relating primarily to the 5 Ni–Cr–Mo–V steels, and (4) a nickel–beryllium alloy. Low cycle fatigue crack propagation studies on several titanium alloys are presented as well as a general review of the status of the titanium casting industry. The new 240,000 ft-lb laboratory drop-weight bulge testing facility is described, and a preliminary correlation of the results obtained with it and the explosion bulge test are presented. The results of a study using fatigue-cracked and side-notched Charpy specimens in impact and slow bend testing on a wide variety of steels is given. The results are compared to those obtained in the standard Charpy test using the same materials. A background statement describing the "philosophy" of testing and evaluation of high strength structural materials which is the basis of the program is included. (auth)

20463 (ORNL-TM-431) COATED-PARTICLE FUEL DEVELOPMENT AT OAK RIDGE NATIONAL LABORATORY. W. O. Harms, comp. (Oak Ridge National Lab., Tenn.). Feb. 14, 1963. Contract W-7405-eng-26. 75p. Dep.(mn); $3.00(cy), 2(mn) CFSTI.

The research program on coated-particle nuclear fuel materials has been concerned with three general problem areas: (1) A broad evaluation of materials involving pyrolytic-carbon-coated fuel carbides with major emphasis on the relationship between measurable properties and behavior during irradiation under simulated gas-cooled power reactor conditions; (2) studies on the compatibility of coated-particle materials with liquid coolants; and (3) chemical processing development for graphite-matrix fuels containing coated particles. The techniques used and the significant results and implications that have evolved in this program are described. (auth)

20464 (SCNC-316) PREPARATION AND PROPERTIES OF $CbAl_3$ AND $CbAl_3$-FUEL BODIES. M. F. Judkins and L. Sama (Sylvania-Corning Nuclear Corp., Bayside, N. Y.). Sept. 1960. Contract AT(30-1)-Gen-366. 51p. Dep.(mn); $3.00(cy), 2(mn) CFSTI.

Niobium aluminide was prepared by eight different methods. Fabricated $NbAl_3$ compound was tested for elevated and intermediate temperature oxidation resistance to air, high temperature stability in vacuum and argon, compatibility with UO_2 and UC in both environments at comparable temperatures for extended times, fabrication capabilities, phase identification, thermal expansion, melting point, and possibility of hot plastic deformation. (auth)

20465 (TID-20344) A STUDY OF THE MATERIAL TRANSPORT MECHANISM IN SINTERING. F. V. Lenel (Rensselaer Polytechnic Inst., Troy, N. Y. Dept. of Materials Engineering). [1963]. Contract AT(30-1)-1995. 35p. (CONF-640618-1). Dep.(mn); $2.00(cy), 1(mn) CFSTI.

From Symposium on Powder Metallurgy, Paris.

Two types of sintering experiments are described. In one type, the growth of interparticle necks in an array of loose spherical silver powder at temperatures near 300°C was determined by measuring changes in the electrical resistance of the array. The activation energy for neck growth of contacts was derived by abruptly changing temperature and noting the change in the rate of neck growth. Since the experiments were run under an external load, the changes in activation energy with stress could be determined. The activation energy was found to decrease rapidly with increasing stress. In the other type of experiments, the isothermal shrinkage rates of compacts formed from spherical copper powder were determined at temperature near 1000°C. The rates for compacts from pure copper powder and from a powder with a dispersion of aluminum oxide in a copper matrix were compared with each other. The pure copper powder compacts had faster shrinkage rates. The experiments were run under a small external load. By varying this load, the stress dependence of the isothermal shrinkage rate could be measured, which was found to be approximately proportional to the fourth power of the stress. On the basis of these results, it is concluded that the material transport mechanism in both the low and high temperature experiments is one of plastic flow by dislocation motion. The variation of activation

energy with stress is typical for cross clip of dislocations. The higher shrinkage rate for pure copper as compared with dispersion strengthened copper powder compacts and the 4th power relationship between shrinkage rate and stress is best interpreted by a dislocation climb mechanism. (auth)

20466 ELECTRON BOMBARDMENT IN METALLURGY. M. Brabers, M. Meulemans, M. Henuset, and P. Groeseneken (Centre d'Etude de l'Energie Nucleaire, Mol, Belg.). Metallurgie (Mons, Belg.), 4: No. 2, 37-41(1963). (In Dutch) (BLG-256)

A review is given of the principles of electron beams and their application to metallurgy. The advantages of a high heating density, easy regulation of the beams, and flexibility in the set-up of electron guns are considered. (auth)

20467 NATURE AND MIGRATION OF PORES IN QUENCHED URANIUM DIOXIDE. K. H. G. Ashbee (Central Electricity Generating Board, Gloucestershire, Eng.). Phil. Mag. (8), 11: 637-41(Mar. 1965).

Pores were produced in foils of quenched uranium dioxide by heating in the beam of an electron microscope. These appear to be open pores and can be made to migrate, at approximately 0.2 μ per second, until they pass near to dislocation lines when a strong elastic interaction occurs. Further heating causes trapped pores to heal up. (auth)

20468 VOPRISY TEORII I PRIMENENIYA REDKOZEMEL'NYKH METALLOV. (Problems in the Theory and Applications of Rare Earth Metals). E. M. Savitskii, and V. F. Terekhova, ed. Moscow, Izdatel'stvo "Nauka," 1964. 272p.

Forty-five papers on the study and use of rare earth metals presented at a meeting held at the A. A. Baikov Metallurgical Institute in March 1963 are given. The topics discussed include physical properties (magnetic, electrical, mechanical, etc.) of the metals and their alloys, phase diagrams, effects of the rare earth metals on the plasticity of many of the refractory metals, and the use of the rare earths in the production of cast iron, steel, and alloys. The sources, mining, production, consumption, costs, and uses of rare earth elements are discussed. (Approximately 350 references). (TTT)

Corrosion

Refer also to abstract 21714.

20469 (EUR-2279.e) EVOLUTION OF CHLORINE IN TERPHENYLS. F. Lanza, G. Marengo, and A. Recrosio (European Atomic Energy Community, Ispra (Italy). Joint Nuclear Research Center). 1965. 28p. Dep.(mn).

Loop experiments showed that the chlorine content in terphenyl varies continuously in long runs. When a chlorinated compound is introduced in a loop, chlorine is taken up by the walls and subsequently slowly released. Corrosion tests were used to identify the trapped chlorine as $FeCl_2$. An influence of $FeCl_2$ solubility on the chlorine concentration was found, and $FeCl_2$ solubility was measured. The influence of chlorine evolution on purification, fouling, and corrosion is discussed. (auth)

20470 (GE-TM-63-7-3) PROPERTIES OF Fe-Cr-Al TYPE ALLOYS CONTAINING ADDITIONS OF YTTRIUM. C. S. Wukusick and J. F. Collins (General Electric Co., Cincinnati, Ohio. Nuclear Materials and Propulsion Operation Services). 1963. Contract AT(40-1)-2847. 39p. Dep.(mn); $2.00(cy), 1(mn) CFSTI.

The development and properties of an Fe-25Cr-4Al-1Y alloy are reviewed. The mechanical properties are similar to those of ferritic stainless steels. The alloy consists of an Fe-Cr-Al matrix containing a dispersion of YFe_3. The dispersion inhibits grain growth but causes incipient melting at 2475°F. Yttrium improves the overall oxidation behavior as a result of improved surface oxide retention during cyclic testing. Kinetic data were obtained for the various reactions occurring during oxidation, i.e., weight gain, surface oxide growth, YFe_3 depletion and internal oxidation. A mechanism for improved oxide adherence based on subscale effects is proposed. (auth)

20471 (HW-SA-3628) THE EFFECTS OF REACTOR DECONTAMINATING SOLUTIONS ON INTERGRANULARLY CORRODED TYPE 304 STAINLESS STEEL. A. P. Larrick (General Electric Co., Richland, Wash. Hanford Atomic Products Operation). Oct. 9, 1964. Contract AT(45-1)-1350. 11p. (CONF-654-55). Dep.(mn); $1.00(cy), 1(mn) CFSTI.

From American Nuclear Society Meeting, San Francisco, Nov.-Dec. 1964.

Severe localized intergranular attack was found in sensitized type 304 stainless steel reactor heat exchanger tubing. Static and pilot plant loop tests were conducted to determine whether the decontaminating solutions would adversely affect the attacked tubing. The results show that the solutions will remove grains from the intergranularly attacked areas (sulfamic acid being the most corrosive), but that no additional damage is produced. (D.L.C.)

20472 (IDO-14651) CORROSION OF TYPE 316 STAINLESS STEEL IN NaK SERVICE — A LITERATURE SURVEY. C. A. Zimmerman (Phillips Petroleum Co., Idaho Falls, Idaho. Atomic Energy Div.). Feb. 1965. Contract AT(10-1)-205. 20p. Dep.; $1.00(cy), 1(mn) CFSTI.

A literature survey of work on corrosion of stainless steel, especially Type 316, by NaK and sodium was made, based on information available through September, 1964. In general, the Type 316 and Type 304 stainless steels should give good performance with NaK. The mechanisms which can lead to failure are attack by impurities at temperatures under 550°C, and carbide precipitation, sigma formation, and mass transfer at higher temperatures. (auth)

20473 (NASA-CR-54269) POTASSIUM CORROSION TEST LOOP DEVELOPMENT. Quarterly Progress Report No. 5, July 15, 1964-October 15, 1964. E. E. Hoffman, ed. (General Electric Co., Cincinnati, Ohio. Space Power and Propulsion Section). Dec. 30, 1964. Contract NAS 3-2547. 51p.

Activities in a program to develop a prototype corrosion test loop for the evaluation of refractory alloys in boiling and condensing K environments are reported. The program is proceeding with the construction and operation of three Nb-Zr test loops. A natural convection loop was operated for 1000 hr to test various components. A single-phase Na forced-circulation loop was operated 1985 hr to evaluate electromagnetic pumps, flow control, and instrumentation. A prototype two-loop corrosion test system was designed and is under construction. Information is included on loop operation, alkali metal vacuum distillation unit development, design of alkali metal purification and handling systems, W/Re thermocouple development, test capsule development for Mo-TZM K reflux experiments, investigation of Nb-Zr alloy grain growth, and development of He analysis systems. (J.R.D.)

20474 (NASA-CR-54281) STUDIES OF ALKALI METAL CORROSION ON MATERIALS FOR ADVANCED SPACE POWER SYSTEMS. Quarterly Progress Report No. 2, September 26, 1964-December 26, 1964. R. W. Harrison (General Electric Co., Cincinnati, Ohio. Space Power and Propulsion Section). Contract NAS 3-6012. 44p.

Stress Corrosion Reflux Capsule Tests. The D-43 alloy bar for the fabrication of the reflux capsules was received and evaluated. Measured creep strengths were higher than those previously reported from the data compilation. The stress corrosion reflux capsule design was completed; engineering drawings were approved by the NASA Technical Manager. Three capsules have been machined and received. With the exception of the LVDT's and the alumina probes, all supporting components for the reflux capsule test facility have been machined and/or are on hand. A boiling nucleator was designed and is to be employed in the capsule tests in order to avoid possible deformation in the reduced wall and/or fracture of the alumina probes as a

result of boiling instabilities. Bimetallic Isothermal Capsule Tests. Two Type 321SS and two type 316SS isothermal capsules, each containing Nb–1 Zr alloy sheet specimens, were filled with potassium and placed on test at 1400°F December 18, 1964. The planned test duration is 1,000 hours. (auth)

20475 (ORNL-3538) SNAP-8 CORROSION PROGRAM. Quarterly Progress Report for Period Ending August 31, 1963. H. W. Savage, E. L. Compere, W. R. Huntley, and A. Taboada (Oak Ridge National Lab., Tenn.). Dec. 19, 1963. Contract W-7405-eng-26. 42p. Dep.(mn); $2.00(cy), 1(mn) CFSTI.

A program was initiated for investigating the compatibility of the structural materials and the NaK coolant in the SNAP-8 primary coolant loop and, also, to provide information on the behavior, control, and disposition of hydrogen, particularly with respect to its diffusion into the power-conversion system. A loop program was planned which entailed operation of 13 reduced-scale forced-flow loops that closely simulate important features of the SNAP-8 primary system. The design of the loops, test stands, and all other appurtenant equipment was 95% completed. Two of the loops and the five test stands to be used in the program are under construction. All materials for constructing the corrosion loops are being characterized and evaluated for conformance with quality specifications. An intense effort is being made to compare the chromizing result on Hastelloy N heater tubes with that on SNAP-8 fuel element cladding. Procedures were developed for the welding of Croloy 9M to austenitic stainless steel and Inconel. An extensive literature survey is being conducted to evaluate the problem of determining the fate and condition of hydrogen in the SNAP-8 primary system. Sufficient data have been found to make preliminary estimates of the steady-state pressure and solubility of hydrogen in the SNAP-8 primary NaK coolant. From these estimates, it appears probable that the hydrogen will diffuse rapidly through the system walls and possibly 70% of it will enter the SNAP-8 secondary mercury system. It was estimated that the steady-state hydrogen pressure in the SNAP-8 primary system will be a fraction of an atmosphere and that the hydrogen will be in dissolved form at NaK temperatures of 1100°F or higher. Experimental determinations of hydrogen solubility in NaK as a function of pressure and temperature are needed to verify the assumptions and to check the accuracy of the estimates. Experiments will also be conducted to determine whether the presence of NaK affects the permeability constants for the passage of hydrogen from NaK through metals. Apparatus for carrying out these experiments was designed and is being constructed. (auth)

20476 (ORNL-3603) NIOBIUM–1% ZIRCONIUM, NATURAL-CIRCULATION, BOILING-POTASSIUM CORROSION LOOP TEST. D. H. Jansen and E. E. Hoffman (Oak Ridge National Lab., Tenn.). May 1964. Contract W-7405-eng-26. 55p. Dep.(mn); $3.00(cy), 2(mn) CFSTI.

A loop fabricated from Nb–1% Zr alloy was tested with naturally circulating boiling potassium for 2800 hr. The purpose of the test was to determine the extent of dissolution of the alloy in the condenser region and the subsequent deposition rate in a subcooled liquid region of the loop. The loop was operated in vacuum at an average pressure of 2.3×10^{-6} torr. A potassium condensing rate of 40 g/min and a condenser temperature of 1130°C were maintained. The results indicate that the Nb–1% Zr alloy adequately contains two-phase potassium at the test conditions. The condenser wall dissolution (0.1 mg/cm^2) corresponded to a removal rate of only 12 μin./yr. Extensive chemical analyses on various loop components indicate some slight contamination of the Nb–1% Zr alloy by residual gases in the vacuum environment, but no evidence of embrittlement was detected. (auth)

20477 (ORNL-3604) SNAP-8 CORROSION PROGRAM. Quarterly Progress Report for Period Ending November 30, 1963. H. W. Savage, E. L. Compere, R. E. MacPherson, W. R. Huntley, and A. Taboada (Oak Ridge National Lab., Tenn.). Mar. 1964. Contract W-7405-eng-26. 51p. Dep.(mn); $3.00(cy), 2(mn) CFSTI.

In the program of tests of corrosion loops simulating the SNAP-8 primary circuit two loops were in operation prior to a month-long strike of craft labor, which deferred completion of construction of additional loops and test stands beyond the end of the quarter. Operation revealed deficiencies in the loop heater arrangement and problems of oxide control. The first loop developed a leak, and operation was terminated for a complete examination. The second loop required heater revision, which was in progress at the end of the quarter. A new heating arrangement was designed and scheduled for use with all loops requiring NaK at 1400°F. The sequence of operation of the loops was rearranged so that the next four loops to be operated will not require NaK above 1300°F. Equipment proposed for injecting hydrogen into the NaK was bench tested with satisfactory results. Tests of equipment for detecting hydrogen after diffusion through loop walls into an argon sweep gas are in progress. Exhaustive examination of all materials used in the test loops continued. Samples of all Hastelloy N tubing to be used in the loops are now being sent to Atomics International to assure adherence to SNAP-8 quality control requirements. The loop which was shut down because of a leak is now undergoing complete postrun metallurgical examination. Detailed procedures for these examinations and for the analysis of results are being prepared. Preliminary measurements of the diffusion of hydrogen from the gas phase and from NaK solution through a Hastelloy N diaphragm were made. The results are tentative and warrant no conclusions. Cells with diaphragms of type 316 stainless steel and of Croloy 9M were fabricated. Apparatus for measuring the solubility of hydrogen in NaK was constructed. (auth)

20478 (ORNL-3618) SNAP-8 CORROSION PROGRAM. Quarterly Progress Report for Period Ending February 29, 1964. H. W. Savage, E. L. Compere, R. E. MacPherson, W. R. Huntley, and A. Taboada (Oak Ridge National Lab., Tenn.). Apr. 1964. Contract W-7405-eng-26. 40p. Dep.(mn); $2.00(cy), 1(mn) CFSTI.

Of the corrosion loops simulating the SNAP-8 primary circuit, one loop continued to operate, three additional loops were started, and construction of a fifth loop was essentially completed. Two loops (10-1 and 9-2) each accumulated over 1000 hr of operation, with temperature profiles at design conditions. The oxide levels in both loops proved difficult to measure because data obtained from the plugging indicators were complex and not completely understood and because the results of chemical analyses for oxide in the NaK were erratic and inconsistent with the plugging-indicator data. Two breaks in the plugging-indicator flow curve were observed, suggesting that more than one material precipitates from the NaK. These problems are being studied further. Hydrogen was injected into loop 8-4 on February 28 and was detected almost immediately by the hydrogen-detection system. Hydrogen monitoring results indicate good agreement with mass spectrographic analysis of the sweep gas. Metallurgical evaluation studies were started on loop 1-1, which ran 701 hr before developing a leak. Posttest examination revealed that the leak occurred in a weldment between a pipe and a pipe reducer that was brittle. Data collected from the first loop clearly reveal the occurrence of extensive carbon migration and a small amount of corrosion in the hot leg. The Croloy 9M material in the loop was essentially decarburized at the hot end of the heat exchanger section and carburized at the cool end. The hot end also exhibited recarburization near the surface. A parametric relationship between the hydrogen partial pressure in heated NaK and the precipitation temperature of alkali metal hydride was derived from separate expressions relating hydrogen gas solubility and pressure, temperature, and decomposition pressure of a solid hydride phase and temperature and solubility of solid hydride in liquid metal. Some estimates were made of precipitation temperatures, and they were compared with those obtained from the literature. The hydrogen permeability of Hastelloy N was measured at

1100, 1300, and 1425°F in the absence of NaK. The data obtained are consistent with earlier measurements at lower temperatures. Achievement of moisture levels of ~1 ppm in the glove box permitted welding to be conducted in the box. NaK was placed in the diffusion cell to check whether it affected the hydrogen diffusion rate. NaK was also placed in a capsule for use in hydride solubility studies. (auth)

20479 (ORNL-3671) SNAP-8 CORROSION PROGRAM. Quarterly Progress Report for Period Ending May 31, 1964. H. W. Savage, E. L. Compere, R. E. MacPherson, W. R. Huntley, and A. Taboada (Oak Ridge National Lab., Tenn.). July 1964. Contract W-7405-eng-26. 35p. Dep.(mn); $2.00(cy), 1(mn) CFSTI.

Operation of two of the eight fractional replicate loops was completed during this reporting period, four loops are in operation, and the remaining two will be in operation in June 1964. Of the two loops comprising a time-study series, one has been deferred, and the other is in long-term operation. Basic parts are available for the two loops for investigating hydrogen-effluent control, and the scope of the investigation is being determined. The 13th loop is to simulate the SNAP-8 hot-spot situations and is being designed. In all loops operated to date, corrosion and mass transfer were found to some extent. Metal was removed from the hot section of the loop and deposited in the cold sections and, particularly, in regions of flow disturbances. Very little corrosion and mass transfer were found in the low-oxygen-content loops, but the amounts were significantly higher in the high-oxygen-content loops. A pronounced difference in the corrosion effects was observed when the oxygen level was increased. Although an increase in corrosion rate with increased oxygen was observed for both the nickel-alloy and the iron-base-alloy specimens, the increase in corrosion rate for the iron-base alloys was dramatically higher, indicating a change in the corrosion mechanism. In addition to metal crystals, a complex oxide of the form $NaMO_2$ was observed throughout the cold region of the loop both as a layer and as crystals intermixed with the metallic mass transferred material. An increase in the resistance of the NaK circuit to flow was observed in high-oxygen-content loop 9-2. A buildup of metallic crystals in the electromagnetic pump cell was at least partly responsible for this flow deterioration. Extensive decarburization, to levels of approximately 0.002 wt %, was observed in the hot section of the Croloy 9M specimens. In some cases the decarburization was accompanied by large grain growth, and carbon pickup was observed throughout the rest of the loop. There is evidence of the presence of a temperature-sensitive precipitate that is apparently unaffected by either the oxygen level in the NaK or hydrides in the loop. The temperature at which this precipitate causes a break in the plugging-indicator flow-rate curves is not affected by hot trapping; however, this temperature decreases somewhat with time of operation and is affected in an erratic manner by cold trapping. The measurement of the NaK oxygen level in the corrosion loops can be made only when this level is held below approximately 80 ppm. Above this level, the break in the plugging-indicator flow-rate curve due to oxygen is masked by the break due to the previously described precipitate. Measurements of the hydrogen effluent from the loop indicate that the hydrogen equilibrium concentration is approximately as predicted. The ratio of hydrogen effluent through Croloy 9M to the effluent through stainless steel indicates that somewhat less hydrogen than anticipated passes through the Croloy 9M, probably due to oxidation of the Croloy. A marked reduction of the hydrogen effluent from the loop can be effected by cold trapping a small stream of the NaK at temperatures as high as 250°F. In laboratory experiments, the hydrogen permeability of Hastelloy N at 1425°F in the presence of NaK was observed to be 0.81 cc (STP) mm cm^{-2} $atm^{-1/2}$. This value is lower than that obtained (1.3) in the absence of NaK. Hydrogen permeability coefficients in the absence of NaK were obtained for type 316 stainless steel and Croloy 9M. The solubility of hydrogen in NaK was determined at 1100°F at pressures of 93, 269.5, and 552.5 mm. The solubility coefficient was 200 ppm $atm^{-1/2}$. (auth)

20480 (ORNL-3730) SNAP-8 CORROSION PROGRAM. Quarterly Progress Report for Period Ending August 31, 1964. H. W. Savage, E. L. Compere, R. E. MacPherson, W. R. Huntley, and A. Taboada (Oak Ridge National Lab., Tenn.). Nov. 1964. Contract W-7405-eng-26. 68p. Dep.(mn); $3.00(cy), 2(mn) CFSTI.

The completion of operation of three loops during this reporting period brought to seven the total number of loops operated. Of the two remaining loops comprising a fractional replicate series, one loop is in operation and one loop was deferred. Of the two-loop time-study series, one loop is in operation and one was deferred. A modified loop that simulates a 1450°F hot-spot condition in the SNAP-8 reactor core was designed, fabricated, and placed in operation. The modifications included a change in the cold finger that mocks up the NaK-filled annulus around the SNAP-8 NaK pump shaft and the installation of a section of type 316 stainless steel-clad Croloy 9M tubing at the high-temperature end of the loop cooler. A second, identical, hot-spot loop will be used to study the effect of continuous cold trapping at 250°F on hydrogen diffusion from the loop. A third hot-spot loop is being designed in which type 316 stainless steel will be substituted for Croloy 9M in the cooler, and the loop NaK will be in contact with the type 316 stainless steel cladding of the duplex tubing section. Flow-through NaK-sampling devices were installed on two loops to study the "precipitate" observed with the plugging indicator. To date only K_2O and Na_2O have been found. There has been no evidence of corrosion products or carbon compounds. Metallographical examinations showed that very little metal migration occurred in loops operated with low-oxygen-content NaK, even when the maximum temperature was 1425°F. Increasing the oxygen content of the NaK increased the corrosion rate of both the nickel- and the iron-base alloys, but the increase was greater in the iron-base alloy. Carbon migration was severe in all loops. The extent of carbon migration was apparently not affected by oxygen content, but some weakly beneficial effects may have resulted from hydrogen additions to the loops. Hydrogen did not adversely affect corrosion and mass transfer. Examination was completed of chromized Hastelloy N piping from the corrosion loops and tubing typical of SNAP-8 fuel element cladding. Chromium enrichment of the surfaces varied in a random fashion from no enrichment to 75% chromium and showed a maximum depth of 0.0015 in. No significant effects on corrosion are expected to be caused by this variation. Studies for defining the fate of hydrogen released from SNAP-8 fuel elements to the primary NaK system were continued. The solubility of hydrogen in NaK was determined at 752, 1009, and 1300°F to augment previous data obtained at 1100°F. The equation $\log_{10}(X/P^{1/2}) = 0.0756 + (274/T)$, where X = hydrogen concentration, cc (STP) per g of NaK; P = hydrogen partial pressure, atm; and T = temperature, °K, expresses the relationship of the Sievert's law coefficient, $S = X/P^{1/2}$, and temperature over this temperature range, that is, 752 to 1300°F. Hydrogen permeability measurements are continuing to provide information on type 316 stainless steel and Croloy 9M in the clean condition, in the presence of NaK, and with the downstream diffusion surface oxidized. Introduction of an Armco iron thimble as a barrier between the upstream diffusion chamber and the hydrogen feed line has eliminated the problems caused by NaK vapor diffusing upstream. Currently measurements are being made on hydrogen fired stainless steel at 1000, 1100, and 1300°F. Equations have been developed to describe the action of a cold trap in reducing the flow of hydrogen from a primary system through a metal wall to a secondary system. Application of solubility data developed during the course of these studies to the SNAP-8 situation indicates that, without cold trapping, the hydrogen partial pressure in the primary NaK system at 1100°F should be approximately 2.4×10^{-5} atm. The use of a bypass cold trap operating at approximately 100°F would reduce the hydrogen partial pressure in the primary system by a factor of 10^{-4} and thus reduce the hydrogen diffusion into the secondary system by a factor of 10^{-2}. Among the difficulties associated with adoption of such a cold trap is the associated loss in

net power output of the SNAP-8 system. If it is assumed that 90% of the sensible heat involved in the temperature transient from 1100 to 100°F can be recovered by the use of an economizer, the cold trap would dissipate 1.3% of the main-stream power at the required bypass flow rate of 3.5 gpm. The possibility of accommodating the hydrogen introduced into the SNAP-8 primary system by the use of hydrogen diffusion windows or getter materials was further examined. It was concluded that excessive window area-to-thickness ratios would be required to produce significant reductions in the hydrogen level. Of the potential solid getter materials, only zirconium and yttrium appear to be adequate. Problems of surface oxidation, compatibility with NaK, and required surface-to-volume ratios make these less attractive than soluble getters which could inhibit hydride activity by forming complexes or filterable precipitates. Lithium and yttrium are being considered as promising soluble getters. (auth)

20481 (ORNL-3787) EVALUATION OF HASTELLOY F AND OTHER CORROSION-RESISTANT STRUCTURAL MATERIALS FOR A CONTINUOUS CENTRIFUGE IN A MULTIPURPOSE FUEL-RECOVERY PLANT. W. E. Clark, L. Rice, and D. N. Hess (Oak Ridge National Lab., Tenn.). Apr. 1965. Contract W-7405-eng-26. 14p. Dep.; $1.00(cy), 1(mn) CFSTI.

Hastelloy F was found suitable as a material of construction for a centrifuge to be used for clarifying solutions generated in various nuclear head-end processing schemes. The maximum corrosion rate was ≦0.7 mil/month in all solutions tested. Test solutions were of the following types: stainless steel dissolved in 4 M H_2SO_4 (from the Sulfex process), stainless steel dissolved in 5 M HNO_3–2 M HCl (from the Darex process), Zircaloy-2 dissolved in 6 M NH_4F–1 M HNO_3 (from the Zirflex process), UO_2–ThO_2 dissolved in 13 M HNO_3–0.04 M NaF–0.04 M $Al(NO_3)_3$ (from the Thorex process), and UO_2 dissolved in 10 M HNO_3–0.01 M Zr–0.05 M NaF (core dissolvent from the Zirflex process). Test temperature was 35°C. Candidate materials besides Hastelloy F included Carpenter 20SCb stainless steel, Hastelloy C, titanium-45A, and a vacuum-melted, low-carbon variation of Ni-o-nel. Hastelloy F was the only one of these materials which was satisfactorily resistant to all of the test solutions. (auth)

20482 (SCNC-314) OXIDATION TESTING OF COATED NIOBIUM ALLOY FUEL ELEMENTS. S. Priceman and L. Sama (Sylvania-Corning Nuclear Corp., Bayside, N. Y.). Sept. 1960. Contract AT(30-1)-Gen-366. 33p. Dep.(mn); $2.00(cy), 1(mn) CFSTI.

Niobium-base fuel elements employing three different aluminum-base coatings were evaluated by several laboratory-type oxidation tests. The static and cyclic oxidation life at 2300°F was determined for the three systems. Effects of temperature and pressure as well as composition and process variables on the rate of oxidation following the initiation of a failure in these coatings were also investigated. (auth)

20483 (SCNC-318) IMPROVED OXIDATION-RESISTANT COATINGS FOR NIOBIUM ALLOYS. L. Sama, B. Brodwin, J. Grubessich, D. Lawthers, and S. Priceman (Sylvania-Corning Nuclear Corp., Bayside, N. Y.). Feb. 1961. Contract AT(30-1)-Gen-366. 45p. Dep.(mn); $2.00 (cy), 1(mn) CFSTI.

Improved coatings were sought for the oxidation protection of niobium and several niobium alloys for 1000 hours at 2300°F. Excellent results were obtained with aluminum alloy dipping baths after screening a large number of bath compositions. Several baths appeared capable of giving approximately 500 hours protection. Protection for 1000 hours appears feasible but has not been attained. Interesting results were obtained by dipping in tin-base baths but these coatings did not appear useful for 100 hours at 2300°F. Pack coating techniques were also investigated with some favorable results. Several samples resisted oxidation for over 500 hours at 2300°F. (auth)

20484 (TID-19978(Vol.I)) SURVEY OF APPLICABLE ELECTROCHEMICAL TECHNOLOGY. Operational and Fabrication Techniques and Materials. Energy Depot Electrolysis System Study. (Allison Div., General Motors Corp., Indianapolis, Ind.). Dec. 1963. Contract AT(30-1)-3101. 19p. Dep.(mn); $1.00(cy), 1(mn) CFSTI.

Construction materials, cell configuration, and fabrication techniques for the Mobile Energy Depot (MED) electrolysis unit are discussed. The MED requires an efficient, rugged, lightweight, and compact electrolysis unit for the generation of hydrogen with a product-to-cell weight ratio approximately an order of magnitude greater than available commercial units. Also, cell components must be lightweight and close electrode spacing must be employed to minimize the weight of electrolyte in the cell. Basically, the electrolysis cell is composed of two electrodes—anode and cathode—immersed in an electrolyte and separated by an ionically conductive separator. The separator divides the cell into two compartments and prevents mixing of the gases generated at each electrode, but being conductive, it allows passage of electrical current. The basic cells are arranged in repeating units and are connected electrically in one of two configurations that will be discussed in a later section. The electrolysis cell construction materials can be divided into four categories: cell container (for tank type construction) and auxiliary equipment; gasket or spacer; electrode; and separator. Cell construction materials are considered from the standpoint of corrosion resistance in both acid and base electrolytes. Two electrolytes, sulfuric acid and potassium hydroxide, are being considered. (P.C.H.)

20485 STUDY OF THE OXIDATION OF THE ALLOY Mg–1% Ce IN HUMID NITROGEN AT HIGH TEMPERATURES. Jean Paiedassi, Raymond Darras, and Michel Perebaskine (Centre d'Etudes Nucleaires, Saclay, France). Compt. Rend., 260: 134-7(Jan. 4, 1965). (In France)

The reaction of the alloy Mg–1 wt% Ce with nitrogen saturated at 25°C with water vapor was studied under isothermal conditions from 475 to 600°C. A long induction period, where the reaction is very slow and the protective film is constituted by the solid solution (Mg, Ce)0, preceeds linear oxidation of the regime for which the compact film subjacent to the porous layer is probably heterogeneous ($\underline{m}MgO + \underline{n}CeO_2$). In the intermediary step, the appearance of porous magnesia by a process of germination and growth was noted following local ruptures of the protector film. (tr-auth)

20486 GENERAL CONCEPTS OF GAS-METAL REACTIONS. Earl A. Gulbransen (Westinghouse Research Labs., Pittsburgh). Corrosion, 21: 76-83(Mar. 1965).

A metal in a gas atmosphere at high temperature is a complex chemical system. The metal usually is not pure but contains in addition to metallic impurities O, N, H, C, S, etc. The gas atmosphere also is usually complex, containing (in addition to O_2) N_2, H_2, CO_2, H_2O, etc. A wide variety of chemical and physical phenomena occur in and on the metal surface in a typical gaseous environment at high temperature. The various phenomena are systematized into five zones of activity: metal, metal-oxide interface, oxide, oxide-gas interface, and gas. The general concepts were considered by setting down classification schemes of diverse observations and phenomena. Eight classification systems are given and discussed. These are: type of reaction, sign and magnitude of free energy change, extent of reaction, crystal structure, empirical and theoretical rate laws, physical and chemical properties of metal and oxide, topology of metal and reaction product, and effect of reaction on metal or environment. (auth)

20487 TYPE 304 STAINLESS STEEL VS FLOWING CO_2 AT ATMOSPHERIC PRESSURE AND 1100-1800F. H. E. McCoy (Oak Ridge National Lab., Tenn.). Corrosion, 21: 84-94(Mar. 1965).

Oxidation characteristics of Type 304 stainless steel in CO_2 were observed over the temperature range from 1100 to 1800°F (593 to 982°C). Although in general oxidation rate curves were parabolic, several periods were observed in which they were approximately linear. These breaks were reproducible and thought to be associated with changes in the rate-controlling step of the oxidation process. Carburi-

zation of Type 304 stainless steel during exposure to CO_2 was observed. Several other alloys were studied to determine the carburization mechanism. These included Type 406 stainless steel, a British 20 Cr–25 Ni, niobium-stabilized steel, Inconel, iron, Fe-1 Cr, Fe-3 Cr, and Fe-10 Cr. Correlation was found between carburization and chromium content, with low chromium favoring and higher chromium inhibiting this reaction. A mechanism was proposed based upon influence of chromium on type of surface oxide formed. (auth)

20488 CORROSION IN NUCLEAR REACTORS AND HOW IT IS COMBATED. R. C. Asher. Corrosion Technol., 11: No. 10, 29-32(Oct. 1964).

Aspects of corrosion where nuclear engineering presents special problems are discussed. Corrosion in graphite-moderated reactors, water-moderated reactors, and liquid metal-cooled reactors is considered. (M.C.G.)

20489 DETERMINATION OF THE REFRACTIVE INDEX AND THICKNESS OF OXIDE FILMS ON ANODIZED ZIRCONIUM FROM TRANSMISSION INTERFERENCE MEASUREMENTS. J. C. Banter (Oak Ridge National Lab., Tenn.). J. Electrochem. Soc., 112: 388-90(Apr. 1965). (ORNL-P-563)

A method is described for determination of the refractive index of thin oxide films stripped from anodized zirconium by dissolution of the metal. This technique involves measurement of the interference patterns produced in the light transmitted through the films at various angles of incidence. The film thickness was also calculated from the data, and results showed that the refractive index does not vary with film thickness for films approximately 3000 to 5000 Å thick. These films exhibited normal dispersion behavior over the ultraviolet, visible, and near infrared regions of the spectrum, with the refractive index varying from 2.07 to 2.50 at wavelengths of 1μ and 250 mμ, respectively. (auth)

20490 GROWTH MECHANISM OF THIN ANODIC OXIDE FILMS ON TANTALUM. I. SELF-ANODIZATION USING AN EXTERNAL RESISTOR. R. Dreiner, K. Lehovec, and J. Schimmel (Sprague Electric Co., North Adams, Mass.). J. Electrochem. Soc., 112: 395-401(Apr. 1965).

The growth of an anodic oxide film on tantalum metal immersed in diluted sulfuric acid was investigated using potential and capacitance measurements. The tantalum metal was connected through an external resistance to a platinum electrode in the electrolyte. An analysis of voltage vs time confirmed the exponential field dependence of the ionic current for the later phases of oxide growth. Analysis of current (I) vs. time (t) measurements provided BF_0 and λF_0 where B is the field coefficient, F_0 is the initial field in the oxide, and λ is the growth rate per unit current, provided that the emf of the reaction, E, is known. E can be determined by matching the B-values derived from I vs. t to those derived from capacitance measurements. For sufficiently thin oxide films the growth rate exceeded the value expected from Faraday's law based on the external current, which indicated the presence of internal electron currents for which the empirical expression, $I_E = I_E^0 e^{-d/l}$, with $I_E^0 \sim 3 \times 10^{-4}$ amp/cm^2 and $l \sim 3.0$Å, was obtained. There were indications that either the inverse Tafel slope, B, or the emf, E, varies with film thickness in the range where the internal electron current is appreciable. (auth)

20491 OXIDATION OF BERYLLIUM IN CO_2 BY AUTORADIOGRAPHIC TECHNIQUES. H. E. McCoy, Jr. (Oak Ridge National Lab., Tenn.). J. Nucl. Mater., 15: 249-62 (1965).

Because of the proposed use of beryllium as a fuel-cladding material in a CO_2-cooled reactor, the compatibility of beryllium and CO_2 at elevated temperatures was studied. The reported breakaway or nonprotective oxidation of beryllium in CO_2 under certain test conditions and the proposed relation of this phenomenon to carbon absorbed during the oxidation stimulated an investigation to determine the reaction products formed and their location. A limited number of tests were run in 200-torr of CO_2 at temperatures between 593 and 815°C for times up to 500 hr. The specimens were examined after test using metallography, autoradiography, and surface counting techniques. It was found that the reaction products of beryllium with CO_2 were BeO and Be_2C. The reaction proceeded along preferred longitudinal directions, which seemed to be influenced by the voids present in the as-received material. The reaction advanced more rapidly in the longitudinal than in the transverse direction. Three possible mechanisms are proposed to account for the greater rate in the longitudinal direction based upon an excess concentration of vacancies in the oxide film from the voids, the segregation of impurity atoms around the voids, and the inability of the material to deform plastically in certain directions due to preferred orientations of the grains. It was found that the beryllium specimens increased in carbon content during exposure to CO_2. The carbon was found to remain associated with the reaction product and did not diffuse into the beryllium. (auth)

20492 FURTHER STUDIES ON THE INHIBITION BY BORIC ACID OF THE OXIDATION OF ZIRCONIUM IN HIGH PRESSURE STEAM. C. F. Britton, J. V. Arthurs, and J. N. Wanklyn (Atomic Energy Research Establishment, Harwell, Berks, Eng.). J. Nucl. Mater., 15: 263-77(1965). (AERE-R-4702)

The rapid oxidation of zirconium in steam at 500°C, 1000 psi is prevented by adding boric acid to the steam. Inhibition was obtained for up to 400 days exposure. Zircaloy-2 however did not show any improvement in inhibited steam. Some alloys, having poor oxidation resistance in steam at 500°C, were improved in inhibited steam, although the effect was not so great as with zirconium. Alloys resistant to steam were not greatly affected. The minimum effective concentration of boric acid could be as low as 0.003 g/g of steam. No inhibition took place at 500°C, 1 atm, or at 400°C, 1000 psi. Anodizing in borate solutions did not inhibit subsequent oxidation in 1 atm or 1000 psi steam at 500°C. (auth)

20493 CORROSION OF CARBON STEEL BY BOILING AND SUPERHEATED MERCURY. A. H. Fleitman, A. J. Romano, and C. J. Klamut (Brookhaven National Lab., Upton, N. Y.). Nucl. Sci. Eng., 22: 24-32(May 1965). (BNL-7607)

Mercury corrosion of Si-deoxidized, low-carbon steel was studied in 5000-hr tests using four natural circulation loops with once-through boilers operating at 593°C and with 111°C of superheat. The relative effects of very small quantities of Ti or Zr additions to the Hg and the effectiveness of steel pretreatment (for 500 hr at 590-620°C with a liquid Hg-Zr solution), prior to contact with boiling Hg, were determined. A fourth loop, which had no additives nor loop pretreatment, was run simultaneously. With the exception of the Hg-Zr pretreated loop, maximum depth of corrosion did not exceed 50 μm and occurred near the superheater exit where the temperature was the highest. Boiler and condenser corrosion were less than 30 μm in these latter loops. Corrosion 300-1000 μm deep was found on the downstream side of the superheater of the Hg-Zr pretreated loop, and the severity of the attack was attributed to boiling instabilities, which caused liquid Hg to come into contact with the superheater walls. Adherent iron deposits were found in the boilers and cooler liquid regions of three of the loops, but no discernible iron deposits were found in the loop with Zr added. The total quantity of mass-transferred iron (deposits and particulate) was estimated to be approximately 0.2 gm in the Zr-added loop, 0.5 gm in the Ti-added loop, 1 gm in the loop with no additions and 2 gm in the loop pretreated with Hg-Zr solution. (auth)

20494 KINETICS OF OXIDATION OF NIOBIUM–NICKEL AND NIOBIUM–ALUMINUM REFRACTORY ALLOYS. R. F. Voytovich. Zh. Fiz. Khim., 38: 2954-7(1964).

The kinetics of oxidation of niobium alloys containing 10, 30, 50, 70, and 90% nickel of aluminum were investigated at 500 to 900°C. Alloying with less than 10% nickel had no effect on the oxidation rate. With increasing nickel content, the scale became dense, adhered firmly to the metal, and protected it against further oxidation. The oxidation became

intensive at about 600°C and follows a parabolic rate. However, the oxidation rate of niobium alloy with 30% Ni at 900°C was linear. In niobium–aluminum alloys, a sharp decrease in the oxidation rate took place at an aluminum content of 10%. With increasing aluminum content, a further decrease in the oxidation rate was observed. The x-ray diffraction patterns showed that the scale of alloys with high Al content consists mostly of γ-Al_2O_3 spinal. Thus, alloying with nickel or aluminum appeared to be an effective method for increasing the oxidation resistance of niobium alloys. (CFSTI)

20495 CORROSION AND PROTECTION OF BERYLLIUM METAL. A. J. Stonehouse and W. W. Beaver (Brush Beryllium Co., Cleveland). 31p. (CONF-492-9)

From National Association of Corrosion Engineers, Chicago, Mar. 1964.

Beryllium readily forms an adherent oxide film on its surface, which is quite protective. There are a number of environments and situations that result in corrosion and attack on the metallic structure despite the protective oxide film. The metal is normally quite resistant to attack by the normal atmosphere to a temperature of 1200°F or slightly higher, but on extended exposure at these temperatures failure of the protective mechanism can occur leading to breakaway oxidation. The metal is quite sensitive to halogen content in aqueous solutions. Long service was experienced in high purity water, but very poor performance was obtained with tap water or otherwise contaminated solutions. The ability of beryllium to withstand corrosive attack by water of varying purity and temperature, moisture, and high-temperature atmospheres is discussed. Suggestions for minimization of corrosion problems with the metal during manufacture of hardware and in actual service are made. Protection from both aqueous and high-temperature atmospheric attack could be achieved by a properly applied anodic coating. The performance of this type of coating in aqueous immersion, humidity cabinet, salt spray, and high-temperature oxidation tests is described. Paints and enamels may also be used to protect the metal. (auth)

20496 A STUDY OF LAMINAR REACTING BOUNDARY LAYERS ON TUNGSTEN, GRAPHITE, AND PYROLYTIC BORON NITRIDE. M. D. Bowen (Lockheed-Georgia Co., Marietta, Ga.) and E. D. Smyly. 28p. (CONF-641208-5).

From 3rd Conference on Performance of High Temperature Systems, Pasadena, Calif.

The results of a study of tungsten, pyrolytic boron nitride, and graphite reacting with air, assuming a frozen, laminar boundary layer, are presented. The heat and mass transfer were calculated for a pressure range of 0.01 to 100 atm over a wide range of wall temperatures. The temperatures associated with the rate-controlled and diffusion-controlled regimes are identified and the points corresponding to saturation of the boundary layer gases by WO_2 for tungsten combustion, and B_2O_3 and free boron for the BN combustion are located. Boron saturation is shown to be a high-temperature phenomena due to the manner in which BN vaporizes. The mass-transfer equations presented, show the differences in combustion of BN, a compound containing an element found in the free stream, and a pure element. The importance of considering elemental oxygen in calculating combustion rates for tungsten at low pressures is demonstrated. (auth)

20497 NUCLEAR REACTOR FUEL MEMBERS. Robert D. Leggett, Robert K. McGeary, and Eber K. Halteman (to General Electric Co. Ltd.). Canadian Patent 701,033. Dec. 29, 1964.

These fuel elements consist of a core containing molybdenum, niobium, platinum, and uranium and a cladding of tin, iron, nickel, chromium, and zirconium. The cladding is at least 3% of the core thickness. The core alloy is in the gamma phase and is said to be highly resistant to corrosion in water up to 650°F. (F.S.A.)

20498 USAGE OF A BERYLLIUM ALLOY FOR MATERIAL FOR GAS-COOLED REACTOR PARTS. Thomas Raine and James Alan Robinson (to Associated Electrical Industries Ltd.). German Patent 1, 181,923. Nov. 19, 1964. Priority date Dec. 2, 1960, Great Britain.

Gas-cooled nuclear reactor parts that must be resistant to the attack of wet carbon dioxide at high temperatures and pressures are made of an alloy of 0.05 to 3% calcium and beryllium. (Gmelin Inst.)

Fabrication

Refer also to abstracts 20437 and 21700.

20499 (AD-606291) COLUMBIUM ALLOY SHEET ROLLING PROGRAM. Final Report, March 7, 1963–September 1, 1964. H. L. Kohn and R. M. Curcio (Fansteel Metallurgical Corp., North Chicago, Ill. Metal Products Div.). Oct. 1964. Contract NOw 63-0231-c. 60p. $3.00 (CFSTI)

Six-inch diameter, 300 lb ingots of Fs-85 (Cb–27Ta–10W–1Zr) and B-66 (Cb–5V–5Mo–1Zr) were processed to produce 0.060-in. × 18-in. wide sheet. The FS-85 was successfully converted to target dimensions while the B-66 sheets did not meet the 18-in. width criteria. The finished sheet was evaluated with respect to chemical and mechanical properties and weldability. The ingot to sheet yield for FS-85 was 51.1% while the yield for B-66 was only 21.5%. FS-85 was considerably easier to fabricate accounting for the greatly superior yield of finished sheet from ingot. The quality of the sheet produced was roughly equivalent for the two alloys except that the FS-85 had better flatness. (CFSTI)

20500 (AFML-TR-64-387) THE PRIMARY WORKING OF REFRACTORY METALS. D. R. Carnahan (Westinghouse Electric Corp., [Blairsville, Pa.]) and V. DePierre (Air Force Materials Lab., Wright-Patterson AFB, Ohio). Nov. 1964. Contract AF33(616)-8325. 130p.

Three-inch diameter billets of sintered W + 2%ThO_2 and cast tungsten, molybdenum, and niobium alloys were heated to temperature ranges of 2400 to 4000°F and extruded by a 700-ton instrumented press through 60, 90, and 120 degree dies into 1.15 to 1.75 in. diameter bars. The extrusion techniques were evaluated by correlating deformation loads and extrusion properties with processing variables. Die load data were evaluated by the relation, die load divided by cross-sectional area of the upset billet equals an extrusion factor, K_d, multiplied by the natural logarithm of the reduction ratio. The following relationship was established between the extrusion factor, K_d, and extrusion temperature: $\ln K_d = \ln K_0 - m T$, where K_d is extrusion factor at temperature, T; K_0 is extrusion factor at 0°F and m = constant for the alloy. Lowest deformation loads were obtained with 60° dies, glass lubricated billets, extrusion speeds below four inches per second and long billet heating times. In some cases, 90° dies gave lower loads than 60° dies. In all cases 120° dies gave the highest loads. Deformation loads varied with billet material compositions and characteristics, e.g., fine grain W + 15%Mo, sintered W + 2%ThO_2, coarse grain W + 15%Mo (50 ppm carbon), and coarse grain W + 15%Mo (100 ppm carbon) require increasing deformation loads in the above order. Surface soundness of extruded bars are a function of processing variables and billet material characteristics. For sintered W + 2%ThO_2 and cast fine grain W + 15%Mo, best surface conditions are obtained by extrusion temperatures below 3600°F; cast coarse grain W + 15%Mo gave poorer surface conditions than either the sintered or fine grain tungsten alloys. For Mo–TZC extrusion temperatures below 3000°F gave the best surfaces. For niobium and tantalum alloys, molybdenum canning techniques were the only means for obtaining satisfactory extrusion surfaces. The canning technique for billets also lowered extrusion loads and provided protection against process contamination. Apparent coefficients of friction in the liner were calculated, ranged from .015 to .205, and tended to increase with extrusion temperature. Bare tungsten alloy billets gave lower coefficients of friction than glass coated billets in the temperature range 3200 to 4000°F. Metallurgical examinations, forging, swaging, and 3000°F tensile tests were made on the tungsten alloys. Metallurgical examinations were also made on Mo–TZC material. Chromium, columbium, molybdenum, tungsten, and tantalum metals

were extruded to provide wrought material of experimental alloys for evaluation by other agencies. These extrusions furnished supplementary data for evaluating processing techniques. (auth)

20501 (BRB-77) QUARTERLY PROGRESS SUMMARY, JANUARY–MARCH 1963. (Bridgeport Brass Co., Seymour, Conn.). Nov. 6, 1963. Contract AT(30-1)-1405. 40p. Dep.(mn); $2.00(cy), 1(mn) CFSTI.

The feasibility of using a traveling mandrel versus a ballistic-type mandrel for the extrusion of I&E tubing was investigated. Better dimensional stability was attained with the traveling mandrel, but mandrel cost versus life was prohibitive. The degree of control of the production variables to eliminate the formation of the duplex grain structure in the Mark V-E reactor fuel inner tubing extrusion process was successfully established. Ram speed and extrusion temperature are the important variables. An evaluation of an infrared optical pyrometer to measure the temperature and thereby control the quality of the uranium as it is being extruded was conducted. A brief initial investigation into the cause of the variation in the length of performance of extrusion dies composed of the same type material indicated a nonuniformity of hardness within the die and among the different samples. The use of a larger extrusion reduction ratio on Mark V-B reactor fuel tubes was found to produce better surface dimensions and grain structures than those currently produced. (W.L.G.)

20502 (DMIC-Memo-198) SURFACE DAMAGE IN MACHINED BERYLLIUM. S. W. Porembka and H. D. Hanes (Defense Metals Information Center, Battelle Memorial Inst., Columbus, Ohio). Jan. 4, 1965. Contract AF33(615)-1121. 14p.

It has been observed that in machining beryllium, microcracking is associated with a mechanically twinned layer caused by the machining. The severity of microcracking appears to be associated with the depth of the machine cut made in a single pass. Actual quantitative data were generated from a study of a machining-damage problem associated with the shingles for the Gemini spacecraft. The influence of this surface damage on the mechanical properties of beryllium is important if the beryllium is employed as a structural material. The damaged surface can be removed by chemical milling, but it may be necessary to remove an appreciable amount of metal (several thousandths of an inch) to eliminate the deepest cracks. Such damage can be reduced by making light finishing cuts. Surface damage can be avoided if electrical-discharge machining or electrochemical milling can be employed to shape the part. (auth)

20503 (EUR-2242.e) THE PREPARATION OF SODIUM SAMPLES FOR NEUTRON SCATTERING EXPERIMENTS. V. Verdingh and K. F. Lauer (European Atomic Energy Community, Ispra (Italy). Joint Nuclear Research Center and European Atomic Energy Community, Geel (Belgium). Central Nuclear Measurements Bureau). 1965. 12p. Dep.(mn).

A technique is described by which aluminium cans of various shapes can be entirely filled with purified, oxygen-free sodium metal. The method consists of melting and filtration of sodium under vacuum, followed by canning, gradual cooling, and/or extrusion. (auth)

20504 (EURAEC-1228) STAINLESS STEEL CLADDING OF VERY THICK STEELS. Quarterly Report No. 1, July 1–September 30, 1964. (Neratoom, N. V., The Hague (Netherlands); Rijksuniversiteit, Ghent (Belgium); and Soudometal, S. A., Brussels (Belgium)). Oct. 22, 1964. Work Performed under United States–Euratom Joint Research and Development Program. Contract 008-63-12 TEEB(RD). 20p. Dep.(mn); $1.00(cy), 1(mn) CFSTI.

Initiation of a research program on various stainless steel cladding parameters is reported. Activities during the period include material procurement and preparation of specimens for the preliminary research phase. (J.R.D.)

20505 (JAERI-1071) DEVELOPMENT OF BONDING METHODS FOR GRAPHITE MATERIALS. Yoshio Ando, Shozo Tobita, Tadato Fujimura, et al. (Japan Atomic Energy Research Inst., Tokyo). Oct. 1964. 43p. (In Japanese). Dep.(mn).

An account is given of bonding methods developed since 1959. (1) Brazing Materials. A new brazing material of Ni–Fe–Ti alloy was found for the bonding of graphite objects. On the other hand, a new type of brazing material, a paste, was also found. (2) Brazing Methods. Vacuum brazing, inert-gas-shielded arc brazing (Tig brazing), and resistance brazing were developed. The new techniques of reinforcement with metallic deposited beads and double-pass Tig brazing were also developed. (3) Bonding of Metallic Terminals on SiC Electric Heaters. In in-pile experiments, a SiC heater is suitable. A new process was found by which a titanium terminal can be bonded to a SiC heater with graphite as rink material. The terminals fabricated by this process are capable of using at 1000°C. (D.L.C.)

20506 (LA-3209) PREPARATION OF TERNARY PLUTONIUM ALLOYS FOR CORE TEST FACILITY PROGRAM. J. A. Leary and L. J. Mullins (Los Alamos Scientific Lab., Univ. of California, N. Mex.). Nov. 9, 1964. Contract W-7405-eng-36. 13p. Dep.; $1.00(cy), 1(mn) CFSTI.

Ternary plutonium-cerium-cobalt alloys are of interest as molten nuclear fuels. In preparing test fuel rods of such alloys, severe segregation of the components occurs unless special rod casting methods are applied. This report summarizes small-scale development work that was done to eliminate the problems associated with alloy segregation. These procedures have been incorporated into large scale fabrication of fuel pins. (auth)

20507 (MAB-206-M) FIRST PROGRESS REPORT BY THE AD HOC COMMITTEE ON METALWORKING PROCESSES AND EQUIPMENT. (Materials Advisory Board, National Academy of Sciences–National Research Council, Washington, D. C.). Mar. 15, 1965. 24p.

The function of the government Metalworking Processes and Equipment Program is to encourage studies of deformation theory which will lead to the improvement of manufacturing technology. An assessment was made of the potential of vibrational energy technology and hydrostatic extrusion which were the subjects of recent government-sponsored symposia, and conclusions and recommendations are submitted as to the value and limitations of these processes and the manner in which the development of each should be undertaken. (D.L.C.)

20508 (NAA-SR-Memo-10625) SNAP SYSTEMS BRAZE JOINT EXPERIENCE. J. R. Crosby (Atomics International, Canoga Park, Calif.). Nov. 5, 1964. Contract AT(11-1)-Gen-8. 13p. Dep.(mn); $1.00(cy), 1(mn) CFSTI.

The SNAP systems utilize a wide variety of braze alloy joints on various components which operate in high temperature-vacuum environments. A compilation of these braze alloy joints and their associated test history is presented. The major part of the discussion and data included is associated with braze applications specific to SNAP systems, particularly the SNAP-10A thermoelectric pump and the Mercury Rankine Program (MRP) thermoelectric pump; however, several material combinations with suggested filler materials are noted for possible utilization in future SNAP material joining problems. (auth)

20509 (NAA-SR-Memo-10633) CLOSURE WELD DEVELOPMENT REACTOR VESSEL, S8DS-12002. E. W. Crow (Atomics International, Canoga Park, Calif.). Oct. 30, 1964. Contract AT(11-1)-Gen-18. 17p. Dep.(mn); $1.00(cy), 1(mn) CFSTI.

Test samples that simulate the closure weld joint in type, thickness of material, and joint design in the Type 316 stainless steel vessel were prepared and welded. After welding, the test samples were subjected to radiographic examination. Specimens containing sections of the welds were prepared and subjected to tensile testing and metallographic evaluation. The welds produced were free of defects within specified limits. (auth)

20510 (NCSC-2663-16) URANIUM INTERSTITIAL PHASES. Quarterly Report, March 1964. J. V. Hamme, R. F. Stoops, and G. S. Sheffield (North Carolina State of the Univ. of North Carolina, Raleigh. Dept. of Engineering

Research). Work Performed under United States–Euratom Joint Research and Development Program. Contract AT(40-1)-2663. 14p. (EURAEC-1053). Dep.(mn); $1.00 (cy), 1(mn) CFSTI.

Specimens of $U(C_{0.75}O_{0.25})$ were sintered by hot pressing with conventional methods and by hot pressing in the presence of liquid uranium. Using conventional methods of pressing, it was found that the $U(C_{0.75}O_{0.25})$ reacted with CO to form UC and UO_2 unless the CO pressure could be maintained near the equilibrium value. Short sintering times and low temperatures (to retard the rate of reaction with CO) were not successful in preserving the oxygen saturated U(C,O). When specimens of $U(C_{0.75}O_{0.25})$ were sintered by hot pressing in the presence of liquid uranium, dense pellets were obtained. The lattice parameter of the U(C,O) phase did not change appreciably in some of these specimens, while in others there was a slight increase in the lattice parameter which indicated some change in composition of the U(C,O) phase. In all cases in which liquid uranium was present during hot pressing, the U(C,O) lattice underwent some distortion as seen by a broadening of the x-ray diffraction lines for the U(C,O) phase. Less UO_2 occurred in these pellets as compared with those obtained by conventional methods of hot pressing; however, some uranium metal remained in each of the pellets. (auth)

20511 (NCSC-2981-1) A NUCLEAR FUEL CONSISTING OF VERY SMALL, UNIFORMLY DISPERSED UC PARTICLES IN A URANIUM MATRIX. Quarterly Report, August 1962. Robert F. Stoops and Anthony J. Mione (North Carolina State Coll., Raleigh. Dept. of Engineering Research). Work Performed under United States–Euratom Joint Research and Development Program. Contract AT(40-1)-2981. 15p. (EURAEC-327). Dep.(mn); $1.00(cy), 1(mn) CFSTI.

All of the necessary equipment for initiating work on this contract has been received and installed. Two glove boxes with purified argon atmospheres are being used for processing the highly pyrophoric materials. The uranium monocarbide obtained for this research appears to be of high purity–especially in freedom from oxygen and nitrogen impurities. Experimental work was started approximately one month ahead of the work schedule. In the initial experiments, difficulties have been encountered with disintegration of the specimens at low temperatures and with oxidation. Changes in processing techniques are being made which are expected to eliminate these difficulties. (auth)

20512 (NCSC-2981-2) A NUCLEAR FUEL CONSISTING OF VERY SMALL, UNIFORMLY DISPERSED UC PARTICLES IN A URANIUM MATRIX. Quarterly Report, December 1962. Robert F. Stoops and Anthony J. Mione (North Carolina State Coll., Raleigh. Dept. of Engineering Research). Work Performed under United States–Euratom Joint Research and Development Program. Contract AT(40-1)-2981. 14p. (EURAEC-334). Dep.(mn); $1.00(cy), 1(mn) CFSTI.

Milling liquids and binders have been investigated. Cyclohexane was found to be suitable for use in milling uranium carbide and uranium hydride since no reactions were detected between this liquid and the uranium compounds. Naphthalene is a satisfactory binder material because it protects the powders from oxidation. It also provides adequate mold release characteristics and green strength to pressed parts and is easily removed at low temperatures. Critical outgassing temperatures were determined. By use of the new preparation techniques and by carefully controlling the rate of heating, samples were sintered without disintegration; but they were quite porous. This equipment should be of great value in achieving the desired density and microstructure. (auth)

20513 (NCSC-2981-3) A NUCLEAR FUEL CONSISTING OF VERY SMALL, UNIFORMLY DISPERSED UC PARTICLES IN URANIUM MATRIX. Progress Report, February 1963. Robert F. Stoops and Anthony J. Mione (North Carolina State Coll., Raleigh. Dept. of Engineering Research). Work Performed under United States–Euratom Joint Research and Development Program. Contract AT(40-1)-2981. 13p. (EURAEC-669). Dep.(mn); $1.00 (cy), 1(mn) CFSTI.

The major problems encountered initially in this research were disintegration and oxidation of the specimens. Special equipment was constructed to study the low temperature reactions which occurred during firing. Disintegration of specimens apparently resulted when the oxygen from adsorbed gases on the particle surfaces reacted with the very small particles of UC and UH_3. The heat from this exothermic reaction caused adsorbed nitrogen to be evolved so rapidly that the pelletized specimens virtually exploded. Since these gases were being adsorbed primarily during processing of the powders, an investigation was initiated to find a milling liquid and a lubricant-binder which would protect the very fine UC and UH_3 powders from oxidation. Of the materials investigated, cyclohexane and naphthalene were found to be most satisfactory. The desired UC particle size and distribution have been obtained in a specimen, but its density was somewhat low. Use of stearic acid as a grinding aid was an important factor in obtaining the very fine UC particles. Hot pressing has not been as successful a technique for producing dense specimens as dry pressing and sintering. On the basis of the results obtained during the first nine months of this research, the probability is high that a nuclear fuel consisting of very small, uniformly dispersed UC particles in a uranium matrix can be developed. (auth)

20514 (NCSC-2981-5) A NUCLEAR FUEL CONSISTING OF VERY SMALL, UNIFORMLY DISPERSED UC PARTICLES IN A URANIUM MATRIX. Quarterly Report, September 1963. Robert F. Stoops (North Carolina State of the Univ. of North Carolina, Raleigh. Dept. of Engineering Research). Work Performed under United States-Euratom Joint Research and Development Program. Contract AT(40-1)-2981. 21p. (EURAEC-868). Dep.(mn); $1.00(cy), 1(mn) CFSTI.

In efforts to fabricate U–UC cermets with the desired microstructure, specimens were prepared by cold pressing and vacuum sintering, by infiltration, and by vacuum hot pressing. Difficulties were encountered with the first two methods because films of UO_2 or UC or both formed on the surfaces of the particles of uranium metal before they melted. These films prevented the molten uranium from flowing between the UC particles and thereby eliminated densification by liquid phase sintering. When a dense specimen was obtained by the cold pressing-vacuum sintering technique, distribution of the uranium metal was not uniform. Therefore, hot pressing appeared to be the most promising technique for producing these cermets. Very dense specimens were produced by this method. The application of pressure during sintering apparently disrupts the films formed on the surfaces of the uranium particles and permits the molten metal to flow between the UC particles. When the uranium metal content of specimens had been high, some of the liquid metal extruded between the die and punches. The UC particles in dense specimens were about twice the desired size, and were not as well separated by the metal matrix as desired. (auth)

20515 (NCSC-2981-6) A NUCLEAR FUEL CONSISTING OF VERY SMALL, UNIFORMLY DISPERSED UC PARTICLES IN A URANIUM MATRIX. Quarterly Report, December 1963. Robert F. Stoops and Mitchell W. Haller (North Carolina State of the Univ. of North Carolina, Raleigh. Dept. of Engineering Research). Work Performed under United States–Euratom Joint Research and Development Program. Contract AT(40-1)-2981. 19p. (EURAEC-981). Dep.(mn); $1.00(cy), 1(mn) CFSTI.

Efforts were devoted to controlling grain growth and to improving the hot pressing technique for producing specimens. When Cr_3C_2 and VC were used as grain growth inhibitors, no reduction in UC particle size in the sintered specimens was observed. It is not known whether these materials were not effective as grain growth inhibitors or whether the particle sizes of the milled powders were larger than expected. Electron microscopy is being used to determine the size of the particles in the milled batches. The grain growth inhibitors, especially VC, apparently did

improve the UC particle separation substantially. Low cost ceramic dies were used for hot pressing U–UC specimens. After repeated use these dies showed little or no wear under the conditions employed. This could bring hot pressing die costs within the range of commercial feasibility. In many cases during the hot pressing operation, the liquid metal extruded from the specimens leaving UC of very nearly theoretical density. This extrusion occurred even when the difference between the OD of the punches and the ID of the die was 0.0127 mm (0.0005 in.). The existing hot press was modified to eliminate punch and thermocouple failures. (auth)

20516 (NCSC-2981-7) A NUCLEAR FUEL CONSISTING OF VERY SMALL UNIFORMLY DISPERSED UC PARTICLES IN A URANIUM MATRIX. Quarterly Report, March 1964. Robert F. Stoops and Mitchell W. Haller (North Carolina State of the Univ. of North Carolina, Raleigh. Dept. of Engineering Research). Work Performed under United States–Euratom Joint Research and Development Program. Contract AT(40-1)-2981. 21p. (EURAEC-1054). Dep.(mn); $1.00(cy), 1(mn) CFSTI.

Investigations showed that vanadium carbide, 0.6% by weight, did not inhibit uranium carbide grain growth, but it apparently promoted separation of the uranium carbide particles by the uranium. High alumina ceramic dies were used for hot pressing, but they apparently did not have sufficient strength under the conditions used. Ceramic dies made from thermocouple protection tubing had been satisfactory in previous experiments under the same conditions. A cursory investigation indicated that a squeeze-out technique is feasible for making dense parts from powders of refractory materials at relatively low temperatures. (P.C.H.)

20517 (NCSC-2981-8) A NUCLEAR FUEL CONSISTING OF VERY SMALL UNIFORMLY DISPERSED UC PARTICLES IN A URANIUM MATRIX. Quarterly Report, June 1964. Robert F. Stoops and Mitchell W. Haller (North Carolina State of the Univ. of North Carolina, Raleigh. Dept. of Engineering Research). Work Performed under United States—Euratom Joint Research and Development Program. Contract AT(40-1)-2981. 23p. (EURAEC-1155). Dep.(mn); $1.00(cy), 1(mn) CFSTI.

Indications were obtained that oxide contamination in specimens was associated with UC additions. Therefore, UC was eliminated from some of the batches, and they were prepared with UH_3 and carbon. When specimens were hot pressed from the latter batches, the UH_3 decomposed to form uranium; and the carbon reacted with part of this uranium to form UC. Use of batches containing UH_3 and carbon did not eliminate the oxidation problem, but it appears to have reduced oxide contamination. Very dense specimens having fine UC particle size were produced by using this combination of materials and by minimizing the time during hot pressing that the specimens were above the temperature of reaction between UC and uranium. The microstructures obtained represent a substantial improvement over those previously obtained, but distribution of the UC particles was not sufficiently uniform. Ceramic dies with thicker walls largely eliminated the problem of die failure during hot pressing. Since there is little or no reaction between the specimens and the ceramic material under the conditions employed, the punches and dies can be reused. A UC specimen with 99.6% of theoretical density was produced by the liquid phase extrusion technique. (auth)

20518 (NMI-TJ-29) HOT EXTRUSION OF METAL POWDERS. P. Loewenstein, L. R. Aronin, and A. L. Geary (Nuclear Metals, Inc., Concord, Mass.). Aug. 9, 1960. 30p.

Hot extrusion is a practical method of consolidating and shaping metal powders into long lengths of various cross sections. It generally yields superior physical properties, and is at present used as the production method for a number of aluminum base alloys. For other metals, however, hot extrusion is still in the laboratory stage. With the continuously increasing demand for metals suitable for higher temperature applications, canned extrusion of metal powders undoubtedly will become an important fabrication method since it permits handling of powders difficult to fabricate by other means. (auth)

20519 (NP-14879) BERYLLIUM COPPER MOLDS. G. G. M. Carr-Harris, comp. Revised by E. N. (Technical Information Service, National Research Council, Ottawa (Ontaric)). Nov. 1951. Revised July 1, 1963. 9p. (TIS-23)

Recent developments in the manufacture of beryllium–copper molds were investigated. It was found that such parts may be produced satisfactorily by sand casting, investment casting, or by pouring the molten metal around a master hob and applying pressure as the metal solidifies, the latter being the method general preferred. Advantages of pressure cast Be–Cu molds are listed. (P.C.H.)

20520 (SC-DC-65-1256) BONDING TO METALLIC FILMS AND SOLID-STATE DEVICES. [E. L. Chavez] (Sandia Corp., Albuquerque, N. Mex.). [Mar. 1965]. Contract AT(29-1)-789 . 23p. (CONF-650308-1). Dep.(mn); $1.00(cy), 1(mn) CFSTI.

From the Calif. Circuits Assn. Symposium, Palo Alto, Calif.

Methods used for making connections to thin-film devices and for bonding to devices that consist of various types of metallic surfaces on substrates or chips of varying thicknesses and composition are discussed. The methods include: soldering; welding; thermocompression bonding; and laser welding or bonding. The different processes described may be combined to form part of a unit or complete system, or they may be used individually, depending on the particular application. (P.C.H.)

20521 (TID-20625(Vol.I(Rev.I)) WELDING PROCEDURES. VOLUME ONE. Procedure Specifications, Welding Procedures, and Procedure Qualification Test Records (HWS-7171 through HWS-7172 Series). (General Electric Co., Richland, Wash. Hanford Atomic Products Operation). [1964]. 298p. (HWS-7170). Dep.(mn); $6.00(cy), 5(mn) CFSTI.

The on-site guide for ASME and ASA code welding is included. Specifications, procedures, and qualification test records are given for the shielded metal-arc welding of carbon steel plate and pipe, and for the oxyacetylene welding of carbon steel pipe. (D.L.C.)

20522 (TID-20625(Vol.II)(Rev.I)) WELDING PROCEDURES. VOLUME TWO. Procedure Specifications, Welding Procedures, and Procedure Qualification Test Records (HWS-7173 through HWS-7177 Series). (General Electric Co., Richland, Wash. Hanford Atomic Products Operation). [1964]. 287p. Dep.(mn); $6.00(cy), 5(mn) CFSTI.

Specifications, procedures, and qualification test records are given for the shielded metal-arc and gas tungsten-arc welding of austenitic stainless steel plate and pipe, and for the submerged arc welding of carbon steel plate and pipe. (D.L.C.)

20523 (TID-20625(Vol.III)(Rev.I)) WELDING PROCEDURES. VOLUME THREE. Procedure Specifications, Welding Procedures, and Procedure Qualification Test Records (HWS-7178 through HWS-7191 Series). (General Electric Co., Richland, Wash. Hanford Atomic Products Operation). [1964]. 282p. Dep.(mn); $6.00(cy), 5(mn) CFSTI.

Specifications, procedures, and qualification test records are given for the following welding processes: shielded metal-arc and gas tungsten-arc welding of austenitic stainless steel plate/pipe to carbon steel plate/pipe with and without consumable insert, gas tungsten-arc and shielded metal-arc welding of carbon steel and austenitic stainless steel pipe/plate, gas tungsten-arc welding of chromium (martensitic) steel plate/pipe to austenitic stainless steel plate/pipe, and shielded metal-arc welding of wrought iron. (D.L.C.)

20524 (TID-20625(Vol.IV)(Rev.I)) WELDING PROCEDURES. VOLUME FOUR. Procedure Specifications, Welding Procedures, and Procedure Qualification Test Records (HWS-7600 through HWS-8091 Series). (General Electric Co., Richland, Wash. Hanford Atomic Products

Operation). [1964]. 265p. Dep.(mn); $6.00(cy), 4(mn) CFSTI.

Specifications, procedures, and qualification test records are given for the following welding processes on plate, sheet, pipe, and tubing: gas tungsten-arc and shielded metal-arc welding of nickel and nickel-base alloys, gas tungsten-arc welding of cobalt-base alloy (Haynes 25) and titanium, and gas tungsten-arc and gas metal-arc welding of aluminum and aluminum alloys. (D.L.C.)

20525 ELECTROLYTIC DEPOSITION OF BERYLLIUM METAL FROM FUSED BERYLLIUM CHLORIDE-ALKALI CHLORIDE BATH. Tadashi Kuroda and Osamu Matsumoto. Bull. Tokyo Inst. Technol., No. 61, 29-41 (1964).

Studies were made of the electrolytic deposition of beryllium. The electromotive force of the cell $Be(s)/BeCl_2(l)-KCl + LiCl(eutectic)(l)/Cl_2(g)$, the current-potential relationship of $BeCl_2$ in alkali metal chloride melt, and the polarization potential of the $BeCl_2$–alkali metal chloride bath during electrolysis were measured. Data are presented in tables and graphs. When the electrolysis was carried out at a lower potential than the decomposition potential of the alkali metal chloride, the deposited metal was dendritic; at a higher potential the deposited metal was a mixture of dendrite and powder. (M.C.G.)

20526 98.2% DENSITY WITH VIBRATING IMPACT PRESSES. Robert F. Stoops (North Carolina State Coll., Raleigh). Ceram. Ind., 82: 54-7; 66; 68(Mar. 1964).

It is considered theoretically possible, with spheres of 3 different sizes, to obtain 98.3% of theoretical density in vibratory or impact forming techniques for ceramic materials. In most dry pressing operations involving hard ceramic particles, green densities in excess of 70% of theoretical were found to be difficult to obtain even under optimum conditions. In vibratory forming, the individual particles of a mixture are placed in vibratory motion in such a way that the particles tend to become arranged in the most dense packing configuration. UO_2 fuel elements were vibrationally compacted at frequencies in the sonic range to densities as high as 90% of theoretical. High-energy impact forming was used to compact UO_2 fuel rods 0.5-in. in dia and 8 ft long to 90% of theoretical density. Packed fuel rods are sometimes swaged to further increase their densities. Equipment for vibratory and impact forming is described. Advantages of these methods are discussed. (M.C.G.)

20527 A NEW METHOD FOR THE PREPARATION OF LARGE GRAINS OF ZIRCONIUM. Marc Billion and Jean-Paul Langeron (Centre d'Etudes de Chimie Metallurgique, Vitry-sur-Seine, France). Compt. Rend., 260: 152-4(Jan.4, 1965). (In French)

In the case of zirconium of sufficient purity, it is possible to prepare large crystals by the changing phase method: the transformation isotherm $\beta \rightarrow \alpha$ is displaced along the sample at a speed of 1 cm/hr. The crystals thus obtained possess a marked substructure. (tr-auth)

20528 SOL-GEL PROCESS FOR PREPARING SPHEROIDAL PARTICLES OF THE DICARBIDES OF THORIUM AND THORIUM–URANIUM MIXTURES. James L. Kelly, A. Todd Kleinsteuber, Sam D. Clinton, and Orlen C. Dean (Oak Ridge National Lab., Tenn.). Ind. Eng. Chem., Process Design Develop., 4: 212-16(Apr. 1965).

Spheroids of dicarbides of thorium and thorium–uranium mixtures were prepared from uranyl and thorium nitrate solutions by a sol-gel process. Thorium dioxide, prepared by the steam denitration of thorium nitrate, is dispersed to a sol in an aqueous nitrate solution. High-surface-area carbon is mixed into this sol. The resultant ThO_2–C is formed into spheroids by dispersing the sol into carbon tetrachloride. The spheroids are set to get by adding isopropyl alcohol to the mixture to extract some water. The resultant 150- to 450-micron spheroids are recovered, washed with an organic solvent, dried, and fired to produce the dicarbide. In a typical firing of the ThO_2–C gels, greater than 98% conversion to ThC_2 was obtained in 1½ hours at 1600°C in vacuum. Kinetic studies indicated that the carburization reaction is pseudo-first order, with an activation energy of about 112 kcal per mole of ThO_2. Thorium–uranium dicarbide spheroids are produced similarly by adding uranyl nitrate solution of an appropriate concentration at the sol preparation step. Coated spheroids of these dicarbides are of interest as fuel particles for graphite-matrix fuel elements, which are favored for high-temperature nuclear reactor fuel. (auth)

20529 ELECTRODEPOSITION OF RHENIUM ON MOLYBDENUM AND TUNGSTEN. I. M. Kvokova and V. I. Layner (Moscow Inst. of Steel and Alloys). Izv. Vysshikh Uchebn. Zavedenii, Tsvetn. Met., No. 4, 142-6 (July-Aug. 1964).

Rhenium was deposited on molybdenum and tungsten by electrolysis, which gave bright, dense deposits. The optimum conditions for obtaining the deposits were determined. A deposit 5 to 10 microns thick was obtained and heated in hydrogen at 1000°C for 15 min; in air at 100°C for 12 hr; in air at 250°C for 6 hr; and in glycerin and castor oil at 150°C for 12 hr. All results were negative. Above a thickness of 2 μ, the Re electrodeposits did not adhere well to Mo and W. It was found that Re deposits could be obtained on Mo and W only after the surface of Mo and W was etched in 15% NaOH with an alternating current at room temperature, a current density of 30 amp/dm^2, and a voltage of 20 v. The following electrolytes are proposed for electrodeposition of rhenium: 60 g/l $HReO_4$, 40 g/l H_2SO_4, 30 g/l $(NH_4)_2SO_4$; or 12 g/l $KReO_4$, 60 g/l H_2SO_4, 100 g/l $(NH_4)_2SO_4$, T = 18 to 20°C, pH 1, and D_c = 20 α/dm^2. In order to obtain deposits thicker than 2 μ it was necessary to grow 2-μ deposits on top of one another, and subject each to a heat treatment in an inert atmosphere at 800 to 1000°C for 10 to 20 min. (CFSTI)

20530 THE PREPARATION OF SINGLE PHASE SINGLE CRYSTALS OF URANIUM DIOXIDE IN THE O/U RANGE 2 TO 2.25. K. T. Scott and K. T. Harrison (Atomic Energy Research Establishment, Harwell, Berks, Eng.). J. Nucl. Mater., 15: 310-11(1965).

Single crystals of crushed fused UO_2 of 1 to 4-mm mean dia and O/U ratio <2.01 were oxidized in a uranium dioxide matrix of O/U ratio up to 2.44 prepared by the low-temperature (180°C) oxidation of ceramic grade UO_2 powder. A 7-day anneal at 800°C in a matrix of O/U = 2.44 produced black friable crystals with an O/U ratio of 2.22 and which showed no sign of grain boundaries or of a second phase. (M.C.G.)

20531 EVALUATION OF EDDY CURRENT INSPECTION FOR HOT SODIUM BONDING IN STAINLESS STEEL CLAD URANIUM CARBIDE REACTOR FUEL ELEMENTS. P. S. Vandervort, J. W. Morris, and S. H. Fitch (Atomics International, Canoga Park, Calif.). Mater. Evaluation, 23: 196-9(Apr. 1965).

Radac Model 440 eddy-current equipment was evaluated as a method for inspecting the sodium bonding of stainless steel-clad uranium carbide fuel rods. Using standard fuel rods containing known simulated defects, experiments were run with numerous machine settings, recorder chart speeds, and rod travel speeds to obtain optimum resolution of discontinuities. Over 80 experimental fuel rods were stripped of the cladding to determine the accuracy of the eddy-current indications. Excellent correlation between visual and eddy-current inspection was obtained. Results of the evaluation indicated that the equipment is capable of reliably detecting and identifying voids, gas bubbles, and lack of bonding or wetting as small as ⅛ in. diameter. Since this is less than the maximum amount of unbonding permissible, the eddy-current technique was demonstrated to be suitable and adequate for the application considered. (auth)

20532 INVESTIGATION OF HIGH-TEMPERATURE SINTERING OF TUNGSTEN. L. S. Vodop'yanov, V. V. Marychev, and Yu. A. Eyduk. Sb. Tr., Vses. Nauchn. Issled. Inst. Tverd. Splavov, No. 5, 221-4(1964).

Tungsten powder, produced by reducing WO_3, was compressed in a hydraulic press under a pressure of 2 ton/cm^2. The resulting low-density compacts were sintered in an atmosphere of H_2 at 750 to 800°C (1 to 1.5 hr). Final sintering of the compacts was accomplished in a vacuum

sintering machine at 10^{-3} mm Hg pressure and a temperature elevation rate of 50°C/min. The compacts began to sinter at 1300 to 1500°C. The sintering rate increased sharply as the temperature was raised to 2400°C. Further increase in temperature produced no appreciable increase in compact density. Impurities of Si and Cu were driven off at 1300°C; Ca, Cr, Fe, and Ni at 1600 to 1800°C; and Al at 2000 to 2200°C. Oxygen was effectively driven off at temperatures above 2200°C. The O_2 content in W sintered at 2200°C did not exceed 0.005%. (CFSTI)

20533 ALUMINOTHERMAL REDUCTION OF EUROPIUM OXIDE. G. G. Gvelesiani, Sh. M. Bezarshvili, and N. P. Mgaloblishvili. Soobshch., Acad. Nauk Gruz. SSR, 35: 379-86(1964).

Earlier studies on aluminothermal reduction were continued. The most promising method of obtaining pure europium is considered to be by the vacuum metallothermal reduction of the oxide. In the case of the reduction of Eu_2O_3 by aluminum, the equilibrium condition is determined solely by the europium vapor pressure since that of aluminum is negligible. This pressure was measured in high-temperature vacuum equipment for the high-temperature form of the oxide and an empirical equation was derived for the pressure and thermodynamic potential of the reaction. The kinetics of the reaction were studied for high- and low-temperature forms of the oxide; gas was evolved more rapidly from the former than from the latter, especially at 1100°C. Graphs show europium output under various conditions of temperature for the aluminothermal reduction process and Ginstling's equation is used to represent the results for the kinetic indices. The mechanism of the reduction process is discussed in terms of wetting, activation centers, crystal structure, and grain size. Unlike the case of ytterbium, no intermediate aluminate was formed, and the metal obtained at 1150°C contained 0.31% aluminum. (CFSTI)

20534 ARGON ARC WELDING OF STAINLESS STEEL TUBING WITH A CARBON DIOXIDE BLOW. F. A. Vagner and V. A. Kazarov. Svarochn. Proizv., No. 12, 28-30(Dec. 1964).

During the construction of the Beloyarsk Atomic Power Station, stainless steel tubing was TIG welded. To protect the reverse side of the root seam from the action of air and to provide for satisfactory forming of the seam inside the tube, argon or helium was supplied at slight excess pressure. The possibility of replacing the inert gases by CO_2 was experimentally tested. Tubing of ten melts with various typical sizes, produced domestically and abroad, was used. Welding was done with a nonconsumable tungsten electrode. The oxidation effect of CO_2 and its decomposition products was found to be insignificant. The thin oxide layer formed during beading, which followed the root seam, was scaled off to a considerable degree, apparently, because of differences in thermal expansion and did not have any effect on either the corrosion properties of the seam or its other properties. In any case the content of α-phase and the satisfactory corrosion resistance of the weld joints did not indicate the possibility of increasing the carbon content in the seam root nor the appearance of hot cracks. The root layer was done by argon-arc welding with a welding wire using dry CO_2 inside the tube. It was concluded that the use of CO_2 during welding of tubes considerably economizes the welding process while preserving the quality of the weld joint. The possibility of replacing inert gases by dry gaseous CO_2 for protecting and forming the reverse bead of the root seam is discussed. (CFSTI)

20535 CUTTING MACHINE AND EXAMINATION FACILITY, CELLS 9 (Engineering Materials). (Du Pont de Nemours (E. I.) & Co. Savannah River Lab., Aiken, S. C.). 26 drawings (CAPE-1165)

A remotely operated machine was designed for use in Cell 9 of the Metallography Facility for cutting specimens of radioactive materials for metallographic examinations and chemical studies. Either an abrasive or diamond wheel may be used for cutting specimens of various sizes and shapes ranging from a 0.5-in. cube to a 3.5 × 3.5 × 35 in. bar. The materials are cut under water in a box to contain the radioactive waste. The cell also contains an ultrasonic cleaner, centrifuge, and scrubber. (For details, see TID-4100) (M.C.G.)

20536 IMPROVEMENTS IN OR RELATING TO THE MANUFACTURE OF GRAPHITISED CARBON ARTICLES. (to Societe le Carbone-Lorraine). British Patent 975,366. Nov. 18, 1964. Priority Jan. 19, 1961, France.

A process is patented whereby carbon is impregnated with a solution of a compound or compounds of rare earths prior to graphitization. The carbon may be in the form of petroleum coke or carbon black in various shapes, and the rare earth may be any element of atomic numbers 57 to 71 inclusive. The process is specifically described using a ceric salt. After impregnation, the carbon is generally baked at temperatures below 1200°C. The rare earth addition greatly increases the graphitization ratio and improves the mechanical, physical, and electrical properties of the graphite produced. (A.G.W.)

20537 METHOD OF PRODUCING URANIUM CARBIDE. Alvin H. Kasberg (to Nuclear Materials and Equipment Corp.). German Patent 1,180,351. Oct. 29, 1964. Priority date Apr. 4, 1960, United States.

Uranium carbide is produced by arc melting a pressed mixture of uranium oxide and coal. The arc is generated between the consumable electrode containing the uranium oxide and the other electrode in an argon gas atmosphere. (Gmelin Inst.)

20538 METHOD FOR THE PRODUCTION OF GRANULATED URANIUM OXIDE. Maurice Delange, Henri Huet, and Paul Vertes (to Commissariat a l'Energie Atomique). German Patent 1,182,218. Nov. 26, 1964. Priority date May 18, 1960, France.

Granulated uranium oxide is produced by the thermal disintegration of ammonium uranate. The method comprises two steps, i.e., a pre-drying phase and a drying and annealing phase. In the first phase small, pulpy pieces of ammonium uranate (with a water content of 50 to 70%) are heated at 150 to 250°C so that the surface of the layers of these pieces become crusty. In the second phase the grains are thoroughly dried at 350 to 450°C to obtain a porosity suited for a treatment by gases, preferably fluorides. (Gmelin Inst.)

20539 METHOD OF PRODUCING DISPERSIONS OF FISSIONABLE MATERIAL FOR NUCLEAR FUEL ELEMENTS. Heinz Eberhard Roellig (to Zentralinstitut fur Kernphysik). German Patent 1,182,363. Nov. 26, 1964. Filed Nov. 22, 1962.

A method of producing stable dispersions of fissionable material in an aluminum matrix is described. A nitride layer is generated on the surface of aluminum powder particles with the help of a gaseous or liquid nitrogen-containing substance, the aluminum powder is mixed with UO_2 powder, and the whole mass pressed. (Gmelin Inst.)

20540 PRESSED BLOCK FOR THE FABRICATION OF NUCLEAR FUEL ELEMENT RODS. Horst Steinkopff and Lotar Loeffler (to Zentralinstitut fur Kernphysik). German Patent 1,185,308. Jan. 14, 1965. Filed Oct. 18, 1962.

A pressed block for the fabrication of encased nuclear fuel element rods by extruding this block is described. This block is composed of an uranium dispersion enclosed in a metallic casing the ends of which are conically strengthened and are provided with two sealed end caps. One end cap has a concavely shaped inner surface. (Gmelin Inst.)

Properties and Structure

Refer also to abstracts 19873, 19933, 20172, 20245, 21187, 21195, and 21703.

20541 (AD-604868) A METALLOGRAPHIC INVESTIGATION OF THE FACTORS AFFECTING THE NOTCH TOUGHNESS OF MARAGING STEELS. A. J. Birkle, D. S. Dabkowski, J. P. Paulina, and L. F. Porter (United

States Steel Corp., Monroeville, Pa. Applied Research Lab.). July 1, 1964. Contract NObs-88540. 58p. $3.00 (CFSTI).

Results are reported of an investigation of nine maraging steels with widely varying notch toughness (25 to 70 ft-lb Charpy V-notch energy at 190 ksi yield strength). Extraction fractography was used in conjunction with such techniques as light microscopy, thin-film electron microscopy, microprobe analysis, and electron-and x-ray-diffraction analysis to identify the causes for the difference in toughness among the nine steels. The results of the investigation indicate that by examining extraction fractographs with metallographic, x-ray- and electron-diffraction, and microprobe techniques it is possible to isolate the major factors responsible for low notch toughness in maraging steels. Thin-film transmission-electron microscopy and analysis of insoluble residue, while generally substantiating the results obtained by analysis of the fractographs, are less definite and therefore less useful than the fractographic studies. (CFSTI)

20542 (AD-606310) MECHANICAL AND PHYSICAL PROPERTIES OF TZM MOLYBDENUM ALLOY SHEET AND OF TUNGSTEN SHEET. Quarterly Progress Report No. 7, May 1–August 31, 1964. Clifford L. Dotson and P. G. Adams (Southern Research Inst., Birmingham, Ala.). Sept. 30, 1964. Contract N600(19)59530. 46p. $2.00 (CFSTI).

Tensile tests were conducted on recrystallized 0.060 in. and 0.100 in. tungsten sheet from room temperature up to 3500°F. Notched- and unnotched-tensile tests were conducted on the 0.060 in. tungsten sheet in the optimum and recrystallized conditions at moderately elevated temperatures (900°F and below) to determine the notched-tensile, brittle-ductile transition temperature. Tensile tests were conducted on recrystallized 0.060 in. and 0.100 in. tungsten sheet from room temperature up to 3500°F. Notched- and unnotched-tensile tests were conducted on the 0.060 in. tungsten sheet in the optimum and recrystallized conditions at moderately elevated temperatures (900°F and below) to determine the notched-tensile, brittle-ductile transition temperature. Tensile tests were completed on the 0.020 in., 0.040 in., and 0.060 in. TZM temperatures for these tests ranged from room temperature to 3000°F. (OTS).

20543 (AERE-GR-101) LOW-TEMPERATURE ELECTRICAL RESISTIVITY OF URANIUM AND BERYLLIUM. W. H. Denton (Atomic Energy Research Establishment, Harwell (England)). Feb. 20, 1947. 24p. Dep.(mn).

For U, the ratio $R_O/R_{273.2}$ was used to monitor the purity of U specimens. The lowest $R_O/R_{273.2}$ value measured was 0.06. At high purities, the physical condition has a large influence on $R_O/R_{273.2}$. Thus, small differences in amounts of impurities can be resolved only if the samples are first prepared in a physically "pure," strain-free condition. The treatment required to produce this physically "pure" condition involves annealing just below the lower transition temperature (647°C) and slow cooling. It is estimated that for chemically pure and strain-free U, the specific resistance at 0°C is $\sim 2.5 \times 10^{-5}$ ohm-cm, and $R_{99}/R_{273.2} \sim 0.36$. For Be, a very large drop in $R_O/R_{273.2}$ from 0.43 to 0.06 results after a heat treatment at 700°C. It appears that the presence of 0.5% metallic impurities causes a rise in $R_O/R_{273.2}$ of about 0.20 and an increase in ρ(0°C) of about 2.4×10^{-6} ohm-cm. The ρ(0°C) of pure strain-free Be at 0°C is estimated to be $\sim 3.2 \times 10^{-6}$ ohm-cm. (D.L.C.)

20544 (AFML-TR-64-388) INVESTIGATION OF THE MECHANICAL CHARACTERISTICS OF ZONE-LEVELED BERYLLIUM. J. A. Carrabine, A. J. Stonehouse, D. G. Fetsko, and W. W. Beaver (Brush Beryllium Co., Cleveland, Ohio). Nov. 1964. Contract AF33(615)-1177. 67p.

Zone-leveling was found to produce beryllium single crystals of intermediate purity, having moderately high basal glide capacity, while retaining reasonably high strength. Properties of the zone-leveled crystals are dependent upon zone travel rate, but not upon the number of zone passes. The enhanced basal glide corresponds to an agglomeration of insoluble impurities, and a retention of the soluble elements in solid solution. The process results in some bulk purification, but does not alter significantly the plastic anisotropy of the crystals. Application of the zone-leveling concepts, in a modified manner, to commercial hot-pressed polycrystalline Be resulted in an improvement in room-temperature tensile elongation, with only minor strength alterations. The implication of these results is that a refinement of the thermal and chemical parameters involved in the process could possibly lead to a materially improved engineering metal of available purity, thus precluding the high-purity approach. (auth)

20545 (BNWL-16) THE FATIGUE BEHAVIOR OF Pu–1.0 w/o Ga DELTA-STABILIZED PLUTONIUM. H. R. Gardner (Battelle-Northwest, Richland, Wash. Pacific Northwest Lab.). Jan. 22, 1965. Contract AT(45-1)-1830. 10p. Dep.(mn); $1.00(cy), 1(mn) CFSTI.

Several metallurgical conditions of Pu–1.0 wt % Ga alloy sheet were fatigue tested at room temperature in cyclic flexure with a superimposed mean stress. It was concluded that fatigue strength was relatively insensitive to yield strength, i.e., metallurgical condition. Over a 0.1% yield strength range of 10,300 to 30,400 psi, fatigue strength varied only from 10,000 to 15,000 psi. The cored, as-cast and homogenized, 94% rolled, 300°C annealed conditions had the lowest fatigue strengths while the cored, 86% rolled sheet had the highest fatigue strength. The presence of alpha phase either initially or introduced during testing seemed to impart increased resistance to fatigue failure. (auth)

20546 (CEA-R-2726) ETUDE DES TRANSFORMATIONS ALLOTROPIQUES DU PLUTONIUM AU MICROSCOPE A PLATINE CHAUFFANTE. (Observation of Allotropic Transformations of Plutonium With a Hot Stage Microscope). Jean Mars and Bernard Spriet (Commissariat à l'Énergie Atomique, Fontenay-aux-Roses (France). Centre de Etudes Nucléaires). Jan. 1965. 56p. Dep.(mn).

A hot stage microscope designed for the examination of plutonium and its alloys is described. This apparatus was used to study the $\alpha \rightleftharpoons \beta$, $\beta \rightleftharpoons \gamma$, $\delta \rightleftharpoons \epsilon$ allotropic transformations of pure or β- and δ-stabilized plutonium. The $\alpha \rightarrow \beta$ transformation is typically a nucleation and growth process. Some particularities caused by the internal stresses due to the volume change during this transformation are examined. The kinetics was studied as a function of these stresses and a temperature dependent activation energy for nucleation was deduced. The $\beta \rightarrow \alpha$ transformation presents a memory effect which implies an orientation relationship between the two phases. This fact is probably caused by the stresses created during the $\beta \rightarrow \alpha$ transition. The $\beta \rightleftharpoons \gamma$ and $\delta \rightleftharpoons \epsilon$ transformations are also diffusion governed processes. (auth)

20547 (CEA-R-2731) VARIATIONS DU PARAMETRE DU MONOCARBURE D'URANIUM EN FONCTION DE SA TENEUR EN CARBONE. (Variations of the Uranium Monocarbide Parameter with Changes in the Carbon Content). Pierre Magnier and Andre Accary (Commissariat à l'Énergie Atomique, Saclay (France). Centre d'Études Nucléaires). Jan. 1965. 5p. Dep.(mn).

It is shown that the chemical species uranium monocarbide is only a particular composition of the uranium–carbon alloy phase containing between 48 and 50 atoms per cent of carbon, and that the crystalline parameter of this phase varies simultaneously from 4.956 Å to 4.961 Å. (auth)

20548 (CONF-640204(p.35-43)) APPLICATION OF HIGH-VOLTAGE ELECTRON MICROSCOPY IN METALLURGICAL RESEARCH. R. M. Fisher (United States Steel Corp., Monroeville, Pa. Research Center).

A survey is presented of the direct examination of metallurgical specimens in the transmission electron microscope. Techniques are described, and image contrast and the effects of high voltage are discussed. Some applications in metallurgy are described briefly. (D.L.C.)

20549 (EURAEC-1282) STUDY OF BASE METAL TO BE USED IN RESEARCH ON BRITTLE FRACTURE OF LARGE WELDED ASSEMBLIES. IMPACT STRENGTH, ROBERTSON AND PELLINI TESTS ON SUPER ELSO

NICKEL–CHROMIUM STEEL. Quarterly Report No. 3, September 1–December 31, 1964. (Institut de Recherches de la Siderugrie, St.-German-Enlaye (France)). Jan. 1965. Work Performed under United States–Euratom Joint Research and Development Program. Contract 031-64-5 TEEF. 12p. Dep.(mn); $1.00(cy), 1(mn) CFSTI.

Impact strength, Robertson, and Pellini tests for brittle fracture were performed on specimens taken from the center and skin of Super Elso chromium–nickel steel plate. All tests show a higher transition temperature for the specimens taken from the center. (W.L.G.)

20550 (HW-84550) A STUDY OF TUNGSTEN–TECHNETIUM ALLOYS. Quarterly Progress Report, October 1, 1964–January 1, 1965. (General Electric Co., Richland, Wash. Hanford Atomic Products Operation). Jan. 1, 1965. Contract AT(45-1)-1350. 28p. Dep.; $2.00(cy), 1(mn) CFSTI.

W and Tc powders were blended and pressed to form compacts for arc melting. The composition was varied from 2.5 to 60 at. % Tc. Hydrogen sintering was found to be required before the compacts could be arc melted successfully. The hardness of the as-cast buttons was measured. No second phase inclusions were observed in the metallographic examination of the H_2-reduced Tc powder. Microstructures of electron-beam-melted pure Tc buttons were observed before and after forging. (D.L.C.)

20551 (IDO-17063) SLOW NEUTRON INELASTIC SCATTERING FROM ALUMINUM POWDER. R. M. Brugger and P. D. Randolph (Phillips Petroleum Co., Idaho Falls, Idaho. Atomic Energy Div.). Feb. 1965. Contract AT(10-1)-205. 27p. Dep.; $2.00(cy), 1(mn) CFSTI.

Measurements of the slow neutron inelastic scattering from a sample of polycrystalline aluminum, of transmission 0.87, have been made using the MTR phased-chopper velocity selector, for wave vector changes between 1.5 and 11 $Å^{-1}$ out to energy transfers of 0.076 ev. Momentum-dependent structure is observed in the scattering. The position and the shift of this structure with increasing energy transfer is explained on the basis of the dispersion relations and the phonon polarization factor. Measurements were made with and without thin cadmium spacers in the sample, in order to examine the effects of multiple scattering. These effects are most pronounced at small momentum transfers, the cadmium producing as much as 40 percent decrease in the elastic scattering data. Multiple scattering is present in the inelastic scattering data but is not as obvious as in the elastic scattering data. Calculations of the frequency distributions in the incoherent approximation were made at several fixed values of momentum transfer in the hope that some value would become apparent at which this calculation would give a valid result. No such value was found. The first moments of the energy transfer were calculated and these agree well with theoretical predictions except at small momentum transfers where multiple scattering is large. (auth)

20552 (IITRI-B6021-6) VANADIUM ALLOY STUDIES. Final Report. F. C. Holtz (IIT Research Inst., Chicago, Ill.). Feb. 24, 1965. Contract NOw 64-0239-c. 31p.

Coated vanadium alloys containing substantial amounts of refractory metal additions have shown promise for application of 2000 to 2400°F; the principal purpose of this program was to improve the short-time rupture strength. Alloys based on V–60Nb, V–40Nb–30 Ta, and V–50 Ta were fabricated to 0.025-in. sheet and evaluated for mechanical properties at room temperature and 2200°F. Arc-melted ingots exhibited excellent cold rollability once the cast structure had been broken down, and nearly all of the alloys had more than 20% tensile elongation at room temperature. The alloy V–40Nb–30Ta–1Ti–0.235Si–0.075C had an ultimate tensile strength of 210,000 psi in the fully recrystallized condition. Room-temperature deformation of most of the alloys was accompanied by extensive twinning. Compositions based on V–50Ta were age hardenable. Creep-rupture data obtained under a 10,000 psi load at 2200°F in vacuo showed that creep rates of the experimental alloys were much lower than the dilute Nb–1Zr alloy, but were somewhat higher than current commercial niobium alloys. Creep rates for some of the experimental alloys were 0.05 in./in./hr during a 2-hr exposure. (auth)

20553 (KFK-262) THE PHONON FREQUENCY DISTRIBUTION OF VANADIUM. W. Glaeser, F. Carvalho, and G. Ehret (Kernforschungszentrum, Karlsruhe (West Germany). Institut fur Angewandte Kernphysik). Dec. 1964. 12p. (CONF-804-28). Dep.(mn)

From Symposium on the Inelastic Scattering of Neutrons, Bombay, Dec. 1964.

The scattering law of vanadium was measured for a relatively large range of momentum transfer ($0<Q<14$ $Å^{-1}$) and energy transfer ($0<\hbar\omega<2k_BT$). Monoenergetic neutrons at ~20, 40, and 80 Mev were used. The frequency distribution function was derived from the scattering law measurements and compared with previous results obtained with the beryllium-filter technique. (D.L.C.)

20554 (LA-3161) CRYOGENIC TENSILE TESTING OF PROJECT ROVER MATERIALS. D. T. Eash (Los Alamos Scientific Lab., Univ. of California, N. Mex.). June 1964. Contract W-7405-eng-36. 64p. Dep.; $3.00(cy), 2(mn) CFSTI.

A tensile cryostat was developed with necessary adaptors to facilitate component testing of materials of interest to Project Rover at ambient, liquid nitrogen, and liquid hydrogen temperatures. A detailed description of the cryostat and types of tests performed, as well as data from testing of approximately 300 specimens, are included. (auth)

20555 (LA-3215) THE OVERDRIVING EFFECT IN DYNAMIC POLYMORPHISM. T. R. Loree, F. S. Minshall, and D. Stirpe (Los Alamos Scientific Lab., Univ. of California, N. Mex.). Nov. 1964. Contract W-7405-eng-36. 20p. Dep.; $2.00(cy), 1(mn) CFSTI.

Experimental investigations on the overdriving effects on the transition and elastic pressure in polymorphism dynamics are presented for three materials: the binary alloy 20 wt % nickel in iron, which showed no effect; 20 wt % chromium in iron, in which a strong effect was found; and 4340 steel of various hardnesses, in which the effect varied with hardness. A model is proposed for the case in which the transition pressure decays as the sample thickness is increased. (P.C.H.)

20556 (NASA-TN-D-2723) THE VAPOR PRESSURE OF MAGNESIUM BETWEEN 223° AND 385°C. William P. Gilbreath (Ames Research Center, National Aeronautics and Space Administration, Moffett Field, Calif.). Mar. 1965. 9p. $1.00(CFSTI).

The vapor pressure of magnesium was determined using a modification of Langmuir's weight-loss method. The vapor pressure of magnesium in the range investigated could be expressed by the equation $\log P_{torr} = 8.6047 - 7560.3/T$ for temperatures between 496 and 658°K. The enthalpy change for the reaction Mg (solid) → Mg (gas) at 298.15°K was found to be 35.3 ± 0.4 kcal/mole. The effect of surface impurities, mainly oxide, in inhibiting the free sublimation of magnesium was found to be especially important in this range. (auth)

20557 (NMI-TJ-60) THE EFFECTS OF PURIFICATION AND REALLOYING ON THE MECHANICAL PROPERTIES OF ZONE-REFINED BERYLLIUM SINGLE CRYSTALS. D. F. Kaufman and L. R. Aronin (Nuclear Metals, West Concord, Mass.). Nov. 27, 1964. Contract AT(30-1)-2784. 18p. (CONF-729-20). Dep.(mn); $1.00 (cy), 1(mn) CFSTI.

From International Conference on Beryllium, Philadelphia, Oct. 1964.

Studies were made on zone-refined Be single crystals to determine the effects of purification on prismatic slip, to learn whether new modes of deformation are activated in high purity Be, and to determine by means of selective realloying the impurity or impurities that might be causing embrittlement. The results showed that the principal benefits from purification by zone-refining are to reduce restrictions on the prismatic and basal glide processes. Significant improvements in deformation behavior seemed to occur after the first few zone-refining passes on a wide variety of starting materials. Purification to very high levels appeared to result in little further change in defor-

mation processes other than lowering of the CRSS's for basal and prismatic slip and an increased resistance to basal cleavage. However, ultimate failure by basal cleavage was still seen even in material of the highest purity. No significant new modes of deformation appeared to be activated as a result of purification. (P.C.H.)

20558 (NP-14888) MACROLAMINATE PARTICLE COMPOSITE MATERIAL DEVELOPMENT. Interim Report No. 5, December 1–February 1, 1965. F. H. Simpson and L. M. Stejskal (Boeing Co., Seattle, Wash. Aero-Space Div.). Contract NOw-64-0194-f. 32p.

Investigation of factors associated with the knife coating process and layer thickness which can cause wide variations in the properties of 93.1 HfO_2 • 4.9 CeO_2 • 2MgO-Mo macrolaminate composites showed: (1) The glass inclusions in the ceramic phase are mainly magnesium • aluminium • silicate with limited amounts of zirconia, hafnia, and ceria (alumina and silica are impurities found in reactor grade II hafnia). (2) Significant segregation of grain into different size fractions from the starting to the finishing ends of laminate panels has not occurred. (3) Magnesium oxide exists as a fine coating around individual hafnium particles or in agglomerates. Oxidation resistance is believed to be closely associated with the manner in which the magnesium oxide is distributed. An evaluation of the effect of particle size on the properties of the composite show: (1) Flexural strength increases with decreasing laminate particle size. (2) Maximum oxidation resistance is obtained from specimens fabricated from –100 + 200 mesh particles. (3) Specimens made from single particle size fractions have better oxidation resistance than those containing a variety of sizes including the fines. (4) Specimens made from a variety of sizes including the fines have higher flexural strength than those made from a single particle size fraction. (5) Maximum deformation in compression is achieved in specimens made from –20 mesh particles and is minimum in specimens made from –100 + 200 mesh particles. The rapid increase in compressive deformation and flexural strength and the rapid decrease in oxidation resistance in specimens made from –200 mesh material could indicate that segregation between the metal and ceramic is occurring in the –200 mesh material and higher ceramic concentration in the –100 + 200 mesh material. Evaluation of particle shape indicates little difference in strength occurs between specimens made from plate-like and the more cubical shaped particles. Specimens made from particles rectangular in cross section with one axis elongated produced flexural strength approximately 40 percent higher than those obtained from specimens made from plate-like or cubical particles. Surface texture of particles as well as the shape factor is suspected of improving the strength of specimens made from the elongated shaped particles. Forming of macrolaminate composites by hot pressing, isostatic pressing, and warm extrusion is discussed. Difficulties in optimizing the sintering cycle have been encountered. They are attributed to variations in the atmosphere and pressure during vacuum sintering. (auth)

20559 (NP-14892) PREPARATION AND PROPERTIES OF TUNGSTEN AND TUNGSTEN–SILVER TEST SPECIMENS FOR U. S. NAVAL ORDNANCE TEST STATION—CHINA LAKE. Report No. 30-144. J. C. Kenney (Mallory Metallurgical Co., Indianapolis, Ind.). Feb. 28, 1963. Contract N60530-7919. 24p.

Three specimen groups of 21 specimens each were prepared from seven different tungsten powders. The first group was hot-pressed tungsten, while the other two groups were infiltrated with silver. The property data presented includes pre-infiltrated density, theoretical density, microstructure, infiltrated density and chemical analysis for the second and third groups, and hardness and compression tests at 1500°F for the third group. (D.L.C.)

20560 (ORNL-3777) EVALUATION OF THORIUM-BASE ALLOYS FOR HIGH-TEMPERATURE STRENGTH. J. A. Burka and J. P. Hammond (Oak Ridge National Lab., Tenn.). Apr. 1965. Contract W-7405-eng-26. 26p. Dep.; $2.00(cy), 1(mn) CFSTI.

An exploratory evaluation of the elevated-temperature properties of thorium-base alloys has been made. Hot hardness and recrystallization temperature up to 750°C were used as screening tests to indicate the effectiveness of the alloying elements in strengthening thorium at high temperature. Zirconium and indium showed the most promise as alloying additions. The Th-5 wt % Zr alloy was four times as hard as unalloyed thorium at 750°C and the Th–4 wt % In alloy five times. At 400°C, the Th–0.2 wt % Be–0.2 wt % C alloy was about three times as hard as unalloyed thorium or about as hard as the indium-containing alloys. Zirconium and indium harden thorium principally by solid-solution strengthening with some contribution by intermetallic hardening in the case of indium. (auth)

20561 (PWAC-380) THE SOLUBILITY OF HELIUM IN LITHIUM AND POTASSIUM. H. Slotnick, S. M. Kapelner, and R. E. Cleary (Pratt and Whitney Aircraft, Middletown, Conn. Connecticut Aircraft Nuclear Engine Lab.). Feb. 24, 1965. Contract AT(30-1)-2789. 26p. Dep.; $2.00(cy), 1(mn) CFSTI.

The solubility of helium in lithium and potassium was determined at temperatures to 871°C and 704°C, respectively, and pressures to 3 atmospheres. The solubility of helium in both alkali metals increases with temperature and pressure. In lithium, the solubility increased from 3.89×10^{-7} moles helium per liter lithium per atmosphere at 649°C to 5.63×10^{-7} moles per liter-atmosphere at 871°C. In potassium, the solubility increased from 5.87×10^{-5} moles per liter-atmosphere at 482°C to 1.71×10^{-4} moles per liter-atmosphere at 704°C. Henry's Law is obeyed in each case. (auth)

20562 (SU-DMS-65-1) DISLOCATION STRUCTURE OBSERVATIONS AT LUDERS FRONTS IN TANTALUM. Technical Report No. 12. Troy W. Barbee, Jr., and Robert A. Huggins (Stanford Univ., Calif. Dept. of Materials Science). Jan. 1965. Contract Nonr-225(34). 27p.

Dislocation configurations at Lüders fronts in tantalum, which deformed by non-uniform discontinuous yielding, were examined. No contrast structure was observed in grain boundaries of recrystallized material unless evidence of sample mishandling or incomplete recrystallization was observed. No classical pileups were seen although slip bands were found in regions just ahead of a Lüders band. Dislocation source action at or near grain boundaries was observed at Lüders fronts and within Lüders bands. The dislocation density was observed to increase during the passage of a Lüders front and grain boundaries were seen to rapidly develop contrast structure during the passage of a Lüders front. These observations are discussed in light of current knowledge concerning the mechanism of discontinuous yielding. (auth)

20563 (TID-21668) THERMAL CONDUCTIVITY OF UO_2 BY A RADIAL HEAT FLOW METHOD. A. D. Feith (General Electric Co., Cincinnati, Ohio. Nuclear Materials and Propulsion Operation). 1963. Contract AT-(40-1)-2847. 25p. (TM-63-9-5). Dep.(mn); $1.00(cy), 1(mn) CFSTI.

The thermal conductivity of high density UO_2 (ρ = 95.6 percent of theoretical) was measured in the temperature range 550 to 2165°C by a radial heat flow technique. Test results at higher temperatures in the temperature range 1600 to 2200°C indicate increasing values of k with T; however, due to increasing difficulties in making measurements at these temperatures, the magnitude of the observed increase is questionable and accurate identification requires some additional experimentation. The variation in conductivity with temperature for this material may be expressed as $k = 11.449/274.77 + T + 2.323 \times 10^{-13} T^3$, where k is in cal/sec-cm-°C and T is in °K. (auth)

20564 (UCRL-12252) MORPHOLOGICAL OBSERVATIONS AFTER DISTILLATION OF BERYLLIUM FROM THE SOLID STATE AT HIGH TEMPERATURES. R. F. Bunshah (Lawrence Radiation Lab., Univ. of California, Livermore). Feb. 15, 1965. Contract W-7405-eng-48.

20p. (CONF-650508-1). Dep.(mn); $1.00(cy), 1(mn) CFSTI.

For Presentation at International Conference on Beryllium Metallurgy, Grenoble, France.

Beryllium was distilled from a 1-in.-dia by 3-in.-long rod that had been premelted and cast in vacuum. The distillate was collected on a hot tantalum collector surrounding the rod. Observations showed that the {0001} planes formed evaporation facets on the distilland rod. Filamentary crystallites oriented orthogonally to the rod axis were found on the surface of the distilland rod. Compared to the starting material and the distillate, these crystallites were rich in low-vapor-pressure impurities such as Fe, Ni, and Cu. Models for the growth of these crystallite networks are proposed. Frequently whiskers of beryllium grew out from the condensate. These were single crystals with the c-axis inclined at a small angle (about 10°) from the whisker axis. (auth)

20565 (WADD-TR-60-37(Pt.V)) PHYSICAL METALLURGY OF TUNGSTEN AND TUNGSTEN-BASE ALLOYS. Heinz G. Sell, George W. King, Randolph H. Schnitzel, and N. Francis Cerulli (Westinghouse Electric Corp., Bloomfield, N. J. Lamp Div.). May 1964. Contract AF33(657)-8347. 106p. CFSTI.

Tensile properties of high purity powder metallurgy tungsten and W-1% ThO_2 alloy were determined at various strain rates and temperatures (800-2400°C). 1% ThO_2 imparts a slight overall increase in strength properties, although above 0.5 T_m these properties are affected by void formation. The tensile properties of pure W and W-0.35% Ta single crystals (worked, and worked and recrystallized) investigated from R.T. to 1200°C were found to be affected by C, particularly in the quenched condition. An alloy screening program was conducted with W-25% Re, and 1% ThO_2 and 1% HfN additions, and with single crystals of W-3.5% Ta-C. The W-Re alloys have superior strength up to 2400°C. A yield stress of 47 kpsi was found at 1600°C in the quenched W-3.5% Ta-C single crystal. Reactions of ThO_2 with W, C, and several carbides were investigated as was the reaction W + TaC. A phase diagram of the W-Ta-C system resulted. (auth)

20566 (IS-Trans-13) A NEW METHOD FOR DETERMINING THE MELTING POINT OF REFRACTORY METALS. Marcello Pirani and Hans Alterthum. Translated for Ames Lab., Ames, Iowa, from Z. Elektrochem., 29: 5-8(1923). 6p. Dep.(mn); $1.10(fs), $0.80(mn) JCL.

A 7-mm thick rod with a fine hole drilled crosswise with respect to its axis, was used for the determination of the melting point of refractory metals, employing the hole as a black body during the temperature measurements. The melting is usually indicated by the formation of a drop of liquid metal in the hole. The melting points of tungsten and molybdenum were determined by this method; they were found to be 3660 ± 60°K and 2840 ± 40°K, respectively, being in good agreement with other recent measurements. The sources of error encountered during the measurement were discussed briefly. (auth)

20567 (LA-tr-65-5) DENSITY OF Co-C AND Ni-C ALLOYS IN SOLID AND LIQUID STATES. E. S. Filippov, A. A. Vertman, and A. M. Samarin. Translated by Helen J. Chick and C. P. Kempter (Los Alamos Scientific Lab., Univ. of California, N. Mex.), from Izv. Vysshikh Uchebn. Zavedenii, Chern. Met., 7: 162-4(1964). 6p. Dep.(mn); $1.00(cy), 1(mn) CFSTI; $1.10(fs), $0.80(mn) JCL.

The temperature and concentration dependence of the density in Co-C and Ni-C systems in the liquid and solid states were investigated. The results of measurements are given in the form of a polytherm of the density. From the polytherms of the density in the region of 1000-1700°C, isotherms were constructed and the effects of carbon on the volume changed during melting were evaluated. Decreases in viscosity and electrical conductivity in proportion to the increase of the concentration of carbon in the systems is explained by the formation of microgroups of carbon. The temperature dependence of the density in semi-logarithmic coordinates for the melts of Co-C and Ni-C can be represented by straight lines (with the exception of the eutectic alloys) such as for pure Ni and Co. (P.C.H.)

20568 THE CRYSTAL STRUCTURE OF TERNARY SILICIDES ThM_2Si (M = Cr, Mn, Fe, Co, Ni AND Cu). Z. Ban and M. Sikirica (Instutute "Rudjer Boskovic," Zagreb). Acta Cryst., 18: 594-9(Apr. 10, 1965).

The existence of well-defined and isomorphous ternary phases of the general composition ThM_2Si_2 (M = Cr, Mn, Fe, Co, Ni, and Cu) was established in the corresponding intermetallic systems. The crystal structure of the isomorphous series of compounds was determined by the x-ray powder method. The compounds crystallize in the tetragonal system in the space group $I4/mmm$ (D_{4h}^{17}), as determined from the systematically absent reflections. The unit cells containing two formula units of ThM_2Si_2, have the dimensions: $ThCr_2Si_2$, a = 4.043 ± 0.001, c = 10.577 ± 0.002 Å; $ThMn_2Si_2$, a = 4.021 ± 0.001, c = 10.493 ± 0.002 Å; $ThFe_2Si_2$, a = 4.038 ± 0.003, c = 9.820 ± 0.005 Å; $ThCo_2Si_2$, a = 4.015 ± 0.003, c = 9.760 ± 0.005 Å; $ThNi_2Si_2$, a = 4.076 ± 0.001, c = 9.551 ± 0.002 Å; and $ThCu_2Si_2$, a = 4.104 ± 0.001, c = 9.864 ± 0.002 Å. (auth)

20569 MIXED OXIDES OF TITANIUM AND NIOBIUM. THE CRYSTAL STRUCTURE OF $TiNb_{24}O_{62}$ ($TiO_2 \cdot 12Nb_2O_5$). R. S. Roth and A. D. Wadsley (C.S.I.R.O., Melbourne). Acta Cryst., 18: 724-30(Apr. 10, 1965).

$TiNb_{24}O_{62}$ is monoclinic, with a = 29.78, b = 3.821, and c = 21.12 Å, β = 94.9°, and space group C2. The structure, refined by two-dimensional Fourier methods, contains ReO_3-type blocks of metal-oxygen octahedra, 3 × 4 and infinite in extension along b. These join up in pairs, and the double blocks pack together by additional edge sharing, with metals in tetrahedral coordination at each of the junctions. The relationship to the structure of high-temperature Nb_2O_5, as well as to other known and hypothetical compounds formed from blocks of the same size, was examined. (auth)

20570 CRYSTAL CHEMISTRY OF HIGHER CARBIDES OF PLUTONIUM. D. M. Chackraburtty and N. C. Jayadevan (Atomic Energy Establishment, Trombay, India). Acta Cryst., 18: 811-12(Apr. 10, 1965).

Plutonium dioxide was heated with carbon from 2200 to 2600°C for 5 to 10 min and cooled rapidly. Carbon monoxide evolved was removed by continuous evacuation. The product was studied by x-ray diffraction. The data could be explained on the basis of a mixture of Pu_2C_3, PuC_2, C, and a phase for which mostly weak lines were recorded. Evidence for the PuC_2 phase is discussed. (M.C.G.)

20571 ON THE THERMAL EXPANSION OF PROTACTINIUM METAL. J. A. C. Marples (Atomic Energy Research Establishment, Harwell, Berks, Eng.). Acta Cryst., 18: 815-17(Apr. 10, 1965).

A disc of protactinium metal was mounted in a high-temperature diffractometer and the x-ray pattern recorded at various temperatures. The lines obtained agreed with the body-centered tetragonal indexing proposed previously by Zachariasen. The mean linear expansion coefficient between room temperature and 700°C was calculated from the data to be 9.9×10^{-6}/°C. (M.C.G.)

20572 SOME SUPERCONDUCTING PROPERTIES OF SEVERAL CARBIDES AND NITRIDES OF THE TRANSITION METALS. L. E. Toth (Univ. of California, Berkeley and Univ. of Minnesota, Minneapolis) V. F. Zackay, M. Wells, J. Olson, and E. R. Parker. Acta Met., 13: 379-85(Apr. 1965). (UCRL-11533(Rev.))

Analogous to the transition elements, their solid solutions, and intermetallic compounds, a correlation is shown to exist between the total number of valence electrons and the superconducting critical temperature for transition metal carbides and nitrides crystallizing in the NaCl structure. The critical temperature increased as the total number of valence electrons increased from eight to about ten. A number of experiments were undertaken to substantiate the correlation. The critical temperature of cubic molybdenum carbide (NaCl structure) was found to be 13.0°K. The critical temperature of the two-phase mixtures of cubic and hexagonal molybdenum carbide was found to be dependent on the relative amounts of the two phases present. This behavior was tentatively explained on the basis of the structural similarities of the two phases. A

critical temperature for the hypothetical compound, cubic TaN, of 12 to 14°K was predicted from the variation of the critical temperature with composition for the cubic solid solutions of TaN and TaC. (auth)

20573 RESEARCH ON THE BERYLLIUM–MANGANESE–OXYGEN AND MAGNESIUM–MANGANESE–OXYGEN SYSTEMS. Cesare Brisi and Maria Lucco Borlera. Atti Accad. Sci. Torino, I, Classe Sci. Fis., Mat. Nat., 99: 157-65(1964-65). (In Italian)

The products obtained by calcination in air or under reducing conditions of mixtures of manganese sesquioxide with beryllium oxide and magnesium oxide were studied. No ternary phase was identified in the Be–Mn–O system. In the Mg–Mn–O system, a phase with the formula $Mg_{3-x}Mn_xO_4$, obtainable from hausmannite by partial substitution of Mn with Mg, was detected. The limit of the series of solid solutions corresponded to an x value of about 1.5 at 900°C and of about 1.2 at 1100°C. Mixed crystals $Mg_xMn_{3-x}O_4$ can coexist in equilibrium with the series of solid solutions extending between manganous oxide and magnesium oxide. At 900°C the existence of the compound Mg_6MnO_8, with a decomposition temperature of about 980°C, was also possible. (auth)

20574 EVIDENCE OF SCREW DISLOCATIONS IN GRAPHITE. A. R. Patel and O. P. Bahl (Sardar Vallabhbhai Vidyapeeth, Vallabh Vidyanagar, India). Brit. J. Appl. Phys., 16: 169-71(Feb. 1965).

Spiral etch pits are produced by etching natural graphite cleavage flakes in sodium peroxide. By etching matched cleavage faces, a correspondence was found between the number, nature, and position of the spiral etch pits on these faces. Similar correspondence was found in the etch patterns produced on the two sides of a thin flake of graphite, 95 μm thick, from which it is inferred that the spiral pits indicate the sites of screw dislocations on the cleavage face and that they run right through the body of the crystal. (auth)

20575 RATE OF EVAPORATION OF THORIUM FROM CARBURIZED THORIATED TUNGSTEN CATHODES MEASURED BY ACTIVATION ANALYSIS. H. Schmied and M. Deak (Brown Boveri and Co. Ltd., Baden, Switzerland). Brit. J. Appl. Phys., 16: 269-70(Feb. 1965).

The rate of evaporation of thorium from carburized thoriated tungsten cathodes has been measured by means of activation analysis at different temperatures. Values found are about ten times higher than those from previous measurements based on the saturated emission of a receptor wire. (auth)

20576 THERMAL DIFFUSIVITY AT INCANDESCENT TEMPERATURES BY A MODULATED ELECTRON BEAM TECHNIQUE. M. J. Wheller (General Electric Co., Ltd., Wembley, Eng.). Brit. J. Appl. Phys., 16: 365-76(Mar. 1965).

An apparatus is described for the determination of the thermal diffusivity by Cowan's method of a thin slab of material heated to incandescence by an electron beam. The electron beam is amplitude modulated to vary sinusoidally with time, and the phase difference between the resulting temperature fluctuations of the two faces of the slab yield the thermal diffusivity of the sample. Results obtained for the thermal diffusivity and, hence, the thermal conductivity of Mo, Pt, Ta, and W are given. The Lorentz functions of all four metals were found to be constant over the temperature ranges studied. Thermal conductivity values determined for three types of graphite, indium oxide, uranium dioxide, a U-49 at. % C alloy, and boron nitride are also given. The results obtained cover a range of thermal conductivities from 0.02 to 1.1 w cm^{-1} deg K^{-1} within various temperature ranges between 1200 and 3000°K. (auth)

20577 CONSTITUTION AND MAGNETIC AND ELECTRICAL PROPERTIES OF PALLADIUM TELLURIDES ($PdTe-PdTe_2$). A. Kjekshus (Univ. of Oslo, Blindern, Norway) and W. B. Pearson. Can. J. Phys., 43: 438-49(Mar. 1965). (NRC-8269)

The region from PdTe to $PdTe_2$ was examined by x-ray methods to establish the phase boundaries. The results confirm the existence of a continuous solid solution at high temperatures and narrow homogeneity regions for PdTe and $PdTe_2$ at low temperatures. PdTe is a nonstoichiometric phase, at least below 500°C. Magnetic susceptibility, electrical resistivity, thermoelectric power, and superconducting transition temperatures of PdTe and $PdTe_2$ were measured. (auth)

20578 EFFECTIVE MAGNETIC FIELDS ACTING ON THE ATOMIC NUCLEI OF FERROMAGNETS. F. M. Gal'perin. Dokl. Akad. Nauk SSSR, 159: 1257-60(Dec. 21, 1964). (In Russian)

In view of the fact that present-day theory cannot account rigorously for the large effective magnetic fields acting on the atomic nuclei of ferromagnets, empirical relations for the calculation of the effective field were derived, with an aim at comparing them with the experimental results. The relation obtained for the pure metals Fe, Co, and Ni is $H_{eff} = -[10^2 m/\mu_B - H_s]$ kOe, where m–atomic magnetic moment, μ_B–Bohr magneton, and H_s is the product of the number of unpaired conduction electrons in the 4s band of the metal (N_s) by the negative contribution (H_A) made by the 4s electron to H_{eff}. The values obtained experimentally for H_{eff} and for N_s are in agreement with experiment and with direct measurements of H_s made by investigating the Mossbauer effect on ^{119}Sn nuclei dissolved in Fe, Co, and Ni. Tables are presented of the magnetic fields on the nuclei ^{57}Fe in ferromagnetic alloys and on the nuclei of diamagnetic elements in Fe, Co, and Ni. In the latter case, the fields depend essentially on the host metal. (ATD)

20579 EFFECT OF CHROMIUM AND IRON ON THE ELASTIC PROPERTIES OF NIOBIUM. I. M. Nedyukha and V. G. Chernyi (Inst. of Foundry, Academy of Sciences, Ukrainian SSR). Fiz. Metal. i Metalloved., 18: 599-603 (Oct. 1964).

The elastic properties of polycrystalline niobium and alloys of niobium with chromium (up to 17% Cr) and iron (up to 10.5% Fe) were studied. From data on the velocity of ultrasonic waves obtained by the pulse method, the modulus of elasticity, shear modulus, bulk compression modulus, Poisson ratio, characteristic temperature, and mean-square deviations of the atoms in the crystal lattice were found. It was established that there is an increase in the strength of atomic bonds in niobium when it is alloyed with chromium and iron. Alloys of niobium containing 1.5, 3.0, 5.0, 7.0, 15.0, 16.0, and 17.0 percent by weight chromium and 1.5, 2.0, 3.5, 4.5, 7.5, and 10.5 percent by weight iron were melted in an arc furnace in an inert atmosphere. As initial materials, 99.4% pure niobium, 99.92% pure electrolytic chromium, and 99.99% pure iron were used. The alloys were studied in the cast state. Each of the characteristics was calculated as the average of 5 to 7 experiments. The modulus of normal elasticity and the shear modulus were increased by alloying of niobium with chromium and iron while the Poisson ratio was reduced. The change in the modulus of bulk compression, depending on the content of chromium and iron, was characterized by curves with a minimum, which corresponded to 3.0 to 6.0% chromium and 1.5 to 2.0% iron. Within the limits of chromium and iron concentrations studied, a considerable increase was observed in the characteristic temperature of niobium and a decrease in the mean-square deviations of its atoms at the nodes of the crystal lattice. The data obtained showed a uniform indication of an increase in the strength of atomic bonds when niobium was alloyed with chromium and iron. (CFSTI)

20580 COALESCENCE OF DISLOCATION LOOPS. A. M. Kosevich, Z. K. Saralidze, and V. V. Slezov (Kharkov State Univ.). Fiz. Tverd. Tela, 6: 3383-91(1964).

Interstitial atoms and the prismatic dislocation loop produced by such defects in a sample subjected to radiation damage are discussed. The final stage of dislocation-loop development, when the loop dimensions are sufficiently large and the supersaturation is very low, so that coalescence (growth of large loops by dissolution of smaller ones) is the predominating mechanism, was considered. Elastic

interaction between loops was assumed negligibly small. Each loop was regarded as growing in an unbounded medium having a certain finite concentration at infinity. By determining the rate of growth of a round prismatic dislocation loop it is shown that for a given concentration of interstitial atoms there exists a critical loop radius, beyond which the loop does not change size. An asymptotic distribution function was obtained for the loop dimensions, and the asymptotic values of the numbers and average dimensions of the loops were determined. (CFSTI)

20581 RESONANT PARAMAGNETIC ABSORPTION IN ALLOYS BASED ON GADOLINIUM. Iuliu Pop and V. I. Chechernikov (Moscow State Univ.). Fiz. Tverd. Tela, 6: 3751-3(1964).

The resonant paramagnetic absorption of gadolinium alloys was investigated using a spectrometer operating in the 3-cm band and in the temperature interval from 20 to 200°C. The compositions of the alloys were: 90, 75, 65, 50, and 25 at. % Gd in Gd–Y alloys, 90, 80, and 70 wt % Gd in Gd–Er alloys, and 90 and 70 wt % Gd in Gd–Tb alloys. The samples were in the form of small particles several microns in size and spheres with diameters up to 1 mm. The variation of the absorption line width and of the spectroscopic splitting factor with the concentration of the second metal was qualitatively the same for Y and for Er, the former reaching a maximum and the latter a minimum near 20 wt %. The increase of the splitting factor with increasing content of the second component is attributed to the influence of the spin-orbit interaction. Other effects of alloy concentration on the paramagnetic resonance signal are also discussed. (ATD)

20582 REGENERATED THORIUM FUEL FOR BREEDING REACTOR. T. Oekava. Genshiryoku Kogyo, 9: No. 2, 20-5(1963). (In Japanese)

Up-to-date data are presented on the $^{232}Th-^{233}U$ fuel cycle and the technology of thorium carbide fuel elements. Experimental studies of the density, vacancies, and microhardness of pressed metallic products showed a great deal of cracks formed during powder compression that were perpendicular to the compression. The variations in the compressed density and compression force and the relation between the pressure and vacancies were analyzed. It is shown that the cracks are the result of elastic deformation in graphites. Experiments revealed identical constant lattices for various graphites and an actual density of 2.25 for all graphites except artificial ones. (R.V.J.)

20583 INTERACTION OF NIOBIUM CARBIDE WITH TUNGSTEN. Yu. N. Vil'k, R. G. Avarbe, V. S. Neshpor, T. P. Ryzhkova, and Yu. A. Omel'chenko (State Inst. of Applied Chemistry, USSR). High Temp. (USSR)(English Transl.), 2: 241-6(Mar.-Apr. 1964). Translated from Teplofiz. Vysokikh Temp., 2: 241-6(Mar.-Apr. 1964).

The phase equilibrium between tungsten and the niobium carbides $NbC_{0.98}$ and $NbC_{0.85}$ at temperatures of 2000, 2600, 2700, and 3000°C was studied by x-ray, metallographical, and visual thermal analysis, and by measuring the microhardness of the phases. It was established that the sections $W-NbC_{0.98}$ and $W-NbC_{0.85}$ studied are not pseudo-binary, and pass through regions of two-phase equilibrium (in the solid state), $\alpha + \delta$ (W and W_2C base solid solutions), $\alpha + \gamma$ (W and NbC base solid solutions), and $\gamma + \beta$ (NbC and Nb_2C base solid solutions) and a region of three-phase equilibrium $\alpha + \delta + \gamma$. The existence of ternary compounds W–Nb–C was not observed in the region of alloy composition studied. The liquid phase appears at temperatures below 2600°C in region of the W–Nb–C ternary system studied. In the region of the W–Nb–C ternary system studied, there exist the binary eutectic $\alpha-\delta$, the ternary eutectic $\alpha-\delta-\gamma$ and the ternary peritectic $\alpha-\beta-\gamma$. On the basis of the results obtained, hypothetical isothermal sections of the concentration triangle W–Nb–C were constructed for temperatures 2000, 2600-2700, and 3000°C, together with a polythermal W–NbC section. (auth)

20584 DUCTILITY AND MELTING POINT OF SINTERED W–Mo–Re ALLOYS. William H. Lenz (Los Alamos Scientific Lab., N. Mex.). Intern. J. Powder Met., 1: No. 1, 42-50(Jan. 1965). (LA-DC-6591)

A ductility test was developed and applied to the entire system of sintered W–Mo and W–Mo–Re alloys up to 20 at. % Re. Ductility is related to composition, sintering temperature up to 2340°C, ThO_2 additive, and furnace atmosphere. Rhenium appeared to activate the tungsten-rich compositions so that only minor molybdenum additions were necessary to contribute to ductility. Melting points of eighteen alloys were determined; possible combinations of melting point and ductility ranges are suggested. (auth)

20585 DESTABILIZATION OF ZIRCONIA. T. W. Smoot and D. S. Whittemore (Harbison-Walker Refractories Co., Pittsburgh, Penna.). J. Am. Ceram. Soc., 48: 163-4 (Mar. 21, 1965).

Thermal cycling was carried out on partly and completely stabilized zirconia samples containing about 0.2% total impurities including hafnia. Prolonged cycling between 1600 and 2100°F resulted in only minor destabilization of partly stabilized samples. The fully stabilized zirconia samples showed no destabilization under the same conditions. It was found that destabilization of zirconia is enhanced by impurities, which apparently have a greater affinity for calcia than for zirconia in cubic solid solution. (M.C.G.)

20586 INFLUENCE OF STRESS ON FISSION-GAS RELEASE. C. S. Morgan, R. B. Fitts, and J. L. Scott (Oak Ridge National Lab., Tenn.). J. Am. Ceram. Soc., 48: 166-7(Mar. 21, 1965). (ORNL-P-307)

To evaluate the possibility that dislocation movement might play a part in fission-gas release, the effects of stress on release of fission gas were determined. UO_2 and ThO_2-UO_2 compacts were irradiated at ~100°C to a burnup of about 1.85×10^{15} fissions/cm^3. After a 7-day decay period these specimens were placed in an apparatus that permitted application of a compressive stress at an elevated temperature. A stream of helium carried fission gas to a liquid-nitrogen trap where radiation from ^{133}Xe was counted. Specimens were annealed for varying lengths of time; then they were stressed and the change in fission-gas release noted. Results are presented in tables and graphs. The application of stress caused a fission-gas release burst and a subsequent increased release rate. The initial release burst was substantially larger than subsequent bursts obtained on reapplication of stress, which were sometimes not detectable. (M.C.G.)

20587 METASTABLE PHASES IN URANIUM ALLOYS WITH HIGH SOLUTE SOLUBILITY IN THE BCC GAMMA PHASE. PART I. THE SYSTEM U–Nb. K. Tangri and D. K. Chaudhuri (Atomic Energy Establishment, Trombay, India). J. Nucl. Mater., 15: 278-87(1965).

Composition limits of metastable phases α', α'', and γ^0 and changes in parameters a, b, c, and angle γ (ab) of the alpha-uranium lattice with increasing niobium additions, were determined. While the parameter a was not affected, the parameters b and c steadily decreased and increased, respectively. The angle γ showed an abrupt change from 90° at 10.00 at. % Nb to 91.07° at 11.93 at. % Nb. From a study of the effect of cooling rates in producing alternative structures, it is shown that the mode of formation of α', α'' and γ^0 in the U–Nb alloy is similar to that observed in the U–Mo system. Based on the size of the solute atom, a relationship was developed to predict the α'/α'' boundary composition in various uranium binary systems with high solute solubility in the gamma phase. (auth)

20588 METASTABLE PHASES IN URANIUM ALLOYS WITH HIGH SOLUTE SOLUBILITY IN THE BCC GAMMA PHASE. PART II. THE SYSTEM U–Ru. K. Tangri, D. K. Chaudhuri, and C. N. Rao (Atomic Energy Establishment, Trombay, India). J. Nucl. Mater., 15: 288-97(1965).

In U–Ru alloys containing up to 9.51 at. % Ru, the metastable phases α' and γ^0 produced on water quenching from the gamma field were studied by x-ray diffraction and metallography. For compositions up to 6.90 at. % Ru only α' phase was produced, whereas for higher compositions (up to the solubility limit of 10 at. % Ru) both the α' and γ^0 phases coexist. The absence of the phase α'', which was found to exist in the U–Mo and U–Nb alloys, may be ascribed to the incompressibility of the b parameter below 5.80 Å. This may be due to the possible variation in the

state of ionization of the ruthenium atoms when present in varying amounts in the uranium matrix. A possible explanation for the coexistence of the phases α' and γ^0 is that the γ^0 phase, which requires more than 10 at. % ruthenium for its formation, is present as small incoherently diffracting nuclei in the gamma phase and that these nuclei grow into larger domains partly depleting the ruthenium content of the surrounding regions thus rendering them more susceptible to shear producing the phase α'. (auth)

20589 THE PSEUDO BINARY PHASE DIAGRAMS OF PuO_2 WITH ALUMINA, BERYLLIA AND MAGNESIA AND THE PSEUDO TERNARY PuO_2-ThO_2-BeO. A. Hough and J. A. C. Marples (Atomic Energy Research Establishment, Harwell, Berks, Eng.). J. Nucl. Mater., 15: 298-309(1965). (AERE-R-4749)

The pseudo-binary phase diagrams of plutonium oxide with alumina, beryllia, and magnesia were examined under oxidizing conditions. All three systems were simple eutectics with no intermediate compounds and limited terminal solid solubility. The compositions and temperatures of the eutectics were determined: the latter were very similar to those reported for the corresponding urania systems. The system $BeO-ThO_2$ was also found to be a simple eutectic, in agreement with the results of previous workers. In the ternary system $BeO-ThO_2-PuO_2$, there was negligible solid solubility of beryllia in the plutonia-thoria solid solution and vice versa and a eutectic valley joined the eutectics in the binaries $BeO-ThO_2$ and $BeO-PuO_2$. (auth)

20590 ANNEALINGS OF THE ELECTRIC RESISTIVITY PRODUCED IN COPPER BY QUENCHING AND BY IRRADIATION. I. COMPARISON OF QUENCHINGS UNDER HELIUM AND UNDER HYDROGEN ATMOSPHERES. A. Lucasson, P. Lucasson, and Cl. Budin (Faculte des Sciences, Paris). J. Phys. (Paris), 25: 1004-12(Dec. 1964). (In French)

A specimen of copper was quenched in hydrogen atmosphere and then in a helium atmosphere. After each of these quenches, isothermal or isochronal anneals were performed in order to compare the mobilities of the point defects produced. Near room temperature, the activation energies for motion were found equal to 0.77 ± 0.10 ev after helium quenches and to 0.80 ± 0.06 ev after hydrogen quenches. Between –30 and +50°C, the isochronal curves (in percent of annealed resistivity) are identical. It is concluded that it is not possible to distinguish a difference in the mobility of the point defects produced in either case. (auth)

20591 ON THE PHASE TRANSITION IN $Sr(FeTa)_xO_3$. Takehiko Nakagawa and Shoichiro Nomura (Tokyo Inst. of Tech.). J. Phys. Soc. Japan, 20: 179(Jan. 1965).

Studies were carried out on the system $Sr(FeTa)_xO_3-SrTiO_3$. Lattice parameters were determined using powder x-ray diffraction; results are presented and compared with those for the $Sr(FeTa)_xO_3-Ba(FeTa)_xO_3$ system. The perovskite tetragonal-cubic transition temperature was determined from the temperature dependence of the electric conductivity; the variation of the transition temperature with the content of the system is presented, and it is indicated that the transition in $Sr(FeTa)_xO_3$ is of the same kind as the nonferroelectric 110°K transition in $SrTiO_3$. (M.J.T.)

20592 THE METALLOGRAPHY OF FRACTURE OF ALPHA URANIUM. D. M. R. Taplin (Univ. of Melbourne) and J. W. Martin. Metallurgia, 71: 83-6(Feb. 1965).

A study was made of the fracture characteristics of alpha uranium between –183 and 400°C with particular reference to the ductile/brittle transition. Ductile failure occurred by void formation at inclusions followed by void growth and interlinkage. A fracture transition to intergranular failure occurred at about room temperature, and with decreasing temperature at gradual transition to a crystallographic failure along twin/matrix interfaces took place. (auth)

20593 EFFECTS OF 1.0% SUPERIMPOSED MEAN STRAIN ON THE BENDING FATIGUE STRENGTH OF ZIRCALOY-4. D. F. Mowbray (Knolls Atomic Power Lab., Schenectady, N. Y.). Nucl. Appl., 1: 39-48(Feb. 1965).

The superposition of 1.0% mean strain on constant-deflection cycled bending-fatigue specimens of Zircaloy-4 plate reduces the fatigue strength at both room temperature and 600°F. The implications of these test results on recommended fatigue design procedures are examined. Limited studies of crack propagation in Zircaloy plate indicated conformance with the hypotheses of Frost and Dugdale. It was also found that an oxide film formed by exposure to 680°F water for 72 hours is detrimental to fatigue strength at room temperature. (auth)

20594 CORRELATION OF TEMPERATURE AND GRAIN SIZE EFFECTS IN DUCTILE-BRITTLE TRANSITION OF MOLYBDENUM. E. M. Passmore (ManLabs, Inc., Cambridge, Mass.). Phil. Mag. (8), 11: 441-50(Mar. 1965).

An experimental investigation of the effects of temperature and grain size on the tensile properties of high purity molybdenum showed that transitions from ductile to brittle behavior occur with both decreasing temperature and increasing grain size. Based on the assumed temperature independence of the critical stress criterion for cleavage fracture, both of these transitions were interpreted largely in terms of the plastic strain dependence of this critical fracture stress (σ_c). The grain size dependence of σ_c at constant strain was found to be of the form $\sigma_c = \sigma_c^0 + k_c l^{-\frac{1}{2}}$, in which σ_c^0 is strain dependent and $k_c = 2 \times 10^8$ dyne-cm$^{-\frac{3}{2}}$. (auth)

20595 THE MAGNETIC SUSCEPTIBILITY OF SCANDIUM. W. E. Gardner and J. Penfold (Atomic Energy Research Establishment, Harwell, Berks, Eng.). Phil. Mag. (8), 11: 549-59(Mar. 1965).

The magnetic susceptibility of scandium metal was measured between 10 and 293°K and the results are compared with previous measurements. An interpretation of the susceptibility behavior is given in terms of a modified density of states curve based on the band structure calculations of Altmann and Bradley. The modification consists of superimposing a narrow peak at the Fermi energy of width 0.22 ev. The importance of electron-electron terms enhancing the susceptibility is demonstrated. In addition a discussion of the temperature-dependent Knight shift measurements of Blumberg et al. is given, in which the temperature dependence is associated with the contact term. (auth)

20596 ON THE INTERMEDIATE PHASES IN THE SYSTEM SAMARIUM–ALUMINIUM. K. H. J. Buschow and J. H. N. van Vucht. Philips Res. Rept., 20: 15-22 (Feb. 1965).

The samarium–aluminum system was found to contain five intermediate phases: Sm_2Al, SmAl, $SmAl_2$, $SmAl_3$, and $SmAl_4$. Sm_2Al and SmAl are orthorhombic and isotypic with Er_2Al and ErAl, respectively; $SmAl_2$ has the cubic $MgCu_2$ (Laves) type of structure; $SmAl_3$ has the Mg_3Cd type of structure; and $SmAl_4$ is isotypic with $BaAl_4$. With the help of thermoanalytical data, part of the phase diagram is constructed. It shows a peculiar three-phase reaction $SmAl_4 \rightarrow SmAl_3$ + liquid on cooling. (auth)

20597 MAGNETIC PROPERTIES OF ORDERING RARE-EARTH ANTIMONIDES. G. Busch, O. Marincek, A. Menth, and O. Vogt (Eidgenossische Technische Hochschule, Zurich). Phys. Letters, 14: 262-4(Feb. 15, 1965).

An investigation was made of the magnetic behavior of NdSb, GdSb, TbSb, DySb, HoSb, and ErSb, using powdered specimens and also GdSb single crystallites. Graphs of the reciprocal molar susceptibilities versus temperature and magnetizations versus internal field are presented. It was found that all antimonides were antiferromagnetic below the Néel-point, and that the spin structure changes suddenly from antiferromagnetism to a spin arrangement with a net magnetic moment under the influence of a sufficiently high field, Hc. The magnetic properties are tabulated. (L.B.S.)

20598 ON THE SUSCEPTIBILITY OF LIQUID GADOLINIUM. R. M. Xavier, X. A. Da Silva, and W. Baltensperger (Centro Brasileiro de Pesquisas Fisicas, Rio de Janeiro). Phys. Letters, 15: 126-7(Mar. 15, 1965).

The effects of a liquid structure and of a short mean free path on the ionic magnetic moments are evaluated for Gd. The results show that at high temperatures the short mean free path drastically decreased the paramagnetic Curie temperature, which is larger in the liquid than in the solid state. (L.B.S.)

20599 MEASUREMENT OF MEAN INNER POTENTIALS OF BERYLLIUM IN ELECTRON INTERFEROMETER. C. Joehsson, H. Hoffmann, and G. Moellenstedt (Universitat, Tubingen, Ger.). Physik Kondensierten Materie, 3: 193-9(1965). (In German)

The mean inner potential in layers of polycrystalline high-purity beryllium (99.99%) was measured using an electron optical bi-prism interferometer. Since supporting foils consisting of Be, C, Al_2O_3, SiO, or collodion were destroyed when Be was evaporated onto them, a method to prepare the step-shaped specimens had to be developed. The following layers were consecutively evaporated onto a glass slide: first a layer of B_2O_3, then a continuous base layer of Be, and last, through a grid stencil, square steps of Be. The compound foil was separated from the slide by solution of the B_2O_3 in water, and mounted on an electron microscopical specimen holder. The experimentally determined mean inner potential value of beryllium Φ_{exp} = 7.8 ± 0.4 v was in good agreement with Y. Siota's theoretical value Φ_{theor} = 7.4 v. (auth)

20600 PERIODICITY OF STRUCTURE AND PROPERTIES OF LANTHANIDES IN CONNECTION WITH THEIR PHASE DIAGRAMS. V. K. Grigorovich. Tr. Inst. Met. im. A. A. Baikova, Akad. Nauk SSSR, No. 14, 212-26(1963).

An examination of the structure of outer electron shells of lanthanides and their valence and ionization potential was used to account for a periodicity in the change of melting and boiling points, heats of vaporization, allotropic transformations, interatomic distances, density, compressibility, coefficient of expansion, elastic moduli, and electron work functions as the atomic number of lanthanides increased. In contrast to the other lanthanides, in Eu and Yb the atomic diameters were large, and marked deviations in other properties were observed, indicating a reduced strength of the interatomic bond caused by reduced electron concentration of Eu and Yb (2 electrons per atom instead of 3 in the other lanthanides). It was postulated that the appearance of high-temperature BCC modifications in Ga, Ce, Pr, Nd, Eu, Yb, Sm, Gd, Tb, and probably in Dy and Ho is due to the fact that their ions in this state have filled, overlapping $5p^6$ shells. In accordance with the views developed by N. V. Belov, it is shown that structures of the type α-La(|AB|AC|...) and α-Sm (|ABABCBCAC|...) represent a combination of the two tightest stackings; the first, a combination of the cubic stacking of Cu (|ABC|...) and the simple hexagonal stacking of Mg (|AB|...), and the second, a combination of stackings like Mg and α-La. Lanthanides with the same Mg structure (yttrium subgroup) of α-La (cerium subgroup) form continuous series of solid solutions with one another, whereas lanthanides from different subgroups form intermediate compounds isomorphous with α-Sm. The nonisomorphism of the hexagonal modification of lanthanides of the cerium and yttrium subgroups, apparently due to the filling of 1st and 2nd half of the 4f shell, respectively, also caused an appreciable difference in their reaction with metals other than the rare earths. (CFSTI)

20601 VAPOR PRESSURE OF GADOLINIUM AND DYSPROSIUM. G. P. Kovtun, A. A. Kruglykh, and V. S. Pavlov (Khar'kov Inst. of Physics and Tech., Ukrainian SSR). Ukr. Fiz. Zh., 9: 1089-91(Oct. 1964). (In Ukrainian)

The pressure of gadolinium and dysprosium vapor was determined over the temperature intervals of 1120–1310 and 850–1075°C respectively, using Knudsen's effusion method by the difference of the weight of the tantalum effusion cell before and after the experiment. The following equations describe the results obtained for Gd and Dy, respectively: $\log P_{mmHg} = 12.03 - 23705/T$, and $\log P_{mmHg} = 0.79 - 15825/T$. The heats of sublimation were calculated: 108.5 and 72.4 kcal/mole for Gd and Dy, respectively. The respective entropies of sublimation equal 42.0 and 31.6 cal/mole degree. (ATD)

20602 A STUDY OF DISLOCATION STRUCTURE OF SUBBOUNDARIES IN MOLYBDENUM SINGLE CRYSTALS. Duan Fong, Chi Li, and Nay-ben Ming (Nanking Univ., China). Wu. Li Hsueh Pao, 21: 431-43(Feb. 1965). (In Chinese)

By means of the etch-figure technique, dislocation structure of subboundaries in electron-beam zone-melted molybdenum single crystals was directly observed. A thorough analysis of experimental results are given, these are further compared with the deductions derived from the Frank's formula for subboundaries, and the theoretical predictions are fully verified. The directions of parallel etch-lines observed on (111) plane are along the intersection lines of glide planes and climb plane, it proves that these are symmetrical tilt subboundaries composed of edge dislocations with Burgers vector $\frac{1}{2}\langle 111\rangle$. The verification of the generalized Read-Shockley formula for intersecting subboundaries revealed by etch-pitting (110) surface proves these to be asymmetrical tilt subboundaries composed of two sets of dislocations. The 15 sets of networks of etch-lines were analyzed, in which 5 sets are proved to be $\frac{1}{2}\langle 111\rangle/\langle 100\rangle$ networks, 9 sets to be $\langle 100\rangle/\langle 110\rangle$ networks. In the network analysis, in addition to the stereographic method used by Carrington et al., a new method by verifying Frank's formula quantitatively was developed, and it proved to be effective in determining Burgers vectors of dislocation networks when the stereographic analysis failed to yield a unique result. Various patterns indicating interactions of singular dislocations with subboundaries, in particular, steps on the subboundaries induced by singular dislocations and also interactions of inclusions with subboundaries were observed. Various types of subboundary junctions and non-equilibrium subboundaries were observed and discussed. All these results prove that the etch-figure method of observing dislocations is an effective means for the quantitative study of dislocation substructure in crystals, comparable in power with that of transmission electron microscopy. (auth)

20603 ELECTRON MICROSCOPE STUDIES OF PRECIPITATES AND FISSION DAMAGE IN VAPOR GROWN UO_2 CRYSTALS. H. Blank (CEN, Brussels) and S. Amelinckx. Z. Metallk., 55: 460-6(1964). (BLG-289)

Observations on defects in vapor grown UO_2 single crystals are reported. Information on the precipitation of excess oxygen in UO_{2+x} and on the damage after neutron irradiation (up to 10^{16} nvt) was gained. (auth)

20604 PARAMETERS OF RECRYSTALLIZATION OF NIOBIUM AND TUNGSTEN. L. N. Larikov, E. E. Zasimchuk, and M. N. Semenenko. p.121-4 of "Nauchnyy Sovet po Probleme Zharoprochnykh Splavov. Issledovaniya Staley i Splavov." Moscow, Izd-vo Nauka, 1964.

The stability of hardened metals at high temperatures may be expressed to some degree by the recrystallization rate parameters. Pure niobium (99.997%) and pure tungsten containing 0.02% C, 0.006% Si, 0.01% P, 0.015% Fe, 0.008% S, 0.0022% Cd, 0.0004% Pb, 0.00008% Bi, and 0.003% Sn were investigated. Niobium was subjected to 94% uniaxial compression at room temperature, and recrystallization annealing was carried out at 960 to 1080°C. Tungsten was rolled (90% compression) at 1200°C in air and annealed at 1300 to 2000°C in a vacuum. The recrystallization rate was determined from the appearance of "punctures" on the x rays, taken after etching with HNO_3 + HF. A linear inverse relationship was obtained in both cases between the logarithm of the growth in recrystallization centers and the reciprocal of the absolute temperature: $G = G_0 \exp(-Q_G/RT)$, where G_0 is 10^{16} and 10^{15} cm/sec for Nb and W, respectively, and Q_G is 130 to 180 kcal/g·atom. The microhardness of tungsten was also measured for different annealing temperatures, and found to decrease sharply at 1200°C. Comparison showed that niobium is weakened prior to recrystallization, while tungsten is weakened during recrystallization. Niobium is thus deformed at rela-

tively lower temperatures in relation to the melting point. (CFSTI)

20605 DEFORMATION BEHAVIORS OF NIOBIUM AND TANTALUM AT LOW TEMPERATURES. Dale Stephen Cowgill. Thesis, Ames, Iowa, Iowa State Univ. of Science and Tech., 1964. 195p.

The deformation behaviors of equivalent niobium and tantalum were investigated over the ductile-to-brittle transition range in niobium. For metals of equivalent composition and structure, tensile testing at equal temperatures and strain rates resulted in virtually the same yield strengths in both niobium and tantalum. Cleavage was observed on {110} and {100} planes in niobium specimens, which fractured after more than 27 per cent reduction in area, but none of the tantalum specimens exhibited cleavage. The niobium ductile-to-brittle (shear-to-cleavage) transition temperature was found to increase from –180°C to –160°C with an increase in nitrogen content from 100 to 250 ppM. Twinning was observed in all tantalum specimens tested at low temperatures, but was observed in only those niobium specimens which subsequently failed by cleavage. In both materials the amount of twinning increased with increasing interstitial impurities and with decreasing temperatures. The only difference detected in slip behavior was that fine complex slip was more often observed in low temperature tantalum test specimens than in equivalent niobium specimens. The apparent slip planes were determined from slip traces on large grains in the polycrystalline specimens and were found to exhibit no systematic variation with material, composition, or temperature. It was concluded that the occurrence of cleavage in niobium is not solely dependent on composition, initial structure, temperature, and strain rate, but is controlled by some mechanism operating during plastic deformation after yielding. (Dissertation Abstr., 25: No. 5, Nov. 1964)

20606 A MATERIALS STUDY OF THE LANTHANUM–TELLURIUM SYSTEM. Thomas Haliburton Ramsey, Jr. Thesis, Austin, Tex., Univ. of Texas, 1964. 206p.

A basic materials study was made of the rare earth, lanthanum, atomic number 57, and the group VI element, tellurium, atomic number 52. The making of diffusion couples by vapor-solid and vapor-liquid reactions of the elements produced all of the compounds existing in the La-Te system. The compounds formed and identified in the system were LaTe, $LaTe_3$, $LaTe_2$, and La_3Te_4. The phase diagram for this system was established by standard techniques supplemented by metallographic, x-ray, differential, thermal, and chemical analyses. A study of the relative stability of these compounds in air at room temperature indicates that $LaTe_2$ is the least stable and La_3Te_4 the most stable. A study of the crystal chemistry of the compounds revealed the following: LaTe, face-centered cubic, NaCl type, space group Fm3m; La_2Te_3–La_3Te_4, body-centered cubic, Th_3P_4 type, space group I$\bar{4}$3d; $LaTe_2$, tetragonal system, Fe_2As type, space group P($\bar{4}$/n)mm; $LaTe_3$, orthorhombic system, space group Bmmb. The measured and theoretical densities are all in the order of 6–7 g/cc. Only small single crystals suitable for x-ray work were obtained for these compounds. The electronic evaluations were, therefore, made on polycrystalline materials which had chemical purities of approximately 99.5% after reaction. The results indicate metallic conductivities for LaTe, $LaTe_2$, and $LaTe_3$. The conductivities of La_2Te_3–La_3Te_4 and the defect $LaTe_2$ compounds reveal some semiconducting character. Values range from 20×10^3 ohm-cm for La_2Te_3 to 0.6×10^3 ohm-cm for La_3Te_4, and a range of 10-150 ohm-cm for the defect $LaTe_2$ compounds. No Hall voltages could be detected; thermal energy gaps were unreliable; and infra-red energy gaps could not be obtained from the absorption curves. A more reliable evaluation of the materials was obtained by thermoelectric power measurements, including carrier type. Some of the deficient $LaTe_2$ compounds have Seebeck coefficients of 100 (μv/°C) and La_2Te_3 has values near 300 (μv/°C). The other compounds show more metallic behavior. (A.G.W.)

20607 GRAIN BOUNDARIES AND THE MECHANICAL BEHAVIOR OF MAGNESIUM OXIDE. R. B. Day and R. J. Stokes (Air Force Systems Command, Wright-Patterson AFB, Ohio). 43p. (CONF-641116-4)

From Conference on the Role of Grain Boundaries and Surfaces in Ceramics, Raleigh, N. C.

The mechanical properties of magnesium oxide single crystals and polycrystals were compared at different temperatures. Single crystals showed increasing interpenetrability and multiplicity of slip systems at elevated temperatures. Above 1700°C slip was very flexible, i.e., slip systems with different Burgers vectors completely interpenetrated each other and slip occurred over a variety of slip planes. Furthermore, above 1600°C rearrangement of dislocations by polygonization was observed and in certain cases recrystallization could be obtained. Polycrystals prepared by the recrystallization of single crystals showed a brittle to ductile transition with increasing temperature. At low temperatures any structural discontinuity capable of blocking slip dislocations, including subgrain and grain boundaries, induced cleavage crack nucleation and brittle fracture. At intermediate temperatures (1400 to 1700°C) more slip occurred but it was not flexible enough for grains to conform to each other's change in shape and constraints developed which could be relaxed only by intergranular sliding. This led to intergranular crack nucleation and brittle fracture. At elevated temperatures (above 1700°C) slip was very flexible and the polycrystalline matrix deformed plastically and necked down to a ductile fracture. Polygonization and recrystallization of the deforming grains also contributed to relaxation of internal stresses. These high temperature deformation processes were remarkably similar to face-centered cubic metals undergoing creep. Slight porosity caused an increase in the brittle to ductile transition temperature. While high-density, hot-pressed magnesia showed plasticity above 2000°C it was limited by intergranular failure. (auth)

20608 COMPUTATION OF COMPONENT VAPOR PRESSURES AND VAPORIZATION RATES IN REFRACTORY METAL-METAL-CARBON SYSTEMS. Larry Kaufman and Gerald L. Stepakoff (ManLabs, Inc., Cambridge, Mass.). 32p. (CONF-641208-1)

From 3rd Conference on Performance of High Temperature Systems, Pasadena, Calif.

The Schottky-Wagner model of non-stoichiometric compound phases, which was applied to the prediction of phase diagrams, vapor pressures, and vaporization in binary metal-carbon systems, was extended to deal with the problem of a ternary metal-metal-carbon system. This approach was utilized to derive explicit equations capable of predicting the temperature and compositional dependencies of the vapor pressure and rates of evaporation of each of the elemental components of ternary NaCl-type carbides. The equations were used to predict these properties for (Ta, Hf) C between 2200 and 3000°K for comparison with available experimental data. In line with the observations, the equations revealed the existence of the composition range in which the rate of evaporation exhibits a minimum. The equations were also used to predict the occurrence or absence of ternary congruencies and to deduce the time dependence of the rate of vaporization for non-congruent vaporization. (auth)

20609 METHOD OF PRODUCING A SUPERCONDUCTING NIOBIUM–ZIRCONIUM ALLOY. Robert Graham Teuting and Jack Wernick (to Western Electric Co. Inc.). German Patent 1,180,955. Nov. 5, 1964. Priority date Oct. 11, 1961, United States.

The superconducting properties of the binary alloy composed of 9.84 to 89.84 wt % zirconium with the rest niobium were improved by treating this alloy for 0.5 to 10 hr at a temperature of at least 300°C and of cooling subsequently with a velocity of at least 30°C/min. (Gmelin Inst.)

20610 APPLICATION OF A MAGNESIUM ALLOY FOR NUCLEAR FUEL ELEMENT CANS. Geoffrey Charles Edward Olds (to Associated Electrical Industries). German Patent 1,184,507. Dec. 31, 1964. Priority date Oct. 25, 1957, Great Britain.

A magnesium alloy used for nuclear fuel element cans is

composed of 0.5 to 1.0 wt % zirconium, 0.05 to 0.5 wt % manganin, and the rest of magnesium. (Gmelin Inst.)

20611 METHOD OF IMPROVING THE DUCTILITY OF BERYLLIUM. Alexander Beillie Brown, Alfred John Martin, and Frederick Morrow (to Babcock and Wilcox Ltd.). German Patent 1,184,511. Dec. 31, 1964. Priority date Aug. 19, 1959, Great Britain.

A method is described for improving the ductility of thermally reduced beryllium containing 0.1% iron and other contaminations by at least 30% between 300 and 400°C and by at least 40% between 400 and 600°C. The semi-finished beryllium is treated in an inert gas atmosphere or under vacuum at a temperature between 600 and 850°C for more than 12 hours and cooled slowly to ambient temperature. (Gmelin Inst.)

Radiation Effects

See also CHEMISTRY — Radiation Chemistry.

Refer also to abstracts 19934, 20421, 21607, and 21686.

20612 (AFCRL-64-839) EFFECTS OF ENERGETIC PHOTON IRRADIATION ON GERMANIUM. Physical Sciences Research Papers No. 57. P. H. Hannaway, H. M. DeAngelis, and E. Y. Wang (Air Force Cambridge Research Labs., L. G. Hanscom Field, Mass.). Mar. 17, 1964. 24p. CFSTI.

N-type germanium samples were exposed at ~30°C to gamma rays from a 6100 Curie ^{60}Co source and x rays (up to 3 Mev) produced by bombardment of a tungsten target with 3-Mev electrons from a Van de Graaff generator (model KN). From the temperature dependence of carrier concentration for defect levels induced by the x irradiation, evidence is presented for defect levels at $E_c - 0.2$ ev and $E_v + 0.26$ ev. These levels were observed in ^{60}Co irradiations. From a study of carrier removal rate as a function of the Fermi level, evidence is also presented for the existence of a very shallow level, $E_c - 0.07$ ev, induced by ^{60}Co gamma rays. (auth)

20613 (CEA-R-2529) CONTRIBUTION A L'ETUDE DE LA PRECIPITATION DE L'HELIUM DANS UN ALLIAGE ALUMINIUM–LITHIUM. (Contribution to the Study of Helium Precipitation in an Aluminium–Lithium Alloy). Viviane Levy, Jacqueline Antolin, Jacqueline Espinasse, and Yves Adda (Commissariat à l'Énergie Atomique, Saclay (France). Centre d'Études Nucléaires). July 1964. 36p. Dep.(mn).

In order to determine the swelling mechanisms, the behavior of helium in aluminium was studied using transmission electron microscopy. The helium was introduced into the aluminium by irradiation of Al–^{6}Li alloys containing small amounts of lithium. The influence of various factors on the nucleation and the swelling of the bubbles was was studied, including: helium concentration; temperature; and number and distribution of crystal defects in the metal. It was found that the precipitation of rare gas bubbles could in certain cases prevent the recrystallization of the metal as a result of a mechanism depending on the anchoring of the dislocations and grain boundaries by the bubbles. (auth)

20614 (HW-81250A) THE H-4, H-5, AND H-6 IRRADIATION EXPERIMENTS: IRRADIATION OF N-REACTOR GRAPHITE — INTERIM REPORT NO. 1. J. W. Helm (General Electric Co., Richland, Wash. Hanford Atomic Products Operation). Oct. 1964. Contract AT(45-1)-1350. 107p. Dep.; $4.00(cy), 3(mn) CFSTI.

Irradiations are being performed in the D7 and F7 positions of the GETR to determine the long-term irradiation behavior of N-Reactor moderator graphite, designated TSX. Results are now available for samples irradiated to a maximum neutron exposure of 4.8×10^{21} nvt, E > 0.18 Mev. Mean sample temperatures, which ranged from 425 to 825°C, agreed within ±50°C from capsule to capsule and from one reactor cycle to the next. The TSX graphite tested was obtained from three separate full-size unmachined blocks. The contraction of the graphite showed a dependence on the temperature of irradiation. The transverse samples showed a large spread in contraction for several samples irradiated at the same temperature to equivalent exposures, with no statistical differences among samples taken from several locations in the block. All TSX samples showed continued contraction upon increased neutron exposure and the parallel samples contracted more and at a faster rate than did the transverse. The TSX graphite showed nearly the same contraction behavior as the CSF graphite in both the transverse and parallel orientations. Data on radiation-induced changes of sample volume, crystallite parameters, Young's modulus, and electrical resistivity are also presented. (auth)

20615 (HW-SA-3212) EXPERIMENTS ON THE THERMAL CONDUCTIVITY OF UO_2 AT HANFORD LABORATORIES. J. L. Bates, D. R. de Halas, J. O. McPartland, M. H. Montgomery, and J. A. Christensen (General Electric Co., Richland, Wash. Hanford Atomic Products Operation). Sept. 23, 1963. Contract AT(45-1)-1350. 15p. Dep.(mn); $1.00(cy), 1(mn) CFSTI.

Preliminary results from a simple, radial heat flow experiment seemed to confirm the hypothesis that internal radiation contributes to heat transfer in large grain, stoichiometric UO_2. Surface temperatures of hollow oxide pellets stacked about a heated tungsten wire were compared to determine relative conductivities. Radial flow thermal conductivity measurements of three series of polycrystalline and single crystal UO_2 specimens were performed at temperatures to 1800°C. The presence of a radiation contribution was strongly suggested in experiments where a thin, tungsten coating was first vapor deposited on the hollow, cylindrical specimens. The opaque surface layer of tungsten intercepted any radiation directly transmitted through the rather thin samples. (P.C.H.)

20616 (IDO-17011) TRANSIENT TESTS OF THE FULLY ENRICHED, STAINLESS STEEL PLATE-TYPE, P CORE IN THE SPERT I REACTOR: DATA SUMMARY REPORT. A. P. Wing (Phillips Petroleum Co., Idaho Falls, Idaho. Atomic Energy Div.). Dec. 1964. Contract AT(10-1)-205. 65p. Dep.; $3.00(cy), 2(mn) CFSTI.

Data obtained from the transient test series performed on the Spert I stainless steel plate-type P core are presented. The tests consisted of step insertions of reactivity under varying conditions ranging from ambient temperature to ≈97°C and resulted in asymptotic reactor periods ranging from 6.0 sec to 4.0 msec. The experimental data obtained from each test are presented in both tabular and graphical form. The graphs include time-history plots of reactor power, fuel plate surface temperature, and pressure. Time-history composite graphs displaying fuel plate surface temperature as a function of reactor core position are included. Correlated graphs displaying fuel test data as functions of asymptotic reactor period also are included. (auth)

20617 (NASA-TN-D-2727) DAMAGE TO GERMANIUM DUE TO 22- AND 40-Mev PROTON BOMBARDMENTS. Roger A. Breckenridge and Chris Gross (Langley Research Center, National Aeronautics and Space Administration, Langley Station, Va.). Mar. 1965. 19p. $1.00(CFSTI).

The effects of 22 and 40 Mev proton bombardments on n- and p-type single-crystal germanium were investigated. Electrical conductivity and the Hall coefficient were measured as a function of proton flux to provide removal rates for majority carriers. A defect energy level was located in n-type germanium 0.20 ev ± 0.01 ev below the bottom of the conduction band from a study of the Hall coefficient as a function of temperature and, also, from a study of the removal rate of electrons as a function of the Fermi level. The rate of introduction of acceptor levels in n-type germanium was found to be 73.5 per cm-proton for irradiation with 22 Mev protons and 41.4 per cm-proton for irradiation with 40 Mev protons. The measured removal rates of holes in p-type germanium were much lower than the removal rates of electrons in n-type germanium at a similar resistivity and for the same bombarding particles. A limiting value of the Fermi level was located between 0.20 ev and 0.25 ev above the top of the valence band. (auth)

20618 (NBS-8614) IRRADIATION INDUCED COLOR CENTERS IN MAGNESIUM FLUORIDE. R. F. Blunt and M. I. Cohen (National Bureau of Standards, Washington, D. C.). Jan. 4, 1965. 28p.

Irradiation-induced color centers in MgF_2, having the rutile structure, were produced and studied, principally at room temperature. Most irradiation was done with 50 kv x rays. The primary effect is a strong, anisotropic band with an E⊥c component at 255 nm and an E∥c component at 265 nm. This "center" is largely and irreversibly bleached with 254 nm light to produce a strong band at 370 nm and weak bands at 300 and 320 nm. All of the latter appear only for E⊥c. Detailed bleaching experiments, in the course of which the 300 nm band is permanently bleached out, indicate that the 370 nm "center" has no component along the c-axis and is cylindrically symmetric about the c-axis, a surprising symmetry for any simple model possible for the rutile structure. The 320 nm band, however, has been shown to be polarized along a [110] direction. Ultraviolet-excited luminescent bands appear at 420 and 560 nm. The former appears for E⊥c, while the latter is isotropic. It is not possible as yet to tell if the responsible centers are electron or hole traps, or as to what role impurities play. Apparent "saturations" with x-ray dosage were readily produced on samples from two sources and the 250 nm band would correspond to at least 10^{17} centers per cm^3. (auth)

20619 (NP-14883) GAMMA-RAY IRRADIATION OF GERMANIUM. EFFECTS OF CHEMICAL IMPURITIES. Herman Shulman and George Ausman, Jr. (Harry Diamond Labs., Washington, D. C.). Nov. 20, 1964. 20p. (TR-1266)

N-type germanium was irradiated in a cobalt-60 gamma source at ambient temperature (~25°C). The effects of donor impurities (arsenic and antimony) upon conduction-electron removal rate ($-dn/d\phi$) and subsequent annealing behavior were investigated experimentally by means of Hall effect and resistivity measurements. With irradiation, carrier-removal rates were observed to decrease markedly in antimony-doped germanium and more slowly in arsenic-doped samples. The rate of introduction of the characteristic 0.21-ev level (below the conduction band) was observed to decrease as the concentration of conduction electrons is increased; it is higher in antimony-doped samples than in those doped with arsenic. A study of the effects of annealing at temperatures near 100°C indicated that recovery of conduction electrons, as measured at 77°K, proceeds much more rapidly in antimony-doped germanium than in arsenic-doped germanium. The fraction of damage remaining unannealed in the latter is, for equal time at equal temperature, proportional to the concentration of arsenic atoms. On the other hand, the 0.21-ev levels anneal out more rapidly in the arsenic-doped material than in material doped with antimony. Recovery of the Hall mobility during thermal anneal proceeds concomitantly with the removal of the 0.21-ev level, although certain anomalies have been noted. It is suggested that the radiation-induced 0.21-ev acceptor level is associated with isolated interstitials, which are electrostatically attracted to donor impurities, where they are trapped during the anneal. This process is presumably more efficient for the smaller arsenic ion than in the case of the larger antimony ion. Recent progress in measuring Hall coefficient of irradiated samples as a function of magnetic field is described. (auth)

20620 (NYO-2024-8) RADIATION DAMAGE STUDIES IN SOLIDS USING THE TECHNIQUES OF ELECTRON-SPIN PARAMAGNETIC RESONANCE AND NUCLEAR MAGNETIC RESONANCE. Annual Progress Report, May 1, 1964 through April 30, 1965. P. J. Bray (Brown Univ., Providence, R. I. Dept. of Physics). Feb. 16, 1965. Contract AT(30-1)-2024. 49p. Dep.(mn); $2.00(cy), 1(mn) CFSTI.

ESR and NMR data were obtained and analyzed for reactor-irradiated crystals of the potassium halides. The results show that the ionizing radiation accompanying the neutron flux is the principal source of the damage, and that the defect system responsible for the NMR spectra perturbations is the interstitial halogen molecule. The decomposition of LiF by reactor irradiation was studied by NMR, and it was found that the formation of a molecular fluorine phase and lithium metal are strong functions of the specimen temperature near 300°C. A study of quadrupole effects in unirradiated NaI was completed, and NMR data from reactor irradiations of NaI crystals at 20°C over a wide dose range are being analyzed. ESR studies were carried out on paramagnetic centers produced in glasses and crystalline compounds by gamma irradiation at room and low temperature. New glass systems studied included alkali halide/boron oxide glasses, borate glasses, phosphate glasses, CABAL glasses, and As_2S_3 glasses. The ESR spectrum of air-quenched $K_2B_2O_4/K_2CO_3$ ceramics indicated a hyperfine interaction with a boron nucleus, and the spin Hamiltonian parameters were determined. The results of NMR, x-ray, and other studies on these materials are described briefly. The ESR study of paramagnetic ions in glasses and polycrystalline compounds was continued, and the spectra of Mn^{2+}, Fe^{3+}, and Cr^{3+} are discussed. The existence of several species of paramagnetic centers in peroxyborate compounds was demonstrated by ESR studies. (D.L.C.)

20621 INFLUENCE OF GAMMA FLUX ON THE ELECTRICAL CONDUCTIVITY OF ZrO_2 FILMS AND ITS RELEVANCE TO CORROSION IN NUCLEAR REACTORS. P. J. Harrop and J. N. Wanklyn (Atomic Energy Research Establishment, Harwell, Berks, Eng.). Brit. J. Appl. Phys., 16: 155-62(Feb. 1965). (AERE-R-4703)

Measurements of the a-c conductivity and thermoelectric power were made on anodic and thermal oxide films on Van Arkel zirconium and Zircaloy 2; and some thermal films were given subsequent anodic treatment. The results point to p-type electronic conductivity being predominant in such films at room temperature. Gamma irradiation at 1.05×10^7 Rad h^{-1} did not affect the instantaneous conductivity of the films at 1592 c/s, other than by a slight warming effect; and dose effects are shown to be unlikely. It is argued, from both experiment and theory, that any effect of gamma irradiation on electron transport in corrosion films in high temperature water reactors is very unlikely. Accordingly, if electron transport controls corrosion, any effect of gamma flux on corrosion is unlikely. (auth)

20622 INFLUENCE OF ELECTRON BOMBARDMENT ON THE SURFACE STATE OF GERMANIUM. V. N. Ovsyuk and L. S. Smirnov (Inst. of Solid State Physics and Semiconductor Electronics, Novosibirsk, USSR). Fiz. Tverd. Tela, 6: 3031-7(1964).

The influence of electron bombardment on the surface state of n-type germanium was investigated in order to derive information on the structure of the surface by determining the dependence of the surface recombination rate on the time. The electron energies were in a range from 1 to 16 kev, which was sufficient for desorption of the physically and chemically adsorbed atoms on the surface. The samples were thin plates, $7 \times 4 \times 0.3$ to 0.5 mm, and had a surface resistivity of 30 to 40 ohm cm. The measurements were carried out in vacuum at $\sim 5 \times 10^{-6}$ mm Hg. The current density employed in the measurements was usually 10^{-6} to 10^{-8} amp/cm^2. The surface state was monitored by measuring the stationary photoconductivity of the samples. The results indicated that the processes occurring on the germanium surface can be of two kinds: redistribution of the charge in the surface layer, and outgassing under the influence of the electron beam. The rate of outgassing depended on the electron energy and exhibited a sharp maximum near 12 to 16 kev. (CFSTI)

20623 IMPURITY PHOTOCONDUCTIVITY PRODUCED IN GERMANIUM BY GAMMA-RAY IRRADIATION. A. B. Gerasimov, B. M. Konovalenko, I. D. Yaroshetskii, and A. A. Barkalaya (Ioffe Inst. of Physics and Tech., Leningrad). Fiz. Tverd. Tela, 6: 3166-8(1964).

Samples of n- and p-type germanium with initial carrier densities of $n = (2-6) \times 10^{13}$ and $p_0 = (0.6-2) \times 10^{13}$ cm^{-3} were used. The samples were exposed to γ rays from ^{60}Co at a dose rate 80 to 90 r/sec. The spectral curves disclosed a large number of bends and ledges, pointing to a

complicated spectrum of the local levels in the forbidden band. Measurements of all the investigated samples indicated the presence of the following energy levels: E_v + 0.52, E_v + 0.48, E_v + 0.43, E_v + 0.41, E_v + 0.37, E_v + 0.33, E_v + 0.31, and E_v + 0.27. This spectrum coincided fully with the spectrum of the local levels produced in the central part of the forbidden band when germanium was irradiated with fast neutrons, to which the levels with energies E_v + 0.31 and E_v + 0.43 eV, which are symmetrical relative to the center of the forbidden band, were added. It was also concluded that the various levels introduced by impurities in the central part of the forbidden band are not due to any clustering of the point defects with the atoms of the doping impurity. (CFSTI)

20624 LOW-TEMPERATURE IRRADIATION OF GERMANIUM WITH FAST ELECTRONS. A. B. Gerasimov and B. M. Konovalenko (Ioffe Inst. of Physics and Tech., Leningrad). Fiz. Tverd. Tela, 6: 3184-6(1964).

Preliminary results are presented on low-temperature irradiation of n-type Ge with $N_d = 2 \times 10^{14}$ to 2×10^{15} cm^{-3}, including samples without and with dislocations (dislocation density 10^7 to 10^8 cm^{-2}), and also of p-type Ge with $N_a = 8 \times 10^{14}$ to 4×10^{15} cm^{-3}. The samples were irradiated with 3.5-Mev electrons at 77°K. The irradiated samples were kept in the liquid nitrogen for several days until their resistance stabilized, and then were subjected to isochronous annealing to room temperature with an interval of 20 to 30°C between annealing points and with an annealing time 15 min. After each annealing, measurements were made at 77°K of the Hall coefficient, the conductivity, and the spectral characteristic of the impurity photoconductivity. All n-type samples were converted by irradiation into p-type with a Fermi level located near $\mu = E_v + 0.1$ ev. The variation of the conductivity during the annealing is shown in graphs. The impurity photoconductivity spectral characteristic was found to be strongly dependent on the annealing stage. Measurements on n-type samples showed that low-temperature irradiation produces entirely different results from irradiation at room temperature. At low temperatures the Fermi level dropped much lower. A noticeable difference in the Fermi level was also observed when a comparison was made between the results of low-temperature irradiation and irradiation at room temperature of samples with and without dislocations. All the results indicated that stepwise isochronous annealing brings about noticeable changes in the structure of the radiation defects produced by low-temperature irradiation of germanium. (CFSTI)

20625 ON THE DEPTH OF PENETRATION AND DISTRIBUTION OF RADIATION DAMAGE WHEN GERMANIUM IS BOMBARDED WITH ARGON AND NITROGEN IONS. P. V. Pavlov, E. I. Zorin, D. I. Tetelbaum, and Yu. S. Popov (Gor'kii State Univ., USSR). Fiz. Tverd. Tela, 6: 3222-6(1964).

The thicknesses of the inversion layers produced on n-type germanium bombarded with argon and nitrogen ions with energies of 46, 67, and 82 kev were measured. The germanium was in the form of plates 5 × 5 × 1 mm with a resistivity of 1 ohm-cm, cut perpendicular to the [111] axis. The plates were carefully ground and chemically polished so that the surface was uniform within 0.2 μ. The ion beams were produced in an accelerator with magnetic ion separation. The samples were etched away layer by layer after irradiation and the surface resistivity was measured after each etching by a four-probe method. The results showed that for argon the thickness of the inversion layer agrees well with the theory of K. O. Nielsen. The thickness of the inversion layer increased with increasing energy and radiation dose, and was larger for nitrogen ions than for argon ions, although the experimental value was smaller for nitrogen than predicted by theory. The depth distributions of the specific conductivities in the inversion layers were determined and it was established that sufficiently large doses of bombarding argon ions produce, on the surface of the inversion layer, a high-resistance region whose thickness increases with the dose. It is suggested that this high-resistance layer is due to disordering of the crystal structure of the germanium; this hypothesis was confirmed by electron diffraction data. (CFSTI)

20626 HIGH-TEMPERATURE ANNEALING OF DEFECTS PRODUCED IN GERMANIUM BY FAST NEUTRONS. R. F. Konopleva, S. R. Novikov, and S. M. Ryvkin. Fiz. Tverd. Tela, 6: 3263-5(1964).

Earlier investigations of the spectrum of energy levels produced in germanium by fast neutrons were continued, and high-temperature annealing of the defects produced by the neutrons was studied. The samples previously investigated were subjected to isochronous and isothermal annealing in the temperature range from 70 to 400°C. The annealing was in air and the temperature was maintained constant within 1.0°C. The electric conductivity and the temperature dependence of the Hall coefficient were measured after each annealing. The measurements disclosed the presence of two stages of annealing, one in the temperature region near 150°C, when about 15% of the defects were annealed, and one above 250°C, when the remaining defects were annealed. The corresponding activation energies were 1.2 and 2.6 ev. These activation energies were characteristic of the diffusion of single and double vacancies in germanium. Therefore, it was concluded that 85% of the defects produced by neutron irradiation are in the form of double vacancies, which are annealed at temperatures above 250°C, and the remainder are the less stable single vacancies, which are annealed at about 150°C. Earlier deductions that the defects have an acceptor character were also confirmed. (A.T.D. Press)

20627 RADIATIVE RECOMBINATION IN Si AND Ge ASSOCIATED WITH RADIATION DEFECTS. Yu. L. Ivanov and A. V. Yukhnevich. Fiz. Tverd. Tela, 6: 3703-4(1964).

Observations were made of recombination radiation from impurity regions of Si and Ge p-n junctions irradiated by gamma rays and fast neutrons, respectively. The Si p-n junctions were obtained by diffusing Al into n-type Si with a resistivity of 150 ohm · cm. The area of the junction was 0.36 mm^3, and the base was 0.2 mm thick. Radiation defects were produced at room temperature by gamma rays from a ^{60}Co source. The integrated dose was 5×10^{17} cm^{-2}. The excess carriers were generated by pulsed injection in the forward direction. The Ge p-n junctions were prepared by diffusing In into n-type Ge with a resistivity of 10 ohm · cm. The amount of dislocations was kept at a minimum. The Ge p-n junctions were irradiated by fast neutrons in a reactor. The recombination spectra of Si and Ge are shown. (ATD)

20628 ENERGY STRUCTURE OF GAMMA-RADIATION DEFECTS IN GERMANIUM. T. V. Mashovets and R. Yu. Khansevarov. Fiz. Tverd. Tela, 7: 308-10(1965).

An investigation was made of the spectral distribution of impurity photoconductivity in specimens containing defects with different charge states and the influence of annealing of irradiated specimens on spectral distribution of photoconductivity. The specimens were cut from different monocrystals with an initial concentration of donors (antimony) ranging from 4×10^{13} to 3×10^{14} cm^{-3}. Irradiation was conducted at 10°C. In addition to the spectral dependence of impurity photoconductivity of specimens before irradiation, after irradiation, and after annealing, the dependence of charge-carrier concentration on temperature was obtained. The rate of irradiation of specimens and the temperature of measurements were selected in such a way that the filling of defect levels with electrons was realized as follows: all defect levels located below the levels of chemical donors were filled with electrons; the $E_c - 0.20$-ev level was partially filled; the E_v + 0.27-ev level was partially filled; the E_v + 0.22-ev level was partially filled; and the E_v + 0.11-ev level was practically filled. Analysis of the energy diagrams showed that the $E_c - 0.27$-ev, E_v + 0.32-ev, and E_v + 0.16-ev levels are always present in all specimens before irradiation and remain after annealing. It is possible that these levels could be attributed to some constantly present impurities. The $E_c - 0.20$-ev, $E_c - 0.34$-ev, E_v + 0.27-ev, E_v + 0.22-ev, and E_v + 0.11-ev levels are produced during irradiation, the last two only during

prolonged irradiation. The stability of radiative defects with regard to annealing increased with increasing radiation dose. (CFSTI)

20629 ABSORPTION OF RADIOWAVES BY A DIELECTRIC IN IONIZING RADIATION FIELD. V. K. Zhuravlev (Tomsk Polytechnic Inst., USSR). Izv. Vysshikh Uchebn. Zavedenii, Fiz., No. 1, 32-6(1965). (In Russian)

Reverse dielectric losses in dielectrics placed in ionizing radiation fields were analyzed on the basis of universal relations for absorption by a system of classical rotators with continuous energy distribution. (tr-auth)

20630 MODIFICATION OF THE STRENGTH OF PAPER BY ROENTGEN IRRADIATION. O. Schwab, K. Nitzl, and H. Klingelhoeffer (Institut der Papiertechnischen Stiftung, Munich). Kolloid-Z., 199: 108-13(Oct. 1964). (In German)

Irradiations were performed using 150-kv x rays, and Schleicher & Schull chromatography paper 2043 in 15 × 35 mm strips irradiated parallel and perpendicular to the fiber orientation. Pretreatment with various atmospheres, such as $H_2O + N_2$, O_2, and N_2 was found to affect breaking loads depending on time and dosage. Dependence of average polymerization degree on length of irradiation was also found. Time, breaking load in kp (parallel and perpendicular), breaking energy in kp m, Cu number, and carboxyl groups as % cellulose were found to be: 0, 12.4, 7.9, 9.2×10^{-3}, 0.6, 0.156; 0.5, 12.6, 8.1, 8.8×10^{-3}, 0.6, –; 1.0, 12.3, 8.1, 9.3×10^{-3}, 0.7, –; 2.0, 12.4, 8.2, 8.1×10^{-3}, 0.9, 0.425; 4.0, 11.3, 7.8, 8.1×10^{-3}, 1.8, 0.955; 8.0, 10.2, 6.9, 5.1×10^{-3}, 3.5, –; 10.0, –, –, –, –, 1.588. A linear relation was found to exist between the logarithm of the breaking energy and the logarithm of the hydroxyl group number. (TCO)

20631 THE EFFECT OF STRESS ON THE RADIATION STABILITY OF ASTM A 302 GRADE B PRESSURE-VESSEL STEEL. M. B. Reynolds (Vallecitos Atomic Lab., Pleasanton, Calif.). Mater. Res. Std., 3: 644-5(Aug. 1963).

Studies were made to determine if radiation stability of reactor pressure vessel steels is altered by simultaneous application of stress. A fixture for holding samples under stress during irradiation was designed to replace one of the plugs used to restrict water flow in unfueled channels of the core of the Vallecitos Boiling Water Reactor. It allows an unstressed control specimen of equivalent length to be installed parallel to the stressed specimen. The specimens tested were cut from a plate of the same heat of ASTM A 302 grade B steel used in fabrication of the Dresden Nuclear Power Station reactor pressure vessel. Analysis of this heat is provided. After irradiation the fixture was removed and the two specimens cut into 5.5-cm lengths, and notched with a remotely operable broach to produce standard Charpy V-notch impact specimens. These specimens were tested in the usual manner. During irradiation for 7 months, the specimen was stressed and unloaded at least 30 times owing to reactor shut-downs and scrams, each of which resulted in loss of coolant pressure. Maximum exposure as indicated by a nickel flux monitor was 4.35×10^{19} per $cm^2 > 1$ Mev for the stressed specimen and 2.64×10^{19} per $cm^2 > 1$ Mev for the unstressed control specimen. Results showed that the impact strength of the stressed material was greater than that of the unstressed material in spite of the somewhat lower exposure on the unstressed bar. As to possible mechanisms of this effect, it appears that stress aids the growth of vacancy clusters beyond the size and spacing at which the maximum effect on mechanical properties occurs. (TCO)

20632 EXPOSURE OF X-RAY FILM TO RADIOACTIVE FALLOUT LEVELS OF GAMMA RAYS. Joseph C. Williamson (Medical Field Service School, Ft. Sam Houston Tex.). Med. Bull. U. S. Army Europe, 20: 69-70(Mar. 1963).

An attempt was made to evaluate protection afforded x-ray film in field medical installations during radioactive fallout situations. During field exercises in which nuclear warfare situations were employed, inadequate protection was being given the stock supply of x-ray film. The method of protecting x-ray film most used by medical installation commanders was a $\frac{1}{32}$ in. lead-lined chest (standard equipment). An attempt was made to determine the extent of protection afforded by the lead-lined chest. X-ray film was placed in the chest while loaded in cassettes or while in its original cardboard container. Cobalt-60 and Ra sources were placed around the outside of the chest to give a rate inside the chest of 25 mR/hr. Film receiving a total dose of γ radiation of 5 to 50 mR showed little effect and could be used later for radiography. Film receiving a total dose of 50 to 100 mR had enough darkening due to the radiation to require cautious use. Film receiving 100 to 200 mR resulted in moderate darkening and limited usefulness; 200 to 300 mR resulted in film of very limited use; and 300 to 500 mR rendered the film useless. Where large parts are to be x rayed, such as chest, abdomen, pelvis, the upper limit of pre-exposure appeared to be 100 mR. It was found that by developing one film from the package to roughly determine the degree of exposure the ma-sec setting could sometimes be adjusted to compensate for the contrast. It was concluded that this protective, $\frac{1}{32}$ in. lead-lined chest will not protect x-ray film from fallout γ rays. Furthermore, the chest will not hold all the film normally on hand in a field medical installation. (BBB)

20633 ON THE FISSION-GAS RETENTION ABILITY OF URANIUM DIOXIDE PELLETS PRODUCED WITH DIFFERENT TECHNIQUES. I. Amato, R. L. Colombo, and G. Frigerio (FIAT, Turin). Nucl. Sci. Eng., 22: 111-13 (May 1965).

The fission gas retention ability of UO_2 pellets sintered in hydrogen was examined. The pellets were irradiated at low temperature in a flux of 5×10^{12} n cm^{-2} sec. They were then tested in a hot cell with 6 hr diffusion anneal at 1400°C in a tantalum crucible under helium atmosphere and subsequent melting in potassium pyrosulfate. Gases released during both stages were carried to a charcoal trap. A scintillation detector was used to determine the ^{133}Xe released from the samples. (C.E.S.)

20634 NEUTRON IRRADIATION DAMAGE IN MOLYBDENUM. M. E. Downey and B. L. Eyre (Atomic Energy Research Establishment, Harwell, Berks, Eng.). Phil. Mag. (8), 11: 53-70(Jan. 1965). (AERE-R-4632)

The technique of transmission electron microscopy was used to study neutron irradiation damage and its behavior on annealing in molybdenum. Microhardness tests were carried out on all specimens before thinning to obtain some indication of the relation between structural effects and the mechanical properties. The results show that part of the damage in molybdenum neutron irradiated to a dose of 2×10^{22}n cm^{-2} (fission) is in the form of point defect clusters which are deduced to be interstitial. The interstitial point defects must therefore be sufficiently mobile during irradiation at 60°C to form into these clusters. However, the experimentally estimated point defect density only accounts for a small proportion of the theoretical number suggesting that most of the interstitials are present singly or as submicroscopic clusters. On annealing there is little change in the observable damage up to 800°C but the microhardness shows a peak at 170°C followed by steady recovery. Above 800°C the loops grow rapidly and finally join up to form dislocation networks. This stage is accompanied by an increase in the rate of recovery of the micro-hardness. The loops are shown to be interstitial in nature with Burgers vector $a/2\langle 111\rangle$, though during the early stages of network formation some $\langle 100\rangle$ type dislocations form through the reaction: $a/2[111] + a/2[1\bar{1}\bar{1}] \rightarrow a[100]$. These results are discussed in conjunction with other more indirect recovery data and a model is proposed for the annealing of irradiation damage in molybdenum above room temperature. The general conclusion is that the initial damage structure and its subsequent behavior on annealing are largely governed by the distribution and mobility of interstitial impurity atoms during irradiation. (auth)

20635 THE EFFECTS OF FAST NEUTRON IRRADIATION ON THE REPEATED YIELDING CHARACTERISTICS OF A COPPER–TIN ALLOY. B. Russell (Univ. of Queensland, Brisbane). Phil. Mag. (8), 11: 139-51(Jan. 1965).

The rate of vacancy formation during straining of irradiated copper-tin alloys was investigated by means of repeated yielding experiments, and was found to increase with neutron doses in excess of 1.6×10^{16} nvt. The rate of formation was very high immediately after yielding, but fell to a constant value after 3% strain. Transmission microscopy was used to identify two distinct types of damage. Small dislocation loops with an average diameter of 40 Å and a density of 10^{16} cm^{-3} were observed, together with large dislocation loops with a diameter of 380 Å and a density of 2×10^{14} cm^{-3}. The overall increase in rate of vacancy formation was attributed to the interaction of glide dislocations with the small dislocation loops and the initial high rate to the presence of heavily jogged dislocation sources. (auth)

20636 INTERSTITIAL LOOPS IN NEUTRON-IRRADIATED MOLYBDENUM. J. D. Meakin and I. G. Greenfield (Franklin Inst., Philadelphia). Phil. Mag. (8), 11: 277-90(Feb. 1965). (TID-21210; F-B 1979-1(App.B))

The irradiation of zone-refined molybdenum to a dose of 8×10^{17} nvt at 600°C produces a low density of large prismatic dislocation loops. The loops which number 2×10^{13}/cm^3 have an average diameter of 1100 Å and are shown to be close to pure edge in character with a Burgers vector a/2⟨111⟩. Diffraction contrast experiments established that the loops are formed by the aggregation of interstitial atoms. An order of magnitude analysis of the behavior of radioinduced defects indicates that vacancies are not sufficiently mobile to aggregate into resolvable loops. (auth)

20637 THE MECHANICAL PROPERTIES OF REACTOR GRAPHITE. W. N. Reynolds (Atomic Energy Research Establishment, Harwell, Berks, Eng.). Phil. Mag. (8), 11: 357-68(Feb. 1965). (AERE-R-4566)

It is shown that after brief neutron irradiation the elastic constants of polycrystalline reactor graphite are reasonably consistent with the single crystal values in a uniform stress (Reuss) approximation. A method is proposed for dealing with the anisotropy of the polycrystalline aggregate by reference to the coefficients of thermal expansion. This leads to a consistent model of the behavior of the elastic constants at higher irradiation doses and temperatures, and also of fracture. The model is extended to cover the phenomenon of irradiation creep. It is shown that reactor Grade A graphite is unlikely to crack at differential strain rates of less than 350 ppm/10^{20} neutrons/cm^2 parallel and 600 ppm/10^{20} neutrons/cm^2 perpendicular to extrusion. It should also withstand respective total differential strains of 0.4 and 0.65% and differential stresses of 0.65 and 0.47 Kg/mm^2 without cracking. In pure compression the fracture stress is estimated at 2.5 kg/mm^2 and the strain at 2.5%. (auth)

20638 THE ABSORPTION SPECTRA AND IRRADIATION OF PLASTICALLY DEFORMED DIAMOND. C. Phaal (Crown Mines, Johannesburg, S. Africa). Phil. Mag. (8), 11: 369-78(Feb. 1965).

Plastically deformed diamond single crystals were irradiated with fast electrons and their optical absorption spectra determined. The results suggest that preferential irradiation damage occurred in regions of high strain and that the group B absorption bands in type I diamonds are associated with strain. (auth)

20639 AN EFFECT OF FAST NEUTRON IRRADIATION ON THE POLISHING OF DIAMOND. Eileen M. Wilks (Oxford Univ.). Phil. Mag. (8), 11: 433-5(Feb. 1965).

A good quality diamond that was irradiated with 10^{19} fast neutrons/cm^2, and whose lattice parameter increased by 0.6%, was polished with diamond powder on a revolving lap. Almost immediately, multiple cracking occurred on the polished cube surface, more or less parallel to {111} planes. This behavior, hitherto unobserved on diamond, probably arises as the result of stresses set up by the partial anneal of the surface layers heated by the polishing action. (auth)

20640 THE ELASTICITY OF POLYCRYSTALLINE GRAPHITE. R. L. Woolley (Central Electricity Generating Board, Gloucestershire, Eng.). Phil. Mag. (8), 11: 475-83(Mar. 1965).

The elastic displacement of screw dislocations bounding the lamellar grains is of the correct order of magnitude to account for the observed elasticity of reactor grade graphite. The change of elastic modulus on irradiation cannot be explained in terms of the pinning of these or of other dislocations by the clusters observed in irradiated single crystals. The pinning is attributed to the population of smaller clusters in the grain boundaries. The fall of elastic modulus at higher irradiation is attributed to vacancies. (auth)

20641 NEUTRON-ACOUSTIC IRRADIATION OF ALUMINIUM SINGLE CRYSTALS. B. Langenecker and C. W. Fountain (Naval Ordnance Test Station, China Lake, Calif.). Phil. Mag. (8), 11: 513-19(Mar. 1965).

Ultrasonic irradiation of ~25 w/cm^2 at 20 kc may increase the critical resolved shear stress by a factor of 4 in 99.999% pure aluminum single crystals. This acoustic hardening is accompanied by a yield-point phenomenon, which, in its graphical appearance, resembles effects by neutron irradiation with no sound applied. Hardening by ultrasound and by neutron irradiation are compared, and effects of the superposition of fast neutrons (>0.1 Mev; ~2×10^{16} n/cm^2) and intense ultrasound (~25 w/cm^2 at 20 kc) in aluminum single crystals having diameters between 0.6 and 1.5 mm are presented. Increases were found to amount to as much as a factor of 14 in the critical resolved shear stress of these crystals compared to untreated samples. Simultaneously, the electric resistivity increased with combined treatment by 3.2 times over untreated samples. The results from these investigations are discussed in the light of present theories of neutron and acoustic radiation damage. (auth)

20642 IRRADIATION OF URANIUM WITH NEUTRONS AT 4.5°K. G. Burger, (Technische Hochschule, Munich), K. Isebeck, H. Wenzl, J. C. Jousset, and Y. Quere. Phil. Mag. (8), 11: 621-5(Mar. 1965).

A liquid helium temperature irradiation of pure uranium is described. The initial resistivity increases are given for various textures of the metal. It is shown that there exists in uranium a very mobile defect which anneals out between 4 and 20°K. (auth)

20643 A STUDY OF FISSION FRAGMENT DAMAGE IN TUNGSTEN WITH THE FIELD-ION MICROSCOPE. K. M. Bowkett (Cambridge Univ., Eng.), L. T. Chadderton, H. Norden, and B. Ralph. Phil. Mag. (8), 11: 651-6(Mar. 1965).

The field-ion microscope was used for the first time to study the atomic details of fission fragment damage in tungsten. Needle-shaped specimens were bombarded with collimated uranium fission fragments and the dose adjusted so that the interaction of a single fission fragment with each specimen can be studied. Large hemispherical craters ~250 Å radius were formed where a fragment interacted with the specimen surface and by using controlled field evaporation the exact geometry of such craters could be found. Field evaporation also enabled the damage in depth to be investigated; and a number of vacancy clusters ~35 Å diameter were found. (auth)

20644 BEHAVIOUR OF HEXAGONAL SELENIUM SINGLE CRYSTAL DURING REACTOR IRRADIATION. T. O. Tuomi (Inst. of Tech., Otaniemi, Finland). Phys. Letters, 14: 282-3(Feb. 15, 1965).

A selenium single crystal was irradiated in the Triga reactor and the conductance was measured as a function of the power. The results show that the behavior during reactor irradiation is completely different from that of Ge and Si semiconductors, which are permanently damaged at room temperature by a fast neutron flux of 6×10^{15} cm^2. Measurements of the gamma heating in the reactor and the measured temperature dependence of the conductance exclude the possibility that the change in conductance is due to gamma heating. (L.B.S.)

20645 DIRECTIONAL EFFECTS IN ELECTRON-IRRADIATED Cu SINGLE CRYSTALS. A. Sosin and K. Garr

(Atomics International, Canoga Park, Calif.). Phys. Status Solidi, 8: 481-5(1965).

Thin copper single crystal samples were irradiated by energetic electrons incident along major crystallographic directions. Appreciable defect production was observed in samples oriented for ⟨100⟩ and ⟨110⟩ incidence in the near-threshold range, indicating that threshold displacement energies for both directions are comparable. Postirradiation studies showed that recovery takes place throughout the entire stage I temperature range, even at the lowest electron energies. (auth)

20646 LENGTH CHANGES IN THE IRRADIATION OF GOLD WITH α-PARTICLES IN THE TEMPERATURE REGION OF −20 TO +90°C. K. Isebeck (Technische Hochschule, Munich). Phys. Status Solidi, 8: 577-92(1965).

The change in length of thin gold foils (99.999% purity) was studied upon irradiation with α particles in the temperature region −20 to +90°C. At temperatures below 0°C about 20 to 50% of the recovery of the change in length was found to be a first-order, diffusion limited reaction with an activation energy of (0.65 ± 0.07) ev. The defect densities were of the order of 10^{-6}. The annealing behavior is interpreted as the recombination of interstitial atoms with vacancies produced within the same defect cascade. Above 0°C, the initial dilatation on irradiation is followed by a gradual contraction of the foil. This behavior is interpreted as due to the migration of interstitial atoms to the surface of the foil. At temperatures between 40 and 65°C the recovery was found to be exponential after prolonged annealing for about 50% of the recovery. The activation energy is (0.81 ± 0.03) ev. The latter portion of the recovery is identified with the migration of vacancies to dislocations. (auth)

20647 MAGNETIC AFTER EFFECTS IN NICKEL AFTER LOW TEMPERATURE IRRADIATION WITH NEUTRONS. E. Balthesen (Kernforschungsanlage, Julich, Ger.), K. Isebeck, and H. Wenzl. Phys. Status Solidi, 8: 593-602(1965).

The magnetic after-effects of structural lattice defects produced by neutron irradiation of nickel at 25°K were investigated in the temperature region of 8 to 400°K. Several very pronounced after-effects were found at low temperatures within the stage I region of the recovery of the residual resistivity. The properties of several after-effects (activation energy and pre-exponential factor) were determined. The main features of the recovery stages of the magnetic after-effects agree with those of the residual resistivity. (auth)

20648 MAGNETIC AFTER EFFECTS IN IRON AFTER LOW TEMPERATURE IRRADIATION WITH NEUTRONS. E. Balthesen (Kernforschungsanlage, Julich, Ger.), K. Isebeck, and H. Wenzl. Phys. Status Solidi, 8: 603-11 (1965).

High-purity iron was irradiated at low temperatures with neutrons to various doses. Magnetic after-effects due to radiation induced defects were investigated in careful annealing experiments from 4.5 to 300°K. A number of pronounced orientation after-effects with complex annealing behavior were found. All relaxation amplitudes were roughly proportional to the dose. The after-effects disappeared on annealing between 130 and 270°K. A comparison with other experiments indicates that an annealing stage of the electrical resistivity or the stored energy may correspond to the annealing of several magnetic after-effects. (auth)

20649 RESISTIVITY OF PLUTONIUM, NEPTUNIUM AND URANIUM DUE TO THE ACCUMULATION OF RADIOACTIVE SELF DAMAGE. E. King (Atomic Energy Research Establishment, Harwell, Berks, Eng.), J. A. Lee, K. Mendelssohn, and D. A. Wigley. Proc. Roy. Soc. (London), Ser. A, 284: 325-43(Mar. 9, 1965).

An increase with time in resistivity occurs in plutonium at low temperatures as a result of radioactive self damage. The effect was studied in experiments at liquid helium temperature lasting over 8000 hr and was found to exist in the α, β and δ phases of the metal. In all cases the resistivity approaches saturation, the rates of increase depending on the crystal structure and isotropic content of the sample. In spite of wide differences in these rates the functional increase is roughly the same. The temperature dependence of the accumulated resistivities in all three modifications deviates very strongly from a simple additive resistance obeying Matthiesen's rule. The resistivity of fully damaged α plutonium is almost temperature independent, becoming smaller than that of the undamaged specimen above about 50°K. Measurements on neptunium and uranium-233 also showed resistivity increases with time at helium temperatures, but the effect is too small to decide whether Matthiesen's rule is obeyed in these metals. The observed effects were discussed under the assumption that in plutonium scattering of electrons at low temperatures is mainly due to a cooperative phenomenon. (auth)

20650 EFFECT OF ANNEALING ON THE RESISTIVITY OF SELF DAMAGED PLUTONIUM. D. A. Wigley (Oxford Univ.). Proc. Roy. Soc. (London), Ser. A, 284: 344-53 (Mar. 9, 1965).

When samples of α plutonium are stored at low temperatures, their resistivities increase owing to the accumulation of defects produced by the radioactive disintegration of the nuclei. Isochronal annealing experiments were performed on α plutonium which show that this additional resistivity recovers in two distinct stages centered at about 75 and 150°K respectively. In δ stabilized plutonium the first annealing stage is more pronounced and occurs at lower temperatures, the values of which are dependent on the concentration of aluminum used to stabilize the δ phase. Isochronal annealing experiments were also performed on heavily damaged samples of α plutonium and yield further information on the anomalous temperature dependence of the resistivity changes brought about by self irradiation at low temperatures. The correlation between the observed resistivity changes and corresponding changes in the concentration of point defects is discussed. (auth)

20651 EFFECTS OF RADIATION ON SEMICONDUCTORS. Viktor Sergeevich Vavilov. Authorized Translation from the Russian by A. Tybulewicz. New York, Consultants Bureau, 1965. 234p. $15.00.

The effects of electromagnetic radiation and high-energy particles on semiconductors are discussed. The processes of absorption of electromagnetic radiation, photoionization and ionization by charged high-energy particles, and recombination processes by which an excited crystal returns to its original equilibrium state are considered. Radiative recombination in semi-conductors is described. The theory of the formation of structural defects in semiconductors by hard radiation, and experimental data on changes in physical properties due to such defects are presented. (M.C.G.)

20652 MAGNETIC AFTER EFFECTS IN NEUTRON IRRADIATED IRON, NICKEL, AND COBALT. P. Moser, P. Peretto, D. Dautreppe, and P. Vigier (Centre d'Etudes Nucleaires, Grenoble, France). 9p. (CONF-794-5)

From Magnetism Conference, Minneapolis, Nov. 1964.

After neutron irradiation of iron at 78°K, four magnetic after-effect zones were observed. All those zones annealed out in different temperature ranges corresponding to the well-known stages of recovery in neutron irradiated iron. If the sample was annealed for 30 min at 500°C after an irradiation at 78°K, a different magnetic after effect zone appeared. The different characteristics of each zone (activation energy for reorientation, spectrum width, defects symmetry, etc) were studied. A model concerning the nature of the defects responsible for these magnetic after effects is proposed. Similar effects were found in neutron-irradiated nickel and cobalt at 28°K. From the results on nickel a great number of arguments are given in favor of the interstitially configuration. (auth)

METEOROLOGY

See also GEOLOGY AND MINERALOGY — Site Survey and Selection.

20653 (ANL-6938(p.209-41)) STACK PLUME RISE DETERMINATIONS AS AFFECTED BY METEOROLOGICAL AND ENGINEERING FACTORS. Harry Moses, Gordon H. Strom, and James E. Carson (Argonne National Lab., Ill.).

Empirical plume-rise formulas of Davidson-Bryant and Holland, and the semitheoretical formula of Bosanquet are discussed. Critical examination of these formulas indicates that a better one is needed. Stümke's generalized formula may be accepted after further tests are made with independent data. It appears that for large stacks with appreciable buoyancy such as those at Gernsheim or Duisburg, Holland's formula with a Stümke correction factor of about 3 may be used, i.e., $\Delta h = 3(1.5\ V_s d + 4 \times 10^{-5} Q_H)/U$. For smaller stacks with little buoyancy such as the Argonne stack, a Stümke K factor of about 2 may be used. The effect of stability on plume rise can be taken into account by adding 10 to 20% of the computed value, under lapse conditions, and subtracting the same amount under stable stratifications. Terrain effects, such as nearby buildings, hills and valleys or forested areas, must be taken into account. In most cases, this can only be done by wind-tunnel tests. Meteorological conditions may also materially affect plume rise. (J.R.D.)

20654 (ANL-6938(p.242-51)) DETERMINATION OF TURBULENCE DISSIPATION BY EULERIAN VARIANCE ANALYSIS. Paul Frenzen (Argonne National Lab., Ill. and Commonwealth Scientific and Industrial Research Organization, Aspendale (Australia). Div. of Meteorological Physics.

Submitted to Quart. J. Roy. Meteorol. Soc.

Using a variance function to specify the variance retained by a time series smoothed via running means, it is shown that the rate of turbulence dissipation can be computed from an Eulerian wind record supplied by a single, 3-cup anemometer through the relation $\epsilon = (A/\overline{U})\ [(u^2_{T_j} - u^2_{T_k})/(T_k^{\frac{2}{3}} - T_j^{\frac{2}{3}})]^{\frac{3}{2}}$. Here $A \approx 3.3$ derives from the Kolmogoroff law, $\overline{U}$ is the mean flow, and the numerator of the bracketed term represents the additional reduction in variance effected by increasing the averaging interval from T_j to T_k. Preliminary verifications of the relation are presented, and an experimental program designed to use the method is outlined. (auth)

20655 (ANL-6938(p.252-6)) INSTRUMENTATION FOR ATMOSPHERIC TRUBULENCE STUDIES. Paul Frenzen (Argonne National Lab., Ill.).

In order to obtain data more suitable to the method of Eulerian variance analysis than those employed for preliminary computations, an unusual 3-cup anemometer was constructed. A wind tunnel was placed in operation for absolute calibration and determination of the step-function response characteristics of this and future wind-measuring devices. Suitable equipment for the measurement of flow velocity was also installed. (J.R.D.)

20656 (ANL-6938(p.257-73)) PLUME-RISE CHARACTERISTICS OF A SCALE MODEL SMOKE PLUME. Gordon H. Strom and Edward J. Kaplin (Argonne National Lab., Ill.).

The development of equipment and techniques for conducting scale-model wind-tunnel experiments on the atmospheric diffusion of smoke plumes is reported. An important feature of the development work is the inclusion of temperature gradient as one of the test variables. Following each series of experiments, various modifications and additions were made in wind-tunnel equipment and instrumentation to correct defects found in experimental results. The last two series (identified as Series III and IV) producing results which showed significant agreement with prototype data obtained with the Argonne Experimental Smoke Stack are reported. Of the meteorological and stack variables measured in these experiments only those significant to plume rise are included. (J.R.D.)

20657 (DASA-1309) PROJECT STAR DUST. Quarterly Report No. 9. Herbert W. Feely, Ben Davidson, James P. Friend, Raymond J. Lagomarsino, and Micah W. M. Leo (Isotopes, Inc., Westwood, N. J.). Sept. 1, 1963. Contract DA-49-146-XZ-079. 336p. (AD-606712) $6.00 (CFSTI).

Work done on Project Star Dust during the preceding contract year is reviewed. Filter samples of stratospheric radioactivity were collected using WU-2, RB-57, and RB-52 aircraft. Lower altitude collections included intensive sampling in the vicinity of extrusions of stratospheric air into the troposphere during the spring of 1963. A number of radiochemical and radiometric procedures used during Project Star Dust and developed since the issuance of the final report on Project HASP are described. (auth)

20658 RADIOACTIVE COPPER AS AN ATMOSPHERIC TRACER. Gilbert S. Raynor (Brookhaven National Lab., Upton, N. Y.). St. Joseph, Mich., American Society of Agricultural Engineers, 1965, Preprint Paper No. 64-823, 36p. (CONF-641207-2). (BNL-8645)

From American Society of Agricultural Engineers, Winter Meeting, New Orleans.

Techniques and instruments were developed for the use of radioactive copper as a tracer in studies of diffusion and dispersion through the atmosphere and of deposition on the ground and vegetation. The copper, in the form of solid, spherical particles, 2 to 12 μ in diameter, or in a soluble compound, is activated by exposure to a slow-neutron flux to produce ^{64}Cu. The particles suspended in a liquid and the compounds in solution are emitted into the air by atomizing nozzles. Air concentrations are measured by filtered or rotating impactor samplers. Material deposited on the ground and vegetation is measured by mobile radiation counters, by sticky paper collectors, by autoradiographs on x ray film or by actual soil and plant samples. Both beta and positron annihilation gamma counting are utilized in analyzing the filters and other samples. Instrument calibration techniques and safety procedures were established. (auth)

PHYSICS

General

Refer also to abstract 20905.

20659 (AD-606490) ELASTIC WAVE INTERACTION WITH CYLINDRICAL CAVITY. J. F. Gilbert (Plesset (E.H.) Associates, Inc., Los Angeles). Dec. 1, 1959. Contract AF04(647)-342. 25p. $1.00(CFSTI).

The interaction of a plane pressure pulse with a smooth, cylindrical cavity in a two dimensional, elastic, homogeneous medium is studied using the high frequency approximation common to geometrical optics. Both a normal and oblique impingement are considered. Reflection and divergence coefficients are computed and plotted as a function of problem geometry. Stresses and displacements along the cylindrical surface are also shown. The maximum stress occurs on the surface near the 70 degree central angle radial when the incidence is normal. Computations of similar divergence and reflection coefficients for oblique impingement are accomplished by geometrical considerations using the computed values for normal impingement. The maximum stress is considerably less than for the normal case. (auth)

20660 (P-1113(RAND)) RANDOM WALK, SCATTERING AND INVARIANT IMBEDDING. I. ONE-DIMENSIONAL DISCRETE CASE. Richard Bellman and Robert Kalaba (RAND Corp., Santa Monica, Calif.). June 27, 1957. 10p. (AD-606439). $1.00(CFSTI).

A method is introduced for treating problems involving random walk processes, based upon the principle of invariant imbedding. Since scattering processes can often be formulated in terms of random walk, the present method can be used for treating scattering processes. (auth)

20661 (RLE-TR-428) DIAGNOSTIC EXPERIMENTS IN A MAGNETICALLY DRIVEN SHOCK TUBE (thesis). John B. Heywood (Research Lab. of Electronics, Massachusetts Inst. of Tech., Cambridge). Dec. 31, 1964. 59p.

Experiments are described in hydrogen in a magnetic annular shock tube with an applied axial magnetic field. Measurements of the front speed were made over as wide a range of initial gas pressure, initial drive bank voltage, and axial magnetic field as possible. These results are compared with the predicted speeds obtained from the Kemp and Petschek solutions and the snowplow model, and agreement is obtained. Measurements were also made on the front properties with magnetic and electric field probes inside the annulus, and with phototubes. It was found that a substantial fraction of the drive current always flows in the front and no shock wave preceding the current sheet was observed. A detailed picture of the current distribution inside the annulus is obtained, and a current loop was found to flow behind the front. It is shown that electric-field measurements substantiate this picture. It is also shown that when the Alfvén speed ahead of the front is comparable with the front speed, the flow pattern changes significantly. (auth)

20662 A MODEL OF THE INSULATOR-METAL TRANSITION. PART I. TWO-BODY CORRELATIONS. G. Kemeny (Kennecott Copper Corp., Lexington, Mass.). Ann. Phys. (N. Y.), 32: 69-99(Mar. 1965).

A simple cubic hydrogenic lattice in the extreme tight binding approximation with only one energy band is set up as a model for an insulator. A two-particle Green's function equation for one full and one empty state is derived with a mutual interaction potential. The model is a generalization of one by Hubbard applying only one particle Green's functions to electrons in narrow energy bands. The model is also a generalization of one by Slater and Koster which applies to electron-impurity interactions. It is shown that the energy of a pair of full and empty states depends on the orientation and magnitude of the relative crystal momentum of the pair. Kohn's criterion for the insulating state is satisfied by all bound pairs. A qualitative discussion of this lattice as a superposition of pairs is also given on the basis of the quasi-chemical equilibrium theory. (auth)

20663 LAMINAR UNSTEADY MAGNETOHYDRODYNAMIC FLOW IN AN ANNULAR CHANNEL UNDER A RADIAL MAGNETIC FIELD. S. C. Gupta and M. L. Mittal (Indian Inst. of Tech., Bombay). Appl. Sci. Res., Sect. B, 11: 161-75(1964).

The unsteady flow of an electrically conducting viscous fluid in the region emanating from the common axis in planes perpendicular to it is discussed. In the special case when the magnetic Reynolds number of the flow is the same as its Reynolds number, an exact solution in terms of Bessel functions was obtained which after infinite time tends to the steady flow discussed by Globe. (auth)

20664 DETERMINATION OF GRADIENTS OF FLOW VARIABLES BEHIND THREE-DIMENSIONAL STATIONARY AND PSEUDO STATIONARY CURVED SHOCK WAVES IN CONDUCTING GASES. J. C. Pant and R. S. Mishra (Univ. of Gorakhpur, India). Appl. Sci. Res., Sect. B, 11: 181-204(1964).

The gradients of magnetic field, velocity, pressure and density behind a shock wave were obtained in three dimensional steady motion of a conducting gas. A continuous differentiable function of coordinates was taken for the shock configuration and it is assumed that the components of the magnetic field H^i, velocity components u^i, pressure p and density ρ behind the shock-surface are differentiable functions. The quantities H^i, u^i, p and ρ in front of the shock-wave were taken as constant quantities. The gradients of flow and field quantities were calculated behind the pseudostationary shockwave and in cases where the normal component of the magnetic field is zero on both sides of the shock wave. The relation between the curvature k of the shock-surface and the curvature K of the stream line just behind the shock surface in two dimensional steady motion was derived. The determination of the ratio K/k for an attached shock in the case of a wedge was considered. (auth)

20665 AN APPLICATION OF THE OPERATIONAL CALCULUS TO THE EQUATIONS OF THE RAYLEIGH PROBLEM IN MHD. J. A. Steketee (Technische Hogeschool, Delft, Netherlands). Appl. Sci. Res., Sect. B, 11: 255-72(1964).

The operational calculus in the form developed by Van der Pol and Bremmer is applied to obtain some solutions for the equations of the Rayleigh Problem in MHD. The diffusivities in these solutions can have arbitrary values. A limiting case of the solutions is studied, and it is shown that the solutions have some advantages as compared to the integrals of Chang and Yen, and of Hide and Roberts. Finally an example of Ludford is used to verify that the integrals obtained here will make their appearance in the solution of some boundary value problems. (auth)

20666 ON LAGRANGIAN FORMALISM AND ITS APPLICATION TO MINKOWSKI THEORIES OF GRAVITATION AND ELECTROMAGNETISM. Sylvie Ledered (Universite, Paris). Cahiers Phys., 18: 233-84(June-July 1964). (In French)

The application of the Lagrangian formalism to the Minkowski theories of gravitation and electromagnetism is investigated. The identities of the canonical tensor and metric tensor are deduced from a Lagrangian. The definition of a gravitational momentum-energy is studied for a phenomenological theory of the gravitation field in the framework of restricted relativity. The Euclidian theories of gravitation are then examined under the angle of Lagrangian coherence. The possibility of building a Euclidian theory of the gravitation field that is not reduced to a linear approximation of general relativity

is investigated in a pentadimension formalism. The particle with maximum total spin 2 is considered. (J.S.R.)

20667 OPTICAL CROSS-SECTIONS AND QUANTUM-KINETIC DEPTHS. Lev Akobjanoff (Sanitation and Radiation Lab., Berkeley, Calif.). Cahiers Phys., 18: 297-302(Aug.-Sept. 1964).

Quantum-kinetics postulates that collisions between particles of light and material obstacles depend, besides the requirement of the passage of photon tracks through the optical cross section of targets, additionally on the generation of photonic activity nodes within the volume of atoms and molecules. An effect of "quantum-kinetic depth" is thus foreseen for any reaction of light, and this effect is experimentally demonstrated in the refraction of alkali halides and other crystals of the O_h^5 group as well as of paraffins. (auth)

20668 RIEMANN WAVES IN RELATIVISTIC MAGNETOHYDRODYNAMICS. I. S. Shikin (Moscow State Univ.). Dokl. Akad. Nauk SSSR, 159: 1240-3(Dec. 21, 1964). (In Russian)

General magnetohydrodynamic equations are considered for a nonviscous non-heat-conducting substance with ideal conductivity and for simple Riemann waves. The equations considered are the energy-momentum conservation law, the induction equation, and the equation for ideal electric conductivity. The heat function is assumed to be either dependent on the pressure and on the number of particles, in which case the system of magnetohydrodynamic equations is not closed and must be supplemented by the particle-number conservation law, or a function of the pressure only, in which case the magnetohydrodynamic equations constitute a closed system. The propagation of a Riemann wave is analyzed for both types of heat functions in question. The various types of resultant waves are described. These are tangential waves, tangential discontinuities, entropy waves, Alfvén waves, and magnetosonic waves, the conditions for the occurrence of which are defined briefly. (ATD)

20669 SECOND SOUND IN A WEAKLY IDEAL BOSE GAS. Yu. A. Tserkovnikov and N. N. Bogolyubov (Steklov Inst. of Mathematics, Academy of Sciences, USSR). Dokl. Akad. Nauk SSSR, 159: 1264-7(Dec. 21, 1964). (In Russian)

The limiting case of the problem of second sound in a weakly ideal Bose gas, when the collision frequency is low, is considered. The interaction is assumed small and the gas density is large. In this case the system of equations for the single-particle Green's function becomes equivalent to the random-phase approximation and can be easily evaluated. The asymptotic behavior of the Green's function as the time increases without limit is obtained, making the results applicable to plasma calculations. (ATD)

20670 EQUATIONS OF AVERAGE TURBULENT MOTION FOR PLANE ELECTROHYDRODYNAMIC FLOWS. V. O. Kasyanov and V. V. Ushakov (Civilian Aeronotic Inst., Kiev). Dopovidi Akad. Nauk Ukr. RSR, No. 11, 1448-51(1964). (In Ukrainian)

Equations of average turbulent motion are obtained for plane electrohydrodynamic flows. They are similar to Reynolds' equations, but have additional terms describing the effect of the turbulent motion of the electric space charge. (auth)

20671 PHONON CORRELATION FUNCTION AND INELASTIC COHERENT SCATTERING OF NEUTRONS BY CRYSTALS CONTAINING SHALLOW ELECTRONIC IMPURITY CENTERS. M. A. Krivoglaz and P. I. Shaldervan. Fiz. Tverd. Tela, 6: 3272-8(1964).

A previous work is extended in that, in addition to interactions with conduction electrons, electron-phonon interactions are considered accompanied by quantum transitions between discrete electron levels, such as occur in crystals containing shallow electronic centers. The phonon correlation function, frequency shift, and attenuation are determined. The calculation is carried out in a higher-order perturbation-theory approximation than is customary, with account taken of the finite lifetimes of the electron states. This makes it possible to eliminate the divergences connected with the resonant character of the interaction. The influence of the interaction between phonons and local centers on the energy distribution of the scattered neutrons is investigated. The estimates made show that this interaction can lead to a noticeable change in the phonon attenuation and in the width and shape of the scattered-neutron energy distribution. (OTS).

20672 INTERACTION OF SUPERSONIC WAVE WITH A BEAM OF CHARGED PARTICLES. Sh. M. Kogan and V. B. Sandomirskii (Inst. of Radio Engineering and Electronics, Moscow). Fiz. Tverd. Tela, 6: 3457-63(1964).

The possible amplification of ultrasound in a piezoelectric crystal by means of a beam of charged particles moving in a slot inside the crystal is investigated analytically. The mechanism of this amplification is similar to that in a traveling-wave tube, and is of particular interest in the amplification of waves with large phase velocities. The coupling between the plasma wave in the beam and the elastic wave in the dielectric is provided by the piezoelectric effect and has a maximum when the frequencies of the two waves coincide and their wave vectors have the same direction as the beam. Analytic expressions are derived for the amplification in two limiting cases, when the amplified wave varies slowly and rapidly in the direction normal to the slot. The resonant character of the effect and its similarity to the process in a traveling wave tube distinguish this type of amplification from that produced by carrier drift. (CFSTI)

20673 PARTICLE DISTRIBUTION IN A CENTRALLY SYMMETRIC FIELD IN THE PRESENCE OF AN INCOMING STREAM. PART II. A. M. Moskalenko (Inst. of Terrestrial Magnetism, Ionosphere and Radio Wave Propagation, Academy of Sciences, USSR). Geomagnetism Aeronomy (USSR) (English Transl.), 4: 404-10(1964).

General expressions are obtained for the concentration and flux of particles in a rarefied gas in a repulsive Coulomb field in the presence of an incoming stream. The concentration and flux of particles are computed for cases when the velocity of the incoming stream is much lower and much higher than the thermal velocity of the particles. Particle absorption on the surface of a body is taken into account. (auth)

20674 EFFECTS OF TEMPERATURE, PRESSURE, AND IONIZATION OF THE FORMATION AND STABILITY OF FISSION TRACKS IN MINERALS AND GLASSES. R. L. Fleischer, P. B. Price, and R. M. Walker (General Electric Research Lab., Schenectady, N. Y.). J. Geophys. Res., 70: 1497-1502(Mar. 15, 1965).

In view of the demonstrated usefulness of the fission-fragment-track technique in geochronology, the effect of various geophysical variables on track formation and stability was studied. Track fading in tektite glass, zircon, olivine, muscovite, phlogopite, and biotite was studied as a function of temperature, pressure, plastic deformation, and highly ionizing radiation. Temperature was found to be the most important parameter, and track-annealing data are given for each material. Hydrostatic pressures up to 80 kb have practically no effect on annealing curves of zircon and olivine. Track annealing in tektites can be accelerated only upon application of an hydrostatic pressure much larger than would ever be encountered by even a well-buried tektite. Purely hydrostatic pressures do not accelerate track annealing in micas, but shear deformations can shorten, distort, or erase tracks. Large doses of ionizing radiation (other than extremely massive nuclear particles) have no effect on track stability in any of the materials. Tracks formed at 77°K have the same appearance as tracks formed at room temperature or higher. (auth)

20675 THE FIREBALL IN AIR. Hans A. Bethe (Cornell Univ., Ithaca, N. Y.). J. Quant. Spectry. Radiative Transfer, 5: 9-12(Jan.-Feb. 1965).

The successive stages of the fireball due to a nuclear ex-

plosion in air are defined. Stage C primarily is considered, from the minimum in the apparent fireball temperature to the point where the fireball becomes transparent. In the first part of this stage (C I), the shock (which previously was opaque) becomes transparent due to decreasing pressure. The radiation comes from a region in which the temperature distribution is given essentially by the Taylor solution; the radiating layer is given by the condition that the mean free path is about $^1/_{10}$ of the radius. The radiating temperature during this stage increases about as $p^{-\frac{1}{4}}$, where p is the pressure. To supply the energy for the radiation, a cooling wave proceeds from the outside into the hot interior. When this wave reaches the isothermal sphere, the temperature is close to its second maximum. Thereafter, the character of the solution changes; it is now dominated by the cooling wave (Stage C II). The temperature would decrease slowly (as $p^{\frac{1}{4}}$) if the problem were one-dimensional, but in fact it is probably nearly constant for the three-dimensional case. The radiating surface shrinks slowly. The cooling wave eats into the isothermal sphere until this is completely used up. The inner part of the isothermal sphere, (the part which has not yet been reached by the cooling wave) continues to expand adiabatically; it therefore cools very slowly and remains opaque. After the entire isothermal sphere is used up, the fireball becomes transparent, and the radiation drops rapidly. The ball will therefore be left at a rather high temperature, about 5000°. The cooling wave reaches the isothermal sphere at a definite pressure $p_c \approx 5(\rho_1/\rho_0)^{\frac{1}{2}}$ bars, where ρ_1 is the ambient and ρ_0 the sea-level density. The radiating temperature at this time is about 10,000°. The slight dependence of physical properties on yield is exhibited in approximate formulas. (auth)

20676 MEASUREMENTS OF THE FREE-BOUND AND FREE-FREE CONTINUA OF NITROGEN, OXYGEN AND AIR. R. A. Allen, A. Textoris, and J. Wilson (Avco-Everett Research Lab., Everett, Mass.). J. Quant. Spectry. Radiative Transfer, 5: 95-108(Jan.-Feb. 1965).

Measurements were made of the equilibrium radiation behind incident and reflected shocks produced in an electric arc-driven shock tube over a temperature range of 8000 to 14,000°K. Experiments are described which used a tungsten photoelectric gauge to make photometric measurements in the vacuum ultraviolet. This gauge was positioned at the axis of the shock tube and cored the oncoming shock wave. By the use of optical stops, this gauge was capable of resolving the shock front. A knowledge of the photoelectric yield of the tungsten provided a photometric measurement. The photoionization cross section for the ground-state nitrogen atom was inferred from these measurements to be of the order of 10^{-17} cm^2. Data were also obtained of the continua at 0.51 μ in nitrogen, oxygen, and air which gave information on the component of the radiation produced by electrons being captured by ions and neutral atoms. The measurements agree well with free-bound calculations assuming a hydrogen-like model for N and O. Measurements were also obtained in the infrared at 6.1 μ in air over a range of shock conditions, which imply an effective $Z_{\bar{g}}^2$(Z^2 times Gaunt factor) of 1.5 for the air-constituent free-free transitions. (auth)

20677 THE ABSORPTION AND SCATTERING OF RADIATION BY SMALL SOLID PARTICLES. N. L. Krascella (United Aircraft Corp. Research Labs., East Hartford, Conn.). J. Quant. Spectry. Radiative Transfer, 5: 245-51 (Jan.-Feb. 1965).

The classical Mie theory, which describes the attenuation of plane wave radiation by small spherical particles, was programmed for an IBM 7094 computer to permit rapid evaluation of the extinction, absorption, and scattering cross sections of particles as functions of wavelength and particle radius. Computational procedures were facilitated by application of the method of logarithmic derivative functions. A comparison of calculated results based on the UACRL machine program and those reported in the current literature was made to assess the program validity and precision. Extinction, absorption, and scattering cross sections for carbon, tungsten, aluminum and platinum are presented for particles with radii from 0.05 to 1.0 μ and in the wavelength range between 0.25 and 4.0 μ. (auth)

20678 LIMITATIONS ON MAGNETIC FIELDS OBTAINED BY FLUX-COMPRESSION. [PART] I. G. Lehner, J. G. Linhart, and J. P. Somon (Euratom-CNEN, Frascati, Italy). Nucl. Fusion, 4: 362-79(Dec. 1964).

Two principal limitations on maximum magnetic fields generated by flux compression are connected with two fundamental processes—magnetic field diffusion and the conversion of kinetic energy of the conductor compressing the field into stored energy of this field. Criteria for maximum fields are obtained, discussed, and applied to typical experimental situations. (auth)

20679 ON THE ESSENTIAL IDENTITY OF THE AMPLIFICATION OF LONGITUDINAL PLASMA WAVES AND THE NEGATIVE ABSORPTION OF ČERENKOV RADIATION IN AN ELECTRON STREAM. V. L. Ginzburg and V. V. Zheleznyakov (Lebedev Inst. of Physics, Moscow). Phil. Mag. (8), 11: 197-203(Jan. 1965).

It is shown that in certain conditions the negative Cherenkov absorption and building up of plasma waves obtained in the quantum treatment of the problem is identical with amplification effect and building up of these waves which is obtained as a result of classical considerations on the basis of the kinetic equation. In this connection a criticism of the paper by Twiss in which a different opinion is expressed is presented. (auth)

20680 STRUCTURE OF RADIATION-RESISTED SHOCK WAVES WITH VIBRATIONAL NONEQUILIBRIUM. George Emanuel (Aerospace Corp., El Segundo, Calif.). Phys. Fluids, 8: 626-35(Apr. 1965).

The continuum equations of gasdynamics are used to study the effect of thermal radiation and vibrational nonequilibrium on the structure of a shock wave. Emphasis is on a description of the gasdynamic phenomena involved rather than on numerical results. For example, a Mollier diagram interpretation, useful for understanding radiation-resisted shock waves, is given. The principal results stem from an analysis of the singular-point structure far upstream and far downstream in the flow. This analysis indicates in a heuristic fashion that a unique solution exists. It also shows that two parameters, a Mach number and the ratio of a radiation length to a relaxation length, primarily govern the qualitative behavior of the flow. Thus, for a specific range of values of these parameters, the vibrational energy overshoots its final equilibrium value. For a different range, a net amount of radiant energy is transferred from the hot gas behind the adiabatic shock to the gas far downstream. (auth)

20681 TRANSPORT EQUATIONS FOR A GAS MIXTURE. B. Samuel Tanenbaum (Case Inst. of Tech., Cleveland). Phys. Fluids, 8: 683-6(Apr. 1965).

The Boltzmann equation is applied to a gas mixture in which each constituent is separately in equilibrium without necessarily being close to equilibrium with the rest of the gas. Exact conservation equations for the number density, momentum, and energy of each constituent in the mixture are derived for inverse power interparticle force laws. In the limit when the differences among the individual flow velocities, $u_s - u_t$, are all small compared to a "sound speed" $a_0 = (2k)^{\frac{1}{2}}[(T_s/m_s) + (T_t/m_t)]^{\frac{1}{2}}$, it is found that the conservation equations reduce, for all force laws, to a form similar (but not identical) to the continuum equations commonly used in plasma physics. For larger relative flow velocities, the equations retain this simple form only for Maxwell molecules. For other inverse power laws all the collisional transfer terms increase relative to the Maxwell molecule results with increasing a_0 or $|u_t - u_s|$ for shorter-range forces (hard spheres, for example) and decrease with increasing a_0 or $|u_t - u_s|$ for longer-range forces (Coulomb, for example). Finally, in the limit when a_0 is small compared to $|u_t - u_s|$ it is shown that, with one exception, all collisional transfer terms become temperature independent. (auth)

20682 ONE-DIMENSIONAL GASES WITH HARD-CORE REPULSION. R. J. Baxter (Australian National Univ., Canberra). Phys. Fluids, 8: 687-92(Apr. 1965).

An elementary mathematical device previously employed to derive the statistical mechanical properties of a classical one-dimensional gas with interaction potential that satisfies a linear differential equation with constant coefficients over the domain $(0,\infty)$ is shown to be also applicable when the potential contains a repulsive hard core. In particular, the thermodynamic properties of a one-dimensional plasma of hard rods and of the gas model of Kac are derived. The infinite-range phase transition obtained in the latter case by Kac, Uhlenbeck, and Hemmer is found to be amenable to investigation by the methods used. (auth)

20683 EQUILIBRIUM DISTRIBUTION FUNCTIONS FOR A CLASSICAL ELECTRON GAS. C. W. Hirt (Los Alamos Scientific Lab., N. Mex.). Phys. Fluids, 8: 693-8(Apr. 1965). (LA-DC-6533)

The cluster expansion techniques of Mayer and Abe are applied to a calculation of the exact equilibrium s-particle distribution function for a classical electron gas in a positive background. The radial distribution function is found to be well approximated by the Boltzmann factor for a Debye–Hückel potential. Corrections to the Debye–Hückel expression are discussed. A simple approximation for the s-particle correlation function is given in terms of a three-fold integral. (auth)

20684 A POWERFUL SOURCE OF MILLIMETRE WAVELENGTH ELECTROMAGNETIC RADIATION. I. B. Bott (Radar Research Establishment, Malvern, Worcs, Eng.). Phys. Letters, 14: 293-4(Feb. 15, 1965).

Results are presented concerning the generation of millimeter wavelength radiation by injecting free electrons from a Pierce gun into a uniform volume of high magnetic field in an overmoded cavity. The schematic of the apparatus and a plot of the corresponding axial magnetic field intensity are presented. The total energy radiated during a current pulse was measured, and a curve of the radiated power versus wavelength is shown. The results were found to be consistent with the theory of Schneider. (L.B.S.)

20685 USING A RECTANGULAR MODEL TO OBTAIN ANALYTICAL EXPRESSIONS FOR SPHERICAL ABERRATION OF ELECTROMAGNETIC QUADRUPOLE LENSES. A. D. Dymnikov, T. Ya. Fishkova, and S. Ya. Yavor (Ioffe Inst. of Physics and Tech., Leningrad). Phys. Letters, 15: 132-4(Mar. 15, 1965).

Expressions for spherical aberration that do not explicitly involve field derivatives were obtained by solving the trajectory equations using the perturbation method. The results of calculation for a parallel beam are compared with experimental data for an electrostatic quadrupole lens. (L.B.S.)

20686 NON-BINARY ATOMIC COLLISIONS IN CRYSTALS. H. H. Andersen (Atomenergikommissionen, Roskilde, Denmark) and P. Sigmund. Phys. Letters, 15: 237-8(Apr. 1, 1965).

The energy losses by atoms in focusing collision sequences and channeling in atoms were studied. The energy loss for a Cu atom in the ⟨100⟩ channel in Cu was calculated in the momentum approximation, the constant velocity approximation, and by using a spherically symmetric Born-Mayer potential. The energy loss of ⟨111⟩ collision sequences in Cu was also calculated in the momentum approximation. (D.C.W.)

20687 ON THE CORRELATION POTENTIALS OF RECTILINEAR STATISTICAL SYSTEMS. B. N. Baranov and I. P. Pavlotskii (Steklov Mathematical Inst., Moscow). Phys. Letters, 15: 242(Apr. 1, 1965).

The distribution functions and correlation potentials of a rectilinear statistical system in thermodynamic equilibrium with a fixed particle order are derived. (D.C.W.)

20688 RADIATIVE TRANSFER IN DISPERSIVE MEDIA. E. G. Harris (General Atomic Div., General Dynamics Corp., San Diego, Calif.). Phys. Rev., 138: B479-85(Apr. 26, 1965).

A radiative transfer equation is derived which is sufficiently general to apply to energy transfer by various types of wave motion, such as electromagnetic waves, sound waves, hydromagnetic waves, etc. Scattering of waves is neglected. The equation is compared to the equation found in the literature of radio astronomy, and the meaning of a term in this equation is clarified. The general solution of the equation is given. A more rigorous derivation of the transfer equation based on a method due to Wigner is given. (auth)

20689 POSSIBILITY OF LONG-RANGE SPIN POLARIZATION IN A DEGENERATE ELECTRON GAS. A. Bardasis (Univ. of Maryland, College Park), D. S. Falk, R. A. Ferrell, M. S. Fullenbaum, R. E. Prange, and D. L. Mills. Phys. Rev. Letters, 14: 298-300(Mar. 1, 1965).

Dreyfus, Maynard, and Quattropani calculated that it is possible for an induced long-range spin-density distribution to exist in a nonferromagnetic metal, contrary to the Ruderman-Kittel theory, in which the spin density generated at large distances from a localized spin perturbation is of an oscillatory nature. The calculation is reexamined in order to reconcile it with the theory. The contribution to the total spin density by the nonevanescing waves is evaluated; it is found that the nonevanescing waves contribute a long-range polarization just canceling that from the evanescing waves, thus leaving only the Ruderman-Kittel spatial dependence. A brief sketch of the calculation is given, and the cancellation between the long-range portions of the spin density is exhibited explicitly. (M.J.T.)

20690 LONG-RANGE MAGNETIC COUPLING IN METALS. Kei Yosida and A. Okiji (Tokyo Univ.). Phys. Rev. Letters, 14: 301-2(Mar. 1, 1965).

Calculations by Dreyfus, Maynard, and Quattropani are considered, which point out that a nonoscillating spin-density fluctuation is induced in a nonmagnetic metal and decreases with the distance from the contact plane with a ferromagnetic metal. Their expression for the electron density in the nonmagnetic metal is rederived, and compared with that obtained taking into consideration contributions from electrons with wave vector greater than a given function of the difference in average potential between the two metals. It is found that, near the contact plane of two kinds of metals, only oscillating density fluctuations are induced, originating from the Ruderman-Kittel interaction. (M.J.T.)

20691 LARGE ISOTOPE EFFECT IN THE FORMATION OF H^- OR D^- BY ELECTRON IMPACT ON H_2, HD, AND D_2. D. Rapp, T. E. Sharp, and D. D. Briglia (Lockheed Missiles and Space Co., Palo Alto, Calif.). Phys. Rev. Letters, 14: 533-5(Apr. 5, 1965).

The total cross sections for the production of negative ions by electron attachment in H_2, HD, and D_2 were measured as a function of electron energy. It was found that the cross section for production of H^- from H_2 exceeds the sum of the cross sections for H^- and D^- from HD, which in turn exceeds that for D^- from D_2. (D.C.W.)

20692 SPIN SUSCEPTIBILITY OF A SUPERFLUID FERMI LIQUID. A. J. Leggett (Univ. of Illinois, Urbana). Phys. Rev. Letters, 14: 536-7(Apr. 5, 1965).

An expression is derived for the spin susceptibility of a superfluid Fermi liquid, taking into account strong-coupling effects. The implications for the detection of superfluidity in liquid ^{3}He are considered. (D.C.W.)

20693 A MASTER EQUATION FOR GASES. J. Schroeter (Philipps-Universitat, Marburg, Ger.). Physica, 31: 1-32(Jan. 1965).

A master equation is derived under the assumption that under macroscopical constraints the exact time propagator of a system can be replaced by one which shows a certain sort of Markoff character. For this purpose the term "macroscopic observation" is treated by inducing a coarse graining with the help of the Boltzmann density functions. For the actual calculation suppositions concerning the interaction of the particles, the mean density and the coarse

graining are made so that the two-collision approximation is valid. Finally, the result is compared with that of Ludwig. (auth)

20694 THE ACTUAL MASS OF POTENTIAL ENERGY, A CORRECTION TO CLASSICAL RELATIVITY. L. Brillouin (Columbia Univ., New York). Proc. Natl. Acad. Sci. U. S., 53: 475-82(Mar. 1965).

The mass connected with the external potential energy of a body in motion is investigated, with particular consideration of the interaction of two charged spheres. The total energy of a particle (charge) interacting with other charges and moving at a small velocity is calculated, taking into account the mass of potential energy. (D.C.W.)

20695 PERTURBATION THEORY AND NUCLEAR FERROMAGNETISM. P. Lal (University Coll., Cardiff, Wales, U.K.). Proc. Phys. Soc. (London), 85: 27-32(Jan. 1965).

The energy of the nuclear ferromagnetic state in the presence of conduction electrons, calculated by using the hyperfine interaction between the electron and the nuclear spins as perturbation, is compared with the energy calculated earlier avoiding the use of perturbation theory. It is shown that the two values do not agree, which means that perturbation theory can not be applied in this case. (auth)

20696 ELECTRON DIFFUSION IN HYDROGEN AT HIGH ELECTRIC FIELDS AND LOW GAS PRESSURES. P. A. Lawson and J. Lucas (Univ. of Liverpool). Proc. Phys. Soc. (London), 85: 177-83(Jan. 1965).

The radial distribution of a stream of electrons after drifting through a gas in a uniform electric field was theoretically analyzed. The solution takes into account electron ionization and the boundary conditions imposed by the electrodes. The distribution was experimentally verified for hydrogen, and values of the ratio of the diffusion coefficient to the mobility coefficient were obtained for $15 < E/p_0 < 100$ v cm^{-1} torr^{-1}. (auth)

20697 ASYMPTOTIC FORM OF CORRELATION FUNCTIONS IN CLASSICAL FLUIDS AND IN LIQUID HELIUM 4. J. E. Enderby, T. Gaskell, and N. H. March (Univ. of Sheffield, Eng.). Proc. Phys. Soc. (London), 85: 217-21(Feb. 1965).

A solution is proposed to the problem of the asymptotic form of the radial distribution function g(r) for both quantal and classical liquids. For the quantal fluid helium-4 at absolute zero, Feynman's result that the structure factor $S(k) = \hbar k/2Mc$ for sufficiently small k is shown to yield $g(r) \sim 1 - (\hbar/2\pi^2 n_0 Mc)\, r^{-4}$ where n_0 is the mean density and c is the sound velocity. For classical liquid insulators, such as argon, where the long-range van der Waals interaction may be written as $\phi(r) \sim -Ar^{-6}$, $g(r) \sim 1 - [1/kT\,\{S(0)\}^2\phi(r)]$ in regions well away from the critical point. For simple liquid metals, such as sodium, neglecting Fermi surface blurring, $\phi(r) \sim Br^{-3} \cos 2k_f r$, and this gives $g(r) \sim 1 - [1/kT\,\{S(2k_f)\}^2\phi(r)]$, where k_f is the magnitude of the Fermi wave vector. (auth)

20698 SOME ELECTRON SPIN RESONANCE OBSERVATIONS OF GADOLINIUM S STATE IONS IN METALS. A. M. Harris, J. Popplewell, and R. S. Tebble (Univ. of Sheffield, Eng.). Proc. Phys. Soc. (London), 85: 513-22 (Mar. 1965).

Measurements of the paramagnetic g factors were made, using electron spin resonance at 8 mm wavelength, in solid solutions of gadolinium in yttrium, palladium, and lutetium at temperatures between 60 and 400°K. The measurements show that the g factor for the trivalent gadolinium ion in the metallic lattice varies significantly from the free ion value and is concentration dependent. For alloys containing more than 30% Gd in the Gd–Y alloy system, 80% Gd in the Gd–Lu alloy system and for all concentrations in the Gd–Pd alloy system, the g factors are less than the free ion value. Lower concentrations of Gd in the Gd–Y and Gd–Lu alloy systems have g factors greater than the free ion value of 1.99. A qualitative attempt was made to explain this variation, using a model proposed by Kondo in which two interactions are considered. (auth)

20699 A TIME DILATION EXPERIMENT BASED ON THE MÖSSBAUER EFFECT. D. C. Champeney, G. R. Isaak, and A. M. Khan (Univ. of Birmingham, Eng.). Proc. Phys. Soc. (London), 85: 583-93(Mar. 1965).

Experiments are described in which the time dilatation at the tip of a high speed rotor is measured and compared with the expectations of relativity theory. Mössbauer sources and absorbers are attached to the center and tip (or vice versa) of the rotor and the time dilatation deduced from the variation of gamma ray transmission with rotor speed. A technique is described whereby using a source absorber combination with an appropriate inherent frequency shift the experiment takes on the features of a null experiment. A result $2.1 \pm 1.9\%$ in excess of the expected dilatation is obtained. (auth)

20700 THE COEFFICIENTS OF VISCOSITY AND THERMAL CONDUCTIVITY OF ATOMIC HYDROGEN FROM 1 TO 400°K. R. A. Buckingham (London Univ.), J. W. Fox, and E. Gal. Proc. Roy. Soc. (London), Ser. A, 284: 237-51(Feb. 23, 1965).

Quantum scattering theory was used to calculate the coefficients of viscosity and thermal conductivity of atomic hydrogen from 1 to 400°K on the basis of the accurate interaction potentials of Dalgarno and Lynn. The wave equation was integrated numerically, and phase shifts with their appropriate multiples of π are presented for L = 0(1) 35. The effect of the identity of the protons on the viscosity cross sections was investigated. The quantal cross sections were compared with the classical values of Dalgarno and Smith and with values estimated by the empirical method of Hirschfelder and Eliason. Correction terms were evaluated for obtaining the second approximation to the coefficient of viscosity in the Chapman-Enskog formulation. (auth)

20701 INTENSE MAGNETIC FIELDS. Henry H. Kolm and Arthur J. Freeman. Sci. Am., 212: No. 4, 66-74; 76; 78(Apr. 1965).

A survey on the production of intense magnetic fields is presented. The basic effects and origin of magnetic fields are reviewed, together with the difficulties of producing intense fields. Magnets designed for production of pulsed and continuous intense fields are then discussed, including superconducting magnets, Bitter magnets, and a water-cooled solenoid magnet that produces a continuous 25×10^4 gauss field. Applications of intense magnetic fields are also considered, together with the new National Magnet Laboratory. (D.C.W.)

20702 COMPARISON OF ENERGY LOSSES OF ELECTRONS WITH OPTICAL PROPERTIES OF KCl AND KBr. M. Creuzburg and H. Raether (Universitat, Hamburg). Solid State Commun., 2: 345-7(Nov. 1964).

Electron energy loss spectra of KCl and KBr were compared with optically measured spectra of $\mathrm{Im}(1/\epsilon)$. Good agreement is shown in the position of the peaks and in the general shape. Also the absolute intensity was found to be in accord with the dielectric theory. (auth)

20703 RADIATIVE RECOMBINATION FROM GaAs DIRECTLY EXCITED BY ELECTRON BEAMS. D. A. Cusano (General Electric Research Lab., Schenectady, N. Y.). Solid State Commun., 2: 353-8(Nov. 1964).

The salient features of radiative recombination near the band edge in GaAs are determined by electron beam excitation of donor and acceptor doped crystals ranging in impurity content from 10^{16} to 10^{20}/cm^3. The results indicate a strong influence of impurities and allow a consistent interpretation of recombination mechanism over the whole impurity range. At optimum doping (2×10^{18} to 10^{19}/cm^3) p-type GaAs at 77°K should exhibit laser action under high intensity electron bombardment. (auth)

20704 NEWTONIAN AND EINSTEINIAN MOTION OF HOMOGENEOUS MATTER. Ya. B. Zel'dovich. Soviet Astron AJ (English Transl.), 8: 700-7(Mar.-Apr. 1965). Translated from Astron. Zh., 41: 873-83(Sept.-Oct. 1964).

Uniformly distributed matter is regarded as moving under its own gravitation at a uniform but anisotropic

linear velocity, including rotation and displacement. A correct Newtonian formulation results in a body with an ellipsoidal boundary. The character of the motion is analyzed, and the Newtonian and Einsteinian treatments are compared. (auth)

20705 PROPAGATION AND FORMATION OF DENSITY AND SHOCK WAVES ALONG CYLINDRICAL ELECTRON BEAMS UNDER CONSIDERATION OF THE SPACE CHARGE FORCES. L. Oertel. Telefunken Ztg., 37: 308-18(Nov. 1964). (In German)

It is shown that the propagation can be described by differential equations of density waves along an electron beam within metal tubes whose diameters are not too large: the differential equations are identical with Euler's equations for the dynamics of gases. This fact allows the implementation of Riemann's shock wave theory for the calculation of high condensation. By means of an example which is easy to calculate for an initial velocity given by a hyperbolic function, the build-up of shock waves is shown. It is shown that it is possible to derive from this simple example an estimation of the a-c amplitudes of an electron beam in a klystron at maximum compression. The estimated values agree well with the values obtained from the ballistic theory with space charge that a much clearer approximation method is possible when, instead of starting with Euler's equations themselves, they are first brought to diagonal form. For the initial conditions prevailing in the klystron, a solution is given of Riemann's differential equation. (auth)

20706 GENERALIZED INERTIAL SYSTEMS IN NEWTONIAN MECHANICS AND IN GENERAL RELATIVITY. II. THE THEORY OF EINSTEIN. Kh. P. Keres. Tr. Inst. Fiz. i Astron., Akad. Nauk Est. SSR, No. 25, 3-35(1964). (In Russian)

If freely falling particles are considered to be moving by inertia, the so called generalized inertial systems may be defined in general-relativistic mechanics in exactly the same way as in nonrigid Newtonian mechanics. In a generalized inertial system the acceleration of a freely moving particle is zero (the law of inertia), as in Newtonian mechanics. Every 3-space R, described by a 3-dimensional congruence of time-like world lines, possesses two dynamical characteristics: a 3-vector b_i and an antisymmetric 3-tensor Ω_{ik}. They are calculated with the aid of some specialized generalized inertial system, but are independent of the choice of the latter. Hence the quantities b_i and Ω_{ik} characterize the motion of space R with respect to the totality of generalized inertial systems. They are the analogues of Newtonian acceleration and rotation of volume elements of the space R with respect to the inertial systems. All spaces fall into four classes. The spaces belonging to the generalized inertial systems are characterized by the equations $b_i = 0$, $\Omega_{ik} = 0$. For a space of a given class there exist preferred time-systems characteristic of that class of spaces. By regarding a given frame of reference as inertial, the 3-dimensional inertial or gravitational forces may be introduced. (auth)

20707 ON STATIC SOLUTIONS OF THE PROBLEM OF MANY PARTICLES IN GENERAL RELATIVITY. PART I. I. Piir. Tr. Inst. Fiz. i Astron., Akad. Nauk Est. SSR, No. 25, 36-46(1964). (In Russian)

Hoffmann's theorem, according to which a Curzon-Silberstein solution with isolated singularities corresponds to an equilibrium (in the Newtonian sense) collinear system of point masses of both signs proved to remain valid in the case of point particles characterized both by masses and by dipole and multipole moments. (auth)

20708 ON STATIC SOLUTIONS OF MANY-PARTICLE PROBLEM IN GENERAL RELATIVITY. PART II. I. Piir. Tr. Inst. Fiz. i Astron., Akad. Nauk Est. SSR, No. 25, 75-84(1964). (In Russian)

A possible axially symmetric one-particle solution of the Einstein's equations is obtained. It contains both the well known solutions of Schwarzschild and of Curzon-Silberstein as special cases. Also a solution describing the gravitational field of a collinear system of such particles is analyzed. (auth)

20709 AN ACCELERATING SYSTEM WITH DRIFT TUBES ON SUPERHIGH FREQUENCY. V. B. Krasovitskii and V. I. Kurilko (Khar'kov Inst. of Physics and Tech.), Ukr. Fiz. Zh., 9: 1134-6(Oct. 1964). (In Ukrainian)

To make the best use of the very intense electric fields which can be obtained by means of lasers for accelerating charged particles, it is necessary to have a system of waveguides for the visible range of frequencies. A cylindrical diffraction grating, which is essentially an optical equivalent of drift tubes, can be such a system. The excitation of a wave having a phase velocity close to the velocity of light in a cylindrical diffraction grating made of infinitely thin rings whose width was equal to half the grating period was analyzed. It is shown that waves whose length approximately equals the period of grating can be excited, and if the system is filled with a dielectric whose dielectric constant is close to unity, the field can be focused in the neighborhood of the axis of the system. It is also shown that such waves, whose attenuation by radiation through the grating is small, can be propagated in such a system. (ATD)

20710 SINGLE-PHONON GREEN'S FUNCTION, PHONON CORRELATION FUNCTION, AND INELASTIC COHERENT SCATTERING OF NEUTRONS BY CRYSTALS CONTAINING SHALLOW ELECTRONIC IMPURITY CENTERS. M. A. Krivoglaz and P. G. Shaldervan (Inst. of Metal Physics, Kiev). Ukr. Fiz. Zh., 9: 1331-44(Dec. 1964). (In Ukrainian)

An attempt is made to show how the interaction between phonons and electrons localized in shallow impurity centers (with Bohr frequencies lower than the maximum oscillation frequency) influences the damping and the frequency shift of the electron levels. The calculations were made by the method of temperature Green's functions, and to eliminate the divergences the chain of equations was uncoupled in a higher order of approximation than customary, thus taking explicit account of the width of the electron level. Formulas are derived for the Green's function with account of single-phonon interaction only, as well as for the general case. These formulas are then used to determine the single-phonon correlation functions and the damping and shift of the phonon oscillations. It is shown that when the frequency of the absorbed or emitted phonon is close to the Bohr frequency of the electron center, the energy distribution of the scattered neutrons exhibits resonant peaks, with a Lorentz line shape when the phonon damping is lower than the electron damping. If the electron damping is higher, the distribution is not Lorentzian and a narrow peak or dip is produced. The damping due to the electron phonon interaction is estimated and is shown to be independent of the nature of the center, being governed only by the density of the localized electrons and the distribution function of the oscillation frequencies near the Bohr frequency. This damping can become appreciable at relatively low density concentrations $\sim 10^{-3} - 10^{-5}$. (ATD)

20711 MEAN ENERGY OF ELECTRON GAS AT ABSOLUTE ZERO. I. R. Yukhnovskii, V. V. Tsiganenko, and M. V. Vavrukh (L'vov State Univ., Ukrainian SSR). Ukr. Fiz. Zh., 10: 135-46(Feb. 1965). (In Ukrainian)

The trace of the operator $\exp(-\beta H)$, given in the representation of the displacement is calculated. The parameter of the expansion at $T = 0$ is $\sqrt{r_s}$, where $r_s = \langle r \rangle / a_0$. It is shown that the mean energy with an accuracy to the diagrams of the second order is the series $\epsilon = (2.21/r_s^2 - 0.916/r_s + 0.354/r_s^{3/2}) + \ldots$. (auth)

20712 GAS IONIZING RADIATION OF A DISCHARGE IN OXYGEN IN A HOMOGENEOUS FIELD. Timm H. Teich (Universitat, Hamburg). Z. Naturforsch., 19a: 1420-1 (Dec. 1964). (In German)

The absorption coefficient and the intensity of gas ionizing radiation emitted by a not self-sustained discharge in oxygen in a homogeneous field were measured by means of

a sub-divided ionization chamber of suitable geometry. It was thus possible to evaluate the dependence on E/p of the emission intensity. An additional pressure dependent effect was found and explained as quenching of excited states by collisions. (auth)

20713 NONSTATIONARY ISOTHERMAL MOTION OF A GAS. M. I. Chibisov. Zh. Tekhn. Fiz., 35: 123-6(Jan. 1965). (In Russian)

The one-dimensional free dispersion of a gas is calculated for the cases of plane, spherical and cylindrical symmetry. The temperature is assumed to be always uniform, but to vary with time. These calculations should be applicable to a plasma in which the electron temperature greatly exceeds the ion temperature, for in this case the rapid heat conduction by the electrons would tend to keep the temperature uniform. The velocity v and density n of the gas are assumed to have the forms $v = ax$, $n = A(b)\exp(-bx^2)$, where x is the coordinate appropriate to the symmetry under discussion, a and b are functions of time to be determined, and A is a function of b, the form of which is assumed at the start (A is a different function for each type of symmetry). These expressions are inserted in the equation of continuity, the hydrodynamic equation of motion, and the equation of energy conservation; and the resulting equations are solved for a and b as functions of time. The limiting velocity of the dispersing gas is found to be close to the velocity of sound in each case. (ATD)

20714 ASTROPHYSICS AND THE MANY-BODY PROBLEM. VOLUME 2. E. N. Parker, J. S. Goldstein, A. A. Maradudin, and V. Ambegaokar. Brandeis University Summer Institute Lectures in Theoretical Physics. New York, W. A. Benjamin, Inc., 1963. 444p.

Separate abstracts were prepared for the four sections of the book. (D.C.W.)

For abstracts of individual sections see: 20715, 20716, 20783, and 20784.

20715 GREEN'S FUNCTIONS IN MANY-BODY PROBLEMS. V. Ambegaokar (Cornell Univ., Ithaca, N. Y.). p.321-438 of "Astrophysics and the Many-Body Problem. Vol. 2." New York, W. A. Benjamin, Inc., 1963.

The equilibrium and transport properties of normal fermion systems are calculated by both the Landau theory and the Green's function approach, demonstrating the equivalence of the two approaches. The d-c conductivity is treated in detail by the Green's function approach. (D.C.W.)

20716 TOPICS IN THE THEORY OF THE VIBRATIONS OF IMPERFECT CRYSTALS. A. A. Maradudin (Westinghouse Electric Corp., Pittsburgh). p.107-320 of "Astrophysics and the Many-Body Problem. Vol. 2." New York, W. A. Benjamin, Inc., 1963.

The in-band frequencies and the localized mode frequency for a linear chain containing a mass defect are calculated first, and the general theory of lattice dynamics for crystals containing isolated defects is outlined. The vibrations of randomly disordered crystals are then studied; and methods for calculating the equilibrium properties of such crystals are described, such as the thermodynamic function and the frequency distribution function. The calculation of the time-dependent properties of disordered crystals is outlined. Expressions are obtained for the optical absorption coefficient of a disordered crystal and the cross section for gamma absorption by an impurity atom in a crystal. The lifetime of a localized impurity mode due to its coupling with the other modes through anharmonic forces is also calculated. (D.C.W.)

20717 COMPRESSION OF MAGNETIC FIELD BY EXPLODING FOILS. J. G. Linhart and G. Schenk (Euratom-CNEN, Frascati, Rome). 19p. (CONF-533-3)

From 3rd Conference on Exploding Wires, Boston, Mar. 1964.

Experiments are described in which a thin cylindrical metallic foil is exploded by passing a pulse of electrical current through it. The plasma generated in such an explosion compresses an axial magnetic field. Initial fields of several kilogauss were comparessed to about 50 kgauss. Interpretation of the details of the explosion and compression processes is attempted. (auth)

Accelerators

Refer also to abstracts 20204, 20282, 20326, and 20422.

20718 (BNL-8968) ENGINEERING DESIGN OF THE AGS FAST BEAM EXTRACTION SYSTEM. E. B. Forsyth and C. Lasky (Brookhaven National Lab., Upton, N. Y.). Mar. 10, 1965. Contract AT-30-2-GEN-16. 9p. (CONF-650306-12). Dep.(mn); $1.00(cy), 1(mn) CFSTI.

From Particle Accelerator Conference, Washington, D. C.

The design of the Brookhaven AGS fast-beam extraction-system components is outlined, including data on the design of the ferrite magnet and pulser, the septum magnet and its power supply, the ejector magnet and its power supply, the hydraulic systems, and the vacuum systems. The extractor provides an external beam with essentially the same structure and intensity as the original beam. (T.F.H.)

20719 (BNL-8970) A PROPOSED AGS ACCELERATING CAVITY. M. Plotkin (Brookhaven National Lab., Upton, N. Y.). [Mar. 5, 1965]. Contract [AT(30-2)-Gen-16]. 5p. (CONF-650306-21). Dep.(mn); $1.00(cy), 1(mn) CFSTI.

From Particle Accelerator Conference, Washington, D. C.

The proposal for the AGS conversion to a higher intensity machine is predicated on 500 Mev injection. This injection energy raises the space charge limit to about 2×10^{13} protons/pulse. The corresponding r-f requirements, if we maintain the twelfth harmonic for acceleration, necessitate a frequency swing from 3.5 to 4.45 Mc. The proposal includes an additional main magnet power supply, which increases the rate-of-rise of field by a factor of two. This sets the requirement of about twice the volts/turn to be developed by the r-f system. A proposed ferrite accelerating cavity is investigated that uses ferrite rings. This cavity can also serve to accelerate protons in the existing AGS, covering the frequency range from 1.4 to 4.45 Mc with a voltage 50% greater than is presently available. The methods of computing impedance, losses, beam loading, and saturation characteristics for a number of possibilities of ring size and permeability are described. (auth)

20720 (BNL-8982) RECENT DEVELOPMENTS IN HIGH-INTENSITY ION BEAM PRODUCTION AND PRE-ACCELERATION. A. van Steenbergen (Brookhaven National Lab., Upton, N. Y.). [1964]. Contract AT-30-2-GEN-16. 23p. (CONF-650306-6). Dep.(mn); $1.00(cy), 1(mn) CFSTI.

From Particle Accelerator Conference, Washington, D. C.

Some high-intensity ion sources, applicable for particle accelerators, are evaluated in terms of extracted beam emittance and source "brightness." Specifically recent results obtained with the duoplasmatron ion source, with and without large plasma expansion cup, are given. It is indicated that a high-intensity "rectilinear" ion beam may be obtained from an expanded plasma with a high gradient accelerator structure. Recent approaches to air-insulated columns are given, mainly related to the BNL preaccelerator design. (auth)

20721 (CEA-R-2749) ETUDE DU GROUPEMENT DES ELECTRONS DANS L'ACCELERATEUR LINEAIRE DE SACLAY. (Study of Electron Bunching in the Saclay Linear Accelerator). Roland Bergere, Andrê Veyssiere, and Hans Beil (Commissariat à l'Énergie Atomique, Saclay (France). Centre d'Études Nucléaires). Feb. 1965. 57p. Dep.(mn).

The classifical theory of the linear accelerator buncher does not fit the experimental measurements of the shape of the bunch of electrons performed at Saclay by the method of the energy spectrum. If the spurious effect of the mode converter at the input of the linac is taken into account the

theory can fit the experimental results and also explain the variations of the phase of the bunch on the accelerating sine wave. (auth)

20722 (JINR-D-1946) ON THE ACCELERATION OF VARIABLY CHARGED PARTICLES IN AN ELECTROSTATIC FIELD. M. M. Fiks and G. N. Vyalov (Joint Inst. for Nuclear Research, Dubna (USSR). Lab. of Nuclear Problems). 1965. 7p. Dep.(mn).

The acceleration of variably charged particles in the electrostatic field is dealt with. The beam intensity that can be reached in accelerators of a certain type is considered. It is shown to be possible in principle to obtain high-intensity ion beams of all the elements with a limiting energy $W_k \simeq 0.125 A_0 Z_0^2$ Mev. (auth)

20723 (JINR-P-1945) ISSLEDOVANIE MAGNITNYKH POLEI V ELENENTAKH IONNO-OPTICHESKOI SISTEMY ANTIPROTONNOGO KANALA Na 5 Gev. (An Investigation of the Magnetic Fields in the Units of the Ionic Optical System for the 5-Gev Antiproton Channel). J. Betko, J. Glasnik, M. Polak, and J. Puzyak (Joint Inst. for Nuclear Research, Dubna (USSR). Lab. of High Energy). 1965. 24p. Dep.(mn).

The results of the magnetic measurements (topography of the magnetic field, magnetization curves, etc.) are presented. The measurements were made by using Hall detectors for the electromagnets and magnetic quadrupoles of the ionic optical system for the 5-Gev antiproton channel of the Laboratory of High Energies. The accuracy of the measurements is not less than 1%. (auth)

20724 (LA-DC-6759) HIGH-POWER TEST ON A CLOVERLEAF CAVITY. J. R. Parker, J. D. Doss, R. W. Freyman, E. A. Knapp, and W. J. Shlaer (Los Alamos Scientific Lab., Univ. of California, N. Mex.). [1964]. Contract [W-7405-eng-36]. 8p. (CONF-650306-36). Dep.(mn); $1.00(cy), 1(mn) CFSTI.

From Particle Accelerator Conference, Washington, D. C.

A one-cell plus two half-cell cloverleaf cavity similar to those suitable for a proton linear accelerator was operated up to four times the design power to investigate sparking and heat distribution problems. This cavity was fabricated of oxygen-free high-conductivity copper forgings using techniques suitable for mass production. The power source used was a 100-kw, 800-Mc power amplifier running at 6% duty factor. No sustained sparking was observed even at the highest power levels. Data taken on cavity cleanup, equilibrating times, x-ray yield, and resonant frequency versus power input are given. Details of the cavity fabrication, waveguide matching, and the waveguide vacuum window are discussed. (auth)

20725 (LA-DC-6760) RESONANTLY COUPLED ACCELERATING STRUCTURES FOR HIGH-CURRENT PROTON LINACS. B. C. Knapp, E. A. Knapp, G. J. Lucas, and J. M. Potter (Los Alamos Scientific Lab., Univ. of California, N. Mex.). [1964]. Contract [W-7405-eng-36]. 19p. (CONF-650306-33). Dep.(mn); $1.00(cy), 1(mn) CFSTI.

From Particle Accelerator Conference, Washington D. C.

The results of model studies and an equivalent circuit analysis of the operation of a chain of cavities in the $\pi/2$ mode are given. Various $\pi/2$ mode structures are described and the performance of models of these structures is discussed. Results of numerical solutions to an equivalent circuit applicable to the problem are also given, which include frequency error tolerances and coupling tolerances, for typical cases of interest. Multiple drive of a long resonator chain is also discussed. (auth)

20726 (LA-DC-6775) TRANSVERSE BEAM BLOW-UP IN A STANDING-WAVE LINAC CAVITY. R. L. Gluckstern (Massachusetts Univ., Amherst) and H. S. Butler (Los Alamos Scientific Lab., Univ. of California, N. Mex.). [1964]. Contract [W-7405-eng-36]. 14p. (CONF-650306-32). Dep.(mn); $1.00(cy), 1(mn) CFSTI.

From Particle Accelerator Conference, Washington, D. C.

The theory of the interaction of a beam with transverse modes in a standing wave linear accelerator is summarized and applied to the design parameters for recently proposed proton linacs. Approximate results are derived for the limiting current and these are checked and extended by detailed numerical calculation of the build-up of transverse fields. For the contemplated linacs, the current limit is of the order of 10 amperes, safely above the design values. (auth)

20727 (LA-DC-6777) BEAM DYNAMICAL CALCULATIONS WITH REALISTIC FIELDS IN A DRIFT TUBE LINEAR ACCELERATOR. Marvin Rich (Los Alamos Scientific Lab., Univ. of California, N. Mex.). [1964]. Contract [W-7405-eng-36]. 9p. (CONF-650306-31). Dep.(mn); $1.00(cy), 1(mn) CFSTI.

From Particle Accelerator Conference, Washington, D. C.

A method for numerical beam dynamics studies of drift tube type linear accelerators using electromagnetic fields similar to those encountered in actual machines is presented. Results of calculations for a 90-Mev accelerator are given, and comparisons are made with similar calculations in which the axial electric field is assumed spatially constant within the accelerating gap. (auth)

20728 (LA-DC-6875) DESIGN OF THE RF PHASE AND AMPLITUDE CONTROL SYSTEM FOR A PROTON LINEAR ACCELERATOR. Robert A. Jameson, Thomas F. Turner, and Ned A. Lindsay (Los Alamos Scientific Lab., Univ. of California, N. Mex.). [1965]. Contract [W-7405-eng-36]. 15p. (CONF-650306-30). Dep.(mn); $1.00 (cy), 1(mn) CFSTI.

From Particle Accelerator Conference, Washington, D. C.

The specifications on r-f amplitude and phase in a proton linear accelerator are reviewed. The expected amplitude and phase disturbances during normal operation are discussed, showing the need for fast control of these parameters during the beam-on period. Analytical expressions are derived for the response of the r-f amplitude and phase envelopes in an accelerator structure to amplitude or phase modulations in the drive. Experimental results verifying the theoretical expressions are presented. (auth)

20729 (MURA-706) ALGORISMS FOR RELAXATION CALCULATION OF FFAG MAGNETOSTATIC FIELDS. S. C. Snowdon (Midwestern Universities Research Assn., Stoughton, Wis.). Feb. 10, 1965. Contract W-31-109-38-1707. 27p. Dep.; $2.00(cy), 1(mn) CFSTI.

A method of developing algorisms for a general second-order differential equation of the elliptic type is given. Application is made to the development of algorisms for an FFAG magnetostatic guide field. Algorism modifications are found for points near a two-dimensional edge of ideal iron that removes the analytical difficulty occasioned by the presence of infinite fields on the edge. (auth)

20730 (ORNL-3760(p.64-8)) PRODUCTION, ACCELERATION, AND INJECTION OF IONIC AND ATOMIC BEAMS. (Oak Ridge National Lab., Tenn.).

After the elimination of a large energy modulation of the beam, 100 ma of H_2^+ can be injected through an exact geometrical duplicate of the DCX-2 injector duct on the 600-kv test stand. Total H ion currents of 350 ma at 600 kv were obtained by using a modified duoplasmatron ion source with an expanded plasma extraction region. The beam emittance from these sources is inferior to the small cup duoplasmatron, which makes a study to improve the H_2^+ production difficult with the present 600-kev analyzing geometry. A series of studies is being made with the 100-kv test stand to evaluate the extraction of large currents with these large plasma surface ion sources. Based on studies with the 100-kv test stand, an increase by a factor of 3 to 5 in the beam available for Lorentz-force dissociation in DCX-1 seems possible. This large cup extraction geometry also has yielded beams of 100 ma of H^+ or H_2^+ at 40 kev which were, by visual observations, ap-

proximately parallel and 3/4 in. in dia. A total current of 200 ma was extracted at 20 kev but with large divergence. (auth)

20731 (UCRL-11684) DESIGN CONSIDERATIONS FOR HIGH-INTENSITY NEGATIVE ION SOURCES. Kenneth W. Ehlers (Lawrence Radiation Lab., Univ. of California, Berkeley). Feb. 11, 1965. Contract W-7405-eng-48. 13p. (CONF-650306-11). Dep.(mn); $1.00(cy), 1(mn) CFSTI.

From Particle Accelerator Conference, Washington, D. C.

The production of negative hydrogen ions (H^-) by an ion source similar to that employed in many cyclotrons has been studied. The negative ions are extracted directly from the arc plasma in a direction normal to the magnetic field, without use of a charge-exchange medium. In an attempt to improve the negative-ion yield, the arc-discharge chamber has been modified to conform to assumptions made as to the probable formation mechanism of the observed negative ions. Outputs of negative hydrogen ions in excess of 5 mA have been obtained. Ion-source operating parameters are discussed, as well as considerations for the utilization of this discharge geometry by negative-ion cyclotrons. (auth)

20732 (UCRL-11796) PROBLEMS OF INDUCED RADIOACTIVITY AROUND THE 200-Bev ALTERNATING-GRADIENT SYNCHROTRON. William S. Gilbert and Ralph H. Thomas (Lawrence Radiation Lab., Univ. of California, Berkeley). Feb. 16, 1965. Contract W-7405-eng-48. 9p. (CONF-650306-14). Dep.(mn); $1.00(cy), 1(mn) CFSTI.

From Particle Accelerator Conference, Washington, D. C.

Starting from the shut-down radiation fields proposed at the Brookhaven AGS, a calculation is made of the fields to be expected from a proposed 200-Bev AGS producing 3×10^{13} protons per pulse with a maximum beam power of 500 kw. Means are discussed for reducing the induced radioactivity in the 200-Bev AGS. (T.F.H.)

20733 (UCRL-11799) HYDROSTATIC LEVELING SYSTEMS. Pierre F. Pellissier (Lawrence Radiation Lab., Univ. of California, Berkeley). Mar. 5, 1965. Contract W-7405-eng-48. 3p. (CONF-650306-20). Dep.(mn); $1.00(cy), 1(mn) CFSTI.

From Particle Accelerator Conference, Washington, D. C.

The feasibility of using a mercury-filled hydrostatic leveling system for vertical positioning of the magnets of the proposed 200-Bev proton synchrotron is discussed. Possible sources of error in this type of system, as well as means for alleviating these sources, are outlined. It is concluded that the hydrostatic system, permanently installed in the synchrotron, should be accurate within 0.001 in. across the 1-mile diameter of the synchrotron. The hydrostatic system is considered to be much more rapid than optical leveling methods. (T.F.H.)

20734 (UCRL-11800) SYNCHROTRON-MAGNET COST STUDIES. Charles G. Dols and Robert A. Kilpatrick (Lawrence Radiation Lab., Univ. of California, Berkeley). Mar. 2, 1965. Contract W-7405-eng-48. 9p. (CONF-650306-9). Dep.(mn); $1.00(cy), 1(mn) CFSTI.

From Particle Accelerator Conference, Washington, D. C.

Cost studies of magnet designs for a 200-Bev synchrotron led to a coil design using cross sections of the conductor that differed for the inner and outer coil sides. The primary basis for estimating costs of magnet construction was the record of the actual costs of the Brookhaven AGS magnet. Determinations of optimum magnetic-flux densities and optimum current densities were made by minimizing the total costs of magnet cores, magnet coils, power supply, operating costs, magnet-support structure, correcting magnets, and tunnel enclosure. The studies depended on the use of computer programs for predicting magnetic fields in air and in iron. Operating costs were capitalized by multiplying the cost per year by 10. (auth)

20735 (UCRL-11807) THE EFFECT OF ACCELERATOR PARAMETERS ON MECHANICAL TUNING OF rf CAVITIES. Michael A. Green (Lawrence Radiation Lab., Univ. of California, Berkeley). Mar. 1, 1965. Contract W-7405-eng-48. 9p. (CONF-650306-15). Dep.(mn); $1.00(cy), 1(mn) CFSTI.

From Particle Accelerator Conference, Washington, D. C.

A frequency modulation system for r-f cavities is described that uses a "loudspeaker" type mechanical r-f tuning device. The modulation system is found to be most suitable for proton synchrotrons having low frequency swing and low repetition rates. A typical mechanically tuned r-f system for a medium-energy high-repetition-rate particle accelerator is used to illustrate the optimization of the moving portion of the tuner, the control system and the response limits on the servo loop, and the mechanical response of the moving part and its effect on tuning accuracy. (T.F.H.)

20736 (UCRL-11828(p.236-41)) 88-INCH CYCLOTRON OPERATION AND DEVELOPMENT. Hermann A. Grunder, Frank B. Selph, Hogil Kim, Elon Close, and David J. Clark (Lawrence Radiation Lab., Univ. of California, Berkeley).

A brief account is given of the development of new beams and facilities in the past year. The phase width and energy spread of the external beam are discussed. The work on the regenerative extraction system is described. (D.L.C.)

20737 (UCRL-11955) SURVEY OF INJECTION-SYSTEM DESIGN. W. A. S. Lamb (Lawrence Radiation Lab., Univ. of California, Berkeley). Feb. 16, 1965. Contract W-7405-eng-48. 16p. (CONF-650306-18). Dep.(mn); $1.00(cy), 1(mn) CFSTI.

From Particle Accelerator Conference, Washington, D. C.

The general problems of injection into particle accelerators are discussed, with the criteria for the choice of injection parameters emphasized. Examples are given of the injection system designed for a 200-Bev proton synchrotron. (auth)

20738 (UCRL-11983) NEUTRINO BEAMS FROM A HIGH-INTENSITY 200-Gev PROTON SYNCHROTRON. V. Z. Peterson and D. Keefe (Lawrence Radiation Lab., Univ. of California, Berkeley). Feb. 12, 1965. Contract W-7405-eng-48. 16p. (CONF-650111-1). Dep.(mn); $1.00(cy), 1(mn) CFSTI.

From CERN Informal Neutrino Conference, Geneva.

Theoretical estimation are presented of the beam intensity, beam transport characteristics, reaction rates, and spectra of neutrino (antineutrino) beams from a 200-Bev proton synchrotron. (T.F.H.)

20739 SURFACES OF CONSTANT SPACE CHARGE FIELD COMPONENTS IN A CYLINDER OF UNIFORM CHARGE DENSITY. Ivan Cherry and Douglas Venable (Los Alamos Scientific Lab., N. Mex.). Am. J. Phys., 33: 243-4(Mar. 1965). (LA-DC-6525)

Poisson's equation was solved using a high-speed digital computer, where the running parameter was the cylinder length-to-diameter ratio; and the space charge field components were obtained. The distribution of the surfaces of constant radial and axial field components, which also represent surfaces of constant force components, are shown. (L.B.S.)

20740 HIGH-CURRENT AIR-CORE BETATRONS. A. I. Pavlovskii, G. D. Kuleshov, G. V. Sklizkov, Yu. A. Zysin, and A. I. Gerasimov. Dokl. Akad. Nauk SSSR, 160: 68-70(Jan. 1, 1965). (In Russian)

A description is given of pulsed air-core betatrons in which circulating currents of about 90 amp (2×10^{12} accelerated electrons per cycle of acceleration) at electron energies up to 100 Mev were obtained. To generate an axially symmetric betatron field, an electromagnet consisting of two flat spirals connected by a central solenoid with a gap in its middle part was used. The azimuthal static inhomogeneity of the magnetic field in the plane of the equilibrium orbit did not exceed 0.5%. The relative dimensions of the stability regions in the radial and axial directions were $\Delta r/r_0 \approx 0.7$ and $\Delta z/r_0 \approx 0.6$, respectively. The electromagnets were supplied with power from capacitor energy accumulators. The maximum intensity of the

magnetic field was limited by the energy of the power supply and the reliability of the electromagnet's structure. The latter limited the intensity of the magnetic field to approximately $2-4 \times 10^4$ Oe. The intensity of the field in the region of the central solenoid was, then, $1-2 \times 10^5$ Oe. Systems for ensuring radiation pulses with a duration of several hundredths of a microsecond to several tens of microseconds were used to direct the accelerated electron beam to the target. In betatrons with $r_0 \leq 11.7$ cm a rapid release of electrons was obtained through azimuthal perturbation of the magnetic field by means of a small induction coil. In accelerators with $r_0 \simeq 23.4$ cm, a dual release system was employed which consisted in a preliminary slow change of the radius of the equilibrium orbit and the subsequent fast translation of the electron beam to the target. With this method it is easier to obtain very short radiation pulses with a duration equal to a time of about 10 revolutions of the electrons ($\sim 5 \times 10^{-8}$ sec). In addition, the structure of the beam during translation is maintained. (ATD)

20741 MEASUREMENT OF SKYSHINE NEUTRONS AROUND THE FRASCATI SYNCHROTRON. M. Ladu, M. Pelliccioni, and E. Rotondi (CNEN, Frascati, Italy). Energia Nucl. (Milan), 12: 98-9(Feb. 1965). (In Italian)

The flux and mean energy of skyshine neutrons in the area around the Frascati synchrotron were measured. The flux measurements were made with a paraffin enclosed BF_3 counter and showed that the neutron flux decreased approximately according to the law $\phi = kr^{-n}$, where r is the distance from the machine and k is a constant depending on the operating conditions of the synchrotron. The mean energy was evaluated from the attenuation curve and varied from 250 to 400 kev. (J.S.R.)

20742 SMASHING THE ATOM. HIGHER POWERED PARTICLE ACCELERATORS ARE NEEDED TO UNLOCK SECRETS OF THE ATOM. John H. Martin (Argonne National Lab., Ill.). Ind. Res., 7: No. 3, 42-9(Mar. 1965).

The trends in accelerators with respect to energy, costs, and acceleration principles are summarized, with reference to particular accelerators. Applications of accelerators in nuclear physics, industry, medicine, chemistry, element production, particle production, and atmospheric research are indicated. (D.C.W.)

20743 FOCUSING OF AN ELECTRON STREAM WITH RADIO-FREQUENCY FIELDS. C. K. Birdsall (Univ. of California, Berkeley) and G. W. Rayfield. J. Electron. Control (1), 17: 601-22(Dec. 1964).

A stream of electrons was focused solely by the fields of a slow ($v_p < c$) electromagnetic wave. An analysis was obtained by transforming to the wave frame in which the equations of motion of electrostatic periodic focusing are valid. By using the well-known results for the static case, and retransforming to the laboratory frame, focusing behavior and design information (circuit size, frequency, power for a given stream) were obtained. A second but more appropriate analysis was made by transforming to the average electron frame in order to predict both fast- and slow-wave results; for the axially symmetric modes considered, the slow-wave focusing requires orders of magnitude less power than for fast waves and has a more favorable field shape. Several experiments were performed using a helix as the slow waveguide. The stream was launched into the helix and was collected both on the helix and by a collector at the opposite end. Typically 10 to 20% of the current would be transmitted with no wave, rising linearly with wave power to a best transmission of over 80%. The best results were obtained with the wave velocity in the same direction and greater than the average velocity of the results. At best, a 1 w stream (roughly 1 mamp at 1000 v) was focused by about 10 w of r-f wave power at 1000 Mc. These results are in rough agreement with the theory. For a given injected stream there appears to be a maximum r-f power beyond which focusing decreases; this effect may be due to either a strong localized lens effect at the point of stream injection or to r-f voltages large compared with the average steam voltage. (auth)

20744 A CALCULATION OF THE SHUNT IMPEDANCE OF A CLOVERLEAF ACCELERATOR STRUCTURE. W. J. Shlaer (Los Alamos Scientific Lab., N. Mex.). J. Nucl. Energy, Pt. C, 7: 133-40(Mar.-Apr. 1965). (LA-DC-6496)

The field in a single cell of a cloverleaf accelerator structure was calculated in a two-dimensional approximation by synthesis from the fields produced by line currents inside a metal cylinder. Effective shunt impedances at $\beta = 0.7$ fall around 25 MΩ/m for the shapes considered. Cells with wide, short lobes give the best shunt impedance. (auth)

20745 NONLINEAR PHASE RESONANCES IN A HIGH-ENERGY SYNCHROTRON. J. Andrade E Silva and G. Lochak (Laboratoire Joliot-Curie de Physique Nucleaire, Orsay, France and Institut Henri-Poincare, Paris). J. Phys. (Paris), 25: 981-8(Dec. 1964). (In French)

Calculations were made on the linear and nonlinear resonances produced by defects in the construction of circular accelerators in which there are fast phase oscillations. The importance of the zones of nonlinear resonance was studied by comparison of their effects with those of the linear resonances; and the amplitude increase of the phase oscillations resulting from the crossing of the exterior and parametric linear resonances was calculated. Conclusions were drawn concerning the precautions which should be taken in the construction of these accelerators. (auth)

20746 AN IMPROVED SYSTEM FOR ENERGY MODULATION OF PARTICLE ACCELERATORS. M. A. Wilson and M. L. Roush (Univ. of Maryland, College Park). Nucl. Instr. Methods, 34: 54-6(Apr. 1965).

The effective energy of an accelerator beam is modulated by applying a saw-tooth voltage function to an appropriately insulated target. An extremely simple means is described for generating an output pulse which is linearly related to the target voltage at the times when selected events are detected. In addition to the excellent stability of the system, an accurate calibration can be obtained by applying known d-c voltages to the target and a means is described for simultaneously recording data and a normalization for any nonlinearities of the saw-tooth voltage function. (auth)

20747 ON THE RELATION BETWEEN BEAM CURRENT AND DEE VOLTAGE IN A CYCLOTRON. J. D. Lawson (Rutherford Lab., Chilton, Berks, Eng.). Nucl. Instr. Methods, 34: 173-4(Apr. 1965).

It was previously suggested that the effect of space charge near the center of the cyclotron is to limit the accelerated current to a value which is proportional to the cube of the dee voltage. Electric focusing was neglected and it was assumed that the magnetic focusing enters suddenly at some radius r_m. It is shown that more realistic assumptions about the magnetic focusing give a less rapidly increasing function of v and in particular the focusing arising from a parabolic field fall-off at the center yields a $v^{\frac{1}{2}}$ dependence. (C.E.S.)

20748 THE CERN RADIO FREQUENCY PARTICLE SEPARATOR— FIRST OPERATION. P. Bramham, R. D. Fortune, E. Keil, H. Lengeler, B. W. Montague (CERN, Geneva), and W. W. Neale. Phys. Letters, 15: 290-1 (Apr. 1, 1965).

The testing of the CERN microwave particle accelerator is summarized, including measurements of the compositions and fluxes of the meson (K^+) and (K^-) beams. Meson (K^+) and (K^-) beams at 10.12 Bev/c were obtained. (D.C.W.)

20749 INVESTIGATION OF NEUTRON AND γ RADIATION BETWEEN CURRENT PULSES OF A 70 Mev ELECTRON LINEAR ACCELERATOR. A. D. Abramenkov, S. S. Kalinichenko, A. A. Krasnikov, and G. K. Khomyakov (Khar'kov Inst. of Physics and Tech.). Ukr. Fiz. Zh., 10: 123-7 (Feb. 1965). (In Ukrainian)

It is shown that the background produced by captured slow neutrons and γ quanta is noticeably present during time intervals between current pulses behind shielding concrete walls of an electron linear accelerator for about 7 msec. The background duration is dependent of the pulse

time. The lifetime of slow neutrons and γ-active isotopes produced by slow neutron capture in different parts of the equipment and shielding is about 3.5 msec. The maximum energy of the quanta is approximately 8 Mev. (auth)

20750 EFFECTS OF FLUCTUATIONS ON THE PRECISION OF SYNCHRONIZATION DEVICES. V. I. Tikhonov. Usp. Fiz. Nauk, 83: 665-94(Aug. 1964). (In Russian)

If, either directly or by means of a special device, an external periodic oscillation acts on a self-oscillating system, the frequency of the natural oscillation will be distributed and within a certain range it will coincide with the frequency of the external oscillation. This synchronization range depends on the parameters of the system and the amplitude of the external oscillation; outside of this range, the natural and external oscillations do not coincide. This phenomenon is of great interest in radiophysics and for the study of nuclear reactions. Such reactions in the cyclotron require a high level of stability in the parameters of the accelerated ion beam and the frequency of the accelerating voltage in order to avoid a voltage drop in the dees. Disturbances in the resonance system may be avoided by automatically subordinating the generator under the natural frequency or the dee circuit, or vice-versa. The motion parameters are usually determined by interferometric or Doppler methods. Investigations of the effect of fluctuations on the synchronization processes and the influence of such fluctuations on the operation of the autonomous generator have helped to clarify the nature of the auto-oscillations. The fluctuations may be due to recurrent or sudden noise of the electronic devices, heat changes, and external random effects, such as pressure, temperature, or humidity changes. The problems encountered in synchronization work are systematically reviewed, attempting to derive generally valid conclusions. (Review article, 52 references). (TTT)

20751 LINEAR ACCELERATOR. Hubert Leboutet and Roger Jean (to CSF Compagnie Generale de Telegraphie sans Fil). German Patent 1,182,369. Nov. 26, 1964. Priority date Sept. 27, 1961, France.

The linear accelerator described consists of a plurality of straight portions connected by magnetic separator devices in which the particle beam is separated into bunches with each bunch having a different high-energy level. The beam has at the separator output essentially the same configuration as the beam applied to the input. For control and adjustment of the accelerator means are provided at the ends of the straight accelerator portions for the injection or extraction of auxiliary beams into or from the straight portions of the accelerator. (Gmelin Inst.)

20752 LINEAR ACCELERATOR. Lawrence Edmond Brown and Carig Spencer Nunan (to Varian Associates). German Patent 1,186,567. Feb. 4, 1965. Priority date June 25, 1958, United States.

The accelerator vessel described has a flared, flat exit portion, which is composed of two thick-walled plates of metal. The inner surface of these plates is recessed in such a way that the cross section of this portion has generally the shape of a rhombus, two edges of which are situated in the plane scanned by the particle rays. (Gmelin Inst.)

20753 MAGNET CONSTRUCTION FOR A VARIABLE ENERGY CYCLOTRON. Richard J. Burleigh, E. L. Kelly, J. H. Dorst, and C. G. Dols (to U. S. Atomic Energy Commission). U. S. Patent 3,175,131. Mar. 23, 1965.

Cyclotron magnets and more particularly pole pieces and pole tips constructed to meet the requirements of variable energy cyclotrons are described. The pole pieces are provided with annular voids of suitable size and location and the pole tips are provided with a plurality of tapped holes in any portion of which iron studs may be threaded. These two features used jointly provide a means for maintaining a suitable field profile when the overall field strength must be changed from a first level to a widely differing second level. (AEC)

Astrophysics and Cosmology

Refer also to abstracts 20439, 20875, 20878, 20890, and 21155.

20754 AN OPTICAL METHOD FOR THE DETECTION OF ANTIMATTER IN THE UNIVERSE. N. A. Vlasov (Lebedev Inst. of Physics, Moscow). Astr. Zh., 41: 893-7(1964).

The possibility of the existence of antimatter in the universe and methods for its detection are discussed in connection with the electromagnetic separation of matter and antimatter proposed by Alfven and Klein. An optical method of observation of protonium and positronium emission is proposed, in addition to the known methods of registration of particles and gamma rays emitted as a result of annihilation. The sources of such emission can be the boundaries of regions of matter and antimatter, where there is a mixture of particles and antiparticles and where the probability of protonium and positronium formation is high. Some of the emission lines of positronium and protonium lie in the visual and infrared regions. The atmosphere is sufficiently transparent for observation of these lines at long exposures with high-speed and narrow-directivity ground telescopes. Emission from the center of the Galaxy is of interest; one of the sources of soft rays from the galactic center may be protonium. (ATD)

20755 ON SOME POSSIBILITIES OF DETECTING THE H-F TURBULENCE OF A COSMIC PLASMA. V. N. Tsytovich (Lebedev Inst. of Physics, Moscow). Astr. Zh., 41: 992-5(1964).

Assuming that the variation in transverse-wave spectrum intensity in a turbulent plasma is due mainly to processes of dissociation or merging of the transverse and plasma waves, it was demonstrated that, during the passage of the 21-cm line near the sun, the spectrum broadens and shifts toward the red region. Simultaneously, a red component appears with a frequency which differs from the mean frequency of the line by approximately the plasma frequency. In a turbulent plasma, in which the wave characteristic phase velocity is much lower than the velocity of light, electromagnetic wave scattering greatly exceeds the shift and broadening of the spectrum. The possibility of using these phenomena to determine the h-f turbulence of a cosmic plasma is noted. (ATD)

20756 EVALUATION OF THE SPECTRUM OF SOLAR IONIZING RADIATION DURING THE AUGUST 22, 1958 BURST USING DATA FROM VERTICAL SOUNDINGS OF THE IONOSPHERE. I. N. Odintosova. Geomagnetizm i Aeronomiya, 4: 1035-42(1964).

A study of the N(h)-profile at heights of 100-320 km showed a significant increase in electron concentration at the F_2- and E-layer levels of the ionosphere during a burst. At heights of 120-200 km, no noticeable increase in electron concentration was detected. Ionosphere data from the Moscow station were used. The equation $\Delta q_t = \beta \Delta N_t = a' N_0 \Delta N_t$ was used to calculate parameter changes at the moment of maximum effect (N_t = ion concentration during burst). On the basis of the data obtained, an evaluation is made of the intensity spectrum of solar radiation during a burst at wavelengths shorter than 1000 Å. Virtual heights are converted to true heights by the tenpoint integral method without calculating interlayer ionization. Values for the change in ionization rate are obtained from the equation of ionization balance for heights at which the electron concentration increased during the burst. Comparisons of the spectrum obtained with rocket measurements made during various bursts are tabulated. (ATD)

20757 CONCERNING THE CHARACTER OF PROPAGATION OF SOLAR COSMIC RAYS IN INTERPLANETARY SPACE. L. I. Dorman and L. I. Miroshnichenko. Izv. Akad. Nauk SSSR, Ser. Fiz., 28: 1978-84(Dec. 1964). (In Russian)

The analysis of some recent experimental (satellite and other) data on solar cosmic rays was undertaken in view of the increasing interest in the nature of propagation of

solar cosmic radiation. On the basis of the now commonly accepted diffusion model the density of solar cosmic ray particles is described by an inhomogeneous equation of the type: $(\partial n/\partial t) = \varkappa\nabla^2 n + F(r,t)$; $n(r,0) = 0$; $-\infty < r < +\infty$; $t > 0$, where n is the density of solar particles, $\varkappa$ is the diffusion coefficient, and $F(r,t)$ is the density of the particle source. Analysis indicates that the density n should have a maximum at $t = r^2/6\varkappa$, and the density should fall off according to the $t^{-\frac{3}{2}}$ law (at a fixed r; for example, the radius of the Earth's orbit). Some data are consistent with this (the solar c.r. burst of 23 Feb. 1956), but some more recent data are better described by an exponential law: $n = ae^{-t/T}$, where T is a time constant that initially is of the order of tens of minutes and later of the order of hours. Further analysis of the data indicates that the coefficient of diffusion may depend not only on the energy of the particles but also on the distance from the sun and the azimuthal angle of emission of the particles. The adduced formulas are used for an approximate analysis of some recent data, including the data from Explorer XII. The analysis indicates that the diffusion coefficient is a power function of the energy. Consideration is given to evaluation of the anisotropy of the solar c.r. flux; mathematical analysis shows that the anisotropy may vary with time, which is borne out by the available data on large solar c.r. bursts. (ATD)

20758 NEW COSMOLOGICAL THEORY. N. Kalitzin. Izv. Fiz. Inst. Aneb, Bulgar. Akad Nauk, 11: 167-77(1963). (In Bulgarian)

A record power cosmic ray shower corresponding to a primary cosmic particle with energy of the order 10^{20} ev was registered in New Mexico in 1961. It follows from the theory of the origin of cosmic rays that this particle must be of an extragalactic origin. The existence of extragalactic cosmic rays with energy of the order 10^{20} ev enables one to presume the existence of extragalactic cosmic rays with much higher energy. If a particle with an energy of 10^{60} ev penetrates into the interior of a star, of the type of our Sun, for instance, rather interesting phenomena may occur. The particle may cause a shower of other particles in the star and thus transfer its entire energy to the star. This may lead to the explosion of the star, similar to that of novae and supernovae. It is suggested that the explosion of some typical novae and supernovae stars is precisely due to this reason. The integral energy spectrum of cosmic rays with energy of the order 10^{60} ev is determined from the frequency of explosion of novae. With the help of this spectrum the frequency of the explosion of supernovae is determined, which proves to be approximately the observed frequency. In the case of a noncentral hit of the super-high energy cosmic particle upon the star, the latter may receive a considerable angular momentum. If it is assumed that the explosions of novae and supernovae give rise to multiple stars and planetary systems, one can explain the strange distribution of the angular momentum in the solar system and some multiple stars. If a particle possessing energy of the order 10^{80} ev penetrates into a denser star, galaxies and anti-galaxies may occur. Perhaps the catastrophic phenomena observed in peculiar radiogalaxies of the type of Swan A, Centaur A and so on are due to a similar reason. With the help of this hypothesis, one can easily eliminate the expansion and thermodynamic paradoxes, as well as the problem of the exhaustion of hydrogen in the universe. The same hypothesis allows the elucidation of the question of the formation of elements after helium in the periodic system. It should be noted that Blokhintsev suggested that particles with super-high energy existed and when these particles met other such particles, stars could be formed. The simple relativistic treatment of this question, however, shows that such a transformation of kinetic energy into rest energy is only possible when the particle enters the interior of a star. (auth)

20759 A RADIO METHOD OF DETECTING SOLAR FLARES. John H. Reid (Dublin Inst. for Advanced Studies). J. Atmospheric and Terrest. Phys., 27: 127-8(Jan. 1965).

A monthly breakdown of data on solar flares, recorded at the Cape of Good Hope, and of observations of sudden increases in the long-wave field intensity (SIL) is given for Aug. 1958 to July 1960. It seems that the radio method used to monitor the SIL's does not detect all solar flare activity, contrary to claims. (M.J.T.)

20760 COSMIC RAY EXPOSURE AGES OF IRON METEORITES BY THE Ne^{21}/Al^{26} METHOD. Michael E. Lipschutz (Univ. of Chicago and Goddard Space Flight Center, Greenbelt, Md.), Peter Signer, and Edward Anders. J. Geophys. Res., 70: 1473-89(Mar. 15, 1965).

The ^{26}Al and ^{44}Ti contents of 10 iron meteorites were determined by γ-γ coincidence counting of separated fractions. The ^{26}Al contents, ranging from 0 to 2.70 dpm/kg, were lower by factors of 1.5 to 3 than literature values obtained by β-counting. This discrepancy is apparently caused by a β-emitting impurity that interferes in β-counting but not in the γ-γ coincidence method. The concentrations of ^{3}He, ^{4}He, ^{21}Ne, ^{36}Ar, and ^{38}Ar were determined mass spectrometrically. From the ^{21}Ne and ^{26}Al content of these meteorites, the following cosmic ray exposure ages, in millions of years, were calculated (relative to Norfolk = 600 m.y.): Arispe = 120, Aroos = 1000, Duchesne = 200, Grant = 590, Odessa, 360, Sandia Mountains $\leq$ 210, Santa Apolonia = 840, Sikhote-Alin = 320, Treysa = 530. In most cases, these values agree rather well with previously determined $^{41}K/^{40}K$ and $^{36}Ar/^{36}Cl$ ages. The agreement with the $^{41}K/^{40}K$ ages, in particular, casts doubt on the notion that the exposure ages of iron meteorites are strongly affected by space erosion. Sandia Mountains and Arispe were found to contain noble gases in anomalous proportions. Apparently both these meteorites contain small amounts of radiogenic or primordial ^{4}He. Arispe, moreover, seems to have suffered a secondary breakup some 100 m.y. ago. Except for the observed falls, Aroos, Sikhote-Alin, and Treysa, none of the above meteorites contained any detectable ^{44}Ti activity. Evidently, the terrestrial ages of these meteorites are long in comparison with the half life of ^{44}Ti, 48 yr. The absence of ^{44}Ti activity in Norfolk shows that it can not have been associated with a 1907 fireball, as had been previously supposed. Sandia Mountains appears to have a low ^{26}Al activity, possibly due to a terrestrial age of the order of 10^6 yr. (auth)

20761 COSMIC RAY EXPOSURE AGES OF TEKTITES BY THE FISSION-TRACK TECHNIQUE. R. L. Fleischer (General Electric Research Lab., Schenectady, N. Y.), C. W. Naeser, P. B. Price, R. M. Walker, and M. Maurette. J. Geophys. Res., 70: 1491-6(Mar. 15, 1965).

Tektites exposed to primary cosmic radiation will contain distinctive, readily identifiable, induced-fission tracks, a large fraction of which will survive the heating that occurs as tektites fall to earth. A search for such events in samples from each of the four chronological tektite groups failed to reveal such events and thereby indicates an average cosmic-ray exposure age of less than 300 yr. By further work a space exposure of 20 yr or less could be detected. (auth)

20762 THE EQUILIBRIUM DISTRIBUTION OF NUCLIDES IN MATTER AT HIGH TEMPERATURES. F. E. Clifford and R. J. Tayler (Department of Applied Mathematics and Theoretical Physics, Cambridge, Eng.). Mem. Roy. Astron. Soc., 69: 21-81(1965).

At temperatures between 10^9 and 10^{10}°K and at suitable densities, nuclear reactions may become so profuse that approximate statistical equilibrium is set up between the concentrations of the different nuclides. Current theories of stellar evolution suggest that this equilibrium can be set up in stars and the resulting e-process elements may be distributed through space by a stellar catastrophe such as a supernova explosion. Complete statistical equilibrium between all the types of particles which occur in a star can not be set up because the neutrinos, which occur in all beta decay reactions, have an effectively infinite mean free path. However, nuclear and electromagnetic interactions occur much more rapidly than beta decays and in a short

time the nuclei and photons come almost into equilibrium while the total numbers of protons and neutrons in the system are essentially constant. Subsequently beta decay reactions gradually change the relative proportions of protons and neutrons and, although the neutrino losses prevent true equilibrium, it is possible that the beta decays and inverse decays come into balance and that the ratio of the total number of protons to the total number of neutrons tends to a limiting value. Calculations are reported for the whole range of values of the physical parameters which are thought to be important, at least in stellar interiors. Nuclidic abundances were found as a function of three parameters: the density, the temperature and the ratio of the total number of protons to the total number of neutrons. In all, results were obtained for 333 sets of values of the three parameters; and detailed nuclidic abundances, before and after beta decay, are tabulated for 96 of these cases. The accuracy of the calculation is limited by the uncertainties of nuclear data. A detailed discussion is given of the possible size of errors arising from these uncertainties. It is also pointed out that, if the properties of only a few nuclides are shown to be seriously in error, it is a relatively simple matter to modify the tabulated results so that they are still solutions of the equilibrium equations, but now refer to different values of the density and the ratio of total number of protons to total number of neutrons. (auth)

20763 DISAPPEARANCE OF THE POLAR CAP ON MARS IN 1956 AFTER A SOLAR FLARE WITH EJECTION OF PARTICLES. L. Krivsky (Astronomical Inst., Czechoslovak Academy of Sciences, Ondrejov), J. Cech, and J. Sadil. Nature, 205: 994(Mar. 6, 1965).

The sudden disappearance of the south polar cap on Mars during its perihelion opposition in 1956 is explained in terms of the effects of radiation from the solar flare of August 31, 1956, on the atmosphere of Mars. (D.C.W.)

20764 SOME EXACT SOLUTIONS IN MAGNETOHYDRODYNAMICS WITH ASTROPHYSICAL APPLICATIONS. Alfred Clark, Jr. (Massachusetts Inst. of Tech., Cambridge). Phys. Fluids, 8: 644-9(Apr. 1965).

The equations describing a class of exact solutions in magnetohydrodynamics are given. The solutions considered are those for which the magnetic field is everywhere parallel to a fixed direction in space. Several velocity fields satisfying the equations are discussed briefly. One example discussed in detail serves as a model for the time development of a vertical magnetic field in a flow resembling the solar supergranulation flow. For this problem, it is shown that the characteristic time scale for finite conductivity diffusion effects to be important is much shorter than the usual dimensional scale of $(\text{length})^2$ divided by diffusivity. In particular, it is shown that under typical conditions of solar supergranulation flow, the time scale for diffusion is comparable with the observed lifetimes of the supergranulation cells. (auth)

20765 GALACTIC X-RAY SOURCES. G. R. Burbidge, R. J. Gould, and W. H. Tucker (Univ. of California, San Diego, La Jolla). Phys. Rev. Letters, 14: 289-92(Mar. 1, 1965).

A review of possible mechanisms for the production of x rays by galactic sources is given. The mechanisms of neutron-star production and Compton scattering are discussed briefly; simple calculations indicate negligible fluxes from these processes. Models based on production by synchrotron emission and by bremsstrahlung are considered. It is found that the energy-loss time scales for the high-energy synchrotron electrons are very short, and very high temperatures are required to produce bremsstrahlung. (M.J.T.)

20766 CONTINUAL ACCELERATION OF SOLAR PROTONS IN THE Mev RANGE. D. A. Bryant, T. L. Cline, U. D. Desai, and F. B. McDonald (Goddard Space Flight Center, Greenbelt, Md.). Phys. Rev. Letters, 14: 481-4 (Mar. 29, 1965).

Evidence obtained from the Explorer-XIV cosmic-ray experiment is reported for the long-term persistence of a new component consisting of protons in the 3 to 20 Mev range. Integral proton intensities are shown for six solar rotations. The counting rate was found to increase rapidly after a sudden commencement and displays a strong asymmetry with the initial increase and partial decay, followed generally by a long plateau region. It is also found that the energy measurements for the recurrent events are best ordered by exponential spectra. The continued presence of the protons is taken as evidence that they are being continually accelerated by the sun. (L.B.S.)

20767 PHYSICAL CONDITIONS IN THE GASEOUS ENVELOPE OF 3C-273. I. S. Shklovskii (Shternberg State Astronomical Inst., USSR). Soviet Astron. AJ (English Transl.), 8: 638-42(Mar.-Apr. 1965). Translated from Astron. Zh., 41: 801-6(Sept.-Oct. 1964).

The absence of a noticeable Balmer discontinuity in the spectrum of the quasi-stellar object 3C-273 leads to the conclusion that the gaseous nebula surrounding the nucleus ($T_e \approx 30{,}000$) should be ionized by the completely absorbed ultraviolet radiation of the nucleus. Ionization in the nebula should be stratified. The spectral distribution of the ionizing ultraviolet radiation of the nucleus is found. The spectral density of this radiation varies slightly up to $h\nu \sim 25$ ev. However in the region $h\nu \sim$ 35-50 ev. It decreases by a factor of 10^3 and then remains constant up to $h\nu \sim 120$ ev. The latter is explained by the inverse Compton effect. Evidence is given for the conclusion that the nebula surrounding the 3C-273 nucleus is a closed expanding shell. The emission of the Mg II resonance lines is discussed. The age of the quasi-stellar source estimated from the expansion of the envelope is of the order of several thousand years. This same age follows from an analysis of the radio source 3C-273-B. At the same time the age of the source 3C-273-A is of the order of several hundred thousand years. It is concluded that energy release by such objects is of a recurrent character. The same is true for radio galaxies and also nuclei for normal galaxies. A hypothesis is proposed that sources of the Cyg A type are quasi-stellar objects observed between two successive outbursts. The recurrence of explosive processes is one of the most essential characteristics of metagalactic sources of radio emission. (auth)

20768 MAGNETIC COLLAPSE AND THE NATURE OF INTENSE SOURCES OF COSMIC RADIO-FREQUENCY EMISSION. N. S. Kardashev (Shternberg State Astronomical Inst., USSR). Soviet Astron. AJ (English Transl.), 8: 643-8(Mar.-Apr. 1965). Translated from Astron. Zh., 41: 807-13(Sept.-Oct. 1964).

Enhancement of the external magnetic field under gravitational contraction of cosmic bodies may account for a whole series of observed characteristics of high-intensity radio sources of nonthermal emission. The contraction of a star is treated here up to the point where rotational instability sets in. The post-contraction star may exert a regular twist effect on the magnetic field of the shell over a protracted time span, resulting in the formation of radio sources having a quasi-regular magnetic field of the type found in the Crab Nebula (in type I supernovas). In the contraction of very massive stars (type II supernovas), the twisting of the field will come to a halt long before that point, because of the breakdown in the magnetic coupling between the star and the shell, after which radio sources exhibiting shell structure will be formed. In the collapse of supermassive bodies formed from the interstellar and intergalactic medium, the conversion of a considerable fraction of the rest energy into the energy of the external magnetic field is entirely possible. Radiation of the external magnetic field will ensue as the contracting body approaches the gravitational radius, and this will entail the generation of relativistic hydromagnetic waves which may bring about explosive events and may be responsible for the acceleration of cosmic rays in radio galaxies. (auth)

20769 GAS DYNAMICAL MODEL OF A TYPE II SUPERNOVA OUTBURST. V. S. Imshenik and D. K. Nadezhin. Soviet Astron. AJ (English Transl.), 8: 664-

73(Mar.-Apr. 1965). Translated from Astron. Zh., 41: 829-41(Sept.-Oct. 1964).

The problem of the disintegration of a main sequence massive star (M = 15 M⊙-50 M⊙) as a result of the instantaneous release of a store of energy comparable to the gravitational energy, near the center of the star, is solved numerically. Spherically symmetrical gas dynamical equations with radiative heat conduction lie at the basis of the treatment. Ionization and recombination processes of hydrogen atoms are considered. The radiative energy flux from the star's surface, the velocity of motion of the stellar matter, the effective temperature, and other parameters are found. All of these data are found to be closely consistent with available observational reports on type II supernovae. The protracted time-invariance of the light-curve (of the order of several ten-day periods) observed in type II supernovae is a particularly interesting result in the calculations. In the model in question, the exhaustion mechanism in the disintegrating star is a narrow cooling and recombination wave propagating throughout the interior of the star. The close agreement between the velocity of the cooling wave relative to the stellar matter and the velocity of the matter ahead of the wave front is the reason for the constant brightness, since under these conditions the radius of the wavefront advanced by the cooling wave will undergo almost no change, while the effective temperature, governed by the opacity and dependent primarily on the ionization potential of hydrogen, will remain practically constant. (auth)

20770 PARTICLE ACCELERATION IN A SHOCK EMERGING FROM A STAR. D. K. Nadezhin and D. A. Frank-Kamenetskii. Soviet Astron. AJ (English Transl.), 8: 674-6(Mar.-Apr. 1965). Translated from Astron. Zh., 41: 842-5(Sept.-Oct. 1964).

A similarity solution is considered for the ejection of nova and supernova envelopes. The results are compared with exact numerical integrations of the partial differential equations. Direct gas-dynamical acceleration of particles to relativistic velocities upon emergence of a shock is discussed. (auth)

20771 THE $p + p \rightarrow d + e^+ + \nu$ REACTION RATE IN THE CRYSTALLINE WHITE-DWARF INTERIOR. V. P. Kopyshev. Soviet Astron. AJ (English Transl.), 8: 691-4(Mar.-Apr. 1965). Translated from Astron. Zh., 41: 863-6(Sept.-Oct. 1964).

Heavy nuclei in the interior of a white dwarf form a crystal lattice, the field of which affects the rate of the $p + p \rightarrow d + e^+ + \nu$ reaction. Since the reaction proceeds above the field barriers, its rate is accelerated by a factor of 3.5 to ~5 over that in an ideal plasma under the same conditions ($\rho \approx 10^6$ g/cm^3, $T \sim 10^7$°K). Kirzhnits had estimated a rate eight orders slower for transitions below the barriers. (auth)

20772 THE NEUTRINO LUMINOSITY OF A STAR AND THE NEUTRAL CURRENT. E. P. Shabalin (Inst. of Theoretical and Experimental Physics, Academy of Sciences, USSR). Soviet Astron. AJ (English Transl.), 8: 695-9(Mar.-Apr. 1965). Translated from Astron. Zh., 41: 867-72(Sept.-Oct. 1964).

The transition of a nucleus from an excited state to ground with emission of a neutrino pair makes only a minor contribution to the neutrino luminosity of a star, compared with other processes. Weak interaction with the neutral current has certain implications here. (auth)

20773 PRESTELLAR EVOLUTION OF THE UNIVERSE. V. B. Yakubov. Soviet Astron. AJ (English Transl.), 8: 708-14(Mar.-Apr. 1965). Translated from Astron. Zh., 41: 884-92(Sept.-Oct. 1964).

An expanding, homogeneous model universe is considered, following Zel'dovich's "cold" variant. In the zero approximation the universe contains p, e^-, and ν_e; the first approximation also includes n, μ^+, and $\nu_\mu(\nu_e,\nu_{\bar{\mu}})$ are the electronic and mesonic neutrinos). At epoch t = 0 (infinite mass density), the temperature and entropy per baryon are assumed to be zero. The relatively slow reaction rates during the expansion prevent the particles from reaching equilibrium concentration at any time, and therefore the entropy rises. The entropy and temperature variations are computed. When nuclear density is approached, equal numbers of p, e^-, and ν_e only will remain; and with continued expansion cold hydrogen will form until star production sets in. Baryon, lepton, and charge conservation are assumed throughout, at all densities. Matter is assumed electrically neutral, with the lepton concentration twice the baryon. Only "slow," weak-interaction reactions are considered, since "fast" electromagnetic and strong-interaction reactions will always reach equilibrium and contribute nothing to the entropy. (auth)

20774 OPTICAL SEARCH FOR ANTIMATTER IN THE UNIVERSE. N. A. Vlasov. Soviet Astron. AJ (English Transl.), 8: 715-18(Mar.-Apr. 1965). Translated from Astron. Zh., 41: 893-7(Sept.-Oct. 1964).

The existence of antimatter in the universe, and methods of its detection, are discussed in connection with the Alfven-Klein mechanism of electromagnetic separation of matter and antimatter. In addition to existing methods of recording of particles and annihilation gamma rays, an optical method is proposed for the observation of characteristic radiation of protonium and positronium. These emissions may be due to the boundaries of regions occupied by matter and antimatter where particles and antiparticles are mixed and there is a high probability of formation of protonium and positronium. The emission spectrum contains lines which lie in the visible and infrared regions. The atmosphere is quite transparent to these lines, and therefore the observations can be carried out with the aid of highly directional, large-aperture telescopes, using long exposures. Other methods require extra-terrestrial observations. The emission of the center of the galaxy is of interest in this connection, since protonium may be one of the sources of soft x rays from the galactic center. (auth)

20775 DETERMINATION OF THE EXCITATION TEMPERATURE IN THE SOLAR ATMOSPHERE. R. B. Teplitskaya (Inst. of Terrestrial Magnetism, Ionosphere and the Propagation of Radio Waves, Academy of Sciences, Siberian SSR). Soviet Astron. AJ (English Transl.), 8: 725-30(Mar.-Apr. 1965). Translated from Astron. Zh., 41: 907-13(Sept.-Oct. 1964).

The excitation temperature for Fe I, Ti I, and Ti II atoms in the solar atmosphere, determined from equivalent line widths, is compared with the mean electron temperature of the corresponding layers. The two temperatures are in agreement to within experimental error. The relative abundance of titanium obtained from Ti II lines is in good agreement with that found from Ti I lines. (auth)

20776 THE H_α RADIATION FIELD IN PROMINENCES. N. A. Yakovkin and M. Yu. Zel'dina (Kiev State Univ.). Soviet Astron. AJ (English Transl.), 8: 731-5(Mar.-Apr. 1965). Translated from Astron. Zh., 41: 914-19(Sept.-Oct. 1964).

The results of the solution of the integral equation for the case of complete noncoherent scattering shows that in spite of the large optical thickness of prominences in H_α, photospheric radiation in this line penetrates into prominences and excites radiation emission. The density of diffuse radiation is higher than the average density of solar radiation in a prominence. The theoretical profile has a saddle-like form, characteristic of H_α profiles obtained from observations. (auth)

20777 PROFILES OF THE STRONGER FRAUNHOFER LINES IN THE SOLAR SPECTRUM. I. HYDROGEN LINES. D. M. Kuli-Zade (Leningrad State Univ.). Soviet Astron. AJ (English Transl.), 8: 736-43(Mar.-Apr. 1965). Translated from Astron. Zh., 41: 920-9(Sept.-Oct. 1964).

The H_α, H_β, H_γ, and H_δ line profiles in the solar-disc spectrum were studied. It is found that the lines are sharper at the limb than at the center of the disc. The equivalent widths increase from H_α to H_δ at the center, while the opposite is observed for the limb. The observed

profiles are compared with theoretical profiles computed under various assumptions concerning the broadening mechanisms. It is shown that the above lines are broadened mainly by the statistical Stark effect due to slow ions and collisional damping by fast electrons. The H_α and H_β lines are broadened also by the pressure of HI atoms. (auth)

20778 PROFILE OF THE LINE Byλ 21655.2 A OF THE HYDROGEN BRACKETT SERIES IN THE SOLAR SPECTRUM. O. N. Mitropol'skaya (Shternberg State Astronomical Inst., USSR). Soviet Astron. AJ (English Transl.), 8: 744-6(Mar.-Apr. 1965). Translated from Astron. Zh., 41: 930-3(Sept.-Oct. 1964).

The B_γ line profile at different distances from the center of the solar disc was obtained from observations with the tower solar telescope of the Shternberg Astronomical Institute and a lead-sulfide photocell. The residual intensities of the line wings are computed for different θ and compared with theoretical values. It is assumed that the line wings are due to true absorption. The agreement is good in the central parts of the disc. At the limb the observed profile is systematically lower than the theoretical profile. This is explained by the increasing role of scattering in the upper photospheric layers. (auth)

20779 TEMPORAL VARIATION IN AREA OF A SUNSPOT GROUP. N. I. Kozhevnikov (Shternberg State Astronomical Inst., USSR). Soviet Astron. AJ (English Transl.), 8: 747-9(Mar.-Apr. 1965). Translated from Astron. Zh., 41: 934-6(Sept.-Oct. 1964).

It is shown that the area of a spot group increases in the same manner as the area of a section of a sphere rising in a liquid with constant velocity. The ascent velocity is proportional to the magnetic field strength of the group. (auth)

20780 INFLUENCE OF SOLAR ACTIVITY ON PROCESSES IN THE EARTH'S LOWER ATMOSPHERE. M. N. Gnevyshev and B. I. Sazonov (Main Astronomical Observatory, Academy of Sciences, USSR). Soviet Astron. AJ (English Transl.), 8: 750-3(Mar.-Apr. 1965). Translated from Astron. Zh., 41: 937-41(Sept.-Oct. 1964).

An analysis of high-level pressure charts of the northern hemisphere for the years 1949–1962 showed that the places of greatest frequency of recurrence of maximum and minimum pressure at the heights of the upper troposphere and lower stratosphere are concentrated in circular zones similar to the auroral zone. In the 11-year cycle the number of these pressure formations has two maxima coinciding with the corresponding maxima in the intensity of emission of the coronal line 5303 A. Therefore, both the geographical distribution of high-level pressure formations and their changes with time indicate that they are determined by solar corpuscular radiation. (auth)

20781 POSSIBLE WAYS OF DETECTING HIGH-FREQUENCY TURBULENCE IN COSMIC PLASMA. V. N. Tsytovich (Lebedev Inst. of Physics, Moscow). Soviet Astron. AJ (English Transl.), 8: 796-7(Mar.-Apr. 1965). Translated from Astron. Zh., 41: 992-5(Sept.-Oct. 1964).

The changes in the wave spectrum and wave scattering due to the passage of waves through turbulent plasma are calculated. It is shown that when 21-cm radiation passes near the sun, the spectrum is broadened and displaced towards the red. Moreover, a red satellite appears which is separated from the mean frequency of the line by an amount of the order of the frequency of plasma oscillations. In a turbulent plasma in which the characteristic phase velocity of waves is much less than the velocity of light, scattering of electromagnetic waves exceeds very considerably the shift and broadening of the spectrum. Possible applications of these effects in the determination of the intensity of high-frequency turbulence of cosmic plasma are discussed. (auth)

20782 ASTROPHYSICS AND SPACE SCIENCE: AN INTEGRATION OF SCIENCES. Allen J. McMahon. Prentice-Hall International Series in Space Technology. Englewood Cliffs, N. J., Prentice-Hall, Inc., 1965. 457p.

Observations and present theories and models in astrophysics are reviewed, including solar emissions and storms, solar flares, sunspots and prominences, solar radio emissions and the corona; the role of supernovae in astrophysics: supernovae in the local galaxy, supernova radio sources, the Crab nebula, and supernova explosions; the formation of the elements and the solar system; the physics of the interplanetary region: solar cosmic radiation, meteorites, coronal phenomena, magnetosphere-solar wind interactions, planetary radio emissions, and planetary structure. 164 references. (M.J.T.)

20783 PLASMA PHYSICS AND ASTROPHYSICS. E. N. Parker (Univ. of Chicago). p.1-81 of "Astrophysics and the Many-Body Problem. Vol. 2." New York, W. A. Benjamin, Inc., 1963.

The general equations of motion of a gross plasma are derived both for a collisionless plasma and a perfectly conducting classical fluid. The application of the equations to astrophysical phenomena is then demonstrated. (D.C.W.)

20784 STELLAR EVOLUTION. Jack S. Goldstein (Brandeis Univ., Waltham, Mass.). p.83-106 of "Astrophysics and the Many-Body Problem. Vol. 2." New York, W. A. Benjamin, Inc., 1963.

The evolution of a star from its formation to its final stages of supernova and white dwarf is traced, with emphasis on the nuclear processes in stars. The experimental bases of the theory are considered. (D.C.W.)

20785 SOLAR RADIATION. Francis S. Johnson (Southwest Center for Advanced Studies, Dallas). p.95-105 of "Satellite Environment Handbook. Second Edition." Stanford, Calif., Stanford Univ. Press, 1965.

Solar spectral irradiance data are given for microwave and ultraviolet radiation from 7.0 microns to 850 Å; ultraviolet spectral line intensities are also tabulated. The solar wind, due to the continuous hydrodynamical expansion of the solar corona, is mentioned. Solar variations are discussed, including variations in sunspot number and in x-ray emission, especially during solar flares. (M.J.T.)

20786 STAR EVOLUTION. COURSE XXVII. PROCEEDINGS OF THE ENRICO FERMI INTERNATIONAL SCHOOL OF PHYSICS, VARENNA, AUGUST 20–SEPTEMBER 1, 1962. L. Gratton, ed. New York, Academic Press, 1963. 495p.

Eighteen papers are included. Separate abstracts were prepared for all of them. (M.J.T.)

For abstracts of individual papers see: 20787, 20788, 20789, 20790, 20791, 20792, 20793, 20794, 20795, 20796, 20797, 20798, 20799, 20800, 20801, 20802, 20803, and 20903.

20787 STELLAR EVOLUTION— INTRODUCTORY LECTURE. L. Gratton (Universita, Rome and Laboratorio Gas Ionizzati, Frascati, Italy). p. 1-10 of "Star Evolution." New York, Academic Press, 1963.

A brief review of the history of ideas on stellar evolution is given, and the present state of stellar-evolution theories is surveyed, with mention of the Hertzsprung-Russell diagram and theories of stellar formation and of the origin of chemical elements. Possible future developments of the theory are speculated upon. (M.J.T.)

20788 OBSERVATIONAL APPROACH TO STELLAR EVOLUTION. A. R. Sandage (Mt. Wilson and Palomar Observatories, Pasadena, Calif.) and L. Gratton. p.11-49 of "Star Evolution." New York, Academic Press, 1963.

The form and terminology of the Hertzsprung-Russell diagram are outlined, and the equation for the main sequence is derived. Observational evidence on stellar evolution and the resulting H-R plots are reviewed. The fitting of observed main sequences of clusters to the theory is discussed, using evidence on interstellar reddening and heavy-element abundances. Correlations between kinematical properties, age, and chemical composition are considered. A brief discussion is given of properties of intrinsic variable stars, mainly connected with the period-luminosity relation in cepheids. (M.J.T.)

20789 CONSTRUCTION OF STELLAR MODELS. M. H. Wrubel (Indiana Univ., Bloomington). p.50-84 of "Star Evolution." New York, Academic Press, 1963.

The differential equations of stellar structure, describing a spherical star in equilibrium, are given. A statistical description of the material in stellar interiors is presented, considering occupation numbers for free and bound electrons, radiation and gas pressure, entropy, the equation of state, and $e^- - e^+$ pair degeneracy. Opacity calculations, on the interaction of radiation and the stellar material, are discussed, considering bound-free, free-free, and bound-bound absorptive processes, conduction, and scattering. Sources of nuclear energy, mainly nuclear interactions and beta decay, are described. The stepwise method and the shell method for computer numerical solutions of the problem of stellar structure and evolution are discussed. (M.J.T.)

20790 STELLAR MODELS. J. Faulkner and K. Griffiths (Cambridge Univ., Eng.). p.85-94 of "Star Evolution." New York, Academic Press, 1963.

A description is given of the computer methods used in an investigation of stellar models; the surface routine, determining the pressure and radius at 10^5°K, and the stepwise method for central stellar regions are discussed. Calculation results on the zero-age main sequence, effects of varying composition, mixed stars, the mass-luminosity relation, and the present-day sun are summarized and compared with observations. (M.J.T.)

20791 NUCLEAR ASTROPHYSICS. G. Burbidge (Univ. of California, San Diego). p.95-173 of "Star Evolution." New York, Academic Press, 1963.

A review of work in the application of nuclear physics to astronomy is presented. The topic of energy generation in stars, treated elsewhere in the book, is briefly surveyed. Studies on synthesis of the elements are extensively reviewed, including the relaton of stellar evolution and nucleosynthesis; H and He burning; the α, s, equilibrium, r, p, and x processes; and supernova explosions. Testing of stellar evolutionary theories by comparison with observed composition of stars is discussed, considering the H/He ratio, stellar ages and composition, and stars giving evidence of current nuclear activity. The role of neutrino emission in stellar evolution is considered. Studies on the behavior of matter at high densities and nuclear reactions and beta decay in high-density matter are described. Astrophysical age determination using radioactive nuclei is discussed. High-energy nuclear astrophysics is considered, with discussions of cosmic radiation and radio galaxies. 262 references. (M.J.T.)

20792 OBSERVED ABUNDANCE ANOMALIES INDICATING NUCLEOSYNTHESIS IN INDIVIDUAL STARS. E. M. Burbidge (Univ. of California, San Diego). p.174-6 of "Star Evolution." New York, Academic Press, 1963.

Observations of H-burning, He-burning, and the s-processes in various stars are reviewed, for stars apparently of spectral type O or B with weak or absent H lines, for A-type stars weak or lacking in H, for Wolf-Rayet stars, and for white dwarfs. (M.J.T.)

20793 THE EARLY STAGES OF STELLAR EVOLUTION. E. Schatzman (Institut d'Astrophysique, Paris). p.177-242 of "Star Evolution." New York, Academic Press, 1963.

Early stages of stellar evolution are studied, taking into account the law of conservation of angular momentum and the observed equatorial velocity distribution of stars in the H-R diagram. The theories of stellar origin from extremely dense matter or by formation of binary stars are mentioned. The mathematical model of a contracting star is developed, and the change of luminosity as a function of temperature is considered. The time scale of contraction and the effect of rotation-induced mass loss on contraction are discussed. The atmospheric structure of a rotating star and the mass flow in the contracting star are examined. The role of magnetic activity during star formation is discussed at length, developing the theory of the acceleration of charged particles by MHD shock waves. Surface nuclear reactions are considered. The difference between early and late-type stars in the H-R diagram is explained. (M.J.T.)

20794 ASSOCIATIONS AND VERY YOUNG CLUSTERS. L. Gratton (Laboratorio di Astrofisica e Laboratorio Gas Ionizzati, Frascati, Italy). p.243-63 of "Star Evolution." New York, Academic Press, 1963.

O and T stellar associations are described, and observations and models on the space distribution, instabilities, expansion, number and rate of formation, stellar content, diffuse matter, and Hertzsprung-Russell diagrams and luminosity functions of associations are reviewed. 85 references. (M.J.T.)

20795 NEBULAR VARIABLES AND RELATED OBJECTS. L. Rosino (Universita, Padua). p.264-79 of "Star Evolution." New York, Academic Press, 1963.

Nebular variables are stars found in stellar associations of clusters, near or in diffuse nebulosities, and having irregular variations of brightness. The frequency and distribution, light curves, and spectra of nebular variables are discussed. The phenomenon of flare stars is described. Peculiar objects in diffuse nebulae — infrared stars, infrared stars embedded in minute nebulosities, small reflection nebulosities without stars, and Herbig-Haro objects — are discussed. The deviation of the nebular variables from the zero-age main sequence in the H-R diagram is considered. The requirements of a theory to explain observations on nebular variables are discussed. (M.J.T.)

20796 THE PROBLEM OF ETA CARINAE. L. Gratton (Laboratorio di Astrofisica e Laboratorio Gas Ionizzati, Frascati, Italy). p.297-311 of "Star Evolution." New York, Academic Press, 1963.

The plausibility of the hypothesis that the southern variable η Carinae shows phenomena associated with the formation of a massive star or group of stars is demonstrated. Observations on η Car are summarized and discussed, including light variation, the spectrum and its variations, the expanding nebula around the variable, the O association in the η-Car region (Carina II), the possible membership of η Car in the association Carina II, and the physical properties of η Car. (M.J.T.)

20797 RELATION BETWEEN THE EVOLUTION OF STARS AND GALAXIES. E. M. Burbidge (Univ. of California, San Diego). p.312-29 of "Star Evolution." New York, Academic Press, 1963.

The Hubble sequence for galaxy classification is described. The relation between stellar-population classifications and galactic evolution is discussed. Methods for estimation of stellar populations in galaxies are summarized. The evolutionary significance of the galactic mass and mass-to-light ratio is considered. Galactic structure — spiral, barred spiral, normal, and nonequilibrium — is discussed. (M.J.T.)

20798 STARS WITH HELIUM-RICH CORES. R. Kippenhahn (Max-Planck-Institut fur Physik und Astrophysik, Munich). p.330-68 of "Star Evolution." New York, Academic Press, 1963.

The phase of stellar evolution is considered in which stars leave the main sequence of the H-R diagram and become giants or supergiants because of the exhaustion of hydrogen in the central region. It is discussed whether the He from H burning in a star is stored in the central region or mixed with matter in the outer regions, by meridional circulation. The physical problems of nonmixed evolution — problems encountered in trying to calculate theoretical evolutionary tracks for inhomogeneous stars — are summarized; it is found that for stars which are not very hot the outer boundary conditions are very important. The outer layers of these stars are considered, especially the theory of the convective regions near the surface. (M.J.T.)

20799 THEORETICAL MODELS FOR THE PULSATIONS OF CEPHEIDS. N. Baker (Goddard Inst. for Space Studies, New York). p.369-88 of "Star Evolution." New York, Academic Press, 1963.

Some general aspects of the theory of pulsational instability are discussed, and physical ideas behind recent treatments of cepheid instability are presented. It is attempted to interpret the pulsations of some of the intrinsic variable stars as phenomena of vibrational instability. The pulsation equations are discussed briefly. Pulsation theory — the linear adiabatic and nonadiabatic forms — is presented. Numerical models of cepheids are discussed. Explanations of the position of variable stars, especially the classical cepheids and the RR-Lyrae stars, on the H-R diagram and of the period-luminosity relation are considered. (M.J.T.)

20800 WHITE DWARFS AND TYPE I SUPERNOVAE. E. Schatzman (Institut d'Astrophysique, Paris). p.389-93 of "Star Evolution." New York, Academic Press, 1963.

Studies of the equation of state of matter at high densities or temperatures and of the rate of thermonuclear reactions at high densities are reviewed. Observations and interpretations on zero- and nonzero-temperature white dwarfs and on type-I supernovae are discussed. (M.J.T.)

20801 STELLAR STABILITY AND STELLAR EVOLUTION. P. Ledoux (Universite, Liege). p.394-445 of "Star Evolution." New York, Academic Press, 1963.

The stability of a purely spherical star in a state of pure hydrostatic equilibrium is considered, using the small perturbation method; effects of rotation, magnetic fields, and gravitational fields due to companions are neglected. General hydrodynamical equations are developed, taking into account conservation of mass, momentum, and mechanical, thermal, and total energy, and the effects of radiation, ionization, and nuclear processes; the linearized equations are obtained. The general equation for the case of purely radial perturbation, neglecting turbulence and viscosity, is derived. Stellar stability and evolution are considered for the cases of dynamical and vibrational stability toward radial and nonradial pulsations and secular stability. 68 references. (M.J.T.)

20802 STELLAR HYDROMAGNETICS. I. W. Roxburgh (Cambridge Univ., Eng.). p.446-51 of "Star Evolution." New York, Academic Press, 1963.

Theories on the origin of stellar magnetic fields are reviewed. The effect of magnetic fields on the internal structure of stars is examined, assuming the existence of such internal fields. The structure of the radiative zones of an upper main sequence magnetic star is examined, and expressions for the velocity of circulation currents are obtained. The effect of mixing between the core and envelope is considered. (M.J.T.)

20803 THE EVOLUTION OF CLOSE BINARY SYSTEMS. M. Hack (Osservatorio Astronomico, Merate, Italy). p.452-88 of "Star Evolution." New York, Academic Press, 1963.

Observational facts on the evolutionary pattern of close pairs are reviewed, including classification of close eclipsing binaries, spectrographic observations, photometric evidence of mass loss and intrinsic variability in brightness, statistical relations between parameters of close binary systems, and rotation of spectroscopic binaries. A table is given of observed and derived parameters of binary stars. The interpretation of these facts is studied especially considering the evolutionary effects of the loss and transfer of mass. Evolutionary stages of various groups of stars are explained. The evolutionary hypotheses of Crawford, Kopal, and Struve are presented and discussed, for cases of overluminosity of the companion and the interaction between the two stars, for binary systems of the ζ Aurigae type, and for close binary systems at the end of the evolutionary path. The most probable evolutionary picture is summarized. (M.J.T.)

Atomic Physics

Refer also to abstracts 21042 and 21092.

20804 (ANL-6938(p.36-45)) INELASTIC COLLISION CROSS SECTIONS OF NEON AND ARGON FROM MEASUREMENTS OF ELECTRON DRIFT VELOCITY. Joseph C. Bowe (Argonne National Lab., Ill.).

The cross section of excitation of Ne and Ar by electron impact is assumed to be given by $Q_1(u) = h(u - u_1)^\gamma$, where u_1 is the excitation energy. Formulas for drift velocity and overshoot, derived previously, are used with the experimental mobility data to evaluate the constant h for each gas for values of $\gamma = 0$, $\frac{1}{2}$, and $\frac{3}{2}$. For Ar at 12 ev, the cross sections found by this procedure lie in the range 0.6 to 7.6 $\times 10^{-17}$ cm^2 compared with Maier-Leibnitz's value of 0.9×10^{-17} cm^2 and in Ne at 16.9 ev the values are in the range from 1.0 to 1.6×10^{-19} cm^2 compared with Maier-Leibnitz's value of 5.6×10^{-18} cm^2. These values are tentative pending the outcome of further work. (auth)

20805 (NASA-CR-54223) INVESTIGATION OF COLLISION PROBABILITY OF ELECTRONS AND IONS WITH ALKALI METAL ATOMS. Semiannual Report, April 22, 1964 to October 21, 1964. R. H. Bullis and W. L. Nighan (United Aircraft Corp., East Hartford, Conn. Research Labs.). Nov. 10, 1964. Contract NAS3-4171. 63p. (UACRL-C-920243-6; N65-12017)

A summary is presented of the experimental research investigations conducted to determine the collision probabilities of electrons and cesium ions with cesium atoms. In previous studies under Contract NASr-112, electron cyclotron resonance techniques were employed to measure the electron-cesium atom collision probability over an energy range from 0.05 to 0.10 ev. A modified Ramsauer beam experiment was employed under the same contract to measure the collision probability of cesium ions with cesium atoms over the energy range from 0.12 to 9.7 ev. The work under this present contract represents an extension of these earlier investigations. A cesium arc discharge is being used in conjunction with electrostatic and r-f conductivity probe techniques to determine the collision probability of electrons with cesium atoms over the energy range from 0.1 to 0.5 ev. Further cesium ion-cesium atom collision probability measurements are being made in the existing modified Ramsauer beam experiment to extend the energy range of these measurements below 0.1 ev. (D.L.C.)

20806 (ORNL-3702) A NEW TECHNIQUE FOR MEASURING RANGE OF LOW ENERGY CHARGED PARTICLES IN CONDUCTING SOLIDS. A. K. Roecklein, M. Y. Nakai, E. T. Arakawa, J. L. Stanford, and R. D. Birkhoff (Oak Ridge National Lab., Tenn.). Mar. 1965. Contract W-7405-eng-26. 57p. Dep.; $3.00(cy), 2(mn) CFSTI.

Thesis submitted to Vanderbilt Univ., Nashville.

A method is described for measuring ranges of charged particles in conducting solids, and experimental data are presented for proton ranges in aluminum at energies less than 10 kev. A thickness of aluminum, greater than the maximum range of protons at this energy, is evaporated onto a glass substrate. This layer is covered by an extremely thin layer of silicon monoxide, which is a good electrical insulator. A second aluminum layer was then evaporated onto the SiO layer and its thickness was accurately measured by optical interferometry. The two aluminum layers were separated by an electrical resistance across the SiO layer of the order of 1 megohm and each was provided with current leads to a galvanometer. The proton beam was extracted from a radio-frequency ion source and accelerated to the desired energy by a series of anodes in an evacuated system. An electrostatic stopping potential analysis was performed to determine the energy distribution in the beam. Protons were incident normally on the top aluminum layer and fractional currents to the top and bottom aluminum layers were measured as the beam energy was increased. Curves for proton transmission as a function of energy were derived from the normalized current data for several aluminum film thicknesses. The energy at which 50% of the current protons were transmitted was determined for several thicknesses. A curve showing the range of charge as a function of energy for 50% transmission was thus derived, and this curve was compared with theory and other empirical range-energy data. (auth)

20807 (UCRL-11828(p.201-4)) APPEARANCE POTENTIALS OF SOME DOUBLY CHARGED MOLECULE

IONS. Amos S. Newton and Aldo F. Sciamanna (Lawrence Radiation Lab., Univ. of California, Berkeley).

Appearance potentials of M^{2+} ions formed by 70-kev electron impact were measured with a mass spectrometer for the following compounds: N_2, NO, O_2, CO_2, COS, CS_2, HCN, C_2N_2, NH_3, furan, thiophene, pyrrole, benzene, pyridine, and aniline. The results are tabulated along with the potential for singly charged ions and the yield of M^{2+} in the total ionization. It is seen that the ratio of the potentials of doubly and singly charged ions is close to 2.75 for most compounds. (D.L.C.)

20808 (UCRL-12054-T) AN APPROXIMATE, FINITE TEMPERATURE, THOMAS-FERMI POTENTIAL. William Zink (Lawrence Radiation Lab., Univ. of California, Livermore). Aug. 1964. Contract W-7405-eng-48. 13p. Dep.(mn); $1.00(cy), 1(mn) CFSTI.

An attempt was made to obtain a simple analytical expression for a potential that closely approximates the Thomas-Fermi potential and is easy to calculate. Such an expression is useful is calculating atomic form factors and energy levels of ionized and compressed atoms. (C.E.S.)

20809 (UCRL-12218) EVALUATION OF THE HYDROGENIC MATRIX ELEMENT $\langle O|e^{i\underset{\sim}{k}\cdot\underset{\sim}{r}}|n\underline{l}\rangle$. Margaret J. Fulton and Marvin H. Mittleman (Lawrence Radiation Lab., Univ. of California, Livermore). Jan. 21, 1965. Contract W-7405-eng-48. 34p. Dep.; $2.00(cy), 1(mn) CFSTI.

A calculation of the matrix element $\int d^3r\ \phi_0\ e^{i\underset{\sim}{k}\cdot\underset{\sim}{r}}\ \phi_{n\underline{l}}$ is performed, where $\phi_{n\underline{l}}$ denotes the normalized wave function for the $(n,\underline{l})$th excited state of hydrogen, and ϕ_0 denotes the ground state. For several values of the wave number k, tables containing contributions from individual $(n,\underline{l})$ matrix elements, $A_{n\underline{l}}$, along with the sum of the squares of these matrix elements, $\Sigma(k)$, are presented. The mathematical derivation of these results is given. On the low end of the energy scale, the contribution from $\underline{l} = 1$ for each n-value is maximum, while at high energies the $\underline{l} = 0$ contribution is seen to dominate. Using this high-energy result, an approximation for $\Sigma(k)$ is derived. (auth)

20810 THE KEPLER PROBLEM IN PARABOLIC COORDINATES ACCORDING TO THE HAMILTON-JACOBI THEORY. Fritz Schweiger (Universitat, Vienna). Acta Phys. Austriaca, 19: 138-63(1965). (In German)

The motion of a particle in a central field with the potential $V(r) = C/r$ was investigated. Whereas this problem has been extensively investigated in spherical coordinates, this is not the case in parabolic coordinates. This problem was investigated in parabolic coordinates by the Hamilton-Jacobi theory. The case of elliptical orbits was considered approximately. (tr-auth)

20811 PHYSICAL BASIS FOR HUND'S RULE. II. N. Karayianis (Harry Diamond Labs., Washington, D. C.). Am. J. Phys., 33: 201-4(Mar. 1965).

A simple model is proposed that is useful for understanding the role played by the Coulomb interaction in determining the total orbital angular momentum of an atomic ground state. An example is given and some possible shortcomings of the model are discussed. (auth)

20812 TWO-BODY PROBLEM IN THE ONE-DIMENSIONAL HEISENBERG MODEL. Shigetoshi Katsura (Tohoku Univ., Sendai). Ann. Phys. (N. Y.), 31: 325-41 (Feb. 10, 1965).

The coupled transcendental equations of Bethe, which determine eigenvalues of the one-dimensional Heisenberg model, are decomposed into uncoupled equations in the case of two reversed spins. The second cluster integral which determines exact behavior in the high field and low temperature region, is calculated by solving these equations. The contribution of bound states is dominant in the case of ferromagnetic interaction. Spin wave theory using Bose statistics gives the low bound of the magnetization, while Frank's and Mannari's theories using Fermi statistics give the upper bound of it in the case of ferromagnetic interaction. (auth)

20813 BOMBARDMENT OF COPPER AND GERMANIUM SURFACES BY LOW ENERGY ARGON IONS. A. Van Itterbeek, G. Forrez, J. Witters, R. Van Audekercke, and W. Van Itterbeek (Technische Fysica, Louvain, Belg.). Appl. Sci. Res., Sect. B, 11: 286-92(1964).

Polycrystalline copper surfaces and germanium single crystals were bombarded with 1000-ev argon ions. The argon ions were produced by means of an electron current between a heated tungsten cathode and an anode at a potential of +300 v. The pressure of the argon gas was maintained at 10^{-3} mm Hg. The whole system could be evacuated to 10^{-6} mm Hg with an oil diffusion pump. Before and after the bombardment, replicas of the surface were made for investigation with the electron-microscope. After sputtering, dislocation steps appear at the surfaces, and the grain dimensions increase with increasing sputtering time. For the germanium single crystals, the dislocations seem to lie all in the same crystallographic direction. (auth)

20814 LASER BEAM-INDUCED ELECTRON AND ION EMISSION FROM METAL FOILS. J. K. Cobb and J. J. Muray (Stanford Univ., Calif.). Brit. J. Appl. Phys., 16: 271-3(Feb. 1965).

An experiment was conducted to determine the mechanism involved in electron and positive ion emission from metal foils using a pulsed ruby laser with an output energy of about 0.2 joule. The metals studied were Al, Ag, Au, Be, Cu and stainless steel. (auth)

20815 SIMULTANEOUS STIMULATED EMISSION IN HELIUM-4 AND HELIUM-3. Roger Der Agobian, Jean-Louis Otto, Roland Cagnard, and Rolland Echard (Laboratoire Central de Telecommunications, Paris). Compt. Rend., 260: 473-6(Jan. 11, 1965). (In French)

The 3^3D-4^3P transition was observed in both ^4He and ^3He. The intensity variations of these two transitions were determined. In a mixture of the two isotopes, the simultaneous oscillation of the two transitions could be obtained in the very narrow composition limits $0.45 < p(^3He)/(p(^3He) + p(^4He)) \leq 0.6$. The ratio of the intensity of the transitions could be changed by varying the composition of the mixture. The isotopic displacement was measured as $\Delta\nu = -288 \pm 3$ mK. (J.S.R.)

20816 EFFECTS OF MULTIPLE STIMULATION IN THE INTERACTION OF SEVERAL WAVES OF BOSONS. Guy Mayer (Compagnie Generale de T.S.F., Orsay, France). Compt. Rend., 260: 477-80(Jan. 11, 1965). (In French)

Elementary interactions between light and matter, where the number of bosons produced can be higher by several units than the number of incident bosons, are considered. Such interactions, often too weak to be detected experimentally in normal conditions can produce considerable phenomena whose excitation is intense enough to cause stimulation effects. The case of a photon producing, by interaction with matter, several identical phonons and one photon is discussed particularly because of its possible incidences on stimulated Raman effects and on the development of stimulated systems with increasing gain. (tr-auth)

20817 OBSERVATION OF A NEW OPTICAL ABSORPTION BAND IN IRRADIATED LITHIUM FLUORIDE CRYSTALS. Yves Farge, Marianne Lambert, Bernard Letellier, and Andre Guinier (Faculte des Sciences, Orsay, France). Compt. Rend., 260: 485-8(Jan. 11, 1965). (In French)

Lithium fluoride crystals irradiated with high energy electrons (1 to 400 Mev) or x rays at high doses show, after annealing, a specific absorption at 5000 A. The color centers responsible for this band seem to be complex defects due to the displacement of the halogen ions of the lattice. (tr-auth)

20818 NATURE OF DIPOLES IN NONSTOICHIOMETRIC PRASEODYMIUM OXIDES. Guiu Grosvald (Faculte des Sciences, Rennes, France). Compt. Rend., 260: 489-91 (Jan. 11, 1965). (In French)

During an attempt at the interpretation of the relaxation phenomena observed in praseodymium oxides, two hypotheses were proposed: the effect of the paramagnetism of

Pr^{4+} and strong electron-phonon interactions. It is shown as the result of some experiments that only the last interpretation should be considered. (tr-auth)

20819 SPUTTERING OF SOLIDS BY ION BOMBARDMENT. Rainer Behrisch (Institut fur Plasmaphysik GmbH, Garching, Ger.). Ergeb. Exakt. Naturw., 35: 295-443 (1964). (In German)

A review is given on the present state of the studies on the sputtering of solids. After a brief explanation of the assumptions for reproducible measurements, the results obtained by various investigators on sputtering measurements on polycrystalline materials and single crystals were discussed. It was shown that measurements on single crystals are still very incomplete. Sputtering measurements on polycrystals always have an uncertainty connected to the texture of the materials. The theory of radiation damage in solids was considered at length. The application of the representations developed for the calculation of the sputtering rates has lead to no satisfactory results. The sputtering phenomena appear to be one of the most important methods of investigation for obtaining data on the radiation damage in solids. (tr-auth)

20820 ON THE ANNIHILATION OF POSITRONS IN ALKALI-HALIDE CRYSTALS. V. I. Gol'danskii and E. P. Propkop'ev (Inst. of Chemical Physics, Moscow). Fiz. Tverd. Tela, 6: 3301-6(1964).

The annihilation of positrons from polaron states in alkali halide crystals was considered within the framework of the Pekar polaron theory. The lifetimes and momentum distributions of the centers of gravity of the annihilating pairs in the case of positron annihilation by polaron states in an "ideal" alkali halide crystal were calculated, and the additional positron annihilation possible in crystals with defects is listed. The contributions made to the short- and long-lived components of the annihilation spectrum (with lifetimes ≈ 2 and $\approx 5 \times 10^{-10}$ sec, respectively) were found to be affected by annihilation from the ground and excited polaron states, respectively. (CFSTI)

20821 ELECTRON CAPTURE BY PROTONS PASSING THROUGH HELIUM GAS. Thomas A. Green (Sandia Lab., Albuquerque, N. Mex.), H. E. Stanley, and You-Chien Chiang. Helv. Phys. Acta, 38: 109-24(1965).

The impact-parameter method, in a two-state moving-atom approximation, is applied to the reaction $H^+ + He \rightarrow H(1s) + He^+(1s)$. The effects of distortion and back coupling are taken into account and are shown to improve the predicted value of the total cross section considerably for energies near that for which the cross section is a maximum. The theory is shown to be inadequate at both high and low energies. (auth)

20822 ASYMMETRY OF SCATTERING INDICATRICES OF TRANSPARENT PARTICLES. T. P. Toropova. Izv. Akad. Nauk Kaz. SSR, Ser. Fiz.-Mat. Nauk, No. 3, 111-16 (1964).

Although theory provides an exact solution to the problem of scattering of light by Mie particles, the results of this theory can not be used fully because the calculations were made and tabulated only for certain limited intervals of the various parameters involved. The asymmetry coefficients of Mie particles were calculated for two values of the refractive index, 1.50 and 1.25. The former value is chosen close to the refractive index of aerosol particles in the atmosphere, which are usually water droplets containing salt. The latter value was chosen to ascertain the effect of the variation of the refractive index on the form of the scattering indicatrix. The results confirm the fact that the asymmetry coefficient is an oscillating function of the ratio of the particle size to the wavelength. It is also found that a change in the refractive index strongly affects the results, except when the particles are quite small, and in some cases the asymmetry coefficient may more than double following a change of 25% in the refractive index. (ATD)

20823 ATOMIC-BEAM SCATTERING STUDIES ON THE Li–Hg SYSTEM: QUANTUM EFFECTS AND VELOCITY DEPENDENCE OF THE CROSS SECTIONS. Peter J. Groblicki and Richard B. Bernstein (Univ. of Michigan, Ann Arbor and Univ. of Wisconsin, Madison). J. Chem. Phys., 42: 2295-2304(Apr. 1, 1965).

Measurements of the velocity dependence of the angular intensity distribution of ^6Li and ^7Li beams scattered by a crossed Hg beam are reported. The Li beams were velocity selected, the Hg beam Maxwellian. Angular intensity distributions were measured at various relative velocities (v_r) from 700 to 1200 m/sec and relative total cross sections (q) from $v_r = 300$ to 1350 m/sec. The differential cross sections showed expected quantum interferences. Scattering patterns for $^6Li-$ and ^7Li-Hg were found to be identical at the same de Broglie wavelength. The over-all angular dependence of the scattering at low angles followed the θ^{-5} relationship characteristic of an r^{-6} long-range potential. Extremes in the total cross sections $q(v_r)$ were also observed. The experimental data were analyzed in terms of a Lennard-Jones (12, 6) potential, but it was not possible to determine a unique set of potential parameters. Comparison of observed and calculated results yielded three nearly equivalent sets of σ, ϵ lying within the ranges $2.5 \leq \sigma \leq 3.5$ Å and $480 \leq \epsilon/k \leq 1000$°K. (auth)

20824 INCOHERENT X-RAY SCATTERING FACTORS. R. F. Pohler and H. P. Hanson (Univ. of Texas, Austin). J. Chem. Phys., 42: 2347-52(Apr. 1, 1965).

Incoherent scattering factors for C, O, Cl, Al, and I were calculated from Hartree–Fock–Slater wavefunctions. Comparison of the values of C and Al with Hartree–Fock values showed good agreement. Results for I, which represent the heaviest element for which calculations of this type were performed, were compared with statistical Thomas-Fermi values. (auth)

20825 CLASSICAL AND QUANTAL SCATTERING. I. THE CLASSICAL ACTION. Felix T. Smith (Stanford Research Inst., Menlo Park, Calif.). J. Chem. Phys., 42: 2419-26(Apr. 1, 1965).

Classical scattering is based on the action $A = S - S_0$, where S is the action over the actual trajectory and S_0 is over the equivalent without interaction. For two-body spherical potential scattering $A = \Delta(L, E) - L\Theta$, where Θ is the deflection angle and Δ is the classical phase, the classical limit of $2\hbar\delta_l(E)$. A rapidly convergent integral expression is given for $\Delta(L, E)$. From this a convergent expansion in $1/E$ valid for fixed $L \neq 0$ and an equivalent form in $1/L$ valid for fixed E were derived. The lowest term in $1/L$ agreed with Massey and Mohr, and higher terms were evaluated. (auth)

20826 PRELIMINARY ELECTRON-DIFFRACTION STUDY OF H_2 AT SMALL SCATTERING ANGLES. R. A. Bonham (Indiana Univ., Bloomington and Tokyo Univ.) and T. Iijima. J. Chem. Phys., 42: 2612-14(Apr. 1, 1965).

Evidence on the molecular charge distribution in H_2 obtained by a diffraction method is presented. Sector electron diffraction photographs of H_2 and He were obtained. (M.C.G.)

20827 INFLUENCE OF THE CHARACTERISTICS OF A PLASMA INITIATOR ON THE FORMATION OF THIN LAYERS OF COPPER OXIDES IN REACTIVE CATHODIC PULVERIZATION. G. Perny and B. Laville-Saint-Martin (Laboratoire de Physico-Chimie des Couches Minces, Mulhouse, France). J. Phys. (Paris), 25: 993-8(Dec. 1964). (In French)

Thin layers of copper oxides are prepared by condensation on fused quartz in a weakly ionized argon-oxygen plasma, of products initiated by cathode sputtering. The influence of discharge potential, and characteristics of the plasma, upon the nature of the layers are studied. (auth)

20828 SPIN SCATTERING. SYNTHESIS OF BIBLIOGRAPHIC REVIEWS. Jacques Pescia (Faculte des Sciences, Orsay, France). J. Phys. (Paris), 25: 1041-4(Dec. 1964). (In French)

A synthesis is given of reviews on the question of spin scattering, and the results are compared with experiment. (auth)

20829 OPACITY OF HIGHLY IONIZED AIR. B. Kivel and H. Mayer (Los Alamos Scientific Lab., N. Mex.). J. Quant. Spectry. Radiative Transfer, 5: 13-38(Jan.-Feb. 1965).

The opacity and thermodynamic properties of air at temperatures above 10 ev and densities below normal were calculated in accordance with the prescriptions given by Mayer. Corresponding to given densities and temperatures, self-consistent distributions of electrons in bound states and their eigenenergies are determined. With this information the thermodynamic properties of air and the frequency-dependent absorption coefficients are calculated. The Rosseland opacity—a weighted average of the absorption coefficient—is calculated, showing the effects of argon and the ionic lines. (auth)

20830 THE PHOTOIONIZATION CONTRIBUTION TO THE RADIATION ABSORPTION COEFFICIENT OF AIR. R. R. Johnston, B. H. Armstrong, and O. R. Platas (Lockheed Research Labs., Palo Alto, Calif.). J. Quant. Spectry. Radiative Transfer, 5: 49-53(Jan.-Feb. 1965).

The photoelectric absorption coefficients of N, O, and air are given for temperatures of 1 to 20 ev, densities $\sim 10^{-5}$ times normal to normal, and photon energies from 1 ev to 1 kev. The photoionization cross section near threshold was evaluated by the method of Burgess and Seaton and continued into a high-energy acceleration Born approximation utilizing Hartree-Fock-Slater bound state wave functions. The edge-shift due to electron collision broadening was included. The absorption coefficients obtained are compared with results of previous calculations. (auth)

20831 THE ATOMIC LINE CONTRIBUTION TO THE RADIATION ABSORPTION COEFFICIENT OF AIR. B. H. Armstrong, R. R. Johnston, and P. S. Kelly (Lockheed Research Labs., Palo Alto, Calif.). J. Quant. Spectry. Radiative Transfer, 5: 55-65(Jan.-Feb. 1965).

An IBM 7094 computer program was developed to compute the atomic line contribution to the spectral absorption coefficient of air. The input to this program consists of a list of the possible atomic states present in the gas, and for each of these, its spectroscopic description, energy, and occupation number or concentration (obtained from a previous calculation). The program compares all pairs of levels, applies selection rules as appropriate and thereby picks out the allowed transitions. The contribution to the absorption coefficient due to each transition is then computed, using Hartree–Fock–Slater radial dipole integrals and Baranger–Stewart electron collision broadening in a Voigt profile. A progressive lumping of the atomic levels is employed. For principal quantum numbers $n = 2$ and 3, most multiplets are treated distinctly. For $n = 4$ to 8 and $l \leq 3$ transition arrays are computed, and for larger l and $n \geq 9$ hydrogenic approximations are made. Line series are terminated by a temperature-density dependent cutoff consistent with our photoelectric calculation. Representative results are presented and comparisons are made with other calculations. A discussion is presented of upper bounds on Rosseland and Planck mean absorption coefficients, including the derivation of a new bound for the Planck mean. (auth)

20832 SPECTRAL ABSORPTION IN HEATED AIR. D. R. Churchill and R. E. Meyerott (Lockheed Missiles and Space Co., Palo Alto, Calif.). J. Quant. Spectry. Radiative Transfer, 5: 69-86(Jan.-Feb. 1965).

Several molecular band systems, which contribute appreciably to the absorption coefficient of heated air, were theoretically reconstructed using a series of digital computer programs. Experimental spectroscopic results were used in these programs whenever such results were available. The band systems are generated on a line-by-line basis up to high rotational quantum numbers, and then stored on magnetic tapes. The tapes are then used by other programs to compute absorption coefficients. Previous results are briefly summarized, and two recently treated band systems are discussed: the Birge–Hopfield No. 1 system of N_2 and the vibration-rotation bands of NO. (auth)

20833 THE CALCULATION OF BOUND-FREE TRANSITION PROBABILITIES AND THEIR APPLICATIONS TO THE CONTINUUM SPECTRA OF THE RARE GASES. Dieter Schlueter (Universitat, Kiel). J. Quant. Spectry. Radiative Transfer, 5: 87-9(Jan.-Feb. 1965).

The quantum defect methods of Bates and Damgaard and of Burgess and Seaton were used to compute the bound-free absorption coefficients of neon, argon, krypton, and xenon in the spectral range from 3600 to 10,000 Å. (auth)

20834 TABLES OF HYDROGENIC PHOTOIONIZATION CROSS-SECTIONS AND RECOMBINATION COEFFICIENTS. A. Burgess (University Coll., London). Mem. Roy. Astron. Soc., 60: Pt. 1, 1-8(1964).

The cross sections for photoionization of a hydrogenic atom or ion initially in the state nl are tabulated to 5 significant figures for n = I(I)20, l = 0(I)n – I and a wide range of energies of the ejected electron. The hydrogenic radiative recombination coefficients for a Maxwellian distribution of electron velocities are tabulated to 4 significant figures for n = I(I)20, l = 0(I)n – I and electron temperatures from T = 0 to ∞. (auth)

20835 AN ANALYTICAL METHOD FOR THE APPROXIMATE DETERMINATION OF THE EIGENFUNCTIONS AND ENERGIES OF ELECTRONS IN ATOMS. T. Tietz (Univ. of Lodz, Poland). Opt. Spectry. (USSR) (English Transl.), 17: 439-40(Dec. 1964). Translated from Optika i Spektroskopiya, 17: 805-8(Dec. 1964).

A solution is given to the single electron Schroedinger equation using the method of Rasetti with precise numerical values for the free neutral atom. Precise values for the Thomas-Fermi function and its derivatives are tabulated and formulas are given, which allow the eigenfunctions and energies of electrons in the lowest energy states s, p, d, and f to be calculated analytically. The Roentgen terms obtained by this method were found to be in good agreement both with terms found experimentally and with terms calculated by the Hartree method. (auth)

20836 SEMIEMPIRICAL METHOD FOR DETERMINING THE ELECTROSTATIC POTENTIAL OF THE MOLECULAR ELECTRON SHELL AT THE ATOMIC NUCLEI. II. CALCULATION OF POTENTIALS AT THE NUCLEI IN SOME DIATOMIC MOLECULES. T. K. Rebane. Opt. Spectry. (USSR) (English Transl.), 17: 450-3(Dec. 1964). Translated from Optika i Spektroskopiya, 17: 825-31(Dec. 1964).

Calculation of the electrostatic potential of the electron shell at the nuclei was carried out for a number of diatomic molecules using a method based on interpolation of the experimental energies of isoelectronic molecules and on the application of the generalized Gelman-Feynman theorem. (auth)

20837 DEDUCTION OF THE INTERATOMIC POTENTIAL IN ALUMINIUM FROM ION RANGE MEASUREMENTS. D. P. Corkhill and G. Carter (Univ. of Liverpool). Phil. Mag. (8), 11: 131-7(Jan. 1965).

The mean range of energetic atoms moving in a target composed of similar atoms in a randomized array may be deduced in terms of collision mean free path, which itself depends upon the form of the potential energy-separation law for the atoms. Earlier calculations of the relation between mean range and mean free path are extended to allow deduction of the interatomic potential between ^{24}Na and ^{27}Al atoms from available experimental range, energy data. An interatomic potential of the form $V(r) = k/r^1$ is found to give a good representation for this case for interatomic separations between 0.17 and 0.36 Å. (auth)

20838 AN INVESTIGATION OF THERMAL SPIKES BY STUDYING THE HIGH ENERGY SPUTTERING OF METALS AT ELEVATED TEMPERATURES. R. S. Nelson (Atomic Energy Research Establishment, Harwell, Berks, Eng.). Phil. Mag. (8), 11: 291-302(Feb. 1965). (AERE-R-4692)

The sputtering ratio of Au, Ag, Cu, Zn, Bi, and Ge polycrystals bombarded with 45 kev Xe^+, Ar^+, and Ne^+ ions was studied as a function of temperature. In every case the

curve of sputtering ratio as a function of temperature was initially constant, but at temperatures approaching the melting-point the curve exhibited an approximately exponential rise. The increase is explained in terms of evaporation from thermal spikes created by the individual ions, and analysis of the results has provided information as to the spikes' size, lifetime, and temperature. (auth)

20839 SPIN RESONANCE LINE SHAPES. A. M. Stoneham (Atomic Energy Research Establishment, Harwell, Berks, Eng.). Phys. Letters, 14: 297-8(Feb. 15, 1965).

The effect of microwave electromagnetic and acoustic fields used as probes for observing spin resonance is investigated. The hamiltonian for the system of spins and for the probe interaction is written, and it is shown that the line shape does not depend on the characteristics of the probe for $S' = \frac{1}{2}$. (L.B.S.)

20840 SIGNIFICANCE OF THE MEASUREMENT ON THE ELECTRIC DIPOLE MOMENT OF THE CESIUM ATOM. M. Sachs (Boston Univ.). Phys. Letters, 14: 302-4(Feb. 15, 1965).

An ambiguity in the interpretation of an experiment on the measurement of the electric dipole moment of the Cs atom is pointed out, and possible experimental tests that might lead to its resolution are suggested. The approach of Salpeter on the effect of the P and T violating covariant term on the energy level structure is discussed; and the outline of a calculation concerning the linear electric field effect in hydrogenic or complex atoms and its implications are given. (L.B.S.)

20841 RESPONSE OF AN ELECTROSTATIC PROBE TO AN ELECTROMAGNETICALLY PRODUCED AIR SHOCK. H. Craig Miller (General Electric Research Lab., Schenectady, N. Y.). Phys. Letters, 14: 307(Feb. 15, 1965).

Electrostatic probe measurements on the total ionization distance behind electromagnetically produced shock waves in air are compared with the microwave and magnetic probe measurements of Lin et al. and the theoretical predictions of Lin and Teare. The results were found to be in agreement. (L.B.S.)

20842 ELASTIC SCATTERING OF LOW-ENERGY ELECTRONS BY ALKALI ATOMS. E. Karule (Inst. of Physics, Riga). Phys. Letters, 15: 137-9(Mar. 15, 1965).

The total cross sections for elastic scattering of electrons by atomic Li, Na, K, and Cs were calculated below the threshold for excitation to 1.8, 2.0, 1.6, and 1.4 ev, respectively, using the close-coupling exchange approximation for the ground and first excited atomic states. Numerical Hartree-Fock wave functions were used for Li, and semi-empirical valence electron wave functions were used for Na, K, and Cs. Phase shifts were calculated in the static and close-coupling approximations and phase shifts versus energy curves are presented. The results are compared with experimental data. (L.B.S.)

20843 QUANTUM THEORY OF LASER COHERENCE AND NOISE. Victor Korenman (Harvard Univ., Cambridge, Mass.). Phys. Rev. Letters, 14: 293-5(Mar. 1, 1965).

Results are reported on a calculation of laser properties, giving insight into the relation between models assuming a pure sinusoidal output and those based on a signal with a finite frequency width. A fully quantum mechanical description of the laser in terms of correlation functions of the quantized radiation and matter fields is used. A gaseous laser, in which the cavity is idealized by boundary conditions, and a uniformly distributed quantum mechanical loss mechanism are considered. The pump is also treated quantum mechanically. (M.J.T.)

20844 EXPERIMENTAL EVIDENCE FOR DOUBLE ELECTRON EMISSION IN AN AUGER PROCESS. Thomas A. Carlson and Manfred O. Krause (Oak Ridge National Lab., Tenn.). Phys. Rev. Letters, 14: 390-2(Mar. 15, 1965). (ORNL-P-957)

Experimental results are presented on the charge spectrum of neon formed from ionization by x rays between 167 and 913 ev, along with results from previous experiments at energies to 1600 ev. The relative amount of double electron emission accompanying the KLL Auger transition was determined from the abundance of Ne^{3+} relative to Ne^{2+} that resulted from K vacancies formed with x ray energies below 913 ev. The possibility of electron shake-off was examined in search for the reason for the double ionization in the Auger process; the greater part of the emission was attributed to the phenomena of electron correlation. (L.B.S.)

20845 SPIN DENSITY OF s ELECTRONS IN IRON. T. A. Kaplan (Massachusetts Inst. of Tech., Lexington). Phys. Rev. Letters, 14: 499-501(Mar. 29, 1965).

A previous experiment by Overhauser and Stearns (Phys. Rev. Letters 13: 316(1964)) on the Mössbauer effect in Fe–Al alloys in which it was concluded that there is a large qualitative difference between the true 4s-electron susceptibility and the free-electron susceptibility due to interactions between 4s electrons is discussed. An argument is presented that their conclusion is premature since their neglect of the k dependence of the periodic part of the 4s Bloch functions is probably serious. A considerable sensitivity of the results to such k dependence is indicated, and it is suggested that a detailed theory neglecting s-s interactions might give approximate agreement with experiment. (C.E.S.)

20846 THREE DISCRETE Q VALUES IN Ar^+–Ar COLLISIONS. Quentin C. Kessel, Arnold Russek, and Edgar Everhart (Univ. of Connecticut, Storrs). Phys. Rev. Letters, 14: 484-6(Mar. 29, 1965).

Coincidence measurements of charge correlation in Ar^+–Ar collisions are described. The results suggest that there are only two excited intermediate levels, A ~ 50 ev and B ~ 310 ev, which can appear in each atom after collision, and that three Q values correspond to 2A, A + B, and 2B. (L.B.S.)

20847 MULTIPHOTON IONIZATION AND THE BREAKDOWN OF NOBLE GASES. Richard G. Tomlinson (Ohio State Univ., Columbus). Phys. Rev. Letters, 14: 489-90 (Mar. 29, 1965).

Experimental evidence is presented, which indicates that the multiphoton process cannot account for the observed temporal dependence, pressure dependence, or absolute or relative intensities of breakdown in Kr, Ar, Ne, and He gases, although multiphoton ionization may trigger the breakdown process. Breakdown thresholds were determined by successively attenuating laser pulses until no visible discharge was produced, and the results were compared with theoretical predictions. (L.B.S.)

20848 MULTICHANNEL RESONANCES IN THE FORWARD SCATTERING OF ELECTRONS BY HELIUM. G. E. Chamberlain (National Bureau of Standards, Washington, D. C.). Phys. Rev. Letters, 14: 581-2(Apr. 12, 1965).

The forward, inelastic scattering of electrons by helium was investigated. At incident electron energies between 22.4 and 22.8 ev, resonance structure was observed in all four of the open channels, corresponding to excitation of the finial-state, neutral helium levels $(1s2s)^3S$,$(1s2s)^1S$, $(1s2p)^3P$, and $(1s2p)^1P$. (D.C.W.)

20849 SPECTROSCOPIC PROPERTIES OF ACTIVATED LASER CRYSTALS. PART III. P. Goerlich, H. Karras, G. Koetitz, and R. Lehmann. Phys. Status Solidi, 8: 385-429 (1965).

A review is given of spectroscopic literature in the field of laser crystals. Spectroscopic data on absorption, spontaneous fluorescence, and stimulated emission are presented for the actinide group, transition metals, and semiconductors. Instrumental set-ups are discussed, including laser arrangements, developments on pumping light sources, modulation and determination of input and output power, and testing instruments for absorption and fluo-

rescence. Literature on optical and thermal properties and on crystal growth is surveyed. 155 references. (M.J.T.)

20850 IONIZATION CROSS SECTIONS FOR ELECTRONS (0.6-20 kev) IN NOBLE AND DIATOMIC GASES. B. L. Schram, F. J. De Heer, M. J. Van der Wiel, and J. Kistemaker (Stichting Voor Fundamenteel Onderzoek der Materie, Amsterdam). Physica, 31: 94-112(Jan. 1965).

Absolute cross sections for the ionization of Ar, He, Kr, Ne, Xe, D_2, H_2, N_2, and O_2 by high-energy electrons (0.6 to 20 kev) were measured. The results were compared with other measurements and with theoretical predictions. (D.C.W.)

20851 CONTINUUM CORRELATION IN C^-. Valerie P. Myerscough (Royal Holloway Coll., Surrey, Eng.). Proc. Phys. Soc. (London), 85: 33-40(Jan. 1965).

The effect of correlation between open shell and continuum electrons on the photodetachment cross section of C^- is examined in a modified central field exchange approximation. The results show improved agreement between the dipole length and dipole velocity formulations, but continue to display an incorrect energy behavior at low energies. (auth)

20852 THE POLARIZABILITIES AND SHIELDING FACTORS OF THE BERYLLIUM SEQUENCE. A. Dalgarno and H. A. J. McIntyre (Queen's Univ., Belfast), Proc. Phys. Soc. (London), 85: 47-50(Jan. 1965).

The fully coupled Hartree–Fock approximation is used to calculate the dipole and quadrupole polarizabilities and shielding factors of Be, B^+ and C^{2+}. (auth)

20853 THE 1s-2p EXCITATION OF HYDROGEN ATOMS. B. L. Moiseiwitsch and R. Perrin (Queen's Univ., Belfast). Proc. Phys. Soc. (London), 85: 51-5(Jan. 1965).

The second Born approximation is used to calculate the cross sections for the excitation of the 2p states of atomic hydrogen by proton, electron and positron impact, allowance being made for the effect of virtual transitions involving the 1s, 2s, and $2p_{0,\pm1}$ intermediate states. In the case of proton impact, provided coupling to the 2s intermediate state is excluded from the second Born approximation calculations, good agreement is obtained at high energies with the cross section given by the exact numerical integration of the coupled differential equations connecting the 1s and 2p states. Satisfactory accord is also obtained with the results of close-coupling calculations in which full allowance is made for the 1s, 2s and $2p_{0,\pm1}$ states, but exchange is neglected, for the scattering of slow electrons. On the other hand, it is found that the agreement with the corss section resulting from analogous calculations for positron impact is not good. (auth)

20854 ELECTRON EXCHANGE IN IMPACT IONIZATION OF ATOMIC HYDROGEN. S. S. Prasad (Queen's Univ., Belfast). Proc. Phys. Soc. (London), 85: 57-9 (Jan. 1965).

Methods hitherto used for allowance for exchange in the treatment of electron impact ionization of atomic hydrogen are discussed. A simple method based upon Ochkur's simplification of the Born–Oppenheimer approximation is also studied and is found to give very good results. (auth)

20855 THE IMPACT PARAMETER METHOD FOR ELECTRON EXCITATION OF ELECTRIC QUADRUPOLE TRANSITIONS. A. D. Stauffer and M. R. C. McDowell (Royal Holloway Coll., Surrey, Eng). Proc. Phys. Soc. (London), 85: 61-9(Jan. 1965).

The semi-classical impact parameter method of Seaton is extended to electric quadrupole transitions. It is justified for $\Delta l = 2$ but not $\Delta l = 0$ transitions, though it is more sensitive to choice of cut-off than for electric dipole transitions. Results are presented for several transitions in hydrogen and helium. Where they can be compared with experiment ($He\ 1^1S \rightarrow n^1D$) they are in reasonable accord, except close to threshold. (auth)

20856 ELECTRON IMPACT SPECTROSCOPY. III. CALCULATED CROSS SECTIONS FOR INELASTIC SCATTERING FROM BENZENE. F. H. Read and G. L. Whiterod (Univ. of Manchester, Eng.). Proc. Phys. Soc. (London), 85: 71-7(Jan. 1965).

The Born approximation is used to obtain differential and total cross sections for inelastic electron scattering from benzene. The three lowest excited singlet states are treated (i.e. those of symmetry $^1B_{1u}$, $^1B_{2u}$, and $^1E_{1u}$). Simple π-electron antisymmetric molecular orbitals are used as the electronic wave functions, and the cross sections are averaged and summed over rotational and vibrational states. The effects of vibronic interactions on the cross sections are included. (auth)

20857 THE IDENTIFICATION OF EMISSION LINES FROM A VAN DE GRAAFF BEAM. L. Kay (Univ. of Manchester, Eng.). Proc. Phys. Soc. (London), 85: 163-6 (Jan. 1965).

Nitrogen ions of velocity 1.6×10^8 to 6.0×10^8 cm sec^{-1} passed through a carbon foil of thickness about 500 Å which served both to increase the degree of ionization and to leave the ions in excited states. It is shown that by measuring the relative intensities of the de-excitation emission lines as a function of ion velocity the degree of ionization of the emitting ions can be determined unambiguously, in confirmation of the suggestion made by Kay in 1963. Measurements of line intensities as a function of distance from the existing foil yield directly the mean lives of excited states in singly and doubly ionized nitrogen. The techniques should be capable of extension to very high degrees of ionization. (auth)

20858 ON THE ELASTIC SCATTERING OF ELECTRONS BY CARBON ATOMS. M. J. Seaton (University Coll., London). Proc. Phys. Soc. (London), 85: 197-9 (Jan. 1965).

A simple expression is obtained for the phase shift produced by an atom having a quadrupole moment, assuming $\{l(l+1)\}^{\frac{1}{2}}/k$ to be large compared with the mean atomic radius. This gives results which are in good agreement with Born phases for scattering by H 2p, but which are not in agreement with phases calculated by Myerscough and McDowell for scattering by carbon. (auth)

20859 THE REFRACTIVE INDEX OF HELIUM. Y. M. Chan and A. Dalgarno (Queen's Univ., Belfast). Proc. Phys. Soc. (London), 85: 227-30(Feb. 1965).

The refractive index of helium for wavelengths longer than 600 Å is calculated by a variational method from the ground state representation of Hart and Herzberg. The results agree very well with the observations which refer to wavelengths between 2700 Å and 9000 Å. (auth)

20860 RECOMBINATION OF POSITIVE IONS AND ELECTRONS IN A DENSE NEUTRAL GAS. D. R. Bates and S. P. Khare (Queen's Univ., Belfast). Proc. Phys. Soc. (London), 85: 231-43(Feb. 1965).

A theory is presented of the recombination of electrons and positive ions in the presence of neutral atoms which act as third bodies, explicit account being taken of the effect of radiative transitions. Comparison is made with the theories of Thomson and of Pitaevskii. Detailed calculations are carried out on recombination in helium gas. It is found that the rate coefficient α is very great when the temperature θ is low and the number density N(He) is high: for example, that α for He^+ is 5×10^{-8} cm^3 sec^{-1} and for Na^+ is 2×10^{-6} cm^3 sec^{-1} when θ is 250°K and N(He) is 3×10^{19} cm^{-3}. (auth)

20861 PHOTOELECTRIC EMISSION IN LOW PRESSURE HELIUM DISCHARGES. F. Llewellyn Jones, C. G. Morgan, and D. Kenneth Davies (University Coll. of Swansea, Wales, U. K.). Proc. Phys. Soc. (London), 85: 351-4 (Feb. 1965).

Values of the photoelectric secondary coefficient δ'/α due to the incidence of delayed nonresonance photons, having energies of approximately 20 ev on a silver cathode in a low pressure ($10 < p_0 < 39$ mm Hg) discharge in helium in the range $9 < E/p_0 < 22$ v cm^{-1} mm Hg^{-1} of electric field E to gas pressure p_0, were obtained from measurements of the ionization growth times. Estimates of absolute photoelectric yield were deduced from the values of δ'/α and

are found to lie between 0.2 and 0.3 electrons per quantum. (auth)

20862 EXCITATION IN RARE GAS ION-ATOM COLLISIONS IN THE ENERGY RANGE 100-400 kev. E. W. Thomas and H. B. Gilbody (University Coll., London). Proc. Phys. Soc. (London), 85: 363-73(Feb. 1965).

Absolute cross sections for the emission of some of the more intense lines induced in various rare gas ion–atom impacts were determined in the spectral range 3900–6000 Å by the analytis of radiation (assumed isotropic) emitted under single-collision conditions. In most cases it is found that the principal emission lines are associated with the singly ionized states of the incident and target particles. Probable excitation mechanisms are discussed with reference to relevant charge-rearrangement collision cross sections. (auth)

20863 ERROR ESTIMATES FOR ATOMIC AND MOLECULAR QUANTITIES. J. C. Y. Chen (Brookhaven National Lab., Upton, N. Y.) and A. Dalgarno. Proc. Phys. Soc. (London), 85: 399-402(Mar. 1965). (BNL-8550)

A procedure for improving the calculation of matrix elements when using approximate wave functions is described, and application is made to the expectation values of several operatora for the ground states of the helium isoelectronic sequence. (auth)

20864 THE IONIZATION OF NEUTRAL HELIUM BY ELECTRON IMPACT. I. H. Sloan (University Coll., London). Proc. Phys. Soc. (London), 85: 435-42(Mar. 1965).

Cross sections for the ionization of neutral helium by electron impact are calculated in two versions of the Born approximation and in the Born exchange approximation, using accurate atomic wave functions. The effect of exchange in the Born exchange approximation is to remove more than half of the discrepancy between the conventional Born (Born (a)) cross sections and the experimental values of Smith. The Born (b) approximation, which is consistent with the Pauli principle, gives results intermediate between the other two. The calculated energy and velocity distributions conflict with previous Born (a) determinations. (auth)

20865 POLARIZATION BY MERCURY OF 100- TO 2000-ev ELECTRONS. P. J. Bunyan and J. L. Schonfelder (Univ. of Melbourne). Proc. Phys. Soc. (London), 85: 455-62(Mar. 1965).

Accurate numerical calculations are presented for the energy and angular dependence of the cross sections and polarizations of electrons scattered by mercury in the energy region 100 to 2000 ev. The results are compared with experiment and found to be in good agreement. (auth)

20866 THE CALCULATION OF EXCHANGE SCATTERING AMPLITUDES. M. R. H. Rudge (Queen's Univ., Belfast). Proc. Phys. Soc. (London), 85: 607-8(Mar. 1965).

It is shown that the approximation of Ochkur is in a certain sense incorrect and an appropriate modification is indicated. (auth)

20867 TEMPERATURE DIFFUSE SCATTERING OF ELECTRONS IN POLYCRYSTALLINE ALUMINUM FOILS. M. Horstmann (Universitat, Hamburg). Solid State Commun., 2: 339-43(Nov. 1964).

The diffuse elastic scattering of 51-kev electrons at a polycrystalline aluminum foil was studied in the temperature range 150-800°K. The integrated intensity as well as the angular distribution of the temperature dependent part of the background intensity is compared with theoretical calculations of the temperature diffuse scattering. The temperature independent part of the background intensity is mainly due to elastic scattering of electrons in the amorphous oxide layer of the aluminum foil. (auth)

20868 CALCULATIONS ON THE WAVELENGTH DEPENDENCE OF THE INTENSITY OF BACK-REFLECTED ELECTRONS FROM NICKEL (111). G. Gafner (Council for Scientific and Industrial Research. Pretoria). Surface Sci., 2: 534-43(1964).

Calculations were made on the intensity of back-reflected radiation from the (111) face of nickel using the kinematic theory. The absorption factor was chosen so as to induce the same peak to background ratio as found in published experimental results. The effects of inter-layer spacing changes were studied and found to be absent from the experimental results. The changes in peak positions brought about by a phase change in the incident beam as it passes through a layer are shown to be very similar to the shifts caused by the inner potential. The conservation of elastically scattered energy, shown to be a possibility by the experimental results, was introduced into the calculations and, notwithstanding an improvement in fit, this was still not good enough to establish the validity of the kinematic theory even in the region of higher (>200 ev) electron energies. (auth)

20869 THE DEPENDENCE OF OVERHAUSER NUCLEAR POLARIZATION ON FREQUENCY AND MOLECULE MOTION IN LIQUIDS. K. D. Kramer. Thesis, Mainz, Universitat, 1963. 93p. $2.00(Gmelin, AED-DISS. 63-735). (In German)

Nuclear polarization of various organic solvents was measured. Dependence of nucleus-electron coupling constants on resonance frequency and correlation time are studied. Temperature dependence of dynamic proton polarization is given. The value of the coupling constant for fast motion and low frequencies indicates a pure magnetic dipole-dipole coupling between electron and proton spin. Results can be explained by translations of the interaction partners. Relaxation data of the solvents for various temperatures and frequencies indicate that it is as a first order approximation for relaxation time calculations sufficient to include volume effects of the diffusing molecules. (Gmelin Inst.)

20870 SHIFT AND BROADENING OF THE FIRST TWO ABSORPTION DOUBLETS OF CESIUM DUE TO THE PRESENCE OF HELIUM AND ARGON. Robert Ogden Garrett. Thesis, Eugene, Ore., Univ. of Oregon, 1964. 112p.

More convenient and more accurate measurement techniques both in the low and high pressure region were developed to obtain accurate quantitative information on the behavior of the absorption lines of cesium broadened by foreign gas atoms. The shift of Cs(1)/Ar has two linear regions, the first ending at r.d. = 2.2, the second beginning at r.d. = 25. The ratio of slopes in the two regions is about 1 : 2 for the $^2P_{\frac{3}{2}}$ component and more than 1 : 4 for the $^2P_{\frac{1}{2}}$ component. Measurements of the shift of Cs(2)/Ar revealed that this shift also has two linear regions. The first region ends at r.d = 0.9 and the second begins at r.d. = 2.5. The slope ratio for both components is about 1 : 4 in the two regions. Measurements of the Cs(1)/He shift revealed two very close linear regions followed by an upward curvature beginning at r.d. = 15. The $^2P_{\frac{3}{2}}$ component curve became linear again above r.d. = 42, the $^2P_{\frac{1}{2}}$ component not becoming linear until r.d. = 140. No unexpected behavior was observed for Cs(2)/He shifts, the two curves starting linearly and then curving upward. The fact that the half width versus r.d. curves for Cs(1)/Ar, Cs(2)/Ar, Cs(1)/He, and Cs(2)/He exhibit non-linear behavior at low pressures was demonstrated. The Cs(1)/Ar graph shows no fine structure effect up to r.d. = 8 with the two components diverging along "S" curves to r.d. = 25 above which they are linear. The Cs(2)/Ar curves follow even more pronounced "S" curves. These "S" curves cross one another at r.d. = 3.2 with the curves becoming linear above r.d. = 4.5 for the $^2P_{\frac{1}{2}}$ component. Half widths for Cs(1)/He show non-linear behavior only up to r.d. = 3. Half widths for Cs(2)He are non-linear throughout the region from r.d. = 0 to 12. The work also showed that half widths for Cs(1)/He and Cs(2)/He show a strong temperature dependence. To a first approximation the dependence was found to be directly proportional to the temperature. Argon-perturbed half widths showed little if any temperature dependence and none of the shift measurements showed any noticeable dependence. (A.G.W.)

20871 AN EXPERIMENTAL INVESTIGATION OF SURFACE IONIZATION. Miles Joel Dresser. Thesis, Ames, Iowa, Iowa State Univ. of Science and Tech., 1964, 156p.

The surface ionization efficiencies of Er, Gd, and Yb from the (112) face of a W single crystal are presented and compared to the Saha-Langmuir equation. The absolute ionization efficiencies were measured in ultrahigh vacuum environment (around 5×10^{-9} torr). The electronic work function of the surface was determined in an auxiliary experiment to be 4.85 ± 0.03 ev. When the surface is clean the degree of ionization, α, was found to follow the general form of the Saha-Langmuir equation, $\alpha = Ae^{-E/kT}$. The magnitudes of A and E, however, are not consistent with the values predicted theoretically. It is demonstrated that the Saha-Langmuir theory is inadequate for the description of the surface ionization of complicated atoms at single crystal tungsten surfaces. (Dissertation Abstr., 25: No. 5, Nov. 1964)

Cosmic Radiation

See *also* Elementary Particles and Radiations. Nuclear Properties and Reactions.

20872 (ANL-6938(p.71-88)) MEASUREMENT OF THE COSMIC-RAY FAST NEUTRON BACKGROUND. Jacob Kastner, Billie G. Oltman, Leonidas D. Marinelli, and Joseph H. Klems (Argonne National Lab., Ill.).

Efforts in a program to develop statistically significant data on fast neutron dose being received by man from the natural environment by man from the natural environment are described. Pulse shape descrimination associated with large hydrogen-rich organic scintillators are being used to provide high efficiency and tissue-like properties. The proton-recoil spectra are analyzed in the usual way for the incident fast neutron flux and spectra. Corrections for self absorption in the scintillator and for multiple scattering are described. A computer program for use in determining cosmic ray neutron background is included. (J.R.D.)

20873 (D2-11608) ANALYSIS OF SOLAR-FLARE HAZARD TO MANNED SPACE SYSTEMS. E. L. Chupp, D. L. Dye, B. W. Mar, L. A. Oncley, and R. W. Williams (Boeing Co., Seattle, Wash.). [1961]. 83p. (AD-606548). $3.00(CFSTI).

An evaluation of the solar-flare proton radiation hazard is presented. By a detailed analysis of all available rocket, balloon, and riometer data for solar-flare proton events from February 1956 to September 1960, an estimate is made of the total proton flux and a power law differential spectrum is estimated for each event. Brief consideration of radiobiological effects of the nonuniform dose distributions resulting from flare proton spectra leads to the assignment of the absorbed dose at 4-centimeter depth in tissue as representative of the medically significant dose for flare events. A typical space vehicle design is analyzed for its solar-flare proton shielding effectiveness, and a factor of three to ten reduction in dose is found. It is concluded that the probability of encountering a dangerous dose level in the course of a week's space flight is comparable to, or less than, the probability of a fatal accident in a week of flying in an operational military aircraft. Use of a solar-flare proton event prediction criterion will reduce the hazard by a factor of three for a short mission; the use of a small amount of extra shielding will reduce the dose encountered by a further factor up to ten. (auth)

20874 (P-1020(RAND)) THE RANDOM FUNCTIONS OF COSMIC-RAY CASCADES. T. E. Harris (RAND Corp., Santa Monica, Calif.). Feb. 7, 1957. 11p. (AD-606268). $1.00(CFSTI).

The usual model for the soft component of cosmic radiation, appropriate to the assumption of complete screening, is studied. First treating the case where collision loss is neglected, the expected values for the number of electrons and photons are related to the probability distribution of a certain nonmultiplicative Markov process, limit-theorems for this process having an interpretation in terms of the original multiplicative process. The total energy in all electrons is shown to converge in probability to a positive constant. If collision loss is included, certain peculiarities are pointed out in the fluctuations of the number of electrons. (auth)

20875 DIFFUSION MECHANISM OF THE DIURNAL VARIATION OF COSMIC RAYS. G. F. Krymskii. Dokl. Akad. Nauk SSSR, 160: 61-3(Jan. 1, 1965). (In Russian)

Solar winds form jet streams of matter with a magnetic field running along their axes. The movement of these particles from the sun is in a radial direction when the kinetic energy of the gas is significantly greater than the energy of the magnetic field. The angle θ between the axis of the stream and the line from the earth to the sun at the point where the terrestrial orbit is intersected depends upon the solar wind velocity. Jet streams of solar wind form a magnetic field in interplanetary space, the force lines of which are Archimedes spirals. The magnetic field diffuses cosmic rays anisotropically, and the diffusion coefficient parallel to the axes of the jet streams is greater than that perpendicular to the axes. The diffusion process causes a convective flux of cosmic rays which flows from the sun. This flux must be compensated by a diffused flux flowing to the sun. The diffusion occurs along the axes of the jet streams, but the compensating flux has a tangential component. In the stationary state the convective flux and the radial component of diffusion of cosmic rays cancel each other, and the resultant flux is perpendicular west of the earth-sun line. This flux creates the anisotropy of cosmic rays, the positive source of which forms a right angle eastward from the sun. The amplitude of the anisotropy is determined by the components of the cosmic-ray flux, depending upon the velocity of the solar winds. (ATD)

20876 LATITUDINAL MEASUREMENTS OF THE INTENSITY OF COSMIC RAYS IN THE STRATOSPHERE. V. K. Babarykin, V. V. Bayarevich, Yu. I. Stozhkov, and T. N. Charakhch'yan (Lebedev Inst. of Physics, Moscow and Moscow State Univ.). Geomagnetism Aeronomy (USSR) (English Transl.), 4: 367-70(1964).

The results are reported of measurements of the intensity of cosmic rays in the upper layers of the atmosphere, made at several latitudes in December 1962 from the ship Estoniya on its crossing from Leningrad to the coast of Antarctica. The results of the measurements are discussed and compared with data obtained earlier by other authors. (auth)

20877 DECREASE IN COSMIC-RAY INTENSITY IN THE STRATOSPHERE DURING GEOMAGNETIC STORMS. A. N. Charakhch'yan and T. N. Charakhch'yan (Lebedev Inst. of Physics, Moscow and Moscow State Univ.). Geomagnetism Aeronomy (USSR) (English Transl.), 4: 371-4 (1964).

Data are presented on decreases in cosmic ray intensity in the stratosphere during nine large magnetic storms in the period from 1957 to 1961. The spectrum of variation of primary radiation with energies of several Bev during the Forbush decrease is investigated. (auth)

20878 EFFECT OF CHROMOSPHERIC FLARES IN THE NEUTRON COMPONENT OF COSMIC RAYS ON MAGNETICALLY QUIET DAYS AND DURING LARGE FLARES ACCOMPANIED BY TYPE-III ABSORPTION. L. I. Dorman, V. I. Ivanov, and E. V. Kolomeyets (Kazakh State Univ., USSR). Geomagnetism Aeronomy (USSR) (English Transl.), 4: 454-5(1964).

The effects of 165 chromospheric flares of class 2 and higher that occurred during the period from July 1957 to December 1958 on the neutron component of cosmic rays were analyzed. Flares were selected that occurred at a time when the geomagnetic field was quiet. The method of superposed epochs was used in the investigation. It was shown that the intensity of the neutron component increased from 0.05 to 0.2%. The data were averaged over latitude

belts to increase statistical accuracy, and the energy spectrum of particles generated during small chromospheric flares was computed. (L.B.S.)

20879 EFFECT OF COSMIC RADIATION ON INFORMATION RECEPTION ABOARD AES'S AND AT GROUND POINTS. E. M. Zhulina. Geomagnetizm i Aeronomiya, 4: 1134-6(1964).

Cosmic-radiation interference in ground-satellite links at 20 M is evaluated. Quantitative information on audio reception aboard the satellite and field strength measurements of relative cosmic-radiation intensity during the Vostok-3 and -4 flights are used. The formula $U = \sqrt{4kT(a/b)\Delta fR}$ is used to convert cosmic-radiation intensity into units of field intensity to facilitate comparisons with measured field strength (U, voltage at receiver input; k, Boltzmann constant; T, effective temperature of total radiation; a and b, amplitude of signal and generator noise above zero level; f, bandpass; R, resistance). Eight satellite passes at about 4000–6000 km were selected for the comparison. It is concluded that to 6000 km the signal field intensity at the receiver point exceeds the cosmic radiation intensity in the zenith direction by several factors. At 6000–15,000 km, the signal field strength gradually decreases to a level comparable to cosmic radiation intensity. Between 15,000 and 20,000 km, the reception of useful signals may be interrupted. (ATD)

20880 THE ORIGIN OF COSMIC RAYS. V. L. Ginzburg and S. I. Syrovatskii. Izv. Akad. Nauk SSSR, Ser. Fiz., 28: 1910-21(Dec. 1964). (In Russian)

If it is assumed that the electron fraction of galactic and metagalactic cosmic rays are the same, the energy density of the metagalactic rays $w_{mg} = 10^{-3}w_g = 1$ ev/cm^3, where w_g is the energy density of cosmic rays within the galaxy. Thus, the galactic rays must originate within the galaxy itself. The "expanding" galaxy theory, under which the cosmic rays originate in metagalactic space, seems improbable because the density of gas near the local group of galaxies is too small, the necessary adiabatic invariance would not occur in the movement of cosmic rays over the last 10^{10} years, and the observed magnetic trapping effect of the local galaxies would not occur. A variant of the expanding galaxy theory, which assumes that $w_{mg} = w_g$ avoids the above problems, but contradicts radio data. According to the galactic theory, cosmic rays originate in the explosion of nova or supernova stars. At present no cosmic rays come from the center of the galaxy, but they may have come from an explosion 3 to 5×10^7 years ago. Particles with energies above 10^{17} ev can only come from the explosion of galactic nuclei. Calculations are presented which indicate that the electron component of cosmic rays is too large to be the result of pion decay, and therefore includes primary electrons. The primary electron source is calculated to be $Q(E)dE = 4.1 \times 10^{41}E^{-1.7}dE$ electrons per second for $0.5 < E < 10$ Bev. If the anomolous muons observed in wide atmospheric showers are really high-energy electrons, then $Q(E) = 1.6 \times 10^{42}\ E^{-2.3}$ for $E > 10$ Bev. Data on cosmic gamma rays are reviewed. (TTT)

20881 GAMMA AND ROENTGEN RADIATION ASSOCIATED WITH THE GALACTIC AND METAGALACTIC COSMIC RAYS. V. L. Ginzburg and S. I. Syrovatskii. Izv. Akad. Nauk SSSR, Ser. Fiz., 28: 1922-5(Dec. 1964). (In Russian)

Sources of galactic gamma rays with $E \geq 5 \times 10^7$ ev are considered from four processes: decay of mesons (π^0) formed from collisions of cosmic rays with interstellar matter, bremsstrahlung from relativistic electrons, reverse Compton effect, and x rays from magnetic bremsstrahlung. The total intensity of cosmic rays $I(E) = 1.5E^{-2.6}$ particles cm^{-2} sec^{-1} steradian^{-1} Bev^{-1}; and the intensity of the electron component $I_e(E) = 0.02E^{-2}$, where E is in Bev. The intensity of gamma rays from meson (π^0) decay $I_{\gamma\pi^0}(>E_\gamma) = 2.8 \times 10^{-4}M(L)E_\gamma^{-1.8}$ for $E_\gamma > 1$ to 3 Bev. M(L) is the mass of gas in the path length L. For interstellar gas $M = 2 \times 10^{-24}$g. The bremstrahlung intensity from the above electron spectrum $I_{\gamma b}(>E_\gamma) = 3 \times 10^{-4}M(L)E_\gamma^{-1}$. The equation for the total gamma flux may be derived from these equations. Most, but not all, of the Galactic gamma rays come from the reverse Compton effect. On the other hand, the metagalactic gamma rays come entirely from the reverse Compton effect. (TTT)

20882 RESULTS OF CALCULATIONS OF THE ENERGY SPECTRUM OF GALACTIC COSMIC RAYS. A. N. Charakhch'yan and T. N. Charakhch'yan. Izv. Akad. Nauk SSSR, Ser. Fiz., 28: 1926-9(Dec. 1964). (In Russian)

The form of the cosmic-ray energy spectrum is almost invariant to solar activity, indicating that most of the cosmic rays come from the galaxy, with only a small component of solar origin. The differential energy spectrum of solar cosmic rays is proportional to $E^{-2.5}$, which is similar to the dependence of galactic cosmic rays. It would appear that both spectra are the same, but direct comparison is difficult because of the lack of data on the proton diffusion coefficient D of interplanetary space. A preliminary estimate gives $D(p) \propto vp^{0.5}/3$, where v and p (0.5-5.0 Bev/c) are the proton velocity and momentum. If the energy loss of cosmic rays by collisions in interstellar space is neglected, the diffusion approximation with an initial injection at the center of the galaxy 10^8 years ago gives a good representation of the experimental spectra for cosmic protons and aipha particles. According to the diffusion theory, cosmic protons reaching the earth with energies <13 Bev are increasing in intensity, while protons with E > 13 Bev are decreasing. (TTT)

20883 A POSSIBILITY OF INVESTIGATING THE COMPOSITION OF THE PRIMARY COSMIC RADIATION OF SUPERHIGH ENERGY. N. M. Nesterova and S. I. Nikol'skii (Inst. of Physics, Academy of Sciences, USSR). Izv. Akad. Nauk SSSR, Ser. Fiz., 28: 1930-3(Dec. 1964). (In Russian)

An analysis of the composition of primary cosmic rays of more than 10^{14} ev was made, based on Cherenkov flashes occurring when a large cosmic shower was passing through the atmosphere and on the number of particles at the observational level. The fluctuations of the ratio of Cherenkov flashes Q versus the number of particles in the shower n obtained at Pamir (elevation 3860 m) were compared with the computations of the composition of primary cosmic radiation based on various assumptions of its components. Using the ratio Q/n, the composition of primary cosmic rays in showers was computed for two assumed types of protons and other heavy particles. The first type contained data about the composition of primary cosmic rays with energies of $10^{10}-10^{12}$ ev at the upper limit of the atmosphere. The second type contained primary cosmic rays with a composition having heavy nuclei with particle energies from 10^{11} to 10^{15} ev. The distribution of particles depends upon the composition of the primary cosmic rays. (ATD)

20884 PRIMARY COSMIC RADIATION OF SUPER HIGH ENERGY. G. B. Khristiansen, A. T. Abrosimov, V. B. Atrashkevich, G. V. Kulikov, V. I. Solev'eva, Yu. Fomin, and B. A. Khrenov. Izv. Akad. Nauk SSSR, Ser. Fiz., 28: 1934-41(Dec. 1964). (In Russian)

The spectrum investigation of large atmospheric showers may be made by means of the number of particles which is possible to study using a complex large-scale facility. The spectrum of large atmospheric showers near sea level changes its form sharply with a change in the total number N of particles. The transition of cosmic radiation from the shower spectrum to the primary energy spectrum is performed using a model of the development of atmospheric showers. The development depends upon the number of particles and their atomic number A. These parameters were obtained by analyzing the fluctuations of meson(μ) flux measurement in the complex facility. The distribution of the meson number depends upon the form of the primary energy spectrum, which is characterized by the exponent γ. Acceleration and diffusion of cosmic rays occur when both a change in the energy spectrum and a change in the composition of rays take place simultaneously. The diffusion of cosmic rays takes place in a magnetic field where the dif-

fusion coefficient is specified by magnetic rigidity, which is equal to $2\epsilon/300H$ for nuclei and $\epsilon/300H$ for protons (ϵ is the energy of a nucleon). The percentage of galactic cosmic radiation of various energies is tabulated. This table shows that the increase of energy causes an increase of heavy nuclei in cosmic radiation of the galaxy. A decrease in the percentage of light nuclei α and L with the increase in energy is caused by the higher diffusion coefficient. The number of mesons(μ) computed theoretically agreed with experimental data up to 10^{15} ev of the primary particles. At energies greater than 10^{17} ev, the experimental data showed more protons and light nuclei than the theory purports. (ATD)

20885 VARIATIONS IN THE INTENSITY OF COSMIC RAYS. L. I. Dorman. Izv. Akad. Nauk SSSR, Ser. Fiz., 28: 1942-58(Dec. 1964). (In Russian)

A combination review and discussion of analysis of the data (reports of the world network of cosmic ray stations, balloon, and satellite data, etc.) on the variations in intensity of cosmic radiation is presented with a view to extracting significant information on conditions in outer space and on the interaction, macroscopic and microscopic, of cosmic rays. For the purpose of isolating extra-terrestrial variations, the observed variations are classified as variations of atmospheric origin (Class I), variations of geomagnetic origin (Class II) and variations of extra-terrestrial origin (Class III). The first two, being fairly well understood, can be allowed for. Class III variations, in turn, are subdivided into modulation effects, solar cosmic radiation, and variations of galactic origin. The various effects involved in the fluctuations in the three subclasses are discussed and some general regularities and pertinent laws are adduced. Among the topics touched upon are 11-year variations, cosmic ray density gradients in space, the Forbush effect, the difference between solar and galactic cosmic rays, retardation of cosmic rays in space, variation of the energy spectrum exponent in the high-energy range, etc. (ATD)

20886 FORBUSH DECREASES IN THE INTENSITY OF COSMIC RAYS ACCORDING TO DATA OBTAINED IN THE ATMOSPHERE. A. N. Charakhch'yan and T. N. Charakhch'yan. Izv. Akad. Nauk SSSR, Ser. Fiz., 28: 1963-5(Dec. 1964). (In Russian)

Thirty-five cases of decreases in the intensity of cosmic rays in the stratosphere which were followed by magnetic storms were recorded at geomagnetic latitudes of 51 and 41°. Data obtained in the stratosphere at 41° lat. agreed with those obtained on the ground. Variations in the particle number obtained on the earth's surface correspond to the variations of primary cosmic rays, the energy of which is between 1.5 Bev and 4.6 Bev. A table is given which contains the ratios of intensities of primary cosmic rays measured on the ground to those measured in the stratosphere at 51 and 41° lat. and also ratios of variations of primary cosmic rays in the stratosphere at 51° lat. to those measured on the ground. The numerical values given in the table do not vary from storm to storm. (ATD)

20887 EFFECT OF THE EQUATORIAL FLUX IN CHANGING THE RIGIDITY OF THE GEOMAGNETIC CUT-OFF OF COSMIC-RAY PARTICLES. L. I. Dorman and M. I. Tyasto. Izv. Akad. Nauk SSSR, Ser. Fiz., 28: 1966-72(Dec. 1964). (In Russian)

Conflicting data on the change of the magnetic rigidity of the earth's field during magnetic storms and the expected effect on the observed intensity of cosmic rays are reviewed. The rigidity of the geomagnetic cutoff is calculated for two simple models of the perturbed field: first that the perturbed field lies in the equatorial plane as a linear ring of flux moving toward the west; secondly that the flux moves along a sphere with a force proportional to the cosine of the latitude. As the radius of the flux ring is decreased, or as the flux in the ring is increased, the threshold of the rigidity decreases for both eastward and westward motion, according to the first model. Calculations according to the second model show that the threshold cutoff depends not only on the decrease of the horizontal component of the flux, but also on its radius. If the flux which is responsible for the main phase of the magnetic storm (D_{st} variation) varies with latitude, then for the same amount of decrease of the horizontal component at the equator, various effects will be observed in the growth of the cosmic-ray intensity in the minimum Forbush effect. (TTT)

20888 INFLUENCE OF MAGNETIC STORMS ON COSMIC RAYS DURING MAXIMUM AND MINIMUM SOLAR ACTIVITY. M. V. Alaniya, L. I. Dorman, V. K. Koiava, T. V. Kebuladze, V. G. Koridze, and A. M. Chkhetiya. Izv. Akad. Nauk SSSR, Ser. Fiz., 28: 1993-6(Dec. 1964). (In Russian)

The parameters which characterize the association between the effects of cosmic rays and the phases of magnetic storms are: the increase of cosmic ray intensity before the magnetic storm, the global distribution of the Forbush effect, and solar diurnal variations. Data for studying the correlations between these two phenomena were taken from observations made during the IGY. Four magnetic storms of world-wide character were discussed. The intensity of cosmic rays for the soft and hard components is represented graphically for magnetic storms from 13 to 31 August 1958. The intensity of the cosmic rays increased before the storm, reaching a maximum during the daytime. The amplitude of the intensity increase was greater at higher elevations than at sea level. Discrepancies between experimental and theoretical results were observed both for sea level and mountain elevations. (ATD)

20889 MODULATION OF COSMIC RAYS BY AN INTERPLANETARY MAGNETIC FIELD. A. I. Kuz'min, G. F. Krymskii, P. A. Krivoshapkin, G. V. Skripin, N. P. Chirkov, and G. V. Shafer (Inst. of Space Physics Research and Aeronomy of the Yakutsk Branch of Siberian Div., Academy of Sciences, USSR). Izv. Akad. Nauk SSSR, Ser. Fiz., 28: 1997-2000(Dec. 1964). (In Russian)

The flux of cosmic rays depends upon the state of chromospheric flares. A reflecting magnetic field can exist inside or outside the terrestrial orbit; this field does not restrict the motion of solar particles. The occurrence of cosmic rays during various phases of Forbush decreases indicates that solar cosmic rays can reach the earth freely. The Forbush effect is evident in a space which is separated from other space by an envelope. In this segregated space, solar cosmic rays may move away from or toward the sun. This segregated space is characterized by a decrease of galactic cosmic rays. The energy spectrum of particle variations with an energy of more than 7 Bev is characterized by an exponential function with an exponent of -0.5 to -1.5. Variations with a maximum exponent are associated with the 11-year solar activity cycle. The degree of variation is greater in the polar regions than at middle latitudes. The delay in the Forbush decrease on the earth as compared with the solar chromospheric flares obtained by experiments indicates an expansion of the magnetic shell of the segregated space with a velocity of 10^8 cm sec^{-1}. This expansion may be identified with the motion of the radial interplanetary magnetic field. The intensity of galactic cosmic rays is less in the vicinity of the solar system than in the free flux in the galaxy. An intensity gradient of cosmic rays must exist at the boundary between the solar system and the unperturbed galaxy. (ATD)

20890 X-RAY BURSTS AND SOLAR COSMIC RAYS. B. M. Vladimirskii and A. K. Pankratov. Izv. Akad. Nauk SSSR, Ser. Fiz., 28: 2019-21(Dec. 1964). (In Russian)

Data taken on solar flares with short wavelength flashes ($\lambda < 8$ Å) (SWF) are compared with solar flares with no SWF. Data taken on the absorption of cosmic rays at low latitudes (SCNA) during the period 1958 to 1961 are correlated with the intensity of the cosmic rays. The percentage absorption increases logarithmically with the intensity up to 80% SCNA, and then levels off. The correlation between the x rays with energies $\geq$1.5 kev and the relativistic part of solar cosmic rays (E > 1 Bev) may be explained in

principle if the x rays responsible for the SWF originate from epithermal electrons (synchrotron radiation), and if the electrons are accelerated at the same velocity as the nuclei in the cosmic rays. (TTT)

20891 COUPLING COEFFICIENTS FOR VARIOUS COSMIC RAY COMPONENTS. E. G. Boos, V. V. Viskov, L. I. Dorman, E. V. Kolomeets, and Zh. S. Takibaev. Izv. Akad. Nauk SSSR, Ser. Fiz., 28: 2022-5(Dec. 1964). (In Russian)

Equations are derived for the energy and angular distributions of mesons(π) and (μ) in the atmosphere. It is assumed that the primary particles lose equal increments of energy at each interaction, forming only mesons(π) and that the transverse momenta of the generated mesons is the same for all interactions. The meson(μ) flux is calculated assuming that only pions generate muons. The equations may be reduced to a previously published one-dimensional form which assumed that the primary nucleons entered the atmosphere vertically. (TTT)

20892 LATITUDINAL MEASUREMENTS OF COSMIC RAY INTENSITIES AND COUPLING COEFFICIENTS IN THE STRATOSPHERE. V. K. Babarykin, V. V. Bayarevich, Yu. I. Stozhkov, and T. N. Charakhch'yan. Izv. Akad. Nauk SSSR, Ser. Fiz., 28: 2026-8(Dec. 1964). (In Russian)

Cosmic-ray intensities in the stratosphere at various latitudes were measured on board the Estonia on its way to the Anarctic from Leningrad by means of radioprobes with counting equipment. Five probes were sent into the stratosphere in the Northern hemisphere, and nine probes in the Southern hemisphere. The same type of counting equipment was used in recording cosmic-ray intensity variations continuously at Murmansk, Moscow, and Alma-Ata. The cosmic-ray intensity at the maximum (latitude effect) is plotted as a function of the critical particle momentum for the vertical direction. The data on the latitude effect were used to calculate coupling coefficients which are useful in reducing observed variations in the stratosphere to variations in the primary spectrum of the cosmic rays. Coupling coefficients are tabulated for momenta of 0.5 to 15 Bev/c at Murmansk, Moscow, Simeiz, and Alma-Ata. (TTT)

20893 STUDIES OF THE NATURE OF COSMIC-RAY PARTICLES BEYOND THE ATMOSPHERE BY MEANS OF NUCLEAR PHOTOEMULSIONS. N. L. Grigorov, D. A. Zhuravlev, M. A. Kondrat'eva, I. D. Rapoport, and I. A. Savenko. Izv. Akad. Nauk SSSR, Ser. Fiz., 28: 2035-8 (Dec. 1964). (In Russian)

The particle flux at a height of 300 km was determined from charged particle traces on a nuclear emulsion 10 × 10 cm with a thickness of 400 microns at geomagnetic latitudes of ±65° on board the second soviet spaceship. The flux was found to be 2.26 ± 0.23 particles cm^{-2} sec^{-1}, which is in good agreement with values of 2.19 ± 0.06 and 2.52 ± 0.11 particles cm^{-2} sec^{-1} obtained by gas counters. An analysis of the grain density showed that 62% of the particles had a minimum ionization ($g < 1.4\ g_{min}$), 23% of the particles had an ionization in the interval 1.4 to 2.4 g_{min}, and 15% of the particles belonged in the ionization interval of 2.4 to 7.8 g_{min}. Since the primary cosmic ray flux is 0.65 particles cm^{-2} sec^{-1}, it can be seen that the interaction of the primary radiation with matter leads to particle multiplication. A total of 2260 ± 170 stars cm^{-3} day^{-1} were observed in the emulsion. High-energy proton interactions in the emulsion are responsible for about 1500 stars cm^{-3} day^{-1}. Nuclear spallation reactions are the source of the strongly ionizing particles. (TTT)

20894 INVESTIGATION OF PRIMARY COSMIC RAYS. V. L. Ginzburg, L. V. Kurnosova, V. I. Logachev, L. A. Razorenov, and M. I. Fradkin. Izv. Akad. Nauk SSSR, Ser. Fiz., 28: 2039-44(Dec. 1964). (In Russian)

Data on primary cosmic rays in the region of light nuclei, obtained during flights of Soviet space vehicles, and comparative data obtained by means of radiosondes are presented. The comparative data were obtained by means of photographic emulsions and Cherenkov counters. A table lists the values of the L/S ratio; another table gives the values of the percentages of Li, Be, B, C, N, and heavier nuclei referred to the total flux with $Z \geq 3$. The satellite and balloon data on the L/S ratio are reasonably consistent; the agreement is somewhat poorer for the percentages. Figures give data on the fluxes of alpha particles, nuclei with $Z \geq 5$ and nuclei with $Z \geq 12$ for different energies; the flight trajectory corresponding to a brief flare-up in solar activity; and variations with time of the counting rates of the space vehicle gas-counter telescope and Cherenkov counter detecting nuclei with $Z > 5$. From a brief analysis of the data it is inferred that there may be different cosmic ray production mechanisms operating on the sun. One should produce cosmic radiation with approximately the chemical composition of the solar atmosphere; another may result in preferential acceleration of heavy nuclei. Further data are needed before one can draw definitive conclusions regarding the nature of the solar cosmic ray production mechanisms. (auth)

20895 STUDIES OF COSMIC RAYS AT HIGH ALTITUDES. S. N. Vernov, I. A. Savenko, P. I. Shavrin, V. E. Nesterov, N. F. Pisarenko, and R. I. Basilova. Izv. Akad. Nauk SSSR, Ser. Fiz., 28: 20 2045-8(Dec. 1964). (In Russian)

The time variations in cosmic-ray count rate at altitudes of 200 to 300 km were determined by means of single shielded STS-5 Geiger-Muller counters for the period from August, 1960 to June, 1963. An analysis of the count rate showed that the variation in count rate with time is analogous to that observed for cosmic rays in the stratosphere. The contribution of particles from the Van Allen radiation belts to the count rate is about 10%. The average count rate in the equatorial region was 1.109 counts cm^{-2} sec^{-1}. At high latitudes (threshold momentum of 0.45 to 4.9 Bev/c) the count rate increases by a factor of 1.2. Minimum count rates were found over the whole interval of longitudes. The observed count rate in counts cm^{-2} sec^{-1} can be related in a well-defined manner with the threshold magnetic strength of the point of measurement as follows: $N \approx 1/p^{3}$ in the interval of strength of 11 to 15 Bev/c; $N \approx 1/p^{4}$ in the interval of strength of 2 to 11 Bev/c; and $N \approx$ const in the interval of strength of 0.2 to 1 Bev/c. This fact indicates that there is a genetic relation between the secondary radiation which is counted and the primary cosmic radiation. (TTT)

20896 A GEOMETRIC PROGRAM FOR THE ANALYSIS OF PENETRATING SHOWERS OF COSMIC RAYS. L. L. Gabuniya, K. V. Mandritskaya, L. A. Razdol'skaya, N. N. Roinishvili, and N. G. Tatalashvili. Izv. Akad. Nauk SSSR, Ser. Fiz., 28: 2077-81(Dec. 1964). (In Russian)

A program for the statistical analysis of penetrating showers of cosmic rays consists of two parts: the analysis of a simple track and finding the origin of the shower. In analyzing a single track, the x-axis is taken along the base of the photograph, and the z-axis is taken along the force lines of the magnetic field. The magnification of a point is determined on going to spatial coordinates. In determining the momentum, the projection of the space curve on a plane perpendicular to the magnetic force lines (xoy) is approximated by a parabola of the type $X = (\sigma/2)\ Y^2 + AY + B$. For small curvatures it is shown that $\Delta x^* \approx m\ \delta x$, where δx is the root mean square error in the measurement of the coordinates on the film. Values of $\Delta x/\Delta x^*$ are plotted against x/d (d is the film base), and it is shown that in most cases $\Delta x/\Delta x^*$ is >1. The parabola parameters σ, A, and B are determined. To find the origin of the shower, a set of equations is solved, where the sum of the square of the distances of all the traces to the origin is a minimum. The shower origins in a lead disk 15 mm thick were found for 12 showers. The root mean square error of the coordinate measurements are $\Delta x = 0.883$, $\Delta y = 2.502$, and $\Delta z = 2.028$ mm. (TTT)

20897 ATMOSPHERIC EFFECTS ON THE COSMIC RAY INTENSITY AT A DEPTH OF 60 M.W.E. UNDERGROUND AT LONDON. J. C. Dutt and T. Thambyahpillai

(Imperial Coll. of Science and Tech., London). J. Atmospheric Terrest. Phys., 27: 349-58(Mar. 1965).

The effects of changes in atmospheric parameters on the meson intensity recorded by two semi-cubical telescopes located at an equivalent depth of 60 m of water below ground were investigated by the method of correlation analysis. The cosmic ray intensity showed significant correlations with sea-level pressure and the upper air temperature (in the range 200–70 mb), but the negative temperature effect due to μ–e decay was too small to lead to significant correlation. The weighted average values of the two regression coefficients are given and the results are discussed in relation to earlier measurements and theoretical estimates. (auth)

20898 ON THE DISTRIBUTION OF INELASTICITY IN HIGH ENERGY (20-100 Gev) NUCLEAR COLLISIONS IN CARBON AND BRASS. S. Lal, A. Subramanian, S. C. Tonwar, and R. H. Vatcha (Tata Inst. of Fundamental Research, Bombay). Phys. Letters, 14: 332-3(Feb. 15, 1965).

The distributions of K_{π^0} in interactions with carbon and brass targets were measured, using a multiplate cloud chamber operated at an altitude of 800 g/cm^2, a total absorption spectrometer, and an air Cherenkov counter. An upper cut-off was observed at $K_{\pi^0} \sim 0.4$, which indicates that there is little probability of all or a large fraction of the incident energy going to π^0-mesons ($K_{\pi^0} \sim K$) at 20-100 Gev. The results are compared with theoretical calculations and other experimental results. (L.B.S.)

20899 ČERENKOV SCINTILLATION COUNTER MEASUREMENTS RELATING TO THE ISOTOPIC COMPOSITION OF HELIUM NUCLEI IN THE PRIMARY COSMIC RADIATION. W. R. Webber and J. F. Ormes (Univ. of Minnesota, Minneapolis). Phys. Rev., 138: B416-19 (Apr. 26, 1965).

A balloon-borne scintillation Cherenkov telescope was used to measure the spectrum and geomagnetic cutoff-transmission effects on the low-energy proton and helium components in the primary cosmic radiation. Differences are found in the cutoff effects (assumed to be rigidity-dependent) of these two components in flights at closely adjacent latitudes. It is shown that these differences can be related to the presence of ^{3}He in the primary radiation. The ratio (^{3}He/^{3}He + ^{4}He) is deduced to be 0.30 ± 0.07, essentially independent of energy in the range 120–300 Mev/nucleon. This result is compared with other measurements and some implications regarding the production of the ^{3}He nuclei are discussed. (auth)

20900 A SURVEY OF ELECTRONS BEYOND 5 R_E WITH EXPLORER XIV. Louis Albert Frank. Thesis, Iowa City, Iowa, State Univ., 1964. 86p.

A comprehensive survey of the spatial distributions of electrons E > 40 kev beyond ~5 R_E with ten months of Explorer XIV observations revealed that the gross features of the spatial distribution of these electron fluxes were (1) a "hard core" of intensities of ~10^7(cm^2-sec)$^{-1}$ extending from ~2 to 8 R_E near the magnetic equatorial plane, which is characterized by relatively small temporal changes and a weak latitude dependence, (2) a "tail" of electron fluxes on the night side of earth confined near the ecliptic plane beyond ~10 R_E, (3) an increasing radial extent of observable electron intensities as the local time of the satellite position increases (decreases) from local noon (~12 R_E) to evening (morning)(≳ 16 R_E), and (4) high intensities of electrons at all latitudes of the Explorer XIV trajectory in the day side of the magnetosphere to ~12 R_E and a relative sparcity of electrons in the night side of the magnetosphere beyond ~8 R_E at high ecliptic latitudes. The B and L coordinates are shown to lose their effectiveness for organizing the observed omnidirectional intensities of electrons, E > 40 kev and E > 1.6 Mev, beyond ~6 R_E; the observations of electrons E > 40 kev beyond ~10 R_E on the night side of the earth can be conveniently summarized in an earth-centered solar-ecliptic coordinate system. Acceleration of electrons E > 40 kev within ~2 or 3 R_E beyond the sunward side of the magnetospheric boundary is suggested by recurrent "spikes" of intensities in these regions. Sample three-point integral energy spectrums of electrons are presented for a typical pass of Explorer XIV through the earth's magnetosphere. It was found that the electron spectrum softens with increasing geocentric radial distance and, if the integral spectrums are represented by kE^{-n}, then $n \simeq 1$ at L = 4.3 and $n \simeq 2$ at L = 7.1. (Dissertation Abstr., 25: No. 5, Nov. 1964)

20901 ISOTOPIC COMPOSITION AND THE ENERGY SPECTRUM OF LOW ENERGY HELIUM NUCLEI IN PRIMARY COSMIC RADIATION. Prabhakar J. Lavakare. Thesis, Rochester, N. Y., Univ. of Rochester, 1964. 109p.

The isotopic composition and the energy spectrum of low-energy helium nuclei were investigated using a nuclear emulsion stack flown from Fort Churchill, Canada, on 4th August 1962. The proportion of ^{3}He nuclei was determined to be 20 ± 5% within the kinetic energy interval of 160-370 Mev/nucleon and within a rigidity interval of 1.1-1.4 Bev/c, this value was found to be 26 ± 8%. The differential energy interval was found to have a maximum around 275-300 Mev/nucleon. Assuming that there is no ^{3}He at the cosmic-ray sources and that the observed abundance is the result of the passage of primary radiation through the interstellar matter, it is concluded that the primary radiation has travelled a total of 7 ± 2 g/cm^2 of this medium. This result is found to be consistent with the values obtained from the lithium, beryllium, and boron experiment. The implications of these results are examined on the basis of different models used for the propagation of cosmic radiation through the interstellar matter. (Dissertation Abstr., 25: No. 5, Nov. 1964)

20902 PENETRATING PARTICLE RADIATION. A. J. Dessler and B. J. O'Brien (Rice Univ., Houston, Tex.). p.53-92 of "Satellite Environment Handbook. Second Edition." Stanford, Calif., Stanford Univ. Press, 1965.

The motion of a charged particle trapped in a dipole-like magnetic field is discussed; the (B,L) and (R,λ) magnetic coordinate systems are explained. Geomagnetically trapped radiation–the Van Allen radiation belt and the Starfish radiation–is described. Observations of relativistic cosmic protons, neutrons, electrons, and heavy nuclei produced by solar flares are summarized. Intensities and energy spectra of nuclei, electrons, and positrons in the galactic cosmic radiation are reviewed. The phenomena of precipitated and auroral particles are discussed. (M.J.T.)

20903 NOTES ON COSMIC RADIATION. M. M. Shapiro (Naval Research Lab., Washington, D. C. and Weizmann Inst. of Science, Rehovoth, Israel). p.280-96 of "Star Evolution." New York, Academic Press, 1963.

Features of the cosmic radiation incident upon the earth are sketched, including composition, particle flux and density, energy spectra of primary cosmic nuclei, magnetic confinement, and isotropy. Implications of the Li-Be-B anomaly and the He-isotope abundances are discussed. Theories of the origin of cosmic rays are considered, and cosmic-ray production in supernovae and possible acceleration mechanisms are discussed. (M.J.T.)

Direct Energy Conversion

Refer also to abstracts 20730 and 21580.

20904 (BLG-317) LA CONVERSION DIRECTE APPLIQUEE AUX SOURCES RADIO-ISOTOPIQUES. (Direct Conversion Applications of Radioisotopic Sources). P. Bemelmans (Centre d'Étude de l'Énergie Nucléaire, Brussels (Belgium)). Sept. 1964. 48p. Dep.(mn).

Taking account of power levels, reliability, and practical performances, a systematic evaluation is made of the various methods that may be used to convert the energy of radioactive decay into useful electrical energy; only three procedures appear as reasonably well fitted to this form of primary energy. In all three cases, the energy evolved from the radioelement is first degraded into heat by self-absorption of the radiation. Thermophotovoltaic conversion seems promising, but it is still in its earliest developmental stage. Thermoelectric conversion is characterized by a well es-

tablished technological status, but, as far as space applications are concerned, it is apparently hindered by limited operational temperatures and by intrinsic limitations owing to the properties of the materials. On the contrary, thermionic generators are essentially high-temperature devices. After a general survey of the problem of cathode materials, different practical approaches to thermionic conversion are reviewed; particular stress is laid upon the possibilities afforded by thermionic cells with rare-gas filling as a means of obviating the difficulties raised by the use of cesium vapor. (auth)

20905 (SC-RR-65-54) SPECIAL MATERIALS TESTS FOR THE HYPERSONIC PLASMA GENERATOR. K. J. Touryan (Sandia Corp., Albuquerque, N. Mex.). Mar. 1965. Contract [AT(29-1)-789]. 13p. Dep.; $1.00(cy), 1(mn) CFSTI.

Cesium- and copper-impregnated tungsten emitters were tested in a 160-kw plasma jet to study: the effects of nose cone seeding upon the power output of a d-c generator utilizing the thermionic emission from a nose cone and upon the kinetic energy of the shock-generated plasma; and the cooling effectiveness of copper evaporation upon emitter surfaces. Nose cone seeding gave an increase in generator output by a factor of two. The tests of emitter materials also included a set of carbide emitters. Of the emitter surfaces tested, hafnium carbide showed the best heat resistance and the ZrC-coated collector registered 40 watt/in.^{2} output in 80%N–20%O plasma arc-jet. (auth)

20906 OPERATING CHARACTERISTICS OF TWO THERMIONIC CONVERTERS HAVING RHENIUM–NICKEL AND TUNGSTEN–NICKEL ELECTRODES. V. C. Wilson and J. Lawrence (General Electric Research Lab., Schenectady, N. Y.). Advan. Energy Conversion, 4: 195-221 (Dec. 1964).

Two parallel plane thermionic converters were tested. One had a rhenium emitter and a nickel collector surrounded by a nickel guard ring. The other had a tungsten emitter and nickel collector and guard. Both had interelectrode spacings of 0.005 in. The collectors and guard rings could be kept in the same temperature and potential. Both converters were capable of delivering large currents. The W–Ni converter at T_E = 2235°K developed over 40 W/cm^2 (68A/cm^2 at 0.6 V) at the electrodes. At each emitter temperature the Re–Ni converter had maximum output at a lower optimum cesium pressure than that for the W–Ni converter. At equal emitter temperatures and current densities the Re–Ni converter had higher output voltages. It is believed this is a result of the lower cesium pressure which enabled the collector work function to be lower. The Re–Ni converter at 2150°K had a usable output at 15 A/cm^2 of 16.8 W/cm^2 and a calculated efficiency of 19.8 per cent. An analysis based on the assumption that at each current density the current is limited by a maximum negative potential in the system, suggests that the variation of output voltage with current is primarily a result of a variation in the maximum potential point. This analysis also suggests that there is a double sheath at the emitter, i.e., negative sheath next to the emitter followed by a positive ion-rich sheath. (auth)

20907 ELECTRON TEMPERATURE IN MAGNETOHYDRODYNAMIC GENERATORS. M. S. Sodha (Republic Aviation Corp., Farmingdale, N. Y.). Brit. J. Appl. Phys., 16: 319-22(Mar. 1965).

Expressions are derived for the electron temperature in a linear magnetohydrodynamic generator for three different electrode configurations. In contrast to earlier investigations (which assumed an electron collision frequency independent of electron velocity v), the electron collision frequency is assumed to be proportional to v^S. Numerical results are presented for the cases in which S = 1 and 2. (auth)

20908 MHD RESEARCH IN THE UNITED KINGDOM. P. D. Dunn (United Kingdom Atomic Energy Authority, [Risley, Lancs, Eng.]), B. C. Lindley, and J. K. Wright. Consulting Engr. (London), 26: 634-6(Dec. 1964).

A review is presented of some research on the electric conductivity of seeded combustion products, duct construction, air heaters, seed recovery, magnets, impurities in monatomic gases, and conditions in the MHD duct. Estimates of the capital costs of MHD plants as a function of efficiency for various preheat temperatures are included, and future research is indicated. (D.C.W.)

20909 EXPERIMENTS IN M.H.D. POWER GENERATION. G. J. Womack. Electron Eng., 37: 7-14(Jan. 1965).

Results obtained with a small gaseous propane-oxygen combustion-driven MHD generator are reported. A comparatively large permanent magnet was used to produce a constant flux density of 9800 gauss. The combustion products were seeded with up to approximately 1.6% by weight potassium. Experiments were carried out with both hot carbon and water-cooled copper electrodes. Electrical conductivity determinations of the working fluid were made, using both types of electrodes, by measuring the current-voltage characteristics under induced and applied electric field conditions. To assist the interpretation of these results, a double-beam sodium line reversal apparatus was built to measure the gas temperature. Good agreement between the measured and theoretically calculated electronic conductivity was obtained for both hot and cold electrodes. For the cold electrodes the mode of the conductivity was electronic and not ionic, therefore the cold cathode must be electron emitting. The exact mechanism of this emission is not fully understood, but is probably due to carbon deposition on the electrode surface. This carbon is probably amorphous and of high porosity and low thermal conductivity. Therefore, this layer will approach the stagnation conditions of the gas stream which would be sufficient to give high thermionic emission. From the electrical conductivity measurements the collision cross-sections were determined and compared to the theoretically predicted values calculated by Frost's method. Reasonably good agreement was obtained. Low-frequency voltage noise was observed. Hall generator measurements were made to determine $\omega_e\tau_e$, where ω_e is the electron angular cyclotron frequency and τ_e is the electron-atom collision mean time. (auth)

20910 PROSPECTS FOR PRODUCING HIGH-POWER MAGNETOHYDRODYNAMIC GENERATORS. E. Ya. Kazovskii, Ya. B. Danilevich, and V. N. Shakhtarin. Elektrotekhnika, No. 9, 8-14(1964).

Basic problems associated with the generation and utilization of MHD power are reviewed, and the theory of the MHD generator is outlined briefly. A simplified expression is obtained for the power output P from one-dimensional MHD considerations $P = \sigma B^2\omega^2\eta(1-\eta)$, where η is the loading parameter. Alkali metals are shown to possess a maximum ionization rate at minimum temperatures (2300-3300°K). Both constant-current and variable-current generators are reviewed. The conduction type is shown to be more practical in the near future as opposed to the pulsed generator. The schematic of an open-cycle MHD power plant is given, and the details of the various components are outlined. The one-dimensional MHD theory for an ideal conducting gas flow is treated in greater detail, and mass, momentum, and energy conservation equations are obtained in a differential form. The effects of Hall currents, boundary losses, end losses, and magnetic losses are mentioned, and segmented electrodes are suggested to minimize some of these losses—especially the Hall currents. A set of efficiency expressions is obtained, including electric, thermodynamic, and power efficiency. A list of materials suitable for withstanding high-temperature corrosive atmospheres is presented. The experimental prototype designed at AVCO Research Center, Mass., USA, is reviewed, and recommendations are made for a 500-megawatt power plant utilizing a combined nuclear reactor and an MHD generator. (ATD)

20911 POSSIBILITY OF NON-THERMAL IONIZATION COMBUSTION PRODUCT MAGNETOHYDRODYNAMIC GENERATORS. D. V. Freck and J. K. Wright (Central

Electricity Research Labs., Surrey, Eng.). Nature, 205: 1192-3(Mar. 20, 1965).

Various methods of obtaining significant reductions in working temperature for a given electrical conductivity in open-cycle combustion product magnetohydrodynamic generators are reviewed, and it is shown that magnetically induced ionization may possibly give a significant increase in conductivity. The methods discussed include: induction of excessive ionization from an external source, for example, uv lamp, radio-frequency breakdown, electron beam injection, etc.; use of currents flowing in the gases to cause an increase in ionization by raising the electron temperature; and use of non-equilibrium effects that occur when chemical reactions occur in flames to raise the electron temperature. (P.C.H.)

20912 EXPERIMENTAL OPEN-CYCLE MHD-GENERATOR. V. S. Bzhozovskii, I. Dul. E. Fuksievich, M. Mikosh, and R. Vang (Inst. of Nuclear Research, Academy of Sciences, Poland). Teplofiz. Vysokikh Temp., 2: 771-9(1964).

An open-cycle MHD generator was designed for a 1-Mw output. The schematic of the generator is given. The generator has two combustion chambers: the 100-300 kw capacity chamber uses oxygen, nitrogen, or air and kerosene fuel. The interior is made of refrax material wound with water-carrying copper tubes for cooling. To enhance ionization, potassium is used as seed material. Fuel consumption ranges between 12-25 kg/hr. A brief description is given of the 1000 kw capacity combustion chamber. The power system also contains a regenerator for heating air to 1100°C, using the hot exhaust from the MHD generator. To improve the heat transfer process in the regenerator, special turbulence and circulation flows are induced. The electromagnet is described. Various materials were tested for use as generator walls. The heat flow through the walls was gauged at 14 to 71 volt/cm^2. Three types of materials were used as electrodes: graphite, zirconium oxide, and metallic borides. The MHD generator itself consists of a nozzle, a channel with segmented electrodes, and a diffuser. The transverse electrodes are of the Faraday type. (ATD)

20913 ON THE OSCILLATIONS OF THE CURRENT IN A THERMOELECTRONIC ENERGY CONVERTER. I. P. Stakhanov and A. S. Stepanov. Zh. Tekhn. Fiz., 35: 132-9 (Jan. 1965). (In Russian)

A method proposed for the investigation of oscillations in a thermoelectronic energy converter offers the advantage of explaining the formation of ion clusters and also takes into account the occurrence of collisions. Because a dispersion formula derived from the kinetic and Poisson equations becomes intractable when the distribution functions of electrons and ions in the near-cathode regions are inserted, f_e is approximated by two electron beams, representing the electrons in a quiescent plasma and the perturbation caused by the passage of the current through the diode. The perturbations of the ion distribution are concentrated in one point, and therefore f_i is represented by a single beam. The use of the above approximation leads to a simplified dispersion function for beam instability which shows that, in the region close to the cathode, the instability sets in at sufficiently strong electron currents, or, when the electron current is small, at strong ion current. It is in this near-cathode region that the instability engenders quasi-neutral longitudinal oscillations of the plasma in the interelectrode spacing, the phase velocity of which is of the order of the thermal ionic velocity, while the damping is determined by the collisions with neutral atoms. The frequency of these oscillations is found, and is shown to be inversely proportional to the interelectrode distance if the pressure is low, and inversely proportional to the square of the interelectrode distance if the pressure is high. The results are shown to be in good agreement with experimental data. (ATD)

20914 MAGNETOHYDRODYNAMIC GENERATORS OF ALTERNATING CURRENT. Elias Zahavi. U. S. Patent 3,154,703. Oct. 27, 1964. Filed Apr. 11, 1960.

An alternating current is generated by producing an alternating magnetic field in an intermittent firing combustion chamber and exhausting the hot products of combustion across the magnetic field. The apparatus includes the combustion chamber, two electrodes inside the chamber, an air supply valve, an exhaust valve, a fuel injector, an igniter, an air compressor, a field winding on an iron core outside the chamber, and an a-c generator for the field winding. Valve control means are so arranged with respect to the alternating magnetic field that the chamber fires with twice the frequency of the field, and exhaust of burned gases occurs when the field is at a maximum. To increase the ionization of the exhaust gases, an aqueous solution of a salt such as potassium carbonate is injected into the chamber before each firing. (A.G.W.)

Elementary Particles and Radiations

Refer also to abstracts 20445, 20448, 20449, 20707, 20708, 21092, 21110, and 21238.

20915 (BNL-8967) THE BROOKHAVEN-COLUMBIA PLASMA LENS. E. B. Forsyth, L. M. Lederman, and J. Sunderland (Brookhaven National Lab., Upton, N. Y.). Oct. 10, 1965. Contract [AT(30-2)-Gen-16]. 9p. (CONF-650306-4). Dep.(mn); $1.00(cy), 1(mn) CFSTI.

From Particle Accelerator Conference, Washington, D. C.

A uniform current density plasma is generated by discharging a high voltage capacitor bank into two electrodes in a low pressure gas. The magnetic field within the plasma produces achromatic focussing of pions and kaons traveling along the electrode axis. (auth)

20916 (CERN-65-7) BARYON RESONANCES. Robert D. Tripp (European Organization for Nuclear Research, Geneva (Switzerland)). Feb. 10, 1965. 63p. Dep.(mn).

Elementary scattering theory is considered, followed by a discussion of the Breit-Wigner equation, with particular emphasis on those characteristic aspects which are identifiable in scattering experiments. The Y*(1520) which, being a multichannel resonance, is sufficiently complex as to contain all interesting aspects of the analysis is discussed as a specific example. Other baryon resonances are discussed with emphasis on those that have been more recently discovered and those whose quantum numbers are still uncertain. (C.E.S.)

20917 (IC/65/3) ON THE MASS DIFFERENCE OF Ξ^- AND Ξ^0. Tetsuo Sawada and Asim O. Barut (International Centre for Theoretical Physics, Trieste (Italy)). Jan. 1965. 15p. Dep.(mn).

As an application of a method for computing coupling constants, the Ξ^--Ξ^0 mass difference is calculated from the consistency requirement of the various determinations of the same coupling constant. Predictions concerning $NN\pi$ and $\Sigma\Sigma\pi$ couplings are made. (auth)

20918 (IC/65/4) A REMARK ON SELECTION RULES IN PARA-FIELD THEORY. S. Kamefuchi (International Centre for Theoretical Physics, Trieste (Italy)). Jan. 19, 1965. 7p. Dep.(mn).

Selection rules are examined within the framework of local field theory, retaining the requirement that the Euler-Lagrange variational equations be consistent with the Heisenberg relations, but allowing general types of variations. (T.F.H.)

20919 (IC/65/5) BROKEN SU(6) SYMMETRY AND NONLEPTONIC BARYON DECAYS. Ken Kawarabayashi and Roscoe White (International Centre for Theoretical Physics, Trieste (Italy)). Jan. 25, 1965. 9p. Dep.(mn).

Nonleptonic baryon decays are studied in a broken-SU(6) scheme, using a simple symmetry-breaking interaction. (T.F.H.)

20920 (IC/65/6) CAN THE COUPLING CONSTANT ASSUME ARBITRARY VALUE IN THE S-MATRIX

THEORY? Tetsuo Sawada (International Centre for Theoretical Physics, Trieste (Italy)). Jan. 1965. 12p. Dep.(mn).

A relation is found between masses and coupling constants, within the framework of S-matrix theory, starting from the assumption of maximal analyticity of the scattering amplitude. (T.F.H.)

20921 (IC/65/7) ON THE FOUNDATIONS OF SU_6. Notes of a Lecture. Christian Fronsdal (International Centre for Theoretical Physics, Trieste (Italy)). Jan. 28, 1965. 11p. Dep.(mn).

An introduction is given to relativistically invariant SU_{2n} theories for elementary particles, and emphasis is placed on the results for n = 3. (T.F.H.)

20922 (IC/65/8) SOME UNITARY REPRESENTATIONS OF A NON-COMPACT FORM OF SU_4. Christian Fronsdal (International Centre for Theoretical Physics, Trieste (Italy)). Feb. 1965. 18p. Dep.(mn).

It has been suggested that certain non-compact groups, among them $\tilde{SU}_{12}$, may be relevant for the theory of elementary particles. In that case it would be of interest to study their unitary representations. As a beginning the noncompact real forms of $\tilde{SU}_4$ of $\tilde{SU}_{12}$ is studied. It is found that among several noncompact real forms of SU_4 only that which is isomorphic to the rotation group $R_{4,2}$ is of interest. For this group, all the unitary irreducible representations for which the energy operator has a positive definite spectrum are determined. The relationship between these representations and those of the Poincaré group are then studied. (auth)

20923 (IC/65/18) DYNAMICAL GROUPS AND MASS FORMULA. A. O. Barut and A. Boehm (International Centre for Theoretical Physics, Trieste (Italy)). Mar. 1965. 20p. Dep.(mn).

The homogeneous Lorentz group and the 4 + 1 de Sitter group are interpreted as the dynamical groups of a nonrelativistic and a relativistic "rotator," respectively. In an irreducible representation of the latter group the mass formula $m^2 = m_0^2 + \lambda^2 j(j+1)$ is obtained for certain states. The contraction of the dynamical groups (Euclidian group in 3 dimensions and Poincaré group, respectively), destroys the energy or mass spectrum and can be associated with the limit $\hbar \to 0$. The model of an elementary particle as a de Sitter "rotator" is discussed. (auth)

20924 (ICTP-64/2) S-MATRIX ELEMENTS IN THE TWO-PARTICLE UNITARITY APPROXIMATION FOR A WORLD OF ONE SPACE DIMENSION. R. Delbourgo (International Centre for Theoretical Physics, Trieste (Italy)). Nov. 1964. 25p. Dep.(mn).

For a world having a single spatial dimension, the unitarity equations are applied in the two-particle approximation to solve for the crossing symmetric scattering amplitude, and thereby determine the form factor and propagator of the theory; comparison of the full amplitude with the "Born approximation" reveals their quite different asymptotic characters. The solution is also used to discuss the problem of overlapping final-state interactions and it is proved that the enhancement is multiplicative in form. (auth)

20925 (ICTP-64/3) PRODUCTION AMPLITUDES. I. CONSTRUCTION OF INVARIANT AMPLITUDES. II. PARTIAL WAVE DECOMPOSITION AND ANALYTIC CONTINUATION IN TOTAL ANGULAR MOMENTUM. A. O. Barut and Y. C. Leung (International Centre for Theoretical Physics, Trieste (Italy)). Dec. 1964. 31p. Dep.(mn).

Lorentz-covariant scattering amplitudes for production processes involving both massive and massless particles are systematically discussed. Explicit form of both the spin and the isotopic spin amplitudes for production processes involving pions, nucleons, photons, and neutrinos, as well as the crossing relations in both spin and isospin variables, are given. (auth)

20926 (ICTP-64/4) SOME PROBLEMS OF SYMMETRY BREAKING. A. Boehm (International Centre for Theoretical Physics, Trieste (Italy)). Dec. 1964. 10p. Dep.(mn).

A possible explanation of the problem of equidistant rule for the masses of the baryon resonances is given. The method is also applied to explain the discrepancy between various calculated values of the $\varphi - \omega$ mixing angle. (auth)

20927 (ICTP-64/7) THE RELATIVISTIC STRUCTURE OF SU(6). R. Delbourgo, Abdus Salam, and J. Strathdee (International Centre for Theoretical Physics, Trieste (Italy)). Dec. 3, 1964. 14p. Dep.(mn).

It is shown that a relativistic basis for invariance under SU(6) exists only if the group structure is extended to $U^+(6) \otimes U^-(6)$ for any interaction terms. The notion of inhomogeneous extension $U_6^+(6) \otimes U_6^-(6)$ is introduced. This extension leaves the kinetic energy terms invariant, though it does not provide a fully satisfactory theory. (auth)

20928 (ICTP-64/10) GAUGE APPROXIMATIONS IN MESODYNAMICS. R. J. Rivers (International Centre for Theoretical Physics, Trieste (Italy)). Dec. 1964. 30p. Dep.(mn).

In a non-perturbative theory for vector and scalar mesodynamics of the kind proposed by Salam, it is found that the "gauge approximations" introduced in this approach are the most sensible of a set of approximation schemes that preserve the scalar gauge invariance of the approximated unitarity equations. In showing this, it is found to be most convenient to work with "one-photon irreducible" and one-photon one-meson irreducible Green's functions. The generalized identities of the Ward-Takahashi kind that these Green's functions satisfy are exhibited, as well as the decomposition of the general n-point function in terms of these Green's functions. (auth)

20929 (ICTP-64/12) THE SCALAR BEHAVIOR OF VECTOR ELECTRODYNAMICS AT HIGH ENERGY. D. A. Akyeampong (International Centre for Theoretical Physics, Trieste (Italy)). Dec. 1964. 20p. Dep.(mn).

Using Salam's gauge approximation technique to the electrodynamics of vector mesons, it is shown using two-particle unitarity, that in its high-energy aspects, the theory is analogous to that for scalar mesons only for particular values of the constants of the theory. (auth)

20930 (JINR-E-1975) INFRARED ASYMPTOTICS OF THE GREEN FUNCTIONS. L. D. Solov'ev (Soloviev) (Joint Inst. for Nuclear Research, Dubna (USSR). Lab. of Theoretical Physics). 1965. 13p. Dep.(mn).

The infrared asymptotics containing all singular terms in all orders in e have been found for the Green function of the charged particle with spin 0 and ½. (auth)

20931 (JINR-P-1951) O VOZMOKHNOM SUSHCHESTVOYANII NOVYKH BOZONNYKH REZONANSOV, RASPADAYUSHCHIKHSYA S UCHASTIEM γ-KVANTOV. (On a Possible Existence of New Boson Resonance Decays Involving γ Quanta). V. G. Grishin (Joint Inst. for Nuclear Research, Dubna (USSR). Lab. of High Energy). 1965. 7p. Dep.(mn).

The properties of the hypothetical mesons (L) are considered for which the decays into other particles via strong coupling are forbidden. It is shown that if L mesons have a mass in the range from 140 up to 560 Mev and S = 0, I = 1, $J \leq 1$, they decay mainly through the electromagnetic channel, γ quanta being involved. A similar situation takes place if the L meson masses are from 500 to 780 Mev and S = 1, I = 1, $J \leq 1$. Such decays are not yet studied experimentally. (auth)

20932 (LNF-64/60) MEASUREMENT OF THE REACTION $\gamma + p \to p + \pi^0$ NEAR THE FIRST RESONANCE FROM THE POLARIZED PHOTONS OF THE FRASCATI 1-Gev COHERENT BREMSSTRAHLUNG BEAM. Note No. 266. G. Barbiellini, G. Bologna, J. DeWire, G. Diambrini, G. P. Murtas, and G. Sette (Laboratori Nazionale di Frascati, Comitato Nazionale per l'Energia Nucleare (Italy)). Nov. 16, 1964. 9p. Dep.(mn).

The cross sections for interactions of polarized, co-

herent bremsstrahlung photons with protons are analyzed at 228 to 325 Mev photon energy. (T.F.H.)

20933 (NP-14828) LECTURES ON ORIGIN OF SYMMETRIES. Matscience Report No. 33. E. C. G. Sudarshan. Notes by T. S. Santhanam (Institute of Mathematical Sciences, Madras (India)). [1964]. 89p. Dep.(mn).

Eight lectures are presented on the building up of particles and the interpretation in field theory. Charge independence of strong interactions, breakdown of charge independence in electromagnetic interactions, isospin group and charge independence, irreducible representations of the group of rotations in complex three dimensions (SU_3), self consistent model of strong interaction symmetry, a mechanism for induction of symmetry in strong interactions and multiplet structure, and Smushkevich Principle and derivation of symmetry and charge conservation in strong interactions are discussed. (C.E.S.)

20934 (NP-14829) LECTURES ON GAUGE INVARIANCE AND MASS OF VECTOR BOSONS. Matscience Report No. 32. B. Zumino. Notes by N. R. Ranganathan, K. Venkatesan, and G. Jagannathan (Institute of Mathematical Sciences, Madras (India)). [1963]. 58p. Dep.(mn).

The mass of vector bosons when the bosons are generated by means of local gauge transformation is considered. Various arguments purporting to prove that either the physical or the bare mass vanishes when there is invariance under gauge groups are reviewed. Johnson's proof as to why the photon should have zero mass, which is based on a sum rule for the mass of vector mesons, is discussed. Schwinger's model and its relativistic covariance are also considered. (C.E.S.)

20935 (NP-14885) EXPERIMENTAL MEASUREMENT OF THE ELECTROMAGNETIC FORM FACTOR OF THE NEGATIVE π MESON (thesis). Technical Report No. 37. David G. Cassel (Princeton Univ., N. J. Elementary Particles Lab.). Jan. 1965. Contract Nonr-1858(06). 178p.

The scattering of π mesons of 21 Bev energy, incident on electrons at rest, was studied in order to determine the electromagnetic form factor of the π meson. The results of an analysis of 4% of the data obtained in the experiment are consistent with a point charge model for the π meson. The data place an upper limit on the root mean square radius due to charge structure effects and radiative effects of R = 3.3 fermi. This limitation on the radius is to be interpreted as a limitation on the absolute value of the slope of the form factor at t = 0. These data do not exclude positive slopes at the origin corresponding to an imaginary value of the radius of the same magnitude. (auth)

20936 (TID-20558) A COMPARISON OF SOME APPROXIMATIONS FOR SELF-BOUND MANY-FERMION SYSTEMS. D. S. Koltun, R. Puff, A. S. Reiner, and L. Wilets (Washington Univ., Seattle). [1964]. Contract AT (45-1)-1388. 45p. Dep.(mn); $2.00(cy), 1(mn) CFSTI.

Within the framework of the Green's-function formalism of the many-fermion problem, three approximations which close the otherwise infinite hierarchy of coupled integral equations are compared. These approximations, each of which attempts to include the important two-body correlations, differ in the choice of two-body propagators for intermediate states ($\Lambda_{00} \sim G_1^0 G_1^0$ $\Lambda_{10} \sim G_1^0 G_1$, or $\Lambda_{11} \sim G_1 G_1$) in the T matrix used to calculate the two-body correlation function. The use of Λ_{10} or Λ_{11} has been generally assumed to be an improvement over the use of Λ_{00}, although the choice between Λ_{10} and Λ_{11} is not clear. The advantages in Λ_{11} from the point of view of exact symmetry relations does not preclude the use of Λ_{10} for calculating bulk properties. Comparisons are made between the results of the Λ_{10} approximation and those obtained by the reference-spectrum method. The observation that, with a reduced Hamiltonian, Λ_{10} yields the correct (BCS) solution for superconductivity (while Λ_{11} and Λ_{00} do not) provides a motivation for using the propagator $\Lambda_{10} \sim G_1^0 G_1$ for the general Hamiltonian. G_1^0 is, crudely, the single particle propagator for the normal state. It remains to be demonstrated that lifetime effects in the normal state do not destroy the gap in the excitation spectrum. It is shown that, in a self-consistent solution of this Λ_{1n} approximation, the energy gap alters G_1^0 in just such a way as to force the width of the spectral function for G^n to be zero in a region around the Fermi surface of the order of the gap. This in turn guarantees that the spectral function for G_1 is indeed zero in the gap region. (auth)

20937 (TID-21672) SUMMARY OF PROGRESS REPORT [ON NUCLEON-NUCLEON INTERACTION] DURING YEARLY PERIOD ENDING IN FEBRUARY 1965. McAllister H. Hull, Jr., and Gregory Breit (Yale Univ., New Haven). Contract AT(30-1)-1807. 13p. Dep.(mn); $1.00 (cy), 1(mn) CFSTI.

A brief review is given of calculations on nucleon-nucleon interactions, nucleon-nucleus scattering, pion-nucleon interactions, photodisintegration of deuterons, higher order effects in Coulomb excitation, and nucleon transfer in heavy ion collisions. (C.E.S.)

20938 (UCRL-11828(p.9-10)) DIGITAL-COMPUTER CALCULATION OF MATRIX ELEMENTS OF NUCLEAR INTERACTIONS. Martin G. Redlich and Robert M. Baer (Lawrence Radiation Lab., Univ. of California, Berkeley).

For the interaction between nucleons 1 and 2, $V(1,2) = V_{X\kappa}(r)P_X Q_\kappa$, a computer program was used to calculate the exact values of coefficients. The coefficients were C_m for given j_1, j_2, j_1', and j_2' in the equation $\langle j_1 j_2 J | V_{X\kappa}(r) P_X Q_\kappa | j_1' j_2' J \rangle = \sum_m C_m(j_1 j_2, j_1' j_2', J, X_1 \kappa) K_m^{(\kappa)}$. The exact values of matrix elements of the zero-range central and tensor interactions were also calculated as a check on the calculated C_m. (D.L.C.)

20939 (UR-875-30) DECAY MODE $K \rightarrow 2\pi + \gamma$. Stephen V. Pepper and Yoshiaki Ueda (Rochester Univ., N. Y. Dept. of Physics and Astronomy). Apr. 6, 1964. Contract AT(30-1)-875. 35p. Dep.(mn); $2.00(cy), 1(mn) CFSTI.

The radiative decay $K^+ \rightarrow \pi^+ + \pi^0 + \gamma$ is considered in the light of the $\Delta T = \frac{1}{2}$ rule. The possibility that the nonradiative and radiative rates are of the same order of magnitude is investigated by constructing mechanisms that obey the $\Delta T = \frac{1}{2}$ rule in the absence of electromagnetic interactions. We consider a boson pole model and a model involving a two-particle intermediate state and find that the former model can give contributions to the radiative rate that are of the same order of magnitude as the internal bremsstrahlung contribution. The pole model also furnishes an estimate of the rate for $K_{2^0} \rightarrow \pi^+ + \pi^- + \gamma$. (auth)

20940 (UR-875-72) THE QUARK MODEL AS A PROBE OF HIGHER SYMMETRIES. S. Okubo and R. E. Marshak (Rochester Univ., N. Y. Dept. of Physics and Astronomy). Jan. 14, 1965. Contract AT(30-1)-875. 25p. (CONF-650105-2). Dep.(mn); $1.00(cy), 1(mn) CFSTI.

From Conference on Symmetry Principles at High Energy, Coral Gables, Fla.

The model based on a triplet of Dirac four-component fields (i.e., quarks) interacting via a four-fermion interaction is discussed. A summary is given of the progress made in utilizing the quark model as a probe to determine the nature of a possible larger mixed Lorentz-internal symmetry group as well as the manner in which this group is broken. (C.E.S.)

20941 INFLUENCE OF A LIMITING OF THE CHARGE NUMBER ON THE EXCHANGE RULE FOR PRODUCTION AND ANNIHILATION OPERATORS. Gerhard Heldmann (Technische Hochschule, Vienna). Acta Phys. Austriaca, 19: 164-7(1965). (In German)

A derivation of the exchange relations for the production and annihilation operators of particles that can have a state $\underline{N}$ times higher was given. In the limiting case, $\underline{N}$ = 1, the exchange relations for Fermi operators were found and for $\underline{N} = \infty$, the exchange operators for Bose operators. In the statistics of the localized spin deviations of a ferromagnet, the upper limit of the occupation number of a state was considered. (tr-auth)

20942 INELASTIC ELECTRON-DEUTERON SCATTERING. K. Hoelzl, P. Urban, and G. Saller (Universitat, Graz). Acta Phys. Austriaca, 19: 168-91(1965). (In German)

The inelastic electron-deuteron scattering was theoretically investigated. The kinematics of the problem were discussed, and the determination of the semi-relativistic interaction operators was described. The wave functions based on the calculations were discussed. The matrix element was calculated, and numerical results are given. The results were compiled and discussed extensively. (J.S.R.)

20943 THE PROBLEM OF CAUSALITY IN S-MATRIX THEORY. R. J. Eden and P. V. Landshoff (Cambridge Univ., Eng.). Ann. Phys. (N. Y.), 31: 370-90(Feb. 10, 1965).

The problem of introducing space and time concepts into scattering theory is considered with a view to stating a causality principle from which it may be possible to derive analytic properties of S-matrix elements. Solutions are given for problems related to: partial localization of interactions in space so that noninteracting terms can be separated out; partial localization in time so that initial and final states can be separated and macroscopic time become meaningful; the use of negative energy states (or off mass-shell states) is superpositions to form wave packets; approximations to multiparticle S-matrix elements and their relevance to "simple" scattering processes; limiting procedures that may relate experiments to the conventional S-matrix elements. (auth)

20944 MULTIPLE-WAVE PROPAGATION AND CAUSALITY. E. Gerjuoy (Univ. of Pittsburgh). Ann. Phys. (N. Y.), 32: 1-45(Mar. 1965).

The implications of the principle of causality (loosely stated, that the response to an incident signal can not begin until the signal arrives) are investigated for the transmission and reflection of electromagnetic waves by multiple-wave media (media, which can propagate waves of several different wave numbers $K(\omega)$ at the same frequency ω). Although many of the results obviously have wider validity, the medium is taken to be in fact a plasma, while for simplicity the analysis is restricted to the special case of one-dimensional wave propagation along z, with the plasma confined to a finite slab $o \leqq z \leqq d$. The plasma may be lossy, need not be uniform, and may be stable or unstable. The conclusions drawn include: causality can be preserved even though the transmission amplitude $T(\omega)$ and reflection amplitude $A(\omega)$ have singularities in the upper half ω-plane. Poles of $A(\omega)$, $T(\omega)$ in $\text{Im}\ \omega > 0$ typically occur with slabs of unstable plasma. In stable plasmas, the existence of a branch point at $\text{Im}\ \omega > 0$ for one $K^2(\omega)$ implies there is at least one other $K^2(\omega)$ with the same branch point. In stable plasmas it is impossible to excite one such nonsingly valued $K^2(\omega)$ wave without exciting at least one other such wave. With isotropic plasmas the singularities of $T(\omega)$, $A(\omega)$ in $\text{Im}\ \omega > 0$ are symmetrically located about the imaginary axis. Despite some complications associated with the limiting behavior of the dispersion equation at infinite $|\omega|$, under ordinary circumstances, with slabs of stable plasma, $A(\omega)$ and $T(\omega) - 1$ each should obey Kramers-Kronig relations. The results are illustrated by reference to two actual plasma dispersion relations—the warm collisionless plasma (stable) and the two-stream plasma (unstable). (auth)

20945 APPLICATION OF BETHE-SALPETER METHODS TO SOME RENORMALIZATION PROBLEMS IN POTENTIAL THEORY. R. Rockmore (Rutgers State Univ., New Brunswick, N. J. and Brookhaven National Lab., Upton, N. Y.). Ann. Phys. (N. Y.), 32: 114-26(Mar. 1965). (BNL-8388)

A direct adaptation of Bethe-Salpeter methods in momentum space to nonrelativistic quantum mechanics is used to reproduce some results of Bertocchi on vertex renormalization in potential theory and to extend such considerations to a discussion of the normalization condition ($Z_3 = 0$) as well. It is shown that the normalization condition may be cast into the usual statement of the square-integrability of bound-state wave functions or alternatively into a form familiar from a dispersion theoretic treatment of scattering with bound states given by Blankenbeeler. The generalized Ward identify is used to indicate briefly the relevance of this discussion to a study of the form factor of the composite. Some remarks are made about other equivalent formulations of the normalization condition in the nonrelativistic theory. (auth)

20946 GENERAL THEORY OF COVARIANT PARTICLE EQUATIONS. D. L. Pursey (Univ. of Glasgow). Ann. Phys. (N. Y.), 32: 157-91(Mar. 1965).

A general procedure is given for constructing infinitely many systems of wave equations and subsidiary conditions for a particle of given spin and nonzero mass. The subsidiary conditions are shown to be precisely the conditions which annihilate solutions of the wave equations corresponding to the wrong spin values. Several different but equivalent sets of subsidiary conditions are derived. Explicit formulas are obtained which relate one set of covariant wave functions to a different set; these relations may be reinterpreted if desired as wave equations. The converse problem of recovering the canonical representation from the manifestly covariant theory is discussed, and three different procedures are derived. The discrete transformations of space inversion, time reversal and particle-antiparticle conjugation are treated, and a proof is given of a result found empirically by Foldy. A brief account is given of the invariant scalar product. A momentum-space representation but an heuristic treatment is given of the transition to a configuration space representation by means of a four-dimensional formal Fourier transformation. The space-time coordinates (introduced as Fourier transform variables conjugate to the momentum and energy) derived from different manifestly covariant descriptions of a given system appear to be inequivalent. (auth)

20947 ON THE ULTRARELATIVISTIC LIMIT OF THE THEORY OF FREE VECTOR MESONS. J. Beckers (Universite, Liege). Bull. Soc. Roy. Sci. Liege, 33: 666-71(1964). (In French)

The extreme-relativistic limit for Kemmer particles, established by Mathews and Sankaranarayanan with the help of a unitary transformation applied to the Hamiltonian equations, is completed by using the transformed initial condition. The equivalence with Strocchi's results and with Maxwell theory is shown. (auth)

20948 INTERNAL GROUPS AND THE HEISENBERG THEORY OF ELEMENTARY PARTICLES. Jules Geheniau (Universite, Brussels). Cahiers Phys., 18: 285-91(June-July 1964). (In French)

Some aspects of the Heisenberg theory of elementary particles are considered. The equations of the same type that can be written on the basis of the SU_3 group and the Lorentz group are examined. These are used as examples. The same idea is applicable to all internal groups. (J.S.R.)

20949 THE POLARIZABILITY OF THE NEUTRON. L. G. Moroz and V. N. Tret'yakov. Dokl. Akad. Nauk Belorussk. SSR, 8: 575-8(1964).

The electric polarizability derived from scattering experiments with slow neutrons seems larger than that supported by other experimental data. The present authors calculate the electric and magnetic meson polarizability at 60 Mev with forward scattering using dispersion relations for six independent amplitudes. The total Compton scattering amplitude in the centroid system is expressed as a linear combination of these amplitudes. The dispersion relations for the real part are then given. By the use of unitarity requirements, the imaginary part is expressed as a bilinear combination of amplitudes for 1-meson production at the nucleon in the S- and P-states. This can then be directly expressed by the angular distribution coefficients of the photomesons created at a proton and the ratio of cross sections for $\pm$-meson production at the threshold of photoproduction. After some manipulations, the polariza-

bilities are given in terms of dispersion integrals which are then integrated by Simpson's method using six points, the numerical results so obtained being then tabulated. The electric polarizability was found to be $(1.23 \pm 0.25) \times 10^{-42}$ cm^3, and the magnetic, $(7.7 \pm 10) \times 10^{-44}$ cm^3. Recoil contributions can be neglected in this region. The values agree for those of the proton in order of magnitude, thus supporting Baldin's assumption. These results favor polarization of the π-meson cloud as the main mechanism of the polarizability of nucleons. (ATD)

20950 SCATTERING THEORY FOR RELATIVISTIC PARTICLES. F. Coester (Argonne National Lab., Ill.). Helv. Phys. Acta, 38: 7-23(1965).

Relativistic particle quantum mechanics is a possible alternative to quantum field theory on the one hand and analytic S-matrix theory on the other. The scattering theory for one or several two-particle channels can be formulated in the rest frame of the center of mass along the same lines as the nonrelativistic scattering theory. The existence and completeness of the scattering states, their asymptotic properties, and the Lorentz invariance of the S operator follow from known mathematical theorems. To be consistent, a multiparticle theory must satisfy the following requirements. The interaction of two particles should be the same when they are alone or when other particles are present at a large distance. Since a particle system may break up into two or more noninteracting clusters, the dynamical description of the entire system must also contain the correct Lorentz-invariant description of each of the clusters. These requirements were satisfied for three-particle systems. (auth)

20951 SYMMETRY BREAKING IN THE STATIC STRONG-COUPLING THEORY. G. Wentzel (Univ. of Chicago). Helv. Phys. Acta, 38: 65-72(1965). (COO-264-216; EFINS-64-48)

The effects on the energy spectra of the nucleon (or baryon) "isobars" of differences in meson masses which violate either charge symmetry or SU(3) symmetry are studied. Scalar theories show a high sensitivity to such symmetry-breaking causes. The situation is markedly different in a pseudoscalar theory (nucleon and pions) where the charge symmetry appears to be stabilized through the interdependence of spin and isospin (J = I). (auth)

20952 ON THE QUANTIZATION OF A SYSTEM OF TWO PARTICLES. C. Piron (Université, Geneva). Helv. Phys. Acta, 38: 104-8(1965). (In French)

Some quantization rules are proposed, leading to a model for a system of two coupled particles with different masses in which stationary states are possible. (D.C.W.)

20953 CAUSALITY AND ONE-PARTICLE SINGULARITIES OF THE S-MATRIX. G. Wanders (Université, Lausanne, Switzerland). Helv. Phys. Acta, 38: 142-9 (1965).

The existence of one-particle singularities located in the physical region of a three-body scattering amplitude is shown to result from suitable requirements of macrocausality. (auth)

20954 CONCERNING ELASTIC PROTON ANTIPROTON INTERACTION. I. G. Golyak. Izv. Akad. Nauk Kaz. SSR, Ser. Fiz.-Mat. Nauk, No. 1, 79-82(1964).

The total antiproton interaction cross sections are difficult to reconcile with those of proton-proton and proton-neutron cross sections at low energies, and there is no theory for them at energies, and there is no theory for them at energies much above 250 Mev. Thus Feynman pole diagrams are used to derive a cross-section equation analogous to that of the elastic positron-electron scattering. This equation agrees with experimental results on the cross sections but diverges greatly for the angular distributions. The difference is attributed to different contributions from the Feynman diagrams for pure and annihilation scattering, respectively, and to the fact that pole terms alone can not describe elastic p-p scattering. (ATD)

20955 REPRESENTATION OF THE SCATTERING AMPLITUDES. I. Nedyalkov. Izv. Fiz. Inst. Aneb. Bulgar. Akad Nauk, 11: 179-92(1963). (In Bulgarian)

The different ways of expressing the dependence of the scattering amplitude h(z) on its argument z are called the representation of the scattering amplitude. In the component representation, h(z) is expressed as a sum of more elementary functions. The component representation is proved to be unique. The determination of h(z) in regions with singularities is carried out in cases which are inaccessible for the Oehmes method. In suitable representations, algebraic equations of the Low type are derived. The equations may have an advantage over dispersion equations because the usual analytical properties of the scattering amplitude are not necessary for their derivation. The possibilities of a natural classification of the scattering amplitudes are discussed. (auth)

20956 ON SEMICLASSICAL SCATTERING. J. A. Barker and C. H. J. Johnson (Commonwealth Scientific and Industrial Research Organization, Melbourne). J. Chem. Phys., 42: 2263-7(Apr. 1, 1965).

The behavior of the quantum-mechanical phase shifts for scattering by a potential well was examined in the classical limit. The phase shifts tended to zero in the classical limit for all cases in which the corresponding classical trajectory did not pass through the well. This disproved by counterexample the result of Curtiss and Powers, which indicated that there should be a contribution to the phase shifts even in the classical limit for classically inaccessible but energetically possible regions between two inner classical turning points. The error in the latter result appeared to arise from the neglect of bound states of positive energy, which exist in the classical limit (and only in that limit). (auth)

20957 EFFECT OF THREE TURNING POINTS ON SEMICLASSICAL SCATTERING. C. F. Curtiss (Univ. of Wisconsin, Madison). J. Chem. Phys., 42: 2267-9(Apr. 1, 1965).

When three turning points occur in the effective potential, the region between the two inner turning points is associated with classically bound trajectories or quantum-mechanically metastable states. The effect of this portion of the effective potential-energy curve on the semiclassical phase shifts and transport cross sections is discussed. (auth)

20958 THE LIMIT DISTRIBUTION OF A BINARY CASCADE PROCESS. P. E. Ney (Stanford Univ., Calif.). J. Math. Anal. Appl., 10: 30-6(Feb. 1965).

The limit distribution of branching stochastic process is investigated. The branching stochastic process is defined as follows: An initial particle undergoes a collision after a random time, yielding two particles. Each offspring parent, independent of the history of the process or of other particles existing at the time undergoes collision, producing further offspring. (C.E.S.)

20959 INVARIANT INBEDDING: PARTICLE INTERACTION, AND CONSERVATION RELATIONS. Richard Bellman and Sherman Lehman (RAND Corp., Santa Monica, Calif.). J. Math. Anal. Appl., 10: 112-22(Feb. 1965).

It is shown that for a quite general class of transport processes involving particle-particle interaction as well as the usual particle-medium interaction, difference approximations can be obtained, which exhibit nonnegativity and boundedness in an immediate fashion. Furthermore, a uniform Lipschitz condition is preserved. (L.B.S.)

20960 HIGH-ORDER LIMIT OF PARA-BOSE AND PARA-FERMI FIELDS. O. W. Greenberg (Univ. of Maryland, College Park) and A. M. L. Messiah. J. Math. Phys. (N. Y.), 6: 500-4(Apr. 1965).

Para-Bose and para-Fermi quantization are schemes of second quantization which generalize the usual Bose and Fermi schemes. The different cases of para-Bose (para-Fermi) quantization are labeled by a positive integer p, which is called the "order." For p = 1, the usual Bose

(Fermi) quantization is recovered. The high-p limit of para-Bose (para-Fermi) quantization is studied, and it is shown that, to a large extent, the high-p limit of a para-Bose (para-Fermi) field is a Fermi (Bose) field. The nature of the limit is studied in detail, and a paradox relating to the connection of spin and statistics is resolved. (auth)

20961 PROOF THAT SCATTERING IMPLIES PRODUCTION IN QUANTUM FIELD THEORY. Stanley O. Aks (Univ. of Maryland, College Park). J. Math. Phys. (N. Y.), 6: 516-32(Apr. 1965).

A proof of the necessity of production processes in quantum field theory is carried out in the axiomatic framework. It is shown that a field theory that is assumed to have a nontrivial scattering amplitude violates crossing symmetry, if production processes are absent. The proof is based on the rigorous analytic properties of the scattering amplitude, particularly the analyticity in the invariant-scattering variables s, t, and u. In the case of a scalar theory with pairing symmetry, the scattering amplitude is known to be analytic within the domain $|stu| < 7168m^6$, except for the usual cuts. Under the working assumption that production processes are null, it is shown that this domain can be enlarged by applying the elastic unitarity conditions beyond the (usual) elastic region. The domain is enlarged sufficiently to include the first Landau singularity of the absorptive part of the scattering amplitude. This singularity is not symmetric in s and t within the extended domain, and this is incompatible with the crossing symmetry of the scattering amplitude. In order to avoid a contradiction, the discontinuity across this Landau singularity must be null. It follows that the scattering amplitude must itself be null. In the course of the proof it is shown that the conclusion is valid for a scattering amplitude satisfying the requirements of an S-matrix theory embodied in the Mandelstam representation. (auth)

20962 CLASSIFICATION OF THREE-PARTICLE STATES ACCORDING TO SU_3. A. J. Dragt (Inst. for Advanced Study, Princeton, N. J.). J. Math. Phys. (N. Y.), 6: 533-53(Apr. 1965).

It is shown that the set of states for three noninteracting particles can be put into a one-to-one correspondence with the set of irreducible representations of SU_3. This classification leads to three-particle angular momentum states which treat all particles on an equal basis. The states exhibit the maximum localization compatible with a given total energy, momentum, and angular momentum. Only nonrelativistic particles are treated. (auth)

20963 UNIQUENESS OF STEADY-STATE SOLUTIONS TO THE FOKKER-PLANCK EQUATION. A. H. Gray, Jr. (Univ. of California, Santa Barbara). J. Math. Phys. (N. Y.), 6: 644-7(Apr. 1965).

The uniqueness of steady-state probability densities in certain continuous Markov processes is proven when the Fokker-Planck or Kolmogorov equation satisfied by the transition probability is of a variety called "steady." The tendency of other probability densities to approach such steady-state densities is formally demonstrated. (auth)

20964 PROPERTY OF THE VERTEX FUNCTION IN POTENTIAL THEORY. R. Rockmore (Rutgers Univ., New Brunswick, N. J. and Brookhaven National Lab., Upton, N. Y.). J. Math. Phys. (N. Y.), 6: 648-51(Apr. 1965). (BNL-8424)

The vertex function of an s-wave bound state in potential theory is discussed in terms of a nonrelativistic Bethe-Salpeter formalism. It is shown that the Born series defining the off-shell amplitude, $\Gamma(k^2,P_0)$, has the property that $\Gamma(k^2,k^2/m) = \Gamma_0/D(k^2,\lambda)$, where $D(k^2,\lambda)$ is the Jost function for potential strength λ, and where the bare (Γ_0) and physical (Γ_c) couplings are related by $\Gamma_0 = \Gamma_c Z_1$, with Z_1, the vertex renormalization constant equal to $D(-\alpha^2, \lambda)$. The particular proof presented drives from a detailed comparison in momentum space of alternative, but equivalent, coordinate space definitions of the Jost function originating with Jost and Pais. (auth)

20965 INTERNAL SYMMETRY AND THE POINCARE GROUP. Yukio Tomozawa (Inst. for Advanced Study, Princeton, N. J. and Univ. of Colorado, Boulder). J. Math. Phys. (N. Y.), 6: 656-7(Apr. 1965).

Theorems concerning the interrelation between the Poincaré group and the symmetry group of elementary-particle interactions were proved under weaker conditions than that of McGlinn. (auth)

20966 NOTE ON POSITRONIUM. George Tiktopoulos (Princeton Univ., N. J.). J. Math. Phys. (N. Y.), 6: 573-7 (Apr. 1965).

By means of an inequality providing an upper bound for the norm of integral operators, it is shown that the Bethe-Salpeter equation for bound states of the electron-positron system (in the ladder approximation) admits solutions associated with a discrete spectrum of binding energies. It is found that in the weak coupling limit the spectrum $B(\alpha)$ approaches asymptotically the Coulomb spectrum in the sense $\lim(B(\alpha)/m\alpha^2) = \{(1/4n^2)|n = 1, 2, 3, \ldots \infty\}$, where α is the fine-structure constant and m the electron rest mass. (auth)

20967 ALGEBRAIC CONSTRUCTION OF THE BASIS FOR THE IRREDUCIBLE REPRESENTATIONS OF ROTATION GROUPS AND FOR THE HOMOGENEOUS LORENTZ GROUP. J. A. Castilho Alcaras and P. Leal Ferreira (Instituto de Fisica Teorica, São Paulo, Brazil). J. Math. Phys. (N. Y.), 6: 578-83(Apr. 1965).

The basic functions for a class of the irreducible representations of the rotation groups in n dimensions (R_n) are explicitly constructed by an algebraic method in which the basic functions are taken to be homogeneous polynomials in the variables of E_n. The solutions correspond to the hyperspherical harmonics of the mathematical literature and are of interest for problems exhibiting invariance under a certain R_n. The method is also applied to derive a basis for the infinite-dimensional irreducible representations of the homogeneous Lorentz group if homogeneous functions are in the variables of the corresponding pseudo-Euclidean space. (auth)

20968 RENORMALIZATION CONSTANT OF ELECTRON GAS IN THE HIGH DENSITY LIMIT. D. J. W. Geldart and S. H. Vosko (McMaster Univ., Hamilton, Ont.). J. Phys. Soc. Japan, 20: 20-5(Jan. 1965).

A detailed derivation of the expressions for the renormalization constant Z for an interacting electron gas in the lowest order of the effective interaction is given. It is clearly demonstrated that the result of Daniel and Vosko is correct in the high density limit, contrary to some recent work of Osaka. Numerical results are included for the renormalization constant. (auth)

20969 STUDY OF THE POSSIBLE EXISTENCE OF THE 3π RESONANCE STATE (625 Mev) AND (1000 Mev) AND OF THE 4π RESONANCE STATE (1050 Mev). Chung-show Kuo and Hsien-chung Sung. K'o Hsueh T'ung Pao, No. 11, 1001-3(1964). (In Chinese)

The existence of the α_1 and β_1 resonance states is reviewed. In addition to the $\eta(548)$ and $\omega(782)$ states, the experiments indicated the possibility of the existence of two resonance states in the 3π system, α_1 resonance ($m = 625 \pm 25$ Mev) and β_1 resonance ($m = 1000 \pm 10$ Mev). In the α_1 resonance (++−) and (+-0) states were observed; in the β_1 resonance only (00−) was noted. From this an isotopic spin of T = 1 was derived. If these particles indeed exist, they must belong to the SU(3) group, according to the formula $m_\gamma^2 = m_\beta^2 + 0.226(\text{Bev})^2$. The corresponding resonance states are $T = 1/2$, $m_{\alpha\gamma} = 785$ Mev, $m_{\beta\gamma} = 1107$ Mev; for T = 0 $m_{\alpha 0} = 854$ Mev, $m_{\beta 0} = 1140$ Mev. The results indicate that the β_γ and α_γ states may exist. As the β_1 band is very broad and its decay constant Q is relatively small and no corresponding peaks were found in the 2π and the 4π systems, it is concluded that 3π is the main decay pattern. The experiments also indicate that a 4π resonance is possible at m = 1050 Mev. Experimental peaks were observed in the 4π system at (++−−), (+−00) and (++−0). On this basis, the possibility of an isotopic spin in the 4π system is admitted. (TTT)

20970 A POTENTIAL MODEL FOR THE Ω^-. Guru Vachan Dass (Delhi Univ.). Nucl. Phys., 67: 654-8(June 1965).

A separable potential previously applied to the 3-3 pion-nucleon resonance was suitably modified and applied to the $\Xi\bar{K}$ system. The baryon exchange force provides the dominant mechanism responsible for the required attraction. The Ω^- (1685 Mev) appears as a bound state in the $\Xi\bar{K}$ system for reasonable values of the F-D mixing parameter f. The calculated mass of the Ω^- is very close to the experimental value. (auth)

20971 ELECTROMAGNETIC FORM FACTORS AND THE GENERALIZED POINCARÉ GROUP, *I*. T. Fulton and J. Wess (Universitat, Vienna). Phys. Letters, 15: 177-9(Mar. 15, 1965).

The contribution of iso-orbit effects to the electromagnetic form factors are discussed. The generalized Poincaré group covariant arguments are used to construct current operators for mesons and baryons. (L.B.S.)

20972 SU(6)-SYMMETRY AND HIGHER ANGULAR MOMENTA. V. G. Kadyshevskii, R. M. Muradyan, A. N. Tavkhelidze, and I. T. Todorov (Joint Inst. for Nuclear Research, Dubna, USSR). Phys. Letters, 15: 180-2 (Mar. 15, 1965).

The procedure for constructing the Lie algebra of generators of SU(6) from those of SU(2) and SU(3) is described. The magnetic moment operator is defined, corresponding to the model of vector addition of magnetic moments of quarks. Wave functions of the proton and the neutron are constructed in terms of the components Ψ^{ABC} of the 56-component tensor, and the proton and neutron magnetic moments are found. It is shown that the algebra of SU(6) can be generalized to the case when the quarks possess an arbitrary orbital angular momentum. (L.B.S.)

20973 RELATIVISTIC GENERALIZATION OF SU(6)-SYMMETRY. V. G. Kadyshevskii, R. M. Muradyan, A. N. Tavkhelidze, and I. T. Todorov (Joint Inst. for Nuclear Research, Dubna, USSR). Phys. Letters, 15: 182-4 (Mar. 15, 1965).

A solution to the problem of unifying the internal symmetry group SU(3) with the Poincaré group is suggested, based on a four-dimensional representation of the Poincaré group. (L.B.S.)

20974 P AND C PROPERTIES OF THE U(12) MULTIPLETS. Abdus Salam (International Centre for Theoretical Physics, Trieste, Italy), J. Strathdee, J. M. Charap, and P. T. Matthews. Phys. Letters, 15: 184-5(Mar. 15, 1965).

The implications are listed of the U(12) scheme regarding parity and charge conjugation properties for strong interactions. Assignments for the basic multiplets are given for mesons and baryons. (L.B.S.)

20975 PARAFERMION MODEL FOR HIGHER BARYONIC RESONANCE. S. Hatsukade (Kyoto Univ.). Phys. Letters, 15: 185-8(Mar. 15, 1965).

It was previously proposed that quarks are parafermions of an order 3, and that the baryon 56-plet is a completely symmetric system composed of three parafermions in an s-state. The model is applied to the higher baryonic resonances, and it is shown that it can only be applied successfully under the assumption that the orbital angular momentum is shared equally by the three parafermions. A rule for addition of equal angular momenta is hypothesized, and the spin and parity of the possible states predicted by the scheme are presented. The second order mass formula in SU(3) is used to test the scheme, and the predictions of the model are compared with experimental data. (L.B.S.)

20976 ANTIPROTON-PROTON ELASTIC SCATTERING AT 4 Gev/c AND DERIVATION OF DIFFRACTION SLOPE AT INFINITE ENERGY. O. Czyzewski, B. Escoubes, Y. Goldschmidt-Clermont, M. Guinea-Moorhead, D. R. O. Morrison, and S. De Unamuno-Escoubes (CERN, Geneva). Phys. Letters, 15: 188-91(Mar. 15, 1965).

A study was made of two-prong interactions observed in the Saclay hydrogen bubble chamber exposed to an antiproton beam of the CERN proton synchrotron. The results were used to calculate the asymptotic value of the slope of the diffraction peak at infinite incident momentum. The total pp and $p\bar{p}$ cross sections were calculated and the asymptotic value of the ratio $\sigma_{el}/\sigma_{total}$ was derived, using the optical model applied to a black sphere. (L.B.S.)

20977 A TEST FOR C CONSERVATION IN STRONG INTERACTION PHYSICS. G. Cohen-Tannoudji and A. M. L. Messiah (Department de Physique Nucleaire et de Physique du Solide, Saclay, France). Phys. Letters, 15: 191-3 (Mar. 15, 1965).

It is pointed out that the $\bar{p}p \to \bar{\Lambda}\Lambda$ interaction provides significant tests for C conservation in strong interactions. It is shown that the interference between C-conserving and C-violating transition amplitudes can be directly calculated from the observed angular correlation data on the decay products of the hyperon pair. (L.B.S.)

20978 IMAGINARY FERMI CONSTANT G AS A MODEL OF CP VIOLATION. L. Wolfenstein (CERN, Geneva). Phys. Letters, 15: 196-8(Mar. 15, 1965).

A model is proposed for CP violation that involves only the standard forms of the interaction hamiltonian and requires no new coupling constant. The basic feature of the model, which consists in replacing G by iG, is that CP violating matrix elements are higher order in the weak interaction than CP conserving ones. The consequences and main disadvantages of the model are noted. (L.B.S.)

20979 TEST OF THE $\Delta S/\Delta Q$ RULE IN K^0_{e3} DECAY. R. Cester, P. T. Eschstruth, F. V. Murphy, G. K. O'Neill, B. Quassiati, R. Wattson, and D. E. Yount (Princeton Univ., N. J.). Phys. Letters, 15: 198-200(Mar. 15, 1965). (PPAD-533E)

An experiment was performed to test the $\Delta S/\Delta Q$ rule in K^0_{e3} decay, using a magnetic field spark chamber, scintillation counters, and Freon gas Cherenkov counters. A diagram of the experimental apparatus is given. Kinematics programs were used to calculate the Q-value, coplanarity and the momentum in the decay plane transverse to the neutral track for each decay. The data were analyzed for K^0_{e3} and $K^0_1 \to \pi^+\pi^-$ decays and the results of the selection of events are tabulated. The integral time distribution is plotted and compared with the graph of the equation for the total K^0_{e3} rate. (L.B.S.)

20980 RENORMALIZATION OF p-p POLARIZATION DATA IN THE 50-150 Mev ENERGY REGION. O. N. Jarvis and B. Rose (Atomic Energy Research Establishment, Harwell, Berks, Eng.). Phys. Letters, 15: 271-3(Apr. 1, 1965).

The absolute polarization in proton–carbon scattering was measured by two independent methods. The results were used to calculate factors by which polarizations quoted in the literature should be multiplied. The variation with energy of the corrected polarization for p-p scattering at a center-of-mass angle of 61.8° was obtained. (D.C.W.)

20981 KINEMATICAL ENHANCEMENTS IN THE FINAL STATE OF PERIPHERAL PROCESSES. U. Maor and T. A. O'Halloran, Jr. (Harvard Univ., Cambridge, Mass.). Phys. Letters, 15: 281-3(Apr. 1, 1965).

The kinematical features of peripheral processes were studied by considering the one-pion-exchange contribution to the $\pi^+ + p \to \rho^0 + \pi^+ + p$ interaction at 3.65 Bev/c and the interaction $K^+ + p \to \pi^+ + p + K^0_1$ at 3.0 Bev/c. An appreciable enhancement of the $\pi^+ - \rho^0$ and $\pi^+ - K^0_1$ mass distributions was obtained near the lower edge of their phase-space distributions. Examination of the ρ exchange diagram for $\pi^+ + p \to \omega^0 + \pi^+ + p$ at 3.5 Bev/c revealed a pronounced peak at 1.2 Bev. The positions of the peaks were energy dependent. (D.C.W.)

20982 NONLEPTONIC HYPERON DECAYS AND BROKEN U_7(12)-SYMMETRY. R. Oehme (Univ. of Chicago). Phys. Letters, 15: 284-6(Apr. 1, 1965).

The nonleptonic decay amplitudes of hyperons are

studied on the basis of a covariant U_7 (12) symmetry scheme. Sum rules for the parity-conserving and parity-violating amplitudes are obtained. (D.C.W.)

20983 TESTS OF RELATIVISTIC SU(6) IN PROTON-ANTIPROTON ANNIHILATION. H. Harari (Israel Atomic Energy Commission, Yavne) and H. J. Lipkin. Phys. Letters, 15: 286-8(Apr. 1, 1965).

The interactions $\bar{p} + p \rightarrow \pi^+ + \pi^-$, $K^+ + K^-$, and $K^0 + \bar{K}^0$ are proposed as tests of relativistic generalizations of SU(6) symmetry. (D.C.W.)

20984 ON $K^* \rightarrow K\pi\pi$ DECAY. V. B. Geshkenbein and B. L. Ioffe (Inst. for Theoretical and Experimental Physics, Moscow). Phys. Letters, 15: 289-90(Apr. 1, 1965).

The probability of the $K^* \rightarrow K + 2\pi$ decay is calculated, assuming that the mesons (ω) and (φ) are the mixing of a unitary singlet and of the component T = 0 and Y = 0 of a unitary octet. (D.C.W.)

20985 EVIDENCE FOR $K_{\mu 4}$ DECAY. D. Cline and W. F. Fry (Univ. of Wisconsis, Madison). Phys. Letters, 15: 293-6(Apr. 1, 1965). (COO-881-46)

A probable $K_{\mu 4}$ decay was observed in mesons (K^+) stopping in liquid freon. The $K_{\mu 4}$ branching ratio was found to be 1.2×10^{-3} per K^+ decay within the 90% confidence level. The branching ratio was also determined by combining this observation with a $K_{\mu 4}$ decay observed in nuclear emulsion. Limits on the additional form factors associated with the $K_{\mu 4}$ decay were also obtained. (D.C.W.)

20986 THREE-NUCLEON PROBLEM WITH SEPARABLE POTENTIALS. M. Bander (Stanford Univ., Calif.). Phys. Rev., 138: B322-5(Apr. 26, 1965). (SLAC-PUB-64; TID-21361)

The low-energy three-nucleon problem with two-particle separable potentials is solved. The formalism of Faddeev in recasting the three-body equations into Fredholm form and subsequent angular-momentum reductions are carried out. Upon searching for a bound state, two poles of the amplitude are found. Upon further examination, one of the poles is found to have a residue whose sign is opposite to those encountered in scattering with local field theory or with local potentials. (auth)

20987 EFFECT OF AN INELASTIC CHANNEL ON THE POSITION AND WIDTH OF A RESONANCE. Pran Nath and Y. N. Srivastava (Univ. of California, Riverside). Phys. Rev., 138: B404-7(Apr. 26, 1965).

The effect of an inelastic channel on the position and width of a resonance is investigated for the case of a two-channel problem using effective-range theory and the uncoupled-phase method. Some estimates are obtained for the shift in the position and reduction in the width of the resonance due to the introduction of the inelastic channel. It is shown that an inelastic channel has, in general, the effect of shifting the resonance maxima towards the first threshold and reducing the asymmetry in width on the high-energy side and the low-energy side of the single-channel resonance. An estimate for the reduction in the asymmetry is also obtained. A two-channel computer experiment is performed to test the quantitative validity of the estimates. Good quantitative agreement of the estimates is obtained with the exact two-channel results. (auth)

20988 NEUTRAL WEAK INTERACTION CURRENTS. F. Curtis Michel (Rice Univ., Houston, Texas). Phys. Rev., 138: B408-15(Apr. 26, 1965).

The consequences of postulating that the strangeness-conserving weak interactions are symmetric in isotope spin space (i.e., the leptons paired in isotopic spin doublets) are traced, with special attention to the resultant neutral weak currents and possible experiments to detect such currents. Far from being excluded experimentally, this theory in fact leads generally to only very difficult-to-detect effects such as elastic neutrino-nucleon scattering (order G in amplitude). Circular dichroism (microwave frequencies) of first excited hydrogen is expected. Other possible experimental subjects are also discussed. (auth)

20989 PROPERTIES OF A MASSIVE NEUTRAL GAUGE PARTICLE. Y. Fujii (Stanford Univ., Calif.). Phys. Rev., 138: B423-9(Apr. 26, 1965).

The properties of a massive neutral vector particle which is assumed to be a gauge particle associated with the baryon number and to bear strong interactions are investigated. The strong resemblance to quantum electrodynamics serves as a guide. Results are as follows: A simple relation between the mass and wave-function renormalizations is obtained. The theory of mixing between two vector particles cannot be applied in its simplest form if one or both of them are gauge particles. There are some restrictions on the form of the interaction with mesons, which can be tested experimentally. The analysis of the production of two vector particles from a pion incident on a nucleon is proposed as an example. (auth)

20990 OBSERVATIONS OF RADIATIVE τ^+ DECAYS. P. Stamer, T. Huetter, E. L. Koller, S. Taylor, and J. Grauman (Stevens Inst. of Tech., Hoboken, N. J.). Phys. Rev., 138: B440-1(Apr. 26, 1965).

Seven examples of the decay mode $K^+ \rightarrow \pi^+ + \pi^+ + \pi^- + \gamma$ were found in a systematic study of 3618 τ^+ decays in nuclear emulsion. The γ energies are 6.3 ± 1.5, 11.4 ± 1.4, 13.4 ± 1.4, 14.2 ± 1.4, 17.8 ± 1.3, 27.5 ± 1.0, and 34.0 ± 0.9 Mev. The experimental branching ratio for γ energies greater than 11 Mev is $P(3\pi + \gamma)/P(3\pi) = (1.7 \pm 0.7) \times 10^{-3}$. (auth)

20991 PARITY CONSERVATION AND BOOTSTRAPS. F. Zachariasen (California Inst. of Tech., Pasadena) and C. Zemach. Phys. Rev., 138: B441-5(Apr. 26, 1965).

It is suggested that parity conservation in the strong interactions may be a consequence of the bootstrap hypothesis. A model is presented to illustrate how this might come about. (auth)

20992 MODEL FOR THE FIRST NUCLEON RECURRENCE. P. R. Auvil and J. J. Brehm (Northwestern Univ., Evanston, Ill.). Phys. Rev., 138: B458-9(Apr. 26, 1965).

A calculation of the position and width of the $\frac{5}{2}^+$ (1688) pion-nucleon resonance is made. Inelastic unitarity is used to generate the dynamics where single-pion exchange coupling $N\pi$ to N_f states provides an approximation for the force. Good agreement with experiment is obtained. A similar mechanism for generating higher $N\pi$ resonances is suggested. (auth)

20993 A STUDY OF TWO-PRONG EVENTS IN PROTON-ANTIPROTON ANNIHILATIONS AT REST. F. N. Ndili (Ibadan Univ., Nigeria). Phys. Rev., 138: B460-5 (Apr. 26, 1965).

Proton-antiproton annihilations at rest yielding two charged mesons were analyzed to search for multimeson resonances. The results show evidence for appreciable production of the ρ, the K^*, and the φ mesons. The data on the ρ-meson production indicate that antiproton annihilation from the singlet S state is not negligible compared to the triplet S state. (auth)

20994 EMPIRICAL MASS RELATIONS INVOLVING THE STRONGLY INTERACTING PARTICLES. R. M. Sternheimer (Brookhaven National Lab., Upton, N. Y.). Phys. Rev., 138: B466-78(Apr. 26, 1965).

Previous work on linear mass relations involving the strongly interacting particles was extended. These results interrelate the masses of the mesons and baryons, and in some cases involve the muon mass m_μ. The mass m of the various particles was expressed in the form of a bilinear expression, into which there enter only the two constants m_π and m_μ. Empirical regularities concerning the isotopic spin I, angular momentum J, and the parity of states whose mass difference is $2m_\pi$ were noted. A systematic investigation was made of the following three types of mass relations: $m_3 = m_1 - m_2$, $m_3 = m_1 + \frac{1}{2}m_2$, and $m_3 = \frac{1}{2}(m_1 + m_2)$, where m_1, m_2, and m_3 are the masses of three strongly interacting particles. A list was made of some of the particle sequences, where a sequence is defined as a group of three or more particles with constant mass spacing Δm. Altogether 27 sequences were found,

for which Δm is a simple linear function of the pion and nucleon masses, m_π and m_N. (auth)

20995 MEASUREMENT OF THE NEUTRON-NEUTRON S-WAVE SCATTERING LENGTH FROM THE REACTION $\pi^- + d \rightarrow 2n + \gamma$. R. P. Haddock (Univ. of California, Los Angeles), R. M. Salter, Jr., M. Zeller, J. B. Czirr, and D. R. Nygren. Phys. Rev. Letters, 14: 318-23(Mar. 1, 1965).

Neutron time-of-flight spectra from the reaction $\pi^- + d \rightarrow 2n + \gamma$ were measured, using coincidence detection of all three final particles by scintillation counters. Results based on 2002 events at four angles from 6 to 17° are given in histograms. The data were fitted to theoretical hypotheses, and a preliminary value for the neutron-neutron S-wave scattering length of −16.4 ± 1.9 f was found. The result is compared with those of previous experiments. (M.J.T.)

20996 TEST OF SU(6) PREDICTIONS IN WEAK N^* PRODUCTION. C. H. Albright and L. S. Liu (Northwestern Univ., Evanston, Ill.). Phys. Rev. Letters, 14: 324-6 (Mar. 1, 1965).

The relation between the elastic process $\nu_\mu + n \rightarrow p + \mu^-$ and the inelastic process $\nu_\mu + n \rightarrow N^{*+} + \mu^-$, through the SU(6) vertex function constructed by Beg and Pais to describe the general semileptonic process $\nu_l + B(1) \rightarrow B(2) + l$ in the nonrelativistic limit, is tested in detail. The eight form factors for the general matrix element of the inelastic process are considered, and the two vector form factors are determined using CVC theory. Numerical results for the total cross section and the invariant differential cross section of the inelastic process are presented. (M.J.T.)

20997 BARYON SPECTROSCOPY BY INELASTIC ELECTRON-PROTON SCATTERING. A. A. Cone, K. W. Chen, J. R. Dunning, Jr., C. Hartwig, N. F. Ramsey, J. K. Walker, and Richard Wilson (Harvard Univ., Cambridge, Mass.). Phys. Rev. Letters, 14: 326-8(Mar. 1, 1965).

The cross section for inelastic electron-proton scattering was measured at 31 and 90° by detecting the scattered electrons. Differential cross sections, corrected for effects of scattering from the target wall, Dalitz pair production, and shower counter efficiency, are given and compared with calculated cross sections due to the radiative tails. Excitation of the resonances $\Delta_\delta(1238)$, $N_\gamma(1512)$, $N_{\alpha_2}(1688)$, and (1920) are discussed. (M.J.T.)

20998 DECAY OF THE ρ^0 MESON, AND THE POSSIBLE EXISTENCE OF A T = 0 SCALAR DI-PION. Loyal Durand, III and Yam-tsi Chiu (Yale Univ., New Haven). Phys. Rev. Letters, 14: 329-32(Mar. 1, 1965).

The suggestion that the anomalies in the decay angular distribution of the ρ^0 meson, observed in the reaction $\pi^- + p \rightarrow \pi^+ + \pi^- + n$, result from the interference of the resonant T = 1, J = 1⁻ amplitude in the $\pi^+\pi^-$ system with a T = 0 amplitude having J = 0⁺ or 2⁺ is explored in detail, using the modified single-pion-exchange model to describe the production process. Results are reported from studies assuming the $\pi^+\pi^-$ system to result from the decay of a superposition of the ρ^0 resonance and a resonant T = 0, J = 0⁺ state ϵ^0 with $m_\epsilon \sim m_\rho$ and $\Gamma_\epsilon \sim \Gamma_\rho$. (M.J.T.)

20999 DECAY $K_1^0 \rightarrow 2\pi$ AND SPONTANEOUS BREAKDOWN OF THE CP SYMMETRY. G. Marx (Stanford Univ., Calif.). Phys. Rev. Letters, 14: 334-6(Mar. 1, 1965).

A possible explanation of the $K_1^0 \rightarrow 2\pi$ decay, using an assumption of spontaneous breakdown of the CP symmetry, is shown. The asymmetric vacuum is characterized by a minimum condition, $\langle 0|H|0\rangle$ = min, using a CP-symmetric Hamiltonian. The principles of relativity and equivalence are maintained in the model. A coupling between the Goldstone model and the kaon field, described by a CP- and Lorentz-symmetrical Lagrangian, is considered in order to show the possibility for spontaneous breakdown of CP. (M.J.T.)

21000 RESONANCE AND HIGH-ENERGY LIMIT OF SCATTERING. Masao Sugawara (Purdue Univ., Lafayette, Ind.). Phys. Rev. Letters, 14: 336-9(Mar. 1, 1965).

It is pointed out that the usual analyticity assumption implies a strong correlation between a pronounced low-energy resonance and the high-energy limit of the scattering amplitude. It is proved that the forward amplitude can not satisfy an unsubtracted dispersion relation, as long as a pronounced low-energy resonance appears in the direct and/or crossed channels, assuming that the forward elastic-scattering amplitude is analytic in the usual sense. It is also proved that, if the forward amplitude becomes purely imaginary rapidly enough in the infinite-energy limit, then the high-energy limit of the total cross section can be only a finite, nonzero limit, if there is a pronounced low-energy resonance. The pion-nucleon 33 resonance and $\pi^0\pi^-$ scattering are discussed. (M.J.T.)

21001 NONEXISTENCE OF "PURE BOOTSTRAP" SOLUTIONS TO THE CHEW-LOW THEORY. Kerson Huang and Alfred H. Mueller (Massachusetts Inst. of Tech., Cambridge). Phys. Rev. Letters, 14: 396-8 (Mar. 15, 1965). (MIT-2098-121)

A proof is given that no bootstrap solution to the Chew-Low theory exists in the one-meson approximation if the scattering amplitudes satisfy unsubtracted dispersion relations, under the assumption that the nucleon is the only pole present. (L.B.S.)

21002 RELATIVISTIC EXTENSION OF SU(6). S. K. Bose and Yu. M. Shirokov (Univ. of Delhi). Phys. Rev. Letters, 14: 398-9(Mar. 15, 1965).

A method of combining the inhomogeneous Lorentz group (P) with internal symmetry is illustrated by explicitly constructing a higher symmetry group (G), which has the following properties: G contains the group P and SU(3) as subgroups, SU(6) as a little group, and irreducible representations of G contain a mass spectrum. (L.B.S.)

21003 PHOTOPRODUCTION OF W^+ MESON. Howard R. Reiss and Moon H. Cha (Naval Ordnance Lab., Silver Spring, Md.). Phys. Rev. Letters, 14: 399-401(Mar. 15, 1965).

The cross section was calculated for $\gamma + p \rightarrow W^+ + n$ interaction for a range of W masses up to six proton masses, using the V-A form for the weak interaction and the photon-meson vertex. The lowest order Feynman diagrams involving only the weak and electromagnetic interactions shown, and the total cross section is given as a function of photon energy for three values of the W mass. The value obtained for all three cases was 10^{-34} cm². (L.B.S.)

21004 FURTHER EVIDENCE FOR A Kπ RESONANCE NEAR 1400 Mev. Lyndon M. Hardy, Suh Urk Chung, Orin I. Dahl, Richard I. Hess, Janos Kirz, and Donald H. Miller (Univ. of California, Berkeley). Phys. Rev. Letters, 14: 401-3(Mar. 15, 1965). (UCRL-11898(Rev.))

An investigation was made of π^- p interactions at 3.9 and 4.2 Bev/c, and the final states were analyzed in search for decay of S = +1 bosons in the mass interval 1.0 to 1.5 Bev. The πK effective mass distribution showed a marked enhancement at 1430 ± 60 Mev. The assignment of I = ½ for K*(1430) was suggested from the lack of corresponding enhancement in other final states, and the spin was deduced for decay angular correlations. The existence of an unstable meson with S = +1, I = ½, M = 1430 ± 20 Mev and a full width Γ = 100 ± 20 Mev is concluded. (L.B.S.)

21005 PHENOMENOLOGICAL APPROACH TO A RELATIVISTIC SU(6) THEORY. B. Sakita and K. C. Wali (Argonne National Lab., Ill.). Phys. Rev. Letters, 14: 404-8(Mar. 15, 1965).

A method for extending the SU(6) symmetry to the relativistic domain is outlined, based on the construction of the symmetry group G, where G is the semidirect product of T_{36} and SL(6,C). The difficulties encountered in the physical interpretation of the 36 translational operators are overcome in the approach, and the physical consequences are discussed. Calculations are made on the effective meson-meson and meson-baryon interactions, using the equation for the interaction lagrangian and the lowest order perturbation theory. The results are tabulated and discussed. (L.B.S.)

21006 $\pi^- + p \rightarrow \pi^0 + n$ CHARGE-EXCHANGE SCATTERING AT HIGH ENERGIES. I. Mannelli (Universita, Pisa, Italy and Istituto Nazionale di Fisica Nucleare, Pisa, Italy), A. Bigi, R. Carrara, M. Wahlig, and L. Sodickson. Phys. Rev. Letters, 14: 408-14(Mar. 15, 1965). (MIT-2098-115)

A detailed analysis was made of differential and total cross section measurements of the elastic charge-exchange interaction $\pi^- + p \rightarrow \pi^0 + n$, at incident pion momenta of 6, 8, 10, 12, 16, and 18 Bev/c. Monte Carlo calculations were made of the angular distributions and were compared with experimental distributions. The square of the amplitude was calculated from the difference between π^- p and π^+ p total cross sections, using the optical theorem and assuming charge independence. The results are tabulated. The predictions of the Regge theory and dispersion relations are discussed. (L.B.S.)

21007 SINGLE REGGE-POLE ANALYSIS OF π^- p CHARGE-EXCHANGE SCATTERING. Robert K. Logan (Massachusetts Inst. of Tech., Cambridge). Phys. Rev. Letters, 14: 414-16(Mar. 15, 1965). (MIT-2098-114)

A Regge-pole analysis was made of π^--p charge exchange scattering, assuming that only the ρ trajectory is exchanged. An expression for the differential cross section was obtained, and the energy dependence of the charge-exchange amplitude was calculated. The analysis established the consistency of two experiments with unitarity, dispersion relations, and the $E^{\alpha t}$ energy dependence of charge-exchange amplitude. (L.B.S.)

21008 SHELL MODEL FOR BARYON RESONANCES. Maurice M. Miller (Lockheed-Georgia Co., Marietta, Ga.). Phys. Rev. Letters, 14: 416-19(Mar. 15, 1965).

The characteristics of the symmetrical jj-coupling shell model is investigated for baryon resonances, and the results are applied to interpretation of current data concerning baryon resonances and shoulders. Supermultiplets of baryon resonances are proposed, which transform according to the three-particle symmetric representation of SU(6j + 3) for a shell of given j. A linear mass formula associated with a chain of symmetry breaking, SU(6j + 3), SU(2j + 1), and SU(3) is proposed. Results of the shell-model classifications for $j = \frac{1}{2}$, $\frac{3}{2}$, and $\frac{5}{2}$ are tabulated, as well as the baryon mass spectrum for the $(p_{\frac{1}{2}})^3$ shell. (L.B.S.)

21009 U(6) ⊗ U(6) AND NONLEPTONIC DECAYS. M. Ademollo (Universita, Florence), G. Altarelli, and R. Gatto. Phys. Rev. Letters, 14: 420-1(Mar. 15, 1965).

The nonleptonic hyperon decays in U(6) ⊗ U(6) are discussed, assuming that the decay interaction is a self-product of the currents of (35,1), CP invariance, and octet enhancement. The ambiguities in the assignment of stable baryons and of stable mesons are solved. The forbiddenness of $\Sigma_{\frac{3}{2}}^{\frac{3}{2}}$ in s wave, Lee's relation of p waves, and two relations connecting s and p waves are found in addition to the expected $\Delta T = \frac{1}{2}$ relations and Gell-Mann's s-wave relation. (L.B.S.)

21010 REGGE POLES AND THE PHASE OF THE FORWARD-SCATTERING AMPLITUDE. Roger J. N. Phillips (Univ. of California, Berkeley) and William Rarita. Phys. Rev. Letters, 14: 502-4(Mar. 29, 1965). (UCRL-11932)

The πN, NN, and $\bar{\text{N}}$N total cross section data from 6 to 26 Bev/c, taken from previous experiments, were used to fix the parameters for the forward-scattering amplitudes, taking three Regge poles for πN and four for NN. The ratio of the real to the imaginary part of the amplitudes is illustrated and compared with experiment. It is shown that simple Regge pole models predict a substantial real part at high energies. (L.B.S.)

21011 EFFECT OF ELECTRIC FIELD ON POSITRON LIFETIMES IN ARGON AND HELIUM. W. R. Falk, P. H. R. Orth, and G. Jones (Univ. of British Columbia, Vancouver). Phys. Rev. Letters, 14: 447-9(Mar. 22, 1965).

An experiment was performed to study the effect of an applied electric field on the positron lifetime characterizing the exponential portion of the annihilation spectrum. A gas pressure chamber with field-defining electrodes, a NaI(Tl) gamma-ray detector in conjunction with a time-to-pulse-height converter, and a multichannel analyzer were used. In argon, the lifetime was found to increase by a factor of two when a strong electric field is applied; in helium little evidence was found for either the shoulder or field dependence of the lifetime. The relation between the experimental results and the elastic scattering and annihilation cross sections was obtained. (L.B.S.)

21012 MEASUREMENT OF THE MOMENTUM SPECTRUM OF POSITRONS FROM MUON DECAY. Marcel Bardon (Columbia Univ., New York), Peter Norton, John Peoples, Allan M. Sachs, and Juliet Lee-Franzini. Phys. Rev. Letters, 14: 449-53(Mar. 22, 1965).

An experiment was performed to measure the momentum spectrum of positrons from muon decay in a plastic scintillator target counter, using a magnetic spectrometer with sonic spark chambers. The momentum and emission angle were determined, and the Michel parameter, which characterizes the shape of the spectrum, was found to be 0.747 ± 0.005. (L.B.S.)

21013 MESON-MESON COUPLINGS IN AN SU(6)-INVARIANT THEORY. I. S. Gerstein (Univ. of Pennsylvania, Philadelphia). Phys. Rev. Letters, 14: 453-6 (Mar. 22, 1965).

The SU(6) invariant theory is applied to boson interactions. A search was made for an SU(6) structure in the static limit of zero momentum transfer, using the Fourier transform of the SU(3)- and Lorentz-invariant interaction lagrangrian. Relations are derived between the SU(3)-independent VVV, VVP, VPP and VφP couplings, based on the 35-dimensional representation of SU(6) joining the pseudoscalar meson octet (P), the vector-meson octet (V) and the vector-meson singlet (φ), and processes such as φ, ω, and ρ decay are correlated. (L.B.S.)

21014 Σ-Λ MASS DIFFERENCE IN THE SU(6)-SYMMETRIC BOOTSTRAP MODEL. Richard H. Capps (Northwestern Univ., Evanston, Ill.). Phys. Rev. Letters, 14: 456-8(Mar. 22, 1965).

The strong (isospin preserving) baryon mass splitting is examined in the SU(6)-symmetric bootstrap model, with particular reference to the Σ-Λ mass difference. Baryon mass ratios were calculated and compared with experiment. Satisfactory agreement was found for the mass splittings within the octet and decuplet. The calculated decuplet-octet mass splittings were found to be half as large as the experimental value, which was attributed to relativistic spin-dependent effects. (L.B.S.)

21015 LORENTZ-COVARIANT SU(6), PARTICLE-ANTIPARTICLE ALGEBRAS, AND SUPERMULTIPLET STRUCTURE. K. T. Mahanthappa (Inst. for Advanced Study, Princeton, N. J.) and E. C. G. Sudarshan. Phys. Rev. Letters, 14: 458-61(Mar. 22, 1965).

The results of an investigation of higher symmetry groups are presented, with particular emphasis on the relativistic invariance of the free lagrangian. The algebra of FW(2) and FW(3) groups generated by the intrinsic spin is identified, and particle-antiparticle doubling of the intrinsic spin group is discussed. The canonical spin group is combined with an internal symmetry group to obtain the FW(6). The relativistic pure particle-particle and particle-antiparticle interactions are represented in terms of the two-component Foldy-Wouthuysen-Tani amplitudes, and the FW(6)-invariant interaction form factors are obtained. (L.B.S.)

21016 QUARK MODEL IN MOMENTUM SPACE AND HIGHER SYMMETRIES. Riazuddin and L. K. Pandit (Univ. of Rochester, N. Y.). Phys. Rev. Letters, 14: 462-6(Mar. 22, 1965). (UR-875-70)

A résumé of the FW representation is given, and its

use in the relativistic completion procedure of Bég and Pais is indicated. The symmetries underlying the three-quark models in momentum space formulation are considered. It is found that the free-field hamiltonian is invariant under a U(12) group. A four-fermion interaction is written which is U(6)-invariant in the limit of large quark mass, but otherwise contains parts which reduce this invariance to U(3). (L.B.S.)

21017 DECAY $Y_1^*(1660) \rightarrow Y_0^*(1405) + \pi$. Philippe Eberhard (Univ. of California, Berkeley), F. T. Shively, Ronald R. Ross, Daniel M. Siegel, J. R. Ficenec, Robert I. Hulsizer, D. W. Mortara, Morris Pripstein, and William P. Swanson. Phys. Rev. Letters, 14: 466-71(Mar. 22, 1965). (UCRL-11934)

Experimental evidence is reported for the decay $Y_1^*(1660) \rightarrow Y_1^*(1405) + \pi$, which can be used as evidence that the $Y_1^*(1660)$ is a member of an octet if $Y_0^*(1450)$ is assumed to be a unitary singlet. An analysis was made of $Y\pi\pi$ invariant mass distributions of events from exposure of the Berkeley hydrogen bubble chamber to 2.45-, 2.65-, and 2.70-Bev/c K^- beams. It is concluded that the $\Sigma\pi\pi$ decay of the $\Sigma(1660)$ is dominated by the intermediate state $\Lambda(1450) + \pi^+$, and that it is at least comparable to the decay $\Sigma(1385) + \pi$. (L.B.S.)

21018 JOHNSON-TREIMAN RELATIONS FROM VECTOR-MESON EXCHANGE. R. F. Sawyer (Massachusetts Inst. of Tech., Cambridge). Phys. Rev. Letters, 14: 471-2(Mar. 22, 1965).

It is shown that the Johnson-Treiman relations in the SU(6) theory between Kp and πp total cross sections follow also from the octet vector meson exchange model. (L.B.S.)

21019 LEPTONIC DECAYS OF THE BARYONS. V. De Santis and W. A. Dunn (Northwestern Univ., Evanston, Ill.). Phys. Rev. Letters, 14: 472-5(Mar. 22, 1965).

The branching ratios for the leptonic decays of the baryons are calculated using the weak iso-spin model, and it is shown under reasonable assumptions that the results can be expressed in terms of three independent parameters. The parameters were determined from the $n \rightarrow p + e + \gamma$, $\Lambda \rightarrow p + e + \nu$, $\Sigma^- \rightarrow n + e + \nu$ decays, and comparison was made between the remaining experimental and predicted branching ratios to test the model under the assumptions made. The results of the $\Delta S = \Delta Q$ rule are compared and discussed. (L.B.S.)

21020 CP-NONCONSERVING DECAY $K_1^0 \rightarrow \pi^+ + \pi^- + \pi^0$. Jared A. Anderson (Univ. of California, Berkeley), Frank S. Crawford, Jr., Robert L. Golden, Donald Stern, Thomas O. Binford, and V. Gordon Lind. Phys. Rev. Letters, 14: 475-7(Mar. 22, 1965). (UCRL-11938)

In a previous paper on the absolute decay rate $\Gamma_2(+-0)$ for $K_2^0 \rightarrow \pi^+ + \pi^- + \pi^0$, the time distribution of the 16 $\pi^+\pi^-\pi^0$ events were found to be completely compatible with $\Gamma_1(+-0) = 0$, where $\Gamma_1(+-0)$ is the rate for $K_1^0 \rightarrow \pi^+ + \pi^- + \pi^0$, and the results were consistent with CP invariance. The constraint $\Gamma_1(+-0) = 0$ was imposed in obtaining the result for $\Gamma_2(+-0)$. Two events are added, and the correct result for $\Gamma_2(+-0)$ is found to be $(2.87 \pm 0.23) \times 10^6$ sec^{-1}. The data are reanalyzed without the assumption that $\Gamma_1(+-0)$ is zero, and without the assumption of CP invariance. A likelihood function is constructed and the amplitude ratio $a_1(+-0)/a_2(+-0)$ is calculated. It is concluded that $\Gamma_1(+-0)/\Gamma_2(+-0)$ is less than five, and that the amplitude ratio of zero cannot be ruled out. (L.B.S.)

21021 DYNAMICAL THEORY OF NONLEPTONIC HYPERON P WAVES IN SU(6) SYMMETRY. E. Borchi, F. Buccella, and R. Gatto (Universita, Florence). Phys. Rev. Letters, 14: 507-9(Mar. 29, 1965).

A dynamical theory of nonleptonic hyperon P waves is proposed. The assumptions of CP invariance and of transformation of the nonleptonic interaction as the 35 of SU(6) are supplemented with the assumption of dominance of the baryon intermediate states of 56 in a one-variable dispersion relation. (L.B.S.)

21022 COVARIANCE, SU(6), AND UNITARITY. M. A. B. Beg and A. Pais (Rockefeller Inst., New York). Phys. Rev. Letters, 14: 509-13(Mar. 29, 1965).

The unitary properties of the effective S matrix are studied to prove that the free kinetic energy breaks the completed SU(6). Broader conditions of validity are also found for results previously obtained with $SU(12)_g$. (L.B.S.)

21023 SELECTION RULES IN RELATIVISTIC $SU(6)_g$ THEORIES. Harry J. Lipkin (Weizmann Inst. of Science, Rehovoth, Israel). Phys. Rev. Letters, 14: 513-14(Mar. 29, 1965).

Selection rules, which were obtained using SU(2) subgroups of SU(6) called quark spins, are shown to be valid in any relativistic theory which satisfies certain conditions. (L.B.S.)

21024 MESON-BARYON SCATTERING IN THE INTRINSICALLY BROKEN M(12) SYMMETRY SCHEME. J. M. Cornwall, P. G. O. Freund, and K. T. Mahanthappa (Inst. for Advanced Study, Princeton, N. J.). Phys. Rev. Letters, 14: 515-17(Mar. 29, 1965).

The projection procedure requiring that the M(12) multiplet fields satisfy the Bargmann-Wigner-type wave equation is applied to the problem of meson-baryon scattering. Sum rules that follow from the meson-baryon reaction amplitudes and the kinematic functions are given, and the significance of these sum rules as tests for the M(12) symmetry scheme is interpreted. (L.B.S.)

21025 SOME TESTS OF RELATIVISTIC SU(6) SCHEMES. R. Blankenbecler, M. L. Goldberger, K. Johnson, and S. B. Treiman (Princeton Univ., N. J.). Phys. Rev. Letters, 14: 518-20(Mar. 29, 1965).

The direct implications of the $SU(12)_g$ scheme are studied for a number of experimentally accessible reactions. The general class of reactions, for arbitrary scattering angle, $M + B \rightarrow M' + B'$, is considered, where M denotes the pseudoscalar octet and B the baryon octet. Predictions on real spatial amplitudes, zero polarizations, and energy-angle dependence between differential cross sections, following from the structure for meson-baryon scattering according to the $SU(12)_g$ prescription, are discussed. (L.B.S.)

21026 $B = \frac{1}{3}$ QUARKS AND SU(9) SYMMETRY. G. Cocho and E. Chacon (International Centre for Theoretical Physics, Trieste). Phys. Rev. Letters, 14: 521-3(Mar. 29, 1965).

Quarks are considered as spinors in a nine-dimensional unitary space and SU(9) is considered as the basic intrinsic group. The dimensions of some of the representations of the group are given, and two SU(3)(T,Y) nonets of spinless particles are obtained by decomposition of the $\underline{80} \oplus \underline{1}$ representations. The components contained in the 80 and 165 representations are tabulated. (L.B.S.)

21027 SU(6) CLEBSCH-GORDAN COEFFICIENTS FOR THE PRODUCT 35×56. J. C. Carter, J. J. Coyne, and S. Meshkov (National Bureau of Standards, Washington, D. C.). Phys. Rev. Letters, 14: 523-6(Mar. 29, 1965).

The SU(6)-multiplet coupling factors for the product $\underline{35} \times \underline{56}$ were obtained independently by two methods, and are tabulated according to the source terms for the SU(3) $\otimes$ SU(2) representations of each SU(6) representation. The complete SU(6) Clebsch-Gordan coefficients for any state considered are obtained by multiplying the appropriate SU(3) coefficients by the SU(6)-multiplet coupling factors. Scattering amplitudes are obtained for meson-baryon initiated amplitudes, according to SU(6), and are listed along with the Johnson-Treiman elastic amplitudes. (L.B.S.)

21028 U(12) SYMMETRY AND WEAK INTERACTIONS. Ken Kawarabayashi and Roscoe White (International Centre for Theoretical Physics, Trieste). Phys. Rev. Letters, 14: 527-30(Mar. 29, 1965).

Some consequences of the assumption that weak interactions also might share symmetry properties of the U(12) group are discussed. It is assumed that the effective hadron currents associated with leptonic decay processes and

the effective nonleptonic interactions each transform according to the 143-dimensional representation of the U(12) group. (L.B.S.)

21029 EXPERIMENTAL TEST OF CHARGE-CONJUGATION INVARIANCE. D. Cline and R. M. Dowd (Univ. of Wisconsin, Madison). Phys. Rev. Letters, 14: 530-1 (Mar. 29, 1965).

A search was made for the $\pi^0 \rightarrow \gamma + \gamma + \gamma$ decay mode from the $K_{\pi 2}$ decay events to test the validity of charge-conjugation invariance for electromagnetic and strong interactions. Mesons(K^+) from the Berkeley Bevatron were stopped in a heavy-liquid bubble chamber, filled with C_3F_8. The detection procedure is described. The upper limit on the decay mode relative to the normal mode was found to be $<3.8 \times 10^{-4}$. The 3γ rate is written, assuming a C-nonconservation parameter G, and the 90% confidence upper limit on $|G|^2$ was found to be <0.12. (L.B.S.)

21030 MESON AND BARYON MASSES IN SU(6) SYMMETRY. H. Harari (Israel Atomic Energy Commission, Yavne) and H. J. Lipkin. Phys. Rev. Letters, 14: 570-2 (Apr. 5, 1965).

The mass relations for members of the SU(6) supermultiplets are discussed, with particular consideration of the transformation properties of the SU(6) symmetry-breaking part of the strong interaction. It is shown that the experimental values of baryon and meson masses are in disagreement with the assumption that the mass splittings in both SU(6) supermultiplets are given by the expectation values of operators having the same definite transformation properties under SU(6). (D.C.W.)

21031 RELATIVISTIC SCATTERING OF TWO EQUAL-MASS CHARGED PARTICLES. William B. Rolnick and R. M. Thaler (Case Inst. of Tech., Cleveland). Phys. Rev. Letters, 14: 572-4(Apr. 5, 1965).

The scattering of two charged particles of equal mass in the relativistic domain is investigated using a Hamiltonian of the form $H = H_0(1) + H_0(2) + V(\vec{r}_1 - \vec{r}_2)$, where $H_0(i)$ is a relativistic free-particle Hamiltonian for particle i. (D.C.W.)

21032 MASS DIFFERENCES AND LIE ALGEBRAS OF FINITE ORDER. L. O'Raifeartaigh (Syracuse Univ., N. Y.). Phys. Rev. Letters, 14: 575-7(Apr. 5, 1965). (NYO-3399-23)

A theorem is proved which shows that if the mass operator is self-adjoint and the masses of the particles are regarded as discrete points in the mass spectrum, then the mass differences can not be explained within the context of any Lie algebra of finite order. (D.C.W.)

21033 PROTON-ANTIPROTON ANNIHILATION IN M(12) SYMMETRY MODEL. Yasuo Hara (Univ. of Chicago). Phys. Rev. Letters, 14: 603-4(Apr. 12, 1965).

The annihilation of proton pairs is proposed as a test of the M(12) symmetry model (a relativistic generalization of the SU(6) symmetry model). Relations among the cross sections for the various annihilation processes are considered. (D.C.W.)

21034 OBSERVATION OF THE LOW-ENERGY Λ-p INTERACTION. A. C. Melissinos (Univ. of Rochester, N. Y.), N. W. Reay, J. T. Reed, T. Yamanouchi, E. Sacharidis, S. J. Lindenbaum, S. Ozaki, and L. C. L. Yuan. Phys. Rev. Letters, 14: 604-7(Apr. 12, 1965).

The momentum spectra of mesons(K^+) produced in p-p interactions at 2.40 and 2.85 Bev were measured using a liquid hydrogen target. The cross sections for meson(K^+) production were obtained by integrating over angles and momentum. A marked deviation at the upper end of the meson(K^+) spectrum was observed, indicating a singularity in the Λ-p s-matrix very close to zero energy. Scattering lengths and an effective range for the Λ-p system were obtained by fitting the data by an s-wave formalism. The possibility that the singularity could be attributed to a decaying resonance was also considered. (D.C.W.)

21035 INTERNAL SYMMETRY AND RELATIVISTIC WAVE FUNCTIONS. C. L. Critchfield (Los Alamos Scientific Lab., N. Mex.). Phys. Rev. Letters, 14: 607-9(Apr. 12, 1965). (LA-DC-6969)

It is shown that the noncompact symplectic group of rank six, Sp(12), permits the same quantum numbers as SU(6) plus that of γ_4 which, when considered to be an infinitesimal operator, is a form of particle gauge operator since the sign of its eigen-values is that of the energy in hole theory. (D.C.W.)

21036 $\overline{U}(12)$ PREDICTIONS FOR $p\bar{p}$ ANNIHILATION INTO MESONS. R. Delbourgo, Y. C. Leung, M. A. Rashid, and J. Strathdee (International Centre for Theoretical Physics, Trieste, Italy). Phys. Rev. Letters, 14: 609-11 (Apr. 12, 1965). (IC/65/26)

The predictions of $\overline{U}(12)$ symmetry—a relativistic generalization of SU(6) symmetry—for annihilations at rest are compared with experimental observations on $p-\bar{p}$ annihilation into mesons. (D.C.W.)

21037 PION PRODUCTION IN HIGH-ENERGY MUON-NUCLEON COLLISIONS. P. L. Jain and P. J. McNulty (State Univ. of New York, Buffalo). Phys. Rev. Letters, 14: 611-14(Apr. 12, 1965).

The interaction of mesons (μ^-) with nucleons at 5 Bev/c was investigated by exposing nuclear emulsions to a meson(μ^-) beam. The total inelastic cross section was found to be $\sim 3 \pm 0.25$ μb/nucleon, and the cross sections for an inelastic process in which charged mesons(π) and strange particles are produced were found to be $\sim 7 \pm 1.4$ and $1 \pm 0.6 \times 10^{-31}$ cm^2/nucleon, respectively. The average transverse momentum of the mesons(π) was 244 ± 35 Mev/c. The distribution of the angular deflection of mesons(μ^-) producing nuclear interactions, the energy spectrum of the mesons(π) produced, and the integral spectrum of the square of the transferred four-momentum were obtained and compared with theoretical predictions. (D.C.W.)

21038 EVIDENCE ON THE EXISTENCE OF SHADOW PIONS IN K^+ DECAY. Allen E. Everett (Tufts Univ., Medford, Mass.). Phys. Rev. Letters, 14: 615-16(Apr. 12, 1965).

In terms of the shadow-matter hypothesis of Nishijima and Saffouri, a decay process with a mode of the form $A \rightarrow B + \pi^0$ may also have the mode $A \rightarrow B + \pi^{0\prime}$, where $\pi^{0\prime} \rightarrow 2\gamma'$. Experimental observations on the branching ratios for meson(K^+) decay are considered in view of this possibility. The data are consistent with the possibility that the meson (K^+) decays by $K^+ \rightarrow \pi^+ + \pi^{0\prime}$ with a branching ratio of about 5%. (D.C.W.)

21039 IMPLICATIONS OF $SU(12)_L$ FOR NN ANNIHILATION AT REST. Ngee-pong Chang (Rockefeller Inst., New York) and Joseph M. Shpiz. Phys. Rev. Letters, 14: 617-21(Apr. 12, 1965).

The annihilation of nucleon pairs at rest is studied by means of the relativistic completion procedures given by Beg and Pais for SU(6). The predictions of $SU(12)_L$ for annihilation at rest into two or three mesons, pseudoscalar as well as vector, are considered. It is found that the assignment of the baryons to the totally symmetric 364 representation of $SU(12)_L$ gives agreement with experimental results. (D.C.W.)

21040 NEW DATA ON RESONANCES. V. B. Mandel'tsveig and A. M. Perelogov. Priroda, No. 11, 64-6 (Nov. 1964).

The hyperon (Ω^-) was discovered by the characteristic multistage decay pattern that appeared in one of 100,000 photographs that were made. The mass was shown to be 1686 ± 12 Mev, but the spin and parity are still not known. The existence of the hyperon (Ω) with necessary mass is a strong argument for the "eightfold way" if the spin and parity turn out to be like those of the other baryons. A number of new meson resonances have also been observed, but the experimental values of the quantum numbers have not been well established, and spin and parity of some of

them are not known. It is now considered that baryon multiplets consist of three triplets and that those with eight and ten particles are constructed similarly. If quarks with approximately equal mass exist, they should be stable to, but could be converted to each other by, weak interactions. They should be observable in cosmic rays, and their mass should be greater than 2000 Mev. (TTT)

21041 THE DENSITY OF STATES AND BOLTZMANN EQUATION FOR ELECTRONS IN DISORDERED SYSTEMS. S. F. Edwards (Univ. of Manchester, Eng.). Proc. Phys. Soc. (London), 85: 1-25(Jan. 1965).

The problem of obtaining the mean density matrix and the Boltzmann equation for an electron in the presence of a random array of weak scatterers of arbitrary density is studied. The density matrix was previously studied by recombining its averaged perturbation expansion, but this is criticized on the grounds that it violates sum rules which are shown to apply to the mean density matrix. A new method is given which gives an integral equation for the mean density matrix having a form very similar in structure to the Boltzmann equation and automatically satisfying the sum rules. This method can be applied at arbitrary densities of scatterers and it is shown that the mean density matrix is Lorentzian near the mean free electron curve $E = (\hbar^2/2m)k^2 + Nu$ but Gaussian far from this curve, and the new form can be applied near band edges. The Boltzmann equation can be easily obtained from the density matrix, and its kernel can be expressed as a graphical series which is not based on the density of scatterers. (auth)

21042 CAPTURE OF NEGATIVE MESONS IN LIQUID HELIUM. J. E. Russell (Oxford Univ.). Proc. Phys. Soc. (London), 85: 245-55(Feb. 1965).

Estimates are made of the rates for the de-excitation of (π^-,α) and (K^-,α) atoms in liquid helium. An estimate is also made of the rate of nuclear capture of K^- mesons from high s states. The calculated Auger and radiative rates give total cascade times which are roughly $\frac{1}{6}$ as large as the experimental values. The approximations which are used are such that this is regarded as satisfactory agreement. For principal quantum number $21 \leq n \leq 24$ the Auger rate for (K^-,α) atoms is approximately equal to the rate for nuclear absorption. The calculations indicate that the amount of K^- absorption from high s states may not be negligibly small. (auth)

21043 THE S-WAVE SCATTERING LENGTHS FOR THE PION-PROTON INTERACTION. D. C. Cundy, R. A. Donald, W. H. Evans, W. Hart, P. Mason, D. E. Plane, J. R. Smith, and J. G. Thomas (Univ. of Liverpool). Proc. Phys. Soc. (London), 85: 257-65(Feb. 1965).

From an analysis of charge exchange and elastic scattering of 35 Mev negative pions using a liquid hydrogen bubble chamber, the charge-exchange total cross section is found to be 5.61 ± 0.40 mb and the s-wave scattering lengths $a_1 = +0.187 \pm 0.009$ and $a_3 = -0.082 \pm 0.011$ in units of $\hbar = c = m_\pi = 1$. The quantity $a_1 - a_3$ is found by a method free from systematic error and independent of Coulomb corrections. It is compared with that of the analysis of pion–proton scattering data, using dispersion relations, by Hamilton and Woolcock. The agreement is reasonable. (auth)

21044 A THIRD POSITRON LIFETIME IN SOLID POLYMERS. S. J. Tao and H. H. Green (Univ. of New South Wales, Sydney). Proc. Phys. Soc. (London), 85: 463-7(Mar. 1965).

Positron lifetimes were measured in Teflon, polyethylene, nylon-6, polypropylene, and paraffin wax. Using equipment of good resolution, $W_{\frac{1}{2}} = 0.7$ nsec, wide range, 30 nsec, and a highly linear response, three components of the lifetimes are found in each case. These are about 0.3, 0.6–1.1, and 1.7–4.1 nsec. Two components only were reported so far. A connection is found between the observed intensities of the longer components and the degree of crystallinity of the polymers, and an explanation is offered. The intensities of the long components vary according to the previous heat treatment of the polymer, especially in Teflon, in a way which depends on the physical structure of the solid. The identification of the three components should permit a useful re-examination of positron lifetimes in molecular materials. (auth)

21045 ON THE INTERMEDIATE BOSON THEORY OF WEAK INTERACTIONS. Kuo-chen Yang and Hung Kuan. Sci. Sinica (Peking), 13: 519-20(1964).

Some branching ratios of strange particle decays (leptonic and nonleptonic) were calculated. The decay rates of eight processes were calculated and used to compute the branching ratios. The results showed that all the calculated values were larger than the observed values by one order of magnitude. This discrepancy was ascribed to the smallness of the hyperon-lepton interaction constant; the possibility of strangeness-conserving and strangeness-changing decay processes being associated with two different sets of intermediate bosons was proposed. Inadequacies of Lee's model and Takeda's model were discussed. The following identity was obtained: $w(\Sigma^- \to ne^-\bar{\nu})/w(\Sigma^- \to n\pi^-) = w(\Sigma^+ \to ne^+\nu)/w(\Sigma^+ \to n\pi^+)$, where w is the decay rate. Using the experimental knowledge that $w(\Sigma^- \to n\pi^-) \approx w(\Sigma^+ \to n\pi^-)$, it was predicted that $w(\Sigma^- \to ne^-\bar{\nu}) \approx w(\Sigma^+ \to ne^+\nu)$. (OTS)

21046 APPLICATION OF THE TREIMAN-YANG CRITERION TO NUCLEON-NUCLEON INTERACTION. Tzu-tzan Huang (Joint Inst. for Nuclear Research, Dubna, USSR). Sci. Sinica (Peking), 14: 363-6(Mar. 1965).

The possibility of applying the Treiman-Yang criterion to the study of such reactions as $n + p \to p + p + \pi^-$ is discussed. The contributions from all possible one-pion exchange Feynman graphs to the definite final state are considered. This allows singling out from the experimental data the events corresponding to some Feynman graph. Such an approach makes it possible to apply the Treiman-Yang criterion also to the processes in which there are identical particles in the final state. (auth)

21047 POLYNOMIAL BASES OF GROUP SU_3 AND AN EXPLICIT EXPRESSION FOR ITS CLEBSCH-GORDAN COEFFICIENTS. Pei-yu Hou. Sci. Sinica (Peking), 14: 367-77(Mar. 1965).

The properties of the Young diagrams were used to construct a complete set of polynomial bases for representing the SU_n group. The basis of irreducible representations in the product space of two irreducible representations is then discussed. Finally by methods of construction of an invariant, an explicit expression for the Clebsch-Gordan coefficients of group SU_3 is obtained. (auth)

21048 COMPLEX ANGULAR MOMENTUM IN π-N SCATTERING. Lian-sou Liu (Peking Univ.). Sci. Sinica (Peking), 14: 466-8(Mar. 1965).

The problem of π-N scattering is treated, using Sawyer's method for summation of the most singular term in every order of approximation and neglecting particle isospin. Expressions for the scattering amplitude are obtained, and high-energy behavior in the crossed channels is discussed. (M.J.T.)

21049 REGGEIZATION OF HADRONS. Yu. M. Malyuta (Inst. of Physics, Kiev). Ukr. Fiz. Zh., 9: 1368-9(Dec. 1964). (In Ukrainian)

Regge trajectories for Ξ^0 hyperons ($\Xi^0 = \overline{K}^0\Lambda$) and for M^0 mesons ($\overline{M}^0 = \overline{K}^0\eta$) were found and calculated using the method previously suggested by the author (Ukr. Fiz. Zh., 10: No. 1, (1965)). With the coupling constant $g_2h_1/4\pi = 26$ the hyperon mass M = 1.28 Bev differs from the observed mass by 3%. With the coupling constant for the $\overline{M}^0$ meson $h_1^2/4\pi$ the M^0 mass coincides with the observed mass. (R.V.J.)

21050 S-MATRIX IN KEMMER-DUFFIN FORMALISM (SPIN 0). M. Koiv and L. Palgi. Tr. Inst. Fiz. i Astron., Akad. Nauk Est. SSR, No. 24, 67-101(1964). (In Russian)

The application of the Kemmer-Duffin and Klein-Gordon formalisms for various interactions is examined. (auth)

21051 THE PAULI-FIERZ TRANSFORMATION GROUP AND FOUR-BOSON INTERACTION LAGRANGIANS (10-ROW

REPRESENTATION). V. Loorits and H. Oiglane. Tr. Inst. Fiz. i Astron., Akad. Nauk Est. SSR, No. 25, 70-4(1964). (In Russian)

Four-boson interaction Lagrangians for vector bosons are constructed as eigenvectors of the Pauli-Fierz group operators. Normalization requirements on the Lagrangians enable the relations between the values of the interaction constants to be calculated. (auth)

21052 ON EXPANSION OF THE SCATTERING AMPLITUDE INTO PARTIAL WAVES. Ya. I. Granovskii. Tr. Inst. Fiz. i Astron., Akad. Nauk Est. SSR, No. 25, 85-101 (1964). (In Russian)

A convenient method for expansion of the scattering amplitude into partial waves on the basis of Jacob-Wick method was developed. The processes $\pi N \to \pi N$, $\pi\pi \to N\overline{N}$, $N\overline{N} \to N\overline{N}$, and $N\overline{N} \to N\overline{N}$ are considered. (auth)

21053 STRUCTURE OF THE g-PLANE IN RELATIVISTIC SCHROEDINGER THEORY. Yu. M. Lomsadze, I. V. Khimich, and I. M. Shuba (Uzhgorod State Univ., Ukrainian SSR). Ukr. Fiz. Zh., 9: 1176-84(Nov. 1964). (In Ukrainian)

The structure of the complex g-plane of the partial wave amplitude is investigated for the scattering of a relativistic spinless particle by a Coulomb potential. The nature of the motion of the poles $g_0(\gamma,E)$ of the partial wave amplitude is studied along two sheets of its g-plane with variation of the energy E along the real axis in the case of an arbitrary physical $\gamma = l + 1/2$. The nature of the motion of the poles $E_0(\gamma,g)$ of this amplitude is also studied along two sheets of its E-plane with variation of g along the real axis. A detailed physical interpretation is given both of the peculiarities of the partial wave amplitude and of the peculiarities of the trajectories $g_0(\gamma,E)$ and $E_0(\gamma,g)$ in their g- and E-planes. The situation arising on transition to the nonrelativistic limit is considered. Considerations are brought about the structure of the g-plane of the partial wave amplitude for the case of scattering of a relativistic spinless particle as well as of a particle with spin by a Yukawa potential. Elucidation of the g-plane structure permits applying the Mittag-Leffler procedure for any $g \neq \gamma$. (auth)

21054 ANALYTICAL PROPERTIES OF THE SCATTERING AMPLITUDE, CORRESPONDING TO A CLASS OF FEYNMAN DIAGRAMS. V. I. Kolomytsev and V. I. Fushchich. Ukr. Mat. Zh., 16: 610-23(1964). (In Russian)

Analytical properties of scattering amplitudes corresponding to a class of Feynman diagrams with initial α concept of scattering amplitude and integration along one parameter fulfilled by means of a δ function were investigated. The diagrams were used in order to determine the influence of the spectral curve properties on the analytical properties of the amplitudes. (R.V.J.)

21055 ON SINGULARITY OF AMPLITUDES OF SCATTERING IN A COMPLEX Z-PLANE. N. T. Mordovets. Ukr. Mat. Zh., 16: 624-30(1964). (In Russian)

Previously O. S. Parasyuk (Doklady Akad. Nauk. 145. 1247 (1962)) investigated analytical properties of scattering amplitudes in quantum field theory using the Leman ellipse, Legendre polynomial, Regge analyticity and LeRua-Lindelef theorem. The analyticity of scattering amplitudes as a function Z behind the Leman ellipse was investigated considering a series of Taylor factors which established the possibility of analytical continuity $F(\xi)$ function beyond the power series convergence circle. (R.V.J.)

21056 EFFECTIVE WAVE EQUATIONS IN THE THEORY OF QUANTUM GREEN'S FUNCTIONS. V. L. Bonch-Bruevich. Ukr. Mat. Zh., 16: 719-29(1964). (In Russian).

Green's functions were used for developing general formulas for the first density matrix, mean energy, and binary correlation function for the system of many interacting particles. (R.V.J.)

21057 THE DECOMPOSITION OF DIRECT PRODUCTS OF IRREDUCIBLE REPRESENTATIONS OF SU_3. Hung-chou Sun and Qi-zhi Han (Peking Univ.). Wu Li Hsueh Pao, 21: 56-66(Jan. 1965). (In Chinese)

The familiar concepts of rotation group were used to obtain the irreducible unitary representations and the reduction coefficients of the group SU_3. (These coefficients may be called the generalized Clebsch-Gordan coefficients.) This method is easier than those given by others. (auth)

21058 THE LOW-ENERGY KAON-PION SCATTERING. Lon-shang Chou and Ting-gin Chen. Wu Li Hsueh Pao, 21: 67-74(Jan. 1965). (In Chinese)

The method suggested by L. A. P. Balázs for solving the problem of the low energy pion-pion scattering is applied to the kaon-pion scattering process. It is found that the position of the K^* resonance is $\sqrt{S_R} = 854$ Mev, the half width $\frac{1}{2}\Gamma_1^{\frac{1}{2}} = 126$ Mev, and the phenomenological constant of the amplitude of the process $\pi + \pi \to K + \overline{K}$ $\xi = 0.3\ \mu^{-2}$. The position of the K^* resonance is in good agreement with experiment. (auth)

21059 ON THE DECAY BRANCHING RATIO OF THE UNSTABLE PARTICLE η: $R(\eta \to \pi\pi\gamma/\eta \to 3\pi)$. Pao-ru Tzu. Wu Li Hsueh Pao, 21: 92-102(Jan. 1965). (In Chinese)

The branching ratio of $\eta \to \pi\pi\gamma$ and $\eta \to 3\pi$ is studied through the analytic continuation of a dispersion relation with respect to the mass of η. It is pointed out that the anomalous threshold and complex singularities are both present. Under the appropriate approximation, the branching ratio $R(\eta \to \pi\pi\gamma/\eta \to 3\pi) \approx 0.65$ is obtained, which is close to recent experimental results. (auth)

21060 DECAY OF K_{l3}. I-shin Tuan and Ch'ung-yuan Chou (Univ. of Lanchao, China). Wu Li Hsueh Pao, 21: 101-13(Jan. 1965). (In Chinese)

The ratios of decay probabilities $\Gamma(K_{\mu 3}^+)/\Gamma(K_{e3}^+)$, $\Gamma(K_2^0 \to \pi\mu + \nu)/\Gamma(K_2^0 \to \pi e + \nu$, $\{\Gamma(K_2^0 \to \pi e + \nu) + \Gamma(K_2^0 \to \pi e^- \nu)\}/\Gamma(K_{e3}^+)$ and μ meson spectrum in $K_{\mu 3}^+$ decay were found using a dispersion relations and by considering intermediate state $K - \pi$. It is shown that with the violation of the selection rule $|\Delta I| = 1/2$, $\Delta S = +\Delta Q$ and unequal amplitudes $I_Z = 1/2$ and $I_Z = 3/2$ the probability ratios and μ-meson spectrum are in a good agreement with the experimental data. The form factors for K_{l3} decay were not constant. (tr-auth)

21061 THE PRINCIPLE OF MAXIMUM ANALYTICITY AND SOME PROPERTIES OF THE REGGE TRAJECTORIES. Pong-cheng Yin, Peng-sheng Yeh, and Chun-ting Chang (Fu-Tai Univ., Shanghai). Wu Li Hsueh Pao, 21: 114-20(Jan. 1965). (In Chinese)

Some properties of the Regge trajectories are investigated on the basis of the principle of maximum analyticity. It was shown that the Regge trajectories corresponding to the different particles are monotonic increasing functions of energy below the threshold and the asymptotic limits of every trajectory are the same for $t \to \pm\infty$. In particular, the vacuum Regge trajectory has nonlinear feature when $-t_0 < t < 0$ and the slope at zero energy $\alpha_p'(0)$ must satisfy the inequality $1/t_0 < \alpha_p'(0) < 1/4$ where t_0 is the value of t when $\alpha_p(-t_0) = 0$. (auth)

21062 INELASTIC COLLISIONS OF 6.8-Bev/c π^--MESONS WITH NUCLEONS. Shih-wei Wang, Tzu-tzen Wang, Zin-rhu Rhen, Chung-suen Lo, Pwu-in Cheng, and Teh-chang Huang. Wu Li Hsueh Pao, 21: 235-46(Feb. 1965). (In Chinese)

An analysis of 317 inelastic interaction events is presented. The angular and momenta distributions, etc., in the pion-nucleon center of mass system, of the secondary charged particles resulted from the collisions agree with the results of previous works and may be compared with the theoretical calculation based on the mechanism of peripheral collision. Those events in which the secondary protons are identified have been analyzed as follows: The total energy ω of all secondary particles except the protons in barycentric system was computed. The ideogram of ω distribution is given and is compared with the modified theoretical distribution calculated by Barashenkov et al. under the approximation of the OPE model. At about $\omega = 1.5$ Bev

a peak was found which is not given by the theoretical curve. Events in this peak were preliminarily analyzed. By using the secondary protons of the events and other events under the same conditions, the coefficients of inelasticity, K_3, in the mirror system were computed. The distribution of K_3 is given and is compared with the modified theoretical distribution calculated by Barashenkov et al. under the approximation of the OPE model. Moreover, the events of different values of K_3 were analyzed and discussed tentatively by means of the concept of target mass and using the method of F plot proposed by Duller Walker. (auth)

21063 HIGH-ENERGY SCATTERING AND α_q-REGGE TRAJECTORY. Pong-cheng Yin, Peng-sheng Yeh, and Chun-ting Chang (Fu-Dan Univ., China). Wu Li Hsueh Pao, 21: 346-54(Feb. 1965). (In Chinese)

A new Regge trajectory, α_q, with vacuum quantum numbers, $\alpha_q(0) = \alpha_p(0) = 1$, but $\alpha_q'(0) \neq \alpha_p'(0)$ was introduced. α_q as well as α_p takes part in the high energy non-exchange processes, and they interfere with each other. The consequence of the two vacuum Regge trajectories is equivalent to an effective trajectory α_e, the slope of which at zero energy $\alpha_e'(0)$ is dependent on the processes. The essential difference of this theory from the old one deduced from a single vacuum trajectory, α_p, is that $\alpha_e'(0)$ will be different for different processes. This does not conflict with the newest experiments. It is expected that $\alpha_e' 0'$ for K–N scattering will take different values from those of π–N and N–N. The existence of α_q may not influence the relations between the total cross sections of the crossed processes, but the polarization of the high energy nucleon after scattering will decrease much more slowly, than absence of α_q, as energy increases. (auth)

21064 RADIATION FROM A POINT CHARGE IN A WAVEGUIDE IN THE PRESENCE OF AN EXTERNAL MAGNETIC FIELD. E. D. Gazazyan and O. S. Mergelyan. Zh. Tekhn. Fiz., 35: 158-9(Jan. 1965). (In Russian)

The radiation from a point charge moving uniformly along the axis of a circular waveguide filled with dielectric material and located in a longitudinal magnetic field was calculated. The equations for the electric field of the moving charge are quoted from the literature, and the calculation reduces to fitting the boundary conditions on the waveguide surface. The energy radiated per unit path length is calculated. The spectrum of the radiation is discrete and the same for both right- and left-hand circularly polarized components, but the intensities of these components and the conditions for their radiation are different. (ATD)

21065 INTRINSIC AND DYNAMIC PROPERTIES OF Ξ HYPERON. Georges Whitney London. Thesis, Rochester, N. Y., Univ. of Rochester, 1964. 118p.

The Brookhaven 20″ hydrogen bubble chamber was exposed to a separated K^- meson beam, with a laboratory momentum of 2.24 Bev/c, at the Alternating Gradient Synchrotron. A total of about 340,000 pictures were studied. The masses of the Ξ^- and Ξ^0 were determined to be 1320.4 ± 0.3 Mev and 1313.5 ± 2.2 Mev, respectively. The lifetime of the Ξ^- was measured by the Bartlett maximum likelihood method modified to include the lambda detection probability. The result is $\tau_{\Xi^-} = (1.80^{+0.16}_{-0.13}) \times 10^{-10}$ sec. The decay parameters, α^-, β^-, and γ^-, were determined for the Ξ^-. There were two determinations, consistent with each other, one spin-independent and one spin-dependent. In the latter analysis, the polarization of the cascade is found to be equal to (85 ± 14)%. Since α^- is non-zero, parity is violated in Ξ^- decay. Taking into account final state interactions, it is found that either charge conjugation (C) invariance or time reversal (T) invariance is violated but not both. Upon the assumption that the phase shifts at a Q = 66.0 Mev are similar to the π-N phase shifts at the same Q, then the data favor T invariance and C violation. A determination of α^0 for the Ξ^0 gave $\alpha^0 = 0.20 \pm 0.37$, consistent with the $|\Delta I| = 1/2$ rule which predicts $\alpha^0 = \alpha^-$. An example of the beta decay of the Ξ^- is described. In the $\Xi\ \pi$ K final states, a $\Xi\ \pi$ resonance was observed in addition to the previously observed Kπ resonances, the K*(885) and n(730). The masses of the Ξ^{*-} and Ξ^{*0} and the true width of the Ξ^* were found to be $M_{\Xi^{*-}} = 1535.7 \pm 4.7$ Mev, $M_{\Xi^{*0}} = 1528.7 \pm 1.1$ Mev, and $\Gamma_{\Xi^*} = 8.5 \pm 3.0$ Mev. An estimate of the electromagnetic mass splitting of the Ξ^* is thus 7.0 ± 4.7 Mev. Isospin $1/2$ is favored over $3/2$ by about three standard deviations. A spin $\geq 3/2$ is indicated, with little or no evidence of background interference. The mass, isospin, and spin, therefore, of the Ξ^* are consistent with the SU(3) prediction of a resonance with the quantum numbers of a $\Xi\ \pi$ system at a mass of about 1530 Mev. No other resonance in the $\Xi\ \pi$ system was detected up to an invariant mass of 1840 Mev. No resonance in the Ξ K system was observed. (Dissertation Abstr., 25: No. 5, Nov. 1964)

21066 QUANTUM NUMBERS OF THE β MESON. Sharashchandra Hanamant Patil. Thesis, San Diego, Calif., Univ. of California, 1964. 72p.

The $\pi\pi$, $\pi\omega$ scattering amplitudes in I = J = 1 state are parameterized in terms of five parameters, which are determined so as to give the ρ meson position and width, the ω-width, and the B meson position and its $\pi\omega$ decay width under the assumption that B has quantum numbers 1^-. These amplitudes are then used to discuss $\pi\pi$, $\pi\omega$ production processes in terms of a simple peripheral model including π, ω exchanges. The model predicts a large $\pi^+\pi^-$ decay rate of B with a cross section comparable to the experimental $\pi^+\pi^-$ resonant cross section (the f^0) observed at approximately the same position as the B meson. On the other hand, since the B is an I = 1 particle this implies that the branching ratio of the $2\pi^0$ decay to that of the $\pi^+\pi^-$ decay should be small. This is incompatible with the experimentally observed large branching ratio. Within the limitations of our model, it is therefore unlikely that the B meson is a 1^- particle. (Dissertation Abstr., 25: No. 5, Nov. 1964)

21067 APPLICATION OF N/D METHOD TO YUKAWA POTENTIAL SCATTERING AND ANALYSIS OF REGGE TRAJECTORIES WITH SPIN EFFECTS. Max Luming. Thesis, San Diego, Univ. of California, 1964. 176p.

The partial wave amplitude for Yukawa potential scattering is evaluated by the N/D method with the approximation of neglecting distant unknown cuts. The N/D solution with only the first Born cut, and the solutions with the first and second Born cuts are obtained. The second solution, which contains the exact left hand discontinuity out to $k^2 = -9\mu^2/4$ (in units where k^2 is the energy, μ is the potential range inverse), is found to give a reasonable approximation to the exact amplitude in the low-energy region up to an energy of the order $3\mu^2$, for potential strengths up to values sufficiently strong to give an S-wave bound state. The solution also gives reasonably good prediction of the S-wave binding energy. The Yukawa amplitude is also evaluated by the determinantal method. The first order solution using only the first Born and the second order solution using the first and second Born terms are obtained. It is found that the first order solution gives poor prediction of binding energy and the second order solution gives no bound state whatsoever. The phase shifts found by the determinantal method are less reliable than the N/D method. The problem of extending the N/D equations to non-integer l is considered. The method of dividing the amplitude by the threshold factor and using a cut-off in the dispersion integrals introduces an essential singularity at infinite l, which raises questions concerning its validity. These questions are clarified by applying the method to find the leading trajectory of the Yukawa potential and comparing with the exact trajectory. The extended N/D equations are used to find the Regge trajectories for the elastic scattering of two spin $1/2$ particles. Different techniques for handling the kinematic singularity in the energy plane are discussed. Considering only the left hand cut from single pion exchange, the Regge continued amplitudes are evaluated, including solutions near the J = 0 pole of the Born terms. Distinction between Regge continued amplitude and the physical amplitude at J = 0 is discussed. It is found that the top Regge trajectory as calculated by the ND^{-1} method lies near the value $J = s_1 + s_2 - 1$ in the weak coupling limit, where s_1 and s_2 are the spins of the scattering particles. Some of the problems that might

arise when higher spins are considered are discussed. (Dissertation Abstr., 25: No. 5, Nov. 1964)

21068 ON BARYON ANTIBARYON SCATTERING. Martin Samuel Spergel. Thesis, Rochester, N. Y., Univ. of Rochester, 1964. 200p.

A method was developed for determining the elastic, charge exchange, and annihilation cross sections for the antibaryon-baryon system in the non-relativistic region of energies. The method involves the use of a boundary condition and an "elastic potential" to represent the strong baryon-antibaryon interaction. The boundary condition is taken to maximize the absorption cross section in each channel of specified isotopic spin, ordinary spin, and total angular momentum. The potentials are constructed by modifying the one- and two-pion nucleon-nucleon potentials in accordance with field theoretic and the SU3 group concepts. The differential elastic cross sections, total elastic, charged exchange, and annihilation cross sections were calculated up to several hundred Mev for nucleon-antinucleon and nucleon-antihyperon scattering, (i.e., $\bar{N}N$ and $\bar{\Sigma}N$). Polarizations as well as the cross sections for the reaction $\bar{\Lambda}N \rightarrow \bar{\Sigma}N$ were calculated. The antinucleon-nucleon results fit the available experimental data. (Dissertation Abstr., 25: Nov. 5, Nov. 1964)

21069 ANGULAR DISTRIBUTION OF THE PRODUCTS OF THE K_{e3} MESONIC DECAY. Paul Edward Condon. Thesis, Princeton, N. J., Princeton Univ., 1963. 103p.

The reaction $K^+ \rightarrow e^+ + \nu + \pi^0$ was studied by bringing K mesons to rest inside an array of scintillation counters, and detecting angular correlations among the electron and two gamma rays from the cascade reaction $K^+ \rightarrow e^+ + \nu + \pi^0$, $\pi^0 \rightarrow \gamma + \gamma$. The gamma rays were detected in scintillation-lead sandwiches, which also identified electrons by showers produced in the lead. The electron-gamma ray detectors involved ninety scintillation counters. The pulses from all these counters were recorded in digital form on teletype tape, and identification of K_{e3} events was carried out on a digital computer. In this reaction it is of particular interest to learn the dynamical character of the reaction and to discover a possible energy dependence of the form factors. The data of this experiment are consistent with vector-axial vector coupling with constant form factor. (Dissertation Abstr., 25: No. 5, Nov. 1964)

21070 SOME GENERALIZATIONS OF THE THRESHOLD-TYPE REGGE TRAJECTORIES. Walter Henry Carnahan. Thesis, Bloomington, Ind., Indiana Univ., 1964. 50p.

The threshold-type Regge poles are examined from the point of view of non-relativistic potential theory. In the second chapter, the formalism to be used is introduced via a simple example of two coupled spin-zero channels. The trajectories of the threshold poles by a numerical single channel calculation for two spin-zero particles interacting via a square well potential are presented in Chapter III. Chapter IV demonstrates the existence of the threshold poles in the case of two spin-particles interacting via a tensor force. Two particles in a bound s-state are allowed to be excited via the incident particle only to a p-wave state with no ionization. It is assumed that the particle-particle interaction is a superposition of Yukawas and thus the j-dependence of the potential can be written. A similarity transformation is introduced, which removes the j-dependence of the potential; with the aid of this transformation it is seen that the transformed Jost function has a simple fixed pole at $j = -\frac{1}{2}$, that the determinant of the Jost function has no poles, and that the transformed S-matrix has no fixed poles. (Dissertation Abstr., 25: No. 5, Nov. 1964)

21071 POLARIZATION CORRELATION OF Λ AND Σ^0 HYPERONS IN THE PROCESS $K^- + p \rightarrow \Sigma^0 + \pi^0$, $\Sigma^0 \rightarrow \Lambda + \gamma$. Moon Hwa Cha. Thesis, College Park, Md., Univ. of Maryland, 1963. 84p.

A generally covariant treatment of polarization correlations in the two-step process $K^- + p \rightarrow \Sigma^0 + \pi^0$, $\Sigma^0 \rightarrow \Lambda + \gamma$, and similar processes, is presented, with both kinematical and dynamical weight factors included. The results are used to compute the Λ polarization, as a function of the Λ momentum, for K^- mesons at a laboratory momentum of 400 Mev/c. The implications of the results for the phenomenological analysis of Watson, Ferro-Luzzi, and Tripp of the $K^- + p \rightarrow \Sigma + \pi$ reaction amplitudes are considered. (Dissertation Abstr., 25: No. 5, Nov. 1964)

21072 FUNDAMENTAL PARTICLES. K. Nishijima. Lecture Notes and Supplements in Physics. New York, W. A. Benjamin, Inc., 1964. 419p.

A historical survey of the discovery of muons and pions in cosmic rays is given. The study of invariance principles and their application to the determination of the pion transformation properties are discussed, with consideration of time reversal, parity, spin, and charge conjugation. Charge symmetry and charge independence in nuclear and pion physics are considered. Covariant perturbation theory and dispersion theory are introduced, and the dynamical properties of the pion-nucleon interaction are described in terms of dispersion relations, emphasizing the analysis of nucleon form factors leading to predictions on the presence of vector mesons. A discussion of strange particles and hyperfragments is presented. The violation of parity in weak interactions is discussed. (M.J.T.)

21073 MOTT EFFECT OF ELEMENTARY PARTICLES AND NUCLEI WITH ELECTROMAGNETIC STRUCTURE. A. Herrmann. Thesis, Munich, Universitat, 1964. 108p. $2.00(Gmelin, AED-DISS. 64-150). (In German)

Calculations of Mott asymmetry for various incident and target particles using Born's approximation of quantum electrodynamics are described. Dependence of Mott effect on structure functions is discussed. Electron-proton scattering is treated in detail. (Gmelin Inst.)

21074 THEORY OF LOW ENERGY PION-PION SCATTERING. Kyungsik Kang. Thesis, Bloomington, Ind., Indiana Univ., 1964. 73p.

A limited examination of the pion-pion scattering problem is made in an effort to shed some light on the conjectures about analyticity and crossing symmetry made by Chew and Mandelstam. The basic conjecture is that the amplitude is a Lorentz invariant, analytic function of all energy variables except for the requirement of unitarity. The crossing symmetry conditions are studied in detail, and the crossing symmetry relations are derived using transformation properties of the scattering amplitudes and analytic continuation only. It appears that the validity of the Chew-Mandelstam crossing relations is restricted only to the nearby region, unless the singularities from the two crossed channels cancel each other in the overlapping region. If the delicate cancellation occurs in the overlapping region, then the Chew-Mandelstam crossing relation is valid up to where the double spectral function begins to contribute, and to where the partial wave expansion of the scattering amplitude fails to converge. It is hoped that the nearest singularities lead to estimation of the most important aspects of the processes. Nearby left-hand singularities are chosen in such a way that the functional forms are correct near the branch point. Inelastic effects and distant left-hand singularities are crudely incorporated by means of regulating dispersion integrals and polynomials (subtraction terms). An amplitude is obtained, which manifestly satisfies the analyticity and unitarity in a single channel at low energy. A detailed satisfaction of the self-consistent conditions around the symmetry point is stressed on the amplitude by adjusting parameters. The amplitude will thus satisfy elastic unitarity exactly and crossing symmetry only approximately. (Dissertation Abstr., 25: No. 5, Nov. 1964)

21075 MESON CONTRIBUTION TO THREE BODY FORCES IN THE TRITON. Norman Edward Holden. Thesis, Washington, D. C., Catholic Univ. of America, 1964. 70p.

The contribution of 3-body forces to the binding energy of the triton was calculated. The static 3-body force obtained by Coury and Frank using Chew-Low methods was used. This includes the effect of 2 p-wave mesons exchanged between recoil-less nuclei. The potential includes an adjustable core parameter to assert the sensitivity of

the binding to the close-up (0.5 fermi) part of the wave function. The wave functions chosen are the Pease-Feshbach two S functions and 3 D functions. A first order perturbation calculation of the 3-body energy was made. The results were found to be attractive and give a contribution of the order of a fraction of a Mev. Thus 3-body forces are not very crucial to the binding and will not explain the discrepancy between experiment and the Blatt-Derrick exhaustive 2-body force calculation. (Dissertation Abstr., 25: No. 5, Nov. 1964)

21076 KINEMATIC ANALYSIS OF PRODUCTION REACTIONS. John Reid Higgins. Thesis, Bloomington, Ind., Indiana Univ., 1964. 53p.

Production reactions of elementary particles (A + B → 1 + 2 + 3) depend on five variables, three of which (internal variables) fix the momenta of the three final particles relative to each other while the other two (orientation variables) fix the orientation of the final three-particle system. It is shown that if the orientation variables are taken to be Euler angles then the production partial wave amplitude b^M_L can be defined in a natural way as $B = \sum b^M_L Y^M_L(\beta,\alpha)$, where B is the production amplitude and b^M_L depends on internal variables only. This definition is extended to the case in which some of the particles have spin. The use of Euler angles as orientation variables has an additional advantage that, in terms of them, the volume element for three-particle phase space takes on a very concise form. It is shown that the partial wave expansion for a production amplitude can simplify the unitarity condition on the elastic amplitude in which the production process is taken into account, and an expression for the imaginary part of the elastic phase shift in terms of production partial wave amplitudes is given. Finally an application is made to the $\pi + N \rightarrow A + \pi + N$ reaction under the assumption that the 3-3 isobar dominates. It is suggested that of the various distributions that can be measured the angular distribution of the normal to the plane formed by the three final particles will be the least complicated. (Dissertation Abstr., 25: No. 5, Nov. 1964)

21077 REGGE POLES IN BOSON-FERMION SCATTERING. Daniel Zissel Freedman. Thesis, Madison, Wis., Univ. of Wisconsin, 1964. 143p.

Two aspects of the problem of Regge poles in boson-fermion scattering are considered. The Bethe-Salpeter equation for the partial wave amplitudes $f_l \pm (w)$ in the scattering of scalar bosons and spin one-half fermions is studied in the ladder approximation. In this approximation the equation sums the ladder graphs in which the scattering takes place by boson exchange. It is proved, using a Fredholm technique, that the scattering amplitudes are meromorphic in half-planes of the angular momentum variable l, and that there is at least one Regge trajectory in each amplitude in these regions. Expressions for the leading Regge trajectories and their residues are obtained, which are valid to lowest order in perturbation theory. The implication of the Regge behavior for the asymptotic limits of the scattering amplitudes at high energies in the crossed channels is investigated. It is shown that the Regge pole predictions coincide exactly, to the order considered, with the predictions of ordinary perturbation theory. The question of whether the nucleon lies on a Regge trajectory is considered. A dynamical mechanism is suggested by which the nucleon is Reggeized in pion-nucleon scattering. The basis of the model is the fourth order box graph for πN scattering in which the nucleon and the T = 1 ρ meson appear in the intermediate state. The analytic interpolating function of the partial wave amplitude for this graph has a fixed pole in the j plane at $j = \frac{1}{2}$. The pole is "nonsense" in the physical partial wave amplitude at $j = \frac{1}{2}$ because of the presence of a non-continuable term. The fixed pole becomes a moving Regge pole when the lowest order N/D method is applied. The nucleon lies on the Regge trajectory generated, and the "elementary" nucleon singularity is cancelled by the non-continuable term. The trajectory has a reasonable slope at the nucleon mass. The model is then generalized to an SU_3 invariant theory of strong interactions and a Regge trajectory of the baryon obtained. The relationship of the N/D and Fredholm methods in models of this type is discussed, and the important role played by the factorability of the Born term is pointed out. (Dissertation Abstr., 25: No. 5, Nov. 1964)

Field Theory and Quantum Mechanics

Refer also to abstract 20812.

21078 (AFOSR-64-1380) A BROUWER-TYPE SPACE TO REPLACE THE CONVENTIONAL PHYSICAL CONTINUUM WHEN PARTICLES ARE REGARDED AS DISTINCTION SYSTEMS. E. W. Bastin and C. W. Kilmister (Cambridge Language Research Unit (England)). Nov. 1963. Contract AF61(052)-331. 34p. (AD-604044). $2.00 (CFSTI).

An ordered distinction system arises when entities specified by a set of properties each of which may be present or absent are considered, and when the growth of knowledge in time is taken into account. It is shown that all such systems have certain sets of integers corresponding to them, and the structure of these sets is considered. (auth)

21079 (IC/65/2) ASYMPTOTIC BEHAVIOUR OF PHASE SHIFT IN λ FOR STRONGLY SINGULAR POTENTIALS. B. Jakšić and N. Limić (International Centre for Theoretical Physics, Trieste (Italy)). Jan. 1965. 31p. Dep.(mn).

The asymptotic form of the phase shift is derived for strongly singular potentials for large complex λ, $|\arg \lambda| < \pi/2$, and real K. It is shown also that the S-matrix for such potentials must have an infinite number of poles in the λ-plane, accumulating along the imaginary axis. (auth)

21080 (IC/65/9) EXTRAPOLATION OF THE S-MATRIX FROM THE LEHMANN'S REPRESENTATION. N. Limić (International Centre for Theoretical Physics, Trieste (Italy)). Feb. 1965. 9p. Dep.(mn).

The extrapolation of the S-matrix to complex angular momenta is obtained using the Lehmann representation of the amplitude for the elastic scattering and the unitarity condition. In the half plane $\mathrm{Re}\ l > l_0$ the S-matrix is analytic regular and satisfies the extended unitarity condition. (auth)

21081 (ICTP-64/9) RIGGED HILBERT SPACES. Arno Boehm (International Centre for Theoretical Physics, Trieste (Italy)). Dec. 1964. 22p. Dep.(mn).

A technique is presented for "rigging" Hilbert spaces in order to make possible the representation of non-compact groups in terms of these spaces. (T.F.H.)

21082 THE STRUCTURE OF THE FIELD AND THE MOTION EQUATIONS FOR N CHARGED, GRAVITATING MASS POINTS IN FIRST AND SECOND APPROXIMATION. Hans Stephani (Universitat, Jena, Ger.). Acta Phys. Polon., 26: 1045-60(Dec. 1964). (In German)

Methods were developed completely for the calculation of the first and second approximation of pure gravitational fields and were used for the coupled Einstein-Maxwell field. The Schwarzschild metric was obtained exactly up to terms in κ^2, using the formula obtained for a static particle. (tr-auth)

21083 THREE-DIMENSIONAL ISOTROPIC HARMONIC OSCILLATOR AND SU_3. D. M. Fradkin (Iowa State Univ., Ames). Am. J. Phys., 33: 207-11(Mar. 1965). (IS-879)

A consideration of the eigenvalue problem for the quantum-mechanical three-dimensional isotropic harmonic oscillator leads to a derivation of a conserved symmetric tensor operator, in addition to the angular momentum vector operator. Upon examining the classical limit, it is found that the symmetric tensor completely specifies the orientation of the elliptical orbit, in a way analogous to the Runge-Lenz vector for the Kepler problem. The tensor operator and the angular momentum vector operator are

then related to the infinitesimal operators for the SU_3 group. (auth)

21084 ELECTROMAGNETIC FIELDS AND CYLINDRICAL SYMMETRY. K. P. Singh, L. Radhakrishna, and R. Sharan (Banaras Hindu Univ., India). Ann. Phys. (N. Y.), 32: 46-8(Mar. 1965).

The relativistic significance of the projective curvature tensor W_{hijk} is discussed. It is found that the vanishing of the divergence of this tensor in an electrovac universe implies a purely electric field. By breaking W_{hijk} into its antisymmetric and symmetric parts, P_{hijk} and Q_{hijk}, respectively, it is shown that the vanishing of the symmetric part is a necessary and sufficient condition for the space to be an Einstein space. In an electromagnetic field P_{hijk} is expressible linearly in terms of the Riemann curvature tensor R_{hijk} and the conformal curvature tensor C_{hijk}. P_{hijk} has all the symmetry and antisymmetry properties of R_{hijk} and also it possesses the cyclic property $P_{h[ijk]}=0$. The vanishing of the contracted tensor P_{ij} implies an Einstein space. This permits extension of the Pirani formalism of gravitational waves to the Einstein space with the help of W_{hijk}. The electromagnetic significance of the cylindrically symmetric metric of Marder is then considered. The Rainich algebraic relations give rise to four possible cases of electromagnetic fields, three of which correspond to electromagnetic wrenches, in the terminology of flat space-time, along one of the spatial coordinate lines. The complexion vector vanishes implying a purely electric field for the cylindrically symmetric electrovac universes. The conditions for the fields in question to be of Petrov type II were found. None of the well-known cylindrical electrovac universes satisfies these conditions. The fourteen scalar invariants of order two were evaluated for the four cases of electromagnetic fields. Two scalar invariant relations and a tensor relation exist as necessary conditions for electromagnetic fields of cylindrical symmetry. The groups of motions admitted by the fields are discussed. An exact nonstatic solution of the Einstein-Maxwell equations in vacuo is obtained, and some of its properties are studied. (auth)

21085 ENTIRE FUNCTIONS OF THE FREE FIELD. Arthur Jaffe (Institut des Hautes Etudes Scientifiques, Bures-sur-Yvette, France). Ann. Phys. (N. Y.), 32: 127-56(Mar. 1965).

The Borchers class is determined for a massive free field in two-dimensional space-time. Properties of the field operators, their closures, and their bounded functions are then discussed. Finally, an extension is made to the equivalence class of a tensor product of n massive free fields. (auth)

21086 ANALYSIS OF QUASI-MAXWELLIAN EQUATIONS DESCRIBING COMPENSATING FIELDS. A. G. Iosif'an, K. P. Stanyukovich, and G. A. Sokolik. Dokl. Akad. Nauk SSSR, 159: 1261-3(Dec. 21, 1964). (In Russian)

General quasi-linear equations for an arbitrary field are considered. These equations were first introduced for the case of gravitation. Equations of this type are derivable in natural fashion from the Noether theorem, and this theorem is formulated for local gauge transformations. Two pairs of quasi-Maxwellian equations are then derived for the case of a gravitational field; having the advantage that their quasi-Maxwellian character is retained even in a strong gravitational field, and the nonlinearity is contained in its entirety in the expression for the current. This nonlinear expression can be used for the description of gravitational waves. (ATD)

21087 WAVE MECHANIZATION OF DYNAMICAL SYSTEMS. Richard Arens (Univ. of California, Los Angeles). J. Math. Anal. Appl., 10: 135-60(Feb. 1965).

The construction of the Schroedinger equations is considered for dynamical systems such as the space-time manifold, the lagrangian, and the clock function. The Hamilton-Jacobi relation is defined, and the harmonic solutions are found. An absolute dynamic system is defined, and discussions are presented on a Minkowski system with a convector potential, exactness and divergence of vector fields, harmonic phase functions, and the differential equations for complex waves. (L.B.S.)

21088 MICROCAUSALITY IN ASYMPTOTIC QUANTUM FIELD THEORY. F. Rohrlich and J. C. Stoddart (Syracuse Univ., N. Y.). J. Math. Phys. (N. Y.), 6: 495-9(Apr. 1965).

Asymptotic quantum field theory can be formulated without the axiom of microcausality, (strong local commutativity). It is shown here that in certain cases microcausality is nevertheless a consequence of the remaining assumptions of the theory. These cases are the ones for which solutions of the basic equations can be obtained in perturbation expansion, i.e., the scalar, spin ½, and neutral vector field. For the charged vector boson, for example, the microscopic causality condition cannot be proved from the basic postulates. In the provable cases the functional derivative in the Bogoliubov causality condition can be defined explicitly, and this condition can then be derived from the postulates of asymptotic quantum field theory. In the other cases, Bogoliubov causality cannot be defined explicitly. (auth)

21089 STATISTICAL MECHANICS OF ASSEMBLIES OF COUPLED OSCILLATORS. G. W. Ford (Univ. of Michigan, Ann Arbor), M. Kac, and P. Mazur. J. Math. Phys. (N. Y.), 6: 504-15(Apr. 1965).

It is shown that a system of coupled harmonic oscillators can be made a model of a heat bath. Thus a particle coupled harmonically to the bath and by an arbitrary force to a fixed center will (in an appropriate limit) exhibit Brownian motion. Both classical and quantum mechanical treatments are given. (auth)

21090 ON A SPECIAL CLASS OF TYPE-I GRAVITATIONAL FIELDS. Manfred Truemper (Yeshiva Univ., New York). J. Math. Phys. (N. Y.), 6: 584-9(Apr. 1965).

An investigation is made of the algebraic structure and the analytic properties of a class of normal hyperbolic Riemannian 4-spaces restricted by the following condition: There exists a timelike unit vector u^a such that the Riemann tensor satisfies ${}^*R_{abcd}u^bu^d=0$. This condition is shown to be equivalent to the statement that the conform tensor is Petrov type I with real eigenvalues, u^a being a principal vector and an eigenvector of the Ricci tensor. This means that there is no flux of nongravitational energy relative to an observer travelling with 4-velocity u^a. The eigen null directions (Debever vectors) of the conform tensor lie in a timelike hyperplane spanned by u^a and the two eigenvectors of $\epsilon_{ac} \equiv -C_{abcd}u^bu^d$ belonging to the eigenvalues with largest absolute value. The conform tensor is degenerate (type D) if and only if a Debever direction projected into the rest space of an observer u^a is an eigendirection of ϵ_{ab}. The complete set of Bianchi identities is examined. It yields an expression for the covariant eigentime derivative of ϵ_{ab} and an algebraic relation linking the rotation and shear of u^a to the curvature tensor of the Reimannian space. The general results are applied to special Einstein spaces ($R_{ab}=0$) admitting a congruence of timelike curves without shear and rotation. We get a new simplified proof of the theorem that in the case of nondegeneracy such are static, the curves of the congruence being paths of an isometric motion. (auth)

21091 NEW HOMOGENEOUS SOLUTIONS OF EINSTEIN'S FIELD EQUATIONS WITH INCOHERENT MATTER OBTAINED BY A SPINOR TECHNIQUE. Istvan Ozsvath (Southwest Center for Advanced Studies, Dallas). J. Math. Phys. (N. Y.), 6: 590-610(Apr. 1965).

Einstein's field equations with incoherent matter are solved for the case of homogeneous space-time, i.e., for metrics allowing a four parametric simply transitive group of motions. Two families of new solutions are obtained by use of a spinor technique. As a special result a proof emerges for Gödel's theorem, which states that there exist only two homogeneous solutions of Einstein's field equations with incoherent matter and rigid rotation, namely the Gödel cosmos and the Einstein static universe. (auth)

21092 UNIFORM ASYMPTOTIC ESTIMATES FOR WAVE PACKETS IN THE QUANTUM THEORY OF SCAT-

TERING. Calvin H. Wilcox (Argonne National Lab., Ill. and Univ. of Wisconsin, Madison). J. Math. Phys. (N. Y.), 6: 611-20(Apr. 1965).

The theory of the scattering of particles by a potential field V(x) according to the classical wave mechanics of Schrödinger is considered. Various conditions on V(x) are known which imply that the wave packets $\psi(x,t)$ describing scattered particles are asymptotically equal in $L_2(R^n)$ to wave packets $\psi_0(x,t)$ for free particles when $t \to \infty$ or $-\infty$. Additional conditions on V(x) and the initial values of the wave packets are given which imply that $\psi(x,t)$ and $\psi_0(x,t)$ have square-integrable (or continuous) partial derivatives of a prescribed order whose difference tends to zero in $L_2(R^n)$(or uniformly in R^n) when $t \to \infty$ or $-\infty$. (auth)

21093 UPPER BOUND FOR THE DOUBLE SPECTRAL FUNCTION IN POTENTIAL SCATTERING. D. Bessis (Centre d'Etudes Nucleaires de Saclay, Gif-sur-Yvette, France). J. Math. Phys. (N. Y.), 6: 637-43(Apr. 1965).

For potentials V(z) holomorphic in Re $z > 0$ and bounded by $|V(z)| < K/|z|^{\rho}$ $\rho < 2$ for $|z| \leq 1$, and $|V(z)| < K|z|^{\gamma} e^{-\mu_0 \operatorname{Re} z}$ for $|z| \geq 1$, $\gamma > 1/4$, it is shown that the double spectral "function" $\rho(s,t)$ is a continuous function of s and t in $s > 0$, $t > 0$, and an upper bound is obtained for it. This upper bound shows clearly that the double integral of the Mandelstam representation in fact exists and defines an analytic function of s and t in two cut planes. The generalization of the results to the case when $\rho(s,t)$ is no longer a function but a distribution is indicated. (auth)

21094 VERTEX MODIFICATION FOR COULOMBIC INTERACTIONS BY EXACT SUMMATION OF LADDER DIAGRAMS. Yoh-han Pao and H. L. Frisch (Bell Telephone Labs., Inc., Murrary Hill, N. J.). J. Math. Phys. (N. Y.), 6: 652-5(Apr. 1965).

A class of ladder diagrams for Coulombic interactions to infinite order was summed exactly, and a "bare" interaction was replaced with a self-consistent effective interaction or equivalently the vertex operator was modified in a manner which may be of particular significance for systems of low particle density in analogy with what can be done for nuclear matter and liquid helium. The method is only valid for nearly free particles, the exact energy being negative but the zero-order description being that of free particles. Effective attractive interactions between two electrons or interaction with an external Coulombic field constitute perturbations which fall within the range of validity of the scheme. Despite the limitation of the specific results, the method is probably of more general use and interest and both the approach and specific results are described. (auth)

21095 NECESSARY CONDITION ON THE RADIAL DISTRIBUTION FUNCTION. Eugene Feenberg (Washington Univ., St. Louis). J. Math. Phys. (N. Y.), 6: 658-9(Apr. 1965).

Trial functions g(r) may be used as radial distribution functions to study the ground-state properties of a uniform extended quantum fluid (liquid He, nuclear matter). A result obtained by Wigner and Seitz in the study of the charged electron gas imposes an integral inequality on any assumed g(r). The relation is $\int_0^\infty [1-g(r)]r\,dr / [\int_0^\infty [1-g(r)]r^2\,dr]^{\frac{1}{2}} < 1.792/3^{\frac{1}{2}} = 1.243$. This inequality places an effective constraint on the location, magnitude, and width of the nearest-neighbor peak. (auth)

21096 HIGH-ENERGY BEHAVIOR AT FIXED ANGLE FOR THE FIVE-POINT FUNCTION IN PERTURBATION THEORY. J. V. Greenman (Cambridge Univ., Eng.). J. Math. Phys. (N. Y.), 6: 660-70(Apr. 1965).

The validity of the d-line method used by Halliday in studying the high-energy behavior at fixed angle of the four-point function is examined in more detail. This is carried out within the context of determining the high-energy behavior at fixed angle for the five-point function. The leading asymptotic behavior of the sum of all planar five-point graphs in a ϕ^3 theory at fixed angle is s^{-2}. (auth)

21097 CLEBSCH-GORDAN COEFFICIENTS ADAPTED TO CUBIC SYMMETRY. Jacques Moret-Bailly (Faculte des Sciences, Dijon, France), Lucienne Gautier, and Jean Montagutelli. J. Mol. Spectr., 15: 355-77(Mar. 1965).

The problems in quantum mechanics often have a spherical symmetry in the first approximation and a lower symmetry in a better approximation. Tables of Clebsch-Gordan coefficients are given for calculations in the cases where this lower symmetry is cubic. The tables were compiled on an IBM 7090 computer. (M.C.G.)

21098 RELATIVE VELOCITY IN RELATIVITY THEORY. L. Essen. Nature, 205: 1199-1200(Mar. 20, 1965).

The validity of the relativistic velocity transformation equation for relative velocity in relativity theory is discussed. (P.C.H.)

21099 EXACT SOLUTION FOR CHARGED PARTICLE TRAJECTORIES IN AN ELECTROMAGNETIC FIELD. M. J. Laird and F. B. Knox (Imperial Coll. of Science and Tech., London). Phys. Fluids, 8: 755-6(Apr. 1965).

The trajectories of electrons are considered in the presence of whistler-mode waves propagating in a region of the magnetosphere small enough for the magnetic field to be essentially uniform. The procedure is modified to obtain exact solutions for the trajectory of a charged particle when the oscillating field is a circularly-polarized plane wave travelling in the direction of the static uniform field. (L.B.S.)

21100 SPHERICAL GRAVITATIONAL COLLAPSE WITH ENERGY TRANSPORT BY RADIATIVE DIFFUSION. C. W. Misner (Univ. of California, Livermore and Univ. of Maryland, College Park) and D. H. Sharp. Phys. Letters, 15: 279-81(Apr. 1, 1965).

A general relativistic theory of radiative diffusion is outlined in which the form of the diffusion law is determined, apart from the expression for the coefficient of radiative transport, by the thermodynamic requirement that the entropy production rate be non-negative. (D.C.W.)

21101 ASYMPTOTIC BEHAVIOUR OF THE VERTEX FUNCTION IN SPINOR-PSEUDOSCALAR THEORY. M. Cassandro (Universita, Rome and Istituto Nazionale di Fisica Nucleare, Rome) and V. Formisano. Phys. Letters, 15: 292-3(Apr. 1, 1965).

The asymptotic behavior of the vertex function in the spinor-pseudoscalar theory is evaluated. The result is different from that obtained previously for electrodynamics involving massive photons. (D.C.W.)

21102 STATISTICAL DESCRIPTIONS OF FREE BOSON FIELDS. Dennis Holliday (Rand Corp., Santa Monica, Calif.) and Martin L. Sage. Phys. Rev., 138: B485-7(Apr. 26, 1965).

Several serious mathematical deficiencies in Sudarshan's probability-functional approach to the statistical description of light beams are demonstrated. In particular, it is shown that all the correlation functions of the beam do not necessarily determine its density matrix. (auth)

21103 ELECTROMAGNETIC SOLUTIONS OF THE FIELD EQUATIONS OF GENERAL RELATIVITY. B. Kent Harrison (Los Alamos Scientific Lab., N. Mex.). Phys. Rev., 138: B488-94(Apr. 26, 1965). (LA-DC-6492)

An investigation of the electromagnetic field in general relativity was undertaken. This study was partially motivated by the recent interest in the intense quasistellar sources and gravitational collapse and relativistic models for such phenomena. Metrics and fields as functions of two or three independent variables are considered. The equations for the case of two independent variables are presented in a simple form, and certain special solutions of these equations are derived, which may have some bearing on gravitational collapse. The major result may be stated as follows. Suppose given a set of metric coefficients g_{ik} which are functions of no more than three independent variables and which satisfy the vacuum field equations. It is assumed that it is possible to express this metric in diagonal form. Then, from this metric, one can find another metric, plus nonzero electromagnetic field, which satisfy the field equations with electromagnetic sources plus Maxwell's equations. (auth)

21104 EFFECTS OF GRAVITATIONAL RADIATION REACTION IN THE GENERAL RELATIVISTIC TWO-BODY PROBLEM BY A LORENTZ-INVARIANT APPROXIMATION METHOD. Stanley F. Smith and Peter Havas (Lehigh Univ., Bethlehem, Penna.). Phys. Rev., 138: B495-? (Apr. 26, 1965).

A Lorentz-invariant approximation method for obtaining the equations of motion of mass points in the general theory of relativity was developed recently. If retarded interactions are assumed, the first-order equations contain radiation reaction terms similar to those appearing in electrodynamics. These equations are used to investigate the question of the existence of gravitational radiation through the examination of selected approximate solutions of the two-body problem, without recourse to the assumption of slow motion. For the case of equal masses, the motion is almost circular; the particles are found to spiral outward in time. This result is in disagreement with Einstein's calculation of the distant field and the resulting energy loss due to quadrupole radiation based on the linear approximation, which, however, did not take proper account of the motion of the particles consistent with the approximate field equations used. These equations lead in a natural manner to an energy-momentum pseudotensor of the field consistent with the approximate equations of motion employed. Using this pseudotensor, the distant outgoing retarded field due to the circular motion of two equal masses is found to correspond to an energy influx of quadrupole type; similar results are found for elliptic motion of unequal masses in slow-motion approximation. On the other hand, the assumption of advanced interactions would lead to inward spiraling and an incoming field with energy outflow. The significance of these discomforting results is discussed; possible objections against the equations of motion used, the method of solution of these equations, or the interpretation of the solutions obtained are examined. The possibility that the calculation of radiation effects on the basis of the higher order equations of motion will yield results differing qualitatively from those obtained here in first order cannot be excluded. (auth)

21105 COHERENT STATES AND THE NUMBER-PHASE UNCERTAINTY RELATION. P. Carruthers (Cornell Univ., Ithaca, N. Y.). Phys. Rev. Letters, 14: 387-9(Mar. 15, 1965).

The number-phase uncertainty relation was derived in terms of Hermitian sine and cosine operators and was evaluated for coherent states having a wide range of the mean excitation using a CDC 1604 computer. It is shown that for large N the coherent states are minimum-uncertainty number-phase states as well as minimum-uncertainty position-momentum states. (L.B.S.)

21106 PROPOSAL FOR AN EXPERIMENT TO TEST THE SIMULTANEITY THEOREM OF THE SPECIAL THEORY OF RELATIVITY. R. Fuerth (London Univ.). Proc. Phys. Soc. (London), 85: 131-3(Jan. 1965).

The indirect evidence for the existence of the Lorentz "local time" effect, which is also a feature of the special theory of relativity, is discussed; and a simple direct experiment, using radio waves in the centimeter region, for testing the theorem of the relativity of simultaneity of events is proposed. (auth)

21107 A SCALAR THEORY OF GRAVITATION. J. S. Dowker (Univ. of Manchester, Eng.). Proc. Phys. Soc. (London), 85: 595-600(Mar. 1965).

A scalar gravitational theory is introduced which gives the correct rotation of the perihelion. (auth)

21108 ZERO REST-MASS FIELDS INCLUDING GRAVITATION: ASYMPTOTIC BEHAVIOUR. R. Penrose (Univ. of Texas, Austin). Proc. Roy. Soc. (London), Ser. A, 284: 159-203(Feb. 23, 1965).

A zero rest-mass field of arbitrary spin s determines, at each event in space-time, a set of 2s principal null directions which are related to the radiative behavior of the field. These directions exhibit the characteristic "peeling-off" behavior of Sachs, namely that to order r^{-k-1} (k = 0, ..., 2s), 2s−k of them coincide radially, r being a linear parameter in any advanced or retarded radial direction. This result is obtained for fields of any spin in special relativity, by means of an inductive spinor argument which depends ultimately on the appropriate asymptotic behavior of a very simple Hertz-type complex scalar potential. Spin $(s-\frac{1}{2})$ fields are used as potentials for spin s fields, etc. Several examples are given to illustrate this. In particular, the method is used to obtain physically sensible singularity-free waves for each spin which can be of any desired algebraic type. A general technique is described then for discussing asymptotic properties of fields in curved space-times, which is applicable to all asymptotically flat or asymptotically de Sitter space-times. This involves the introduction of "points at infinity" in a consistent way. These points constitute a hypersurface boundary $\mathscr{I}$ to a manifold whose interior is conformally identical with the original space-time. Zero rest-mass fields exhibit an essential conformal invariance, so their behavior at "infinity" can be studied at this hypersurface. Continuity at $\mathscr{I}$ for the transformed field implies that the "peeling-off" property holds. Furthermore, if the Einstein empty-space equations hold near $\mathscr{I}$ then continuity at $\mathscr{I}$ for the transformed gravitational field is a consequence. This leads to generalizations of results owing to Bondi and Sachs. The case when the Einstein-Maxwell equations hold near $\mathscr{I}$ is also similarly treated here. The hypersurface $\mathscr{I}$ is space-like, time-like or null according as the cosmological constant is positive, negative or absent. The technique affords a covariant approach to the definition of radiation fields in general relativity. If $\mathscr{I}$ is not null, however, the radiation field concept emerges as necessarily origin dependent. Further applications of the technique are also indicated. (auth)

21109 ROTATION IN GENERAL RELATIVITY WITH APPLICATIONS TO THE CASE OF A ROTATING PARTICLE. P. C. Bartrum. Proc. Roy. Soc. (London), Ser. A, 284: 204-23(Feb. 23, 1965).

A method is developed for dealing with rotations in general relativity. Formulas are derived, which are used for obtaining equations of motion of a rotating "particle" by a Lagrangian method in which the Lagrangian is a function of the co-ordinates, velocity, acceleration, and angular velocity of the particle. In order that the particle shall have only three rotational degrees of freedom and that the equations shall refer to the center of mass, it is found that the Lagrangian should be a function of a quantity $\Omega^{\mu\nu}$ which represents the apparent angular velocity minus the "relativity precession." (auth)

21110 THE LITTLE LORENTZ GROUP AND WAVE EQUATIONS OF FREE MASSLESS FIELDS WITH ARBITRARY SPIN. Yu. P. Stepanovskii (Inst. of Physics and Tech. Kiev). Ukr. Fiz. Zh., 9: 1165-8(Nov. 1964). (In Ukrainian)

An elementary particle with spin S other than zero and described by a 2S + 1 component wave function is investigated. It is assumed that if the 4-momentum of the particle is known, its wave function can be determined with the exactness of a multiplier. Thus, the wave function of the particle must satisfy certain linear equations, such as $(iS_{\mu\nu} + S\delta_{\mu\nu})\,\partial/\partial\chi_\nu\,\psi(\chi) = 0$, where $S_{\mu\nu}$ is the matrix of an infinitesimal transformation characterizing the Lorentz group, according to which the ψ wave function is transformed. From the equations it is evident that the mass of the particles is equal to zero. For $S = \frac{1}{2}$, 1, and 2, these equations describe neutrinos, a free electromagnetic field, and weak gravitational waves, respectively. (ATD)

21111 MOTION OF THE POLES OF THE BETHE-SALPETER PARTIAL WAVE AMPLITUDE IN THE g^2-PLANE. Yu. M. Lomsadze, S. S. Tokar, and J. M. Shuba (Uzhgorod State Univ., [Ukrainian SSR]). Ukr. Fiz. Zh., 9: 1277-82(Dec. 1964). (In Ukrainian)

The structure of the complex g^2-plane (g is a physical, renormalized, coupling constant) of the partial wave amplitude $f_g(l,s)$ is studied within the framework of the Bethe-Salpeter approach in the first non-vanishing (ladder), as

well as in the arbitrary, but finite in g^2, approximation for the Bethe-Salpeter kernel. For the field-theory interaction hamiltonians of class I, $f_g(l,s)$ is meromorphic in the entire finite g^2-plane. For hamiltonians of class II in the ladder approximation root branch points arise, apart from the poles. In all these cases the structure of the g^2-plane permits application of the Mittag-Leffler procedure. Consideration of a finite number of approximations for the Bethe-Salpeter kernel in the case of class II hamiltonians leads to an immovable singularity of $f_g(l,s)$ at the point $g^2 = 0$ forbidding any application of this procedure whatever. The only constructive possibility of preserving the Mandelstam or even one-dimensional dispersion relation consists in the assumption that the vicinity $\epsilon(R)$ of convergence of the power in the g^2 expansion for an exact Bethe-Salpeter potential $V(g^2,R)$ vanishes as $R \to 0$. This assumption may (at least under certain conditions) make it possible to apply the Mittag-Leffler procedure to class II field-theory hamiltonians as well. As to field-theory hamiltonians of higher classes, there are grounds for believing that $f_g(l,s)$ in this case has an immovable singularity at the point $g^2 = 0$ which hinders the application of the Mittag-Leffler procedure and makes both the Mandelstam and the one-dimensional dispersion relations impossible. (auth)

21112 STÜCKELBERG'S FORMALISM FOR A FIELD OF SPIN $^3/_2$. G. L. Stavraki (Inst. of Physics, Kiev). Ukr. Fiz. Zh., 10: 10-15(Jan. 1965). (In Ukrainian)

Stückelberg's formalism for local fields of higher spins is considered on the example of a field of spin $^3/_2$. In this method the field of spin $^3/_2$ is described by a set of auxiliary Heisenberg tensor operators. Additional conditions necessary to ensure positive probabilities are imposed on the amplitude of the state and not on these operators. It is shown that such a formalism of description of the fields reduces the theory of fields of higher spins to that of fields with higher derivatives in the interaction lagrangian and with such additional conditions as do not change on including the interaction. As is known, a field of spin s transfers an entire spectrum of spins s, s−1, etc. It is shown that from this point of view Stückelberg's method may be interpreted as a method of description where the interaction of the given field with other fields is explicitly arranged along the spectrum of transferred spins. (auth)

21113 ANALYTIC PROPERTY OF SCATTERING AMPLITUDES CORRESPONDING TO A CLASS OF FEYNMAN DIAGRAMS. V. I. Kolomy'tsev and V. I. Fushchich. Ukr. Mat. Zh., 16: 610-23(1964).

The analytic property of Feynman amplitudes is studied. A theorem is obtained proving the absence of complex singularities in a Feynman scattering amplitude of a specific type. A class of diagrams is considered where the scattering amplitude satisfies the theorem. The Feynman amplitude is given by $F(s,t) = \int \prod_{i=1}^{n} d\alpha_i \delta\{1 - \sum_{i=1}^{n} \alpha_i\} \{C(\alpha)\}^{\rho} / \{D(\alpha; s, t)\}^{\gamma}$, where $D(\alpha; s,t) = f(\alpha)\, s + g(\alpha)\, t - K(\alpha; m_i^2 M_j^2)$ satisfying the conditions $f(\alpha) = \alpha_n f_1(\alpha_{n-2}) \geq 0$, $g(\alpha) = \alpha_{n-1} g_1(\alpha_{n-3}) \geq 0$, $-K(\alpha; m_i^2, M_j^2) = \alpha_n \alpha_{n-1} k_1(\alpha_{n-3})\, M_j^2 + \alpha_n k_2(\alpha_{n-3}, m_i^2, M_j^2) + \alpha_{n-1} k_3(\alpha_{n-2}, m_i^2, M_j^2) + k_4(\alpha_{n-2}, m_i^2 M_j^2)$. It is shown that for $M_j^2 \leq 0$, $F(s,t)$, forms an analytic function in s and t in the domain of two arbitrary planes with the exclusion of a branch cut along the real axis. The results are applied to Feynman diagrams of fourth and sixth order. (ATD)

21114 PCT, SPIN AND STATISTICS, AND ALL THAT. R. F. Streater and A. S. Wightman. The Mathematical Physics Monograph Series. New York, W. A. Benjamin, Inc., 1964. 188p. $9.00.

Transformation properties of physical states in relativistic quantum mechanics are summarized, with discussions of super-selection rules, symmetry operations, and the Lorentz and Poincaré groups. Necessary mathematical tools, including the definition of distribution, Fourier transforms, LaPlace transforms and holomorphic functions, tubes and extended tubes, the edge of the wedge theorem, and Hilbert space, are introduced. It is shown that a field theory is defined by the vacuum expectation values of products of field operators. General theorems of quantum field theory are obtained, including theorems on the global nature of local commutativity, on properties of the polynomial algebra of an open set, the PCT theorem, the theorem on the connection of spin with statistics, Haag's theorem and generalizations, and theorems on the equivalence classes of local fields. (M.J.T.)

21115 INTERMEDIATE QUANTUM MECHANICS. Hans A. Bethe. Lecture Notes and Supplements in Physics. New York, W. A. Benjamin, Inc., 1964. 286p. $4.95.

Quantum mechanics is applied to atomic structure and the theory of atomic collisions, giving a knowledge of Clebsch-Gordan coefficients and a detailed treatment of optical transition probabilities. Discussions are presented of the Schroedinger equation, identical particles and symmetry, perturbation and variation calculations on two-electron atoms, the self-consistent field, the Thomas-Fermi statistical model, the theory of multiplets, molecules, the theory of radiation, and the photoelectric effect. Relativistic wave equations are treated, including the Klein-Gordan and Dirac equations. An introduction to field theory, including field quantization, second quantization, and quantum electrodynamics, is given. (M.J.T.)

21116 INTRODUCTION TO THE THEORY OF RELATIVITY AND THE PRINCIPLES OF MODERN PHYSICS. Hueseyin Yilmaz. A Blaisdell Book in the Pure and Applied Sciences. New York, Blaisdell Publishing Company, 1965. 230p.

The basic ideas of relativity, causality, positive definiteness of energy, quantum nature of energy, and equivalence of inertial and gravitational mass are used to present the principles of modern physics for the advanced undergraduate or first-year graduate level. Discussions are given of Galilean relativity, experiments on the constancy of the velocity of light, Lorentz transformations and their consequences, Minkowski space and particle dynamics, the field concept and consequences, electromagnetic fields, spinor fields, the action principle, quantum field theory, general-covariance principle, equivalence principle, field equations and the three experimental tests, and topics in general relativity. (M.J.T.)

21117 TABLES OF COULOMB WAVE FUNCTIONS (WHITTAKER FUNCTIONS). A. V. Luk'yanov, I. V. Teplov, and M. K. Akimova. A Pergamon Press Book. Mathematical Tables Series. Volume 24. Translation by D. E. Brown of "Tablitsy Volnovykh Kulonovskikh Funktsii." New York, The Macmillan Company, 1965. 234p.

Tables of Coulomb wave functions or Whittaker functions — solutions of the radial part of the Schroedinger equation for the motion of a particle in a Coulomb field — are given. The tables are designed for computation of the Coulomb functions on the boundary of the nucleus and for computation of integrals of products of radial functions, encountered in the theory of direct nuclear reactions. Values are given of $F_l(\eta,\rho)$ and $G_l(\eta,\rho)$ for $l = 0$ (1) 15, $\rho = 1$ (0.2) 20, and $0 \leq \eta \leq 6.3096$ and of the derivatives $G_l'(\eta,\rho)$ with respect to ρ for the same values of ρ and η and for $l = 0, 1$. Methods used in the computer compilation of the tables and the use of the tables are described. (M.J.T.)

21118 STUDIES IN THE STATISTICAL PROPERTIES OF ELECTROMAGNETIC RADIATION. Chandra Lal Mehta. Thesis, Rochester, N. Y., Univ. of Rochester, 1964, 202p.

Statistical re-formulation of quantum mechanics in terms of phase space distribution functions, as given by Moyal (1949) using Weyl's (1931) correspondence rule between classical functions and operators, has been extended to various different correspondence rules. A law of multiplication, which is associative and distributive with respect to addition, is also introduced in each case; it gives correct correspondence between operator multiplication and the multiplication of classical functions. The dynamical brackets obtained in each case are found to be Lie brackets. Conditions on the phase space distribution functions to describe pure states are given. This formulation is then

applied to a quantized system of independent harmonic oscillators. In such systems the eigenstates of the destruction operator play an important role. Some of the properties of these eigenstates are investigated in detail. Next, the general description of the statistical electromagnetic radiation is studied in detail, both in terms of semi-classical theory (Wolf 1963 b) and the theory of quantized field (Glauber 1963 a,c). A one-to-one correspondence between the two descriptions first established by Sudarshan (1963 a,b) is derived in a new way. As an illustration of the general theory, coherence properties of blackbody radiation are discussed. Semiclassical as well as quantum field theoretical methods are used to derive explicit expressions for the second order complex electric, magnetic and mixed correlation tensors and identical results are obtained in each case. Correlation tensors of higher orders are also considered. In one of the appendices, some properties of the multivariate Gaussian distribution are considered and a proof of the moment theorem for a Gaussian random process (real as well as complex one) is given. (Dissertation Abstr., 25: No. 5, Nov. 1964)

21119 GAUGE INVARIANT CALCULATION OF VACUUM POLARIZATION PHENOMENA IN QUANTUM ELECTRODYNAMICS. John Chardon Herrera. Thesis, Seattle, Univ. of Washington, 1964. 77p.

A technique capable of describing in detail the various phenomena arising in the limit of low energy photons because of the polarization of the vacuum is obtained by quantizing the gauge invariant effective interaction Lagrangian. This approach then permits the use of the standard covariant calculational tools of quantum electrodynamics. This technique is first applied to the computation of the differential cross section for low energy photon-photon scattering. The well known Euler cross section is thereby derived in a direct manner. As a second example, the probability of the triple breakup of a free photon because of vacuum polarization is explicitly shown to vanish. This, however, is primarily due to the kinematics of the photon breakup. For a third application the differential cross section for the scattering of a low energy photon from the Coulomb field of a nucleus, that is, Delbrück scattering is calculated. Here the exact low-energy differential cross section is obtained. However, though the present technique determines completely the angular dependence, it is necessary to introduce a momentum cutoff in the Coulomb field in order to obtain a finite value for the coefficient in front of the angular dependence. A comparison of the resulting expression for the cross section with that for forward scattering given by Rohrlich and Gluckstern (1952) gives the numerical value of this coefficient. A brief comparison between the angular distribution for Delbrück scattering and that for a combination of an electric and magnetic dipole radiator is presented. (Dissertation Abstr., 25: No. 5, Nov. 1964)

21120 DEGENERATE FIELDS WITH TWISTING RAYS. Joseph David Zund. Thesis, Austin, Tex., Univ. of Texas, 1964. 59p.

The structure of the Einstein vacuum field equations of general relativity is investigated in detail when the space-time contains a twisting ray congruence. Let V_4 be a four-dimensional Riemann Space. Let $K^r = dx^r/d\rho$ be the tangent vector to a null geodesic congruence $x^r = x^r(\rho)$, then $k^r k_r = 0$ (1) and $k_r;_s k^s = 0$ (2) where ρ is an affine parameter. If $k_{(r|s|} k^{r|s} = \frac{1}{2}(k^r;\ r)^2$ (3) then the congruence is said to be shear-free. The term "ray" refers to a congruence which satisfies equations (1), (2) and (3). The congruence is said to be "twisting" if $k_{[r|s|} k^{r|s} \neq 0$. The most general line element is investigated for the space-time that admits a twisting ray congruence, namely $ds^2 = 2p^2(d\xi + A\, d\Sigma)(d\eta + B d\Sigma) + 2d\rho\, d\Sigma + C\, d\bar{\Sigma}^2$ where $x^r = (\xi, \eta, \sigma, \rho)$, $d\Sigma = K(L d\xi + M d\eta + d\sigma) = k_r dx^r$, and p, A, B, C are unknown functions of ξ, η, σ, and ρ; K, L, M are unknown functions of ξ, η, and σ. The vacuum field equations are calculated by using the tetrad formalism and it is shown that the first seven field equations determine the complete ρ dependence of the metric. The last three equations determine the ξ, η, σ dependence and must be solved for each degenerate Petrov type separately. The conditions for the various degenerate Petrov types are given and several examples of previously unknown exact solutions are constructed. (Dissertation Abstr., 25: No. 5, Nov. 1964)

21121 QUANTUM STATISTICAL THEORY OF RELAXATION IN ISOLATED SPIN SYSTEMS. John Alexander Tjon Joe Gin. Thesis, Utrecht, Rijksuniversiteit, [1964]. 45p.

The long time approach to statistical equilibrium of a spin system, isolated from the lattice vibrations, is studied, starting from the relaxation function of Kubo and Tomita. Only the behavior of the longitudinal magnetization is considered. The formalism used is based on the fact that in general a coarse grained description of the behavior of macroscopic variables is sufficient. For this purpose quantum-mechanical phase cells are introduced, which are characterized by the macro energy and the longitudinal magnetization. The asymptotic behaviour of the system is described in terms of these phase cells by a first order differential equation, the so-called master equation. From the derivation the important condition follows that the master equation is only valid in the presence of either a large magnetic field or a strong exchange interaction between the spins. In investigating the relaxation function with the aid of the master equation use is also made of a linearity condition, which implies that the system is not far from statistical equilibrium. The result for the spin-spin relaxation time, computed in this way, disagrees with that of Caspers, but is the same as found by Hartmann and Anderson. Finally the theories of these authors on spin-spin relaxation are discussed. (auth)

21122 TWO-GROUP THEORY OF A FERMION SYSTEM WITH INTERACTION AND ITS APPLICATIONS. M. Heim. Thesis, Erlangen-Nuremburg, Universitat, 1964. 34p. $2.00(Gmelin, AED-DISS- 64-149). (In German)

Two-group theory can be used for calculations of expectation values of systems, which cannot be treated by perturbation theory. Limitations of the application of two-group theory are described. It is concluded that a formalism including hard-core interactions of nucleons is needed. (Gmelin Inst.)

Geophysics

Refer also to abstracts 20782, 20888, 20902, and 21099.

21123 (D1-82-0398) AMPLIFICATION OF HYDROMAGNETIC WAVES IN THE MAGNETOSPHERE BY A CYCLOTRON INSTABILITY PROCESS WITH APPLICATIONS TO THE THEORY OF HYDROMAGNETIC WHISTLERS. J. A. Jacobs and T. Watanabe (Boeing Scientific Research Labs., Seattle, Wash. Geo-Astrophysics Lab.). Jan. 1965. 75p.

Cyclotron instability is an instability process caused by resonance between a circularly polarized electromagnetic wave and a stream of charged particles. The resonance is determined by the condition that the polarization and the angular frequency of the electromagnetic wave viewed from the reference system moving with the streaming particles are the same as the sense of the gyrating motion of the particles and their cyclotron frequency. Cyclotron instabilities that take place in magnetospheric hydromagnetic waves coupled with a stream of either electrons or protons are investigated. The physical nature of the instabilities is examined, upon the basis of the general theory of growing waves, in which there are two kinds of instabilities, convective and nonconvective. Convective instability, which is synonymous with a traveling amplifying wave, is obtained in the case of the combination of an ion resonance mode of hydromagnetic waves and a stream of electrons, and also in the case of the combination of an electron resonance mode and a stream of ions. For other combinations, an ion resonance mode plus an ion stream and an electron resonance mode plus an electron stream, nonconvective instability arises, and behaves as if it were a self-excited oscillator. In order to have the resonance

frequency in a range from one-tenth to one-half the ion cyclotron frequency, the streaming velocity of ions must lie in the range from a value comparable to the Alfvén velocity to a value about ten times larger, while the streaming velocity of electrons must be a thousand to ten thousand times larger than the Alfvén velocity. The growth time of an instability is computed for a typical example representing an actual situation in the magnetosphere. The growth time can be of the order of ten seconds, if ions are responsible for the instability in an ion resonance mode of hydromagnetic waves. An attempt is made to apply the theory to hydromagnetic whistlers, where some kind of amplification process seems to take place fairly often. (auth)

21124 (P-1121(RAND)) IONOSPHERIC ELECTRIC CURRENT-SYSTEMS DERIVED USING INTERNATIONAL POLAR YEAR DATA. E. H. Vestine and T. Nagata (RAND Corp., Santa Monica, Calif.). July 1, 1957, Revised Oct. 1, 1957. 47p. (AD-606444). $2.00(CFSTI).

The present state of knowledge of the electric-current systems flowing within the upper atmosphere is summarized. Accounts on the general subject of geomagnetic observations made during the Second International Polar Year, 1932-1933, are also considered. (auth)

21125 (RAD-TR-64-27) A PROTON-COLLISION MECHANISM FOR THE PRODUCTION OF SPREAD F IRREGULARITIES. Antarctic Research and Data Analysis. Scientific Report No. 16. John R. Herman (Avco Corp., Wilmington, Mass. Research and Advanced Development Div.). Aug. 24, 1964. Contract NSF-C255. 30p. (AD-606400). $2.00(CFSTI).

The spread echoes observed on Arctic and Antarctic ionograms arise from reflections or scattering from irregularities in the F region. The formation mechanism for such irregularities is explained. The assumption is made that field-aligned irregularities are caused by low energy (≤20 kev) charged particles spiralling along magnetic field lines and penetrating to F-region heights. Ionization is created along the field lines by collisions, and it remains field-aligned because of diffusion. It is suggested that this mechanism is operative at all times but with some variation in intensity. During daytime the irregularities produced in this manner are usually masked by higher electron densities given by photoionization. Supporting evidence for the proposed production mechanism is given by the diurnal, seasonal, and geographical variations in spread-F occurrence, and its correlation with magnetic activity. (auth)

21126 OBSERVATIONS USING THE ARTIFICIAL SATELLITE ELECTRON-2 OF THE CORRELATION BETWEEN VARIATIONS OF THE MAGNETIC FIELD AND STREAMS OF POSITIVE IONS INSIDE THE TERRESTRIAL MAGNETOSPHERE. K. I. Gringauz, Sh. Sh. Dolginov, V. V. Bezrukikh, E. G. Eroshenko, L. N. Zhuzgov, L. S. Musatov, E. K. Solomatina, and U. V. Fastovskii. Dokl. Akad. Nauk SSSR, 159; 1272-5(Dec. 21, 1964). (In Russian)

The artificial satellite Electron-2, equipped with magnetometers and a trap for charged particles, recorded positive ions of all energies, their fluxes with energies of more than 100 ev, and measured all three components of the geomagnetic field in the magnetosphere and at the radiation belts. Recorded data showed a correlation between the variations of the magnetic activity on the terrestrial surface and the intensities of fluxes of positive ions and the magnetic field far from the earth. This correlation was observed on quiet days and on days with magnetic disturbances. Numerous negative ion fluxes were recorded on magnetically quiet days. During this time, the magnetometer recorded a magnetic field of regular intensity although it exceeded the theoretical field by 20 γ. The maximum deflection from the theoretical field was detected at the apogee of the satellite. On 12 February 1964, all magnetic observatories on the earth recorded magnetic disturbances of sudden commencement while the trap in the satellite recorded positive ion fluxes exclusively of an intensity of 4×10^{-10} amp. At this time the satellite was at apogee. The magnetometer recorded a rapid increase in the magnetic field. (ATD)

21127 INVESTIGATION OF ELECTRON CONCENTRATION IN THE LOWER PART OF THE IONOSPHERE (D REGION). REVIEW. G. S. Ivanov-Kholodnyi (Inst. of Applied Geophysics, Moscow). Geomagnetism Aeronomy (USSR) (English Transl.), 4: 337-50(1964).

A review is given of the rocket determinations of the electron concentration in the ionosphere at heights of <100 km. Methods associated with the propagation of radio waves and plasma probe methods are examined, and compared with ground measurements. The conclusions are listed. 81 references. (L.B.S.)

21128 DYNAMICS OF THE RADIATION BELTS OF THE EARTH. PART II. B. A. Tverskoi (Moscow State Univ.). Geomagnetism Aeronomy (USSR) (English Transl.), 351-66(1964).

The motion of charged particles in the magnetosphere during magnetic storms is examined with an accuracy up to the square of the amplitude of the quadrupole term of the disturbance, inclusive. It is shown that a continuous flow of particles toward the earth and diffusion take place under the influence of such disturbances. A general equation is obtained, which takes into account these effects and Coulomb particle losses. Several solutions of this problem are examined. The average distribution of relativistic electrons in time in the outer radiation belt and its variations, associated with the solar cycle, are computed. It is shown that rapid variations are reversible and caused by the appearance of ring currents in the magnetosphere. An estimate is made of the position of the inner boundary and of the average energy of particles of the outer proton-helium belt. It is shown that intensity in the inner proton belt decreases from a maximum as the 10th power of the distance from the center of the earth. The theoretical results are compared with experimental data. (auth)

21129 SPATIAL DISTRIBUTION OF ANOMALOUS IONIZATION IN THE F_2-LAYER AT HIGH LATITUDES. L. A. Yudovich (Inst. of Terrestrial Physics, Ionosphere and Radio Wave Propagation, Academy of Sciences, USSR). Geomagnetism Aeronomy (USSR) (English Transl.), 4: 411-15(1964).

The spatial distribution of anomalous ionization in the F_2-layer on the dark side of the ionosphere at high-latitude stations in the northern and southern hemispheres and the influence of anomalous ionization on f_0F_2, caused by ultraviolet solar radiation, are examined. It is shown that the critical frequencies of anomalous ionization reach their maximum values at geomagnetic latitudes 82–87°. The space-time variations of $f_0F_{2_a}$ can be explained in the framework of the theory of magnetospheric circulation developed by Axford and Hines. The latitudinal distribution of ionization in the noon hours during the winter solstice obeys the laws of a simple layer both in the northern and in the southern hemispheres. (auth)

21130 SPATIAL STRUCTURE OF THE GEOMAGNETIC FIELD AND SOME ASPECTS OF THE INNER STRUCTURE OF THE EARTH. PART II. I. M. Pudovkin (Inst. of Terrestrial Magnetism, Ionosphere and Radio Propagation, Academy of Sciences, USSR). Geomagnetism Aeronomy (USSR) (English Transl.). 4: 427-33(1964).

The spatial structure of the geomagnetic field is investigated. Problems involved in the construction of normal fields and the results of an analysis of the spatial structure of the residual Bauer field, constructed for the levels h = 0, 500, 1000, 15,000, 3000, 5000, and 10,000 km, are discussed. (auth)

21131 WESTERN DRIFT OF THE GEOMAGNETIC FIELD. N. V. Adam, N. P. Ben'kova, V. P. Orlov, and L. O. Tyurmina (Inst. of Terrestrial Magnetism, Ionosphere and Radio Wave Propagation, Academy of Sciences, USSR). Geomagnetism Aeronomy (USSR) (English Transl.), 4: 434-41(1964).

Methods of computing the velocity ν of the western geomagnetic drift are reviewed. Spherical analyses of the

total field and of secular variations are used to estimate drift velocity for individual harmonics. The rate of movement of the centers of world anomalies and of the zero isodynams outlining them is estimated on the basis of maps of non-dipole fields for several epochs. The longitudinal distribution of ν is shown. It is assumed that different drift velocities are associated with the different depths of current vortices in the core. The high velocities of the western drift and their regular nature indicate that the drift is not associated with processes in the mantle. (auth)

21132 STATE OF THE IONOSPHERE AT MIDDLE LATITUDES DURING MAGNETIC STORMS ASSOCIATED WITH ANOMALOUS ABSORPTION IN THE POLAR CAP. R. G. Gachechiladze and G. M. Khocholava (Tbilisi State Univ., USSR). Geomagnetism Aeronomy (USSR) (English Transl.), 4: 479-81(1964).

The main patterns of the anomalous absorption in the polar cap were determined and explained from the viewpoint of the general theory of magnetic-ionospheric disturbances. The state of the ionosphere was investigated at high, middle, and low latitudes. The study confirmed the assumption that the state of the F_2 layer at middle latitudes is normal during anomalous absorption in the polar cap preceding a magnetic storm. The anomalous polar cap absorption was found to be local, and the ionospheric disturbances associated with it were found to be single-phase negative disturbances. (L.B.S.)

21133 SPATIAL DISTRIBUTION OF IONOSPHERIC DISTURBANCES IN THE F_2-LAYER. E. V. Lavrova. Geomagnetism Aeronomy (USSR) (English Transl.), 4: 482-5(1964).

The ionospheric data were analyzed from the world network of stations for July, September, and December 1957, and the planetary distribution of ionospheric disturbances in the F_2 layer were investigated as a function of season, geomagnetic coordinates, time of a storm, and local time. (L.B.S.)

21134 LUNAR-DIURNAL GEOMAGNETIC VARIATIONS AND THEIR RELATION TO THE LEVEL OF ACTIVITY OF SOLAR WAVE EMISSION. N. Z. Nodia, N. A. Katsiashvili, and G. M. Khocholava (Geophysical Inst., Academy of Sciences, Georgian SSR). Geomagnetism Aeronomy (USSR) (English Transl.), 4: 488-9(1964).

A study was made of lunar-diurnal variations (L-variations) for the clarification of the influence of tide-producing forces of the geomagnetic field and for verification of the dynamo theory. The L-variations were computed for the three elements H, D, and Z, using the Chapman-Miller method. The amplitudes and phases of the first harmonics were determined by harmonic analysis. Similar computations for years of maximum solar activity showed no significant differences in the L-variations of all three elements. (L.B.S.)

21135 DEPENDENCE OF THE ENERGY OF A MAGNETIC STORM ON THE DISTANCE TO THE CORPUSCULAR STREAM. V. I. Afanas'eva, E. I. Mogilevskii, and Yu. D. Kalinin (Inst. of Terrestrial Magnetism, Ionosphere, and Radio Wave Propagation, Academy of Sciences, USSR). Geomagnetism Aeronomy (USSR) (English Transl.), 4: 495-6(1964).

Calculations are made on the energy dependence of a magnetic storm on the distance from the center of the earth to the solar corpuscular stream. It was found that a deformation of $6R_E$ (where R_E is the radius of the earth) of a magnetosphere of radius 20 R_E is sufficient to transfer to the magnetosphere an energy corresponding to the energy of a geomagnetic storm. (L.B.S.)

21136 DATA ON THE EARTH'S RADIATION BELTS OBTAINED DURING THE COSMOS FLIGHTS AT ALTITUDES OF 200–400 km. S. N. Vernov, I. A. Savenko, P. I. Shavrin, V. E. Nesterov, N. F. Pisarenko, and K. N. Sharvina. Izv. Akad. Nauk SSSR, Ser. Fiz., 28: 2049-57 (Dec. 1964). (In Russian)

Data on the earth's radiation belts collected during the Cosmos series in 1960-1963 at altitudes below 400 km are presented. Data obtained from Cosmos-4 indicate a maximum density shift within the outer radiation belt over a broad interval of longitude during magnetically quiet days. At the same time, an increase of average density was also noted within the radiation belts. From data of Cosmos-7 and Cosmos-15 the geographical distribution of electron density in the Brazilian anomaly at an altitude of approx. 300 km was determined. This distribution roughly coincided with electron distribution in the inner radiation belt measured by Discoverer-31. The existence of electrons with energies exceeding 2 Mev within the inner radiation belt are indirectly indicated. During the flight of Cosmos-4 in April 1962, the counting rate of the Geiger counter showed a four-fold increase over satellite measurements made in August 1960. The rate of increase coincided with the proton-density change within the inner belt during the period of the transition to minimum solar activity (and decreased atmospheric density). (ATD)

21137 FAST PARTICLE CAPTURE FROM INTERPLANETARY SPACE. B. A. Tverskoi. Izv. Akad. Nauk SSSR, Ser. Fiz., 28: 2032-4(Dec. 1964). (In Russian)

The pressure of the solar wind perturbs the magnetic field around the earth. The resulting asymmetry of the magnetic sphere around the earth has an effect on the movement of particles in the Van Allen radiation belts. The displacement of charged particles is greater on the day side of the magnetic sphere than on the night side. This distribution of particle intensities in the equatorial plane at the beginning of a solar storm was observed by means of the satellite Explorer XIV. The particle displacement also depends on the longitude. It is pointed out that the quadrupole terms of the perturbed magnetic field represent the greatest contribution to the particle motion. Detailed calculations show that after a solar storm the particles in a radiation belt come closer to the earth on the average. An estimate of the particle flux is given. (TTT)

21138 THE F-LAYER AT SUNRISE NEAR THE MAGNETIC EQUATOR. A. J. Lyon and O. A. Awojobi (Univ. of Ibadan, Nigeria). J. Atmospheric and Terrest. Phys., 27: 53-6(Jan. 1965).

The rapid increase of ionization in the F region following sunrise is investigated using data obtained from ionospheric soundings at Ibadan during the IGY. The various factors which influence this rise are considered, and estimates of production and loss rates are made. (auth)

21139 v.l.f. RADIATION FROM THE HIGH ALTITUDE NUCLEAR EXPLOSIONS AT JOHNSTON ISLAND, AUGUST 1958. D. L. Croom (Cambridge Univ., Eng.). J. Atmospheric and Terrest. Phys., 27: 111-12(Jan. 1965).

Atmospheric recording equipment at Cambridge, England, was used to investigate changes in the earth's vertical electric field produced by radiation from the U. S. nuclear tests above Johnston Island. Records are given of observations made on a wide-band atmospheric waveform recorder and on two narrow-band receivers tuned to 320 and 80 cps. It is not possible from the results to determine whether the radiation from a nuclear device can be distinguished from that due to lightning discharges. (M.J.T.)

21140 THE RELATION BETWEEN THE DISPERSION OF A WHISTLER AND THE ELECTRON TEMPERATURE IN THE PROTONOSPHERE. J. E. Geisler and S. A. Bowhill (Univ. of Illinois, Urbana). J. Atmospheric Terrest. Phys., 27: 122-5(Jan. 1965).

Whistler dispersion is defined, and the effect on the whistler dispersion from the redistribution of electrons resulting from a change of temperature in an isothermal protonosphere is reported. An integral expression for the dispersion is derived and evaluated numerically for temperatures from 500 to 2000°K and geomagnetic latitudes of 40 and 60°. (M.J.T.)

21141 DIFFUSIVE EQUILIBRIUM OF THE TOPSIDE ELECTRON DENSITY IN THE F2-REGION. R. G. Baxter

and P. C. Kendall (Univ. of Sheffield, Eng.). J. Atmospheric Terrest. Phys., 27: 129-32(Feb. 1965).

An assumption of diffusive equilibrium with variable scale height gives good global agreement with satellite Alouette observations of the topside F2-layer. The theory also gives information on the vertical variation of the scale height, and may be applied to topside data in reduced form, as given by King et al. A recent criticism of the theory by Duncan is discussed. (auth)

21142 THE DYNAMICS OF THE AURORA. II. WESTWARD TRAVELING SURGES. S.-I. Akasofu, D. S. Kimball, and Ching-I. Meng (Univ. of Alaska, College). J. Atmospheric Terrest. Phys., 27: 173-87(Feb. 1965).

During an auroral substorm, a violent expanding motion of an auroral system located around the midnight sector generates rapid wavy motions of auroral arcs or bands that lie in the evening sector. This particular type of motion is called the westward traveling surge. Various characteristics of the surges are described in detail and their geomagnetic and ionospheric effects are examined. (auth)

21143 THE DYNAMICS OF THE AURORA. III. WESTWARD DRIFTING LOOPS. S.-I. Akasofu, D. S. Kimball, and Ching-I. Meng (Univ. of Alaska, College). J. Atmospheric Terrest. Phys., 27: 189-96(Feb. 1965).

Westward traveling surges generated by a violent expanding motion of an auroral system during an auroral substorm degenerate sometimes into a loop or a group of loops after they are propagated westwards a certain distance. The loop (or the group of loops) thus formed drifts westwards with various speeds. Characteristics of the westward drifting loops are studied. (auth)

21144 DIFFUSION OF LOW ENERGY AURORAL ELECTRONS IN THE ATMOSPHERE. Kaichi Maeda (Goddard Space Flight Center, Greenbelt, Md.). J. Atmospheric Terrest. Phys., 27: 259-75(Feb. 1965).

The work of Spencer on the energy dissipation of electrons in air is extended below 25 kev by means of the Monte Carlo method, and the results are applied to the diffusion of monoenergetic electrons in the polar atmosphere. The results show significant effect of straggling, not only on the distribution of the most penetrating flux but also on the height of maximum dissipation and on the back-scattering. The dependence of back-scattering on the angular distributions as well as the energies of incident electrons are calculated, indicating that it decreases rapidly below 10 kev and that a maximum of back-scattering seems to occur at energies around 20 kev, with values of the order of 7 to 20 per cent for vertical and isotropic incidence, respectively for intensity. Corresponding energy back-scattering coefficients (albedos) are approximately half of these values. (auth)

21145 PRODUCTION RATES AND ELECTRON DENSITIES IN THE LOWER IONOSPHERE DUE TO SOLAR COSMIC RAYS. G. W. Adams and A. J. Masley (Douglas Aircraft Co., Inc., Santa Monica, Calif.). J. Atmospheric Terrest. Phys., 27: 289-98(Mar. 1965).

The ratio, ψ, of Q (the production rate of electron-ion pairs) to N^2 (the steady-state electron density squared) was calculated for solar cosmic-ray event conditions over the altitude range $40 < Z < 80$ km. The calculations were accomplished by determining the production rate from direct measurements of the particle spectra and using electron density values determined by multifrequency riometers. The ratio, ψ, is shown as a function of altitude and of the number density of neutral molecules. A comparison with theoretical values for ψ shows a disagreement not easily explained. (auth)

21146 CENTRIFUGAL EFFECTS OF THE FLOW OF PLASMA ROUND THE GEOMAGNETIC HOLLOW. Angela M. Downs (Univ. of Sheffield, Eng.). J. Atmospheric Terrest. Phys., 27: 299-302(Mar. 1965).

A method of calculating the shape and position of the geomagnetic hollow, taking into account centrifugal effects in the flow of plasma round the hollow, is considered. Comparison is made with the results of Chapman and Kendall, who investigated a cylindrical sheet problem in which centrifugal effects are also present, and with the hollow calculated by Beard (1960), who assumed specular reflection of the plasma. In view of recent satellite results indicating an outward flaring of the magnetopause surface on the night side of the earth, it is suggested that centrifugal effects should be included in further three-dimensional calculations of the hollow. (auth)

21147 THICKNESS OF ZENITHAL AURORAL ARC OVER ALASKA. J. S. Kim and R. A. Volkman (Univ. of Idaho, Moscow). J. Atmospheric Terrest. Phys., 27: 321-8(Mar. 1965).

The thicknesses of the auroral arcs were measured on thirty, twenty-four and six independent homogeneous auroral arcs which occurred during 1958 directly above three IGY stations in Alaska: College, Kotzebue and Farewell. The measured thicknesses over the three Alaskan stations were in the range from 1.7 to 23.1 km; the average was 8.8 km. The thicknesses were related to the geomagnetic and earth-current activities. No significant daily, seasonal, or latitudinal variation of thickness was found. (auth)

21148 DYNAMICAL BEHAVIOUR OF MAGNETOSPHERE BOUNDARY FOLLOWING IMPACT BY DISCONTINUITY IN THE SOLAR WIND. John R. Spreiter and Audrey L. Summers (Ames Research Center, Moffett Field, Calif.). J. Atmospheric Terrest. Phys., 27: 359-65(Mar. 1965).

Time histories of the development of the magnetosphere boundary following impact of a sharp-fronted plasma cloud and of the compression of the magnetosphere following impact by a discontinuity in the solar wind are calculated. Results are presented for initially planar discontinuities having their normals either aligned with or inclined 30° to the wind direction. Although several minutes are generally required for a discontinuity in the solar wind to sweep past the geophysically significant portion of the magnetosphere, it is found that any individual element of the magnetosphere boundary usually completes the major part of its adjustment to the new conditions within a period of about a minute. (auth)

21149 PULSATING AURORAL RADAR ECHOES AND THEIR POSSIBLE HYDROMAGNETIC ASSOCIATION. J. G. Keys (P. E. L. Auroral Station, Omakau, N. Z.). J. Atmospheric Terrest. Phys., 27: 385-93(Mar. 1965).

Pulsating radar echoes observed from Bluff, New Zealand, during the IGY are examined. The pulsations exhibit a diurnal variation in occurrence, periods dependent on latitude, and onset times dependent on planetary K-index. These features, combined with the observed period range of 1 to 9 min and an association with magnetic activity, suggest a hydromagnetic excitation mechanism in the outer magnetosphere. (auth)

21150 ENERGY SOURCE FOR BALL LIGHTNING. W. H. Andersen (Shock Hydrodynamics, Inc., Sherman Oaks, Calif.). J. Geophys. Res., 70: 1291-3(Mar. 15, 1965).

It is shown that the electromagnetic radiation frequencies from external sources required to form ball lightning (according to the Kapitza theory) are emitted during the collision of charged water drops. Calculations show that a reasonable volume of nominally charged droplets will provide the energy necessary for the lightning ball, but a prohibitively large volume of ordinary rain drops is required. It is hypothesized that shock from ordinary bolt lightning may provide the requisite droplet-charging energy, either through liquid breakup in a polarizing field or by gas friction. Interactions or convergence of the electromagnetic radiation may be of importance in producing the required localized energy densities. (auth)

21151 MAGNETO-ATMOSPHERIC WAVES IN A HORIZONTALLY STRATIFIED CONDUCTING MEDIUM. C. P. Yu (Purdue Univ., Lafayette, Ind.). Phys. Fluids, 8: 650-6 (Apr. 1965).

The propagation of magneto-atmospheric waves in an inviscid, compressible and perfectly electrically conducting medium in the presence of a vertical gravitational field and

a horizontal magnetic field is investigated. If the medium is isothermal and its magnetic pressure is proportional to its mechanical pressure, it is found that the convective instability arises when the ratio of the Alfvén speed to the sound speed exceeds $[2(1-1/\gamma)]^{\frac{1}{2}}$ where γ is the adiabatic index. When the medium is found to be stable, a disturbance in the medium will travel as waves in three different modes. For small wavenumbers, two of these modes are similar to the acoustic and gravity modes found in the nonmagnetic case. For very large wavenumbers, the acoustic mode becomes the modified sound wave found in the case of a uniform medium, while the gravity wave behaves as the corresponding modified hydromagnetic wave unless the component of the wavenumber in the direction of the magnetic lines is sufficiently small. The third mode which does not appear in the nonmagnetic case behaves nearly as a pure hydromagnetic wave; it is influenced only to a minor extent by compressibility and gravity. The damping of each mode due to viscosity, finite electrical and thermal conductivity is discussed. (auth)

21152 ELECTRON BREMSSTRAHLUNG AND AURORAL LUMINOSITY PULSATIONS. R. S. Iyengar (Mount Allison Univ., Sackville, Can.). Phys. Letters, 15: 135-6(Mar. 15, 1965).

Evidence is presented of similar x-ray effects and effects in auroral luminosity during disturbed periods. A comparison is given of the magnitudes of energy in several processes. It is concluded that the eddy processes near the 100-km level provide an atmospheric source-mechanism with which to link some of the concurrent events of the auroral zone, such as pulsations in the x rays and in auroral luminosity. (L.B.S.)

21153 INCOHERENT SCATTER FROM PLASMA OSCILLATIONS IN THE IONOSPHERE. F. W. Perkins, E. E. Salpeter, and K. O. Yngvesson (Cornell Univ., Ithaca, N. Y.). Phys. Rev. Letters, 14: 579-80(Apr. 12, 1965).

The incoherent backscattering of radar pulses (430 Mcps) from the ionosphere between 150 and 600 km was observed. Scattering from weakly damped longitudinal electrostatic plasma oscillations was detected. The observations were compared with the predictions of a non-equilibrium theory which allows for the presence of photoelectrons. (D.C.W.)

21154 PROPOSAL FOR AN EXPERIMENT FOR EXCITATION OF CHARGED PARTICLES IN THE VAN ALLEN BELTS BY A SATELLITE-BORNE ELECTROMAGNETIC FIELD EMITTER. Raumfahrtforschung, 8: 168-70(Oct.-Dec. 1964). (In German)

An experiment for the excitation of charged particles in one of the Van Allen belts by a satellite-borne electromagnetic field emitter is proposed. The emitter frequency would be of the order of magnitude of the Larmor frequency. This would give a supplementary modulation motion to the electrons. The whistler signs and the long echoes would be measured. The data that could be obtained from these measurements are described and discussed. (J.S.R.)

21155 SOLAR CORPUSCULAR STREAMS AND GEOMAGNETISM. E. R. Mustel (Astronomical Council, Academy of Sciences, USSR). Soviet Astron. AJ (English Transl.), 8: 619-37(Mar.-Apr. 1965). Translated from Astron. Zh., 41: 777-800(Sept.-Oct. 1964).

An analysis is presented of the physical properties of solar corpuscular streams. Various properties of recurrent and sporadic geomagnetic disturbances are compared for this purpose, as well as disturbances (at the polar caps of the earth) on geomagnetically quiet days when K_p is small. Particular stress is laid on the study of the diurnal variation of geomagnetic disturbances of diverse types as monitored by high-latitude stations. The following topics are discussed: geomagnetic disturbance with the phase of the cycle, and in the course of the year; the 27-day sequence of disturbances; the nature of geomagnetic disturbances (presence of D_{st} and SC); diurnal variation of geomagnetic disturbances; and short-period variations of the magnetic field. Several general properties of quasistationary and nonstationary corpuscular streams are studied, with particular emphasis on the presence of a leading (lateral) front in quasistationary corpuscular streams from active solar regions. Some inferences are drawn on the interaction between corpuscular streams of different types and the earth's magnetosphere. Corpuscular streams emanating from high-intensity chromospheric flares interact in the first instance with the subsolar points on the earth. (auth)

21156 ATMOSPHERIC RADIATION. I. THEORETICAL BASIS. R. M. Goody. Oxford Monographs on Meteorology. Oxford, Clarendon Press, 1964. 445p. 75s.

A systematic theoretical treatment is given of the interaction of solar electromagnetic energy with a planetary atmosphere, the subsequent redistribution of this energy, and its ultimate return to space in the form of low-temperature terrestrial radiation. All levels of a planet from the surface boundary layer to the exosphere are considered. Discussions are given of the theory of radiative transfer, the theory of gaseous absorption, band models, absorption by atmospheric gases, computation of fluxes and heating rates, extinction by molecules and droplets, radiative equilibrium of atmospheres, and radiative transfer and fluid motions. (M.J.T.)

21157 SATELLITE ENVIRONMENT HANDBOOK. SECOND EDITION. Francis S. Johnson, ed. Stanford, California, Stanford University Press, 1965. 204p. $7.50.

Data describing the geophysical environment encountered by artificial earth satellites are summarized. Eight articles are included; separate abstracts were prepared for five. Articles not abstracted are on micrometeoroids, radio noise, and thermal radiation from the earth. (M.J.T.)

For abstracts of individual papers see: 20785, 20902, 21158, 21159, and 21160.

21158 STRUCTURE OF THE UPPER ATMOSPHERE. Francis S. Johnson (Southwest Center for Advanced Studies, Dallas). p.3-20 of "Satellite Environment Handbook. Second Edition." Stanford, Calif., Stanford Univ. Press, 1965.

The thermal structure of the atmosphere is outlined, and expressions for the variation of the physical properties of the atmosphere in space and time are obtained. Graphs are presented of data on atmospheric temperature and density distributions, concentrations of major atmospheric constituents (He, H, O, N_2, O_2, Ar), and mean molecular weight distributions. Sunspot-cycle, diurnal, solar-activity, magnetic-activity, and seasonal atmospheric variations are discussed. Tables are given of atmospheric parameters as a function of altitude for low-, medium, and high-density atmospheres. (M.J.T.)

21159 STRUCTURE OF THE IONOSPHERE. W. B. Hanson (Southwest Center for Advanced Studies, Dallas). p.23-49 of "Satellite Environment Handbook. Second Edition." Stanford, Calif., Stanford Univ. Press, 1965.

A description is given of the various regions of the ionosphere—D, E, F_1, and F_2 regions, and the outer ionosphere and protonosphere—and their properties—height, electron concentration, height of peak concentration, and critical frequency for peak concentration. Diffusive-equilibrium distributions of main ionic constituents and ionospheric temperatures are discussed. Expressions for ionospheric conductivities and collision frequencies are given, and values calculated from them are plotted. (M.J.T.)

21160 GEOMAGNETISM. A. J. Dessler (Rice Univ., Houston, Tex.). p.153-82 of "Satellite Environment Handbook. Second Edition." Stanford, Calif., Stanford Univ. Press, 1965.

Diagrams of the main geomagnetic field at the surface of the earth are presented, giving total intensity, horizontal and vertical intensity, declination, and inclination. Sperical harmonic analysis of the field at the surface is described, and results of calculations of the field above the earth are shown. Transient variations in the geomagnetic field are discussed, including solar-wind distortions and phases of

geomagnetic storms. Hydromagnetic-wave propagation in the outer ionosphere is reviewed. (M.J.T.)

Low Temperature Physics

Refer also to abstract 21486.

21161 (JINR-P-1953) URAVNENIYA GIDRODINAMIKI SVERKHTEKUCHEI FERMI-ZHIDKOSTI I DVUKHCHASTICHNYE FUNKTSII. (Hydrodynamical Equations for the Superfluid Fermi-Liquid and the Two-Particle Green Functions. [Part] I.). Z. Galyasevich (Joint Inst. for Nuclear Research, Dubna (USSR). Lab. of Theoretical Physics). 1965. 34p. Dep.(mn).

The hydrodynamical equations for a system of identical Fermi particles with pairing forces (in the system there is a condensate of the coupled pairs) are obtained. In the case of the small deviation from the thermodynamic equilibrium, using the connection between the variations of the mean values (which are found from the linearized hydrodynamical equations) and the Green functions, the expressions for the poles of the two-particle Green functions are obtained. The expressions describe elementary excitations of two kinds, viz. first and second sound. In the computations the method proposed by Bogoliubov for obtaining the one-particle Green functions for superfluid Bose systems is applied. (auth)

21162 (UCRL-11828(p.199-201)) THE CERIUM MAGNESIUM NITRATE TEMPERATURE SCALE. R. B. Frankel, N. J. Stone, and D. A. Shirley (Lawrence Radiation Lab., Univ. of California, Berkeley).

The $(1/T^* - 1/T)$ correlation for cerium magnesium nitrate (CMN) is discussed, where T^* = temperature obtained from the Curie's law susceptibility of CMN, and T = absolute temperature. The anisotropy of the 255-kev γ ray of aligned ^{137m}Ce in CMN was measured as a function of $1/T^*$. The results indicate breakdown of the available correlation at $1/T = 300$, and a new $(1/T^* - 1/T)$ correlation was made which is valid down to 0.002°K. (D.L.C.)

21163 SUPERCONDUCTIVITY AND OBSERVABILITY OF THE ELECTROMAGNETIC POTENTIALS. F. Rothen, C. Gruber, and D. Rivier (Universite, Lausanne, Switzerland). Helv. Phys. Acta, 38: 125-36(1965). (In French)

An elementary model for the superconductor is proposed, which uses a Lorentz-invariant scalar function derived from the relativistic form of London equations. Uniformity of this wave function gives the quantization of an invariant quantity (the generalized fluxoid), of which the usual fluxoid and "the periodic action" are two special forms. The quantization of the period of the supercurrents of Josephson is shown to be a particular consequence of the latter. In the light of the proposed model, the connection is discussed between the observability of the vector and scalar electromagnetic potentials on one hand, and of the quantization of the fluxoid and of the period of Josephson's supercurrents on the other hand. (auth)

21164 ON ELECTRON TUNNELING FROM A HARD SUPERCONDUCTOR IN THE MIXED STATE. Sadao Nakajima and Yuri Nakao (Tokyo Univ.). J. Phys. Soc. Japan, 20: 8-14(Jan. 1965).

Gorkov's derivation of the Ginzburg-Landau equation from BCS theory is reformulated so it can be applied to dynamical processes involving quasiparticle excitations. The method is applied to electron tunneling from an intrinsic hard superconductor in Abrikosov's mixed state. It is shown that near the transition point the usual tunneling current averaged over Abrikosov's energy-gap distribution is obtained. Some numerical estimates are made of the dependence of I-V characteristics on magnetic field in the case of Nb. (auth)

21165 HIGH-FIELD SUPERCONDUCTIVITY. J. E. Kunzler. Mater. Res. Std., 5: 161-71(Apr. 1965).

A review on superconductivity is presented, with emphasis on high-field superconductors and their use in magnets. The GLAG theory which accounts for the high critical field of type-II superconductors is reviewed, together with the properties and fabrication of high field-high current density materials. The fabrication and performance of Nb_3Sn and Nb–Zr magnets are discussed, together with applications of high field-high current superconductors. 55 references. (D.C.W.)

21166 ON THE ORIGIN OF RESISTANCE IN THE MIXED STATE OF TYPE-II SUPERCONDUCTORS. R. G. Jones, E. H. Rhoderick, and A. C. Rose-Innes (Manchester Coll. of Science and Tech., Manchester, Eng.). Phys. Letters, 15: 214-15(Apr. 1, 1965).

It was previously proposed that the voltage appearing in a type-II superconductor in the mixed state above a critical value of the current is an induced emf produced by the motion of the magnetic flux through the superconductor. It is suggested that this mechanism is not compatible with the laws of electromagnetism. (D.C.W.)

21167 PRECESSIONAL MODES OF FLUX TUBES IN TYPE I SUPERCONDUCTORS. P. G. de Gennes (Faculte des Sciences, Orsay, France). Phys. Letters, 15: 216-18 (Apr. 1, 1965).

The energy and momentum of a vortex ring in a pure superconductor are calculated and are used to derive the drift velocity of the ring. The result is in agreement with the magnus force concept for both type-I and -II superconductors. For macroscopic flux tubes in type-I superconductors, it leads to slow precessional motions of the type recently observed by DeSorbo in pure indium. (D.C.W.)

21168 VISCOSITY × NORMAL DENSITY OF LIQUID HELIUM IN A TEMPERATURE INTERVAL ABOUT THE LAMBDA POINT. R. W. H. Webeler and D. C. Hammer (Lewis Research Center, Cleveland). Phys. Letters, 15: 233-4(Apr. 1, 1965).

The temperature dependence of the product of viscosity and normal density of liquid helium was measured in a temperature interval around the lambda point for both increasing and decreasing temperatures. The temperature dependence of the viscosity alone was determined by using normal density values calculated elsewhere. (D.C.W.)

21169 AMPLITUDE-DEPENDENT ULTRASONIC ATTENUATION IN SUPERCONDUCTING LEAD. B. R. Tittmann and H. E. Boemmel (Univ. of California, Los Angeles). Phys. Rev. Letters, 14: 296-8(Mar. 1, 1965).

An explanation is proposed for the observed increase in attenuation for increasing ultrasonic amplitudes in superconducting Pb; this behavior is not explicable in terms of a simple modification of the BCS theory. The Granato-Luecke mechanism is described, in which the dislocations are pinned down by impurity atoms and the nodes of the dislocation network; thermal phonons assist the unpinning processes; the higher the sound-wave amplitudes, the more unpinning occurs and the higher is the damping of the ultrasonic waves. An expression for the attenuation is given, and results of experiments testing this hypothesis are surveyed. (M.J.T.)

21170 DEPENDENCE OF THE SUPERCONDUCTING TRANSITION TEMPERATURE ON CARRIER CONCENTRATION IN SEMICONDUCTING $SrTiO_3$. J. F. Schooley (National Bureau of Standards, Washington, D. C.), W. R. Hosler, E. Ambler, J. H. Becker, Marvin L. Cohen, and C. S. Koonce. Phys. Rev. Letters, 14: 305-7(Mar. 1, 1965).

The superconducting transition temperature of reduced $SrTiO_3$ was measured as a function of electronic carrier concentration from 10^{18} to 10^{21} carriers/cm^3. The transition temperature exhibits a maximum in this concentration range. The dependence of the transition temperature on carrier concentration is explained on the basis of the assumption that the superconductivity arises primarily from the attractive interaction from the exchange of intervalley phonons between time-reversed electron pairs; the dependence shows screening effects produced by the free carriers. (M.J.T.)

21171 SUPERCONDUCTING SURFACE SHEATH OF A TYPE-II SUPERCONDUCTOR BELOW THE UPPER CRITI-

CAL FIELD H_{c2}. H. J. Fink (Atomics International, Canoga Park, Calif.). Phys. Rev. Letters, 14: 309-12(Mar. 1, 1965).

The order parameter of a bulk type-II superconductor near its surface (bounded by a vacuum) is calculated for magnetic fields parallel to the surface and close to the upper critical field H_{c2} when the Ginzburg-Landau parameter $\kappa \gg 1$. It is found that the energy gap near the surface is larger than its zero-field value for fields just below H_{c2}. The maximum value of the order parameter is in general not at the surface but is field dependent and occurs within about one coherence length from the surface. The superconducting properties—order parameter, energy gap, superconducting electron concentration—of the metal near its surface do not show abrupt changes near H_{c2}. (M.J.T.)

21172 OBSERVATION OF THE ANALOG OF THE ac JOSEPHSON EFFECT IN SUPERFLUID HELIUM. P. L. Richards and P. W. Anderson (Bell Telephone Labs., Murray Hill, N. J.). Phys. Rev. Letters, 14: 540-3(Apr. 5, 1965).

An observation in superfluid liquid helium of the effect analogous to the a–c Josephson effect of superconductivity is reported. (D.C.W.)

21173 GAUGE-INVARIANT HAMILTONIAN OF SUPERCONDUCTIVITY AND THE FLUX QUANTIZATION. Alfred Zawadowski (Central Research Inst. for Physics, Budapest). Phys. Rev. Letters, 14: 557-8(Apr. 5, 1965).

A gauge-invariant Hamiltonian for treating the electromagnetic properties of superconductors is proposed and is used to treat the flux quantization. (D.C.W.)

21174 PHONON EFFECTS ON NUCLEAR SPIN RELAXATION IN SUPERCONDUCTORS. M. Fibich (Yeshiva Univ., New York). Phys. Rev. Letters, 14: 561-4(Apr. 5, 1965).

A broadening of the energy levels must be introduced into the BCS theory to obtain agreement with the measured ratio of the relaxation rates in superconducting aluminum to those in the normal metal. It is shown that an effective broadening of the energy levels is brought about by absorption processes of thermal phonons. (D.C.W.)

21175 REMOVAL OF MODE DEGENERACY IN A ROTATING SECOND-SOUND RESONATOR. Kenneth A. Shapiro (Univ. of California, Los Angeles). Phys. Rev. Letters, 14: 429-31(Mar. 22, 1965).

The differential equation for second sound in rotating He II is derived, based on the reversible thermohydrodynamics of Lin. Application is made to the doubly and triply degenerate modes, and good agreement is found with experimental observations on the coupled second-sound waves. (L.B.S.)

21176 THERMOMECHANOELECTRICAL—EFFECTS FOR SUPERFLUID HELIUM. W. J. Neidhardt (Newark Coll. of Engineering, N. J.). Phys. Rev. Letters, 14: 488-9 (Mar. 29, 1965).

The possibility of verifying thermomechanoelectrical effects for superfluid helium is investigated. The equilibrium condition is obtained for two containers filled with liquid helium and thermally isolated from each other and the outside; the containers are connected by a super leak which allows no normal helium to pass. It was found that a difference in electric field between the two chambers results in temperature and pressure difference or a pressure or temperature difference, and that superfluid helium will flow from one container to the other until the equilibrium condition is fulfilled. (L.B.S.)

21177 CAPTURE CROSS SECTIONS FOR NEGATIVE IONS IN ROTATING HELIUM II. B. E. Springett, D. J. Tanner, and R. J. Donnelly (Univ. of Chicago). Phys. Rev. Letters, 14: 585-7(Apr. 12, 1965).

The cross section for the capture of a negative ion by a vortex line in rotating helium II was measured as a function of temperature and of the potential between the collector and the grid in front of an alpha source electroplated on a copper electrode. The entire assembly was immersed in a cryostat. The results were compared with theoretical predictions. (D.C.W.)

21178 MICROWAVE-PHONON-ASSISTED TUNNELING IN SUPER-CONDUCTING DIODES. B. Abeles and Y. Goldstein (Radio Corp. of America, Princeton, N. J.). Phys. Rev. Letters, 14: 595-8(Apr. 12, 1965).

An extra tunneling current was observed in Al–Pb tunnel diodes deposited on one end of a crystal rod in which sound waves were excited by microwave techniques. The extra current depends strongly on the voltage bias across the diode, and the dependence of the extra current on the acoustic power is different for longitudinal and transverse phonons. An interpretation was attempted on the basis of a model in which the tunnel diode acts as a quantum detector of sound. (D.C.W.)

21179 ON THE EXISTENCE OF A MAXIMUM IN THE FOUNTAIN PRESSURE VS TEMPERATURE RELATIONSHIP IN LIQUID HELIUM II. E. F. Hammel and W. E. Keller (Los Alamos Scientific Lab., N. Mex.). Physica, 31: 89-93(Jan. 1965). (LA-DC-6499)

The fountain pressure was calculated as a function of temperature for a 3.36-μ slit, using the Gorter-Mellink theory. The maximum in the curve below 1.5°K was obtained, together with good agreement with the experimental curve. (D.C.W.)

21180 THE CAPTURE OF HOT ELECTRONS BY Au^- AND Au^{2-} CENTERS IN GERMANIUM AT 20°K. R. G. Pratt and B. K. Ridley (Mullard Research Labs., Redhill, Surrey, Eng.). Proc. Phys. Soc. (London), 85: 293-300 (Feb. 1965).

The time constants associated with the capture of hot electrons by gold centers in germanium at 20°K were measured as a function of electric field in specimens containing N_{Sb} antimony and N_{Au} gold atoms per cubic centimeter where $N_{Au} < N_{Sb} < 2N_{Au}$. Capture by Au^{2-} centers dominated at high fields. The capture rate per Au^{2-} center at high fields was a factor 2×10^3 higher than the zero-field value, confirming previous results. A direct measurement of the capture rate per Au^- center at high fields was not possible, and the value was estimated from current density measurements. This estimate gave an increase of capture rate per Au^- center over the zero-field value by a factor of about 20. The zero-field value of the capture rate per Au^- center at 20°K was found to be 3×10^{-12} cm^3 sec^{-1}. The hot electron results for both Au^- and Au^{2-} centers were conveniently summarized by assuming an energy dependence of the capture rate $\alpha(E)$ of the form $\alpha(E) = AS(E)E^{p+\frac{1}{2}}$, where A was temperature dependent and S(E) was the coulomb tunneling factor for the transverse effective mass. For Au^{2-} centers $p = 0.8 \pm 0.1$. For Au^- centers $p = 1.0 \pm 0.1$ from 77°K results, and this was adequate to explain the 20°K results. For low electron energies the approximate formula of Bonch-Bruevitch for the zero-field capture rate, $\alpha = \exp\{-(T_0/T)^{\frac{1}{2}}\}$, was applicable, with $T_0 = 1.34 \times 10^4$°K for Au^- centers and $T_0 = 5.35 \times 10^4$°K for Au^{2-} centers. (auth)

21181 EFFECT OF IMPURITIES ON SUPERCONDUCTING TRANSITIONS. D. M. Brink and M. J. Zuckermann (Oxford Univ.). Proc. Phys. Soc. (London), 85: 329-41(Feb. 1965).

It is shown that Thouless' method for finding the critical temperature of a pure superconductor can be extended to include nonmagnetic impurities in the superconductor. Explicit expressions for the critical temperature, anisotropy, and jump in specific heat of a superconductor doped with small quantities of nonmagnetic impurities are given. The method is extended to include paramagnetic impurities in the superconductor, and the results for the critical temperature are compared with experimental work on aluminum doped with iron-group impurities. (auth)

21182 PROGRESS IN CRYOGENICS. Volume 4. K. Mendelssohn, ed. Progr. Cryog., 4: 1-231(1964). New York, Academic Press, 1964.

Seven articles on low-temperature technology and on physical phenomena important in cryogenic applications are included. Separate abstracts were prepared for five. Arti-

cles not abstracted are on radial-flow low-temperature expansion turbines and ferrimagnetism. (M.J.T.)

For abstracts of individual papers see: 21183, 21184, 21185, 21186, and 21187.

21183 LIQUID HELIUM SUPPLIES IN GREAT BRITAIN. P. L. Smith (National Physical Lab., Teddington, Middx, Eng.). Progr. Cryog., 4: 11-24(1964).

The history of He liquefaction, the establishment of a He liquefier at the National Physical Laboratory, the quantity and cost of liquid-He production at the NPL, and the construction of a new plant at NPL are reviewed. The transfer of the He-liquefaction scheme to the British Oxygen Company is mentioned. Information on the cost of liquid-He production, on plant room layout, and on He liquefiers in Britain by Feb., 1963, is included. (M.J.T.)

21184 HELIUM-3 AT LOW TEMPERATURES. D. F. Brewer (Univ. of Sussex, Eng.). Progr. Cryog., 4: 25-71 (1964).

Basic properties of ^{3}He are discussed and compared with those of ^{4}He. Theories of liquid ^{3}He are reviewed, including the ideal Fermi-gas theory, the Fermi-liquid phenomenological and microscopic theories, and the prediction of a superfluid liquid phase transition. Theories of solid ^{3}He are mentioned. Properties of the liquid are discussed, including the variation of density with pressure and temperature, specific heat, entropy, transport properties, sound propagation, and surface tension. The melting curve and the production of solid ^{3}He are considered. Nuclear susceptibility and diffusion and nuclear spin relaxation in the solid and liquid are surveyed, and general features of liquid ^{3}He-^{4}He mixtures are mentioned. 128 references. (M.J.T.)

21185 MAGNETIC COOLING. W. A. Little (Stanford Univ., Calif.). Progr. Cryog., 4: 99-121(1964).

An introduction to the field of magnetic cooling or adiabatic demagnetization is given, and recent developments are reviewed. The theory of magnetic cooling is described briefly, including removal of spin entropy by a magnetic field, internal interactions, and temperature determination. Properties of paramagnetic salts acceptable for use in magnetic cooling are given. Experimental considerations are discussed, including cryostat design, He transfer, Dewar flasks, production of low initial temperatures, magnets, vacuum chamber, thermal isolation and contact, thermal valves, and thermometry. 85 references. (M.J.T.)

21186 SUPERCONDUCTING RESONANT CAVITIES. E. Maxwell (Massachusetts Inst. of Tech., Lexington). Progr. Cryog., 4: 123-58(1964).

Properties of cavity resonators are described. Theory and experimental observations of the anomalous skin effect in normal metals are discussed. Empirical and theoretical descriptions of superconducting surface impedance are given. Materials for and design and fabrication of superconducting resonators are considered. 54 references. (M.J.T.)

21187 SUPERCONDUCTIVE MATERIALS AND SOME OF THEIR PROPERTIES. B. W. Roberts (General Electric Research Lab., Schenectady, N. Y.). Progr. Cryog., 4: 159-217(1964).

A review of superconductor properties is given, and high-field superconductivity, superconductor criteria (especially Matthias' rules, and metallurgical aspects are discussed. Tables are given of superconductive properties of elements, critical properties of all known superconductive materials and data on all materials known to have been checked for a superconducting transition down to a given temperature, superconductive materials in order of increasing critical temperature and in order of increasing critical field, and high-field superconductors. 530 references. (M.J.T.)

21188 ULTRASONIC AND THERMAL BEHAVIOR OF Nb-25% Zr IN STRONG MAGNETIC FIELDS. L. J. Neuringer and Y. Shapira (Massachusetts Inst. of Tech., Cambridge, Mass.). Solid State Commun., 2: 349-51(Nov. 1964).

An absorption edge for ultrasonic shear waves has been observed at the upper critical field of Nb-25% Zr. The temperature variation of the field at which this edge occurs was compared with several theoretical models. (auth)

21189 SOME CHARACTERISTICS OF SUPERCONDUCTING THIN FILMS OF LEAD AND INDIUM. I. A. Artemenko and G. A. Mikhailov. Ukr. Fiz. Zh., 9: 1369-71 (Dec. 1964). (In Ukrainian)

Superconductivity of Pb and In films were studied with 6000 Å thick, 1 mm wide, and 10 mm long 99.999% pure specimens vacuum deposited on glass, quartz, and mica base. The properties of the specimens were measured at room and liquid helium temperatures at constant currents. Indium films exhibited much faster superconducting transitions than lead films indicating a more uniform structure than lead. Measurements of Pb and In film conductivity as a function of the base material and temperature showed that the superconducting transition on quartz increased with lower temperature. (R.V.J.)

21190 INVESTIGATION OF AN EQUATION FOR A GAP IN AN ENERGETIC SPECTRUM OF A SUPERCONDUCTOR. A. V. Svidzinskii. Ukr. Mat. Zh., 16: 544-50(1964). (In Russian)

The Bogolyubov energy gap function in one-dimensional superconductor excitation spectrum was investigated using a simplified universal model taking into account the nucleus as a function of energy variables. Considering that the function is of the same order as the function for pulse direction, both functions were considered simultaneously. Resolution asymptotics for the Bogolyubov energy gap function were developed at temperatures close to critical. (R.V.J.)

21191 BOUND STATE IN SUPERCONDUCTORS WITH PARAMAGNETIC IMPURITIES. Luh Yu. Wu Li Hsueh Pao, 21: 75-91(Jan. 1965). (In Chinese)

A generalized canonical transformation and a SCF method were used to investigate the influence of isolated impurity atoms on the properties of superconductors. It was found that a bound state of excitation exists around a paramagnetic impurity with its energy level in the energy gap. An analytical expression was obtained for the corresponding wave function. The effect of electromagnetic absorption due to the bound state should appear as a precursory peak. The possible experimental verifications of the bound state through tunnelling effect and infrared absorption are discussed. Furthermore, the excitations of continuous spectra around a nonmagnetic impurity and the spatial variation of the energy gap parameter were considered. (auth)

21192 CRITICAL MAGNETIC FIELD OF A SUPERCONDUCTING ALLOY FILM. Hang-sheng Wu (Peking Univ.). Wu Li Hsueh Pao, 21: 132-9(Jan. 1965). (In Chinese)

The theory developed previously is extended to a thin superconducting film containing impurities. The critical magnetic field for the second order phase transition of the superconducting alloy film was obtained. The results obtained are reduced to those of the Ginzburg-Landau theory when $2d \gg \xi_0$ with arbitrary l or $2d \ll \xi_0$ with $l \ll 2d$, but are different when $2d < \xi_0$ with $l > 2d$, l being the mean free path of the electrons. The theory agrees with Blumberg's experiment. (auth)

21193 SUPERCONDUCTIVE MEMORIES. Richard W. Ahrons. Thesis, Brooklyn, Polytechnic Inst., 1963. 243p.

An investigation into superconductive memories with emphasis on the random-access memory and the associative memory is described. Since the field on one side of a film is all that is known for the case of superconducting memories, an approximate field solution for several geometries is found by using a minimum energy principle and an approximate relationship for the energy stored in the volume outside the superconductor. An experiment on a continuous film memory (CFM) cell showed that two bits can be sotred independently in one cell. This experiment tends to substantiate a speculation that storage is an edge phenomena. The model of the CFM describes an induced storage current.

This model can explain the effects of snap-action sense, hysteresis, and the onset of a second sense signal corresponding to the trailing edge in addition to a sense signal corresponding to the leading edge. When the CFM cells are incorporated in an array, there are constraints such as operating speeds and noise. Superconductive associative memories appear attractive because of large capacities inherent to film memories. However the term associative memory must not only be characterized by the type of interrogation as described by McDermid and Petersen but also by the type of (1) readout of multiple responses and (2) write process. A cryotron implementation of both parallel and Modified Lewin readout schemes shows the Modified Lewin scheme to be inherently faster for larger arrays than parallel readout although the Modified Lewin scheme requires almost four times as many cycles to readout. Both readout schemes in the cryotron implementation require approximately the same write time. (A.G.W.)

21194 QUANTIZED FLUX IN SUPERCONDUCTING CYLINDERS. Alvin L. Kwiram and Bascom S. Deaver, Jr. (Stanford Univ., Calif.). 7p. (CONF-651-69)

From 9th International Conference on Low Temperature Physics, Columbus, Ohio, Aug.-Sept. 1964.

The flux change occurring in small hollow superconducting cylinders of Sn, In, Pb, and V cyclically cooled through the transition temperature in an applied axial magnetic field at frequencies up to 80 kcps was observed. A periodic variation as a function of applied field was found at all frequencies tried indicating the quantized flux is established in the cylinders at least as fast as 10^{-5} seconds. The period was measured and it was found that it corresponds to a flux change of hc/2e through the cylinder. (P.C.H.)

21195 SUPERCONDUCTIVITY IN THE NIOBIUM–SELENIUM SYSTEM. E. Revolinsky, G. A. Spiering, and D. J. Beerntsen (Allis-Chalmers Research Labs., Milwaukee). 19p. (CONF-524-19)

From American Inst. of Mining, Metallurgical and Petroleum Engineers Annual Meeting, New York, Feb. 1964.

The dependence of superconducting transition temperatures on changes in composition and structure was observed in the Nb-Se system. Within the composition limits of $Nb_{1.05}Se_2$ to $NbSe_2$, a hexagonal two-layer structure of the NbS_2 type and a hexagonal four-layer structure of a new structure type were found to be superconducting. They were formed by heating at temperatures of 600 to 800°C and 850 to 1000°C respectively. For the two-layer phase, T_c varied from 7.0°K at $NbSe_2$ to 2.2°K at $Nb_{1.05}Se_2$. For the four-layer phase, the transition temperature varied between 6.3 and 5.9°K over the same approximate composition range. Double transitions indicating a four-layer to two-layer phase transformation were associated with samples quenched from the four-layer phase region. Periodic measurement of transition temperature of individual samples indicated that the transformation continued at room temperature. (auth)

Neutron Physics

See also REACTOR TECHNOLOGY — Criticality Studies.

Refer also to abstracts 20551, 20671, 21612, 21613, 21638, 21735, and 21742.

21196 (AWRE-O-81/64) DICE MK.IV — THE PREPARATION OF NUCLEAR DATA INTO A FORM SUITABLE FOR MONTE CARLO CALCULATIONS USING THE IBM7030 COMPUTER. W. M. M. Kerr — J. B. Parker, ed. (Atomic Weapons Research Establishment, Aldermaston (England)). Dec. 1964. 47p. Dep.(mn).

DICE Mk.IV is a system which automatically converts basic nuclear data into a form suitable for Monte Carlo calculations. Its constituent components MOULD, ABSYNTH, EGMV and CR are separately described. (auth)

21197 (CEA-R-2747) SPECIFICATION D'UN CODE DE DIFFUSION MULTIGROUPE A DEUX DIMENSIONS: ALCI. (Specifications for a Multi-Group Scattering Code of Two Dimensions ALCI). Jean-Paul Bayard, André Guillou, Bernard Lago, Marie-Josèphe Bureau du Colombier, Ginette Guillou, and Chantal Vasseur (Commissariat à l'Énergie Atomique, Saclay (France). Centre d'Études Nucléaires). Feb. 1965. 48p. Dep.(mn).

The specifications of the ALCI program are given. This program resolves the system of difference equations similar to the homogeneous problem of multigroup neutron scattering, with two dimensions in space, in the three geometries XY, RZ, RΘ. It is possible with this method to calculate geometric and composition criticalities and also to calculate the accessory problem on demand. The maximum number of points dealt with is 6000. The maximum permissible number of groups is 12. The internal iterations are treated by the method of alternating directions. The external iterations are accelerated using the extrapolation method due to Tchebychev. (auth)

21198 (CEA-R-2759) SPECIFICATION D'UN CODE DE DIFFUSION EN GEOMETRIE XY: DAIXY. (Specifications for a Scattering Code for an XY Geometry: DAIXY). Chantal Vasseur, Robert Bruyere, Andre Guillou, and Paul Quilichini (Commissariat à l'Énergie Atomique, Saclay (France). Centre d'Études Nucléaires). Feb. 1965. 25p. Dep.(mn).

The specifications of the DAIXY program which resolves the difference equations system analog to the homogeneous problem of multigroup neutron scattering, in a two-dimensional space with XY geometry are described. The maximum number of points treated is 10,050. The number of groups must be less than 4. The internal iterations are dealt with by the alternating directions method; the external iterations are accelerated by the extrapolation method due to Chebyshev. (auth)

21199 (CEX-65.02) TECHNICAL CONCEPT — OPERATION HENRE. F. F. Haywood and J. A. Auxier (Oak Ridge National Lab., Tenn.). Feb. 1965. Contract W-7405-eng-26. 25p. Dep.; $1.00(cy), 1(mn) CFSTI.

A small but intense source of 14-Mev neutrons is to be mounted in the hoisting mechanism of the 1500-ft BREN tower at the Nevada Test Site. The experimental program, designated Operation HENRE, will be conducted during the spring and summer of 1965 and will be sufficiently comprehensive to characterize the radiation fields. In addition, a series of applied shielding experiments will include configurations of interest to both military and civilian laboratories. It is important that data be accumulated that will assist in understanding the apparent uncertainties in existing transport calculations, especially data that will give approximate values for effective neutron cross sections for air-over-ground transport. The neutron source will be operated at heights from about 25 to 1500 ft above the air-ground interface. The average neutron yield during operational periods of about 4 hours is expected to be equal to or greater than 10^{13} n/sec. (auth)

21200 (KFK-264) RECENT MEASUREMENTS OF THE SCATTERING LAWS OF SOME HYDROGENEOUS MODERATORS. W. Glaeser, G. Ehret, and A. Merkel (Kernforschungszentrum, Karlsruhe (West Germany). Institut fur Angewandte Kernphysik). Dec. 1964. 14p. (CONF-804-27). Dep.(mn).

From Symposium on the Inelastic Scattering of Neutrons, Bombay, Dec. 1964.

Experimental studies are carried out of the distributions of neutrons scattered by benzene, ZrH, and water vapor at incident energies of 0.018 to 0.080 ev. The experimental results are compared with theoretical scattering-law predictions. (T.F.H.)

21201 (KFK-tr-164) UBER DIE TOTALREFLEXION VON NEUTRONEN AN KOBALTSPIEGELN. (On the Total Reflection of Neutrons in Cobalt Mirrors). R. Rypjanu, M. Popovic, B. Grabcev, and V. Vasiliu. Translated into German by Franz Weitzenmiller (Kernforschungzentrum,

Karlsruhe, Germany), from Rev. Phys., Acad. Rep. Populaire Roumaine, 8: 277-84(1963). 12p. Dep.(mn); $1.60 (fs), $0.80(mf) JCL.

The total reflection of monochromatic neutrons on two cobalt mirrors was determined. The reflection coefficient of the beam on the mirror was determined as a function of the incident angle of the beam and the magnetizing field. The results are shown graphically and their significance is discussed. (J.S.R.)

21202 DISTRIBUTION OF NEUTRONS THERMALIZED IN THE RETARDER OF A LONG COUNTER. G. Robaye. Bull. Soc. Roy. Sci. Liege, 33: 558-62(1964). (In French)

A simulation program by the Monte-Carlo method was developed, which makes it possible to determine the distribution after thermalization in a hydrogenous moderator of incident neutrons under given conditions of energy, direction, and point of entry. First results are presented in graphic form. The utilization of the results for the study of the response of long counters is sketched. (tr-auth)

21203 ON A PROBLEM IN NEUTRON TRANSPORT THEORY. Kennard W. Reed, Jr. (New York Univ., New York). J. Math. Anal. Appl., 10: 161-5(Feb. 1965).

A mixed initial and boundary-valued problem for the linearized Boltzmann equation is formulated and solved for the distribution of neutrons in a fixed three-dimensional body. (L.B.S.)

21204 NEUTRON THERMALIZATION BASED ON THERMODYNAMICS. M. Grmela (Inst. for Nuclear Research, Czechoslovak Academy of Sciences, Rez). J. Nucl. Energy: Pt. A and B, 19: 81-90(Feb. 1965).

The space-energy distribution of neutrons in a weakly absorbing medium with constant temperature is studied from principles of thermodynamics of irreversible processes. The entropy production rate is calculated for thermalization process. Simultaneously are demonstrated limits of thermodynamics applicability. Further, on the principle of minimization of entropy production rate for stationary processes, the equations for temperature and density of neutron gas in dependence on the space coordinates are obtained. The results show connections between the parameters characterizing thermalization and between kinetic and fluctuation parameters. The elaborated method can be used for study of general dense gases thermalization. (auth)

21205 EQUILIBRIUM NEUTRON ENERGY SPECTRA IN FINITE BLOCKS OF GRAPHITE. S. K. Trikha and L. S. Kothari (Univ. of Delhi). J. Nucl. Energy: Pt. A and B, 19: 101-2(Feb. 1965).

The equilibrium neutron energy spectra in graphite assemblies of different bucklings were calculated, using numerical iteration to solve the energy-dependent Boltzmann diffusion equation. The decay constants for the different assemblies were determined and were compared with experimental values. The average energy of the neutron distribution was also obtained, together with the diffusion and diffusion cooling coefficients. (D.C.W.)

21206 DIFFUSION COEFFICIENT OF THERMAL NEUTRONS IN BERYLLIUM AT DIFFERENT TEMPERATURES. I. C. Goyal (Univ. of Delhi). J. Nucl. Energy: Pt. A and B, 19: 103-5(Feb. 1965).

The diffusion coefficient for thermal neutrons in beryllium at 60, 100, 150, 200, 250, 300, and 400°K was calculated as a function of neutron energy. The average diffusion coefficient at 60, 100, 200, and 300°K was also obtained. (D.C.W.)

21207 NEUTRON TEMPERATURES ACROSS THE INTERFACE BETWEEN WATER AND BORON — POISONED WATER. A PRELIMINARY NOTE. L. M. Caspers and A. J. Meerburg (Technical Univ., Delft, Netherlands). Koninkl. Ned. Akad. Wetenschap., Proc., Ser. B, 68: 1-7(1965).

Spatially dependent neutron temperatures were measured across the interface between water and boron-poisoned water, using Lu–Mn foils. The temperature remained practically constant in approaching the interface from the water side, rising sharply by several tens of degrees at the interface and increasing gradually to the infinite medium temperature in the poisoned water. The temperature distribution was calculated by two-group (thermal) diffusion theory with and without diffusion heating-cooling of the neutrons. The model with diffusion heating-cooling gave substantially better agreement. (D.C.W.)

21208 A PULSED NEUTRON SOURCE BASED ON THE ORBITRON. L. Ruby and D. K. Wells (Univ. of California, Berkeley). Nucl. Instr. Methods, 34: 66-8(Apr. 1965). (UCRL-11727)

A pulsed neutron generator was developed which employs an Orbitron ion source and is capable of producing 10^8 neutrons in pulses of 3 μsec. The ion source, which is usually simple in design, requires no magnet and operates at pressures as low as 3μ. Operating characteristics were determined for a 3 in. dia. tube in which deuterons are extracted radially from the ion source. (auth)

21209 NEUTRON DEPOLARISATION EFFECTS IN PRECESSION MAGNETS. J. Atkinson and J. E. Sherwood (Univ. of California, Livermore). Nucl. Instr. Methods, 34: 137-40(Apr. 1965). (UCRL-12113)

The measurement of the polarization of neutron beams is greatly facilitated by the magnetic precession technique, in which a reversal of the polarization vector is achieved by allowing the neutrons to precess about a suitable magnetic field. However, in general, a depolarization of the beam occurs because of unwanted magnetic field components. The behavior of a 100% polarized beam of classical non-relativistic neutrons which pass through the bore of a simple solenoid was studied. The amount of the depolarization was calculated for several geometries by following in detail the motion of the neutron spin vector. Assuming the beam fills the bore of the solenoid and considering only trajectories parallel to the solenoid axis, it was found that a beam depolarization of 1% occurs for a solenoid length-to-radius ratio of 10. However, if the length equals the radius, the depolarization is 21%. (auth)

21210 COMPARISONS OF MEASURED AND CALCULATED NEUTRON FLUXES IN LAMINATED IRON AND HEAVY WATER. Erkki J. Aalto (Aktiebolaget Atomenergi, Stockholm). Nucl. Sci. Eng., 22: 33-9(May 1965).

Measurements of neutron fluxes were performed in configurations depicting the regions extending radially and axially outwards from the core of a PHWR Reactor, in order to test the accuracy of the available methods in shield design on thin alternating laminas of Fe and D_2O. The results are compared to fluxes calculated by the British 18-group removal-diffusion method and by the NRN method developed at AB Atomenergi. The results show that the values predicted may be expected to be within a factor of 2 from the true values in most cases. The predicted relative flux distributions follow the observed ones with fairly good accuracy in spite of the apparent misuse of diffusion theory for the thin regions in question. It is also shown that the predicted change in the fast spectrum while penetrating these setups should be confirmable with certain threshold detectors. (auth)

21211 NEUTRON THERMALIZATION STUDIES IN GRAPHITE. K. Serdula and J. Young (Univ. of Birmingham, Eng.). Nucl. Sci. Eng., 22: 40-50(May 1965).

The neutron diffusion and integral scattering properties of graphite were measured by the pulsed-neutron-source technique. Measurements were performed on assemblies with geometric bucklings from 0.0036 to 0.0151 cm^{-2}. The time of attainment of asymptotic neutron-energy spectra was determined from transmission measurements. Results from these latter measurements indicated that the minimum thermalization time, for the assemblies investigated, was ≈2 msec. Asymptotic average neutron velocities, measured both internally and externally, were obtained as a function of assembly size. Results indicated that an asymptotic neutron spectrum did not exist for as-

semblies with $B^2 \approx 0.015$ cm^{-2} at a time $\gtrsim 2$ msec after the neutron pulse. A value of the diffusion cooling coefficient, $C = 45.6 \pm 4.7 \times 10^5$ cm^4/sec was derived from the measured thermal neutron decay constants. (auth)

21212 ABOUT THE GENERALIZATION OF AMOUYAL-BENOIST'S METHOD FOR CALCULATING DISADVANTAGE FACTORS AND FLUX DISTRIBUTIONS IN TWO-REGION CELLS. Z. Weiss (Institutt for Atomenergi, Kjeller, Norway). Nucl. Sci. Eng., 22: 60-77(May 1965).

Making use of the isotropic incident flux approximation, the disadvantage factor ζ for a two-region unit cell can be written as a linear combination of two so-called X functions, each of them depending on the properties of one region only. A general variational approach, based on Ritz-Galerkin's method, is used to find a closed expression for X in terms of the weighted collision probabilities, $P^{ij} = 1/V \int_V \int_V P(r \rightarrow r')\, q_i(r)\, q_j(r')\, dr\, dr'$. From this expression the properties of X will be deduced once more, but then in a general way. An analytical calculation of X in slab geometry and a numerical one in cylindrical geometry are given. The results of the first were used for a comparison with Theys' generalization of the Amouyal-Benoist-Horowitz theory; the results of the second example were compared with Leslie's calculation of the same X function by means of successive collision probabilities. It is furthermore shown that the same procedure that serves to calculate X functions gives, as an important by-product, the constant production and the isotropic albedo solutions of Peierl's integral transport theory. From these solutions the flux distribution in the unit cell (of arbitrary geometry) can be constructed. Sauer's simple recipe for calculating the X function is discussed and is shown to be inaccurate for weakly absorbing media. (auth)

21213 THE EFFECTS OF FLUX ANISOTROPY ON THERMAL-NEUTRON FLUX PERTURBATIONS. J. V. Walker (Agricultural and Mechanical Coll. of Texas, College Station). Nucl. Sci. Eng., 22: 94-101(May 1965).

The effects of neutron flux anisotropy upon thermal-neutron flux perturbations were found by experimentally determining the perturbations induced by foils placed in fluxes of known nonuniformities. Anisotropies in the magnitude of the vector flux were introduced by placing a black cadmium absorber sheet in an isotropic flux produced by a uniform slowing-down source in water. The resulting angular and spatial distributions of the thermal-neutron flux were computed by using Yvon's method to solve the Boltzmann equation for an absorbing half space containing a uniform slowing-down source. Using indium foils with thicknesses from 14 mg/cm^2 to 184.9 mg/cm^2, the relative flux perturbations were measured to within ±1% in regions which varied from a highly directional flux at the cadmium surface to essentially an isotropic distribution several mean free paths from the absorber. The experimental data indicated that the flux perturbations remained constant at all distances greater than about three mean free paths from the non-reentrant boundary, but that the flux depression decreased in the region near and vanished at the boundary. It was concluded, contrary to earlier predictions, that flux perturbation theories, based upon isotropic flux models, cannot be used to correct flux perturbations induced in all anisotropic fluxes. It was pointed out that, if this effect is overlooked, significant errors may exist in some relative or absolute flux measurements made in the region near a boundary or absorber. (auth)

21214 COMPARISONS OF EXACT AND S_N SOLUTIONS OF THE MONOENERGETIC CRITICAL EQUATION WITH ANISOTROPIC SCATTERING. K. D. Lathrop (Los Alamos Scientific Lab., N. Mex.) and A. Leonard. Nucl. Sci. Eng., 22: 115-18(May 1965). (LA-DC-6587)

One of the useful applications of the method of singular integral equations is to provide exact solutions of the Boltzmann transport equation against which numerical code solutions can be compared. Such a comparison was made by calculating the critical thickness of a plane homogeneous slab in the monoenergetic approximation. The anisotropic scatterer is represented by a three-term Legendre expansion in a form that maintains the anisotropic-scattering cross section as a separate free parameter. (C.E.S.)

21215 ON THE GREEN'S FUNCTION OF MONOENERGETIC NEUTRON TRANSPORT THEORY. A. M. Jacobs and J. J. McInerney (Pennsylvania State Univ., University Park). Nucl. Sci. Eng., 22: 119-20(May 1965).

Several misleading aspects which were generated by previous developments of the angular Green's function for monoenergetic neutron transport are discussed. (C.E.S.)

21216 NEUTRON GENERATOR AT THE ATOMIC ENERGY CENTRE, LAHORE. S. A. Durrani, ed. Nucleus (Lahore), 1: No. 3, 20-6(July-Sept. 1964).

A pulsed neutron source is described, which can produce up to 1.2×10^{7} neutrons/sec in the 4π solid angle by the T(d,n) ^{4}He reaction. The neutron energy ranges from 13.4 to 14.7 Mev, depending on the neutron emission angle. With a deuterium target, neutrons from 2.1 to 2.8 Mev can be obtained from the D(d,n) ^{3}He reaction, the yield being 3×10^8 sec^{-1}. The research program for the installation is outlined, and health physics aspects are discussed. (D.C.W.)

21217 MEASUREMENT OF THE NEUTRON DIFFUSION PARAMETERS OF BENZENE WITH THE PULSE METHOD. Marko Kuechle and Guenter Kussmaul (Kernforschungszentrum, Karlsruhe, Ger.). Nukleonik, 6: 329-30(Nov. 1964). (In German)

The neutron diffusion parameter of benzene was determined and compared with an earlier measurement on diphenyl. The decay constant, absorption cross section, transport cross section, and the mean quadratic energy loss per collision were determined. There is no significant difference between the two compounds. The deviations between various studies arise from incomplete elimination of the harmonics. (J.S.R.)

21218 SMALL-ANGLE SCATTERING OF SUBTHERMAL NEUTRONS ON HEAVY ICE. O. Dengel, J. Christ, and W. Schmatz (Technisch Hochschule, Munich and Kernforschungsanlage, Julich, Ger.). Phys. Letters, 15: 231-2(Apr. 1, 1965).

The temperature dependence of the small-angle scattering of subthermal neutrons on mono- and poly-crystalline heavy ice was measured, using neutrons with an average wavelength of 6 Å. An increase in scattering observed while raising the sample temperature was attributed to rearrangement of a low-temperature structure at about −80°C. The results indicate microstructures with an average size of 1000 Å. (D.C.W.)

21219 HARMONIC FREE DETERMINATION OF THE THERMAL NEUTRON ABSORPTION CROSS SECTION OF HYDROGEN BY A PULSED SOURCE TECHNIQUE. M. J. Harris and R. E. Kay (Univ. of Manchester, Eng.). Proc. Phys. Soc. (London), 85: 79-86(Jan. 1965).

A method, based on Fourier analysis of harmonics, was developed for measuring the rate of decay of the fundamental mode of the thermal neutron density distribution which is established in a cylinder of water after thermalization of an injected burst of fast neutrons. Measurement of this decay for a range of water depths enables determination, by extrapolation, of the decay constant $v\Sigma_a$ of an infinitely large system. The 2200 m sec^{-1} thermal neutron microscopic absorption cross section of hydrogen was measured. The value obtained, 326 ± 3 mbn, is in good agreement with that obtained by most previous workers by a variety of other methods. The thermal neutron diffusion coefficient was also measured, although the experiment was not optimized for this. The value obtained, D = 35,200 ± 400 at 22°C, also agrees very well with previous results. (auth)

21220 NEUTRON FLUX PERTURBATIONS DUE TO INFINITE PLANE ABSORBERS. I. SPATIALLY CONSTANT SOURCE. M. M. R. Williams (Univ. of Birmingham, Eng.). Proc. Phys. Soc. (London), 85: 413-33(Mar. 1965).

Exact solutions were obtained for several problems in

one-velocity neutron transport theory by means of the Wiener-Hopf technique. The basic problem concerns the calculation of the neutron flux and angular distribution at the surface of an infinite, purely absorbing foil or control plate embedded in a moderator. Solutions are obtained for the cases of isotropic and linear anisotropic scattering in the moderator. An approximate solution was obtained for an infinite lattice of such absorbers by the end-point method. Numerical results are compared with those from approximate theories such as P_{13}, double P_3, and variational methods. It is found that the double P_3 and variational methods are very accurate indeed, whereas the P_{13} method, which although adequate, shows some unexpected errors for such a high order polynomial approximation. An approximate formula was developed which allows a certain amount of scattering in the foil; the limitations of this are discussed. (auth)

21221 INVESTIGATION OF THE SCATTERING OF NEUTRONS ON HEAVY WATER AT SMALL ANGLES. W. Gissler (Kernforschungsanlage, Julich, Ger.). Z. Naturforsch., 19a: 1422-4(Dec. 1964). (In German)

The existence of large molecular conglomerates was investigated by means of the measurement of the differential effective cross section of long-wave neutrons on heavy water at small scattering angles. The elastic coherent scattering cross section for various molecular conglomerate models was calculated. The experimental results showed no agreement with the theoretical results. Therefore, within the accuracy of measurements there was no indication of the existence of conglomerates. (J.S.R.)

21222 QUASIDIFFUSION METHOD FOR SOLVING THE KINETIC EQUATION. V. Ya. Goldin. Zh. Vychislitel. Mat. i Mat. Fiz., 4: 1078-87(Nov.-Dec. 1964). (In Russian)

The Boltzmann linear integro-differential equation $(1/v)(\partial\varphi/\partial t) + \Omega\nabla\varphi + \Sigma\varphi = \int\varphi(r, \Omega', v', t)\, w(\mu_0, v' \rightarrow v)\, dv'd\Omega' + s(r, \Omega, v, t)$ is treated, subject to the condition that the exterior surface S is convex and the neutron flow onto S from the outside is equal to zero. By a series of transformations, this problem is converted to a generalization of that of solving the diffusion problem. These can be handled by any one of a number of standard methods. The quasidiffusion method proposed makes it possible to decrease significantly the number of iterations of the whole equation, transferring a large part of the work in defining the critical parameters to a system of equations of the diffusion type. Two examples are given to illustrate convergence of the iterative method in the case of an inhomogeneous diffusion equation; results are given for neutron flow in a system which is a homogeneous sphere of radius R_1 (1-st zone) surrounded by a homogeneous spherical shell, of thickness in $R_2 - R_1$ (2-nd zone). (ATD)

21223 AN ITERATIVE SOLUTION METHOD FOR THE NEUTRON TRANSPORT EQUATION WITH ANISOTROPIC SCATTERING. Bruce W. Crawford (Univ. of California, Berkeley). 40p. (CONF-654-78)

From American Nuclear Society Meeting, San Francisco, Nov.-Dec. 1964.

An iterative method is presented for solution of the monoenergetic neutron transport equation with an anistropic scattering kernel for arbitrary geometry. The method is demonstrated by solving the monenergetic, one-dimensional, infinite-medium, Green's function problem with anisotropic scattering for isotropic sources. (D.C.W.)

Nuclear Properties and Reactions

Refer also to abstracts 19958, 20342, 20937, and 21678.

21224 (AECL-2160) THE ENERGY RELEASE IN LOW-ENERGY FISSION. J. S. Fraser (Atomic Energy of Canada Ltd., Chalk River (Ontario)). Feb. 1965. 21p. (SM-60/34). $1.00(AECL).

Studies are reported of the mass deficit, energy release, and fine structure in low-energy and spontaneous fission. The relations between the total kinetic energy, the neutron energy, and the slope of the ν (neutrons produced/fission) curve are also studied. (T.F.H.)

21225 (AECL-2168) FISSION DATA AND NUCLEAR TECHNOLOGY. G. C. Hanna (Atomic Energy of Canada Ltd., Chalk River (Ontario)). Feb. 1965. 17p. (SM-60/50). $1.00(AECL).

The availability, necessity, and uses of nuclear data on nuclei used in reactors is discussed, from the viewpoints of the disseminator of the data and the user of the data. Representative cross section values are tabulated for ^{233}U, ^{235}U, and ^{239}Pu. (T.F.H.)

21226 (AEET/HP/Th-19) CHAIN ELEMENT ACTIVITY IN INTERMITTENT IRRADIATION. P. P. Damle and K. Santhanam (Atomic Energy Establishment, Trombay (India)). 1964. 18p. Dep.(mn).

A method is developed for calculating the activity of neutron induced chain elements or fission products in intermittent irradiation in a reactor. General expressions for the activity of the nth member in such chains were obtained taking account of depletion of parent element and daughters by radioactive decay and neutron capture. By regrouping terms, the activity is expressed as a summation of products of a constant times a growth (or decay) term. In going from one cycle of irradiation and decay to the next, the constants remain the same while the growth (or decay) terms alone vary. The concept of an irradiation time equivalent to a cycle of operation and decay is used. The equivalent irradiation time for the first cycle is used as the reference point for the second cycle. First and second cycles can then be represented by an equivalent irradiation time which is to be used for the third cycle, and so on. By repetition of this procedure, an entire complex irradiation history is simplified. The method is also applicable to cases where power level varies from cycle to cycle provided it is constant during each cycle. Examples are presented to illustrate the method. (auth)

21227 (ANL-6941) A RE-EVALUATION OF FISSION RATIOS MEASURED IN ZPR-III CRITICAL ASSEMBLIES. William G. Davey and Paul I. Amundson (Argonne National Lab., Idaho Falls, Idaho). Oct. 1964. Contract W-31-109-eng-38. 20p. Dep.; $1.00(cy), 1(mn) CFSTI.

A recent comparison of measured and calculated fission ratios for 18 ZPR-III fast critical assemblies showed that the interpretation of these data contained ambiguities that suggested that the intercalibration of the fission chambers should be re-examined. Hence, an independent intercalibration was carried out in which the relative masses of fissile materials were estimated in terms of the fission rates in a thermal flux and the well-known thermal cross sections of certain fissile isotopes. The original mass calibrations were generally confirmed with corrections being of the order of only 3%, but the ^{234}U chambers required corrections of 9 to 12%. Additional small corrections of up to 1% were also established to allow for certain errors in the techniques used for the fission ratio measurements. The original measured data were corrected and recompared with calculations. These revised experimental data are shown to be in better agreement with calculated values. (auth)

21228 (ANL-6970) THE GENERALIZED RIEMANN ZETA FUNCTIONS AND THEIR APPLICATIONS IN THE CALCULATIONS OF NEUTRON CROSS SECTIONS. M. Atoji and F. L. Clark (Argonne National Lab., Ill.). Dec. 1964. Contract W-31-109-eng-38. 53p. Dep.; $3.00(cy), 1(mn) CFSTI.

The generalized Riemann Zeta function of incomplete mode is introduced. The values of the generalized Riemann function and those of the incomplete mode are given for a specific range of the variables. The calculation was initiated in order to fulfill a need in the neutron cross-section study. Other physical applications of the tables in a wider scope are also suggested. (auth)

21229 (BNL-8841) X-RAYS EMITTED IN COINCIDENCE WITH THE FISSION OF Cf^{252}. T. Darrah Thomas, Richard A. Atneosen (Princeton Univ., N. J.), Walter M.

Gibson (Bell Telephone Labs., Inc., Murray Hill, N. J.), and Morris L. Perlman (Brookhaven National Lab., Upton, N. Y.). [1964]. Contract [AT(30-2)-Gen-16]. 21p. (PPA-2137-536; CONF-650301-6). Dep.(mn); $1.00(cy), 1(mn) CFSTI.

From Symposium on the Physics and Chemistry of Fission, Salzburg, Austria.

Measurements of the lifetimes of the K x rays emitted in coincidence with the fission of ^{252}Cf are described. Information on the spectrum and yield of K x rays per fission is also included. It is found that measurement of the K x rays emitted by ^{252}Cf fission fragments, in conjunction with measurements of the masses of these fission fragments, is a valid method for determining the charge distribution for a given fission-fragment mass. The spectrum and yield of electrons emitted in coincidence with the fission of ^{252}Cf is measured as a function of the mass division. (T.F.H.)

21230 (CEA-R-2552) CONTRIBUTION A L'ETUDE PAR LA METHODE DU TEMPS DE VOL DE L'INTERACTION DES NEUTRONS LENTS AVEC L'U^{235}. (Contribution to the Study of the Interaction of Slow Neutrons with ^{235}U Using Time-of-Flight Methods). Michaudon Andre (Commissariat a l'Energie Atomique, Saclay (France). Centre d'Etudes Nucleaires). 1964. 381p. Dep.(mn).

Thesis submitted to Paris Univ., France.

The properties of the excited levels of uranium-236 obtained by interaction of slow neutrons with uranium-235 are studied. The experiments have been carried out at the Saclay linear electron accelerator by the time-of-flight method. The technical and physical conditions which rule the experiments: compromise between resolution and counting rate; time dispersion due to the slowing down of the neutrons; and crystalline binding effects. The experimental total, fission, and ternary fission cross sections are given. The resonance parameters, their statistical distribution, and their correlations are analyzed. Some classifications of the resonances are carried out according to their parameters, and these classifications are compared with each other and with other results. The evidence of a cross section correlation with a range smaller than 100 ev seems to be confirmed. (auth)

21231 (COO-1198-255) ADVANCES IN MÖSSBAUER EFFECT METHODOLOGY HIGH-PRESSURE TECHNIQUES. R. Ingalls (Illinois Univ., Urbana). [1964]. Contracts ONR-1834(05) and AT(11-1)-1198. 12p. Dep.(mn); $1.00 (cy), 1(mn) CFSTI.

Development of a high-pressure cell for Mössbauer measurements permits investigation of isomer shifts, hyperfine fields, and recoilless fractions as a function of lattice parameter. The method employed, that of supported pistons, is applicable to the study of Mössbauer sources, in the form of a foil or powder, over the pressure range of 0 to 300 kb. Because of the amount of support material and sample size, the method has only been applied to sources. The pressure cell and its loading and calibration are discussed. (auth)

21232 (JEN-141-DF/I-45) INTERACCIONES DE UN HAZ DE PARTICULAS ^{3}He DE 29 Mev SOBRE NUCLEOS LIGEROS. (Interactions of 29-Mev He^3 Particles with Light Nuclei). J. de la Rubia Pacheco (Junta de Energia Nuclear, Madrid (Spain). Division de Fisica). 1964. 24p. Dep.(mn).

The interactions of 29-Mev ^{3}He particles with ^{32}S, ^{19}F, and ^{12}C, irradiated in a cyclotron, have been studied using the nuclear emulsion technique. The first excitation levels of ^{12}C and ^{32}S have been obtained, and the pick-up reaction ^{12}C(^{3}He,^{4}He)^{11}C has been studied and used to calculate its Q-value and the first levels of ^{11}C. Angular distributions of the elastic differential cross section of ^{3}He from ^{32}S and ^{19}F have been studied and the parameters of the corresponding interaction optical model have been obtained. The agreement between theoretical and experimental results is quite good. The interaction radii for both processes have been determined and the approximate angular distribution of the pick-up cross section was calculated. (auth)

21233 (JINR-E-1992) ON THE SMALL-ANGLE SCATTERING OF CHARGED PARTICLES. L. D. Solov'ev (Joint Inst. for Nuclear Research, Dubna (USSR). Lab. of Theoretical Physics). 1965. 8p. Dep.(mn).

For the high energy scattering of charged elementary particles the relativistic formula for the forward elastic cross section and the optical theorem for the nuclear scattering amplitude are obtained taking into account the interference between nuclear and Coulomb interaction. (auth)

21234 (JINR-P-1908) NEUPRUGOE RASSEYANIE TYAZHELYKH CHASTITS S VOZBUZHDENIEM KOLLEKTIVIYKH SOSTOYANII YADER. (Inelastic Scattering of Heavy Particles With Excitation of Collective Nuclear States). V. K. Luk'yanov and I. Zh. Petkov (Joint Inst. for Nuclear Research, Dubna (USSR). Lab. of Theoretical Physics). 1964. 9p. Dep.(mn).

The inelastic scattering of heavy particles, with excitation of collective nuclear levels, has been considered at energies above barrier. An expression for the excitation cross section of any n-phonon transition has been obtained. The contribution of both the Coulomb and nuclear part of the interaction is taken into account. If this interaction is small, then in the first approximation a usual variant treated in the diffraction theory method is obtained. (auth)

21235 (JINR-P-1950) O "BIENIYAKH" IZLUCHENIYA YADER, VOZBUZHDAEMYKH POTOKOM CHASTITS PEREMENNOI INTENSIVNOSTI. (On "Beating" of Nuclear Radiation Due to a Particle Flux of Variable Intensity). V. G. Baryshevskii and M. I. Podgorentskii (Joint Inst. for Nuclear Research, Dubna (USSR). Lab. of High Energy and Joint Inst. for Nuclear Research, Dubna (USSR). Lab. of Theoretical Physics). 1965. 5p. Dep.(mn).

The behavior of a system of nuclei that is bombarded with a flux of particles with variable intensity is investigated. A possibility of a resonance enhancement of the radiation "beating" of this system is indicated. A comparison is made with γ-γ coincidences. (auth)

21236 (JINR-P-1952) O YADERNYKH FORMFAKTORAKH V PROTSESSE ZAKHVATA MYUONOV GELIEM-3. (Nuclear Form-Factors in Muon-Capture by Helium 3). O. A. Zaimidoroga, B. V. Struminskii, R. M. Sulyaev, I. V. Falomkin, V. M. Tsulko-S tinkov, and Yu. A. Shcherbakov (Joint Inst. for Nuclear Research, Dubna (USSR). Lab. of Nuclear Problems). 1965. 7p. Dep.(mn).

The $\mu^- + {}^3\mathrm{He} \rightarrow {}^3\mathrm{H} + \nu$ reaction rate (Λ) has been calculated on the basis of data on form-factors obtained in experiments on pion capture by ^{3}He and the scattering of electrons on ^{3}He and ^{3}H. Its value turned out to be 1515 ± 55 sec^{-1} with $g_A^s|g_V^s - 1.16$ and $g_P^\mu|g_A^\mu = 7$. From the comparison of experimental and theoretical results, the pseudoscalar constant $g_P^\mu = (8 \pm 3)g_A^\mu$ has been evaluated. (auth)

21237 (KFK-265) EINE MESSUNG DES ISOMEREN AUFSPALTVERHALTNISSES BEIN AKTIVIERUNG IN DEN ERSTEN 3 INDIUM-RESONANZEN. (A Measurement of Isomeric Splitting Ratios by Activation in the First 3 Indium Resonances). E. Albold and P. v. Blankenhagen (Kernforschungszentrum, Karlsruhe (West Germany). Institut fur Angewandte Kernphysik). Dec. 1964. 12p. (EANDC-E-55). Dep.(mn).

The reaction ^{115}In(n,γ)^{116}In produces 3 isomers of ^{116}In. The ratios R of the β-active states were determined. The experimental technique and the evaluation method were described. A comparison is made of the results with the static cascade theory. (J.S.R.)

21238 (LA-3205) BIBLIOGRAPHY OF NUCLEAR INTERACTIONS OF He^3 WITH d, n, OR p AND OF d WITH n, p, OR T AT 3-30 Mev. Betty S. Jackson (Los Alamos Scientific Lab., Univ. of California, N. Mex.). Oct. 9, 1964. Contract W-7405-eng-36. 14p. Dep.; $1.00(cy), 1(mn) CFSTI.

A bibliography is presented, consisting of 99 references to material on ^{3}He interactions with d, n, and p; d interactions with n, p, and t; and nuclear reactions involving pairs of these particles at 3 to 30 Mev. (T.F.H.)

21239 (LA-3206) STATUS OF THE LASL MONTE CARLO INTRANUCLEAR CASCADE CALCULATION (1964). S. L. Whetstone (Los Alamos Scientific Lab., Univ. of California, N. Mex.). Dec. 10, 1964. Contract W-7405-eng-36. 26p. Dep.; $2.00(cy), 1(mn) CFSTI.

Described briefly are the changes made from the original version of the LASL Monte Carlo intranuclear cascade calculation published (Phys. Rev., 110: 185-204 (1958)) by Metropolis et al. Changes include improved pion-production dynamics and the introduction of a Fermi-type non-uniform nuclear density distribution. A few intercomparisons between the results of the present and the original version are made. Some comparisons are also given between the present calculations and experiment. (auth)

21240 (LA-DC-6232) THE (He^3,d) REACTION ON THE N = 28 NUCLEI (thesis). Dale D. Armstrong (Los Alamos Scientific Lab., Univ. of California, N. Mex.). 1965. Contract W-7405-eng-36. 94p. Dep.(mn); $3.00(cy), 2(mn) CFSTI.

Submitted to Univ. of New Mexico.

A beam of 22-Mev ^{3}He ions was used to investigate the (^{3}He,d) reaction on ^{48}Ca, ^{51}V, ^{52}Cr, and ^{54}Fe. A solid-state E-ΔE mass-identification detector system was used. The use of a summing preamplifier for performing the coherent addition of the E and ΔE pulses allowed the energy resolution to be reduced to the inherent energy spread of the cyclotron beam, which is 100 to 120 kev. Levels or groups of levels were resolvable up to an excitation of 5 to 6 Mev for all the nuclei that were studied, and angular distributions were obtained for the deuterons corresponding to these levels. A modified version of the Gibbs-Tobocman distorted-wave calculation was used to extract spectroscopic information concerning the levels. The formalism developed for the j-j coupling version of the nuclear shell model was used to assign the levels to the various single-particle states. The isobaric-spin splitting of the single-particle strength was observed for the $2p_{\frac{3}{2}}$ proton single-particle state in ^{55}Co. However, only the lower isobaric spin components of the SP states were observed for all the other nuclei studied. The seniority mixing of the two 4^+ states in ^{52}Cr belonging to the $(f_{\frac{7}{2}})^4$ configuration was determined and compares favorably with the predictions made by Komoda. Elastic-scattering date for 22-Mev ^{3}He ions elastically scattered from ^{40}Ca, ^{48}Ca, ^{51}V, ^{52}Cr, ^{54}Fe, and ^{56}Fe were obtained. Optical-model fits to the elastic-scattering data provided the optical-model parameters for ^{3}He ions that were required for the distorted-wave calculation. (auth)

21241 (LA-DC-6639) SYMMETRY OF NEUTRON-INDUCED Pu^{239} FISSION IN RESONANCE REGION. G. A. Cowan, B. P. Bayhurst, R. J. Prestwood, J. S. Gilmore, and G. W. Knobeloch (Los Alamos Scientific Lab., Univ. of California, N. Mex.). [1963]. Contract [W-7405-eng-36]. 13p. (CONF-650301-7). Dep.(mn); $1.00(cy), 1(mn) CFSTI.

From Symposium on the Physics and Chemistry of Fission, Salzburg, Austria.

Symmetry of fission in ^{239}Pu by energy-resolved neutrons has been radiochemically measured in the resonance region by a neutron time-of-flight method, dubbed the "wheel" method. Data were obtained from 200 to 600 ev in energy intervals ranging from 10 ev to 25 ev in width, containing three to twelve resonances per sample. Both increases and decreases in symmetry of fission were observed as compared with thermal neutron fission of ^{239}Pu. Measured by the ratio of ^{115}Cd, a "valley" fission product, to ^{99}Mo, a "peak" fission product, the symmetric yield decreased by 18% at 250 ± 4 ev, 29% at 307 ± 5 ev, and 33% at 395 ± 6 ev. The symmetric yield increased by 16% ev to 206 ev. The average symmetry of fission over the energy region 196 ev to 585 ev showed a decrease of 8% from the thermal value. Changes in the ratio ^{111}Ag/^{99}Mo appeared to be about one-third as great as changes in the ^{115}Cd/^{99}Mo ratio from level to level. The ratio ^{140}Ba/^{99}Mo showed no systematic changes from the thermal value within analytical error and the average is within 1% of the thermal ratio, which permits the assumption that ^{99}Mo and ^{140}Ba yields are not variable for resonance fission and are the same as in thermal fission. (auth)

21242 (NP-14837) SECONDARY NUCLEONS PRODUCED IN HIGH-ENERGY NUCLEAR REACTIONS. W. R. Yucker (Douglas Aircraft Co., Inc., Santa Monica, Calif. Missile and Space Systems Div.). Dec. 1964. 124p. (SM-46334). Dep.(mn).

The results of a study to provide some of the basic nuclear data necessary for space radiation shielding calculations are presented. Both experimental data and information generated by Monte Carlo calculations are used in the analysis. Empirical relations derived from these data are presented for non-elastic cross sections, cascade yields, residual nuclear excitation, evaporation yields, and secondary energy and angular distributions. These results provide a model for calculating the cross sections for production of secondary nucleons by high energy nucleons striking complex nuclei. (auth)

21243 (ORNL-3506) SPECTRA OF GAMMA RAYS PRODUCED BY THE INTERACTION OF ~160-Mev PROTONS WITH Be, C, O, Al, Co, AND Bi. W. Zobel, F. C. Maienschein, and R. J. Scroggs (Oak Ridge National Lab., Tenn.). Apr. 1965. Contract W-7405-eng-26. 75p. Dep.; $3.00(cy), 2(mn) CFSTI.

A measurement of the gamma rays in the energy range from 0.6 to 11 Mev resulting from bombardment of Be, C, H_2O, Al, Co, and Bi targets with ~160-Mev protons has been completed. A three-crystal scintillation spectrometer was used as a pair spectrometer for photons having energies above 2 Mev and as a total-absorption, anticoincidence spectrometer for photons having energies below 2.5 Mev. A time-of-flight method was used to reject neutrons, with an average rejection efficiency of 0.70 ± 0.01. Data were obtained in the form of pulse-height spectra, which were converted to photon spectra by a computer-programmed "unscrambling" technique, resulting in the assignment of upper and lower spectral bounds representing a 68% confidence interval. The bulk of the data was obtained at 136° from the direction of the proton beam; other data obtained with aluminum targets at 44 and 20.5° gave no evidence of anisotropy. Discrete gamma rays were found for all materials except bismuth. Cross sections for the production of these gamma rays were computed and plausible assignments were made for the transitions giving rise to these lines. In the case of Al, Co, and Bi a continuum was observed, underlying the discrete spectrum for the aluminum and cobalt targets. The total gamma-ray production cross sections for photons in the energy range from 0.6 to 11 Mev were calculated to be: Be, (6.8 ± 1.3) mb; C, (41.4 ± 6.3) mb; O, (115 ± 22) mb; Al, (434 ± 97) mb; and Co, (1050 ± 220) mb. (auth)

21244 (ORNL-P-844) COMPARISON OF MEASURED NEUTRON AND PROTON SPECTRA WITH CALCULATED SPECTRA IN THE ENERGY REGION BETWEEN 50 AND 160 Mev. W. A. Gibson, W. R. Burrus, W. E. Kinney, J. W. Wachter (Oak Ridge National Lab., Tenn.); and C. F. Johnson (General Dynamics/Fort Worth, Tex.). [1964]. Contract W-7405-eng-26. 8p. (CONF-720-5). Dep.(mn); $1.00(cy), 1(mn) CFSTI.

From 2nd Symposium on Protection Against Radiation Hazards in Space, Gatlinburg, Tenn., Oct. 1964.

The energy spectra of secondary protons and neutrons emerging from targets bombarded by a collimated beam of 160-Mev protons were obtained with a proton recoil spectrometer covering the energy range between 50 and 160 Mev. Secondary neutron production cross sections and yields are presented for targets of Al, Co, and Bi. The results are compared with previous Monte Carlo calculations. (C.E.S.)

21245 (ORNL-TM-196) EVAP—A FORTRAN PROGRAM FOR CALCULATING THE EVAPORATION OF VARIOUS PARTICLES FROM EXCITED COMPOUND NUCLEI. Lawrence Dresner (Oak Ridge National Lab., Tenn.). Apr. 11, 1962. Contract W-7405-eng-26. 13p. Dep.(mn); $1.00(cy), 1(mn) CFSTI.

A program (EVAP) is written in FORTRAN in order to calculate (among other things) the number of neutrons emitted and the neutron energy spectrum, from any compound nucleus. (T.F.H.)

21246 (TID-21697) COMPUTER PROGRAM FOR NUCLEAR MAGNETIC AND QUADRUPOLE RESONANCE FREQUENCIES AND INTENSITIES, I = ½ TO 9. Edward H. Carlson (Alabama Univ., University. Dept. of Physics). Feb. 1, 1965. Contract AT(40-1)-3090. 14p. Dep.(mn); $1.00(cy), 1(mn) CFSTI.

Two computer programs are described: HERDAG gives the eigenvalues and eigenvectors of a complex Hermitian matrix of any size; and ZEEMAN uses HERDAG to find the energy level schemes of any nuclear system having I = ½ to 9 in a magnetic field that is arbitrarily oriented with respect to the principal axis of the quadrupole interaction tensor. ZEEMAN also calculates the frequencies and relative intensities of transitions, in the case in which an arbitrarily oriented oscillating r-f field is present. (T.F.H.)

21247 (UCRL-11828(p.10-11)) ENERGY LEVELS OF Pb^{210} FROM SHELL THEORY. Martin G. Redlich (Lawrence Radiation Lab., Univ. of California, Berkeley).

Calculations for ^{210}Pb, made on the basis of the double-closed-shell core model, are reported. The agreement with experimental results is discussed briefly. (D.L.C.)

21248 (UCRL-11828(p.21-5)) ALPHA ACTIVITIES IN PLATINUM. A. Siivola (Lawrence Radiation Lab., Univ. of California, Berkeley).

Nine alpha-emitting Pt isotopes with mass numbers from 173 to 181 were prepared by ^{16}O bombardments of Yb isotopes and ^{20}Ne bombardments of Er isotopes. Alpha energies, half lives, branching ratios, and reduced widths are tabulated and compared with these of the other Pt isotopes. Alpha spectra and excitation functions are given for the reactions ^{170}Yb(^{16}O,xn), ^{172}Yb(^{16}O,xn), and ^{162}Er(^{20}Ne,xn). (D.L.C.)

21249 (UCRL-11828(p.25)) ALPHA-ACTIVE GOLD ISOTOPES. A. Siivola (Lawrence Radiation Lab., Univ. of California, Berkeley).

Six new Au isotopes with mass numbers 177, 178, 179, 181, 183, and 185 were prepared by bombardment of targets with heavy beams. Their alpha energies and half lives are tabulated. (D.L.C.)

21250 (UCRL-11828(p.26)) LIGHT POLONIUM ISOTOPES. A. Siivola (Lawrence Radiation Lab., Univ. of California, Berkeley).

The reactions ^{185,187}Re(^{19}F,xn)Po were used to produce Po isotopes with the mass numbers from 193 to 200, there being two isomers each for the 195 and 197 isotopes. Their alpha energies and half lives are listed and compared with earlier data. (D.L.C.)

21251 (UCRL-11828(p.31-4)) MEASUREMENTS OF INTERNAL-CONVERSION COEFFICIENTS IN THE DECAY OF U^{237}. T. Yamazaki and J. M. Hollander (Lawrence Radiation Lab., Univ. of California, Berkeley).

The gamma spectrum from ^{237}U decay was measured with a Li-drifted Ge detector and used to calculate internal-conversion coefficients. The coefficients are compared with theoretical values, and a proposed decay scheme is given. (D.L.C.)

21252 (UCRL-11828(p.35-8)) MEASUREMENT OF PAIR-PRODUCTION CROSS SECTIONS NEAR THRESHOLD. T. Yamazaki and J. M. Hollander (Lawrence Radiation Lab., Univ. of California, Berkeley).

Pair-production cross sections were measured near threshold using Li-drifted Ge γ-ray detectors, for the following isotopes: ^{60}Co, ^{22}Na, ^{24}Na, ^{140}La, ^{88}Y, and ^{90}Nb. The experimental results are compared with the theoretical Bethe-Heitler curve, which is seen to drop below experiment as the energy decreases. (D.L.C.)

21253 (UCRL-11828(p.38-40)) ENERGY LEVELS OF $_{97}Bk^{249}$. M. D. Holtz, J. M. Hollander, T. Novakov, and R. L. Graham (Lawrence Radiation Lab., Univ. of California, Berkeley).

The decay scheme of ^{253}Es is given. Theoretical half lives of the first two excited states were calculated and compared with experimental values. Branching ratios of M1 transitions were also calculated and compared with experiment. (D.L.C.)

21254 (UCRL-11828(p.55-6)) NUCLEAR MAGNETIC MOMENT OF THE 2084-kev STATE IN CERIUM-140. R. M. Levy and D. A. Shirley (Lawrence Radiation Lab., Univ. of California, Berkeley).

The 329- to 487-kev cascade in ^{140}Ce was studied, and a half life of 3.52 ± 0.10 nsec was found. Modulation at twice the Larmor precision frequency was used to measure the g factor (magnetic moment/spin) for the 2084-kev state. The g factor was determined to be +1.014 ± 0.038, which lies between the quasi-particle and single-particle predictions. With a spin of 4, the magnetic moment is +4.056 ± 0.152 nm. (D.L.C.)

21255 (UCRL-11828(p.57-8)) NUCLEAR ZEEMAN EFFECT IN IRIDIUM-193. J. J. Huntzicker, E. Matthias, S. S. Rosenblum, and D. A. Shirley (Lawrence Radiation Lab., Univ. of California, Berkeley).

A Li-drifted Ge γ-ray detector was used to observe the Mössbauer effect for ^{193}Ir sources in Fe, Co, and Ni lattices and natural Ir metal absorber at 4°K. Hyperfine structure was observed, and a proposed hyperfine-level scheme is given. Hyperfine fields of ^{193}Ir were calculated to be 1210 ± 250, 980 ± 200, and 450 ± 100 kG in Fe, Co, and Ni, respectively. The spin-½ first-excited-state moment is anomalously small, 0.56 ± 0.11 nm. (D.L.C.)

21256 (UCRL-11828(p.58-62)) AN INVESTIGATION OF THE LEVEL SCHEME OF TELLURIUM-125 AND MEASUREMENT OF THE MAGNETIC DIPOLE MOMENT OF ANTIMONY-125 BY NUCLEAR POLARIZATION. N. J. Stone, R. B. Frankel, J. J. Huntzicker, and D. A. Shirley (Lawrence Radiation Lab., Univ. of California, Berkeley).

The Li-drifted Ge gamma detector was used to study the nucleus ^{125}Sb and its decay to ^{125}Te. Angular momentum coupling constants were measured and compared with theory for gamma transitions in ^{125}Sb, and the nuclear magnetic moment was found to be 2.72 ± 0.15 nm. The spin assignments are discussed. (D.L.C.)

21257 (UCRL-11828(p.63-6)) THE DECAY SCHEME OF EINSTEINIUM-254. W. McHarris, F. S. Stephens, F. Asaro, and I. Perlman (Lawrence Radiation Lab., Univ. of California, Berkeley).

Added information on the alpha decay of ^{254}Es resulted in a more refined decay scheme. The higher-energy γ rays were resolved with a germanium gamma detector, and data on alpha and factors are listed for the alpha groups, and the properties of rotational bands in ^{250}Bk are compared with predictions. (D.L.C.)

21258 (UCRL-11828(p.67-71)) DECAY OF MOLYBDENUM-90. J. A. Cooper, J. M. Hollander, M. I. Kalkstein, and J. O. Rasmussen (Lawrence Radiation Lab., Univ. of California, Berkeley).

A study of the conversion electron and gamma spectra in the decay of ^{90}Mo to ^{90}Nb was made in an attempt to resolve inconsistencies in the transitions. Analysis of the conversion lines show the multipolarities of the 122- and 257-kev transitions to be E2 and E3, respectively. A decay scheme is proposed in which a very-low-energy (<2 kev) transition is used to explain the very long half life (24 sec) measured for the 122-kev transition. (D.L.C.)

21259 (UCRL-11828(p.77-80)) FISSION BARRIERS OF W, Re, Os, Ir, AND Hg ISOTOPES. Torbjoern Sikkeland, Victor E. Viola, Jr., Jack E. Clarkson, and Naftali H. Steiger (Lawrence Radiation Lab., Univ. of California, Berkeley).

Fission excitation functions were measured for the systems ^{159}Tb + ^{19}F, ^{165}Ho + ^{14}N, ^{174}Yb + ^{12}C, ^{175}Lu + ^{12}C, ^{182}W + ^{12}C, ^{169}Tm + ^{11}B, and ^{175}Lu + ^{11}B. The quantity $\sigma_f/(\sigma_{CF} - \sigma_i)$ was plotted versus the excitation energy of the compound nucleus formed in a complete fusion (CF) of ion and target.

The graphs are used to show the effects of target, neutron binding energy, and fission barrier E_f on Γ_f/Γ_n. Experimental and liquid-drop-metal E_f values are compared for each of the systems. (D.L.C.)

21260 (UCRL-11828(p.81)) FISSION BARRIER OF THALLIUM-201. Donald S. Burnett, Raymond C. Gatti, Franz Plasil, P. Buford Price, Wladyslaw J. Swiatecki, and Stanley G. Thompson (Lawrence Radiation Lab., Univ. of California, Berkeley).

The fission barrier of the compound nucleus ^{201}Tl, formed by helium-ion bombardment of ^{197}Au, was determined to be 22.5 ± 1.5 Mev. The following equation was derived: x (fissionability parameter) = $(Z^2/A)/(48.5 \pm 0.5)$. The saddle-point mass of ^{201}Tl was determined to be 200.9949 ± 0.0015 mass units on the carbon scale. (D.L.C.)

21261 (UCRL-11828(p.81-3)) FISSION BARRIERS OF POLONIUM-210 AND ANTIMONY-119, 117. R. C. Gatti, A. Khodai-Joopary, and S. G. Thompson (Lawrence Radiation Lab., Univ. of California, Berkeley).

The fission excitation functions of ^{210}Po and ^{119,117}Sb produced by proton bombardment of ^{209}Bi and alpha bombardment of natural In were determined. Graphs of fission cross section and log Γ_f/Γ_n vs excitation energy are given. The results indicate that the fission barrier is ~21.5 ± 1.0 Mev for ^{210}Po and ~38 Mev for ^{119}Sb. (D.L.C.)

21262 (UCRL-11828(p.84-6)) FISSION OF URANIUM-238 AND PLUTONIUM-240 NUCLEI EXCITED BY INELASTIC α-PARTICLE SCATTERING. Harold C. Britt, Franz Plasil, and Stanley G. Thompson (Lawrence Radiation Lab., Univ. of California, Berkeley).

A study was made of the general properties of $(\alpha,\alpha'f)$ reactions on ^{238}U and ^{240}Pu targets, using alpha energies of 40.0 and 38.1 Mev, respectively. Fission fragment anisotropies, coincident energy spectra, and angular correlations of fission fragments are given and discussed. (D.L.C.)

21263 (UCRL-11828(p.90-2)) ENERGY-MASS DISTRIBUTIONS OF Bi, Au, AND W IN He-ION-INDUCED FISSION. F. Plasil, H. C. Britt, and S. G. Thompson (Lawrence Radiation Lab., Univ. of California, Berkeley).

Energy-mass distributions have been measured in the fission of ^{209}Bi, ^{197}Au, and ^{182}Au induced by ^{4}He ions, and some of the results for ^{209}Bi and ^{182}W are discussed. The distributions for ^{182}W are compared with theory and with heavy-ion bombardments resulting in the same compound nucleus, ^{186}Os. The distributions for ^{209}Bi are also compared with theory. The factors involved in the disagreements between experiment and theory are discussed. (D.L.C.)

21264 (UCRL-11828(p.92-4)) ANALYSIS OF FISSION-EXCITATION FUNCTIONS OF LIGHT ELEMENTS. Franz Plasil and S. G. Thompson (Lawrence Radiation Lab., Univ. of California, Berkeley).

The data obtained by Sikkeland on the fission of ^{182}W induced by ^{16}O were analyzed in an attempt to include the effects of angular momentum and fission after neutron emission. The calculated and measured fission barriers were compared, and the parameters are tabulated. (D.L.C.)

21265 (UCRL-11828(p.95-7)) INVESTIGATIONS OF THE K X RAYS EMITTED IN THE SPONTANEOUS FISSION OF CALIFORNIUM-252. H. R. Bowman, S. S. Kapoor, and S. G. Thompson (Lawrence Radiation Lab., Univ. of California, Berkeley).

The kinetic energies of the pair fragments and the energies of the K x rays emitted by the fragments were measured with a high-resolution Li-drifted silicon detector. The results were analyzed to obtain the most probable charge vs the initial mass of the fragments, and they are currently being analyzed for the intensities of the x rays per fragment and the average time of emission of the x rays. (D.L.C.)

21266 (UCRL-11828(p.108-9)) NUCLEAR SPECTROSCOPY WITH TWO-NUCLEON TRANSFER REACTIONS. Norman K. Glendenning (Lawrence Radiation Lab., Univ. of California, Berkeley).

The correlation of the transfer of a pair of nucleons between a nucleus and a light nuclide is discussed. An example using the $^{12}C(\alpha,d)^{14}N$ is used to show that a wave function containing only small admixtures of other configurations contains important correlations that are absent in the dominant configuration. The projection of the relevant part of the center-of-mass motion is given. (D.L.C.)

21267 (UCRL-11828(p.113-16)) INELASTIC SCATTERING OF 50.9-Mev ALPHA PARTICLES FROM Ne^{20}. A. Springer and B. G. Harvey (Lawrence Radiation Lab., Univ. of California, Berkeley).

Inelastic alpha scattering was used to study the complex rotational band structure of the deformed nucleus ^{20}Ne. Energy spectra were measured at 1-degree intervals from 11 to 43° c.m. Cross sections for the members of the ground state rotational band and of the low-lying negative parity bands are compared with the Austern and Blair model for single and double excitation. (D.L.C.)

21268 (UCRL-11828(p.129-31)) OCTUPOLE STATES IN N^{15} AND O^{16}. André Bussiere, Norman K. Glendenning, Bernard G. Harvey, Jeannette Mahoney, John R. Meriwether, and Daniel J. Horen (Lawrence Radiation Lab., Univ. of California, Berkeley). (UCRL-11633)

The elastic and inelastic scattering of 40.6-Mev helium ions by ^{15}N and ^{16}O was studied. The 5.276- and 7.57-Mev levels of ^{15}N were found to be strongly excited. The angular distributions for elastically scattered particles are given, and optical-model fits to the data were made. Inelastic angular distributions were calculated. The octupole levels and the interpretation of the results are discussed. (D.L.C.)

21269 (UCRL-11828(p.132-3)) ENERGY VARIATION OF THE PHASE RULE IN α-PARTICLE SCATTERING. J. R. Meriwether, A. Bussiere de Nercy, B. G. Harvey, J. Mahoney, and D. J. Horen (Lawrence Radiation Lab., Univ. of California, Berkeley).

The phase predictions of the diffraction model for the inelastic and elastic angular distributions of scattered alpha particles are discussed. An experimental study was made to determine the energy dependence of the various mechanisms proposed. Angular distributions for the scattering of alpha particles at 25 to 100 Mev were measured for the first 2+, second 2+, and first 4+ levels in ^{62}Ni. The in- and out-phase relationships are discussed and compared with the diffraction model. (D.L.C.)

21270 (UCRL-11828(p.214-16)) OBSERVATION OF ELECTRONIC RELAXATION IN MÖSSBAUER SPECTROSCOPY. H. Hollis Wickman, Melvin P. Klein, and D. A. Shirley (Lawrence Radiation Lab., Univ. of California, Berkeley).

The extreme cases where $\tau\Delta\nu > 1$ and $\tau\Delta\nu < 1$ (τ = electron correlation time, $\Delta\nu$ = frequency difference between hfs components) are considered. An experimental study was made of the Mössbauer spectra of ^{57}Fe in ferrichrome and ferrichrome A at 300 to 2.5°K. Relaxation spectra were obtained from modified Bloch equations. It is concluded that an intermediate case of exchange ($\tau\Delta\nu \sim 1$) was observed. (D.L.C.)

21271 (KFK-tr-161) UBER DEN MECHANISMUS DES PROTONENZERFALLS. (On the Mechanisms of Proton Decays). V. I. Gol'danskii (Akademiya Nauk S.S.S.R.). Translated into German by Peter Buriks (Kernforschungzentrum, Karlsruhe, Germany). 1964. 11p. Dep.(mn); $1.60(fs), $0.80(mf) JCL.

In neutron-poor isotopes with $Z \leq 50$ three variants of proton decay are possible: proton decay, double proton decay, and a process consisting of two processes, i.e., the emission of delayed protons. It is concluded from experimental studies that the emission of delayed protons, but not one of the two first variants, and no proton isomerism, was observed. The "light" emitter observed was apparently ^{21}Mg and the "heavy" emitter ^{70}Kr. (tr-auth)

21272 DECAY OF Eu^{157} AND Tm^{174}. K. Kantele (Univ. of Helsinki), K. M. Broom, and D. M. Chittenden, II. Ann. Acad. Sci. Fennicae, Ser. A VI, 162: 1-17(1964).

The decay of 15.1-hr ^{157}Eu and 5.2-min ^{174}Tm was investigated with scintillation spectrometers, radiochemical separations having been used in element indentification and source preparation. Decay schemes are proposed incorporating 0.46 and 850-μsec isomeric states in the daughter nuclei ^{157}Gd and ^{174}Yb, respectively. The results are discussed in the framework of the Nilsson scheme and the pairing correlation model. (auth)

21273 ENERGY GAP AT THE FERMI SURFACE OF NUCLEAR MATTER. Donald W. L. Spring (McMaster Univ., Hamilton, Ont., Can. and Cornell Univ., Ithaca, N. Y.). Ann. Phys., 31: 342-69(Feb. 10, 1965).

It is shown that there is an energy gap at the Fermi surface of nuclear matter, due to the definition of the G matrix off the energy shell for an interacting particle and hole. This gap was evaluated self-consistently as $0.16\ \hbar^2k_F^2/Mm^* = 13\ MeV/m^*$, when $k_F = 1.4\ F^{-1}$. The calculation is carried out within the framework of the reference spectrum method. The average energy denominator—the amount by which the G matrix is off the energy shell—was carefully evaluated for a particle just above the Fermi surface as a function of the energy gap D. The average denominator is shown to depend on the gap D almost linearly, but to be exceedingly independent of the forces acting. Restricted Euler functions, by means of which the calculations may be carried out trivially, are defined and tabulated. (auth)

21274 QUASI-DEUTERON PRODUCTION BY γ RAYS IN HEAVY NUCLEI. Erlend Oestgaard (Institutt for Teoretisk Fysikk, N.T.H., Trondheim, Norway). Arkiv Fys. Seminar Trondheim, No. 1, 1-41(1965).

The total cross section for direct absorption of gamma rays by neutron–proton pairs is evaluated for nuclear matter in the approximation of effective mass for photon energies from 20 Mev to 200 Mev. Electric dipole and quadrupole and magnetic dipole transitions are taken into account. The results are compared with other theoretical results. (auth)

21275 NUCLEAR ENERGY. WHAT IT IS AND HOW IT ACTS. Andrew W. Kramer, ed. Atomics, [18:] 32-6 (Mar.-Apr. 1965).

The shell theory of nuclear structure, its origin, and its correlation with the electron theory of atomic structure are discussed. Empirical evidence for magic numbers and their relation to the stability of nuclei are considered. Application of the Pauli exclusion principle to the nuclear shell model is described. (M.C.G.)

21276 STUDY OF THE REACTIONS $K^{39}(\gamma,n)K^{38,38m}$ AND $K^{39}(\gamma,np)A^{37}$ UP TO 80 Mev. S. Costa and F. Ferrero (Universita, Turin). Atti Accad. Sci. Torino, I. Classe Sci. Fis., Mat. Nat., 99: 85-93(1965). (In Italian)

The experimental apparatus and the analytical method developed in the Synchrotron Laboratory of the University of Turin for the measurement of the short-lived β^+ activity obtained from photonuclear reactions are described. The cross sections of the reactions $^{39}K(\gamma,n)^{38}K$ and $^{39}K(\gamma,n)^{38m}K$ were measured outside the giant resonance. Information was obtained on the reaction $^{39}K(\gamma,np)^{37}Ar$ and on the possibility of the formation of the 0.95-sec isomeric state of ^{38m}K. (tr-auth)

21277 DETERMINATION OF THE SPIN IN THE 0.416 Mev ENERGY LEVEL OF THE Fe-55 NUCLEUS FROM THE (d,p) AND (n,γ) REACTIONS. E. A. Rudak and E. I. Firsov. Dokl. Akad. Nauk Belorussk. SSR, 8: 514-15 (1964).

The possibility is discussed of a single-valued determination of the spin in the 0.416-Mev level of ^{55}Fe by juxtaposing the intensity of the protons from the $^{54}Fe(d,p)^{55}Fe$ reaction and the intensity of the γ rays from the $^{54}Fe(n,\gamma)^{55}Fe$ reaction, which correspond to transitions to identical levels of the product nucleus. (OTS)

21278 INVESTIGATION OF THE DECAY OF Rh-100. N. M. Antoneva, B. S. Dzhelepov, G. S. Katykhin, and V. B. Smirnov (Leningrad State Univ.). Dokl. Akad. Nauk SSSR, 159: 1252-4(Dec. 21, 1964). (In Russian)

The emission from the isotope ^{100}Rh was investigated with the aid of a "ketron" type magnetic spectrometer with scintillation recording of the electrons ($\Delta H\xi/H\xi$ = 0.5%) and with scintillation γ spectrometers used singly, doubly, and to measure total absorption with NaI crystals in a barrel. The isotope ^{100}Rh was obtained either from the reaction Ag + p (660 Mev) or as the daughter product of ^{100}Pd decay. The observed transitions were identified by observing the growth and decrease in the intensities of the γ lines and some conversion lines in the Pd and Rh fractions. Approximately 16 new γ transitions belonging to the decay of ^{100}Rh were observed, and it is pointed out that previously observed lines actually constitute groups of lines. The research covered in detail the energy range from 200 to 2500 kev. A complete level scheme and tables of the γ transition energies and the results of the investigation of the γ-γ coincidence spectra are presented. (ATD)

21279 CROSS SECTIONS FOR CERTAIN REACTIONS IN WHICH FAST π^+ MESONS ARE ABSORBED BY LIGHT NUCLEI. B. P. Afanasev and V. I. Ostroumov (Leningrad Polytechnic Inst.). Dokl. Akad. Nauk SSSR, 159: 1255-6 (Dec. 21, 1964). (In Russian)

Photoemulsion stars formed during meson (π^+) absorption by C, N, and O nuclei were examined in a fine grain emulsion irradiated in a synchrocyclotron by 80 ± 6 Mev meson (π^+) beams. Seven hundred and eighty nine events of spallation with one or two gray tracks belonging to < 20-Mev protons and 2 to 4 tracks of heavy particles (probably α particles) were observed in the 1.32 cm^3 emulsion. An analysis was made of the possible reactions in the selected events: $\pi + {}^{14}N \rightarrow 2p + 3\alpha$, $\pi + {}^{14}N \rightarrow p + d + 2\alpha + {}^3He$, $\pi + {}^{14}N \rightarrow \pi' + d + 3\alpha$, $\pi + {}^{16}O \rightarrow 2p + 2\alpha + {}^6Li$, $\pi + {}^{16}O \rightarrow p + {}^3He + 3\alpha$, and $\pi + {}^{12}C \rightarrow p + {}^3He + 2\alpha$. The energy of gray track particles was determined by the method of least squares using 4 conservation equations, the energy of other particles was estimated by their paths in the nuclear emulsion. Cross sections of examined reactions were determined using the known bombarding meson (π) flux with consideration for meson (μ) admixtures in it and by the number of observed spallation events. The content of C, N, and O in the emulsion was 0.277, 0.087, and 0.283 g/cm^3, respectively. (R.V.J.)

21280 A STUDY OF THE DECAY OF Pd^{101}, Rh^{101*}, AND Rh^{101}. N. M. Antonieva, B. S. Dzhelepov, M. K. Nikitin, and V. B. Smirnov (Leningrad State Univ.). Dokl. Akad. Nauk SSSR, 160: 57-60(Jan. 1, 1965). (In Russian)

The decay of ^{101}Pd, ^{101*}Rh, and ^{101}Rh was investigated with the aid of a magnetic spectrometer of the "ketron" type (resolution 0.5%) with the electrons registered with the aid of scintillation gamma spectrometers: single, double (for the study of gamma-gamma coincidences), and total absorption spectrometer with a 70 × 70 mm NaI crystal in a barrel. The target preparation methods and the precautions taken to exclude background are described. The gamma transitions belonging to the various decays were identified and level schemes are proposed. (ATD)

21281 ON Pi-MESIC ATOM PROCESSES IN HYDROGEN-CONTAINING SUBSTANCES. V. I. Petrukhin and Yu. D. Prokoshkin (Joint Inst. for Nuclear Research, Dubna, USSR). Dokl. Akad. Nauk SSSR, 160: 71-2(Jan. 1, 1965). (In Russian)

An attempt was made to determine the mechanism of the transfer of pions from hydrogen atoms to heavier atoms in hydrogen-containing substances such as styrene. The negative pions passed through scintillation counters, were slowed down, and stopped in the target. The resultant gamma quanta were registered by Cherenkov total-absorption spectrometers. Various gases and solutions were used as the targets. The results showed that a probability of capture of pions by nuclei of bound hydrogen does not depend on the density of the material employed (ethane). Similar results were obtained also with solutions. It follows therefore that the transfer of pions in hydrogen-containing substances is a process which occurs with large

intensity only when the distances between the hydrogen atoms and the heavy atoms are small. It is also concluded that the mechanism is more complicated than assumed previously by Panofsky et al. It is to be expected, in particular, that the intensity of the transfer depends essentially on the molecular structure of the substance. (ATD)

21282 THE POSSIBILITY OF USING NUCLEAR MAGNETIC RESONANCE FOR THE STUDY OF THE FINE STRUCTURE OF PHOTONUCLEAR REACTIONS. V. A. Shkoda-Ul'yanov. Dokl. i Soobshch. Uzhgorodsk. Gos. Univ., Ser. Fiz. Mat. Nauk No. 4, 7-8(1961).

Two important nuclear properties are the spin and the magnetic moment, characterized by the gyromagnetic ratio. It is therefore to be expected that in the energy region where the nuclear properties vary sharply, the gyromagnetic ratio, characterizing the initial unexcited state, will also change. A technique is described for studying this phenomenon by means of nuclear magnetic resonance, using a betatron to produce intense bundles of polarized γ quanta which impinge on appropriate targets in a strong pulsating magnetic field; the target may also be polarized. (ATD)

21283 THE COMPOUND NUCLEUS AND ASYMMETRIC FISSION. Lennart Simons. Fys. Tidsskr., 60: 85-9 (1962). (In Swedish)

The history of the experimental results and the theoretical speculations leading to the theory of the compound nucleus and asymmetric fission is briefly summarized. (J.S.R.)

21284 THEORETICAL AND EXPERIMENTAL PROBABILITIES OF RADIATIVE TRANSITIONS IN THE DEFORMED NUCLEUS Yb-173. O. D. Kovrigin, G. D. Laty'shev, and G. A. Londarenko. Izv. Akad. Nauk Kaz. SSR, Ser. Fiz.-Mat. Nauk, No. 1, 51-9(1964).

Theoretical calculations are based on the formulas of Weisskopf and Moszkowski. The required Clebsch-Gordan coefficients not published elsewhere are calculated and tabulated. The experimental partial probabilities were obtained by measuring the spectrum of the internal conversion electrons, using for the lifetimes of the excited levels the values obtained by Berlovich et al. The conversion electron spectrum was measured with a large double-focusing magnetic beta spectrometer. The source was the lutetium fraction obtained by chromatographic separation of a tantalum target bombarded with 660-Mev protons. Comparison of the theoretical and experimental data disclosed a strong hindrance of γ transitions to the ground state, indicating that ^{173}Yb is a strongly deformed nucleus and the γ transitions are of the electric dipole type. (ATD)

21285 MEASUREMENTS OF TOTAL NEUTRON CROSS SECTIONS IN In AND Sm. R. B. Bergzhanov, D. A. Gladyshev, S. V. Starodubtsev, and T. Khaidarov (Inst. of Nuclear Physics, Academy of Sciences, USSR). Izv. Akad. Nauk Kaz. SSR, Ser. Fiz.-Mat. Nauk, No. 4, 32-6(1964). (In Russian)

The results of a measurement of the total cross sections for the interaction of neutrons with In and Sm at energies from 0.7 to 14 ev are reported. (J.S.R.)

21286 THE QUESTION OF INTERPRETATION OF ELASTIC SCATTERING OF DEUTERONS WITH ENERGY OF 10.3 Mev ON He^4. L. S. Sokolov and A. P. Mamontov. Izv. Tomsk. Politekhn. Inst., 122: 11-13(1962).

The elastic-scattering cross section of deuterons with energy of 10.3 Mev on ^{4}He is calculated from an optical model with a rectangular complex potential. The agreement between calculation and experiment is considerably worse for the region of large angles than for small angles. The best correlation between the calculation and experimental curves for the entire range of angles is obtained for $V_0 = -41$ Mev, $W_0 = -5$ Mev (when $r_0 = 1.5 \cdot 10^{-13}$ cm). Comparison of these parameters of the interaction potential with the corresponding parameters for proton and neutron scattering makes it possible to assume that only one of the nucleons of the deuteron interacts with a nucleus, while the second nucleon, in all probability, passes outside the range of nuclear forces. (tr-auth)

21287 THE CONNECTION BETWEEN THE WIDTH OF THE GIANT RESONANCE OF THE (γ,n)-REACTION AND FILLING OF THE ENERGY LEVELS OF THE NUCLEUS. A. K. Berzin, R. P. Meshcheryakov, S. I. Shornikov, and B. M. Yakovlev. Izv. Tomsk. Politekhn. Inst., 122: 14-18(1962).

Threshold energies for certain Mo and Nd isotopes were measured. Threshold energies in the (γ,n) reaction for the isotopes ^{92}Mo, ^{94}Mo, ^{100}Mo, ^{142}Nd, and ^{150}Nd were determined by the method of induced activity, and for the isotopes ^{97}Mo and ^{145}Nd—by the method of direct neutron registration. The values of the threshold energies of the other isotopes were determined while processing the general curve of the yield of photoneutrons from all isotopes of a given element. It was found that for isotopes containing 8 neutrons above the filled shell there are observed somewhat too high values of the threshold energies of the (γ,n) reaction. Cross sections of (γ,n) reactions on isotopes of La, Ce, and ^{141}Pr, Nd, ^{142}Nd, and ^{150}Nd were also studied. It was noted that the insignificant difference in the widths of the giant resonances for the ^{150}Nd isotope and nuclei having a filled neutron shell indicates slight deformation of the ^{150}Nd nucleus, since strongly deformed nuclei have high values for the giant resonance width. From this fact, together with data on the thresholds of the (γ,n) reaction, it is concluded that for the ^{150}Nd isotope there is no filling of the $2f_{\frac{5}{2}}$ level or realization of any other configuration. (tr-auth)

21288 ANGULAR DISTRIBUTION OF PHOTONEUTRONS FROM Ta^{181} AND Bi^{209}. A. K. Berzin and A. E. Kolchin. Izv. Tomsk. Politekhn. Inst., 122: 19-20(1962).

The angular distributions of photoneutrons from ^{181}Ta and ^{209}Bi were studied. A betatron with maximum energy 24 Mev is used as a γ source. Neutrons were recorded by means of recoil protons in nuclear photoemulsions of type NIKFI Ya-2 100 microns thick. In the case of Ta, the photographic plates were set at angles of 30, 60, 90, 120, and 150° to the direction of the γ beam; in the case of Bi these angles were 30, 60, 90, 115, 135, and 150°. The experimental points for ^{181}Ta, within limits of error, lie quite well on the curve $0.35 + (0.65 \pm 0.1)\sin^2\theta$, and for ^{209}Bi—on the curve $0.45 + 0.55 \sin^2\theta$. (tr-auth)

21289 EXCITATION OPERATORS AND INTRINSIC HAMILTONIANS. R. K. Nesbet (International Business Machines Corp., San Jose, Calif.). J. Math. Phys. (N. Y.), 6: 621-9(Apr. 1965).

An operator $A^\dagger$ that satisfies $[H,A^\dagger] = \hbar\omega A^\dagger$ converts a stationary-state eigenfunction of the hamiltonian H into another eigenfunction with energy eigenvalue increased by $\hbar\omega$. Such operators describe collective excitations of many-particle systems, and their properties can be used to construct an intrinsic hamiltonian that is dynamically independent of the collective degrees of freedom, without introducing subsidiary conditions. The procedure developed by Lipkin, valid when $\hbar\omega$ is real and positive, is extended to make possible the construction of an intrinsic hamiltonian when $\hbar\omega$ vanishes and $A^\dagger$ is Hermitian, and also when $\hbar\omega$ is complex. The nuclear cranking model is shown to be a special case of the proposed general method for vanishing $\hbar\omega$ in which effective moments of inertia occur as eigenvalues of linear equations. Several examples are worked out in detail, all dealing with an interacting phonon-electron system in the random-phase approximation. Results derived are the explicit screened Coulomb interaction from electronic plasma excitations, a verification of the renormalized phonon frequency spectrum and phonon–electric interaction derived in the adiabatic approximation, and the resulting screened Coulomb and phonon-induced electronic interactions obtained when plasma and phonon exciations are treated simultaneously. (auth)

21290 CROSS-SECTION MEASUREMENT FOR THE THRESHOLD REACTIONS ^{56}Fe(n,p)^{56}Mn, ^{59}Co(n,α)^{56}Mn, AND ^{63}Cu(n,2n)^{62}Cu BETWEEN 12.6 AND 19.6 Mev NEUTRON ENERGY. H. Liskien and A. Paulsen (Euratom, Geel, Belg.). J. Nucl. Energy: Pt. A and B, 73-80(Feb. 1965).

Absolute cross-section data for the threshold reactions $^{56}Fe(n,p)^{56}Mn$, $^{59}Co(n,\alpha)^{56}Mn$, and $^{63}Cu(n,2n)^{62}Cu$ were determined using the activation method. Monoenergetic neutrons between 12.6 and 19.6 Mev were obtained from the $T(d,n)^4He$ reaction by the use of a 3-Mev Van de Graaff accelerator. The error on the cross sections falls between ±6 and 7%. The half lives of the product nuclei ^{56}Mn and ^{62}Cu were remeasured. (auth)

21291 MEASUREMENT OF THE MEAN LIVES OF EXCITED STATES OF OSMIUM-186, THALLIUM-203, TUNGSTEN-182, AND LEAD-207. R. Rougny, J. J. Samueli, and A. Sarazin (Institut de Physique Nucleaire, Lyon). J. Phys. (Paris), 25: 989-92(Dec. 1964). (In French)

Half lives of excited states were measured by mean of the time analyzing technique in the range of 10^{-10} sec. for Os-186, Tl-203, W-182, W-182, and Pb-207. (auth)

21292 STUDY OF γ-γ CASCADES IN THE CAPTURE OF THERMAL NEUTRONS PRODUCING THE FIRST EXCITED STATES IN ^{200}Hg. P. Carlos, H. Nifenecker, J. Fagot, and J. Matuszek (Centre d'Etudes Nucleaires, Saclay, France). J. Phys. (Paris), 25: 1013-16(Dec. 1964). (In French)

The γ-γ cascades following thermal neutron capture in Hg-199 were studied using a Hoogenboom circuit, with a 4'' × 6'' NaI(Tl) crystal inside a large 8'' × 12'' NaI(Tl) crystal annulus for the high energy gamma ray spectrum, and a single 4'' × 4'' NaI(Tl) crystal for detecting the lower energy radiation. Results on γ-γ cascades which go down from the capturing state to the first excited state are given. (auth)

21293 DETERMINATION OF THE K CONVERSION COEFFICIENT OF THE 400-Mev TRANSITION IN THE DECAY OF ^{203}Pb IN USE IN A SEMICONDUCTOR COUNTER. H. E. Bosch (Instituto de Investigacion Aeronautica y Espacial, DINFIA, Buenos Aires), F. Krmpotic, and A. Plastino. J. Phys. (Paris), 25: 1023-5(Dec. 1964). (In French)

An example of the possibilities of applying solid state detectors for the determination of conversion coefficients is described. The conversion coefficient corresponding to the 0.400-Mev transition in the decay of ^{203}Pb was determined. The electron-gamma coincidence method, replacing the magnetic spectrometer by a solid state counter, was used. The value of the K-conversion coefficient for the E2 + M1 transition is $\alpha_K(0.400) = 0.121 \pm 0.010$. (auth)

21294 ABSOLUTE MEASUREMENTS OF [PAIR] PRODUCTION CROSS SECTIONS OF γ RAYS IN NaI(Tl) CRYSTALS. J. Huck (Universite, Lyon). J. Phys. (Paris), 25: 1029-34(Dec. 1964). (In French)

An experimental method for measuring the total pair production cross section near the threshold is given. Applications are made with γ rays from ^{24}Na, ^{60}Co, ^{59}Fe, ^{65}Zn, ^{86}Rb, and a NaI(Tl) target. (auth)

21295 ELASTIC AND INELASTIC SCATTERINGS OF POLARIZED PROTONS FROM Be^9 AND Al^{27}. Kiyoji Fukunaga (Kyoto Univ.). J. Phys. Soc. Japan. 20: 1-7 (Jan. 1965).

The angular dependence of the asymmetry of the polarized protons scattered from ^9Be and ^{27}Al was measured. The data for elastic scattering at 7 Mev for both nuclei and 12 Mev for ^9Be are consistent with other published data. The asymmetry of 7-Mev protons inelastically scattered from ^9Be which remained in the excited state at 2.43 Mev has a sign opposite to that in elastic scattering, and the maximum asymmetry is about 35% at 50° in the cms. (auth)

21296 FISSION FRAGMENT ENERGY SPECTRUM AFTER PROMPT NEUTRON EMISSION. Hisao Kobayashi, Atsushi Nakamoto, and Masanao Hosoe (St. Paul's Univ., Yokosuka, Japan). J. Phys. Soc. Japan, 20: 176-7(Jan. 1965).

The fragment energy-energy correlation distribution after thermal-neutron fission of ^{235}U was measured, using surface barrier Si-Au detectors. The initial mass distribution was deduced and is compared with that from time-of-flight measurements. The average energy loss of the fragment due to prompt neutron emission and the energy distribution of the fragments before and after prompt neutron emission are given. Errors involved in the approximation used in the computation are discussed. (M.J.T.)

21297 NEW KIND OF RADIOACTIVE DECAY: PROTON EMISSION. H. Schneider (Universitat, Giessen, Ger.). Kerntechnik, 6: 583(Dec. 1964). (In German)

The irradiation of ^{27}Al with protons at 97 Mev produces the nuclear reaction $^{27}Al(p,3n)^{25}Si$. A proposed decay scheme for ^{25}Si includes a delayed proton emission. The experimental apparatus for the detection and measurement of the delayed proton was described. The pulse spectrum obtained shows 3 maxima corresponding to delayed protons with energies at 4.65, 4.10, and 3.39 Mev. (J.S.R.)

21298 A THICK TARGET METHOD FOR THE MEASUREMENT OF DIFFERENTIAL NEUTRON SCATTERING CROSS-SECTIONS. E. Barnard, A. T. G. Ferguson, W. R. McMurray, and I. J. Van Heerden (Atomic Energy Research Establishment, Harwell, Berks, Eng.). Nucl. Instr. Methods, 34: 29-32(Apr. 1965).

Bombarding a thick lithium target with protons produces neutrons with a continuous energy spectrum. The application of this spectrum to the measurement of differential elastic scattering cross sections over a wide range of energies is described. Essential aspects of the analysis of the time of flight measurements are outlined. Results are presented and discussed for elastic scattering from Bi, Al, Fe, and Ni at 75° for neutron energies between 85 and 700 kev. Structure due to resonance scattering from compound states is clearly observable. (auth)

21299 THE INFLUENCE OF RADON DAUGHTER CONCENTRATION IN AIR ON GAMMA SPECTROMETER BACKGROUND. F. C. Kloke, E. T. Smith, and B. Kahn (Robert A. Taft Sanitary Engineering Center, Cincinnati). Nucl. Instr. Methods, 34: 61-5(Apr. 1965).

The contribution of the radon-222 daughters lead-214 and bismuth-214 to the background count rate of a NaI(Tl) gamma spectrometer was determined at radon concentrations between 100 and 1200 pC/cm³ of air. The effect was measured at five characteristic gamma energy regions in a system consisting of a cylindrical detector 10 cm in diameter and 10 cm long and a 60 × 60 × 90 cm airspace. It was confirmed by calculations for spherical detector and airspace of the same volume. The count rate from the radon-222 daughters was 2.7×10^{-3} count/min per C/m³ in both the 0.08 Mev region at 0.35 Mev and the 0.12 Mev region at 0.61 Mev. The background count rates for these energy regions were 29.7 and 17.5 count/min, respectively, in the absence of radon daughters. (auth)

21300 ON THE INVESTIGATION OF THE ADIABATIC AND NONADIABATIC REVERSAL OF THE THERMAL NEUTRON SPIN. A. D. Gulko, S. S. Trostin, and A. Hudoklin (Inst. for Theoretical and Experimental Physics, Moscow). Nucl. Instr. Methods, 34: 88-92(Apr. 1965).

The adiabatic and nonadiabatic reversal of the spin of polarized thermal neutrons produced by the reflection from a magnetized cobalt mirror was investigated. The adiabatic reversal of the neutron spin in the guide magnetic fields used caused no depolarization. A nonadiabatic reversal of the neutron spin with respect to the guide field was achieved by means of a sharp reversal of the direction of the magnetic field produced by a current in a thin aluminum foil. The polarization flipping efficiency for foils of different sizes was measured. For neutrons reflected from the polarizer at angles of 5.3, 9.9, and 17.6′ the polarization flipping efficiency was found to be −0.993 ± 0.005, −0.993 ± 0.004, and −0.983 ± 0.006 respectively. (auth)

21301 COMPARISON OF THE NEUTRON YIELD FROM DEUTERIDED ERBIUM AND TITANIUM TARGETS. L. N. Large and H. Hill (Services Electronics Research Lab., Baldock, Herts, Eng.). Nucl. Instr. Methods, 34: 100-2 (Apr. 1965).

The neutron yield from deuterided erbium and titanium targets was directly compared by bombarding a number of these targets with a beam of deuterons of energy between 60–130 kev. The average neutron yield for the rare earth targets even after vacuum baking at 420°C was found to be very similar to that for titanium targets loaded to an atomic ratio of 1.4. The percentage spread in yield after baking is considerably lower than for the titanium targets assessed. The use of rare earth targets, which can be run at higher temperatures than titanium without losing the occluded gas enables higher target dissipation to be used, thus resulting in greater total neutron yield. (auth)

21302 DIFFERENTIAL INTERNAL BREMSSTRAHLUNG SPECTRA FROM Y^{90} AND Y^{91}. Boerje Persson (Univ. of Lund, Sweden). Nucl. Phys., 67: 121-32(May 1965).

Internal bremsstrahlung spectra were measured in a coincidence experiment at two fixed angles with respect to the direction of emission of the electron. Energy selection was used in the electron channel. At low photon energies, the experiment is in agreement with the theory for $Z = 0$. At higher energies there is a considerable experimental photon excess, which cannot be accounted for by Coulomb corrections to the theory according to available methods. The discrepancies are strongly dependent on the angle and the photon energy, but have a comparatively small dependence on the electron energy. (auth)

21303 NEUTRON POLARIZATION IN THE $T(d,n)He^4$ REACTION AT E_d = 2.1 AND 2.9 Mev. J. Christiansen, F. W. Buesser, F. Niebergall, and G. Soehngen (Institut fur Experimentalphysik, Hamburg). Nucl. Phys., 67: 133-44(May 1965).

The angular distributions of the polarization of the neutrons from the $T(d,n)^4He$ reaction were investigated at incident deuteron energies of 2.1 and 2.9 Mev. The asymmetries of the neutrons scattered by helium were determined by measuring the energy and the direction of the recoil α particles by means of a counter telescope consisting of two parallel-plate avalanche counters. The measurements were performed in open geometry. The angular distributions of the polarization show maximum values at $\theta_{n\,lab} = 75°$ of $P = -(16.9 \pm 4.0)\%$ and $P = -(19.2 \pm 4.6)\%$ at $E_d = 2.1$ and 2.9 Mev respectively. In both cases a second zero crossing appears at $\theta_{n\,lab} = 105°$ leading to positive polarization values at backward angles. The experimental results are compared with previous measurements in the energy region of the deuterons from 1.8 to 10.0 Mev. The characteristic features of the angular distributions and the energy dependence of the polarization are discussed. (auth)

21304 EXISTENCE OF ISOBARIC STATES AND BETA DECAY OF HEAVIER NUCLEI. Jun-ichi Fujita (Tokyo Univ.) and Kiyomi Ikeda. Nucl. Phys., 67: 145-77(May 1965).

It was already pointed out that the experimental discovery of well-defined isobaric states suggests that the heavier nuclei have the supermultiplet structure to a certain extent. The systematics of nuclear matrix elements for the allowed beta decay are investigated on the basis of the pairing model including nuclear interactions between unlike nucleons. Two different approaches were used: the conventional pairing model, which additionally includes the effect of the short or long range residual proton-neutron interactions; the modified pairing model, in which the supermultiplet-like structure is assumed in the zeroth approximation and partially destroyed by the spin-dependent interactions such as the spin-orbit forces. The results are compared with experimental data on the Sn–Sb transitions. It is concluded that the main part of the hindrance factor can be attributed to the p-n interaction. The theory of isobaric peaks in (p,n) reactions is reformulated by using the so-called Ahrens-Feenberg approximation method. Several formulas of a general validity are derived, which are especially useful in treating the normal allowed matrix elements. (auth)

21305 PHOTONEUTRON CROSS SECTIONS FOR Co, Ni, Cu, AND Ga. G. Baciu, G. C. Bonazzola, B. Minetti, C. Molino, L. Pasqualini, and G. Piragino (Universita, Turin and Instituto Nazionale di Fisica Nucleare, Turin). Nucl. Phys., 67: 178-86(May 1965).

The results of measurements from the threshold to 28 Mev of photoneutron cross sections for natural cobalt, nickel, copper, and gallium are given. The targets of the natural elements were exposed to the γ-ray beam of the 31-Mev betatron. The photoneutrons were detected by means of a 4π thermalized neutron counter. For the four elements, the integrated cross sections (in mb · Mev) are: $\sigma(Co) = 657 \pm 89$; $\sigma(Ni) = 313 \pm 48$; $\sigma(Cu) = 733 \pm 105$; $\sigma(Ga) = 947 \pm 98$. The particularly low value of the integrated cross section for nickel is explained by taking into account the shell structure effects in the statistical model theory. For the level density the expression given by Rosenzweig was used. (auth)

21306 THE 6.02 Mev LEVEL OF B^{10}. G. Fricke (Technische Hochschule, Darmstadt, Ger.), G. R. Bishop, and D. B. Isabelle. Nucl. Phys., 67: 187-92(May 1965).

The 6.02-Mev level in ^{10}B was investigated by means of inelastic electron scattering. It is shown that this level is excited by an E2 transition whose transition probability is collectively enhanced. (auth)

21307 POLARIZATION OF THE NEUTRONS FROM THE $Be^9(\alpha,n_0)C^{12}$ AND $Be^9(\alpha,n_1)C^{12*}$ REACTIONS. G. P. Lietz, S. F. Trevino, A. F. Behof, and S. E. Darden (Univ. of Notre Dame, Ind.). Nucl. Phys., 67: 193-202(May 1965).

The polarizations of the neutrons from the $^9Be(\alpha,n)^{12}C$ reactions leading to the ground and first excited states of ^{12}C were measured as a function of neutron emission angle for several bombarding energies between 1.90 and 4.50 Mev. Polarization of the neutrons was measured by scattering from a ^4He analyzer in the form of a high pressure gas scintillator. Asymmetries in the scattering of the neutrons from the helium were measured with the aid of an electromagnet which could rotate the polarization vector of the neutrons between the source and the scatterer. Values of the polarization as large as 40% were observed for the ground-state neutrons, while the maximum polarization of the excited-state neutrons was about 25%. In general, the polarizations vary appreciably with energy and angle. (auth)

21308 THE E2 CONVERSION COEFFICIENTS OF ROTATIONAL TRANSITIONS. S. C. Pancholi (Rijksuniversiteit, Groningen, Netherlands). Nucl. Phys., 67: 203-8 (May 1965).

A survey of the E2 conversion coefficients of rotational transitions was made. In addition to the direct measurements of K and total conversion coefficients, values of α_{tot} are given which were derived from lifetime and Coulomb excitation measurements. Comparison of α_K and α_{tot} with theory indicates that the existing discrepancies are mostly due to the B(E2) Coulomb excitation values being probably in error. (auth)

21309 THE BINDING ENERGY OF THE TRITON WITH A VELOCITY-DEPENDENT POTENTIAL. B. K. Srivastava (Cornell Univ., Ithaca, N. Y.). Nucl. Phys., 67: 236-48(May 1965).

A variational calculation of the binding energy of the triton was made using a two-body velocity-dependent central potential adjusted to fit two-body low and high energy scattering data and the binding energy of the deuteron. A set of one, two, and three parameter trial functions were used. The values of the binding energy of the triton obtained with these trial functions suggest that convergence was nearly obtained. Obviously, the highest value for the binding energy is obtained with the three-parameter trial function and is equal to 7.17 Mev. The Coulomb energy of ^3He was calculated by the usual perturbation method and a value equal to 0.663 Mev was obtained. These values of the binding energy of the triton and the Coulomb energy of ^3He agree reasonably well with similar calculations using repulsive hard core potentials but are lower than the experimental values. (auth)

21310 ELASTIC SCATTERING OF 17 TO 21 Mev NEUTRONS FROM ^{12}C. M. V. Harlow, Jr. (Oak Ridge National Lab., Tenn.), R. L. Robinson, and B. B. Kinsey. Nucl.

Phys., 67: 249-56(May 1965). (ORNL-P-700)

A search for a resonance in the yield of elastically scattered 17- to 21-Mev neutrons from ^{12}C was made. The differential cross section was measured for laboratory angles of 36, 51, 60, 86, 123.5, and 139°. The total cross section was also measured for the same range of neutron energies. In the differential cross sections which were measured at 36, 51, and 60°, a broad peak was present at a laboratory neutron energy of 19.5 ± 0.2 Mev. Its total width at half maximum was approximately 1.1 Mev and its height was between 14 and 21% of the value of the continuum. Within the 4.5% statistical error of the measurements, the peak does not appear at 86°. At 123.5 and 139°, the cross section decreases monotonically by a factor of three between 17.5 and 20.5 Mev. The total cross section data, which exhibit a weak resonance at 19.6 ± 0.2 Mev having a total width at half maximum of about 1.2 Mev, are consistent with the differential cross section results. The resonance, which presumably results from a state or states in the compound nucleus ^{13}C, appears similar to the known resonance in the yield of elastically scattered 22.5-Mev protons from ^{12}C. (auth)

21311 THE ANGULAR DISTRIBUTIONS OF THE (t,p), (d,p) AND (d,d′) REACTIONS LEADING TO ^{26}Mg. S. Hinds, H. Marchant, and R. Middleton (Atomic Weapons Research Establishment, Aldermaston, Berks, Eng.). Nucl. Phys., 67: 257-70(May 1965).

The $^{24}Mg(t,p)^{26}Mg$ and $^{25}Mg(d,p)^{26}Mg$ reactions were studied at incident energies of 11.0 and 10.0 Mev respectively using the multi-angle spectrograph. Angular distributions of 20 proton groups were measured from the former reactions and 18 from the (d,p) reaction. Plane wave stripping curves were fitted to the angular distributions and where possible spin and parity assignments were made. Relative reduced widths were extracted from the (d,p) measurements. The inelastic scattering of deuterons from ^{26}Mg was also investigated at an incident energy of 12 Mev. Only the deuteron groups leading to the first and second excited states showed appreciable intensity, and angular distributions of these are presented. Previous results from the $^{27}Al(t,\alpha)^{26}Mg$ reaction are analyzed in the light of the (2J + 1) rule and have enabled some spin ambiguities, arising from the stripping investigation, to be removed. The possible occurrence of collective effects in ^{26}Mg is discussed. (auth)

21312 SPIN OF THE 1821 kev LEVEL IN Kr^{82}. Jan P. Roalsvig and Karl J. Casper (Western Reserve Univ., Cleveland). Nucl. Phys., 67: 271-6(May 1965).

The angular correlation data for the ^{82}Kr decay were re-analyzed after a discrepancy was noted in the arguments leading to the assignment of spin 4 for the 1821-kev level. Additional analytical techniques not previously used on these data show that the spin of this state must be 3. (auth)

21313 A STUDY OF THE REACTION $C^{12}(O^{16},\alpha)Mg^{24}$ BELOW AND NEAR THE COULOMB BARRIER. D. E. Groce and G. P. Lawrence (Australian National Univ., Canberra). Nucl. Phys., 67: 277-88(May 1965).

Angular distributions of alpha particles from the reaction $^{12}C(^{16}O,\alpha)^{24}Mg$ were measured for the ground state and first six excited states of ^{24}Mg at ^{16}O bombarding energies between 15.0 and 22.5 Mev in 250 kev steps. Considerable complicated structure was observed. Although the angular distributions appeared to change rapidly with energy, some gross features did persist over a range of 1 to 2 Mev. Especially prominent was the high degree of asymmetry about 90°. From the angular distributions integrated cross sections were extracted in the form of excitation functions. These exhibit peaks which occur in several of the groups simultaneously. The most prominent appear to be at 7.1, 7.7, 8.6, 8.8, and 9.3 Mev center-of-mass energy. (auth)

21314 ON THE DECAY OF ^{142}La. W. V. Prestwich and T. J. Kennett (McMaster Univ, Hamilton, Ont.). Nucl. Phys., 67: 302-8(May 1965).

Evidence is presented that the beta transition from the ^{142}La ground state to the ^{142}Ce ground state has a unique character. On the basis of the evidence a spin and parity assignment of 2^- is made for the ^{142}La ground state. Angular correlation studies leading to spin assignments for four excited states in ^{142}Ce are also discussed. The assignments are 1.54 Mev, 2^+, 2.41 Mev, 2, 2.55 Mev, 1, and 2.71 Mev, 3 or 4. (auth)

21315 NEUTRAL RADIATIONS FOLLOWING PION CAPTURE IN COMPLEX NUCLEI. P. M. Hattersley, H. Muirhead, and J. N. Woulds (Univ. of Liverpool). Nucl. Phys., 67: 309-14(May 1965).

A time-of-flight technique was used to measure the energy spectra of neutrons emitted following pion capture in nuclei of widely varying atomic weight. The spectra are characterized by a low-energy evaporation part and a high-energy direct component. Nuclear temperatures were calculated from the former. The apparatus also detected γ radiation, and relative photon yields are given. (auth)

21316 COLLECTIVE EXCITED STATES IN EVEN XENON ISOTOPES. H. Morinaga and Neil L. Lark (Instituut voor Kernphysisch Onderzoek, Amsterdam). Nucl. Phys., 67: 315-20(May 1965).

Ground state collective bands in neutron deficient even xenon isotopes were observed by the measurements of low-energy gamma rays emitted following the $(\alpha,4n)$ and $(\alpha,2n)$ reactions on separated tellurium isotopes. The energy of the states up to the 10^+ state in ^{128}Xe was observed as well as those up to 8^+ in ^{124}Xe, ^{126}Xe, and ^{130}Xe and up to 4^+ in ^{132}Xe. The energy of the corresponding states in neighboring isotopes decreases smoothly with the decreasing number of neutrons. The ratios of the energy of successive gamma rays indicate that these nuclei are in between vibrational (equal gamma ray energy) and rotational (equal difference between gamma ray energies). These isotopes were expected to belong to a new region of deformed nuclei. (auth)

21317 γ-RAYS FROM THE CAPTURE IN Ta AND Au OF NEUTRONS FROM 1 TO 4 Mev. B. Lundberg and N. Starfelt (Research Inst. of National Defence, Stockholm). Nucl. Phys., 67: 321-32(May 1965).

The γ-ray spectra emitted in the capture of neutrons of energies from 1 to 4 Mev in Ta and Au were measured. In both elements the shape of the spectrum was found to vary only slightly with neutron energy. Using statistical nuclear theory γ-ray spectra were calculated and compared with measurements. Good agreement with experiment was obtained for Au at all neutron energies employing a γ-ray strength function which depends only on the photon energy. In Au the strength function has a peak at 5.5 Mev with a magnitude of about 2% of the integrated γ-ray strength predicted by the E1 sum rule. In Ta the peak in the strength function is much weaker and it was not possible to separate it from the low-energy tail of the giant resonance. (auth)

21318 ANGULAR DISTRIBUTIONS BY LEVELS IN THE REACTION $^{28}Si(n,\alpha)^{25}Mg$ AT 14.8 Mev. B. Leroux, J. Dalmas, Ph. Th. Doan, Ph. Le Thanh, and R. Chastel (Laboratoire de Physique Nucleaire de la Faculte des Sciences, Bordeaux). Nucl. Phys., 67: 333-6(May 1965).

The $^{28}Si(n,\alpha)^{25}Mg$ reaction induced by 14.8-Mev neutrons was studied with the help of the nuclear emulsion method. The angular distributions of the groups of alpha particles leaving the residual nucleus in its ground state and in its two first excited levels (0.584 and 0.976 Mev) were obtained; they show a predominance of backward emission. (auth)

21319 LIFETIME OF 120 kev LEVEL OF Lu^{177}. A. Schwarzschild and L. Grodzins (Brookhaven National Lab., Upton, N. Y.). Nucl. Phys., 67: 336-41(May 1965). (BNL-8690)

The lifetime of the 120-kev state of ^{177}Lu was measured using plastic scintillators and a fast time-to-amplitude converter. The lifetime was derived from the observed exponential decay of the time spectrum. It is

$\tau_5 = (1.16 \pm 0.08) \times 10^{-10}$ sec. Values of B(E2), g_K and g_R for this first excited state of the ground state rotational band are presented. They are close to those previously obtained in neighboring nuclei. (auth)

21320 THE MEASUREMENT OF THE K SHELL PARTICLE PARAMETER IN THE 272 kev E1 TRANSITION OF Yb^{173}. P. Hornshoej and B. I. Deutch (Univ. of Aarhus, Denmark). Nucl. Phys., 67: 342-52(May 1965).

The 272-kev K-allowed, 8×10^4 hindered E1 transition in ^{173}Yb was studied with a single-gap electron-gamma angular correlation spectrometer. Using the K conversion coefficient of the 279-kev transition in ^{203}Tl for calibration, the K conversion coefficient of the 272 kev transition in ^{173}Yb was determined to be $\alpha_K(272) = (1.97 \pm 0.10) \times 10^{-2}$ indicating the transition to be pure E1. Directional correlations with either 272-kev K electrons or 272-kev gamma rays and 79-kev gamma rays were measured. They are of the form $W(\theta) = 1 + A_2P_2(\cos\theta)$, where $A_2(272\gamma - 79\gamma) = -0.330 \pm 0.006$, and $A_2(272\ Ke^- - 79\gamma) = +0.531 \pm 0.032$. It follows that the mixing amplitude in the 79-kev transition δ_{79} is negative. The results of γ-γ angular correlation measurements with liquid sources were similar to those obtained with a plated spectrometer source. The E1 K particle parameter deduced from the A_2 terms is $b_2(272K) = -1.61 \pm 0.10$, in agreement with the point nucleus approximation result (−1.53) of Biedenharn and Rose. A list of 11 particle parameters extracted from published angular correlation data with pure transitions is included. There is only one serious disagreement with the particle parameters of Biedenharn and Rose. There is no evidence of dynamic nuclear structure effects below hindrances of 10^6. (auth)

21321 POSITRON SHAPE FACTOR OF $Co^{56}(4^+ \rightarrow 4^+)$. C. P. Bhalla (Univ. of Alabama, Huntsville). Nucl. Phys., 67: 353-7(May 1965).

The experimental beta shape factor of $^{56}Co(4^+ \rightarrow 4^+)$, as reported to be represented by (1 + b/W) by Hamilton, Langer, and Smith, was analyzed by the inclusion of the second-order effects. Within the framework of the V-A theory, several excellent fits to the experimental positron shape factor are obtained; thus, the need for a large P interaction and/or for the Uhlenbeck-Konopinski gradient coupling is unnecessary. (auth)

21322 THE MAGNETIC DIPOLE MOMENTS OF CONJUGATE NUCLEI. C. Mahaux (Universite, Liege). Nucl. Phys., 67: 358-68(May 1965).

The deviations from the Schmidt values of the experimental magnetic dipole moments of odd-mass nuclei are somewhat larger for odd-proton nuclei than for the conjugate odd-neutron nuclei, except for the $^3H - ^3He$ and $^{13}N - ^{13}C$ pairs. These features are explained on the basis of the Schmidt-Margenau-Wigner model, taking into account the spin-orbit correction to the magnetic dipole moment operator. It is also shown that the results predicted by the odd-group model are contradicted by experiment when the Jensen-Mayer approximation is adopted for the spin-orbit correction. This discrepancy is less important when Philpott's approximation is adopted. (auth)

21323 RETARDATIONS IN l-ALLOWED M1 TRANSITIONS IN ODD-MASS NUCLEI. A. S. Venkatesha Murthy, S. M. Brahmavar, and M. K. Ramaswamy (Karnatak Univ., India). Nucl. Phys., 67: 369-76(May 1965).

Various theories developed in recent years to understand the nuclear structure of low-lying excited states of odd-mass nuclei and other proposed interactions are briefly mentioned. An attempt, based on the experimental and single-particle transition probabilities, was made to derive further information about these states. The analysis of l-allowed and l-forbidden transitions between these low-lying states brings out a new feature of retardation in l-allowed transitions. These retardations give some evidence of configuration mixing or other possible interactions in the pure single-particle shell model states. (auth)

21324 E2/M1 MIXING RATIOS AND K CONVERSION COEFFICIENTS OF SOME ROTATIONAL TRANSITIONS. D. Ashery, A. E. Blaugrund, R. Kalish, J. S. Sokolowski, and Z. Vager (Weizmann Inst. of Science, Rehovoth, Israel). Nucl. Phys., 67: 385-94(May 1965).

The E2/M1 mixing ratios and K conversion coefficients of the first two rotational transitions in ^{153}Eu and ^{165}Ho were measured by observing the decay of the second rotational level in these nuclei. This level was Coulomb excited, and its decay by two cascade transitions was detected in a coincidence arrangement. The mixing ratios were determined from the angular distributions of the two gamma rays. The same coincidence arrangement was used to measure the K conversion coefficients of these transitions. The E2/M1 mixing ratio of the 110-kev transition in ^{169}Tm was also determined. The following results were obtained: $^{153}Eu - \delta(109\ kev) = 0.585 \pm 0.050$, $\alpha_K(83.4\ kev) = 2.34 \pm 0.13$, $\alpha_K(109\ kev) = 1.15 \pm 0.09$; $^{165}Ho - \delta(95\ kev) = 0.173 \pm 0.036$, $\delta(114\ kev) = 0.171 \pm 0.032$, $\alpha_K(95\ kev) = 2.64 \pm 0.10$, $\alpha_K(114\ kev) = 1.49 \pm 0.07$; $^{169}Tm - \delta(110\ kev) = -0.146 \pm 0.016$. In the case of ^{165}Ho and ^{169}Tm the experimental mixing ratios agree with predictions of the rotational model. This is not true for ^{153}Eu. The measured K conversion coefficients are in good agreement with theoretically calculated values. (auth)

21325 THE $Ge^{73}(n,\alpha)Zn^{70}$ REACTION AT 14 Mev OBSERVED IN A LITHIUM DRIFTED GERMANIUM DETECTOR. J. H. Aitken and W. R. Dixon (National Research Council, Ottawa). Nucl. Phys., 67: 395-400(May 1965).

The (n,α) reactions induced in germanium by 14-Mev neutrons were observed in a germanium semiconductor detector. Values of the cross section of the ground-state transition of $^{73}Ge(n,\alpha)^{70}Zn$ at 14.1 and 14.8 Mev are presented along with possible evidence for the existence of excited states of ^{70}Zn at 1.95 ± 0.1 and at 2.3 ± 0.1 Mev. Evidence for a reduced response of the detector to the Zn recoil atoms is discussed. (auth)

21326 STUDY OF THE (d,t) REACTION ON Be, Ar, Y, Zr, AND Pb AT 11.8 Mev. R. Jahr and R. Santo (Max-Planck-Institut fur Kernphysik, Heidelberg). Nucl. Phys., 67: 401-12(May 1965). (In German)

Using the counter telescope technique, angular distributions of tritons from (d,t) reactions on ^9Be, ^{40}Ar, ^{89}Y, ^{91}Zr, ^{92}Zr, ^{94}Zr, ^{96}Zr, and ^{208}Pb were measured between 20 and 90° in steps of 5°. Besides the excitation of the ground state, transitions to the lowest excited states were observed in several cases. The data were analyzed in terms of the DWBA and PWBA theory. In several cases l values, spectroscopic factors, and values of the parameter Λ were determined. (auth)

21327 NEUTRON S-WAVE STRENGTH FUNCTIONS OF SPHERICAL NUCLEI. M. Z. Rahman Khan (Muslim Univ., Aligarh, India). Nucl. Phys., 67: 413-16(May 1965).

Using a distorted wave approximation some remarks are made about fits to neutron S-wave strength functions of spherical nuclei. These indicate that good fits to low-energy data, especially sensitive to the imaginary part, are facilitated by using a surface-peaked imaginary distribution having, in addition to strength and width parameters, a variable location parameter. These considerations should be helpful in improving theoretical fits to the strength function data. It is also indicated that, at present, a phenomenological fit to the S-wave strength function data can hardly give a unique imaginary distribution. (auth)

21328 THE ELASTIC SCATTERING OF 5.5−10.0 Mev ^3He PARTICLES BY ^{27}Al NUCLEI. K. H. Bray (Australian National Univ., Canberra), J. Nurzynski, and G. R. Satchler. Nucl. Phys., 67: 417-27(May 1965).

Angular distributions for the elastic scattering of 5.5, 7.0, 8.0, 9.0, and 10.0 Mev ^3He particles by ^{27}Al nuclei were measured for scattering angles between 15 and 165° in the laboratory system. The 5.5-Mev results are significantly different from those published by Parry et al. The data were analyzed using simple optical model Woods-Saxon potentials. (auth)

21329 PROPERTIES OF LOW-ENERGY TRANSITIONS IN Dy^{161}. R. T. Brockmeier and John D. Rogers (California Inst. of Tech., Pasadena). Nucl. Phys., 67: 428-32(May 1965).

The decay of ^{161}Tb to ^{161}Dy was studied using the bent crystal spectrometer. Energies and intensities of ten gamma transitions were determined, and the results were used to derive the reduced multipole transition probabilities of the various transitions. (auth)

21330 ENERGIES AND CHARACTER OF LOW-LYING LEVELS IN Nb^{94}. U. Gruber (Technische Hochschule, Munich and Research Establishment, Riso, Denmark), R. Koch, B. P. Maier, O. W. B. Schult, J. B. Ball, K. H. Bhatt, and Raymond K. Sheline. Nucl. Phys., 67: 433-42(May 1965). (ORNL-P-731)

Utilizing the Riso bent crystal spectrometer, 47 transitions were observed from 54 kev to ~1 Mev from the reaction $^{93}Nb(n,\gamma)^{94}Nb$. These transitions determine the following levels in ^{94}Nb (energy in kev, spin-parity in parentheses): G. S. (6^+), ≈40.7 (3^+), 58.724 (4^+), 78.675 (7^+), 113.404 (5^+), 314.64 (5^+), ≈334 (2^+) and 640.5 (6^+). The 315- and 641-kev states probably correspond primarily to the $J = 5/2$ state of the three neutron configuration coupling to the $g_{9/2}$ proton configuration. The other six states result primarily from the coupling of the $J = 5/2$ state of the three neutron configuration and the $g_{9/2}$ proton configuration. Energies of the levels and transition probability ratios are consistent with this interpretation. (auth)

21331 INVESTIGATION OF THE ENERGY DEPENDENCE OF THE ISOMERIC CROSS-SECTION RATIO IN $Br^{79}(n,\gamma)Br^{80,80m}$ REACTIONS. J. Basco (Inst. of Nuclear Research, Debrecen, Hungary), J. Csikai, B. Kardon, and D. Kiss. Nucl. Phys., 67: 443-8(May 1965).

The isomeric cross section ratio was measured for the $^{79}Br(n,\gamma)^{80}Br$, ^{80m}Br reaction, and the results were compared with the values predicted by the method of Huizenga and Vandenbosch. It can be inferred from the measured values that the average number of steps in the γ cascades varies with the exciting energies. The value of $\sigma \approx 4$ obtained for the spin density parameter in the investigated energy range of 0–3 Mev is in good agreement with those computed from the Fermi-gas model. The ratio of the effective to the rigid body moment of inertia was estimated to be about 0.8. It seems from the comparison of the measured and calculated cross section ratios that thermal neutron capture occurs into the $I + 1/2$ state. (auth)

21332 THE $^{40}Ca(p,p')$ REACTION AT 150 Mev. D. Newton, A. B. Clegg, and G. L. Salmon (Nuclear Physics Lab., Oxford). Nucl. Phys., 67: 449-65(May 1965).

The $^{40}Ca(p,p')$ reaction was studied by observing coincidences between scattered protons and decay gamma radiation from the states excited. Measurements were made of the variation of the gamma spectrum with scattered proton energy, measured with coarse resolution, and of the angular correlations between gamma rays and scattered protons. These have made possible a detailed investigation of which states of ^{40}Ca are excited strongly: at 3.73($J = 3^-$), 4.48, 6.76, 6.9 ($J = 2^+$) Mev. The assignments in brackets are deduced from this experiment. It is also shown that the 6.76-Mev state cannot have $J = 2^+$; the results are consistent with it having $J = 3^-$. Upper limits are placed on the cross sections for excitation of other states and a comparison made between measurements of the $^{40}Ca(p,p')$ and $^{40}Ca(e,e')$ reactions. (auth)

21333 DECAY OF ^{103}Ru. Ambuj Mukerji, David N. McNelis, and John W. Kane, Jr. (Univ. of Alabama, Tuscaloosa). Nucl. Phys., 67: 466-78(May 1965).

The decay of ^{103}Ru to ^{103}Rh was investigated with the help of scintillation spectrometers. Employing gamma-gamma coincidences and sum-coincidence measurements as well as successive peel off procedure, the following gamma rays were resolved: 53 kev (0.7), 65 kev (–), 297 kev (0.6), 362 kev (–), 440 kev (0.9), 498 kev (88), 555 kev (2), and 610 kev (5). The following gamma ray cascades were established: 555-53 kev, 440-53 kev, and 297-65 kev. Beta-gamma coincidences revealed two inner beta-ray groups of maximum energies 112 ± 6 kev (7) and 214 ± 12 kev (89) emitted in coincidence with the 610- and 498-kev gamma rays, respectively. The figure in parentheses represents the relative intensity in arbitrary units. The maximum energy of the highest energy beta ray group was measured to be 716 ± 40 kev. From gamma-gamma coincidences the internal conversion coefficient of the 53-kev gamma ray was found to be $\alpha_K = 2.74 \pm 0.03$ indicating a mixture of M1 + E2 with $\delta^2 = 0.15 \pm 0.02$. A decay scheme is presented. (auth)

21334 MEASUREMENTS OF THE EPICADMIUM CAPTURE-TO-FISSION CROSS-SECTION RATIO IN U^{235}. D. E. Conway, H. D. Cook, and S. B. Gunst (Westinghouse Electric Corp., Pittsburgh). Nucl. Sci. Eng., 22: 20-3 (May 1965).

The epicadmium capture-to-fission cross section ratio in ^{235}U is obtained from post-irradiation measurements on bare and cadmium-covered samples exposed in the beryllium reflector of the Materials Testing Reactor. Relative capture-to-fission rates are determined from measurements of the quantities of ^{236}U and of fission product ^{137}Cs produced. The bare experiment measurements are used in combination with the cadmium-covered measurements to eliminate the need to know the yield and half life of ^{137}Cs. For the irradiation spectrum, the experiment gives a value of 0.51 ± 0.03 for the ^{235}U epicadmium α (above 0.51 ev). (auth)

21335 A SIMPLE ESTIMATE OF THE EFFECTS OF RESONANCE INTERFERENCE. Charles N. Kelber (Argonne National Lab., Ill.). Nucl. Sci. Eng., 22: 120-1(May 1965).

An approximate method for computing the effects of resonance interference is presented. It is supposed that there are two resonances, labeled I and II, close together and that by reason of nuclide abundance or level parameters, resonance I dominates the shape of the flux near the resonant energy. A simple estimate of the capture rate in resonance II may be obtained by integrating the capture cross section from resonance II times the flux determined by the presence of resonance I in the absence of resonance II. (C.E.S.)

21336 RESONANCE INTEGRALS FOR U^{233} FISSION AND Th^{232} CAPTURE. J. Hardy, Jr. (Westinghouse Electric Corp., Pittsburgh). Nucl. Sci. Eng., 22: 121-4(May 1965). (WAPD-T-1748)

The resonance integrals of ^{233}U fission and ^{232}Th capture were measured relative to the resonance capture integral of ^{197}Au by means of the cadmium-ratio-activation technique. Dilute detector foils were irradiated in the TRX critical facility. The epithermal flux spectrum was approximately proportional to 1/E except for the flux peak above 25 kev. (C.E.S.)

21337 ANOMALOUS ISOMER SHIFT RATIOS IN Eu^{151} AND Eu^{153}. U. Atzmony and S. Ofer (Hebrew Univ., Jerusalem). Phys. Letters, 14: 284-5(Feb. 15, 1965).

Results of recoiless absorption measurements carried out with $EuSO_4$, Eu_2O_3, and Eu metal absorbers at 20°K of the 97- and 103-kev gamma transitions of Eu^{153} and the 21.7-kev transition of ^{151}Eu obtained in previous measurement show that the isomer shift ratio is different for the various transitions. Possible explanations for the results are proposed. (L.B.S.)

21338 THE IRON-57 MÖSSBAUER EFFECT IN SOME STAINLESS STEELS. C. W. Kocher (Budd Co., Downingtown, Penna.). Phys. Letters, 14: 287-9(Feb. 15, 1965).

The Mössbauer effect in ^{57}Fe found in types 210, 301, 316, and AM 355 stainless steels was measured at room temperature, using a hydraulic constant-velocity transducer. Transmission spectra were measured in cold rolled and annealed samples, using a ^{57}Co source electroplated on a copper foil. No magnetic splitting was observed for cold worked or annealed stainless steels 301 and 316. The magnetic phase in the cold worked 201 and AM 255 steels, which showed a six-line magnetic spectra, was identified by x-ray

diffraction measurements, and the spectra were ascribed to the presence of martensite. The difference in nuclear magnetic fields in AM 355 and 201 was ascribed to the dilution of iron in the martensite by the alloying elements. (L.B.S.)

21339 ANGULAR DEPENDENCE OF CONVERSION ELECTRONS FROM A MONOCRYSTALLINE SOURCE. G. Astner, I. Berstroem, B. Domeij, L. Eriksson, and A. Persson (Forskningsinstitutet för Atomfysik, Stockholm). Phys. Letters, 14: 308-10(Feb. 15, 1965).

A tantalum single crystal was bombarded by 60-kev ^{133}Xe ions in the ⟨100⟩-direction using an isotope beam separator. A double focusing permanent magnet spectrometer was used to measure the angular dependence of the K- and L-conversion electrons of the 81.0-kev γ ray. It was observed that the gross structure of the angular pattern is the same for both the K- and L-conversion lines. (L.B.S.)

21340 SHAPES OF β-RAY SPECTRA AND PARTIALLY CONSERVED AXIAL-VECTOR CURRENT. H. Daniel and G. Th. Kaschl (Max-Planck-Institut für Kernphysik, Heidelberg). Phys. Letters, 14: 310-11(Feb. 15, 1965).

The result of studies of the $0 \rightarrow 0$ transitions with parity change, $^{144}Ce \rightarrow {}^{144}Pr$ and $^{166}Ho \rightarrow {}^{166}Er$, is reported; and plots of the shape factors for these transitions are shown. The spectra of ^{144}Ce, ^{144}Pr, ^{166}Ho and of ^{22}Na and ^{114}In are discussed in the light of Tadic's calculations. It is concluded that the experimental data do not support the concept of a partially-conserved axial vector current. (L.B.S.)

21341 ANALOGUES OF EXCITED STATES IN TIN ISOTOPES. D. L. Allan (Atomic Energy Research Establishment, Harwell, Berks, Eng.). Phys. Letters, 14: 311-13 (Feb. 15, 1965).

The inelastic scattering proton energy spectra of ^{118}Sn were measured at 10.3 to 12 Mev for more than 60 different incident proton energies, using a broad-range spectrograph and photographic plates. Excitation cross sections were measured, and intensity variations for several groups were studied in detail to give the shape and resonant energy of the analog states. It is concluded that levels with similar properties have similar excitation energies in ^{118}Sn and ^{119}Sn. (L.B.S.)

21342 NEW RESULTS FOR THE $Li^7(p,\gamma)Be^*$ REACTION. M. Wilson and J. B. Marion (Univ. of Maryland, College Park). Phys. Letters, 14: 313-15(Feb. 15, 1965).

A LiF target was bombarded with protons at 0.4 to 2.4 Mev to study the formation of the 16.62 and 16.92 Mev excited levels of ^8Be by the $^7Li(p,\gamma)^8Be^*$ reaction. The alpha emission was analyzed with a double focusing magnetic spectrometer and was detected by a nuclear emulsion or solid state counter. The branching ratio of the 16.62 and 16.92 Mev transitions was measured and the absolute cross section for the transition from the 17.6 to the 16.6 Mev level was determined. It was found that the cross section increases gradually with bombarding energy above the 0.44 Mev resonance. (L.B.S.)

21343 INAPPROPRIATENESS OF AN ISOTOPIC SPIN DESCRIPTION FOR HIGHLY-EXCITED LEVELS IN Be^8. J. B. Marion (Univ. of Maryland, College Park). Phys. Letters, 14: 315-17(Feb. 15, 1965).

A model of the 16.62 and 16.9 Mev states of ^8Be is proposed. The $^{10}B(d,\alpha)^8Be$, $^7Li(d,n)^8Be$, $^9Be(He^3,\alpha)^8Be$, and $^8B(\beta^+)Be^8$ reactions were examined and compared with the single-particle description. It is concluded that all experimental evidence favors an interpretation of the 16.62 and 16.92 Mev levels in ^8Be as relatively pure single particle states and that no definite isotopic spin can be assigned to these levels. (L.B.S.)

21344 MEASUREMENTS AND ANALYSIS OF MUONIC X-RAY SPECTRA IN THE SPHERICAL NUCLEI Au, Pb, AND Bi AND THE DEFORMED NUCLEI W AND U. H. L. Acker (Universität, Freiburg i. B.), G. Backenstoss, C. Daum, J. C. Sens, and S. A. De Wit. Phys. Letters, 14: 317-20(Feb. 15, 1965).

The energies and relative intensities of the muonic x-ray spectra in natural Au, Pb, Bi, W, and U were measured, using a Li-drifted germanium detector and the muons channel of the CERN synchrotron. Energy values were obtained as a function of the radial constant and skin thickness for Au, Pb, and Bi from a numerical solution of the Dirac equation for the 1s, 2p, and 3d levels, using a Fermi-type nuclear charge distribution. The energy spectra of the strongly deformed nuclei U and W were calculated and compared with the experimental results. (L.B.S.)

21345 MÖSSBAUER EFFECT AND ISOMER SHIFT ON Eu^{153}. E. Steichele, S. Huefner, and P. Kienle (Technische Hochschule, Darmstadt, Ger.). Phys. Letters, 14: 321-2 (Feb. 15, 1965).

Isomer shift data are reported for the 97 and 103 kev γ transitions in ^{153}Eu for Eu_2O_3, EuS, and $EuCl_2$. The relative transmission or the γ rays were measured as a function of the Doppler shift with a Na(Tl) spectrometer, using $^{153}Gd_2O_3$ and $^{152}Sm_2O_3$ sources. The change of the mean square radius for proton transitions in a deformed nucleus is deduced and discussed. The resonance absorption spectra for Eu_2O_3 and EuS are presented, and the ^{153}Eu isomer shifts relative to Eu_2O_3 are tabulated. (L.B.S.)

21346 ENERGY LEVELS IN Ti^{48} AND Ti^{50} OBSERVED FROM INELASTIC PROTON SCATTERING AT 7 Mev. T. A. Belote, W. E. Dorenbusch, O. Hansen, and A. Sperduto (Massachusetts Inst. of Tech., Cambridge). Phys. Letters, 14: 323-5(Feb. 15, 1965). (MIT-2098-111)

The low-lying part of the Ti level scheme was investigated from proton inelastic scattering at 7 Mev. The protons were momentum analyzed in a multiple-gap spectrograph and were detected in photographic emulsions. Eleven levels were observed, and the spin and parity of a previously unidentified level at 3.004 Mev are discussed. Two levels were observed in a similar experiment on the $^{50}Ti(p,p')$ reaction, which correspond to the first and second excited states of ^{50}Ti. (L.B.S.)

21347 NUMBER DEPENDENCE OF THE ACCURACY OF BCS CALCULATIONS IN THE THEORY OF DEFORMED NUCLEI. R. W. Richardson (New York Univ., New York). Phys. Letters, 14: 325-7(Feb. 15, 1965).

The exact eigenvalues of the pairing-force hamiltonian are investigated for N pairs of particles in 2N equispaced, doubly degenerate, single-particle levels for N = 4, 8, 12, and 16, and for interaction strengths in the ranges that reproduce nuclear pairing energies. It is found that the accuracy of the BCS ground state energy does not improve as the number of particles increases from 8 to 32. The calculated values for the pairing energies, the ground state energy shifts and the excitation energies are tabulated, and the errors are discussed. (L.B.S.)

21348 MESONIC EXCHANGE EFFECTS AND THE EFFECTIVE COUPLING CONSTANT G_A IN β-DECAY. R. J. Blin-Stoyle and S. Papageorgiou (Univ. of Sussex, Brighton, Eng.). Phys. Letters, 14: 343-4(Feb. 15, 1965).

The mesonic exchange effects in β decay are calculated for ^{15}O, ^{17}F, ^{39}Ca, and ^{41}Sc, using fully anti-symmetrical LS-coupled wave functions and assuming the density distribution obtained for nucleons in an oscillator potential. The results are tabulated. It is concluded that mesonic exchange effects lead to an increase on the order of 6 to 11% in allowed axial vector matrix elements, and in order to take these effects into account the axial vector coupling constant can be replaced by an effective coupling constant incorporating an enhancement of this order of magnitude. (L.B.S.)

21349 CRANK MODEL AND PERTURBATION CALCULATION. G. Lehmann and W. Macke (Universitat, Dresden). Phys. Letters, 15: 141-2(Mar. 15, 1965). (In German)

A description is given of the rotational state of deformed nuclei, using the cranking model and a perturbation calculation. Relations are given for the hamiltonian operator, the ground state energy, and the S-matrix. The energy of the rotational state is given as a function of the angular veloc-

ity, and the exact ground state energy is calculated by the vacuum-bound graphs. (L.B.S.)

21350 AN ODD-ODD NUCLEUS WITH 0^+ GROUND STATE (Eu^{156}). E. T. Williams, P. G. Hansen, J. Lippert, H. L. Nielsen, and K. Wilsky (Atomenergikomissionen, Risø, Denmark). Phys. Letters, 15: 143-4(Mar. 15, 1965).

Results are presented on an experimental study of the β^- decay of ^{156}Sm. Measurements were made using a six-gap spectrometer, $e^- - \gamma$ and $e^- - \beta$ coincidence techniques, a xenon-filled proportional counter, and a Li-drifted-germanium semiconductor counter. Multipole orders were obtained from measured internal conversion coefficients and from shell and subshell ratios, and spins and parities of the ^{156}Eu states are assigned. Emphasis is given to the identification of the 2.24-Mev beta group depopulating ^{156}Eu as a pure Fermi ($0^+ \rightarrow 0^+$) transition to ^{156}Gd. The decay scheme is presented. (L.B.S.)

21351 THE ISOSPIN STRUCTURE OF LOW LYING COLLECTIVE OCTUPOLE VIBRATIONS. C. J. Veje (Universitet, Copenhagen). Phys. Letters, 15: 145-7 (Mar. 15, 1965).

The collective octupole modes of vibrations (isoscalar and isovector) are investigated for low energy vibrational states in inelastic scattering processes. Reduced transition probabilities are obtained from the reduced matrix elements, neglecting electromagnetic excitations or assuming the isospin of the incoming particle is zero. The isospin structure of the one-phonon octupole density vibrations in spherical nuclei is investigated using a shell-model potential interacting with pairing plus octupole-octupole forces and the quasi-boson approximation. The resulting energy and transition probabilities for the two strongest, low lying one-phonon octupole states for some nuclei are tabulated. (L.B.S.)

21352 MASS-SPECTROMETRIC DETERMINATION OF Li^6 AND Li^7 PRODUCTION IN C^{12} AND O^{16} BY HIGH ENERGY PROTONS. R. Bernas, M. Epherre, E. Gradsztajn, R. Klapisch, and F. Yiou (Laboratoire Joliot-Curie, Orsay, France). Phys. Letters, 15: 147-9(Mar. 15, 1965).

High-purity graphite slabs and cylinders of ice were bombarded by high-energy protons from the Orsay and CERN synchrocyclotrons, and mass spectrometric analysis was made of ^6Li and ^7Li production. Results are tabulated on the ratio of $^6Li/^7Li$, which was determined a short time after irradiation and after a sufficiently long period of time corresponding to the decay of ^7Be; the cross sections for ^{12}C were obtained from previous measurements and the cross sections for ^{16}O were determined by isotopic dilution with natural lithium. The accuracy of the measurements is discussed, and the significance for astrophysics and spallation or fragmentation processes is considered. (L.B.S.)

21353 ON INELASTIC SCATTERING OF HEAVY PARTICLES WITH EXCITATION OF THE COLLECTIVE STATES OF NUCLEI. V. K. Lukyanov and I. Z. Petkov (Joint Inst. for Nuclear Research, Dubna, USSR). Phys. Letters, 15: 149-51(Mar. 15, 1965).

The scattering amplitude and excitation cross section are calculated for the inelastic scattering of heavy particles above the barrier, using an adiabatic approximation and the method of stationary phase. An expression is obtained which yields the excitation cross section for any n-phonon transition (multipole transition) and also resembles in form the expression which underlies the theory of multiple Coulomb excitation. (L.B.S.)

21354 ON A MECHANISM OF PRODUCTION OF FAST CHARGED PARTICLES IN REACTIONS BETWEEN COMPLEX NUCLEI. S. P. Ivanova and B. N. Kalinkin (Joint Inst. for Nuclear Research, Dubna, USSR). Phys. Letters, 15: 152(Mar. 15, 1965).

A model is suggested to account for the emission of high energy protons and other fast particles and the anisotropy in the angular distribution observed in reactions between complex nuclei. Estimates were obtained for the $^{16}O + ^{197}Au$ reaction, which show that the suggested accelerating mechanism of fast particle production does contradict experimental data. (L.B.S.)

21355 THE EMISSION OF K X-RAYS IN SPONTANEOUS FISSION OF Cf^{252}. L. E. Glendenin and H. C. Griffin (Argonne National Lab., Ill.). Phys. Letters, 15: 153-5 (Mar. 15, 1965).

The yield, energy distribution, and time distribution of K x rays accompanying spontaneous fission of ^{252}Cf were measured, using a surface barrier semiconductor detector, a NaI(Tl) detector, and a fast-slow coincidence and linear gate circuit, and delayed coincidence and time-of-flight methods. The yield and time distribution indicate that internal conversion is the primary mechanism for producing K vacancies in the fragments. The energy spectrum expected from internal conversion of the prompt γ rays in ^{252}Cf fission was also calculated, using an IBM 1620 computer, and was compared with the observed spectrum. The results were found to be in fair agreement except for the heavy group between $Z \sim 54$ and 58. (L.B.S.)

21356 THE $Y^{89}(p,n)Zr^{89}$ REACTION. D. B. Lightbody, G. E. Mitchell, and A. Sayres (Columbia Univ., New York). Phys. Letters, 15: 155-7(Mar. 15, 1965).

An yttrium target was bombarded by proton beams at 4.6 to 5.6 Mev and the yield and angular distributions of the neutrons were measured, using a ^3He neutron spectrometer. Excitation curves are given for the n_0 and n_1 groups (leaving the residual nucleus in its ground and first excited states, respectively). Isobaric analog states at 4.83 and 5.03 Mev are investigated. (L.B.S.)

21357 GAMMA TRANSITIONS TO THE 16.6- AND 16.9-Mev STATES IN Be^8. D. Kohler and P. Paul (Stanford Univ., Calif.). Phys. Letters, 15: 157-9(Mar. 15, 1965).

An experiment was performed in search of 1.0- and 0.70-Mev gamma rays originating in the bombardment of a thin ^7Li target with 440 kev protons, in coincidence with two alpha particles of combined energies of 16.6 and 16.9 Mev, respectively, using two silicon surface barrier counters and a NaI(Tl) crystal. The summed alpha spectrum recorded in a pulse height analyzer without any coincidence showed that the main alpha peak due to the direct break-up of ^8Be following proton capture has a small satellite peak due to the delayed break-up of primarily the 16.62-Mev state following gamma emission. The gamma spectrum in coincidence with the summed alpha spectrum showed a strong gamma peak corresponding to a transition from the 17.64- to the 16.62-Mev state. A transition to the 16.94-Mev state was also observed, and the ratio of the peak areas was determined. A model is proposed for the configurations of the 16.6- and 16.9-Mev states. (L.B.S.)

21358 SINGLE PARTICLE STRENGTHS IN THE $Cu^{63}(d,He^3)Ni^{62}$ REACTION. J. C. Hiebert, E. Newman, and R. H. Bassel (Oak Ridge National Lab., Tenn.). Phys. Letters, 15: 160-2(Mar. 15, 1965).

A ^{63}Cu target was bombarded with deuteron beams at 34.2 Mev from ORIC, and the scattered deuteron and reaction products were detected with a transmission-mounted surface barrier detector and a lithium-drifted silicon detector. Angular distributions of the transitions to the ground state, first excited 2^+ state, and the 0^+, 2^+, 4^+ triplet were analyzed, using a DWBA calculation, assuming a single particle pickup mechanism and a least-squares analysis of the data. The optimum percentages of the $p_{\frac{3}{2}}$ and $f_{\frac{7}{2}}$ strength were determined, and spectroscopic factors were calculated. The results are discussed. (L.B.S.)

21359 SIGN CHANGE OF INDUCED HYPERFINE FIELDS IN THE 5p SHELL. R. B. Frankel, J. Huntzicker, E. Matthias, S. S. Rosenblum, D. A. Shirley, and N. J. Stone (Univ. of California, Berkeley). Phys. Letters, 15: 163-5(Mar. 15, 1965). (UCRL-11882)

The systematic variation of hyperfine fields with atomic number was investigated for Ru in Ni, and Cd and Te in both Ni and Fe. The induced fields were found to go systematically through zero and become positive in the 5p shell. (L.B.S.)

21360 SHELL MODEL AND DEFORMED STATES IN O^{18}. P. Federman and I. Talmi (Weizmann Inst. of Science, Rehovoth, Israel). Phys. Letters, 15: 165-7 (Mar. 15, 1965).

The nondiagonal matrix elements of the nuclear interaction between the deformed J = 0, J = 2 states and the corresponding shell states in ^{18}O are calculated. The admixtures in the various eigenstates are estimated. (L.B.S.)

21361 COLLECTIVE ADMIXTURES IN THE ODD-PARITY STATES OF O^{16}. G. E. Brown and A. M. Green (Princeton Univ., N. J.). Phys. Letters, 15: 168-9(Mar. 15, 1965).

The admixture of a deformed odd parity state with low-lying states as lp-lh excitations in a spherical basis is investigated. An interpretation is given to the lowest-lying T = 0 states in ^{16}O. (L.B.S.)

21362 CORE EXCITATION: Au^{197} REVISITED. A. De-Shalit (Weizmann Inst. of Science, Rehovoth, Israel). Phys. Letters, 15: 170-2(Mar. 15, 1965).

A description is given of the electromagnetic properties of the first five excited states in ^{197}Au, using the core-excitation model. Static moments are explained in terms of transition probabilities, and single-particle moments are calculated and compared with experimental values. (L.B.S.)

21363 CORIOLIS ANTI-PAIRING EFFECTS ON HIGH SPIN ROTATIONAL STATES IN DEFORMED NUCLEI. T. Udagawa and R. K. Sheline (Florida State Univ., Tallahassee). Phys. Letters, 15: 172-5(Mar. 15, 1965).

A method is presented for treating the Coriolis anti-pairing effect using a variational calculation within the framework of the cranking model. The expectation value and the moment of inertia are evaluated for the hamiltonian of the pair interaction for proton and neutrons. Numerical calculations were performed for ^{170}Hf and ^{172}Hf, and contributions for centrifugal stretching are considered. (L.B.S.)

21364 PAIRING CORRELATION AND ODD-EVEN EFFECT IN THE NUCLEAR LEVEL DENSITY. P. Brovetto (Universita, Cagliari, Italy), L. Fassio, and V. Canuto. Phys. Letters, 15: 175-6(Mar. 15, 1965).

The effect of the pairing correlation on the nuclear level density was investigated for an odd assembly of nucleons, and the ratio of the level densities for the odd and even case was calculated. A factor of four was found between the level density of a nucleus with the energy gap equal to zero and that of a nucleus equal to 1 Mev. It is shown that the pairing effect decreases for increasing excitation energy. (L.B.S.)

21365 THE PRODUCTION OF HYPERFRAGMENTS BY THE INTERACTIONS IN FLIGHT OF LOW ENERGY K^- MESONS WITH EMULSION NUCLEI. H. Henrotin (Universite Libre, Brussels), J. Lemonne, J. Sacton, D. H. Davis, M. A. Shaukat, J. E. Allen, and M. M. Kasim. Phys. Letters, 15: 193-6(Mar. 15, 1965).

An experiment was performed using two stacks of 600 μm thick Ilford K5 emulsion pellicles exposed to low energy K^- mesons from the degraded 800-Mev/c K beam at the CERN proton synchrotron, and the production rate of hypernuclei was determined. The variation of the non-mesonic to mesonic decay ratio is tabulated as a function of the range of the hyperfragment. The hypernuclei originating from interactions with the light and heavy nuclei are separated, and it was found that 76% are attributed to heavy spallation hypernuclei. The emission frequencies were calculated and compared with other results. (L.B.S.)

21366 NUCLEAR MAGNETIC RESONANCE LINEWIDTH IN β-Mn. J. Butterworth, L. E. Drain, and J. Penfold (Atomic Energy Research Establishment, Harwell, Berks, Eng.). Phys. Letters, 15: 215-16(Apr. 1, 1965).

The magnetic susceptibility and NMR linewidth of beta manganese powders formed by crushing in air and argon were studied over a range of temperature. The results indicate that the previously observed anomalous increase in line width at low temperatures can be explained in terms of contamination by a strongly magnetic manganese compound. Several previously unreported features were observed in preliminary measurements of the ^{55}Mn resonance at 10 kgauss. (D.C.W.)

21367 GROUND STATE WAVE FUNCTION OF H^3 AND He^3. R. Boesch, J. Lang, R. Mueller, and W. Woelfli (Eidgenossische Technische Hochschule, Zurich). Phys. Letters, 15: 243-5(Apr. 1, 1965).

The total cross section for the reaction $^3H(\gamma,n)^2H$ was calculated, together with the contribution of the interference term of the electric dipole transitions from the S and S′ state, using the wave function of Gunn and Irving. The product of the neutron velocity and the capture cross section for thermal neutrons in deuterium was also calculated, as well as the charge radii, form factors, and photoabsorption cross sections of ^3H and ^3He. Comparisons with experimental values indicate that the Gunn-Irving wave function, with a certain admixture of the S′ state, gives a good approximation to the ground state of 3-body nuclei. (D.C.W.)

21368 MUON CAPTURE IN Li^6 AS A TOOL FOR TESTING NUCLEAR MODELS. A. Lodder and C. C. Jonker (Vrije Universiteit, Amsterdam). Phys. Letters, 15: 245-8 (Apr. 1, 1965).

The meson (μ^-) capture probability for ^6Li leading to the ground state of ^6He was calculated in the harmonic oscillator shell model, the cluster model, and the three-particle model. It was concluded that the capture probability provides an independent way for testing the tail of the ^6Li wave functions. (D.C.W.)

21369 A DIRECT MEASUREMENT OF A SHORT NUCLEAR LIFETIME ($\sim 10^{-20}$ s) USING PROXIMITY SCATTERING. J. Lang, R. Mueller, W. Woelfli, R. Boesch, and P. Marmier (Eidgenossische Technische Hochschule, Zurich). Phys. Letters, 15: 248-9(Apr. 1, 1965).

The proximity scattering of the nucleon emitted in the decay of an excited nuclei by the primary nucleon produced in the reaction along with the excited state causes the line in the energy spectrum of the primary nucleon to acquire a heel. The use of this effect to determine the lifetime of the excited state was studied by measuring the proton energy spectra for the $^{12}C + {}^2H \rightarrow {}^{12}C + p + n$ reaction. The mean lifetime of the level group at 3.5 Mev was determined to be 0.6×10^{-20} sec, in agreement with values obtained from level widths. (D.C.W.)

21370 WHY IS THE GALLAGHER-MOSZKOWSKI RULE SO WELL VERIFIED? A. G. De Pinho and J. Picard (Centre d'Etudes Nucleaires, Saclay, France). Phys. Letters, 15: 250-2(Apr. 1, 1965). (In French)

The origin of the degeneracy of the K^+ doublet in deformed odd-odd nuclei in the Nilsson model was investigated in terms of the residual interaction between the two single nucleons. The bases and predictions of the Gallagher-Moszkowski rule were considered. (D.C.W.)

21371 EFFECT OF ELASTIC UNITARITY ON THE REACTIONS $d(n,\gamma)H^3$ AND $d(p,\gamma)He^3$. G. Barucchi (Università, Turin), B. Bosco, and P. Nata. Phys. Letters, 15: 252-5(Apr. 1, 1965).

The corrections due to elastic unitarity in the radiative capture of neutrons and protons by deuterons through the dipole magnetic moment are evaluated, using a model in which ^3H and ^3He are described as a deuteron bound to a neutron or proton, respectively. (D.C.W.)

21372 CALCULATION OF NUCLEON-ALPHA CASCADES. J. P. Cohen, G. Albouy, M. Gusakow, and L. Valentin (Institut du Radium, Orsay, France). Phys. Letters, 15: 255-8(Apr. 1, 1965). (In French)

The effects in spallation reactions of alpha emission by direct interaction were investigated in a Monte Carlo calculation. The total inelastic cross section and the cross section for formation of compound nuclei were calculated for proton bombardment of ^{197}Au at 155 Mev, together with the angular and energy distributions of the alpha particles

emitted by direct interaction. The results were compared with experimental values. (D.C.W.)

21373 CHARGE DEPENDENCE OF THE INTERNUCLEON POTENTIAL. R. J. Blin-Stoyle and C. Yalgin (Univ. of Sussex, Eng.). Phys. Letters, 15: 258-60(Apr. 1, 1965).

The parameters describing the charge dependence in a phenomenological, charge-dependent potential are estimated. It is shown that some features of the potential can arise from the one-boson-exchange description of the internucleon potential. (D.C.W.)

21374 NEW LEVELS IN V^{47}. H. Albinsson and J. Dubois (Chalmers Univ. of Tech., Goteborg). Phys. Letters, 15: 260-1(Apr. 1, 1965).

Gamma coincidence and pair spectra from the $^{46}Ti(p,\gamma)^{47}V$ reaction at 1020, 1095, 1127, 1208, 1252, 1358, and 1365 kev were measured. Previously unreported levels at 665 ± 3, 1650 ± 3, 1963 ± 4, 2071 ± 4, 2172 ± 7, 2204 ± 7, 2428 ± 7, 2712 ± 10, and 3362 ± 10 kev were observed, and a decay scheme was proposed. The Q-value of the reaction was determined to be 5177 ± 5 kev. (D.C.W.)

21375 DECAY OF Sn^{121m} AND MÖSSBAUER ABSORPTION IN Sb^{121}. R. E. Snyder and G. B. Beard (Wayne State Univ., Detroit). Phys. Letters, 15: 264-6(Apr. 1, 1965).

The beta spectrum of the long-lived isomer of ^{121}Sn was investigated; and the Mössbauer absorption of the 37-kev gamma ray in ^{121}Sb was studied, using absorbers of Sb, SnO_2, and Sb_2O_3. (D.C.W.)

21376 THE $Si^{30}(d,n)P^{31}$ REACTION. B. Cujec, W. G. Davies, W. K. Dawson, T. B. Grandy, G. C. Neilson, and K. Ramavataram (Univ. of Alberta, Edmonton). Phys. Letters, 15: 266-9(Apr. 1, 1965).

Neutron time-of-flight spectra from the $^{30}Si(d,n)^{31}P$ reaction at 3.0, 3.5, and 4.0 Mev were measured, and the angular distributions of neutrons leading to various levels of ^{31}P were obtained. Nine previously unreported levels in the region of excitation from 5 to 7 Mev were identified. Assignments of $\frac{1}{2}^+$ were made for the ^{31}P levels at 3.13 and 5.25 Mev. (D.C.W.)

21377 HYPERFINE SPLITTING AND g FACTOR OF THE 84-kev STATE IN Yb^{170}. A. Hueller (Technische Hochschule, Munich), W. Wiedemann, P. Kienle, and S. Huefner. Phys. Letters, 15: 269-71(Apr. 1, 1965).

The gyromagnetic ratio of the 84-kev, I = 2 state of ^{170}Yb was determined to be 0.334 ± 0.005 from its magnetic hyperfine splitting in $YbCl_3 \cdot 6H_2O$ as obtained by Mössbauer measurements. This value is in excellent agreement with the value calculated by Nilsson and Prior with pairing correlations taken into account. (D.C.W.)

21378 γ-NEUTRINO CORRELATION IN FIRST FORBIDDEN NUCLEAR μ-MESON CAPTURE. Z. Oziewicz and N. P. Popov (Ioffe Inst. of Physics and Tech., Leningrad). Phys. Letters, 15: 273-5(Apr. 1, 1965).

The angular gamma-neutrino correlation in meson (μ) capture is investigated for the case of first-forbidden transitions. The reaction $\mu + {}^{12}C \rightarrow {}^{12}B^* + \nu_\mu$ is considered as an example. (D.C.W.)

21379 LOG ft VALUES AND T = $\frac{3}{2}$ ANALOGUE STATES. J. C. Hardy and B. Margolis (McGill Univ., Montreal). Phys. Letters, 15: 276-8(Apr. 1, 1965).

The log ft values were calculated for the mirror ($T = \frac{1}{2} \rightarrow T = \frac{1}{2}$) transitions of ^{17}F, ^{19}Ne, ^{21}Na, ^{23}Mg, ^{25}Al, ^{27}Si, ^{29}P, ^{31}S, ^{33}Cl, ^{35}Ar, ^{37}K, and ^{39}Ca. The results were in remarkably good agreement with experimental values. The deformations were obtained primarily from the measured magnetic dipole moments. The log ft values for T = $\frac{3}{2}$ superallowed transitions in ^{17}Ne, ^{21}Mg, ^{25}Si, ^{29}S, ^{33}Ar, and ^{37}Ca were calculated, using these deformations. The values clustered around 3.3, which was used to calculate log ft values for the positron decay branches of delayed proton precursors (^{21}Mg, ^{25}Si, ^{29}S, ^{33}Ar, and ^{37}Ga). (D.C.W.)

21380 ENERGY LEVELS IN ^{32}S FROM THE REACTION $^{31}P(p,\gamma)^{32}S$. S. L. Andersen (Universitetet, Oslo). Phys. Norvegica, 1: No. 5, 247-71(1965).

The spins of eight levels in ^{32}S and parities for four of them were determined, together with the branching ratios and the multipole mixings of the gamma transitions. The gamma yield of six resonances in ^{31}P in the energy region 1147 to 1581 kev was measured, and the values of $|M|^2$ for several gamma transitions were calculated. The reduced proton width θ_p^2 is given for the resonances at 1246 and 1436 kev. A description of the method of analysis of the gamma angular correlations is included, together with a discussion of its limitations. (auth)

21381 TREATMENT OF NEUTRON-PROTON PAIRING CORRELATIONS. B. Banerjee and J. C. Parikh (Tata Inst. of Fundamental Research, Bombay). Phys. Rev., 138: B303-5(Apr. 26, 1965).

The short-range correlation between neutrons and protons in the configuration $(j)^N$ is discussed in the BCS approximation. The interaction is assumed to exist only in the J = 0 and T = 1 state of two nucleons. The ground- and excited-state energies are calculated and compared with the exact values. (auth)

21382 HYPERFINE STRUCTURES OF Re^{186} AND Re^{188}. Richard G. Schlecht, Matthew B. White, and Douglas W. McColm (Univ. of California, Berkeley). Phys. Rev., 138: B306-9(Apr. 26, 1965). (UCRL-11705)

The atomic-beam magnetic-resonance flop-in technique was used to determine the hyperfine-structure separations of the isotopes ^{186}Re and ^{188}Re. The magnetic-dipole interaction constant a and the electric-quadrupole interaction constant b were measured for these two radioactive isotopes in the $J = \frac{1}{2}$ ground state. Beams were produced by electron bombardment of irradiated rhenium wires. The spins of both isotopes were determined previously to be 1. For the interaction constants of ^{186}Re the values $a_{186} = \pm 78.3058(24)$ Mc, $b_{186} = \mp 8.3601(50)$ Mc were obtained. These give values for the two hyperfine-structure separations of $\Delta\nu_{186}(\frac{7}{2},\frac{5}{2}) = \pm 265.292(14)$ Mc, $\Delta\nu_{186}(\frac{5}{2},\frac{3}{2}) = \pm 208.305(14)$ Mc. For the interaction constants of ^{188}Re the values $a_{188} = \pm 80.4320(32)$ Mc, $b_{188} = \pm 7.7455(60)$ Mc were obtained. These give values for the two hyperfine-structure separations of $\Delta\nu_{188}(\frac{7}{2},\frac{5}{2}) = \pm 273.379(13)$ Mc, $\Delta\nu_{188}(\frac{5}{2},\frac{3}{2}) = \pm 212.698(17)$ Mc. The nuclear moments of both isotopes were determined to be positive. Also obtained was an improved value for the electronic Landé g factor for rhenium: $g_J = -1.95203(8)$. (auth)

21383 MAGNETIC MOMENTS OF RHENIUM-186 AND RHENIUM-188 AND ANALYSIS OF THE RHENIUM HYPERFINE STRUCTURE. Lloyd Armstrong, Jr., and Richard Marrus (Univ. of California, Berkeley). Phys. Rev., 138: B310-15(Apr. 26, 1965). (UCRL-11750)

The nuclear moments of rhenium-186 and rhenium-188 were measured by the method of triple resonance in an atomic beam. They are found to be $\mu_I(186) = +1.728(.003)$ nm and $\mu_I(188) = +1.777(.005)$ nm, including the correction for diamagnetic shielding. With these values, an analysis based on the wave function of Trees was undertaken of the hyperfine structure (hfs) in the $^6S_{5/2}$ ground state arising from the half-filled 5d shell. Calculations are made of contributions arising from the breakdown of Russell-Saunders coupling within the configuration $(5d)^5(6s)^2$ and configuration mixing by $(5d)^6(6s)$. It is shown that the principal contribution to the magnetic dipole hfs comes from relativistic effects in $^6S_{5/2}$. This is consistent with the small value obtained for the hyperfine anomaly $^{186}\Delta^{188} = 0.1(0.4)\%$. It is found that if the radial wave functions of Cohen for 5d electrons are used to calculate relativistic corrections, then good agreement is obtained with the measured A constant. The correction factors of Casimir are shown to be too small by a factor tor of four. The quadrupole hyperfine structure is found to arise primarily from the cancellation of two off-diagonal matrix elements: a nonrelativistic element $\langle {}^4P_{5/2}|q_J|{}^4D_{5/2}\rangle$ and a relativistic element $\langle {}^6S_{5/2}|q_J|{}^4P_{5/2}\rangle$. Unfortunately, the accuracy is insufficient to permit a reliable determination of even the sign of the quadrupole moment. The measured nuclear moments are compared with the predictions of the Nilsson model. Good agreement is found if free-nucleon g factors are used, and excellent agreement is obtained with quenched g factors. (auth)

21384 EFFECT OF DEFORMATION VIBRATIONS ON E2 BRANCHING RATIOS IN DEFORMED EVEN-EVEN NUCLEI. J. P. Davidson and M. G. Davidson (Rensselaer Polytechnic Inst., Troy, N. Y.). Phys. Rev., 138: B316-21(Apr. 26, 1965). (UCRL-11600)

Ratios of electric-quadrupole reduced transition probabilities are calculated using a collective model. For transitions between positive-parity states the asymmetric-core model with β vibrations is used, while for negative-parity states a similar model with ζ vibrations is used. The reduced transition probability can be divided into two factors, the first an adiabatic term, and the second due to the vibration on the deformation parameter. For small values of the stiffness parameter μ, the vibrational contribution to the ratios is found to be a factor close to unity. However, this factor can be large for greater μ. Experimental branching ratios of several deformed even-even nuclei are compared with theory. (auth)

21385 "SENIORITY-ZERO" EXCITED STATES OF THE PAIRING HAMILTONIAN. R. R. Chasman (Argonne National Lab., Ill.). Phys. Rev., 138: B326-33(Apr. 26, 1965).

The seniority-zero excited-state spectrum of the hamiltonian $H = \Sigma_{k>0}\epsilon_k(a_k^\dagger a_k + a_{-k}^\dagger a_{-k}) - G\,\Sigma_{k,l>0}\, a_k^\dagger a_{-k}^\dagger a_{-l}a_l$ is studied in detail. Approximate excited-state wave functions of the form $\psi^\lambda = \Sigma_\alpha\, F(\lambda,\alpha)\Sigma_i D(\alpha,i)a_i^\dagger a_{-i}^\dagger \Sigma_{j>i} D(\alpha,j)\, a_j^\dagger a_{-j}^\dagger \ldots|0\rangle$ are developed. These solutions are compared with exact solutions of a small system and the agreement is quite good. A somewhat larger system is studied in order to see how the excited-state spectrum changes as the number of separable functions is increased. The method is applied to heavy nuclei and is in good agreement with observed 0^+ excited states for nuclei having 144 to 150 neutrons. A theoretical 0^+ spectrum is displayed for each even neutron system from 144 to 152 neutrons. (auth)

21386 COLLECTIVE EXCITATIONS IN THE ZIRCONIUM ISOTOPES. H. W. Broek and J. L. Yntema (Argonne National Lab., Ill.). Phys. Rev., 138: B334-9(Apr. 26, 1965).

Angular distributions were derived for the scattering of 43-Mev alpha particles by ^{90}Zr, ^{91}Zr, ^{92}Zr, and ^{94}Zr. Angular distributions for elastic scattering for the l = 2 transitions, for the l = 3 transitions, and for many other peaks are presented. The collective excitations in ^{92}Zr and ^{94}Zr are quite similar, and resemble those of the Ni and Zn isotopes. However, the l = 3 transition is more prominent than the l = 2 transition in all four zirconium isotopes. (auth)

21387 DETERMINATION OF NEUTRON REDUCED WIDTHS BY THE ^{14}N(^{14}N,^{13}N)^{15}N REACTION. L. C. Becker and J. A. McIntyre (Yale Univ., New Haven). Phys. Rev., 138: B339-45(Apr. 26, 1965).

Measurements were made of cross sections for the neutron transfer reaction ^{14}N(^{14}N,^{13}N)^{15}N at energies below the Coulomb barrier. It is shown that the tunneling theory for neutron transfer is consistent with the angular distribution function, $d\sigma(\theta)/d\Omega$, at the center-of-mass energy of 6.62 Mev. By using the tunneling theory, the single-particle reduced width θ_0^2 is found to be $(4.5 \pm 1.0) \times 10^{-2}$ for the transferred neutron at a radius of 5 F by assuming that θ_0^2 is the same for ^{14}N and ^{15}N. This value is to be compared to $\theta_0^2 = (4.0 \pm 1.0) \times 10^{-2}$ as determined from (d,p) stripping and $\theta_0^2 = (5.2 \pm 1.0) \times 10^{-2}$ as determined from shell-model calculations. Good agreement is thus obtained between reduced widths determined by neutron transfer and by (d,p) reactions. (auth)

21388 ^{14}N(^{14}N,^{13}N)^{15}N REACTION AND THE NEUTRON TUNNELING MECHANISM. J. C. Hiebert (Oak Ridge National Lab., Tenn.), J. A. McIntyre, and J. G. Couch. Phys. Rev., 138: B346-9(Apr. 26, 1965). (ORNL-P-909)

Angular-distribution and total-cross-section measurements were made for the ^{14}N(^{14}N,^{13}N)^{15}N reaction over a range of energies. For center-of-mass energies below about 6.5 Mev, the tunneling theory of neutron transfer is shown to give a good account of the data. At higher energies, nuclear absorption occurs for the close collisions and spoils the tunneling description. These results show why earlier descriptions of this reaction by the tunneling theory were unsuccessful. (auth)

21389 EMISSION OF Li^8 FRAGMENTS IN THE INTERACTIONS OF 3.0-Gev/c K$^-$ MESONS WITH NUCLEI IN NUCLEAR EMULSION. G. Baumann (Centre de Recherches Nucleaires, Strasbourg), J. P. Gerber, A. Bechdolff, H. Braun, P. Cueer, and D. M. Harmsen. Phys. Rev., 138: B350-2(Apr. 26, 1965).

The experimental results of the emission of hammer tracks (^{8}Li, ^{9}Li, ^{8}B nuclei) from 3-Bev/c K$^-$-meson interactions are compared with the theory of nuclear evaporation. The results are only in partial agreement with this theory. The production rate increases with incident energy from 0.8 up to 3 Bev/c. The forward-to-backward ratios decrease when the energy of the incident particle rises. (auth)

21390 RATIOS OF INDEPENDENT YIELDS OF THE ISOMERS Te$^{131-131m}$ AND Te$^{133-133m}$ IN FISSION. Demetrios G. Sarantites, Glen E. Gordon, and Charles D. Coryell (Massachusetts Inst. of Tech., Cambridge). Phys. Rev., 138: B353-64(Apr. 26, 1965). (MIT-905-24)

The independent yield ratios of (30-h ^{131m}Te)/(25-min ^{131}Te) and of (53-min ^{133m}Te)/(12.5-min ^{133}Te) were measured in the following types of fission: ^{235}U with thermal neutrons, and ^{232}Th and ^{238}U with 18-Mev deuterons and with 33-Mev ^{4}He ions. The fractional independent chain yields of the isomers were measured by determining the growth curves of the daughter iodine activities extracted at successive time intervals from aliquots of samples containing tellurium activities quickly separated from fission induced in short irradiations, and correcting for contributions from precursors. The isomer-yield ratios for independent formation for 30-h ^{131m}Te/25-min ^{131}Te and for 53-min ^{133m}Te/12.5-min ^{133}Te, respectively, are as follows: 1.8 ± 0.4 and 1.55 ± 0.5 for ^{235}U(n_{th},F), 3.3 ± 0.5 and 2.8 ± 1.7 for ^{232}Th(α_{33},F), 2.7 ± 0.5 and 1.7 ± 0.9 for ^{232}Th(d_{18},F), 5.0 ± 1.0 and 3.1 ± 2.0 for ^{238}U(α_{33},F), and 3.3 ± 0.5 and 1.8 ± 1.1 for ^{238}U(d_{18},F). The fractional independent chain yield of ^{131m}Te + ^{131}Te was measured as 0.124 ± 0.014 for ^{235}U(n_{th},F). The fraction of decay of ^{131}Sb to ^{131m}Te was measured and found to be $6.8 \pm 1\%$. On the basis of the measured isomer ratios, the intrinsic spin of the primary fragment (leading by the emission of neutrons and γ rays to the secondary fragments studied) was estimated. The calculations indicate that in thermal-neutron fission an appreciably larger spin ($\sim 5\hbar$) than that of the compound nucleus must be assigned to the heavy primary fragment in order to explain the observed isomer ratios in ^{131}Te and ^{133}Te. Similar reasoning in the 33-Mev ^{4}He ion fission of ^{232}Th indicates that the primary fragment must be given an intrinsic spin value roughly $7\hbar$. (auth)

21391 PROTON POLARIZATION IN THE Sr^{88}(d,p)Sr^{89*} (1.05-Mev) REACTION. E. J. Ludwig and D. W. Miller (Indiana Univ., Bloomington). Phys. Rev., 138: B364-71 (Apr. 16, 1965).

The polarization of protons from the ^{88}Sr(d,p)^{89*}Sr reaction exciting the 1.05-Mev state in ^{89}Sr was measured at 14 laboratory angles from 12 to 131° using a deuteron bombarding energy of 11 Mev. In this reaction, which involves no orbital-angular-momentum transfer by the captured neutron, spin-orbit terms in the optical-model potentials describing the interactions of the incident and exit particles are considered to be responsible for the polarization. The measurements were made using a heavy-particle magnetic spectrometer to select the desired proton group and focus it on the carbon second scatterer. This scatterer was viewed to the right and the left by a pair of scintillation counters set at a mean laboratory angle of 40°. The sign of the polarization seems to correspond to the sign of the slope of the angular distribution, being negative at the forward angles with apparent sign changes at the subsequent minima and maxima. This behavior is in approximate agreement with the derivative rule for stripping reactions with $l_n = 0$ orbital-angular-momentum transfer. The po-

larization changes most rapidly near the stripping minima and becomes largest at the backward angles (−28% at 95°). (auth)

21392 RATIO OF THE FORMATION CROSS SECTIONS OF ^{44g}Sc AND ^{44m}Sc IN NITROGEN-INDUCED REACTIONS. I. R. Williams and K. S. Toth (Oak Ridge National Lab., Tenn.). Phys. Rev., 138: B382-8(Apr. 26, 1965).

Thick targets of P, ZnS, and $CuCl_2$ were bombarded with 30- to 42-Mev ^{14}N ions, and excitation functions were obtained for the compound-nucleus reactions with ^{31}P, ^{32}S, and ^{35}Cl producing ^{44m}Sc, ^{44g}Sc, and ^{43}Sc. The reaction products were identified by means of their characteristic gamma rays and half lives, and quantitatively studied by radioactive assay. The data were combined with some previously obtained at ^{14}N energies below 28 Mev. The isomer ratio ^{44m}Sc/^{44g}Sc was found to rise with increasing excitation energy and angular momentum for all three targets. The ratios were compared with compound-nucleus theory as treated by Huizenga and Vandenbosch to test assumptions concerning the multipolarity and multiplicity of the gamma quanta emitted by the final nucleus. (auth)

21393 DENSITY PROPAGATOR FOR A SELF-BOUND FERMION SYSTEM. II. LINEAR RESPONSE AND INELASTIC ELECTRON SCATTERING. A. S. Reiner (Weizmann Inst. of Science, Rehovoth, Israel). Phys. Rev., 138: B389-98(Apr. 26, 1965).

Using the Green's-function technique of Martin, Schwinger, and Puff, a calculation is made of the total linear response of nuclear matter, as measurable, for instance, in an inelastic electron or muon scattering experiment. In the independent-pair approximation used, two contributions stand out: the quasielastic response of properly dressed particles with well-defined lifetimes, and the contribution due to the scattering between those particles. An extensive analysis is made of the importance of the transverse component of the electromagnetic interaction as well as of the two mentioned contributions. The properly defined quasielastic scattering is predicted to dominate the scattering. A comparison is made with previous calculations by Czyz and Gottfried. (auth)

21394 $Kr^{86}(d,p)Kr^{87}$ REACTIONS AND COMPARISONS WITH (d,p) REACTIONS ON Sr^{88}, Zr^{90}, AND Mo^{92}. Richard E. Sass, Baruch Rosner, and Edward J. Schneid (Univ. of Pittsburgh). Phys. Rev., 138: B399-404(Apr. 26, 1965).

Eleven energy levels in ^{87}Kr were located by the ^{86}Kr(d,p)^{87}Kr reaction. The excitation energies of the levels are ground state, 0.55, 1.52, 2.17, 2.34, 2.57, 2.89, 3.09, 3.31, 3.65, and 3.97 Mev. The orbital-angular-momentum transfer as well as the spectroscopic factors were deduced for the predominant transitions with the aid of distorted-wave Born-approximation calculations. A comparison between the proton spectra obtained by the (d,p) reaction on the ^{86}Kr, ^{88}Sr, ^{90}Zr, and ^{92}Mo isotones all of which have a closed shell (N = 50) of neutrons, but different numbers of proton pairs, is discussed. (auth)

21395 VACUUM POLARIZATION CORRECTIONS TO HYPERFINE STRUCTURE IN MUONIC ATOMS. Morton M. Sternheim (Yale Univ., New Haven). Phys. Rev., 138: B430-2(Apr. 26, 1965).

Measurement of the hyperfine-structure splitting in muonic atoms would be interesting in view of the discrepancies in electronic atoms. In muonic atoms, nuclear-structure effects are much larger than the uncertainty in the fine-structure constant and may therefore be observed unambiguously. The various corrections are briefly discussed, and the large vacuum-polarization correction is calculated. (auth)

21396 STRUCTURE OF THE PROTON AND THE HYPERFINE SHIFT IN HYDROGEN. C. K. Iddings (Stanford Univ., Calif.). Phys. Rev., 138: B446-58(Apr. 26, 1965).

The proton-size correction to the hyperfine structure in the ground state of atomic hydrogen is re-examined. It is shown by means of dispersion relations that this correction can be expressed as an integral over experimentally measurable cross sections for electron-proton scattering. This clarifies the physical nature of the correction, puts it on a rigorous basis, and lends support to previous analyses. In the absence of experimental data, theoretical estimates for the correction are given. They agree with previous estimates, and therefore the present experimental value for the hyperfine splitting cannot be explained. Possible implications of this disagreement are discussed, and experiments which would clarify the situation are suggested. (auth)

21397 EXPERIMENTAL EVIDENCE FOR PARITY IMPURITY IN A NUCLEAR GAMMA TRANSITION. F. Boehm and E. Kankeleit (California Inst. of Tech., Pasadena). Phys. Rev. Letters, 14: 312-15(Mar. 1, 1965).

A measurement of the circular polarization of the 482-kev gamma transition in ^{181}Ta is reported, and evidence of a small parity admixture is found. Polarization was measured by a scintillation counter after the passage of the gamma ray through an electromagnet core, and a table of the observed asymmetry is presented. The observed sign and magnitude of the admixture parity nonconserving agree with estimates based on the current-current hypothesis of weak interactions, which predicts a strangeness-preserving nonleptonic weak coupling. (M.J.T.)

21398 REORIENTATION EFFECT IN Cd^{114}. J. de Boer, R. G. Stokstad, G. D. Symons, and A. Winther (California Inst. of Tech., Pasadena). Phys. Rev. Letters, 14: 564-7(Apr. 5, 1965).

The reorientation effect in ^{114}Cd, arising from the dependence of the Coulomb excitation process on the static moments of the energy levels, was determined by evaluating the measured cross sections for the scattering of ^{4}He and ^{16}O ions in terms of the quadrupole moment of the first 2^+ state. A rather large quadrupole moment for the 2^+ state was required to explain the experimental results. (D.C.W.)

21399 ANOMALOUS E2 PARTICLE PARAMETERS IN DEFORMED NUCLEI. J. H. Hamilton, E. F. Zganjar, T. M. George, and W. H. Hibbitts (Vanderbilt Univ., Nashville). Phys. Rev. Letters, 14: 567-70(Apr. 5, 1965).

The K-shell particle parameters, which transform gamma-gamma into electron-gamma directional correlations, of E2 transitions in ^{152}Gd, ^{154}Gd, and ^{152}Sm were determined by comparing gamma-gamma and electron-gamma directional correlation measurements made with the same source. The results were compared with values obtained with a point-nucleus approximation; disagreements were obtained for the deformed nuclei. (D.C.W.)

21400 ROUGH COMPUTATION OF THE SEPARATION ENERGY OF STRONGLY BOUND NUCLEONS. D. M. Brink (Oxford Univ.) and N. Sherman. Phys. Rev. Letters, 14: 393-5(Mar. 15, 1965).

A model is presented for estimating the adiabatic energy of a nucleon in the 1s and 1p levels, under general assumptions on the nuclear hamiltonian, the two-body internucleon potential, and the nuclear wave functions and using special properties of harmonic-oscillator wave functions. A comparison is made of the theoretical and experimental values of the separation energies for some nuclei ^{7}Li and ^{40}Ca. (L.B.S.)

21401 HIGH-RESOLUTION STUDY OF THE REACTION $C^{12}(p,2p)B^{11}$ AT 50 Mev. H. G. Pugh, D. L. Hendrie, Marc Chabre, and E. Boschitz (Univ. of California, Berkeley). Phys. Rev. Letters, 14: 434-6(Mar. 22, 1965). (UCRL-11940)

The energy spectra and differential cross section for the ground state transition were measured for the $^{12}C(p,2p)^{11}B$ reaction, using two counter telescopes, each consisting of a pair of lithium-drifted silicon detectors. The summed spectrum showed four excited states of ^{11}B with appreciable intensity. The mechanism for production of the $\frac{5}{2}^-$ and $\frac{7}{2}^-$ states was investigated. The $^{12}C(p,d)^{11}C$ reaction was also studied, and the results support the assumption that the unresolved doublet at 6.8 Mev in ^{11}B for the (p,2p) reaction consists mainly of the $\frac{7}{2}^-$ state. (L.B.S.)

21402 INTRANUCLEAR CASCADE AND FERMI-MODEL BREAKUP CALCULATIONS ON THE PRODUCTION OF Li, Be, AND B ISOTOPES IN C^{12} BY 156-Mev PROTONS. E. Gradsztajn, F. Yiou, R. Klapisch, and R. Bernas (Laboratoire Joliot-Curie, Orsay, France). Phys. Rev. Letters, 14: 436-9(Mar. 22, 1965).

A calculation was performed for the production cross sections of ^{6}He, ^{6}Li, ^{7}Li, ^{8}Li, ^{9}Li, ^{9}Be, ^{10}Be, ^{10}B, ^{11}B, ^{10}C, and ^{11}C from 156-Mev proton-irradiated carbon, using the hypothesis of a two-step mechanism of which the first step is the intranuclear cascade initiated by the incident proton and leading to a particular excited residual nucleus, and the second step is the breakup of the residual nucleus into various particles. The results are tabulated and compared with experimental absolute cross sections. (L.B.S.)

21403 SPONTANEOUS FISSION IN VERY NEUTRON-RICH ISOTOPES. D. W. Dorn and R. W. Hoff (Univ. of California, Livermore). Phys. Rev. Letters, 14: 440-1 (Mar. 22, 1965).

Samples obtained from the underground nuclear explosion test (Par) were analyzed for isotopes produced by multiple neutron captures in the ^{238}U target. The mass yields calculations were performed and the results are given. A possible explanation is given for the depletion of even-mass isotopes, and the implied spontaneous fission half lives are tabulated. (L.B.S.)

21404 INFORMATION ABOUT THE NEUTRON-NEUTRON SCATTERING LENGTH FROM THE REACTION $H^3(n,d)2n$. V. Ajdacic, M. Cerineo, B. Lalovic, G. Paic, I. Slaus, and P. Tomas (Institut "Rudjer Boskovic," Zagreb and Institut "Boris Kidric," Belgrade). Phys. Rev. Letters, 14: 442-4(Mar. 22, 1965).

The deuteron spectra from the ^{3}H(n,d)2n reaction were measured at 14.4 Mev and were analyzed to determine the neutron-neutron scattering length, a_{nn}. The cross sections were calculated in the Born approximation for the pickup process with $a_{nn} = -17, -22$, and -27 F, and were compared with the Watson curve with $a_{nn} = -17$ and the experimental curve with $a_{nn} = -18$. The shape of the spectrum in the high-energy region indicates that the influence of distortive effects is small. (L.B.S.)

21405 REACTIONS $H^3(n,p)3n$ AND $H^3(n,H^4)\gamma$ AT E_n = 14.4 Mev. V. Ajdacic, M. Cerineo, B. Lalovic, G. Paic, I. Slaus, and P. Tomas (Institut "Rudjer Boskovic," Zagreb and Institut "Boris Kidric," Belgrade). Phys. Rev. Letters, 14: 444-6(Mar. 22, 1965).

The proton spectra were measured from the reaction $n + H^3$ at 14.4 Mev, using a semiconductor counter telescope with multidimensional analyzers. The cross section for ^{3}H(n,p)3n reactions, integrated from 3.8 to 5.1 Mev at 0°, was found to be 12 mb/sr, which was smaller than the cross section for the breakup ^{3}H(n,d)3p. The failure to reproduce the experimental data on the simultaneous breakup into three neutrons and a proton is interpreted as an indication of strong final interactions. A 6.4-Mev proton group was found, and was assigned to the $n + H^3$ interaction. The assignment implied the existence of a bound state of three neutrons, with binding energy of 1 Mev and cross section of 3.8 mb/sr. An attempt was made to detect ^{4}H from the reaction ^{3}H(n,^{4}H)γ, and the upper limit of the cross section was found to be 0.2 mb/sr. The probable nonexistence of ^{4}H and ^{5}H was interpreted as evidence that the existence of n^3 and n^4 is highly improbable. (L.B.S.)

21406 $\pi^{\pm}$ AND $K^{\pm}$ PRODUCTION CROSS SECTIONS FOR 12.5-Bev PROTONS ON Be. R. A. Lundy (Argonne National Lab., Ill.), T. B. Novey, D. D. Yovanovitch, and V. L. Telegdi. Phys. Rev. Letters, 14: 504-7(Mar. 29, 1965).

A slow extracted proton beam from the Argonne ZGS, ~100 msec duration and 12.5 Bev, was focused onto a Be target, and a precise measurement of meson production was performed. The experimental arrangement, using plastic scintillation counters and Cherenkov counters, is described. Differential production cross sections obtained for π^+, π^-, K^+ and K^- at 2° to 16° are presented, and errors are discussed. (L.B.S.)

21407 NUCLEAR SUPERRADIANCE IN SOLIDS. J. H. Terhune and G. C. Baldwin (General Electric Co., Schenectady, N. Y.). Phys. Rev. Letters, 14: 589-91 (Apr. 12, 1965).

An analysis is outlined of spontaneous gamma emission from nuclei with only two nondegenerate internal energy states coupled by a radiative transition in a perfect crystal lattice. The results are interpreted as showing that spontaneous decay in a perfect crystalline solid can lead to a superradiant condition. (D.C.W.)

21408 MÖSSBAUER EFFECT IN K^{40} USING AN ACCELERATOR. S. L. Ruby and R. E. Holland (Argonne National Lab., Ill.). Phys. Rev. Letters, 14: 591-3(Apr. 12, 1965).

The resonant absorption spectrum for the 29-kev gamma ray from ^{40}K was measured, using the ^{39}K(d,p)^{40}K reaction to excite the 29-kev level. Average values of -0.02 ± 0.09 and 4.1 ± 0.35 mm/sec were obtained for the isomer shift and the linewidth, respectively. (D.C.W.)

21409 MÖSSBAUER EFFECT OF THE 29.4-kev NEUTRON CAPTURE GAMMA RAY OF K^{40}. D. W. Hafemeister and E. Brooks Shera (Los Alamos Scientific Lab., N. Mex.). Phys. Rev. Letters, 14: 593-5(Apr. 12, 1965).

The resonant absorption of the 29.4-kev gamma ray resulting from the decay of the 29.4-kev level excited in ^{40}K by thermal neutron capture in ^{39}K was observed at 4 and 78°K, using targets of K, KCl, and KF, together with enriched KCl absorbers of two different thicknesses. The isomer shifts (essentially zero) and linewidths were obtained, and an upper limit was established for the change in nuclear radius between the ground and first excited states of ^{40}K. (D.C.W.)

21410 MAGNETIC DIPOLE TRANSITIONS AND g_R FACTORS IN DEFORMED EVEN-EVEN NUCLEI. Walter Greiner (Universitat, Frankfurt am Main). Phys. Rev. Letters, 14: 599-602(Apr. 12, 1965).

The lowering of the rotational g_R factors from the value Z/A for deformed even-even nuclei is investigated, together with the magnetic dipole transitions from the second to the first 2^+ state. It is shown that the lowering of the g_R factor indicates a smaller proton deformation and a nonvanishing value of the neutron deformation, which is responsible for magnetic transitions between rotational bands. It is also found that the g factor becomes a g tensor. Theoretical predictions for the g_R factor of the first rotational 2^+ state and the M1−E2 mixing parameter for the $2^{+\prime} \rightarrow 2^+$ transition are compared with each other and with experimental observations. The results indicate that some structure for the magnetic dipole transitions is related to the structure of the g_R factors. (D.C.W.)

21411 ON BARRIER PENETRABILITIES IN ALPHA DECAY. A. Saendulescu (Inst. for Atomic Physics, Bucharest) and T. Voeroes. Physica, 31: 83-8(Jan. 1965).

The barrier penetrabilities for some nuclei were calculated by numerical integration in the WKB approximation. The existence of nuclear, coulomb and centrifugal potentials for both even-even and odd nuclei was assumed. The relative intensities of favored alpha transitions for five odd nuclei were calculated by using the intensities of favored alpha transitions of the corresponding five even-even nuclei. The theoretical results are in good agreement with the experimental data. (auth)

21412 THE ENERGIES OF N-NUCLEON SYSTEMS BY BOPP'S APPROXIMATION. J. D. Patterson and R. K. Anderson (South Dakota School of Mines and Tech., Rapid City). Proc. Phys. Soc. (London), 85: 41-5(Jan. 1965).

The energies of levels in ^{204}Pb and ^{205}Pb were calculated by a modified Bopp's method, which was shown to be equivalent to the thirty-year-old method of Bacher and Goudsmit. (D.C.W.)

21413 MULTI-LEVEL ANALYSIS OF RESONANCES IN ^{6}Li(d,α)α AND ^{7}Li(p,α)α REACTIONS. R. M. Freeman (Centre d'Etudes Nucleaires, Saclay, France) and G. S. Mani. Proc. Phys. Soc. (London), 85: 267-80(Feb. 1965).

The resonances observed in $^{6}Li(d,\alpha)\alpha$ reactions are fitted using the multi-level formalism of Wigner and Eisenbud's R-matrix theory. Three levels in ^{8}Be around 22 Mev excitation are predicted at excitation energies of 22.542, 24.02, and 25.227 Mev having spins 2^+, 0^+, and 2^+ respectively. The 0^+ level has a large deuteron width which is about 75% of the Wigner limit, while the two 2^+ levels show smaller deuteron widths, about 25% and 3% of the Wigner limit for the lower and higher levels respectively. The alpha reduced widths for all these levels are small compared with the Wigner limit, the 0^+ level having the maximum alpha width. The use of this reaction as a detector of polarized deuterons is discussed. Preliminary analysis of the $^{7}Li(p,\alpha)\alpha$ resonances is also presented. (auth)

21414 AN EXPERIMENTAL STUDY OF THE $^{6}Li(d,\alpha)\alpha$ REACTION. G. S. Mani (Univ. of Manchester, Eng.), R. M. Freeman, F. Picard, D. Redon, and A. Sadeghi. Proc. Phys. Soc. (London), 85: 281-4(Feb. 1965).

The $^{6}Li(d,\alpha)\alpha$ reaction was studied in the region between 4 and 12 Mev deuteron energy. No new resonances were found although the angular distributions show that the reaction mechanism is predominantly compound nuclear. No evidence was found for any direct interaction. (auth)

21415 COLLECTIVE STATES OF CLOSED-SHELL NUCLEI. R. Phythian (Univ. of Manchester, Eng.). Proc. Phys. Soc. (London), 85: 403-12(Mar. 1965).

A variational method is developed to find certain low-lying collective states of a closed-shell nucleus using the random-phase approximation with an effective particle-hole attraction of zero range. A numerical calculation is carried out to illustrate the use of this method for a very simple model nucleus and the significance of the results is discussed. (auth)

21416 ft VALUES OF $0^+ \rightarrow 0^+$, $\Delta T = 0$, β DECAYS: IMPLICATIONS FOR THE CONSERVED VECTOR CURRENT THEORY. R. J. Blin-Stoyle, S. C. K. Nair, and S. Papageorgiou (Univ. of Sussex, Brighton, Eng.). Proc. Phys. Soc. (London), 85: 477-91(Mar. 1965).

Calculations are made of the magnitude of charge-dependent corrections to the polar vector matrix elements of a number of $J = 0^+$, $T = 1 \rightarrow J = 0^+$, $T = 1$ beta decays. Both the Fermi gas model and jj coupled shell model are used, and with a most optimistic treatment it is not found possible to resolve the present difference between the experimentally determined polar vector β-decay coupling constant G_V and the μ-decay coupling constant G_μ. The role played by mesonic exchange corrections, should conserved vector current theory not hold, is also investigated, and it is found that experiment is consistent with zero contribution from such effects. It is finally concluded that the measured ft values are in agreement with conserved vector current theory only if it is formulated along the lines suggested by Cabbibo. (auth)

21417 ASYMPTOTIC FORM OF THE ELECTRON CAPTURE CROSS SECTION IN THE CLASSICAL APPROXIMATION. D. R. Bates and R. A. Mapleton (Queen's Univ., Belfast). Proc. Phys. Soc. (London), 85: 605-7(Mar. 1965).

If the protons are treated as distinguishable particles classical mechanics gives the asymptotic electron capture cross section in $H^+ - H(1s)$ collisions to be proportional to the inverse cube of the impact energy just as does quantum mechanics and in addition gives almost the correct constant of proportionality. (auth)

21418 ALPHA DECAY STUDIES OF Pa-230, Pa-228, Pa-226, AND THEIR DESCENDANTS. Jerome D. McCoy (Univ. of Tulsa, Okla.). Soc. Sci. Fennica, Commentationes Phys.-Math., 30: 1-37(1964).

Alpha particles from ^{230}Pa were observed for the first time and an alpha-to-total branching ratio of $4.3 \pm 0.7 \times 10^{-5}$ was measured for this nuclide. New alpha fine structure groups were observed; two of these were assigned to ^{230}Pa, four to ^{218}At, three to ^{226}Pa, two to ^{222}Ac, four to ^{218}Fr, and two to ^{214}At. Previous results on alpha fine structure were confirmed for seven alpha groups of ^{224}Ac, six groups of ^{220}Fr, and one group of ^{216}At. Electron capture decay of ^{226}Pa was observed for the first time and an electron capture-to-total branching ratio of $26 \pm 5\%$ was measured. (auth)

21419 E2/M1 MIXING RATIOS OF $2^+ \rightarrow 2^+$ IN EVEN-EVEN NUCLEI. P. Holmberg and E. Spring (Univ. of Helsinki). Soc. Sci. Fennica, Commentationes Phys.-Math., 30: No. 2, 5-12(1964).

A survey is made of the mixing ratio E2/M1 of $2^+ \rightarrow 2^+$ transitions in even-even nuclei. Within the mass region $52 \leq A \leq 200$, the ratio shows systematic behaviour for the intervals between nuclei with magic neutron numbers. A sine-shaped curve is given fitting the experimental points in the various regions between the neutron numbers 28, 50, 82 and 126. The radiative width is calculated for M1-radiation of the transitions. The values are found to center on $|M|^2 \approx 0.1$ for spherical or nearly spherical nuclei (neutron number near a magic number), $|M|^2 \approx 4 \times 10^{-4}$ for deformed nuclei ($150 \leq A \leq 190$), and $|M|^2 \approx 5 \times 10^{-4}$ for other nuclei. (auth)

21420 INFLUENCE OF INTERMEDIATE VECTOR BOSON ON MUON CAPTURE RATE. M. Koiv, J. Meitre, and L. Palgi. Tr. Inst. Fiz. i Astron., Akad. Nauk Est. SSR, No. 25: 63-9(1964). (In Russian)

Nonlocal corrections due to the intermediate charged vector boson to muon capture in He, H, and C are examined. The results are compared with experimental data. (auth)

21421 POLARIZATION DENSITY MATRIX WITH CONVERSION BETWEEN μ-MESIC ATOM HYPERFINE STRUCTURE STATES. M. Koiv. Tr. Inst. Fiz. i Astron., Akad. Nauk Est. SSR, No. 25, 102-5(1964). (In Russian)

An expression for the density matrix for the polarized state after $(I + \frac{1}{2}) \rightarrow (I - \frac{1}{2})$ conversion with Auger-electron emission, where I is the nuclear spin, is obtained, using the density matrix for the effect of the K-shell hyperfine structure on the muon and nucleus polarization. (M.J.T.)

21422 ANHARMONICITY EFFECT IN THE MÖSSBAUER LINE SHIFT. V. Hizhnyakov. Tr. Inst. Fiz. i Astron., Akad. Nauk Est. SSR, No. 25, 106-8(1964). (In Russian)

The combined effect of the change of nuclear mass after gamma emission and the anharmonicity of lattice oscillations on the Mössbauer effect was studied. The effect of these factors on the position and width of phononless and phonon transitions was calculated. (M.J.T.)

21423 APPROXIMATE CALCULATION OF THE PATH OF RELATIVISTIC ELECTRONS BY THE STOPPING POWER OF MATTER. A. A. Ostroukhov and N. G. Nakhodkin (Kiev State Univ.). Ukr. Fiz. Zh., 9: 1151-3(Oct. 1964). (In Ukrainian)

Simple approximation formulas were developed for calculating electron paths in terms of the stopping power of matter for initial energy in the range of 100 kev $\leq E_{\beta^-} <$ 5 Mev with the order of error not exceeding 2%. (R.V.J.)

21424 ON THE EFFECT OF NUCLEAR BOUNDARY DIFFUSION. E. V. Inopin and A. V. Shebeko (Khar'kov Inst. of Physics and Tech., Academy of Sciences, Ukrainian SSR). Ukr. Fiz. Zh., 9: 1161-4(Nov. 1964). (In Ukrainian)

A method is proposed for taking into account the diffusion of the nuclear boundary which permits obtaining a simple analytical solution and investigating the effect of diffusion on a number of scattering characteristics. An expression is obtained determining the magnitude of the resonance shift in the cross section of scattering of slow neutrons by nuclei, and its role becomes more significant with an increase in the mass of the scattered particles, which agrees with the known facts. (auth)

21425 SCATTERING AMPLITUDES OF CHARGED PARTICLES AT SMALL MOMENTA. Yu. L. Mentkovskii (Inst. of Physics, Kiev). Ukr. Fiz. Zh., 9: 1169-75 (Nov. 1964). (In Ukrainian)

As is known, the partial amplitudes of nuclear Coulomb scattering $S_l(k)$ prove singular at zero. To construct dispersion relations it is, therefore, important to know the

asymptotic of $S_l(k)$ for small k. It is known that on the first Riemann sheet (the upper k-half-plane) $S_l^n(k)$ has the form $\Gamma^2(l + 1 + (ia/2k)) \cdot f_l(k)$ (24), the function $f_l(k)$ being regular at zero. (auth)

21426 INELASTIC SCATTERING OF PROTONS BY Mg^{24} NUCLEI. V. Yu. Storizhko and A. I. Popov (Khar'kov Inst. of Physics and Tech., Academy of Sciences, Ukrainian SSR). Ukr. Fiz. Zh., 9: 1283-5(Dec. 1964). (In Ukrainian)

The differential cross section of the inelastic scattering $^{24}Mg(pp'\gamma)^{24}Mg$ was measured in the range of proton energies from 2000 to 4200 kev. Resonances were observed at energies 2015, 2345, 2415, 2760, 2920, 2970, 3600, 3669, and 4022 kev. A resonance was found for the first time at E_p = 2345 kev. Measurements were made of the angular distributions of γ rays at resonance energies. (auth)

21427 ON DIFFRACTION SCATTERING OF DEUTERONS BY NON-SPHERICAL TRANSLUCENT NUCLEI WITH DIFFUSE FRINGES. E. Ismatov (Inst. of Physics, Kiev). Ukr. Fiz. Zh., 9: 1373-6(Dec. 1964). (In Ukrainian)

The influence of diffuse fringes and nuclear transparency on the angular distribution of elastic and inelastic deuteron scattering by nuclei was studied by means of a diffraction scattering model. Inelastic scattering with excitation of nuclear oscillations was investigated without considering Coulomb interactions. Formulas were developed for inelastic scattering of deuterons on nuclei with diffused fringes. A formula for the diffraction cross section for scattering with the excitation of initial even-even nuclei is given. Scattering of deuterons on ^{27}Mg at 19.6 and 21 Mev was used as an example. Diagrams are given of the angular distributions for elastic and inelastic scattering. (R.V.J.)

21428 RESONANCE ABSORPTION OF γ-QUANTA WITH 23.8-kev ENERGY BY SnO_2 SUSPENSION IN GLYCERINE. V. I. Lisichenko (Dnepropetrovsk State Univ., Ukrainian SSR). Ukr. Fiz. Zh., 9: 1376-8(Dec. 1964). (In Ukrainian)

Resonance absorption of γ quanta with 23.8 kev energy by a SnO_2 suspension in glycerine enriched by ^{118}Sn was measured at temperatures from 300 to 336°K. The Mössbauer spectra indicated that the shape of the resonance absorption line depends on the preparation technology of the suspension. Measurements of a thin suspension showed that the shape and the intensity of the resonance absorption line changed with the duration of the heating. Simultaneously with reduced width and increased intensity there was observed a certain deviation from the Lorentz shape. (R.V.J.)

21429 PRODUCTION OF HYPERFRAGMENTS FROM THE INTERACTIONS OF 3.0 Gev/c K^- MESONS WITH EMULSION NUCLEI K^- COLLABORATION. J. Lemonne, J. Sacton, G. Schorochoff, et al. (Universite Libre, Brussels). Univ. Bruxelles, Inst. Phys., Bull. No. 18, 25p. (Nov. 1964).

The production of hyperfragments by the interactions of mesons(K^-) at 3.0 Bev/c in nuclear emulsion was studied. The observed frequency of production, 3.0 ± 0.1%, is significantly smaller than at lower meson(K^-) momenta, while the range distribution shows a relative increase in the number of hyperfragments of range greater than 5 μm. This increase is attributed to an increased contribution from the fragmentation process. The great majority of hyperfragments of range less than 10 μm are the heavy spallation products of silver and bromine nuclei; their mass numbers differ on the average by about 30 nucleon masses from those of the parent nuclei. Three further examples of the meson(π^-) decays of heavy spallation hyperfragments were observed. (auth)

21430 PULSE METHOD FOR INVESTIGATING NUCLEAR QUADRUPOLE RESONANCE. B. N. Pavlov, I. A. Safin, G. K. Semin, E. I. Fedin, and Ya. D. Shtern. Vestn. Akad. Nauk SSSR, No. 11, 40-3(1964).

The advantages of pulse methods for investigating nuclear quadrupole resonance (NQR) over steady-state methods are discussed. Steady-state methods can be used successfully only for samples with very perfect crystal structure. In these cases the equivalent Q of the line $Q_{eq_0} = (\nu_0/\Delta\nu) \sim 10^1$, where ν_0 is the NQR frequency and $\Delta\nu$ is the line width. Broadening of the NQR line, caused by disorder in the crystal structure leads not only to a decrease in signal amplitude but also to a decrease in sensitivity. The latter is caused by spurious effects with the strong modulations of frequency and magnetic field which are required. As a result, steady-state methods are useless when $Q_{eq_0} \leq 10^3$. However, the sensitivity of a pulse spectrometer remains practically constant with line width, since the initial amplitude of the nuclear induction signal and the maximum amplitude of the quadrupole spin echo signal are proportional to the integral NQR signal intensity and are only slightly dependent on the line width. An expression for the gain in sensitivity of the pulse method over the steady-state method is given. The quadrupole echo signal from ^{75}As in As_2S_3 is shown; this signal is unobserved when using the steady-state method. Examples are also given which show that frequency measurements and resolution using the pulse spectrometer are as good as those obtained using the steady-state spectrometer. (ATD)

21431 CROSS SECTIONS FOR ABSORPTION OF HIGH-ENERGY π^+, K^+ MESONS, AND PROTONS BY C, Al, Cu, Sn, AND Pb NUCLEI. Nai-sen Chang (Univ. of Nankao, China). Wu Li Hsueh Pao, 21: 121-31(Jan. 1965). (In Chinese)

Cross sections for absorption of 2.72-, 3.70-, and 4.75-Bev/c mesons(π^+) by Al, C, Cu, Pb, and Sn nuclei, 4.75-Bev/c mesons(K^+) by Al, C, and Cu nuclei, and 2.75-Bev/c protons by C, Pb, and Sn nuclei were measured. Nuclear radii obtained on the basis of the data on meson(π^+) reactions agreed with the data based on the reactions of low-energy neutron with nuclei but do not agree with the data based on 1.5-Bev meson(π^-) reactions with nuclei. The mean total cross section for interactions of 4.75-Bev/c mesons(K^+) with nucleons based on the optical model for absorption of mesons(K^+) by nuclei was equal to $\bar{\sigma}_{KN}$= 16.5 mb. (tr-auth)

21432 THE α-REDUCED WIDTH OF 1p SHELL NUCLEI. Fan Wang, Chin-chuan Chen, and Shih-yuan Sze (Nanking Univ., China). Wu Li Hsueh Pao, 21: 140-53 (Jan. 1965). (In Chinese)

Using shell model wave functions the α reduced width of some 1p shell nuclei is calculated. From the results of calculation it is noticed that for normal parity levels, the calculated values are in agreement with the experimental values, while for nonnormal parity levels, the calculated values are always much less than the experimental values. This means that at least for describing the nonnormal parity states, shell model wave functions without suitable modification are not sufficient. (auth)

21433 THE (dp) STRIPPING REACTIONS WITH THE TARGET CORE EXCITATION. Sih-tjuen Chiu. Wu Li Hsueh Pao, 21: 208-17(Jan. 1965). (In Chinese)

The (d,p) stripping reactions with the target core excitation are studied. In this case it is assumed that the target nucleus and the residual nucleus contain the conventional shell model configuration and other configurations mixed by the nucleon-nucleon residual interaction. The differential cross section formula is derived for the reaction process based on the above assumption. The formula shows that the contribution to the reaction cross section is mainly due to the configuration mixing of target nucleus. One may expect that the cross section values are rather small, because the admixture in general is weak. The formula also shows that the characteristic peak of the reaction angular distribution is determined by the orbital angular momentum quantum number of the hole state which is created during the core excitation. These two conclusions are consistent with experimental results for this type of reactions. This formula is used to calculate the spectroscopic factors for six reaction events. The theoretical values of the spectroscopic factors, within the experimental errors, agree with those extracted from the experimental data. (auth)

21434 THE INFLUENCES OF PAIRING FORCE ON THE PROPERTIES OF RARE-EARTH NUCLEI. Chin-yen Tseng, Jian-hua Cheng, and Hei-gang Wie (Peking Univ.). Wu Li Hsueh Pao, 21: 266-315(Feb. 1965). (In Chinese)

The various properties of the rare-earth even-even nuclei (intrinsic excitation spectra, β-decay, and even-odd mass differences, etc.) are analyzed with a new method. For this purpose, the single-particle levels have to be determined. It is found that on the basis of Nilsson's level scheme, with suitably chosen parameters μ and κ, the spins and parities of the low-lying intrinsic spectra and the level spacing of odd-A nuclei may be explained, after taking account of the influence of pairing force. The parameters chosen are as follow: $\kappa \sim 0.067-0.072$, $\eta \sim 4-4.6$, $\mu \sim 0.59$(N = 4), $\mu \sim 0.45$(N = 5) for proton, and $\mu \sim 0.40-0.45$(N = 5), $\mu \sim 0.33$(N = 6) for neutron. The variation of the energy eigenvalue induced by the change of parameter μ is estimated with the perturbation method, and the results are close to the exact eigenvalues. The nuclei ^{166}Er, ^{168}Er, ^{170}Yb, ^{172}Yb, ^{174}Yb, ^{176}Hf, ^{182}W, ^{160}Dy, and ^{162}Dy were analyzed. (auth)

21435 ANGULAR DISTRIBUTION OF RESONANTLY SCATTERED γ QUANTA. F. Wittmann (Technische Hochschule, Munich). Z. Naturforsch., 19a: 1409-12(Dec. 1964). (In German)

With the help of the Mössbauer effect, the 129-kev level in ^{191}Ir was excited, and the angular distribution $W(\theta)$ of the scattered radiation was measured. It was $W(\theta) = 1 + (0.85 \pm 0.15)\ P_2(\cos\theta) + (0.02 \pm 0.18)\ P_4(\cos\theta)$. The mixing ratio of M1 and E2 radiation of the transition and the sign of δ was found together with results from Coulomb excitation measurements. (tr-auth)

21436 ENERGY DETERMINATION OF PROTONS FROM RANGE MEASUREMENTS. L. Koschmieder (Universitat, Bonn). Z. Naturforsch., 19a: 1414-16(Dec. 1964). (In German)

A study was made to determine whether the integral range curve could be completely described with use of the empirical constant, the mean ionization energy or whether deviations occur as a result of secondary processes. Electrolytic copper plates were used as absorbers in the experimental study with proton energies at 57.0, 88.9, and 144.3 Mev. The measured and calculated values were compared and agree with each other. Below 60 Mev deviations occur that are larger than the to-be-expected increase of the absorption cross section. A significant effect at the end of the range curve could be established. (J.S.R.)

21437 GENERAL STRUCTURE OF AND SYMPLECTIC SYMMETRY IN $f_{\frac{7}{2}}$ NUCLEI. Joseph Natale Ginocchio. Thesis, Rochester, N. Y., Univ. of Rochester, 1964. 214p.

By using a two-body interaction determined from the best available evidence concerning the $f^2_{\frac{7}{2}}$ system, and assuming pure $f^n_{\frac{7}{2}}$ configurations, the energy spectra, spectroscopic factors, beta decays, and magnetic dipole properties of nuclei in the range of atomic masses $40 < A \leq 56$ are calculated. The basic set of states used have definite isospin, angular momentum, and symplectic symmetry. Coefficients of fractional parentage are calculated in this representation and are used to calculate the nuclear properties. These calculated properties are then compared with the empirical ones. For states lying low in the energy spectrum the agreement is satisfactory and represents a considerable improvement over that given by the simple seniority model. The status of symplectic symmetry (seniority s, reduced isospin t) as a conserved quantum number is then investigated. Ignoring the contribution to the energy dispersion due to the trivial J^2 and T^2 part of the interaction, it is found that 64% of the energy dispersion is due to the symplectic-symmetry-violating part of the interaction as compared to 89% for a pure quadrupole force. Inspection of the wave functions of the j^n system reveals that the weight of a given symplectic representation in the wave function never exceeds 82%, except for the trivial cases in which there is only one symplectic representation allowed. Predominant weights as low as 32% are found. The general conclusion is that deviations of measured quantities from the seniority predictions do not necessarily imply configuration admixing, but might well be explained by models that do not mix configurations but do mix symplectic representations. (Disseration Abstr., 25: No. 5, Nov. 1964)

21438 THE PRODUCTION OF TRITIUM AND HELIUM-3 BY PROTON BOMBARDMENT OF METALS. SOLAR ORIGIN OF TERRESTRIAL TRITIUM. Roger Henry Ide. Thesis, Los Angeles, Univ. of California, 1964. 109p.

Radiochemical analyses of recovered satellites have generated considerable interest in nuclear reactions initiated by relatively low-energy (<150-Mev) solar protons. Of particular interest are the results obtained for the Discoverer XVII satellite, which was in orbit during the intense solar flare of November 12, 1960. The amounts of tritium and helium-3 found in portions of the recovered satellite appear to be one and two orders of magnitude too large respectively to be explained as products of reactions induced by solar protons. The fact that the helium-3 content was roughly ten times that of tritium is especially interesting, since proton-induced nuclear reactions were expected to produce roughly equal amounts of these two isotopes. In order to help explain these results, measurements of the cross sections for the production of tritium and helium-3, and especially of the ratio of these cross sections, for proton energies in the vicinity of 30–50 Mev were desired. Accordingly, targets of aluminum and iron were bombarded with 30–45 Mev protons. Each target was then split, and the relative gross gamma activity of the two portions was determined. One portion of each target, together with blanks of the target materials, was then exposed to a thermal neutron flux of about 5×10^{19} n/cm^2. The tritium content of all the samples was determined by a system of vacuum extraction and gas counting. The results indicate that the ratio $\sigma_{He^3}/\sigma_{H^3}$ for bombardment of both aluminum and iron with 35–50 Mev protons lies in the range 0.8–1.5. The results conclusively show that the tritium and helium-3 in Discoverer XVII were not produced by solar protons. (A.G.W.)

21439 $C^{12}(d,p)C^{13}$: DISTORTED WAVE BORN APPROXIMATION ANALYSIS OF PROTON ANGULAR DISTRIBUTION AND PROTON–GAMMA ANGULAR CORRELATIONS. David George Gerke. Thesis, Durham, N. C., Duke Univ., 1964. 115p.

DWBA fits were made to existing $^{12}C(d,p_{2,3})^{13}C$ proton angular distribution and proton–gamma angular correlation data. The optical model potentials used in the distorted wave calculations were found by fitting $^{12}C(d,d)^{12}C$ and $^{13}C(p,p)^{13}C$ angular distributions measured at the appropriate energies. The results of the DWBA analysis were also compared with the predictions of the Butler theory. Bombarding energies of 2.8, 3.2, and 3.7 Mev were used during the $^{12}C(d,d)^{12}C$ measurements. The $^{13}C(p,p)^{13}C$ measurements were made at energies of 1.365, 1.548, 1.734, 1.917, 2.195, and 2.378 Mev. In addition to the elastic scattering angular distributions, $^{12}C(d,d)$, (d,p_0), (d,p_1), (d,p_2), and (d,p_3) yield curves were measured between 2.6 and 4.0 Mev at laboratory angles of 30° and 90°. The DWBA fits to the stripping angular distribution data are better than the Butler fits. Absolute reduced widths of 0.21 ± 0.05 and 1.03 ± 0.25 single particle units were found for the transitions to the second and third excited states of ^{13}C respectively. The DWBA fits to the angular correlation parameters reproduced the trend of the data much better than the Butler curves but are not in quantative agreement with the data. The anomalies observed in the elastic deuterium and reaction product yield curves show considerable correlation, which indicates that compound nucleus effects are present at the energies used in this work. (Dissertation Abstr., 25: No. 5, Nov. 1964)

21440 STABILITY OF THE HARTREE-FOCK APPROXIMATION IN NUCLEAR MATTER. Chindhu Sona Warke. Thesis, San Diego, Calif., Univ. of California, 1964. 129p.

The equivalence of the collective oscillation and Fermi-sphere deformation approaches for the determination of the stability conditions of the plane-wave Hartree-Fock

state is shown. The merits and demerits of each method are pointed out. An attempt is made to give the physical interpretation of each unstable mode of collective oscillation with the use of this equivalence. The tensor force interaction is put to test for the stability of the plane-wave Hartree-Fock state. It is found that the plane-wave Hartree-Fock state is stable, both in low as well as in the high density region; however, it becomes unstable in the intermediate density region, in the neighborhood of p_f^{-1} approximately equal to the range of the interaction. The formal Overhauser solution is derived in this case, and it is found that the single-particle energy is not spherically symmetric. It is shown that in small |q| (collective excitation momentum) approximation, the stability conditions do not depend on the shape of the potential. It is found that for a finite range repulsive interaction (in the small |q| approximation) the longer tail potential favors the Hartree-Fock instability in the high-density region, while the shorter tail potential favors the Hartree-Fock instability in the low-density region. A discussion about the choice of the collective excitation momentum |q| is given. An attempt is made to study the temperature effect on the stability condition. It is found that, as the temperature is increased, the unstable region decreases as it should. The general derivation of the stability conditions, in the |q| approximation, is given in the Appendices. Starting from the Brueckner-Goldstone ground-state energy, some physical quantities which are related to stability are also derived in the Appendices. (Dissertation Abstr., 25: No. 5, Nov. 1964)

21441 ELASTIC AND INELASTIC SCATTERING OF 14 Mev NEUTRONS BY C^{12}, Si^{28}, AND O^{16}. H. Aichinger. Thesis, Erlangen-Nuremburg, Universitat, 1963. 49p. $2.00(Gmelin, AED-DISS. 63-719). (In German)

Design and construction of an apparatus for the measurement of scattering cross sections for 14-Mev neutrons are described. Results of a nuclear resonance fluorescence experiment using the 4.43-Mev level of ^{12}C are given. Theoretical data disagree with experimental results indicating that scattering of ^{12}C plays an important role. Cross sections for inelastic and elastic scattering by ^{28}Si and ^{16}O are given. (Gmelin Inst.)

21442 THE ONE PARTICLE RADIATION TRANSITIONS IN THE OPTICAL MODEL OF THE NUCLEUS. K. Urankar. Thesis, Munich, Universitat, 1963. 64p. $2.00(Gmelin, AED-DISS. 63-721). (In German)

Theoretical expressions for proton capture cross sections including Coulomb interaction are given. Interaction in the interior of the nucleus is described by a complex potential. Radiation transition cross sections are computed using the distorted wave approximation. Calculated cross sections of ^{60}Ni for proton energies between 10 and 20 Mev are lower than experimental data. (Gmelin Inst.)

21443 THE EMISSION OF DELAYED NEUTRONS IN NUCLEAR FISSION. H. J. V. Fiedler. Thesis, Mainz, Universitat, 1963. 140p. $2.00(Gmelin, AED-DISS. 63-739). (In German)

Delayed-neutron data are reviewed. Yields of delayed neutrons for various fission processes are explained by cumulated fission yields of the known precursors. Yields of the first 4 delayed neutron groups for low-energy fission are in agreement with calculations based on the fission yields of halogen precursors. Neutron yields in ^{232}Th fission with neutron energies between 3 and 14 Mev were measured. (Gmelin Inst.)

21444 GRUPPENTHEORETISCHE METHODEN IM SCHALENMODELL DER KERNE. TEIL I. (Group Theoretical Methods in Shell Models of the Nucleus. Part I.). Guenter Flach and Roland Reif. Berlin, Akademie-Verlag, 1964. 239p.

The principles of the modern representation of the shell model of the nucleus are presented for physicists and mathematicians. Only introductory group theoretical methods are treated. The shell model of the nucleus, group theoretical principles, abstract groups, representation theory, and symmetrical groups and their irreducible representation, the classical Lie groups and their representation, the character of the irreducible representations, and products and limitation to subgroups are discussed. (J.S.R.)

21445 FISSION PRODUCT YIELDS AND THEIR MASS DISTRIBUTION. Yu. A. Zysin, A. A. Lbov, and L. I. Sel'chenkov. Authorized Translation from the Russian. Translated from "Vykhody Produktov Deleniya i Ikh Raspredelenie po Massam." New York, Consultants Bureau, 1964. 124p.

This book was previously abstracted from the original language, NSA 18: 9439. (M.C.G.)

21446 PROTONS RESONANCES IN INTERMEDIATE NUCLEI. Granvil Charles Kyker, Jr. Thesis, Durham, N. C., Duke Univ., 1964. 149p.

The yield of the deexcitation gamma ray following inelastic proton scattering to the first excited states of ^{46}Ti, ^{48}Ti, ^{50}Cr, ^{54}Fe, and ^{56}Fe was studied for proton energies between 2.5 and 3 Mev with energy resolution of approximately 700 ev. For all targets except ^{54}Fe, angular distributions of the gamma-ray yield were measured as a means of assigning spins and parities to resonances observed in the excitation functions. A total of approximately 160 resonances were observed and assigned in this way. Results showed the first excited state of ^{50}Cr to have spin 2. In addition, the spacings of $5/2^+$ levels in the compound nuclei ^{47}V, ^{51}Mn, and ^{57}Co are consistent with the dependences on neutron excess and shell structure observed in neutron total cross section measurements. There are also indications of a maximum in the D-wave proton strength function in the neighborhood of mass number 47. Finally, the shape of the observed resonances was compared with the prediction of the straggling theory of Symon, and the agreement between the data and the theory is quite good. (Dissertation Abstr., 25: No. 5, Nov. 1964)

21447 PROTON POLARIZATION IN THE $Sr^{88}(d,p)Sr^{89}$ REACTION. Edward James Ludwig. Thesis, Bloomington, Ind., Indiana Univ., 1964. 141p.

The polarization of protons emitted from the $^{88}Sr(d,p)$ $^{89*}Sr_{1.04Mev}$ reaction was measured at 14 laboratory scattering angles using 11-Mev incident deuterons. The deuteron beam from the Indiana University Cyclotron bombarded a thick strontium target centered in a 16" scattering chamber. A heavy-particle magnetic spectrometer was used to select the desired proton group from the (d,p) reaction, while a carbon polarimeter "analyzed" the polarization of protons in the group. The measured polarization angular distribution verifies the importance of including spin-orbit terms in the optical-model potential. In addition, it appears to be in agreement with the "derivative relation," which has been applied to deuteron stripping reactions with zero orbital angular momentum transfer by Biedenharn and Satchler (Bi 61). The fact that this relation has failed to apply to polarization angular distributions taken at other laboratories for similar reactions in lighter elements suggests that heavier elements may be more useful for investigating spin-orbit contributions to the optical-model potential. Successful attempts have been made by Satchler at Oak Ridge to extract a consistent set of proton and deuteron optical-model parameters from theoretical fits to the elastic-deuteron data of the present experiment and the (d,p) angular distribution data of Preston et al. Spin-orbit terms were added to the optical potentials obtained in this way to attempt an analysis of the proton polarization distribution. Preliminary attempts to fit the data have already indicated that the sign of the spin-orbit potentials are in agreement with those used in shell-model calculations and in theoretical analyses of elastic proton scattering data. (Dissertation Abstr., 25: No. 5, Nov. 1964)

21448 THEORETICAL CONSIDERATIONS OF THE INVESTIGATION OF NUCLEAR STRUCTURE BY INELASTIC ELECTRON SCATTERING. John Terrence Reynolds. Thesis, Durham, N. C., Duke Univ., 1964, 178p.

The problem of the inelastic scattering of electrons by nuclei is approached by using a distorted partial-wave de-

scription of the initial and final electron states and a multipole expansion of the interaction with the nucleus. General cross section formulas are derived and the evaluation of these is reduced essentially to evaluating radial integrals involving the partial-wave components of the electron wave functions and the nuclear transition charge and current densities. An important feature of the present method is to display that those integrals corresponding to partial waves that do not appreciably penetrate the nuclear charge distribution can be approximated by the corresponding integrals for a point nucleus, and moreover, that these integrals have a closed analytic form. The contribution of those partial waves that do penetrate is found by numerical evaluation of the various matrix elements using electron wave functions obtained by numerical integration of the radial part of the Dirac equation for a central field. An extensive analysis of experimental data using a phenomenological vibrator model of the nucleus shows that the observed cross sections can be accounted for by a pronounced peak in the transition charge density at the nuclear surface and that this shape can be simply related to the ground state charge density. A detailed analysis of the range of validity of the plane-wave Born approximation shows that it is grossly inadequate for analyzing data at angles past the first diffraction minimum, but it may be improved for analyzing forward angle scattering by changing the effective radius of the nucleus to partially correct for the distortion effects. Calculations based on the shell model with residual pairing and long range forces are performed and it is shown how excited nuclear states may be identified in terms of this model and how the strengths of the residual interactions may be deduced. It is also demonstrated how situations can occur, in which deductions about the detailed structure of the single-particle energy levels may be made. (Dissertation Abstr., 25: No. 5, Nov. 1964)

21449 L/K X-RAY INTENSITY RATIO IN THE DECAY OF Tl^{204} AND L-SHELL FLUORESCENCE YIELDS OF Hg. Pemmaraju Venugopala Rao. Thesis, Eugene, Ore., Univ. of Oregon, 1964. 65p.

The Hg L/K x-ray intensity ratio in the decay of ^{204}Tl was determined with proportional and scintillation counters, using Ag K x rays for intercomparison of detector efficiencies. Beta rays were stopped before entering the detectors. The shape of the bremsstrahlung spectrum under the x-ray peaks was determined with ^{36}Cl beta rays. The result is $I_L/I_K = 0.52 \pm 0.02$. The mean L-fluorescence yield of Hg following electron-capture decay of ^{204}Tl then is $\bar{\omega}_L = 0.40 \pm 0.05$. The partial L-shell fluorescence yield of Hg following K_α x-ray emission was measured as $\omega_{KL} = 0.41 \pm 0.02$ from K and L x-ray coincidences. The partial L-shell fluorescence yield of Hg following L capture only of ^{204}Tl is $\omega_{LL} = 0.39 \pm 0.06$, as determined by the same method. Subshell fluorescence yields $\omega_{LII} = 0.55 \pm 0.06$ and $\omega_{LIII} = 0.33 \pm 0.03$ were found. The relationship of these fluorescence yields to each other and to Coster-Kronig transition probabilities is discussed. The close agreement between $\bar{\omega}_L$ and ω_{KL} confirms that, in the region about Z = 80, precise L-shell fluorescence yields obtainable by x-ray coincidence measurements can be used to derive electron capture ratios from x-ray intensity ratios. (Dissertation Abstr., 25: No. 5, Nov. 1964)

21450 LEVEL SCHEMES OF Ga^{69}, I^{129}, AND Sb^{119}. Akunuri Venkata Ramayya. Thesis, Bloomington, Ind., Indiana Univ., 1964. 122p.

The decay of ^{69}Ge(38.5 ± 0.5hr) to the levels in ^{69}Ga was investigated by means of beta-gamma, and gamma-gamma coincidence and the sum peak techniques. Gamma rays of energies 240, 260, 300, 323, 420, 576, 770, 800, 880, 1065, 1120, 1220, 1355, 1560, 1910, and 2040 kev were found to depopulate the levels at 0, 323, 576, 880, 1120, 1340, 1540, 1880, 1910, 1945, 2040 kev. The beta-ray feedings and the log ft values were calculated. A decay scheme consistent with the experimental results is presented. Spins are assigned to some of the levels. The decay of 33d ^{129m}Te to the levels in ^{129}I was studied by the same techniques. Gamma rays were observed at 27, 120, 210, 250, 280, 335, 465, 550, 635, 690, 710, 820, 980, 1045, 1100, and 1255 kev. The analysis of the coincidence spectra suggests that the 210-, 280-, and 820-kev gamma rays are each composed of two transitions of nearly the same energies. Levels were constructed at 27, 280, 492, 570, 710, 840, 1045, 1127, 1255, and 1400 kev. The log ft values were calculated. The ratio of the intensity of the isomeric transition to that of the total decay from ^{129m}Te calculated from the beta-ray feedings was 71%. Some of the experimentally observed levels are compared with the theoretically calculated levels. In the case of ^{119}Sb, the 153-1220 kev and 270-2090 kev gamma-gamma angular correlations are measured. The directional correlation coefficients for the 153-1220 kev gamma rays are $A_2 = -0.069 \pm 0.005$ and $A_4 = 0.002 \pm 0.005$. The spins of $^{11}/_2$, $^{9}/_2$, $^{7}/_2$, and $^{5}/_2$ are assigned to the 1.37, 1.22, 0.27, and 0 Mev levels respectively. It is concluded that the 153- and 1220-kev transitions are pure dipole radiations. The angular correlation coefficients for the 270-2090 kev gamma rays are $A_2 = 0.083 \pm 0.015$ and $A_4 = 0.012 \pm 0.015$. The 2.37-Mev level is assigned to the spin of $^{11}/_2$. Assuming 2090-kev transition is pure E2 the 270-kev transition is found to be a mixture of M1 and E2. (Dissertation Abstr., 25: No. 5, Nov. 1964)

21451 MEASUREMENT AND SHELL MODEL INTERPRETATION OF THE LOW-LYING NUCLEAR ENERGY LEVELS OF NIOBIUM-92. Richard Franklyn Sweet. Thesis, Austin, Tex., Univ. of Texas, 1964. 103p.

The levels of ^{92}Nb were studied with the 22-Mev proton beam of the Oak Ridge 86-inch cyclotron by means of the $^{93}Nb(p,d)^{92}Nb$ reaction. The deuterons are detected with a magnetic analysis system having an overall resolution of about 30 kev for deuterons of this energy. The energies of the observed levels are 0, 137, 289, 360, and 492 kev. Only five of the expected six levels are observed, but since the level at 492 kev is about twice the half-width of the other four levels, it is apparently not a single level. The next group of levels excited by this reaction is at an excitation of about 3 Mev. Explicit calculations of the energy levels arising from the coupling of a $g_{9/2}$ proton to a $d_{5/2}$ neutron have been performed by de-Shalit using a zero-range interaction, and by Kim using a finite-range interaction. A comparison of the level spacings with the results of de-Shalit suggests a spin sequence of either 7, 2, 5, 3, 4, 6, or 2, 7, 5, 3, 4, 6. The results of Kim suggest a sequence of 7, 2, 5, 3, 4, 6 with the spin 7 and 2 levels very close together. The correct spin sequence among various assumed sequences can be found by comparison of theoretical and experimental spectroscopic factors. As expected from de-Shalit and Kim's results, the sequence 7, 2, 5, 3, 4, 6 for the ^{92}Nb levels gives excellent agreement, as does the 7, 2, 5, 3, 6, 4 assignment, while all other assignments yield considerably poorer results. The conclusion, therefore, is that the energies, spins and parities of the low-lying levels of ^{92}Nb are: 0 kev (7+), 137 kev (2+), 289 kev (5+), 360 kev (3+), and 492 kev (4+, 6+). A.G.W.)

21452 NUCLEAR PAIR-CORRELATION FUNCTION VIA ELECTRON SCATTERING. Yogendra Narain Srivastava. Thesis, Bloomington, Ind., Indiana Univ., 1964. 61p.

A theoretical analysis is made of the differential cross section for the process of inelastic scattering of electrons by a nucleus accompanied by the emission of two nucleons. The analysis is two-fold. First, assuming a purely EM interaction and invoking closure and impulse approximations, the above cross section is seen to be proportional to the Fourier transform of the nucleon-nucleon correlation function in the nucleus. Secondly, following a physical idea due to Gottfried and employed in a similar context, the nuclear cross section is compared to that of the electrodisintegration of a deuteron. This has the advantage that it eliminates the need to introduce an explicit Hamiltonian (as in the first case), and also it allows the inclusion of some very important mesonic effects due to the virtual pion exchange between the two outgoing nucleons. The cross section, which is rather low, is shown to be within the reach of the present experimental techniques. Detailed kinematical

questions are explored and the optimal experimental setup indicated. The corrections due to final state interactions and real-meson production channels are also discussed. (Dissertation Abstr., 25: No. 5, Nov. 1964)

21453 CIRCULAR POLARIZATION OF EXTERNAL BREMSSTRAHLUNG PRODUCED BY BETA RAYS FROM Bi^{210}. Mary Elizabeth Cunningham. Thesis, Eugene, Ore., Univ. of Oregon, 1964. 112p.

The degree of circular polarization of bremsstrahlung produced in lead by ^{210}Bi beta rays was measured as a function of photon energy from 285 to 851 kev. The polarization was determined by Compton scattering of the bremsstrahlung photons through an average angle of 51° from a 30-cm ID hollow cylinder of Armco magnetic ingot iron. The scatterer was magnetized to saturation, and the field was reversed every 5 minutes. The results are consistent with a beta-particle longitudinal polarization of -0.71 (v/c) over the entire energy range. This value is in agreement with the electron scattering measurements by Ullman, et al., made at energies above 600 kev, and also with the electron scattering measurements of Alikhanov, et al., and of Harmsen and Holm, covering lower energies. (Dissertation Abstr., 25: No. 5, Nov. 1964)

21454 NEUTRON RESONANCES IN THE NICKEL ISOTOPES AND OTHER INTERMEDIATE NUCLEI. John Alden Farrell. Thesis, Durham, N. C., Duke Univ., 1964. 95p.

High-resolution neutron total cross sections of separated isotopes of ^{42}Ca, ^{44}Ca, ^{50}Cr, ^{54}Cr, ^{58}Ni, ^{60}Ni, ^{62}Ni, and ^{64}Ni were measured using the ^{7}Li (p,n)^{7}Be reaction as the source of neutrons. The data were fitted with a multilevel formula derived from the R matrix formalism. Widths were obtained for all recognizable s-wave resonances and a few of the widest p-wave resonances. The distributions of the reduced widths and local spacings of the s-wave resonances were found to be in good agreement with the respective Porter-Thomas and Wigner distributions. The average s-wave level spacings were corrected to an excitation energy of 6 Mev and combined with data for other nuclei in this region in order to compare the behavior of the average level spacings with the predictions of various shell models. Reasonably good agreement with both the Rosensweig model and the model of Newson and Duncan if it is assumed that, at the excitation energies involved, a major shell is closed at 16 nucleons instead of 20. The data indicate that a dependence of the average level spacing on neutron excess exists but that it probably is not a simple exponential. (Dissertation Abstr., 25: No. 5, Nov. 1964)

21455 NUCLEAR EXCITATION BY 1 Mev TO 3 Mev ELECTRONS. Benson Tilbert Chertok. Thesis, Boston Univ., 1964. 125p.

The Robl theory of nuclear excitation by low-energy electrons was experimentally tested and the experimental possibilities and limitations of using low-energy electron scattering for measuring lifetimes and multipolarities of nuclear electromagnetic transitions were investigated. Two separate experiments were performed: one was electron scattering from a low-Z nucleus, ^{7}Li, and the other was both electron and photon scattering from a high-Z nucleus, ^{115}In. The ^{7}Li experiment satisfied all of the criteria used by Robl, but in the ^{115}In experiment the criterion of $Z/137 \beta \ll 1$ was not satisfied. The differential cross section for inelastic electron scattering from ^{7}Li agrees with Robl's prediction. The results of the electron excitation of ^{115}In are in serious disagreement with the theory. The experimental excitation function is a factor of six larger than theory at 10 per cent above the threshold and 3.5 larger than theory at 30 per cent above threshold. The disagreement is believed to be primarily due to the breakdown of the Born approximation. When the theory is corrected by multiplying the Dirac plane waves by the nuclear Coulomb factor F(Z,p), there is excellent agreement between the experimental and theoretical excitation functions for the 1.07-Mev level of ^{115}In. This correction is made by using the nuclear Coulomb function for both the incident and scattered electron wave functions. If the Robl theory with the distorted wave correction is adequate to describe high-Z experiments, then a new tool has been developed for assigning multipolarities to nuclear transitions that have a finite branching ratio, both to the isomer and ground levels. (Dissertation Abstr., 25: No. 5, Nov. 1964)

21456 A SPARK CHAMBER MEASUREMENT OF THE POLARIZATION OF HIGH-ENERGY PHOTOPROTONS FROM DEUTERIUM, LITHIUM, AND CARBON. Thomas Otis White, Jr. Thesis, Lafayette, Ind., Purdue Univ., 1964. 76p.

The polarization of photoprotons from deuterium, lithium, and carbon was measured by means of a carbon-plate spark chamber polarimeter at 58° in the laboratory system. The photon source was the bremsstrahlung from the Purdue synchrotron operating at a peak energy of 310 Mev. The protons whose tracks were observed were produced with energies between 155 and 179 Mev. The scanning and measurement of about 225,000 photographs yielded about 1500 acceptable scattering events for each target element. Event reconstruction and polarization calculations were carried out using programs for the IBM 7090 computer. The polarizations were found to be $-.10 \pm .17$, $-.15 \pm .12$, and $-.18 \pm .16$ for deuterium, lithium, and carbon respectively. A comparison is made in terms of other experimental results and existing theory. (Dissertation Abstr., 25: No. 5, Nov. 1964)

21457 ALPHA–GAMMA ANGULAR CORRELATION STUDIES OF THE REACTIONS $Si^{28}(\alpha,\alpha')Si^{28}_{1.77}(\gamma)Si^{28}$ AND $O^{16}(\alpha,\alpha')O^{6}_{6.13}(\gamma)O^{16}$. Donald Errol Blatchley. Thesis, Bloomington, Ind., Indiana Univ., 1964. 95p.

The 22.5-Mev alpha-particle beam from the Indiana University cyclotron was used in conjunction with standard fast-slow coincidence techniques to study angular correlations between inelastically scattered alpha particles and de-excitation gamma rays in the reactions $^{28}Si(\alpha,\alpha')^{28}Si_{1.77}(\gamma)^{28}Si$ and $^{16}O(\alpha,\alpha')^{16}O_{6.13}(\gamma)^{16}O$. The predictions for these two angular correlations are discussed in terms of simple direct-reaction theories. A direct reaction will single out a specific recoil direction for the target nucleus, and this recoil direction serves as an axis of symmetry for the subsequent gamma-ray correlation pattern. The plane-wave Born approximation predicts that the symmetry axis lies along the actual nuclear recoil direction; the adiabatic approximation predicts that the recoil direction for elastic scattering will serve as the symmetry axis. The experimental data from both of the reactions studied are found to disagree with these predictions. The results of three distorted-wave Born approximation (DWBA) calculations on the ^{28}Si reaction are presented. These results show that the DWBA prediction for the angular correlation behavior is strongly dependent on the optical model parameters used in the distorted-wave calculation. Only one of the three sets of optical model parameters is found to be consistent with the experimental data, and this consistency only holds for scattering angles less than 80° (cms). (Dissertation Abstr., 25: No. 5, Nov. 1964)

21458 SOME NUCLEAR REACTIONS OF Cu^{63} WITH 60 TO 420-Mev PROTONS. Virginia Bayard Fonda Caress. Thesis, Rochester, N. Y., Univ. of Rochester, 1964. 95p.

The $^{63}Cu(p,p2n)^{61}Cu$, $^{63}Cu(p,3p)^{61}Co$, and $^{63}Cu(p,2n)^{62}Zn$ absolute cross sections were measured using protons of 60-420 Mev in energy. In addition, the theoretical values of these cross sections and of the $^{63}Cu(p,3n)^{61}Zn$ reaction cross section were calculated using cascade-evaporation calculations based on the Serber model of a nuclear reaction. The ^{61}Cu and ^{61}Co excitation functions and the ratios $\sigma\,^{61}Cu/\sigma\,^{61}Co$ were compared with the theoretical predictions. The experimental ^{61}Cu excitation function agreed very well with the calculated curve above 150 Mev; however, below this point the calculated cross section values were slightly low. It was suggested that the disagreement below 150 Mev might be attributed to the fact that the Monte Carlo cascade calculations did not include a diffuse edge for the nucleus nor refraction effects, or to the fact that the experimental curve included contributions from the (p,t) evaporation and pickup reactions and the (p,d) pickup reaction followed by neutron evaporation. The agreement

between the experimental and calculated ^{61}Co excitation functions was not as good as for ^{61}Cu. The experimental ^{61}Co curve was flat up to about 250 Mev, and then rose. The theoretical curve was lower than the experimental curve and remained flat. The calculations indicated that above 250 Mev the dominant process producing ^{61}Co was the direct knock out of three protons. It was proposed that this direct reaction process was causing the rise in the experimental curve, but that the calculations did not appear to give enough weight to it. The experimental and theoretical ratios, $\sigma\,^{61}\text{Cu}/\sigma\,^{61}\text{Co}$, were in agreement over the entire range of incident proton energies. The ratios showed that the cross section for ^{61}Cu was greater than that for ^{61}Co at all energies. (Dissertation Abstr., 25: No. 5, Nov. 1964)

21459 ELASTIC AND INELASTIC SCATTERING OF ALPHA PARTICLES BY Fe^{56}, Zn^{64}, Zn^{66}, AND Zn^{68}. Howard Lynn Wilson. Thesis, Bloomington, Ind., Indiana Univ., 1964. 123p.

Angular distributions for elastic scattering and for inelastic scattering to the lowest 2^+ and 3^- states in ^{56}Fe, ^{64}Zn, ^{66}Zn, and ^{68}Zn were obtained using 22.2-Mev alpha particles. The elastic distributions extend from 20° to 167° while the 2^+ distributions go from 30° to 167°. In ^{56}Fe the 3^- distribution extends from 30° to 107° whereas for the Zn isotopes the range is from 60° to 167°. The characteristics of these distributions suggest that the reaction is direct in nature. The optical model was used to fit the elastic distributions and the parameters thus found were used in fitting the 2^+ distributions with the distorted-wave Born approximation (DWBA). Although three values of V_0 were found that would fit the elastic distributions (for $\theta \gtrsim 125°$), viz., $V_0 = -20, -40, -70$ Mev, it was found that only for $V_0 = -20$ Mev could good fits also be obtained for the 2^+ distributions. For $\theta \gtrsim 125°$ the fits were found to be quite poor. Two suggestions are proposed to explain the failure of the theory at such large scattering angles. As a check on the DWBA, a coupled channels calculation was done on ^{64}Zn with $V_0 = -20$ Mev in which the ground state and first excited state were coupled together. The results were found to agree very well with those of the DWBA. (Dissertation Abstr., 25: No. 5, Nov. 1964)

21460 RADIOACTIVE DECAYS OF Fe^{59}, Nb^{95}, AND Ca^{47} WITH EMPHASIS ON THE UNUSUALLY FAST, NON-UNIQUE TWICE-FORBIDDEN BETA TRANSITIONS. Donald Eugene Wortman. Thesis, Bloomington, Ind., Indiana Univ., 1964. 92p.

The study of the decay of ^{59}Fe indicated that the highest energy beta group results from 0.30% of the decays and has an end point energy of 1.573 ± 0.003 Mev. The experimental data could be fitted with a shape factor $p^2 + 3.3\,q^2$, which is consistent in form with that expected for a twice-forbidden $\Delta I = 2$, no transition. The comparative half life is relatively short. The two more intense beta transitions are 0.475 ± 0.003 Mev, 51.2%, log ft = 6.74 and 0.273 ± 0.005 Mev, 48.5%, log ft = 5.92. The study of the decay of ^{95}Nb likewise yielded a very low relative intensity and short comparative half life for the highest energy group. It was found that the 0.924-Mev beta group has an abundance of no more than 0.075% (log ft ≥ 10.8 rather than 9.7). The very low intensity does not permit a definitive shape measurement. The main decay is by a (159.7 ± 0.5)-kev beta transition followed by a (764.5 ± 0.5)-kev gamma ray with a K/(L + M) internal conversion ratio of 7.5 ± 0.1 and $\alpha_k = (1.1 \pm 0.1) \times 10^{-3}$. The investigation of the beta-ray spectrum of ^{47}Ca indicated that the highest energy transition to the ground state of ^{47}Sc does not have a unique shape, and therefore a $\frac{3}{2}^+$ assignment to the ground state of ^{47}Ca is not possible. The ground state to ground state transition is probably from a $\frac{7}{2}^-$ initial to a $\frac{7}{2}^-$ final state. Evidence was found for a beta transition to the first excited state of ^{47}Sc, which appears to be a twice-forbidden transition from $\frac{7}{2}^-$ to $\frac{3}{2}^-$ with an energy of 1.486 ± 0.005 Mev and an intensity of 1.3-1.8%. The comparative half life for this $\Delta I = 2$, no transition is also relatively short with log ft = 9.0. The beta transition to the second excited state of ^{47}Sc is 0.671 ± 0.010 Mev, 82.4%, and log ft = 6.0. The observations are consistent with an assignment $\frac{7}{2}^-$ to $\frac{5}{2}^-$. The energies of the three gamma rays that follow the decay of ^{47}Ca were found to be 1.308 ± 0.005, 0.815 ± 0.005, and 0.493 ± 0.010 Mev. The half life for the beta decay was found to be 4.7 ± 0.1 days. (Dissertation Abstr., 25: No. 5, Nov. 1964)

21461 A SOLUTION TO THE RELATIVISTIC DISPERSION RELATIONS OF PHOTOPRODUCTION ACCORDING TO THE METHODS OF OMNES. Paul Finkler. Thesis, Lafayette, Ind., Purdue Univ., 1964. 127p.

The 3-3 photoproduction partial wave amplitudes are determined by means of a modified Omnès solution for the singular integral equations under the assumption that inelastic effects are negligible. The method requires a knowledge of the unknown high-energy phases taken into account by means of a construction that simulates their effect on the low-energy scattering amplitudes. A modified Chew-Low type effective range formula is derived, which should satisfactorily represent the 3-3 amplitude throughout the region of the giant resonance. A formula is derived for computing the non-singular integrals appearing in the invariant amplitudes. Finally, the formulas used for calculating the cross sections are displayed and the results are compared with experiments. (Dissertation Abstr., 25: No. 5, Nov. 1964)

21462 INTERPRETATION OF NMR SPECTRA. AN EMPIRICAL APPROACH. Roy H. Bible, Jr. New York, Plenum Press, 1965. 156p. $12.50.

It is proposed to teach the organic chemist how to interpret proton magnetic resonance spectra, and to provide reference data needed in the use of proton spectra. Discussions are given of first-order spin patterns, coupling of protons with other nuclei, nonequivalence of protons, higher-order spin patterns and multiple resonance, and complications in spectrum interpretation. A systematic approach to NMR spectrum interpretation is described, and suggested operating procedure for the Varian A-60 NMR spectrometer is considered. (M.J.T.)

21463 CONTEMPORARY MODELS OF THE ATOMIC NUCLEUS. P. E. Nemirovskii. A Pergamon Press Book. Translation by S. [Nikolic] and M. Nikolic of "Sovremennye Modeli Atomnogo Yadra." New York, The Macmillan Company, 1963. 340p.

Basic nuclear properties—spin-parity, magnetic and electric moments, isospin, and nuclear size and shape—are reviewed. Descriptions of nuclei using the shell model, the unified or collective model, and the optical model are presented, based on previous works. A theoretical analysis of the shell model is given, considering the connection between the optical and shell model, many-particle configurations, and the stripping reaction. Radiative transitions and alpha decay are discussed in terms of the shell and unified models. 390 references. (M.J.T.)

21464 CALCULATED FAST NEUTRON CAPTURE CROSS SECTIONS FOR Ta^{181}, W, W^{182}, W^{183}, W^{184}, W^{186}. A. Prince. 17p. (CONF-654-72)

From American Nuclear Society Meeting, San Francisco, Nov.-Dec. 1964.

The results of calculations of fast neutron capture cross sections of ^{181}Ta and the four main isotopes of tungsten in the energy range of 1 to 200 kev are presented. The method of analysis is similar to that of Lane and Lynn in which the detailed formulation for the contributions to the capture from the various partial neutron waves are provided by low-energy resonance data. (auth)

Plasma Physics and Thermonuclear Processes

Refer also to abstracts 20755, 20783, 20905, and 21289.

21465 (AFCRL-63-779) THE HYDROMAGNETIC WAVE TUBE. Instrumentation for Geophysics and Astrophysics No. 30. Randall E. Murphy and Marshall H.

Bruce (Air Force Cambridge Research Labs., L. G. Hanscom Field, Mass.). Nov. 1963. 20p. (AD-424939) $2.60(OTS).

An experimental study of the production of magnethydrodynamic waves is reported. This investigation attempts to experimentally answer the questions of energy coupling, modes of propagation, and to explore the possibility of cross modulation between electromagnetic and hydromagnetic waves. A laboratory device, called the Hydromagnetic Wave Tube, was constructed to accomplish this program. The physical construction of this device is outlined and a theoretical analysis of the anticipated ionization characteristics is presented. (auth)

21466 (AFCRL-64-550) TRANSIENT REFLECTION AND TRANSMISSION OF A PLANE WAVE NORMALLY INCIDENT UPON A SEMI-INFINITE ANISOTROPIC PLASMA. Physical Sciences Research Papers No. 33. Carl T. Case (Air Force Cambridge Research Labs., L. G. Hanscom Field, Mass.). July 1964. 44p. (AD-606559). $2.00(CFSTI).

General solutions for the transmitted and reflected waves in integral form are obtained for a plane wave of arbitrary time dependence, normally incident upon a semi-infinite, cold, collisionless, homogeneous, anisotropic, ionized medium. The special case of an isotropic plasma with an incident wave of harmonic time dependence is also investigated. (auth)

21467 (ARL-63-203) TWIN-CHANNEL INSTABILITY IN A TOROIDAL PLASMA AT B_z FIELD REVERSAL. S. Berglund, G. B. Jyoti, and S. Westerlund (Uppsala Univ., (Sweden). Inst. of Physics). [1963]. 4p. (AD-422407). $1.10(CFSTI).

It is proposed that pinch discharge columns within which a longitudinal magnetic field is caused to change sign should have a better stability than discharges with an internal stabilizing field only. A series of experiments with programming of the B_z field in toroidal Z-pinches is described. The filling gas was hydrogen, and a porcelain torus of 102 cm major diameter and 22 cm minor diameter was used. Two independent B_z fields were generated from coils evenly spaced along the torus periphery. (C.E.S.)

21468 (BSD-TDR-64-164) RADIATION FROM A GAS CONTAINING ALKALI METAL VAPORS. Robert H. Thomas (Avco-Everett Research Lab., Everett, Mass.). Jan. 1965. Contract AF04(694)-414. 24p. (AMP-152)

An approximate analytic expression is derived for the radiant energy flux from a plasma contained in an infinite plane parallel enclosure. (auth)

21469 (CEA-R-2713) STABILITE DES PLASMAS OBTENUS DANS E.P.P.E. (Stability of Plasmas Obtained in EPPE). Jean Adam, Paul-Henri Rebut, and André Torossian (Commissariat à l'Énergie Atomique, Fontenay-aux-Roses (France). Centre de Études Nucléaires). Nov. 1964. 32p. (EUR-2176 f). Dep.(mn).

A plasma stable during its whole confinement time has been observed. This confinement time seems to be limited by the resistive diffusion of the magnetic fields through the plasma. (auth)

21470 (IPP-1/14) UNTERSUCHUNGEN UBER DEN EINFLUSS VON NEUTRALGAS AUF DIE DYNAMIK DER THETA-PINCH-ENTLADUNGEN. (Investigation of the Effects of Neutral Gas on the Dynamics of Theta Pinch Discharges). D. Duechs (Institut fur Plasmaphysik, G.m.b.H., Garching (West Germany)). Oct. 1963. 126p. (IPP-6/10). Dep.(mn).

The effect of the electrical neutral gas components in fast, high-current gas discharges was investigated. In the discharge tube of a theta field, the magnetic field–spatially and temporally resolved–was measured in the initial phases where the ionization degree is still low. A three-liquid model for a mixture of electrons, ions, and neutral atoms leads to an equation system for the calculation of the discharge. The coefficients used are valid for a hydrogen plasma. The system of coupled partial differential equations was numerically solved on an IBM-7090 computer. The plasma (electron and ion) density, the density of atoms, the plasma and neutral gas velocities, the temperature of electrons, ions, and neutral particles, and the magnetic field as functions of a space coordinate and time were calculated. The results of the calculations are given for several sets of initial values and compared with the results of the magnetic field measurement. (tr-auth)

21471 (IPP-1/24) UNTERSUCHUNG DER BEI HEISSEN PLASMEN AUFTRETENDEN "PRECURSOR-IONISIERUNG" MIT EINEM MIKROWELLEN-INTERFEROMETER. (Investigation of the "Precursor Ionization" Occurring in Hot Plasmas With Microwave Interferometer). A. Hirt (Institut fur Plasmaphysik, G.m.b.H., Garching (West Germany)). June 1964. 54p. Dep.(mn).

Precursor ionization was investigated with 4-mm and 2-cm microwave interferometers in a conical z-pinch shock tube (6.25 kJ), and in a relatively weak (6.25 kJ) and a relatively strong (32 kJ) theta pinch. With the interferometer the variation of the refraction index of the plasma–and therefore the electron density–was determined as phase alteration between a wave going through the plasma and an unperturbed comparison wave. The results show that the insertion point of the ionization is independent of the place of the measurement and that neither a magnet placed perpendicular to the propagation direction nor a capacitive coupling produced intentionally alters the percursor ionization. It appears that the measured electron density arises through volume ionization of the neutral gas. The origin of the precursor effect is ionizing radiation from the discharge plasma. By estimation of the radiation loss of a plasma it is seen that line radiation of impurities is the most effective constituent for an ionization. Studies with highly unpurified plasmas confirm this. The electron density is 5×10^{13} cm^{-3} in H_2 at 85 cm distance from the discharge (conical z pinch) and in He at 50 cm distance. The measured ionization decreases with increasing distance sharper than $1/x^2$ and shows in the pressure dependence a sharply expressed maximum between 0.1 and 0.2 Torr. Time, position, and pressure dependence can be explained satisfactorily with volume ionization by line radiation. (tr-auth)

21472 (IPP-1/25) EIN DIFFERENTIAL-INTERFEROMETER UND SEINE ANWENDUNG ZUR BESTIMMUNG VON ELEKTRONENDICHTEGRADIENTEN. (A Differential Interferometer and its Application to the Determination of Electron Density Gradients). A. Heiss (Institut fur Plasmaphysik, G.m.b.H., Garching, (West Germany)). June 1964. 82p. Dep.(mn).

After some fundamental remarks on the application of interference method in plasma physics and the task that the differential interferometer should fulfill in this connection, the construction and performance of such a device is described. The application for measurements on plasma was described and the conditions to be fulfilled were discussed. The measurement of electron density gradients on a theta pinch with the differential interferometer was described. (tr-auth)

21473 (IPP-1/28) DIMENSIONIERUNG UND VERGLEICH VON Z-PINCH ANTIPINCH UND THETAPINCH ALS ANORDNUNGEN ZUR ERZEUGUNG STARKER STOSSWELLEN. (Dimensioning and Comparison of Z-Pinch, Antipinch, and Theta Pinch as Apparatus for the Production of Strong Collision Waves). W. Koeppendoerfer (Institut fur Plasmaphysik, G.m.b.H., Garching, (West Germany)). July 1964. 24p. Dep.(mn).

The question of the dimensioning of shock tubes to be used to heat a plasma in a short time with the help of strong waves was considered. The three linear configurations—z-pinch, antipinch, and theta pinch—were investigated and compared with respect to the maximum attainable velocity of the propelling piston. (tr-auth)

21474 (LA-3189) THE POWER CROWBAR ENERGY SYSTEM FOR SCYLLA IV. E. L. Kemp and W. E. Quinn (Los Alamos Scientific Lab., Univ. of California, N. Mex.). June 10, 1964. Contract W-7405-eng-36. 21p. Dep.; $1.00(cy), 1(mn) CFSTI.

The energy storage system of Scylla IV has four capacitor banks, which are applied in the following order: the reverse bias bank—10 kv, 280 kJ, with a rise time of 60 μsec; the preionization bank—40 kv, 9 kJ, that rings at 300 kc; the primary bank—50 kv, 540 kJ, with a rise time of 3.7 μsec; and the power crowbar bank—20 kv, 3 MJ, with a rise time of 25 μsec. The first three banks have been in operation for over a year, and their performance is discussed. The main problem with the power crowbar bank is the switch. This switch must hold off the pulse voltages applied by the other three banks while also holding off the d-c voltage of the power crowbar bank. It must also fire with low jitter when the voltage across it is near zero. Three types of switches were considered for this application: a 20-kv ignitron, a developmental 50-kv ignitron, and a vacuum spark gap. The characteristics of each switch are discussed, and the choice of the vacuum switch is discussed in detail. The discussion also includes the various methods of triggering vacuum switches. A washer gun is chosen as the trigger for each gap. This gun is shown and discussed. The 3-MJ capacitor bank is discussed as a system, including the capacitor protection scheme, the prefire protection circuit, and the complete firing system. (auth)

21475 (LA-DC-6383) EXPERIMENTAL STUDIES OF THE PENETRATION OF A PLASMA STREAM INTO A TRANSVERSE MAGNETIC FIELD. D. A. Baker and J. E. Hammel (Los Alamos Scientific Lab., Univ. of California, N. Mex.). [1964]. Contract [W-7405-eng-36]. 38p. Dep. (mn); $2.00(cy), 1(mn) CFSTI.

The interaction of a dense ($n \simeq 3 \times 10^{13}$ cm^{-3}), fast ($v \simeq 4 \times 10^7$ cm/sec) plasma stream with a transverse magnetic field is studied experimentally by injecting a plasma from a coaxial gun perpendicular to the magnetic field of a pair of mirror coils. The experiments show that the stream from such a gun can penetrate magnetic fields up to ~9 kG. A rapid field-plasma intermixing takes place and the injected stream crosses the magnetic field by electrically polarizing and producing an E × B drift. It was found that the forward motion of the stream can be stopped by draining the polarization charge by current flow along field lines to a shorting conductor located outside a magnetic mirror. Measurements of stream thickness normal to the magnetic field and of the effectiveness of the depolarizing conductors have been made, as functions of the strength of the transverse field. The exclusion of the plasma from high magnetic fields, and the variation of stream width with magnetic field intensity, are due to plasma polarization effects rather than plasma diamagnetism. Observations on electrons having energies above 200 kev, which are produced during the experiment, are discussed. (auth)

21476 (MATT-283) EQUILIBRIUM OF A PLASMA IN A TOROID WITH FINITE RESISTIVITY, INERTIA AND DENSITY GRADIENT DRIFT. Georg Knorr (Princeton Univ., N. J. Plasma Physics Lab.). June 1964. Contract AT(30-1)-1238. 18p. (CONF-640606-22). Dep.(mn); $1.00(cy), 1(mn) CFSTI.

From American Physical Society Summer Meeting, Denver.

A theoretical study of the equilibrium of a dilute plasma in toroidal geometry with rotational transform has been carried out, taking into account finite resistivity and finite inertia. If an additional nonvanishing density gradient drift of the plasma perpendicular to the magnetic field is assumed, the plasma drifts out of the toroid. The characteristic time of this process is found to be a factor of 2 r/R (R = major radius of the toroid; r = minor radius) smaller than the time associated with the diffusion from a toroid. (auth)

21477 (MATT-290) ELECTRON CYCLOTRON HARMONIC RADIATION FROM A PLASMA. A. F. Kuckes and J. M. Dawson (Princeton Univ., N. J. Plasma Physics Lab.). July 1964. Contract AT(30-1)-1238. 7p. (CONF-641108-13). Dep.(mn); $1.00(cy), 1(mn) CFSTI.

From American Physical Society, New York.

Microwave emission by plasma in magnetic fields, at harmonics of the electron cyclotron frequency, is studied. It is assumed that this emission results from gyration of electrons in regions of plasma hybrid resonance. The intensities of the resonance peaks predicted by this analysis are compared with the experimentally observed peak intensities. (T.F.H.)

21478 (NP-14880) OSCILLATIONS IN A ONE-DIMENSIONAL, INHOMOGENOUS PLASMA. E. A. Jackson and M. Raether (Illinois Univ., Urbana. Coordinated Science Lab.). Jan. 1965. Contract DA-28-043-AMC-00073(E). 24p. (R-239)

A one-dimensional, finite, cold or warm, inhomogeneous plasma is considered. A rigorous formulation of the resonance problem for such a plasma is presented. Calculations of the eigenfrequencies and their damping rates are carried out in detail for the long-wavelength regime. (T.F.H.)

21479 (ORNL-3760) THERMONUCLEAR DIVISION SEMIANNUAL PROGRESS REPORT FOR PERIOD ENDING OCTOBER 31, 1964. (Oak Ridge National Lab., Tenn.). Feb. 1965. Contract W-7405-eng-26. 114p. Dep.; $4.00 (CFSTI).

Research and development are reported in sections on single pass experiments (DCX-1), multipass experiments (DCX-2), electron cyclotron heating, plasma physics, cross section measurements, production, acceleration, and injection of ionic and atomic beams, plasma theory and computation, magnetics and superconductivity, vacuum systems, and fusion chain reactions. Separate abstracts were prepared for each section. (J.R.D.)

For abstracts of individual sections see: 20140, 20730, 21480, 21481, 21482, 21483, 21484, 21485, and 21487.

21480 (ORNL-3760(p.1-9)) INJECTION AND ACCUMULATION—SINGLE-PASS EXPERIMENTS (DCX-1). J. L. Dunlap, R. S. Edwards, G. R. Haste, L. A. Massengill, C. E. Nielsen, H. Postma, L. H. Reber, R. G. Reinhardt, W. J. Schill, and E. R. Wells (Oak Ridge National Lab., Tenn.).

Experiments with plasmas established by Lorentz-force trapping at low pressures were emphasized during this report period. Essentially parallel investigations of the radiofrequency (r-f) signals generated by plasma instabilities, and of the anomalous proton losses suggested by earlier data were conducted. The use of panoramic receivers and intensity-modulated oscilloscope displays provided simultaneous time-resolved spectra of both polarizations of magnetic signals and led to the recognition of several modes of r-f signal behavior. The experiments on anomalous proton losses were for verification that the trapping fraction does not decrease with the increase of injected-beam current and charge-exchange decay time. Studies with radial probes are also reported that showed radial losses of fast protons. An inconclusive search was made for mirror-loss of fast protons. The radial losses were found to be time-correlated with r-f signals which can be interpreted as the result of unstable clusters in that portion of the trapped proton population which precesses so as to contribute to density near the outer radius of the plasma. (auth)

21481 (ORNL-3760(p.10-22)) INJECTION AND ACCUMULATION—MULTIPLE-PASS EXPERIMENTS (DCX-2). P. R. Bell, J. S. Culver, R. C. Davis, et al. (Oak Ridge National Lab., Tenn.).

Studies of the plasma in DCX-2 were continued, as previously, with the 600-kev H_2^+ beam dissociated in a Li arc. The density, as estimated from the integrated charge-exchange neutral flux following beam turnoff, was only ~2×10^9 ions/cm^3, and the energy spread was also smaller than had been found during the previous report period. This variation in plasma behavior was not explained. From the evidence of the scanning energy analyzer, the plasma appears to consist of two parts: a group of ions which maintain their injected longitudinal energy (with, however, a rather wide spread in total energy), and a group with very low longitudinal energy. This latter group is trapped

in a very weak mirror (mirror ratio $1 + 10^{-3}$) produced by the careful adjustment of the magnetic field. The energy distribution of this group shows a mean value considerably higher (~500 to 800 kev) than the injected energy. The loss rate of plasma from the machine was not completely established, but experiments have ruled out losses to the walls. Fluctuations seen in the foil detector signals were established as fluctuations in the neutral flux. Strong correlations in these signals along the field, with poorer correlations in azimuthally distributed detectors, suggest radially limited perturbations in the charge-exchange rate which extended from one end of the volume to the other. Correlation studies of the radio-frequency emission at the cyclotron frequency and its harmonics were undertaken, but the variation of frequency content for large probe separations makes analysis difficult. An attempt to establish a correlation distance has so far been unsuccessful, although when the probes are very close (less than 5 cm), fairly good correlation is seen. An experimental estimate of the charge-exchange cross section of the Li arc was made. Assuming a density of 5×10^{12} ions/cm^3 and a reasonable arc diameter, the cross section was not very different from that for protons in H and agreed with a similar estimate made by the OGRA workers. (auth)

21482 (ORNL-3760(p.23-9)) ELECTRON-CYCLOTRON HEATING. (Oak Ridge National Lab., Tenn.).

Bremsstrahlung measurements were continued on the electron-cyclotron plasma in the EPA Facility. The present measurements show that the electron temperature is constant under a wide variety of conditions. The electron density shows some increase with microwave heating power and a strong dependence on a gas pressure. The neutral beam experiment was initiated. A 20-ma beam of neutral H has been injected into the EPA plasma. Preliminary measurements showed a factor of 15 increase in trapped proton lifetime due to neutral density reduction in the hot-electron plasma. The first experiments to be performed on the redesigned ELMO Facility will be electron-cyclotron heating at 8 and 5.5 mm, with ELMO operated with a mirror field. The facility will also be operated as a double-folded cusp with 3-cm microwave power. (auth)

21483 (ORNL-3760(p.30-56)) PLASMA PHYSICS. (Oak Ridge National Lab., Tenn.).

The method of fully ionizing plasma was further examined in successively larger devices called "Burnout I" through "Burnout V." A reflex electron beam interacts with the self-generated plasma within the anode region of the pressure gradient discharge. After initial ionization and stripping of light ions, the beam appears to continue to lose energy to the plasma. Preliminary Burnout IV data indicate ion and electron temperatures above thermal at densities of above 10^{12} cm^{-3}. A simple momentum probe—a wire carrying a high current—was used to study plasma properties. An improved coherent detector that is much more free of slow drift than was the earlier device is being used making sound wave studies easier. Measurements of ionic sound wave velocities as a function of ionic mass and electron temperature are reported. Measurements of γ, the adiabatic compression coefficient of the electron gas are also reported along with the thickness of sheaths on the emitting and detecting ion-wave probes, and the radial drift velocity of the plasma to the walls of the container. Studies of the effect of boundary condition on beam focus were continued. A comparison between the flat plate wall and the boundary impedance network was made. Either boundary wall treatment extends the pressure range where the beam imperfection value remains in the operable range of ~1.2. This extension of the operable pressure holds for a variety of positions of the boundary surface walls with respect to the beam. A reflexive discharge was operated in BPF at input powers from 10 to 25 kw. The neutrons observed when operating with a deuterium discharge appear to originate predominantly at the anticathode. There is evidence for resonances in the neutron intensity at certain ratios of the electron oscillation frequency to the ion cyclotron frequency. The flutes emitted from the deuterium arc core which were described in earlier progress reports were stabilized by moving the arc anode toward the cathode. This new electrode geometry results in the arc running through a field whose average radial gradient is apparently positive. Stabilization is determined by a discontinuous change in the average saturation ion current to a probe, 1 cm radially from the arc core, and a simultaneous reduction in the frequency and amplitude of current spikes in the time-resolved signals. Studies of the H arc in the long solenoid were continued. A density of 1.5×10^{13} ions cm^{-3} is obtained from water-cooled Cu probe measurements. The ion saturation currents to baffles placed around the arc are found to vary with the type of cathode used and to decrease with increasing magnetic field. Langmuir probe measurements of the ion density as a function of radius show a decrease in the radial e-folding distance from about 0.8 to 0.6 cm with an increase in field from 5500 to 9625 gauss. Transverse observations of a high-current-density H arc in the long solenoid gave spectral line broadening and slant (Doppler effect due to ordered rotation about arc axis) on the H 4340-Å line. In a relatively diffuse H arc the slant effect on the H line was absent or undetected, and there was only a very slight slant of the ionic impurity spectrum lines in the main body of the arc. However, in the peripheral region of the arc the ionic impurities had a typically large slant. (auth)

21484 (ORNL-3760(p.57-63)) CROSS-SECTION MEASUREMENTS. C. F. Barnett, J. A. Ray, and J. C. Thompson (Oak Ridge National Lab., Tenn.).

Measurements were completed for the production of excited H atoms resulting from the dissociation of 500-kev H_2^+ by C arc. The optimum ratio of H^0/H_2^+ for arc production was 0.20 compared with Ar gas production of 0.14. The fraction of H^0 in principal quantum numbers $n > 8$ compared with the total neutral yield was 0.0046, which may be compared with a fraction of 0.0127 produced by Ar gas collisions. Attempts to measure resonances in the cross section for electron capture into excited states by passing of protons through atomic H were unsuccessful due to mechanical failure of the W oven used to produce atomic H. By passing protons through molecular H and He, the fraction of H^0 with principal quantum number $n = 12$ or greater was determined at 16 to 34 kev. The fraction increases monotonically with energy, with values at 34 kev of 0.002 and 0.0014 for H and He respectively. Evaluation of the Bendix magnetic electron multiplier indicates variations in gains of 10^5 over the surface of the ¾- by ¾-in. W cathode. Orders of magnitude in the change of gain render the multiplier useless as an absolute particle detector, and it can be used for relative measurements only if the spatial distribution of the particles remains constant during the measurements. (auth)

21485 (ORNL-3760(p.69-76)) PLASMA THEORY AND COMPUTATION. (Oak Ridge National Lab., Tenn.).

Energy spread in injection machines, a manifestation of microinstabilities, is analyzed from the thermodynamic point of view applied previously to diffusion in a torus. In this light, the observed energy spread is seen to be relatively small. In particular, the potentially large energy reservoir in plasma anisotropy makes a small contribution to the ultimate growth of electric fields. The dispersion relation derived by Harris was analyzed for distributions which simulate the loss-cone effect of mirror confinement. Amplification of electrostatic waves at frequencies near harmonics of the ion gyrofrequency can occur for waves propagating almost perpendicular to the magnetic field. Stability zone diagrams are presented, and their interpretation is discussed. It was shown that a system described by a bi-Maxwellian distribution function, situated in a constant magnetic field, is stable against electrostatic instabilities if $T_{\parallel}/T_{\perp} > \frac{1}{2}$. Numerical computation of the decay of neutral particle current from DCX-2 was attempted. Effects included are charge exchange, ion cooling by arc electrons, ion-ion diffusion (Coulomb), and ion scattering out mirrors. Diffusion across a magnetic field is calculated for a given fluctuating electric field. The field may

arise from microinstabilities, or, as in the example treated, it may represent two-body collisions. It is shown that the plasma potential to be expected with mirror confinement should not destroy flute stabilization by magnetic wells. The stabilization of flutes in arcs by very shallow average wells may provide experimental confirmation. (auth)

21486 (ORNL-3760(p.77-93)) MAGNETICS AND SUPERCONDUCTIVITY. (Oak Ridge National Lab., Tenn.).

The injection duct (snout) of DCX-2 in its original form must be operated with additional helical coils in order to compensate the influence of the radial change of the main magnetic field. In cooperation with the DCX-2 group, a new snout was built using an improved design with a helical coil of variable pitch which is arranged inside the can of the injection duct. The new injection duct design is an appreciable technical improvement; furthermore, having a new snout leaves the old one as a spare for the operation of DCX-2. In the previous semiannual report a new analytical method was presented for optimizing the power of solenoid systems which produce homogeneous fields. Recently this method was applied to the design of a 7-Mw, 60-kilogauss magnet coil with 13 in. inner diameter. In general, calculations of magnetic fields containing ferromagnetic materials are involved. Two previously reported general utility codes for computing magnetic properties of electric current systems were extended to permit the inclusion of magnetostatic elements. A list was prepared containing brief descriptions of magnetic field computer codes used at this laboratory. In superconductivity research the measurement of magnetic moments is of great importance. Vibrating-coil magnetometers were built which allow continuous measurements with relatively high signal-to-noise ratios. A design of a vibrating-coil magnetometer which differs from the known types in that the flux is measured in the homogeneous middle zones of samples with demagnetization factors $n \sim 1$ is described. Such an instrument was built, and tests in fields, produced by a superconducting 50-kilogauss magnet, showed encouraging results. (J.R.D.)

21487 (ORNL-3760(p.98-9)) FUSION CHAIN REACTIONS. J. R. McNally, Jr. (Oak Ridge National Lab., Tenn.).

A qualitative discussion is presented on the concept of fusion chain reactions in which protons (deuterons, tritons, ^{3}He, or energetic alphas) may catalyze the burning of ^{6}Li or other nuclear fuels, quite analogous to chemical chain reactions except for the energy scale of the events. (auth)

21488 (PIBMRI-1208-64) DIAGNOSTICS OF PULSED PLASMAS AND ELECTRON BEAM-PLASMA INTERACTIONS. Robert R. Pepper (Polytechnic Inst. of Brooklyn, Farmingdale, N. Y. Graduate Center). Apr. 27, 1964. Contract AF33(657)-10820. 23p. (AL-TDR-64-65; AD-606514). $1.00(CFSTI).

A microwave phase bridge or interferometer was constructed and tested for the purpose of measuring high electron densities in pulsed plasmas. The initiation and growth, both in time and space, of a pulsed plasma (1 torr) were studied by observations of intensity and line shape of several spectral lines. Measurement of Stark splitting yielded plots of electric field intensity and hence space charge distribution as functions of axial position and time. The discharge started near the anode and propagated towards the cathode. The electric field near the cathode reached 45 kv/cm in 25 nanoseconds and remained at about 58 kv/cm during almost the total pulse duration of 500 nanoseconds. The total optical radiation after 24 nanoseconds is only 5% of its value after 500 nanoseconds. A set-up was constructed for studying interactions between an electron beam and a plasma. The plasma was produced by electron impact in the beam when the gas pressure was between 0.0001 and 0.01 torr. Some electronic gain was observed but no quantitative results were obtained because of experimental difficulties in maintaining a strong beam and an appropriate plasma. (auth)

21489 (TID-4005(Pt.5)) SUMMARIES OF THE USAEC RESEARCH PROGRAM ON CONTROLLED THERMONUCLEAR REACTIONS. (Division of Research (AEC), Washington, D. C. and Division of Technical Information Extension (AEC), Oak Ridge, Tenn.). Feb. 1965. 68p. Dep.; $3.00(cy), 2(mn) CFSTI.

Summaries are presented of USAEC-sponsored studies aimed at containment and control of thermonuclear reactions. The topics covered include experimental hot- and cold-plasma studies, theoretical investigations, cross-section analyses, materials and component evaluation, diagnostic techniques, and cryogenic-systems design. (T.F.H.)

21490 (TID-21698) RESEARCH ON INSTABILITIES IN HIGHLY IONIZED LOW-PRESSURE METAL-VAPOR PLASMAS. Progress Report, October 1–December 31, 1964. M. F. Hoyaux, G. W. Penney, F. J. Young, V. M. M. Glaude, G. D. Linton, and E. M. Williams (Carnegie Inst. of Tech., Pittsburgh, Pa.). Contract AT(30-1)-3100. 5p. (EAC-4). Dep.(mn); $1.00(cy), 1(mn) CFSTI.

Plasma instability caused by constriction in the positive column of a mercury arc discharge is studied. Refinements in apparatus completed during this quarter comprised a direct semi-logarithmic oscillographic display for Langmuir probe characteristics, an isolated probe driver for double-probe characteristics and a decreased strobe-pulse length in the swept time-sampled probe instrumentation (plasmograph). It has been found that the hard-tube pulse source is more nearly a constant-current source than the delay-line pulse source so that the discharge current is considerably more stable in the instability interval. Consequently, it has been possible to use the Langmuir probe measurements over a time interval that includes not only the entire pre-instability interval but also a small interval after the onset of instability. Theoretical studies of the plasma sac region have been directed toward the beam-plasma interaction; some initial plans for the modelling of the interaction have been made. (auth)

21491 (UCRL-12057(Rev.I)) MICROWAVE EXCITATION OF A LIVERMORE PUFFATRON PLASMA AT THE ELECTRON CYCLOTRON FREQUENCY. J. L. Shohet and J. F. Steinhaus (Lawrence Radiation Lab., Univ. of California, Livermore). Jan. 13, 1965. Contract W-7405-eng-48. 15p. Dep.; $1.00(cy), 1(mn) CFSTI.

A Livermore Puffatron device was operated in conjunction with a microwave signal at the electron cyclotron frequency. The Puffatron is essentially a coaxial $\vec{E} \times \vec{B}$ plasma gun. Two wavelengths were used: 8 mm and 3 cm (X-band). The 3-cm radiation was pulsed at 40 kw for 2 μsec, while the 8-mm radiation was operated continuously at 15 w. The most informative results were obtained with the 3-cm radiation. When the radiation was applied during the afterglow of the Puffatron discharge, a burst of light and a signal on Langmuir loop and capacitance probes were observed. (auth)

21492 (FTD-TT-64-102) THE CONTROLLED PLASMA. J. Lominadze and N. Tsintsadze. Translated from Metanierеba Tekhn., No. 12, 25-8(1961). 11p. CFSTI.

A brief outline of the problems associated with controlled thermonuclear reactions is presented. (C.E.S.)

21493 KINETIC THEORY OF PLASMA AND ELECTROMAGNETIC FIELDS. N. Rostoker, R. Aamodt, and O. Eldridge (General Atomic Div., General Dynamics Corp., San Diego, Calif.). Ann. Phys. (N. Y.), 31: 243-91(Feb. 10, 1965).

The oscillator treatment of the transverse electromagnetic fields originally developed by Simon and Harris was re-examined. An essential feature of the previous treatment was that the electromagnetic energy changed on a long collisional time scale. It is established that this quantity in fact changes on a short time scale of the order of the inverse plasma frequency. This invalidates the previous expansion procedure. A new treatment is developed that involves only moments of the oscillator functions. The resultant correlation equations have been solved by a test-particle method which provides a simple physical interpretation of the solutions. Fluctuations, radiation, and the

Fokker-Planck equation are obtained for a spatially homogeneous plasma with a constant unperturbed magnetic field. This calculation assumes the adiabatic approximation. The corresponding problem with zero-magnetic field is also discussed. (auth)

21494 INTERACTION OF OPTICAL AND ACOUSTIC PHONONS WITH LONGITUDINAL PLASMA WAVES. Raphael Tsu and Donald L. White (Bell Telephone Labs., Inc., Murray Hill, N. J.). Ann. Phys. (N. Y.), 32: 100-13(Mar. 1965).

The interaction between the longitudinal plasma wave and the lattice waves is examined by a self-consistent field approach. The propagation characteristic of a longitudinal plasma wave under the influence of an applied longitudinal electric field is examined by means of the Boltzmann transport equation. The solutions for the lattice waves are derived by using a linear chain model. This approach leads to a combined dispersion relation consisting of three branches representing respectively, electron plasma, optical phonons and acoustic phonons; and give a clear exposition of the interaction between the collective electron modes and the lattice modes. The combined dispersion relation reduces essentially to the acoustical and optical cases where some special cases have been obtained previously. Due to the strong interaction between the optical phonons and plasma waves, the optical reststrahlen frequency is raised while the plasma frequency is lowered. The acoustic phonons can have gain under application of a suitable drift field. The form of the attenuation constant suggests that the optical phonons can also have gain; however, theory can not apply due to the large drift field required. (auth)

21495 A THERMODYNAMICAL MODEL OF CONDUCTIVITY DISPERSION IN PLASMAS AND SEMICONDUCTORS. P. H. Fang (Goddard Space Flight Center, Greenbelt, Md.). Appl. Sci. Res., Sect. B, 11: 231-8(1964).

A relation between the kinetic energy and the relaxation time, given by the Arrhenius equation, is introduced into the electric conductivity equation of plasmas and semiconductors. The change of the conductivity in the frequency and the time domains and the nature of the distribution of relaxation times, of this new model of conductivity dispersion, was investigated mathematically. (auth)

21496 TRANSIENT CONDUCTIVITY OF SOME SEMICONDUCTORS AND PLASMAS. P. H. Fang (Goddard Space Flight Center, Greenbelt, Md.). Appl. Sci. Res., Sect. B, 11: 239-46(1964).

The decay function of transient conductivity for some cases of semiconductors and plasmas is numerically computed. The results are useful in analyzing experimental data on conductivity dispersion and to determine the nature of the dispersion mechanism. (auth)

21497 TEMPERATURE DETERMINATION ON THE LOW-CURRENT CARBON ARC BY MEANS OF BLACKENING COMPARISON WITH A CARBON ARC OF KNOWN TEMPERATURE DISTRIBUTION. H. G. Kloss and K. Rademacher (Physikalisch-Technisches Institut, Deutsche Akademie der Wissenschaften, Berlin). Beitr. Plasmaphysik, 4: 221-30(1964). (In German)

A method for the determination of the temperature profile of a low-current carbon arc was described, which provides a high time resolution. The method depends on the photographic measurement of the radiation intensity of the arc plasma by blackening comparison with a carbon arc of known temperature distribution. The knowledge of the concentration distribution of the CN molecules in the arc, which are the important carriers of the radiation emission, is necessary. This concentration distribution was calculated by a diffusion expression. Since the concentration enters only slightly in the temperature, nonstationary arcs are to be detected largely through a stationary approximation. The accuracy of the method is ±300°. (tr-auth)

21498 THE TEMPERATURE FIELD OF A LOW-CURRENT ARC IN AIR. H. G. Kloss and K. Rademacher (Physikalisch-Technisches Institut, Deutsche Akademie der Wissenschaften, Berlin). Beitr. Plasmaphysik, 4: 231-7(1964). (In German)

The temperature field of a 10-amp carbon arc was measured by the method of blackening comparison with a carbon arc of known temperature distribution. A comparison of the temperature profile of arcs between carbon or metal cathodes shows that electrode materials with ionization energies over 7.5 ev exert no effect on the temperature field of the arc within the measurement accuracy. (tr-auth)

21499 FAST ELECTRONS IN THE NEGATIVE GLOW OF LOW-VOLTAGE COLD-CATHODE DISCHARGES IN HELIUM. H. M. Grimley and K. G. Emeleus (Queens Univ., Belfast). Brit. J. Appl. Phys., 16: 281(Feb. 1965).

The spectrum of the negative glow of a helium discharge tube with a cold sodium cathode includes the He II line at 4686 Å, with excitation potential 75 v, when the cathode fall is 80 v. The presence of the line, and the distance into the negative glow for which it can be traced with cathode fall 140 v, provide confirmatory evidence for the presence in the negative glow of fast electrons which have traversed a large part of the cathode dark space. (auth)

21500 NEUTRINO GENERATION AND ACCELERATION IN A TURBULENT PLASMA. V. N. Tsytovich (Lebedev Inst. of Physics, Moscow). Dokl. Akad. Nauk SSSR, 159: 1268-71(Dec. 21, 1964). (In Russian)

It is shown that, in the presence of weak $(e\nu)(e\nu)$ interaction, neutrino production in a turbulent plasma should be accompanied also by neutrino acceleration, with the number of the neutrinos (and also the number of the antineutrinos) conserved as their average energy increases. Taking advantage of the fact that plasma turbulence can be described in terms of low frequency (hydrodynamic) and high frequency (Langmuir) plasmons, which have been shown to be capable of being absorbed and emitted by neutrinos (low frequency plasmons) or of generating neutrino-antineutrino pairs (high frequency plasmons), the effect of acceleration of the neutrinos by plasmons is analyzed and the energy lost by a turbulent plasma to production of neutrino antineutrino pairs is calculated. The results show that for waves whose phase velocity tends to the velocity of light the acceleration tends to zero, indicating that absorption and emission of electromagnetic waves in vacuum is forbidden. High frequency turbulence (Langmuir plasmons) are shown to accelerate the neutrinos more effectively than hydrodynamic plasmons. It is also shown that nonlinear effects in plasmon interaction make it possible for waves to be effectively pumped over into the region of phase velocities exceeding the velocity of light. The relation between the rate of neutrino generation and star evolution is discussed in connection with results of several recent papers. (ATD)

21501 RECOMBINATION DECAY OF NONEQUILIBRIUM NONISOTHERMAL PLASMA. K. N. Ul'yanov (Lenin All-Union Electrotechnical Inst., [Academy of Sciences,] USSR). High Temp. (USSR) (English Transl.), 2: 121-5(Mar.-Apr. 1964). Translated from Teplofiz. Vysokikh Temp., 2: 137-41(Mar.-Apr. 1964).

The recombination decay of a nonequilibrium nonisothermal plasma is analyzed. The entire set of discrete states is taken into account. A study is made of the distribution of atoms over the states of the discrete and continuous energy spectra during the decay process. The condition for the quasistability of excited states and the contribution from the excited states to the effective recombination coefficient are discussed. The role of inelastic processes in the energy balance of free electrons is investigated. (auth)

21502 THE PROCESS OF ESTABLISHING AN ELECTRIC CURRENT IN AN IONIZED GAS. A. K. Musin (Lenin All-Union Electrotechnical Inst., [Academy of Sciences,] USSR). High Temp. (USSR)(English Transl.), 2: 126-38 (Mar.-Apr. 1964). Translated from Teplofiz. Vysokikh Temp., 2: 142-55(Mar.-Apr. 1964).

The establishment of space-charge zones close to elec-

trodes and of the electric current due to the flow of gas ions in the space between electrodes is investigated. The basic stages of the process of establishing an electric current are described. (auth)

21503 METHOD OF MEASURING HEAT FLUXES IN A PLASMA. Yu. V. Makarov and Yu. A. Polyakov (Krzhizhanovskii Power Inst., USSR). High Temp. (USSR)(English Transl.), 2: 151-4(Mar.-Apr. 1964). Translated from Teplofiz. Vysokikh Temp., 2: 170-5(Mar.-Apr. 1964).

It is shown that a thin copper wire with glass insulation can be used to measure heat fluxes from a plasma with a short lifetime. (auth)

21504 DETERMINATION OF THE INHOMOGENEITY IN THE CONCENTRATION OF ATOMS IN A LOW-VOLTAGE PULSE DISCHARGE. P. A. Naumenkov (Inst. of Physics, Academy of Sciences, Belorussian SSR). High Temp.(USSR)(English Transl.), 2: 155-8(Mar.-Apr. 1964). Translated from Teplofiz. Vysokikh Temp., 2: 176-80 (Mar.-Apr. 1964).

It is shown that Cowan and Dicke's theory of an inhomogeneous source is applicable to some types of low-voltage spark discharge. The degree of inhomogeneity and the neutral-atom concentration are determined. The former is n = 1.25, and the concentration of electrode atoms is 2.4×10^{17} cm^{-3}, for a discharge of duration 0.04 sec. It is considered that the initial stage of a strong discharge may occur in the vapor of the electrode material. (auth)

21505 RADIATION OF CESIUM PLASMA. V. A. Abramov and Yu. A. Tarasov. High Temp.(USSR)(English Transl.), 2: 160-9(Mar.-Apr. 1964). Translated from Teplofiz. Vysokikh Temp., 2: 160-9(Mar.-Apr. 1964).

The radiation losses of a cesium plasma in the temperature range from 3000 to 4000°K are calculated, including both the bright-line and continuous radiation. (D.C.W.)

21506 REFLECTION AND TRANSMISSION PROPERTIES OF A STRATIFIED PLASMA. J. Basu (Univ. of Calcutta). Indian J. Phys., 38: 435-52(Sept. 1964).

Equations are derived for the reflection and transmission coefficients of a plane electromagnetic wave incident normally on a plasma having a homogeneous layer in the middle and inhomogeneous layers on both sides. The equations are expressed in terms of parameters which can be calculated from the characteristic properties of the plasma by applying a numerical method and using a digital computer. It is found to be possible to simplify the calculations if the inhomogeneous layers are identical. A plasma with a trapezoidal distribution of electron density along its thickness is discussed. The reflection and transmission coefficients for a number of such plasmas can be directly calculated from the results reported. The results refer to a few typical thicknesses of the inhomogeneous layers of the plasma, for which approximate methods that have been generally used in the past for determining the coefficients turn out to be unsatisfactory. (auth)

21507 COMMENTS ON THE VALIDITY OF TREATING A DENSE PLASMA AS A METAL. H. W. Lorber (Edgerton, Germeshausen and Grier, Inc., Las Vegas, Nev.). J. Electron. Control (1), 17: 635-48(Dec. 1964).

The pressure exerted by an electromagnetic field against the surface of a plasma is discussed for the case where the plasma is sufficiently dense to exclude the field. It is shown under rather general conditions that the electromagnetic boundary conditions are the same at the plasma surface as they are at a metallic surface and that the pressure exerted by the electromagnetic field against the surface of the plasma is the same as that exerted against a metal surface, except for an extra term $-\rho v_n^2$ that involves the motion of the plasma surface under the influence of the time-varying electromagnetic field. In an example, this extra term is shown to account for 19% of the pressure required to confine the plasma. (auth)

21508 PLASMA CONFINEMENT WITH A ROTATING MAGNETIC FIELD. Hiromichi Kondo and Katsushi Toshioka (Mitsubishi Electric Mfg. Co., Japan). J. Inst. Elec. Engrs. Japan, 84: 267-72(Feb. 1964). (In Japanese)

A new method of plasma confinement in a cylindrical shape is described with the rotating field produced by the axial currents given as $i_z = I \sin(wt + m\theta)$, m = 3, 4, ... in the region b < r < c; r, θ and Z indicate the cylindrical co-ordinates. The plasma column to be confined is approximated by a solid cylinder of metal whose permeability and conductivity are μ_0 and σ, respectively, and is assumed to be still; this is realized by the application of two kinds of field whose rotating directions are selected contrary to each other so that the azimuthal forces counterbalance. The electromagnetic field is calculated by neglecting the effect of displacement currents. The simple Ohm's law $j = \sigma E$ is assumed, and the time average of the confining force ($j \times B$), is obtained, which is negative at every point in the cylinder so that it is directed inward. If the axis of the rotating field is selected to be a circle, such a field will provide a new configuration for the plasma confinement in a toroidal shape. The confining force is shown to be reinforced by the insertion of high-permeability material in the outer region r > c. The proposed scheme can be expected to provide an essentially stable confinement, since in this the electromagnetic potential energy increases rapidly as the plasma deviates from its equilibrium position. (auth)

21509 APPROACH TO STABILITY OF A PLASMA. B. W. Abraham (Universite Libre, Brussels). J. Math. Phys. (N. Y.), 6: 630-6(Apr. 1965).

The stabilization of a spatially homogeneous plasma by the collision term of the new kinetic equation of Balescu for a weakly unstable plasma is shown for a simplified model. The one-particle velocity distribution consists of two symmetrically displaced Lorentz distribution functions in which the displacement velocity and velocity spread are functions of time. For this distribution function, the collision term decreases the displacement velocity and increases the velocity spread until the plasma is quite stable. Physically this process can be viewed as conversion of relative energy to kinetic energy. This is demonstrated to be equivalent to the passage of the zero of the plus dielectric constant from the upper half complex plane, characterizing an unstable plasma, to the lower half complex plane, characterizing a stable plasma. (auth)

21510 GAS-LASER DETERMINATION OF THE ELECTRON DENSITY IN THE AFTERGLOW OF A HYDROGEN DISCHARGE. J. M. P. Quinn (Culham Lab., Abingdon, Berks, Eng.). J. Nucl. Energy, Pt. C, 7: 113-22(Mar.-Apr. 1965). (CLM-P-60)

A helium–neon gas laser was used to determine the electron density variation, both spatial and temporal, in the afterflow of a Z-pinch in hydrogen at 100 mtorr. The percentage ionization, defined as the ratio of the electron density to the initial gas density, was found to drop from approximately 100 to 1% in two phases. During the first phase, lasting 10 μsec, the dominating process was recombination. In the second phase, lasting a further 90 μsec, ambipolar diffusion took over completely. Further, the results obtained for the density variation on the axis are compared with similar determinations using completely independent techniques. (auth)

21511 PERPENDICULAR TEMPERATURE OF THE HELIUM DISCHARGE IN THE C-STELLARATOR. K. A. Uo (Princeton Univ., N. J.). J. Nucl. Energy, Pt. C, 7: 123-32(Mar.-Apr. 1965).

The perpendicular pressure and temperature of a current-carrying helium plasma in the C-STELLARATOR were measured by means of a diamagnetic coil. In order to reduce recycling a pulsed gas feed was used. The perpendicular temperature shows fairly good agreement with the resistivity temperature. The particle velocity distribution is essentially isotropic. The proportionality between these two temperatures is very good until in the late discharge. The discrepancy late in the discharge suggests that some runaway electrons are produced. These tend to increase the apparent resistivity temperature, but do not affect the perpendicular temperature greatly. The resistivity temperature would then appear higher than the true temperature. (auth)

21512 THE ANOMALOUS DIFFUSION OF THE CURRENT SHEATH IN A TOROIDAL DISCHARGE. D. J. Lees, G. D. Hobbs, M. G. Rusbridge, and P. A. H. Saunders (Culham Lab., Abingdon, Berks, Eng.). J. Nucl. Energy, Pt. C, 7: 141-60(Mar.-Apr. 1965).

The diffusion of the current sheath in ZETA is shown to be incompatible with classical resistive diffusion at high rates of energy input or low pressures. In the anomalous region the diffusion time is approximately proportional to mass density and inversely proportional to the applied electric field. There are considerable asymmetries in the toroidal discharge and complicated convective motions during the diffusion phase, but these appear not to be the primary cause of the enhanced diffusion. Evidence has been obtained that the enhanced diffusion is not due to the presence of a probe in the plasma. It is therefore probable that there must be an enhanced resistivity, depending on the local values of mass density and electric field, which is presumably due to some form of turbulence, but none of the simple models of such turbulence considered account for the results. (auth)

21513 THE REFLECTION OF MICROWAVES FROM AN ANISOTROPIC PLASMA SURFACE. L. C. Robinson (Univ. of Sydney). J. Nucl. Energy, Pt. C, 7: 167-73(Mar.-Apr. 1965).

The problem of reflection of an incident linearly polarized microwave signal from a plasma surface oriented at right angles to a magnetic induction field is analyzed. The reflection coefficient is sensitive to high electron densities; with 3-cm waves it offers a means of measurement in the density region 10^{13} to 10^{15} cm^{-3}. (auth)

21514 ELECTRON TEMPERATURE MEASUREMENT OF A PLASMA FROM A PLASMA GUN BY MEANS OF A TRIPLE PROBE. S. Kunieda, N. Kawashima, and S. Mori (Japan Atomic Energy Research Inst., Ibaraki). J. Nucl. Energy, Pt. C, 7: 175-7(Mar.-Apr. 1965).

The electron temperature of a plasma (density of 10^{13} to $10^{14}/cm^3$ and velocity of about 10^6 cm/sec) from a coaxial gun was measured by the triple-probe method proposed by Chen. The temperature obtained was in satisfactory agreement with that obtained by the double-probe method. The time variation of the electron temperature was also measured. (D.C.W.)

21515 TIME-RESOLVED LANGMUIR PROBE MEASUREMENTS OF PLASMA DENSITY AND TEMPERATURE IN ELECTROMAGNETIC SHOCK-TUBES. W. Fucks and R. Theenhaus (Technische Hochschule, Aachen). J. Nucl. Energy, Pt. C, 7: 177-81(Mar.-Apr. 1965).

The electron density and temperature behind the luminous front in a theta-pinch shock tube were measured by spectroscopic methods and Langmuir probe techniques. The results obtained by the two methods were in reasonable agreement. (D.C.W.)

21516 THE LONGITUDINAL COMPRESSION IN A COMPRESSIONAL IOFFE MIRROR MACHINE. M. G. Rusbridge (Culham Lab., Abingdon, Berks, Eng.). J. Nucl. Energy, Pt. C, 7: 183-5(Mar.-Apr. 1965).

If the multipole and mirror field are increased in the same proportion, a particular line of force is displaced inwards; and the relative contribution of the multipole field decreases, so that the length between mirror points increases. It is shown that, depending on the multipolarity of the field, this effect can cancel or even reverse the longitudinal compression due to the changing energy of the particle. (D.C.W.)

21517 MICROWAVE GENERATION OF HARMONICS IN A STATIC MAGNETIC FIELD. Makoto Moriyama and Masao Sumi (Electrical Communication Lab., Tokyo). J. Phys. Soc. Japan, 20: 138-52(Jan. 1965).

By assuming the spatial variation of electron density and introducing an inner plasma field, the microwave generation of harmonics in the presence of a static magnetic field is analyzed. By solving the Boltzmann and Poisson equations using the perturbation technique, the electron distribution function, the inner electric field strength, and the current density of the harmonics are obtained for special cases. It is found that the output power of the second harmonic does not vanish even when the plasma has complete geometrical symmetry and that the resonance which maximizes the output of the second harmonic occurs when the microwave frequency is nearly equal to the cyclotron frequency. (auth)

21518 AN INSTABILITY OF THE ACCELERATED PLASMA. Masatoshi Tanaka (Japan Atomic Energy Research Inst., Tokyo). J. Phys. Soc. Japan, 20: 177(Jan. 1965).

Photographs from axial and transverse directions and magnetic probes indicated that a plasma current sheet, initially azimuthally symmetric, is swept into a spoke in about 2 μsec after discharge ignition. The phenomenon is interpreted theoretically as resulting from the unstable character of an accelerated plasma in a magnetic field. (M.J.T.)

21519 RADIO-FREQUENCY OPACITY OF A NON-UNIFORM PLASMA. E. T. Florance (Geophysics Corp. of America, Bedford, Mass.). J. Quant. Spectry. Radiative Transfer, 5: 271-80(Jan.-Feb. 1965).

The validity of a radiative transfer model applied to radio wave propagation in a nonuniform plasma is investigated with Maxwell field correlation functions. It is found that Oster's quasi-particle model of photon propagation in a general dispersive medium yields a different dependence of the absorption coefficient on refreactive index than predicted by phenomenological electrodynamics. This discrepancy is traced to the fact that dispersion affects the dynamics of the Maxwell field. The probabilities of absorption and emission thus depend on the refractive index contrary to the assumption of Oster. (auth)

21520 STABILITY OF NON-LINEAR STATIONARY PLASMA OSCILLATIONS. V. N. Oraevskii (Inst. of Nuclear Physics, Academy of Sciences, Novosibirsk, Siberian SSR). Nucl. Fusion, 4: 263-71(Dec. 1964). (In Russian)

The method of investigation of the stability of stationary oscillations of not too large amplitude (the ratio of the hydrodynamic wave velocity to phase velocity serves as a small parameter) is reviewed first. Instabilities arise because of the presence of a positive feedback between small sinusoidal oscillations propagating in the "background" of the finite-amplitude wave. Instabilities recall quasi-particle decays: frequencies and wave vectors of developing oscillations are related to the frequency and wave vector of the initial wave by relations typical of the laws of energy and momentum conservation. A characteristic peculiarity of growth rates of developing oscillations is their proportionality to the value of the initial wave amplitude. An example of finding the growth rate of small perturbations is discussed; the stability of a sinusoidal Alfvén wave of small amplitude is investigated. Instability of such a wave is related to compressibility of the medium (for incompressible media instability disappears). For large-amplitude oscillations there is no general method for stability studies. However, even here a positive feedback between small oscillations can appear. For this reason an Alfvén wave is unstable (in a compressible medium) if it has an arbitrary amplitude with a sawtooth profile for the magnetic field lines (the chosen profile of the magnetic field lines enables one to solve the problem precisely). Finally, the results of investigations of the stability of other oscillation modes are given, such as ion-acoustic oscillations of an non-isothermal plasma, electron Langmuir oscillations, magneto-acoustic oscillations, etc. (auth)

21521 PLASMA-WAVE PROPAGATION ACROSS A MAGNETIC FIELD. A. B. Kitsenko and K. N. Stepanov (Kharkov Inst. of Physics and Tech., Academy of Sciences, Ukrainian SSR). Nucl. Fusion, 4: 272-8(Dec. 1964). (In Russian)

The effect of thermal electron and ion motion on wave propagation in a non-relativistic, low-pressure plasma ($\kappa_\alpha = 4\pi n_0 \tau_\alpha / H_0^2 \ll 1$) across a magnetic field was investigated. The dispersion equation for an ordinary wave has the solutions $\omega_s(k)$ close to $s\omega_\alpha (s = 1,2...)$ for any ratio of

wavelength ($\lambda = 1/k$) to the Larmor radius ρ_α of the α type particles having thermal velocity. In order of magnitude $\omega_s(k) - s\omega_\alpha \approx \kappa_\alpha\omega_\alpha$ for $k\rho_\alpha \approx 1$. The dispersion equation for an extraordinary wave has also an analogous solution in the high-frequency region ($\omega \approx \omega_e$), and also a solution corresponding to longitudinal plasma oscillations for $k^2\rho_\alpha^2 \gg \kappa_\alpha$. Longitudinal-oscillation frequencies for the case of a dense plasma, when $\Omega_e \gg \omega_e$ (Ω_e is the electron Langmuir frequency, and ω_e their gyro-frequency) decrease for an increase of $k\rho_e$, diminishing from the values $\omega \approx s\omega_e$ ($s = 2, 3 \ldots$) for $k\rho_e \ll 1$, down to $\omega \approx (s-1)\omega_e$ for $k\rho_e \gg 1$. For a low-density plasma ($\Omega_e \leq \omega_e$), plasma-frequency behavior is shown. In the low-frequency region ($\omega \lesssim \omega_i$), the dispersion equation for an extraordinary wave determines (for the case of a cold plasma) the frequency $\omega = kV_A$ corresponding to a magneto-acoustic wave (V_A is the Alfvén velocity). This expression is inapplicable for $k\rho_i \approx s$ ($s = 1,2 \ldots$) when $\omega \approx s\omega_i$. In this region it is necessary to take into account thermal ion motion. Behavior of the various branch frequencies of an extraordinary hot-plasma wave for $\omega \approx \omega_i$ is comparatively complex. Investigation has been carried out of the self-excitation (caused by beam instability) of electron (high-frequency) branches of the oscillations discussed, for the passage of an ion cyclotron wave through a plasma. (auth)

21522 ELECTRON RADIATION IN PLASMA-MAGNETIC-FIELD BOUNDARY LAYER. V. V. Dolgopolov, V. I. Pakhomov, and K. N. Stepanov (Kharkov Inst. of Physics and Tech., Academy of Sciences, Ukrainian SSR). Nucl. Fusion, 4: 279-80(Dec. 1964). (In Russian)

It is shown that the intensity of cyclotron radiation of electrons in the plasma-magnetic-field boundary layer decreases by mc^2/T times (T is plasma temperature) in comparison with radiation in the void, because dielectric permeability is large in a frequency range of the order of cyclotron frequency. The radiation intensity per unit plasma surface equals $I \approx e^3 n_0^{1/2} T^3/c^6 m^{3/2}$ in order of magnitude, where n_0 is plasma density. Because of plasma resonance in a non-uniform layer, bremsstrahlung in frequency ranges lower than the maximum Langmuir frequency is mc^2/T times as large as cyclotron radiation, even for the case of rare collisions. If Langmuir oscillations in the layer are unstable because of the presence of electron drift velocity, radiation of the layer exceeds thermal radiation at the Langmuir frequency by $(mc^2T^2/e^6n_0)^{1/4}$ times. (auth)

21523 LOW-FREQUENCY PLASMA OSCILLATIONS FOR QUASI-TRANSVERSE PROPAGATION. D. G. Lominadze (Physics Inst., Academy of Sciences, Georgia SSR) and K. N. Stepanov. Nucl. Fusion: 4: 281-6(Dec. 1964). (In Russian)

The spectra and damping of some new branches of hot-plasma oscillations propagating perpendicular to or almost perpendicular to the external magnetic field H_0 are discussed. An investigation was made of an oscillation branch adjoining longitudinal ion-cyclotron oscillations, extraordinary ion-cyclotron and magneto-acoustic waves, and ordinary ion-cyclotron and hybrid waves. The phase velocity of these waves along the magnetic field $V = \omega/k_\parallel$ is considerably larger than ion thermal velocity ($k_\parallel$ is the wave-vector projection in the magnetic-field direction). Waves adjoining longitudinal cyclotron oscillations have a wavelength of the order of the Larmor radius of an ion with thermal velocity and frequencies of the order of ion cyclotron frequency; the phase velocity of these waves along the magnetic field is considerably smaller than thermal electron velocity v_e. These waves can be separated from the general dispersion equation for the case of a low-pressure plasma when $\kappa \ll 1$, where $\kappa = 4\pi n_0 T_i/H_0^2$ (n_0 is the density; T_i, the plasma ion temperature). For $\kappa \ll \cos^2\theta \ll 1$ (θ is the angle between H_0 and the propagation direction) this branch changes to longitudinal ion cyclotron oscillations. The dispersion equation for an ordinary wave for $V \ll V_c$ has two solutions, corresponding to the hybrid wave with frequency $\omega = \omega_0 = k_\parallel kV_s V_A/\omega_i)$, where $V_s = (T_e/m_i)^{1/2}$, $\omega_i = eH_0/m_iC$ and $V_A = H_0/(4\pi n_0 m_i)^{1/2}$ and the ion-cyclotron wave with $\omega \approx s\omega_i$ ($s = 1, 2, \ldots$). For the oscillations pointed out the damping rates which are caused by Cherenkov absorption by plasma electrons and ions and cyclotron absorption by plasma ions were found. Oscillation excitation by fluxes of low-density charged particles passing through plasma along a magnetic field was also examined. Cherenkov and cyclotron wave excitation by both a hot and a cold beam were investigated. (auth)

21524 DIFFUSION OF TRAPPED REVERSED MAGNETIC FIELD IN A THETA PINCH IN THE PRESENCE OF A PROBE. M. Keilhacker (Institut fur Plasmaphysik G.m.b.H., Garching, Ger.). Nucl. Fusion, 4: 287-95(Dec. 1964). (CLM-P-47)

The trapped reversed flux a 26-kjoule theta pinch with known initial conditions was measured as a function of time with a radial multiple probe and compared with numerical calculations. The measured flux agreed with the numerical calculations during the implosion of the plasma but decreased rapidly after the maximum compression whereas the calculated flux remains almost constant because of the increasing plasma temperature. It is shown that radiation cooling by probe impurities can explain this enhanced field diffusion in the neighborhood of the probe. The numerical calculations can be fitted to the experimental results by increasing the radiation loss due to hydrogenic continuum radiation by a few times 10^4. It is estimated that the heat flow to the probe, which is mainly carried by ions (with an energy according to the floating potential of the probe), liberates enough oxygen to account for this factor due to line radiation. Radial framing-camera photographs show a tearing mode resistive instability developing near the probe which seems to be started off by this radiation cooling. A limit on the reliability of probe measurements is given as a function of plasma density and temperature. (auth)

21525 STUDIES ON MACROINSTABILITIES IN A THETA PINCH WITH ANTIPARALLEL MAGNETIC FIELD. A. Eberhagen and H. Glaser (Institut fur Plasmaphysik, Garching, Ger.). Nucl. Fusion, 4: 296-9(Dec. 1964).

The plasma column of a theta pinch with an antiparallel trapped magnetic field has a tendency to break up into several discrete plasma rings. With a smaller theta-pinch apparatus experiments were done to search for mechanisms responsible for triggering such macroinstabilities. Probe ports inserted into the plasma and also external side pockets on the discharge tube cause an early and drastic breakup of the plasma column. But even in smooth tubes discrete plasma rings occur. They could be suppressed by having some discharges with a parallel magnetic field preceding those with a reversed one. This "memory" effect could be explained by the contamination of the inner tube wall by water after each discharge. In this way the plasma column with an antiparallel trapped magnetic field was stable until peak magnetic field. This stability proved to be insensitive to adding amounts of oxygen— as much as 4.6% —to the hydrogen gas and also to lowering the degree of pre-ionization. Finally comparison has been made for the observed formation time of the plasma rings and their number with theoretical predictions. With plasma temperatures derived from the appearance of O IV lines, the formation time can be explained by the resistive diffusion time whereas the theoretical predictions of Furth, Killeen and Rosenbluth for tearing-mode resistive instabilities seem rather to give too small values. (auth)

21526 ENERGY EXCHANGE BETWEEN HIGH- AND LOW-FREQUENCY OSCILLATIONS IN A PLASMA. V. L. Fedorchenko, V. I. Muratov, and B. N. Rutkevich (Kharkov Inst. of Physics and Tech., Academy of Sciences, Ukrainian SSR). Nucl. Fusion, 4: 300-4(Dec. 1964). (In Russian)

Oscillations of frequency $\nu \approx 100$ kcps were detected in a plasma created by an electron beam in a magnetic field. The amplitude of these oscillations depends on the strength of the external field of frequency $\omega \gg \nu$. The high-frequency field is in turn modulated by the low frequency, and this

produces combination frequencies ($\omega \pm \nu$). The oscillation amplitudes at the combination frequencies $\omega + \nu$ and $\omega - \nu$ are not equal; as in the case of the Raman effect, this may be related to the effectiveness of the interaction of various frequencies and to the direction of energy transfer. (auth)

21527 PENETRATION OF AN ALTERNATING MAGNETIC FIELD INTO PLASMA IN THE PRESENCE OF THE HALL EFFECT. T. F. Volkov (Kurchatov Inst. of Atomic Energy, Moscow). Nucl. Fusion, 4: 305-11(Dec. 1964). (In Russian)

The depth of penetration of a travelling magnetic field into plasma in the presence of an electron increase due to Hall effect was found. Since the electrons move in the direction of the field displacement, the penetration depth increases in comparison with the case of electrons that are motionless on the average and is determined by the effective frequency $\Omega = k|V - v^0|$; V is field velocity, v^0 electron velocity (that is, there occurs a peculiar "Doppler effect"). Velocity v^0 for a nonlinear case is a function of the coordinates and depends on the magnitude of the field, its displacement velocity and also on conduction. The electrons are entrained in the direction of the field motion, which always leads to skin-depth increase. A rough calculation of the penetration depth can be made according to the formula $\delta = \delta_0 (1 - \langle B \rangle^2 |B_0^2)^{-1}$, where $\delta_0 = c|(4\pi\sigma kV)^{1/2}$ is the "normal" skin depth; B_0 is the alternating magnetic field amplitude on the plasma surface; and $\langle B \rangle$ is the magnetic-field magnitude on the plasma surface. This field creates a current of entrained electrons. The calculation is applicable in order of magnitude up to $\langle B \rangle \approx B_0$. (auth)

21528 PROBING OF A HIGH-FREQUENCY-DISCHARGE PLASMA WITH ATOMIC BEAMS. O. V. Kozlov and V. D. Rusanov (Kurchatov Inst. of Atomic Energy, Moscow). Nucl. Fusion, 4: 312-20(Dec. 1964). (In Russian)

Probing of a helium plasma of a high-frequency pulsed-discharge was performed with helium (8 and 15 kev) and argon (10 kev) beams, permitting determination of the ion and neutral distributions in time, as well as the electron temperature. The plasma parameters so obtained coincide satisfactorily with microwave and probe measurements. (auth)

21529 DIAGRAM-ADDITION METHOD IN TURBULENT-PLASMA THEORY. A. B. Mikhailovskii (Kurchatov Inst. of Atomic Energy, Moscow). Nucl. Fusion, 4: 321-34(Dec. 1964). (In Russian)

The use for plasma-turbulence description of a diagram technique analogous to the one suggested by Wyld for hydrodynamic turbulence is proposed. Such an approach enables one to abandon the perturbation theory limits used for the study of weakly turbulent pulsations and to obtain approximate equations with the aid of which turbulence with $\gamma \approx \omega$ can be investigated. A precise solution of the Vlasov equation was found for some types of turbulent-plasma pulsations in a magnetic field without assumption of smallness of the pulsation amplitude. This solution has the appearance of an infinite series in powers of the potential of the electric field. Each term of this series has a corresponding graphical picture. Series expansion is performed with respect to a random potential as well as averaging of the products of the random potentials over a Gaussian statistical ensemble and addition of infinite diagram subseries. The resulting equations represent a system of an infinite number of integral equations of infinite order for an infinite number of functions. By way of one or another reasonable discontinuity of this system of equations, a closed system of a finite number of finite-order equations can be obtained. One of these approximate equation systems is constructed, representing a certain analogy with the hydrodynamic equations of Kraichnan. (auth)

21530 THE TOROIDAL THETA PINCH IN M-AND-S CONFIGURATION. W. Lotz, E. Remy, and G. Wolf (Max-Planck-Institut fur Physik und Astrophysik, Munich). Nucl. Fusion, 4: 335-43(Dec. 1964).

For certain toroidal closed surfaces (M-and-S surfaces) of a $\beta = 1$ plasma without resultant azimuthal currents, theory predicts equilibrium. A toroidal plasma was produced by means of a toroidal theta pinch discharge (B_{max} = 10 kgauss, frequency of main discharge, 30 kcps). By adding periodic, additional windings the azimuthal field was corrugated, thus approaching M-and-S surfaces. Smear-camera and image-converter investigations of discharges in helium and hydrogen show that in approaching the theoretical surface, equilibrium is approximated. This could be observed over time intervals more than three times as long as the drift time in a purely azimuthal field under otherwise identical conditions. The electron densities are in the range of 10^{15} to 10^{17} cm^{-3}, the temperature 5 to 10 ev and beta (β) between 0.1 and 1. (auth)

21531 PROPERTIES OF A HIGH-BETA PLASMA PRODUCED BY ELECTRON-CYCLOTRON HEATING. R. A. Dandl, A. C. England, W. B. Ard, H. O. Eason, M. C. Becker, and G. M. Haas (Oak Ridge National Lab., Tenn.). Nucl. Fusion, 4: 344-53(Dec. 1964).

The sequence of experiments resulting in the development of steady-state dense hot-electron plasmas is briefly described. These plasmas are produced in magnetic-mirror machines by radiation at the electron-cyclotron frequency. The electron-cyclotron plasma with the greatest stored energy to date has a volume of about 50 liters, an electron temperature of 120 kev, a density of 4 to 7×10^{11}/cm^3, and an average beta of about 0.4. This plasma is created in the EPA Facility by a 50-kw, 10.6-Bcps microwave power source. The construction and operation of the machine are briefly discussed. The analysis and interpretation of the bremsstrahlung and diamagnetic measurements employed to determine these parameters are given. Diamagnetic and particle decay measurements on a smaller machine, the Physics Test Facility, are also described. (auth)

21532 NON-LINEAR THEORY OF CONVECTIVE INSTABILITY. A. V. Timofeev (Kurchatov Inst. of Atomic Energy, Moscow). Nucl. Fusion, 4: 354-61(Dec. 1964). (In Russian)

The convective instability of a dilute plasma that occurs when the plasma density exceeds a certain critical value is discussed in the quasi-linear approximation. It is shown that the equations determining the frequency and amplitude of nonlinear oscillations permit introduction of an effective potential energy. The oscillations themselves are in a certain sense equivalent to the oscillations of a nonlinear, two-dimensional, axially symmetric oscillator (rotator) that moves without friction. Consideration of nonlinear effects made possible considerable specification of the instability criterion found in the linear approximation. It is shown that plasma stability with respect to finite-amplitude oscillations depends on the quantity $d^3n/d(r^2)^3$, where n is plasma density and r is the distance from the axis of the system. (auth)

21533 VALIDITY OF THE KADOMTSEV-NEDOSPASOV APPROXIMATION FOR A SIMPLE GEOMETRY PLASMA. Eugene V. Ivash (Univ. of Texas, Austin). Phys. Fluids, 8: 699-703(Apr. 1965).

The problem of the instability of a weakly ionized plasma between two infinite parallel plates in crossed uniform electric and magnetic fields was considered for a simple set of boundary conditions. The primary purpose was to investigate the validity of the Kadomtsev-Nedospasov type of simplifying approximation for the perturbed particle density and potential for a relatively simple case. It was found that the approximation in the form introduced by Simon is valid under some, though not all, plasma conditions. The effect of ionization on stability was also investigated, and may be appreciable. (auth)

21534 CALCULATION OF THE SINGULARITIES OF A MAGNETIC FIELD. John M. Greene (Princeton Univ., N. J.). Phys. Fluids, 8: 704-7(Apr. 1965). (MATT-246)

One problem which arises when finding the external magnetic field necessary to support a hydromagnetic configuration is considered. If the hydromagnetic configuration is given without regard to the vacuum field that contains it, then that external vacuum field will in general have singu-

larities at a finite distance from the fluid-vacuum boundary. The location of these singularities is considered. This provides the essential limitation to the position of the external current system that ultimately contains the fluid. (auth)

21535 MAGNETIC-DIPOLE-INDUCED PLASMA MOTIONS. H. Yoshihara and H. Thommen (General Dynamics/Astronautics, San Diego, Calif.). Phys. Fluids, 8: 708-12 (Apr. 1965).

A supersonic flow of an electron plasma past a weak magnetic dipole is examined using a linearized set of two-species continuum plasma equations. The resulting perturbations were found to exhibit both a hyperbolic as well as an elliptic behavior. The results as found are not directly applicable to the solar wind interaction with the geomagnetic dipole, but they strongly suggest the necessity of re-examining the validity of magnetospheric models of the interaction, starting from the full two-species plasma equations. (auth)

21536 WAVE PROPAGATION IN HOT PLASMA WAVEGUIDES WITH INFINITE MAGNETOSTATIC FIELDS. H. H. Kuehl, G. E. Stewart, and C. Yeh (Univ. of Southern California, Los Angeles). Phys. Fluids, 8: 723-9(Apr. 1965).

Solutions of the "dispersion relation" for an unbounded Maxwellian electron plasma, $2k^2/k_D^2 = Z'(\omega/kv_{th})$ for ω real are given. Solutions of the corresponding relation for a circular waveguide filled with a hot plasma with an infinite magnetostatic field are also presented. It is shown that these solutions are of importance in evaluating the fields in such waveguides since they determine the poles of the integrands which arise in the integral formulation of the problem. The integral solution for the field in the waveguide due to a general symmetric excitation at the wall of the waveguide is given. (auth)

21537 PLASMA DEPOLARIZATION AND HEATING IN THE COLLISIONS OF POLARIZED PLASMAS. Everet H. Beckner (Sandia Lab., Albuquerque, N. Mex.). Phys. Fluids, 8: 730-8(Apr. 1965).

A study was conducted of the deceleration and depolarization phenomena which occurred when oppositely-directed plasma streams were caused to collide in the presence of a transverse magnetic field. The depolarization which followed collision of these oppositely-polarized plasmas resulted primarily from plasma deceleration through $j \times B$ forces. Translational kinetic energy was found to be efficiently converted to thermal energy in such processes. In addition, Ohmic heating effects were quite important, particularly late in time. Ohmic potential drops were found to be unimportant, even for these highly tensor plasmas. The presence of the transverse magnetic field during collision resulted in significant increase in the assembled plasma temperature, density, and "lifetime," compared to those which occurred when the field was absent. (auth)

21538 CHARGE SEPARATION EFFECTS IN THE FERRARO-ROSENBLUTH COLD PLASMA SHEATH MODEL. Arrigo Sestero (New York Univ., New York). Phys. Fluids, 8: 739-44(Apr. 1965).

An exact treatment is given of the Ferraro-Rosenbluth cold plasma sheath model, to improve on the charge neutral approximation considered previously in the literature. It is found that the turning points of the ion stream and of the electron stream are actually separated in space. It is found also, somewhat unexpectedly, that there exists a certain range of parameters for which the ions are turned back sooner than the electrons, due to the combined effect of the electric and magnetic forces in the sheath. The change of behavior in the solution occurs discontinuously, allowing for no intermediate case with the two species of particles turning together. Finally, it is found that the sheath is not, in general, over-all charge-neutral, and that the excess charge can actually be of either sign, depending on the values of the parameters. (auth)

21539 PLASMA VORTICES IN THE COAXIAL PLASMA ACCELERATOR. W. H. Bostick, W. Prior, and E. Farber (Stevens Inst. of Tech., Hoboken, N. J.). Phys. Fluids, 8: 745-7(Apr. 1965).

Considerations of conservation of mass and momentum flow in the plasma coaxial accelerator make it apparent that plasma eddies or vortices should be produced behind the current sheet. Measurements of axial and radial electric fields of radial current density and ion flow density, show experimentally that these vortices are present. (auth)

21540 EFFECT OF SHEATHS ON DRIFT INSTABILITIES IN THERMIONIC PLASMAS. Francis F. Chen (Princeton Univ., N. J.). Phys. Fluids, 8: 752-4(Apr. 1965).

The effect of electron and ion sheaths on drift instabilities was investigated for a cylindrically symmetric, thermally ionized plasma created between two hot cathodes in a strong magnetic field. The sheath conditions at the boundary are given. The dispersion relation was derived for waves with arbitrary axial wavelengths, and eigenvalues are found from the boundary conditions for any machine condition. The relation is generalized to include field curvature and finite Larmor radius stabilization. A numerical example is given for the lowest azimuthal mode of a 2300°K potassium plasma. (L.B.S.)

21541 EFFECTS OF PASSING CURRENT ON PLASMA LOSSES IN A Q-DEVICE. N. D'Angelo and A. Y. Wong (Princeton Univ., N. J.). Phys. Fluids, 8: 757-8(Apr. 1965). (MATT-284)

An experiment was performed in a Q-3 device to test the dependence of the density fall-off, n/n_0, on the ratio of the ion temperature to the plate temperature. It was found that heating of the plasma ions by the current enhances the recombination mechanism at the plate, and results in a decrease of plasma density, as predicted by the equation for $\ln n$ vs $(x-1)(x+1)$. (L.B.S.)

21542 METHOD OF INTEGRATION OF THE BOLTZMANN EQUATION IN THE PRESENCE OF SPATIAL GRADIENTS. Akira Hasegawa (Bell Telephone Labs., Murray Hill, N. J.). Phys. Fluids, 8: 761-2(Apr. 1965).

A method of integration of the Boltzmann equation is introduced for a linearized part of the electron distribution function in a nonuniform magnetized plasma. The function, f_1, is obtained in terms of the linearized field quantities and the stationary density function through operators involving spatial gradients, and is used together with Maxwell's equations to yield a set of differential equations with current and charge density being expressed as functions of spatial derivatives of the fields. (L.B.S.)

21543 COMMENT ON "TIME DEPENDENCE OF THE TWO-PARTICLE CORRELATION FUNCTION IN A ONE-COMPONENT PLASMA." Ralph L. Guernsey (Univ. of Maryland, College Park). Phys. Fluids, 8: 766-7(Apr. 1965).

Comments are made on the meaningfulness of Lamb's expansion of t, in powers of the plasma parameter, and the asymptotic behavior of the explicitly time-dependent Landau damped contributions. (L.B.S.)

21544 COMMENTS ON "THERMOELECTRIC EFFECTS IN A JOULE-HEATED PLASMA." Malcolm Haines (Imperial Coll. of Science and Tech., London). Phys. Fluids, 8: 768-9(Apr. 1965).

The large difference in the physical results that are obtained for the thermoelectric effects in a Joule-heated plasma is pointed out for the case in which the transport coefficients of Marshall are used instead of Spitzer and Haim or Robinson and Bernstein. Other changes in the theoretical model that can produce a limiting heat flow to the cathode are indicated. (L.B.S.)

21545 HIGH FREQUENCY WAVE-VECTOR DEPENDENT CONDUCTIVITY OF A DEGENERATE ELECTRON GAS. M. Suffczynski (Michigan State Univ., East Lansing). Phys. Letters, 14: 305-6(Feb. 15, 1965).

The leading asymptotic corrections to the conductivity of a degenerate electron gas is calculated for the case in which the electromagnetic wave frequency is higher than the electron collision frequency. The Kubo expression for conductivity is given in terms of the autocorrelation function of the current operators, and the diagram technique of

the temperature-dependent Green functions is applied. (L.B.S.)

21546 ON NON-LINEAR RESONANT LIGHT MIXING IN PLASMAS. A. Salat (Institut fur Plasmaphysik GmbH, Garching, Ger.). Phys. Letters, 15: 139-41(Mar. 15, 1965).

Density fluctuations stimulated by two beams of laser light in a plasma and the scattering signal obtained by scattering a third laser beam on the fluctuations are investigated. Calculations are made which show the essential differences in the intensity of the scattering signal and the accuracy of the adjustment of the beams between a two and three laser system. Numerical results are presented for a ruby light. It is concluded that non-linear light mixing is detectable with present lasers in two and three laser systems, and the latter gives higher intensities but requires a more careful experimental adjustment. (L.B.S.)

21547 INTERACTION OF LIGHT WITH LIGHT IN A PLASMA. H. Cheng (Bell Telephone Labs., Murray Hill, N. J.) and Y. C. Lee. Phys. Rev. Letters, 14: 426-8 (Mar. 22, 1965).

The processes contributing to scattering of a light beam incident on a plasma which is excited by two light beams are investigated. The hamiltonian of the plasma-photon system is given and the scattering amplitude is obtained. It is shown that the cross section not only includes contributions from the process of elastic light-light scattering, but also from inelastic light-light scattering and from other inelastic processes. (L.B.S.)

21548 ROTATIONAL INSTABILITY IN A PENNING-TYPE DISCHARGE. K. I. Thomassen (Stanford Univ., Calif.). Phys. Rev. Letters, 14: 587-9(Apr. 12, 1965).

The results of an investigation of a low-pressure, hot-cathode hydrogen discharge are presented. A dominant m = 1 structure was observed in the discharge noise above the critical value of the magnetic field, together with an increase in the noise amplitude of the m = 1 mode at the critical magnetic field above which the diffusion is anomalous. Further, a dominant m = 3 structure was observed below the critical field, as well as damping of the m = 1 flute below the critical field. (D.C.W.)

21549 HARMONIC GENERATION AND FREQUENCY MIXING AT PLASMA RESONANCE. R. A. Stern (Bell Telephone Labs., Whippany, N. J.). Phys. Rev. Letters, 14: 538-40(Apr. 5, 1965).

Oscillations were generated in the positive column of a low-pressure mercury glow discharge by microwave signals. At signal frequencies corresponding to the excitation of the Tonks-Dattner resonances, the generation of the second harmonic of the excitation signal and of beat frequencies (linear sums) of the fundamental frequencies of two simultaneously excited oscillations was observed. The observations were found to be consistent with solutions of the nonlinear Vlasov equation and to represent the inherent nonlinear properties of plasma-electron oscillations. (D.C.W.)

21550 RADIATION-INDUCED INSTABILITY OF ELECTRON PLASMA OSCILLATIONS. D. F. DuBois (Hughes Research Labs., Malibu, Calif.). Phys. Rev. Letters, 14: 544-6(Apr. 5, 1965).

The absorption of radiation by electrons in plasma is studied. It is shown that, for radiation frequencies near the plasma frequency, electron oscillations can become unstable and grow in amplitude when they gain energy faster than they can dissipate it by their dominant damping mechanism. (D.C.W.)

21551 ANALYSIS OF STATISTICAL CURRENT FLUCTUATIONS IN A TOWNSEND DISCHARGE. C. J. Evans (University Coll. of Swansea, Wales, U. K.). Proc. Phys. Soc. (London), 85: 185-90(Jan. 1965).

An expression is derived for the frequency spectrum of the electron current fluctuations in a gas discharge, with a uniform electric field and steady illumination of the cathode. The expression is modified for those cases in which the positive ion current must be taken into account, and it is shown how the distribution of frequencies depends on the type of secondary process present. The application of the results to experimental measurements is discussed. (auth)

21552 AN EXPERIMENTAL STUDY OF HELICON WAVE PROPAGATION IN A GASEOUS PLASMA. J. A. Lehane and P. C. Thonemann (United Kingdom Atomic Energy Authority, Abingdon, Berks, Eng.). Proc. Phys. Soc. (London), 85: 301-16(Feb. 1965). (CLM-P-64)

The results of an experimental study of helicon wave propagation in a partially ionized cylindrical plasma are reported. Conditions were chosen so that the phase velocity of the wave was independent of both the electron and ion mass. The phase velocity, the attenuation, and the structure of the plasma magnetic fields are compared with the theoretical treatment of Klozenberg, McNamara, and Thonemann in 1964. The agreement is satisfactory. In particular, evidence is presented which supports the anomalously high attenuation due to surface currents predicted by the theory. (auth)

21553 A STUDY OF HELICON WAVES IN INDIUM. G. N. Harding and P. C. Thonemann (United Kingdom Atomic Energy Authority, Abingdon, Berks, Eng.). Proc. Phys. Soc. (London), 85: 317-28(Feb. 1965). (CLM-P-54)

Measurements were made of the phase velocity and the attenuation of helicon waves propagated parallel to the axis of a long cylinder of indium metal at 4.2°K. A constant magnetic field was applied parallel to the axis of the cylinder. Both the axisymmetric (m = 0) and dipole (m = ±1) modes were studied. The experimental results are compared with the predictions of theory for two different assumptions concerning the boundary conditions. It is shown that the theoretical predictions which include non-zero vacuum fields give the best agreement with the experiment. The Hall coefficient derived from these measurements is consistent with that calculated on the assumption of one hole per atom within the experimental error (~1.5%). (auth)

21554 THE STARTING MECHANISM OF THE FIRST STAGE OF THE RING DISCHARGE. K. Chandrakar and A. von Engel (Oxford Univ.). Proc. Roy. Soc. (London), Ser. A, 284: 442-54(Mar. 9, 1965).

When the high-frequency magnetic field of a coil surrounding a cylindrical vessel filled with hydrogen is increased above a critical value, a faint discharge starts which emits the H_2-band spectrum. If the current in the coil is raised further, an intense ring discharge suddenly develops showing predominantly the atomic hydrogen lines. The first stage is shown to be initiated by the axial component of the electric field of the coil, even when conventional electrostatic screens are used. When the axial component is suppressed, a circumferential component of even twice the axial starting field fails to initiate the discharge. This axial uniform field is calculated for low pressures, at which the mean free electron path exceeds the size of the vessel, by assuming that electrons are multiplied by collisions with the glass wall; it is thus independent of the gas and its density. The dependence of the starting field on length, pressure and frequency is measured using a vessel of variable length and 4 cm radius. Values of 9 and 5 v/cm peak at 15 and 5 Mc/s respectively are found between 10^{-4} and 10^{-2} mmHg at 20 cm length, in agreement with theory. For pressures between 0.1 and 1 mmHg the starting field is calculated by balancing the rate of gas ionization by electron collisions and the loss of charge by diffusion to the wall, field-dependent energy losses being allowed for. Its value, now depending on the nature of the gas, rises with increasing pressure and becomes frequency-independent at higher pressures. Again, theory and experiment agree quantitatively. (auth)

21555 OPTICAL METHODS OF DETERMINING SOME CHARACTERISTICS OF AN ARC DISCHARGE. E. V. Il'ina. Sb. Tr. Leningr. Mekhan. Inst., No. 33, 135-41 (1963).

The outward drift of Li, Na, and Ba atoms injected into

an arc and the change in the temperature of the arc plasma following introduction of small amounts of Na between carbon electrodes were investigated experimentally. The diffusion of material from the arc was observed using an SKS-1 camera. The investigated substances ($NaNO_3$, $BaCO_3$, $LiCO_3$) in the form of granules, were introduced into the discharge on the point of a quartz needle which crossed the discharge at a speed of 60 cm/sec. The glow of the atoms of the introduced substance was separated by interference light filters. The curves showing the variation of the blackening from frame to frame made it possible to determine the average time that the atoms stayed in the arc and the diffusion coefficient. The diffusion coefficient was also calculated from the rate of displacement of the boundary of the glowing region in the plasma, or from the rate of displacement of a surface having a definite glow intensity. The temperature of the arc was determined from the ratio of the intensities of the spectral lines. A decrease in the arc temperature was observed when sodium atoms were introduced into the arc. (tr-auth)

21556 PROPERTIES OF ARGON–CESIUM PLASMA IN AN ELECTRIC FIELD. V. A. Abramov and Yu. A. Tarasov. Teplofiz. Vysokikh Temp., 2: 313-20(1964).

To determine the efficiency gain from increasing the conductivity of a MHD-generator plasma stream above its equilibrium value with the aid of an electric field, the electric field necessary to heat electrons in an argon–cesium plasma to 3000–4000°K was estimated. The energy lost in elastic collisions by the cesium ions and atoms and by the argon atoms and by inelastic collisions is taken into account. Some of the losses, such as radiation losses, included in the energy balance were evaluated elsewhere. The values of the optimal plasma conductivity are obtained for different cesium concentrations and argon pressures in the electron temperature range 3000–4000°K. Some possible causes of plasma instability are mentioned. (ATD)

21557 RECOMBINATION DECAY IN NONISOTHERMAL PLASMA. K. N. Ul'yanov. Teplofiz. Vysokikh Temp., 2: 510-16(1964).

The theory of recombination decay in nonequilibrium nonisothermal plasmas is considered, including electron and heavy-particle temperature variations. The normalized equation for the time rate of change of the concentration of electrons and atoms in all states and the differential form of Saha's equation are given. These equations and the energy conservation equation are combined to obtain expressions for the electron and heavy-particle temperatures. The limiting cases of electron temperature reduction without change in electron concentration and of slow rate of change of electron temperature, such that variations in excited atom concentrations depend only slightly on electron concentration, are considered. The decay of nonequilibrium, optically transparent H plasma is analyzed, using the developed formulas. (ATD)

21558 LOWERING NEGATIVE ION-ELECTRON DETACHMENT POTENTIAL IN PLASMA. I. V. Avilova and G. E. Norman. Teplofiz. Vysokikh Temp., 2: 517-24(1964).

The effect of nonideal conditions on the concentration and spectra of photodissociation of negative ions in a plasma is investigated. Three factors affecting negative-ion and electron concentrations are studied: Debye-Hückel change in free energy, statistical weight corrections for upper excitation states, and continuous lowering of ionization potential. In homogeneous electric fields, the lowering of the potential barrier ΔA (A is the electron-negative ion affinity potential) is obtained by the equation $\Delta A(E) = \frac{5}{4}eE(2ae/E)^{\frac{1}{5}}$ where, for $\Delta A = A$, $E = E_1$. For micropoles with potentials greater than E_1, no negative ions can exist. Saha's equation is modified to include the potential $A - A(E)$ instead of A and integrated over all micropole distributions to yield $\int_0^{E_1} \exp[-\Delta A(E)/kT]f(E)dE + \gamma\beta$, where f(E) is the micropole distribution function. The value of γ is calculated for Li^- and Cs^- ions, in a pressure range $p = 0.1 - 100$ atm and temperature range $T = 3000$-6000°K, and represented graphically. The results show a significant departure in γ from unity. Similar calculations are made for β which is shown to indicate the lowering of the average electron-affinity potential of negative ions. An expression is derived for the long wavelength shift in the photodissociation spectrum, which in turn is shown to be an indication of a lowering in the electron dissociation potential. (ATD)

21559 INSTABILITY OF ELECTROMOTIVE FORCES IN WEAKLY IONIZED PLASMAS. B. V. Eliseev. Teplofiz. Vysokikh Temp., 2: 852-9(1964).

Instabilities in electromotive forces generated by currents flowing perpendicular to the magnetic field are investigated. The instabilities are produced either by electron current speeds or ion slipping speeds exceeding the speed of sound in the neutral gas. A dispersion relation is obtained from the governing hydromagnetic and Maxwell's equations. Effects of viscosity and heat conduction are considered as perturbations, and the growth rate of sonic oscillations is shown to be of order γ_m. Ionization instabilities in a nonhomogeneous plasma are discussed and are shown to lie within the straight line $\delta^2_{MIN} = (4/a^2)(1 + a)$ and the curve $\tau' = \tau + (T_e/N_s)(dN_s/dT_e)(\varphi\sigma N_s/j_0^2)$. Instabilities in the region below the curve are predominantly caused by electron motion. The limit of stability with respect to ion slip is given by $V_T/V_S = 1/\delta_+$. (ATD)

21560 EFFECT OF NITROGEN IMPURITY ON ELECTRON ENERGY LOSS IN NONEQUILIBRIUM ARGON–CESIUM PLASMA. V. K. Zhibritskii. Teplofiz. Vysokikh Temp., 2: 945-6(1964).

To study the effect of impurities on the electron energy balance in a plasma, a steady-state discharge in argon was investigated with various nitrogen concentrations $\alpha(P_{N_2}/P_{Ar})$ and addition of cesium ($P_{Cs} = 0.1$ mm Hg). The total gas pressure in the discharge tube was maintained at 100 mm Hg and the current at a constant value of 0.5 amp. Electron temperatures were plotted as conductivity ($S = W/\sigma$, volt · cm^{-2} · ohm) and electron temperature T_e versus concentration α. The S versus α curve shows a sudden increase for values of α above 5×10^{-3}. The S versus T_e curve shows a two-fold rise between $\alpha = 10^{-4}$ to 10^{-3}, followed by a subsequent decrease to the original level at $\alpha = 10^{-2}$. These results show that the effects of molecular impurities are significant on the nonequilibrium conductivity of argon–cesium plasmas. (ATD)

21561 ON THE EXCITATION OF SOUND WAVES IN A WEAKLY IONIZED PLASMA. V. V. Angeleiko and A. B. Kitsenko (Inst. of Physics and Tech., Kiev.). Ukr. Fiz. Zh., 10: 16-20(Jan. 1965). (In Ukrainian)

The low-frequency electron-ion oscillations of a weakly ionized plasma were investigated. It is assumed that the equilibrium distribution function of electrons satisfy by velocities the kinetic equation with the collision integral in Davidov's form. It is shown that the electron drift with respect to ions may lead, in the presence of a strong external electric field, to the instability of distribution obtained by Davidov. This instability is associated with excitation of electron-ion oscillations. (auth)

21562 A HOLLOW-CATHODE-FED HOLLOW CONDUCTOR FOR PLASMA. S. Ahlbom and H. Neuhaus (Univ. of Stockholm). Z. Naturforsch., 19a: 1419-20(Dec. 1964). (In German)

The suitability of a hollow cathode for plasma injection is investigated. The design and construction of the hollow conductor is described. It is filled with helium at a pressure of about 1 torr. The transmission factor is very sensitive to changes in gas pressure and current strength. The hollow conductor can also be used as an amplitude modulator for microwaves. Studies with hydrogen or neon gave qualitatively similar transmission curves. (J.S.R.)

21563 NONLINEAR THEORY OF INTERACTION BETWEEN ELECTRON BEAMS IN PLASMA AND THE TRANSVERSE WAVES. L. M. Kovrozhnykh and V. N. Tsytovich. Zh. Tekhn. Fiz., 35: 14-25(Jan. 1965). (In Russian)

A self-consistent problem of nonlinear interaction between an electron beam propagated in plasma and a longitudinal or transverse wave, characterized as a noise, was

solved. Both the "inherent" radiation generated by the beam itself and the external radiation were taken into account. The interaction of a nonrelativistic electron beam propagated with a velocity much greater than thermal velocity and the interaction of an ultrarelativistic electron beam were considered. The second case is of interest since the radiation frequencies at which nonlinear effects appear can be in a region of very high frequencies adjacent to the visible range. Three different cases were investigated: a beam existing in plasma for a sufficiently long time, in which there are only "inherent" noises; the presence of sufficiently intense external noise sources (transverse noises); and a beam passing momentarily through a bounded system (a radiation generated by the beam). (ATD)

21564 INTERACTION OF A TRAVELLING ELECTROMAGNETIC WAVE WITH A PLASMA. R. A. Demirkhanov, I. A. Kossyi, N. I. Leont'ev, S. N. Lozovskii, Yu. K. Udovichenko, and T. M. Filatova. Zh. Tekhn. Fiz., 35: 43-6 (Jan. 1965).

An experimental investigation was undertaken to test the possibility of confining a plasma by means of a traveling electromagnetic wave as proposed by Osovets. A toroidal pulsed machine was used, similar to that described by Demirkhanov. Hydrogen plasma was investigated at a pressure of 0.06 mm Hg. One megacycle/sec traveling waves were produced with a delay line terminated in its surge impedance. The phase velocity was 5.6×10^7 cm/sec and the maximum amplitude of the magnetic field was 230 gauss. The electron density and temperature and the longitudinal component of the high-frequency magnetic field were measured at various distances from the axis to the discharge tube by means of probes. The electron temperature was approximately constant at 60,000°K; and the electron density was of the order of 10^{14} cm^{-3}. From the measured data, the gradients of the plasma pressure and the magnetic pressure were calculated. The plasma pressure gradient everywhere exceeded the magnetic; confinement of the plasma was accordingly not achieved. Some calculations are presented concerning the behavior of a plasma in a high-frequency magnetic field. To achieve confinement it is not sufficient simply to increase the magnetic field strength, for the high-frequency field tends to heat the plasma. It is concluded that confinement can be achieved only in an incompletely ionized plasma with a large electron density, in which energy can be transferred from the electrons to the walls of the chamber via the ions and the neutral particle. (ATD)

21565 RESONANCE INTERACTION BETWEEN A PLASMA BUNCH AND AN ELECTROMAGNETIC WAVE IN A WAVEGUIDE. B. P. Kononov. Zh. Tekhn. Fiz., 35: 47-50(Jan. 1965). (In Russian)

The reflection of H_{01} and H_{11} waves from a stationary plasma bunch of quasi-spherical form in a circular waveguide was investigated. H_{01} and H_{11} modes, which are easily excited and can be employed in radiative plasma acceleration, were generated in a circular waveguide 14 cm in diameter. A plasma bunch was formed with the aid of a pulsed gas discharge in a spherical glass bulb placed on the axis of the waveguide. Basic measurements were performed with a bulb 3.5 cm in diameter in the 1 to 2×10^{-1} mm Hg pressure range. The calculated dependence of electric and magnetic moments on plasma density coincided with the experimental results. Resonance wave scattering can play an essential role in radiative acceleration of plasma. When the wave is scattered by a relatively large plasma bunch, the "radiative friction" is large, and the resonance is relatively weak. However, when the wave is scattered by small objects, the resonance effect is intensified considerably and can be used for increasing the effectiveness of radiative acceleration. (ATD)

21566 PLASMA ACCELERATION WITH THE AID OF AN ELECTROMAGNETIC H_{11}-TYPE WAVE IN A CIRCULAR WAVEGUIDE. B. P. Kononov, K. A. Sarksyan, V. A. Silin, and L. E. Tsopp. Zh. Tekhn. Fiz., 35: 51-5(Jan. 1965). (In Russian)

The acceleration of plasma bunches with the aid of a strong electromagnetic H_{11} wave in the decimeter range in a circular waveguide was experimentally investigated. The plasma was generated by a source with a pressure drop. An external magnetic field was used to confine the plasma bunch. The experimental setup consisted of an ultrahigh-frequency generator, a plasma source, an accelerating waveguide with a focusing magnetic field, and measuring devices. The generator produced single 1.5-Mw pulses of 10-μsec duration. An H_{01} wave from a rectangular waveguide was transformed into an H_{11} wave in a circular waveguide. The pressure in the waveguide was 1 to 2×10^{-6} mm Hg. The measurements showed that during a radiative plasma acceleration the ions acquired different energies. The character of the interaction of the wave with the plasma depends on the relation between the frequency of the incident wave (ω) and the frequency of the Langmuir oscillations in the plasma (ω_e). At $\omega > \omega_e$ the plasma bunch is transparent, and if its size is smaller than the wavelength a coherent interaction takes place and the total acting force is proportional to the number of electrons in the plasma bunch. It is suggested that ions with energies of 50 kev and higher appear as a result of resonance acceleration of plasma bunches of small effective size. Such bunches can appear during plasma decay. (ATD)

21567 SPECTROSCOPIC INVESTIGATION OF THE PLASMA IN COLLIDING BURSTS. V. G. Zykov, I. A. Stepanenko, L. A. Dushin, I. K. Nikol'skii, O. S. Pavlichenko, and V. T. Tolok. Zh. Tekhn. Fiz., 35: 56-61(Jan. 1965). (In Russian)

The processes taking place in colliding plasma bursts were investigated. Plasma bursts were injected from one or more of four conical plasma guns equally disposed about the periphery of a 20 cm diameter stainless steel tube, and the spectra were observed in both the longitudinal and transverse directions. The time-integrated spectrum was recorded photographically in the range from 2000 to 6000 Å, and the time dependence of the intensity of certain lines was determined with a photoelectric instrument. The plasma bursts had a maximum density of 2×10^{14} cm^{-3}, and the electron temperature was 4 to 4.5 ev. The velocity of the fast component of a bursts was 1.4×10^7 cm/sec; this was followed by a slower "tail." The collision of two plasma bursts led to an increase in the intensity of all spectrum lines and the appearance of lines that were not observed in single bursts. Velocity measurements performed with the photoelectric instrument using the H_β 4861, C I 4371 and C II 4267 lines showed that both the carbon ions and the hydrogen atoms moved more rapidly than the carbon atoms. The presence of excited ions in the plasma burst at a considerable distance from the source is discussed, and it is suggested that these are continually formed by a charge exchange mechanism. The ion temperature was determined from the Doppler broadening of the C II 4267 line. Collision of the plasma bursts was found to be accompanied by an increase of the ion temperature. It is concluded that the strong interaction between plasma bursts observed in this and the previous work can be accounted for by Coulomb interaction. (ATD)

21568 INVESTIGATION OF THE CAPTURE OF PLASMA IN A MAGNETIC TRAP WITH OPPOSING FIELDS. V. G. Zykov, I. A. Stepanenko, V. T. Tolok, and K. D. Sinel'nikov (Inst. of Physics and Tech., Kharkov) Zh. Tekhn. Fiz., 35: 62-71(Jan. 1965). (In Russian)

The confinement of plasma by a three-cusp magnetic field produced in a 20-cm-diameter stainless steel cylinder by four windings was investigated. The maximum magnetic field at the wall of the chamber in the cusps was 1200 gauss. Hydrogen plasma was injected at one or more of the cusps by four conical plasma guns equally spaced about the periphery. The ion density and electron temperature were measured with probes, and the magnetic properties of the plasma were studied with a magnetic probe. Particular attention was given to the density and persistence of the plasma in the plane of the central cusp. It was found that when the plasma was injected only in the central cusp the

magnetic field did not tend to confine it to this region. The magnetic field did, however, tend to confine to the central region plasma that was injected at one of the side cusps, and this tendency was markedly increased (the decay time increased from 30 to 55 microsec) when plasma was injected at both side cusps simultaneously. This behavior is ascribed to interaction between the opposing plasma streams entering the central region from the two sides. The maximum density reached by the plasma on the axis in the plane when it was simultaneously injected at all three cusps was 7.5×10^{14} cm^{-3}. In all cases the electron temperature (approximately 4.5 ev) was independent of time. (ATD)

21569 INSTABILITY AND ANOMALOUS DIFFUSION IN A POTASSIUM PLASMA. N. S. Buchel'nikova, A. M. Kudryavtsev, and R. A. Salimov. Zh. Tekhn. Fiz., 35: 72-83 (Jan. 1965). (In Russian)

In order to investigate the instability of a nonuniform plasma in a magnetic field when the ion Larmor radius is comparable with the dimensions of the plasma, the electromagnetic oscillations and diffusion of a potassium plasma column were measured. The plasma was formed in a 4-cm-diameter, 50-cm-long cylindrical chamber by surface ionization of K atoms on a 2-cm-diameter hot tungsten spiral. A longitudinal magnetic field up to 1200 gauss was applied, and plasmas of density from 10^7 to 5×10^{11} cm^{-3} were investigated. The plasma column was most dense on the axis of the chamber, and the radius of the column at half-maximum density was ordinarily about 6 mm. Electromagnetic oscillations were observed with a fundamental frequency between 60 and 70 Kc/sec and an intensity exceeding the noise level by a factor of 100. The second and third harmonics of these oscillations were also observed with somewhat lower intensity. The wavelength was determined by measuring the phase shift between the signals received by two movable probes. The wavelength of the fundamental in the azimuthal direction was found to be equal to the circumference of the plasma column; the wavelength in the longitudinal direction was approximately 20 cm. The frequency and wavelength of these oscillations were independent of the magnetic field strength, but the oscillations disappeared when the magnetic field was increased to such an extent that the ion Larmor radius became considerably smaller than the radius of the plasma column. The diffusion constant of the plasma transversely to the magnetic field was measured by the method of Alikhanov. The diffusion constant was found to be of the order of 5×10^4 cm^2/sec; it decreased slowly with increasing magnetic field and plasma density. The experimental data are discussed at some length; and, by a process of elimination, it is concluded that the observed oscillations represent a new type of plasma instability associated with the large ion Larmor radius and that the anomalous diffusion (which is about an order of magnitude greater than can be accounted for by the classical processes), is due to this new instability. (ATD)

21570 INVESTIGATION OF THE STEADY FLOW OF A WEAKLY IONIZED PLASMA IN THE HOMOPOLAR DEVICE. K. V. Donskoi and E. M. Drobsyhevskii (Ioffe Inst. of Physics and Tech., Leningrad). Zh. Tekhn. Fiz., 35: 84-93(Jan. 1965). (In Russian)

The radial pressure drop and velocity profile were measured in a mass of rotating plasma confined between two coaxial cylindrical electrodes in a longitudinal magnetic field. The radii of the water-cooled aluminum electrodes were 3.4 and 9.8 cm, and the annular region occupied by the plasma was bounded axially by two dielectric walls 3.6 cm apart. The plasma was formed by electric breakdown of the gas (usually air at a pressure between 0.125 and 1.0 torr) and was caused to rotate by the magnetohydrodynamic force due to the interaction of the radial current with the longitudinal magnetic field. Magnetic fields up to 5500 gauss were used. The temperature of the plasma was estimated to be 700°K. The pressure drop between the outer and inner electrodes was measured with an inclined oil manometer, and the velocity profile was determined by measuring the viscous drag on 0.5-cm-diameter spheres. Both the pressure drop and the radial distribution of azimuthal velocity was found to depend markedly on the polarity of the electrodes. When the inner electrode was the cathode, the pressure drop was much less than with the opposite polarity; in some cases it even became negative, the pressure at the inner electrode then being greater than at the outer. The velocity profile was more sharply peaked in this case (inner electrode the cathode) and the maximum velocity occurred at a smaller radius. The possible origin of the polarity sensitive body forces responsible for this behavior is discussed, and it is concluded that they are principally due to an "ionic wind" effect, which arises from the fact that the magnetic field hinders the motion of the electrons parallel to the electric field more than that of the ions. The stability of the flow was investigated, and it is concluded that the flow was laminar in most of the experiments. When the gas pressure was sufficiently increased, instability set in, as evinced by fluctuating forces on the probe sphere. This is ascribed to "destruction of the symmetry of the electric and hydrodynamic parameters of the system with respect to the central plane of the chamber as a consequence of the inhomogeneity of the magnetic field." When the gas pressure was sufficiently reduced, the potential on the electrodes suddenly increased or the current decreased. The cause of this instability is obscure. (ATD)

21571 FORMATION OF A QUASINEUTRAL BEAM OF ACCELERATED IONS IN THE PLASMA ISSUING FROM AN ION SOURCE. M. D. Gabovich, L. I. Romanyuk, and E. A. Lozovaya (Inst. of Physics, Academy of Sciences, Ukrainian SSR). Zh. Tekhn. Fiz., 35: 94-100(Jan. 1965). (In Russian)

A reflex-discharge ion source was operated under a variety of conditions. The current-voltage characteristics were measured, and particular attention was given to the potential gradient in the plasma beam issuing from the source. The principal conclusion is that the following conditions are requisite for obtaining ions with energies corresponding to the cathode drop: the issuing plasma must contain an intense beam of primary electrons with appropriate velocity distribution; the plasma must issue from the chamber into a region of sufficiently high vacuum; and there must not be a positively charged electrode outside the discharge chamber that could remove electrons from the issuing plasma. (ATD)

21572 ULTRAHIGH FREQUENCY INVESTIGATION OF PLASMA DEIONIZATION AT ATMOSPHERIC PRESSURE. S. I. Andreev and B. M. Sokolov. Zh. Tekhn. Fiz., 35: 101-7(Jan. 1965). (In Russian)

An ultrahigh frequency method is described by which the time variation of the electron density and temperature of a plasma can be determined and some information can be obtained concerning the distribution of these quantities along the plasma column. This method was used to investigate the deionization following a spark discharge in air at atmospheric pressure, and the results are presented and discussed. A 76-ohm coaxial resonator was used, loaded with an adjustable internal capacitance so that its resonant frequency could be varied slightly from the 750 Mc/sec exciting frequency. The spark discharge took place within the resonator, and the characteristics of the resulting plasma were determined from the shift in resonant frequency and the change in the Q of the cavity. The theory of these effects is discussed, and it is shown that an average value of the electron concentration and temperature can be determined and some information can be obtained concerning the deviation from uniform electron density distribution. It was found that the electron density following a spark discharge in air is very unevenly distributed over the length of the gap. The volume recombination coefficient at electron concentrations between 10^9 and 10^{10} cm^{-3} was found to vary from 2×10^{-6} to 1.5×10^{-5} cm^3/sec, depending on the length of the gap and the energy of the discharge. (ATD)

21573 ON THE ELECTRON AND ION DISTRIBUTION FUNCTIONS FOR A PLASMA IN A SLIGHTLY NONUNI-

FORM HIGH-FREQUENCY FIELD. A. G. Litvak, M. I. Petelin, and E. I. Yakubovich. Zh. Tekhn. Fiz., 35: 108-16 (Jan. 1965). (In Russian)

The electron and ion distribution functions for a completely ionized plasma confined in a high-frequency potential well are calculated with collisions taken into account. The thermal velocities are assumed to be small compared with the velocity of light. The kinetic equations are employed with collision integrals in the form given by Landau. The equations of motion include the forces due to the applied high-frequency field and to the electric field arising from the average separation of charge. The coordinates and velocities of the particles are separated into oscillatory and drift components, and by suitably averaging over the former, kinetic equations are derived for the quasiparticles represented by the latter. These are solved on the assumptions that the number of particles in the body of the plasmoid is much greater than the number in the skin layer and that the mean free path of a particle greatly exceeds the dimensions of the region in which it is localized (the amplitude of the corresponding oscillatory component of the corresponding coordinate), and the distributions are found to be Maxwellian. The time variation of the ion and electron temperatures is calculated in the quasistationary approximation, and it is found that both ultimately increase with time, the electron temperature more rapidly than the ion temperature. The effects of loss of particles through the potential barrier and heating due to space dispersion are estimated, and the H theorem is derived for particles described by Landau's collision integrals in a third. (ATD)

21574 A MULTIPLE BEAM RADIOINTERFEROMETER FOR PLASMA DIAGNOSTICS. V. Ya. Balakhanov, V. D. Rusanov, and A. R. Striganov. Zh. Tekhn. Fiz., 35: 127-31 (Jan. 1965). (In Russian)

A multiple beam microwave interferometer of the Fabry-Perot type is proposed for plasma diagnostics. The multiple beam instrument should have the advantage over the usual two-beam interferometer of greater sensitivity, and it should also permit the measurement of the electron collision frequency. The partially reflecting surfaces would consist of silvered mica sheets from which the silver has been removed in parallel strips to provide the requisite transparency. The theory of the instrument is discussed briefly, and it is concluded that it should be possible to measure electron concentrations as low as 1.7×10^9 cm^{-3}. By observing the change in the Q of the instrument due to the introduction of the plasma, it should be possible to measure electron collision frequencies as low as 1.4×10^6 sec^{-1}. Either a reflector may be moved as in the usual Fabry-Perot interferometer or the exciting frequency may be modulated. In the latter case it would be possible to follow the time development of processes in a pulsed plasma. The use of the confocal Fabry-Perot interferometer is also briefly discussed. This should have some advantages in the case of a cylindrically or spherically symmetric plasma. (ATD)

21575 ON THE EXCITATION OF MAGNETOACOUSTIC WAVES IN COLLIDING PLASMA STREAMS. D. G. Lominadze and K. N. Stepanov (Inst. of Physics, Academy of Sciences, Georgia SSR and Inst. of Physics and Tech., Academy of Sciences, Ukrainian SSR). Zh. Tekhn. Fiz., 35: 148-51(Jan. 1965). (In Russian)

The stability against low-frequency long-wavelength oscillations of two interpenetrating plasma streams moving in opposite directions parallel to a magnetic field is discussed theoretically. The temperatures of the two streams are assumed greatly to exceed the ion temperature. The dispersion equation is written for waves for which the frequency is low compared with the ion Larmor frequency, the wavelength is considerably greater than the electron and ion Larmor radii, and the component of the phase velocity parallel to the magnetic field is low compared with the electron and high compared with the ion thermal velocity. The antihermitian part of the dielectric tensor, describing Cherenkov absorption and radiation, is neglected. The roots of this dispersion equation are discussed; and the region of stability which was calculated numerically, is presented graphically in terms of coordinates representing essentially the relative velocity of the two streams and the strength of the magnetic field. The effect of Cherenkov absorption and radiation on the stability region is discussed briefly. (ATD)

21576 SPACE CHARGE FORMATION IN HIGH FREQUENCY ELECTRIC FIELD IN AIR. A. A. Zhukov. Zh. Tekhn. Fiz., 35: 151-3(Jan. 1965). (In Russian)

The formation of space charge in a high-frequency field between plane-parallel electrodes in air at atmospheric pressure was investigated experimentally. Gap lengths from 0.6 to 1.8 mm and frequencies from 1.5 to 10 Mc/sec were employed. The initial ionization was produced by ultraviolet illumination of one electrode through an opening in the other. A jet of air was blown through the gap and the ions blown from the interelectrode region were collected on a (positively or negatively) charged electrode and were measured with an electrometer. The positive ion current was found to increase rapidly with field strength, but the negative ion current showed one or two maxima before the surge preceding breakdown. Theoretical expressions for the ion currents are derived and compared with the experimental data. Good agreement is found for the positive ion current and for the negative ion current at field strengths well beyond the first maximum but before the second. The first maximum of the negative ion current occurs at the field strength at which electrons first penetrate the whole gap between the electrodes. The second maximum always occurs at the same field strength $E/p \approx$ 45 v/cm mm Hg. It is suggested that this maximum may be due to a decrease of the electron attachment probability beginning with this value of E/p, although the data of Harrison and Geballe indicate that the attachment probability increases in this region. (ATD)

21577 ON POSSIBLE DEVELOPMENT OF INSTABILITIES IN A PLASMA CAPTURED BY A TRANSVERSE MAGNETIC FIELD. I. I. Demidenko, N. S. Lomino, V. G. Padalka, B. G. Safronov, and K. D. Sinel'nikov (Inst. of Physics and Tech., Kharkov). Zh. Tekhn. Fiz., 35: 154-6 (Jan. 1965). (In Russian)

The development of instabilities in plasma bursts trapped by a transverse magnetic field and traveling parallel to it were investigated. The apparatus and the peculiarities of the capture and propagation of the plasma bursts were previously described. The plasma bursts passed through a 1.5 cm diameter circular aperture in a screen located 30 cm from the point of capture and were observed at various distances from the screen with a "plasmascope." When the screen was of dielectric material, or when it was of metal but floating, a tongue emerged from the more dense side of the plasma, grew, and reached the wall of the chamber after the plasma burst had traveled some 60 cm from the screen. This instability is assumed to be of the Rayleigh-Taylor type and due to the rotation of the plasma, its inhomogeneity, and the presence within it of a net negative charge. When the screen was of metal and grounded, the development of this instability was almost entirely suppressed. Experiments were also performed with a screen containing a 4 mm wide slot instead of a circular aperture. In this case the instability did not develop. The failure of flute instability to develop in the plasma sheets that passed through the slot is discussed briefly. (ATD)

21578 ELECTRIC BREAKDOWN THROUGH A SLOT IN GLASS IN A CESIUM VAPOR ATMOSPHERE. Yu. K. Gus'kov, S. Ya. Lebedev, and V. G. Rodionova. Zh. Tekhn. Fiz., 35: 156-7(Jan. 1965). (In Russian)

The breakdown potential between a 1.1 cm diameter hot cylindrical cathode and a 1.8 cm diameter coaxial cylindrical anode was measured in cesium vapor at pressures from 0.001 to 3 mm Hg and at cathode temperatures from 430 to 650°C. In the interelectrode space was located a glass cylinder, coaxial with the electrodes and containing a circular slot of adjustable width. The plane of the slot was perpendicular to the axis of the system. The width of this

slot was varied from 0.03 to 0.3 mm. The results are tabulated. The breakdown potential decreased somewhat with increasing slot width, and as a function of pressure it was minimum at about 0.1 mm Hg. (ATD)

21579 ENERGY DISTRIBUTION OF ELECTRONS IN THE POSITIVE COLUMN OF A DISCHARGE IN A MIXTURE OF MERCURY WITH INERT GASES. V. B. Khalfin. Zh. Tekhn. Fiz., 35: 160-2(Jan. 1965). (In Russian)

The electron energy distribution in a mercury discharge containing Ar, Ne or Xe was calculated by the method proposed by Kagan and Lyagushchenko in order to interpret the experimental results of Vorobyeva, Kagan, and Milenin, who found that the presence of an inert gas reduced the number of high energy electrons below the Maxwellian value. The calculation is described in some detail, but no intermediate formulas are given. The distribution function was evaluated numerically for two cases for which experimental data are available, and the results are compared with the experimental values. The calculated distributions deviate from the Maxwellian in the same direction, but not quite so far as the experimental curves. The agreement is considered satisfactory. (ATD)

21580 ON THE INFLUENCE OF THE PLASMA DENSITY NEAR THE ELECTRODE ON THE CONDUCTIVITY IN A TRANSVERSE MAGNETIC FIELD. V. P. Pashchenko, I. P. Stakhanov, and A. S. Stepanov. Zh. Tekhn. Fiz., 35: 165-7(Jan. 1965). (In Russian)

A magnetic field affects the conductivity of a plasma not only by altering the diffusion constant but also by influencing the density of the plasma in the neighborhood of the electrode. This latter effect is calculated. The electron distribution function in the electrode region is computed separately for strong and weak fields; the distribution function for intermediate fields, where the electron Larmor radius is comparable with the mean free path, is obtained by interpolation. The difference between the electron temperature and the cathode temperature was neglected, and the solution of the kinetic equation without the collision term was fitted to the solution of the diffusion equation at a distance from the cathode of the order of the mean free path. The results of the calculations were compared with measurements performed with a mock thermoelectric converter by plotting the ratio of the saturation current to the equilibrium current (obtained by extrapolation from the low temperature region) against the strength of the applied transverse magnetic field. Moderately good agreement between theory and experiment was obtained. The differences between the theoretical and experimental values are ascribed to the neglect of the temperature difference between the electrons and the cathode and to a possibly incorrect determination of the overcompensation factor. The plasma density near the cathode was found to increase with increasing magnetic field and to approach the equilibrium value in strong fields. The conductivity, accordingly, decreases less rapidly with increasing magnetic field than does the diffusion constant, and under some conditions it may even increase. (ATD)

21581 ON OHMIC HEATING OF A PARTIALLY IONIZED PLASMA BY A UNIFORM HIGH-FREQUENCY FIELD. A. G. Litvak, M. I. Petelin, and E. I. Yakubovich. Zh. Tekhn. Fiz., 35: 168-9(Jan. 1965). (In Russian)

The heating of a three-component non-relativistic plasma (electrons, ions and atoms) by a high-frequency field is discussed briefly. The field is assumed directly to heat only the electrons. It is pointed out that a steady state is possible only when the concentration of neutral atoms greatly exceeds that of the charged particles and that in the steady state the electron temperature exceeds the ion temperature, which in turn exceeds the atom temperature. The energy loss by the neutral atoms, requisite for the existence of such a steady state, is not discussed nor do the equations presented contain a term describing it. It is pointed out that the results of Gurevich, who neglected collisions between electrons and neutral particles and assumed that the ions and neutral particles had the same temperature, are valid only in a very narrow temperature interval. In a fully ionized plasma the sum of the electron and ion temperatures increases without limit, but their difference approaches a constant value. (ATD)

21582 ON DEVELOPMENT OF INSTABILITY IN A PLASMA BURST DURING ITS MOTION IN A LONGITUDINAL MAGNETIC FIELD. A. A. Kalmykov, S. A. Trubchaninov, and V. A. Naboka (Inst. of Physics and Tech., Kharkov). Zh. Tekhn. Fiz., 35: 169-72(Jan. 1965). (In Russian)

Plasma bursts from a coaxial plasma gun fired by the 18-kv discharge of a 12-μf capacitor bank were observed with a "plasmascope" as they moved in a (not always uniform) longitudinal magnetic field. The purpose of the observations was to investigate such instabilities of the plasma bursts as might develop. When a plasma burst traversed a magnetic barrier in which the field strength increased to a maximum value of 1600 gauss and decreased again to a low value in a distance of 50 cm, the core of the burst decreased in size, but a halo of presumably less dense plasma formed and grew. At certain values of the magnetic field, a spiral protuberance formed and increased in size. Such protuberances continued to develop when the plasma burst was moving in a uniform field. The direction of the spiral protuberance depended on the direction of the magnetic field and corresponded to a rotation of the plasma in the direction of the Larmor rotation of the ions. The observed instability is believed to be of the Rayleigh-Taylor type and a consequence of rotation of the plasma burst. The cause of the plasma rotation is not known, but drift forces due to the crossed fields resulting from uncompensated space charge in the plasma may be involved. The instability develops under a wide variety of conditions and is expected to complicate the problem of injecting plasma into a magnetic mirror system. (ATD)

21583 ON THE ANISOTROPY OF THE ELECTRON ENERGY DISTRIBUTION IN THE "ALPHA" INSTALLATION. B. V. Galaktionov, M. M. Larionov, and K. A. Podushnikova. Zh. Tekhn. Fiz., 35: 172-4(Jan. 1965). (In Russian)

The electron energy distribution in the plasma of the "alpha" installation was measured at the instant of maximum discharge current with a triple-grid probe. The probe was oriented so that its electrodes were perpendicular to the magnetic field at the instant of maximum current; by rotating the probe through 180° it was possible to determine separately the energy distribution of the electrons that were accelerated or retarded, respectively, by the circuital electric field. Although no anisotropy of the ion energy distribution had been detected in previous measurements, the electron energy distribution was found to be indeed anisotropic. The observed electron energy distribution could be represented by a displaced Maxwellian curve in which the energy of the directed motion was from 3 to 15% of the thermal energy. These results are similar to those obtained by Gibson and Mason for the "zeta" installation. The interpretation of the results is discussed very briefly, and it is suggested that reflection from field fluctuations prevent any considerable number of electrons from being continuously accelerated, so that the effect of the longitudinal electric field is merely to render the electron velocity distribution slightly anisotropic. (ATD)

21584 TRANSFORMATION OF LONGITUDINAL HIGH-FREQUENCY FIELD BY THE IONIC-ACOUSTIC SPECTRUM. I. A. Daneliya (Tbilisi State Univ., USSR). Zh. Tekhn. Fiz., 35: 174-5(Jan. 1965). (In Russian)

On the basis of previous results the cross sections are calculated for the transformation of an extraneous Langmuir wave into a transverse wave and for the scattering of the Langmuir wave with the production of another longitudinal wave of different frequency as a result of the nonlinear interaction of the Langmuir wave with the ionic-acoustic waves. The result should be of interest in connection with plasma diagnostics. (ATD)

21585 ON THE KINETIC THEORY OF THE BOUNDARY LAYER BETWEEN A RAREFIED PLASMA AND A MAGNETIC FIELD. Yu. S. Sigov. Zh. Vychislitel. Mat. i Mat. Fiz., 4: 1065-77(Nov.-Dec. 1964). (In Russian)

The problem of a steady boundary layer between a rarefied plasma and a magnetic field is considered. A mathematical formulation of the general steady-state problem of the self-consistent structure of an electromagnetic field in the transition boundary layer is presented. The plasma configuration considered is described by a system of Vlasov equations, and boundary conditions are established. Qualitative analysis of the solutions is carried out. The law of self-consistent field decay is established on the assumption that there are no trapped particles. It is shown that for a wide range of particle distribution functions there exists a sharp boundary between a plasma and an electromagnetic field. An attempt is made to formulate precisely all physical assumptions and mathematical restrictions in the same order as they arise in the theory. It is concluded that any processes leading to the appearance of particles with finite trajectories will cause an additional penetration of the electromagnetic field in the plasma and, ultimately, violation of the exponential law of field decay. (ATD)

21586 ELECTRON ENERGY DISTRIBUTION IN HYDROGEN. Terry Morrone. Thesis, Brooklyn, Polytechnic Inst., 1964. 120p.

The electron energy distribution for a high or low density molecular hydrogen plasma, with constant or high frequency field applied, is described by the Boltzmann equation. Its solution is obtained using harmonic expansions of the velocity and time dependence of the distribution function. The first three Legendre polynomials represent the velocity dependence, and a Fourier series, with harmonics higher than the second neglected, represents the time dependence. Using these expansions the Boltzmann equation is written as a set of eight equations in eight unknowns. The equations may be manipulated to give a single equation in a single unknown if the applied field frequency is either much greater or much less than the relaxation frequency for energy change, which is about equal to the sum of inelastic collision frequencies. Under these conditions the energy distribution for a particular weakly ionized gas is determined by a single parameter, the effective field divided by the pressure. The collision integrals for electron-neutral inelastic collisions are evaluated using the latest and most accurate collision cross section curves available in the literature. The Coulomb collision integral is evaluated by means of an expansion of the distribution in powers of the change in velocity on collision. The ionization frequency and average energy are computed and compared with the low density values corresponding to the same applied field. It was found that the ionization frequency increases and the average energy decreases. The analysis applies at densities where electron-neutral collisions out-number Coulomb collisions. The average ionization frequency is calculated as a function of the applied fields and the result is compared with an experiment in which the ionization frequency was determined by measurement of the time required for a microwave beam to cause electrical breakdown in hydrogen. Theory and experiment agreed to within ten percent. (A.G.W.)

21587 STATISTICAL THERMODYNAMICS OF THE ONE DIMENSIONAL PLASMA AND RELATED SYSTEMS. Allan Michael Salzberg. Thesis, Minneapolis, Univ. of Minnesota, 1964. 123p.

The exact statistical thermodynamics of five related systems were obtained. The first system treated is the finite one-dimensional plasma composed of a mixture of two species of positive ions and one species of negative ions, where the number of each species present is given by N_1, N_2, and N_3 and the respective ionic lengths are λ_1, λ_2, and λ_3. Each member of this system carries a charge of magnitude q and, as there are an equal number of positive and negative ions, the system is in a state of electroneutrality. This potential energy of the system, U, is in general given by the relation $U = \Sigma_{i<j} U_{ij}$. Employment of the constant pressure partition function gives $\mu_1 = \mu_1(\mu_2, T, P)$ where μ is the chemical potential, T is the temperature, and P the pressure. From this relationship the thermodynamics of a single component system is obtained in the limit $\mu_2 \to -\infty$ both in the presence and absence of an external field. The excess thermodynamic functions of mixing are obtained from this relation in conjunction with the Gibbs-Duhem relations. Finally the general relations were extended to a multi-component system. The second case, the dipole plasma, differs from case one in the limit $N_2 \to 0$ only in the fact that the positive ions can carry dipoles of moment M in addition to the positive charge q. The thermodynamics of the system is obtained through the use of the constant pressure partition function subject to certain restrictions. The potential of a system comprised of 2N particles of mass m and length λ is given by $U = \Sigma U_{ij}$ where for $x < \lambda$ $U_{ij} = \infty$ and for $x > \lambda$ $U_{ij} = gm_1m_2|x|$. Once again the constant pressure partition function is employed. Behavior attributed to a gradual condensation of the 2N particles into one superparticle is found in this system. The two-dimensional systems cannot be completely characterized as it is not possible to integrate the formal expression of the canonical partition function Q. However, Q can be separated into a product of two functions, one of which is independent of the area. This leads immediately to the equation of state of the two systems. (A.G.W.)

21588 NONLINEAR PLASMA WAVES. Jeffrey Philip Freidberg. Thesis, Brooklyn, Polytechnic Inst., 1964. 108p.

Nonlinear wave propagation in an infinite homogeneous plasma, particularly one-dimensional longitudinal waves propagating in a plasma consisting of mobile ions and electrons, is studied. At first the effects of a non-zero thermal spread in the energy distributions of the particles is neglected. However, the electrons are allowed to stream freely past the ions, thereby creating an environment in which the two-stream instability can be excited. Exact periodic solutions to the nonlinear equations and a nonlinear dispersion relation, which is a function of the wave amplitude, are found. For sufficiently large values of the wavenumber, k, the dispersion relation has four real roots corresponding to four bounded periodic waves. For smaller values of k, the dispersion relation yields two real and two complex roots. To obtain a more realistic representation of a plasma both the electrons and ions are allowed to have a small thermal spread in their energy distributions. For this case the equations are too complicated to yield exact solutions. Hence, a perturbation procedure for solving a nonlinear second order differential equation with an additional small nonlinear term is devised. Then, by making use of this procedure the first order correction to the dispersion relation is calculated. As expected, the inclusion of a "temperature" term allows an acoustic type wave to be propagated in the plasma. With regard to the two stream instability, the temperature effects cause a slight decrease and a slight shift in the range of k where stabilization occurs before overtaking. Finally it is shown that the maximum amplitude of these waves is determined by the condition that there be no trapped particles. (A.G.W.)

21589 E-MODE PROPAGATION IN PLANE-STRATIFIED PLASMA. Peter Hirsch. Thesis, Brooklyn, Polytechnic Inst., 1964. 144p.

Some phenomena of electromagnetic plane wave propagation in a plane-stratified, isotropic plasma are studied by way of the wave equation. The complexity of this problem depends on the polarization of the wave. If the wave possesses a component of electric field in the direction of the gradient of the stratification, then the wave equation is of the form $(d^2y/dx^2) - (1/x)(dy/dx) - (x + B)y = 0$. Approximate solutions of the wave equation are derived. These predict resonant absorption of electromagnetic energy at the plane in the plasma where the electron density has a certain critical value that depends on the wave frequency. This absorption causes the electric field strength at the critical plane to grow linearly in time after the source is turned on. Further, the magnitude of the reflection coefficient from a stratified region which includes a critical plane can never be unity, and no lossless surface waves can propagate along the stratification. (Dissertation Abstr., 25: No. 5, Nov. 1964)

21590 THE METASTABLE ABNORMAL GLOW DISCHARGE IN HYDROGEN. Martin David Nahemow. Thesis, Brooklyn, Polytechnic Inst., 1964. 64p.

In an effort to trace the progress of a glow discharge from the time the initial breakdown starts to the time when the stable glow configuration is reached, a series of time-resolved spectroscopic studies of a wall-bounded pulsed discharge in hydrogen was undertaken. By examination of the Stark-splitting of the spectral lines of the hydrogen spectrum, the electric field was mapped in space and time within the cathode-fall region of the discharge. The initial breakdown was examined by mapping the intensity of the spectral lines of hydrogen in space and time across the entire interelectrode gap. Data is presented for pressures from 0.2 to 3.0 torr, interelectrode spacings from 1.5 to 48 centimeters, and applied potentials from breakdown to 6000 volts. The mapping has a spacial resolution of 0.2 millimeters and a temporal resolution of nanoseconds. The experimental data is compared to theoretical calculations made by A. L. Ward. Ward's calculations are based on a formulation of the avalanche theory of breakdown. The agreement between the experimental data and the results of the theoretical calculations is such that the avalanche theory can be considered sufficient to account for the electrical breakdown of hydrogen at large overvoltages. There is no apparent need to invoke any other mechanism to account for the propagating luminous fronts observed and the formative times, which may be as short as 40 nanoseconds. (Dissertation Abstr., 25: No. 5, Nov. 1964)

21591 MEASUREMENT OF THE DENSITIES OF PLASMAS BY THE METHOD OF HYPERFREQUENCY INTERFEROMETRY. Maurice Favre (C.S.F., Paris). Paper 5, Session 7, 5p. of "Mesucora 63. Congres International Mesure-Controle Regulation-Automatisme. Tome I." Paris, Mesucora, [1964]. (In French)

A brief review was made on the principles and limitations of the electrical or optical methods for the examination of the state of plasmas. The characteristics of the investigation methods resting on the use of hyperfrequencies, one of the most advantageous forms being that of hyperfrequency interferometry, were examined. A device for the measurement of the characteristics of plasmas based on this method is described. (J.S.R.)

21592 DEVICE FOR THE GENERATION OF A HIGH-TEMPERATURE PLASMA. Max Steenbeck (to VEB Atomkraftwerk Rheinsberg mit Betriebsteil, Berlin). German Patent 1,184,023. Dec. 23, 1964. Filed Sept. 18, 1959.

The device for generation of a high-temperature plasma comprises dipoles arranged on the inner surface of the reaction vessel. The dipoles radiate transverse waves into a central reaction zone. These dipoles are located in two different zones of a cylinder wall in such a way that the focal area is either a sphere or a cylinder. (Gmelin Inst.)

21593 ROTATING PLASMA DEVICE. J. G. Gorman and L. H. Rietjens (to U. S. Atomic Energy Commission). U. S. Patent 3,171,788. Mar. 2, 1965.

Means are described for heating and confining high-temperature plasma. An exposed electrical conductor having a large positive potential draws a large electron current through the conductor to disturb the charge neutrality of a particular portion of the plasma. In a stellarator, this disturbance imposes a strong annular radial electric field in the plasma that is rapidly reacted with an externally imposed magnetic field to rotate the plasma in the electric field region thereby greatly decreasing the loss rate of the plasma to the discharge tube wall of the stellarator. (AEC)

Shielding

Refer also to abstracts 21242 and 21614.

21594 (AD-424387) RADIATION SHIELDING STUDIES AT NCEL. C. M. Huddleston (Naval Civil Engineering Lab., Port Hueneme, Calif.). Nov. 18, 1963. 6p. $1.10 (CFSTI).

An intensive study was carried out on the streaming of gamma radiation through air ducts in concrete because of the importance of such studies to the shelter entranceway problem. Results of findings to date are presented, and the current shielding research program at NCEL is discussed. (auth)

21595 (TID-7698(Pt.I)(p.33-248)) HANDBOOK OF SHIELDING REQUIREMENTS AND RADIATION CHARACTERISTICS OF ISOTOPIC POWER SOURCES FOR TERRESTRIAL, MARINE, AND SPACE APPLICATIONS. E. D. Arnold (Oak Ridge National Lab., Tenn.).

This handbook is intended primarily for use in preparation of preliminary design estimates by design engineers in the field of isotopic source development and application. The calculated radiation intensities are probably slightly pessimistic in that they are overestimated no more than 50%. Calculations have been made of the radiation intensities from shielded and unshielded sources fabricated from seventeen isotopes that show promise for use in isotopic power or radiation applications. Source sizes in the range of 100 to 20,000 thermal watts were evaluated. All shielded sources were assumed to be attenuated by iron, lead, and uranium; and in those cases where the source also emitted neutrons, neutron and gamma attenuation through water was determined. The isotopes studied and their physical form are as follows: ^{60}Co (metal), ^{85}Kr (liquefied gas), ^{90}Sr (oxide and titanate), Zr–^{95}Nb (oxide), ^{106}Ru (metal), ^{137}Cs (glass), ^{144}Ce (oxide), ^{147}Pm (oxide), ^{170}Tm and ^{171}Tm (both as oxides), ^{204}Tl (metal), ^{210}Po (metal matrix with void space for gas collection), ^{232}U (oxide), ^{228}Th (oxide matrix with void space for gas collection), ^{238}Pu (oxide), ^{243}Cm (oxide matrix with void space for gas collection), and ^{244}Cm (oxide). Several examples of how the graphical results may be used to calculate separation distance, shield thickness, and shield weight are included. (D.L.C.)

21596 (UCRL-12005) YOGI-G: A GAMMA-RAY MONTE CARLO PROGRAM. Simon Kellman (Lawrence Radiation Lab., Univ. of California, Livermore). Aug. 4, 1964. Contract W-7405-eng-48. 159p. Dep.(mn); $5.00 (cy), 3(mn) CFSTI.

YOGI-G is a gamma-ray Monte Carlo program written in FORTRAN II language for the IBM 7090/7094 computer with LRL monitor control. The code computes gamma energy deposition in selected rectangular and cylindrical systems. In relatively simple geometries, the program processes more than 5000 collisions per minute. Pair production, Compton collision, and photoelectric absorption processes are treated. Energy transferred to electrons in these processes is assumed to be absorbed at the point of collision since the ranges of the electrons are small. Energy deposition per zone and the corresponding variance are computed. In addition to the straight tally, two expected-value calculations of gamma energy absorption in each zone and in each energy sector of every material region are available in order to improve statistical accuracy. (auth)

21597 THE EFFECT OF ABSORBER POSITION ON SCATTERING IN MEASUREMENT OF β RAY ABSORPTION. Taikichi Hattori (Muroran Inst. of Tech., Japan). Muroran Kogyo Daigaku Kenkyu Hokoku, 4: 845-53(June 1964). (In Japanese)

A method is described by which the counting rate of radiated beta particles is kept constant regardless of absorber position. The curves of the counting rate plotted against the absorber position can be classified into three fundamental types: (1) V type with a minimum in the counting rate, (2) inverted V type with a maximum, and (3) monotonously increasing (or decreasing) type. Experiments show that the degree of collimation has a remarkable influence on the form of the curves. The monotonously increasing type gradually transfers into the inverted V type, and the same thing happens to the V type as the hole diameter of the collimator is made small. Thus the optimum diameter for flattening the curves is obtained. By using this optimum diameter the

measurement of thickness or density of continuously moving materials could be performed with higher precision. In case of the extremely collimated radiation the curves ultimately become the monotonously decreasing type. These experimental results agree with simple theoretical calculations. (auth)

21598 NOMOGRAM FOR DETERMINING SHIELD THICKNESS FOR POINT AND LINE SOURCES OF GAMMA RAYS. C. Joenemalm (Aktiebolaget Atomenergi, Studsvik, Sweden). Nucl. Struct. Eng., 1: 324-31(Mar. 1965).

A set of nomograms is given for the determination of the required shield thickness against gamma radiation. The sources handled are point and infinite line sources with shields of Pb, Fe, magnetite concrete (ρ = 3.6), ordinary concrete (ρ = 2.3), or water. The gamma energy range covered is 0.5 to 10 Mev. The nomograms are directly applicable for source and dose points on the surfaces of the shield. They can easily be extended to source and dose points in other positions by applying a geometrical correction. (auth)

21599 EFFECT OF BREMSSTRAHLUNG ON THE MEASUREMENT OF LARGE ANGLE COHERENT SCATTERING OF γ RAYS. A. Nath (Bose Inst., Calcutta). Sci. Culture (Calcutta), 30: 502-5(Oct. 1964).

The possibility of Delbrueck scattering and the contributions of hard Compton and bremsstrahlung photons in observations of excess γ-scattering cross sections over theoretical values at 1 to 2.80 Mev are reviewed. Results are reported on investigations on the effect of bremsstrahlung in measurements of coherent scattering of hard γ rays. Relative bremsstrahlung contribution to the coherent scattering intensity was estimated theoretically, and results were compared with measurements using a Pb scatterer and ^{60}Co source; measured spectra and the derived bremsstrahlung spectrum are presented. (M.J.T.)

Solid State Physics

See also CHEMISTRY — Inorganic and Physical Chemistry
METALS, CERAMICS, AND OTHER MATERIALS — Properties and Structure

Refer also to abstracts 19849, 20555, 21407, 21495, and 21496.

21600 (IS-968) NATURE OF THE ENERGY LEVELS IN HYDRATED THULIUM ETHYLSULPHATE. Lewis C. Bartel and Frank H. Spedding (Ames Lab., Iowa State Univ. of Science and Tech.). Aug. 1964. Contract W-7405-eng-82. 193p. Dep.; $5.00(cy), 4(mn) CFSTI.

In order to discuss the absorption spectra taken in this work, several theoretical discussions are presented. These discussions include the crystal field theory, theory for the effect on the spectra of a magnetic field parallel to the c-axis of a thulium ethylsulphate crystal, and a recent theory explaining the spectra when the magnetic field is in the basal plane and perpendicular to the light path. The theory for the interaction of the lattice vibrations with the 4f electrons linear in the boson creation and annihilation operators is also discussed. The absorption spectra were taken in high orders on a 3.4 meter Ebert mounting spectrograph. The dispersions ranged from 1.23 cm^{-1}/mm in the seventh order to 2.39 cm^{-1}/mm in the sixteenth order. Transitions from the ground $^3H_6$ multiplet to the $^3F_4$, $^3F_3$, $^3F_2$, $^1D_2$ multiplets were photographed. Line energies are reported for zero magnetic field and for various magnetic fields in both the parallel and perpendicular field directions. From the line energies and splittings, the zero field level energies and the level splittings with magnetic field are determined. The parallel and perpendicular magnetic field splitting factors are listed for various levels. Theoretical splitting factors of the levels for both magnetic field directions are calculated and are found to be in qualitative agreement with the experimental ones. A recent theory of Murao, Spedding, and Good for the even numbered electron rare earth ions in crystal fields with C_{3h} point group symmetry predicts: (a) the energies of the lines in the spectra are independent of the angle the transverse magnetic field makes with the a-axis; (b) some of the line intensities vary as the angle the transverse field makes with the a-axis is varied, but the intensities are a maximum or a minimum at the same angle defining a direction of a new axis. This new axis is the x-axis of a coordinate system in which the lattice sums of the terms proportional to $Y_{6,6} - Y_{6-6}$ vanish. The theoretical predictions are experimentally verified and the angle between the x-axis and the a-axis is found to be 9° ± 2° for a 10 per cent concentration of Tm in Y ethylsulphate. (auth)

21601 (ORNL-tr-490) RELATIONSHIP BETWEEN THE ELECTRICAL PROPERTIES OF IONIC COMPOUNDS OF GROUP II ELEMENTS AND THE ENERGY OF INTERACTION IONS IN A CRYSTALLINE LATTICE. A. P. Nakhodnova. Translated by A. L. Monks (Oak Ridge National Lab., Tenn.), from Izv. Tomsk. Politekhn. Inst., 91: 209-18(1956). 15p. Dep.(mn); $1.00(cy), 1(mn) CFSTI; $1.60(fs), $0.80(mf) JCL.

Measurements were made on the temperature dependence of the electroconductivity, dielectric penetrability, and tgδ of oxides of Group II metals and halide compounds of alkali earth metals; comparisons with the crystalline lattice energy were also made. The results showed that the temperature dependence of the electroconductivity increases according to an exponential law characteristic for the ionic conductivity; it increases with a decrease in the crystalline lattice energy of the substance. The activation energy values of the current carriers calculated from the slope of the straight lines in $\sigma = f(1/T)$ decrease uniformly with the crystalline lattice energy. The dielectric penetrability and tgδ of the ionic compounds of Group II elements as well as the electroconductivity, increased with temperature. It was concluded that the electric properties of compounds of Group II elements are in close connection with the physical properties of a substance and are determined by the crystalline lattice energy. (P.C.H.)

21602 EXCITON ABSORPTION IN THE PRESENCE OF EXCITED F CENTERS. Dietmar Froehlich and Herbert Mahr (Cornell Univ., Ithaca, N. Y.). Phys. Rev. Letters, 14: 494-6(Mar. 29, 1965).

A pulse-transmission experiment was performed to measure the optical absorption of crystals containing defects in excited states. The experiment provides a new method for studying the excited F center in alkali halides. An optical absorption band was observed in KI which exists only during the lifetime of the excited electronic state of the F center. The position and strength of the absorption band suggests that it is due to an exciton state formed in the vicinity of the relaxed F center. The absorption then depends on the crystal field surrounding the center and thus gives direct evidence of its symmetry properties. (L.B.S.)

21603 LATTICE DYNAMICS OF WHITE TIN. J. M. Rowe, B. N. Brockhouse, and E. C. Svensson (McMaster Univ., Hamilton, Ont.). Phys. Rev. Letters, 14: 554-6 (Apr. 5, 1965).

The dispersion relations for lattice vibrations in white tin with wave vector along the (00ζ) direction of the reduced zone and along its continuation, the (10ζ) direction, were measured at 100 and 296°K. The results indicate that no short-range force model can adequately describe the lattice vibrations of beta tin. Evidence was obtained for interference effects in the electron-phonon interaction. (D.C.W.)

REACTOR TECHNOLOGY

General

21604 (EUR-2202.e) SYNTHESIS OF OPTIMAL CONTROL AND HYBRID COMPUTATION. W. de Backer (European Atomic Energy Community, Ispra (Italy). Joint Nuclear Research Center and European Atomic Energy Community, Ispra (Italy). European Scientific Data Processing Center). 1964. 13p. (CONF-640912). Dep.(mn).

From 4th International Analogue Computation Meeting, Brighton, Eng.

The implementation of Pontryagin's necessary conditions for optimal control on analog and hybrid computers is considered. The computational difficulties of the programming of the adjoint variables and the maximization of the hamiltonian are analyzed. Restricted state variables are treated on the basis of implicit computing of Lagrange multipliers with penalty functions. The limitations of the proposed methods are discussed. Attention is devoted to the solution of the two-point boundary problem, being the final but most difficult step of the synthesis. The specific needs for hybrid computation are underlined. Computational results are obtained in the field of nuclear reactor control. (auth)

21605 (HW-SA-3560) REACTOR DECONTAMINATION AND THE HEALTH PHYSICIST. L. R. Wallis, M. L. Smith, and F. E. Owen (General Electric Co., Richland, Wash. Hanford Atomic Products Operation). [1963]. Contract AT(45-1)-1350. 9p. (CONF-642-30). Dep.(mn); $1.00(cy), 1(mn) CFSTI.

From Health Physics Society, Cincinnati, June 1964.

A procedure for the removal of the radioactive scale from the internal surface of a reactor's rear face piping and nozzles without corroding the process tubes was developed and tested at the 100-H area reactor. A chemical reagent that removed the scale at fairly dilute concentrations and a system for backflushing the solution out the nozzles without putting it through the process tubes were employed. The effects of decontamination on radiation dose in the reactor area and the radiation dose to personnel during the operation were evaluated. (C.H.)

21606 (WCAP-3269-9) EFFECTS OF CHEMICAL SHIM ENVIRONMENTS ON THE WEAR OF REACTOR MATERIALS. D. G. Sammarone (Westinghouse Electric Corp., Pittsburgh, Pa. Atomic Power Div.). May 1964. Contract AT(30-1)-3269. 59p. Dep.(mn); $3.00(cy), 2(mn) CFSTI.

The effects of chemical shim environments on the wear of reactor material were investigated. A total of six material combinations normally employed for wear applications in nuclear power reactors were used in this study. Variables consisted of two temperatures (600 and 200°F), and three water chemistries (demineralized water, boric acid, and boric acid plus lithium hydroxide). This resulted in 36 individual tests being run. A piston-cylinder wear test rig was used. Combined and individual wear factors as well as specific wear values were determined. Results showed that the amount of wear with chemical shim solutions was generally the same as with demineralized water. Changes in wear due to temperature could not be detected except for the 410 s/s vx. 304 s/s piston-cylinder combination. In this case the amount of wear was higher at the 200°F temperature than at the 600°F temperature. (auth)

Auxiliaries and Components

Refer also to abstract 20110.

21607 (APED-4773) PRESSURE VESSEL STEEL SURVEILLANCE PROGRAM FOR GENERAL ELECTRIC POWER REACTORS. F. A. Brandt (General Electric Co., San Jose, Calif. Atomic Power Equipment Dept.). Jan. 8, 1965. 55p. (65APE1)

Pressure vessel steel surveillance programs are performed in nuclear power reactors to provide knowledge of the mechanical properties of the pressure vessel material as neutron irradiation proceeds. A standard surveillance program is described. Design of specimens, capsules, and associated equipment, as well as selection of test material and techniques for special preparation and testing, are discussed. (auth)

21608 (AWRE-R-2/65) THE PRESSURE RISE IN THE BIOLOGICAL SHIELD OF A SMALL SCALE MODEL OF A GAS-COOLED REACTOR FOLLOWING A SIMULATED PRESSURE VESSEL FAILURE. F. J. Walford (Atomic Weapons Research Establishment, Aldermaston (England)). Apr. 1965. 15p. Dep.; $0.60(BIS), 3s.Od.(HMSO).

A model of a typical gas circuit and biological shield was constructed in which it was possible to simulate a failure of the reactor vessel. Measurements of the pressure distribution within the model following failure of the reactor vessel are reported as well as the measurements made when some of the model parameters were varied. (auth)

21609 (GAMD-5001(Rev.2)) TARGET—AN IBM COMPUTER CODE FOR THE STRESS ANALYSIS OF BODIES OF REVOLUTION INPUT INSTRUCTIONS. D. C. Cornell and C. Riparbelli (General Atomic, San Diego, Calif.). Aug. 19, 1964. Contract AT(04-3)-167. 93p. Dep.(mn); $3.00(cy), 3(mn) CFSTI.

The IBM code TARGET, written in the FORTRAN IV language and compiled for the 7044 digital computer, is described and discussed. The TARGET program is a numerical method for calculating the deformation of bodies of revolution and the consequent stress distribution. The method employs the concept of stiffness coefficients. Example problems of a thick plate in pure bending and a reinforced concrete pressure vessel are treated. (C.E.S.)

21610 (GAMD-6109) A METHOD FOR DETERMINING THE OPTIMAL TENDON CONFIGURATION IN A PRESTRESSED CONCRETE REACTOR STRUCTURE. D. C. Cornell (General Atomic, San Diego, Calif.). Oct. 23, 1964. Contract AT(04-3)-167. 57p. Dep.(mn); $3.00(cy), 2(mn) CFSTI.

A rapid method for determining the optimum tendon configuration in a pre-stressed concrete reactor structure is presented. The problem is formulated as a system of inequalities that span a field of feasible solutions which is defined by predetermined constraints. The optimum solution is then determined by linear programming techniques. Results indicate that this method is readily applicable to the analysis of prestressed concrete reactor structures. (auth)

21611 (NAA-SR-9826) FINAL DESIGN OF SODIUM-HEATED, MODULAR, STEAM GENERATORS FOR THE SCTI. D. F. Casey, J. J. Hammer, D. Logan, and M. C. Williams (Atomics International, Canoga Park, Calif.). Feb. 1, 1965. Contract AT-11-1-GEN-8. 100p. Dep.; $3.00(cy) 2(mn) CFSTI.

In July 1963, design of a 37-tube, modular-type, low-temperature evaporator and high-temperature superheater for testing in the Sodium Component Test Installation was initiated. The evaporator and superheater modules, when combined, would be capable of generating 2400-psi, 1050°F steam. The final design of the modular steam generators is reported. (auth)

21612 (NAA-SR-Memo-10557(Pt.I)) MONTE CARLO EVALUATION OF COLLIMATOR EFFICIENCY. PART I. DESCRIPTION OF THE CLUB COMPUTER CODE. W. B. Green and R. S. Hubner (Atomics International, Canoga

Park, Calif.). Oct. 13, 1964. Contract [AT(11-1)-Gen-8]. 32p. Dep.(mn); $2.00(cy), 1(mn) CFSTI.

The CLUB code is a Monte Carlo computer program designed to assist in the evaluation of neutron collimator efficiency. The theory on which the code is based is described, along with the code input and output. (auth)

21613 (NAA-SR-Memo-10557(Pt.II)) MONTE CARLO EVALUATION OF COLLIMATOR EFFICIENCY. PART 2. LISTING OF THE CLUB CODE. W. B. Green and R. S. Hubner (Atomics International, Canoga Park, Calif.). Oct. 26, 1964. Contract [AT(11-1)-Gen-8]. 56p. Dep. (mn); $3.00(cy), 2(mn) CFSTI.

A complete listing of the CLUB code is given. The code computes direct and scattered fluxes incident on a detector at a specified position in a collimator system, using the Monte Carlo method. The mathematical theory of the code, and a description of the code input and output, are given. The results of the collimator design study are outlined. (auth)

21614 (NAA-SR-Memo 10559) ANALYSIS OF SHIELD TEST FACILITY EXPERIMENTS USING THE TWO COMPONENT METHOD. W. B. Green (Atomics International, Canoga Park, Calif.). Oct. 13, 1964. Contract AT(11-1)-Gen-8. 10p. Dep.(mn); $1.00(cy), 1(mn) CFSTI.

The two-component method of shield analysis is reviewed and discussed, and the experimental configuration is described; the study indicates that results obtained from removal theory are as good as those obtained using the two component method, for obtaining dose rate estimates at points within about 6 feet of the shield surface; other results are cited, which indicate that the two-component method is a valuable tool of analysis for dose points greater than this distance. (auth)

21615 (NASA-CR-54282) PNEUMATIC NUTATOR ACTUATOR MOTOR. Quarterly Report No. 2. C. N. High, G. R. Howland, and J. R. Williamson (Bendix Products Aerospace Div., Bendix Corp., South Bend, Ind.). Dec. 31, 1964. Contract NAS3-5214. 46p. (BPAD-864-15598R) $2.00(CFSTI).

Fabrication of a prototype pneumatic nutator actuator motor for drum control of a nuclear reactor is described. Photographs of the component parts are shown. Test results of the breadboard commutation circuit are given. (auth)

21616 THE DETERMINATION OF LONG-LIVED KRYPTON AND XENON ISOTOPES IN MAGNOX REACTOR COOLANTS, AS A MEANS OF DETECTING CERTAIN FUEL ELEMENT FAILURES. R. L. D. French and D. W. Ockenden (United Kingdom Atomic Energy Authority, Seascale, Cumberland, Eng.). J. Nucl. Energy: Pt. A and B, 19: 91-100(Feb. 1965).

A technique is described for the determination of small concentrations of 4-hr ^{85m}Kr, 5-day ^{133}Xe and 9-hr ^{135}Xe in the carbon dioxide coolant of Magnox reactors. This involves a gas chromatographic separation of the residual gas sample obtained by bubbling the coolant through 60% potassium hydroxide, followed by gamma spectrometric analysis of the resulting krypton and xenon fractions. The variations in the levels of these isotopes during several fuel element failures are presented and discussed. This monitoring technique is shown to be complementary to the normal burst cartridge detection system and provides an early warning of certain failures. (auth)

21617 EXCURSION-LIMITING FUSE FOR THE MIXED SPECTRUM CRITICAL ASSEMBLY. K. Hikido (General Electric Co., San Jose, Calif.), G. V. Brynsvold, and H. F. Johnston. Nucl. Appl., 1: 33-8(Feb. 1965).

An excursion-limiting fuse incorporated into the design of the Mixed Spectrum Critical Assembly to provide an ultimate shutdown mechanism, backing up the safety system, is described. The development tests and the results of excursion analyses are summarized. (D.C.W.)

21618 DYNAMIC THERMAL STRESSES IN REACTOR SHELLS. Pawel Rafalski (Inst. of Nuclear Research, Warsaw). Nucl. Struct. Eng., 1: 265-76(Mar. 1965).

A method for determination of the temperature and thermal stress distributions in a plane reactor shell was derived. The transient operation of the reactor was considered. It was assumed that the material of the shell is homogeneous and isotropic and satisfied the Boltzmann principle of superposition. As an example of application of the derived method two problems, elastic shell and viscoelastic shell, were solved for the case of reactor shutdown. The effects of inertia forces were taken into account. (auth)

21619 THERMAL ANALYSIS OF CYLINDRICAL SHELLS. F. J. Witt (Oak Ridge National Lab., Tenn.). Nucl. Struct. Eng., 1: 276-84(Mar. 1965).

An analysis of a cylindrical shell subjected to an axisymmetric temperature distribution, which varied along the axis and linearly through the thickness, is presented. The differential equation pertinent to the analysis was derived, and all of the stress components are set forth for a particular form of the temperature distribution. The analysis is of sufficient generality to be applicable to almost any axisymmetrically, thermally loaded cylindrical shell. (auth)

21620 EXPERIMENTAL INVESTIGATION OF THE NONLINEAR BEHAVIOR OF SHALLOW SPHERICAL SHELLS. J. D. W. Hossack (Univ. of Strathclyde, Glasgow). Nucl. Struct. Eng., 1: 285-94(Mar. 1965).

Some studies in the field of instability of shallow spherical shells are reviewed. The causes of the apparent inconclusive nature of earlier experimental investigations are examined. Work carried out in such a manner as to eliminate, as far as possible, some of the factors responsible for experimental error is reported. The results of an experimental investigation of the nonlinear stress and deformation characteristics of shallow shell behavior are presented. Good experimental agreement with theory is shown to be dependent on the preparation of uniform stress free specimens of accurate geometry and on the requirement that the shell be supported in a manner consistent with the assumptions of relevant theory. (auth)

21621 IMPROVEMENTS IN OR RELATING TO NUCLEAR REACTOR CONTROL ROD OPERATING DEVICES. Anatole Dmitrieff (to Commissariat à l'Energie Atomique). British Patent 975,599. Nov. 18, 1964. Priority date Mar. 28, 1960, France.

A device for permitting the transmission of a translatory movement through a fluid-tight wall is applied to control of control rods and safety rods inside the core of nuclear reactors. A cylindrical sleeve is located outside of and connected to a reactor casing. A rod longitudinally movable in the sleeve is connected at one end to a control rod or safety rod and also to a gear rack through which movement is achieved. To prevent radioactive products from accumulating inside the sleeve, a circulation of fluid is established between the two ends of the sleeve in the annular space defined by the sleeve and the movable rod or the gear rack. (A.G.W.)

21622 NEUTRON ABSORBING ROD FOR NUCLEAR REACTORS. Maurice Lechevallier (to Groupement Atomique Alsacienne Atlantique). British Patent 975,648. Nov. 18, 1964. Priority date Nov. 12, 1962, France.

A control rod for a nuclear reactor consists essentially of a plurality of nested elements capable of sliding one inside the other without any risk of separation. When the rod is needed, the suspension device holding the rod in the ready position is released and the rod falls of its own weight into the core channel. The rod head is secured by a flange and shoulder arrangement at the top of the channel and each element slides over the adjacent element until it reaches its own stop. The shocks that absorb the kinetic energy of the rod are thus numerous and too small to cause apparent deformation or require additional braking. (A.G.W.)

21623 IMPROVEMENTS IN OR RELATING TO NUCLEAR REACTOR CONTROL. Philippe Flachs, Georges Lapicque, and George Nicolo (to Commissariat à l'Énergie

Atomique). British Patent 975,742. Nov. 18, 1964. Priority date June 22, 1961, France.

A process is patented for indicating in a subcritical reactor any rise in the excess reactivity above a predetermined threshold value. A source of neutrons the intensity of which decays exponentially is provided within the reactor. Measurement of the neutron flux after the neutrons have traversed the reactor core by a detector produces a potential that is a function of the reactivity of the core. A reference potential is provided by a time-scaled potentiometric device. The potential produced by the neutron detector and the reference potential are compared by an electronic device arranged to produce a signal when the first potential is greater than the second. (A.G.W.)

21624 IMPROVEMENTS IN OR RELATING TO SYSTEMS FOR DETECTING LEAKS IN FUEL ELEMENTS IN A NUCLEAR REACTOR. Jane Cicely Thompson and Robert Vincent Ingham (to Nuclear Power Plant Co. Ltd. and AEI-John Thompson Nuclear Energy Co. Ltd.). British Patent 976,367. Nov. 25, 1964. Filed July 20, 1962.

A leak detector system is patented wherein at least two tapping points for monitoring the cooling fluid are provided per channel in at least some of the fuel-containing channels of the reactor. Samples from each tapping point are conveyed to fission product detection systems operating independently of each other. One tapping point of a channel may be connected to a system for monitoring single channels or to a group monitoring system for mixed samples from one group of channels. At the same time the second tapping point may be connected to a system for monitoring mixed samples from the same group of channels or to a further group monitoring system for mixed samples of a different group of channels. This arrangement of two tapping points per channel allows parts of one monitoring system to be removed for maintenance or other purposes without interrupting the other system. (A.G.W.)

21625 METHOD AND MEANS FOR REPLACING FUEL ELEMENTS IN NUCLEAR REACTOR. Ernst Bosshard (to Sulzer Freres, S. A.). Canadian Patent 698,484. Nov. 24, 1964. Priority date Mar. 4, 1960, Switzerland.

In the method of reactor fuel changing described, the fuel rod is received in a tube manipulated in a space below the calandria. The spent fuel element is then moved aside and lifted out of the tube into a vertical channel still inside the concrete shielding. The containing tube is next moved out of the way and the fuel rod lowered in a water-filled storage bay. The entire assembly consisting of receiving tube, vertical channel, and fuel bay are part of the concrete shielding enclosing the calandria. Provision is made for maintaining coolant flow during fuel shifting. During the entire operation the fuel is never withdrawn from shielding so no heavy lead flask is needed. (F.S.A.)

21626 APPARATUS FOR DETECTING THE PRESENCE OF FISSION PRODUCTS IN A GASEOUS MEDIUM, e.g. FOR DETECTING LEAKS IN THE CANS OF NUCLEAR FUEL ELEMENTS. Andre Roguin (to Commissariat a l'Energie Atomique). German Patent 1,177,258. Sept. 3, 1964. Priority date June 2, 1960, France.

The apparatus comprises a cylindrical electrostatic precipitation chamber, a plate-like collector electrode mounted on a piston arranged for axial movement between the two ends of the chamber, and a scintillator arranged at one end of the chamber. (Gmelin Inst.)

21627 PILLAR FOR A VERTICALLY STACKED, SOLID MODERATOR STRUCTURE OF A NUCLEAR REACTOR. Pierre Rouge and Roger Manes (to Commissariat a l'Energie Atomique). German Patent 1,177,750. Sept. 10, 1964. Priority date Oct. 26, 1961, France.

The pillar comprises a central, metallic portion, which is concentrically surrounded by cylindrically shaped, piled ring elements, and centering rings for positioning the central portion in the surrounding ring elements. The centering rings are arranged in such a way between two ring elements that they are spaced by an annular slit. (Gmelin Inst.)

21628 SUPPORTING STRUCTURE FOR A VERTICAL MODERATOR STRUCTURE OF A NUCLEAR REACTOR. Gerard Dupuy (to Commissariat a l'Energie Atomique). German Patent 1,177,751. Sept. 10, 1964. Priority date May 25, 1962, France.

The supporting structure described is for heterogeneous gas-cooled reactors with a solid moderator composed of vertically arranged moderator pillars held together by a system of longitudinally arranged springs. The support structure comprises a plurality of supporting plates arranged in a common level on each of which a group of pillars is mounted. From each of the groups only the central pillar is attached to the supporting plate. The plates rest on pillars arranged symmetrically around the central axis and are thermally insulated from the hot core. (Gmelin Inst.)

21629 ELECTROMAGNETIC DRIVE FOR CONTROL RODS IN NUCLEAR REACTORS. Franz Schreiber (to Siemens-Schuckertwerke AG). German Patent 1,182,364. Nov. 26, 1964. Filed Jan. 26, 1961.

The electromagnetic drive for control rods in nuclear reactors is based on the principle of mechanical spindle drives. The control rod comprises a tube made of magnetizable material and is provided with a layer of neutron-absorbing material the surface of which is in the form of a spindle thread. The tubular housing of the control rod is composed of annular magnetic pole shoes axially spaced by rings of unmagnetic material. Axial movement of the rod is achieved by rotating the housing about the common axis of symmetry (magnetic thread). (Gmelin Inst.)

21630 MEANS FOR EMERGENCY COOLING OF A NUCLEAR REACTOR. Walter Geipel (to Licentia Patent-Verwaltungs GmbH). German Patent 1,185,309. Jan. 14, 1965. Filed Apr. 11, 1961.

The equipment for the removal of shutdown heat consists of three cooling circuits such as the primary cooling circuit of the reactor, the emergency cooling circuit for the removal of shutdown heat, and an idling circuit for cooling the core when the reactor is not in use. In case of an accident when the emergency cooling circuit is in operation the cooler arranged in this circuit is cooled by the idling circuit. After the core is cooled sufficiently further cooling of the core is carried solely by the idling circuit. (Gmelin Inst.)

21631 CONTROL ELEMENT FOR NUCLEAR REACTORS. Karl Janner (to Siemens-Schuckertwerke AG). German Patent 1,185,310. Jan. 14, 1965. Filed Mar. 21, 1959.

The control element consists of two cooperating neutron balance means displaceable relative to one another between a first extreme position and a second extreme position. Each control means includes a support member adapted to support one or more neutron-balance-disturbing members each of which consists of at least two substances that disturb the neutron balance in different ways. These substances are disposed in a manner such that, when the control element is in use in one extreme position, there occurs the minimum exposure of one of the substances to neutrons and in the other of the extreme positions there occurs the minimum exposure of the other substance to neutrons. (Gmelin Inst.)

21632 CONTROL DEVICE FOR NUCLEAR REACTORS. Christoph Steinert (to Deutsche Babcock and Wilcox-Dampfkesselwerke Aktiengesellschaft). German Patent 1,186,565. Feb. 4, 1965. Filed Apr. 4, 1960.

The device described includes two bodies movable longitudinally one within the other. The outer surface of the inner body and the inner surface of the outer body are shaped to provide, throughout the range of movement, an annular space between the two bodies. The annular space between the two bodies is filled with a neutron-absorbing fluid. (Gmelin Inst.)

21633 MEANS FOR SECURING PRESSURE TUBES CONTAINING FUEL ELEMENTS IN A NUCLEAR REACTOR. Eugen Guidi (to Sulzer Freres, S. A.). U. S. Patent

3,154,474. Oct. 27, 1964. Priority date June 8, 1960, Switzerland.

A device for securing pressure tubes containing fuel rods and coolant ducts to the moderator part of a nuclear reactor and for connecting supply and relief pipes for the coolant to the pressure tube is patented. The device includes stationary connecting means with coolant connections on the moderator part, a movable element adapted to press the pressure tube against the stationary element, and an elastic element for pressing the movable element against the pressure tube. Means are provided for adjusting the pressure exerted by the elastic element on the movable element. (A.G.W.)

Criticality Studies

See also PHYSICS — Criticality Studies.

21634 (BNL-9010) CENTERS AND LIMIT CYCLES IN REACTOR KINETICS. Louis M. Shotkin (Brookhaven National Lab., Upton, N. Y.). Mar. 1965. Contract AT-30-2-GEN-16. 33p. (CONF-650406-3). Dep.(mn); $2.00 (cy), 1(mn) CFSTI.

From Symposium on Neutron Dynamics and Control, Tucson, Ariz.

A practical method for computing the amplitude and frequency of centers and limit cycles is given. This is an extension of a method of Krylov and Bogoliubov. The method considers stable periodic solutions that arise from linear solutions of the form exp $(b \pm i\omega t)$. Two asymptotic series are derived: one for $b/\omega = O(\mu)$, $\mu \ll 1$; and the other for $b/\omega = O(1)$. Analytic results are obtained with these series for two specific problems in reactor kinetics, namely the two-temperature problem with no prompt power coefficient, and the xenon problem with no temperature feedback. (auth)

21635 (BNL-9011) EVOLUTION OF THE FINITE ESCAPE TIME CONCEPT IN REACTOR KINETICS. Jack Chernick (Brookhaven National Lab., Upton, N. Y.). Mar. 1965. Contract AT-30-2-GEN-16. 13p. (CONF-650406-4). Dep.(mn); $1.00(cy), 1(mn) CFSTI.

From Symposium on Neutron Dynamics and Control, Tucson, Ariz.

The usefulness of the finite-escape-time concept in reactor kinetics is discussed. The general problem for a reactor with several temperature coefficients is treated. For adiabatic conditions, exact criteria for the existence of solutions of finite escape time are given. If all temperature coefficients are positive, it is shown that the solutions of the reactor excursion problem diverge in a finite time. The method of expansion in a small parameter is explored. (auth)

21636 (CONF-654-32) SELF-SHIELDING IN CLOSELY SPACED SLAB LATTICES. S. W. Kitchen and K. R. Edgar (Knolls Atomic Power Lab., Schenectady, N. Y.). [1964]. Contract W-31-109-eng-52. 21p. Dep.(mn); $1.00(cy), 1(mn) CFSTI.

From American Nuclear Society Meeting, San Francisco, Nov.-Dec. 1964.

Since the underlying assumption in most reactor calculations is the homogeneous distribution of fuel, the comparison of flat plate fuel reactor measurements to calculations requires a knowledge of the effectiveness of this heterogeneous fuel relative to homogeneous fuel. For closely spaced (0.1 to 0.4 in.) lattices with slab thickness ranging up to ~0.2 mean free paths, calculations indicate self-shielding factors several per cent higher than for isolated plane absorbing foils. An experiment devised as a means for reducing the uncertainty in the effectiveness of fuel in slab lattices to acceptable limits is described. A special sub-lattice was constructed in the central region of the Flexible Plastic Reactor. This sub-lattice consisted of four aluminum trays. Each tray was loaded with an identical array of polyethylene strips and aluminum strips. Forty-five strips of 93% enriched fuel coated with Teflon were loaded into this array in groups of three to form fifteen fuel slabs. (C.E.S.)

21637 (CONF-650406-2) THE SPATIAL DEPENDENCE OF PULSED-NEUTRON REACTIVITY MEASUREMENTS. Martin Becker and Karl S. Quisenberry (Knolls Atomic Power Lab., Schenectady, N. Y.). [1964]. Contract W-31-109-eng-52. 50p. Dep.(mn); $2.00(cy), 1(mn) CFSTI.

From Symposium on Neutron Dynamics and Control, Tucson, Ariz.

A series of pulsed neutron reactivity measurements is reported, in which strong spatial dependence of the results is observed. The difference between prompt and delayed fundamental mode shapes is found to account for this dependence. The major pulsed-neutron techniques are derived using a kinetics analysis in which the prompt and delayed fluxes are each assumed to be separable in space and time, but in which the total flux is not. It is concluded that standard experimental methods yield a meaningful reactivity if an easily-obtained spatial correction factor is applied. (auth)

21638 (CONF-650501-4) VARIATIONAL SYNTHESIS WITH DISCONTINUOUS TRIAL FUNCTIONS. E. L. Wachspress and M. Becker (Knolls Atomic Power Lab., Schenectady, N. Y.). Feb. 1965. Contract W-31-109-eng-52. 22p. Dep.(mn); $1.00(cy), 1(mn) CFSTI.

From the Application of Computing Methods to Reactor Problems, Argonne, Ill.

The multichannel flux synthesis method for treating neutron-diffusion problems in several dimensions is considered. In this method, regions are represented by nodes, and nodal difference equations are derived with the aid of the lower-dimensional results. By suitably choosing a functional and trial functions, nodal difference equations are derived from variational principles. Discontinuous trial functions are used. Methods for obviating the difficulties presented by these discontinuities are discussed. (T.F.H.)

21639 (IA-988) THE XENON MINIMAX PROBLEM. M. Ash (Israel Atomic Energy Commission, Yavne. Soreq Research Establishment). Sept. 1964. 78p. Dep.(mn)

A high flux thermal reactor possesses hundreds of dollars of negative reactivity, following shutdown from equilibrium, due to the large concentration of xenon-135 present. Using the methods of Dynamic Programming, optimal flux shutdown programs were obtained, from a computerized algorithm, that minimize the 11 hour xenon maximum and/or the xenon concentration itself at a given post shutdown time. Such programs, with constraints on the flux magnitude only, are found to consist of pulsing the reactor at given intervals depending on the parameters involved. (auth)

21640 (IDO-16983) SOME METHODS OF CALCULATION OF THE PARAMETERS IN THE REACTOR KINETICS EQUATIONS. G. E. Putnam (Phillips Petroleum Co., Idaho Falls, Idaho. Atomic Energy Div.). Feb. 1965. Contract AT(10-1)-205. 87p. Dep.; $3.00(cy), 2(mn) CFSTI.

The spatially independent form of the reactor kinetics equations is written in terms of several time-dependent parameters, namely, the reactivity, the delayed neutron fraction, the prompt neutron lifetime, the concentration of the ith species of delayed neutron precursor, and the source. Ways of computing the values of the parameters according to these formulae are described in detail with the emphasis given entirely to methods which utilize practically any of the commonly available reactor computer codes without recourse to the calculation of neutron importance functions. Methods are outlined that lead to an indirect evaluation of the commonly encountered integrals of functions weighted by the importance function: that is, the methods involve no integration. The arbitrariness of the definitions of some of the parameters is discussed and several different but equally valid sets of definitions are given by way of example. The criterion for the consistency of a set of definitions is given. (auth)

21641 (JINR-P-1996) STATISTICHESKAYA TEORIYA RAZMNOZHENIYA NEITRONOV I SHUMY V STATSIONARNYKH YADERNYKH REAKTORAKH. (Statistical Theory of Neutron Multiplication and Noises in Stationary Nuclear Reactors). B. Kozik (Joint Inst. for Nuclear Research, Dubna (USSR). Lab. of Neutron Physics). 1965. 20p. Dep.(mn).

The stochastic linear model of the neutron multiplication process is used to derive equations for neutron correlation functions which, for stationary systems, are solved by the Laplace transformation. A direct Fourier transformation of these equations yields an exact expression for the spectral density power of noise in the reactor. This expression gives grounds, from the statistical viewpoint, for application of the dynamical models of linear systems with white noise "at output" to zero power reactor systems. (auth)

21642 (MMPP-FRPC-64-3) NONLINEAR REACTOR KINETICS. Elias P. Gyftopoulos (Massachusetts Inst. of Tech., Cambridge. Dept. of Nuclear Engineering). 1964. Contract AT(11-1)-1372. 47p. (CONF-640615-2). Dep.(mn); $2.00(cy), 1(mn) CFSTI.

From Fast Reactor Physics Conference, Ann Arbor, Mich.

The nonlinear reactor kinetics equations are derived in order to determine their applicability in studies of very fast transients, and in order to analyze their usefulness in studies of stability. The nonlinear stability criteria of the reactor are found in terms of experimentally accessible linear properties that can be calculated. (T.F.H.)

21643 (WAPD-T-1728) THE ANALYTICAL AND MONTE CARLO ANALYSIS OF AN EXPERIMENT DESIGNED TO ILLUSTRATE SPATIAL AND ENERGY INTERFERENCE AMONG RESONANCE NUCLIDES. N. R. Candelore and R. C. Gast (Bettis Atomic Power Lab., West Mifflin, Pa.). Dec. 1964. Contract AT(11-1)-Gen-14. 18p. (CONF-654-51). Dep.(mn); $1.00(cy), 1(mn) CFSTI.

From American Nuclear Society Meeting, San Francisco, Nov.-Dec. 1964.

A series of light water moderated critical experiments were performed to illustrate spatial and energy interference among resonance nuclides. The nuclides chosen appear in composite fuel plates, i.e., plates of parasitic resonance nuclides (hafnium) held adjacent to plates of ^{235}U. Experiment analysis using an analytical resonance capture program and using a Monte Carlo resonance capture program is discussed. (C.E.S.)

21644 (WAPD-TM-478) HARMONY: SYSTEM FOR NUCLEAR REACTOR DEPLETION COMPUTATION. R. J. Breen, O. J. Marlowe, C. J. Pfeifer (Bettis Atomic Power Lab., Pittsburgh). Jan. 1965. Contract AT(11-1)-Gen-14. 108p. Dep.(mn); $4.00(cy), 3(mn) CFSTI.

The Harmony system consists of an integrated set of computer programs which facilitate the diffusion-depletion calculations required in the design and analysis of nuclear reactors. The system design emphasizes flexibility in order to allow the description of a wide range of problems. The user is able to tailor the system to describe his reactor. This flexibility includes the cross section treatment as well as the number and type of nuclides which can be represented. The initial application has been with two-dimensional spatial programs for x-y and r-z geometries in PDQ-5 and hexagonal geometries in PDQ-6. (auth)

21645 EXPERIMENTAL STUDIES ON NATURAL URANIUM–LIGHT WATER EXPONENTIAL PILE. [PART] II. Eiichi Takeda, Eiichi Arai, Keiji Kanda, and Shinichi Wakabayashi. Bull. Tokyo Inst. Technol., No. 61, 59-66 (1964).

The material buckling of the natural uranium-light water exponential pile was measured in two lattice piches on the basis that the values of material buckling and reflector saving are independent of the core size with the same core composition. The neutron multiplication factor calculated was compared with the theoretical values calculated by the four-factor formula. (auth)

21646 EXPERIMENTAL STUDIES OF SUBCRITICAL REACTOR WITH GRAPHITE MODERATOR. R. Anakhara, Genshiryoku Kogyo, No. 3, 54-7(1963). (In Japanese)

Experiments with the subcritical graphite moderated reactor indicated a comparatively simple method for changing the shape of the fuel element lattice into tetragonal or hexagonal and the feasibility of using native graphite, fuel, and measuring instruments. The results of all experiments including the exponential functions coincided with published data. The thermal neutron diffusion length in a graphite moderator was found to be α = 51.7 and 54.4 cm for graphite of density 1.68 and 1.6 g/cm^2, respectively. The length of fast neutron moderation by metal foils was α_s^2 = 315.1 ± 1 cm^2 for Cd-coated ^{197}Au and $\alpha_{\frac{1}{4}}^2$ = 330 ± 5 cm^2 for Cd-coated ^{115}In. Data are also given on the neutron distribution in fuel rods and the radioactivity of the area surrounding the reactor. The maximum distribution of thermal neutrons was 50 neutrons/cm^2 sec and the maximum for fast neutrons was 10 neutrons/cm^2 sec and γ rays 0.9 mr/h. The total dose of all radiation did not exceed the permissible dosage. (R.V.J.)

21647 STABLE NUMERICAL SOLUTIONS OF THE REACTOR KINETICS EQUATIONS. K. F. Hansen, B. V. Koen, and W. W. Little, Jr. (Massachusetts Inst. of Tech., Cambridge). Nucl. Sci. Eng., 22: 51-9(May 1965).

A numerical procedure for the integration of the reactor kinetics equation is developed. It has the property of being numerically unconditionally stable for all values of the reactivity or integration-step size. The basic assumption of the method is that the neutron and precursor densities behave exponentially with a frequency characteristic of the asymptotic frequency corresponding to the reactivity. As a consequence of the assumption, and the factoring of the kinetics equation, it is then shown that for constant reactivity the asymptotic numerical eigensolution is exactly the asymptotic eigensolution of the differential kinetics equations. Thus, for constant reactivity, the asymptotic numerical solution can be shown to differ from the asymptotic analytic solution by at most a constant factor, proportional to h_t^2, for all time. (auth)

21648 IMPROVEMENTS TO THE THEORY OF RESONANCE ESCAPE IN HETEROGENEOUS FUEL. I. REGULAR ARRAYS OF FUEL RODS. D. C. Leslie (Atomic Energy Establishment, Winfrith, Dorset, Eng.). J. G. Hill, and A. Jonsson. Nucl. Sci. Eng., 22: 78-86(May 1965). (AEEW-R-353)

A new and very simple method of calculating Dancoff factors in regular arrays of cylindrical fuel rods is presented. This method is readily applicable to canned fuel, and comparisons with Monte Carlo calculations show that its accuracy is adequate for practical purposes. An extension of the standard equivalence theorem which, unlike the theorem itself, is accurate enough for practical work is given. This extension enables the resonance integrals of regular arrays to be calculated from the Dancoff factor and from calculations of the resonance integral in homogeneous mixtures. These methods were compared with the very accurate Monte Carlo calculations of Levine; the result is most satisfactory. (auth)

21649 THE EXTRAPOLATION DISTANCE AT THE SURFACE OF A GREY CYLINDRICAL CONTROL ROD. N. Spinks (Australian Atomic Energy Commission, Lucas Heights, New South Wales). Nucl. Sci. Eng., 22: 87-93 (May 1965).

The extrapolation distance ϵ at the surface of a grey cylindrical control rod of given size is found in terms of the blackness β of the rod and in terms of the extrapolation distance ϵ_b at the surface of a black rod of the same size. The formula is $(\epsilon/\lambda_e) = (\epsilon_b/\lambda_e) + [4(1-\beta)/3\beta]$, where λ_e is the transport mean free path in the region external to the rod. Tables are provided for β, and an empirical expression for ϵ_b/λ_e is given. (auth)

21650 LARGE REACTOR EXCURSIONS STARTING AT OPERATING CONDITIONS. Jose Canosa (General Electric Co., Pleasanton, Calif.). Nucl. Sci. Eng., 22: 113-15 (May 1965).

An extension of previous work (Nucl. Sci. Eng., 19: 329 (1964)) on large excursions in reactors is presented, which includes those starting at operating, steady-state conditions. The previous work was limited to excursions starting at zero power. (C.E.S.)

21651 A NOTE ON THE INVERSE KINETICS ANALYSIS. P. Kovanic (Inst. of Nuclear Research, Czechoslovak Academy of Sciences, Rez). Nucl. Sci. Eng., 22: 118-19 (May 1965).

It is proposed that for the reactor power function of the type $n = n_0 \exp(\alpha t)(1 + A \sin \omega t)$ the corresponding reactivity function can be found by solving reactor point kinetics equations. (C.E.S.)

21652 CORRELATION OF IN-PILE TRANSIENT PRESSURE MEASUREMENTS. C. E. Dickerman and W. Stephany (Argonne National Lab Ill.). Nucl. Struct. Eng., 1: 342-4 (Mar. 1965).

Theoretical studies were made of the effects of physical parameters on transient pressures and coolant expulsion from typical fast reactor coolant channel geometries, using representations in which detailed heat transfer phenomena do not enter explicitly but could be included when appropriate. An analytical model was developed for correlation of computer pressure pulse calculations performed using a code based on a model developed by Mehta, Rosenberg, and Ray for calculation of pressure transients in the large sodium loop being constructed for fast reactor safety experiments in TREAT. (M.C.G.)

21653 ON THE DELAY TIME FOR BUBBLE FORMATION IN WATER-MODERATED REACTORS. H. William McCurdy (Pennsylvania State Univ., University Park). Nucl. Struct. Eng., 1: 345-6(Mar. 1965).

The wait time for bubble formation in the power burst following a large insertion of reactivity in a water-moderated reactor is associated with the growth of a very thin thermal layer adjacent to the heating surface. It can be treated as a transient-conduction phenomenon, described by Fourier's equation along with the appropriate boundary and initial conditions. Equations are given for calculating delay time for any water-moderated reactor where void formation is the primary shutdown mechanism. The peak power and energy release at peak power may also be calculated. (M.C.G.)

21654 SOLUTION OF A TWO-DIMENSIONAL NEUTRON DIFFUSION PROBLEM BY FLUX SYNTHESIS. Peter Kilian (AEG-Kernenergieanlagen, Frankfurt am Main). Nukleonik, 6: 340-4(Nov. 1964). (In German)

The calculation of the two-dimensional distribution of the thermal neutron flux in the large cell of a water-moderated reactor was reduced with the help of a variation method to the calculation of the one-dimensional flux distribution. The position-dependent superposition of a second one-dimensional asymptotic flux gives a good approximation of the flux distribution. Iterations improved the results only slightly. (tr-auth)

21655 CALCULATION OF NEUTRON FLUX OF A GIVEN REACTOR CELL USING THE RELAXATION METHOD. Olaf Abeln (Universität, Innsbruck). Nukleonik, 6: 344-7(Nov. 1964). (In German)

The relaxation method as an approximation solution of differential equations was especially developed by Southwell for physics and technology. This method was shown also advantageous for reactor physics as it gives in a relatively simple and rapid fashion a survey of the solutions of the differential equations given. This proves correct especially for the neutron flux distribution of complicated reactor cells whose multiple boundary conditions can not be fulfilled by analytical solutions. The application possibilities of the relaxation method were shown on the calculation of a cell of the Kahl power reactor. (tr-auth)

21656 HEAT TRANSFER MODEL OF A REACTOR WITH A REFLECTOR ZONE. W. Humbach and U. Jauernik (Technische Hochschule, Darmstadt, Ger.). Nukleonik, 6: 367-8(Nov. 1964). (In German)

A previously reported method that applied the analogy between the distribution of the neutron current density of a stationary reactor determined by the one-group theory and the temperature distribution of a cooling body to the determination of the geometric buckling and spatial flux density distribution in reactors with spatially constant nuclear data is discussed. It is shown that this method can be used to represent regions without neutron production (as reflectors) with the help of a heat transfer model. Confirmation of the theoretical expression was obtained on a paraffin cylinder. (J.S.R.)

21657 METHOD AND MEANS FOR THE PULSATION OF NUCLEAR REACTORS. Ronald Dierckx, Gustav Kistner, and Herbert Meister (to Europaische Atomgemeinschaft (EURATOM)). German Patent 1,184,873. Jan. 7, 1965. Filed Sept. 10, 1963.

The pulsation of the nuclear reactor is carried out by circulating a rolling body of fissionable and magnetizable material through an annular channel partially arranged in the neutron field of the core. The power for movement of the rolling body is provided by a traveling wave which is generated by coils wound on the housing of channel. (Gmelin Inst.)

Design and Feasibility

21658 IMPROVEMENTS IN OR RELATING TO NUCLEAR REACTORS. (to Gutehoffnungshutte Sterkrade AG). British Patent 975,908. Nov. 25, 1964. Priority date Apr. 16, 1960, Germany.

The reactor patented has two moderator zones, one containing heavy water and the other containing a different moderator, for example graphite. The heavy water moderator is contained in tubes distributed in a mass of the second moderator, and fuel elements are disposed inside the tubes containing the heavy water. The second moderator is a solid material and is formed with holes containing fuel elements. When heavy water is used as a second moderator, a higher ^{238}U-to-^{239}Pu conversion ratio is obtained than in purely graphite-moderated reactors. (A.G.W.)

21659 COMBINED BOILING WATER AND SUPERHEATED NUCLEAR REACTORS. Hans Kluge and Erhard Fisher (to Licentia Paten- Verwaltungs- GmbH). Canadian Patent 701,192. Jan. 5, 1965. Priority date Feb. 12, 1960, Germany.

Fuel rods are attached to a plate and contained in tubes open at the bottom. As the cooling water moves upward over the rods it boils and steam passes into the steam chamber above, which is also immersed in water. At the top is the superheated steam dome, which is connected to the saturated steam chamber by external pipes. Control rods are inserted from below and are driven by the varying pressure of the superheated steam, which depends on the turbine demands. Special means are used to control corrosion. Only one passage of coolant takes place through the cooling channels in the reactor core in one direction, during which preheating, vaporization, and superheating occur. (F.S.A.)

21660 NUCLEAR REACTOR CONTROLLED BY VARYING THE LEVEL OF THE LIQUID MODERATOR. Wolfgang Keller (to Siemens-Schuckertwerke AG). German Patent 1,184,024. Dec. 23, 1964. Filed June 28, 1963.

In a nuclear reactor controlled by varying the level of the liquid moderator special fuel elements are located above the normal fuel elements within the control range of the moderator level between the maximum and minimum level. These special fuel elements were more highly enriched in fissionable material than the normal fuel elements. (Gmelin Inst.)

21661 BOILING WATER NUCLEAR REACTORS. George Howard Forsyth (to Vickers-Armstrongs (Engineers) Ltd.). German Patent 1,184,025. Dec. 23, 1964. Priority date Nov. 25, 1960, Great Britain.

A boiling-water reactor is described, which has a steam space in the reactor vessel in which the steam evolved from the boiling moderator accumulates. This reactor is provided with a steam circulating system for drawing steam from this space and circulating it through the reactor core thereby controlling the reactivity of the core over the load range of the reactor. (Gmelin Inst.)

21662 METHOD FOR COOLING NUCLEAR REACTORS WITH STEAM. Walter Geipel (to Gesellschaft fur Kernforschung mbH). German Patent 1,184,430. Dec. 31, 1964. Filed Aug. 16, 1963.

The method consists of evaporating the feedwater before it enters the nuclear reactor, and of superheating the steam within the reactor. In order to ensure that the steam entering the nuclear reactor is dry the feedwater is evaporated under critical pressure and expanded to a predetermined working pressure. (Gmelin Inst.)

21663 FAST-NEUTRON PASTE-FUELED REACTOR. R. W. Dickinson and D. T. Eggen (to U. S. Atomic Energy Commission). U. S. Patent 3,169.117. Feb. 9, 1965.

A fast nuclear reactor is described in which the fuel is in paste form. The paste consists of a liquid metal and a fissionable fuel selected from the class consisting of UC, PuC, ThC-UC, and PuC-UC. The paste is held within a core vessel by fuel-containing members, and liquid metal is used as the coolant. (AEC)

Fuels

Refer also to abstracts 19833 and 20036.

21664 (CEND-3336-229) DEVELOPMENT AND TESTING OF A TEMPERATURE TRANSIENT METHOD FOR PERFORMING IN-PILE THERMAL CONDUCTANCE TESTING. Progress Report, October 1–December 31, 1964. C. E. Burdg, J. R. Parrette, R. I. Brockett, and W. P. Chernock (Combustion Engineering, Inc., Windsor, Conn. Nuclear Div.). Feb. 1965. Work Performed under United States–Euratom Joint Research and Development Program. Contract AT(30-1)-3336. 19p. (EURAEC-1307). Dep.(mn); $1.00(cy), 1(mn) CFSTI.

The concept now being investigated is one whereby measurement of the transient temperature response at the surface of an operating fuel element, following a reactor power change, will yield thermal conductance values. This two-phase investigation consists first of out-of-pile demonstrations of feasibility, followed by in-pile confirmation of the method. Concurrent mathematical analyses of the thermal model will provide the bases for data interpretation, as well as guides for the design of the experimental portions of the program. A digital computer study of the expected transient characteristics of the proposed in-pile element has been made. The predicted behavior is somewhat similar to that predicted for the out-of-pile element, in that the clad response to cyclically varying input may yield both effective conductivity and fuel-clad conductance values. An important difference is that the in-pile element is expected to be less sensitive to changes in the thermal parameters, a direct result of distributed power generation as opposed to axial line heating. With the aid of these analyses of the thermal models, out-of-pile experiments are being designed to permit verification of the predicted performance. (auth)

21665 (GAMD-5535) GAIL IV IRRADIATION ASSEMBLY DESIGN SUMMARY AND INFORMATION DATA PACKAGE. E. O. Winkler (General Atomic, San Diego, Calif.). Aug. 11, 1964. Contract AT(04-3)-167. 71p. Dep.(mn); $3.00(cy), 2(mn) CFSTI.

The experimental fuel element designated GAIL IV, to be irradiated at the General Electric Test Reactor in the General Atomic In-pile Loop, is a 12-hole, radially purged "telephone dial" graphite body containing packed beds of "triplex" coated fuel particles. The purpose of the irradiation is to study the thermal, mechanical, and fission-product-release characteristics of an essentially full-scale packed-particle-bed fuel element operating at reactor conditions. Predicted operating conditions and limits of operation are presented. Design of the fabrication of the experiment are described. (auth)

21666 (GEAP-4640) SODIUM-COOLED REACTORS PROGRAM. FAST CERAMIC REACTOR DEVELOPMENT PROGRAM. Eleventh Quarterly Report, April–June 1964. C. E. Breizy, ed. (General Electric Co., San Jose, Calif. Atomic Power Equipment Dept.). July 1964. Contract AT(04-3)-189. 57p. Dep.(mn); $3.00(cy), 2(mn) CFSTI.

A fission product plugging capsule experienced local temperature excursions, caused perhaps by a gas bubble rising through the NaK annulus within the capsule. Irradiation was continued with temperatures within operating limits at 70% of full power. During the next two operating cycles the capsule was irradiated at full power with temperatures again normal. Exposure of three high-burnup pre-irradiated mixed-oxide fuel series capsules was completed after obtaining the target burnup of ~60,000 Mwd/t. Preliminary post-irradiation examination by gamma scanning indicated breaching of the fuel specimen's cladding, which was verified on disassembly of the capsule. All components for modification of an unirradiated capsule for transient irradiation in TREAT were completed and hydrostatic testing of the outer pressure vessel containment successfully accomplished. Irradiation of another high-burnup capsule was halted when, with an accumulated burnup of approximately 80,000 Mwd/t, temperature readings indicated a 45 percent overpower condition on the lower fuel pin. A plutonium migration capsule was finished and irradiated. Thermal conductivity of $UO_{2.000}$ was determined, using the "hot-rod" rig, with excellent precision and agreement with prior data. A first draft of the specifications for the two-dimensional synthesis code, MUSY2, has been written and preliminary problem characteristics established. (auth)

21667 (GEAP-4776) ACCURATE NUCLEAR FUEL BURNUP ANALYSES. Quarterly Progress Report No. 12, September–November 1964. B. F. Rider, F. R. Smith, J. L. Jaech, C. P. Ruiz, and J. P. Peterson, Jr. (Vallecitos Atomic Lab., General Electric Co., San Jose, Calif.). Dec. 1, 1964. Contract AT(04-3)-189. 30p. Dep.(mn); $2.00(cy), 1(mn) CFSTI.

The development of accurate methods for the determination of nuclear fuel burnup is studied. Mass-spectrometric analysis of stable fission product isotopes is studied as a means to improve accuracy. One of the most promising of such isotopes for the U-235–Pu-239 fuel system is Nd-148. The method for separating fission product Nd-148 from irradiated UO_2 has been simplified to three columns from the five columns previously employed. The detailed procedure is described in which neodymium is: isolated from the fuel and cladding constituents on a Dowex-1 column from methanolic nitric acid; purified by reverse-phase chromatography on a column of di(2-ethylhexyl) phosphoric acid on silica (Chromosorb); and finally adsorbed on Dowex-50 and freed of actinide contamination by washing with ethanolic HCl and recovered in 6M HCl for mass analysis. Calculation of the Nd-148 content from the resultant mass ratios has been rearranged mathematically to facilitate machine computation. A statistical evaluation was made of magnetic and voltage scanning with the mass spectrometer to determine the contribution of the scanning mode to precision and bias. Little difference could be found between the two methods as long as the biases were small and accurately known. The optimum allocation of effort was determined from an analysis of variance. To achieve the best accuracy in mass spectrometric analysis, it was found necessary to minimize at least three sources of error (i.e., separation-to-separation, filament-to-filament, and scan-to-scan variation). An optimized allocation was found to be two chemical separations per sample, three filaments per separation, and two scans per filament. It was found more accurate to obtain 12 scans in this manner than to obtain a greater number of scans on a single filament or on a single chemical separation. (auth)

21668 (HW-84196) RECLAIMING OF INNER FUELS WITH CRACKED SUPPORTS. W. G. Hudson (General Electric Co., Richland, Wash. Hanford Atomic Products Operation). Sept. 18, 1964. Contract AT(45-1)-1350. 11p. Dep.(mn); $1.00(cy), 1(mn) CFSTI.

Two methods of recovery were developed for inner fuels held because of cracked supports. The first method used was to remove the support arch and leave the tabs on the fuels. New supports were welded on top of the old tabs. This method was satisfactory process-wise but was not approved because of a potential hot spot problem created by the superimposed support tabs. In the second method, the support arch was removed and the tabs left in place in the same way as before. A new support was relocated radially on the fuel halfway between the old support positions. It was felt that this method would be more restrictive to coolant flow but would not create a potential hot spot area. In initial experiments, attempts were made to remove only the defected support and partially remove the oxide film, followed by re-etching and re-autoclaving. These were only partially successful because of problems that developed in support welding and in the etching and autoclave process. The most successful method was to remove all the supports by sawing them off leaving the taps in place and removing only the autoclave film on the external clad to preserve inner clad thickness. Oxide film is removed on the cap to a point midway between the inner and outer weld. This leaves the film break-off line (prone to entrap etchant and leave a white oxide line) in an area where more rapid corrosion rates would not be deleterious to the fuels. During abrasive blasting of the outer surface, the inner weld is protected from abrasive by rubber gaskets held in place by a rod in the fuel bore (Figure 4). During subsequent etching, the inner weld must be protected from the solution because of the preferential attack of fluoride etchant on zircaloy oxide films containing beryllium. This produces a rough surface which entraps fluoride and turns the original black oxide weld to a white or light gray when autoclaved. The same rod and gasket equipment is used as for protection during abrasive blasting except that the rubber gaskets are modified to provide a liquid-tight seal protecting the inner weld area during etching. (auth)

21669 THERMAL BOWING OF REACTOR FUEL ELEMENTS. A. C. Rapier and T. M. Jones (United Kingdom Atomic Energy Authority, Windscale, Cumb., Eng.). J. Nucl. Energy, Pts. A & B, 19: 145-91(Mar. 1965).

Every fuel element becomes bowed because of initial inaccuracies in manufacture and inevitable temperature asymmetries around its circumference which develop in operation. This initial bow causes changes in the heat transfer conditions around the circumference, inducing temperature changes and hence changing the bow. A general theoretical expression is derived for the amplification of the initial bow in terms of the physical properties of the coolant, fuel, and can, the dimensions of the system, and the power rating. It is shown that some combinations of these parameters will lead to complete instability; i.e., the element will continue to bow until it touches the channel wall or another element, leading to serious local overheating of the can. The maximum bow and corresponding excess can temperature must be limited to an acceptable value. Usually the only convenient way to do this is to reduce the unsupported axial length of the element. The determination of the maximum safe value is discussed. Experiments are reported which confirm the predicted variation of induced bowing with the more important parameters over the range of general interest. (auth)

21670 CERAMIC AND DISPERSION TYPE FUEL FOR REACTORS. Elek Szabo and Miklos Fodor. Magy. Kem. Lapja, 19: 413-23(Aug. 1964). (In Hungarian)

The interest in ceramic and dispersion type fuels for reactors, due to their advantages in the operation of nuclear power stations, is discussed. A survey is given on the various ceramic, dispersion, cermet, and coated-particle fuel types considering production methods, characteristics, recent developments, and possible utilization in a variety of nuclear reactors. (auth)

21671 "CERAMIC" NUCLEAR MATERIALS. T. J. Davies (Manchester Coll. of Science and Tech., Eng.). Mutech Chem. Eng. J., No. 9, 45-8(1964).

Advantages in using ceramic instead of metallic fuels for reactors are discussed. Uranium carbides and oxides, thorium oxides, and dispersion fuels are discussed. Fission product damage is also considered. (M.C.G.)

21672 FAST REACTOR FUEL BURNUP. F. R. Channon, J. D. Luoma, and E. D. Frankhouser (Associated Midwest Universities, Lemont, Ill.). Nucl. Appl., 1: 55-61 (Feb. 1965).

Burnup equations based upon isotopic analyses of the fuel are derived for fast reactors. Initial concentrations of ^{235}U, ^{236}U, ^{238}U, ^{239}Pu, ^{240}Pu and ^{241}Pu are considered. Relative reaction rates are used to simplify the isotopic network into an analyzable form. (auth)

21673 PLUTONIUM FUEL FOR THERMAL REACTORS. Nucl. News, 8: No. 4, 11-14(Apr. 1965).

The difficulties in using Pu in thermal reactors are indicated first. Methods for fabrication and chemical processing of Pu fuel elements are then summarized, together with the differences in reactor physics with Pu and ^{235}U fuel systems. The use of ^{240}Pu as a burnable poison and the use of Pu in nuclear rockets are mentioned, together with the addition of fissionable material to irradiated fuel elements. The economics of Pu fuel are considered. (D.C.W.)

21674 TEMPERATURE DISTRIBUTIONS IN END CAPS OF CYLINDRICAL REACTOR FUEL ELEMENTS. Benjamin M. Ma (Iowa State Univ., Ames). Nucl. Struct. Eng., 1: 259-64(Mar. 1965).

The temperature distributions in bonded end caps of solid cylindrical reactor fuel elements with an internal, uniform heat source were determined theoretically. The solution for the temperature distributions was expressed by products of Bessel functions with hyperbolic functions. An illustrative example was chosen for enriched uranium oxide fuel elements with Zircaloy cladding and bonded Zircaloy end caps. The lengths of the end caps were 0.5, 1.0, and 1.5 times the fuel-rod radius. The results of the example indicated that relatively long end caps have somewhat lower maximum temperatures and lower radial temperature gradients than short end caps. These maximum temperatures and radial temperature gradients tended to approach constants as the lengths of the end caps increased. The maximum surface temperature of the end caps was checked against corrosion temperature limit of Zircaloy in water coolant of nuclear reactors. (auth)

21675 IMPROVEMENTS IN AND RELATING TO NUCLEAR REACTOR FUEL ELEMENTS. James Alastair Pearson (to C. A. Parsons & Co. Ltd.). British Patent 975,929. Nov. 25, 1964. Filed June 13, 1961.

A fuel element designed for insertion in a bore in a reactor core consists of a plurality of spaced tubes containing nuclear fuel so arranged as to form a tubular framework. A support member extends axially through the framework, and its walls in conjunction with the tubes form several ducts for coolant flow. The portions of the walls adjacent to the tubes are disposed at an oblique angle to the tubes and baffle the spaces between the tubes. A sheath closely fitted over the tubes extends over substantially the whole axial length of the element and has apertures in the surface to permit the cooling fluid flowing over the outer surface to join that flowing inside the sheath in the reverse direction. (A.G.W.)

21676 GRADIENT FUEL PLATES. R. D. Cheverton (to U. S. Atomic Energy Commision). U. S. Patent 3,175,955. Mar. 30, 1965.

A neutronic reactor fuel element plate containing a fissionable fuel distributed in a concentration gradient across the width of the element is described. A burnable poison is distributed in a concentration gradient which differs in magnitude and direction from the fissionable fuel concentration gradient. (AEC)

Power and Power-Breeder Reactors

Refer also to abstracts 20103, 20509, and 21732.

21677 (ANL-6864) EBR-II WET CRITICAL EXPERIMENTS. F. S. Kirn (Argonne National Lab., Idaho Falls, Idaho) and W. B. Loewenstein (Argonne National Lab., Ill.). Oct. 1964. Contract W-31-109-eng-38. 46p. Dep.; $2.00 (cy) 1 mn (CFSTI).

Criticality studies of the EBR-II were conducted with sodium coolant in the reactor system. The wet critical experiments were designed to provide two general, but not mutually exclusive types of information. First there are the data that are essential for operating the power reactor system, including control rod worth, neutron source strength, nuclear instrument response, etc. The second type of data are of general interest and include the total worth of the sodium coolant, critical size, and the isothermal temperature coefficient of reactivity. (C.E.S.)

21678 (ANL-6972) CONSISTENT HEAVY-ATOM CROSS-SECTION EVALUATION FOR PLUTONIUM RECYCLE CALCULATIONS. D. P. Moon (Argonne National Lab., Ill.). Dec. 1964. Contract W-31-109-eng-38. 11p. Dep.; $1.00(cy), 1(mn) CFSTI.

The EBWR Plutonium Recycle Experiment has been initiated to provide data for the creation of a computational model that will permit accurate prediction of isotopic behavior and reactivity changes with burnup for plutonium-fueled, light-water, thermal reactors. A preliminary model has been tested against data from a number of cold critical experiments. Data from hot criticals and from the EBWR central plutonium region at various burnups are necessary before a complete model can be formulated. This model utilizes the GAM, RIC, SOFOCATE, (or TEMPEST), DSN, and REX codes. This model has been tested against data both from the YANKEE critical experiments (with stainless-steel-clad UO_2 rods) and from Hanford Laboratories' critical experiments with zirconium-clad PuO_2-UO_2 rods and with plutonium–aluminum rods. Good agreement between the model and the experimental data was obtained for the above-mentioned systems. (auth)

21679 (BLG-261) FONCTIONNEMENT D'UNE CENTRALE NUCLEAIRE DE TYPE PWR. RESULTATS DE LA PREMIERE ANNEE DE FONCTIONNEMENT DE LA CENTRALE BELGE BR3. (Operation of a PWR-Type Nuclear Powerplant. Results of the First Year of Operation of the Belgian BR3 Power Station). H. Dresse, M. Gueben, L. Maesen, and M. Potemans (Centre d'Étude de l'Énergie Nucléaire, Brussels (Belgium)). June 1964. 48p. Dep. (mn).

The BR3, first Belgian nuclear power station, was brought into industrial operation on January 1, 1963, after a complete set of tests of the main characteristics of the plant. During the entire year 1963, the station ran without any difficulty and the power operation was satisfactory. The behavior of the equipment was quite good. The gross energy production at the end of 1963 reached 50 kMwh. The utilization factor during the period of power operation was 72%. Some special tests were conducted, including incident simulation and the replacing of a main coolant system pump. The plant was also used for the theoretical and practical training of Belgian and foreign staff. In order to extend the core life and to allow some experiments, the reactor was defuelled after 3800 E.F.P.H. It was then refuelled following a new core configuration. Eight new fuel assemblies, including a newly conceived fuel assembly containing some initially enriched plutonium dioxide fuel elements, were placed in the core. In general, the operation took place without any difficulty; contamination and radiation exposure problems were limited to some extent owing to, among other things, some pre-operative precautions. (auth)

21680 (COO-1402-1) CRITICAL REVIEW OF THE DESIGN OF THE HALLAM MODERATOR ELEMENT, PHASE I. K. R. Stearns and Zenons Zudans (Franklin Inst., Philadelphia, Pa. Labs. for Research and Development). Aug. 28, 1964. Contract AT(11-1)-1402. 66p. (I-B2254-1). Dep.(mn); $3.00(cy), 2(mn) CFSTI.

A number of documents dealing with the Hallam moderator element development and design were critically reviewed. Comments clarifying some specific points of the reviewed documents were listed. Critical areas needing further investigation were depicted and a brief outline of the required analysis given. (auth)

21681 (COO-1402-2) CRITICAL REVIEW OF THE DESIGN OF THE HALLAM MODERATOR ELEMENT, PHASE II. TASK 1. THE CONCENTRATION OF STRESS IN THE CAN AT A JOINT IN GRAPHITE CAUSED BY TEMPERATURE GRADIENTS ACROSS A DIAMETER OF THE MODERATOR ELEMENT. TASK 2. POSSIBILITY OF MECHANISM OF THERMAL STRESS RATCHET. K. R. Stearns and L. Berkowitz (Franklin Inst., Philadelphia, Pa. Labs. for Research and Development). Dec. 14, 1964. Contract AT(11-1)-1402. 60p. (F-B2254). Dep.(mn); $3.00(cy), 2(mn) CFSTI.

The concentration of stress in the can, at a joint in graphite, caused by temperature gradients across a diameter of the moderator element is analyzed. The stiff graphite logs will not bow perceptibly and would be expected to compel a considerable distortion of the can at the gaps between graphite sections. The theory of a beam on elastic foundation is appropriate for the study of a single flat with a temperature gradient across its width. Solution by computer indicated that high stresses would be expected near the joint between logs. The probability of a thermal-stress ratchet mechanism that would tend to increase the separation between the graphite sections is considered. The cause would be differences in the temperature distributions and slipping patterns during scram as opposed to startup. At a level of intensity of friction indicated by the tests, it is shown that neither temperature dependence nor kinetic variation of friction would result in sufficient displacement of the sections of graphite to be likely to indicate damage to the sheaths in the small number of scrams from high power levels logged at HNPF if the coolant temperature at any given point on a moderator element drops monotonically during scram. The violent observed temperature fluctuations, however, suggest that a number of successive waves of racheting might conceivably accompany a single scram-from-power incident. (auth)

21682 (GAMD-4732) PRELIMINARY TARGET STEAM GENERATOR DESIGN STUDY. H. F. Menzel (General Atomic, San Diego, Calif.). Oct. 29, 1963. Contract AT(04-3)-167. 31p. Dep.(mn); $2.00(cy), 1(mn) CFSTI.

The total steam generating capacity of the power plant is divided into six steam generator modules. The steam generator design data of the various steam cycles can be compared. The advantage of a single-gas-reheat cycle, as far as capital investment for steam generators is concerned, is shown. A disadvantage associated with this scheme is the possibility of outflow from the primary system in case of a tube rupture in the reheater section. Such outflow could occur whenever the steam pressure in the reheater section is lower than the helium pressure, i.e., during operation at low loads. The use of suitable detection and control circuits, however, makes this system perfectly satisfactory. This problem can be overcome by using a double steam-reheat cycle, which, unfortunately, is accompanied by a large increase in capital expenditure for steam generators. This increase is caused by the additional equipment cost for reheat exchangers and added heat transfer surface in the steam generator, which is required as a result of a lower temperature efficiency. Single gas/single steam reheat is a compromise between the two steam cycles. This design requires less capital investment than the double reheat cycle. Although the danger of reverse flow still exists, the operational characteristic of this steam cycle limits that possibility to the very low load range, during which an accident causing reverse flow seems rather unlikely. (auth)

21683 (GAMD-5272(Rev.2)) TARGET PRESTRESSED CONCRETE STRUCTURE NUMERICAL STRESS ANALYSIS OF PLEXIGLAS CEILING MODEL. D. C. Cornell (General Atomic, San Diego, Calif.). Nov. 20, 1964. Contract AT(04-3)-167. 34p. Dep.(mn); $2.00(cy), 1(mn) CFSTI.

The numerical analysis described in this report deals specifically with the PCRS for the 1000 Mw(e) TARGET reactor, but the method is general and the results will, in principle, be applicable to other designs. The analysis presented is the counterpart to the experimental stress studies. The aims of the analysis are: to compare the numerical results with the experimental values, in order to verify the correctness of the analysis; and to obtain by both approaches (numerical and experimental) a "stress concentration function" associated with the penetrations in the ceiling of the TARGET pressure vessel. (auth)

21684 (GEAP-4061) WATER SURFACE WAVES IN BOILING WATER REACTORS. C. L. Howard and R. G. Hamilton (General Electric Co., San Jose, Calif. Atomic Power Equipment Dept.). Aug. 31, 1962. Contract AT(04-3)-189. 96p. Dep.(mn); $3.00(cy), 3(mn) CFSTI.

Water surface waves are discussed as a possible factor in the dynamic performance of boiling water reactors. This theory was developed as an attempt to explain some of the results of the VBWR stability experiment. The reactor flux, fuel channel flow rate, and recirculation loop flow rate all had "noise" or random oscillations at a frequency of 0.4 to 1.0 cycles per second. With the exception of fuel channel flow rate, the noise frequency was essentially independent of reactor flow rate. Also, the flux noise amplitude increased with increasing reactor flow rate. These results were partly unexpected, and study of their implications resulted in the surface wave theory. (C.E.S.)

21685 (HASL-152) OPERATIONAL SAFETY EVALUATION OF REMOTE REACTOR PLANTS. Alfred J. Rizzo, Martin S. Weinstein, James E. McLaughlin, and Wesley M. Johnson (Health and Safety Lab., New York Operations Office (AEC), N. Y.) Dec. 1964. 28p. Dep.; $2.00(cy), 1(mn) CFSTI.

Operational safety evaluations at two remote reactors, the PM-1 located at Sundance, Wyoming, and the PM-3A at McMurdo Sound, Antarctica, are described in light of unique problems of communications, weather conditions, and accessibility associated with these sites. The procedure used in performing continuous safety surveillance offsite and periodic rigorous on-site inspections is discussed. It includes analyzing equipment and operational problems, determining the qualifications of operating personnel, and examining the adequacy of communications for proper safety control. The major problems found in these evaluations stemmed mainly from unanticipated equipment design shortcomings such as control rod actuator corrosion, potential disability of fail-safe circuitry in the event of component failure, and local accumulations of radiolytic hydrogen gas to explosive concentrations in the PM-3A containment system. Modifications in design to correct these problems are appraised. Overall results of operating safety evaluations at both reactors indicate that they conformed satisfactorily to established safety criteria of the U. S. Atomic Energy Commission and that all personnel are effectively protected against undue exposure to radiation and other potential hazards arising from their operation. (auth)

21686 (HW-84540) POSTIRRADIATION EVALUATION OF ZIRCALOY-2 PRTR PRESSURE TUBES. PART III. M. C. Fraser (General Electric Co., Richland, Wash. Hanford Atomic Products Operation). Dec. 15, 1964. Contract AT(45-1)-1350. 15p. Dep.(mn); $1.00(cy), 1(mn) CFSTI.

PRTR Surveillance Program work performed and information obtained since the last status report is reported. In addition to more burst test strength and circumferential elongation data, zirconium hydride concentration values from all tubes examined and crack propagation data for irradiated and unirradiated specimens are presented. The burst test strength data show that strength increases with neutron exposure and they indicate that this trend will not be substantially changed by a factor of two increase in neutron exposure. The burst test circumferential elongation data show decreasing elongation values with increasing neutron exposure. The curves indicate that a factor of two increase in neutron exposure will produce a small additional ductility decrement. Zirconium hydride concentration data indicate generally low levels, but at flaws high concentrations, 300 to 500 ppm maximum, have been found. Crack propagation data indicate that neutron irradiation of 5×10^{20} nvt has no effect on critical crack lengths. The indicated PRTR operational critical crack length is about ten inches. Criteria for selection of PRTR Zircaloy-2 pressure tubes to be discharged for examination are proposed. Their bases are the above conclusions. It is recommended that the tube examination portion of the PRTR surveillance program be directed toward crack initiation and propagation studies. (auth)

21687 (IDO-28637) ARMY GAS-COOLED REACTOR SYSTEMS PROGRAM. Quarterly Progress Report, July 1–September 30, 1964. (Aerojet-General Nucleonics, San Ramon, Calif.). Nov. 13, 1964. Contract AT(10-1)-880. 85p. Dep.; $3.00(cy), 2(mn) CFSTI.

The technical progress of the Army Gas-Cooled Reactor Systems Program to develop a mobile, low-power, nuclear power plant for military field operation is summarized. The ML-1 power plant testing was resumed on 1 September 1964; the onstream factor for the month was 77%. Laboratory studies of corrosion of aluminum in shield solution were completed; corrosion was attributed to heavy metal ions and chlorides in the shield solution. Limits were established for ML-1 operation. The final report of the full power and limited endurance run of the ML-1 (ANSOP 16625A) indicates that the power output of the t-c set during this test was lower than predicted; the shielding performed somewhat better than predicted. Burst tests of improved precooler samples indicated a design deficiency. The final design of the improved air-side cooling arrangement for the precooler was completed. A subcontract was awarded for the design and manufacture of a 3600/1800 rpm gear set for use with the new alternator. The final design of the improved starting system was initiated. The design of the overspeed scram chassis was completed and development of the improved speed and temperature control system continued. Metallurgical examination of IB-17R-2 cladding samples revealed an unanticipated second phase. The IB-17R-3 test continued without incident. Tests indicated that fuel pin tip plating is not required for ML-1-II elements. Burst tests indicate that the finned cladding is satisfactory for the ML-1-II elements. The ML-1 Technology Program was initiated with a series of tests to define the limits of the Hastelloy X cladding technology. The ML-1A preliminary safety analysis was published. The modification of the GCRE facility continued. (auth)

21688 (JAERI-1067) INITIAL CRITICAL AND POWER TESTS OF THE JAPAN POWER DEMONSTRATION REACTOR PLANT. (Japan Atomic Energy Research Inst., Tokyo). Dec. 1964. 211p. Dep.(mn). (In Japanese)

JPDR tests are reported. Tests are roughly divided into two parts; first is zero-power physics test; and second is power tests for physics and engineering. The tests was originally programmed and proposed by the main contractor of JPDR. This proposed tests program was modified and supplemented with request of JAERI and tests themselves were conducted by engineers from both parties. In general, the tests were completed successfully and rapidly. (auth)

21689 (JAERI-1068) JPDR MINIMUM CRITICALITY CALCULATION. Yasushi Kuge, Akira Hirata, Yoshihde Yamasaki, Keiichi Mochizuki, and Satoru Katsuragi (Japan Atomic Energy Research Inst., Tokyo). July 1964. 80p. Dep.(mn). (In Japanese)

The minimum-criticality core configurations of the JPDR core are estimated with and without poison curtains,

and the theoretical results are compared with the results of criticality experiments of the JPDR core. Computational methods and their results for the fast- and thermal-neutron spectra, spectrum-averaged cross sections, thermal neutron disadvantage factor in the fuel rod cell, average cross sections and infinite multiplication factor in the fuel assembly cell, and reactivity effect of the connector region are also presented. (auth)

21690 (LA-3244) QUARTERLY STATUS REPORT ON ADVANCED REACTOR TECHNOLOGY (ART) FOR PERIOD ENDING JANUARY 31, 1965. (Los Alamos Scientific Lab., Univ. of California, N. Mex.). Feb. 1965. Contract W-7405-eng-36. 55p. Dep.; $3.00(cy), 1(mn) CFSTI.

Research and development are reported on LAMPRE, Fast Reactor Core Test Facility, Omega West Reactor Experiment, ultra-high Temperature Reactor Experiment, and MHD applications. Results of studies on Pu compounds are summarized, and efforts devoted to fabrication of a satellite heat transfer pipe are described. (J.R.D.)

21691 (NAA-SR-Memo-9492) COMPUTER CALCULATION OF FUEL CLADDING TEMPERATURES, HEAT FLUXES AND POWER DISTRIBUTION IN THE PNPF CORE. D. F. Hausknecht (Atomics International, Canoga Park, Calif.). Apr. 4, 1964. Contract [AT(11-1)-Gen-8]. 69p. Dep.(mn); $3.00(cy), 2(mn) CFSTI.

A computer program has been written to monitor fuel cladding temperatures, heat fluxes and overall power distribution in the PNPF core on a routine basis. Computation of the quantities of interest is based on an extension of theoretical analyses of the fission power distribution and heat conduction in the core. Axial fission power distributions have been fitted with transcendental functions using the method of least squares so that they can be expressed in analytical form, thereby permitting the maximum values of related quantities to be determined expediently by machine computation. Data from routine survey of the outlet thermocouples of all the fuel elements, a total flow rate, and the temperature rise across the core are the primary pieces of input information required by the program. Results from each case run include tabulation by element and contour maps of maximum cladding temperature, maximum heat flux and relative power. (auth)

21692 (NAA-SR-Memo-9976) EXPONENTIAL EXPERIMENTS TO DETERMINE MATERIAL BUCKLING FOR UC-FUELED GRAPHITE-MODERATED ASSEMBLIES. O. R. Hillig, E. J. Johnson, and V. A. Swanson (Atomics International, Canoga Park, Calif.). June 25, 1964. Contract AT-11-1-GEN-8. 100p. Dep.(mn); $3.00(cy), 3(mn) CFSTI.

Material buckling measurements have been carried out to provide physics information directly applicable to the Advanced Sodium Graphite Reactor (ASGR) concept. This concept includes slightly enriched (3.02 w/o), uranium carbide fuel elements, sodium coolant, and graphite moderator. Three triangular lattice pitches, 9, 11, and 12 inches have been studied. These studies included control channel mockups of "wet" (sodium-filled channels) and "dry" (empty channels) control rod arrangements for each lattice pitch. Measurements were carried out in subcritical assemblies of varying sizes (assemblies containing 19, 23, and 31 channels) to study two effects: diffusion anisotropy and the finite assembly size dependence. The diffusion anisotropy was caused by void streaming and assembly heterogeneities. The apparent size dependence was due to the inability to measure the radial component of buckling. The experimental results, a brief description of the theoretical interpretation of these results, and the corrected results are presented. These material buckling values are also compared to results inferred from two-region critical mass studies and to calculated values using few-group and multigroup theories. (auth)

21693 (NP-14896) O.E.C.D. HALDEN REACTOR PROJECT. Fifth Annual Report, 1963/64. (European Nuclear Energy Agency, Paris (France)). 196p. Dep.(mn).

A series of experiments was conducted to measure the reactor transfer functions at both low and high power, using sinusoidal reactivity perturbations. The reactor reached its maximum design power of 20 Mw for the first time. Subsequent power experiments were concerned with such functions as integral void reactivity, reactor stability with induced reactivity perturbations (including investigations of non-linear effects), noise measurements, steam load variations, and automatic control of the vessel pressure. Analysis of the results of these experiments has revealed certain unresolved aspects in the dynamic behavior of HBWR. It has been concluded that the phenomenon of moderator flashing instability observed in HBWR is of sufficiently low frequency to be controlled by an automatic control system. The influence of steam voids on the thermal neutron flux distribution was found to be small in the second fuel charge. Water chemistry experiments designed to study the radiolytic decomposition of heavy water and the problems associated with pH control by ammonia addition have shown that radiolytic gas formation is dependent on gas stripping efficiency in the fuel channels, and can be reduced significantly by deuterium additions. Furthermore, the feasibility of pH control by ammonia addition has been demonstrated. Four heavily instrumented fuel assemblies (IFA 1, 2, 3, and 4) have been installed in the reactor, and these have been used to determine the thermal and hydraulic operating characteristics of the fuel channels over a wide range of conditions. A modified sinusoidal reactivity oscillator was installed in the reactor and was used extensively along with the automatic transfer function analyzer, for dynamic experiments. Means were also developed to use the control rod system to produce small-amplitude step changes in reactivity. The electrically heated boiling test loop was successfully commissioned and was operated with two different instrumented dummy fuel assemblies for determination of channel steady state hydraulic characteristics and for an investigation of the downcomer flashing void phenomenon. A gravity-flow cold test loop was completed and was used for calibration of the turbine flow meter. A Beckman EASE analog computer was installed, and circuits were developed to enable on-line digestion of raw data and automatic plotting of meaningful parameters. The analog-to-digital converter EVA was substantially improved for rapid registration of data and computed parameters on punch tape. A digital computer, GIER, was installed and a great number of programs were made available to permit rapid analysis of dynamics experiments. A statistical analog computer, ISAC, was used to record data on magnetic tape and to compute auto- and cross-correlations. An existing xenon simulator and an analog reactivity meter were improved. (auth)

21694 (P-1076(RAND)) THE SOVIET ATOMIC POWER PROGRAM: LARGE OR SMALL? Arnold Kramish (RAND Corp., Santa Monica, Calif.). May 1, 1957. 9p. (AD-606374). $1.00(CFSTI)

At the Twentieth Party Congress in January, 1956, a directive was given to "build atomic power plants with a total capacity of 2,000,000 to 2,500,000 kw in 1956 to 1960." When this order was published, observers questioned whether "total" referred to the rated thermal or electrical capacity of the atomic power stations. The thermal figure would be more than three times the electrical rating, depending on the thermodynamic efficiency of the system. The dangers inherent in utilizing the ambiguous Soviet data are discussed. (auth)

21695 ECONOMIC INTEGRATION OF NUCLEAR POWER PLANTS INTO THE SYSTEMS OF PRODUCTION AND DISTRIBUTION OF ELECTRIC ENERGY. M. Pierre Ailleret (Electricite de France, Paris). Bull. Inform. A.T.E.N. (Assoc. Tech. Energie Nucl.), No. 49, 65-72 (Sept.-Oct. 1964). (In French)

The integration of nuclear power plants into the production systems of electrical energy is discussed. Questions of the magnitude of the units in relation to the risk of failure, size of investments and interest rate, cost of transport of the fuels, and cost of storing the fuels are considered. The utilization of nuclear power plants is considered in the light of the discussion of these problems. (J.S.R.)

21696 CONSIDERATION ON THE DESIGN OF THE FAST POWER REACTOR WITH A CENTRAL BLANKET. Yoshie Ebizuka, Hiroshi Mizuta, Nagayasu Ikeda, and Masuo Shindo. Bull. Tokyo Inst. Technol., No. 54, 41-50(1963).

The effects of the central blanket on static performance of fast power reactors were investigated. Calculations and a discussion of the results are presented. Although the calculations represent preliminary phase, the results indicate general trends of various quantities and the effects of the central blanket from the viewpoint of engineering design of fast power reactors. (auth)

21697 LIQUID METAL BREEDER REACTOR (LIMB) NUCLEAR EVALUATION. Robert J. Teitel and John B. Brown (Douglas Aircraft Co., Inc., Santa Monica, Calif.). Nucl. Appl., 1: 13-24(Feb. 1965).

The Liquid Metal Breeder reactor is an internally cooled fluid fuel reactor based upon a $^{232}Th-^{233}U$ thermal breeder cycle. It employs a molten lead coolant, a uranium–bismuth solution fuel, a thorium bismuthide dispersion in lead–bismuth blanket fluid and a graphite moderator. Heat from the fuel is transferred through a graphite fuel element to the coolant which transports the heat to an external boiler and pump. Equilibrium concentrations of uranium isotopes heavier than ^{233}U and other reasonable assumptions were derived from existing information and then used to develop a broad survey of LIMB reactor sizes. Two sizes, 200 and 1000 Mw(th), were chosen for more detailed evaluation. The 200-Mw(th) reactor has a potential breeding ratio of 1.08 and an 8 year doubling time. The 1000-Mw(th) reactor has a breeding ratio of 1.05 and a 12 year doubling time. Using the most pessimistic estimates on processing could reduce the breeding ratio, while improvements in design and the utilization of low-cross-section coolants can counteract these losses. (auth)

21698 EXPERIENCE WITH HIGH PRESSURE HEAVY-WATER SYSTEMS AT NPD. A. C. Hoyle and G. R. Howey (Canadian General Electric Co. Ltd. and Hydro Electric Power Commission of Ontario). Nucl. Appl., 1: 25-32 (Feb. 1965).

Two innovations in the design of the NPD primary system were to use carbon steel for piping and to fill and test with heavy water only. Resulting savings were $400,000 and $100,000, respectively. Specifications ensured satisfactory surface and fluid states following commissioning. Operation of the carbon steel system has been very satisfactory except for a fueling-machine failure when foreign materials were introduced into the system. The pD of the system has been maintained between 10–11, the dissolved O_2 concentration at < 0.01 parts/10^6 and the crud level during steady-state operation at < 0.01 parts/10^6 with peak crud concentrations of < 0.1 parts/10^6. During pressure testing, 496 lbs of reactor grade D_2O were lost at a cost of $12,400 at today's prices; nevertheless this loss is acceptably low. Significantly, the corrosion rate, the radiolytic damage, and the gas formation were never as great as had been expected. Carbon steel is therefore recommended for other pressurized water systems. The experience gained in operating NPD for two years showed the economic feasibility of pressurized D_2O as a reactor coolant and pointed out the improvements required. Consequently, the target figure of 10 lb/day loss of D_2O for a 200-MWe reactor now appears feasible. (auth)

21699 REVIEW OF PRESSURIZED WATER REACTOR TECHNOLOGY DEVELOPMENTS. J. C. Rengel (Westinghouse Electric Corp., Pittsburgh). Nucl. Energy, 12-14 (Jan. 1965).

Developments in pressurized water reactor technology reviewed at the Third U. N. Conference on Peaceful Uses of Atomic Energy are summarized. Technical advances in chemical shim control, spectral shift control, control-rod design, redesign of internal components, pressure vessels, motor pumps, steam generators, safety aspects, fuel development, turbine generators, and reliability are reviewed briefly. A table of present PWR applications is given. (M.J.T.)

21700 WELDING EXPERIENCE OF THE REACTOR PRESSURE VESSEL FOR TOKAI NUCLEAR POWER STATION. Toshio Takaichi (Tokai Construction Office of Fuji Electric Co., Ltd., Tokyo) and Yoshio Ando. Nucl. Struct. Eng., 1: 295-307(Mar. 1965).

A nuclear power station is being constructed at Tokai-mura in Ibaraki Prefecture. The station is an advanced Calder Hall type. The electrical output is 166 Mw. The pressure vessel was fabricated using 80 and 92-mm thick aluminum killed steel. Each part of the pressure vessel was prefabricated, then lifted into the reactor building and assembled. Single-sided welding of skirt to skirt forging, C/D nozzle to shell welding, and C/D standpipe to nozzle welding were difficult, particularly to get good penetration and to keep accurate positioning and verticality. (auth)

21701 ADVANTAGES OF THE BINARY MERCURY–WATER VAPOR CYCLE FOR THE SODIUM REACTOR. J. K. Davidson, L. E. Phillips, and A. H. Gage. Rivoluzione Ind., No. 143, 21-5(Dec. 1964). (In Italian)

In order to solve the problem of the direct heat exchange between sodium and water, the use of mercury was suggested. Preliminary studies on a mercury–water vapor cycle are reported. The yield of such a cycle, examination of the cycle components, and economic considerations are discussed. (J.S.R.)

21702 BLOCK-TYPE ATOMIC REACTOR. K. Polushkin and Yu. Tokarev. Tekhn. Molodezhi, No. 9, 6-8(1964).

The nuclear power station ARBUS, placed in operation Aug. 11, 1963, at Melekess, is described. The advantages and disadvantages of the organic coolant, compared to water, are discussed. The generator produced 750 kwe, of which 250 kw are used to drive the pumps, compressors, electrolyzer, etc. The ARBUS is delivered in separate completely mounted blocks, which have already undergone all necessary tests at the manufacturing plant. The complete station consists of 19 of these blocks, weighing from 6 to 19 tons and dimensioned to permit conventional transport. Assembly—mainly interconnecting the blocks using pipelines—requires 2 to 3 months. Inexpensive carbon steel is used in the construction, and all conventional parts are standard mass-produced items. The ARBUS is housed in a small building, with the electrolysis unit and the coolant overflow tanks set up outside. The radioactivity ejected into the ventilation stack (7×10^{-8} C/day) is below the standard for residential communities. (ATD)

21703 ANALYSIS OF THERMOELECTRIC MATERIALS FOR THE DIRECT CONVERSION OF NUCLEAR ENERGY. Glenn Earl Russcher. Thesis, Ames, Iowa, Iowa State Univ. of Science and Tech., 1964. 97p.

An analysis is conducted to select a group of best possible thermoelectric materials for consideration in a direct power conversion system incorporated into a nuclear reactor core. A search for semiconductor materials with specific desirable combinations of parameters is pursued by the analysis of continuity in electron band gap energies and melting temperatures of compounds in chemical groups as a function of the molecular weight of the compound. Eighteen possible thermoelectric materials are predicted in this manner. The figure of merit was not measured for these materials, but calculations based on theoretical and empirical relations indicate that some of these show great promise. High-temperature thermoelectric materials are utilized in the detailed reactor calculations outlined in the appendices. These calculations show that high-temperature materials are superior to the conventional materials such as PbTe. The analysis of an integral direct conversion system also indicates that an optimization of reactor core power density can be achieved by matching the thermal conductivity of the nuclear fuel to that of the thermoelectric material. Heterogeneous reactor cell calculations are outlined which show that materials other than PbTe may be incorporated into a reactor core in quantities compatible with the design of an integral direct conversion system. It is concluded that high temperature operation of thermoelectric materials, above their dislocation annealing temperature, would preclude a major radiation damage prob-

lem for the direct conversion system. (Dissertation Abstr., 25: No. 5, Nov. 1964)

21704 PRTR FUEL ELEMENT RUPTURE TESTING FACILITY (Engineering Materials). (General Electric Co. Hanford Atomic Products Operation, Richland, Wash.). 25 drawings. (CAPE-1153)

The facility was designed to permit testing of high-risk or defective fuel elements with either single pass or recirculating coolant to maximum conditions of 600°F and 2000 psi. It is used to permit determination of the real operating limits of Plutonium Research Test Reactor (PRTR) and future power reactor fuel elements. The test loop activity can be monitored and loop cool-down rates can be controlled and programmed. The high temperature and pressure segment of the facility is located in the experimental (B) cell of the PRTR. The remainder of the equipment is located outside the cell. (For details, see TID-4100) (M.C.G.)

21705 IMPROVEMENTS IN OR RELATING TO THE GENERATION OF POWER BY THE OPERATION OF A NUCLEAR REACTOR. John Rodney Dyson Fuller (Bristol Aerojet Ltd.). British Patent 976,467. Nov. 25, 1964. Filed Sept. 23, 1959.

A method is described for generating power by the operation of a graphite-moderated nuclear reactor whereby each repeated cycle of operation time is divided into three equal periods. One period is devoted to the axial shuffling of the partly used fuel elements in each of "X" channels, all subject to approximately the same flux intensity; the second period is devoted to removal and replacement by new elements in each of "Y" channels, all subject to approximately the same flux intensity; and the third period is devoted to servicing the charge machine. Two plans are patented for the axial shuffling of the partly used fuel elements. If the number of fuel elements in a channel is divisible by two, and when the fuel elements have reacted their half life, the upper half and the lower half of the column of elements are changed about so that the two ends of the column become the middle of the column. Likewise, if the number of fuel elements in a channel is divisible by three and when the elements have reacted one third of their life, the top third of the column of elements is moved to the bottom of the channel, the other two thirds being lifted to the top of the column; the process is repeated when the elements have reacted two thirds of their life. (A.G.W.)

21706 APPARATUS FOR PRODUCING CONTROLLABLE SLOW NEUTRON CHAIN REACTION. Arthur F. Martin (to Hercules Powder Co.). U. S. Patent 3,154,473. Oct. 27, 1964. Filed Mar. 7, 1958.

The core of the reactor patented contains a critical mass of fissionable material suspended as a powder in a coolant gas and is substantially surrounded by a moderator. The suspension of fissionable material is continuously cycled from the core through heat exchangers located outside the moderator and back to the core. Preferably a cyclone-type separator is included in the circuit to remove the fissionable material from the gas between the fission zone and the heat exchanger; the gas is again mixed with previously separated fissionable material before return to the fission zone. The system is described with uranium oxide in the form of a powder of about 0.5 to 10μ with an enrichment of at least 20% ^{235}U as the fissionable material, but other compounds of U and Pu may be used. The coolant gas is a low neutron cross section inert gas or an organic compound. The system may be arranged to utilize fission fragment energy and reactor radiations to initiate desirable chemical reactions in the gas phase or in the moderator at the same time power is being produced. (A.G.W.)

Process Heat Reactors

Refer also to abstract 20120.

21707 (ORNL-TM-432) PRELIMINARY BACKGROUND STUDIES OF THE PROSPECTS FOR ECONOMICAL DESALINATION OF SEA WATER USING NUCLEAR ENERGY. R. P. Hammond, et al. (Oak Ridge National Lab., Tenn.). Nov. 1, 1962. Contract W-7405-eng-26. 33p. Dep.(mn); $2.00(cy), 1(mn) CFSTI.

Very large reactors supplying heat to evaporators seem likely to be capable of producing fresh water from the sea which is cheaper than can be anticipated from any other presently proposed method, and possibly cheap enough for irrigation. This likelihood is especially strong if production of electric power is combined with production of water. The low cost could be achieved, however, only if quantities of water are produced which are much larger than have heretofore been considered in the saline water program. The cost of such a project and the amounts of water and power concerned tend to approach the scale of large river development projects. It is probably economically practical for municipalities to construct dual-purpose plants for production of power and city water using current technology. These moderate-sized plants could be either nuclear or fossil-fueled. Intermediate size nuclear water plants might be useful as an instrument of foreign aid. Once constructed, such plants would be cheap to operate, especially if existing U. S. reactor fueling facilities were utilized. The small plants would serve as pilot plants for developing larger stations. (auth)

21708 (ORNL-TM-465) PROSPECTS FOR SEA-WATER DESALINATION WITH NUCLEAR ENERGY. AN EVALUATION PROGRAM. Gale Young, R. Philip Hammond, and I. Spiewak (Oak Ridge National Lab., Tenn.). Jan. 1963. Contract W-7405-eng-26. 32p. Dep.(mn); $2.00(cy), 1(mn) CFSTI.

An evaluation and preliminary design program is proposed for the application of large nuclear reactors to the distillation of sea water. The applicable technology of evaporation processes and low-fuel-cost reactors is surveyed and applied to the projection of the cost of producing fresh water in large plants. (auth)

21709 REACTOR DEVELOPMENT PROGRAMME FOR LARGE-SCALE DESALTING PLANTS. REPORT BY U. S. ATOMIC ENERGY COMMISSION. Nucl. Energy, 16-20(Jan. 1965).

The objectives and achievements of the Civilian Nuclear Power Program are reviewed. The history of the use of nuclear energy for process heat and desalting is discussed, and international activities in this field are summarized. The proposed AEC reactor-development program for large-scale desalting is presented; the heavy-water moderated, organic cooled reactor offers the best potential for meeting the energy needs for large power-water situations. Estimated program costs through 1975 are summarized. (M.J.T.)

21710 USING LIGHT OBTAINED FROM NUCLEAR REACTORS DIRECTLY TO CARRY OUT UNDERGROUND PROCESSES. John J. Grebe (Dow Chemical Co., [Midland, Mich.]). 21p. (CONF-718-2)

From American Institute of Chemical Engineers Meeting, Las Vegas, Nev., Sept. 1964.

A high-temperature nuclear reactor was planned. It is made of graphite, ZrC, and nuclear fuel and it can radiate part of its heat output as light through mirror systems. It should make low-cost, high-temperature, clean heat available to chemical, metallurgical, and mining engineers. A large radiating surface can be produced by circulating a wave of liquid metal fuel in channels over a large mass of graphite. Thermal conduction, metal vapor condensation, and radiation provide for heat transfer. Shielded windows and reflecting mirror systems permit light to shine onto the surface to be heated. The maximum reactor temperature may be limited by the boiling point of metals like Mg, Pb, Bi, Ga, Ce, and Sn. Boiling and foaming disperses the fuel to a less active configuration for inherent self-regulating characteristics. A sequence of possible applications for such a source of light is presented to emphasize the need of very-high-temperature reactors emitting their energy as light. (auth)

Production Reactors

Refer also to abstracts 20137, 20475, 20477, 20478, 20479, 20480, and 20508.

21711 (DPSPU-63-30-40) IMPURITIES IN MODERATOR OF SAVANNAH RIVER PLANT REACTORS. F. B. Longtin (Du Pont de Nemours (E. I.) & Co., Aiken, S. C. Savannah River Plant). Jan. 1964. Contract AT(07-2)-1. 9p. (CONF-179-18). Dep.(mn); $1.00(cy), 1(mn) CFSTI.

From American Chemical Society Radionuclidic Exchange on Soils, Minerals, and Resin, Philadelphia, Apr. 1964.

Chemical and physical analyses of quite pure (< 3 micromhos/cm) reactor moderator (heavy water of the Savannah River Plant Reactors are discussed. The analyses are useful in diagnosing such troubles as high moderator radioactivity and high activity release from material carried by discharged fuel. The basic information they yield has helped in developing methods of operation (such as pD control) which will prevent recurrence of troublesome conditions. (C.E.S.)

21712 (HW-61979) LEAKAGE FROM ZONE I AND II OF 105-N. G. E. Wade (General Electric Co., Richland, Wash. Hanford Atomic Products Operation). Sept. 16, 1959. Contract AT(45-1)-1350. 13p. Dep.(mn); $1.00 (cy), 1(mn) CFSTI.

A brief survey is made of the problems associated with the minimization of leakage from zones I and II of the 105-N building. This survey is an outgrowth of the confinement concept used in the design of the NPR. Leakage through concrete walls, leakage through penetrations, and permissible leakage are discussed. (C.E.S.)

21713 (HW-83092(Rev.)) TIME-VARIABLE TIME DELAY FOR ANALOG COMPUTER SIMULATIONS. R. A. Walker (General Electric Co., Richland, Wash. Hanford Atomic Products Operation). Dec. 1964. Contract AT(44-1)-1350. 29p. Dep.; $2.00(cy), 1(mn) CFSTI.

Analog simulation studies of the N-Reactor at Hanford indicated a need for a method of delaying analog signals over varying time periods. The requirement included the ability to vary the time delay period during the simulation by means of a control voltage from the analog computer. A time-variable time delay system was designed and built that accepts analog signals in the range of 0.0 to −10 V and delays them from 15 to 150 sec. The control voltage for determining the time delay period must be in the range of 0.0 to +10 V. (auth)

21714 (RL-REA-592) PERFORMANCE OF SELECTED INHIBITORS IN REACTOR COOLANT BACKUP SERVICE. L. D. Gustafson (General Electric Co., Richland, Wash. Hanford Atomic Products Operation). Feb. 15, 1965. Contract AT(45-1)-1350. 11p. Dep.(mn); $1.00(cy), 1(mn) CFSTI.

A test program was conducted to evaluate the carbon-steel corrosion-inhibiting effects of sodium silicate, sodium nitrite, and sodium dichromate in the feedwater supply for five of the reactor high tanks. The concentration of inhibitor was 100 to 200 ppm, and the duration of the tests ranged from 3.5 to 5 months. The results showed that each inhibitor was partially effective, reducing the coupon weight loss by 10 to 50%. However, there was no improvement in pitting corrosion. It was concluded that none of the inhibitors at the concentrations tested will provide the required corrosion inhibition on carbon steel surfaces exposed to low-flow to stagnant reactor water. (D.L.C.)

Propulsion and Space

See also ENGINEERING — Space Propulsion.

21715 (AD-605574) A PRELIMINARY PARAMETRIC SURVEY OF URANIUM–CARBON NUCLEAR REACTOR ROCKET SYSTEMS. Earl W. Allen (Space Technology Labs., Inc., Los Angeles, Calif.). June 29, 1960. 206p. $6.00 CFSTI.

Data obtained during a parametric study of single-pass, bare, uranium–carbon reactors using hydrogen as a coolant fluid are presented. The reactor compositions, dimensions, and weights are related to outlet temperatures and ideal thrusts. It is necessary to point out that many of the assumptions are quite crude, and that these data are to be used primarily to gain some insight into the problems and to provide guidance in the preparation of more detailed studies. Certain performance restraints, possible alternate approaches to studies of this type, and the usefulness of such studies are discussed. (auth)

21716 (GEAP-3514) N. S. SAVANNAH FUEL DESIGN AND DEVELOPMENT PROGRAM. CORE II CRITICAL ASSEMBLY ANALYSIS. H. A. Brammer (General Electric Co., San Jose, Calif. Atomic Power Equipment Dept.). Nov. 15, 1961. Contract AT(04-3)-189. 119p. Dep.(mn); $4.00(cy), 3(mn) CFSTI.

Analysis was made of experimental results of a limited comparative critical assembly program performed to augment physics analyses of the General Electric Company second core (Core II) loading for the N. S. Savannah. Interpretation of comparative nuclear measurements between General Electric simulated Core II fuel and Babcock & Wilcox MARTY critical fuel is made. Measured reactivity effects of various mechanical parts of the assemblies are compared to calculated results. All experimental results previously published by Babcock & Wilcox are given for reference purposes. (auth)

21717 (IDO-17019) SNAPTRAN 2/10A-3 DESTRUCTIVE TEST RESULTS. W. E. Kessler, O. L. Cordes, G. A. Dinneen, R. D. Fletcher, and G. F. Brockett (Phillips Petroleum Co., Idaho Falls, Idaho. Atomic Energy Div.). Jan. 1965. Contract AT(10-1)-205. 136p. Dep.; $4.00 (cy), 3 mn (CFSTI).

The radiological hazards and dynamic reactor behavior in the SNAPTRAN 2/10A-3 destruction by rapid water immersion were investigated. Conclusions drawn from the destructive test analysis indicate that the radiological hazards were considerably less than were calculated. (C.E.S.)

21718 (IDO-17071) SNAPTRAN 2/10A-3 POST-DESTRUCTIVE TEST REACTOR EXAMINATION, CLEANUP, AND SAFETY CONSIDERATIONS. R. D. Fletcher (Phillips Petroleum Co., Idaho Falls, Idaho. Atomic Energy Div.). Jan. 1964. Contract [AT(10-1)-205]. 43p. Dep.(mn); $2.00(cy), 1(mn) CFSTI.

The SNAPTRAN 2/10A-3 reactor, a slightly modified version of the SNAP 2/10A reactor, was designed for investigating the nuclear safety aspects associated with immersion of the reactor core in water which is expected to result in a destructive power excursion. The post-test examination program to be carried out on the reactor fuel and components and the test area cleanup procedures to be employed following the destructive test are described. In addition, the nuclear safety considerations are also presented for all phases of the recovery operation, transportation to the examination area, and during examination of fuel materials in the hot cells and laboratories. The post-test examination is intended to supply information which will aid in understanding the nature of the reactor disassembly process, provides supplemental data on the magnitude of the nuclear and mechanical energy released, and defines the physical condition and radiation levels of the reactor and its environs following a destructive power excursion. Procedures are also presented for the safe test site cleanup including location and removal of all intact fuel elements and fuel fragments, recovery of structural parts of the reactor, and decontamination of the test area. (auth)

21719 (NAA-SR-9780) ANALYSIS OF SNAPTRAN-3 DESTRUCTIVE EXPERIMENT. K. E. Buttrey, L. I. Moss, D. F. Paddleford, A. Weitzberg, and J. O. Zane (Atomics International, Canoga Park, Calif.). Feb. 1, 1965. Contract AT-11-1-GEN-8. 82p. Dep.; $3.00(cy), 2(mn) CFSTI.

The SNAPTRAN (SNAP Transient)-3 destructive experiment was conducted at the National Reactor Testing Station

as one of the major projects in the Aerospace Safety Program. Data obtained from the experiment are reported, and the analysis of the data is discussed from the standpoint of determining the nuclear energy release and reactivity feedback effects. The results are comparable with those obtained by theoretical means. Devices called energy probes were employed as a new technique for measuring the detailed history of the energy density in the fuel-moderator. Using these devices to calibrate the nuclear power detectors, the total yield for the transient was 1.22×10^{18} fissions. (auth)

21720 (NAA-SR-10318) APPLICATION OF NUCLEAR POWER PLANTS (SNAP UNITS) TO THE MANNED ORBITING RESEARCH LABORATORY (MORL). W. V. Botts, M. Marko, P. E. McCourt, V. Keshishian, A. R. Piccot, and G. S. Budney (Atomics International, Canoga Park, Calif.). Feb. 1, 1965. Contract AT(11-1)-Gen-8. 91p. Dep.; $2.25 (cy), 2(mn) CFSTI.

Two designs of a nominal 6-kwe Nuclear Power Plant (NPP), one using thermoelectrics for power conversion and the other using the Mercury-Rankine cycle NPP are described. The integration of the NPP into the Manned Orbiting Research Laboratory (MORL) is given. In addition, detailed discussions are presented on the NPP operational and integration requirements as defined by the MORL mission, nuclear shielding parametric and design data, nuclear hazards and safety criteria and design, NPP deployment subsystem design and analysis, and the developmental requirements to meet the MORL schedule. (auth)

21721 (NAA-SR-Memo-10160) SCALP—SNAP-8 DRM1 CONVERSION PROGRAM. Katharine W. Medeiros (Atomics International, Canoga Park, Calif.). Aug. 24, 1964. Contract [AT(11-1)-Gen-8]. 25p. Dep.(mn); $1.00 (cy), 1(mn) CFSTI.

SCALP is a special purpose program designed to convert the thermocouple data from SNAP 8 DRM1 test runs, draw linear graphs in optional groupings, and record the converted data on magnetic tape for storage and retrieval. (auth)

21722 (NAA-SR-Memo-10767) TEST CONTROL DEVICES—SNAP-10A VIBRATION TEST PROGRAM. R. M. Oliva and E. L. Gardner (Atomics International, Canoga Park, Calif.). Dec. 10, 1964. Contract AT-11-1-GEN-8. 13p. (CONF-641020-1). Dep.(mn); $1.00(cy), 1(mn) CFSTI.

From 34th Symposium on Shock, Vibration, and Associated Environments, Pacific Grove, Calif.

The solutions to various test control problems are recorded. The input, response, and safety control devices employed during vibration testing on past and current SNAP 10A vehicles are discussed. Each device's description, function, and operation are discussed in detail. (auth)

21723 (NASA-CR-193) RESEARCH IN AND APPLICATION OF MODERN AUTOMATIC CONTROL THEORY TO NUCLEAR ROCKET DYNAMICS AND CONTROL. [Progress Report]. Lynn E. Weaver, Donald G. Schultz, David L. Hetrick, James L. Melsa, Hugh S. Murray, and Phillip A. Secker (Arizona Univ., Tucson). Mar. 1965. 96p. $5.00(CFSTI).

Results of investigations of the application and extension of modern automatic control theory to nuclear rocket dynamics and control are summarized. In investigation of closed-loop sub-optimal control employing the second method of Liapunov, an approach to the synthesis problem is discussed in which an attempt is made to combine the Second Method of Liapunov and Pontryagin's Maximum Principle resulting in a closed-loop control, as compared with open-loop control obtained using the Maximum Principle. The research was mainly concerned with developing the foundation for this approach. In work on nonlinear stability of coupled-core reactors, a study of the application of the Second Method of Liapunov to the stability of clustered nuclear rocket engines was conducted. Previous stability analysis of coupled-core systems was based on linear reactor models, with approximations to the neutron transport delay times. More realistic system models are being considered with true delay times to determine regions of stability. In work on synthesis of optimal closed-loop controls for nuclear rocket systems, the realization of a closed control for an optimal control law determined by the Maximum Principle is considered. In physical systems various types of disturbance are encountered which makes open-loop control impractical. The determination of a closed-loop control in the presence of measurement noise and external disturbances is examined. Several approaches to the problem are discussed and an example is worked. Investigations of limits of validity for some approximations in reactor dynamics are reported. Various approximations to the response of reactors to constant rates of reactivity increase are discussed. Such approximations are of particular interest during strat-up. Research in which insufficient progress has been made to warrant a report is the work on the stability of loosely-coupled higher order system. (auth)

21724 NUCLEAR MERCHANT SHIPS. Wolfgang Rojahn. Euratom Bull., 4: No. 1, 12-23(Mar. 1965).

A survey of the Euratom program for the development of nuclear merchant ships is presented, with emphasis on the vessel Otto Hahn, which was launched in June, 1964. (D.C.W.)

21725 FACILITY DESIGN PROBLEMS ASSOCIATED WITH STATIC FIRING OF LARGE NUCLEAR ROCKET STAGES. Maxwell R. Morton (Vitron Engineering Co., New York). Nucl. Struct. Eng., 1: 308-23(Mar. 1965).

Problems encountered in the design of static firing facilities for large nuclear rocket stages are discussed. Layout of the facility, maximum credible accident, transporter, static firing pit, neutron shield tank, propellant heating, altitude simulation, remote connections, diffuser removal, mate or demate facility, stage tank countdown area, cold flow and vacuum test facility, and engine assembly and disassembly building are described. Gamma doses from operational and incident exhaust clouds were calculated and are shown on graphs. (M.C.G.)

Research and Test Reactors

21726 (ANL-6849) EXPERIMENTS ON BOILING CORE B-2, BORAX-V. (Argonne National Lab., Idaho Falls, Idaho). Nov. 1964. Contract W-31-109-eng-38. 138p. Dep.; $4.00(cy), 3(mn) CFSTI.

A description is given of the core B-2 fuel loading in BORAX-V. Measurements are reported of the reactivity, power distributions, water chemistry, transfer function, and plant performance for this core. Results of stability analyses, in-pile tests, and special experiments are discussed. Data from in-pile instruments are analyzed. (T.F.H.)

21727 (BNL-7661(Vol.II)) FINAL SAFETY ANALYSIS REPORT ON THE BROOKHAVEN HIGH FLUX BEAM RESEARCH REACTOR. J. M. Hendrie (Brookhaven National Lab., Upton, N. Y.). Apr. 1964. Contract [AT(30-2)-Gen-16]. 297p. Dep.(mn); $6.00(cy), 6(mn) CFSTI.

21728 (BNL-7661(Vol.I)) FINAL SAFETY ANALYSIS REPORT ON THE BROOKHAVEN HIGH FLUX BEAM RESEARCH REACTOR. J. M. Hendrie (Brookhaven National Lab., Upton, N. Y.). Apr. 1964. Contract [AT(30-2)-Gen-16]. 327p. Dep.(mn); $7.00(cy), 7(mn) CFSTI.

A safety analysis of the HFBR is presented that takes into account a wide variety of environmental hazards, reactor system accidents and malfunctions, and human errors. Volume I contains information on the reactor site, reactor building and containment system, reactor core, primary coolant system, secondary coolant system, and auxiliary systems. In Volume II the experimental facilities, instrumentation and control, shielding, radioactive wastes and effluents, initial tests and operating procedures, administration, and accident analysis are discussed. (C.E.S.)

21729 (CEA-R-2442) DÉTERMINATION EXPÉRIMENTALE DU SPECTRE DES NEUTRONS DANS LE RÉFLECTEUR D'UNE PILE A EAU LÉGÈRE. (Experimental Measurement of Neutron Spectra in the Reflector of a Light Water Reactor). Pierre Bretheé. Commissariat à l'Énergie Atomique, Grenoble (France). Centre d'Études Nucléaires). 1964. 96p. Dep.(mn);

Thesis submitted to Université, Grenoble, France.

The temperature of the thermal neutron spectrum was calculated using Au–Lu foils. This temperature varies from 300°K (temperature of the moderator) at 30 cm of the core to 350°K in a hole of the core. Four resonance detectors were used (Au, In, Co, Mn). The linking up energy E_m between thermal neutron spectrum and slowing down spectrum is about 0.23 ev and is free from the Maxwell spectrum temperature. The decrease of slowing down flux regarding thermal flux, farther from the core, was showed. Three threshold detectors (Ni, Al, Mg) were used A $E^{\lambda}e^{-\beta E}$ form of the spectrum above 3 Mev was assumed. The values of β are in a range from 0.775, at the center of the core and in a loop-hole, to 0.64 at about 30 cm of the core. The following interpolations give useful informations between the field where measurements were made: between 340 ev and 10 kev: 1/E form, between 10 kev and 330 kev: 1/(E, σ_s (E)) form (σ_s (E) = elastic scattering section on hydrogen), and between 330 kev and 3 Mev: calculated form by the moments method. (auth)

21730 (CEA-R-2557) PREMIERS RESULTATS D'ESSAIS INTERESSANT LE BLOC PILE DE RAPSODIE. (First Results of Interesting Tests of the Rapsodie Block Pile). Andre Chalot, Rene Ginier, and Michel Sauvage (Commissariat à l'Énergie Atomique, Cadarache (France). Centre d'Études Nucléaires). June 1964. 118p. (EUR-2232.f). Dep.(mn).

Experiments carried out on the engineering model of Rapsodie and on an associated sodium facility set in a laboratory hall of Cadarache are described. The difficulties encountered during the erection and assembly of the engineering model and the results of the first series of experiments and tests carried out on this installation (loading of the subassemblies, preheating, thermal shocks, etc.) are detailed. The experiments and tests carried out on two prototype control-rod-drive mechanisms, which led to the definitive design of the drive mechanism are reported. The results proved the validity of the general design principles adopted for Rapsodie. (auth)

21731 (KFK-242) A MULTIPLE INPUT DATA ACQUISITION SYSTEM USING A SMALL ON-LINE COMPUTER. A DISPLAY SYSTEM FOR USE WITH AN ON-LINE COMPUTER. G. Krueger and G. Dimmler (Kernforschungzentrum, Karlsruhe (West Germany). Institut für Angewandte Kernphysik, Karlsruhe). July 1964. 14p. (CONF-593-7). Dep.(mn).

From Conference on the Automatic Acquisition and Reduction on the Automatic Acquisition and Reduction of Nuclear Data, Karlsruhe, Ger., July 1964.

The data from several independent multiparameter experiments at the Karlsruhe FR2 reactor are simultaneously recorded by an on-line computer system. The system involves: remote control and buffer stations on each experiment, data communication lines for parallel data transfer from each individual experiment to the computer, a multiplexer unit, involving a 4 × 24-bit buffer store, a computer Control Data 160-A with 8K memory, two magnetic tape units, and a specially designed display system. All operations are governed by one control program. After transferring the input data from the buffer store to the computer memory, they are checked and reduced using different data handling routines for each experiment. Finally the information is stored onto magnetic tape or directly accumulated in the core storage. Design and performance of the whole system are discussed. (auth)

21732 (NAA-SR-10379) SODIUM REACTOR EXPERIMENT. POWER EXPANSION PROGRAM—HEAT TRANSFER SYSTEMS MODIFICATIONS. W. J. Freede and J. K. Roberts, eds. (Atomics International, Canoga Park, Calif.). Oct. 9, 1964. Contract AT(11-1)-Gen-8. 53p. Dep.; $1.25(cy), 2(mn) CFSTI.

Modifications have been made to the Sodium Reactor Experiment facility to improve plant reliability and permit an increase in power to 30 Mwt. with a reactor coolant outlet temperature up to 1200°F. Pertinent changes in the heat transfer systems include: installation of a new main intermediate heat exchanger; replacement of sodium coolant pumps; increase in diameter of certain main primary sodium coolant lines from 6 to 8 in.; reduction in number of valve and freeze traps; utilization of flowing vent lines; and installation of a circulating nitrogen atmosphere cooling system for removing excess incidental heat from galleries. (auth)

21733 (NAA-SR-Memo-10532) EVALUATION TESTING OF FILTORS DPDT RELAYS. M. W. Christian (Atomics International, Canoga Park, Calif.). Oct. 7, 1964. Contract [AT(11-1)-Gen-8]. 20p. Dep.(mn); $1.00(cy), 1(mn) CFSTI.

Twenty-five Filtors latching (PL26V3A6A-1) and twenty-five nonlatching (PR26V3H6A-1) relays were tested to provide data to aid in the selection of back-up DPDT relays for SNAP 10A use. After analyzing the results of the initial performance test and the destructive examination, it was decided that the Filtors DPDT Relays did not warrant any further testing. (auth)

21734 (NAA-SR-Memo-10666) SNAP-10A MALFUNCTION DETECTION SUBSYSTEM—OPERATION AND ANALYSIS. L. E. Fort, G. Drucker, and B. R. Wade (Atomics International, Canoga Park, Calif.). Nov. 2, 1964. Contract AT(11-1)-Gen-11. 38p. Dep.(mn); $2.00(cy), 1(mn) CFSTI.

The SNAP 10A malfunction detection subsystem is designed to initiate a tape recorder sequence for obtaining diagnostic data to assess the cause of failure during power operation. An automatic malfunction detection system is required so that failure diagnostic data are acquired even when the vehicle is not in a normal acquisition zone. The malfunction detection circuits monitoring: NaK volume containment; high reactor outlet temperature; low reactor outlet temperature; and low voltage on the 28 v unregulated bus are shown to be sufficient to enable identification of a major component failure. (auth)

21735 (ORNL-P-1092) MEASUREMENTS AND CALCULATIONS OF ENERGY AND ANGULAR DETAILS OF FAST NEUTRON FLUX IN WATER FROM A POOL-TYPE REACTOR. V. V. Verbinski and M. S. Bokhari (Oak Ridge National Lab., Tenn.). [1963]. Contract [W-7405-eng-26]. 41p. (CONF-654-54). Dep.(mn); $2.00(cy), 1(mn) CFSTI.

From American Nuclear Society Meeting, San Francisco, Nov.-Dec. 1964.

Measurements have been made of the spectral, spatial, and angular details of the fast-neutron flux at one position within the Bulk Shielding Reactor I (BSR-I) and at several positions in the water medium surrounding the reactor. A shielded-diode spectrometer, developed especially for these measurements, was used to obtain the angular flux. The measurements were made in a gamma flux as high as 10^6 r/hr. The spectra for the O^0 (forward) angular flux initially harden with increasing neutron-penetration depth in water up to about 30 cm, after which the spectral shape remains nearly constant. The spectra at 40.5 and 51° are much softer and are nearly constant at depths in water where the spectrometer does not view the edge of the reactor. The reactor power was calibrated against thin uranium foils, and the spectral data were compared with predictions of two neutron transport codes, NIOBE and DTK, all normalized to a reactor power of 2.4×10^{-11} watts. The experimental and calculational results were everywhere within about a factor-of-two agreement with the measurements over a range of attenuation of about 10^4 for angles of O to 52^0 and energies of 1.5 to 12 Mev. (auth)

21736 (ORNL-tr-539) SODIUM PILE LOOP FOR IRRADIATION OF A FISSIONABLE NEEDLE. Translated

by Gregory L. Boisvert from [Paper Presented at the 8th Meeting of the "Reactor and Irradiation Devices Working Group, Grenoble, France, Oct. 1964."]. 32p. $3.60(fs), $1.16(mf) JCL.

The present report describes in general terms a loop designed and constructed for the irradiation of a sheathed fissionable material cooled by the circulation of a molten metal. One of the main irradiation studies which must be pursued with the experimental facilities constructed, is that of the behavior of one or more needles of fissionable material in operating conditions simulating as closely as possible those encountered in the molten metals fast reactor series. These facilities were designed to be incorporated into one of the main channels of the BR2 high flux research reactor. It provides a certain amount of flexibility in adapting to the operating conditions required, especially as regards the hydraulics, thermionics, and geometry of the experimental section. The loop described is presented in one of its applications, namely, the irradiation of a fissionable needle, which contains a mixture of plutonium and uranium oxides. Preliminary studies and trials indicated the choice of the engineering design; the results obtained thus far indicate that the specifications have been realized. (auth)

21737 ANALYSIS OF NUCLEAR REACTOR NOISE. K. Kurusyna. Genshiryoku Kogyo, 8: No. 11, 49-53(1962). (In Japanese)

Amplitude modulations of a certain irregular shape wave were studied in a JRR-1 reactor and reactor characteristics were determined. The reactor noise (fluctation of neutron density in a reactor) is expressed by Poisson deviation. The Rossi-α method producing a mean square number of neutrons $V^2 = 7.8 \pm 0.6$ was used for measuring neutron lifetime. The neutron lifetime was $L = 36.8 \pm 4.0$ μsec. The neutron lifetime determined by the noise energy spectra was 38.8 ± 1.8 μsec. Band filtration and correlation methods were used for obtaining reactor noise energy spectra. (P.V.J.)

21738 RADIOACTIVITY OF JRR-2 REACTOR. Kato and Fakuda. Genshiryoku Kogyo, 9: No. 2, 55-9(1963). (In Japanese)

Data are given on measurements of radioactivity in the reactor building and surrounding area fater JRR-2 startup. The results showed that radiation leaking from the reactor vessel was taking place mainly through the heavy concrete shielding, through the experimental channels, and channels used for instrumentation. The γ-ray energy was below 0.3 Mev. In the pump room the highest γ activity (15R/w) was found near the heavy water entrance into the active reactor zone, the connecting pipe, and heat exchanger at 2 m height from the bottom. The radiation intensity and ^{41}Ar concentration in the radioactive gas increased in proportion to the reactor power. The emission of ^{41}Ar and concentration at the top of the stack for the reactor was 850 μC/sec and 7×10^{-5} μC/ml, respectively. The concentration of aerosols containing the daughter nucleid Rn and Th was 7×10^{-2} μC/ml in the reactor room and 1×10^{-2} μC/ml in remote points. In the waste water the concentration of ^{24}Na was 1×10^{-3} μC/mn and the solid waste activity was less than 50 mR/hr. (R.V.J.)

21739 SHIELDING WALL FOR NUCLEAR INSTALLATION. T. Nai. Genshiryoku Kogyo, 9: No. 4, 55-60(1963). (In Japanese)

Economic aspects, construction problems, and various materials for shielding nuclear installations are discussed. The relation between the specific densities of the filler and concrete and the ratio between a heavy filler and a heavy specific density concrete were studied. Tables are given of various types of concretes, and practical suggestions are made for handling and mixing the material. Calculations are also given for shielding designed for 100 kw swimming pool reactor. (R.V.J.)

21740 IRRADIATIONS IN THE RESEARCH REACTOR. Janos Toerko. Magy. Kem. Lapja, 19: 409-12(Aug. 1964). (In Hungarian)

Experience obtained in connection with irradiations performed in a research reactor are summarized. The mathematical relations regarding the expectable activity of isotopes produced by nuclear reactions and the principal standpoints of the selection and preparation of targets for irradiation are discussed. (auth)

21741 DESIGN OF EQUIPMENT FOR RAPID HANDLING OF IRRADIATED SOLUTIONS. C. E. Bemis, Jr. and J. W. Irvine, Jr. (Massachusetts Inst. of Tech., Cambridge). Nucl. Instr. Methods, 34: 57-60(Apr. 1965). (MIT-905-21)

Details and operating experience are presented for a rapid handling system designed to transfer irradiated solutions and liquids from irradiation containers to apparatus for subsequent chemical processing. The system described is the receiver station for a pneumatic tube which runs between the M.I.T. Reactor and adjoining Nuclear Chemistry Laboratories. Handling times as short as 2 sec are achieved with minimal manipulation and with safety to operating personnel. The transfer is accomplished by piercing the irradiation container with a needle assembly and drawing the liquid into an evacuated system. (auth)

21742 A FLUX CONVERTER FOR IRRADIATION WITH FAST NEUTRONS AT FRF. E. Boehm and E. Roessle (Johann-Wolfgang-Goethe-Universitat, Frankfurt am Main). Nukleonik, 7: 14-18(Jan. 1965). (In German)

For irradiation and activation with fast neutrons at the FRF, a flux converter was built that makes possible irradiation with fast neutrons without perturbation of the reactor, while simultaneously carrying out experiments. Its principal component is a beaker of 10% enriched metallic uranium in a vertical radiation channel in the reactor reflector, which converts the thermal neutrons by fission in ^{235}U into fast fission neutrons. By conversion of the thermal flux of 2×10^{11} n/cm^2 sec, a fast flux (E > 0.1 Mev) at the interior of the uranium cylinder of 8×10^{10} n/cm^2 sec was obtained. This corresponds to an increase of the fast flux by a factor of 40. (tr-auth)

21743 FUEL ELEMENT TYPE KD FOR THE HFBRR (Engineering Materials). (Brookhaven National Lab., Upton, N. Y.). 2 drawings, 1 spec. (CAPE-1179)

Fuel elements used in the High Flux Beam Research Reactor (HFBRR) at the Brookhaven National Laboratory are described. The reactor is used to provide intense beams of neutrons for research purposes, such as resonance measurement with neutron choppers, diffraction studies on complicated structures, low-temperature neutron alignment measurements using polarization neutrons, and a series of solid-state problems involving low-lying excitation states in solids. Each fuel element consists of 19 curved, Al-U alloy fuel plates attached to grooved side-plates by roll swaging, an inlet shroud assembly above the fuel plates, and a supporting structure below the fuel plate section. The two outside fuel plates are thicker than the inner plates and each outside plate contains half the U loading of an inner plate. (For details, see TID-4100) (M.C.G.)

21744 SWIMMING POOL REACTOR. Arno Mueller (to Deutsche Babcock and Wilcox-Dampfkesselwerke). German Patent 1,182,361. Nov. 26, 1964. Filed Aug. 28, 1961.

The swimming pool reactor described is provided with a forced-convection primary cooling circuit. The water is circulated downward through the core and from there via a heat exchanger through a cooler and back to the core region of the tank. The heat absorbed in operation in the reactor core is partially transferred in the heat exchanger to a stream of water circulated from the tank through the exchanger and back to the upper portion of the tank. By this arrangement of the cooling circuits a breakthrough of contaminated water from the vicinity of the core to the surface of the tank is avoided. (Gmelin Inst.)

21745 PULSED NEUTRON SOURCE PRODUCED FROM A FAST REACTOR. Gustav Kistner, Rolf Misenta, and Victor Raievski (to Europaische Atomgemeinschaft (EURA-

TOM)). German Patent 1,184,872. Jan. 7, 1965. Filed Aug. 15, 1963.

The pulsed neutron source consists of a fast nuclear reactor with two exit windows for the neutrons located in the reflector, and with separate shields of a material with reactivity-raising properties, e.g., a fissionable material, which are moved past the windows. The reactivity is pulsed in two steps, in which the reactivity is raised at one window up to criticality (preliminary pulse) and at the other window above prompt criticality (excess pulse). The window at which the excess pulse is generated has the form of at least one slit which is narrow compared with the window for generating the preliminary pulse. (Gmelin Inst.)

21746 PULSED NEUTRON SOURCE PRODUCED FROM A FAST REACTOR. Gustav Kistner, Herbert Meister, and Victor Raievski (to Europaische Atomgemeinschaft (EURATOM)). German Patent 1,185,307. Jan. 14, 1965. Filed Aug. 15, 1963.

The pulsed neutron source consists of a fast nuclear reactor with one exit window for the neutrons located in the reflector, and two adjacent, synchronized shields of a material with reactivity-raising properties, e.g., a fissionable material, which are moved in front of and past the window. The reactivity is pulsed in two steps, in which the reactivity is raised by one of the shields up to criticality (preliminary pulse), and by the other shield above prompt criticality (excess pulse). The shield generating the preliminary pulse is provided with at least one opening which is small compared with the width of the window. The area on the shield generating the excess pulse, which is covered by fissionable material, is equal to the area of the opening in the other shield. (Gmelin Inst.)

WASTE DISPOSAL AND PROCESSING

See also BIOLOGY AND MEDICINE — Ecology.
CHEMISTRY — Radiochemistry.
CHEMISTRY — Separation Processes and Procedures.
HEALTH AND SAFETY.

Refer also to abstracts 20042, 20196, 20220, 20234, 20431, and 20653.

21747 (DP-942) BURNING OF RADIOACTIVE PROCESS SOLVENT. D. Whitney Tharin, Jr. (Du Pont de Nemours (E. I.) & Co., Aiken, S. C. Savannah River Lab.). Feb. 1965. Contract AT(07-2)-1. 16p. Dep.; $1.00(cy), 1(mn) CFSTI.

Spent solvent from radiochemical separations processes is accumulated and burned in burial ground facilities. Between mid-1955 and February 1964, 290,000 gallons were stored or burned with negligible release of radionuclides. (auth)

21748 (DPSPU-64-30-8B) A METHOD FOR DISPOSAL OF LARGE QUANTITIES OF DEGRADED AND LOW-LEVEL CONTAMINATED SOLVENT. J. A. Harper and L. Jolly, Jr. (Du Pont de Nemours (E.I.) Co., Aiken, S. C. Savannah River Plant). May 1964. Contract AT-(07-2)-1. 12p. (CONF-642-31). Dep.(mn); $1.00(cy), 1(mn) CFSTI.

From Health Physics Society, Cincinnati, June 1964.

Solvent used in radiochemical separations processes is degraded during exposure to radiation, and retains certain fission products. Disposal of large quantities of degraded solvent is a waste disposal problem of considerable magnitude. Of several disposal methods considered, controlled open pan burning was selected as the safest and most economical. An extensive air sampling program showed that more than 99% of all the solvent radioactivity, primarily fission products and plutonium, remained in a gummy residue. Over a period of two years, 80,000 gallons of solvent was burned which contained about 8 curies of gamma emitting isotopes and about 60 millicuries of alpha emitting isotopes. No adverse effect on the environment adjacent to the burning operations was detected. (auth)

21749 (HW-84549) CHEMICAL EFFLUENTS TECHNOLOGY WASTE DISPOSAL INVESTIGATIONS, JANUARY–DECEMBER 1964. D. J. Brown (General Electric Co., Richland, Wash. Hanford Atomic Products Operation). 1964. Contract AT(45-1)-1350. 23p. Dep.(mn); $1.00(cy), 1(mn) CFSTI.

Results of radioactive nuclide surveillance in the ground at Hanford are reported. Sections are included on analysis of ground water monitoring data from 200-east, 200-west, and 600 areas. Information is also included on fission-product tritium in ground water and proposed well drilling. Data are included on the average concentration of radioisotopes in various wells, and on concentration of radioisotopes found in ground water that exceed the routine detection limit of 0.08 pCβ cc. (J.R.D.)

21750 (LA-3150) DISPOSAL OF Am^{241}–Pu^{239} RAFFINATE SOLUTIONS BY FIXATION WITH CEMENT. L. A. Emelity, C. W. Christenson, and E. B. Fowler (Los Alamos Scientific Lab., Univ. of California, N. Mex.). Aug. 1964. Contract W-7405-eng-36. 20p. Dep.; $1.00(cy), 1(mn) CFSTI.

In 1959 it became necessary to develop a means of disposal of a raffinate solution containing ^{241}Am and ^{239}Pu with some parent materials and daughter products. Research led to a decision to neutralize the waste and fix it in cement-vermiculite for land burial. Development of the physical plant to treat the wastes on a continuing basis is described in detail. Data on the first 4½ years operation are presented. For control of the operation, systems for sampling the fresh mortar mixes and for conducting a study of the rate of radioactivity leach from the cured sample blocks were established. The problem of activity plating on the interior surface of the glass leach-test container is discussed and a decision to conduct leach water counting in the acid phase is explained. Leach water activity data are presented which demonstrate the excellent retention of activity by the mortar over periods extending to 2 years. The data verify that leach rate during the first few weeks immersion exceeds that of following periods due to the accessibility of block surface activity. The per gallon cost of material for disposal of the raffinate waste solution is $0.984 (prices as of August 21, 1964). (auth)

21751 (ORNL-P-1064) DISPOSAL OF HIGH-LEVEL POWER REACTOR WASTES IN A SALT MINE. W. J. Boegly, Jr., R. L. Bradshaw, F. M. Empson, W. C. McClain, F. L. Parker, and W. F. Schaffer, Jr. (Oak Ridge National Lab., Tenn.). [1964]. Contract [W-7405-eng-26]. (CONF-650203-3). Dep.(mn); $2.00(cy), 1(mn) CFSTI.

From National AIME Meeting, Chicago.

The major conclusions of previous studies on the disposal of high-level liquid and solid wastes in salt mines are outlined. A field experiment called Project Salt Vault is being planned to demonstrate the feasibility of such disposal. The experiment, using irradiated fuel assemblies in lieu of actual wastes, will be conducted in the Carey salt mine at Lyons, Kansas. The objectives, design, instrumentation, etc., of the experiment are described. (D.L.C.)

21752 DETERMINATION OF CONCENTRATION OF WASTE WATER FROM LOW-ACTIVITY INSTALLATIONS AND LIQUID WASTE STORAGE TANK. T. Sekiny. Genshiryoku Kogyo, 10: No. 1, 54-7(1964). (In Japanese)

Experiments were carried out to demonstrate that process water may be safely stored in tanks. Becasue of the relatively high permissible concentrations of ^{35}S, ^{131}I, and ^{32}P, process water from equipment where these isotopes are present need not be treated prior to storage. Water from equipment used with long-lived isotopes may be higher than permissible. The possibility of leakage into the ground through the walls of concrete tanks, both unlined and lined with epoxy resin, was studied. The first tank contained ^{32}P in a concentration 200 times the MPC in water, and although water seeped through, no activity appeared outside. No leakage occurred with the second type, and, because ^{32}P would precipitate along with impurities, the ^{32}P concentration would be greater near the bottom. (IIC-M.G.)

21753 PIPE RADIOACTIVE WASTES TO SHALE BEDS. H. O. Weeren (Oak Ridge National Lab., Tenn.). Heating, Piping, Air Conditioning, 36: 122-3(Nov. 1964).

Piping employed in a radioactive waste disposal method, in which waste liquids are piped and injected into shale beds, is described. The experiment consists of injecting several 40,000 gal batches of intermediate level waste solution, mixed with cement and other additives, into a shale formation at a depth of approximately 900 ft. The mixer, surge tank, injection pump, and wallhead valving are installed in cells to reduce radiation exposure to operators. The process requires handling of radioactive and nonradioactive solutions at low pressure (up to 300 psi), slurries of sand or cement at high pressure (up to 7500 psi), and bulk cement. The greater part of the waste transfer

line is cast iron pipe with mechanical joints. Some of it is welded carbon steel. (M.C.G.)

21754 METHOD FOR THE PRODUCTION OF GLASS. Bo Kurt Wilhelm Simmingskold (to Aktiebolaget Atomenergi). British Patent 975,718. Nov. 18, 1964. Priority date Mar. 17, 1962, Sweden.

By the process described, radioactive waste solutions such as those resulting from processing of used reactor fuel elements may be converted into a form of glass suitable for storing for an unlimited time. Diatomaceous earth or other solid silica material of equivalent porosity is stirred into the solution and elements from the solution are absorbed on it. The silica material is then separated, dried, and melted. The silica material may be used in powdered form or in the form of stones produced by use of a binder material such as clay, and insoluble ingredients may be mixed with the silica material before the absorption step. (A.G.W.)

21755 DEACTIVATION OF RADIOACTIVE WASTE LIQUIDS. Vladmir Vesely, Jiri Napravnik, and Jindrich Jansa. Czech Patent 109,734. Jan. 15, 1964.

The radioactive waste liquid is extracted by means of colloidal sorbent (bentonite clay 2 g/l) operating in an inactivation system of 2 to 10 stages. The waste is fed into the system from one side, while the colloidal sorbent suspension is introduced periodically, alternating from the opposite side. In each deactivation stage the radioactive waste is stirred with the sorbent coming from the next higher deactivation stage and the suspension is subjected to coagulation in an electric field. After separation of the solid and liquid phases the liquid is conducted to the higher stage, while the mud of coagulated sorbent, meanwhile thickened by sedimentation, is led into the lower deactivation stage; the process is repeated in each stage of the system. After a 6-stage treatment, approximately 99% of ^{90}Sr, ^{90}Y, ^{137}Cs, ^{137}Ba, ^{106}Ru, and ^{106}Rh is removed.
Public Health Eng. Abstr., 45: (Feb.-Mar. 1965).

GENERAL AND MISCELLANEOUS

21756 (BNL-8934) GENE DIFFERENTIATION. M. Demerec (Brookhaven National Lab., Upton, N. Y.). [1964]. Contract AT-30-2-GEN-16. 8p. (CONF-734-5). Dep.(mn); $1.00(cy), 1(mn) CFSTI.

From Symposium on Genes and Chromosomes Structure and Function, Buenos Aires, Nov.-Dec. 1964.

Data are reviewed on the evolutionary events responsible for observed similarities and divergencies between the genetic material of Salmonella typhimurium, and that of Escherichia coli, S. montevideo, and S. abony. Emphasis is placed on genetic divergence between S. typhimurium and S. montevideo or S. abony. (C.H.)

21757 (BNL-7918) EXCITATION OF A PARALLEL RESONANT LRC CIRCUIT FROM A FAST-SWEEPING SIGNAL SOURCE. J. G. Cottingham (Brookhaven National Lab., Upton, N. Y.). [nd]. Contract AT(30-2)-Gen-16. 8p. Dep.(mn); $1.00(cy), 1(mn) CFSTI.

When a sweep frequency current source is used to excite a parallel resonant LRC circuit, the maximum response occurs late. This apparent frequency shift is numerically analyzed and the relation to frequency sweep rate determined. (auth)

21758 (BNL-8864) TRANSFERS OF ^{14}C AND TRITIUM FROM SUBSTRATES TO CO_2, WATER, AND LIPIDS IN OBESE AND DIABETIC SUBJECTS IN VIVO. Walton W. Shreeve (Brookhaven National Lab., Upton, N. Y.). [1964]. Contract AT-30-2-GEN-16. 24p. (CONF-641213-1). Dep.(mn); $1.00(cy), 1(mn) CFSTI.

From New York Academy of Sciences, New York City.

A discussion is presented of radioisotopic studies of lipogenesis in natural diabetes and sources of metabolic hydrogen for reduction of fatty acid intermediates. The studies include conversion of ^{14}C-labeled acetate and ^{3}H-labeled carbohydrates to fatty acids in diabetic patients, formation of $^{14}CO_2$ and ^{3}HOH from glucose-1-^{14}C, -1-^{3}H in obese patients, and conversion of ^{3}H- and ^{14}C-labeled carbohydrates to fatty acids in obese-hyperglycemic mice. (D.L.C.)

21759 (NYO-3402-1) MAGNETO-THERMODYNAMICS OF PARA- AND ANTIFERRO-MAGNETS. Annual Report, June 1, 1964–March 1, 1965. R. A. Butera (Pittsburgh Univ., Pa. Dept. of Chemistry). Mar. 1, 1965. Contract AT(30-1)-3402. 25p. Dep.(mn); $1.00(cy), 1(mn) CFSTI.

Activities in a program to determine the exchange interaction strength in magnetic systems in which ordering occurs below 4°K are reported. Studies of magnetothermodynamic properties of salts containing transition metal ions and intermetallics which exhibit appropriate cooperative magnetic effects at low temperatures in high magnetic fields are in progress. Progress is reported on assembly of the magnetothermodynamic apparatus, preparation of high-purity $MnBr_2 \cdot 4H_2O$ single crystals, studies of $MnBr_2 \cdot 4H_2O$ single crystal magnetic properties, and measurement of $MnBr_2 \cdot 4H_2O$ thermal conductivity at cryogenic temperatures. (J.R.D.)

21760 (NYO-2728-4) RATES OF HYDROGEN ABSTRACTION FROM VARIOUS SUBSTRATES BY FREE RADICALS. FINAL REPORT. PART I. A STUDY OF RELATIVE RATES OF HYDROGEN ATOM ABSTRACTION FROM AROMATIC MOLECULES BY METHYL RADICALS (thesis). Alan Campbell Eachus. PART II. ADDITIONAL DATA FOR TRIPHENYLMETHANE, 1,2-DIPHENYLETHANE AND PARA-T-BUTYLCUMENE. (State Univ. of New York, Syracuse. Coll. of Forestry). Mar. 1, 1965. Contract AT(30-1)-2728. 106p. Dep.(mn); $4.00(cy), 2(mn) CFSTI.

The method of measuring rates of hydrogen abstraction from aromatic compounds is based on competitive abstraction by methyl radicals of tritium atoms from a reference compound (toluene) and of hydrogen atoms from aromatic substrates. The method was used to study the reactivity of the following aromatic compounds at 0 to 95°C: o-xylene, m-xylene, p-xylene, ethylbenzene, cumene, mesitylene, tetralin, cyclohexylbenzene, indan, diphenylmethane, triphenylmethane, 1,2-diphenylethane, and para-t-butylcumene. Conclusions on the variables affecting the reactivity of carbon-hydrogen bonds are given. (D.L.C.)

21761 (P-1134(RAND)) INTERNATIONAL REGISTRATION OF THE ATOM. Arnold Kramish (RAND Corp., Santa Monica, Calif.). July 26, 1957. 10p. (AD-606453). $1.00(CFSTI).

In view of the Universal Declaration of Human Rights which proclaims the individual's right to life, liberty, and security of person, it is not within the province of the United Nations to enunciate the principle that nations and individuals engaged in nuclear research and development operations of any sort have an obligation to do so at minimum risk to other nations and to the individuals of all nations. It is the common right to know of any such operations which possess a potential of harm or could conceivably magnify themselves to a stage dangerous to individual life and security. The last decade has shown a discouraging lack of progress in disarmament negotiations. This is due, in large measure, to the comprehensive, sweeping nature of the plans submitted. And if we are now beginning to make any progress in this field, it is because emphasis has been changed to the achievement of step-by-step goals. But the final goal, disarmament in its absolute sense, may never be achieved. The common goal must be the disciplined manufacture and use of armaments. (auth)

21762 (RM-2163(RAND)) THE SOVIET UNION AND THE ATOM: TOWARD NUCLEAR MATURITY. Arnold Kramish (RAND Corp., Santa Monica, Calif.). Apr. 25, 1958. Project RAND. 116p. (AD-606766). $4.00(CFSTI).

The Soviet Union has never issued formal periodic reports on the organization and progress of the atomic energy program. It is consequently with the greatest of difficulty that information on the Soviet program can be obtained. General descriptive information from publicly available materials on the USSR atomic energy program is summarized. (242 references) (C.H.)

21763 (SC-DR-64-1741) ENVIRONMENTAL TESTING OF THE RFD-2 RE-ENTRY VEHICLE. D. L. Krenz (Sandia Corp., Albuquerque, N. Mex.). Feb. 1965. Contract AT(29-1)-789. 35p. Dep.; $2.00(cy), 1(mn) CFSTI.

The environmental testing of Re-entry Flight Demonstration Number Two (RFD-2) re-entry vehicle–the environments, the test parameters, the testing techniques and the results–are discussed. (auth)

21764 (SC-DR-64-2135) DESIGN PRINCIPLES FOR MOLDED PLASTIC POTTING SHELLS. Edward A. Salazar (Sandia Corp., Albuquerque, N. Mex.). Feb. 1965. Contract AT(29-1)-789. 9p. Dep.(mn); $1.00(cy), 1(mn) CFSTI.

Information is given on the good design in molded plastic potting shells. Some common pitfalls are discussed, and fundamental principles that should be followed for economy and maximum serviceability are described. (auth)

21765 (SC-DR-65-74) AUTOMATIC INDUCTION SOLDERING. M. J. Davis (Sandia Corp., Albuquerque, N. Mex.). Mar. 1965. Contract AT(29-1)-789. 12p. Dep.; $1.00(cy), 1(mn) CFSTI.

A description is given of the development of an induction soldering process which is controlled by an infrared radiometer. A method of measuring and controlling the power level of the induction unit is described. The effects of part rotation, joint design, and joint location with respect to the induction coil are discussed with respect to maintaining a low part temperature during soldering. (auth)

21766 (SC-TM-64-921) A SWEEP-FREQUENCY MULTIPOINT CALIBRATOR FOR FREQUENCY-MEASUR-

ING DEVICES. R. G. Bemis (Sandia Corp., Albuquerque, N. Mex.). Mar. 1965. Contract AT(29-1)-789. 19p. Dep.(mn); $1.00(cy), 1(mn) CFSTI.

A system is described for rapid and accurate calibration of frequency measuring devices over the frequency range of 1000 to 12,000 megacycles. This system is composed of a sweep-frequency oscillator, a harmonic transfer oscillator, a standard-frequency source, an r-f detector, and a readout oscilloscope. This system can increase the efficiency of calibrating frequency-measuring devices. (auth)

21767 (SC-TM-65-44) CLOSE-IN TRACKING ERROR IN INTERFEROMETER TRACKING SYSTEMS. W. D. Gutscher (Sandia Corp., Albuquerque, N. Mex.). Feb. 1965. Contract AT(29-1)-789. 12p. Dep.(mn); $1.00(cy), 1(mn) CFSTI.

It is frequently necessary to track objects with an electronic trajectory-measuring system when the object being tracked passes close by the tracking station. In systems that obtain angular information in the same manner as the Stare and Midot systems, an error is introduced into the data because of the proximity of the tracked object. An analysis is presented of the magnitude and characteristics of this error as a function of both range and direction of the tracked object. (auth)

21768 (SC-TM-65-48) AN ADJUSTABLE POSITIVE-LIMIT MAGNETIC TORQUE WRENCH. J. H. Walker (Sandia Corp., Albuquerque, N. Mex.). Mar. 1965. Contract AT(29-1)-789. 15p. Dep.; $1.00(cy), 1(mn) CFSTI.

Design and test results are described for prototype torque wrenches which incorporate electromagnets and permanent magnets to provide positive-limit torque output with no possibility of exceeding a preset torque value. (auth)

21769 (TID-21661) LONG RANGE BALLOON TRACKING. Final Report. John Chisholm (Sierra Nevada Corp., Reno) and Norman Kennedy (Weather Bureau Research Station, Las Vegas, Nev.). Sept. 1964. Contract AT(26-1)-114. 115p. Dep.(mn); $4.00(cy), 3(mn) CFSTI.

A radar system is outlined for extended tracking of constant-altitude balloons (tetroons) in the vicinity of Nevada Test Site. The radar networks around the site and their difficulties in skin tracking tetroons are discussed. The possible use of a beacon system to improve the tracking capability is considered. Typical track data and recommendations for future development are given. (D.L.C.)

21770 (TID-21677) RELAXATION BEHAVIOR, MOLECULAR MOTION, AND STRUCTURE IN POLYMERS AND RELATED MATERIALS. Progress Report, June 1964–February 1965. J. A. Sauer (Rutgers–The State Univ. of New Jersey, New Brunswick. Bureau of Engineering Research). Contract AT(30-1)-3384. 15p. Dep.(mn); $1.00(cy), 1(mn) CFSTI.

Nuclear magnetic resonance T_1 measurements are being used to study motion at the resonant frequency in polymer chains. Equipment for measuring the complex elastic and shear moduli over a wide temperature range are briefly described. The structure of individual polyethylene crystals is discussed, and the successful preparation of single lamellar crystals of polypropylene is reported. The formation of bands and striations in the fracture studies of polypropylene is noted. Relaxation studies on polyvinyl stearate and its monomer are underway. (D.L.C.)

21771 (TID-21684) STUDIES OF THE LUMINESCENCE OF SOLUTIONS OF BENZENE AND SOME SIMPLE BENZENE DERIVATIVES (thesis). William Phillip Helman (Minnesota Univ., Minneapolis). Dec. 1964. Contract AT(11-1)-913. 135p. Dep.(mn); $4.00(cy); 3(mn) CFSTI.

The emission spectra of benzene in the pure state and in cyclohexane solutions of concentration ranging from 0.1 to 11 M, were measured at temperatures from 10 to 50°C. Similar measurements were made for toluene, p-xylene, and mesitylene. The long-wavelength emission band (LWE) in benzene was identified with a state of several interacting benzene molecules (excimer), while the short-wavelength emission band (SWE) is fluorescence from "monomer" states in dilute solution. Absolute quantum yields were computed for LWE and SWE, and models relating LWE and SWE are discussed. (D.L.C.)

21772 (TID-21709) THE MOLECULAR BASE OF MUTATION AND RELATED GENETIC PHENOMENA. Final Report. A. Gib DeBusk (Florida State Univ., Tallahassee. Dept. of Biological Science). [1964]. Contract AT(40-1)-2788. 20p. Dep.(mn); $1.00(cy), 1(mn) CFSTI.

Desoxyribonucleic acid isolated from Neurospora crassa was used in studies of genetic transformation and characterization of messenger DNA. Pulse labeling-centrifugation studies revealed what is probably messenger RNA associated in aggregates of up to 50 single 805 ribosome units. These polysome structures were verified by electron microscopy and it is suggested that they represent polycistromic messengers. Various crude and purified RNA fractions were employed without success in attempts to demonstrate phenotypic transformations in Neurospora. Data are included from studies of an inducible extracellular α-amylose from Neurospora, and application of a forward mutation technique for mosaic analysis of Neurospora. (C.H.)

21773 (UCRL-11308) MOLECULAR ORIENTATION IN QUANTASOMES. III. A FLOW DICHROISM APPARATUS AND ITS APPLICATION TO THE STUDY OF THE STRUCTURE OF SPINACH QUANTASOMES. Kenneth Sauer (Lawrence Radiation Lab., Univ. of California, Berkeley). Feb. 10, 1964. Contract W-7405-eng-48. 27p. Dep.(mn); $2.00(cy), 1(mn) CFSTI.

A new apparatus is described for measuring dichroism spectra with very high sensitivity for macromolecular structures oriented in a hydrodynamic gradient. The method has been used to explore the dichroism spectrum of quantasome aggregates isolated from spinach chloroplasts. The quantasome flow dichroism resembles qualitatively that observed previously using electric field orientation, in that a pigment absorbing at wavelengths longer than 680 mμ exhibits appreciably greater dichroism than those absorbing at shorter wavelengths. It is shown that the absorption oscillator for this long wavelength absorption lies parallel to the streamlines of the sheer gradient, which is assumed to be the direction in which the planes of the chloroplast lamellae are oriented. (auth)

21774 (UCRL-11858) DISLOCATION ARRANGEMENTS IN DEFORMED COPPER POLYCRYSTALS (thesis). Gopinathan Vellaikal (Lawrence Radiation Lab., Univ. of California, Berkeley). Jan. 1965. Contract W-7405-eng-48. 25p. Dep.(mn); $1.00(cy), 1(mn) CFSTI.

The very early stages of plastic deformation were studied by means of etch pit techniques in large grained copper polycrystals deformed in compression. Special attention was given to regions near grain boundaries in an attempt to clarify the role of grain boundaries in plastic deformation. Their role as barriers to slip during the early stages of plastic deformation was clearly demonstrated. One of the first indications that plastic deformation had taken place was the operation of Frank Read sources. The resulting dislocation loops frequently traversed the entire cross section of the grain and piled up against the grain boundary. (auth)

21775 (UCRL-12307) PREPARATION AND PROPERTIES OF FLUOROCARBON ALCOHOL 3,5-DINITROBENZOATES FOR STUDY AS SURFACE-ACTIVE AGENTS. Eugene R. Bissell (Lawrence Radiation Lab., Univ. of California, Livermore). Dec. 21, 1964. Contract W-7405-eng-48. 10p. Dep.; $1.00(cy), 1(mn) CFSTI.

The use of esters of 3,5-dinitrobenzoic acid with various monohydric fluorocarbon alcohols, as surfactants in HMX-fluoropolymer PBX explosives is suggested. Seven esters of this type were prepared from the C_3 to C_{11} fluorocarbon alcohols by pyridine-catalyzed esterification with 3,5-dinitrobenzoyl chloride. Their yields, melting points, densities, and analyses are tabulated. The purity was studied using chromatography and calorimetry. Solubility and infrared spectra were also determined. (D.L.C.)

21776 (UCRL-12389) MAGNETIC FIELDS, VAGAL INHIBITION, AND ACETYLCHOLINESTERASE ACTIVITY. Wei Young and John W. Gofman (Lawrence Radiation Lab., Univ. of California, Livermore). Feb. 1965. Contract W-7405-eng-48. 18p. Dep.; $1.00(cy), 1(mn) CFSTI.

The application of a nonuniform magnetic field (4000 to 15,000 oersteds) produces several effects upon the isolated frog vagal heart preparation, including a consistent decrease in the duration of vagal inhibition, a decrease in cardiac contractility and cardiac work per cycle, and a high frequency of cardiac irregularity arising after cessation of the field. The decreased duration of vagal inhibition is interpreted as an increased rate of acetylcholine hydrolysis. Whatever the mechanism(s) involved, the magnetic field further decreases the vagal inhibition period even after a marked decrease has already been produced by partial replacement of potassium ions by cesium ions in the bathing fluid medium. The data are consistent with, but do not prove, the concept that the magnetic field provokes a major increase in catalytic activity of the enzyme, acetylcholinesterase, at the myoneural junction. (auth)

21777 (UR-662) CHANGES IN KINETICS OF ERYTHROPOIESIS AS REFLECTED IN FREQUENCY DISTRIBUTION OF ERYTHROCYTE VOLUMES OF ACUTELY BLED DOGS. G. F. Orthey and M. Ingram (Rochester Univ., N. Y. Atomic Energy Project). Dec. 4, 1964. Contract W-7401-eng-49. 35p. Dep.; $2.00(cy), 1(mn) CFSTI.

A study was made of the frequency distribution of erythrocyte volumes in normal and acutely bled dogs. Cell volumes were measured and graphed with a model B Coulter Counter with size distribution plotter. Size distribution of erythrocytes of different ages were evaluated by obtaining frequency distribution graphs (histograms) for various fractions of a centrifuged column of red cells. The normal dog is shown to have a bimodal distribution of erythrocyte volumes and the cell volume distribution curves of both newly formed and old erythrocytes are virtually identical. The dogs that were studied responded to acute blood loss by producing abnormally sized erythrocytes as well as by marked acceleration of erythrocyte production. Data are presented to show that the two populations of erythrocytes normally present may vary independently in response to erythropoietic stress. The observations reported are interpreted in the light of Lajtha's model for erythropoiesis. (auth)

21778 (JPRS-28835 JAPANESE EVALUATION OF COMMUNIST CHINA'S NUCLEAR EXPLOSION. Junnosuke Kishida. Translated from p.23-8 of "Asahi Kagaku," Dec. 1964. 15p. (TT-65-30364). $1.00(CFSTI).

An account is given of several predictions of the Chinese nuclear explosion. The use of reconnaissance aircraft and satellites is discussed. Fragmentary information is pieced together to determine the steps leading to the production of the bomb, and preparations for a second test are discussed. (C.E.S.)

21779 (JPRS-29037) TRANSLATIONS ON COMMUNIST CHINA'S SCIENCE AND TECHNOLOGY NO. 156. Mar. 9, 1965. 107p. (TT-65-30464). $4.00(CFSTI).

For an abstract of the individual paper see: 19778.

21780 (JPRS-29200) TRANSLATIONS ON COMMUNIST CHINA'S SCIENCE AND TECHNOLOGY NO. 161. [1964]. 143p. (TT-65-30547). $4.00(CFSTI).

A separate abstract was prepared for one paper. Other papers review China's achievements in internal medicine during the past 5 yr, medical service in rural China, the combined use of traditional Chinese medicine and modern Western medicine for the treatment of various pathological conditions, the development of an antidote for poisoning by organophosphate insecticides, and the development of lasers, analog computers, and transistorized circuits. (C.H.)

For an abstract of the individual paper see: 19620.

21781 NUCLEAR ENERGY IN CANADA. Comit. Nazl. Energia Nucl., Notiziario, 10: No. 12, 69-85(Dec. 1964). (In Italian)

The nuclear energy program in Canada (nuclear power plants, mining development, and the development of nuclear fuels) is briefly reviewed, with emphasis on the current trends. (J.S.R.)

21782 DRAWING APPARATUS. C. H. Bean (to U. S. Atomic Energy Commission). U. S. Patent 3,173,284. Mar. 16, 1965.

A drawing apparatus only about twice as long as the tube being drawn is described. This is made possible by using a stationary piston and a movable hydraulic cylinder to pull the tube through the drawing apparatus. Because the cylinder rather than the piston is movable, the tube being drawn may extend along side of the cylinder. This side-by-side arrangement of tube and cylinder keeps the over-all length of the drawing apparatus to about twice the length of the tube. (AEC)

21783 MOISTURE INDICATOR AND METHOD OF MAKING THE SAME. W. S. Pappas and C. W. Weber (to U. S. Atomic Energy Commission). U. S. Patent 3,173,880. Mar. 16, 1965.

A moisture indicator for liquids of low water solubility, such as halogenated hydrocarbon coolants, was prepared. Activated silica gel was impregnated with 2 to 3 wt % cobaltous bromide and at least 0.5 wt % hydrobromic acid. The impregnated silica gel exhibited a pink color when exposed to dichlorotetrafluoroethane containing more than approximately 15 ppm of moisture at a temperature of 90 to 120°F and a green color when exposed to the same liquid containing less than 15 ppm of moisture. (AEC)

21784 SWEEPING IMAGE MIRROR CAMERA. Thure Anderson (to U. S. Atomic Energy Commission). U. S. Patent 3,174,153. Mar. 16, 1965.

A sweeping-image camera employing a reflecting mirror optical system for photographing rapidly varying events is described. The optical system of the camera includes a concave spherical objective mirror positioned with its principle axis at an angle to the path of the incident light and a convex cylindrical mirror disposed outside the margin of the path of the incident light to receive the reflected image from the objective mirror and direct it on a rotating mirror, which in turn sweeps the image onto a film. To correct for the astigmatism introduced into the reflected image by the tilting of the objective mirror, the curvature of the cylindrical mirror is adjusted to cause the tangential and sagittal components of the astigmatic image to coincide and thereby provide a faithful image. (AEC)

21785 THREE STATE MEMORY DEVICE. Forrest O. Salter (to U. S. Atomic Energy Commission). U. S. Patent 3,176,154. Mar. 30, 1965.

A three-state memory device was designed, which consisted of a tunnel diode with an inductance connected to it in series. The input and output of the device are taken across the series-connected diode and inductance. The inductance has a value to permit the diode to oscillate in the negative resistance portion of its characteristic curve, so that the output of the device is caused to have a characteristic curve with three positive slopes. Means are provided for operating the device on each of the positive slopes of the characteristic curve of the device responsive to predetermined input voltages. (AEC)

CORPORATE AUTHOR INDEX

This index contains entries for this period for all report literature and, in addition, for certain published literature items for which it is felt that a corporate approach is especially desirable, e.g., symposia, conference proceedings, and meetings.

Each entry under a corporate author is a shortened version of the title of the publication, followed by the *NSA* volume and abstract number. Report numbers are given in parentheses.

The phrase "Progress report" is abbreviated as "Prog. rpt.," permitting a more rapid and complete alphabetical arrangement of the titles without changing the location of the progress report titles in relation to the other titles.

A

AEROJET-GENERAL CORP., AZUSA, CALIF.

Solar-heated H propulsion system. I., 19: 20137 (NASA-CR-59332)

AEROJET-GENERAL NUCLEONICS, SAN RAMON, CALIF.

Prog. rpt. on AGCR systems, 7–9/64, 19: 21687 (IDO-28637)

AEROSPACE CORP., EL SEGUNDO, CALIF.

Prog. rpt. on ceramic materials, semiannual, 1–6/62, 19: 20455 (DCAS-TDR-62-192)

AIR FORCE CAMBRIDGE RESEARCH LABS., L. G. HANSCOM FIELD, MASS.

Effects of energetic photon irradiation on Ge, 19: 20612 (AFCRL-64-839)

Hydromagnetic wave tube, 19: 21465 (AFCRL-63-779)

Reflection and transmission of plane wave normally incident upon semi-infinite anisotropic plasma, 19: 21466 (AFCRL-64-550)

AIR FORCE MATERIALS LAB., WRIGHT-PATTERSON AFB, OHIO.

Primary working of refractory metals, 19: 20500 (AFML-TR-64-387)

AKADEMIYA NAUK SSSR.

Mechanisms of proton decays, 19: 21271 (KFK-tr-161)

AKTIEBOLAGET ATOMENERGI, STOCKHOLM (SWEDEN).

Bibliography on radiation-induced graft polymerization on cellulose, 19: 19960 (VDDIT-93)

ALABAMA UNIV., UNIVERSITY. DEPT. OF PHYSICS.

Computer program for nuclear magnetic and quadrupole resonance frequencies and intensities, I = ½ to 9, 19: 21246 (TID-21697)

ALLISON DIV., GENERAL MOTORS CORP., INDIANAPOLIS, IND.

Electrochemical technology, 19: 20484 (TID-19978(Vol.I))

AMES LAB., IOWA STATE UNIV. OF SCIENCE AND TECH.

Application of adiabatic calorimeter to determination of heats of fusion and formation of metallic compounds, 19: 19838 (IS-1070)

Concentration of Cs from pollucite, 19: 20044 (IS-T-1)

Energy levels in hydrated Tm ethylsulfate, 19: 21600 (IS-968)

Environmental radioactivity, 19: 20156 (IS-1098)

Preparation and some analytical applications of tri-n-octylphosphine sulfide, 19: 19753 (IS-T-3)

Reversed-phase chromatographic separation of Zr and Hf, 19: 19752 (IS-T-2)

Writing topological programs for GUTS, 19: 20320 (IS-989)

ARGONNE NATIONAL LAB., IDAHO FALLS, IDAHO.

EBR-II wet critical experiments, 19: 21677 (ANL-6864)

Experiments on boiling core B-2, BORAX-V, 19: 21726 (ANL-6849)

Fission ratios in ZPR-III critical assemblies, 19: 21227 (ANL-6941)

ARGONNE NATIONAL LAB., ILL.

Aberrations of quadrupole magnets, 19: 20252 (CONF-640204 (p.82-92))

Application of high-voltage electron microscopy in metallurgical research, 19: 20548 (CONF-640204(p.35-43))

Biological applications of electron microscopy, 19: 19455 (CONF-640204(p.44-62))

Calcium accretion and bone formation in dogs, 19: 19470 (ANL-6938 (p.141-61))

Conference on high-voltage electron microscopes, ANL, 2/64, 19: 20246 (CONF-640204)

Cosmic-ray fast neutron background, 19: 20872 (ANL-6938(p.71-88))

Determination of Th and P in Th phosphides, 19: 19740 (ANL-7005)

Determination of turbulence dissipation by Eulerian variance analysis, 19: 20654 (ANL-6938(p.242-51))

Diurnal variations in metabolic activity of bone and cartilage, 19: 19472 (ANL-6938(p.179-93))

EBR-II wet critical experiments, 19: 21677 (ANL-6864)

Elastic and inelastic scattering of electrons at high accelerating voltages, 19: 20254 (CONF-640204(p.123-36))

Electron microscopy at MIT, 19: 20249 (CONF-640204(p.20-5))

Electron microscopy at ORNL, 19: 20250 (CONF-640204(p.26-34))

General technical problems in radiological physics, 19: 19657 (ANL-6938(p.97-119))

Generalized Riemann zeta functions and applications in calculations of neutron cross sections, 19: 21228 (ANL-6970)

Heavy-atom cross-section evaluation for Pu recycle calculations, 19: 21678 (ANL-6972)

High-voltage electron microscopy, 19: 20253 (CONF-640204(p.106-22))

High-voltage power supplies and their regulation, 19: 20085 (CONF-640204(p.93-105))

Inelastic collision cross sections of Ne and Ar, 19: 20804 (ANL-6938 (p.36-45))

Instrumentation for atmospheric turbulence studies, 19: 20655 (ANL-6938(p.252-6))

Internal Sr-90 β dosimetry with fluorods, 19: 20314 (ANL-6938(p.62-70))

Intramolecular excimer formation in diphenyl- and triphenyl alkanes, 19: 19956 (ANL-6938(p.27-35))

Iterative unfolding method for response matrices, 19: 20316 (ANL-6984)

Lead-210 in inhabitants of Caribbean island, 19: 20193 (ANL-6938 (p.120-4))

Low-level γ counting room, 19: 20092 (ANL-6938(p.91-6))

Measuring photoionization efficiencies as function of energy, 19: 19955 (ANL-6938(p.21-2))

Multichannel analyzer data processing on CDC 160-A computer, 19: 20315 (ANL-6938(p.206-8))

Osteolathyrism and inhibition of endosteal bone reaction in estrogen-treated mice by AAN, 19: 19471 (ANL-6938(p.162-78))

Plume rise characteristics of scale-model smoke plume, 19: 20656 (ANL-6938(p.257-73))

Prog. rpt. on radiological physics, 7/63–6/64, 19: 20192 (ANL-6938)

Program catalog with permuted description index for CDC CO-OP computers, 19: 20438 (ANL-7016)

Recovery from division delay in irradiated gametes of *Arbacia punctulata*, 19: 19496 (ANL-6938(p.49-56))

Relative activities of Th daughter isotopes in tissues of Thorotrast patients, 19: 19497 (ANL-6938(p.127-39))

Scanning techniques for high-voltage microscopes, 19: 20251 (CONF-640204(p.63-81))

Scintillations in Ar–N mixtures, 19: 20313 (ANL-6938(p.9-20))

Stack plume rise determinations as affected by meteorological and engineering factors, 19: 20653 (ANL-6938(p.209-41))

State of the art of conventional commercial instruments, 19: 20247 (CONF-640204(p.1-16))

Supervoltage electron microscopy outside U. S., 19: 20248 (CONF-640204(p.17-19))

Underground laboratory for high-sensitivity γ counting, 19: 20093

(ANL-6938(p.194-205))

ARIZONA UNIV., TUCSON.
Prog. rpt. on application of automatic control theory to nuclear rocket, 2–9/64, 19: 21723 (NASA-CR-193)

ARMA DIV., AMERICAN BOSCH ARMA CORP., GARDEN CITY, N. Y.
Feasibility of nuclear gyro, 19: 20279 (RTD-TDR-63-4001)

ARMED FORCES INST. OF PATHOLOGY, WASHINGTON, D. C.
High-voltage electron microscopy, 19: 20253 (CONF-640204(p.106-22))

ARMY ENGINEER WATERWAYS EXPERIMENT STATION, VICKSBURG, MISS.
Predicting shape of explosion-produced craters, 19: 20089 (NP-14887)

ATOMIC ENERGY ESTABLISHMENT, TROMBAY (INDIA).
Chain element activity in intermittent irradiation, 19: 21226 (AEET/HP/Th-19)

ATOMIC ENERGY OF CANADA LTD., CHALK RIVER (ONTARIO).
Energy release in low-energy fission, 19: 21224 (AECL-2160)
Fission data and nuclear technology, 19: 21225 (AECL-2168)

ATOMIC ENERGY RESEARCH ESTABLISHMENT, HARWELL (ENGLAND).
Decomposition potential of system K_2ZrF_6–NaCl–KCl, 19: 19850 (NP-tr-1230)
Determination of radiostrontium in biological materials, 19: 19739 (AERE-AM-101)
Effect of H_2 and H_2O on radiation-induced reaction of CO_2, 19: 19954 (AERE-R-4839)
Fast neutron dose-equivalent rate monitor, 19: 20312 (AERE-R-4525)
Inhibitors for CO_2–graphite reaction in reactors, 19: 19953 (AERE-R-4201)
Low-temperature electrical resistivity of U and Be, 19: 20543 (AERE-GR-101)
Resuspension factor of Pu from various surfaces, 19: 20191 (AERE-R-4635)

ATOMIC WEAPONS RESEARCH ESTABLISHMENT, ALDERMASTON (ENGLAND).
Preparation of nuclear data into form suitable for Monte Carlo calculations, 19: 21196 (AWRE-O-81/64)
Pressure rise in biological shield of GCR, 19: 21608 (AWRE-R-2/65)

ATOMICS INTERNATIONAL, CANOGA PARK, CALIF.
Analysis of shield test facility experiments using two-component method, 19: 21614 (NAA-SR-Memo-10559)
Analysis of SNAPTRAN-3 destructive experiment, 19: 21719 (NAA-SR-9780)
Application of SNAP units to Manned Orbiting Research laboratory, 19: 21720 (NAA-SR-10318)
Closure weld development reactor vessel, S8DS-12002, 19: 20509 (NAA-SR-Memo-10633)
Comparative fuel cycle evaluation. II., 19: 20048 (NAA-SR-9335)
Computer calculation of fuel cladding temperatures, 19: 21691 (NAA-SR-Memo-9492)
Evaluation testing of Filtors DPDT relays, 19: 21733 (NAA-SR-Memo-10532)
Gantry and trolley for fuel handling cask, 19: 20099 (TID-21644)
Harmonic analysis Fourier series curve fit, 19: 20442 (NAA-SR-Memo-9729)
Heat transfer systems modification for SRE, 19: 21732 (NAA-SR-10379)
Material buckling for UC-fueled graphite-moderated assemblies, 19: 21692 (NAA-SR-Memo-9976)
Mercury Rankine program thermoelectric pump data analysis, 19: 20096 (NAA-SR-Memo-10729)
Mercury wetting and its effects on heat transfer, 19: 20112 (NAA-SR-Memo-10315)
Monte Carlo evaluation of collimator efficiency, 19: 21612 (NAA-SR-Memo-10557(Pt.I))
Monte Carlo evaluation of collimator efficiency, 19: 21613 (NAA-SR-Memo-10557(Pt.II))
Preparation of ceramographic sections of BeO, 19: 20460 (NAA-SR-Memo-9761)
SNAP systems braze joint experience, 19: 20508 (NAA-SR-Memo-10625)
SNAP-8 DRM1 conversion program, 19: 21721 (NAA-SR-Memo-10160)
SNAP-10A malfunction detection subsystem, 19: 21734 (NAA-SR-Memo-10666)
Sodium-heated, modular, steam generators for SCTI, 19: 21611 (NAA-SR-9826)
Test control devices—SNAP-10A vibration tests, 19: 21722 (NAA-SR-Memo-10767)
Wetting of Mercury-Rankine boiler tube surface, 19: 20111 (NAA-SR-Memo-10224)

AVCO CORP., TULSA, OKLA.
Biological tool for study of cellular radiation damage, 19: 19457 (NP-14886)

AVCO CORP., WILMINGTON, MASS. RESEARCH AND ADVANCED DEVELOPMENT DIV.
Proton-collision mechanism for production of spread F irregularities, 19: 21125 (RAD-TR-64-27)

AVCO-EVERETT RESEARCH LAB., EVERETT, MASS.
Radiation from gas containing alkali metal vapors, 19: 21468 (BSD-TDR-64-164)

B

BABCOCK AND WILCOX CO., BARBERTON, OHIO. BOILER DIV.
Prog. rpt. on Na-heated steam generator, 12/64, 19: 20107 (BAW-1280-22)

BATTELLE-NORTHWEST, RICHLAND, WASH. PACIFIC NORTHWEST LAB.
Fatigue behavior of Pu–1.0 w/o Ga δ-stabilized Pu, 19: 20545 (BNWL-16)
Flow visualization, 19: 20108 (BNWL-31)
Recovery of Sr from Purex waste, 19: 20035 (BNWL-4)
Values in fuel from power reactors, 19: 20036 (BNWL-25)

BELL TELEPHONE LABS., MURRAY HILL, N. J.
Elastic and inelastic scattering of electrons at high accelerating voltages, 19: 20254 (CONF-640204(p.123-36))
X rays emitted in coincidence with fission of Cf-252, 19: 21229 (BNL-8841)

BENDIX PRODUCTS AEROSPACE DIV., BENDIX CORP., SOUTH BEND, IND.
Prog. rpt. on pneumatic nutator actuator motor, 12/64, 19: 21615 (NASA-CR-54282)

BETTIS ATOMIC POWER LAB., PITTSBURGH.
HARMONY—system for nuclear reactor depletion computation, 19: 21644 (WAPD-TM-478)
Raman spectrum of ZrO_2, 19: 19849 (WAPD-T-1760)

BETTIS ATOMIC POWER LAB., WEST MIFFLIN, PA.,
Spatial and energy interference among resonance nuclides, 19: 21643 (WAPD-T-1728)

BOEING CO., SEATTLE, WASH.
Solar-flare hazard to manned space systems, 19: 20873 (D2-11608)

BOEING CO., SEATTLE, WASH. AERO-SPACE DIV.
Prog. rpt. on macrolaminate particle composite material, 12/64–2/65, 19: 20558 (NP-14888)

BOEING SCIENTIFIC RESEARCH LABS., SEATTLE, WASH. GEO-ASTROPHYSICS LAB.
Amplification of hydromagnetic waves in magnetosphere by cyclotron instability process, 19: 21123 (D1-82-0398)

BRIDGEPORT BRASS CO., SEYMOUR, CONN.
Prog. rpt. on fuels, 1–3/63, 19: 20501 (BRB-77)

BROOKHAVEN NATIONAL LAB., UPTON, N. Y.
Brookhaven-Columbia plasma lens, 19: 20915 (BNL-8967)
Centers and limit cycles in reactor kinetics, 19: 21634 (BNL-9010)
Cobalt-60 research irradiators, 19: 20095 (BNL-8976)
Cost estimate for Co-60 radiation-induced ethylene polymerization process, 19: 19957 (BNL-8993)
Design of AGS fast beam extraction system, 19: 20718 (BNL-8968)
Electronic peakers, 19: 20094 (BNL-8969)
Evolution of finite escape time concept in reactor kinetics, 19: 21635 (BNL-9011)
Excitation of parallel resonant LRC circuit from fast-sweeping signal source, 19: 21757 (BNL-7918)
Gene differentiation, 19: 21756 (BNL-8934)
High-intensity ion beam production and preacceleration, 19: 20720 (BNL-8982)
Mechanism of thermal decomposition of α-phenylethylazomethane, 19: 19943 (BNL-8243)
Proposed AGS accelerating cavity, 19: 20719 (BNL-8970)
Safety analysis on Brookhaven HFBR, 19: 21727 (BNL-7661(Vol.II))
Safety analysis on Brookhaven HFBR, 19: 21728 (BNL-7661(Vol.I))
Transfer of C-14 and tritium from substrates to CO_2, water, and lipids in obese and diabetic subjects, 19: 21758 (BNL-8864)
X rays emitted in coincidence with fission of Cf-252, 19: 21229 (BNL-8841)

BROWN UNIV., PROVIDENCE, R. I. DEPT. OF PHYSICS.
Prog. rpt. on radiation damage in solids, annual, 5/64–4/65, 19: 20620 NYO-2024-8)

BRUSH BERYLLIUM CO., CLEVELAND, OHIO.
Mechanical characteristics of zone-leveled Be, 19: 20544 (AFML-TR-64-388)

C

CAMBRIDGE LANGUAGE RESEARCH UNIT (ENGLAND).
Brouwer-type space for particles as distinction systems, 19: 21078 (AFOSR-64-1380)

CAMILLE DREYFUS LAB., RESEARCH TRIANGLE INST., DURHAM, N. C.
Radiation polymerization of crystalline trithiane, 19: 19959 (CONF-571-37)
CARNEGIE INST. OF TECH., PITTSBURGH, PA.
Prog. rpt. on instabilities in metal-vapor plasmas, 10–12/64, 19: 21490 (TID-21698)
CENTRE D'ETUDE DE L'ENERGIE NUCLEAIRE, BRUSSELS (BELGIUM).
Direct conversion applications of radioisotopic sources, 19: 20904 (BLG-317)
Operation of PWR-type powerplant, 19: 21679 (BLG-261)
Production of radioisotopes. Study of maximum possible accident, 19: 20195 (BLG-281)
Tritium laboratory—maximum possible accident, 19: 20194 (BLG-280)
CHICAGO OPERATIONS OFFICE (AEC), ILL.
Radiological assistance plan handbook, 19: 20197 (COO-281)
CHICAGO UNIV., ILL. INST. FOR COMPUTER RESEARCH.
Prog. rpt. on computer research, 2/65, 19: 20439 (COO-614-31)
COLLINS RADIO CO., DALLAS, TEX.
Prog. rpt. on antennas for 1- to 50-psi overpressure range, final, 7/62–9/63, 19: 20109 (CER-D1703)
COMBUSTION ENGINEERING, INC., WINDSOR, CONN. NUCLEAR DIV.
Prog. rpt. on performing in-pile thermal conductance testing, 10–12/64, 19: 21664 (CEND-3336-229)
COMISION NACIONAL DE ENERGIA ATOMICA, BUENOS AIRES (ARGENTINA).
Preparation of carrier-free P-32, 19: 20021 (NP-14900)
Prog. rpt. on Sr-90 levels in diets and bones of children, 1965, 19: 20165 (TID-21711)
COMMISSARIAT A L'ENERGIE ATOMIQUE, CADARACHE (FRANCE). CENTRE D'ETUDES NUCLEAIRES.
First results of tests of Rapsodie block pile, 19: 21730 (CEA-R-2557)
COMMISSARIAT A L'ENERGIE ATOMIQUE, CHUSCLAN (FRANCE). CENTRE DE PRODUCTION DE PLUTONIUM DE MARCOULE.
Safety in processing irradiated fuels, 19: 20037 (CEA-R-2654)
COMMISSARIAT A L'ENERGIE ATOMIQUE, FONTENAY-AUX-ROSES (FRANCE).
Allotropic transformations of Pu, 19: 20546 (CEA-R-2726)
Determination of amounts of nuclides during radioactive transformations. II., 19: 19958 (CEA-R-2348)
Preparation of nuclear-pure beryllium oxalate tri-hydrate, 19: 19832 (CEA-R-2591)
Stability of plasmas obtained in EPPE, 19: 21469 (CEA-R-2713)
Thermodynamic study of treatment of U–Zr alloys, 19: 19742 (CEA-R-2592)
X-ray microanalysis—determination of correction factors, 19: 19746 (CEA-R-2728)
COMMISSARIAT A L'ENERGIE ATOMIQUE, GRENOBLE (FRANCE). CENTRE D'ETUDES NUCLEAIRES.
Measurement of neutron spectra in reflector of light water reactor, 19: 21729 (CEA-R-2442)
COMMISSARIAT A L'ENERGIE ATOMIQUE, SACLAY (FRANCE). CENTRE D'ETUDES NUCLEAIRES.
Apparatus for high-temperature measurement of interior friction in rigid samples, 19: 20245 (CEA-R-2718)
Comparison of cascades with total minimum flux, 19: 19744 (CEA-R-2622)
Detection of critical accidents at Commissariat a l'Energie Atomique, 19: 20330 (AEC-tr-6547)
Electron bunching in Saclay linear accelerator, 19: 20721 (CEA-R-2749)
Exchange reactions between molten salt and TBP in liquid silicone, 19: 19833 (CEA-R-2628)
Helium precipitation in Al–Li alloy, 19: 20613 (CEA-R-2529)
Improvement of spectrographic analyses, 19: 19743 (CEA-R-2619)
Interaction of slow neutrons with U-235, 19: 21230 (CEA-R-2552)
Radiochemical separation of Ca-45, Sr-89, and Ba-140, 19: 19745 (CEA-R-2712)
Resistance of metallic U tubes to external pressure, 19: 20453 (CEA-R-2572)
Specifications for scattering code for XY geometry: DAIXY, 19: 21198 (CEA-R-2759)
Specifications for multi-group scattering code of two dimensions: ALCI, 19: 21197 (CEA-R-2747 & Add.)
Variations of U parameter with changes in C content, 19: 20547 (CEA-R-2731)
X-ray fluorescence analysis of light elements, 19: 19741 (CEA-R-2539)

D

DEFENSE METALS INFORMATION CENTER, BATTELLE MEMORIAL INST., COLUMBUS, OHIO.
Surface damage in machined Be, 19: 20502 (DMIC-Memo-198)
DEPARTMENT OF NATIONAL HEALTH AND WELFARE, OTTAWA (ONTARIO). RADIATION PROTECTION DIV.
Data from Radiation Protection Programs, Vol. 3, No. 1, 19: 20161 (NP-14869)
DIVISION OF ISOTOPES DEVELOPMENT (AEC), WASHINGTON, D. C.
Conference on isotopic power development, Germantown, Maryland, 6/64, 19: 20426 (TID-7698(Pt.I))
Fission products, 19: 20431 (TID-7698(Pt.I)(p.1-16))
Isotopic power data sheets, 19: 20402 (TID-7698(Pt.I)(p.17-30))
Nuclear safety—standards and evaluation, 19: 20206 (TID-7698 (Pt.I)(p.31-2))
Radioisotope space propulsion systems, 19: 20428 (TID-7698 (Pt.I)(p.257-76))
Shielding requirements and radiation characteristics of isotopic power sources, 19: 21595 (TID-7698(Pt.I)(p.33-248))
SNAPS 9A and 19, 19: 20427 (TID-7698(Pt.I)(p.249-56))
DIVISION OF REACTOR DEVELOPMENT (AEC), WASHINGTON, D. C.
Nuclear safety—standards and evaluation, 19: 20206 (TID-7698 (Pt.I)(p.31-2))
DIVISION OF RESEARCH (AEC), WASHINGTON, D. C.
Summaries of research in controlled thermonuclear reactions, 19: 21489 (TID-4005(Pt.5))
DIVISION OF TECHNICAL INFORMATION EXTENSION, (AEC), OAK RIDGE, TENN.
Bibliography on biological applications of γ radiation, 19: 19505 (TID-3580)
Bibliography on radioactive fallout, 19: 20164 (TID-3086(Suppl.2))
Summaries of research in controlled thermonuclear reactions, 19: 21489 (TID-4005(Pt.5))
DOUGLAS AIRCRAFT CO., INC., SANTA MONICA, CALIF. MISSILE AND SPACE SYSTEMS DIV.
Secondary nucleons produced in high-energy nuclear reactions, 19: 21242 (NP-14837)
DU PONT DE NEMOURS (E. I.) & CO., AIKEN, S. C. SAVANNAH RIVER LAB.
Burning of radioactive process solvent, 19: 21747 (DP-942)
Determination of Zr-95 and Nb-95 in mixtures, 19: 19748 (DP-933)
DU PONTE DE NEMOURS (E. I.) & CO., AIKEN, S. C. SAVANNAH RIVER PLANT.
Disposal of large quantities of degraded and low-level contaminated solvent, 19: 21748 (DPSPU-64-30-8B)
Impurities in moderator of Savannah River reactors, 19: 21711 (DPSPU-63-30-40)
Nondestructive testing of reactor fuel, target, and control elements, 19: 20126 (DPSPU-65-30-11)

E

EUROPEAN ATOMIC ENERGY COMMUNITY.
Diluent influence on liquid-liquid extraction by trilaurylamine hydrochloride, 19: 20039 (EUR-2246.e)
Distribution law of product of random variables according to new composition law, 19: 20440 (EUR-2251.i)
Evolution of chlorine in terphenyls, 19: 20469 (EUR-2279.e)
First results of tests of Rapsodie block pile, 19: 21730 (CEA-R-2557)
Liquid-liquid extraction of $FeCl_3$, 19: 20038 (EUR-2245.e)
Magnetic tape instrumentation for on-line recording and off-line analysis, 19: 20255 (EUR-2119.e)
Plating U and Al with Nb, 19: 20456 (EUR-2111.d)
Preparation of Na samples for neutron scattering experiments, 19: 20503 (EUR-2202.e)
Synthesis of optimal control and hybrid computation, 19: 21604 (EUR-2202.e)
EUROPEAN ATOMIC ENERGY COMMUNITY, GEEL (BELGIUM). CENTRAL NUCLEAR MEASUREMENTS BUREAU.
Magnetic tape instrumentation for on-line recording and off-line analysis, 19: 20255 (EUR-2119.e)
Preparation of Na samples for neutron scattering experiments, 19: 20503 (EUR-2242.e)
EUROPEAN ATOMIC ENERGY COMMUNITY, ISPRA (ITALY). EUROPEAN SCIENTIFIC DATA PROCESSING CENTER.
Synthesis of optimal control and hybrid computation, 19: 21604 (EUR-2202.e)
EUROPEAN ATOMIC ENERGY COMMUNITY, ISPRA (ITALY). JOINT NUCLEAR RESEARCH CENTER.
Determination of Al, Al_2O_3, Fe, Si, Zn, C in SAP powders, 19: 19750 (EUR-2286.f)
Determination of waste water radioactivity, 19: 19749 (EUR-2118.f)
Evolution of chlorine in terphenyls, 19: 20469 (EUR-2279.e)

Magnetic tape instrumentation for on-line recording and off-line analysis, 19: 20255 (EUR-2119.e)
Plating U and Al with Nb, 19: 20456 (EUR-2111.d)
Preparation of Na samples for neutron scattering experiments, 19: 20503 (EUR-2242.e)
Synthesis of optimal control and hybrid computation, 19: 21604 (EUR-2202.e)

EUROPEAN NUCLEAR ENERGY AGENCY, PARIS (FRANCE).
Prog. rpt. on Halden reactor project, annual, 1963–64, 19: 21693 (NP-14896)

EUROPEAN ORGANIZATION FOR NUCLEAR RESEARCH, GENEVA (SWITZERLAND).
Baryon resonances, 19: 20916 (CERN-65-7)

F

FANSTEEL METALLURGICAL CORP., NORTH CHICAGO, ILL. METAL PRODUCTS DIV.
Prog. rpt. on Nb alloy sheet rolling, final 3/7/63–9/1/64, 19: 20499 (AD-606291)

FLORIDA STATE UNIV., TALLAHASSEE. DEPT. OF BIOLOGICAL SCIENCE.
Prog. rpt. on molecular bases of mutation, final 1965, 19: 21772 (TID-21709)

FRANKLIN INST., PHILADELPHIA, PA. LABS. FOR RESEARCH AND DEVELOPMENT.
Design of Hallam moderator element. I., 19: 21680 (COO-1402-1)
Design of Hallam moderator element. II., 19: 21681 (COO-1402-2)

G

GENERAL ATOMIC, SAN DIEGO, CALIF.
GAIL IV irradiation assembly design summary, 19: 21665 (GAMD-5535)
Gas transport properties and pore structure of nuclear graphites, 19: 20457 (GAMD-4814)
Iterative technique for stress analysis of PCR structures, 19: 20086 (GAMD-5926)
Neutron activation analysis procedures for determination of O in K, 19: 19751 (GA-5982)
Numerical stress analysis of PCRS for TARGET, 19: 21683 (GAMD-5272 (Rev.2))
TARGET—IBM computer code for stress analysis of bodies of revolution, 19: 21609 (GAMD-5001(Rev.2))
TARGET steam generator design, 19: 21682 (GAMD-4732)
Tendon configuration in prestressed concrete reactor structure, 19: 21610 (GAMD-6109)
Thermal protection of concrete pressure vessel, 19: 20110 (GAMD-5432)

GENERAL DYNAMICS/FORT WORTH, TEX.
Comparison of measured neutron and proton spectra with calculated spectra in energy region between 50 and 160 Mev, 19: 21244 (ORNL-P-844)
Induced-voltage studies in Co-60 γ irradiator, 19: 20398 (FZK-214)

GENERAL ELECTRIC CO., CINCINNATI, OHIO. NUCLEAR MATERIALS AND PROPULSION OPERATION.
Electromagnetic testing of thin-wall, refractory metal tubing, 19: 20454 (CONF-650212-1)
Properties of Fe–Cr–Al type alloys containing Y, 19: 20470 (GE-TM-63-7-3)
Thermal conductivity of UO_2, 19: 20563 (TID-21668)

GENERAL ELECTRIC CO., CINCINNATI, OHIO. SPACE POWER AND PROPULSION SECTION.
Prog. rpt. on alkali metal corrosion, 9/26–12/26/64, 19: 20474 (NASA-CR-54281)
Prog. rpt. on K corrosion test loop, 7/15–10/15/64, 19: 20473 (NASA-CR-54269)

GENERAL ELECTRIC CO., PHILADELPHIA, PA. MISSILE AND SPACE DIV.
Prog. rpt. on surface contouring applied to semiconductor radiation detectors, semiannual, 6/64–1/65, 19: 20323 (NYO-3246-4)

GENERAL ELECTRIC CO., RICHLAND, WASH. HANFORD ATOMIC PRODUCTS OPERATION.
Effects of reactor decontaminating solutions on intergranularly corroded type 304 stainless steel, 19: 20471 (HW-SA-3628)
Fission products, 19: 20431 (TID-7698(Pt.I)(p.1-16))
Increased processing flexibility—Purex, 19: 20040 (HW-84085)
Ion exchange purification of Am-241, 19: 20041 (HW-84352)
Irradiation of N-reactor graphite, 19: 20614 (HW-81250A)
Leakage from Zone I and II of 105-N, 19: 21712 (HW-61979)
Neutron spectrum measurements, 19: 20201 (HW-SA-3525)
Performance of selected inhibitors in reactor coolant backup service, 19: 21714 (RL-REA-592)
Personnel neutron dosimeter development, 19: 20318 (HW-SA-3526)
Plutonium releases during overheating and fires, 19: 20200 (HW-83668)
Postirradiation evaluation of Zy-2 pressure tubes. III., 19: 21686 (HW-84540)
Prog. rpt. on W–Tc alloys, 10/64–1/65, 19: 20550 (HW-84550)
Prog. rpt. on waste disposal, 1–12/64, 19: 21749 (HW-84549)
Radiation monitoring of personnel by dose rate telemetering, 19: 20317 (HW-82369)
Rate and formation constants from oxidation-reduction reaction data, 19: 19836 (HW-SA-3476)
Reactor decontamination and the health physicist, 19: 21605 (HW-SA-3560)
Reclaiming of inner fuels with cracked supports, 19: 21668 (HW-84196)
Thermal conductivity of UO_2, 19: 20615 (HW-SA-3212)
Time-variable time delay for computer simulations, 19: 21713 (HW-83092 (Rev.))
Welding procedures, 19: 20521 (TID-20625(Vol.I(Rev.I)))
Welding procedures, 19: 20522 (TID-20625(Vol.II)(Rev.I))
Welding procedures, 19: 20523 (TID-20625(Vol.III)(Rev.I))
Welding procedures, 19: 20524 (TID-20625(Vol.IV)(Rev.I))
709/7090 program for indexing x-ray diffraction powder patterns. I., 19: 19834 (HW-74393)
709/7090 program for indexing x-ray diffraction powder patterns. III., 19: 19835 (HW-89062)

GENERAL ELECTRIC CO., SAN JOSE, CALIF. ATOMIC POWER EQUIPMENT DEPT.
Core II critical assembly analysis for NS *Savannah*, 19: 21716 (GEAP-3514)
Sodium logging in fast ceramic reactor fuels, 19: 20458 (GEAP-4283)
Water surface waves in BWR, 19: 21684 (GEAP-4061)
Pressure vessel steel for reactors, 19: 21607 (APED-4773)
Prog. rpt. on fast ceramic reactor program, 4–6/64, 19: 21666 (GEAP-4640)

GENERAL ELECTRIC CO., SAN JOSE, CALIF. VALLECITOS ATOMIC LAB.
Prog. rpt. on nuclear fuel burnup analyses, 9–11/64, 19: 21667 (GEAP-4776)

GEOLOGICAL SURVEY, WASHINGTON, D. C.
Geologic map and sections of Thirsty Canyon, Nye County, Nevada, 19: 20150 (TEI-859)
Geologic map of Quartet Dome Quadrangle, Nye County, Nevada, 19: 20151 (TEI-860)

GEOSCIENCE LTD., SOLANA BEACH, CALIF.
Prog. rpt. on heat transfer for space nuclear power systems, 9/63–8/64, (SAN-409-12)

GOODYEAR ATOMIC CORP., PIKETON, OHIO.
Can you afford your cooling water treatment program?, 19: 20087 (GAT-P-33)

GOSUDARSTVENNYI KOMITET PO ISPOL'ZOVANIYU ATOMNOI ENERGII SSSR.
Concentration of radioactive products over Indian and Pacific Oceans, 19: 20158 (NP-14712)
Radioactivity of ground-level air on Hayes Island, 19: 20157 (NP-14697)
Strontium-90 in fresh-water reservoirs in Soviet Union, 1961–62, 19: 20160 (NP-14728)
Strontium-90 in Pacific Ocean, 19: 20159 (NP-14726)

GRENOBLE UNIV. (FRANCE).
Measurement of neutron spectra in reflector of light water reactor, 19: 21729 (CEA-R-2442)

H

HARRY DIAMOND LABS., WASHINGTON, D. C.
Gamma irradiation of Ge. Impurity effects, 19: 20619 (NP-14883)

HEALTH AND SAFETY LAB., NEW YORK OPERATIONS OFFICE (AEC), N. Y.
Boundary effect of γ transport from point source, 19: 20198 (HASL-157)
Carbon-14 measurements in atmosphere, 1953–64, 19: 20155 (HASL-159)
Energy distribution of x-ray beams from 250-kv constant potential machine, 19: 20256 (HASL-151)
Operational safety evaluation of remote reactor plants, 19: 21685 (HASL-152)
Prog. rpt. on fallout program, 12/64–3/65, 19: 20154 (HASL-158)
Prog. rpt. on high-altitude balloon sampling, 7–12/64, 19: 20162 (NYO-3276-9)

HUDSON INST., INC., HARMON-ON-HUDSON, N. Y.
Aspects of environment resulting from various kinds of nuclear wars, 19: 20199 (HI-388-RR(Pt.III))

I

IIT RESEARCH INST., CHICAGO, ILL.
Prog. rpt. on nondestructive evaluation of coating-metal, 19: 20127 (IITRI-N213-23)
Prog. rpt. on V alloy studies, final, 2/65, 19: 20552 (IITRI-B6021-6)
Prog. rpt. on V-base alloys, final, 10/63–9/64, 19: 20459 (IITRI-B6019-6)
ILLINOIS UNIV., URBANA.
Advances in Mössbauer effect methodology high-pressure techniques, 19: 21231 (COO-1198-255)
ILLINOIS UNIV., URBANA. COORDINATED SCIENCE LAB.
Oscillations in one-dimensional, inhomogeneous plasma, 19: 21478 (NP-14880)
INDUSTRIAL RESEARCH ORGANIZATION, ASPENDALE (AUSTRALIA). DIV. OF METEOROLOGICAL PHYSICS.
Determination of turbulence dissipation by Eulerian variance analysis, 19: 20654 (ANL-6938(p.242-51))
INSTITUT DE RECHERCHES DE LA SIDERUGRIE, ST.-GERMAN-ENLAYE (FRANCE).
Prog. rpt. on tests on super ELSO Ni–Cr steel, 9–12/64, 19: 20549 (EURAEC-1282)
INSTITUT FUR PLASMAPHYSIK, G.M.B.H., GARCHING, (WEST GERMANY).
Differential interferometer and application to determination of electron density gradients, 19: 21472 (IPP-1/25)
Effects of neutral gas on dynamics of theta-pinch discharges, 19: 21470 (IPP-1/14)
Magnetic field measurements with help of Zeeman effect, 19: 20257 (IPP-1/19)
"Precursor ionization" occurring in hot plasmas, 19: 21471 (IPP-1/24)
Z-pinch, antipinch, and theta pinch as apparatus for production of strong collision waves, 19: 21473 (IPP-1/28)
INSTITUT NATIONAL DES SCIENCES ET TECHNIQUES NUCLEAIRES, PARIS (FRANCE).
Exchange reactions between molten salt and TBP in liquid silicone, 19: 19833 (CEA-R-2628)
INSTITUT ZA NUKLEARNE NAUKE "BORIS KIDRIC," BELGRADE (YUGOSLAVIA).
Prog. rpt. on hematopoietic regeneration of irradiated animals, final, 19: 19499 (NP-14899)
INSTITUTE OF MATHEMATICAL SCIENCES, MADRAS (INDIA).
Gauge invariance and mass of vector bosons, 19: 20934 (NP-14829)
Origin of symmetries, 19: 20933 (NP-14828)
INSTITUTE OF NUCLEAR RESEARCH, WARSAW (POLAND).
Theoretical investigation of O hydrides, 19: 19844 (PAN-550/XVII)
INSTITUTO DE ENERGIA ATOMICA, SAO PAULO (BRAZIL).
Pulsed sieve-plate extraction columns. I and II., 19: 20043 (IEA-77)
INTERNATIONAL ATOMIC ENERGY AGENCY, VIENNA (AUSTRIA).
Deposition of Ba or Sr in aortic tissue, 19: 19500 (NP-14907)
Symposium on medical radioisotope scanning, Athens, 4/64. II., 19: 19709
Tables of thermodynamic data, 19: 19933
INTERNATIONAL CENTRE FOR THEORETICAL PHYSICS, TRIESTE (ITALY).
Asymptotic behavior of phase shift in λ for strongly singular potentials, 19: 21079 (IC/65/2)
Broken SU(6) symmetry and nonleptonic baryon decays, 19: 20919 (IC/65/5)
Can coupling constant assume arbitrary value in S-matrix theory?, 19: 20920 (IC/65/6)
Dynamical groups and mass formula, 19: 20923 (IC/65/18)
Extrapolation of S matrix from Lehmann's representation, 19: 21080 (IC/65/9)
Foundations of SU_6, 19: 20921 (IC/65/7)
Gauge approximations in mesodynamics, 19: 20928 (ICTP-64/10)
Mass difference of Ξ and Ξ^0, 19: 20917 (IC/65/3)
Problems of symmetry breaking, 19: 20926 (ICTP-64/4)
Production amplitudes. I and II., 19: 20925 (ICTP-64/3)
Relativistic structure of SU(6), 19: 20927 (ICTP-64/7)
Rigged Hilbert spaces, 19: 21081 (ICTP-64/9)
S-matrix elements in two-particle unitarity approximation for one-dimensional world, 19: 20924 (ICTP-64/2)
Scalar behavior of vector electrodynamics at high energy, 19: 20929 (ICTP-64/12)
Selection rules in para-field theory, 19: 20918 (IC/65/4)
Some unitary representations of non-compact form of SU_3, 19: 20922 (IC/65/8)
ISOTOPES, INC., WESTWOOD, N. J.
Prog. rpt. on Project Star Dust, 9/63, 19: 20657 (DASA-1309)
ISRAEL ATOMIC ENERGY COMMISSION, YAVNE. SOREQ NUCLEAR RESEARCH ESTABLISHMENT.
Criterion for selectivity in recoil labeling, 19: 20020 (IA-907)
Effects of Co-60 γ rays on oranges, 19: 20404 (IA-999)
Ion exchange studies of complex formation, 19: 19837 (IA-1000)
Xenon minimax problem, 19: 21639 (IA-988)
ISTITUTO SUPERIORE DI SANITA', ROME (ITALY). LABORATORI DI FISICA.
Circuit diagrams and standard electronic equipment, 19: 20321 (ISS-64/28)

J

JAPAN ATOMIC ENERGY RESEARCH INST., TOKYO.
Initial critical and power tests of JPDR, 19: 21688 (JAERI-1067)
Bonding methods for graphite materials, 19: 20505 (JAERI-1071)
Flowmeter for F gas and vapors of reactive fluorides, 19: 20259 (JAERI-1074)
Minimum criticality calculation for JPDR, 19: 21689 (JAERI-1068)
Recording thermobalance for F gas and vapors of reactive fluorides, 19: 20258 (JAERI-1070)
JOHNS HOPKINS UNIV., BALTIMORE, MD.
Biological applications of electron microscopy, 19: 19455 (CONF-640204(p.44-62))
JOINT INST. FOR NUCLEAR RESEARCH, DUBNA (USSR). LAB. OF HIGH ENERGY.
"Beating" of nuclear radiation due to particle flux of variable intensity, 19: 21235 (JINR-P-1950)
Magnetic fields in units of ionic optical system for 5-Bev antiproton channel, 19: 20723 (JINR-P-1945)
Possible existence of new boson resonance decays involving γ quanta, 19: 20931 (JINR-P-1951)
Reduction of minimization of quadratic functional, 19: 20441 (JINR-P-1958)
JOINT INST. FOR NUCLEAR RESEARCH, DUBNA (USSR). LAB. OF NEUTRON PHYSICS.
Theory of neutron multiplication and noises in nuclear reactors, 19: 21641 (JINR-P-1996)
JOINT INST. FOR NUCLEAR RESEARCH, DUBNA (USSR). LAB. OF NUCLEAR PROBLEMS.
Acceleration of variably charged particles in electrostatic field, 19: 20722 (JINR-D-1946)
Nuclear form-factors in μ capture in He-3, 19: 21236 (JINR-P-1952)
JOINT INST. FOR NUCLEAR RESEARCH, DUBNA (USSR). LAB. OF NUCLEAR REACTIONS.
Electromagnetic mass-separator. I., 19: 20260 (JINR-P-1948)
Electromagnetic mass-separator. II., 19: 20261 (JINR-P-1949)
JOINT INST. FOR NUCLEAR RESEARCH, DUBNA (USSR). LAB. OF THEORETICAL PHYSICS.
"Beating" of nuclear radiation due to particle flux of variable intensity, 19: 21235 (JINR-P-1950)
Hydrodynamical equations for superfluid Fermi-liquid and two particle Green functions. I., 19: 21161 (JINR-P-1953)
Inelastic scattering of heavy particles with excitation of collective nuclear states, 19: 21234 (JINR-P-1908)
Infrared asymptotics Green functions, 19: 20930 (JINR-E-1975)
Small-angle scattering of charged particles, 19: 21233 (JINR-E-1992)
JUNTA DE ENERGIA NUCLEAR, MADRID (SPAIN).
Production of radioactive isotopes in Spain, 19: 20432 (ORNL-tr-295)
JUNTA DE ENERGIA NUCLEAR, MADRID (SPAIN). DIVISION DE QUIMICA.
Determination of Nb, Ta, and U in tantalite–columbite ores, 19: 19754 (JEN-134-DQ/I-39)
JUNTA DE ENERGIA NUCLEAR, MADRID (SPAIN). DIVISION DE FISICA.
Interactions of 29-Mev He-3 particles with light nuclei, 19: 21232 (JEN-141-DF/I-45)
JUNTA DE ENERGIA NUCLEAR, MADRID (SPAIN). LABORATORIO DE MINERALOGIA.
Genesis of uraniferous deposits. I., 19: 20185 (JEN-132-SIG/I-3)

K

KERNFORSCHUNGSZENTRUM, KARLSRUHE (WEST GERMANY).
Instrument and unit program, 19: 20262 (KFK-259)
KERNFORSCHUNGSZENTRUM, KARLSRUHE (WEST GERMANY). INSTITUT FUR ANGEWANDTE KERNPHYSIK.
Measurement of isomeric splitting ratios by activation, 19: 21237 (KFK-265)
Multiple input data acquisition system using small on-line computer, 19: 21731 (KFK-242)
Phonon frequency distribution of V, 19: 20553 (KFK-262)
Scattering laws of some hydrogenous moderators, 19: 21200 (KFK-264)
KERNFORSCHUNGSZENTRUM, KARLSRUHE (WEST GERMANY).

INSTITUT FUR RADIOCHEMIE.
Absolute measurement of radionuclides with 4π counter, 19: 19755 (KFK-252)
KNOLLS ATOMIC POWER LAB., SCHENECTADY, N. Y.
Self-shielding in closely spaced slab lattices, 19: 21636 (CONF-654-32)
Spatial dependence of pulsed-neutron reactivity measurements, 19: 21637 (CONF-650406-2)
Variational synthesis with discontinuous trial functions, 19: 21638 (CONF-650501-4)
X-ray emission analysis, 19: 19747 (CONF-650214-1)

L

LABORATORI NAZIONALI DI FRASCATI, COMITATO NAZIONALE PER L'ENERGIA NUCLEARE (ITALY).
Reaction $\gamma + p \rightarrow p + \pi^0$ near first resonance from polarized photons, 19: 20932 (LNF-64/60)
LAWRENCE RADIATION LAB., UNIV. OF CALIFORNIA, BERKELEY.
Alpha activities in Pt, 19: 21248 (UCRL-11828(p.21-5))
Alpha-active Au isotopes, 19: 21249 (UCRL-11828(p.25))
Appearance potentials of some doubly charged molecule ions, 19: 20807 (UCRL-11828(p.201-4))
Artificial construction of particle tracks by Monte Carlo method, 19: 20325 (UCRL-11624)
Automatic spectrogram measuring and recording, 19: 20288 (UCRL-11828(p.232-3))
Beam integrator, 19: 20284 (UCRL-11828(p.222-3))
Cerium magnesium nitrate temperature scale, 19: 21162 (UCRL-11828 (p.199-201))
Chemical evolution, 19: 19946 (UCRL-11950)
Computational studies of transients in packed tubular chemical reactors, 19: 19734 (UCRL-11757)
Control of response sensitivity in gas chromatography, 19: 20281 (UCRL-11828(p.204-7))
Crystal structure of Cs aquopentachlororuthenate, 19: 19845 (UCRL-11828(p.146))
Crystal structure of OsO_4, 19: 19846 (UCRL-11828(p.158-9))
Decay scheme of Es-254, 19: 21257 (UCRL-11828(p.63-6))
Decay of Mo-90, 19: 21258 (UCRL-11828(p.67-71))
Digital-computer calculation of matrix elements of nuclear interactions, 19: 20938 (UCRL-11828(p.9-10))
Dislocation arrangements in deformed Cu polycrystals, 19: 21774 (UCRL-11858)
Effect of accelerator parameters on mechanical tuning of r-f cavities, 19: 20735 (UCRL-11807)
Energy levels of Bk-249, 19: 21253 (UCRL-11828(p.38-40))
Energy levels of Pb-210, 19: 21247 (UCRL-11828(p.10-11))
Energy-mass distributions of Bi, Au, and W in He-ion-induced fission, 19: 21263 (UCRL-11828(p.90-2))
Energy variation of phase rule in α-particle scattering, 19: 21269 (UCRL-11828(p.132-3))
ESR spectra of radical anions in liquid ammonia, 19: 19945 (UCRL-11864)
Experimental instrumentation for 88-inch cyclotron, 19: 20282 (UCRL-11828(p.218-19))
Fission barrier of Tl-201, 19: 21260 (UCRL-11828(p.81))
Fission barriers of Po-210 and Sb-119, and Sb-117, 19: 21261 (UCRL-11828(p.81-3))
Fission barriers of W, Re, Os, Ir, and Hg isotopes, 19: 21259 (UCRL-11828(p.77-80))
Fission of U-238 and Pu-240 nuclei excited by inelastic α-particle scattering, 19: 21262 (UCRL-11828(p.84-6))
Fission-excitation functions of light elements, 19: 21264 (UCRL-11828(p.92-4))
Flow dichroism apparatus and its application to study of structure of spinach quantasomes. III., 19: 21773 (UCRL-11308)
Hewlett-Packard digital recorder model 562A insignificant-zero suppression, 19: 20285 (UCRL-11828(p.229))
Hewlett-Packard digital recorder model 562A modification to produce leader paper, 19: 20286 (UCRL-11828(p.230))
High-intensity negative ion sources, 19: 20731 (UCRL-11684)
Hydrostatic leveling systems, 19: 20733 (UCRL-11799)
Inelastic scattering of 50.9-Mev α particles from Ne-20, 19: 21267 (UCRL-11828(p.113-16))
Injection-system design, 19: 20737 (UCRL-11955)
Instrument development program, 19: 20287 (UCRL-11828(p.230-2))
Internal-conversion coefficients in decay of U-237, 19: 21251 (UCRL-11828(p.31-4))
K x rays emitted in spontaneous fission of Cf-252, 19: 21265 (UCRL-11828(p.95-7))
Level decay of Te-125 and magnetic dipole moment of Sb-125, 19: 21256 (UCRL-11828(p.58-62))
Light Po isotopes, 19: 21250 (UCRL-11828(p.26))
Molecular beam electric resonance experiments on LiF, LiCl, LiBr, LiI, and NaF, 19: 19848 (UCRL-11828(p.193-7))
Mössbauer effect instrumentation, 19: 20327 (UCRL-11828(p.221-2))
Neutrino beams from high-intensity 200-Bev proton synchrotron, 19: 20738 (UCRL-11983)
Nondestructive activation analysis with Li-drifted Ge detectors, 19: 19775 (UCRL-11828(p.197-9))
Nuclear magnetic moment of 2084-kev state in Ce-140, 19: 21254 (UCRL-11828(p.55-6))
Nuclear spectroscopy with two-nucleon transfer reactions, 19: 21266 (UCRL-11828(p.108-9))
Nuclear Zeeman effect in Ir-193, 19: 21255 (UCRL-11828(p.57-8))
Observation of electronic relaxation in Mössbauer spectroscopy, 19: 21270 (UCRL-11828(p.214-16))
Octupole states in N-15 and O-16, 19: 21268 (UCRL-11828(p.129-31))
Pair-production cross sections near threshold, 19: 21252 (UCRL-11828(p.35-8))
Problems of induced radioactivity around 200-Bev AGS, 19: 20732 (UCRL-11796)
Prog. rpt. on nuclear chemistry, annual, 1964, 19: 19735 (UCRL-11828)
Silicon radiation detectors, 19: 20328 (UCRL-11828(p.225-6))
Stability of XeO_3 in basic solutions, 19: 19847 (UCRL-11828(p.182-3))
Subgrouping multichannel analyzers on periodic basis, 19: 20283 (UCRL-11828(p.221))
Synchrotron-magnet coat studies, 19: 20734 (UCRL-11800)
Velocity spectrometers used in Bevatron deflected-beam research, 19: 20326 (UCRL-11787)
88-Inch cyclotron operation and development, 19: 20736 (UCRL-11828 (p.236-41))
LAWRENCE RADIATION LAB., UNIV. OF CALIFORNIA, LIVERMORE.
Approximate, finite temperature, Thomas-Fermi potential, 19: 20808 (UCRL-12054-T)
Evaluation of hydrogenic matrix element $\langle 0|e^{ik \cdot r}|n\ell\rangle$, 19: 20809 (UCRL-12218)
Explosively driven pipe closure, 19: 20100 (UCRL-12203)
Gallium oxide in spectrographic procedures, 19: 19774 (UCRL-7962)
Gas analytical apparatus for project Dribble, 19: 19776 (UCRL-12169)
Magnetic fields, vagal inhibition, and acetylcholinesterase activity, 19: 21776 (UCRL-12389)
Microwave excitation of Puffatron plasma at electron cyclotron frequency, 19: 21491 (UCRL-12057(Rev.I))
Morphological observations after distillation of Be from solid state, 19: 20564 (UCRL-12252)
OCTOPUS/6600 users' manual, 19: 20443 (UCRL-12256)
Parallelism in computing systems, 19: 20444 (UCRL-12293-T)
Preparation and properties of fluorocarbon alcohol 3,5-dinitrobenzoates, 19: 21775 (UCRL-12307)
YOGI-G—gamma-ray Monte Carlo program, 19: 21596 (UCRL-12005)
LIEGE UNIV. (BELGIUM).
Diluent influence on liquid-liquid extraction by trilaurylamine hydrochloride, 19: 20039 (EUR-2246.e)
Liquid-liquid extraction of $FeCl_3$, 19: 20038 (EUR-2245.e)
LOS ALAMOS SCIENTIFIC LAB., UNIV OF CALIFORNIA, N. MEX.
Beam dynamical calculations with realistic fields in drift-tube linear accelerator, 19: 20727 (LA-DC-6777)
Bibliography of nuclear interactions of He-3 with d, n, or p, 19: 21238 (LA-3205)
Compressibility of gaseous mixtures of He–N and He–D at high pressures, 19: 19840 (LA-3250)
Cryogenic tensile testing of Rover materials, 19: 20554 (LA-3161)
Determination of boric acid in admixture with cyanuric acid, 19: 19756 (LA-3193)
Disposal of Am^{241}–Pu^{239} raffinate solutions, 19: 21750 (LA-3150)
Gravimetric determination of H in Mo metal, 19: 19758 (LA-3225)
High-power test on cloverleaf cavity, 19: 20724 (LA-DC-6759)
Monte Carlo intranuclear cascade calculation, 19: 21239 (LA-3206)
Overdriving effect in dynamic polymorphism, 19: 20555 (LA-3215)
Penetration of plasma stream into transverse magnetic field, 19: 21475 (LA-DC-6383)
Power crowbar energy system for Scylla IV, 19: 21474 (LA-3189)
Processing of Pu by ion exchange. III., 19: 20045 (LA-2838)
Processing of Pu by ion exchange. V., 19: 20046 (LA-3188)
Prog. rpt. on advanced reactor technology, 1/31/65, 19: 21690 (LA-3244)
R-f phase and amplitude control system for proton linear accelerator, 19: 20728 (LA-DC-6875)
Reaction (He^3,d) on N = 28 nuclei, 19: 21240 (LA-DC-6232)
Resonantly coupled accelerating structures for high-current proton linacs, 19: 20725 (LA-DC-6760)
Retinal dose due to visible radiation from nuclear explosions, 19: 19498

(LA-3204)
Semiconductor anticoincidence detector system, 19: 20322 (LA-DC-6397)
Spectrophotometric determination of Re in Ta–Re alloys, 19: 19757 (LA-3213)
Spectrophotometric determination of U in mixtures of U and Mo, 19: 19759 (LA-3226)
Symmetry of neutron-induced Pu-239 fission in resonance region, 19: 21241 (LA-DC-6639)
Ternary Pu alloys for core test facility, 19: 20506 (LA-3209)
Transverse beam blow-up in standing-wave linac cavity, 19: 20726 (LA-DC-6775)

LOUISIANA STATE UNIV., BATON ROUGE. DEPT. OF FOOD AND SCIENCE AND TECHNOLOGY.
Prog. rpt. on radiation pasteurization of shrimp and oysters, final, 1–12/64, 19: 20407 (ORO-626)

LOVELACE FOUNDATION FOR MEDICAL EDUCATION AND RESEARCH, ALBUQUERQUE, N. MEX.
Transport of relatively insoluble materials from lung to lymph nodes, 19: 19456 (LF-21)

M

MAINZ UNIV. (WEST GERMANY).
Separation of rare earths on ion exchangers, 19: 20049 (NP-14834)

MALLORY METALLURGICAL CO., INDIANAPOLIS, IND.
Preparation and properties of W and W–Ag specimens, 19: 20559 (NP-14892)

MARINE BIOLOGICAL LAB., WOODS HOLE, MASS.
Recovery from division delay in irradiated gametes of *Arbacia punctulata*, 19: 19496 (ANL-6938(p.49-56))

MASSACHUSETTS INST. OF TECH., CAMBRIDGE.
Electron microscopy at MIT, 19: 20249 (CONF-640204(p.20-5))
Studies of complex ions, 19: 19841 (MIT-1965-18)

MASSACHUSETTS INST. OF TECH., CAMBRIDGE. DEPT. OF MECHANICAL ENGINEERING.
Entrance flow and transition from laminar-to-turbulent flow in vertical tubes, 19: 20114 (NP-14920)
Film boiling of liquid flowing upward through heated tube, 19: 20113 (NP-14895)

MASSACHUSETTS INST. OF TECH., CAMBRIDGE. DEPT. OF NUCLEAR ENGINEERING.
Nonlinear reactor kinetics, 19: 21642 (MMPP-FRPC-64-3)

MASSACHUSETTS UNIV., AMHERST.
Transverse beam blow-up in standing-wave linac cavity, 19: 20726 (LA-DC-6775)

MARTIN CO., BALTIMORE, MD. NUCLEAR DIV.
Radioisotope-powered underwater acoustic beacon, 19: 20405 (MND-3180-1)
SNAPS 9A and 19, 19: 20427 (TID-7698(Pt.I)(p.249-56))

MATERIALS ADVISORY BOARD, NATIONAL ACADEMY OF SCIENCES–NATIONAL RESEARCH COUNCIL, WASHINGTON, D. C.
Prog. rpt. on metalworking processes and equipment, 3/65, 19: 20507 (MAB-206-M)

MEDICAL RESEARCH COUNCIL, LONDON (ENGLAND).
Assay of Sr-90 in human bone in UK, 1963, 19: 20170

MELBOURNE UNIV., PARKVILLE (AUSTRALIA).
Prog. rpt. on effects of radiation and radiomimetic chemicals on *Pseudomonas aeruginosa*, 12/60–6/61, 19: 19501 (NP-14931)
Prog. rpt. on effects of radiation and radiomimetic chemicals on *Pseudomonas aeruginosa*, 6–12/61, 19: 19502 (NP-14932)
Prog. rpt. on effects of radiation and radiomimetic chemicals on *Pseudomonas aeruginosa*, final, 6–12/62, 19: 19503 (NP-14933)

MICHIGAN UNIV., ANN ARBOR. ACOUSTICS AND SEISMICS LAB.
Conference on Vela Uniform borehole research, Dallas, 3/64, 19: 20173 (VESIAC-4410-83-X)

MIDWEST RESEARCH INST., KANSAS CITY, MO.
Advanced valve technology, 19: 20097 (NASA-SP-5019)

MIDWESTERN UNIVERSITIES RESEARCH ASSN., STOUGHTON, WIS.
Aberrations of quadrupole magnets, 19: 20252 (CONF-640204(p.82-92))
Relaxation calculation of FFAG magnetostatic fields, 19: 20729 (MURA-706)

MINNESOTA UNIV., MINNEAPOLIS.
Luminescence of solutions of benzene and some simple benzene derivatives, 19: 21771 (TID-21684)

MOUND LAB., MIAMISBURG, OHIO.
Bismuth recovery process, 19: 20047 (MLM-734)
Photochemical method of separating Hg isotopes, 19: 20429 (MLM-1214)

N

NATIONAL AERONAUTICS AND SPACE ADMINISTRATION, CLEVELAND, OHIO. LEWIS RESEARCH CENTER.
Analysis of O in K, 19: 19760 (NASA-TM-X-1085)
Evaluation of filament deterioration in electron-bombardment ion sources, 19: 20138 (NASA-TN-D-2173)

NATIONAL AERONAUTICS AND SPACE ADMINISTRATION, LANGLEY STATION, VA. LANGLEY RESEARCH CENTER.
Damage to Ge due to proton bombardments, 19: 20617 (NASA-TN-D-2727)

NATIONAL AERONAUTICS AND SPACE ADMINISTRATION, MOFFETT FIELD, CALIF. AMES RESEARCH CENTER.
Equilibrium thermodynamic properties of CO_2, 19: 19842 (NASA-SP-3014)
Vapor pressure of Mg, 19: 20556 (NASA-TN-D-2723)

NATIONAL BUREAU OF STANDARDS, WASHINGTON, D. C.
Irradiation induced color centers in MgF_2, 19: 20618 (NBS-8614)

NATIONAL LEAD CO. OF OHIO, CINCINNATI.
Analytical chemistry manual of FMPC, 19: 19772 (TID-7022(Vol.I)(Bk.2))

NAVAL CIVIL ENGINEERING LAB., PORT HUENEME, CALIF.
Applications of radioisotopes, 19: 20403 (AD-606253)
Radiation shielding studies, 19: 21594 (AD-424387)

NAVAL RADIOLOGICAL DEFENSE LAB., SAN FRANCISCO, CALIF.
Nitrous oxide dosimeter—influence of cell diameter on nitrogen yield, 19: 20329 (USNRDL-TR-806)
Radiochemical procedure for In, 19: 19777 (USNRDL-TR-819)
Removal of simulated fallout from pavements, 19: 20207 (USNRDL-TR-797)

NAVAL RESEARCH LAB., WASHINGTON, D. C.
Prog. rpt. on metallurgical characteristics of high-strength structural materials, 9–12/64, 19: 20462 (NRL-6258)

NERATOOM, N. V., THE HAGUE (NETHERLANDS).
Prog. rpt. on stainless steel cladding of steels, 7–9/64, 19: 20504 (EURAEC-1228)

NEW MEXICO UNIV., ALBUQUERQUE.
Reaction (He^3,d) on N = 28 nuclei, 19: 21240 (LA-DC-6232)
Response of buried cylinders to quasi-static overpressures, 19: 20136 (AFWL-TDR-64-13)

NORTH CAROLINA STATE COLL., RALEIGH. DEPT. OF ENGINEERING RESEARCH.
Prog. rpt. on fuel of UC particles in U matrix, 8/62, 19: 20511 (NCSC-2981-1)
Prog. rpt. on fuel of UC particles in U matrix, 12/62, 19: 20512 (NCSC-2981-2)
Prog. rpt. on fuel of UC particles in U matrix, 2/63, 19: 20513 (NCSC-2981-3)

NORTH CAROLINA STATE OF THE UNIV. OF NORTH CAROLINA, RALEIGH. DEPT. OF ENGINEERING RESEARCH.
Prog. rpt. on fuel of UC particles in U matrix, 9/63, 19: 20514 (NCSC-2981-5)
Prog. rpt. on fuel of UC particles in U matrix, 12/63, 19: 20515 (NCSC-2981-6)
Prog. rpt. on fuel UC particles in U matrix, 3/64, 19: 20516 (NCSC-2981-7)
Prog. rpt. on fuel of UC particles in U matrix, 6/64, 19: 20517 (NCSC-2981-8)
Prog. rpt. on U interstitial phases, 3/64, 19: 20510 (NCSC-2663-16)

NUCLEAR METALS, INC., CONCORD, MASS.
Hot extrusion of metal powders, 19: 20518 (NMI-TJ-29)

NUCLEAR METALS, WEST CONCORD, MASS.
Effects of purification and realloying on mechanical properties of zone-refined Be single crystals, 19: 20557 (NMI-TJ-60)

O

OAK RIDGE GASEOUS DIFFUSION PLANT, TENN.
Kinetics and mechanism of fluorination of Cu(I) and Cu(II) oxides, 19: 19839 (K-1627)

OAK RIDGE INST. OF NUCLEAR STUDIES, INC., TENN.
Cobalt molybdate catalyst for synthesis of benzene for liquid scintillation radiocarbon dating, 19: 19944 (ORINS-50)

OAK RIDGE NATIONAL LAB., TENN.
Adsorption of Pa on unfired Vicor, 19: 20051 (ORNL-3773)
Boiling-K corrosion loop test, 19: 20476 (ORNL-3603)
Civil defense research at ORNL, 19: 20202 (ORNL-P-1093)
Coated-particle fuel development, 19: 20463 (ORNL-P-431)
Comparison of measured neutron and proton spectra with calculated spectra in energy region between 50 and 160 Mev, 19: 21244 (ORNL-P-844)
Computer program for flow calculations, 19: 20115 (ORNL-TM-1093)
Cross-section measurements, 19: 21484 (ORNL-3760(p.57-63))
Desalination of sea water using nuclear energy, 19: 21707 (ORNL-TM-432)
Disposal of high-level power reactor wastes in salt mine, 19: 21751

(ORNL-P-1064)
Dissolution of high-density UO_2, PuO_2, and UO_2–PuO_2 pellets in inorganic acids, 19: 20050 (ORNL-3695)
Dynamic gas thermometry, 19: 20277 (ORNL-P-1068)
Electron microscopy at ORNL, 19: 20250 (CONF-640204(p.26-34))
Electron-cyclotron heating, 19: 21482 (ORNL-3760(p.23-9))
Energy and angular details of fast neutron flux in water from pool-type reactor, 19: 21735 (ORNL-P-1092)
Evaluation of Hastelloy F and other materials for centrifuge in fuel recovery plant, 19: 20481 (ORNL-3787)
Evaluation of Th-base alloys for high-temperature strength, 19: 20560 (ORNL-3777)
EVAP—program for calculating evaporation of particles from nuclei, 19: 21245 (ORNL-TM-196)
Facility radiation and contamination alarm systems, 19: 20203 (ORNL-TM-988)
Fusion chain reactions, 19: 21487 (ORNL-3760(p.98-9))
High-purity KCl, 19: 19843 (ORNL-TM-1071)
High-temperature high-vacuum thermocouple drift tests, 19: 20278 (ORNL-P-1069)
High-temperature thermocouples used in ORNL-GCR program fuel irradiation experiments, 19: 20401 (ORNL-P-1065)
Isotopic power data sheets, 19: 20402 (TID-7698(Pt.I)(p.17-30))
Magnetics and superconductivity, 19: 21486 (ORNL-3760(p.77-93))
Measuring range of low-energy charged particles in conducting solids, 19: 20806 (ORNL-3702)
Multiple-pass experiments (DCX-2), 19: 21481 (ORNL-3760(p.10-22))
Plasma physics, 19: 21483 (ORNL-3760(p.30-56))
Plasma theory and computation, 19: 21485 (ORNL-3760(p.69-76))
Production, acceleration, and injection of ionic and atomic beams, 19: 20730 (ORNL-3760(p.64-8))
Prog. rpt. on SNAP-8 corrosion, 6–8/63, 19: 20475 (ORNL-3538)
Prog. rpt. on SNAP-8 corrosion, 9–11/63, 19: 20477 (ORNL-3604)
Prog. rpt. on SNAP-8 corrosion, 12/63–2/64, 19: 20478 (ORNL-3618)
Prog. rpt. on SNAP-8 corrosion, 3–5/64, 19: 20479 (ORNL-3671)
Prog. rpt. on SNAP-8 corrosion, 6–8/64, 19: 20480 (ORNL-3730)
Prog. rpt. on thermonuclear research, semiannual, 10/64, 19: 21479 (ORNL-3760)
Quenching variables from biomedical samples in liquid scintillator systems, 19: 20324 (ORNL-P-1094)
Sea-water desalination with nuclear energy, 19: 21708 (ORNL-TM-465)
Separation of long-lived fission product elements using EDTA, 19: 20052 (ORNL-TM-1035)
Shielding requirements and radiation characteristics of isotopic power sources, 19: 21595 (TID-7698(Pt.I)(p.33-248))
Single-pass experiments (DCX-1), 19: 21480 (ORNL-3760(p.1-9))
Smoothed thermocouple tables, alumel–chromel cryogenic, 19: 20274 (ORNL-3649(Vol.2)(Sect.2.12))
Smoothed thermocouple tables, Au–2.1% Co vs. Cu cryogenic, 19: 20272 (ORNL-3649(Vol.2)(Sect.2.10))
Smoothed thermocouple tables, chromel–alumel, 19: 20265 (ORNL-3649(Vol.2)(Sect.2.3))
Smoothed thermocouple tables, chromel–constantan, 19: 20268 (ORNL-3649(Vol.2)(Sect.2.6))
Smoothed thermocouple tables, constantan–Cu cryogenic, 19: 20273 (ORNL-3649(Vol.2)(Sect.2.11))
Smoothed thermocouple tables, constantan (JN)–Fe (JP) cryogenic, 19: 20275 (ORNL-3649(Vol.2)(Sect.2.13))
Smoothed thermocouple tables, constantan (YN)–Fe(YP) cryogenic, 19: 20276 (ORNL-3649(Vol.2)(Sect.2.14))
Smoothed thermocouple tables, Cu–constantan, 19: 20267 (ORNL-3649 (Vol.2)(Sect.2.5))
Smoothed thermocouple tables, Fe–constantan, 19: 20266 (ORNL-3649 (Vol.2)(Sect.2.4))
Smoothed thermocouple tables, Pt vs. Pt–10% Rh, 19: 20263 (ORNL-3649(Vol.2)(Sect.2.1))
Smoothed thermocouple tables, Pt vs. Pt–13% Rh, 19: 20264 (ORNL-3649(Vol.2)(Sect.2.2))
Smoothed thermocouple tables, W vs. W–26% Re, 19: 20269 (ORNL-3649(Vol.2)(Sect.2.7))
Smoothed thermocouple tables, W–3% Re vs. W–25% Re, 19: 20271 (ORNL-3649(Vol.2)(Sect.2.9))
Smoothed thermocouple tables, W–5% Re vs. W–26% Re, 19: 20270 (ORNL-3649(Vol.2)(Sect.2.8))
Spectra of γ rays produced by interaction of ~160-Mev protons with Be, C, O, Al, Co, and Bi, 19: 21243 (ORNL-3506)
Technical concept—Operation HENRE, 19: 21199 (CEX-65.02)
Vacuum systems, techniques, and materials studies, 19: 20140 (ORNL-3760(p.94-7))

P

PARIS UNIV., FRANCE.
Interaction of slow neutrons with U-235, 19: 21230 (CEA-R-2552)
PHILLIPS PETROLEUM CO., IDAHO FALLS, IDAHO. ATOMIC ENERGY DIV.
Calculation of parameters in reactor kinetics equations, 19: 21640 (IDO-16983)
Corrosion of type 316 stainless steel in NaK service, 19: 20472 (IDO-14651)
Prog. rpt. on chemical processing, 4–6/64, 19: 20042 (IDO-14646)
Slow neutron inelastic scattering from Al powder, 19: 20551 (IDO-17063)
SNAPTRAN 2/10A-3 destructive test, 19: 21717 (IDO-17019)
SNAPTRAN 2/10A-3 post-destructive test reactor examination, 19: 21718 (IDO-17071)
Transient tests of fully enriched, stainless steel plate-type, P core in Spert I reactor, 19: 20616 (IDO-17011)
Transistorized bidirectional decade counter, 19: 20319 (IDO-17059)
PITTSBURGH UNIV., PA. DEPT. OF CHEMISTRY.
Prog. rpt. on magneto-thermodynamics of para- and antiferromagnets, 6/64–3/65, 19: 21759 (NYO-3402-1)
PLESSET (E. H.) ASSOCIATES, INC., LOS ANGELES.
Elastic wave interaction with cylindrical cavity, 19: 20659 (AD-606490)
POLYTECHNIC INST. OF BROOKLYN, FARMINGDALE, N. Y. GRADUATE CENTER.
Pulsed plasmas and electron beam-plasma interactions, 19: 21488 (PIBMRI-1208-64)
PRATT AND WHITNEY AIRCRAFT, MIDDLETOWN, CONN. CONNECTICUT AIRCRAFT NUCLEAR ENGINE LAB.
Solubility of He in Li and K, 19: 20561 (PWAC-380)
PRINCETON UNIV., N. J.
X rays emitted in coincidence with fission of Cf-252, 19: 21229 (BNL-8841)
PRINCETON UNIV., N. J. ELEMENTARY PARTICLES LAB.
Electromagnetic form factor of the π^- meson, 19: 20935 (NP-14885)
PRINCETON UNIV., N. J. PLASMA PHYSICS LAB.
Electron cyclotron harmonic radiation from a plasma, 19: 21477 (MATT-290)
Equilibrium of plasma in toroid, 19: 21476 (MATT-283)

R

RADIATION RESEARCH ASSOCIATES, INC., FORT WORTH, TEX.
Gamma energy and angular distributions near air/ground interface from plane fallout, 19: 20163 (RRA-M42)
RADIO CORP. OF AMERICA, CAMDEN, N. J.
State of the art of conventional commercial instruments, 19: 20247 (CONF-640204(p.1-16))
RAND CORP., SANTA MONICA, CALIF.
Ecological problems and postwar recuperation, 19: 19504 (RM-2801-PR)
Gaseous-diffusion isotope-separation process, 19: 20430 (P-1231(RAND))
International registration of atom, 19: 21761 (P-1134(RAND))
Ionospheric electric current systems, 19: 21124 (P-1121(RAND))
Random functions of cosmic-ray cascades, 19: 20874 (P-1020(RAND))
Random walk, scattering, and invariant imbedding. I., 19: 20660 (P-1113(RAND))
Soviet atomic power program, 19: 21694 (P-1076(RAND))
Soviet Union and the atom, 19: 21762 (RM-2163(RAND))
RENSSELAER POLYTECHNIC INST., TROY, N. Y. DEPT. OF MATERIALS ENGINEERING.
Electrode kinetic studies of Th, 19: 19762 (RPI-2714-6)
Study of the material transport mechanism in sintering, 19: 20465 (TID-20344)
RENSSELAER POLYTECHNIC INST., TROY, N. Y. DEPT. OF NUCLEAR ENGINEERING AND SCIENCE.
Radioactive gas production from R.P.I. Linac, 19: 20204 (RPI-328-25)
RESEARCH LAB. OF ELECTRONICS, MASSACHUSETTS INST. OF TECH., CAMBRIDGE.
Diagnostic experiments in magnetically driven shock tube, 19: 20661 (RLE-TR-428)
RIJKSUNIVERSITEIT GHENT (BELGIUM).
Prog. rpt. on stainless steel cladding of steels, 7–9/64, 19: 20504 (EURAEC-1228)
ROCHESTER UNIV., N. Y. ATOMIC ENERGY PROJECT.
Frequency distribution of erythrocyte volumes of acutely bled dogs, 19: 21777 (UR-662)
Retention of Sr-90 by fetal and newborn rate, 19: 19473 (UR-661)
ROCHESTER UNIV., N. Y. DEPT. OF PHYSICS AND ASTRONOMY.
Decay mode $K \to 2\pi + \gamma$, 19: 20939 (UR-875-30)
Quark model as probe of higher symmetries, 19: 20940 (UR-875-72)

RUTGERS–THE STATE UNIV. OF NEW JERSEY, NEW BRUNSWICK. BUREAU OF ENGINEERING RESEARCH.
Prog. rpt. on basic studies in gas-solid suspensions, 4–10/64, 19: 20098 (TID-21633)
Prog. rpt. on polymers and related materials, 6/64–2/65, 19: 21770 (TID-21677)
RUTGERS–THE STATE UNIV. OF NEW JERSEY, NEW BRUNSWICK. SCHOOL OF CERAMICS.
Development of refractory ceramics, 19: 20461 (NP-14893)

S

SAINT LOUIS UNIV., MO.
Billiken calibration shot in southeast Missouri, 19: 20171 (AFCRL-64-659)
SAINT MARGARET'S HOSPITAL, BOSTON, MASS.
Prog. rpt. on effect of radiation on changes accompanying phagocytosis by leukocytic cells, 19: 19507 (TID-21712)
SANDIA CORP., ALBUQUERQUE, N. MEX.
Adjustable positive-limit magnetic torque wrench, 19: 21768 (SC-TM-65-48)
Automatic induction soldering, 19: 21765 (SC-DR-65-74)
Bonding to metallic films and solid-state devices, 19: 20520 (SC-DC-65-1256)
Close in tracking error in interferometer tracking systems, 19: 21767 (SC-TM-65-44)
Constructing low-relief earth-fill dams using nuclear explosives, 19: 20090 (SC-RR-65-41)
Design for molded plastic potting shells, 19: 21764 (SC-DR-64-2135)
Environmental testing of RFD-2 re-entry vehicle, 19: 21763 (SC-DR-64-1741)
Indium adhesion test for surface cleanliness, 19: 20205 (SC-TM-64-1722)
Materials tests for hypersonic plasma generator, 19: 20905 (SC-RR-65-54)
Sweep-frequency multipoint calibrator for frequency-measuring devices, 19: 21766 (SC-TM-64-921)
SANDIA CORP., LIVERMORE, CALIF.
Transistorized, 25-ampere constant-current battery discharger, 19: 20280 (SCL-DR-64-128)
SIERRA NEVADA CORP., RENO.
Long-range balloon tracking, 19: 21769 (TID-21661)
SOUTHERN RESEARCH INST., BIRMINGHAM, ALA.
Prog. rpt. on properties of TZM Mo alloy and W, 5–8/64, 19: 20542 (AD-606310)
SOUTHWEST RESEARCH INST., SAN ANTONIO, TEX.
Low-level radioactive waste containers in accident environment, 19: 20196 (CONF-650103-6)
SPACE TECHNOLOGY LABS., INC., LOS ANGELES, CALIF.
Uranium–carbon nuclear reactor rocket systems, 19: 21715 (AD-605574)
STANFORD UNIV., CALIF. DEPT. OF MATERIALS SCIENCE.
Dislocation structure at Luders fronts in Ta, 19: 20562 (SU-DMS-65-1)
STANFORD UNIV., CALIF. NUCLEAR TECHNOLOGY LAB.
Effect of large temperature gradients on turbulent flow of gases in thermal entrance region of tubes, 19: 20117 (SU-247-4)
STATE UNIV. OF NEW YORK, SYRACUSE. COLL. OF FORESTRY.
Rates of hydrogen abstraction from various substrates by free radicals. I and II., 19: 21760 (NYO-2728-4)
SWIFT AND CO., CHICAGO, ILL. RESEARCH LABS.
Ready-to-eat ration-type beef items, 19: 20406 (NP-14928)
SYLVANIA-CORNING NUCLEAR CORP., BAYSIDE, N. Y.
Oxidation testing of coated Nb alloy fuel elements, 19: 20482 (SCNC-314)
Oxidation-resistant coatings for Nb alloys, 19: 20483 (SCNC-318)
Preparation and properties of $CbAl_3$ and $CbAl_3$-fuel bodies, 19: 20464 (SCNC-316)

T

TECHNICAL INFORMATION SERVICE, NATIONAL RESEARCH COUNCIL, OTTAWA (ONTARIO).
Beryllium–copper molds, 19: 20519 (NP-14879)
TEXAS AGRICULTURAL AND MECHANICAL UNIV., COLLEGE STATION. ACTIVATION ANALYSIS RESEARCH LAB.
Activation analysis as applied to petroleum exploration industry, 19: 19773 (TID-20467)
TEXAS ENGINEERING EXPERIMENT STATION, COLLEGE STATION.
Application of linear estimation to chemical mixture problem, 19: 19769 (TEES-2671-4(Chap.7))
Communication theory in neutron activation analysis, 19: 19766 (TEES-2671-4(Chap.3))
Detector research, 19: 19767 (TEES-2671-4(Chap.4))
Mark II automatic computer-coupled activation analysis system, 19: 19765 (TEES-2671-4(Chap.2))
Neutron activation analysis, 19: 19764 (TEES-2671-4(Chap.1))
Prog. rpt. on automated activation analysis, annual, 1964, 19: 19763 (TEES-2671-4)
Program for digital computer analysis of pulse-height spectra, 19: 19770 (TEES-2671-4(Chap.8))
Public benefit demonstrations using nuclear activation analysis, 19: 19771 (TEES-2671-4(Chap.9))
Sodium separation, 19: 19768 (TEES-2671-4(Chap.6))
THOMAS A. EDISON RESEARCH LAB., WEST ORANGE, N. J.
Nuclear-resistant transmitter, 19: 20400 (NP-14955)
TRW SPACE TECHNOLOGY LABS., THOMPSON RAMO WOOLDRIDGE INC., REDONDO BEACH, CALIF.
Radioisotope space propulsion systems, 19: 20428 (TID-7698(Pt.I) (p.257-76))
TUNG-SOL ELECTRIC INC., BLOOMFIELD, N. J. ELECTRON TUBE DIV.
Prog. rpt. on radiation-resistant electron tubes, 10–11/64, 19: 20399 (NP-14946)

U

UNION CARBIDE RESEARCH INST., TARRYTOWN, N. Y.
Determination of B in refractory borides, 19: 19761 (NP-14876)
UNITED AIRCRAFT CORP., EAST HARTFORD, CONN. RESEARCH LABS.
Prog. rpt. on collision probability of electrons and ions with alkali metal atoms, 4/22–10/21/64, 19: 20805 (NASA-CR-54223)
UNITED ELECTRODYNAMICS, INC., ALEXANDRIA, VA. EARTH SCIENCES DIV.
Prog. rpt. on seismic research, semiannual, 4–9/64, 19: 20172 (NP-14877)
UNITED STATES–EURATOM JOINT RESEARCH AND DEVELOPMENT PROGRAM.
Prog. rpt. on fuel of UC particles in U matrix, 8/62, 19: 20511 (NCSC-2981-1)
Prog. rpt. on fuel of UC particles in U matrix, 12/62, 19: 20512 (NCSC-2981-2)
Prog. rpt. on fuel of UC particles in U matrix, 2/63, 19: 20513 (NCSC-2981-3)
Prog. rpt. on fuel of UC particles in U matrix, 9/63, 19: 20514 (NCSC-2981-5)
Prog. rpt. on fuel of UC particles in U matrix, 12/63, 19: 20515 (NCSC-2981-6)
Prog. rpt. on fuel UC particles in U matrix, 3/64, 19: 20516 (NCSC-2981-7)
Prog. rpt. on fuel of UC particles in U matrix, 6/64, 19: 20517 (NCSC-2981-8)
Prog. rpt. on stainless steel cladding of steels, 7–9/64, 19: 20504 (EURAEC-1228)
Prog. rpt. on tests on super ELSO Ni–Cr Steel, 9–12/64, 19: 20549 (EURAEC-1282)
Prog. rpt. on U interstitial phases, 3/64, 19: 20510 (NCSC-2663-16)
UNITED STATES STEEL CORP., MONROEVILLE, PA. APPLIED RESEARCH LAB.
Factors affecting notch toughness of maraging steels, 19: 20541 (AD-604868)
UNITED STATES STEEL CORP., MONROEVILLE, PA. RESEARCH CENTER.
Application of high-voltage electron microscopy in metallurgical research, 19: 20548 (CONF-640204(p.35-43))
UNIVERSITA COMMERCIALE LUIGI BOCCONI, MILAN (ITALY).
Distribution law of product of random variables according to new composition law, 19: 20440 (EUR-2251.i)
UPPSALA UNIV., (SWEDEN). INST. OF PHYSICS.
Twin-channel instability in toroidal plasma at B_z field reversal, 19: 21467 (ARL-63-203)
USTAV JADERNEHO VYZKUMU, CESKOSLOVENSKA AKADEMIE VED, REZ (CZECHOSLOVAKIA).
Extraction of U from ores, 19: 20053 (UJV-1202/64)

V

VANDERBILT UNIV., NASHVILLE, TENN.
Measuring range of low-energy charged particles in conducting solids, 19: 20806 (ORNL-3702)
VIRGINIA UNIV., CHARLOTTESVILLE. RADIOBIOLOGY AND BIOPHYSICS LAB.
Radiation dose rate dependence of DNA synthesis, 19: 19506 (TID-21703)

W

WASHINGTON UNIV., SEATTLE.
Comparison of some approximations for self-bound many-fermion systems, 19: 20936 (TID-20558)
WEATHER BUREAU RESEARCH STATION, LOS VEGAS, NEV.
Long-range balloon tracking, 19: 21769 (TID-21661)
WESTINGHOUSE ELECTRIC CORP., BLAIRSVILLE, PA.
Primary working of refractory metals, 19: 20500 (AFML-TR-64-387)
WESTINGHOUSE ELECTRIC CORP., BLOOMFIELD, N. J. LAMP DIV.
Physical metallurgy of W and W-base alloys, 19: 20565 (WADD-TR-60-37(Pt.V))
WESTINGHOUSE ELECTRIC CORP., PITTSBURGH, PA. ATOMIC POWER DIV.
Effects of chemical shim environments on wear of reactor materials, 19: 21606 (WCAP-3269-9)
WISCONSIN UNIV., MADISON.
Supervoltage electron microscopy outside U. S., 19: 20248 (CONF-640204(p.17-19))

Y

YALE UNIV., NEW HAVEN.
Prog. rpt. on nucleon-nucleon interactions, annual, 2/65, 19: 20937 (TID-21672)

PERSONAL AUTHOR INDEX

Each entry after an author's name is a shortened version of the title of the report or article, followed by the *NSA* volume and abstract number. Report numbers are given in parentheses.

The phrase "Progress report" is abbreviated as "Prog. rpt.," permitting a more rapid and complete alphabetical arrangement of the titles without changing the location of the progress report titles in relation to the other titles.

Because of problems involving the mechanical preparation of this index, all accent marks are omitted. The following changes in spelling have been introduced to reduce some of the confusion which might result from omitting the accents:

ä	becomes	ae
ö		oe
ø		oe
ü		ue (except in transliterated Chinese names)

A

AALTO, Erkki J., Neutron fluxes in laminated Fe and heavy water, 19: 21210

AAMODT, R., Kinetic theory of plasma and electromagnetic fields, 19: 21493

ABBOTT, R. P., OCTOPUS/6600 users' manual, 19: 20443 (UCRL-12256)

ABELES, B., Tunneling in superconducting diodes, 19: 21178

ABELN, Olof, Calculation of neutron flux, 19: 21655

ABIL'DAEV, A. Kh., Gamma-gamma coincidence with energy analysis of coinciding radiations, 19: 20342

ABRAHAM, B. W., Approach to stability of a plasma, 19: 21509

ABRAMENKOV, A. D., Neutron and γ radiation between current pulses of 70-Mev accelerator, 19: 20749

ABRAMOV, V. A., Argon–Cs plasma in an electric field, 19: 21556

ABRAMOV, V. A., Radiation of Cs plasma, 19: 21505

ABRASHKIN, S., Preparation of I-131 from irradiated U oxide, 19: 20029

ABROSIMOV, A. T., Complex installation for study of extensive air showers, 19: 20347

ABROSIMOV, A. T., Primary cosmic radiation of superhigh energy, 19: 20884

ACCARY, Andre, Variations of U parameter with changes in C content, 19: 20547 (CEA-R-2731)

ACKER, H. L., Analysis of muonic x-ray spectra, 19: 21344

ACKERMANN, R. J., Pressure of U over U–UO_2 system, 19: 19890

ADAM, Jean, Stability of plasmas obtained in EPPE, 19: 21469 (CEA-R-2713)

ADAM, N. V., Western drift of the geomagnetic field, 19: 21131

ADAMIC, K., ESR study of irradiated anhydrous maltose, 19: 19994

ADAMS, F., Neutron-activation analysis of Cu in Pb, 19: 19815

ADAMS, G. E., Spectroscopic studies of reactions of OH radical in aqueous solutions, 19: 20009

ADAMS, G. W., Electron densities in lower ionosphere due to solar cosmic rays, 19: 21145

ADAMS, J. M., Low threshold neutron detector, 19: 20355

ADAMS, P. G., Prog. rpt. on properties of TZM Mo alloy and W, 5–8/64, 19: 20542 (AD-606310)

ADAMS, R. K., Smoothed thermocouple tables, Pt vs. Pt–10% Rh, 19: 20263 (ORNL-3649(Vol.2)(Sect.2.1))

ADAMS, R. K., Smoothed thermocouple tables, Pt vs. Pt–13% Rh, 19: 20264 (ORNL-3649(Vol.2)(Sect.2.2))

ADAMS, R. K., Smoothed thermocouple tables, chromel–alumel, 19: 20265 (ORNL-3649(Vol.2)(Sect.2.3))

ADAMS, R. K., Smoothed thermocouple tables, Fe–constantan, 19: 20266 (ORNL-3649(Vol.2)(Sect.2.4))

ADAMS, R. K., Smoothed thermocouple tables, Cu–constantan, 19: 20267 (ORNL-3649(Vol.2)(Sect.2.5))

ADAMS, R. K., Smoothed thermocouple tables, chromel–constantan, 19: 20268 (ORNL-3649(Vol.2)(Sect.2.6))

ADAMS, R. K., Smoothed thermocouple tables, W vs. W–26% Re, 19: 20269 (ORNL-3649(Vol.2)(Sect.2.7))

ADAMS, R. K., Smoothed thermocouple tables, W–5% Re vs. W–26% Re, 19: 20270 (ORNL-3649(Vol.2)(Sect.2.8))

ADAMS, R. K., Smoothed thermocouple tables, W–3% Re vs. W–25% Re, 19: 20271 (ORNL-3649(Vol.2)(Sect.2.9))

ADAMS, R. K., Smoothed thermocouple tables, Au–2.1% Co vs. Cu cryogenic, 19: 20272 (ORNL-3649(Vol.2)(Sect.2.10))

ADAMS, R. K., Smoothed thermocouple tables, constantan–Cu cryogenic, 19: 20273 (ORNL-3649(Vol.2)(Sect.2.11))

ADAMS, R. K., Smoothed thermocouple tables, alumel–chromel cryogenic, 19: 20274 (ORNL-3649(Vol.2)(Sect.2.12))

ADAMS, R. K., Smoothed thermocouple tables, constantan (JN)–Fe (JP) cryogenic, 19: 20275 (ORNL-3649(Vol.2)(Sect.2.13))

ADAMS, R. K., Smoothed thermocouple tables, constantan (YN)–Fe (YP) cryogenic, 19: 20276 (ORNL-3649(Vol.2)(Sect.2.14))

ADAMSON, Martyn G., Crystal structure of Cs aquopentachlororuthenate, 19: 19845 (UCRL-11828(p.146))

ADDA, Yves, Helium precipitation in Al–Li alloy, 19: 20613 (CEA-R-2529)

ADEMOLLO, M., U(6) ⊗ U(6) and nonleptonic decays, 19: 21009

ADLOFF, Jean-Pierre, Rare earths—nuclear chemistry, 19: 19738

AFANASEV, B. P., Cross sections for reactions in which π^+ mesons are absorbed by light nuclei, 19: 21279

AFANAS'EVA, V. I., Energy of a magnetic storm, 19: 21135

AGARBICEANU, I., Color centers produced by electrons in KCl and KBr, 19: 19979

AGATI, G., Histochemical findings in irradiated rat placenta. II., 19: 19557

AHARONI, Y., Effects of Co-60 γ rays on oranges, 19: 20404 (IA-999)

AHLBOM, S., Hollow conductor for plasma, 19: 21562

AHRONS, Richard W., Superconductive memories, 19: 21193

AICHINGER, H., Scattering of 14-Mev neutrons by C-12, Si-28, and O-16, 19: 21441

AILLERET, M. Pierre, Economic integration of nuclear power plants into the systems of production and distribution of electric energy, 19: 21695

AIMONE, V., Histochemical findings in irradiated rat placenta. II., 19: 19557

AITKEN, J. H., Reaction $^{74}Ge(n,\alpha)^{69}Zn$ at 14 Mev, 19: 21325

AITKEN, Th. W., Energy dependence of Cornell thick-walled ionization chamber, 19: 20367

AJDACIC, V., Neutron-neutron scattering length from $^2H(n,d)2n$ reaction, 19: 21404

AJDACIC, V., Reactions $H^3(n,p)3n$ and $H^3(n,H^4)\gamma$ at E_n = 14.4 Mev, 19: 21405

AKASOFU, S.-I., Dynamics of the aurora. II., 19: 21142

AKASOFU, S.-I., Dynamics of the aurora. III., 19: 21143

AKATSUKA, Syunichi, Brain injuries resulting from radiotherapy for eye tumors, 19: 19701

AKERS, L. K., Cobalt molybdate catalyst for synthesis of benzene for liquid scintillation radiocarbon dating, 19: 19944 (ORINS-50)

AKHTAR, Sayeed, Separation and analysis of H by adsorption and gas chromatography, 19: 20435

AKIMOVA, M. K., Tables of Coulomb wave functions, 19: 21117

AKOBJANOFF, Lev, Optical cross sections and quantum-kinetic depths, 19: 20667

AKS, Stanley O., Proof that scattering implies production in quantum field

theory, 19: 20961
AKSENOVA, A. S., Effectiveness of preventive tetanus vaccination in monkeys after prolonged irradiation, 19: 19608
AKUTSU, Sumiyoshi, Brain injuries resulting from radiotherapy for eye tumors, 19: 19701
AKYEAMPONG, D. A., Scalar behavior of vector electrodynamics at high energy, 19: 20929 (ICTP-64/12)
ALANIYA, M. V., Influence of magnetic storms on cosmic rays, 19: 20888
ALBERT, C., Kidney homografts, 19: 19519
ALBINSSON, H., New levels in V-47, 19: 21374
ALBOLD, E., Measurement of isomeric splitting ratios by activation, 19: 21237 (KFK-265)
ALBOUY, G., Calculation of nucleon-α cascades, 19: 21372
ALBRIGHT, C. H., Test of SU(6) predictions in weak N* production, 19: 20996
ALCARAS, J. A. Castilho, Basis for irreducible representations of rotation groups, 19: 20967
ALCOCK, C. B., Solubility of O in liquid metals, 19: 19918
ALEKSANDROV, A. F., Impedance of plane capacitor filled with plasma. I., 19: 20301
ALEKSANDROV, N. N., Direct measuring of air β activity, 19: 20169
ALEVIZOU, V., Photoscanning of spleen, 19: 19725
ALEXANDER, J. L., Program for digital computer analysis of pulse-height spectra, 19: 19770 (TEES-2671-4(Chap.8))
ALI, S. M., Titration of Be in glacial acetic acid, 19: 19803
ALIKHANOVA, Z. M., Infrared spectra of uranyl compounds with hydroxy acids, 19: 19911
ALLAN, D. L., Analogs of excited states in Sn isotopes, 19: 21341
ALLEN, E. A., Complex compounds of quadrivalent and tervalent Mo, 19: 19892
ALLEN, Earl W., Uranium–carbon nuclear reactor rocket systems, 19: 21715 (AD-605574)
ALLEN, J. E., Interactions in flight of low-energy K^- mesons with emulsion nuclei, 19: 21365
ALLEN, R. A., Measurements of continua of N, O, and air, 19: 20676
ALLEN, R. A., Standardization of electron capture nuclides, 19: 20384
ALLENDEN, D., Surveillance monitor for U and Pu in atmosphere, 19: 20381
ALTARELLI, G., U(6) ⊗ U(6) and nonleptonic decays, 19: 21009
ALTERTHUM, Hans, Determining melting point of refractory metals, 19: 20566 (IS-Trans-13)
ALTVATER, W., Trapping of dust by foils, 19: 20236
ALUKER, E. D., Radioluminescence of some Tl-activated alkali halides, 19: 19966
ALVAREZ, F., Kidney homografts, 19: 19519
ALVAREZ, F., Modification of immunologic tolerance with transplantation of allogenic hematopoietic cells, 19: 19493
ALVAREZ BARTOLOME, M. L., Use of EDTA in quantitative analysis. III., 19: 19779
AMATO, I., Fission-gas retention ability of UO_2 pellets, 19: 20633
AMBEGAOKAR, V., Green's functions in many-body problem, 19: 20715
AMBEGAOKAR, V., Lectures on astrophysics and the many-body problem. II., 19: 20714
AMBLER, E., Carrier concentration in semiconducting $SrTiO_3$, 19: 21170
AMELINCKX, S., Electron microscope studies of precipitates, 19: 20603
AMIEL, S., Criterion for selectivity in recoil labeling, 19: 20020 (IA-907)
AMIEL, S., Radioactive analysis of Mn, 19: 19806
AMPELOGOVA, N. I., Complexing of Po with chloride ions, 19: 19906
AMPELOGOVA, N. I., Hydrolysis of Po in perchloric acids, 19: 19905
AMUNDSON, Paul I., Fission ratios in ZPR-III critical assemblies, 19: 21227 (ANL-6941)
ANAKHARA, R., Subcritical reactor with graphite moderator, 19: 21646
ANDERS, Edward, Cosmic-ray exposure ages of Fe meteorites, 19: 20760
ANDERSEN, H. H., Non-binary atomic collisions in crystals, 19: 20686
ANDERSEN, S. L., Energy levels in S-32 from reaction $^{31}P(p,\gamma)^{32}S$, 19: 21380
ANDERSEN, W. H., Energy source for ball lightning, 19: 21150
ANDERSON, Jared A., CP-nonconserving decay $K_1^0 \to \pi^+ + \pi^- + \pi^0$, 19: 21020
ANDERSON, P. W., A-c Josephson effect in superfluid He, 19: 21172
ANDERSON, R. E., Geologic map and sections of Thirsty Canyon, Nye County, Nevada, 19: 20150 (TEI-859)
ANDERSON, R. K., Energies of n-nucleon systems by Bopp's approximation, 19: 21412
ANDERSON, Robert E., Autopsy study of leukemia in Hiroshima, 19: 19526
ANDERSON, Thure, Sweeping-image mirror camera, 19: 21784
ANDO, Yoshio, Bonding methods for graphite materials, 19: 20505 (JAERI-1071)
ANDRADE E SILVA, J., Nonlinear phase resonances in high-energy synchrotron, 19: 20745
ANDRE, Michaudon, Interaction of slow neutrons with U-235, 19: 21230 (CEA-R-2552)
ANDREEV, S. I., Ultrahigh frequency investigation of plasma deionization at atmospheric pressure, 19: 21572
ANDRIANOVA, L. A., Effect of radiation on neurosecretion of nuclei in hypothalamic area, 19: 19509 (JPRS-29250(p.9-13))
ANGELEIKO, V. V., Sound waves in weakly ionized plasma, 19: 21561
ANGERSTEIN, Wilfried, Dosage reduction in x-ray diagnosis, 19: 20229
ANOKHINA, I. N., Radiation effects on thermal properties of alkali-halide crystals, 19: 19986
ANTOLIN, Jacqueline, Helium precipitation in Al–Li alloy, 19: 20613 (CEA-R-2529)
ANTON'EVA, N. M., Decay of Rh-100, 19: 21278
ANTON'EVA, N. M., Decay of Pd-101, Rh-101*, and Rh-101, 19: 21280
AOKI, Shigebumi, Turbulent heat transfer in pipe, 19: 20118
ARAI, Eiichi, Studies on natural U–H_2O exponential pile. II., 19: 21645
ARAKAWA, E. T., Measuring range of low-energy charged particles in conducting solids, 19: 20806 (ORNL-3702)
ARD, W. B., Properties of high-β plasma, 19: 21531
ARENS, Richard, Wave mechanization of dynamical systems, 19: 21087
ARMBRUSTER, P., Measurement of gas concentration in methane, 19: 20376
ARMSTRONG, B. H., Atomic line contribution to radiation absorption coefficient of air, 19: 20831
ARMSTRONG, B. H., Photoionization contribution to radiation absorption coefficient of air, 19: 20830
ARMSTRONG, DALE D., Reaction (He^3,d) on N = 28 nuclei, 19: 21240 (LA-DC-6232)
ARMSTRONG, Lloyd, Jr., Magnetic moments of Re-186 and Re-188, 19: 21383
ARNOLD, E. D., Shielding requirements and radiation characteristics of isotopic power sources, 19: 21595 (TID-7698(Pt.I)(p.33-248))
ARONIN, L. R., Effects of purification and realloying on mechanical properties of zone-refined Be single crystals, 19: 20557 (NMI-TJ-60)
ARONIN, L. R., Hot extrusion of metal powders, 19: 20518 (NMI-TJ-29)
ARRIBAS JIMENO, S., Use of EDTA in quantitative analysis. III., 19: 19779
ARTEMENKO, I. A., Characteristics of superconducting films of Pb and In, 19: 21189
ARTHURS, J. V., Oxidation of Zr in high-pressure steam, 19: 20492
ASARO, F., Decay scheme of Es-254, 19: 21257 (UCRL-11828(p.63-6))
ASAVINEI, Ionca, Measurement of activity of radionuclides by 4π β-γ coincidences, 19: 20385
ASH, M., Xenon minimax problem, 19: 21639 (IA-988)
ASHBEE, K. H. G., Migration of pores in quenched UO_2, 19: 20467
ASHER, R. C., Corrosion in nuclear in nuclear reactors, 19: 20488
ASHERY, D., E2/M1 mixing ratios and K conversion coefficients of some rotational transitions, 19: 21324
ASHIZAWA, Takashi, Solvent extractions of Cs and Fr, 19: 20058
ASHLEY, R. W., Determination of H in Zr alloys, 19: 19831
ASHLEY, William H., Gravimetric determination of H in Mo metal, 19: 19758 (LA-3225)
ASPERGER, S., Secondary α-deuterium isotope effects in reaction of 2-phenylethyltrimethylammonium ion by hydroxide ion, 19: 19947
ASPIN, N., Determination of Cu in biological materials, 19: 19807
ASTNER, G., Conversion electrons from monocrystalline source, 19: 21339
ATHERTON, D. R., Radium contamination at the Jordan River delta of the Great Salt Lake, 19: 20220
ATKINSON, J., Neutron depolarization effects in precession magnets, 19: 21209
ATNEOSEN, Richard A., X rays emitted in coincidence with fission of Cf-252, 19: 21229 (BNL-8841)
ATOJI, M., Generalized Riemann zeta functions and applications in calculations of neutron cross sections, 19: 21228 (ANL-6970)
ATRASHKEVICH, V. B., Complex installation for study of extensive air showers, 19: 20347
ATRASHKEVICH, V. B., Primary cosmic radiation of superhigh energy, 19: 20884
ATZMONY, U., Anomalous isomer shift ratios in Eu-151 and Eu-153, 19: 21337
AUGENSTEIN, Leroy G., Advances in radiation biology. I., 19: 19461
AUGENSTEIN, Leroy G., Ionization and excitation in radiation inactivation of enzymes, 19: 19517
AULD, Harry E., Technique for simulating air-blast-induced ground motions, 19: 20184
AUSMAN, George, Jr., Gamma irradiation of Ge. Impurity effects, 19: 20619 (NP-14883)
AUVIL, P. R., Model for the first nucleon recurrence, 19: 20992
AUXIER, J. A., Technical concept—Operation HENRE, 19: 21199 (CEX-65.02)
AVARBE, R. G., Interaction of NbC with W, 19: 20583
AVILOVA, I. V., Lowering negative ion-electron detachment potential in

plasma, 19: 21558
AWOJOBI, O. A., F layer at sunrise near the magnetic equator, 19: 21138
AYRAPETYANTS, M. G., Higher nervous activity of adult dogs subjected to ionizing radiation in antenatal development, 19: 19536
AYRES, Robert U., Aspects of environment resulting from various kinds of nuclear wars, 19: 20199 (HI-388-RR(Pt.III))
AYSCOUGH, P. B., Elementary processes in radiation- and photo-chemistry, 19: 20002

B

BABARYKIN, V. K., Intensity of cosmic rays in stratosphere, 19: 20876
BABARYKIN, V. K., Latitudinal measurements of cosmic-ray intensities in stratosphere, 19: 20892
BACIU, G., Photoneutron cross sections for Co, Ni, Cu, and Ga, 19: 21305
BACKENSTOSS, G., Analysis of munoic x-ray spectra, 19: 21344
BAEHR, Werner, Method of pre-decontaminating fuel to be reprocessed, 19: 20084
BAER, Robert M., Digital-computer calculation of matrix elements of nuclear interactions, 19: 20938 (UCRL-11828(p.9-10))
BAES, C. F., Jr., Hydrolysis of Th(IV) at 0 and 95°C, 19: 19878
BAES, C. F., Jr., Purification of Be, 19: 20070
BAGGE, E., Neutron chopper for measurement of total cross sections. II., 19: 20331
BAHL, O. P., Evidence of screw dislocations in graphite, 19: 20574
BAHM, Edward L., Modified hoke valve for ultrahigh-vacuum use, 19: 20145
BAHR, G. F., High-voltage electron microscopy, 19: 20253 (CONF-640204(p.106-22))
BAILEY, Harry E., Equilibrium thermodynamic properties of CO_2, 19: 19842 (NASA-SP-3014)
BAILY, W. E., Sodium logging in fast ceramic reactor fuels, 19: 20458 (GEAP-4283)
BAKER, D. A., Penetration of plasma stream into transverse magnetic field, 19: 21475 (LA-DC-6383)
BAKER, N., Theoretical models for the pulsations of cepheids, 19: 20799
BAKH, N. A., Properties of irradiated and heat-treated polyethylene, 19: 20017
BAKLANOVSKII, E. D., Complexing of uranyl with salicylic acid. II., 19: 19904
BALAKHANOV, V. Ya., Multiple beam radiointerferometer for plasma diagnostics, 19: 21574
BALANDIN, A. A., Effect of S-35 radiation on dehydration of cyclohexanol, 19: 20013
BALDWIN, G. C., Nuclear superradiance in solids, 19: 21407
BALINT, Andor, Cytological and physiological investigation of maize lines treated with irradiation, 19: 19527
BALL, J. B., Energies and character of low-lying levels in Nb-94, 19: 21330
BALLESTRACCI, R., Crystallographic study of sulfides of rare earths and of Na, 19: 19862
BALTENSPERGER, W., Susceptibility of liquid Gd, 19: 20598
BALTHESEN, E., Magnetic after-effects in Ni after irradiation with neutrons, 19: 20647
BALTHESEN, E., Magnetic after-effects in Fe after irradiation with neutrons, 19: 20648
BAMBERGER, C. E. L., Purification of Be, 19: 20070
BAN, Z., Crystal structure of ternary silicides ThM_2Si_2, 19: 20568
BAN, Z., Ternary silicides containing U and transition metals, 19: 19871
BANDER, M., Three-nucleon problem with separable potentials, 19: 20986
BANERJEE, B., Treatment of neutron-proton pairing correlations, 19: 21381
BANTER, J. C., Thickness of oxide films on anodized Zr, 19: 20489
BAPTISTA, A. M., Localization of iodine in stomach, 19: 19717
BARANOV, B. N., Correlation potentials of rectilinear statistical systems, 19: 20687
BARANY, Janos, Protecting children against radiation injury in pelvic x-ray examinations, 19: 19677
BARBEE, Troy W., Jr., Dislocation structure at Luders fronts in Ta, 19: 20562 (SU-DMS-65-1)
BARBIELLINI, G., Reaction $\gamma + p \rightarrow p + \pi^0$ near first resonance from polarized photons, 19: 20932 (LNF-64/60)
BARDASIS, A., Possibility of long-range spin polarization in a degenerate electron gas, 19: 20689
BARDON, Marcel, Momentum spectrum of positrons from muon decay, 19: 21012
BARENBOIM, G. M., Interaction of excited biomolecules with O. II., 19: 19970
BARKALAYA, A. A., Impurity photoconductivity produced in Ge by γ irradiation, 19: 20623
BARKAS, Walter H., Artificial construction of particle tracks by Monte Carlo method, 19: 20325 (UCRL-11624)
BARKER, J. A., Semiclassical scattering, 19: 20956
BARNARD, E., Low threshold neutron detector, 19: 20355
BARNARD, E., Measurement of differential neutron scattering cross sections, 19: 21298
BARNES, Harold, Oceanography and marine biology. II., 19: 19467
BARNETT, C. F., Cross-section measurements, 19: 21484 (ORNL-3760(p.57-63))
BARRINGTON, A. E., Helium memory effects observed with tandem mass spectrometer, 19: 20146
BARTEL, Lewis C., Energy levels in hydrated Tm ethylsulfate, 19: 21600 (IS-968)
BARTHOUX, A., Detection of critical accidents at Commissariat a l'Energie Atomique, 19: 20330 (AEC-tr-6547)
Bartolome, M. L. Alvarez
see Alvarez Bartolome, M. L.
BARTON, Harry L., Splenic transplantation in the dog, 19: 19521
BARTRUM, P. C., Rotation in general relativity, 19: 21109
BARUCCHI, G., Effect of elastic unitarity on reactions $d(n,\gamma)^3H$ and $d(p,\gamma)^3He$, 19: 21371
BARUT, A. O., Dynamical groups and mass formula, 19: 20923 (IC/65/18)
BARUT, A. O., Production amplitudes. I and II, 19: 20925 (ICTP-64/3)
BARUT, Asim O., Mass difference of Ξ^- and Ξ^0, 19: 20917 (IC/65/3)
BARYSHEVSKII, V. G., "Beating" of nuclear radiation due to particle flux of variable intensity, 19: 21235 (JINR-P-1950)
BASCO, J., Isomeric cross-section ratio in $^{79}Br(n,\gamma)^{80,80m}Br$ reactions, 19: 21331
BASIAGO, R., Nuclear-resistant transmitter, 19: 20400 (NP-14955)
BASILOVA, R. I., Cosmic rays at high altitudes, 19: 20895
BASKIN, Y., Determination of Th and P in Th phosphides, 19: 19740 (ANL-7005)
BASSE, R., Improved pulse shape discriminator, 19: 20370
BASSEL, R. H., Reaction $^{63}Cu(d,^3He)^{62}Ni$, 19: 21358
BASSENGE, E., Measurement of coronary circulation with new isotope technique, 19: 19668
BASTIN, E. W., Brouwer-type space for particles as distinction systems, 19: 21078 (AFOSR-64-1380)
BASU, J., Transmission properties of a stratified plasma, 19: 21506
BATES, D. R., Asymptotic form of electron capture cross sections, 19: 21417
BATES, D. R., Recombination of positive ions and electrons in dense neutral gas, 19: 20860
BATES, J. L., Thermal conductivity of UO_2, 19: 20615 (HW-SA-3212)
BATSANOV, S. S., Optical properties of rare earth oxides. II., 19: 19928
BAUER, A. W., Electromagnetic testing of thin-wall, refractory metal tubing, 19: 20454 (CONF-650212-1)
BAUER, Franz K., Salivary secretion of Cs-131, 19: 19486
BAUER, U., Detection of liver metastases following rectal administration of I-131, 19: 19662
BAUMANN, G., Interactions of 3.0-Bev/c K⁻ mesons with nuclei, 19: 21389
BAXTER, R. C., Retention of Sr-90 by fetal and newborn rats, 19: 19473 (UR-661)
BAXTER, R. G., Topside electron density in the F2 region, 19: 21141
BAXTER, R. J., One-dimensional gases with hard-core repulsion, 19: 20682
BAYARD, Jean-Paul, Specifications for multi-group scattering code of two dimensions: ALCI, 19: 21197 (CEA-R-2747 & Add.)
BAYAREVICH, V. V., Intensity of cosmic rays in stratosphere, 19: 20876
BAYAREVICH, V. V., Latitudinal measurements of cosmic-ray intensities in stratosphere, 19: 20892
BAYHURST, B. P., Symmetry of neutron-induced Pu-239 fission in resonance region, 19: 21241 (LA-DC-6639)
BEAL, B. T., Spin lattice relaxation time of F-19 in CaF_2 below 1°K, 19: 19897
BEAN, C. H., Drawing apparatus, 19: 21782
BEARD, G. B., Decay of Sn-121m and Mössbauer absorption in Sb-121, 19: 21375
BEAVER, W. W., Corrosion and protection of Be, 19: 20495
BEAVER, W. W., Mechanical characteristics of zone-leveled Be, 19: 20544 (AFML-TR-64-388)
BECCHINI, M. F., Radioiodinated (^{125}I and ^{131}I) fibrinogen for detection of malignant tumors, 19: 19716
BECHDOLFF, A., Interactions of 3.0-Bev/c K⁻ mesons with nuclei, 19: 21389
BECKER, J. H., Carrier concentration in semiconducting $SrTiO_3$, 19: 21170
BECKER, L. C., Determination of neutron reduced widths by the $^{14}N(^{14}N,^{13}N)^{15}N$ reaction, 19: 21387
BECKER, M., Variational synthesis with discontinuous trial functions, 19: 21638 (CONF-650501-4)
BECKER, M. C., Properties of high-β plasma, 19: 21531
BECKER, Martin, Spatial dependence of pulsed-neutron reactivity measurements, 19: 21637 (CONF-650406-2)
BECKERS, J., Ultrarelativistic limit of theory of free vector mesons,

19: 20947
BECKNER, Everet H., Heating in collision of polarized plasmas, 19: 21537
BEER, Michael, Biological applications of electron microscopy, 19: 19455 (CONF-640204(p.44-62))
BEERNTSEN, D. J., Superconductivity in Nb–Se system, 19: 21195
BEETS, C., Spectrometry of fast neutrons by surface barrier junctions and Li-6, 19: 20334
BEG, M. A. B., Covariance, SU(6), and unitarity, 19: 21022
BEHOF, A. F., Neutrons from $^{9}Be(\alpha,n_0)^{12}C$ and $^{9}Be(\alpha,n_1)^{12m}C$ reactions, 19: 21307
BEHRISCH, Rainer, Sputtering of solids by ion bombardment, 19: 20819
BEIL, Hans, Electron bunching in Saclay linear accelerator, 19: 20721 (CEA-R-2749)
BEKETOV, A. R., Structure of α-UO_3–U_3O_8 region, 19: 19929
BEKETOV, A. R., Structure of gamma UO_3, 19: 19930
BELFORD, T. N., Solubility of O in liquid metals, 19: 19918
BELL, P. R., Multiple-pass experiments (DCX-2), 19: 21481 (ORNL-3760(p.10-22))
BELLMAN, Richard, Invariant imbedding, particle interaction, and conservation relations, 19: 20959
BELLMAN, Richard, Random walk, scattering, and invariant imbedding. I., 19: 20660 (P-1113(RAND))
BELLOCH-ZIMMERMANN, V., Radium-226 in human embryonic tissue, 19: 20216
BELOTE, T. A., Energy levels in Ti-48 and Ti-50, 19: 21346
BELOV, N. V., Structure refinement for $Pr(NO_3)_3 \cdot 6H_2O$, 19: 19914
BELYAEV, V. A., Increase of O assimilation during irradiation, 19: 19584
BELYAEVA, I. F., Complex installation for study of extensive air showers, 19: 20347
BEMELMANS, P., Direct conversion applications of radioisotopic sources, 19: 20904 (BLG-317)
BEMIS, C. E., Jr., Equipment for rapid handling of irradiated solutions, 19: 21741
BEMIS, R. G., Sweep-frequency multipoint calibrator for frequency-measuring devices, 19: 21766 (SC-TM-64-921)
BEN'KOVA, N. P., Western drift of the geomagnetic field, 19: 21131
BENNETT-CORNIEA, Winifred, Radiolysis of poly-α-L-glutamic acid in aqueous solution, 19: 19990
BEN-PORATH, M., Scanning with I-125, 19: 19711
BENVENISTE, M., Influence of impurities on optical properties of irradiated LiF, 19: 19998
BENVENUTI, A., Somatic mutations in potatoes induced by radiation, 19: 19518
BERARD, C. W., Wound healing: effect of ascorbic acid and D_2O, 19: 19484
BERDNIKOVA, A. V., Uranium content in surrounding medium and human elimination, 19: 19490
BERGE, P., Influence of impurities on optical properties of irradiated LiF, 19: 19998
BERGER, J.-A., Measurement of β activities on thin chromatographic layers, 19: 19792
BERGER, M., Exploration of cardiac dynamics with radioactive tracers, 19: 19705
BERGERE, Roland, Electron bunching in Saclay linear accelerator, 19: 20721 (CEA-R-2749)
BERGLUND, S., Twin-channel instability in toroidal plasma at B_z field reversal, 19: 21467 (ARL-63-203)
BERGONZINI, R., Radioprotective power of prochlorperazine, 19: 19631
BERGONZINI, R., Weight changes in albino mice after total-body irradiation, 19: 19632
BERGSTRESSER, K. S., Spectrophotometric determination of Re in Ta–Re alloys, 19: 19757 (LA-3213)
BERGSTRESSER, Paul, Gravimetric determination of H in Mo metal, 19: 19758 (LA-3225)
BERGZHANOV, R. B., Neutron cross sections in In and Sm, 19: 21285
BERKOWITZ, L., Design of Hallam moderator element. II., 19: 21681 (COO-1402-2)
BERMUDEZ POLONIO, J., Determination of Nb, Ta, and U in tantalite–columbite ores, 19: 19754 (JEN-134-DQ/I-39)
BERNAS, R., Intranuclear cascade and breakup calculations on production of Li, Be, and B isotopes in C-12 by 156-Mev protons, 19: 21402
BERNAS, R., Lithium-6 and Li-7 production in C-12 and O-16 by high-energy protons, 19: 21352
BERNHARD, Michael, The atom fishers, 19: 19469
BERNSTEIN, Richard B., Atomic-beam scattering studies on Li–Hg system, 19: 20823
BERSIN, Richard L., Radiometric sensing of atomic H in trace quantities, 19: 19825
BERSTROEM, I., Conversion electrons from monocrystalline source, 19: 21339
BERTAUT, E.-F., Crystallographic study of sulfides of rare earths and of Na, 19: 19862
BERTEIG, L., Exposure to radiation from medical procedures, 19: 19597
BERTSCH, G. F., Lumped delay line spark chamber, 19: 20372
BERZIN, A. K., Angular distribution of photoneutrons from Ta-181 and Bi-209, 19: 21288
BERZIN, A. K., Connection between width of giant resonance of (γ,n) reaction and filling of energy levels of the nucleus, 19: 21287
BESSENT, R. G., Paramagnetic resonance of H in CaF_2 and KCl, 19: 19896
BESSIS, D., Double spectral function in potential scattering, 19: 21093
BETHE, Hans A., Intermediate quantum mechanics, 19: 21115
BETHE, Hans A., The fireball in air, 19: 20675
BETKO, J., Magnetic fields in units of ionic optical system for 5-Bev antiproton channel, 19: 20723 (JINR-P-1945)
BEVEGE, Eleanor E., Detection and estimation of trace elements by d-c arc excitation, 19: 19827
BEZARSHVILI, Sh. M., Aluminothermal reduction of Eu_2O_3, 19: 20533
BEZRUKIKH, V. V., Correlation between variations of magnetic field and positive ions inside magnetosphere, 19: 21126
BHALLA, C. P., Positon shape factor of $^{56}Co(4^+ \rightarrow 4^+)$, 19: 21321
BHATT, K. H., Energies and character of low-lying levels in Nb-94, 19: 21330
BIBERGAL, A. V., Problems of investigation of parameters of powerful γ devices for radiotherapy, 19: 19704
BIBIKOVA, A. F., Biological action of protons of 510-Mev energy in irradiation of dogs, 19: 19578
BIBLE, Roy H., Jr., Interpretation of NMR spectra, 19: 21462
BIELINSKI, Edward, Effect of γ radiation on red blood cells in stored human blood, 19: 19513
BIGI, A., Charge-exchange scattering at high energies for $\pi^- + p \rightarrow \pi^0 + n$, 19: 21006
BILDSTEIN, H., Method of cyclohexane dosimetry, 19: 20341
BILLION, Marc, Preparation of large grains of Zr, 19: 20527
BINFORD, Thomas O., CP-nonconserving decay $K_1^0 \rightarrow \pi^+ + \pi^- + \pi^0$, 19: 21020
BING, R. J., Measurement of coronary circulation with new isotope technique, 19: 19668
BINOPOULOS, D., Photoscanning of spleen, 19: 19725
BIRD, P. M., Film monitoring procedures for radiation workers, 19: 20243
BIRD, P. M., Radiation exposure trends from film monitoring data, 19: 20241
BIRDSALL, C. K., Focusing of electron stream with fields, 19: 20743
BIRKHOFF, R. D., Diffusion pump oil deposition measurements, 19: 20143
BIRKHOFF, R. D., Measuring range of low-energy charged particles in conducting solids, 19: 20806 (ORNL-3702)
BIRKLE, A. J., Factors affecting notch toughness of maraging steels, 19: 20541 (AD-604868)
BISHOP, G. R., 6.02-Mev level of B-10, 19: 21306
BISSELL, Eugene R., Preparation and properties of fluorocarbon alcohol 3,5-dinitrobenzoates, 19: 21775 (UCRL-12307)
BITYUKOV, V. D., Properties of irradiated and heat-treated polyethylene, 19: 20017
BLACKETT, N. M., Recovery in erythropoiesis and erythropoietic capacity following whole-body irradiation, 19: 19644
BLANC, G., Influence of impurities on optical properties of irradiated LiF, 19: 19998
BLANK, H., Electron microscope studies of precipitates, 19: 20603
BLANKENBECLER, R., Tests of relativistic SU(6) schemes, 19: 21025
BLATCHLEY, Donald Errol, Alpha–γ angular correlation studies, 19: 21457
BLAU, M., Pancreas scanning with ^{75}Se-selenomethionine, 19: 19722
BLAUGRUND, A. E., E2/M1 mixing ratios and K conversion coefficients of some rotational transitions, 19: 21324
BLINC, R., ESR study of irradiated anhydrous maltose, 19: 19994
BLIN-STOYLE, R. J., Charge dependence of internucleon potential, 19: 21373
BLIN-STOYLE, R. J., Effective coupling constant G_A in β decay, 19: 21348
BLIN-STOYLE, R. J., ft Values of $0^+ \rightarrow 0^+$, $\Delta T = 0$, β decays: conserved vector current theory, 19: 21416
BLONDEL, A., Industrial applications of radioelements, 19: 20417
BLOXSOM, D. E., Jr., Dissociated and ionized H hypersonic flows, 19: 20124
BLUEMCHEN, G., Measurement of coronary circulation with new isotope technique, 19: 19668
BLUMENSTOCK, David A., Lung transplantation in the dog, 19: 19523
BLUNT, R. F., Irradiation induced color centers in MgF_2, 19: 20618 (NBS-8614)
BOAG, J. W., Spectroscopic studies of reactions of OH radical in aqueous solutions, 19: 20009
BOBOVNIKOVA, Ts. I., Strontium-90 in fresh-water reservoirs in Soviet Union, 1961–62, 19: 20160 (NP-14728)
BOCK, C. D., Feasibility of nuclear gyro, 19: 20279 (RTD-TDR-63-4001)

BODEN, R., Separation of Bk from Ce, 19: 20071
BOEGLY, W. J., Jr., Disposal of high-level power reactor wastes in salt mine, 19: 21751 (ORNL-P-1064)
BOEHM, A., Dynamical groups and mass formula, 19: 20923 (IC/65/18)
BOEHM, A., Problems of symmetry breaking, 19: 20926 (ICTP-64/4)
BOEHM, Arno, Rigged Hilbert spaces, 19: 21081 (ICTP-64/9)
BOEHM, E., Flux converter for irradiation with fast neutrons at FRF, 19: 21742
BOEHM, F., Parity impurity in nuclear γ transition, 19: 21397
BOEMMEL, H. E., Amplitude-dependent ultrasonic attenuation in superconducting Pb, 19: 21169
BOESCH, R., Direct measurement of short nuclear lifetime, 19: 21369
BOESCH, R., Ground state wave function of H-3 and He-3, 19: 21367
BOESSENROTH, Ivo H., Writing topological programs for GUTS, 19: 20320 (IS-989)
BOGOLYUBOV, N. N., Second sound in weakly ideal Bose gas, 19: 20669
BOHR, H. H., Effect of cortisone and anabolic steroids on retention of of Ca-47 and Sr-85 in rats, 19: 19476
BOHUN, A., Luminescence and electronic emission of alkali chlorides with Cu, 19: 19964
BOIKO, V. A., Manganese, Ni, and Cr in experimental radiation sickness in growing animals, 19: 19540
BOISVERT, Gregory L., Sodium pile loop for irradiation of fissionable needle, 19: 21736 (ORNL-tr-539)
BOJAN, N., Determination of U and elements that accompany it. I., 19: 19811
BOKHARI, M. S., Energy and angular details of fast neutron flux in water from pool-type reactor, 19: 21735 (ORNL-P-1092)
BOLLINI, V., Renal scintiscanning with ^{203}Hg–neohydrin, 19: 19721
BOLOGNA, G., Reaction $\gamma + p \rightarrow p + \pi^0$ near first resonance from polarized photons, 19: 20932 (LNF-64/60)
BONAZZOLA, G. C., Photoneutron cross sections for Co, Ni, Cu, and Ga, 19: 21305
BONCH-BRUEVICH, V. L., Effective wave equations in theory of quantum Green's functions, 19: 21056
BONHAM, R. A., Preliminary electron-diffraction study of H_2, 19: 20826
BONILLA, Charles F., Out-of-pile steam-fraction determination, 19: 20294
BOOS, E. G., Coupling coefficients for cosmic components, 19: 20891
BORANIC, M., Counteracting killing effect of foreign cells, 19: 19651
BORBAS, J. R., Nuclear-resistant transmitter, 19: 20400 (NP-14955)
BORCHI, E., Nonleptonic hyperon P waves in Su(6) symmetry, 19: 21021
BORESKOV, G. K., Isotopic exchange of O in γ-Al_2O_3–O_2 system, 19: 19872
BORISENKO, L. F., Scandium separation from pyroxenites, 19: 20081
BORLERA, Maria Lucco, Research on Be–Mn–O and Mg–Mn–O systems, 19: 20573
BOSCH, H. E., K conversion coefficient of 400-Mev transition in decay of Pb-203, 19: 21293
BOSCHITZ, E., Reaction ^{12}C(p,2p)^{11}B at 50 Mev, 19: 21401
BOSCO, B., Effect of elastic unitarity on reactions d(n,γ)^{3}H and d(p,γ)^{3}He, 19: 21371
BOSE, S. K., Relativistic extension of SU(6), 19: 21002
BOSSHARD, Ernst, Replacing fuel elements in nuclear reactor, 19: 21625
BOST, William E., Bibliography on radioactive fallout, 19: 20164 (TID-3086(Suppl. 2))
BOSTICK, W. H., Plasma vortices in coaxial plasma accelerator, 19: 21539
BOTHE, H.-K., Determinations of body water in humans, 19: 19480
BOTT, I. B., Source of millimeter EM radiation, 19: 20684
BOTTGER, Gary Lee, Infrared spectra of solid acetylene, 19: 19935
BOTTS, W. V., Application of SNAP units to Manned Orbiting Research laboratory, 19: 21720 (NAA-SR-10318)
BOUJOT, Jean-Paul, Determination of amounts of nuclides during radioactive transformations. II., 19: 19958 (CEA-R-2348)
BOULIGAND, Georges-Marie, Comparison of cascades with total minimum flux, 19: 19744 (CEA-R-2622)
BOURRET, J., Personnel exposed to x rays in hospitals, 19: 19525
BOVE, Joseph C., Inelastic collision cross sections of Ne and Ar, 19: 20804 (ANL-6938(p.36-45))
BOWEN, M. D., Laminar reacting boundary layers on W, graphite, and pyrolytic B nitride, 19: 20496
BOWER, J. D., Studies of renal homotransplantation in man, 19: 19463
BOWER, J. R., Prog. rpt. on chemical processing, 4–6/64, 19: 20042 (IDO-14646)
BOWERS, Eveline G., Protective actions of AET or serotonin in radiation injury, 19: 19635
BOWHILL, S. A., Relation between dispersion of whistler and electron temperature in protonosphere, 19: 21140
BOWKETT, K. M., Study of fission fragment damage in W, 19: 20643
BOWMAN, H. R., K x rays emitted in spontaneous fission of Cf-252, 19: 21265 (UCRL-11828(p.95-7))
BOWRING, R. W., Stability and burnout tests with H_2O, 19: 20120
BRABERS, M., Electron bombardment in metallurgy, 19: 20466
BRADBURY, S., Amyloidosis in radiation chimeras and its relationship to lymphoid hypoplasia, 19: 19650
BRADLEY, Mildred J., Effect of W on the hydrolysis of UC_2, 19: 19882
BRADSHAW, R. L., Disposal of high-level power reactor wastes in salt mine, 19: 21751 (ORNL-P-1064)
BRAHMAVAR, S. M., Retardations in l-allowed M1 transitions in odd-mass nuclei, 19: 21323
BRAININA, Kh. Z., Determination of Ce in rare earths, 19: 19821
BRAMBILLA, F., Distribution law of product of random variables according to new composition law, 19: 20440 (EUR-2251.i)
BRAMBLETT, Elizabeth Lee, Harmonic analysis Fourier series curve fit, 19: 20442 (NAA-SR-Memo-9729)
BRAMHAM, P., CERN r-f particle separator—first operation, 19: 20748
BRAMMER, H. A., Core II critical assembly analysis for NS *Savannah*, 19: 21716 (GEAP-3514)
BRANDT, F. A., Pressure vessel steel for reactors, 19: 21607 (APED-4773)
BRAUN, H., Interactions of 3.0-Bev/c K$^-$ mesons with nuclei, 19: 21389
BRAY, K. H., Elastic scattering of 5.5- to 10.0-Mev He-3 particles by Al-27, 19: 21328
BRAY, P. J., Prog. rpt. on radiation damage in solids, annual, 5/64–4/65, 19: 20620 (NYO-2024-8)
BRECKENRIDGE, Roger A., Damage to Ge due to proton bombardments, 19: 20617 (NASA-TN-D-2727)
BREEN, R. J., HARMONY—system for nuclear reactor depletion computation, 19: 21644 (WAPD-TM-478)
BREGADZE, I. F., Weakening of irradiation damage by amino acids, 19: 19636
BREHM, J. J., Model for the first nucleon recurrence, 19: 20992
BREIT, Gregory, Prog. rpt. on nucleon-nucleon interactions, annual, 2/65, 19: 20937 (TID-21672)
BREIVOGEL, Francis W., Jr., Molecular beam electric resonance experiments on LiF, LiCl, LiBr, LiI, and NaF, 19: 19848 (UCRL-11828 (p.193-7))
BREIZY, C. E., Prog. rpt. on fast ceramic reactor program, 4–6/64, 19: 21666 (GEAP-4640)
BRENNAN, James T., "Knee" of a fallout decay curve, 19: 20223
BRESEE, J. C., Civil defense research at ORNL, 19: 20202 (ORNL-P-1093)
BRESLER, S. E., Mutagenesis in isolated DNA induced by uv and chemical agents, 19: 19542
BRETHE, Pierre, Measurement of neutron spectra in reflector of light water reactor, 19: 21729 (CEA-R-2442)
BREWER, D. F., Helium-3 at low temperatures, 19: 21184
BREYSSE, Michele, Thorium oxalate precipitation and thermal decomposition, 19: 19861
BRICE, J., Brain-tumor localization, 19: 19714
BRIGGS, N. H., High-temperature thermocouples used in ORNL-GCR program fuel irradiation experiments, 19: 20401 (ORNL-P-1065)
BRIGLIA, D. D., Formation of H$^-$ or D$^-$ by electron impact on H_2, HD, and D_2, 19: 20691
BRIL, Kazimierz J., Pulsed sieve-plate extraction columns. I and II., 19: 20043 (IEA-77)
BRILLOUIN, L., Actual mass of potential energy, 19: 20694
BRINK, D. M., Effect of impurities on superconducting transitions, 19: 21181
BRINK, D. M., Separation energy of strongly bound nucleons, 19: 21400
BRINKMAN, R., Deposition of Ba or Sr in aortic tissue, 19: 19500 (NP-14907)
BRINKMANN, E., Properties of a secondary emission multiplier, 19: 20388
BRISI, Cesare, Research on Be–Mn–O and Mg–Mn–O systems, 19: 20573
BRITT, H. C., Energy-mass distributions of Bi, Au, and W in He-ion-induced fission, 19: 21263 (UCRL-11828(p.90-2))
BRITT, Harold C., Fission of U-238 and Pu-240 nuclei excited by inelastic α-particle scattering, 19: 21262 (UCRL-11828(p.84-6))
BRITTON, C. F., Oxidation of Zr in high-pressure steam, 19: 20492
BROCKETT, G. F., SNAPTRAN 2/10A-3 destructive test, 19: 21717 (IDO-17019)
BROCKETT, R. I., Prog. rpt. on performing in-pile thermal conductance testing, 10–12/64, 19: 21664 (CFND-3336-229)
BROCKHOUSE, B. N., Lattice dynamics of white Sn, 19: 21603
BROCKMEIER, R. T., Properties of low-energy transitions in Dy-161, 19: 21329
BRODIN, M. S., Circular luminescence of Na uranyl acetate crystal, 19: 19921
BRODIN, M. S., Luminescence appearing in Na uranyl acetate irradiated laser beam, 19: 20010
BRODSKII, A. M., Transformations of normal alkanes, 19: 19980
BRODWIN, B., Oxidation-resistant coatings for Nb alloys, 19: 20483 (SCNC-318)
BROEK, H. W., Collective excitations in Zr isotopes, 19: 21386

BROOM, K. M., Decay of Eu-157 and Tm-174, 19: 21272
BROVETTO, P., Odd-even effect in nuclear level density, 19: 21364
BROWN, Alexander Baillie, Improving ductility of Be, 19: 20611
BROWN, D. E., Tables of Coulomb wave functions, 19: 21117
BROWN, D. J., Prog. rpt. on waste disposal, 1–12/64, 19: 21749 (HW-84549)
BROWN, G. E., Collective admixtures in odd-parity states of O-16, 19: 21361
BROWN, James Robert, Devices for detecting radiation, 19: 20392
BROWN, James Robert, Devices for detecting radiation, 19: 20393
BROWN, John B., Liquid metal breeder reactor, 19: 21697
BROWN, Lawrence Edmond, Linear accelerator, 19: 20752
BRUCE, Marshall H., Hydromagnetic wave tube, 19: 21465 (AFCRL-63-779)
BRUGGER, R. M., Slow neutron inelastic scattering from Al powder, 19: 20551 (IDO-17063)
BRUNE, D., Simultaneous determination of 30 trace elements, 19: 19793
BRUSTAD, Tor, Ionization and excitation in radiation inactivation of enzymes, 19: 19517
BRUYERE, Robert, Specifications for scattering code for XY geometry: DAIXY, 19: 21198 (CEA-R-2759)
BRYANT, D. A., Continual acceleration of solar protons in Mev range, 19: 20766
BRYNSVOLD, G. V., Excursion-limiting fuse for critical assembly, 19: 21617
BRYUNFO, M., Effect of radiation on RNA and RNA metabolism in human cancerous tumor cells, 19: 19602
BUCCELLA, F., Nonleptonic hyperon P waves in SU(6) symmetry, 19: 21021
BUCHEL'NIKOVA, N. S., Instability and anomalous diffusion in K plasma, 19: 21569
BUCHTELA, K., Thin-layer chromatography in salts of heteropolyacids, 19: 20069
BUCKINGHAM, J. S., Ion exchange purification of Am-241, 19: 20041 (HW-84352)
BUCKINGHAM, R. A., Thermal conductivity of atomic H from 1 to 400°K, 19: 20700
BUDIN, Ch., Annealings of electric resistivity produced in Cu by quenching and by irradiation. I., 19: 20590
BUDNEY, G. S., Application of SNAP units to Manned Orbiting Research laboratory, 19: 21720 (NAA-SR-10318)
BUDNITSKAYA, E. V., Effect of radiation on RNA and RNA metabolism in human cancerous tumor cells, 19: 19602
BUDY, A. M., Osteolathyrism and inhibition of endosteal bone reaction in estrogen-treated mice by AAN, 19: 19471 (ANL-6938(p.162-78))
BUESSER, F. W., Neutron polarization in T(d,n)^{4}He reaction, 19: 21303
BUETTNER, K., Determinations of body water in humans, 19: 19480
BUFFEREAU, Michel, Improvement of spectrographic analyses, 19: 19743 (CEA-R-2619)
BUIATTI, M., Somatic mutations in potatoes induced by radiation, 19: 19518
BULGAK, V. I., Daily mitotic activity in regenerating liver during acute radiation sickness, 19: 19510 (JPRS-29250(p.27-32))
BULLIS, R. H., Prog. rpt. on collision probability of electrons and ions with alkali metal atoms, 4/22–10/21/64, 19: 20805 (NASA-CR-54223)
BUNSHAH, R. F., Morphological observations after distillation of Be from solid state, 19: 20564 (UCRL-12252)
BUNYAN, P. J., Polarization by Hg of 100- to 2000-ev electrons, 19: 20865
BURBIDGE, E. M., Evolution of stars and galaxies, 19: 20797
BURBIDGE, E. M., Observed abundance anomalies, 19: 20792
BURBIDGE, G., Nuclear astrophysics, 19: 20791
BURBIDGE, G. R., Galactic x-ray sources, 19: 20765
BURDG, C. E., Prog. rpt. on performing in-pile thermal conductance testing, 10–12/64, 19: 21664 (CEND-3336-229)
BUREAU DU COLOMBIER, Marie-Josephe, Specifications for multi-group scattering code of two dimensions: ALCI, 19: 21197 (CEA-R-2747 & Add.)
BURGER, G., Irradiation of U with neutrons at 4.5°K, 19: 20642
BURGESS, A., Tables of hydrogenic photoionization cross sections and recombination coefficients, 19: 20834
BURIKS, Peter, Mechanisms of proton decays, 19: 21271 (KFK-tr-161)
BURKA, J. A., Evaluation of Th-base alloys for high-temperature strength, 19: 20560 (ORNL-3777)
BURLAKOVA, E. V., Erythrograms of rats subjected to action of synthetic radiomimetric embikhin, 19: 19489
BURLEIGH, Richard J., Magnet construction for variable-energy cyclotron, 19: 20753
BURMISTROV, V. R., Gamma-gamma coincidence with energy analysis of coinciding radiations, 19: 20342
BURNETT, Donald S., Fission barrier of Tl-201, 19: 21260 (UCRL-11828 (p.81))
BURRUS, W. R., Comparison of measured neutron and proton spectra with calculated spectra in energy region between 50 and 160 Mev, 19: 21244 (ORNL-P-844)
BUSCH, G., Magnetic properties of the rare earth nitrides, 19: 19895
BUSCH, G., Magnetic properties of ordering rare earth antimonides, 19: 20597
BUSCHOW, K. H. J., Intermediate phases in Sm–Al, 19: 20596
BUSSIERE, André, Octupole states in N-15 and O-16, 19: 21268 (UCRL-11828(p.129-31))
BUTERA, R. A., Prog. rpt. on magneto-thermodynamics of para- and anti-ferromagnets, 6/64–3/65, 19: 21759 (NYO-3402-1)
BUTLER, A. P., Isotopic fractionation of U in sandstone, 19: 20187
BUTLER, H. S., Transverse beam blow-up in standing-wave linac cavity, 19: 20726 (LA-DC-6775)
BUTTERWORTH, J., NMR linewidth in beta Mn, 19: 21366
BUTTREY, K. E., Analysis of SNAPTRAN-3 destructive experiment, 19: 21719 (NAA-SR-9780)
BZHOZOVSKII, V. S., Open-cycle MHD generator, 19: 20912

C

CACCIARI, Alberto, Producing Th oxide–U oxide mixtures, 19: 19942
CAGNARD, Roland, Simultaneous stimulated emission in He-4 and He-3, 19: 20815
CALAIS, Daniel, Chemical diffusion in Pu–U system, 19: 19869
CALAIS, Daniel, X-ray microanalysis—determination of correction factors, 19: 19746 (CEA-R-2728)
CALVIN, Melvin, Chemical evolution, 19: 19946 (UCRL-11950)
CAMPBELL, Alan, Rates of hydrogen abstraction from various substrates by free radicals. I and II., 19: 21760 (NYO-2728-4)
CAMPBELL, B. L., Development of oil-soluble Au-198 compounds, 19: 20030
CAMPBELL, E. M., Isodose charts for Co-60 teletherapy beams, 19: 19733
CANDELORE, N. R., Spatial and energy interference among resonance nuclides, 19: 21643 (WAPD-T-1728)
CANOSA, Jose, Large reactor excursions, 19: 21650
CANOSSI, C., Radioprotective power of prochlorperazine, 19: 19631
CANUTO, V., Odd-even effect in nuclear level density, 19: 21364
CAPPS, Richard H., Σ-Λ mass difference in SU(6)-symmetric bootstrap model, 19: 21014
CARAZZONE, P. F., Histochemical findings in irradiated rat placenta. II., 19: 19557
CARESS, Virginia Bayard Fonda, Reactions of Cu-63 with protons at 60- to 420 Mev, 19: 21458
CARLOS, P., Cascades (γ-γ) in first excited state of Hg-200, 19: 21292
CARLSON, Edward H., Computer program for nuclear magnetic and quadrupole resonance frequencies and intensities, I = ½ to 9, 19: 21246 (TID-21697)
CARLSON, Thomas A., Double electron emission in an Auger process, 19: 20844
CARNAHAN, D. R., Primary working of refractory metals, 19: 20500 (AFML-TR-64-387)
CARNAHAN, Walter Henry, Threshold-type Regge trajectories, 19: 21070
CARR, W. J., Geologic map and sections of Thirsty Canyon, Nye County, Nevada, 19: 20150 (TEI-859)
CARRARA, R., Charge-exchange scattering at high energies for $\pi^- + p \rightarrow \pi^0 + n$, 19: 21006
CARR-HARRIS, G. G. M., Beryllium–copper molds, 19: 20519 (NP-14879)
CARRUTHERS, P., Coherent states and the number-phase uncertainty relation, 19: 21105
CARSON, James E., Stack plume rise determinations as affected by meteorological and engineering factors, 19: 20653 (ANL-6938(p.209-41))
CARTER, G., Deduction of interatomic potential in Al, 19: 20837
CARTER, J. C., SU(6) Clebsch-Gordan coefficients for the product 35 × 56, 19: 21027
CARTER, J. G., Diffusion pump oil deposition measurements, 19: 20143
CARTER, R. A., Problems in establishing radioactive I uptake diagnostic service, 19: 19682
CARVALHO, F., Phonon frequency distribution of V, 19: 20553 (KFK-262)
CASE, Carl T., Reflection and transmission of plane wave normally incident upon semi-infinite anisotropic plasma, 19: 21466 (AFCRL-64-550)
CASEY, D. F., Sodium-heated, modular, steam generators for SCTI, 19: 21611 (NAA-SR-9826)
CASPER, Karl J., Spin of 1821-kev level in Kr-82, 19: 21312
CASPERS, L. M., Neutron temperatures across the interface between H_2O and B, 19: 21207
CASSANDRO, M., Vertex function in spinor-pseudoscalar theory, 19: 21101
CASSEL, David G., Electromagnetic form factor of the π^- meson, 19: 20935 (NP-14885)
CAVALLARO, L., Thermal protection of concrete pressure vessel, 19: 20110 (GAMD-5432)

CECH, J., Disappearance of polar cap on Mars, 19: 20763
CEREBONNET, G., Treatment of uterine fibromas outside pregnancy, 19: 19700
CERINEO, M., Neutron-neutron scattering length from $^{3}H(n,d)2n$ reaction, 19: 21404
CERINEO, M., Reactions $H^{3}(n,p)3n$ and $H^{3}(n,H^{4})\gamma$ at $E_n = 14.4$ Mev, 19: 21405
CERRAI, Enrico, Liquid ion exchangers, 19: 20061
CERULLI, N. Francis, Physical metallurgy of W and W-base alloys, 19: 20565 (WADD-TR-60-37(Pt.V))
CESTER, R., Test of $\Delta S/\Delta Q$ rule in K^{0}_{2} decay, 19: 20979
CHA, Moon H., Photoproduction of W^{+} mesons, 19: 21003
CHA, Moon Hwa, Polarization correlation of Λ and Σ^{0} hyperons, 19: 21071
CHABRE, Marc, Reaction $^{12}C(p,2p)^{11}B$ at 50 Mev, 19: 21401
CHABRILLAC, M., Irradiation of cellulose and cellulose derivatives, 19: 19961 (CEA-tr-A-1741)
CHACKERIAN, Charles, Jr., Infrared absorption spectrum of $^{12}C^{18}O_2$, 19: 19936
CHACKRABURTTY, D. M., Crystal chemistry of higher carbides of Pu, 19: 20570
CHACON, E., B = ⅓ quarks and SU(9) symmetry, 19: 21026
CHADDERTON, L. T., Study of fission fragment damage in W, 19: 20643
CHALLIS, B. C., Hydrogen exchange of azulenes. V., 19: 19883
CHALOT, Andre, First results of tests of Rapsodie block pile, 19: 21730 (CEA-R-2557)
CHAMBERLAIN, G. E., Forward scattering of electrons by He, 19: 20848
CHAMBERLAIN, N. V., Radium contamination at the Jordan River delta of the Great Salt Lake, 19: 20220
CHAMPENEY, D. C., Time dilation experiment based on Mössbauer effect, 19: 20699
CHAN, Y. M., Refractive index of He, 19: 20859
CHANDRAKAR, K., Starting mechanism of first stage of ring discharge, 19: 21554
CHANG, Chun-ting, High-energy scattering and α_q-Regge trajectory, 19: 21063
CHANG, Chun-ting, Principle of maximum analyticity and properties of Regge trajectories, 19: 21061
CHANG, Nai-sen, Absorption of high-energy π^{+}, K^{+} mesons, and protons C, Al, Cu, Sn, and Pb, 19: 21431
CHANG, Ngee-pong, Implications of SU(12) for $\bar{N}N$ annihilation at rest, 19: 21039
CHANNON, F. R., Fast reactor fuel burnup, 19: 21672
CHARAKHCH'YAN, A. N., Calculations of energy spectrum of galactic cosmic rays, 19: 20882
CHARAKHCH'YAN, A. N., Decrease in cosmic-ray intensity in stratosphere, 19: 20877
CHARAKHCH'YAN, A. N., Forbush decreases in intensity of cosmic rays, 19: 20886
CHARAKHCH'YAN, T. N., Calculations of energy spectrum of galactic cosmic rays, 19: 20882
CHARAKHCH'YAN, T. N., Decrease in cosmic-ray intensity in stratosphere, 19: 20877
CHARAKHCH'YAN, T. N., Forbush decreases in intensity of cosmic rays, 19: 20886
CHARAKHCH'YAN, T. N., Intensity of cosmic rays in stratosphere, 19: 20876
CHARAKHCH'YAN, T. N., Latitudinal measurements of cosmic-ray intensities in stratosphere, 19: 20892
CHARAP, J. M., P and C properties of U(12) multiplets, 19: 20974
CHARKES, N. David, Diagnosis of bone metastasis by photoscanning with Sr-85, 19: 19666
CHAROENKWAN, P., Studies of β spectra using solid-state spectrometer, 19: 20360
CHARREL, J., Contamination of Mediterranean shellfish, 19: 20230
CHARVAT, J., Pentose cycle and radiation diseases, 19: 19538
CHASMAN, R. R., "Seniority-zero" excited states of the pairing hamiltonian, 19: 21385
CHASTEL, R., Levels in reaction $^{29}Si(n,\alpha)^{26}Mg$, 19: 21318
CHAUDHURI, D. K., Metastable phases in U alloys. I., 19: 20587
CHAUDHURI, D. K., Metastable phases in U alloys. II., 19: 20588
CHAVEZ, E. L., Bonding to metallic films and solid-state devices, 19: 20520 (SC-DC-65-1256)
CHECHERNIKOV, V. I., Resonant paramagnetic absorption in alloys based on Gd, 19: 20581
CHEN, Chin-chuan, Alpha-reduced width of 1p shell nuclei, 19: 21432
CHEN, Francis F., Drift instabilities in thermionic plasmas, 19: 21540
CHEN, Fu-ming, Electron coupling of nuclear spins, 19: 19888
CHEN, J. C. Y., Error estimates for atomic and molecular quantities, 19: 20863
CHEN, K. W., Baryon spectroscopy by inelastic e-p scattering, 19: 20997
CHEN, Kuo-chun, Genetics of *Sordaria brevicollis*. I., 19: 19547
CHEN, Ting-gin, Low-energy K-π scattering, 19: 21058
CHENG, H., Interaction of light with light in a plasma, 19: 21547
CHENG, Jian-hua, Influences of pairing force on properties of rare-earth nuclei, 19: 21434
CHENG, Pwu-in, Inelastic collisions of 6.8 Bev/c π^{-} mesons with nucleons, 19: 21062
CHENG, Shoo-chong, Formation of antiendotoxins against *E. coli* for involution of hemorrhagic syndrome in radiation sickness, 19: 19487
CHERNICK, Jack, Evolution of finite escape time concept in reactor kinetics, 19: 21635 (BNL-9011)
CHERNOCK, W. P., Prog. rpt. on performing in-pile thermal conductance testing, 10–12/64, 19: 21664 (CEND-3336-229)
CHERNYAK, A. S., Extraction of Sc by alkyl phosphoric acids, 19: 20082
CHERNYI, V. G., Effect of Cr and Fe on elastic properties of Nb, 19: 20579
CHERRY, Ivan, Surfaces of constant space charge field components, 19: 20739
CHERTOK, Benson Tilbert, Nuclear excitation by 1- to 3-Mev electrons, 19: 21455
CHEVERTON, R. D., Gradient fuel plates, 19: 21676
CHIANG, You-Chien, Electron capture by protons passing through He, 19: 20821
CHIBISOV, M. I., Nonstationary isothermal motion of a gas, 19: 20713
CHIBISOV, M. I., Resonance charge exchange in inert gases, 19: 19931
CHICK, Helen J., Density of Co–C and Ni–C alloys in solid and liquid states, 19: 20567 (LA-tr-65-5)
CHIEN, Guan-yin, Thermoluminescence of irradiated high polymers. I., 19: 20007
CHIEN, Pao-kung, Thermoluminescence of irradiated high polymers. I., 19: 20007
CHIKISHEV, Yu. G., Radiation synthesis of polymers based on dimethylphosphinoborine, 19: 19982
CHIOTTI, Premo, Application of adiabatic calorimeter to determination of heats of fusion and formation of metallic compounds, 19: 19838 (IS-1070)
CHIOTTI, Premo, Transfer of solutes between liquid alloys in mutual contact with a fused salt, 19: 20066
CHIRKOV, N. P., Modulation of cosmic rays by interplanetary magnetic field, 19: 20889
CHISHOLM, John, Long-range balloon tracking, 19: 21769 (TID-21661)
CHITTENDEN, D. M., II, Decay of Eu-157 and TM-174, 19: 21272
CHIU, Sih-tjuen, Stripping reactions (dp) with target core excitation, 19: 21433
CHIU, Yam-tsi, Decay of the ρ^{0} meson; possible existence of T = 0 scalar di-pion, 19: 20998
CHKHETIYA, A. M., Influence of magnetic storms on cosmic rays, 19: 20888
CHOLIN, V. V., Half lethal dose ($LD_{50/30}$) and age of irradiated rats, 19: 19575
CHOPPIN, Gregory R., Parent-daughter radioactive equilibrium, 19: 20031
CHOU, Ch'ung-yuan, Decay of K_{13}, 19: 21060
CHOU, Lon-shang, Low-energy K-π scattering, 19: 21058
CHOU, Shing-ting, Chromosomal aberrations of irradiated human leukocytes, 19: 19596
CHRIST, J., Scattering of subthermal neutrons on heavy ice, 19: 21218
CHRISTENSEN, J. A., Thermal conductivity of UO_2, 19: 20615 (HW-SA-3212)
CHRISTENSON, C. W., Disposal of Am^{241}–Pu^{239} raffinate solutions, 19: 21750 (LA-3150)
CHRISTIAN, M. W., Evaluation testing of Filtors DPDT relays, 19: 21733 (NAA-SR-Memo-10532)
CHRISTIANSEN, J., Neutron polarization in T(d,n)^{4}He reaction, 19: 21303
CHUDAKOV, A. E., Radiation study by Cosmos 17, 19: 20343
CHUKHLANTSEV, V. G., Sodium zirconosilicate and hafnosilicate crystals, 19: 19916
CHUNG, Suh Urk, Further evidence for Kπ resonance near 1400 Mev, 19: 21004
CHUPP, E. L., Solar-flare hazard to manned space systems, 19: 20873 (D2-11608)
CHURCHILL, D. R., Spectral absorption in heated air, 19: 20832
CLARK, Alfred, Jr., Some exact solutions in MHD, 19: 20764
CLARK, D. E., Jr., Removal of simulated fallout from pavements, 19: 20207 (USNRDL-TR-797)
CLARK, David J., 88-Inch cyclotron operation and development, 19: 20736 (UCRL-11828(p.236-41))
CLARK, F. L., Generalized Riemann zeta functions and applications in calculations of neutron cross sections, 19: 21228 (ANL-6970)
CLARK, J. P., Electromagnetic testing of thin-wall, refractory metal tubing, 19: 20454 (CONF-650212-1)
CLARK, W. E., Evaluation of Hastelloy F and other materials for centrifuge in fuel recovery plant, 19: 20481 (ORNL-3787)
CLARKSON, Jack E., Fission barriers of W, Re, Os, Ir, and Hg isotopes,

19: 21259 (UCRL-11828(p.77-80))
CLAUDEL, Bernard, Thorium oxalate precipitation and thermal decomposition, 19: 19861
CLEARY, R. E., Solubility of He in Li and K, 19: 20561 (PWAC-380)
CLEGG, A. B., Reaction $^{40}Ca(p,p')$ at 150 Mev, 19: 21332
CLEVELAND, J. M., Trifluoride processing of Pu metal recycle, 19: 20065
CLEVELAND, R. H., Studies of renal homotransplantation in man, 19: 19463
CLIFFORD, F. E., Equilibrium distribution of nuclides in matter at high temperatures, 19: 20762
CLINE, D., Evidence for $K_{\mu 4}$ decay, 19: 20985
CLINE, D., Experimental test of charge-conjugation invariance, 19: 21029
CLINE, T. L., Continual acceleration of solar protons in Mev range, 19: 20766
CLINTON, Sam D., Preparing spheroidal particles of dicarbides of Th and Th–U mixtures, 19: 20528
CLODE, W. H., Localization of iodine in stomach, 19: 19717
CLOSE, Elon, 88-inch cyclotron operation and development, 19: 20736 (UCRL-11828(p.236-41))
COBB, J. K., Electron and ion emission from metal foils, 19: 20814
COBBIN, W. C., Removal of simulated fallout from pavements, 19: 20207 (USNRDL-TR-797)
COCHE, A., Emission spectrum and time constants of organic scintillators, 19: 19962
COCHO, G., B = ⅓ quarks and SU(9) symmetry, 19: 21026
COESTER, F., Scattering theory for relativistic particles, 19: 20950
COFFEY, D. L., Photochemical method of separating Hg isotopes, 19: 20429 (MLM-1214)
COGLIATI, Guido, Producing Th oxide–U oxide mixtures, 19: 19942
COHEN, A., Measurement of coronary circulation with new isotope technique, 19: 19668
COHEN, J. P., Calculation of nucleon-α cascades, 19: 21372
COHEN, M. I., Irradiation induced color centers in MgF_2, 19: 20618 (NBS-8614)
COHEN, Marvin L., Carrier concentration in semiconducting $SrTiO_3$, 19: 21170
COHEN-TANNOUDJI, G., Test for C conservation in strong-interaction physics, 19: 20977
COLAS, R., Industrial applications of radioelements, 19: 20417
COLBY, L. J., Jr., Comparative fuel cycle evaluation. II., 19: 20048 (NAA-SR-9335)
COLE, Leonard J., Hepatomas in mice after irradiation, 19: 19594
COLLIN, J. L., Determination of Al, Al_2O_3, Fe, Si, Zn, C in SAP powders, 19: 19750 (EUR-2286.f)
COLLINS, J. F., Properties of Fe–Cr–Al type alloys containing Y, 19: 20470 (GE-TM-63-7-3)
COLLINS, John A., Lung transplantation in the dog, 19: 19523
COLLINS, R. G., Elementary processes in radiation- and photochemistry, 19: 20002
COLLINS, Vincent P., Splenic transplantation in the dog, 19: 19521
COLOMBO, R. L., Fission-gas retention ability of UO_2 pellets, 19: 20633
COMPERE, E. L., Prog. rpt. on SNAP-8 corrosion, 6–8/63, 19: 20475 (ORNL-3538)
COMPERE, E. L., Prog. rpt. on SNAP-8 corrosion, 9–11/63, 19: 20477 (ORNL-3604)
COMPERE, E. L., Prog. rpt. on SNAP-8 corrosion, 12/63–2/64, 19: 20478 (ORNL-3618)
COMPERE, E. L., Prog. rpt. on SNAP-8 corrosion, 3–5/64, 19: 20479 (ORNL-3671)
COMPERE, E. L., Prog. rpt. on SNAP-8 corrosion, 6–8/64, 19: 20480 (ORNL-3730)
CONDON, Paul Edward, Products of the $K_{\mu 3}$ mesonic decay, 19: 21069
CONE, A. A., Baryon spectroscopy by inelastic e-p scattering, 19: 20997
CONIGLIO, John G., Lipid metabolism in acute radiation injury, 19: 19610
CONNELL, St. James, Changes in germ-free mice following whole-body x irradiation, 19: 19619
CONNOR, Thomas B., Pre-operative localization of parathyroid adenomata, 19: 19732
CONWAY, D. E., Epicadmium capture-to-fission cross section, 19: 21334
CONZEMIUS, R. J., Source of ions in mass spectrometer, 19: 20292
COOK, H. D., Epicadmium capture-to-fission cross section, 19: 21334
COOK, Judy, Recovery from lethal effects of cross-linking alkylation, 19: 19485
COOKSON, G. G., Spark source mass spectrograph, 19: 19830
COOLEY, G., Synthesis of [^{3}H-labeled steroids], 19: 20025
COOPER, J. A., Decay of Mo-90, 19: 21258 (UCRL-11828(p.67-71))
COOPER, R. S., Processing of Pu by ion exchange. III., 19: 20045 (LA-2838)
CORBISIER, O., Production of radioisotopes. Study of maximum possible accident, 19: 20195 (BLG-281)
CORBISIER, O., Tritium laboratory—maximum possible accident, 19: 20194
CORCORAN, J. B., Multichannel analyzer data processing on CDC 160-A computer, 19: 20315 (ANL-6938(p.206-8))
CORCORAN, John B., Underground laboratory for high-sensitivity γ counting, 19: 20093 (ANL-6938(p.194-205))
CORDES, O. L., SNAPTRAN 2/10A-3 destructive test, 19: 21717 (IDO-17019)
CORKHILL, D. P., Deduction of interatomic potential in Al, 19: 20837
CORMACK, D. V., Radiation sensitivity of *Serratia marcescens*, 19: 19649
CORNELL, D. C., Iterative technique for stress analysis of PCR structures, 19: 20086 (GAMD-5926)
CORNELL, D. C., Numerical stress analysis of PCRS for TARGET, 19: 21683 (GAMD-5272(Rev.2))
CORNELL, D. C., TARGET—IBM computer code for stress analysis of bodies of revolution, 19: 21609 (GAMD-5001(Rev.2))
CORNELL, D. C., Tendon configuration in prestressed concrete reactor structure, 19: 21610 (GAMD-6109)
CORNUET, R., Industrial applications of radioelements, 19: 20417
CORNWALL, J. M., Meson-baryon scattering in intrinsically broken M(12) symmetry scheme, 19: 21024
CORYELL, Charles D., Yields of Te-131 and Te-133 isomers in fission, 19: 21390
COSTA, Eduardo C., Pulsed sieve-plate extraction columns. I and II., 19: 20043 (IEA-77)
COSTA, S., Measurement of angular distribution of photoneutrons by high-efficiency detector, 19: 20333
COSTA, S., Reactions $K^{39}(\gamma,n)K^{38}$ ^{38m} and $K^{39}(\gamma,np)A^{37}$ up to 80 Mev, 19: 21276
COTTINGHAM, J. G., Excitation of parallel resonant LRC circuit from fast-sweeping signal source, 19: 21757 (BNL-7918)
COUCH, J. G., Reaction $^{14}N(^{14}N,^{13}N)^{15}N$ and the neutron tunneling mechanism, 19: 21388
COUCOURDE, F., Use of new drug in treatment of radiodermatitis, 19: 19633
COUTAREL, Y., Measurement device for low β activities, 19: 20382
COWAN, C. A., Symmetry of neutron-induced Pu-239 fission in resonance region, 19: 21241 (LA-DC-6629)
COWAN, J. J., Outdoor γ irradiation facility, 19: 20102
COWAN, Robert D., Retinal dose due to visible radiation from nuclear explosions, 19: 19498 (LA-3204)
COWGILL, Dale Stephen, Deformation behaviors of Nb and Ta, 19: 20605
COYNE, J. J., SU(6) Clebsch-Gordan coefficients for the product 35 × 56, 19: 21027
CRAMER, James D., Compressibility of gaseous mixtures of He–N and He–D at high pressures, 19: 19840 (LA-3250)
CRAWFORD, Bruce W., Iterative solution method for neutron transport equation with anisotropic scattering, 19: 21223
CRAWFORD, Frank S., Jr., CP-nonconserving decay $K_2^0 \to \pi^+ + \pi^- + \pi^0$, 19: 21020
CREUZBURG, M., Energy losses of electrons, 19: 20702
CREWE, Albert V., Scanning techniques for high-voltage microscopes, 19: 20251 (CONF-640204(p.63-81))
CRIDER, John Earl, Computational studies of transients in packed tubular chemical reactors, 19: 19734 (UCRL-11757)
CRITCHFIELD, C. L., Internal symmetry and relativistic wave functions, 19: 21035
CROOM, D. L., Vlf radiation from high-altitude nuclear explosions, 19: 21139
CROSBY, G. A., Crystal-field splitting in Tm^{3+} chelates, 19: 19886
CROSBY, J. R., SNAP systems braze joint experience, 19: 20508 (NAA-SR-Memo-10625)
CROW, E. W., Closure weld development reactor vessel, S8DS-12002, 19: 20509 (NAA-SR-Memo-10633)
CROWLEY, L. V., Wound healing: effect of ascorbic acid and D_2O, 19: 19484
CRUCHAUD, A., Inhibition of immune response, 19: 19589
CSIKAI, J., Isomeric cross-section ratio in $^{79}Br(n,\gamma)^{80,80m}Br$ reactions, 19: 21331
CUEER, P., Interactions of 3.0-Bev/c K⁻ mesons with nuclei, 19: 21389
CUJEC, B., Reaction $^{30}Si(d,n)^{31}P$, 19: 21376
CULVER, J. S., Multiple-pass experiments (DCX-2), 19: 21481 (ORNL-3760(p.10-22))
CUNDY, D. C., S-wave scattering lengths for n-p interaction, 19: 21043
CUNNINGHAM, B. B., Prog. rpt. on nuclear chemistry, annual, 1964, 19: 19735 (UCRL-11828)
CUNNINGHAM, Mary Elizabeth, Bremsstrahlung produced by β rays from Bi-210, 19: 21453
CURCIO, R. M., Prog. rpt. on Nb alloy sheet rolling, final 3/7/63–9/1/64, 19: 20499 (AD-606291)
CURRY, R. Bruce, Scandium as tracer of movement of clay suspensions, 19: 20183
CURTISS, C. F., Effect of three turning points on semiclassical scattering,

19: 20957
CUSANO, D. A., Radiative recombination from GaAs, 19: 20703
CUYPERS, M. Y., Public benefit demonstrations using nuclear activation analysis, 19: 19771 (TEES-2671-4(Chap.9))
CVORIC, Jelisaveta, Production of radioactive colloidal Au-198, 19: 20022 (JPRS-29258)
CZEIZEL, E., Effect of x irradiation on liver regeneration, 19: 19512
CZERNIAK, P., Scanning study of livers, 19: 19730
CZIRR, J. B., Neutron-neutron S-wave scattering length from reaction $\pi^- + d \to 2n + \gamma$, 19: 20995
CZYZEWSKI, O., Antiproton-proton elastic scattering, 19: 20976

D

DABKOWSKI, D. S., Factors affecting notch toughness of maraging steels, 19: 20541 (AD-604868)
DA COSTA, H., Effect of blood transfusions on subsequent marrow transplant in irradiated mice, 19: 19653
DAHL, Orin I., Further evidence for Kπ resonance near 1400 Mev, 19: 21004
DAHLER, A., Environmental γ radiation in Norwegian houses, 19: 20218
DAINTON, F. S., Elementary processes in radiation- and photochemistry, 19: 20002
DALGARNO, A., Error estimates for atomic and molecular quantities, 19: 20863
DALGARNO, A., Polarizabilities and shielding factors of Be sequence, 19: 20852
DALGARNO, A., Refractive index of He, 19: 20859
DALMAS, J., Levels in reaction $^{28}Si(n,\alpha)^{25}Mg$, 19: 21318
DALY, N. R., Isotopic analysis of U using internal standard, 19: 20188
D'AMATO, F., Somatic mutations in potatoes induced by radiation, 19: 19518
DAMLE, P. P., Chain element activity in intermittent irradiation, 19: 21226 (AEET/HP/Th-19)
DAMMIN, Gustave J., Human kidney transplantation, 19: 19520
DAMYANOVICH, Sandor, Effect of SH-inhibitors on radiation sensitivity of proteins and amino acids, 19: 19621
DANBARA, H., Distribution of Sr-90 and Cs-137 concentration in Japanese bulls, 19: 20215
DANDL, R. A., Properties of high-β plasma, 19: 21531
DANELIYA, I. A., Transformation of longitudinal h-f field by ionic-acoustic spectrum, 19: 21584
D'ANGELO, N., Effects of passing current on plasma losses in a Q device, 19: 21541
DANIEL, H., Shapes of β spectra and partially conserved axial-vector current, 19: 21340
DANILEVICH, Ya. B., Production of high-power MHD generators, 19: 20910
D'ARCY, Gerald P., Technique for simulating air-blast-induced ground motions, 19: 20184
DARDEN, S. E., Neutrons from $^9Be(\alpha,n_0)^{12}C$ and $^9Be(\alpha,n_1)^{12m}C$ reactions, 19: 21307
DARENSKAYA, N. G., Biological action of protons of 510-Mev energy in irradiation of dogs, 19: 19578
DARENSKAYA, N. G., Comparative radiosensitivity of Wistar and non-pedigree rats, 19: 19585
DARRAS, Raymond, Oxidation of alloy Mg–1% Ce in humid N at high temperatures, 19: 20485
DA SILVA, X. A., Susceptibility of liquid Gd, 19: 20598
DASS, Guru Vachan, Potential model for the Ω^-, 19: 20970
DAUM, C., Analysis of munoic x-ray spectra, 19: 21344
DAUTREPPE, D., Magnetic after-effects in neutron-irradiated Fe, Ni, and Co, 19: 20652
DAVEY, William G., Fission ratios in ZPR-III critical assemblies, 19: 21227 (ANL-6941)
DAVIDSON, Ben, Prog. rpt. on Project Star Dust, 9/63, 19: 20657 (DASA-1309)
DAVIDSON, Franklin D., Commercial spectrometer modified for x-ray spectroscopy, 19: 19801
DAVIDSON, J. K., Advantages of Hg–H_2O vapor cycle for Na reactor, 19: 21701
DAVIDSON, J. P., Effect of deformation vibrations on E2 branching ratios in deformed even-even nuclei, 19: 21384
DAVIDSON, M. G., Effect of deformation vibrations on E2 branching ratios in deformed even-even nuclei, 19: 21384
DAVIES, D., Approximate functional equation for Dirichlet L functions, 19: 20450
DAVIES, D. Kenneth, Photoelectric emission in low-pressure He discharges, 19: 20861
DAVIES, T. J., "Ceramic" nuclear materials, 19: 21671
DAVIES, W. G., Reaction $^{28}Si(d,n)^{29}P$, 19: 21376
DAVIS, D. H., Interactions in flight of low-energy K^- mesons with emulsion nuclei, 19: 21365
DAVIS, James T., Lipid metabolism in acute radiation injury, 19: 19610
DAVIS, M. J., Automatic induction soldering, 19: 21765 (SC-DR-65-74)
DAVIS, R. C., Multiple-pass experiments (DCX-2), 19: 21481 (ORNL-3760(p.10-22))
DAVIS, V. C., Preparation of ceramographic sections of BeO, 19: 20460 (NAA-SR-Memo-9761)
DAVISSON, E. G., Computer program for flow calculations, 19: 20115 (ORNL-TM-1095)
DAVISSON, E. G., Smoothed thermocouple tables, Pt vs. Pt–10% Rh, 19: 20263 (ORNL-3649(Vol.2)(Sect.2.1))
DAVISSON, E. G., Smoothed thermocouple tables, Pt vs. Pt–13% Rh, 19: 20264 (ORNL-3649(Vol.2)(Sect.2.2))
DAVISSON, E. G., Smoothed thermocouple tables, chromel–alumel, 19: 20265 (ORNL-3649(Vol.2)(Sect.2.3))
DAVISSON, E. G., Smoothed thermocouple tables, Fe–constantan, 19: 20266 (ORNL-3649(Vol.2)(Sect.2.4))
DAVISSON, E. G., Smoothed thermocouple tables, Cu–constantan, 19: 20267 (ORNL-3649(Vol.2)(Sect.2.5))
DAVISSON, E. G., Smoothed thermocouple tables, chromel–constantan, 19: 20268 (ORNL-3649(Vol.2)(Sect.2.6))
DAVISSON, E. G., Smoothed thermocouple tables, W vs. W–26% Re, 19: 20269 (ORNL-3649(Vol.2)(Sect.2.7))
DAVISSON, E. G., Smoothed thermocouple tables, W–5% Re vs. W–26% Re, 19: 20270 (ORNL-3649(Vol.2)(Sect.2.8))
DAVISSON, E. G., Smoothed thermocouple tables, W–3% Re vs. W–25% Re, 19: 20271 (ORNL-3649(Vol.2)(Sect.2.9))
DAVISSON, E. G., Smoothed thermocouple tables, Au–2.1% Co vs. Cu cryogenic, 19: 20272 (ORNL-3649(Vol.2)(Sect.2.10))
DAVISSON, E. G., Smoothed thermocouple tables, constantan–Cu cryogenic, 19: 20273 (ORNL-3649(Vol.2)(Sect.2.11))
DAVISSON, E. G., Smoothed thermocouple tables, alumel–chromel cryogenic, 19: 20274 (ORNL-3649(Vol.2)(Sect.2.12))
DAVISSON, E. G., Smoothed thermocouple tables, constantan (JN)–Fe (JP) cryogenic, 19: 20275 (ORNL-3649(Vol.2)(Sect.2.13))
DAVISSON, E. G., Smoothed thermocouple tables, constantan (YN)–Fe (YP) cryogenic, 19: 20276 (ORNL-3649(Vol.2)(Sect.2.14))
DAVYDOV, E. N., Radioactivity of ground-level air on Hayes Island, 19: 20157 (NP-14697)
DAWIDS, S. G., Effect of cortisone and anabolic steroids on retention of Cs-47 and Sr-85 in rats, 19: 19476
DAWSON, J. M., Electron cyclotron harmonic radiation from a plasma, 19: 21477 (MATT-290)
DAWSON, W. K., Reaction $^{28}Si(d,n)^{29}P$, 19: 21376
DAY, R. B., Grain boundaries and mechanical behavior of MgO, 19: 20607
DEAK, M., Evaporation of Th from carburized thoriated tungsten cathodes, 19: 20575
DEAN, M. H., Isotpic analysis of U using internal standard, 19: 20188
DEAN, Orlen C., Preparing spheroidal particles of dicarbides of Th and Th–U mixtures, 19: 20528
DE ANGELIS, H. M., Effects of energetic photon irradiation on Ge, 19: 20612 (AFCRL-64-839)
DE ARRIETA, J., Gantry and trolley for fuel handling cask, 19: 20099 (TID-21644)
DEAVER, Bascom S., Jr., Quantized flux in superconducting cylinders, 19: 21194
DE BACKER, W., Synthesis of optimal control and hybrid computation, 19: 21604 (EUR-2202.e)
DE BOER, J., Reorientation effect in Cd-114, 19: 21398
DEBRIE, G., Detection of critical accidents at Commissariat a l'Energie Atomique, 19: 20330 (AEC-tr-6547)
DE BUSK, A. Gib, Prog. rpt. on molecular bases of mutation, final 1965, 19: 21772 (TID-21709)
de Carvalho, R. A. Guedes
see Guedes de Carvalho, R. A.
DE GENNES, P. G., Flux tubes in type-I superconductors, 19: 21167
DEGNER, W., Comparative physical considerations of modern ways of irradiation, 19: 19688
DE GROUCHY, J., Risks for embryo, fetus, and infant from medical radiology, 19: 19699
DE HALAS, D. R., Thermal conductivity of UO_2, 19: 20615 (HW-SA-3212)
DE HEER, F. J., Ionization cross sections for electrons in gases, 19: 20850
DE LA CRUZ, F., Production of radioactive isotopes in Spain, 19: 20432 (ORNL-tr-295)
DELALOYE, B., Indirect lymphography and oncology, 19: 19719
DELANGE, Maurice, Production of granulated UO_2, 19: 20538
DELAPLACE, Jean, Apparatus for high-temperature measurement of interior friction in rigid samples, 19: 20245 (CEA-R-2718)
DELAY, Alain, Radiochemical method for analysis of Sr-90 in bones, 19: 19789

DELBOURGO, R., Relativistic structure of SU(6), 19: 20927 (ICTP-64/7)
DELBOURGO, R., S-matrix elements in two-particle unitarity approximation for one-dimensional world, 19: 20924 (ICTP-64/2)
DELBOURGO, R., U(12) Predictions for $p\bar{p}$ annihilation into mesons, 19: 21036
DELCORTE, Michele, Preparation of nuclear-pure beryllium oxalate trihydrate, 19: 19832 (CEA-R-2591)
DE LEEUW, S., Spectrometry of fast neutrons by surface barrier junctions and Li-6, 19: 20334
DE LEONE, Ruggero, Producing Th oxide–U oxide mixtures, 19: 19942
DELMAROVA, V., Volumetric determination of micro amounts of fluoride, 19: 19788
DELORENZI, E., Behavior of fungal spores in confined irradiated environment, 19: 19559
DELORENZI, E., Effects of irradiation on fungal spores, 19: 19558
DELPEYROUX, Paul, Resistance of metallic U tubes to external pressure, 19: 20453 (CEA-R-2572)
DEL VAL, M., Production of radioactive isotopes in Spain, 19: 20432 (ORNL-tr-295)
DE MAEYER, Edward, Virus plaque development in mammalian cell cultures after uv irradiation, 19: 19563
DE MAEYER-GUIGNARD, Jaqueline, Virus plaque development in mammalian cell cultures after uv irradiation, 19: 19563
DE MARIA, D., Radioprotective power of prochlorperazine, 19: 19631
DE MARIA, D., Weight changes in albino mice after total-body irradiation, 19: 19632
DEMEREC, M., Gene differentiation, 19: 21756 (BNL-8934)
DEMIDENKO, I. I., Development of instabilities in plasma captured by transverse magnetic field, 19: 21577
DEMIRKHANOV, R. A., Interaction of traveling EM wave with plasma, 19: 21564
DEMKOV, Yu. N., Resonance dissociative capture of electrons, 19: 19899
DE MONTPREVILLE, Claude Thomas, Resistance of metallic U tubes to external pressure, 19: 20453 (CEA-R-2572)
DEM'YANOV, A. V., Electromagnetic mass-separator. I., 19: 20260 (JINR-P-1948)
DEM'YANOV, A. V., Electromagnetic mass-separator. II., 19: 20261 (JINR-P-1949)
DE MERCY, A. Bussière, Energy variation of phase rule in α-particle scattering, 19: 21269 (UCRL-11828(p.132-3))
DENGEL, O., Scattering of subthermal neutrons on heavy ice, 19: 21218
DENIAUD, Suzanne, Improvement of spectrographic analyses, 19: 19743 (CEA-R-2619)
DENISENKO, E. A., Determination of radiogenic Ar activation, 19: 20166
DENOVAN, A. S., Determination of H in Zr alloys, 19: 19831
DENTON, W. H., Low-temperature electrical resistivity of U and Be, 19: 20543 (AERE-GR-101)
DEPASQUALI, G., Highly charged states following Co-57 electron capture in hydrated Co compounds, 19: 20032
DE PIERRE, V., Primary working of refractory metals, 19: 20500 (AFML-TR-64-387)
DE PINHO, A. G., Why is Gallagher-Moszkowski rule so well verified?, 19: 21370
DER AGOBIAN, Roger, Simultaneous stimulated emission in He-4 and He-3, 19: 20815
DEREIGNE, André, Analysis of $[Ce_2(SO_4)_3 \cdot 9H_2O]$ and $[Ce_2(SO_4)_3 \cdot 8H_2O]$, 19: 19857
DERINGER, Margaret K., Comparative survival of substrains C3HeB and C3HfB following midlethal irradiation and allogenic marrow inoculation, 19: 19648
DERMENTZOGLOU, F., Diagnosis of intraspinal neurological syndromes, 19: 19720
DERWISH, G. A. W., Ion-molecule reactions in acetylene, 19: 19988
DESAI, U. D., Continual acceleration of solar protons in Mev range, 19: 20766
DE SANTIS, V., Leptonic decays of the baryons, 19: 21019
DE-SHALIT, A., Core excitation: Au-197 revisited, 19: 21362
DESNEIGES, P., Detection of critical accidents at Commissariat a l'Energie Atomique, 19: 20330 (AEC-tr-6547)
DESPOTOVIC, R., Preparation of Na perchlorate labeled with Cl-36, 19: 20028
DESSLER, A. J., Geomagnetism, 19: 21160
DESSLER, A. J., Penetrating particle radiation, 19: 20902
DETRY, R., Personnel exposed to x rays in hospitals, 19: 19525
DE UNAMUNO-ESCOUBES, S., Antiproton-proton elastic scattering, 19: 20976
DEUTCH, B. I., K-shell particle parameter in 272-kev E1 transition of Yb-173, 19: 21320
DEVANI, Muljibhai, Dephosphorylation of sugar phosphates and nucleotides by group-IV metal ions, 19: 19876
DE VRIES, Dale Bryon, Recoil reactions of C-11 in hydrocarbons, 19: 20018
DE VRIES, H., Radiation absorption and charge separation in crystal counters, 19: 20389
DE WIRE, J., Reaction $\gamma + p \rightarrow p + \pi^0$ near first resonance from polarized photons, 19: 20932 (LNF-64/60)
DE WIT, S. A., Analysis of munoic x-ray spectra, 19: 21344
DIAMBRINI, G., Reaction $\gamma + p \rightarrow p + \pi^0$ near first resonance from polarized photons, 19: 20932 (LNF-64/60)
DIANA, Massimo, Problems of chemical engineering in high-temperature technology, 19: 19868
DICKERMAN, C. E., Correlation of in-pile transient pressure measurements, 19: 21652
DICKINSON, R. W., Fast-neutron paste-fueled reactor, 19: 21663
DIENER, E., Alteration of carcinogenesis by radiation, 19: 19606
DIENSTBIER, Z., Pentose cycle and radiation diseases, 19: 19538
DIERCKX, Ronald, Pulsation of reactors, 19: 21657
DIETL, J., Luminescence of Fe-57 in ZnS phosphors, 19: 19855
DIMITROV, L., Delayed changes in animals which survived lethal irradiations, 19: 19627
DIMMLER, G., Multiple input data acquisition system using small on-line computer, 19: 21731 (KFK-242)
DINNEEN, G. A., SNAPTRAN 2/10A-3 destructive test, 19: 21717 (IDO-17019)
DIXON, W. R., Reaction $^{72}Ge(n,\alpha)^{69}Zn$, 19: 21324
DMITRIEFF, Anatole, Improvements in control rod operating devices, 19: 21621
DMITRIEV, V. A., Complex installation for study of extensive air showers, 19: 20347
DOAN, Ph. Th., Levels in reaction $^{28}Si(n,\alpha)^{25}Mg$, 19: 21318
DOBROSEL'SKAYA, N. P., Effect of S-35 radiation on dehydration of cyclohexanol, 19: 20013
DOBRYNINA, T. A., Lithium peroxide, 19: 19932
DOBRZANSKI, W. T., Effect of chloramphenicol on uv-induced streptomycin-, novobiocin-, and penicillin resistance in staphylococcus, 19: 19531
DOBRZANSKI, W. T., Effect of post-irradiation treatments on uv-induced mutations to antibiotic-resistance in Staphylococcus, 19: 19532
DODD, R. A., Supervoltage electron microscopy outside U. S., 19: 20248 (CONF-640204(p.17-19))
DOLEJSI, J., Luminescence and electronic emission of alkali chlorides with Cu, 19: 19964
DOLGINOV, Sh. Sh., Correlation between variations of magnetic field and positive ions inside magnetosphere, 19: 21126
DOLGOPOLOV, V. V., Electron radiation in plasma-magnetic-field boundary layer, 19: 21522
DOLS, C. G., Magnet construction for variable-energy cyclotron, 19: 20753
DOLS, Charles G., Synchrotron-magnet cost studies, 19: 20734 (UCRL-11800)
DOMANSKII, A. N., Interaction of excited biomolecules with O. II., 19: 19970
DOMEIJ, B., Conversion electrons from monocrystalline source, 19: 21339
DOMINGUEZ, G., Production of radioactive isotopes in Spain, 19: 20432 (ORNL-tr-295)
DOMSHLAK, M. P., Biological action of protons of 510-Mev energy in irradiation of dogs, 19: 19578
DONALD, R. A., S-wave scattering lengths for π-p interaction, 19: 21043
DONNAN, M. Yates, Determination of Zr-95 and Nb-95 in mixtures, 19: 19748 (DP-933)
DONNELLAN, B. A., Response of buried cylinders to quasi-static overpressures, 19: 20136 (AFWL-TDR-64-13)
DONNELLY, R. J., Capture cross sections for negative ions in rotating He(II), 19: 21177
DONSKOI, K. V., Steady flow of weakly ionized plasma in homopolar device, 19: 21570
DORE, E. K., Organ visualization by photoscanning using radioalbumin, 19: 19710
DORENBUSCH, W. E., Energy levels in Ti-48 and Ti-50, 19: 21346
DORMAN, L. I., Coupling coefficients for cosmic components, 19: 20891
DORMAN, L. I., Effect of equatorial flux on geomagnetic cutoff of cosmic-ray particles, 19: 20887
DORMAN, L. I., Influence of magnetic storms on cosmic rays, 19: 20888
DORMAN, L. I., Neutron component of cosmic rays, 19: 20878
DORMAN, L. I., Propagation of solar cosmic rays in interplanetary space, 19: 20757
DORMAN, L. I., Variations in intensity of cosmic rays, 19: 20885
DORN, D. W., Spontaneous fission in very neutron-rich isotopes, 19: 21403
DOROBISZ, Tadeusz, Effect of γ radiation on red blood cells in stored human blood, 19: 19513
DORST, J. H., Magnet construction for variable-energy cyclotron, 19: 20753

DOSS, J. D., High-power test on cloverleaf cavity, 19: 20724 (LA-DC-6759)
DOSTAL, M., Influence of 19-norandrostenolone upon acute irradiation disease in rats, 19: 19624
DOTSON, Clifford L., Prog. rpt. on properties of TZM Mo alloy and W, 5-8/64, 19: 20542 (AD-606310)
DOUSSET, M., Dose delivered to tissue contaminated with α emitter, 19: 19482
DOUSSET, M., Safety standards, 19: 20221
DOWD, R. M., Experimental test of charge-conjugation invariance, 19: 21029
DOWKER, J. S., Scalar theory of gravitation, 19: 21107
DOWLING, John, Billiken calibration shot in southeast Missouri, 19: 20171 (AFCRL-64-659)
DOWNES, A. M., Chromium-51 complex of EDTA, 19: 20026
DOWNEY, M. E., Neutron irradiation damage in Mo, 19: 20634
DOWNS, Angela M., Flow of plasma round the geomagnetic hollow, 19: 21146
DOXIADES, T., Scanning in diagnosis of echinococcus disease of liver, 19: 19729
DRAGT, A. J., Classification of three-particle states according to SU_3, 19: 20962
DRAGULESCU, C., Separation of Nb from Ta, 19: 20054
DRAIN, L. E., NMR linewidth in beta Mn, 19: 21366
DRASKOVIC, Rade, Production of radioactive colloidal Au-198, 19: 20022 (JPRS-29258)
DREINER, R., Growth mechanism of thin anodic oxide films on Ta. I., 19: 20490
DRESNER, Lawrence, EVAP—program for calculating evaporation of particles from nuclei, 19: 21245 (ORNL-TM-196)
DRESSE, H., Operation of PWR-type powerplant, 19: 21679 (BLG-261)
DRESSER, Miles Joel, Investigation of surface ionization, 19: 20871
DREW, D. D., Program for digital computer analysis of pulse-height spectra, 19: 19770 (TEES-2671-4(Chap.8))
DROBYSHEVSKII, E. M., Steady flow of weakly ionized plasma in homopolar device, 19: 21570
DROWART, J., Vapor pressure of U, 19: 19889
DRUCKER, G., SNAP-10A malfunction detection subsystem, 19: 21734 (NAA-SR-Memo-10666)
DU BOIS, D. F., Instability of electron plasma oscillations, 19: 21550
DUBOIS, J., New levels in V-47, 19: 21374
DUBOIS, M., Influence of impurities on optical properties of irradiated LiF, 19: 19998
DUBROVIN, V. S., Complexing of uranyl with salicylic acid. I., 19: 19903
DUCATI, Adriano C., High-temperature acceleration of propellants, 19: 20139
DUCOUSSO, R., Effect of ionizing radiations on methylene blue in glycerol solution, 19: 20016
DUECHS, D., Effects of neutral gas on dynamics of theta-pinch discharges, 19: 21470 (IPP-1/14)
DUGGAN, M. H., Brain-tumor localization, 19: 19714
DUKES, E. Kenneth, Determination of Zr-95 and Nb-95 in mixtures, 19: 19748 (DP-933)
DUL, I., Open-cycle MHD generator, 19: 20912
DUNLAP, J. L., Single-pass experiments (DCX-1), 19: 21480 (ORNL-3760(p.1-9))
DUNN, P. D., MHD research in the United Kingdom, 19: 20908
DUNN, W. A., Leptonic decays of the baryons, 19: 21019
DUNNE, F. T., Mechanism of thermal decomposition of α-phenylethylazomethane, 19: 19943 (BNL-8243)
DUNNING, J. R., Jr., Baryon spectroscopy by inelastic e-p scattering, 19: 20997
DUNSTER, H. J., Responsibilities of health physicist, 19: 20219
DUPUIS, Marie-Claire, Radiochemical separation of Ca-45, Sr-89, and Ba-140, 19: 19745 (CEA-R-2712)
DUPUIS, Michel, Radiochemical separation of Ca-45, Sr-89, and Ba-140, 19: 19745 (CEA-R-2712)
DUPUY, Gerard, Supporting structure for vertical moderator structure of reactor, 19: 21628
DUPUY, Michel, Chemical diffusion in Pu–U system, 19: 19869
DURAND, Loyal, III, Decay of the ρ^0 meson; and possible existence of T=0 scalar di-pion, 19: 20998
DURRANI, S. A., Neutron generator, 19: 21216
DUSHIN, L. A., Spectroscopic investigation of plasma in colliding bursts, 19: 21567
DUTT, J. C., Cosmic-ray intensity at depth of 60.0 m.w.e. underground at London, 19: 20897
DU VAL, V., Gas analytical apparatus for project Dribble, 19: 19776 (UCRL-12169)
DUYCKAERTS, G., Diluent influence on liquid-liquid extraction by trilaurylamine hydrochloride, 19: 20039 (EUR-2246.e)
DUYCKAERTS, G., Liquid-liquid extraction of $FeCl_3$, 19: 20038 (EUR-2245.e)
D'YACHKIKHIN, Yu. A., Electromagnetic mass-separator. II., 19: 20261 (JINR-P-1949)
DYE, D. L., Solar-flare hazard to manned space systems, 19: 20873 (D2-11608)
DYMNIKOV, A. D., Spherical aberration of EM quadrupole lenses, 19: 20685
DZHANIKULOV, F., Cultivation of cotton mutants under influence of P-32, 19: 19580
DZHELEPOV, B. S., Decay of Rh-100, 19: 21278
DZHELEPOV, B. S., Decay of Pd-101, Rh-101*, and Rh-101, 19: 21280
DZHIKIDZE, E. K., Effectiveness of preventive tetanus vaccination in monkeys after prolonged irradiation, 19: 19608
DZVONYAR, J., Iodine storage by human fetal thyroid, 19: 19491

E

EACHUS, Alan Campbell, Rates of hydrogen abstraction from various substrates by free radicals. I and II., 19: 21760 (NYO-2728-4)
EASH, D. T., Cryogenic tensile testing of Rover materials, 19: 20554 (LA-3161)
EASON, H. O., Properties of high-β plasma, 19: 21531
EBERHAGEN, A., Macroinstabilities in theta pinch, 19: 21525
EBERHARD, Philippe, Decay $Y_1^*(1660) \rightarrow Y_0^*(1405) + \pi$, 19: 21017
EBIHARA, Hiroshi, Chemical effects of $^{35}Cl(n,p)^{35}S$ reaction. I., 19: 20004
EBIZUKA, Yoshie, Design of the fast power reactor, 19: 21696
ECHARD, Rolland, Simultaneous stimulated emission in He-4 and He-3, 19: 20815
EDEN, R. J., Problem of causality in S-matrix theory, 19: 20943
EDGAR, K. R., Self-shielding in closely spaced slab lattices, 19: 21636 (CONF-654-32)
EDWARDS, George W., Velocity spectrometers used in Bevatron deflected-beam research, 19: 20326 (UCRL-11787)
EDWARDS, R. S., Single-pass experiments (DCX-1), 19: 21480 (ORNL-3760(p.1-9))
EDWARDS, S. F., Boltzmann equation for electrons in discolored systems, 19: 21041
EGER, I., Determination of U and elements that accompany it. I., 19: 19811
EGGEN, D. T., Fast-neutron paste-fueled reactor, 19: 21663
EGGERS, S. H., Preparation of deuterium-labeled O–methyl groups, 19: 20034
EGLIT, A. Kh., Transformations of normal alkanes, 19: 19980
EHLERS, Kenneth W., High-intensity negative ion sources, 19: 20731 (UCRL-11684)
EHRET, G., Phonon frequency distribution of V, 19: 20553 (KFK-262)
EHRET, G., Scattering laws of some hydrogenous moderators, 19: 21200 (KFK-264)
EHRLICH, R. D., Increased processing flexibility—Purex, 19: 20040 (HW-84085)
EICHELBERGER, R. L., Preparation of ceramographic sections of BeO, 19: 20460 (NAA-SR-Memo-9761)
EICHHORN, H.-J., Medical requirements of irradiation plan, 19: 19687
EICHNEROVA, R., Protective effect of fat in radiation sickness, 19: 19625
EISENHOWER, E. H., Electron accelerators for food processing, 19: 20422
EL-BISI, Hamed M., Microbiological safety and stability of radiation-sterilized foods, 19: 20420
ELDER, J. A., Diffusion pump oil deposition measurements, 19: 20143
ELDRIDGE, O., Kinetic theory of plasma and electromagnetic fields, 19: 21493
ELIAS, C., Photoscanning of spleen, 19: 19725
ELINSON, S. V., Uranium: methods for determination, 19: 19823
ELISEEV, B. V., Instability of electromotive forces in weakly ionized plasmas, 19: 21559
ELLIOTT, Donald Edward, Preparation and some analytical applications of tri-n-octylphosphine sulfide, 19: 19753 (IS-T-3)
ELLIS, W. R., Development of oil-soluble Au-198 compounds, 19: 20030
ELSHUNI, K. A., Recovery from irradiation damage of barley seeds, 19: 19639
EMANUEL, George, Structure of radiation-resisted shock waves, 19: 20680
EMANUEL, N. M., Decay of peroxides in irradiated DNA solutions, 19: 19541
EMANUEL, N. M., Long afterglow in proteins and synthetic polymers irradiated by x rays, 19: 19983
EMELEUS, K. G., Low-voltage cold-cathode discharges in He, 19: 21499
EMELITY, L. A., Disposal of Am^{241}–Pu^{239} raffinate solutions, 19: 21750 (LA-3150)
EMERT, C. J., Raman spectrum of ZrO_2, 19: 19849 (WAPD-T-1760)
EMERY, F. E., Calibration techniques used with semiconductor detectors, 19: 20371
EMPSON, F. M., Disposal of high-level power reactor wastes in salt mine,

19: 21751 (ORNL-P-1064)
ENDERBY, J. E., Asymptotic form of correlation functions in liquid He-4, 19: 20697
ENDRES, G. W. R., Neutron spectrum measurements, 19: 20201 (HW-SA-3525)
ENGLAND, A. C., Properties of high-β plasma, 19: 21531
ENGLE, P. M., Bismuth recovery process, 19: 20047 (MLM-734)
EPHERRE, M., Lithium-6 and Li-7 production in C-12 and O-16 by high-energy protons, 19: 21352
ERDELSKY, Karol, Influence of γ irradiation on maize, 19: 19528
EREMENKO, Yu. A., Accuracy of locating particle in spark chamber and determining ion drift in Wilson chamber, 19: 20344
ERIKSSON, L., Conversion electrons from monocrystalline source, 19: 21339
ERJAVEC, M., Contrast-increasing electronic device for scintillation scanner, 19: 19696
ERJAVEC, M., Localization of bone tumors by Sr-85, 19: 19675
ERJAVEC, M., Scintillation scanning of bone tumors and metastases, 19: 19697
ERMOLAEVA, N. V., DNA localization on lymphoid tissue after γ irradiation, 19: 19583
ERNST, H., Detection of liver metastases following rectal administration of I-131, 19: 19662
EROSHENKO, E. G., Correlation between variations of magnetic field and positive ions inside magnetosphere, 19: 21126
ERRERA, M., Effect of radiation on RNA and RNA metabolism in human cancerous tumor cells, 19: 19602
ERSHOV, B. G., Radiolysis of aqueous nitrate solutions, 19: 19981
ESCHSTRUTH, P. T., Test of $\Delta S/\Delta Q$ rule in K^0_{l3} decay, 19: 20979
ESCOUBES, B., Antiproton-proton elastic scattering, 19: 20976
ES'KOVA, E. M., Mineralogy and geochemistry of rare elements (Urals), 19: 20190
ESPE, W., Synthetic zeolites in high vacuum technology, 19: 20141
ESPINASSE, Jacqueline, Helium precipitation in Al–Li alloy, 19: 20613 (CEA-R-2529)
ESSEN, L., Relative velocity in relativity theory, 19: 21098
ETTINGER, K. W., New fast quenching circuit for self-quenched G-M counters, 19: 20349
EVANS, C. J., Statistical current fluctuations in Townsend discharge, 19: 21551
EVANS, W. H., S-wave scattering lengths for π-p interaction, 19: 21043
EVERETT, Allen E., Existence of shadow pions in K^+ decay, 19: 21038
EVERHART, Edgar, Three discrete Q values in Ar^+–Ar collisions, 19: 20846
EYDUK, Yu. A., High-temperature sintering of W, 19: 20532
EYRE, B. L., Neutron irradiation damage in Mo, 19: 20634

F

FABOT, J., Cascades (γ-γ) in first excited state of Hg-200, 19: 21292
FACCHINI, A., Separation of long-lived fission product elements using EDTA, 19: 20052 (ORNL-TM-1035)
FAILLA, Patricia McClement, Recovery from division delay in irradiated gametes of *Arbacia punctulata*, 19: 19496 (ANL-6938(p.49-56))
FAKUDA, Radioactivity of JRR-2 reactor, 19: 21738
FALCONER, David G., Attainment of high resolutions in holography, 19: 20297
FALK, D. S., Possibility of long-range spin polarization in a degenerate electron gas, 19: 20689
FALK, K., Charge transport time in semiconductor detectors, 19: 20366
FALK, W. R., Positron lifetimes in Ar and He, 19: 21011
FALLOWFIELD, T. L., Management of irradiation casualties, 19: 19630
FALOMKIN, I. V., Nuclear form-factors in μ capture in He-3, 19: 21236 (JINR-P-1952)
FAN, Fui-k'ang, Polymorphism of ZrO_2 and rare earth zirconate production, 19: 19925
FANG, P. H., Model of conductivity dispersion in plasmas, 19: 21495
FANG, P. H., Transient conductivity of plasmas, 19: 21496
FARBER, E., Plasma vortices in coaxial plasma accelerator, 19: 21539
FARGE, Yves, New absorption band in irradiated LiF, 19: 20817
FARNELL, Daniel R., Toxicity of intravenously injected U in guinea pigs, 19: 19488
FARRELL, John Alden, Neutron resonances in the Ni isotopes, 19: 21454
FARSKY, J., Changes of electroshock seizures in rats after irradiation, 19: 19514
FASSIO, L., Odd-even effect in nuclear level density, 19: 21364
FASTOVSKII, U. V., Correlation between variations of magnetic field and positive ions inside magnetosphere, 19: 21126
FAULKNER, J., Stellar models, 19: 20790
FAURE, G., Strontium-87 abundance in Hawaiian volcanic rocks, 19: 20168
FAVRE, Maurice, Measurement of densities of plasmas by hyperfrequency interferometry, 19: 21591

FAVRE, Robert, Device for simulation of influence of radioactivity in environment on tracking apparatus for radiation, 19: 20244
FEDERMAN, P., Shell model and deformed states in O-18, 19: 21360
FEDIN, E. I., Pulse method for nuclear quadrupole resonance, 19: 21430
FEDORCHENKO, V. L., Energy exchange between oscillations in plasma, 19: 21526
FEDOROV, A. A., Determination of heavy elements in rocks from γ radiation emitted, 19: 20180
FEELY, Herbert W., Prog. rpt. on Project Star Dust, 9/63, 19: 20657 (DASA-1309)
FEENAN, K., Complex compounds of quadrivalent and tervalent Mo, 19: 19892
FEENBERG, Eugene, Necessary condition on radial distribution function, 19: 21095
FEITH, A. D., Thermal conductivity of UO_2, 19: 20563 (TID-21668)
FEOFILOV, P. P., Luminescence of rare earths in crystals of fluorite type, 19: 19854
FERGUSON, A. T. G., Low threshold neutron detector, 19: 20355
FERGUSON, A. T. G., Measurement of differential neutron scattering cross sections, 19: 21298
FERNANDEZ, M. A. Perez, Localization of iodine in stomach, 19: 19717
FERNBACH, S., Parallelism in computing systems, 19: 20444 (UCRL-12293-T)
FERRARI, Sergio, Producing Th oxide–U oxide mixtures, 19: 19942
FERREBEE, Joseph W., Lung transplantation in the dog, 19: 19523
FERREIRA, P. Leal, Basis for irreducible representations of rotation groups, 19: 20967
FERRELL, R. A., Possibility of long-range spin polarization in a degenerate electron gas, 19: 20689
FERRERO, F., Reactions $K^{39}(\gamma,n)K^{38,38m}$ and $K^{39}(\gamma,np)A^{37}$ up to 80 Mev, 19: 21276
FERRIS, Leslie M., Effect of W on the hydrolysis of UC_2, 19: 19882
FESHCHENKO, V. G., Decomposition potential of system K_2ZrF_6–NaCl–KCl, 19: 19850 (NP-tr-1230)
FETSKO, D. G., Mechanical characteristics of zone-leveled Be, 19: 20544 (AFML-TR-64-388)
FIBICH, M., Phonon effects on nuclear spin relaxation in superconductors, 19: 21174
FICENEC, J. R., Decay $Y_1^0(1660) \rightarrow Y_0^0(1405) + \pi$, 19: 21017
FIEDLER, H. J. V., Emission of delayed neutrons in fission, 19: 21443
FIKS, M. M., Acceleration of variably charged particles in electrostatic field, 19: 20722 (JINR-D-1946)
FILATOVA, T. M., Interaction of traveling EM wave with plasma, 19: 21564
FILIPPOV, A. P., Oxidizing activity of HNO_3 during reaction with UO_2, 19: 19912
FILIPPOV, E. S., Density of Co–C and Ni–C alloys in solid and liquid states, 19: 20567 (LA-tr-65-5)
FILIPPOV, V. K., Heterogeneous equilibrates in $UO_2(NO_3)_2$–HNO_3–H_2O system. III., 19: 19908
FILIPPOV, V. K., Heterogeneous equilibrates in $UO_2(NO_3)_2$–HNO_3–H_2O system. IV., 19: 19909
FINK, Charles R., SNAPS 9A and 19, 19: 20427 (TID-7698(Pt.I)(p.249-56))
FINK, H. J., Superconducting surface sheath of a type-II superconductor, 19: 21171
FINK, Robert M., Enzymic preparation of radioactive orotidine 5'-phosphate, 19: 20024
FINKLER, Paul, Solution to the relativistic dispersion relations, 19: 21461
FINN, R. J., Photopeak efficiencies of NaI(Tl) crystals, 19: 20358
FIRSOV, E. I., Determination of the spin in 0.416-Mev energy level of Fe-55 nucleus from (d,p) and (n,γ) reactions, 19: 21277
FISCHER, Erhard, Combined boiling water and superheater nuclear reactors, 19: 21659
FISCHER, J., Scintillation scanning of spleen, 19: 19726
FISCHOFF, Robert L., Relationship between dimensions of U particles dispersed in air and excretion of U in urine, 19: 19478
FISCUS, W. Guy, Splenic transplantation in the dog, 19: 19521
FISHER, R. M., Application of high-voltage electron microscopy in metallurgical research, 19: 20548 (CONF-640204(p.35-43))
FISHKOVA, T. Ya., Spherical aberration of EM quadrupole lenses, 19: 20685
FITCH, Richard Anthony, Improvements in pulse generators, 19: 20309
FITCH, S. H., Eddy-current inspection for stainless steel-clad U carbide, 19: 20531
FITE, L. E., Mark II automatic computer-coupled activation analysis system, 19: 19765 (TEES-26714(Chap.2))
FITE, Lloyd E., Activation analysis as applied to petroleum exploration industry, 19: 19773 (TID-20467)
FITE, Lloyd E., Prog. rpt. on automated activation analysis, annual, 1964, 19: 19763 (TEES-2671-4)

FITTS, R. B., Influence of stress on fission-gas release, 19: 20586
FLACH, Guenter, Group theoretical methods in shell models. I., 19: 21444
FLACHS, Philippe, Improvements in nuclear reactor control, 19: 21623
FLANARY, J. R., Adsorption of Pa on unfired Vycor, 19: 20051 (ORNL-3773)
FLATBY, J., Exposure to radiation from medical procedures, 19: 19597
FLEISCHER, R. L., Cosmic-ray exposure ages of tektites, 19: 20761
FLEISCHER, R. L., Stability of fission tracks in minerals and glasses, 19: 20674
FLEITMAN, A. H., Corrosion of C steel by Hg, 19: 20493
FLETCHER, Gilbert H., Radiation therapy for cancer of uterine cervix, 19: 19681
FLETCHER, R. D., SNAPTRAN 2/10A-3 destructive test, 19: 21717 (IDO-17019)
FLETCHER, R. D., SNAPTRAN 2/10A-3 post-destructive test reactor examination, 19: 21718 (IDO-17071)
FLETCHER, W., Spark source mass spectrograph, 19: 19830
FLORANCE, E. T., Radio-frequency opacity of nonuniform plasma, 19: 21519
FOCHT, Elizabeth Florence, RBE of γ and x irradiation for cataract induction, 19: 19612
FODOR, Miklos, Ceramic- and dispersion-type fuel for reactors, 19: 21670
FOELDES, Janos, Radiation hazard in use of radioactive isotopes, 19: 19670
FOMIN, Yu., Primary cosmic radiation of superhigh energy, 19: 20884
FONG, Duan, Dislocation structure of subboundaries in Mo single crystals, 19: 20602
FORAGE, A. J., Restoration of *E. coli* strain B after γ irradiation, 19: 19550
FORD, G. W., Statistical mechanics of assemblies of coupled oscillators, 19: 21089
FORMISANO, V., Vertex function in spinor-pseudoscalar theory, 19: 21101
FORREST, A. P. M., Use of Y-90 for destruction of pituitary gland, 19: 19660
FORREZ, G., Bombardment of Cu and Ge by low-energy Ar ions, 19: 20813
FORSSBERG, Arne, Effects of small doses of ionizing radiations, 19: 19516
FORSYTH, E. B., Brookhaven-Columbia plasma lens, 19: 20915 (BNL-8967)
FORSYTH, E. B., Design of AGS fast beam extraction system, 19: 20718 (BNL-8968)
FORSYTH, George Howard, Control of BWR, 19: 21661
FORT, Donald, Gaseous-diffusion isotope-separation process, 19: 20430 (P-1231(RAND))
FORT, L. E., SNAP-10A malfunction detection subsystem, 19: 21734 (NAA-SR-Memo-10666)
FORTUNE, R. D., CERN r-f particle separator—first operation, 19: 20748
FOSS, Alan S., Computational studies of transients in packed tubular chemical reactors, 19: 19734 (UCRL-11757)
FOSTER, George B., Selective ray energy utilization in radiation gaging systems, 19: 20311
FOSTER, Riley P., Splenic transplantation in the dog, 19: 19521
FOUNTAIN, C. W., Neutron-acoustic irradiation of Al single crystals, 19: 20641
FOWLER, E. B., Disposal of Am^{241}–Pu^{239} raffinate solutions, 19: 21750 (LA-3150)
FOWLES, G. W. A., Complex compounds of quadrivalent and tervalent Mo, 19: 19892
FOX, J. W., Thermal conductivity of atomic H from 1 to 400°K, 19: 20700
FRADKIN, D. M., Three-dimensional isotropic harmonic oscillator and SU_3, 19: 21083
FRADKIN, M. I., Investigation of primary cosmic rays, 19: 20894
FRAENZ, K., High-speed binary analog-digital converter, 19: 20299
FRANCESCONI, Aldo, Reprocessing of ceramics by volatilization, 19: 20060
FRANK, Louis Albert, Survey of electrons beyond 5 R_E, 19: 20900
FRANKE, H. G., Discharge broadening in counting tubes, 19: 20379
FRANKEL, R. B., Cerium magnesium nitrate temperature scale, 19: 21162 (UCRL-11828(p.199-201))
FRANKEL, R. B., Induced hyperfine fields in 5p shell, 19: 21359
FRANKEL, R. B., Level scheme of Te-125 and magnetic dipole moment of Sb-125, 19: 21256 (UCRL-11828(p.58-62))
FRANKHOUSER, E. D., Fast reactor fuel burnup, 19: 21672
FRANK-KAMENETSKII, D. A., Particle acceleration in shock emerging from star, 19: 20770
FRANTSUZ, E. T., Radio probe for measurement of cosmic-ray density in stratosphere, 19: 20346
FRANZGROTE, Ernest, Chemical analysis of surfaces using α particles, 19: 19795
FRASER, J. S., Energy release in low-energy fission, 19: 21224 (AECL-2160)
FRASER, M. C., Postirradiation evaluation of Zy-2 pressure tubes. III., 19: 21686 (HW-84540)
FRASER, R., Therapeutic pituitary ablation by Y-90 or Au-198, 19: 19667
FRAZEE, Russell Thomas, Reversed-phase chromatographic separation of Zr and Hf, 19: 19752 (IS-T-2)
FRAZER, J., Gas analytical apparatus for project Dribble, 19: 19776 (UCRL-12169)
FRECK, D. V., Non-thermal ionization combustion product MHD generators, 19: 20911
FREEDE, W. J., Heat transfer systems modification for SRE, 19: 21732 (NAA-SR-10379)
FREEDMAN, Daniel Zissel, Regge poles in boson-fermion scattering, 19: 21077
FREEMAN, Arthur J., Intense magnetic fields, 19: 20701
FREEMAN, R. M., Reaction $^6Li(d,\alpha)\alpha$, 19: 21414
FREEMAN, R. M., Resonances in $^6Li(d,\alpha)\alpha$ and $^7Li(p,\alpha)\alpha$ reactions, 19: 21413
FREIDBERG, Jeffrey Philip, Nonlinear plasma waves, 19: 21588
FRENCH, R. L., Gamma energy and angular distributions near air/ground interface from plane fallout, 19: 20163 (RRA-M42)
FRENCH, R. L. D., Determination of long-lived Kr and Xe isotopes in Magnox reactor coolants, 19: 21616
FRENZEN, Paul, Determination of turbulence dissipation by Eulerian variance analysis, 19: 20654 (ANL-6938(p.242-51))
FRENZEN, Paul, Instrumentation for atmospheric turbulence studies, 19: 20655 (ANL-6938(p.252-6))
FREUND, P. G. O., Meson-baryon scattering in intrinsically broken M(12) symmetry scheme, 19: 21024
FREVERT, L., Transistorized stabilized high-voltage power supply, 19: 20357
FREYMAN, R. W., High-power test on cloverleaf cavity, 19: 20724 (LA-DC-6759)
FRICKE, G., 6.02-Mev level of B-10, 19: 21306
FRIEDELL, Morris T., Radioactive iodine and surgery of thyroid, 19: 19665
FRIEDMAN, L., Intramolecular isotope effects in AB–HD ion-molecule reactions, 19: 19995
FRIEDMAN, L., Small-cross-section exothermic ion-molecule reactions, 19: 19887
FRIEDRICH, H. C., Treatment of ulcerated after-effects of x ray, 19: 19605
FRIEND, James P., Prog. rpt. on Project Star Dust, 9/63, 19: 20657 (DASA-1309)
FRIGERIO, G., Fission-gas retention ability of UO_2 pellets, 19: 20633
FRISCH, H. L., Vertex modification for Coulombic interactions, 19: 21094
FRISCHBIER, H.-J., Telecobalt treatment of uterine carcinoma, 19: 19663
FRITZE, K., Determination of Cu in biological materials, 19: 19807
FROEHLICH, Dietmar, Exciton absorption in presence of excited F centers, 19: 21602
FRONSDAL, Christian, Foundations of SU_3, 19: 20921 (IC/65/7)
FRONSDAL, Christian, Some unitary representations of non-compact form of SU_3, 19: 20922 (IC/65/8)
FRY, W. F., Evidence for $K_{\mu 4}$ decay, 19: 20985
FUCKS, W., Time-resolved Langmuir probe measurements of plasma density, 19: 21515
FUDENBERG, Hugh, Splenic homotransplantation, 19: 19522
FUEREDI, H., Precipitation and hydrolysis of U(VI). II., 19: 19870
FUERTH, R., Experiment to test simultaneity theorem of special theory of relativity, 19: 21106
FUJII, Y., Properties of massive neutral gauge particle, 19: 20989
FUJIMURA, Tadato, Bonding methods for graphite materials, 19: 20505 (JAERI-1071)
FUJIO, Yoshihisa, Hemagglutinin production in vaccinia virus, 19: 19549
FUJISAWA, Ginji, Flowmeter for F gas and vapors of reactive fluorides, 19: 20259 (JAERI-1074)
FUJISAWA, Ginji, Recording thermobalance for F gas and vapors of reactive fluorides, 19: 20258 (JAERI-1070)
FUJITA, Jun-ichi, Beta decay of heavier nuclei, 19: 21304
FUKSIEVICH, E., Open-cycle MHD generator, 19: 20912
FUKUNAGA, Kiyoji, Scatterings of polarized protons from Be-9 and Al-27, 19: 21295
FUKUTOMI, Hiroshi, Distribution of D between water and anion exchanger. I., 19: 19864
FUKUTOMI, Hiroshi, Distribution of D between H_2O and anion exchanger. II., 19: 19865
FULLENBAUM, M. S., Possibility of long-range spin polarization in a degenerate electron gas, 19: 20689
FULLER, John Rodney Dyson, Generation of power by reactor operation, 19: 21705
FULTON, Margaret J., Evaluation of hydrogenic matrix element $<0|e^{ik\cdot r/n}|>$, 19: 20809 (UCRL-12218)
FULTON, T., Electromagnetic form factors and generalized Poincaré

group, 19: 20971
FURCHTGOTT, Ernest, Postscript to behavioral effects of ionizing radiations, 19: 19572
FURSENKO, M. V., Variability of *penicillium nigricans* on uv and x irradiation, 19: 19556
FUSHCHICH, V. I., Analytical properties of scattering amplitude corresponding to class of Feynman diagrams, 19: 21054
FUSHCHICH, V. I., Analytic property of scattering amplitudes corresponding to Feynman diagrams, 19: 21113

G

GABOR, J. D., Pilot plant studies of direct fluorination process, 19: 20059
GABOVICH, M. D., Formation of quasineutral beam in plasma issuing from ion source, 19: 21571
GABRIEL, A. H., Two-meter grazing-incidence spectrometer, 19: 20348
GABUNIYA, L. L., Geometric program for analysis of penetrating showers of cosmic rays, 19: 20896
GACHECHILADZE, R. G., Ionosphere at middle latitudes during magnetic storms, 19: 21132
GAEUMANN, Tino, Radiation chemistry, 19: 19977
GAFNER, G., Intensity of back-reflected electrons from Ni(111), 19: 20868
GAGE, A. H., Advantages of Hg–H_2O vapor cycle for Na reactor, 19: 21701
GAL, E., Thermal conductivity of atomic H from 1 to 400°K, 19: 20700
GALAKTIONOV, B. V., Anisotropy of electron energy distribution in alpha installation, 19: 21583
GALLAGHER, J., Measurement of coronary circulation with new isotope technique, 19: 19668
GALLI, A., Ion-molecule reactions in acetylene, 19: 19988
GALLION, Robert E., Detection and estimation of trace elements by d-c arc excitation, 19: 19827
GAL'PERIN, F. M., Effective magnetic fields acting on nuclei of ferromagnets, 19: 20578
GALYASEVICH, Z., Hydrodynamical equations for superfluid Fermi-liquid and two-particle Green functions. I., 19: 21161 (JINR-P-1953)
GANSHINA, A. N., Biological action of protons of 510-Mev energy in irradiation of dogs, 19: 19578
GARDINER, Donald M., Radiological assistance plan handbook, 19: 20197 (COO-281)
GARDNER, E. L., Test control devices —SNAP-10A vibration tests, 19: 21722 (NAA-SR-Memo-10767)
GARDNER, H. R., Fatigue behavior of Pu–1.0 w/o Ga δ-stabilized Pu, 19: 20545 (BNWL-16)
GARDNER, Leonard B., Applications of radioisotopes, 19: 20403 (AD-606253)
GARDNER, Ross D., Gravimetric determination of H in Mo metal, 19: 19758 (LA-3225)
GARDNER, W. E., Magnetic susceptibility of Sc, 19: 20595
GARLAND, L. Henry, Current status of radiotherapy in carcinoma laryngis, 19: 19659
GARNER, E. L., Isotopic fractionation of U in sandstone, 19: 20187
GARR, K., Directional effects in electron-irradiated Cu single crystals, 19: 20645
GARRATT, C. W., Gamma energy and angular distributions near air/ground interface from plane fallout, 19: 20163 (RRA-M42)
GARRETT, Robert Ogden, First two absorption doublets of Cs, 19: 20870
GARRISON, Warren M., Radiolysis of poly-α-L-glutamic acid in aqueous solution, 19: 19990
GARTNER, Gerald J., Application of adiabatic calorimeter to determination of heats of fusion and formation of metallic compounds, 19: 19838 (IS-1070)
GASKELL, T., Asymptotic form of correlation functions in liquid He-4, 19: 20697
GAST, R. C., Spatial and energy interference among resonance nuclides, 19: 21643 (WAPD-T-1728)
GATSOU, P., Scanning in diagnosis of echinococcus disease of liver, 19: 19729
GATTI, R. C., Fission barriers of Po-210 and Sb-119, and Sb-117, 19: 21261 (UCRL-11828(p.81-3))
GATTI, Raymond C., Fission barrier of Tl-201, 19: 21260 (UCRL-11828 (p.81))
GATTO, R., Nonleptonic hyperon P waves in SU(6) symmetry, 19: 21021
GATTO, R., U(6) ⊗ U(6) and nonleptonic decays, 19: 21009
GAUTIER, Lucienne, Clebsch-Gordan coefficients adapted to cubic symmetry, 19: 21097
GAZAZYAN, E. D., Radiation from point charge in waveguide in presence of external magnetic field, 19: 21064
GEARY, A. L., Hot extrusion of metal powders, 19: 20518 (NMI-TJ-29)
GEERING, Jean-Jacques, Radiochemical method for analysis of Sr-90 in bones, 19: 19789
GEEVER, E. F., Wound healing: effect of ascorbic acid and D_2O, 19: 19484
GEHENIAU, Jules, Internal groups and Heisenberg theory of elementary particles, 19: 20948
GEIPEL, Walter, Means for emergency cooling of nuclear reactor, 19: 21630
GEIPEL, Walter, Method for cooling reactors with steam, 19: 21662
GEISLER, J. E., Relation between dispersion of whistler and electron temperature in protonosphere, 19: 21140
GELDART, D. J. W., Renormalization constant of electron gas, 19: 20968
GEORGE, T. M., Anomalous E2 particle parameters in deformed nuclei, 19: 21399
GERASIMOV, A. B., Impurity photoconductivity produced in Ge by γ irradiation, 19: 20623
GERASIMOV, A. B., Low-temperature irradiation of Ge with fast electrons, 19: 20624
GERASIMOV, A. I., High-current air-core betatrons, 19: 20740
GERBER, J. P., Interactions of 3.0-Bev/c K⁻ mesons with nuclei, 19: 21389
GERJUOY, E., Multiple-wave propagation and causality, 19: 20944
GERKE, David George, $C^{12}(d,p)C^{13}$: distorted-wave Born approximation analysis, 19: 21439
GERMAI, Georges, Measurement of weak activities of $^{137}CsClO_4$, $^{90}SrSO_4$, and $Ag^{131}I$ in scintillation gels, 19: 20335
GERRARD, Martha, Preparation of In-115m, 19: 20023 (ORNL-tr-556)
GERSTEIN, I. S., Meson-meson couplings in SU(6)-invariant theory, 19: 21013
GESHKENBEIN, B. V., $K^* \to K\pi\pi$ decay, 19: 20984
GESKE, G., Intensity and final energy of bremsstrahlung of betatron using ionization chambers, 19: 20337
GHOSE, A. M., Uniform-spectral-sensitivity photon counter, 19: 20356
GIANNINI, Gabriel M., High-temperature acceleration of propellants, 19: 20139
GIARDINI-GUIDONI, A., Ion-molecule reactions in acetylene, 19: 19988
GIBBONS, A. B., Geologic map of Quartet Dome Quadrangle, Nye County, Nevada, 19: 20151 (TEI-860)
GIBSON, W. A., Comparison of measured neutron and proton spectra with calculated spectra in energy region between 50 and 160 Mev, 19: 21244 (ORNL-P-844)
GIBSON, Walter M., X rays emitted in coincidence with fission of Cf-252, 19: 21229 (BNL-8841)
GIERTS, G., Spectrometry of fast neutrons by surface barrier junctions and Li-6, 19: 20334
GILBERT, J. F., Elastic wave interaction with cylindrical cavity, 19: 20659 (AD-606490)
GILBERT, William S., Problems of induced radioactivity around 200-Bev AGS, 19: 20732 (UCRL-11796)
GILBODY, H. B., Excitation in rare gas ion–atom collisions, 19: 20862
GILBREATH, William P., Vapor pressure of Mg, 19: 20556 (NASA-TN-2723)
GILLIES, N. E., Restoration of *E. coli* strain B after γ irradiation, 19: 19550
GILMER, G. H., Diffuse interface in critical fluid mixture, 19: 19952
GILMORE, J. S., Symmetry of neutron-induced Pu-239 fission in resonance region, 19: 21241 (LA-DC-6639)
GILMORE, W., Diffuse interface in critical fluid mixture, 19: 19952
GIN, John Alexander Tjon Joe, Quantum statistical theory of relaxation in isolated spin systems, 19: 21121
GINIER, Rene, First results of tests of Rapsodie block pile, 19: 21730 (CEA-R-2557)
GINOCCHIO, Joseph Natale, Symplectic symmetry in $f_{7/2}$ nuclei, 19: 21437
GINZBURG, V. L., Gamma and x radiation associated with cosmic rays, 19: 20881
GINZBURG, V. L., Investigation of primary cosmic rays, 19: 20894
GINZBURG, V. L., Negative absorption of Cherenkov radiation in an electron stream, 19: 20679
GINZBURG, V. L., Origin of cosmic rays, 19: 20880
GIPSON, Donald H., Explosively driven pipe closure, 19: 20100 (UCRL-12203)
GIRARDI, Francesco, Determination of Co in steel by neutron activation and γ spectrometry, 19: 19784
GISSLER, W., Scattering of neutrons on heavy water, 19: 21221
GIZA, T., Effect of Sr-90 on treatment of experimental rickets, 19: 19680
GLADYSHEV, D. A., Neutron cross sections in In and Sm, 19: 21285
GLAESER, W., Phonon frequency distribution of V, 19: 20553 (KFK-262)
GLAESER, W., Scattering laws of some hydrogenous moderators, 19: 21200 (KFK-264)
GLASER, H., Macroinstabilities in theta pinch, 19: 21525
GLASNIK, J., Magnetic fields in units of ionic optical system for 5-Bev antiproton channel, 19: 20723 (JINR-P-1945)
GLAUDE, V. M. M., Prog. rpt. on instabilities in metal-vapor plasmas, 10–12/64, 19: 21490 (TID-21698)
GLAZUNOV, P. Yu., Radiation synthesis of polymers based on dimethylphosphinoborine, 19: 19982

GLENDENIN, L. E., Emission of K x-rays in spontaneous fission of Cf-252, 19: 21355
GLENDENNING, Norman K., Nuclear spectroscopy with two-nucleon transfer reactions, 19: 21266 (UCRL-11828(p.108-9))
GLENDENNING, Norman K., Octupole states in N-15 and O-16, 19: 21268 (UCRL-11828(p.129-31))
GLUCKSTERN, R. L., Transverse beam blow-up in standing-wave linac cavity, 19: 20726 (LA-DC-6775)
GNEVYSHEV, M. N., Solar activity in earth's lower atmosphere, 19: 20780
GODON, C., Use of radioactive I in thyroid pathology, 19: 19587
GOEBEL, J. B., 709/7090 program for indexing x-ray diffraction powder patterns. I., 19: 19834 (HW-74393)
GOEBEL, J. B., 709/7090 program for indexing x-ray diffraction powder patterns. III., 19: 19835 (HW-89062)
GOEKGOER, S., Response measurement of magnetic probe, 19: 20293
GOERLICH, P., Spectroscopic properties of activated laser crystals. III., 19: 20849
GOFMAN, John W., Magnetic fields, vagal inhibition, and acetylcholinesterase activity, 19: 21776 (UCRL-12389)
GOHEEN, Milton Ward, Inorganic salts of 5-nitrobarbituric acid, 19: 19824
GOLD, Raymond, Iterative unfolding method for response matrices, 19: 20316 (ANL-6984)
GOL'DANSKII, V. I., Annihilation of positrons in alkali-halide crystals, 19: 20820
GOL'DANSKII, V. I., Mechanisms of proton decays, 19: 21271 (KFK-tr-161)
GOLDBERGER, M. L., Tests of relativistic SU(6) schemes, 19: 21025
GOLDEN, Robert L., CP-nonconserving decay $K_1^0 \to \pi^+ + \pi^- + \pi^0$, 19: 21020
GOLDIN, V. Ya., Quasidiffusion method for solving kinetic equation, 19: 21222
GOLDMAN, Ernest H., Automatic translation, 19: 20452
GOLDSCHMIDT-CLERMONT, Y., Antiproton-proton elastic scattering, 19: 20976
GOLDSTEIN, J. S., Lectures on astrophysics and the many-body problem. II., 19: 20714
GOLDSTEIN, Jack S., Stellar evolution, 19: 20784
GOLDSTEIN, N. D., Isotopic exchange of O in γ-Al_2O_3–O_2 system, 19: 19872
GOLDSTEIN, Y., Tunneling in superconducting diodes, 19: 21178
GOLDSWORTHY, W. W., Instrument development program, 19: 20287 (UCRL-11828(p.230-2))
GOLUB, V. A., Formation of complexes from Y, La, and rare-earth elements with serine, 19: 19874
GOLUTVINA, M. M., Concentration of radioactive Sr and Cs from H_2O by electrodialysis, 19: 19809
GOLYAK, I. G., Elastic proton-antiproton interaction, 19: 20954
GONCHARENKO, E. N., Erythrograms of rats subjected to action of synthetic radiomimetic embikhin, 19: 19489
GONGORA, R., Scintigraphic method in morphological exploration of liver, 19: 19728
GONZALEZ, C. G., Paper electrophoresis of Y in HCl, 19: 19810
GOOD, Mary L., 5,5'Thiodisalicyclic acid as analytical reagent, 19: 19812
GOODE, J. H., Adsorption of Pa on unfired Vycor, 19: 20051 (ORNL-3773)
GOODE, R. J., Prog. rpt. on metallurgical characteristics of high-strength structural materials, 9–12/64, 19: 20462 (NRL-6258)
GOODY, R. M., Atmospheric radiation. I., 19: 21156
GORDON, B. E., Determination of Cl by instrumental neutron activation analysis, 19: 19826
GORDON, Glen E., Yields of Te-131 and Te-133 isomers in fission, 19: 21390
GORMAN, J. G., Rotating plasma device, 19: 21593
GOSO, R. P., Preparation of carrier-free P-32, 19: 20021 (NP-14900)
GOULD, R. J., Galactic x-ray sources, 19: 20765
GOULDING, F. S., Beam integrator, 19: 20284 (UCRL-11828(p.222-3))
GOULDING, F. S., Experimental instrumentation for 88-inch cyclotron, 19: 20282 (UCRL-11828(p.218-19))
GOV, H. B. F., Effect of H_2 and H_2O on radiation-induced reaction of CO_2, 19: 19954 (AERE-R-4839)
GOYAL, I. C., Diffusion coefficient of thermal neutrons in Be, 19: 21206
GRABCEV, B., Total reflection of neutrons in Co mirrors, 19: 21201 (KFK-tr-164)
GRADSZTAJN, E., Intranuclear cascade and breakup calculations on production of Li, Be, and B isotopes in C-12 by 156-Mev protons, 19: 21402
GRADSZTAJN, E., Lithium-6 and Li-7 production in C-12 and O-16 by high-energy protons, 19: 21352
GRADZINSKI, Andrzej, Effect of γ radiation on red blood cells in stored human blood, 19: 19513
[GRAFF VON] REICHENBACH, H., Sorption of Sr in Schleswig-Holstein soils, 19: 19474 (CEA-tr-A-1616)
GRAHAM, R. L., Energy levels of Bk-249, 19: 21253 (UCRL-11828(p.38-40))
GRANDY, T. B., Reaction $^{30}Si(d,n)^{31}P$, 19: 21376
GRANGER, H. C., Uranium ore rolls—an analysis, 19: 20186
GRANOVSKII, Ya. I., Expansion of scattering amplitude into partial waves, 19: 21052
GRASHIN, Yu. M., Time analyzer based on AI-100, 19: 20298
GRATTON, L., Associations and very young clusters, 19: 20794
GRATTON, L., Observational approach to stellar evolution, 19: 20788
GRATTON, L., Problem of Eta Carinae, 19: 20796
GRATTON, L., Star evolution, 19: 20786
GRATTON, L., Stellar evolution—introductory lecture, 19: 20787
GRAUMAN, J., Observations of radiative τ^+ decays, 19: 20990
GRAY, A. H., Jr., Uniqueness of steady-state solutions to the Fokker-Planck equation, 19: 20963
GRAY, James, Jr., Carbon-14 measurements in atmosphere, 1953–64, 19: 20155 (HASL-159)
GRAYBEAL, Jack D., Nuclear quadrupole resonance of Bi-209 in $BiBr_3$, 19: 19940
GREBE, John J., Using light obtained from nuclear reactors directly to carry out underground processes, 19: 21710
GREEN, A. M., Collective admixtures in odd-parity states of O-16, 19: 21361
GREEN, H. H., Third positron lifetime in solid polymers, 19: 21044
GREEN, Michael A., Effect of accelerator parameters on mechanical tuning of r-f cavities, 19: 20735 (UCRL-11807)
GREEN, Paul J., Nuclear quadrupole resonance of Bi-209 in $BiBr_3$, 19: 19940
GREEN, R. M., Photopeak efficiencies of NaI(Tl) crystals, 19: 20358
GREEN, Thomas A., Electron capture by protons passing through He, 19: 20821
GREEN, W. B., Analysis of shield test facility experiments using two-component method, 19: 21614 (NAA-SR-Memo-10559)
GREEN, W. B., Monte Carlo evaluation of collimator efficiency, 19: 21612 (NAA-SR-Memo-10557(Pt.I))
GREEN, W. B., Monte Carlo evaluation of collimator efficiency, 19: 21613 (NAA-SR-Memo-10557(Pt.II))
GREENBERG, O. W., High-order limit of para-Bose and para-Fermi fields, 19: 20960
GREENE, John M., Calculation of singularities of magnetic field, 19: 21534
GREENE, N. D., Electrode kinetic studies of Th, 19: 19762 (RPI-2714-6)
GREENFIELD, I. G., Interstitial loops in neutron-irradiated Mo, 19: 20636
GREENMAN, J. V., Five-point function in perturbation theory, 19: 21096
GREINER, Norman Roy, Reactions of hydrocarbons initiated by excited He, 19: 19937
GREINER, Walter, Magnetic dipole transitions and g_n factors in deformed even-even nuclei, 19: 21410
GRIFFIN, D. S., Stresses and deflections of thick, curved plates, 19: 20130
GRIFFIN, H. C., Emission of K x-rays in spontaneous fission of Cf-252, 19: 21355
GRIFFITHS, K., Stellar models, 19: 20790
GRIGORESCU, Leon, Measurement of activity of radionuclides by 4π β-γ coincidences, 19: 20385
GRIGORESCU, Leon, Measurement of activity of radionuclides by β-γ coincidence method, 19: 20386
GRIGOR'EVA, V. S., Optical properties of rare earth oxides. II., 19: 19928
GRIGOROV, N. L., Nature of cosmic-ray particles beyond atmosphere, 19: 20893
GRIGOROVICH, V. K., Periodicity of structure and properties of lanthanides in connection with their phase diagrams, 19: 20600
GRIMLEY, H. M., Low-voltage cold-cathode discharges in He, 19: 21499
GRIMM, John, Prog. rpt. on radiation-resistant electron tubes, 10–11/64, 19: 20399 (NP-14946)
GRINGAUZ, K. I., Correlation between variations of magnetic field and positive ions inside magnetosphere, 19: 21126
GRISHIN, V. G., Possible existence of new boson resonance decays involving γ quanta, 19: 20931 (JINR-P-1951)
GRMELA, M., Neutron thermalization based on thermodynamics, 19: 21204
GROBLICKI, Peter J., Atomic-beam scattering studies on Li–Hg system, 19: 20823
GROCE, D. E., Reaction $^{14}C(^{16}O,\alpha)^{26}Mg$, 19: 21313
GRODZINS, L., Lifetime of 120-kev level of Lu-177, 19: 21319
GROESENEKEN, P., Electron bombardment in metallurgy, 19: 20466
GROSS, Chris, Damage to Ge due to proton bombardments, 19: 20617 (NASA-TN-D-2727)
GROSS, J., Scanning with I-125, 19: 19711
GROSSE-RYUKEN, Kh., Isolation of neutron-deficient isotopes of elements in Ce group of rare earths, 19: 20078
GROSVALD, Guiu, Nature of dipoles in Pr oxides, 19: 20818
GRUBER, C., Superconductivity and electromagnetic potentials, 19: 21163
GRUBER, U., Energies and character of low-lying levels in Nb-94,

19: 21330
GRUBESSICH, J., Oxidation-resistant coatings for Nb alloys, 19: 20483 (SCNC-318)
GRUNDER, Hermann A., 88-Inch cyclotron operation and development, 19: 20736 (UCRL-11828(p.236-41))
GRZYBEK, H., Skeletal muscles at different stages of radiation disease, 19: 19574
GUARINO, M., Changes induced by radiations in some subcutaneous nervous, structures, 19: 19591
GUEBEN, M., Operation of PWR-type powerplant, 19: 21679 (BLG-261)
GUEDES DE CARVALHO, R. A., Paper electrophoresis of Y in HCl, 19: 19810
GUERNSEY, Ralph L., Comment on two-particle correlation function in plasma, 19: 21543
GUGAN, K., Fine focus x-ray source, 19: 20291
GUIDI, Eugen, Pressure tubes containing fuel elements in reactor, 19: 21633
GUILLAUMONT, Robert, Hydrolysis of Pa(IV), 19: 20063
GUILLAUMONT, Robert, Ionic species of protactinium in aqueous solution. II., 19: 20055
GUILLAUMONT, Robert, Ionic species of Pa in aqueous solution. III., 19: 20056
GUILLON, A., Energy resolution in liquid scintillation counting, 19: 20351
GUILLOU, Andre, Determination of amounts of nuclides during radioactive transformations. II., 19: 19958 (CEA-R-2348)
GUILLOU, Andre, Specifications for multi-group scattering code of two dimensions: ALCI, 19: 21197 (CEA-R-2747 & Add.)
GUILLOU, Andre, Specifications for scattering code for XY geometry: DAIXY, 19: 21198 (CEA-R-2759)
GUILLOU, Ginette, Determination of amounts of nuclides during radioactive transformations. II., 19: 19958 (CEA-R-2348)
GUILLOU, Ginette, Specifications for multi-group scattering code of two dimensions: ALCI, 19: 21197 (CEA-R-2747 & Add.)
GUINARD, Albert, Observing specimens contained in fluid-tight chamber, 19: 20105
GUINEA-MOORHEAD, M., Antiproton-proton elastic scattering, 19: 20976
GUINIER, Andre, New absorption band in irradiated LiF, 19: 20817
GUINN, V. P., Neutron activation analysis procedures for determination of O in K, 19: 19751 (GA-5982)
GULBRANSEN, Earl A., General concepts of gas-metal reactions, 19: 20486
GULKO, A. D., Reversal of the thermal neutron spin, 19: 21300
GUNST, S. B., Epicadmium capture-to-fission cross section, 19: 21334
GUPTA, S. C., Laminar unsteady MHD flow, 19: 20663
GUREEV, E. S., Extraction of actinide elements with dialkyl phosphoric acids, 19: 20075
GUSAKOW, M., Calculation of nucleon-α cascades, 19: 21372
GUS'KOV, Yu. K., Electric breakdown through slot in glass in Cs vapor, 19: 21578
GUSTAFSON, L. D., Performance of selected inhibitors in reactor coolant backup service, 19: 21714 (RL-REA-592)
GUTOWSKY, H. S., Electron coupling of nuclear spins, 19: 19888
GUTSCHER, W. D., Close in tracking error in interferometer tracking systems, 19: 21767 (SC-TM-65-44)
GVELESIANI, G. G., Aluminothermal reduction of Eu_2O_3, 19: 20533
GYFTAKI, H., Photoscanning of spleen, 19: 19725
GYFTOPOULOS, Elias P., Nonlinear reactor kinetics, 19: 21642 (MMPP-FRPC-64-3)

H

HAAS, F. X., Photochemical method of separating Hg isotopes, 19: 20429 (MLM-1214)
HAAS, G. M., Properties of high-β plasma, 19: 21531
HAASE, D. J., Crystal chemistry of rare earth group VI systems. I., 19: 19879
HAASE, D. J., Crystal chemistry of rare earth group VI systems. II., 19: 19880
HACK, M., Evolution of close binary systems, 19: 20803
HADDOCK, R. P., Neutron-neutron S-wave scattering length from reaction $\pi^- + d \rightarrow 2n + \gamma$, 19: 20995
HAFEMEISTER, D. W., Mössbauer effect of 29.4-kev neutron-capture γ ray of K-40, 19: 21409
HAGEMANN, F. T., Carbon-14 measurements in atmosphere, 1953–64, 19: 20155 (HASL-159)
HAGEN, E. W., Dynamic gas thermometry, 19: 20277 (ORNL-P-1068)
HAGER, Edward B., Human kidney transplantation, 19: 19520
HAINES, Malcolm, Comments on thermoelectric effects in Joule-heated plasma, 19: 21544
HAINSKI, Z., Analysis of purified U compounds, 19: 19800
HAJDUKOVIC, Srdan, Prog. rpt. on hematopoietic regeneration of irradiated animals, final, 19: 19499 (NP-14899)
HALLER, Mitchell W., Prog. rpt. on fuel of UC particles in U matrix, 12/63, 19: 20515 (NCSC-2981-6)
HALLER, Mitchell W., Prog. rpt. on fuel UC particles in U matrix, 3/64, 19: 20516 (NCSC-2981-7)
HALLER, Mitchell W., Prog. rpt. on fuel of UC particles in U matrix, 6/64, 19: 20517 (NCSC-2981-8)
HALTEMAN, Eber K., Nuclear reactor fuel members, 19: 20497
HALVORSEN, Sten, Injury to bone marrow after Thorotrast, 19: 19567
HAMILTON, J. H., Anomalous E2 particle parameters in deformed nuclei, 19: 21399
HAMILTON, R. G., Water surface waves in BWR, 19: 21684 (GEAP-4061)
HAMLET, Peter, Radiolysis of hexafluoroethane, 19: 19991
HAMME, J. V., Prog. rpt. on U interstitial phase, 3/64, 19: 20510 (NCSC-2663-16)
HAMMEL, E. F., Fountain pressure vs. temperature relationship in liquid He II, 19: 21179
HAMMEL, J. E., Penetration of plasma stream into transverse magnetic field, 19: 21475 (LA-DC-6383)
HAMMER, D. C., Viscosity x normal density of liquid He, 19: 21168
HAMMER, J. J., Sodium-heated, modular, steam generators for SCTI, 19: 21611 (NAA-SR-9826)
HAMMOND, J. P., Evaluation of Th-base alloys for high-temperature strength, 19: 20560 (ORNL-3777)
HAMMOND, R. P., Desalination of sea water using nuclear energy, 19: 21707 (ORNL-TM-432)
HAMMOND, R. Philip, Sea-water desalination with nuclear energy, 19: 21708 (ORNL-TM-465)
HAMPL, V., Preparation of labeled condensation aerosols. I., 19: 20027
HAN, Qi-zhi, Decomposition of direct products of irreducible representation of SU_3, 19: 21057
HANES, H. D., Surface damage in machined Be, 19: 20502 (DMIC-Memo-198)
HANICKA, M., Effect of Sr-90 on treatment of experimental rickets, 19: 19680
HANNA, G. C., Fission data and nuclear technology, 19: 21225 (AECL-2168)
HANNAWAY, P. H., Effects of energetic phonon irradiation on Ge, 19: 20612 (AFCRL-64-839)
HANSEN, K. F., Solutions of reactor kinetics equations, 19: 21647
HANSEN, O., Energy levels in Ti-48 and Ti-50, 19: 21346
HANSEN, P. G., Odd-odd nucleus with 0^+ ground state (^{156}Eu), 19: 21350
HANSON, H. P., Incoherent x-ray scattering factors, 19: 20824
HANSON, W. B., Structure of the ionosphere, 19: 21159
HARA, Yasuo, Proton-antiproton annihilation in M(12) symmetry model, 19: 21033
HARARI, H., Meson and baryon masses in SU(6) symmetry, 19: 21030
HARARI, H., Tests of relativistic SU(6) in p-$\bar{p}$ annihilation, 19: 20983
HARDING, G. N., Study of helicon waves in In, 19: 21553
HARDY, Edward P., Jr., Prog. rpt. on fallout program, 12/64–3/65, 19: 20154 (HASL-158)
HARDY, J. C., Log ft values and T = ½ analog states, 19: 21379
HARDY, J., Jr., Resonance integrals for U-233 fission and Th-232 capture, 19: 21336
HARDY, Lyndon M., Further evidence for Kπ resonance near 1400 Mev, 19: 21004
HARE, G. E., Revolution in power generation, 19: 20415
HARLAN, J. W., Ready-to-eat ration-type beef items, 19: 20406 (NP-14920)
HARLING, O. K., Detector time jitter in He-3 and BF_3 proportional counters, 19: 20364
HARLOW, M. V., Jr., Elastic scattering of 17- to 21-Mev neutrons from C-12, 19: 21310
HARMS, W. O., Coated-particle fuel development, 19: 20463 (ORNL-TM-431)
HARMSEN, D. M., Interactions of 3.0-Bev/c K⁻ mesons with nuclei, 19: 21389
HARPER, J. A., Disposal of large quantities of degraded and low-level contaminated solvent, 19: 21748 (DPSPU-64-30-8B)
HARRIS, A. M., Gadolinium S state ions in metals, 19: 20698
HARRIS, E. G., Radiative transfer in dispersive media, 19: 20688
HARRIS, J. A., Nondestructive activation analysis with Li-drifted Ge detectors, 19: 19775 (UCRL-11828(p.197-9))
HARRIS, M. J., Thermal neutron absorption cross section of H, 19: 21219
HARRIS, T. E., Random functions of cosmic-ray cascades, 19: 20874 (P-1020(RAND))
HARRISON, B. Kent, Electromagnetic solutions of field equations of general relativity, 19: 21103
HARRISON, J. Hartwell, Human kidney transplantation, 19: 19520
HARRISON, K. T., Preparation of single-phase single crystals of UO_2, 19: 20530
HARRISON, R. W., Prog. rpt. on alkali metal corrosion, 9/26–12/26/64,

19: 20474 (NASA-CR-54281)
HARROP, P. J., Electrical conductivity of ZrO_2, 19: 20621
HART, Edwin J., Gamma-induced chain reaction between formic acid and H_2O_2, 19: 19989
HART, W., S-wave scattering lengths for n-p interaction, 19: 21043
HARTLEY, H. O., Application of linear estimation to chemical mixture problem, 19: 19769 (TEES-2671-4(Chap.7))
HARTWELL, Shattuck W., Jr., Radiogenic neoplasms of the hands, 19: 19524
HARTWIG, C., Baryon spectroscopy by inelastic e-p scattering, 19: 20997
HARUYAMA, Kenji, Solvent extractions of Cs and Fr, 19: 20058
HARVEY, B. G., Energy variation of phase rule in α-particle scattering, 19: 21269 (UCRL-11828(p.132-3))
HARVEY, B. G., Inelastic scattering of 50.9-Mev α particles from Ne-20, 19: 21267 (UCRL-11828(p.113-16))
HARVEY, Bernard G., Octupole states in N-15 and O-16, 19: 21268 (UCRL-11828(p.129-31))
HASEGAWA, Akira, Integration of the Boltzmann equation in presence of spatial gradients, 19: 21542
HASTE, G. R., Single-pass experiments (DCX-1), 19: 21480 (ORNL-3760(p.1-9))
HATSUKADE, S., Parafermion model for higher baryonic resonance, 19: 20975
HATTERSLEY, P. M., Pion capture in complex nuclei, 19: 21315
HATTON, J., Spin lattice relaxation time of F-19 in CaF_2 below 1°K, 19: 19897
HATTORI, Toikichi, Effect of absorber position on scattering in measurement of β absorption, 19: 21597
HAUSKNECHT, D. F., Computer calculation of fuel cladding temperatures, 19: 21691 (NAA-SR-Memo-9492)
HAVAS, Peter, Effects of gravitational radiation reaction in general relativistic two-body problem, 19: 21104
HAVLENA, Joan M., X irradiation of the 36-hour rat embryo, 19: 19618
HAYAKAWA, Sohachiro, Luminescence of uranyl ions dissolved in H_2O, 19: 19863
HAYES, W., Paramagnetic resonance of H in CaF_2 and KCl, 19: 19896
HAYWOOD, F. F., Spatial dose distribution in air-over-ground geometry, 19: 20217
HAYWOOD, F. F., Technical concept—Operation HENRE, 19: 21199 (CEX-65.02)
HEADRIDGE, J. B., Polarographic determination of Mo in Nb-base alloys, 19: 19781
HEBERT, Alvin J., Molecular beam electric resonance experiments on LiF, LiCl, LiBr, LiI, and NaF, 19: 19848 (UCRL-11828(p.193-7))
HECHTMAN, Herbert B., Lung transplantation in the dog, 19: 19523
HEGEWALD, H., Comparative physical considerations of modern ways of irradiation, 19: 19688
HEIDENREICH, Robert D., Elastic and inelastic scattering of electrons at high accelerating voltages, 19: 20254
HEIM, M., Two-group theory of fermion system, 19: 21122
HEINTZELMAN, J. T., Protective actions of AET or serotonin in radiation injury, 19: 19635
HEISS, A., Differential interferometer and application to determination of electron density gradients, 19: 21472 (IPP-1/25)
HELDMANN, Gerhard, Influence of limiting of charge number on exchange, 19: 20941
HELM, J. W., Irradiation of N-reactor graphite, 19: 20614 (HW-81250A)
HELMAN, William Phillip, Luminescence of solutions of benzene and some simple benzene derivatives, 19: 21771 (TID-21684)
HENDERSON, E. H., Determination of radiostrontium in biological materials, 19: 19739 (AERE-AM-101)
HENDRICKS, J. W., High-temperature high-vacuum thermocouple drift tests, 19: 20278 (ORNL-P-1069)
HENDRIE, D. L., Reaction $^{12}C(p,2p)^{11}B$ at 50 Mev, 19: 21401
HENDRIE, J. M., Safety analysis on Brookhaven HFBR, 19: 21727 (BNL-7661(Vol.II))
HENDRIE, J. M., Safety analysis on Brookhaven HFBR, 19: 21728 (BNL-7661(Vol.I))
HENDRON, A. J., Jr., Predicting shape of explosion-produced craters, 19: 20089 (NP-14887)
HENICKSMAN, A. L., Spectrophotometric determination of U in mixtures of U and Mo, 19: 19759 (LA-3226)
HENROTIN, H., Interactions in flight of low-energy K⁻ mesons with emulsion nuclei, 19: 21365
HENUSET, M., Electron bombardment in metallurgy, 19: 20466
HERAK, J. N., ESR study of irradiated anhydrous maltose, 19: 19994
HEREMANS, R., Conversion of UO_2 to UF_4, 19: 19867
HEREMANS, Rene, Reprocessing of ceramics by volatilization, 19: 20060
HERMAN, John R., Proton-collision mechanism for production of spread F irregularities, 19: 21125 (RAD-TR-64-27)
HERRERA, John Chordon, Vacuum polarization phenomena in quantum electrodynamics, 19: 21119
HERRMANN, A., Mott effect of elementary particles and nuclei, 19: 21073
HERRMANN, Guenter, 25 Years of nuclear fission, 19: 20033
HERTZOG, Daniel, Exchange reactions between molten salt and TBP in liquid silicone, 19: 19833 (CEA-R-2628)
HERZOG, R. F. K., Helium memory effects observed with tandem mass spectrometer, 19: 20146
HESS, D. N., Evaluation of Hastelloy F and other materials for centrifuge in fuel recovery plant, 19: 20481 (ORNL-3787)
HESS, Paul, Underground laboratory for high-sensitivity γ counting, 19: 20093 (ANL-6938(p.194-205))
HESS, Richard I., Further evidence for Kπ resonance near 1400 Mev, 19: 21004
HETRICK, David L., Prog. rpt. on application of automatic control theory to nuclear rocket, 2–9/64, 19: 21723 (NASA-CR-193)
HETTER, Britia, Salivary secretion of Cs-131, 19: 19486
HEYWOOD, John B., Diagnostic experiments in magnetically driven shock tube, 19: 20661 (RLE-TR-428)
HIBBERT, P., Determination of Po-210 in urine, 19: 19791
HIBBITTS, W. H., Anomalous E2 particle parameters in deformed nuclei, 19: 21399
HIEBERT, J. C., Reaction $^{63}Cu(d,^3He)^{62}Ni$, 19: 21358
HIEBERT, J. C., Reaction $^{14}N(^{14}N,^{13}N)^{15}N$ and the neutron tunneling mechanism, 19: 21388
HIGBY, William J., Writing topological programs for GUTS, 19: 20320 (IS-989)
HIGGINS, John Reid, Kinematic analysis of production reactions, 19: 21076
HIGH, C. N., Prog. rpt. on pneumatic nutator actuator motor, 12/64, 19: 21615 (NASA-CR-54282)
HIKIDO, K., Excursion-limiting fuse for critical assembly, 19: 21617
HILL, H., Neutron yield from deuterided Er and Ti targets, 19: 21301
HILL, J. G., Theory of resonance escape in heterogeneous fuel. I., 19: 21648
HILLAIRET, Jacques, Apparatus for high-temperature measurement of interior friction in rigid samples, 19: 20245 (CEA-R-2718)
HILLIG, O. R., Material buckling for UC-fueled graphite-moderated assemblies, 19: 21692 (NAA-SR-Memo-9976)
HINDS, S., Angular distributions of (t,p) and (d,d′) reactions leading to Mg-26, 19: 21311
HIRAI, Takako, Solid-state polymerization of binary component system, 19: 19972
HIRAMOTO, Toshiyuki, Whole-body counter. I., 19: 20377
HIRATA, Akira, Minimum criticality calculation for JPDR, 19: 21689 (JAERI-1068)
HIRATA, Masao, Luminescence of uranyl ions dissolved in H_2O, 19: 19863
HIRATA, Masao, Luminescence of uranyl ions dissolved in H_2O, 19: 19863
HIRAYAMA, Fumio, Intramolecular excimer formation in diphenyl- and triphenyl alkanes, 19: 19956 (ANL-6938(p.27-35))
HIRLEA, I., Radiation effects on live substances, 19: 19562
HIRONO, Y., Induced premeiotic exchange of linked markers in the angiosperm arabidopsis, 19: 19548
HIRSCH, Peter, E-mode propagation in plane-stratified plasma, 19: 21589
HIRT, A., "Precursor ionization" occurring in hot plasmas, 19: 21471 (IPP-1/24)
HIRT, C. W., Equilibrium distribution functions for a classical electron gas, 19: 20683
HIZHNYAKOV, V., Anharmonicity effect in the Mössbauer line shift, 19: 21422
HOBBS, G. D., Diffusion of current sheath in toroidal discharge, 19: 21512
HOBSON, J. P., Low-pressure limits of hot-filament ionization gages, 19: 20147
HOCHMAN, A., Scanning with I-125, 19: 19711
HOCHMAN, J. M., Mercury Rankine program thermoelectric pump data analysis, 19: 20096 (NAA-SR-Memo-10729)
HOCHMAN, J. M., Mercury wetting and its effects on heat transfer, 19: 20112 (NAA-SR-Memo-10315)
HODBY, J. W., Paramagnetic resonance of H in CaF_2 and KCl, 19: 19896
HOEHN, R., Effect of γ radiation on leather, 19: 20414
HOELZL, K., Inelastic electron-deuteron scattering, 19: 20942
HOFF, R. W., Spontaneous fission in very neutron-rich isotopes, 19: 21403
HOFFMAN, E. E., Boiling-K corrosion loop test, 19: 20476 (ORNL-3603)
HOFFMAN, E. E., Prog. rpt. on K corrosion test loop, 7/15–10/15/64, 19: 20473 (NASA-CR-54269)
HOFFMANN, H., Measurement of mean inner potentials of Be, 19: 20599
HOIGNE, J., Application of high-energy radiation to chemical production, 19: 20409
HOLDEN, F. R., Radiation control regulations of state of California, 19: 19655
HOLDEN, Norman Edward, Three-body forces in the triton, 19: 21075

HOLLAND, R. E., Mössbauer effect in K-40 using an accelerator, 19: 21408
HOLLANDER, J. M., Decay of Mo-90, 19: 21258 (UCRL-11828(p.67-71))
HOLLANDER, J. M., Energy levels of Bk-249, 19: 21253 (UCRL-11828 (p.38-40))
HOLLANDER, J. M., Internal-conversion coefficients in decay of U-237, 19: 21251 (UCRL-11828(p.31-4))
HOLLANDER, J. M., Nondestructive activation analysis with Li-drifted Ge detectors, 19: 19775 (UCRL.11828(p.197-9))
HOLLANDER, J. M., Pair-production cross sections near threshold, 19: 21252 (UCRL-11828(p.35-8))
HOLLANDER, J. M., Prog. rpt. on nuclear chemistry, annual, 1964, 19: 19735 (UCRL-11828)
HOLLIDAY, Dennis, Statistical descriptions of free boson fields, 19: 21102
HOLLISTER, Charlotte, Ion exchange on natural clay mineral, 19: 19794
HOLLOWAY, B., Prog. rpt. on effects of radiation and radiomimetic chemicals on *Pseudomonas aeruginosa*, final, 6–12/62, 19: 19503 (NP-14933)
HOLLOWELL, Craig D., Molecular beam electric resonance experiments on LiF, LiCl, LiBr, LiI, and NaF, 19: 19848 (UCRL-11828(p.193-7))
HOLM, Dale M., Semiconductor anticoincidence detector system, 19: 20322 (LA-DC-6397)
HOLM, Hans I., Bibliography on radiation-induced graft polymerization on cellulose, 19: 19960 (VDDIT-93)
HOLMBERG, P., E2/M1 mixing ratios of $2^+ \rightarrow 2^+$ transitions in even-even nuclei, 19: 21419
HOLMES, T. H., Determination of Cu in biological materials, 19: 19807
HOLROYD, R. A., Radiolysis of saturated and unsaturated hydrocarbons, 19: 19985
HOLTZ, F. C., Prog. rpt. on V alloy studies, final, 2/65, 19: 20552 (IITRI-B6021-6)
HOLTZ, M. D., Energy levels of Bk-249, 19: 21253 (UCRL-11828(p.38-40))
HOLTZMAN, Richard B., Lead-210 in inhabitants of Caribbean island, 19: 20193 (ANL-6938(p.120-4))
HONJO, T., Dynamic viscoelastic properties of graft copolymers. II., 19: 20001
HONKONEN, David L., Nondestructive testing of reactor fuel, target, and control elements, 19: 20126 (DPSPU-65-30-11)
HOOVER, D. L., Geologic map of Quartet Dome Quadrangle, Nye County, Nevada, 19: 20151 (TEI-860)
HOPKINS, B. J., Retention of Sr-90 by fetal and newborn rats, 19: 19473 (UR-661)
HOPKINS, Ted E., Crystal structure of Cs aquopentachlororuthenate, 19: 19845 (UCRL-11828(p.146))
HOREN, D. J., Energy variation of phase rule in α-particle scattering, 19: 21269 (UCRL-11828(p.132-3))
HOREN, Daniel J., Octupole states in N-15 and O-16, 19: 21268 (UCRL-11828(p.129-31))
HORNIK, N., Effect of Sr-90 on treatment of experimental rickets, 19: 19680
HORNSHOEJ, P., K-shell particle parameter in 272-kev E1 transition of Yb-173, 19: 21320
HORSTMANN, M., Scattering of electrons in polycrystalline Al foils, 19: 20867
HORVATH, P. J., Radiation monitoring of personnel by dose rate telemetering, 19: 20317 (HW-82369)
HOSBEIN, David J., Lung transplantation in the dog, 19: 19523
HOSLER, W. R., Carrier concentration in semiconducting $SrTiO_3$, 19: 21170
HOSOE, Masanao, Fission fragment energy spectrum, 19: 21296
HOSSACK, J. D. W., Nonlinear behavior of shallow spherical shells, 19: 21620
HOSTE, J., Neutron-activation analysis of Cu in Pb, 19: 19815
HOU, Pei-yu, Polynomial bases of group SU_3, 19: 21047
HOUGH, A., Pseudo binary phase diagrams of PuO_2, 19: 20589
HOUTERMANS, H., Measurement of radioactivity at laboratory of Agence Internationale de l'Energie Atomique, 19: 20387
HOWARD, C. L., Water surface waves in BWR, 19: 21684 (GEAP-4061)
HOWELL, Vernon Thomas Seymour, Improvements in pulse generators, 19: 20309
HOWEY, G. R., High-pressure D_2O systems, 19: 21698
HOWLAND, G. R., Prog. rpt. on pneumatic nutator actuator motor, 12/64, 19: 21615 (NASA-CR-54282)
HOYAUX, M. F., Prog. rpt. on instabilities in metal-vapor plasmas, 10–12/64, 19: 21490 (TID-21698)
HOYLE, A. C., High-pressure D_2O systems, 19: 21698
HOZAKA, Tokuo, Two kinds of Zr carbide, 19: 19866
HRABOVSKY, Zoltan, X-ray screening of pelvic dysplasia, 19: 19678
HRSAK, I., Counteracting killing effect of foreign cells, 19: 19651
HSIAO, Chi-chick, Chemical protective drugs against radiation, 19: 19620 (JPRS-29200(p.96-106))
HSIUNG, Vera, Lipid metabolism in acute radiation injury, 19: 19610
HUANG, J., Diffuse interface in critical fluid mixture, 19: 19952
HUANG, Kerson, Nonexistence of "pure bootstrap" solutions to Chew-Low theory, 19: 21001
HUANG, Teh-chang, Inelastic collisions of 6.8 Bev/c π^- mesons with nucleons, 19: 21062
HUANG, Ting-chio, Chemical effects of $^{38}Cl(n,p)^{38}S$ reaction. I., 19: 20004
HUANG, Tzu-tzan, Application of Treiman-Yang criterion to N-N interaction, 19: 21046
HUBAUX, A., Determination of Al, Al_2O_3, Fe, Si, Zn, C in SAP powders, 19: 19750 (EUR-2286.f)
HUBBARD, D. P., Polarographic determination of Mo in Nb-base alloys, 19: 19781
HUBER, R. W., Prog. rpt. on metallurgical characteristics of high-strength structural materials, 9–12/64, 19: 20462 (NRL-6258)
HUBNER, R. S., Monte Carlo evaluation of collimator efficiency, 19: 21612 (NAA-SR-Memo-10557(Pt.I))
HUBNER, R. S., Monte Carlo evaluation of collimator efficiency, 19: 21613 (NAA-SR-Memo-10557(Pt.II))
HUCK, J., Pair production cross sections of γ rays in NaI(Tl) crystals, 19: 21294
HUDDLESTON, C. M., Radiation shielding studies, 19: 21594 (AD-424387)
HUDOKLIN, A., Reversal of the thermal neutron spin, 19: 21300
HUDSON, W. G., Reclaiming of inner fuels with cracked supports, 19: 21668 (HW-84196)
HUEBNER, H., Nomenclature of isotopes of chemical elements, 19: 19736
HUEBNER, K., Magnetic field measurements with help of Zeeman effect, 19: 20257 (IPP-1/19)
HUEFNER, S., Hyperfine splitting and g factor of 84-kev state in Yb-170, 19: 21377
HUEFNER, S., Mössbauer effect and isomer shift on Eu-153, 19: 21345
HUELLER, A., Hyperfine splitting and g factor of 84-kev state in Yb-170, 19: 21377
HUES, A. D., Spectrophotometric determination of U in mixtures of U and Mo, 19: 19759 (LA-3226)
HUET, Henri, Production of granulated UO_2, 19: 20538
HUETTER, T., Observations of radiative τ^+ decays, 19: 20990
HUGER, William, Jr., Radiogenic neoplasms of the hands, 19: 19524
HUGGINS, Robert A., Dislocation structure at Luders fronts in Ta, 19: 20562 (SU-DMS-65-1)
HULL, McAllister H., Jr., Prog. rpt. on nucleon-nucleon interactions, annual, 2/65, 19: 20937 (TID-21672)
HULSIZER, Robert I., Decay $Y_1^0(1660) \rightarrow Y_0^0(1405) + \pi$, 19: 21017
HULTBERG, S., Automatic acquisition and reduction of nuclear data, 19: 20447
HUMBACH, W., Heat transfer model of reactor, 19: 21656
HUMBEL, Franz, Device for calibration of radiation detection instruments, 19: 20395
HUME, D. M., Studies of renal homotransplantation in man, 19: 19463
HUNSTEIN, W., Radiation-induced leukemia in Wistar rats, 19: 19530
HUNT, S. E., Surveillance monitor for U and Pu in atmosphere, 19: 20381
HUNT, V. R., Gonadal exposure to Po-210 in mouse and man, 19: 19495
HUNTLEY, W. R., Prog. rpt. on SNAP-8 corrosion, 6–8/63, 19: 20475 (ORNL-3538)
HUNTLEY, W. R., Prog. rpt. on SNAP-8 corrosion, 9–11/63, 19: 20477 (ORNL-3604)
HUNTLEY, W. R., Prog. rpt. on SNAP-8 corrosion, 12/63–2/64, 19: 20478 (ORNL-3618)
HUNTLEY, W. R., Prog. rpt. on SNAP-8 corrosion, 3–5/64, 19: 20479 (ORNL-3671)
HUNTLEY, W. R., Prog. rpt. on SNAP-8 corrosion, 6–8/64, 19: 20480 (ORNL-3730)
HUNTZICKER, J., Induced hyperfine fields in 5p shell, 19: 21359
HUNTZICKER, J. J., Level scheme of Te-125 and magnetic dipole moment of Sb-125, 19: 21256 (UCRL-11828(p.58-62))
HUNTZICKER, J. J., Nuclear Zeeman effect in Ir-193, 19: 21255 (UCRL-11828(p.57-8))
HURD, John, Isthmian sea-level canal, 19: 20091
HURLEY, P. M., Strontium-87 abundance in Hawaiian volcanic rocks, 19: 20168
HUSAIN, Athar, Gamma-induced chain reaction between formic acid and H_2O_2, 19: 19989
HUSTER, E., Discharge broadening in counting tubes, 19: 20379
HUTH, Gerald C., Prog. rpt. on surface contouring applied to semiconductor radiation detectors, semiannual, 19: 20323 (NYO-3246-4)
HVOSTOVA, V. V., Recovery from irradiation damage of barley seeds, 19: 19639

I

IBRAGIMOV, A. P., Radiolysis of frozen solutions of amino acids and

peptides, 19: 20012
IDDINGS, C. K., Structure of proton and hyperfine shift in H, 19: 21396
IDE, Roger Henry, Proton bombardment of metals, 19: 21438
IDZERDA, B., Magnetic tape instrumentation for on-line recording and off-line analysis, 19: 20255 (EUR-2119.e)
IGALI, Sandor, Genetic effects of x irradiation, 19: 19568
IIJIMA, T., Preliminary electron-diffraction study of H_2, 19: 20826
IIJIMA, Tsutomu, Measurement of anisotropic fast-neutron spectrum, 19: 20374
IIMURA, Takeshi, Whole-body counter. I., 19: 20377
IKEDA, Kiyomi, Beta decay of heavier nuclei, 19: 21304
IKEDA, Nagayasu, Design of the fast power reactor, 19: 21696
IKKOS, D., Scanning in diagnosis of echinococcus disease of liver, 19: 19729
ILIC, Ratko, Production of radioactive colloidal Au-198, 19: 20022 (JPRS-29258)
IL'INA, E. V., Optical methods of determining characteristics of an arc discharge, 19: 21555
IL'INA, G. V., Effects of radioactive fission products on harvest, 19: 19508 (JPRS-28977)
IMSHENIK, V. S., Gas dynamical model of type II supernova outburst, 19: 20769
INGALLS, R., Advances in Mössbauer effect methodology high-pressure techniques, 19: 21231 (COO-1198-255)
INGALLS, R., Highly charged states following Co-57 electron capture in hydrated Co compounds, 19: 20032
INGHAM, Robert Vincent, Systems for detecting leaks in fuel elements, 19: 21624
INGRAM, M., Frequency distribution of erythrocyte volumes of acutely bled dogs, 19: 21777 (UR-662)
INOPIN, E. V., Nuclear boundary diffusion, 19: 21424
IOFFE, B. L., $K^* \to Kn\gamma$ decay, 19: 20984
IOSIF'AN, A. G., Analysis of quasi-Maxsellian equations describing compensating fields, 19: 21086
IPPOLITOVA, E. A., Investigation of system UO_3–UO_2, 19: 19873
IRVINE, J. W., Jr., Equipment for rapid handling of irradiated solutions, 19: 21741
ISAAK, G. R., Time dilation experiment based on Mössbauer effect, 19: 20699
ISABELLE, D. B., 6.02-Mev level of B-10, 19: 21306
ISEBECK, K., Irradiation of U with neutrons at 4.5°K, 19: 20642
ISEBECK, K., Length changes on irradiation of Au, 19: 20646
ISEBECK, K., Magnetic after-effects in Ni after irradiation with neutrons, 19: 20647
ISEBECK, K., Magnetic after-effects in Fe after irradiation with neutrons, 19: 20648
ISENBURGER, Herbert R., Filmbadge monitoring for radiation, 19: 20242
ISHIDA, Yoichi, Dielectric behavior of poly(β-propiolactone), 19: 20000
ISHIHARA, Tomio, Whole-body counter. I., 19: 20377
ISMATOV, E., Scattering of deuterons by non-spherical translucent nuclei, 19: 21427
ISRAELI, Yigal Julius, Complex of uranic acid with monosodium dimethylglyoxime, 19: 19860
ISRAELI, Yigal Julius, Mechanism of hydrolysis of uranyl ion, 19: 19858
ISRAELI, Yigal Julius, Ultraviolet and visible spectra of uranyl ion, 19: 19859
ITO, Shizuko, Isomeric transition of Br-80m in pentamminecobalt(III) bromides, 19: 19973
IVANKINA, M. S., Radiation effects on thermal properties of alkali-halide crystals, 19: 19986
IVANOV, Ivan, Hemopoiesis in sheep exposed to sublethal doses of x rays, 19: 19600
IVANOV, V. I., Neutron component of cosmic rays, 19: 20878
IVANOV, V. I., Octahydrates of sulfates of lanthanides and Y, 19: 19915
IVANOV, V. I., Versene-protective action against uv damages of *Bacterium coli*, 19: 19638
IVANOV, Yu. L., Radiative recombination in Si and Ge associated with radiation defects, 19: 20627
IVANOVA, K. S., Radioactive equilibrium in accessory monazites, 19: 20189
IVANOVA, S. P., Production of fast charged particles in reactions between complex nuclei, 19: 21354
IVANOV-KHOLODNYI, G. S., Electron concentration in the D region, 19: 21127
IVANOV-SMOLENSKII, A. V., Similitude criterion of MHD phenomena and EM power losses, 19: 20119
IVASH, Eugene V., Validity of the Kadomtsev-Nedospasov approximation for a simple geometry plasma, 19: 21533
IVERSEN, James Delano, Magnetogasdynamic laminar compressible boundary layers, 19: 20122
IWAO, H., Nutrition and effect of γ-ray exposure, 19: 19628
IWATA, Masahisa, Removal of astringency in Kaki by γ radiation, 19: 19571
IYENGAR, R. S., Electron bremsstrahlung and auroral luminosity pulsations, 19: 21152
IYER, R. H., Electrodeposition of Ac, 19: 19902
IZVEKOVA, A. V., Chemotherapy of radiation sickness, 19: 19622

J

JACH, K., Appliances protecting against ionizing radiations, 19: 19634
JACKSON, Betty S., Bibliography of nuclear interactions of He-3 with d, n, or p, 19: 21238 (LA-3205)
JACKSON, E. A., Oscillations in one-dimensional, inhomogenous plasma, 19: 21478 (NP-14880)
JACKSON, Wayne H., Billiken calibration shot in southeast Missouri, 19: 20171 (AFCRL-64-659)
JACOBS, A. M., Green's function of monoenergetic neutron transport theory, 19: 21215
JACOBS, J. A., Amplification of hydromagnetic waves in magnetosphere by cyclotron instability process, 19: 21123 (D1-82-0398)
JAECH, J. L., Prog. rpt. on nuclear fuel burnup analyses, 9–11/64, 19: 21667 (GEAP-4776)
JAFFE, Arthur, Entire functions of the free field, 19: 21085
JAGANNATHAN, G., Gauge invariance and mass of vector bosons, 19: 20934 (NP-14829)
JAHR, R., Reaction (d,t) on Be, Ar, Y, Zr, and Pb at 11.8 Mev, 19: 21326
JAIN, H. C., Electrodeposition of Ac, 19: 19902
JAIN, P. L., Pion production in high-energy μ-N collisions, 19: 21037
JAKSIC, B., Asymptotic behavior of phase shift in λ for strongly singular potentials, 19: 21079 (IC/65/2)
JAMES, D. B., Processing of Pu by ion exchange. III., 19: 20045 (LA-2838)
JAMES, D. B., Processing of Pu by ion exchange. V., 19: 20046 (LA-3188)
JAMES, Paul E., Soil profile measurements with radioactivity, 19: 20182
JAMESON, Robert A., R-f phase and amplitude control system for proton linear accelerator, 19: 20728 (LA-DC-6875)
JAMMET, H., General principles of organization of protection, 19: 20222
JAMMET, H., Scintigraphic method in morphological exploration of liver, 19: 19728
JANNER, Karl, Control element for reactors, 19: 21631
JANSA, Jindrich, Deactivation of radioactive waste liquids, 19: 21755
JANSEN, D. H., Boiling-K corrosion loop test, 19: 20476 (ORNL-3603)
JARVIS, O. N., Renormalization of p-p polarization data, 19: 20980
JAUERNIK, U., Heat transfer model of reactor, 19: 21656
JAYADEVAN, N. C., Crystal chemistry of higher carbides of Pu, 19: 20570
JEAN, Roger, Linear accelerator, 19: 20751
JELONEK, A., Effect of Sr-90 on treatment of experimental rickets, 19: 19680
JENEY, E., Radioactivity of atmospheric sediments, 19: 20235
JENKIN, J. G., High-pressure gas scintillation counters. II., 19: 20361
JERCHEL, D., Radio thin-layer chromatography, 19: 19808
JEWETT, John G., Hydrogen participation in cis-4-*t*-butylcyclohexyl brosylate solvolysis, 19: 19949
JIMENEZ, P., Public benefit demonstrations using nuclear activation analysis, 19: 19771 (TEES-2671-4(Chap.9))
Jimeno, S. Arribas
see Arribas Jimeno, S.
JIRGAL, G. H., Jr., Effects of x irradiation on self-friction of KCl, 19: 20011
JOEHSSON, C., Measurement of mean inner potentials of Be, 19: 20599
JOENEMALM, C., Shielding thickness for sources of γ rays, 19: 21598
JOERGENSEN, Chr. Klixbuell, Absorption spectra of Tc(IV) and Re(IV) hexahalides, 19: 19924
JOHNSON, C. F., Comparison of measured neutron and proton spectra with calculated spectra in energy region between 50 and 160 Mev, 19: 21244 (ORNL-P-844)
JOHNSON, C. H. J., Semiclassical scattering, 19: 20956
JOHNSON, D. E., Organ visualization by photoscanning using radioalbumin, 19: 19710
JOHNSON, E. J., Material buckling for UC-fueled graphite-moderated assemblies, 19: 21692 (NAA-SR-Memo-9976)
JOHNSON, Francis S., Satellite environment handbook, 2nd Ed., 19: 21157
JOHNSON, Francis S., Solar radiation, 19: 20785
JOHNSON, Francis S., Structure of the upper atmosphere, 19: 21158
JOHNSON, K., Tests of relativistic SU(6) schemes, 19: 21025
JOHNSON, M. L., Sodium logging in fast ceramic reactor fuels, 19: 20458 (GEAP-4283)
JOHNSON, R. A., Determination of Cl by instrumental neutron activation analysis, 19: 19826
JOHNSON, Wesley M., Operational safety evaluation of remote reactor plants, 19: 21685 (HASL-152)
JOHNSTON, H. F., Excursion-limiting fuse for critical assembly, 19: 21617
JOHNSTON, R. R., Atomic line contribution to radiation absorption coefficient of air, 19: 20831

JOHNSTON, R. R., Photoionization contribution to radiation absorption coefficient of air, 19: 20830
JOLLY, L., Jr., Disposal of large quantities of degraded and low-level contaminated solvent, 19: 21748 (DPSPU-64-30-8B)
JONAK, J., Skeletal muscles at different stages of radiation disease, 19: 19574
JONAS, J., Electron coupling of nuclear spins, 19: 19888
JONES, D. B., Can you afford your cooling water treatment program?, 19: 20087 (GAT-P-33)
JONES, E., Brain-tumor localization, 19: 19714
JONES, F. Llewellyn, Photoelectric emission in low-pressure He discharges, 19: 20861
JONES, G., Positron lifetimes in Ar and He, 19: 21011
JONES, I. S., Resuspension factor of Pu from various surfaces, 19: 20191 (AERE-R-4635)
JONES, J. T., Determination of Zr in Nb, 19: 19780
JONES, R. G., Mixed state of type-II superconductors, 19: 21166
JONES, T. M., Thermal bowing of reactor fuel elements, 19: 21669
JONKE, A. A., Pilot plant studies of direct fluorination process, 19: 20059
JONKER, C. C., Muon capture in Li-6 for testing nuclear models, 19: 21368
JONSSON, A., Theory of resonance escape in heterogeneous fuel. I., 19: 21648
JONSSON, I., Bone-marrow scanning after Au-198 injection, 19: 19718
JORDAN, George L., Jr., Splenic transplantation in the dog, 19: 19521
JOUSSET, J. C., Irradiation of U with neutrons at 4.5°K, 19: 20642
JUDKINS, M. F., Preparation and properties of $NbAl_3$ and $NbAl_3$-fuel bodies, 19: 20464 (SCNC-316)
JUNOD, P., Magnetic properties of the rare earth nitrides, 19: 19895
JUSTIN-BESANCON, L., Pharmacogenic teratogenic hazard detection in the clinic, 19: 19533
JYOTI, G. B., Twin-channel instability in toroidal plasma at B_z field reversal, 19: 21467 (ARL-63-203)

K

KABACHENKO, A. P., Electromagnetic mass-separator. II., 19: 20261 (JINR-P-1949)
KAC, M., Statistical mechanics of assemblies of coupled oscillators, 19: 21089
KADLEC, J., Extraction of U from ores, 19: 20053 (UJV-1202/64)
KADYSHEVSKII, V. G., Relativistic generalization of SU(6) symmetry, 19: 20973
KADYSHEVSKII, V. G., SU(6) symmetry and higher angular momenta, 19: 20972
KAHAN, R. S., Effects of Co-60 γ rays on oranges, 19: 20404 (IA-999)
KAHN, B., Influence of Rn daughter concentration of γ-spectrometer background, 19: 21299
KAJIKAWA, R., Direct recording of particle tracks of spark chamber, 19: 20368
KAKIHANA, Hidetake, Distribution of D between water and anion exchanger. I., 19: 19864
KAKIHANA, Hidetake, Distribution of D between H_2O and anion exchanger. II., 19: 19865
KAKIHANA, Hidetake, Separation factors of N isotopes with ion exchangers, 19: 20433
KAKIHANA, Hidetake, Thermodynamic theory of ion exchange. III., 19: 20057
KAKUSHKINA, M. L., Formation of toxic lipids in radiation sickness, 19: 19599
KALABA, Robert, Random walk, scattering, and invariant imbedding. I., 19: 20660 (P-1113(RAND))
KALINICHENKO, S. S., Neutron and γ radiation between current pulses of 70-Mev accelerator, 19: 20749
KALININ, Yu. D., Energy of a magnetic storm, 19: 21135
KALINKIN, B. N., Production of fast charged particles in reactions between complex nuclei, 19: 21354
KALISH, R., E2/M1 mixing ratios and K conversion coefficients of some rotational transitions, 19: 21324
KALITZIN, N., New cosmological theory, 19: 20758
KALKSTEIN, M. I., Decay of Mo-90, 19: 21258 (UCRL-11828(p.67-71))
KALMYKOV, A. A., Instability in plasma burst during its motion in longitudinal magnetic field, 19: 21582
KALMYKOVA, I. S., Extraction separation of Sc, 19: 20080
KAMEFUCHI, S., Selection rules in para-field theory, 19: 20918 (IC/65/4)
KAMINSKII, D. L., Optical properties of magnets focusing atomic beam into cavity of maser, 19: 20302
KANDA, Keiji, Studies on natural U–H_2O exponential pile. II., 19: 21645
KANE, John W., Jr., Decay of Ru-103, 19: 21333
KANEVSKII, E. A., Oxidizing activity of HNO_3 during reaction with UO_2, 19: 19912
KANG, Kyungsik, Theory of low-energy π-π scattering, 19: 21074
KANITZ, S., Determination of mixed fission products in sea water, 19: 19790
KANKELEIT, E., Parity impurity in nuclear γ transition, 19: 21397
KANTELE, K., Decay of Eu-157 and Tm-174, 19: 21272
KAPELNER, S. M., Solubility of He in Li and K, 19: 20561 (PWAC-380)
KAPLAN, Ch., Automatic safety control equipment for power plants, 19: 20103
KAPLAN, H. S., Organ visualization by photoscanning using radioalbumin, 19: 19710
KAPLAN, T. A., Spin density of s electrons in Fe, 19: 20845
KAPLIN, Edward J., Plume rise characteristics of scale-model smoke plume, 19: 20656 (ANL-6938(p.257-73))
KAPOOR, S. S., K x rays emitted in spontaneous fission of Cf-252, 19: 21265 (UCRL-11828(p.95-7))
KAPUSTIN, I. N., Reduction of errors due to misses and accidental coincidences in counter telescopes, 19: 20345
KARAYIANIS, N., Physical basis for Hund's rule. II., 19: 20811
KARDASHEV, N. S., Intense sources of cosmic r-f emission, 19: 20768
KARDON, B., Isomeric cross-section ratio in $^{79}Br(n,\gamma)^{80,80m}Br$ reactions, 19: 21331
KARRAS, H., Spectroscopic properties of activated laser crystals. III., 19: 20849
KARTUZHANSKII, A. L., Effect of polyethylene glycols on nuclear photographic emulsions, 19: 20014
KARULE, E., Elastic scattering of low-energy electrons by alkali atoms, 19: 20842
KASBERG, Alvin H., Method of producing UC, 19: 20537
KASCHL, G. Th., Shapes of β spectra and partially conserved axial-vector current, 19: 21340
KASIM, M. M., Interactions in flight of low-energy K⁻ mesons with emulsion nuclei, 19: 21365
KASTNER, Jacob, Cosmic-ray fast neutron background, 19: 20872 (ANL-6938(p.71-88))
KASTNER, Jacob, Internal Sr-90 β dosimetry with fluorods, 19: 20314 (ANL-6938(p.62-70))
KASYANOV, V. O., Equations for plane EHD flows, 19: 20670
KATO, Radioactivity of JRR-2 reactor, 19: 21738
KATSIASHVILI, N. A., Lunar-diurnal geomagnetic variations, 19: 21134
KATSURA, Shigetoshi, Two-body problem in one-dimensional Heisenberg model, 19: 20812
KATSURAGI, Satoru, Minimum criticality calculation for JPDR, 19: 21689 (JAERI-1068)
KATYKHIN, G. S., Decay of Rh-100, 19: 21278
KAUFFMAN, F. L., Ready-to-eat ration-type beef items, 19: 20406 (NP-14928)
KAUFFMAN, H. M., Jr., Studies of renal homotransplantation in man, 19: 19463
KAUFMAN, Aaron, Dating (^{230}Th–^{234}U) of carbonates from lakes, 19: 20181
KAUFMAN, D. F., Effects of purification and realloying on mechanical properties of zone-refined Be single crystals, 19: 20557 (NMI-TJ-60)
KAUFMAN, Larry, Vaporization rates in refractory metal–metal–C systems, 19: 20608
KAUT, V., Oxygen requirements of irradiated rats of various age, 19: 19539
KAWAMATSU, Shunji, Solid-state polymerization of binary component system, 19: 19972
KAWARABAYASHI, Ken, Broken SU(6) symmetry and nonleptonic baryon decays, 19: 20919 (IC/65/5)
KAWARABAYASHI, Ken, U(12) Symmetry and weak interactions, 19: 21028
KAWASE, Akira, Derivatives of 2-(2-thiazolylazo)phenol as analytical reagents. VII., 19: 19814
KAWASHIMA, N., Electron temperature measurement of a plasma from a plasma gun, 19: 21514
KAY, H. E. M., Fetal hemopoietic cells, 19: 19468
KAY, L., Emission lines from Van de Graaff beam, 19: 20857
KAY, R. E., Thermal neutron absorption cross section of H, 19: 21219
KAZAKOVA, T. A., Concentration of radioactive Sr and Cs from H_2O by electrodialysis, 19: 19809
KAZAROV, V. A., Argon arc welding of stainless steel tubing, 19: 20534
KAZOVSKII, E. Ya., Production of high-power MHD generators, 19: 20910
KEBULADZE, T. V., Influence of magnetic storms on cosmic rays, 19: 20888
KEEFE, D., Neutrino beams from high-intensity 200-Bev proton synchrotron, 19: 20738 (UCRL-11983)
KEENAN, Robert G., Recent advances in physical methods of analysis, 19: 19782
KEIL, E., CERN r-f particle separator—first operation, 19: 20748
KEILHACKER, M., Diffusion of trapped reversed magnetic field in theta pinch, 19: 21524
KELBER, Charles N., Effects of resonance interference, 19: 21335
KELER, E. K., Polymorphism of ZrO_2 and rare earth zirconate production,

19: 19925
KELLER, H. L., Dose distribution and dose rate in pendulum irradiation, 19: 19691
KELLER, H. L., Tissue factor with different radiation qualities, 19: 19689
KELLER, W. E., Fountain pressure vs. temperature relationship in liquid He II, 19: 21179
KELLER, Wolfgang, Reactor controlled by varying level of liquid moderator, 19: 21660
KELLIE, A. E., Synthesis of [^{3}H-labeled steroids], 19: 20025
KELLMAN, Simon, YOGI-G—gamma-ray Monte Carlo program, 19: 21596 (UCRL-12005)
KELLY, E. L., Magnet construction for variable-energy cyclotron, 19: 20753
KELLY, James L., Preparing spheroidal particles of dicarbides of Th and Th–U mixtures, 19: 20528
KELLY, P. S., Atomic line contribution to radiation absorption coefficient of air, 19: 20831
KEMENY, G., Model of the insulator-metal transition. I., 19: 20662
KEMP, E. L., Power crowbar energy system for Scylla IV, 19: 21474 (LA-3189)
KEMPTER, C. P., Density of Co–C and Ni–C alloys in solid and liquid states, 19: 20567 (LA-tr-65-5)
KENDALL, E. G., Prog. rpt. on ceramic materials, semiannual, 1–6/62, 19: 20455 (DCAS-TDR-62-192)
KENDALL, P. C., Topside electron density in the F2 region, 19: 21141
KENMOKU, A., Nutrition and effect of γ-ray exposure, 19: 19628
KENNEDY, Norman, Long-range balloon tracking, 19: 21769 (TID-21661)
KENNETT, T. J., Decay of La-142, 19: 21314
KENNEY, J. C., Preparation and properties of W and W–Ag specimens, 19: 20559 (NP-14892)
KERES, Kh. P., Generalized inertial systems. II., 19: 20706
KERNAHAN, D. A., Review of the literature on burns and trauma, 19: 19555
KERNAN, William J., Writing topological programs for GUTS, 19: 20320 (IS-989)
KERR, W. M. M., Preparation of nuclear data into form suitable for Monte Carlo calculations, 19: 21196 (AWRE-O-81/64)
KERSLAKE, William R., Evaluation of filament deterioration in electron-bombardment ion sources, 19: 20138 (NASA-TN-D-2173)
KERTAI, P., Effect of x irradiation on liver regeneration, 19: 19512
KERTESZ, L., Iodine storage by human fetal thyroid, 19: 19491
KESHISHIAN, V., Application of SNAP units to Manned Orbiting Research laboratory, 19: 21720 (NAA-SR-10318)
KESSEL, Quentin C., Three discrete Q values in Ar^+–Ar collisions, 19: 20846
KESSEL, W., Improved pulse shape discriminator, 19: 20370
KESSLER, W. E., SNAPTRAN 2/10A-3 destructive test, 19: 21717 (IDO-17019)
KEVAN, Larry, Radiolysis of hexafluoroethane, 19: 19991
KEYS, J. G., Pulsating auroral radar echoes, 19: 21149
KHAIDAROV, T., Neutron cross sections in In and Sm, 19: 21285
KHALFIN, V. B., Energy distribution of electrons in positive column of discharge, 19: 21579
KHALKIN, V. A., Isolation of neutron-deficient isotopes of elements in Ce group of rare earths, 19: 20078
KHAN, A. M., Time dilation experiment based on Mössbauer effect, 19: 20699
KHAN, M. Z. Rahman, Neutron S-wave strength functions of spherical nuclei, 19: 21327
KHANSEVAROV, R. Yu., Energy structure of γ radiation defects in Ge, 19: 20628
KHARE, S. P., Recombination of positive ions and electrons in dense neutral gas, 19: 20860
KHARITONOV, Yu. Ya., Infrared spectra of uranyl compounds with hydroxy acids, 19: 19911
KHENOKH, M. A., Effects of ionizing radiation on glycogen, 19: 20015
KHERRMANN, E., Isolation of neutron-deficient isotopes of elements in Ce group of rare earths, 19: 20078
KHIMICH, I. V., Structure of g plane relativistic Schroedinger theory, 19: 21053
KHITEV, P. P., Determination of heavy elements in rocks from γ radiation emitted, 19: 20180
KHOCHOLAVA, G. M., Ionosphere at middle latitudes during magnetic storms, 19: 21132
KHOCHOLAVA, G. M., Lunar-diurnal geomagnetic variations, 19: 21134
KHODAI-JOOPARY, A., Fission barriers of Po-210 and Sb-119, and Sb-117, 19: 21261 (UCRL-11828(p.81-3))
KHOMYAKOV, G. K., Neutron and γ radiation between current pulses of 70-Mev accelerator, 19: 20749
KHRENOV, B. A., Primary cosmic radiation of superhigh energy, 19: 20884
KHRISTIANSEN, G. B., Complex installation for study of extensive air showers, 19: 20347
KHRISTIANSEN, G. B., Primary cosmic radiation of superhigh energy, 19: 20884
KHVOSTIKOV, V. D., Alpha-solid solution of nitrogen in Zr, 19: 19877
KIENLE, P., Hyperfine splitting and g factor of 84-kev state in Yb-170, 19: 21377
KIENLE, P., Mössbauer effect and isomer shift on Eu-153, 19: 21345
KIKUCHI, K., Direct recording of particle tracks of spark chamber, 19: 20368
KIL'CHEVSKAYA, M. A., Cholesterol metabolism in liver and lungs during radiation and hypothyreosis, 19: 19511 (JPRS-29364(p.1-4))
KILIAN, Peter, Two-dimensional neutron diffusion problem, 19: 21654
KILMISTER, C. W., Brouwer-type space for particles as distinction systems, 19: 21078 (AFOSR-64-1380)
KILPATRICK, Robert A., Synchrotron-magnet cost studies, 19: 20734 (UCRL-11800)
KIM, Hogil, 88-Inch cyclotron operation and development, 19: 20736 (UCRL-11828(p.236-41))
KIM, J. S., Thickness of zenithal auroral arc over Alaska, 19: 21147
KIM, Stephen M., Cobalt molybdate catalyst for synthesis of benzene for liquid scintillation radiocarbon dating, 19: 19944 (ORINS-50)
KIMBALL, D. S., Dynamics of the aurora. II., 19: 21142
KIMBALL, D. S., Dynamics of the aurora. III., 19: 21143
KIMURA, Kikuzi, Radiation scattering and leakage from x-ray, 19: 20232
KIMURA, Shiushichi, Two kinds of Zr carbide, 19: 19866
KINDLIMANN, L. E., Electrode kinetic studies of Th, 19: 19762 (RPI-2714-6)
KING, E., Resistivity of Pu, Np, and U, 19: 20649
KING, E. N., Beryllium–copper molds, 19: 20519 (NP-14879)
KING, E. R., Radioisotope therapy in nuclear medicine, 19: 19706
KING, George W., Physical metallurgy of W and W-base alloys, 19: 20565 (WADD-TR-60-37(Pt.V))
KING, P. J., Efficiency of stainless steel packings, 19: 20068
KINNEY, W. E., Comparison of measured neutron and proton spectra with calculated spectra in energy region between 50 and 160 Mev, 19: 21244 (ORNL-P-844)
KINSEY, B. B., Elastic scattering of 17- to 21-Mev neutrons from C-12, 19: 21310
KIPPENHAHN, R., Stars with He-rich cores, 19: 20798
KIRN, F. S., EBR-II wet critical experiments, 19: 21677 (ANL-6864)
KIRRMANN, Jean-Michel, Teratogenic effects of ionizing radiations on embryonic development, 19: 19466
KIRSCHNER, Marvin A., Isotope effects in gas-liquid chromatography of steroids, 19: 19893
KIRZ, Janos, Further evidence for $K\pi$ resonance near 1400 Mev, 19: 21004
KISELEV, P. N., Formation of antiendotoxins against *E. coli* for involution of hemorrhagic syndrome in radiation sickness, 19: 19487
KISHIDA, Junnosuke, Japanese evaluation of Communist China's nuclear explosion, 19: 21778 (JPRS-28835)
KISLYAK, G. M., Phosphorescence of B–U phosphors, 19: 19919
KISS, D., Isomeric cross-section ratio in $^{79}Br(n,\gamma)^{80,80m}Br$ reactions, 19: 21331
KISTEMAKER, J., Ionization cross sections for electrons in gases, 19: 20850
KISTLER, R. W., Ages of La Sal Mountains rocks, Utah, 19: 20178
KISTNER, Gustav, Pulsation of reactors, 19: 21657
KISTNER, Gustav, Pulsed neutron source produced from fast reactor, 19: 21745
KISTNER, Gustav, Pulsed neutron source produced from fast reactor, 19: 21746
KITAGAWA, Hirotoshi, Removal of astringency in Kaki by γ radiation, 19: 19571
KITCHEN, S. W., Self-shielding in closely spaced slab lattices, 19: 21636 (CONF-654-32)
KITSENKO, A. B., Plasma-wave propagation across magnetic field, 19: 21521
KITSENKO, A. B., Sound waves in weakly ionized plasma, 19: 21561
KIVEL, B., Opacity of highly ionized air, 19: 20829
KJEKSHUS, A., Constitution and properties of Pd tellurides, 19: 20577
KLAMUT, C. J., Corrosion of C steel by Hg, 19: 20493
KLAPISCH, R., Intranuclear cascade and breakup calculations on production of Li, Be, and B isotopes in C-12 by 156-Mev protons, 19: 21402
KLAPISCH, R., Lithium-6 and Li-7 production in C-12 and O-16 by high-energy protons, 19: 21352
KLAPPER, F., Intensity and final energy of bremsstrahlung of betatron using ionization chambers, 19: 20337
KLASINC, L., Secondary α-deuterium isotope effects in reaction of 2-phenylethyltrimethylammonium ion by hydroxide ion, 19: 19947
KLEIBEL, F., Anabolic steroids during radiation therapy, 19: 19669
KLEIN, G. W., Radiolysis of saturated and unsaturated hydrocarbons, 19: 19985
KLEIN, Georges, Measurements in nanosecond electronics, 19: 20304

KLEIN, Melvin P., Observation of electronic relaxation in Mössbauer spectroscopy, 19: 21270 (UCRL-11828(p.214-16))
KLEINSTEUBER, A. Todd, Preparing spheroidal particles of dicarbides of Th and Th–U mixtures, 19: 20528
KLEMS, Joseph H., Cosmic-ray fast neutron background, 19: 20872 (ANL-6938(p.71-88))
KLEPFER, J. S., Transfer of solutes between liquid alloys in mutual contact with a fused salt, 19: 20066
KLEVTSOV, P. P., Determination of heavy elements in rocks from γ radiation emitted, 19: 20180
KLINGELHOEFFER, H., Modification of strength of paper by irradiation, 19: 20630
KLOKE, F. C., Influence of Rn daughter concentration on γ-spectrometer background, 19: 21299
KLOSS, H. G., Temperature determination on low-current C arc, 19: 21497
KLOSS, H. G., Temperature field of low-current arc in air, 19: 21498
KLUG, W., Radiation damage and tumor growth following thorotrast pyelography, 19: 19707
KLUGE, Hans, Combined boiling water and superheater nuclear reactors, 19: 21659
KLYGIN, A. E., Uranium: methods for determination, 19: 19823
KNAPP, B. C., Resonantly coupled accelerating structures for high-current proton linacs, 19: 20725 (LA-DC-6760)
KNAPP, E. A., High-power test on cloverleaf cavity, 19: 20724 (LA-DC-6759)
KNAPP, E. A., Resonantly coupled accelerating structures for high-current proton linacs, 19: 20725 (LA-DC-6760)
KNOBELOCH, G. W., Symmetry of neutron-induced Pu-239 fission in resonance region, 19: 21241 (LA-DC-6639)
KNOLL, P., Manufacture of open radioactive preparations, 19: 20436
KNORR, Georg, Equilibrium of plasma in toroid, 19: 21476 (MATT-283)
KNOWLES, Alan K., Resistor employing irradiated gas, 19: 20310
KNOWLES, D. J., Facility radiation and contamination alarm systems, 19: 20203 (ORNL-TM-988)
KNOX, F. B., Charged particle trajectories in an EM field, 19: 21099
KOBAYASHCHI, M., Neutron radiation photography, 19: 20129
KOBAYASHI, Hisao, Fission fragment energy spectrum, 19: 21296
KOBAYASHI, Shigeo, Luminescence of uranyl ions dissolved in H_2O, 19: 19863
KOBAYASHI, Takatoshi, Slit-type screen for telecobalt therapy, 19: 19674
KOCH, Charles W., Stability of XeO_3 in basic solutions, 19: 19847 (UCRL-11828(p.182-3))
KOCH, H. W., Electron accelerators for food processing, 19: 20422
KOCH, R., Energies and character of low-lying levels in Nb-94, 19: 21330
KOCHER, C. W., Iron-57 Mössbauer effect in some stainless steels, 19: 21338
KOEN, B. V., Solutions of reactor kinetics equations, 19: 21647
KOENIG, Harold, Studies of brain lysosomes, 19: 19611
KOENIG, John H., Development of refractory ceramics, 19: 20461 (NP-14893)
KOEPPENDOERFER, W., Z-pinch, antipinch, and theta pinch as apparatus for production of strong collision waves, 19: 21473 (IPP-1/28)
KOETITZ, G., Spectroscopic properties of activated laser crystals. III., 19: 20849
KOGAN, Sh. M., Interaction of supersonic wave with beam of charged particles, 19: 20672
KOHLER, D., Gamma transitions in Be-8, 19: 21357
KOHLMANNSPERGER, J., Luminescence decay of pyrene-, dibenzyl-, and dibenzyl tetracene crystals, 19: 19963
KOHN, H. L., Prog. rpt. on Nb alloy sheet rolling, final 3/7/63–9 /1/64, 19: 20499 (AD-606291)
KOIAVA, V. K., Influence of magnetic storms on cosmic rays, 19: 20888
KOIV, M., Conversion between μ-mesic atom hfs states, 19: 21421
KOIV, M., Influence of intermediate vector boson on muon capture rate, 19: 21420
KOIV, M., S matrix in Kemmer-Duffin formalism (spin 0), 19: 21050
KOJIMA, Takashi, Distribution of D between water and anion exchanger. I., 19: 19864
KOJIMA, Takashi, Distribution of D between H_2O and anion exchanger. II., 19: 19865
KOJIMA, Takashi, Thermodynamic theory of ion exchange. II., 19: 20057
KOLCHIN, A. E., Angular distribution of photoneutrons from Ta-181 and Bi-209, 19: 21288
KOLLER, E. L., Observations of radiative π^+ decays, 19: 20990
KOLM, Henry H., Intense magnetic fields, 19: 20701
KOLOMEETS, E. V., Coupling coefficients for cosmic components, 19: 20891
KOLOMEYETS, E. V., Neutron component of cosmic rays, 19: 20878
KOLOMY'TSEV, V. I., Analytical properties of scattering amplitude corresponding to class of Feynman diagrams, 19: 21054
KOLOMY'TSEV, V. I., Analytic property of scattering amplitudes corresponding to Feynman diagrams, 19: 21113
KOLTUN, D. S., Comparison of some approximations for self-bound many-fermion systems, 19: 20936 (TID-20558)
KOMENDA, S., Changes of electroshock seizures in rats after irradiation, 19: 19514
KOMISSAROVA, L. N., Scandium separation from pyroxenites, 19: 20081
KOMLEV, L. V., Radioactive equilibrium in accessory monazites, 19: 20189
KOMMUNARSKAYA, A. D., Variability of *penicillium nigricans* on uv and x irradiation, 19: 19556
KONDO, Hiromichi, Plasma confinement with a rotating magnetic field, 19: 21508
KONDRAT'EVA, M. A., Nature of cosmic-ray particles beyond atmosphere, 19: 20893
KONONOV, B. P., Plasma acceleration with aid of EM H_{11}-type wave in circular waveguide, 19: 21566
KONONOV, B. P., Resonance interaction between plasma bunch and EM wave, 19: 21565
KONOPLEVA, R. F., High-temperature annealing of defects produced in Ge by fast neutrons, 19: 20626
KONOVALENKO, B. M., Impurity photoconductivity produced in Ge by γ irradiation, 19: 20623
KONOVALENKO, B. M., Low-temperature irradiation of Ge with fast electrons, 19: 20624
KOOI, J., Separation of Bk from Ce, 19: 20071
KOONCE, C. S., Carrier concentration in semiconducting $SrTiO_3$, 19: 21170
KOPOLDOVA, J., Radiation chemistry of amino acids, 19: 19969
KOPYSHEV, V. P., Reaction rate of $p + p \rightarrow d + e^+ + \nu$ in white dwarf, 19: 20771
KORDIOLIS, N., Diagnosis of intraspinal neurological syndromes, 19: 19720
KORECZ, Karoly, Influence of β radiation on metabolism of the cornea, 19: 19552
KOREN, K., Exposure to radiation from medical procedures, 19: 19597
KORENMAN, Victor, Quantum theory of laser coherence and noise, 19: 20843
KORIDZE, V. G., Influence of magnetic storms on cosmic rays, 19: 20888
KOROTKOVA, G. V., X-ray breakdown of deoxynucleoprotein of intestinal bacteria, 19: 19576
KORSHAK, V. V., Radiation synthesis of polymers based on dimethylphosphinoborine, 19: 19982
KOSCHMIEDER, L., Energy determination of protons, 19: 21436
KOSEVICH, A. M., Coalescence of dislocation loops, 19: 20580
KOSMIDER, S., Skeletal muscles at different stages of radiation disease, 19: 19574
KOSS, F. W., Radio thin-layer chromatography, 19: 19808
KOSSYI, I. A., Interaction of traveling EM wave with plasma, 19: 21564
KOSTROMINA, K. N., Dose field in telegamma therapy of collum carcinoma, 19: 19686
KOSYAKOV, V. N., Extraction of actinide elements with dialkyl phosphoric acids, 19: 20075
KOTHARI, L. S., Equilibrium neutron energy spectra in finite blocks of graphite, 19: 21205
KOTLYAROV, I. I., Treatment of radiation skin lesions with fresh autofibrin films, 19: 19642
KOTOV, A. G., EPR study of radiolysis of ammonia adsorbed on solids, 19: 19984
KOVACS, Geza, Cytological and physiological investigation of maize lines treated with irradiation, 19: 19527
KOVAL'SKAYA, L. P., Storage time of fruit and vegetables treated with γ rays, 19: 20413
KOVANIC, P., Inverse kinetics analysis, 19: 21651
KOVBA, L. M., Investigation of system UO_3–UO_2, 19: 19873
KOVRIGIN, O. D., Radiative transitions in Yb-173 deformed nucleus, 19: 21284
KOVROZHNYKH, L. M., Theory of interaction between electron beams in plasma and transverse waves, 19: 21563
KOVTUN, G. P., Vapor pressure of Gd and Dy, 19: 20601
KOVYAZIN, N. V., Influence of temperature on recovery of reproductive function of uv-damaged yeast cells, 19: 19626
KOZHEVNIKOV, N. I., Temporal variation in area of sunspot group, 19: 20779
KOZIK, B., Theory of neutron multiplication and noises in nuclear reactors, 19: 21641 (JINR-P-1996)
KOZLOV, O. V., Probing of high-frequency-discharge plasma, 19: 21528
KRAEV, D., Tissue activation during mixed neutron irradiation, 19: 19601
KRAFFT, O., Discharge broadening in counting tubes, 19: 20379
KRAMER, Andrew W., Nuclear energy. XX., 19: 21275
KRAMER, K. D., Dependence of Overhauser nuclear polarization on frequency and molecule motion in liquids, 19: 20869
KRAMISH, Arnold, International registration of atom, 19: 21761 (P-1134

(RAND))
KRAMISH, Arnold, Soviet atomic power program, 19: 21694 (P-1076(RAND))
KRAMISH, Arnold, Soviet Union and the atom, 19: 21762 (RM-2163(RAND))
KRASCELLA, N. L., Scattering of radiation by small solid particles, 19: 20677
KRASNIKOV, A. A., Neutron and γ radiation between current pulses of 70-Mev accelerator, 19: 20749
KRASNOPEVTSEV, Yu. V., Concentration of radioactive products over Indian and Pacific Oceans, 19: 20158 (NP-14712)
KRASOVITSKII, V. B., Accelerating system with drift tubes on superhigh frequency, 19: 20709
KRASZNAI, Istvan, Radiation hazard in use of radioactive isotopes, 19: 19670
KRAUSE, Manfred O., Double electron emission in an Auger process, 19: 20844
KRAYBILL, H. F., Wholesomeness in radiation preservation of foods, 19: 20423
KREFELD, R., Analysis of purified U compounds, 19: 19800
KREISEL, W. D., Transistorized stabilized high-voltage power supply, 19: 20357
KRENZ, D. L., Environmental testing of RFD-2 re-entry vehicle, 19: 21763 (SC-DR-64-1741)
KRIEGER, G. L., Indium adhesion test for surface cleanliness, 19: 20205 (SC-TM-64-1722)
KRIEGER, Herman L., Measurement of long-lived activation products in soil by γ spectroscopy, 19: 19829
KRIVISKII, A. S., Versene-protective action against uv damages of *Bacterium coli*, 19: 19638
KRIVOGLAZ, M. A., Phonon correlation function and inelastic coherent scattering of neutrons by crystals, 19: 20671
KRIVOGLAZ, M. A., Single-phonon Green's function, phonon correlation function, and inelastic coherent scattering of neutrons, 19: 20710
KRIVOSHAPKIN, P. A., Modulation of cosmic rays by interplanetary magnetic field, 19: 20889
KRIVSKY, L., Disappearance of polar cap on Mars, 19: 20763
KRMPOTIC, F., K conversion coefficient of 400-Mev transition in decay of Pb-203, 19: 21293
KRONRAD, L., Chemical state of I in Te compounds after neutron irradiation, 19: 20005
KRUEGER, G., Multiple input data acquisition system using small on-line computer, 19: 21731 (KFK-242)
KRUEGER, R., Effect of γ radiation on leather, 19: 20414
KRUGERS, J., Ionization detectors in gas chromatography, 19: 19804
KRUGLYAKOVA, K. E., Decay of peroxides in irradiated DNA solutions, 19: 19541
KRUGLYKH, A. A., Vapor pressure of Gd and Dy, 19: 20601
KRYMSKII, G. F., Diffusion mechanism of diurnal variation of cosmic rays, 19: 20875
KRYMSKII, G. F., Modulation of cosmic rays by interplanetary magnetic field, 19: 20889
KRZHIVOKOL'SKII, V. A., Change in cholinesterase activity after immunization and irradiation, 19: 19609
KUAN, Hung, Intermediate boson theory of weak interactions, 19: 21045
KUBOSE, D. A., Nitrous oxide dosimeter—influence of cell diameter on nitrogen yield, 19: 20329 (USNRDL-TR-806)
KUCKES, A. F., Electron cyclotron harmonic radiation from a plasma, 19: 21477 (MATT-290)
KUDRITSKAYA, L. N., Hydroxo complexes of Th(IV), 19: 19922
KUDRITSKAYA, L. N., State of Th in solutions $HClO_4$, HCl, and HNO_3, 19: 19923
KUDRYASHOV, Yu. B., Erythrograms of rats subjected to action of synthetic radiomimetic embikhin, 19: 19489
KUDRYAVTSEV, A. M., Instability and anomalous diffusion in K plasma, 19: 21569
KUECHLE, Marko, Neutron diffusion parameters of benzene, 19: 21217
KUEHL, H. H., Wave propagation in hot plasma waveguides, 19: 21536
KUGE, Yasushi, Minimum criticality calculation for JPDR, 19: 21689 (JAERI-1068)
KUHL, O., Cobalt-60 research irradiators, 19: 20095 (BNL-8976)
KUHN, Endre, Dosage problems in Co-60 treatment of uterine carcinoma, 19: 19708
KUKACKA, L. E., Cobalt-60 research irradiators, 19: 20095 (BNL-8976)
KUKACKA, L. E., Cost estimate for Co-60 radiation-induced ethylene polymerization process, 19: 19957 (BNL-8993)
KULESHOV, G. D., High-current air-core betatrons, 19: 20740
KULIKOV, G. V., Primary cosmic radiation of superhigh energy, 19: 20884
KULI-ZADE, D. M., Fraunhofer lines in the solar spectrum. I., 19: 20777
KUNIEDA, S., Electron temperature measurement of a plasma from a plasma gun, 19: 21514
KUNZLER, J. E., High-field superconductivity, 19: 21165
KUO, Chung-shou, Possible existence of 3π resonance state, 19: 20969
KUO, De-liang, ESR spectra of γ-irradiated cyanoacetic acid, 19: 20006
KURILKO, V. I., Accelerating system with drift tubes on superhigh frequency, 19: 20709
KURNOSOVA, L. V., Investigation of primary cosmic rays, 19: 20894
KURODA, Tadashi, Electrolytic deposition of Be metal, 19: 20525
KURUSYNA, K., Nuclear reactor noise, 19: 21737
KUSSMAUL, Guenter, Neutron diffusion parameters of benzene, 19: 21217
KUSTOVA, G. N., Optical properties of rare earth oxides. II., 19: 19928
KUTTIG, H., Telecobalt treatment of uterine carcinoma, 19: 19663
KUZICHEVA, E. A., Effects of ionizing radiation on glycogen, 19: 20015
KUZ'MIN, A. I., Modulation of cosmic rays by interplanetary magnetic field, 19: 20889
KUZ'MINA, A. V., Stored energy of alkali-halide crystals following γ irradiation, 19: 19987
KUZNETSOV, A. K., Polymorphism of ZrO_2 and rare earth zirconate production, 19: 19925
KUZNETSOV, B. S., Complexing of Po with chloride ions, 19: 19906
KUZNETSOV, B. S., Hydrolysis of Po in perchloric acids, 19: 19905
KUZNETSOVA, G. A., Concentration of radioactive Sr and Cs from H_2O by electrodialysis, 19: 19809
KUZNETSOVA, N. N., Effects of radioactive fission products on harvest, 19: 19508 (JPRS-28977)
KUZNETSOVA, Z. M., Isothermal solubility in NH_4F–UO_2–H_2O system, 19: 19913
KVETINA, J., Influence of pethidine upon breathing and metabolism of rats during acute irradiation disease, 19: 19481
KVOKOVA, I. M., Electrodeposition of Re on Mo and W, 19: 20529
KWIRAM, Alvin L., Quantized flux in superconducting cylinders, 19: 21194
KYKER, Granvil Charles, Jr., Proton resonances in intermediate nuclei, 19: 21446
KYRI, I., Separation of Nb from Ta, 19: 20054

L

LADU, M., Measurement of Skyshine neutrons around Frascati synchrotron, 19: 20741
LADU, M., Mixed radiation field measurement, 19: 20373
LAETSCH, F., Radiation damage and tumor growth following thorotrast pyelography, 19: 19707
LAFUMA, Diagnosis and treatment of radioactive contamination, 19: 19656
LAGO, Bernard, Specifications for multi-group scattering code of two dimensions: ALCI, 19: 21197 (CEA-R-2747 & Add.)
LAGOMARSINO, Raymond J., Prog. rpt. on Project Star Dust, 9/63, 19: 20657 (DASA-1309)
LAI, Guang-chi, Thermoluminescence of irradiated high polymers. I., 19: 20007
LAI, Tsai-teh, Polarographic study of uranyl pyrophosphate complex, 19: 19816
LAIRD, M. J., Charged particle trajectories in an EM field, 19: 21099
LAL, P., Perturbation theory and nuclear ferromagnetism, 19: 20695
LAL, S., Distribution of inelasticity in high-energy collisions in C and brass, 19: 20898
LALOVIC, B., Neutron-neutron scattering length from $^3H(n,d)2n$ reaction, 19: 21404
LALOVIC, B., Reactions $H^3(n,p)3n$ and $H^3(n,H^4)\gamma$ at E_n = 14.4 Mev, 19: 21405
LAM, C. F., Detector research, 19: 19767 (TEES-2671-4(Chap.4))
LAMB, W. A. S., Injection-system design, 19: 20737 (UCRL-11955)
LAMBERT, B. E., Determination of Po-210 in urine, 19: 19791
LAMBERT, Marianne, New absorption band in irradiated LiF, 19: 20817
LAMBERTS, H. B., Deposition of Ba or Sr in aortic tissue, 19: 19500 (NP-14907)
LAMI, H., Emission spectrum and time constants of organic scintillators, 19: 19962
LAMPE, L., Iodine storage by human fetal thyroid, 19: 19491
LANDIS, D. A., Beam integrator, 19: 20284 (UCRL-11828(p.222-3))
LANDIS, D. A., Experimental instrumentation for 88-inch cyclotron, 19: 20282 (UCRL-11828(p.218-19))
LANDO, J. B., Radiation polymerization of crystalline trithiane, 19: 19959 (CONF-571-37)
LANDSHOFF, P. V., Problem of causality in S-matrix theory, 19: 20943
LANG, J., Direct measurement of short nuclear lifetime, 19: 21369
LANG, J., Ground state wave function of H-3 and He-3, 19: 21367
LANGAN, J. K., Diagnosis of massive pulmonary embolism by radioisotope scanning, 19: 19724
LANGE, J., Absolute measurement of radionuclides with 4π counter, 19: 19755 (KFK-252)
LANGE, W. J., Outgassing procedures for glass ultrahigh-vacuum systems, 19: 20148
LANGENECKER, B., Neutron-acoustic irradiation of Al single crystals, 19: 20641

LANGER, H., Determinations of body water in humans, 19: 19480
LANGERON, Jean-Paul, Preparation of large grains of Zr, 19: 20527
LANGMANN, H. J., Mobility of hot electrons and influence on pulse rise time, 19: 20359
LANZA, F., Evolution of chlorine in terphenyls, 19: 20469 (EUR-2279.e)
LAPEYRAQUE, F., Effect of blood transfusions on subsequent marrow transplant in irradiated mice, 19: 19653
LAPICQUE, Georges, Improvements in nuclear reactor control, 19: 21623
LARGE, L. N., Neutron yield from deuterided Er and Ti targets, 19: 21301
LARIKOV, L. N., Parameters of recrystallization of Nb and W, 19: 20604
LARIONOV, M. M., Anisotropy of electron energy distribution in alpha installation, 19: 21583
LA RIVIERE, J. R., Increased processing flexibility—Purex, 19: 20040 (HW-84085)
LARK, Neil L., Collective excited states in even Xe isotopes, 19: 21316
LARRICK, A. P., Effects of reactor decontaminating solutions on intergranularly corroded type 304 stainless steel, 19: 20471 (HW-SA-3628)
LARSSON, I.-G., Bone-marrow scanning after Au-198 injection, 19: 19718
LASKY, C., Design of AGS fast beam extraction system, 19: 20718 (BNL-8968)
LASSNER, Erik, Determination of Ni in Mo and W, 19: 19799
LATHROP, K. D., Solutions of the monoenergetic critical equation with anisotropic scattering, 19: 21214
LATORRE, O., Determination of Nb, Ta, and U in tantalite–columbite ores, 19: 19754 (JEN-134-DQ/I-39)
LATTAR, S. F., Effects of Co-60 γ rays on oranges, 19: 20404 (IA-999)
LATY'SHEV, G. D., Radiative transitions in Yb-173 deformed nucleus, 19: 21284
LAUER, K. F., Preparation of Na samples for neutron scattering experiments, 19: 20503 (EUR-2242.e)
LAURENT, H., Preparation of In-115m, 19: 20023 (ORNL-tr-556)
LAUSTRIAT, G., Emission spectrum and time constants of organic scintillators, 19: 19962
LAVAKARE, Prabhakar J., Helium nuclei in primary cosmic radiation, 19: 20901
LA VALLE, D. E., High-purity KCl, 19: 19843 (ORNL-TM-1071)
LAVERTY, WILLIAM F., Film boiling of liquid flowing upward through heated tube, 19: 20113 (NP-14895)
LAVIE, J. M., Detection of critical accidents at Commissariat a l'Energie Atomique, 19: 20330 (AEC-tr-6547)
LAVILLE-SAINT-MARTIN, B., Formation of thin layers of Cu oxides in reactive cathodic pulverization, 19: 20827
LAVROVA, E. V., Ionospheric disturbances in the F_2 layer, 19: 21133
LAVROVSKII, K. P., Transformations of normal alkanes, 19: 19980
LAWRENCE, G. P., Reaction $^{12}C(^{16}O,\alpha)^{24}Mg$, 19: 21313
LAWRENCE, J., Operating characteristics of two thermionic converters, 19: 20906
LAWRENCE, W. Thompson, Entrance flow and transition from laminar-to-turbulent flow in vertical tubes, 19: 20114 (NP-14920)
LAWRIE, W. E., Prog. rpt. on nondestructive evaluation of coating-metal, 19: 20127 (IITRI-N213-23)
LAWSON, J. D., Beam current and dee voltage in cyclotron, 19: 20747
LAWSON, P. A., Electron diffusion in H at high electric fields and low gas pressures, 19: 20696
LAWTHERS, D., Oxidation-resistant coatings for Nb alloys, 19: 20483 (SCNC-318)
LAYNER, V. I., Electrodeposition of Re on Mo and W, 19: 20529
LAZAROVICI, Cristion, Measurement of activity of radionuclides by 4π β-γ coincidences, 19: 20385
LAZUTIN, L. L., Radio probe for measurement of cosmic-ray density in stratosphere, 19: 20346
LBOV, A. A., Fission-product yields and mass distribution, 19: 21445
LEAKE, J. W., Fast neutron dose-equivalent rate monitor, 19: 20312 (AERE-R-4525)
LEANDRI, M., Contamination of Mediterranean shellfish, 19: 20230
LEARY, J. A., Ternary Pu alloys for core test facility, 19: 20506 (LA-3209)
LEBEDEV, B. I., Biological action of protons of 510-Mev energy in irradiation of dogs, 19: 19578
LEBEDEV, N. A., Isolation of neutron-deficient isotopes of elements in Ce group of rare earths, 19: 20078
LEBEDEV, S. Ya., Electric breakdown through slot in glass in Cs vapor, 19: 21578
LEBEDINSKII, A. V., Mechanism of inhibiting effect of radiation on cell division, 19: 19613
LEBOUTET, Hubert, Linear accelerator, 19: 20751
LECHEVALLIER, Maurice, Neutron absorbing rod for reactors, 19: 21622
LECOCQ, Alfred, Preparation of nuclear-pure beryllium oxalate tri-hydrate, 19: 19832 (CEA-R-2591)
LECOCQ, Alfred, Thermodynamic study of treatment of U–Zr alloys, 19: 19742 (CEA-R-2592)
LEDERED, Sylvie, Lagrangian formalism and application to Minkowski theories of gravitation and electromagnetism, 19: 20666
LEDERMAN, L. M., Brookhaven-Columbia plasma lens, 19: 20915 (BNL-8967)
LEDOUX, P., Stellar stability and stellar evolution, 19: 20801
LEE, H. M., Studies of renal homotransplantation in man, 19: 19463
LEE, J. A., Resistivity of Pu, Np, and U, 19: 20649
LEE, Phillip B., Special problems from viewpoint of Bridge, Tunnel, and Turnpike Authorities, 19: 20239
LEE, W. R., Calcium accretion and bone formation in dogs, 19: 19470 (ANL-6938(p.141-61))
LEE, Y. C., Interaction of light with light in a plasma, 19: 21547
LEE-FRANZINI, Juliet, Momentum spectrum of positrons from muon decay, 19: 21012
LEES, D. J., Diffusion of current sheath in toroidal discharge, 19: 21512
LEGGETT, A. J., Spin susceptibility of superfluid Fermi liquid, 19: 20692
LEGGETT, Robert D., Nuclear reactor fuel members, 19: 20497
LE GRAND, J., Dose delivered to tissue contaminated with α emitter, 19: 19482
LEHANE, J. A., Helicon wave propagation in gaseous plasma, 19: 21552
LEHMAN, Sherman, Invariant imbedding, particle interaction, and conservation relations, 19: 20959
LEHMANN, G., Crank model and perturbation calculation, 19: 21349
LEHMANN, R., Spectroscopic properties of activated laser crystals. III., 19: 20849
LEHNER, G., Limitations on magnetic fields obtained by flux-compression. I., 19: 20678
LEHOVEC, K., Growth mechanism of thin anodic oxide films on Ta. I., 19: 20490
LEIGH, Gerald G., Technique for simulating air-blast-induced ground motions, 19: 20184
LEJEUNE, J., Risks for embryo, fetus, and infant from medical radiology, 19: 19699
LEMONNE, J., Interactions in flight of low-energy K^- mesons with emulsion nuclei, 19: 21365
LEMONNE, J., Production of hyperfragments from interactions of K^- mesons with nuclei, 19: 21429
LEMPERT, Neil, Lung transplantation in the dog, 19: 19523
LE NAGARD, Monique, Radiochemical separation of Ca-45, Sr-89, and Ba-140, 19: 19745 (CEA-R-2712)
LENEL, F. V., Study of the material transport mechanism in sintering, 19: 20465 (TID-20344)
LENGELER, H., CERN r-f particle separator—first operation, 19: 20748
LENZ, William H., Melting point of sintered W–Mo–Re alloys, 19: 20584
LEO, Micah W. M., Prog. rpt. on Project Star Dust, 9/63, 19: 20657 (DASA-1309)
LEONARD, A., Solutions of the monoenergetic critical equation with anisotropic scattering, 19: 21214
LEONT'EV, N. I., Interaction of traveling EM wave with plasma, 19: 21564
LERCH, Pierre, Radiochemical method for analysis of Sr-90 in bones, 19: 19789
LERES, Richard G., Subgrouping multichannel analyzers on periodic basis, 19: 20283 (UCRL-11828(p.221))
LEROUX, B., Levels in reaction $^{28}Si(n,\alpha)^{25}Mg$, 19: 21318
LESIGANG, Margrit, Thin-layer chromatography in salts of heteropolyacids, 19: 20069
LESLIE, D. C., Theory of resonance escape in heterogeneous fuel. I., 19: 21648
LETELLIER, Bernard, New absorption band in irradiated LiF, 19: 20817
LE THANH, Ph., Levels in reaction $^{28}Si(n,\alpha)^{25}Mg$, 19: 21318
LEUNG, Y. C., Production amplitudes. I and II, 19: 20925 (ICTP-64/3)
LEUNG, Y. C., U(12) Predictions for $p\bar{p}$ annihilation into mesons, 19: 21036
LEVENSON, S. M., Wound healing: effect of ascorbic acid and D_2O, 19: 19484
LEVINSKAYA, M. Kh., Alpha-solid solution of nitrogen in Zr, 19: 19877
LEVINSKII, Yu. V., Alpha-solid solution of nitrogen in Zr, 19: 19877
LEVY, Donald Harris, ESR spectra of radical anions in liquid ammonia, 19: 19945 (UCRL-11864)
LEVY, F., Magnetic properties of the rare earth nitrides, 19: 19895
LEVY, Ira S., Systems of LiH with alkaline earth and rare earth hydrides, 19: 19881
LEVY, R. M., Nuclear magnetic moment of 2084-kev state in Ce-140, 19: 21254 (UCRL-11828(p.55-6))
LEVY, Viviane, Helium precipitation in Al–Li alloy, 19: 20613 (CEA-R-2529)
LEWICKI, Z., Morphologic changes in thyroid of rats treated with ionizing radiation, 19: 19569
LEWIS, Jerry P., Transplantation potential of marrow frozen at programmed cooling rates, 19: 19645
LI, Chi, Dislocation structure of subboundaries in Mo single crystals,

19: 20602
LICHTMAN, David, Adsorption-desorption of residual gases in high vacuum, 19: 20144
LIEBERMAN, J. A., Nuclear safety—standards and evaluation, 19: 20206 (TID-7698(Pt.I)(p.31-2))
LIEBNER, Edwin J., Intralymphatic radioactive therapy for pelvic cancer, 19: 19658
LIEBSTER, J., Radiation chemistry of amino acids, 19: 19969
LIESTOEL, I., Environmental γ radiation in Norwegian houses, 19: 20218
LIETZ, G. P., Neutrons from $^{9}Be(\alpha,n_0)^{12}C$ and $^{9}Be(\alpha,n_1)^{12m}C$ reactions, 19: 21307
LIGHTBODY, D. B., Reaction $^{89}Y(p,n)^{89}Zr$, 19: 21356
LIKHACHEVA, A. G., State of blood coagulating system and basic hematological indices during continuous work with various particle accelerators, 19: 20237
LILJENZIN, J. O., Determination of size distribution of particles in suspension, 19: 19901
LIMIC, N., Asymptotic behavior of phase shift in λ for strongly singular potentials, 19: 21079 (IC/65/2)
LIMIC, N., Extrapolation of S matrix from Lehmann's representation, 19: 21080 (IC/65/9)
LINCOLN, T. A., Decontamination of radioactive materials from the skin, 19: 19494
LIND, V. Gordon, CP-nonconserving decay $K_2^0 \rightarrow \pi^+ + \pi^- + \pi^0$, 19: 21020
LINDENBAUM, S. J., Observation of the low-energy Λ-p interaction, 19: 21034
LINDLEY, B. C., MHD research in the United Kingdom, 19: 20908
LINDNER, R., Determination of size distribution of particles in suspension, 19: 19901
LINDSAY, Ned A., R-f phase and amplitude control system for proton linear accelerator, 19: 20728 (LA-DC-6875)
LINHART, J. G., Compression of magnetic field by exploding foils, 19: 20717
LINHART, J. G., Limitations on magnetic fields obtained by flux-compression. I., 19: 20678
LINTON, G. D., Prog. rpt. on instabilities in metal-vapor plasmas, 10-12/64, 19: 21490 (TID-21698)
LIPANOVICH, Marko I., Portable γ-intensity time recorder, 19: 20397
LIPIS, V. L., Problems of investigation of parameters of powerful γ devices for radiotherapy, 19: 19704
LIPKIN, H. J., Meson and baryon masses in SU(6) symmetry, 19: 21030
LIPKIN, H. J., Tests of relativistic SU(6) in p-$\bar{p}$ annihilation, 19: 20983
LIPKIN, Harry J., Selection rules in relativistic SU(6) theories, 19: 21023
LIPMAN, P. W., Geologic map and sections of Thirsty Canyon, Nye County, Nevada, 19: 20150 (TEI-859)
LIPPERT, J., Odd-odd nucleus with 0+ ground state (^{156}Eu), 19: 21350
LIPSCHUTZ, Michael E., Cosmic-ray exposure ages of Fe meteorites, 19: 20760
LIPSETT, Mortimer B., Isotope effects in gas-liquid chromatography of steroids, 19: 19893
LISICHENKO, V. I., Resonance absorption of γ quanta by SnO_2, 19: 21428
LISKIEN, H., Cross-section measurement for $^{56}Fe(n,p)^{56}Mn$, $^{59}Co(n,\alpha)^{56}Mn$, and $^{63}Cu(n,2n)^{62}Cu$, 19: 21290
LITTLE, J. P., Gonadal exposure to Po-210 in mouse and man, 19: 19495
LITTLE, W. A., Magnetic cooling, 19: 21185
LITTLE, W. W., Jr., Solutions of reactor kinetics equations, 19: 21647
LITVAK, A. G., Electron and ion distribution functions for plasma in slightly nonuniform high-frequency field, 19: 21573
LITVAK, A. G., Ohmic heating of partially ionized plasma by a uniform h-f field, 19: 21581
LIU, L. S., Test of SU(6) predictions in weak N^* production, 19: 20996
LIU, Lian-sou, Complex angular momentum in π-N scattering, 19: 21048
LIVDAHL, P., High-voltage power supplies and their regulation, 19: 20085 (CONF-640204(p.93-105))
LLOYD, R. D., Radium contamination at the Jordan River delta of the Great Salt Lake, 19: 20220
LO, Chung-tsuen, Inelastic collisions of 6.8 Bev/c π^- mesons with nucleons, 19: 21062
LOCHAK, G., Nonlinear phase resonances in high-energy synchrotron, 19: 20745
LOCKER, Robert J., Prog. rpt. on surface contouring applied to semiconductor radiation detectors, semiannual, 6/64-1/65, 19: 20323 (NYO-3246-6)
LODDER, A., Muon capture in Li-6 for testing nuclear models, 19: 21368
LOEBE, J., Experiences in treatment of euthyroid goiters with I-131, 19: 19685
LOEBER, Christian, Measuring dosage rate of particle or EM radiation, 19: 20396
LOEFFLER, Lotar, Pressed block for fabrication of fuel element rods, 19: 20540
LOEHR, E., Radium-226 in human embryonic tissue, 19: 20216
LOEWENSTEIN, P., Hot extrusion of metal powders, 19: 20518 (NMI-TJ-29)
LOEWENSTEIN, W. B., EBR-II wet critical experiments, 19: 21677 (ANL-6864)
LOGACHEV, V. L., Investigation of primary cosmic rays, 19: 20894
LOGAN, D., Sodium-heated, modular, steam generators for SCTI, 19: 21611 (NAA-SR-9826)
LOGAN, Robert K., Single Regge-pole analysis of π^-p charge-exchange scattering, 19: 21007
LOMINADZE, D. G., Excitation of magnetoacoustic waves in colliding plasma streams, 19: 21575
LOMINADZE, D. G., Low-frequency plasma oscillations, 19: 21523
LOMINADZE, J., Controlled plasma, 19: 21492 (FTD-TT-64-102)
LOMINO, N. S., Development of instabilities in plasma captured by transverse magnetic field, 19: 21577
LOMSADZE, Yu. M., Poles of the Bethe-Salpeter partial wave amplitude in the g^2-plane, 19: 21111
LOMSADZE, Yu. M., Structure of g plane relativistic Schroedinger theory, 19: 21053
LONDARENKO, G. A., Radiative transitions in Yb-173 deformed nucleus, 19: 21284
LONDON, Georges Whitney, Intrinsic and dynamic properties, 19: 21065
LONG, E. L., Jr., High-temperature thermocouples used in ORNL-GCR program fuel irradiation experiments, 19: 20401 (ORNL-P-1065)
LONG, F. A., Hydrogen exchange of azulenes. V., 19: 19883
LONGTIN, F. B., Impurities in moderator of Savannah River reactors, 19: 21711 (DPSPU-63-30-40)
LOONEY, W. B., Radiation dose rate dependence of DNA synthesis, 19: 19506 (TID-21703)
LOORITS, V., Pauli-Fierz transformation group, 19: 21051
LORBER, H. W., Validity of treating a dense plasma as a metal, 19: 21507
LOREE, T. R., Overdriving effect in dynamic polymorphism, 19: 20555 (LA-3215)
LOTHROP, R. P., Experimental instrumentation for 88-inch cyclotron, 19: 20282 (UCRL-11828(p.218-19))
LOTHROP, Robert P., Silicon radiation detectors, 19: 20328 (UCRL-11828(p.225-6))
LOTZ, W., Toroidal theta pinch in M-and-S configuration, 19: 21530
LOVE, D. L., Radiochemical procedure for In, 19: 19777 (USNRDL-TR-819)
LOVELESS, A., Recovery from lethal effects of cross-linking alkylation, 19: 19485
LOZOVAYA, E. A., Formation of quasineutral beam in plasma issuing from ion source, 19: 21571
LOZOVSKII, S. N., Interaction of traveling EM wave with plasma, 19: 21564
LUBYANI, V. V., Spark chamber, 19: 20378
LUCAS, G. J., Resonantly coupled accelerating structures for high-current proton linacs, 19: 20725 (LA-DC-6760)
LUCAS, Henry F., Jr., Low-level γ counting room, 19: 20092 (ANL-6938 (p.91-6))
LUCAS, J., Electron diffusion in H at high electric fields and low gas pressures, 19: 20696
LUCASSON, A., Annealings of electric resistivity produced in Cu by quenching and by irradiation. I., 19: 20590
LUCASSON, P., Annealings of electric resistivity produced in Cy by quenching and by irradiation. I., 19: 20590
LUCHNER, K., Luminescence of Fe-57 in ZnS phosphors, 19: 19855
LUDWIG, E. J., Proton polarization in $^{88}Sr(d,p)^{89m}Sr$ (1.05-Mev) reaction, 19: 21391
LUDWIG, Edward James, Proton polarization in reaction $^{88}Sr(d,p)^{89}Sr$, 19: 21447
LUEDENBACH, J., Influence of radiation on electrical conductivity of glasses, 19: 19976
LUEHRS, R. E., Radiation hazard from contaminated aircraft, 19: 20208
LUFT, S. J., Geologic map of Quartet Dome Quadrangle, Nye County, Nevada, 19: 20151 (TEI-860)
LUKENS, H. R., Jr., Neutron activation analysis procedures for determination of O in K, 19: 19751 (GA-5982)
LUKIN, Yu. T., Accuracy of locating particle in spark chamber and determining ion drift in Wilson chamber, 19: 20344
LUK'YANOV, A. V., Tables of Coulomb wave functions, 19: 21117
LUK'YANOV, V. K., Inelastic scattering of heavy particles, 19: 21353
LUK'YANOV, V. K., Inelastic scattering of heavy particles with excitation of collective nuclear states, 19: 21234 (JINR-P-1908)
LUMING, Max, Analysis of Regge trajectories, 19: 21067
LUNDBERG, B., Gamma rays from neutron capture in Ta and Au, 19: 21317
LUNDY, R. A., Production cross sections for $\pi^{\pm}$ and $K^{\pm}$ for 12.5-Bev protons on Be, 19: 21406
LUOMA, J. D., Fast reactor fuel burnup, 19: 21672
LUTHER, Lars. Christian, Diffusion of He in solids, 19: 19934
LUZSA, Gyoergy, Radiation exposure of inhabitants of Mosonmagyarovar in 1961, 19: 20227

LYKO, J., Effect of acute chemical intoxications and protracted ionizing radiations on alkaline phosphatase activity in human granulocytes, 19: 19570
LYON, A. J., F layer at sunrise near the magnetic equator, 19: 21138
LYSENKO, G. M., Phosphorescence of B–U phosphors, 19: 19919

M

MA, Benjamin M., Temperature distributions in end caps of fuel elements, 19: 21674
MACHEKHIN, A. M., Accuracy of locating particle in spark chamber and determining ion drift in Wilson chamber, 19: 20344
MACHTA, Lester, Carbon-14 measurements in atmosphere, 1953–64, 19: 20155 (HASL-159)
MACHU, L., Volumetric determination of micro amounts of fluoride, 19: 19788
MACIEL, Gary E., Carbon-13 chemical shifts in substituted benzenes, 19: 19951
MACKE, W., Crank model and perturbation calculation, 19: 21349
MAC PHERSON, R. E., Prog. rpt. on SNAP-8 corrosion, 9–11/63, 19: 20477 (ORNL-3604)
MAC PHERSON, R. E., Prog. rpt. on SNAP-8 corrosion, 12/63–2/64, 19: 20478 (ORNL-3618)
MAC PHERSON, R. E., Prog. rpt. on SNAP-8 corrosion, 3–5/64, 19: 20479 (ORNL-3671)
MAC PHERSON, R. E., Prog. rpt. on SNAP-8 corrosion, 6–8/64, 19: 20480 (ORNL-3730)
MAC QUEEN, K. F., Sprout inhibition of vegetables using γ radiation, 19: 20424
MADAKBAS, M., Charge transport time in semiconductor detectors, 19: 20366
MAEDA, Koichi, Diffusion of low-energy auroral electrons, 19: 21144
MAEDA, Morimasa, Slit-type screen for telecobalt therapy, 19: 19674
MAEH, To-on, Determination of P by fast neutron activation analysis, 19: 19828
MAESEN, L., Operation of PWR-type powerplant, 19: 21679 (BLG-261)
MAESEN, L., Operation of PWR-type powerplant, 19: 21679 (BLG-261)
MAGEE, J. H., Studies of renal homotransplantation in man, 19: 19463
MAGEE, Patrick M., Effect of large temperature gradients on turbulent flow of gases in thermal entrance region of tubes, 19: 20117 (SU-247-4)
MAGISTRIS, A., Electrode reaction kinetics for H evolution in molten KHF_2, 19: 19875
MAGNENAT, P., Indirect lymphography and oncology, 19: 19719
MAGNIER, Pierre, Variations of U parameter with changes in C content, 19: 20547 (CEA-R-2731)
MAHANTHAPPA, K. T., Lorentz-covariant SU(6), particle-antiparticle algebras, and supermultiplet structure, 19: 21015
MAHANTHAPPA, K. T., Meson-baryon scattering in intrinsically broken M(12) symmetry scheme, 19: 21024
MAHAUX, C., Magnetic dipole moments of conjugate nuclei, 19: 21322
MAHONEY, J., Energy variation of phase rule in α-particle scattering, 19: 21259 (UCRL-11828(p.132-3))
MAHONEY, Jeannette, Octupole states in N-15 and O-16, 19: 21268 (UCRL-11828(p.129-31))
MAHR, Herbert, Exciton absorption in presence of excited F centers, 19: 21602
MAIENSCHEIN, F. C., Spectra of γ rays produced by interaction of ~160-Mev protons with Be, C, O, Al, Co, and Bi, 19: 21243 (ORNL-3506)
MAIER, B. P., Energies and character of low-lying levels in Nb-94, 19: 21330
MAINO, F., Liquid-liquid extraction of $FeCl_3$, 19: 20038 (EUR-2245.e)
MAIRE, M., Sorption of Sr in Schleswig-Holstein soils, 19: 19474 (CEA-tr-A-1616)
MAJONI, G., Improved pulse shape discriminator, 19: 20370
MAKAROV, N. M., Chronic γ-irradiation effects on pea and vetch, 19: 19586
MAKAROV, Yu. V., Method of measuring heat fluxes in a plasma, 19: 21503
MAKINO, F., Direct recording of particle tracks of spark chamber, 19: 20368
MALAKHOV, S. G., Radioactivity of ground-level air on Hayes Island, 19: 20157 (NP-14697)
MALINOVSKY, M., Volumetric determination of micro amounts of fluoride, 19: 19788
MALLARD, J. R., Brain-tumor localization, 19: 19714
MALVICINI, A., Determination of waste water radioactivity, 19: 19749 (EUR-2118.f)
MALYUTA, Yu. M., Reggeization of hadrons, 19: 21049
MAMONTOV, A. P., Elastic scattering of deuterons with energy of 10.3 Mev on He-4, 19: 21286
MANDEL'TSVEIG, V. B., New data on resonances, 19: 21040
MANDRITSKAYA, K. V., Geometric program for analysis of penetrating showers of cosmic rays, 19: 20896
MANES, Roger, Pillar for vertically stacked, solid moderator structure of reactor, 19: 21627
MANI, G. S., Reaction $^6Li(d,\alpha)\alpha$, 19: 21414
MANI, G. S., Resonances in $^6Li(d,\alpha)\alpha$ and $^7Li(p,\alpha)\alpha$ reactions, 19: 21413
MANLEY, T. R., Scattering filters in the far infrared, 19: 19917
MANNELLI, I., Charge-exchange scattering at high energies for $\pi^- + p \to \pi^0 + n$, 19: 21006
MANOWITZ, B., Cobalt-60 research irradiators, 19: 20095 (BNL-8976)
MANOWITZ, B., Cost estimate for Co-60 radiation-induced ethylene polymerization process, 19: 19957 (BNL-8993)
MANSIKKA, Kauko, Transition energy for polymorphic transformation of CsCl, 19: 19900
MAOR, U., Final state of peripheral processes, 19: 20981
MAPLETON, R. A., Asymptotic form of electron capture cross sections, 19: 21417
MAR, B. W., Solar-flare hazard to manned space systems, 19: 20873 (D2-11608)
MARADUDIN, A. A., Lectures on astrophysics and the many-body problem. II., 19: 20714
MARADUDIN, A. A., Vibrations of imperfect crystals, 19: 20716
MARCH, N. H., Asymptotic form of correlation functions in liquid He-4, 19: 20697
MARCHANT, H., Angular distributions of (t,p) and (d,d′) reactions leading to Mg-26, 19: 21311
MARCHIORO, Thomas L., Splenic homotransplantation, 19: 19522
MARCUS, Y., Ion exchange studies of complex formation, 19: 19837 (IA-1000)
MARENGO, G., Evolution of chlorine in terphenyls, 19: 20469 (EUR-2279.e)
MARGOLINAS, S., Industrial applications of radioactive isotopes in automation, 19: 20416
MARGOLIS, B., Log ft values and $T = \frac{1}{2}$ analog states, 19: 21379
MARINCEK, O., Magnetic properties of ordering rare-earth antimonides, 19: 20597
MARINELLI, Leonidas D., Cosmic-ray fast neutron background, 19: 20877 (ANL-6938(p.71-88))
MARINELLI, Leonidas D., General technical problems in radiological physics, 19: 19657 (ANL-6938(p.97-119))
MARION, J. B., Isotopic spin description of highly excited levels in Be-8, 19: 21343
MARION, J. B., New results for $^7Li(p,\gamma)^{8**}Be$ reaction, 19: 21342
MARKO, M., Application of SNAP units to Manned Orbiting Research laboratory, 19: 21720 (NAA-SR-10318)
MARKOV, V. K., Uranium: methods for determination, 19: 19823
MARKOVSKII, L. Ya., Application of CS_2 in synthesis of rare earth sulfides, 19: 19927
MARKOVSKII, L. Ya., Lanthanum borocarbides, 19: 19926
MARLOWE, O. J., HARMONY—system for nuclear reactor depletion computation, 19: 21644 (WAPD-TM-478)
MARMIER, P., Direct measurement of short nuclear lifetime, 19: 21369
MAROVSKI, Th., Influence of x-ray therapy on hepatic function, 19: 19684
MARPLES, J. A. C., Pseudo binary phase diagrams of PuO_2, 19: 20589
MARPLES, J. A. C., Thermal expansion of Pa metal, 19: 20571
MARRUS, Richard, Magnetic moments of Re-186 and Re-188, 19: 21383
MARS, Jean, Allotropic transformations of Pu, 19: 20546 (CEA-R-2726)
MARSH, W. R., Effect of H_2 and H_2O on radiation-induced reaction of CO_2, 19: 19954 (AERE-R-4839)
MARSHAK, R. E., Quark model as probe of higher symmetries, 19: 20940 (UR-875-72)
MARSHALL, J. H., Calcium accretion and bone formation in dogs, 19: 19470 (ANL-6938(p.141-61))
MARSHALL, Louise R., Ion exchange on natural clay mineral, 19: 19794
MARTELL, E. A., Radiochemical evidence for Antler shot contribution to September 1961 fallout, 19: 20167
MARTIN, Alfred John, Improving ductility of Be, 19: 20611
MARTIN, Arthur F., Apparatus for producing controllable slow neutron chain reaction, 19: 21706
MARTIN, J. W., Metallography of fracture of alpha U, 19: 20592
MARTIN, John H., Need of higher-powered accelerators, 19: 20742
MARTINEZ, John S., Radioisotope space propulsion systems, 19: 20428 (TID-7698(Pt.I)(p.257-76))
MARTINI, M., Rise time of pulses supplied by semiconductor detectors, 19: 20369
MARTYSH, G. G., Effect of polyethylene glycols on nuclear photographic emulsions, 19: 20014
MARX, G., Decay $K_L^0 \to 2n$ and spontaneous breakdown of the CP symmetry, 19: 20999
MARYCHEV, V. V., High-temperature sintering of W, 19: 20532
MASAIKE, A., Direct recording of particle tracks of spark chamber, 19: 20368
MASHOVETS, T. V., Energy structure of γ radiation defects in Ge,

19: 20628
MASIAK, Michal, Effect of γ radiation on red blood cells in stored human blood, 19: 19513
MASLEY, A. J., Electron densities in lower ionosphere due to solar cosmic rays, 19: 21145
MASON, P., S-wave scattering lengths for n-p interaction, 19: 21043
MASON, Ronald, Advances in radiation biology. I., 19: 19461
MASON, Ronald, Ionization and excitation in radiation inactivation of enzymes, 19: 19517
MASSENGILL, L. A., Single-pass experiments (DCX-1), 19: 21480 (ORNL-3760(p.1-9))
MASSIMILLA, Leopoldo, Problems of chemical engineering in high-temperature technology, 19: 19868
MASTRYUKOVA, V. M., Mechanism of inhibiting effect of radiation on cell division, 19: 19613
MASUDA, Akimasa, Size effect of O anion on partition coefficients, 19: 20152
MATEEV, B., Radiation response of lung after intensive telecobalt therapy, 19: 19683
MATSUI, Noriyoshi, Brain injuries resulting from radiotherapy for eye tumors, 19: 19701
MATSUMOTO, Osamu, Electrolytic deposition of Be metal, 19: 20525
MATSUO, Masato, Dielectric behavior of poly(β-propiolactone), 19: 20000
MATSUOKA, O., Radiation injury to animals by radioactive materials. II., 19: 19565
MATSUZAWA, Taiju, Changes in germ-free mice following whole-body x irradiation, 19: 19619
MATTERN, K. L., Comparative fuel cycle evaluation. II., 19: 20048 (NAA-SR-9335)
MATTHEWS, P. T., P and C properties of U(12) multiplets, 19: 20974
MATTHIAS, E., Induced hyperfine fields in 5p shell, 19: 21359
MATTHIAS, E., Nuclear Zeeman effect in Ir-193, 19: 21255 (UCRL-11828 (p.57-8))
MATUSZEK, J., Cascades (γ-γ) in first excited state of Hg-200, 19: 21292
MATUSZEK, John M., Jr., Prog. rpt. on high-altitude balloon sampling, 7-12/64, 19: 20162 (NYO-3276-9)
MAUCHLINE, J., Radioisotopes in the marine environment, 19: 20226
MAUDAL, S., Exposure to radiation from medical procedures, 19: 19597
MAURETTE, M., Cosmic-ray exposure ages of tektites, 19: 20761
MAXWELL, E., Superconducting resonant cavities, 19: 21186
MAY, F., Preamplifier-amplifier system for proportional counters, 19: 20362
MAY, Harold A., Underground laboratory for high-sensitivity γ counting, 19: 20093 (ANL-6938(p.194-205))
MAY, Kenneth D., Advanced valve technology, 19: 20097 (NASA-SP-5019)
MAYER, Guy, Effects of multiple stimulation in interaction of bosons, 19: 20816
MAYER, H., Opacity of highly ionized air, 19: 20829
MAYER, M., Risks for embryo, fetus, and infant from medical radiology, 19: 19699
MAYS, C. W., Radium contamination at the Jordan River delta of the Great Salt Lake, 19: 20220
MAZUR, P., Statistical mechanics of assemblies of coupled oscillators, 19: 21089
MC CLAIN, W. C., Disposal of high-level power reactor wastes in salt mine, 19: 21751 (ORNL-P-1064)
MC COLM, Douglas W., Hyperfine structures of Re-186 and Re-188, 19: 21382
MC COURT, P. E., Application of SNAP units to Manned Orbiting Research laboratory, 19: 21720 (NAA-SR-10318)
MC COY, H. E., Type 304 stainless steel vs. flowing CO_2, 19: 20487
MC COY, H. E., Jr., Oxidation of Be in CO_2, 19: 20491
MC COY, Jerome D., Alpha-decay studies of Pa-230, Pa-228, and Pa-226, 19: 21418
MC CULLOCH, E. A., Host-cell interactions in mice bearing isologous hemopoietic grafts, 19: 19615
MC CURDY, H. William, Bubble formation in water-moderated reactors, 19: 21653
MC DERMOTT, Mark Arthur, Flow instability in a BWR, 19: 20121
MC DONALD, F. B., Continual acceleration of solar protons in Mev range, 19: 20766
MC DONALD, I. W., Chromium-51 complex of EDTA, 19: 20026
MC DONALD, T. F., Importance of edema in acute radiation injury to cerebral cortex of rats, 19: 19607
MC DOWELL, M. R. C., Electron excitation of electric quadrupole transition, 19: 20855
MC DUFFIE, H. F., Purification of Be, 19: 20070
MC ELROY, D. L., High-temperature high-vacuum thermocouple drift tests, 19: 20278 (ORNL-P-1069)
MC EWEN, M., Bismuth recovery process, 19: 20047 (MLM-734)
MC GEARY, Robert K., Nuclear reactor fuel members, 19: 20497
MC GINNIS, J. T., Outdoor γ irradiation facility, 19: 20102
MC HARRIS, W., Decay scheme of Es-254, 19: 21257 (UCRL-11828(p.63-6))
MC INERNEY, J. J., Green's function of monoenergetic neutron transport theory, 19: 21215
MC INTYRE, H. A. J., Polarizabilities and shielding factors of Be sequence, 19: 20852
MC INTYRE, J. A., Determination of neutron reduced widths by the $^{14}N(^{14}N,^{13}N)^{15}N$ reaction, 19: 21387
MC INTYRE, J. A., Reaction $^{14}N(^{14}N,^{13}N)^{15}N$ and the neutron tunneling mechanism, 19: 21388
MC KANE, Robert H., Nondestructive testing of reactor fuel, target, and control elements, 19: 20126 (DPSPU-65-30-11)
MC KINLEY, G. J., Determination of B in refractory borides, 19: 19761 (NP-14876)
MC KINNEY, Russell A., Prog. rpt. on surface contouring applied to semiconductor radiation detectors, semiannual, 6/64-1/65, 19: 20323 (NYO-3246-4)
MC KOWN, Gary L., Nuclear quadrupole resonance of Bi-209 in $BiBr_3$, 19: 19940
MC LAREN, K. G., Irradiation effects in polytetrafluoroethylene, 19: 19971
MC LAUGHLIN, James E., Boundary effect of γ transport from point source, 19: 20198 (HASL-157)
MC LAUGHLIN, James E., Operational safety evaluation of remote reactor plants, 19: 21685 (HASL-152)
MC MAHON, Allen J., Astrophysics and space science, 19: 20782
MC MURRAY, W. R., Low threshold neutron detector, 19: 20355
MC MURRAY, W. R., Measurement of differential neutron scattering cross sections, 19: 21298
MC NALLY, J. R., Jr., Fusion chain reactions, 19: 21487 (ORNL-3760 (p.98-9))
MC NELIS, David N., Decay of Ru-103, 19: 21333
MC NULTY, P. J., Pion production in high-energy μ-N collisions, 19: 21037
MC PARTLAND, J. O., Thermal conductivity of UO_2, 19: 20615 (HW-SA-3212)
MC QUILKIN, F. R., High-temperature thermocouples used in ORNL-GCR program fuel irradiation experiments, 19: 20401 (ORNL-P-1065)
MEADS, Philip F., Jr., Aberrations of quadrupole magnets, 19: 20252 (CONF-640204(p.82-92))
MEAKIN, J. D., Interstitial loops in neutron-irradiated Mo, 19: 20636
MECHALI, Acute radiation syndrome, 19: 19553
MECHAM, W. J., Pilot plant studies of direct fluorination process, 19: 20059
MEDEIROS, Katharine W., SNAP-8 DRM1 conversion program, 19: 21721 (NAA-SR-Memo-10160)
MEDVEDEV, Yu. A., Increase of O assimilation during irradiation, 19: 19584
MEERBURG, A. J., Neutron temperatures across the interface between H_2O and B, 19: 21207
MEHTA, Chandra Lal, Statistical properties of EM radiation, 19: 21118
MEINZER, R., Electron coupling of nuclear spins, 19: 19888
MEISELS, G. G., Radiolysis of ethylene. IV., 19: 19993
MEISTER, Herbert, Pulsation of reactors, 19: 21657
MEISTER, Herbert, Pulsed neutron source produced from fast reactor, 19: 21746
MEITRE, J., Influence of intermediate vector boson on muon capture rate, 19: 21420
MEL, Howard C., Stable-flow free boundary fractionation of spleen-colony-forming cells from mouse bone marrow, 19: 19617
MELISSINOS, A. C., Observation of the low-energy Λ-p interaction, 19: 21034
MELSA, James L., Prog. rpt. on application of automatic control theory to nuclear rocket, 2-9/64, 19: 21723 (NASA-CR-193)
MENDELSSOHN, K., Resistivity of Pu, Np, and U, 19: 20649
MENDELSSOHN, K., Progress in cryogenics. IV., 19: 21182
MENG, Ching-I., Dynamics of the aurora. II., 19: 21142
MENG, Ching-I., Dynamics of the aurora. III., 19: 21143
MENON, M. P., Neutron activation analysis, 19: 19764 (TEES-2671-4 (Chap.1))
MENON, M. P., Sodium separation, 19: 19768 (TEES-2671-4(Chap.6))
MENON, Manchery P., Prog. rpt. on automated activation analysis, annual, 1964, 19: 19763 (TEES-2671-4)
MENTH, A., Magnetic properties of the rare earth nitrides, 19: 19895
MENTH, A., Magnetic properties of ordering rare-earth antimonides, 19: 20597
MENTKOVSKII, Yu. L., Scattering amplitudes of charged particles at small momenta, 19: 21425
MENZEL, H. F., TARGET steam generator design, 19: 21682 (GAMD-4732)
MEREDITH, O. M., Protective actions of AET or serotonin in radiation injury, 19: 19635
MERGELYAN, O. S., Radiation from point charge in waveguide in presence of external magnetic field, 19: 21064

MERIKAS, G., Scanning in diagnosis of echinococcus disease of liver, 19: 19729
MERIWETHER, J. R., Energy variation of phase rule in α-particle scattering, 19: 21269 (UCRL-11828(p.132-3))
MERIWETHER, John R., Octupole states in N-15 and O-16, 19: 21268 (UCRL-11828(p.129-31))
MERKEL, A., Scattering laws of some hydrogenous moderators, 19: 21200 (KFK-264)
MERRILL, John P., Human kidney transplantation, 19: 19520
MESHCHERYAKOV, R. P., Connection between width of giant resonance of (γ,n) reaction and filling of energy levels of the nucleus, 19: 21287
MESHKOV, S., SU(6) Clebsch-Gordan coefficients for the product 35 × 56, 19: 21027
MESSER, Charles E., Systems of LiH with alkaline earth and rare earth hydrides, 19: 19881
MESSIAH, A. M. L., High-order limit of para-Bose and para-Fermi fields, 19: 20960
MESSIAH, A. M. L., Test for C conservation in strong-interaction physics, 19: 20977
METROPOLIS, Nicholas, Prog. rpt. on computer research, 2/65, 19: 20439 (COO-614-31)
MEULEMANS, M., Electron bombardment in metallurgy, 19: 20466
MEYER, Norman J., Hydrolysis of Th(IV) at 0 and 95°C, 19: 19878
MEYER, O., Mobility of hot electrons and influence on pulse rise time, 19: 20359
MEYEROTT, R. E., Spectral absorption in heated air, 19: 20832
MEYNIEL, G., Measurement of β activities on thin chromatographic layers, 19: 19792
MEZINA, I. P., Radioluminescence of some Tl-activated alkali halides, 19: 19966
MGALOBLISHVILI, N. P., Aluminothermal reduction of Eu_2O_3, 19: 20533
MICHAEL, B. D., Spectroscopic studies of reactions of OH radical in solutions, 19: 20009
MICHAELSON, W., Electronic peakers, 19: 20094 (BNL-8969)
MICHEL, F. Curtis, Neutral weak interaction currents, 19: 20988
MICHOT, Helene, Radiochemical separation of Ca-45, Sr-89, and Ba-140, 19: 19745 (CEA-R-2712)
MICKLEM, H. S., Amyloidosis in radiation chimeras and its relationship to lymphoid hypoplasia, 19: 19650
MIDDLETON, R., Angular distributions of (t,p) and (d,d′) reactions leading to Mg-26, 19: 21311
MIDGLEY, A. R., Jr., Use of labeled antibodies in ultrastructural studies, 19: 19465
MIKAMI, Hisashi, Separation of isotope gas mixture in supersonic jet, 19: 20434
MIKHAILENKO, I. E., Effect of S-35 radiation on dehydration of cyclohexanol, 19: 20013
MIKHAILOV, A. P., Effect of uv radiation on dark phase of actinorythmic reaction, 19: 19543
MIKHAILOV, G. A., Characteristics of superconducting films of Pb and In, 19: 21189
MIKHAILOVSKII, A. B., Diagram-addition method in turbulent-plasma theory, 19: 21529
MIKOSH, M., Open-cycle MHD generator, 19: 20912
MIKROPOULOS, H., Diagnosis of intraspinal neurological syndromes, 19: 19720
MILANI, S., Raman spectrum of ZrO_2, 19: 19849 (WAPD-T-1760)
MILDER, Nelson L., Evaluation of filament deterioration in electron-bombardment ion sources, 19: 20138 (NASA-TN-D-2173)
MILLER, D. W., Proton polarization in $^{88}Sr(d,p)^{89}Sr$ (1.05-Mev) reaction, 19: 21391
MILLER, Donald H., Further evidence for Kπ resonance near 1400 Mev, 19: 21004
MILLER, H. Craig, Response of electrostatic probe to EM-produced air shock, 19: 20841
MILLER, Maurice M., Shell model for baryon resonances, 19: 21008
MILLS, D. L., Possibility of long-range spin polarization in a degenerate electron gas, 19: 20689
MILOVSKII, A. V., Absolute age of pegmatite, 19: 20176
MINDER, W., Dosimetry and radiation protection, 19: 20213
MINETTI, B., Photoneutron cross sections for Co, Ni, Cu, and Ga, 19: 21305
MING, Hoy-ben, Dislocation structure of subboundaries in Mo single crystals, 19: 20602
MINGARRO, E., Genesis of uraniferous deposits. I., 19: 20185 (JEN-132-SIG/I-3)
MINOR, Joseph E., Low-level radioactive waste containers in accident environment, 19: 20196 (CONF-650103-6)
MINSHALL, F. S., Overdriving effect in dynamic polymorphism, 19: 20555 (LA-3215)
MIONE, Anthony J., Prog. rpt. on fuel of UC particles in U matrix, 8/62, 19: 20511 (NCSC-2981-1)
MIONE, Anthony J., Prog. rpt. on fuel of UC particles in U matrix, 12/62, 19: 20512 (NCSC-2981-2)
MIONE, Anthony J., Prog. rpt. on fuel of UC particles in U matrix, 2/63, 19: 20513 (NCSC-2981-3)
MIROPOL'SKII, Z. L., Radioisotopic methods for investigation of processes inside boilers, 19: 20418
MIROSHNICHENKO, L. I., Propagation of solar cosmic rays in interplanetary space, 19: 20757
MISENTA, Rolf, Pulsed neutron source produced from fast reactor, 19: 21745
MISHIMA, J., Plutonium releases during overheating and fires, 19: 20200 (HW-83668)
MISHIN, V. Ya., Heterogeneous equilibrates in $UO_2(NO_3)_2$–HNO_3–H_2O system. II., 19: 19907
MISHIN, V. Ya., Heterogeneous equilibrates in $UO_2(NO_3)_2$–HNO_3–H_2O system. III., 19: 19908
MISHIN, V. Ya., Heterogeneous equilibrates in $UO_2(NO_3)_2$–HNO_3–H_2O system. IV., 19: 19909
MISHRA, R. S., Curved shock waves in conducting gases, 19: 20664
MISNER, C. W., Spherical gravitational collapse, 19: 21100
MITCHELL, G. E., Reaction $^{89}Y(p,n)^{89}Zr$, 19: 21356
MITCHELL, H. H., Ecological problems and postwar recuperation, 19: 19504 (RM-2801-PR)
MITROPOL'SKAYA, O. N., Hydrogen Brackett series in solar spectrum, 19: 20778
MITSUHASHI, T., Distribution of Sr-90 and Cs-137 concentration in Japanese bulls, 19: 20215
MITTAL, M. L., Laminar unsteady MHD flow, 19: 20663
MITTLEMAN, Marvin H., Evaluation of hydrogenic matrix element $\langle 0|e^{ik\cdot r/n!}|\rangle$, 19: 20809 (UCRL-12218)
MIURA, Masatoshi, Solid-state polymerization of binary component system, 19: 19972
MIURA, Toyohiko, Radiation scattering and leakage from x-ray, 19: 20232
MIYAMOTO, Shigenori, Method for measuring the ionizing power of an incident charged particle, 19: 20339
MIZUTA, Hiroshi, Design of the fast power reactor, 19: 21696
MOCHIZUKI, Koiichi, Minimum criticality calculation for JPDR, 19: 21689 (JAERI-1068)
MOELLENSTEDT, G., Measurement of mean inner potentials of Be, 19: 20599
MOGILEVSKII, E. I., Energy of a magnetic storm, 19: 21135
MOHLER, H., Conservation of foods and sterilization of medical and pharmaceutical products, 19: 20410
MOISEENKO, E. V., X-ray breakdown of deoxynucleoprotein of intestinal bacteria, 19: 19576
MOISEEV, I. V., Uranium: methods for determination, 19: 19823
MOISEIWITSCH, B. L., Excitation 1s-2p of H atoms, 19: 20853
MOLE, R. H., Cancer production by chronic exposure to irradiation, 19: 19561
MOLINO, C., Photoneutron cross sections for Co, Ni, Cu, and Ga, 19: 21305
MONASTERIO, G., Radioiodinated (^{125}I and ^{131}I) fibrinogen for detection of malignant tumors, 19: 19716
MONCMANOVA, A., Volumetric determination of micro amounts of fluoride, 19: 19788
MONFILS, A., Absorption spectra of H_2, HD, and D_2. VI., 19: 19894
MONKS, A. L., Centrifugal pump for sampling radioactive liquids, 19: 20101 (ORNL-tr-442)
MONKS, A. L., Dielectric losses in oxides and halide compounds of group II elements, 19: 19851 (ORNL-tr-491)
MONKS, A. L., Production of radioactive isotopes in Spain, 19: 20432 (ORNL-tr-295)
MONKS, A. L., Relationship between electrical properties of ionic compounds of group-II elements and energy of interaction ions, 19: 21601 (ORNL-tr-490)
MONTAGUE, B. W., CERN r-f particle separator—first operation, 19: 20748
MONTAGUTELLI, Jean, Clebsch-Gordan coefficients adapted to cubic symmetry, 19: 21097
MONTGOMERY, M. H., Thermal conductivity of UO_2, 19: 20615 (HW-SA-3212)
MOON, D. P., Heavy-atom cross-section evaluation for Pu recycle calculations, 19: 21678 (ANL-6972)
MOORE, J. G., Adsorption of Pa on unfired Vycor, 19: 20051 (ORNL-3773)
MORAN, T. F., Intramolecular isotope effects in AB–HD ion-molecule reactions, 19: 19995
MORAN, T. F., Small-cross-section exothermic ion-molecule reactions, 19: 19887
MORCZEK, A., Medical supervision of personnel occupationally exposed to radiation, 19: 20214
MORDOVETS, N. T., Singularity of amplitudes of scattering in complex s

plane, 19: 21055
MOREAU, Guy, X-ray microanalysis—determination of correction factors, 19: 19746 (CEA-R-2728)
MORET-BAILLY, Jacques, Clebsch-Gordan coefficients adapted to cubic symmetry, 19: 21097
MORGAN, C. G., Photoelectric emission in low-pressure He discharges, 19: 20861
MORGAN, C. S., Influence of stress on fission-gas release, 19: 20586
MORI, Nobutane, Physicochemical studies of irradiated DNA, 19: 19566
MORI, S., Electron temperature measurement of a plasma from a plasma gun, 19: 21514
MORINAGA, H., Collective excited states in even Xe isotopes, 19: 21316
MORINI, M., Radioprotective power of prochlorperazine, 19: 19631
MORINI, M., Weight changes in albino mice after total-body irradiation, 19: 19632
MORIYAMA, Makoto, Microwave generation of harmonics in static magnetic field, 19: 21517
MORLEY, T. P., Design and function of brain scanner, 19: 19712
MOROZ, L. G., Polarizability of the neutron, 19: 20949
MOROZ, V. I., Reduction of minimization of quadratic functional, 19: 20441 (JINR-P-1958)
MORRIS, Clarence, Gas analytical apparatus for project Dribble, 19: 19776 (UCRL-12169)
MORRIS, J. W., Eddy-current inspection for stainless steel-clad U carbide, 19: 20531
MORRIS, W., Gallium oxide in spectrographic procedures, 19: 19774 (UCRL-7962)
MORRISON, D. R. O., Antiproton-proton elastic scattering, 19: 20976
MORRISON, Gail, Radiation sensitivity of *Serratia marcescens*, 19: 19649
MORRONE, Terry, Electron energy distribution in H, 19: 21586
MORROW, Frederick, Improving ductility of Be, 19: 20611
MORSE, Jerome G., SNAPS 9A and 19, 19: 20427 (TID-7698(Pt.I)(p.249-56))
MORTARA, D. W., Decay $Y_1^*(1660) \rightarrow Y_0^*(1405) + \pi$, 19: 21017
MORTON, Maxwell R., Static firing of large nuclear rocket stages, 19: 21725
MOSER, P., Magnetic after-effects in neutron-irradiated Fe, Ni, and Co, 19: 20652
MOSES, Alfred J., Nuclear techniques in analytical chemistry, 19: 19822
MOSES, Harry, Stack plume rise determinations as affected by meteorological and engineering factors, 19: 20653 (ANL-6938(p.209-41))
MOSHKOV, B. S., Effect of uv radiation on dark phase of actinorythmic reaction, 19: 19543
MOSKALENKO, A. M., Particle distribution in centrally symmetric field. II., 19: 20673
MOSS, L. I., Analysis of SNAPTRAN-3 destructive experiment, 19: 21719 (NAA-SR-9780)
MOSS, William T., Radiotherapy and surgery, 19: 19703
MOWBRAY, D. F., Bending fatigue strength of Zircaloy-4, 19: 20593
MUCCI, Joseph F., Ion exchange on natural clay mineral, 19: 19794
MUEHLBERGER, Erich, High-temperature acceleration of propellants, 19: 20139
MUELLER, Alfred H., Nonexistence of "pure bootstrap" solutions to Chew-Low theory, 19: 21001
MUELLER, Arno, Swimming pool reactor, 19: 21744
MUELLER, R., Direct measurement of short nuclear lifetime, 19: 21369
MUELLER, R., Ground state wave function of H-3 and He-3, 19: 21367
MUELLER, S., Techniques for ensuring compliance with the 1st SSVO. II., 19: 20211
MUELLER, W., Diluent influence on liquid-liquid extraction by trilaurylamine hydrochloride, 19: 20039 (EUR-2246.e)
MUELLER, W., Liquid-liquid extraction of $FeCl_3$, 19: 20038 (EUR-2245.e)
MUENZEL, F., Radiation sources for research and industry, 19: 20408
MUENZEL, H., Absolute measurement of radionuclides with 4π counter, 19: 19755 (KFK-252)
MUIRHEAD, H., Pion capture in complex nuclei, 19: 21315
MUKERJI, Ambuj, Decay of Ru-103, 19: 21333
MUKHITDINOV, G. N., Mineralogy and geochemistry of rare elements (Urals), 19: 20190
MULLINS, L. J., Ternary Pu alloys for core test facility, 19: 20506 (LA-3209)
MUNNICH, K. O., Tritium of atomic bombs as indicator in hydrology, 19: 20174 (CEA-tr-A-1729)
MUNZEL, F., Irradiation of cellulose and cellulose derivatives, 19: 19961 (CEA-tr-A-1741)
MURADYAN, R. M., Relativistic generalization of SU(6) symmetry, 19: 20973
MURADYAN, R. M., SU(6) symmetry and higher angular momenta, 19: 20972
MURATOV, V. I., Energy exchange between oscillations in plasma, 19: 21526
MURAY, J. J., Electron and ion emission from metal foils, 19: 20814
MURPHY, F. V., Test of $\Delta S/\Delta Q$ rule in $K_{\mu 3}^+$ decay, 19: 20979
MURPHY, Randall E., Hydromagnetic wave tube, 19: 21465 (AFCRL-63-779)
MURRAY, Hugh S., Prog. rpt. on application of automatic control theory to nuclear rocket, 2–9/64, 19: 21723 (NASA-CR-193)
MURRAY, Joseph E., Human kidney transplantation, 19: 19520
MURTAS, G. P., Reaction $\gamma + p \rightarrow p + \pi^0$ near first resonance from polarized photons, 19: 20932 (LNF-64/60)
MURTEIRA, M. A., Localization of iodine in stomach, 19: 19717
MURTHY, A. S. Venkatesha, Retardations in l-allowed M1 transitions in odd-mass nuclei, 19: 21323
MUSATOV, L. S., Correlation between variations of magnetic field and positive ions inside magnetosphere, 19: 21126
MUSIL, J., Effect of repeated chest x-ray examinations of women, 19: 19592
MUSIN, A. K., Electric current in an ionized gas, 19: 21502
MUSTEL, E. R., Solar corpuscular streams and geomagnetism, 19: 21155
MUZYKA, I. D., Adsorption of complex U compounds from aqueous solutions, 19: 20074
MUZYKANTOV, V. S., Isotopic exchange of O in γ-Al_2O_3–O_2 system, 19: 19872
MYERS, M. I., Brain-tumor localization, 19: 19714
MYERSCOUGH, Valerie P., Continuum correlation in C^-, 19: 20851

N

NABIVANETS, B. I., Hydroxo complexes of Th(IV), 19: 19922
NABIVANETS, B. I., State of Th in solutions $HClO_4$, HCl, and HNO_3, 19: 19923
NABOKA, V. A., Instability in plasma burst during its motion in longitudinal magnetic field, 19: 21582
NACHTIGALL, D., Measurement of flux density and neutron dose, 19: 20375
NADEZHIN, D. K., Gas dynamical model of type II supernova outburst, 19: 20769
NADEZHIN, D. K., Particle acceleration in shock emerging from star, 19: 20770
NAESER, C. W., Cosmic-ray exposure ages of tektites, 19: 20761
NAGAMATSUYA, Takaaki, Reduction of γ-irradiated Ni oxide by H, 19: 19975
NAGATA, T., Ionospheric electric current systems, 19: 21124 (P-1121 (RAND))
NAHEMOW, Martin David, Metastable abnormal glow discharge in H, 19: 21590
NAHILNITSKAYA, Z. N., Ionic penetrability of irradiated erythrocytes, 19: 19577
NAI, T., Shielding for nuclear installation, 19: 21739
NAIR, S. C. K., *ft* Values of $0^+ \rightarrow 0^+$, $\Delta T = 0$, β decays: conserved vector current theory, 19: 21416
NAITO, Setsuya, Late liver cirrhosis from Thorotrast, 19: 19560
NAKAGAWA, Takehiko, Phase transition in $Sr(FeTa)_{1/2}O_3$, 19: 20591
NAKAI, M. Y., Measuring range of low-energy charged particles in conducting solids, 19: 20806 (ORNL-3702)
NAKAJIMA, Sadao, Electron tunneling from hard superconductor, 19: 21164
NAKAMOTO, Atsushi, Fission fragment energy spectrum, 19: 21296
NAKAMURA, Kazuo, Brain injuries resulting from radiotherapy for eye tumors, 19: 19701
NAKAMURA, Michiyuki, Automatic spectrogram measuring and recording, 19: 20288 (UCRL-11828(p.232-3))
NAKAMURA, Tokihisa, Luminescence of uranyl ions dissolved in H_2O, 19: 19863
NAKANO, Toru, Determination of formation energy of M center in KCl, 19: 19999
NAKAO, Yuri, Electron tunneling from hard superconductor, 19: 21164
NAKATSUKA, Jiro, Slit-type screen for telecobalt therapy, 19: 19673
NAKHODKIN, N. G., Calculation of path of relativistic electrons, 19: 21423
NAKHODNOVA, A. P., Relationship between electrical properties of ionic compounds of group-II elements and energy of interaction ions, 19: 21601 (ORNL-tr-490)
NAKHODNOVA, A. P., Dielectric losses in oxides and halide compounds of group II elements, 19: 19851 (ORNL-tr-491)
NAPRAVNIK, Jiri, Deactivation of radioactive waste liquids, 19: 21755
NASTOU, A., Scanning in diagnosis of echinococcus disease of liver, 19: 19729
NATA, P., Effect of elastic unitarity on reactions $d(n,\gamma)^3H$ and $d(p,\gamma)^3He$, 19: 21371
NATH, A., Coherent scattering of γ rays, 19: 21599
NATH, Pran, Effect of inelastic channel on position and width of resonance, 19: 20987
NATTERSTAD, J. John, Carbon-13 chemical shifts in substituted benzenes, 19: 19951
NAUMENKOV, P. A., Concentration of atoms in a low-voltage pulse

discharge, 19: 21504
NAVTANOVICH, M. L., Extraction of Sc by alkyl phosphoric acids, 19: 20082
NAWAZ, Rab, Titration of Be in glacial acetic acid, 19: 19803
NAZIROV, N. N., Cultivation of cotton mutants under influence of P-32, 19: 19580
NDILI, F. N., Two-prong events in p-p annihilations at rest, 19: 20993
NEALE, W. W., CERN r-f particle separator—first operation, 19: 20748
NEALY, Carson L., Parent-daughter radioactive equilibrium, 19: 20031
NEDYALKOV, I., Numerical solution of one class of nonlinear integral equations of dispersion type, 19: 20445
NEDYALKOV, I., Representation of scattering amplitudes, 19: 20955
NEDYUKHA, I. M., Effect of Cr and Fe on elastic properties of Nb, 19: 20579
NE'EMAN, Y., Invariant derivation of SU(6) symmetry, 19: 20448
NEFEDOV, Yu. G., Biological action of protons of 510-Mev energy in irradiation of dogs, 19: 19578
NEICHARDT, W. J., Thermomechanoelectrical effects for superfluid He, 19: 21176
NEILSON, G. C., Reaction $^{30}Si(d,n)^{31}P$, 19: 21376
NELKEN, S., Radiopelvimetry, 19: 19698
NELMS, L. W., Induced-voltage studies in Co-60 γ irradiator, 19: 20398 (FZK-214)
NELSON, R. S., High-energy sputtering of metals at elevated temperatures, 19: 20838
NEMEC, V., Protective effect of fat in radiation sickness, 19: 19625
NEMIROVSKII, P. E., Models of the atomic nucleus, 19: 21463
NEMODA, D., Polonium-210 production, 19: 20008
NEMODRUK, A. A., Extraction of U as uranyl acetate, 19: 19817
NEMTSEVA, L. S., Fast neutron after-effects on *Crepis capillaris* seeds, 19: 19581
NESBET, R. K., Excitation operators and intrinsic hamiltonians, 19: 21289
NESHPOR, V. S., Interaction of NbC with W, 19: 20583
NESTEROV, V. E., Cosmic rays at high altitudes, 19: 20895
NESTEROV, V. E., Data on earth's radiation belts obtained during Cosmos flights, 19: 21136
NESTEROVA, N. M., Investigating composition of primary cosmic radiation of superhigh energy, 19: 20883
NEUBURGER, E., Instrument and unit program, 19: 20262 (KFK-259)
NEUHAUS, H., Hollow conductor for plasma, 19: 21562
NEURINGER, L. J., Thermal behavior of Nb-25% Zr in strong magnetic fields, 19: 21188
NEWCOMBE, Howard B., Radiation protection in Canada. VI., 19: 19654
NEWELL, M. F., Ages of La Sal Mountains rocks, Utah, 19: 20178
NEWMAN, E., Reaction $^{63}Cu(d,^3He)^{62}Ni$, 19: 21358
NEWTON, Amos S., Appearance potentials of some doubly charged molecule ions, 19: 20807 (UCRL-11828(p.201-4))
NEWTON, Amos S., Control of response sensitivity in gas chromatography, 19: 20281 (UCRL-11828(p.204-7))
NEWTON, Amos S., Formation of metastable states of rare gases by electron impact, 19: 19992
NEWTON, D., Reaction $^{63}Cu(p,p')$ at 150 Mev, 19: 21332
NEY, P. E., Limit distribution of binary cascade process, 19: 20958
NICHOLS, George, Jr., Diurnal variations in metabolic activity of bone and cartilage, 19: 19472 (ANL-6938(p.179-93))
NICOLO, George, Improvements in nuclear reactor control, 19: 21623
NIEBERGALL, F., Neutron polarization in $T(d,n)^4He$ reaction, 19: 21303
NIELSEN, C. E., Single-pass experiments (DCX-1), 19: 21480 (ORNL-3760(p.1-9))
NIELSEN, H. L., Odd-odd nucleus with 0^+ ground state (^{156}Eu), 19: 21350
NIELSEN, J. M., Sodium-22 and Cs-134 in foods, man, and air, 19: 20225
NIFENECKER, H., Cascades (γ-γ) in first excited state of Hg-200, 19: 21292
NIGHAN, W. L., Prog. rpt. on collision probability of electrons and ions with alkali metal atoms, 4/22–10/21/64, 19: 20805 (NASA-CR-54223)
NIKITIN, M. K., Decay of Pd-101, Rh-101*, and Rh-101, 19: 21280
NIKITINA, K. I., Formation of antiendotoxins against *E. coli* for involution of hemorrhagic syndrome in radiation sickness, 19: 19487
NIKOLAEV, Yu. M., Concentration of radioactive Sr and Cs from H_2O by electrodialysis, 19: 19809
NIKOLIC, M., Models of the atomic nucleus, 19: 21463
[NIKOLIC], S., Models of the atomic nucleus, 19: 21463
NIKOLOV, K., Tissue activation during mixed neutron irradiation, 19: 19601
NIKOL'SKII, I. K., Spectroscopic investigation of plasma in colliding bursts, 19: 21567
NIKOL'SKII, S. I., Investigating composition of primary cosmic radiation of superhigh energy, 19: 20883
NIKULIN, Yu. P., Problems of investigation of parameters of powerful γ devices for radiotherapy, 19: 19704
NISHIJIMA, K., Fundamental particles, 19: 21072
NITZL, K., Modification of strength of paper by irradiation, 19: 20630

NOAKES, John E., Cobalt molybdate catalyst for synthesis of benzene for liquid scintillation radiocarbon dating, 19: 19944 (ORINS-50)
NODIA, N. Z., Lunar-diurnal geomagnetic variations, 19: 21134
NOEL, J.-P., Spectrometry of fast neutrons by surface barrier junctions and Li-6, 19: 20334
NOHARA, Norimoso, Whole-body counter. I., 19: 20377
NOMOTO, Shoji, Measurement of anisotropic fast-neutron spectrum, 19: 20374
NOMURA, Shoichiro, Phase transition in $Sr(FeTa)_{1/2}O_3$, 19: 20591
NOMURA, Terunosuke, Separation factors of N isotopes with ion exchangers, 19: 20433
NORDAHL, J. H., Increased processing flexibility—Purex, 19: 20040 (HW-84085)
NORDEN, H., Study of fission fragment damage in W, 19: 20643
NORIN, Marvin P., Radioisotope-powered underwater acoustic beacon, 19: 20405 (MND-3180-1)
NORMAN, G. E., Lowering negative ion-electron detachment potential in plasma, 19: 21558
NORTON, Harry William, Closure means for pressure vessels, 19: 20106
NORTON, Peter, Momentum spectrum of positrons from muon decay, 19: 21012
NOSOVA, N. F., Heterogeneous equilibrates in $UO_2(NO_3)_2$–HNO_3–H_2O system. IV., 19: 19909
NOVAK, Arthur F., Prog. rpt. on radiation pasteurization of shrimp and oysters, final, 1–12/64, 19: 20407 (ORO-626)
NOVAK, P. E., Sodium logging in fast ceramic reactor fuels, 19: 20458 (GEAP-4283)
NOVAKOV, T., Energy levels of Bk-249, 19: 21253 (UCRL-11828(p.38-40))
NOVEY, T. B., Production cross sections for $\pi^\pm$ and $K^\pm$ for 12.5-Bev protons on Be, 19: 21406
NOVIKOV, S. R., High-temperature annealing of defects producted in Ge by fast neutrons, 19: 20626
NOWELL, Peter C., Hepatomas in mice after irradiation, 19: 19594
NOWIK, I., Relaxation phenomena in Dy_2O_3, 19: 19898
NOZAKI, H., Distribution of Sr-90 and Cs-137 concentration in Japanese bulls, 19: 20215
NUNAN, Craig Spencer, Linear accelerator, 19: 20752
NURZYNSKI, J., Elastic scattering of 5.5- to 10.0-Mev He-3 particles by Al-27, 19: 21328
NYGREN, D. R., Neutron-neutron S-wave scattering length from reaction $\pi^- + d \to 2n + \gamma$, 19: 20995

O

O'BRIEN, B. J., Penetrating particle radiation, 19: 20902
O'BRIEN, Keran, Boundary effect of γ transport from point source, 19: 20198 (HASL-157)
OCKENDEN, D. W., Determination of long-lived Kr and Xe isotopes in Magnox reactor coolants, 19: 21616
ODINTOSOVA, I. N., Spectrum of solar ionizing radiation during August 22, 1958 burst, 19: 20756
OEHME, R., Nonleptonic hyperon decays, 19: 20982
OEKAVA, T., Thorium fuel for breeding reactor, 19: 20582
OERTEL, L., Density and shock waves along cylindrical electron beams, 19: 20705
OESTGAARD, Erlend, Quasi-deuteron production by γ rays in heavy nuclei, 19: 21274
OFER, S., Anomalous isomer shift ratios in Eu-151 and Eu-153, 19: 21337
OGAWA, S., Dynamic viscoelastic propertids of graft copolymers. II., 19: 20001
OGILVIE, Robert E., Electron microscopy at MIT, 19: 20249 (CONF-640204(p.20-5))
OGUR, M., Tricarboxylic acid cycle mutants in saccharomyces, 19: 19593
OGUR, S., Tricarboxylic acid mutants in saccharomyces, 19: 19593
O'HALLORAN, T. A., Jr., Final state of peripheral processes, 19: 20981
OHARA, Hiroyoshi, Brain injuries resulting from radiotherapy for eye tumors, 19: 19701
OHASHI, Y., Direct recording of particle tracks of spark chamber, 19: 20368
OIGLANE, H., Pauli-Fierz transformation group, 19: 21051
OKIJI, A., Long-range magnetic coupling in metals, 19: 20690
OKUBO, S., Quark model as probe of higher symmetries, 19: 20940 (UR-875-72)
OLDS, Geoffrey Charles Edward, Magnesium alloy for fuel element cans, 19: 20610
OLIVA, H., Kidney homografts, 19: 19519
OLIVA, R. M., Test control devices—SNAP-10A vibration tests, 19: 21722 (NAA-SR-Memo-10767)
OLMSTED, John, III, Formation of metastable states of rare gases by electron impact, 19: 19992
OLSON, J., Superconducting properties of carbides and nitrides, 19: 20572

OLTMAN, Billie G., Cosmic-ray fast neutron background, 19: 20872 (ANL-6938(p.71-88))
OLTMANN, A., Cobalt-60 research irradiators, 19: 20095 (BNL-8976)
OMEL'CHENKO, Yu. A., Interaction of NbC with W, 19: 20583
OMES, D., Contamination of Mediterranean shellfish, 19: 20230
ONCESCU, Mircea, Measurement of activity of radionuclides by 4π β-γ coincidences, 19: 20385
ONCLEY, L. A., Solar-flare hazard to manned space systems, 19: 20873 (D2-11608)
O'NEILL, G. K., Test of $\Delta S/\Delta Q$ rule in $K^0_{\mu 3}$ decay, 19: 20979
O'NEILL, G. L., Sodium logging in fast ceramic reactor fuels, 19: 20458 (GEAP-4283)
ONGA, Masao, Dielectric behavior of poly(β-propiolactone), 19: 20000
OPALOVSKII, A. A., Isothermal solubility in NH_4F–UO_2–H_2O system, 19: 19913
OPRESCU, M., Separation of Nb from Ta, 19: 20054
ORAEVSKII, V. N., Stability of non-linear stationary plasma oscillations, 19: 21520
O'RAIFEARTAIGH, L., Internal symmetry and Lorentz invariance, 19: 20449
O'RAIFEARTAIGH, L., Mass differences and Lie algebras of finite order, 19: 21032
ORLANDO, G., Determination of mixed fission products in sea water, 19: 19790
ORLOV, V. P., Western drift of the geomagnetic field, 19: 21131
ORNES, J. F., Isotopic composition of He nuclei in primary cosmic radiation, 19: 20899
ORTH, P. H. R., Positron lifetimes in Ar and He, 19: 21011
ORTHEY, G. F., Frequency distribution of erythrocyte volumes of acutely bled dogs, 19: 21777 (UR-662)
OSTROM, Thomas R., Nuclear weapons, war, and survival, 19: 19554
OSTROUKHOV, A. A., Calculation of path of relativistic electrons, 19: 21423
OSTROUMOV, V. I., Cross sections for reactions in which π^+ mesons are absorbed by light nuclei, 19: 21279
OTROSCHENKO, V. A., Comparison of mitosis supression by separate irradiation of nucleus and cytoplasmic structures, 19: 19579
OTTAVIANI, G., Rise time of pulses supplied by semiconductor detectors, 19: 20369
OTTO, Jean-Louis, Simultaneous stimulated emission in He-4 and He-4, 19: 20815
OVECKS, M., Protective effect of fat in radiation sickness, 19: 19625
OVERTURF, G. E., Transistorized, 25-ampere constant-current battery discharger, 19: 20280 (SCL-DR-64-128)
OVSYUK, V. N., Influence of electron bombardment on surface state of Ge, 19: 20622
OWEN, F. E., Reactor decontamination and the health physicist, 19: 21605 (HW-SA-3560)
OWENS, B. B., Melting properties of alkali nitrates, 19: 19884
OZAKI, S., Observation of the low-energy Λ-p interaction, 19: 21034
OZIEWICZ, Z., First-forbidden nuclear μ-meson capture, 19: 21378
OZSVATH, Istvan, New homogeneous solutions of Einstein's field equations, 19: 21091

P

PACHECO, J. de la Rubia, Interactions of 29-Mev He-3 particles with light nuclei, 19: 21232 (JEN-141-DF/I-45)
PADALKA, V. G., Development of instabilities in plasma captured by transverse magnetic field, 19: 21577
PADDLEFORD, D. F., Analysis of SNAPTRAN-3 destructive experiment, 19: 21719 (NAA-SR-9780)
PAERISCH, M., Determinations of body water in humans, 19: 19480
PAIG, G., Neutron-neutron scattering length from $^3H(n,d)2n$ reaction, 19: 21404
PAIC, G., Reactions $H^3(n,p)3n$ and $H^3(n,H^4)\gamma$ at $E_n = 14.4$ Mev, 19: 21405
PAIEDASSI, Jean, Oxidation of alloy Mg–1% Ce in humid N at high temperatures, 19: 20485
PAIS, A., Covariance, SU(6), and unitarity, 19: 21022
PAISS, Y., Criterion for selectivity in recoil labeling, 19: 20020 (IA-907)
PAK, M. I., Accuracy of locating particle in spark chamber and determining ion drift in Wilson chamber, 19: 20344
PAKHOMOV, V. I., Electron radiation in plasma-magnetic-field boundary layer, 19: 21522
PALGI, L., Influence of intermediate vector boson on muon capture rate, 19: 21420
PALGI, L., S matrix in Kemmer-Duffin formalism (spin 0), 19: 21050
PAMASYUK, V. D., Formation of complexes from Y, La, and rare-earth elements with serine, 19: 19874
PANCHOLI, S. C., E2 conversion coefficients of rotational transitions, 19: 21308
PANDIT, L. K., Quark model in momentum space and higher symmetries, 19: 21016
PANKOVICH, A. M., Osteolathyrism and inhibition of endosteal bone reaction in estrogen-treated mice by AAN, 19: 19471 (ANL-6938(p.162-78))
PANKRATOV, A. K., X-ray bursts and cosmic rays, 19: 20890
PANNETIER, Guy, Analysis of $[Ce_2(SO_4)_3 \cdot 9H_2O]$ and $[Ce_2(SO_4)_3 \cdot 8H_2O]$, 19: 19857
PANT, J. C., Curved shock waves in conducting gases, 19: 20664
PANTAZIS, G., Diagnosis of intraspinal neurological syndromes, 19: 19720
PAO, Yeh-hsu, Vertex modification for Coulombic interactions, 19: 21094
PAPAGEORGIOU, S., Effective coupling constant G_A in β decay, 19: 21348
PAPAGEORGIOU, S., ft Values of $0^+ \rightarrow 0^+$, $\Delta T = 0$, β decays: conserved vector current theory, 19: 21416
PAPPAS, W. S., Moisture indicator, 19: 21783
PARAMONOVA, V. I., Complexing of uranyl with salicylic acid. I., 19: 19903
PARAMONOVA, V. I., Complexing of uranyl with salicylic acid. II., 19: 19904
PARASCHOU, E., Diagnosis of intraspinal neurological syndromes, 19: 19720
PARCHER, Jon F., Deactivation of gas chromatographic support, 19: 19997
PARIKH, J. C., Treatment of neutron-proton pairing correlations, 19: 21381
PARKACHEVA, V. V., Colorimetric determination of Ce, 19: 19819
PARKANYI, C., Nomenclature of organic labeled molecules, 19: 19737
PARKER, A., Determination of radiostrontium in biological materials, 19: 19739 (AERE-AM-101)
PARKER, E. N., Lectures on astrophysics and the many-body problem. II., 19: 20714
PARKER, E. N., Plasma physics and astrophysics, 19: 20783
PARKER, E. R., Superconducting properties of carbides and nitrides, 19: 20572
PARKER, F. L., Disposal of high-level power reactor wastes in salt mine, 19: 21751 (ORNL-P-1064)
PARKER, J. B., Preparation of nuclear data into form suitable for Monte Carlo calculations, 19: 21196 (AWRE-O-81/64)
PARKER, J. R., High-power test on cloverleaf cavity, 19: 20724 (LA-DC-6759)
PARR, Robert M., Relative activities of Th daughter isotopes in tissues of Thorotrast patients, 19: 19497 (ANL-6938(p.127-39))
PARRA, J., Kidney homografts, 19: 19519
PARRA, J., Modification of immunologic tolerance with transplantation of allogenic hematopoietic cells, 19: 19493
PARRETTE, J. R., Prog. rpt. on performing in-pile thermal conductance testing, 10–12/64, 19: 21664 (CEND-3336-229)
PASHCHENKO, V. P., Influence of plasma density near electrode on conductivity in transverse magnetic field, 19: 21580
PASQUALINI, L., Photoneutron cross sections for Co, Ni, Cu, and Ga, 19: 21305
PASSE, S., Spectrometry of fast neutrons by surface barrier junctions and Li-6, 19: 20334
PASSMORE, E. M., Temperature and grain size effects in ductile-brittle transition of Mo, 19: 20594
PASSOVOY, Mitchell, Transplantation potential of marrow frozen at programmed cooling rates, 19: 19645
PASTUSKA, G., Effect of γ radiation on leather, 19: 20414
PATEL, A. R., Evidence of screw dislocations in graphite, 19: 20574
PATIL, Sharashchandra Hanumant, Quantum numbers of the B meson, 19: 21066
PATIN, S. A., Strontium-90 in Pacific Ocean, 19: 20159 (NP-14726)
PATTERSON, J. D., Energies of n-nucleon systems by Bopp's approximation, 19: 21412
PATTERSON, James H., Chemical analysis of surfaces using α particles, 19: 19795
PATTORET, A., Vapor pressure of U, 19: 19689
PAUL, P., Gamma transitions in Be-8, 19: 21357
PAUL, W., Design and function of brain scanner, 19: 19712
PAULINA, J. P., Factors affecting notch toughness of maraging steels, 19: 20541 (AD-604868)
PAULSEN, A., Cross-section measurement for $^{56}Fe(n,p)^{56}Mn$, $^{59}Co(n,\alpha)^{56}Mn$, and $^{63}Cu(n,2n)^{62}Cu$, 19: 21290
PAULY, Jules, Determination of Co in steel by neutron activation and γ spectrometry, 19: 19784
PAVANELLO, R., Determination of mixed fission products in sea water, 19: 19790
PAVLICHENKO, O. S., Spectroscopic investigation of plasma in colliding bursts, 19: 21567
PAVLOTSKII, I. P., Correlation potentials of rectilinear statistical systems, 19: 20687

PAVLOV, B. N., Pulse method for nuclear quadrupole resonance, 19: 21430
PAVLOV, P. V., Depth of penetration and distribution of radiation damage when Ge is bombarded with Ar and N ions, 19: 20625
PAVLOV, V. S., Vapor pressure of Gd and Dy, 19: 20601
PAVLOVIC, D., Secondary α-deuterium isotope effects in reaction of 2-phenylethyltrimethylammonium ion by hydroxide ion, 19: 19947
PAVLOVSKII, A. I., High-current air-core betatrons, 19: 20740
PAYNE, George O., Jr., Packaging aspects of radiation preservation of foods, 19: 20421
PCHELKIN, V. A., Strontium-90 in Pacific Ocean, 19: 20159 (NP-14726)
PEARSON, F. J., Jr., Isotope effect in the benzene synthesis for radiocarbon dating, 19: 20179
PEARSON, James Alastair, Improvements in reactor fuel elements, 19: 21675
PEARSON, W. B., Constitution and properties of Pd tellurides, 19: 20577
PECA, O., Influence of pethidine upon breathing and metabolism of rats during acute irradiation disease, 19: 19481
PECUL, Krzysztof, Theoretical investigation of O hydrides, 19: 19844 (PAN-550/XVII)
PEINCENAT, M. R., Quick counting scales for nuclear physics, 19: 20380
PEKHOV, A. P., Effects of x irradiation on frequency of genetic recombinations and recombinations in *E. coli*, 19: 19537
PELLICCIONI, M., Measurement of Skyshine neutrons around Frascati synchrotron, 19: 20741
PELLICCIONI, M., Mixed radiation field measurement, 19: 20373
PELLINI, W. S., Prog. rpt. on metallurgical characteristics of high-strength structural materials, 9–12/64, 19: 20462 (NRL-6258)
PELLISSIER, Pierre F., Hydrostatic leveling systems, 19: 20733 (UCRL-11799)
PENCHEV, G., Numerical solution of one class of nonlinear integral equations of dispersion type, 19: 20445
PENDLETON, Robert C., Radium contamination at the Jordan River delta of the Great Salt Lake, 19: 20220
PENELLE, G., Production of radioisotopes. Study of maximum possible accident, 19: 20195 (BLG-281)
PENELLE, G., Tritium laboratory—maximum possible accident, 19: 20194
PENFOLD, J., Magnetic susceptibility of Sc, 19: 20595
PENFOLD, J., NMR linewidth in beta Mn, 19: 21366
PENG, C. T., Quenching correction in liquid scintillation counting, 19: 20332
PENNEY, G. W., Prog. rpt. on instabilities in metal-vapor plasmas, 10–12/64, 19: 21490 (TID-21698)
PENROSE, R., Zero rest-mass fields including gravitation, 19: 21108
PEOPLES, John, Momentum spectrum of positrons from muon decay, 19: 21012
PEPPER, Robert R., Pulsed plasmas and electron beam-plasma interactions, 19: 21488 (PIBMRI-1208-64)
PEPPER, Stephen V., Decay mode $K \to 2\pi + \gamma$, 19: 20939 (UR-875-30)
PEQUIGNOT, H., Pharmacogenic teratogenic hazard detection in the clinic, 19: 19533
PEREBASKINE, Michel, Oxidation of alloy Mg–1% Ce in humid N at high temperatures, 19: 20485
PERELOGOV, A. M., New data on resonances, 19: 21040
PERETTO, P., Magnetic after-effects in neutron-irradiated Fe, Ni, and Co, 19: 20652
PERKINS, F. W., Incoherent scatter from plasma oscillations in the ionosphere, 19: 21153
PERKINS, R. W., Sodium-22 and Cs-134 in foods, man, and air, 19: 20225
PERKINS, W. G., Crystal-field splitting in Tm^{3+} chelates, 19: 19886
PERLMAN, I., Decay scheme of Es-254, 19: 21257 (UCRL-11828(p.63-6))
PERLMAN, Morris L., X rays emitted in coincidence with fission of Cf-252, 19: 21229 (BNL-8841)
PERNY, G., Formation of thin layers of Cu oxides in reactive cathodic pulverization, 19: 20827
PERONI, L., Changes induced by radiations in some subcutaneous nervous structures, 19: 19591
PERRIN, J., Measurement of β activities on thin chromatographic layers, 19: 19792
PERRIN, R., Excitation 1s-2p of H atoms, 19: 20853
PERRINE, Laurence A., Portable γ-intensity time recorder, 19: 20397
PERSON, James C., Measuring photoionization efficiencies as function of energy, 19: 19955 (ANL-6938(p.21-2))
PERSSON, A., Conversion electrons from monocrystalline source, 19: 21339
PERSSON, Boerje, Bremsstrahlung spectra from Y-90 and Y-91, 19: 21302
PERUMOV, D. A., Mutagenesis in isolated DNA induced by uv and chemical agents, 19: 19542
PESCIA, Jacques, Spin scattering. Synthesis of bibliographic reviews, 19: 20828
PESINA, E. Ya., Application of CS_2 in synthesis of rare earth sulfides, 19: 19927
PESKIN, Richard L., Prog. rpt. on basic studies in gas-solid suspensions, 4–10/64, 19: 20098 (TID-21633)
PETELIN, M. I., Electron and ion distribution functions for plasma in slightly nonuniform high-frequency field, 19: 21573
PETELIN, M. I., Ohmic heating of partially ionized plasma by a uniform h-f field, 19: 21581
PETER, F., Radioactivity of atmospheric sediments, 19: 20235
PETERSON, J. P., Jr., Prog. rpt. on nuclear fuel burnup analyses, 9–11/64, 19: 21667 (GEAP-4776)
PETERSON, V. Z., Neutrino beams from high-intensity 200-Bev proton synchrotron, 19: 20738 (UCRL-11983)
PETKOV, I. Z., Inelastic scattering of heavy particles, 19: 21353
PETKOV, I. Zh., Inelastic scattering of heavy particles with excitation of collective nuclear states, 19: 21234 (JINR-P-1908)
PETRAN, V. I., Spark chamber, 19: 20378
PETRUKHIN, V. I., Pi-mesic atom processes in H-containing substances, 19: 21281
PETRYSHYN, W. V., On a class of K-p.d and non-K-p.d operators and operator equations, 19: 20446
PFEFFER, G., Emission spectrum and time constants of organic scintillators, 19: 19962
PFEIFER, C. J., HARMONY—system for nuclear reactor depletion computation, 19: 21644 (WAPD-TM-478)
PHAAL, C., Absorption spectra and irradiation of plastically deformed diamond, 19: 20638
PHILLIPS, H. R., Program for digital computer analysis of pulse-height spectra, 19: 19770 (TEES-2671-4(Chap.8))
PHILLIPS, L. E., Advantages of Hg–H_2O vapor cycle for Na reactor, 19: 21701
PHILLIPS, Roger J. N., Regge poles and phase of forward-scattering amplitude, 19: 21010
PHYTHIAN, R., Collective states of closed-shell nuclei, 19: 21415
PICARD, F., Reaction $^6Li(d,\alpha)\alpha$, 19: 21414
PICARD, J., Why is Gallagher-Moszkowski rule so well verified?, 19: 21370
PICCOT, A. R., Application of SNAP units to Manned Orbiting Research laboratory, 19: 21720 (NAA-SR-10318)
PICHOTIN, Bernard, Improvement of spectrographic analyses, 19: 19743 (CEA-R-2619)
PICKRELL, Kenneth, Radiogenic neoplasms of the hands, 19: 19524
PIERCE, G. B., Use of labeled antibodies in ultrastructural studies, 19: 19465
PIIR, I., Many particles problem in general relativity. II., 19: 20708
PIIR, I., Problem of many particles in general relativity. I., 19: 20707
PIKAEV, A. K., Radiolysis of aqueous nitrate solutions, 19: 19981
PINAJIAN, J. J., Preparation of In-115m, 19: 20023 (ORNL-tr-556)
PINCOCK, Richard E., Deuterium isotope effects in ionic decomposition of *t*-butylperoxy formate, 19: 19948
PINTENA, J., Energy resolution in liquid scintillation counting, 19: 20351
PIONTKOVSKII, I. A., Higher nervous activity of adult dogs subjected to ionizing radiation in antenatal development, 19: 19536
PIPPIG, Werner, Separation of rare earths on ion exchangers, 19: 20049 (NP-14834)
PIRAGINO, G., Photoneutron cross sections for Co, Ni, Cu, and Ga, 19: 21305
PIRANI, Marcello, Determining melting point of refractory metals, 19: 20566 (IS-Trans-13)
PIRON, C., Quantization of system of two particles, 19: 20952
PISARENKO, N. F., Cosmic rays at high altitudes, 19: 20895
PISARENKO, N. F., Data on earth's radiation belts obtained during Cosmos flights, 19: 21136
PIVNIK, L. Yo., Sodium zirconosilicate and hafnosilicate crystals, 19: 19916
PIZZINI, S., Electrode reaction kinetics for H evolution in molten KHF_2, 19: 19875
PLANE, D. E., S-wave scattering lengths for *n*-p interaction, 19: 21043
PLANQUE, M., Detection of critical accidents at Commissariat a l'Energie Atomique, 19: 20330 (AEC-tr-6547)
PLASIL, F., Energy-mass distributions of Bi, Au, and W in He-ion-induced fission, 19: 21263 (UCRL-11828(p.90-2))
PLASIL, Franz, Fission barrier of Tl-201, 19: 21260 (UCRL-11828(p.81))
PLASIL, Franz, Fission of U-238 and Pu-240 nuclei excited by inelastic α-particle scattering, 19: 21262 (UCRL-11828(p.84-6))
PLASIL, Franz, Fission-excitation functions of light elements, 19: 21264 (UCRL-11828(p.92-4))
PLASTINO, A., K conversion coefficient of 400-Mev transition in decay of Pb-203, 19: 21293
PLATAS, O. R., Photoionization contribution to radiation absorption coefficient of air, 19: 20830
PLATT, R. B., Outdoor γ irradiation facility, 19: 20102
PLATUNOVA, N. B., Complexing of uranyl with salicylic acid. I., 19: 19903
PLATUNOVA, N. B., Complexing of uranyl with salicylic acid. II.,

19: 19904
PLIESS, G., Problems of so-called radiation protective agents, 19: 19643
PLOTKIN, M., Proposed AGS accelerating cavity, 19: 20719 (BNL-8970)
PLUTE, E. F., Treatment of radiation skin lesions with fresh autofibrin films, 19: 19642
POCHIN, E. E., Counting studies of hepatic uptake, 19: 19492
POCHTAREVA, V. I., Influence of temperature on recovery of reproductive function of uv-damaged yeast cells, 19: 19626
PODGORENTSKII, M. I., "Beating" of nuclear radiation due to particle flux of variable intensity, 19: 21235 (JINR-P-1950)
PODOL'NYI, V. Z., Effect of radiation on growth of plants, 19: 19545
PODUSHNIKOVA, K. A., Anisotropy of electron energy distribution in alpha installation, 19: 21583
POECZE, L., Activation analysis of metals, 19: 19796
POEYHOENEN, Jorma, Transition energy for polymorphic transformation of CsCl, 19: 19900
POHLER, R. F., Incoherent x-ray scattering factors, 19: 20824
POLAK, M., Magnetic fields in units of ionic optical system for 5-Bev antiproton channel, 19: 20723 (JINR-P-1945)
POLCAKOVA, J., Effect of x rays on mechanical resistance of erythrocytes, 19: 19595
POLEVOI, R. M., Strontium-90 in Pacific Ocean, 19: 20159 (NP-14726)
POLEZHAEV, Yu. M., Sodium zirconosilicate and hafnosilicate crystals, 19: 19916
Polonio, J. Bermudez
see Bermudez Polonio, J.
POLUEKTOV, N. S., Extraction of rare-earth elements as ternary salicylate–pyridine complexes, 19: 20079
POLUSHKIN, K., Block-type atomic reactor, 19: 21702
POLYAKOV, Yu. A., Method of measuring heat fluxes in a plasma, 19: 21503
POLYKOVA, I. N., Influence of temperature on recovery of reproductive function of uv-damaged yeast cells, 19: 19626
POND, S. F., Resuspension factor of Pu from various surfaces, 19: 20191 (AERE-R-4635)
PONKSHE, M. R., Low-background gas-flow counter assembly, 19: 20353
PONTHUS, P., Irradiation and incompatible grafts, 19: 19588
POP, Iulio, Resonant paramagnetic absorption in alloys based on Gd, 19: 20581
POPOV, A. I., Inelastic scattering of protons by Mg-24, 19: 21426
POPOV, N. I., Strontium-90 in Pacific Ocean, 19: 20159 (NP-14726)
POPOV, N. P., First-forbidden nuclear μ-meson capture, 19: 21378
POPOV, Yu. S., Depth of penetration and distribution of radiation damage when Ge is bombarded with Ar and N ions, 19: 20625
POPOVIC, M., Total reflection of neutrons in Co mirrors, 19: 21201 (KFK-tr-164)
POPOVSKII, V. V., Isotopic exchange of O in γ-Al_2O_3–O_2 system, 19: 19872
POPPLEWELL, J., Gadolinium S state ions in metals, 19: 20698
POREMBKA, S. W., Surface damage in machined Be, 19: 20502 (DMIC-Memo-198)
PORTER, L. F., Factors affecting notch toughness of maraging steels, 19: 20541 (AD-604868)
POSPISIL, J., Pentose cycle and radiation diseases, 19: 19538
POSTMA, H., Single-pass experiments (DCX-1), 19: 21480 (ORNL-3760(p.1-9))
POTEMANS, M., Operation of PWR-type powerplant, 19: 21679 (BLG-261)
POTTER, J. M., Resonantly coupled accelerating structures for high-current proton linacs, 19: 20725 (LA-DC-6760)
POWELL, J. L., Strontium-87 abundance in Hawaiian volcanic rocks, 19: 20168
POZDNYAKOV, A. A., Analytical chemistry of Tc, 19: 19820
POZDNYAKOV, A. L., DNA localization on lymphoid tissue after γ irradiation, 19: 19583
POZDNYAKOV, A. L., Use of embryonic blood-making liver cells in acute radiation syndrome, 19: 19637
PRANGE, R. E., Possibility of long-range spin polarization in a degenerate electron gas, 19: 20689
PRASAD, S. S., Impact ionization of atomic H, 19: 20854
PRATT, R. G., Capture of hot electrons by Au^- and Au^{2-} centers in Ge, 19: 21180
PRAVDINA, G. M., Comparative radiosensitivity of Wistar and non-pedigree rats, 19: 19585
[PREIMERR VON DEM] BUSSCHE, G., Sorption of Sr in Schleswig-Holstein soils, 19: 19474 (CEA-tr-A-1616)
PREPEJCHAL, William, Internal Sr-90 β dosimetry with fluorods, 19: 20314 (ANL-6938(p.62-70))
PRESTWICH, W. V., Decay of La-142, 19: 21314
PRESTWOOD, R. J., Symmetry of neutron-induced Pu-239 fission in resonance region, 19: 21241 (LA-DC-6639)
PRIBIL, R., Separation and determination of Zr, Th, Ti, and rare-earth metals, 19: 19802
PRIBIL, Rudolf, Tetrathylenepentamine-N,N,N′,N″,N‴,N⁗,N⁗′-heptaacetic acid as a titrimetric reagent, 19: 19813
PRICE, P. B., Cosmic-ray exposure ages of tektites, 19: 20761
PRICE, P. B., Stability of fission tracks in minerals and glasses, 19: 20674
PRICE, P. Buford, Fission barrier of Tl-201, 19: 21260 (UCRL-11828 (p.81))
PRICEMAN, S., Oxidation testing of coated Nb alloy fuel elements, 19: 20482 (SCNC-314)
PRICEMAN, S., Oxidation-resistant coatings for Nb alloys, 19: 20483 (SCNC-318)
PRINCE, A., Calculated fast neutron capture cross sections for Ta-181, W, W-182, W-183, W-184, and W-186, 19: 21464
PRIOR, W., Plasma vortices in coaxial plasma accelerator, 19: 21539
PRIPSTEIN, Morris, Decay $Y_1^*(1660) \rightarrow Y_0^*(1405) + \pi$, 19: 21017
PRODIC, B., Crystal structure of double nitrate octahydrates of Th, 19: 19852
PROKOPCHUK, A. Ya., Protein fractions of blood serum in radioinduced dermatitis, 19: 19598
PROKOSHKIN, Yu. D., Pi-mesic atom processes in H-containing substances, 19: 21281
PROKSCH, E., Method of cyclohexane dosimetry, 19: 20341
PRON, G. F., Lanthanum borocarbides, 19: 19926
PROPKOP'EV, E. P., Annihilation of positrons in alkali-halide crystals, 19: 20820
PROPSTL, George, Radioisotopes and radiations in the textile industry, 19: 20411
PROUKAKIS, C., Photoscanning of spleen, 19: 19725
PROUT, G. R., Jr., Studies of renal homotransplantation in man, 19: 19463
PRUSSIN, S. G., Nondestructive activation analysis with Li-drifted Ge detectors, 19: 19775 (UCRL-11828(p.197-9))
PRZESTALSKI, Stanislaw, Effect of γ radiation on red blood cells in stored human blood, 19: 19513
PSHEZHETSKII, S. Ya., EPR study of radiolysis of ammonia adsorbed on solids, 19: 19984
PUDOVKIN, I. M., Spatial structure of the geomagnetic field. II., 19: 21130
PUESCHEL, Richard, Determination of Ni in Mo and W, 19: 19799
PUFF, R., Comparison of some approximations for self-bound many-fermion systems, 19: 20936 (TID-20558)
PUGH, H. G., Reaction $^{13}C(p,2p)^{11}B$ at 50 Mev, 19: 21401
PURCELL, N. J., Program catalog with permuted description index for CDC CO-OP computers, 19: 20438 (ANL-7016)
PURSEY, D. L., General theory of covariant particle equations, 19: 20946
PUSHKAR, N. S., Transplantation of bone marrow to animals with acute radiation sickness, 19: 19641
PUSHLENKOV, M. F., Complexing of Am with neutral organophosphorus compounds. II., 19: 20076
PUSHLENKOV, M. F., Formation of transuranic nitrates with phosphorus compounds, 19: 20077
PUTNAM, G. E., Calculation of parameters in reactor kinetics equations, 19: 21640 (IDO-16983)
PUZYAK, J., Magnetic fields in units of ionic optical system for 5-Bev antiproton channel, 19: 20723 (JINR-P-1945)
PYNADATH, Thomas I., Enzymic preparation of radioactive orotidine 5′-phosphate, 19: 20024

Q

QUARANTA, A. Alberigi, Rise time of pulses supplied by semiconductor detectors, 19: 20369
QUASSIATI, B., Test of $\Delta S/\Delta Q$ rule in K_{β}^0 decay, 19: 20979
QUASTLER, Henry, Advances in radiation biology. I., 19: 19461
QUERE, Y., Irradiation of U with neutrons at 4.5°K, 19: 20642
QUILICHINI, Paul, Specifications for scattering code for XY geometry: DAIXY, 19: 21198 (CEA-R-2759)
QUINCY, R. B., Jr., High-purity KCl, 19: 19843 (ORNL-TM-1071)
QUINLIVAN, W. D., Geologic map and section of Thirsty Canyon, Nye County, Nevada, 19: 20150 (TEI-859)
QUINN, J. M. P., Electron density in afterglow of H discharge, 19: 21510
QUINN, W. E., Power crowbar energy system for Scylla IV, 19: 21474 (LA-3189)
QUISENBERRY, Karl S., Spatial dependence of pulsed-neutron reactivity measurements, 19: 21637 (CONF-650406-2)

R

RABSON, T. A., Calibration techniques used with semiconductor detectors, 19: 20371
RACHEV, V. V., Investigation of system UO_2–UO_3, 19: 19873
RADEMACHER, K., Temperature determination on low-current C arc,

19: 21497
RADEMACHER, K., Temperature field of low-current arc in air, 19: 21498
RADFORD, E. P., Jr., Gonadal exposure to Po-210 in mouse and man, 19: 19495
RADHAKRISHNA, L., Electromagnetic fields and cylindrical symmetry, 19: 21084
RADICELLA, R., Preparation of carrier-free P-32, 19: 20021 (NP-14900)
RADICELLA, R., Preparation of I-131 from irradiated U oxide, 19: 20029
RAETHER, H., Energy losses of electrons, 19: 20702
RAETHER, M., Oscillations in one-dimensional, inhomogenous plasma, 19: 21478 (NP-14880)
RAFALSKI, Pawel, Dynamic thermal stresses in reactor shells, 19: 21618
RAFAL'SON, A. E., Quadrupole mass analyzer and application to chemical and isotopic analysis, 19: 20300
RAFIKOV, S. R., Radiation synthesis of polymers based on dimethylphosphinoborine, 19: 19982
RAFTER, T. A., Interpretation and reporting of C-14 activity measurements, 19: 20238
RAGAZZINI, R., Somatic mutations in potatoes induced by radiation, 19: 19518
RAIEVSKI, Victor, Pulsed neutron source produced from fast reactor, 19: 21745
RAIEVSKI, Victor, Pulsed neutron source produced from fast reactor, 19: 21746
RAIFF, W. J., Bismuth recovery process, 19: 20047 (MLM-734)
RAINE, Thomas, Beryllium alloy for GCR parts, 19: 20498
RAINEY, R. H., Adsorption of Pa on unfired Vycor, 19: 20051 (ORNL-3773)
RAINEY, R. H., Separation of long-lived fission product elements using EDTA, 19: 20052 (ORNL-TM-1035)
RAINEY, Robert H., Dissolution of high-density UO_2, PuO_2, and UO_2–PuO_2 pellets in inorganic acids, 19: 20050 (ORNL-3695)
RAJEWSKY, B., Radium-226 in human embryonic tissue, 19: 20216
RAKOVIC, M., Determination of Na content of filter papers, 19: 19786
RAKOW, A., Determination of dose distribution for irradiation planning, 19: 19693
RALPH, B., Study of fission fragment damage in W, 19: 20643
RAM, J. Sri, Use of labeled antibodies in ultrastructural studies, 19: 19465
RAMANIAH, M. V., Electrodeposition of Ac, 19: 19902
RAMASWAMY, M. K., Retardations in l-allowed M1 transitions in odd-mass nuclei, 19: 21323
RAMAVATARAM, K., Reaction $^{30}Si(d,n)^{31}P$, 19: 21376
RAMAYYA, Akunuri Venkata, Level schemes of Ga-69, I-129, and Sb-119, 19: 21450
RAMSEY, N. F., Baryon spectroscopy by inelastic e-p scattering, 19: 20997
RAMSEY, Thomas Halliburton, Jr., Materials study of the La–Te system, 19: 20606
RANDALL, I. E., Wetting of Mercury-Rankine boiler tube surface, 19: 20111 (NAA-SR-Memo-10224)
RANDOLPH, P. D., Slow neutron inelastic scattering from Al powder, 19: 20551 (IDO-17063)
RANGANATHAN, N. R., Gauge invariance and mass of vector bosons, 19: 20934 (NP-14829)
RAO, C. L., Electrodeposition of Ac, 19: 19902
RAO, C. N., Metastable phases in U alloys. II., 19: 20588
RAO, M. N., Low-background gas-flow counter assembly, 19: 20353
RAO, Pemmaraju Venugopala, L/K intensity ratio in decay of Tl-204, 19: 21449
RAPIER, A. C., Thermal bowing of reactor fuel elements, 19: 21669
RAPOPORT, I. D., Nature of cosmic-ray particles beyond atmosphere, 19: 20893
RAPP, D., Formation of H^- or D^- by electron impact on H_2, HD, and D_2, 19: 20691
RARITA, William, Regge poles and phase of forward-scattering amplitude, 19: 21010
RASHID, M. A., U(12) Predictions for $p\bar{p}$ annihilation into mesons, 19: 21036
RASMUSSEN, J. O., Decay of Mo-90, 19: 21258 (UCRL-11828(p.67-71))
RASTRELLI, Leonard U., Low-level radioactive waste containers in accident environment, 19: 20196 (CONF-650103-6)
RATNER, T. G., Problems of investigation of parameters of powerful γ devices for radiotherapy, 19: 19704
RAUH, E. G., Pressure of U over U–UO_2 system, 19: 19890
RAY, J. A., Cross-section measurements, 19: 21484 (ORNL-3760(p.57-63))
RAYFIELD, G. W., Focusing of electron stream with fields, 19: 20743
RAYNOR, Gilbert S., Radioactive Cu as atmospheric tracer, 19: 20658
RAZDOL'SKAYA, L. A., Geometric program for analysis of penetrating showers of cosmic rays, 19: 20896
RAZORENOV, L. A., Investigation of primary cosmic rays, 19: 20894
READ, F. H., Electron impact spectroscopy. III., 19: 20856
REAY, N. W., Observation of the low-energy Λ-p interaction, 19: 21034
REBANE, T. K., Electrostatic potential of the molecular electron shell at the atomic nuclei. II., 19: 20836
REBER, L. H., Single-pass experiments (DCX-1), 19: 21480 (ORNL-3760(p.1-9))
REBUT, Paul-Henri, Stability of plasmas obtained in EPPE, 19: 21469 (CEA-R-2713)
RECROSIO, A., Evolution of chlorine in terphenyls, 19: 20469 (EUR-2279.e)
REDEI, G. P., Induced premeiotic exchange of linked markers in the angiosperm arabidopsis, 19: 19548
REDHEAD, P. A., Low-pressure limits of hot-filament ionization gages, 19: 20147
REDLICH, Martin G., Digital-computer calculation of matrix elements of nuclear interactions, 19: 20938 (UCRL-11828(p.9-10))
REDLICH, Martin G., Energy levels of Pb-210, 19: 21247 (UCRL-11828 (p.10-11))
REDON, D., Reaction $^6Li(d,\alpha)\alpha$, 19: 21414
REED, J. T., Observation of the low-energy Λ-p interaction, 19: 21034
REED, Konnard W., Jr., Problem in neutron transport theory, 19: 21203
REGGIANI, R., Weight changes in albino mice after total-body irradiation, 19: 19632
REID, John H., Radio method of detecting solar flares, 19: 20759
REIF, Roland, Group theoretical methods in shell models. I., 19: 21444
REINCKE, U., Radiation-induced leukemia in Wistar rats, 19: 19530
REINER, A. S., Comparison of some approximations for self-bound many-fermion systems, 19: 20936 (TID-20558)
REINER, A. S., Density propagator for a self-bound Fermion system. II., 19: 21393
REINHARDT, H., Determination of size distribution of particles in suspension, 19: 19901
REINHARDT, R. G., Single-pass experiments (DCX-1), 19: 21480 (ORNL-3760(p.1-9))
REISNER, John H., State of the art of conventional commercial instruments, 19: 20247 (CONF-640204(p.1-16))
REISS, Howard R., Photoproduction of W^+ mesons, 19: 21003
REISTAD, A., Environmental γ radiation in Norwegian houses, 19: 20218
REMBIESOWA, H., Effect of Sr-90 on treatment of experimental rickets, 19: 19680
REMY, E., Toroidal theta pinch in M-and-S configuration, 19: 21530
RENGEL, J. C., Review of pressurized water reactor technology developments, 19: 21699
RETHORE, O., Risks for embryo, fetus, and infant from medical radiology, 19: 19699
REVIS, V. A., Incorporation of methionine-S^{35} into proteins of bone marrow and spleen in acute radiation sickness, 19: 19604
REVOLINSKY, E., Superconductivity in Nb–Se system, 19: 21195
REYNOLDS, F., Prog. rpt. on nuclear chemistry, annual, 1964, 19: 19735 (UCRL-11828)
REYNOLDS, John Terrence, Investigation of nuclear structure by electron scattering, 19: 21448
REYNOLDS, M. B., Radiation stability of ASTM A 302 grade B pressure-vessel steel, 19: 20631
REYNOLDS, W. N., Mechanical properties of reactor graphite, 19: 20637
REZNICHENKO, V. Ya., Circular luminescence of Na uranyl acetate crystal, 19: 19921
REZNIKOV, M. I., Radioisotopic methods for investigation of processes inside boilers, 19: 20418
RHEN, Zin-rhu, Inelastic collisions of 6.8 Bev/c π^- mesons with nucleons, 19: 21062
RHODERICK, E. H., Mixed state of type-II superconductors, 19: 21166
RIAZUDDIN, Quark model in momentum space and higher symmetries, 19: 21016
RICCIONI, N., Radioiodinated (^{131}I and ^{125}I) fibrinogen for detection of malignant tumors, 19: 19716
RICE, L., Evaluation of Hastelloy F and other materials for centrifuge in fuel recovery plant, 19: 20481 (ORNL-3787)
RICH, Marvin, Beam dynamical calculations with realistic fields in drift-tube linear accelerator, 19: 20727 (LA-DC-6777)
RICHARDS, A. G., Dental x-ray exposure of sites within head and neck, 19: 19676
RICHARDS, Clement John, Improvements in heat-exchanging elements, 19: 20125
RICHARDS, P. L., A-c Josephson effect in superfluid He, 19: 21172
RICHARDSON, D. M., Vacuum systems, techniques, and materials studies, 19: 20140 (ORNL-3760(p.94-7))
RICHARDSON, G. L., Recovery of Sr from Purex waste, 19: 20035 (BNWL-4)
RICHARDSON, R. W., Accuracy of BCS calculations in theory of deformed nuclei, 19: 21347
RICHERT, Raymond, Detection of center of gravity of current pulses of scintillation counter, 19: 20336
RICHTER, G., Neutron chopper for measurement of total cross sections.

II., 19: 20331
RICHTER, J., Determination of isodoses with computers, 19: 19692
RIDER, B. F., Prog. rpt. on nuclear fuel burnup analyses, 9–11/64, 19: 21667 (GEAP-4776)
RIDLEY, B. K., Capture of hot electrons by Au^- and Au^{2-} centers in Ge, 19: 21180
RIDLEY, R. G., Isotopic analysis of U using internal standard, 19: 20188
RIEDINGER, A., Gas transport properties and pore structure of nuclear graphites, 19: 20457 (GAMD-4814)
RIETJENS, L. H., Rotating plasma device, 19: 21593
RIFKIND, David, Splenic homotransplantation, 19: 19522
RIGAUD, Andre, Preparation of nuclear-pure beryllium oxalate tri-hydrate, 19: 19832 (CEA-R-2591)
RINSHAW, S. J., Isotopic power data sheets, 19: 20402 (TID-7698(Pt.I) (p.17-30))
RIPAN, Raluca, Determination of U and elements that accompany it. I., 19: 19811
RIPARBELLI, C., TARGET—IBM computer code for stress analysis of bodies of revolution, 19: 21609 (GAMD-5001(Rev.2))
RITTER, A. J., Treatment of radiation skin lesions with fresh autofibrin films, 19: 19642
RITTER, Robert Lucien, Kinetics and mechanism of fluorination of Cu(I) and Cu(II) oxides, 19: 19839 (K-1627)
RIVERA, Joseph, Prog. rpt. on fallout program, 12/64–3/65, 19: 20154 (HASL-158)
RIVERS, R. J., Gauge approximations in mesodynamics, 19: 20928 (ICTP-64/10)
RIVIER, D., Superconductivity and electromagnetic potentials, 19: 21163
RIZZO, Alfred J., Operational safety evaluation of remote reactor plants, 19: 21685 (HASL-152)
ROACH, Morris D., Silicon radiation detectors, 19: 20328 (UCRL-11828 (p.225-6))
ROALSVIG, Jan P., Spin of 1821-kev level in Kr-82, 19: 21312
ROBAYE, G., Thermal neutrons in retarder of long counter, 19: 21202
ROBERT, Andre, X-ray fluorescence analysis of light elements, 19: 19741 (CEA-R-2539)
ROBERTS, B. W., Superconductive materials, 19: 21187
ROBERTS, C. E., Hydrolysis of Th(IV) at 0 and 95°C, 19: 19878
ROBERTS, Donald R., Internal Sr-90 β dosimetry with fluorods, 19: 20314 (ANL-6938(p.62-70))
ROBERTS, E., Jr., Two-uranium-foil system for accident dosimetry, 19: 20340
ROBERTS, J. K., Heat transfer systems modification for SRE, 19: 21732 (NAA-SR-10379)
ROBERTS, Richard W., Modified hoke valve for ultrahigh-vacuum use, 19: 20145
ROBERTS, Richard W., Ultrahigh vacuum, 19: 20149
ROBINSON, James Alan, Beryllium alloy for GCR parts, 19: 20498
ROBINSON, L. C., Reflection of microwaves from an anisotropic plasma surface, 19: 21513
ROBINSON, R. L., Elastic scattering of 17- to 21-Mev neutrons from C-12, 19: 21310
ROCCELLA, M., Mixed radiation field measurement, 19: 20373
ROCHE, Franck, Determination of amounts of nuclides during radioactive transformations. II., 19: 19958 (CEA-R-2348)
ROCKMORE, R., Property of vertex function in potential theory, 19: 20964
ROCKMORE, R., Renormalization problems in potential theory, 19: 20945
RODIER, Jean, Safety in processing irradiated fuels, 19: 20037 (CEA-R-2654)
RODIONOVA, V. G., Electric breakdown through slot in glass in Cs vapor, 19: 21578
RODRIGUES, M. Simoe, Localization of iodine in stomach, 19: 19717
ROECKLEIN, A. K., Diffusion pump oil deposition measurements, 19: 20143
ROECKLEIN, A. K., Measuring range of low-energy charged particles in conducting solids, 19: 20806 (ORNL-3702)
ROEHNSCH, W., Activation determination of P, S, and Cl, 19: 19798
ROELLIG, Heinz Eberhard, Producing dispersions of fissionable material for fuel elements, 19: 20539
ROEPPISCHER, H., Influence of infrared radiation on roentgeno-luminescence, 19: 19965
ROESSLE, E., Flux converter for irradiation with fast neutrons at FRF, 19: 21742
ROGERS, John D., Properties of low-energy transitions in Dy-161, 19: 21329
ROGERS, Raymond N., Determination of boric acid in admixture with cyanuric acid, 19: 19756 (LA-3193)
ROGUIN, Andre, Apparatus for detecting leaks in cans of fuel elements, 19: 21626
ROHE, K. H., Discharge broadening in counting tubes, 19: 20379
ROHLOFF, F., Measurement of flux density and neutron dose, 19: 20375
ROHRLICH, F., Microcausality in asymptotic quantum field theory, 19: 21088
ROHRMANN, C. A., Fission products, 19: 20431 (TID-7698(Pt.I)(p.1-16))
ROHRMANN, C. A., Values in fuel from power reactors, 19: 20036 (BNWL-25)
ROHSENOW, Warren M., Film boiling of liquid flowing upward through heated tube, 19: 20113 (NP-14895)
ROINISHVILI, N. N., Geometric program for analysis of penetrating showers of cosmic rays, 19: 20896
ROITSIN, A. B., Theory of electron-nuclear double resonance (ENDOR) of F centers, 19: 19920
ROJAHN, Wolfgang, Nuclear merchant ships, 19: 21724
ROLNICK, William B., Relativistic scattering of two equal-mass charged particles, 19: 21031
ROMANENKO, E. D., Adsorption of complex U compounds from aqueous solutions, 19: 20074
ROMANKOVA, A. G., Variability of *penicillium nigricans* on uv and x irradiation, 19: 19556
ROMANO, A. J., Corrosion of C steel by Hg, 19: 20493
ROMANOVA, O. V., Treatment of radiation skin lesions with fresh autofabrin films, 19: 19642
ROMANYUK, L. I., Formation of quasineutral beam in plasma issuing from ion source, 19: 21571
ROSE, B., Renormalization of p-p polarization data, 19: 20980
ROSE-INNES, A. C., Mixed state of type-II superconductors, 19: 21166
ROSEN, H., Wound healing: effect of ascorbic acid and D_2O, 19: 19484
ROSENBLUM, S. S., Induced hyperfine fields in 5p shell, 19: 21359
ROSENBLUM, S. S., Nuclear Zeeman effect in Ir-193, 19: 21255 (UCRL-11828(p.57-8))
ROSHANMANESH, A., Tricarboxylic acid cycle mutants in saccharomyces, 19: 19593
ROSHOLD, J. N., Isotopic fractionation of U in sandstone, 19: 20187
ROSINO, L., Nebular variables and related objects, 19: 20795
ROSNER, Baruch, Reactions $^{86}Kr(d,p)^{87}Kr$, 19: 21394
ROSS, Harley H., Quenching variables from biomedical samples in liquid sciatillator systems, 19: 20324 (ORNL-P-1094)
ROSS, Ronald R., Decay $Y_1^0(1660) \rightarrow Y_0^0(1405) + \pi$, 19: 21017
ROSSI, G., Analysis of purified U compounds, 19: 19800
ROSTOKER, N., Kinetic theory of plasma and electromagnetic fields, 19: 21493
ROTH, R. S., Mixed oxides of Ti and Nb, 19: 20569
ROTHEN, F., Superconductivity and electromagnetic potentials, 19: 21163
ROTONDI, E., Measurement of Skyshine neutrons around Frascati synchrotron, 19: 20741
ROUCAYROL, J. C., Measurement of β activities on thin chromatographic layers, 19: 19792
ROUGE, Pierre, Pillar for vertically stacked, solid moderator structure of reactor, 19: 21627
ROUGNY, R., Mean lives of excited states of Os-186, Tl-203, W-182, and Pb-207, 19: 21291
ROUSH, M. L., Energy modulation of particle accelerators, 19: 20746
ROUSSEAU, Pierre, Observing specimens contained in fluid-tight chamber, 19: 20105
ROUX, C., Pharmacogenic teratogenic hazard detection in the clinic, 19: 19533
ROWE, J. M., Lattice dynamics of white Sn, 19: 21603
ROWLANDS, David T., Jr., Splenic homotransplantation, 19: 19522
ROXBURGH, I. W., Stellar hydromagnetics, 19: 20802
ROYLANCE, P. J., Recovery in erythropoiesis and erythropoietic capacity following whole-body irradiation, 19: 19644
RUBY, L., Pulsed neutron source based on the Orbitron, 19: 21208
RUBY, S. L., Mössbauer effect in K-40 using an accelerator, 19: 21408
RUCHKIN, E. D., Optical properties of rare earth oxides. II., 19: 19928
RUDAK, E. A., Determination of the spin in 0.416-Mev energy level of Fe-55 nucleus from (d,p) and (n,γ) reactions, 19: 21277
RUDGE, M. R. H., Calculation of exchange scattering amplitudes, 19: 20866
RUDJORD, T., Environmental γ radiation in Norwegian houses, 19: 20218
RUIZ, C. P., Prog. rpt. on nuclear fuel burnup analyses, 9–11/64, 19: 21667 (GEAP-4776)
RUMANOVA, I. M., Structure refinement for $Pr(NO_3)_3 \cdot 6H_2O$, 19: 19914
RUSANOV, V. D., Multiple beam radiointerferometer for plasma diagnostics, 19: 21574
RUSANOV, V. D., Probing of high-frequency-discharge plasma, 19: 21528
RUSBRIDGE, M. G., Diffusion of current sheath in toroidal discharge, 19: 21512
RUSBRIDGE, M. G., Longitudinal compression in a compressional Ioffe mirror machine, 19: 21516
RUSSCHER, Glenn Earl, Analysis of thermoelectric materials, 19: 21703
RUSSEK, Arnold, Three discrete Q values in Ar^+–Ar collisions, 19: 20846
RUSSELL, B., Effects of fast neutron irradiation on Cu–Sn alloy, 19: 20635

RUSSELL, J. A., Jr., Facility radiation and contamination alarm systems, 19: 20203 (ORNL-TM-988)
RUSSELL, J. E., Capture of negative mesons in liquid He, 19: 21042
RUSSELL, James E., Radioactive gas production from R.P.I. Linac, 19: 20204 (RPI-328-25)
RUTKEVICH, B. N., Energy exchange between oscillations in plasma, 19: 21526
RUZICKA, J., Substoichiometry in radiochemical analysis, 19: 19783
RYABCHIKOVA, G. G., Radiolysis of aqueous nitrate solutions, 19: 19981
RYAN, Robert M., Radioactive gas production from R.P.I. Linac, 19: 20204 (RPI-328-25)
RYDKII (RYDKIY), S. G., Effects of radioactive fission products on on harvest, 19: 19508 (JPRS-28977)
RYGAILO, T. A., Determination of Ce in rare earths, 19: 19821
RYPJANU, R., Total reflection of neutrons in Co mirrors, 19: 21201 (KFK-tr-164)
RYVKIN, S. M., High-temperature annealing of defects produced in Ge by fast neutrons, 19: 20626
RYZHKOVA, T. P., Interaction of NbC with W, 19: 20583
RYZHOV, N. I., Biological action of protons of 510-Mev energy in irradiation of dogs, 19: 19578

S

SABBIONI, Enrico, Determination of Co in steel by neutron activation and γ spectrometry, 19: 19784
SABISTON, D. C., Jr., Diagnosis of massive pulmonary embolism by radio-isotope scanning, 19: 19724
SACHARIDIS, E., Observation of the low-energy Λ-p interaction, 19: 21034
SACHS, Allan M., Momentum spectrum of positrons from muon decay, 19: 21012
SACHS, M., Electric dipole moment of the Cs atom, 19: 20840
SACTON, J., Interactions in flight of low-energy K⁻ mesons with emulsion nuclei, 19: 21365
SACTON, J., Production of hyperfragments from interactions of K⁻ mesons with nuclei, 19: 21429
SADEGHI, A., Reaction ^{6}Li(d,α)n, 19: 21414
SADIL, J., Disappearance of polar cap on Mars, 19: 20763
SAENDULESCU, A., Barrier penetrabilities in α decay, 19: 21411
SAFIN, I. A., Pulse method for nuclear quadrupole resonance, 19: 21430
SAFRONOV, B. G., Development of instabilities in plasma captured by transverse magnetic field, 19: 21577
SAGE, Martin L., Statistical descriptions of free boson fields, 19: 21102
SAHAROV, V. N., Comparison of mitosis supression by separate irradiation of nucleus and cytoplasmic structures, 19: 19579
ST. PIERRE, Leon E., Ultrahigh vacuum, 19: 20149
SAITO, Nobufusa, Isomeric transition of Br-80m in pentamminecobalt(III) bromides, 19: 19973
SAITO, Nobufusa, Radiolysis of cobaltammine complexes, 19: 19974
SAKITA, B., Phenomenological approach to relativistic SU(6) theory, 19: 21005
SALAM, Abdus, P and C properties of U(12) multiplets, 19: 20974
SALAM, Abdus, Relativistic structure of SU(6), 19: 20927 (ICTP-64/7)
SALAT, A., Non-linear resonant light mixing in plasmas, 19: 21546
SALAZAR, Edward A., Design for molded plastic potting shells, 19: 21764 (SC-DR-64-2135)
SALIBEKOV, S. E., Alpha-solid solution of nitrogen in Zr, 19: 19877
SALIMOV, R. A., Instability and anomalous diffusion in K plasma, 19: 21569
SALLER, G., Inelastic electron-deuteron scattering, 19: 20942
SALMON, G. L., Reaction ^{40}Ca(p,p') at 150 Mev, 19: 21332
SALPETER, E. E., Incoherent scatter from plasma oscillations in the ionosphere, 19: 21153
SALTER, Forrest O., Three-state memory device, 19: 21785
SALTER, R. M., Jr., Neutron-neutron S-wave scattering length from reaction $\pi^- + d \rightarrow 2n + \gamma$, 19: 20995
SALZBERG, Allan Michael, Statistical thermodynamics of the one dimensional plasma, 19: 21587
SAM, D., Radiochemical procedure for In, 19: 19777 (USNRDL-TR-819)
SAMA, L., Oxidation testing of coated Nb alloy fuel elements, 19: 20482 (SCNC-314)
SAMA, L., Oxidation-resistant coating for Nb alloys, 19: 20483 (SCNC-318)
SAMA, L., Preparation and properties of $NbAl_3$ and $NbAl_3$-fuel bodies, 19: 20464 (SCNC-316)
SAMARAS, V., Diagnosis of intraspinal neurological syndromes, 19: 19720
SAMARIN, A. M., Density of Co–C and Ni–C alloys in solid and liquid states, 19: 20567 (LA-tr-65-5)
SAMMARONE, D. G., Effects of chemical shim environments on wear of reactor materials, 19: 21606 (WCAP-3269-9)
SAMSAHL, K., Simultaneous determination of 30 trace elements, 19: 19793
SAMUEL, J. K., Low-background gas-flow counter assembly, 19: 20353
SAMUELI, J. J., Mean lives of excited states of Os-186, Tl-203, W-182, and Pb-207, 19: 21291
SAMUELS, L. D., Gonadal exposure to Po-210 in mouse and man, 19: 19465
SANDAGE, A. R., Observational approach to stellar evolution, 19: 20788
SANDER, Sten, Injury to bone marrow after Thorotrast, 19: 19567
SANDERS, William Mort, Semiconductor anticoincidence detector system, 19: 20322 (LA-DC-6397)
SANDERSON, Colin G., Prog. rpt. on high-altitude balloon sampling, 7–12/64, 19: 20162 (NYO-3276-9)
SANDOMIRSKII, V. B., Interaction of supersonic wave with beam of charged particles, 19: 20672
SANIELEVICI, A., Measurement of radioactivity at laboratory of Agence Internationale de l'Energie Atomique, 19: 20387
SANTHANAM, K., Chain element activity in intermittent irradiation, 19: 21226 (AEET/HP/Th-19)
SANTHANAM, T. S., Origin of symmetries, 19: 20933 (NP-14828)
SANTO, R., Reaction (d,t) on Be, Ar, Y, Zr, and Pb at 11.8 Mev, 19: 21326
SAN'YU, Kholi, Uranium defects in linear accelerator, 19: 20128
SAPEZHINSKII, I. I., Long afterglow in proteins and synthetic polymers irradiated by x rays, 19: 19983
SARALIDZE, Z. K., Coalescence of dislocation loops, 19: 20580
SARANTITES, Demetrios G., Yields of Te-131 and Te-133 isomers in fission, 19: 21390
SARAZIN, A., Mean lives of excited states of Os-186, Tl-203, W-182, and Pb-207, 19: 21291
SARGENT, K. A., Geologic map of Quartet Dome Quadrangle, Nye County, Nevada, 19: 20151 (TEI-860)
SARKISYAN, A. S., Arsenate method for iodimetric determination of Zr, 19: 19818
SARKSYAN, K. A., Plasma acceleration with aid of EM H_{11}-type wave in circular waveguide, 19: 21566
SASS, Richard E., Reactions ^{86}Kr(d,p)^{87}Kr, 19: 21394
SATO, F., Life span shortening induced by radiation. IV., 19: 19564
SATO, Toichi, Extraction of U(VI) from HNO_3 solutions, 19: 20067
SATO, Yoshiki, Determination of formation energy of M center in KCl, 19: 19999
SAUER, J. A., Prog. rpt. on polymers and related materials, 6/64–2/65, 19: 21770 (TID-21677)
SAUER, Kenneth, Flow dichroism apparatus and its application to study of structure of spinach quantasomes. III., 19: 21773 (UCRL-11308)
SAUERMANN, G. O., Helium memory effects observed with tandem mass spectrometer, 19: 20146
SAUNDERS, P. A. H., Diffusion of current sheath in toroidal discharge, 19: 21512
SAUVAGE, Michel, First results of tests of Rapsodie block pile, 19: 21730 (CEA-R-2557)
SAUVAGNAC, R., Energy resolution in liquid scintillation counting, 19: 20351
SAVAGE, H. W., Prog. rpt. on SNAP-8 corrosion, 6–8/63, 19: 20475 (ORNL-3538)
SAVAGE, H. W., Prog. rpt. on SNAP-8 corrosion, 9–11/63, 19: 20477 (ORNL-3604)
SAVAGE, H. W., Prog. rpt. on SNAP-8 corrosion, 12/63–2/64, 19: 20478 (ORNL-3618)
SAVAGE, H. W., Prog. rpt. on SNAP-8 corrosion, 3–5/64, 19: 20479 (ORNL-3671)
SAVAGE, H. W., Prog. rpt. on SNAP-8 corrosion, 6–8/64, 19: 20480 (ORNL-3730)
SAVENKO, I. A., Cosmic rays at high altitudes, 19: 20895
SAVENKO, I. A., Data on earth's radiation belts obtained during Cosmos flights, 19: 21136
SAVENKO, I. A., Nature of cosmic-ray particles beyond atmosphere, 19: 20893
SAVINTSEV, P. A., Radiation effects on thermal properties of alkali-halide crystals, 19: 19986
SAVITSKII, E. M., Problems in theory and applications of rare earth metals, 19: 20468
SAVOSKINA, G. P., Complexing of Am with neutral organophosphorus compounds. II., 19: 20076
SAVOSKINA, G. P., Formation of transuranic nitrates with phosphorus compounds, 19: 20077
SAVVAS, C., Diagnosis of intraspinal neurological syndromes, 19: 19720
SAWADA, Tetsuo, Can coupling constant assume arbitrary value in S-matrix theory?, 19: 20920 (IC/65/6)
SAWADA, Tetsuo, Mass difference of Ξ⁻ and Ξ⁰, 19: 20917 (IC/65/3)
SAWYER, R. F., Johnson-Treiman relations from vector-meson exchange, 19: 21018
SAYRES, A., Reaction ^{89}Y(p,n)^{89}Zr, 19: 21356
SAZONOV, B. I., Solar activity in earth's lower atmosphere, 19: 20780
SCAVNICAR, S., Crystal structure of double nitrate octahydrates of Th,

19: 19852
SCHAFFER, W. F., Jr., Disposal of high-level power reactor wastes in salt mine, 19: 21751 (ORNL-P-1064)
SCHAGEN, P., Alternatives to thermionic emission, 19: 20289
SCHATZMAN, E., Early stages of stellar evolution, 19: 20793
SCHATZMAN, E., White dwarfs and type-I supernovae, 19: 20800
SCHENK, G., Compression of magnetic field by exploding foils, 19: 20717
SCHENKEL, J., Effects obtainable by irradiation of polymers, 19: 19978
SCHENKEL, J., Irradiation of cellulose and cellulose derivatives, 19: 19961 (CEA-tr-A-1741)
SCHIFF, Erwin, Determination of U(VI) in aqueous solutions in presence of SO_4^{--}, NO_3^- and CH_3COO^- anions, 19: 19797
SCHIFFMACHER, Gerard, Purification of Eu by distillation of halogenides, 19: 20062
SCHIFINO, A., Use of new drug in treatment of radiodermatitis, 19: 19633
SCHILL, W. J., Single-pass experiments (DCX-1), 19: 21480 (ORNL-3760(p.1-9))
SCHIMMEL, J., Growth mechanism of thin anodic oxide films on Ta. I., 19: 20490
SCHIRRMEISTER, D., Determination of isodoses with computers, 19: 19692
SCHLECHT, Richard G., Hyperfine structures of Re-186 and Re-188, 19: 21382
SCHLUETER, Dieter, Bound-free transition probabilities and continuum spectra of rare gases, 19: 20833
SCHMATZ, W., Scattering of subthermal neutrons on heavy ice, 19: 21218
SCHMETS, J., Conversion of UO_2 to UF_4, 19: 19867
SCHMETS, Jean, Reprocessing of ceramics by volatilization, 19: 20060
SCHMIED, H., Evaporation of Th from carburized thoriated tungsten cathodes, 19: 20575
SCHMILLEN, A., Luminescence decay of pyrene-, dibenzyl-, and dibenzyl tetracene crystals, 19: 19963
SCHNEID, Edward J., Reactions $^{86}Kr(d,p)^{87}Kr$, 19: 21394
SCHNEIDER, H., New kind of radioactive decay: proton emission, 19: 21297
SCHNEIDER, W., Trapping of dust by foils, 19: 20236
SCHNEIDERMAN, S. B., Viscosities and diffusivities of ionized H–U mixtures, 19: 19941
SCHNITZEL, Randolph H., Physical metallurgy of W and W-base alloys, 19: 20565 (WADD-TR-60-37(Pt.V))
SCHOBER, B., Changes of electroshock seizures in rats after irradiation, 19: 19514
SCHONFELDER, J. L., Polarization by Hg of 100- to 2000-ev electrons, 19: 20865
SCHOOLEY, J. F., Carrier concentration in semiconducting $SrTiO_3$, 19: 21170
SCHOOLEY, John C., Stable-flow free boundary fractionation of spleen-colony-forming cells from mouse bone marrow, 19: 19617
SCHOROCHOFF, G., Production of hyperfragments from interactions of K⁻ with nuclei, 19: 21429
SCHRAM, B. L., Ionization cross sections for electrons in gases, 19: 20850
SCHREIBER, Franz, Electromagnetic drive for reactor control rods, 19: 21629
SCHROETER, J., Master equation for gases, 19: 20693
SCHULT, O. W. B., Energies and character of low-lying levels in Nb-94, 19: 21330
SCHULTZ, Donald G., Prog. rpt. on application of automatic control theory to nuclear rocket, 2–9/64, 19: 21723 (NASA-CR-193)
SCHULTZ, H. A., Scintillations in Ar–N mixtures, 19: 20313 (ANL-6938 (p.9-20))
SCHULZ, J., High-speed binary analog-digital converter, 19: 20299
SCHWAB, O., Modification of strength of paper by irradiation, 19: 20630
SCHWABE, K., Influence of radiation on electrical conductivity of glasses, 19: 19976
SCHWARZ, Harold A., Radiation chemistry of aqueous solutions, 19: 19968
SCHWARZ, K. K., Radioluminescence of some Tl-activated alkali halides, 19: 19966
SCHWARZSCHILD, A., Lifetime of 120-kev level of Lu-177, 19: 21319
SCHWEIGER, Fritz, Kepler problem in parabolic coordinates according to Hamilton-Jacobi theory, 19: 20810
SCHWENKER, R. P., Transition probability of $^3\Pi_u \rightarrow X\ ^3\Pi_g$ system of CO_2^+, 19: 19996
SCHWOCHAU, Klaus, Absorption spectra of Tc(IV) and Re(IV) hexahalides, 19: 19924
SCIAMANNA, Aldo F., Appearance potentials of some doubly charged molecule ions, 19: 20807 (UCRL-11828(p.201-4))
SCIAMANNA, Aldo F., Control of response sensitivity in gas chromatography, 19: 20281 (UCRL-11828(p.204-7))
SCOTT, J. L., Influence of stress on fission-gas release, 19: 20586
SCOTT, K. T., Preparation of single-phase single crystals of UO_2, 19: 20530
SCROGGS, R. J., Spectra of γ rays produced by interactions of ~160-Mev protons with Be, C, O, Al, Co, and Bi, 19: 21243 (ORNL-3506)
SEATON, M. J., Elastic scattering of electrons by C atoms, 19: 20858
SECKER, Phillip A., Prog. rpt. on application of automatic control theory to nuclear rocket, 2–9/64, 19: 21723 (NASA-CR-193)
SEIDEL, W., New results of measurements of high-energy electrons, 19: 19695
SEIDMAN, A., Filmless automatic processing of nuclear tracks, 19: 20354
SEKINY, T., Determination of concentration of waste water from low-activity installations, 19: 21752
SEL'CHENKOV, L. I., Fission-product yields and mass distribution, 19: 21445
SELL, Heinz G., Physical metallurgy of W and W-base alloys, 19: 20565 (WADD-TR-60-37(Pt.V))
SELPH, Frank B., 88-Inch cyclotron operation and development, 19: 20736 (UCRL-11828(p.236-41))
SELTZER, Stanley, Mechanism of thermal decomposition of α-phenyl-ethylazomethane, 19: 19943 (BNL-8243)
SEMENENKO, M. N., Parameters of recrystallization of Nb and W, 19: 20604
SEMIN, G. K., Pulse method for nuclear quadrupole resonance, 19: 21430
SEMTURS, F., Preamplifier-amplifier system for proportional counters, 19: 20362
SENNETT, Roy S., Resistor employing irradiated gas, 19: 20310
SENS, J. C., Analysis of munoic x-ray spectra, 19: 21344
SERDULA, K., Neutron thermalization studies in graphite, 19: 21211
SEREDA, G. A., Strontium-90 in fresh-water reservoirs in Soviet Union, 1961–62, 19: 20160 (NP-14728)
SESTERO, Arrigo, Ferraro-Rosenbluth cold plasma sheath model, 19: 21538
SETTE, G., Reaction $\gamma + p \rightarrow p + \pi^0$ near first resonance from polarized photons, 19: 20932 (LNF-64/60)
SHA, William T., Out-of-pile steam-fraction determination, 19: 20294
SHABALIN, E. P., Neutrino luminosity of a star, 19: 20772
SHAFER, G. V., Modulation of cosmic rays by interplanetary magnetic field, 19: 20889
SHAHID, M. Ahmad, Labeled triiodothyronine *in vitro* test for thyroid function, 19: 19679
SHAKHTAKHTINSKII, G. B., Arsenate method for iodimetric determination of Zr, 19: 19818
SHAKHTARIN, V. N., Production of high-power MHD generators, 19: 20910
SHALDERVAN, P. G., Single-phonon Green's function, phonon correlation function, and inelastic coherent scattering of neutrons, 19: 20710
SHALDERVAN, P. I., Phonon correlation function and inelastic coherent scattering of neutrons by crystals, 19: 20671
SHAMBON, Arthur, Energy distribution of x-ray beams from 250-kv constant potential machine, 19: 20256 (HASL-151)
SHAMU, R. E., High-pressure gas scintillation counters. II., 19: 20361
SHAPIRA, Y., Thermal behavior of Nb-25% Zr in strong magnetic fields, 19: 21188
SHAPIRO, Removal of mode degeneracy in a rotating second-sound resonator, 19: 21175
SHAPIRO, M. M., Notes on cosmic radiation, 19: 20903
SHARAN, R., Electromagnetic fields and cylindrical symmetry, 19: 21084
SHARP, D. H., Spherical gravitational collapse, 19: 21100
SHARP, T. E., Formation of H⁻ or D⁻ by electron impact on H_2, HD, and D_2, 19: 20691
SHARPATYI, V. A., Radiolysis of frozen solutions of amino acids and peptides, 19: 20012
SHARVINA, K. N., Data on earth's radiation belts obtained during Cosmos flights, 19: 21136
SHATSKII, V. M., Scandium separation from pyroxenites, 19: 20081
SHAUKAT, M. A., Interactions in flight of low-energy K⁻ mesons with emulsion nuclei, 19: 21365
SHAVRIN, P. I., Cosmic rays at high altitudes, 19: 20895
SHAVRIN, P. I., Data on earth's radiation belts obtained during Cosmos flights, 19: 21136
SHAWE, D. R., Ages of La Sal Mountains rocks, Utah, 19: 20178
SHAWE, D. R., Uranium ore rolls—an analysis, 19: 20186
SHCHERBAKOV, Yu. A., Nuclear form-factors in μ capture in He-3, 19: 21236 (JINR-P-1952)
SHEBEKO, A. V., Nuclear boundary diffusion, 19: 21424
SHEDLOVSKY, J. P., Radiochemical evidence for Antler shot contribution to September 1961 fallout, 19: 20167
SHEFFIELD, G. S., Prog. rpt. on U interstitial phases, 3/64, 19: 20510 (NCSC-2663-16)
SHEIKO, I. N., Decomposition potential of system K_2ZrF_6–NaCl–KCl, 19: 19850 (NP-tr-1230)
SHELINE, R. K., High-spin rotational states in deformed nuclei, 19: 21363
SHELINE, Raymond K., Energies and character of low-lying levels in Nb-94, 19: 21330
SHEPPARD, J. C., Rate and formation constants from oxidation-reduction

reaction data, 19: 19836 (HW-SA-3476)
SHERA, E. Brooks, Mössbauer effect of 29.4-kev neutron-capture γ ray of K-40, 19: 21409
SHERMAN, N., Separation energy of strongly bound nucleons, 19: 21400
SHERWOOD, J. E., Neutron depolarization effects in precession magnets, 19: 21209
SHIBATA, Nagao, Chemical effects of $^{35}Cl(n,p)^{35}S$ reaction. I., 19: 20004
SHIELDS, W. R., Isotopic fractionation of U in sandstone, 19: 20187
SHIGA, Koji, Late liver cirrhosis from Thorotrast, 19: 19560
SHIKIN, I. S., Riemann waves in relativistic MHD, 19: 20668
SHILIN, V. A., Gamma-gamma coincidence with energy analysis of coinciding radiations, 19: 20342
SHIMAZU, Hisashi, Turbulent heat transfer in pipe, 19: 20118
SHINDO, Masao, Design of the fast power reactor, 19: 21696
SHINER, V. J., Jr., Hydrogen participation in cis-4-*t*-butylcyclohexyl brosylate solvolysis, 19: 19949
SHIRLEY, D. A., Cerium magnesium nitrate temperature scale, 19: 21162 (UCRL-11828(p.199-201))
SHIRLEY, D. A., Induced hyperfine fields in 5p shell, 19: 21359
SHIRLEY, D. A., Level scheme of Te-125 and magnetic dipole moment of Sb-125, 19: 21256 (UCRL-11828(p.58-62))
SHIRLEY, D. A., Nuclear magnetic moment of 2084-kev state in Ce-140, 19: 21254 (UCRL-11828(p.55-6))
SHIRLEY, D. A., Nuclear Zeeman effect in Ir-193, 19: 21255 (UCRL-11828 (p.57-8))
SHIRLEY, D. A., Observation of electronic relaxation in Mössbauer spectroscopy, 19: 21270 (UCRL-11828(p.214-16))
SHIROKOV, Yu. M., Relativistic extension of SU(6), 19: 21002
SHIVELY, F. T., Decay $Y_1^*(1660) \rightarrow Y_0^*(1405) + \pi$, 19: 21017
SHKLOVSKII, I. S., Physical conditions in gaseous envelope of 3C-273, 19: 20767
SHKODA-UL'YANOV, V. A., Use of nuclear magnetic resonance for study of structure of photonuclear reactions, 19: 21282
SHLAER, W. J., High-power test on cloverleaf cavity, 19: 20724 (LA-DC-6759)
SHLAER, W. J., Shunt impedance of cloverleaf accelerator structure, 19: 20744
SHOHET, J. L., Microwave excitation of Puffatron plasma at electron cyclotron frequency, 19: 21491 (UCRL-12057(Rev.I))
SHORNIKOV, S. I., Connection between width of giant resonance of (γ,n) reaction and filling of energy levels of the nucleus, 19: 21287
SHOTKIN, Louis M., Centers and limit cycles in reactor kinetics, 19: 21634 (BNL-9010)
SHPETNII, A. I., Spark chamber, 19: 20378
SHPIZ, Joseph M., Implications of SU(12) for $\bar{N}N$ annihilation at rest, 19: 21039
SHREEVE, Walton W., Transfer of C-14 and tritium from substrates to CO_2, water, and lipids in obese and diabetic subjects, 19: 21758 (BNL-8864)
SHTERN, Yu. D., Pulse method for nuclear quadrupole resonance, 19: 21430
SHUBA, I. M., Structure of g plane relativistic Schroedinger theory, 19: 21053
SHUBA, J. M., Poles of the Bethe-Salpeter partial wave amplitude in the g^2-plane, 19: 21111
SHUL'GIN, I. A., Effect of radiation on growth of plants, 19: 19545
SHULMAN, Herman, Gamma irradiation of Ge. Impurity effects, 19: 20619 (NP-14883)
SHUR, L. I., Effect of polyethylene glycols on nuclear photographic emulsions, 19: 20014
SHWE, Hla, Artificial construction of particle tracks by Monte Carlo method, 19: 20325 (UCRL-11624)
SIEGEL, Daniel M., Decay $Y_1^*(1660) \rightarrow Y_0^*(1405) + \pi$, 19: 21017
SIEGEL, Peter, Intralymphatic radioactive therapy for pelvic cancer, 19: 19658
SIERRO, Jerome, Paramagnetic resonance of V_F center in CaF_2, 19: 20003
SIEVERT, Rolf Maximilian, Measuring and recording ionizing radiation, 19: 20394
SIFFERLEN, Raymond, Resistance of metallic U tubes to external pressure, 19: 20453 (CEA-R-2572)
SIGMUND, P., Non-binary atomic collisions in crystals, 19: 20686
SIGNER, Peter, Cosmic-ray exposure ages of Fe meteorites, 19: 20760
SIGOV, Yu. S., Kinetic theory of boundary layer between rarefied plasma and magnetic field, 19: 21585
SIIVOLA, A., Alpha activities in Pt, 19: 21248 (UCRL-11828(p.21-5))
SIIVOLA, A., Alpha-active Au isotopes, 19: 21249 (UCRL-11828(p.25))
SIIVOLA, A., Light Po isotopes, 19: 21250 (UCRL-11828(p.26))
SIKIRICA, M., Crystal structure of ternary silicides ThM_2Si_2, 19: 20568
SIKIRICA, M., Ternary silicides containing U and transition metals, 19: 19871
SIKKELAND, Torbjoern, Fission barriers of W, Re, Os, Ir, and Hg isotopes, 19: 21259 (UCRL-11828(p.77-80))
SIKOV, Melvin R., X irradiation of the 36-hour rat embryo, 19: 19618
SILAEV, Yu. V., Long afterglow in proteins and synthetic polymers irradiated by x rays, 19: 19983
SILIN, V. A., Plasma acceleration with aid of EM H_{11}-type wave in circular waveguide, 19: 21566
SIMINOVITCH, L., Host-cell interactions in mice bearing isologous hemopoietic grafts, 19: 19615
SIMMINGSKOLD, Bo Kurt Wilhelm, Method for the production of glass, 19: 21754
SIMMONS, D. J., Osteolathyrism and inhibition of endosteal bone reaction in estrogen-treated mice by AAN, 19: 19471 (ANL-6938(p.162-78))
SIMMONS, David J., Diurnal variations in metabolic activity of bone and cartilage, 19: 19472 (ANL-6938(p.179-93))
SIMONOVA, L. I., Transplantation of bone marrow to animals with acute radiation sickness, 19: 19641
SIMONS, John Wesley, Secondary isotope effects in chemical activation systems, 19: 19938
SIMONS, Lennart, Compound nucleus and asymmetric fission, 19: 21283
SIMPSON, F. H., Prog. rpt. on macrolaminate particle composite material, 12/64–2/65, 19: 20558 (NP-14888)
SINEL'NIKOV, K. D., Capture of plasma in magnetic trap with fields, 19: 21568
SINEL'NIKOV, K. D., Development of instabilities in plasma captured by transverse magnetic field, 19: 21577
SINGER, Evzen, Analysis of UF_4, 19: 19785
SINGH, K. P., Electromagnetic fields and cylindrical symmetry, 19: 21084
SINGLETON, J. H., Outgassing procedures for glass ultrahigh-vacuum systems, 19: 20148
SINISTRERO, G., Histochemical findings in irradiated rat placenta. II., 19: 19557
SINMAN, A., Response measurement of magnetic probe, 19: 20293
SINMAN, S., Fast scale-of-five circuit and its applications, 19: 20296
SINMAN, S., Response measurement of magnetic probe, 19: 20293
SIRAHAMA, Shigekuni, Late liver cirrhosis from Thorotrast, 19: 19560
SISSONS, H. A., Calcium accretion and bone formation in dogs, 19: 19470 (ANL-6938(p.141-61))
SKADCHENKO, N. M., Effects of K_3PO_4 *N and lime on Sr-90 accumulation by plants, 19: 19475 (JPRS-27940(p.10-17))
SKLAROFF, David M., Diagnosis of bone metastasis by photoscanning with Sr-85, 19: 19666
SKLAROFF, David S., Clinical use of radioisotopes, 19: 19661
SKLIZKOV, G. V., High-current air-core betatrons, 19: 20740
SKOBLO, A. I., Uranyl perchlorate complexes, 19: 19910
SKOWRONSKI, S., Appliances protecting against ionizing radiations, 19: 19634
SKRIPIN, G. V., Modulation of cosmic rays by interplanetary magnetic field, 19: 20889
SLAUS, I., Neutron-neutron scattering length from $^3H(n,d)2n$ reaction, 19: 21404
SLAUS, I., Reactions $H^3(n,p)3n$ and $H^3(n,H^4)\gamma$ at E_n = 14.4 Mev, 19: 21405
SLEZOV, V. V., Coalescence of dislocation loops, 19: 20580
SLOAN, I. H., Ionization of neutral He by electron impact, 19: 20864
SLOTNICK, H., Solubility of He in Li and K, 19: 20561 (PWAC-380)
SMIRNOV, B. M., Resonance charge exchange in inert gases, 19: 19931
SMIRNOV, L. S., Influence of electron bombardment on surface state of Ge, 19: 20622
SMIRNOV, V. B., Decay of Rh-100, 19: 21278
SMIRNOV, V. B., Decay of Pd-101, Rh-101*, and Rh-101, 19: 21280
SMIRNOVA, R. I., Application of CS_2 in synthesis of rare earth sulfides, 19: 19927
SMITH, E. T., Influence of Rn daughter concentration of γ-spectrometer background, 19: 21299
SMITH, F. R., Prog. rpt. on nuclear burnup analyses, 9–11/64, 19: 21667 (GEAP-4776)
SMITH, Felix T., Classical and quantal scattering. I., 19: 20825
SMITH, Francis M., Artificial construction of particle tracks by Monte Carlo method, 19: 20325 (UCRL-11624)
SMITH, Harry E., Silicon radiation detectors, 19: 20328 (UCRL-11828 (p.225-6))
SMITH, Hilton A., Separation and analysis of H by adsorption and gas chromatography, 19: 20435
SMITH, J. R., S-wave scattering lengths for *n*-p interaction, 19: 21043
SMITH, K. D., Transistorized bidirectional decade counter, 19: 20319 (IDO-17059)
SMITH, L. H., Application of linear estimation to chemical mixture problem, 19: 19769 (TEES-2671-4(Chap.7))
SMITH, M. L., Radiation monitoring of personnel by dose rate telemetering, 19: 20317 (HW-82369)
SMITH, M. L., Reactor decontamination and the health physicist, 19: 21605 (HW-SA-3560)

SMITH, P. L., Liquid He supplies in Great Britain, 19: 21183
SMITH, Stanley F., Effects of gravitational radiation reaction in general relativistic two-body problem, 19: 21104
SMOES, S., Vapor pressure of U, 19: 19889
SMOKE, Edward J., Development of refractory ceramics, 19: 20461 (NP-14893)
SMOOT, T. W., Destabilization of zirconia, 19: 20585
SMYLY, E. D., Laminar reacting boundary layers on W, graphite, and pyrolytic B nitride, 19: 20496
SNAJDER, J., Contrast-increasing electronic device for scintillation scanner, 19: 19696
SNOWDON, S. C., Relaxation calculation of FFAG magnetostatic fields, 19: 20729 (MURA-706)
SNYDER, R. E., Decay of Sn-121m and Mössbauer absorption in Sb-121, 19: 21375
SOBOTTKA, Emory E., Environmental radioactivity, 19: 20156 (IS-1098)
SODEE, D. B., Radioisotope scanning of pancreas, 19: 19723
SODEE, D. B., Selective neoplasm localization, 19: 19715
SODHA, M. S., Electron temperature in MHD generators, 19: 20907
SODICKSON, L., Charge-exchange scattering at high energies for $\pi^- + p \rightarrow n^0 + n$, 19: 21006
SOEHNGEN, G., Neutron polarization in T(d,n)^{4}He reaction, 19: 21303
SOKOL, Harvey A., Radiolysis of poly-α-L-glutamic acid in aqueous solution, 19: 19990
SOKOLIK, G. A., Analysis of quasi-Maxwellian equations describing compensating fields, 19: 21086
SOKOLOV, B. M., Ultrahigh frequency investigation of plasma deionization at atmospheric pressure, 19: 21572
SOKOLOV, L. S., Elastic scattering of deuterons with energy of 10.3 Mev on He-4, 19: 21286
SOKOLOV, M. M., Determination of heavy elements in rocks from γ radiation emitted, 19: 20180
SOKOLOWSKI, J. S., E2/M1 mixing ratios and K conversion coefficients of some rotational transitions, 19: 21324
SOLOMATINA, A. I., Radiation synthesis of polymers based on diethylphosphinoborine, 19: 19982
SOLOMATINA, E. K., Correlation between variations of magnetic field and positive ions inside magnetosphere, 19: 21126
SOLOV'EV (SOLOVIEV), L. D., Infrared asymptotics Green functions, 19: 20930 (JINR-E-1975)
SOLOV'EV, L. D., Small-angle scattering of charged particles, 19: 21233 (JINR-E-1992)
SOLOV'EVA, V. I., Primary cosmic radiation of superhigh energy, 19: 20884
SOMON, J. P., Limitations on magnetic fields obtained by flux-compression. I., 19: 20678
SONKA, J., Pentose cycle and radiation diseases, 19: 19538
SOROKIN, Yu. A., EPR study of radiolysis of ammonia adsorbed on solids, 19: 19984
SOSIN, A., Directional effects in electron-irradiated Cu single crystals, 19: 20645
SOSOVA, V. F., Fatal shock in irradiated rabbits as response to administration of homologous γ-globulin, 19: 19535
SOWBY, F. D., Radiation protection in Canada. VII., 19: 20212
SPAEPEN, Jozef, Nuclear measurements, 19: 20088
SPECHT, H. J., Measurement of gas concentration in methane, 19: 20376
SPEDDING, Frank H., Energy levels in hydrated Tm ethylsulfate, 19: 21600 (IS-968)
SPEECKAERT, Philippe, Reprocessing of ceramics by volatilization, 19: 20060
SPERDUTO, A., Energy levels in Ti-48 and Ti-50, 19: 21346
SPERGEL, Martin Samuel, Baryon-antibaryon scattering, 19: 21068
SPICER, G. S., Determination of radiostrontium in biological materials, 19: 19739 (AERE-AM-101)
SPICER, W. E., Radiation effects in optical materials, 19: 20019
SPIEGL, Charles J., Packaging aspects of radiation preservation of foods, 19: 20421
SPIERING, G. A., Superconductivity in Nb–Se system, 19: 21195
SPIEWAK, I., Sea-water desalination with nuclear energy, 19: 21708 (ORNL-TM-465)
SPIGT, C. L., Stability and burnout tests with H_2O, 19: 20120
SPINELLI-RESSI, F., Scanning of spleen with Cr-51, 19: 19727
SPINKS, H., Extrapolation distance at surface of grey cylindrical control rod, 19: 21649
SPITSYN, Vict. I., Radiolysis of aqueous nitrate solutions, 19: 19981
SPITSYN, Vikt. I., Effect of S-35 radiation on dehydration of cyclohexanol, 19: 20013
SPOOR, H. L., Toxic hazard associated with $BaCl_2$, 19: 20210
SPREITER, John R., Dynamical behavior of magnetosphere boundary, 19: 21148
SPRIET, Bernard, Allotropic transformations of Pu, 19: 20546 (CEA-R-2726)
SPRING, E., E2/M1 mixing ratios of $2^+ \rightarrow 2^+$ transitions in even-even nuclei, 19: 21419
SPRINGER, A., Inelastic scattering of 50.9-Mev α particles from Ne-20, 19: 21267 (UCRL-11828(p.113-16))
SPRINGETT, B. E., Capture cross sections for negative ions in rotating He(II), 19: 21177
SPRUNG, Donald W. L., Energy gap at Fermi surface of nuclear matter, 19: 21273
SPURNY, K., Preparation of labeled condensation aerosols. I., 19: 20027
SPURNY, Kvetoslav, Filtration materials for respirators for radioactive aerosols, 19: 20228
SRIVASTAVA, B. K., Binding energy of the triton, 19: 21309
SRIVASTAVA, Suresh C., 5,5'Thiodisalicyclic acid as analytical reagent, 19: 19812
SRIVASTAVA, Y. N., Effect of inelastic channel on position and width of resonance, 19: 20987
SRIVASTAVA, Yogendra Narain, Nuclear pair-correlation function, 19: 21452
SATCHLER, G. R., Elastic scattering of 5.5- to 10.0-Mev He-3 particles by Al-27, 19: 21328
STAHLHOFEN, W., Radium-226 in human embryonic tissue, 19: 20216
STAKHANOV, I. P., Influence of plasma density near electrode on conductivity in transverse magnetic field, 19: 21580
STAKHANOV, I. P., Oscillations of current in thermoelectronic energy converter, 19: 20913
STAMENOV, Boris, Hemopoiesis in sheep exposed to sublethal doses of x rays, 19: 19600
STAMER, P., Observations of radiative π^+ decays, 19: 20990
STANFORD, J. L., Measuring range of low-energy charged particles in conducting solids, 19: 20806 (ORNL-3702)
STANKOVIC, V., Counteracting killing effect of foreign cells, 19: 19651
STANLEY, H. E., Electron capture by protons passing through He, 19: 20821
STANNETT, V., Radiation polymerization of crystalline trithiane, 19: 19959 (CONF-571-37)
STANYUKOVICH, K. P., Analysis of quasi-Maxwellian equations describing compensating fields, 19: 21086
STARFELT, N., Gamma rays from neutron capture in Ta and Au, 19: 21317
STARIK, I. E., Complexing of Po with chloride ions, 19: 19906
STARIK, I. E., Hydrolysis of Po in perchloric acids, 19: 19905
STARODUBTSEV, S. V., Neutron cross sections in In and Sm, 19: 21285
STARY, J., Substoichiometry in radiochemical analysis, 19: 19783
STARZL, Thomas E., Splenic homotransplantation, 19: 19522
STAUDER, William, Billiken calibration shot in southeast Missouri, 19: 20171 (AFCRL-64-659)
STAUFFER, A. D., Electron excitation of electric quadrupole transitions, 19: 20855
STAVRAKI, G. L., Stuckelberg's formalism for field of spin ½, 19: 21112
STEARNS, K. R., Design of Hallam moderator element. I., 19: 21680 (COO-1402-1)
STEARNS, K. R., Design of Hallam moderator element. II., 19: 21681 (COO-1402-2)
STEBLER, Alfred, Device for calibration of radiation detection instruments, 19: 20395
STECKELMACHER, W., Review of low-pressure measurement, 19: 20142
STEELE, E. L., Neutron activation analysis procedures for determination of O in K, 19: 19751 (GA-5982)
STEENBECK, Max, Device for generation of high-temperature plasma, 19: 21592
STEICHELE, E., Mössbauer effect and isomer shift on Eu-153, 19: 21345
STEIGER, Naftali H., Fission barriers of W, Re, Os, Ir, and Hg isotopes, 19: 21259 (UCRL-11828(p.77-80))
STEINBERG, M., Cobalt-60 research irradiators, 19: 20095 (BNL-8976)
STEINBERG, M., Cost estimate for Co-60 radiation-induced ethylene polymerization process, 19: 19957 (BNL-8993)
STEINERT, Christoph, Control device for reactors, 19: 21632
STEINFINK, H., Crystal chemistry of rare earth group VI systems. I., 19: 19879
STEINFINK, H., Crystal chemistry of rare earth group VI systems. II., 19: 19880
STEINHAUS, J. F., Microwave excitation of Puffatron plasma at electron cyclotron frequency, 19: 21491 (UCRL-12057(Rev.I))
STEINKOPFF, Horst, Pressed block for fabrication of fuel element rods, 19: 20540
STEJSKAL, L. M., Prog. rpt. on macrolaminate particle composite material, 12/64–2/65, 19: 20558 (NP-14888)
STEKETEE, J. A., Rayleigh problem in MHD, 19: 20665
STELLMANN, Chr., Radiosensitivity of microorganisms: practical consequences, 19: 19590
STEPAKOFF, Gerald L., Vaporization rates in refractory metal–metal–C systems, 19: 20608

STEPANENKO, I. A., Capture of plasma in magnetic trap with fields, 19: 21568
STEPANENKO, I. A., Spectroscopic investigation of plasma in colliding bursts, 19: 21567
STEPANOV, A. S., Influence of plasma density near electrode on conductivity in transverse magnetic field, 19: 21580
STEPANOV, A. S., Oscillations of current in thermoelectronic energy converter, 19: 20913
STEPANOV, K. N., Electron radiation in plasma-magnetic-field boundary layer, 19: 21522
STEPANOV, K. N., Excitation of magnetoacoustic waves in colliding plasma streams, 19: 21575
STEPANOV, K. N., Low-frequency plasma oscillations, 19: 21523
STEPANOV, K. N., Plasma-wave propagation across magnetic field, 19: 21521
STEPANOVSKII, Yu. P., Lorentz group and wave equations of free massless fields, 19: 21110
STEPHANI, Hans, Structure of field and motion equations for n charged, gravitating mass points, 19: 21082
STEPHANY, W., Correlation of in-pile transient pressure measurements, 19: 21652
STEPHENS, F. S., Decay scheme of Es-254, 19: 21257 (UCRL-11828(p.63-6))
STERN, Donald, CP-nonconserving decay $K_2^0 \to \pi^+ + \pi^- + \pi^0$, 19: 21020
STERN, R. A., Frequency mixing at plasma resonance, 19: 21549
STERN, T. W., Ages of La Sal Mountains rocks, Utah, 19: 20178
STERNHEIM, Morton M., Vacuum polarization corrections to hfs in muonic atoms, 19: 21395
STERNHEIMER, R. M., Empirical mass relations involving the strongly interacting particles, 19: 20994
STEWART, G. E., Wave propagation in hot plasma waveguides, 19: 21536
STEWART, H. J., Use of Y-90 for destruction of pituitary gland, 19: 19660
STEYN, P. S., Preparation of deuterium-labeled O–methyl groups, 19: 20034
STIRPE, D., Overdriving effect in dynamic polymorphism, 19: 20555 (LA-3215)
STODDART, J. C., Microcausality in asymptotic quantum field theory, 19: 21088
STOKES, R. J., Grain boundaries and mechanical behavior of MgO, 19: 20607
STOKSTAD, R. G., Reorientation effect in Cd-114, 19: 21398
STONE, N. J., Cerium magnesium nitrate temperature scale, 19: 21162 (UCRL-11828(p.199-201))
STONE, N. J., Induced hyperfine fields in 5p shell, 19: 21359
STONE, N. J., Level scheme of Te-125 and magnetic dipole moment of Sb-125, 19: 21256 (UCRL-11828(p.58-62))
STONEHAM, A. M., Spin resonance line shapes, 19: 20839
STONEHOUSE, A. J., Corrosion and protection of Be, 19: 20495
STONEHOUSE, A. J., Mechanical characteristics of zone-leveled Be, 19: 20544 (AFML-TR-64-388)
STOOPS, R. F., Prog. rpt. on U interstitial phases, 3/64, 19: 20510 (NCSC-2663-16)
STOOPS, Robert F., Prog. rpt. on fuel of UC particles in U matrix, 8/62, 19: 20511 (NCSC-2981-1)
STOOPS, Robert F., Prog. rpt. on fuel of UC particles in U matrix, 12/62, 19: 20512 (NCSC-2981-2)
STOOPS, Robert F., Prog. rpt. on fuel of UC particles in U matrix, 2/63, 19: 20513 (NCSC-2981-3)
STOOPS, Robert F., Prog. rpt. on fuel of UC particles in U matrix, 9/63, 19: 20514 (NCSC-2981-5)
STOOPS, Robert F., Prog. rpt. on fuel of UC particles in U matrix, 12/63, 19: 20515 (NCSC-2981-6)
STOOPS, Robert F., Prog. rpt. on fuel UC particles in U matrix, 3/64, 19: 20516 (NCSC-2981-7)
STOOPS, Robert F., Prog. rpt. on fuel of UC particles in U matrix, 6/64, 19: 20517 (NCSC-2981-8)
STOOPS, Robert F., 98.2% Density with vibrating impact presses, 19: 20526
STOPPA, I. M., Histochemical findings in irradiated rat placenta. II., 19: 19557
STORIZHKO, V. Yu., Inelastic scattering of protons by Mg-24, 19: 21426
STORRUSTE, A., Environmental γ-radiation in Norwegian houses, 19: 20218
STORY, Troy L., Jr., Molecular beam electric resonance experiments on LiF, LiCl, LiBr, LiI, and NaF, 19: 19848 (UCRL-11828(p.193-7))
STOZHKOV, Yu. I., Intensity of cosmic rays in stratosphere, 19: 20876
STOZHKOV, Yu. I., Latitudinal measurements of cosmic-ray intensities in stratosphere, 19: 20892
STRAKHOVA, M. P., State of blood coagulating system and basic hematological indices during continuous work with various particle accelerators, 19: 20237
STRANGE, J. N., Predicting shape of explosion-produced craters, 19: 20089 (NP-14887)
STRATHDEE, J., P and C properties of U(12) multiplets, 19: 20974
STRATHDEE, J., Relativistic structure of SU(6), 19: 20927 (ICTP-64/7)
STRATHDEE, J., U(12) Predictions for $p\bar{p}$ annihilation into mesons, 19: 21036
STREATER, R. F., PCT, spin and statistics, and all that, 19: 21114
STREET, K., Jr., Formation of metastable states of rare gases by electron impact, 19: 19992
STREET, Kenneth, Jr., Molecular beam electric resonance experiments on LiF, LiCl, LiBr, LiI, and NaF, 19: 19848 (UCRL-11828(p.193-7))
STREHLOW, R. A., Vacuum systems, techniques, and materials studies, 19: 20140 (ORNL-3760(p.94-7))
STREKALOVSKII, V. N., Structure of α-UO_3–U_3O_8 region, 19: 19929
STREKALOVSKII, V. N., Structure of gamma UO_3, 19: 19930
STRIGANOV, A. R., Multiple beam radiointerferometer for plasma diagnostics, 19: 21574
STROKE, George W., Attainment of high resolutions in holography, 19: 20297
STROM, Gordon H., Plume rise characteristics of scale-model smoke plume, 19: 20656 (ANL-6938(p.257-73))
STROM, Gordon H., Stack plume rise determinations as affected by meteorological and engineering factors, 19: 20653 (ANL-6938(p.209-41))
STRUMINSKII, B. V., Nuclear form-factors in μ capture in He-3, 19: 21236 (JINR-P-1952)
STRZHIZHOVSKII, A. D., Mechanism of inhibiting effect of radiation on cell division, 19: 19613
STUHL, Z., Radioactive analysis of Mn, 19: 19806
STUPNIKOVA, N. I., Absolute age of pegmatite, 19: 20176
STUTZ, E., Radiation-induced leukemia in Wistar rats, 19: 19530
SUBRAMANIAN, A., Distribution of inelasticity in high-energy collisions in C and brass, 19: 20898
SUDARSHAN, E. C. G., Lorentz-covariant SU(6), particle-antiparticle algebras, and supermultiplet structure, 19: 21015
SUDARSHAN, E. C. G., Origin of symmetries, 19: 20933 (NP-14828)
SUFFCZYNSKI, M., Conductivity of a degenerate electron gas, 19: 21545
SUGAWARA, Masao, Resonance and high-energy limit of scattering, 19: 21000
SUGLOBOV, D. N., Solubility of $UO_2(ClO_4)_2 \cdot 3H_2O$ in mixed solvents, 19: 20073
SUGLOBOV, D. N., Uranyl nitrate solubility in mixed solvents, 19: 20072
SUGLOBOVA, I. G., Solubility of $UO_2(ClO_4)_2 \cdot 3H_2O$ in mixed solvents, 19: 20073
SUGLOBOVA, I. G., Uranyl nitrate solubility in mixed solvents, 19: 20072
SUGLUBOV, D. N., Uranyl perchlorate complexes, 19: 19910
SULYAEV, R. M., Nuclear form-factors in μ capture in He-3, 19: 21236 (JINR-P-1952)
SUMI, Masao, Microwave generation of harmonics in static magnetic field, 19: 21517
SUMMERS, Audrey L., Dynamical behavior of magnetosphere boundary, 19: 21148
SUN, Hung-chou, Decomposition of direct products of irreducible representations of SU_3, 19: 21057
SUNDBOM, L., Individual filter technique in Co-60 radiation therapy, 19: 19690
SUNDERLAND, J., Brookhaven-Columbia plasma lens, 19: 20915 (BNL-8967)
SUNG, Hsien-chung, Possible existence of 3π resonance state, 19: 20969
SURTMADZHIEV, Krusto, Hemopoiesis in sheep exposed to sublethal doses of x rays, 19: 19600
SURYRIN, Yu. E., Extraction of Sc by alkyl phosphoric acids, 19: 20082
SUTKA, Jozsef, Cytological and physiological investigation of maize lines treated with irradiation, 19: 19527
SUZUKI, Hiroshige, Two kinds of Zr carbide, 19: 19866
SUZUKI, Keizo, Flowmeter for F gas and vapors of reactive fluorides, 19: 20259 (JAERI-1074)
SVEC, H. J., Source of ions in mass spectrometer, 19: 20292
SVENSSON, E. C., Lattice dynamics of white Sn, 19: 21603
SVIDZINSKII, A. V., Equation for gap in energetic spectrum of superconductor, 19: 21190
SVORCOVA, S., Oxygen requirements of irradiated rats of various age, 19: 19539
SWAIN, J. R., Two-meter grazing-incidence spectrometer, 19: 20348
SWANSON, V. A., Material buckling for UC-fueled graphite-moderated assemblies, 19: 21692 (NAA-SR-Memo-9976)
SWANSON, William P., Decay $Y_1^1(1660) \to Y_0^0(1405) + \pi$, 19: 21017
SWEET, Richard Franklyn, Low-lying nuclear energy levels of Nb-92, 19: 21451
SWIATECKI, Wladyslaw J., Fission barrier of Tl-201, 19: 21260 (UCRL-11828(p.81))
SWIGER, Elizabeth D., Nuclear quadrupole resonance of Bi-209 in $BiBr_3$, 19: 19940

SYMONS, G. D., Reorientation effect in Cd-114, 19: 21398
SYROVATSKII, S. I., Gamma and x radiation associated with cosmic rays, 19: 20881
SYROVATSKII, S. I., Origin of cosmic rays, 19: 20880
SZABO, Elek, Ceramic- and disperaion-type fuel for reactors, 19: 21670
SZABOLCS, Marton, Effect of SH-inhibitors on radiation sensitivity of proteins and amino acids, 19: 19621
SZATI, Imre, Effect of SH-inhibitors on radiation sensitivity of proteins and amino acids, 19: 19621
SZE, Shih-yuan, Alpha-reduced width of 1p shell nuclei, 19: 21432
SZIRMAK, Eva, Influence of β radiation on metabolism of the cornea, 19: 19552

T

TABOADA, A., Prog. rpt. on SNAP-8 corrosion, 6–8/63, 19: 20475 (ORNL-3538)
TABOADA, A., Prog. rpt. on SNAP-8 corrosion, 9–11/63, 19: 20477 (ORNL-3604)
TABOADA, A., Prog. rpt. on SNAP-8 corrosion, 12/63–2/64, 19: 20478 (ORNL-3618)
TABOADA, A., Prog. rpt. on SNAP-8 corrosion, 3–5/64, 19: 20479 (ORNL-3671)
TABOADA, A., Prog. rpt. on SNAP-8 corrosion, 6–8/64, 19: 20480 (ORNL-3730)
TAKAHASHI, Akira, Flowmeter for F gas and vapors of reactive fluorides, 19: 20259 (JAERI-1074)
TAKAHASHI, Akira, Recording thermobalance for F gas and vapors of reactive fluorides, 19: 20258 (JAERI-1070)
TAKAHASHI, Tadao, Turbulent heat transfer in pipe, 19: 20118
TAKAICHI, Toshio, Welding reactor pressure vessel for Tokai Station, 19: 21700
TAKASHIMA, Yoichi, Separation of isotope gas mixture in supersonic jet, 19: 20434
TAKAYANAGI, Motow, Dielectric behavior of poly(β-propiolactone), 19: 20000
TAKEDA, Eiichi, Studies on natural U–H_2O exponential pile. II., 19: 21645
TAKESHITA, Kenji, Personal monitoring of exposure to radiation, 19: 20338
TAKETA, S. Tom, Biological effects of protons and neutrons in large animals, 19: 19615
TAKIBAEV, Zh. S., Coupling coefficients for cosmic components, 19: 20891
TALMI, I., Shell model and deformed states in O-18, 19: 21360
TALPOVA, H., Determination of Na content of filter papers, 19: 19786
TAMERS, M. A., Isotope effect in the benzene synthesis for radiocarbon dating, 19: 20179
TAMOYAN, G. S., Similitude criterion of MHD phenomena and EM power losses, 19: 20119
TANAKA, Eiichi, Whole-body counter. I., 19: 20377
TANAKA, Masatoshi, Instability of accelerated plasma, 19: 21518
TANANAEVA, N. N., Adsorption of complex U compounds from aqueous solutions, 19: 20074
TANENBAUM, B. Samuel, Transport equations for gas mixture, 19: 20681
TANGRI, K., Metastable phases in U alloys. I., 19: 20587
TANGRI, K., Metastable phases in U alloys. II., 19: 20588
TANNER, D. J., Capture cross sections for negative ions in rotating He(II), 19: 21177
TAO, S. J., Third positron lifetime in solid polymers, 19: 21044
TAPLIN, D. M. R., Metallography of fracture of alpha U, 19: 20592
TAPLIN, G. V., Organ visualization by photoscanning using radioalbumin, 19: 19710
TAPTAS, J., Diagnosis of intraspinal neurological syndromes, 19: 19720
TARANTIN, N. I., Electromagnetic mass-separator. I., 19: 20260 (JINR-P-1948)
TARANTIN, N. I., Electromagnetic mass-separator. II., 19: 20261 (JINR-P-1949)
TARASOV, Yu. A., Argon–Cs plasma in an electric field, 19: 21556
TARASOV, Yu. A., Radiation of Cs plasma, 19: 21505
TATALASHVILI, N. G., Geometric program for analysis of penetrating showers of cosmic rays, 19: 20896
TAVKHELIDZE, A. N., Relativistic generalization of SU(6) symmetry, 19: 20973
TAVKHELIDZE, A. N., SU(6) symmetry and higher angular momenta, 19: 20972
TAYLER, R. J., Equilibrium distribution of nuclides in matter at high temperatures, 19: 20762
TAYLOR, M. P., Determination of Po-210 in urine, 19: 19791
TAYLOR, S., Observations of radiative τ^+ decays, 19: 20990
TEBBLE, R. S., Gadolinium S state ions in metals, 19: 20698
TEICH, Timm H., Gas ionizing radiation of discharge in O, 19: 20712
TEITEL, Robert J., Liquid metal breeder reactor, 19: 21697
TELEGDI, V. L., Production cross sections for $\pi^\pm$ and $K^\pm$ for 12.5-Bev protons on Be, 19: 21406
TELFER, Nancy, Salivary secretion of Cs-131, 19: 19486
TELFORD, R. E., Determination of Th and P in Th phosphides, 19: 19740 (ANL-7005)
TELTSCHAROV, L., Influence of x-ray therapy on hepatic function, 19: 19684
TEMPLETON, David H., Crystal structure of Cs aquopentachloro-ruthenate, 19: 19845 (UCRL-11828(p.146))
TEMPLETON, David H., Crystal structure of OsO_4, 19: 19846 (UCRL-11828(p.158-9))
TEMPLETON, W. L., Radioisotopes in the marine environment, 19: 20226
TEODORESCU, G., Color centers produced by electrons in KCl and KBr, 19: 19979
TEPLITSKAYA, R. B., Excitation temperature in solar atmosphere, 19: 20775
TEPLOV, I. V., Tables of Coulomb wave functions, 19: 21117
TEPTIN, A. L., Behavior of Green function of finite-difference analog of Sturm-Liouville boundary-value, 19: 20451
TEREKHOVA, V. F., Problems in theory and applications of rare earth metals, 19: 20468
TERHUNE, J. H., Nuclear superradiance in solids, 19: 21407
TETELBAUM, D. I., Depth of penetration and distribution of radiation damage when Ge is bombarded with Ar and N ions, 19: 20625
TEUTING, Robert Graham, Method of producing superconducting Nb–Zr alloy, 19: 20609
TEXTORIS, A., Measurements of continua of N, O, and air, 19: 20676
TEZAK, B., Precipitation and hydrolysis of U(VI). II., 19: 19870
THALER, R. M., Relativistic scattering of two equal-mass charged particles, 19: 21031
THAMBYAHPILLAI, T., Cosmic-ray intensity at depth of 60 m.w.e. underground at London, 19: 20897
THARIN, D. Whitney, Jr., Burning of radioactive process solvent, 19: 21747 (DP-942)
THEENHAUS, R., Time-resolved Langmuir probe measurements of plasma density, 19: 21515
THIELHEIM, K. O., Properties of retina-like counter, 19: 20352
THIRLAWAY, H. I. S., Detecting explosions, 19: 20177
THOMAS, E. Donnell, Lung transplantation in the dog, 19: 19523
THOMAS, E. W., Excitation in rare gas ion–atom collisions, 19: 20862
THOMAS, J., Treatment of ulcerated after-effects of x ray, 19: 19605
THOMAS, J. G., S-wave scattering lengths for n-p interaction, 19: 21043
THOMAS, R. G., Transport of relatively insoluble materials from lung to lymph nodes, 19: 19456 (LF-21)
THOMAS, R. N., Pulse-lengthening circuit, 19: 20350
THOMAS, Ralph H., Problems of induced radioactivity around 200-Bev AGS, 19: 20732 (UCRL-11796)
THOMAS, Robert H., Radiation from gas containing alkali metal vapors, 19: 21468 (BSD-TDR-64-164)
THOMAS, T. Darrah, X rays emitted in coincidence with fission of Cf-252, 19: 21229 (BNL-8841)
THOMASSEN, K. I., Rotational instability in a Penning-type discharge, 19: 21548
THOMMEN, H., Magnetic-dipole-induced plasma motions, 19: 21535
THOMPSON, J. C., Cross-section measurements, 19: 21484 (ORNL-3760(p.57-63))
THOMPSON, Jane Cicely, Systems for detecting leaks in fuel elements, 19: 21624
THOMPSON, S. G., Energy-mass distributions of Bi, Au, and W in He-ion-induced fission, 19: 21263 (UCRL-11828(p.90-2))
THOMPSON, S. G., Fission barriers of Po-210 and Sb-119, and Sb-117, 19: 21261 (UCRL-11828(p.81-3))
THOMPSON, S. G., Fission-excitation functions of light elements, 19: 21264 (UCRL-11828(p.92-4))
THOMPSON, S. G., K x rays emitted in spontaneous fission of Cf-252, 19: 21265 (UCRL-11828(p.95-7))
THOMPSON, Stanley G., Fission barrier of Tl-201, 19: 21260 (UCRL-11828 (p.81))
THOMPSON, Stanley G., Fission of U-238 and Pu-240 nuclei excited by inelastic α-particle scattering, 19: 21262 (UCRL-11828(p.84-6))
THON, W. J., Design for radiation safety, 19: 20209
THONEMANN, P. C., Helicon wave propagation in gaseous plasma, 19: 21552
THONEMANN, P. C., Study of helicon waves in In, 19: 21553
THORELL, C. B., Secretion of I-131 in milk, 19: 19477
THORN, R. J., Pressure of U over U–UO_2 system, 19: 19890
TIETZ, T., Eigenfunctions and energies of electrons in atoms, 19: 20835
TIGYI, Jozsef, Biological effect of ionizing radiation, 19: 19551
TIKHONOV, V. I., Precision of synchronization devices, 19: 20750

TIKTOPOULOS, George, Note on positronium, 19: 20966
TILL, J. E., Host-cell interactions in mice bearing isologous hemopoietic grafts, 19: 19615
TIMOFEEV, A. V., Non-linear theory of convective instability, 19: 21532
TITOV, V. B., Transformations of normal alkanes, 19: 19980
TITTMANN, B. R., Amplitude-dependent ultrasonic attenuation in superconducting Pb, 19: 21169
TOBITA, Shozo, Bonding methods for graphite materials, 19: 20505 (JAERI-1071)
TOCHILIN, E., Radiation control regulations of state of California, 19: 19655
TODD, Frank A., Protecting foods and water against radioactive contamination, 19: 20240
TODD, James P., High-temperature acceleration of propellants, 19: 20139
TODOROV, I. T., Relativistic generalization of SU(6) symmetry, 19: 20973
TODOROV, I. T., SU(6) symmetry and higher angular momenta, 19: 20972
TOELGYESSY, J., Use of reflected β radiation for determination of end-points in precipitation titrations, 19: 19787
TOERKO, Janos, Irradiations in the research reactor, 19: 21740
TOKAR, S. S., Poles of the Bethe-Salpeter partial wave amplitude in the g^4-plane, 19: 21111
TOKAREV, Yu., Block-type atomic reactor, 19: 21702
TOLOK, V. T., Capture of plasma in magnetic trap with fields, 19: 21568
TOLOK, V. T., Spectroscopic investigation of plasma in colliding bursts, 19: 21567
TOLU, Kanoti, Uranium defects in linear accelerator, 19: 20128
TOMAS, P., Neutron-neutron scattering length from $^3H(n,d)2n$ reaction, 19: 21404
TOMAS, P., Reactions $H^3(n,p)3n$ and $H^3(n,H^4)\gamma$ at E_n = 14.4 Mev, 19: 21405
TOMINAGA, Takeshi, Isomeric transition of Br-80m in pentamminecobalt (III) bromides, 19: 19973
TOMINAGA, Takeshi, Radiolysis of cobaltammine complexes, 19: 19974
TOMLINSON, M., Inhibitors for CO_2–graphite reaction in reactors, 19: 19953 (AERE-R-4201)
TOMLINSON, Richard G., Multiphoton ionization and breakdown of noble gases, 19: 20847
TOMOZAWA, Yukio, Internal symmetry for Poincaré group, 19: 20965
TONWAR, S. C., Distribution of inelasticity in high-energy collisions in C and brass, 19: 20898
TOPCHIEV, A. V., Radiolysis of frozen solutions of amino acids and peptides, 19: 20012
TORI, G., Renal scintiscanning with ^{203}Hg–neohydrin, 19: 19721
TOROPOVA, T. P., Asymmetry of scattering indicatrices of transparent particles, 19: 20822
TOROSSIAN, Andre, Stability of plasmas obtained in EPPE, 19: 21469 (CEA-R-2713)
TORRES, J. A., Kidney homografts, 19: 19519
TORRES, J. A., Modification of immunologic tolerance with transplantation of allogenic hematopoietic cells, 19: 19493
TOSCO, U., Behavior of fungal spores in confined irradiated environment, 19: 19559
TOSCO, U., Effects of irradiation on fungal spores, 19: 19558
TOSHIOKA, Katsushi, Plasma confinement with a rotating magnetic field, 19: 21508
TOTH, K. S., Formation cross sections of Sc-44g and Sc-44m in N-induced reactions, 19: 21392
TOTH, L. E., Superconducting properties and nitrides, 19: 20572
TOURYAN, K. J., Materials tests for hypersonic plasma generator, 19: 20905 (SC-RR-65-54)
TOVE, P. A., Charge transport time in semiconductor detectors, 19: 20366
TRABUT, Louis, Apparatus for high-temperature measurement of interior friction in rigid samples, 19: 20245 (CEA-R-2718)
TRAMBOUZE, Yves, Thorium oxalate precipitation and thermal decomposition, 19: 19861
TRAPMANN, Heinz, Dephosphorylation of sugar phosphates and nucleotides by group-IV metal ions, 19: 19876
TREIMAN, S. B., Tests of relativistic SU(6) schemes, 19: 21025
TRENTIN, John J., Splenic transplantation in the dog, 19: 19521
TRET'YAKOV, V. N., Polarizability of the neutron, 19: 20949
TREVINO, S. F., Neutrons from $^9Be(\alpha,n_0)^{12}C$ and $^9Be(\alpha,n_1)^{12m}C$ reactions, 19: 21307
TRICE, James B., Prog. rpt. on surface contouring applied to semiconductor radiation detectors, semiannual, 6/64–1/65, 19: 20323 (NYO-3246-4)
TRIKHA, S. K., Equilibrium neutron energy spectra in finite blocks of graphite, 19: 21205
TRIPP, Robert D., Baryon resonances, 19: 20916 (CERN-65-7)
TROBAUGH, Frank E., Jr., Transplantation potential of marrow frozen at grammed cooling rates, 19: 19645
TROSTIN, S. S., Reversal of the thermal neutron spin, 19: 21300
TRUBCHANINOV, S. A., Instability in plasma burst during its motion in longitudinal magnetic field, 19: 21582
TRUEMPER, Manfred, Special class of type-I gravitational fields, 19: 21090
TRUSHINA, M. N., Use of embryonic blood-making liver cells in acute radiation syndrome, 19: 19637
TSENG, Chia-yen, Influences of pairing force on properties of rare-earth nuclei, 19: 21434
TSERKOVNIKOV, Yu. A., Second sound in weakly ideal Bose gas, 19: 20669
TSETLIN, B. L., Radiation synthesis of polymers based on dimethylphosphinoborine, 19: 19982
TSIGANENKO, V. V., Mean energy of electron gas at absolute zero, 19: 20711
TSINTSADZE, N., Controlled plasma, 19: 21492 (FTD-TT-64-102)
TSOCHEV, Ts. N., Biological prophylaxis of acute radiation disease with lyophilized royal jelly, 19: 19629
TSOI, A. Kh., Accuracy of locating particle in spark chamber and determining ion drift in Wilson chamber, 19: 20344
TSOPP, L. E., Plasma acceleration with aid of EM H_{11}-type wave in circular waveguide, 19: 21566
TSU, Raphael, Interaction of optical and acoustic phonons with plasma waves, 19: 21494
TSUCHIMOTO, Michiko, Isotopic exchange of Tl(III) between Tl(III) ion and Tl N-2-hydroxyethylethylenediamine-N,N',N'-triacetate complex in water, 19: 19856
TSUJIMURA, Shigeo, Flowmeter for F gas and vapors of reactive fluorides, 19: 20259 (JAERI-1074)
TSUJIMURA, Shigeo, Recording thermobalance for F gas and vapors of reactive fluorides, 19: 20258 (JAERI-1070)
TSULKO-SITINKOV, V. M., Nuclear form-factors in μ capture in He-3, 19: 21236 (JINR-P-1952)
TSYTOVICH, V. N., Detecting h-f turbulence of cosmic plasma, 19: 20755
TSYTOVICH, V. N., High-frequency turbulence in cosmic plasma, 19: 20781
TSYTOVICH, V. N., Neutrino generation and acceleration in turbulent plasma, 19: 21500
TSYTOVICH, V. N., Theory of interaction between electron beams in plasma and transverse waves, 19: 21563
TUAN, I-shin, Decay of K_{13}, 19: 21060
TUBIANA, M., Risks for embryo, fetus, and infant from medical radiology, 19: 19699
TUCHKOVA, S. J., Loss of regeneration capacity by salamander extremities after exposure to x rays, 19: 19544
TUCHKOVA, S. J., Regeneration of extremities in salamanders following x-ray treatment, 19: 19546
TUCKER, W. H., Galactic x-ray sources, 19: 20765
TUMANYAN, M. A., Chemotherapy of radiation sickness, 19: 19622
TUN, Than, Isodose charts for Co-60 teletherapy beams, 19: 19733
TUOMI, T. O., Behavior of Se during reactor irradiation, 19: 20644
TURKEVICH, Anthony L., Chemical analysis of surfaces using α particles, 19: 19795
TURNER, Thomas F., R-f phase and amplitude control system for proton linear accelerator, 19: 20728 (LA-DC-6875)
TUSHINGHAM, R., Spark source mass spectrograph, 19: 19830
TUSL, M., Oxygen requirements of irradiated rats of various age, 19: 19539
TUTTLE, L. W., Retention of Sr-90 by fetal and newborn rats, 19: 19473 (UR-661)
TVERSKOI, B. A., Dynamics of radiation belts. II., 19: 21128
TVERSKOI, B. A., Fast particle capture from interplanetary space, 19: 21137
TYASTO, M. I., Effect of equatorial flux on geomagnetic cutoff of cosmic-ray particles, 19: 20887
TYBULEWICZ, A., Radiation effects on semiconductors, 19: 20651
TYURMINA, L. O., Western drift of the geomagnetic field, 19: 21131
TZU, Pao-ru, Branching ratio of unstable particle η, 19: 21059

U

UDAGAWA, T., High-spin rotational states in deformed nuclei, 19: 21363
UDOVICHENKO, Yu. K., Interaction of traveling EM wave with plasma, 19: 21564
UEDA, Yoshiaki, Decay mode $K \to 2\pi + \gamma$, 19: 20939 (UR-875-30)
UEKI, Totzuo, Crystal structure of OsO_4, 19: 19846 (UCRL-11828(p.158-9))
ULLMANN, J. W., Adsorption of Pa on unfired Vycor, 19: 20051 (ORNL-3773)
UL'YANOV, K. N., Recombination decay of nonequilibrium nonisothermal plasma, 19: 21501
UL'YANOV, K. N., Recombination decay in nonisothermal plasma, 19: 21557
UNRUH, C. M., Personnel neutron dosimeter development, 19: 20318 (HW-SA-3526)

UO, K. A., Temperature of the discharge in C stellarator, 19: 21511
UPHOFF, Delta E., Comparative survival of substrains C3HeB and C3HfB following midlethal irradiation and allogenic marrow inoculation, 19: 19648
URANKAR, K., One particle radiation transitions in optical model, 19: 21442
URBAIN, Walter M., Radiation preservation of fresh meat and poultry, 19: 20425
URBAN, P., Inelastic electron-deuteron scattering, 19: 20942
URIARTE, Armando L., Dissolution of high-density UO_2, PuO_2, and UO_2–PuO_2 pellets in inorganic acids, 19: 20050 (ORNL-3695)
URONE, Paul, Deactivation of gas chromatographic support, 19: 19997
USHAKOV, V. V., Equations for plane EHD flows, 19: 20670
UVAROV, E. B., Decomposition potential of system K_2ZrF_6–NaCl–KCl, 19: 19850 (NP-tr-1230)

V

VACEK, L., Effect of x rays on mechanical resistance of erythrocytes, 19: 19595
VACZO, G., Effect of x irradiation on liver regeneration, 19: 19512
VAGER, Z., E2/M1 mixing ratios and K conversion coefficients of some rotational transitions, 19: 21324
VAGNER, F. A., Argon arc welding of stainless steel tubing, 19: 20534
VAKULOV, P. V., Radiation study by Cosmos 17, 19: 20343
VALENTIN, L., Calculation of nucleon-α cascades, 19: 21372
VALEVA, S. A., Radiosensitivities of kindred plants. II., 19: 19582
VAN ANDEL, J. G., Deposition of Ba or Sr in aortic tissue, 19: 19500 (NP-14907)
VAN AUDEKERCKE, R., Bombardment of Cu and Ge by low-energy Ar ions, 19: 20813
VAN BEKKUM, D. W., Immunologic reactivity and specific tolerance of graft in radiation chimeras and influence of thymus, 19: 19652
VAN CRAEYNEST, Annick, X-ray microanalysis—determination of correction factors, 19: 19746 (CEA-R-2728)
VAN DER MERWE, K. F., Preparation of deuterium-labeled O–methyl groups, 19: 20034
VAN DER STRICHT, E., Rapid determination of Cs-137 in radioactive dusts, 19: 19805
VANDERVORT, P. S., Eddy-current inspection for stainless steel-clad U carbide, 19: 20531
VAN DER WIEL, M. J., Ionization cross sections for electrons in gases, 19: 20850
VANG, R., Open-cycle MHD generator, 19: 20912
VAN HEERDEN, I. J., Low threshold neutron detector, 19: 20355
VAN HEERDEN, I. J., Measurement of differential neutron scattering cross sections, 19: 21298
VANIKOV, A. V., Properties of irradiated and heat-treated polyethylene, 19: 20017
VAN ITTERBEEK, A., Bombardment of Cu and Ge by low-energy Ar ions, 19: 20813
VAN ITTERBEEK, W., Bombardment of Cu and Ge by low-energy Ar ions, 19: 20813
VAN PUTTEN, L. M., Secondary disease in different species and its modification, 19: 19647
VAN STEENBERGEN, A., High-intensity ion beam production and preacceleration, 19: 20720 (BNL-8982)
VAN VUCHT, J. H. N., Intermediate phases in Sm–Al, 19: 20596
VARGA, S., Use of reflected β radiation for determination of end-points in precipitation titrations, 19: 19787
VARLAMOV, V. G., Time analyzer based on Al-100, 19: 20298
VARTOLOMEI, M., Exposure of drugs to nuclear bomb explosion, 19: 20231
VASHCHINU, T., Radioactive measuring devices, 19: 20412
VASILEV, G. A., Increase of O assimilation during irradiation, 19: 19584
VASILIU, V., Total reflection of neutrons in Co mirrors, 19: 21201 (KFK-tr-164)
VASKOV, L. S., Therapy of chronic radiation injuries, 19: 19623
VASSEUR, Chantal, Specifications for multi-group scattering code of two dimensions: ALCI, 19: 21197 (CEA-R-2747 & Add.)
VASSEUR, Chantal, Specifications for scattering code for XY geometry: DAIXY, 19: 21198 (CEA-R-2759)
VATCHA, R. H., Distribution of inelasticity in high-energy collisions in C and brass, 19: 20898
VATUL'OV, V. M., Luminescence appearing in Na uranyl acetate irradiated laser beam, 19: 20010
VAVILOV, Viktor Sergeevich, Radiation effects on semiconductors, 19: 20651
VAVRUKH, M. V., Mean energy of electron gas at absolute zero, 19: 20711
VDOVENKO, V. M., Solubility of $UO_2(ClO_4)_2 \cdot 3H_2O$ in mixed solvents, 19: 20073
VDOVENKO, V. M., Uranyl perchlorate complexes, 19: 19910
VDOVENKO, V. M., Uranyl nitrate solubility in mixed solvents, 19: 20072
VEDENEEV, G. V., Complex installation for study of extensive air showers, 19: 20347
VEJE, C. J., Isospin structure of low-lying collective octupole vibrations, 19: 21351
VEKSHINA, N. V., Lanthanum borocarbides, 19: 19926
VELA, R., Kidney homografts, 19: 19519
VELA, R., Modification of immunologic tolerance with transplantation of allogeneic hematopoietic cells, 19: 19493
VELLAIKAL, Gopinathan, Dislocation arrangements in deformed Cu polycrystals, 19: 21774 (UCRL-11858)
VENABLE, Douglas, Surfaces of constant space charge field components, 19: 20739
VENDRAME, L., Radioprotective power of prochlorperazine, 19: 19631
VENDRAME, L., Weight changes in albino mice after total-body irradiation, 19: 19632
VENKATESAN, K., Gauge invariance and mass of vector bosons, 19: 20934 (NP-14829)
VENKER, H., Plating U and Al with Nb, 19: 20456 (EUR-2111.d)
VERBINSKI, V. V., Energy and angular details of fast neutron flux in water from pool-type reactor, 19: 21735 (ORNL-P-1092)
VERDINGH, V., Preparation of Na samples for neutron scattering experiments, 19: 20503 (EUR-2242.e)
VERHEIJKE, M. L., Coincidence spectrometer for positron annihilation radiation, 19: 20363
VERNOV, S. N., Complex installation for study of extensive air showers, 19: 20347
VERNOV, S. N., Cosmic rays at high altitudes, 19: 20895
VERNOV, S. N., Data on earth's radiation belts obtained during Cosmos flights, 19: 21136
VERNOV, S. N., Radiation study by Cosmos 17, 19: 20343
VERNYI, E. A., Uranium: methods for determination, 19: 19823
VERTES, Paul, Production of granulated UO_2, 19: 20538
VERTMAN, A. A., Density of Co–C and Ni–C alloys in solid and liquid states, 19: 20567 (LA-tr-65-5)
VESELY, Vladimir, Tetraethylenepentamine-N,N,N′,N″,N‴,N⁗,N⁗′-heptaacetic acid as a titrimetric reagent, 19: 19813
VESELY, Vladmir, Deactivation of radioactive waste liquids, 19: 21755
VESTINE, E. H., Ionospheric electric current systems, 19: 21124 (P-1121(RAND))
VEYSSIERE, Andre, Electron bunching in Saclay linear accelerator, 19: 20721 (CEA-R-2749)
VIALLET, Henri, Resistance of metallic U tubes to external pressure, 19: 20453 (CEA-R-2572)
VIGIER, P., Magnetic after-effects in neutron-irradiated Fe, Ni, and Co, 19: 20652
VIL'K, Yu. N., Interaction of NbC with W, 19: 20583
VINOGRADOV, A. V., Uranium: methods for determination, 19: 19823
VIOLA, Victor E., Jr., Fission barriers of W, Re, Os, Ir, and Hg isotopes, 19: 21259 (UCRL-11828(p.77-80))
VIOLET, Regis, Improvement of spectrographic analyses, 19: 19743 (CEA-R-2619)
VISKOV, V. V., Coupling coefficients for cosmic components, 19: 20891
VLACHOV, K., Influence of x-ray therapy on hepatic function, 19: 19684
VLADIMIRSKII, B. M., X-ray bursts and cosmic rays, 19: 20890
VLASENKO, V. G., Spark chamber, 19: 20378
VLASOV, N. A., Optical method for detection of antimatter in universe, 19: 20754
VLASOV, N. A., Optical search for antimatter in the universe, 19: 20774
VLASOV, V. G., Structure of α-UO_3–U_3O_8 region, 19: 19929
VLASOV, V. G., Structure of gamma UO_3, 19: 19930
VLATKOVIC, M., Preparation of Na perchlorate labeled with Cl-36, 19: 20028
VODICKA, I., Influence of 19-norandrostenolone upon acute irradiation disease in rats, 19: 19624
VODOP'YANOV, L. S., High-temperature sintering of W, 19: 20532
VOEROES, T., Barrier penetrabilities in α decay, 19: 21411
VOGG, Hubert, Method of pre-decontaminating fuel to be reprocessed, 19: 20084
VOGT, O., Magnetic properties of the rare earth nitrides, 19: 19895
VOGT, O., Magnetic properties of ordering rare-earth antimonides, 19: 20597
VOLKMAN, R. A., Thickness of zenithal auroral arc over Alaska, 19: 21147
VOLKOV, T. F., Penetration of alternating magnetic field into plasma, 19: 21527
VOLODINA, G. F., Structure refinement for $Pr(NO_3)_3 \cdot 6H_2O$, 19: 19914
VOLPI, G. G., Ion-molecule reactions in acetylene, 19: 19988
VON BLANKENHAGEN, P., Measurement of isomeric splitting ratios by activation, 19: 21237 (KFK-265)
VON ENGEL, A., Starting mechanism of first stage of ring discharge,

19: 21554
VORESS, Hugh E., Bibliography on radioactive fallout, 19: 20164 (TID-3086(Suppl.2))
VOROBEV, A. A., Dielectric losses in oxides and halide compounds of group II elements, 19: 19851 (ORNL-tr-491)
VORONKOVA, L. N., Comparison of mitosis supression by separate irradiation of nucleus and cytoplasmic structures, 19: 19579
VORTMAN, L. J., Constructing low-relief earth-fill dams using nuclear explosives, 19: 20090 (SC-RR-65-41)
VOSKO, S. H., Renormalization constant of electron gas, 19: 20968
VOSS, Milo D., Environmental radioactivity, 19: 20156 (IS-1098)
VOYTOVICH, R. F., Kinetics of oxidation of Nb–Ni and Nb–Al refractory alloys, 19: 20494
VRIGAZOV, Angel, Hemopoiesis in sheep exposed to sublethal doses of x rays, 19: 19600
VUCCINO, S., Measurement of α and β radioactivity, 19: 20383
VUKICEVIC, Sreten, Production of radioactive colloidal Au-198, 19: 20022 (JPRS-29258)
VYALOV, G. N., Acceleration of variably charged particles in electrostatic field, 19: 20722 (JINR-D-1946)
VYSOCHINA, I. V., Reversible attachment of O to hemoglobin, 19: 19529

W

WACHSMANN, F., Tissue factor with different radiation qualities, 19: 19689
WACHSMANN, Felix, Betatron in modern radiotherapy, 19: 19673
WACHSPRESS, E. L., Variational synthesis with discontinuous trial functions, 19: 21638 (CONF-650501-4)
WACHTER, J. W., Comparison of measured neutron and proton spectra with calculated spectra in energy region between 50 and 160 Mev, 19: 21244 (ORNL-P-844)
WADDELL, William R., Splenic homotransplantation, 19: 19522
WADE, B. R., SNAP-10A malfunction detection subsystem, 19: 21734 (NAA-SR-Memo-10666)
WADE, G. E., Leakage from Zone I and II of 105-N, 19: 21712 (HW-61979)
WADSLEY, A. D., Mixed oxides of Ti and Nb, 19: 20569
WAGNER, H. N., Jr., Diagnosis of massive pulmonary embolism by radioisotope scanning, 19: 19724
WAHLIG, M., Charge-exchange scattering at high energies for $\pi^- + p \rightarrow \pi^0 + n$, 19: 21006
WAINERDI, Richard Elliott, Activation analysis as applied to petroleum exploration industry, 19: 19773 (TID-20467)
WAINERDI, Richard E., Prog. rpt. on automated activation analysis, annual, 1964, 19: 19763 (TEES-2671-4)
WAKABAYASHI, Shinichi, Studies on natural U–H_2O exponential pile. II., 19: 21645
WALFORD, F. J., Pressure rise in biological shield of GCR, 19: 21608 (AWRE-R-2/65)
WALI, K. C., Phenomenological approach to relativistic SU(6) theory, 19: 21005
WALKER, J. H., Adjustable positive-limit magnetic torque wrench, 19: 21768 (SC-TM-65-48)
WALKER, J. K., Baryon spectroscopy by inelastic e-p scattering, 19: 20997
WALKER, J. V., Effects of flux anisotropy on thermal-neutron flux perturbations, 19: 21213
WALKER, R. A., Time-variable time delay for computer simulations, 19: 21713 (HW-83092(Rev.))
WALKER, R. M., Cosmic-ray exposure ages of tektites, 19: 20761
WALKER, R. M., Stability of fission tracks in minerals and glasses, 19: 20674
WALLACE, Richard M., Determination of Zr-95 and Nb-95 in mixtures, 19: 19748 (DP-933)
WALLER, W. A., Two-meter grazing-incidence spectrometer, 19: 20348
WALLIS, L. R., Reactor decontamination and the health physicist, 19: 21605 (HW-SA-3560)
WALMSLEY, P. N., Efficiency of stainless steel packings, 19: 20068
WALTER, E., Radiation physical problems of therapy with high-energy electrons, 19: 19694
WANDERS, G., Causality and one-particle singularities of S matrix, 19: 20953
WANG, E. Y., Effects of energetic photon irradiation on Ge, 19: 20612 (AFCRL-64-839)
WANG, Fan, Alpha-reduced width of 1p shell nuclei, 19: 21432
WANG, I-Wei, Uranyl nitrate solubility in mixed solvents, 19: 20072
WANG, Shih-wei, Inelastic collisions of 6.8 Bev/c π^- mesons with nucleons, 19: 21062
WANG, Tzu-tzen, Inelastic collisions of 6.8 Bev/c π^- mesons with nucleons, 19: 21062
WANG, Yen, Thyroid uptake of disassociated I-131, 19: 19731
WANKLYN, J. N., Electrical conductivity of ZrO_2, 19: 20621
WANKLYN, J. N., Oxidation of Zr in high-pressure steam, 19: 20492
WARD, Helen L., Bibliography on biological applications of γ radiation, 19: 19505 (TID-3580)
WARD, Kenneth C., Automatic spectrogram measuring and recording, 19: 20288 (UCRL-11828(p.232-3))
WARKE, Chindhu Sona, Hartree-Fock approximation in nuclear matter, 19: 21440
WATANABE, T., Amplification of hydromagnetic waves in magnetosphere by cyclotron instability process, 19: 21123 (D1-82-0398)
WATKINS, C. A., Radiochemical evidence for Antler shot contribution to September 1961 fallout, 19: 20167
WATT, Robert D., Velocity spectrometers used in Bevatron deflected-beam research, 19: 20326 (UCRL-11787)
WATTSON, R., Test of $\Delta S/\Delta Q$ rule in K^0_{β} decay, 19: 20979
WEAVER, Lynn E., Prog. rpt. on application of automatic control theory to nuclear rocket, 2–9/64, 19: 21723 (NASA-CR-193)
WEBB, S. J., Radiation sensitivity of *Serratia marcescens*, 19: 19649
WEBB, W. W., Diffuse interface in critical fluid mixture, 19: 19952
WEBBER, R. L., Dental x-ray exposure of sites within head and neck, 19: 19676
WEBBER, W. R., Isotopic composition of He nuclei in primary cosmic radiation, 19: 20899
WEBELER, R. W. H., Viscosity x normal density of liquid He, 19: 21168
WEBER, C. W., Moisture indicator, 19: 21783
WEEREN, H. O., Pipe radioactive wastes to shale beds, 19: 21753
WEIJER, D. L., Beta radiation from radioactive I-131, 19: 19483
WEINSTEIN, Martin S., Operational safety evaluation of remote reactor plants, 19: 21685 (HASL-152)
WEISS, E. J., Crystal chemistry of rare earth group VI systems. I., 19: 19879
WEISS, Z., Disadvantage factors and flux distributions in two-region cells, 19: 21212
WEITZBERG, A., Analysis of SNAPTRAN-3 destructive experiment, 19: 21719 (NAA-SR-9780)
WEITZENMILLER, Franz, Total reflection of neutrons in Co mirrors, 19: 21201 (KFK-tr-164)
WELLS, D. K., Pulsed neutron source based on the Orbitron, 19: 21208
WELLS, E. R., Single-pass experiments (DCX-1), 19: 21480 (ORNL-3760(p.1-9))
WELLS, M., Superconducting properties of carbides and nitrides, 19: 20572
WELTON, T. A., Electron microscopy at ORNL, 19: 20250 (CONF-640204(p.26-34))
WENCLEWSKI, A., Effects of radiation on activity of aryl-sulfate sulphohydrolase in the brain, 19: 19573
WENDELL, A., Radiological assistance plan handbook, 19: 20197 (COO-281)
WENDER, M., Effects of radiation on activity of aryl-sulfate sulphohydrolase in the brain, 19: 19573
WENDER, M., Radiation effects on components in brain, 19: 19534
WENDT, H. F., Determination of B in refractory borides, 19: 19761 (NP-14876)
WENTZEL, G., Symmetry breaking in static strong-coupling theory, 19: 20951
WENZL, H., Irradiation of U with neutrons at 4.5°K, 19: 20642
WENZL, H., Magnetic after-effects in Ni after irradiation with neutrons, 19: 20647
WENZL, H., Magnetic after-effects in Fe after irradiation with neutrons, 19: 20648
WERBOFF, Jack, X irradiation of the 36-hour rat embryo, 19: 19618
WERNER, M., Digital decimal pulse ratemeter, 19: 20295
WERNICK, Jack, Method of producing superconducting Nb–Zr alloy, 19: 20609
WESS, J., Electromagnetic form factors and generalized Poincaré group, 19: 20971
WESTER, P. O., Simultaneous determination of 30 trace elements, 19: 19793
WESTERLUND, S., Twin-channel instability in toroidal plasma at B_z field reversal, 19: 21467 (ARL-63-203)
WESTON, Ralph E., Jr., Equilibrium between H_2O and D_2O, 19: 19891
WEY, Song-jey, Polarographic study of uranyl pyrophosphate complex, 19: 19816
WHEATLEY, Pamela, Recovery from lethal effects of cross-linking alkylation, 19: 19485
WHELLER, M. J., Thermal diffusivity at incandescent temperatures, 19: 20576
WHETSTONE, S. L., Monte Carlo intranuclear cascade calculation, 19: 21239 (LA-3206)
WHIPPLE, Harold E., Conference on transplantation, New York, 11/64. II., 19: 19462
WHITE, D. H., Flow visualization, 19: 20108 (BNWL-31)
WHITE, Donald L., Interaction of optical and acoustic phonons with plasma

waves, 19: 21494
WHITE, Matthew B., Hyperfine structures of Re-186 and Re-188, 19: 21382
WHITE, Roscoe, Broken SU(6) symmetry and nonleptonic baryon decays, 19: 20919 (IC/65/5)
WHITE, Roscoe, U(12) Symmetry and weak interactions, 19: 21028
WHITE, Thomas Otis, Jr., Polarization of photoprotons from D, Li, and C, 19: 21456
WHITEROD, G. L., Electron impact spectroscopy. III., 19: 20856
WHITTEMORE, D. S., Destabilization of zirconia, 19: 20585
WICKMAN, H. Hollis, Observation of electronic relaxation in Mössbauer spectroscopy, 19: 21270 (UCRL-11828(p.214-16))
WIDMAYER, Dorotheo J., Interpretation of kappa in *Paramecium aurelia*, 19: 19464
WIE, Hoi-guang, Influences of pairing force on properties of rare-earth nuclei, 19: 21434
WIEDEMANN, W., Hyperfine splitting and g factor of 84-kev state in Yb-170, 19: 21377
WIGHTMAN, A. S.,PCT, spin and statistics, and all that, 19: 21114
WIGLEY, D. A., Resistivity of Pu, Np, and U, 19: 20649
WIGLEY, D. A., Resistivity of self-damaged Pu, 19: 20650
WILCKE, O., Positron scanning for diagnosis of intracranial lesions, 19: 19713
WILCOX, Calvin H., Wave packets in quantum theory of scattering, 19: 21092
WILDMAN, P. J. L., Device for measuring electric field in presence of ionization, 19: 20290
WILETS, L., Comparison of some approximations for self-bound many-fermion systems, 19: 20936 (TID-20558)
WILKINS, Dale E., Soil profile measurements with radioactivity, 19: 20182
WILKINS, W. W., Communication theory in neutron activation analysis, 19: 19766 (TEES-2671-4(Chap.3))
WILKS, Eileen M., Effect of fast neutron irradiation on polishing of diamond, 19: 20639
84085)
WILL, Drake W., Autopsy study of leukemia in Hiroshima, 19: 19526
WILLI, J. C., Increased processing flexibility—Purex, 19: 20040 (HW-
WILLIAMS, D. A., Scattering filters in the far infrared, 19: 19917
WILLIAMS, E. M., Prog. rpt. on instabilities in metal-vapor plasmas, 10-12/64, 19: 21490 (TID-21698)
WILLIAMS, E. T., Odd-odd nucleus with 0+ ground state (^{156}Eu), 19: 21350
WILLIAMS, I. R., Formation cross sections of Sc-44g and Sc-44m in N-induced reactions, 19: 21392
WILLIAMS, M. C., Sodium-heated, modular, steam generators for SCTI, 19: 21611 (NAA-SR-9826)
WILLIAMS, M. M. R., Neutron flux perturbations due to infinite plane absorbers. I., 19: 21220
WILLIAMS, R. W., Solar-flare hazard to manned space systems, 19: 20873 (D2-11608)
WILLIAMSON, J. R., Prog. rpt. on pneumatic nutator actuator motor, 12/64, 19: 21615 (NASA-CR-54282)
WILLIAMSON, Joseph C., Exposure of x-ray film to radioactive fallout, 19: 20632
WILLIAMSON, Stanley M., Stability of XeO_3 in basic solutions, 19: 19847 (UCRL-11828(p.182-3))
WILLIS, D. E., Seismic measurements of large underwater shots, 19: 20175
WILSKY, K., Odd-odd nucleus with 0+ ground state (^{156}Eu), 19: 21350
WILSON, A. S., 709/7090 program for indexing x-ray diffraction powder patterns. I., 19: 19834 (HW-74393)
WILSON, A. S., 709/7090 program for indexing x-ray diffraction powder patterns. III., 19: 19835 (HW-89062)
WILSON, Howard Lynn, Scattering of α particles by Fe-56, Zn-64, Zn-66, and Zn-68, 19: 21459
WILSON, J., Measurements of continua of N, O, and air, 19: 20676
WILSON, M., New results for ^{7}Li(p,γ)^{8*} Be reaction, 19: 21342
WILSON, M. A., Energy modulation of particle accelerators, 19: 20746
WILSON, Raphael, Changes in germ-free mice following whole-body x irradiation, 19: 19619
WILSON, Richard, Baryon spectroscopy by inelastic e-p scattering, 19: 20997
WILSON, Richard E., Human kidney transplantation, 19: 19520
WILSON, V. C., Operating characteristics of two thermionic converters, 19: 20906
WIMBER, Donald E., Effects of intracellular irradiation with tritium, 19: 19515
WIND, H., Electron energy for H_2^+ in ground state, 19: 19885
WINDLER, Frank, Lipid metabolism in acute radiation injury, 19: 19610
WING, A. P., Transient tests of fully enriched, stainless steel plate-type, P core in Spert I reactor, 19: 20616 (IDO-17011)
WINKLER, E. O., GAIL IV irradiation assembly design summary, 19: 21665 (GAMD-5535)
WINKLER, H., Influence of infrared radiation on roentgenoluminescence, 19: 19965
WINTHER, A., Reorientation effect in Cd-114, 19: 21398
WIRSCHING, Joseph E., Parallelism in computing systems, 19: 20444 (UCRL-12293-T)
WITT, F. J., Thermal analysis of cylindrical shells, 19: 21619
WITTERS, J., Bombardment of Cu and Ge by low-energy Ar ions, 19: 20813
WITTMANN, F., Angular distribution of resonantly scattered γ quanta, 19: 21435
WOELFLI, W., Direct measurement of short nuclear lifetime, 19: 21369
WOELFLI, W., Ground state wave function of H-3 and He-3, 19: 21367
WOLF, G., Toroidal theta pinch in M-and-S configuration, 19: 21530
WOLF, R., Scintillation scanning of spleen, 19: 19726
WOLFENSTEIN, L., Imaginary Fermi constant G as model of CP violation, 19: 20978
WOLFF, Etienne, Teratogenic effects of ionizing radiations on embryonic development, 19: 19466
WOMACK, G. J., Experiments in MHD power generation, 19: 20909
WONG, A. Y., Effects of passing current on plasma losses in a Q device, 19: 21541
WONG, An-chi, Chromosomal aberrations of irradiated human leukocytes, 19: 19596
WOOD, D. F., Determination of Zr in Nb, 19: 19780
WOOLLEY, R. L., Elasticity of polycrystalline graphite, 19: 20640
WORKMAN, Joseph B., Pre-operative localization of parathyroid adenomata, 19: 19732
WORTMAN, Donald Eugene, Radioactive decays of Fe-59, Nb-95, and Ca-47, 19: 21460
WOULDS, J. N., Pion capture in complex nuclei, 19: 21315
WRIGHT, E. A., Site of uptake of I by hair, 19: 19479
WRIGHT, J., Inhibitors for CO_2–graphite reaction in reactors, 19: 19953 (AERE-R-4201)
WRIGHT, J. K., MHD research in the United Kingdom, 19: 20908
WRIGHT, J. K., Non-thermal ionization combustion product MHD generators, 19: 20911
WRUBEL, M. H., Construction of stellar models, 19: 20789
WRZESINSKA, A., Influence of fast neutrons on luminescence of ZnS, 19: 19967
WU, Hung-sheng, Critical magnetic field of superconducting alloy film, 19: 21192
WUKUSICK, C. S., Properties of Fe–Cr–Al type alloys containing Y, 19: 20470 (GE-TM-63-7-3)
WYCKOFF, Ralph W. G., Commercial spectrometer modified for x-ray spectroscopy, 19: 19801
WYDLER, A. A., Hewlett-Packard digital recorder model 562A insignificant-zero suppression, 19: 20285 (UCRL-11828(p.229))
WYDLER, A. A., Hewlett-Packard digital recorder model 562A modification to produce leader paper, 19: 20286 (UCRL-11828(p.230))

X

XAVIER, R. M., Susceptibility of liquid Gd, 19: 20598

Y

YAGI, K., Third-order aberrations in broad-range spectrometer, 19: 20365
YAKIMOV, M. A., Heterogeneous equilibrates in $UO_2(NO_3)_2$–HNO_3–H_2O system. II., 19: 19907
YAKIMOV, M. A., Heterogeneous equilibrates in $UO_2(NO_3)_2$–HNO_3–H_2O system. III., 19: 19908
YAKIMOV, M. A., Heterogeneous equilibrates in $UO_2(NO_3)_2$–HNO_3–H_2O system. IV., 19: 19909
YAKOVKIN, N. A., H_α radiation field in prominences, 19: 20776
YAKOVLEV, B. M., Connection between width of giant resonance of (γ,n) reaction and filling of energy levels of the nucleus, 19: 21287
YAKOVLEV, G. N., Extraction of actinide elements with dialkyl phosphoric acids, 19: 20075
YAKUBOV, V. B., Prestellar evolution of the universe, 19: 20773
YAKUBOVICH, E. I., Eleetron and ion distribution functions for plasma in slightly nonuniform high-frequency field, 19: 21573
YAKUBOVICH, E. I., Ohmic heating of partially ionized plasma by a uniform h-f field, 19: 21581
YALGIN, C., Charge dependence of internucleon potential, 19: 21373
YAMADA, Atsushi, Autopsy study of leukemia in Hiroshima, 19: 19526
YAMADA, Chikahisa, Slit-type screen for telecobalt therapy, 19: 19674
YAMAMOTO, Tsutomu, Autopsy study of leukemia in Hiroshima, 19: 19526
YAMANE, Hiroyasu, Removal of astringency in Kaki by γ radiation, 19: 19571
YAMANOUCHI, T., Observation of the low-energy Λ-p interaction, 19: 21034
YAMASAKI, Yoshihde, Minimum criticality calculation for JPDR, 19: 21689

(JAERI-1068)
YAMASHINA, Toshiro, Reduction of γ-irradiated Ni oxide by H, 19: 19975
YAMASHITA, Nobuo, Dose distribution in tumors. I., 19: 19671
YAMASHITA, Nobuo, Dose distribution in tumors. II., 19: 19672
YAMAZAKI, T., Internal-conversion coefficients in decay of U-237, 19: 21251 (UCRL-11828(p.31-4))
YAMAZAKI, T., Pair-production cross sections near threshold, 19: 21252 (UCRL-11828(p.35-8))
YANG, Kuo-chen, Intermediate boson theory of weak interactions, 19: 21045
YANG, Wen-shang, Thermoluminescence of irradiated high polymers. I., 19: 20007
YANOVA, K. G., Radiolysis of frozen solutions of amino acids and peptides, 19: 20012
YAROSHETSKII, I. D., Impurity photoconductivity produced in Ge by γ irradiation, 19: 20623
YAVOR, S. Ya., Spherical aberration of EM quadrupole lenses, 19: 20685
YEH, C., Wave propagation in hot plasma waveguides, 19: 21536
YEH, Pong-sheng, High-energy scattering and a_q-Regge trajectory, 19: 21063
YEH, Pong-sheng, Principle of maximum analyticity and properties of Regge trajectories, 19: 21061
YENICAY, F., Response measurement of magnetic probe, 19: 20293
YILMAZ, Huseyin, Theory of relativity and principles of modern physics, 19: 21116
YIN, Pong-chen, Principle of maximum analyticity and properties of Regge trajectories, 19: 21061
YIN, Pong-cheng, High-energy scattering and a_q-Regge trajectory, 19: 21063
YIOU, F., Intranuclear cascade and breakup calculations on production of Li, Be, and B isotopes in C-12 by 156-Mev protons, 19: 21402
YIOU, F., Lithium-6 and Li-7 production in C-12 and O-16 by high-energy protons, 19: 21352
YNGVESSON, K. O., Incoherent scatter from plasma oscillations in the ionosphere, 19: 21153
YNTEMA, J. L., Collective excitations in Zr isotopes, 19: 21386
YOKOI, K., Direct recording of particle tracks of spark chamber, 19: 20368
YOSHIHARA, H., Magnetic-dipole-induced plasma motions, 19: 21535
YOSHIHARA, Kenji, Chemical effects of $^{35}Cl(n,p)^{35}S$ reaction. I., 19: 20004
YOSIDA, Koi, Long-range magnetic coupling in metals, 19: 20690
YOUNG, F. J., Prog. rpt. on instabilities in metal-vapor plasmas, 10–12/64, 19: 21490 (TID-21698)
YOUNG, Gale, Sea-water desalination with nuclear energy, 19: 21708 (ORNL-TM-465)
YOUNG, J., Neutron thermalization studies in graphite, 19: 21211
YOUNG, Tommy Lee, Concentration of Cs from pollucite, 19: 20044 (IS-T-1)
YOUNG, Wei, Magnetic fields, vagal inhibition, and acetylcholinesterase activity, 19: 21776 (UCRL-12389)
YOUNT, D. E., Test of $\Delta S/\Delta Q$ rule in K^0_{β} decay, 19: 20979
YOVANOVITCH, D. D., Production cross sections for $\pi^{\pm}$ and $K^{\pm}$ for 12.5-Bev protons on Be, 19: 21406
YU, C. P., Magneto-atmospheric waves in horizontally stratified conducting medium, 19: 21151
YU, Kuo-t'sai, Colorimetric determination of rare earth elements and Th in ore, 19: 19778 (JPRS-29037(p.56-68))
YU, Lieh, Bound state in superconductors with paramagnetic impurities, 19: 21191
YU, Wen-shi, Heat transfer to turbulent liquid metals in eccentric annuli, 19: 20123
YUAN, L. C. L., Observation of the low-energy Λ-p interaction, 19: 21034
YUBEREV, N. N., Behavior of Green function of finite-difference analog of Sturm-Liouville boundary-value problem, 19: 20451
YUCKER, W. R., Secondary nucleons produced in high-energy nuclear reactions, 19: 21242 (NP-14837)
YUDIN, E. V., Effects of x irradiation on frequency of genetic recombinations in *E. coli*, 19: 19537
YUDOVICH, L. A., Ionization in the F_2 layer, 19: 21129
YUKHNEVICH, A. V., Radiative recombination in Si and Ge associated with radiation defects, 19: 20627
YUKHNOVSKII, I. R., Mean energy of electron gas at absolute zero, 19: 20711

Z

ZAALBERG, O. Brocades, Allogenic chimeric bone marrow: capacity to repopulate the lymphatic tissue of irradiated syngeneic host, 19: 19646
ZACHARIASEN, F., Parity conservation and bootstraps, 19: 20991
ZACHVEJ, J., Influence of 19-norandrostenolone upon acute irradiation disease in rats, 19: 19624
ZACKAY, V. F., Superconducting properties of carbides and nitrides, 19: 20572
ZAGORITES, Harry A., Portable γ-intensity time recorder, 19: 20397
ZAHAVI, Elias, Magnetohydrodynamic generators of alternating current, 19: 20914
ZAIMIDOROGA, O. A., Nuclear form-factors in μ capture in He-3, 19: 21236 (JINR-P-1952)
ZAKREVSKII, S. V., Luminescence appearing in Na uranyl acetate irradiated laser beam, 19: 20010
ZALESKI, E., Measurement of coronary circulation with new isotope technique, 19: 19668
ZALKIN, Allan, Crystal structure of Cs aquopentachlororuthenate, 19: 19845 (UCRL-11828(p.146))
ZALKIN, Allan, Crystal structure of OsO_4, 19: 19846 (UCRL-11828 (p.158-9))
ZAMYATINA, V. A., Radiation synthesis of polymers based on dimethylphosphinoborine, 19: 19982
ZAMYATKINA, O. G., Impairment of synthesis of serum albumin in rat liver in acute radiation sickness, 19: 19603
ZANARINI, G., Rise time of pulses supplied by semiconductor detectors, 19: 20369
ZANE, J. O., Analysis of SNAPTRAN-3 destructive experiment, 19: 21719 (NAA-SR-9780)
ZANE, Ronald, Mossbauer effect instrumentation, 19: 20327 (UCRL-11828(p.221-2))
ZASIMCHUK, E. E., Parameters of recrystallization of Nb and W, 19: 20604
ZASTAWNY, A., New fast quenching circuit for self-quenched G-M counters, 19: 20349
ZAVADOVSKAYA, E. K., Stored energy of alkali-halide crystals following γ irradiation, 19: 19987
ZAVILGELSKII, G. B., Versene-protective action against uv damages of *Bacterium coli*, 19: 19638
ZAWADOWSKI, Alfred, Superconductivity and flux quantization, 19: 21173
ZDRAFCOVICI, R., Exposure of drugs to nuclear bomb explosion, 19: 20231
ZEITLER, E. H., High-voltage electron microscopy, 19: 20252 (CONF-640204(p.106-22))
ZEL'DINA, M. Yu., H_{α} radiation field in prominences, 19: 20776
ZEL'DOVICH, Ya. B., Newtonian and Einsteinian motion of homogeneous matter, 19: 20704
ZELLER, M., Neutron-neutron S-wave scattering length from reaction $\pi^- + d \rightarrow 2n + \gamma$, 19: 20995
ZEMACH, C., Parity conservation and bootstraps, 19: 20991
ZEMANY, P. D., X-ray emission analysis, 19: 19747 (CONF-650214-1)
ZEMLYANUKHIN, V. I., Complexing of Am with neutral organophosphorus compounds. II., 19: 20076
ZEMLYANUKHIN, V. I., Formation of transuranic nitrates with phosphorus compounds, 19: 20077
ZGANJAR, E. F., Anomalous E2 particle parameters in deformed nuclei, 19: 21399
ZHABIN, A. G., Mineralogy and geochemistry of rare elements (Urals), 19: 20190
ZHDANOV, A. P., Effect of polyethylene glycols on nuclear photographic emulsions, 19: 20014
ZHELEZNYAKOV, V. V., Negative absorption of Cherenkov radiation in an electron stream, 19: 20679
ZHIBRITSKII, V. K., Effect of N impurity on electron energy loss in nonequilibrium Ar–Cs plasma, 19: 21560
ZHIVOPISTSEV, V. P., Colorimetric determination of Ce, 19: 19819
ZHIVOPISTSEV, V. P., Extraction separation of Sc, 19: 20080
ZHIZHINA, G. P., Decay of peroxides in irradiated DNA solutions, 19: 19541
ZHUKOV, A. A., Space charge formation in h-f electric field in air, 19: 21576
ZHULINA, E. M., Effect of cosmic radiation on information reception aboard AES's and at ground points, 19: 20879
ZHURAVLEV, D. A., Nature of cosmic-ray particles beyond atmosphere, 19: 20893
ZHURAVLEV, V. K., Absorption of radiowaves by dielectric in radiation field, 19: 20629
ZHUZGOV, L. N., Correlation between variations of magnetic field and positive ions inside magnetosphere, 19: 21126
ZIEGLER, Charles A., X-ray analysis system with means to detect only coherently scattered x-rays, 19: 20135
ZIMMERMAN, C. A., Corrosion of type 316 stainless steel in NaK service, 19: 20472 (IDO-14651)
ZINK, William, Approximate, finite temperature, Thomas-Fermi potential, 19: 20808 (UCRL-12054-T)
ZOBEL, W., Spectra of γ rays produced by interaction of ~160-Mev protons with Be, C, O, Al, Co, and Bi, 19: 21243 (ORNL-3506)
ZOLOTNIKOVA, G. P., Change in cholinesterase activity after immuniza-

tion and irradiation, 19: 19609
ZOLTAN, L., Isotope hypophysectomy, 19: 19664
ZORIN, E. I., Depth of penetration and distribution of radiation damage when Ge is bombarded with Ar and N ions, 19: 20625
ZSEBOK, Z. R., Sulfhydryl compounds as radioprotective substances, 19: 19640
ZUCKERMANN, M. J., Effect of impurities on superconducting transitions, 19: 21181
ZUDANS, Zenons, Design of Hallam moderator element. I., 19: 21680 (COO-1402-1)
ZUMINO, B., Gauge invariance and mass of vector bosons, 19: 20934 (NP-14829)
ZUND, Joseph David, Degenerate fields with twisting rays, 19: 21120
ZUPPINGER, A., Problems of radiobiology in radiotherapy, 19: 19702
ZWICKER, Earl, Effects of x irradiation on self-friction of KCl, 19: 20011
ZYBINA, D. L., Decay of peroxides in irradiated DNA solutions, 19: 19541
ZYKOV, S. I., Absolute age of pegmatite, 19: 20176
ZYKOV, V. G., Spectroscopic investigation of plasma in colliding bursts, 19: 21567
ZYKOV, V. G., Capture of plasma in magnetic trap with fields, 19: 21568
ZYSIN, Yu. A., Fission-product yields and mass distribution, 19: 21445
ZYSIN, Yu. A., High-current air-core betatrons, 19: 20740

SUBJECT INDEX

Main entries in this index are generally specific materials, things, and processes. These are followed by modifiers that describe the properties of, and processes applied to, the main entries.

The number preceding the colon is the *NSA* volume number, and the number following is the abstract number. The designation (R) following the abstract number indicates that the abstract is of a progress report; (P) indicates a patent; and (T) indicates a translation. Abstracts for reports other than progress reports carry no letter designation. References to report numbers, where appropriate, are included after the abstract number of the citation. Published literature (journal article or book) is identifiable by the absence of a report number.

The user should bear in mind that the ideas presented in the original literature, rather than key words, have been indexed. The indexers have tried to select what seemed the most probable and logical place to look for typical information. Since it is not possible to anticipate where a user would look for information, numerous cross references are included to assist him in his search.

Experience in using an index of this type will be the best guide in obtaining the desired information, and a consideration of synonymous or closely related terms will prove valuable.

Information must be so indexed as to be of the greatest use to the greatest number of users. This requires that a topic be indexed to headings that most specifically describe it and not ordinarily to the headings that describe its ultimate use, nor to the general class headings that include the specific headings. For example, information on the treatment of thyroid disease with I-131 would be indexed under Thyroid Diseases and under Iodine Isotopes I-131, but not necessarily under Radiotherapy. A study of the effects of x radiation on hair would be indexed under both X Radiation and Hair.

The broad, general class headings are used only for general information or for comprehensive reports or articles.

Subject Heading Styles

Generally, the direct form of subject entry is used rather than inverted headings or, in some cases, subheadings; e.g., Amino Acids rather than Acids, amino; Helium Isotopes He-4 rather than Helium—isotopes He-4 or Helium—He-4 isotopes. Note, however, that in some cases modifying terms are used parenthetically in preference to a more direct type of entry which would result in the scattering of information. Organic compounds, however, are usually entered in the index in the inverted form so that substituted compounds can be listed near the parent compound; e.g., Benzene, Bromo- rather than Bromobenzene. In general, the style of nomenclature used is that of *Chemical Abstracts*, except that some items listed in that publication as subheadings are elevated to form part of the main heading; e.g., Butyric Acid, Methyl Ester rather than Butyric Acid—methyl ester.

Alphabetization

Main headings are arranged according to the widely accepted word-by-word alphabetic system. A parenthetic qualifier following a main heading is disregarded in alphabetizing unless there are two or more headings identical except for the parenthetic qualifier, in which case the qualifier determines the order. Headings involving Greek letters are arranged as if the names of the letters were spelled out, e.g., Mesons (π), Mesons (ξ).

Nomenclature of Inorganic Compounds

Inorganic compounds are indexed in the direct form, listing cations in the order of increasing valence in the case of polycationic salts of varying valence and in alphabetic order for polycationic salts in which all cations have the same valence; e.g., Sodium Aluminum Silicates and Potassium Sodium Sulfates.

Multicomponent Systems

Multicomponent alloys, except well-known trade names are indexed under each element in the alloy.

Example: Aluminum–Chromium Alloys are indexed

ALUMINUM ALLOYS
Al–Cr ...
CHROMIUM ALLOYS
Al–Cr ...

Well-known alloys such as Hastelloy are indexed directly. Cross references appear in the index cumulations. Multicomponent systems of elements are indexed similarly.

Example: Silicon–Tungsten Systems are indexed

SILICON SYSTEMS
Si–W ...
TUNGSTEN SYSTEMS
Si–W ...

Multicomponent systems of compounds are similarly indexed under the compound.

Physical States of Materials

Specification of the physical state of the material, if other than normal, is included in the modifying phrase.

Modifying Phrases (Subheadings)

Whenever it appears that such information would be useful, descriptive phrases (modifiers), rather than ordinary subheadings, are used under the main headings to give a better indication of the material covered in an abstract. Such phrases are written so that the idea considered most important is presented first. However, when using this index, the reader is advised to scan all modifiers under a main heading to determine whether any abstracts in addition to the most obvious should be consulted for the desired information. Many of the modifiers are designed to be read in inverted order or to be read with the main heading inserted at the position of the comma in order to obtain a meaningful phrase; e.g., Uranium—allotropic transformation temperatures of, effect of cooling rate on is read "effect of cooling rate on allotropic transformation temperatures of uranium." In many cases, the prepositions have been omitted from such phrases provided no ambiguity results from the omission.

For entries concerned with physics, if the modifier does not indicate whether the reference is experimental or theoretical, a symbol E or T or E/T is given.

Conferences

Proceedings of conferences and conference papers are included in the Report Number Index.

A

ABDOMEN
radiodiagnosis of infant, protective measures for, 19: 19677
radiotherapy of cancer of, method for intralymphatic, 19: 19658
ABSTRACTS
on radioinduced graft polymerization on cellulose, 19: 19960 (VDDIT-93)
ACCELERATORS
beam injection systems for, design, (E), 19: 20737 (UCRL-11955)
ion preaccelerators and sources for, (E), 19: 20720 (BNL-8982)
performance of electrostatic, for variably charged particles, (T), 19: 20722 (JINR-D-1946)
principles and uses of, review on, 19: 20742
radiation protection in use of electron, 19: 20213
space charge distribution in uniformly charged circular cylinder for, 19: 20739
use for food processing, 19: 20422
uses as radiation sources in industry and research, 19: 20408
ACETATES
effects on spectrophotometric determination of zinc using 1-(2-thiazolylazo)-2-naphthol, 19: 19814
ACETIC ACID
effects on polarographic determination of uranium, 19: 19797
ACETIC ACID, [(CARBOXYMETHYL)IMINO] BIS[[ETHYLENE [(CARBOXYMETHYL)IMINO] ETHYLENE] NITRILO] TETRA-
analytical uses as titrimetric reagent, 19: 19813
ACETIC ACID, [(CARBOXYMETHYLIMINO) BIS(ETHYLENENITRILO)] TETRA-
analytical uses in determination of rare earths, thorium, titanium, and zirconium, 19: 19802
ACETIC ACID, CYANO-
radiolysis of single crystal, ESR spectra of free radicals produced by gamma, 19: 20006
ACETIC ACID, [ETHYLENEBIS[(CARBOXYMETHYLIMINO)ETHYLENE-NITRILO]]TETRA-
analytical uses in determination of rare earths, thorium, titanium, and zirconium, 19: 19802
ACETIC ACID, (ETHYLENEDIAMINE) TETRA-
analytical uses in determination of magnesium, uranium, and zinc, 19: 19779
analytical uses in determination of rare earths, thorium, titanium, and zirconium, 19: 19802
effects on spectrophotometric determination of zinc using 1-(2-thiazolylazo)-2-naphthol, 19: 19814
preparation of chromium-51-labeled, use as tracer for gastrointestinal function studies in animals, 19: 20026
protective effects against uv radiation damage in *E. coli* bacteriophages, 19: 19638
solvent properties for beryllium hydroxide purification, 19: 20070
ACETIC ACID, (ETHYLENEDIAMINE) TETRA- COMPLEXES
with long-lived fission products, electrodialytic migration, 19: 20052 (ORNL-TM-1035)
ACETONE
effects on radioinduced carbon dioxide-graphite reactions, (E), 19: 19953 (AERE-R-4201)
effects on stability of polonium chloride complexes, 19: 19906
ACETONE, THENOYLTRIFLUORO-
reactions with protactinium hydroxide complexes, 19: 20056
solvent properties for protactinium, 19: 20055
solvent properties for protactinium, 19: 20063
4-methyl-2-pentanone–thenoyltrifluoroacetone, use in preparation of pure potassium chloride, 19: 19843 (ORNL-TM-1071)
ACETONITRILE
amino, effects on bone formation in mice, 19: 19471(R) (ANL-6938 (p.162-78))
effects on ionic decomposition of *t*-butylperoxy formate, 19: 19948
ACETYLENE
conversion to benzene for radiocarbon dating, using cobalt molybdate alumina catalyst, 19: 19944 (ORINS-50)
effects on radioinduced carbon dioxide-graphite reactions, (E), 19: 19953 (AERE-R-4201)
radiation effects of electron bombardment on ion-molecule reactions in, 19: 19988
spectra of solid deuterated and normal, infrared, 19: 19935
yields in carbon-11 recoil reactions with hydrocarbons, 19: 20018
ACTINIUM
electrodeposition on platinum, conditions for quantitative, 19: 19902
ACTINIUM ISOTOPES Ac-222
alpha decay, (E), 19: 21418
ACTINIUM ISOTOPES Ac-224
alpha decay, (E), 19: 21418
ACTINIUM ISOTOPES Ac-226
alpha decay, (E), 19: 21418
ACTINIUM ISOTOPES Ac-228
content in blood and bones of humans injected with thorotrast, 19: 19497(R) (ANL-6938(p.127-39))
content in tissue of rats injected with thorotrast, 19: 19497(R) (ANL-6938(p.127-39))
ACTIVATION ANALYSIS
counting losses in, statistical analysis of, 19: 19766(R) (TEES-2671-4(Chap.3))
development of automated, 19: 19763(R) (TEES-2671-4)
development of automated, 19: 19764(R) (TEES-2671-4(Chap.1))
development of neutron-, for potassium analysis for oxygen, (E), 19: 19751 (GA-5982)
gamma spectra in, reduction of, 19: 19767(R) (TEES-2671-4(Chap.4))
industrial uses of, book, 19: 20417
interference in, removal of sodium, 19: 19768(R) (TEES-2671-4 (Chap.6))
methods of, review of, 19: 19822
of rat tissues, 19: 19601
of trace elements in normal and tumor tissues, 19: 19793
spectra in, computer program for pulse-height, 19: 19770(R) (TEES-2671-4(Chap.8))
statistical procedures for, 19: 19769(R) (TEES-2671-4(Chap.7))
substoichiometric separation in, theory and uses of, 19: 19783
system for, design and operation of computer-coupled, 19: 19765(R) (TEES-2671-4(Chap.2))
use of automatic, in petroleum exploration, 19: 19773 (TID-20467)
uses for determining impurities in metals, 19: 19796
ACTIVATION DETECTORS
development of, with reduced Compton background, 19: 19767(R) (TEES-2671-4(Chap.4))
ADRENAL GLANDS
radiation effects on oxygen assimilation, steroid hormone content, and weight of, 19: 19584
ADRENOCORTICOTROPIC HORMONE
effects on bone marrow and organ graft tolerance, 19: 19588
AEROSOLS
analysis for manganese, activation, 19: 19771(R) (TEES-2671-4 (Chap.9))
light scattering by transparent Mie-particle, asymmetry in, (T), 19: 20822
preparation of radioisotope-labeled silver iodide, sodium chloride, and sulfuric acid, 19: 20027
sorption of radioactive, by chlorinated polyvinyl chloride filters, 19: 20228
AGE ESTIMATION
isotope effects in, by carbon-14-labeled benzene synthesis, 19: 20179
lead isotope method of, for pegmatites, 19: 20176
methods for marine carbonate, comparison of radiometric, 19: 20181
nuclear methods for, 19: 19822
radiocarbon dating, method for benzene synthesis for liquid-scintillation, 19: 19944 (ORINS-50)
AIR
absorption coefficients at high temperatures, molecular band contribution to optical, (T), 19: 20832
carbon arcs in, temperature profile of low-current, (E), 19: 21498
effects on radioinduced carbon dioxide-graphite reactions, (E), 19: 19953 (AERE-R-4201)
flow in thermal entrance region of heated tubes, effects of large temperature gradients on turbulent, 19: 20117 (SU-247-4)
gamma transport in, near air/ground interface, (T), 19: 20163 (RRA-M42)
ionization by electromagnetic shock, probe response to, (E), 19: 20841
neutron transport in, analysis of fast, (E), 19: 21199 (CEX-65.02)
opacity and thermodynamic properties at high temperatures, (T), 19: 20829
plasma of, recombination in, (E), 19: 21572
radiation absorption coefficient of, photoionization contribution to, (T), 19: 20830
radiation absorption coefficient of, atomic line contribution to, (T), 19: 20831
spectra of, between shock waves, (E), 19: 20676
uranium dispersion in plant, relation of particle size and human urinary excretion to, 19: 19478
AIRCRAFT
fallout contamination on, 19: 20208
ALANINE
protective effects against radiation damage in Ehrlich ascites carcinoma cells, 19: 19636
radiolysis in frozen aqueous solutions, 19: 20012
ALARM SYSTEMS

description of radiochemical processing plant, for contamination and radiation, 19: 20203 (ORNL-TM-988)
performance in mixed gamma and neutron fields, 19: 20330(T) (AEC-tr-6547)
ALBUMINS
radiation effects on synthesis of rat liver serum, effects of food ingestion on, 19: 19603
radiation effects on thermoluminescence, 19: 19983
use of iodine-131-labeled human serum, for liver-spleen photoscanning, 19: 19710
ALGAE
radiation effects on penicillin production by *Penicillium nigricans*, 19: 19556
ALKALI METAL CHLORIDES
radioinduced formation of sulfur-35 in, chemical effects from, 19: 20004
ALKALI METAL HALIDES
light refraction in crystals of, 19: 20667
positron annihilation reactions in, polaron theory of, 19: 20820
radiation effects on, mechanisms in, 19: 20019
ALKALI METAL HYDRIDES
precipitation in potassium–sodium alloy, 19: 20478(R) (ORNL-3618)
ALKALI METALS
distillation of, vacuum unit for, 19: 20473(R) (NASA-CR-54269)
radiant energy flux from plasma seeded with, in infinite-plane parallel enclosure, (T), 19: 21468 (BSD-TDR-64-164)
ALKALINE EARTH METALS
separation of strontium from mixtures of, 19: 19789
ALKANES
light refraction in, (E), 19: 20667
radiolysis of, thermal transformations and yields in, 19: 19980
ALKANES, DIPHENYL-
intermolecular excimer formation in, 19: 19956(R) (ANL-6938(p.27-35))
ALKANES, TRIPHENYL-
intermolecular excimer formation in, 19: 19956(R) (ANL-6938(p.27-35))
ALLANITES
age estimation in pegmatites by lead isotope method, 19: 20176
ALLANTOIN
radiation effects on rat urinary excretion of, protective effects of casein diets against, 19: 19628
ALLOYS
development of high-strength, for naval structures, 19: 20462(R) (NRL-6258)
preparation directly from low-grade ores by radiant heating using light from reactor, 19: 21710
properties of superconducting, data on, 19: 21187
purification by transfer of solutes to liquid scrub alloy in fused salt, 19: 20066
superconducting critical fields of, (T), 19: 21192
ALPHA BEAMS
characteristics of, from 88-inch cyclotron, 19: 20736(R) (UCRL-11828 (p.236-41))
ALPHA DECAY
barrier penetration factors for, (T), 19: 21411
ALPHA PARTICLES
charge transfer from hydrogen atoms to, calculation of, 19: 19937
detection and measurement of, design of air pulse chamber for, 19: 20383
detection and measurement of, sensitivity of nuclear emulsion for, 19: 20014
detection of, gas scintillation detector for, 19: 20361
dosage to superficially contaminated tissues, theoretical calculation of, 19: 19482
effects on length changes in gold, 19: 20646
effects on luminescence of bibenzyl and pyrene, 19: 19963
emission in proton reactions (p,α) and (p,γ) with lithium-7 at 0.4 to 2.4 Mev, spectra of, 19: 21342
emission in proton reactions (p,$\alpha\gamma$) with lithium-7 at 440 kev, spectra of, 19: 21357
reactions (α,α') with oxygen-16 and silicon-28, alpha-gamma angular correlations in, 19: 21457
reactions (α,d) with carbon-12, wave functions for, (E/T), 19: 21266(R) (UCRL-11828(p.108-9))
reactions (α,n) with beryllium-9 at 1.9 to 4.5 Mev, polarization from, (E), 19: 21307
reactions (α,2nγ) and (α,4nγ) with tellurium isotopes at 34 to 52 Mev, collective levels from, (E), 19: 21316
reactions with argon–nitrogen mixtures, scintillation spectra from, 19: 20313(R) (ANL-6938(p.9-20))
reactions with thorium-232 and uranium-238 at 33 Mev, tellurium-131 and -133 isomer pair yields from fission, (E), 19: 21390
scattering by iron-56 and zinc isotopes, angular distribution of elastic, 19: 21459
scattering by nuclei, study of phase rule in angular distributions, (E/T), 19: 21269(R) (UCRL-11828(p.132-3))
scattering by nuclei at 3.1 Mev, conversion coefficients and mixing ratios for rotational transitions in inelastic, (E), 19: 21324
scattering by plutonium -240 and uranium-238, fission in inelastic, (E), 19: 21262(R) (UCRL-11828(p.84-6))
scattering by rotational bands in neon-20 at 50.9 Mev, inelastic, (E/T), 19: 21267(R) (UCRL-11828(p.113-16))
scattering by zirconium isotopes, collective excitation in elastic, (E) 19: 21386
scattering from surfaces, chemical analysis by, (E/T), 19: 19795
ALPHA SOURCES
monitoring atmospheric, device for, 19: 20381
ALUMINUM
analysis for hafnium or zirconium using catechol violet, colorimetric, 19: 19780
analysis for impurities by activation methods, 19: 19796
analysis for trace elements, activation, 19: 19775(R) (UCRL-11828 (p.197-9))
coating with niobium, development of methods for, 19: 20456 (EUR-2111.d)
deposition on vanadium-base alloys for oxidation protection, 19: 20459(R) (IITRI-B6019-6)
determination by titration, suitability of tetraethylenepentamine hepta-acetic acid for, 19: 19813
determination in alloys with iron, nickel, and uranium, correction factors for x-ray micro-, 19: 19746 (CEA-R-2728)
determination in ppm range by d-c arc excitation, spectrochemical, 19: 19827
determination in SAP powders by different laboratories, statistics on, 19: 19750 (EUR-2286.f)
determination in uranium and its compounds and alloys, methods for, 19: 19823
dispersion of uranium dioxide in, 19: 20539(P)
effects on determination of zirconium using arsenate method, 19: 19818
effects on phosphorus determination by neutron activation methods, 19: 19828
effects on strength of thorium at high temperatures, 19: 20560 (ORNL-3777)
electromagnetic wave absorption and scattering by particles of, (T), 19: 20677
electron and ion emission from foils of, laser-induced, (E), 19: 20814
electron diffuse scattering at 51 kev, temperature dependence of, (E), 19: 20867
meson (K^+) absorption at 4.75 Bev/c, cross sections for, (E), 19: 21431
meson (π^-) reactions (π^-,nγ) with, energy spectra from, (E), 19: 21315
meson (π^+) absorption at 2.72, 3.70, and 4.75 Bev/c, cross sections for, (E), 19: 21431
neutron elastic scattering at 85 to 700 kev, differential cross sections for, (E), 19: 21298
neutron inelastic scattering by powdered, distributions from slow, (E), 19: 20551 (IDO-17063)
nuclear spin relaxation in superconducting, phonon effects on, (T), 19: 21174
nucleon reactions at high energies, secondary nucleon yields from, (E/T), 19: 21242 (NP-14837)
proton range-energy relations in, (E), 19: 20806 (ORNL-3702)
proton reactions at 160 Mev, 0.6- to 11-Mev gamma rays from, (E), 19: 21243 (ORNL-3506)
proton reactions at 160 Mev, secondary nucleon spectra from, (E/T), 19: 21244 (ORNL-P-844)
proton reactions at 30–40 Mev, helium-3 and tritium production in, 19: 21438
radioinduced hardening of single crystals of, fast neutron, 19: 20641
response of buried hollow cylinders of, to quasi-static overpressures, 19: 20136 (AFWL-TDR-64-13)
separation from plutonium processing solutions, 19: 20065
separation from scandium by solvent extraction of diantipyrinylmethane complex, 19: 20080
sodium-24 ranges in, interatomic potential from, (T), 19: 20837
ultrasonic hardening of single crystals of, 19: 20641
uses in metallothermal reduction of europium oxide, 19: 20533
welding of pipes and plates of, Hanford procedures for, 19: 20524 (TID-20625(Vol.IV)(Rev.I))
x-radiation scattering by, Hartree-Fock calculations of incoherent, 19: 20824
ALUMINUM ALLOYS
corrosion in reactors, 19: 20488
deposition on niobium alloys for oxidation protection at 2300°F, 19: 20483 (SCNC-318)
fracture tests of, 19: 20462(R) (NRL-6258)

welding of pipes and plates of, Hanford procedures for, 19: 20524 (TID-2625(Vol.IV)(Rev.I))
Al–Cr–Fe–Y, oxidation mechanism, 19: 20470 (GE-TM-63-7-3)
Al–Cr–Fe–Y, properties of oxidation-resistant, 19: 20470 (GE-TM-63-7-3)
Al–Fe, internal friction measurements at high temperatures, 19: 20245 (CEA-R-2718)
Al–Fe, magnetic fields at iron-57 nuclei in, (E), 19: 20578
Al–Li, nondestructive testing of control rods and targets of, 19: 20126 (DPSPU-65-30-11)
Al–Li, radiation effects on helium precipitation in, 19: 20613 (CEA-R-2529)
Al–Mo–Sn–Ti–V–Zr, beta transus temperature of, 19: 20462(R) (NRL-6258)
Al–Mo–Sn–Ti–V, beta transus temperature of, 19: 20462(R) (NRL-6258)
Al–Mo–Ti, beta transus temperature of, 19: 20462(R) (NRL-6258)
Al–Mo–Ti–V, mechanical properties of diffusion-bonded plates of, 19: 20462(R) (NRL-6258)
Al–Mo–Ti–V, mechanical properties of solution-annealed and aged T-19, 19: 20462(R) (NRL-6258)
Al–Mo–Ti–Zr, beta transus temperature of, 19: 20462(R) (NRL-6258)
Al–Nb, oxidation kinetics at 500 to 900°C, 19: 20494
Al–Nb, preparation and properties of $NbAl_3$ for possible use as reactor material, 19: 20464 (SCNC-316)
Al–Nb–Ta–Ti, fatigue crack propagation in, study of low-cycle, 19: 20462(R) (NRL-6258)
Al–Nb–Ta–Ti, mechanical properties of, effects of processing on, 19: 20462(R) (NRL-6258)
Al–Sn, phase studies, 19: 20596
Al–Sn–Ti–V, beta transus temperature of, 19: 20462(R) (NRL-6258)
Al–Sn–Ti–Zr, mechanical properties of diffusion-bonded plates of, 19: 20462(R) (NRL-6258)
Al–Ti–V, fatigue crack propagation in, study of low-cycle, 19: 20462(R) (NRL-6258)
Al–Ti–V, mechanical properties of diffusion-bonded plates of, 19: 20462(R) (NRL-6258)
Al–Ti–V–Zr, beta transus temperature of, 19: 20462(R) (NRL-6258)
Al–Ti–Zr, mechanical properties of diffusion-bonded plates of, 19: 20462(R) (NRL-6258)
Al–U, nondestructive testing of fuel tubes of, 19: 20126 (DPSPU-65-30-11)

ALUMINUM ISOTOPES Al-26
beta decay of, CVC theory and ft values for, (T), 19: 21416
content in iron meteorites, (E), 19: 20760

ALUMINUM ISOTOPES Al-27
energy levels of, nucleon separation energy in 1p and 1s, 19: 21400
helium-3 elastic scattering at 5.5 to 10.0 Mev, angular distributions from, (E), 19: 21328
performance in nuclear gyroscopes, (T), 19: 20279 (RTD-TDR-63-4001)
proton reactions (p,3n) at 97 Mev, (E), 19: 21297
proton scattering at 7 Mev, polarized, (E), 19: 21295

ALUMINUM NITRATES
effects on dissolution of plutonium dioxide and uranium dioxide pellets in nitric acid, 19: 20050 (ORNL-3695)
solubility in nitric acid solutions, 19: 20042(R) (IDO-14646)
$Al(NO_3)_3$–HNO_3–H_2O, distribution coefficients for plutonium between anion exchange resin and, calculation, 19: 20046 (LA-3188)

ALUMINUM OXIDES
determination in SAP powders by different laboratories, statistics on, 19: 19750 (EUR-2286.f)
effects on thermal stability of zirconium oxide, 19: 20585
oxygen isotopic exchange with molecular oxygen, 19: 19872
particle size distribution in suspensions of powders of, diffusion technique for determining, 19: 19901
removal of calcined, from waste calcination facility, 19: 20042(R) (IDO-14646)
sintering characteristics of, effects of magnesia on, 19: 20461 (NP-14893)
spectra of suspensions of, in thin polyethylene films, infrared transmission, 19: 19917
Al_2O_3–BaO–CaO–MgO–SiO_2, presintering of compositions in, 19: 20461 (NP-14893)
Al_2O_3–CoO–MoO_3, catalytic properties for benzene synthesis from acetylene, for radiocarbon dating, 19: 19944 (ORINS-50)
Al_2O_3–Cu, sintering of dispersion compacts of, near 1000°C, 19: 20465 (TID-20344)
Al_2O_3–MgO–SiO_2, devitrification, 19: 20461 (NP-14893)
Al_2O_3–PuO_2, phase diagrams, 19: 20589

ALUMINUM STEEL
welding of, for Tokai-mura Power Reactor, 19: 21700

ALUMINUM SYSTEMS
Al–Polyethylene–U, neutron self-shielding in closely packed slab lattices of, (E), 19: 21636 (CONF-654-32)

ALUMS
alums–U, boric acid–U, phosphorescence in, 19: 19919

AMERICIUM
separation from nitric acid solutions by solvent extraction using dialkyl phosphoric acid, 19: 20075
separation from nitric acid solutions by solvent extraction using organophosphorus compounds, 19: 20076
solvent extraction by tridodecylamine hydrochloride, 19: 20039 (EUR-2246.e)
solvent extraction from chloride solutions by tridodecylamine hydrochloride, mechanism, 19: 20038 (EUR-2245.e)

AMERICIUM ISOTOPES Am-241
purification by chromatographic ion exchange, flowsheet for, 19: 20041 (HW-84352)
separation from power reactor fuels, economics of, 19: 20036 (BNWL-25)
waste fixation of raffinate solutions containing, 19: 21750 (LA-3150)

AMERICIUM ISOTOPES Am-242
separation from power reactor fuels, economics of, 19: 20036 (BNWL-25)

AMERICIUM ISOTOPES Am-243
separation from power reactor fuels, economics of, 19: 20036 (BNWL-25)

AMES LAB., AMES, IOWA
environs monitoring, 1964, 19: 20156 (IS-1098)

AMIDE POLYMERS
positron lifetime in nylon-6, (E), 19: 21044

AMINES
development of gold-198, for industrial tracers, 19: 20030
use for metal extraction, review, 19: 20053 (UJV-1202/64)

AMINO ACIDS
protective effects against radiation damage to serum albumin in rat liver, 19: 19603
radiation chemistry of, 19: 19969
radiolysis of frozen aqueous solutions of, 19: 20012
radiosensitivity of, effects of SH-inhibitors on, 19: 19621

AMMONIA
dissociation constants of, effects of isotopic difference of, 19: 20433
effects on radioinduced carbon dioxide-graphite reactions, (E), 19: 19953 (AERE-R-4201)
ionization by electron impact, appearance potential for doubly charged molecule ions in, 19: 20807(R) (UCRL-11828(p.201-4))
radical anions in liquid, electron spin resonance spectra of, 19: 19945 (UCRL-11864)
radiolysis of adsorbed, EPR study of gamma, 19: 19984

AMMONIUM ACID PHOSPHATES
analysis for phosphorus by neutron activation methods, 19: 19828

AMMONIUM CERIUM NITRATES
effects on dissolution of plutonium dioxide pellets in nitric acid, 19: 20050 (ORNL-3695)

AMMONIUM COBALT SULFATES
cobalt-57 Mossbauer spectra in hydrated, (E), 19: 20032

AMMONIUM COMPOUNDS, QUATERNARY
complexes of tetramethylammonium salt with molybdenum salt, bonding in, 19: 19841 (MIT-1965-18)
reactions of 2-phenylethyltrimethyl ammonium iodide with ethoxide and hydroxide ions, deuterium isotope effects on, 19: 19947
tetradecylammonium complexes with uranyl perchlorates, spectra of, infrared, 19: 19910

AMMONIUM FLUORIDES
reactions with molybdenum, tungsten, and uranium oxides in aqueous solutions, 19: 19913

AMMONIUM PHOSPHOMOLYBDATES
analytical uses in determination of cesium-137, 19: 19805

AMMONIUM URANATES
reduction of, for preparation of granulated uranium oxide, 19: 20538(P)

AMMONIUM URANYL FLUORIDES
preparation by dissolution of uranium dioxide in aqueous solutions of ammonium fluoride, 19: 19913

AMPLIFIERS
description of modular-packaged linear, 19: 20287(R) (UCRL-11828 (p.230-2))
description of semilogarithmic, 19: 20287(R) (UCRL-11828(p.230-2))
design, 19: 20321 (ISS-64/28)

ANALYSIS
beta reflection determination of end points in precipitation titrations, 19: 19787
book: *Nuclear Techniques in Analytical Chemistry*, 19: 19822
radiochemical, substoichiometry in, 19: 19783
radiometric, methods and uses in combination with thin-layer

chromatography, 19: 19808
ANEMIA
effects on erythropoietin content of blood plasma, 19: 19499(R) (NP-14899)
radiodiagnosis of hemolytic, by photoscanning of spleen using chromium-51-labeled heat-treated erythrocytes, 19: 19725
radioinduced by Thorotrast injections, 19: 19567
ANEMOMETERS
design for cooling and heat transfer research, 19: 20098(R) (TID-21633)
design of high-torque low-inertia, 19: 20655(R) (ANL-6938(p.252-6))
wind turbulence dissipation by, mathematical analysis of, 19: 20654(R) (ANL-6938(p.242-51))
ANILINE
ionization by electron impact, appearance potential for doubly charged molecule ions in, 19: 20807(R) (UCRL-11828(p.201-4))
solvent properties for uranium, 19: 19817
ANIMAL CELLS
effects of embryonic blood-forming liver, on radiation sickness in rats, 19: 19637
globulin production by fetal hemopoietic, review on, 19: 19468
immune reactions of virus-infected, in tissue cultures, 19: 19549
radiation effects on, small-dose, 19: 19516
radiation effects on, 19: 19562
radiation effects on interferon synthesis and virus plaque development in rat embryo cells, 19: 19563
radiation effects on physicochemistry of DNA in, review on, 19: 19566
radiation effects on RNA metabolism and synthesis in HeLa tumor cells, 19: 19602
radiation effects on replication of, 19: 19613
radiation effects on, 19: 19614
radiation effects on Ehrlich ascites carcinoma protective effects of α- and β-alanine and arginine against, 19: 19636
recovery of irradiated, effects of heavy water, nitrogen, and puromycin on sea urchin, 19: 19496(R) (ANL-6938(p.49-56))
tritium incorporation in, biological effects of beta particles on, 19: 19515
ANIMALS
radiation effects on, small-dose, 19: 19516
radiation injuries, role of glucose metabolism in, 19: 19538
radioactivity of marine, in contaminated lake, 19: 20220
radioisotope content in marine, effects and source of artificial and natural, 19: 20226
ANION EXCHANGE MATERIALS
deuterium exchange with water, 19: 19865
distribution coefficients for plutonium between aluminum nitrate–nitric acid solutions and Dowex 1 × 4, calculation, 19: 20046 (LA-3188)
performance of fixed-bed nitrate-form Dowex 1 × 4 column for plutonium sorption from nitric acid solution, calculation, 19: 20045 (LA-2838)
ANIONS
dissociation potential in plasma, (T), 19: 21558
ANTENNAS
development of blast-resistant, for 1- to 50-psi overpressures, (E), 19: 20109(R) (CER-D1703)
ANTHRANILIC ACID
asthranilic acid–boric acid, phosphorescence in, 19: 19919
ANTIBARYONS
interactions with baryons, calculation of cross sections for, 19: 21068
ANTIBIOTIC THERAPY
of infectious complications of radiation sickness in rabbits and rats, 19: 19622
ANTIBIOTICS
resistance of bacteria to, effects of ultraviolet radiation in *Staphylococcus aureus*, 19: 19531
resistance of bacteria to, effects of ultraviolet radiation in *Staphylococcus aureus*, 19: 19532
ANTIBODIES
labeled, preparation and use in electron microscopic studies, 19: 19465
radiation effects on formation of, 19: 19589
ANTIFERROMAGNETIC MATERIALS
properties of, apparatus for measuring, 19: 21759(R) (NYO-3402-1)
ANTIHYPERONS (Λ)
production in p$\bar{p}$ interactions, charge conjugation conservation in, (T), 19: 20977
ANTIHYPERONS (Ξ^+)
decay of, branching ratios for leptonic, (T), 19: 21019
ANTIMONY
analysis for impurities by activation methods, 19: 19796
determination as impurity in pure bismuth by activation methods, 19: 19796
effects on radioinduced defects in n-type germanium, 19: 20619 (NP-14883)
ANTIMONY ALLOYS
Sb–Dy, magnetic properties of, (E), 19: 20597
Sb–Er, magnetic properties of, (E), 19: 20597
Sb–Gd, magnetic properties of, (E), 19: 20597
Sb–Ho, magnetic properties of, (E), 19: 20597
Sb–Nd, magnetic properties of, (E), 19: 20597
Sb–Tb, magnetic properties of, (E), 19: 20597
ANTIMONY ISOTOPES Sb-119
energy level scheme, 19: 21450
fission barrier of compound nucleus, (E), 19: 21261(R) (UCRL-11828(p.81-3))
ANTIMONY ISOTOPES Sb-121
energy level transitions in, retardations in l-allowed M1, (T), 19: 21323
Mössbauer effect in, (E), 19: 21375
ANTIMONY ISOTOPES Sb-122
magnetic fields acting on, in ferromagnetic materials, 19: 20578
ANTIMONY ISOTOPES Sb-124
content in stratosphere, 19: 20657(R) (DASA-1309)
production using Rossendorf Reactor in East Germany, 19: 20436
ANTIMONY ISOTOPES Sb-125
content in stratosphere, 19: 20657(R) (DASA-1309)
decay of, nuclear orientation study of levels in, (E), 19: 21256(R) (UCRL-11828(p.58-62))
ANTINUCLEONS
interactions with nucleons, phase of forward amplitudes for, (T), 19: 21010
interactions with nucleons, selection rules for final states in, (T), 19: 21023
interactions with nucleons at rest, SU(12) symmetry model predictions for annihilation, (T), 19: 21039
interactions with nucleons, Jacob-Wick method for scattering amplitude in, (T), 19: 21052
ANTIPARTICLES
detection of antimatter in universe, optical method for, 19: 20754
symmetry groups for particle-antiparticle algebras, supermultiplet structure and SU(6), 19: 21015
ANTIPROTON BEAMS
optical systems for 5-Gev, magnetic field distributions in, (E), 19: 20723 (JINR-P-1945)
ANTIPROTONS
interactions with protons in universe, optical method for protonium detection in, 19: 20754
interactions with protons, Feynman diagrams for cross sections of elastic, (T), 19: 20954
interactions with protons at 4 Bev/c, diffraction slope at infinite energy in elastic, (E/T), 19: 20976
interactions with protons, charge conjugation conservation in strong, (T), 19: 20977
interactions with protons, multimeson resonances in annihilation, (E), 19: 20993
interactions with protons, M(12) symmetry model testing by annihilation, (T), 19: 21033
interactions with protons, U(12) symmetry predictions for annihilation, (T), 19: 21036
ANTIPYRINE, 4,4'-METHYLENEDI-
solvent properties for scandium, 19: 20080
ANTIPYRINE, 4,4'-(*p*-NITROBENZYLIDENE)DI-
analytical uses in determination of cerium, 19: 19819
ARCO CHEMICAL PLANT
operation, April-June 1964, 19: 20042(R) (IDO-14646)
ARGENTINA
fallout monitoring, 1964, 19: 20165(R) (TID-21711)
ARGININE
protective effects against radiation damage in Ehrlich ascites carcinoma cells, 19: 19636
ARGON
absorption coefficient from 3.6 to 10×10^3 Å, (T), 19: 20833
argon ion reactions at 25 kev, discrete Q values in, (E), 19: 20846
argon-ion reactions at 100 to 400 kev, excitation in, (E), 19: 20862
charge exchange in, atom-ion resonance, (T), 19: 19931
collisions with excited cyclopropane, energy transfer in, 19: 19938
effects on radioinduced carbon dioxide-graphite reactions, (E), 19: 19953 (AERE-R-4201)
effects on spectral lines of cesium, 19: 20870
efficiency of argon–cesium MHD-generator plasma in electric field, (T), 19: 21556
electron energy loss in nonequilibrium argon–cesium plasma, nitrogen effect on, (E), 19: 21560
electron reactions with, excitation cross sections for, 19: 20804(R) (ANL-6938(p.36-45))
electron reactions with, excitation functions for metastable state formation in, 19: 19992

ionization by electrons at 0.6 to 20 kev, (E/T), 19: 20850
photoionization of, dielectric breakdown from, (E), 19: 20847
plasma of, development of emitter electrodes for, (E), 19: 20905 (SC-RR-65-54)
positron annihilation in, effect of electric field on rate of, (E), 19: 21011
separation from minerals, determination of activation energy for, 19: 20166
ARGON IONS
reactions with argon at 25 kev, discrete Q values in, (E), 19: 20846
reactions with argon at 100 to 400 kev, excitation in, (E), 19: 20862
reactions with germanium at 46, 67, and 82 kev, inversion layer production in, 19: 20625
sputtering on copper and germanium at 1000 ev, 19: 20813
sputtering on copper, copper oxide production in, 19: 20827
sputtering on metals at 45 kev, thermal spikes in, (E), 19: 20838
ARGON ISOTOPES Ar-33
decay of, log ft values for, (T), 19: 21379
ARGON ISOTOPES Ar-36
content in iron meteorites, (E), 19: 20760
ARGON ISOTOPES Ar-38
content in iron meteorites, (E), 19: 20760
ARGON ISOTOPES Ar-40
activation energy in minerals, 19: 20166
content in rocks of La Sal Mountains, Utah, (E), 19: 20178
deuteron reactions (d,t) at 11.8 Mev, angular distributions from, (E), 19: 21326
ARGON SYSTEMS
Ar–hexafluoroethane, radiolysis of, yields from, 19: 19991
Ar–N, scintillation from alpha-excited, pulse-height spectra of, 19: 20313(R) (ANL-6938(p.9-20))
ARMY REACTORS (ML-1)
development, 19: 21687(R) (IDO-28637)
ARMY REACTORS (PM-1)
safety evaluation of, 19: 21685 (HASL-152)
ARMY REACTORS (PM-3)
safety evaluation of PM-3A, 19: 21685 (HASL-152)
ARSENIC
determination as impurity in pure bismuth by activation methods, 19: 19796
determination in uranium and its compounds and alloys, methods for, 19: 19823
effects on radioinduced defects in n-type germanium, 19: 20619 (NP-14883)
ARSENIC ISOTOPES As-74
analytical uses for determination of trace amounts of atomic hydrogen, 19: 19825
use in positron scanning for brain tumors, 19: 19713
use in positron scanning for brain tumors, 19: 19714
ARSENIC ISOTOPES As-75
nuclear quadrupole resonance in arsenic sulfides, (E), 19: 21430
ARSENIC SULFIDES
arsenic-75 NQR in, (E), 19: 21430
radioinduced centers in glasses of, electron spin resonance study of gamma, 19: 20620(R) (NYO-2024-8)
ASCORBIC ACID
effects on wound healing in rats, 19: 19484
radiation effects on content of, in adrenal cortex, 19: 19584
ASPHALT
fallout decontamination of areas paved with, 19: 20207 (USNRDL-TR-797)
ASTATINE ISOTOPES At-214
alpha decay, (E), 19: 21418
ASTATINE ISOTOPES At-216
alpha decay, (E), 19: 21418
ASTROPHYSICS
book: *Astrophysics and Space Science*, 19: 20782
book: *Astrophysics and the Many-Body Problem*, 19: 20714
envelope ejection by novas and supernovas, (T), 19: 20770(T)
evolution in, relation between galactic and stellar, 19: 20797
model of type-II supernova outburst, (T), 19: 20769(T)
proton-proton interaction in white dwarfs, (T), 19: 20771(T)
review of nuclear, 19: 20791
ATMOSPHERE
beta activity in, method for direct measurement of, 19: 20169
book: *Atmospheric Radiation. I. Theoretical Basis*, 19: 21156
carbon-14 activity in New Zealand, interpretation of, 19: 20238
carbon-14 content of, total and fallout, 1953 to 1964, 19: 20155 (HASL-159)
carbon-14 content of carbon dioxide in ground-level, 19: 20657(R) (DASA-1309)
cosmic ray intensity in, Forbush decreases in, (E), 19: 20886
diffusion of particles in, tracer studies using copper-64 of, 19: 20658
effects on cosmic-ray intensity in earth, (E), 19: 20897
electron diffusion in, low-energy auroral, (T), 19: 21144
hydromagnetic wave propagation in, (T), 19: 21151
monitoring for plutonium and uranium, device for, 19: 20381
monitoring for radioactivity in, in Canada, 19: 20224
pressure distribution in lower, solar activity effects on, (E), 19: 20780(T)
radiation dose distribution in air-over-ground geometry, spatial gamma and neutron, 19: 20217
radioactive fallout in 1964 and 1965 in, prognosis of, 19: 20233
radioactivity due to fallout in, 1964 and 1965, 19: 20154(R) (HASL-158)
radioactivity monitoring of, in Canada, 19: 20161 (NP-14869)
radioactivity of, methods of monitoring for compliance with regulations, 19: 20211
structure of upper, review and data on, 19: 21158
turbulence in, instrumentation for studies of, 19: 20655(R) (ANL-6938 (p.252-6))
ATMOSPHERES
radioactivity of dusts in, in Debrecen, Hungary, 19: 20235
ATOMIC BEAMS
focusing of hydrogen, using six-pole magnetis, (T), 19: 20302
injection into magnetic mirrors, 19: 21482(R) (ORNL-3760(p.23-9))
scattering of, quantum effects and velocity dependence of cross section in, 19: 20823
use in plasma diagnostics, (E), 19: 21528
ATOMIC ENERGY
development in Soviet Union, 19: 21762 (RM-2163(RAND))
ATOMIC ENERGY, LEGAL ASPECTS
in industrial uses of radioisotopes, 19: 20417
ATOMIC EXPLOSIONS
blast effects of, on underground cylindrical cavities, (T), 19: 20659 (AD-606490)
blast effects of, on hardened radio antennas, (E), 19: 20109(R) (CER-D1703)
development in Soviet Union, 19: 21762 (RM-2163(RAND))
effects on drugs, review of, 19: 20231
evaluation of Chinese, 19: 21778(T) (JPRS-28835)
fallout from Antler vented underground, (E), 19: 20167
fireball from, radiation from, (T), 19: 20675
international control, 19: 21761 (P-1134(RAND))
radioactivity from, device for simulation of performance of radiation detectors in monitoring, 19: 20244(P)
shock-wave-induced ground motions from atmospheric, simulation of, 19: 20184
use in construction of earth-fill dams, feasibility, 19: 20090 (SC-RR-65-41)
use in excavation of sea-level Isthmian canal, 19: 20091
vented gases in Dribble project, apparatus for analysis of, 19: 19776 (UCRL-12169)
ATOMIC MODELS
Hund's rule for Coulomb interaction for ground state orbital angular momentum, 19: 20811
ATOMIC PHYSICS
two-body problem in the one-dimensional Heisenberg model, 19: 20812
ATOMIC STRUCTURE
book: *Intermediate Quantum Mechanics*, 19: 21115
of lanthanides, periodicity in, 19: 20600
orbital angular momentum of atomic ground state, Hund's rule for, 19: 20811
ATOMS
acceleration of variably charged, by electrostatic fields, (T), 19: 20722 (JINR-D-1946)
collisions in crystals, non-binary, (T), 19: 20686
distribution in low-voltage pulse discharge, (E/T), 19: 21504(T)
electron eigenfunctions and energies in, (T), 19: 20835(T)
elementary particle scattering by, equations for classical and quantal, 19: 20825
energy levels and form factors for, approximate Thomas-Fermi potential for, (T), 19: 20808 (UCRL-12054-T)
energy levels of, Hund's rule for orbital angular momentum of ground state, 19: 20811
scattering of, wave packets in quantum theory for, 19: 21092
transitions in, electron impact excitation of electric quadrupole, (T), 19: 20855
AUGER ELECTRONS
emission in x ray reactions with neon, double, (E), 19: 20844
AURORAL STORMS
charged-particle fluxes in, review of, 19: 20902
dynamics of, westward traveling surges in, (E), 19: 21142
dynamics of, westward drifting loops, (E), 19: 21143

luminosity of, production of pulsations in, (E), 19: 21152
thickness of auroral arcs, over Alaska, (E), 19: 21147
AUTORADIOGRAPHY
industrial uses of, book, 19: 20417
AZOMETHANE, 1-ETHYL-1-PHENYL-
thermal decomposition of, mechanism, 19: 19943 (BNL-8243)
AZULENE
hydrogen isotopic exchange to and from, in acid solutions, 19: 19883

B

BACTERIA
gene differentiation in, 19: 21756 (BNL-8934)
radiation and chemical effects on mutagenesis in isolated DNA of *B. subtilis*, 19: 19542
radioinduced antibiotic-resistant mutations of *Staphylococcus aureus*, 19: 19531
radioinduced antibiotic-resistant mutations of *Staphylococcus aureus*, 19: 19532
radioinduced transduction in *Pseudomonas aeruginosa*, 19: 19501(R) (NP-14931)
radioinduced transduction in *Pseudomonas aeruginosa*, 19: 19502(R) (NP-14932)
radioinduced transduction in *Pseudomonas aeruginosa*, 19: 19503(R) (NP-14933)
radiosensitivity of *Serratia marcescens*, effects of humidity and inositol on, 19: 19649
radiosensitivity of, causing food spoilage, 19: 20420
radiosensitivity of, causing meat spoilage, 19: 20425
BACTERIOPHAGES
effects on transduction in *Pseudomonas aeruginosa*, 19: 19501(R) 14931)
effects on transduction in *Pseudomonas aeruginosa*, 19: 19502(R) (NP-14932)
effects on transduction in *Pseudomonas aeruginosa*, 19: 19503(R) (NP-14933)
radiation effects on *E. coli*, protective effects of Versene against uv, 19: 19638
BALANCES
description of recording thermo-, for reactions of fluorine and fluoride vapors, 19: 20258 (JAERI-1070)
BALLOONS
tracking of tetroons in vicinity of Nevada Test Site, long-range, 19: 21769 (TID-21661)
BARBITURIC ACIDS
diethyl-, effects of barbital on alkaline phosphatase activity in human granulocytes, 19: 19570
5-nitro-, analytical uses of, 19: 19824
5-nitro-, thermogravimetric properties of inorganic salts of, 19: 19824
BARIUM
determination by precipitation as diliturate, 19: 19824
diffusion of atoms of, in arc discharge, (E), 19: 21555
geochemistry and mineralogy of, in Cherry Mountains (Urals), USSR, book, 19: 20190
metabolism in rats, 19: 19500 (NP-14907)
BARIUM CHLORIDES
dielectric losses in, temperature dependence of, 19: 19851(T) (ORNL-tr-491)
electric properties of, effects of lattice energy and temperature on, 19: 21601(T) (ORNL-tr-490)
precipitation of uranium(VI) with, in presence of sodium carbonate, 19: 19870
toxic hazards to personnel from use in fire extinguishant, 19: 20210
BARIUM COMPOUNDS
thermolysis of diliturate, 19: 19824
BARIUM FLUORIDES
dielectric losses in, frequency and temperature dependences of, 19: 19851(T) (ORNL-tr-491)
electric properties of, effects of lattice energy and temperature on, 19: 21601(T) (ORNL-tr-490)
luminescence spectra of rare earth ions in, 19: 19854
BARIUM HYDRIDES
BaH_2–LiH, phase studies, 19: 19881
BARIUM IONS
solvent extraction from molten nitrate by liquid silicone–TBP at 150°C, 19: 19833 (CEA-R-2628)
BARIUM ISOTOPES Ba-137
decay and growth as daughter product of cesium-137, relation of half life to, 19: 20031
BARIUM ISOTOPES Ba-140
content in stratosphere, 19: 20657(R) (DASA-1309)
determination in air by beta measurement, efficiency of counter for, 19: 20169
separation from fission products solution for radiochemical determination, 19: 19745 (CEA-R-2712)
BARIUM OXIDES
dielectric losses in, frequency and temperature dependences of, 19: 19851(T) (ORNL-tr-491)
electric properties of, effects of lattice energy and temperature on, 19: 21601(T) (ORNL-tr-490)
Al_2O_3–BaO–CaO–MgO–SiO_2, presintering of compositions in, 19: 20461 (NP-14893)
BARLEY
radiation effects on chromosome rearrangements in seed of, partial recovery from, 19: 19639
BARYONS
charge conjugation and parity of U(12) multiplets for, 19: 20974
decay of, broken-SU(6)-symmetry models for nonleptonic, (T), 19: 20919 (IC/65/5)
form factors and generalized Poincaré group for, electromagnetic, 19: 20971
interactions with mesons, relativistic SU(6) theory for, 19: 21005
interactions with mesons, Johnson-Treiman relations from vector-meson exchange in, 19: 21018
interactions with mesons, M(12) symmetry scheme for, (T), 19: 21024
interactions with pseudoscalar mesons, predictions of relativistic SU(6) scheme for, (T), 19: 21025
interactions with mesons, amplitudes in SU(6) scheme for, 19: 21027
interactions with antibaryons, calculation of cross sections for, 19: 21068
mass relations for, empirical, 19: 20994
masses of, in SU(6) symmetry, (T), 19: 21030
BARYONS, RESONANCE
decay of Y_1^* (1660), Y_0^* (1405) production in, (E), 19: 21017
excitation of Δ (1238), N (1512), N (1688), and (1920), in electron-proton scattering, (E/T), 19: 20997
mass relations for, empirical, 19: 20994
mass spectrum of, symmetry-breaking effects in, (T), 19: 20951
model for N* (1688), (T), 19: 20992
model for, parafermion, 19: 20975
production and properties of, (T), 19: 20916 (CERN-65-7)
production of N*, SU(6) for neutrino-neutron, (T), 19: 20996
production of $N_{3/2}^*$, (T), 19: 21000
properties of, shell model for, (T), 19: 21008
symmetry properties of, (T), 19: 20926 (ICTP-64/4)
BEACONS
feasibility of radioisotope-powered acoustic, 19: 20405 (MND-3180-1)
BEHAVIOR
radiation effects on, 19: 19572
BELGIAN REACTOR-2
experimental facilities for irradiation of fissionable needle, sodium-loop, 19: 21736(T) (ORNL-tr-539)
BELGIAN REACTOR-3
operations, (E), 19: 21679 (BLG-261)
BENTONITES
sorptive properties in radioactive waste liquids, 19: 21755(P)
BENZENE
carbon-11 recoil reactions in, effects of oxygen and radiation dose on, 19: 20018
effects on ionic decomposition of *t*-butylperoxy formate, 19: 19948
effects on radioinduced carbon dioxide-graphite reactions, (E), 19: 19953 (AERE-R-4201)
electron inelastic scattering by, cross sections for, (T), 19: 20856
ionization by electron impact, appearance potential for doubly charged molecule ions in, 19: 20807(R) (UCRL-11828(p.201-4))
luminescence spectra and quantum yields of pure and cyclohexane solutions of, 19: 21771 (TID-21684)
neutron diffusion in, cross sections and decay constants for, 19: 21217
neutron scattering by, at 0.018 to 0.080 ev, (E), 19: 21200 (KFK-264)
nuclear magnetic resonance of carbon-13 in, chemical shifts of, 19: 19951
solvent properties for hydrochloric acid, tridodecylamine hydrochloride, and water, 19: 20039 (EUR-2246.e)
solvent properties in mixtures with butyl, dichlorodiethyl, and ethyl ethers for uranyl nitrates, 19: 20072
solvent properties in mixtures with butyl ether for uranyl perchlorate, 19: 20073
synthesis for radiocarbon dating by liquid scintillation, isotope effects in, 19: 20179
synthesis from acetylene for radiocarbon dating, using cobalt molybdate alumina catalyst, 19: 19944 (ORINS-50)
vaporization lifetimes of droplets of, 19: 20116(R) (SAN-409-12)
BENZENE, CHLORO-

effects on ionic decomposition of *t*-butylperoxy formate, 19: 19948
BENZENE, CYCLOHEXYL-
hydrogen abstraction from, by methyl radicals, 19: 21760 (NYO-2728-4)
BENZENE, DIETHYL-
solvent properties for hydrochloric acid, tridodecylamine hydrochloride, and water, 19: 20039 (EUR-2246.e)
BENZENE, DIISOPROPYL-
solvent properties for hydrochloric acid, tridodecylamine hydrochloride, and water, 19: 20039 (EUR-2246.e)
BENZENE, ETHYL-
hydrogen abstraction from, by methyl radicals, 19: 21760 (NYO-2728-4)
BENZENE, FLUORO-
nuclear magnetic resonance of carbon-13 and fluorine-19, chemical shifts of, 19: 19951
BENZENE, NITRO-
effects on ionic decomposition of *t*-butylperoxy formate, 19: 19948
solvent properties for hydrochloric acid, tridodecylamine hydrochloride, and water, 19: 20039 (EUR-2246.e)
spectra of radical anions in liquid ammonia, electron spin resonance, 19: 19945 (UCRL-11864)
BENZENE, NITROSO-
spectra of radical anions in liquid ammonia, electron spin resonance, 19: 19945 (UCRL-11864)
BENZENESULFONIC ACID, BROMO-, BUTYLCYCLOHEXYL ESTER
solvolysis of, deuterium isotope effects on, 19: 19949
solvolysis of, deuterium isotope effects on, 19: 19950
BENZOIC ACID, 3,5-DINITRO- ESTERS
synthesis and properties of fluorocarbon alcohol 3,5-dinitrobenzoates, 19: 21775 (UCRL-12307)
BENZYLAMINE, DIDODECYL-
deuterium exchange with water, 19: 19864
BERKELIUM
separation from cerium in trace amounts by extraction chromatography, 19: 20071
BERKELIUM ISOTOPES Bk-249
energy levels, (T), 19: 21253(R) (UCRL-11828(p.38-40))
BERKELIUM ISOTOPES Bk-250
energy levels, (E/T), 19: 21257(R) (UCRL-11828(p.63-6))
BERYLLIUM
content in primary cosmic radiation, 19: 20894
corrosion protection of, survey on, 19: 20495
crystal structure of, after distillation from solid state at high temperatures, 19: 20564 (UCRL-12252)
determination in glacial acetic acid by titration using perchloric acid, 19: 19803
determination in purified uranium compounds by chromatography and spectrography, 19: 19800
determination in uranium and its compounds and alloys, methods for, 19: 19823
ductility at 300 to 600°C, method for improving, 19: 20611(P)
effects on fabrication and mechanical properties of niobium–tantalum–titanium–vanadium alloy sheet, 19: 20552(R) (IITRI-B6021-6)
effects on strength of thorium at high temperatures, 19: 20560 (ORNL-3777)
electric conductivity at low temperatures, effects of purity on, 19: 20543 (AERE-GR-101)
electrolytic deposition from fused chloride bath, 19: 20525
electron and ion emission from foils of, laser-induced, (E), 19: 20814
electron shielding factors and polarizabilities of, (T), 19: 20852
geochemistry and mineralogy of, in Cherry Mountains (Urals), USSR, book, 19: 20190
inner potential in polycrystalline layers of, method of measuring mean, 19: 20599
internal friction measurements at high temperatures, 19: 20245 (CEA-R-2718)
mechanical properties of zone-refined, purification and realloying effects on, 19: 20557 (NMI-TJ-60)
mechanical properties of zone-leveled, 19: 20544 (AFML-TR-64-388)
neutron diffusion coefficient at 60 to 400°K, thermal, (T), 19: 21206
nucleon reactions at high energies, secondary nucleon yields from, (E/T), 19: 21242 (NP-14837)
oxidation by carbon dioxide at 593 to 815°C and 200 torr, tracer studies of, 19: 20491
properties for use in gas-cooled reactors, effects of calcium on, 19: 20498(P)
proton reactions at 160 Mev, 0.6- to 11-Mev gamma rays from, (E), 19: 21243 (ORNL-3506)
proton reactions at 12.5 Bev, mesons (K) and (π) production in, (E), 19: 21406
surface damage in machined, 19: 20502 (DMIC-Memo-198)
BERYLLIUM ALLOYS
Be–Ca, corrosion resistance to wet carbon dioxide at high temperatures and pressures, 19: 20498(P)
Be–Ca, properties for use in gas-cooled reactors, 19: 20498(P)
Be–Cu, fabrication of molds of, 19: 20519 (NP-14879)
Be–Cu, tensile properties of, testing, (E), 19: 20554 (LA-3161)
Be–Ni, fracture studies, 19: 20462(R) (NRL-6258)
BERYLLIUM CHLORIDES
electrolysis in fused alkali metal chloride system, 19: 20525
BERYLLIUM HYDROXIDES
purification by acetylacetone-EDTA solvent extraction, 19: 20070
BERYLLIUM ISOTOPES Be-7
content in stratosphere, 19: 20657(R) (DASA-1309)
BERYLLIUM ISOTOPES Be-8
energy level transitions in, (E), 19: 21357
energy levels from alpha decay in lithium-7 (p,γ) reactions, 19: 21342
energy levels in, single particle description of excited, 19: 21343
energy levels of, lithium-6 (d,α) and lithium-7 (p,α) reactions for resonance, (T), 19: 21413
BERYLLIUM ISOTOPES Be-9
alpha reactions (α,n) at 1.9 to 4.5 Mev, polarization from, (E), 19: 21307
deuteron reactions (d,t) at 11.8 Mev, angular distributions from, (E), 19: 21326
production in proton reactions with carbon-12 at 156 Mev, cross sections for, (T), 19: 21402
proton scattering at 7 and 12 Mev, polarized, (E), 19: 21295
BERYLLIUM ISOTOPES Be-10
production in proton reactions with carbon-12 at 156 Mev, cross sections for, (T), 19: 21402
BERYLLIUM OXALATES
preparation of pure trihydrate of, 19: 19832 (CEA-R-2591)
BERYLLIUM OXIDES
analysis for impurities, spectrographic method using gallium oxide, 19: 19774 (UCRL-7962)
dielectric losses in, frequency and temperature dependences of, 19: 19851(T) (ORNL-tr-491)
electric properties of, effects of lattice energy and temperature on, 19: 21601(T) (ORNL-tr-490)
preparation of polished and thin sections of, for microscopic examination, 19: 20460 (NAA-SR-Memo-9761)
BeO–PuO_2, phase diagrams, 19: 20589
BeO–PuO_2–ThO_2, phase diagrams, 19: 20589
BeO–ThO_2, phase diagrams, 19: 20589
BERYLLIUM SYSTEMS
Be–Mn–O, phase studies of, 19: 20573
BETA DECAY
coupling constant and mesonic exchange effects in, effective, 19: 21348
theory of, in heavy nuclei with isobaric states, 19: 21304
BETA PARTICLES
absorption of, effects of absorber position on measurement of, 19: 21597
activity in human blood, blood plasma, and ovaries from iodine-131 uptake, 19: 19483
detection and measurement in Hanford ground water, 19: 21749(R) (HW-84549)
detection and measurement *in vitro* and *in vivo* using fluororod dosimeters, 19: 20314(R) (ANL-6938(p.62-70))
detection and measurement of activity on this chromatographic layers, equipment and method for, 19: 19792
detection and measurement using scintillation gels, (E), 19: 20335
detection and measurement of, methods for, 19: 20383
detection and measurement of, sensitivity of nuclear emulsion for, 19: 20014
detection of, proportional counter anticoincidence assembly for, 19: 20353
effects from phosphorus-32 on digestive tract of rats, 19: 19565
effects of incorporated tritium, in cells, 19: 19515
effects on blood vessel permeability of, from deposited barium-140 or strontium-85, 19: 19500 (NP-14907)
effects on dehydration of cyclohexanol from sulfur-35-labeled catalyst, 19: 20013
effects on metabolism in rabbit cornea, 19: 19552
reactions with lead, polarization of bremsstrahlung from, 19: 21453
uses of reflected, for end-point determination in precipitation titrations, 19: 19787
BETA SOURCES
detection and measurement in air, efficiency of counter for, 19: 20169
detection and measurement of low-activity, device for, 19: 20382
preparation of cerium-144, engineering drawings of equipment for, 19: 20437
shielding for 80-C strontium-90, engineering drawings of, 19: 20134
use in thickness gaging, 19: 20311
BETA SPECTRA

shapes of, and partially conserved axial-vector current, (E/T), 19: 21340
BETA SPECTROMETERS
performance of lithium-drifted semiconductor, 19: 20360
BETATRONS
bremsstrahlung energy and intensity in, method for determining, 19: 20337
development of high-current air-core, (E), 19: 20740
BEVATRON
beam velocity spectrometers for, design of, (E), 19: 20326 (UCRL-11787)
BIBENZYL
radioinduced luminescence of, comparison of alpha and electron, 19: 19963
radioinduced luminescence of tetracene-doped, comparison of alpha and electron, 19: 19963
BIBLIOGRAPHIES
on advanced valves, 19: 20097 (NASA-SP-5019)
on atomic energy program of Soviet Union, publicly-available publications, 19: 21762 (RM-2163(RAND))
on automatic collection and processing of nuclear data, 19: 19766(R) (TEES-2671-4(Chap.3))
on biological applications of gamma radiation, 19: 19505 (TID-3580)
on bone and cartilage formation, 19: 19472(R) (ANL-6938(p.179-93))
on bone growth, 19: 19471(R) (ANL-6938(p.162-78))
on chemical evolution, 19: 19946 (UCRL-11950)
on chemistry of rare earths, French, 1956 to 1961, 19: 19738(T)
on corrosion of stainless steel by potassium–sodium alloy and sodium, 19: 20472 (IDO-14651)
on diagnosis and therapy of chronic radiation injuries, 19: 19623
on dosimeters, 19: 20314(R) (ANL-6938(p.62-70))
on fallout, 19: 20154(R) (HASL-158)
on fallout, 19: 20164 (TID-3086(Suppl.2))
on high-field superconductivity, 19: 21165
on hot extrusion of metal powders, 19: 20518 (NMI-TJ-29)
on interactions of nuclei having A = 1 to 3, (E/T), 19: 21238 (LA-3205)
on ion exchange in complex formation studies, 19: 19837 (IA-1000)
on isotope hypophysectomy, 19: 19664
on lithium peroxide, 19: 19932
on nuclear chemistry, French, 1956 to 1961, 19: 19738(T)
on plutonium release due to overheating or fires, 19: 20200 (HW-83668)
on radiation chemistry of cellulose and its derivatives, 19: 19961(T) (CEA-tr-A-1741)
on radiation injury models, 19: 19564
on radioactivity measurement in waste waters, 19: 19749 (EUR-2118.f)
on radioinduced graft polymerization on cellulose, 19: 19960 (VDDIT-93)
on radioprotective compounds, 19: 19620(T) (JPRS-29200(p.96-106))
on reactor control theory, 19: 21723(R) (NASA-CR-193)
on spin scattering, synthesis of, 19: 20828
on stack disposal meteorology, 19: 20653(R) (ANL-6938(p.209-41))
on thermodynamics of nuclear materials, 19: 19933
on uranium extraction from leach solutions by amines and acidic organo-phosphorus compounds, 19: 20053 (UJV-1202/64)
on wetting effects in mercury heat transfer, 19: 20112 (NAA-SR-Memo-10315)
BIOCHEMISTRY
applications in studies of radiation effects on muscles, 19: 19551
BIOLOGICAL MATERIALS
analysis for phosphorus by neutron activation methods, 19: 19828
analysis for potassium, activation, 19: 19771(R) (TEES-2671-4(Chap.9))
analysis for strontium-89 and -90, radiochemical, 19: 19739 (AERE-AM-101)
analysis of, developments in physical methods for, 19: 19782
radiation effects on, 19: 19614
BIOLOGICAL SYSTEMS
radiation effects on, tritium beta, 19: 19515
radiation effects on, small-dose, 19: 19516
radiation effects on, 19: 19562
radiation effects, gamma, bibliography on, 19: 19505 (TID-3580)
BIOLOGY
book: *Oceanography and Marine Biology*. Vol. 2, 19: 19467
electron microscopy in structural studies in molecular, 19: 19455 (CONF-640204(p.44-62))
BIOMETRY
logarithmical relation of concentration of inhaled insoluble particles in lungs to that in pulmonary lymph nodes, 19: 19456 (LF-21)
BIOPHYSICS
applications in studies of radiation effects on muscles, 19: 19551
BIOTITES
argon-40 activation energy in, 19: 20166
2,2'-BIQUINOLINE
solvent properties for copper, 19: 19815
BIREFRINGENCE
use in flow visualization, 19: 20108 (BNWL-31)
BISMUTH
analysis for impurities by activation methods, 19: 19796
determination by titration, suitability of tetraethylenepentamine heptaacetic acid for, 19: 19813
neutron elastic scattering at 85 to 700 kev, differential cross sections for, (E), 19: 21298
neutron reactions with, polonium-210 production in, 19: 20008
nucleon reactions at high energies, secondary nucleon yields from, (E/T), 19: 21242 (NP-14837)
proton reactions at 160 Mev, 0.6- to 11-Mev gamma rays from, (E), 19: 21243 (ORNL-3506)
proton reactions at 160 Mev, secondary nucleon spectra from, (E/T), 19: 21244 (ORNL-P-844)
separation from mercury by solvent extraction using tri-n-octylphosphine oxide, 19: 19753 (IS-T-3)
separation from polonium by electrolysis, 19: 20008
separation from waste solutions by electrolytic deposition, evaluation of, 19: 20047 (MLM-734)
sputtering by ions at 45 kev, thermal spikes in, (E), 19: 20838
x-ray spectra in, muonic, (E), 19: 21344
BISMUTH BROMIDES
crystal structure of, nuclear quadrupole resonance studies of, coupling in solid bismuth, 19: 19940
BISMUTH ISOTOPES Bi-206
use in scanning for brain tumors, 19: 19714
BISMUTH ISOTOPES Bi-209
alpha fission of, energy-mass distributions in, (E/T), 19: 21263(R) (UCRL-11828(p.90-2))
nuclear quadrupole coupling in solid bismuth bromide, 19: 19940
photon reactions (γ,n), angular distributions from, (E), 19: 21288
proton fission of, excitation energy, (E), 19: 21261(R) (UCRL-11828(p.81-3))
BISMUTH ISOTOPES Bi-212
content in blood and bones of humans injected with thorotrast, 19: 19497(R) (ANL-6938(p.127-39))
content in tissue of rats injected with thorotrast, 19: 19497(R) (ANL-6938(p.127-39))
BISMUTH ISOTOPES Bi-214
effects on radon-222 gamma spectra, 19: 21299
BISMUTH OXYCHLORIDES
spectra of suspensions of, in thin polyethylene films, infrared transmission, 19: 19917
BLAST EFFECTS
hazards of, in nuclear warfare, 19: 19554
hazards of, in nuclear warfare, 19: 19555
on buried hollow cylinders, quasi-static overpressure study, 19: 20136 (AFWL-TDR-64-13)
BLOOD
iodine-131 uptake by human, beta activity from, 19: 19483
radiation effects on erythrocytes in stored, 19: 19513
BLOOD CELLS
globulin production by fetal hemopoietic cells, review on, 19: 19468
radiation effects of simulated space situation on monkey, gamma and proton, 19: 19616
BLOOD PICTURE
effects of nitrogen mustard on, in rats, 19: 19489
effects of work in betatron and cyclotron labs on human, 19: 20237
radiation effects on, chronic, low-level, 19: 19525
radiation effects on dog, proton, 19: 19578
radiation effects on conventional and germfree mouse, whole-body, 19: 19619
BLOOD PLASMA
erythropoietin content of, effects of anemia and irradiation on, 19: 19499(R) (NP-14899)
iodine-131 uptake by human, beta activity from, 19: 19483
BLOOD SERUM
radiation and immunization effects on cholinesterase activity in rabbits, 19: 19609
radiation effects on albumin synthesis in rat liver, effects of food ingestion, 19: 19603
radiodermatitis effects on protein fractions in human and rabbit, 19: 19598
BLOOD TRANSFUSIONS
effects on bone marrow transplants in irradiated mice, 19: 19653
radiation effects on erythrocytes in stored blood for use in, 19: 19513
BLOOD VESSELS
radiation effects from deposited barium-140 or strontium-85 on permeability of, 19: 19500 (NP-14907)
BLOWERS
testing helium, for Turret Reactor, 19: 21690(R) (LA-3244)

BODY WATER
determination in man, radiometric, using tritium, 19: 19480
BOILERS
book: *Radioisotopic Methods for Investigation of Processes Inside Boilers*, in Russian, 19: 20418
design for liquid metal heat transfer studies, 19: 20116(R) (SAN-409-12)
design for TARGET gas-cooled power reactor, (E), 19: 21682 (GAMD-4732)
development of sodium-heated, 19: 20107(R) (BAW-1280-22)
feasibility of radioisotope-heated underwater, for acoustic beacon, 19: 20405 (MND-3180-1)
wetting Rankine tubes by mercury in, effects of surface treatment on, 19: 20111 (NAA-SR-Memo-10224)
BOILING
film, of saturated liquid nitrogen flowing upward in heated tube at high vapor qualities, 19: 20113 (NP-14895)
steam void determination in, method for, 19: 20294
BOILING REACTOR EXPERIMENTS
operations of BORAX-V Core B-2, (E), 19: 21726 (ANL-6849)
BOILING REACTORS
control of, utilizing evolved steam circulated through core, 19: 21661(P)
coolant flow instability in, calculation of, 19: 20121
design of superheating, 19: 21659(P)
BONDING
methods for graphite, development of, 19: 20505 (JAERI-1071)
of metallic films and solid-state devices, methods for, 19: 20520 (SC-DC-65-1256)
testing of, nondestructive method for, 19: 20127(R) (IITRI-N213-23)
BONE DISEASES
localization of, by whole-body counting and scanning after administration of gold-198, 19: 19718
radiography of pelvic dysplasia in infants, radiation hazards of, 19: 19678
BONE MARROW
effects of allogenic chimeric, on repopulation of lymphatic tissues in irradiated mice, 19: 19646
gold-198 uptake by human, whole-body counting and scanning of, 19: 19718
immunologic reactivity and tolerance of radiation mouse chimeras to grafts of, thymus effects on, 19: 19652
preservation of, effects of low temperature on antigenic properties, 19: 19641
protective effects of injections of fresh and frozen, against radiation injuries in rats, 19: 19641
protective effects of allogenic, against radiation mortality in mice, 19: 19648
protective effects of transplants in irradiated mice, effects of blood transfusions on, 19: 19653
radiation chimeras of, effects on kidney grafts in dogs, 19: 19493
radiation effects on uptake of sulfur-35-labeled methionine by proteins in rabbit, 19: 19604
radiation effects on host-cell interactions in mice with grafts of, 19: 19615
radiation effects on fractionation of spleen-colony-forming cells in mouse, 19: 19617
radiation effects on erythropoiesis in rat, effects of transplants on recovery from, 19: 19644
radiation injuries of, induced by injected Thorotrast, 19: 19567
radiation, drug and hormone effects on graft tolerance for, 19: 19588
transplantation effects on secondary disease in monkeys, methods for modification of, 19: 19647
transplantation potential of frozen, at programmed cooling rates, 19: 19645
BONE TUMORS
localization of primary and secondary, using strontium-85, 19: 19675
radiodiagnosis by scintillation scanning using strontium-85, 19: 19697
radiodiagnosis of metastatic, by external scanning of strontium-85, 19: 19666
BONES
analysis for strontium-89 and -90, radiochemical, 19: 19739 (AERE-AM-101)
analysis for strontium-90 by radiochemical methods, 19: 19789
calcium metabolism in dog, tracer studies of, 19: 19470(R) (ANL-6938 (p.141-61))
lead-210 content in, of Puerto Ricans, 19: 20193(R) (ANL-6938(p.120-4))
metabolic activity of rat, diurnal variations of, 19: 19472(R) (ANL-6938(p.179-93))
strontium-90 content in, of Argentine children, 19: 20165(R) (TID-21711)
strontium-90 content in, in Great Britain, 1963, 19: 20170
BORANES, ARYL-
solvent properties for cesium, francium, and thallium, 19: 20058
BORANES, PHOSPHINO-
radioinduced polymerization of trimeric cyclic, 19: 19982
BORATE GLASS
paramagnetic ions in, electron spin resonance studies of, 19: 20620(R) (NYO-2024-8)
radioinduced centers in, electron spin resonance study of gamma, 19: 20620(R) (NYO-2024-8)
BORIC ACID
determination in mixtures with cyanuric acid, 19: 19756 (LA-3193)
effects on coolant pump wear in water-cooled reactors, 19: 21606 (WCAP-3269-9)
effects on oxidation of zirconium and its alloys by steam at 500°C and 1000 psi, 19: 20492
anthranilic acid–boric acid, phosphorescence in, 19: 19919
boric acid–U, phosphorescence in, 19: 19919
boric acid–sulfanilic acid, phosphorescence in, 19: 19919
BORIDES
analysis for boron by pyrohydrolysis, 19: 19761 (NP-14876)
BORON
analysis for impurities, spectrographic method using gallium oxide, 19: 19774 (UCRL-7962)
content in primary cosmic radiation, 19: 20894
determination in ppm range by d-c arc excitation, spectrochemical, 19: 19827
determination in refractory borides by pyrohydrolysis, 19: 19761 (NP-14876)
determination in uranium and its compounds and alloys, methods for, 19: 19823
effects on fabrication and mechanical properties of niobium–tantalum–titanium–vanadium alloy sheet, 19: 20552(R) (IITRI-B6021-6)
purification, 19: 20455(R) (DCAS-TDR-62-192)
BORON IONS
electron shielding factors and polarizabilities of monovalent, (T), 19: 20852
BORON ISOTOPES B-8
emission in meson (K^-) reactions with emulsion nuclei at 0.8 to 3.0 Bev/c, (E), 19: 21389
BORON ISOTOPES B-10
electron inelastic scattering at 100 to 220 Mev, excitation of 6.02-Mev level in, (E), 19: 21306
energy levels of, reduced width of, (T), 19: 21432
energy levels of, nucleon separation energy in 1p and 1s, 19: 21400
neutron reactions (n,α) with, cross section for thermal, (E), 19: 20088
production in proton reactions with carbon-12 at 156 Mev, cross sections for, (T), 19: 21402
BORON ISOTOPES B-11
energy levels from carbon-12 (p,2p) reactions, 19: 21401
energy levels of, reduced width of, (T), 19: 21432
production in proton reactions with carbon-12 at 156 Mev, cross sections for, (T), 19: 21402
reactions with lutetium-175 and thulium-169, fission, (E/T), 19: 21259(R) (UCRL-11828(p.77-80))
BORON NITRIDES
oxidation in air at 0.01 to 100 atm, assuming frozen laminar boundary layer, 19: 20496
thermal conductivity at high temperatures, (E), 19: 20576
BORON OXIDES
spectra of suspensions of, in thin polyethylene films, infrared transmission, 19: 19917
BORON SYSTEMS
B–C–La, phase studies, 19: 19926
B–C–rare earths, phase studies, 19: 19926
BOROSILICATE GLASS
radioinduced centers in, electron spin resonance study of gamma, 19: 20620(R) (NYO-2024-8)
BOSONS
form factors and generalized Poincaré group for, electromagnetic, 19: 20971
interactions of four vector, Pauli-Fierz transformation group and Lagrangians for, 19: 21051
interactions of intermediate vector, effect on meson (μ) capture rate, (T), 19: 21420
interactions of spin-0, Kemmer-Duffin and Klein-Gordon formalisms for, 19: 21050
interactions with fermions, Regge poles in, 19: 21077
mass of vector, gauge invariance for, 19: 20934 (NP-14829)
photoproduction of intermediate vector (W^+), on protons, (T), 19: 21003
quantization of para-Bose fields, 19: 20960
reactions with matter, multiple-boson production in, (T), 19: 20816
sound in weakly ideal gases of, second, (T), 19: 20669

statistics of free fields of, (T), 19: 21102

BRAIN
radiation effects on secretion from nuclei of hypothalamic area in rabbits, 19: 19509(T) (JPRS-29250(p.9-13))
radiation effects on physiology of mineral contents in developing guinea pig, 19: 19534
radiation effects on 3,1,5,1-aryl-sulfate sulfohydrolase activity in guinea pig, *in utero*, 19: 19573
radiation effects on edema in cerebral cortex in rat, 19: 19607
radiation effects on lipid metabolism in newborn and weanling rat, 19: 19610
radiation effects on lysosomes in, hypothesis on, 19: 19611
radiation injuries of, induced by radiotherapy of eye tumors, 19: 19701

BRAIN TUMORS
localization by positron scanning after administration of arsenic-74 or copper-64, 19: 19713
localization by scintillation after administration of mercury-197, 19: 19715
localization of developments in scanning methods for, 19: 19714
localization of, design and function of scanner for, 19: 19712

BRASS
cosmic particle reactions with, K_{π_0} inelasticity distribution in, (E), 19: 20898

BRAZED JOINTS
development for Rover project, (E), 19: 20554 (LA-3161)
experience on SNAP components, review, 19: 20508 (NAA-SR-Memo-10625)

BRAZING ALLOYS
experience on SNAP components, review, 19: 20508 (NAA-SR-Memo-10625)
performance with Rover-reactor materials, (E), 19: 20554 (LA-3161)

BREEDER REACTORS
analysis of lead-cooled liquid-metal-fueled, nuclear and parametric, (T), 19: 21697
fuel elements for, technology of thorium, 19: 20582

BREMSSTRAHLUNG
energy and intensity of high-energy, method for determining, 19: 20337
interactions with protons at 228 to 325 Mev, cross sections, (E), 19: 20932 (LNF-64/60)
polarization of, produced in lead by bismuth-210 beta particles, 19: 21453
production in auroral storms, mechanism for, (E), 19: 21152
reactions (γ,n) and (γ,np) with potassium-39 to 80 Mev, (E), 19: 21276
reactions (γ,n) with bismuth-209 and tantalum-181, angular distributions from, (E), 19: 21288
reactions (γ,n) with nuclei at 10 to 28 Mev, cross sections for, (E), 19: 21305
spectra of magnetic mirror plasma, 19: 21482(R) (ORNL-3760(p.23-9))

BROMIDE IONS
solvent extraction from molten nitrate by liquid silicone–TBP at 150°C, 19: 19833 (CEA-R-2628)

BROMINE
effects on radioinduced carbon dioxide-graphite reactions, (E), 19: 19953 (AERE-R-4201)

BROMINE ISOTOPES
effects on molecular properties of lithium bromide, 19: 19848(R) (UCRL-11828(p.193-7))

BROMINE ISOTOPES Br-79
neutron reactions (n,γ) at 0.024 to 3.1 Mev, isomeric cross section ratio for, (E), 19: 21331

BROMINE ISOTOPES Br-80
isomeric transition in bromine-80m-labeled pentamminecobalt bromides, recoil reactions from, 19: 19973
production of isomer pairs of, in bromine-79 (n,γ) reactions at 0.024 to 3.1 Mev, (E), 19: 21331
production using Rossendorf Reactor in East Germany, 19: 20436

BROMINE ISOTOPES Br-82
production using Rossendorf Reactor in East Germany, 19: 20436

BROMINE ISOTOPES Br-87
decay scheme, 19: 21275

BROOKHAVEN ALTERNATING-GRADIENT SYNCHROTRON
accelerating cavity for beam injector of, (E), 19: 20719 (BNL-8970)
beam extraction system for, design of, (E), 19: 20718 (BNL-8968)
magnet current control systems for, (E), 19: 20094 (BNL-8969)

BROOKHAVEN BEAM RESEARCH REACTOR
fuel element design for, engineering drawings of, 19: 21743
safety analysis, 19: 21728 (BNL-7661(Vol.I))
safety analysis, 19: 21727 (BNL-7661(Vol.II))

BROWNIAN MOVEMENT
theory for assemblies of coupled oscillators, 19: 21089

BUBBLE CHAMBERS
data analysis from, computer program for, (T), 19: 20320 (IS-989)

BUBBLES
formation delay time in water-moderated reactors after large insertion of reactivity, 19: 21653

BUILDING MATERIALS
gamma dose from brick, concrete, and wood, 19: 20218
radiography of, neutron, 19: 20129

BULK SHIELDING FACILITY
neutron distributions in shielding of, at 1.5 to 12 Mev, (E), 19: 21735 (ORNL-P-1092)

BUTADIENE
spectra of radical anions in liquid ammonia, electron spin resonance, 19: 19945 (UCRL-11864)

BUTADIENE, 2,3-DIMETHYL-
spectra of radical anions in liquid ammonia, electron spin resonance, 19: 19945 (UCRL-11864)

1,3-BUTADIENE, 2-METHYL-
spectra of radical anions in liquid ammonia, electron spin resonance, 19: 19945 (UCRL-11864)

BUTYL ETHER
solvent properties in mixtures with benzene, carbon tetrachloride, chloroform, heptane, toluene, and xylene for uranyl nitrate, 19: 20072
solvent properties in mixtures with chlorinated hydrocarbons for uranyl perchlorate trihydrate, 19: 20073

BUTYL GROUP
decomposition of chemically activated, isotope effects in, 19: 19938

BUTYL PHOSPHATES
solvent properties for protactinium, 19: 20055
solvent properties for americium, 19: 20076
solvent properties for neptunium, plutonium, and uranium in aqueous nitrate solutions, role of complex formation in, 19: 20077
$LiNO_3$–KNO_3–$NaNO_3$, distribution of ions between liquid–TBP and silicone–TBP, solvent properties for ions from molten nitrate at 150°C, 19: 19833 (CEA-R-2628)
TBP–Varsol, solvent properties for nitric acid from aqueous solution, pulse column studies of, 19: 20043 (IEA-77)

C

CADARACHE REACTORS (RAPSODIE)
testing engineering mockup of, (E), 19: 21730 (CEA-R-2557)

CADMIUM
determination by titration, suitability of tetraethylenepentamine heptaacetic acid for, 19: 19813
effects on spectrophotometric determination of zinc using 1-(2-thiazolylazo)-2-naphthol, 19: 19814
separation from indium, 19: 20023(T) (ORNL-tr-556)
separation from uranium by sorption of uranium complexes on activated charcoal, 19: 20074

CADMIUM ALLOYS
Cd–Ag, tensile properties of, testing, (E), 19: 20554 (LA-3161)

CADMIUM ISOTOPES Cd-109
content in stratosphere, 19: 20657(R) (DASA-1309)

CADMIUM ISOTOPES Cd-111
energy level transitions in, retardations in l-allowed M1, (T), 19: 21323
hyperfine fields in 5p shell of, induced, 19: 21359

CADMIUM ISOTOPES Cd-113
content in stratosphere, 19: 20657(R) (DASA-1309)
energy level transitions in, retardations in l-allowed M1, (T), 19: 21323

CADMIUM ISOTOPES Cd-114
Coulomb excitation of 0.5578-Mev energy level of, reorientation effect in, (E), 19: 21398

CADMIUM ISOTOPES Cd-115
content in stratosphere, 19: 20657(R) (DASA-1309)
production using Rossendorf Reactor in East Germany, 19: 20436

CADMIUM SULFIDES
radiation effects on, mechanisms in, 19: 20019
spectra of suspensions of, in thin films of polyethylene, infrared transmission, 19: 19917

CADMIUM ZINC SULFIDES
radioinduced luminescence of manganese- and indium-activated, effects of infrared radiation on x-ray, 19: 19965

CALCIUM
determination by precipitation as diliturate, 19: 19824
determination by titration, suitability of tetraethylenepentamine heptaacetic acid for, 19: 19813
effects on properties of beryllium for use in gas-cooled reactors, 19: 20498(P)
meson (π^-) reactions (π^-,nγ) with, energy spectra from, (E), 19: 21315
metabolism in dog bones, tracer studies of, 19: 19470(R) (ANL-6938 (p.141-61))

CALCIUM ALLOYS
Be–Ca, corrosion resistance to wet carbon dioxide at high temperatures and pressures, 19: 20498(P)
Be–Ca, properties for use in gas-cooled reactors, 19: 20498(P)
Ca–Mg_2, heats of formation and fusion of intermetallic compound $CaMg_2$ in, 19: 19838 (IS-1070)
CALCIUM CARBONATES
spectra of suspensions of, in thin polyethylene films, infrared transmission, 19: 19917
CALCIUM CHLORIDES
dielectric losses in, temperature dependence of, 19: 19851(T) (ORNL-tr-491)
electric properties of, effects of lattice energy and temperature on, 19: 21601(T) (ORNL-tr-490)
precipitation of uranium(VI) with, in presence of sodium carbonate, 19: 19870
CALCIUM COMPOUNDS
thermolysis of diliturate, 19: 19824
CALCIUM FLUORIDES
dielectric losses in, frequency and temperature dependences of, 19: 19851(T) (ORNL-tr-491)
electric properties of, effects of lattice energy and temperature on, 19: 21601(T) (ORNL-tr-490)
fluorine-19 spin lattices relaxation time in, below 1°K, (E), 19: 19897
hydrogen EPR spectra in, 19: 19896
luminescence spectra of rare earth ions in, 19: 19854
radioinduced V_F centers in, EPR studies of x, 19: 20003
spectra of suspensions of, in thin films of polyethylene, infrared transmission, 19: 19917
CALCIUM HYDROXIDES
content in soil, effects on strontium-90 accumulation in oats, 19: 19475(T) (JPRS-27940(p.10-17))
CALCIUM IONS
solvent extraction from molten nitrate by liquid silicone–TBP at 150°C, 19: 19833 (CEA-R-2628)
CALCIUM ISOTOPES
neutron reactions with, resonances in, 19: 21454
CALCIUM ISOTOPES Ca-37
decay of, log ft values for, (T), 19: 21379
CALCIUM ISOTOPES Ca-39
beta decay of, mesonic exchange effect in, 19: 21348
CALCIUM ISOTOPES Ca-40
deuteron reactions (d,p) with, target core excitation in, (T), 19: 21433
energy levels of, nucleon separation energy in 1p and 1s, 19: 21400
helium-3 scattering at 22 Mev, models for, (E/T), 19: 21240 (LA-DC-6232)
proton inelastic scattering at 150 Mev, energy levels from, (E), 19: 21332
CALCIUM ISOTOPES Ca-42
deuteron reactions (d,p) with, target core excitation in, (T), 19: 21433
CALCIUM ISOTOPES Ca-45
separation from fission products solution for radiochemical determination, 19: 19745 (CEA-R-2712)
use in bone formation rate determination, 19: 19470(R) (ANL-6938 (p.141-61))
CALCIUM ISOTOPES Ca-47
beta decay, 19: 21460
uptake and retention in rats, effects of cortisone and anabolic steroids on, 19: 19476
CALCIUM ISOTOPES Ca-48
helium-3 elastic scattering and reactions (He-3,d) at 22 Mev, (E), 19: 21240 (LA-DC-6232)
CALCIUM OXIDES
dielectric losses in, frequency and temperature dependences of, 19: 19851(T) (ORNL-tr-491)
effects on thermal stability of zirconium oxide, 19: 20585
electric properties of, effects of lattice energy and temperature on, 19: 21601(T) (ORNL-tr-490)
Al_2O_3–BaO–CaO–MgO–SiO_2, presintering of compositions in, 19: 20461 (NP-14893)
CaO–NaOH, sorptive properties of soda lime for fluorine and hydrofluoric acid, thermobalance study, 19: 20258 (JAERI-1070)
CALIFORNIUM ISOTOPES Cf-252
fission of, charge and mass distributions from, (E), 19: 21229 (BNL-8841)
fission of, K x-ray emission in spontaneous, (E), 19: 21355
fission of, x rays emitted by fragments from, (E), 19: 21265(R) (UCRL-11828(p.95-7))
CALORIMETERS
use of adiabatic, for determining thermodynamic properties of intermetallic compounds, 19: 19838 (IS-1070)
CALUTRONS
beam stabilization in, 19: 21483(R) (ORNL-3760(p.30-56))
CAMERAS
design of sweeping-image, 19: 21784(P)
mirrors for use with, engineering drawings of turbine-driven, 19: 20308
CAMPHOR
effects on polarography of uranyl pyrophosphate complexes, 19: 19816
CANADA
fallout monitoring, 1964, 19: 20161 (NP-14869)
nuclear energy program in, 19: 21781
radiation monitoring program of, 19: 20243
radiation protection programs in, 19: 20224
radiation protection standards in, 19: 20212
CANADIAN REACTORS
environs monitoring, 1964, 19: 20161 (NP-14869)
CARBIDES
vaporization rates of ternary, equations for predicting, 19: 20608
CARBOHYDRATES
metabolism in diabetic and obese subjects, tracer studies of, 19: 21758 (BNL-8864)
CARBON
compatibility of pyrolytic, with water under high heat flux conditions, 19: 20463 (ORNL-TM-431)
content in primary cosmic radiation, 19: 20894
cosmic particle reactions with, K_{π_0} inelasticity distribution in, (E), 19: 20898
determination in SAP powders by different laboratories, statistics on, 19: 19750 (EUR-2286.f)
determination in uranium and its compounds and alloys, methods for, 19: 19823
diffusion of uranium in pyrolytic, 19: 20463 (ORNL-TM-431)
effects on fabrication and mechanical properties of niobium–tantalum–titanium–vanadium alloy sheet, 19: 20552(R) (IITRI-B6021-6)
effects on strength of thorium at high temperatures, 19: 20560 (ORNL-3777)
electromagnetic wave absorption and scattering by particles of, (T), 19: 20677
electron elastic scattering by atoms of, phase shift for, (T), 19: 20858
evaluation of coatings of pyrolytic, on fuel particles, 19: 20463 (ORNL-TM-431)
graphitization of, effects of impregnation with rare earths on, 19: 20536(P)
mass transfer between potassium–sodium alloy and structural alloys at high temperatures, 19: 20478(R) (ORNL-3618)
meson (K^+) absorption at 4.75 Bev/c, cross sections for, (E), 19: 21431
meson (μ) capture by, intermediate vector boson in, (T), 19: 21420
meson (π^-) reactions (π^-,nγ) with, energy spectra from, (E), 19: 21315
meson (π^+) absorption at 2.72, 3.70, and 4.75 Bev/c, cross sections for, (E), 19: 21431
nucleon reactions at high energies, secondary nucleon yields from, (E/T), 19: 21242 (NP-14837)
photon reactions with, polarization of protons from, 19: 21456
proton reactions at 160 Mev, 0.6- to 11-Mev gamma rays from, (E), 19: 21243 (ORNL-3506)
proton reactions at 2.72 Bev/c, cross sections for, (E), 19: 21431
proton scattering by, polarization in, (E), 19: 20980
reactions with hydrogen atoms and ions in electron-bombarded acetylene, 19: 19988
reactions with plutonium dioxide at 2200 to 2600°C, 19: 20570
reactions with uranium hydrides, preparation of dense, fine particle uranium carbides by, 19: 20517(R) (NCSC-2981-8)
separation from plutonium processing solutions, 19: 20065
thermal conductivity, 19: 21690(R) (LA-3244)
x-radiation scattering by, Hartree-Fock calculations of incoherent, 19: 20824
CARBON ARCS
temperature profile of low-current, method for determining, 19: 21497
temperature profile of low-current, in air, (E), 19: 21498
CARBON DIOXIDES
content in atmosphere, 19: 20155 (HASL-159)
content in glass ultrahigh vacuum systems, method for lowering, 19: 20148
corrosive effects on graphite at high temperatures, 19: 21690(R) (LA-3244)
corrosive effects on iron, Inconel, stainless steel, and other steels, 19: 20487
corrosive effects on beryllium, tracer studies of, 19: 20491
determination in vented gases from underground nuclear explosion, apparatus for, 19: 19776 (UCRL-12169)
ionization by electron impact, appearance potential for doubly charged molecule ions in, 19: 20807(R) (UCRL-11828(p.201-4))
production from labeled glucose in obese patients, 19: 21758 (BNL-8864)

radiation effects of 200-ev electrons on, 19: 19996
radioinduced reactions with graphite, inhibition of, (E), 19: 19953 (AERE-R-4201)
radioinduced reactions with graphite at 100 to 600°C, effects of hydrogen and water vapor on neutron, 19: 19954 (AERE-R-4389)
spectra of electron-excited, transition probabilities in, 19: 19996
spectra of oxygen-18 enriched, infrared, 19: 19936
thermodynamic properties of, graphs of equilibrium, 19: 19842 (NASA-SP-3014)
uses in argon-arc welding of stainless steel tubing, 19: 20534
yields from radiolysis of formic acid–hydrogen peroxide solutions, effects of pH on, 19: 19989
CO_2–DH, electron reactions with, cross sections for secondary ion formation in, 19: 19995

CARBON IONS
electron shielding factors and polarizabilities of divalent, (T), 19: 20852
photon reactions with monovalent, electron emission in, (T), 19: 20851
reactions with hydrogen atoms and ions in electron-bombarded acetylene, 19: 19988

CARBON ISOTOPES C-10
production in proton reactions with carbon-12 at 156 Mev, cross sections for, (T), 19: 21402

CARBON ISOTOPES C-11
energy levels, (E), 19: 21232 (JEN-141-DF/I-45)
energy levels from carbon-12 (p,d) reactions, 19: 21401
energy levels of, reduced width of, (T), 19: 21432
production in proton reactions with carbon-12 at 156 Mev, cross sections for, (T), 19: 21402
recoil reactions in hydrocarbons, effects of oxygen and radiation dose on, 19: 20018

CARBON ISOTOPES C-12
alpha reactions (α,d), correlations in wave functions for, (E/T), 19: 21266(R) (UCRL-11828(p.108-9))
deuteron reactions (d,p), distorted wave Born approximation analysis of, 19: 21439
energy levels of, reduced width of, (T), 19: 21432
energy levels of, lifetime of short-lived, (E), 19: 21368
energy levels of, nucleon separation energy in 1p and 1s, 19: 21400
helium-3 reactions at 29 Mev, (E), 19: 21232 (JEN-141-DF/I-45)
meson (π^+) reactions at 80 Mev, cross section for, (E), 19: 21279
neutron elastic scattering at 17 to 21 Mev, resonances in, (E), 19: 21310
neutron scattering at 14 Mev by, cross sections for, (E/T), 19: 21441
oxygen-16 reactions (O-16,α) at 15.0 to 22.5 Mev, angular distributions from, (E), 19: 21313
proton reactions (p,d) and (p,2p) at 50 Mev, cross sections for, 19: 21401
proton reactions at 44 to 25,000 Mev, lithium-6 and -7 production in, (E), 19: 21352
proton reactions at 156 Mev, cross sections for intranuclear cascade and breakup in, (T), 19: 21402
reactions with lutetium-175, tungsten-182, and ytterbium-174, fission, (E/T), 19: 21259(R) (UCRL-11828(p.77-80))

CARBON ISOTOPES C-13
content in stratosphere, 1953 to 1964, 19: 20155 (HASL-159)
content in troposphere, 1953 to 1964, 19: 20155 (HASL-159)
effects on thermal decomposition of 1-ethyl-1-phenylazomethane, 19: 19943 (BNL-8243)
nuclear magnetic dipole moment, (T), 19: 21322
nuclear magnetic resonance chemical shifts in substituted benzenes, 19: 19951

CARBON ISOTOPES C-14
activity in atmosphere, Kauri tree, and surface ocean water in New Zealand, interpretation of, 19: 20238
age estimation using, isotope effects in benzene synthesis for, 19: 20179
content in carbon dioxide in ground-level air, 19: 20657(R) (DASA-1309)
content in stratosphere, 1953 to 1964, 19: 20155 (HASL-159)
content in troposphere, 1953 to 1964, 19: 20155 (HASL-159)
incorporation in orotidine-5'-phosphate, method for, 19: 20024
measurement on thin-layer chromatograms, equipment and method for, 19: 19792
production using Rossendorf Reactor in East Germany, 19: 20436
tracer use in studies of fatty acid synthesis in diabetic and obese subjects, 19: 21758 (BNL-8864)
use in age estimation of marine carbonates, 19: 20181

CARBON MONOXIDES
content in atmosphere, 19: 20155 (HASL-159)
determination in vented gases from underground nuclear explosion, apparatus for, 19: 19776 (UCRL-12169)
effects on radioinduced carbon dioxide-graphite reactions, (E), 19: 19953 (AERE-R-4201)
electron reactions with, excitation functions for metastable state formation in, 19: 19992
radioinduced production in carbon dioxide-graphite systems, effects of hydrogen and water vapor on, 19: 19954 (AERE-R-4839)
sorption and desorption of residual, in high vacuum, (E), 19: 20144
yields from radiolysis of formic acid–hydrogen peroxide solutions, effects of pH on, 19: 19989
CO–DH, electron reactions with, cross sections for secondary ion formation in, 19: 19995

CARBON STEEL
corrosion by boiling and superheated mercury, 19: 20493
corrosion by Hanford reactor feedwater, tests of inhibitors for, 19: 21714 (RL-REA-592)
welding of pipes and plates of, Hanford procedures for, 19: 20521 (TID-20625(Vol.I(Rev.I))
welding of pipes and plates of, Hanford procedures for, 19: 20522 (TID-20625(Vol.II)(Rev.I))
welding of pipes and plates of, Hanford procedures for, 19: 20523 (TID-20625(Vol.III)(Rev.I))

CARBON SULFIDES
ionization by electron impact, appearance potential for doubly charged molecule ions in, 19: 20807(R) (UCRL-11828(p.201-4))
reactions with rare earth oxides to prepare sulfides, 19: 19927

CARBON SYSTEMS
B–C–La, phase studies, 19: 19926
B–C–rare earths, phase studies, 19: 19926
C–Co, concentration and temperature effects on density of, 19: 20567(T) (LA-tr-65-5)
C–Mo–Ti–Zr, extrusion of molybdenum-TZC, 19: 20500 (AFML-TR-64-387)
C–Nb–W–Zr, creep properties of D-43, 19: 20474(R) (NASA-CR-54281)
C–Nb–W–Zr, stress corrosion of D-43 by refluxing potassium, research program on, 19: 20474(R) (NASA-CR-54281)
C–Ni, concentration and temperature effects on density of, 19: 20567(T) (LA-tr-65-5)
C–Ta–V–Zr, coating for oxidation protection, 19: 20459(R) (IITRI-B6019-6)
C–Ta–W, phase diagram, 19: 20565 (WADD-TR-60-37(Pt.V))
C–U, thermal conductivity at high temperatures, (E), 19: 20576

CARBON TETRACHLORIDE
effects on alkaline phosphatase activity in human granulocytes, 19: 19570
effects on radioinduced carbon dioxide-graphite reactions, (E), 19: 19953 (AERE-R-4201)
solvent properties for hydrochloric acid, tridodecylamine hydrochloride, and water, 19: 20039 (EUR-2246.e)
solvent properties in mixtures with butyl, dichlorodiethyl, and ethyl ethers for uranyl nitrates, 19: 20072
solvent properties in mixtures with butyl ether for uranyl perchlorate, 19: 20073

CARBONATES
age estimation of marine, comparison of radiometric methods for, 19: 20181

CARBONYL SULFIDE
ionization by electron impact, appearance potential for doubly charged molecule ions in, 19: 20807(R) (UCRL-11828(p.201-4))

CARBOX PROCESS
evaluation, 19: 20048 (NAA-SR-9335)

CARCINOGENS
tumors induced in rats by, synergistic effects of x radiation, 19: 19606

CARCINOMAS
localization by scintillation after administration of mercury-197, 19: 19715
radiotherapy of human, effects on liver function, 19: 19684
radiotherapy of pelvic and vulvar, method for intralymphatic, 19: 19658
radiotherapy of uterine, 19: 19663
radiotherapy of uterine, dose field distribution in telegamma, 19: 19686
radiotherapy of uterine, radiation dose from cobalt-60 bead implants, 19: 19708

CARTILAGE
metabolic activity of rat, diurnal variations of, 19: 19472(R) (ANL-6938(p.179-93))

CASCADE SHOWERS
calculations of intranuclear, (T), 19: 21239 (LA-3206)
statistical properties of cosmic electromagnetic, (T), 19: 20874 (P-1020(RAND))
statistics for binary, limit distribution in, 19: 20958

CASCADES
parameters of gaseous diffusion, of total minimum flux, 19: 19744 (CEA-R-2622)

CASEIN
protective effects of dietary, against radiation damage in rats, 19: 19628

CATARACTS
radioinduced in rats, RBE of gamma and x radiation for, 19: 19612
CATHODES
design of hollow, for plasma injection devices, 19: 21562
sputtering of copper, oxide production in argon–oxygen plasma, 19: 20827
thorium evaporation from carburized tungsten, at 1900 to 2200°K, (E), 19: 20575
CATIONS
recombination with electrons in dense neutral gas, (T), 19: 20860
CATTLE
cesium-137 and strontium-90 content in muscles and organs in bulls from fallout, 19: 20215
iodine-131 secretion in milk of, after single dose, 19: 19477
CAVES
radiation protection in use of gamma, 19: 20213
CAVITY RESONATORS
description of r-f, used for frequency modulation of synchrotron beams, (E), 19: 20735 (UCRL-11807)
design for accelerating charged-particle beams, (E), 19: 20719 (BNL-8970)
fabrication, properties, and theory of superconducting, 19: 21186
performance of chains of, for proton linacs, 19: 20725 (LA-DC-6760)
testing of cloverleaf, for proton linacs, 19: 20724 (LA-DC-6759)
CELLULOSE
radiation chemistry of, review, 19: 19961(T) (CEA-tr-A-1741)
radioinduced graft polymerization on, bibliography, 19: 19960 (VDDIT-93)
CELLULOSES
radiation chemistry of, review, 19: 19961(T) (CEA-tr-A-1741)
CEMENTS
preparation of, uses of radioisotopes in industrial, 19: 20417
CENTRIFUGAL PUMPS
design for sampling radioactive liquids, 19: 20101(T) (ORNL-tr-442)
CENTRIFUGES
materials evaluation for continuous, in multipurpose fuel recovery plant, 19: 20481 (ORNL-3787)
CERAMIC MATERIALS
development of refractory, with lowered firing temperature, 19: 20461 (NP-14893)
fabrication by vibratory and impact methods, 19: 20526
research program on, 19: 20455(R) (DCAS-TDR-62-192)
CERIUM
determination by titration, suitability of tetraethylenepentamine heptaacetic acid for, 19: 19813
determination in mixture of rare earths by polarography, 19: 19821
determination using 5,5'-thiodisalicylic acid, gravimetric, 19: 19812
determination using diantipyrinyl-*p*-nitrophenylmethane, colorimetric, 19: 19819
nucleon reactions at high energies, secondary nucleon yields from, (E/T), 19: 21242 (NP-14837)
separation from aqueous solution by solvent extraction as salicylate pyridine complex, 19: 20079
separation from berkelium in trace amounts by extraction chromatography, 19: 20071
separation from irradiated fuels, 19: 20084(P)
separation from magnesium–thorium alloy by transfer to liquid scrub alloy in fused salt, 19: 20066
separation from nitric acid solutions by solvent extraction using dialkyl phosphoric acid, 19: 20075
separation from other light lanthanides by partition chromatography following production by proton bombardment of erbium, 19: 20078
separation from scandium by solvent extraction of diantipyrinylmethane complex, 19: 20080
CERIUM ALLOYS
Ce–Co–Pu, corrosion by sodium at 650°C, 19: 21690(R) (LA-3244)
Ce–Co–Pu, corrosive effects on tantalum and tantalum–tungsten alloys at 600 to 1100°C, 19: 21690(R) (LA-3244)
Ce–Co–Pu, preparation of homogeneous, 19: 21690(R) (LA-3244)
Ce–Co–Pu, production of uniform rods of, by chill casting, 19: 20506 (LA-3209)
Ce–Mg, oxidation by moist nitrogen at 475 to 600°C, 19: 20485
CERIUM COMPLEXES
with EDTA, migration in electrodialysis cell, 19: 20052 (ORNL-TM-1035)
with serine, stability and composition, 19: 19874
CERIUM HYDRIDES
CeH_x–LiH, phase studies, 19: 19881
CERIUM IONS
solvent extraction from molten nitrate by liquid silicone–TBP at 150°C, 19: 19833 (CEA-R-2628)
CERIUM ISOTOPES
determination in air by beta measurement, efficiency of counter for, 19: 20169
photon reactions (*y*,n), cross sections for, (E), 19: 21287
CERIUM ISOTOPES Ce-137
gamma ray of metastable, low-temperature anisotropy in cerium magnesium nitrate of 255-kev, 19: 21162(R) (UCRL-11828(p.199-201))
CERIUM ISOTOPES Ce-140
energy levels of, nuclear magnetic moment of 2084-kev, (E/T), 19: 21254(R) (UCRL-11828(p.55-6))
CERIUM ISOTOPES Ce-141
content in air over Indian and Pacific Oceans in 1961–62, 19: 20158 (NP-14712)
content in stratosphere, 19: 20657(R) (DASA-1309)
CERIUM ISOTOPES Ce-142
energy levels of, parity and spin for, (E), 19: 21314
CERIUM ISOTOPES Ce-144
beta decay spectra, 19: 21340
content in air on Hayes Island, 1960–61, 19: 20157 (NP-14697)
content in air over Indian and Pacific Oceans in 1961–62, 19: 20158 (NP-14712)
content in stratosphere, 19: 20657(R) (DASA-1309)
properties of, nuclear and physical, 19: 20402 (TID-7698(Pt.I)(p.17-30))
separation from power reactor fuels, economics of, 19: 20036 (BNWL-25)
separation from wastes in Hanford isotope plant, feasibility study, 19: 20431 (TID-7698(Pt.I)(p.1-16))
shielding power sources of, 19: 21595 (TID-7698(Pt.I)(p.33-248))
CERIUM OXIDES
CeO_2–HfO_2–MgO–Mo, preparation and properties of macrolaminate particle composites of, 19: 20558(R) (NP-14888)
CERIUM SULFATES
crystal structure of octahydrates and nonahydrates, 19: 19857
CERIUM SULFIDES
preparation by sulfonation of oxide using carbon disulfide, 19: 19927
CERIUM ZIRCONATES
preparation and properties of, 19: 19925
CESIUM
collision with cesium ions and electrons, measurement of probabilities of, 19: 20805(R) (NASA-CR-54223)
determination by precipitation as diliturate, 19: 19824
effects as impregnant on performance of tungsten emitters in hypersonic plasma generators, (E), 19: 20905 (SC-RR-65-54)
efficiency of argon–cesium MHD-generator plasma in electric field, (T), 19: 21556
electric dipole moment of atomic, 19: 20840
electron elastic scattering at 0.1 to 2.0 ev, cross sections for, (T), 19: 20842
electron energy loss in nonequilibrium argon–cesium plasma, nitrogen effect on, (E), 19: 21560
geochemistry and mineralogy of, in Cherry Mountains (Urals), USSR, book, 19: 20190
plasma of, radiation losses from high-temperature, (T), 19: 21505(T)
separation from aqueous solutions by solvent extraction using tetraphenylboron, 19: 20058
separation from cobalt by ion exchange on montmorillonite, 19: 19794
separation from other fission products by thin-layer chromatography, 19: 20069
separation from pollucite ores, development of processes for, 19: 20044 (IS-T-1)
separation from water and snow by electrodialysis, 19: 19809
spectra of, resonance oscillator strengths of, 19: 21690(R) (LA-3244)
spectral lines of, effects of argon and helium on, 19: 20870
thermodynamic properties of vaporous, 19: 20116(R) (SAN-409-12)
use in seeding plasma in magnetohydrodynamic cells, 19: 21690(R) (LA-3244)
CESIUM ALLOYS
Ce–Zn, heats of formation and fusion of intermetallic compound $CeZn_2$ in, 19: 19838 (IS-1070)
CESIUM ALUMINUM SILICATES
separation of cesium from pollucite, development of processes for, 19: 20044 (IS-T-1)
CESIUM CHLORIDES
crystal structure polymorphic transformation of, transition energy for, 19: 19900
CESIUM CHLORORUTHENATES
structure of $Cs_2RuCl_5H_2O$, 19: 19845(R) (UCRL-11828(p.146))
CESIUM COMPLEXES
with EDTA, migration in electrodialysis cell, 19: 20052 (ORNL-TM-1035)
CESIUM COMPOUNDS
solubility and thermolysis of diliturate, 19: 19824

CESIUM IONS
collision with cesium atoms, measurement of probability of, 19: 20805(R) (NASA-CR-54223)
CESIUM ISOTOPES Cs-131
secretion in human saliva, 19: 19486
CESIUM ISOTOPES Cs-134
content in man, relation of content in milk and food to, 19: 20225
determination in soil after nuclear detonation, gamma spectroscopic, 19: 19829
gamma spectrum, (E), 19: 20342
CESIUM ISOTOPES Cs-137
contamination of food chain by, from fallout, 19: 20240
content in air on Hayes Island, 1960–61, 19: 20157 (NP-14697)
content in air over Indian and Pacific Oceans in 1961–62, 19: 20158 (NP-14712)
content in diet in U. S., 1964, 19: 20154(R) (HASL-158)
content in man, relation of content in milk and food to, 19: 20225
content in milk in Canada, 1964, 19: 20161 (NP-14869)
content in muscles and organs in bulls from fallout, 19: 20215
content in stratosphere, 19: 20657(R) (DASA-1309)
detection and measurement in solution, use of 4π counter in absolute, 19: 19755 (KFK-252)
detection and measurement of, performance of whole-body plastic scintillation detector for, 19: 20377
determination by collection on ammonium phosphomolybdate and counting, 19: 19805
determination in air by beta measurement, efficiency of counter for, 19: 20169
determination in natural water reservoirs, rain water, and snow using electrodialysis and gamma spectroscopy, 19: 19809
determination in rain water, using scintillation gels, (E), 19: 20335
determination in waste waters, methods for, 19: 19749 (EUR-2118.f)
distribution in soils in Kansas, 19: 20657(R) (DASA-1309)
half life of, relation of decay rate and growth of barium-137 daughter to, 19: 20031
properties of, nuclear and physical, 19: 20402 (TID-7698(Pt.I)(p.17-30))
separation from food and water, 19: 20240
separation from power reactor fuels, economics of, 19: 20036 (BNWL-25)
separation from storage basin water, 19: 20042(R) (IDO-14646)
separation from wastes in Hanford isotope plant, feasibility study, 19: 20431 (TID-7698(Pt.I)(p.1-16))
shielding power sources of, 19: 21595 (TID-7698(Pt.I)(p.33-248))
CESIUM NITRATES
melting points and volumes of fusion at 0 to 10,000 atm, 19: 19884
CHARCOAL
sorptive properties for uranium complexes, 19: 20074
CHARGED PARTICLE BEAMS
extraction from Brookhaven AGS, design of systems for, (E), 19: 20718 (BNL-8968)
injection into accelerators, systems for, (E), 19: 20737 (UCRL-11955)
integrator circuit design for cyclotron, 19: 20284(R) (UCRL-11828 (p.222-3))
interaction with ultrasonic waves in piezoelectric crystals, (T), 19: 20672
separator for, testing of r-f, (E), 19: 20748
spectroscopy of Bevatron, instruments for, (E), 19: 20326 (UCRL-11787)
CHARGED PARTICLES
absorption by conductors, range-energy relations for, (E), 19: 20806 (ORNL-3702)
acceleration by electrostatic fields, (T), 19: 20722 (JINR-D-1946)
acceleration using lasers, drift tubes for, (T), 19: 20709
book: *Tables of Coulomb Wave Functions (Whittaker Functions)*, 19: 21117(T)
Cherenkov emission by, in dielectric in longitudinal magnetic field, (T), 19: 21064
detection and measurement using h-f alternating-voltage crystal counters, 19: 20389
distribution in Van Allen Radiation Belts, solar storm effects on, (T), 19: 21137
excitation in Van Allen radiation belts, 19: 21154
flux in magnetosphere, effects of geomagnetic field variations on, 19: 21126
ionization by, method for measuring, 19: 20339
motion in central potential field, (T), 19: 20810
motion in electromagnetic fields, trajectories for, (T), 19: 21099
motion in magnetosphere and radiation belts during magnetic storms, (T), 19: 21128(T)
production in reactions between complex nuclei, high energy, (T), 19: 21354
properties of elementary, l-r asymptotics of Green's functions for, (T), 19: 20930 (JINR-E-1975)
reactions with lithium-6, energy production in, 19: 21487(R) (ORNL-3760(p.98-9))
scattering by nuclei, amplitudes and cross sections for small-angle, (T), 19: 21233 (JINR-E-1992)
scattering by nuclear Coulomb fields, amplitudes for, (T), 19: 21425
CHELATES
use in decontamination of radioactive substances, review on, 19: 19656
CHEMICAL ANALYSIS
developments in physical methods of, 19: 19782
methods used at Feed Materials Production Center, manual on, 19: 19772 (TID-7022(Vol.I)(Bk.2))
of surfaces, using alpha scattering, (E/T), 19: 19795
CHEMICAL ENGINEERING
for high-temperature systems, review of problems in, 19: 19868
transients in packed tubular chemical, models for computation of, 19: 19734 (UCRL-11757)
CHEMICAL RADIATION DETECTORS
cell diameter effect on nitrogen yield in nitrous oxide, 19: 20329 (USNRDL-TR-806)
properties of cyclohexane, 19: 20341
CHEMICALS AND REAGENTS
preparation of, uses of radiation in, 19: 20409
CHEMISTRY
radioisotope uses in industrial, 19: 20417
research program of Nuclear Chemistry Division of Lawrence Radiation Laboratory, 19: 19735(R) (UCRL-11828)
CHEMOTHERAPY
of tumors, evaluation of results, 19: 19702
CHERENKOV RADIATION
absorption in electron streams, negative, (T), 19: 20679
emission by point charge in dielectric in longitudinal magnetic field, (T), 19: 21064
CHICKENS
radiation effects on developing embryos, 19: 19466
radiation effects on ionic permeability of rooster erythrocytes, 19: 19577
CHIMERAS
effects of allogenic bone marrow, on repopulation of lymphatic tissues in irradiated mice, 19: 19646
radiation bone marrow and lymph cell, effects on kidney grafts in dogs, 19: 19493
radiation mouse, amyloidosis and relation to lymphoid hypoplasia in, 19: 19650
radiation mouse, thymus effects on immunological reactivity and tolerance to marrow grafts in, 19: 19652
CHLORAMPHENICOL
effects on ultraviolet-induced mutants of *Staphylococcus aureus*, 19: 19531
CHLORIDE COMPLEXES
with polonium, stability of, effects of acetone on, 19: 19906
CHLORIDE IONS
reactions with cobalt ions, equilibrium constant for, 19: 19833 (CEA-R-2628)
solvent extraction from molten nitrate by liquid silicone–TBP at 150°C, 19: 19833 (CEA-R-2628)
CHLORIDES
effects on spectrophotometric determination of zinc using 1-(2-thiazolylazo)-2-naphthol, 19: 19814
CHLORINE
determination by neutron activation-gamma spectrometry method, 19: 19826
determination in presence of phosphorus and sulfur by activation methods, 19: 19798
determination in selenium by activation methods, 19: 19798
effects on radioinduced carbon dioxide-graphite reactions, (E), 19: 19953 (AERE-R-4201)
evolution from terphenyl in loop corrosion test, 19: 20469 (EUR-2279.e)
x-radiation scattering by, Hartree-Fock calculations of incoherent, 19: 20824
CHLORINE ISOTOPES
effects on molecular properties of lithium chloride, 19: 19848(R) (UCRL-11828(p.193-7))
CHLORINE ISOTOPES Cl-34
beta decay of, CVC theory and ft values for, (T), 19: 21416
CHLORINE ISOTOPES Cl-35
neutron reactions (n,p) with, in various chlorides, protective effects against oxidation of sulfur produced in, 19: 20004
nitrogen-14 reactions at 30 to 42 Mev, scandium-44 isomer pair production in, (E), 19: 21392
performance in nuclear gyroscopes, (T), 19: 20279 (RTD-TDR-63-4001)
CHLORINE ISOTOPES Cl-36

incorporation in sodium perchlorate, 19: 20028
CHLOROFORM
solvent properties for hydrochloric acid, tridodecylamine hydrochloride, and water, 19: 20039 (EUR-2246.e)
solvent properties in mixtures with butyl, dichlorodiethyl, and ethyl ethers for uranyl nitrates, 19: 20072
solvent properties in mixtures with butyl ether for uranyl perchlorate, 19: 20073
solvent properties for rare earth complexes with salicylic acid and pyridine, 19: 20079
solvent properties for scandium complexes with diantipyrinylmethane, 19: 20080
CHLOROPLASTS
dichroism spectrum of quantasome aggregates from, measurement of, 19: 21773 (UCRL-11308)
CHLORTETRACYCLINE
protective effects against radiation sickness in rats, 19: 19637
CHOLESTEROL
metabolism in rats, effects of hypothyroidism on, 19: 19511(T) (JPRS-29364(p.1-4))
radiation effects on metabolism of, in rats, 19: 19511(T) (JPRS-29364(p.1-4))
radiation effects on content of, in adrenal cortex, 19: 19584
CHOLINESTERASES
radiation and immunization effects on activity of, in rabbits, 19: 19609
CHROMATOGRAPHY
column preparation for gas, by radioinduced polymerization of hexamethyldisilazane on firebrick, 19: 19997
equipment for analysis of vented gases from underground nuclear explosion, 19: 19776 (UCRL-12169)
gas, ionization detector development for use in, 19: 19804
isotope effects of deuterium and hydrogen in gas-liquid, of acetylated steroids, 19: 19893
liquid ion exchanger applications in, 19: 20061
radioactivity of thin-layer chromatograms, equipment and method for measuring beta, 19: 19792
response sensitivity of hot-wire thermal conductivity detector for gas, variables affecting, 19: 20281(R) (UCRL-11828(p.204-7))
thin-layer, methods and uses in combination with radiometric analysis, 19: 19808
thin-layer, uses of oxine germanomolybdate and pyridine germanomolybdate in, 19: 20069
CHROMIUM
determination by titration, suitability of tetraethylenepentamine heptaacetic acid for, 19: 19813
determination in ppm range by d-c arc excitation, spectrochemical, 19: 19827
determination in uranium and its compounds and alloys, methods for, 19: 19823
effects on strength of thorium at high temperatures, 19: 20560 (ORNL-3777)
radiation effects on content in dog tissues, 19: 19540
CHROMIUM ALLOYS
Al–Cr–Fe–Y, oxidation mechanism, 19: 20470 (GE-TM-63-7-3)
Al–Cr–Fe–Y, properties of oxidation-resistant, 19: 20470 (GE-TM-63-7-3)
Cr–Fe, corrosion by carbon dioxide at 1100 to 1800°F, 19: 20487
Cr–Fe, magnetic fields at iron-57 nuclei in, (E), 19: 20578
Cr–Fe, overdriving effects on polymorphism dynamics in, 19: 20555 (LA-3215)
Cr–Fe–Ni–Sn–Zr, properties for use as fuel element cladding, 19: 20497(P)
Cr–Nb, elastic properties, 19: 20579
Cr–Nb–V, fabrication and mechanical properties of sheet of, 19: 20552(R) (IITRI-B6021-6)
CHROMIUM CARBIDES
effects on grain growth of uranium carbides, 19: 20515(R) (NCSC-2981-6)
superconducting properties, 19: 20572
use in nozzles for high-temperature thermometry in gases, 19: 20277 (ORNL-P-1068)
CHROMIUM IONS
electron spin resonance spectrum in borate glass, 19: 20620(R) (NYO-2024-8)
CHROMIUM ISOTOPES
neutron reactions with, resonances in, 19: 21454
CHROMIUM ISOTOPES Cr-50
energy levels of, spin of first, 19: 21446
proton reactions at 2.5–3 Mev, resonances in, 19: 21446
CHROMIUM ISOTOPES Cr-51
incorporation in EDTA, use as tracer for gastrointestinal function studies in animals, 19: 20026
production in Spain, 19: 20432(T) (ORNL-tr-295)
use in diagnosis of pulmonary embolism in dogs and man, 19: 19724
use in diagnosis of hemolytic anemia by photoscanning of spleen, 19: 19725
use in scintiscanning of spleen, 19: 19726
use in scintiscanning of spleen, 19: 19727
use in therapy by intra-arterial injection, method for, 19: 19661
CHROMIUM ISOTOPES Cr-52
helium-3 elastic scattering and reactions (He-3,d) at 22 Mev, (E), 19: 21240 (LA-DC-6232)
CHROMIUM OXIDES
spectra of suspensions of, in thin polyethylene films, infrared transmission, 19: 19917
CHROMIUM STEEL
corrosion of Croloy 9M by potassium–sodium alloy, research program on, 19: 20477(R) (ORNL-3604)
corrosion of Croloy 9M by potassium–sodium alloy at high temperatures, carbon mass transfer in, 19: 20478(R) (ORNL-3618)
corrosion of Croloy 9M by potassium–sodium alloy at high temperatures, loop experiments, 19: 20479(R) (ORNL-3671)
corrosion of Croloy 9M by potassium–sodium alloy at high temperatures, mass transfer in, 19: 20480(R) (ORNL-3730)
diffusion of hydrogen in Croloy 9M at 1100 to 1425°F, 19: 20479(R) (ORNL-3671)
diffusion of hydrogen in Croloy 9M at 1100 to 1300°F, 19: 20480(R) (ORNL-3730)
welding of Croloy 9M to austenitic stainless steel, 19: 20475(R) (ORNL-3538)
welding to stainless steel pipe and plate, Hanford procedures for, 19: 20523 (TID-20625(Vol.III)(Rev.I))
Cr–Mo, corrosion of Croloy 2¼ in sodium-heated steam generator after 4000 hr, 19: 20107(R) (BAW-1280-22)
Cr–Mo–Ni–V, development, 19: 20462(R) (NRL-6258)
Cr–Ni, brittle fracture of super ELSO, 19: 20549(R) (EURAEC-1282)
CHROMIUM SYSTEMS
Cr–Si–Th, crystal structure of compound in, 19: 20568
Cr–Si–U, preparation and crystal structure of compounds in, 19: 19871
CHROMOSOMES
radiation effects on *Crepis capillaris* seeds, moisture effects on fast neutron post-, 19: 19581
radiation effects on barley seed, partial recovery from, 19: 19639
radioinduced aberrations of, in maize, 19: 19527
radioinduced aberrations in human leukocytes, 19: 19596
radioinduced aberrations, 19: 19614
CIRCUITS
design for computer-coupled activation analysis system, 19: 19765(R) (TEES-2671-4(Chap.2))
excitation of parallel resonant LRC, from fast-sweeping signal source, 19: 21757 (BNL-7918)
for radiation dose rate telemetering systems, 19: 20317 (HW-82369)
CITRATES
effects on spectrophotometric determination of zinc using 1-(2-thiazolylazo)-2-naphthol, 19: 19814
CIVILIAN DEFENSE
medical aspects of, 19: 19554
medical aspects of, 19: 19555
post-attack recovery from nuclear warfare, ecological problems, 19: 19504 (RM-2801-PR)
shelters for urban populations, design and cost of tunnel-grid, 19: 20202 (ORNL-P-1093)
CLAYS
movement in porous media, tracer studies of, 19: 20183
CLOUD CHAMBERS
ion drift in, (E), 19: 20344
COAL
mining of, use of radioisotopes in, 19: 20417
mining of, uses of light from nuclear reactors in, 19: 21710
reactions with uranium oxide, uranium carbide preparation by, 19: 20537(P)
COATINGS
bonding process for stainless steel on steel, development of, 19: 20504(R) (EURAEC-1228)
deposition on refractory materials, ultrasonic method for nondestructive testing of, 19: 20127(R) (IITRI-N213-23)
development for oxidation protection of niobium alloys at 2300°F, 19: 20483 (SCNC-318)
development of oxidation-protective, for vanadium-base alloys at 1800 to 2500°F, 19: 20459(R) (IITRI-B6019-6)
COBALT
analysis of, x-ray emission, 19: 19747 (CONF-650214-1)
bremsstrahlung reactions (γ,n) at 10 to 28 Mev, cross sections for, (E), 19: 21305

determination in animal food, activation, 19: 19771(R) (TEES-2671-4 (Chap.9))
determination in steel by activation methods, 19: 19784
determination in uranium and its compounds and alloys, methods for, 19: 19823
effects of spectrophotometric determination of zinc using 1-(2-thiazolylazo)-2-naphthol, 19: 19814
iridium-193 Mössbauer effect in, (E), 19: 21255(R) (UCRL-11828 (p.57-8))
magnetic fields at nuclei in, (E), 19: 20578
neutron reflection by, analysis of total, (E), 19: 21201(T) (KFK-tr-164)
neutron scattering from magnetized mirrors of, spin reversal in thermal, 19: 21300
proton reactions at 160 Mev, 0.6- to 11-Mev gamma rays from, (E), 19: 21243 (ORNL-3506)
proton reactions at 160 Mev, secondary nucleon spectra from, (E/T), 19: 21244 (ORNL-P-844)
radiation effects on magnetism of, at 28°K, neutron, 19: 20652
separation from cesium by ion exchange on montmorillonite, 19: 19794
separation of magnesium from, by complex formation and solvent extraction, 19: 19833 (CEA-R-2628)

COBALT ALLOY COUPLES
Co–Au/Cu, thermocouple tables for cryogenic, smoothed, 19: 20272 (ORNL-3649(Vol.2)(Sect.2.10))

COBALT ALLOYS
Ce–Co–Pu, corrosion by sodium at 650°C, 19: 21690(R) (LA-3244)
Ce–Co–Pu, corrosive effects on tantalum and tantalum–tungsten alloys at 600 to 1100°C, 19: 21690(R) (LA-3244)
Ce–Co–Pu, preparation of homogeneous, 19: 21690(R) (LA-3244)
Ce–Co–Pu, production of uniform rods of, by chill casting, 19: 20506 (LA-3209)
Co–Fe, magnetic fields at iron-57 nuclei in, (E), 19: 20578

COBALT BROMIDES
use with silica gel as moisture indicator, 19: 21783(P)

COBALT CHLORIDES
cobalt-57 Mossbauer spectra in hydrated, (E), 19: 20032

COBALT COMPLEXES
ammine, radiolysis, 19: 19974

COBALT(III) COMPLEXES
ammine bromide, recoil reactions from isomeric transition of bromine-80m in, 19: 19973

COBALT(II) FLUOSILICATES
cobalt-57 Mossbauer spectra in hydrated, (E), 19: 20032

COBALT IONS
reactions with chloride and cyanide ions, equilibrium constants for, 19: 19833 (CEA-R-2628)
solvent extraction from molten nitrate by liquid silicone–TBP at 150°C, 19: 19833 (CEA-R-2628)

COBALT ISOTOPES Co-54
beta decay of, CVC theory and ft values for, (T), 19: 21416

COBALT ISOTOPES Co-55
energy levels of, properties of $2p_{3/2}$ single-particle, (E/T), 19: 21240 (LA-DC-6232)

COBALT ISOTOPES Co-56
beta decay shape factor, (T), 19: 21321

COBALT ISOTOPES Co-57
content in stratosphere, 19: 20657(R) (DASA-1309)
energy level spacings in, 19: 21446
Mössbauer spectra in hydrated cobalt compounds, (E), 19: 20032

COBALT ISOTOPES Co-58
content in stratosphere, 19: 20657(R) (DASA-1309)
production in Spain, 19: 20432(T) (ORNL-tr-295)

COBALT ISOTOPES Co-59
magnetic fields acting on, in ferromagnetic materials, 19: 20578
neutron reactions (n,α) at 12.6 to 19.6 Mev, cross sections for, (E), 19: 21290

COBALT ISOTOPES Co-60
activity determination by 4π beta-gamma coincidence method, corrections for, 19: 20385
content in stratosphere, 19: 20657(R) (DASA-1309)
determination in soil after nuclear detonation, gamma spectroscopic, 19: 19829
dosimetry of gamma radiation from teletherapy unit using, 19: 19733
electron pair production cross section near threshold, (E), 19: 21252(R) (UCRL-11828(p.35-8))
gamma emission by, intensities near air/ground interface, (T), 19: 20163 (RRA-M42)
gamma spectrum, (E), 19: 20342
production using Rossendorf Reactor in East Germany, 19: 20436
properties of, nuclear and physical, 19: 20402 (TID-7698(Pt.I)(p.17-30))
separation from power reactor fuels, economics of, 19: 20036 (BNWL-25)
shielding power sources of, 19: 21595 (TID-7698(Pt.I)(p.33-248))
therapeutic use in treatment of uterine carcinoma, 19: 19663

COBALT NITRATES
$Co(NO_3)_2$–$Th(NO_3)_4$, crystal structure of octahydrates, 19: 19852

COBALT OXIDES
spectra of suspensions of, in thin films of polyethylene, infrared transmission, 19: 19917
Al_2O_3–CoO–MoO_3, catalytic properties for benzene synthesis from acetylene, for radiocarbon dating, 19: 19944 (ORINS-50)

COBALT SULFATES
cobalt-57 Mossbauer spectra in hydrated, (E), 19: 20032

COBALT SYSTEMS
C–Co, concentration and temperature effects on density of, 19: 20567(T) (LA-tr-65-5)
Co–Si–Th, crystal structure of compound in, 19: 20568

COINCIDENCE CIRCUITS
design, 19: 20321 (ISS-64/28)

COINCIDENCE COUNTERS
design for measuring cosmic ray density in stratosphere, 19: 20346
design of γ-γ, with energy analysis, 19: 20342
distribution function of retina-like, (T), 19: 20352
performance as dosimeters in mixed gamma and neutron fields, 19: 20330(T) (AEC-tr-6547)
performance of, reduction of accidental coincidences and misses in, 19: 20345

COINCIDENCE MEASUREMENTS
corrections for 4π β-γ, 19: 20385
corrections in β-γ, of radioisotope activities, 19: 20386

COLLIMATORS
efficiency of neutron, computer analysis of, (T), 19: 21612 (NAA-SR-Memo-10557(Pt.I))
efficiency of neutron, computer analysis of, (T), 19: 21613 (NAA-SR-Memo-10557(Pt.II))

COLLOIDS
production of radioactive gold-198, procedures for, 19: 20022(T) (JPRS-29258)
radioactive, particle size distribution in, diffusion technique for determining, 19: 19901
use of scintillation, for weak beta counting, (E), 19: 20335

COLORADO
uranium isotopic fractionation in sandstone of Slick Rock District, 19: 20187

COLUMBITES
analysis for niobium, tantalum, and uranium by x-ray fluorescence spectrometry, 19: 19754 (JEN-134-DQ/I-39)

COLUMN PACKING
preparation for gas chromatography by radioinduced polymerization of hexamethyldisilazane on firebrick, 19: 19997

COMMUNICATION THEORY
development of statistical, for activation analysis, 19: 19766(R) (TEES-2671-4(Chap.3))

COMPLEXES
composition and stability of, use of ion exchange in studies on, 19: 19837 (IA-1000)

COMPUTER PROGRAMS
AA-6, for analysis of pulse-height spectra in activation analysis, 19: 19770(R) (TEES-2671-4(Chap.8))
ALCI, neutron two-dimensional multigroup scattering code, (T), 19: 21197 (CEA-R-2747 and Add.)
Algal compiler modifications, 19: 20439(R) (COO-614-31)
CLUB, for efficiency of neutron collimators, (T), 19: 21612 (NAA-SR-Memo-10557(Pt.I))
CLUB, for efficiency of neutron collimators, (T), 19: 21613 (NAA-SR-Memo-10557(Pt.II))
DAIXY, for multigroup neutron scattering in two-dimensional space with XY geometry, 19: 21198 (CEA-R-2759)
DYNPROG, for xenon minimax problem in thermal reactors, for Philco 2000, 19: 21639 (IA-988)
ESR IV, for electron spin resonance spectra of organic radical anions, Fortran II, 19: 19945 (UCRL-11864)
EVAP, evaporation of neutrons from compound nuclei, FORTRAN, (T), 19: 21245 (ORNL-TM-196)
for calculations of intranuclear cascades, (T), 19: 21239 (LA-3206)
for CDC computers, catalog of, 19: 20438 (ANL-7016)
for complex magnetic systems, 19: 21486(R) (ORNL-3760(p.77-93))
for cosmic-ray neutron background, 19: 20872(R) (ANL-6938(p.71-88))
for determining optimal tendon configuration in pre-stressed concrete reactor structure, 19: 21610 (GAMD-6109)
for Euler coefficients of Fourier series of discrete functions, FORTRAN II for IBM 709/7090/7094, (T), 19: 20442 (NAA-SR-Memo-9729)

for fields of magnetic cylinders and rings, 19: 21486(R) (ORNL-3760 (p.77-93))
for fuel cladding temperatures in Piqua reactor, (E), 19: 21691 (NAA-SR-Memo-9492)
for gas, liquid, steam, and vapor flow calculations, FORTRAN, 19: 20115 (ORNL-TM-1093)
for indexing x-ray diffraction powder patterns for cubic case, FORTRAN for IBM 709/7090, 19: 19834 (HW-74393)
for indexing x-ray diffraction powder patterns for orthorhombic case, FORTRAN for IBM 709/7090, 19: 19835 (HW-89062)
for magnetic fields of FFAG accelerators, (E), 19: 20729 (MURA-706)
GUTS, analysis of bubble-chamber data, FORTRAN, (T), 19: 20320 (IS-989)
HARMONY, package for reactor depletion calculations, in FORTRAN II for Philco 2000, 19: 21644 (WAPD-TM-478)
HERDAG, analysis of nuclear magnetic and quadrupole resonances, (T), 19: 21246 (TID-21697)
MO, for molecular orbital calculations for organic radical anions, Fortran IV, 19: 19945 (UCRL-11864)
MUSY2, reactor physics code, (T), 19: 21666(R) (GEAP-4640)
SCALP, analysis of SNAP-8 DRM1 test data, (E), 19: 21721 (NAA-SR-Memo-10160)
SPECTRA, for bremsstrahlung spectra from shielded isotopic power sources, 19: 21595 (TID-7698(Pt.I)(p.33-248))
TARGET, for stress analysis of prestressed concrete structures by finite element method, 19: 20086 (GAMD-5926)
TARGET, for stress analysis of bodies of revolution, in FORTRAN IV for IBM 7044, 19: 21609 (GAMD-5001(Rev.2))
YOGI-G, gamma energy deposition in matter, FORTRAN II for IBM 7090/7094, (T), 19: 21596 (UCRL-12005)
ZEEMAN, analysis of nuclear magnetic and quadrupole resonances, (T), 19: 21246 (TID-21697)

COMPUTERS
description of TRASK, with 24 K 40-bit word memory (5 μsec cycle) for reduction of nuclear data, 19: 20447
development of parallelism in, for efficiency and speed, (T), 19: 20444 (UCRL-12293-T)
DICE Mk. IV, for preparation of nuclear data for Monte Carlo calculations, in S2 for IBM 7030, 19: 21196 (AWRE-O-81/64)
operation of Maniac III, 19: 20439(R) (COO-614-31)
programming for hybrid computation for optimal reactor control, 19: 21604 (EUR-2202.e)
programming system for CDC 6600, OCTOPUS/6600, 19: 20443 (UCRL-12256)
use for determination of isodoses in radiotherapy, 19: 19692
use for translations, development and equipment for, 19: 20452
use of CDC 160-A, for multi-channel analyzer data processing, 19: 20315(R) (ANL-6938(p.206-8))
use of IBM 709, in Mark II activation analysis system, 19: 19765(R) (TEES-2671-4(Chap.2))
use on-line for data acquisition from FR2 research reactor experimental facilities, 19: 21731 (KFK-242)
uses of conference on, 19: 20305

CONCRETES
fallout decontamination of areas paved with, 19: 20207 (USNRDL-TR-797)
gamma shielding by, nomograms for determining thicknesses for, 19: 21598
gamma streaming through air duct in, 19: 21594 (AD-424387)
performance of prestressed, in reactor pressure vessels, (T), 19: 21683 (GAMD-5272(Rev.2))
properties for reactor shielding, 19: 21739
stress analysis of prestressed, finite element method for, 19: 20086 (GAMD-5926)
stress analysis of pressure vessel reinforced, computer program for, 19: 21609 (GAMD-5001(Rev.2))
tendon configuration for pre-stressed, optimum, 19: 21610 (GAMD-6109)
thermal protection of structures of, 19: 20110 (GAMD-5432)
waste fixation in, raffinate, 19: 21750 (LA-3150)

CONDENSERS
design for measurement of boiling potassium condensation conductances, 19: 20116(R) (SAN-409-12)

CONFERENCES
see also introduction to Report Number Index
Analysis of Oxygen in Potassium, NASA Round-Robin Meeting, Lewis Research Center, June 4, 1964, 19: 19760 (NASA-TM-X-1085)
High-Voltage Electron Microscope Meeting, AMU-ANL, Argonne National Lab., Feb. 13 to 14, 1964, 19: 20246 (CONF-640204)
Isotopic Power Development, Conference on, Germantown, Maryland, May 18 to 19, 1964, 19: 20426 (TID-7698(Pt.I))
Luminescence, International Conference on, Torun, Poland, Sept. 1963, 19: 19853
Measurement, Control, Regulation, and Automation, International Congress on, Paris, Nov. 15–22, 1963, Vol. I, 19: 20303
Measurement, Control, Regulation, and Automation, International Congress on, Paris, Nov. 15–22, 1963, Vol. II, 19: 20305
Medical Radioisotope Scanning, Athens, April 20–24, 1964, 19: 19709
Rare Earth Metals, Meeting on Problems in Theory and Applications of, Moscow, March 1963, 19: 20468
Sixth International Transplantation Conference, New York City, Nov. 1964, 19: 19462
Vela Uniform Borehole Research, VESIAC conference on progress in, Dallas, Texas, March 9 to 10, 1964, 19: 20173 (VESIAC-4410-83-X)

CONSTANTS AND CONVERSION FACTORS
Coulomb wave functions, 19: 21117(T)

CONTAMINATION
monitoring radiochemical plant, alarm system for, 19: 20203 (ORNL-TM-988)
testing for surface, modification in indium adhesion, 19: 20205 (SC-TM-64-1722)

CONVECTION
entrance flow in vertical tubes with combined free-forced, laminar-turbulent transition in, 19: 20114 (NP-14920)

CONVERSION ELECTRONS
angular dependence of, from monocrystalline source, (E), 19: 21339

CONVEYERS
design for facility for separation of plutonium from leachable residues, 19: 20083

COPPER
analysis for hafnium or zirconium using catechol violet, colorimetric, 19: 19780
analysis for impurities by spark source mass spectrography, 19: 19830
bremsstrahlung reactions (γ,n) at 10 to 28 Mev, cross sections for, (E), 19: 21305
copper atom energy losses in, (T), 19: 20686
deposition on vanadium-base alloys for oxidation protection, 19: 20459(R) (IITRI-B6019-6)
determination as impurity in pure bismuth by activation methods, 19: 19796
determination in lead by neutron activation methods, 19: 19815
determination in pure aluminum, activation, 19: 19775(R) (UCRL-11828(p.197-9))
determination in ppm range by d-c arc excitation, spectrochemical, 19: 19827
determination in tissue samples by activation methods, 19: 19807
determination using 5,5′ thiodisalicylic acid, spectrophotometric, 19: 19812
dislocation arrangements in deformed polycrystals of, 19: 21774 (UCRL-11858)
effects as impregnant on performance of tungsten emitters in hypersonic plasma generators, (E), 19: 20905 (SC-RR-65-54)
effects on determination of zinc, 19: 19779
effects on photometric determination of nickel traces in pure molybdenum and tungsten, 19: 19799
effects on spectrophotometric determination of zinc using 1-(2-thiazolylazo)-2-naphthol, 19: 19814
electric conductivity of, effects of quenching in hydrogen and helium on, 19: 20590
electron and ion emission from foils of, laser-induced, (E), 19: 20814
meson (K^+) absorption at 4.75 Bev/c, cross sections for, (E), 19: 21431
meson (π^-) reactions (π^-,$n\gamma$) with, energy spectra from, (E), 19: 21315
nucleon reactions at high energies, secondary nucleon yields from, (E/T), 19: 21242 (NP-14837)
proton ranges in, energy determination by, 19: 21436
radiation effects on defects in monocrystalline, electron, 19: 20645
separation from lead by solvent extraction using cuproine, 19: 19815
separation from silver by solvent extraction using tri-*n*-octylphosphine sulfide, 19: 19753 (IS-T-3)
sintering of powder compacts of, near 1000°C, 19: 20465 (TID-20344)
sputtering by argon ions at 1000 ev, 19: 20813
sputtering by argon and oxygen ions, copper oxide production in, 19: 20827
sputtering by ions at 45 kev, thermal spikes in, (E), 19: 20838

COPPER ALLOY COUPLES
Chromel/constantan, thermocouple tables, smoothed, 19: 20268 (ORNL-3649(Vol.2)(Sect.2.6))
constantan/Cu, thermocouple tables, smoothed, 19: 20267 (ORNL-3649(Vol.2)(Sect.2.5))
constantan/Fe, thermocouple tables, smoothed, 19: 20266 (ORNL-3649(Vol.2)(Sect.2.4))
constantan/iron, thermocouple tables for cryogenic JN/JP, smoothed, 19: 20275 (ORNL-3649(Vol.2)(Sect.2.13))

constantan/iron, thermocouple tables for cryogenic YN/YP, smoothed, 19: 20276 (ORNL-3649(Vol.2)(Sect.2.14))
Cu/constantan, thermocouple tables for cryogenic, smoothed, 19: 20273 (ORNL-3649(Vol.2)(Sect.2.11))

COPPER ALLOYS
Be–Cu, fabrication of molds of, 19: 20519 (NP-14879)
Be–Cu, tensile properties of, testing, (E), 19: 20554 (LA-3161)
Cu–Mn–Zn, effects on properties of magnesium and magnesium–zirconium alloy for use as fuel element can, 19: 20610(P)
Cu–Sn, radiation effects on vacancy repeated yielding characteristics of, 19: 20635

COPPER COUPLES
constantan/Cu, thermocouple tables, smoothed, 19: 20267 (ORNL-3649(Vol.2)(Sect.2.5))
Cu/constantan, thermocouple tables for cryogenic, smoothed, 19: 20273 (ORNL-3649(Vol.2)(Sect.2.11))
Co–Au/Cu, thermocouple tables for cryogenic, smoothed, 19: 20272 (ORNL-3649(Vol.2)(Sect.2.10))

COPPER ISOTOPES Cu-62
half life of, (E), 19: 21290

COPPER ISOTOPES Cu-63
deuteron reactions (d,He-3) at 34.2 Mev, single particle strengths in, 19: 21358
magnetic fields acting on, in ferromagnetic materials, 19: 20578
neutron reactions (n,2n) at 12.6 to 19.6 Mev, cross sections for, (E), 19: 21290
proton reactions at 60–420 Mev, comparison of experiment and theory, 19: 21458

COPPER ISOTOPES Cu-64
use in positron scanning for brain tumors, 19: 19713
uses as atmospheric tracer, 19: 20658

COPPER OXIDES
fluorination of monovalent and divalent, kinetics and mechanism of, 19: 19839 (K-1627)
production in copper cathode sputtering by argon–oxygen plasma, 19: 20827
spectra of suspensions of, in thin polyethylene films, infrared transmission, 19: 19917

COPPER SYSTEMS
Al_2O_3–Cu, sintering of dispersion compacts of, near 1000°C, 19: 20465 (TID-20344)
Cu–Si–Th, crystal structure of compound in, 19: 20568

CORDIERITES
devitrification, 19: 20461 (NP-14893)

CORROSION INHIBITORS
testing dichromate, nitrite, and silicate as, in Hanford reactor tanks, 19: 21714 (RL-REA-592)

CORROSION LOOPS
design and operation of potassium–sodium alloy, for studies of SNAP-8 coolant circuit materials, 19: 20480(R) (ORNL-3730)
design and operation of niobium–zirconium, for potassium, 19: 20473(R) (NASA-CR-54269)
operation of potassium–sodium alloy, for studies of SNAP-8 coolant circuit materials, 19: 20477(R) (ORNL-3604)
operation of potassium–sodium alloy, for studies of SNAP-8 primary circuit, 19: 20478(R) (ORNL-3618)
operation of potassium–sodium alloy, for studies of SNAP-8 coolant circuit materials, 19: 20479(R) (ORNL-3671)
program of potassium–sodium alloy, for studies of SNAP-8 coolant circuit materials, 19: 20475(R) (ORNL-3538)
test of boiling-potassium niobium–1% zirconium alloy, 19: 20476 (ORNL-3603)
tests on chlorine evolution from terphenyl in, 19: 20469 (EUR-2279.e)

CORTISONE
effects on calcium-47 and strontium-85 retention in rats, 19: 19476

COSMIC ALPHA PARTICLES
energy spectra of primary, (T), 19: 20882

COSMIC ELECTRONS
bremsstrahlung emission from relativistic, (T), 19: 20881
distribution in space, Explorer XIV survey of, 19: 20900
source of primary, (T), 19: 20880

COSMIC MESONS (μ)
flux in EAS, 19: 20884
intensity in earth, atmospheric effects on, (E), 19: 20897

COSMIC MESONS (π)
decay of, gamma radiation from, (T), 19: 20881
production in nucleon reactions with carbon and brass, inelastic, (E), 19: 20898

COSMIC NEUTRONS
detection and measurement of background of fast, 19: 20872(R) (ANL-6938(p.71-88))
intensity of, effects of solar flares on, 19: 20878(T)

COSMIC PARTICLES
acceleration in shock propropagation from stars, 19: 20770(T)
composition of primary, 19: 20894
composition of ultra-high energy, 19: 20883
detection of, spark chamber efficiency for, 19: 20378
emission in galactic explosions, (T), 19: 20880
energy spectra of primary, (T), 19: 20882
flux at 300 km, (E), 19: 20893
flux in EAS, 19: 20884
helium component of, isotopic composition of, (E), 19: 20899
interactions in nuclear emulsion at 300 km, (E), 19: 20893
reactions with carbon and brass, K_{ee}, inelasticity distribution in, (E), 19: 20898
spectra of galactic and solar-flare, review of, 19: 20902

COSMIC PROTONS
effects of solar, in manned spacecraft, (T), 19: 20873 (D2-11608)
energy spectra of primary, (T), 19: 20882
flux in EAS, 19: 20884
intensity, 19: 20899
interactions in ionospheric F region, (T), 19: 21125 (RAD-TR-64-27)
interactions in nuclear emulsion at 300 km, (E), 19: 20893

COSMIC RADIATION
composition of ultra-high energy, 19: 20883
coupling coefficients for, 19: 20892
coupling factors for components of, (T), 19: 20891
density in stratosphere, radio probe for measuring, 19: 20346
detection and measurement of, laboratory for, 19: 20347
energy spectra of primary, (T), 19: 20882
flux at 200 to 300 km, time variations in, (E), 19: 20895
flux of, diffusion mechanism of diurnal variations of, (E/T), 19: 20875
helium nuclei in, content and energy spectrum of, 19: 20901
intensity during solar activity maximum and minimum, geomagnetic storm effects on, 19: 20888
intensity in atmosphere, Forbush decreases in, (E), 19: 20886
intensity in earth, atmospheric effects on, (E), 19: 20897
intensity in stratosphere, (E), 19: 20876(T)
intensity in stratosphere, latitude dependence of, (E), 19: 20892
intensity of, geomagnetic cutoff effects on, (T), 19: 20887
intensity of, modulation by interplanetary magnetic fields, 19: 20889
intensity variations in stratosphere during geomagnetic storms, (E), 19: 20877(T)
intensity variations, 19: 20885
interactions in stars at 10^{60} ev, stellar explosions from, 19: 20758
interference in ground-satellite links at 20 Mc, (E), 19: 20879
origin, (T), 19: 20880
origin and properties of, review of, 19: 20903
sources of galactic gamma, (T), 19: 20881
sources of r-f, (T), 19: 20768(T)

COSMIC SHOWERS
analysis of, geometric method for statistical, 19: 20896
composition of ultra-high energy, 19: 20883
detection and measurement of, laboratory for, 19: 20347
statistical properties of electromagnetic-cascade, (T), 19: 20874 (P-1020(RAND))

COSMOLOGY
antimatter in universe, optical method for detecting, 19: 20774(T)
evolution of stars, (T), 19: 20758
evolution of universe, prestellar, 19: 20773(T)
field equations in, homogeneous solutions of Einstein's, 19: 21091
gravitational collapse of cosmic bodies, energy release in, (T), 19: 20768(T)
model of type-II supernova outburst, (T), 19: 20769(T)
nebula of 3C-273, (T), 19: 20767(T)

COTTON
analysis of seed from, activation, 19: 19771(R) (TEES-2671-4(Chap.9))
effects of phosphorus-32 on mutation development in, 19: 19580

COUNTING DEVICES
design and performance in determination of pulse losses in activation analysis, 19: 19766(R) (TEES-2671-4(Chap.3))
design of digital decimal pulse ratemeter, 19: 20295

CRATERS
formation by underground explosions, 19: 20090 (SC-RR-65-41)
shape of explosion-produced, method for predicting, 19: 20089 (NP-14887)

CRITICAL ASSEMBLIES
neutron self-shielding in closely packed slab lattices of, (E), 19: 21636 (CONF-654-32)
neutron transport in water-moderated hafnium–uranium-235, resonance interference in, (E/T), 19: 21643 (WAPD-T-1728)

CRUSTACEA

radiation processing of shrimp, effects on storage life, 19: 20407(R) (ORO-626)
radioactive contamination of, 19: 20230
CRYOGENICS
book: *Progress in Cryogenics*, Vol. 4, 19: 21182
magnetic cooling, review of, 19: 21185
CRYSTAL DETECTORS
charged particle absorption and charge separation in h-f alternating-voltage, 19: 20389
CRYSTAL STRUCTURE
radioinduced dislocation loop coalescence in, 19: 20580
CRYSTALS
atom collisions in, non-binary, (T), 19: 20686
gamma emission from isomeric nuclei in perfect, (T), 19: 21407
lattice vibrations of imperfect, (T), 19: 20716
neutron inelastic scattering by doped, electron-phonon interaction effects in, 19: 20671
neutron scattering in, single-phonon Green's function for, (T), 19: 20710
oscillation anharmonicity in, effect on Mössbauer spectrum, (T), 19: 21422
spectroscopic properties of activated laser, review of, 19: 20849
sputtering by ion bombardment, review of, 19: 20819
CUMENE
hydrogen abstraction from, by methyl radicals, 19: 21760 (NYO-2728-4)
CUMENE, *p*-*tert*-BUTYL-
hydrogen abstraction from, by methyl radicals, 19: 21760 (NYO-2728-4)
CURIUM ISOTOPES Cm-242
properties of, nuclear and physical, 19: 20402 (TID-7698(Pt.I)(p.17-30))
separation from power reactor fuels, economics of, 19: 20036 (BNWL-25)
shielding power sources of, 19: 21595 (TID-7698(Pt.I)(p.33-248))
CURIUM ISOTOPES Cm-244
properties of, nuclear and physical, 19: 20402 (TID-7698(Pt.I)(p.17-30))
separation from power reactor fuels, economics of, 19: 20036 (BNWL-25)
shielding power sources of, 19: 21595 (TID-7698(Pt.I)(p.33-248))
CURIUM ISOTOPES Cm-245
separation from power reactor fuels, economics of, 19: 20036 (BNWL-25)
CURRENT INTEGRATORS
design for cyclotron beams, 19: 20284(R) (UCRL-11828(p.222-3))
design for ionization chambers, 19: 20367
CUTTING TOOLS
design of remotely operated, for radioactive materials, engineering drawings of, 19: 20535
CYANIDE IONS
effects on spectrophotometric determination of zinc using 1-(2-thiazolylazo)-2-naphthol, 19: 19814
reactions with cobalt ions, equilibrium constant for, 19: 19833 (CEA-R-2628)
solvent extraction from molten nitrate by liquid silicone–TBP at 150°C, 19: 19833 (CEA-R-2628)
CYANOGEN
ionization by electron impact, appearance potential for doubly charged molecule ions in, 19: 20807(R) (UCRL-11828(p.201-4))
CYANURIC ACID
separation of boric acid from, 19: 19756 (LA-3193)
CYCLOHEPTATRIENE
spectra of radical anions in liquid ammonia, electron spin resonance, 19: 19945 (UCRL-11864)
1,3-CYCLOHEXADIENE
spectra of radical anions in liquid ammonia, electron spin resonance, 19: 19945 (UCRL-11864)
CYCLOHEXANE
carbon-11 recoil reactions in, effects of oxygen and radiation dose on, 19: 20018
effects on luminescence of benzene, mesitylene, toluene, and *p*-xylene, 19: 21771 (TID-21684)
properties as radiation dosimeter, 19: 20341
solvent properties for hydrochloric acid, tridodecylamine hydrochloride, and water, 19: 20039 (EUR-2246.e)
solvent properties in mixtures with butyl ether for uranyl perchlorate, 19: 20073
use as milling medium in preparation of dispersions of uranium carbide in uranium, 19: 20512(R) (NCSC-2981-2)
use as milling medium in preparation of dispersions of uranium carbide in uranium, 19: 20513(R) (NCSC-2981-3)
cyclohexane–methanol, interface in critical fluids of, reflectivity of diffuse, 19: 19952
CYCLOHEXANOL
radiation effects on dehydration of, from sulfur-35-labeled magnesium sulfate–sodium sulfate catalyst, 19: 20013
radiation effects on dehydration of, fast electron, 19: 20013
CYCLOOCTATETRAENE
spectra of radical anions in liquid ammonia, electron spin resonance, 19: 19945 (UCRL-11864)
CYCLOPROPANE
deactivation of vibrationally excited, by collisions with argon, ethylene, helium, and nitrogen, 19: 19938
CYCLOPROPANE, 1,2-DIMETHYL-
isomerization of chemically activated, isotope effects in, 19: 19938
CYCLOTRONS
beam current and dee voltage in, relation between, (T), 19: 20747
beam current integrator for, 19: 20284(R) (UCRL-11828(p.222-3))
emission from magnetic field-plasma boundary layer, (T), 19: 21522
instrumentation for 88-inch, 19: 20282(R) (UCRL-11828(p.218-19))
magnet construction for variable-energy, 19: 20753(P)
operation and development of 88-inch, 19: 20736(R) (UCRL-11828 (p.236-41))
operation of, effects of fluctions on precision of, 19: 20750
CYLINDERS
interactions of hollow, with shock waves in elastic media, 19: 20659 (AD-606490)
response of buried hollow aluminum, to quasi-static overpressures, 19: 20136 (AFWL-TDR-64-13)
CYSTEINE
effects on radiation effects on electroshock seizures in rats, 19: 19514
effects on thermoluminescence of x-irradiated polymers and proteins, 19: 19983
CYTOCHROME C
radiation effects on thermoluminescence, 19: 19983
CYTOLOGY
radiation effects on cell division in sea urchin zygotes, 19: 19496(R) (ANL-6938(p.49-56))
CYTOPLASM
radiation effects on mitosis suppression in *Tradescantia paludosa*, 19: 19579

D

DAREX PROCESS
corrosive effects of solutions from, on candidate alloys for centrifuge, 19: 20481 (ORNL-3787)
DATA RECORDING SYSTEMS
circuit for spacing data groups in Hewlett-Packard Model 562A digital, 19: 20286(R) (UCRL-11828(p.230))
circuit for suppressing insignificant zeros in Hewlett-Packard Model 562A digital, 19: 20285(R) (UCRL-11828(p.229))
description of spectrogram, for use with comparator, 19: 20288(R) (UCRL-11828(p.232-3))
development for multi-channel analyzers, 19: 20315(R) (ANL-6938 (p.206-8))
statistical analysis of punch card records of radiation doses measured by film dosimeters, 19: 20241
DATA TABULATIONS
computer program catalog for CDC, 19: 20438 (ANL-7016)
smoothed emf tables for platinum/platinum–10% rhodium thermocouples, 19: 20263 (ORNL-3649(Vol.2)(Sect.2.1))
smoothed emf tables for platinum/platinum–13% rhodium thermocouples, 19: 20264 (ORNL-3649(Vol.2)(Sect.2.2))
smoothed emf tables for Chromel/Alumel thermocouples, 19: 20265 (ORNL-3649(Vol.2)(Sect.2.3))
smoothed emf tables for iron/constantan thermocouples, 19: 20266 (ORNL-3649(Vol.2)(Sect.2.4))
smoothed emf tables for copper/constantan thermocouples, 19: 20267 (ORNL-3649(Vol.2)(Sect.2.5))
smoothed emf tables for Chromel/constantan thermocouples, 19: 20268 (ORNL-3649(Vol.2)(Sect.2.6))
smoothed emf tables for tungsten/tungsten–26% rhenium thermocouples, 19: 20269 (ORNL-3649(Vol.2)(Sect.2.7))
smoothed emf tables for tungsten–5% rhenium/tungsten–26% rhenium thermocouples, 19: 20270 (ORNL-3649(Vol.2)(Sect.2.8))
smoothed emf tables for tungsten–3% rhenium/tungsten–25% rhenium thermocouples, 19: 20271 (ORNL-3649(Vol.2)(Sect.2.9))
smoothed emf tables for gold–2.1% cobalt/copper cryogenic thermocouples, 19: 20272 (ORNL-3649(Vol.2)(Sect.2.10))
smoothed emf tables for constantan/copper cryogenic thermocouples, 19: 20273 (ORNL-3649(Vol.2)(Sect.2.11))
smoothed emf tables for Alumel/Chromel cryogenic thermocouples, 19: 20274 (ORNL-3649(Vol.2)(Sect.2.12))
smoothed emf tables for constantan(JN)/iron(JP) cryogenic thermocouples, 19: 20275 (ORNL-3649(Vol.2)(Sect.2.13))

smoothed emf tables for constantan(YN)/iron(YP) cryogenic thermocouples, 19: 20276 (ORNL-3649(Vol.2)(Sect.2.14))
superconducting properties of materials, 19: 21187
thermodynamic data on nuclear materials, 19: 19933

DECONTAMINATING SOLUTIONS
effects on intergranularly attacked areas in type 304 stainless steel, 19: 20471 (HW-SA-3628)

DECONTAMINATION
of fallout from paved areas, 19: 20207 (USNRDL-TR-797)
use of chelates in, review on, 19: 19656

DENSITOMETERS
descriptions of radiometric, 19: 20412
radiometric, for sediment measurements by gamma scattering, engineering drawings of, 19: 20419

DENSITY
measurement in ocean-bottom sediments by gamma scattering, 19: 20419

DEUTERIUM
effects on exothermic ion-molecule reactions, 19: 19887
effects on gas-liquid chromatography of acetylated steroids, 19: 19893
effects on ion-molecule reactions under electron bombardment, 19: 19995
effects on ionic decomposition of *t*-butylperoxy formate, 19: 19948
effects on reactions of 2-phenylethyltrimethylammonium iodide with ethoxide and hydroxide ions, 19: 19947
effects on solvolysis of cis-4-*t*-butylcyclohexyl-*p*-bromobenzenesulfonate, 19: 19949
effects on solvolysis of trans-4-*t*-butylcyclohexyl-*p*-bromobenzenesulfonate, 19: 19950
electron attachment in, negative ion production by dissociative, (E), 19: 20691
exchange between water and salts of trioctylamine or benzyldilaurylamine, 19: 19864
exchange between water and anion exchange resin, 19: 19865
exchange to and from azulene in acid solutions, 19: 19883
incorporation in methoxy groups for mass spectrometry, method for, 19: 20034
ionization by electrons at 0.6 to 20 kev, (E/T), 19: 20850
isotope effects in chemical activation systems, 19: 19938
isotope effects on thermal decomposition of 1-ethyl-1-phenylazomethane, 19: 19943 (BNL-8243)
isotope effects on infrared spectra of solid acetylene, 19: 19935
photon reactions with, polarization of protons from, 19: 21456
separation from hydrogen and tritium by adsorption and gas chromatography, 19: 20435
spectra of, rotational analysis B′, B″, D, D′, and D″ states in absorption, 19: 19894
uses in hydrogen determination in metals by isotopic equilibration, 19: 19831

DEUTERIUM HYDRIDES
electron attachment in, negative ion production by dissociative, (E), 19: 20691
spectra of, rotational analysis B′, B″, D, D′, and D″ states in absorption, 19: 19894
CO_2–DH, electron reactions with, cross sections for secondary ion formation in, 19: 19995
CO–DH, electron reactions with, cross sections for secondary ion formation in, 19: 19995
DH–N, electron reactions with, cross sections for secondary ion formation in, 19: 19995
DH–O, electron reactions with, cross sections for secondary ion formation in, 19: 19995

DEUTERIUM IONS
production of monovalent, by electron attachment in deuterium and deuterium hydride, (E), 19: 20691

DEUTERIUM SYSTEMS
D–He, compressibility at high pressures at 25°C, 19: 19840 (LA-3250)

DEUTERONS
emission from neutron reactions with tritium at 14.4 Mev, spectra of, (E), 19: 21404
interactions with photons, parameters for disintegration in, (T), 19: 20937(R) (TID-21672)
interactions with helium-3, nucleons, and tritons, bibliography, (E/T), 19: 21238 (LA-3205)
interactions with electrons, inelastic, (T), 19: 20942
interactions with mesons (π^-), neutron-neutron scattering length from, (E), 19: 20995
nucleon capture by, elastic unitarity effects in radiative, (T), 19: 21371
production of quasi-[illegible] photon absorption in nuclei, (T), 19: 21274
reactions (d,α) with lithium, multi-level analysis of resonances in, (T), 19: 21413
reactions (d,α) at 4 to 12 Mev, (E), 19: 21414
reactions (d,He-3) with copper-63 at 34.2 Mev, single particle strengths in, 19: 21358
reactions (d,n) with tritium at 2.1 and 2.9 Mev, polarization distributions from, (E), 19: 21303
reactions (d,n) with silicon-30, 19: 21376
reactions (d,p) with strontium-88, proton polarization in, 19: 21447
reactions (d,p) with iron-54, energy levels from, (T), 19: 21277
reactions (d,p) with magnesium-24 at 10 and 11 Mev, angular distributions 19: 21311
reactions (d,p) with nuclei, target core excitation in, (T), 19: 21433
reactions (d,p) with carbon-12, distorted wave Born approximation analysis of, 19: 21439
reactions (d,p) with strontium-88 at 11 Mev, polarization from, (E), 19: 21391
reactions (d,p) with krypton-86 at 15 Mev, energy levels from, (E), 19: 21394
reactions (d,p) with nuclei, proton spectra from, 19: 21394
reactions (d,t) with nuclei at 11.8 Mev, angular distributions from, (E), 19: 21326
reactions with deuterided erbium and titanium, neutron yields from, (E), 19: 21301
reactions with thorium-232 and uranium-238 at 18 Mev, tellurium-131 and -133 isomer pair yields from fission, (E), 19: 21390
scattering by helium-4 at 10.3 Mev, cross sections for elastic, (T), 19: 21286
scattering by magnesium-26 at 12 Mev, angular distributions from inelastic, (E), 19: 21311
scattering by nonspherical translucent nuclei, diffraction, (T), 19: 21427

DIABETES
fatty acid synthesis in, tracer studies of, 19: 21758 (BNL-8864)

DIALYSIS
use of electro-, in separation of long-lived fission products, 19: 20052 (ORNL-TM-1035)

DIAMONDS
diffusion of helium in, 19: 19934
radiation effects on plastically deformed, electron, 19: 20638
radiation effects on polishing of, fast neutron, 19: 20639

DIATOMACEOUS EARTH
use as sorptive agent in waste-solution fixation in glass, 19: 21754(P)

DIELECTRIC BREAKDOWN
in cesium vapor through slot in glass, (E), 19: 21578

DIELECTRICS
model of, (T), 19: 20662
radiation effects on radio wave absorption by, 19: 20629

DIES
design for use in preparing radiation sources, engineering drawings of, 19: 20437

DIET
effects on radiation damage to serum albumin in rat liver, 19: 19603
protective effects of fatty, against radiation sickness in rats, 19: 19625
protective effects of casein, against radiation damage in rats, 19: 19628
radioactivity due to fallout in, 1964 and 1965, 19: 20154(R) (HASL-158)
strontium-90 content in, of Argentine children, 19: 20165(R) (TID-21711)

DIFFERENTIAL EQUATIONS
Green-function behavior in finite-difference boundary value problem, 19: 20451

DIFFRACTION GRATINGS
use as drift tubes for charged particle acceleration by lasers, (T), 19: 20709

DIFFUSION
in high-temperature ionized mixtures, calculation of, 19: 19941

DIOCTYLAMINE
solvent properties for uranium, 19: 20067

DIODES
electric current in tunnel, microwave phonon effects on, (E), 19: 21178
plasma oscillations in thermionic, (T), 19: 20913
uses of tunnel, in three-state memory device, 19: 21785(P)

DISASTERS
handling of, involving radioactive contamination, 19: 20197 (COO-281)
medical management of casualties of reactor accident, 19: 19630
radiation dosimeter for use in criticality accidents, 19: 20330(T) (AEC-tr-6547)

DISEASES
radiotherapy of, use of radioisotopes for, 19: 19706

DISILAZANE
hexamethyl-, radioinduced polymerization on firebrick for use as gas chromatographic support, 19: 19997

DISSOLVERS
studies of electrolytic, in Arco Plant, 19: 20042(R) (IDO-14646)

DISTILLATION APPARATUS
development for alkali metals, 19: 20473(R) (NASA-CR-54269)

DODECYLAMINE
solvent properties for uranium, 19: 20067
DOGS
erythropoiesis in normal and acutely-bled, 19: 21777 (UR-662)
kidney transplantation in, effects of bone marrow and lymph cell radiation chimeras on, 19: 19493
kidney transplantation in, evaluation of methods for suppression of immune reactions, 19: 19519
lung transplantation in, 19: 19523
radiation effects on nervous activity of, antenatal, 19: 19536
radiation effects on content of chromium, magnesium, and nickel in tissues of, 19: 19540
radiation effects on blood picture in, proton, 19: 19578
radiodiagnosis of pulmonary embolism in, by photoscanning using chromium-51 or iodine-131, 19: 19724
spleen transplantation in, 19: 19521
spleen transplantation in, 19: 19522
DOSIMETERS
cell diameter effect on nitrogen yield in nitrous oxide, 19: 20329 (USNRDL-TR-806)
design of portable two-capacitor, 19: 20391(P)
development and performance of medical, 19: 19657(R) (ANL-6938 (p.97-119))
development and use of fluororod, for beta particles and gamma radiation, 19: 20314(R) (ANL-6938(p.62-70))
development and uses in radiation protection methods, 19: 20213
development for gamma counting using cyclohexane radiolysis, 19: 20341
development for particle or electromagnetic radiation, 19: 20396(P)
development of uranium-foil, for neutrons, 19: 20340
DRAWING
equipment for, with stationary piston and movable cylinder, 19: 21782(P)
DRUGS
effects of immunosuppressive, on reactions to spleen transplants, 19: 19522
effects of immunosuppressive, on reactions to lung transplants, 19: 19523
effects on bone marrow and organ graft tolerance, 19: 19588
radiation effects on, from exposure to nuclear explosion, review of data on, 19: 20231
skeletal anomalies in fetuses induced by, 19: 19533
DRY BOXES
design for facility for separation of plutonium from leachable residues, 19: 20083
specimen viewing in, design of apparatus for, 19: 20105(P)
DUSTS
analysis for cesium-137, rapid method for, 19: 19805
collection of radioactive, efficiency of foils for, 19: 20236
radioactivity of atmospheric, in Debrecen, Hungary, 19: 20235
DYES
color quenching in liquid scintillation systems, 19: 20324 (ORNL-P-1094)
effects of acridine orange on transduction in *Pseudomonas aeruginosa*, 19: 19502(R) (NP-14932)
DYSPROSIUM
determination in purified uranium compounds by chromatography and spectrography, 19: 19800
separation from other light lanthanides by partition chromatography following production by proton bombardment of erbium, 19: 20078
vapor pressure, 19: 20601
DYSPROSIUM ALLOYS
Sb–Dy, magnetic properties of, (E), 19: 20597
DYSPROSIUM IONS
spectra in barium, calcium, and strontium fluorides, absorption and luminescence, 19: 19854
DYSPROSIUM ISOTOPES Dy-160
energy level transitions in, E2 conversion coefficients of rotational, (T), 19: 21308
properties of, effects of pairing forces on, (T), 19: 21434
DYSPROSIUM ISOTOPES Dy-161
energy level transitions in, probabilities for, (E), 19: 21329
DYSPROSIUM ISOTOPES Dy-162
energy level transitions in, E2 conversion coefficients of rotational, (T), 19: 21308
properties of, effects of pairing forces on, (T), 19: 21434
DYSPROSIUM ISOTOPES Dy-164
energy level transitions in, E2 conversion coefficients of rotational, (T), 19: 21308
DYSPROSIUM NITRIDES
magnetic properties of, influence of crystal field on, 19: 19895
DYSPROSIUM OXIDES
magnetic hyperfine interactions and relaxation times in, (T), 19: 19898
DYSPROSIUM SULFATES
crystal structure and bond types of octahydrates, 19: 19915(T)

E

EARTHQUAKES
epicenter location in southeast Missouri, calibration explosion for, 19: 20171 (AFCRL-64-659)
seismic waves from, model of, 19: 20172(R) (NP-14877)
seismic waves from FALLON, comparison with waves from HARDHAT and SHOAL explosions, 19: 20172(R) (NP-14877)
ECOLOGY
nuclear warfare and, 19: 20199 (HI-388-RR(Pt.III))
problems in post-attack environment of nuclear warfare, 19: 19504 (RM-2801-PR)
EINSTEINIUM ISOTOPES Es-253
alpha decay of, energy levels from, (E/T), 19: 21253(R) (UCRL-11828(p.38-40))
EINSTEINIUM ISOTOPES Es-254
decay scheme, (E), 19: 21257(R) (UCRL-11828(p.63-6))
ELECTRIC ARCS
dissociation of molecular hydrogen ions in, 19: 21484(R) (ORNL-3760(p.57-63))
electrode development for, (E), 19: 20905 (SC-RR-65-54)
measurements of long-solenoid hydrogen, 19: 21483(R) (ORNL-3760 (p.30-56))
proton charge-exchange cross sections in hydrogen and lithium, 19: 21481(R) (ORNL-3760(p.10-22))
stability of, in metal vapors, (E), 19: 21490(R) (TID-21698)
stabilization of deuterium, 19: 21483(R) (ORNL-3760(p.30-56))
ELECTRIC CONDENSERS
impedance of plasma-filled, (T), 19: 20301
ELECTRIC CONDUCTORS
charged-particle range-energy relations in, (E), 19: 20806 (ORNL-3702)
radioinduced currents in insulated, gamma, 19: 20398 (FZK-214)
ELECTRIC CONTROL SYSTEMS
description of, for currents in Brookhaven AGS magnets, (E), 19: 20094 (BNL-8969)
ELECTRIC CURRENTS
formation in plasma flow between electrodes, (T), 19: 21502(T)
ionospheric distributions of, (E), 19: 21124 (P-1121(RAND))
radioinduced in insulated conductor, 19: 20398 (FZK-214)
ELECTRIC DISCHARGE
atom distribution in low-voltage spark, (E/T), 19: 21504(T)
current sheath in toroidal, diffusion of, (E), 19: 21512
electron current fluctuations in Townsend, (T), 19: 21551
electron energy in negative glow of cold-cathode helium, (E), 19: 21499
in h-f magnetic fields, starting mechanism for ring, (E/T), 19: 21554
kinetics of theta-pinch, effects of neutral gas on, (T), 19: 21470 (IPP-1/14)
neutron production by deuterium-gas, 19: 21483(R) (ORNL-3760 (p.30-56))
optical determination of properties of arc, 19: 21555
ELECTRIC FIELDS
effects on electron energy distribution in plasma, (E), 19: 21583
ionizing effects on hydrogen, 19: 21484(R) (ORNL-3760(p.57-63))
measurement in ionosphere, device for, 19: 20290
space charge formation in h-f, in air, (E), 19: 21576
ELECTRIC GENERATORS
design and performance of high-power MHD, (T), 19: 20910
design of 1-Mw open-cycle MHD, 19: 20912
electrode development for hypersonic plasma generator, (E), 19: 20905 (SC-RR-65-54)
ionization in combustion product MHD, methods for non-thermal, 19: 20911
performance of radioisotope-heated thermionic, thermoelectric, and thermophotovoltaic, (E/T), 19: 20904 (BLG-317)
ELECTRIC POWER
generation by magnetohydrodynamic a-c generator, 19: 20914
ELECTRIC PROBES
development, 19: 21480(R) (ORNL-3760(p.1-9))
development for plasma momentum measurements, 19: 21483(R) (ORNL-3760(p.30-56))
response to electromagnetically produced air shock, (E), 19: 20841
ELECTRODES
deterioration of tantalum filaments in electron-bombardment mercury ion thruster, 19: 20138 (NASA-TN-D-2173)
development of emitter, for hypersonic plasma generators, 19: 20905 (SC-RR-65-54)
electric breakdown in coaxial cylindrical geometry, through glass

slot, (E), 19: 21578
performance of tungsten-nickel, in thermionic converters, 19: 20906
plasma flow between, electric current and space charge formation in, (T), 19: 21502(T)
ELECTRODYNAMICS
stability of emf's in weakly ionized plasma, (T), 19: 21559
ELECTROHYDRODYNAMICS
turbulent plane flow in, equations of average, 19: 20670
ELECTROLYTIC CELLS
construction materials for, corrosion resistance of, 19: 20484 (TID-19978(Vol.I))
ELECTROMAGNETIC FIELDS
charged-particle trajectories in, (T), 19: 21099
electron-beam focusing by r-f, (E/T), 19: 20743
plasma boundary layer with, (T), 19: 21585
plasma heating by h-f, (T), 19: 21581
plasma kinetics in, (T), 19: 21493
pressure on dense plasma, metal analog for, (T), 19: 21507
symmetry of, cylindrical, (T), 19: 21084
wave equations for free fields of, (T), 19: 21110
ELECTROMAGNETIC LENSES
aberration of quadrupole, calculation of spherical, (T), 19: 20685
aberrations of quadrupole, 19: 20252 (CONF-640204(p.82-92))
design of plasma, for focusing meson-neutrino beam, 19: 20915 (BNL-8967)
design requirements for high-voltage electron microscopes, 19: 20249 (CONF-640204(p.20-5))
field distributions in optical system of 5-Gev antiproton beam, (E), 19: 20723 (JINR-P-1945)
ELECTROMAGNETIC WAVES
absorption and scattering by solid particles, (T), 19: 20677
emission from fireball of atomic explosion in air, 19: 20675
emission in collisions of charged water drops, ball lightning from, (T), 19: 21150
energy transfer in dispersive media, (T), 19: 20688
interactions with plasma pulses in waveguide, resonance, (E), 19: 21565
interactions with cosmic plasma, h-f turbulence in, (T), 19: 20755
plasma acceleration by, (E), 19: 21566
plasma containment by traveling, (E), 19: 21564
production of vlf, in high-altitude nuclear explosions, (E), 19: 21139
propagation in multiple-wave media, (T), 19: 20944
propagation in plane-stratified isotropic plasma, 19: 21589
propagation in stratified plasma, (T), 19: 21506
propagation in turbulent plasma in space, (T), 19: 20781(T)
propagation of helicon, in partially ionized plasma, (E), 19: 21552
propagation of helicon, in indium metal at 4.2°K, (E), 19: 21553
propagation of r-f, in nonuniform plasma, (T), 19: 21519
refraction by helium at wavelengths longer than 6000 Å, (T), 19: 20859
statistical properties of, 19: 21118
transformation in plasma, (T), 19: 21584
transport in anisotropic plasma, (T), 19: 21466 (AFCRL-64-550)
ELECTROMAGNETISM
Minkowski theory of, Lagrangian formalism for, 19: 20666
ELECTRON BEAMS
bunching of, in Saclay linear accelerator, (T), 19: 20721 (CEA-R-2749)
Cherenkov radiation absorption in, negative, (T), 19: 20679
density and shock wave propagation along cylindrical, (T), 19: 20705
effects in mice, pathological, 19: 19635
effects on defects in copper single crystals, directional, 19: 20645
effects on ion-molecule reactions in acetylene, 19: 19988
effects on magnesium fluoride crystals, 19: 20618 (NBS-8614)
effects on preservation of food, 19: 20410
electromagnetic wave generation by, 19: 20684
focusing by r-f fields, (E/T), 19: 20743
interactions with plasma, diagnostics of, (E), 19: 21488 (PIBMRI-1208-64)
interactions with plasma waves, (T), 19: 21563
properties in food processing, 19: 20422
reaction with quenched uranium dioxide foils, pore production and migration in, 19: 20467
space-charge wave amplification in, longitudinal, (T), 19: 20679
therapeutic uses of, 19: 19673
uses in metallurgy, 19: 20466
ELECTRON CAPTURE
x-ray emission in, method for measuring, 19: 20384
ELECTRON MICROSCOPES
description of scanning high-voltage, 19: 20251 (CONF-640204(p.63-81))
description of supervoltage, outside U. S., 19: 20248 (CONF-640204 (p.17-19))
magnetic lenses for high-voltage, 19: 20249 (CONF-640204(p.20-5))
survey of commercial, 19: 20247 (CONF-640204(p.1-16))
ELECTRON MICROSCOPY
conference on high-voltage, 19: 20246 (CONF-640204)
contrast in high-voltage, effects of electron scattering on, 19: 20254 (CONF-640204(p.123-36))
resolution improvement in, studies, 19: 20250 (CONF-640204(p.26-34))
review of high-voltage, 19: 20253 (CONF-640204(p.106-22))
use in structural studies in molecular biology, 19: 19455 (CONF-640204(p.44-62))
use of high-voltage, in metallurgy, 19: 20548 (CONF-640204(p.35-45))
use of labeled antibodies for studies of ultrastructure, 19: 19465
ELECTRON MULTIPLIER TUBES
dynode materials for, properties of Allen-type, 19: 20388
performance in measurement of charged and neutral beams, 19: 21484(R) (ORNL-3760(p.57-63))
ELECTRON PAIRS
production in gamma reactions in sodium iodide crystals, cross sections for, (E), 19: 21294
production near threshold, cross sections for, (E), 19: 21252(R) (UCRL-11828(p.35-8))
ELECTRON SHOWERS
statistical properties of cosmic, (T), 19: 20874 (P-1020(RAND))
ELECTRON TUBES
radiation effects on, hardening against gamma and neutron, 19: 20399(R) (NP-14946)
ELECTRONIC EQUIPMENT
design, 19: 20321 (ISS-64/28)
design for calibrating frequency-measuring devices, (E), 19: 21766 (SC-TM-64-921)
design for increasing contrast in automatic scintillation scanner, 19: 19696
development of surface-field-controlled semiconductor, (E), 19: 20323(R) (NYO-3246-4)
electron emission in, alternatives to thermionic, 19: 20289
performance of tracking stations for close-in transits, (E), 19: 21767 (SC-TM-65-44)
standardization of, for nuclear-physics studies, (E), 19: 20262 (KFK-259)
ELECTRONICS
nanosecond measurements in, problems in, 19: 20304
ELECTRONS
angular distribution from meson ($K_{\mu 4}$) decay, 19: 21069
attachment in deuterium, deuterium hydride, and hydrogen, negative ion production in, (E), 19: 20691
Boltzmann equation and density matrix for, in disordered systems, (T), 19: 21041
capture by molecules, dissociative resonance, (T), 19: 19899
capture by protons in helium, (T), 19: 20821
capture of hot, by gold-ion impurities in germanium at 20°K, (E/T), 19: 21180
collision in seeded combustion products, (E), 19: 20909
collision with cesium atoms, measurement of probability of, 19: 20805(R) (NASA-CR-54223)
cyclotron radiation from, in magnetic field-plasma boundary layer, (T), 19: 21522
density and temperature in electromagnetic shock tube, Langmuir probe measurement of, (E), 19: 21515
density and temperature in plasma, method for determining, 19: 21572
density in afterglow of hydrogen z-discharge, (E), 19: 21510
density in ionospheric D region, methods for determining, 19: 21127(T)
density in ionospheric F2 region, diffusive equilibrium of topside, (T), 19: 21141
density in lower ionosphere, during solar cosmic ray events, (T), 19: 21145
density in magnetized plasma, microwave measurement of, (E/T), 19: 21513
density in Van Allen belts at 200 to 400 km, 19: 21136
detection of, gas scintillation detector for, 19: 20361
diffusion in gas, at high electric fields and low pressures, (E/T), 19: 20696
diffusion of low-energy auroral, in atmosphere, (T), 19: 21144
dissociation potential in plasma, (T), 19: 21558
distribution function for plasma in high-frequency magnetic field, (T), 19: 21573
distribution functions for gases of, equilibrium, 19: 20683
distribution in protonosphere, whistler dispersion from temperature, (T), 19: 21140
distributions in plasma, interferometer design for analyses of, (E), 19: 21472 (IPP-1/25)
effects of thermal, on plasma wave propagation across magnetic field, (T), 19: 21521

effects on carbon dioxide at 200 ev, 19: 19996
effects on color center formation in potassium bromide and chloride crystals, 19: 19979
effects on dehydration of cyclohexanol, 19: 20013
effects on ethylene, 19: 19993
effects on germanium at 77°K, 19: 20624
effects on ion-molecule reactions in deuterium hydride mixtures with carbon dioxide, carbon monoxide, nitrogen, and oxygen, 19: 19995
effects on luminescence of bibenzyl and pyrene, 19: 19963
effects on metastable state formation in carbon monoxide, hydrogen, nitrogen, and rare gases, 19: 19992
effects on optical absorption bands in lithium fluorides, 19: 20817
effects on oxygenated aqueous solutions of ferrocyanide ions, 19: 20009
effects on plastically deformed diamonds, 19: 20638
effects on surface state of n-type germanium at 1 to 16 kev, 19: 20622
effects on trimeric cyclic dimethylphosphinoborine, 19: 19982
eigenfunctions and energies in atoms, (T), 19: 20835(T)
electric conductivity in degenerate gases of, h-f, 19: 21545
electrostatic potential of shells of, at nuclei in diatomic molecules, (T), 19: 20836(T)
emission from metal foils, laser-induced, (E), 19: 20814
emission of, alternatives to thermionic, 19: 20289
energy distribution in mercury discharge plasma containing inert gases, (T), 19: 21579
energy distribution in alpha Soviet thermonuclear experiment, (E), 19: 21583
energy distribution in hydrogen plasma, equations for, 19: 21586
energy in negative glow of cold-cathode helium discharges, (E), 19: 21499
energy of gases of, at absolute zero, (T), 19: 20711
exchange in proton reactions with hydrogen atoms, cross sections for, (T), 19: 21417
interactions in geomagnetic fields, effects on hydromagnetic wave propagation, (T), 19: 21123 (D1-82-0398)
interactions in hydrogen plasma, equations for, 19: 21586
interactions with phonons in beta tin, (E), 19: 21603
interactions with protons in Overhauser nuclear polarization, 19: 20869
interactions with mesons (π^-) at 21 Bev, meson structure from, (E), 19: 20935 (NP-14885)
interactions with deuterons, inelastic, (T), 19: 20942
interactions with protons, baryon resonances in, (E/T), 19: 20997
interactions with protons, Born approximation for Mott asymmetry in, 19: 21073
interactions with Coulomb fields, vertex modification for, 19: 21094
interactions with phonons in doped crystals, (T), 19: 20671
ionization of diatomic and rare gases at 0.6 to 20 kev, (E/T), 19: 20850
ionization of hydrogen atoms by, electron exchange in, (T), 19: 20854
mobility in silicon detectors, effects on pulse rise time in, 19: 20359
motion in central potential field, (T), 19: 20810
motion in presence of magnetospheric whistler-mode waves, trajectories for, (T), 19: 21099
motion of plasma of, magnetic-dipole-induced, (T), 19: 21535
nuclear excitation by 1- to 3-Mev, test of Robl theory of, 19: 21455
oscillations in plasma, radiation from, (T), 19: 21477 (MATT-290)
oscillations in plasma, harmonic generation and frequency mixing from, (E), 19: 21549
oscillations in plasma, radioinduced instability of, (T), 19: 21550
polarization in degenerate gas of, long-range spin, (T), 19: 20689
production by photo- and radiation chemistry in glasses, ESR spectra of, 19: 20002
reactions with Allen-type dynodes, yields from, 19: 20388
reactions with argon and neon, excitation cross sections for, 19: 20804(R) (ANL-6938(p.36-45))
reactions with compounds by 70-kev, appearance potential for doubly charged molecule ions in, 19: 20807(R) (UCRL-11828(p.201-4))
reactions with gallium arsenides, radiative recombination in, (E), 19: 20703
reactions with helium, ionization cross sections for, (T), 19: 20864
reactions with hydrogen atoms, 2p level excitation in, (T), 19: 20853
reactions with matter at 100 kev to 5 Mev, energy losses in, (T), 19: 21423
recombination with positive ions in dense neutral gas, (T), 19: 20860
renormalization constant of interacting gas of, (T), 19: 20968
scattering by (111) face of nickel, kinematic theory calculations of, 19: 20868
scattering by aluminum at 51 kev, temperature dependence of diffuse, (E), 19: 20867
scattering by benzene, cross sections for inelastic, (T), 19: 20856
scattering by boron-10 at 100 to 220 Mev, excitation of 6.02-Mev level in inelastic, (E), 19: 21306
scattering by carbon atoms, phase shift for elastic, (T), 19: 20858
scattering by helium and hydrogen, evidence for molecular charge distribution in, 19: 20826
scattering by helium, multichannel resonances in forward inelastic, (E), 19: 20848
scattering by hydrogen atoms, exchange amplitudes for excitation in, (T), 19: 20866
scattering by lithium, sodium, potassium, and cesium at 0.1 to 2.0 ev, cross sections for elastic, (T), 19: 20842
scattering by mercury at 100 to 2000 ev, polarization from, (T), 19: 20865
scattering by nuclei, theory of, 19: 21448
scattering by nuclei, analysis of cross section for inelastic, 19: 21452
scattering by nuclear matter, linear response to inelastic, (T), 19: 21393
scattering in high-voltage electron microscopy, elastic and inelastic, 19: 20254 (CONF-640204(p.123-36))
spin interactions with nuclei, energy of, (T), 19: 20695
spin scattering of, bibliography on, 19: 20828
temperature in h-f helium discharge plasma, (E), 19: 21528
temperature in linear MHD generator, (T), 19: 20907
temperature in solar atmosphere, (E), 19: 20775(T)
temperature in transient plasma, triple-probe method for measuring, (E), 19: 21514
use in radiotherapy, physical problems in, 19: 19694
use in radiotherapy, dose distributions in, 19: 19695

ELECTROSTATIC FIELDS
charged particle acceleration in, (T), 19: 20722 (JINR-D-1946)

ELECTROSTATIC PRECIPITATORS
uses in detecting leaks in fuel element cans, 19: 21626(P)

ELEMENTARY PARTICLES
angular momenta and SU(6) symmetry for, 19: 20972
annihilation and production operators for, exchange relations for, (T), 19: 20941
book: *Fundamental Particles*, 19: 21072
charge conjugation and parity of U(12) multiplets for, 19: 20974
coupling constants and masses of, S-matrix theory for, 19: 20920 (IC/65/6)
form factors and generalized Poincaré group for, electromagnetic, 19: 20971
Heisenberg theory and internal groups for, 19: 20948
interactions in many-body systems of, Green's quantum functions for, 19: 21056
interactions of many, Hoffman theorem in general relativity for, 19: 20707
interactions of many, in general relativity, (T), 19: 20708
interactions of, asymptotic phase shifts for, (T), 19: 21079 (IC/65/2)
interactions of, bootstrap hypothesis for parity conservation in strong, (T), 19: 20991
interactions of, bootstrap solution to Chew-Low theory for, 19: 21001
interactions of, effect of inelastic channel on position and width of resonance in, (T), 19: 20987
interactions of, Jacob-Wick method for scattering amplitude in, (T), 19: 21052
interactions of, kinematical effects in peripheral, (T), 19: 20981
interactions of, kinematic analysis of production, 19: 21076
interactions of, model of CP violation in weak, 19: 20978
interactions of, production amplitudes in, (T), 19: 20925 (ICTP-64/3)
interactions of, production processes in, (T), 19: 20961
interactions of, Poincaré symmetry and groups for, 19: 20965
interactions of, Regge trajectories with spin effects in, 19: 21067
interactions of, SU$_3$ classification of three-body states in, (T), 19: 20962
interactions of, structure of g-plane in relativistic Schroedinger theory for, 19: 21053
interactions of, threshold-type Regge trajectories in, 19: 21070
interactions of, unitary amplitudes in one-dimensional worlds, (T), 19: 20924 (ICTP-64/2)
interactions of, U(12) symmetry for weak, (T), 19: 21028
mass differences in multiplets of, Lie algebra for, (T), 19: 21032
model in momentum space and higher symmetries for, three-quark, 19: 21016
models for, combined internal-symmetry and Lorentz-invariant, (T), 19: 20449
models for, relativistic structure of SU(6), (T), 19: 20927 (ICTP-64/7)
models for, using de Sitter and Lorentz groups, (T), 19: 20923 (IC/65/18)
properties of charged, i-r asymptotics of Green's functions for, (T), 19: 20930 (JINR-E-1975)
properties of, in SU(6) theory, 19: 20921 (IC/65/7)
properties of, in $\tilde{SU}_4$ group of $\tilde{SU}_{12}$ theory, 19: 20922 (IC/65/8)
scattering by atoms, equations for classical and quantal, 19: 20825
scattering by potential well, quantum mechanical phase shifts in semiclassical, (T), 19: 20956

scattering of, phase shifts and transport cross sections in, (T), 19: 20957
scattering of, wave packets in quantum theory for, 19: 21092
SU(6) symmetry, invariant derivation of, 19: 20448
symmetries for, origin of, 19: 20933 (NP-14828)
symmetries for, quark model as probe of higher, 19: 20940 (UR-875-72)
symmetries of, testing of relativistic SU(6), (T), 19: 20983
symmetry for B = ⅓ quarks, SU(9), 19: 21026
symmetry for, Clebsch-Gordan coefficients for 35 × 56 in SU(6), 19: 21027
symmetry for, covariance, unitarity, and SU(6), 19: 21022
symmetry for, decomposition of direct products of irreducible representations of SU_n, 19: 21057
symmetry for, irreducible representations for homogeneous Lorentz and rotation groups in, 19: 20967
symmetry for, relativistic generalization of SU(6), 19: 20973
symmetry for, relativistic generalization of SU(6), 19: 21002
symmetry group for, Clebsch-Gordan coefficients of SU(3), (T), 19: 21047
symmetry groups for particle-antiparticle algebras, supermultiplet structure and SU(6), 19: 21015
symmetry model for, relativistic SU(6), 19: 21005
symmetry of, internal, (T), 19: 21035
theory of, in Brouwer spaces, 19: 21078 (AFOSR-64-1380)
transitions of, selection rules in para-field theory, 19: 20918 (IC/65/4)
transport of, conservation relations, interactions, and invariant imbedding in, (T), 19: 20959
wave equations for, method for constructing covariant, (T), 19: 20946

ELEMENTS
abundances in matter at high temperature, (T), 19: 20762
determination of light, by x-ray fluorescence excited by radioisotopes, 19: 19741 (CEA-R-2539)
partition coefficients in basic rocks, effects of oxygen anion size on, 19: 20152

EMBRYOS
radiation effects on developing, 19: 19466
radiation effects on interferon synthesis and virus plaque development in cells of rat, 19: 19563
radiation effects on rat, exposed at 36 hours, 19: 19618
radiosensitivity of developing, 19: 19592
radiosensitivity of, 19: 19699

ENGINEERING
design principles for molded plastic potting shells, 19: 21764 (SC-DR-64-2135)

ENZYMES
effects of magnetic fields on activity of, in frog heart, 19: 21776 (UCRL-12389)
radiation effects on 3,1,6,1-aryl-sulfate sulfohydrolase activity in guinea pig brain and liver, *in utero*, 19: 19573
radiation effects on thermoluminescence, 19: 19983
radioinduced inactivation of, 19: 19517

EQUIPMENT AND PROCEDURES
design and tests of adjustable positive-limit magnetic torque wrench, 19: 21768 (SC-TM-65-48)

ERBIUM
determination in purified uranium compounds by chromatography and spectrography, 19: 19800
deuteron reactions with deuterided, neutron yields from, (E), 19: 21301
ionization at single-crystal tungsten surfaces, 19: 20871
proton reactions at 680 Mev, production of neutron-deficient isotopes of light lanthanides in, 19: 20078
separation from aqueous solution by solvent extraction as salicylate pyridine complex, 19: 20079
separation from other rare earths by partition chromatography, 19: 20078

ERBIUM ALLOYS
Er–Gd, paramagnetic resonance absorption in, at 20 to 200°C, 19: 20581
Sb–Er, magnetic properties of, (E), 19: 20597

ERBIUM COMPLEXES
with serine, stability and composition, 19: 19874

ERBIUM IONS
spectra in barium, calcium, and strontium fluorides, absorption and luminescence, 19: 19854

ERBIUM ISOTOPES Er-162
neon-20 reactions (Ne-20,xn), alpha spectra, (E), 19: 21248(R) (UCRL-11828(p.21-5))

ERBIUM ISOTOPES Er-164
energy level transitions in, E2 conversion coefficients of rotational, (T), 19: 21308

ERBIUM ISOTOPES Er-166
energy level transitions in, E2 conversion coefficients of rotational, (T), 19: 21308
properties of, effects of pairing forces on, (T), 19: 21434

ERBIUM ISOTOPES Er-168
energy level transitions in, E2 conversion coefficients of rotational, (T), 19: 21308
properties of, effects of pairing forces on, (T), 19: 21434

ERBIUM NITRIDES
magnetic properties of, influence of crystal field on, 19: 19895

ERBIUM SULFATES
crystal structure and bond types of octahydrates, 19: 19915(T)

ERBIUM SYSTEMS
Er–Se, phase equilibria and crystal chemistry, 19: 19879
Er–Te, phase equilibria and crystal chemistry, 19: 19880

ERYTHROCYTES
effects of nitrogen mustard on content in rat blood, 19: 19489
hemolysis of, induced by radioinduced toxins in rabbit liver lipids, 19: 19599
radiation effects on, in stored blood, 19: 19513
radiation effects on ionic permeability of rat and rooster, 19: 19577
radiation effects on mechanical resistance of human, 19: 19595

ERYTHROPOIESIS
kinetics in normal and acutely-bled dogs, 19: 21777 (UR-662)
radiation effects on, in rabbits and rats, 19: 19499(R) (NP-14899)
radiation effects on rat bone marrow, effects of bone marrow transplants on recovery from, 19: 19644

ERYTHROPOIETIN
radiation effects on activity and formation of, in rabbits and rats, 19: 19499(R) (NP-14899)

ESCHERICHIA COLI
effects of endotoxins of, on hemorrhagic syndrome in guinea pigs, 19: 19487
gene differentiation in, 19: 21756 (BNL-8934)
radiation effects on frequency and properties of genetic recombinations in, 19: 19537
radiation effects on deoxynucleoproteins in, 19: 19576
radiation effects on phages of, protective effects of Versene against uv, 19: 19638
radiosensitivity of, effects of proline on, 19: 19550
toxic effects of mustard gas on, recovery from lethal, 19: 19485

ESTERASES
radiation effects on activity of, in guinea pig skeletal muscle, 19: 19574

ESTROGENS
effects on bone formation in mice, 19: 19471(R) (ANL-6938(p.162-78))

ETHANE
determination in vented gases from underground nuclear explosion, apparatus for, 19: 19776 (UCRL-12169)
effects on radioinduced carbon dioxide-graphite reactions, (E), 19: 19953 (AERE-R-4201)
meson (π^-) transfer from hydrogen to heavier atoms in, (E), 19: 21281
yields in carbon-11 recoil reactions with hydrocarbons, 19: 20018

ETHANE, 1,2-DICHLORO-1,1,2,2-TETRAFLUORO-
analysis for moisture, use of silica gel impregnated with cobalt bromide for, 19: 21783(P)

ETHANE, DIPHENYL-
hydrogen abstraction from, by methyl radicals, 19: 21760 (NYO-2728-4)

ETHANE, HEXAFLUORO-
Ar–hexafluoroethane, radiolysis of, yields from, 19: 19991
radiolysis at 3 atm, yields from, 19: 19991

ETHANE, TRICHLORO-
effects on radioinduced carbon dioxide-graphite reactions, (E), 19: 19953 (AERE-R-4201)

ETHANE, 1,1,1-TRICHLORO-2,2-BIS(*p*-CHLOROPHENYL)-
effects on alkaline phosphatase activity in human granulocytes, 19: 19570

ETHANETHIOL, 2-AMINO-
protective effects of, against radiation injury of rat placenta, 19: 19557
protective effects of, against radiation injuries in rat liver, 19: 19599
protective effects with serotonine against radiation lethality in mice, 19: 19627

ETHANOL
effects on pulse radiolysis of ferrocyanide solutions, 19: 20009
effects on radioinduced carbon dioxide-graphite reactions, (E), 19: 19953 (AERE-R-4201)

ETHER, BIS(CHLOROETHYL)
solvent properties in mixtures with benzene, carbon tetrachloride, chloroform, heptane, toluene, and xylene for uranyl nitrate, 19: 20072

ETHYL ETHER
solvent properties in mixtures with benzene, carbon tetrachloride, chloroform, heptane, toluene, and xylene for uranyl nitrate, 19: 20072

ETHYLAMINE, 2,2'-DITHIOBIS-
protective effects with royal jelly against radiation damage in rats, 19: 19629

ETHYLENE
collisions with excited cyclopropane, energy transfer in, 19: 19938

radiation effects on, scavenging effects of carbon-14-labeled methyl radical on, 19: 19985
radioinduced polymerization of, economics of gamma-, 19: 19957 (BNL-8993)
radiolysis of, kinetic analysis of free radical reactions in, 19: 19993
yields in carbon-11 recoil reactions with hydrocarbons, 19: 20018
ETHYLENE, CHLORO- POLYMERS
sorptive properties of chlorinated, for radioactive aerosols, 19: 20228
ETHYLENE, FLUORO- POLYMERS
with styrene, radiation effects on viscoelastic properties at 20 to 170°C, 19: 20001
ETHYLENE GLYCOL POLYMERS
effects on sensitivity of nuclear emulsions, 19: 20014
ETHYLENE OXIDE POLYMERS
radiation effects on thermoluminescence, 19: 19983
ETHYLENE POLYMERS
positron lifetime in, (E), 19: 21044
radiation effects on, glow peaks and their activation energies in, 19: 20007
radiation effects on electric conductivity, 19: 20017
radioinduced from ethylene, economics of gamma-, 19: 19957 (BNL-8993)
spectra of suspensions of metal halides and oxides in thin films of, infrared transmissions, 19: 19917
Al–polyethylene–U, neutron self-shielding in closely packed slab lattices of, (E), 19: 21636 (CONF-654-32)
ETHYLENE, TETRAFLUORO- POLYMERS
positron lifetime in, (E), 19: 21044
radiation effects on mechanical properties of, gamma, (E), 19: 19971
ETHYLENIMINE
effects on penicillin production by *Penicillium nigricans*, 19: 19556
EUROPIUM
determination in purified uranium compounds by chromatography and spectrography, 19: 19800
europium-153 gamma resonance absorption in, 19: 21337
preparation by aluminothermal reduction of oxide, 19: 20533
purification by halide distillation processes, 19: 20062
separation from other light lanthanides by partition chromatography following production by proton bombardment of erbium, 19: 20078
EUROPIUM BROMIDES
vapor pressure, 19: 20062
EUROPIUM CHLORIDES
europium-153 Mössbauer effect in, (E), 19: 21345
vapor pressure, 19: 20062
EUROPIUM COMPLEXES
with EDTA, migration in electrodialysis cell, 19: 20052 (ORNL-TM-1035)
with serine, stability and composition, 19: 19874
EUROPIUM HYDRIDES
EuH_2–LiH, phase studies, 19: 19881
EUROPIUM IODIDES
vapor pressure, 19: 20062
EUROPIUM IONS
spectra in barium, calcium, and strontium fluorides, absorption and luminescence, 19: 19854
EUROPIUM ISOTOPES Eu-151
isomer shift ratios in europium-153 and, 19: 21337
EUROPIUM ISOTOPES Eu-152
determination in soil after nuclear detonation, gamma spectroscopic, 19: 19829
EUROPIUM ISOTOPES Eu-153
alpha inelastic scattering at 3.1 Mev, conversion coefficients and mixing ratios for rotational transitions in, (E), 19: 21324
isomer shift and Mössbauer effect in, (E/T), 19: 21345
isomer shift ratios in europium-151 and, 19: 21337
EUROPIUM ISOTOPES Eu-154
determination in soil after nuclear detonation, gamma spectroscopic, 19: 19829
EUROPIUM ISOTOPES Eu-156
energy levels of, spin, parity, and transitions of, (E), 19: 21350
EUROPIUM ISOTOPES Eu-157
decay of 15.1-hr, (E), 19: 21272
EUROPIUM OXIDES
europium-153 gamma resonance absorption in, 19: 21337
europium-153 Mössbauer effect in, (E), 19: 21345
reduction to metal by metallothermal reduction using aluminum, 19: 20533
EUROPIUM SULFATES
crystal structure and bond types of octahydrates, 19: 19915(T)
europium-153 gamma resonance absorption in, 19: 21337
EUROPIUM SULFIDES
europium-153 Mössbauer effect in, (E), 19: 21345
EVOLUTION
chemical, review of evidence for, 19: 19946 (UCRL-11950)
of gene differentiation in bacteria, 19: 21756 (BNL-8934)
EXPERIMENTAL BOILING WATER REACTOR
reactivity changes with fuel burnup, model for calculating, 19: 21678 (ANL-6972)
EXPERIMENTAL BREEDER REACTOR-II
criticality studies, (E), 19: 21677 (ANL-6864)
EXPERIMENTAL GAS COOLED REACTOR
temperature measurement in, nozzle development for, 19: 20277 (ORNL-P-1068)
EXPLOSIONS
use of eight pound charges in construction of earth-fill dams, 19: 20090 (SC-RR-65-41)
EXPLOSIVES
use in pipe closure system, 19: 20100 (UCRL-12203)
EXPONENTIAL PILES
buckling measurements in, for advanced sodium-graphite power reactors, (E), 19: 21692 (NAA-SR-Memo-9976)
design of graphite-moderated, with changeable core configuration, 19: 21646
neutron buckling in natural uranium-light water, 19: 21645
EXTRACTION APPARATUS
design for facility for separation of plutonium from leachable residues, 19: 20083
EXTRUSION
equipment for uranium-tube, 19: 20501(R) (BRB-77)
of metal powders, review of hot, 19: 20518 (NMI-TJ-29)
EYES
radiation effects on metabolism of cornea, beta, 19: 19552
radiosensitivity of, to visible radiation from nuclear explosion, 19: 19498 (LA-3204)
radiotherapy of tumors of, radiation injury of brain from, 19: 19701

F

FALLOUT
bibliography on, 19: 20154(R) (HASL-158)
bibliography on, 19: 20164 (TID-3086(Suppl.2))
contamination of aircraft by, 19: 20208
contamination of food and water supplies by, 19: 20240
content in atmosphere in 1964 and 1965, prognosis of, 19: 20233
decontamination of paved areas, 19: 20207 (USNRDL-TR-797)
effects of gamma radiation in, on x-ray film in lead-lined chest, 19: 20632
from vented Antler shot, (E), 19: 20167
gamma emission by, intensities near air/ground interface, (T), 19: 20163 (RRA-M42)
hazards from, "knee and zone" concepts for estimating, 19: 20223
monitoring in air over Indian and Pacific Oceans, 1961–62, 19: 20158 (NP-14712)
monitoring in Argentina, 1964, 19: 20165(R) (TID-21711)
monitoring in Canada, 1964, 19: 20161 (NP-14869)
monitoring in Great Britain, 1963, 19: 20170
monitoring in ground air on Hayes Island, 1960–61, 19: 20157 (NP-14697)
monitoring in Iowa, 1964, 19: 20156 (IS-1098)
monitoring in stratosphere and troposphere, 1953 to 1964, 19: 20155 (HASL-159)
monitoring in stratosphere, 19: 20162(R) (NYO-3276-9)
monitoring programs in Canada, 19: 20224
monitoring stratospheric, in Star Dust Project, 19: 20657(R) (DASA-1309)
monitoring, 1964 and 1965, 19: 20154(R) (HASL-158)
radiation hazards from, in nuclear warfare, 19: 19554
FAST REACTORS
core test facility for, design and development of, 19: 21690(R) (LA-3244)
design for use as pulsed neutron source, 19: 21745(P)
design for use as pulsed neutron source, 19: 21746(P)
design of liquid-metal-cooled, paste-fueled, 19: 21663(P)
fuel burnup equations for, (T), 19: 21672
fuel development and testing for sodium-cooled ceramic, (E), 19: 21666(R) (GEAP-4640)
performance of power breeder, effects of central blanket on static, 19: 21696
safety analysis of transient pressure and coolant expulsion for, 19: 21652
FATS
protective effects of dietary, against radiation sickness in rats, 19: 19625
FATTY ACIDS
synthesis in diabetic and obese subjects, tracer studies of, 19: 21758

(BNL-8864)
FEED MATERIALS PRODUCTION CENTER, FERNALD, OHIO
analytical chemistry manual, 19: 19772 (TID-7022(Vol.I)(Bk.2))
FELDSPARS
age estimation in pegmatites by lead isotope method, 19: 20176
age of, La Sal Mountain, Utah, (E), 19: 20178
FERMIONS
density propagation for self-bound system of, (T), 19: 21393
Green function formalism for normal systems of, 19: 20715
interactions of many, approximations in calculations of, (T), 19: 20936 (TID-20558)
interactions with bosons, Regge poles in, 19: 21077
quantization of para-Fermi fields, 19: 20960
spin susceptibility of superfluid system of, (T), 19: 20692
superfluidity of liquids of, (T), 19: 21161 (JINR-P-1953)
systems of interacting, two-group theory for, 19: 21122
FERRITIN
use as label for antibodies for electron microscopic studies of ultrastructure, 19: 19465
FERROCYANIDES
radiolysis of oxygenated aqueous solutions of, reactions of hydroxyl radicals in, 19: 20009
FERROMAGNETIC MATERIALS
electron-nuclear spin interaction in, energy of, (T), 19: 20695
FERTILIZERS
analysis for phosphorus by neutron activation methods, 19: 19828
FETUSES
globulin production by hemopoietic cells in animal, review on, 19: 19468
iodine uptake and storage by thyroid in human, 19: 19491
radioinduced skeletal anomalies in, 19: 19533
radiosensitivity of developing, 19: 19592
radiosensitivity of, 19: 19698
radiosensitivity of, 19: 19699
radium-226 content in skeleton of human, 19: 20216
skeletal anomalies induced by drugs in, 19: 19533
strontium metabolism in rat, tracer study, 19: 19473 (UR-661)
FFAG ACCELERATORS
magnetic field calculations for, relaxation methods for, (E), 19: 20729 (MURA-706)
FIBRINOGEN
use of autofibrin films for treatment of radioinduced skin lesions on man, 19: 19642
use of iodine-125 and -131-labeled, for localization of malignant tumors, 19: 19716
FIELD THEORY
amplitudes for production processes in, (T), 19: 20925 (ICTP-64/3)
analogies between scalar and vector mesodynamics, 19: 20929 (ICTP-64/12)
asymptotic behavior of complex phase shifts in, (T), 19: 21079 (IC/65/2)
asymptotic properties of charged-particle Green's functions in, 19: 20930 (JINR-E-1975)
baryon nonleptonic decay in broken-SU(6), 19: 20919 (IC/65/5)
book: *Intermediate Quantum Mechanics*, 19: 21115
book: *Introduction to the Theory of Relativity and the Principles of Modern Physics*, 19: 21116
book: *PCT, Spin and Statistics, and All That*, 19: 21114
boson mass in, gauge invariance for vector, 19: 20934 (NP-14829)
elementary particle coupling constants and masses in, 19: 20920 (IC/65/6)
elementary particle properties in SU(6), 19: 20921 (IC/65/7)
elementary particle models in, using de Sitter and Lorentz groups, 19: 20923 (IC/65/18)
equations for degenerate fields with twisting rays, 19: 21120
equations in, solutions of Einstein's, 19: 21091
extrapolation of S matrix to complex angular momenta, representations for, (T), 19: 21080 (IC/65/9)
Feynman scattering amplitudes in, analytic property of, 19: 21113
fields with arbitrary spin and zero rest-mass, asymptotic behavior of, 19: 21108
many-body problems in, uses of fermion, 19: 21122
mesodynamics in, gauge approximations in non-perturbative, 19: 20928 (ICTP-64/10)
operators of massive free fields, 19: 21085
quantization of Bose and Fermi fields in, 19: 20960
quantum, microcausality in asymptotic, 19: 21088
quantum, production processes from scattering in, (T), 19: 20961
relativistic structure of SU(6), 19: 20927 (ICTP-64/7)
representation of non-compact groups in, using rigged Hilbert spaces, 19: 21081 (ICTP-64/9)
selection rules in para-, 19: 20918 (IC/65/4)
spaces in, description of Brouwer, 19: 21078 (AFOSR-64-1380)
spin-3/2 fields in, Stuckelberg formalism for, 19: 21112
symmetry properties of baryon resonances in, (T), 19: 20926 (ICTP-64/4)
unitary representations of noncompact $\bar{SU}_*$ group of $\bar{SU}_{12}$ in, 19: 20922 (IC/65/8)
unitary scattering amplitudes in one-dimensional worlds, 19: 20924 (ICTP-64/2)
vertex function in pseudoscalar-spinor theory, asymptotic behavior of, 19: 21101
wave equations for free massless fields with arbitrary spin, 19: 21110
FILTER PAPERS
analysis for fallout fission products, gamma spectrometric, 19: 20162(R) (NYO-3276-9)
analysis for sodium by neutron activation methods, 19: 19786
FILTERS
design for use in preparing radiation sources, engineering drawings of, 19: 20437
effects on dose distribution in cobalt-60 radiotherapy, 19! 19690
sorptive properties of chlorinated polyvinyl chloride, for radioactive aerosols, 19: 20228
FIRE EXTINGUISHING AGENTS
toxic hazards of barium chloride in Ternary Eutectic Salt, 19: 20210
FIRES
ecological effects of, resulting from nuclear warfare, 19: 19504 (RM-2801-PR)
hazards of radioisotope production laboratory, 19: 20195 (BLG-281)
FISH
analysis for cesium-137, rapid method for, 19: 19805
FISSION
delayed-neutron emission in, 19: 21443
distributions of charge and mass from californium-252, (E), 19: 21229 (BNL-8841)
energy release in low-energy, (E/T), 19: 21224 (AECL-2160)
of heavy nuclei, chemical studies of low-energy, 19: 20033
symmetries in plutonium-239 resonance-neutron-induced, (E), 19: 21241 (LA-DC-6639)
theory of asymmetric, review on, 19: 21283
FISSION CHAMBERS
performance as personnel fast-neutron dosimeters, (E), 19: 20318 (HW-SA-3526)
FISSION FRAGMENTS
distributions of charges and masses of, from californium-252, (E), 19: 21229 (BNL-8841)
energy spectrum of, after prompt-neutron emission in uranium-235 thermal-neutron fission, (E), 19: 21296
reactions with tungsten, damage in, 19: 20643
x-ray emission by spontaneous, of californium-252, (E), 19: 21265(R) (UCRL-11828(p.95-7))
FISSION PRODUCTS
activity of chain element, in intermittent irradiation in reactors, (T), 19: 21226 (AEET/HP/Th-19)
determination in filter paper samples, quality control of gamma spectrometric, 19: 20162(R) (NYO-3276-9)
determination in Ligurian Sea, methods for, 19: 19790
diffusion from fuel element cans, apparatus for detecting, 19: 21626(P)
diffusion from thorium dioxide–uranium dioxide and uranium dioxide compacts, effects of stress on, 19: 20586
effects on harvest and grain quality of field crops, 19: 19508(T) (JPRS-28977)
processing for isotope recovery, 19: 20431 (TID-7698(Pt.I)(p.1-16))
release from irradiated pyrolytic-carbon-coated particles, 19: 20463 (ORNL-TM-431)
release to atmosphere in SNAPTRAN 2/10A-3 destruct, (E), 19: 21717 (IDO-17019)
separation by thin-layer chromatography on oxine germanomolybdate and pyridine germanomolybdate, 19: 20069
separation from irradiated fuels, 19: 20084(P)
separation from power reactor fuels, economics of, 19: 20036 (BNWL-25)
separation from technetium, 19: 19820
separation of barium-140, calcium-45, and strontium-89 from solutions of, 19: 19745 (CEA-R-2712)
separation of indium from, by radiochemical precipitation, 19: 19777 (USNRDL-TR-819)
separation of long-lived, by electrodialytic migration of EDTA complexes, 19: 20052 (ORNL-TM-1035)
track formation and stability in glass and minerals, (E), 19: 20674
volatization from ceramic fuels, 19: 20060
FISSIONABLE MATERIAL
content in reactor fuel plates, variable-gradient, 19: 21676(P)
FLOWMETERS

design and characteristics of, for fluorine gas and reactive fluoride vapors, 19: 20259 (JAERI-1074)
FLUID FLOW
calculation of, computer program for, 19: 20115 (ORNL-TM-1093)
entrance flow in vertical tubes with combined free-forced convection, laminar-turbulent transition in, 19: 20114 (NP-14920)
in boiling reactors, calculation of instability in, 19: 20121
magnetohydrodynamic, equations solutions for, 19: 20764
of liquid helium II through slit, pressure-temperature relation for, (T), 19: 21179
two-phase, in film boiling of saturated liquid nitrogen flowing upward through heated tube at high vapor qualities, 19: 20113 (NP-14895)
visualization by streaming birefringence of bentonite clay solution, comparison with other techniques, 19: 20108 (BNWL-31)
FLUID FLOW (LAMINAR)
magnetic field effects on compressible boundary layers in, 19: 20122
magnetohydrodynamic, in annular channel with radial fields, (T), 19: 20663
FLUID FLOW (TURBULENT)
heat transfer to liquid metals in, in eccentric annuli, 19: 20123
FLUID FUEL REACTORS
analysis of lead-cooled liquid-metal-fueled, nuclear and parametric, 19: 21697
design of fast paste-fueled, liquid-metal-cooled, 19: 21663(P)
design using powder suspended in gas, 19: 21706(P)
FLUORESCENCE
spectra of diphenyl- and triphenylalkane intramolecular excimer-excited, 19: 19956(R) (ANL-6938(p.27-35))
FLUORIDE IONS
determination of microamounts by volumetric methods using thorium nitrate, 19: 19788
solvent extraction from molten nitrate by liquid silicone–TBP at 150°C, 19: 19833 (CEA-R-2628)
FLUORIDE VOLATILITY PROCESSES
development, 19: 20059
FLUORINE
determination in uranium tetrafluoride, methods for, 19: 19785
determination in uranium and its compounds and alloys, methods for, 19: 19823
flowmeter design for, 19: 20259 (JAERI-1074)
nuclear magnetic resonance in perfluorotoluene, coupling constants for, 19: 19888
reactions with copper(I) and (II) oxides, kinetics and mechanism of, 19: 19839 (K-1627)
reactions with uranium tetrafluoride, thermobalance study, 19: 20258 (JAERI-1070)
sorption by soda lime, thermobalance study of, 19: 20258 (JAERI-1070)
FLUORINE ISOTOPES F-17
beta decay of, mesonic exchange effect in, 19: 21348
FLUORINE ISOTOPES F-19
helium-3 reactions at 29 Mev, (E), 19: 21232 (JEN-141-DF/I-45)
nuclear magnetic resonance chemical shifts in fluorobenzenes, 19: 19951
performance in nuclear gyroscopes, (T), 19: 20279 (RTD-TDR-63-4001)
reactions (F-19,xn) with rhenium-185 and -187, production of light polonium isotopes by, (E), 19: 21250(R) (UCRL-11828(p.26))
reactions with terbium-159, fission, (E/T), 19: 21259(R) (UCRL-11828(p.77-80))
spin lattice relaxation time in calcium fluorides, below 1°K, (E), 19: 19897
FLUOROORGANIC COMPOUNDS
synthesis and properties of fluorocarbon alcohol 3,5-dinitrobenzoates, 19: 21775 (UCRL-12307)
FOILS
magnetic field compression by exploding, (E), 19: 20717
use of, for collection of radioactive dusts, 19: 20236
FOOD
analysis of animal, for cobalt by activation, 19: 19771(R) (TEES-2671-4(Chap.9))
cesium-134, -137, and sodium-22 content in, relation of content in man to, 19: 20225
contamination by fallout, 19: 20240
radiation effects on wholesomeness, 19: 20410
radiation processing of oysters and shrimp, effects on storage life, 19: 20407(R) (ORO-626)
radiation processing of oranges, effects on quantity, 19: 20404 (IA-999)
radiation processing of beef, product treatments for flavor in, 19: 20406 (NP-14928)
radiation processing of, 19: 20420
radiation processing of, testing polymeric film packaging for, 19: 20421
radiation processing of, cost factors in electron accelerator, 19: 20422
radiation processing of, effects on wholesomeness, 19: 20423
radiation processing of carrots, onions, and potatoes for inhibition of sprouting, 19: 20424
radiation processing of fresh meat and poultry, 19: 20425
radioisotope uptake by marine organisms, research program on, 19: 19469
radiopreservation of fruits, effects of radiation dose on storage life in, 19: 20413
radiosterilization and radiopasteurization at high, medium, and low doses, 19: 20410
uranium content in, effects of soil and water content on, 19: 19490
FOOD IRRADIATION FACILITIES
cost of, for processing fresh meat and poultry, 19: 20425
design for processing carrots, onions, and potatoes for sprout inhibition, 19: 20424
economics of electron accelerator, 19: 20422
FORMATES
t-butylperoxy-, decomposition of, deuterium isotope effects on, 19: 19948
FORMIC ACID
formic acid–H_2O_2, radiolysis of, effects of pH on yields from chain, 19: 19989
FRANCIUM
separation from aqueous solutions by solvent extraction using tetraphenylboron, 19: 20058
FRANCIUM ISOTOPES Fr-218
alpha decay, (E), 19: 21418
FRANCIUM ISOTOPES Fr-220
alpha decay, (E), 19: 21418
FREE RADICALS
electron paramagnetic resonance of, in irradiated frozen solutions of amino acids and peptides, 19: 20012
electron spin resonance spectra of organic anions produced in liquid ammonia by electrolysis, 19: 19945 (UCRL-11864)
radioinduced in aqueous solutions and water, nature of, 19: 19968
radioinduced in single crystal cyanoacetic acid, ESR spectra of, 19: 20006
radioinduced, electron paramagnetic resonance studies, 19: 19614
reactions in irradiated ethylene, kinetic analysis of, 19: 19993
FREQUENCY ANALYZERS
calibration systems for, design, (E), 19: 21766 (SC-TM-64-921)
FREQUENCY METERS
calibration systems for, design, (E), 19: 21766 (SC-TM-64-921)
FREQUENCY MODULATION
systems for synchrotrons, design of, (E), 19: 20735 (UCRL-11807)
FROGS
effects of magnetic fields on heart function in, 19: 21776 (UCRL-12389)
FRUITS
radiation effects on astringency of oriental persimmons, 19: 19571
radiation effects on storage of, 19: 20413
radiation processing of oranges, effects on quality, 19: 20404 (IA-999)
FUNGI
radiation effects on spores of, 19: 19558
radiation effects on spores of, 19: 19559
radiation effects on, in fruit, 19: 20413
radioinduced mutations of *Sordaria brevicollis*, ultraviolet, 19: 19547
radiosensitivity of, causing food spoilage, 19: 20420
FURAN
ionization by electron impact, appearance potential for doubly charged molecule ions in, 19: 20807(R) (UCRL-11828(p.201-4))

G

GADOLINIUM
determination in purified uranium compounds by chromatography and spectrography, 19: 19800
ionization at single-crystal tungsten surfaces, 19: 20871
magnetic susceptibility of liquid, 19: 20598
separation from other light lanthanides by partition chromatography following production by proton bombardment of erbium, 19: 20078
vapor pressure, 19: 20601
GADOLINIUM ALLOYS
Er–Gd, paramagnetic resonance absorption in, at 20 to 200°C, 19: 20581
Gd–Lu, gadolinium ion ESR in, g-factors from, (E), 19: 20698
Gd–Pd, gadolinium ion ESR in, g-factors from, (E), 19: 20698
Gd–Tb, paramagnetic resonance absorption in, at 20 to 200°C, 19: 20581
Gd–Y, gadolinium ion ESR in, g-factors from, (E), 19: 20698
Gd–Y, paramagnetic resonance absorption in, at 20 to 200°C, 19: 20581
Sb–Gd, magnetic properties of, (E), 19: 20597
GADOLINIUM COMPLEXES
with serine, stability and composition, 19: 19874
GADOLINIUM IONS
electron spin resonance in metals, g-factors from, (E), 19: 20698
GADOLINIUM ISOTOPES Gd-152

transitions in, particle parameters of E2, (E), 19: 21399
GADOLINIUM ISOTOPES Gd-154
energy level transitions in, E2 conversion coefficients of rotational, (T), 19: 21308
transitions in, particle parameters of E2, (E), 19: 21399
GADOLINIUM ISOTOPES Gd-156
energy level transitions in, E2 conversion coefficients of rotational, (T), 19: 21308
energy levels of, beta transition to ground state, (E), 19: 21350
GADOLINIUM ISOTOPES Gd-157
energy levels, (E), 19: 21272
GADOLINIUM ISOTOPES Gd-158
energy level transitions in, E2 conversion coefficients of rotational, (T), 19: 21308
GADOLINIUM ISOTOPES Gd-160
energy level transitions in, E2 conversion coefficients of rotational, (T), 19: 21308
GADOLINIUM NITRIDES
magnetic properties of, influence of crystal field on, 19: 19895
GADOLINIUM SULFATES
crystal structure and bond types of octahydrates, 19: 19915(T)
GALAXIES
formation of, (T), 19: 20758
GALLIC ACID
effects of propyl esters of, on thermoluminescence of x-irradiated polymers and proteins, 19: 19983
GALLIUM
bremsstrahlung reactions (γ,n) at 10 to 28 Mev, cross sections for, (E), 19: 21305
determination in pure aluminum, activation, 19: 19775(R) (UCRL-11828(p.197-9))
geochemistry and mineralogy of, in Cherry Mountains (Urals), USSR, book, 19: 20190
GALLIUM ALLOYS
Ga–Pu, fatigue strength of delta-stabilized, 19: 20545 (BNWL-16)
GALLIUM ARSENIDES
electron reactions with, radiative recombination from, (E), 19: 20703
GALLIUM ISOTOPES Ga-69
energy level scheme, 19: 21450
performance in nuclear gyroscopes, (T), 19: 20279 (RTD-TDR-63-4001)
GALLIUM OXIDES
analytical use in spectrographic methods, 19: 19774 (UCRL-7962)
GAMMA RADIATION
absorption by europium oxides, europium sulfides, recoiless, 19: 21337
absorption by tin oxide suspension in glycerol at 23.8 kev, resonance, (E), 19: 21428
angular distribution from meson (K_{μ_3}) decay, 19: 21069
background count in underground low-level counting laboratory, 19: 20093(R) (ANL-6938(p.194-205))
cataract induction in rats by, effectiveness relative to x radiation, 19: 19612
detection and measurement of low-level, underground counting room for, 19: 20092(R) (ANL-6938(p.91-6))
detection and measurement of low-level, underground counting room for, 19: 20093(R) (ANL-6938(p.194-205))
detection and measurement of, calibration of fluororod dosimeters, 19: 20314(R) (ANL-6938(p.62-70))
detection and measurement of high-level, performance of ionization chamber and scintillation detector for, 19: 20330(T) (AEC-tr-6547)
detection and measurement of, performance of whole-body plastic scintillation detector for, 19: 20377
detection of, scintillation counters for, 19: 20356
detection of, scintillation counter efficiency for, 19: 20358
dose distribution in air-over-ground geometry, spatial, 19: 20217
dose distributions from static firing of nuclear rockets, 19: 21725
dose rates from shielded isotopic power sources, 19: 21595 (TID-7698(Pt.I)(p.33-248))
dosimetry in Norwegian houses, 19: 20218
dosimetry of, from cobalt-60 teletherapy unit, 19: 19733
dosimetry of, uses of cyclohexane in, 19: 20341
effects from fallout on x-ray film in lead-lined chest, 19: 20632
effects in *Escherichia coli*, effects of proline on, 19: 19550
effects in mice, carcinogenic, 19: 19594
effects in rats, carcinogenic, 19: 19561
effects on anhydrous maltose at 77 and 293°K, electron spin resonance studies of, 19: 19994
effects on animals and plants, small-dose, 19: 19516
effects on aqueous nitrate solutions, 19: 19981
effects on astringency of oriental persimmons, 19: 19571
effects on β-propiolactone, 19: 20000
effects on blood cells in monkeys, space simulated, 19: 19616
effects on carbon and graphite materials in contact with heavy water, 19: 20463 (ORNL-TM-431)
effects on carbon dioxide-graphite reactions, (E), 19: 19953 (AERE-R-4201)
effects on chain reaction between formic acid and hydrogen peroxide, 19: 19989
effects on chromosome rearrangements in barley seed, partial recovery from, 19: 19639
effects on cobaltammine complexes, 19: 19974
effects on cyanoacetic acid crystal, ESR spectra of free radicals produced in, 19: 20006
effects on defects in germanium, 19: 20628
effects on developing embryos, 19: 19466
effects on electric conductivity of polyethylene, 19: 20017
effects on electric conductivity of zirconium oxide films, (E), 19: 20621
effects on electron tubes, hardening against, 19: 20399(R) (NP-14946)
effects on erythrocytes in stored blood, 19: 19513
effects on fractionation of spleen-colony-forming cells from bone marrow in mice, 19: 19617
effects on germination of maize seeds, 19: 19528
effects on glasses, electron spin resonance study of centers induced in, 19: 20620(R) (NYO-2024-8)
effects on glasses, ESR spectra of electron production in, 19: 20002
effects on glycogen, 19: 20015
effects on hexafluoroethane, 19: 19991
effects on hexamethyldisilazane on firebrick, 19: 19997
effects on impurity photoconductivity in germanium, 19: 20623
effects on induction of electronic energy levels in n-type germanium, 19: 20612 (AFCRL-64-839)
effects on insulated conductor, electric currents induced by, 19: 20398 (FZK-214)
effects on leather and air-dried sheepskins, 19: 20414
effects on lipid metabolism in newborn and weanling rats, 19: 19610
effects on liver lipids in rabbits, 19: 19599
effects on M-center formation energy in potassium chloride, 19: 19999
effects on mechanical properties of polytetrafluoroethylene, (E), 19: 19971
effects on n-type germanium, effects of antimony and arsenic on, 19: 20619 (NP-14883)
effects on nitrous oxide dosimeter, cell diameter effect on nitrogen yield in, 19: 20329 (USNRDL-TR-806)
effects on operation of pressure transmitter at high temperatures, 19: 20400 (NP-14955)
effects on pea and vetch plants, chronic, 19: 19586
effects on plastic film packaging, 19: 20421
effects on polyethylene, glow peaks and their activation energies in, 19: 20007
effects on polyglutamic acid in aqueous solution, 19: 19990
effects on polymerization of ethylene, economics of, 19: 19957 (BNL-8993)
effects on polymerization of crystalline trithiane, chemical, 19: 19959 (CONF-571-37)
effects on polymerization of binary solid solutions and mixed crystals, 19: 19972
effects on preservation of food, 19: 20410
effects on rats, protective effects of casein diets against, 19: 19628
effects on reduction of nickel oxide by hydrogen, 19: 19975
effects on secretory activity of nuclei of brain hypothalamic area in rabbits, 19: 19509(T) (JPRS-29250(p.9-13))
effects on silicon p-n junctions, 19: 20627
effects on soluble DNA localization in rabbit lymphoid appendix, 19: 19583
effects on somatic mutation induction in potatoes, 19: 19518
effects on sprouting of carrots, onions, and potatoes, 19: 20424
effects on storage time of fruits, 19: 20413
effects on stored energy of alkali-halide crystals, 19: 19987
effects on thermal properties of alkali-halide crystals and solid solutions, 19: 19986
effects on transduction in *Pseudomonas aeruginosa*, 19: 19501(R) (NP-14931)
effects on transduction in *Pseudomonas aeruginosa*, 19: 19502(R) (NP-14932)
effects on transduction in *Pseudomonas aeruginosa*, 19: 19503(R) (NP-14933)
effects on viscoelastic properties of polyvinyl fluoride–styrene, copolymers, 19: 20001
emission by fallout and point sources, near air/ground interface, (T), 19: 20163 (RRA-M42)
emission by nuclei exposed to variable-intensity particle bombardment, intensity variations of, (T), 19: 21235 (JINR-P-1950)
emission in proton reactions (p,αγ) with lithium-7 at 440 kev, spectra of,

19: 21357
emission in thermal neutron capture reactions with mercury-199, (E), 19: 21292
energy deposition by, in matter, (T), 19: 21596 (UCRL-12005)
enzyme inactivation by, 19: 19517
intensities from point sources on ground, boundary effect in, 19: 20198 (HASL-157)
measurement and recording as function of time, device for, 19: 20397
production in 70-Mev electron linear accelerator shielding, 19: 20749
reactions (γ,np) with heavy nuclei, (T), 19: 21274
reactions in Na(Tl) crystals, electron pair production cross sections for, (E), 19: 21294
scattering by iridium-191, angular distributions from resonance, (E), 19: 21435
scattering by lead, bremsstrahlung effect in large-angle coherent, (E/T), 19: 21599
shielding against 0.5 to 10 Mev, nomograms for determining thicknesses of various materials for, 19: 21598
spectra in activation analysis, detector design for reduction of, 19: 19767(R) (TEES-2671-4(Chap.4))
streaming through air duct in concrete, 19: 21594 (AD-424387)
therapeutic uses of, 19: 19673
use in biological and medical research, bibliography on, 19: 19505 (TID-3580)

GAMMA SHIELDING
heating of, Monte Carlo computer program for, (T), 19: 21596 (UCRL-12005)
performance of lithium hydride as, (T), 19: 21614 (NAA-SR-Memo-10559)
thicknesses of, nomograms for determining, 19: 21598

GAMMA SOURCES
description and costs of Brookhaven cobalt-60, 19: 20095 (BNL-8976)
design and operation of 2500-C cesium-137, 19: 20102
preparation of strontium-90, engineering drawings of equipment for, 19: 20437
radiation dose from implanted cobalt-60 beads, 19: 19708
therapeutic uses of, design of slit-type lead screen for, 19: 19674
use in sterilizing hides and improving leather quality, 19: 20414
use of cobalt-60, for radiotherapy of uterine carcinomas, 19: 19663
uses in densitometers for *in situ* measurement of ocean-bottom sediments, 19: 20419

GAMMA SPECTROMETERS
design of coincidence, 19: 20342
efficiency of coincidence scintillation, for positron annihilation radiation, 19: 20363
performance in analysis of filter paper samples for fallout fission products, 19: 20162(R) (NYO-3276-9)
use for measurement of electron pair production cross sections in Na(Tl) crystals, (E), 19: 21294

GAMMA SPECTROSCOPY
uses in determination of heavy elements in uranium-containing rocks, 19: 20180

GAS ANALYZERS
design and operation of chromatographic, for analysis of vented gases from underground nuclear explosion, 19: 19776 (UCRL-12169)
development of helium, 19: 20473(R) (NASA-CR-54629)

GAS COOLED REACTORS
design using powder suspended in gas as fuel, 19: 21706(P)
materials for, properties of beryllium–calcium alloy as, 19: 20498(P)
moderator support structure for heterogeneous, 19: 21628(P)
pressure vessel failure in, simulation using models, (E), 19: 21608 (AWRE-R-2/65)
steam generator design for TARGET power, (E), 19: 21682 (GAMD-4732)
vessels for TARGET thermal, design analysis for prestressed-concrete, (T), 19: 21683 (GAMD-5272(Rev.2))

GAS FLOW
calculation of, computer program for, 19: 20115 (ORNL-TM-1093)
hypersonic, equilibrium of dissociated and ionized hydrogen in, 19: 20124

GAS FLOW (TURBULENT)
in thermal entrance region of heated tubes, effects of large temperature gradients on, 19: 20117 (SU-247-4)

GASEOUS DIFFUSION PROCESS
model for uranium isotope separation, linear programming, 19: 20430 (P-1231(RAND))
parameters of cascades for, with total minimum flux, 19: 19744 (CEA-R-2622)

GASES
determination in solids by spark source mass spectrography, 19: 19830
distribution functions for classical electron, equilibrium, 19: 20683
effects of neutral, on dynamics of theta-pinch discharges, (T), 19: 21470 (IPP-1/14)
electromagnetic wave transport in anisotropic ionized, (T), 19: 21466 (AFCRL-64-550)
electron diffusion in, in electric fields, (T), 19: 20696
electron-positive ion recombination in dense neutral, (T), 19: 20860
energy of electron, at absolute zero, (T), 19: 20711
evolution from sputter-ion pumps, 19: 20140(R) (ORNL-3760(p.94-7))
motion of, nonstationary isothermal, (T), 19: 20713
particle distribution in repulsive Coulomb field in rarefied, effect of incoming stream on, (T), 19: 20673(T)
probability density of, equation for, (T), 19: 20693
reactions with metals at high temperatures, classification of, 19: 20486
shock propagation in conducting, gradients of flow variables behind, (T), 19: 20664
sorption and desorption of residual, in high-vacuum, (E), 19: 20144
sound in weakly ideal Bose, second, (T), 19: 20669
thermodynamic equilibrium and transport of ionized, problems of high temperature in studies of, 19: 19868
thermodynamic properties of one-dimensional, with hard-core repulsion, 19: 20682
transport equations for mixtures of, Boltzmann, 19: 20681

GASTROINTESTINAL TRACT
function in sheep, preparation of chromium-51-labeled EDTA for studies on, 19: 20026
radiation effects of phosphorus-32 on rat, 19: 19565

GATING SYSTEMS
description of, for periodic subgrouping of multichannel analyzers, 19: 20283(R) (UCRL-11828(p.221))

GEIGER-MUELLER TUBES
quenching circuit for, design of fast, 19: 20349

GELATIN
effects on polarography of uranyl pyrophosphate complexes, 19: 19816

GENES
differentiation of, role of evolution in bacteria, 19: 21756 (BNL-8934)

GENETICS
of *Neurospora crossa*, 19: 21772(R) (TID-21709)
radiation effects on frequency and properties of recombinations of, in *E. coli*, 19: 19537
radiation effects on human, exposed as infants, 19: 19568
radiation effects on population, problems in assessment of, 19: 19654
radioinduced transduction in *Pseudomonas aeruginosa*, 19: 19501(R) (NP-14931)
radioinduced transduction in *Pseudomonas aeruginosa*, 19: 19502(R) (NP-14932)
radioinduced transduction in *Pseudomonas aeruginosa*, 19: 19503(R) (NP-14933)

GEOCHEMISTRY
book: *Mineralogy and Geochemistry of Rare Elements in Cherry Mountains (Urals)*, in Russian, 19: 20190

GEOLOGY
genesis of uranium deposits, deposition, source, and transport in, 19: 20185 (JEN-132-SIG/I-3)
map of Quartet Dome Quadrangle, Nye County, Nevada, 19: 20151 (TEI-860)
map of Thirsty Canyon SE Quadrangle, Nye County, Nevada, 19: 20150 (TEI-859)
Mohole Project review, 19: 20153

GEOMAGNETIC FIELDS
book: *Astrophysics and Space Science*, 19: 20782
charged-particel confinement in, review of, 19: 20902
description, 19: 21160
disturbances in, solar plasma effects in, (E), 19: 21155(T)
effects on charged-particle streams in magnetosphere, 19: 21126
effects on hydromagnetic wave propagation in atmosphere, (E), 19: 21151
interactions with hydromagnetic waves, amplification processes in, (T), 19: 21123 (D1-82-0398)
interactions with cosmic protons, ionospheric effects of, (T), 19: 21125 (RAD-TR-64-27)
motion of, western drift, (T), 19: 21131(T)
solar wind effects on, (T), 19: 21137
structure of, spatial, (E/T), 19: 21130(T)
variations of, lunar-diurnal, 19: 21134(T)

GEOMAGNETIC STORMS
cosmic ray intensity during Forbush decrease, (E), 19: 20877(T)
effects on charged-particle motion in magnetosphere and radiation belts, (T), 19: 21128(T)
effects on cosmic radiation during solar activity maximum and minimum, 19: 20888
effects on ionospheric F2 layer, (E), 19: 21132(T)
energy of, dependence on distance to solar corpuscular stream of, (T),

19: 21135(T)
GEOPHYSICS
book: *Satellite Environment Handbook*, 19: 21157
ionospheric electric-current distributions, (E), 19: 21124 (P-1121(RAND))
GERMANIUM
diffusion of helium in, 19: 19934
electron capture by gold-ion impurities in, at 20°K, (E/T), 19: 21180
geochemistry and mineralogy of, in Cherry Mountains (Urals), USSR, book, 19: 20190
performance of lithium-drifted, in anticoincidence detector system, 19: 20322 (LA-DC-6397)
properties of lithium-drifted, as detector in activation analysis, 19: 19775(R) (UCRL-11828(p.197-9))
radiation damage by protons at 22 and 40 Mev, defects induced by, 19: 20617 (NASA-TN-D-2727)
radiation effects on surface state of n-type, electron, 19: 20622
radiation effects on impurity photoconductivity in, gamma, 19: 20623
radiation effects on Fermi levels at 77°K, electron, 19: 20624
radioinduced defects in n-type, effects of antimony and arsenic on gamma, 19: 20619 (NP-14883)
radioinduced defects in, annealing of fast-neutron, 19: 20626
radioinduced defects in crystal structure of, energy structure of, 19: 20628
radioinduced inversion layer production on, by argon and nitrogen ions at 46, 67, and 82 kev, 19: 20625
sputtering by argon ions at 1000 ev, 19: 20813
sputtering by ions at 45 kev, thermal spikes in, (E), 19: 20838
GERMANIUM COMPLEXES
with molybdenum and pyridine or 8-quinolinol, properties for use as thin-layer chromatograms, 19: 20069
GERMANIUM ISOTOPES Ge-73
neutron reactions (n,α) at 14 Mev, cross sections for, (E), 19: 21325
GERMANIUM JUNCTIONS
radiation effects on p-n, fast neutron, 19: 20627
radioinduced electronic energy levels in n-type, methods for determining gamma and x-ray, 19: 20612 (AFCRL-64-839)
GERMANY
radiation protection regulations in, 19: 20211
radiation sources and radioisotope production in East, 19: 20436
GLASS
fission product tracks in, formation and stability of, (E), 19: 20674
photochemistry and radiolysis of aqueous acid and alkaline and non-aqueous, ESR spectra of, 19: 20002
preparation of, uses of radioisotopes in industrial, 19: 20417
radiation effects on electric conductivity, 19: 19976
radioinduced centers in, electron spin resonance study of gamma, 19: 20620(R) (NYO-2024-8)
sorptive properties of unfired Vycor powdered, for protactinium-233 from solutions of irradiated fuel, 19: 20051 (ORNL-3773)
waste fixation in, process for, 19: 21754(P)
GLASS ELECTRODES
radiation effects, 19: 19976
GLOBULIN
effects of gamma, on fatal shock in irradiated rabbits, 19: 19535
production by fetal hemopoietic cells, review on, 19: 19468
radiodermatitis effects on blood serum, in humans and rabbits, 19: 19598
GLOW DISCHARGES
properties of metastable abnormal, in hydrogen, 19: 21590
GLUCOSE
conversion of labeled, into carbon dioxide and water in obese patients, 19: 21758 (BNL-8864)
radiation effects on metabolism of, 19: 19538
GLUTAMIC ACID POLYMERS
radiolysis in aqueous solutions, effects of pH on gamma, 19: 19990
GLUTARIC ACID
trioxy-, reactions with uranyl ions, spectra of complexes formed in, 19: 19911
GLYCEROL
effects on fluorescence of uranyl ions, 19: 19863
gamma resonance absorption by tin oxides suspended in, at 23.8 kev, (E), 19: 21428
GLYCINE
radiolysis in frozen aqueous solutions, 19: 20012
GLYCOGEN
radiolysis of, role of hydroxyl radical in gamma, 19: 20015
GLYOXIME, DIMETHYL-
effects on spectrophotometric determination of zinc using 1-(2-thiazolylazo)-2-naphthol, 19: 19814
GLYOXIME, DIMETHYL- COMPLEXES
with uranic acid, formation constant and uranium coordination number of, 19: 19860
GOITER
iodine-131 treatment of euthyroid, in man, 19: 19685
GOLD
analysis for impurities by activation methods, 19: 19796
determination using 5,5′ thiodisalicylic acid, spectrophotometric, 19: 19812
electron and ion emission from foils of, laser-induced, (E), 19: 20814
neutron reactions (n,γ) at 1 to 4 Mev, spectra from, (E/T), 19: 21317
radiation effects on length changes in, alpha, 19: 20646
separation by reversed-phase chromatography using tri-n-octylphosphine sulfide, 19: 19753 (IS-T-3)
sputtering by ions at 45 kev, thermal spikes in, (E), 19: 20838
x-ray spectra in, muonic, (E), 19: 21344
GOLD ALLOY COUPLES
Co–Au/Cu, thermocouple tables for cryogenic, smoothed, 19: 20272 (ORNL-3649(Vol.2)(Sect.2.10))
GOLD IONS
electron capture by impurity, in germanium at 20°K, (E/T), 19: 21180
GOLD ISOTOPES Au-177
alpha energy and half life, (E), 19: 21249(R) (UCRL-11828(p.25))
GOLD ISOTOPES Au-178
alpha energy and half life, (E), 19: 21249(R) (UCRL-11828(p.25))
GOLD ISOTOPES Au-179
alpha energy and half life, (E), 19: 21249(R) (UCRL-11828(p.25))
GOLD ISOTOPES Au-181
alpha energy and half life, (E), 19: 21249(R) (UCRL-11828(p.25))
GOLD ISOTOPES Au-183
alpha energy and half life, (E), 19: 21249(R) (UCRL-11828(p.25))
GOLD ISOTOPES Au-185
alpha energy and half life, (E), 19: 21249(R) (UCRL-11828(p.25))
GOLD ISOTOPES Au-193
energy level transitions in, retardations in l-allowed M1, (T), 19: 21323
GOLD ISOTOPES Au-197
energy level transitions in, retardations in l-allowed M1, (T), 19: 21323
energy levels of, core excitation model for, (T), 19: 21362
magnetic fields acting on, in ferromagnetic materials, 19: 20578
oxygen-16 reactions with, charged-particle production in, (T), 19: 21354
proton reactions at 155 Mev, nucleon-alpha cascades from, (T), 19: 21372
GOLD ISOTOPES Au-198
amine salts of, development for industrial tracers, 19: 20030
magnetic fields acting on, in ferromagnetic materials, 19: 20578
production of colloidal and granular, in Spain, 19: 20432(T) (ORNL-tr-295)
production of colloidal, procedures for, 19: 20022(T) (JPRS-29258)
therapeutic effects for pituitary ablation, 19: 19667
uptake by human bone marrow, whole-body counting and scanning of, 19: 19718
uptake by human liver, profile counting studies on, 19: 19492
uptake by human lymph system, indirect lymphography of, 19: 19719
use in diagnosis of liver diseases by scanning, 19: 19730
use in scintiscanning of liver during amebiasis, 19: 19728
use in therapy by intra-arterial injection, method for, 19: 19661
GONADS
iodine-131 uptake by human ovaries, beta activity from, 19: 19483
polonium-210 content in, of smokers and non-smokers, 19: 19495
radiation exposure to, in inhabitants of Mosonmagyarovar, Hungary from medical examinations in 1961, 19: 20227
radiation hazards to human, by infant exposure, 19: 19568
radiosensitivity of female, 19: 19592
GRAPHITE
analysis for impurities by spark source mass spectrography, 19: 19830
bonding methods for, development of, 19: 20505 (JAERI-1071)
compatibility with water under high flux conditions, 19: 20463 (ORNL-TM-431)
corrosion by carbon dioxide at high temperatures, 19: 21690(R) (LA-3244)
corrosion in reactors, 19: 20488
diffusion of rare gases in, effects of pore structure on, 19: 20457 (GAMD-4814)
dislocations in, screw, (E), 19: 20574
neutron diffusion and thermalization in, (E), 19: 21646
neutron energy spectra in blocks of, equilibrium, (T), 19: 21205
neutron thermalization in, (E), 19: 21211
oxidation by air and helium, 19: 21690(R) (LA-3244)
oxidation in air at 0.01 to 100 atm, assuming frozen laminar boundary layer, 19: 20496
preparation by graphitization of carbon containing rare earths, 19: 20536(P)
radiation effects on properties of CSF, TSGBF, and TSX, neutron, 19: 20614 (HW-81250A)
radiation effects on mechanical properties of reactor, neutrons, 19: 20637

radiation effects on elasticity of polycrystalline, neutron, 19: 20640
radioinduced reactions with carbon dioxide, inhibition of, (E), 19: 19953 (AERE-R-4201)
radioinduced reactions with carbon dioxide at 100 to 600°C, effects of hydrogen and water vapor on neutron, 19: 19954 (AERE-R-4839)
reactions with zirconium oxide to prepare carbide, 19: 19866
testing of, engineering drawings of phase-sensitive eddy-current concentrator for, 19: 20132
thermal conductivity, 19: 21690(R) (LA-3244)
thermal conductivity at high temperatures, (E), 19: 20576
GRAPHITE MODERATED REACTORS
corrosion problems in, review of, 19: 20488
design using heavy water as second moderator, 19: 21658(P)
exponential experiments for advanced sodium-cooled power, (E), 19: 21692 (NAA-SR-Memo-9976)
heat transfer and neutron kinetics in nuclear rocket, (T), 19: 21715 (AD-605574)
GRASS
analysis of, activation, 19: 19771(R) (TEES-2671-4(Chap.9))
GRAVITATION
effects on general relativistic two-body problem, 19: 21104
effects on hydromagnetic wave propagation in atmosphere, (E), 19: 21151
energy transport in gravitational collapse, radiative, (T), 19: 21100
field equations for, analysis of quasi-Maxwellian, (T), 19: 21086
graviton field and motion equations in, charged, 19: 21082
Minkowski theory of, Lagrangian formalism for, 19: 20666
motion of homogeneous matter under, (T), 19: 20704
properties and structure of type-I fields in Reimann space, 19: 21090
theory of, scalar, 19: 21107
wave equations for free fields of, (T), 19: 21110
GREAT BRITAIN
fallout monitoring, 1963, 19: 20170
GROUND
blast effects on cylindrical cavities in, 19: 20659 (AD-606490)
gamma intensities from point sources on, effects of air interface on, 19: 20198 (HASL-157)
gamma transport in, near air/ground interface, (T), 19: 20163 (RRA-M42)
motions of, simulation of air-blast-induced, 19: 20184
neutron transport in, analysis of fast, (E), 19: 21199 (CEX-65.02)
radiation dose distribution in air-over-ground geometry, spatial gamma and neutron, 19: 20217
GROUND WATERS
monitoring for beta and tritium contamination at Hanford, 19: 21749(R) (HW-84549)
GROWTH
radiation effects on wheat, photoperiod and temperature effects on uv, 19: 19545
GUINEA PIGS
effects of *E. coli* endotoxins on hemorrhagic syndrome in, relation of radiation sickness to, 19: 19487
radiation effects on phagocytic activity of leukocytes in, 19: 19507(R) (TID-21712)
radiation effects on physiology of mineral contents in developing brain in, 19: 19534
radiation effects on 3,1,6,1-aryl-sulfate sulfohydrolase activity in brain and liver of, *in utero*, 19: 19573
radiation effects on acid and alkaline phosphatase and esterase activity in skeletal muscles in, 19: 19574
uranium toxicity in, 19: 19488

H

HAFNIUM
determination in other metals using catechol violet, colorimetric, 19: 19780
effects on fabrication and mechanical properties of niobium–tantalum–titanium–vanadium alloy sheet, 19: 20552(R) (IITRI-B6021-6)
geochemistry and mineralogy of, in Cherry Mountains (Urals), USSR, book, 19: 20190
separation from zirconium by reversed-phase chromatography, 19: 19752 (IS-T-2)
HAFNIUM BORIDES
analysis for boron by pyrohydrolysis, 19: 19761 (NP-14876)
HAFNIUM CARBIDES
performance as emitter in hypersonic plasma generators, (E), 19: 20905 (SC-RR-65-54)
superconducting properties, 19: 20572
HfC–TaC, vaporization rates and vapor pressures at 2200 to 3000°K, equations for predicting, 19: 20608
HAFNIUM ISOTOPES Hf-170
energy levels of, Coriolis anti-pairing effects on high spin rotational, (T), 19: 21363
HAFNIUM ISOTOPES Hf-172
energy levels of, Coriolis anti-pairing effects on high spin rotational, (T), 19: 21363
HAFNIUM ISOTOPES Hf-176
energy level transitions in, E2 conversion coefficients of rotational, (T), 19: 21308
HAFNIUM ISOTOPES Hf-178
energy level transitions in, E2 conversion coefficients of rotational, (T), 19: 21308
properties of, effects of pairing forces on, (T), 19: 21434
HAFNIUM ISOTOPES Hf-180
energy level transitions in, E2 conversion coefficients of rotational, (T), 19: 21308
HAFNIUM NITRIDES
superconducting properties, 19: 20572
HfN–W, tensile properties at 800 to 2400°C, 19: 20565 (WADD-TR-60-37(Pt.V))
HAFNIUM OXIDES
effects on thermal stability of zirconium oxide, 19: 20585
CeO_2–HfO_2–MgO–Mo, preparation and properties of macrolaminate particle composites of, 19: 20558(R) (NP-14888)
HAFNIUM SYSTEMS
Hf–U-235–H_2O, neutron transport in critical assemblies of, resonance interference in, (E/T), 19: 21643 (WAPD-T-1728)
HAIR
iodine isotope and sulfur-35 uptake by mouse vibrissal, origin of, 19: 19479
HALDEN BOILING REACTOR
heat transfer burnout and stability in, 19: 20120
operations, (E/T), 19: 21693(R) (NP-14896)
HALLAM POWER REACTOR
fuel handling in, specification for gantry and trolley for, 19: 20099 (TID-21644)
moderator elements for, design review, (E/T), 19: 21680 (COO-1402-1)
moderator elements for, mechanical design of, (E), 19: 21681 (COO-1402-2)
HANDBOOKS AND MANUALS
for use of OCTOPUS/6600, 19: 20443 (UCRL-12256)
on analytical methods used at Feed Materials Production Center, 19: 19772 (TID-7022(Vol.I)(Bk.2))
on shielding requirements and radiation characteristics of isotopic power sources, 19: 21595 (TID-7698(Pt.I)(p.33-248))
HANDS
radiation injuries of, 19: 19524
HANFORD PRODUCTION REACTORS
cooling system-decontamination, 19: 21605 (HW-SA-3560)
corrosion in, tests of inhibitors for carbon steel, 19: 21714 (RL-REA-592)
fuel element reclamation when supports are cracked, 19: 21668 (HW-84196)
neutron spectra outside, (E), 19: 20201 (HW-SA-3525)
simulation of N, computer components for, (E), 19: 21713 (HW-83092 (Rev.))
HANFORD PRODUCTION REACTORS (N)
containment building for, leakage from Zone I and II of, 19: 21712 (HW-61979)
moderator, irradiation studies of graphite, 19: 20614 (HW-81250A)
HANFORD WORKS, RICHLAND, WASH.
neutron spectrum measurements at, for health physics applications, (E), 19: 20201 (HW-SA-3525)
radioisotope production at, feasibility study, 19: 20431 (TID-7698(Pt.I)(p.1-16))
radiological monitoring of ground water, 19: 21749(R) (HW-84549)
welding procedures for carbon steel pipe and plate, 19: 20521 (TID-20625(Vol.I(Rev.I))
welding procedures for carbon steel and stainless steel pipe and plate, 19: 20522 (TID-20625(Vol.II)(Rev.I))
welding procedures for pipe and plate, 19: 20523 (TID-20625(Vol.III) (Rev.I))
welding procedures for pipe, plate, tubing, and sheet, 19: 20524 (TID-20625(Vol.IV)(Rev.I))
HARMONIC ANALYSIS
Euler coefficients of Fourier series of discretely defined functions, (T), 19: 20442 (NAA-SR-Memo-9729)
HASTELLOY B
welding of pipes and plates of, Hanford procedures for, 19: 20524 (TID-20625(Vol.IV)(Rev.I))
HASTELLOY C
corrosion by potassium–sodium alloy, research program on, 19: 20477(R) (ORNL-3604)

corrosion by potassium–sodium alloy at high temperatures, carbon mass transfer in, 19: 20478(R) (ORNL-3618)
corrosion by solutions produced in head-end processes for fuel, 19: 20481 (ORNL-3787)
welding of pipes and plates of, Hanford procedures for, 19: 20524 (TID-20625(Vol.IV)(Rev.I))
HASTELLOY F
corrosion by solutions produced in head-end processes for fuel, 19: 20481 (ORNL-3787)
welding of pipes and plates of, Hanford procedures for, 19: 20524 (TID-20625(Vol.IV)(Rev.I))
HASTELLOY RZ35
tensile properties of, testing, (E), 19: 20554 (LA-3161)
HASTELLOY X
welding of pipes and plates of, Hanford procedures for, 19: 20524 (TID-20625(Vol.IV)(Rev.I))
HAYNES 25 ALLOY
welding of pipes and plates of, Hanford procedures for, 19: 20524 (TID-20625(Vol.IV)(Rev.I))
wetting by mercury, effects of surface treatment on, 19: 20111 (NAA-SR-Memo-10224)
HEAD
phantom of, for use in radiation dosimetry, 19: 19676
radiation dose to, during diagnostic dental radiography, 19: 19676
HEALTH PHYSICS
aims and responsibilities of health physicists, 19: 20219
maximum permissible doses for personnel and populations, external and internal, 19: 20221
neutron spectrum measurements at Hanford plant areas, (E), 19: 20201 (HW-SA-3525)
research programs at ANL, July 1962 to July 1963, 19: 20192(R) (ANL-6938)
HEART
cesium-137 and strontium-90 content in bulls from fallout, 19: 20215
effects of magnetic fields on function in frogs, 19: 21776 (UCRL-12389)
function of, tracer technique for dynamic exploration of, 19: 19705
HEART DISEASES
radiodiagnosis of coronary insufficiency and myocardial circulation using rubidium-86, 19: 19668
HEAT EXCHANGERS
design of tube and baffle, 19: 20125(P)
HEAT TRANSFER
effects on reactor kinetics, 19: 20116(R) (SAN-409-12)
from plasma, method for measuring, 19: 21503(T)
in boiling forced-flow liquid metals, analysis of, 19: 20116(R) (SAN-409-12)
in concrete pressure vessel, evaluation of, 19: 20110 (GAMD-5432)
in gas-solid suspension, equipment for studying, 19: 20098(R) (TID-21633)
in graphite–uranium rocket reactor, (T), 19: 21715 (AD-605574)
in pipe when heat flow varies sinusoidally, 19: 20118
in turbulent gas flow in thermal entrance region of heated tubes, 19: 20117 (SU-247-4)
to liquid metals flowing turbulently in eccentric annuli, 19: 20123
wetting effects on mercury, literature review, 19: 20112 (NAA-SR-Memo-10315)
HEAT TRANSFER SYSTEMS
development for satellites, 19: 21690(R) (LA-3244)
steam void determination in, method for, 19: 20294
HEATERS
design and construction of radiant, 19: 20098(R) (TID-21633)
HEAVY WATER REACTORS
design using graphite as second moderator, 19: 21658(P)
development for large-scale desalting, 19: 21709
HELIUM
analysis of, development of apparatus for, 19: 20473(R) (NASA-CR-54629)
charge exchange in, atom-ion resonance, (T), 19: 19931
collisions with excited cyclopropane, energy transfer in, 19: 19938
compressibility at high pressures at 25°C, 19: 19840 (LA-3250)
density and viscosity of liquid, around lambda point, (E), 19: 21168
diffusion and precipitation in irradiated aluminum–lithium alloys, 19: 20613 (CEA-R-2529)
diffusion in diamond, germanium, and silicon, 19: 19934
diffusion in gas-solid suspensions, equipment for measuring, 19: 20098(R) (TID-21633)
diffusion in graphite, effects of pore structure on, 19: 20457 (GAMD-4814)
diffusion in tourmalines, 19: 19934
diffusion into solids induced by ion and neutron bombardment, 19: 19934
effects on radioinduced carbon dioxide-graphite reactions, (E), 19: 19953 (AERE-R-4201)
effects on spectral lines of cesium, 19: 20870
electron diffraction by, 19: 20826
electron inelastic scattering by, multichannel resonances in forward, (E), 19: 20848
electron reactions with, ionization cross sections for, (T), 19: 20864
electron-positive ion recombination in dense neutral gaseous, (T), 19: 20860
energy levels of, expectation values of operators for ground state, (T), 19: 20863
flow in thermal entrance region of heated tubes, effects of large temperature gradients on turbulent, 19: 20117 (SU-247-4)
flow of liquid II, pressure-temperature relation for fountain, (T), 19: 21179
helium-ion reactions at 100 to 400 kev, excitation in, (E), 19: 20862
hydrogen ion reactions with, electron capture in, (T), 19: 20821
ion capture in rotating liquid II, negative, (E), 19: 21177
ionization by electrons at 0.6 to 20 kev, (E/T), 19: 20850
ionization in pinch devices and shock tubes, (E/T), 19: 21471 (IPP-1/24)
meson (K^-) and (π^-) de-excitation capture in liquid, (T), 19: 21042
meson (μ) capture by, intermediate vector boson in, (T), 19: 21420
performance in scintillation detectors for alpha particles and electrons, 19: 20361
photoelectric emission in low-pressure discharge of, (E), 19: 20861
photoionization cross section of, (T), 19: 20830
photoionization of, dielectric breakdown from, (E), 19: 20847
plasma of, perpendicular pressure and temperature in stellarators (C), (E), 19: 21511
positron annihilation in, effect of electric field on rate of, (E), 19: 21011
preparation and supplies of liquid, in Great Britain, 19: 21183
production in ionization gages in vacuum systems, (E), 19: 20146
reactions of excited, with hydrocarbons, 19: 19937
refractive index, (T), 19: 20859
solubility in lithium and potassium, 19: 20561 (PWAC-380)
sound, propagation in rotating liquid II, mode degeneracy in second, 19: 21175
superfluid flow of liquid, thermomechanoelectrical effects for, 19: 21176
superfluidity of, Josephson effect analog in, (E), 19: 21172
transitions in, electron impact excitation of electric quadrupole, (T), 19: 20855
HELIUM IONS
reactions with helium at 100 to 400 kev, excitation in, (E), 19: 20862
reactions with hydrogen, deuterium isotope effects on, 19: 19887
recombination with electrons in dense neutral gas, (T), 19: 20860
scattering by octupole levels in nitrogen-15 and oxygen-16 at 40.6 Mev, (E/T), 19: 21268(R) (UCRL-11828(p.129-31))
HELIUM ISOTOPES He-3
content and energy spectrum of, in cosmic radiation, 19: 20901
content in Discoverer XVII, origin of, 19: 21438
content in iron meteorites, (E), 19: 20760
content in primary cosmic radiation, 19: 20899
density and viscosity of liquid, around lambda point, (E), 19: 21168
energy of, Coulomb, (T), 19: 21309
hyperfine structure of μ-mesic atoms of, vacuum polarization corrections to, (T), 19: 21395
interactions with deuterons and nucleons, bibliography, (E/T), 19: 21238 (LA-3205)
meson (μ^-) capture ^{3}y, nuclear form factors from, (T), 19: 21236 (JINR-P-1952)
nuclear magnetic dipole moment, (T), 19: 21322
performance in nuclear gyroscopes, (T), 19: 20279 (RTD-TDR-63-4001)
production by proton reactions with metals, 19: 21438
properties and theory of, at low temperatures, 19: 21184
reactions (He-3,d) and scattering with N = 28 nuclei, (E), 19: 21240 (LA-DC-6232)
reactions with light nuclei at 29 Mev, (E), 19: 21232 (JEN-141-DF/I-45)
scattering by aluminum-27 at 5.5 to 10.0 Mev, angular distributions from, (E), 19: 21328
spectral emission in, helium-3 and -4 simultaneous stimulated, (E), 19: 20815
wave function of, ground-state, (T), 19: 21367
HELIUM ISOTOPES He-4
content in iron meteorites, (E), 19: 20760
content in primary cosmic radiation, 19: 20899
density and viscosity of liquid, around lambda point, (E), 19: 21168
deuteron elastic scattering at 10.3 Mev, cross sections for, (T), 19: 21286
distribution function in quantal liquid, asymptotic form of radial, 19: 20697
spectral emission in, helium-3 and -4 simultaneous stimulated, (E),

19: 20815
HELIUM ISOTOPES He-6
production in proton reactions with carbon-12 at 156 Mev, cross sections for, (T), 19: 21402
HELIUM SYSTEMS
D–He, compressibility at high pressures at 25°C, 19: 19840 (LA-3250)
He–N, compressibility at high pressures at 25°C, 19: 19840 (LA-3250)
He–Xe, performance in scintillation detectors, 19: 20361
HEMATOPOIETIC SYSTEM
radiation effects on, in rabbits and rats, 19: 19499(R) (NP-14899)
radiation effects on sheep, 19: 19600
HEMOGLOBIN
radiation effects on oxygen attachment in rabbit equation for calculating, 19: 19529(T)
radiation effects on thermoluminescence, 19: 19983
reactions of oxygen in, equation for reversible attachment and transition process in, 19: 19529(T)
HEMORRHAGE
effects of *E. coli* endotoxin on syndrome of, in guinea pigs, 19: 19487
hematological response of dogs to artificial, 19: 21777 (UR-662)
HEPTANE
effects on ionic decomposition of *s*-butylperoxy formate, 19: 19948
solvent properties in mixtures with butyl, dichlorodiethyl, and ethyl ethers for uranyl nitrates, 19: 20072
HETEROGENEOUS REACTORS
moderator support structure for gas-cooled, 19: 21628(P)
HEXANE
carbon-11 recoil reactions in, effects of oxygen and radiation dose on, 19: 20018
HIGH-ALTITUDE EXPLOSIONS
electromagnetic radiation from, vif, (E), 19: 21139
radiation dose calculation for eyes exposed to visible radiation from nuclear, 19: 19498 (LA-3204)
HIGH ENERGY INJECTION DEVICES
beam injection duct for DCX-2, 19: 21486(R) (ORNL-3760(p.77-93))
development at ORNL, 19: 21479(R) (ORNL-3760)
development of DCX-1, 19: 21480(R) (ORNL-3760(p.1-9))
ion sources for DCX-2, 19: 20730(R) (ORNL-3760(p.64-8))
operation of DCX-2, 19: 21481(R) (ORNL-3760(p.10-22))
plasma stability in DCX, calculation of, 19: 21485(R) (ORNL-3760 (p.69-76))
HIGH-TEMPERATURE CORROSION
of metals in gas atmosphere, 19: 20486
HIGH-TEMPERATURE REACTIONS
chemical engineering problems in, 19: 19868
HIROSHIMA
leukemia incidence in, correlation of age, degree, duration, exposure, and type in, 19: 19526
HISTOLOGY
use of labeled antibodies in electron microscopic studies, 19: 19465
HOISTS
design specification for gantry and trolley for fuel handling cask, 19: 20099 (TID-21644)
HOLMIUM ALLOYS
Sb–Ho, magnetic properties of, (E), 19: 20597
HOLMIUM COMPLEXES
with serine, stability and composition, 19: 19874
HOLMIUM IONS
spectra in barium, calcium, and strontium fluorides, absorption and luminescence, 19: 19854
HOLMIUM ISOTOPES Ho-165
alpha inelastic scattering at 3.1 Mev, conversion coefficients and mixing ratios for rotational transitions in, (E), 19: 21324
nitrogen-14 fission, excitation energy, (E/T), 19: 21259(R) (UCRL-11828(p.77-80))
HOLMIUM ISOTOPES Ho-166
beta decay spectra, 19: 21340
HOLMIUM NITRIDES
magnetic properties of, influence of crystal field on, 19: 19895
HOLMIUM SULFATES
crystal structure and bond types of octahydrates, 19: 19915(T)
HOSPITALS
equipment for staff protection during radiotherapy, 19: 19634
HUMIDITY
effects on radiosensitivity of *Serratia marcescens*, 19: 19649
HUNGARY
monitoring atmospheric dusts in Debrecen, 19: 20235
radiation exposure to Mosonmagyarovar in habitants from medical examinations in 1961, 19: 20227
HYALURONIDASES
radiation effects on thermoluminescence, 19: 19983
HYDRACRYLIC ACID, β-LACTONE
radioinduced polymerization at −78°C, dielectric properties of products from, 19: 20000
HYDRAZINE HYDROCHLORIDE
radioinduced formation of sulfur-35 in, chemical effects from, 19: 20004
HYDROAROMATIC COMPOUNDS
reactions with excited helium, 19: 19937
HYDROBROMIC ACID
use with silica gel as moisture indicator, 19: 21783(P)
HYDROCARBONS
radiolysis of, use of carbon-14-labeled methyl radical as scavenger in, 19: 19985
separation of mixtures of by distillation, efficiency of Stedman stainless steel packings for, 19: 20068
HYDROCHLORIC ACID
effects on dissolution of plutonium dioxide pellets in nitric acid, 19: 20050 (ORNL-3695)
equilibrium with tridodecylamine, 19: 20039 (EUR-2246.e)
solubility in organic diluents, 19: 20039 (EUR-2246.e)
HYDROCYANIC ACID
ionization by electron impact, appearance potential for doubly charged molecule ions in, 19: 20807(R) (UCRL-11828(p.201-4))
HYDRODYNAMICS
equations for superfluidity of Fermi liquids, (T), 19: 21161 (JINR-P-1953)
of thermal protection of concrete pressure vessels, 19: 20110 (GAMD-5432)
system for closure of pipes, 19: 20100 (UCRL-12203)
HYDROFLUORIC ACID
effects on dissolution of plutonium dioxide and uranium dioxide pellets in nitric acid, 19: 20050 (ORNL-3695)
flowmeter design for, 19: 20259 (JAERI-1074)
reactions with molybdenum, tungsten, and uranium oxides in aqueous solutions, 19: 19913
sorption by soda lime, thermobalance study of, 19: 20258 (JAERI-1070)
HYDROFLUORINATION
of plutonium oxides, engineering drawings of equipment for, 19: 19939
HYDROGEN
abstraction from aromatic compounds by methyl radicals, 19: 21760 (NYO-2728-4)
atomic matrix elements and wave functions for, (T), 19: 20809 (UCRL-12218)
beams of atomic, reactions in EPA plasma, 19: 21482(R) (ORNL-3760(p.23-9))
behavior in potassium–sodium alloy corrosion loops, 19: 20480(R) (ORNL-3730)
charge transfer to alpha particles, calculation of, 19: 19937
decay in nonequilibrium optically transparent plasma of, recombination, (T), 19: 21557
detection in potassium–sodium alloy loops, test of system for, 19: 20478(R) (ORNL-3618)
determination in molybdenum metal, combustion-gravimetric, 19: 19758 (LA-3225)
determination in potassium–sodium alloy loop, using detector-sleeve sweep gas, 19: 20480(R) (ORNL-3730)
determination in titanium and Zircaloy-2 by isotopic equilibration, 19: 19831
determination in uranium and its compounds and alloys, methods for, 19: 19823
determination in vented gases from underground nuclear explosion, apparatus for, 19: 19776 (UCRL-12169)
determination of trace amounts of atomic, by reaction with arsenic-74, 19: 19825
diffusion in Croloy 9M and type 316 stainless steel at high temperatures, 19: 20479(R) (ORNL-3671)
diffusion in Croloy 9M and type 316 stainless steel at 1100 to 1300°F, 19: 20480(R) (ORNL-3730)
diffusion in Hastelloy N in absence and presence of potassium–sodium alloy at 1100 to 1425°F, 19: 20478(R) (ORNL-3618)
diffusion in INOR-8 at 1425°F in presence of potassium–sodium alloy, 19: 20479(R) (ORNL-3671)
diffusion through SNAP-8 coolant system, 19: 20475(R) (ORNL-3538)
diffusion through INOR-8 diaphragm at high temperatures in absence and presence of potassium–sodium alloy, 19: 20477(R) (ORNL-3604)
effects on gas-liquid chromatography of acetylated steroids, 19: 19893
effects on radioinduced carbon dioxide-graphite reactions, (E), 19: 19953 (AERE-R-4201)
effects on radioinduced reactions of carbon dioxide with graphite, 19: 19954 (AERE-R-4839)
effluent measurements in potassium–sodium alloy corrosion loops, 19: 20479(R) (ORNL-3671)

electric discharges in, unstable plasma rotation in Penning, (E), 19: 21548
electric discharges in, in h-f magnetic fields, (E/T), 19: 21554
electron attachment in, negative ion production by dissociative, (E), 19: 20691
electron density in afterglow of z-discharge in, (E), 19: 21510
electron diffraction by, evidence for molecular charge distribution in, 19: 20826
electron diffusion in, at low pressures in strong electric fields, (E/T), 19: 20696
electron dissociative resonance capture in molecular, (T), 19: 19899
electron energy distribution in plasmas of, equations for, 19: 21586
electron paramagnetic resonance in calcium fluoride and potassium chloride crystals, spectra of, 19: 19896
electron reactions with, excitation functions for metastable state formation in, 19: 19992
electron scattering by atomic, exchange amplitudes for excitation in, (T), 19: 20866
energy level excitation by electron, positron, and proton impact, 2p, (T), 19: 20853
exchange to and from azulene in acid solutions, 19: 19883
flow in wind tunnel nozzles at 13,000°K and 1000 atm, 19: 20124
glow discharges in, properties of metastable abnormal, 19: 21590
hyperfine structure of, proton-size effects on, (T), 19: 21396
injection and detection in potassium–sodium alloy corrosion loops, 19: 20477(R) (ORNL-3604)
ionization by electric fields, 19: 21484(R) (ORNL-3760(p.57-63))
ionization by electrons at 0.6 to 20 kev, (E/T), 19: 20850
ionization by electron impact, electron exchange, (T), 19: 20854
ionization in pinch devices and shock tubes, (E/T), 19: 21471 (IPP-1/24)
meson (μ) capture by, intermediate vector boson in, (T), 19: 21420
meson (π^-) transfer to heavier atoms in ethane and styrene, (E), 19: 21281
neutron absorption cross section of, thermal, (E), 19: 21219
performance as space-vehicle propellant with solar heating, 19: 20137 (NASA-CR-59332)
performance in nuclear gyroscopes, (T), 19: 20279 (RTD-TDR-63-4001)
photoionization cross sections and recombination coefficients of, (T), 19: 20834
production of atomic, by molecular ion reactions with protons, 19: 21484(R) (ORNL-3760(p.57-63))
proton reactions with atomic, electron capture cross sections for, (T), 19: 21417
reactions with carbon atoms and ions in electron-bombarded acetylene, 19: 19988
reactions with helium and neon ions, deuterium isotope effects on, 19: 19887
reactions with irradiated nickel oxides, effects of radiation dose on reduction rates in, 19: 19975
removal from SNAP-8 coolant system, 19: 20480(R) (ORNL-3730)
shock wave propagation in, in magnetically driven shock tubes, (E), 19: 20661 (RLE-TR-428)
solubility in potassium–sodium alloy, apparatus for measurement of, 19: 20477(R) (ORNL-3604)
solubility in potassium–sodium alloy at 1100°F, 19: 20479(R) (ORNL-3671)
solubility in potassium–sodium alloy at 752 to 1300°F, 19: 20480(R) (ORNL-3730)
sorption and desorption of residual, in high vacuum, (E), 19: 20144
spectra in sun, Brackett gamma line in, (E/T), 19: 20778(T)
spectra in sun, Fraunhofer lines in, (E/T), 19: 20777(T)
spectra of solar prominences, alpha line in, (T), 19: 20776(T)
spectra of, rotational analysis B', B'', D, D', and D'' states in absorption, 19: 19894
spin isomer separation in, by absorption and gas chromatography, 19: 20435
stability in toroidal plasma of, twin-channel, (E), 19: 21467 (ARL-63-203)
thermal conductivity and viscosity coefficients of atomic, from 1 to 400°K, (T), 19: 20700
transitions in atomic, electron impact excitation of electric quadrupole, (T), 19: 20855
yields from electrolysis of molten potassium and fluoride, 19: 19875
yields from radiolysis of formic acid–hydrogen peroxide solutions, effects of pH on, 19: 19989

HYDROGEN COMPOUNDS
neutron energy distribution in moderating, in long counter, (T), 19: 21202

HYDROGEN IONS
beams of molecular, production and injection in DCX-2, 19: 20730(R) (ORNL-3760(p.64-8))
dissociation of molecular, neutral atoms from, 19: 21484(R) (ORNL-3760(p.57-63))
electron capture by monovalent, from helium, (T), 19: 20821
electronic energy for two-Coulomb center in molecular, 19: 19885
photoionization cross sections and recombination coefficients of, (T), 19: 20834
production of high-intensity beams of atomic negative, (E), 19: 20731 (UCRL-11684)
production of monovalent, by electron attachment in hydrogen and deuterium hydride, (E), 19: 20691
reactions with carbon atoms and ions in electron-bombarded acetylene, 19: 19988

HYDROGEN ISOTOPES
separation by adsorption and gas chromatography, 19: 20435
separation by ion exchange, 19: 19865

HYDROGEN ISOTOPES H-4
production in neutron reactions with tritium at 14.4 Mev, (E), 19: 21405

HYDROGEN PEROXIDES
effects on dissolution of plutonium dioxide pellets in nitric acid, 19: 20050 (ORNL-3695)
effects on radiolysis of glycogen, 19: 20015
effects on spectrophotometric determination of zinc using 1-(2-thiazolylazo)-2-naphthol, 19: 19814
formic acid–H_2O_2, radiolysis of, effects of pH on yields from chain, 19: 19989

HYDROGEN SYSTEMS
H–O, calculation of bond energies and wave functions by united atom method for ions in, 19: 19844 (PAN-550/XVII)
H–U, diffusion and viscosity coefficients of high-temperature ionized, 19: 19941

HYDROLOGY
use of tritium in, 19: 20174(T) (CEA-tr-A-1729)

HYDROMAGNETIC WAVES
effects of magnetospheric, on auroral radar echoes, (T), 19: 21149
energy transfer in dispersive media, (T), 19: 20688
interactions with geomagnetic fields, amplification processes in, (T), 19: 21123 (D1-82-0398)
production and propagation of, equipment for, 19: 21465 (AFCRL-63-779)
propagation from stellar collapse, (T), 19: 20768(T)
propagation in atmosphere in gravitational and magnetic fields, 19: 21151
theory of Riemann, 19: 20668

HYDROXIDES
bond energies and wave functions of, calculation by united atom method, 19: 19844 (PAN-550/XVII)

HYDROXYL IONS
bond energies and wave functions of, calculation by united atom method, 19: 19844 (PAN-550/XVII)
reactions with 2-phenylethyltrimethylammonium iodide, deuterium isotope effects on, 19: 19947

HYDROXYL RADICAL
effects on yields from radiolysis of glycogen, 19: 20015
reactions in irradiated ferrocyanide solutions, 19: 20009

HYDROXYLAMINE
effects on mutagenesis in isolated DNA from *B. subtilis*, 19: 19542

HYDROXYLAMINE HYDROCHLORIDE
radioinduced formation of sulfur-35 in, chemical effects from, 19: 20004

HYPERFRAGMENTS
book: *Fundamental Particles*, 19: 21072
production in meson (K^-) reactions with emulsion nuclei at 3.0 Bev/c, (E), 19: 21429
production in meson (K^-) reactions with emulsion nuclei, (E), 19: 21365

HYPERONS
decay of, amplitudes for nonleptonic, (T), 19: 20982
decay of, broken-SU(6)-symmetry models for nonleptonic, (T), 19: 20919 (IC-65/5)

HYPERONS (Λ)
decay of, branching ratios for leptonic, (T), 19: 21019
decay of, broken-SU(6)-symmetry models for nonleptonic, (T), 19: 20919 (IC/65/5)
interactions with protons at low energy, (E), 19: 21034
mass relative to hyperons (Σ), SU(6)-symmetric bootstrap model for difference in, 19: 21014
polarization correlation of hyperons (Σ^0) and, from meson (K^-)-proton interactions, 19: 21071
production in $p\bar{p}$ interactions, charge conjugation conservation in, (T), 19: 20977

HYPERONS (Λ^0)
decay of, p-wave amplitudes for nonleptonic, (T), 19: 21021
decay of, U(12) symmetry for weak interactions in, (T), 19: 21028
decay of, U(6) ⊗ U(6) for nonleptonic, (T), 19: 21009

HYPERONS (Ω^-)

decay of, broken-SU(6)-symmetry models for nonleptonic, (T), 19: 20919 (IC/65/5)
decay of, p-wave amplitudes for nonleptonic, (T), 19: 21021
properties, 19: 21040
properties of, potential model for, (T), 19: 20970
HYPERONS (Σ)
decay of, branching ratios for leptonic, (T), 19: 21019
interactions with hyperons (Σ) and mesons (π), coupling constants for, (T), 19: 20917 (IC/65/3)
mass relative to hyperons (Λ), SU(6)-symmetric bootstrap model for difference in, 19: 21014
HYPERONS (Σ^-)
decay of, branching ratios for leptonic, (T), 19: 21019
decay of, branching ratios and rates of, (T), 19: 21045
decay of, p-wave amplitudes for nonleptonic, (T), 19: 21021
decay of, U(12) symmetry for weak interactions in, (T), 19: 21028
decay of, U(6) ⊗ U(6) for nonleptonic, (T), 19: 21009
HYPERONS (Σ^0)
decay of, branching ratios for leptonic, (T), 19: 21019
polarization correlation of hyperons (Λ) and, from meson (K^-)-proton interactions, 19: 21071
HYPERONS (Σ^+)
decay of, branching ratios for leptonic, (T), 19: 21019
decay of, branching ratios and rates of, (T), 19: 21045
decay of, broken-SU(6)-symmetry models for nonleptonic, (T), 19: 20919 (IC/65/5)
decay of, U(6) ⊗ U(6) for nonleptonic, (T), 19: 21009
HYPERONS (Ξ)
interactions with mesons (K), hyperons (Ω^-) as bound state in, (T), 19: 20970
properties of, dynamic and intrinsic, 19: 21065
HYPERONS (Ξ^-)
decay of, branching ratios for leptonic, (T), 19: 21019
decay of, broken-SU(6)-symmetry models for nonleptonic, (T), 19: 20919 (IC/65/5)
decay of, p-wave amplitudes for nonleptonic, (T), 19: 21021
decay of, U(12) symmetry for weak interactions in, (T), 19: 21028
decay of, U(6) ⊗ U(6) for nonleptonic, (T), 19: 21009
mass difference ($\Xi^- - \Xi^0$), (T), 19: 20917 (IC/65/3)
HYPERONS (Ξ^0)
decay of, branching ratios for leptonic, (T), 19: 21019
decay of, U(6) ⊗ U(6) for nonleptonic, (T), 19: 21009
mass and Regge trajectories for, (T), 19: 21049
mass difference ($\Xi^- - \Xi^0$), (T), 19: 20917 (IC/65/3)

I

ICE-d_2
neutron scattering at small angles, temperature dependence of cold, (E), 19: 21218
IGNEOUS ROCKS
separation of scandium from pyroxenite, 19: 20081
IMMUNE REACTIONS
of animal cells in tissue culture, to virus infections, 19: 19549
of radiation mouse chimeras to bone marrow grafts, thymus effects on, 19: 19652
of spleen cells in irradiated mice, protection of killing effect of, 19: 19651
radiation effects on, to spleen transplants in dogs, 19: 19521
radiation effects on, to spleen transplants, 19: 19522
radiation effects on, to lung transplants, 19: 19523
radiation effects on, 19: 19589
radiation, drug, and hormone effects on, of bone marrow and organ grafts, 19: 19588
to kidney transplants in dogs, 19: 19519
to kidney transplants in man, 19: 19520
to lung transplants, effects of immunosuppressive drugs, 19: 19523
to spleen transplants, effects of immunosuppressive drugs, 19: 19522
use of labeled antibodies for studies of ultrastructure, 19: 19465
IMMUNITY
effects of bone marrow and lymph cell radiation chimeras on, in kidney grafts in dogs, 19: 19493
in animal fetuses, review on, 19: 19468
radiation effects on tetanus vaccination in monkeys, 19: 19608
IMMUNIZATION
effects with and without radiation on cholinesterase activity in rabbits, 19: 19609
IN-PILE LOOPS
description and operation of sodium-cooled, for irradiation of fissionable needle, 19: 21736(T) (ORNL-tr-539)
design for testing defective or high-risk fuel elements in PRTR, engineering drawings of, 19: 21704
INCONEL
corrosion by carbon dioxide at 1100 to 1800°F, 19: 20487
corrosion in reactors, 19: 20488
tensile properties of 718, testing, (E), 19: 20554 (LA-3161)
use in nozzles for high-temperature thermometry in gases, 19: 20277 (ORNL-P-1068)
welding of pipes and plates of, Hanford procedures for, 19: 20524 (TID-20625(Vol.IV)(Rev.I))
INDAN
hydrogen abstraction from, by methyl radicals, 19: 21760 (NYO-2728-4)
INDIAN OCEAN
radioactivity of air in, 1961–62, 19: 20158 (NP-14712)
INDIUM
determination using 5,5′thiodisalicylic acid, gravimetric, 19: 19812
effects on spectrophotometric determination of zinc using 1-(2-thiazolylazo)-2-naphthol, 19: 19814
effects on strength of thorium at high temperatures, 19: 20560 (ORNL-3777)
electromagnetic-wave propagation in metallic, helicon, (E), 19: 21553
geochemistry and mineralogy of, in Cherry Mountains (Urals), USSR, book, 19: 20190
magnetic flux quantization in superconducting cylinders of, 19: 21194
neutron flux perturbations in foils of, effects of flux anisotropies on, (E), 19: 21213
neutron total cross section at 0.7 to 14 ev, (E), 19: 21285
separation from cadmium, 19: 20023(T) (ORNL-tr-556)
separation from mixed fission products by radiochemical precipitation, 19: 19777 (USNRDL-TR-819)
superconducting transition temperature of films of, (E), 19: 21189
use in adhesion test for cleanliness, modifications in method for, 19: 20205 (SC-TM-64-1722)
INDIUM ALLOYS
In–Pu, phase studies, 19: 21690(R) (LA-3244)
INDIUM ISOTOPES In-113
alpha fission of, excitation energy, (E), 19: 21261(R) (UCRL-11828(p.81-3))
INDIUM ISOTOPES In-114
magnetic fields acting on, in ferromagnetic materials, 19: 20578
INDIUM ISOTOPES In-115
alpha fission of, excitation energy, (E), 19: 21261(R) (UCRL-11828(p.81-3))
electron and photon scattering from, excitation in, 19: 21455
neutron inelastic scattering by, isomeric states from, (E), 19: 21237 (KFK-265)
production of metastable, 19: 20023(T) (ORNL-tr-556)
INDIUM ISOTOPES In-116
energy levels of, properties of isomeric, (E), 19: 21237 (KFK-265)
INDIUM OXIDES
thermal conductivity at high temperatures, (E), 19: 20576
5-INDOLOL, 3-(2-AMINOETHYL)-
protective effects with AET and MEA against radiation lethality in mice, 19: 19627
protective effects of, against radiation injuries in mice, 19: 19635
INERTIAL NAVIGATION
development of nuclear gyroscopes for, (T), 19: 20279 (RTD-TDR-63-4001)
INFECTIONS
antibiotic therapy of, associated with radiation sickness in rabbits and rats, 19: 19622
of radiodermatitis lesions, 19: 19605
INFRARED RADIATION
effects on x-ray-induced luminescence of cadmium zinc sulfide phosphors, 19: 19965
INOR-8
corrosion by potassium–sodium alloy, research program on, 19: 20477(R) (ORNL-3604)
corrosion by potassium–sodium alloy at high temperatures, carbon mass transfer in, 19: 20478(R) (ORNL-3618)
corrosion of chromized, by potassium–sodium alloy at high temperatures, loop experiments, 19: 20479(R) (ORNL-3671)
corrosion of chromized, by potassium–sodium alloy at high temperatures, mass transfer in, 19: 20480(R) (ORNL-3730)
diffusion of hydrogen through diaphragm of, at high temperatures in absence of potassium–sodium alloy, 19: 20477(R) (ORNL-3604)
diffusion of hydrogen in, in absence and presence of potassium–sodium alloy at 1100 to 1425°F, 19: 20478(R) (ORNL-3618)
diffusion of hydrogen in, at 1425°F in presence of potassium–sodium alloy, 19: 20479(R) (ORNL-3671)
metallographic examination of chromized tubing of, 19: 20480(R) (ORNL-3730)

metallurgical study of chromized tubing of, 19: 20475(R) (ORNL-3538)
metallurgical study of chromized tubing of, 19: 20477(R) (ORNL-3604)
INOSITOL
effects on radiosensitivity of *Serratia marcescens*, 19: 19649
INSPECTION AND CONTROL
conference on automatic, 19: 20303
conference on automatic, 19: 20305
equipment for power plant, design of automatic safety, 19: 20103
INSTRUMENTATION
conference on automatic, 19: 20303
conference on automatic, 19: 20305
developments for 88-inch cyclotron, 19: 20282(R) (UCRL-11828 (p.218-19))
INSTRUMENTS
design for calibrating frequency-measuring devices, (E), 19: 21766 (SC-TM-64-921)
design for constant-current discharge-testing of batteries, (E), 19: 20280 (SCL-DR-64-128)
development of nuclear gyroscopes, (T), 19: 20279 (RTD-TDR-63-4001)
developments in, for physical methods of analysis, 19: 19782
modular packaging of, 19: 20287(R) (UCRL-11828(p.230-2))
performance of tracking stations for close-in transits, (E), 19: 21767 (SC-TM-65-44)
standardization of, for nuclear-physics studies, (E), 19: 20262 (KFK-259)
INTERFEROMETERS
design for plasma electron-density gradient measurements, (E), 19: 21472 (IPP-1/25)
design of hyperfrequency, for plasma density measurements, 19: 21591
design of multiple-beam microwave, for plasma diagnostics, 19: 21574
INTERNAL FRICTION
measurement in rigid samples at high temperatures, apparatus for, 19: 20245 (CEA-R-2718)
INTESTINE
cesium-137 and strontium-90 content in bulls from fallout, 19: 20215
radiation effects on desoxyribonucleic acid metabolism in rat, 19: 19506 (TID-21703)
IODATES
solvent extraction from molten nitrate by liquid silicone–TBP at 150°C, 19: 19833 (CEA-R-2628)
solvent extraction from molten nitrate by liquid silicone–TBP at 150°C, 19: 19833 (CEA-R-2628)
IODIDE IONS
reactions with methyl iodide, selectivity of labeling in recoil, 19: 20020 (IA-907)
solvent extraction from molten nitrate by liquid silicone–TBP at 150°C, 19: 19833 (CEA-R-2628)
IODINE
chemical properties of, formed in irradiation of tellurium compounds, 19: 20005
effects on radioinduced carbon dioxide-graphite reactions, (E), 19: 19953 (AERE-R-4201)
uptake and storage in human fetal thyroid, 19: 19491
x-radiation scattering by, Hartree-Fock calculations of incoherent, 19: 20824
IODINE ISOTOPES
uptake by vibrissal hairs of mice, origin of, 19: 19479
IODINE ISOTOPES I-125
use in human fibrinogen for detection of malignant tumors in man, 19: 19716
use in photoscanning of liver and thyroid, 19: 19711
IODINE ISOTOPES I-129
energy level scheme, 19: 21450
IODINE ISOTOPES I-131
activity distribution and chemical states in irradiated tellurium compounds, 19: 20005
contamination of food chain by, from fallout, 19: 20240
determination in air by beta measurement, efficiency of counter for, 19: 20169
incorporation in silver iodide aerosols, 19: 20027
preparation of carrier-free, from irradiated uranium trioxide, 19: 20029
production in Spain, 19: 20432(T) (ORNL-tr-295)
production using Rossendorf Reactor in East Germany, 19: 20436
radiation hazards from diagnostic uses of, 19: 19587
separation from food and water, 19: 20240
stability of compounds labeled with, used in clinical studies, 19: 19731
therapeutic uses during human pregnancy, hazards in, 19: 19491
therapeutic uses of, in thyroid diseases, 19: 19665
uptake and secretion by cow milk after single dose, 19: 19477
uptake by human blood, blood plasma, and ovaries, beta activity from, 19: 19483
uptake by human liver, profile counting studies on, 19: 19492
uptake by shellfish, 19: 20230
use in diagnosis of liver tumors in man by infusion in bowel, 19: 19662
use in diagnosis of pulmonary embolism in dogs and man, 19: 19724
use in diagnosis of echinococcus disease of liver by scanning, 19: 19729
use in diagnosis of liver diseases by scanning, 19: 19730
use in diagnostic clinic in Great Britain, 19: 19682
use in fractionated treatment of euthyroid goiters in man, 19: 19685
use in human fibrinogen for detection of malignant tumors in man, 19: 19716
use in human serum albumin for liver-spleen photoscanning, 19: 19710
use in iodide for localization of stomach tumors and ulcers, 19: 19717
use in myeloscintigraphy of intraspinal neurological syndromes, 19: 19720
use in scanning for brain tumors, 19: 19714
use in scintiscanning of liver during amebiasis, 19: 19728
use in therapy by intra-arterial injection, method for, 19: 19661
ION BEAMS
accelerating cavities for, for Brookhaven AGS, (E), 19: 20719 (BNL-8970)
acceleration and production of high-intensity, devices for, (E), 19: 20720 (BNL-8982)
injection into accelerators, systems for, (E), 19: 20737 (UCRL-11955)
production and injection of molecular hydrogen, in DCX-2, 19: 20730(R) (ORNL-3760(p.64-8))
production of high-intensity negative-hydrogen-atom, (E), 19: 20731 (UCRL-11684)
production of quasi-neutral, using reflex-discharge ion source, (E), 19: 21571
ION EXCHANGE
equilibrium of, in mixed solvents, equations for, 19: 20057
use in complex formation studies, 19: 19837 (IA-1000)
ION EXCHANGE MATERIALS
efficiency of liquid, 19: 20061
use of artificial zeolites in high vacuum systems, review on, 19: 20141
ION EXCHANGE PROCESSES
separation of rare earths by, use of polyphosphates as elution medium in, 19: 20049 (NP-14834)
ION PUMPS
gas evolution from sputter, 19: 20140(R) (ORNL-3760(p.94-7))
ION SOURCES
accelerating cavities for, for Brookhaven AGS, (E), 19: 20719 (BNL-8970)
description of high-intensity, (E), 19: 20720 (BNL-8982)
design of high-intensity negative-hydrogen-atom, (E), 19: 20731 (UCRL-11684)
design of, using piezoelectric vacuum vibrator, 19: 20292
deterioration of tantalum filaments in electron-bombardment mercury, for space propulsion, 19: 20138 (NASA-TN-D-2173)
development for production of molecular hydrogen ions, 19: 20730(R) (ORNL-3760(p.64-8))
ion beam formation from reflex-discharge, quasi-neutral, (E), 19: 21571
use of Orbitron, for neutron sources, 19: 21208
IONIZATION
in combustion product MHD generators, methods for non-thermal, 19: 20911
measurement of photo-, apparatus for molecular, 19: 19955(R) (ANL-6938(p.21-2))
production of precursor, in pinch devices and shock tubes, (E/T), 19: 21471 (IPP-1/24)
IONIZATION CHAMBERS
current integrator for, design of, 19: 20367
design of portable two-capacitor, 19: 20391(P)
performance and uses in gas chromatography, 19: 19804
performance as dosimeters in mixed gamma and neutron fields, 19: 20330(T) (AEC-tr-6547)
use in determination of bremsstrahlung energy and intensity in betatrons, 19: 20337
IONOSPHERE
disturbances in F region of, mechanisms for, (T), 19: 21125 (RAD-TR-64-27)
disturbances in F2 layer of, spatial distribution of, 19: 21133(T)
disturbances of F2 layer during magnetic storms, (E), 19: 21132(T)
electric currents in, (E), 19: 21124 (P-1121(RAND))
electric fields in, device for measuring, 19: 20290
electron concentration in D region of, review on rocket determinations of, 19: 21127(T)
electron density in F2 region of, diffusive equilibrium of topside, (T), 19: 21141
ionization in F region of, at sunrise near magnetic equator, 19: 21138
ionization in F2 layer, spatial distribution of anomalous, (E/T), 19: 21129(T)
ionization of lower, by solar cosmic radiation, (T), 19: 21145

plasma oscillations in, incoherent radar scattering from, (E), 19: 21153
structure and properties of, review of, 19: 21159
IONS
acceleration of variably charged, by electrostatic fields, (T), 19: 20722 (JINR-D-1946)
capture of negative, by vortex line in rotating helium II, (E), 19: 21177
distribution function for plasma in high-frequency magnetic field, (T), 19: 21573
distribution in h-f helium discharge plasma, (E), 19: 21528
effects of thermal, on plasma wave propagation across magnetic field, (T), 19: 21521
emission from metal foils, laser-induced, (E), 19: 20814
energy levels for, approximate Thomas-Fermi potential for, (T), 19: 20808 (UCRL-12054-T)
interactions in geomagnetic fields, effects on hydromagnetic wave propagation, (T), 19: 21123 (D1-82-0398)
ionization in beams, determination from spectral emission lines, (E), 19: 20857
production in lower ionosphere, during solar cosmic-ray events, (T), 19: 21145
reactions of heavy, nucleon transfer in, (T), 19: 20937(R) (TID-21672)
scattering by nuclei, excitation of collective states in inelastic, (T), 19: 21353
sputtering on solids, review of, 19: 20819
IOWA
fallout monitoring, 1964, 19: 20156 (IS-1098)
IRIDIUM ISOTOPES Ir-187
fission barrier of compound nucleus, (E/T), 19: 21259(R) (UCRL-11828(p.77-80))
IRIDIUM ISOTOPES Ir-191
gamma resonant scattering by, angular distribution of, (E), 19: 21435
IRIDIUM ISOTOPES Ir-193
hyperfine levels of, Mössbauer study of, (E/T), 19: 21255(R) (UCRL-11828(p.57-8))
IRON
analysis for hafnium or zirconium using catechol violet, colorimetric, 19: 19780
analysis for uranium by photocolorimetric methods, 19: 19811
corrosion by carbon dioxide at 1100 to 1800°F, 19: 20487
determination by titration, suitability of tetraethylenepentamine heptaacetic acid for, 19: 19813
determination in alloys with uranium, correction factors for x-ray micro-, 19: 19746 (CEA-R-2728)
determination in ppm range by d-c arc excitation, spectrochemical, 19: 19827
determination in SAP powders by different laboratories, statistics on, 19: 19750 (EUR-2286.f)
determination in uranium, photocolorimetric, 19: 19811
determination in uranium and its compounds and alloys, methods for, 19: 19823
determination using 5,5′thiodisalicylic acid, spectrophotometric, 19: 19812
effects on determination of zirconium using arsenate method, 19: 19818
effects on photometric determination of nickel traces in pure molybdenum and tungsten, 19: 19799
effects on spectrophotometric determination of zinc using 1-(2-thiazolylazo)-2-naphthol, 19: 19814
electron spin density in, s-, 19: 20845
gamma shielding by, nomograms for determining thicknesses for, 19: 21598
iridium-193 Mössbauer effect in, (E), 19: 21255(R) (UCRL-11828 (p.57-8))
magnetic fields at nuclei in, (E), 19: 20578
neutron elastic scattering at 85 to 700 kev, differential cross sections for, (E), 19: 21298
neutron flux in laminates with heavy water, (E/T), 19: 21210
proton reactions at 30–40 Mev, helium-3 and tritium production in, 19: 21438
radiation effects on magnetic properties of defects in, neutron, 19: 20648
radiation effects on magnetism of, at 78°K, neutron, 19: 20652
separation from plutonium processing solutions, 19: 20065
solvent extraction by tridodecylamine hydrochloride, 19: 20039 (EUR-2246.e)
solvent extraction from chloride solutions by tridodecylamine hydrochloride, mechanism, 19: 20038 (EUR-2245.e)
spectral lines in solar atmosphere, excitation temperature for, (E), 19: 20775(T)
welding of wrought, Hanford procedures for, 19: 20523 (TID-20625(Vol.III) (Rev.I))
IRON ALLOY COUPLES
Invar/Ni, tensile properties of, testing, (E), 19: 20554 (LA-3161)
IRON ALLOYS
corrosion inhibition by pertechnate ions, 19: 19820
Al–Cr–Fe–Y, oxidation mechanism, 19: 20470 (GE-TM-63-7-3)
Al–Cr–Fe–Y, properties of oxidation-resistant, 19: 20470 (GE-TM-63-7-3)
Al–Fe, internal friction measurements at high temperatures, 19: 20245 (CEA-R-2718)
Al–Fe, magnetic fields at iron-57 nuclei in, (E), 19: 20578
Co–Fe, magnetic fields at iron-57 nuclei in, (E), 19: 20578
Cr–Fe, corrosion by carbon dioxide at 1100 to 1800°F, 19: 20487
Cr–Fe, magnetic fields at iron-57 nuclei in, (E), 19: 20578
Cr–Fe, overdriving effects on polymorphism dynamics in, 19: 20555 (LA-3215)
Cr–Fe–Ni–Sn–Zr, properties for use as fuel element cladding, 19: 20497(P)
Fe–Nb, elastic properties, 19: 20579
Fe–Ni, magnetic fields at iron-57 nuclei in, (E), 19: 20578
Fe–Ni, overdriving effects on polymorphism dynamics in, 19: 20555 (LA-3215)
Fe–Pu, corrosive effects on tantalum and tantalum–tungsten alloys at 600 to 1100°C, 19: 21690(R) (LA-3244)
Fe–V, magnetic fields at iron-57 nuclei in, (E), 19: 20578
IRON COMPOUNDS
iron-57 Mössbauer spectra in ferrichrome and ferrichrome A, 19: 21270(R) (UCRL-11828(p.214-16))
IRON COUPLES
constantan/Fe, thermocouple tables, smoothed, 19: 20266 (ORNL-3649(Vol.2)(Sect.2.4))
constantan/iron, thermocouple tables for cryogenic JN/JP, smoothed, 19: 20275 (ORNL-3649(Vol.2)(Sect.2.13))
constantan/iron, thermocouple tables for cryogenic YN/YP, smoothed, 19: 20276 (ORNL-3649(Vol.2)(Sect.2.14))
IRON CYANIDES
determination by titration using lead nitrate, end-point determination by beta reflection in, 19: 19787
IRON IONS
electron spin resonance spectrum in borate glass, 19: 20620(R) (NYO-2024-8)
formation of highly charged, by electron capture in hydrated cobalt compounds, (E), 19: 20032
IRON ISOTOPES Fe-54
deuteron reactions (d,p), energy levels from, (T), 19: 21277
helium-3 elastic scattering and reactions (He-3,d) at 22 Mev, (E), 19: 21240 (LA-DC-6232)
neutron capture by, energy levels from, (T), 19: 21277
proton reactions at 2.5–3 Mev, resonances in, 19: 21446
IRON ISOTOPES Fe-55
beta decay of, x radiation from, (E), 19: 20323(R) (NYO-3246-4)
content in stratosphere, 19: 20657(R) (DASA-1309)
energy levels of, spin of 0.416 Mev, (T), 19: 21277
use to excite x-ray fluorescence in analysis of light elements, 19: 19741 (CEA-R-2539)
IRON ISOTOPES Fe-56
alpha elastic scattering by, angular distribution of, 19: 21459
helium-3 scattering at 22 Mev, models for, (E/T), 19: 21240 (LA-DC-6232)
neutron reactions (n,p) at 12.6 to 19.6 Mev, cross sections for, (E), 19: 21290
proton reactions at 2.5–3 Mev, resonances in, 19: 21446
IRON ISOTOPES Fe-57
energy level transitions in, retardations in l-allowed M1, (T), 19: 21323
magnetic fields acting on, in ferromagnetic materials, 19: 20578
Mössbauer effect in, use for time dilation experiments, 19: 20699
Mössbauer effect in types 201, 301, 316, and AM 355 stainless steels, (E), 19: 21338
Mössbauer spectra in ferrichrome and ferrichrome A, 19: 21270(R) (UCRL-11828(p.214-16))
nuclear resonance absorption spectra of, in zinc sulfide phosphors, 19: 19855
IRON ISOTOPES Fe-59
beta decay, 19: 21460
content in stratosphere, 19: 20657(R) (DASA-1309)
uptake by shellfish, 19: 20230
IRON OXIDES
analysis for impurities by activation methods, 19: 19796
effects on thermal stability of zirconium oxide, 19: 20585
IRON SYSTEMS
Fe–Si–Th, crystal structure of compound in, 19: 20568
Fe–Si–U, preparation and crystal structure of compounds in, 19: 19871
IRRADIATION FACILITIES
description and costs of Brookhaven cobalt-60, 19: 20095 (BNL-8976)
design and operation of 2500-C cesium-137 gamma, 19: 20102
IRRADIATION TECHNIQUES

development for research reactors, 19: 21740
ISONIPECTOIC ACID, 1-METHYL-4-PHENYL-
effects on breathing and metabolism in rats with radiation sickness, 19: 19481
ISOTOPE EFFECTS
in gas-liquid chromatography of acetylated steroids, 19: 19893
of deuterium on exothermic ion-molecule reactions, 19: 19887
of deuterium on ion-molecule reactions under electron bombardment, 19: 19995
of deuterium on ionic decomposition of *t*-butylperoxy formate, 19: 19948
of deuterium on reactions of 2-phenylethyltrimethylammonium iodide with ethoxide and hydroxide ions, 19: 19947
of deuterium on solvolysis of cis-4-*t*-butylcyclohexyl-*p*-bromobenzenesulfonate, 19: 19949
of deuterium on solvolysis of trans-4-*t*-butylcyclohexyl-*p*-bromobenzenesulfonate, 19: 19950
on spectra of carbon diodide, infrared, 19: 19936
on spectra of deuterated acetylene, infrared, 19: 19935
ISOTOPE SEPARATION METHODS
effusion, efficiency calculations for, 19: 20434
ISOTOPES
abundances in stars, (T), 19: 20762
ISOTOPIC EQUILIBRATION
substoichiometric separation in, theory and uses of, 19: 19783
uses in analysis, 19: 19822
uses in determination of hydrogen in metals, 19: 19831
ISOTOPIC EXCHANGE
between thallium(III) ions and thallium hydroxyethylenediamine triacetate complex in water, 19: 19856
of deuterium between water and salts of trioctylamine or benzyldilaurylamine, 19: 19864
of deuterium between water and anion exchange resin, 19: 19865
of hydrogen by azulene in acid solutions, 19: 19883
of oxygen-18 between aluminum oxide and molecular oxygen, 19: 19872

J

JAPANESE POWER DEMONSTRATION REACTOR
criticality, (T), 19: 21689 (JAERI-1068)
startup and power tests in, (E), 19: 21688 (JAERI-1067)
JETS
arc-, development for space propulsion, 19: 20139
resisto-, development for space propulsion, 19: 20139

K

KEROSENE
TBP–Varsol, solvent properties for nitric acid from aqueous solution, pulse column studies of, 19: 20043 (IEA-77)
KETENE POLYMERS
radioinduced polymerization with 3-chloromethyl-3-ethyloxetane, 19: 19972
KIDNEYS
cesium-137 and strontium-90 content in bulls from fallout, 19: 20215
radiation effects on immune reactions to transplanted, in dogs, 19: 19519
radiodiagnosis of urologic diseases by scintiscanning of, using mercury-203, 19: 19721
radiodiagnosis using thorotrast, tumor development from, 19: 19707
transplantation in man, 19: 19463
transplantation in dogs, effects of bone marrow and lymph cell radiation chimeras on, 19: 19493
transplantation in man, 19: 19520
KILNS
design for facility for separation of plutonium from leachable residues, 19: 20083
KRYPTON
absorption coefficient from 3.6 to 10 × 10^3 Å, (T), 19: 20833
charge exchange in, atom-ion resonance, (T), 19: 19931
diffusion in graphite, effects of pore structure on, 19: 20457 (GAMD-4814)
electron reactions with, excitation functions for metastable state formation in, 19: 19992
ionization by electrons at 0.6 to 20 kev, (E/T), 19: 20850
krypton-ion reactions at 100 to 400 kev, excitation in, (E), 19: 20862
photoionization of, dielectric breakdown from, (E), 19: 20847
KRYPTON IONS
reactions with krypton at 100 to 400 kev, excitation in, (E), 19: 20862
KRYPTOH ISOTOPES Kr-70
proton decay, (E), 19: 21271(T) (KFK-tr-161)
KRYPTON ISOTOPES Kr-82
energy levels of, spin of 1821-kev, (T), 19: 21312
KRYPTON ISOTOPES Kr-85
determination in magnox reactor coolant, method for, 19: 21616
separation from power reactor fuels, economics of, 19: 20036 (BNWL-25)
shielding power sources of, 19: 21595 (TID-7698(Pt.I)(p.33-248))
KRYPTON ISOTOPES Kr-86
deuteron reactions (d,p) at 15 Mev, energy levels from, (E), 19: 21394
KRYPTON ISOTOPES Kr-87
energy levels, (E), 19: 21394

L

LA SAL MOUNTAINS (UTAH)
rock ages in, 19: 20178
LABORATORIES
accident in, radiation hazards from tritium release in, 19: 20194 (BLG-280)
background count in underground low-level gamma-counting, 19: 20093(R) (ANL-6938(p.194-205))
design for cosmic ray studies, 19: 20347
fire in radioisotope production, radiation hazards of, 19: 20195 (BLG-281)
ventilation system for low-level gamma-counting, 19: 20092(R) (ANL-6938(p.91-6))
LABORATORY EQUIPMENT
description of, for research on ceramic materials, 19: 20455(R) (DCAS-TDR-62-192)
standardization of, for nuclear-physics studies, (E), 19: 20262 (KFK-259)
LAMINATES
preparation and properties of ceria–hafnia–magnesia–molybdenum particulate macro-, 19: 20558(R) (NP-14888)
LANGUAGE
translation using computers, developments in, 19: 20452
LANTHANUM
determination by titration, suitability of tetraethylenepentamine heptaacetic acid for, 19: 19813
determination in purified uranium compounds by chromatography and spectrography, 19: 19800
separation from aqueous solution by solvent extraction as salicylate pyridine complex, 19: 20079
separation from scandium by solvent extraction of diantipyrinylmethane complex, 19: 20080
LANTHANUM COMPLEXES
with EDTA, migration in electrodialysis cell, 19: 20052 (ORNL-TM-1035)
with serine, stability and composition, 19: 19874
LANTHANUM HYDRIDES
LaH_x–LiH, phase studies, 19: 19881
LANTHANUM IONS
solvent extraction from molten nitrate by liquid silicone–TBP at 150°C, 19: 19833 (CEA-R-2628)
LANTHANUM ISOTOPES
photon reactions (γ,n), cross sections for, (E), 19: 21287
LANTHANUM ISOTOPES La-140
determination in air by beta measurement, efficiency of counter for, 19: 20169
electron pair production cross section near threshold, (E), 19: 21252(R) (UCRL-11828(p.35-8))
LANTHANUM ISOTOPES La-142
beta decay of, gamma angular correlations in, (E), 19: 21314
LANTHANUM NITRIDES
superconducting properties, 19: 20572
LANTHANUM SULFIDES
preparation by sulfonation of oxide using carbon disulfide, 19: 19927
LANTHANUM SYSTEMS
B–C–La, phase studies, 19: 19926
La–Te, phase studies and properties of compounds in, 19: 20606
LANTHANUM ZIRCONATES
preparation and properties of, 19: 19925
LARYNX
radiotherapy of cancer of, 19: 19659
LEAD
analysis for copper by neutron activation methods, 19: 19815
beta reactions in, polarization of bremsstrahlung from, 19: 21453
determination by titration, suitability of tetraethylenepentamine heptaacetic acid for, 19: 19813
determination in uranium-containing rocks from composition of gamma radiation emitted, 19: 20180
determination using 5,5'-thiodisalicylic acid, gravimetric, 19: 19812
gamma coherent large-angle scattering by, bremsstrahlung effect in,

(E/T), 19: 21599
gamma shielding by, nomograms for determining thicknesses for, 19: 21598
magnetic flux quantization in superconducting cylinders of, 19: 21194
meson (π^-) reactions (π^-,nγ) with, energy spectra from, (E), 19: 21315
meson (π^+) absorption at 2.72, 3.70, and 4.75 Bev/c, cross sections for, (E), 19: 21431
nucleon reactions at high energies, secondary nucleon yields from, (E/T), 19: 21242 (NP-14837)
protective effects of, against radiation injury of rat placenta, 19: 19557
proton reactions at 2.72 Bev/c, cross sections for, (E), 19: 21431
separation from copper by solvent extraction using cuproine, 19: 19815
separation from mercury and silver by solvent extraction using tri-n-octylphosphine oxide, 19: 19753 (IS-T-3)
superconducting transition temperature of films of, (E), 19: 21189
ultrasonic attenuation in superconducting, amplitude-dependent, (T), 19: 21169
x-ray spectra in, muonic, (E), 19: 21344

LEAD FLUORIDES
spectra of suspensions of, in thin polyethylene films, infrared transmission, 19: 19917

LEAD ISOTOPES Pb-203
decay of, K conversion coefficient of 400 Mev transition in, (E), 19: 21293

LEAD ISOTOPES Pb-204
content in rocks of La Sal Mountains, Utah, (E), 19: 20178
energy levels of, energies of, (T), 19: 21412

LEAD ISOTOPES Pb-205
energy levels of, energies of, (T), 19: 21412

LEAD ISOTOPES Pb-206
content in rocks of La Sal Mountains, Utah, (E), 19: 20178

LEAD ISOTOPES Pb-207
content in rocks of La Sal Mountains, Utah, (E), 19: 20178
energy levels of, half life of 570-kev excited, 19: 21291

LEAD ISOTOPES Pb-208
content in rocks of La Sal Mountains, Utah, (E), 19: 20178
deuteron reactions (d,t) at 11.8 Mev, angular distributions from, (E), 19: 21326

LEAD ISOTOPES Pb-210
content in stratosphere, 19: 20657(R) (DASA-1309)
content in vertebrae of Puerto Ricans, 19: 20193(R) (ANL-6938(p.120-4))
energy levels of, calculations, (T), 19: 21247(R) (UCRL-11828(p.10-11))

LEAD ISOTOPES Pb-212
content in blood and bones of humans injected with thorotrast, 19: 19497(R) (ANL-6938(p.127-39))
content in tissue of rats injected with thorotrast, 19: 19497(R) (ANL-6938(p.127-39))

LEAD ISOTOPES Pb-214
effects on radon-222 gamma spectra, 19: 21299

LEATHER
radiation effects on tensile strength and water permeability, 19: 20414

LECTURES
book: *Lectures on Astrophysics and the Many-Body Problem*, 19: 20714
on astrophysical phenomena, 19: 20783
on Green's functions in many-body problems, 19: 20715
on star evolution, 19: 20786
on stellar evolution, 19: 20784
on theory of vibrations of imperfect crystals, 19: 20716

LEPTONS
interactions of, neutral currents in, (T), 19: 20988
interactions of, U(12) symmetry for weak, (T), 19: 21028

LEUKEMIA
incidence in Hiroshima, correlation of age, degree, duration, exposure, and type in, 19: 19526
radioinduced in rats, 19: 19530
radioinduced in rats, 19: 19561
radiotherapy of, by intra-arterial injection of radioisotopes, 19: 19661

LEUKOCYTES
metabolism in, tracer studies, 19: 19507(R) (TID-21712)
radiation and toxic chemical effects on alkaline phosphatase activity in human granulocytes, 19: 19570
radiation effects on phagocytosis by, 19: 19507(R) (TID-21712)
radioinduced chromosome aberrations in human, 19: 19596

LEVEL INDICATORS
descriptions of radiometric, 19: 20412
design of hydrostatic, for 200-Bev proton synchrotron, (E), 19: 20733 (UCRL-11799)
radiometric, for studies of boilers, 19: 20418

LEVEL REGULATORS
performance of conductivity-probe interface, in pulse column, 19: 20043 (IEA-77)

LIFE SPANS
radiation effects of simulated space situation on monkey, gamma and proton, 19: 19616

LIGHT
dose calculation for eye of, from nuclear explosion, 19: 19498 (LA-3204)
effects on transduction in *Pseudomonas aeruginosa*, 19: 19502(R) (NP-14932)
interactions with light in plasma, (T), 19: 21547
interactions with matter, (E/T), 19: 20667
production by nuclear reactors, use in underground processes of, 19: 21710
reactions with matter, multiple-boson production in, (T), 19: 20816
refraction in alkanes and alkali halides, (E), 19: 20667
scattering by plasma, nonlinear resonant mixing by, (T), 19: 21546
scattering by transparent Mie particles, asymmetry in, (T), 19: 20822

LIGHTNING
energy source for ball, electromagnetic, (T), 19: 21150

LIMBS
radiation effects on loss of regeneration capacity in salamander, 19: 19544

LINEAR ACCELERATORS
beam dynamics in drift tube type, (T), 19: 20727 (LA-DC-6777)
beam interactions with transverse modes in standing-wave in proton, (T), 19: 20726 (LA-DC-6775)
cavity resonator chains for proton, model analysis of, (T), 19: 20725 (LA-DC-6760)
cavity resonators for proton, high-power test on cloverleaf, 19: 20724 (LA-DC-6759)
design of, for separation beam into bunches with different energy levels, 19: 20751(P)
design of, with exit of two thick-walled metal plates, 19: 20752(P)
electromagnetic field amplitude and phase in proton, control of, (E/T), 19: 20728 (LA-DC-6875)
electron beam bunching in Saclay, (T), 19: 20721 (CEA-R-2749)
gamma and neutron production in shielding of 70-Mev electron, 19: 20749
radioactivity control at electron, 19: 20204 (RPI-328-25)
use for uranium radiography, 19: 20128
waveguide structures for, shunt impedance of cloverleaf, (T), 19: 20744

LIPIDS
radiation effects on metabolism of, in newborn and weanling rat brain, 19: 19610
radioinduced toxins in, of rabbit liver, 19: 19599

LIQUID METAL COOLED REACTORS
analysis of lead-cooled liquid-metal-fueled, nuclear and parametric, 19: 21697
coolant cycle in sodium, binary mercury–water vapor, (E), 19: 21701
corrosion problems in, review of, 19: 20488
design of fast paste-fueled, 19: 21663(P)
exponential experiments for advanced sodium-graphite power, (E), 19: 21692 (NAA-SR-Memo-9976)
fuel development and testing for fast, sodium-cooled, ceramic, (E), 19: 21666(R) (GEAP-4640)
steam generators for sodium, design of modular, 19: 21611 (NAA-SR-9826)

LIQUIDS
distribution function in classical, asymptotic form of radial, 19: 20697
moisture content in, of low water solubility, method of determining, 19: 21783(P)
performance as working media in nuclear gyroscopes, (T), 19: 20279 (RTD-TDR-63-4001)
phase concentrations in boiling, use of radiation for determining, 19: 20418
sampling radioactive, equipment for, 19: 20101(T) (ORNL-tr-442)
spin susceptibility of superfluid Fermi, (T), 19: 20692

LITHIUM
content in primary cosmic radiation, 19: 20894
diffusion of atoms of, in arc discharge, (E), 19: 21555
electron elastic scattering at 0.1 to 2.0 ev, cross sections for, (T), 19: 20842
geochemistry and mineralogy of, in Cherry Mountains (Urals), USSR, book, 19: 20190
photon reactions with, polarization of protons from, 19: 21456
solvent properties for helium at 649 to 871°C, 19: 20561 (PWAC-380)
thermodynamic properties of vaporous, 19: 20116(R) (SAN-409-12)

LITHIUM ALLOYS
Al–Li, nondestructive testing of control rods and targets of, 19: 20126 (DPSPU-65-30-11)
Al–Li, radiation effects on helium precipitation in, 19: 20613 (CEA-R-2529)

LITHIUM BROMIDES

molecular properties of, beam electric resonance studies of, 19: 19848(R) (UCRL-11828(p.193-7))
LITHIUM CHLORATES
effects on ionic decomposition of *t*-butylperoxy formate, 19: 19948
LITHIUM CHLORIDES
molecular properties of, beam electric resonance studies of, 19: 19848(R) (UCRL-11828(p.193-7))
LITHIUM COMPOUNDS
solubility and thermolysis of diliturate, 19: 19824
LITHIUM FLUORIDES
molecular properties of, beam electric resonance studies of, 19: 19848(R) (UCRL-11828(p.193-7))
radiation damage in, nuclear magnetic resonance study of reactor, 19: 20620(R) (NYO-2024-8)
radiation effects on optical absorption band in, electron and x-, 19: 20817
radiation effects on optical properties of, effect of impurities on x, 19: 19998
spectra of suspensions of, in thin polyethylene films, infrared transmission, 19: 19917
LiF–NaF, effects on coated-particle fuels at 800 to 1000°C, 19: 20463 (ORNL-TM-431)
LITHIUM HYDRIDES
performance as reactor shielding, (T), 19: 21614 (NAA-SR-Memo-10559)
BaH_2–LiH, phase studies, 19: 19881
CeH_2–LiH, phase studies, 19: 19881
EuH_2–LiH, phase studies, 19: 19881
LaH_2–LiH, phase studies, 19: 19881
LiH–ScH_2, phase studies, 19: 19881
LiH–SmH_2, phase studies, 19: 19881
LiH–SrH_2, phase studies, 19: 19881
LiH–YbH_2, phase studies, 19: 19881
LITHIUM HYDROXIDES
effects on coolant pump wear in water-cooled reactors, 19: 21606 (WCAP-3269-9)
LITHIUM IODIDES
molecular properties of, beam electric resonance studies of, 19: 19848(R) (UCRL-11828(p.193-7))
LITHIUM IONS
solvent extraction from molten nitrate by liquid silicone–TBP at 150°C, 19: 19833 (CEA-R-2628)
LITHIUM ISOTOPES
effects on molecular properties of lithium halides, 19: 19848(R) (UCRL-11828(p.193-7))
LITHIUM ISOTOPES Li-6
deuteron reactions (d,α) with, multi-level analysis of resonances in, (T), 19: 21413
deuteron reactions (d,α) at 4 to 12 Mev, (E), 19: 21414
meson (μ) capture probability in, lithium-6 model testing by, (T), 19: 21368
meson (π^-) reactions (π^-,nγ) with, energy spectra from, (E), 19: 21315
neutron reactions (n,α) with, fast neutron spectrometry using, (E), 19: 20334
performance in nuclear gyroscopes, (T), 19: 20279 (RTD-TDR-63-4001)
production in proton reactions with carbon-12 and oxygen-16 at high energies, (E), 19: 21352
production in proton reactions with carbon-12 at 156 Mev, cross sections for, (T), 19: 21402
reactions with charged particles, energy production in, 19: 21487(R) (ORNL-3760(p.98-9))
scattering of atomic beam of, by crossed mercury beam, quantum effects and cross sections for, 19: 20823
LITHIUM ISOTOPES Li-7
electron inelastic scattering from, excitation in, 19: 21455
energy levels of, nucleon separation energy in 1p and 1s, 19: 21400
meson (π^-) reactions (π^-,nγ) with, energy spectra from, (E), 19: 21315
performance in nuclear gyroscopes, (T), 19: 20279 (RTD-TDR-63-4001)
production in proton reactions with carbon-12 and oxygen-16 at high energies, (E), 19: 21352
production in proton reactions with carbon-12 at 156 Mev, cross sections for, (T), 19: 21402
proton reactions (p,γ) at 0.4 to 2.4 Mev, beryllium-8 levels from, 19: 21342
proton reactions (p,$\alpha\gamma$) at 440 kev, gamma transitions in, 19: 21357
proton reactions (p,d) with, multi-level analysis of resonances in, (T), 19: 21413
scattering of atomic beam of, by crossed mercury beam, quantum effects and cross sections for, 19: 20823
LITHIUM ISOTOPES Li-8
emission in meson (K$^-$) reactions with emulsion nuclei at 0.8 to 3.0 Bev/c, (E), 19: 21389
production in proton reactions with carbon-12 at 156 Mev, cross sections for, 19: 21402
LITHIUM ISOTOPES Li-9
emission in meson (K$^-$) reactions with emulsion nuclei at 0.8 to 3.0 Bev/c, (E), 19: 21389
production in proton reactions with carbon-12 at 156 Mev, cross sections for, (T), 19: 21402
LITHIUM NITRATES
effects on dissolution of plutonium dioxide and uranium dioxide pellets in nitric acid, 19: 20050 (ORNL-3695)
melting points and volumes of fusion at 0 to 10,000 atm, 19: 19884
$LiNO_3$–KNO_3–$NaNO_3$, distribution of ions between liquid–TBP and molten, at 150°C, 19: 19833 (CEA-R-2628)
LITHIUM PEROXIDES
preparation and properties of, book, 19: 19932
LIVER
analysis for selenium, activation, 19: 19771(R) (TEES-2671-4(Chap.9))
cesium-137 and strontium-90 content in bulls from fallout, 19: 20215
cirrhosis induced by Thorotrast in, 19: 19560
gold-198, iodine-131 and yttrium-90 uptake by human, profile counting studies on, 19: 19492
radiation and immunization effects on cholinesterase activity in rabbits, 19: 19609
radiation effects on desoxyribonucleic acid metabolism in rat, 19: 19506 (TID-21703)
radiation effects on mitotic activity in regenerating, of rats, 19: 19510(T) (JPRS-29250(p.27-32))
radiation effects on regeneration after partial hepatectomy, 19: 19512
radiation effects on 3,1,6,1-aryl-sulfate sulfohydrolase activity in guinea pig, *in utero*, 19: 19573
radiation effects on serum albumin synthesis in rat, effects of food ingestion on, 19: 19603
radiation effects on amyloidosis in hyaline deposits in mouse, after liver and marrow injections, 19: 19650
radiation effects on function of human, from cancer therapy, 19: 19684
radiodiagnosis of tumors of human, by iodine-131 infusion in bowel, 19: 19662
radiodiagnosis of, by photoscanning using iodine-131-labeled human serum albumin, 19: 19710
radiodiagnosis of, by photoscanning using iodine-125, 19: 19711
radioinduced toxins in lipids of rabbit, 19: 19599
LIVER DISEASES
radiodiagnosis by scanning using gold-198 and iodine-131, evaluation of, 19: 19730
radiodiagnosis of amebiasis in man by scintiscanning using gold-198 and iodine-131, 19: 19728
radiodiagnosis of echinococcus, by scanning using iodine-131, 19: 19729
LOS ALAMOS MOLTEN PLUTONIUM REACTOR EXPERIMENTS
development and operation, 19: 21690(R) (LA-3244)
LOS ALAMOS OMEGA WEST REACTOR
development, 19: 21690(R) (LA-3244)
LOS ALAMOS TURRET REACTOR
design and development, 19: 21690(R) (LA-3244)
LUBRICANTS
analysis for phosphorus by neutron activation methods, 19: 19828
LUMINESCENCE
conference on, Torun, Poland, Sept. 1963, 19: 19853
measurement of radio-, from organic liquids and plastics, (E), 19: 19962
of iron-57 in zinc sulfide phosphors, 19: 19855
radiation effects on, in copper-doped potassium and sodium chloride crystals, 19: 19964
radiation effects on, in zinc sulfide, 19: 19967
radioinduced, in bibenzyl and pyrene, 19: 19963
radioinduced, in cadmium zinc sulfide phosphors in presence of infrared radiation, 19: 19965
radioinduced, temperature quenching of, 19: 19966
LUMINESCENT DETECTORS
performance as personnel fast-neutron dosimeters, (E), 19: 20318 (HW-SA-3526)
LUMINESCENT MATERIALS
tritium leakage from luminous points, 19: 20161 (NP-14869)
LUNG DISEASES
radiodiagnosis of embolism in dogs and man by photoscanning using chromium-51 or iodine-131, 19: 19724
LUNGS
cesium-137 and strontium-90 content in bulls from fallout, 19: 20215
particle transport in, 19: 19456 (LF-21)
radiation and immunization effects on cholinesterase activity in rabbits, 19: 19609
radiation effects on healthy tissue in human, after therapy of tumor,

19: 19683
transplantation in dogs, 19: 19523
LUTETIUM ALLOYS
Gd–Lu, gadolinium ion ESR in, g-factors from, (E), 19: 20698
LUTETIUM COMPLEXES
with serine, stability and composition, 19: 19874
LUTETIUM ISOTOPES Lu-175
boron-11 fission, excitation energy, (E/T), 19: 21259(R) (UCRL-11828(p.77-80))
carbon-12 fission, excitation energy, (E/T), 19: 21259(R) (UCRL-11828(p.77-80))
LUTETIUM ISOTOPES Lu-177
energy levels of, lifetime of 120-kev, (E), 19: 21319
LUTETIUM SULFATES
crystal structure and bond types of octahydrates, 19: 19915
LYMPH SYSTEM
deposition of inhaled insoluble particles in pulmonary lymph nodes, 19: 19456 (LF-21)
effects of allogenic chimeric bone marrow on repopulation of lymphatic tissues in irradiated mice, 19: 19646
effects on immune reactions in dogs, 19: 19519
gold-198 uptake by human, indirect lymphography of, 19: 19719
radiation chimeras of, effects on kidney grafts in dogs, 19: 19493
radiation effects on soluble DNA localization in rabbit appendix, 19: 19583
LYSOSOMES
radiation effects on brain, hypothesis on, 19: 19611

M

MAGNESIUM
analysis for hafnium or zirconium using catechol violet, colorimetric, 19: 19780
analysis for trace amounts of zinc using 1-(2-thiazolylazo)-2-naphthol, spectrophotometric, 19: 19814
determination by titration, suitability of tetrathylenepentamine heptaacetic acid for, 19: 19813
determination in uranium and its compounds and alloys, methods for, 19: 19823
determination using titanium yellow and EDTA, 19: 19779
effects on optical properties of x-irradiated lithium fluorides, 19: 19998
meson (π^-) reactions (π^-,nγ) with, energy spectra from, (E), 19: 21315
properties for use as fuel element can, effects of manganin and zirconium on, 19: 20610(P)
radiation effects on content in dog tissues, 19: 19540
separation from cobalt, nickel, and zinc by complex formation and solvent extraction, 19: 19833 (CEA-R-2628)
vapor pressure at 223 to 385°C, 19: 20556 (NASA-TN-D-2723)
MAGNESIUM ALLOYS
Ca–Mg, heats of formation and fusion of intermetallic compound $CaMg_2$ in, 19: 19838 (IS-1070)
Ce–Mg, oxidation by moist nitrogen at 475 to 600°C, 19: 20485
Mg–Th, purification by transfer to liquid magnesium–zinc alloy in fused salt, 19: 20066
Mg–Zn, heats of formation and fusion of intermetallic compound $MgZn_2$ in, 19: 19838 (IS-1070)
Mg–Zn, sorption of impurities in magnesium–thorium alloy by liquid, in fused salt, 19: 20066
Mg–Zr, properties for use as fuel element can, effects of manganin on, 19: 20610(P)
MAGNESIUM CERIUM NITRATES
use as low-temperature scale, correlation for, 19: 21162(R) (UCRL-11828(p.199-201))
MAGNESIUM CHLORIDES
precipitation of uranium(VI) with, in presence of sodium carbonate, 19: 19870
MAGNESIUM FLUORIDES
radioinduced color centers in rutile crystals of, 19: 20618 (NBS-8614)
MAGNESIUM IONS
solvent extraction from molten nitrate by liquid silicone–TBP at 150°C, 19: 19833 (CEA-R-2628)
MAGNESIUM ISOTOPES Mg-21
decay of, log ft values for, (T), 19: 21379
proton decay, (E), 19: 21271(T) (KFK-tr-161)
MAGNESIUM ISOTOPES Mg-24
deuteron diffraction scattering at 19.6 and 21 Mev, (T), 19: 21427
proton inelastic scattering at 2.015 to 4.20 Mev, differential cross sections for, (E), 19: 21426
triton reactions (t,p) at 10 and 11 Mev, angular distributions from, (E), 19: 21311
MAGNESIUM ISOTOPES Mg-25
deuteron reactions (d,p) at 10 and 11 Mev, angular distributions from, (E), 19: 21311
MAGNESIUM ISOTOPES Mg-26
deuteron inelastic scattering at 12 Mev, angular distributions from, (E), 19: 21311
energy levels of, parity and spin of, (E), 19: 21311
MAGNESIUM NITRATES
$Mg(NO_3)_2$–$Th(NO_3)_4$, crystal structure of octahydrates, 19: 19852
MAGNESIUM OXIDES
dielectric losses in, frequency and temperature dependences of, 19: 19851(T) (ORNL-tr-491)
effects on sintering of alumina, 19: 20461 (NP-14893)
effects on thermal stability of zirconium oxide, 19: 20585
electric properties of, effects of lattice energy and temperature on, 19: 21601(T) (ORNL-tr-490)
mechanical properties of polycrystals and single crystals of, at room temperature to 2000°C, 19: 20607
spectra of suspensions of, in thin polyethylene films, infrared transmission, 19: 19917
Al_2O_3–BaO–CaO–MgO–SiO_2, presintering of compositions in, 19: 20461 (NP-14893)
Al_2O_3–MgO–SiO_2, devitrification, 19: 20461 (NP-14893)
CeO_2–HfO_2–MgO–Mo, preparation and properties of macrolaminate particle composites of, 19: 20558(R) (NP-14888)
MgO–PuO_2, phase diagrams, 19: 20589
MAGNESIUM SULFATES
$MgSO_4$–Na_2SO_4, surface area and radioactivity of sulfur-35-labeled, 19: 20013
MAGNESIUM SYSTEMS
Mg–Mn–O, phase studies of, 19: 20573
MAGNETIC FIELDS
calculations for FFAG accelerators, using relaxation methods, (E), 19: 20729 (MURA-706)
compression by exploding foils, (E), 19: 20717
cosmic radiation modulation by interplanetary, 19: 20889
effects of transverse, on electric conductivity of plasma in thermionic cells, (T), 19: 21580
effects on heart function in frogs, 19: 21776 (UCRL-12389)
fluid flow in, laminar compressible boundary layers in, 19: 20122
measurement in optical system of 5-Gev antiproton beam, (E), 19: 20723 (JINR-P-1945)
measurement of time-varying, using Zeeman effect, (E), 19: 20257 (IPP-1/19)
penetration into plasma with Hall effect, (T), 19: 21527
plasma collisions in transverse, depolarization and heating in, (T), 19: 21537
plasma containment by rotating, 19: 21508
plasma containment in, configuration singularities for, 19: 21534
plasma containment by three-cusp, (E), 19: 21568
plasma diffusion across, (E), 19: 21475 (LA-DC-6383)
plasma stability in transverse, (E), 19: 21577
plasma wave propagation across, (T), 19: 21521
production of strong, by flux compression, (T), 19: 20678
production of strong, survey on, 19: 20701
ultrasonic attenuation in superconductors in strong, (E), 19: 21188
MAGNETIC MIRROR MACHINES
bremsstrahlung spectra from, 19: 21482(R) (ORNL-3760(p.23-9))
compression in multipole, longitudinal, (T), 19: 21516
design of ELMO, 19: 21482(R) (ORNL-3760(p.23-9))
energy storage and delivery systems performance in Scylla IV, (E), 19: 21474 (LA-3189)
plasma density in Q-3, effect of current heating on, (E), 19: 21541
MAGNETIC MIRRORS
plasma diffusion across, (E), 19: 21475 (LA-DC-6383)
MAGNETIC PROBES
effects on magnetic field diffusion in theta pinch, (E/T), 19: 21524
response of, method for measuring, 19: 20293
MAGNETIC RECORDING SYSTEMS
description of instrumentation for tape, for multiparameter nuclear experiments, 19: 20255 (EUR-2119.e)
design of gamma intensity time recorder, 19: 20397
MAGNETIC RESONANCE
of radioinduced free radicals, 19: 19614
spin resonance line shapes, effect of probes on, (T), 19: 20839
theory of ENDOR, of F-centers in sodium chloride type crystals, 19: 19920
use of electron spin, in studies of radiation damage in solids, 19: 20620(R) (NYO-2024-8)
MAGNETITE CONCRETES
gamma shielding by, nomograms for determining thicknesses for, 19: 21598

MAGNETOHYDRODYNAMIC CELLS
design and performance of high-power, (T), 19: 20910
design of a-c, 19: 20914
design of closed-Brayton-cycle, 19: 21690(R) (LA-3244)
design of 1-Mw open-cycle, 19: 20912
electric conductivity of seeded combustion products in, (E), 19: 20909
electrode development for hypersonic plasma generator, (E), 19: 20905 (SC-RR-65-54)
electron temperature in linear, (T), 19: 20907
research program in United Kingdom, review on, 19: 20908
MAGNETOHYDRODYNAMICS
flow of rotating weakly ionized plasma, (E), 19: 21570
fluid flow in annular channel with radial fields, laminar, (T), 19: 20663
fluid flow in, equations solutions for, 19: 20764
fluid flow in, laminar compressible boundary layers in, 19: 20122
Rayleigh problem in, operational calculus for, (T), 19: 20665
wave propagation in relativistic, Riemann, (T), 19: 20668
MAGNETOMETERS
design for measuring superconducting samples, 19: 21486(R) (ORNL-3760(p.77-93))
MAGNETOSPHERE
boundary of, solar wind discontinuity effects on, (T), 19: 21148
charged-particle motion during magnetic storms, (T), 19: 21128(T)
charged-particle streams in, effects of geomagnetic field variations on, 19: 21126
electron trajectories in presence of whistler-mode waves in, (T), 19: 21099
solar wind interaction with, geomagnetic cavity from, (T), 19: 21146
MAGNETS
aberrations of quadrupole, 19: 20252 (CONF-640204(p.82-92))
cost analysis for, for 200-Bev alternating-gradient synchrotron, (T), 19: 20734 (UCRL-11800)
current control systems for, in Brookhaven AGS, (E), 19: 20094 (BNL-8969)
design and construction for variable-energy cyclotrons, 19: 20753(P)
hydrogen atomic beam focusing by six-pole, (T), 19: 20302
neutron depolarization effects in precession, fast, 19: 21209
review on high-field superconducting, 19: 21165
survey on high-field, 19: 20701
MAGNOX ALLOYS
corrosion in reactors, 19: 20488
MAIZE
radiation effects on genetic, 19: 19527
radiation effects on germination of seeds of, 19: 19528
radiosensitivity of sprouting seed of, effects of 2,4-dinitrophenol on fast neutron and gamma, 19: 19582
MALIC ACID COMPLEXES
with uranyl ions, spectra of, infrared, 19: 19911
MALTOSE
radiation effects on anhydrous, electron spin resonance studies of gamma, 19: 19994
MAMMALS
radiation effects on developing embryos, 19: 19466
radiation injuries, protective effects of chemical agents, 19: 19643
MAN
body water measurements using tritium, 19: 19480
cesium-131 secretion in saliva of, as compared to potassium-39, 19: 19486
cesium-134, -137, and sodium-22 content in, 19: 20225
destruction of pituitary gland in, use of yttrium-90 for, 19: 19660
ecological effects of nuclear warfare on, 19: 19504 (RM-2801-PR)
ecology of, effects of nuclear warfare on, 19: 20199 (HI-388-RR(Pt.III))
effects of work in betatron and cyclotron labs on blood picture of, 19: 20237
gold-198 uptake by bone marrow in, whole-body counting and scanning of, 19: 19718
gold-198 uptake by lymph system, in lymphography of, 19: 19719
iodine-131 uptake by blood, blood plasma, and ovaries in, beta activity from, 19: 19483
kidney transplantation in, 19: 19463
kidney transplantation in, clinical evaluation, 19: 19520
liver cirrhosis induced by Thorotrast in, 19: 19560
radiation and toxic chemical effects on alkaline phosphatase activity in granulocytes in, 19: 19570
radiation effects on phagocytic activity of leukocytes in, 19: 19507(R) (TID-21712)
radiation effects on developing embryos, 19: 19466
radiation effects on genetics of, exposed as infants, 19: 19568
radiation effects on mechanical resistance of erythrocytes in, 19: 19595
radiation effects on healthy lung tissue in, after therapy of tumor, 19: 19683
radiation injuries in infants from diagnoses, protective measures for, 19: 19677
radiation protection during radiographic examinations, 19: 20229
radiation sickness in, diagnosis, syndrome, and treatment of, 19: 19553
radiodermatitis in, effects on blood serum protein fractions, 19: 19598
radiodiagnosis of pulmonary embolism in, by photoscanning using chromium-51 or iodine-131, 19: 19724
radiography of pelvic dysplasia in infants, radiation hazards of, 19: 19678
radioinduced skin lesions on, use of fresh blood autofibrin films for treatment of, 19: 19642
radiosensitivity of skin of, 19: 19605
radiotherapy of cancer in, effects on liver function, 19: 19684
radiotherapy of euthyroid goiters in, using iodine-131, 19: 19685
radiotherapy of tumors in, anabolic effects of steroids in, 19: 19669
radium-226 content in placenta and fetal skeleton in, 19: 20216
spleen transplantation in, 19: 19522
strontium-90 content in bones and diet of Argentine children, 19: 20165(R) (TID-21711)
thorium-232 decay products in tissue of thorotrast-injected, 19: 19497(R) (ANL-6938(p.127-39))
uranium content in, effects of content in food, soil, and water supplies on, 19: 19490
MANGANESE
determination by activation methods, 19: 19806
determination by precipitation as diliturate, 19: 19824
determination by titration, suitability of tetraethylenepentamine heptaacetic acid for, 19: 19813
determination in aerosols, activation, 19: 19771(R) (TEES-2671-4 (Chap.9))
determination in manganese–plutonium–uranium alloys, x-ray-fluorescent, 19: 21690(R) (LA-3244)
determination in pure aluminum, activation, 19: 19775(R) (UCRL-11828(p.197-9))
determination in presence of nickel by activation methods, 19: 19796
determination in ppm range by d-c arc excitation, spectrochemical, 19: 19827
determination in uranium and its compounds and alloys, methods for, 19: 19823
effects on spectrophotometric determination of zinc using 1-(2-thiazolylazo)-2-naphthol, 19: 19814
manganese-55 NMR linewidth in beta, (E), 19: 21366
MANGANESE ALLOY COUPLES
Chromel/constantan, thermocouple tables, smoothed, 19: 20268 (ORNL-3649(Vol.2)(Sect.2.6))
constantan/Cu, thermocouple tables, smoothed, 19: 20267 (ORNL-3649(Vol.2)(Sect.2.5))
constantan/Fe, thermocouple tables, smoothed, 19: 20266 (ORNL-3649(Vol.2)(Sect.2.4))
constantan/iron, thermocouple tables for cryogenic JN/JP, smoothed, 19: 20275 (ORNL-3649(Vol.2)(Sect.2.13))
constantan/iron, thermocouple tables for cryogenic YN/YP, smoothed, 19: 20276 (ORNL-3649(Vol.2)(Sect.2.14))
Cu/constantan, thermocouple tables for cryogenic, smoothed, 19: 20273 (ORNL-3649(Vol.2)(Sect.2.11))
Invar/Ni, tensile properties of, testing, (E), 19: 20554 (LA-3161)
MANGANESE ALLOYS
Cu–Mn–Zn, effects on properties of magnesium and magnesium–zirconium alloy for use as fuel element can, 19: 20610(P)
Mn–Pu–U, analysis for manganese, x-ray-fluorescent, 19: 21690(R) (LA-3244)
MANGANESE BROMIDES
magnetic properties of crystalline, 19: 21759(R) (NYO-3402-1)
preparation of high-purity crystalline, 19: 21759(R) (NYO-3402-1)
thermal conductivity at cryogenic temperatures, 19: 21759(R) (NYO-3402-1)
MANGANESE COMPOUNDS
solubility and thermolysis of diliturate, 19: 19824
MANGANESE IONS
electron spin resonance spectrum in borate glass, 19: 20620(R) (NYO-2024-8)
MANGANESE ISOTOPES Mn-51
energy level spacings in, 19: 21446
MANGANESE ISOTOPES Mn-54
content in stratosphere, 19: 20657(R) (DASA-1309)
MANGANESE ISOTOPES Mn-55
nuclear magnetic resonance linewidth in beta manganese, (E), 19: 21366
spectra of, measurement of Kα x, (E), 19: 20323(R) (NYO-3246-4)
MANGANESE ISOTOPES Mn-56
determination by photoneutron production in heavy water by gamma decay, 19: 19806

half life of, (E), 19: 21290
MANGANESE NITRATES
$Mn(NO_3)_2$–$Th(NO_3)_4$, crystal structure of octahydrates, 19: 19852
MANGANESE SYSTEMS
Be–Mn–O, phase studies of, 19: 20573
Mg–Mn–O, phase studies of, 19: 20573
Mn–Si–Th, crystal structure of compound in, 19: 20568
Mn–Si–U, preparation and crystal structure of compounds in, 19: 19871
MANOMETERS
development of micro-, for low pressure measurement, 19: 20142
MARITIME PRESSURIZED WATER REACTOR
critical assembly study of Core II loading, analysis, 19: 21716 (GEAP-3514)
MARITIME REACTORS
development of, Euratom program for, 19: 21724
MASERS (OPTICAL)
activation of, using light from nuclear reactor, 19: 21710
beam reactions with noble gases, ionization and dielectric breakdown in, (E), 19: 20847
beam reactions with sodium uranyl acetate crystals, luminescence from, 19: 20010
beam scattering by plasma, nonlinear resonant mixing by, (T), 19: 21546
crystals for, review of spectroscopic properties of activated, 19: 20849
quantum theory of coherence and noise in, 19: 20843
use for accelerating charged particles, drift tubes for, (T), 19: 20709
MASS SPECTROGRAPHY
performance for accurate determination of reactor-fuel burnup, (E), 19: 21667(R) (GEAP-4776)
uses of spark source, for analysis in atomic energy programs, 19: 19830
MASS SPECTROMETERS
description and characteristics of Russian, 19: 20261 (JINR-P-1949)
ion source for, using piezoelectric vacuum vibrator, 19: 20292
magnetic analyzer calculations for Russian, 19: 20260 (JINR-P-1948)
theory and uses of quadrupole, review on, 19: 20300
MATERIALS TESTING
Charpy tests of steels, correlation of, 19: 20462(R) (NRL-6258)
eddy-current methods of, for hot sodium bonding in stainless steel-clad uranium carbide, 19: 20531
eddy-current nondestructive, engineering drawings for phase-sensitive concentrate for, 19: 20132
equipment and methods for nondestructive, of reactor control fuel, and target elements, 19: 20126 (DPSPU-65-30-11)
equipment for drop-weight bulge testing of high-strength materials, 19: 20462(R) (NRL-6258)
equipment for electromagnetic inspection of thin-wall refractory-metal tubing, 19: 20454 (CONF-650212-1)
methods for nondestructive, of coating-metal bonds, 19: 20127(R) (IITRI-N213-23)
nondestructive method for reactor fuel elements, 19: 20135(P)
temperature verification systems for, engineering drawings of, 19: 20133
MATHEMATICAL TABLES
of Riemann Zeta function of incomplete mode, (T), 19: 21228 (ANL-6970)
MATHEMATICS
analysis of quadded logic, 19: 20439(R) (COO-614-31)
Clebsch-Gordan coefficients adapted to cubic symmetry in quantum mechanics problems, 19: 21097
equations for degenerate fields with twisting rays, 19: 21120
equations in, reduction of minimization of quadratic, (T), 19: 20441 (JINR-P-1958)
Eulerian variance analysis of turbulence dissipation, 19: 20654(R) (ANL-6938(p.242-51))
formula for Dirichlet L-functions, asymptotic, (T), 19: 20450
groups in, combination of internal-symmetry and Lorentz-invariant, 19: 20449
logarithmical relation of concentration of inhaled insoluble particles in lungs to that in pulmonary lymph nodes, 19: 19456 (LF-21)
models for computation of transients in packed tubular chemical reactors, 19: 19734 (UCRL-11757)
operators in, nonsymmetric linear and unbounded, 19: 20446
operators in, relation between three-dimensional isotropic harmonic oscillator and SU(3) group, 19: 21083
representation of non-compact groups in, using rigged Hilbert spaces, 19: 21081 (ICTP-64/9)
solution of dispersion-type nonlinear integral equations, numerical, 19: 20445
solution of linear equations with unbounded operators, 19: 20439(R) (COO-614-31)
solution to relativistic dispersion relations for photoproduction by Omnès method, 19: 21461
spaces in, description of Brouwer, 19: 21078 (AFOSR-64-1380)
SU(6) symmetry, invariant derivation of, 19: 20448
validity limits for approximations in reactor dynamics, 19: 21723(R) (NASA-CR-193)
MATTER
detection of anti-, optical method for, 19: 20774(T)
electron and meson (μ) inelastic scattering by nuclear, linear response to, (T), 19: 21393
electron reactions at 100 kev to 5 Mev, energy losses in, (T), 19: 21423
element abundances in, at high temperatures, (T), 19: 20762
Hartree-Fock state of nuclear, stability of, 19: 21440
motion of homogeneous, under gravitation, (T), 19: 20704
neutron diffusion in, variational flux-synthesis analysis of, (T), 19: 21638 (CONF-650501-4)
photon reactions with, multiple-boson production in, (T), 19: 20816
shock wave interactions with cylindrical cavities in, (T), 19: 20659 (AD-606490)
MECHANICS
oscillators in, statistics of systems of coupled, 19: 21089
MEDICAL SUPPLIES
radiosterilization, 19: 20410
MEDICINE
management of casualties of reactor accident, 19: 19630
organization of facilities for nuclear warfare, 19: 19554
organization of facilities for nuclear warfare, 19: 19555
recommendation for physician in decontamination of radioactive materials from skin, 19: 19494
MELTING
point measurement for refractory metals, 19: 20566(T) (IS-Trans-13)
MEMORY DEVICES
design of three-state, 19: 21785(P)
properties of superconductive, 19: 21193
MERCAPTO GROUP
protective effects of, against radiation injuries, 19: 19640
MERCHANT VESSELS
nuclear-powered, Euratom development program on, 19: 21724
MERCURY
corrosive effects on carbon steel, 19: 20493
determination in ppm range by d-c arc excitation, spectrochemical, 19: 19827
determination in wheat, activation, 19: 19771(R) (TEES-2671-4 (Chap.9))
effects on spectrophotometric determination of zinc using 1-(2-thiazolylazo)-2-naphthol, 19: 19814
electric arc discharges in, stability of, (E), 19: 21490(R) (TID-21698)
electron energy distribution in discharge plasma of, inert gas effects on, (T), 19: 21579
electron scattering at 100 to 2000 ev, polarization from, (T), 19: 20865
fluorescence yield from L-shell of, following electron-capture decay of thallium-204, 19: 21449
heat transfer and pressure drop in forced-flow boiling, models of, 19: 20116(R) (SAN-409-12)
heat transfer by, literature review of wetting effects in, 19: 20112 (NAA-SR-Memo-10315)
properties as intermediate coolant in sodium–water reactor systems, 19: 21701
pumping of, development of thermoelectric pumps for, (E), 19: 20096 (NAA-SR-Memo-10729)
scattering of atomic beams of lithium-6 and lithium-7 by crossed thermal beam of, quantum effects and cross sections in, 19: 20823
separation by reversed-phase chromatography and solvent extraction using tri-*n*-octylphosphine sulfide, 19: 19753 (IS-T-3)
separation from bismuth and lead by solvent extraction using tri-*n*-octylphosphine sulfide, 19: 19753 (IS-T-3)
vaporization lifetimes of droplets of, 19: 20116(R) (SAN-409-12)
wetting Rankine boiler tubes by, effects of surface treatment on, 19: 20111 (NAA-SR-Memo-10224)
MERCURY IONS
solvent extraction from molten nitrate by liquid silicone–TBP at 150°C, 19: 19833 (CEA-R-2628)
MERCURY ISOTOPES
separation by photochemical reaction with water vapor, feasibility of, 19: 20429 (MLM-1214)
MERCURY ISOTOPES Hg-194
fission barrier of compound nucleus, (E/T), 19: 21259(R) (UCRL-11828(p.77-80))
MERCURY ISOTOPES Hg-197
use in carcinoma localization by scintillation, 19: 19715
MERCURY ISOTOPES Hg-199
energy level transitions in, retardations in l-allowed M1, (T), 19: 21323
neutron capture by, γ-γ cascades in thermal, (E), 19: 21292

MERCURY ISOTOPES Hg^{200}
production in neutron capture by mercury-199, γ-γ cascades from, (E), 19: 21292
MERCURY ISOTOPES Hg^{203}
use in renal scintiscanning of urologic diseases, 19: 19721
MESIC ATOMS
hyperfine structure of meson (μ), vacuum polarization corrections to, (T), 19: 21395
internal conversion between hyperfine states of μ, polarization density matrix in, (T), 19: 21421
meson (π^-) transfer from hydrogen, to heavier atoms, (E), 19: 21281
x-ray emission from gold, lead, bismuth, uranium, and tungsten, 2p-1s and 3p-2p energies for, (E/T), 19: 21344
MESITYLENE
hydrogen abstraction from, by methyl radicals, 19: 21760 (NYO-2728-4)
luminescence spectra and quantum yields of pure and cyclohexane solutions of, 19: 21771 (TID-21684)
MESON BEAMS
focusing of, using plasma lens, 19: 20915 (BNL-8967)
separator for K^1, testing of CERN r-f, (E), 19: 20748
MESON SHOWERS
calculations of intranuclear, (T), 19: 21239 (LA-3206)
MESONS
book: *Fundamental Particles*, 19: 21072
charge conjugation and parity of U(12) multiplets for, 19: 20974
contribution to three-body forces in tritons, 19: 21075
exchange of vector, in meson-baryon interactions, 19: 21018
form factors and generalized Poincaré group for, electromagnetic, 19: 20971
interactions of, SU(6)-invariant theory for couplings in, (T), 19: 21013
interactions with baryons and mesons, relativistic SU(6) theory for, 19: 21005
interactions with baryons, Johnson-Treiman relations from vector-meson exchange in, 19: 21018
interactions with baryons, M(12) symmetry scheme for, (T), 19: 21024
interactions with baryons, predictions of relativistic SU(6) scheme for, (T), 19: 21025
interactions with baryons, amplitudes in SU(6) scheme for, 19: 21027
mass relations for, empirical, 19: 20994
mass spectrum of, symmetry violations in, (T), 19: 20951
masses of, in SU(6) symmetry, (T), 19: 21030
properties of scalar and vector, electrodynamic theory for, 19: 20929 (ICTP-64/12)
theory for, gauge approximations in non-perturbative mesodynamics, 19: 20928 (ICTP-64/10)
theory of free vector, 19: 20947
MESONS, RESONANCE
decay of K*, (K-2π), (T), 19: 20984
decay of mesons (L), existence of radiative, (T), 19: 20931 (JINR-P-1951)
mass and Regge trajectories for M^2, (T), 19: 21049
production of K* (1430), in mesons (π^-)–proton interactions at 3.9 and 4.2 Bev/c, (E), 19: 21004
production of K*, in antiproton-proton annihilation, (E), 19: 20993
production of K*, in meson (K) interactions with mesons (π), (T), 19: 21058
properties of, data on, 19: 21040
review on three -and four-pi, 19: 20969
MESONS (B)
quantum numbers of, 19: 21066
MESONS (η)
decay of, branching ratios for, (T), 19: 21059
MESONS (K)
decay of K*, (K-2π), (T), 19: 20984
interactions with hyperons (Ξ), hyperons (Ω^-) as bound state in, (T), 19: 20970
interactions with mesons (π) at low energies, K* production in, (T), 19: 21058
interactions with nucleons at high energies, Regge trajectories for, (T), 19: 21063
MESONS (K^-)
capture in liquid helium, de-excitation, (T), 19: 21042
interactions with protons at 2.45 to 2.70 Bev/c, Y_1^* (1660) production in, (E), 19: 21017
interactions with protons at 2.24 Bev, hyperon (Ξ) production in, 19: 21065
interactions with protons at 400 Mev, polarization correlation of hyperons (Λ) and hyperons (Σ^0) in, 19: 21071
production in proton reactions with beryllium at 12.5 Bev, cross sections for, (E), 19: 21406
reactions with emulsion nuclei at 3.0 Bev/c, hyperfragment production in, (E), 19: 21429
reactions with emulsion nuclei, hyperfragment production in, (E), 19: 21365
reactions with emulsion nuclei at 0.8 to 3.0 Bev/c, lithium-8 emission in, (E), 19: 21389
MESONS (K^0)
decay of (K_1^0), spontaneous breakdown of CP symmetry in (2π), (T), 19: 20999
decay of (K_2^0), into two mesons (π) and a photon, (T), 19: 20939 (UR-875-30)
decay of K_2^0, CP-nonconserving, (T), 19: 21020
decay of K_2^0, branching ratios for three-body leptonic, (T), 19: 21060
decay of, CP violation in 2π, (T), 19: 20978
MESONS (K^+)
absorption by aluminum, carbon, and copper at 4.75 Bev/c, (E), 19: 21431
decay into two mesons (π) and a photon, (T), 19: 20939 (UR-875-30)
decay of, branching ratios for 3π, (E), 19: 20990
decay of, branching ratios for three-body leptonic, (T), 19: 21060
decay of, probability ratio for, (T), 19: 21060
decay of, shadow mesons (π^0) in, (T), 19: 21038
interactions with protons, kinematical effects in peripheral, (T), 19: 20981
production in proton-proton interactions at 2.40 and 2.85 Bev, (E), 19: 21034
production in proton reactions with beryllium at 12.5 Bev, cross sections for, (E), 19: 21406
MESONS ($K_{\mu 3}^0$)
decay of, $\Delta S/\Delta Q$ rule in, (E/T), 19: 20979
MESONS (K_{e3}^+)
decay of, angular distribution of products of, 19: 21069
decay of, probability ratio for, (T), 19: 21060
MESONS ($K_{\mu 3}$)
form factors and branching ratio for, (E), 19: 20985
MESONS ($K_{\pi 3}$)
branching ratios, (E), 19: 20990
MESONS (L)
decay of, existence of radiative, (T), 19: 20931 (JINR-P-1951)
MESONS (μ)
background in underground low-level gamma-counting laboratory, 19: 20093(R) (ANL-6938(p.194-205))
book: *Fundamental Particles*, 19: 21072
capture by helium, hydrogen, and carbon, intermediate vector boson in, (T), 19: 21420
capture by nuclei, gamma-neutrino correlation in first-forbidden, (T), 19: 21378
distributions and flux in atmosphere, angular and energy, (T), 19: 20891
mass relations for, empirical, 19: 20994
scattering by nuclear matter, linear response to inelastic, (T), 19: 21393
MESONS (μ^-)
capture by helium-3, nuclear form factors from, (T), 19: 21236 (JINR-P-1952)
capture probability in lithium-6, lithium-6 model testing by, (T), 19: 21368
interactions with nucleons at 5 Bev/c meson (π) production in, (E), 19: 21037
MESONS (μ^+)
decay of, positron momentum spectrum in, (E), 19: 21012
MESONS (ω)
decay of, SU(6)-invariant theory for couplings in, 19: 21013
properties as massive neutral gauge particle, 19: 20989
MESONS (ϕ)
decay of, selection rules in relativistic SU(6) theory for, 19: 21023
decay of, SU(6)-invariant theory for couplings in, 19: 21013
production in antiproton-proton annihilation, (E), 19: 20993
properties as massive neutral gauge particle, 19: 20989
MESONS (π)
book: *Fundamental Particles*, 19: 21072
distributions in atmosphere, angular and energy, (T), 19: 20891
interactions with nucleons, parameters for, (T), 19: 20937(R) (TID-21672)
interactions with hyperons (Σ) and nucleons, coupling constants for, (T), 19: 20917 (IC/65/3)
interactions with elementary particles, production amplitudes in, (T), 19: 20925 (ICTP-64/3)
interactions with protons, kinematical effects in peripheral, (T), 19: 20981
interactions with nucleons, production of massive neutral gauge particle, (T), 19: 20989
interactions with nucleons, position and width of N* (1688) in, (T), 19: 20992
interactions with nucleous, N_3^*, resonance in, (T), 19: 21000

interactions with nucleons, phase of forward amplitudes for, (T), 19: 21010
interactions with nucleons, selection rules for final states in, (T), 19: 21023
interactions with nucleons, complex angular momentum in, (T), 19: 21048
interactions with mesons (π), Jacob-Wick method for scattering amplitude in, (T), 19: 21052
interactions with nucleons, Jacob-Wick method for scattering amplitude in, (T), 19: 21052
interactions with mesons (K) at low energies, K* production in, (T), 19: 21058
interactions with nucleons at high energies, Regge trajectories for, (T), 19: 21063
interactions with mesons (π), theory of low-energy, 19: 21074
interactions with nucleons, kinematic analysis of, 19: 21076
interactions with nucleons, Regge trajectories in, 19: 21077
interactions with nucleons, numerical solution of integral equation for, 19: 20445
polarizability of, neutron-polarizability contribution from, (T), 19: 20949
production in meson (μ^-)-proton interactions at 5 Bev/c, 19: 21037

MESONS (π^-)
capture in liquid helium, de-excitation, (T), 19: 21042
electromagnetic structure of, (E), 19: 20935 (NP-14885)
interactions with electrons at 21 Bev, meson structure from, (E), 19: 20935 (NP-14885)
interactions with deuterons, neutron-neutron scattering length from, (E), 19: 20995
interactions with protons, T = 0 scalar di-pion in ($\pi^+\pi^-$n), (T), 19: 20998
interactions with mesons (π^0), (T), 19: 21000
interactions with protons at 3.9 and 4.2 Bev/c, K* (1430) production in, 19: 21004
interactions with protons at 6 to 18 Bev/c, charge-exchange cross sections for, (E), 19: 21006
interactions with protons, Regge-pole analysis of charge-exchange, (T), 19: 21007
interactions with protons at 35 Mev, s-wave scattering length for, (E), 19: 21043
interactions with nucleons at 6.8 Bev/c, angular and momentum distributions in, (E), 19: 21062
production in proton reactions with beryllium at 12.5 Bev, cross sections for, (E), 19: 21406
reactions (π^-,nγ) with nuclei, energy spectra from, (E), 19: 21315
transfer from hydrogen to heavier atoms in ethane and styrene, (E), 19: 21281

MESONS (π^0)
decay of, charge-conjugation invariance in 3γ, (E), 19: 21029
emission of shadow, in meson (K+) decay, (T), 19: 21038
interactions with mesons (π^-), (T), 19: 21000

MESONS (π^+)
absorption by aluminum, carbon, copper, lead, and tin, at 2.72, 3.70, and 4.75 Bev/c, (E), 19: 21431
production in proton reactions with beryllium at 12.5 Bev, cross sections for, (E), 19: 21406
reactions with carbon, nitrogen, and oxygen at 80 Mev, cross sections for, (E), 19: 21279

MESONS (ρ)
decay of, SU(6)-invariant theory for couplings in, 19: 21013
production in antiproton-proton annihilation, (E), 19: 20993

MESONS (ρ^0)
decay of, T = 0 scalar di-pion in, (T), 19: 20998

METABOLISM
diurnal rate variation in rat bone and cartilage, 19: 19472(R) (ANL-6938(p.179-93))
effects of pethidine on, in rats with radiation sickness, 19: 19481
of glucose, role in radiation injury, 19: 19538
radiation effects on, in rabbit cornea, 19: 19552
radiation effects on lipid, in newborn and weanling rat brain, 19: 19610
radiation effects on, in animal cells, 19: 19613

METAL-FOIL DETECTORS
development of neutron, using normal and depleted uranium, 19: 20340

METAL POWDERS
hot extrusion of, review, 19: 20518 (NMI-TJ-29)

METALLIC FILMS
bonding to solid-state devices, methods for, 19: 20520 (SC-DC-65-1256)

METALLURGY
electron beam uses in, 19: 20466
electron microscopy in, use of high-voltage, 19: 20548 (CONF-640204 (p.35-43))
metalworking, ad hoc committee report on, 19: 20507(R) (MAB-206-M)
radioisotope uses in, 19: 20417

METALS
analysis by activation methods, 19: 19796
book: *Mineralogy and Geochemistry of Rare Elements in Cherry Mountains (Urals)*, in Russian, 19: 20190
containment of boiling, properties of tantalum for, 19: 21690(R) (LA-3244)
corrosion by gases, classification of phenomena in, 19: 20486
development of high-strength, for naval structures, 19: 20462(R) (NRL-6258)
heat transfer to liquid, flowing turbulently in eccentric annuli, 19: 20123
magnetic coupling in ferromagnetic and nonmagnetic, long-range spin-density, (T), 19: 20690
melting point measurement for refractory, method for, 19: 20566(T) (IS-Trans-13)
polarization in nonferromagnetic, long-range spin, (T), 19: 20689
properties of superconducting, data on, 19: 21187

METEORITES
cosmic-ray exposure ages of iron, (E), 19: 20760

METEOROLOGY
formulas for calculating plume rise from stacks, 19: 20653(R) (ANL-6938(p.209-41))

METHANE
determination in vented gases from underground nuclear explosion, apparatus for, 19: 19776 (UCRL-12169)
effects on radioinduced carbon dioxide-graphite reactions, (E), 19: 19953 (AERE-R-4201)
ionization by fission products in proportional detector, (E), 19: 20376
reactions with excited helium, 19: 19937
yields in carbon-11 recoil reactions with hydrocarbons, 19: 20018

METHANE, DIPHENYL-
hydrogen abstraction from, by methyl radicals, 19: 21760 (NYO-2728-4)

METHANE, IODO-
reactions with recoil iodide, selectivity of labeling in, 19: 20020 (IA-907)

METHANE, TRICHLOROFLUORO-
heat transfer in forced-flow boiling, 19: 20116(R) (SAN-409-12)
vaporization lifetimes of droplets of, 19: 20116(R) (SAN-409-12)

METHANE, TRIPHENYL-
hydrogen abstraction from, by methyl radicals, 19: 21760 (NYO-2728-4)

METHANOL
effects on radioinduced carbon dioxide-graphite reactions, (E), 19: 19953 (AERE-R-4201)
cyclohexane–methanol, interface in critical fluids of, reflectivity of diffuse, 19: 19952

METHIONINE
radiation effects on uptake of sulfur-35-labeled, by rabbit marrow and spleen proteins, 19: 19604

METHYL GROUP
preparation of deuterated, attached to oxygen, 19: 20034

METHYL RADICALS
hydrogen abstraction reactions with aromatic compounds, 19: 21760 (NYO-2728-4)
use of carbon-14-labeled, as radiolysis scavenger for hydrocarbons, 19: 19985

METHYLENE BLUE
radiolysis of, in glycerol solution, 19: 20016

METROLOGY
equipment for automatic, conference on, 19: 20303

MICA
fission product tracks in, formation and stability of, (E), 19: 20674

MICE
bone formation in, effects of aminoacetonitrile and estrogen on, 19: 19471(R) (ANL-6938(p.162-78))
iodine isotope and sulfur-35 uptake by vibrissal hairs of, origin of, 19: 19479
radiation effects on host-cell interactions of hemopoietic grafts in, 19: 19615
radiation effects on fractionation of spleen-colony-forming cells from bone marrow in, 19: 19617
radiation effects on blood picture in conventional and germfree, whole-body, 19: 19619
radiation effects on, protective effects of AET or MEA with serotonine against lethal, 19: 19627
radiation effects on, protective effects of frozen bone marrow grafts against, 19: 19645
radiation effects on, effects of allogenic chimeric bone marrow on repopulation of lymphatic tissue in, 19: 19646
radiation effects on, protective effects of allogenic marrow inoculation against, 19: 19648
radiation effects on, amyloidosis in chimeras and relation to lymphoid hypoplasia in whole-body, 19: 19650

radiation effects on, effects of blood transfusions on subsequent marrow transplants in, 19: 19653
radiation injuries, protective effects of prochlorperazine, 19: 19631
radiation injuries, protective effects of prochlorperazine, 19: 19632
radiation injuries in, protective effects of aminoethylisothiourea and serotonin in, 19: 19635
radioinduced tumors in, 19: 19594
transplantation of spleen cells in irradiated, protection from killing effect of, 19: 19651

MICROANALYSIS
correction factors for electron penetration in x-ray, 19: 19746 (CEA-R-2728)
properties of electron probe, 19: 19747 (CONF-650214-1)

MICROORGANISMS
radiosensitivity of, factors affecting, 19: 19590

MICROSCOPES
description of hot-stage, for studying plutonium, 19: 20546 (CEA-R-2726)

MICROSCOPY
of brain tissues, sample preparation, 19: 19509(T) (JPRS-29250(p.9-13))

MICROWAVE EQUIPMENT
microwave propagation in plasma-filled waveguides, 19: 21536

MICROWAVE SPECTROSCOPY
spin resonance line shapes in, effect of probes on, 19: 20839

MICROWAVES
emission by plasma, at electron-cyclotron harmonic frequencies, (T), 19: 21477 (MATT-290)
harmonic generation by, in plasma, (T), 19: 21517
interactions with Puffatron plasma, excitation from, (E), 19: 21491 (UCRL-12057(Rev.I))
production by injection of free electrons into high magnetic fields, (E), 19: 20684
propagation in hot plasma waveguides with infinite magnetostatic fields, (T), 19: 21536
reflection from anisotropic plasma surface, (E/T), 19: 21513
spectrum in solar radiation, review of, 19: 20785

MILITARY PERSONNEL
protection from fallout, decay-curve estimates for, 19: 20223

MILK
analysis for cesium-137, rapid method for, 19: 19805
analysis for selenium, activation, 19: 19771(R) (TEES-2671-4(Chap.9))
analysis for strontium-89 and -90, radiochemical, 19: 19739 (AERE-AM-101)
cesium-134, -137, and sodium-22 content in, relation of content in man to, 19: 20225
cesium-137 and strontium-90 content in Canadian, 1964, 19: 20161 (NP-14869)
iodine-131 secretion in cow, after single dose, 19: 19477
radioactivity due to fallout in, 1964 and 1965, 19: 20154(R) (HASL-158)

MINERALOGY
book: *Mineralogy and Geochemistry of Rare Elements in Cherry Mountains (Urals)*, in Russian, 19: 20190

MINERALS
fission product tracks in, formation and stability of, (E), 19: 20674
radiation effects on physiology of content of, in developing guinea pig brain, 19: 19534
separation of argon-40 from, determination of activation energy for use in, 19: 20166

MINING
methods of, using light from nuclear reactors, 19: 21710

MIRRORS
design of turbine-driven, engineering drawings of, 19: 20308
neutron total reflection by cobalt, (E), 19: 21201(T) (KFK-tr-164)

MISSILES
detection by tracking stations near trajectories, (E), 19: 21767 (SC-TN-65-44)

MISSOURI
seismic data from BILLIKEN calibration explosion in southeast, 19: 20171 (AFCRL-64-659)

MIT RESEARCH REACTOR
equipment for transferring irradiated solutions from, pneumatic, 19: 21741

MITOSIS
radiation effects on, in regenerating rat liver cells, 19: 19510(T) (JPRS-29250(p.27-32))
radiation effects on suppression of, in cytoplasmic structures and nucleus of *Tradescantia paludosa*, 19: 19579
radiation effects on, in animal cells, 19: 19613
radiation effects on, in animal cells, 19: 19614

MIXED SPECTRUM CRITICAL ASSEMBLY
shutdown of, excursion-limiting fuse for, 19: 21617

MIXERS
transients in packed tubular chemical, models for computation of, 19: 19734 (UCRL-11757)

MOLDS
design principles for plastic potting shells, 19: 21764 (SC-DR-64-2135)
fabrication of beryllium–copper, methods for, 19: 20519 (NP-14879)

MOLECULES
appearance potentials for doubly charged ionic, in ionization by 70-kev electrons, 19: 20807(R) (UCRL-11828(p.201-4))
dissociation by ionization, theory of, 19: 19937
electron dissociative capture by, resonance, (T), 19: 19899
electron shell electrostatic potential at nuclei in diatomic, (T), 19: 20836(T)
labeling with radioisotopes, rules for formulas and nomenclature following, 19: 19736
photoionization of, equipment for measuring, 19: 19955(R) (ANL-6938 (p.21-2))
scattering of, wave packets in quantum theory for, 19: 21092

MOLLUSKS
radiation processing of oysters, effects on storage life, 19: 20407(R) (ORO-626)
radioactive contamination of, 19: 20230

MOLYBDENUM
analysis for hydrogen, combustion-gravimetric, 19: 19758 (LA-3225)
analysis for trace amounts of nickel, photometric, 19: 19799
coating with rhenium by electrolysis, optimum conditions for, 19: 20529
crystal structure of, dislocation subboundaries in, 19: 20602
determination in niobium alloys, polarographic, 19: 19781
determination in uranium and its compounds and alloys, methods for, 19: 19823
determination using 5,5′ thiodisalicylic acid, spectrophotometric, 19: 19812
effects on fabrication and mechanical properties of niobium–tantalum–titanium–vanadium alloy sheet, 19: 20552(R) (IITRI-B6021-6)
effects on strength of thorium at high temperatures, 19: 20560 (ORNL-3777)
melting point measurement by black-body method, 19: 20566(T) (IS-Trans-13)
radiation effects on, annealing of neutron, 19: 20634
radioinduced interstitial loops in, neutron, 19: 20636
separation from technetium, 19: 19820
tensile properties of, grain size and temperature effects on, 19: 20594
thermal conductivity at high temperatures, (E), 19: 20576

MOLYBDENUM ALLOYS
Al–Mo–Sn–Ti–V–Zr, beta transus temperature of, 19: 20462(R) (NRL-6258)
Al–Mo–Sn–Ti–V, beta transus temperature of, 19: 20462(R) (NRL-6258)
Al–Mo–Ti, beta transus temperature of, 19: 20462(R) (NRL-6258)
Al–Mo–Ti–V, mechanical properties of diffusion-bonded plates of, 19: 20462(R) (NRL-6258)
Al–Mo–Ti–V, mechanical properties of solution-annealed and aged T-19, 19: 20462(R) (NRL-6258)
Al–Mo–Ti–Zr, beta transus temperature of, 19: 20462(R) (NRL-6258)
Mo–Nb, extrusion, 19: 20500 (AFML-TR-64-387)
Mo–Nb–Pt–U, corrosion resistance in water, 19: 20497(P)
Mo–Nb–Pt–U, properties for use as reactor fuel, 19: 20497(P)
Mo–Nb–Ti, coating of, for oxidation protection at 2300°F, 19: 20483 (SCNC-318)
Mo–Nb–Ti–V, coating for oxidation protection, 19: 20459(R) (IITRI-B6019-6)
Mo–Nb–V–Zr, fabrication and properties of B-66 sheet, 19: 20499(R) (AD-606291)
Mo–Nb–W, extrusion, 19: 20500 (AFML-TR-64-387)
Mo–Re–W, ductility and melting points of sintered, 19: 20584
Mo–Ti–Zr, corrosion by potassium vapor, design of test capsule for, 19: 20473(R) (NASA-CR-54629)
Mo–Ti–Zr, tensile properties of TZM sheet, 19: 20542(R) (AD-606310)
Mo–U, spectrophotometric analysis for uranium, 19: 19759 (LA-3226)
Mo–W, ductility and melting points of sintered, 19: 20584
Mo–W, extrusion, 19: 20500 (AFML-TR-64-387)

MOLYBDENUM CARBIDES
superconducting properties, 19: 20572

MOLYBDENUM CHLORIDES
complexes with tetramethylammonium salt, bonding in, 19: 19841 (MIT-1965-18)

MOLYBDENUM COMPLEXES
magnetic susceptibility and spectra, 19: 19892
with germanium and pyridine or 8-quinolinol, properties for use as thin-layer chromatograms, 19: 20069

MOLYBDENUM IONS
coordination chemistry of quadrivalent and tervalent, 19: 19892

MOLYBDENUM ISOTOPES
photon reactions (y,n), threshold energy for, (E), 19: 21287
MOLYBDENUM ISOTOPES Mo-99
decay of, gamma transitions in, (E), 19: 21258(R) (UCRL-11828 (p.67-71))
MOLYBDENUM ISOTOPES Mo-92
deuteron reactions (d,p) with, spectra from, 19: 21394
photon reactions (y,n), threshold energy for, (E), 19: 21287
MOLYBDENUM ISOTOPES Mo-94
photon reactions (y,n), threshold energy for, (E), 19: 21287
MOLYBDENUM ISOTOPES Mo-97
photon reactions (y,n), threshold energy for, (E), 19: 21287
MOLYBDENUM ISOTOPES Mo-99
content in stratosphere, 19: 20657(R) (DASA-1309)
MOLYBDENUM ISOTOPES Mo-100
photon reactions (y,n), threshold energy for, (E), 19: 21287
MOLYBDENUM OXIDES
reactions in ammonium fluoride and hydrofluoric acid solutions, 19: 19913
Al_2O_3–CoO–MoO_3, catalytic properties for benzene synthesis from acetylene, for radiocarbon dating, 19: 19944 (ORINS-50)
MOLYBDENUM STEEL
Cr–Mo, corrosion of Croloy 2¼ in sodium-heated steam generator after 4000 hr, 19: 20107(R) (BAW-1280-22)
Cr–Mo–Ni–V, development, 19: 20462(R) (NRL-6258)
MOLYBDENUM SYSTEMS
CeO_2–HfO_2–MgO–Mo, preparation and properties of macrolaminate particle composites of, 19: 20558(R) (NP-14888)
C–Mo–Ti–Zr, extrusion of molybdenum-TZC, 19: 20500 (AFML-TR-64-387)
Mo–Si–U, preparation and crystal structure of compounds, 19: 19871
MONAZITES
radioactivity equilibrium between radium, thorium, and uranium in, in Ukraine, 19: 20189
MONKEYS
effects of bone marrow grafts on secondary disease in, methods for modification of, 19: 19647
radiation effects on effectiveness of tetanus vaccination in, 19: 19608
radiation effects of simulated space situation on blood cells in, gamma and proton, 19: 19616
MONTE CARLO METHOD
for grain coordinates for artificial construction of particle tracks, 19: 20325 (UCRL-11624)
use in calculation of intranuclear cascades, (T), 19: 21239 (LA-3206)
MONTMORILLONITES
ion exchange properties of, 19: 19794
MÖSSBAUER EFFECT
analysis at high pressures, methods for, (E), 19: 21231 (COO-1198-255)
measurement using multiscaler mode of pulse-height analyzer, 19: 20327(R) (UCRL-11828(p.221-2))
of iridium-193 in cobalt, iron, and nickel, (E), 19: 21255(R) (UCRL-11828(p.57-8))
spectra of iron-57 in ferrichrome and ferrichrome A, 19: 21270(R) (UCRL-11828(p.214-16))
spectral position and width in, lattice-oscillation anharmonicity effect on, (T), 19: 21422
use for time dilation experiments, 19: 20699
MOTORS
development of pneumatic-nutator, for actuating reactor control drums, (E), 19: 21615(R) (NASA-CR-54282)
power losses in liquid between rotor and stator of induction, MHD and EM, (E/T), 19: 20119
MUSCLES
cesium-137 and strontium-90 content in bulls from fallout, 19: 20215
radiation effects on, 19: 19551
radiation effects on acid and alkaline phosphatase and esterase activity in guinea pig skeletal, 19: 19574
MUSCOVITES
argon-40 activation energy in, 19: 20166
MUSTARD GAS
toxic effects on *E. coli*, recovery from lethal, 19: 19485
MUTATIONS
effects of phosphorus-32 on development of, in cotton plants, 19: 19580
induced by sulfonate in maize, 19: 19527
of kappa in *Paramecium aurelia*, 19: 19464
of *Neurospora crossa*, 19: 21772(R) (TID-21709)
radiation and chemical effects on, in *B. subtilis* isolated DNA, 19: 19542
radioinduced antibiotic-resistant, of *Staphylococcus aureus*, 19: 19531
radioinduced antibiotic-resistant, of *Staphylococcus aureus*, 19: 19532
radioinduced in *Arabidopsis thaliana*, 19: 19548
radioinduced in maize, 19: 19527
radioinduced in potatoes, gamma, 19: 19518
radioinduced in *Sordaria brevicollis*, ultraviolet, 19: 19547

N

NAPHTHACENE
effects on radioinduced luminescence of Bibenzyl, 19: 19963
NAPHTHALENE
use as binder in preparation of dispersions of uranium carbide in uranium, 19: 20512(R) (NCSC-2981-2)
use as binder in preparation of dispersions of uranium carbide in uranium, 19: 20513(R) (NCSC-2981-3)
NAPHTHALENE, 1,2,3,4-TETRAHYDRO-
hydrogen abstraction from, by methyl radicals, 19: 21760 (NYO-2728-4)
NAPHTHOL
effects on polarography of uranyl pyrophosphate complexes, 19: 19816
2-NAPHTHOL, 1-(2-PYRIDYLAZO)-
analytical uses in determination of nickel traces in molybdenum and tungsten, 19: 19799
2-NAPHTHOL, 1-(2-THIAZOLYLAZO)-
analytical uses in determination of trace amounts of nickel, 19: 19814
NATURAL WATERS
analysis for cesium-137, strontium-89, and strontium-90 by electrodialysis and gamma spectroscopy, 19: 19809
radioactivity of, methods of monitoring for compliance with regulations, 19: 20211
NEBULAE
isophotometer tracings of, errors in, 19: 20439(R) (COO-614-31)
NEODYMIUM
determination by titration, suitability of tetraethylenepentamine heptaacetic acid for, 19: 19813
separation from aqueous solution by solvent extraction as salicylate pyridine complex, 19: 20079
separation from magnesium–thorium alloy by transfer to liquid scrub alloy in fused salt, 19: 20066
separation from other light lanthanides by partition chromatography following production by proton bombardment of erbium, 19: 20078
separation from scandium by solvent extraction of diantipyrinylmethane complex, 19: 20080
NEODYMIUM ALLOYS
Sb–Nd, magnetic properties of, (E), 19: 20597
NEODYMIUM COMPLEXES
with serine, stability and composition, 19: 19874
NEODYMIUM IONS
spectra in barium, calcium, and strontium fluorides, absorption and luminescence, 19: 19854
NEODYMIUM ISOTOPES
photon reactions (y,n), cross sections for, (E), 19: 21287
NEODYMIUM ISOTOPES Nd-142
photon reactions (y,n), cross sections for, (E), 19: 21287
NEODYMIUM ISOTOPES Nd-145
photon reactions (y,n), threshold energy for, (E), 19: 21287
NEODYMIUM ISOTOPES Nd-147
determination in air by beta measurement, efficiency of counter for, 19: 20169
NEODYMIUM ISOTOPES Nd-148
uses in calculations of reactor-fuel burnup, (E), 19: 21667(R) (GEAP-4776)
NEODYMIUM ISOTOPES Nd-150
photon reactions (y,n), cross sections for, (E), 19: 21287
NEODYMIUM NITRATES
thermal decomposition, 19: 19928
NEODYMIUM OXIDES
preparation by decomposition of nitrate, oxalate, and sulfate, 19: 19928
NEODYMIUM OXYSULFATES
preparation and properties, 19: 19928
NEODYMIUM SULFATES
crystal structure and bond types of octahydrates, 19: 19915(T)
thermal decomposition, 19: 19928
NEODYMIUM ZIRCONATES
preparation and properties of, 19: 19925
NEON
absorption coefficient from 3.6 to 10×10^3 Å, (T), 19: 20833
charge exchange in, atom-ion resonance, (T), 19: 19931
electron reactions with, excitation cross sections for, 19: 20804(R) (ANL-6938(p.36-45))
electron reactions with, excitation functions for metastable state formation in, 19: 19992
ionization by electrons at 0.6 to 20 kev, (E/T), 19: 20850
neon-ion reactions at 100 to 400 kev, excitation in, (E), 19: 20862
photoionization of, dielectric breakdown from, (E), 19: 20847

x-ray reactions at 167 to 913 ev, double Auger electron emission in, (E), 19: 20844
NEON IONS
reactions with hydrogen, deuterium isotope effects on, 19: 19887
reactions with neon at 100 to 400 kev, excitation in, (E), 19: 20862
sputtering on metals at 45 kev, thermal spikes in, (E), 19: 20838
NEON ISOTOPES Ne-17
decay of, log ft values for, (T), 19: 21379
NEON ISOTOPES Ne-20
alpha inelastic scattering at 50.9 Mev by rotational bands in, (E/T), 19: 21267(R) (UCRL-11828(p.113-16))
reactions (Ne-20,xn) with erbium isotopes, (E), 19: 21248(R) (UCRL-11828(p.21-5))
NEON ISOTOPES Ne-21
content in iron meteorites, (E), 19: 20760
NEPTUNIUM
electric conductivity at low temperature, radioactive self-damage effects on, (E), 19: 20649
separation from nitric acid solutions by solvent extraction using dialkyl phosphoric acid, 19: 20075
separation from nitrate solutions by solvent extraction using organo-phosphorus compounds, 19: 20077
NEPTUNIUM ISOTOPES Np-237
energy levels, (T), 19: 21251(R) (UCRL-11828(p.31-4))
separation from power reactor fuels, economics of, 19: 20036 (BNWL-25)
NEPTUNIUM NITRATES
separation from nitric acid solutions by complex formation with organic phosphorus compounds, 19: 20077
NERVES
effects of magnetic fields on vagal inhilition in frogs, 19: 21776 (UCRL-12389)
NERVOUS SYSTEM
morphology of subcutaneous, in radiodermatitis, 19: 19591
radiation effects on control center of autonomic, in rabbits, 19: 19509(T) (JPRS-29250(p.9-13))
radiation effects on dog, antenatal, 19: 19536
radiation effects on, 19: 19572
NEUROSPORA
genetic studies of, 19: 21772(R) (TID-21709)
NEUTRINOS
emission from stars, neutral current effects in, (T), 19: 20772(T)
interactions with elementary particles, production amplitudes in, (T), 19: 20925 (ICTP-64/3)
interactions with nucleons, neutral weak currents in, (T), 19: 20988
interactions with neutrons, SU(6) for N* production in, (T), 19: 20996
production and acceleration in plasma, (T), 19: 21500
production by meson beam focused by plasma lens, 19: 20915 (BNL-8967)
production by 200-Bev proton synchrotron, (T), 19: 20738 (UCRL-11983)
wave equations for free fields of, (T), 19: 21110
NEUTRON PHOTOGRAPHY
use for irradiated fuel elements and building materials, 19: 20129
NEUTRON SCATTERING CROSS SECTIONS
measurement of differential, thick target method for, 19: 21298
NEUTRON SHIELDING
neutron transport in, analysis of fast, (E), 19: 21199 (CEX-65.02)
performance of lithium hydride as, (T), 19: 21614 (NAA-SR-Memo-10559)
NEUTRON SOURCES
design and uses of pulsed, 19: 21216
development using Orbitron ion sources, 19: 21208
pulsed, fast reactor design for use as, 19: 21745(P)
pulsed, fast reactor design for use as, 19: 21746(P)
use in steam void determination in loops, 19: 20294
uses of fast, in Operation HENRE transport studies, (E), 19: 21199 (CEX-65.02)
NEUTRON SPECTRA
measurement at various Hanford plant areas, (E), 19: 20201 (HW-SA-3525)
NEUTRON SPECTROMETERS
design of scintillation time-of-flight, 19: 20355
resolution function of neutron chopper, for total cross section measurements, (T), 19: 20331
NEUTRON TOTAL CROSS SECTIONS
measurement for indium and samarium at 0.7 to 14 ev, (E), 19: 21285
measurement of, neutron chopper for, 19: 20331
NEUTRONS
activation of elements in rat tissues by, 19: 19601
angular distribution of, high-efficiency detector for, 19: 20333
binding energy in nuclei, 19: 21275
capture by iron-54, energy levels from, (T), 19: 21277
capture by nuclei, effects of resonance interference in, (T), 19: 21335
capture by uranium-238, spontaneous fission of isotopes produced in, (E), 19: 21403
capture-to-fission ratio for uranium-235, epicadmium, (E), 19: 21334
collimation of, computer analysis of efficiency of collimators, (T), 19: 21612 (NAA-SR-Memo-10557(Pt.I))
collimation of, computer analysis of efficiency of collimators, (T), 19: 21613 (NAA-SR-Memo-10557(Pt.II))
decay of, branching ratios for leptonic, (T), 19: 21019
decay of, U(12) symmetry for weak interactions in, (T), 19: 21028
detection and measurement at various Hanford plant areas, (E), 19: 20201 (HW-SA-3525)
detection and measurement using semiconductor and scintillation detectors, 19: 20330(T) (AEC-tr-6547)
detection and measurement of, use of LiI(Eu) scintillation counter for, 19: 20375
detection and measurement of, development of nuclear emulsion dosimeter for, 19: 20161 (NP-14869)
diffusion in benzene, cross sections and decay constants for, 19: 21217
diffusion in grey control rods, extrapolation length for, (T), 19: 21649
diffusion in matter, variational flux-synthesis analysis of, (T), 19: 21638 (CONF-650501-4)
diffusion in two-dimensional space with XY geometry, computer program for, 19: 21198 (CEA-R-2759)
distributions in reactors, calculation using centers and limit cycles, (T), 19: 21634 (BNL-9010)
distributions in reactors, calculations of, (T), 19: 21640 (IDO-16983)
dose distribution in air-over-ground geometry, spatial, 19: 20217
dosimetry of, development of metal-foil detector for, 19: 20340
effects on carbon dioxide-graphite reactions, (E), 19: 19953 (AERE-R-4201)
effects on carbon dioxide-graphite reactions, effects of hydrogen and water vapor on chemical, 19: 19954 (AERE-R-4839)
effects on elasticity of graphite polycrystals, 19: 20640
effects on electric conductivity of glass, 19: 19976
effects on electric conductivity of polyethylene, 19: 20017
effects on electron tubes, hardening against, 19: 20399(R) (NP-14946)
effects on graphite moderator, 19: 20614 (HW-81250A)
effects on high-temperature thermocouples, 19: 20401 (ORNL-P-1065)
effects on luminescence of thallium-activated alkali halides, 19: 19966
effects on magnetic properties of defects in nickel, 19: 20647
effects on magnetic properties of defects in iron, 19: 20648
effects on magnetism of cobalt, iron, and nickel, 19: 20652
effects on mechanical properties of reactor graphite, 19: 20637
effects on molybdenum, annealing of, 19: 20634
effects on pyrolytic-carbon-coated uranium carbide particles, 19: 20463 (ORNL-TM-431)
effects on thermal properties of alkali-halide crystals and solid solutions, 19: 19986
effects on vacancy repeated yielding characteristics of copper–tin alloys, 19: 20635
effects on vapor-grown single crystals of uranium dioxide, 19: 20603
emission by compound nuclei, computer analysis of, (T), 19: 21245 (ORNL-TM-196)
emission from plasma, 19: 21483(R) (ORNL-3760(p.30-56))
energy and flux of skyshine, around synchrotron, (E), 19: 20741
energy distribution in hydrogenous moderator of long counter, (T), 19: 21202
energy spectra in reflector of Melusine, (E), 19: 21729 (CEA-R-2442)
energy spectra in finite graphite blocks, equilibrium, (T), 19: 21205
escape in regular arrays of fuel rods, resonance, (T), 19: 21648
flux distribution in Kahl power reactor, relaxation method for calculating, 19: 21655
flux distributions in reactors, computer programs for, 19: 21644 (WAPD-TM-478)
flux distributions and disadvantage factors in two-region cells, (T), 19: 21212
flux in heavy water–iron laminates, (E/T), 19: 21210
flux in JRR-1, analysis of variations in, 19: 21737
flux perturbations due to infinite plane absorbers, (T), 19: 21220
fluxes of, method for solving Boltzmann equation for, 19: 21222
interactions with deuterons and helium-3, bibliography, (E/T), 19: 21238 (LA-3205)
interactions with neutrinos, SU(6) for N* production in, (T), 19: 20996
interactions with protons, Treiman-Yang criterion for, (T), 19: 21046
interactions with protons in nuclei, isobaric states in, (T), 19: 21304
interactions with protons, pairing correlations in, (T), 19: 21381
kinetics in graphite–uranium rocket reactors, (T), 19: 21715 (AD-605574)
multiplication and fluctuations in reactors, (T), 19: 21641 (JINR-P-1996)
multiplication in natural uranium-light water exponential pile,

calculations from material buckling, 19: 21645
photoproduction in heavy water, 19: 19806
photoproduction on busmuth-209 and tantalum-181, angular distributions from, (E), 19: 21288
photoproduction on nuclei at 10 to 28 Mev, cross sections for, (E), 19: 21305
polarizability of meson (π) contribution to, (T), 19: 20949
production of secondary, in proton reactions with nuclei at 160 Mev, (E/T), 19: 21244 (ORNL-P-844)
reactions (n,α) with cobalt-59 at 12.6 to 19.6 Mev, (E), 19: 21290
reactions (n,α) with silicon-28 at 14.8 Mev, angular distributions from, (E), 19: 21318
reactions (n,α) with germanium-73 at 14 Mev, cross sections for, (E), 19: 21325
reactions (n,γ) with gold and tantalum at 1 to 4 Mev, spectra from, (E/T), 19: 21317
reactions (n,γ) with niobium-93, spectra from, (E), 19: 21330
reactions (n,γ) with bromine-79 at 0.024 to 3.1 Mev, isomeric cross section ratio for, (E), 19: 21331
reactions (n,γ) with deuterons, elastic unitarity effects in, (T), 19: 21371
reactions (n,d) with tritium at 14.4 Mev, neutron-neutron scattering length from, (E), 19: 21404
reactions (n,p) and (n,γ) with tritium at 14.4 Mev, (E), 19: 21405
reactions (n,p) with iron-56 at 12.6 to 19.6 Mev, (E), 19: 21290
reactions (n,p) with chlorine-35 in various chlorides, protective effects against oxidation of sulfur produced in, 19: 20004
reactions (n,2n) with copper-63 at 12.6 to 19.6 Mev, (E), 19: 21290
reactions with bismuth, polonium-210 production in, 19: 20008
reactions with calcium, chromium, and nickel isotopes, resonances in, 19: 21454
reactions with carbon-12, oxygen-16, and silicon-28 at 14 Mev, cross sections for scattering, (E/T), 19: 21441
reactions with molybdenum, interstitial loops in, 19: 20636
reactions with nuclei, cross sections for, (T), 19: 21228 (ANL-6970)
reactions with nuclei, availability of cross section data for, (E), 19: 21225 (AECL-2168)
reactions with nuclei, chain element activity in intermittent, (T), 19: 21226 (AEET/HP/Th-19)
reactions with nuclei at high energies, secondary nucleon yields from, (E/T), 19: 21242 (NP-14837)
reactions with plutonium and uranium isotopes, fission ratios for, (E), 19: 21227 (ANL-6941)
reactions with plutonium-239 at 200 to 600 ev, symmetries in fission, (E), 19: 21241 (LA-DC-6639)
reactions with thorium-232 at 3 to 14 Mev, delayed-neutron yields in fission, 19: 21443
reactions with uranium at 4.5°K, point defects in, 19: 20642
reflection by cobalt mirrors, analysis of total, (E), 19: 21201(T) (KFK-tr-164)
scattering by carbon-12 at 17 to 21 Mev, resonances in, (E), 19: 21310
scattering by doped crystals, electron-phonon interaction effects in inelastic, (T), 19: 20671
scattering by heavy water, molecular conglomerates in, 19: 21221
scattering by indium-115, isomeric states from inelastic, (E), 19: 21237 (KFK-265)
scattering by nuclei at 85 to 700 kev, differential cross sections for elastic, (E), 19: 21298
scattering in crystals with electron impurity centers, single-phonon Green's function for, (T), 19: 20710
scattering length from deuteron-meson (π^-) interactions, neutron-neutron, (E), 19: 20995
scattering of, two-dimensional multigroup analysis of, (T), 19: 21197 (CEA-R-2747 and Add.)
shielding in closely packed slab lattices, self-, (E), 19: 21636 (CONF-654-32)
spectroscopy of, using iterative unfolding method, (T), 19: 20316 (ANL-6984)
temperature distribution across water-boron-poisoned water interface, (E/T), 19: 21207
thermalization in weakly absorbing medium, (T), 19: 21204
thermalization in graphite, (E), 19: 21211
transport equation with anisotropic scattering, iterative method for solving, (T), 19: 21223
transport in fixed three-dimensional body, equations for, 19: 21203
transport in hafnium–uranium-235-water systems, resonance interference in, (E/T), 19: 21643 (WAPD-T-1728)
transport in reactor reflectors, heat transfer model for, 19: 21656
transport of pulsed, in reactors, (T), 19: 21637 (CONF-650406-2)
transport of, computer program for preparing data for Monte Carlo calculations for, 19: 21196 (AWRE-O-81/64)
transport of, Green's function for monoenergetic, (T), 19: 21215
transport of, monoenergetic critical equation for, (T), 19: 21214
yields from deuteron reactions with deuterided erbium and titanium, (E), 19: 21301
yields of secondary, in nucleon reactions with nuclei at high energies, (E/T), 19: 21242 (NP-14837)

NEUTRONS, COLD
scattering by heavy ice, temperature dependence of small-angle, (E), 19: 21218

NEUTRONS, DELAYED
emission in fission, 19: 21443

NEUTRONS, EPITHERMAL
capture by thorium-232, resonance integrals for, (E), 19: 21336
reactions with uranium-233, resonance integrals for fission, (E), 19: 21336
scattering by hydrogenous materials at 0.018 to 0.080 ev, (E), 19: 21200 (KFK-264)

NEUTRONS, FAST
background count in underground low-level gamma-counting laboratory, 19: 20093(R) (ANL-6938(p.194-205))
capture by tantalum-181, tungsten-182, tungsten-183, tungsten-184, and tungsten-186, (T), 19: 21464
detection and measurement using surface-barrier junctions and lithium-6, (E), 19: 20334
distribution and thermalization in reactor graphite, 19: 21646
distributions in water of swimming-pool reactors, (E), 19: 21735 (ORNL-P-1092)
dosimetry of, design of scintillation ratemeter for, (E), 19: 20312 (AERE-R-4525)
dosimetry of, development of instruments for personnel, (E), 19: 20318 (HW-SA-3526)
effects on chromosome aberrations in *Crepis capillaris* seeds, moisture effects on post-, 19: 19581
effects on diamonds, stresses in, 19: 20639
effects on germanium, annealing of, 19: 20626
effects on hardness of aluminum single crystals, 19: 20641
effects on luminescence of zinc sulfide, 19: 19967
effects on operation of pressure transmitter at high temperatures, 19: 20400 (NP-14955)
effects on reactor pressure vessel steel under stress, 19: 20631
effects on tantalum hardness, 19: 21690(R) (LA-3244)
effects on Zircaloy-2 pressure tubes in PRTR, 19: 21686 (HW-84540)
polarization in precession magnets, 19: 21209
production in thermal reactor channels, method for, 19: 21742
radiation effects on germanium p-n junctions, 19: 20627
scattering by vanadium, phonon frequency distribution from, 19: 20553 (KFK-262)
spectra of, nuclear emulsions for measuring, 19: 20374
transport in air, ground, and shielding, studies in HENRE Operation, (E), 19: 21199 (CEX-65.02)

NEUTRONS, THERMAL
absorption by hydrogen, cross section for, (E), 19: 21219
capture by mercury-199, γ-γ cascades in, (E), 19: 21292
diffusion coefficient in beryllium at 60 to 400°K, (T), 19: 21206
diffusion in reactor graphite, length of, (E), 19: 21646
diffusion in water-moderated lattices, two-dimensional, (T), 19: 21654
flux in indium foils, effects of flux anisotropies on perturbations in, (E), 19: 21213
production in 70-Mev electron linear accelerator shielding, 19: 20749
reactions (n,α) with boron-10, cross section for, (E), 19: 20088
reactions with nuclei, energy release in fission, (E/T), 19: 21224 (AECL-2160)
reactions with plutonium and uranium isotopes, cross sections for, (T), 19: 21678 (ANL-6972)
reactions with uranium-235, cross sections for, (E), 19: 21230 (CEA-R-2552)
reactions with uranium-235, fragment energy spectrum in fission, (E), 19: 21296
reactions with uranium-235, tellurium-131 and -133 isomer pair yields from fission, (E), 19: 21390
scattering by aluminum powder, distributions from inelastic, (E), 19: 20551 (IDO-17063)
scattering by nuclei, boundary diffusion effects on cross sections for, (T), 19: 21424
scattering from magnetized cobalt mirrors, spin reversal in, 19: 21300

NEVADA (NYE CO.)
geologic map of Quartet Dome Quadrangle, 19: 20151 (TEI-860)
geologic map of Thirsty Canyon SE Quadrangle, 19: 20150 (TEI-859)

NEVADA TEST SITE
balloon tracking in vicinity of, long-range, 19: 21769 (TID-21661)

NI-O-NEL
corrosion of low-carbon, by solutions produced in head-end processes

for fuel, 19: 20481 (ORNL-3787)
NICKEL
analysis for impurities by activation methods, 19: 19796
bremsstrahlung reactions (γ,n) at 10 to 28 Mev, cross sections for, (E), 19: 21305
determination by titration, suitability of tetraethylenepentamine heptaacetic acid for, 19: 19813
determination in pure molybdenum and tungsten, photometric, 19: 19799
determination in presence of manganese by activation methods, 19: 19796
determination in uranium and its compounds and alloys, methods for, 19: 19823
effects on spectrophotometric determination of zinc using 1-(2-thiazolylazo)-2-naphthol, 19: 19814
electron backscattering by (111) face, kinematic theory calculations of, 19: 20868
iridium-193 Mössbauer effect in, (E), 19: 21255(R) (UCRL-11828 (p.57-8))
magnetic fields at nuclei in, (E), 19: 20578
meson (π^-) reactions (π^-,nγ) with, energy spectra from, (E), 19: 21315
neutron elastic scattering at 85 to 700 kev, differential cross sections for, (E), 19: 21298
nucleon reactions at high energies, secondary nucleon yields from, (E/T), 19: 21242 (NP-14837)
performance of electrodes of, in thermionic converters, 19: 20906
radiation effects on content in dog tissues, 19: 19540
radiation effects on magnetic properties of defects in, neutron, 19: 20647
radiation effects on magnetism of, at 28°K, neutron, 19: 20652
separation from palladium by solvent extraction using tri-n-octylphosphine oxide, 19: 19753 (IS-T-3)
separation of magnesium from, by complex formation and solvent extraction, 19: 19833 (CEA-R-2628)
tensile properties of, testing, (E), 19: 20554 (LA-3161)
welding of pipes and plates of, Hanford procedures for, 19: 20524 (TID-20625(Vol.IV)(Rev.I))
NICKEL ALLOY COUPLES
Alumel/Chromel, thermocouple tables, smoothed, 19: 20265 (ORNL-3649(Vol.2)(Sect.2.3))
Alumel/Chromel, thermocouple tables for cryogenic, smoothed, 19: 20274 (ORNL-3649(Vol.2)(Sect.2.12))
Chromel/constantan, thermocouple tables, smoothed, 19: 20268 (ORNL-3649(Vol.2)(Sect.2.6))
constantan/Cu, thermocouple tables, smoothed, 19: 20267 (ORNL-3649(Vol.2)(Sect.2.5))
constantan/Fe, thermocouple tables, smoothed, 19: 20266 (ORNL-3649(Vol.2)(Sect.2.4))
constantan/iron, thermocouple tables for cryogenic JN/JP, smoothed, 19: 20275 (ORNL-3649(Vol.2)(Sect.2.13))
constantan/iron, thermocouple tables for cryogenic YN/YP, smoothed, 19: 20276 (ORNL-3649(Vol.2)(Sect.2.14))
Cu/constantan, thermocouple tables for cryogenic, smoothed, 19: 20273 (ORNL-3649(Vol.2)(Sect.2.11))
Invar/Ni, tensile properties of, testing, (E), 19: 20554 (LA-3161)
NICKEL ALLOYS
analysis for hafnium or zirconium using catechol violet, colorimetric, 19: 19780
Be–Ni, fracture studies, 19: 20462(R) (NRL-6258)
Cr–Fe–Ni–Sn–Zr, properties for use as fuel element cladding, 19: 20497(P)
Fe–Ni, magnetic fields at iron-57 nuclei in, (E), 19: 20578
Fe–Ni, overdriving effects on polymorphism dynamics in, 19: 20555 (LA-3215)
Ni–Nb, oxidation kinetics at 500 to 900°C, 19: 20494
NICKEL COUPLES
Invar/Ni, tensile properties of, testing, (E), 19: 20554 (La-3161)
NICKEL IONS
solvent extraction from molten nitrate by liquid silicone–TBP at 150°C, 19: 19833 (CEA-R-2628)
NICKEL ISOTOPES
neutron reactions with, resonances in, 19: 21454
NICKEL ISOTOPES Ni-60
proton capture cross sections at 10 to 20 Mev, (E/T), 19: 21442
NICKEL ISOTOPES Ni-61
magnetic fields acting on, in ferromagnetic materials, 19: 20578
NICKEL ISOTOPES Ni-62
alpha scattering at 25 to 100 Mev, angular distributions, (E/T), 19: 21269(R) (UCRL-11828(p.132-3))
NICKEL ISOTOPES Ni-63
energy levels of, from copper-63 (d,He-3) reactions, 19: 21358
NICKEL NITRATES
$Ni(NO_3)_2$–$Th(NO_3)_4$, crystal structure of octahydrates, 19: 19852
NICKEL OXIDES
analysis for impurities by activation methods, 19: 19796
radiation effects on reduction by hydrogen, 19: 19975
NICKEL STEEL
Cr–Mo–Ni–V, development, 19: 20462(R) (NRL-6258)
Cr–Ni, brittle fracture of super ELSO, 19: 20549(R) (EURAEC-1282)
NICKEL SYSTEMS
C–Ni, concentration and temperature effects on density of, 19: 20567(T) (LA-tr-65-5)
Ni–Si–Th, crystal structure of compound in, 19: 20568
NIOBIUM
analysis for hafnium or zirconium using catechol violet, colorimetric, 19: 19780
coating of, for oxidation protection at 2300°F, 19: 20483 (SCNC-318)
corrosion in reactors, 19: 20488
crystallization rate after uniaxial compression and annealing, 19: 20604
deformation at low temperatures, 19: 20605
deposition of coatings of, development of methods for, 19: 20456 (EUR-2111.d)
deposition on vanadium-base alloys for oxidation protection, 19: 20459(R) (IITRI-B6019-6)
determination in columbite–tantalite ores, x-ray fluorescence spectrometric, 19: 19754 (JEN-134-DQ/I-39)
determination in uranium and its compounds and alloys, methods for, 19: 19823
effects on strength of thorium at high temperatures, 19: 20560 (ORNL-3777)
elastic properties, 19: 20579
geochemistry and mineralogy of, in Cherry Mountains (Urals), USSR, book, 19: 20190
properties as control rods, 19: 21690(R) (LA-3244)
separation from irradiated fuels, 19: 20084(P)
separation from tantalum by ion exchange, 19: 20054
NIOBIUM ALLOYS
analysis for molybdenum, polarographic, 19: 19781
Al–Nb, oxidation kinetics at 500 to 900°C, 19: 20494
Al–Nb, preparation and properties of $NbAl_3$ for possible use as reactor material, 19: 20464 (SCNC-316)
Al–Nb–Ta–Ti, fatigue crack propagation in, study of low-cycle, 19: 20462(R) (NRL-6258)
Al–Nb–Ta–Ti, mechanical properties of, effects of processing on, 19: 20462(R) (NRL-6258)
Cr–Nb, elastic properties, 19: 20579
Cr–Nb–V, fabrication and mechanical properties of sheet of, 19: 20552(R) (IITRI-B6021-6)
Fe–Nb, elastic properties, 19: 20579
Mo–Nb, extrusion, 19: 20500 (AFML-TR-64-387)
Mo–Nb–Pt–U, corrosion resistance in water, 19: 20497(P)
Mo–Nb–Pt–U, properties for use as reactor fuel, 19: 20497(P)
Mo–Nb–Ti, coating of, for oxidation protection at 2300°F, 19: 20483 (SCNC-318)
Mo–Nb–Ti–V, coating for oxidation protection, 19: 20459(R) (IITRI-B6019-6)
Mo–Nb–V–Zr, fabrication and properties of B-66 sheet, 19: 20499(R) (AD-606291)
Mo–Nb–W, extrusion, 19: 20500 (AFML-TR-64-387)
Nb–Ta–Ti, coating of, for oxidation protection at 2300°F, 19: 20483 (SCNC-318)
Nb–Ta–Ti–V, coating for oxidation protection, 19: 20459(R) (IITRI-B6019-6)
Nb–Ta–Ti–V, fabrication and mechanical properties of sheet of, 19: 20552 (IITRI-B6021-6)
Nb–Ta–V, fabrication and mechanical properties of sheet of, 19: 20552(R) (IITRI-B6021-6)
Nb–Ta–W–Zr, fabrication and properties of FS-85 sheet, 19: 20499(R) (AD-606291)
Nb–Ti, coating of, for oxidation protection at 2300°F, 19: 20483 (SCNC-318)
Nb–Ti–V, coating for oxidation protection at 1800 to 2500°F, 19: 20459(R) (IITRI-B6019-6)
Nb–Ti–V, fabrication and mechanical properties of sheet of, 19: 20552(R) (IITRI-B6021-6)
Nb–Ti–W–V, coating for oxidation protection, 19: 20459(R) (IITRI-B6019-6)
Nb–U, phase studies, 19: 20587
Nb–V, coating for oxidation protection, 19: 20459(R) (IITRI-B6019-6)
Nb–V, fabrication and mechanical properties of sheet of, 19: 20552(R) (IITRI-B6021-6)
Nb–Zr, corrosion by boiling potassium in loop test, 19: 20476 (ORNL-3603)
Nb–Zr, extrusion, 19: 20500 (AFML-TR-64-387)
Nb–Zr, grain growth of, effects of cold working and annealing on,

19: 20473(R) (NASA-CR-54629)
Nb–Zr, mass transfer from type 316 and 321 stainless steel to, in liquid potassium, research program on, 19: 20474(R) (NASA-CR-54281)
Nb–Zr, strength properties, 19: 20474(R) (NASA-CR-54281)
Nb–Zr, superconducting properties of, effects of heating to 300°C for 10 hr on, 19: 20609(P)
Nb–Zr, ultrasonic attenuation in superconducting, in strong magnetic fields, (E), 19: 21188
Ni–Nb, oxidation kinetics at 500 to 900°C, 19: 20494
NIOBIUM BORIDES
analysis for boron by pyrohydrolysis, 19: 19761 (NP-14876)
NIOBIUM CARBIDES
superconducting properties, 19: 20572
NbC–W, phase studies at 2000 to 3000°C, (E), 19: 20583(T)
NIOBIUM CHLORIDES
reduction of, for deposition of niobium coatings, 19: 20456 (EUR-2111.d)
NIOBIUM COMPLEXES
with EDTA, migration in electrodialysis cell, 19: 20052 (ORNL-TM-1035)
NIOBIUM ISOTOPES Nb-90
electron pair production cross section near threshold, (E), 19: 21252(R) (UCRL-11828(p.35-8))
energy levels, (E/T), 19: 21258(R) (UCRL-11828(p.67-71))
NIOBIUM ISOTOPES Nb-92
energy levels of, spins and parities of low-lying, 19: 21451
NIOBIUM ISOTOPES Nb-93
neutron reactions (n,γ) with, spectra from, (E), 19: 21330
NIOBIUM ISOTOPES Nb-94
energy levels of, parity and spin of, (E), 19: 21330
NIOBIUM ISOTOPES Nb-95
beta decay, 19: 21460
content in air over Indian and Pacific Oceans in 1961–62, 19: 20158 (NP-14712)
content in air over Indian and Pacific Oceans, 1961–62, 19: 20158 (NP-14712)
determination in mixtures with zirconium-95, radiometric, 19: 19748 (DP-933)
shielding power sources of, 19: 21595 (TID-7698(Pt.I)(p.33-248))
NIOBIUM NITRIDES
superconducting properties, 19: 20572
NIOBIUM OXIDES
Nb_2O_5–TiO_2, crystal structure and equilibria of phases in system, 19: 20569
NIOBIUM SELENIDES
superconductivity in, transition temperatures for, (E), 19: 21195
NIOBIUM SYSTEMS
C–Nb–W–Zr, creep properties of D-43, 19: 20474(R) (NASA-CR-54281)
C–Nb–W–Zr, stress corrosion of D-43 by refluxing potassium, research program on, 19: 20474(R) (NASA-CR-54281)
NITRATE IONS
effects on polarographic determination of uranium, 19: 19797
NITRATES
effects on spectrophotometric determination of zinc using 1-(2-thiazolylazo)-2-naphthol, 19: 19814
radiolysis of aqueous solutions of, mechanism of gamma, 19: 19981
NITRIC ACID
oxidizing activity in sulfuric acid solutions during reactions with uranium dioxide, 19: 19912
solvent extraction from aqueous solution into TBP–Varsol, pulse column studies of, 19: 20043 (IEA-77)
solvent properties for aluminum nitrate, 19: 20042(R) (IDO-14646)
solvent properties for pellets of plutonium dioxide, uranium dioxide, and their mixtures, effects of additives on, 19: 20050 (ORNL-3695)
$Al(NO_3)_3$–HNO_3–H_2O, distribution coefficients for plutonium between anion exchange resin and, calculation, 19: 20046 (LA-3188)
HNO_3–H_2SO_4–UO_3, oxidation-reduction potentials in, 19: 19912
HNO_3–$UO_2(NO_3)_2$, chemical potentials and solution-vapor equilibrium in, at 25, 35, and 50°C, 19: 19907
NITROGEN
boiling of upwardly flowing, in heated tube at high vapor qualities, film, 19: 20113 (NP-14895)
collisions with excited cyclopropane, energy transfer in, 19: 19938
content in primary cosmic radiation, 19: 20894
determination in uranium and its compounds and alloys, methods for, 19: 19823
determination in vented gases from underground nuclear explosion, apparatus for, 19: 19776 (UCRL-12169)
effect on electron energy loss in argon–cesium plasma, (E), 19: 21560
effects in optical absorption by air at high temperatures, 19: 20832
electron reactions with, excitation functions for metastable state formation in, 19: 19992
ionization by electron impact, appearance potential for doubly charged molecule ions in, 19: 20807(R) (UCRL-11828(p.201-4))
ionization by electrons at 0.6 to 20 kev, (E/T), 19: 20850
plasma of, development of emitter electrodes for, (E), 19: 20905 (SC-RR-65-54)
radiation absorption coefficient of, photoionization contribution to, (T), 19: 20830
radiation effects on rat urinary excretion of, protective effects of casein diets against, 19: 19628
reactions with cerium–magnesium alloys at 475 to 600°C, effects of water vapor on, 19: 20485
reactions with zirconium at 1400 to 1700°C, 19: 19877
spectra of, behind shock waves, (E), 19: 20676
NITROGEN IONS
ionization in beams, determination from spectral emission lines, (E), 19: 20857
reactions with germanium at 46, 67, and 82 kev, inversion layer production in, 19: 20625
NITROGEN ISOTOPES
separation factors for, on ion exchangers, 19: 20433
NITROGEN ISOTOPES N-13
production in linear electron accelerator, concentration guides and monitoring for, 19: 20204 (RPI-328-25)
NITROGEN ISOTOPES N-14
meson (π^+) reactions at 80 Mev, cross section for, (E), 19: 21279
nitrogen-14 reactions (N-14,N-13) at 6.62 Mev, neutron reduced widths from, (E), 19: 21387
nitrogen-14 reactions (N-14,N-13) at 4.7 to 9.4 Mev, neutron tunneling mechanism in, (E), 19: 21388
reactions with chlorine-35, phosphorus-31, and sulfur-32 at 30 to 42 Mev, scandium-44 isomer pair production in, (E), 19: 21392
reactions with holmium-165, fission, (E/T), 19: 21259(R) (UCRL-11828(p.77-80))
separation from nitrogen-15 by ion exchange, effects of ion exchange material and solvent on, 19: 20433
NITROGEN ISOTOPES N-15
alpha scattering by octupole levels in, at 40.6 Mev, (E/T), 19: 21268(R) (UCRL-11828(p.129-31))
nuclear magnetic dipole moment, (T), 19: 21322
separation from nitrogen-14 by ion exchange, effects of ion exchange material and solvent on, 19: 20433
NITROGEN MUSTARDS
effects on erythrocyte content in rat blood, 19: 19489
toxic effects on *E. coli*, recovery from lethal, 19: 19485
NITROGEN OXIDES
effects in optical absorption by air at high temperatures, 19: 20832
effects on pulse radiolysis of ferrocyanide solutions, 19: 20009
effects on radioinduced carbon dioxide-graphite reactions, (E), 19: 19953 (AERE-R-4201)
ionization by electron impact, appearance potential for doubly charged molecule ions in, 19: 20807(R) (UCRL-11828(p.201-4))
quenching effects of nitric oxide on radiofluorescence of tryptophan and tyrosine, 19: 19970(T)
radiolysis of nitrous oxide, effects of cell diameter on nitrogen yield in gamma, 19: 20329 (USNRDL-TR-806)
NITROGEN SYSTEMS
Ar–N, scintillation from alpha-excited, pulse-height spectra of, 19: 20313(R) (ANL-6938(p.9-20))
DH–N, electron reactions with, cross sections for secondary ion formation in, 19: 19995
He–N, compressibility at high pressures at 25°C, 19: 19840 (LA-3250)
N–O, plasma of, development of emitter electrodes for, (E), 19: 20905 (SC-RR-65-54)
NITROUS ACID
effects on mutagenesis in isolated DNA from *B. subtilis*, 19: 19542
19-NORANDROSTENOLONE
effects on acute radiation disease in rats, 19: 19624
NORWAY
dose in houses in, 19: 20218
NOZZLES
development of refractory, for high-temperature thermometry in gases, 19: 20277 (ORNL-P-1068)
flow of dissociated and ionized hydrogen in, equilibrium in, 19: 20124
isotope separation in gases in supersonic jet, calculations of, 19: 20434
NPD REACTOR
cooling system of, operating experience with, 19: 21698
NUCLEAR BATTERIES
performance for thermionic, thermoelectric, and thermophotovoltaic energy conversion, (E/T), 19: 20904 (BLG-317)
use of radioisotopes in, economics of, 19: 20415
NUCLEAR CHEMISTRY

bibliography on, French publications, 1956 to 1961, 19: 19738(T)
book: *Nuclear Techniques in Analytical Chemistry*, 19: 19822
NUCLEAR ELECTRIC MOMENTS
analysis of quadrupole, using computers, (T), 19: 21246 (TID-21697)
NUCLEAR EMULSIONS
cosmic particle interactions in, at 300 km, (E), 19: 20893
meson (K^-) reactions with, hyperfragment production in, (E), 19: 21365
meson (K^-) reactions at 0.8 to 3.0 Bev/c, lithium-8 emission in, (E), 19: 21389
sensitivity of, effects of polyethylene glycols on, 19: 20014
use for measuring anisotropic fast neutron spectra, 19: 20374
NUCLEAR ENGINEERING
book: *Radioisotopic Methods for Investigation of Processes Inside Boilers*, in Russian, 19: 20418
development in Soviet Union, 19: 21762 (RM-2163(RAND))
shell structure stability in, to nonlinear stress and deformation, 19: 21620
thermodynamic properties of nuclear materials, tables of, 19: 19983
NUCLEAR MAGNETIC MOMENTS
alignment of, in nuclear gyroscopes, (T), 19: 20279 (RTD-TDR-63-4001)
analysis using computers, (T), 19: 21246 (TID-21697)
NUCLEAR MAGNETIC RESONANCE
book: *Interpretation of NMR Spectra*, 19: 21462
internuclear coupling constants in, effects of temperature and solvents on, 19: 19888
use in studies of radiation damage in solids, 19: 20620(R) (NYO-2024-8)
NUCLEAR MATERIALS MANAGEMENT
fuel burnup determination in reactors, methods for accurate, (E), 19: 21667(R) (GEAP-4776)
NUCLEAR MODELS
book: *Contemporary Models of the Atomic Nucleus*, 19: 21463
for lithium-6, testing of, (T), 19: 21368
NUCLEAR MODELS (COLLECTIVE)
book: *Contemporary Models of the Atomic Nucleus*, 19: 21463
excitation of collective states by heavy-particle inelastic scattering, (T), 19: 21234 (JINR-P-1908)
NUCLEAR MODELS (OPTICAL)
book: *Contemporary Models of the Atomic Nucleus*, 19: 21463
single-particle radiation transitions in, 19: 21442
NUCLEAR MODELS (SHELL)
book: *Contemporary Models of the Atomic Nucleus*, 19: 21463
book: *Group Theoretical Methods in Shell Models of the Nucleus*, 19: 21444
Pauli exclusion principle in, development and application of, 19: 21275
NUCLEAR PHYSICS
book: *Tables of Coulomb Wave Functions (Whittaker Functions)*, 19: 21117(T)
development in Soviet Union, 19: 21762 (RM-2163(RAND))
instrumentation for, description of standardized, (E), 19: 20262 (KFK-259)
research program of Nuclear Chemistry Division of Lawrence Radiation Laboratory, 19: 19735(R) (UCRL-11828)
NUCLEAR POWER
safety in space, outline of standards and evaluation of, 19: 20206 (TID-7698(Pt.I)(p.31-2))
use for desalination of sea water, economics of, 19: 21707 (ORNL-TM-432)
use for sea water desalination, evaluation, 19: 21708 (ORNL-TM-465)
NUCLEAR POWER PLANTS
control equipment for, design of automatic safety, 19: 20103
development in Soviet Union, 19: 21762 (RM-2163(RAND))
development of Canadian, 19: 21781
economic integration into electric systems, 19: 21695
NUCLEAR QUADRUPOLE RESONANCE
detection and measurement of, pulse method for, 19: 21430
NUCLEAR REACTIONS
amplitudes for production processes in, (T), 19: 20925 (ICTP-64/3)
calculations of intranuclear-cascades in, (T), 19: 21239 (LA-3206)
data recording for multiparameter, magnetic tape, 19: 20255 (EUR-2119.e)
fine structure of photo, NMR method for, 19: 21282
neutron emission in compound-nucleus, (T), 19: 21245 (ORNL-TM-196)
nucleon pair transfer between light nuclide and nucleus, correlations in, (E/T), 19: 21266(R) (UCRL-11828(p.108-9))
properties of, involving incident and outgoing particles having A = 1 to 3, (E/T), 19: 21238 (LA-3205)
NUCLEAR SHOWERS
calculations of intranuclear, (T), 19: 21239 (LA-3206)
NUCLEAR SPIN
interactions with electron spin, energy of, (T), 19: 20695
NUCLEAR STRUCTURE
eigenstates of pairing-force hamiltonian for deformed nuclei, (T), 19: 21347
theory of, inelastic electron scattering in, 19: 21448
NUCLEAR THEORY
beta spectra and partially-conserved axial-vector current, 19: 21340
compound nuclear states in, 19: 21283
eigenstates of pairing-force hamiltonian for deformed nuclei, (T), 19: 21347
energy gap at Fermi surface of nuclear matter, 19: 21273
excitation operators and intrinsic hamiltonians in, 19: 21289
Hartree-Fock approximation in, stability of, 19: 21440
NUCLEI
alpha decay of, barrier penetrabilities in, (T), 19: 21411
alpha scattering by, study of phase rule in angular distributions, (E/T), 19: 21269(R) (UCRL-11828(p.132-3))
charged-particle scattering by, amplitudes and cross sections for small-angle, (T), 19: 21233 (JINR-E-1992)
charged-particle scattering by Coulomb fields of, amplitudes for, (T), 19: 21425
decay of $T = -\frac{3}{2}$, log ft values for, (T), 19: 21379
electron inelastic scattering by, analysis of cross section for, 19: 21452
electron scattering by, theory of, 19: 21448
electron shell electrostatic potential at, in diatomic molecules, (T), 19: 20836(T)
energy gap at Fermi surface of, 19: 21273
energy level deformation vibrations in even-even, effects on E2 branching ratios in, (T), 19: 21384
energy level density in, odd-even effect of pairing correlation in, (T), 19: 21364
energy level energies in Bopp approximation, (T), 19: 21412
energy levels of closed-shell, collective, (T), 19: 21415
energy levels of deformed, cranking model and perturbation calculation for rotational, (T), 19: 21349
energy levels of deformed odd-odd, doublet $K^{\pm}$, (T), 19: 21370
energy levels of, isospin structure of low lying collective octupole vibrations in, (T), 19: 21351
energy levels of, lifetime measurements on short-lived, 19: 21369
energy levels of, pairing hamiltonian for seniority-zero excited, (T), 19: 21385
excitation by low-energy electrons, test of Robl theory of, 19: 21455
fission of heavy, review of chemical studies of low-energy, 19: 20033
fission of, energy release in low-energy, (E/T), 19: 21224 (AECL-2160)
gamma emission by, mass-change effect on Mössbauer spectrum after, (T), 19: 21422
gamma resonance absorption at high pressures, methods for analyzing, (E), 19: 21231 (COO-1198-255)
gyromagnetic ratios and magnetic dipole transitions of deformed even-even, (T), 19: 21410
ion inelastic scattering by, excitation of collective states in, (T), 19: 21353
magnetic and quadrupole resonances in, computer analysis of, (T), 19: 21246 (TID-21697)
magnetic dipole moments of conjugate, (T), 19: 21322
meson (K^-) reactions with emulsion, hyperfragment production in, (E), 19: 21365
meson (K^-) reactions at 0.8 to 3.0 Bev/c, lithium-8 emission in, (E), 19: 21389
meson (μ) capture by, gamma-neutrino correlation in first-forbidden, (T), 19: 21378
neutron capture by, effects of resonance interference in, (T), 19: 21335
neutron cross sections of, availability for reactor calculations, (E), 19: 21225 (AECL-2168)
neutron emission by compound, computer analysis of, (T), 19: 21245 (ORNL-TM-196)
neutron reactions with, cross sections for, (T), 19: 21228 (ANL-6970)
neutron reactions with, chain element activity in intermittent, (T), 19: 21226 (AEET/HP/Th-19)
neutron S-wave strength functions of spherical, (T), 19: 21327
neutron scattering by, boundary diffusion effects on cross sections for slow, (T), 19: 21424
neutron-proton interactions in, isobaric states in, (T), 19: 21304
nucleon pair transfer between light nuclide and, correlations in, (E/T), 19: 21266(R) (UCRL-11828(p.108-9))
nucleon pairing correlations in, (T), 19: 21381
nucleon reactions with, nucleon-alpha cascades from, (T), 19: 21372
nucleon scattering by, parameters for, (T), 19: 20937(T) (TID-21672)
nucleon-nucleon interaction in, charge dependence of, (T), 19: 21373
particle inelastic scattering by, collective-state excitation in, (T), 19: 21234 (JINR-P-1908)
particle reactions at variable beam intensities, radiation from, (T), 19: 21235 (JINR-P-1950)

photon absorption by neutron-proton pairs in, (T), 19: 21274
photon scattering by Coulomb field of, gauge invariant calculation of, 19: 21119
polarization in organic solvents, Overhauser effect in, 19: 20869
proton decay, (E), 19: 21271(T) (KFK-tr-161)
radiation from, intensity variations produced by variable-intensity particle bombardment, (T), 19: 21235 (JINR-P-1950)
reactions of, nucleon transfer in, (T), 19: 20937(R) (TID-21672)
spin interactions with electrons, energy of, (T), 19: 20695
spin scattering of, bibliography on, 19: 20828
stability of, relation of magic numbers to, 19: 21275
structure and symplectic symmetry of, in region $40 \leq A \leq 56$, 19: 21437
theory of compound, review on, 19: 21283
transitions in deformed, particle parameters of E2, (E), 19: 21399
transitions in even-even, E2/E1 mixing ratios of $2^+ \rightarrow 2^+$, 19: 21419

NUCLEI (CELLS)
radiation effects on secretory activity of, in brain hypothalamic area of rabbits, 19: 19509(T) (JPRS-29250(p.9-13))
radiation effects on mitosis suppression in *Tradescantia paludosa*, 19: 19579

NUCLEIC ACIDS
content in *Pseudomonas aeruginosa*, 19: 19503(R) (NP-14933)
metabolism of, tracer studies using tritium, 19: 19515
structure of, use of electron microscopy in studies of, 19: 19455 (CONF-640204(p.44-62))

NUCLEON SHOWERS
alpha emission in, by direct interaction, (T), 19: 21372
calculations of intranuclear, (T), 19: 21239 (LA-3206)

NUCLEONS
book: *Fundamental Particles*, 19: 21072
energies of many-body systems of, in Bopp approximation, 19: 21412
interactions at high energies, Regge trajectories for, (T), 19: 21063
interactions in three-body systems of, with separable potentials, (T), 19: 20986
interactions with mesons (π) and nucleons, parameters for, (T), 19: 20937(R) (TID-21672)
interactions with nucleons, computer calculation of matrix elements of, (T), 19: 20938(R) (UCRL-11828(p.9-10))
interactions with mesons (π) and nucleons, coupling constants for, (T), 19: 20917 (IC/65/3)
interactions with elementary particles, production amplitudes in, (T), 19: 20925 (ICTP-64/3)
interactions with neutrinos, neutral weak currents in, (T), 19: 20988
interactions with mesons (π), production of massive neutral gauge particle in, (T), 19: 20989
interactions with mesons (π), position and width of N* (1688) in, (T), 19: 20992
interactions with mesons (π), N^*_{33} resonance in, (T), 19: 21000
interactions with antinucleons, mesons (π), and nucleons, phase of forward amplitudes for, (T), 19: 21010
interactions with antinucleons, mesons (π), and nucleons, selection rules for final states in, (T), 19: 21023
interactions with mesons (μ^-) at 5 Bev/c, meson (π) production in, (E), 19: 21037
interactions with antinucleons at rest, SU(12) symmetry model predictions for annihilation, (T), 19: 21039
interactions with nucleons, Treiman-Yang criterion for, (T), 19: 21046
interactions with mesons (π), complex angular momentum in, (T), 19: 21048
interactions with mesons (π), Jacob-Wick method for scattering amplitude in, (T), 19: 21052
interactions with nucleons, Jacob-Wick method for scattering amplitude in, (T), 19: 21052
interactions with antinucleons, Jacob-Wick method for scattering amplitude in, (T), 19: 21052
interactions with mesons (π^-) at 6.8 Bev/c, angular and momentum distributions in, (E), 19: 21062
interactions with mesons (K) and (π) at high energies, Regge trajectories for, (T), 19: 21063
interactions with mesons (π), kinematic analysis of, 19: 21076
interactions with mesons (π), Regge trajectories in, 19: 21077
interactions with nucleons, charge dependence of, (T), 19: 21373
interactions with mesons (π), solution of integral equation for, 19: 20445
pair transfer between nucleus and light nuclide, correlations in, (E/T), 19: 21266(R) (UCRL-11828(p.108-9))
scattering by nuclei, parameters for, (T), 19: 20937(R) (TID-21672)
transfer in heavy ion collisions, parameters for, (T), 19: 20937(R) (TID-21672)

NUCLEOPROTEINS
deoxy-, radiation effects on *E. coli*, 19: 19576

NUCLEOTIDES
dephosphorylation by thorium and zirconium ions, 19: 19876

O

OATS
strontium-90 metabolism in, effects of soil treatment on, 19: 19475(T) (JPRS-27940(p.10-17))

OCEANOGRAPHY
book: *Oceanography and Marine Biology*. Vol. 2, 19: 19467

OILS
mass transport in vacuum pumps, 19: 20140(R) (ORNL-3760(p.94-7))

OLIVINES
fission product tracks in, formation and stability of, (E), 19: 20674

OPTICAL MATERIALS
radiation effects on, mechanisms in, 19: 20019

OPTICAL SYSTEMS
for measurement of dichroism spectra, 19: 21773 (UCRL-11308)

ORES
analysis for rare earths and thorium, colorimetric, 19: 19778(T) (JPRS-29037(p.58-68))

ORGANIC COMPOUNDS
analysis for impurities, spectrographic method using gallium oxide, 19: 19774 (UCRL-7962)
formation on earth during chemical evolution period, evidence for, 19: 19946 (UCRL-11950)
labeling with radioisotopes, rules for formulas and nomenclature following, 19: 19736
labeling with radioisotopes, rules for formulas and nomenclature following, 19: 19737
radioluminescence properties of liquid, (E), 19: 19962

ORGANIC COOLED REACTORS
construction and design of Soviet ARBUS, 19: 21702
development for large-scale desalting, 19: 21709

ORGANISMS
radioisotope uptake by marine, research program on, 19: 19469

ORGANS
radiation, drug and hormone effects on graft tolerance for, 19: 19588

OROTIDINE-5'-PHOSPHATE
preparation of carbon-14-labeled, method for, 19: 20024

OSCILLOGRAPHS
use in plasma diagnostics, 19: 21483(R) (ORNL-3760(p.30-56))

OSMIUM ISOTOPES Os-186
energy level transitions in, E2 conversion coefficients of rotational, (T), 19: 21308
energy levels of, half life of 137-kev excited, 19: 21291
fission barrier of compound nucleus, (E/T), 19: 21259(R) (UCRL-11828(p.77-80))

OSMIUM ISOTOPES Os-188
energy level transitions in, E2 conversion coefficients of rotational, (T), 19: 21308

OSMIUM OXIDES
structure of tetroxide, 19: 19846(R) (UCRL-11828(p.158-9))

OXALATES
effects on spectrophotometric determination of zinc using 1-(2-thiazolylazo)-2-naphthol, 19: 19814

OXETANES
radioinduced polymerization of binary mixtures of substituted, 19: 19972
3-chloromethyl-3-ethyl-, radioinduced polymerization with 3,3-bis-(chloromethyl)oxetane, diketene, 3-fluoromethyl-3-ethyloxetane, and trioxane, 19: 19972

OXONIUM IONS
bond energies and wave functions of, calculation by united atom method, 19: 19844 (PAN-550/XVII)

OXYGEN
determination in potassium, neutron-activation, (E), 19: 19751 (GA-5982)
determination in potassium, round-robin meeting on, 19: 19760 (NASA-TM-X-1085)
determination in uranium and its compounds and alloys, methods for, 19: 19823
determination in vented gases from underground nuclear explosion, apparatus for, 19: 19776 (UCRL-12169)
effects on carbon-11 recoil reactions with hydrocarbons, 19: 20018
effects on heat of sublimation of uranium, 19: 19889
effects on radiolysis of glycogen, 19: 20015
effects on radiosensitivity of cells, 19: 19614
effects on thermoluminescence of x-irradiated polymers and proteins, 19: 19983
effects on vapor pressure of uranium, 19: 19890
electric discharge in, ionizing radiation of, 19: 20712
ionization by electron impact, appearance potential for doubly charged molecule ions in, 19: 20807(R) (UCRL-11828(p.201-4))

ionization by electrons at 0.6 to 20 kev, (E/T), 19: 20850
isotopic exchange with aluminum oxide, 19: 19872
meson (π^-) reactions (π^-,ny) with, energy spectra from, (E), 19: 21315
proton reactions at 160 Mev, 0.6 to 11-Mev gamma rays from, (E), 19: 21243 (ORNL-3506)
quenching effects on radiofluorescence of tryptophan and tyrosine, 19: 19970(T)
radiation absorption coefficient of, photoionization contribution to, (T), 19: 20830
radiation effects on attachment in rabbit hemoglobin, equation for calculating, 19: 19529(T)
radiation effects on requirements of, by rats, 19: 19539
radiation effects on assimilation of, in adrenal cortex, 19: 19584
reactions in blood, equation for reversible attachment and transition process in, 19: 19529(T)
reactions with aluminum–chromium–iron–yttrium alloy, mechanism, 19: 20470 (GE-TM-63-7-3)
solubility and thermodynamics in liquid tin at 536, 600, 700, and 751°C, 19: 19918
spectra of, behind shock waves, (E), 19: 20676
x-radiation scattering by, Hartree-Fock calculations of incoherent, 19: 20824
DH–O, electron reactions with, cross sections for secondary ion formation in, 19: 19995

OXYGEN IONS
effects of size of, on partition coefficients of elements in basic rocks, 19: 20152
sputtering on copper, copper oxide production in, 19: 20827

OXYGEN ISOTOPES O-14
beta decay of, CVC theory and ft values for, (T), 19: 21416

OXYGEN ISOTOPES O-15
beta decay of, mesonic exchange effect in, 19: 21348
production in linear electron accelerator, concentration guides and monitoring for, 19: 20204 (RPI-328-25)

OXYGEN ISOTOPES O-16
alpha reactions (α,α') at 22.5 Mev, alpha-gamma angular correlations in, 19: 21457
alpha scattering by octupole levels in, at 40.6 Mev, (E/T), 19: 21268(R) (UCRL-11828(p.129-31))
deuteron reactions (d,p) with, target core excitation in, (T), 19: 21433
energy levels of, reduced width of, (T), 19: 21432
energy levels of, collective admixtures in odd-parity, (T), 19: 21361
energy levels of, nucleon separation energy in 1p and 1s, 19: 21400
meson (π^+) reactions at 80 Mev, cross section for, (E), 19: 21279
neutron scattering at 14 Mev by, cross sections for, (E/T), 19: 21441
proton reactions at 155 and 600 Mev, lithium-6 and -7 production in, (E), 19: 21352
reactions (O-16,α) with carbon-12 at 15.0 to 22.5 Mev, angular distributions from, (E), 19: 21313
reactions (O-16,xn) with ytterbium isotopes, (E), 19: 21248(R) (UCRL-11828(p.21-5))
reactions with gold-197, charged-particle production in, (T), 19: 21354
reactions with tungsten-182, analysis of excitation function for fission, (E/T), 19: 21264(R) (UCRL-11828(p.92-4))

OXYGEN ISOTOPES O-18
energy levels in, deformed, (T), 19: 21360
exchange between aluminum oxide and molecular oxygen, 19: 19872
isotope effects on infrared spectra of carbon dioxide, 19: 19936

OXYGEN SYSTEMS
Be–Mn–O, phase studies of, 19: 20573
H–O, calculation of bond energies and wave functions by united atom method for ions in, 19: 19844 (PAN-550/XVII)
Mg–Mn–O, phase studies of, 19: 20573
N–O, plasma of, development of emitter electrodes for, (E), 19: 20905 (SC-RR-65-54)

OZONE
effects on dissolution of plutonium dioxide pellets in nitric acid, 19: 20050 (ORNL-3695)

P

PACIFIC OCEAN
radioactivity of air in, 1961–62, 19: 20158 (NP-14712)
strontium-90 content in surface waters of, 1961, 19: 20159 (NP-14726)

PACKAGING
of instruments into modular units, 19: 20287(R) (UCRL-11828(p.230-2))
radiation effects on plastic film, 19: 20421
standards of, for shipment of radioactive materials on toll facilities, 19: 20239

PACKED COLUMNS
efficiency of Stedman stainless steel gauge packing for, effects of surface treatment on, 19: 20068

PAINTS
luminous containing tritium, safety of, 19: 20161 (NP-14869)
radiation effects on, mechanisms in, 19: 20019

PAIR PRODUCTION
cross sections near threshold for photo-, (E), 19: 21252(R) (UCRL-11828(p.35-8))
electron, in gamma reactions with sodium iodide crystals, (E), 19: 21294

PALLADIUM
determination using 5,5′ thiodisalicylic acid, spectrophotometric, 19: 19812
separation by reversed-phase chromatography and solvent extraction using tri-n-octylphosphine sulfide, 19: 19753 (IS-T-3)
separation from nickel by solvent extraction using tri-n-octylphosphine sulfide, 19: 19753 (IS-T-3)
separation from power reactor fuels, economics of, 19: 20036 (BNWL-25)

PALLADIUM ALLOYS
Gd–Pd, gadolinium ion ESR in, g-factors from, (E), 19: 20698

PALLADIUM ISOTOPES Pd-101
decay of, gamma spectra from, (E), 19: 21280

PALLADIUM TELLURIDES
electric, magnetic, and phase properties of, (E), 19: 20577

PANCREAS
cesium-137 and strontium-90 content in bulls from fallout, 19: 20215
radiodiagnosis of tumors of, by scanning using selenium-75-labeled selenomethionine, 19: 19722
radiodiagnosis of tumors of, by photoscanning using selenium-75-labeled selenomethionine, 19: 19723

PAPER
radiation effects on strength of chromatography, 19: 20630

PARAFFIN
positron lifetime in, (E), 19: 21044

PARAMAGNETIC MATERIALS
properties of, apparatus for measuring, 19: 21759(R) (NYO-3402-1)

PARAMECIUM
kappa mutations in, 19: 19464

PARTICLE STATISTICS
correlation potentials of rectilinear systems, (T), 19: 20687
Fokker-Planck equation in, steady-state solutions to, 19: 20963
formalism for binary cascade processes, limit distribution in, 19: 20958
formalism for free boson fields, (T), 19: 21102
quantum, para-Bose and para-Fermi fields in, 19: 20960

PARTICLE TRACKS
analysis of bubble-chamber, computer program for, (T), 19: 20320 (IS-989)
construction of, Monte Carlo method for generation of grain coordinates for artificial, 19: 20325 (UCRL-11624)
determination in spark chambers, filmless digitization system for, 19: 20354
determination in spark chambers using x-ray film, 19: 20368

PARTICLE TRAJECTORIES
detection by, of macroscopic, tracking station near orbit, (E), 19: 21767 (SC-TM-65-44)

PARTICLES
distribution in repulsive Coulomb field in rarefied gases, effect of incoming stream on, (T), 19: 20673(T)
electromagnetic wave absorption and scattering by solid, (T), 19: 20677
interactions of many, Hoffman theorem in general relativity for, 19: 20707
interactions of many, in general relativity, (T), 19: 20708
light scattering by transparent Mie, asymmetry in, (T), 19: 20822
reactions with nuclei, radiations from, (T), 19: 21235 (JINR-P-1950)
scattering by nuclei, collective-state excitations in inelastic, (T), 19: 21234 (JINR-P-1908)
size distribution in suspension, diffusion technique for determining, 19: 19901
transport of inhaled insoluble, from lung to lymph nodes, 19: 19456 (LF-21)

PEAS
radiation effects on, chronic gamma, 19: 19586

PEGMATITES
age estimation of, by lead isotope method, 19: 20176

PENICILLIN
radiation effects on production by *Penicillium nigricans*, ultraviolet and x, 19: 19556

2,4-PENTANEDIONE
reactions with polonium hydroxy ions, 19: 19905
solvent properties for beryllium hydroxide purification, 19: 20070

2,4-PENTANEDIONE COMPLEXES
thulium benzoyl-, spectra of, crystal-field splitting in absorption and emission, 19: 19886

2-PENTANONE, 4-METHYL-
solvent properties for cesium, francium, and thallium, 19: 20058
4-methyl-2-pentanone–thenoyltrifluoroacetone, use in preparation of pure potassium chloride, 19: 19843 (ORNL-TM-1071)
PENTOSES
radiation effects on metabolism of, 19: 19538
PEPTIDES
radiolysis of frozen aqueous solutions of, 19: 20012
PERBORATES
paramagnetic centers in, electron spin resonance studies of, 19: 20620(R) (NYO-2024-8)
PERCHLORIC ACID
analytical uses in determination of beryllium, 19: 19803
PERIODATES
effects on spectrophotometric determination of zinc using 1-(2-thiazolylazo)-2-naphthol, 19: 19814
PEROXIDES
radiation effects on decay of, in rat spleen DNA, 19: 19541
PERSONNEL
decontamination of radioactive materials from skin of, recommendations for physician in, 19: 19494
effects of work in betatron and cyclotron labs on blood picture of, 19: 20237
radiation dosimetry of, performance of film badges and pocket chambers for, 19: 20338
radiation effects on blood picture of hospital, 19: 19525
radiation exposure of medical and industrial, trends for 6 occupational classifications, 19: 20241
radiation exposure to, maximum permissible doses for external and internal, 19: 20221
radiation monitoring of medical and x-ray, in radiology work, 19: 20232
radiation monitoring by film badges, review on, 19: 20242
radiation monitoring of, use of film dosimeters, 19: 20243
radiation protection of dental, regulation for, 19: 19655
radiation protection of, organization for, 19: 20222
radiation protection of nuclear industry, 19: 20214
toxic hazards to from use of barium chloride in fire extinguishant, 19: 20210
urinary excretion of uranium by, relation of particle size dispersion in air to, 19: 19478
PERTECHNETATE IONS
effects on corrosion of iron alloys, 19: 19820
PERTURBATION THEORY
for electron-nuclear spin interaction, 19: 20695
scattering in, high-energy behavior of five-point function for ladder diagrams in, 19: 21096
PETROLEUM
production of, uses of light from nuclear reactors in underground processes for, 19: 21710
prospecting for and refining of, uses of radioisotopes in, 19: 20417
PHANTOMS
of head, for use in radiation dosimetry, 19: 19676
PHENOL, DINITRO-
effects on fast neutron and gamma radiosensitivity of sprouting maize seed, 19: 19582
PHONONS
frequency distribution function in vanadium, 19: 20553 (KFK-262)
interactions with longitudinal plasma waves, (T), 19: 21494
interactions with electrons in beta tin, (E), 19: 21603
interactions with electrons in doped crystals, (T), 19: 20671
production in interactions of bosons and matter, (T), 19: 20816
PHOSPHATASE ACTIVITY
radiation and toxic chemical effects on alkaline in human granulocytes, 19: 19570
radiation effects on, in guinea pig skeletal muscle, 19: 19574
PHOSPHATE GLASS
beta and gamma dosimetry using, 19: 20314(R) (ANL-6938(p.62-70))
radiation effects on alumina-containing, 19: 20042(R) (IDO-14646)
radioinduced centers in, electron spin resonance study of gamma, 19: 20620(R) (NYO-2024-8)
PHOSPHATE ROCKS
analysis for phosphorus by neutron activation methods, 19: 19828
PHOSPHATES
analysis of soluble, for phosphorus, by neutron activation methods, 19: 19828
preparation of phosphorus-32-labeled ortho-, 19: 20021 (NP-14900)
PHOSPHATIDES
radioinduced toxins in, of rabbit liver, 19: 19599
PHOSPHINE SULFIDE, TRIOCTYL-
solvent properties for metals, 19: 19753 (IS-T-3)
PHOSPHINIC ACID, BUTYL-, BUTYL ESTER
solvent properties for neptunium, plutonium, and uranium in aqueous nitrate solutions, role of complex formation in, 19: 20077
PHOSPHINIC ACID, DIBUTYL, BUTYL ESTER
solvent properties for neptunium, plutonium, and uranium in aqueous nitrate solutions, role of complex formation in, 19: 20077
PHOSPHORIC ACID, ALKYL ESTERS
solvent properties for americium, cerium, neptunium, plutonium, and uranium, 19: 20075
solvent properties for americium, 19: 20076
solvent properties for light lanthanides, 19: 20078
solvent properties for scandium, 19: 20082
PHOSPHORS
color quenching in liquid, 19: 20324 (ORNL-P-1094)
luminescence of iron-57 in zinc sulfide, 19: 19855
performance of liquid, for measurement of cosmic-ray fast neutron background, 19: 20872(R) (ANL-6938(p.71-88))
radioluminescence of organic liquid and plastic, (E), 19: 19962
PHOSPHORUS
determination by neutron activation methods, effects of aluminum and silicon on, 19: 19828
determination in presence of chlorine and sulfur by activation methods, 19: 19798
determination in selenium by activation methods, 19: 19798
determination in thorium phosphides, gravimetric, 19: 19740 (ANL-7005)
determination in uranium and its compounds and alloys, methods for, 19: 19823
PHOSPHORUS COMPOUNDS
organic, use for metal extraction, review, 19: 20053 (UJV-1202/64)
PHOSPHORUS ISOTOPES P-31
energy levels, (E), 19: 21376
nitrogen-14 reactions at 30 to 42 Mev, scandium-44 isomer pair production in, (E), 19: 21392
performance in nuclear gyroscopes, (T), 19: 20279 (RTD-TDR-63-4001)
proton reactions (p,γ) with, sulfur-32 energy levels from, (E), 19: 21380
PHOSPHORUS ISOTOPES P-32
effects on digestive tract in rats, 19: 19565
effects on mutation development in cotton plants, 19: 19580
preparation of carrier-free, as orthophosphate, 19: 20021 (NP-14900)
production in Spain, 19: 20432(T) (ORNL-tr-295)
storage in underground tanks in liquid solutions, activity in seepage from, 19: 21752
use in therapy by intra-arterial injection, method for, 19: 19661
PHOTOELECTRIC CELLS
for measurement of dichroism spectra, 19: 21773 (UCRL-11308)
performance of radioisotope-heated thermophotovoltaic, (E/T), 19: 20904 (BLG-317)
PHOTOELECTRIC EFFECT
emission in low-pressure helium discharges, (E), 19: 20861
PHOTOGRAPHIC FILM
radiation effects from fallout on x-ray, in lead-lined chest, 19: 20632
sensitivity of, 19: 20229
use for direct recording of particle tracks in spark chambers, 19: 20368
PHOTOGRAPHIC FILM DETECTORS
analysis of data from, for 6 occupational classifications, 19: 20241
automatic handling procedures for, 19: 20243
development of, for use as neutron dosimeter, 19: 20161 (NP-14869)
performance as personnel dosimeters, 19: 20243
performance for personnel monitoring, testing of, 19: 20338
use in personnel monitoring, review on, 19: 20242
PHOTOGRAPHY
use in determining dose distributions in radiotherapy, 19: 19693
PHOTOMETERS
systematic errors in nebular isophote tracing, estimation of, 19: 20439(R) (COO-614-31)
PHOTOMULTIPLIER TUBES
dynode materials for, properties of Allen-type, 19: 20388
power supplies for, design of transistorized, 19: 20357
uses for measurement of radioluminescence of organic phosphors, (E), 19: 19962
PHOTON SHOWERS
statistical properties of cosmic, (T), 19: 20874 (P-1020(RAND))
PHOTONS
absorption by neutron-proton pairs in heavy nuclei, (T), 19: 21274
detection and measurement of, sensitivity of nuclear emulsions for, 19: 20014
interactions of, solution to relativistic dispersion relations for, 19: 21461
interactions with deuterons, parameters for disintegration in, (T), 19: 20937(R) (TID-21672)
interactions with elementary particles, production amplitudes in, (T), 19: 20925 (ICTP-64/3)

interactions with protons at 228 to 325 Mev, cross sections, (E), 19: 20932 (LNF-64/60)
interactions with protons, intermediate vector boson production in, (T), 19: 21003
interactions with photons, gauge invariant calculation of, 19: 21119
interactions with matter, (E/T), 19: 20667
ionization of hydrogen atoms and ions by, (T), 19: 20834
ionizing effects on molecules, apparatus for measuring, 19: 19955(R) (ANL-6938(p.21-2))
mass of, gauge invariance for zero, 19: 20934 (NP-14829)
reactions (γ,n) with nuclei, giant-resonance width and energy-level filling in, (E), 19: 21287
reactions with carbon, deuterium, and lithium, polarization of protons from, 19: 21456
reactions with matter, multiple-boson production in, (T), 19: 20816
reactions with monovalent carbon ions, bound-free electron correlation in, (T), 19: 20851
reactions with nuclei, NMR method for fine structure of, 19: 21282
scattering by Coulomb fields, gauge invariant calculation of, 19: 21119

PHOTOPROTONS
polarization of, from carbon, deuterium, and lithium, 19: 21456

PHYSICAL CHEMISTRY
Overhauser dynamic nuclear polarization in, 19: 20869

PHYSIOLOGY
of muscles, radiation effects on, 19: 19551
use of labeled antibodies in electron microscopic studies, 19: 19465

PINCH DEVICES
magnetic field diffusion in theta, magnetic probe effects on, (E/T), 19: 21524
plasma stability in EppE hard-core, (E), 19: 21469 (CEA-R-2713)
plasma stability in theta, with antiparallel magnetic field, (E), 19: 21525
plasma stability in toroidal theta, (E), 19: 21530

PINCH EFFECT
electron density gradients in, interferometer design for analyses of, (E), 19: 21472 (IPP-1/25)
electron density variation in afterglow of z, in hydrogen, (E), 19: 21510
kinetics of theta, effects of neutral gas on, (T), 19: 21470 (IPP-1/14)
plasma instability in Z, twin-channel, (E), 19: 21467 (ARL-63-203)
plasma precursor ionization in, (E/T), 19: 21471 (IPP-1/24)
shock waves in, heating effects of, (E), 19: 21473 (IPP-1/28)

PIPES
closure system for, design of explosively driven, 19: 20100 (UCRL-12203)
flow in, computer program for gas and liquid, 19: 20115 (ORNL-TM-1093)
heat transfer when heat flux varies sinusoidally in, 19: 20118
performance in radioactive waste deposition at depth of 900 ft in shale beds, 19: 21753
welding of carbon steel, Hanford procedures for, 19: 20521 (TID-20625 (Vol.I(Rev.I))
welding of carbon steel and stainless steel, Hanford procedures for, 19: 20522 (TID-20625(Vol.II)(Rev.I))
welding of steel, Hanford procedures for, 19: 20523 (TID-20625(Vol.III) (Rev.I))
welding of, Hanford procedures for, 19: 20524 (TID-20625(Vol.IV)(Rev.I))

PIQUA POWER REACTOR
fuel cladding temperatures in, computer analysis of, (E), 19: 21691 (NAA-SR-Memo-9492)

PITUITARY GLAND
destruction by yttrium-90, therapeutic effects of, 19: 19664
destruction of, use of yttrium-90 for, 19: 19660
radiotherapy of, using gold-198 and yttrium-90, 19: 19667

PLACENTA
radium-226 content in human, 19: 20216

PLACENTAL TISSUES
radiosensitivity of rat, effects of cysteamine on lead shielding, 19: 19557

PLANETS
book: *Astrophysics and Space Science*, 19: 20782
polar cap on, 1956 disappearance of, (E/T), 19: 20763

PLANT CELLS
radiation effects on, small-dose, 19: 19516
tritium incorporation in, biological effects of beta particles on, 19: 19515

PLANTS
analysis for cesium-137, rapid method for, 19: 19805
analysis for strontium-89 and -90, radiochemical, 19: 19739 (AERE-AM-101)
particle deposition from atmosphere on, tracer studies using copper-64 on, 19: 20658
radiation effects on, small-dose, 19: 19516
radiation effects on dark phase of actinorhythmic reaction in, uv, 19: 19543
radiation effects on chromosome aberrations in *Crepis capillaris* seeds, moisture effects on post-, 19: 19581
radiation effects on pea and vetch, chronic gamma, 19: 19586
radioactivity of marine, in contaminated lake, 19: 20220
radioinduced mutations in *Arabidopsis thaliana*, 19: 19548
radiosensitivity of, 19: 19504 (RM-2801-PR)
strontium metabolism in, effects of soil conditions on, 19: 19474(T) (CEA-tr-A-1616)
uranium content in, effects of soil and water content on, 19: 19490

PLASMA
acceleration by electromagnetic waves, (E), 19: 21566
accelerators for, vortices in coaxial, (E), 19: 21539
boundary layer between electromagnetic field and rarified, (T), 19: 21585
boundary layer with magnetic field, electron cyclotron radiation from, (T), 19: 21522
charge separation effects in cold sheath model for, 19: 21538
collapse of accelerated current sheet of, (E/T), 19: 21518
collisions in transverse magnetic fields, depolarization and heating in, (T), 19: 21537
containment and heating of, in stellarator, 19: 21593(P)
containment by magnetic fields, configuration singularities for, (T), 19: 21534
containment by three-cusp magnetic field, (E), 19: 21568
containment by traveling electromagnetic waves, (E), 19: 21564
containment of cylindrical, by rotating magnetic fields, 19: 21508
containment of, problems in, 19: 21492(T) (FTD-TT-64-102)
containment programs for, summaries of AEC, (E/T), 19: 21489 (TID-4005(Pt.5))
current sheath in toroidal discharge, (E), 19: 21512
decay in nonequilibrium nonisothermal, recombination, (T), 19: 21557
decay of nonequilibrium nonisothermal, recombination, (T), 19: 21501(T)
density in Q-device, effect of current heating on, (E), 19: 21541
density measurements on, by hyperfrequency interferometry, 19: 21591
diagnostics of, (E), 19: 21488 (PIBMRI-1208-64)
diagnostics of h-f discharge, using atomic beams, (E), 19: 21528
diagnostics using multiple-beam microwave interferometer, 19: 21574
diffusion across magnetic fields, (E), 19: 21475 (LA-DC-6383)
diffusion and instability in potassium, in magnetic field, (E), 19: 21569
dissociation potential in, electron-negative ion, (T), 19: 21558
efficiency of argon–cesium MHD-generator, in electric field, (T), 19: 21556
electric conductivity dispersion in, thermodynamical model of, 19: 21495
electric conductivity of, transient, 19: 21496
electric conductivity of degenerate electron-gas, h-f, 19: 21545
electric conductivity in transverse magnetic field in thermionic cells, (T), 19: 21580
electric conductivity in combustion-driven MHD generator, (E), 19: 20909
electromagnetic fields and kinetic theory of, 19: 21493
electromagnetic radiation by, at electron-cyclotron harmonics, (T), 19: 21477 (MATT-290)
electromagnetic wave transport in anisotropic, (T), 19: 21466 (AFCRL-64-550)
electromagnetic wave propagation in stratified, (T), 19: 21506
electromagnetic wave propagation in nonuniform, r-f, (T), 19: 21519
electromagnetic wave interactions with pulses of, in waveguide, (E), 19: 21565
electromagnetic wave propagation in, (T), 19: 20944
electromagnetic-field pressure against dense, metal analog for, (T), 19: 21507
electromagnetic-wave propagation in partially ionized, helicon, (E), 19: 21552
electron and ion distribution functions for, in high-frequency magnetic field, (T), 19: 21573
electron density and temperature in electromagnetic shock tube, Langmuir probe measurement of, (E), 19: 21515
electron density and temperature of, method for determining, 19: 21572
electron density gradients in, interferometer design for analyses of, (E), 19: 21472 (IPP-1/25)
electron distribution function in, integration of Boltzmann equation for, 19: 21542
electron energy distribution in, in alpha Soviet thermonuclear experiment, (E), 19: 21583
electron energy distribution in hydrogen, equations for, 19: 21586
electron energy loss in nonequilibrium argon–cesium, nitrogen effect on, (E), 19: 21560
electron oscillations in, radioinduced instability of, (T), 19: 21550
electron temperature measurements on transient, triple-probe method for,

(E), 19: 21514
excitation of Puffatron, by microwaves at electron-cyclotron frequency, (E), 19: 21491 (UCRL-12057(Rev.I))
excitation operators and intrinsic hamiltonians in, 19: 21289
flow around geomagnetic hollow, (T), 19: 21146
flow between plane electrodes, electric current and space charge formation in, (T), 19: 21502(T)
flow of rotating weakly ionized, (E), 19: 21570
heat transfer from, method for measuring, 19: 21503(T)
heating of partially ionized, by h-f electromagnetic fields, (T), 19: 21581
hydromagnetic wave production and propagation in, equipment for, 19: 21465 (AFCRL-63-779)
injection devices for, design of hollow conductor, 19: 21562
interactions of bunches of, (E), 19: 21567
interactions with electron beams, diagnostics of, (E), 19: 21488 (PIBMRI-1208-64)
ionization of pinch- and shock-generated, (E/T), 19: 21471 (IPP-1/24)
kinetics of theta-pinch, effects of neutral gas on, (T), 19: 21470 (IPP-1/14)
kinetics of toroidal dilute, in equilibrium state, (T), 19: 21476 (MATT-283)
light interactions with light in, (T), 19: 21547
light scattering by, nonlinear resonant mixing by, (T), 19: 21546
magnetic field penetration into, with Hall effect, (T), 19: 21527
microwave generation of harmonics in, (T), 19: 21517
microwave propagation in waveguides of hot, 19: 21536
microwave reflection from anisotropic, (E/T), 19: 21513
motion equations for, astrophysical uses of, 19: 20783
motion of electron, magnetic-dipole-induced, (T), 19: 21535
neutral particle energy in DCX-2, 19: 21481(R) (ORNL-3760(p.10-22))
neutrino production and acceleration in, (T), 19: 21500
neutron emission from, 19: 21483(R) (ORNL-3760(p.30-56))
oscillations in inhomogeneous finite, (T), 19: 21478 (NP-14880)
oscillations in ionospheric, incoherent radar scattering from, (E), 19: 21153
oscillations in thermionic cells, (T), 19: 20913
oscillations in, energy exchange between high- and low-frequency, (E), 19: 21526
oscillations in, electron beam interactions with, (T), 19: 21563
oscillations in, phonon interactions with, (T), 19: 21494
oscillations in, stability of nonlinear stationary, 19: 21520
particle correlation function in one-component, time dependence of two-body, (T), 19: 21543
pressure and temperature of helium, in stellarators (C), (E), 19: 21511
production and properties, 19: 21479(R) (ORNL-3760)
production and properties of ionized, in burnout experiments, 19: 21483(R) (ORNL-3760(p.30-56))
production of high-density high-temperature, by electron cyclotron heating, (E), 19: 21531
production of high-temperature, dipole arrangement for, 19: 21592(P)
properties of hydrogen-ion-dissociation induced, 19: 21481(R) (ORNL-3760(p.10-22))
radiant energy flux from alkali metal-seeded, in infinite-plane parallel enclosure, (T), 19: 21468 (BSD-TDR-64-164)
radiation losses from cesium, at 3000 to 4000°K, (T), 19: 21505(T)
radiofrequency emission by, 19: 21480(R) (ORNL-3760(p.1-9))
resonances in, harmonic generation and frequency mixing at, (E), 19: 21549
shock heating of, in pinch configuration, (E), 19: 21473 (IPP-1/28)
sound propagation in, 19: 21483(R) (ORNL-3760(p.30-56))
sound wave excitation in weakly ionized, (T), 19: 21561
stability in EppE hard-core pinch device, (E), 19: 21469 (CEA-R-2713)
stability in Penning discharge, rotational, (E), 19: 21548
stability in thermionic, effect of sheaths on drift, (T), 19: 21540
stability in theta pinch with antiparallel magnetic field, (E), 19: 21525
stability in toroidal, twin-channel, (E), 19: 21467 (ARL-63-203)
stability in toroidal theta pinch, (E), 19: 21530
stability in transverse magnetic fields, (E), 19: 21577
stability of contra-streaming, in magnetic field, (T), 19: 21575
stability of dilute, nonlinear theory of convective, 19: 21532
stability of emf's in weakly ionized, (T), 19: 21559
stability of metal-vapor, (E), 19: 21490(R) (TID-21698)
stability of pulses of, in longitudinal magnetic fields, (E), 19: 21582
stability of weakly ionized, Kadomtsev-Nedospasov approximation for, 19: 21533
stability of, calculation and theory of, 19: 21485(R) (ORNL-3760 (p.69-76))
stability of, kinetic equations and Lorentz distribution function for, (T), 19: 21509
temperature of electron-cyclotron, 19: 21482(R) (ORNL-3760(p.23-9))
thermodynamic properties of one-dimensional, with hard-core repulsion, 19: 20682
thermodynamics of one-dimensional, statistical, 19: 21587
thermoelectric effects in Joule-heated, 19: 21544
turbulence in cosmic, detection of h-f, (T), 19: 20781(T)
turbulence in, diagram technique for describing, (T), 19: 21529
turbulence of cosmic, h-f, (T), 19: 20755
use as lens for focusing meson-neutrino beam, 19: 20915 (BNL-8967)
wave propagation across magnetic fields, (T), 19: 21521
wave propagation in magnetic fields, low-frequency, (T), 19: 21523
wave propagation in infinite homogeneous, nonlinear, 19: 21588
wave propagation in plane-stratified, wave equations for, 19: 21589
wave transformation in, Langmuir, (T), 19: 21584

PLASMA JETS
electrode development for, (E), 19: 20905 (SC-RR-65-54)
excitation of plasma from Puffatron gun, by microwaves at electron-cyclotron frequency, (E), 19: 21491 (UCRL-12057(Rev.I))
use in space propulsion, 19: 20139
vortices in coaxial, (E), 19: 21539

PLASTIC DEFORMATION
of metals and alloys, ad hoc committee report on, 19: 20507(R) (MAB-206-M)

PLASTICS
molds for potting shells, design principles of, 19: 21764 (SC-DR-64-2135)
radiation effects on package-film, gamma, 19: 20421
radioluminescence properties of, (E), 19: 19962

PLATES
stress analysis of bent, computer program for, 19: 21609 (GAMD-5001 (Rev.2))
stresses in long, thick, uniformly curved, methods of calculating, 19: 20130
welding of carbon steel, Hanford procedures for, 19: 20521 (TID-20625 (Vol.I(Rev.I))
welding of carbon steel and stainless steel, Hanford procedures for, 19: 20522 (TID-20625(Vol.II)(Rev.I))
welding of steel, Hanford procedures for, 19: 20523 (TID-20625(Vol.III) (Rev.I))
welding of, Hanford procedures for, 19: 20524 (TID-20625(Vol.IV)(Rev.I))

PLATINUM
electromagnetic wave absorption and scattering by particles of, (T) 19: 20677
separation by reversed-phase chromatography using tri-n-octylphosphine sulfide, 19: 19753 (IS-T-3)
thermal conductivity at high temperatures, (E), 19: 20576

PLATINUM ALLOY COUPLES
Pt/Pt–Rh, performance in gas-cooled reactor fuel irradiation experiments, 19: 20401 (ORNL-P-1065)
Pt/Pt–Rh, thermocouple tables, smoothed, 19: 20263 (ORNL-3649 (Vol.2)(Sect.2.1))
Pt/Pt–Rh, thermocouple drift at high temperatures in vacuum, 19: 20278 (ORNL-P-1069)
Pt/Pt–Rh, thermocouple tables, smoothed, 19: 20264 (ORNL-3649 (Vol.2)(Sect.2.2))
Pt–Rh/Pt–Rh, thermocouple drift at high temperatures in vacuum, 19: 20278 (ORNL-P-1069)

PLATINUM ALLOYS
Mo–Nb–Pt–U, corrosion resistance in water, 19: 20497(P)
Mo–Nb–Pt–U, properties for use as reactor fuel, 19: 20497(P)

PLATINUM COUPLES
Pt/Pt–Rh, performance in gas-cooled reactor fuel irradiation experiments, 19: 20401 (ORNL-P-1065)
Pt/Pt–Rh, thermocouple tables, smoothed, 19: 20263 (ORNL-3649 (Vol.2)(Sect.2.1))
Pt/Pt–Rh, thermocouple drift at high temperatures in vacuum, 19: 20278 (ORNL-P-1069)
Pt/Pt–Rh, thermocouple tables, smoothed, 19: 20264 (ORNL-3649 (Vol.2)(Sect.2.2))

PLATINUM ISOTOPES Pt-173
production and alpha decay properties, (E), 19: 21248(R) (UCRL-11828(p.21-5))

PLATINUM ISOTOPES Pt-174
production and alpha decay properties, (E), 19: 21248(R) (UCRL-11828(p.21-5))

PLATINUM ISOTOPES Pt-175
production and alpha decay properties, (E), 19: 21248(R) (UCRL-11828(p.21-5))

PLATINUM ISOTOPES Pt-176
production and alpha decay properties, (E), 19: 21248(R) (UCRL-11828(p.21-5))

PLATINUM ISOTOPES Pt-177

production and alpha decay properties, (E), 19: 21248(R) (UCRL-11828(p.21-5))
PLATINUM ISOTOPES Pt-178
production and alpha decay properties, (E), 19: 21248(R) (UCRL-11828(p.21-5))
PLATINUM ISOTOPES Pt-179
production and alpha decay properties, (E), 19: 21248(R) (UCRL-11828(p.21-5))
PLATINUM ISOTOPES Pt-180
production and alpha decay properties, (E), 19: 21248(R) (UCRL-11828(p.21-5))
PLATINUM ISOTOPES Pt-181
production and alpha decay properties, (E), 19: 21248(R) (UCRL-11828(p.21-5))
PLOWSHARE PROJECT
Isthmian Canal excavation, 19: 20091
PLUTONIUM
contamination of floors by, resuspension factors for, 19: 20191 (AERE-R-4635)
determination in uranium and its compounds and alloys, methods for, 19: 19823
electric conductivity at low temperature, radioactive self-damage effects on, (E), 19: 20649
monitoring atmospheric, device for, 19: 20381
neutron spectra of, measurement at Hanford, (E), 19: 20201 (HW-SA-3525)
phase transformations of, microscopic study of allotropic, 19: 20546 (CEA-R-2726)
processing irradiated, operation of Windscale plant for, 19: 20064
radiation self-damage in, annealing of, (E), 19: 20650
release due to overheating or fires, review, 19: 20200 (HW-83668)
separation from leachable residues, engineering drawings of facility for, 19: 20083
separation from nitric acid solutions by solvent extraction using dialkyl phosphoric acid, 19: 20075
separation from nitrate solutions by solvent extraction using organo-phosphorus compounds, 19: 20077
separation from processing solutions by trifluoride precipitation and filtration, 19: 20065
separation from spent fuel elements, development of direct fluoride volatility process for, 19: 20059
sorption on anion exchange resin from nitric acid solution, calculation of fixed-bed column performance in, 19: 20045 (LA-2838)
sorption on anion exchange resin from aluminum nitrate–nitric acid solutions, calculation of equilibrium distribution coefficients for, 19: 20046 (LA-3188)
use in thermal reactors, 19: 21673
PLUTONIUM ALLOYS
Ce–Co–Pu, corrosion by sodium at 650°C, 19: 21690(R) (LA-3244)
Ce–Co–Pu, corrosive effects on tantalum and tantalum–tungsten alloys at 600 to 1100°C, 19: 21690(R) (LA-3244)
Ce–Co–Pu, preparation of homogeneous, 19: 21690(R) (LA-3244)
Ce–Co–Pu, production of uniform rods of, by chill casting, 19: 20506 (LA-3209)
Fe–Pu, corrosive effects on tantalum and tantalum–tungsten alloys at 600 to 1100°C, 19: 21690(R) (LA-3244)
Ga–Pu, fatigue strength of delta-stabilized, 19: 20545 (BNWL-16)
In–Pu, phase studies, 19: 21690(R) (LA-3244)
Mn–Pu–U, analysis for manganese, x-ray-fluorescent, 19: 21690(R) (LA-3244)
Pu–Ti–U, phase studies, 19: 21690(R) (LA-3244)
Pu–U, diffusion coefficients in, 19: 19869
PLUTONIUM BORIDES
crystal structure, 19: 21690(R) (LA-3244)
PLUTONIUM CARBIDES
crystal structure, 19: 21690(R) (LA-3244)
preparation and crystal structure of higher, 19: 20570
PLUTONIUM CHLORIDES
thermodynamic properties, 19: 21690(R) (LA-3244)
PLUTONIUM(IV) FLUORIDES
neutron spectra of, measurement at Hanford, (E), 19: 20201 (HW-SA-3525)
preparation by fluorination of oxide, engineering drawings of equipment for, 19: 19939
PLUTONIUM ISOTOPES Pu-238
separation from power reactor fuels, economics of, 19: 20036 (BNWL-25)
shielding power sources of, 19: 21595 (TID-7698(Pt.I)(p.33-248))
PLUTONIUM ISOTOPES Pu-239
burnup in reactors, accurate determination of, 19: 21667(R) (GEAP-4776)
content in stratosphere, 19: 20657(R) (DASA-1309)
neutron cross sections for, model for thermal, (T), 19: 21678 (ANL-6972)
neutron cross sections of, availability for reactor calculations, (E), 19: 21225 (AECL-2168)
neutron fission at 200 to 600 ev, symmetries in, (E), 19: 21241 (LA-DC-6639)
neutron fission rates relative to uranium-235, (E), 19: 21227 (ANL-6941)
separation from power reactor fuels, economics of, 19: 20036 (BNWL-25)
waste fixation of raffinate solutions containing, 19: 21750 (LA-3150)
PLUTONIUM ISOTOPES Pu-240
fission induced by alpha inelastic scattering, (E), 19: 21262(R) (UCRL-11828(p.84-6))
fission of, neutron spectra from spontaneous, (E), 19: 20201 (HW-SA-3525)
neutron cross sections for, model for thermal, (T), 19: 21678 (ANL-6972)
neutron fission rates relative to uranium-235, (E), 19: 21227 (ANL-6941)
separation from power reactor fuels, economics of, 19: 20036 (BNWL-25)
PLUTONIUM ISOTOPES Pu-241
neutron cross sections for, model for thermal, (T), 19: 21678 (ANL-6972)
separation from power reactor fuels, economics of, 19: 20036 (BNWL-25)
PLUTONIUM ISOTOPES Pu-242
separation from power reactor fuels, economics of, 19: 20036 (BNWL-25)
PLUTONIUM ISOTOPES Pu-244
separation from power reactor fuels, economics of, 19: 20036 (BNWL-25)
PLUTONIUM NITRATES
contamination of floors by, resuspension factors for, 19: 20191 (AERE-R-4635)
separation of plutonium from solutions of, by trifluoride precipitation, 19: 20065
PLUTONIUM(IV) NITRATES
separation from nitric acid solutions by complex formation with organic phosphorus compounds, 19: 20077
PLUTONIUM (VI) NITRATES
separation from nitric acid solutions by complex formation with organic phosphorus compounds, 19: 20077
PLUTONIUM NITRIDES
preparation methods, 19: 21690(R) (LA-3244)
PLUTONIUM OXIDES
contamination of floors by, resuspension factors for, 19: 20191 (AERE-R-4635)
fluorination of, engineering drawings of equipment for, 19: 19939
PLUTONIUM(IV) OXIDES
dissolution of high-density pellets of, in nitric acid with and without additives, 19: 20050 (ORNL-3695)
reactions with carbon to prepare higher carbides, 19: 20570
sintering of, procedure for, 19: 21690(R) (LA-3244)
Al_2O_3–PuO_2, phase diagrams, 19: 20589
BeO–PuO_2, phase diagrams, 19: 20589
BeO–PuO_2–ThO_2, phase diagrams, 19: 20589
MgO–PuO_2, phase diagrams, 19: 20589
PuO_2–UO_2, dissolution of high-density pellets of, in nitric acid, 19: 20050 (ORNL-3695)
PuO_2–UO_2, sodium logging in fuel elements of, 19: 20458 (GEAP-4283)
PLUTONIUM RECYCLE TEST REACTOR
fuel element testing facility for, engineering drawings of, 19: 21704
pressure tubes, postirradiation evaluation of Zircaloy-2, 19: 21686 (HW-84540)
PNEUMATIC SYSTEMS
design for irradiated solutions transfer from MIT research reactor, 19: 21741
POCKET CHAMBERS
development of personnel fast-neutron dosimeters, (E), 19: 20318 (HW-SA-3526)
performance for personnel monitoring, testing of, 19: 20338
POLONIUM
separation from bismuth by electrolysis, 19: 20008
POLONIUM COMPLEXES
chloride, stability of, effects of acetone on, 19: 19906
hydroxy-, hydrolysis in perchloric acid, 19: 19905
with acetylacetone, formation constants and hydrolysis reactions, 19: 19905
POLONIUM ISOTOPES Po-193
alpha energy and half life, (E), 19: 21250(R) (UCRL-11828(p.26))

POLONIUM ISOTOPES Po-194
alpha energy and half life, (E), 19: 21250(R) (UCRL-11828(p.26))
POLONIUM ISOTOPES Po-195
alpha energy and half life, (E), 19: 21250(R) (UCRL-11828(p.26))
POLONIUM ISOTOPES Po-196
alpha energy and half life, (E), 19: 21250(R) (UCRL-11828(p.26))
POLONIUM ISOTOPES Po-197
alpha energy and half life, (E), 19: 21250(R) (UCRL-11828(p.26))
POLONIUM ISOTOPES Po-198
alpha energy and half life, (E), 19: 21250(R) (UCRL-11828(p.26))
POLONIUM ISOTOPES Po-199
alpha energy and half life, (E), 19: 21250(R) (UCRL-11828(p.26))
POLONIUM ISOTOPES Po-200
alpha energy and half life, (E), 19: 21250(R) (UCRL-11828(p.26))
POLONIUM ISOTOPES Po-210
content in stratosphere, 19: 20657(R) (DASA-1309)
content in tobacco smoke, 19: 19495
determination in urine by autoradiography, 19: 19791
distribution in tissues of man and mouse, 19: 19495
fission barrier of compound nucleus, (E), 19: 21261(R) (UCRL-11828(p.81-3))
production by neutron irradiation of bismuth, 19: 20008
separation from power reactor fuels, economics of, 19: 20036 (BNWL-25)
shielding power sources of, 19: 21595 (TID-7698(Pt.I)(p.33-248))
use to excite x-ray fluorescence in analysis of light elements, 19: 19741 (CEA-R-2539)
POLONIUM ISOTOPES Po-214
determination in air by beta measurement, efficiency of counter for, 19: 20169
POLYCYTHEMIA
radiotherapy of, by intra-arterial injection of radioisotopes, 19: 19661
POLYMERS
preparation of, use of radiation in, 19: 20417
radiation effects on, review of, 19: 19978
relaxation and molecular motion in, research program on, 19: 21770(R) (TID-21677)
POLYPHOSPHATES
use as elution medium in ion-exchange separation of rare earths, 19: 20049 (NP-14834)
POPULATIONS
ecology of human, effects of nuclear warfare on, 19: 20199 (HI-388-RR(Pt.III))
protection of, from hazards of nuclear weapons, disarmament and international control programs for, 19: 21761 (P-1134(RAND))
radiation effects on genetic damage in, problems in assessment of, 19: 19654
radiation exposure to inhabitants in Mosonmagyarovar, Hungary from medical examinations in 1961, 19: 20227
radiation exposure to, maximum permissible doses for external and internal, 19: 20221
radiation protection of, organization for, 19: 20222
POSITRONIUM
detection in universe, optical method for, 19: 20754
energy levels of, from Bethe-Salpeter equation, 19: 20966
radiation from, detection of optical, 19: 20774(T)
POSITRONS
annihilation in alkali metal halide crystals, polaron theory of, 19: 20820
annihilation in argon and helium, effect of electric field on rate of, (E), 19: 21011
annihilation of, coincidence spectrometer for radiation from, 19: 20363
emission in meson (μ^+) decay, momentum spectra of, (E), 19: 21012
lifetime in solid polymers, (E), 19: 21044
reactions with hydrogen atoms, 2p level excitation in, (T), 19: 20853
use in localization of brain tumors after administration of arsenic-74 or copper-64, 19: 19713
POTASSIUM
analysis for oxygen, neutron-activation, (E), 19: 19751 (GA-5982)
analysis for oxygen, round-robin meeting on, 19: 19760 (NASA-TM-X-1085)
corrosive effects of boiling, on niobium–1% zirconium alloy loop, 19: 20476 (ORNL-3603)
corrosive effects on refractory alloys, 19: 20473(R) (NASA-CR-54629)
corrosive effects on refractory alloys, research program on, 19: 20474(R) (NASA-CR-54281)
determination in biological materials, activation, 19: 19771(R) (TEES-2671-4(Chap.9))
determination in cottonseed, activation, 19: 19771(R) (TEES-2671-4 (Chap.9))
electron elastic scattering at 0.1 to 2.0 ev, cross sections for, (T), 19: 20842
heat transfer in forced-flow boiling, 19: 20116(R) (SAN-409-12)
plasma of, diffusion and stability in magnetic field, (E), 19: 21569
purification of corrosion-loop, system for, 19: 20473(R) (NASA-CR-54629)
radiation effects on physiology of content of, in developing guinea pig brain, 19: 19534
solvent properties for helium at 482 to 704°C, 19: 20561 (PWAC-380)
stability of thermionic plasma of, effect of sheaths on drift, (T), 19: 21540
thermodynamic properties of vaporous, 19: 20116(R) (SAN-409-12)
vaporization lifetimes of droplets of, 19: 20116(R) (SAN-409-12)
POTASSIUM ACID FLUORIDES
electrolysis of molten, kinetics of hydrogen evolution in, 19: 19875
POTASSIUM ALLOYS
K–Na, corrosive effects on stainless steels, literature survey, 19: 20472 (IDO-14651)
K–Na, corrosive effects on structural alloys, research program on, 19: 20477(R) (ORNL-3604)
K–Na, corrosive effects on structural alloys at high temperatures, loop experiments, 19: 20478(R) (ORNL-3618)
K–Na, corrosive effects on structural alloys at high temperatures, loop experiments, 19: 20479(R) (ORNL-3671)
K–Na, corrosive effects on structural alloys at high temperatures, mass transfer in, 19: 20480(R) (ORNL-3730)
K–Na, hydride precipitation in, 19: 20478(R) (ORNL-3618)
K–Na, pumping of, development of thermoelectric pumps for, (E), 19: 20096 (NAA-SR-Memo-10729)
K–Na, solvent properties for hydrogen, apparatus for measurement of, 19: 20477(R) (ORNL-3604)
K–Na, solvent properties for hydrogen at 752 to 1300°F, 19: 20480(R) (ORNL-3730)
K–Na, solvent properties for hydrogen at 1100°F, 19: 20479(R) (ORNL-3671)
POTASSIUM BORATES
$K_2B_2O_4$–K_2CO_3, paramagnetic defects in air-quenched ceramics of, electron spin resonance study of, 19: 20620(R) (NYO-2024-8)
POTASSIUM BROMIDES
electron energy losses in, 19: 20702
optical properties, 19: 20702
radiation damage in, electron-spin and nuclear-magnetic resonance studies of reactor, 19: 20620(R) (NYO-2024-8)
radiation effects on thermal properties of crystals and solid solutions of, gamma and neutron, 19: 19986
radiation effects on stored energy in, gamma, 19: 19987
radioinduced color center formation in, 19: 19979
radioinduced luminescence of thallium-activated, quenching effects of temperature on, 19: 19966
POTASSIUM CARBONATES
use in combustion chamber of magnetohydrodynamic generator, 19: 20914
$K_2B_2O_4$–K_2CO_3, paramagnetic defects in air-quenched ceramics of, electron spin resonance study of, 19: 20620(R) (NYO-2024-8)
POTASSIUM CHLORIDES
electron energy losses in, 19: 20702
hydrogen EPR spectra in, 19: 19896
optical properties, 19: 20702
preparation of high-purity, 19: 19843 (ORNL-TM-1071)
radiation effects on luminescence of copper-doped, 19: 19964
radiation effects on thermal properties of crystals and solid solutions of, gamma and neutron, 19: 19986
radiation effects on stored energy in, gamma, 19: 19987
radiation effects on M-center formation in, gamma, 19: 19999
radiation effects on sliding and static friction of, x, 19: 20011
radioinduced color center formation in, 19: 19979
radioinduced luminescence of thallium-activated, quenching effects of temperature on, 19: 19966
spectra of suspensions of, in thin polyethylene films, infrared transmission, 19: 19917
KCl–K_2ZrF_6–NaCl, decomposition potentials in electrolysis of, 19: 19850(T) (NP-tr-1230)
POTASSIUM CHROMATES
spectra of suspensions of, in thin polyethylene films, infrared transmission, 19: 19917
POTASSIUM FLUOZIRCONATES
decomposition potentials in electrolysis of, 19: 19850(T) (NP-tr-1230)
KCl–K_2ZrF_6–NaCl, decomposition potentials in electrolysis of, 19: 19850(T) (NP-tr-1230)
POTASSIUM HALIDES
radiation damage in, electron-spin and nuclear-magnetic resonance studies of reactor, 19: 20620(R) (NYO-2024-8)

POTASSIUM HYDROXIDES
corrosive effects on electrolytic cell materials, 19: 20484 (TID-19978 (Vol.I))
reactions with xenon trioxide in solution, 19: 19847(R) (UCRL-11828 (p.182-3))
POTASSIUM IODIDES
color centers in, exciton absorption in the presence of excited F, 19: 21602
radiation effects on thermal properties of crystals and solid solutions of, gamma and neutron, 19: 19986
radiation effects on stored energy in, gamma, 19: 19987
radioinduced luminescence of thallium-activated, quenching effects of temperature on, 19: 19966
POTASSIUM IONS
solvent extraction from molten nitrate by liquid silicone–TBP at 150°C, 19: 19833 (CEA-R-2628)
POTASSIUM ISOTOPES K-38
beta decay of ground-state and isomeric, from potassium-39 (γ,n) reactions, (E), 19: 21276
POTASSIUM ISOTOPES K-39
photoreactions (γ,n) and (γ,np) to 80 Mev, (E), 19: 21276
secretion in human saliva, 19: 19486
POTASSIUM ISOTOPES K-40
content in rocks of La Sal Mountains, Utah, (E), 19: 20178
detection and measurement of, performance of whole-body plastic scintillation detector for, 19: 20377
Mössbauer effect for 29.4-kev gamma ray of, (E), 19: 21409
Mössbauer spectra for 29-kev gamma ray from, (E), 19: 21408
POTASSIUM ISOTOPES K-42
secretion in human saliva, 19: 19486
POTASSIUM NITRATES
melting points and volumes of fusion at 0 to 10,000 atm, 19: 19884
$LiNO_3$–KNO_3–$NaNO_3$, distribution of ions between liquid–TBP and molten, at 150°C, 19: 19833 (CEA-R-2628)
POTASSIUM PHOSPHATES
content in soil, effects on strontium-90 accumulation in oats, 19: 19475(T) (JPRS-27940(p.10-17))
POTATOES
radiation effects on sprouting of, gamma, 19: 20424
radioinduced somatic mutations in, gamma, 19: 19518
POTENTIOMETERS
design, 19: 20321 (ISS-64/28)
POWDER RIVER BASIN (WYO.)
uranium isotopic fractionation in sandstone of, 19: 20187
POWER BREEDER REACTORS
performance of fast, effects of central blanket on static, 19: 21696
POWER PLANTS
control equipment for, design of automatic safety, 19: 20103
pump development for mercury Rankine-cycle, (E), 19: 20096 (NAA-SR-Memo-10729)
POWER REACTORS
construction and design of Soviet ARBUS, 19: 21702
design using powder suspended in gas as fuel, 19: 21706(P)
exponential experiments for advanced sodium-graphite, (E), 19: 21692 (NAA-SR-Memo-9976)
fuel processing for, economics of fission product recovery in, 19: 20036 (BNWL-25)
loading schedule for, 19: 21705(P)
materials for use in, analysis of thermoelectric, 19: 21703
neutron flux distribution in Kahl, relaxation method for calculating, 19: 21655
output of Soviet, evaluation of total, (T), 19: 21694 (P-1076(RAND))
stability of coupled-core, analysis of nonlinear, 19: 21723(R) (NASA-CR-193)
steam generator design for TARGET gas-cooled, (E), 19: 21682 (GAMD-4732)
vessels for TARGET gas-cooled, design analysis for prestressed-concrete, (T), 19: 21683 (GAMD-5272(Rev.2))
POWER SUPPLIES
design of transistorized, for photomultipliers, 19: 20357
development of radioisotopic, conference on, 19: 20426 (TID-7698 (Pt.I))
performance of radioisotope-heated thermionic, thermoelectric, and thermophotovoltaic, (E/T), 19: 20904 (BLG-317)
shielding isotopic, 19: 21595 (TID-7698(Pt.I)(p.33-248))
survey of high-voltage, 19: 20085 (CONF-640204(p.93-105))
PRASEODYMIUM
determination by titration, suitability of tetraethylenepentamine heptaacetic acid for, 19: 19813
separation from other light lanthanides by partition chromatography following production by proton bombardment of erbium, 19: 20078
separation from scandium by solvent extraction of diantipyrinylmethane complex, 19: 20080
PRASEODYMIUM COMPLEXES
with serine, stability and composition, 19: 19874
PRASEODYMIUM ISOTOPES Pr-141
photon reactions (γ,n), cross sections for, (E), 19: 21287
PRASEODYMIUM NITRATES
crystal structure of hexahydrate, 19: 19914(T)
PRASEODYMIUM NITRIDES
magnetic properties of, influence of crystal field on, 19: 19895
PRASEODYMIUM OXIDES
dipole relaxation in nonstoichiometric, (E/T), 19: 20818
PRASEODYMIUM SULFATES
crystal structure and bond types of octahydrates, 19: 19915(T)
PRASEODYMIUM SULFIDES
preparation by sulfonation of oxide using carbon disulfide, 19: 19927
PREDNISOLONE
anabolic effects in radiotherapy of human tumors, 19: 19669
PREGNANCY
radiation hazards to fetuses during, 19: 19533
radiation hazards from diagnostic chest x-ray examination during, 19: 19592
radiation hazards to fetus during, 19: 19698
radiation hazards of diagnostic radiography during, 19: 19699
therapeutic use of iodine-131 during human, hazards of, 19: 19491
PRESSURE TRANSMITTERS
radiation and temperature effects on operation of, 19: 20400 (NP-14955)
PRESSURE VESSELS
closure design for, 19: 20106(P)
design analysis for prestressed-concrete, for reactors, (T), 19: 21683 (GAMD-5272(Rev.2))
failure of gas-cooled-reactor, simulation using models, (E), 19: 21608 (AWRE-R-2/65)
materials surveillance program for steel reactor, 19: 21607 (APED-4773)
stress analysis of, computer program for, 19: 21609 (GAMD-5001 (Rev.2))
tendon configuration in pre-stressed concrete, program for determining optimal, 19: 21610 (GAMD-6109)
thermal protection system for concrete, economics and evaluation of, 19: 20110 (GAMD-5432)
welding of closure joint in Type 316 stainless steel, tests of, 19: 20509 (NAA-SR-Memo-10633)
welding of, for Tokai-mura Power Reactor, 19: 21700
PRESSURIZED WATER REACTORS
technology developments, 19: 21699
PROCESS HEAT REACTORS
development for large-scale desalting, 19: 21709
economics for sea water desalination, 19: 21707 (ORNL-TM-432)
evaluation of large, for sea water desalination, 19: 21708 (ORNL-TM-465)
PROLINE
effects on radiosensitivity of *Escherichia coli*, 19: 19550
PROMETHIUM
separation from other light lanthanides by partition chromatography following production by proton bombardment of erbium, 19: 20078
PROMETHIUM ISOTOPES Pm-147
properties of, nuclear and physical, 19: 20402 (TID-7698(Pt.I)(p.17-30))
separation from power reactor fuels, economics of, 19: 20036 (BNWL-25)
separation from wastes in Hanford isotope plant, feasibility study, 19: 20431 (TID-7698(Pt.I)(p.1-16))
shielding power sources of, 19: 21595 (TID-7698(Pt.I)(p.33-248))
PROMETHIUM SULFATES
crystal structure and bond types of octahydrates, 19: 19915(T)
PROPANE, 1-CHLORO-
solvent properties in mixtures with butyl ether for uranyl perchlorate, 19: 20073
PROPANE, 2-CHLORO-
solvent properties in mixtures with butyl ether for uranyl perchlorate, 19: 20073
PROPENE POLYMERS
positron lifetime in, (E), 19: 21044
preparation and fracture studies of single lamellar crystals of, 19: 21770(R) (TID-21677)
PROPORTIONAL DETECTORS
design of anticoincidence assembly of, for beta particles, 19: 20353
design of high-efficiency neutron, for angular-distribution measurement, 19: 20333
design of methane-filled, for fission products, 19: 20376
pulse amplifier and discriminator system for, design of, 19: 20362
response of long-counter, neutron energy distribution in hydrogenous

moderator for study of, (T), 19: 21202
time jitter in boron trifluoride and helium-3, 19: 20364
use of 4π, for standardization of electron capture radioisotope, 19: 20384
PROPULSION
electrothermal, for space applications, 19: 20139
ion thrustor for space, study of tantalum filament deterioration in electron-bombardment mercury, 19: 20138 (NASA-TN-D-2173)
radioisotope systems for space, POODLE program for, 19: 20428 (TID-7698(Pt.I)(p.257-76))
systems for space, mission analysis for solar-heated hydrogen, 19: 20137 (NASA-CR-59332)
PROTACTINIUM
separation from perchloric solutions by solvent extraction using thenoyltrifluoroacetone and tributylphosphate, synergistic effects in, 19: 20055
separation from perchlorate solutions by solvent extraction using thenoyltrifluoroacetone, 19: 20063
thermal expansion from 18 to 1055°C, 19: 20571
PROTACTINIUM COMPLEXES
hydroxyl, reactions with thenoyltrifluoroacetone, 19: 20056
PROTACTINIUM IONS
hydrolysis of pentavalent, 19: 20056
hydrolysis of tetravalent, 19: 20063
PROTACTINIUM ISOTOPES Pa-226
alpha decay, (E), 19: 21418
PROTACTINIUM ISOTOPES Pa-228
alpha decay, (E), 19: 21418
PROTACTINIUM ISOTOPES Pa-230
alpha decay, (E), 19: 21418
PROTACTINIUM ISOTOPES Pa-231
separation from power reactor fuels, economics of, 19: 20036 (BNWL-25)
PROTACTINIUM ISOTOPES Pa-233
separation from solutions of irradiated thorium–uranium fuel by sorption on unfired Vycor, 19: 20051 (ORNL-3773)
PROTEINS
radiation effects on uptake of sulfur-35-labeled methionine by rabbit marrow and spleen, 19: 19604
radiation effects on thermoluminescence, 19: 19983
radiodermatitis effects on blood serum, in humans and rabbits, 19: 19598
radiosensitivity of, effects of SH-inhibitors on, 19: 19621
PROTON BEAMS
injection into 200-Bev synchrotrons, systems for, (E), 19: 20737 (UCRL-11955)
PROTON CAPTURE CROSS SECTIONS
calculation in optical model, 19: 21442
PROTON PAIRS
annihilation at rest, SU(12) symmetry model predictions for, (T), 19: 21039
annihilation into mesons, Ū(12) symmetry predictions for, (T), 19: 21036
annihilation of, M(12) symmetry model testing by, (T), 19: 21033
annihilation of, testing of relativistic SU(6) symmetry by, (T), 19: 20983
PROTON SHIELDING
gamma-ray production in, (E), 19: 21243 (ORNL-3506)
performance of space vehicles as solar, for manned missions, (T), 19: 20873 (D2-11608)
PROTONS
absorption by aluminum, range-energy relations for, (E), 19: 20806 (ORNL-3702)
absorption by carbon, lead, and tin at 2.72 Bev/c, (E), 19: 21431
angular distribution from carbon-12 (d,p) reactions, distorted wave Born approximation analysis of, 19: 21439
binding energy in nuclei, 19: 21275
charge-exchange cross sections in hydrogen and lithium arcs, 19: 21481(R) (ORNL-3760(p.10-22))
effects on blood cells in monkeys, space simulated, 19: 19616
effects on blood picture in dogs, 19: 19578
effects on germanium at 22 and 40 Mev, 19: 20617 (NASA-TN-D-2727)
effects on hyperfine shift in hydrogen, size, (T), 19: 21396
electron capture from helium, (T), 19: 20821
emission from neutron reactions with tritium at 14.4 Mev, spectra of, (E), 19: 21405
emission in nuclear decay, (E), 19: 21271(T) (KFK-tr-161)
interactions with deuterons and helium-3, bibliography, (E/T), 19: 21238 (LA-3205)
interactions with antiprotons in universe, optical method for protonium detection in, 19: 20754
interactions with protons in white dwarfs, (T), 19: 20771(T)
interactions with bremsstrahlung photons at 228 to 325 Mev, cross sections, (E), 19: 20932 (LNF-64/60)
interactions with antiprotons, Feynman diagrams for cross sections of elastic, (T), 19: 20954
interactions with antiprotons at 4 Bev/c, diffraction slope at infinite energy in elastic, (E/T), 19: 20976
interactions with antiprotons, charge conjugation conservation in strong, (T), 19: 20977
interactions with protons at 50 to 150 Mev, polarization in, (E), 19: 20980
interactions with antiprotons, multimeson resonances in annihilation, (E), 19: 20993
interactions with electrons, baryon resonances in, (E/T), 19: 20997
interactions with mesons (π^-), T = 0 scalar di-pion in ($\pi^+\pi^-$n), (T), 19: 20998
interactions with photons, intermediate vector boson production in, (T), 19: 21003
interactions with mesons (π^-) at 3.9 and 4.2 Bev/c, K* (1430) production in, 19: 21004
interactions with mesons (π^-) at 6 to 18 Bev/c, charge-exchange cross sections for, (E), 19: 21006
interactions with mesons (π^-), Regge-pole analysis of charge-exchange, (T), 19: 21007
interactions with mesons (K-) at 2.45 to 2.70 Bev/c, Y$_1^*$ (1660) production in, 19: 21017
interactions with antiprotons, M(12) symmetry model testing by annihilation, (T), 19: 21033
interactions with hyperons (Λ) at low energy, (E), 19: 21034
interactions with protons at 2.40 and 2.85 Bev, meson (K+) production in, (E), 19: 21034
interactions with antiprotons, Ū(12) symmetry predictions for annihilation, (T), 19: 21036
interactions with mesons (π^-) at 35 Mev, s-wave scattering length for, (E), 19: 21043
interactions with neutrons, Treiman-Yang criterion for, (T), 19: 21046
interactions with mesons (K-) at 2.24 Bev, hyperon (Ξ) production in, 19: 21065
interactions with mesons (K-), polarization correlation of hyperons (Λ) and hyperons (Σ°) in, 19: 21071
interactions with electrons, Born approximation for Mott asymmetry in, 19: 21073
interactions with neutrons in nuclei, isobaric states in, (T), 19: 21304
interactions with neutrons, pairing correlations in, (T), 19: 21381
polarization in strontium-88 (d,p) reactions at 11 Mev, 19: 21447
production in reactions between complex nuclei, high energy, (T), 19: 21354
production of secondary, in proton reactions with nuclei at 160 Mev, (E/T), 19: 21244 (ORNL-P-844)
ranges in copper, energy determination by, 19: 21436
reactions (p,αγ) with lithium-7 at 440 kev, gamma transitions in, (E) 19: 21357
reactions (p,γ) with lithium-7, beryllium-8 levels from, 19: 21342
reactions (p,γ) with deuterons, elastic unitarity effects in, (T), 19: 21371
reactions (p,γ) with titanium-46, (E), 19: 21374
reactions (p,γ) with phosphorus-31, sulfur-32 energy levels from, (E), 19: 21380
reactions (p,d) and (p,2p) with carbon 12 at 59 Mev, energy spectra of, 19: 21401
reactions (p,d) with lithium-7, multi-level analysis of resonances in, (T), 19: 21413
reactions (p,n) with yttrium-89 at 4.6 to 5.6 Mev, angular distributions in, (E), 19: 21356
reactions (p,3n) with aluminum-27 at 97 Mev, (E), 19: 21297
reactions with aluminum and iron at 30–40 Mev, helium-3 and tritium production in, 19: 21438
reactions with beryllium at 12.5 Bev, mesons (K) and (π) production in, (E), 19: 21406
reactions with carbon-12 and oxygen-16 at high energies, lithium-6 and -7 production in, (E), 19: 21352
reactions with carbon-12 at 156 Mev, intranuclear cascade and breakup in, (T), 19: 21402
reactions with copper-63, comparison of experiment and theory, 19: 21458
reactions with erbium at 680 Mev, production of neutron deficient isotopes of light lanthanides in, 19: 20078
reactions with gold-197 at 155 Mev, nucleon-alpha cascades from, (T), 19: 21372
reactions with hydrogen atoms, 2p level excitation in, (T), 19: 20853
reactions with hydrogen atoms, electron capture cross sections for, (T), 19: 21417
reactions with intermediate nuclei, resonances in, 19: 21446
reactions with molecular hydrogen ions, production of excited neutral atoms in, 19: 21484(R) (ORNL-3760(p.57-63))
reactions with nuclei at 160 Mev, 0.6- to 11-Mev gamma rays from, (E), 19: 21243 (ORNL-3506)

reactions with nuclei at 160 Mev, secondary nucleon spectra from, (E/T), 19: 21244 (ORNL-P-844)
reactions with nuclei at high energies, secondary nucleon yields from, (E/T), 19: 21242 (NP-14837)
scattering by calcium-40 at 150 Mev, energy levels from inelastic, (E), 19: 21332
scattering by magnesium-24 at 2.015 to 4.20 Mev, differential cross sections for inelastic, (E), 19: 21426
scattering by tin-118, analog states from inelastic, 19: 21341
scattering by titanium-48 and titanium-50 at 7 Mev, energy levels from inelastic, (E), 19: 21346
scattering of polarized, by aluminum-27 and beryllium-9 at 7 and 12 Mev, (E), 19: 21295
trapping in DCX-1 by Lorentz dissociation of hydrogen ions, losses in, 19: 21480(R) (ORNL-3760(p.1-9))
yields of secondary, in nucleon reactions with nuclei at high energies, (E/T), 19: 21242 (NP-14837)

PSEUDOUREA, 2-(2-AMINOETHYL)-2-THIO-
protective effects with serotonine against radiation lethality in mice, 19: 19627
protective effects of, against radiation injuries in mice, 19: 19635

PUERTO RICO
lead-210 content in population of, 19: 20193(R) (ANL-6938(p.120-4))

PULMONARY ABSORPTION
of inhaled insoluble particles, 19: 19456 (LF-21)

PULSE ANALYZERS
analog-digital converter for multichannel, fast binary, 19: 20299
data processing for multi-channel, computer system for, 19: 20315(R) (ANL-6938(p.206-8))
description of pulse shape discriminator for particle separation and pile-up suppression, 19: 20370
design of 100-channel time analyzer, 19: 20298
subgrouping multichannel, gating device for periodic, 19: 20283(R) (UCRL-11828(p.221))
use of multiscaler mode of, for Mössbauer effect studies, 19: 20327(R) (UCRL-11828(p.221-2))

PULSE COLUMNS
performance of cartridges for sieve-plate, 19: 20043 (IEA-77)

PULSE GENERATORS (ELECTRONICS)
description of, for firing Brookhaven AGS ignitrons, (E), 19: 20094 (BNL-8969)
design of high-voltage single-unit, 19: 20309

PULSE GENERATORS (PNEUMATICS)
model of air pulser, 19: 20042(R) (IDO-14646)

PUMPS
design for facility for separation of plutonium from leachable residues, 19: 20083
performance in radioactive waste deposition at depth of 900 ft in shale beds, 19: 21753
wear of coolant-circulating, in water-cooled reactors with chemical shims, 19: 21606 (WCAP-3269-9)

PUMPS (LIQUID METAL)
development of thermoelectric, (E), 19: 20096 (NAA-SR-Memo-10729)

PUREX PROCESS
plant modifications for increased processing flexibility, 19: 20040 (HW-84085)
separation of strontium from stored waste from, by lead sulfate carrier precipitation, 19: 20035 (BNWL-4)

PYRENE
radioinduced luminescence of, comparison of alpha and electron, 19: 19963

PYRIDINE
effects on ionic decomposition of *t*-butylperoxy formate, 19: 19948
ionization by electron impact, appearance potential for doubly charged molecule ions in, 19: 20807(R) (UCRL-11828(p.201-4))
reactions with rare earths in presence of salicylic acid for their separation from aqueous solutions, 19: 20079

PYRIDINE COMPLEXES
with germanium and molybdenum, properties for use as thin-layer chromatograms, 19: 20069

PYROCATECHOL
analytical uses of violet complex of, for determination of hafnium and zirconium, 19: 19780

PYROPHOSPHATES
effects on spectrophotometric determination of zinc using 1-(2-thiazolylazo)-2-naphthol, 19: 19814

PYRROLE
ionization by electron impact, appearance potential for doubly charged molecule ions in, 19: 20807(R) (UCRL-11828(p.201-4))

PYRROLIDONE, VINYL- POLYMERS
radiation effects on thermoluminescence, 19: 19983

Q

QUANTUM ELECTRODYNAMICS
analogies between scalar and vector mesodynamics, 19: 20929 (ICTP-64/12)
uncertainty relation in, coherent states and number-phase, 19: 21105
vacuum polarization phenomena in, gauge invariant calculation of, 19: 21119

QUANTUM MECHANICS
book: *Intermediate Quantum Mechanics*, 19: 21115
book: *Tables of Coulomb Wave Functions (Whittaker Functions)*, 19: 21117(T)
Clebsch-Gordan coefficients for cubic symmetry in problems in, 19: 21097
field theory in, microcausality in asymptotic, 19: 21088
field theory in, production processes from scattering in, (T), 19: 20961
formalism for excitation operators and intrinsic hamiltonians, 19: 21289
harmonic oscillator and SU(3) group, three-dimensional isotropic, 19: 21083
many-body problem in, radial distribution function for, 19: 21095
model for superconductors, (T), 19: 21163
model for two-particle system, 19: 20952
oscillators in, statistics of systems of coupled, 19: 21089
scattering by potential well, phase shifts in semiclassical, (T), 19: 20956
scattering in, wave packets in, (T), 19: 21092
scattering semiclassical phase shifts and transport cross sections, effects of three turning points on, (T), 19: 20957
statistical formulation of, in terms of phase space distribution functions, 19: 21118
statistical theory of relaxation in isolated spin systems, 19: 21121
two-body problem in the one-dimensional Heisenberg model, 19: 20812
uncertainty relation in, coherent states and number-phase, 19: 21105
wave mechanization of dynamical systems, 19: 21087

QUARTZ
radiation effects on, mechanisms in, 19: 20019

8-QUINOLINOL COMPLEXES
with germanium and molybdenum, properties for use as thin-layer chromatograms, 19: 20069

R

RABBITS
radiation and immunization effects on cholinerase activity in, 19: 19609
radiation effects on phagocytic activity of leukocytes in, 19: 19507(R) (TID-21712)
radiation effects on hematopoietic system in, 19: 19499(R) (NP-14899)
radiation effects on secretory activity of nuclei of brain hypothalamic area, 19: 19509(T) (JPRS-29250(p.9-13))
radiation effects on oxygen attachment in hemoglobin in, equation for calculating, 19: 19529(T)
radiation effects on, gamma globulin effects on fatal shock in, 19: 19535
radiation effects on metabolism in cornea of, 19: 19552
radiation effects on soluble DNA localization in lymphoid appendix tissue in, 19: 19583
radiation sickness in, effects on sulfur-35-labeled methionine uptake by marrow and spleen proteins in, 19: 19604
radiation sickness in, antibiotic therapy of infections during, 19: 19622
radioinduced dermatitis in, effects on blood serum protein fractions, 19: 19598
radioinduced toxins in liver lipids in, 19: 19599

RADAR
reflection in auroral zone, pulsations in, (E/T), 19: 21149
scattering from ionospheric plasma oscillations, incoherent, (E), 19: 21153
use to track balloons over long distances, 19: 21769 (TID-21661)

RADIATION
chimeras of bone marrow and lymph cells, effects on kidney grafts in dogs, 19: 19493
chimeras of mice, thymus effects on immunological reactivity and tolerance to bone marrow grafts in, 19: 19652
coherence properties of blackbody, 19: 21118
detection and measurement of, in analytical chemistry applications, 19: 19822
detection and measurement of mixed fields of ionizing, spark chambers for, 19: 20373
dose estimates of, after reactor accident, 19: 19630
dose rate measurements for electromagnetic or particle, method of, 19: 20396(P)
dosimetry of, review of difficulties in, 19: 20213
effects of nuclear warfare, ecological, 19: 19504 (RM-2801-PR)

effects of, bibliography on chemical, French, 1956 to 1961, 19: 19738(T)
effects on alkali halides, electron-spin and nuclear-magnetic resonance studies of, 19: 20620(R) (NYO-2024-8)
effects on alkaline phosphatase activity in human granulocytes, 19: 19570
effects on alumina–phosphate glass, 19: 20042(R) (IDO-14646)
effects on behavior, 19: 19572
effects on biological systems, 19: 19562
effects on biological materials and cells, 19: 19614
effects on bone marrow and organ graft tolerance, 19: 19588
effects on brain lysosomes, hypothesis on, 19: 19611
effects on cell replication, 19: 19613
effects on cellulose, bibliography on graft polymerization induced by, 19: 19960 (VDDIT-93)
effects on cellulose and its derivatives, review of chemical, 19: 19961(T) (CEA-tr-A-1741)
effects on cholinesterase activity in rabbits, effects of immunization on, 19: 19609
effects on dislocation loops in crystals, 19: 20580
effects on Ehrlich ascites carcinoma cells, protective effects of α- and β-alanine and arginine against, 19: 19636
effects on erythropoiesis in rat bone marrow, effects of bone marrow transplants on recovery from, 19: 19644
effects on genetic damage in populations, problems in assessment of 19: 19654
effects on host-cell interactions of hemopoietic grafts in, 19: 19615
effects on hydrocarbons, use of carbon-14-labeled methyl radical as scavenger in, 19: 19985
effects on immune reactions, 19: 19589
effects on maize, genetic, 19: 19527
effects on methylene blue in glycerol solution, 19: 20016
effects on mice, effects of allogenic chimeric bone marrow on repopulation of lymphatic tissue in, 19: 19646
effects on mice, protective effects of AET or MEA with serotonine against lethal, 19: 19627
effects on mice, protective effects of frozen bone marrow grafts against, 19: 19645
effects on morphology of rat thyroid, 19: 19569
effects on muscles, 19: 19551
effects on oxygen assimilation, steroid hormone content and weight of adrenal cortex, 19: 19584
effects on physicochemistry of DNA, review on, 19: 19566
effects on polymers, review of, 19: 19978
effects on rabbits, gamma globulin effects on fatal shock in, 19: 19535
effects on radio wave absorption by dielectrics, 19: 20629
effects on rats, leukemogenic, 19: 19530
effects on rats, oxygen requirements in, 19: 19539
effects on rats, protective effects of cystamine and royal jelly against, 19: 19629
effects on rats, relation between age and half lethal dose in, 19: 19575
effects on reactor pressure vessel steel, surveillance program for, 19: 21607 (APED-4773)
effects on semiconductors, book, 19: 20651(T)
effects on skin lesion formation on man, use of fresh blood autofibrin films for treatment of, 19: 19642
effects on tetanus vaccination in monkeys, 19: 19608
effects on thermal conductivity of uranium dioxide, 19: 20615 (HW-SA-3212)
effects on zygote cell division in sea urchins, gamma, 19: 19496(R) (ANL-6938(p.49-56))
emission from electric discharges in oxygen in homogeneous fields, 19: 20712
exposure to inhabitants in Mosonmagyarovar, Hungary from medical examinations in 1961, 19: 20227
exposure trends for 6 occupational classifications, 19: 20241
flux from alkali-seeded plasma in infinite-plane parallel enclosure, (T), 19: 21468 (BSD-TDR-64-164)
hazards from tritium release in laboratory accident, 19: 20194 (BLG-280)
hazards of, in fires in radioisotope production laboratories, 19: 20195 (BLG-281)
hazards of, in nuclear warfare, 19: 19554
hazards of, in nuclear warfare, 19: 19555
monitoring radiochemical plant, alarm system for, 19: 20203 (ORNL-TM-988)
skeletal anomalies in fetuses induced by, 19: 19533
use in textile industry, Euratom program on, 19: 20411
uses in production of compounds, economics of, 19: 20409

RADIATION CHEMISTRY
chemicals production using radiation, comparison with catalytic and photochemical methods, 19: 20409
energy absorption processes in, review of, 19: 19977
of alkanes, 19: 19980
of amino acids, 19: 19969
of amino acids and peptides in frozen aqueous solutions, 19: 20012
of aqueous solutions and water, 19: 19968

RADIATION DETECTION INSTRUMENTS
design and performance for detection of gamma radiation and neutrons from criticality accidents, 19: 20330(T) (AEC-tr-6547)
design for atmospheric monitoring for plutonium and uranium, 19: 20381
design for cosmic ray studies, 19: 20347
design for low beta activities, 19: 20382
design for measuring and recording radiation intensity, 19: 20394(P)
development of personnel fast-neutron dosimeters, (E), 19: 20318 (HW-SA-3526)
performance in monitoring radiation from nuclear explosion, device for simulation of, 19: 20244(P)
response matrices of, iterative unfolding method for, (T), 19: 20316 (ANL-6984)
standardization of, 19: 20262 (KFK-259)

RADIATION DETECTION INSTRUMENTS (ION CURRENT TYPE)
electric discharge broadening in self-quenching, 19: 20379

RADIATION DETECTION INSTRUMENTS (PULSE TYPE)
calibration of, device for use in, 19: 20395(P)
contrast in, electronic device for increasing, 19: 19696
design and function of, for localization of brain tumors, 19: 19712
design for Cosmos 17, 19: 20343
design of scintillation, 19: 20392(P)
design of scintillation, 19: 20393(P)
design of, for low alpha activities, 19: 20383
development of surface-field-controlled semiconductor, (E), 19: 20323(R) (NYO-3246-4)
development of, for monitoring of personnel by dose rate telemetering, 19: 20317 (HW-82369)
efficiency for direct measurement of air beta activity, 19: 20169
pulses for, transistor circuit for lengthening, 19: 20350

RADIATION DETECTORS
calibration of, x-ray facility for, 19: 20256 (HASL-151)
transmitter system for telemetering dose to remotely-located, 19: 20317 (HW-82369)
use of 4π, in absolute measurement of radionuclides in solution, 19: 19755 (KFK-252)

RADIATION INJURIES
classification of, after reactor accident, 19: 19630
diagnosis and therapy of chronic, review of, 19: 19623
effects on edema in cerebral cortex of rat brain, 19: 19607
emergency treatment of, after reactor accident, 19: 19630
in cells, reparation of, 19: 19614
in infants irradiated *in utero*, 19: 19699
model for, considering effects on organs and organ-organ interactions, 19: 19564
of bone marrow induced by injected Thorotrast, 19: 19567
of brain, induced by radiotherapy of eye tumors, 19: 19701
of embryos, protective effects of chemical agents on, 19: 19466
of liver induced by deposited Thorotrast, 19: 19560
pathology of, induced by electron beam exposure in mice, 19: 19635
pathology of, of hands, 19: 19524
protection against, effects of cysteamine or lead shielding of rat placenta, 19: 19557
protection against, effects of prochlorperazine in mice, 19: 19631
protection against, effects of prochlorperazine in mice, 19: 19632
protection against, effects of aminoethylisothiourea and serotonin in mice, 19: 19635
protection against, effects of injections of fresh and frozen bone marrow in rats, 19: 19641
protection against, effects of chemical agents, 19: 19643
protection against, effects of sulfhydryl compounds, 19: 19640
protective effects of shielding against, in pelvic diagnoses in infants, 19: 19677
role of glucose metabolism in, of animals, 19: 19538

RADIATION MONITORING
alarm system for radiochemical plant, 19: 20203 (ORNL-TM-988)
equipment for alpha, 19: 20381
equipment performance in nuclear explosion, simulation of, 19: 20244(P)
of medical and x-ray personnel in radiology work, 19: 20232
of personnel by dose rate telemetering system, 19: 20317 (HW-82369)

RADIATION PROTECTION
aims and responsibilities of health physicists, 19: 20219
development of personnel fast-neutron dosimeters, (E), 19: 20318 (HW-SA-3526)
during accidents involving radioactive materials, organization plan for, 19: 20197 (COO-281)
equipment for, of hospital staff during radiotherapy, 19: 19634

in atomic energy facilities, 19: 20209
methods of, survey of, 19: 20213
monitoring methods for, in Germany, 19: 20211
of patients during radiography, 19: 20229
of personnel in nuclear industry, 19: 20214
of personnel in static firing of nuclear rockets, 19: 21725
of populations from hazards of nuclear weapons, 19: 21761 (P-1134 (RAND))
personnel monitoring program for, 19: 20243
principles of personnel and population, organization for, 19: 20222
program in Canada, 19: 20161 (NP-14869)
programs in Canada, 19: 20224
standards for, in Canada, 19: 20212

RADIATION SICKNESS
antibiotic therapy of infectious complications of, in rabbits and rats, 19: 19622
diagnosis and treatment of, 19: 19630
effects of biomycin and embryonic blood-forming liver cells on, in rats, 19: 19637
effects of pethidine on breathing and metabolism in rat, 19: 19481
effects on sulfur-35-labeled methionine uptake by marrow and spleen proteins in rabbits, 19: 19604
hemorrhagic syndrome in guinea pig, relation of *E. coli* endotoxin involution to, 19: 19487
protective effects of fatty diet against, in rats, 19: 19625
syndrome of human, diagnosis and treatment of, 19: 19553

RADIATION SOURCES
book: *Industrial Applications of Radioelements*, in French, 19: 20417
industrial and research uses of, economics of, 19: 20408
regulations for control of, in California, 19: 19655
use in million megohm resistor, 19: 20310

RADIATION TARGETS
testing of, nondestructive, 19: 20126 (DPSPU-65-30-11)

RADIO WAVES
absorption by dielectrics in ionizing radiation field, 19: 20629
emission by DCX-1 plasma, 19: 21480(R) (ORNL-3760(p.1-9))
emission by DCX-2 plasma, 19: 21481(R) (ORNL-3760(p.10-22))
scattering from ionospheric plasma oscillations, incoherent, (E), 19: 21153

RADIOACTIVE CONTAMINATION
diagnosis and treatment of alpha, beta, and gamma, 19: 19656
of floors by plutonium, resuspension factors for, 19: 20191 (AERE-R-4635)

RADIOACTIVE MATERIALS
contamination of human skin by, recommendations for, 19: 19494
cutting of, engineering drawings of remotely operated machine for, 19: 20535
regulations for control of, in California, 19: 19655
sampling liquid, equipment for, 19: 20101(T) (ORNL-tr-442)
shipping of, on toll facilities, 19: 20239
transport and disposal of low-level wastes, structural integrity of containers for, 19: 20196 (CONF-650103-6)

RADIOACTIVE WATERS
radioactivity measurement in, review of methods for, 19: 19749 (EUR-2118.f)

RADIOACTIVITY
calculations for chain element, in intermittent irradiation in reactors, (T), 19: 21226 (AEET/HP/Th-19)
distribution in soil profile after plowing under radioactive dust, methods of measuring, 19: 20182
distributions of induced, in 200-Bev alternating-gradient synchrotron, (T), 19: 20732 (UCRL-11796)
measurement in solutions, methods for, 19: 20387
measurement in waste waters, review of methods for, 19: 19749 (EUR-2118.f)
monitoring atmospheric dusts in Debrecen, Hungary, 19: 20235
monitoring methods for compliance with regulations on, 19: 20211
monitoring nuclear explosion, device for simulation of, 19: 20244(P)
monitoring of ground air, in Hayes Island, 19: 20157 (NP-14697)
monitoring stratospheric, Star Dust Project, 19: 20657(R) (DASA-1309)
of marine environment, research program on, 19: 19469

RADIOAPPLICATORS
radiation dose from cobalt-60 beads, 19: 19708
use of yttrium-90, for destruction of pituitary gland, 19: 19660

RADIOBIOLOGY
book: *Advances in Radiation Biology*. Vol. 1, 19: 19461
book: *Mechanisms of the Inhibiting Effect of Ionizing Radiation on Cell Division*, 19: 19613

RADIOCHEMICAL PROCESSING PLANTS
alarm systems for, contamination and radiation, 19: 20203 (ORNL-TM-988)
design for separation of plutonium from leachable residues, engineering drawings of, 19: 20083
neutron spectrum measurements at Hanford plant areas, (E), 19: 20201 (HW-SA-3525)
operation of Windscale, for plutonium, 19: 20064
safety experience at Marcoule plant for reprocessing irradiated fuels, from six years' operation, 19: 20037 (CEA-R-2654)
waste solvent burning, 19: 21747 (DP-942)
waste solvent disposal by burning, 19: 21748 (DPSPU-64-30-8B)

RADIOCHEMISTRY
of low-energy fission of heavy nuclei, 19: 20033

RADIODERMATITIS
blood serum protein fraction changes in human and rabbit, 19: 19598
induced by radiotherapy, morphology of nervous structures in, 19: 19591
pathology and treatment of, 19: 19605
pathology of, 19: 19524
treatment with Solcoseryl, 19: 19633

RADIODIAGNOSIS
clinic for, in Great Britain using iodine-131, 19: 19682
development and hazards of, 19: 19657(R) (ANL-6938(p.97-119))
effects on human genetics by infant exposure, 19: 19568
of amebiasis in human, by scintiscanning using gold-198 and iodine-131, 19: 19728
of bone tumors by external scanning of strontium-85, 19: 19666
of bone tumors by scintillation scanning using strontium-85, 19: 19697
of bone tumors using strontium-85, 19: 19675
of bone tumors, evaluation of radioisotopes for tracer use in, 19: 19666
of coronary insufficiency and myocardial circulation using rubidium-86, 19: 19668
of echinococcus liver disease by scanning using iodine-131, 19: 19729
of hemolytic anemia by photoscanning of spleen using heat-treated chromium-51-labeled erythrocytes, 19: 19725
of liver and spleen by photoscanning using iodine-131-labeled human serum albumin, 19: 19710
of liver and thyroid by photoscanning using iodine-125, 19: 19711
of liver diseases by scanning using gold-198 and iodine-131, evaluation of, 19: 19730
of liver tumors in man by iodine-131 infusion in bowel, 19: 19662
of pancreatic tumors by scanning using selenium-75-labeled seleno-methionine, 19: 19722
of pancreatic tumors by photoscanning using selenium-75-labeled selenomethionine, 19: 19723
of pulmonary embolism in dogs and man by photoscanning using chromium-51 or iodine-131, 19: 19724
of spinal neurology syndromes by myeloscintigraphy after administration of iodine-131, 19: 19720
of spleenic defects and tumors by scintiscanning using chromium-51, 19: 19726
of spleenic function by scintiscanning using chromium-51, 19: 19727
of thyroid tumor by external counting of cobalt-57- or cobalt-58-labeled vitamin B-12, 19: 19732
of urologic diseases by renal scintiscanning using mercury-203, 19: 19721
radiation exposure to inhabitants of Mosonmagyarovar, Hungary from, in 1961, 19: 20227
radiation hazards from use of iodine-131 for, 19: 19587
radiation hazards from use of radioisotopes for, 19: 19670
use of iodine-131-labeled compounds for, 19: 19731
use of radioisotopes in, conference on, 19: 19709

RADIOGRAPHY
of pelvic regions during pregnancy, radiation hazards to fetus of, 19: 19698
radiation exposure of head during dental diagnostic, 19: 19676
radiation hazards of diagnostic chest, in pregnant women, 19: 19592
radiation hazards from diagnostic uses in infants, 19: 19678
radiation hazards during pregnancy of diagnostic, 19: 19699
radiation monitoring of personnel engaged in, 19: 20232
radiation protection of patients during, 19: 20229

RADIOISOTOPES
activity determination by 4π beta-gamma coincidence method, corrections for, 19: 20385
activity of solutions of, methods for measuring, 19: 20387
activity of, corrections in β-γ-coincidence measurement of, 19: 20386
book: *Industrial Applications of Radioelements*, in French, 19: 20417
characteristics of heat sources of, 19: 20431 (TID-7698(Pt.I)(p.1-16))
content in marine environment, effects and source of artificial and natural, 19: 20226
distributions in 200-Bev alternating-gradient synchrotron, (T), 19: 20732 (UCRL-11796)
incorporation in compounds, rules for formulas and nomenclature following, 19: 19736

incorporation in organic compounds, rules for formulas and nomenclature following, 19: 19737
production in pile irradiation, resolution of matrix equation for calculating, 19: 19958 (CEA-R-2348)
production using Rossendorf Reactor in East Germany, review of, 19: 20436
radiation protection programs for users of, in Canada, 19: 20224
standardization of electron-capture, method for, 19: 20384
uptake by marine organisms, research program on, 19: 19469
use in diagnostic scanning, conference on, 19: 19709
use in industrial automation, 19: 20416
use in nuclear batteries, economics of, 19: 20415
use in power sources, conference on, 19: 20426 (TID-7698(Pt.I))
use in radiotherapy, complications and dosages in, 19: 19706
use in space propulsion, POODLE program for, 19: 20428 (TID-7698 (Pt.I)(p.257-76))
use in textile industry, Euratom program on, 19: 20411
use to excite x-ray fluorescence in analysis of light elements, 19: 19741 (CEA-R-2539)
use to power underwater acoustic beacon with fluid-mechanical energy conversion, feasibility study, 19: 20405 (MND-3180-1)
uses as radiation sources in industry and research, 19: 20408
uses for investigation of processes in boilers, book, 19: 20418
uses in medicine, control and hazards of, 19: 19657(R) (ANL-6938 (p.97-119))
uses of, bibliography on, French, 1956 to 1961, 19: 19738(T)
uses of, literature review for Naval use in field and research, 19: 20403 (AD-606253)

RADIOLOGICAL DEFENSE
organization of medical facilities for, 19: 19554
organization of medical facilities for, 19: 19555

RADIOLOGICAL TELEMETERING SYSTEMS
design for monitoring personnel, 19: 20317 (HW-82369)

RADIOLOGICAL WARFARE
ecological problems of post-attack recovery, 19: 19504 (ZM-2801-PR)
effects on ecosystem, 19: 20199 (HI-388-RR(Pt.III))
international control, 19: 21761 (P-1134(RAND))
medical aspects of, 19: 19554
medical aspects of, 19: 19555

RADIOLOGICAL WARFARE AGENTS
development in Soviet Union, 19: 21762 (RM-2163(RAND))
international control, 19: 21761 (P-1134(RAND))

RADIOLOGY
of human lymph system using gold-198, 19: 19719
of kidneys using thorotrast, tumor development from, 19: 19707
radiation monitoring of personnel engaged in, 19: 20232
regulations for control in dental, 19: 19655
research programs at ANL, July 1962 to July 1963, 19: 20192(R) (ANL-6938)

RADIOMETRIC ANALYSIS
of filter paper samples for fission products, quality control of gamma spectrometric, 19: 20162(R) (NYO-3276-9)
of labeled biological samples, effects of color quenching variables, 19: 20324 (ORNL-P-1094)
substoichiometric separation in, theory and uses of, 19: 19783

RADIOMIMETIC SUBSTANCES
effects on erythrocyte content in rat blood, 19: 19489

RADIOPROTECTIVE COMPOUNDS
chemical structure of, review, 19: 19620(T) (JPRS-29200(p.96-106))
criteria for, 19: 19620(T) (JPRS-29200(p.96-106))
evaluation of prochlorperazine in mice, 19: 19631
evaluation of prochlorperazine in mice, 19: 19632
evaluation of sulfhydryl compounds as, 19: 19640
protective effects against radiation injuries of developing embryos, 19: 19466
protective effects against 19-norandrostenolone effects on acute radiation disease in rats, 19: 19624
reaction mechanisms in cells, 19: 19614
toxic effects in man of, 19: 19643

RADIOSENSITIVITY
of amino acids and proteins, effects of SH-inhibitors on, 19: 19621
of animal cells, factors affecting, 19: 19614
of microörganisms, 19: 19590
of nonpedigreed and Wistar strain rats, 19: 19585
of seed from grain crops grown on fission product-contaminated soil, 19: 19508(T) (JPRS-28977)
of *Serratia marcescens*, effects of humidity and inositol on, 19: 19649
of sprouting maize seed, effects of 2,4-dinitrophenol on fast neutron and gamma, 19: 19582

RADIOSTERILIZATION
of beef, product treatment for flavor in, 19: 20406 (NP-14928)
of carrots, onions, and potatoes, for inhibition of sprouting, 19: 20424
of food and medical supplies, 19: 20410
of foods, effects on plastic film packaging in, 19: 20421
of foods, effects on wholesomeness, 19: 20423
of foods, microbiological safety of, 19: 20420
of foods, use of electron accelerators for, 19: 20422
of meats and poultry, 19: 20425
of oranges, effects on quality, 19: 20404 (IA-999)
of oysters and shrimp, effects on storage life, 19: 20407(R) (ORO-626)

RADIOTHERAPY
development and hazards of, 19: 19657(R) (ANL-6938(p.97-119))
dose distribution in cobalt-60, effects of filters on, 19: 19690
dose distribution and rate in pendulum, method for determining, 19: 19691
dose distributions in, use of computers for calculating, 19: 19692
dose distributions in, photographic method for determining, 19: 19693
dose distributions in high-energy electron, energy dependence of, 19: 19695
equipment for properties of Russian Volfram, 19: 19704
evaluation of results, 19: 19702
of cancer of larynx, 19: 19659
of cancer of uterine cervix, 19: 19681
of cancer, effects on liver function, 19: 19684
of cancer, radiation dose evaluation, 19: 19597
of carcinomas of uterus, radiation dose from implanted cobalt-60 beads, 19: 19708
of euthyroid goiters in man using iodine-131, 19: 19685
of eye tumors, radiation injuries of brain induced by, 19: 19701
of gynecologic cases using radium, protective equipment for hospital personnel in, 19: 19634
of human tumors, anabolic effects of steroids in, 19: 19669
of lung tumors in man, effects on healthy lung tissue, 19: 19683
of pelvic and vulvar cancer, method for intralymphatic, 19: 19658
of pituitary using gold-198 and yttrium-90 seeds, 19: 19667
of thyroid diseases using iodine-131, 19: 19665
of tumors using electron beams, 19: 19673
of tumors, design of slit-type lead screen for use with cobalt-60 gamma sources, 19: 19674
of tumors, dose distribution in, 19: 19671
of tumors, dose distribution in, 19: 19672
of tumors, effects of surgery, 19: 19703
of uterine carcinomas, 19: 19663
of uterine carcinomas, dose field distribution in telegamma, 19: 19686
of uterine tumors, 19: 19700
requirements and sources for, relation between, 19: 19688
requirements for, medical, 19: 19687
techniques for use of radioisotopes in, by intra-arterial injection, 19: 19661
tissue factors in, measurements on betatron and gamma, 19: 19689
use of isotopes in, complications and dosages in, 19: 19706
using cobalt-60 teletherapy unit, isodose charts for obliquely incident wedge-filtered beams, 19: 19733
using high-energy electrons, physical problems in, 19: 19694

RADIUM
content in bones of muskrats in contaminated lake, 19: 20220

RADIUM ISOTOPES Ra-224
content in blood and bones of humans injected with thorotrast, 19: 19497(R) (ANL-6938(p.127-39))
content in tissues of humans and rats injected with thorotrast, 19: 19497(R) (ANL-6938(p.127-39))

RADIUM ISOTOPES Ra-226
content in human placenta and fetal skeleton, 19: 20216
content in plants and silts in contaminated lake, 19: 20220
use in age estimation of marine carbonates, 19: 20181

RADIUM ISOTOPES Ra-228
content in blood and bones of humans injected with thorotrast, 19: 19497(R) (ANL-6938(p.127-39))
content in tissues of humans and rats injected with thorotrast, 19: 19497(R) (ANL-6938(p.127-39))

RADIUM ORES
radioactivity equilibrium in, in accessory monazites of Ukraine, 19: 20189

RADON ISOTOPES Rn-222
gamma spectra of, effects of daughter products on, 19: 21299
separation from air in low-level gamma counting rooms, 19: 20092(R) (ANL-6938(p.91-6))

RAIN WATER
analysis for cesium-137, strontium-89, and strontium-90 by electrodialysis and gamma spectroscopy, 19: 19809
radioactivity from tritium content in, 19: 20174(T) (CEA-tr-A-1729)
radioactivity monitoring of, in Canada, 19: 20161 (NP-14869)

RARE EARTH COMPLEXES

with serine, stability and composition, 19: 19874

RARE EARTH COMPOUNDS
solubility and thermolysis of dilitunte, 19: 19824

RARE EARTH HALIDES
vapor pressure differences in, separation by, 19: 20062

RARE EARTH NITRIDES
magnetic properties of, influence of crystal field on, 19: 19895

RARE EARTH SYSTEMS
B–C–rare earths, phase studies, 19: 19926

RARE EARTHS
analysis for cerium by polarography, 19: 19821
book: *Problems in Theory and Applications of Rare Earth Metals*, in Russian, 19: 20468
chemistry of, bibliography on, French publication, 1956 to 1961, 19: 19738(T)
determination as impurities in pure bismuth by activation methods, 19: 19796
determination by complex formation with substituted acetic acids, 19: 19802
determination by precipitation as dilituate, 19: 19824
determination by spark source mass spectrography, 19: 19830
determination in ores, colorimetric, 19: 19778(T) (JPRS-29037(p.58-68))
determination using 5,5′-thiodisalicylic acid, gravimetric, 19: 19812
effects on graphitization of carbon, 19: 20536(P)
geochemistry and mineralogy of, in Cherry Mountains (Urals), USSR, book, 19: 20190
partition coefficients in basic rocks, effects of oxygen anion size on, 19: 20152
phase diagrams of, effects of atomic structure on, 19: 20600
physical properties of, effects of periodicity of electron shell structure on, 19: 20600
production of neutron-deficient isotopes of light lanthanides in proton bombardment of erbium, 19: 20078
separation by distillation of halides, 19: 20062
separation by ion exchange, use of polyphosphates as elution medium in, 19: 20049 (NP-14834)
separation from aqueous solution by solvent extraction as salicylate pyridine complex, 19: 20079
separation from magnesium–thorium alloy by transfer to liquid magnesium–zinc alloy in fused salt, 19: 20066
separation from strontium, 19: 19789

RARE GASES
charge exchange in, atom-ion resonance, (T), 19: 19931
effects on electron energy distribution in mercury discharge plasma, (T), 19: 21579

RATE METERS
design of gamma intensity time recorder, 19: 20397
design of scintillation, for fast-neutron dosimetry, (E), 19: 20312 (AERE-R-4525)

RATS
barium metabolism in, tracer study, 19: 19500 (NP-14907)
bone and cartilage formation in, diurnal variations of, 19: 19472(R) (ANL-6938(p.179-93))
calcium-47 and strontium-85 retention in, effects of cortisone and anabolic steroids on, 19: 19476
cholesterol metabolism in, effects of hypothyroidism, 19: 19511(T) (JPRS-29364(p.1-4))
effects of nitrogen mustard on erythrocytes in, 19: 19489
effects of strontium-90 on treatment of rickets in, with vitamin D_2, 19: 19680
healing of wounds in, effects of ascorbic acid and water-d_2 on, 19: 19484
neutron activation of elements in tissues of, 19: 19601
radiation effects on desoxyribonucleic acid metabolism in liver and intestine of, 19: 19506 (TID-21703)
radiation effects on hematopoietic system in, 19: 19499(R) (NP-14899)
radiation effects on mitotic activity in regenerating liver of, 19: 19510(T) (JPRS-29250(p.27-32))
radiation effects on cholesterol metabolism in, 19: 19511(T) (JPRS-29364(p.1-4))
radiation effects on electroshock seizures in, cysteine and dose effects on, 19: 19514
radiation effects on, oxygen requirements in, 19: 19539
radiation effects on peroxide decay in spleen DNA in, 19: 19541
radiation effects on interferon synthesis and virus plaque development in embryonic cells of, 19: 19563
radiation effects on morphology of thyroid in, 19: 19569
radiation effects on, relation between age and half-lethal dose in, 19: 19575
radiation effects on ionic permeability of erythrocytes in, 19: 19577
radiation effects on serum albumin synthesis in liver of, effects of food ingestion on, 19: 19603
radiation effects on lipid metabolism in brain of newborn and weanling, 19: 19610
radiation effects on activity, learning, mortality, and seizure susceptibility of, exposed *in utero*, 19: 19618
radiation effects on, effects of 19-norandrostenolone on acute, 19: 19624
radiation effects on, protective effects of casein diets against, 19: 19628
radiation effects on bone marrow erythropoiesis in, effects of bone marrow transplants on recovery from, 19: 19644
radiation effects on, protective effects of cystamine and royal jelly against, 19: 19629
radiation effects of phosphorus-32 on digestive tract in, 19: 19565
radiation effects, carcinogenic, 19: 19561
radiation injuries of placenta, protective effects of cysteamine or lead shielding, 19: 19557
radiation injuries in, effects on edema in cerebral cortex, 19: 19607
radiation injuries, protective effects of injections of fresh and frozen bone marrow, 19: 19641
radiation sickness in, effects of pethidine on breathing and metabolism in, 19: 19481
radiation sickness in, antibiotic therapy of infections during, 19: 19622
radiation sickness in, protective effects of fatty diet against, 19: 19625
radiation sickness in, effects of biomycin and embryonic blood-forming liver cells on, 19: 19637
radioinduced cataracts in, 19: 19612
radioinduced leukemia in, 19: 19530
radioinduced tumors in, effects of chemical carcinogens on, 19: 19606
radiosensitivity of nonpedigreed and Wistar strain, 19: 19585
strontium metabolism in fetal and newborn, tracer study, 19: 19473 (UR-661)
strontium metabolism in, tracer study, 19: 19500 (NP-14907)
thorium-232 decay products in tissue of thorotrast-injected, 19: 19497(R) (ANL-6938(p.127-39))

REACTION MECHANISMS
formation constants of oxidation-reduction reactions, calculation, 19: 19836 (HW-SA-3476)
rate constant measurements for reactions of free radicals with solutes in aqueous solutions, 19: 19968

REACTOR BREEDING BLANKETS
effects of central, on static performance of fast power reactor, 19: 21696

REACTOR COMPONENTS
design analysis for prestressed-concrete vessels, (T), 19: 21683 (GAMD-5272(Rev.2))
stress analysis of prestressed concrete, computer program for, 19: 20086 (GAMD-5926)
tendon configuration in pre-stressed concrete, program for determining optimal, 19: 21610 (GAMD-6109)

REACTOR CONTROL RODS
design of telescopic, 19: 21622(P)
design of, containing two neutron-balance-disturbing substances, 19: 21631(P)
drive mechanism for, 19: 21621(P)
drive mechanism for, design of electromagnetic, 19: 21629(P)
neutron extrapolation distance at surface of grey, (T), 19: 21649
testing of aluminum–lithium alloy, equipment and methods for nondestructive, 19: 20126 (DPSPU-65-30-11)
testing of, drop, 19: 21690(R) (LA-3244)

REACTOR CONTROL SYSTEMS
actuator motors for, development of pneumatic-nutator, (E), 19: 21615(R) (NASA-CR-54282)
design for boiling-water reactors, 19: 21661(P)
design for indicating excess reactivity at startup, 19: 21623(P)
design of, utilizing neutron-absorbing fluid, 19: 21632(P)
development of, utilizing variations in level of liquid moderator, 19: 21660(P)
theory of automatic, for rockets, 19: 21723(R) (NASA-CR-193)

REACTOR COOLANTS
circulation in swimming pool reactor, forced-convection, 19: 21744(P)
heat transfer burnout and stability of natural-circulation water, in seven-rod bundle, 19: 20120
steam void determination in, method for, 19: 20294

REACTOR COOLING SYSTEMS
decontamination of, 19: 21605 (HW-SA-3560)
design of emergency, for removal of shutdown heat, 19: 21630(P)

REACTOR ENGINEERING
control theory in nuclear rocket control and dynamics, 19: 21723(R) (NASA-CR-193)
corrosion problems in, review of, 19: 20488
design analysis for prestressed-concrete vessels, (T), 19: 21683 (GAMD-5272(Rev.2))

thermal analysis of cylindrical shells, (T), 19: 21619
thermal stress distributions in elastic and viscoelastic shells in reactor shutdown, 19: 21618
REACTOR FUEL ALLOYS
preparation of cerium–cobalt–plutonium, 19: 21690(R) (LA-3244)
REACTOR FUEL ELEMENTS
cans for, properties of magnesium–0.5 to 1.0 wt% zirconium alloy for, 19: 20610(P)
core-position determination in clad, apparatus for, 19: 20135(P)
design for use in reactor controlled by varying level of liquid moderator, 19: 21660(P)
design of tube assembly for high-temperature reactors, 19: 21675(P)
dissolution of APPR and HTRE-3, in Arco Plant, 19: 20042(R) (IDO-14646)
fabrication of clad, by extrusion of pressed block, 19: 20540(P)
failure in magnox reactors, detection of, 19: 21616
failure in reactors, detection system for, 19: 21624(P)
fission product release by, apparatus for detecting, 19: 21626(P)
processing at Arco Plant, aqueous, 19: 20042(R) (IDO-14646)
processing of irradiated, development of direct fluoride volatility process for, 19: 20059
processing of irradiated, fission product separation in, 19: 20084(P)
radiography of irradiated, neutron, 19: 20129
reclaiming inner, with cracked supports, 19: 21668 (HW-84196)
temperature distributions in end caps of cylindrical, (T), 19: 21674
testing for fast, sodium-cooled, ceramic reactors, (E), 19: 21666(R) (GEAP-4640)
testing of defective or high-risk, engineering drawings of in-pile loop for, 19: 21704
testing of uranium, equipment and methods for nondestructive, 19: 20126 (DPSPU-65-30-11)
thermal bowing, (E/T), 19: 21669
thermal conductance measurement in-pile, development of transient temperature method for, 19: 21664(R) (CEND-3336-229)
REACTOR FUEL ELEMENTS (CERAMIC)
buckling of uranium-carbide, in sodium-graphite lattices, (E), 19: 21692 (NAA-SR-Memo-9976)
design of GAIL-IV experimental, 19: 21665 (GAMD-5535)
development, performance, and uses of, survey of, 19: 21670
performance of, review, 19: 21671
processing of irradiated, by volatilization, 19: 20060
processing of uranium carbide, evaluation of aqueous and pyro-, 19: 20048 (NAA-SR-9335)
sodium logging in, effects of, 19: 20458 (GEAP-4283)
testing for fast sodium-cooled reactors, (E), 19: 21666(R) (GEAP-4640)
REACTOR FUEL ELEMENTS (DISPERSION)
development of coated-particle graphite-matrix, 19: 20463 (ORNL-TM-431)
development of uranium matrix containing very small uranium carbide particles, 19: 20511(R) (NCSC-2981-1)
development of uranium matrix containing very small uranium carbide particles, 19: 20512(R) (NCSC-2981-2)
development of uranium matrix containing very small uranium carbide particles, 19: 20513(R) (NCSC-2981-3)
development, performance, and uses of, survey of, 19: 21670
fabrication, 19: 20539(P)
oxidation tests of aluminum alloy-coated niobium-alloy, 19: 20482 (SCNC-314)
performance of, review, 19: 21671
processing of graphite-base coated-particle, development of methods for, 19: 20463 (ORNL-TM-431)
testing of stainless steel–uranium dioxide, in Spert I, 19: 20616 (IDO-17011)
REACTOR FUEL PLATES
design of aluminum–uranium alloy, engineering drawings of, 19: 21743
design of, with concentration gradients of fissionable material and burnable poisons, 19: 21676(P)
oxidation tests of aluminum alloy-coated niobium-alloy, 19: 20482 (SCNC-314)
testing of stainless steel–uranium dioxide, in Spert I, 19: 20616 (IDO-17011)
REACTOR FUEL RODS
fabrication by vibratory and impact forming and swaging, 19: 20526
neutron resonance escape in regular arrays of heterogeneous, (T), 19: 21648
REACTOR FUEL TUBES
deformation of uranium, by external pressure, 19: 20453 (CEA-R-2572)
extrusion of I&E, traveling mandrel for, 19: 20501(R) (BRB-77)
extrusion of Mark V-E, effects of variables on duplex grain structure formation in, 19: 20501(R) (BRB-77)
extrusion of Mark V-B, effects of reduction ratio on, 19: 20501(R) (BRB-77)
testing of aluminum–uranium alloy, equipment and methods for nondestructive, 19: 20126 (DPSPU-65-30-11)
REACTOR FUELS
burnup in fast reactors, equations for, 19: 21672
burnup of, accurate determination of, (E), 19: 21667(R) (GEAP-4776)
compatibility of coated-particle, with molten fluoride, 19: 20463 (ORNL-TM-431)
development for fast reactor, 19: 21690(R) (LA-3244)
development in Canada, 19: 21781
development of coated-particle, 19: 20463 (ORNL-TM-431)
development, performance, and uses of coated-particle, survey of, 19: 21670
processing of, economics of fission product recovery in, 19: 20036 (BNWL-25)
radiation effects testing, experience with high-temperature thermocouples in, 19: 20401 (ORNL-P-1065)
reprocessing at Marcoule, safety experience in, 19: 20037 (CEA-R-2654)
separation of protactinium-233 from irradiated thorium–uranium, by sorption on unfired Vycor, 19: 20051 (ORNL-3773)
REACTOR MATERIALS
neutron cross sections of, availability of data on, (E), 19: 21225 (AECL-2168)
thermodynamic properties of, tables of, 19: 19933
REACTOR MATRICES
neutron multiplication and material buckling in natural uranium-light water, 19: 21645
REACTOR MODERATORS
level of liquid, reactor control by variations of, 19: 21660(P)
support structure for vertically stacked, solid, 19: 21627(P)
support structure for solid, in gas-cooled heterogeneous reactors, 19: 21628(P)
REACTOR REFLECTORS
neutron transport in, heat transfer model for, 19: 21656
REACTOR SAFETY
evaluation of PM-1 and PM-3A, 19: 21685 (HASL-152)
in transient pressures and coolant expulsion, 19: 21652
pressure distributions in gas-cooled-reactor shielding following pressure-vessel failure, (E), 19: 21608 (AWRE-R-2/65)
radiation monitoring of personnel by dose rate telemetering, 19: 20317 (HW-82369)
testing RFD-2 re-entry vehicle, (E), 19: 21763 (SC-DR-64-1741)
REACTOR SAFETY EXPERIMENTS
fuel element testing in Spert I, fully enriched stainless steel plate, 19: 20616 (IDO-17011)
loop meltdown experiments in TREAT, analysis of sodium, 19: 21652
pressure effects in, from vaporizing coolant, 19: 21652
REACTOR SHIELDING
performance of lithium-hydride, (T), 19: 21614 (NAA-SR-Memo-10559)
pressure distributions in, following pressure-vessel failure, (E), 19: 21608 (AWRE-R-2/65)
properties of concrete, evaluation of, 19: 21739
thermal protection system for concrete, evaluation and economics of, 19: 20110 (GAMD-5432)
REACTOR SIMULATORS
time delays for, design of time-variable, (E), 19: 21713 (HW-83092 (Rev.))
REACTOR TUBES
neutron production in thermal, method for fast, 19: 21742
radiation effects on Zircaloy-2 PRTR, 19: 21686 (HW-84540)
securing in reactor, device for, 19: 21633(P)
REACTORS
control of, hybrid computation for optimal, 19: 21604 (EUR-2202.e)
design with variable moderator level, 19: 21660(P)
development in Soviet Union, 19: 21762 (RM-2163(RAND))
kinetics of, calculations of parameters involved in, (T), 19: 21640 (IDO-16983)
kinetics of, centers and limit cycles for, (T), 19: 21634 (BNL-9010)
kinetics of, effects of heat transfer on, 19: 20116(R) (SAN-409-12)
kinetics of, finite-escape-time concept for, (T), 19: 21635 (BNL-9011)
kinetics of, nonlinear analysis of, (T), 19: 21642 (MMPP-FRPC-64-3)
light production by, in underground processes of, 19: 21710
loading equipment and methods for, 19: 21625(P)
neutron diffusion in, variational flux-synthesis analysis of, (T), 19: 21638 (CONF-650501-4)
neutron fluctuations and multiplication in, (T), 19: 21641 (JINR-P-1996)
neutron flux distributions in, computer program for, 19: 21644 (WAPD-TM-478)
neutron transport in reflectors of, heat transfer model for, 19: 21656
physics calculations on, availability of nuclear data for, (E), 19: 21225 (AECL-2168)
pulsation of, by movement of body of fissionable and magnetizable

material through neutron field of core, 19: 21657(P)
radioactivity of chain elements in, with intermittent irradiation, (T), 19: 21226 (AEET/HP/Th-19)
radioinduced carbon dioxide-graphite reactions in, inhibition of, (E), 19: 19953 (AERE-R-4201)
reactivity excursions starting at operating conditions, (T), 19: 21650
reactivity of, inverse kinetics analysis of, (T), 19: 21651
reactivity of, pulsed-neutron measurements of, (T), 19: 21637 (CONF-650406-2)
reactivity of, solutions of kinetic equations for, (T), 19: 21647
uses as radiation sources in industry and research, 19: 20408

RECOIL IONS
labeling by, selectivity in, 19: 20020 (IA-907)

RECTIFIERS
firing Brookhaven AGS ignitrons by variable-phase pulses, (E), 19: 20094 (BNL-8969)

REFRACTORY MATERIALS
coatings on, ultrasonic method for nondestructive testing of, 19: 20127(R) (IITRI-N213-23)
melting point measurement for metallic, method for, 19: 20566(T) (IS-Trans-13)

RELATIVITY THEORY
book: *Introduction to the Theory of Relativity and the Principles of Modern Physics*, 19: 21116
curvature tensor in electromagnetic field, projective, 19: 21084
Einstein theory for generalized inertial systems in general, 19: 20706
Einstein vacuum field equations of, for space-time containing twisting ray congruence, 19: 21120
energy in, potential, 19: 20694
field equations in general, electromagnetic solutions of, 19: 21103
fields with arbitrary spin and zero rest-mass, asymptotic behavior of, 19: 21108
gravitational collapse in general, radiative diffusion in, 19: 21100
gravitational radiation reaction effects on two-body problem in general, 19: 21104
motion equations for rotating particles in general, 19: 21109
relative velocity in, validity of relativistic velocity transformation equation for, 19: 21098
simultaneity theorem of special, testing of, 19: 21106
time dilation in, use of Mössbauer effect for measuring, 19: 20699

RELAYS
evaluation of DPDT, for SNAP-10A, (E), 19: 21733 (NAA-SR-Memo-10532)

REMOTE-CONTROL EQUIPMENT
design for cutting radioactive materials, engineering drawings of, 19: 20535
design specification for gantry and trolley for fuel handling cask, 19: 20099 (TID-21644)

REMOTE-VIEWING EQUIPMENT
design observations in fluid-tight chambers, 19: 20105(P)

RESEARCH REACTORS
experimental facilities of FR2, data acquisition system using on-line computer for, 19: 21731 (KFK-242)
neutron density fluctuation in JRR-1, measurement of, 19: 21737
radioactivity from JRR-2, measurements of, 19: 21738
testing in, mathematical expressions for, 19: 21740

RESINS
radioactivity of thin chromatographic layers of, equipment and method for measuring beta, 19: 19792

RESISTANCE THERMOMETERS
resistance bridge design for low-temperature, engineering drawings of, 19: 20307

RESISTORS
calibration of, engineering drawings of resistance bridge for, 19: 20307
design of million-megohm, using radiation source between terminals, 19: 20310

RESPIRATION
effects of pethidine on, in rats with radiation sickness, 19: 19481

RESPIRATORY TRACTS
transport of insoluble particles in, 19: 19456 (LF-21)

RHENIUM
determination in rhenium–tantalum alloys, spectrophotometric, 19: 19757 (LA-3213)
electrodeposition on molybdenum and tungsten, optimum conditions for, 19: 20529
geochemistry and mineralogy of, in Cherry Mountains (Urals), USSR, book, 19: 20190
performance of electrodes of, in thermionic converters, 19: 20906
separation from technetium, 19: 19820

RHENIUM ALLOY COUPLES
Re–W/Re–W, performance in gas-cooled reactor fuel irradiation experiments, 19: 20401 (ORNL-P-1065)
Re–W/Re–W, thermocouple tables, smoothed, 19: 20270 (ORNL-3649 (Vol.2)(Sect.2.8))
Re–W/Re–W, thermocouple drift at high temperatures in vacuum, 19: 20278 (ORNL-P-1069)
Re–W/Re–W, thermocouple tables, smoothed, 19: 20271 (ORNL-3649 (Vol.2)(Sect.2.9))
Re–W/W, thermocouple tables, smoothed, 19: 20269 (ORNL-3649 (Vol.2)(Sect.2.7))
Re–W/W, thermocouple drift at high temperatures in vacuum, 19: 20278 (ORNL-P-1069)

RHENIUM ALLOYS
Mo–Re–W, ductility and melting points of sintered, 19: 20584
Re–Ta, spectrophotometric analysis for rhenium, 19: 19757 (LA-3213)
Re–W, tensile properties at 800 to 2400°C, 19: 20565 (WADD-TR-60-37(Pt.V))
Re–W, testing of thin-wall tubes of, electromagnetic, 19: 20454 (CONF-650212-1)

RHENIUM BORIDES
crystal structure, 19: 19841 (MIT-1965-18)

RHENIUM BROMIDES
spectra of rhenium(IV) hexabromides, absorption, 19: 19924

RHENIUM CHLORIDES
crystal structure, 19: 19841 (MIT-1965-18)
spectra of rhenium(IV) hexachlorides, absorption, 19: 19924

RHENIUM COMPLEXES
with organic compounds, preparation on, 19: 19841 (MIT-1965-18)

RHENIUM COUPLES
Re/W, development, 19: 20473(R) (NASA-CR-54629)
Re/W, performance in gas-cooled reactor fuel irradiation experiments, 19: 20401 (ORNL-P-1065)

RHENIUM FLUORIDES
spectra of rhenium(IV) hexafluorides, absorption, 19: 19924

RHENIUM IODIDES
spectra of rhenium(IV) hexaiodides, absorption, 19: 19924

RHENIUM ISOTOPES Re-185
fluorine-19 reactions (F-19,xn), production of light polonium isotopes by (E), 19: 21250(R) (UCRL-11828(p.26))

RHENIUM ISOTOPES Re-186
hyperfine structure, (E), 19: 21382
nuclear magnetic moments, (E), 19: 21383

RHENIUM ISOTOPES Re-187
fluorine-19 reactions (F-19,xn), production of light polonium isotopes by (E), 19: 21250(R) (UCRL-11828(p.26))

RHENIUM ISOTOPES Re-188
hyperfine structure, (E), 19: 21382
nuclear magnetic moments, (E), 19: 21383

RHODIUM
determination using 5,5′thiodisalicylic acid, spectrophotometric, 19: 19812
separation from power reactor fuels, economics of, 19: 20036 (BNWL-25)

RHODIUM ALLOY COUPLES
Pt/Pt–Rh performance in gas-cooled reactor fuel irradiation experiments, 19: 20401 (ORNL-P-1065)
Pt/Pt–Rh, thermocouple tables, smoothed, 19: 20263 (ORNL-3649 (Vol.2)(Sect.2.1))
Pt/Pt–Rh, thermocouple drift at high temperatures in vacuum, 19: 20278 (ORNL-P-1069)
Pt/Pt–Rh, thermocouple tables, smoothed, 19: 20264 (ORNL-3649 (Vol.2)(Sect.2.2))
Pt–Rh/Pt–Rh, thermocouple drift at high temperatures in vacuum, 19: 20278 (ORNL-P-1069)

RHODIUM ISOTOPES Rh-100
beta decay scheme, (E), 19: 21278

RHODIUM ISOTOPES Rh-101
decay of, gamma spectra from, (E), 19: 21280
energy levels of, parity and spin of, (E), 19: 21280

RHODIUM ISOTOPES Rh-102
content in stratosphere, 19: 20657(R) (DASA-1309)

RHODIUM ISOTOPES Rh-103
energy levels of, parity and spin for, (E), 19: 21333

RIBONUCLEASE
radiation effects on thermoluminescence, 19: 19983

RIBONUCLEIC ACID
content in differentiating cells in regeneration of extremities by irradiated salamanders, 19: 19546
properties of, in *Neurospora crassa*, 19: 21772(R) (TID-21709)
radiation effects on metabolism and synthesis of, in HeLa tumor cells, 19: 19602

RIBONUCLEIC ACID, DESOXY-

content in differentiating cells in regeneration of extremities by irradiated salamanders, 19: 19546
isolation and genetic role of, in *Neurospora crossa*, 19: 21772(R) (TID-21709)
radiation and chemical effects on mutagenesis of isolated *B. subtilis*, 19: 19542
radiation effects on metabolism of, in rat liver and intestinal cells, 19: 19506 (TID-21703)
radiation effects on peroxide decay in rat spleen, 19: 19541
radiation effects on physicochemistry of, review on, 19: 19566
radiation effects on localization of soluble, in rabbit lymphoid appendix, 19: 19583
radiation effects on synthesis of, in animal cells, 19: 19613
radiation effects on synthesis of, 19: 19614
RICKETS
treatment in rats using strontium-90 with vitamin D_3, 19: 19680
ROCKET REACTORS
control of, theory of automatic, 19: 21723(R) (NASA-CR-193)
facility design for, 19: 21725
heat transfer and neutron kinetics in graphite–uranium, (T), 19: 21715 (AD-605574)
mission analysis for hydrogen propelled, 19: 20137 (NASA-CR-59332)
ROCKET REACTORS (KIWI)
materials evaluation for, (E), 19: 20554 (LA-3161)
ROCKET REACTORS (TORY)
gamma heating in outer sections of IIC, (T), 19: 21596 (UCRL-12005)
ROCKETS
nuclear, static firing of, design of facility for, 19: 21725
propulsion of, development of methods for, 19: 20139
use in ionospheric electron density measurements, 19: 21127(T)
ROCKS
age estimation of, from La Sal Mountains, Utah, (E), 19: 20178
analysis of uranium-containing, for heavy elements by spectrometry of natural gamma radiation, 19: 20180
analysis, systems for automatic activation, 19: 19773 (TID-20467)
element partition coefficients in, effects of oxygen anion size on, 19: 20152
spalling of, uses of light from nuclear reactors for, 19: 21710
strontium-87 abundance in volcanic, from Hawaii, (E), 19: 20168
ROYAL JELLY
protective effects with cystamine against radiation damage in rats, 19: 19629
RUBIDIUM
determination by precipitation as diliturate, 19: 19824
geochemistry and mineralogy of, in Cherry Mountains (Urals), USSR, book, 19: 20190
thermodynamic properties of vaporous, 19: 20116(R) (SAN-409-12)
RUBIDIUM COMPOUNDS
solubility of diliturate, 19: 19824
RUBIDIUM ISOTOPES Rb-86
secretion in human saliva, 19: 19486
use in diagnosis of coronary insufficiency and myocardial circulation, 19: 19668
RUBIDIUM NITRATES
melting points and volumes of fusion at 0 to 10,000 atm, 19: 19884
RUSSIAN REACTORS
construction and design of ARBUS power, 19: 21702
power output of, evaluation of total, (T), 19: 21694 (P-1076(RAND))
RUTHENIUM
determination using 5,5′thiodisalicylic acid, spectrophotometric, 19: 19812
nucleon reactions at high energies, secondary nucleon yields from, (E/T), 19: 21242 (NP-14837)
separation from irradiated fuels, 19: 20084(P)
separation from power reactor fuels, economics of, 19: 20036 (BNWL-25)
separation from technetium, 19: 19820
RUTHENIUM ALLOYS
Ru–U, phase studies, 19: 20588
RUTHENIUM COMPLEXES
with EDTA, migration in electrodialysis cell, 19: 20052 (ORNL-TM-1035)
RUTHENIUM ISOTOPES Ru-99
hyperfine fields in 5p shell of, induced, 19: 21359
RUTHENIUM ISOTOPES Ru-100
energy levels, (E), 19: 21278
RUTHENIUM ISOTOPES Ru-101
energy levels of, parity and spin of, (E), 19: 21280
RUTHENIUM ISOTOPES Ru-103
beta decay of, spectra from, (E), 19: 21333
content in air over Indian and Pacific Oceans, 1961–62, 19: 20158 (NP-14712)
detection and measurement in solution, use of 4π counter in absolute, 19: 19755 (KFK-252)
determination in air by beta measurement, efficiency of counter for, 19: 20169
RUTHENIUM ISOTOPES Ru-106
content in air over Indian and Pacific Oceans, 1961–62, 19: 20158 (NP-14712)
shielding power sources of, 19: 21595 (TID-7698(Pt.I)(p.33-248))

S

SAFETY
analysis of low-level radioactive waste containers in accident environment, 19: 20196 (CONF-650103-6)
criteria for shipment of radioactive materials on toll facilities, 19: 20239
during accidents involving radioactive materials, organization plan for, 19: 20197 (COO-281)
experience at Marcoule irradiated fuel reprocessing plant, 19: 20037 (CEA-R-2654)
in aerospace nuclear power, outline of standards and evaluation of, 19: 20206 (TID-7698(Pt.I)(p.31-2))
in atomic energy facilities, 19: 20209
plutonium release due to overheating or fires, 19: 20200 (HW-83668)
SAFETY HAZARDS
analysis of, from solar flares during manned space missions, (T), 19: 20873 (D2-11608)
testing RFD-2 re-entry vehicle for, (E), 19: 21763 (SC-DR-64-1741)
SALAMANDERS
radiation effects on loss of regeneration capacity in extremities of, 19: 19544
radiation effects on DNA and RNA variations in regeneration of extremities, 19: 19546
SALICYLIC ACID
reactions with rare earths in presence of pyridine for their separation from aqueous solutions, 19: 20079
reactions with uranyl ions, spectrophotometric studies of complex formation in, 19: 19903
reactions with uranyl ions, stability of complexes formed in, 19: 19904
SALICYLIC ACID, THIO-
analytical uses in determination of metal ions, 19: 19812
SALIVA
cesium-131 secretion in human, as compared to potassium-39, 19: 19486
SALMONELLA
gene differentiation in, 19: 21756 (BNL-8934)
SALT DEPOSITS
waste disposal in Lyons, Kansas, mine, field experiment, 19: 21751 (ORNL-P-1064)
SAMARIUM
determination in purified uranium compounds by chromatography and spectrography, 19: 19800
neutron total cross section at 0.7 to 14 ev, (E), 19: 21285
separation from magnesium–thorium alloy by transfer to liquid scrub alloy in fused salt, 19: 20066
separation from other light lanthanides by partition chromatography following production by proton bombardment of erbium, 19: 20078
SAMARIUM ALLOYS
Al–Sm, phase studies, 19: 20596
SAMARIUM COMPLEXES
with serine, stability and composition, 19: 19874
SAMARIUM HYDRIDES
LiH–SmH_2, phase studies, 19: 19881
SAMARIUM IONS
spectra in barium, calcium, and strontium fluorides, absorption and luminescence, 19: 19854
SAMARIUM ISOTOPES Sm-152
energy level transitions in, E2 conversion coefficients of rotational, (T), 19: 21308
transitions in, particle parameters of E2, (E), 19: 21399
SAMARIUM ISOTOPES Sm-154
energy level transitions in, E2 conversion coefficients of rotational, (T), 19: 21308
SAMARIUM ISOTOPES Sm-156
beta decay scheme, (E), 19: 21350
SAMARIUM SULFIDES
preparation by sulfonation of oxide using carbon disulfide, 19: 19927
SAMPLING
equipment for potassium–sodium alloy corrosion loops, 19: 20477(R) (ORNL-3604)
equipment for radioactive-liquid, 19: 20101(T) (ORNL-tr-442)
SANDSTONE DEPOSITS (COLO.)

uranium isotopic fractionation in, 19: 20187
SANDSTONE DEPOSITS (WYO.)
uranium isotopic fractionation in, 19: 20187
SAP (SINTERED ALUMINUM PRODUCTS)
analysis for aluminum, carbon, iron, silicon, and zinc at different laboratories, statistics on, 19: 19750 (EUR-2286.f)
SATELLITES
book: *Satellite Environment Handbook*, 19: 21157
cosmic-electron survey by Explorer XIV, 19: 20900
cosmic-radiation interference in communication with, at 20 Mc, (E), 19: 20879
detection by tracking stations near trajectories, (E), 19: 21767 (SC-TM-65-44)
helium-3 and tritium content in Discoverer XVII, origin of, 19: 21438
radiation detection equipment for Cosmos 17, design of, 19: 20343
SAVANNAH RIVER PRODUCTION REACTORS
moderator purity in, monitoring of, 19: 21711 (DPSPU-63-30-40)
SCALERS
design and characteristics of 100 MH_3 pre-, 19: 20380
design of digital decimal pulse ratemeter, 19: 20295
design of fast scale-of-five circuit, 19: 20296
design of transistorized bidirectional decade, (E), 19: 20319 (IDO-17059)
design of 10-Mc, engineering drawings for, 19: 20306
SCANDIUM
determination by complex formation with diantipyrinylmethane, 19: 20080
determination by titration, suitability of tetraethylenepentamine heptaacetic acid for, 19: 19813
geochemistry and mineralogy of, in Cherry Mountains (Urals), USSR, book, 19: 20190
magnetic susceptibility at 10 to 293°K, 19: 20595
separation from concentrates and slags by solvent extraction using alkyl phosphoric acids, 19: 20082
separation from other elements by solvent extraction of diantipyrinylmethane complex, 19: 20080
separation from pyroxenites by solvent extraction, precipitation of oxalate, and reduction, 19: 20081
SCANDIUM HYDRIDES
LiH–ScH_x, phase studies, 19: 19881
SCANDIUM ISOTOPES Sc-41
beta decay of, mesonic exchange effect in, 19: 21348
SCANDIUM ISOTOPES Sc-43
production in nitrogen-14 reactions with chlorine-35, phosphorus-31, and sulfur-32, (E), 19: 21392
SCANDIUM ISOTOPES Sc-44
production of isomer pairs of, in nitrogen-14 reactions with chlorine-35, phosphorus-31, and sulfur-32, (E), 19: 21392
SCANDIUM ISOTOPES Sc-46
tracer uses in clay movement in porous media, 19: 20183
SCANDIUM NITRIDES
superconducting properties, 19: 20572
SCATTERING
amplitude for production processes in quantum field theory, (T), 19: 20961
amplitude for three-body, one-particle singularities of, (T), 19: 20953
amplitude for, equations for classical and quantal, 19: 20825
amplitudes corresponding to Feynman diagrams in, analytical properties of, 19: 21054
amplitudes for production processes in, (T), 19: 20925 (ICTP-64/3)
amplitudes for Yukawa potential, use of N/D method in, 19: 21067
amplitudes for, representation of, (T), 19: 20955
amplitudes in complex z plane, singularity of, 19: 21055
amplitudes in, motion of poles of Bethe-Salpeter p-wave, (T), 19: 21111
analysis by invariant-imbedding approach to random-walk method, (T), 19: 20660 (P-1113(RAND))
asymptotic behavior of complex phase shifts in, (T), 19: 21079 (IC/65/2)
electromagnetic structure functions in, Mott effect on, 19: 21073
extrapolation of S matrix to complex angular momenta, representations for, (T), 19: 21080 (IC/65/9)
Feynman amplitudes of, analytic property of, 19: 21113
of relativistic particles, quantum theory of, 19: 20950
of two charged particles of equal mass, relativistic, (T), 19: 21031
perturbation theory for, high-energy behavior of five-point function for ladder diagrams in, 19: 21096
phase shifts and transport cross sections in, effects of three turning points on, (T), 19: 20957
phase shifts for potential-well, quantum mechanical, (T), 19: 20956
potential, double spectral function in, 19: 21093
potential, property of vertex function in, (T), 19: 20964
Regge trajectories in, principle of maximum analyticity for properties of, 19: 21061
renormalization in potential, (T), 19: 20945
resonance and high-energy limit of amplitude for, 19: 21000
S-matrix theory for, causality in, 19: 20943
theory of, structure of g-plane in relativistic Schroedinger, 19: 21053
theory of, wave packets in quantum, 19: 21092
unitary amplitudes for, in one-dimensional worlds, 19: 20924 (ICTP-64/2)
SCINTILLATION
spectra from alpha excitation of argon–nitrogen mixtures, pulse-height, 19: 20313(R) (ANL-6938(p.9-20))
SCINTILLATION DETECTORS
current-pulse center of gravity in, determination of, (T), 19: 20336
design and performance of whole-body plastic, for gamma rays, 19: 20377
design for Cosmos 17, 19: 20343
design for fast-neutron dosimetry, (E), 19: 20312 (AERE-R-4525)
design for neutron time-of-flight spectrometry, 19: 20355
design of gas, for alpha particles and electrons, 19: 20361
development for gamma rays, 19: 20356
efficiency of sodium iodide, for gamma rays, 19: 20358
energy resolution in liquid, factors affecting, 19: 20351
performance as dosimeters in mixed gamma and neutron fields, 19: 20330(T) (AEC-tr-6547)
performance of LiI(Eu), for measurement of neutron flux density and dose, 19: 20375
performance of, effects of color quenching variables due to sample preparation, 19: 20324 (ORNL-P-1094)
quenching corrections for liquid, in sample counting, 19: 20332
uses in detecting leaks in fuel element cans, 19: 21626(P)
SCRUBBERS
design for facility for separation of plutonium from leachable residues, 19: 20083
SEA URCHINS
radiation effects on zygote cell division in, gamma, 19: 19496(R) (ANL-6938(p.49-56))
SEA WATER
analysis for mixed fission products in Ligurian, method for, 19: 19790
carbon-14 activity in New Zealand, interpretation of, 19: 20238
content of radioisotopes in animals and plants in, effects and source of artificial and natural, 19: 20226
desalination of, evaluation of nuclear, 19: 21708 (ORNL-TM-465)
desalination of, reactor program for, 19: 21709
desalination using nuclear energy, economics of, 19: 21707 (ORNL-TM-432)
SEALS AND GLANDS
closure system design, explosively driven, 19: 20100 (UCRL-12203)
SEED
analysis of, activation, 19: 19771(R) (TEES-2671-4(Chap.9))
radiation effects from fission products in soil on, of grain crops, 19: 19508(T) (JPRS-28977)
radiation effects on germination and plant growth from maize, 19: 19528
radiation effects on chromosome aberrations in *Crepis capillaris*, moisture effects on fast neutron post-, 19: 19581
radiation effects on chromosome rearrangements in barley, partial recovery from, 19: 19639
radiosensitivity of sprouting maize, effects of 2,4-dinitrophenol on fast neutron and gamma, 19: 19582
SEEDLINGS
radiation effects on development of maize, 19: 19528
SEISMIC WAVES
amplitude and spectra of, from underwater explosions, 19: 20175
detection and discrimination 2000 to 6000 miles from source, 19: 20177
propagation of surface and underground, models of, 19: 20172(R) (NP-14877)
SEISMOLOGY
air-blast-induced ground motions, method of simulating, 19: 20184
borehole research in, Vela Uniform project, 19: 20173 (VESIAC-4410-83-X)
data from BILLIKEN calibration explosion in southeast Missouri, 19: 20171 (AFCRL-64-659)
developments in, for distinguishing underground explosions from earthquakes, 19: 20177
error determination in seismic event location, 19: 20172(R) (NP-14877)
of underwater explosions, 19: 20175
wave equation development, 19: 20172(R) (NP-14877)
SELENIUM
analysis for chlorine, phosphorus and sulfur by activation methods, 19: 19798
determination in liver and milk, activation, 19: 19771(R) (TEES-2671-4(Chap.9))
geochemistry and mineralogy of, in Cherry Mountains (Urals), USSR, book, 19: 20190

radiation effects on electric conductivity of crystalline reactor, gamma, 19: 20644
SELENIUM ISOTOPES Se-75
use in pancrease scanning, 19: 19722
use in photoscanning of pancreas, 19: 19723
SELENIUM SYSTEMS
Er–Se, phase equilibria and crystal chemistry, 19: 19879
SEMICONDUCTOR DETECTORS
calibration of, accuracy of techniques for, 19: 20371
charge transport time in, effect of non-constant carrier mobility on, 19: 20366
design and performance of anticoincidence lithium-drifted germanium, 19: 20322 (LA-DC-6397)
development for measurement of charge-exchange neutral particles, 19: 21482(R) (ORNL-3760(p.23-9))
development of surface-field-controlled, (E), 19: 20323(R) (NYO-3246-4)
fabrication of diffused and lithium-drifted silicon, 19: 20328(R) (UCRL-11828(p.225-6))
performance as dosimeters in mixed gamma and neutron fields, 19: 20330(T) (AEC-tr-6547)
performance of lithium-drifted, in beta spectrometers, 19: 20360
pulse rise time in silicon, electron mobility effects on, 19: 20359
pulse rise times in, charged-particle discrimination by, 19: 20369
use of lithium-drifted germanium, in activation analysis, 19: 19775(R) (UCRL-11828(p.197-9))
SEMICONDUCTORS
bonding thin metallic films to, methods for, 19: 20520 (SC-DC-65-1256)
book: *Effects of Radiation on Semiconductors*, 19: 20651(T)
electric conductivity dispersion in, thermodynamical model of, 19: 21495
electric conductivity of, transient, 19: 21496
performance of surface-field-controlled, (E), 19: 20323(R) (NYO-3246-4)
SERINE
reactions with rare earths, composition and stability of complexes formed in, 19: 19874
SHALE DEPOSITS
waste disposal at depth of 900 ft in, equipment for, 19: 21753
SHEEP
gastrointestinal function in, preparation of chromium-51-labeled EDTA for studies on, 19: 20026
SHEETS
welding of, Hanford procedures for, 19: 20524 (TID-20625(Vol.IV)(Rev.I))
SHELLS
deformation and stress stability of shallow spherical, nonlinear, 19: 21620
response of buried aluminum cylindrical, to quasi-static overpressures, 19: 20136 (AFWL-TDR-64-13)
thermal stress and temperature distributions in plane, for reactors, (T), 19: 21618
thermal stress and temperature distributions in cylindrical, (T), 19: 21619
SHELTERS
blast effects on cylindrical underground, 19: 20659 (AD-606490)
design and cost of tunnel-grid, for urban populations, 19: 20202 (ORNL-P-1093)
gamma streaming through air duct in concrete, 19: 21594 (AD-424387)
response of buried hollow cylinders to quasi-static overpressures, 19: 20136 (AFWL-TDR-64-13)
role in radiological defense of, 19: 19554
underground, uses of light from nuclear reactors in clearing space for, 19: 21710
SHIELDED CONTAINERS
handling reactor fuel casks, equipment for, 19: 20099 (TID-21644)
SHIELDING
design for 80-C strontium-90 beta source, engineering drawings of, 19: 20134
development for space radiation, calculations for, 19: 21242 (NP-14837)
gamma streaming through air duct in concrete, 19: 21594 (AD-424387)
of infants in pelvic examinations, protective effects of, 19: 19677
of isotopic power sources, handbook on, 19: 21595 (TID-7698(Pt.I) (p.33-248))
performance of, use of radioisotopes for studying, 19: 20417
protective effects of, against radiation injury of rat placenta, 19: 19557
stress analysis of prestressed concrete, finite element method for, 19: 20086 (GAMD-5926)
SHIELDING MATERIALS
for gamma sources, nomograms for determining thicknesses for, 19: 21598
neutron transport in, analysis of fast, (E), 19: 21199 (CEX-65.02)
SHIPPING
of low-level radioactive wastes, structural integrity of containers for, 19: 20196 (CONF-650103-6)
SHOCK
induced in irradiated rabbits by gamma globulin, 19: 19535
radiation effects on electroshock seizures in rat cysteine and dose effects on, 19: 19514
SHOCK TUBES
electron density and temperature in electromagnetic, (E), 19: 21515
plasma heating in, by pinch effects, (E), 19: 21473 (IPP-1/28)
plasma precursor ionization in, (E/T), 19: 21471 (IPP-1/24)
shock wave diagnostics in magnetically driven, (E), 19: 20661 (RLE-TR-428)
SHOCK WAVES
effects of explosion-produced, on h-f, uhf, and vhf antennas, (E), 19: 20109(R) (CER-D1703)
ground motions induced by air-blast, simulation of, 19: 20184
interactions with plasma in pinch devices, heating effects of, (E), 19: 21473 (IPP-1/28)
interactions with cylindrical cavities in elastic media, 19: 20659 (AD-606490)
ionization of air, electrostatic probe measurement of, 19: 20841
plasma precursor ionization in, (E/T), 19: 21471 (IPP-1/24)
propagation along cylindrical electron beams, (T), 19: 20705
propagation from atomic explosions in air, (T), 19: 20675
propagation in conducting gases, gradients of flow variables behind, (T), 19: 20664
propagation in hydrogen, in magnetically driven shock tubes, (E), 19: 20661 (RLE-TR-428)
propagation in outer layers of type-II supernova, (T), 19: 20769(T)
structure of thermal radiation-resisted, with vibrational nonequilibrium, (T), 19: 20680
SILICON
deposition on vanadium-base alloys for oxidation protection, 19: 20459(R) (IITRI-B6019-6)
determination by activation methods, 19: 19796
determination in SAP powders by different laboratories, statistics on, 19: 19750 (EUR-2286.f)
determination in uranium and its compounds and alloys, methods for, 19: 19823
diffusion of helium in, 19: 19934
effects on fabrication and mechanical properties of niobium–tantalum–titanium–vanadium alloy sheet, 19: 20552(R) (IITRI-B6021-6)
effects on phosphorus determination by neutron activation methods, 19: 19828
fabrication of diffused and lithium-drifted detectors of, 19: 20328(R) (UCRL-11828(p.225-6))
pulse rise time in detectors of, electron mobility effects on, 19: 20359
SILICON CARBIDES
bonding to titanium, 19: 20505 (JAERI-1071)
SILICON ISOTOPES Si-25
decay of, log ft values for, (T), 19: 21379
proton-emission decay of, spectrum of, (E), 19: 21297
SILICON ISOTOPES Si-28
alpha reactions (α,α') at 22.5 Mev, alpha-gamma angular correlations in, 19: 21457
deuteron reactions (d,p) with, target core excitation in, (T), 19: 21433
neutron reactions (n,α) at 14.8 Mev, angular distributions from, (E), 19: 21318
neutron scattering at 14 Mev by, cross sections for, (E/T), 19: 21441
SILICON ISOTOPES Si-29
performance in nuclear gyroscopes, (T), 19: 20279 (RTD-TDR-63-4001)
SILICON ISOTOPES Si-30
deuteron reactions (d,n) with, (E), 19: 21376
SILICON JUNCTIONS
radiation effects on p-n, gamma, 19: 20627
use of surface-barrier, in fast neutron spectrometry, (E), 19: 20334
SILICON OXIDES
effects on thermal stability of zirconium oxide, 19: 20585
radioactive of thin chromatographic layers of, equipment and method for measuring beta, 19: 19792
use of colloidal, impregnated with cobalt bromide and hydrobromic acid, as moisture indicator, 19: 21783(P)
Al_2O_3–BaO–CaO–MgO–SiO_2, presintering of compositions in, 19: 20461 (NP-14893)
Al_2O_3–MgO–SiO_2, devitrification, 19: 20461 (NP-14893)
SILICON SYSTEMS
Co–Si–Th, crystal structure of compound in, 19: 20568
Cr–Si–Th, crystal structure of compound in, 19: 20568
Cr–Si–U, preparation and crystal structure of compounds in, 19: 19871
Cu–Si–Th, crystal structure of compound in, 19: 20568
Fe–Si–Th, crystal structure of compound in, 19: 20568
Fe–Si–U, preparation and crystal structure of compounds in, 19: 19871

Mn–Si–Th, crystal structure of compound in, 19: 20568
Mn–Si–U, preparation and crystal structure of compounds in, 19: 19871
Mo–Si–U, preparation and crystal structure of compounds, 19: 19871
Ni–Si–Th, crystal structure of compound in, 19: 20568

SILICONES
$LiNO_3$–KNO_3–$NaNO_3$, distribution of ions between liquid–TBP and silicone–TBP, solvent properties for ions from molten nitrate at 150°C, 19: 19833 (CEA-R-2628)

SILTS
density of ocean-bottom, equipment for measurement by gamma scattering, 19: 20419

SILVER
analysis for impurities by activation methods, 19: 19796
corrosive effects on tantalum–tungsten alloys at 1900°C, 19: 21690(R) (LA-3244)
deposition on vanadium-base alloys for oxidation protection, 19: 20459(R) (IITRI-B6019-6)
determination by titration using hydrochloric acid, end-point determination by beta reflection in, 19: 19787
electron and ion emission from foils of, laser-induced, (E), 19: 20814
nucleon reactions at high energies, secondary nucleon yields from, (E/T), 19: 21242 (NP-14837)
separation by reversed-phase chromatography and solvent extraction using tri-n-octylphosphine sulfide, 19: 19753 (IS-T-3)
separation from copper, lead, and zinc by solvent extraction using tri-n-octylphosphine sulfide, 19: 19753 (IS-T-3)
sintering of loose powder of, near 300°C, 19: 20465 (TID-20344)
sputtering by ions at 45 kev, thermal spikes in, (E), 19: 20838

SILVER ALLOYS
Ag–W, preparation and properties of infiltrated, 19: 20559 (NP-14892)
Cd–Ag, tensile properties of, testing, (E), 19: 20554 (LA-3161)

SILVER COMPOUNDS
thermolysis of diliturate, 19: 19824

SILVER IODIDES
labeling with iodine-131 and aerosol preparation, 19: 20027

SILVER ISOTOPES Ag-107
energy level transitions in, retardations in l-allowed M1, (T), 19: 21323

SILVER ISOTOPES Ag-109
energy level transitions in, retardations in l-allowed M1, (T), 19: 21323

SILVER ISOTOPES Ag-110
incorporation in silver iodide aerosols, 19: 20027
production using Rossendorf Reactor in East Germany, 19: 20436

SINGLE CRYSTALS
preparation and properties of manganous bromide, 19: 21759(R) (NYO-3402-1)

SINTERING
material transport mechanism in, studies, 19: 20465 (TID-20344)

SKELETON
development of, effects of aminoacetonitrile on, 19: 19471(R) (ANL-6938(p.162-78))
radiation effects on acid and alkaline phosphatase and esterase activity in muscle of guinea pig, 19: 19574
radioinduced anomalies in fetal, 19: 19533
radium-226 content in human fetal, 19: 20216

SKIN
contamination by radioactive materials, recommendation for physician in removal of, 19: 19494
radiosensitivity of human, 19: 19605

SKIN LESIONS
radioinduced human, use of fresh blood autofibrin films for treatment of, 19: 19642

SLAGS
separation of scandium from blast-furnace, 19: 20081

SLICK ROCK DISTRICT (COLO.)
uranium isotopic fractionation in sandstone of, 19: 20187

SLUG CANNING
of sodium for neutron scattering experiments, 19: 20503 (EUR-2242.e)

SLUG CANS
materials for, evaluation of magnesium-0.5 to 1.0 wt% zirconium alloy for, 19: 20610(P)

SMOKES
diffusion of, equipment for scale-model experiments on, 19: 20656(R) (ANL-6938(p.257-73))
rise from stacks, formulas for, 19: 20653(R) (ANL-6938(p.209-41))

SNOW
analysis for cesium-137, strontium-89, and strontium-90 by electrodialysis and gamma spectroscopy, 19: 19809

SODIUM
analysis for impurities by spark source mass spectrography, 19: 19830
canning for neutron scattering experiments, method for, 19: 20503 (EUR-2242.e)
corrosive effects on materials in steam generator, 19: 20107(R) (BAW-1280-22)
corrosive effects on cerium–cobalt–plutonium alloys at 650°C, 19: 21690(R) (LA-3244)
corrosive effects on stainless steels, literature survey, 19: 20472 (IDO-14651)
determination in cottonseed, activation, 19: 19771(R) (TEES-2671-4 (Chap.9))
determination in filter papers by neutron activation methods, 19: 19786
determination in pure aluminum, activation, 19: 19775(R) (UCRL-11828(p.197-9))
diffusion of atoms of, in arc discharge, (E), 19: 21555
effects on ceramic reactor fuels, 19: 20458 (GEAP-4283)
electron elastic scattering at 0.1 to 2.0 ev, cross sections for, (T), 19: 20842
radiation effects on physiology of content of, in developing guinea pig brain, 19: 19534
reactions with water in steam generators, studies of problems produced by, 19: 20107(R) (BAW-1280-22)
separation of radioactive, from activation samples, 19: 19768(R) (TEES-2671-4(Chap.6))
thermodynamic properties of vaporous, 19: 20116(R) (SAN-409-12)
uses for bonding stainless steel to uranium carbide, eddy-current evaluation of, 19: 20531

SODIUM ALLOYS
K–Na, corrosive effects on stainless steels, literature survey, 19: 20472 (IDO-14651)
K–Na, corrosive effects on structural alloys, research progmm on, 19: 20477(R) (ORNL-3604)
K–Na, corrosive effects on structural alloys at high temperatures, loop experiments, 19: 20478(R) (ORNL-3618)
K–Na, corrosive effects on structural alloys at high temperatures, loop experiments, 19: 20479(R) (ORNL-3671)
K–Na, corrosive effects on structural alloys at high temperatures, mass transfer in, 19: 20480(R) (ORNL-3730)
K–Na, hydride precipitation in, 19: 20478(R) (ORNL-3618)
K–Na, pumping of, development of thermoelectric pumps for, (E), 19: 20096 (NAA-SR-Memo-10729)
K–Na, solvent properties for hydrogen, apparatus for measurement of, 19: 20477(R) (ORNL-3604)
K–Na, solvent properties for hydrogen at 1100°F, 19: 20479(R) (ORNL-3671)
K–Na, solvent properties for hydrogen at 752 to 1300°F, 19: 20480(R) (ORNL-3730)

SODIUM CARBONATES
precipitation of uranium(VI) with, in presence of alkaline earth chlorides, 19: 19870

SODIUM CHLORIDES
color centers in, ENDOR of, (T), 19: 19920
effects on radiation effects on ionic permeability of rooster erythrocytes, 19: 19577
labeling with sodium-24 and aerosol preparation, 19: 20027
radiation effects on luminescence of copper-doped, 19: 19964
radiation effects on thermal properties of crystals and solid solutions of, gamma and neutron, 19: 19986
radiation effects on stored energy in, gamma, 19: 19987
sorption of labeled, by chlorinated polyvinyl-chloride filters, 19: 20228
spectra of suspensions of, in thin polyethylene films, infrared transmission, 19: 19917
KCl–K_2ZrF_6–NaCl, decomposition potentials in electrolysis of, 19: 19850(T) (NP-tr-1230)

SODIUM CHROMATES
corrosion inhibiting effects on carbon steel, 19: 21714 (RL-REA-592)
effects on dissolution of plutonium dioxide pellets in nitric acid, 19: 20050 (ORNL-3695)

SODIUM COMPOUNDS
solubility and thermolysis of diliturate, 19: 19824

SODIUM ETHOXIDE
reactions with 2-phenylethyltrimethylammonium iodide, deuterium isotope effects on, 19: 19947

SODIUM FLUORIDES
molecular properties of, beam electric resonance studies of, 19: 19848(R) (UCRL-11828(p.193-7))
LiF–NaF, effects on coated-particle fuels at 800 to 1000°C, 19: 20463 (ORNL-TM-431)
NaF–UF_4, decomposition of, thermobalance study of, 19: 20258 (JAERI-1070)

SODIUM HAFNIUM SILICATES
crystal structure, 19: 19916(T)

SODIUM HYDROXIDES
CaO–NaOH, sorptive properties of soda lime for fluorine and hydro-

fluoric acid, thermobalance study, 19: 20258 (JAERI-1070)
SODIUM IODIDES
gamma reactions with tallium-activated crystals of, electron pair production cross sections for, (E), 19: 21294
performance of thallium-activated, for gamma detection, 19: 20358
quadrupole effects in, nuclear magnetic resonance study of, 19: 20620(R) (NYO-2024-8)
SODIUM IONS
solvent extraction from molten nitrate by liquid silicone–TBP at 150°C, 19: 19833 (CEA-R-2628)
SODIUM ISOTOPES Na-22
content in man, relation of content in milk and food to, 19: 20225
electron pair production cross section near threshold, (E), 19: 21252(R) (UCRL-11828(p.35-8))
SODIUM ISOTOPES Na-23
performance in nuclear gyroscopes, (T), 19: 20279 (RTD-TDR-63-4001)
SODIUM ISOTOPES Na-24
activity determination by 4π beta-gamma coincidence method, corrections for, 19: 20385
electron pair production cross section near threshold, (E), 19: 21252(R) (UCRL-11828(p.35-8))
incorporation in sodium chloride aerosols, 19: 20027
production using Rossendorf Reactor in East Germany, 19: 20436
ranges in aluminum, interatomic potential from, (T), 19: 20837
SODIUM NITRATES
corrosion inhibiting effects on carbon steel, 19: 21714 (RL-REA-592)
effects on dissolution of plutonium dioxide and uranium dioxide pellets in nitric acid, 19: 20050 (ORNL-3695)
melting points and volumes of fusion at 0 to 10,000 atm, 19: 19884
SODIUM NITRITES
effects on dissolution of uranium dioxide pellets in nitric acid, 19: 20050 (ORNL-3695)
SODIUM PERCHLORATES
labeling with chlorine-36, 19: 20028
SODIUM RARE-EARTH SULFIDES
crystal structure, 19: 19862
SODIUM REACTOR EXPERIMENT
performance upgrading to 30 Mwt, modifications for, (E), 19: 21732 (NAA-SR-10379)
SODIUM SILICATES
corrosion inhibiting effects on carbon steel, 19: 21714 (RL-REA-592)
SODIUM SULFATES
$MgSO_4$–Na_2SO_4, surface area and radioactivity of sulfur-35-labeled, 19: 20013
SODIUM URANYL ACETATES
luminescence of crystals of, circular, 19: 19921
radioinduced luminescence in crystals of, laser beam, 19: 20010
SODIUM ZIRCONIUM SILICATES
crystal structure, 19: 19916(T)
SOILS
analysis for cesium-137, rapid method for, 19: 19805
analysis for cesium-134, cobalt-60, and europium-152 and -154 after nuclear detonation, gamma spectroscopic, 19: 19829
analysis for strontium-89 and -90, radiochemical, 19: 19739 (AERE-AM-101)
fallout contamination of, ecological effects, 19: 19504 (RM-2801-PR)
fission product contamination of, effects on seeds of grain plants, 19: 19508(T) (JPRS-28977)
particle deposition from atmosphere on, tracer studies using copper-64 on, 19: 20658
radioactivity distribution in Kansas, cesium-137 and strontium-90, 19: 20657(R) (DASA-1309)
radioactivity distribution in, after plowing under radioactive dust, methods of determining, 19: 20182
strontium distribution in, effects of various conditions on, 19: 19474(T) (CEA-tr-A-1616)
strontium-90 transfer to oats, effects of content of stable strontium, potassium phosphate, and lime, 19: 19475(T) (JPRS-27940(p.10-17))
uranium content in, effects on content in man, 19: 19490
SOLAR FLARES
detection of, radio method for, 19: 20759
effects on charged particle distribution in radiation belts, (T), 19: 21137
effects on cosmic neutron intensity, 19: 20878(T)
effects on polar cap on mass, (E/T), 19: 20763
proton acceleration from, at 3 to 20 Mev, (E), 19: 20766
protons from, effects on manned space missions, (T), 19: 20873 (D2-11608)
x-ray emission from, (T), 19: 20890
SOLAR RADIATION
acceleration of proton, at 3 to 20 Mev, (E), 19: 20766
book: *Atmospheric Radiation. I. Theoretical Basis*, 19: 21156
effects of corpuscular stream, on energy of geomagnetic storms, (T), 19: 21135(T)
effects of solar wind discontinuity on magnetospheric boundary, (T), 19: 21148
effects on pressure distribution in lower atmosphere, (E), 19: 20780(T)
flux of, diffusion mechanism of diurnal variations of, (E/T), 19: 20875
interactions of solar wind with magnetosphere, geomagnetic cavity from, (T), 19: 21146
propagation in interplanetary space, (T), 19: 20757
properties of corpuscular streams, (E), 19: 21155(T)
spectra of, data on microwave, uv, and x-ray, 19: 20785
spectrum during solar burst, (E), 19: 20756
SOLDERING
process for automatic induction, using infrared radiometer, 19: 21765 (SC-DR-65-74)
SOLENOIDS
design of homogeneous power-optimized, 19: 21486(R) (ORNL-3760 (p.77-93))
neutron depolarization effects in precession magnets of, fast, 19: 21209
SOLIDS
analysis for gases by spark source mass spectrography, 19: 19830
gamma emission from isomeric nuclei in, (T), 19: 21407
performance as working media in nuclear gyroscopes, (T), 19: 20279 (RTD-TDR-63-4001)
sputtering by ion bombardment, review of, 19: 20819
SOLUTIONS
rate constant measurements for reactions of free radicals with solutes in aqueous, 19: 19968
SOLVENT EXTRACTION PROCESSES
study of diluent influence in extraction by tridodecylamine hydrochloride, 19: 20039 (EUR-2246.e)
use of amines and acidic organophosphorus compounds in, review, 19: 20053 (UJV-1202/64)
SOLVENTS
burning of radioactive, from radiochemical separations processes, 19: 21747 (DP-942)
disposal of degraded contaminated, by burning, 19: 21748 (DPSPU-64-30-8B)
SONIC INSPECTION
of small-diameter tubing, engineering drawings of equipment for, 19: 20131
SOUND
effects on tunneling current in superconducting diodes, (E), 19: 21178
energy transfer in dispersive media, (T), 19: 20688
excitation in weakly ionized plasma, (T), 19: 21561
interactions of ultra-, with charged particle beam in piezoelectric crystal, (T), 19: 20672
SOUND GENERATORS
feasibility of radioisotope-powered underwater, 19: 20405 (MND-3180-1)
SOVIET UNION
atomic energy program, summary based on publicly-available materials, 19: 21762 (RM-2163(RAND))
mineralogy and geochemistry of rare elements in Cherry Mountains (Urals), 19: 20190
pegmatite age estimation in Biryusa, 19: 20176
strontium-90 content in fresh water basins in, 1961–62, 19: 20160 (NP-14728)
SOVIET UNION (UKRAINE)
radioactivity equilibrium between radium, thorium, and uranium in accessory monazites in, 19: 20189
SPACE
nuclear safety in, outline of standards and evaluation of, 19: 20206 (TID-7698(Pt.I)(p.31-2))
solar radiation propagation in interplanetary, 19: 20757
SPACE FLIGHT
mission analysis for solar-heated hydrogen propulsion system, 19: 20137 (NASA-CR-59332)
safety hazards in manned, from solar flares, (T), 19: 20873 (D2-11608)
SPACE VEHICLES
performance as solar-proton shielding, for manned missions, (T), 19: 20873 (D2-11608)
power plants for Manned Orbiting Research Laboratory, SNAP-8, 19: 21720 (NAA-SR-10318)
power plants for, development of pumps for mercury Rankine-cycle, 19: 20096 (NAA-SR-Memo-10729)
propulsion by radioisotope-heated thrusters, POODLE program for, 19: 20428 (TID-7698(Pt.I)(p.257-76))
propulsion systems for, mission analysis for solar-heated hydrogen, 19: 20137 (NASA-CR-59332)
testing hulls for, in hypersonic flow of dissociated and ionized hydrogen, 19: 20124

testing RFD-2 re-entry vehicle, (E), 19: 21763 (SC-DR-64-1741)

SPAIN
radioisotope production in, 19: 20432(T) (ORNL-tr-295)

SPARK CHAMBERS
charged particle ionization power in, 19: 20339
design and performance of lumped delay line, 19: 20372
efficiency for cosmic particles, 19: 20378
particle track recording on x-ray film, 19: 20368
particle tracks in, filmless digitizing of location of, 19: 20354
spark displacement in, determination of, (E), 19: 20344
use for mixed fields of ionizing radiation, 19: 20373

SPECTRA
detection and measurement of, using iterative unfolding method (T), 19: 20316 (ANL-6984)

SPECTROGRAM COMPARATORS
description of automatic measuring and recording system for, 19: 20288(R) (UCRL-11828(p.232-3))

SPECTROMETERS
design of grazing-incidence, for photographic and photoelectric recording, 19: 20348
design of velocity, for Bevatron beams, (E), 19: 20326 (UCRL-11787)
magnetic field aberrations in charged-particle, 19: 20365
performance of neutral-particle energy analyzing, 19: 21481(R) (ORNL-3760(p.10-22))

SPECTROSCOPY
analysis using carrier distillation technique, use of mechanical packer in, 19: 19743 (CEA-R-2619)
methods using gallium oxide, 19: 19774 (UCRL-7962)
uses of Zeeman, for measurement of time-varying magnetic fields, (E), 19: 20257 (IPP-1/19)

SPINAL CORD
radiodiagnosis of neurological syndromes in, by myeloscintigraphy after administration of iodine-131, 19: 19720

SPINELS
sintering characteristics of, 19: 20461 (NP-14893)

SPLEEN
radiation and immunization effects on cholinesterase activity in rabbits, 19: 19609
radiation effects on peroxide decay in DNA in rat, 19: 19541
radiation effects on uptake of sulfur-35-labeled methionine by proteins in rabbit, 19: 19604
radiation effects on host-cell interactions in mice with grafts of, 19: 19615
radiation effects on amyloidosis in hyaline deposits in mouse, after liver and marrow injections, 19: 19650
radiodiagnosis of hemolytic anemia by photoscanning of, using heat-treated chromium-51-labeled erythrocytes, 19: 19725
radiodiagnosis of defects and tumors of, by scintiscanning using chromium-51, 19: 19726
radiodiagnosis of function of, by scintiscanning using chromium-51, 19: 19727
radiodiagnosis of, by photoscanning using iodine-131-labeled human serum albumin, 19: 19710
transplantation in dogs, 19: 19521
transplantation in dogs and man, 19: 19522
transplantation in irradiated mice, protection from killing effect of, 19: 19651

SPORES
radiation effects on fungal, 19: 19558
radiation effects on fungal, 19: 19559

SPUTTERING
properties of, review of, 19: 20819

STACK DISPOSAL
plume rise formulas for, 19: 20653(R) (ANL-6938(p.209-41))

STAINLESS STEEL
analysis for hafnium or zirconium using catechol violet, colorimetric, 19: 19780
analysis for impurities by spark source mass spectrography, 19: 19830
bonding to uranium carbide by sodium, eddy-current inspection of, 19: 20531
corrosion by carbon dioxide at 1100 to 1800°F, 19: 20487
corrosion by potassium–sodium alloy and sodium, literature survey, 19: 20472 (IDO-14651)
corrosion by terphenyls, chlorine evolution in, 19: 20469 (EUR-2279.e)
corrosion in reactors, 19: 20488
corrosion of Carpenter 20SCb, by solutions produced in head-end processes for fuel, 19: 20481 (ORNL-3787)
corrosion of type 316, in sodium-heated steam generator after 4000 hr, 19: 20107(R) (BAW-1280-22)
corrosion of types 316 and 347, by potassium–sodium alloy, research program on, 19: 20477(R) (ORNL-3604)
corrosion of Types 316 and 347 by potassium–sodium alloy at high temperatures, carbon mass transfer in, 19: 20478(R) (ORNL-3618)
corrosion of types 347 and 316, by potassium–sodium alloy at high temperatures, loop experiments, 19: 20479(R) (ORNL-3671)
corrosion of types 316 and 347, by potassium–sodium alloy at high temperatures, mass transfer in, 19: 20480(R) (ORNL-3730)
decontamination effects on intergranularly attacked areas in type 304, 19: 20471 (HW-SA-3628)
deposition on steel, methods development for, 19: 20504(R) (EURAEC-1228)
diffusion of hydrogen in type 316, at 1000 to 1300°F, 19: 20479(R) (ORNL-3671)
diffusion of hydrogen in type 316, at 1100 to 1300°F, 19: 20480(R) (ORNL-3730)
electron and ion emission from foils of, laser-induced, (E), 19: 20814
mass transfer from type 316 and 321 to niobium–1% zirconium alloy in liquid potassium, research program on, 19: 20474(R) (NASA-CR-54281)
plume rise behavior in scale-model tests, 19: 20656(R) (ANL-6938(p.257-73))
tensile properties of 17-7PH, A286, and 347, testing, (E), 19: 20554 (LA-3161)
testing of, engineering drawings of phase-sensitive eddy-current concentrator for, 19: 20132
use in nozzles for high-temperature thermometry in gases, 19: 20277 (ORNL-P-1068)
welding by argon-arc method, uses of carbon dioxide in, 19: 20534
welding of closure joint in reactor vessels of Type 316, tests of, 19: 20509 (NAA-SR-Memo-10633)
welding of pipes and plates of, Hanford procedures for, 19: 20523 (TID-20625(Vol.III)(Rev.I))
stainless steel–UO_2, testing in Spert I, 19: 20616 (IDO-17011)

STAINLESS STEEL (AUSTENITIC)
iron-57 Mössbauer effect in 201, 301, 316, and AM 355, (E), 19: 21338
welding of pipes and plates of, Hanford procedures for, 19: 20522 (TID-20625(Vol.II)(Rev.I))
welding to Croloy 9M, 19: 20475(R) (ORNL-3538)

STANDARDS
Euratom Bureau for Nuclear Measurements, activities of, 19: 20088
specification for gantry and trolley for fuel handling cask, 19: 20099 (TID-21644)

STARS
associations of, review of O and T, 19: 20794
atmosphere and plasma winds of, (T), 19: 20783
book: *Astrophysics and Space Science*, 19: 20782
book: *Star Evolution*, 19: 20786
contraction of, energy release in gravitational, (T), 19: 20768(T)
cosmic-ray production in supernovae, 19: 20903
density and temperature of white dwarfs and type-I supernovae, review of, 19: 20800
element abundances in, (T), 19: 20762
evolution and stability of spherical, in hydrostatic equilibrium, (T), 19: 20801
evolution of, (T), 19: 20784
evolution of close binary systems of, review of, (E/T), 19: 20803
evolution of Eta Carinae, 19: 20796
evolution of, contraction and magnetic activity in, (T), 19: 20793
evolution of, observational approach to, 19: 20788
evolution of, relation to galactic evolution, 19: 20797
evolution of, review of theories of, 19: 20787
evolution of, with helium-rich cores, 19: 20798
explosions of, from cosmic-ray interactions at 10^{80} ev, 19: 20758
magnetic-field effect on structure of, (T), 19: 20802
models for pulsational instability of cepheid, (T), 19: 20799
models of, numerical calculations for, 19: 20790
nebula of 3C-273, (T), 19: 20767(T)
nebular variables and nebulosities, 19: 20795
neutrino emission from, neutral current effects in, (T), 19: 20772(T)
nucleosynthesis in, observed abundance anomalies indicating, 19: 20792
positional correlations of nearby, 19: 20439(R) (COO-614-31)
proton-proton interaction in white dwarfs, (T), 19: 20771(T)
radiation emission by galaxies, bremsstrahlung and synchrotron x-, (T), 19: 20765
review of nuclear astrophysics, 19: 20791
shock wave propagation from, particle acceleration in, (T), 19: 20770(T)
structure of, review of models for, 19: 20789

STATISTICS
analysis of punch card records of film dosimeter data for radiation exposure trends, 19: 20241
distribution law for random variables, using composition law for elementary measures, (T), 19: 20440 (EUR-2251.i)
linear estimation of chemical mixtures, 19: 19769(R) (TEES-2671-4

(Chap.7))
models for cosmic electromagnetic cascades in, (T), 19: 20874 (P-1020(RAND))
of counting losses in activation analysis, 19: 19766(R) (TEES-2671-4(Chap.3))
of electron current fluctuations in Townsend discharges, (T), 19: 21551
on determination of aluminum, carbon, iron, silicon, and zinc in SAP at different laboratories, 19: 19750 (EUR-2286.f)
quantum theory of relaxation in isolated spin systems, 19: 21121
random-walk processes in, analysis using invariant imbedding, (T), 19: 20660 (P-1113(RAND))
theory for neutron noise in reactors, (T), 19: 21641 (JINR-P-1996)

STEAM
corrosive effects on zirconium and its alloys at 500°C and 1000 psi in presence of boric acid, 19: 20492
water content in boiler, use of radioisotopes for determining, 19: 20418

STEARIC ACID
use as grinding aid in producing very fine uranium carbide particles, 19: 20513(R) (NCSC-2981-3)

STEEL
analysis for cobalt by activation methods, 19: 19784
coating with stainless steel, methods development for, 19: 20504(R) (EURAEC-1228)
corrosion by carbon dioxide at 1100 to 1800°F, 19: 20487
corrosion in reactors, 19: 20488
fracture tests of high-strength, 19: 20462(R) (NRL-6258)
notch toughness of maraging, metallographic study of, 19: 20541 (AD-604868)
polymorphism in, overdriving effects on dynamics of, 19: 20555 (LA-3215)
radiation effects on reactor pressure vessel, surveillance program for, 19: 21607 (APED-4773)
radiation stability of reactor pressure vessel, stress effects on, 19: 20631
tests of high-strength, correlation of Charpy, 19: 20462(R) (NRL-6258)

STELLARATORS
plasma containment by rotation in, 19: 21593(P)

STELLARATORS (C)
plasma pressure and temperature in, perpendicular, (E), 19: 21511

STEROIDS
chromatography of acetylated, deuterium and hydrogen isotope effects in gas-liquid, 19: 19893
effects of anabolic, on calcium-47 and strontium-85 retention in rats, 19: 19476
preparation of tritium-labeled, method for, 19: 20025

STOMACH
cesium-137 and strontium-90 content in bulls from fallout, 19: 20215
tumor and ulcer localization in, by photoscanning after administration of iodine-131-labeled iodide, 19: 19717

STORAGE BATTERIES
testing output of telemetry-system, (E), 19: 20280 (SCL-DR-64-128)

STRANGE PARTICLES
book: *Fundamental Particles*, 19: 21072
decay of, branching ratios and rates of, (T), 19: 21045

STRATOSPHERE
carbon-14 content of, total and fallout, 1953 to 1964, 19: 20155 (HASL-159)
cosmic radiation density in, radio probe for measuring, 19: 20346
cosmic ray intensity in, (E), 19: 20876(T)
cosmic ray intensity variations during geomagnetic storms, (E), 19: 20877(T)
cosmic-ray intensity in, latitude dependence of, (E), 19: 20892
fallout monitoring, 19: 20162(R) (NYO-3276-9)
fallout monitoring, in Star Dust Project, 19: 20657(R) (DASA-1309)

STREPTOMYCIN
protective effects against 19-norandrostenolone effects on acute radiation disease in rats, 19: 19624

STRESS ANALYSIS
computer program for bodies of revolution, 19: 21609 (GAMD-5001 (Rev.2))
of long, thick, uniformly curved plates, 19: 20130
of prestressed concrete structures by finite element method, computer program for, 19: 20086 (GAMD-5926)
of shallow spherical shells, 19: 21620

STRONTIUM
content in soil, effects on strontium-90 accumulation in oats, 19: 19475(T) (JPRS-27940(p.10-17))
determination by precipitate as diliturate, 19: 19824
distribution in soil, effects of various conditions on, 19: 19474(T) (CEA-tr-A-1616)
geochemistry and mineralogy of, in Cherry Mountains (Urals), USSR, book, 19: 20190
metabolism by plants, effects of soil conditions on, 19: 19474(T) (CEA-tr-A-1616)
metabolism in fetal and newborn rats, tracer study, 19: 19473 (UR-661)
metabolism in rats, 19: 19500 (NP-14907)
separation from other alkaline earths and rare earths, 19: 19789
separation from stored Purex waste by lead sulfate carrier precipitation, 19: 20035 (BNWL-4)
separation from water and snow by electrodialysis, 19: 19809

STRONTIUM CHLORIDES
dielectric losses in, temperature dependence of, 19: 19851(T) (ORNL-tr-491)
electric properties of, effects of lattice energy and temperature on, 19: 21601(T) (ORNL-tr-490)
precipitation of uranium(VI) with, in presence of sodium carbonate, 19: 19870

STRONTIUM COMPLEXES
with EDTA, migration in electrodialysis cell, 19: 20052 (ORNL-TM-1035)

STRONTIUM COMPOUNDS
thermolysis of diliturate, 19: 19824

STRONTIUM FLUORIDES
dielectric losses in, frequency and temperature dependences of, 19: 19851(T) (ORNL-tr-491)
electric properties of, effects of lattice energy and temperature on, 19: 21601(T) (ORNL-tr-490)
luminescence spectra of rare earth ions in, 19: 19854

STRONTIUM HYDRIDES
LiH–SrH_2, phase studies, 19: 19881

STRONTIUM IONS
solvent extraction from molten nitrate by liquid silicone–TBP at 150°C, 19: 19833 (CEA-R-2628)

STRONTIUM IRON TANTALATES
phase transition, 19: 20591

STRONTIUM ISOTOPES Sr-85
radiodiagnostic use of, in external scanning for bone tumor localization, 19: 19666
uptake and retention in rats, effects of cortisone and anabolic steroids on, 19: 19476
use in diagnosis of bone tumors by scintillation scanning, 19: 19697
use in localization of primary and secondary bone tumors in man, 19: 19675

STRONTIUM ISOTOPES Sr-86
content in volcanic rocks of Hawaii, (E), 19: 20168

STRONTIUM ISOTOPES Sr-87
content in volcanic rocks of Hawaii, (E), 19: 20168

STRONTIUM ISOTOPES Sr-88
deuteron (d,p) reactions, proton polarization in, 19: 21447
deuteron reactions (d,p) at 11 Mev, polarization from, (E), 19: 21391
deuteron reactions (d,p) with, spectra from, 19: 21394

STRONTIUM ISOTOPES Sr-89
content in stratosphere, 19: 20657(R) (DASA-1309)
determination in air by beta measurement, efficiency of counter for, 19: 20169
determination in biological materials, radiochemical, 19: 19739 (AERE-AM-101)
determination in natural water reservoirs, rain water, and snow using electrodialysis and gamma spectroscopy, 19: 19809
separation from fission products solution for radiochemical determination, 19: 19745 (CEA-R-2712)

STRONTIUM ISOTOPES Sr-90
contamination of food chain by, from fallout, 19: 20240
content in air on Hayes Island, 1960–61, 19: 20157 (NP-14697)
content in bone in Great Britain, 1963, 19: 20170
content in bones and diet of Argentine children, 19: 20165(R) (TID-21711)
content in diet in U. S., 1964, 19: 20154(R) (HASL-158)
content in fresh water basins in USSR, 1961–62, 19: 20160 (NP-14728)
content in milk in Canada, 1964, 19: 20161 (NP-14869)
content in muscles and organs in bulls from fallout, 19: 20215
content in Pacific Ocean surface waters, 1961, 19: 20159 (NP-14726)
content in stratosphere, 19: 20657(R) (DASA-1309)
detection and measurement in solution, use of 4π counter in absolute, 19: 19755 (KFK-252)
determination in air by beta measurement, efficiency of counter for, 19: 20169
determination in biological materials, radiochemical, 19: 19739 (AERE-AM-101)
determination in bones in presence of radioactive contaminants, 19: 19789
determination in natural water reservoirs, rain water, and snow using electrodialysis and gamma spectroscopy, 19: 19809
determination in rain water, using scintillation gels, (E), 19: 20335

determination in waste waters, methods for, 19: 19749 (EUR-2118.f)
distribution in soils in Kansas, 19: 20657(R) (DASA-1309)
effects on harvest and grain quality of field crops, 19: 19508(T) (JPRS-28977)
effects on treatment of rickets in rats with vitamin D_3, 19: 19680
metabolism in oats, effects of soil treatment on, 19: 19475(T) (JPRS-27940(p.10-17))
properties of, nuclear and physical, 19: 20402 (TID-7698(Pt.I)(p.17-30))
separation from food and water, 19: 20240
separation from power reactor fuels, economics of, 19: 20036 (BNWL-25)
separation from storage basin water, 19: 20042(R) (IDO-14646)
separation from wastes in Hanford isotope plant, feasibility study, 19: 20431 (TID-7698(Pt.I)(p.1-16))
shielding power sources of, 19: 21595 (TID-7698(Pt.I)(p.33-248))

STRONTIUM OXIDES
dielectric losses in, frequency and temperature dependences of, 19: 19851(T) (ORNL-tr-491)
electric properties of, effects of lattice energy and temperature on, 19: 21601(T) (ORNL-tr-490)

STRONTIUM TITANATES
phase transition, 19: 20591
superconducting transition temperature in semiconducting, carrier-concentration effects on, (E/T), 19: 21170

STRUCTURES
gamma dose rate residential, in Norway, 19: 20218
stress analysis of prestressed concrete, finite element method for, 19: 20086 (GAMD-5926)
tendon configuration in pre-stressed concrete, optimal, 19: 21610 (GAMD-6109)

STYRENE POLYMERS
with polyvinyl fluoride, radiation effects on viscoelastic properties at 20 to 170°C, 19: 20001

STYRENES
meson (π^-) transfer from hydrogen to heavier atoms in, (E), 19: 21281

SUCROSE
effects on radiation effects on ionic permeability of rooster erythrocytes, 19: 19577

SUGAR PHOSPHATES
dephosphorylation by thorium and zirconium ions, 19: 19876

SULFANILIC ACID
boric acid–sulfanilic acid, phosphorescence in, 19: 19919

SULFATE IONS
effects on polarographic determination of uranium, 19: 19797
solvent extraction from molten nitrate by liquid silicone–TBP at 150°C, 19: 19833 (CEA-R-2628)

SULFATES
effects on spectrophotometric determination of zinc using 1-(2-thiazolylazo)-2-naphthol, 19: 19814

SULFEX PROCESS
corrosive effects of solutions from, on candidate alloys for centrifuge, 19: 20481 (ORNL-3787)

SULFONATES
effects on transduction in *Pseudomonas aeruginosa*, 19: 19501(R) (NP-14931)
effects on transduction in *Pseudomonas aeruginosa*, 19: 19502(R) (NP-14932)
mutagenic effects in maize, 19: 19527

SULFUR
determination in presence of chlorine and phosphorus by activation methods, 19: 19798
determination in selenium by activation methods, 19: 19798
meson (π^-) reactions (π^-,ny) with, energy spectra from, (E), 19: 21315
oxidation of, in irradiated chlorides, 19: 20004

SULFUR DIOXIDES
determination in vented gases from underground nuclear explosion, apparatus for, 19: 19776 (UCRL-12169)
effects on radioinduced carbon dioxide-graphite reactions, (E), 19: 19953 (AERE-R-4201)

SULFUR ISOTOPES S-29
decay of, log ft values for, (T), 19: 21379

SULFUR ISOTOPES S-32
energy levels, (E), 19: 21380
energy levels of, nucleon separation energy in 1p and 1s, 19: 21400
helium-3 reactions at 29 Mev, (E), 19: 21232 (JEN-141-DF/I-45)
nitrogen-14 reactions at 30 to 42 Mev, scandium-44 isomer pair production in, (E), 19: 21392

SULFUR ISOTOPES S-35
detection and measurement in solution, use of 4π counter in absolute, 19: 19755 (KFK-252)
formation in neutron reactions with chlorine-35 in various chlorides, 19: 20004
incorporation in catalysts used in dehydration of cyclohexanol, 19: 20013
incorporation in sulfuric acid aerosols, 19: 20027
production in Spain, 19: 20432(T) (ORNL-tr-295)
production using Rossendorf Reactor in East Germany, 19: 20436
radiation effects on uptake in methionine by rabbit marrow and spleen proteins, 19: 19604
uptake by vibrissal hairs of mice, origin of, 19: 19479

SULFURIC ACID
corrosive effects on electrolytic cell materials, 19: 20484 (TID-19978 (Vol.I))
labeling with sulfur-35 and aerosol preparation, 19: 20027
HNO_3–H_2SO_4–UO_2, oxidation-reduction potentials in, 19: 19912

SUN
activity of, effects on pressure distribution in Earth's atmosphere, (E), 19: 20780(T)
book: *Astrophysics and Space Science*, 19: 20782
bursts from, solar-radiation spectrum during, (E), 19: 20756
corona of, expansion and heating of, (T), 19: 20783
granulation flow in, MHD equations for super-, (T), 19: 20764
spectra of prominences, hydrogen alpha line in, (T), 19: 20776(T)
spectra of, Brackett hydrogen gamma line in, (E/T), 19: 20778(T)
spectra of, Fraunhofer lines in, (E/T), 19: 20777(T)
spot group area on, time variation in, (T), 19: 20779(T)

SUPERCONDUCTIVITY
calculations of, using approximate many-fermion interactions, (T), 19: 20936 (TID-20558)
of transition metal carbides and nitrides crystalizing is sodium chloride structure, 19: 20572

SUPERCONDUCTORS
critical fields of alloy, (T), 19: 21192
electron tunneling from hard, (T), 19: 21164
energy gap of, Bogolyubov equation for, (T), 19: 21190
fabrication, properties, and theory of resonant-cavity, 19: 21186
flux quantization in, gauge-invariant Hamiltonian formalism for, (T), 19: 21173
flux tube motion in type-I, precessional, (T), 19: 21167
magnetic flux quantization in cylindrical, measurement of, 19: 21194
magnetic moments of, magnetometer for measurement of, 19: 21486(R) (ORNL-3760(p.77-93))
model for, quantum, (T), 19: 21163
nuclear spin relaxation in aluminum, phonon effects on, (T), 19: 21174
properties in memory devices, 19: 21193
properties of, data on, 19: 21187
properties of, paramagnetic impurity effects on, (T), 19: 21191
review on type-II, 19: 21165
surface sheath of type-II, below upper critical field, (T), 19: 21171
transition temperatures of indium and lead film, (E), 19: 21189
transitions in, effects of nonmagnetic and paramagnetic impurities on, (T), 19: 21181
ultrasonic attenuation in niobium–zirconium alloy, in strong magnetic fields, (E), 19: 21188
voltage along type-II, in mixed state, (T), 19: 21166

SUPERFLUIDITY
flow of helium, thermomechanoelectrical effects for, (T), 19: 21176
hydrodynamic equations for, in Fermi liquids, (T), 19: 21161 (JINR-P-1953)

SUPERHEATERS
design of sodium-heated, modular, steam generators, 19: 21611 (NAA-SR-9826)

SUPERHEATERS (NUCLEAR)
design, 19: 21659(P)

SUPERSONIC FLOW
equilibrium of dissociated and ionized hydrogen in, 19: 20124

SURFACE-ACTIVE AGENTS
effects on polarography of uranyl pyrophosphate complexes, 19: 19816
synthesis and properties of fluorocarbon alcohol 3,5-dinitrobenzoates, 19: 21775 (UCRL-12307)

SURFACE WATERS
radioactive contamination of, review of conference on, 19: 20234
strontium-90 content in USSR, 1961–62, 19: 20160 (NP-14728)

SURFACES
contamination of floors by plutonium, resuspension factors for, 19: 20191 (AERE-R-4635)
fallout decontamination of paved, 19: 20207 (USNRDL-TR-797)

SURGERY
effects on results of radiotherapy of tumors, 19: 19703
radiation effects on liver regeneration after partial hepatectomy, 19: 19512

SUSPENSIONS

diffusion of helium in gas-solid, equipment for measuring, 19: 20098(R) (TID-21633)
SWIMMING POOL REACTORS
design with forced-convection primary cooling circuit, 19: 21744(P)
neutron spectra in reflector of Melusine, (E), 19: 21729 (CEA-R-2442)
shielding for, evaluation of, 19: 21739
SWITCHES
performance in power crowbar banks of Scylla IV, (E), 19: 21474 (LA-3189)
SYNCHROTRONS
accelerating potential in, frequency modulation systems for, (E), 19: 20735 (UCRL-11807)
beam injection systems for 200-Bev protron, design, (E), 10: 20737 (UCRL-11955)
beam separator for CERN proton, testing of r-f, (E), 19: 20748
leveling systems for 200-Bev, design of hydrostatic, (E), 19: 20733 (UCRL-11799)
magnet costs for 200-Bev alternating-gradient, (T), 19: 20734 (UCRL-11800)
neutrino beams from 200-Bev proton, (T), 19: 20738 (UCRL-11983)
neutron energy and flux around Frascati, skyshine, (E), 19: 20741
oscillations in high-energy, phase, (T), 19: 20745
radioactivity distributions in 200-Bev AGS, (T), 19: 20732 (UCRL-11796)
SYSTEMS FOR NUCLEAR AUXILIARY POWER
braze joint experience on components for, review, 19: 20508 (NAA-SR-Memo-10625)
heat transfer systems for, analysis of, 19: 20116(R) (SAN-409-12)
testing RFD-2 re-entry vehicle, (E), 19: 21763 (SC-DR-64-1741)
SYSTEMS FOR NUCLEAR AUXILIARY POWER (SNAP-2)
energy release and reactivity feedback effects in SNAP-2/10A destruct, 19: 21719 (NAA-SR-9780)
examination and safety program for SNAPTRAN 2/10A-3, post-destruct, 19: 21718 (IDO-17071)
fission product release and reactor kinetics in SNAPTRAN 2/10A-3 destruct, (E), 19: 21717 (IDO-17019)
SYSTEMS FOR NUCLEAR AUXILIARY POWER (SNAP-7)
feasibility study of underwater 7E, acoustic beacon with fluid-mechanical energy conversion, 19: 20405 (MND-3180-1)
SYSTEMS FOR NUCLEAR AUXILIARY POWER (SNAP-8)
coolant circuit materials, corrosion loop experiments on, 19: 20475(R) (ORNL-3538)
coolant circuit materials, corrosion loop experiments on, 19: 20477(R) (ORNL-3604)
coolant circuit materials, corrosion loop experiments on, 19: 20479(R) (ORNL-3671)
coolant circuit materials, corrosion loop experiments on, 19: 20480(R) (ORNL-3730)
coolant circuit, corrosion loop experiments on matrials for primary, 19: 20478(R) (ORNL-3618)
development for Manned Orbiting Research Laboratory, 19: 21720 (NAA-SR-10318)
hydrogen diffusion through coolant system of, 19: 20475(R) (ORNL-3538)
hydrogen removal from primary coolant system of, studies of possible, 19: 20480(R) (ORNL-3730)
reactor vessel, welding tests of closure joint in Type 316 stainless steel, 19: 20509 (NAA-SR-Memo-10633)
testing of, computer analysis of data from, (E), 19: 21721 (NAA-SR-Memo-10160)
SYSTEMS FOR NUCLEAR AUXILIARY POWER (SNAP-9)
debris from 9A, 19: 20154(R) (HASL-158)
review of 9A, 19: 20427 (TID-7698(Pt.I)(p.249-56))
SYSTEMS FOR NUCLEAR AUXILIARY POWER (SNAP-10)
energy release and reactivity feedback effects in SNAP-2/10A destruct, 19: 21719 (NAA-SR-9780)
examination and safety program for SNAPTRAN 2/10A-3, post-destruct, 19: 21718 (IDO-17071)
fission product release and reactor kinetics in SNAPTRAN 2/10A-3 destruct, (E), 19: 21717 (IDO-17019)
malfunction-detection systems for 10A, (E), 19: 21734 (NAA-SR-Memo-10666)
relays for 10A, evaluation of DPDT, (E), 19: 21733 (NAA-SR-Memo-10532)
testing 10A, control devices for vibrational, (E), 19: 21722 (NAA-SR-Memo-10767)
SYSTEMS FOR NUCLEAR AUXILIARY POWER (SNAP-19)
review of, 19: 20427 (TID-7698(Pt.I)(p.249-56))

T

TANTALITES
analysis for niobium, tantalum, and uranium by x-ray fluorescence spectrometry, 19: 19754 (JEN-134-DQ/I-39)
TANTALUM
analysis for hafnium or zirconium using catechol violet, colorimetric, 19: 19780
analysis for yttrium, spectrographic, 19: 21690(R) (LA-3244)
corrosion by cerium–cobalt–plutonium alloys at 600 to 1100°C, 19: 21690(R) (LA-3244)
corrosion by iron–plutonium alloys at 600 to 1100°C, 19: 21690(R) (LA-3244)
corrosion by iron–plutonium alloys at high temperatures, effects of yttrium on, 19: 21690(R) (LA-3244)
corrosion in reactors, 19: 20488
deformation at low temperatures, 19: 20605
deterioration of filament electrodes of, in electron-bombardment mercury ion thrustor, 19: 20138 (NASA-TN-D-2173)
determination in columbite–tantalite ores, x-ray fluorescence spectrometric, 19: 19754 (JEN-134-DQ/I-39)
determination in uranium and its compounds and alloys, methods for, 19: 19823
geochemistry and mineralogy of, in Cherry Mountains (Urals), USSR, book, 19: 20190
neutron reactions (n,γ) at 1 to 4 Mev, spectra from, (E/T), 19: 21317
oxidation of, growth mechanism of thin oxide film in anodic, 19: 20490
properties as container for boiling metals, 19: 21690(R) (LA-3244)
radiation effects on hardness of, fast neutron, 19: 21690(R) (LA-3244)
separation from niobium by ion exchange, 19: 20054
structure of dislocations at Luders fronts in, 19: 20562 (SU-DMS-65-1)
testing of thin-wall tubes of, electromagnetic, 19: 20454 (CONF-650212-1)
thermal conductivity at high temperatures, (E), 19: 20576
TANTALUM ALLOYS
Al–Nb–Ta–Ti, fatigue crack propagation in, study of low-cycle, 19: 20462(R) (NRL-6258)
Al–Nb–Ta–Ti, mechanical properties of, effects of processing on, 19: 20462(R) (NRL-6258)
Nb–Ta–Ti, coating of, for oxidation protection at 2300°F, 19: 20483 (SCNC-318)
Nb–Ta–Ti–V, coating for oxidation protection, 19: 20459(R) (IITRI-B6019-6)
Nb–Ta–Ti–V, fabrication and mechanical properties of sheet of, 19: 20552(R) (IITRI-B6021-6)
Nb–Ta–V, fabrication and mechanical properties of sheet of, 19: 20552(R) (IITRI-B6021-6)
Nb–Ta–W–Zr, fabrication and properties of Fs-85 sheet, 19: 20499(R) (AD-606291)
Re–Ta, spectrophotometric analysis for rhenium, 19: 19757 (LA-3213)
Ta–V, coating for oxidation protection, 19: 20459(R) (IITRI-B6019-6)
Ta–V, fabrication and mechanical properties of sheet of, 19: 20552(R) (IITRI-B6021-6)
Ta–V–Zr, coating for oxidation protection, 19: 20459(R) (IITRI-B6019-6)
Ta–W, analysis for yttrium, spectrographic, 19: 21690(R) (LA-3244)
Ta–W, corrosion by cerium–cobalt–plutonium alloys at 600 to 1100°C, 19: 21690(R) (LA-3244)
Ta–W, corrosion by iron–plutonium alloys at 600 to 1100°C, 19: 21690(R) (LA-3244)
Ta–W, corrosion by iron–plutonium alloys at high temperatures, effects of yttrium on, 19: 21690(R) (LA-3244)
Ta–W, corrosion by silver at 1900°C, 19: 21690(R) (LA-3244)
Ta–W, tensile properties at 800 to 2400°C, 19: 20565 (WADD-TR-60-37(Pt.V))
TANTALUM BORIDES
analysis for boron by pyrohydrolysis, 19: 19761 (NP-14876)
TANTALUM CARBIDES
reactions with tungsten, 19: 20565 (WADD-TR-60-37(Pt.V))
superconducting properties, 19: 20572
HfC–TaC, vaporization rates and vapor pressures at 2200 to 3000°K, equations for predicting, 19: 20608
TANTALUM ISOTOPES Ta-181
gamma transition in, parity impurity in 482-kev, (E/T), 19: 21397
neutron capture cross section from 1 to 200 kev, (T), 19: 21464
photon reactions (γ,n), angular distributions from, (E), 19: 21288
TANTALUM NITRIDES
superconducting properties, 19: 20572
TANTALUM OXIDES
formation of thin films of, in anodic oxidation of tantalum, 19: 20490
TANTALUM SYSTEMS
C–Ta–V–Zr, coating for oxidation protection, 19: 20459(R) (IITRI-B6019-6)
C–Ta–W, phase diagram, 19: 20565 (WADD-TR-60-37(Pt.V))
TARTARIC ACID COMPLEXES
with uranyl ions, spectra of, infrared, 19: 19911

TECHNETIUM
determination of, evaluation of methods for, 19: 19820
microstructure of electron-beam-melted, effects of forging on, 19: 20550(R) (HW-84550)
separation from dilute solutions containing high concentrations of other salts by ion exchange chromals, 19: 19820
separation from molybdenum and uranium fission products, 19: 19820
superconducting properties, 19: 19820
TECHNETIUM ALLOYS
Tc–W, fabrication and hardness of, 19: 20550(R) (HW-84550)
TECHNETIUM BROMIDES
spectra of technetium(IV) hexabromides, absorption, 19: 19924
TECHNETIUM CHLORIDES
crystal structure, 19: 19841 (MIT-1965-18)
spectra of technetium(IV) hexachlorides, absorption, 19: 19924
TECHNETIUM FLUORIDES
spectra of technetium(IV) hexafluorides, absorption, 19: 19924
TECHNETIUM IODIDES
spectra of technetium(IV) hexaiodides, absorption, 19: 19924
TECHNETIUM ISOTOPES Tc-99
detection and measurement in solution, use of 4π counter in absolute, 19: 19755 (KFK-252)
separation from power reactor fuels, economics of, 19: 20036 (BNWL-25)
TEETH
analysis for strontium-89 and -90, radiochemical, 19: 19739 (AERE-AM-101)
TEKTITES
cosmic-ray exposure ages of, 19: 20761
fission product tracks in, formation and stability of, (E), 19: 20674
TELEMETERING SYSTEMS
batteries for, testing of, (E), 19: 20280 (SCL-DR-64-128)
TELEVISION EQUIPMENT
use for observing personnel in reactor area, 19: 20317 (HW-82369)
TELLURIUM
geochemistry and mineralogy of, in Cherry Mountains (Urals), USSR, book, 19: 20190
TELLURIUM ISOTOPES Te-122
alpha reactions $(\alpha,2n\gamma)$ and $(\alpha,4n\gamma)$ at 34 to 52 Mev, collective levels from, (E), 19: 21316
TELLURIUM ISOTOPES Te-124
alpha reactions $(\alpha,2n\gamma)$ and $(\alpha,4n\gamma)$ at 34 to 52 Mev, collective levels from, (E), 19: 21316
TELLURIUM ISOTOPES Te-125
energy levels, (E/T), 19: 21256(R) (UCRL-11828(p.58-62))
hyperfine fields in 5p shell of, induced, 19: 21359
TELLURIUM ISOTOPES Te-126
alpha reactions $(\alpha,2n\gamma)$ and $(\alpha,4n\gamma)$ at 34 to 52 Mev, collective levels from, (E), 19: 21316
TELLURIUM ISOTOPES Te-128
alpha reactions $(\alpha,2n\gamma)$ and $(\alpha,4n\gamma)$ at 34 to 52 Mev, collective levels from, (E), 19: 21316
TELLURIUM ISOTOPES Te-130
alpha reactions $(\alpha,2n\gamma)$ and $(\alpha,4n\gamma)$ at 34 to 52 Mev, collective levels from, (E), 19: 21316
TELLURIUM ISOTOPES Te-131
yields of isomer pairs of, in fission, (E), 19: 21390
TELLURIUM ISOTOPES Te-133
yields of isomer pairs of, in fission, (E), 19: 21390
TELLURIUM OXIDES
radiation effects on, activity distribution of iodine-131 in various chemical states from, 19: 20005
TELLURIUM SYSTEMS
Er–Te, phase equilibria and crystal chemistry, 19: 19880
La–Te, phase studies and properties of compounds in, 19: 20606
TEMPERATURE
effects on radiation injury recovery in zygotes, 19: 19496(R) (ANL-6938(p.49-56))
effects on transduction in *Pseudomonas aeruginosa*, 19: 19502(R) (NP-14932)
measurement of low, cerium magnesium nitrate correlation for, 19: 21162(R) (UCRL-11828(p.199-201))
TEMPERATURE CONTROL
in materials testing, engineering drawings of temperature verification system for, 19: 20133
TERBIUM
separation from other light lanthanides by partition chromatography following production by proton bombardment of erbium, 19: 20078
TERBIUM ALLOYS
Gd–Tb, paramagnetic resonance absorption in, at 20 to 200°C, 19: 20581
Sb–Tb, magnetic properties of, (E), 19: 20597
TERBIUM COMPLEXES
with serine, stability and composition, 19: 19874
TERBIUM ISOTOPES Tb-159
fluorine-19 fission, excitation energy, (E/T), 19: 21259(R) (UCRL-11828(p.77-80))
TERBIUM ISOTOPES Tb-161
beta decay of, gamma transitions in, (E), 19: 21329
TERBIUM NITRIDES
magnetic properties of, influence of crystal field on, 19: 19895
TERBIUM SULFATES
crystal structure and bond types of octahydrates, 19: 19915(T)
TERPHENYL
corrosive effects on stainless steel and zirconium loops, chlorine evolution in, 19: 20469 (EUR-2279.e)
TESTOSTERONE
chromatography of acetylated, deuterium and hydrogen isotope effects in gas-liquid, 19: 19893
4-chloro-, anabolic effects in radiotherapy of human tumors, 19: 19669
4-hydroxy-17-methyl-, anabolic effects in radiotherapy of human tumors, 19: 19669
TETRACYCLINE
use in bone growth studies, 19: 19470(R) (ANL-6938(p.141-61))
TEXTILES
preparation of, uses of radioisotopes in industrial, 19: 20417
radiation in, industrial use of, 19: 20411
THALLIUM
geochemistry and mineralogy of, in Cherry Mountains (Urals), USSR, book, 19: 20190
separation from aqueous solutions by solvent extraction using tetraphenylboron, 19: 20058
THALLIUM CHLORIDES
spectra of suspensions of, in thin films of polyethylene, infrared transmission, 19: 19917
THALLIUM COMPLEXES
hydroxyethylenediamine triacetate, isotopic exchange with thallium(III) ions in water, 19: 19856
THALLIUM IODIDES
spectra of suspensions of, in thin polyethylene films, infrared transmission, 19: 19917
THALLIUM IONS
isotope exchange with thallium hydroxyethylenediamine triacetate complex in water, 19: 19856
THALLIUM ISOTOPES Tl-201
fission barrier of compound nucleus, (E/T), 19: 21260(R) (UCRL-11828(p.81))
mass, (E), 19: 21260(R) (UCRL-11828(p.81))
THALLIUM ISOTOPES Tl-203
energy level transitions in, retardations in l-allowed M1, (T), 19: 21323
energy levels of, half life of 279-kev excited, 19: 21291
separation from thallium-205, mass spectrometric, 19: 20261 (JINR-P-1949)
THALLIUM ISOTOPES Tl-204
content in stratosphere, 19: 20657(R) (DASA-1309)
decay of, L/K x-ray intensity ratio in, 19: 21449
determination in air by beta measurement, efficiency of counter for, 19: 20169
exchange between thallium(III) and thallium hydroxyethylenediamine triacetate complex in water, 19: 19856
separation from power reactor fuels, economics of, 19: 20036 (BNWL-25)
shielding power sources of, 19: 21595 (TID-7698(Pt.I)(p.33-248))
THALLIUM ISOTOPES Tl-205
energy level transitions in, retardations in l-allowed M1, (T), 19: 21323
separation from thallium-205, mass spectrometric, 19: 20261 (JINR-P-1949)
THALLIUM ISOTOPES Tl-208
detection and measurement of, performance of whole-body plastic scintillation detector for, 19: 20377
THERMAL CONDUCTIVITY
determination at high temperature, electron-beam system for, 19: 20576
measurement in in-pile fuel element, development of transient temperature method for, 19: 21664(R) (CEND-3336-229)
THERMAL CONDUCTIVITY CELLS
response sensitivity of hot-wire detector for gas chromatography, variables affecting, 19: 20281(R) (UCRL-11828(p.204-7))
THERMAL INSULATION
design for concrete pressure vessels, economics and evaluation of, 19: 20110 (GAMD-5432)
THERMAL RADIATION
hazards of, in nuclear warfare, 19: 19554
hazards of, in nuclear warfare, 19: 19555

THERMAL REACTORS
fuel cycle evaluations for, uranium carbide, 19: 20048 (NAA-SR-9335)
fuel for, review on plutonium, 19: 21673
steam generator design for TARGET gas-cooled power, (E), 19: 21682 (GAMD-4732)
vessels for TARGET gas-cooled, design analysis for prestressed-concrete, (T), 19: 21683 (GAMD-5272(Rev.2))
xenon buildup in, optimal flux shutdown programs for, 19: 21639 (IA-988)
THERMAL STRESSES
distribution in plane reactor shells, (T), 19: 21618
distributions in cylindrical shells, 19: 21619
THERMIONIC CELLS
electric conductivity of plasma in, in transverse magnetic field, (T), 19: 21580
electrode development for hypersonic plasma generator, (E), 19: 20905 (SC-RR-65-54)
operation of cesium, with rhenium-nickel and tungsten-nickel electrodes, 19: 20906
performance of radioisotope-heated, (E/T), 19: 20904 (BLG-317)
plasma drift instability in, effect of sheaths on, (T), 19: 21540
plasma oscillations in, (T), 19: 20913
THERMOCOUPLES
development of rhenium–tungsten, 19: 20473(R) (NASA-CR-54629)
drift of platinum–rhodium- and tungsten–rhenium-base, high-temperature high-vacuum tests of, 19: 20278 (ORNL-P-1069)
electromotive force-temperature tables for platinum/platinum–10% rhodium, smoothed, 19: 20263 (ORNL-3649(Vol.2)(Sect.2.1))
electromotive force-temperature tables for platinum/platinum–13% rhodium, smoothed, 19: 20264 (ORNL-3649(Vol.2)(Sect.2.2))
electromotive force-temperature tables for Chromel/Alumel, smoothed, 19: 20265 (ORNL-3649(Vol.2)(Sect.2.3))
electromotive force-temperature tables for iron/constantan, smoothed, 19: 20266 (ORNL-3649(Vol.2)(Sect.2.4))
electromotive force-temperature tables for copper/constantan, smoothed, 19: 20267 (ORNL-3649(Vol.2)(Sect.2.5))
electromotive force-temperature tables for Chromel/constantan, smoothed, 19: 20268 (ORNL-3649(Vol.2)(Sect.2.6))
electromotive force-temperature tables for tungsten/tungsten–26% rhenium, smoothed, 19: 20269 (ORNL-3649(Vol.2)(Sect.2.7))
electromotive force-temperature tables for tungsten–5% rhenium/tungsten–26% rhenium, smoothed, 19: 20270 (ORNL-3649(Vol.2)(Sect.2.8))
electromotive force-temperature tables for tungsten–3% rhenium/tungsten–25% rhenium, smoothed, 19: 20271 (ORNL-3649(Vol.2)(Sect.2.9))
electromotive force-temperature tables for gold–2.1% cobalt/copper cryogenic, smoothed, 19: 20272 (ORNL-3649(Vol.2)(Sect.2.10))
electromotive force-temperature tables for constantan/copper cryogenic, smoothed, 19: 20273 (ORNL-3649(Vol.2)(Sect.2.11))
electromotive force-temperature tables for Alumel/Chromel cryogenic, smoothed, 19: 20274 (ORNL-3649(Vol.2)(Sect.2.12))
electromotive force-temperature tables for constantan(JN)/iron(JP) cryogenic, smoothed, 19: 20275 (ORNL-3649(Vol.2)(Sect.2.13))
electromotive force-temperature tables for constantan(YN)/iron(YP) cryogenic, smoothed, 19: 20276 (ORNL-3649(Vol.2)(Sect.2.14))
performance of high-temperature, in gas-cooled reactor fuel irradiations, 19: 20401 (ORNL-P-1065)
THERMODYNAMIC PROPERTIES
of carbon dioxide, graphs of equilibrium, 19: 19842 (NASA-SP-3014)
of nuclear materials, tables of, 19: 19933
THERMODYNAMICS
condensing coefficient equation derivation, 19: 20116(R) (SAN-409-12)
gases with hard-core repulsion in, properties of one-dimensional, 19: 20682
of one-dimensional plasma, statistical, 19: 21587
THERMOELECTRIC CELLS
performance of radioisotope-heated, (E/T), 19: 20904 (BLG-317)
THERMOELECTRIC MATERIALS
properties in reactors, analysis of, 19: 21703
THERMOMETRY
nozzle development for high-temperature gas, 19: 20277 (ORNL-P-1068)
THERMONUCLEAR EXPLOSIONS
effects on ecosystem, 19: 20199 (HI-388-RR(Pt.III))
international control, 19: 21761 (P-1134(RAND))
pathological effects of, 19: 19554
pathological effects, 19: 19555
radiation dose calculations for eyes exposed to visible radiation from high-altitude, 19: 19498 (LA-3204)
THERMONUCLEAR REACTIONS
catalysis of lithium-6, by charged particles, 19: 21487(R) (ORNL-3760(p.98-9))
containment programs for, summaries of AEC, (E/T), 19: 21489 (TID-4005(Pt.5))
control of, problems in, 19: 21492(T) (FTD-TT-64-102)
THERMONUCLEAR REACTORS
design and operation of, chemical engineering high-temperature problems in, 19: 19868
development at ORNL, 19: 21479(R) (ORNL-3760)
development programs for, summaries of AEC, (E/T), 19: 21489 (TID-4005(Pt.5))
THICKNESS GAGES
design of beta, with selective energy utilization, 19: 20311
radiometric, industrial uses of, 19: 20417
THIOLS
effects on radiosensitivity of amino acids and proteins, 19: 19621
THIOPHENE
ionization by electron impact, appearance potential for doubly charged molecule ions in, 19: 20807(R) (UCRL-11828(p.201-4))
THIOSULFATES
effects on spectrophotometric determination of zinc using 1-(2-thiazolylazo)-2-naphthol, 19: 19814
THOREX PROCESS
corrosive effects of solutions from, on candidate alloys for centrifuge, 19: 20481 (ORNL-3787)
THORIUM
bibliography on, French, 1956 to 1961, 19: 19738(T)
chemical properties in hydrochloric, nitric, and perchloric acids, 19: 19923
determination by complex formation with substituted acetic acids, 19: 19802
determination by precipitation as diliturate, 19: 19824
determination by titration, suitability of tetraethylenepentamine heptaacetic acid for, 19: 19813
determination in ores, colorimetric, 19: 19778(T) (JPRS-29037(p.58-68))
determination in thorium phosphides, gravimetric, 19: 19740 (ANL-7005)
determination in uranium and its compounds and alloys, methods for, 19: 19823
determination using 5,5'-thiodisalicylic acid, gravimetric, 19: 19812
electrode kinetics of, in acid and alkaline solutions, 19: 19762 (RPI-2714-6)
evaporation from carburized tungsten cathodes at 1900 to 2200°K, (E), 19: 20575
geochemistry and mineralogy of, in Cherry Mountains (Urals), USSR, book, 19: 20190
separation from coated-particle fuel elements, processes for, 19: 20463 (ORNL-TM-431)
separation from uranium by anodic dissolution, 19: 19762 (RPI-2714-6)
strength at high temperatures, effects of alloying additives on, 19: 20560 (ORNL-3777)
THORIUM ALLOYS
Mg–Th, purification by transfer to liquid magnesium–zinc alloy in fused salt, 19: 20066
THORIUM CARBIDES
development as fuel for breeder reactors, 19: 20582
preparation of spheroidal particles of, by sol-gel process, 19: 20528
ThC–UC, performance as reactor fuels, 19: 21665 (GAMD-5535)
ThC–UC, preparation of spheroidal particles of, by sol-gel process, 19: 20528
THORIUM CARBONATES
use in age estimation of marine carbonates, 19: 20181
THORIUM CHLORIDE COMPLEXES
stability of, electrodialysis and ion exchange studies of, 19: 19923
THORIUM COMPOUNDS
solubility and thermolysis of diliturate, 19: 19824
THORIUM HYDROXIDES
solubility and stability constants of, effects of pH on, 19: 19922
THORIUM IONS
effects on dephosphorylation of nucleotides and sugar phosphates, 19: 19876
hydrolysis of tetravalent, in sodium perchlorate at 0 and 95°C, 19: 19878
THORIUM ISOTOPES Th-228
content in blood and bones of humans injected with thorotrast, 19: 19497(R) (ANL-6938(p.127-39))
content in plants and silts in contaminated lake, 19: 20220
content in tissues of humans and rats injected with thorotrast, 19: 19497(R) (ANL-6938(p.127-39))
separation from power reactor fuels, economics of, 19: 20036 (BNWL-25)
shielding power sources of, 19: 21595 (TID-7698(Pt.I)(p.33-248))
THORIUM ISOTOPES Th-232

alpha fission at 33 Mev, tellurium-131 and -133 isomer pair yields from, (E), 19: 21390
content in rocks of La Sal Mountains, Utah, (E), 19: 20178
content in tissues of humans injected with thorotrast, 19: 19497(R) (ANL-6938(p.127-39))
deuteron fission at 18 Mev, tellurium-131 and-133 isomer pair yields from, (E), 19: 21390
neutron capture by, resonance integrals for epithermal, (E), 19: 21336
neutron fission at 3 to 14 Mev, delayed-neutron yields in, 19: 21443

THORIUM MINERALS
radioactivity equilibrium in, in accessory monazites of Ukraine, 19: 20189

THORIUM NITRATE COMPLEXES
stability of, electrodialysis and ion exchange studies of, 19: 19923

THORIUM NITRATES
analytical uses in determination of microamounts of fluoride, 19: 19788
$Co(NO_3)_2$–$Th(NO_3)_4$, crystal structure of octahydrates, 19: 19852
$Mg(NO_3)_2$–$Th(NO_3)_4$, crystal structure of octahydrates, 19: 19852
$Mn(NO_3)_2$–$Th(NO_3)_4$, crystal structure of octahydrates, 19: 19852
$Ni(NO_3)_2$–$Th(NO_3)_4$, crystal structure of octahydrates, 19: 19852
$Th(NO_3)_4$–$Zn(NO_3)_2$, crystal structure of octahydrates, 19: 19852

THORIUM OXALATES
precipitation from nitrate solution and calcination to prepare oxide, 19: 19861

THORIUM OXIDES
analysis for trace amounts of zinc using 1-(2-thiazolylazo)-2-naphthol, spectrophotometric, 19: 19814
properties as reactor fuel, 19: 21671

THORIUM(IV) OXIDES
distribution in tissues of, after Thorotrast injections, 19: 19567
effects of injected, on humans and rats, 19: 19497(R) (ANL-6938 (p.127-39))
pathological effects in liver, 19: 19560
pathological effects of, on bone marrow, 19: 19567
preparation by calcination of oxalate, relation of crystal sizes in, 19: 19861
solubility in perchlorate solution, 19: 19878
use in radiology of kidneys, tumor development from, 19: 19707
BeO–PuO_2–ThO_2, phase diagrams, 19: 20589
BeO–ThO_2, phase diagrams, 19: 20589
ThO_2–UO_2, diffusion of fission gases from, effects of stress on, 19: 20586
ThO_2–UO_2, preparation from mixture of thorium and uranyl nitrates, 19: 19942(P)
ThO_2–UO_2, separation of protactinium-233 from irradiated, by sorption on unfired Vycor, 19: 20051 (ORNL-3773)
ThO_2–W, extrusion of sintered, 19: 20500 (AFML-TR-64-387)
ThO_2–W, tensile properties at 800 to 2400°C, 19: 20565 (WADD-TR-60-37(Pt.V))

THORIUM PHOSPHIDES
analysis for phosphorus and thorium, gravimetric, 19: 19740 (ANL-7005)

THORIUM SILICIDES
crystal structure of ternary, 19: 20568

THORIUM SYSTEMS
Co–Si–Th, crystal structure of compound in, 19: 20568
Cr–Si–Th, crystal structure of compound in, 19: 20568
Cu–Si–Th, crystal structure of compound in, 19: 20568
Fe–Si–Th, crystal structure of compound in, 19: 20568
Mn–Si–Th, crystal structure of compound in, 19: 20568
Ni–Si–Th, crystal structure of compound in, 19: 20568

THRESHOLD DETECTORS
container for, engineering drawings of, 19: 20390

THULIUM COMPLEXES
trisbenzoylacetonate, spectra of, crystal-field splitting in absorption and emission, 19: 19886

THULIUM ETHYL SULFATES
energy levels in hydrated, from absorption spectra, (T/E), 19: 21600 (IS-968)

THULIUM IONS
spectra in barium, calcium, and strontium fluorides, absorption and luminescence, 19: 19854

THULIUM ISOTOPES Tm-169
alpha inelastic scattering at 3.1 Mev, conversion coefficients mixing ratios for rotational transitions in, (E), 19: 21324
boron-11 fission, excitation energy, (E/T), 19: 21259(R) (UCRL-11828(p.77-80))

THULIUM ISOTOPES Tm-170
separation from power reactor fuels, economics of, 19: 20036 (BNWL-25)
shielding power sources of, 19: 21595 (TID-7698(Pt.I)(p.33-248))

THULIUM ISOTOPES Tm-171
separation from power reactor fuels, economics of, 19: 20036 (BNWL-25)
shielding power sources of, 19: 21595 (TID-7698(Pt.I)(p.33-248))

THULIUM ISOTOPES Tm-174
decay of 5.2-min, (E), 19: 21272

THULIUM NITRIDES
magnetic properties of, influence of crystal field on, 19: 19895

THULIUM SULFATES
crystal structure and bond types of octahydrates, 19: 19915

THYMOLS
effects on polarography of uranyl pyrophosphate complexes, 19: 19816

THYMUS
effects on immunologic reactivity and tolerance of marrow grafts in radiation mouse chimeras, 19: 19652

THYROID DISEASES
effects on cholesterol metabolism in rats, 19: 19511(T) (JPRS-29364(p.1-4))
radiodiagnosis of, radiation hazards, 19: 19587
radiotherapy of, intra-arterial injection of iodine-131 in, 19: 19661
radiotherapy using iodine-131, 19: 19665

THYROID GLAND
function of, use of labeled-triiodothyronine *in vitro* test for evaluation of, 19: 19679
iodine uptake and storage in human fetal, 19: 19491
radiation effects on morphology of rat, 19: 19569
radiodiagnosis of, by photoscanning using iodine-125, 19: 19711
tumor localization in, by external counting of cobalt-57- or cobalt-58-labeled vitamin B-12, 19: 19732

THYRONINE, TRIIODO-
use of labeled-, for evaluation of thyroid function *in vitro*, 19: 19679

TIMING CIRCUITS
design of 100-channel time analyzer, 19: 20298

TIN
deposition on vanadium-base alloys for oxidation protection, 19: 20459(R) (IITRI-B6019-6)
determination in ppm range by d-c arc excitation, spectrochemical, 19: 19827
effects on strength of thorium at high temperatures, 19: 20560 (ORNL-3777)
magnetic flux quantization in superconducting cylinders of, 19: 21194
meson (π^+) absorption at 2.72, 3.70, and 4.75 Bev/c, cross sections for, (E), 19: 21431
phonon dispersion curves of beta, (E), 19: 21603
proton reactions at 2.72 Bev/c, cross sections for, (E), 19: 21431
solubility and thermodynamics of oxygen in liquid tin at 536, 600, 700, and 751°C, 19: 19918

TIN ALLOYS
deposition on niobium alloys for oxidation protection at 2300°F, 19: 20483 (SCNC-318)
Al–Mo–Sn–Ti–V–Zr, beta transus temperature of, 19: 20462(R) (NRL-6258)
Al–Mo–Sn–Ti–V, beta transus temperature of, 19: 20462(R) (NRL-6258)
Al–Sn–Ti–V, beta transus temperature of, 19: 20462(R) (NRL-6258)
Al–Sn–Ti–Zr, mechanical properties of diffusion-bonded plates of, 19: 20462(R) (NRL-6258)
Cr–Fe–Ni–Sn–Zr, properties for use as fuel element cladding, 19: 20497(P)
Cu–Sn, radiation effects on vacancy repeated yielding characteristics of, 19: 20635

TIN ISOTOPES Sn-118
proton inelastic scattering by, analog of excited states from, 19: 21341

TIN ISOTOPES Sn-119
energy levels in, tin-118 analog excited states of, 19: 21341
magnetic fields acting on, in ferromagnetic materials, 19: 20578

TIN ISOTOPES Sn-121
beta spectra of long-lived, (E), 19: 21375

TIN OXIDES
gamma resonance absorption by glycerol suspensions of, at 23.8 kev, (E), 19: 21428
thermodynamics of formation in oxygen–liquid tin systems, 19: 19918

TISSUE CULTURES
effects of virus infections on immune reactions of L cell, 19: 19549
radiation effects on interferon synthesis and virus plaque development in rat embryo cell, 19: 19563

TISSUES
analysis for copper by activation methods, 19: 19807
analysis for trace elements in normal and tumor, neutron activation, 19: 19793
neutron activation of elements in rat, during mixed neutron and gamma exposure, 19: 19601
preparation of simulated, using *Bacillus megaterium* embedded in poly-

ethylene glycol, 19: 19457 (NP-14886)
radiation dose to superficially contaminated, theoretical calculation of alpha, 19: 19482
radiation effects on, small-dose, 19: 19516
radiation effects on differentiation of, in regeneration of extremities in salamanders, 19: 19546
radiation effects on, 19: 19562
radiation effects on physicochemistry of DNA in, review on, 19: 19566
TITANIUM
abundance in solar atmosphere, spectral line determination of, (E), 19: 20775(T)
analysis for hafnium or zirconium using catechol violet, colorimetric, 19: 19780
analysis for hydrogen by isotopic equilibration, 19: 19831
bonding to silicon carbide heater, 19: 20505 (JAERI-1071)
casting of, review, 19: 20462(R) (NRL-6258)
corrosion by solutions produced in head-end processes for fuel, 19: 20481 (ORNL-3787)
determination by complex formation with substituted acetic acids, 19: 19802
determination in uranium and its compounds and alloys, methods for, 19: 19823
deuteron reactions with deuterided, neutron yields from, (E), 19: 21301
effects on carbon steel corrosion by mercury, 19: 20493
effects on strength of thorium at high temperatures, 19: 20560 (ORNL-3777)
fatigue crack propagation in, study of low-cycle, 19: 20462(R) (NRL-6258)
geochemistry and mineralogy of, in Cherry Mountains (Urals), USSR, book, 19: 20190
spectral lines in solar atmosphere, excitation temperature for, (E), 19: 20775(T)
welding of pipes and plates of, Hanford procedures for, 19: 20524 (TID-20625(Vol.IV)(Rev.I))
TITANIUM ALLOYS
casting of, review, 19: 20462(R) (NRL-6258)
Al–Mo–Sn–Ti–V–Zr, beta transus temperature of, 19: 20462(R) (NRL-6258)
Al–Mo–Sn–Ti–V, beta transus temperature of, 19: 20462(R) (NRL-6258)
Al–Mo–Ti, beta transus temperature of, 19: 20462(R) (NRL-6258)
Al–Mo–Ti–V, mechanical properties of diffusion-bonded plates of, 19: 20462(R) (NRL-6258)
Al–Mo–Ti–V, mechanical properties of solution-annealed and aged T-19, 19: 20462(R) (NRL-6258)
Al–Mo–Ti–Zr, beta transus temperature of, 19: 20462(R) (NRL-6258)
Al–Nb–Ta–Ti, fatigue crack propagation in, study of low-cycle, 19: 20462(R) (NRL-6258)
Al–Nb–Ta–Ti, mechanical properties of, effects of processing on, 19: 20462(R) (NRL-6258)
Al–Sn–Ti–V, beta transus temperature of, 19: 20462(R) (NRL-6258)
Al–Sn–Ti–Zr, mechanical properties of diffusion-bonded plates of, 19: 20462(R) (NRL-6258)
Al–Ti–V, fatigue crack propagation in, study of low-cycle, 19: 20462(R) (NRL-6258)
Al–Ti–V, mechanical properties of diffusion-bonded plates of, 19: 20462(R) (NRL-6258)
Al–Ti–V–Zr, beta transus temperature of, 19: 20462(R) (NRL-6258)
Al–Ti–Zr, mechanical properties of diffusion-bonded plates of, 19: 20462(R) (NRL-6258)
Mo–Nb–Ti, coating of, for oxidation protection at 2300°F, 19: 20483 (SCNC-318)
Mo–Nb–Ti–V, coating for oxidation protection, 19: 20459(R) (IITRI-B6019-6)
Mo–Ti–Zr, corrosion by potassium vapor, design of test capsule for, 19: 20473(R) (NASA-CR-54629)
Mo–Ti–Zr, tensile properties of TZM sheet, 19: 20542(R) (AD-606310)
Nb–Ta–Ti, coating of, for oxidation protection at 2300°F, 19: 20483 (SCNC-318)
Nb–Ta–Ti–V, coating for oxidation protection, 19: 20459(R) (IITRI-B6019-6)
Nb–Ta–Ti–V, fabrication and mechanical properties of sheet of, 19: 20552(R) (IITRI-B6021-6)
Nb–Ti, coating of, for oxidation protection at 2300°F, 19: 20483 (SCNC-318)
Nb–Ti–V, coating for oxidation protection at 1800 to 2500°F, 19: 20459(R) (IITRI-B6019-6)
Nb–Ti–V, fabrication and mechanical properties of sheet of, 19: 20552(R) (IITRI-B6021-6)
Nb–Ti–W–V, coating for oxidation protection, 19: 20459(R) (IITRI-B6019-6)
Pu–Ti–U, phase studies, 19: 21690(R) (LA-3244)
TITANIUM BORIDES
analysis for boron by pyrohydrolysis, 19: 19761 (NP-14876)
TITANIUM CARBIDES
preparation and casting of, 19: 20455(R) (DCAS-TDR-62-192)
superconducting properties, 19: 20572
TITANIUM ISOTOPES Ti-44
content in iron meteorites, (E), 19: 20760
TITANIUM ISOTOPES Ti-46
proton reactions (p,γ) with, (E), 19: 21374
proton reactions at 2.5–3 Mev, resonances in, 19: 21446
TITANIUM ISOTOPES Ti-48
proton inelastic scattering at 7 Mev, energy levels from, (E), 19: 21346
proton reactions at 2.5–3 Mev, resonances in, 19: 21446
TITANIUM ISOTOPES Ti-50
proton inelastic scattering at 7 Mev, energy levels from, (E), 19: 21346
TITANIUM NITRIDES
superconducting properties, 19: 20572
TITANIUM OXIDES
analysis for vanadium, activation, 19: 19771(R) (TEES-2671-4(Chap.9))
effects on thermal stability of zirconium oxide, 19: 20585
Nb_2O_5–TiO_2, crystal structure and equilibria of phases in system, 19: 20569
TITANIUM SYSTEMS
C–Mo–Ti–Zr, extrusion of molybdenum-TZC, 19: 20500 (AFML-TR-64-387)
TOBACCO
polonium-210 content in smoke from, 19: 19495
TOKAI-MURA POWER REACTOR
pressure vessel welding for, 19: 21700
TOLUENE
hydrogen abstraction from, by methyl radicals, 19: 21760 (NYO-2728-4)
luminescence spectra and quantum yields of pure and cyclohexane solutions of, 19: 21771 (TID-21684)
solvent properties for hydrochloric acid, tridodecylamine hydrochloride, and water, 19: 20039 (EUR-2246.e)
solvent properties in mixtures with butyl, dichlorodiethyl, and ethyl ethers for uranyl nitrates, 19: 20072
TOLUENE, OCTAFLUORO-
nuclear magnetic resonance of fluorine in, intermolecular coupling constants in, 19: 19888
TOURMALINES
helium evolution from, 19: 19934
TOXINS
effects of *E. coli* endotoxins on hemorrhagic syndrome in guinea pigs, 19: 19487
radioinduced, in liver lipids in rabbits, 19: 19599
TRACER TECHNIQUES
for measurement of diffusion pump oil deposition in vacuum systems, 19: 20143
scintillation counting in, quenching corrections in, 19: 20332
TRACER TECHNIQUES (BIOLOGY)
calcium metabolism in dog bones, 19: 19470(R) (ANL-6938(p.141-61))
color quenching in liquid scintillation systems, 19: 20324 (ORNL-P-1094)
fatty acid synthesis in diabetic and obese subjects, 19: 21758 (BNL-8864)
use of tritium in, 19: 19515
TRACER TECHNIQUES (CHEMISTRY)
development of oil-soluble gold-198, 19: 20030
evaluation of radiosodium separation from activation samples, 19: 19768(R) (TEES-2671-4(Chap.6))
uses in analysis, 19: 19822
TRACER TECHNIQUES (GEOLOGY)
movement of clay suspensions in porous media, 19: 20183
tritium in hydrology, 19: 20174(T) (CEA-tr-A-1729)
TRACER TECHNIQUES (MEDICINE)
for body water determinations, 19: 19480
for exploration of heart function dynamics, 19: 19705
radiation hazards of diagnostic uses of, 19: 19670
use of cobalt-57- or cobalt-58-labeled vitamin B-12 for localization of thyroid tumor, 19: 19732
using iodine-131, 19: 19731
TRACER TECHNIQUES (METEOROLOGY)
development using copper-64, 19: 20658
TRADESCANTIA
radiation effects on mitosis suppression in cytoplasmic structures and nucleus of, uv, 19: 19579
TRANSISTORS
development of surface-field-controlled, (E), 19: 20323(R) (NYO-3246-4)
TRANSURANIC ELEMENTS
fission of neutron-rich, spontaneous, (E), 19: 21403
production of neutron-rich, in neutron capture by uranium-238, (E),

19: 21403
TREES
carbon-14 activity in Kauri, in New Zealand, 19: 20238
TRIDODECYLAMINE
equilibrium with hydrochloric acid, 19: 20039 (EUR-2246.e)
solubility of hydrochloride of, in organic diluents, 19: 20039 (EUR-2246.e)
solvent properties of hydrochloride of, for americium and iron, 19: 20039 (EUR-2246.e)
solvent properties of hydrochloride of, for americium and iron from chloride solutions, 19: 20038 (EUR-2245.e)
TRIETHYLAMINE
effects on ionic decomposition of s-butylperoxy formate, 19: 19948
TRIOCTYLAMINE
deuterium exchange with water, 19: 19864
solvent properties for uranium, 19: 20067
TRIOXANES
radioinduced polymerization with 3-chloromethyl-3-ethyloxetane, 19: 19972
TRIS(2-ETHYLHEXYL)AMINE
solvent properties for uranium, 19: 20067
TRITHIANE
radioinduced polymerization of crystalline, gamma, 19: 19959 (CONF-571-37)
TRITIUM
content in Discoverer XVII, origin of, 19: 21438
detection and measurement in Hanford ground water, 19: 21749(R) (HW-84549)
detection and measurement of leakage of, from luminous points, 19: 20161 (NP-14869)
deuteron reactions (d,n) at 2.1 and 2.9 Mev, polarization distributions from, (E), 19: 21303
effects of incorporated, in cells, 19: 19515
exchange to and from azulene in acid solutions, 19: 19883
incorporation in steroids, method for, 19: 20025
metabolism and distribution in body water of man, 19: 19480
neutron reactions (n,d) at 14.4 Mev, neutron-neutron scattering length from, (E), 19: 21404
neutron reactions (n,p) and (n,γ) at 14.4 Mev, (E), 19: 21405
nuclear magnetic dipole moment, (T), 19: 21322
production by proton reactions with metals, 19: 21438
properties of, 19: 19515
release to atmosphere in laboratory accident, hazards in, 19: 20194 (BLG-280)
separation from deuterium and hydrogen by adsorption and gas chromatography, 19: 20435
tracer use in studies of fatty acid synthesis in diabetic and obese subjects, 19: 21758 (BNL-8864)
tracer use of nuclear explosion produced, in hydrology, 19: 20174(T) (CEA-tr-A-1729)
tracer uses in studies of nucleic acid metabolism, 19: 19515
use to excite x-ray fluorescence in analysis of light elements, 19: 19741 (CEA-R-2539)
wave function of, ground-stage, (T), 19: 21367
TRITONS
binding energy of, three-body forces in, 19: 21075
binding energy of, with velocity-dependent potential, (T), 19: 21309
interactions with deuterons, bibliography, (E/T), 19: 21238 (LA-3205)
reactions (t,p) with magnesium-24 at 10 and 11 Mev, angular distributions from, (E), 19: 21311
TROPOSPHERE
carbon-14 content of, total and fallout, 1953 to 1964, 19: 20155 (HASL-159)
TRYPSIN
inactivation mechanisms for, in acid solutions, 19: 19968
radiation effects on thermoluminescence, 19: 19983
TRYPTOPHAN
radiofluorescence of, quenching effects of nitric oxide and oxygen on, 19: 19970(T)
TUBES
boiling upward flow of saturated liquid nitrogen at high vapor qualities in heated, film, 19: 20113 (NP-14895)
deformation of uranium, by external pressure, 19: 20453 (CEA-R-2572)
drawing of, design of equipment for, 19: 21782(P)
fluid-entrance flow in vertical, with combined free-forced convection, 19: 20114 (NP-14920)
gas flow in thermal entrance region of heated, effects of large temperature gradients on turbulent, 19: 20117 (SU-247-4)
testing of thin-wall refractory-metal, electromagnetic, 19: 20454 (CONF-650212-1)
testing small-diameter, engineering drawings of ultrasonic device for, 19: 20131
welding of, Hanford procedures for, 19: 20524 (TID-20625(Vol.IV)(Rev.I))
wetting Haynes-25 boiler, by mercury, 19: 20111 (NAA-SR-Memo-10224)
TUMORS
analysis for trace elements, neutron activation, 19: 19793
chemotherapy, evaluation of results, 19: 19702
development in kidneys after thorotrast radiology, 19: 19707
localization in stomach by photoscanning after administration of iodine-131-labeled iodide, 19: 19717
localization of malignant, using iodine-125 and -131-labeled fibrinogen, 19: 19716
localization of thyroid adenomata by external counting of cobalt-57- or cobalt-58-labeled vitamin B-12, 19: 19732
radiation effects on physicochemistry of DNA in, review on, 19: 19566
radiation effects on RNA metabolism and synthesis in HeLa cells, 19: 19602
radiodiagnosis of human liver, by iodine-131 infusion in bowel, 19: 19662
radiodiagnosis of pancreatic, by scanning using selenium-75-labeled selenomethionine, 19: 19722
radiodiagnosis of pancreatic, by photoscanning using selenium-75-labeled selenomethionine, 19: 19723
radiodiagnosis of spleenic, by scintiscanning using chromium-51, 19: 19726
radioinduced in mice, 19: 19594
radioinduced in rats, 19: 19561
radioinduced in rats, effects of chemical carcinogens on, 19: 19606
radioinduced, on hands, 19: 19524
radiotherapy of human, anabolic effects of steroids in, 19: 19669
radiotherapy of human lung, effects on healthy lung tissue, 19: 19683
radiotherapy of laryngeal cancers, 19: 19659
radiotherapy of uterine, 19: 19681
radiotherapy of uterine, 19: 19700
radiotherapy of, by intra-arterial injection of radioisotopes, 19: 19661
radiotherapy of, dose distribution in, 19: 19671
radiotherapy of, dose distribution in, 19: 19672
radiotherapy of, design of slit-type lead screen for use with cobalt-60 gamma sources, 19: 19674
radiotherapy of, effects of surgery on, 19: 19703
radiotherapy of, radiation dose evaluation, 19: 19597
radiotherapy of, use of radioisotopes for, 19: 19706
radiotherapy using electron beams, 19: 19673
radiotherapy, evaluation of results, 19: 19702
TUNGSTEN
analysis for hafnium or zirconium using catechol violet, colorimetric, 19: 19780
analysis for trace amounts of nickel, photometric, 19: 19799
coating with rhenium by electrolysis, optimum conditions for, 19: 20529
crystallization rate after rolling and annealing, 19: 20604
determination in uranium and its compounds and alloys, methods for, 19: 19823
effects on hydrolysis of uranium carbide, 19: 19882
electromagnetic wave absorption and scattering by particles of, (T), 19: 20677
electron emission in monocrystalline, angular dependence of xenon-133 conversion, (E), 19: 21339
evaporation from carburized thoriated electrodes of, at 1900 to 2200°K, 19: 20575
ionization of erbium, gadolinium, and ytterbium at surfaces of, 19: 20871
melting point measurement by black-body method, 19: 20566(T) (IS-Trans-13)
nucleon reactions at high energies, secondary nucleon yields from, (E/T), 19: 21242 (NP-14837)
oxidation in air at 0.01 to 100 atm, assuming frozen laminar boundary layer, 19: 20496
performance as emitter in hypersonic plasma generators, (E), 19: 20905 (SC-RR-65-54)
performance of cesium- and copper-impregnated, as emitter in hypersonic plasma generators, (E), 19: 20905 (SC-RR-65-54)
preparation and properties of hot-pressed, 19: 20559 (NP-14892)
radiation damage in, fission fragment, 19: 20643
reactions with tantalum carbides, 19: 20565 (WADD-TR-60-37(Pt.V))
sintering at 750 to 2200°C, 19: 20532
tensile properties of sheet of, 19: 20542(R) (AD-606310)
tensile properties at 800 to 2400°C, 19: 20565 (WADD-TR-60-37(Pt.V))
thermal conductivity at high temperatures, (E), 19: 20576
x-ray spectra in, muonic, (E), 19: 21344
TUNGSTEN ALLOY COUPLES
Re–W/Re–W, performance in gas-cooled reactor fuel irradiation experiments, 19: 20401 (ORNL-P-1065)
Re–W/Re–W, thermocouple tables, smoothed, 19: 20270 (ORNL-3649 (Vol.2)(Sect.2.8))

Re–W/Re–W, thermocouple tables, smoothed, 19: 20271 (ORNL-3649 (Vol.2)(Sect.2.9))
Re–W/Re–W, thermocouple drift at high temperatures in vacuum, 19: 20278 (ORNL-P-1069)
Re–W/W, thermocouple tables, smoothed, 19: 20269 (ORNL-3649 (Vol.2)(Sect.2.7))
Re–W/W, thermocouple drift at high temperatures in vacuum, 19: 20278 (ORNL-P-1069)
TUNGSTEN ALLOYS
tensile properties at 800 to 2400°C, 19: 20565 (WADD-TR-60-37(Pt.V))
Ag–W, preparation and properties of infiltrated, 19: 20559 (NP-14892)
Mo–Nb–W, extrusion, 19: 20500 (AFML-TR-64-387)
Mo–Re–W, ductility and melting points of sintered, 19: 20584
Mo–W, ductility and melting points of sintered, 19: 20584
Mo–W, extrusion, 19: 20500 (AFML-TR-64-387)
Nb–Ta–W–Zr, fabrication and properties of FS-85 sheet, 19: 20499(R) (AD-606291)
Nb–Ti–W–V, coating for oxidation protection, 19: 20459(R) (IITRI-B6019-6)
Re–W, tensile properties at 800 to 2400°C, 19: 20565 (WADD-TR-60-37(Pt.V))
Re–W, testing of thin-wall tubes of, electromagnetic, 19: 20454 (CONF-650212-1)
Ta–W, analysis for yttrium, spectrographic, 19: 21690(R) (LA-3244)
Ta–W, corrosion by cerium–cobalt–plutonium alloys at 600 to 1100°C, 19: 21690(R) (LA-3244)
Ta–W, corrosion by iron–plutonium alloys at 600 to 1100°C, 19: 21690(R) (LA-3244)
Ta–W, corrosion by iron–plutonium alloys at high temperatures, effects of yttrium on, 19: 21690(R) (LA-3244)
Ta–W, corrosion by silver at 1900°C, 19: 21690(R) (LA-3244)
Ta–W, tensile properties at 800 to 2400°C, 19: 20565 (WADD-TR-60-37(Pt.V))
Tc–W, fabrication and hardness of, 19: 20550(R) (HW-84550)
TUNGSTEN CARBIDES
superconducting properties, 19: 20572
use in nozzles for high-temperature thermometry in gases, 19: 20277 (ORNL-P-1068)
TUNGSTEN COUPLES
Re/W, development, 19: 20473(R) (NASA-CR-54629)
Re/W, performance in gas-cooled reactor fuel irradiation experiments, 19: 20401 (ORNL-P-1065)
Re–W/W, thermocouple tables, smoothed, 19: 20269 (ORNL-3649 (Vol.2)(Sect.2.7))
Re–W/W, thermocouple drift at high temperatures in vacuum, 19: 20278 (ORNL-P-1069)
TUNGSTEN ISOTOPES W-178
fission barrier of compound nucleus, (E/T), 19: 21259(R) (UCRL-11828(p.77-80))
TUNGSTEN ISOTOPES W-179
fission barrier of compound nucleus, (E/T), 19: 21259(R) (UCRL-11828(p.77-80))
TUNGSTEN ISOTOPES W-180
energy level transitions in, E2 conversion coefficients of rotational, (T), 19: 21308
fission barrier of compound nucleus, (E/T), 19: 21259(R) (UCRL-11828(p.77-80))
TUNGSTEN ISOTOPES W-181
content in stratosphere, 19: 20657(R) (DASA-1309)
TUNGSTEN ISOTOPES W-182
alpha fission of, energy-mass distributions in, (E/T), 19: 21263(R) (UCRL-11828(p.90-2))
carbon-12 fission, excitation energy, (E/T), 19: 21259(R) (UCRL-11828(p.77-80))
energy level transitions in, E2 conversion coefficients of rotational, (T), 19: 21308
energy levels of, half life of 100- and 290-kev excited, 19: 21291
neutron capture cross section from 1 to 200 kev, (T), 19: 21464
oxygen-16 fission of, analysis of excitation function for, (E/T), 19: 21264(R) (UCRL-11828(p.92-4))
properties of, effects of pairing forces on, (T), 19: 21434
TUNGSTEN ISOTOPES W-183
neutron capture cross section from 1 to 200 kev, (T), 19: 21464
TUNGSTEN ISOTOPES W-184
energy level transitions in, E2 conversion coefficients of rotational, (T), 19: 21308
neutron capture cross section from 1 to 200 kev, (T), 19: 21464
TUNGSTEN ISOTOPES W-185
content in stratosphere, 19: 20657(R) (DASA-1309)
TUNGSTEN ISOTOPES W-186
energy level transitions in, E2 conversion coefficients of rotational, (T), 19: 21308
neutron capture cross section from 1 to 200 kev, (T), 19: 21464
TUNGSTEN OXIDES
reactions in ammonium fluoride and hydrofluoric acid solutions, 19: 19913
spectra of suspensions of, in thin polyethylene films, infrared transmission, 19: 19917
TUNGSTEN SYSTEMS
C–Nb–W–Zr, creep properties of D-43, 19: 20474(R) (NASA-CR-54281)
C–Nb–W–Zr, stress corrosion of D-43 by refluxing potassium, research program on, 19: 20474(R) (NASA-CR-54281)
C–Ta–W, phase diagram, 19: 20565 (WADD-TR-60-37(Pt.V))
HfN–W, tensile properties at 800 to 2400°C, 19: 20565 (WADD-TR-60-37(Pt.V))
NbC–W, phase studies at 2000 to 3000°C, (E), 19: 20583(T)
ThO_2–W, extrusion of sintered, 19: 20500 (AFML-TR-64-387)
ThO_2–W, tensile properties at 800 to 2400°C, 19: 20565 (WADD-TR-60-37(Pt.V))
TYROSINE
radiofluorescence of, quenching effects of nitric oxide and oxygen on, 19: 19970(T)

U

ULCERS
localization in stomach by photoscanning after administration of iodine-131-labeled iodide, 19: 19717
ULTRASONICS
amplification by interaction with charged particle beam in piezoelectric crystal, (T), 19: 20672
attenuation in superconductors in strong magnetic fields, (E), 19: 21188
attenuation in superconducting lead, amplitude-dependent, (T), 19: 21169
effects on hardness of aluminum single crystals, 19: 20641
technique for nondestructive testing of coating-metal bonds, development of, 19: 20127(R) (IITRI-N213-23)
uses in nondestructive testing of small-diameter tubing, 19: 20131
ULTRAVIOLET RADIATION
effects on dark phase of actinorhythmic reaction in plants, 19: 19543
effects on development and growth of wheat, photoperiod and temperature effects on, 19: 19545
effects on *E. coli* bacteriophages, protective effects of Versene against, 19: 19638
effects on glasses, ESR spectra of electron production in, 19: 20002
effects on interferon synthesis and virus plaque development in rat embryo cells, 19: 19563
effects on magnesium fluoride crystals, 19: 20618 (NBS-8614)
effects on mitosis suppression of cytoplasmic structure and nucleus in *Tradescantia paludosa*, 19: 19579
effects on mutagenesis in isolated DNA from *B. subtilis*, 19: 19542
effects on mutation of yeasts, 19: 19593
effects on penicillin production by *Penicillium nigricans*, 19: 19556
effects on *Sordaria brevicollis*, genetic, 19: 19547
effects on *Staphylococcus aureus*, genetic, 19: 19531
effects on *Staphylococcus aureus*, genetic, 19: 19532
effects on thermoluminescence afterglow of proteins and synthetic polymers, 19: 19983
effects on transduction in *Pseudomonas aeruginosa*, 19: 19501(R) (NP-14931)
effects on transduction in *Pseudomonas aeruginosa*, 19: 19502(R) (NP-14932)
effects on transduction in *Pseudomonas aeruginosa*, 19: 19503(R) (NP-14933)
effects on vaccinia virus, genetic, 19: 19549
effects on yeast cell survival, temperature effects on, 19: 19626
spectrum in solar radiation, review of, 19: 20785
UNDERGROUND EXPLOSIONS
craters produced by, prediction of shape of, 19: 20089 (NP-14887)
detection of, by seismic waves 2000 to 6000 miles from source, 19: 20177
fallout from Antler, (E), 19: 20167
identification of nuclear, by p-phase wave shapes, 19: 20172(R) (NP-14877)
seismic data from BILLIKEN calibration shot in southeast Missouri, 19: 20171 (AFCRL-64-659)
seismic waves from HARDHAT, comparison with waves from FALLON earthquake and SHOAL explosion, 19: 20172(R) (NP-14877)
seismic waves from SHOAL, comparison with waves from FALLON earthquake and HARDHAT explosion, 19: 20172(R) (NP-14877)
use in construction of earth-fill dams, 19: 20090 (SC-RR-65-41)
vented gases in Dribble project, apparatus for analysis of, 19: 19776 (UCRL-12169)

UNDERGROUND STRUCTURES
blast effects on hollow cylindrical, (T), 19: 20659 (AD-606490)
response of buried hollow cylinders to quasi-static overpressures, 19: 20136 (AFWL-TDR-64-13)
site preparation using light from reactors, 19: 21710
UNDERWATER EXPLOSIONS
seismic wave amplitude and spectra from, 19: 20175
URAL MOUNTAINS (SOVIET UNION)
mineralogy and geochemistry of rare elements in, book, 19: 20190
URANIC ACID
reactions with monosodium dimethylglyoxime, 19: 19860
URANIUM
analysis for impurities by spark source mass spectrography, 19: 19830
analysis for iron by photocolorimetric methods, 19: 19811
analysis methods for, book, 19: 19823
bibliography on, French, 1956 to 1961, 19: 19738(T)
book: *Uranium: Methods for Determination*, in Russian, 19: 19823
coating with niobium, development of methods for, 19: 20456 (EUR-2111.d)
content in man, effects of content in food, soil, and water supplies on, 19: 19490
deformation of tubes of, by external pressure, 19: 20453 (CEA-R-2572)
determination as hexavalent ion using EDTA, 19: 19779
determination in columbite–tantalite ores, x-ray fluorescence spectrometric, 19: 19754 (JEN-134-DQ/I-39)
determination in iron, photocolorimetric, 19: 19811
determination in presence of molybdenum, spectrophotometric, 19: 19759 (LA-3226)
determination in presence of acetic acid and sulfate and nitrate ions, polographic, 19: 19797
determination, solvent extraction processes for photometric, 19: 19817
diffusion in pyrolytic carbon, 19: 20463 (ORNL-TM-431)
dispersion in air and urinary excretion by personnel, relation of particle size to, 19: 19478
effects on spectrophotometric determination of zinc using 1-(2-thiazolylazo)-2-naphthol, 19: 19814
effects on strength of thorium at high temperatures, 19: 20560 (ORNL-3777)
electric conductivity at low temperatures, effects of purity on, 19: 20543 (AERE-GR-101)
electric conductivity at low temperature, radioactive self-damage effects on, (E), 19: 20649
extrusion of tubes of, 19: 20501(R) (BRB-77)
fluorometric determination in biological materials, 19: 19490
fracture of alpha-phase, at −183 to 400°C, metallography of, 19: 20592
geochemistry and mineralogy of, in Cherry Mountains (Urals), USSR, book, 19: 20190
heat of sublimation and partial pressures in presence of oxygen, 19: 19889
isotopic analysis using internal standard technique, 19: 20188
isotopic fractionation in sandstone, Powder River Basin, Wyoming and Slick Rock District, Colorado, 19: 20187
monitoring atmospheric, device for, 19: 20381
nucleon reactions at high energies, secondary nucleon yields from, (E/T), 19: 21242 (NP-14837)
radiography using linear accelerator bremsstrahlung beam, 19: 20128
radioinduced point defects at 4.5°K, neutron, 19: 20642
separation from acetic acid solutions by solvent extraction using aniline, 19: 19817
separation from aqueous solutions by adsorption on activated charcoal, 19: 20074
separation from coated-particle fuel elements, processes for, 19: 20463 (ORNL-TM-431)
separation from leach solutions by solvent extraction using amines and acidic organophosphorus compounds, review, 19: 20053 (UJV/1202/64)
separation from nitric acid solutions by solvent extraction using aliphatic amines, 19: 20067
separation from nitric acid solutions by solvent extraction using dialkyl phosphoric acid, 19: 20075
separation from nitrate solutions by solvent extraction using organophosphorus compounds, 19: 20077
separation from spent fuel elements, development of direct fluoride volatility process for, 19: 20059
separation from technetium, 19: 19820
separation from thorium by anodic dissolution, 19: 19762 (RPI-2714-6)
separation from uranium–zirconium alloys by Zircex process, thermodynamics of, 19: 19742 (CEA-R-2592)
testing fuel elements of, equipment and methods for nondestructive, 19: 20126 (DPSPU-65-30-11)
toxic effects of injected, in guinea pigs, 19: 19488
use in neutron dosimeters, 19: 20340
vapor pressure of, effects of oxygen on, 19: 19890
x-ray spectra in, muonic, (E), 19: 21344
URANIUM ALLOYS
analysis methods for, book, 19: 19823
Al–U, nondestructive testing of fuel tubes of, 19: 20126 (DPSPU-65-30-11)
Mn–Pu–U, analysis for manganese, x-ray-fluorescent, 19: 21690(R) (LA-3244)
Mo–Nb–Pt–U, corrosion resistance in water, 19: 20497(P)
Mo–Nb–Pt–U, properties for use as reactor fuel, 19: 20497(P)
Mo–U, spectrophotometric analysis for uranium, 19: 19759 (LA-3226)
Nb–U, phase studies, 19: 20587
Pu–Ti–U, phase studies, 19: 21690(R) (LA-3244)
Pu–U, diffusion coefficients in, 19: 19869
Ru–U, phase studies, 19: 20588
U–Zr, thermodynamics of uranium separation by Zircex process from, 19: 19742 (CEA-R-2592)
URANIUM CARBIDES
bonding stainless steel cladding to, by sodium, eddy-current inspection of, 19: 20531
buckling in sodium-graphite lattices, (E), 19: 21692 (NAA-SR-Memo-9976)
grain growth in, effects of chromium and vanadium carbides on, 19: 20515(R) (NCSC-2981-6)
grain growth of, effects of vanadium carbide on, 19: 20516(R) (NCSC-2981-7)
hydrofluorination of, chemistry of, 19: 20060
hydrolysis of, effects of tungsten on, 19: 19882
lattice parameter of mono-, effects of carbon content on, 19: 20547 (CEA-R-2731)
oxidation of, chemistry of, 19: 20060
preparation by arc melting uranium oxides and coal, 19: 20537(P)
preparation of dense, fine particle, by carbon reactions with uranium hydrides, 19: 20517(R) (NCSC-2981-8)
processing of spent fuels of, evaluation of aqueous and pyro-, 19: 20048 (NAA-SR-9335)
properties as reactor fuel, 19: 21671
radiation effects on pyrolytic-carbon-coated particles of, 19: 20463 (ORNL-TM-431)
reactions of pyrolytic-carbon-coated particles of, with water vapor at temperatures up to 1100°C, 19: 20463 (ORNL-TM-431)
ThC–UC, performance as reactor fuels, 19: 21665 (GAMD-5535)
ThC–UC, preparation of spheroidal particles of, by sol-gel process, 19: 20528
U–UC, development of uniform dispersion of very small carbide particles in uranium matrix, 19: 20511(R) (NCSC-2981-1)
U–UC, development of uniform dispersion of very small carbide particles in uranium matrix, 19: 20512(R) (NCSC-2981-2)
U–UC, development of uniform dispersion of very small carbide particles in uranium matrix, 19: 20513(R) (NCSC-2981-3)
U–UC, fabrication of dense cermets by hot pressing, 19: 20514(R) (NCSC-2981-5)
U–UC, hot pressing of, 19: 20515(R) (NCSC-2981-6)
U–UC, hot pressing of, 19: 20516(R) (NCSC-2981-7)
URANIUM CARBONATES
sintering by hot pressing in presence of liquid uranium, 19: 20510(R) (NCSC-2663-16)
URANIUM COMPLEXES
sorption on activated charcoal from aqueous solutions, 19: 20074
with dimethylglyoxime, formation constant and uranium coordination number of, 19: 19860
with malic tartaric, and trioxyglutaric acids, spectra of infrared, 19: 19911
with salicylic acid, preparation and stability of, spectrophotometric studies of, 19: 19903
with salicylic acid, stability studies by ion exchange, 19: 19904
URANIUM COMPOUNDS
analysis for trace amounts of beryllium and rare earths by chromatography and spectrography, 19: 19800
analysis methods for, book, 19: 19823
URANIUM DEPOSITS
genesis of, deposition, source, and transport in, 19: 20185 (JEN-132-SIG/I-3)
occurrence, formation, and characteristics of roll-type, 19: 20186
URANIUM(IV) FLUORIDES
analysis for impurities for quality control in production, method for, 19: 19785
reactions with fluorine, thermobalance study, 19: 20258 (JAERI-1070)
URANIUM(VI) FLUORIDES
preparation from uranium dioxide by fluidized-bed method, 19: 19867
$NaF–UF_6$, decomposition of, thermobalance study of, 19: 20258

(JAERI-1070)
URANIUM HYDRIDES
reactions with carbon, preparation of dense, fine particle uranium carbides by, 19: 20517(R) (NCSC-2981-8)
URANIUM IONS
precipitation and hydrolysis of hexavalent, in sodium carbonate–alkaline earth chloride systems, 19: 19870
URANIUM ISOTOPES
separation by gaseous diffusion, linear programming model for, 19: 20430 (P-1231(RAND))
use in age estimation of marine carbonates, 19: 20181
URANIUM ISOTOPES U-232
separation from power reactor fuels, economics of, 19: 20036 (BNWL-25)
shielding power sources of, 19: 21595 (TID-7698(Pt.I)(p.33-248))
URANIUM ISOTOPES U-233
neutron cross sections of, availability for reactor calculations, (E), 19: 21225 (AECL-2168)
neutron fission of, resonance integrals for epithermal, (E), 19: 21336
URANIUM ISOTOPES U-234
content in roll ore bodies, Powder River Basin, Wyoming and Slick Rock District, Colorado, 19: 20187
neutron fission rates relative to uranium-235, (E), 19: 21227 (ANL-6941)
URANIUM ISOTOPES U-235
burnup in reactors, accurate determination of, 19: 21667(R) (GEAP-4776)
content in natural uranium, 19: 20188
content in rocks of La Sal Mountains, Utah, (E), 19: 20178
neutron capture-to-fission ratio for, epicadmium, (E), 19: 21334
neutron cross sections for, model for thermal, (T), 19: 21678 (ANL-6972)
neutron cross sections of, availability for reactor calculations, (E), 19: 21225 (AECL-2168)
neutron fission of, fragment energy spectrum in thermal, (E), 19: 21296
neutron fission of, tellurium-131 and -133 isomer pair yields from thermal, (E), 19: 21390
neutron reactions with, cross sections for, (E), 19: 21230 (CEA-R-2552)
Hf–U-235–H_2O, neutron transport in critical assemblies of, resonance interference in, (E/T), 19: 21643 (WAPD-T-1728)
URANIUM ISOTOPES U-236
energy levels, (E), 19: 21230 (CEA-R-2552)
neutron fission rates relative to uranium-235, (E), 19: 21227 (ANL-6941)
separation from power reactor fuels, economics of, 19: 20036 (BNWL-25)
URANIUM ISOTOPES U-237
decay of, gamma spectra and internal conversion coefficients, (E/T), 19: 21251(R) (UCRL-11828(p.31-4))
URANIUM ISOTOPES U-238
alpha fission at 33 Mev, tellurium-131 and -133 isomer pair yields from, (E), 19: 21390
content in natural uranium, 19: 20188
content in rocks of La Sal Mountains, Utah, (E), 19: 20178
deuteron fission at 18 Mev, tellurium-131 and -133 isomer pair yields from, (E), 19: 21390
fission induced by alpha inelastic scattering, (E), 19: 21262(R) (UCRL-11828(p.84-6))
neutron capture by, spontaneous fission of isotopes produced in, (E), 19: 21403
neutron cross sections for, model for thermal, (T), 19: 21678 (ANL-6972)
neutron fission rates relative to uranium-235, (E), 19: 21227 (ANL-6941)
separation from power reactor fuels, economics of, 19: 20036 (BNWL-25)
URANIUM LEACH SOLUTIONS
separation of uranium from, by solvent extraction using amines and acidic organophosphorus compounds, 19: 20053 (UJV-1202/64)
URANIUM MINERALS
mining in Canada, 19: 21781
radioactivity equilibrium in, in accessory monazites of Ukraine, 19: 20189
URANIUM ORE PROCESSING PLANTS
wastes from, radium contamination of Great Salt Lake by, 19: 20220
URANIUM OXIDES
properties as reactor fuel, 19: 21671
reactions in ammonium fluoride and hydrofluoric acid solutions, 19: 19913
reactions with coal, uranium carbide preparation by, 19: 20537(P)
reduction of, chemistry of, 19: 20060
thermal conductivity at high temperatures, (E), 19: 20576
URANIUM OXIDES (Zr ALLOY CLAD)
temperature distribution in Zircaloy end caps for rods of, 19: 21674
URANIUM(IV) OXIDES
crystal structure defects in vapor-grown single crystals, 19: 20603
determination in uranium tetrafluoride, methods for, 19: 19785
diffusion of fission gases from, effects of stress on, 19: 20586
dispersion in aluminum matrix, 19: 20539(P)
dissolution in nitric acid–sulfuric acid solutions, oxidizing activity of nitric acid in, 19: 19912
dissolution of high-density pellets of, in nitric acid with and without additives, 19: 20050 (ORNL-3695)
fabrication by vibratory and impact methods, 19: 20526
fission gas release from irradiated pellets of, 19: 20633
fluorination by fluidized-bed method, 19: 19867
heating by electron beams, pore production and migration in, 19: 20467
oxidation of sintered, chemistry of, 19: 20060
preparation of granulated, by reduction of ammonium uranate, 19: 20538(P)
preparation of single-phase single crystals of, in oxygen to uranium ratio range from 2 to 2.25, 19: 20530
radiation effects on thermal conductivity of, 19: 20615 (HW-SA-3212)
radiation effects on defects in vapor-grown single crystals of uranium dioxide, 19: 20603
sodium logging in fuel elements of, effects of, 19: 20458 (GEAP-4283)
thermal conductivity, (E), 19: 21666(R) (GEAP-4640)
thermal conductivity of high-density, at 550 to 2165°C, 19: 20563 (TID-21668)
vapor pressure, 19: 19890
HNO_3–H_2SO_4–UO_2, oxidation-reduction potentials in, 19: 19912
PuO_2–UO_2, dissolution of high-density pellets of, in nitric acid, 19: 20050 (ORNL-3695)
PuO_2–UO_2, sodium logging in fuel elements of, 19: 20458 (GEAP-4283)
stainless steel–UO_2, testing in Spert I, 19: 20616 (IDO-17011)
ThO_2–UO_2, diffusion of fission gases from, effects of stress on, 19: 20586
ThO_2–UO_2, preparation from mixture of thorium and uranyl nitrates, 19: 19942(P)
ThO_2–UO_2, separation of protactinium-233 from irradiated, by sorption on unfired Vycor, 19: 20051 (ORNL-3773)
UO_2–U_3O_8, crystal structure, 19: 19873
UO_2–UO_3, phase diagram, 19: 19873
U–UO_2, vapor pressure of uranium over, 19: 19890
URANIUM(IV-VI) OXIDES
spectra of suspensions of, in thin films of polyethylene, infrared transmission, 19: 19917
UO_2–U_3O_8, crystal structure, 19: 19873
U_3O_8–UO_3, crystal structure, 19: 19929
URANIUM(VI) OXIDES
crystal structure of gamma phase, 19: 19930
distillation of irradiated, preparation of iodine-131 by dry, 19: 20029
U_3O_8–UO_3, crystal structure, 19: 19929
UO_2–UO_3, phase diagram, 19: 19873
URANIUM SYSTEMS
Al–polyethylene–U, neutron self-shielding in closely packed slab lattices of, (E), 19: 21636 (CONF-654-32)
alums–U, boric acid–U, phosphorescence in, 19: 19919
boric acid–U, phosphorescence in, 19: 19919
Cr–Si–U, preparation and crystal structure of compounds in, 19: 19871
Cu–U, thermal conductivity at high temperatures, (E), 19: 20576
Fe–Si–U, preparation and crystal structure of compounds in, 19: 19871
H–U, diffusion and viscosity coefficients of high-temperature ionized, 19: 19941
Mn–Si–U, preparation and crystal structure of compounds in, 19: 19871
Mo–Si–U, preparation and crystal structure of compounds, 19: 19871
U–UC, development of uniform dispersion of very small carbide particles in uranium matrix, 19: 20511(R) (NCSC-2981-1)
U–UC, development of uniform dispersion of very small carbide particles in uranium matrix, 19: 20512(R) (NCSC-2981-2)
U–UC, development of uniform dispersion of very small carbide particles in uranium matrix, 19: 20513(R) (NCSC-2981-3)
U–UC, fabrication of dense cermets by hot pressing, 19: 20514(R) (NCSC-2981-5)
U–UC, hot pressing of, 19: 20515(R) (NCSC-2981-6)
U–UC, hot pressing of, 19: 20516(R) (NCSC-2981-7)
U–UO_2, vapor pressure of uranium over, 19: 19890
URANYL COMPOUNDS
structural properties of complex, 19: 19911
URANYL FLUORIDES
determination in uranium tetrafluoride, methods for, 19: 19785
URANYL IONS
determination using EDTA, 19: 19779
determination using 5,5′ thiodisalicylic acid, spectrophotometric, 19: 19812

fluorescence and dielectric properties in water and water–glycerol mixtures at –190 to 0°C, 19: 19863
hydrolysis of, equilibrium constants and mechanisms for, 19: 19858
solvent extraction from molten nitrate by liquid silicone–TBP at 150°C, 19: 19833 (CEA-R-2628)
spectra of, ultraviolet and visible, 19: 19859

URANYL NITRATES
chemical potentials and thermodynamic properties in nitric acid solutions at 25 and 50°C, 19: 19909
effects on dissolution of uranium dioxide pellets in nitric acid, 19: 20050 (ORNL-3695)
precipitation from aqueous solutions with alkaline earth chlorides and sodium carbonates, 19: 19870
separation from nitric acid solutions by complex formation with organic phosphorus compounds, 19: 20077
solubility in mixtures of ethers with benzene, carbon tetrachloride, chloroform, heptane, toluene, and xylene, 19: 20072
thermodynamics of formation of hydrates of, at 25 and 50°C, 19: 19908
HNO_3–$UO_2(NO_3)_2$, chemical potentials and solution-vapor equilibrium in, at 25, 35, and 50°C, 19: 19907

URANYL PERCHLORATES
reactions with tetradecylammonium, spectra of complexes formed in, 19: 19910
solubility in butyl ether mixtures with chlorinated hydrocarbons, 19: 20073

URANYL PYROPHOSPHATES
polarography of complexes of, effects of surface-active substances on, 19: 19816

URANYL SALICYLATES
preparation and stability of, spectrophotometric studies of, 19: 19903
stability of, ion exchange studies of, 19: 19904

UREA
radiation effects on rat urinary excretion of, protective effects of casein diets against, 19: 19628

URETHAN POLYMERS
analysis for impurities by spark source mass spectrography, 19: 19830

URINARY TRACT
radiodiagnosis of diseases of, by renal scintiscanning using mercury-203, 19: 19721

URINE
analysis for polonium-210 by autoradiography, 19: 19791
radiation effects on excretion of allantoin, nitrogen, and urea in rat, protective effects of casein diets against, 19: 19628
uranium excretion by human, relation of particle size dispersion in plant air to, 19: 19478

UTAH
radium contamination of Great Salt Lake by wastes from uranium ore processing plant, 19: 20220
rock ages in La Sal Mountain, 19: 20178

UTERUS
radiotherapy of carcinomas of, 19: 19663
radiotherapy of cancer of, 19: 19681
radiotherapy of carcinomas of, dose field distribution in telegamma, 19: 19686
radiotherapy of carcinoma, radiation dose from cobalt-60 bead implants, 19: 19708
radiotherapy of tumors of, 19: 19700
radiotherapy of vulvar cancer, method for intralymphatic, 19: 19658

V

VACCINES
radiation effects on tetanus, in monkeys, 19: 19608

VACUUM
applications of ultrahigh, 19: 20149

VACUUM GAGES
development and uses, 19: 20149
development of, review of, 19: 20142
helium production in, (E), 19: 20146
pressure limits of hot-filament ionization, low-, 19: 20147

VACUUM PUMPS
development and uses, 19: 20149

VACUUM SEALS
development and uses, 19: 20149

VACUUM SYSTEMS
carbon dioxide content in glass, method for lowering, 19: 20148
diffusion pump oil deposition in, method for measuring, 19: 20143
gas sorption and desorption in high, residual, (E), 19: 20144
helium production in ionization gages in, (E), 19: 20146
mass transport of oil in, 19: 20140(R) (ORNL-3760(p.94-7))
ultrahigh, preparation and uses, 19: 20149
use of artificial zeolites in high, review on, 19: 20141
values for ultrahigh, modification of Hoke, 19: 20145

VALLECITOS BOILING WATER REACTOR
coolant surface waves in, (E/T), 19: 21684 (GEAP-4061)

VALVES
design of 12-in. 250-psi ball-type, engineering drawings for, 19: 20104
technology of advanced, review, 19: 20097 (NASA-SP-5019)

VAN ALLEN RADIATION BELTS
charged particle distribution in, solar storm effects on, (T), 19: 21137
charged particle excitation in, 19: 21154
charged-particle confinement in, review of, 19: 20902
charged-particle motion during magnetic storms, (T), 19: 21128(T)
charged-particle streams in, effects of geomagnetic field variations on, 19: 21126
electron density at 200 to 400 km, 19: 21136

VAN DE GRAAFF ACCELERATORS
beam energy of, system for modulating, 19: 20746

VANADIUM
analysis for hafnium or zirconium using catechol violet, colorimetric, 19: 19780
corrosion in reactors, 19: 20488
determination in titanium dioxide, activation, 19: 19771(R) (TEES-2671-4(Chap.9))
determination in uranium and its compounds and alloys, methods for, 19: 19823
effects on strength of thorium at high temperatures, 19: 20560 (ORNL-3777)
magnetic flux quantization in superconducting cylinders of, 19: 21194
phonon frequency distribution function, 19: 20553 (KFK-262)

VANADIUM ALLOYS
Al–Mo–Sn–Ti–V, beta transus temperature of, 19: 20462(R) (NRL-6258)
Al–Mo–Sn–Ti–V–Zr, beta transus temperature of, 19: 20462(R) (NRL-6258)
Al–Mo–Ti–V, mechanical properties of diffusion-bonded plates of, 19: 20462(R) (NRL-6258)
Al–Mo–Ti–V, mechanical properties of solution-annealed and aged T-19, 19: 20462(R) (NRL-6258)
Al–Sn–Ti–V, beta transus temperature of, 19: 20462(R) (NRL-6258)
Al–Ti–V, fatigue crack propagation in, study of low-cycle, 19: 20462(R) (NRL-6258)
Al–Ti–V, mechanical properties of diffusion-bonded plates of, 19: 20462(R) (NRL-6258)
Al–Ti–V–Zr, beta transus temperature of, 19: 20462(R) (NRL-6258)
Cr–Nb–V, fabrication and mechanical properties of sheet of, 19: 20552(R) (IITRI-B6021-6)
Fe–V, magnetic fields at iron-57 nuclei in, (E), 19: 20578
Mo–Nb–Ti–V, coating for oxidation protection, 19: 20459(R) (IITRI-B6019-6)
Mo–Nb–V–Zr, fabrication and properties of B-66 sheet, 19: 20499(R) (AD-606291)
Nb–Ta–Ti–V, coating for oxidation protection, 19: 20459(R) (IITRI-B6019-6)
Nb–Ta–Ti–V, fabrication and mechanical properties of sheet of, 19: 20552 (IITRI-B6021-6)
Nb–Ta–V, fabrication and mechanical properties of sheet of, 19: 20552(R) (IITRI-B6021-6)
Nb–Ti–V, coating for oxidation protection at 1800 to 2500°F, 19: 20459(R) (IITRI-B6019-6)
Nb–Ti–V, fabrication and mechanical properties of sheet of, 19: 20552(R) (IITRI-B6021-6)
Nb–Ti–W–V, coating for oxidation protection, 19: 20459(R) (IITRI-B6019-6)
Nb–V, coating for oxidation protection, 19: 20459(R) (IITRI-B6019-6)
Nb–V, fabrication and mechanical properties of sheet of, 19: 20552(R)
Ta–V, coating for oxidation protection, 19: 20459(R) (IITRI-B6019-6)
Ta–V, fabrication and mechanical properties of sheet of, 19: 20552(R) (IITRI-B6021-6)
Ta–V–Zr, coating for oxidation protection, 19: 20459(R) (IITRI-B6019-6)

VANADIUM CARBIDES
effects on grain growth of uranium carbides, 19: 20515(R) (NCSC-2981-6)
effects on grain growth of uranium carbides, 19: 20516(R) (NCSC-2981-7)
superconducting properties, 19: 20572

VANADIUM ISOTOPES V-46
beta decay of, CVC theory and ft values for, (T), 19: 21416

VANADIUM ISOTOPES V-47
energy level spacings in, 19: 21446
energy levels, (E), 19: 21374

VANADIUM ISOTOPES V-51
helium-3 elastic scattering and reactions (He-3,d) at 22 Mev, (E), 19: 21240 (LA-DC-6232)

VANADIUM NITRIDES
superconducting properties, 19: 20572
VANADIUM STEEL
Cr–Mo–Ni–V, development, 19: 20462(R) (NRL-6258)
VANADIUM SYSTEMS
C–Ta–V–Zr, coating for oxidation protection, 19: 20459(R) (IITRI-B6019-6)
VELA PROJECT
borehole research in, conference on, 19: 20173 (VESIAC-4410-83-X)
vented gases in Dribble project, apparatus for analysis of, 19: 19776 (UCRL-12169)
VESSELS
analysis of low-level radioactive waste containers in accident environment, 19: 20196 (CONF-650103-6)
VINYL ALCOHOL POLYMERS
radiation effects on thermoluminescence, 19: 19983
VIRUSES
radiation effects on development of, in rat embryo cell cultures, 19: 19563
radioinduced mutations of, ultraviolet, 19: 19549
VISCOMETERS
development of, review of, 19: 20142
VISCOSITY
of high-temperature ionized mixtures, calculation of, 19: 19941
VITAMIN D_2
use with strontium-90 in treatment of rickets in rats, 19: 19680

W

WASTE DISPOSAL
burning degraded solvents from radiochemical processes, 19: 21748 (DPSPU-64-30-8B)
containers for low-level, structural integrity of, 19: 20196 (CONF-650103-6)
fixation of americium-241–plutonium-239 raffinate solutions in cement, 19: 21750 (LA-3150)
ground, piping intermediate-level liquids to shale beds, equipment for, 19: 21753
liquid storage in underground tanks, activity in seepage from, 19: 21752
salt mine, field experiment for demonstration of high-level, 19: 21751 (ORNL-P-1064)
WASTE PROCESSING
burning spent solvent from radiochemical separations processes, 19: 21747 (DP-942)
calcination facility operation at Arco Plant, April-June 1964, 19: 20042(R) (IDO-14646)
calcination of zirconium fluoride wastes, 19: 20042(R) (IDO-14646)
fixation in glass, process for, 19: 21754(P)
sorption on clay, 19: 21755(P)
WASTE SOLUTIONS
contamination of surface waters by, review of conference on, 19: 20234
monitoring and treatment of, review of conference on, 19: 20234
radioactivity measurement in, review methods for, 19: 19749 (EUR-2118.f)
separation and purification of americium-241 from, by chromatographic ion exchange, 19: 20041 (HW-84352)
separation of bismuth from, by electrolytic deposition, 19: 20047 (MLM-734)
separation of strontium from stored Purex, by lead sulfate carrier precipitation, 19: 20035 (BNWL-4)
storage in underground tanks, activity in seepage from, 19: 21752
WATER
analysis for cesium-137, rapid method for, 19: 19805
analysis for impurities, spectrographic method using gallium oxide, 19: 19774 (UCRL-7962)
determination in liquids of low water solubility, using impregnated silica gel, 19: 21783(P)
determination in uranium tetrafluoride, methods for, 19: 19785
determination in vented gases from underground nuclear explosion, apparatus for, 19: 19776 (UCRL-12169)
deuterium exchange with salts of trioctylamine or benzyldilaurylamine, 19: 19864
deuterium exchange with anion exchange resin, 19: 19865
effects on fluorescence of uranyl ions, 19: 19863
effects on graphite and pyrolytic carbon under high heat flux conditions, 19: 20463 (ORNL-TM-431)
equilibrium with heavy water, evaluation of constant for, 19: 19891
gamma shielding by, nomograms for determining thicknesses for, 19: 21598
heat transfer burnout and stability of natural circulation, in seven-rod bundle, 19: 20120
neutron distributions at 1.5 to 12 Mev in, from swimming-pool reactors, (E), 19: 21735 (ORNL-P-1092)
neutron scattering by vaporized, at 0.018 to 0.080 ev, (E), 19: 21200 (KFK-264)
neutron temperature across interface with boron-poisoned water, (E/T), 19: 21207
production from labeled glucose in obese patients, 19: 21758 (BNL-8864)
proton reactions at 160 Mev, 0.6- to 11-Mev gamma rays from, (E), 19: 21243 (ORNL-3506)
radiolysis of, nature of free radicals induced by, 19: 19968
reactions with sodium in steam generators, studies of problems produced by, 19: 20107(R) (BAW-1280-22)
solubility in organic diluents, 19: 20039 (EUR-2246.e)
sorption and desorption of residual, in high vacuum, (E), 19: 20144
steam void determination in, method for, 19: 20294
$Al(NO_3)_3$–HNO_3–H_2O, distribution coefficients for plutonium between anion exchange resin and, calculation, 19: 20046 (LA-3188)
Hf–U-235–H_2O, neutron transport in critical assemblies of, resonance interference in, (E/T), 19: 21643 (WAPD-T-1728)
WATER-d_2
analytical uses in determination of manganese, 19: 19806
effects on wound healing in rats, 19: 19484
equilibrium with light water, evaluation of constant for, 19: 19891
neutron flux in laminates with iron, (E/T), 19: 21210
neutron scattering by, molecular conglomerates in, 19: 21221
separation from light water by distillation, efficiency of Stedman stainless steel packings for, 19: 20068
WATER COOLED REACTORS
control of boiling, utilizing evolved steam circulated through core, 19: 21661(P)
coolant pump wear in, effects of chemical shim environments on, 19: 21606 (WCAP-3269-9)
design of boiling superheating, 19: 21659(P)
design of superheating steam-cooled, 19: 21662(P)
WATER MODERATED REACTORS
bubble formation delay time after large insertion of reactivity in, 19: 21653
corrosion problems in, review of, 19: 20488
WATER SUPPLIES
costs of treatment programs for, possible reduction of, 19: 20087 (GAT-P-33)
decontamination of, 19: 20240
radioactivity due to fallout in, 1964 and 1965, 19: 20154(R) (HASL-158)
uranium content in, effects on content in man, 19: 19490
WATER VAPOR
effects on oxidation of cerium–magnesium alloys by nitrogen at 475 to 600°C, 19: 20485
effects on radioinduced reactions of carbon dioxide with graphite, 19: 19954 (AERE-R-4839)
reactions with mercury isotopes, photochemical, 19: 20429 (MLM-1214)
reactions with pyrolytic-carbon-coated uranium carbide particles at temperatures up to 1100°C, 19: 20463 (ORNL-TM-431)
WELDING
argon-arc method of, uses of carbon dioxide in, 19: 20534
procedures, specifications, and qualification test records for use at Hanford, 19: 20524 (TID-20625(VolIV)(Rev.I))
procedures, specifications, and qualification test records for use at Hanford, 19: 20521 (TID-20625(Vol.I(Rev.I))
procedures, specifications, and qualification test records for use at Hanford, 19: 20522 (TID-20625(Vol.II)(Rev.I))
procedures, specifications, and qualification test records for use at Hanford, 19: 20523 (TID-20625(Vol.III)(Rev.I))
WELL LOGGING
activation analysis, systems for automatic, 19: 19773 (TID-20467)
WHEAT
analysis for mercury, activation, 19: 19771(R) (TEES-2671-4(Chap.9))
cesium-134, -137, and sodium-22 content in, relation of content in man to, 19: 20225
radiation effects on development and growth of, photoperiod and temperature effects on uv, 19: 19545
WHISTLERS
dispersion of, protonosphere electron temperature effects on, (T), 19: 21140
electron trajectories in presence of magnetospheric waves from, (T), 19: 21099
WIND
turbulence of, formulas for anemometer dissipation of, 19: 20654(R) (ANL-6938(p.242-51))
WIND TUNNELS

design for calibration of wind-measuring devices, 19: 20655(R) (ANL-6938(p.252-6))
flow of hydrogen at 13,000°K and 1000 atm in, equilibrium in, 19: 20124
use in scale-model smoke plume-rise tests, 19: 20656(R) (ANL-6938 (p.257-73))
WOUNDS
healing of rat, effects of ascorbic acid and water-d_2 on, 19: 19484
radiation effects on tetanus vaccination in monkey, 19: 19608
WYOMING
uranium isotopic fractionation in sandstone of Powder River Basin, 19: 20187

X

X RADIATION
cataract induction in rats by, effectiveness relative to gamma radiation, 19: 19612
dose distribution in tumors, 19: 19672
dose measurements in head of, from diagnostic dental radiography, 19: 19676
effects in *Arabidopsis thaliana*, genetic, 19: 19548
effects in mice, carcinogenic, 19: 19594
effects in rats, carcinogenic, 19: 19606
effects of, on developing embryos and fetuses, 19: 19699
effects on acid and alkaline phosphatase and esterase activity in guinea pig skeletal muscle, 19: 19574
effects on activity, learning, mortality, and seizure susceptibility of rats exposed *in utero*, 19: 19618
effects on animals and plants, small-dose, 19: 19516
effects on blood picture of hospital personnel, 19: 19525
effects on blood picture of conventional and germfree mice, whole-body, 19: 19619
effects on cholesterol metabolism in rats, 19: 19511(T) (JPRS-29364(p.1-4))
effects on chromosome aberrations in human leukocytes, 19: 19596
effects on content of chromium, magnesium, and nickel in dog tissues, 19: 19540
effects on deoxynucleoproteins in *Bacterium coli*, 19: 19576
effects on desoxyribonucleic acid metabolism in rat liver and intestinal cells, 19: 19506 (TID-21703)
effects on developing embryos, 19: 19466
effects on electric conductivity of polyethylene, 19: 20017
effects on electroshock seizures in rats, cysteine and dose effects on, 19: 19514
effects on frequency and properties of genetic recombinations in *E. coli*, 19: 19537
effects on fungal spores, 19: 19558
effects on fungal spores, 19: 19559
effects on hands, pathological, 19: 19524
effects on hematopoietic system in rabbits and rats, 19: 19499(R) (NP-14899)
effects on hemopoiesis in sheep, 19: 19600
effects on human genetics by infant exposure, 19: 19568
effects on immune reactions to transplanted kidney in dogs, 19: 19519
effects on immune reactions to kidney transplants, 19: 19520
effects on immune reactions to spleen transplants in dogs, 19: 19521
effects on immune reactions to spleen transplants, 19: 19522
effects on immune reactions to lung transplants, 19: 19523
effects on induction of electronic energy levels in n-type germanium, 19: 20612 (AFCRL-64-839)
effects on ionic permeability of rat and rooster erythrocytes, 19: 19577
effects on liver regeneration after partial hepatectomy, 19: 19512
effects on loss of regeneration capacity in extremities of salamanders, 19: 19544
effects on luminescence of copper-doped potassium and sodium chloride crystals, 19: 19964
effects on luminescence of cadmium zinc sulfide phosphors in presence of infrared radiation, 19: 19965
effects on luminescence of thallium-activated alkali halides, 19: 19966
effects on magnesium fluoride crystals, 19: 20618 (NBS-8614)
effects on mechanical resistance of human erythrocytes, 19: 19595
effects on mice, amyloidosis in chimeras and relation to lymphoid hypoplasia in whole-body, 19: 19650
effects on mice, effects of blood transfusions on subsequent marrow transplants, 19: 19653
effects on mice, protective effects of allogenic marrow inoculation against, 19: 19648
effects on mice, protection from killing effect of spleen cells in, 19: 19651
effects on mitotic activity in regenerating rat liver cells, 19: 19510(T) (JPRS-29250(p.27-32))
effects on nervous activity of dogs, antenatal, 19: 19536
effects on optical absorption bands in lithium fluorides, 19: 20817
effects on optical properties of lithium fluorides, impurity effects in, 19: 19998
effects on oxygen attachment in rabbit hemoglobin, equation for calculating, 19: 19529(T)
effects on penicillin production by *Penicillium nigricans*, 19: 19556
effects on peroxide decay in rat spleen DNA, 19: 19541
effects on phagocytosis by leukocytes, 19: 19507(R) (TID-21712)
effects on physiology of mineral contents in developing guinea pig brain, 19: 19534
effects on rats, effects of 19-norandrostenolone on acute, 19: 19624
effects on regeneration of extremities in salamanders, 19: 19546
effects on RNA metabolism and synthesis in HeLa tumor cells, 19: 19602
effects on self-friction of potassium chloride, 19: 20011
effects on serum albumin synthesis in rat liver, effects of food ingestion on, 19: 19603
effects on strength of chromatography paper, 19: 20630
effects on thermoluminescence afterglow of proteins and synthetic polymers, 19: 19983
effects on 3,1,6,1-aryl-sulfate sulfohydrolase activity in guinea pig brain and liver, *in utero*, 19: 19573
emission by californium-252 fission fragments, (E), 19: 21229 (BNL-8841)
emission by fission fragments from spontaneous fission of californium-252, (E), 19: 21265(R) (UCRL-11828(p.95-7))
emission from solar flares, (T), 19: 20890
emission in electron capture, measurement of, 19: 20384
enzyme inactivation by, 19: 19517
production in galactic sources, bremsstrahlung and synchrotron-emission, (T), 19: 20765
reactions with calcium fluorides, EPR studies of V_F centers in, 19: 20003
reactions with neon at 167 to 913 ev, double Auger electron emission in, (E), 19: 20844
scattering by atoms, Hartree-Fock calculations of incoherent, 19: 20824
spectrum in solar radiation, review of, 19: 20785
use in determination of core position in reactor fuel elements, 19: 20135(P)
uses in medicine, control and hazards of, 19: 19657(R) (ANL-6938 (p.97-119))
X-RAY BEAMS
energy distribution of, from 250-kv constant-potential machine, 19: 20256 (HASL-151)
X-RAY-DIFFRACTION ANALYSIS
computer program for indexing powder patterns of, for cubic case, 19: 19834 (HW-74393)
computer program for indexing powder patterns of, for orthorhombic case, 19: 19835 (HW-89062)
resolution in holography, method for improving, 19: 20297
X-RAY EQUIPMENT
description of fine focus medium energy tube for radiobiology and crystallography, 19: 20291
description of 250-kv facility for calibrating radiation detectors, 19: 20256 (HASL-151)
X-RAY FLUORESCENCE ANALYSIS
of light elements, using radioisotopes, 19: 19741 (CEA-R-2539)
X-RAY SPECTROMETERS
beam emission in, characteristics of, 19: 19747 (CONF-650214-1)
modification of commercial, for analysis of light elements, 19: 19801
X-RAY SPECTROSCOPY
correction factors for electron penetration in microanalysis, 19: 19746 (CEA-R-2728)
XENON
absorption coefficient from 3.6 to 10×10^3 Å, (T), 19: 20833
buildup in thermal reactors, optimal flux shutdown programs for, 19: 21639 (IA-988)
charge exchange in, atom-ion resonance, (T), 19: 19931
distributions in reactors, calculation using centers and limit cycles, (T), 19: 21634 (BNL-9010)
electromagnetic-wave propagation in partially ionized, helicon, (E), 19: 21552
ionization by electrons at 0.6 to 20 kev, (E/T), 19: 20850
performance in scintillation detectors for alpha particles and electrons, 19: 20361
separation from power reactor fuels, economics of, 19: 20036 (BNWL-25)
XENON IONS
sputtering on metals at 45 kev, thermal spikes in, (E), 19: 20838
XENON ISOTOPES Xe-122
energy levels of, parity and spin of collective, (E), 19: 21316
XENON ISOTOPES Xe-124

energy levels of, parity and spin of collective, (E), 19: 21316
XENON ISOTOPES Xe-126
energy levels of, parity and spin of collective, (E), 19: 21316
XENON ISOTOPES Xe-128
energy levels of, parity and spin of collective, (E), 19: 21316
XENON ISOTOPES Xe-130
energy levels of, parity and spin of collective, (E), 19: 21316
XENON ISOTOPES Xe-131
energy level transitions in, retardations in l-allowed M1, (T), 19: 21323
XENON ISOTOPES Xe-132
energy levels of, parity and spin of collective, (E), 19: 21316
XENON ISOTOPES Xe-133
determination in magnox reactor coolant, method for, 19: 21616
electron emission in monocrystalline tungsten, angular dependence of conversion, (E), 19: 21339
release from irradiated uranium dioxide pellets, 19: 20633
XENON ISOTOPES Xe-135
determination in magnox reactor coolant, method for, 19: 21616
XENON OXIDES
reactions of tri-, with potassium hydroxide in solution, 19: 19847(R) (UCRL-11828(p.182-3))
XENON SYSTEMS
He–Xe, performance in scintillation detectors, 19: 20361
XYLENE
hydrogen abstraction from, by methyl radicals, 19: 21760 (NYO-2728-4)
luminescence spectra and quantum yields of pure and cyclohexane solutions of, 19: 21771 (TID-21684)
solvent properties in mixtures with butyl, dichlorodiethyl, and ethyl ethers for uranyl nitrates, 19: 20072

Y

YEASTS
radiation effects on survival of, temperature effects on uv, 19: 19626
radioinduced mutation of glutamate auxotroph, 19: 19593
YTTERBIUM
ionization at single-crystal tungsten surfaces, 19: 20871
YTTERBIUM COMPLEXES
with serine, stability and composition, 19: 19874
YTTERBIUM HYDRIDES
LiH–YbH_2, phase studies, 19: 19881
YTTERBIUM IONS
spectra in barium, calcium, and strontium fluorides, absorption and luminescence, 19: 19854
YTTERBIUM ISOTOPES Yb-170
energy level transitions in, E2 conversion coefficients of rotational, (T), 19: 21308
energy levels of, gyromagnetic ratio of 84-kev, (E), 19: 21377
oxygen-16 reactions (O-16,xn), alpha spectra and excitation functions, (E), 19: 21248(R) (UCRL-11828(p.21-5))
properties of, effects of pairing forces on, (T), 19: 21434
YTTERBIUM ISOTOPES Yb-172
energy level transitions in, E2 conversion coefficients of rotational, (T), 19: 21308
oxygen-16 reactions (O-16,xn), excitation functions, (E), 19: 21248(R) (UCRL-11828(p.21-5))
properties of, effects of pairing forces on, (T), 19: 21434
YTTERBIUM ISOTOPES Yb-173
energy level transitions in, K-shell particle parameter in 272-kev E1, (E), 19: 21320
gamma transitions and internal conversion in, probabilities of, (E/T), 19: 21284
YTTERBIUM ISOTOPES Yb-174
carbon-12 fission, excitation energy, (E/T), 19: 21259(R) (UCRL-11828(p.77-80))
energy level transitions in, E2 conversion coefficients of rotational, (T), 19: 21308
energy levels, (E), 19: 21272
properties of, effects of pairing forces on, (T), 19: 21434
YTTERBIUM ISOTOPES Yb-176
energy level transitions in, E2 conversion coefficients of rotational, (T), 19: 21308
YTTERBIUM SULFATES
crystal structure and bond types of octahydrates, 19: 19915
YTTRIUM
determination in tantalum and tantalum–tungsten alloys, spectrographic, 19: 21690(R) (LA-3244)
electrophoresis in hydrochloric acid, mobility and spot area in paper, 19: 19810
geochemistry and mineralogy of, in Cherry Mountains (Urals), USSR, book, 19: 20190
separation from magnesium–thorium alloy by transfer to liquid scrub alloy in fused salt, 19: 20066
separation from scandium by solvent extraction of diantipyrinylmethane complex, 19: 20080
YTTRIUM ALLOYS
Al–Cr–Fe–Y, oxidation mechanism, 19: 20470 (GE-TM-63-7-3)
Al–Cr–Fe–Y, properties of oxidation-resistant, 19: 20470 (GE-TM-63-7-3)
Gd–Y, gadolinium ion ESR in, g-factors from, (E), 19: 20698
Gd–Y, paramagnetic resonance absorption in, at 20 to 200°C, 19: 20581
YTTRIUM COMPLEXES
with serine, stability and composition, 19: 19874
YTTRIUM ISOTOPES Y-88
electron pair production cross section near threshold, (E), 19: 21252(R) (UCRL-11828(p.35-8))
YTTRIUM ISOTOPES Y-89
deuteron reactions (d,t) at 11.8 Mev, angular distributions from, (E), 19: 21326
proton reactions (p,n) at 4.6 to 5.6 Mev, angular distributions in, (E), 19: 21356
YTTRIUM ISOTOPES Y-90
beta decay of, internal bremsstrahlung spectra from, 19: 21302
determination in air by beta measurement, efficiency of counter for, 19: 20169
effects on harvest and grain quality of field crops, 19: 19508(T) (JPRS-28977)
therapeutic effects for pituitary ablation, 19: 19667
uptake by human liver, profile counting studies on, 19: 19492
use for destruction of pituitary gland, method of, 19: 19660
use for destruction of pituitary gland, therapeutic effects of, 19: 19664
use in therapy by intra-arterial injection, method for, 19: 19661
YTTRIUM ISOTOPES Y-91
beta decay of, internal bremsstrahlung spectra from, 19: 21302
content in stratosphere, 19: 20657(R) (DASA-1309)
determination in air by beta measurement, efficiency of counter for, 19: 20169
YTTRIUM NITRIDES
superconducting properties, 19: 20572
YTTRIUM SULFATES
crystal structure and bond types of octahydrates, 19: 19915

Z

ZINC
determination by titration, suitability of tetraethylenepentamine heptaacetic acid for, 19: 19813
determination in ppm range by d-c arc excitation, spectrochemical, 19: 19827
determination in SAP powders by different laboratories, statistics on, 19: 19750 (EUR-2286.f)
determination of trace amounts of, using 1-(2-thiazolylazo)-2-naphthol, spectrophotometric, 19: 19814
determination using mercury cyanate and EDTA, 19: 19779
separation from silver by solvent extraction using tri-n-octylphosphine sulfide, 19: 19753 (IS-T-3)
separation of magnesium from, by complex formation and solvent extraction, 19: 19833 (CEA-R-2628)
sputtering by ions at 45 kev, thermal spikes in, (E), 19: 20838
ZINC ALLOYS
Ce–Zn, heats of formation and fusion of intermetallic compound $CeZn_3$ in, 19: 19838 (IS-1070)
Cu–Mn–Zn, effects on properties of magnesium and magnesium–zirconium alloy for use as fuel element can, 19: 20610(P)
Mg–Zn, heats of formation and fusion of intermetallic compound $MgZn_2$ in, 19: 19838 (IS-1070)
Mg–Zn, sorption of impurities in magnesium–thorium alloy by liquid, in fused salt, 19: 20066
ZINC IONS
solvent extraction from molten nitrate by liquid silicone–TBP at 150°C, 19: 19833 (CEA-R-2628)
ZINC ISOTOPES
alpha elastic scattering by, angular distribution of, 19: 21459
ZINC ISOTOPES Zn-65
detection and measurement of, performance of whole-body plastic scintillation detector for, 19: 20377
gamma spectrum, (E), 19: 20342
production using Rossendorf Reactor in East Germany, 19: 20436
ZINC NITRATES
$Th(NO_3)_4$–$Zn(NO_3)_2$, crystal structure of octahydrates, 19: 19852
ZINC OXIDES
dielectric losses in, frequency dependence of, 19: 19851(T) (ORNL-tr-491)

electric properties of, effects of lattice energy and temperature on, 19: 21601(T) (ORNL-tr-490)
radiation effects on, mechanisms in, 19: 20019
spectra of suspensions of, in thin polyethylene films, infrared transmission, 19: 19917

ZINC SULFIDES
luminescence and nuclear resonance absorption spectra of iron-57 in phosphors, 19: 19855
radiation effects on luminescence, 19: 19967

ZIRCALOY-2
analysis for hydrogen by isotopic equilibration, 19: 19831
oxidation by steam at 500°C and 1000 psi, inhibiting effects of boric acid on, 19: 20492
radiation effects on PRTR pressure tubes, 19: 21686 (HW-84540)
radiation effects on electric conductivity of corrosion films on, gamma, (E), 19: 20621

ZIRCALOY-4
fatigue strength of, oxide film and additional strain effects on, (E), 19: 20593
temperature distributions in fuel element end cap of, 19: 21674

ZIRCEX PROCESS
thermodynamics, 19: 19742 (CEA-R-2592)

ZIRCONIUM
determination by complex formation with substituted acetic acids, 19: 19802
determination in other metals using catechol violet, colorimetric, 19: 19780
determination in presence of iron and zirconium using arsenate method, 19: 19818
determination in uranium and its compounds and alloys, methods for, 19: 19823
effects on carbon steel corrosion by mercury, 19: 20493
effects on properties of magnesium for use as fuel element can, 19: 20610(P)
effects on strength of thorium at high temperatures, 19: 20560 (ORNL-3777)
geochemistry and mineralogy of, in Cherry Mountains (Urals), USSR, book, 19: 20190
nitrogen at 1400 to 1700°C, formation of alpha-solid solutions in, 19: 19877
oxidation by steam at 500°C and 1000 psi, inhibiting effects of boric acid on, 19: 20492
oxidation of, refractive index and thickness of films formed in anodic, 19: 20489
preparation of large crystals of, by phase transformation method, 19: 20527
separation from hafnium by reversed-phase chromatography, 19: 19752 (IS-T-2)
separation from irradiated fuels, 19: 20084(P)

ZIRCONIUM ALLOYS
corrosion by terphenyls, chlorine evolution in, 19: 20469 (EUR-2279.e)
corrosion in reactors, 19: 20488
oxidation by steam at 500°C and 1000 psi, inhibiting effects of boric acid on, 19: 20492
Al–Mo–Sn–Ti–V–Zr, beta transus temperature of, 19: 20462(R) (NRL-6258)
Al–Mo–Ti–Zr, beta transus temperature of, 19: 20462(R) (NRL-6258)
Al–Sn–Ti–Zr, mechanical properties of diffusion-bonded plates of, 19: 20462(R) (NRL-6258)
Al–Ti–V–Zr, beta transus temperature of, 19: 20462(R) (NRL-6258)
Al–Ti–Zr, mechanical properties of diffusion-bonded plates of, 19: 20462(R) (NRL-6258)
Cr–Fe–Ni–Sn–Zr, properties for use as fuel element cladding, 19: 20497(P)
Mg–Zr, properties for use as fuel element can, effects of manganin on, 19: 20610(P)
Mo–Nb–V–Zr, fabrication and properties of B-66 sheet, 19: 20499(R) (AD-606291)
Mo–Ti–Zr, corrosion by potassium vapor, design of test capsule for, 19: 20473(R) (NASA-CR-54629)
Mo–Ti–Zr, tensile properties of TZM sheet, 19: 20542(R) (AD-606310)
Nb–Ta–W–Zr, fabrication and properties of FS-85 sheet, 19: 20499(R) (AD-606291)
Nb–Zr, corrosion by boiling potassium in loop test, 19: 20476 (ORNL-3603)
Nb–Zr, extrusion, 19: 20500 (AFML-TR-64-387)
Nb–Zr, grain growth of, effects of cold working and annealing on, 19: 20473(R) (NASA-CR-54629)
Nb–Zr, mass transfer from type 316 and 321 stainless steel to, in liquid potassium, research program on, 19: 20474(R) (NASA-CR-54281)
Nb–Zr, strength properties, 19: 20474(R) (NASA-CR-54281)
Nb–Zr, superconducting properties of, effects of heating to 300°C for 10 hr on, 19: 20609(P)
Nb–Zr, ultrasonic attenuation in superconducting, in strong magnetic fields, (E), 19: 21188
Ta–V–Zr, coating for oxidation protection, 19: 20459(R) (IITRI-B6019-6)
U–Zr, thermodynamics of uranium separation by Zircex process from, 19: 19742 (CEA-R-2592)

ZIRCONIUM BORIDES
analysis for boron by pyrohydrolysis, 19: 19761 (NP-14876)

ZIRCONIUM CARBIDES
performance as emitter in hypersonic plasma generators, (E), 19: 20905 (SC-RR-65-54)
preparation by reaction of graphite with zirconium oxide, 19: 19866
superconducting properties, 19: 20572

ZIRCONIUM COMPLEXES
with EDTA, migration in electrodialysis cell, 19: 20052 (ORNL-TM-1035)

ZIRCONIUM HYDRIDES
neutron scattering by, at 0.018 to 0.080 ev, (E), 19: 21200 (KFK-264)

ZIRCONIUM IONS
effects on dephosphorylation of nucleotides and sugar phosphates, 19: 19876

ZIRCONIUM ISOTOPES Zr-89
energy levels from yttrium-89 (p,n) reactions, 4.83- and 5.03-Mev isobaric analog, (E), 19: 21356

ZIRCONIUM ISOTOPES Zr-90
alpha elastic scattering at 43 Mev, collective excitations in, (E), 19: 21386
deuteron reactions (d,p) with, spectra from, 19: 21394

ZIRCONIUM ISOTOPES Zr-91
alpha elastic scattering at 43 Mev, collective excitations in, (E), 19: 21386
deuteron reactions (d,t) at 11.8 Mev, angular distributions from, (E), 19: 21326

ZIRCONIUM ISOTOPES Zr-92
alpha elastic scattering at 43 Mev, collective excitations in, (E), 19: 21386
deuteron reactions (d,t) at 11.8 Mev, angular distributions from, (E), 19: 21326

ZIRCONIUM ISOTOPES Zr-94
alpha elastic scattering at 43 Mev, collective excitations in, (E), 19: 21386
deuteron reactions (d,t) at 11.8 Mev, angular distributions from, (E), 19: 21326

ZIRCONIUM ISOTOPES Zr-95
content in air over Indian and Pacific Oceans in 1961–62, 19: 20158 (NP-14712)
content in stratosphere, 19: 20657(R) (DASA-1309)
determination in mixtures with niobium-95, radiometric, 19: 19748 (DP-933)
shielding power sources of, 19: 21595 (TID-7698(Pt.I)(p.33-248))

ZIRCONIUM ISOTOPES Zr-96
deuteron reactions (d,t) at 11.8 Mev, angular distributions from, (E), 19: 21326

ZIRCONIUM NITRIDES
superconducting properties, 19: 20572

ZIRCONIUM OXIDES
crystal structure polymorphic conversion of, effects of heat on, 19: 19925
radiation effects on electric conductivity of films of, gamma, (E), 19: 20621
reactions with graphite to prepare carbide, 19: 19866
spectra of, Raman, 19: 19849 (WAPD-T-1760)
stability in thermal cycling between 1600 and 2100°F, effects of impurities on, 19: 20585
thickness and refractive index of films of, on anodized zirconium, 19: 20489

ZIRCONIUM SYSTEMS
C–Mo–Ti–Zr, extrusion of molybdenum-TZC, 19: 20500 (AFML-TR-64-387)
C–Nb–W–Zr, creep properties of D-43, 19: 20474(R) (NASA-CR-54281)
C–Nb–W–Zr, stress corrosion of D-43 by refluxing potassium, research program on, 19: 20474(R) (NASA-CR-54281)
C–Ta–V–Zr, coating for oxidation protection, 19: 20459(R) (IITRI-B6019-6)

ZIRCONS
age of, La Sal Mountain, Utah, (E), 19: 20178
fission product tracks in, formation and stability of, (E), 19: 20674

ZIRCONYL IONS
determination using 5,5'-thiodisalicylic acid, gravimetric, 19: 19812

ZIRFLEX PROCESS
corrosive effects of solutions from, on candidate alloys for centrifuge, 19: 20481 (ORNL-3787)

REPORT NUMBER INDEX

Reports, conference papers and proceedings, numbered translations, and patents abstracted during the period are included in this index. Each item is listed by report number; this is followed by the abstract number and a brief notation regarding public availability. The index entries show, when known, which reports are on file in the depository libraries, which reports have been published in open-literature journals (journal citation given), and which reports can be purchased (source and price). Whenever a report is identified by more than one number, cross references from secondary to primary report numbers are cited.

The report number codes apply to AEC reports unless designated otherwise. Non-AEC reports are identified by parenthetical notes after the report codes; e.g., (non-AEC), (British), (Canadian), (French). The note (Misc.) identifies those codes used for both USAEC and non-AEC reports. Patents are listed under the heading "PATENTS"; the country of origin is included in parentheses.

A comprehensive listing of both AEC and non-AEC report codes is contained in TID-85(3rd Rev.), *Report Number Series Used by the Division of Technical Information in Cataloging Reports*. This information is also included in the Cumulative Report Number Index (issued annually).

Public Availability of USAEC Reports

All USAEC reports abstracted in *NSA* are available to the public through one or more of the following sources:

(1) Depository libraries in the United States, in other countries, and in international agencies. A list of these depositories appears on the inside covers of each issue of *NSA*.

(2) Scientific and technical journals or other publications.

(3) Microcard Editions, Inc., in Microcard and micronegative form. Orders and inquiries should be sent to: Accounting and Shipping Department, West Salem, Wisconsin 54669.

(4) Clearinghouse for Federal Scientific and Technical Information, U. S. Department of Commerce, Springfield, Virginia 22151.

(5) Superintendent of Documents, U. S. Government Printing Office, Washington, D. C. 20402.

Public Availability of Non-AEC Reports

U. S. Reports. Many reports of U. S. Government agencies are available to the public from the Clearinghouse for Federal Scientific and Technical Information (CFSTI). This availability is given when known. Such reports should be ordered by AD number or NASA-N number. If availability is not shown, inquiries may be directed to CFSTI. In the case of NP numbers, inquiries should be by title and author.

Non-U. S. Reports. Many reports of atomic energy establishments of other countries are deposited in the libraries listed on the inside covers of each issue of *NSA*.

Additionally, the following countries have made their reports available as indicated.

AUSTRALIA

Australian Atomic Energy Commission Research Establishment. Available upon request from the Library, Australian Atomic Research Establishment, Private Mail Bag, Sutherland, New South Wales, Australia.

BELGIUM

Centre d'Étude de l'Énergie Nucléaire. Available upon request to individuals and organizations, from the Centre d'Étude de l'Énergie Nucléaire (CEN), 31, Rue Belliard, Bruxelles, Belgium.

CANADA

Atomic Energy of Canada Limited. For sale by the Technical Information Officer, Atomic Energy of Canada Limited, Chalk River, Ontario, Canada. Copies are also deposited in libraries in the United Kingdom.

National Research Council of Canada. Available from the National Research Council of Canada, Ottawa 2, Ontario, Canada.

DENMARK

Atomic Energy Commission Research Establishment, Risø. Available on exchange from the Library, Danish Atomic Energy Commission, Risø, Roskilde, Denmark. Also for sale by Jul. Gjellerup, Booksellers, 87 Sölvgade, København K., Denmark.

Danatom. Available on loan from Research Establishment, Risø, Roskilde, Denmark. Copies are available from Danatom, Aurehøjvej 2, Hellerup, Denmark.

FRANCE

Commissariat à l'Énergie Atomique. Inquiries for reports numbered 1-2199 should be addressed to Commissariat à l'Énergie Atomique, Service Central de Documentation, Centre d'Études Nucléaires de Saclay, Boite Postale No. 2, Gif-sur-Yvette (S. et O.), France. Reports numbered 2200 and above are available from La Documentation Francaise, 16 Rue Lord-Byron, Paris VIII, France.

Service Central de Protection contre les Rayonnements Ionisants. Copies are available from Ministère de la Santé Publique, Service Central de Protection contre les Rayonnements Ionisants, B. P. n° 35-LE VESINET (S. et O.), France.

GERMANY

Deutsches Elektronen-Synchrotron DESY. Copies are available from Deutsches Elektronen-Synchrotron Desy, Dokumentation, 2000 Hamburg-Gr. Flottbek 1, Notkestieg 1, Germany.

Kernforschungsanlage. Copies may be ordered from Zentralbibliothek der Kernforschungsanlage Jülich, Jülich, Bundesrepublik Deutschland.

Hahn-Meitner-Institute für Kernforschung. Available without charge from Hahn-Meitner-Institute für Kernforschung Berlin, Bibliothek, Glienicker Strasse 100, 1 Berlin 39, Germany. Copies are deposited in many national nuclear centers in the world.

Johann-Wolfgang-Goethe Universität, Frankfurt Am Main, Institut für Kernphysik, (IKF). Copies are available from Gmelin Institut, 40-42 Varrentrappstrasse, Frankfurt (Main), West Germany.

ISRAEL

Israel Atomic Energy Commission. Available without charge from Ministry of Defence/Atomic Energy Com-

mission, Soreq Research Establishment, Yavne, Israel. Copies are deposited in libraries in Israel and in other countries.

ITALY

Centro Informazioni Studi Esperienze (CISE). For sale at CISE Press Office, Casella Postale 3986, Milano, Italy. Copies are deposited in libraries in Italy.

Comitato Nazionale per l'Energia Nucleare. Copies are available from Comitato Nazionale per l'Energia Nucleare, Divisione Affari Internazionali e Studi Economici, Ufficio Pubblicazioni, Via Belisario, 15, Roma, Italy.

JAPAN

Japan Atomic Energy Research Institute (JAERI). Available from the Staff Supply Cooperative of Japan Atomic Energy Research Institute (JAERI), 1-1 Tamura-Cho, Shiba, Minato-Ku, Tokyo, Japan. Copies are deposited in depositories in Tokyo, Nagoya, and Osaka.

Nagoya University. Copies are available from Research Information Center, Institute of Plasma Physics, Nagoya University, Nagoya, Japan.

University of Tokyo. Available free of charge from Institute for Nuclear Study, University of Tokyo, Tanashi-Machi, Kitatama-gun, Tokyo, Japan.

NETHERLANDS

Reactor Centrum Nederland. For sale by Reactor Centrum Nederland, 112 Scheveningseweg, 's-Gravenhage, The Netherlands. Copies are deposited in university libraries in Holland and in many national nuclear centers in the world.

NEW ZEALAND

Institute of Nuclear Sciences. Copies are available from Librarian, Institute of Nuclear Sciences, D.S.I.R., Private Bag, Lower Hutt, New Zealand. Copies are deposited in other countries.

NORWAY

Forsvarets Forskningsinstitutt. Copies available from Norwegian Defence Research Establishment, Library, P. O. Box 25, Kjeller, Norway.

Institutt for Atomenergi. "KR" reports are available on an exchange basis from the Library, Institutt for Atomenergi, Box 40, Kjeller, Norway. Other series are not generally available to the public.

Norwegian Reactor School. Copies are available from The Library, Institutt for Atomenergi, P. O. Box 40, Kjeller, Norway.

PAKISTAN

Atomic Energy Center. Copies are available from Atomic Energy Center, P. O. Box 658, Lahore, (West Pakistan).

POLAND

Reports of the Polish nuclear institutes are published by the Nuclear Energy Information Center of the Government Commissioner for Use of Nuclear Energy. Copies are available from Ośrodek Informacji o Energii Jądrowej, Warszawa, PKiN, Poland.

SPAIN

Junta de Energia Nuclear. "JEN" reports are available without charge from Servicio de Documentation, Junta de Energia Nuclear, Ciudad Universitaria, Madrid (3), Spain.

SWEDEN

Aktiebolaget Atomenergi. "AE" reports are for sale from Aktiebolaget Atomenergi, Library Section, Box 43041, Stockholm 43, Sweden. Bibliographies and literature surveys of the VDDIT- series may be obtained from Aktiebolaget Atomenergi, Information Office, Scientific and Technical Information, Box 43041, Stockholm 43, Sweden. Other series are not generally available to the public. Organizations in the atomic energy field may obtain copies from Aktiebolaget Atomenergi. Microcopy of AE reports is available from the International Documentation Centre, Tumba, Sweden.

SWITZERLAND

CERN European Organization for Nuclear Research. Available without charge from CERN European Organization for Nuclear Research, Geneva 23, Switzerland. Copies are deposited in libraries in 13 countries.

Eidgenössisches Institut für Reaktorforschung. "EIR" reports are available from Eidgenössiches Institut für Reaktorforschung, c/o Bibliothek, Würenlingen/Ag, Switzerland.

TURKEY

Turkish Atomic Energy Commission. Copies are available free of charge from T.A.E.C., Çekmece Nuclear Research Center, P. O. Box 1, Airport, İstanbul, Turkey.

UNITED KINGDOM

United Kingdom Atomic Energy Authority. Some reports are for sale in the United States by the British Information Service (BIS), 845 Third Avenue, New York, N. Y. 10022. United Kingdom reports generally may be purchased from Her Majesty's Stationery Office, London. Copies not for sale by Her Majesty's Stationery Office may be purchased in microcopy form from Micro Methods Limited, East Ardsley, Wakefield, Yorks, England. Report copies are deposited in a large number of libraries in England.

Conferences

Published conference proceedings as well as individual unpublished papers from conferences are included in this index. A CONF number is assigned to the conference if published proceedings are received and also if only a single paper is received. The base number used is year-month-sequence. Thus, the number CONF-650101 would indicate that the conference was held in 1965, in January, and that this was the first January 1965 conference so received. This number would be assigned to complete published proceedings, or if individual papers are received, the base number would be extended to include a paper number, i.e., CONF-650101-1. As additional papers are received, they will be assigned consecutive numbers in the series, CONF-650101-1, 2, 3, 4, etc. This numbering system ensures that all papers received from a conference will be associated with that conference in this index.

If published proceedings are received after the receipt of individual papers, the complete proceedings will be abstracted and the abstract number will appear in this index with the base CONF number.

Abbreviations Used in Availability Column

AECL	For sale by Atomic Energy of Canada Ltd., Chalk River, Ontario, Canada.
BIS	For sale by British Information Service, 845 Third Avenue, New York, N. Y. 10022
CFSTI	For sale by the Clearinghouse for Federal Scientific and Technical Information, U. S. Department of Commerce, Springfield, Virginia 22151. The symbol "cy" indicates that the format of the item sold may be either a printed document or a photographic reproduction (two-thirds of original size) depending upon the availability of printed stock. The indicated price is for either format. The symbol "mn" is used to indicate

that copy is available in the form of micronegatives (microfiche). The number preceding the "mn" symbol indicates the number of micronegatives in the set. Micronegatives are available at the following prices: One micronegative, $0.50; each additional micronegative of the set, $0.25. For additional micronegative copies of the same report requested at the time of the original order, $0.25 per micronegative. Prices are reduced on micronegatives if subscription distribution is purchased.

Dep.	AEC reports: Full-size copy is on deposit in the depository libraries both inside and outside the United States. These reports are also for sale by Microcard Editions, Inc., Accounting and Shipping Department, West Salem, Wisconsin 54669. Non-AEC reports: Full-size copy on deposit in the depository libraries in the United States only.
Dep.(mn)	Same as for Dep., except copy is in micronegative (microfiche) form.
DSIR	For sale by the National Lending Library for Science and Technology (D.S.I.R.), Boston Spa, Yorkshire, England.
DTI Extension	Available from the U. S. Atomic Energy Commission, Division of Technical Information Extension, P. O. Box 62, Oak Ridge, Tennessee 37831.
EM	Blueprints and Microcopy of AEC engineering drawings are available from Clearinghouse for Federal Scientific and Technical Information, U. S. Department of Commerce, Springfield, Virginia 22151. Current prices of the CAPE- packages may be obtained from this address. TID-4100, available from the Division of Technical Information Extension, P. O. Box 62, Oak Ridge, Tennessee 37831, contains information on all the CAPE- packages for sale.
Gmelin	Available at a nominal charge and under the AED- number shown from Atomic Energy Documentation Center, Gmelin Institute, 40-42 Varrentrappstrasse, Frankfurt (Main), West Germany.
GPO	For sale by the Superintendent of Documents, Government Printing Office, Washington, D. C. 20402.
HMSO	Her Majesty's Stationery Office, London.
IAEA	Available from the International Atomic Energy Agency, Vienna, Austria.
JCL	For sale by the Special Libraries Association Translation Center, John Crerar Library, 35 West 33rd Street, Chicago, Illinois 60616.
LC	For sale by the Library of Congress, Photoduplication Service, Washington, D. C. 20540.
NAS	National Academy of Sciences, National Research Council, Washington, D. C. 20418.
NRC	For sale by the National Research Council of Canada, Ottawa, Ontario, Canada.
ORINS	Available on interlibrary loan from the Library, Oak Ridge Institute of Nuclear Studies, Post Office Box 117, Oak Ridge, Tennessee 37831.
UKAEA, London	Available from United Kingdom Atomic Energy Authority, 11 Charles II Street, London, S. W. 1.
USGS	Available free of charge from the U. S. Geological Survey, Washington, D. C. 20242.

[The symbols "ph," "mf," and "fs" are used to designate that copy is available only in photostat, microfilm, or facsimile form. The symbol "mn" is used to designate that copy is available in micronegative (microfiche) form. The symbol "cy" is used to designate full size or photographically enlarged copy (two-thirds of original size).]

Report No.	Abstract No.	Availability
NUMERICAL	**(Misc.)**	
65APE1	19-21607	See APED-4773
A-AC-	**(Misc.)**	
82/G/L.973	19-20170	Medical Research Council Monitoring Report Series No. 9. (Medical Research Council, London (England)) $0.40(BIS); 2s. (HMSO)
AAEC-TM-	**(Australian)**	
247	19-20030	Intern. J. Appl. Radiation Isotopes, 16: 257-9(1965)
AD-	**(Misc.)**	
422407	19-21467	See ARL-63-203
422652	19-20109	See CER-D1703
424387	19-21594	$1.10(CFSTI)
424670	19-20279	See RTD-TDR-63-4001
424939	19-21465	See AFCRL-63-779
456495	19-20207	See USNRDL-TR-797
456725	19-20619	See NP-14883
457075	19-20329	See USNRDL-TR-806
457992	19-20558	See NP-14888
604044	19-21078	See AFOSR-64-1380
604868	19-20541	$3.00(CFSTI)
605574	19-21715	$6.00(CFSTI)
606253	19-20403	$1.00(CFSTI)
606268	19-20874	See P-1020(RAND)
606291	19-20499	$3.00(CFSTI)
606310	19-20542	$2.00(CFSTI)
606326	19-19504	See RM-2801-PR
606374	19-21694	See P-1076(RAND)
606400	19-21125	See RAD-TR-64-27
606422	19-20455	See DCAS-TDR-62-192
606439	19-20660	See P-1113(RAND)
606444	19-21124	See P-1121(RAND)
606453	19-21761	See P-1134(RAND)
606490	19-20659	$1.00(CFSTI)
606514	19-21488	See PIBMRI-1208-64
606548	19-20873	See D2-11608
606559	19-21466	See AFCRL-64-550
606573	19-20171	See AFCRL-64-659
606605	19-20430	See P-1231(RAND)
606685	19-20136	See AFWL-TDR-64-13
606712	19-20657	See DASA-1309
606766	19-21762	See RM-2163(RAND)
609153	19-21492	See FTD-TT-64-102
610756	19-21478	See NP-14880
610583	19-20661	See RLE-TR-428
610709	19-20502	See DMIC-Memo-198
611127	19-21468	See BSD-TDR-64-164
611376	19-20459	See IITRI-B6019-6
611822	19-20552	See IITRI-B6021-6
AEC-tr-	**(For complete listing see TID-4025)**	
6547	19-20330	Dep.(mn); $1.10(fs), $0.80(mf) JCL
AECL-	**(Canadian)**	
2160	19-21224	$1.00(AECL)
2168	19-21225	$1.00(AECL)
AEET-HP-	**(Indian)**	
Th-19	19-21226	Dep.(mn)
AEEW-R-	**(British)**	
353	19-21648	Nucl. Sci. Eng., 22: 78-86(1965)
AERE-GR-	**(British)**	
101	19-20543	Dep.(mn)
AERE-M-	**(British)**	
101	19-19739	Dep.; $1.10(BIS), 5s. 6d. (HMSO)
AERE-R-	**(British)**	
4201	19-19953	Dep.; $0.80(BIS); 4s. (HMSO)
4525	19-20312	Dep.; $0.80(BIS); 4s. (HMSO)
4566	19-20637	Phil. Mag. (8), 11: 357-68(1965)
4632	19-20634	Phil. Mag. (8), 11: 53-70(1965)
4635	19-20191	Dep.(mn); Gmelin, AED-CONF-64-083-18
4692	19-20838	Phil. Mag. (8), 11: 291-302(1965)
4702	19-20492	J. Nucl. Mater., 15: 263-77(1965)
4703	19-20621	Brit. J. Appl. Phys., 16: 155-62(1965)
4749	19-20589	J. Nucl. Mater., 15: 298-309(1965)
4839	19-19954	Dep.; $1.00(BIS); 5s. (HMSO)
AFCRL-	**(Non-AEC)**	
63-779	19-21465	$2.60(CFSTI)
64-550	19-21466	$2.00(CFSTI)
64-659	19-20171	$2.00(CFSTI)
64-839	19-20612	CFSTI
AFML-TR-	**(Non-AEC)**	
64-387	19-20500	
64-388	19-20544	
AFOSR-	**(Misc.)**	
64-1380	19-21078	$2.00(CFSTI)
AFWL-TDR-	**(Non-AEC)**	
64-13	19-20136	$3.00(CFSTI)
AHSB(RP)-	**(British)**	
M-24	19-20210	Ann. Occupational Hyg., 7: 369-72(1964)
AL-TDR-	**(Non-AEC)**	
64-65	19-21488	See PIBMRI-1208-64
AMP-	**(Non-AEC)**	
152	19-21468	See BSD-TDR-64-164
ANL-		
6849	19-21726	Dep.; $4.00(cy), 3(mn) CFSTI
6864	19-21677	Dep.; $2.00(cy), 1(mn) CFSTI
6938	19-20192	Dep.; $6.00(cy), 5(mn) CFSTI
6941	19-21227	Dep.; $1.00(cy), 1(mn) CFSTI
6970	19-21228	Dep.; $3.00(cy), 1(mn) CFSTI
6972	19-21678	Dep.; $1.00(cy), 1(mn) CFSTI
6984	19-20316	Dep.; $2.00(cy), 1(mn) CFSTI
7005	19-19740	Dep.; $1.00(CFSTI)
7016	19-20438	Dep.; $3.00(cy), 3(mn) CFSTI
APED-	**(Misc.)**	
4773	19-21607	
ARL-	**(Non-AEC)**	
63-203	19-21467	$1.10(CFSTI)
AWRE-O-	**(British)**	
81/64	19-21196	Dep.(mn)
AWRE-R-	**(British)**	
2/65	19-21608	Dep.; $0.60(BIS); 3s. 0d. (HMSO)
BAW-	**(Misc.)**	
1280-22	19-20107	Dep.(mn); $3.00(cy), 1(mn) CFSTI
BLG-	**(Belgian)**	
256	19-20466	Metallurgie (Mons, Belg.), 4: No. 2, 37-41(1963)
261	19-21679	Dep.(mn)
280	19-20194	Dep.(mn)
281	19-20195	Dep.(mn)
287	19-19867	Chem. Eng. Progr., Symp. Ser., 60: No. 47, 90-5(1964)
288	19-20060	Chem. Eng. Progr., Symp. Ser., 60: No. 47, 20-30(1964)
289	19-20603	Z. Metallk., 55: 460-6(1964)
317	19-20904	Dep.(mn)
BNL-		
7607	19-20493	Nucl. Sci. Eng., 22: 24-32(1965)
7661(Vol.I)	19-21728	Dep.(mn); $7.00(cy), 7(mn) CFSTI
7661(Vol.II)	19-21727	Dep.(mn); $6.00(cy), 6(mn) CFSTI
7918	19-21757	Dep.(mn); $1.00(cy), 1(mn) CFSTI
8243	19-19943	Dep.(mn); $2.00(cy), 1(mn) CFSTI; Gmelin, AED-CONF-64-002-26
8388	19-20945	Ann. Phys. (N. Y.), 32: 114-26(1965)
8424	19-20964	J. Math. Phys. (N. Y.), 6: 648-51(1965)
8550	19-20863	Proc. Phys. Soc. (London), 85: 399-402 (1965)

Report No.	Abstract No.	Availability
8586	19-19891	J. Chem. Phys., 42: 2635-6(1965)
8598	19-19995	J. Chem. Phys., 42: 2391-2405(1965)
8645	19-20658	See CONF-641207-2
8684	19-19887	J. Chem. Phys., 42: 2624-5(1965)
8690	19-21319	Nucl. Phys., 67: 336-41(1965)
8841	19-21229	$1.00(cy), 1(mn) CFSTI
8864	19-21758	Dep.(mn); $1.00(cy), 1(mn) CFSTI
8934	19-21756	Dep.(mn); $1.00(cy), 1(mn) CFSTI
8967	19-20915	Dep.(mn); $1.00(cy), 1(mn) CFSTI
8968	19-20718	Dep.(mn); $1.00(cy), 1(mn) CFSTI
8969	19-20094	Dep.(mn); $1.00(cy), 1(mn) CFSTI
8970	19-20719	Dep.(mn); $1.00(cy), 1(mn) CFSTI
8976	19-20095	Dep.(mn); $2.00(cy), 1(mn) CFSTI
8982	19-20720	Dep.(mn); $1.00(cy), 1(mn) CFSTI
8993	19-19957	Dep.(mn); $2.00(cy), 1(mn) CFSTI
9010	19-21634	Dep.(mn); $2.00(cy), 1(mn) CFSTI
9011	19-21635	Dep.(mn); $1.00(cy), 1(mn) CFSTI
BNWL–		
4	19-20035	Dep.(mn); $2.00(cy), 1(mn) CFSTI
16	19-20545	Dep.(mn); $1.00(cy), 1(mn) CFSTI
25	19-20036	Dep.; $3.00(cy), 1(mn) CFSTI
31	19-20108	Dep.; $3.00(cy), 2(mn) CFSTI
BPAD–	(Non-AEC)	
864-15598R	19-21615	See NASA-CR-54282
BRB–		
77	19-20501	Dep.(mn); $2.00(cy), 1(mn) CFSTI
BSD-TDR–	(Misc.)	
64-164	19-21468	$1.00(cy), 1(mn) CFSTI as AD-611127
CAPE–		
926	19-20390	EM
1058	19-20306	EM
1115	19-20307	EM
1120	19-20104	EM
1139	19-20132	EM
1140	19-20131	EM
1153	19-21704	EM
1165	19-20535	EM
1175	19-20437	EM
1176	19-20419	EM
1179	19-20083	EM
1181	19-19939	EM
1184	19-20308	EM
1186	19-20133	EM
1193	19-20134	EM
1197	19-21743	EM
CEA-R–	(French)	
2348	19-19958	Dep.(mn)
2442	19-21729	Dep.(mn)
2529	19-20613	Dep.(mn)
2539	19-19741	Dep.(mn)
2552	19-21230	Dep.(mn)
2557	19-21730	Dep.(mn)
2572	19-20453	Dep.(mn)
2591	19-19832	Dep.(mn)
2592	19-19742	Dep.(mn)
2619	19-19743	Dep.(mn)
2622	19-19744	Dep.(mn)
2628	19-19833	Dep.(mn)
2654	19-20037	Dep.(mn)
2712	19-19745	Dep.(mn)
2713	19-21469	Dep.(mn)
2718	19-20245	Dep.(mn)
2726	19-20546	Dep.(mn)
2728	19-19746	Dep.(mn)
2731	19-20547	Dep.(mn)
2747 & Add.	19-21197	Dep.(mn)
2749	19-20721	Dep.(mn)
2759	19-21198	Dep.(mn)
CEA-tr–	(French)	
A-1616	19-19474	Dep.(mn)
A-1729	19-20174	Dep.(mn); $1.10(fs), $0.80(mf) JCL
A-1741	19-19961	Dep.(mn); $2.60(fs), $0.83(mf) JCL

Report No.	Abstract No.	Availability
CEND–	(Misc.)	
3336-229	19-21664	Dep.(mn); $1.00(cy), 1(mn) CFSTI
CER–	(Non-AEC)	
D1703	19-20109	$19.75(CFSTI)
CERN–	(European Organization for Nuclear Research)	
65-7	19-20916	Dep.(mn)
CEX–		
65.02	19-21199	Dep.; $1.00(cy), 1(mn) CFSTI
CLM-P–	(British)	
47	19-21524	Nucl. Fusion, 4: 287-95(1964)
54	19-21553	Proc. Phys. Soc. (London), 85: 317-28 (1965)
58	19-19885	J. Chem. Phys., 42: 2371-3(1965)
60	19-21510	J. Nucl. Energy, Pt. C, 7: 113-22(1965)
64	19-21552	Proc. Phys. Soc. (London), 85: 301-16 (1965)
CONF-179–	(American Chemical Society Radionuclidic Exchange on Soils, Minerals, and Resins, Philadelphia, Apr. 1964)	
18	19-21711	See DPSPU-63-30-40
CONF-313–	(2nd National Meeting of the Society for Applied Spectroscopy, San Diego, Calif., Oct. 1963)	
12	19-19827	ORINS. Gmelin, AED-CONF-63-175-27
CONF-322–	(American Chemical Society Production Technology of Np 237 and Pu 238, Denver, Jan. 1964)	
16	19-19943	See BNL-8243
CONF-453–	19-19709	(IAEA Symposium on Medical Radioisotope Scanning, Athens, Apr. 1964) See STI/PUB/82 Vol. II
CONF-492–	(National Association of Corrosion Engineers, Chicago, Mar. 1964)	
9	19-20495	ORINS. Gmelin, AED-CONF-64-035-15
10	19-20087	See GAT-P-33
CONF-524–	(American Institute of Mining, Metallurgical and Petroleum Engineers Annual Meeting, New York, Feb. 1964)	
19	19-21195	ORINS. Gmelin, AED-CONF-64-006-28
CONF-533–	(3rd Conference on Exploding Wires, Boston, Mar. 1964)	
3	19-20717	ORINS. Gmelin, AED-CONF-64-012-14
CONF-555–	(International Symposium on Surface Contamination, Gatlinburg, Tenn., June 1964)	
16	19-20191	See AERE-R-4635
CONF-556–	(12th Annual Meeting of the Radiation Research Society, Miami, Fla., May 1964)	
19	19-19618	ORINS. Gmelin, AED-CONF-64-078-21
21	19-19649	ORINS. Gmelin, AED-CONF-64-078-23
22	19-19619	ORINS. Gmelin, AED-CONF-64-078-27
CONF-571–	(American Chemical Society 148th National Meeting, Chicago, Aug.–Sept. 1964)	
29	19-19940	ORINS. Gmelin, AED-CONF-64-155-38
37	19-19959	Dep.(mn); $1.00(cy), 1(mn) CFSTI; Gmelin, AED-CONF-64-155-50
CONF-592–	(9th Symposium on Ballistics Missile and Space Technology, San Diego, Calif., Aug. 1964)	
2	19-20184	ORINS
CONF-593–	(Conference on the Automatic Acquisition and Reduction of Nuclear Data, Karlsruhe, Ger., July 1964)	
7	19-21731	See KFK-242
CONF-606–	(American Chemical Society, Northwest Regional Meeting, Spokane, Wash., June 1964)	
5	19-19836	See HW-SA-3476
CONF-642–	(Health Physics Society, Cincinnati, June 1964)	
27	19-19829	ORINS. Gmelin, AED-CONF-64-082-53
28	19-20163	See RRA-M42

Report No.	Abstract No.	Availability
30	19-21605	See HW-SA-3560
31	19-21748	See DPSPU-64-30-8B
32	19-20317	See HW-82369
33	19-20201	See HW-SA-3525
34	19-20318	See HW-SA-3526
CONF-651–		(9th International Conference on Low Temperature Physics, Columbus, Ohio, Aug. 31–Sept. 4, 1964)
69	19-21194	ORINS. Gmelin, AED-CONF-64-140-84
CONF-654–	19-2907 19-6030	(American Nuclear Society Meeting, San Francisco, Nov. 30–Dec. 3, 1964)
32	19-21636	Dep.(mn); $1.00(cy), 1(mn) CFSTI
51	19-21643	See WAPD-T-1728
54	19-21735	See ORNL-P-1092
55	19-20471	See HW-SA-3628
72	19-21464	ORINS. Gmelin, AED-CONF-64-219-31
78	19-21223	ORINS. Gmelin, AED-CONF-64-219-91
80	19-19825	ORINS. Gmelin, AED-CONF-64-219-74
81	19-19826	ORINS. Gmelin, AED-CONF-64-219-75
83	19-19828	ORINS. Gmelin, AED-CONF-64-219-67
CONF-705–		(14th International Congress of Occupational Health, Madrid, Sept. 16–21, 1963)
2	19-20242	ORINS
3	19-19494	ORINS
CONF-717–		(CNRS Meeting on Graft of Allogenic Hematopoietic Cells, Paris, Sept. 7–9, 1964)
4	19-19648	ORINS
5	19-19651	ORINS
6	19-19652	ORINS
7	19-19646	ORINS
8	19-19650	ORINS
9	19-19647	ORINS
10	19-19653	ORINS
11	19-19468	ORINS
12	19-19617	ORINS
13	19-19645	ORINS
14	19-19615	ORINS
15	19-19644	ORINS
16	19-19493	ORINS
CONF-718–		(American Institute of Chemical Engineers Meeting, Las Vegas, Nev., Sept. 21, 1964)
2	19-21710	ORINS. Gmelin, AED-CONF-64-163-8
CONF-720–		(2nd Symposium on Protection Against Radiation Hazards in Space, Gatlinburg, Oct. 1964)
5	19-21244	See ORNL-P-844
15	19-19616	ORINS. Gmelin, AED-CONF-64-190-20
19	19-20019	ORINS. Gmelin, AED-CONF-64-190-14
CONF-721–		(8th Conference on Analytical Chemistry in Nuclear Technology, Gatlinburg, Tenn., Oct. 6–8, 1964)
9	19-19830	ORINS. Gmelin, AED-CONF-64-189-6
11	19-19831	ORINS. Gmelin, AED-CONF-64-189-2
CONF-729–		(International Conference on Beryllium, Philadelphia, Oct. 1964)
20	19-20557	See NMI-TJ-60
CONF-734–		(Symposium on Genes and Chromosomes Structure and Function, Buenos Aires, Nov.–Dec. 1964)
5	19-21756	See BNL-8934
CONF-763–		(American Society of Mechanical Engineers Winter Meeting, New York, Nov. 29–Dec. 4, 1964)
44	19-20130	ORINS
CONF-794–		(Magnetism Conference, Minneapolis, Nov. 1964)
5	19-20652	ORINS. Gmelin, AED-CONF-64-204-15
CONF-804–		(Symposium on the Inelastic Scattering of Neutrons, Bombay, Dec. 15–19, 1964)
27	19-21200	See KFK-264
28	19-20553	See KFK-262
CONF-641020–		(34th Symposium on Shock, Vibration, and Associated Environments, Pacific Grove, Calif., Oct. 13–15, 1964)
1	19-21722	See NAA-SR-Memo-10767
CONF-630907–	19-19853	(International Conference on Luminescence, Torun, Poland, Sept. 1963)
CONF-631105–		(Seminar on Protection of the Public in the Event of Radiation Accidents, Geneva, Nov. 18–22, 1963)
1	19-20240	ORINS
CONF-640204–	19-20246	(High Voltage Electron Microscope Meeting, Argonne, Ill., Feb. 13–14, 1964)
CONF-640506–		(Symposium on Methods of Analysis of the Control of Contaminated Surface Waters, Milan, May 12–14, 1964)
1	19-19749	See EUR-2118.f
CONF-640606–		(American Physical Society Summer Meeting, Denver, Colo., June 25–27, 1964)
22	19-21476	See MATT-283
CONF-640609–		(Society of Nuclear Medicine, 11th Annual Meeting, Berkeley, Calif., June 17–20, 1964)
2	19-19732	ORINS. Gmelin, AED-CONF-64-111-7
4	19-19731	ORINS. Gmelin, AED-CONF-64-111-2
CONF-640611–		(Canadian Assn. of Physicists, Division of Medical and Biological Physics, Annual Meeting, Halifax, Nova Scotia, Canada, June 11–13, 1964)
2	19-20241	ORINS. Gmelin, AED-CONF-64-108-3
3	19-20243	ORINS. Gmelin, AED-CONF-64-108-4
5	19-19733	ORINS. Gmelin, AED-CONF-64-108-1
CONF-640615–		(Fast Reactor Physics Conference, Ann Arbor, Mich., June 8–12, 1964)
2	19-21642	See MMPP-FRPC-64-3
CONF-640618–		(Symposium on Powder Metallurgy, Paris, June 15–17, 1964)
1	19-20465	See TID-20344
CONF-640802–		(American Institute of Biological Sciences, 15th Annual Meeting, Boulder, Colo., Aug. 23–28, 1964)
2	19-19495	ORINS. Gmelin, AED-CONF-64-158-8
CONF-640809–		(10th International Botanical Congress, Edinburgh, Aug. 3–12, 1964)
1	19-19946	See UCRL-11950
CONF-640909–		(International Conference on Radiation Preservation of Foods, Boston, Sept. 27–30, 1964)
1	19-20424	ORINS. Gmelin, AED-CONF-64-168-9
3	19-20421	ORINS. Gmelin, AED-CONF-64-168-6
4	19-20425	ORINS. Gmelin, AED-CONF-64-168-5
6	19-20420	ORINS. Gmelin, AED-CONF-64-168-13
8	19-20423	ORINS. Gmelin, AED-CONF-64-168-1
9	19-20422	ORINS. Gmelin, AED-CONF-64-168-2
CONF-640912–		(4th International Analogue Computation Meeting, Brighton, England, Sept. 14–18, 1964)
1	19-21604	See EUR-2202.e
CONF-641001–		(Symposium on Radiochemical Methods of Analysis, Salzburg, Austria, Oct. 19–23, 1964)
54	19-20322	See LA-DC-6397
CONF-641108–		(American Physical Society, New York, Nov. 4–8, 1964)
13	19-21477	See MATT-290
CONF-641113–	19-17445 19-19462	(6th International Transplantation Conference on Transplantation, New York, Nov. 1964)
CONF-641116–		(Conference on the Role of Grain Boundaries and Surfaces in Ceramics, Raleigh, N. C., Nov. 16–18, 1964)
4	19-20607	ORINS. Gmelin, AED-CONF-64-224-5
CONF-641207–		(American Society of Agricultural Engineers, Winter Meeting, New Orleans, La., Dec. 7–10, 1964)
1	19-20182	ORINS

Report No.	Abstract No.	Availability
2	19-20658	ORINS
3	19-20183	ORINS
CONF-641208–	**(3rd Conference on Performance of High Temperature Systems, Pasadena, Calif., Dec. 1964)**	
1	19-20608	ORINS
5	19-20496	ORINS
6	19-20139	ORINS
7	19-20124	ORINS
8	19-19941	ORINS
CONF-641213–	**(New York Academy of Sciences, New York, Dec. 14–17, 1964)**	
1	19-21758	See BNL-8864
CONF-650103–	**(International Symposium on Packaging and Transportation of Radioactive Material, Albuquerque, N. Mex., Jan. 11, 1965)**	
6	19-20196	Dep.(mn); $2.00(cy), 1(mn) CFSTI; Gmelin, AED-CONF-65-001-8
8	19-20239	ORINS. Gmelin, AED-CONF-65-001-12
CONF-650111–	**(CERN Informal Neutrino Conference, Geneva, Jan. 1965)**	
1	19-20738	See UCRL-11983
CONF-650203–	**(National AIME Meeting, Chicago, Feb. 14–18, 1965)**	
3	19-21751	See ORNL-P-1064
CONF-650204–	**(Meeting on Thermocouple Technology and the Effects of Nuclear Radiation on Thermocouples, Washington, D. C., Feb. 24–26, 1965)**	
3	19-20278	See ORNL-P-1069
5	19-20277	See ORNL-P-1068
6	19-20401	See ORNL-P-1065
CONF-650211–	**(New York State Radiological Officers Conference, Albany, Feb. 25, 1965)**	
1	19-20202	See ORNL-P-1093
CONF-650212–	**(The Society for Non-Destructive Testing Spring Convention, Los Angeles, Feb. 22–26, 1965)**	
1	19-20454	Dep.(mn); $1.00(cy), 1(mn) CFSTI
CONF-650213–	**(IEEE Sixth Winter Convention on Military Electronics, Los Angeles, Feb. 3–5, 1965)**	
1	19-20444	See UCRL-12293-T
CONF-650214–	**(American Chemical Society, Troy, N. Y., Feb. 18, 1965)**	
1	19-19747	Dep.(mn); $1.00(cy), 1(mn) CFSTI
CONF-650301–	**(Symposium on the Physics and Chemistry of Fission, Salzburg, Mar. 22–26, 1965)**	
6	19-21229	See BNL-8841
7	19-21241	See LA-DC-6639
CONF-650306–	**(Particle Accelerator Conference, Washington, D. C., Mar. 10–12, 1965)**	
4	19-20915	See BNL-8967
7	19-20720	See BNL-8982
9	19-20734	See UCRL-11800
10	19-20326	See UCRL-11787
11	19-20731	See UCRL-11684
12	19-20718	See BNL-8968
14	19-20732	See UCRL-11796
15	19-20735	See UCRL-11807
17	19-20094	See BNL-8969
18	19-20737	See UCRL-11955
20	19-20733	See UCRL-11799
21	19-20719	See BNL-8970
22	19-20204	See RPI-328-25
30	19-20728	See LA-DC-6875
31	19-20727	See LA-DC-6777
32	19-20726	See LA-DC-6775
33	19-20725	See LA-DC-6760
36	19-20724	See LA-DC-6759
CONF-650308–	**(The Calif. Circuits Assn. Symposium, Palo Alto, Calif., Mar. 25–26, 1965)**	
1	19-20520	See SC-DC-65-1256
CONF-650406–	**(Symposium on Neutron Dynamics and Control, Tucson, Ariz., Apr. 5–7, 1965)**	
2	19-21637	Dep.(mn); $2.00(cy), 1(mn) CFSTI
3	19-21634	See BNL-9010
4	19-21635	See BNL-9011
CONF-650501–	**(The Application of Computing Methods to Reactor Problems, Argonne, Ill., May 17–19, 1965)**	
4	19-21638	Dep.(mn); $1.00(cy), 1(mn) CFSTI
CONF-650507–	**(IAEA Symposium on Radioisotope Sample Measurement Techniques in Medicine and Biology, Vienna, May 24–28, 1965)**	
1	19-20324	See ORNL-P-1094
CONF-650508–	**(International Conference on Beryllium Metallurgy, Grenoble, France, May 20, 1965)**	
1	19-20564	See UCRL-12252
CONF-650509–	**(IAEA Symposium on Nondestructive Testing in Nuclear Technology, Bucharest, May 17–21, 1965)**	
1	19-20126	See DPSPU-65-30-11
COO–		
235-16	19-19464	Genetics, 51: 613-23(1965)
264-216	19-20951	Helv. Phys. Acta, 38: 65-72(1965)
281	19-20197	Dep.(mn); $3.00(cy), 2(mn) CFSTI
614-31	19-20439	Dep.(mn); $3.00(cy), 2(mn) CFSTI
881-46	19-20985	Phys. Letters, 15: 293-6(1965)
1198-254	19-20032	Phys. Letters, 15: 262-4(1965)
1198-255	19-21231	Dep.(mn); $1.00(cy), 1(mn) CFSTI
1365-2	19-19991	J. Chem. Phys., 42: 2255-8(1965)
1402-1	19-21680	Dep.(mn); $3.00(cy), 2(mn) CFSTI
1402-2	19-21681	Dep.(mn); $3.00(cy), 2(mn) CFSTI
D–	**(Misc.)**	
1-82-0398	19-21123	
2-11608	19-20873	$3.00(CFSTI)
DASA–	**(Misc.)**	
1309	19-20657	$6.00(CFSTI)
DCAS-TDR–	**(Non-AEC)**	
62-192	19-20455	$2.00(CFSTI)
DMIC-Memo–	**(Non-AEC)**	
198	19-20502	$1.00(cy), 1(mn) CFSTI as AD-610709
DP–		
933	19-19748	Dep.; $1.00(cy), 1(mn) CFSTI
942	19-21747	Dep.; $1.00(cy), 1(mn) CFSTI
DPSPU–		
63-30-40	19-21711	Dep.(mn); $1.00(cy), 1(mn) CFSTI
64-30-8B	19-21748	Dep.(mn); $1.00(cy), 1(mn) CFSTI
65-30-11	19-20126	Dep.(mn); $1.00(cy), 1(mn) CFSTI
DS–	**(Non-AEC)**	
63-R531-55	19-20279	See RTD-TDR-63-4001
DSR–	**(Non-AEC)**	
9365	19-20114	See NP-14920
DUBNA REPORTS	**(Russian)**	
See JINR (Russian)		
EAC–		
4	19-21490	See TID-21698
EFINS–	**(Misc.)**	
64-48	19-20951	See COO-264-216
EUR–	**(European Atomic Energy Community)**	
935.f	19-20334	Bull. Inform. Sci. Tech. (Paris), No. 81, 1-14(1964)
2111.d	19-20456	Dep.(mn)
2118.f	19-19749	Dep.(mn)
2119.e	19-20255	Dep.(mn)
2123.e	19-19875	Electrochim. Acta, 9: 1189-96(1964)
2134.f	19-19784	Bull. Soc. Chim. France, 1439-45(1964)

Report No.	Abstract No.	Availability
2176.f	19-21469	See CEA-R-2713
2202.e	19-21604	Dep.(mn)
2232.f	19-21730	See CEA-R-2557
2242.e	19-20503	Dep.(mn)
2245.e	19-20038	Dep.(mn)
2246.e	19-20039	Dep.(mn)
2251.i	19-20440	Dep.(mn)
2279.e	19-20469	Dep.(mn)
2286.f	19-19750	Dep.(mn)
EURAEC–		
327	19-20511	See NCSC-2981-1
334	19-20512	See NCSC-2981-2
669	19-20513	See NCSC-2981-3
868	19-20514	See NCSC-2981-5
981	19-20515	See NCSC-2981-6
1053	19-20510	See NCSC-2663-16
1054	19-20516	See NCSC-2981-7
1155	19-20517	See NCSC-2981-8
1228	19-20504	Dep.(mn); $1.00(cy), 1(mn) CFSTI
1282	19-20549	Dep.(mn); $1.00(cy), 1(mn) CFSTI
1307	19-21664	See CEND-3336-229
F–	**(Misc.)**	
B1979-1(App.B)	19-20636	See TID-21210
B2254	19-21681	See COO-1402-2
FTD-TT–	**(Non-AEC)**	
64-102	19-21492	$1.00(cy), 1(mn) CFSTI as AD-609153
FZK–	**(Non-AEC)**	
214	19-20398	CFSTI
GA–	**(Misc.)**	
5982	19-19751	
GAMD–	**(Misc.)**	
4732	19-21682	Dep.(mn); $2.00(cy), 1(mn) CFSTI
4814	19-20457	Dep.(mn); $2.00(cy), 1(mn) CFSTI
5001(Rev.2)	19-21609	Dep.(mn); $3.00(cy), 3(mn) CFSTI
5272(Rev.2)	19-21683	Dep.(mn); $2.00(cy), 1(mn) CFSTI
5432	19-20110	Dep.(mn); $1.00(cy), 1(mn) CFSTI
5535	19-21665	Dep.(mn); $3.00(cy), 2(mn) CFSTI
5926	19-20086	Dep.(mn); $1.00(cy), 1(mn) CFSTI
6109	19-21610	Dep.(mn); $3.00(cy), 2(mn) CFSTI
GAT-P–		
33	19-20087	Dep.(mn); $1.00(cy), 1(mn) CFSTI; Gmelin, AED-CONF-64-035-6
GE-TM–		
63-7-3	19-20470	Dep.(mn); $2.00(cy), 1(mn) CFSTI
GEAP–	**(Misc.)**	
3514	19-21716	Dep.(mn); $4.00(cy), 3(mn) CFSTI
4061	19-21684	Dep.(mn); $3.00(cy), 3(mn) CFSTI
4283	19-20458	Dep.; $4.00(cy), 2(mn) CFSTI
4640	19-21666	Dep.(mn); $3.00(cy), 2(mn) CFSTI
4776	19-21667	Dep.(mn); $2.00(cy), 1(mn) CFSTI
GLR–		
27	19-20116	See SAN-409-12
HASL–		
151	19-20256	Dep.; $2.00(cy), 1(mn) CFSTI
152	19-21685	Dep.; $2.00(cy), 1(mn) CFSTI
157	19-20198	Dep.; $2.00(cy), 1(mn) CFSTI
158	19-20154	Dep.; $4.00(cy), 9(mn) CFSTI
159	19-20155	Dep.; $4.00(cy), 4(mn) CFSTI
HI–	**(Non-AEC)**	
388-RR(Pt.III)	19-20199	
HW–		
61979	19-21712	Dep.(mn); $1.00(cy), 1(mn) CFSTI
74393	19-19834	Dep.(mn); $1.00(cy), 1(mn) CFSTI
81250A	19-20614	Dep.; $4.00(cy), 3(mn) CFSTI
82369	19-20317	Dep.(mn); $1.00(cy), 1(mn) CFSTI; Gmelin, AED-CONF-64-082-30
83092(Rev.)	19-21713	Dep.; $2.00(cy), 1(mn) CFSTI
83668	19-20200	Dep.; $2.00(cy), 1(mn) CFSTI
84085	19-20040	Dep.(mn); $3.00(cy), 2(mn) CFSTI
84196	19-21668	Dep.(mn); $1.00(cy), 1(mn) CFSTI
84352	19-20041	Dep.(mn); $1.00(cy), 1(mn) CFSTI
84540	19-21686	Dep.(mn); $1.00(cy), 1(mn) CFSTI
84549	19-21749	Dep.(mn); $1.00(cy), 1(mn) CFSTI
84550	19-20550	Dep.; $2.00(cy), 1(mn) CFSTI
89062	19-19835	Dep.(mn); $2.00(cy), 2(mn) CFSTI
HW-SA–		
3212	19-20615	$1.00(cy), 1(mn) CFSTI
3366	19-20364	Nucl. Instr. Methods, 34: 141-5(1965)
3476	19-19836	Dep.(mn); $1.00(cy), 1(mn) CFSTI; Gmelin, AED-CONF-64-112-5
3525	19-20201	Dep.(mn); $2.00(cy), 1(mn) CFSTI; Gmelin, AED-CONF-64-082-40
3526	19-20318	Dep.(mn); $1.00(cy), 1(mn) CFSTI; Gmelin, AED-CONF-64-082-34
3560	19-21605	Dep.(mn); $1.00(cy), 1(mn) CFSTI; Gmelin, AED-CONF-64-082-32
3628	19-20471	Dep.(mn); $1.00(cy), 1(mn) CFSTI; Gmelin, AED-CONF-64-219-16
HWS–		
7170	19-20521	See TID-20625(Vol.I(Rev.I))
I–	**(Misc.)**	
B2254-1	19-21680	See COO-1402-1
IA–	**(Non-AEC)**	
907	19-20020	Dep.(mn)
988	19-21639	Dep.(mn)
999	19-20404	Dep.(mn)
1000	19-19837	Dep.(mn)
IC–	**(Non-AEC)**	
65/2	19-21079	Dep.(mn)
65/3	19-20917	Dep.(mn)
65/4	19-20918	Dep.(mn)
65/5	19-20919	Dep.(mn)
65/6	19-20920	Dep.(mn)
65/7	19-20921	Dep.(mn)
65/8	19-20922	Dep.(mn)
65/9	19-21080	Dep.(mn)
65/18	19-20923	Dep.(mn)
65/26	19-21036	Phys. Rev. Letters, 14: 609-11(1965)
ICTP–	**(Italian)**	
64/2	19-20924	Dep.(mn)
64/3	19-20925	Dep.(mn)
64/4	19-20926	Dep.(mn)
64/7	19-20927	Dep.(mn)
64/9	19-21081	Dep.(mn)
64/10	19-20928	Dep.(mn)
64/12	19-20929	Dep.(mn)
IDO–		
14646	19-20042	Dep.; $2.00(cy), 1(mn) CFSTI
14651	19-20472	Dep.; $1.00(cy), 1(mn) CFSTI
16983	19-21640	Dep.; $3.00(cy), 2(mn) CFSTI
17011	19-20616	Dep.; $3.00(cy), 2(mn) CFSTI
17019	19-21717	Dep.; $4.00(cy), 3(mn) CFSTI
17059	19-20319	Dep.; $1.00(cy), 1(mn) CFSTI
17063	19-20551	Dep.; $2.00(cy), 1(mn) CFSTI
17071	19-21718	Dep.(mn); $2.00(cy), 1(mn) CFSTI
28637	19-21687	Dep.; $3.00(cy), 2(mn) CFSTI
IEA–	**(Brazilian)**	
77	19-20043	Dep.(mn)
IITRI–	**(Misc.)**	
B6019-6	19-20459	$2.00(cy), 1(mn) CFSTI as AD-611376
B6021-6	19-20552	$2.00(cy), 1(mn) CFSTI as AD-611822
N213-23	19-20127	
IPP–	**(Non-AEC)**	
1/14	19-21470	Dep.(mn)
1/19	19-20257	Dep.(mn)
1/24	19-21471	Dep.(mn)
1/25	19-21472	Dep.(mn)

Report No.	Abstract No.	Availability
1/28	19-21473	Dep.(mn)
6/10	19-21470	See IPP-1/14
IS–		
879	19-21083	Am. J. Phys., 33: 207-11(1965)
953	19-20292	J. Sci. Instr., 42: 136-9(1965)
968	19-21600	Dep.; $5.00(cy), 4(mn) CFSTI
989	19-20320	Dep.; $2.00(cy), 1(mn) CFSTI
1070	19-19838	Dep.; $3.00(cy), 2(mn) CFSTI
1098	19-20156	Dep.(mn); $2.00(cy), 1(mn) CFSTI
IS-T–		
1	19-20044	Dep.(mn); $4.00(cy), 3(mn) CFSTI
2	19-19752	Dep.(mn); $2.00(cy), 1(mn) CFSTI
3	19-19753	Dep.(mn); $3.00(cy), 1(mn) CFSTI
IS-Trans–		
13	19-20566	Dep.(mn); $1.10(fs), $0.80(mn) JCL
ISS–	(Italian)	
64/28	19-20321	Dep.(mn)
JAERI–	(Japanese)	
1067	19-21688	Dep.(mn)
1068	19-21689	Dep.(mn)
1070	19-20258	Dep.(mn)
1071	19-20505	Dep.(mn)
1074	19-20259	Dep.(mn)
JEN–	(Spanish)	
132-SIG/I-3	19-20185	Dep.(mn)
134-DQ/I-39	19-19754	Dep.(mn)
141-DF/I-45	19-21232	Dep.(mn)
JINR–	(Russian)	
D-1946	19-20722	Dep.(mn)
E-1975	19-20930	Dep.(mn)
E-1992	19-21233	Dep.(mn)
P-1908	19-21234	Dep.(mn)
P-1945	19-20723	Dep.(mn)
P-1948	19-20260	Dep.(mn)
P-1949	19-20261	Dep.(mn)
P-1950	19-21235	Dep.(mn)
P-1951	19-20931	Dep.(mn)
P-1952	19-21236	Dep.(mn)
P-1953	19-21161	Dep.(mn)
P-1958	19-20441	Dep.(mn)
P-1996	19-21641	Dep.(mn)
JPRS–	(Non-AEC)	
27940	19-19458	$2.00(CFSTI)
28835	19-21778	$1.00(CFSTI)
28977	19-19508	$1.00(CFSTI)
29037	19-21779	$4.00(CFSTI)
29200	19-21780	$4.00(CFSTI)
29250	19-19459	$2.00(CFSTI)
29258	19-20022	$1.00(CFSTI)
29364	19-19460	$1.00(CFSTI)
K–		
1627	19-19839	Dep.; $6.00(cy), 5(mn) CFSTI
KFK–	(German)	
242	19-21731	Dep.(mn)
252	19-19755	Dep.(mn)
259	19-20262	Dep.(mn)
262	19-20553	Dep.(mn)
264	19-21200	Dep.(mn)
265	19-21237	Dep.(mn)
KFK-tr–	(German)	
161	19-21271	Dep.(mn); $1.60(fs), $0.80(mf) JCL
164	19-21201	Dep.(mn); $1.60(fs), $0.80(mf) JCL
L–	(Misc.)	
0774-01-9(Vol.I)	19-20137	See NASA-CR-59332
LA–		
2838	19-20045	Dep.; $1.00(cy), 1(mn) CFSTI
3150	19-21750	Dep.; $1.00(cy), 1(mn) CFSTI
3161	19-20554	Dep.; $3.00(cy), 2(mn) CFSTI
3188	19-20046	Dep.; $1.00(cy), 1(mn) CFSTI
3189	19-21474	Dep.; $1.00(cy), 1(mn) CFSTI
3193	19-19756	Dep.; $1.00(cy), 1(mn) CFSTI
3204	19-19498	Dep.; $4.00(cy), 2(mn) CFSTI
3205	19-21238	Dep.; $1.00(cy), 1(mn) CFSTI
3206	19-21239	Dep.; $2.00(cy), 1(mn) CFSTI
3209	19-20506	Dep.; $1.00(cy), 1(mn) CFSTI
3213	19-19757	Dep.; $1.00(cy), 1(mn) CFSTI
3215	19-20555	Dep.; $2.00(cy), 1(mn) CFSTI
3225	19-19758	Dep.; $1.00(cy), 1(mn) CFSTI
3226	19-19759	Dep.; $2.00(cy), 1(mn) CFSTI
3244	19-21690	Dep.; $3.00(cy), 1(mn) CFSTI
3250	19-19840	Dep.; $2.00(cy), 1(mn) CFSTI
LA-DC–		
6232	19-21240	Dep.(mn); $3.00(cy), 2(mn) CFSTI
6383	19-21475	Dep.(mn); $2.00(cy), 1(mn) CFSTI
6397	19-20322	Dep.(mn); $1.00(cy), 1(mn) CFSTI
6492	19-21103	Phys. Rev., 138: B488-94(1965)
6496	19-20744	J. Nucl. Energy, Pt. C, 7: 133-40(1965)
6499	19-21179	Physica, 31: 89-93(1965)
6525	19-20739	Am. J. Phys., 33: 243-4(1965)
6533	19-20683	Phys. Fluids, 8: 693-8(1965)
6587	19-21214	Nucl. Sci. Eng., 22: 115-18(1965)
6591	19-20584	Intern. J. Powder Met., 1: No. 1, 42-50(1965)
6639	19-21241	Dep.(mn); $1.00(cy), 1(mn) CFSTI
6759	19-20724	Dep.(mn); $1.00(cy), 1(mn) CFSTI
6760	19-20725	Dep.(mn); $1.00(cy), 1(mn) CFSTI
6775	19-20726	Dep.(mn); $1.00(cy), 1(mn) CFSTI
6777	19-20727	Dep.(mn); $1.00(cy), 1(mn) CFSTI
6875	19-20728	Dep.(mn); $1.00(cy), 1(mn) CFSTI
6969	19-21035	Phys. Rev. Letters, 14: 607-9(1965)
LA-tr–		
65-5	19-20567	Dep.(mn); $1.00(cy), 1(mn) CFSTI; $1.10(fs), $0.80(mf) JCL
LF–		
21	19-19456	Dep.; $0.50(cy), 1(mn) CFSTI
LNF–	(Italian)	
64/60	19-20932	Dep.(mn)
MAB–	(Non-AEC)	
206-M	19-20507	
MATT–		
246	19-21534	Phys. Fluids, 8: 704-7(1965)
283	19-21476	Dep.(mn); $1.00(cy), 1(mn) CFSTI; Gmelin, AED-CONF-64-113-11
284	19-21541	Phys. Fluids, 8: 757-8(1965)
290	19-21477	Dep.(mn); $1.00(cy), 1(mn) CFSTI; Gmelin, AED-CONF-64-196-20
MIT–	(Misc.)	
905-21	19-21741	Nucl. Instr. Methods, 34: 57-60(1965)
905-24	19-21390	Phys. Rev., 138: B353-64(1965)
1965-18	19-19841	Dep.(mn); $1.00(cy), 1(mn) CFSTI
2098-111	19-21346	Phys. Letters, 14: 323-5(1965)
2098-114	19-21007	Phys. Rev. Letters, 14: 414-16(1965)
2098-115	19-21006	Phys. Rev. Letters, 14: 408-14(1965)
2098-121	19-21001	Phys. Rev. Letters, 14: 396-8(1965)
MLM–		
734	19-20047	Dep.(mn); $2.00(cy), 1(mn) CFSTI
1214	19-20429	Dep.; $1.00(cy), 1(mn) CFSTI
MMPP-FRPC–		
64-3	19-21642	Dep.(mn); $2.00(cy), 1(mn) CFSTI
MND–	(Misc.)	
3180-1	19-20405	Dep.(mn); $3.00(cy), 2(mn) CFSTI
MP–	(Misc.)	
1-677	19-20089	See NP-14887
MURA–	(Misc.)	
706	19-20729	Dep.; $2.00(cy), 1(mn) CFSTI

Report No.	Abstract No.	Availability
N–	**(Misc.)**	
64-33809	19-20137	See NASA-CR-59332
65-12017	19-20805	See NASA-CR-54223
NAA-SR–		
9335	19-20048	Dep.; $1.00(cy), 1(mn) CFSTI
9780	19-21719	Dep.; $3.00(cy), 2(mn) CFSTI
9826	19-21611	Dep.; $3.00(cy), 2(mn) CFSTI
10318	19-21720	Dep.; $2.25(cy), 2(mn) CFSTI
10379	19-21732	Dep.; $1.25(cy), 2(mn) CFSTI
NAA-SR-Memo–		
9492	19-21691	Dep.(mn); $3.00(cy), 2(mn) CFSTI
9729	19-20442	Dep.(mn); $1.00(cy), 1(mn) CFSTI
9761	19-20460	Dep.(mn); $1.00(cy), 1(mn) CFSTI
9976	19-21692	Dep.(mn); $3.00(cy), 3(mn) CFSTI
10160	19-21721	Dep.(mn); $1.00(cy), 1(mn) CFSTI
10224	19-20111	Dep.(mn); $2.00(cy), 1(mn) CFSTI
10315	19-20112	Dep.(mn); $2.00(cy), 1(mn) CFSTI
10532	19-21733	Dep.(mn); $1.00(cy), 1(mn) CFSTI
10557(Pt.I)	19-21612	Dep.(mn); $2.00(cy), 1(mn) CFSTI
10557(Pt.II)	19-21613	Dep.(mn); $3.00(cy), 2(mn) CFSTI
10559	19-21614	Dep.(mn); $1.00(cy), 1(mn) CFSTI
10625	19-20508	Dep.(mn); $1.00(cy), 1(mn) CFSTI
10633	19-20509	Dep.(mn); $1.00(cy), 1(mn) CFSTI
10666	19-21734	Dep.(mn); $2.00(cy), 1(mn) CFSTI
10729	19-20096	Dep.(mn); $1.00(cy), 1(mn) CFSTI
10767	19-21722	Dep.(mn); $1.00(cy), 1(mn) CFSTI
NASA-CR–	**(Misc.)**	
193	19-21723	$5.00(CFSTI)
54100	19-19751	See GA-5982
54223	19-20805	
54269	19-20473	
54281	19-20474	
54282	19-21615	$2.00(CFSTI)
59332	19-20137	$6.00(CFSTI)
NASA-SP–	**(Misc.)**	
3014	19-19842	$3.00(CFSTI)
5019	19-20097	$5.00(CFSTI)
NASA-TM–	**(Non-AEC)**	
X-1085	19-19760	$2.00(CFSTI)
NASA-TN–	**(Misc.)**	
D-2173	19-20138	$1.00(CFSTI)
D-2723	19-20556	$1.00(CFSTI)
D-2727	19-20617	$1.00(CFSTI)
NBS–	**(Misc.)**	
8514	19-20618	
NCSC–	**(Misc.)**	
2663-16	19-20510	Dep.(mn); $1.00(cy), 1(mn) CFSTI
2981-1	19-20511	Dep.(mn); $1.00(cy), 1(mn) CFSTI
2981-2	19-20512	Dep.(mn); $1.00(cy), 1(mn) CFSTI
2981-3	19-20513	Dep.(mn); $1.00(cy), 1(mn) CFSTI
2981-5	19-20514	Dep.(mn); $1.00(cy), 1(mn) CFSTI
2981-6	19-20515	Dep.(mn); $1.00(cy), 1(mn) CFSTI
2981-7	19-20516	Dep.(mn); $1.00(cy), 1(mn) CFSTI
2981-8	19-20517	Dep.(mn); $1.00(cy), 1(mn) CFSTI
NMI-TJ–	**(Misc.)**	
29	19-20518	
60	19-20557	Dep.(mn); $1.00(cy), 1(mn) CFSTI
NP–	**(AEC File No. for Non-AEC Reports)**	
14697	19-20157	Dep.(mn)
14712	19-20158	Dep.(mn)
14726	19-20159	Dep.(mn)
14728	19-20160	Dep.(mn)
14828	19-20933	Dep.(mn)
14829	19-20934	Dep.(mn)
14834	19-20049	
14837	19-21242	Dep.(mn)
14869	19-20161	Dep.(mn)
14876	19-19761	
14877	19-20172	
14879	19-20519	
14880	19-21478	$1.00(cy), 1(mn) CFSTI as AD-610756
14883	19-20619	
14885	19-20935	
14886	19-19457	
14887	19-20089	
14888	19-20558	
14892	19-20559	
14893	19-20461	
14895	19-20113	
14896	19-21693	Dep.(mn)
14899	19-19499	Dep.(mn)
14900	19-20021	Dep.(mn)
14907	19-19500	Dep.(mn)
14920	19-20114	
14928	19-20406	
14931	19-19501	Dep.(mn)
14932	19-19502	Dep.(mn)
14933	19-19503	Dep.(mn)
14946	19-20399	
14955	19-20400	
NP-tr–	**(AEC File No. for Non-AEC Translations)**	
1230	19-19850	Dep.(mn); $1.00(cy), 1(mn) CFSTI; $1.60(fs), $0.80(mf) JCL
NRC–	**(Canadian)**	
8269	19-20577	Can. J. Phys., 43: 438-49(1965)
NRL–	**(Misc.)**	
6258	19-20462	$2.25(CFSTI)
NYO–		
2024-8	19-20620	Dep.(mn); $2.00(cy), 1(mn) CFSTI
2728-4	19-21760	Dep.(mn); $4.00(cy), 2(mn) CFSTI
3246-4	19-20323	Dep.(mn); $3.00(cy), 2(mn) CFSTI
3276-9	19-20162	Dep.(mn); $1.00(cy), 1(mn) CFSTI
3399-15	19-20449	Phys. Rev. Letters, 14: 332-4(1965)
3399-23	19-21032	Phys. Rev. Letters, 14: 575-7(1965)
3402-1	19-21759	Dep.(mn); $1.00(cy), 1(mn) CFSTI
ORINS–		
50	19-19944	Dep.; $1.00(cy), 1(mn) CFSTI
ORNL–		
3506	19-21243	Dep.; $3.00(cy), 2(mn) CFSTI
3538	19-20475	Dep.(mn); $2.00(cy), 1(mn) CFSTI
3603	19-20476	Dep.(mn); $3.00(cy), 2(mn) CFSTI
3604	19-20477	Dep.(mn); $3.00(cy), 2(mn) CFSTI
3618	19-20478	Dep.(mn); $2.00(cy), 1(mn) CFSTI
3649(Vol.2) (Sect.2.1)	19-20263	Dep.; $3.00(cy), 2(mn) CFSTI
3649(Vol.2) (Sect.2.2)	19-20264	Dep.; $3.00(cy), 1(mn) CFSTI
3649(Vol.2) (Sect.2.3)	19-20265	Dep.; $3.00(cy), 1(mn) CFSTI
3649(Vol.2) (Sect.2.4)	19-20266	Dep.; $2.00(cy), 1(mn) CFSTI
3649(Vol.2) (Sect.2.5)	19-20267	Dep.; $2.00(cy), 1(mn) CFSTI
3649(Vol.2) (Sect.2.6)	19-20268	Dep.; $2.00(cy), 1(mn) CFSTI
3649(Vol.2) (Sect.2.7)	19-20269	Dep.; $3.00(cy), 2(mn) CFSTI
3649(Vol.2) (Sect.2.8)	19-20270	Dep.; $3.00(cy), 2(mn) CFSTI
3649(Vol.2) (Sect.2.9)	19-20271	Dep.; $3.00(cy), 2(mn) CFSTI
3649(Vol.2) (Sect.2.10)	19-20272	Dep.; $1.00(cy), 1(mn) CFSTI
3649(Vol.2) (Sect.2.11)	19-20273	Dep.; $1.00(cy), 1(mn) CFSTI
3649(Vol.2) (Sect.2.12)	19-20274	Dep.; $1.00(cy), 1(mn) CFSTI
3649(Vol.2) (Sect.2.13))	19-20275	Dep.; $1.00(cy), 1(mn) CFSTI
3649(Vol.2) (Sect.2.14)	19-20276	Dep.; $1.00(cy), 1(mn) CFSTI
3671	19-20479	Dep.(mn); $2.00(cy), 1(mn) CFSTI
3695	19-20050	Dep.; $3.00(cy), 2(mn) CFSTI
3702	19-20806	Dep.; $3.00(cy), 2(mn) CFSTI

Report No.	Abstract No.	Availability
3730	19-20480	Dep.(mn); $3.00(cy), 2(mn) CFSTI
3760	19-21479	Dep.; $4.00(CFSTI)
3773	19-20051	Dep.; $2.00(cy), 1(mn) CFSTI
3777	19-20560	Dep.; $2.00(cy), 1(mn) CFSTI
3787	19-20481	Dep.; $1.00(cy), 1(mn) CFSTI
ORNL-P-	**(Misc.)**	
307	19-20586	J. Am. Ceram. Soc., 48: 166-7(1965)
563	19-20489	J. Electrochem. Soc., 112: 388-90(1965)
663	19-20070	Nucl. Sci. Eng., 22: 14-19(1965)
700	19-21310	Nucl. Phys., 67: 249-56(1965)
725	19-19882	Inorg. Chem., 4: 597-9(1965)
731	19-21330	Nucl. Phys., 67: 433-42(1965)
844	19-21244	Dep.(mn); $1.00(cy), 1(mn) CFSTI
909	19-21388	Phys. Rev., 138: B346-9(1965)
957	19-20844	Phys. Rev. Letters, 14: 390-2(1965)
1064	19-21751	Dep.(mn); $2.00(cy), 1(mn) CFSTI
1065	19-20401	Dep.(mn); $1.00(cy), 1(mn) CFSTI
1068	19-20277	Dep.(mn); $1.00(cy), 1(mn) CFSTI
1069	19-20278	Dep.(mn); $2.00(cy), 1(mn) CFSTI
1092	19-21735	Dep.(mn); $2.00(cy), 1(mn) CFSTI
1093	19-20202	Dep.(mn); $2.00(cy), 1(mn) CFSTI
1094	19-20324	Dep.(mn); $1.00(cy), 1(mn) CFSTI
ORNL-TM-		
196	19-21245	Dep.(mn); $1.00(cy), 1(mn) CFSTI
431	19-20463	Dep.(mn); $3.00(cy), 2(mn) CFSTI
432	19-21707	Dep.(mn); $2.00(cy), 1(mn) CFSTI
465	19-21708	Dep.(mn); $2.00(cy), 1(mn) CFSTI
988	19-20203	Dep.(mn); $1.00(cy), 1(mn) CFSTI
1035	19-20052	Dep.(mn); $2.00(cy), 1(mn) CFSTI
1071	19-19843	Dep.(mn); $1.00(cy), 1(mn) CFSTI
1093	19-20115	Dep.(mn); $2.00(cy), 1(mn) CFSTI
ORNL-tr-		
295	19-20432	Dep.(mn); $3.60(fs), $1.16(mf) JCL
442	19-20101	Dep.(mn); $1.10(fs), $0.80(mf) JCL
490	19-21601	Dep.(mn); $1.00(cy), 1(mn) CFSTI; $1.60(fs), $0.80(mf) JCL
491	19-19851	Dep.(mn); $1.00(cy), 1(mn) CFSTI; $1.10(fs), $0.80(mf) JCL
539	19-21736	$3.60(fs), $1.16(mf) JCL
556	19-20023	Dep.(mn); $1.10(fs), $0.80(mf) JCL
ORO-		
626	19-20407	Dep.; $2.00(cy), 1(mn) CFSTI
P-	**(Misc.)**	
1020(RAND)	19-20874	$1.00(CFSTI)
1076(RAND)	19-21694	$1.00(CFSTI)
1113(RAND)	19-20660	$1.00(CFSTI)
1121(RAND)	19-21124	$2.00(CFSTI)
1134(RAND)	19-21761	$1.00(CFSTI)
1231(RAND)	19-20430	$2.00(CFSTI)
PAN-	**(Polish)**	
550/XVII	19-19844	Dep.
PATENTS	**(British)**	**(3s. 6d. each, U. K. Patent Office)**
975,366	19-20536	
975,468	19-20391	
975,554	19-20392	
975,555	19-20393	
975,599	19-21621	
975,648	19-21622	
975,718	19-21754	
975,742	19-21623	
975,908	19-21658	
975,911	19-20309	
975,929	19-21675	
975,934	19-20125	
975,956	19-20394	
976,045	19-20105	
976,367	19-21624	
976,467	19-21705	
976,501	19-20106	
PATENTS	**(Canadian)**	
679,254	19-20310	
698,484	19-21625	
701,033	19-20497	
701,192	19-21659	
PATENTS	**(Czechoslovakian)**	
109,734	19-21755	
PATENTS	**(German)**	
1,176,632	19-19942	
1,177,258	19-21626	
1,177,750	19-21627	
1,177,751	19-21628	
1,178,150	19-20244	
1,180,351	19-20537	
1,180,465	19-20395	
1,180,955	19-20609	
1,181,923	19-20498	
1,182,218	19-20538	
1,182,361	19-21744	
1,182,363	19-20539	
1,182,364	19-21629	
1,182,369	19-20751	
1,184,023	19-21592	
1,184,024	19-21660	
1,184,025	19-21661	
1,184,430	19-21662	
1,184,503	19-20084	
1,184,507	19-20610	
1,184,511	19-20611	
1,184,872	19-21745	
1,184,873	19-21657	
1,185,307	19-21746	
1,185,308	19-20540	
1,185,309	19-21630	
1,185,310	19-21631	
1,186,563	19-20396	
1,186,565	19-21632	
1,186,567	19-20752	
PATENTS	**(U. S.)**	**($0.25 each, U. S. Patent Office)**
3,154,473	19-21706	
3,154,474	19-21633	
3,154,684	19-20135	
3,154,685	19-20311	
3,154,686	19-20397	
3,154,703	19-20914	
3,169,117	19-21663	
3,171,788	19-21593	
3,173,284	19-21782	
3,173,880	19-21783	
3,174,153	19-21784	
3,175,131	19-20753	
3,175,955	19-21676	
3,176,154	19-21785	
PIBMRI-	**(Non-AEC)**	
1208-64	19-21488	$1.00(CFSTI)
PPA-		
2137-536	19-21229	See BNL-8841
PPAD-		
533E	19-20979	Phys. Letters, 15: 198-200(1965)
2137-538	19-20372	Nucl. Instr. Methods, 34: 175-6(1965)
PWAC-	**(Misc.)**	
380	19-20561	Dep.; $2.00(cy), 1(mn) CFSTI
R-	**(Misc.)**	
239	19-21478	See NP-14880
RAD-TR-	**(Non-AEC)**	
64-27	19-21125	$2.00(CFSTI)
RL-REA-		
592	19-21714	Dep.(mn); $1.00(cy), 1(mn) CFSTI
RLE-TR-	**(Non-AEC)**	
428	19-20661	$3.00(cy), 2(mn) CFSTI as AD-610583
RM-	**(Misc.)**	

Report No.	Abstract No.	Availability
2163(RAND)	19-21762	$4.00(CFSTI)
2801-PR	19-19504	$2.00(CFSTI)
RPI–	**(Misc.)**	
328-25	19-20204	Dep.(mn); $1.00(cy), 1(mn) CFSTI
2714-6	19-19762	Dep.(mn); $1.00(cy), 1(mn) CFSTI
RRA–	**(Misc.)**	
M42	19-20163	
RRL–		
129	19-19985	Intern. J. Appl. Radiation Isotopes, 15: 633-40(1964)
RTD-TDR–	**(Non-AEC)**	
63-4001	19-20279	$4.00(CFSTI)
SAN–		
409-12	19-20116	Dep.(mn); $5.00(cy), 3(mn) CFSTI
SC-DC–		
65-1256	19-20520	Dep.(mn); $1.00(cy), 1(mn) CFSTI
SC-DR–		
64-1741	19-21763	Dep.; $2.00(cy), 1(mn) CFSTI
64-2135	19-21764	Dep.(mn); $1.00(cy), 1(mn) CFSTI
65-74	19-21765	Dep.; $1.00(cy), 1(mn) CFSTI
SC-RR–		
65-41	19-20090	Dep.; $2.00(cy), 1(mn) CFSTI
65-54	19-20905	Dep.; $1.00(cy), 1(mn) CFSTI
SC-TM–		
64-921	19-21766	Dep.(mn); $1.00(cy), 1(mn) CFSTI
64-1722	19-20205	Dep.(mn); $1.00(CFSTI)
65-44	19-21767	Dep.(mn); $1.00(cy), 1(mn) CFSTI
65-48	19-21768	Dep.; $1.00(cy), 1(mn) CFSTI
SCL-DR–		
64-128	19-20280	Dep.(mn); $1.00(cy), 1(mn) CFSTI
SCNC–	**(Misc.)**	
314	19-20482	Dep.(mn); $2.00(cy), 1(mn) CFSTI
316	19-20464	Dep.(mn); $3.00(cy), 2(mn) CFSTI
318	19-20483	Dep.(mn); $2.00(cy), 1(mn) CFSTI
SLAC-PUB–		
64	19-20986	Phys. Rev., 138: B322-5(1965)
SM–	**(Misc.)**	
60/34	19-21224	See AECL-2160
60/50	19-21225	See AECL-2168
63/43	19-20126	See DPSPU-65-30-11
46334	19-21242	See NP-14837
STI-DOC–	**(International Atomic Energy Agency)**	
10/38	19-19933	Technical Reports Series No. 38, 1964. $2.50; S 52.50; 15/-stg; F.Fr.10,-; DM 8 (IAEA)
STI-PUB–	**(International Atomic Energy Agency)**	
82(Vol.II)	19-19709	$9.50; S 199,50; £2.17.0; F.Fr. 38,-; DM 33,25 (IAEA)
SU–		
247-4	19-20117	Dep.(mn); $6.00(cy), 5(mn) CFSTI
SU-DMS–	**(Non-AEC)**	
65-1	19-20562	
TEES–		
2671-4	19-19763	Dep.; (CFSTI)
TEI–		
859	19-20150	Dep.(mn); $1.00(cy), 1(mn) CFSTI
860	19-20151	Dep.(mn); $1.00(cy), 1(mn) CFSTI
TID–		
3086(Suppl.2)	19-20164	Dep.; $6.00(cy), 5(mn) CFSTI
3580	19-19505	Dep.; $3.00(cy), 2(mn) CFSTI
4005(Pt.5)	19-21489	Dep.; $3.00(cy), 2(mn) CFSTI
7022(Vol.I)(Bk.2)	19-19772	Dep.; $3.50(cy), 5(mn) CFSTI
7698(Pt.I)	19-20426	Dep.; $6.00(cy), 5(mn) CFSTI
18958	19-19610	p.377-87 of "Response of the Nervous System to Ionizing Radiation." Boston, Little, Brown and Co., Inc., 1964
19978(Vol.I)	19-20484	Dep.(mn); $1.00(cy), 1(mn) CFSTI
20261	19-20435	Chem. Rev., 64: 261-76(1964)
20344	19-20465	Dep.(mn); $2.00(cy), 1(mn) CFSTI
20467	19-19773	Dep.(mn); $1.00(cy), 1(mn) CFSTI
20558	19-20936	Dep.(mn); $2.00(cy), 1(mn) CFSTI
20625(Vol.I) (Rev.I)	19-20521	Dep.(mn); $6.00(cy), 5(mn) CFSTI
20625(Vol.II) (Rev.I)	19-20522	Dep.(mn); $6.00(cy), 5(mn) CFSTI
20625(Vol.III) (Rev.I)	19-20523	Dep.(mn); $6.00(cy), 5(mn) CFSTI
20625(Vol.IV) (Rev.I)	19-20524	Dep.(mn); $6.00(cy), 4(mn) CFSTI
20907	19-19881	Inorg. Chem., 4: 543-8(1965)
21162	19-19812	Talanta, 12: 181-5(1965)
21210	19-20636	Phil. Mag. (8), 11: 277-90(1965)
21361	19-20986	See SLAC-PUB-64
21633	19-20098	Dep.(mn); $1.00(cy), 1(mn) CFSTI
21644	19-20099	Dep.(mn); $1.00(cy), 1(mn) CFSTI
21661	19-21769	Dep.(mn); $4.00(cy), 3(mn) CFSTI
21668	19-20563	Dep.(mn); $1.00(cy), 1(mn) CFSTI
21672	19-20937	Dep.(mn); $1.00(cy), 1(mn) CFSTI
21677	19-21770	Dep.(mn); $1.00(cy), 1(mn) CFSTI
21684	19-21771	Dep.(mn); $4.00(cy), 3(mn) CFSTI
21697	19-21246	Dep.(mn); $1.00(cy), 1(mn) CFSTI
21698	19-21490	Dep.(mn); $1.00(cy), 1(mn) CFSTI
21703	19-19506	$1.00(cy), 1(mn) CFSTI
21709	19-21772	Dep.(mn); $1.00(cy), 1(mn) CFSTI
21711	19-20165	Dep.(mn); $1.00(cy), 1(mn) CFSTI
21712	19-19507	Dep.(mn); $2.00(cy), 1(mn) CFSTI
TIS–	**(Non-AEC)**	
23	19-20519	See NP-14879
TM–	**(Misc.)**	
63-9-5	19-20563	See TID-21668
TR–	**(Misc.)**	
1266	19-20619	See NP-14883
TT–	**(Canadian)**	
64-51982	19-19458	See JPRS-27940
65-30364	19-21778	See JPRS-28835
65-30432	19-19508	See JPRS-28977
65-30464	19-21779	See JPRS-29037
65-30547	19-21780	See JPRS-29200
65-30569	19-19459	See JPRS-29250
65-30572	19-20022	See JPRS-29258
65-30622	19-19460	See JPRS-29364
UACRL-C–	**(Non-AEC)**	
920243-6	19-20805	See NASA-CR-54223
UCRL–		
7962	19-19774	Dep.; $1.00(cy), 1(mn) CFSTI
11308	19-21773	Dep.(mn); $2.00(cy), 1(mn) CFSTI
11533(Rev.)	19-20572	Acta Met., 13: 379-85(1965)
11600	19-21384	Phys. Rev., 138: B316-21(1965)
11624	19-20325	Dep.(mn); $1.00(cy), 1(mn) CFSTI
11631	19-19992	J. Chem. Phys., 42: 2321-7(1965)
11633	19-21268	See UCRL-11828(p.129-31)
11684	19-20731	Dep.(mn); $1.00(cy), 1(mn) CFSTI
11705	19-21382	Phys. Rev., 138: B306-9(1965)
11727	19-21208	Nucl. Instr. Methods, 34: 66-8(1965)
11733	19-19990	J. Am. Chem. Soc., 87: 1391-2(1965)
11750	19-21383	Phys. Rev., 138: B310-15(1965)
11757	19-19734	Dep.(mn); $5.00(cy), 3(mn) CFSTI
11787	19-20326	Dep.(mn); $1.00(cy), 1(mn) CFSTI
11796	19-20732	Dep.(mn); $1.00(cy), 1(mn) CFSTI
11799	19-20733	Dep.(mn); $1.00(cy), 1(mn) CFSTI
11800	19-20734	Dep.(mn); $1.00(cy), 1(mn) CFSTI
11807	19-20735	Dep.(mn); $1.00(cy), 1(mn) CFSTI
11828	19-19735	Dep.; $6.00(cy), 5(mn) CFSTI
11858	19-21774	Dep.(mn); $1.00(cy), 1(mn) CFSTI

Report No.	Abstract No.	Availability
11864	19-19945	Dep.(mn); $4.00(cy), 3(mn) CFSTI
11898(Rev.)	19-21004	Phys. Rev. Letters, 14: 401-3(1965)
11932	19-21010	Phys. Rev. Letters, 14: 502-4(1965)
11934	19-21017	Phys. Rev. Letters, 14: 466-71(1965)
11938	19-21020	Phys. Rev. Letters, 14: 475-7(1965)
11940	19-21401	Phys. Rev. Letters, 14: 434-6(1965)
11950	19-19946	Dep.(mn); $1.00(cy), 1(mn) CFSTI
11955	19-20737	Dep.(mn); $1.00(cy), 1(mn) CFSTI
11983	19-20738	Dep.(mn); $1.00(cy), 1(mn) CFSTI
12005	19-21596	Dep.(mn); $5.00(cy), 3(mn) CFSTI
12054-T	19-20808	Dep.(mn); $1.00(cy), 1(mn) CFSTI
12057(Rev.I)	19-21491	Dep.; $1.00(cy), 1(mn) CFSTI
12113	19-21209	Nucl. Instr. Methods, 34: 137-40(1965)
12169	19-19776	Dep.; $1.00(cy), 1(mn) CFSTI
12203	19-20100	Dep.; $1.00(cy), 1(mn) CFSTI
12218	19-20809	Dep.; $2.00(cy), 1(mn) CFSTI
12252	19-20564	Dep.(mn); $1.00(cy), 1(mn) CFSTI
12256	19-20443	Dep.(mn); $3.00(cy), 2(mn) CFSTI
12293-T	19-20444	Dep.(mn); $1.00(cy), 1(mn) CFSTI
12307	19-21775	Dep.; $1.00(cy), 1(mn) CFSTI
12389	19-21776	Dep.; $1.00(cy), 1(mn) CFSTI
UJV–	**(Czechoslovakian)**	
1202/64	19-20053	
UR–		
661	19-19473	Dep.; $1.00(cy), 1(mn) CFSTI
662	19-21777	Dep.; $2.00(cy), 1(mn) CFSTI
875-30	19-20939	Dep.(mn); $2.00(cy), 1(mn) CFSTI
875-70	19-21016	Phys. Rev. Letters, 14: 462-6(1965)
875-72	19-20940	Dep.(mn); $1.00(cy), 1(mn) CFSTI
USNRDL-TR–	**(Misc.)**	
797	19-20207	
806	19-20329	
819	19-19777	Dep.(mn); $1.00(cy), 1(mn) CFSTI
VDDIT–	**(Swedish)**	
93	19-19960	Dep.(mn)
VESIAC–	**(Non-AEC)**	
4410-83-X	19-20173	
WADD-TR–	**(Non-AEC)**	
60-37(Pt.V)	19-20565	CFSTI
WAPD-T–		
1728	19-21643	Dep.(mn); $1.00(cy), 1(mn) CFSTI
1748	19-21336	Nucl. Sci. Eng., 22: 121-4(1965)
1760	19-19849	Dep.(mn); $1.00(cy), 1(mn) CFSTI
WAPD-TM–	**(Misc.)**	
478	19-21644	Dep.(mn); $4.00(cy), 3(mn) CFSTI
WCAP–	**(Misc.)**	
3269-9	19-21606	Dep.(mn); $3.00(cy), 2(mn) CFSTI
WL-TR–	**(Non-AEC)**	
64-149	19-20398	See FZK-214
Y-KB–		
32	19-20340	Health Phys., 11: 255-60(1965)

DEPOSITORIES OF USAEC REPORTS

In Countries Other than the U.S.

ARGENTINA
Buenos Aires, Comisión Nacional de Energía Atómica
AUSTRALIA
Canberra, Australian National Library
Sutherland, New South Wales, Australian Atomic Energy Commission
AUSTRIA
Vienna, Zentral Bibliothek der Physikalischen Institute der Universität
BELGIUM
Mol-Donk, Centre d'Etude de l'Energie Nucleaire
BOLIVIA
La Paz, Comisión Nacional de Energiá Nuclear
BRAZIL
Rio de Janeiro, Instituto Brasileiro de Bibliografia e Documentacao
São Paulo, Instituto de Energia Atomica, Cidade Universitaria São Paulo
BURMA
Rangoon, Union of Burma Applied Research Institute, Atomic Energy Center Library
CANADA
Hamilton, McMaster University
Ottawa, National Research Council Library
Vancouver, University of British Columbia
CEYLON
Colombo, University of Ceylon
CHILE
Santiago, Instituto de Fisica y Matematicas, Universidad de Chile
CHINA
Hsinchu, Taiwan, Free China, National Tsing Hua University
COLOMBIA
Bogota, Instituto De Asuntos Nucleares
COSTA RICA
San Pedro, University of Costa Rica Library
DENMARK
Risö, Danish Atomic Energy Commission
ECUADOR
Quito, Escuela Politécnica Nacional
EL SALVADOR
San Salvador, Universidad de El Salvador, Biblioteca de Energia Nuclear
FINLAND
Helsinki, Teknillisen Korkeakoulun Kirjasto
FRANCE
Gif-sur-Yvette, Centre d'Etudes Nucléaires de Saclay
Paris, Académie des Sciences
GERMANY
Berlin, Hahn-Meitner-Institut für Kernforschung Berlin
Frankfurt/Main, Gmelin-Institut
Munich, Technische Hochschule, Bibliothek
GHANA
Accra, University College of Ghana
GREECE
Athens, Nuclear Research Center "Democritus"
GUATEMALA
Guatemala, Comisión Nacional de Energía Nuclear
HAITI
Port au Prince, University of Haiti
ICELAND
Reykjavik, University of Iceland, Atomic Energy Library
INDIA
Bombay, Department of Atomic Energy
INDONESIA
Bandung, Java, Bandung Institute of Technology
Djogjakarta, Java, Science Faculty, Gadjah Mada University
IRAN
Tehran, Tehran University Nuclear Centre
IRAQ
Baghdad, Iraqi Atomic Energy Commission
IRELAND
Dublin, University College
ISRAEL
Rehovoth, Israel Atomic Energy Commission
ITALY
Rome, Centro di Studi Nucleari della Casaccia
Rome, Comitato Nazionale per l'Energia Nucleare
JAPAN
Tokyo, National Diet Library
KOREA
Seoul, Office of Atomic Energy
LEBANON
Beirut, Lebanese National Council for Scientific Research
LUXEMBOURG
Luxembourg, Ministry of Transport and Electricity
MALAYSIA
Kuala Lumpur, University of Malaysia
MEXICO
Mexico, D.F., Comisión Nacional de Energía Nuclear
NETHERLANDS
The Hague, Reactor Centrum Nederland
NEW ZEALAND
Wellington, Department of Scientific and Industrial Research
NIGERIA
Ibadan, University of Ibadan
NORWAY
Lillestrøm, Institutt för Atomenergi
PAKISTAN
Lahore, West Pakistan, Atomic Energy Centre
PERU
Lima, Junta de Control de Energia Atomica
PHILIPPINE REPUBLIC
Manila, Philippine Atomic Energy Commission
POLAND
Warsaw, Biura Pelnomocnika Rzadu do Spraw Wykorzystania Energii Jadrowej
PORTUGAL
Sacavem, Junta de Energía Nuclear
REPUBLIC OF SOUTH AFRICA
Pretoria, Atomic Energy Board Library
REPUBLIC OF THE CONGO
Leopoldville, Université Lovanium
SPAIN
Madrid, Junta de Energía Nuclear, Biblioteca Documentación y Publicaciones, Ciudad Universitaria
SWEDEN
Nyköping, Aktiebolaget Atomenergi
SWITZERLAND
Zürich, Eidgenössische Technische Hochschule, Bibliothek
THAILAND
Bangkok, Office of the Thai Atomic Energy Commission, Department of Science
TURKEY
Ankara, Turkish Atomic Energy Commission, Atomic Energy Library
UNITED ARAB REPUBLIC
Cairo, Atomic Energy Commission
UNITED KINGDOM
Belfast, City Library
Birmingham, Central Library
Boston Spa, National Lending Library for Science and Technology
Bristol, Central Library
Glasgow, Mitchell Library
Kingston upon Hull, Central Library
Leeds, Central Library
Liverpool, Central Library
London, Central Library, Acton
London, Science Museum Library, South Kensington
Manchester, Central Library
Newcastle upon Tyne, Central Library
Nottingham, Central Library
Sheffield, Central Library
URUGUAY
Montevideo, Comision Nacional de Energia Atomica
VENEZUELA
Caracas, Instituto Venezolano de Investigaciones Científicas
VIET-NAM
Saigon, Atomic Energy Office
YUGOSLAVIA
Belgrade, Federal Commission for Nuclear Energy

In International Agencies

AUSTRIA
Vienna, International Atomic Energy Agency
BELGIUM
Brussels, La Bibliotheque EURATOM
FRANCE
Paris, European Nuclear Energy Agency, O.E.C.D.
ITALY
Ispra, EURATOM Research Center
SWITZERLAND
Geneva, United Nations Library

UNITED STATES
GOVERNMENT PRINTING OFFICE
DIVISION OF PUBLIC DOCUMENTS
WASHINGTON, D.C. 20402

OFFICIAL BUSINESS

POSTAGE AND FEES PAID
U.S. GOVERNMENT PRINTING OFFICE

MIAMI UNIVERSITY LIBRARY